ACTA CHEMICA SCANDINAVICA 11 (1957) 1—4

A Chemical Method for the Quantitative Determination of Male Sperm Antagglutin

P. E. LINDAHL, J.-E. KIHLSTRÖM and S. ROSS

Institute of Zoophysiology, Uppsala, Sweden

A chemical method for the quantitative determination of male sperm antagglutin has been worked out, allowing determinations in the range of 0.5 to 3.5 μg antagglutin.

Since it had been understood that the agglutination of spermatozoa in mammals is prevented by certain substances, named sperm antagglutins, and produced in the male and female genitalia [1–5], the quantitative determination of these substances has been of great interest. For the male antagglutin a biological test method was elaborated [2], giving within certain limits and under favourable conditions certain rough quantitative values. Some variable and unknown factor, located probably in the spermatozoa used as test objects, limits, however, this method to be as yet a mere qualitative one. Still, it has the great advantage of permitting tests on very small samples (about 0.1 ml of normal sperm plasm), and making possible a differentiation between antagglutin in the reduced, biologically active and the oxidized, biologically inactive state. Because of the above mentioned disadvantages we have tried to develop a method, based only on chemical reactions and physical measurements, and rendering possible the determination of 2.0 μg of antagglutin with a reasonable error. Such a method would *e. g.*, allow a study of the physiological variation of the antagglutin content in sperm plasm, using only 0.1 ml samples.

The male sperm antagglutin is a complex, made up by protein, sugar, sulphuric acid residues, and a carbocyclic substance. After attempts to use colour reactions on protein or sugar for the quantitative determination of antagglutin in spots obtained by chromatography on different kinds of threads we intended to convert the antagglutin into a compound with a sufficiently high molar extinction to allow spectrophotometric determinations. It was found that heating of the antagglutin to 220°C with potassium bisulphate (melting point 210°C) results in the formation of a compound which is soluble in ethanol but not in ethyl ether, and which by oxidation with manganese dioxide is transformed into a substance with a high molar extinction in ultra-

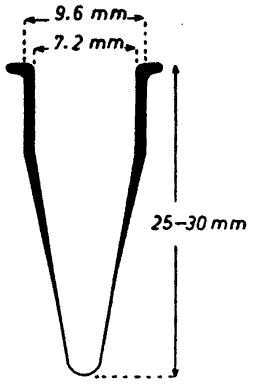


Fig. 1. Micro reaction tube. Note thickening of the edge supporting the tube in the centrifuge.

violet. The solubility of the intermediary product in ethanol but not in ethyl ether makes possible the removal of ether-soluble breakdown products which otherwise disturb the spectrophotometric determination. The extinction maximum disappears at further oxidation, *i. e.* aeration or prolonged standing in contact with air. This process, being slower in ethanol than in water, is, however, retarded by manganese ions. As the extinction of the end-product is much higher in water than in ethanol solution, the former solvent is preferred for the determination of the absorption.

Procedure. Of the sample to be analyzed * 0.1 ml is put into a pointed micro reaction tube (Fig. 1) of pyrex fitting into the micro-comb centrifuge (Laboratoriemaskiner Ltd, Stockholm). By addition of 0.03 ml saturated solution of potassium sulphate the antagglutin is precipitated, and spun down at 7 000 *g* for 5 min. The precipitate is dissolved in 0.1 ml distilled water, and the salting out repeated. The supernatant is removed, and the precipitate dissolved in 0.2 ml distilled water, occupying about two thirds of the height of the conical part of the tube. The water is evaporated at 40°C under vacuum whereby the antagglutin is deposited as a very thin film at the wall of the tube. The latter is then filled up with dry, powdered potassium bisulphate ** till slightly above the edge of the film, the powder pressed down tightly with a small glass pestle, and the filling completed if necessary. The reaction tube is then placed in a big test-tube (18 cm length) with a layer of glass beads at the bottom to keep the reaction tube upright, and the test tube immersed for one hour in an oil-bath of 220°C. Under these conditions the potassium bisulphate melts within 5 min.

After the reaction tube has cooled down it is taken out of the test-tube, its outside is cleaned with ethyl ether, and the tube with its hard content powdered in a mortar. The whole material is transferred to a centrifuge tube with a ground stopper, the mortar being washed out with 3 ml absolute ethanol ("Spectroscopically pure", Vin- och Sprit-centralen Ltd) which is then used for extraction of the salt powder. About 5 mg of manganese dioxide is added, and the closed centrifuge tube shaken vigorously lengthwise for 12 h. The solids are then brought down by centrifugation, and the supernatant poured into a 10 ml flask. The solids in the centrifuge tube are washed out with another half ml ethanol, which is added to the extract in the flask. From this the ethanol is driven off

* If the sample is semen the biologically active part of the antagglutin sticking to the surface of the spermatozoa (*cf.* Ref. [2]) is released by oxidation with 0.01 ml $8 \cdot 10^{-2}$ M hydrogen peroxide per 0.1 ml of semen, and the spermatozoa spun down.

** As commercial preparations of this salt often contain a surplus of sulphuric acid which is deleterious to the method, it is recommended to extract the potassium bisulphate for 12 h in a Soxhlet apparatus with dry freshly distilled ethyl ether.

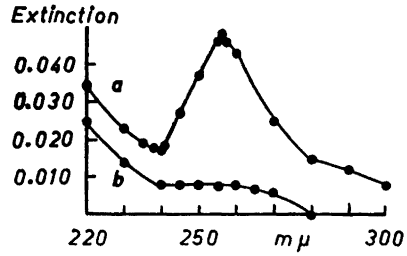


Fig. 2. Absorption curves: analytical procedure applied to *a* antagglutin containing sample, *b* to equal quantity distilled water.

under vacuum at 50°C. As soon as the liquid has disappeared 3 ml freshly distilled dry ethyl ether are poured into the flask which is then shaken for a moment, and left for 5—10 min. The ether is drawn off, and the rest of it quickly evaporated. The remainder in the flask is dissolved in 3.0 ml redistilled water. The UV-absorption of this extract should be read within one h with distilled water as a blank. This determination was carried out by means of a Beckman spectrophotometer, Model DU.

The absorption maximum of the product, obtained with the described procedure is at 256—257, the minimum at 240—242 mμ (Fig. 2a). A blank treated in the same way gives the extinction curve b (Fig. 2). Here the extinction values at 240—242 and 256—257 mμ do not differ significantly. The difference between the extinction maximum and minimum is 0.012 per μg bull antagglutin in the range 0.5 — 3.5 μg (Fig. 3). Above 3.5 μg this difference is not proportional to the amount of antagglutin treated, the straight line in Fig. 3 becoming parallel to the abscissa.

The standard deviation (s) calculated from 20 duplicate determinations on bull semen in the range 0.5 to 3.5 μg (*cf.* Hald [6], p. 244) is 0.103. The duplicate determinations with values below 1.0 μg give a somewhat higher standard deviation than those with values above 1.0 μg (*cf.* below).

Range μg antagglutin	Number of determinations	s
0.5—1.0	8	0.111
1.1—3.4	12	0.097

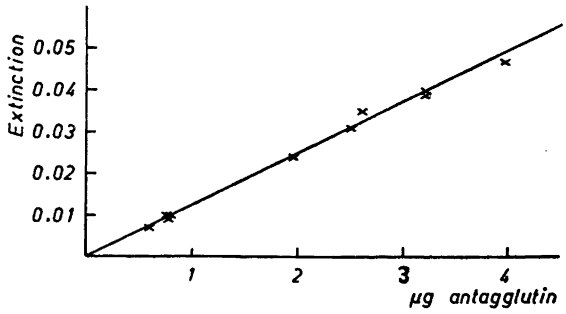


Fig. 3. Differences between extinction maximum at 256—257 mμ and extinction minimum at 240—242 mμ plotted against quantities of antagglutin.

It is essential that no other substances occurring in the sperm plasm give rise to an extinction maximum at 256—257 mμ when treated in the same way. This was controlled by performing the procedure of analysis on samples of sperm plasm from which the antagglutin had been removed by salting out. Further different appropriate quantities of antagglutin were added to equal samples of a sperm plasm with its original antagglutin, and the total antagglutin content analysed. The values obtained fell all on a straight line parallel with that in Fig. 3.

The reactions upon which the described method is based are being studied.

The financial support of the *Swedish Agricultural* and *Natural Science Research Councils*, the *Population Council*, Inc., New York, and *Pharmacia, Ltd.*, Uppsala, is gratefully acknowledged. We thank Mr. O. Heidenberger for valuable technical assistance.

REFERENCES

1. Lindahl, P. E. and Kihlström, J.-E. *Rep. 2nd Internal. Congr. Physiol. Pathol. Animal. Repr.* Copenhagen **1** (1952) 70.
2. Lindahl, P. E. and Kihlström, J.-E. *Fertility and Sterility* **5** (1954) 241.
3. Lindahl, P. E. and Kihlström, J.-E. *Nature* **174** (1954) 600.
4. Lindahl, P. E. and Nilsson, A. *Arkiv Zool. Ser. 2* **7** (1954) 223.
5. Lindahl, P. E., Ingelman-Sundberg, A., Furuhjelm, M. and Nilsson, A. *J. Obstet. Gynaecol. Brit. Empire* **63** (1956) 363.
6. Hald, A. *Statistiske Metoder*, Copenhagen, 1948.

Received September 13, 1956.

ACTA CHEMICA SCANDINAVICA 11 (1957) 5—10

On the Isomerism of Hydroxyurea

VIII. A Polarographic Study of the Formation Process in Aqueous Solution

HELMER KOFOD

Royal Danish School of Pharmacy, Dept. of Organic Chem. Copenhagen, Denmark

The formation of the isomeride, melting at 72°C, from hydroxylammonium chloride and potassium cyanate in aqueous solution, has been followed at 25°C and at 0°C by a polarographic method. The maximum wave height obtained corresponded to a mole fraction of approximately 0.6, not varying markedly with temperature. The rest of the stoichiometric yield — 0.4 in mole fraction — probably consists of the polarographically inactive higher melting isomeride. It is proposed that the isomerides are formed by a mechanism of concurrent reactions rather than by one of consecutive reactions.

In aqueous solution, buffered at pH 9.2, no formation of the lower melting isomeride was detectable. The preliminary results, reported in this paper, may be of interest in connection with the controversial views on the mechanism of the classical urea synthesis.

In the first paper in this series [1] the ionic reaction

$$HONH_3^+ + Cl^- + K^+ + {}^-OCN = \underset{\text{hydroxyurea isomerides}}{CH_4O_2N_2} + K^+ + Cl^- \qquad (1)$$

was subjected to a preliminary kinetic investigation at 0°C. The advancement of the reaction was followed conductometrically. The data indicated a bimolecular, second order process with a rate constant approximately 8 l mole^{-1} min^{-1}. The ultimate conductivity value, arrived at after 20 h, could be accounted for by the potassium ions alone, from which it may be inferred that the hydroxylammonium ion and the cyanate ion react practically completely to yield products, which are only slightly, if at all, ionized. This method obviously could provide no information on the relative amounts of hydroxyurea isomerides formed.

In a previous publication [2] it was shown that the lower melting hydroxyurea (72°C), which in the following will be denoted OU_{72}, is reduced at the dropping mercury electrode, whereas the higher melting one, OU_{140}, is not.

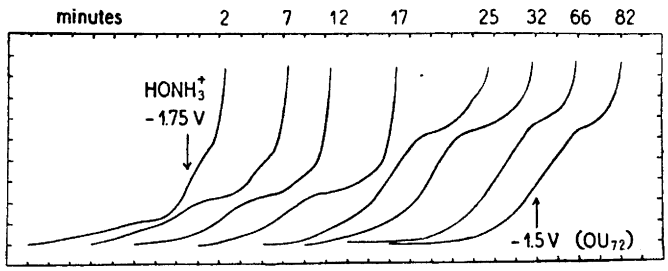


Fig. 1. Formation of hydroxyurea OU_{72} (reaction 1) at 25°C in aqueous solution. Initial concentration of reactants c_0 = 4.0 mM. Dilutions 1:10 with buffer at pH 9.2, polarographed at 25.0°C. Drop time 3.3 sec., height of mercury column 45 cm, rate of mercury outflow 2.66 mg/sec. One unit on the abscissa corresponds to 0.1 volt; the first four curves begin at −1.0 volt *vs.* SCE ("saturated calomel electrode"), one unit on the ordinate corresponds to 0.66 μA. The last four curves begin at −0.8 V *vs.* SCE and were recorded with a sensitivity, increased by a factor 2; one unit on the ordinate corresponds to 0.33 μA.

The polarographic method was worked out in detail for determination of OU_{72} in the presence of OU_{140}.

The present paper is devoted to a further investigation into reaction (1) by following the formation of OU_{72} polarographically.

As a supporting electrolyte potassium borate buffer at pH 9.2 was selected. In a more acid solution the hydroxylammonium wave would interfere severely, and in a more basic solution OU_{72} becomes increasingly unstable [2, Fig. 1].

THE FORMATION OF OU_{72} AT 25°C IN DILUTE AQUEOUS SOLUTION.

A 5 mM aqueous solution of hydroxylammonium chloride and a 20 mM aqueous solution of potassium cyanate, both freshly prepared, were separately equilibrated in a water-thermostat at 25.00±0.02 °C, dissolved oxygen being at the same time removed by passing a stream of moist, oxygen-free nitrogen through the solutions for five minutes. 40.00 ml of the hydroxylammonium solution and 10 ml of the cyanate solution were then rapidly mixed in a flask, which was kept in the thermostat during the reaction. The initial concentration of the reactants was thus 4 mM. 0.5 ml samples were withdrawn at intervals with a pipette, quickly mixed with 4.5 ml of previously deaerated buffer, and polarographed at 25.00°C. The recorded series of current-voltage curves is reproduced in Fig. 1. They clearly show the gradually vanishing hydroxylammonium wave at approximately —1.75 V and the growing hydroxyurea wave at about —1.5 V. The cyanate ion is polarographically inactive in this voltage region. The number appearing above each curve indicates the time in min from the mixing of the reactants and until the recording of the respective polarogram was begun. The wave height, produced by hydroxyurea has previously been demonstrated to be directly proportional to the concentration [2, Fig. 4]. The relation $i = 8.0\ c$ (i being the wave height in μA and c the concentration in mM) was found to apply also at pH 9.2, other conditions being identical. The observed maximum wave height of hydroxyurea OU_{72} is about

1.8 μA, and it corresponds to a concentration of 0.22 mM in the analytical dilution or 2.2 mM in the original reaction mixture. This is slightly more than half the total value, 4.0 mM, expected from stoichiometry, if OU_{72} were the only product. It corresponds to a mole fraction of OU_{72} of *ca.* 0.6; while a mole fraction of *ca.* 0.4 of the polarographically inactive OU_{140} has probably been formed simultaneously.

THE FORMATION OF OU_{72} AT 0°C IN DILUTE AQUEOUS SOLUTION

It was desirable to repeat the above experiment at 0°C. This is the most favourable reaction temperature for preparative work[3], and the data would be directly comparable with the conductometric data, reported earlier for the overall reaction [1], and finally, at the low temperature the slowed-down reaction would be better fit for the polarographic method of analysis.

A rapid withdrawal of well-defined sample-volumes from a reaction mixture at 0°C, followed by dilution and measurement at the standard temperature, 25°C, presented certain experimental difficulties, particularly with the available slow method of analysis. To overcome these obstacles it was first decided to carry out the reaction in the polarographic cell itself, properly thermostated at 0°C, and to work out a concentration-wave-height curve for this particular temperature. Since a pH of about 9.2 is the only region, in which the hydroxylammonium wave and the hydroxyurea wave may be independently and reproducibly measured [2, Fig. 3], the reaction had to be carried out in a buffer having this pH.

Introductory experiments of this kind showed, however, that at pH 9.2 and 0°C the reaction (1) is too slow for practical work. With an initial concentration of 10 mM of the reactants no hydroxyurea-wave was observable and no decrease in the height of the hydroxylammonium-wave was perceptible within 2 h. In unbuffered aqueous solution under otherwise identical conditions this space of time would correspond to more than 90 % reaction, as calculated [1] from $8\ t = \frac{1}{c} - \frac{1}{0.01}$. The temperature of the reaction mixture was raised to 25°C and polarographic measurements were carried out for another hour, still without detection of any hydroxyurea wave.

The failure of reaction (1) in the basic buffer unexpectedly solved the experimental difficulties, met with in the study of the reaction at low temperature, since it provided a convenient means of quenching the reaction in withdrawn samples for subsequent polarographic analysis at the standard temperature, 25°C. It was, therefore, decided to reproduce the experimental technique applied in the first experiment, except that the reaction was carried out at 0°C.

100 ml of an 8.0 mM aqueous solution of hydroxylammonium chloride and 100 ml of an 8.0 mM aqueous solution of potassium cyanate were freshly prepared and cooled separately to 0°C in an ice-water bath. During the temperature equilibration dissolved oxygen was removed in the way previously described. The cyanate solution was poured into the flask containing the hydroxylamine solution, and rapid mixing ensured ($t = 0$). The reaction mixture was maintained at 0°C during the experiment. From time to time 0.5 ml

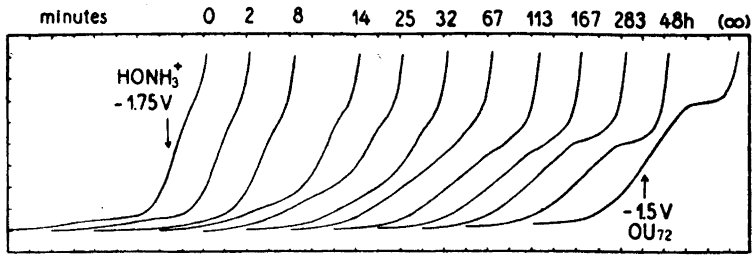


Fig. 2. Formation of hydroxyurea OU_{72} (reaction 1) at 0°C in aqueous solution. Initial concentration of reactants c_0 = 4.0 mM. Dilutions 1:10 with buffer of pH 9.2 polarographed at 25.0°C. Drop time 3.0 sec., height of mercury column 24 cm, rate of mercury outflow 3.02 mg/sec. One unit on the abscissa corresponds to 0.1 V. All curves begin at −1.0 volt *vs.* SCE. One unit on the ordinate represents 0.66 μA.

The first current-voltage curve, marked "0" was obtained with a 4.0 mM aqueous solution of hydroxylammonium chloride, without the addition of cyanate. The last curve ("∞") was obtained with a 4.0 mM aqueous solution of isolated hydroxyurea OU_{72}.

samples were withdrawn with a fast-draining pipette, quickly mixed with 4.5 ml of potassium borate buffer, pH 9.2, previously deaerated and equilibrated at 25.0°C in the polarographic cell. The analytical dilution was further deaerated, and proper mixing and temperature equilibration was ensured by passing a stream of nitrogen through the cell for another minute. The dilutions were then polarographed as previously described in detail [2].

The current-voltage curves are reproduced in Fig. 2. They present the same general picture as Fig. 1, deviating only in the reaction velocity. The initial concentration of the reactants is c_0 = 4.0 mM (0.4 mM in the dilutions). For comparison a 4.0 mM aqueous solution of hydroxylammonium chloride, denoted 0, has been recorded first in the same dilution 1:10. The hydroxylamine wave at −1.75 V is seen to decrease in height as the reaction proceeds, being replaced by a hydroxyurea wave at −1.5 V. The time for the maximum wave-height attained (curve "48 h") corresponds to almost 99 % reaction, as calculated from the conductometric rate constant k = 8 l · mole^{-1}min^{-1}, *vide* Ref. [1]. For comparison a 4.0 mM aqueous solution of authentic OU_{72} has been recorded (last curve in Fig. 2) under identical conditions (dilution 1:10). This curve represents the stoichiometric wave-height for 100 % reaction, if the lower melting hydroxyurea OU_{72} were the only product. We thus arrive at the same conclusion as from the experiment performed at 25°C, *i.e.* that somewhat more than half the reaction product is OU_{72}, mole fraction *ca.* 0.6, the rest being probably the polarographically inactive OU_{140}, in other words the ratio OU_{72}/OU_{140} is well over one. This agreement was to be expected. If follows from simple kinetic arguments that the ratio of isomeric products formed in a process should not vary markedly with temperature, provided the same reaction mechanism applies.

DISCUSSION

The above experimental material is not of sufficient accuracy to justify a detailed kinetic treatment. The individual wave heights, particularly those recorded for degrees of advancements round 50 %, can only be roughly estimated. In the experiment (Fig. 2) there has inevitably been a short rise of temperature during the transfer of samples to the arresting buffer solution. This error grows smaller as the reaction proceeds and becomes insignificant in the last curves. Frequent re-recording showed that the error due to undesired further reaction in the polarographic cell, during the recording of a curve (about 2 min), was negligible. The withdrawal of 0.5 ml samples was made with a fast-draining pipette, which was calibrated at 20°C as usual, and obviously no temperature equilibration could be permitted. The volume mixed with 4.5 ml buffer (measured out at 20°C), therefore, corresponded to slightly more than 0.5 ml at the standard temperature of measurement. Since, however, the same procedure was strictly adhered to, also in preparing the dilutions, recorded in curve 0 and ∞, this error does not invalidate the qualitative conclusions drawn in the following.

The actual mechanism of reaction (1) will be considered in a forthcoming publication, but it may be briefly mentioned here that *a priori* there seems to exist two possibilities, either a mechanism of concurrent reactions (Fig. 3 a) or one of consecutive reactions (Fig. 3b). In the figures 1 denotes the starting materials in reaction (1), 2 and 3 the isomeric hydroxyureas. According to the mechanism depicted in Fig. 3a the isomerides are formed simultaneously and side by side, whereas in Fig. 3b OU_{72} is the primary product, which is then partly isomerized to OU_{140}. Preliminary experiments [2, Fig. 1] have shown that in neutral aqueous solution at room temp. the isomerization 23 is incomparably slower than the formation 12, and this has been confirmed in unpublished work on the kinetics and mechanism of reaction 23 under various conditions. Under such circumstances the mechanism b would manifest itself as a polarographic hydroxyurea wave rapidly rising to almost the stoichiometric height and subsequently falling off very slowly. What actually was observed, however, (Figs. 1 and 2) was a maximum wave height slightly more than half the stoichiometric one, which seems to be in favour of mechanism a.

The apparent failure of reaction 12 in alkaline buffer pH 9.2 (*vide* p. 7) raises the question, as to whether the actual mechanism of the overall reaction (1) is ionic, as indicated in the stoichiometric equation, or rather involves free hydroxylamine and free cyanic acid. For the analogous process leading to

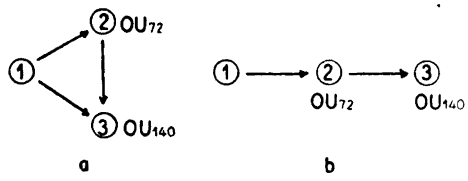


Fig. 3. Possible mechanisms of the formation of the hydroxyurea isomerides (reaction 1). 1 stands for the reactants; a. concurrent formation, b consecutive formation.

urea a non-ionic mechanism has recently been given priority [4] for steric reasons. Weil and Morris [5] have emphasized that the ionic and non-ionic mechanisms are kinetically indistinguishable, owing to the mobile equilibrium $NH_3 + HOCN \rightleftharpoons NH_4^+ + {}^-OCN$, and the same would probably apply to the reaction (1). It is, therefore, highly improbable that any useful information can be obtained from an examination of the pH-dependency of the rate constant of (1), and apart from that such measurements are impracticable with the polarographic method, because the hydroxylammonium wave and the hydrogen wave would interfere with the hydroxyurea wave in neutral and acid solution.

Materials, apparatus and general technique have been described in detail in previous publications [1,2].

REFERENCES

1. Kofod, H. *Acta Chem. Scand.* **7** (1953) 274.
2. Kofod, H. *Acta Chem. Scand.* **9** (1955) 455.
3. Kofod, H. *Acta Chem. Scand.* **7** (1953) 938.
4. Frost, A. A. and Pearson, R. G. *Kinetics and Mechanism.* New York 1953, p. 257.
5. Weil, J. and Morris, J. C. *J. Am. Chem. Soc.* **71** (1949) 1664.

Received September 25, 1956.

ACTA CHEMICA SCANDINAVICA 11 (1957) 11—16

Utilization of Doubly Labeled Pyrimidine Ribosides and Deoxyribosides by the Rat

PETER REICHARD

Biochemical Department, Karolinska Institutet, Stockholm, Sweden

Cytidine, uridine, deoxycytidine and thymidine were prepared from ^{14}C-labeled polynucleotides. The doubly labeled nucleosides were separately injected into partially hepatectomized rats and their incorporation into the pyrimidine part and the sugar moiety of polynucleotide pyrimidines was studied.

The intact incorporation of each administered labeled compound into the corresponding nucleoside was demonstrated. After injection of the labeled pyrimidine ribosides the ratio between the specific activities of pyrimidine and deoxyribose of the isolated deoxyribosides was very close to the corresponding pyrimidine/ribose ratio of the precursor, indicating a relatively direct conversion of the ribosides to deoxyribosides. No utilization of deoxyribosides for the synthesis of ribosides was observed.

In no case did the purine ribosides contain significant activity.

^{15}N-labeled pyrimidine ribosides and deoxyribosides are incorporated by the rat into polynucleotide pyrimidines [1,2]. Free pyrimidines, however, are very poorly or not at all utilized [3–7]. This was taken as evidence that the labeled nucleosides were incorporated as intact molecules into both pentose nucleic acid (PNA) and deoxypentose nucleic acid (DNA) [1,2]. Rose and Schweigert [8] subsequently demonstrated that the ribose and pyrimidine of doubly labeled cytidine-^{14}C were incorporated to the same extent into the pyrimidine and carbohydrate moiety of PNA and DNA pyrimidine nucleosides. This established that the postulated intact incorporation of the labeled nucleosides had taken place at least with cytidine.

In the present investigation cytidine, uridine, deoxycytidine and thymidine were prepared from over all ^{14}C-labeled polynucleotides. The nucleosides, which were accordingly labeled in both the pyrimidine ring and the carbohydrate moiety, were injected into partially hepatectomized rats, and their utilization for polynucleotide biosynthesis in the liver and the intestine was studied.

EXPERIMENTAL

Preparation of labeled ribosides. ^{14}C-yeast nucleic acid was purchased from Schwarz laboratories, Inc. After alkaline hydrolysis the labeled mononucleotides were prepared by gradient elution chromatography on a Dowex-2 formate column [9]. The pyrimidine nucleotides were dephosphorylated with prostatic phosphatase and the formed ribosides were then prepared by starch chromatography [10].

Preparation of labeled deoxyribosides. Labeled DNA was obtained by extraction [11] from *E. coli* grown in the presence of lactate-3-^{14}C *. Labeled deoxynucleotides were prepared by the combined action of deoxyribonuclease and snake venom diesterase [12]. After chromatography [9] the pyrimidine deoxynucleotides were dephosphorylated with snake venom monoesterase and the formed deoxycytidine and thymidine were chromatographed on starch [13].

The purity of all the labeled compounds used for the animal experiments was checked from light absorption data in the ultraviolet [14] and paper chromatography [15].

Before use each labeled compound was diluted with the corresponding nonlabeled riboside or deoxyriboside. The ratio between the specific activities of the pyrimidine ring and the carbohydrate was determined in duplicate experiments as described below.

Animal experiments. Rats weighing 150—200 g were subjected to partial hepatectomy according to the technique used in this laboratory [16]. Starting 20 h after the operation each nucleoside, dissolved in 0.9% NaCl, was injected into one rat at two hours interval. A total of five injections (0.5 ml each) was given to each rat. The rats were killed 42 h after the operation, the livers and the thoroughly washed small intestines were removed and separately placed in alcohol.

Isolation of polynucleotide compounds for ^{14}C-determinations. PNA and DNA were prepared and separated according to Hammarsten [11]. The ribosides and deoxyribosides, respectively, were obtained by a combination of ion exchange and starch chromatography as outlined above for the preparation of the isotopic compounds.

Degradation of nucleosides. In order to determine the ratio between the specific activities of the pyrimidine ring and of the sugar the following procedure was adopted:

Each nucleoside was dissolved in 5 ml of water. The amount of substance was measured by light absorption [14] after dilution of aliquots with 0.1 N HCl. Radioactivity was measured on infinitely thin samples (less than 0.2 μmoles/cm^2) in a Tracerlab Sc-18 windowless flow counter and the specific activity of the whole nucleoside was calculated.

The rest of the pyrimidine nucleoside containing solution was evaporated to dryness *in vacuo*. The residue was transferred to a bomb tube with a small amount of conc. formic acid (1—2 ml) and hydrolyzed at 175° [17], deoxyribosides for 1 h, ribosides for 3 h. This treatment liberated the free pyrimidines. The only nucleoside which was not quantitatively split was uridine. The formic acid was removed by repeated evaporation *in vacuo*, the residue was dissolved in butanol-water and chromatographed on starch [18].

The specific activities of the pyrimidines obtained in this way was calculated after light absorption measurements and determinations of radioactivity as described for the nucleosides.

This method gave the specific activity of the sugar moiety as the difference between that of the nucleoside and that of the pyrimidine ring.

RESULTS

Cytidine-^{14}C. Three different animal experiments were carried out and are recorded in Table 1. In accordance with earlier observations [1,8] cytidine was incorporated into all pyrimidines of both PNA and DNA. The ratios between the specific activities of the pyrimidine ring and of the carbohydrate moiety showed some variations for each nucleoside in the different experiments probably largely depending on the fact that the specific activity of the sugar was determined by difference. The average ratio for all cytidines from both

* I am much indebted to Dr. H. Palmstierna for a gift of the labeled bacteria.

Table 1. Incorporation of doubly labeled cytidine-^{14}C into polynucleotides of the rat.
The specific activity of the precursor was 172 000 ct/min/μmole. The ratio between the specific activities of ribose and cytosine was 1.85.
Each rat received a total of 10 μmoles of cytidine in expts. 1 and 2, 5 μmoles of cytidine in expt. 3.

	Liver						Intestine					
	counts/min/μmole			specific act. of sugar / specific act. of pyrim.			counts/min/μmole			specif. act. of sugar / specific act. of pyrim.		
	Experiment No.						Experiment No.					
	1	2	3				1	2	3			
PNA:												
Cytidine	1 950	1 520	1 110				1 520	2 480	1 420			
Cytosine	660	540	440	1.95;	1.81;	1.53	550	840	570	1.77;	1.85;	1.49
Ribose *	1 290	980	670				970	1 640	850			
Uridine	500	330	250				520	700	420			
Uracil	200	140	100	1.50;	1.36;	1.50	200	250	170	1.60;	1.80;	1.47
Ribose *	300	190	150				320	450	250			
DNA:												
Deoxycytidine	1 340	1 200	720				1 070	750	610			
Cytosine	550	490	240	1.44;	1.45;	2.00	410	310	230	1.61;	1.42;	1.65
Deoxyribose *	790	710	480				660	440	380			
Thymidine	330	280	160				130	220	195			
Thymine	140	110	65	1.36;	1.55;	1.46	50	90	75	1.60;	1.44;	1.60
Deoxyribose *	190	170	95				80	130	120			

* Calc. by difference

liver and intestinal polynucleotides, however, was clearly very close to the corresponding value in the administered precursor.

The uracil/ribose ratios in the polynucleotide uridines were slightly lower than the corresponding values for cytidine. This was also true for the two deoxyribosides. The incorporation into the purine nucleosides is not recorded in the table, since it was insignificant in all cases (less than 10 counts/μmole).

Uridine-^{14}C. Relatively large amounts of the isotopic riboside were administered in order to obtain high enough counts in the isolated compounds (Table 2). In this experiment the pyrimidine/ribose ratios in the PNA ribosides were quite close to that of the administered precursor, and this was also true for the pyrimidine/deoxyribose ratios. Again only very low counts were found in the purine compounds.

Labeled deoxyribosides. The results of experiments with deoxycytidine-^{14}C and thymidine-^{14}C are demonstrated in Table 3. The former compound was incorporated into both deoxycytidine and thymidine of DNA, while the latter was utilized exclusively for thymidine synthesis. In no case was there significant incorporation into PNA pyrimidine ribosides or purine compounds.

Degradation of the isolated deoxyribosides showed that in all cases pyrimidine and deoxyribose were incorporated to about the same extent into DNA.

Table 2. Incorporation of doubly labeled uridine-^{14}C into polynucleotides of the rat. 100 μmoles of uridine (71 000 cts/min/μmole) were injected into one rat. The ratio between the specific activities of ribose and uracil was 1.46.

	Liver		Intestine	
	counts/min/μmole	spec. act. of sugar / spec. act. of pyrim.	ct/min/μmole	spec. act. of sugar / spec. act. of pyrim.
PNA:				
Cytidine	320		330	
Cytosine	130	1.38	120	1.75
Ribose *	180		210	
Uridine	380		330	
Uracil	150	1.53	140	1.36
Ribose *	230		190	
DNA:				
Deoxycytidine	290		130	
Cytosine	125	1.32	60	1.17
Deoxyribose *	165		70	
Thymidine	220		110	
Thymine	105	1.10	45	1.45
Deoxyribose *	115		65	

* Calc. by difference.

DISCUSSION

It is quite clear from the results that the rat has the capacity to incorporate pyrimidine ribosides and deoxyribosides into tissue polynucleotides without a more pronounced breakage of the pyrimidine-sugar bond.

Most experiments were carried out with labeled cytidine, since this compound, when administered in small amounts, was incorporated best into all pyrimidine ribosides and deoxyribosides. The fact that the ratio between the specific activities of cytosine and of ribose within experimental limits was the same in the injected precursor and in the isolated polynucleotide cytidine demonstrates the intact incorporation of the precursor. Such a finding would be extremely improbable if the glycoside linkage of the injected compound were first split and the split products were subsequently utilized for polynucleotide synthesis.

The uracil/ribose ratio was in all cases slightly lower than the cytosine/ribose ratio. Unless this finding depends on some unknown systematic experimental error, it might indicate that a small amount of pyrimidine was incorporated into uridine without being attached to ribose.

The pyrimidine/deoxyribose ratios in the isolated deoxycytidines and thymidines were on the average slightly lower than the pyrimidine/ribose ratios in the isolated ribosides. The difference was, however, not very significant. It is clear that the main route for the incorporation involved a reduction of the

Table 3. Incorporation of doubly labeled deoxyribosides into polynucleotides of the rat. In two experiments 25 μmoles of each deoxyriboside (deoxycytidine = 13 500 ct/min/μmole; thymidine = 13 200 ct/min/μmole) were injected into one rat. The ratios between the specific activities of pyrimidine and deoxyribose were for deoxycytidine 0.97 and for thymidine 0.99.

Isolated	Deoxycytidine injected				Thymidine injected			
	Liver		Intestine		Liver		Intestine	
	ct/min/μmole	sp.act. sugar / sp.act pyrim.	ct/min/μmole	sp.act. sugar / sp.act. pyrim.	ct/min/μmole	sp.act. sugar / sp.act. pyrim.	ct/min/μmole	sp.act. sugar / sp.act. pyrim.
PNA:								
Cytidine	8		9		6		0	
Uridine	5		6		3		2	
DNA:								
Deoxycytidine	1 120		480		11		7	
Cytosine	510	1.20	250	0.92				
Deoxyribose *	610		230					
Thymidine	375		375		620		375	
Thymine	195	0.92	185	1.03	330	0.88	145	0.89
Deoxyribose *	180		190		290		130	

* Calc. by difference.

ribose of the *intact riboside* molecule or a derivative of it. The results definitely exclude a mechanism by which only a smaller part of the ribose molecule was attached to the pyrimidine during the reduction *, as might be visualized in analogy with known enzyme reactions [19]. Furthermore, transglycosidation mechanisms, as demonstrated for microorganisms [20], are also excluded. In this connection the absence of label from the purine bound ribose is of importance.

The data from the incorporation experiments with labeled uridine, deoxycytidine and thymidine all demonstrate the intact incorporation of the administered nucleosides.

Uridine-^{14}C behaved similar to cytidine-^{14}C and showed the transformation of the intact riboside to all polynucleotide pyrimidine nucleosides. Roll *et al.*[21] found some preferential incorporation of uracil from over all labeled uridylic acid-^{14}C into deoxycytidylic and thymidylic acids of the mixed internal organs of the rat. Our data do not show a more pronounced effect of this kind.

The results with the ^{14}C-labeled deoxyribosides confirm the conclusions drawn from earlier experiments with ^{15}N-labeled deoxyribosides that the conversion of ribosides to deoxyribosides *in vivo* is essentially irreversible.

* The loss of one carbon atom of the ribose chain during the reduction is not excluded from the results.

REFERENCES

1. Hammarsten, E., Reichard, P. and Saluste, E. *J. Biol. Chem.* **183** (1950) 105.
2. Reichard, P. and Estborn, B. *J. Biol. Chem.* **188** (1951) 839.
3. Plentl, A. A. and Schoenheimer, R. *J. Biol. Chem.* **153** (1944) 203.
4. Rutman, R. J., Cantarow, A. and Paschkis, K. E. *Cancer Research* **14** (1954) 119.
5. Bendich, A., Getler, H. and Brown, G. B. *J. Biol. Chem.* **177** (1949) 565.
6. Brown, G. B., Roll, P. M. and Weinfeld, H. in Mc Elroy, W. D. and Glass, B. *Phosphorus Metabolism* **II** (1952) 385.
7. Holmes, W. L., Prusoff, W. H. and Welch, A. D. *J. Biol. Chem.* **209** (1954) 503.
8. Rose, I. A. and Schweigert, B. S. *J. Biol. Chem.* **202** (1953) 635.
9. Hurlbert, R. B., Schmitz, H., Brumm, A. F. and Potter, V. R. *J. Biol. Chem.* **209** (1954) 23.
10. Reichard, P. *J. Biol. Chem.* **179** (1949) 763.
11. Hammarsten, E. *Acta Med. Scand. Suppl.* **196** (1947) 634.
12. Sinsheimer, R. L. and Koerner, J. F. *J. Biol. Chem.* **198** (1952) 293.
13. Reichard, P. and Estborn, B. *Acta Chem. Scand.* **4** (1950) 1047.
14. Beaven, G. H., Holiday, E. R. and Johnson, E. A. in Chargaff, E. and Davidson, J. N. *The Nucleic Acids* **I** (1955) 493.
15. Wyatt, G. R. in Chargaff, E. and Davidson, J. N. *The Nucleic Acids* **I** (1955) 243.
16. Bergstrand, A., Eliasson, N. A., Hammarsten, E., Norberg, B., Reichard, P. and v. Ubisch, H. *Cold Spring Harbor Symposia Quant. Biol.* **13** (1948) 22.
17. Vischer, E. and Chargaff, E. *J. Biol. Chem.* **176** (1948) 715.
18. Reichard, P. *Acta Chem. Scand.* **3** (1949) 422.
19. Racker, E. *J. Biol. Chem.* **196** (1952) 347.
20. Macnutt, W. S. *Biochem. J. London* **50** (1952) 384.
21. Roll, P. M., Weinfeld, H. and Carroll, E. *J. Biol. Chem.* **220** (1956) 455.

Received October 9, 1956.

ACTA CHEMICA SCANDINAVICA 11 (1957) 17—23

Formation of Uridine Phosphates from Uracil in Extracts of Ehrlich Ascites Tumor

PETER REICHARD and OLA SKÖLD

Biochemical Department, Karolinska Institutet, Stockholm, Sweden

The enzymic formation of uridine monophosphate from uracil in extracts from Ehrlich ascites tumor has been demonstrated to proceed according to two different mechanisms. The first involved the formation of uridine from uracil + ribose-1-phosphate by the action of nucleoside phosphorylase and the subsequent phosphorylation of uridine with ATP. This mechanism was by far the predominant one in the acetone powder extracts.

The second mechanism involved the direct condensation of uracil with phosphoribosyl pyrophosphate. In this case only very small amounts of UMP synthesis were observed.

The work of Plentl and Schoenheimer [1] originally demonstrated that uracil-^{15}N when injected into rats was not utilized for the biosynthesis of polynucleotide pyrimidines. Even though later work from different laboratories with uracil-^{14}C showed that there was a slight incorporation of the pyrimidine especially into fast growing organs [2,3], comparison of the incorporation data with results obtained with labeled nucleosides or orotic acid [4] demonstrated that the utilization of uracil was very much smaller than that of the other compounds. In the mouse, however, the incorporation of uracil and orotic acid was of the same order of magnitude [5].

The present investigation was started with the aim to investigate the pathway of uracil incorporation in the mouse. *In vivo* experiments demonstrated that labeled uridine phosphates appeared in the acid soluble fraction of mouse liver after injection of uracil-^{14}C in a similar manner as after injection [6] of orotic acid-^{14}C. It seemed justified to assume that the incorporation of uracil into polynucleotide pyrimidines proceeded *via* uridine phosphates. Our investigation was therefore confined to a study of the enzymic formation of uridine monophosphate (UMP)* from uracil.

* The following abbreviations are used throughout this paper: UMP = uridine-5′-phosphate, ATP = adenosine triphosphate, PGA = 3-phosphoglyceric acid, PCA = perchloric acid, PRPP = phosphoribosyl pyrophosphate.

EXPERIMENTAL

Uracil-^{14}C (80 000 ct/min/μmole) was synthesized according to Johnson and Flint [7]. Ribose-5-phosphate, ATP and PGA were commercial products (Schwarz Laboratories, Inc. and Sigma Chemical Company). *Ribose-1-phosphate* was a gift from Dr. H. Klenow, Copenhagen, for which we are very much indebted. *Phosphoribosyl pyrophosphate* was prepared enzymically as described earlier [8]. The preparation was 62 % pure judged from ribose analysis and had a ratio of ribose: acid labile phosphate of 1:1.96. It contained no ATP.

Preparation of enzyme extract. The ascites tumor was originally obtained through the courtesy of Dr. G. Klein, Institute of Cell Research, Karolinska Institutet. Routinely, it was kept by transfer of 0.1 ml of ascitic fluid 8—10 days after the previous inoculation. For the preparation of the acetone powder the ascitic fluid from 20—50 mice on the tenth day after inoculation was pooled and centrifuged cold at 1 000 *g* for 10 min. The sediment was washed twice with physiological sodium chloride and finally suspended in enough sodium chloride solution to give the original ascites volume. The solution was mixed in a Waring blendor with 10 volumes of acetone (−15°), filtered by suction and washed with cold acetone. The residue was dried in a desiccator and kept dehydrated at −15°. *Ca.* 4 g of acetone powder was obtained per 100 ml of ascites.

Immediately before use the powder was extracted with ice cold 0.05 M potassium phosphate buffer, pH 7.4 (10—50 ml per g powder) in a Potter-Elvehjem homogenizer. Three treatments were carried out at 10 min intervals. After centrifugation (15 000 *g* for 15 min) at 0° a clear red extract was obtained which was directly used for the experiments.

Assay of enzyme activity. The enzyme reaction was stopped by addition of 0.1 volume of 4.4 M PCA to the cold solution. The protein precipitate was centrifuged and washed once with 1 ml of 0.6 M PCA.

Two different methods were used after that. In *method 1* the combined supernatants were neutralized with 4 M KOH (phenol red) and the perchlorate was allowed to precipitate overnight in the refrigerator. The supernatant was then chromatographed on a Dowex-2 column according to Hurlbert *et al.*[9] Fractions within the different radioactive peaks were combined and the total radioactivity of each compound was determined on infinitely thin samples. This method gave the amount of the different radioactive uridine phosphates formed from uracil-^{14}C. The identity of the uridine phosphates was based on their localization on the chromatogram.

In *method 2* pyrophosphate linkages were hydrolyzed with acid so that all uridine phosphates were converted to UMP. This was achieved by heating the PCA supernatant at 100° for 1 h. Neutralization with KOH was then carried out as described above. The neutralized solution was then adsorbed on a Dowex-2-formate column (diameter 0.9 cm, length 5 cm). The column was washed with 50 ml of water which removed all uracil and uridine. Thereafter UMP was removed from the column with 60 ml of 6 N formic acid. The total radioactivity of the UMP fraction was determined and from this value and the specific activity of the uracil-^{14}C the amount of UMP formation could be calculated.

A blank which contained no enzyme was carried through the whole procedure and a small correction for "UMP formation" in the blank was applied.

Uracil and uridine could be separated and their specific activities determined by the following procedure: The first fraction from the Dowex-2 column was passed through a Dowex-50-H^+ column (0.9 cm diameter, 5 cm length). After washing with 30 ml of water the eluent was evaporated to dryness *in vacuo*. The dry residue was dissolved in butanol-water and chromatographed on a starch column (2 cm diameter, 20 cm length). The amount of the separated uracil and uridine was determined by light absorption and their specific activities were calculated after determination of radioactivities on infinitely thin samples.

Experiments with whole cells. (*cf.*[5]). In each of two 200 ml Erlenmeyer flasks 6 ml of ascites was mixed with 10 ml of Krebs-Henseleit substrate, from which $CaCl_2$ had been omitted. 50 μmoles of fructose diphosphate was added to each flask, and 25 μmoles of orotic acid-^{15}N to one vessel. The flasks were filled with an atmosphere of oxygen:carbon dioxide (95:5) and kept in an ice bath for 2 h in order to permit orotic acid to penetrate into the cells.[5] After that 25 μmoles of uracil-^{14}C was added and incubation carried out at 37° for another 2 h period.

The reaction was stopped by addition of 1.6 ml of 4.4 M PCA and the solution was mixed in a Waring blendor. The cell mass was filtered, washed with cold 0.2 M PCA and dried with alcohol and ether.

The PCA filtrate was neutralized with KOH and the acid soluble uridine phosphates were prepared from it as described above.

The polynucleotides from the ascites cells were prepared according to Hammarsten [10]. The pyrimidine ribosides were obtained by starch chromatography as described earlier [11]. The different compounds were analyzed for ^{15}N in the mass spectrometer and for ^{14}C in a Tracerlab SC-18 windowless flow counter (infinitely thin samples).

RESULTS

Extracts from acetone powder of Ehrlich ascites tumor showed a small but readily demonstrable capacity to form UMP from uracil in the presence of ribose-5-phosphate, ATP, Mg^{++} and an ATP regenerating system. The *same experimental conditions*, however, did not allow UMP synthesis in extracts from mouse liver acetone powder. All our subsequent experiments were carried out with the ascites tumor.

When starting our investigation we visualized three different pathways which might explain UMP formation: (1) Uracil might be carboxylated to orotic acid and orotic acid might subsequently by known enzymic pathways [12] be converted to UMP. (2) Uracil might replace orotic acid in the condensation with Kornberg's phosphoribosylpyrophosphate [12] and UMP be formed directly. (3) Uracil might react with ribose-1-phosphate [13] (formed from the added ribose-5-phosphate[14]) and form uridine. After that uridine might be phosphorylated by ATP with the formation of UMP, a reaction which we had earlier observed in rat liver extracts.

Formation of orotic acid

The influence of the presence of orotic acid-^{15}N on the formation of acid soluble uridine phosphates and polynucleotide pyrimidines from uracil^{14}-C is demonstrated in Table 1. Freshly obtained tumor cells were incubated with

Table 1. Non-involvement of orotic acid in UMP formation from uracil.

	Uracil + orotic acid			Uracil	
	μmoles formed	ct/min/μmole	atom per cent excess ^{15}N	μmoles formed	ct/min/μmole
Acid soluble fraction:					
UMP	0.12			0.15	
Uridine pyrophosphates	0.02			0.02	
Pentose nucleic acid:					
Uridine		1 290	0.252		1 330
Cytidine		410	0.063		570
Deoxypentose nucleic acid:					
Thymine		210	0.078		170
Cytosine		120	—		150

Ascites cells were incubated with uracil-^{14}C (80 000 ct/min/μmole) and orotic acid-^{15}N (16 atom per cent excess). For further explanation see text.

Krebs-Henseleit solution together with orotic acid. After 2 h at 0° uracil was added and incubation continued for two more hours. In the control vessel preincubation was carried out without orotic acid. The acid soluble nucleotides and the pyrimidines from polynucleotides were prepared in both experiments and the amount of ^{14}C in the different fractions was measured. Clearly the presence of orotic acid very little influenced the incorporation of uracil. The ^{15}N-data show that orotic acid did penetrate into the cells.

A similar experiment was carried out with an acetone powder extract from the tumor in a bicarbonate buffer. Again the presence of orotic acid did not influence the formation of radioactive uridine phosphates from uracil-^{14}C.

Reaction of uracil with phosphoribosyl pyrophosphate

The formation of UMP was greatly stimulated by the inclusion of ribose-5-phosphate and ATP in the medium (Table 2). Our experiments had to be carried out with an undialyzed extract since dialysis almost completely destroyed the ability of the system to synthesize UMP. It was conceivable that the requirement for ATP and ribose-5-phosphate indicated the intermediate formation of PRPP from these compounds. In Table 2 are also recorded two experiments, in which PRPP had been substituted for ATP and ribose-5-phosphate. More than six times the amount of "background synthesis" was observed. Inclusion of fluoride (to inhibit enzymic breakdown of PRPP) did not increase UMP synthesis.

Table 2. Involvement of PRPP.

Additions	μmoles UMP formed
Ribose-5-phosphate	0.007
ATP, PGA	0.007
Ribose-5-phosphate, ATP, PGA	0.092
PRPP	0.047
PRPP, NaF	0.037

Each vessel contained 75 μmoles of $MgCl_2$, 10 μmoles of uracil-^{14}C, 150 μmoles of phosphate buffer, pH 7.4 and enzyme (corresponding to 190 mg of acetone powder). Incubation 40 minutes at 37°. Final volume 4.5 ml.

Where indicated ribose-5-phosphate (40 μmoles), ATP (20 μmoles) PGA (60 μmoles), PRPP (17 μmoles) and NaF (200 μmoles) were added.

In these and the following experiments method 2 was used for enzyme assay. In order to ascertain the identity of the analyzed compound with UMP the radioactive fractions obtained by the acid washing from the PRPP experiments were combined and rechromatographed according to method 1. The main part of the radioactivity was localized in the UMP region of the chromatogram.

Intermediate formation of uridine

The possible participation of uridine during the reaction was tested in one experiment in which nonlabeled uridine was included during the incubation of the tumor extract with uracil-^{14}C, ribose-5-phosphate and ATP. With

method 2 it was found that a considerable increase of radioactivity appeared in the UMP fractions as compared to the control. The specific activity and the total amount of the formed UMP were determined after rechromatography. Uracil and uridine were purified by starch chromatography and the total amounts and specific activities of the two compounds were determined. The results (Table 3) show that a large amount of UMP had been formed, while most of the added uridine had disappeared. The specific activity of uracil had been lowered to about half of its original value. Uridine had received isotope during the incubation and its specific activity was between that of uracil and UMP.

Table 3. Uridine as intermediate in UMP formation.

Isolated after incubation	Addition		
	Uridine		None
	μmoles	ct/min/μmoles	μmoles
Uracil	9.0	49 000	*ca.* 7.5
Uridine	0.5	29 000	—
UMP	5.9	10 700	0.07

Each vessel contained 75 μmoles of $MgCl_2$, 20 μmoles of ATP, 60 μmoles of PGA, 40 μmoles of ribose-5-phosphate, 10 μmoles of uracil-^{14}C (80 000 ct/min/μmole) 150 μmoles of phosphate buffer, pH 7.4, and enzyme (corresponding to 190 mg acetone powder). Incubation 40 min at 37°. Volume = 4.5 ml.
Where indicated 10 μmoles of uridine was added.

This experiment gave strong support to the idea that uridine indeed was an intermediate in UMP formation. The fact that the *total amount* of ^{14}C in UMP was very much increased indicated that uridine was not only an intermediate in the formation of UMP from uracil but also had supplied the substrate for the conversion of uracil-^{14}C to uridine-^{14}C. In order to test this possibility inosine was substituted for ribose-5-phosphate in one experiment (Table 4). Good synthesis of UMP was obtained, but only in the presence of ATP.

Table 4 also includes results obtained with ribose-1-phosphate. Good synthesis of UMP was observed in the presence of ATP and Mg^{++}. When uracil and uridine were purified from the incubation mixture it was found that uridine was formed in the absence of ATP and Mg^{++}, while there was little nucleoside in the presence of these substances.

The localization of the phosphate group on the 5′-position of ribose was demonstrated by enzymic dephosphorylation of the formed UMP with snake venom (*Crotalus adamanteus*) 5′-nucleotidase. Complete liberation of the phosphate group was observed under conditions which allowed no dephosphorylation of the 2′- or 3′-phosphates of uridine.

Table 4. Formation of UMP and uridine from ribose-1-phosphate.

Additions	μmoles UMP formed from ^{14}C	μmoles uridine formed		μmoles uracil left	
		from light absorpt.	from ^{14}C	from light absorpt.	from ^{14}C
Inosine, ATP, PGA, Mg^{++}, phosphate	0.37				
Inosine, Mg^{++}, phosphate	0				
Ribose-1-phosphate, ATP, PGA, Mg^{++}	1.32	0		7.1	6.9
Ribose-1-phosphate, ATP, versene	0.05	2.6	2.4	5.0	4.8
Ribose-1-phosphate, versene	0	2.5	2.5	5.8	5.6

Each experiment contained enzyme (corresp. to 60 mg acetone powder), 10 μmoles of uracil-^{14}C and 150 μmoles of tris buffer, pH 7.4. Volume = 4.5 ml, incubation 40 min at 37°.

Where indicated ATP (20 μmoles), PGA (30 μmoles), inosine (10 μmoles), $MgSO_4$ (75 μmoles), versene (10 μmoles), ribose-1-phosphate (7 μmoles), and phosphate, (100 μmoles, pH 7,4) were added.

DISCUSSION

The results obtained by Hurlbert *et al.* [6] from *in vivo* experiments with orotic acid-^{14}C have made it very probable that uridine phosphates from the acid soluble fraction of cells are intermediates in the biosynthesis of polynucleotide pyrimidines. An investigation of the mechanism of uracil incorporation into polynucleotides in the Ehrlich ascites tumor should consequently start with the elucidation of uridine phosphate formation from uracil.

Three possibilities were from the beginning envisaged for the formation of uridine phosphate from uracil. Of these, transformation of uracil to orotic acid is clearly ruled out from our experiments, both with whole tumor cells and with extracts of acetone powder.

The results with acetone powder extracts demonstrated that UMP formation from uracil could take place in the presence of ATP and ribose-5-phosphate. The latter two compounds could be replaced by phosphoribosyl pyrophosphate, a compound which is an intermediate in UMP formation from orotic acid[12,8]. This resulted, however, in a lower synthesis of UMP than in the presence of ATP + ribose-5-phosphate. It seemed therefore unlikely that the function of these compounds was merely to form PRPP. We interpret the results to indicate that a quite low formation of UMP through direct condensation of uracil + PRPP did take place, though the reaction did only account for a fraction of the UMP formed. It is not probable that PRPP broke down to ribose-1-phosphate and that UMP was formed from this compound, since no ATP was added in these experiments and since UMP was not formed from ribose-1-phosphate in the absence of added ATP.

It is evident, however, that the main pathway of the reaction involved the intermediate formation of uridine. Uridine was formed either from uracil+ribose-1-phosphate or from uracil+inosine+phosphate. The enzyme for

uridine formation, pyrimidine nucleoside phosphorylase [13], is well known. In the presence of ATP, uridine was then phosphorylated and formed UMP. This second reaction required Mg^{++}. The reaction sequence is represented below:

$$\text{Uracil} + \text{ribose-1-phosphate} \xrightarrow[\text{phosphorylase}]{\text{nucleoside}} \text{uridine} + \text{phosphate}$$

$$\text{Uridine} + \text{ATP} \xrightarrow[\text{kinase, } Mg^{++}]{\text{nucleoside}} \text{uridine monophosphate} + (\text{ADP})$$

It is not quite clear why uracil is very poorly utilized for polynucleotide and UMP synthesis in many tissues, *e.g.* rat liver, while it is well utilized by the mouse. Nucleoside phosphorylase is a wide spread enzyme in rat tissues and also the kinase has been found by us in rat liver. Canellakis [15] has suggested that the enzymic reduction of uracil to dihydrouracil in rat liver proceeds at such a fast rate that very little uracil is available for synthetic reactions, unless large amounts are administered. Other explanations might also be considered, such as the availability of ribose-1-phosphate in the different tissues or the concentration of the nucleoside kinase.

REFERENCES

1. Plentl, A. A. and Schoenheimer, R. *J. Biol. Chem.* **153** (1944) 203.
2. Leibman, K. C. and Heidelberger, C. *Federation Proc.* **14** (1955) 243.
3. Canellakis, E. S. *Federation Proc.* **14** (1955) 324.
4. Reichard, P. *Acta Chem. Scand.* **9** (1955) 1275.
5. Lagerkvist, U., Reichard, P., Carlsson, B. and Grabosz, J. *Cancer Research* **15** (1955) 164.
6. Hurlbert, R. B. and Potter, V. R. *J. Biol. Chem.* **209** (1954) 1.
7. Johnson, T. B. and Flint, R. B. *J. Am. Chem. Soc.* **53** (1931) 1077.
8. Hurlbert, R. B. and Reichard, P. *Acta Chem. Scand.* **9** (1955) 251.
9. Hurlbert, R. B., Schmitz, H., Brumm, A. F. and Potter, V. R. *J. Biol. Chem.* **209** (1954) 23.
10. Hammarsten, E. *Acta Med. Scand. Suppl.* **196** (1947) 634.
11. Reichard, P. *Acta Chem. Scand.* **3** (1949) 422.
12. Kornberg, A., Lieberman, I. and Simms, E. S. *J. Am. Chem. Soc.* **76** (1954) 2027.
13. Friedkin, M. and Roberts, D. *J. Biol. Chem.* **207** (1954) 245.
14. Klenow, H. *Arch. Biochem. Biophys.* **46** (1953) 186.
15. Canellakis, E. S. *J. Biol. Chem.* **221** (1956) 315.

Received October 9, 1956.

ACTA CHEMICA SCANDINAVICA 11 (1957) 24—27

Separation of Purines and Pyrimidines by Paper Electrophoresis

GIORGIO SEMENZA*

Institute of Biochemistry, Uppsala University, Uppsala, Sweden

An accurate and fairly rapid method has been worked out for the quantitative determination of purine and pyrimidine bases by paper electrophoresis.

Paper electrophoresis does not seem to have been widely used for the quantitative determination of purines and pyrimidines in nucleic acids hydrolysates. Dimroth *et al*[1]. have reported the separation of adenine from the mixture of the other purines and pyrimidines at pH 3.2, in acetate buffer. Burma [2] reported a successful separation of the four bases in nucleic acid hydrolysates at pH 2 (citrate-phosphate buffer), with 220 V, during 8 hours. Karyone and Inoue [3] also reported a separation of purines and pyrimidines, but no detailed data on their work are available.

In the following, a procedure for the quantitative estimation of purines and pyrimidines by paper electrophoresis is described. As it will be shown, it has some advantages, especially over paper chromatography, but also over other electrophoretic procedures, since it is both more rapid and more accurate, even with very little material.

Electrophoretic separation of the bases from a nucleic acid hydrolysate can only be performed at acidic pH's, because the low solubility of A and G ** leads to a considerable tailing at neutral and alkali pH's. Separation is possible at pH 3.8 (order of travelling towards the cathode: C, A, T+U, G) and at pH 3 (order of travelling: C, A, G, T+U). At intermediate pH values, a separation between G and U+T is not possible; at pH lower than 3, A and C tend to travel together.

---

* Fellow of the Lega Italiana per la Lotta contro i Tumori, Rome. Present address: Physiologisch-chemisches Institut, Zürichbergstrasse 4, Zürich (Switzerland).

** Abbreviations: A, Adenine; C, Cytosine; G, Guanine; T, Thymine; U, Uracil; WS, Levy and Snellbaker's substance [4]; DNA, deoxyribonucleic acid; RNA, ribonucleic acid.

pH 3 was chosen, because at pH 3.8 a certain tailing of G was often observed. Table 1 reports the pK's of dissociation of the amino groups of the bases and their percent dissociation at pH 3.

Table 1. Dissociation constants of the amino groups of the bases and their percent dissociation at pH 3.

	pK's of the amino groups [5]	Percent dissociation at pH 3
Cytosine	4.6	98
Adenine	4.1	92.5
Guanine	3.2	61.5
Thymine	—	—
Uracil	—	—

The relative electrophoretic mobilities, at pH 3, agree fairly well with those calculated from the figures of Table 1.

Although not tested, it is to be expected that 5-methylcytosine should travel with C.

When a hydrolysate of DNA (Wyatt method [6]) is separated by the method described here, a white-fluorescent spot travels with G. This contaminating substance is likely to be identified with the WS (white spot) described by Levy and Snellbaker [4], since the dissociation constants of its groups are very close to those of guanine. Moreover, the UV spectrum of G + WS eluted after paper electrophoresis, corresponds to that of a mixture of G + WS (*e. g.*, the E_{280}/E_{260} ratios are: for G[7], 0.84; for WS [4], about 0.40, and for the eluted mixed spot: 0.74). Since it has been shown [8] that WS is likely formed from G during the hydrolysis of DNA according to Wyatt, eluting and determining the WS together with its parent substance reduces this source of error.

A high electroosmotic flow was found, when Whatman paper No. 1 was used. This is an advantage, as it helps to avoid contamination of the T and U spots with the dark-coloured material formed during the hydrolysis, which remains at the starting point.

Citrate buffer was chosen, because of its low UV extinction.

PROCEDURE

DNA (prepared from calf thymus according to Kay *et al.*[11]) was hydrolysed according to Wyatt [6]. The hydrolysate was brought to dryness, and taken up in enough 1 N HCl, to have 5 to 50 μg of each base in 5 μl.

A humid chamber horizontal electrophoresis apparatus with Whatman No. 1 paper strips (10 cm wide and 42 cm long) and citrate-HCl buffer, pH 3 (Sørensen), diluted to an ionic strength of 0.02 ($\varkappa^{-1} = 0.175 \times 10^4$ ohms at 21° C) was used.

Samples of 5 μl were applied at the starting line, in a narrow zone, after the paper strips had been equilibrated in the apparatus. A part of the paper



Fig. 1. Separation of purines and pyrimidines from a DNA hydrolysate by paper electrophoresis (citrate-HCl buffer, pH 3, μ 0.02, 440 V, during 3 hours on Whatman No.1).

strip was left free for the blanks. A voltage of 440 V, 7—8 mA, was applied during about 3 h at room temperature. The paper was then dried in an oven at 100° C for 5 min. The spots were located with a UV television set [9] or according to Holiday and Johnson [10]. The spots were very compact, without any tailing, in all runs (see Fig. 1).

The spots were eluted overnight with 3.5 ml (or 1.2 ml; in this case, semi-micro cuvettes were used for UV readings) 0.1 N HCl (1 N HCl for G). Readings were taken against water at 250, 260, 280 and 290 mμ. A Beckman DU spectrophotometer was used; the values were corrected for the blanks of the paper (which ranged usually between 0.010 and 0.030).

The comparison between the ratios of the optical densities at these wavelenghts, and those reported by Volkin and Cohn [7] showed excellent agreement, except in the case of G, for the reasons reported above. The extinction coefficents at 260 (for A, G and T) or 280 mμ (for C) reported by Volkin and Cohn [7] were used.

As an example of determination of purine and pyrimidine composition of DNA, the following figures are reported (Table 2), dealing with calf thymus DNA. Ten separate runs were made from a single hydrolysate; each spot contained 5 to 10 μg of each base.

Table 2. Composition of calf thymus DNA, as determined by paper electrophoresis. The values ($\bar{x}$) are expressed as moles per 100 moles of total bases recovered, and represent the averages of ten determinations, on a single hydrolysate. The standard deviation (σ) are expressed as percent of $\bar{x}$.

	$\bar{x}$	σ
Adenine	29.0	± 1.67 %
Thymine	28.5	± 2.64 %
Guanine (+ WS)	21.2	± 3.75 %
Cytosine (+ 5-methyl-cyt.)	21.3	± 4.75 %

As it can be seen, the standard deviations σ in this method are very low. The $\frac{A+T}{G+C+5MeC}$ ratio is 1.35. It agrees fairly well with the figures reported in the literature: 1.20—1.22 [12]; 1.27 [13]; 1.28 [14]; 1.37 [15].

For quantitative purposes, the method described above seems to have some advantages over other methods:

1) It is quite accurate: in the author's hands no other method tested has given standard deviations $< 5\ \%$, when as little as 5—10 μg of each base were used. The method described here can therefore be recommended even when little material is available, as in column chromatography of DNA.

2) Levy and Snellbaker's substance (WS) [4] is determined with its parent substance, *i. e.* guanine [8]. In this way, too low guanine values, as well as too high values of other bases (contaminated by WS) are avoided.

3) Because of the high electroosmotic flow, contamination with the insoluble material formed during the hydrolysis (and not moving from the starting line) is also avoided.

4) It is quite rapid: a 3 hours' run gives a complete separation.

5) This procedure can also be used to separate the four bases (U, G, A, C) obtained from a strong acid hydrolysis of RNA.

I wish to express my sincere thanks to Prof. A. Tiselius and the members of his staff for working facilities, advice and stimulating discussions during the course of this work. I also want to thank Prof. E. Hammarsten for fruitful discussions.

This work was financially supported by the *Rockefeller Foundation* and the *Lega Italiana per la Lotta contro i Tumori*, to whom due thanks are expressed.

REFERENCES

1. Dimroth, K., Jaenicke, L. and Vollbrechtshausen, I. *Hoppe Seylers Z. physiol. Chem.* **289** (1952) 71.
2. Burma, D. P. *Science* **118** (1953) 694.
3. Karyone, T. and Inoue, T. *J. Pharm. Soc. Japan* **74** (1954) 301; *Chem. Abstracts* **48** (1954) 7710.
4. Levy, H. B. and Snellbaker, L. F. *Arch. Biochem. and Biophys.* **54** (1955) 549.
5. Cohn, W. E. in Chargaff, E. and Davidson, J. N. *Nucleic Acids*, Acad. Press, New York 1955. Vol. I, p. 217.
6. Wyatt, G. R. and Cohen, S. S. *Biochem. J. London* **55** (1953) 774.
7. Volkin, E. and Cohn, W. E. in Glick, D. *Methods of Biochemical Analysis*, Interscience Publ., New York 1954. Vol. I p. 304—305.
8. Dunn, D. B. *Biochim. et Biophys. Acta* **18** (1955) 317.
9. Tiselius, A., Hjertén, S. and Levin, Ö. *Arch. Biochem. and Biophys.* **65** (1956) 132.
10. Holiday, E. R. and Johnson, E. A. *Nature* **163** (1949) 216.
11. Kay, E. R. M., Simmons, N. S. and Dounce, A. L. *J. Am. Chem. Soc.* **74** (1952) 1724.
12. Lucy, J. A. and Butler, J. A. V. *Nature* **174** (1954) 32.
13. Wyatt, G. R. *Biochem. J. London* **48** (1951) 584.
14. Frick, G. *Studies on Desoxyribonucleoprotein and Desoxyribonucleic Acid.* Diss. Uppsala 1954.
15. Chargaff, E. and Lipshitz, R. *J. Am. Chem. Soc.* **75** (1953) 3658.

Received October 19, 1956.

ACTA CHEMICA SCANDINAVICA 11 (1957) 28—33

Studies on Rhenium Oxides

ARNE MAGNÉLI

Institute of Inorganic and Physical Chemistry, University of Stockholm, Stockholm, Sweden

The existence of the rhenium oxides ReO_3 and ReO_2 (MoO_2 type) has been confirmed. When rhenium metal and rhenium trioxide are heated together at 800° C only one intermediary phase forms, *viz.* an orthorhombic modification of the dioxide, which is the stable form of ReO_2 in the temperature interval 300° — 1 050° C.

The structure of orthorhombic ReO_2 has been studied by X-ray methods. The metal atom positions have been determined and a probable oxygen atom arrangement is proposed. The structure contains zigzag strings of ReO_6 octahedra joined by edges, the strings being mutually connected by octahedra sharing corners. The short Re-Re distance within the strings suggests the existence of covalent bonds between the metal atoms.

Rhenium trioxide was the first oxide of this metal to be studied by X-ray methods. Thus Meisel [1] found the crystal structure of this compound to be a cubic arrangement of ReO_6 octahedra joined by sharing corners (ReO_3-type structure). Rhenium dioxide, prepared by heating ammonium perrhenate at 500° C *in vacuo*, was investigated by Zachariasen [2], who was able to assign to this phase the MoO_2-structure type. Preliminary structural data on rhenium(VII) oxide have been reported by Wilhelmi [3].

The structural similarity between rhenium dioxide and wolfram dioxide (MoO_2 type) and between rhenium trioxide and wolfram trioxide (distorted ReO_3 type) made it of interest to find out if there exist intermediate oxides of rhenium as is the case with wolfram [4].

PHASE ANALYSIS

Starting materials were rhenium metal powder (Mackay, 99.9 % pure), rhenium trioxide and dirhenium heptoxide prepared from the metal according to Ref.[5] and ammonium perrhenate obtained by treating the latter oxide with ammonia.

Mixtures of rhenium metal and trioxide of gross compositions ranging from $ReO_{1.5}$ to $ReO_{2.5}$ were sealed in evacuated silica tubes and heated for a day at 300° C and then a day at 800° C. The results are summarized in Table 1.

Table 1. Results of the phase analysis.

Composition of the preparation	Appearance of the preparation	Evidence of X-ray powder pattern
Re	Dark, greyish powder	Re
$ReO_{1.50}$	» » »	X + Re
$ReO_{1.93}$	» » »	X + (Re)
$ReO_{2.00}$	» » »	X
$ReO_{2.14}$	» » » + small red grains	X + ReO_3
$ReO_{2.50}$	» » » »	X + ReO_3
ReO_3	Red powder	ReO_3

The only rhenium oxides that form under the conditions applied are the trioxide and the phase of composition close to $ReO_{2.0}$. The powder diagram of the latter is not in agreement with a MoO_2-type structure (*cf.* Table 2).

The powder patterns showed no displacements of the lines for samples of various compositions, which indicates that the ranges of homogeneity are narrow. The following unit cell dimensions were obtained *:

Re (hexagonal) $a = 2.762 \pm 0.001$ Å, $c = 4.457 \pm 0.001$ Å,
ReO_3 (cubic) $a = 3.7510 \pm 0.0005$ Å,

and for the new phase, the powder pattern of which could be indexed with an orthorhombic unit cell

$a = 4.8094 \pm 0.0005$ Å, $b = 5.6433 \pm 0.0005$ Å, $c = 4.6007 \pm 0.0005$ Å.

The density calculated for a cell content of four formula units of ReO_2 is 11.61 in excellent agreement with the density of 11.4 measured by Lehrer (in Biltz [7]) for a sample giving $ReO_{2.01}$ on analysis and prepared from rhenium and rhenium(VII) oxide at 600—650° C.

Rhenium dioxide evidently is dimorphic, forming a monoclinic and also an orthorhombic modification. Samples of the two phases, the former prepared according to Zachariasen [2], were sealed in evacuated silica tubes and heat-treated at various temperatures. While the orthorhombic form did not change within the interval 300—1 050° C, the monoclinic modification transformed into the former which is evidently the stable one in this region. At 300° C this reaction was almost completed in 3 days.

STRUCTURE OF ORTHORHOMBIC RHENIUM DIOXIDE

By heating rhenium dioxide at 1 050° C for a few weeks it was possible to grow crystals suitable for single crystal X-ray investigations. Rotation and Weissenberg photographs were taken with CuK radiation with [101] as rota-

* The X-ray powder data reported in this paper were obtained with a Guinier focusing camera of 80 mm diameter with strictly monochromatized CuKa_1 radiation. The temperature was about 20° C. Potassium chloride (Analar, British Drug Houses, $a = 6.2919$ Å) [6] was added to the specimens as an internal standard. Photographs of samples without admixture were used to reveal superpositions of lines.

Table 2. Powder photograph of orthorhombic rhenium dioxide. Cu$K\alpha_1$ radiation.

I_{obs}	$\sin^2\Theta_{obs}$	*hkl*	$\sin^2\Theta_{calc}$	$p\|F\|^2_{calc} \cdot 10^{-3}$
v st	0.04430	110	0.04428	170
v st	0.07236	111	0.07231	210
v w	0.07438	020	0.07452	3
st	0.10259	021	0.10255	180
		200	0.10260	80
st	0.11216	002	0.11212	160
v w	0.12832	121	0.12820	6
v w	0.13789	102	0.13777	5
—	—	211	0.14926	0
st	0.15651	112	0.15640	250
v w	0.17717	220	0.17712	8
v w	0.18644	022	0.18664	7
w	0.19331	130	0.19332	45
v st	0.20517	221	0.20515	440
—	—	122	0.21229	0
st	0.21466	202	0.21472	180
st	0.22137	131	0.22135	280
—	—	212	0.23335	0
m	0.24945	310	0.24947	100
m	0.27751	311	0.27750	140
v w	0.28930	222	0.28924	12
m	0.29649	113	0.29655	130
w	0.29798	040	0.29807	90
		231	0.29830	0
w	0.30539	132	0.30544	70
m	0.32669	041	0.32610	25
		023	0.32679	170
—	—	321	0.33339	2
—	—	302	0.34296	2
—	—	141	0.35175	0.3
—	—	123	0.35244	2
m	0.36159	312	0.36159	170
—	—	213	0.37350	0
—	—	232	0.38239	0
v w	0.39853	330	0.39851	30
w	0.40073	240	0.40067	90
m	0.41025	042	0.41019	120
		400	0.41039	80
—	—	322	0.41748	0.1
m	0.42638	331	0.42654	200
m	0.42903	241	0.42870	30
		223	0.42939	210
m	0.44562	133	0.44559	200
w	0.44854	004	0.44848	50

tion axis. The intensities were estimated visually and the intensity scales of the various photographs were correlated by means of reflexions, equivalent on account of symmetry relations. The structure amplitudes were calculated using the nomograms given by Lu [8].

The following reflexions were found to be systematically missing:

$$\begin{array}{lll} 0kl & \text{for } k & = 2n + 1 \\ h0l & \text{for } l & = 2n + 1 \\ hk0 & \text{for } h + k & = 2n + 1 \end{array}$$

This is characteristic of the space group *Pbcn* (No. 60).

The linear Harker sections suggested by this symmetry were calculated and found to have the following appearance:

$$\begin{array}{lll} \mathrm{P}(u\tfrac{1}{2}0): & \text{maximum at } u & = \tfrac{1}{2} \\ \mathrm{P}(0v\tfrac{1}{2}): & \text{maximum at } v & = 0.220 \\ \mathrm{P}(\tfrac{1}{2}\tfrac{1}{2}w): & \text{maximum at } w & = 0 \end{array}$$

This locates the rhenium atoms at the point position 4(*c*) with $y = v/2 = 0.110$, which corresponds to an arrangement of zigzag chains of metal atoms running parallel to the *c* axis. The distance between rhenium atoms within the chain is 2.61 Å, while adjacent rhenium atoms of different chains are 3.68 and 3.71 Å apart.

It is of interest to compare the interatomic distances thus obtained with those present in monoclinic rhenium dioxide, the atomic parameters of which, however, have not been determined. The close similarity between the unit cell dimensions of this phase and molybdenum dioxide seem to justify the assumption that the parameter values of these compounds are approximately the same. This leads to Re-Re distances within the straight chains of 2.48 and 3.08 Å and Re-Re distances between neighbouring chains of 3.7 Å.

The similar metal-metal distances present in the two forms of rhenium dioxide suggest that the arrangement of the oxygen atoms around the rhenium atoms in the orthorhombic modification is essentially the same as in the MoO_2-type form, *viz.* in ReO_6 octahedra with shared edges corresponding to the shorter rhenium-rhenium distances and shared corners corresponding to the longer ones. These conditions are fullfilled by the following structure:

Space group: *Pbcn* (No. 60)

4 Re in 4(*c*): $0,y,\tfrac{1}{4}$; $0,\bar{y},\tfrac{3}{4}$; $\tfrac{1}{2},\tfrac{1}{2}+y,\tfrac{1}{4}$; $\tfrac{1}{2},\tfrac{1}{2}-y,\tfrac{3}{4}$. $y = 0.110$

8 O in 8(*d*): x,y,z; $\tfrac{1}{2}-x,\tfrac{1}{2}-y,\tfrac{1}{2}+z$; $\tfrac{1}{2}+x,\tfrac{1}{2}-y,\bar{z}$; $\bar{x},y,\tfrac{1}{2}-z$; $\bar{x},\bar{y},\bar{z}$; $\tfrac{1}{2}+x,\tfrac{1}{2}+y,\tfrac{1}{2}-z$; $\tfrac{1}{2}-x,\tfrac{1}{2}+y,z$; $x,\bar{y},\tfrac{1}{2}+z$. $x = 0.25$, $y = 0.36$, $z = 0.125$.

The interatomic distances have reasonable values throughout, *viz.* Re—O 1.95 and 2.1 Å and O—O 2.6—3.1 Å. The distance of 3.1 Å is that of edges shared by two ReO_6 octahedra.

The influence of the oxygen atoms on the intensities of the X-ray reflexions is very low compared with that of the rhenium atoms. However, for reflexions *hkl* with $h+k = 2n+1$, the contributions of the metal atoms cancel out. The proposed oxygen arrangement gives fair agreement between calculated and observed intensities for this type of reflexions (*cf.* Table 2). As these reflexions are very weak and rather few, it is not, however, possible to improve the oxygen parameters from the experimental data.

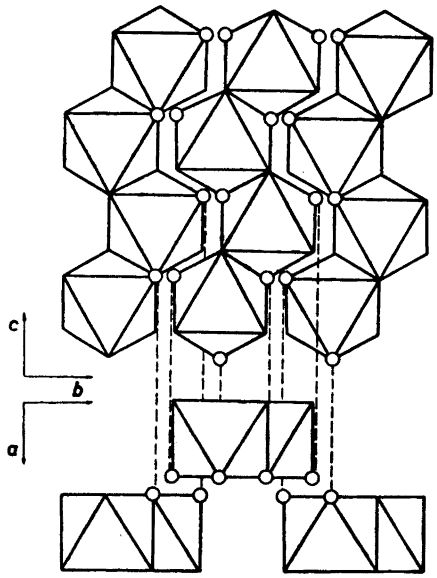


Fig. 1. The coupling of the ReO_6 octahedra of orthorhombic rhenium dioxide viewed along [100] and [001]. The strings of octahedra have been separated in order to reveal superimposed corners and edges. Corners shared by the strings are indicated by rings.

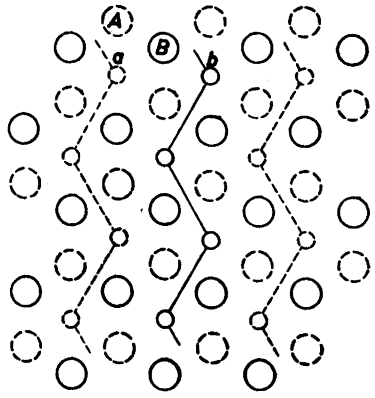


Fig. 2. The idealized structure of orthorhombic rhenium dioxide represented as hexagonal close-packing of the oxygen atoms (large circles). The rhenium atoms (small circles) are situated in octahedral holes. The sequence of the atoms normal to the plane of the figure is AaBbA.

The structure thus derived (*cf.* Fig. 1) has features in common with both the brookite and the rutile types. Thus both rhenium dioxide and brookite contain staggered strings formed by metal-oxygen octahedra having edges in common. While the strings of brookite are mutually connected by octahedra sharing edges and corners, those of rhenium dioxide are exclusively joined by corners as are the straight strings of rutile. No representative of this structure type seems to have been known before. However, as pointed out in a preliminary note [9] Pauling and Sturdivant [10] in connection with the determination of the brookite structure discussed a hypothetic structure, which is actually the same as the one now found for orthorhombic rhenium dioxide. The columbite structure is a superstructure of this type [11].

It is also possible to describe the structure as an hexagonal closepacking of oxygen atoms with rhenium atoms occupying certain of the octahedral interstices as illustrated in Fig. 2.

The pairwise arrangement of the metal atoms within the strings of the MoO_2 structure type has been ascribed to the existence of a homopolar bond between the metal atoms of the doublet [12]. In orthorhombic rhenium dioxide, the rhenium atoms within the staggered strings are uniformly distributed and at intervals (2.61 Å) which are longer than the short distance present in

Table 3. Metal-metal bond distances in some dioxides.

Compound	Structure type	Number of valence electrons available per metal-metal bond	Metal-metal distance Å
TiO_2	rutile	0	2.959
VO_2	MoO_2	2	2.65
ReO_2	ReO_2 (orthorhombic)	3	2.61
MoO_2	MoO_2	4	2.50
WO_2	MoO_2	4	2.49
TcO_2	MoO_2	6	(2.48)
ReO_2	MoO_2	6	(2.49)

the monoclinic rhenium dioxide (2.48 Å). However, if no intermetallic bond is present, the repulsion between the highly charged metal atoms would lead to metal-metal distances of octahedra sharing edges considerably longer than the ideal geometrical value (the normal oxygen-oxygen distance). This effect has actually been observed in several molybdenum and wolfram oxides, where distances of about 3.25 Å frequently occur [4]. Bonds are thus likely to be present also between the metal atoms of the strings of orthorhombic rhenium dioxide. Considering the fact that in this compound every metal atom is bound to two neighbours and the number of valence electrons per bond is thus only half that present in the MoO_2-type rhenium dioxide, the bond distance in the former compound fits in nicely in the qualitative relation between bond distance and number of valence electrons pointed out in a previous communication [13] (*cf.* Table 3).

The author is indebted to Mrs. Stina Nord for her valuable assistance in the experimental work.

These studies form part of a research program on metal oxides and related compounds financially supported by the *Swedish Natural Science Research Council.*

REFERENCES

1. Meisel, K. *Z. anorg. Chem.* **217** (1932) 121.
2. Zachariasen, W. H. *A. C. A. Program and Abstracts of Winter Meeting* (1951) F-4. *(Also private communication.)*
3. Wilhelmi, K.-A. *Acta Chem. Scand.* **8** (1954) 693.
4. Magnéli, A. *Nova Acta Regiae Soc. Sci. Upsaliensis* [4] **14** (1950) No. 8.
5. *Inorganic Syntheses, Vol. III,* New York-Toronto-London 1950.
6. Hambling, P. G. *Acta Cryst.* **6** (1953) 98.
7. Biltz, W. *Z. anorg. Chem.* **214** (1933) 225.
8. Lu, C. S. *Rev. Sci. Instr.* **14** (1943) 331.
9. Magnéli, A. *Acta Cryst.* **9** (1956) 1038.
10. Pauling, L. and Sturdivant, J. H. *Z. Krist.* **68** (1928) 239.
11. Sturdivant, J. H. *Z. Krist.* **75** (1930) 88.
12. Pauling, L. *Chem. Eng. News* **25** (1947) 2970.
13. Magnéli, A. and Andersson, G. *Acta Chem. Scand.* **9** (1955) 1378.

Received October 22, 1956.

ACTA CHEMICA SCANDINAVICA 11 (1957) 34—43

Determination of α-Tocopherol by Chromatography on Secondary Magnesium Phosphate

(With Collaborative Tests in Four Laboratories)

FINN BRO-RASMUSSEN and WILLY HJARDE

Statens Vitamin Laboratorium, Copenhagen, Denmark

A description is given of a method for quantitative determination of α-tocopherol in natural and enriched products. The method, which is generally applicable and suitable for routine examinations, consists in isolation of α-tocopherol by chromatography on secondary magnesium phosphate of the unsaponifiable fraction of the sample with subsequent Emmerie and Engel reaction in equal parts of alcohol and petroleum ether. The chromatography results in a complete separation in one step of α-tocopherol from other tocopherols as well as from carotinoids, vitamin A, sterols and other reducing substances without any time-consuming preliminary treatment. The results obtained by the described method are given and shown to be in close agreement with previously published results.

The chemical methods originally used for the estimation of the vitamin E content of a product aimed in principle at a determination of the total content of vitamin E active tocopherols. When it was found, however, that the biological potency of the individual tocopherols varied considerably, it was realized that methods of this nature were highly unsatisfactory. The vitamin E activity of most of the natural vitamin E sources is chiefly due to their content of α-tocopherol, since the vitamin E activity of some of the other tocopherols is so low that considerable amounts are required to make the activity comparable to that of α-tocopherol (this applies, *e.g.*, to γ- and δ-tocopherol), while in the case of others they occur very sparsely in nature (*e.g.* β-tocopherol, which has so far been found in wheat germ and wheat germ oil only). In practice the determination of the value of a certain product as a source of vitamin E must therefore take the form of a determination of its content of α-tocopherol. When further bearing in mind the growing appreciation of the importance of vitamin E, *e.g.* in feeding stuffs, which has led to the marketing of a steadily increasing number of products enriched with

synthetic α-tocopherol, it will be understood that there is an urgent need of a method for the determination of α-tocopherol for routine purposes.

In the course of time a number of attempts have been made in order to determine the proportion of individual tocopherols present. Hove and Hove [1] thus developed a method for the determination of the total content of tocopherols and the content of α-tocopherol based on the varying rates of reaction displayed by the individual tocopherols with Emmerie and Engel's reagent. Quaife [2] determines the content of α-tocopherol as the difference between the total content of tocopherols and the content of β-, γ- and δ-tocopherol on the basis of the conversion of the latter into nitroso derivatives which are chromatographed on zinc carbonate-Celite. Tosic and Moore [3] determine the content of α-tocopherol by chromatography on alumina of the unsaponifiable matter. By this chromatographic process α-tocopherol is collected together with carotene, however, necessitating a correction for the contribution to the $FeCl_3$-dipyridyl reaction provided by the latter substance. It is further stated that β-tocopherol is not separated completely, involving an overestimation of the content of α-tocopherol.

The best methods for the estimation of the individual tocopherols hitherto developed seem to be those based on paper chromatography which have recently found comparatively extensive application [4-7]. Most of these methods, however, require the removal of certain substances prior to the chromatography to prevent interference with the running of the tocopherols on the chromatogram. It is, *e.g.*, necessary to remove sterols by crystallization from methanol, while vitamin A and carotene are removed by adsorption to Floridin Earth. It seems, furthermore, that one-dimensional, reversed-phase chromatography involves certain losses. Brown [4] has thus ascertained recoveries of only about 80 % of tocopherols. Eggitt and Ward [5] state that the recoveries achieved by them by chromatography were about 95 %. Frequently, however, recoveries of only 90 % are obtainable [7]. A number of the difficulties mentioned above seem, however, to have been overcome by applying two-dimensional chromatography as devised by Green *et al.*[7] By subjecting the extract to initial chromatography on paper impregnated with zinc carbonate it will in many cases be possible to eliminate a number of the time-consuming preliminary treatments, and the duration of the subsequent reversed-phase chromatography may be cut down and the losses consequently diminished. Any statement of the total loss involved in this cromatographic determination is not given, however.

In the following a description will be given of a column chromatographic method for the determination of α-tocopherol in natural and enriched products. In principle the method is simple, and it is readily applicable in routine examinations. The chromatography, in which quantitative recovery of α-tocopherol (98—100 %) is obtained, serves to remove in one step both carotene and vitamin A as well as other tocopherols without any preceding reduction of the quantity of sterols present being required.

For special purposes the method can readily be modified so as to be applicable to the determination of the individual tocopherols. This will be accounted for elsewhere [8].

EXPERIMENTAL

The principle of the method. The material is saponified by means of alcoholic potassium hydroxide to which pyrogallol has been added to protect the tocopherols against oxidation. The saponified solution is extracted repeatedly with ether, and the combined ether extracts washed with water and subsequently dried with anhydrous sodium sulphate. The ether extract is now evaporated to dryness in a carbon dioxide atmosphere and the residue is dissolved in petroleum ether. From this solution α-tocopherol is isolated from the remaining reducing components by chromatography on secondary magnesium phosphate. The amount of α-tocopherol present is finally determined colorimetrically by means of ferric chloride and α,α-dipyridyl (Emmerie and Engel's reaction).

Equipment

Saponification flask with reflux condenser } size to be applied depends on the content of
Separatory funnels } tocopherol in the sample
Evaporation equipment arranged for connection to carbon dioxide supply.
Various volumetric flasks and pipettes.
Chromatographic tube (see Fig. 1).
Spectrophotometer.

Reagents

1. *Pyrogallol*
2. *Potassium hydroxide solution, about 60 %.* Dissolve 60 g potassium hydroxide pellets in 40 ml water.
3. *Absolute alcohol.*
4. *96 % alcohol.*
5. *Ethyl ether.* Render peroxide free by allowing to stand over potassium hydroxide pellets. Distill before use.
6. *About 0.5 N potassium hydroxide solution in about 30 % alcohol.* To 30 ml of potassium hydroxide solution, about 60 % (2) add 300 ml 96 % alcohol and water to make 1 l.
7. *Sodium sulphate.* Anhydrous.
8. *Petroleum ether.* Boiling point below 70°C.
9. *Secondary magnesium phosphate* for chromatography (Merck: Magnesium phosphoricum purum — *cf.* subsequent comments). The commercial product is activated as follows: Dry a quantity of magnesium phosphate corresponding to 200 g anhydrous substance for 24 h at not less than 176°C and cool over concentrated sulphuric acid. Boil the powder for 15 min with a solution of 20 g secondary sodium phosphate (Na_2HPO_4, $2H_2O$) in 1.6 l distilled water. Cool somewhat and separate on Büchner funnel, washing with about 1 l water. Dry the magnesium phosphate for not less than 48 h at not less than 176°C and cool to room temperature over concentrated sulphuric acid. Grind gently in a mortar and sieve through a 120 mesh sieve. Store in a dry place in a well-closed container.
10. *0.1 % ferric chloride solution in absolute alcohol* } store in brown bottles at room
11. *0.25 % alcoholic solution of α,α-dipyridyl* } temperature. Will keep for at least two months.

Procedure

Saponification and extraction. Weigh into the saponification flask a quantity of the sample equivalent to 0.4—4 mg α-tocopherol, but not less than 2 g. Add one fourth of the sample's weight of pyrogallol and as many ml of 60 % potassium hydroxide solution as denoted by the weight of the sample in g and four times its volume of 96 % alcohol.

Saponify by bringing to the boil on water bath and boiling for 10 min. Cool somewhat and add a volume of water equal to three times the volume of alcohol used. Transfer into a separatory funnel, rinsing the flask with ether, using 100—200 ml according to the volume of the sample. When working with larger quantities of feeding stuffs, the alcoholic saponification solution may be decanted into a separatory funnel into which the required volume of water has already been transferred. In this case wash the precipitate successively with all the ether used for the extraction. Shake or swirl the separatory funnel for

one minute, allow the layers to separate and run the aqueous phase into another separatory funnel in which extraction is performed by means of 50—100 ml fresh ether. After a third extraction process, transfer the three ether extracts into one separatory funnel and wash with 100 ml water, 100 ml 0.5 N potassium hydroxide in 30 % alcohol and finally with three 100—200 ml portions of water.

Dry the ether extract by filtering through a 2—3 cm thick layer of anhydrous sodium sulphate placed on a glass filter, and reduce the volume by evaporation in a carbon dioxide atmosphere on water bath until only a few ml remain. Remove the last traces of ether by means of a current of carbon dioxide, but do not heat.

By means of petroleum ether transfer the residue into a volumetric flask of suitable size and fill to volume with petroleum ether.

Chromatography. A column is prepared from the activated magnesium phosphate by suspending a suitable quantity in petroleum ether and running the mixture into a chromatographic tube, the effective length of which is 20 cm and the internal diameter 12 mm (Fig. 1). This tube is connected by means of a rubber tube to a nitrogen cylinder, the nitrogen pressure being regulated so as to provide a suitable rate of flow (2—4 ml per min). When the column of magnesium phosphate has settled, it is covered with a thin layer of anhydrous sodium sulphate. The petroleum ether level must never be allowed to fall below the top of the magnesium phosphate column.

An aliquot of the petroleum ether extract corresponding to about 0.4 mg α-tocopherol (quantities down to 0.1 mg may, however, be determined) is now transferred to the column.

After rinsing with 50 ml petroleum ether, the receiver is exchanged and α-tocopherol is eluted with altogether 150 ml 2 % ethyl ether in petroleum ether. Carotene will not be adsorbed to the column, but may be collected with the petroleum ether. β-, γ-, and δ-tocopherol as well as vitamin A are adsorbed, but require to be eluted an ether concentration higher than 2 % (*cf.* Bro-Rasmussen and Hjarde [8]).

The α-tocopherol fraction is evaporated on a water bath (30°C) until a residue of 5—10 ml remains. This residue is transferred into a volumetric flask (if the quantity of α-tocopherol chromatographed is 0.4 mg, a 30 ml volumetric flask will be suitable), several portions of absolute alcohol and petroleum ether are used for rinsing, the rinsings are added and the flask filled up with absolute alcohol and petroleum ether resulting in an α-tocopherol solution in a solvent consisting of equal parts of alcohol and petroleum ether.

To check the effectivity of the chromatography the last 5 ml petroleum ether eluate plus the first 5 ml petroleum ether-ethyl ether eluate are collected in a 20 ml volumetric flask with 10 ml absolute alcohol. Now the main fraction is collected as described above and, finally, 10 ml eluate likewise in a 20 ml volumetric flask with 10 ml absolute alcohol. Eluate collected in this way before and after the main fraction must not give any reaction for α-tocopherol (*cf.* the subsequent comments).

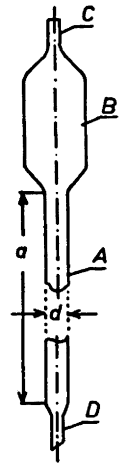


Fig. 1. Chromatographic column. A: column. B: reservoir for eluent. C: connection to pressure. D: outlet tube to retain plug of cottonwool at base of A.

The colorimetric measurement. To a 5 ml sample of the solution containing the isolated α-tocopherol are added 0.25 ml ferric chloride solution (reagent No. 10) and 0.25 ml α,α-dipyridyl solution (reagent No. 11).

The intensity of the colour is measured in a spectrophotometer (or suitable colorimeter) at 520 mμ exactly two min after the addition of the reagents, at which time the intensity must have reached a constant value.

A blank determination is run on 2.5 ml petroleum ether +2.5 ml absolute alcohol + 0.25 ml ferric chloride solution + 0.25 ml α,α-dipyridyl solution.

The value of $E^{1\%}_{1\,cm}$ 520 mμ for the sample can now be calculated and the content of α-tocopherol in the sample examined can be found. By measurements on spectrophotometer at 520 mμ the value of $E^{1\%}_{1\,cm}$ for pure α-tocopherol is taken to equal 400.

Comments

re secondary magnesium phosphate. It seems to be difficult to establish any certain criteria as regards the suitability of a commercial product for the purpose of chromatography. Examination of a number of products has shown that it is possible frequently, but not invariably from products of the above mentioned quality to obtain charges which can be activated. It appears to be necessary to test each charge directly by chromatographing pure α-tocopherol. In this process the α-tocopherol must not be eluted from a 20 cm column by means of 100 ml petroleum ether followed by 100 ml 0.5 % ethyl ether in petroleum ether, while elution should be quantitative when about 125 ml 2 % ethyl ether in petroleum ether is used. If α-tocopherol is eluted by means of petroleum ether or 0.5 % ethyl ether in petroleum ether, the charge of magnesium phosphate is unsuitable for the purpose, its activity being too low to allow for the adsorption of α-tocopherol from low-potency products with a large content of impurities.

re saponification. According to the method used in this case the sample to be tested is saponified directly without any preceding extraction of the fats. Pyrogallol is used to protect the tocopherol against oxidation in the alkaline solution. In agreement with previous investigations [3] pyrogallol was observed to have a marked effect, as will appear from Table 1.

However, even when using pyrogallol, it is not possible completely to eliminate losses in the α-tocopherol determination.

The losses involved in the analyses of individual products may be determined by parallel experiments in which known quantities of tocopherol corresponding to the contents in the products are added and recoveries determined. The following section on the results obtained by the present method gives examples of the losses involved in such determinations.

re chromatography. If the magnesium phosphate fulfills the above requirements, the efficiency of a chromatographic separation may be judged in the following way:

If the eluate collected before the main fraction gives reaction for reducing substances, this may be due either to a content in the extract of reducing substances which are eluted

Table 1. The protective effect of pyrogallol in the determination of α-tocopherol

	Quantity of α-tocopherol found (μg/g)		
	Butter	Wheat germ oil	Enriched fat emulsion
With pyrogallol	23.3	2 060	180
Without pyrogallol	21.5	1 570–1 720	139
Difference in %	8	17–24	20

immediately before α-tocopherol, or to an incomplete adsorption of α-tocopherol. If necessary, the identity of the reducing substances must be determined by chromatography of a parallel sample of the extract to which α-tocopherol has been added. According to the experiences gained hitherto it seems that in cases where this problem has been significant the reason has been an incomplete adsorption of α-tocopherol on account of extreme contents of impurities, chiefly sterols. In such cases a column of 5—10 cm greater length of the column is used.

If the fraction collected immediately after the main fraction displays a reducing action this indicates that tocopherol-like substances are eluted immediately after α-tocopherol.

The latter condition will generally manifest itself in the course of the colorimetric measurement in the form of an increase of the intensity of colour, since only α-tocopherol has been found to produce a colour of constant intensity in the course of 2 min in the mixture of alcohol and petroleum ether used here.

If it is not feasible in this way to eliminate the possibility that impurities have been collected together with α-tocopherol, the chromatography must be repeated, the eluate being collected in fractionation flasks half full of absolute alcohol. From each of the fractions which contain α-tocopherol an aliquot is drawn. These are combined and taken up with a suitable volume of equal parts of absolute alcohol and petroleum ether. If it is not immediately possible to ascertain which of the fractions contain α-tocopherol, parallel chromatography on part of the extract to which pure α-tocopherol has been added must, as referred to above, be resorted to.

RESULTS AND DISCUSSION

As mentioned above a number of determinations of the losses involved in the use of the method have been made in the course of the present work. Table 2 lists the total percentage recoveries for a number of samples with different α-tocopherol contents. It appears from this that the total recovery for the whole procedure decreases with decreasing content of α-tocopherol, the recovery in the case of wheat germ oil with a content of 2 100 μg/g being 98 %, while in the case of chicken feed containing 11 μg/g the loss is 15 %. It should be noted that the loss deriving from the chromatography only constitutes a small and constant part of the total loss (0—2 %), it having been endeavoured in all cases to use for the cromatography a quantity of the product containing about 0.4 mg α-tocopherol (in the case of chicken feed the quantity was only about 0.2 mg). The chief part of the losses in the case of the low-potency samples thus derive from the saponification and the extraction.

As already mentioned, the colorimetric measurement of the content of α-tocopherol is performed in solution in equal parts of alcohol and petroleum ether. For the purpose of the described method this solvent offers two advan-

Table 2. Total percentage recoveries in the α-tocopherol determination

Sample	α-Tocopherol found (μg/g)	Total recovery (%)	Corrected content (μg/g)
Wheat germ oil	2 060	98	2 100
Enriched feeding stuff	550	97	565
Enriched fat emulsion	180	95	189
Butter	23.5	90	26.1
Chicken feed	9.1	85	11

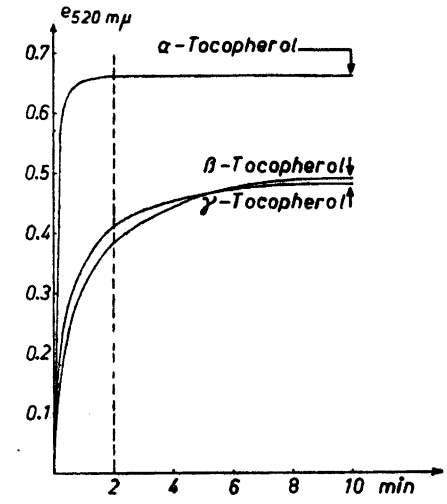


Fig. 2. The colour development at the Emmerie—Engel reaction for α-, β- and γ-tocopherol in petroleum ether/ethanol = 1/1.

tages above alcohol which is the solvent generally used. In the first place it is possible to use the eluate directly for the colorimetric measurement if it is collected in fractionation flasks half full of absolute alcohol, a procedure which is not feasible if petroleum ether only is used. This is of importance in cases when it proves to be necessary to perform a fractionate collection of α-tocopherol as mentioned above, and further in cases when a determination of the other tocopherols is required (*cf.* Bro-Rasmussen and Hjarde [8]). In the second place the use of this solvent gives a fairly certain criterion as to whether the reducing substance collected in the routine cromatography is identical with α-tocopherol, since, as already mentioned, it has been found that it is only the reduction by α-tocopherol of the ferric ions in Emmerie and Engel's reaction which is completed in less than 2 min. To illustrate this, Fig. 2 shows the relationship between colour intensity and time in the case of α-, β-, and γ-tocopherol. As it appears, most clearly in the case of β- and γ-tocopherol, the rate of reaction is reduced as compared to that prevailing in the case of corresponding measurements in alcohol. In the solvent used in this case full colour development is only obtained in the course of 7—10 min in the case of β- and γ-tocopherol, while in alcohol all the three tocopherols mentioned show full colour development in the course of less than 2 min [9].

The fact that the rate of reaction is thus less than when the reaction takes place in alcohol has no influence on the final colour intensity. In the case of synthetic α-, β-, and γ-tocopherol the $E^{1\%}_{1\,cm}$ 520 mμ values have thus in all cases been found to equal about 400 when measured after periods of 2, 10, and 10 min, *i.e.* the same value as that generally given for the reaction in alcohol. It should finally be mentioned that Lambert-Beer's law also applies unchanged when Emmerie and Engel's reaction is performed in a mixture of equal parts of alcohol and petroleum ether. δ-Tocopherol is the only tocopherol which does not show linear dependence on the concentration, for which reason a standard curve should be used in this case.

While the results of collaborative tests made in four laboratories to examine the reproducibility of the method are given in an addendum, a number of determinations of the α-tocopherol content of natural products will be given in the following (Table 3).

Table 3. Content of α-tocopherol in natural products (μg/g)

Material	Results obtained by present method	Results obtained by other workers
Wheat germ oil	2 100	1 680[4]
Wheat germ	220	—
Soybean oil	110	124[4]
Rapeseed oil	225	151[7]
Cottonseed oil	325	470[7]
Corn germ meal	73	—
Butter (summer)	26	24.8[10]
Lucerne	27	22—28[11]
Lucerne silage	36	30—31[11]
Chicken feed	11	—

Among the values given in the table only the determinations made on soybean oil and chicken feed have required additional chromatography with fractionate collection of α-tocopherol, since in these cases it has been found that α-tocopherol is followed immediately by a reducing substance which cannot be identified as a tocopherol [8]. In the case of all the other materials α-tocopherol has been collected directly in one fraction with 150 ml 2 % ether in petroleum ether.

With respect to some of the materials Table 3 lists α-tocopherol contents determined by other workers. A comparison shows that the values found in the present investigation agree well with those previously found.

The present method meets the demand for a simple and readily reproducible method for the determination of α-tocopherol independently of other tocopherols and other reducing constituents of natural and enriched products. The method has another advantage, *viz.* that it is generally applicable and at the same time provides a fairly good criterion as to the specificity of the method. Only in the case of products of very low potency will appreciable losses due to the saponification and extraction processes occur, necessitating parallel experiments with known α-tocopherol additions to correct for such losses. The chromatography, on the other hand, is practically quantitative.

Acknowledgements. We wish to express our thanks to Professor P. Karrer for a sample of synthetic β-tocopherol and to A/S Dansk Sojakagefabrik, Copenhagen, for the cottonseed oil and rapeseed oil used in the investigation.

REFERENCES

1. Hove, E. L. and Hove, Z. *J. Biol. Chem.* **156** (1944) 601.
2. Quaife, M. L. *J. Biol. Chem.* **175** (1948) 605.
3. Tosic, J. and Moore, T. *Biochem. J. London* **39** (1945) 498.

4. Brown, F. *Biochem. J. London* **52** (1952) 523.
5. Eggitt, P. W. R. and Ward, L. D. *J. Sci. Food Agr.* **4** (1953) 176.
6. Eggitt, P. W. R. and Ward, L. D. *J. Sci. Food Agr.* **4** (1953) 569.
7. Green, I., Marcinkiewicz, S. and Watt, P. R. *J. Sci. Food Agr.* **6** (1955) 274.
8. Bro-Rasmussen, F. and Hjarde, W. *Acta Chem. Scand.* **11** (1957) 44.
9. Stern, M. H. and Baxter, J. G. *Anal. Chem.* **19** (1947) 902.
10. Hellström, V. and Andersson, R. *Vår Föda* **7** (1955) 33.
11. Brown, F. *J. Sci .Food Agr.* **4** (1953) 161.

Received September 25, 1956.

Addendum

COLLABORATIVE EXAMINATIONS OF A METHOD FOR THE DETERMINATION OF α-TOCOPHEROL BY CHROMATOGRAPHY ON SECONDARY MAGNESIUM PHOSPHATE

K. Bondrup, A/S Ferrosan, Finn Bro-Rasmussen, Statens Vitamin Laboratorium, E. Jensen, F.D.B.'s centrallaboratorium, and E. Jespersen, Leo Pharmaceutical Products, Copenhagen, Denmark.

The method described above for the determination of α-tocopherol has been checked through collaborative examinations in four laboratories.

The examinations comprised two experimental series as difficulties were experienced as regards the acquisition of suitable magnesium phosphate for the first series. The difficulties manifested themselves in particular with regard to the results obtained in one of the laboratories, for which reason these results have been omitted from Table 4.

Table 4. Results of collaborative tests

Experimental series	Sample of	Calculated addition of α-tocopherol	Results of tests in μg α-tocopherol per g			
			Laboratory			
			A	B	C	D
1	Wheat germ oil	0	2 040	1 800	1 960	2 020
	Soybean oil	0	—	180	240	165
	Soybean oil with an addition of 0.469 mg α-tocopherol acetate per g	410	—	530	580	540
	Feeding stuff x	0	—	70	65	60
	Feeding stuff x with an addition of 0.624 mg α-tocopherol acetate per g	546	—	480	560	570
	Feeding stuff x with an addition of 4.61 per cent wheat germ oil	90	—	160	130	145
2	Feeding stuff y (chiefly ground cereals)	0	6	6	6.6	9
	Feeding stuff y with an addition of 0.0486 mg α-tocopherol acetate per g	42.5	36	44	47	46—38
	Feeding stuff y with an addition of 0.481 mg α-tocopherol acetate per g	420	350	460	440	430

The materials selected for the tests as well as the results of the latter appear from Table 4. As it will be seen, some of the samples have been given an addition of known quantities of tocopherol acetate. For this purpose a commercial, synthetic preparation has been used, analysis of which showed it to contain 875 mg tocopherol per g, corresponding to 96 % pure α-tocopherol acetate. The figures given in the table as regards quantities of tocopherol added have been calculated on the basis of this analysis.

Results of the examinations

Consideration of the results of series 1 shows that maximum deviation occurs in connection with the examination of soybean oil. The reason is that this oil contains reducing substances which are eluted with 2 % ether immediately after α-tocopherol [8] and thus give rise to results which are too high when, as done here, the α-tocopherol fraction is delimited by the collection of a stipulated quantity of eluate. As already mentioned, the presence of this impurity in the α-tocopherol fraction will disclose itself, in that the intensity of the colour does not reach a constant value in the course of 2 min and, further, in that the fraction collected immediately after the main fraction will give a colour reaction with ferric chloride-dipyridyl. If collection in small fractions, as described above, is applied, enabling a delimitation of the α-fraction in each individual case, this source of error will be eliminated.

The presence of the impurities does not make itself felt so much in soybean oil to which α-tocopherol has been added, *i.a.* because a smaller amount of extract is required on the column due to the greater content of α-tocopherol with a correspondingly smaller content of interfering reducing substances.

As regards the results of series 2 the agreement is better although the values obtained by Laboratory A are lower than those of the other laboratories. However, Laboratory A's examinations were made at a somewhat later time than those of the other three laboratories, and it is possible that the lower results are caused by storage losses. The examinations made by Laboratory D of one of the samples suggest that this may be the case, the two values having been obtained by examinations performed at an interval of three months.

It will be seen that it is possible to determine a content of α-tocopherol of less than 10 μg per g, but the accuracy of this determination would no doubt have been better if collection in small fractions had been used for the delimitation of the volume of the α-fraction.

It should be added that the results of repeated examinations of the same material in one laboratory show considerably smaller variations than might have been expected from the discrepancies between the examinations in the four laboratories as given in the table.

From the examinations made the conclusion must be drawn that complete agreement cannot always be obtained from determinations made according to the present method in different laboratories. In cases of doubt, and always when dealing with feeding stuffs with a low content of α-tocopherol, the chromatography should comprise collection in small fractions so as to make it possible to plot the fractionation curve.

ACTA CHEMICA SCANDINAVICA 11 (1957) 44—52

Quantitative Determination of the Individual Tocopherols by Chromatography on Secondary Magnesium Phosphate

FINN BRO-RASMUSSEN and W. HJARDE

Statens Vitamin Laboratorium, Copenhagen, Denmark

A method is given for the determination of the distribution of tocopherols in natural products. The method depends on columnar chromatographic separation of the natural tocopherols in three groups in which the chief components are α-, $\beta+\gamma$-, and δ-tocopherol.

With regard to the recently described and more rarely occurring tocopherols, ζ-tocopherol (5,7-dimethyltocol) will be found together with α-tocopherol, while ε-tocopherol (5-methyltocol) is estimated together with β- and γ-tocopherol.

The possibility of obtaining further separation of the individual tocopherols and the importance in practice of such a separation are discussed, both with a view to the vitamin E activity of the tocopherols and to their action as antioxidants.

Examples are mentioned and the results discussed.

For the majority of practical purposes, in estimating the vitamin E activity of natural products, the greatest significance will be attached to the contents of α-tocopherol. The reasons for this are the higher biological potency of α-tocopherol and the fact that it is the most abundant of the tocopherols. Likewise, in the case of enriched products the tocopherol used will generally be α-tocopherol.

In spite of these facts, the problem of determining the content of other tocopherols in a certain product will at times be of considerable interest. It is thus well-known that the content of α-tocopherol in certain vegetable oils is fairly low compared to their content of other tocopherols, so that to obtain a reliable estimate of the value of such a product as a vitamin E source the contribution to the activity due to each individual tocopherol should be taken into consideration.

The same applies to some extent to tocopherol determinations, the purpose of which is to establish the antioxidant activity of natural products. In this connection it should be noted, however, that it is not possible concerning the antioxidant activity to ascribe a predominating effect to any one of the tocopherols as is possible with respect to the vitamin E potency. When

determining the antioxidant activity of the tocopherols of a certain product, it will thus frequently be insufficient to account for the content of α-tocopherol only.

In such cases a method for the determination of the individual tocopherols is essential. The development of methods for this purpose has commanded great interest during recent years. So far the best results seem to have been obtained by the application of paper chromatography [1-3]. These methods have made it possible to make quantitative determinations of the tocopherols hitherto found (α, β-, γ-, and δ-tocopherol) and also to demonstrate the presence of two new natural tocopherols, *viz.* ε-tocopherol (5-methyltocol) and ζ-tocopherol (5,7-dimethyltocol). On the basis of experience drawn from the paper chomatographic methods Eggitt and Norris [4] have quite recently developed a method for the separation of tocopherol mixtures by means of partition chromatography on paraffin-impregnated kieselguhr columns. This reversed-phase technique allows a separation of the tocopherols into three groups of isomers, *i.e.* mono-, di-, and tri-methyltocols. The authors of the present article have, however, only learned of this method after the conclusion of the present work.

In the following a description will be given of a method for the determination of the individual tocopherols depending on cromatography on secondary magnesium phosphate. This method is a further development of a method for the determination of α-tocopherol published previously (Bro-Rasmussen and Hjarde [5]). When chromatographing tocopherol mixtures on secondary magnesium phosphate, the tocopherols are adsorbed from a solution in petroleum ether. Elution with ethyl ether in petroleum ether in concentrations increasing gradually from 2 % to 6—7 % will result in successive elution of the individual tocopherols in the following order: α-, $\beta+\gamma$-, δ-tocopherol. Any carotene present will not be adsorbed, but will pass through the column with the petroleum ether, while any vitamin A present will require an eluent containing 10—15 % ether, *i.e.* it will be eluted after δ-tocopherol.

EXPERIMENTAL

The present investigations have all been performed according to the technique used for the determination of α-tocopherol as previously described [5] with the exception that the chromatography of the unsaponifiable fraction of the sample has been continued beyond elution with 2 % ether, using gradually increasing ether concentrations as mentioned in connection with each individual experiment.

In certain cases it proved to be convenient, in order to obtain maximum separation, to use a column of greater length than 20 cm. In such cases a 30 cm column has generally been used. This means that α-tocopherol is only eluted quantitatively when slightly more than 150 ml eluent with 2 % ether has been used, but it does not give rise to greater losses in connection with the chromatography than the 0—2 % losses usually met with.

It should finally be stated that fractional collection has been applied in all cases. Fractions have been collected by volume in volumetric flasks half-full of absolute alcohol. The Emmerie-Engel reaction has subsequently been applied to each individual fraction, the measurement being made in the case of α-tocopherol after a 2 min interval, in the case of β- and γ-tocopherol after 10 min, and in the case of δ-tocopherol after 20 min.

The adsorption of α- and β-tocopherol. The unsaponifiable fraction of about 2.5 g wheat germ was chromatographed on a 20 cm column. Elution with 2—4 % ether in petroleum ether. Fig. 1 shows the fractionation curve, the extinction at 520 mμ after the reaction with ferric chloride and α,α-dipyridyl being plotted for each individual fraction.

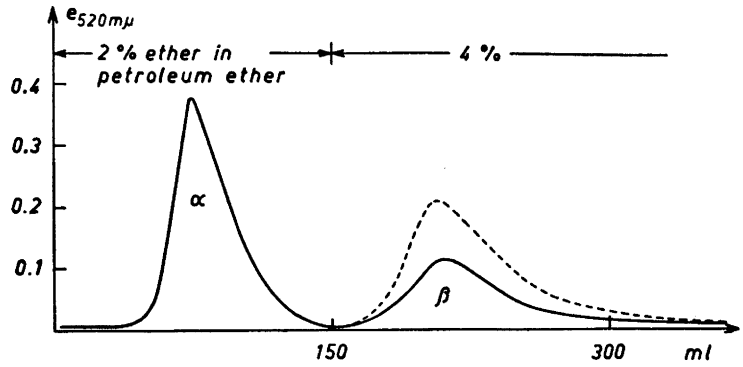


Fig. 1. Fractionation curve for wheat germ with a column 200 mm long. The dotted curve represents the result of addition of synthetic β-tocopherol.

It will be seen from the curve that the separation between the α- and β-tocopherol of wheat germ is complete, α-tocopherol being eluted with 2 % ether and β-tocopherol with about 4 % ether in petroleum ether. Summation shows the total contents in wheat germ to be:

α-tocopherol: 220 μg/g~66 %
β-tocopherol: 112 μg/g~34 %
Altogether: 332 μg/g~100 %

The identification of the two tocopherols of wheat germ was made by parallel runs with addition of the pure substances. To illustrate this the dotted curve in Fig. 1 represents the fractionation of wheat germ to which synthetic β-tocopherol (5,8-dimethyltocol) has been added.

The adsorption of γ-tocopherol. Experiments made with pure synthetic γ-tocopherol * show that this substance is adsorbed on secondary magnesium phosphate and that it is eluted with petroleum ether with about 4 % ether.

Chromatography on a 30 cm column of the unsaponifiable fraction of about 2.5 g wheat germ + about 0.5 mg γ-tocopherol was used to examine the adsorption of γ-toco-

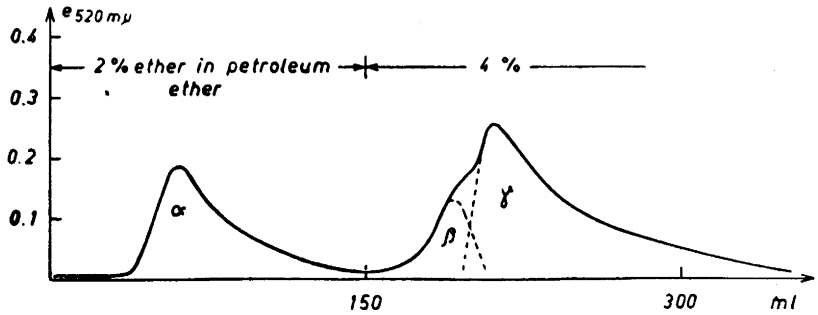


Fig. 2. Fractionation curve for wheat germ after addition of synthetic γ-tocopherol. Column 300 mm long.

* Bought from Distillation Products Industries.

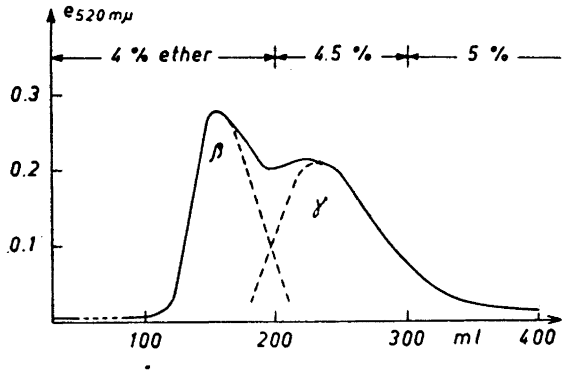


Fig. 3. Fractionation curve for mixture of synthetic β- and γ-tocopherol with a column 500 mm long.

pherol relative to that of β-tocopherol. Fig. 2 shows that β- and γ-tocopherol are on the whole eluted together by means of about 4 % ether. It appears from the figure, however, that there is a tendency towards separation, β-tocopherol being eluted together with the front of the γ-tocopherol zone.

That this tendency is an actual one appears more clearly from Fig. 3 which shows the fractionation curve obtained by chromatography of approximately equal quantities of pure β- and γ-tocopherol on a 50 cm column.

The adsorption of ζ-tocopherol. By means of two-dimensional paper chromatography Green *et al.*[3] have shown that 5,7-dimethyltocol is occasionally found in natural products, and they have given this substance the name of ζ-tocopherol. Since this tocopherol is known to possess a biological potency of the same order of magnitude as that of α-tocopherol (Jacob, Sutcliffe and Todd [6]), it is essential to examine the adsorption exhibited by this substance on chromatography with a view to vitamin E estimation.

By preliminary experiments it is found that synthetic 5,7-dimethyltocol is adsorbed on magnesium phosphate and eluted by means of 2 % ether in petroleum ether, *i.e.* as α-tocopherol. Chromatography on a 20 cm column together with α-tocopherol confirms

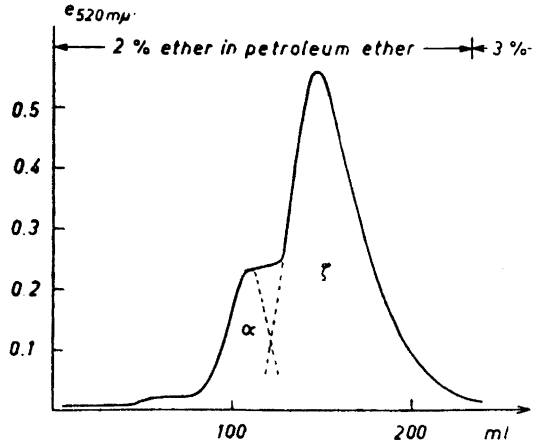


Fig. 4. Fractionation curve for mixture of synthetic α- and ζ-tocopherol with a column 300 mm long.

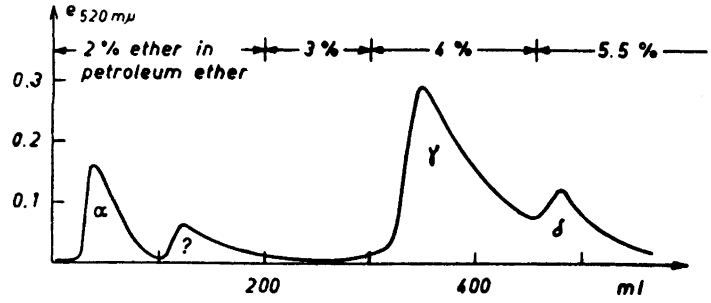


Fig. 5. Fractionation curve for unsaponifiable fraction of soybean oil with a column 300 mm long.

these results, α- as well as ζ-tocopherol being eluted quantitatively by means of 150 ml of 2 % ether in petroleum ether. In routine determinations of α-tocopherol any ζ-tocopherol present will thus be included in the estimate, a result which shows good agreement with the biological activities.

However, chromatography on a 30 cm column shows that there is a certain tendency towards separation between α- and ζ-tocopherol (Fig. 4), the adsorption of α-tocopherol being slightly weaker than that of ζ-tocopherol. Complete separation by this method does not seem to be possible, however.

δ-Tocopherol. Chromatography of soybean oil. To examine the asorption of δ-tocopherol the unsaponifiable fraction of about 2.5 g soybean oil was subjected to chromatography on a 30 cm column.

As appears from the fractionation curve (Fig. 5), a separation into four reducing substances is observed. Out of the four substances three may be identified as above in the case of β-tocopherol (Fig. 1) and are found to be α-, γ-, and δ-tocopherol, which may thus be separated completely, δ-tocopherol not being eluted until the ether concentration in the eluent has reached 6—7 %. The three tocopherols are found to be present in the following quantities:

α-tocopherol:	110 μg/g~13 %
γ-tocopherol:	430 μg/g~51.5 %
δ-tocopherol:	295 μg/g~35.5 %
Altogether:	835 μg/g~100 %

The possibility that the fourth reducing substance which is separated in the chromatography of soybean oil (marked with a ? in Fig. 5) is a tocopherol must apparently be ruled out. Judging from the course of the adsorption ζ-tocopherol is the only possibility, but chromatography of soybean oil with an addition of 5,7-dimethyltocol shows that the unknown substance is not identical with this substance. On the contrary, it appears from Fig. 6 that it is adsorbed between α-tocopherol and 5,7-dimethyltocol. By acting as "displacement carrier" the substance causes the above-mentioned, very incomplete separation between the two tocopherols to become complete. Thus there is no doubt that the unknown substance is not a tocopherol.

ε-Tocopherol. Chromatography of wheat bran. The last of the known natural tocopherols, 5-methyltocol, has hitherto been found in wheat bran and wheat germ only, in the former case in larger quantities, in the latter in small quantities [2,3]. It has been given the name ε-tocopherol.

Chromatography of the unsaponifiable fraction of about 10 g wheat bran showed that the total tocopherol content of 83 μg/g distributes itself between two elution peaks (Fig. 7), *viz*:

"α-tocopherol":	12.5 μg/g~15 %
"β-tocopherol":	70.5 μg/g~85 %
Altogether	83 μg/g~100 %

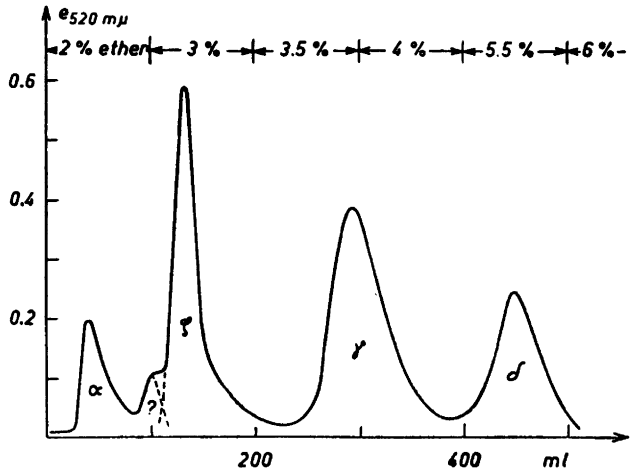


Fig. 6. Fractionation curve for soybean oil after addition of synthetic ζ-tocopherol. Column 300 mm long.

As previously shown, the "α-peak" may contain both α- and ζ-tocopherol. For the examination of the "β-peak" chromatography on paper impregnated with liquid paraffin was applied, the solvent used being 75 % alcohol. This showed that the "β-tocopherol" consisted of two components with $R_F = 0.55$ and $R_F = 0.75$, respectively. By means of parallel experiments in which pure β-tocopherol had been added the spot with $R_F = 0.55$ was identified as being due to β-tocopherol. The other spot ($R_F = 0.75$) thus seems to be identical with Brown's "fast spot" [1] as well as with the ε-tocopherol found by Eggitt and Ward [2] and by Green *et al.*[3]

The quantitative distribution of the components o f "β-tocopherol" was found to be as follows:

β-tocopherol: 11.5 μg/g~14 % of the total in wheat germ
ε-tocopherol: 59 μg/g~71 % » » » » » »

in good agreement with the results obtained by Green *et al.*[3]

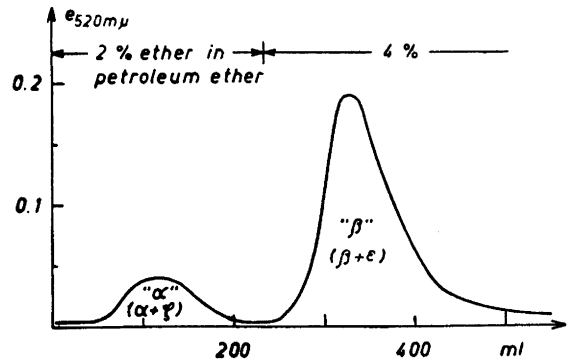


Fig. 7. Fractionation curve for wheat bran with a column 300 mm long.

DISCUSSION

The present experiments show that chromatography of mixtures of the known natural tocopherols on secondary magnesium phosphate results in a separation into three main groups, the number of methyl groups in *ortho* positions in relation to the 6-hydroxy group being the factor which chiefly determined the affinity to the adsorbent magnesium phosphate:

α-, and ζ-tocopherol are eluted with 2 % ether,
β-, γ-, and ε-tocopherol are eluted with 4 % ether,
δ-tocopherol is eluted with 6—7 % ether.

This separation is in perfect analogy with the conditions prevailing in chromatography on zinc carbonate-impregnated paper [3].

The possibility of obtaining further separation by means of the described chromatographic technique has been considered. The tendency, which is shown by Figs. 3 and 4, towards a separation of β- from γ-tocopherol and of α- from ζ-tocopherol suggests that the use of longer columns might enable further separation. In agreement with this attempts at a separation between β- and γ-tocopherol on a 50 cm column have shown improved separation as compared to that obtained on a 30 cm column. As, however, the separation on the 50 cm column is still very incomplete, the experiments have not so far been continued.

Another theoretical possibility of further separation has been demonstrated in connection with the chromatography of soybean oil. When, as shown in the case of α- and ζ-tocopherol there is a slight difference in the adsorption of the tocopherols, suitable substances may be used with success as "displacement carriers", causing a complete separation by being adsorbed between the two substances. The artefact found in soybean oil presents an example. Lacking knowledge of the chemical structure of this substance makes it impossible, however, at present to utilize this fact.

According to the technique used for the present investigations a more complete separation is apparently possible only when applying additional chromatography on paraffin-impregnated paper, as mentioned in connection with the adsorption of ε-tocopherol, a procedure which does not present any difficulties. In this connection it should be noted that by the chromatography on magnesium phosphate the sterols have been removed from the extract so that paper chromatography can be applied directly to the obtained tocopherol fractions. It should also be mentioned that a combination of the recently published reversed-phase partition chromatography on paraffin-impregnated kieselguhr [4] and chromatography on magnesium phosphate will give a separation corresponding to that obtained by two-dimensional paper chromatography. The determination might, *e.g.*, also be made by means of two parallel chromatographic separations of the unsaponifiable matter with subsequent calculation of the contents.

If the problem dealt with is the vitamin E activity of the tocopherols, it is a question, however, considering the biological activity of the individual tocopherols, whether there is any need of further differentiation beyond the three groups referred to above. As regards the biological activity of ζ-tocopherol it

is known that it is almost identical with that of α-tocopherol [6]. Even if the biological potency of ε-tocopherol has not as yet been determined, a consideration of its chemical structure will show that there is every reason to expect that it approximates that of γ- and β-tocopherol, which is generally stated to be 20—30 % of that of α-tocopherol [7]. Finally the biological potency of δ-tocopherol is taken to be 1 % (or less) of that of α-tocopherol. It will thus be seen that the separation obtained corresponds closely to the order of the biological potencies, so that when it is necessary to consider other tocopherols than α-tocopherol, a chromatographic separation on magnesium phosphate will be quite sufficient for most practical purposes.

Of course, it is not possible to apply these findings directly to the question of the antioxidant properties of the tocopherols. It cannot be excluded that for this purpose a complete elucidation of the composition of the tocopherol content may be of interest. In that case chromatography on magnesium phosphate may be combined with chromatography on paraffin-impregnated paper or reversed-phase partition chromatography on kieselguhr columns. It should be emphasized, however, in this connection that definite, quantitative figures for the relative antioxidant potencies of the tocopherols can hardly be given, since the values found depend to a great extent on methods of examination, temperature and criteria applied. [8,9] When taken together with our present lack of knowledge with regard to the antioxidant properties of the most recently described tocopherols, these circumstances tend to cause a determination of the content of each individual tocopherol to be rather illusory.

As mentioned previously in connection with the determination of α-tocopherol [5], column chromatography does not give rise to losses of any magnitude. Chromatography of a mixture of β- and γ-tocopherol on a 50 cm column and elution with 4—5 % ether in petroleum ether thus results in recoveries of 97—98 %.

Table 1. Distribution of tocopherols in natural products

Product	Total tocopherols (μg/g)	$\alpha+\zeta$ (%)	$\beta+\gamma+\varepsilon$ (%)	δ (%)
Wheat germ	332	66	34	
Wheat germ oil	2 300	91	9	
Wheat bran	83	15	85	
Corn germ meal	307	24	76	
Soybean oil	835	13	51.5	35.5
Rapeseed oil	691	32.5	68	
Cottonseed oil	888	36	64	
Mustard oil	525	16	84	

Table 1 lists the results of a number of examinations of natural products which are known to contain considerable quantities of the other tocopherols in addition to α-tocopherol.

Among the products mentioned in Table 1 both soybean oil and mustard oil contain artefacts which are eluted between α- and γ-tocopherol fractions. In soybean oil these substances occur in quantities corresponding to 8 % of

the total reducing power. Corresponding observations have been made by Green *et al.*[3] in twodimensional paper chromatography.

When considering the adsorption data, the artefacts observed in the course of the present investigation do not appear to be identical with those found by Green *et al.*, the latter authors stating that the reducing substances move beyond the α-tocopherol position on zinc carbonate paper, which should correspond to elution before α-tocopherol from the magnesium phosphate column.

The relative contents of α- and β-tocopherol in wheat germ correspond exactly to the values previously found [1,3]. It is remarkable, therefore, that the wheat germ oil examined displays such a low content of β-tocopherol, both as regards absolute and relative values. As the oil in question is a refined wheat germ oil, it cannot, of course, be excluded that the refining process has destroyed part of the β-tocopherol. Since, however, the content of α-tocopherol in the sample examined is slightly above the values usually found (values from 1 250 to 1 900 μg/g are given by Green *et al.*[3], Hove and Hove [10], Quaife [11], and Brown [1]), and since a *selective* destruction of β-tocopherol can hardly be expected to take place, it seems more probable that we are faced with individual variations in the tocopherol composition depending on the origin of the samples. This seems also to apply to cottonseed oil in the case of which Green *et al.*[3] find 58 % α-tocopherol (in the present investigation 36 %) and 42 % γ-tocopherol (in the present investigation 64 %).

Unlike previous researchers [3] the authors of the present work found no δ-tocopherol in mustard oil. It should be noted, however, that the present investigation has comprised one sample of mustard oil only.

Acknowledgements. We wish to express our thanks to Professor P. Karrer for samples of synthetic 5,7- and 5,8-dimethyltocol and to A/S Dansk Sojakagefabrik, Copenhagen, for the cottonseed oil, rapeseed oil and mustard oil used in the investigation.

REFERENCES

1. Brown, F. *Biochem. J. London* **52** (1952) 523.
2. Eggitt, P. W. R. and Ward, L. D. *J. Sci. Food Agr.* **4** (1953) 569.
3. Green, J., Marcinkiewicz, S. and Watt, P. R. *J. Sci. Food Agr.* **6** (1955) 282.
4. Eggitt, P. W. R. and Norris, F. W. *J. Sci. Food Agr.* **6** (1955) 689.
5. Bro-Rasmussen, F. and Hjarde, W. *Acta Chem. Scand.* **11** (1957) 34.
6. Jacob, A., Sutcliffe, F. K. and Todd, A. R. *J. Chem. Soc.* (**1940**) 327.
7. Embree, N. D. *Ann. Rev. Biochem.* **16** (1947) 323.
8. Hove, E. L. and Hove, Z. *J. Biol. Chem.* **156** (1944) 623.
9. Stern, M. H. Robeson, C. D., Weisler, L. and Baxter, J. G. *J. Am. Chem. Soc.* **69** 1947) 869.
10. Hove, E. L. and Hove, Z. *J. Biol. Chem.* **156** (1944) 601.
11. Quaife, M. L. *J. Biol. Chem.* **175** (1948) 605.

Received September 25, 1956.

ACTA CHEMICA SCANDINAVICA 11 (1957) 53—72

Comparative Ligand Field Studies

III. The Decrease of the Integrals F^k for Manganese(II) Complexes as Evidence for Partly Covalent Bonding

CHR. KLIXBÜLL JØRGENSEN

Chemistry Department A, Technical University of Denmark, Copenhagen, Denmark

The relative energy differences between the terms of an electron configuration with a partly filled l-shell can be expressed as multipla of the integrals F^2, F^4, ...F^{2l}. Tanabe and Sugano, Owen, and Orgel pointed out that the ligand field theory agrees much better with absorption spectra of octahedral d^n-complexes, if the values of F^k are assumed to be only 40—90 % of the values found for gaseous ions. This decrease of F^k can have two causes: the central field is decreased by electrons, donated from the ligands, and the partly filled shell is partly present in the ligands. The latter effect is proven by the extrapolation from F^k to values of the average radius $r_0 \sim 0.8-2$ Å of the partly filled shell, which are larger than the ionic radii 0.5—0.8 Å. Manganese(II) complexes are especially discussed with respect to Schläfer's investigation.[34,41] The present author assumes (1) that chloro complexes are formed, (2) that the aquo ion is octahedral and not tetrahedral, (3) that Schläfer's matrix for $^4\Gamma_5$ is wrong, and (4) that the red shifts of the bands of strong $MnCl_2$-solutions only can be interpreted by partly covalent bonding. Generally, anion complexes are shown to have smaller values of F^k than complexes with neutral ligands. The principle of electroneutrality and the Pauling theory of covalent bonding are discussed. The explanation by Orgel of band widths is further discussed. The highly fluorescent tetraethylammonium manganese(II) bromide with tetrahedral environment of Mn(II) is described.

THE INTEGRALS F^k FOR PARTLY FILLED SHELLS

The ligand field theory for a regular octahedral complex describes the energy levels as function of one ligand field * parameter Δ and of linear combinations of the energy levels of the gaseous ion. The latter energy levels cor-

* Orgel, Nyholm, J. Bjerrum and the present author proposed at the Xth Solvay Conference, Bruxelles, May 1956, to use the word "ligand field theory" to denote the crystal field theory extended with the molecular orbital theory for partly intermixing with the orbitals of the ligands, when applied especially to the action of the first co-ordination sphere on the partly filled d-shell in a transition group complex.

† Further, it was proposed to denote the energy difference between the partly filled γ_3- and γ_5-orbitals in a regular octahedral complex by Δ (as proposed by Owen [1]) rather than 10 Dq (*cf.* Schlapp and Penney [2]) or $(E_1—E_2)$ (*cf.* Hartmann and Ilse [3]).

respond to more or less favourable average positions of the electrons, relative to each other, within the same shell. Slater, Condon, and Shortley [4] calculated the relative l^n-term energies as multipla

$$f_2F^2 + f_4F^4 + \ldots + f_{2l}F^{2l} \tag{1}$$

of the integrals

$$F^k = e^2\int_0^\infty \left[\int_0^{r_2} \frac{r_1^k}{r_2^{k+1}} R^2\, dr_1 + \int_{r_2}^\infty \frac{r_2^k}{r_1^{k+1}} R^2\, dr_1\right] R^2\, dr_2 \tag{2}$$

e is the electronic charge, R^2 the square of the radial function of the l-electron, and r_1 and r_2 are the variable distance of the electron from the nucleus.

For convenience, several linear combinations of the integrals F_k are used. For obtaining integral values of the coefficients f_k of eqn. 1, Condon and Shortley [4] defined for d-electrons:

$$F^2 = 49\ F_2 \text{ and } F^4 = 441\ F_4 \tag{3}$$

while Racah [5] later defined the linear combinations:

$$B = F_2 - 5\ F_4 \text{ and } C = 35\ F_4 \tag{4}$$

The energy differences between the terms with the maximum value of the total spin S (among which the term with the highest L is the lowest in the free ion, according to Hund's rule) are multipla of B alone.

When applying the matrices [6] for d^n-systems in ligand fields with the symmetry O_h, Tanabe and Sugano [6], Owen [1], and Orgel [7,8] reported the possibility of smaller values of the term distances (and thus of F^k) for complexes than for the gaseous ions. Fig. 1 is a plot of the ligand field parameter Δ as function of B for the complex divided by B for the gaseous ion. It is seen that a rough linear correlation exist for all the considered elements. However, for a given central ion, the complexes with anions, such as chloride, oxalate or cyanide, have much smaller values of B than complexes with neutral molecules, such as water or ammonia.

Thus, the Orgel diagram, *i. e.* the energy levels as function of Δ, will be partly distorted by the new variables F^k. For nickel(II) complexes, it has been demonstrated in the two earlier papers of this series [9,10] that the slopes of the lines in the Orgel diagram deviate rather much from the values, predicted from the simple ligand field theory [11]. This was originally [9,12] ascribed to the interaction with other electron configurations, *viz.* $3d^{n-1}4s$. The perturbation of the d^n-states of the gaseous ion, when imbedded in the complex, can formally be described as a complicated interaction with many other states with the same $^{2S+1}\Gamma_n$ of other electron configurations.* On the other

* The ligand field [44] can be expanded in a series of contributions: G_0, G_2, G_4. Two orbitals with defined values of l equal to l_1 and l_2 can only be intermixed by quantities F^k or G_k, where $|l_1 - l_2| \leqq k \leqq l_1 + l_2$ and k has the same parity as $l_1 + l_2$. Thus, the spherically symmetrical contribution G_0 can only intermix orbitals with the same l, but different n. As discussed elsewhere [57], this corresponds to a variation of the central field [4] and hence a decrease of F^k for the partly filled shell. It is not believed that the characteristic cubic contribution G_4 is so large that the physical significance of the treatment in terms of F^k-values is invalidated.

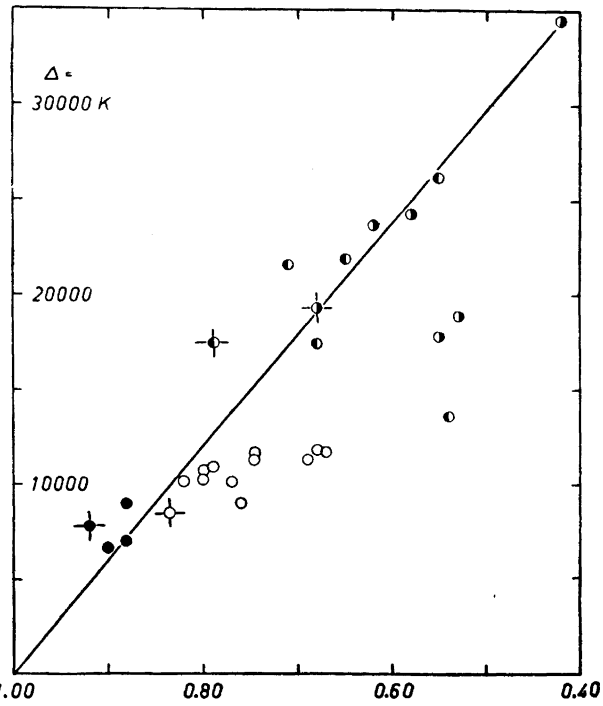


Fig. 1. The correlation between the ligand field parameter △ *and the ratio B in the complex: B in the gaseous ion. Filled circles correspond to manganese (II) complexes, empty circles to nickel (II),* ◐ *to chromium(III) and* ◑ *to cobalt(III). The hexaaquo ions, which have inter alia the highest values of* B, *i.e. the smallest decrease relative to the gaseous ion, are marked by a cross outside the circle.*

hand, it can also to a first-order approximation be described as an interaction between the *d*-orbitals and the other molecular orbitals with the same γ_n and parity, *i. e.* the even γ_3- and even γ_5-orbitals in octahedral complexes [1,13,14]. In the latter approximation, the effects of partly covalent bonding will only appear as a contribution to △ and as decreased values of F^k, as discussed below.

The analogous description of configuration interaction [4] by statistical methods in atomic spectroscopy was given by Trees [15], who added a correction term to the energies of d^n-terms:

$$f_2F^2 + f_4F^4 + \alpha L(L+1) \qquad (5)$$

and improved the agreement much by assuming values of $\alpha \sim 100$ K*. Racah [16] pointed out that this empirical correction corresponds to a mutual polarization of the *d*-orbitals by the electrons, which occupy them. It can be seen from eqn. 2 that isomorphous wavefunctions R^2, which are only differing by

* The unit cm^{-1} for wavenumber σ will now be called K = Kayser, as proposed by the Joint Committee for spectroscopy.

a multiplication factor in the distance r, correspond to values of F^k which are inversely proportional to r_{max} or another characteristic distance. Thus, the average distance of d-electrons from the nucleus must be larger in complexes than in the corresponding gaseous ions.

The perturbation theory states that the energy of two wavefunctions, totally imbedded in a sphere of negative charge, is increased by the same constant amount, thus not changing the energy difference [17]. If the excited wavefunction is partly present outside the sphere, the energy difference will be decreased. Thus, it must be assumed that a more negative charge is present in average between the central nucleus and the d-electron in the complexes than in the gaseous ion. This effect can be realized in two different ways:

I. Electrons from orbitals of arbitrary symmetry (*e. g.* the σ-bonding even γ_1 or odd γ_4) are donated from the ligands to the central ion, thus decreasing the effective charge by decreasing the central field in the theory of Condon and Shortley [4].

II. Linear combinations of atomic orbitals are formed with the symmetries γ_3 and γ_5 from d-electrons and respectively σ- and π-orbitals from the ligands. Orgel [7,8] discussed possibility I on the analogy of the influence of $4s$-electrons on the term distances of $3d^n$-configurations, while most authors have suggested II from Van Vleck's old discovery [18] that the molecular orbital theory and Bethe's electrostatic theory both lead to a considerable value of Δ, implying magnetically anomalous complexes when Δ in octahedral d^4- and d^7- or 2 Δ in d^5- and d^6-systems is larger than the necessary spin-pairing energy. The latter multipla of F^k, which are reported by Tanabe and Sugano [6], were discussed by Griffith [19]. The present author has found that the average spin-pairing energy (when the terms are weighted by factors $2L + 1$) to go from q to $q - 2$ spins is:

$$\begin{aligned} &q \cdot 15/4\ F_2 && \text{for } p^n\text{-systems} \\ &q\left(\frac{35}{12}\ F_2 + \frac{105}{4}\ F_4\right) && \text{for } d^n\text{-systems} \\ &q\left(\frac{35}{4}\ F_2 + \frac{231}{8}\ F_4 + \frac{1001}{4}\ F_6\right) && \text{for } f^n\text{-systems} \end{aligned} \qquad (6)$$

if no restriction is made on the seniority number [5]. These energies are multiplied by the factor $\frac{2l+2}{2l+3}$, if only the maximum values of the seniority numbers are considered. Thus, the average spin pairing energy is $q \cdot 0.15\ F^2$, $\sim q \cdot 0.10\ F^2$, and $\sim q \cdot 0.08\ F^2$ in the three cases.

Owen [1] has given experimental evidence for the possibility II from paramagnetic resonance, partly from hyperfine-structure*, due to the halogen nuclei and iridium nucleus in $IrCl_6^{--}$ and $IrBr_6^{--}$, and partly from the g-values in complexes, which can be written [1]

$$g = 2.00229 + \frac{k\zeta_{nd}}{\Delta} \qquad (7)$$

* Recently, Tinkham [54] reported similar evidence for partly covalent bonding to fluoride ligands of Mn(II), Fe(II), Co(II), and Cr(III) imbedded in ZnF_2. Tinkham proposes that both $2s$, $2p$, $3s$ and $3p$ orbitals of the fluoride ions are involved.

k is a constant, characteristic for the number of d-electrons, and ζ_{nd} is the Landé multiplet splitting factor. The measured g-values of complexes can be made compatible with eqn. 7 by assuming ζ_{nd} being between 10 and 40 % less in the aquo ions than in the gaseous ions of the first transition group. Owen [1] assumes that this can be directly translated to the partly filled shell containing 10—40 % of the ligands' orbitals in the squares of the wavefunction.

However, another evidence for partly covalent bonding can be obtained from the actual values of F^k of complexes. It is possible [17] to extrapolate from the values of F^k to the integral:

$$W = e^2 \int_0^\infty \frac{R^2}{r_i} \, dr \tag{8}$$

and to define an average radius of the partly filled shell:

$$r_0 = \frac{e^2}{W} \left(\text{in Å } r_0 = \frac{116\,000 \text{ K}}{W} \right) \tag{9}$$

If the partly filled shell was concentrated on a spherical surface, all the integrals W and F^k would be equal. For a broader radial function R^2 the inequalities

$$W > F^2 > F^4 > F^6 > \ldots \tag{10}$$

will be valid. For most actual ions [17], F^2 will be $\simeq \frac{1}{2} W$. The present author [17] calculated the values of W and F^k for a rectangular function

$$R^2 = \frac{1}{n-1} \text{ for } 1 \leq r \leq n \text{ and elsewhere } R^2 = 0 \tag{11}$$

Thus, if n is written $1 + \delta$, the series can be expanded:

$$\frac{F^k}{e^2} = \frac{1}{(n-1)^2} \left[\frac{2n}{k+1} - \frac{2}{k} + \frac{2}{n^k k(k+1)} \right] = \\ = 1 - \frac{k+2}{3} \delta + \frac{(k+2)(k+3)}{3 \cdot 4} \delta^2 - \ldots \tag{12}$$

while $$W = \frac{\ln n}{n-1} e^2$$

If R^2 is distributed on several peaks with the areas A_n, arranged according to increasing values of r_n, it is approximately valid [17]:

$$\frac{F^k}{e^2} \simeq \sum_n \frac{A_n^2}{r_n} \{1 - \frac{k+2}{3} \delta_n + \ldots\} + \sum_{m>n} \frac{2 A_n A_m r_n^k}{r_m^{k+1}} \tag{14}$$

Eqn. 14 is useful for anti-bonding combinations of atomic orbitals, which have at least two maxima of R^2, one in the central ion and one in the ligands.

Table 1 gives the values of r_0 for gaseous ions and complexes under the assumption $W = 2\ F^2$. While the analogous values [17] of r_0 for 4f-shells in trivalent lanthanide complexes vary between 0.80 Å for Pr^{+++} and 0.58

Å for Tm^{+++}, somewhat smaller than the ionic radii (and are increased slightly in anion complexes, at most to 0.84 Å in the *A*-form of Pr_2O_3), it is seen from Table 1 that the values of r_0 are distinctly larger than the ionic radii given by Goldschmidt [20].

Table 1.

Electron configuration		F^2 for the gaseous ion	Decrease of F^2 in complexes	r_0 of gaseous ion	r_0 of complexes	Ionic radius
3 d^3	Chromium(III)	74 000 K	21–47 %	0.78 Å	0.99–1.43 Å	0.55 Å
3 d^5	Manganese(II)	66 000	8–12	0.87	0.94–0.99	0.80
3 d^6	Cobalt(III)	~82 000	32–58	0.71	1.04–1.68	0.47
3 d^8	Nickel(II)	88 000	17–35	0.66	0.79–0.99	0.68
4 d^6	Rhodium(III)	~62 000	38–62	0.93	1.3–2.5	0.69

Thus, the gaseous ion will be strongly perturbed, if it is surrounded by other ligands in the distance ~ 2 Å known from crystallography. The maximum of the 3*d*-radial function will approximately be situated* on the boundary between the central ion and the ligand in the crystals. If the approximation of distinct molecular orbitals is assumed, the anti-bonding orbitals γ_3 and γ_5 (corresponding to the partly filled *d*-shell) will achieve a minimum of the square of the radial function between the ligand and the central ion, because the anti-bonding wavefunction will have one node more than the corresponding bonding wavefunction.

OVERLAP INTEGRALS BETWEEN ATOMIC ORBITALS OF THE LIGANDS AND THE CENTRAL ION

If the overlap integral is $S = \int \psi_1 \psi_2 \, d\tau$ between the two wavefunctions ψ_1 and ψ_2, their linear combinations can be written

$$\begin{aligned} \psi_b &= a\,\psi_1 + b\,\psi_2 \qquad & a^2 + b^2 + 2\,ab\,S &= 1 \\ \psi_a &= c\,\psi_1 - d\,\psi_2 \qquad & c^2 + d^2 - 2\,cd\,S &= 1 \end{aligned} \tag{15}$$

It must be realized that the orthogonalization condition

$$ac - db + (bc - ad)\,S = 0 \tag{16}$$

can be satisfied in infinitely many different ways. Thus, both functions do not need to differ from the unperturbed functions, *e. g.* ψ_1 and $\frac{1}{1-S}\psi_2 - \frac{S}{1-S}\psi_1$ are orthogonal. Only when the energy is minimized, the bonding orbital ψ_b with lowest energy may contain large coefficients *a* and *b* of eqn. 15.

* Recently, Hartree [55] has calculated the self-consistent 3*d*-wavefunctions in several divalent transition group ions in the gaseous state. The deviation of the radial functions from the hydrogen-like corresponds to higher electron densities both for small and large values of the distance *r* from the nucleus, while they are lower for intermediate values of *r*. Thus, the maximum occurs at a smaller value than at r_0 given above, while on the other hand, the tail for large *r* is very long. The conclusions on partly covalent bonding are not essentially altered from those presented above.

The secular determinant for wavefunctions with overlap integrals S_{mn} has the diagonal elements $E_{nn} - E$ and the symmetrical non-diagonal elements $E_{mn} - S_{mn}E$. For two levels, the eigenvalues of the energy will be given by the roots E of the equation

$$(E_{11}-E)\ (E_{22}-E) - (E_{12}-S_{12}E)^2 = 0 \tag{17}$$

It is often assumed [21,22] that

$$E_{12} = kS_{12} \cdot \frac{E_{11} + E_{22}}{2} \tag{18}$$

with k a constant between 1.6 and 2. The diagonal sum rule (which always is valid for $S_{mn} = 0$), *viz.*, that the sum of the roots of E is equal to the sum of E_{nn} is only valid, if $k = 1$.

The sum of the roots of eqn. 17 is:

$$E_a + E_b = (E_{11} + E_{22}) \cdot \frac{1 - kS_{12}^2}{1 - S_{12}^2} \tag{19}$$

Since $E_{11} + E_{22}$ generally is negative, $k > 1$ corresponds to relatively increased values of the average energy of the levels.

It is very difficult to derive quantitative information about the parameters S_{mn} and E_{nn} of eqns. 17—19. Many authors have discussed Slater's proposal [23]

$$R^2 = r^{2n} \exp\left(-\frac{2Z_* r}{n}\right) \tag{20}$$

which has the maximum value at

$$r_{max} = \frac{n^2}{Z_*} \text{ (in atomic units)} \tag{21}$$

If $r_0 \sim 1.5$ atomic unit ($= 1.5 \cdot 0.528$ Å) from Table 1 is identified with r_{max} of eqn. 21 with $n = 3$, then Z_* equals 6. (*Cf.* the foot-note p. 58).

Fig. 2 gives the two radial functions R_1 and R_2 from the central ion and the ligand under the assumption that R_2 has the same dependence on distance as R_1, but is distributed on two halves, one in the direction towards the central ion and one in the opposite direction. This is of course a rather rough approximation to the actual radial function. It is seen that the overlap between R_1 and the left-hand half part of R_2 is rather complete. While S_{12} in bi-nuclear complexes with a ligand between two metal ions might achieve large values near 1, S_{12} cannot exceed the upper limit $\sqrt{0.5}$ in mono-nuclear complexes as seen of Fig. 2, and will probably [24] be near 0.5. Fig. 2 gives further R_1^2 and the bonding orbital R_1^2 and anti-bonding orbital R_b^2, normalized to the same area. Due to the normalization factors, R_a^2 will contain most of the right-hand part of R_2, which does not overlap appreciably with R_1. Thus, F^k of R_a^2 (which is the partly filled shell of the complex) would be 20 % of the value for R_1^2, because only about a third of R_1^2 is refound as the first of the three maxima of R_a^2 (however, nearer to the central nucleus). This is not very different from the value 25—30 % implied by more simple reasoning on linear combination of atomic orbitals without consideration of overlap integrals.

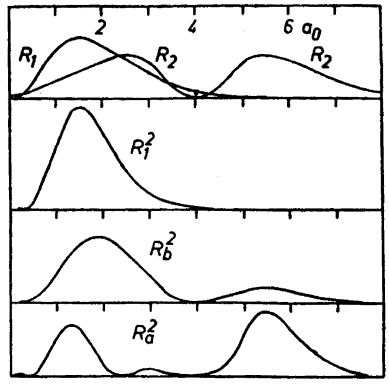


Fig. 2. The radial wavefunctions R_1 *and* R_2 *in a complex with the centres of the central ion at 0 and of the ligand at 4* a_0. *The squares of the bonding,* R_b^2, *and the anti-bonding radial function* R_a^2 *are given below after intermixing of* R_1 *and* R_2. *The partly filled* d-*shell in a complex near the Pauling case corresponds to* R_a^2 *on the figure, while a complex near the electrostatic limiting case has the partly filled shell nearly as* R_1^2.

Fig. 2 represents the Pauling hybridization case with equal energies of the two orbitals and equal radial dependences. Since F^k in complexes actually is decreased 8—62 % (Table 1) and not 80 %, all the complexes exemplify intermediate cases between the electrostatic model with pure d-wavefunctions and the Pauling case. This is the situation, described by Pauling [25] in the somewhat cumbersome language of valence-bond orbitals applied to the groundstates. Thus, Pauling [25] does not recognize the magnetic criterion as distinguishing ionic and covalent complexes, but rather between complexes, where the resistance towards spin-pairing of the d-electrons is larger or smaller than the tendency towards more favourable use of the orbitals for covalent bonding. This is described by the ligand field theory as the competition between spin-pairing energy, *i. e.* multipla of F^k-integrals, and ligand field strength Δ in the cases, where the slopes of the levels with low total spin are more negative in the Orgel diagram than the slope of the lowest level with the maximum spin [6,19,26].

It may be questioned, if σ-bonding is much more important than π-bonding in the d^n-complexes. Since the bond lengths [27,28] to the first approximation are an increasing linear function of the number of γ_3-electrons, the σ-anti-bonding character of these electrons seem well established. However, the F^k-integrals seem to be decreased by the same amount for the levels $^2\Gamma_3$ (G) of γ_5^3 in chromium(III) complexes * and $^1\Gamma_3$ (D) of $\gamma_5^6\,\gamma_3^2$ in nickel(II) complexes as for the levels $^4\Gamma_4$ and $^3\Gamma_4$, respectively, which contains in average 1.5 γ_3-electron more than the groundlevels. Thus, the delocalization of γ_5-electrons (which are π-anti-bonding with respect to filled molecular orbitals with less energy and π-bonding with respect to empty molecular orbitals with higher energy) does not seem to be less than of γ_3-electrons.

* as also Mo(III) and Re(IV). *Cf.* this journal **11** (1957) 82.

Probably, the large overlap integrals make π-bonding more important [24] than usually believed. Williams [29] assumes that the small values of Δ for iodo-, bromo, and chloro-complexes and high values of Δ for cyanide complexes are due to the influence of donation of π-electrons respectively, in the direction from the ligands to the central ion and in the opposite direction. Wolfsberg and Helmholz [21] assume so strong π-bonding in CrO_4^{--} and MnO_4^- that the negative sign of Δ for tetrahedral complexes, implied by both the electrostatic and the σ-bonding models, is reversed.

The experimental evidence from the absorption spectra that the degree of intermixing of d-electrons with γ_3- and γ_5-electrons of the ligands is 10—30 % rather than 50 % corresponds to higher energy of the unperturbed d-electrons than of the ligands' electrons. It can be estimated from Latimer's data [29] that the energy necessary for the reaction in aqueous solution

$$\tfrac{1}{2}\ H_2 \rightarrow H_3O^+\ aq + e^- \qquad (22)$$

is between 4.5 and 5 eV $\sim$ 40 000 K). Thus, it can be estimated from the oxidation potentials (when entropy effects are neglected) that the removal of a $3d$-electron from $Co(NH_3)_6^{++}$ demands $\sim$ 4eV and from $Co(H_2O)_6^{++}$ $\sim$ 6 eV. However, the optical transitions to states of a nearly free electron are not possible with so small an energy, because the ligands have not sufficient time for finding the new equilibrium positions, due to the Franck-Condon principle [28]. Further, it is only approximatively valid that the ionization potentials are equal to the energies of the orbitals, since the other orbitals rearrange slightly during the ionization process. The ionization potentials of most ligands will be $\sim$ 8 eV, but this value refers probably to π-electrons, while the σ-electrons have somewhat lower energies [14]. (1 eV = 8 067 K).

If complexes with $\sim$ 50 % intermixing of γ_3-electrons exist (*i. e.* the Pauling case), weak Laporte-forbidden electron transfer bands would be observed due to transition of bonding γ_3-electrons to γ_5 at nearly the same wavenumbers as the ligand field bands, which are caused by $\gamma_5 \rightarrow \gamma_3$ transitions within the partly filled shell. This case has not been observed, and only in systems, which have a strong tendency towards internal redox processes, such as [14] $IrBr_6^{--}$ or PtI_6^{--}, the electron transfer bands occur at lower wavenumber than the predicted ligand field bands.

The donation of electrons from the ligands, *e. g.* the σ-bonding γ_1- and odd γ_4-electrons, corresponding to the sp^3-part of the Pauling $d^2\,sp^3$-hybridization in octahedral complexes, decrease the effective charge on the central ion. Since the integrals F^k are roughly proportional to Z_0, where $Z_0 - 1$ is the external charge, this effect co-operates in decreasing F^k for complexes. The "principle of electroneutrality", as discussed by Pauling [25], seems to allow a residual charge between +1 and +2 in the domain of the central ion. Since the potential energy of a sphere with the electrical charge z and the radius r is proportional to z^2/r, one would expect small ions with high charges to be unstable. However, chemistry is remarkably unsymmetric with respect to the existence of cations and anions. While elementary anions are not easily provided with more negative charge than −2 (and even divalent anions seem to be highly polarized and only stable near cations), thorium(IV) aquo ions are definite entities. Since the ionic radius increases with negative charge and

decreases with positive charge, the effect can perhaps be described as the breakdown of highly negative anions with large radius, due to the presence of small cations with strong electrostatic fields. However, only the molecular orbital theory can explain the actual complicated behaviour of complexes, and recent investigations [25,27,30] have emphasized the importance of mutual donation of *e. g.* σ-electrons from the ligands and π-electrons to the ligands. That these subtle effects have strong influence on the chemistry of ions without inert gas configurations is evident from the highly different *cyclo*pentadienide complexes formed by thorium(IV) and uranium(IV) [31].

The increased acidity of water or ammonia, when bound to cations, might be taken as evidence for partly covalent bonding. However, pK of the complexes is probably not a linear function of the induced charge of the ligands, assuming *e. g.* the charge $+\frac{1}{2}$ on each water molecule of an aquo ion with p$K = 7$. It is necessary to consider the possibility of stronger covalent bonding of the hydroxo- or amido-group than of ammonia and water. Thus, the acidity [14] of $Pt(NH_3)_6^{+4}$, which is stronger than of NH_4^+, does not imply with certainty a charge above $+1$ of each ligand. Of purely electrostatic reasons, complex-bound H_2O and NH_3 would have the same energy of proton dissociation as H_3O^+ and NH_4^+, when the charge of the central ion is $\frac{3.3\ \text{Å}}{1.3\ \text{Å}} \sim 2.5$, since the distances from the proton to the hydroxyl group and the central ion are roughly 1.3 Å and 3.3 Å, respectively.

MANGANESE(II) COMPLEXES

The absorption spectra measured by Gielessen [32] of manganese(II) salt hydrates and by the present author [33] of the aqueous solution of $MnSO_4$ were interpreted by Orgel [8] on basis of the ligand field theory for an octahedral d^5-system [6,7] (*cf.* Fig. 3). Ten transitions from the groundstate $^6\Gamma_1$ (S) to quartet levels are predicted, and the present author [12] reported later the missing weak bands in the ultraviolet. Table 2 gives the bands with the identification of their excited levels of $MnCl_2$ and $MnSO_4$ in aqueous solution and the other complexes with ethylenediaminetetraacetate, ethylenediamine, and tartrate. The hexaaquo ion has nearly the same spectrum (found in dilute $MnCl_2$) as the un-ionized complex $MnSO_4(H_2O)_5$ probably occurring in strong sulfate solutions.

Schläfer [34] applied also the ligand field theory to the absorption spectra of $MnCl_2$, 4 H_2O and $NH_4Fe(SO_4)_2$, 12 H_2O, which were assumed to contain the ions $Mn(H_2O)_4^{++}$ and $Fe(H_2O)_6^{+++}$. Schläfer's assignment of levels deviate rather much from that of Orgel [8] and the present author [26]. The three levels $^4\Gamma_5$ seem to be shifted erroneously $\sim$ 6 000 K towards lower wavenumbers. The problem, whether the manganese(II) aquo ion is tetrahedral or octahedral, cannot be decided from the quantum numbers Γ_n, since the matrices for d^5-systems are symmetrical [6] with respect to a change of sign of Δ. However, the value of $\Delta = 7\,800$ K for manganese(II) suggests an octahedral co-ordination, when compared to $\Delta = 10\,400$ K for iron(II), 9 300 K for cobalt(II) and 8 500 K for nickel(II) hexaaquo ions. In a tetrahedral complex with purely electrostatic ligand fields, Δ would be [35] multiplied by

Table 2. The absorption bands of manganese(II) complexes, assigned to the excited levels (*cf.* Fig. 3). Wavelength λ in mμ, wavenumber σ in K, one-sided halfwidth δ in K, and molar extinction coefficient ε of each band maximum. Shoulders in parenthesis.

		$^4\Gamma_4(G)$	$^4\Gamma_5(G)$	$^4\Gamma_1(G)$ and $^4\Gamma_3(G)$	$^4\Gamma_5(D)$	$^4\Gamma_3(D)$	$^4\Gamma_4(P)$	$^4\Gamma_3(F)$	$^4\Gamma_4(F)$	$^4\Gamma_5(F)$
1. 8M $MnSO_4$	λ	532	435	400, (396)	356	337	304	279	262	248
$\triangle$ = 7 800 K	σ	18 800	23 000	25 000, (25 250)	28 100	29 700	32 800	(35 800)	(38 400)	(40 400)
	δ	1 200	900	200 200	600	400	1 500	400	—	—
	ε	0.017	0.014	0.036 0.018	0.023	0.021	0.04	—	—	—
2. 3M $MnCl_2$	λ	528	435	(405), 400, (395)	359	340	313	283	272 (268)	247
	σ	18 900	23 000	(24 700), 25 000, (25 300)	27 800	29 400	32 000	(35 400)	36 800 (37 400)	40 500
	δ	1 150	1 000	—	600	—	1 300	—	—	
	ε	0.018	0.014	0.029	0.039	0.024	0.022	0.01	0.04	0.08
1M $MnCl_2$, 6M HCl	λ	521	428	412, 408	360	345	319	285	274	253
	σ	19 200	(23 400)	24 300, 24 500	27 800	29 000	31 400	(35 100)	(36 500)	(39 600)
	δ	1 200	1 200	—	800	—	—	—	—	—
	ε	0.023	0.027	0.040	0.08	0.04	0.038	—	0.07	—
1M $MnCl_2$, 9M HCl	λ	517	442	425, 412	362	347	320	—	—	—
	σ	19 300	22 700	23 500, 24 300	27 700	28 900	31 300	—	—	—
	δ	1 200	—	—	—	—	—	—	—	—
	ε	0.023	0.035	0.048, 0.046	0.12	0.06	0.06	—	—	—
1M $MnCl_2$,	λ	546	440	(410), 405, (401)	361	339	—	—	—	—
1.5M KSCN	σ	18 300	22 800	(24 400), 24 700, (24 900)	27 700	29 500	—	—	—	—
$\triangle$ = 7 900 K	δ	1 400	—	—	—	—	—	—	—	—
	ε	0.021	0.018	0.036, 0.050, 0.034	0.080	0.028	—	—	—	—
Mn enta^{--}	λ	532	471	411	367	343	—	—	—	—
$\triangle$ = 6 800 K	σ	18 800	(21 200)	24 300	27 200	29 200	—	—	—	—
	δ	1 500	—	(—) = 400, (+) = 100	—	—	—	—	—	—
	ε	0.044	0.04	0.25	0.03	0.03	—	—	—	—
Mn++ in tartrate	λ	550	462	425, 415	—	—	—	—	—	—
$+NH_3$	σ	18 200	21 700	23 500, 24 100	—	—	—	—	—	—
$\triangle$ = 7 000 K	δ	1 600	900	400, 400	—	—	—	—	—	—
	ε	0.09	0.12	0.32, 0.36	—	—	—	—	—	—
Mn en_3++	λ	630	494	422	372	—	—	—	—	—
$\triangle$ = 9 100 K	σ	15 900	20 300	23 700	26 900	—	—	—	—	—
	δ	1 500	1 500	300	—	—	—	—	—	—
	ε	0.055	0.063	0.10	0.05	—	—	—	—	—

a factor $-\frac{4}{9}$. The molecular orbital theory may cause strong deviations from this ratio, as discussed p. 61, but the evidence from $CoCl_4^{--}$ suggests very low values of Δ in tetrahedral complexes. Hartmann and Fischer-Wasels [36] assume also tetrahedral co-ordination of paramagnetic nickel(II) complexes. However, the only certain case of this is found by Weyl [37] as a purple nickel glass in rubidium silicate. J. Bjerrum [38] demonstrated a regular development in the absorption spectra of Ni^{++} with from zero to six ammonia molecules. The latter type of argument can also be applied to manganese(II): as can be calculated from Table 2, $\Delta = 9\,100$ K of the tris(ethylenediamine) complex [38] is only 18 % larger than for the aquo ion, agreeing well with the usual effects of exchanging water and amines in octahedral complexes.

The terms of the gaseous Mn^{++} are known from atomic spectroscopy [39]:

^6S	0 K
^4G	26 800
^4P	29 200
^4D	32 300
^4F	43 600

The levels $^4\Gamma_1(G)$, $^4\Gamma_3(G)$ and $^4\Gamma_3(D)$ should have the same wavenumbers as ^4G and ^4D, respectively, if the integrals F^k and thus the term distances were not decreased in complexes. It is seen from Table 2 that these energy differences are decreased 8 % in $Mn(H_2O)_6^{++}$, 12 % in Mn enta^{--} and 12 % in Mn en_3^{++}.

Orgel [7,8] assumed that the presence of two 4*s*-electrons is sufficient to explain this effect, thus applying possibility I on p. 56. However, with the value of r_0 from Table 1, it is probable that ~5 % intermixing with the ligands' orbitals occur. The highest term ^4F seems more decreased, ~19 % in $Mn(H_2O)_6^{++}$. It seems generally valid that high terms are systematically depressed, thus the ratio between the wavenumbers of the spinforbidden transitions to $^2\Gamma_3$ and $^2\Gamma_5$ in chromium(III) complexes [40] is only ~1.5 rather than [6] 1.66 . . . This effect in Mn^{++} is perhaps caused by interaction with other electron configurations, which are situated above 50 000 K. It cannot be certainly decided, if an extra band does not occur of $Mn(H_2O)_6^{++}$ at 37 400 K. It may be due to a doublet level *, which is highly intermixed with the quartet levels. $^2\Gamma_5$ is predicted at 28 000 K of $Mn(H_2O)_6^{++}$ and at 23 000 K of Mn en_3^{++}, while the doublet levels of γ_5 $^4\gamma_3$ are distributed ~8 000 K above these wavenumbers.

Schläfer [41] studied the absorption spectra of crystalline $MnCl_2$, 4 H_2O and aqueous solutions between 1 M and 4.8 M $MnCl_2$. The bands separated in

* It will be a rather difficult task to observe the doublet levels of manganese(II) complexes, corresponding to bands with $\varepsilon \sim 10^{-4}$. Especially, the high overtones of vibration frequencies in the infra-red may produce similar bands. The intensity of quartet bands, even though only 1 % of spin-allowed bands of divalent $3d^n$-complexes, is rather high [26]. Since ζ_{3d} can be interpolated to 300 K, and the distances to the nearets sextet are ~ 20 000 K (either $^6\Gamma_1(S)$ or from other electron configurations), the spin intermixing would be expected to be only $\sim \left(\frac{300}{20\,000}\right)^2 \sim 2 \times 10^{-4}$. Probably, the intensity is borrowed from some other configuration, where the total spin is less strictly defined than in $[A]\ 3d^5$.

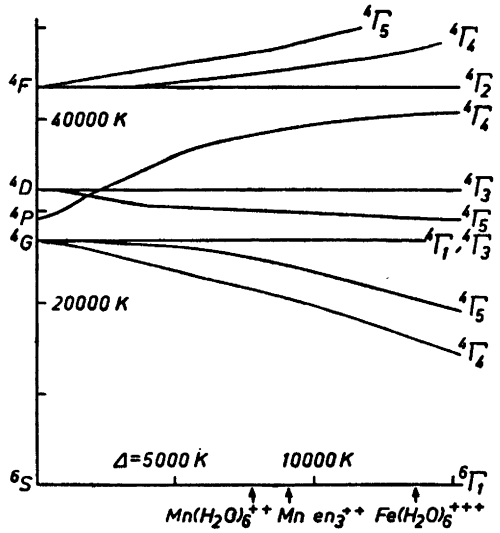


Fig. 3. The Orgel diagram of d^5*-systems, assuming no variation of the term distances* i.e. *the values of* B *and* C *from those of gaseous* Mn^{++}. *Since the term distances are decreased to the latter values in* $Fe(H_2O)_6^{+++}$, *this ion can also find a place in this diagram with* $\Delta =$ *13 700 K. The slopes of the levels can be compared with the observed band widths and with the variation of the wavenumbers of the individual bands as function of* Δ *in Table 2.*

several components, whose intensities change as function of the chloride concentration. The general result is a shift ~2 % towards lower wavenumbers, relative to the aquo ion. This was explained as a physical salt effect, caused by increasing concentration of the anion atmosphere around the manganese(II) ion. The present author believes that the spectral changes rather can be described to the consecutive formation of chloro complexes, and it is demonstrated [17] that Schläfer's electrostatic model for the red shift of the bands of strong salt solutions actually is a translation of partly covalent bonding (*cf.* p. 57). If the values of the molar extinction coefficient ε, reported by Schläfer [41] for the solid, which has a scattering back-ground, are decreased 0.04, the mani-fold of spectra can mainly be explained by the presence of two new complexes besides the hexaaquo ion:

Excited level	$MnCl(H_2O)_5^+$		$MnCl_2(H_2O)_4$	
	λ	ε	λ	ε
$^4\Gamma_1(G)$ and $^4\Gamma_3(G)$	405 mμ	0.038	405 and 408 mμ	0.04
$^4\Gamma_5(D)$	359	0.05	362 and 366	0.07
$^4\Gamma_3(D)$	339	0.023	343	0.06
$^4\Gamma_4(P)$	313	0.017	317	0.04

The two last bands have a minimum of ε in 2.5 M $MnCl_2$, where the monochloro complex probably is dominating. The absence of isosbestic points is not a strong argument against exchange of water with chloride in the first co-

ordination sphere, because the existence of three complexes and the small second-sphere effects probably will disturb the linear combinations of the absorption spectra.

While manganese(II) chloride solutions always will have $\bar{n}$ well below 2, due to the presence of free chloride, which determines the formation curve of mono-nuclear chloride complexes [38], strong hydrochloric acid can produce higher values of $\bar{n}$. Table 2 gives the spectra of $MnCl_2$ in 6 M HCl and in 9 M HCl. In these solutions the red shifts are stronger than in $MnCl_2$, 4 H_2O except when the decreasing value of Δ shifts the band, *e.g.* to ${}^4\Gamma_4(G)$ in the opposite direction. The present author assumes that these complexes are all octahedral. However, in anhydrous solutions, the tetrahedral $MnCl_4^{--}$ may perhaps occur. If $MnCl_2$ in 30 % ethanol +60 % *t*-butanol is treated with PCl_3, yellow solutions are obtained with higher bands at 440, 428, 424, 376 and 356 mμ, while the bands at 406 and 400 mμ reversibly re-appear by addition of a few per cent of water. The yellow solutions exhibit much smaller Δ than the aquo ion and the F^k-integrals are decreased ~13 %, resembling the conditions in $CoCl_4^{--}$. Mr. Palle Andersen [48] has kindly informed me that yellow-green Cs_3MnCl_5 probably has tetrahedral co-ordination of manganese, while the octahedrally co-ordinated double chlorides are pink.

Cs_3MnCl_5 fluoresces yellowish green in ultraviolet radiation, as also the yellow-green salt $[N(C_2H_5)_4]_2$ $MnBr_4$ described in the experimental section. The latter salt does not deliquesce in air and can be prepared from aqueous solution of the components. The intensity of the fluorescence light by 366 mμ excitation is higher than that of uranyl salts. The reflection spectrum corresponds closely to that predicted of Mn(II) in tetrahedral environment *. A narrow peak at 448 mμ, surrounded by a peak at 434 mμ and a shoulder at 476 mμ implies 17 % decrease of F^k, relative to gaseous Mn^{++}. The small value of Δ cannot be evaluated exactly, since the ligand field splitting is less conspicuous than the F^k-decrease. However, Δ seems to be between — 2 000 and — 3 000 K, when the hypothesis of negative sign is assumed. The fluorescent level is ${}^4\Gamma_4(G)$, as discussed by Orgel [28]. A band at 382 mμ and a shoulder at 365 mμ correspond probably to ${}^4\Gamma_4(P)$ and ${}^4\Gamma_4(D)$, while the measured reflectance increases above 100 % below 350 mμ (perhaps caused by the fluorescence). As discussed in the experimental section, a broad, low band ~560 mμ may be due to octahedrally co-ordinated impurities, and a narrow band at 905 mμ to the vibrational over-tone 4 σ(CH).

The decrease of F^k-integrals in anion complexes compared to aquo ions, was demonstrated for other manganese(II) complexes as seen from Table 2. Thus, 1.5 M KSCN produces 1.5 % smaller term distances, but the same Δ as the aquo ion, Mn ata_2^{-4} (these strong manganese solutions are only clear with a large excess of sodium nitrogentriacetate) resembles much Mn $enta^{--}$; tartrate in aqueous ammonia gives a rather strong red shift; etc. These effects resemble much the red shifts of lanthanide complexes [17] with citrate, tartrate,

* Similar arguments apply to $FeCl_4^-$ of which Schläfer [56] reports the reflection spectrum. The narrow band ~525 mμ implies ~40 % decrease of F^k, while the broader ${}^4\Gamma_5(G)$ at ~610 mμ and ${}^4\Gamma_4(G)$ at ~680 mμ implies Δ about —5 000 K. Cobalt-free $FeCl_3$ in 12 M HCl exhibit these bands at 600 and 684 mμ, while a broad shoulder ~740 mμ probably is caused by another iron(III) complex.

and ethylenediaminetetraacetate, which are ~1 % in Pr^{+++}, ~0.7 % in Nd^{+++} and Sm^{+++}, and ~0.3 % in Gd^{+++}, while they vanish in the heavy lanthanides.

Kleiner [42] abandoned the electrostatic ligand field theory, because the Hartree self-consistent field 3*d*-wavefunction for chromium [43] produces a very small and even negative value of Δ for Cr^{+++} in the alums. This is a translation of the large overlap between 3*d*-electrons and the ligands, as seen from Fig. 2. Thus, the electrostatic model of Ilse and Hartmann [44] can be shown to lead to a contradiction, caused by the spatial extensions of the hydrogen-like wavefunctions [12]. However, it is interesting to see that practically all information available on the energy levels of transition group complexes has been found by the electrostatic theory without taking partly covalent bonding into account (for a review, see Ref. [26]). This is due to several reasons of quantum-mechanical nature: (1) The number of levels with a given value of $^{2S+1}\Gamma_n$ is independent of the intermixing and can be found, *e.g.*, from the strong field sub-shell configurations [11]; (2) in complexes with high symmetry, such as O_h, the group-theoretical classification of levels and orbitals is very important; and (3) the molecular orbital theory without interaction of configurations is, contrary to the case of many simple molecules [45], able to predict the excited levels of transition group complexes with ~2 % uncertainty with Δ and the decreased F^k-integrals as the only parameters (*cf.* Fig. 3 and Table 2). The success of the electrostatic theory with Δ as empirical parameter cannot be found only in the general feature of the perturbation theory that the energy levels usually are predicted much better than the wavefunctions; even the squares of the wavefunctions must be highly intermixed in highly covalent complexes such as $Co(CN)_6^{-3}$ or $RhCl_6^{-3}$ with small F^k-integrals. The problem is rather connected with the nearly equal energies of the purely ionic and purely covalent (*i.e.* 50 % intermixing) limiting cases. It is very fortunate that complexes exist with partly filled shells, which can be in more than one state. It is possible in these cases to obtain much information from the excited levels, which is not available in general for closed shells. Especially, the absorption spectra can inform about the geometrical extension of partly filled shells. The only other type of experiment, which so far has presented such evidence, is the d-wavefunction, reported by Shull, Wollan, and Strausser [46] from neutron diffraction of manganese(II) salts. The maximum at 0.6 Å and the narrow half-width might suggest that the wavefunction is actually an anti-bonding combination of the type given in Fig. 2, but with a smaller density in the ligands, corresponding to much less than 50 % intermixing.

The molecular orbital theory gives a much more unified theory for all the energy levels of all the transition group complexes than might earlier have been predicted. The valence bond-theory, which is cumbersome [47] even for simple molecules such as CO or O_2, evolves extreme resonance possibilities for the groundstates of transition group complexes [25], and it is practically without value for the description of the excited levels. On the other hand, the electrostatic theory gives surprisingly good agreement with the observed energy levels, and the intermixing of the *d*-electrons with the ligands' orbitals can be said to be initiated by the perturbing effects of the ligands on the partly filled *d*-shell.

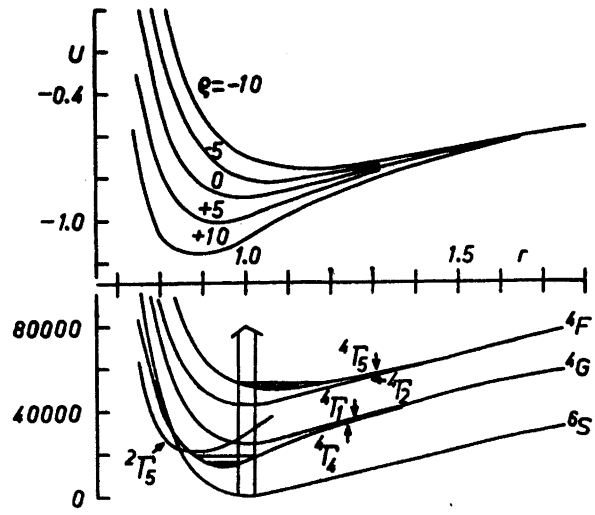


Fig. 4. The potential curve of eqn. (23) with different values of the ligand field stabilization parameter ϱ. The lowest part of the figure exhibits several levels of manganese (II) complexes under the assumption of the same form of potential curves as given above and with the terms of gaseous Mn^{++} at the dissociation limit. The mechanism of band-widths is indicated by the vertical projection of the vibration of the ground-level on the potential curves of the excited levels.

THE WIDTH OF MANGANESE(II) ABSORPTION BANDS AND VIBRATIONAL EXCITATION DUE TO THE FRANCK-CONDON PRINCIPLE

Orgel[8] pointed out that the width of absorption bands is roughly proportional to $\frac{d\sigma}{d\Delta}$, the difference in slope of the excited and the groundlevel in the Orgel diagram, using manganese(II) complexes [33] as examples. This effect is connected with the fact that the equilibrium distance between the central ion and the ligand increases regularly with the number of γ_3-electrons. Thus, a transition between two levels with a different number of γ_3-electrons corresponds to a broad absorption band, because the excited level will be vibrationally excited, since the Franck-Condon principle does not allow the complex to adjust itself to the new equilibrium distances during the very rapid optical excitation. Fig. 4 gives the potential curves $U(r)$ with the polynomial approximation in r^{-1}:

$$U = \frac{1}{9r^9} - \frac{0.02\,\varrho}{r^5} - \frac{1}{r} \qquad (23)$$

where the unit of r is chosen such that for $\varrho = 0$, the minimum of U occurs at $r = 1$. The first of the three parts of the expression represents the mutual repulsion between the closed shells, the second the ligand field effects (with the ligand field stabilization parameter $\varrho = 2n_5 - 3n_3$, n_3 and n_5 being the num-

ber of γ_3- and γ_5-electrons) and the third the electrostatic attraction of the ligand. The equilibrium distances r_L occur for:

ϱ	= +10	+5	0	—5	—10	
r_L	= 0.887	0.940	1.000	1.064	1.128	(24)

Thus, the present author is no longer inclined to assume, as earlier [50], that the equilibrium distances cannot increase ~6 % for each new γ_3-electron, even though the crystallographic distances suggest slightly smaller differences. The vibrational wavenumber 150 K found [50] of $ReCl_6^{--}$ cannot with certainty be identified with a definite one of the six fundamental frequencies of a regular octahedron. However, the order of magnitude of the frequencies is probably not very different from 200 K (*cf.* the recent results [51,52] for UF_6 and PuF_6), and the amplitude of the zero-point vibration thus ~0.08 Å, corresponding to 0.04 units on Fig. 4. Since the differential quotient of U (eqn. 23) at $r = 1$ is $0.1\,\varrho$ (while at $r = 0.9$, it is $-1.63+0.188\varrho$), the manganese(II) complexes are expected to exhibit bandwidths $\delta \sim 1\,500$ K for a difference in $\varrho = 5$.

Generally, the projection [53] of the lowest vibrational state of the ground-level on the potential curve U of the excited level is likely to produce an almost Gaussian-shaped absorption band

$$\varepsilon = \frac{\sigma}{\sigma_0} \cdot \varepsilon_0 \cdot 2^{-\frac{(\sigma_0-\sigma)^2}{\delta^2}} \tag{25}$$

with the half-width δ of the Gaussian part

$$\delta = 0.834\ x_c \cdot \frac{\mathrm{d}U}{\mathrm{d}r} \tag{26}$$

since the square of the wavefunction of the lowest level of a harmonic oscillator is a Gauss-curve with the half-width $x_c\sqrt{\ln 2}$, where x_c is the classical amplitude. If the difference between the potential curves of two levels with ϱ differing 5, *i.e.* Δ, is assumed to be proportional to r^{-5}, it will be valid for small values of x_c

$$\delta = 4.17\ \frac{x_c}{r_L}\ \Delta \tag{27}$$

Since x_c is proportional to $(k\mu)^{-\frac{1}{4}}$, k being the force constant $\frac{\mathrm{d}^2U}{\mathrm{d}r^2}$ of the ground-level, and μ the reduced mass (the existence of more vibrational quanta in molecules with more than two atoms necessitates a more detailed treatment), x_c is not expected to vary more than between 0.03—0.08 Å. Actually, manganese(II) and nickel(II) complexes have $\delta\sim0.15\ \Delta$, while [14] rhodium(III) has $\delta\sim0.09\ \Delta$ and iridium (III) $\delta\sim0.08\ \Delta$, corresponding to higher values of $k\mu$ in the platinum group complexes.

However, if the vibrational wavenumber

$$\sigma_c = \frac{1}{2\pi c}\sqrt{\frac{k}{\mu}} \tag{28}$$

is not much larger than 210 K (the mean Boltzmann energy at room temperature), transitions will occur from the n'th vibrational state of the groundlevel, which has two strong maxima near $r_L \pm x_c\sqrt{2n+1}$ for $n = 1, 2 \ldots$ The feet of the absorption bands will thus be too high and show a strong increase with the temperature T, while δ will be approximately proportional to $\sqrt{T}$ for small σ_c. On the other hand, all bands will vanish too quickly towards low wavenumbers, because $\frac{dU}{dr}$ of eqn. 26 is no constant, but approaches 0 in the bottom of the potential hole. Since no vibrational structure generally can be observed, all the excited states discussed here must be rather diffuse, at least $\sim 0.2\ \sigma_c$. It has earlier been discussed [50], if this broadening may be caused by collisions.

The lower part of Fig. 4 illustrates the potential curves of some manganese(II) levels with the assumption of eqn. 23. For decreasing values of r, corresponding to steeply increasing values of Δ, the levels with different values of ϱ cross each other in a rather complicated way, actually depicting an Orgel diagram such as Fig. 3. Especially, the groundstates of magnetically anomalous complexes (*viz.* $^2\Gamma_5$ in Fig. 4) have intrinsically small values of r_L and high values of Δ, as pointed out by Orgel [27]. The broad vertical arrow represents the possible transitions to excited levels, producing vibrational excitation of levels with r_L differing from that of the groundstate. Especially, excitations to $^4\Gamma_4(G)$, which may be fluorescent in manganese(II) complexes [28], correspond to a decreased value of r_L. The relatively long life of the excited state is made possible by this weak interaction with the environment, while excited states with increased values of r_L rapidly decay by transfer of energy to the thermal motion of other molecules.

EXPERIMENTAL

The stock solution of 2.3 M $MnCl_2$ was prepared from Merck's p.a., which was found to be free of iron. It was added to hydrochloric acid and to 3 M KSCN. Mn enta^{--} was prepared from $MnSO_4$, 4 H_2O (Merck's p.a.), 1.1 mole H_4 enta (Complexon II) and 2 moles Na_2CO_3. The chamois solution is not oxidized by air or H_2O_2, but turns brown (with a maximum at 450 and a narrow hump at 470 mμ) of Mn enta OH^{--} by addition of $KMnO_4$. This solution turns purple [49] (a maximum at 500 mμ) by addition of $HClO_4$ under formation of Mn enta H_2O^-. However, this colour disappears after some minutes.

On the other hand, it is difficult to prevent the oxidation of most other manganese(II) complexes in alkaline solution, thereby forming brown precipitates. The greyish green solution of Mn en_3^{++} (1 M Mn en_3^{++}, 1 M en H^+ and 3 M free en) can be protected against oxidation by a minute amount of ascorbic acid; however, especially in alkaline solution, this compound produces slowly a yellow decomposition product with a high maximum at 384 mμ. Also manganese(II) and ammonium tartrate dissolved in aqueous NH_3 is oxidized by air to a brown solution, which can be reduced by ascorbic acid.

Tetraethylammonium manganese(II) bromide can be prepared by evaporation of a solution of manganese(II) bromide with slightly more than two moles of tetraethylammonium bromide in aqueous hydrobromic acid. After cooling, yellowish green crystals separate, which are washed with ethanol on a glass-sintered funnel and dried, *e. g.* by heating with an ultraviolet "black" mercury lamp, causing a bright green illumination. The yield is $\sim$60 %. The analysis indicates the formula $[N(C_2H_5)_4]_2$ Mn Br_4:exp. 8.8 % Mn, 49.2 Br; theor. 8.7 % Mn, 50.4 % Br. In some cases, the content of Mn is higher, $\sim$10 %, and the reflection spectrum then exhibits a very broad band 560 mμ. It is

presumably caused by a complex with octahedral environment of Mn(II), either $[N(C_2H_5)_4]$ $MnBr_3$ or a solvate. In one sample containing 0.08 mole % cobalt, bands were observed at 645, 670, 705 and 720 mμ of $CoBr_4^{--}$. A narrow band at 900–910 mμ was found in all samples. It cannot be a Mn(II) ligand field band, but is rather four times the CH-stretching frequency, since it also appears in $N(C_2H_5)_4Br$.

The spectra of the solutions were measured in 10 cm silica cells on a Cary Recording Spectrophotometer, model 11 MS–50.

Acknowledgements. I am very much indebted to Professor Jannik Bjerrum for many interesting discussions.

REFERENCES

1. Owen, J. *Proc. Roy. Soc. London* **A 227** (1955) 183.
2. Schlapp, R. and Penney, W. G. *Phys. Rev.* **42** (1932) 666.
3. Hartmann, H. and Ilse, F. E. *Z. Naturforsch.* **6a** (1951) 751.
4. Condon, E. U. and Shortley, G. H. *Theory of Atomic Spectra.* Cambridge 1953.
5. Racah, G. *Phys. Rev.* **62** (1942) 438; **63** (1943) 367.
6. Tanabe, Y. and Sugano, S. *J. Phys. Soc. Japan* **9** (1954) 753, 766.
7. Orgel, L. E. *J. Chem. Phys.* **23** (1955) 1004.
8. Orgel, L. E. *J. Chem. Phys.* **23** (1955) 1824.
9. Jørgensen, C. Klixbüll, *Acta Chem. Scand.* **9** (1955) 1362.
10. Jørgensen, C. Klixbüll, *Acta Chem. Scand.* **10** (1956) 887.
11. Jørgensen, C. Klixbüll, *Acta Chem. Scand.* **9** (1955) 116.
12. Jørgensen, C. Klixbüll, *Acta Chem. Scand.* **9** (1955) 717.
13. Orgel, L. E. *J. Chem. Phys.* **23** (1955) 1819.
14. Jørgensen, C. Klixbüll, *Acta Chem. Scand.* **10** (1956) 500, 518.
15. Trees, R. E. *Phys. Rev.* **83** (1951) 756; **84** (1951) 1089; **85** (1952) 382.
16. Racah, G. *Kgl. Fysiograf. Sällskap. Lund* Handl. **65** (1954) No. 21, p. 31.
17. Jørgensen, C. Klixbüll, *Kgl. Danske Videnskab. Selskab. Mat. Fys. Medd.* **30** (1956) No. 22.
18. Van Vleck, J. H. *J. Chem. Phys.* **3** (1935) 803, 807.
19. Griffith, J. S. *J. Inorg. Nucl. Chem.* **2** (1956) 1, 229.
20. Goldschmidt, V. M. *et al. Geochemische Verteilungsgesetze der Elemente,* IV, V and VII, Oslo 1925–26.
21. Wolfsberg, M. and Helmholz, L. *J. Chem. Phys.* **20** (1952) 837.
22. Ito, K. and Kuroda, Y. *J. Chem. Soc. Japan* **76** (1955) 545, 762, 766, 934.
23. Slater, J. C. *Phys. Rev.* **36** (1930) 57.
24. Craig, D. P., Maccoll, A., Nyholm, R. S., Orgel, L. E. and Sutton, L. E. *J. Chem. Soc.* **1954** 332. 354.
25. Pauling, L. *J. Chem. Soc.* **1948** 1461.
26. Jørgensen, C. Klixbüll, *Reports of the Xth Solvay Conference,* Bruxelles, May 1956.
27. Orgel, L. E. *Reports of the Xth Solvay Conference,* Bruxelles, May 1956.
28. Orgel, L. E. *J. Chem. Phys.* **23** (1955) 1958.
29. Latimer, W. M. *J. Chem. Phys.* **23** (1955) 90.
30. Orgel, L. E. and Sutton, L. E. *Proc. Symposium on Co-ordination Chemistry,* Copenhagen 1953, p. 17.
31. Reynolds, L. T. and Wilkinson, G. *J. Inorg. Nucl. Chem.* **2** (1956) 246.
32. Gielessen, J. *Ann. Physik* [5] **22** (1935) 537.
33. Jørgensen, C. Klixbüll, *Acta Chem. Scand.* **8** (1954) 1502.
34. Schläfer, H. L. *Z. physik. Chem.* **4** (1955) 116.
35. Ballhausen, C. J. *Kgl. Danske Videnskab.Selskab. Mat.fys. Medd.* **29** (1954) No. 4.
36. Hartmann, H. and Fischer-Wasels, H. *Z. physik. Chem.* **4** (1955) 297.
37. Weyl, W. A. *Reports of the Xth Solvay Conference,* Bruxelles, May 1956.
38. Bjerrum, J. *Metal Ammine Formation . . .* Thesis, Copenhagen 1941.
39. Moore, C. E. *Atomic Energy Levels. Natl. Bur. Standards, Circ.* No. 467, Vol. II.
40. Schäffer, C. E. *Acta Chem. Scand. To be published.*
41. Schläfer, H. L. *Z. physik Chem.* **6** (1956) 201.
42. Kleiner, W. H. *J. Chem. Phys.* **20** (1952) 1784.

43. Mooney, R. L. *Phys. Rev.* **55** (1939) 557.
44. Ilse, F. E. and Hartmann, H. *Z. physik. Chem.* **197** (1951) 239.
45. Coulson, C. A., Craig, D. P. and Jacobs, J. *Proc. Roy. Soc. London* **A 206** (1951) 297.
46. Shull, C. G., Strauser, W. A. and Wollan, E. O. *Phys. Rev.* **83** (1951) 333.
47. Coulson, C. A. *Quart. Rev. London* **1** (1947) 144.
48. Andersen, P. *Det 9. nordiske Kemikermøde*, Århus 1956, p. 7.
49. Schwarzenbach, G. *Helv. Chim. Acta* **32** (1949) 839.
50. Jørgensen, C. Klixbüll, *Acta Chem. Scand.* **9** (1955) 710.
51. Hawkins, N. J., Mattraw, H. C. and Sabol, W. W. *J. Chem. Phys.* **23** (1955) 2191.
52. Malm, J. G., Weinstock, B., and Claasen, H. H. *J. Chem. Phys.* **23** (1955) 2192.
53. Herzberg, G. *Molecular Spectra and Molecular Structure. I. Spectra of Diatomic Molecules*. 2. Ed. 1950, p. 392.
54. Tinkham, M. *Proc. Roy. Soc. London* **A236** (1956) 535 and 549.
55. Hartree, D. R. *J. Opt. Soc. Am.* **46** (1956) 350.
56. Schläfer, H. L. *Z. Physik. Chem.* **3** (1955) 221.
57. Jørgensen, C. Klixbüll, *Energy Levels of Complexes and Gaseous Ions*. Gjellerups Forlag, Copenhagen. 1957.

Received August 15, 1956.

ACTA CHEMICA SCANDINAVICA 11 (1957) 73—85

Comparative Ligand Field Studies

IV. Vanadium(IV), Titanium(III), Molybdenum(V) and other Systems with one d-Electron

CHR. KLIXBÜLL JØRGENSEN

Chemistry Department A, Technical University of Denmark, Copenhagen, Denmark

The vanadium(IV) complexes can deviate so much from cubic symmetry that all the four possible bands are observed in the tartrate complex. The absorption spectra of VO enta^{--}, VO ox$_2^{--}$, VO^{++} and several other complexes suggest a tetragonal symmetry with stronger ligand field along one axis than along the two other axes. Thus, the oxygen atom is probably placed on the former axis and is not aquated to two hydroxyl ions. The titanium(III) complexes exhibit smaller deviations from octahedral symmetry, corresponding to shoulders on the principal band. The dark coloured binuclear complex, which is formed between Ti(III) and Ti(IV) in concentrated hydrochloric acid, is investigated. In strong HCl, molybdenum(V) occurs as $MoOCl_5^{--}$, which exhibits two ligand field bands, corresponding to levels analogous to those of VO^{++}. The behaviour of one d-electron in ligand fields and the Jahn-Teller effect is compared with the opposite tetragonality of copper(II) complexes. Other oxidation states of molybdenum, wolfram, and niobium, are shortly discussed.

Systems with only one d-electron do not exhibit levels with different values of the spin S, and thus, spin-forbidden bands do not occur as in d^2—d^8 systems. Further, the integrals F^k of electrostatic interaction between the electrons in the partly filled shell cannot be evaluated; only one multiplet term, ^2D, occurs in the gaseous ion. If the splitting between $^2D_3/_2$ and $^2D_5/_2$ is neglected (it amounts to 384 K in Ti^{+3} and 620 K in V^{+4}), only one absorption band is expected of an octahedral complex with the symmetry O_h. One of the historical foundations of the ligand field theory is that Ilse and Hartmann [1] interpreted the band 20 300 K of $Ti(H_2O)_6^{+++}$ as the transition of the d-electron from the state γ_5 to γ_3, thus exemplifying the parameter [2] Δ, also called $(E_1—E_2)$ or 10 Dq. However, if the ligand field has a symmetry lower than O_h, more than one absorption band is predicted. Kramers' degeneracy cannot allow more than five energy levels of a single d-electron, corresponding to four absorption bands caused by transitions from the groundstate. The low symmetry of the ligand field is not necessarily caused by differences among

Table 1. Absorption bands of vanadyl complexes. Wavelength λ_n in mμ, wavenumber σ_n in K (= cm^{-1}), and molar extinction coefficient ε_n of each maximum and the half-widths $\delta(-)$ and $\delta(+)$ in K towards lower and higher wavenumbers. Shoulders are given in parentheses. The ligands are abbreviated: $enta^{-4}$ = ethylenediaminetetraacetate, ox^{-2} = oxalate, aca^{-} = acetylacetonate, and $tart^{-4}$ = tartrate (with four protons removed from D-tartaric acid).

	λ_n	σ_n	ε_n	$\delta(-)$	$\delta(+)$
VO^{++} in 1 M $HClO_4$	765	13 100	16.5	1 400	—
	(625)	16 000	7.5	—	1 400
	240	41 700	240	4 600	—
VO^{++} in 10 M $HClO_4$	735	13 600	15.5		—
	(635)	15 800	10.5	—	1 500
VO^{++} in 12 M HCl	728	13 700	18.5	—	2 300
VO^{++} in 8 M H_2SO_4	750	13 300	18	—	—
VO $enta^{--}$	780	12 800	23	1 400	—
	582	17 200	19	—	1 400
	(336)	29 800	22	2 000	—
VO ox_2^{--}	792	12 600	25	—	2 200
	605	16 500	9	—	1 700
	(340)	29 400	170	2 000	—
VO aca_2 in C_2H_5OH	780	12 800	34	1 400	1 900
	578	17 300	13	—	1 700
VO $tart^{--}$	910	11 000	22	1 600	1 700
	(587)	17 100	21	1 400	—
	531	18 800	25	—	1 900
	396	25 300	45	2 000	—
VO tart H^{-}	770	13 000	28	—	2 200
	565	17 700	14	—	2 000
	(348)	28 800	30	—	—
VO citrate in 2 M NH_3	850	11 800	15	—	1 800
	533	18 800	6	—	—
	(416)	24 000	3	—	—
VO SCN^{+} (Ref. 24)	720	13 900	58	1 700	—
	580	17 200	27	—	1 400

the six ligands of an octahedral complex; the Jahn-Teller effect produces a distortion to lower symmetry [3], when the cubic groundstate is either Γ_3, Γ_4, or Γ_5. The latter case of $Ti(H_2O)_6^{+++}$ was discussed by Van Vleck [4], who found that the absolute value of the distortion was not large. The present paper demonstrates that the effect is more important for vanadium(IV) complexes.

VANADIUM(IV)

The parameter Δ is 50—80 % larger for trivalent than for divalent ions of the first transition group. Since the pairs Cr(III)—Mn(IV)[5] and Ir(III)—Pt(IV)[6] demonstrate a further increase of Δ from trivalent to quadrivalent ions, Δ of a vanadium(IV) hexaaquo ion would be expected to be $\sim$ 25 000 K. However, VO^{++} in acidic aqueous solution exhibits a band at 13 100 K and a shoulder at 16 000 K, as seen from Fig. 1 and Table 1 and previously measured by Furman and Garner [7] and Rossotti [8].

The external charge + 2 of the vanadyl ion seems well established, *e. g.* by the potentiometric measurements by Ducret [9]. Since the equilibrium

$$O^{--} + H_2O \rightleftharpoons 2\ OH^-$$

is highly shifted towards the right-hand side, one might assume [65] that oxide and water cannot occur as ligands of a complex at the same time, but will exchange the hydrogen atom. Generally, the oxo-ions of the text-books seem to have seen their best time; the hydrolysis of uranium (IV)[10,11] does not produce UO^{++}, and CrO_2^- is undoubtedly $Cr(OH)_4(H_2O)_2^-$ or a polymer. However, the dioxo ions of quinquevalent and sexivalent actinides seem to retain their linear form in aqueous solution [12] and one must conclude that oxygen can be so strongly bound in a complex, probably by forming also π-bonds [13], that the proton affinity disappears.

A priori, one may consider three possibilities for the geometrical configuration of the vanadyl ion: tetrahedral (with two hydroxo- or one oxo-group), trigonal bipyramidic (with two *trans*-hydroxo groups or one perpendicular oxo group) and distorted octahedral (with two *trans*-hydroxo groups or one oxo group). The tetrahedral $V(OH)_2(H_2O)_2^{++}$ can be supported by many argu-

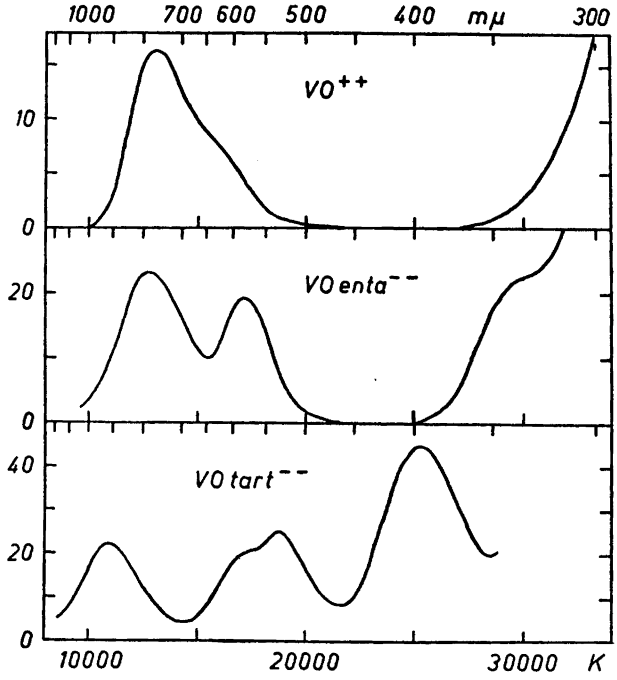


Fig. 1. Absorption spectra of vanadyl complexes.

0.1 M VO++ in 0.5 M to 2 M $HClO_4$.
0.05 M $VOenta^{--}$ from 0.1 M VO++ and 0.12 M Na_4enta mixed together.
0.05 M $(NH_4)_2$ [VO tart], $2H_2O$ in 0.1 M NH_3.

ments; Orgel [14] identified the band at 9 000 K of anhydrous VCl_4 as the transition from $^2\Gamma_3$ to $^2\Gamma_5$ of a tetrahedral complex. Eventhough the intermixing of molecular orbitals [15] can produce deviations from the ratio-4/9 predicted from the electrostatic model [16] between the values of Δ for tetrahedral and octahedral complexes, the absorption bands of the vanadyl ion resemble much those predicted of a split excited state $^2\Gamma_5$. The only known values of Δ for a tetrahedral complex [17], *viz.* those of $CoCl_4^{--}$ and the other cobalt(II) tetrahalides [14], are rather small.* The instantaneously reversible equilibrium between vanadium(IV) and vanadium(V), found by Ducret [9], might suggest the latter to occur in acidic solution as $V(OH)_4^+$. However, it is difficult to understand, why the $V(H_2O)_4^{+4}$ should be so acidic for the two first protons, while the third proton [8,18,19] has pK between 5 and 6, after which the polymerisation to brown hydroxides and anions soon follows. As seen from Fig. 1 and Table 1, a change in the absorption spectrum can actually be observed by going from 2 to 10 M $HClO_4$. However, the shift is so small that it might rather be ascribed to association with perchlorate ions than to a radical change of the first co-ordination sphere. Since the fourth excited level is reported below of VO enta^{--} and other complexes, these cannot be tetrahedral; however, it is not totally disproven that the vanadyl ion itself has a distorted tetrahedral structure. The trigonal bipyramidic structure would produce three levels of the d-electron [3], *i. e.* two absorption bands, and can at most be accepted for VO^{++}, but not for the complexes. Jones [20] discussed the possible equilibria between 5- and 6-co-ordinated vanadyl complexes. However, the X-ray structure [21] of VO_2 shows a distorted (hemiedric) octahedral environment and VO SO_4, 5 H_2O contains monomer vanadium, surrounded by six oxygen atoms [22]. Thus, the ionic radius of V^{+4} does not seem to be so small that the tetrahedral or trigonal bipyramidic configuration is more favoured **, except in the anhydrous VCl_4 and VBr_4.

As seen from Table 1 and Fig. 1, most vanadyl complexes exhibit the two absorption bands more clearly separated than VO^{++} itself, as already reported by Furman and Garner [24] for $VOSCN^+$. One of the most interesting spectra is found in the blue VO enta^{--}, discovered by Schwarzenbach [25]. It has the third band at 29 800 K, a wavenumber comparable to the expected Δ of a cubic vanadium(IV) complex. Thus, the two tetragonal components of $^2\Gamma_3$ in the ligand field of the distorted octahedron seem to be observed at 17 200 K and 29 800 K, a considerable distance. The second band of the complexes VO ox_2^{--}, VO aca_2, $VOSCN^+$, etc. must thus be considered as the first part of a tetragonal splitting of which the second part is hidden by the carboxylate band and other electron transfer bands in the ultraviolet. Actually, a shoulder was observed by Bürger [26] for VO $ox_2^{--} \sim 30\,000$ K besides the two bands at 12 600 and 16 200 K.

---

* *Cf.* the approximate values [2] of Δ in $MnBr_4^{--}$ (—2 000 K) and in $FeCl_4^-$ (—5 000 K).

** Even vanadium(V) appears to be hexa-coordinated in the black 8-hydroxyquinolinate [23] $(C_9H_6ON)_2VOOH$, which turns red with alcohols, yellow with amines, and which forms a blue $[(C_9H_6ON)_2V(OH)_2]Cl$ and a green dimeric anhydride. However, perhaps the nitrogen and the oxygen of the 8-hydroxyquinoline are not both co-ordinated as in other complexes.

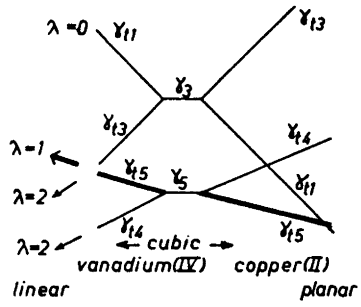


Fig. 2. The two opposite types of tetragonality. The behaviour of copper(II) and vanadium(IV) complexes is qualitatively described as a tetragonal distortion of the energy levels for ligand fields of exact cubic symmetry O_h. In the case of the vanadyl complexes, the energy levels can be extrapolated to those of a linear molecule with a negative value of $E\lambda$, as discussed in Ref. 29.

It is possible to determine the sign of the tetragonality by comparing the spectra of VO^{++} and the other complexes with four ligand atoms attached. Either the ligand field along two axes of a Cartesian co-ordinate is stronger than along the third axis (as is the case of copper(II) complexes [16,66]), or one axis has a stronger ligand field than the two others [27,3]. The latter seems distinctly to be the case; when enta^{-4} occupies the tetragonal plane, the tetragonal splitting is decreased. As seen from Fig. 2, the behaviour is opposite to that of the copper(II) complexes. When they have low tetragonality, two or three bands are observed in the near infra-red and in the visible [5,28] corresponding to transitions from $^2\Gamma_{t3}$ to $^2\Gamma_{t1}$, $^2\Gamma_{t4}$, and $^2\Gamma_{t5}$. When the tetragonality is very pronounced [5], such as in $Cu(NH_3)_4^{++}$ or $Cu\ en_2^{++}$, only one band is observed, probably due to superposition of the three excited levels.

This result supports strongly the classical composition VO^{++} of the vanadyl ion, with the oxygen on the tetragonal axis of strong ligand field. Even though O^{--} can occur on both sides of H_2O in the spectrochemical series (*cf.* the series green Cr_2O_3, violet $Cr(H_2O)_6^{+++}$, and red ruby), a similar strong ligand field would never be expected of two hydroxyl ions. As seen from Fig. 2, the strong bonding of the oxygen may be explained by the results for an electron in a linear ligand field [29]. If the influence of the ligands in the tetragonal plane vanished, $^2\Gamma_{t4}$ and $^2\Gamma_{t3}$ would correspond to the lowest energy level with $\lambda = 2$, $^2\Gamma_{t5}$ to $\lambda = 1$, and $^2\Gamma_{t1}$ of highest energy to $\lambda = 0$. Since the vanadyl ion contains only a single d-electron, it can remain in the groundstate in the level with $\lambda = 2$, while formation of both σ- and π-bonds, which increase the energy of the empty orbitals with $\lambda = 0$ and 1, respectively, does not destabilize the complex. Oxygen seem remarkably apt to π-bonding [13], which would explain the existence of oxo complexes with mainly linear ligand field in the beginning of the transition groups (VO^{++}, $MoOCl_5^{--}$ discussed below, UO_2^{++} etc.). The octahedral complexes in the middle of the transition groups (*e. g.* diamagnetic d^6) and the square-planar tetragonal d^9- and diamagnetic d^8-systems (which have high energy of the γ_{t3}-orbital) are more stable with σ-bonding ligands with high values of Δ, and in the case of low oxidation states, perhaps also by π-bonding in the direction from the central ion to the ligand. Thus, the general tendency to prefer oxygen in the beginning of a transition group (even though Δ is large and electrostatic effects does not dominate, as for Mn^{++} and Ca^{++}) and nitrogen in the end may have a profound connection

with the number of d-electrons, which are destabilized because they are in anti-bonding orbitals.

The transition of VO^{++} to $^2\Gamma_{t1}$ was expected $\sim$ 32 000 K. However, it seems to have a somewhat higher wavenumber and is masked by the broad band at 41 700 K ($\varepsilon = 240$) which was also reported by Furman and Garner [7]. The latter band is not due to hydrolysis, since it is the same in 0.1 M and 1 M $HClO_4$, nor to oxidation of VO^{++}, since it is not changed by addition of a small amount of V^{+++}. The intensity does not suggest that it is allowed; but it can hardly be the ligand field band sought for, since the other complexes do not have high intensity for their transitions to $^2\Gamma_{t1}$. Jones and Colvin [69] have shown by potentiometric measurements that VO^{++} is not more dimeric than V^{+++}; the band is thus not due to an oxygen bridge.

Jones [20] made a valuable contribution to the vanadyl problem by showing that VO aca_2 can be made anhydrous and is soluble as a monomer in benzene; and that the solvation with one molecule of H_2O, NH_3 etc. does not change the properties of VO aca_2 to such a degree that a di-hydroxo complex could be suggested.

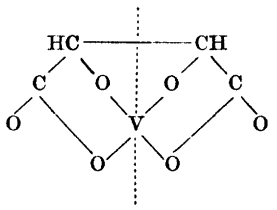
The tetragonal splitting can be made even smaller than for VO $enta^{--}$, and a rhombic splitting, producing in total four ligand bands, seems probable: It has previously [30] been noted that tartrates and citrates in aqueous ammonia produce a purple colour with vanadium(IV). In weakly acidic solution, tartrates produce a dark blue solution, of which the spectrum resembles the other carboxylate complexes such as VO ox_2^{--} (Table 1), and a weak shoulder is observed $\sim$ 28 600 K. The complexes of VO^{++} with organic anions exhibit a different behaviour, according to whether they contain hydroxo (alcohol) functions or not. VO ox_2^{--} and the analogous dark blue complex with succinate decompose in aqueous ammonia to brown precipitates, while the malate with a single hydroxo function forms a violet solution at not too high a concentration of NH_3. Vanadyl tartrates, citrates, and gluconates are soluble even in concentrated NH_3. This suggests a Fehling's solution-type complex, where the metal ion is bound to alcoxo groups of the ligand which have released protons also from the alcohol functions.

Actually, Barbieri [62] prepared a solid purple salt $(NH_4)_2[VOC_4H_2O_6]$, 2 H_2O, which later was studied by Rosenheim and Yu-Mong [63], who also prepared $Ba[VOC_4H_2O_6]$, 5 H_2O, demonstrating that no ammonia of constitution occurs in the anion. The anion must have two carboxylate groups and two alcoxo groups bound to vanadium in the tetragonal plane with the vanadyl oxygen on the perpendicular axis. Ducret [9] reports two pK values = 6.85 and 2.8 for the consecutive uptake of two protons on VO $tart^{--}$. Mr. Kjeld Rasmussen has kindly titrated a sample of ammonium vanadyl tartrate *, prepared [63] by the author, and found the values of p$K \sim 6.1$ and ~ 2.9. It cannot easily be decided whether the protons go on the carboxyl or alcoxo groups; vanadyl ions seem to have a strong affinity to alcoxo and phenoxo groups analogous to

* However, this purple salt turns blue with an excess of tartrate, even in 1 M NH_3, suggesting the formation of a complex with two tartrates and high absorption in the range 800—600 mμ, analogous to $VOtartH^-$.

iron(III), as shown by the preparation of vanadyl bis(salicylates) * and bis(pyrocatechinates) [63].

The tetragonal splitting between the two highest levels ** of VO tart^{--} is decreased to 6 500 K, while the rhombic splitting of $^2\Gamma_{t5}$ amounts to 6 100 K (Table 1). This is rather remarkable, since if the complex had orthogonal axes, its symmetry would be tetragonal with two equivalent axes in the electrostatic perturbation model [3]. The complex can hardly lack a plane of symmetry, intersecting the plane of the paper along the dotted line:



However, the two lines OVO in the plane do not need to be orthogonal ***. The resulting low symmetry C_s no longer presents degenerate electronic levels, and all five possible energy levels are then separated. It must be emphasized that planar platinum(II) complexes, *trans*-Pt A_2B_2, generally exhibit a genuine rhombic splitting [64] which is not found in *cis*-Pt A_2B_2 in agreement with Ballhausen's and the author's predictions for complexes with orthogonal axes [3]. Actually, the d^1-systems such as vanadium(IV), and the d^9-systems, such as copper(II), seem much more liable to exhibit effects of low symmetry than the regular d^3-, paramagnetic d^8-, and diamagnetic d^6-systems, which maintain nearly the energy levels predicted for cubic symmetry O_h, even with sets of highly different ligands.

Small tetragonal splittings might also occur in vanadium(IV) complexes with six equal ligands. The dark red hexachlorides, *e. g.* $[N(CH_3)_4]_2VCl_6$ prepared by Gutmann [31], probably have electron transfer bands in the visible. The pink K_2VF_6 prepared by Hoppe [32] may have $^2\Gamma_{t3} \sim 20\,000$ K and $^2\Gamma_{t1}$ at slightly higher wavenumbers.

Vanadium(III) is also soluble in tartrate and aqueous ammonia with a dark green colour [30]. The solution has maxima at 612, 440 and 424 mμ, the latter forming a broad band. Vanadium(III) in 12 M HCl has the bands at 675 and 448 mμ, while they are situated at 588 and 396 mμ of the solution in 2 M HCl. There is no doubt that the pure hexaaquo ion is still more hypsochromic, resembling the values 562 and 389 mμ, found by Hartmann and Schläfer [33] for vanadium(III) alum crystals. The spectrum of V enta$^-$ is rather peculiar [5].

---

* The pale purplish pink ammonium vanadyl salicylate dissolves with dark green colour in water or ethanol and can be easily re-crystallized. It decomposes with aqueous ammonia, and thus, the purple complex cannot be measured in solution.

** an alternative possibility might be $^2\Gamma_{t5}$ at 17 100 and 18 800 K, thus implying the distance 14 300 K between $^2\Gamma_{t3}$ and $^2\Gamma_{t1}$.

*** Hartmann, Furlani and Bürger [67,68] have recently discussed the deviations from orthogonal axes. Their case, Vox_3^{-3}, exhibits surprisingly small deviations from the spectrum, predicted for an octahedral complex with the symmetry O_h.

TITANIUM(III)

Hartmann and Schläfer [34] observed strong variations in the absorption spectrum of titanium(III), which was ascribed to hydrolysis at low acid concentrations and formation of chloro complexes in strong hydrochloric acid. Recently, Hartmann, Schläfer, and Hansen [35] have investigated the spectrum of anhydrous $TiCl_3$ in different solvents in order to avoid some of these difficulties.

As previously discussed [36], the hexaaquo ion is the dominating species in the reddish purple solution in 2 M HCl. The band at 492 mμ is very broad and has a shoulder at 575 mμ, which was interpreted [3] as distortions caused by the Jahn-Teller effect. The large half-width may be connected with the large value of Δ and the large amplitude of the ligand's vibrations in the relatively weakly bound complex [2], where $\delta \sim 0.15\ \Delta$. However, with the picture given in Ref. 2, it is peculiar, why the bands with highest wavenumbers of the purple vanadyl tartrate and of $MoOCl_5^{--}$ are so narrow.

In stronger hydrochloric acid titanium(III) turns sky-blue with a shift of the double band to about 660 and 525 mμ. These spectra resemble much the spectra reported by Hartmann [35] of $TiCl_3$ in anhydrous alcohols. It may be questioned [37,38] whether these effects are caused solely by solvation or by the partial formation of chloro complexes in the first co-ordination sphere. The hexa(alcohol) solvates seem much more unstable towards uptake of anions than hexaaquo ions. In anhydrous ethanol (but not in 90 % C_2H_5OH), cerium(III) chloro complexes are formed at a chloride concentration $\sim$0.005 M, while 10 M HCl is necessary for the same effect in aqueous hydrochloric acid [39].

However, if the sky-blue solutions of titanium(III) in strong HCl are slightly oxidized, they turn much darker purplish black. This oxidation may be effected by, *e. g.*, a platinum wire, catalyzing the evolution of hydrogen. Table 2 gives the molar extinction coefficients at several wavelengths for mixtures of Ti(III) and Ti(IV) in 12 M HCl. The spectra are seen to be a linear combination of the sky-blue titanium(III) and the dark colour, which has a maximum at 482 mμ and a shoulder at 670 mμ. Further, a strong absorption in the ultraviolet appears, which is absent in pure Ti(III) (which has $\varepsilon = 8$ at 310 mμ).

The dark-coloured complex is similar to the "interaction colours" found in the pair of oxidation states: copper(I, II)[40], tin(II, IV) [41] and antimony-

Table 2. Molar extinction coefficients of titanium(III) and (IV) in 12 M HCl. For mixtures, ε is calculated solely with respect to the total concentration C_{Ti+3} of trivalent titanium. Wavelengths in mμ.

C_{Ti+3}	C_{Ti+4}	C_{Ti+4}: C_{Ti+3}	650	600	550	500	475	$\frac{[III, IV]}{C_{Ti+3}}$
0.1 M	0	0	4.2	5.2	6.0	5.9	5.4	—
0.100	0.02 M	0.2	6.8	8.3	9.9	10.8	10.6	0.12
0.091	0.036	0.4	9.4	11.3	13.6	15.6	15.5	0.24
0.083	0.067	0.8	12.8	15.6	19.0	22.1	22.2	0.40
0.072	0.114	1.6	19.8	23.8	28.7	34.3	34.3	0.71
0.062	0.151	2.4	22.7	27.2	33.1	39.2	39.2	0.85
0.050	0.20	4.0	24.8	29.6	35.8	42.8	42.6	0.95
0.020	0.32	16	26.5	31.5	38	45	44.5	1.00
0	0.4	—	0.1	0.1	0.1	0.15	0.25	—

(III, V) [42] in concentrated HCl. Thus, from the variation of ε in Table 2, the existence of a bi-nuclear complex containing equal amounts of Ti(III) and Ti(IV) is demonstrated. The formation constant of this complex in 12 M HCl, relative to the concentrations [III], [IV], and [III, IV], having the ε values of pure Ti(III), pure Ti(IV) and the limiting value of ε for mixtures and with the known concentrations $C\mathrm{Ti}^{+3} = [\mathrm{III}] + [\mathrm{III, IV}]$ and $C\mathrm{Ti}^{+4} = [\mathrm{IV}] + [\mathrm{III, IV}]$, can be inferred from Table 2 to

$$\frac{[\mathrm{III, IV}]}{[\mathrm{III}]\ [\mathrm{IV}]} = 12$$

Since the pure oxidation states probably occur mainly as $TiCl^{++}$ and $TiCl_6^{--}$ in concentrated HCl, (*cf.* Ref. 61) the composition of the mixed complex [III, IV] may perhaps be rather near to the neutral form Ti_2Cl_7.

The interaction colours, due to titanium in both oxidation states (analogous to molybdenum blue, ferroferricyanides etc.) occur probably also in the black precipitate of $Ti(OH)_3$ from $Ti(H_2O)_6^{+++}$ and alkali. The precipitate is probably oxidized by a spontaneous evolution of hydrogen, analogous to the air oxidation of white $Fe(OH)_2$ to greenish black forms. Also titanium(III, IV) solutions in strong sulphuric acid are black, while the similar phenomenon is not observed in phosphoric acid. Neither do Zr^{+4}, Th^{+4} or U^{+4} interact visibly with Ti^{+3} in strong HCl. It may be remarked that while the pale green $U(OH)_4$ on partial oxidation produces dark brown intermediates, it does not interact with U^{+3}. If the red solution * in HCl is added to aqueous ammonia, a pale orange-red precipitate of $U(OH)_3$ can be observed one second before the evolution of H_2 and the change to pale green.

Titanium (IV) complexes have a strong electron transfer band in the ultraviolet. Thus, TiO_2 is much more absorbing [43] than ZrO_2. Even while the liquid $TiCl_4$ is free of iron (the absorption band of the vapour has recently been measured [44]), its solution in 12 M HCl is pale yellow. Much more conspicuous is the reaction with thiocyanate. While a yellow solution is obtained with this reagent in water, a dark red-brown compound (probably un-ionized $Ti(SCN)_4$) can be extracted with diethyl ether. If titanium(III) is free from impurities of (IV), thiocyanate produces a clear purple colour (the maximum at 528 mμ has $\varepsilon_n = 12$ and $\delta = 3\,000$ K) which is not shifted by extraction with diethyl ether and thus probably is caused by $Ti(SCN)_3(H_2O)_3$.

The purple Ti enta$^-$ has been made several times by cautious addition of Na_4enta and NaOH to Ti(III) in 2 M HCl. Besides the broad maximum at the rather large wavelength 543 mμ, a band one-fourth as strong is observed $\sim$760 mμ, thus corresponding to large deviations from the cubic symmetry O_h.

These examples show that titanium(III) has by no means the strong tendency to form regular octahedral complexes as have d^3-, d^8- and diamagnetic d^6-systems. Thus, no Ti ox_3^{-3} is known; the brown [45] Ti ox_2^- has a strong absorption band $\sim$405 mμ. However, these bands are often electron transfer bands (perhaps also causing the strong colour of violet $TiCl_3$, which was rather expected to have $\Delta \sim 15\,000$ K) rather than ligand field bands.

* of chloro complexes.[70] Below a HCl-concentration 6 M, or in $HClO_4$, uranium(III) is grey.

MOLYBDENUM(V)

When molybdenum(VI) is reduced with zinc in strong HCl, a green colour is observed, which can be ascribed to $MoOCl_5^{--}$, of which Klason [46] and Nordenskjöld [47] prepared several salts, among those some anhydrous. Further reduction yields a red solution of Mo(III), which probably contains $MoCl_6^{-3}$ and $MoCl_5(H_2O)^{--}$. Chilesotti [48] proved by potentiometric measurements that Mo(IV) is not formed in 9 M HCl, while the reduction in more dilute acid may yield all three consecutive oxidation states +5, +4 and +3.

The behaviour seems less complicated in HCl than in other acids. In dilute sulphuric acid, molybdenum(V, VI) blue is invariably formed, and the reduction proceeds with formation of brownish black solutions. Even dilute HCl is highly different from strong HCl in respect to the colour of molybdenum(V). Hiskey, Meloche, and Springer [49,50] studied spectrophotometrically the change of colour from pale green in 8 M HCl to strong amber yellow in 2 M HCl. Table 3 gives the absorption bands of $MoOCl_5^{--}$. Even though the second narrow

Table 3. Absorption bands of $MoOCl_5^{--}$ in 9—12 M HCl. Notation as in Table 1.

λ_n	σ_n	ε_n	$\delta(-)$	$\delta(+)$
712	14 050	16	1 500	1 900
445	22 500	14	1 100	—
355	28 200	500	1 400	—
310.5	32 200	4 400	1 600	1 700
240	40 700	5 500	2 100	—

band has nearly the same position as the much higher, but broader, band which appears in the brown solutions by dilution with water, the present author is inclined to believe that it actually belongs to the undecomposed $MoOCl_5^{--}$. Thus, the intensity ratio between the two first bands is constant in the range 9 M—12 M HCl. Analogous to the levels of VO^{++} (see Fig. 2), the excited level of the band at 14 050 K is $^2\Gamma_{t5}$, while the band at 22 600 K is $^2\Gamma_{t3}$. The cubic contribution $\triangle$ predicted of the hypothetical $MoCl_6^-$ is ~30 000 K. If the spontaneous Jahn-Teller distortion is not very large, the latter ion will be nearly colourless. The second band of $MoOCl_5^{--}$ is much narrower than the first; this may be explained by the influence of intermediate coupling, splitting $^2\Gamma_{t5}$ in the two levels $^2\Gamma_{t6}$ and $^2\Gamma_{t7}$.

The third band of $MoOCl_5^{--}$ is much higher ($\varepsilon = 500$) than the first two ($\varepsilon = 16$ and 14). It is probably a relatively weak electron transfer band. When molybdenum(III) in HCl is slightly oxidized, the third band of this impurity appears strongly. Thus, it can be applied as an indicator for the presence of +5, proving that the broad shoulder at 728 mμ on the red side of the sharp maximum at 673 mμ ($\varepsilon = 1.7$)* is not caused by molybdenum(III). Schmidt [26] observed the behaviour of molybdenum(III) in strong

* The present author [15] has previously identified the excited doublet levels as $^2\Gamma_3$ and $^2\Gamma_4$. However, the absence of $^2\Gamma_5$ is so surprising that it might be assigned to these levels in the red, implying B ~450 K as also the quartet levels do. Actually, the reflection spectrum of $(NH_4)_2[MoCl_5(H_2O)]$ exhibits low bands at 1 050,678 and a shoulder at 652 mμ, while the high bands occur at 506 and 406 mμ. The solution in 12 M HCl shows a band at 1 035 mμ ($\varepsilon = 0.5$). Professor R. W. Asmussen and Mr. Potts Jensen have previously measured a band at 1 100 mμ of solid K_2ReCl_6.

and dilute HCl, which resembles much that of rhodium(III) [6], except that the equilibria are established rapidly. Thus, the bands at 522 and 418 mμ ($\varepsilon = 25$ and 35) are shifted towards 475 and 385 mμ by dilution with water.

The brown solutions of molybdenum(V) in 6 M HCl have $\varepsilon \sim 20$ at 720 mμ and $\varepsilon \sim 150$ at 445 mμ, while the shoulder at 352 mμ is blurred out. There is some evidence that the brown hydrolysis product is more easily formed at high Mo concentrations, indicating at least two Mo atoms per complex. Sacconi and Cini [51] have found that the paramagnetism, corresponding to $S = \frac{1}{2}$ of $MoOCl_5^{--}$, is changed to diamagnetism of Mo(V) in dilute HCl, probably due to formation of oxygen bridges of the type [52] encountered in $Cl_5RuORuCl_5^{-4}$ and $Cl_5ReOReCl_5^{-4}$, of which the latter is in equilibrium [53] with the monomer $ReCl_5(OH)^{--}$.

WOLFRAM(V)

When tungstates(VI) are dissolved in very strong HCl, they can be reduced by amalgamated zinc at first to a blue solution, which perhaps contains the monomer $WOCl_5^{-}$ together with some tungsten(V, VI) blue. It has a maximum (655 mμ, $\varepsilon \sim 7$). By further reduction, a purple solution of tungsten(IV) with $\varepsilon \sim 600$ in a maximum at 19 100 K, is formed. After some time, the more robust yellow-green $W_2Cl_9^{-3}$ are formed (they are oxidized by air much more slowly than W(IV)). The spectrum of this does not exhibit two spin-allowed ligand field transitions to $^4\Gamma_5$ and $^4\Gamma_4$ such as the monomeric Mo(III) does. The first two bands (at 13 200 K, $\varepsilon \sim 25$ and at 16 300 K, $\varepsilon \sim 40$) are probably the spin-forbidden transitions to $^2\Gamma_3$ and $^2\Gamma_5$ with the high intensity perhaps caused by the absence of a centre of inversion in each tungsten atom. Further, a high band occurs at 22 200 K ($\varepsilon \sim 1\,200$). Laudise and Young [54] recognize further a pale red form of tungsten(III) in addition to $W_2Cl_9^{-3}$.

NIOBIUM(IV)

Cozzi and Vivarelli [55] investigated the absorption spectra of niobium(IV), (III) and (II) in hydrochloric acid of different concentrations. Thus, the red-orange niobium(IV) complex in 13 M HCl has a maximum at 478 mμ ($\varepsilon \sim 120$), while the blue Nb(IV) solution in 8—9 M HCl has a broad band ~ 700 mμ ($\varepsilon \sim 150$). It is assumed [55] that these complexes are analogous to VO^{++}, $VOCl_4^{--}$ and VCl_6^{--}. However, it is doubtful whether VO^{++} takes many chloride ligands up in HCl (see Table 1), since the maximum is only slightly shifted. *Cf.* the ion exchange measurements by Kraus, Moore and Nelson [61].

GENERAL REMARKS

Even though the d^1-systems in some cases (VO^{++}, $MoOCl_5^{--}$) exhibit the opposite sign of tetragonality to that of the d^9-systems (*e. g.* Cu^{++}), it is only in a limited range of oxidation states that the typically linear molecules occur. While titanium(III) does not deviate so much from the cubic symmetry as vanadium(IV), the higher oxidation states assume tetrahedral configuration with the necessary Jahn-Teller distortion. Thus, MnO_4^{--} has three bands of nearly equal intensity at 605, 435 and 355 mμ, which must be caused by transfer of π-electrons from the oxygen atoms, analogous to the two strong bands [13]

of MnO_4^-. With the larger ionic radii of the 4d-elements, it has become possible for molybdenum(V) to retain hexa-coordination in $MoOCl_5^{--}$, while ruthenium(VII) in RuO_4^- is tetrahedral with electron transfer bands [56] at 385 and 310 mμ.

It is interesting to see how much more important inherent Jahn-Teller distortion is for the development of typical tetragonal symmetry of titanium(III), vanadium(IV), molybdenum(V) and copper(II) complexes than the tetragonality of mixed complexes, *e. g.* of chromium(III) [57], cobalt(III) [57], nickel(II)[5,58], rhodium(III)[6,59] and iridium(III)[6,59] which often is difficult to detect.

EXPERIMENTAL

The spectra were measured in the range 800—210 mμ on a Cary recording spectrophotometer, Model 11-MS-50, and above 800 mμ on a Beckman DU.

Vanadium solutions. AnalaR NH_4VO_3 was directly, or after ignition to V_2O_5, dissolved in 2 M $HClO_4$ and reduced electrolytically to VO^{++}, or in 10 M HCl and reduced with amalgamated zinc to a mixture of V^{++} and V^{+++}. A 0.5 M solution of the latter kind was diluted with water to 0.1 M and used directly for vanadium(III) measurements and after spontaneous oxidation by air for vanadium(IV) measurements.

0.1 M Na_4enta, 0.6 M $(NH_4)_2$ox, 1 M tartaric acid, 1 M citric acid, 12 M aqueous ammonia etc. were made from analytical or C. P. reagents, and added to vanadium and titanium solutions in measuring flasks.

Solid $(NH_4)_2[VO\ C_4H_2O_6]$, $2H_2O$ and $VO\ aca_2$, H_2O were prepared according to Rosenheim and Yu-Mong [63].

Titanium solutions. Colourless $TiCl_4$ was mixed with 12 M HCl giving a 2 M solution. This solution was diluted to 0.2 M or 0.1 M $TiCl_4$ with different concentrations of HCl and reduced to the clearest shade of purple titanium(III) with zinc.

Molybdenum solutions. Merck's $(NH_4)_6Mo_7O_{24}$ was dissolved in 6 M HCl giving a 0.5 M solution. This was diluted with HCl to 0.1 M or lower concentrations and reduced with amalgamated zinc. Solid K_3MoCl_6 and $(NH_4)_2MoCl_5(H_2O)$[60] were also used for some experiments.

Acknowledgments. I thank Professor Jannik Bjerrum for his kind interest in the investigations.

REFERENCES

1. Ilse, F. E. and Hartmann, H. *Z. physik. Chem.* **197** (1951) 239.
2. Jørgensen, C. Klixbüll, *Acta Chem. Scand.* **11** (1957) 53.
3. Ballhausen, C. J. and Jørgensen, C. Klixbüll, *Kgl. Danske Videnskab Selskab Mat.-fys. Medd.* **29** (1955) No. 14.
4. Van Vleck, J. H. *J. Chem. Phys.* **7** (1939) 61, 72.
5. Jørgensen, C. Klixbüll, *Acta Chem. Scand.* **9** (1955) 1362.
6. Jørgensen, C. Klixbüll, *Acta Chem. Scand.* **10** (1956) 500, 518.
7. Furman, S. C. and Garner, C. S. *J. Am. Chem. Soc.* **72** (1950) 1785.
8. Rossotti, F. J. C. and Rossotti, H. S. *Acta Chem. Scand.* **9** (1955) 1177.
9. Ducret, L. P. *Thesis.* Université de Paris 1951.
10. Kraus, K. A. and Nelson, F. AECD—1888, and *J. Am. Chem. Soc.* **72** (1950) 3901.
11. Hietanen, S. *Rec. trav. chim.* **75** (1956) 711 and *Acta Chem. Scand.* **10** (1956) 1531.
12. Seaborg, G. T. and Katz, J. J. *The Actinide Elements. Natl. Nuclear Energy Ser.* Div. IV, Vol. 14 A.
13. Wolfberg, M. and Helmholz, L. *J. Chem. Phys.* **20** (1952) 837.
14. Orgel, L. E. *J. Chem. Phys.* **23** (1955) 1004.
15. Jørgensen, C. Klixbüll, *Reports of the Xth Solvay Conference*, Bruxelles, May 1956.
16. Ballhausen, C. J. *Kgl. Danske Videnskab. Selskab Mat. fys. Medd.* **29** (1954) No. 4.
17. Ballhausen, C. J. and Jørgensen, C. Klixbüll, *Acta Chem. Scand.* **9** (1955) 397.
18. Jones, G. and Ray, W. A. *J. Am. Chem. Soc.* **66** (1944) 1571.
19. Ducret, L. *Bull. soc. chim. France* **1948** 658.

20. Jones, M. M. *J. Am. Chem. Soc.* **76** (1954) 5995.
21. Anderson, G. *Acta Chem. Scand.* **10** (1956) 623.
22. Lundgren, G. *Rec. trav. chim.* **75** (1956) 585.
23. Blair, A. J. and Pantony, D. A. *Anal. Chim. Acta* **13** (1955) 1.
24. Furman, S. C. and Garner, C. S. *J. Am. Chem. Soc.* **73** (1951) 4528.
25. Schwarzenbach, G. and Sandera, J. *Helv. Chim. Acta* **36** (1953) 1089.
26. Hartmann, H. and Schläfer, H. L. *Angew. Chem.* **66** (1954) 768.
27. Bethe, H. *Ann. Physik* [5] **3** (1929) 133.
28. Belford, R. L. *Bonding and Spectra of Metal Chelates. Thesis.* University of California 1955 (UCRL—3051).
29. Jørgensen, C. Klixbüll, *Acta Chem. Scand.* **11** (1957) 166.
30. Jørgensen, C. Klixbüll, *Naturviden (Ungdommens naturvidenskabelige forening)* **6** (1952) 61.
31. Gutmann, V. *Monatsh.* **85** (1954) 286.
32. Hoppe, R. *Rec. trav. chim.* **75** (1956) 569.
33. Hartmann, H. and Schläfer, H. L. *Z. Naturforsch.* **6a** (1951) 754.
34. Hartmann, H. and Schläfer, H. L. *Z. physik. Chem.* **197** (1951) 116.
35. Hartmann, H. Schläfer, H. L. and Hansen, K. H. *Z. anorg. Chem.* **284** (1956) 153.
36. Jørgensen, C. Klixbüll, *Acta Chem. Scand.* **9** (1955) 405.
37. Jørgensen, C. Klixbüll, *Acta Chem. Scand.* **8** (1954) 175.
38. Jørgensen, C. Klixbüll and Bjerrum, J. *Nature* **175** (1955) 426.
39. Jørgensen, C. Klixbüll, *Kgl. Danske Videnskab. Selskab Mat. fys. Medd.* **30** (1956) No. 22.
40. Mc Connell, H. and Davidsen, N. *J. Am. Chem. Soc.* **72** (1950) 3168, 5557.
41. Browne, C. I., Craig, N. and Davidson, N. *J. Am. Chem. Soc.* **73** (1951) 1946.
42. Whitney, J. E. and Davidson, N. *J. Am. Chem. Soc.* **71** (1949) 3809.
43. Treiber, E., Stenius, A. S., Lang, W. and Berndt, W. *Acta Chem. Scand.* **8** (1954) 1865.
44. Mason, D. M. and Vango, S. P. *J. Phys. Chem.* **60** (1956) 622.
45. Pecsok, R. L. *J. Am. Chem. Soc.* **73** (1951) 1304.
46. Klason, P. *Ber.* **34** (1901) 149.
47. Nordenskjöld, I. *Ber.* **34** (1901) 1572.
48. Chilesotti, A. *Z. Elektrochem.* **12** (1906) 173.
49. Hiskey, C. F., Springer, V. F. and Meloche, V. W. *J. Am. Chem. Soc.* **61** (1939) 3125.
50. Hiskey, C. F. and Meloche, V. W. *J. Am. Chem. Soc.* **62** (1940) 1565.
51. Sacconi, L. and Cini, R. *J. Am. Chem. Soc.* **76** (1954) 4239.
52. Nyholm, R. S. *Reports of the Xth Solvay Conference*, Bruxelles, May 1956.
53. Jezowska-Trzebiatowska, B. and Wajda, S. *Bull. acad. polon. sci. Classe III* **2** (1954) 249 (cf. *Chem. Abstracts* **1954** 13518).
54. Laudise, R. A. and Young, R. C. *J. Am. Chem. Soc.* **77** (1955) 5288.
55. Cozzi, D. and Vivarelli, S. *Z. anorg. Chem.* **279** (1955) 165.
56. Connick, R. E. and Herley, C. R. *J. Am. Chem. Soc.* **74** (1954) 5012.
57. Schäffer, C. E. *Acta Chem. Scand.* **11** (1957). *To be published.*
58. Jørgensen, C. Klixbüll, *Acta Chem. Scand.* **10** (1956) 887.
59. Jørgensen, C. Klixbüll, *Acta Chem. Scand.* **11** (1957) 151.
60. Lohmann, K. H. and Young, R. C. *Inorganic Syntheses* **4** (1953) 97.
61. Kraus, K. A., Moore, G. E. and Nelson, F. *J. Am. Chem. Soc.* **78** (1956) 2692.
62. Barbieri, G. A. *Atti accad. nazl. Lincei* [2] **23** (1914) 47.
63. Rosenheim, A. and Yu-Mong, Hsien *Z. anorg. Chem.* **148** (1925) 25.
64. Babaeva, A. *Izvest. Sektora Platiny i Drug. Blagorod Metal. Inst. Obschchei i Neorg. Khim. Akad. Nauk. SSSR* **25** (1950) 56.
65. Bjerrum, J. *Metal Ammine Formation. Thesis*, Copenhagen 1941, p. 70.
66. Bjerrum, J., Ballhausen, C. J. and Jørgensen, C. Klixbüll, *Acta Chem. Scand.* **8** (1954) 1275.
67. Hartmann, H., Furlani, C. and Bürger, A. *Z. physik. Chem.* **9** (1956) 62.
68. Hartmann, H. and Furlani, C. *Z. physik. Chem.* **9** (1956) 162.
69. Jones, G. and Colvin, J. H. *J. Am. Chem. Soc.* **66** (1944) 1563 and 1573.
70. Jørgensen, C. Klixbüll *Acta Chem. Scand.* **10** (1956) 1503.

Received October 12, 1956.

ACTA CHEMICA SCANDINAVICA 11 (1957) 86—97

Studies on the Extraction of Metal Complexes

XXVII. The Distribution of Some Actinides and Fission Products between Methyl *Iso*butyl Ketone and Aqueous Solutions of HNO_3 and $Ca(NO_3)_2$

JAN RYDBERG and BRITA BERNSTRÖM

Research Institute of National Defence, Dept. 1, Sundbyberg 4, Sweden

The distribution ratios of U(VI), Pu(VI), Pu(IV), Th(IV), Zr(IV), La(III), Ca(II), Na(I) and HNO_3 between methyl *iso*butyl ketone (hexone) and aqueous solutions of varying HNO_3 and $Ca(NO_3)_2$ concentrations have been determined and are given in Figs. 2—10. Some possible methods of separating uranium and plutonium from certain fission products are discussed.

Recently, a considerable number of papers [1] have been released on the separation of uranium, plutonium and mixed fission products from each other by means of different liquid-liquid extraction methods. The two most used organic solvents seem to be hexone (methyl *iso*butyl ketone) and TBP (tributyl phosphate), both of which are used for the extraction of the metal nitrates.

The present work * deals with the extraction of U(VI), Pu(VI), Pu(IV), Th(IV), Zr(IV), La(III), Ca(II), and Na(I) nitrates from aqueous solutions with various concentrations of HNO_3 and $Ca(NO_3)_2$ as salting-out agents. The elements studied represent about 90 % of the β- and γ-activity from the fission products of natural uranium ** which has been irradiated in a pile for several months and cooled for about the same time; the rest of the radioactivity is mainly due to Ru-Rh, which elements are not considered here.

In the present study, distribution experiments were run with each metal separately. The metal concentration of each phase was determined after equilibration. The ratio of the metal concentration in the organic phase to that in the aqueous phase gives the distribution ratio q of the metal. It was

* Based on Report FOA1, No. H 1149—8509, 1954.

** Cs and Rb are assumed to accompany Na, Sr and Ba to accompany Ca while all the rare earths resemble La. Nb is assumed to follow Zr.

generally found that q increases with the HNO_3 or $Ca(NO_3)_2$ concentration of the aqueous phase. Since very little $Ca(NO_3)_2$ dissolves in the organic phase, the variation of q with increasing HNO_3 concentration has been determined at a constant $Ca(NO_3)_2$ concentration in the aqueous phase. In the following, q_{Ca}, q_{La}, etc. will be used as abbreviations for the distribution ratios of the metals given by the subscripts.

EXPERIMENTAL

Chemicals. Hexone (methyl *iso*butyl ketone, $C_4H_9COCH_3$) of technical quality was purchased from the Svenska Shell AB; after filtration it was washed with $NaHCO_3$ and water to remove acid and water-soluble impurities and to saturate it with water.

^{234}Th was prepared according to Dyrssen [4].

^{140}La was obtained as the neutron-irradiated oxide, which was dissolved in HNO_3.

U(VI) solutions were prepared by dissolving UO_3 of high purity in HNO_3.

Zirconium nitrate of puriss. quality was dissolved in 1 M HNO_3. The solution was filtered and standardized by weighing the ignited oxide.

$Ca(NO_3)_2$ and $NaNO_3$ were of analytical grade.

General procedure. All distribution experiments were carried out at room temperature (20 ± 2° C). The metal nitrate and $Ca(NO_3)_2$ were mixed with varying amounts of HNO_3 and shaken with an equal volume of hexone. In all systems, equilibrium was established within 5 min. At high HNO_3 concentrations, the phases were found to undergo large volume changes. This is due to an appreciable extraction of HNO_3 into hexone whereas only negligible amounts of $Ca(NO_3)_2$ are extracted. In order to maintain the $Ca(NO_3)_2$ concentration of the aqueous phase constant throughout a series of distribution experiments, distilled water was added with repeated shaking up to the original volume of the aqueous phase. The two phases were then separated by centrifuging and samples were withdrawn for metal analysis and the titration of nitric acid.

Solubility of $Ca(NO_3)_2$ in HNO_3—H_2O. The addition of HNO_3 to concentrated $Ca(NO_3)_2$ solutions causes $Ca(NO_3)_2$ to crystallize out because its solubility product is exceeded. Solutions of varying HNO_3 content were saturated with $Ca(NO_3)_2$ and allowed to stand for a couple of days to attain equilibrium. Calcium was determined by weighing the ignited oxide after careful evaporation of a definite volume. The acid concentration was determined by titration. Fig. 1 shows the solubility of $Ca(NO_3)_2$ in water solutions as a function of the HNO_3 concentration. As a consequence, the distribution experiments are limited to a smaller acid concentration range at high $Ca(NO_3)_2$ concentrations.

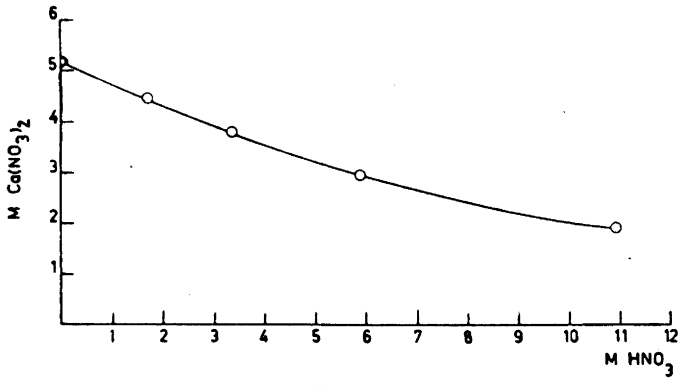


Fig. 1. The solubility of $Ca(NO_3)_2$ in HNO_3 solutions.

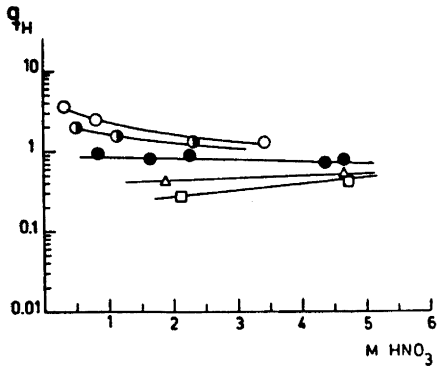


Fig. 2. The distribution ratio q_H of HNO_3 as a function of the equilibrium concentration of HNO_3 in the aqueous phase. Concentrations of $Ca(NO_3)_2$: ○ 4—3.8 M*, ◑ 3 M, ● 2 M, △ 1 M, □ no $Ca(NO_3)_2$ present.

The molal solubility of $Ca(NO_3)_2$ in solutions of varying HNO_3 content has been investigated by Basset and Taylor [5]. By determining the density of the aqueous solutions, a check was made that our results were in agreement with those obtained by Basset and Taylor.

The distribution ratio of HNO_3, q_H. The distribution ratio q_H of HNO_3 between the organic and aqueous phases was determined by titration of the acid in each phase with NaOH. In Fig. 2, q_H is plotted against the equilibrium concentration of HNO_3 in the aqueous phase for different $Ca(NO_3)_2$ concentrations *.

The distribution ratio of sodium, q_{Na}. A gravimetrical determination of the distribution of $NaNO_3$ gave an upper limit of $q_{Na} \leqq 10^{-3}$.

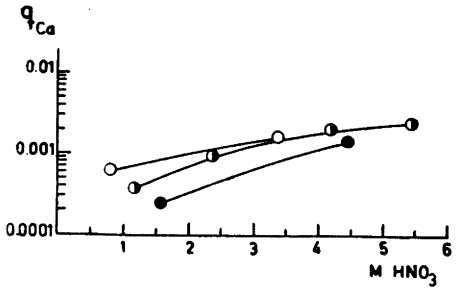


Fig. 3. The distribution ratio q_{Ca} of calcium as a function of the equilibrium concentration of HNO_3 in the aqueous phase. Total concentrations of $Ca(NO_3)_2$: ○ 4—3.8 M*, ◑ 3 M, ● 2 M.

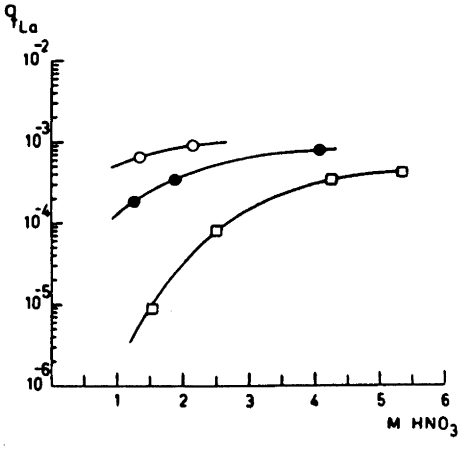


Fig. 4. The distribution ratio q_{La} of lanthanum as a function of the equilibrium concentration of HNO_3 in the aqueous phase. Concentrations of $Ca(NO_3)_2$: ○ 4—3.8 M*, ● 2 M, □ no $Ca(NO_3)_2$ present.

* The $Ca(NO_3)_2$ concentration can be kept constant at 4 M only for acid concentrations $\leqq$ 1 M. To obtain a higher acidity one is forced to start the distribution experiment with an initially acid hexone phase. After equilibrium the aqueous phase has increased in volume due to the distribution of HNO_3, thus causing a decrease of the $Ca(NO_3)_2$ concentration.

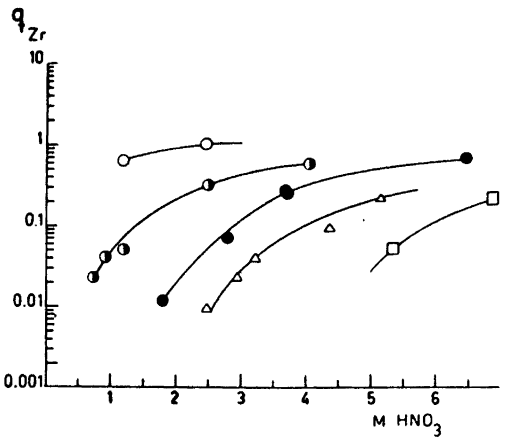


Fig. 5. The distribution ratio q_{Zr} of zirconium as a function of the equilibrium concentration of HNO_3 in the aqueous phase. Concentrations of $Ca(NO_3)_2$: ○ 4—3.7 M*, ◑ 3 M, ◉ 2 M, △ 1 M, □ no $Ca(NO_3)_2$ present.

The distribution ratio of calcium, q_{Ca}. The distribution ratio of Ca between hexone and water is very low. In order to determine the Ca concentration of the hexone phase, a known volume of the phase was taken and evaporated to dryness, whereupon the residue was dissolved in distilled water. Ca was determined by a substitution titration with EDTA (ethylenediamine tetraacetic acid) at pH = 10 using Eriochrome Black T as indicator [6,7]. Blanks were run in the same way. The distribution data obtained are plotted in Fig. 3.

The distribution ratio of lanthanum, q_{La}. The distribution was followed by means of ^{140}La as a tracer. Dry samples of each phase were counted. The La solution used was of very high specific activity, which made it possible to count the aqueous phase after a 100-fold dilution thus avoiding vitiating salt residues of $Ca(NO_3)_2$. In Fig. 4, q_{La} is plotted versus the equilibrium HNO_3 concentration of the aqueous phase.

The distribution ratio of zirconium, q_{Zr}. With an original zirconium concentration of 0.1 M in the aqueous phase, it was possible to determine the distribution of zirconium by gravimetrical analysis. Since $Ca(NO_3)_2$ was present in the aqueous phase, only samples of the hexone phase were weighed after the evaporation and ignition to the oxide. The weights were corrected for the small amounts of calcium coextracted into the hexone phase according to Fig. 3. The phase volumes were measured after equilibrium so that the zirconium content of the aqueous phase could be calculated from the difference between the total amount of zirconium added and that found in the organic phase. The data are given in Fig. 5.

The distribution ratio of thorium, q_{Th}. By means of ^{234}Th (UX_1), the distribution of thorium was followed radiometrically. The thorium concentration in these experiments was $\leq 10^{-5}$.

Liquid counting was used, which involved corrections due to the different absorptions of the radiation in the hexone phase and in the aqueous phases of varying $Ca(NO_3)_2$ concentrations. Using the same liquid counter, these corrections were measured experimentally in the following manner:

a) the counting rate of a definite amount of ^{234}Th was measured in 1 M HNO_3 and in 1 M HNO_3 solutions containing 1, 2, 3 and 4 M $Ca(NO_3)_2$.

b) the counting rate of the same amount of ^{234}Th was measured in hexone after an extraction with 0.2 M TTA (thenoyltrifluoroacetone) in hexone from a 0.05 M $HClO_4$ phase; in this case $q_{Th} > 500$.

The results for q_{Th} are plotted in Fig. 6.

The distribution ratio of hexavalent uranium, q_U, *at* U *concentrations* ≤ 0.1 *M*. After equilibration, samples were withdrawn and evaporated to dryness whereupon the residues were dissolved in 0.1 M $HClO_4$. The uranium content was determined colorimetrically by means of the thiocyanate method [8]. The residues sometimes contained appreciable amounts of Ca but it was found that this did not interfere with the method.

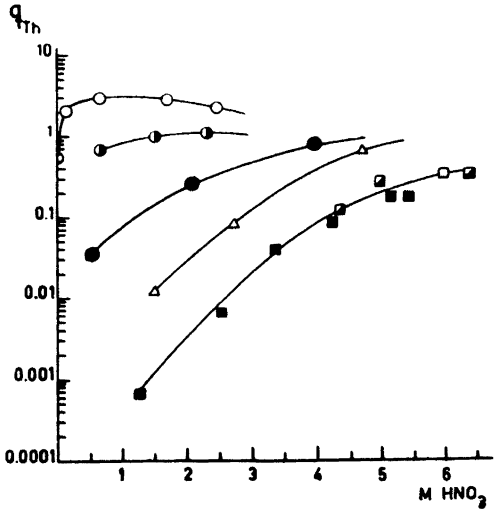


Fig. 6. The distribution ratio q_{Th} of thorium as a function of the equilibrium concentration of HNO_3 in the aqueous phase. Initial concentration of Th $\leq 10^{-5}$ M, except for ◪ where Th concentration is 0.1 M. Concentrations of $Ca(NO_3)_2$: ○ 4—3.7 M*, ◑ 3 M, ● 2 M, △ 1 M, □ ◪ ■ no $Ca(NO_3)_2$ present. (□ radiometrical, ◪ gravimetrical, ■ radiometrical with 0.1 M U present).

The titration of HNO_3 was carried out with methyl orange as indicator in order to avoid titration errors due to the uranium present. The curves for different $Ca(NO_3)_2$ concentrations are found in Fig. 7.

The distribution ratio of thorium and hexavalent uranium at U *concentrations between 0.1 and 1 M.* The experiments were carried out with uranium (UI) in radioactive equilibrium with ^{234}Th (UX_1). It was then possible to determine the distribution of the two

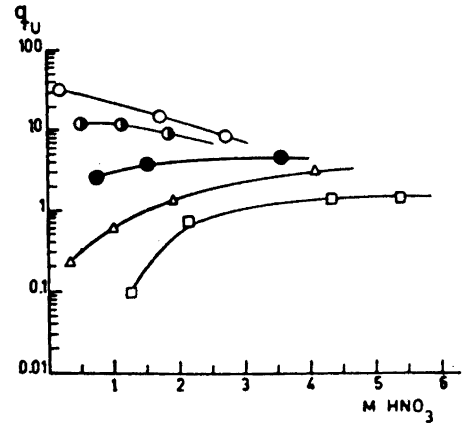


Fig. 7. The distribution ratio q_U of hexavalent uranium as a function of the equilibrium concentration of HNO_3 in the aqueous phase. Concentration of $Ca(NO_3)_2$: ○ 4—3.6 M*, ◑ 3 M, ● 2 M, △ 1 M, □ no $Ca(NO_3)_2$ present.

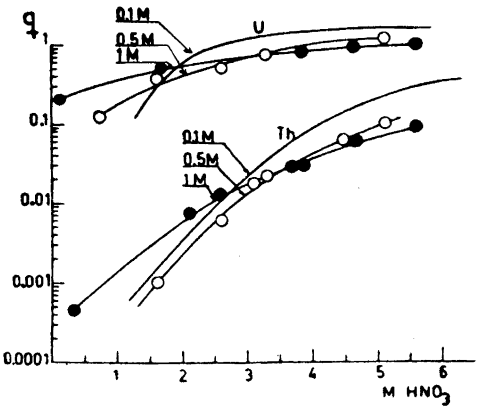


Fig. 8. The distribution ratios q_U of hexavalent uranium and q_{Th} of thorium as functions of the equilibrium concentration of HNO_3 in the aqueous phase. No $Ca(NO_3)_2$ added. Total concentration of U(VI): ● 1 M, ○ 0.5 M. For comparison the curves for 0.1 M U are drawn.

* See footnote, p. 88.

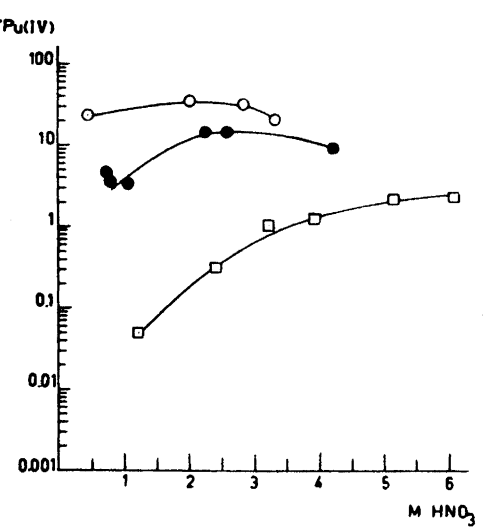


Fig. 9. The distribution ratio $q_{Pu(IV)}$ of Pu(IV) as a function of the equilibrium concentration of HNO_3 in the aqueous phase. Concentrations of $Ca(NO_3)_2$: ○ 4—3.5 M*, ● 2 M, □ no $Ca(NO_3)_2$ present.

metals separately in the solutions using the same analytical procedures as before. The HNO_3 concentration of the aqueous phase was determined by a NaOH titration after removing the uranyl ions by running the sample through the hydrogen form of a cation exchange column (Dowex 50). It is noted that for each UO_2^{2+} that is adsorbed 2 H^+ are removed and must be subtracted in the NaOH titration. The data are given in Fig. 8 where q_U and q_{Th} have been plotted against the HNO_3 concentration of the aqueous phase at equilibrium.

The distribution of tetravalent plutonium, $q_{Pu(IV)}$. A solution of Pu(IV) in 10 M HNO_3 (3×10^{-3} mg Pu/ml) was available. A TTA extraction was employed to confirm the tetrapositive state of plutonium [13].

In the distribution experiments with Pu(IV), 1 ml of this solution was added to a 4 ml aqueous phase of varying HNO_3 content and the resulting solution was then mixed with an equal volume of hexone. After the separation of the phases by centrifugation, samples of 0.1 ml were taken from the two phases and evaporated on Pt-dishes. The pipets were rinsed with 1 M HNO_3 solutions and the washings were also added to the dishes. The dry samples were measured internally in an argon-methane proportional counter. With $Ca(NO_3)_2$ present in the aqueous phase, direct radiochemical analysis of the aqueous phase was not possible. The procedure used was therefore to extract plutonium from the $Ca(NO_3)_2$ solution with a 0.05 M solution of dibutyl phosphate in $CHCl_3$. Tests were made to show that plutonium(IV) was extracted quantitatively under the conditions in question, *i. e.* from acid solutions of 2 M and 4 M $Ca(NO_3)_2$. The results are plotted in Fig. 9.

The distribution of hexavalent plutonium, $q_{Pu(VI)}$. To obtain Pu(VI), different oxidizing agents can be used, *cf.* Refs.[2,11]. The symbols in Fig. 10 represent the following procedures:

◑. A plutonium solution kept in 5 M HNO_3 was treated for 5 min with solid $NaBiO_3$; the excess bismuthate was removed by centrifugation. The oxidized plutonium solution was then immediately used in distribution experiments with hexone, pretreated only as described under "Chemicals".

□. The plutonium solution was treated with 0.001 M $Cr_2O_7^{2-}$ in 1 M HNO_3 with Co^{2+} as catalyst for 10 min at 90° C. The hexone used in the distribution experiments was pretreated with dichromate solutions in the same way but at room temperature. Dry, thin samples could not be obtained in the distribution experiments when more concentrated dichromate solutions were used.

* See footnote, p. 88.

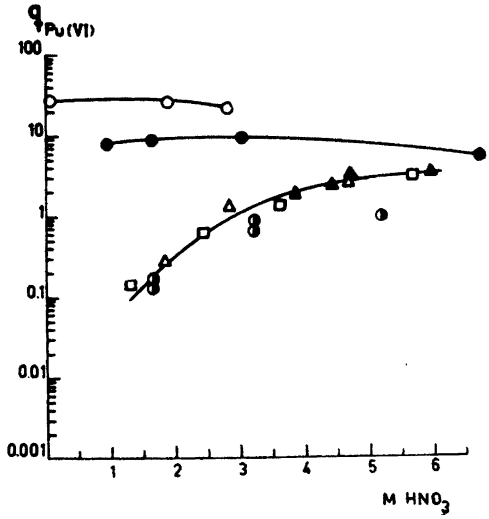


Fig. 10. The distribution ratio $q_{Pu(VI)}$ of Pu(VI) as a function of the equilibrium concentration of HNO_3 in the aqueous phase. Concentrations of $Ca(NO_3)_2$: O 4—3.6 M *, ● 2 M, □ ◑ △ ▲ no $Ca(NO_3)_2$ present (for explanation of symbols see text).

▲. The plutonium solution was made 10 M in HNO_3 and 0.67 M in $KBrO_3$; the hexone was shaken immediately before the distribution experiments with an equal volume of 10 M HNO_3 and 0.1 M $KBrO_3$.

△. The plutonium solution was made 1 M in HNO_3 and 0.2 M in $KBrO_3$ and kept at 95° C for 30 min; the hexone was pretreated with 0.1 M $Cr_2O_7^{=}$ in 1 M HNO_3 followed by washing with sodium hydroxide and finally steam distilliaton of the hexone (*cf.* Ref.[1] Paper 541, Vol. 9).

For the curves with 2 M (symbol ●) and 4 M (symbol O) $Ca(NO_3)_2$, 0.2 M $KBrO_3$ was used as oxidant. The plutonium analysis of the two phases was performed in the following manner: a) a dry, thin sample of the hexone phase could be obtained directly by evaporation, b) when no $Ca(NO_3)_2$ was present, 0.1 ml of the aqueous phase was evaporated and counted; when $Ca(NO_3)_2$ was present, 3 ml of the aqueous phase was adjusted to approximately 0.05 M in H^+ by adding concentrated NH_3 and then shaken with 2 ml hexone 0.05 M in dibutyl phosphate; preliminary tests showed that plutonium(VI) is extracted quantitatively under these conditions. The results are found in Fig. 10.

DISCUSSION OF RESULTS

The results obtained above are collected in Figs. 11—15, from which it is possible to choose conditions for separating the different metals from each other.

When uranium and plutonium are dissolved in hot, concentrated HNO_3, one gets mainly U(VI), Pu(IV) and Pu(VI). Now it can be seen from Figs. 11, 13 and 15 that the distribution ratios of these species are close together, which makes it difficult to separate them from each other. If it is desired to separate uranium from plutonium, one should make use of the facts that plutonium can be reduced to Pu(III) without the reduction of U(VI) [1,2] and that Pu(III) behaves much similar to La(III) [3], which is easily separated from U(VI) [1,2].

The following discussion will only deal with the separation of uranium together with plutonium from the other metals, which represent most of the

* See footnote, p. 88.

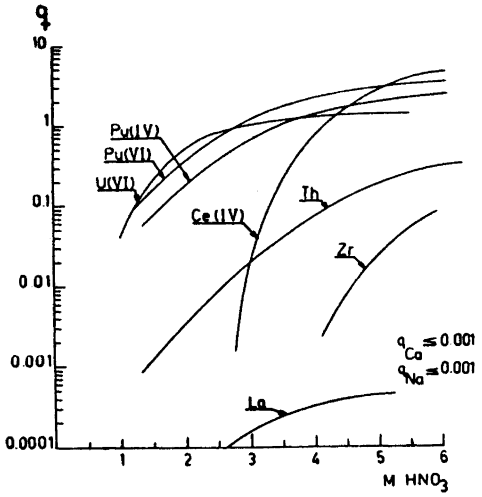


Fig. 11. The distribution ratios of U, Pu(IV) and Pu(VI), Th, Zr, Ce(IV) and La as functions of the equilibrium concentration of HNO_3 in the aqueous phase. No $Ca(NO_3)_2$ added. The Ce(IV) curve is taken from Glendenin *et al.*[12].

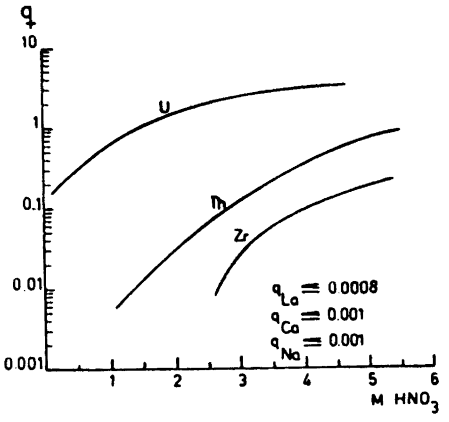


Fig. 12. The distribution ratios of U, Th and Zr as functions of the equilibrium concentration of HNO_3 in the aqueous phase. Concentration of $Ca(NO_3)_2$ 1 M.

undesired impurities in pile irradiated uranium. In order to avoid complications due to hydrolyses of some of the metals, the discussion will be limited to acidities ≤ 1 M in H^+.

Extraction formulas and definition of the decontamination factor

For batchwise extractions of a single (stationary) aqueous phase with fresh organic solvent (also called "multiple extraction"), the equation

$$P = 100 \cdot q \cdot r_v \sum_{1}^{n} (1 + q \cdot r_v)^{-n} \qquad (1)$$

gives the percentage P of the metal obtained in the combined organic phases after n extractions when the ratio between the volumes of the organic and aqueous phases is r_v. It is seen that the larger $q \cdot r_v$ is, the more complete will the extraction be.

For counter-current extractions (batchwise or continuous) with n extracting and m stripping stages and introduction of the feed at the stage $m = n = 1$, the ratio R of the amount of the metal leaving in the organic phase to that leaving in the aqueous phase is given by

$$R = \frac{E^m(E^n - 1)}{E^m - 1} \qquad (2)$$

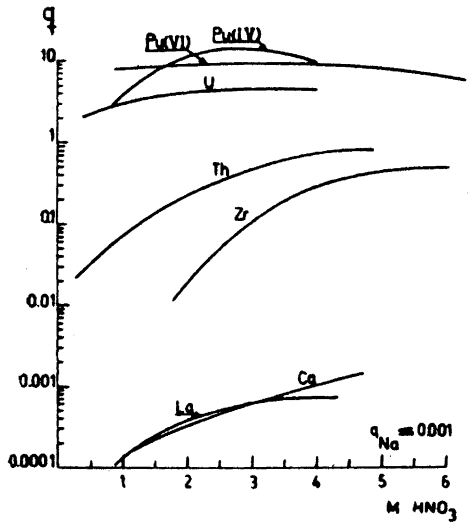


Fig. 13. The distribution ratios of U, Pu(IV) and Pu(VI), Th, Zr, La and Ca as functions of the equilibrium concentration of HNO_3 in the aqueous phase. Concentration of $Ca(NO_3)_2$ 2 M.

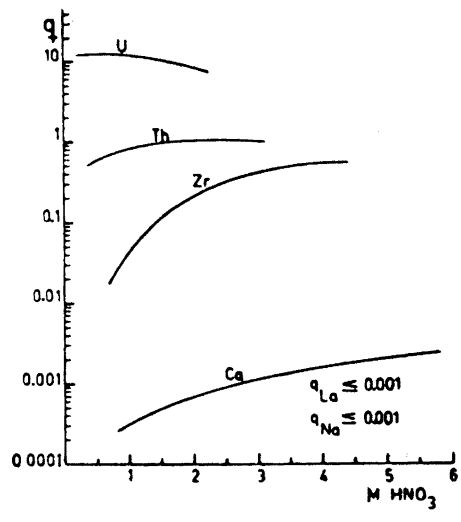


Fig. 14. The distribution ratios of U, Th, Zr and Ca as functions of the equilibrium concentration of HNO_3 in the aqueous phase. Concentration of $Ca(NO_3)_2$ 3 M.

where $E = q \cdot r_v$ (E is called extraction factor). Eqn. 2 is valid provided r_v is constant throughout all stages, which implies that the volume of the feed is negligible. Convenient graphs of this equation have been given by Bartels and Kleiman [9].

The decontamination factor (*D. F.*) is here defined as the ratio of the desired product (A) to the contaminants (B) in the organic phase at the n:th stage divided by the corresponding ratio in the original aqueous phase (= feed),

$$D.\,F. = \frac{(A)_n/(B)_n}{(A)_0/(B)_0} \qquad (3)$$

The extraction of uranium and plutonium into hexone without the addition of $Ca(NO_3)_2$

In Fig. 11, the distribution ratios q of the different metals are compared for the case where no $Ca(NO_3)_2$ is added. Since the distribution ratios are fairly low for uranium and plutonium, the ratio r_v of the volume of the organic phase to that of the aqueous phase must be considerably greater than 1 in order that a good yield of these ions shall be obtained in the combined organic phases for a reasonably small number of extraction stages.

As an example, a multiple extraction using a HNO_3 equilibrium concentration of 2 M, where the decontamination factor is large, will be described. (*Cf.* Fig. 16 which illustrates how the separation factor between U and Th (*i.e.* q_U/q_{Th}) varies with the HNO_3 and $Ca(NO_3)_2$ concentration). Let us assume according to Fig. 11 that $q_{Pu(IV)} \approx q_{Pu(VI)} \approx q_{U(VI)} \geq 0.2$ at 2 M HNO_3. If $r_v = 5$, then

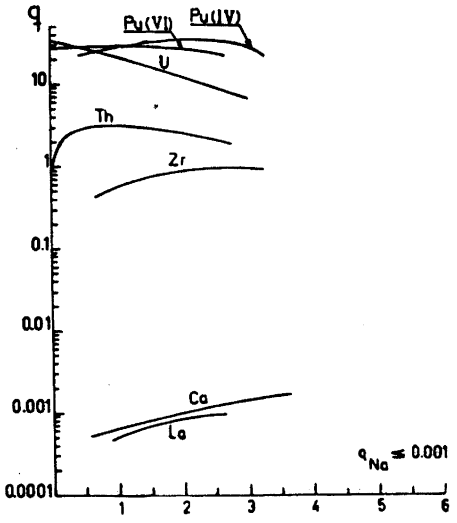


Fig. 15. The distribution ratios of U, Pu(IV) and Pu(VI), Th, Zr, La and Ca as functions of the equilibrium concentration of HNO_3 in the aqueous phase. Concentration of $Ca(NO_3)_2$ 4—3.5 M *.

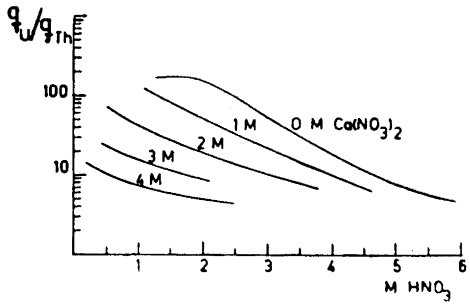


Fig. 16. The separation factor q_U/q_{Th} as a function of the equilibrium concentration of HNO_3 in the aqueous phase at varying $Ca(NO_3)_2$ concentrations.

eqn. 1 indicates that, with 6 extractions ($n = 6$), more than 98 % of U(VI), Pu(IV) and Pu(VI) is extracted. The decontamination factor will be > 8 with respect to thorium and $> 10^3$ with respect to La and probably also to the other elements in Fig. 11 (Ce, Zr, Ca and Na).

In a counter-current extraction, E in eqn. 2 must be > 1 in order to get any appreciable extraction of an element. Thus either q or r_v must be increased compared to the multiple extraction above. Since $r_v = 5$ is about the practical upper limit with hexone, q must be increased, which is possible by going to higher HNO_3-concentrations. Let us assume that $q_{U(VI)} \approx q_{Pu(IV)} \approx q_{Pu(VI)} \geq 0.6$ in 3 M HNO_3 while, for the other elements in Fig. 11, $q \leq 0.02$. For $n = 4$ and $m = 3$ (*i. e.* 6 stages altogether since $m = 1$ and $n = 1$ is the feed stage) and $r_v = 5$, it is found that more than 99 % of U(VI), Pu(IV) and Pu(VI) will be extracted with a decontamination factor $> 10^3$.

This shows that with a counter-current technique it is feasible to get a good separation of uranium and plutonium from fission products. However, a drawback of these extractions is the large volumes of organic solvent needed.

The extraction of uranium and plutonium into hexone from $Ca(NO_3)_2$ solution

By comparing Figs. 12—15, where 1, 2, 3 and 4 M $Ca(NO_3)_2$ was present in the aqueous phase, it is seen that the distribution ratios of all metals increase with the $Ca(NO_3)_2$ concentration. This makes it possible to use $r_v \approx 1$ at high

* See footnote, p. 88.

$Ca(NO_3)_2$ concentrations. It is also noted that the curves for the different metals become closer to each other which means that the separation between the elements becomes less efficient (*cf.* Fig. 16). For the separation of U(VI), Pu(IV) and Pu(VI) from the fission products, it is necessary to consider primarily the decontamination due to zirconium.

Let us assume that a multiple extraction is carried out at 1.5 M HNO_3 and with 3 M $Ca(NO_3)_2$, where we estimate from Figs. 13 and 15 that $q_{Pu(IV)} \approx \approx q_{Pu(VI)} > q_{U(VI)} = 10$ (Fig. 14). It can be calculated from eqn. 1 with $r_v = 1$ that 3 multiple extractions will yield 99.9 % U(VI), Pu(IV) and Pu(VI) in the hexone phase. However, at the same time about 25 % of the zirconium present will go into the hexone phase ($q_{Zr} = 0.1$).

If the extractions instead are carried out in a counter-current manner with $n = 3$, $m = 3$, one can calculate, using eqn. 2, that > 99 % of U(VI), Pu(IV) and Pu(VI) will be extracted with < 1 % zirconium.

The advantage of using high salt concentrations is that the ratio r_v of the volume of the organic phase to that of the aqueous phase can be kept ≈ 1. An easier separation of the hexone and aqueous phase with high salt concentration is also obtained due to the increased density of the aqueous phase. A drawback of the method is that more difficulties are in general encountered in taking care of salt-rich radioactive wastes.

The extraction of uranium and thorium at higher uranium concentrations

In most practical separation processes, one has to start with a high concentration of uranium. Since uranium nitrate will act as a salting-out agent and increase the distribution ratios, a separate investigation was made in which the initial uranium concentration was increased to 1 M and q_U and q_{Th} were determined (Fig. 8). In agreement with the results obtained with $Ca(NO_3)_2$, an increased uranium concentration increases the distribution ratios most at HNO_3 concentrations < 1 M. At high acidities, the distribution ratios q_U and q_{Th} show a tendency to decrease with increasing uranium concentration.

However, for the case discussed above where the extraction is made from a $Ca(NO_3)_2$-free solution at 3 M HNO_3, one can assume that the same separation of uranium and plutonium from the bulk of the fission products will be obtained when starting with higher initial uranium concentrations.

Acknowledgements. The authors wish to thank the head of this institute, Professor G. Ljunggren, for his continuous interest and support of this work. We also wish to thank Professor L. G. Sillén and Dr. D. Dyrssen for valuable discussions and Miss V. Dahlberg for generous experimental assistance. The English in this paper has been revised by Dr. D. Gillam.

REFERENCES

1. *Proceedings of the International Conference on the Peaceful Uses of Atomic Energy*, Geneva, August 1955, Vol. 7 and 9, New York 1956.
2. Rydberg, J. and Sillén, L. G. *Acta Chem. Scand.* **9** (1955) 1241.
3. Seaborg, G. T. *The Actinide Elements, National Nuclear Energy Series IV — 14A* (1954), Chapter 17.

4. Dyrssen, D. *Svensk Kem. Tidskr.* **62** (1950) 153.
5. Basset, H. Jr. and Taylor, H. S. *J. Chem. Soc.* **101** (1912) 576.
6. Schwarzenbach, G. and Biederman, W. *Chimica* **2** (1948) 56.
7. Schwarzenbach, G. *Die komplexometrische Titration*, Stuttgart 1955.
8. Rodden, C. J. and Warf, J. C. *Analytical Chemistry of the Manhattan Project, Nati nal Nuclear Energy Series VIII-1* (1950) Chapter 1. (Hök, B. *Svensk Kem. Tidskr.* **65** (1953) 105).
9. Bartels, C. R. and Kleiman, G. *Chem. Eng. Progr.* **45** (1949) 589.
10. Hindman, J. C. *The Actinide Elements, N.N.E.S. IV—14A* (1954), Chapter 9.
11. Connick, R. E. *The Actinide Elements, N.N.E.S. IV—14A* (1954), Chapter 8.
12. Glendenin, L. E., Flynn, K. F., Buchanan, R. F. and Steinberg, E. P. *Anal. Chem.* **27** (1955) 59.
13. Rydberg, J. *Arkiv Kemi* **9** (1956) 109; Cunninghame, J. G. and Miles, G. L. *J. Inorg. Nucl. Chem.* **3** (1956) 54.

Received October 17, 1956.

ACTA CHEMICA SCANDINAVICA 11 (1957) 98—100

The Non-occurrence of Cedrene and Cedrol in *Juniperus communis* L.

JOHAN B-SON BREDENBERG

Department of Chemistry, Institute of Technology, Helsingfors, Finland

It is proposed that the presence or absence of cedrene and cedrol can be used to differentiate between the sections *Sabina* and *Oxycedrus* in the genus *Juniperus*. Neither cedrene nor cedrol have been detected in the ethereal oil from the wood of *Juniperus communis* L., which belongs to the section *Oxycedrus*.

The genus *Juniperus*, which comprises about 60 species, is divided into three sections: *Caryocedrus*, *Oxycedrus* and *Sabina* [1]. No investigation of the extraneous matter of the monotypic section *Caryocedrus* has been made. Most of the investigations of the species belonging to *Oxycedrus* and *Sabina* have been concentrated on the ethereal oil. Erdtman [2] quotes cedrene and cedrol as typical constituents of the wood of junipers. It was of interest to check this statement in the case of the ethereal oil from the wood of *Juniperus communis* L. The oil was fractionally distilled. From the fraction (No. 3, Table 2) corresponding to the boiling point of cedrene no cedrene glycol could be obtained. An infrared spectrum of the fraction showed that it did not contain cedrene. From a higher boiling fraction (No. 10, Table 2) crystals, m.p. 75—76°, were slowly deposited. The infrared spectrum of this compound was not identical with the spectrum of cedrol. No additional crystalline substances could be obtained in spite of prolonged cooling or storage at room temperature (two years). As cedrol crystallizes well, these results are taken as evidence of the absence of cedrene and cedrol from the oil.

In the light of this discovery a closer scrutiny of the literature was made, with interesting results (Table 1).

It has been claimed that cedrene occurs in *J. oxycedrus* L.[19]. The constants given for this cedrene, however, show such a great divergence from those for natural cedrene that this claim is not worthy of consideration. It must be remarked that a negative sign does not necessarily exclude the presence of the substances, since the investigations are far from complete. This is especially true of cedrene, a liquid hydrocarbon. Nevertheless it seems possible to differentiate the sections *Sabina* and *Oxycedrus* by the presence or absence of cedrene and cedrol in the ethereal oil from the wood.

Table 1. Occurrence of cedrene and cedrol in junipers. The species have been arranged according to Pilger [3].

		Species	Part	Cedrol	Cedrene	Ref.
Oxycedrus		*J. communis* L.	Wood	–	–	This paper
		J. communis L. var. *saxatilis* Pall.	Branches	–	–	4
		J. oxycedrus L.	Wood	–	–	5
		J. taxifolia Hook. et Arn.	Branches	–	–	6
Sabina	The Old World	*J. sabina* L.	Branches	–	–	7
		J. semiglobosa Regel	»	+	–	8
		J. seravschanica Komarov	»	+	(+)	9
		J. excelsa Bieb.	»	+	+	10
		J. polycarpos C. Koch	»	(+)	–	11
		J. procera Hochst.	Wood	+	(+)	12, 13
		J. chinensis L.	»	+	(+)	14
		J. phoenicea L.	Branches	–	–	15
		J. turkestanica Komarov	»	+	–	8
	America	*J. mexicana* Schiede	Wood	(+)	(+)	16
		J. occidentalis Hook.	»	+	+	17
		J. virginiana L.	»	+	+	18

+ The substance has been isolated.
(+) The substance is either incompletely characterized or the method of identifying it is unknown.
– The substance has not been found.

EXPERIMENTAL

The ethereal oil was obtained, in connection with other work [20], by extraction of wood meal (13 kg) with ether, separation of the acidic components, and steam distillation of the neutral oil. The steam distillate (234 g, 1.8 % of the air-dried wood) had the following constants: d_{15}^{15} 0.937, n_D^{20} 1.507, α_D^{20} −24°, E. No. 7.2. It was fractionated in a 1 m spinning band column, giving the fractions in Table 2.

Table 2. Fractional distillation of 234 g of ethereal oil. Yield 185 g, 79 %.

Distillate,	g	B.p. °C,	mm Hg	d_4^{20}	n_D^{20}	α_D^{18}
1.	5.4	116–26	14	0.9172	1.4980	−27.7
2.	14.1	126–27	14	9238	5014	−44.8
3.	52.8	127–28	14	9273	5031	−62.3
4.	19.6	128–38	14	9207	5074	−34.0
5.	16.3	138–40	14	9250	5125	+3.0
6.	25.8	140–42	14	9252	5143	+2.3
7.	7.9	130–32	9	9259	5154	−1.5
8.	9.4	132–43	9	9498	5135	−4.1
9.	7.7	143–45	9	9737	5069	−7.3
10.	7.4	145–47	9	9779	5068	−7.7
11.	8.8	147–54	9	9815	5102	−10.2
12.	4.1	154–58	9	9870	5138	−8.3
13.	3.7	158–68	9	9970	5197	−21.1
14.	2.1	168–72	9	9972	5235	+0.7

The constants of the fraction No. 3 corresponded fairly well with those reported for natural cedrene [21]. Five grams of this fraction were oxidized with $KMnO_4$ according to a method described in the literature [22]. No cedrene glycol could be found. Comparison of the infrared spectrum of the fraction with a spectrum given by Plattner *et al.*[23] showed that no cedrene was present.

After two months, crystals were slowly formed in fraction No. 10. Four months later the crystals were filtered (yield 90 mg, m.p. 70—75°). Recrystallisation from methanol-water raised the melting point to 75—76°. An infrared spectrum established that the compound was not cedrol.

All attempts to obtain additional crystalline substances by prolonged cooling or storage of the fractions at room temperature for a long time (two years) failed.

The author is indebted to Professor H. Erdtman, who has supplied the IR-spectrum of authentic cedrol and to Mr. B. C. Fogelberg, Centrallaboratorium Ab., Helsingfors, who has taken the other IR-spectra.

REFERENCES

1. Krüssmann, G. *Die Nadelgehölze*, Paul Parey, Berlin 1955, p. 29.
2. Cook, J. W. (Ed.) *Progress in Organic Chemistry* **1** (1952) 22.
3. Engler, A. and Prantl, K. (Ed.) *Die natürlichen Pflanzenfamilien*, Wilhelm Engelmann, Leipzig 1926, Vol. XIII, p. 396.
4. Tsukervanik, I. and Grach, L. *Acta Univ. Asiae Mediae Tashkent, Ser. VI* **1937**, No. 37.
5. Mousseron, M., Granger, R. and Ronayroux, M. *Compt. rend.* **208** (1939) 1411.
6. Shinozaki, Y. *J. Chem. Ind. Japan* **24** (1921) 202; *Chem. Zentr.* **1922: IV**, 763.
7. Guenther, E. *The Essential Oils*, Van Nostrand Co., New York 1952, Vol. VI, p. 386.
8. Tsukervanik, I. and Danilevskiĭ, L. *Trudy sredneaziatskoi opytnoi stantsii ef.-maslichnyh rastenii* **1934**, No. 3.
9. Tsukervanik, I. and Danilevskiĭ, L. *Trudy sredneaziatskoi opytnoi stantsii ef.-maslichnyh rastenii* **1935**, No. 5.
10. Rutovskiĭ, B. N. and Vinogradova, I. V. *Trans. Sci. Chem.-Pharm. Inst. (U.S.S.R.)* **1927**, No. 17, 142.
11. Sokolnikov, N. P. *Pishchevaya Prom.* **1944**, No. 5—6, 22.
12. Schimmel & Co. *Ber. Schimmel & Co. Akt.-Ges.* **1911: II**, 105.
13. Dumont, H. M. *Soap, Perfumery & Cosmetics* **13** (1940) 127.
14. Uchida, S. *J. Soc. Chem. Ind. Japan* [*Suppl.*] **31** (1928) 190 B; *Chem. Zentr.* **1928: II**, 2198.
15. Rodie, J. *Bull. soc. chim.* [4] **1** (1907) 492.
16. Windemuth, N. *Pharm. Arch.* **16** (1945) 17; *Chem. Abstracts* **39** (1945) 3879.
17. Kurth, E. F. and Lackey, H. B. *J. Am. Chem. Soc.* **70** (1948) 2206.
18. Rousset, L. *Bull. soc. chim.* [3] **17** (1897) 485.
19. Sontag, D. *Rev. marques-Parfums France* **17** (1939) 5.
20. Bredenberg, J. B. and Gripenberg, J. *Acta Chem. Scand.* **8** (1954) 1728.
21. Naves, Y. R., Papazian, G. and Perrottet, E. *Helv. Chim. Acta* **26** (1943) 302.
22. Etablissements A. Chiris. *Parfums France* **1925** No. 28, 168; *Chem. Abstracts* **19** (1925) 2726.
23. Plattner, Pl. A., Fürst, A., Eschenmoser, A., Keller, W., Kläui, H., Meyer, St. and Rosner, M. *Helv. Chim. Acta* **36** (1953) 1845.

Received October 8, 1956.

ACTA CHEMICA SCANDINAVICA 11 (1957) 101—104

On the Occurrence of Folic Acid, Folic Acid Conjugates and Folic Acid Conjugases in Pollen

NIELS NIELSEN and BJÖRN HOLMSTRÖM

Research Department, AB Kabi, Stockholm, Sweden

The contents of folic acid and folic acid conjugates of 10 different pollen samples were determined. The folic acid content ranged between 0.42 and 2.2 μg per g pollen. The amount of folic acid conjugates was in most cases considerably higher — 4 to 12 times as high. In two samples of pollen from grasses, *viz. Zea mays* and *Secale cereale*, the content of folic acid and of folic acid conjugates was of the same magnitude. Compared to other vegetable materials the pollen is relatively rich in folic acid and folic acid conjugates.

The presence of conjugases was established for pollen from *Pinus montana*, *Zea mays*, *Phleum pratense* and *Secale cereale*. For pollen from *Zea mays* the conjugase(s) was found to have its pH-optimum at 4.5 being active between pH 4 and 6. This conjugase must therefore be different from the conjugases in chicken pancreas. The effect obtained is stronger than that obtained with hog kidney and for this reason the conjugase in pollen can hardly be the same as in hog kidney. The content of conjugase in pollen is sufficient to convert all the conjugates in the pollen.

Continuing previous studies on the vitamin content of different pollen samples[1] we have studied the occurrence of folic acid. Very little is known regarding the presence of this vitamin in pollen. As folic acid is believed to be an important component of the so called vitamin T [2] which is reported to be an important growth factor for insects [3], investigations on the occurrence of this vitamin in pollen seemed of *a priori* interest.

In this investigation we wanted to determine both the amount of folic acid * and the amount of folic acid conjugates. As considerable amounts of folic acid conjugates were found (in most pollen samples the content of folic acid conjugates was much greater than the content of folic acid) we also studied the occurrence of folic acid conjugases in the pollen.

* In accordance with Welch and Nichol [4] we understand by folic acid the compounds able to promote the growth of *Streptococcus faecalis* and *Lactobacillus casei, viz.* pteroyl glutamic acid and pteroyl diglutamic acid.

Table 1. The occurrence of folic acid and folic acid conjugates in pollen.

Source of pollen	Folic acid µg/g pollen dry weight	Folic acid + folic acid conjugates	Folic acid in percentage of folic acid + conjugates
Pinus contorta	0.74	3.1	24
Pinus montana	0.42	2.5	17
Picea canadensis	1.4	12.8	11
Alnus glutinosa	0.53	4.3	12
Alnus incana	0.84	10.1	8
Betula alba	1.1	4.3	26
Fagus silvatica	1.9	7.3	26
Zea mays	2.2	4.5	49
Phleum pratense	1.1	5.6	20
Secale cereale	1.1	2.3	48

For the determination of folic acid, 5 g of pollen was suspended in 30 ml of water and heated to 120° for 5 min. Due to this heating the conjugases which might be present in the pollen are inactivated [5]. After heating, the suspension was centrifuged and the pollen residue washed twice with 20 ml of water. The combined extracts were made up to 100 ml for assay.

For the determination of the total content of folic acid plus folic acid conjugates the samples were treated with chicken pancreas conjugase according to the method described by Teply and Elvehjem [6]. The treatment with hog kidney or almond conjugases [7] was also tried, but the values obtained with chicken pancreas conjugase were found to be somewhat higher and this method was therefore preferred. For the assay, *Streptococcus faecalis* ATCC 8043 was used applying the paper-disc method.

Ten pollen samples were analyzed. The samples were collected directly from the plants. The purity of the samples was high, the amount of foreign pollen not exceeding 1 %. The pollen samples were collected in 1955 and stored in a cool and dry place until they were analyzed.

As can be seen from Table 1 the sum of folic acid and folic acid conjugates varied between 2.3 and 12.8 µg per g dry material. These values are relatively high in comparison with those of other vegetable materials [8]. No connection can be seen between the folic acid content and the systematic position of the plant from which the pollen was derived. The pollen samples from the closely related species *Alnus glutinosa* and *A. incana* show a marked deviation in their contents of folic acid and folic acid conjugates. Earlier it was found that the content of six other B-vitamins in pollen from these two species was rather similar [1].

The content of folic acid calculated as per cent of the sum of the contents of folic acid and folic acid conjugates varies considerably. For most of the pollen samples it varied between 10 and 25 %, *i.e.* the folic acid conjugates were present in considerably higher amounts than was folic acid. For two of the samples, however, the relative amounts of folic acid were very high. In the pollen from the two grasses *Zea mays* and *Secale cereale* the folic acid content was as high as that of the folic acid conjugates. In the third sample of grass-pollen investigated, *i.e.* pollen from *Phleum pratense*, the amount of folic acid

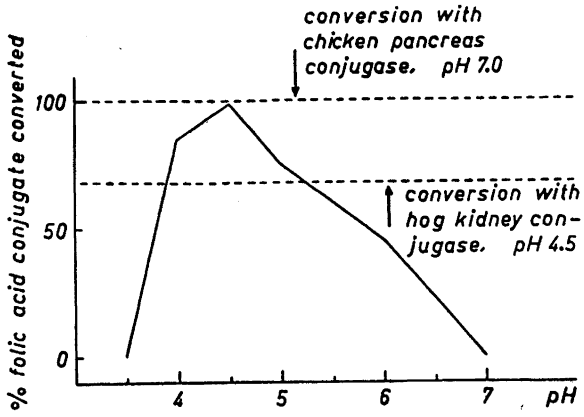


Fig. 1. Conversion of folic acid conjugates.

was low compared to the value for the folic acid conjugates. The number of pollen samples investigated was to small to justify any conclusion as to whether pollen from grasses have a tendency to be relatively rich in folic acid compared to folic acid conjugates.

Weygand and Hofmann [9] studied the content of folic acid in some pollen samples and found the amount to vary between 3.4 and 6.4 μg per g pollen. It is uncertain whether the folic acid conjugates are included.

As the content of folic acid conjugates appeared to be high in pollen it was of interest to investigate the presence of conjugates in the pollen. Since conjugases are widely distributed in nature [7] their occurrence in pollen was to be expected.

The investigation of pollen conjugases was performed mainly with pollen from *Zea mays*. A number of samples were prepared, each containing 5 g pollen in 25 ml of water. One of the samples was heated to 100° immediately in order to inactivate the conjugases, and was then used to determine the amount of folic acid present. One other sample was similarly heated and chicken pancreas conjugase added to determine the total content of folic acid and folic acid conjugates. Other samples were kept for 18 h at 25° at different pH values.

As can be seen from Fig. 1, the amount of folic acid was unaltered in the samples kept at pH 3.5 and 7.0 whereas there was an increase in the folic acid activity of the other samples. This indicates that the pollen contains conjugase (or conjugases) active between approximately pH 4.0 and pH 6.0, the optimum being about pH 4.5.

The conjugase present in the pollen from *Zea mays* differs from the conjugase in chicken pancreas in having the optimum at pH 4.5. The chicken pancreas conjugase has the optimum at pH 7-8 [5]. Although the conjugase extracted from hog kidney has its optimum at pH 4.5 [7,10] it can, however, hardly be the same conjugase as that in pollen. Our experiments showed that the hog kidney conjugase cannot split the conjugates in pollen to the same extent as

can the pollen conjugase. Thus the conjugase found in pollen must differ from both the conjugase in chicken pancreas and that in hog kidney.

It is seeen from Fig. 1 that at pH 4.5 the same amount of folic acid was obtained with pollen conjugases as with chicken pancreas conjugase. If it be assumed that chicken pancreas conjugase can split all the conjugates, then the amount of conjugase present in the pollen would suffice to convert all the conjugates of the pollen into folic acid.

It is of interest that pollen conjugase has its optimum at a pH not naturally occurring in pollen.

Experiments with other pollen samples, *viz.* pollen from *Pinus montana*, *Phleum pratense* and *Secale cereale*, demonstrated that the content of folic acid increased and that the content of folic acid conjugates decreased when the pollen was incubated in water at 25° and at pH 5. This indicates that conjugases are also present in these pollen samples.

REFERENCES

1. Nielsen, N., Grömmer, J. and Lundén, R. *Acta Chem. Scand.* **9** (1955) 1100.
2. Walker, A., Dellweg, H. and Rowold, E. *Klin. Wochschr.* **29** (1951) 780.
3. Goetsch, W. *Experientia* **3** (1947) 326.
4. Welch, A. D. and Nichol, C. A. *Ann. Rev. Biochem.* **21** (1952) 633.
5. Laskowski, M., Mims, V. and Day, P. L. *J. Biol. Chem.* **157** (1945) 731.
6. Teply, L. J. and Elvehjelm, C. A. *J. Biol. Chem.* **157** (1945) 303.
7. Bird, O. D., Binkley, S. B., Bloom, E. S., Emmet, A. D. and Pfiffner, J. J. *J. Biol. Chem.* **157** (1945) 413.
8. Stokstad, E. L. R. *The Vitamins* **3** (1954) 168.
9. Weygand, F. and Hofmann, H. *Chem. Ber.* **83** (1950) 405.
10. Bird, O. D., Robbins, M., Vandenbelt, J. M. and Pfiffner, J. J. *J. Biol. Chem.* **163** (1946) 649.

Received October 11, 1956.

ACTA CHEMICA SCANDINAVICA 11 (1957) 105—119

An Investigation of Conditions for Precipitation of Uranium(IV) Orthophosphate

ERIK STRANDELL

Department of Applied Inorganic Chemistry, Royal Institute of Technology, Stockholm, Sweden

The precipitation of uranium as uranium(IV) orthophosphate from low concentrated acid solutions depends greatly on the possible presence of aluminium salts in the solutions. At high concentrations of aluminium ion, no precipitation is obtained. In chloride solutions consisting of uranium(IV) chloride, aluminium chloride, orthophosphoric and hydrochloric acids, the precipitation is prevented due to the formation of soluble double complexes between uranium, aluminium and phosphate ions. In sulfate solutions consisting of uranium(IV) sulfate, aluminium sulfate, orthophosphoric and sulfuric acids, the precipitate is formed only within a relatively narrow pH range around pH 1. At higher pH values, precipitation is prevented probably by the same double complexes as in chloride solutions. At lower pH values, precipitation is prevented mainly by soluble complexes between uranium and sulfate.

Some investigations were performed in order to clarify the conditions for the precipitation of uranium(IV) orthophosphate from low concentrated acid solutions. It was then proved that the presence of aluminium salts in the solutions has a great effect.

PRECIPITATION EXPERIMENTS

To perform the precipitation experiments, solutions were prepared containing 0.0017 M uranyl chloride, 0.042 M orthophosphoric acid and various amounts of aluminium chloride. The pH was adjusted to various values using hydrochloric acid. Analogous sulfate solutions were prepared from uranyl sulfate, orthophosphoric acid, aluminium sulfate and sulfuric acid. The solutions were heated to 35° C and reduced with a suitable reducing agent. The solutions were kept under slight stirring at 35° C for about 24 h. The time elapsing before a precipitate could be clearly seen was noted. After 24 h, the solutions were filtered and the amounts of uranium in the mother liquors were determined by analysis.

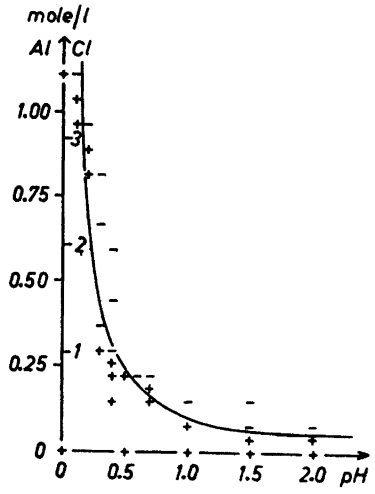


Fig. 1. Precipitation of uranium(IV) phosphate from chloride solutions with various concentrations of $AlCl_3$. + indicates precipitation, — no precipitation.

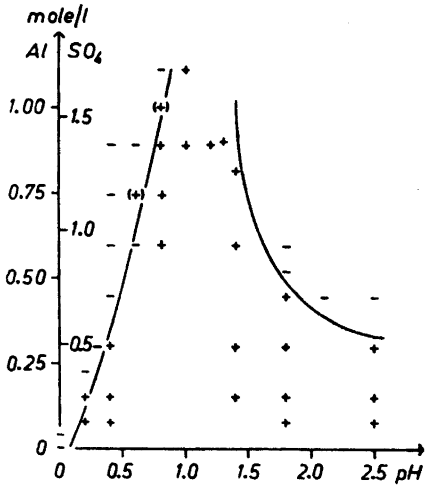


Fig. 2. Precipitation of uranium(IV) phosphate from sulfate solutions with various concentrations of $Al_2(SO_4)_3$. (+) indicates precipitation after 5 h.

In Figs. 1 and 2, where the axes are the concentration of aluminium in the various solutions and pH, the precipitation experiments on the above mentioned chloride and sulfate solutions have been plotted. Cases where a precipitate is obtained within 5 h have been marked with + on the figures. If precipitation occurs after 5 h, this is marked with (+). Cases where no precipitation occurs within 24 h have been marked with — on the figures. The approximate boundary between precipitation and no precipitation is drawn.

Figs. 1 and 2 show that no uranium(IV) phosphate precipitates from low concentrated solutions at high aluminium concentrations. Fig. 1 shows that, in chloride solutions, the boundary between precipitation and no precipitation decreases with increasing pH. Gelin [1] has in an unpublished article given an account of precipitation experiments with uranium chloride solutions with various concentrations of aluminium chloride and phosphoric acid. In diagrams with the aluminium concentration plotted against the phosphate concentration, Gelin obtained precipitation boundaries similar to those of Fig. 1. According to Fig. 2, a boundary with a pronounced peak within pH interval 0.7—1.2 is obtained in sulfate solutions.

Precipitation experiments have been performed on sulfate solutions with an addition of sodium, magnesium or iron(II) sulfate as ionic medium, Figs. 3, 4 and 5. These additions were so calculated that, at various concentrations of aluminium sulfate, the total concentration of sulfate in the different solutions remained constant = 1.4 mole/l. The experiments were carried out as before.

Figs. 2—5 show that the area for precipitation of uranium(IV) phosphate in sulfate solutions depends greatly on the ionic medium. The difference between sodium and magnesium sulfate as ionic medium is especially remarkable.

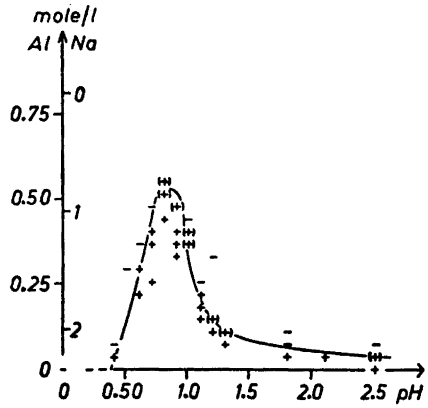


Fig. 3. Precipitation of uranium(IV) phosphate from sulfate solutions at various concentrations of aluminium. Sulfate concentration kept at 1.4 mole/l using Na_2SO_4.

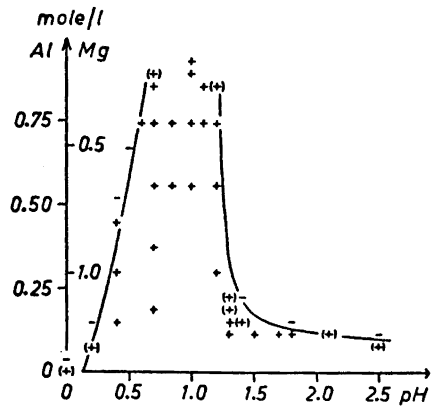


Fig. 4. Precipitation of uranium(IV) phosphate from sulfate solutions at various concentrations of aluminium. Sulfate concentration kept at 1.4 mole/l using $MgSO_4$.

PRECIPITATION YIELDS

In the above mentioned chloride solutions, the yield of precipitate is over 90 % in the greater part of the region where a precipitate is obtained. Not until the precipitation boundary is reached does the yield quickly decrease to zero. Corresponding conditions are obtained with sulfate solutions, with sodium, magnesium or iron(II) sulfate as ionic medium, on the right hand side of the peak. With magnesium sulfate as ionic medium, the following yields at pH 1.3, 1.8 and 2.5 were obtained, corresponding to the precipitation experiments shown in Fig. 4:

Al	Yield, %		
mole/l	pH 1.3	pH 1.8	pH 2.5
0.07			93
0.11	97	94	0
0.15	72	0	
0.19	90		
0.22	35		

In sulfate solutions without an extra addition of sulphate salt, the yields of uranium decrease more slowly with increasing concentration of aluminium. The corresponding precipitation experiments are shown in Fig. 2.

Al	Yield, %	
mole/l	pH 1.8	pH 2.5
0.07	97	96
0.15	95	66
0.30	85	40
0.45	30	
0.52	0	

On the left side of the peak in Figs. 2—5, the yields decrease slowly with increasing concentration of aluminium. In solutions without an extra addition of sulfate salt and also in solutions with magnesium sulfate, the following yields were obtained at pH 0.4. The corresponding points are found in Figs. 2 and 4.

Al mole/l	Yield, % No extra addition of sulfate	With $MgSO_4$ as ionic medium
0.07	94	
0.15	75	92
0.30	15	45
0.45		15

PRECIPITATE ANALYSES

Examinations in a Norelco Geiger-Counter X-Ray Diffractometer and in an electron microscope (10 000 ×) showed the precipitate to be amorphous.

A number of precipitates deposited from solutions at pH 0.4 have been analysed. The results are shown in Figs. 6—9. By means of the chloride analyses of the precipitates and the mother liquors, the compositions of the precipitates have been corrected for the amount of enclosed mother liquor using the rough assumption that Cl^- was not adsorbed on the precipitates to any appreciable extent. In chloride solutions containing 0.0025 M uranium(IV) chloride, 2.8 M sodium chloride, orthophosphoric and hydrochloric acids, the uranium phosphate precipitates with a composition of 2.1 mole phosphate/mole

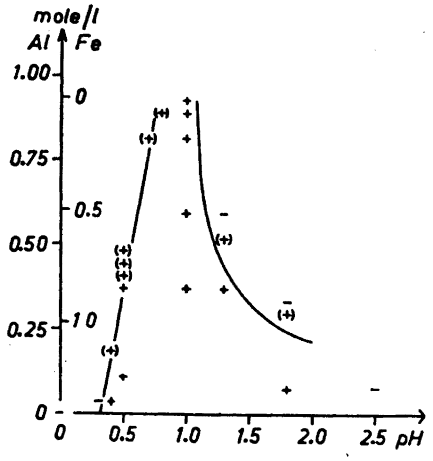


Fig. 5. Precipitation of uranium(IV) phosphate from sulfate solutions at various concentrations of aluminium. Sulfate concentration kept at 1.4 mole/l using $FeSO_4$.

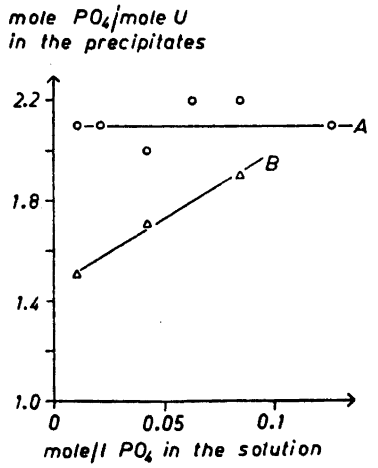


Fig. 6. Composition of uranium precipitates: A) The ratio PO_4:U in precipitates from solutions of uranium chloride with 2.8 M NaCl and various proportions of H_3PO_4. pH 0.4. B) The same solutions with an addition of 0.7 M $FeSO_4$.

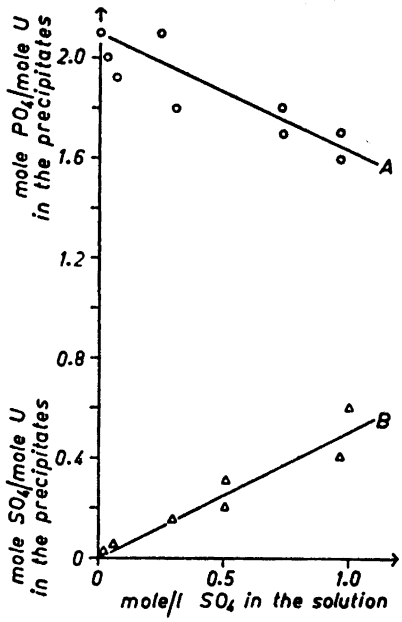


Fig. 7. The compositions of precipitates from solutions containing 0.0025 M UCl_4, 2.8 M NaCl, 0.04 M H_3PO_4 and various concentrations of sulfate. pH 0.4. A) The ratio PO_4:U in the precipitates. B) The ratio SO_4:U.

uranium irrespective of the phosphoric acid concentration in the solution (*cf.* Fig. 6). From the same chloride solutions but with an addition of *ca.* 0.7 M iron(II) sulfate, precipitates are obtained with a phosphate/uranium ratio which decreases as the phosphate concentration in the solution decreases. In solutions with the same phosphate concentration but with different sulfate concentrations, the precipitates according to Fig. 7 deposit, where the ratio mole phosphate/mole uranium decreases with increasing amount of sulfate in the solution. However, the ratio sulfate/uranium increases to the same extent so that the ratio (phosphate + sulfate)/uranium remains constant at 2.1.

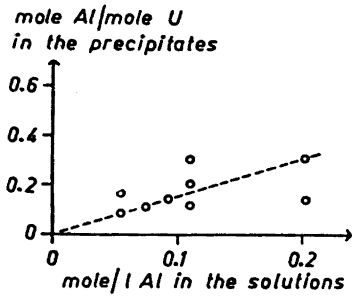


Fig. 8. The ratio Al:U in the precipitates from uranium chloride solutions with 2.8 M NaCl, 0.04 M H_3PO_4, various concentrations of $AlCl_3$ and pH 0.4.

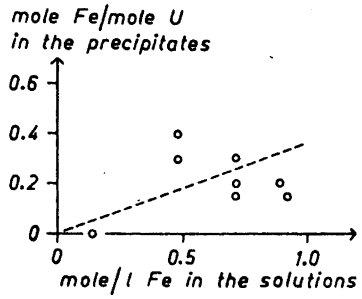


Fig. 9. The ratio Fe:U in the precipitates from solutions of uranium chloride with 2.8 M NaCl, 0.04 M H_3PO_4, various concentrations of $FeSO_4$ and pH 0.4.

According to Fig. 8, a larger amount of aluminium is obtained in the precipitate as the concentration of aluminium in the solution increases. With iron(II) sulfate in the solution, iron is also found in the precipitates. A comparison between washed and unwashed precipitates showed that the iron, but not the aluminium, can be removed by water.

EXTINCTIOMETRIC MEASUREMENTS

It was found that, in the greater part of the precipitation regions in Figs. 1—5, an initial opalescence or precipitation develops to complete visibility within 0.5—1.5 h. The time required has been measured from the moment when the reducing agent was added. In the chloride solutions, the precipitate shows a tendency to develop more rapidly than in the corresponding sulfate solutions. In the vicinity of the precipitation boundary, the precipitates do not become visible until after *ca.* 1.5—3.5 h.

Some preliminary complex investigations and measurements of reduction speed have been performed to find the reason for these long precipitation times. The experiments were performed in a Beckman spectrophotometer, model DU. The concentrations of the solutions were selected so that no precipitation was obtained during the reduction.

First, the extinction was measured at various wave-lengths on unreduced as well as reduced solutions containing 0.0075 M uranium chloride or uranium sulfate dissolved in 0.4 N hydrochloric acid or sulfuric acid respectively. Then the extinction was measured on the same solutions after the addition of the remaining components. The state of reduction and complexity for uranium were estimated by comparing the extinction curves obtained. These experiments were supplemented by a few measurements of the reduction speed, where the extinction was measured at 649 mμ as a function of the time elapsed from the addition of the reducing agent. In Fig. 10, where a few of the extinction curves obtained are shown, the curves A and B refer to the above mentioned reduced solutions containing uranium chloride and sulfate, respectively. Curve C is the extinction curve for the same reduced uranium chloride solution as in curve A but with an addition of 0.5 M aluminium chloride and 0.1 M orthophosphoric acid.

According to Rodden [4], curve A is typical for the extinction of uranium(IV) chloride in strong hydrochloric acid solutions. Not only are the extinction peaks at 429.5 mμ, 549 mμ and 649 mμ characteristic but also the shape of the peak at 485—495 mμ and the small extra peak at 672 mμ. The same curves are obtained with uranium(IV) perchlorate. This indicates that uranium(IV) is present mainly as free ions in the solutions.

According to Betts and Leigh [2], uranium(IV) forms very strong complexes with sulfate. Curve B is characteristic for these complexes. The shape of the peak at 485—495 mμ is especially remarkable. In addition, the highest peak is lower than that for the chloride solutions and moved from 649 mμ to 651 mμ. The small peak at 672 mμ was not found.

During measurements on 0.0075 M uranium(IV) chloride solutions containing 2.8 M sodium chloride, it was proved that the extinction curve typical for sulfate solutions was obtained on the addition of 0.1 M sodium sulfate. This is also evidence for no, or only weak, complexes between uranium(IV) and chloride.

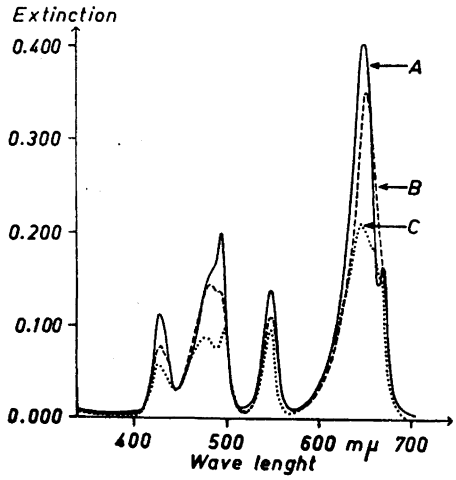


Fig. 10. Extinction curves of a few uranium(IV) solutions. A) 0.0075 M UCl_4 in 0.4 N HCl. B) 0.0075 M $U(SO_4)_2$ in 0.4 N H_2SO_4. C) 0.0075 M UCl_4, 0.5 M $AlCl_3$, 0.1 M H_3PO_4 and HCl to pH 0.4. The measurements were performed in 10 mm cuvettes.

Curve C, Fig. 10 is characteristic for the soluble uranium(IV) phosphate complexes that were obtained in connection with the precipitation experiments. Especially notable is the double peak at 479 and 498 mμ and the great decrease in the peak at 650 mμ. In those cases where it was impossible to determine whether the change in the extinction curves was due to incomplete reduction or complex formation, measurements were performed on solutions where the uranium was reduced before as well as after the addition of the remaining components. If the extinction curves from solutions reduced *before* the addition of remaining components agree with those from solutions reduced *after* the addition, then any differences between these extinction curves and the corresponding curves from solutions *without* addition cannot be caused by incomplete reduction. The difference must then be due to complex formation in the solutions.

The important results from experiments on precipitation of uranium as uranium(IV) orthophosphate from acid solution can be summed up as follows:

a) In the solutions used for precipitation experiments according to Figs. 1—5, uranium(IV) is reduced completely or almost completely to uranium(IV) even in the cases where no precipitate is obtained.

b) The long times for precipitation are due not to the rate of reduction but to difficulties of precipitate development.

c) In chloride solutions, the extinction curves typical for the actual uranium(IV) phosphate complexes are found in the region where, according to Fig. 1, no precipitate is formed.

d) In sulfate solutions, the uranium is complex-bound in the region for no precipitation on the right hand side of the peak in Figs. 2—5, in the same way as in chloride solutions. However, on the left hand side of the peak, the uranium in sulfate solutions mainly exists as soluble uranium(IV) sulfate complexes.

CALCULATION OF THE PRECIPITATION BOUNDARY IN FIG. 1 VALID FOR CHLORIDE SOLUTIONS

Figs. 1 and 2 show that the precipitation conditions are simpler in chloride solutions than in corresponding sulfate solutions. The extinction curves obtained do not indicate that uranium(IV) forms complexes with chloride. However, uranium does form very strong complexes with sulfate [2]. When calculating the complex ratio of uranium in chloride solutions, the possible presence of uranium(IV) chloride complexes may therefore be disregarded, whereas the complexes between uranium(IV) and sulfate must be considered when calculating the ratio in sulfate solutions. Only the conditions in chloride solutions are discussed here. The calculations below should give an explanation of the form of the precipitation boundary in Fig. 1 as well as of the precipitation yield, which is over 90 % within the whole precipitation region except for a small section near the precipitation boundary where the yield quickly decreases to zero.

The calculations have been based upon the assumption that soluble double complexes between uranium(IV), aluminium and phosphate prevent the uranium phosphate from precipitating.

In the calculations, consideration has been taken only of possible complexes between uranium, aluminium and phosphate, while all the possible complexes with remaining ions are neglected. No consideration has been taken of activity factors, hydrolysis (the actual pH-range is below 2) or of the fact that the salt concentrations have not been kept constant in the experiments in Fig. 1 with which the calculated precipitation boundaries are compared.

The following complexes between uranium and phosphate are conceivable: With one uranium ion in each complex, such as $U(H_2PO_4)_n$, $U(HPO_4)_n$ and $U(PO_4)_n$, with several uranium ions such as $U_m(H_2PO_4)_n$, $U_m(HPO_4)_n$ and $U_m(PO_4)_n$ or mixed complexes such as $U_m(H_2PO_4)_n(HPO_4)_{n'}(PO_4)_{n''}$. The complexes found in the solutions can be designated by the formula $U_m(H_pPO_4)_n$ where $m = 1, 2, 3, \ldots$, $n = 1, 2, 3, \ldots$ and p is continuously variable between 0 and 2. The total concentration is denoted here by $\Sigma[U_m(H_pPO_4)_n]$.

The corresponding complexes between aluminium and phosphate are conceivable and may be collected together in the general formula $Al_q(H_tPO_4)_r$. The total concentration of these complexes is written $\Sigma[Al_q(H_tPO_4)_r]$.

Conceivable complexes between uranium, aluminium and phosphate may be collected together in the general formula:

$$U_xAl_y(H_zPO_4)_w^{+4x+3y+wz-3w},$$

which is shortened below to $U-Al-PO_4$. The total concentration of these complexes is written $\Sigma[U-Al-PO_4]$. The complexity constants are obtained from the formula:

$$[U-Al-PO_4] \,/\, [U^{4+}]^x \cdot [Al^{3+}]^y \cdot [H_zPO_4^{-3+z}]^w = K_{x,y,w} \qquad (1)$$

According to Fig. 6, uranium(IV) precipitates from a chloride solution as phosphate with a composition approximately corresponding to the formula $U(HPO_4)_2$. Hence we obtain the following equation for the solubility product L:

$$[U^{4+}] \cdot [HPO_4^{2-}]^2 = L \qquad (2)$$

If the complexity constants for the aluminium phosphate complexes are denoted by $k_{q,r}$, the following equation is obtained:

$$[Al_q(H_tPO_4)_r] = k_{q,r} \cdot [Al^{3+}]^q \cdot [H_tPO_4^{-3+t}]^r \qquad (3)$$

If the total concentrations of uranium, aluminium and phosphoric acid are written C_U, C_{Al} and C_{PO_4}, respectively, the following formulas are obtained:

$$C_U = [U^{4+}] + \Sigma m[U_m(H_pPO_4)_n] + \Sigma x[U-Al-PO_4] \quad (4)$$

$$C_{Al} = [Al^{3+}] + \Sigma q[Al_q(H_tPO_4)_r] + \Sigma y[U-Al-PO_4] \quad (5)$$

$$C_{PO_4} = [H_3PO_4] + [H_2PO_4^-] + [HPO_4^{2-}] + [PO_4^{3-}] + \\ + \Sigma r[Al_q(H_tPO_4)_r] + \Sigma n[U_m(H_pPO_4)_n] + \Sigma w[U-Al-PO_4] \quad (6)$$

In uranium(IV) chloride solutions not containing aluminium, the uranium phosphate precipitates almost to 100 %. In sulfate solutions not containing aluminium, a complete yield is also obtained within a favourable pH range. According to Betts and Leigh [2], uranium(IV) forms very strong complexes with sulfate. Consequently the solubility product must be very small and the concentration of soluble uranium phosphate complexes must be low. In eqn. (4), $[U^{4+}]$ and $\Sigma m[U_m(H_pPO_4)_n]$ may be disregarded in comparison with the double complexes. Since it cannot be determined from the empirically found precipitation boundary whether one or several uranium ions are found in each double complex, it may be assumed that only one uranium ion is present in each complex, consequently $x = 1$. The low uranium concentrations in the solutions are in evidence for this assumption. It may further be assumed that one of the double complexes present is so dominant that the remainder can be overlooked. On applying these simplifications we obtain:

$$C_U \approx [U-Al-PO_4] \quad (7)$$

Similarly, one of the aluminium phosphate complexes present in the solutions may be assumed so dominant that the remainder can be neglected. This complex is assumed as simple as possible, *i. e.* $AlHPO_4^+$. Eqn. (3) is then:

$$\Sigma[Al_q(H_tPO_4)_r] \approx [AlHPO_4^+] = k_{1,1} \cdot [Al^{3+}] \cdot [HPO_4^{2-}] \quad (8)$$

In eqn. (6), $[HPO_4^{2-}]$ and $[PO_4^{3-}]$ may be neglected since the pH range is below 2.5. The uranium phosphate complexes may be neglected for the same reason as in eqn. (3). On applying these simplifications the following equations are obtained:

1) For soluble complexes of the type $UAl_y(PO_4)_w^{+4+3y-3w}$:

$$C_{Al} = \left(\frac{C_U}{K_{1,y,w} \cdot L}\right)^{\frac{1}{y}} \cdot [HPO_4^{2-}]^{\frac{2-w}{y}} \cdot (1 + k_{1,1} \cdot [HPO_4^{2-}]) \cdot \left(\frac{k_s'''}{\{H^+\}}\right)^{\frac{y}{w}} + yC_U \quad (9)$$

2) For soluble complexes of the type $UAl_y(HPO_4)_w^{+4+3y-2w}$:

$$C_{Al} = \left(\frac{C_U}{K_{1,y,w} \cdot L}\right)^{\frac{1}{y}} \cdot [HPO_4^{2-}]^{\frac{2-w}{y}} \cdot (1 + k_{1,1} \cdot [HPO_4^{2-}]) + yC_U \quad (10)$$

3) For soluble complexes of the type $UAl_y(H_2PO_4)_w^{+4+3y-w}$:

$$C_{Al} = \left(\frac{C_U}{K_{1,y,w} \cdot L}\right)^{\frac{1}{y}} \cdot [HPO_4^{2-}]^{\frac{2-w}{y}} \cdot (1 + k_{1,1} \cdot [HPO_4^{2-}]) \cdot \left(\frac{k_s''}{\{H^+\}}\right)^{\frac{w}{y}} + yC_U \quad (11)$$

$[HPO_4^{2-}]$ is obtained from the equation:

$$k_{1,1} \cdot \left(\frac{\{H^+\}^2}{k_s' \cdot k_s''} + \frac{\{H^+\}}{k_s''}\right) \cdot [HPO_4^{2-}]^2 + \\ + \left(\frac{\{H^+\}^2}{k_s' \cdot k_s''} + \frac{\{H^+\}}{k_s''} + k_{1,1} \cdot (C_{Al} - C_{PO_4} + wC_U - yC_U)\right) \cdot [HPO_4^{2-}] = C_{PO_4} - wC_U \quad (12)$$

where $k_s' = \{H^+\} \cdot [H_2PO_4^-]/[H_3PO_4]$, $k_s'' = \{H^+\} \cdot [HPO_4^{2-}] / [H_2PO_4^-]$,

$k_s''' = \{H^+\} \cdot [PO_4^{3-}] / [HPO_4^{2-}]$ and $-\log\{H^+\} = pH$.

From eqns. (9)—(12), $C_{Al} = f(\{H^+\})$ is obtained by inserting various values for y and w at constant concentrations of uranium and phosphate. In Figs. 13—15, precipitation boundaries with 0% yields are shown, calculated with $C_U = 0.0017$ mole/l and $C_{PO_4} = 0.042$ mole/l. In eqns. (9)—(12), the complexity constant for aluminium phosphate is included. Bjerrum and Dahm [3] have examined complex formations in acid solutions with low concentrations of aluminium, an excess of phosphate and low salt concentrations. From the complexity constants obtained, $k_{1,1}$ is calculated to be 7.2×10^7 l/mole. A determination in solutions containing 2.8 M sodium chloride as ionic medium, made for the calculations mentioned below, gave $k_{1,1} = 3.3 \times 10^7$ l/mole. In the precipitation experiments according to Fig. 1, the salt concentrations in the solutions varied between the concentrations used in the two determinations of $k_{1,1}$ mentioned above. Thus the average value 5×10^7 l/mole is used here.

The dissociation constant of the orthophosphoric acid k_s' was taken to be 8×10^{-2} l/mole, k_s'' to be 6×10^{-8} l/mole and k_s''' to be 5×10^{-13} l/mole.

In eqn. (12), the factors wC_U and $(w-y) \cdot k_{1,1} \cdot C_U$ can be neglected. In this equation, C_{Al} is included as a correction factor. These values of C_{Al} at various pH values are taken from Fig. 1. Such a correction is not accurate in cases where the calculated precipitation boundary does not agree with the experimental one but this is of course of no importance here.

The factor $(C_U/K_{1,y,w}.L)^{\frac{1}{y}} = a_{y,w}$ included in eqns. (9)—(11) is calculated from these equations at $C_{Al} = 0.31$ mole/l, $C_{PO_4} = 0.042$ mole/l and pH = 0.4 corresponding to point A in Figs. 13—15.

In Fig. 11, some precipitation boundaries for uranium(IV) orthophosphate, based on point A and under the assumption of a few simple soluble double complexes of the type $UAl_y(HPO_4)_w^{+4+3y-2w}$, are found. The figure shows that soluble complexes of this type give a boundary close to the experimental one

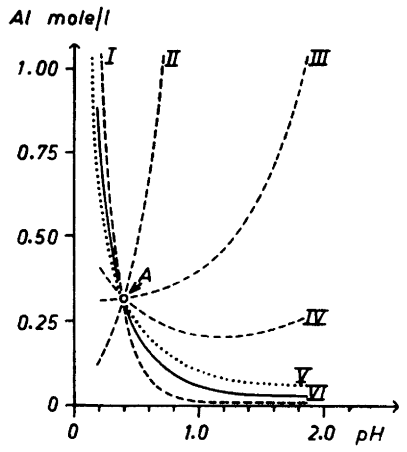


Fig. 11. A few calculated precipitation boundaries under assumption of soluble complexes of the type $UAl_y(HPO_4)_w^{+4+3y-2w}$. I) $UAl(HPO_4)_4^-$; II) $UAlHPO_4^{5+}$; III) $UAl_2(HPO_4)_2^{6+}$; $UAl(HPO_4)_2^{3+}$; IV) $UAl_3(HPO_4)_3^{7+}$; V) By Fig. 1; VI) $UAl(HPO_4)_3^+$, $UAl_y(HPO_4)_{y+2}^{+y}$.

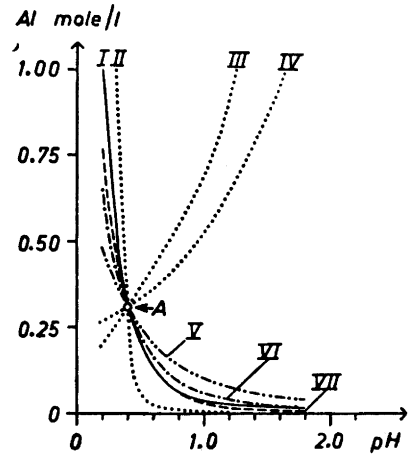


Fig. 12. A few precipitation boundaries calculated under the assumption of soluble complexes of the type $UAl_y(PO_4)_w^{+4+3y-3w}$. I) $UAl_8(PO_4)_8^{4+}$; II) $UAl(PO_4)_3^{2-}$; III) $UAlPO_4^{4+}$; IV) $UAl_2PO_4^{7+}$; V) $UAl_2(PO_4)_2^{4+}$; VI) $UAl_3(PO_4)_3^{4+}$; VII) $UAl(PO_4)_2^+$.

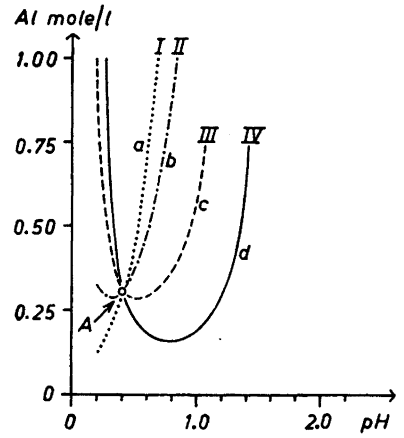


Fig. 13. A few precipitation boundaries calculated under the assumption of soluble complexes of the type $UAl_y(H_2PO_4)_w^{+4+3y-w}$. I) $UAl(H_2PO_4)_2^{5+}$; II) $UAl(H_2PO_4)_4^{3+}$, III) $UAl(H_2PO_4)_6^{+}$; IV) $UAl(H_2PO_4)_8^{-}$.

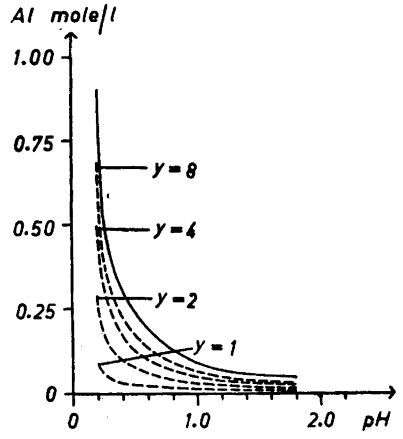


Fig. 14. A few calculated boundaries for 90 % precipitate yield (dashed curves). The continuous line is the experimentally found boundary for a 0 % yield.

if $w \approx y + 2$, *i. e.* the following complex: $UAl_y(HPO_4)_{y+2}^{+y}$. If $w > y + 2$, the curve increases too rapidly with decreasing pH compared with the experimental one while, if $w < y + 2$, it increases too slowly.

If a different point than point A in Figs. 11—13 is chosen as basis for the calculations, only a parallel shift of the calculated precipitation boundary is obtained.

In Fig. 12, the precipitation boundaries for uranium phosphate have been calculated under the assumption of a few soluble complexes of the type $UAl_y(PO_4)_w^{+4+3y-3w}$. The figure shows, that complexes of this type give a precipitation boundary close to the experimental one for the following cases: a) when $y = 1$, $w = 1$, *i. e.* $UAl(PO_4)_2^{+}$, b) when $y = w \geqq 3$ and c) for higher values of y and w when $y \approx w$, *i. e.* the following complexes: $UAl_y(PO_4)_y^{4+}$.

According to eqn. (11), the following equation applies for soluble complexes of the type $UAl_y(H_2PO_4)_w^{+4+3y-w}$:

$$C_{Al} = \beta_{y,w}\,[HPO_4^{2-}]^2 \cdot (1 + k_{1,1}\,[HPO_4^{2-}]) \cdot ([HPO_4^{2-}] \cdot \{H^+\})^{-\frac{w}{y}} + yC_U \quad (13)$$

$$\text{where } \beta_{y,w} = (C_U/K_{1,y,w} \cdot L)^{\frac{w}{y}} = \text{a constant.}$$

In eqn. (13), the expression $[HPO_4^{2-}]^2 \cdot (1 + k_{1,1} \cdot [HPO_4^{2-}])$ increases rapidly with increasing pH. However, the expression $([HPO_4^{2-}] \cdot \{H^+\})$ increases slowly with pH. In order that C_{Al} in eqn. (13) shall decrease with increasing pH, it is necessary that quotient w/y should be large. In Fig. 13, curve a shows the calculated precipitation boundary for $w/y = 2$, curve b for $w/y = 4$, curve c

for $w/y = 6$ and curve d for $w/y = 8$. It is seen that soluble complexes of the type $UAl_y(H_2PO_4)_w^{+4+3y-w}$ cannot give a precipitation boundary similar to the experimental one.

In Figs. 11—13, the precipitation boundaries are calculated so that precipitation just begins for the appropriate solution or *i. e.* so that the yield is 0 %. In the following, the boundary is calculated on the basis of a yield of 90 %.

In Fig. 1, the yield is more than 90 % for the precipitation region and decreases rapidly near the boundary to zero. When calculating the HPO_4^{2-} concentration at various pH, C_{Al} is included only as a term of correction. Hence, during the calculation of the precipitation boundary, the same HPO_4^{2-} concentrations can be used in eqns. (9)—(11) independent of the yield.

If the total uranium(IV) concentration in the solutions at a certain precipitate yield is denoted by C'_U, the corresponding a-value by $a'_{y,w}$ and the corresponding values at 0 % yield by C_U^{tot} and a_U^{tot}, respectively, the following equation is obtained from the relation $a_{y,w} = (C_U/K_{1,y,w} \cdot L)^{\frac{1}{y}}$:

$$a'_{y,w} = \left(\frac{C'_U}{C_U^{tot}}\right)^{\frac{1}{y}} \cdot a_{y,w}^{tot} \tag{14}$$

The precipitation boundary at a certain yield is obtained from eqn. (10):

$$C'_{Al} = a'_{y,w} \, [HPO_4^{2-}]^{\frac{2-w}{y}} (1 + k_{1,1} \cdot [HPO_4^{2-}]) + yC'_U \tag{15}$$

If the aluminium concentration in the solutions at 0 % yield is denoted by C_{Al}^{tot}, one obtains:

$$C_{Al}^{tot} = a_{y,w}^{tot} \cdot [HPO_4^{2-}]^{\frac{2-w}{y}} \cdot (1 + k_{1,1} \cdot [HPO_4^{2-}]) + yC_U^{tot} \tag{16}$$

From eqns. (14), (15) and (16) one obtains the expression:

$$C'_{Al} = (C_{Al}^{tot} - y \cdot C_U^{tot}) \cdot \left(\frac{C'_U}{C_U^{tot}}\right)^{\frac{1}{y}} + yC'_U \tag{17}$$

If eqn. (9) or (11) is used instead of eqn. (10), it is seen that eqn. (17) is true for the three complex types $UAl_y(PO_4)_w^{+4+3y-3w}$, $UAl_y(HPO_4)_w^{+4+3y-2w}$ and $UAl_y(H_2PO_4)_w^{+4+3y-w}$.

At a 90 % precipitation yield the following values apply at the concentrations used in the experiments: $C_U^{tot} = 0.0017$ mole/l and $C'_U = 0.00017$ mole/l. C_{Al}^{tot} at various pH values is obtained from Fig. 1.

Eqn. (17) shows that the greater the number of aluminium ions in the double complexes the closer the boundary for 90 % precipitate yield approaches the boundary for 0 % yield. In Fig. 14 the boundary for a 90 % yield is calculated for complexes with 1, 2, 4 and 8 aluminium ions. Complexes with 6—8 aluminium or more correspond best with the experimentally found precipitate yields.

According to Figs. 11 and 12, both $UAl_y(HPO_4)_w^{+4+3y-2w}$ and $UAl_y(PO_4)_w^{+4+3y-3w}$ can be used to explain the precipitation boundary in chloride solutions. The main part of the double complexes is probably of the type $UAl_y(HPO_4)_w^{+4+3y-2w}$ since the actual pH range is 0.1—2.5. The precipitate yields obtained indicate indirectly a maximum number of phosphate around each

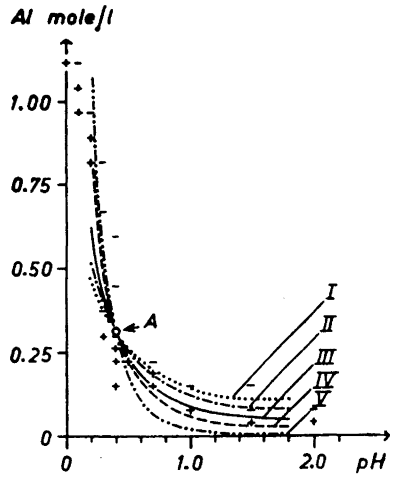


Fig. 15. Calculated precipitation boundaries under assumption of soluble complexes of the type $UAl_y(HPO_4)_8^{+3y-12}$. I) $UAl_{12}(HPO_4)_8^{24+}$; II) $UAl_{10}(HPO_4)_8^{18+}$; III) $UAl_8(HPO_4)_8^{12+}$; IV) $UAl_6(HPO_4)_8^{6+}$; V) $UAl_4(HPO_4)_8$.

uranium atom. The distance U—O in uranium dioxide [5] is 2.34 Å and distance P—O in phosphate [6] 1.56—1.69 Å. This shows that around each uranium(IV), there is sufficient space for a maximum of 8 phosphate groups. This would correspond to complexes of the type $UAl_y(HPO_4)_8^{+3y-12}$. Fig. 15 shows a few precipitation boundaries calculated using complexes of this type. The figure shows that the formulas $UAl_6(HPO_4)_8^{6+}$ and $UAl_8(HPO_4)_8^{12+}$ give the best fit with the experimentally found precipitation boundary.

The distances between the aluminium ions and the phosphate groups in the above mentioned complexes are too great for a stable complex to be formed. According to tests with models on the other hand, a stable complex with the formula $UAl_8(HPO_4)_8(H_2O)_{12}^{12+}$ is possible, where each aluminium is surrounded octahedrally by 2 water units and 4 oxygens from 2 phosphate groups.

In a solution with 0.0025 M uranium(IV)sulfate, 0.8 M sodium sulfate and sulfuric acid to pH 0.4, no precipitate was obtained with a concentration of 0.0105 M phosphoric acid, with 0.046 M 86 % yield and with 0.084 M phosphoric acid 96 %. If the complexity constant for $[USO_4^{2+}] / [U^{4+}] . [SO_4^{2-}] =$ 1 740 l/mole (Betts and Leigh [2]) and the dissociation constant for $HSO_4^- = 10^{-2}$ l/mole and the dissociation constant for $H_3PO_4 = 7.5 \times 10^{-3}$ l/mole and that for $H_2PO_4^- = 6.2 \times 10^{-8}$, then the solubility product may be estimated from the above mentioned precipitation yields:

$$L = [U^{4+}] . [HPO_4^{2-}]^2 \approx 10^{-25} \text{ (mole/l)}^3$$

If the complex $UAl_8(HPO_4)_8^{12+}$ represents all the forms of double complexes that may give an explanation of the precipitation boundary obtained in chloride solutions, then the complexity constant for this complex may be estimated to be:

$$K_{1,8,8} = \frac{[UAl_8(HPO_4)_8^{12+}]}{[U^{4+}] . [Al^{3+}]^8 . [HPO_4^{2-}]^8} \approx 10^{82} \text{ (l/mole)}^{16}$$

CONCLUSIONS

In acid *chloride* solutions containing 0.0017 M uranium(IV) chloride and 0.042 M orthophosphoric acid but different concentrations of aluminium chloride and different pH values, it was found that uranium phosphate precipitates only within an area marked with + in Fig. 1. Within the greater part of this area, the precipitate yield is over 90 %. The precipitates are amorphous with a somewhat variable composition, corresponding approximately to the formula $U(HPO_4)_2$. According to certain extinction measurements, the uranium phosphate is prevented from precipitating by some soluble uranium(IV) phosphate complexes. A plausible explanation of the precipitation boundary in Fig. 1 is that these complexes are double complexes of uranium, aluminium and phosphate. Calculations show that the following types of complexes give a precipitation boundary corresponding well with the experimental one, considering the conditions under which this boundary was obtained:

a) $UAl_y(HPO_4)_w^{+4+3y-2w}$ where $\frac{2-w}{y} = -0.9 \pm 0.3$

b) $UAl_y(PO_4)_w^{+4+3y-3w}$ where $w/y = -1 \pm 0.3$

Complexes of the type $UAl_y(H_2PO_4)_w^{+4+3y-w}$ cannot give a precipitation boundary similar to the experimental one.

Since the actual pH range is 0.1—2.5 the double complexes are probably mainly of the type $UAl_y(HPO_4)_w^{+4+3y-2w}$. The more aluminium ions there are in the complex, the smaller is that region in the neighbourhood of the precipitation boundary where the precipitation yield falls from over 90 % to zero. Thus, in order to correspond to the precipitation yields obtained, the number of aluminium ions in the complex and hence also the number of phosphate groups must be considered to be as large as possible. Since 8 phosphate groups is the maximum number which can be accommodated around each uranium(IV) ion, this indicates that complexes of the type $UAl_y(HPO_4)_8^{+3y-12}$. Of these complexes, $UAl_6(HPO_4)_8^{6+}$ and $UAl_8(HPO_4)_8^{12+}$ fit in best with the experimentally determined precipitation boundary in acid chloride solutions.

From *sulfate* solutions containing 0.0017 M uranium(IV) sulfate and 0.042 M orthophosphoric acid but different concentrations of aluminium sulfate and different pH values, it was found that there exists a boundary (*cf.* Fig. 2) for the precipitation of uranium phosphate which has a pronounced peak at pH 0.7—1.2. Corresponding precipitation boundaries were found on adding sodium, magnesium or iron(II) sulfate as ionic medium.

A plausible explanation of the precipitation boundary in Figs. 2—5 is that, at pH values to the *right* of the peak, the uranium is prevented from precipitating because of the same soluble double complexes between uranium(IV), aluminium and phosphate as those in the chloride solutions. The shape of the curve, the precipitate yields and the extinction measurements are all in favour of this. A calculation on this part of the boundary may however be more complicated than for chloride solutions since, besides allowing for the presence of uranium and aluminium sulfate complexes, it must also be considered that the uranium does not precipitate as pure phosphate but as phosphate-sulfate: $U(HPO_4,SO_4)_2$.

At pH values to the *left* of the peak, the uranium is prevented from precipitating by uranium(IV) complexes with sulfate. With decreasing pH, the HPO_4^{2-} content decreases faster than the SO_4^{2-} content, for which reason the possibility of reaching the solubility product of the uranium(IV) phosphate decreases quicker than that for forming soluble uranium sulfate complexes. From Figs. 2—5, it is clear that, even in this part of the pH range other factors must play a part, *inter alia* the double complexes mentioned above.

The author wishes to thank the head of the Department, Professor Otto Stelling, for suggesting this topic of research, for his encouraging help and advice during the investigations and for his kind permission to publish this article. Thanks are also due to Professor Arne Ölander for many helpful discussions. Financial aid for this investigation has been provided by *A/B Atomenergi*, Stockholm. Tekn. lic. Erik Svenke is thanked for his kind help with the application for A/B Atomenergi's authorization for publication.

REFERENCES

1. Gelin, R. *Report G2, A/B Atomenergi,* Stockholm.
2. Betts, R. and Leigh, R. *Can. J. Research* **28B** (1950) 514.
3. Bjerrum, N. and Dahm, C. *Z. physik. Chem. Bodenstein-Festband* (1931) 62.
4. Rodden, C. *Anal. Chem., National Nuclear Energy Series, Div. VIII*, Vol. 1, 543, who refers to Howland, J. J., *Report CN-2888*, April 1945, Hindman, J. C., Kraus, K. A. and Howland, J. J. Jr., *Report CK-1371*, March 1944.
5. Magnéli, A. and Kihlborg, L. *Acta Chem. Scand.* **5** (1951) 578.
6. Mori, H. and Ito, T *Acta Chryst.* **3** (1950) 1.

Received October 15, 1956.

ACTA CHEMICA SCANDINAVICA 11 (1957) 120—124

Haemoglobin Present in the Nuclear Fraction of the Liver

R. BONNICHSEN, G. EHRENSTEIN, G. HEVESY and J. SCHLIACK

Institute for Organic Chemistry and Biochemistry, University of Stockholm, Sweden

The nuclear fraction of 1 g of rat and rabbit liver contains 0.34 and 0.58 mg of in aqueous medium non-extractable haemoglobin. The corresponding figure for the nuclei of the red corpuscles of 1 ml of hen's blood is 0.9 mg.

The haemoglobin content of the nuclear fraction of 1 g of foetal rabbit liver is 100 times as large as that of 1 g of maternal liver. The ratio of their ^{59}Fe content 11 to 17 h after labelling the maternal plasma iron, works out to be 100.

One day or more after exposure of the rat to 500 r, incorporation of ^{59}Fe into the non-extractable haemoglobin of the liver nucleus fraction is strongly depressed.

As mentioned in a previous note (Bonnichsen *et al.*[1]) the nuclear fraction of the liver of the guinea-pig contains small amounts of haemoglobin not extractable by saline or other aqueous solutions. This paper contains data on the incorporation of ^{59}Fe into this fraction isolated from the liver of adult rats and rabbits and of that of the rabbit embryo. This fraction was furthermore located in the nuclei of the erythrocytes of the hen.

That in the basophilic erythroblasts of human and rat bone marrow the site of haemoglobin synthesis is primarily the nucleus, was repeatedly suggested. The methods applied in these investigations were ultraviolet absorption microspectroscopy and cytochemical staining procedures [2–9].

EXPERIMENTAL

In 15 experiments with male rats an aggregate number of 173 animals, weighing between 150—280 g were injected intraperitoneally with 0.25 ml of a 3.8 % ammonium-citrate solution containing 0.5—12 μg of with ^{59}Fe labelled iron of 0.1—12 μC activity. Half the number of rats was exposed to 150 *r* — 500 *r* of X-rays. Injection took place 15 min to 5 days after exposure.

The animals were killed from 2 to 48 h after injection. The livers were perfused first with 0.145 M NaCl and then with 0.25 M sucrose containing 0.018 m $CaCl_2$. The weighed livers were homogenized in 9 vols. of 0.25 M sucrose — 0.0018 M $CaCl_2$. The further procedure was carried out according to Hogeboom *et al.*[10]

The nuclear fraction isolated by this procedure was cytologically inhomogeneous. The fraction contained about 60—80 % of the cell nuclei, it also contained erythrocytes, connective tissue, residual intact cells and free mitochondria.

In order to haemolyze the erythrocytes, the fraction was homogenized with 10 vols. distilled water and allowed to stand several hours. This last step was repeated at least three times more.

After clearing the suspension of nuclei obtained in this way by adding 3 % of deoxycholate, the haemoglobin bands were steadily visible in the handspectroscope. The CO-band was that of haemoglobin. The pyridine-haemochromogen band was located at 557 mμ.

The haemin was extracted with a mixture of acetone and HCl (10 ml 20 % HCl in 1 l of acetone). After filtration, the acetone was evaporated *in vacuo*. The haemin was crystallized twice from conc. acetic acid, and the crystals washed with 1 N HCl. The haemin was then combusted and the solution analyzed as described by Bonnichsen *et al.*[11]

In order to know in which part of the above nuclear fraction the non-extractable haemoglobin is located, we separated the fraction, prior to haemolyzing the red cells with distilled water, in the counter-streaming centrifuge of Lindahl [12] in five fractions containing particles of different size and different specific gravity. The fractions were examined with the phase-contrast microscope and with the handspectroscope. Thereafter, the specific activity of their haemin was determined. The result of one of these experiments is seen in Fig. 1.

In five of the above experiments of the liver nuclei have been isolated both in aqueous medium and in organic solvents of low polarity according to the methods described by Dounce *et al.*[13] and Allfrey *et al.*[14] The nuclear preparations obtained in this way were treated and analysed as described above. No difference was found in the properties of the non-extractable haemoglobin of the nuclear fraction prepared either in aqueous or in organic medium.

The liver ferritin was prepared as previously described by Loftfield *et al.*[15]

In experiments with 2—3 kg rabbits 8 animals were investigated. Their plasma was labelled with ^{59}Fe as described by Ehrenstein *et al.*[16] and reinjected. The animals were killed 3—24 h after injection.

Simultaneously, in all our experiments haemin of the circulating haemoglobin was analysed as well.

In two experiments with hens 100 ml of hen blood were incubated *in vitro* for 3 h at 37° C with 2 ml of 3.8 % ammonium citrate solution containing 2 μg labelled iron of 25 μC activity. The plasma was centrifuged off and the red cells washed four times with 5 vols. or more of isotonic saline.

The erythrocyte nuclei were prepared according to Hogeboom *et al.*[10] However, as the red cells are not sufficiently broken down by the homogenization procedure usually employed for the disintegration of other tissues, we haemolyzed the cells by freezing at —20° C and thawing them three times or more, suspended in a mixture of 0.25 M sucrose — 0.00018 m $CaCl_2$. The nuclei were then centrifuged down (International Refrigerated centrifuge head No. 269) for 10 min at 2 000 r.p.m. Thereafter, the procedure of Hogeboom *et al.*[10] was applied. Samples were taken from the whole washed red cells, the stroma-free haemolysate and from the final nucleus preparation. The haemin was extracted as described above.

RESULTS AND DISCUSSION

a) *Experiments with rats.*

The amount of ^{59}Fe present in one μg of iron of the nuclear haemoglobin fraction of the liver varied in experiments on rats between 0.6×10^{-4} and 10×10^{-4} % of that injected.

The liver of our rats contained 10 μg of nuclear haemin iron out of 2.5 mg of total iron present in the liver. This fraction makes out 0.4 % of its total iron content.

In the course of the purification process in aqueous medium extractable haemoglobin may have been removed. However, the non-extractable haemoglobin content of the nuclei was not found to be larger when the nuclei were

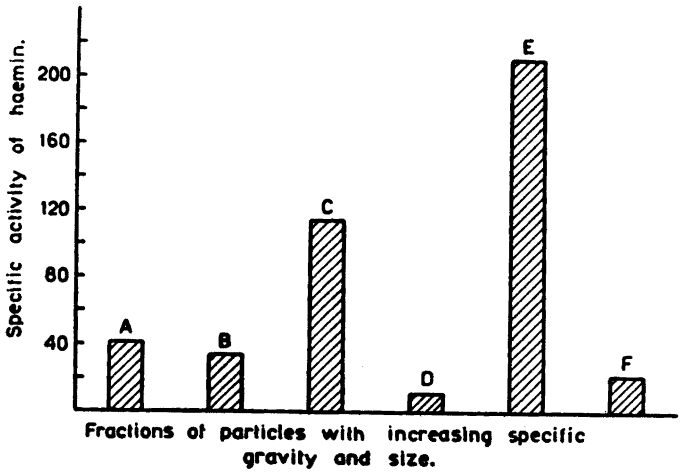


Fig. 1. Results of separation of nuclear components of the liver cells of the rat in Lindahls counter-streaming centrifuge.

A = Total nuclear fraction, prepared according to Hogeboom.
B = Impure mitochondria containing erythrocytes.
C = Erythrocytes and small fibers of connective tissue.
D = Cell membranes.
E = Small nuclei.
F = Large nuclei.

isolated after lyophilisation in organic medium. In the haemoglobin content of the nuclear fraction of the red cells of the hen, when these were isolated in an organic medium, Stern *et al.*[17] found a haemoglobin-iron content of 19 % of that of the total red corpuscle, while we find after isolation of the nuclei in an aqueous medium 1 % of the total haemoglobin-iron content to be non-extractable. This 1 % compares with 0.4 % found by us in the liver nuclei of rats and 2 % in those of the rabbit.

We compared also the effect of irradiation with 500 *r* of X-rays on rats on the incorporation of ^{59}Fe into the liver nuclear haemoglobin fraction. As seen in Table 1 the X-ray effect is shortly after exposure a very restricted one for both haemoglobin fractions. The X-ray effect as seen in Fig. 2 doesn't seem as pronounced as that on the circulating haemoglobin. If we, however, take into account the enhanced activity of the liver of the exposed animal, this difference is strongly reduced.

b) *Experiments with rabbits.*

The amount of ^{59}Fe present 4 h after injection in one μg iron of the non-extractable haemoglobin of the nuclear fraction of the rabbit liver varied between 2×10^{-4} and 6×10^{-4} % of that injected.

The iron content of the non-extractable liver nucleus fraction haemoglobin varied between 0.5 and 3.8 μg with a mean value of 1.9 μg per one g liver.

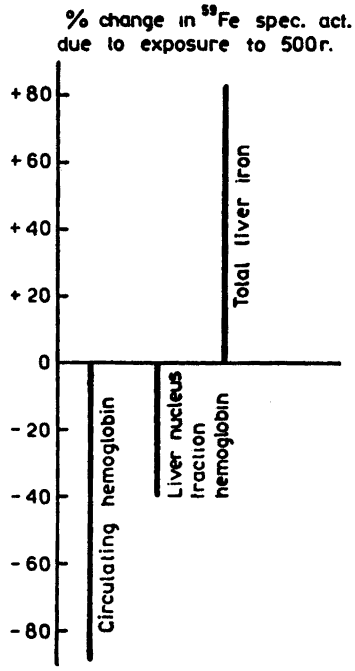


Fig. 2. Effect of exposure of the rat to whole body irradiation on the incorporation of intraperitoneally injected ^{59}Fe as citrate into liver fractions and the circulating haemoglobin.

For the nuclear haemoglobin content of 1 g of rat and rabbit liver the corresponding figures are 0.38 mg and 0.56 mg.

We also carried out experiments with pregnant rabbits 21 days after mating. A plasma sample of the mother was labelled as described by Ehrenstein *et al.*[16] The livers of the mothers and foetuses were investigated 11 to 17 h after labelling the maternal plasma. The results are seen in Table 2.

Table 1. Ratio of specific activities of iron fractions of to 500 *r* exposed and control rats.

Injected with ^{59}Fe shortly after exposure			Injected with ^{59}Fe 1 day or more after exposure		
Liver nucleus fraction haemoglobin	Circulating haemoglobin	Total liver iron	Liver nucleus fraction haemoglobin	Circulating haemoglobin	Total liver iron
1.16	0.53	1.60	0.915	0.161	1.15
0.97	1.04	1.41	0.503	0.063	2.48
1.15	0.84	0.93	0.570	0.238	1.72
0.78	0.46	1.27	0.727	0.072	1.92
			0.318	0.029	2.44
Mean value 1.01	0.72	1.30	0.605	0.112	1.94

Table 2.

	Mother	Foetus
Total liver iron	13.9 mg	1.5 mg
Total non-extractable liver nuclear haemoglobin iron	24 μg	41 μg
Total liver activity in % of that injected	8	20
Total non-extractable liver nuclear haemoglobin activity in % of that injected	3.4×10^{-3}	3.4×10^{-1}

Both the iron content of the nuclear fraction and its specific activity is much higher in the foetus than in the mother.

Three of the pregnant rabbits were exposed 1 day prior to injecting them with ^{59}Fe to an X-ray dose of 500 *r*. The effect of the radiation on the incorporation of ^{59}Fe into the liver nuclear fraction is discussed in a paper by Ehrenstein *et al.*[16]

The generous support to this investigation by *Riksföreningen för kräftsjukdomarnas bekämpande*, *Cancernämnden* and the *Alice och Knut Wallenbergs Stiftelse* is gratefully acknowledged. We are also much indebted to Professor P. E. Lindahl for kindly putting his centrifuge at our disposal.

REFERENCES

1. Bonnichsen, R. and Hevesy, G. *Acta Chem. Scand.* **9** (1955) 1045.
2. Villa, L. *Haematologica* **10** (1929) 327.
3. Villa, L. *Haematologica* **10** (1929) 355.
4. Riecker, H. H. *J. Exptl. Med.* **49** (1929) 937.
5. Knoll, W. *Folia Haematol.* **44** (1931) 310.
6. Hermansky, F. *Casopis Lékaru. Ceskych.* **90** (1951) 988.
7. De Carvalho, S. and Wilkins, M. F. H. *Proc. 4th Internat. Congr. Int. Soc. Haematol.*, Grune & Stratton, New York, 1954, p. 119.
8. De Carvalho, S. *Ed. Gaz. Med. Portug.*, Lisbon, 1954.
9. De Carvalho, S. *Blood* **10** (1955) 453.
10. Hogeboom, G. H., Schneider, W. C. and Striebich, M. J. *J. Biol. Chem.* **196** (1952) 111.
11. Bonnichsen, R. and Hevesy, G. *Acta Chem. Scand.* **9** (1955) 509.
12. Lindahl, P. E. and Nyberg, E. *Iva* **26** (1955) 309.
13. Dounce, A. L., Tishkoff, G. H., Barnett, S. R. and Freer, R. M. *J. Gen. Physiol.* **33** (1950) 629.
14. Allfrey, V. G., Stern, H., Mirsky, A. E. and Saetren, H. *J. Gen. Physiol.* **35** (1952) 529.
15. Loftield, R. B. and Bonnichsen, R. *Acta Chem. Scand.* **10** (1956) 1547.
16. Ehrenstein, G. and Hevesy, G. *Acta Physiol. Scand.* **38** (1956) 184.
17. Stern, H., Allfrey, V. G., Mirsky, A. E. and Saetren, H. *J. Gen. Physiol.* **35** (1952) 559.

Received October 15, 1956.

ACTA CHEMICA SCANDINAVICA 11 (1957) 125—131

The Acidity Function in Solutions of Hydrogen Chloride in Methanol-Water Mixtures

PENTTI SALOMAA

Department of Chemistry, University of Turku, Turku, Finland

Values of Hammett's acidity function H_0 for solutions of hydrogen chloride in water and methanol and in their binary mixtures have been measured spectrophotometrically for the concentration range from 0.08 to 0.8 N. The proton-donating power of the solution decreases at first with increasing methanol content, passes through a minimum when the mole fraction of methanol is approximately 0.5, and then increases as pure methanol is approached. The acidic properties of the solutions are more pronounced in anhydrous methanol than in water, but the addition of even relatively small amounts of water to methanol is able to lower appreciably the proton-availability. The value of the equilibrium constant for the distribution of protons between methanol and water calculated from the values of the acidity function in methanol solutions containing low concentrations of water has been found to be in agreement with the value derived from kinetic data.

The acidity function H_0 introduced by Hammett and co-workers [1,2] makes possible a comparison of the protolytic properties of a wide range of acid solutions. Values of this quantity have already been determined for aqueous solutions of several inorganic acids [1-6] and for solutions of hydrogen chloride in dioxan, ethanol and acetone [7], and in their binary mixtures with water [8]. The values of the acidity function for solutions of hydrogen chloride in water-methanol mixtures presented in this paper have been measured for use in connection with kinetic data [9].

RESULTS AND DISCUSSION

The measurement of Hammett's acidity function H_0 involves the determination of the ratio of the concentration of a suitably chosen uncharged indicator base to that of its conjugate acid in the acid solution under study. If B denotes the indicator base and BH^+ its conjugate acid, the thermodynamic constant of the equilibrium

$$B + H^+ \rightleftharpoons BH^+ \qquad (I)$$

is given by the mass-law expression:

$$\frac{[BH^+]\, f_{BH^+}}{[B]\, [H^+]\, f_B\, f_{H^+}} = K_B \qquad (1)$$

in which the f's are the respective activity coefficients. The acidity function H_0 is defined by

$$H_0 = \log K_B - \log \frac{[BH^+]}{[B]} = - \log \frac{f_B\, f_{H^+}}{f_{BH^+}} [H^+] \qquad (2)$$

In order to obtain a common basis for the comparison of the proton-availabilities in different solvents, pure water can be taken as the reference solvent, in which case K_B is the constant for the indicator equilibrium in dilute aqueous acid.

The acidities of the solutions examined in the present study were such that only one indicator, *p*-nitroaniline, was required, since the ratio of concentrations of the base and conjugate acid forms of the indicator could be spectrophotometrically measured with sufficient accuracy in all cases. Measurements of the equilibrium ratio for *p*-nitroaniline in dilute aqueous hydrochloric acid solutions gave the value 1.02 for log K_B. This value is intermediate between the value 1.11 obtained by Hammett and Paul [2] and the value 0.95 reported by Braude [7] for the same indicator. The slight differences between the values for the indicator constant which may be due to differences in apparatus and technique are of no practical significance when the data for a given binary solvent system are compared, as even the selection of the reference solvent is in principle arbitrary.

The recorded values of the indicator ratio in water-methanol mixtures of varying hydrogen chloride content are presented in Table 1. The values λ are the wavelengths of the absorption maxima and ε the corresponding molar extinction coefficients. The indicator ratio has been computed by the equation

$$\frac{[BH^+]}{[B]} = \frac{\varepsilon_N - \varepsilon_A}{\varepsilon_A - \varepsilon_s} \qquad (3)$$

where ε_N and ε_A are the extinction coefficients of the indicator solutions at the wavelengths of maximum absorption in the neutral solvent and in the acid solution in question, respectively, and ε_s is a small correction term which denotes the extinction coefficient of the conjugate acid of *p*-nitroaniline in the acid solution. For estimating ε_s, which cannot be measured directly, Braude and Stern [7,8] took advantage of the fact that in the near ultraviolet region the absorption of the conjugate acid of an aromatic amine is of the same order of magnitude as that of the corresponding hydrocarbon lacking the amino group, and substituted the extinction coefficients of nitrobenzene for those of the conjugate acid of *p*-nitroaniline. The molar extinction coefficients of nitrobenzene varied from 20 to 90 in ethanol-water mixtures in the wavelength range in question. Since the values of ε_s are evidently of the same order of magnitude also in methanol-water mixtures, and since the experimental errors when measuring ε_A were approximately of the same order of magnitude, a

Table 1. Values of the indicator ratio of *p*-nitroaniline and of the acidity function H_0 in solutions of hydrogen chloride in methanol-water mixtures. a is the approximate slope of the plot of H_0 against log [HCl].

% MeOH by wt.	[HCl]	λ in mμ	ε	$\log\frac{[BH^+]}{[B]}$	H_0	a
0	—	378	12 920			
0	0.0792	382	7 100	−0.08	+1.10	
0	0.198	380	4 070	+0.34	+0.68	−1.08
0	0.396	378	2 310	+0.67	+0.35	
0	0.792	379	1 220	+1.00	+0.02	
8.10	—	380	13 830			
8.10	0.0798	384	8 350	−0.18	+1.20	
8.10	0.199	381	4 890	+0.27	+0.75	−1.10
8.10	0.399	381	2 870	+0.59	+0.43	
8.10	0.798	386	1 550	+0.92	+0.10	
16.55	—	380	14 100			
16.55	0.0804	385	9 630	−0.33	+1.35	
16.55	0.201	384	5 700	+0.17	+0.85	−1.12
16.55	0.402	385	3 620	+0.47	+0.55	
16.55	0.804	386	1 950	+0.81	+0.21	
25.37	—	380	14 450			
25.37	0.0811	388	10 700	−0.45	+1.47	
25.37	0.203	387	7 210	+0.01	+1.01	−1.16
25.37	0.406	388	4 520	+0.35	+0.67	
25.37	0.811	388	2 410	+0.71	+0.31	
34.59	—	380	14 880			
34.59	0.0817	385	11 860	−0.59	+1.61	
34.59	0.204	388	8 560	−0.13	+1.15	−1.17
34.59	0.408	390	5 990	+0.18	+0.84	
34.59	0.817	391	3 150	+0.58	+0.44	
44.23	—	381	15 020			
44.23	0.0820	380	12 910	−0.78	+1.80	
44.23	0.205	383	10 590	−0.38	+1.40	−1.14
44.23	0.410	384	7 940	−0.05	+1.07	
44.23	0.820	381	4 580	+0.36	+0.66	
54.33	—	381	15 880			
54.33	0.0821	378	13 920	−0.85	+1.87	
54.33	0.205	382	11 850	−0.47	+1.49	−1.04
54.33	0.411	382	9 430	−0.16	+1.18	
54.33	0.821	380	6 280	+0.19	+0.83	
64.92	—	380	16 270			
64.92	0.0820	381	14 240	−0.84	+1.86	
64.92	0.205	382	12 420	−0.51	+1.53	−1.03
64.92	0.410	382	10 340	−0.24	+1.26	
64.92	0.820	381	6 560	+0.17	+0.85	
76.03	—	379	17 000			
76.03	0.0814	376	14 860	−0.84	+1.86	
76.03	0.204	379	12 900	−0.50	+1.52	−1.04
76.03	0.407	380	10 550	−0.21	+1.23	
76.03	0.814	379	6 880	+0.17	+0.85	
87.71	—	377	17 080			
87.71	0.0805	374	14 640	−0.78	+1.80	
87.71	0.201	376	12 270	−0.40	+1.42	−1.03
87.71	0.403	377	9 420	−0.09	+1.11	
87.71	0.805	377	6 000	+0.27	+0.75	
100	—	365	17 210			
100	0.100	371	3 830	+0.55	+0.47	
100	0.200	375	2 030	+0.89	+0.13	−1.12
100	0.300	379	1 350	+1.09	−0.07	
100	0.400	380	1 040	+1.22	−0.20	

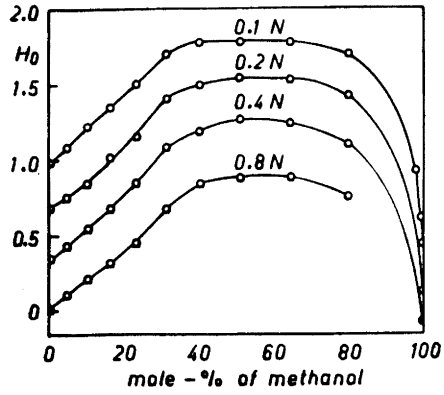


Fig. 1. The variation of H_0 with solvent composition in solutions of hydrogen chloride in methanol-water mixtures.

mean value $\varepsilon_s = 60$ was used in all cases to correct for the absorption by the conjugate acid when calculating the indicator ratio by eqn. (3).

The values of the acidity function H_0 calculated by substituting in eqn. (2) the measured values of the indicator ratio and the value 1.02 given above for log K_B were found to vary approximately linearly with the logarithm of the hydrogen chloride concentration in each solvent mixture. In order to facilitate the calculation of H_0-values for different acid concentrations by interpolation, the slopes of the plots of H_0 against log[HCl] for the different solvents are included in Table 1.

In Fig. 1 H_0 is plotted against the solvent composition in methanol-water mixtures for hydrogen chloride concentrations of 0.1, 0.2, 0.4 and 0.8 N. From the curves it is seen that H_0 increases at first and hence the proton-donating power of the solution decreases when methanol is added to water. The acidity function has its highest values when the mole fraction of methanol is between 0.4—0.7 and remains practically constant over this range. When pure methanol is approached, H_0 decreases rapidly and in anhydrous methanol its values are smaller than in water solution at the same hydrogen chloride concentrations. The variation of H_0 with solvent composition is similar in methanol-water as in ethanol-water mixtures, investigated by Braude and Stern [8], but is not quite so marked in the former mixtures, which is natural since methanol resembles water more closely in its properties. In the methanol-water mixtures at 0.1 N hydrogen chloride concentration the maximum value of H_0 is by 0.79 unit higher than in water, whereas in the ethanol-water mixtures the corresponding increase is 1.24 units [8]. The value of the acidity function for 0.1 N hydrogen chloride in anhydrous methanol, +0.47, is slightly smaller than the value, +0.61, in anhydrous ethanol. Thus the proton-availability is somewhat higher in methanol than in ethanol solution, which is in accordance with the greater basicity of ethanol as compared with methanol [10].

The data in Table 2 illustrate the effect of small additions of water to methanol on the value of H_0. Owing to the method of preparing the solutions, the hydrogen chloride concentrations varied slightly for different additions of water, and the indicator ratios have been corrected to apply to the same

Table 2. The effect of low concentrations of water on the value of H_0 in methanol and the evaluation of the constant $K_{H_2O}^{MeOH}$ for the equilibrium of proton distribution between methanol and water. In neutral solution, ε = 17 210.

$[H_2O]_{tot.}$	[HCl]	λ	ε	[BH+]/[B]	$\{[BH^+]/[B]\}_{0\cdot1}$	$\{H_0\}_{0\cdot1}$	$x_{0\cdot1}$	$K_{H_2O}^{MeOH}$
0.000	0.1000	371	3 830	3.55	3.55	+0.47	—	
0.051	0.0990	372	4 400	2.95	2.98	+0.55	0.20	(5.8)
0.101	0.0980	373	4 720	2.68	2.73	+0.58	0.32	4.2
0.150	0.0971	374	5 120	2.39	2.46	+0.63	0.48	4.1
0.198	0.0962	375	5 550	2.12	2.20	+0.68	0.67	4.2
0.245	0.0952	375	6 030	1.87	1.96	+0.73	0.89	4.5
0.291	0.0943	376	6 500	1.66	1.76	+0.77	1.13	4.7
0.336	0.0935	376	6 740	1.57	1.68	+0.79	1.24	4.4
0.380	0.0926	375	7 220	1.40	1.51	+0.84	1.52	4.8
0.424	0.0917	374	7 610	1.27	1.38	+0.88	1.79	5.0
0.467	0.0909	372	8 580	1.01	1.11	+0.97	2.60	(6.6)

concentration, 0.1 N, of hydrogen chloride that was present in anhydrous methanol by taking into account that the indicator ratio is approximately proportional to the acid concentration, at least in the narrow concentration range in question. The values with subscript 0.1 are the corrected values. The data in Table 2 show that small additions of water to methanol effect a pronounced increase in H_0, *i.e.* the proton-availability is appreciably reduced by the additions. This result is in accordance with the observations of Goldschmidt and Thuesen [11] who found that the equivalent conductance of hydrogen chloride falls rapidly when small quantities of water are added to methanol.

As Braude and Stern [8] have shown, the values of the indicator ratio determined for acid solutions in alcohol containing small amounts of water can be employed in a study of the alkoxonium-hydroxonium ion equilibrium. If a proton solvated by methanol is denoted by (mMeOH ,H^+) (m, the number of methanol molecules in the complex) and a proton solvated by water by ($n H_2O$, H^+) (n, the number of water molecules in the complex), the following equilibrium may be written:

$$(m\text{MeOH},H^+) + n\,H_2O \rightleftharpoons (nH_2O,H^+) + m\ \text{MeOH} \qquad \text{(II)}$$

The equilibrium constant for the reaction is given by

$$K_{H_2O}^{MeOH} = \frac{[nH_2O,H^+]}{[m\text{MeOH},H^+]\,[H_2O]^n} \qquad (4)$$

when the methanol concentration is taken to be constant. If hydrogen chloride can be assumed to be completely dissociated in methanol and in methanol-water mixtures, and it is written

$$x = \frac{[nH_2O,\ H^+]}{[m\text{MeOH},H^+]} \qquad (5)$$

eqn. (4) takes the form

$$K_{H_2O}^{MeOH} = \frac{x\ (1+x)^n}{\{(1+x)\ [H_2O]_{tot.} - nx[HCl]\}^n} \qquad (6)$$

In this equation, $[H_2O]_{tot.}$ denotes the total concentration of water present. The values of x can be computed if it is assumed that the minimum value of the indicator ratio $[BH^+]/[B]$ occurs in methanol-water mixtures in a region where the hydrogen ions have been completely transferred from methanol molecules to water molecules. The values of x can then be calculated by the equation

$$x = \frac{I_0 - I}{I - I_{min.}} \tag{7}$$

where I_0, I and $I_{min.}$ are the indicator ratios for the same concentration of acid in pure methanol, in the methanol solution containing a small amount of added water under study, and in the mixture where it has a minimum value, respectively. By interpolation from the data in Table 1, the value of $I_{min.}$ for 0.1 N hydrogen chloride is found to be 0.17, while the value of I_0 given in Table 2 is 3.55. Using these values, and the indicator ratios for 0.1 N hydrogen chloride solutions in methanol-water mixtures of low water content, the values of x given in Table 2 are obtained by eqn. (7).

The number of water molecules, n, which participate in the solvation of proton (eqn. II) in methanol-water mixtures of low water content can be determined by eqn. (6). For the mixtures studied, it is found that n is equal to unity as the values of the equilibrium constant computed by eqn. (6), by substituting $n = 1$, remain constant within the limits of experimental error, as shown by the figures in the last column of Table 2. The value of n was found to be unity also for ethanol-water mixtures of low water content, investigated by Braude and Stern [8].

The average value of $K_{H_2O}^{MeOH}$, 4.5 l mole^{-1}, in Table 2 is in excellent agreement with the value 4.8 l mole^{-1} derived by Goldschmidt and Thuesen [11] from their kinetic data on the effect of small water concentrations on the rate of esterification in methanol.

EXPERIMENTAL

Chemicals. Methanol, *pro analysi* from E. Merck, Darmstadt, was dried with magnesium according to Lund and Bjerrum [12], refluxed over anhydrous cupric sulphate, and distilled. The *p*-nitroaniline, of *purum* grade from E. Merck, was crystallised twice from anhydrous ethanol; it melted at 149°C.

Solutions. The solutions, which contained 20 moles per cent or more water were prepared by mixing measured volumes of water, aqueous hydrochloric acid and methanol to which the indicator had been dissolved to give the chosen concentration. When calculating the concentrations of indicator and hydrogen chloride in the mixed solutions, the data for the contraction of methanol-water mixtures given in the International Critical Tables [13] were employed. In a few cases the hydrogen chloride concentrations were checked also by titration, whereupon values in agreement with those calculated were obtained. The indicator concentration was varied from 1.5×10^{-5} M to 1.5×10^{-4} M depending upon the acidity of the solution. The solutions in pure methanol were prepared by passing carefully dried hydrogen chloride into anhydrous methanol. The methanol-water mixtures of low water content were prepared by mixing anhydrous methanol and methanol containing 5 moles per liter of water. The measurements on the solutions were made immediately after their preparation, in order that the slow reaction between hydrogen chloride and methanol could not influence the results.

Spectrophotometric measurements. The absorptions of the solutions required for the calculation of the indicator ratios were measured at 25±2°C with a Beckman Model DU

Quartz Spectrophotometer. The solutions containing *p*-nitroaniline exhibited maximum absorptions at wavelengths close to 380 mμ. A slit width of 0.15 mm was employed in the measurements; in the spectral range in question this corresponds to a half-intensity band width of about 1.3 mμ. The absorbance of the indicator solution was in each case measured against the same solution without added indicator because the solvents were found to differ appreciably in their absorption in the wavelength range where the measurements were made.

The value of the indicator constant K_B of *p*-nitroaniline in water which was used for the calculation of the values of the acidity function was determined by measuring the indicator ratio in dilute aqueous hydrochloric acid solutions by the method described above. Table 3 gives the results from which the values of the indicator constants have been calculated according to eqn. (1) by taking into account that the activity coefficient ratio remains practically unity in dilute aqueous solutions.

Table 3. The determination of the indicator constant of *p*-nitroaniline in dilute aqueous hydrochloric acid solutions.

[HCl]	0.0158	0.0317	0.0475	0.0634	0.0792	
$[BH^+]/[B]$	0.170	0.320	0.500	0.680	0.827	
K_B	10.8	10.1	10.5	10.7	10.4	*average* $K_B = 10.5$

REFERENCES

1. Hammett, L. P. and Deyrup, A. J. *J. Am. Chem. Soc.* **54** (1932) 2721.
2. Hammett, L. P. and Paul, M. A. *J. Am. Chem. Soc.* **56** (1934) 827, 830.
3. Bell, R. P., Dowling, A. L. and Noble, J. A. *J. Chem. Soc.* **1955** 3106.
4. Bell, R. P., Bascombe, K. N. and McCoubrey, J. C. *J. Chem. Soc.* **1956** 1286.
5. Harbottle, G. *J. Am. Chem. Soc.* **73** (1951) 4024.
6. Heilbronner, E. and Weber, S. *Helv. Chim. Acta* **32** (1949) 1513.
7. Braude, E. A. *J. Chem. Soc.* **1948** 1971.
8. Braude, E. A. and Stern, E. S. *J. Chem. Soc.* **1948** 1976.
9. Salomaa, P. *Acta Chem. Scand.* **11** (1957) 141.
10. Dewar, M. J. S. *The Electronic Theory of Organic Chemistry*, Oxford 1949, pp. 91—96.
11. Goldschmidt, H. and Thuesen, A. *Z. physik. Chem.* **81 B** (1913) 30.
12. Lund, H. and Bjerrum, J. *Ber.* **64 B** (1931) 210.
13. *International Critical Tables*, New York 1928, Vol. III, pp. 115—116.

Received October 1, 1956.

ACTA CHEMICA SCANDINAVICA 11 (1957) 132—140

The Acid-Catalysed Solvolysis of Alkoxymethyl Esters. Part I. The Relation between the Rate of Hydrolysis and the Acidity Function

PENTTI SALOMAA

Department of Chemistry, University of Turku, Turku, Finland

Kinetic measurements are made of the rate of hydrolysis of methoxymethyl acetate, ethoxymethyl acetate and methoxymethyl formate in different aqueous acids up to 5 N acid concentration. In all cases, the velocity of hydrolysis is more closely related to the acidity function H_0 of the solution than to its acid concentration, thus indicating that the critical complex behaves like the conjugate acid of the ester and does not contain a water molecule. The plots of the logarithms of the first-order rate constants against $-H_0$ give straight lines with slopes varying between 1.00 and 1.15. The results suggest that the reactions take place predominantly according to a mechanism, which in the rate-determining reaction stage involves the formation of an alkoxymethyl cation from the conjugate acid of the ester. This mechanism is identical with the unimolecular alkyl-oxygen fission mechanism of acid-catalysed ester hydrolysis, designated $A_{AL}1$ by Ingold.

The acid-catalysed hydrolysis reaction of alkoxymethyl esters

$$RCOOCH_2OR' + H_2O \xrightarrow{H^+} RCOOH + HCHO + R'OH \qquad (I)$$

provides an interesting problem for kinetic investigations. Owing to the fact that these compounds are as well esters as acetals, various reaction mechanisms may be expected to be involved. The hydrolysis by dilute aqueous hydrochloric acid has been previously investigated by Palomaa and co-workers [1-3] and by Salmi [4]. As the temperature dependence of the rate of hydrolysis was more closely related to that of dialkyl formals than to that of simple alkyl esters, the latter author suggested that the point of initial rupture was on the alkoxyl side of the ester.

The acidity function H_0, first introduced by Hammett and co-workers [5,6], has furnished a criterion which has been frequently used to obtain information about the mechanisms of acid-catalysed hydrolysis reactions[e.g.7-11]. Its use

necessarily involves the extension of the rate measurements up to relatively high acid concentrations in which the difference between the values of H_0 and pH becomes significant. The present paper describes the results obtained for the hydrolysis of some constitutionally simple alkoxymethyl esters in different aqueous acids.

RESULTS AND DISCUSSION

The basic idea about the application of the acidity function H_0 to acid-catalysed hydrolysis reactions originates from Zucker and Hammett [7]. The authors showed that if the critical complex contains only a proton in addition to the substrate molecule, there exist a linear relation between the logarithm of the first-order rate constant and $-H_0$ with a slope of nearly unity. On the other hand, if the critical complex contains also a water molecule, such a dependence of the reaction rate on the acidity function is not to be expected. In the latter case, the reaction velocity is more closely related to the acid concentration of the solution. The former type of mechanism is to be termed unimolecular, because only one reacting species, the conjugate acid of the substrate, is undergoing a change of covalency in the rate-determining reaction stage, whereas the latter mechanism is bimolecular, two molecular species being involved in the rate-determining reaction [12].

Our kinetic method to follow reactions (I) was based on the determination of formaldehyde produced at various reaction times. The experimental results are given in Tables 1, 2 and 3. In the tables, k denotes the first-order rate constant, and k_c the rate constant reduced to 1 N catalyst concentration by dividing k by the normality of the acid. The tables also include the values of the Hammett acidity function H_0 for the solutions used. The latter values have been obtained by interpolation from the data given by Hammett and Deyrup [5] and by Bell, Dowling and Noble [10] for aqueous hydrochloric acid, and by Hammett and Paul [6] for aqueous sulphuric acid, and by Harbottle [13] for aqueous perchloric acid containing added sodium perchlorate, respectively. Since the values given by Hammett and co-workers refer to molal concentrations of the solute, the corresponding molar concentrations were calculated from the data given by Harned and Ehlers [14] and in the International Critical Tables [15].

The values obtained for k_c at relatively low acid concentrations show but slight differences from the corresponding values determined earlier by Palomaa and co-workers [2,3]. These authors measured the velocity of reaction (I) by a titrimetrical determination of the acid produced, and found for k_c at 25°C the values: 0.00247 l mole^{-1}sec.$^{-1}$ for methoxymethyl acetate, 0.00875 l mole^{-1}sec.$^{-1}$ for ethoxymethyl acetate, and 0.00918 l mole^{-1}sec.$^{-1}$ for methoxymethyl formate, respectively. In the present case, the determination of the rate constants by an alkalimetric titration was not possible, because the concentration of the catalyst acid was usually relatively high in comparison to that of the acid formed during the reaction. In addition, the formaldehyde analysis allowed to bring the reactions to stop, and the end points of the titrations were sharp, whereas in the alkalimetric titration the rapidity of the alkaline hydrolysis of alkoxymethyl esters is a source of error in analysis. In the

Table 1. Hydrolysis of methoxymethyl acetate in various aqueous acid solutions at 25°C. Acid concentrations in moles/l of solution.

Solution	Acid concn.	$10^3 \times k$ sec.$^{-1}$	$10^3 \times k_c$ l mole^{-1}sec.$^{-1}$	H_0
Hydrochloric acid	0.0998	0.237	2.37	+1.07
» »	0.450	1.30	2.89	+0.33
» »	0.632	2.09	3.31	+0.18
» »	0.866	3.16	3.65	0.00
» »	1.245	6.23	5.00	−0.24
» »	1.549	9.14	5.90	−0.35
» »	2.42	22.0	9.09	−0.71
» »	2.62	25.6	9.77	−0.77
» »	2.91	36.4	12.5	−0.89
» »	3.42	62.8	18.4	−1.09
» »	3.83	99.2	25.9	−1.22
» »	4.29	170	39.6	−1.38
» »	5.01	290	57.9	−1.64
Sulphuric acid	0.740	3.11	2.10	+0.08
» »	1.166	6.16	2.64	−0.22
» »	1.99	18.2	4.57	−0.66
» »	2.41	28.7	5.95	−0.89
» »	3.28	104	15.9	−1.33
0.300 M perchloric acid + 5.700 M sodium perchlorate	0.300	14.4	48.0	−0.74
0.500 M perchloric acid + 5.500 M sodium perchlorate	0.500	24.5	49.0	−1.00
1.000 M perchloric acid + 5.000 M sodium perchlorate	1.000	54.9	54.9	−1.35

Table 2. Hydrolysis of ethoxymethyl acetate in aqueous hydrochloric acid at 25°C. Acid concentrations in moles/l of solution.

Acid concn.	$10^3 \times k$ sec.$^{-1}$	$10^3 \times k_c$ l mole^{-1}sec.$^{-1}$	H_0
0.1066	0.929	8.71	+1.05
0.632	8.04	12.7	+0.18
0.947	15.7	16.6	−0.03
1.245	24.4	19.6	−0.24
1.549	37.2	24.0	−0.35
1.851	50.0	27.0	−0.48
2.42	95.5	39.5	−0.71

Table 3. Hydrolysis of methoxymethyl formate in aqueous hydrochloric acid at 25°C. Acid concentrations in moles/l of solution.

Acid concn.	$10^3 \times k$ sec.$^{-1}$	$10^3 \times k_c$ l mole^{-1}sec.$^{-1}$	H_0
0.1066	0.916	8.59	+1.05
0.632	6.77	10.7	+0.18
0.947	11.6	12.2	−0.03
1.245	16.9	13.6	−0.24
1.549	23.7	15.3	−0.35
1.851	28.6	15.5	−0.48
2.42	51.3	21.2	−0.71

case of methoxymethyl acetate, the present method allowed an accurate determination of rate constants up to nearly 5 N hydrochloric acid concentration, whereas the rapidity of the reactions of ethoxymethyl acetate and methoxymethyl formate limited the measurements to a narrower range of concentrations.

The values of k_c given in Tables 1, 2 and 3 show that the rate of hydrolysis increases much more rapidly than the acid concentration of the solution. For instance, in the case of methoxymethyl acetate, the value of k_c increases by a factor of about 25 when the hydrochloric acid concentration is increased from 0.1 N to 5 N. In the case of ethoxymethyl acetate, the relative increase in the values of k_c with hydrochloric acid concentration is nearly of the same order of magnitude, whereas the increase is less pronounced in the hydrolysis of methoxymethyl formate.

Like the hydrolysis reactions of methylal [8] and trioxan [11], the hydrolysis of alkoxymethyl esters shows a close relation between the reaction velocity and the acidity function of the solution. This is seen from Figs. 1 and 2 in which the values of log k are plotted against the Hammett acidity function. The plots follow an approximately linear course as shown by the straight lines drawn in the diagrams which have slopes of 1.15 in the cases of methoxymethyl acetate and ethoxymethyl acetate, and a slope of 1.00 in the case of methoxymethyl formate, respectively. In the hydrolysis of methoxymethyl acetate (Fig. 1), the points corresponding to hydrochloric and sulphuric acids lie approximately on the same straight line, whereas the points referring to perchloric acid solutions containing added sodium perchlorate show systematic deviations from the former solutions. This may be due to small systematic differences between the values of H_0 determined by different authors, and to the limitations involved in assuming that the ratio of the activity coefficients of the substrate ester and the critical complex would vary with the solvent composition in an exactly similar way as the activity coefficient ratio of the indicator base and its conjugate acid, which have been used in the determination of H_0 [cf.8,13,16]. Systematic deviations between the results for different acids were also observed in the hydrolysis of trioxan, investigated by Bell, Bascombe and McCoubrey [11].

From the relationship between the hydrolysis rate of alkoxymethyl esters and the acidity function it may be concluded that the reactions take place by a mechanism, in which no water molecule is undergoing a change of covalency on the attainment of the transition state, *i.e.* the slow, rate-determining stage of the reaction is unimolecular and involves the formation of a carbonium ion from the conjugate acid of the ester. Similar conclusions were reached by McIntyre and Long [8] for the hydrolysis of methylal, and by Bell, Bascombe and McCoubrey [11] for the hydrolysis of trioxan. The plots corresponding to those of Figs. 1 and 2 gave a slope of 1.15 for methylal, and a slope of 1.2 for trioxan. In the case of acetal hydrolysis, the unimolecular mechanism has been also supported by other lines of experimental evidence [17,18].

The similarity of alkoxymethyl ester hydrolysis to acetal hydrolysis is not confined to a similar dependence of the reaction rate on the acidity function of the solution. In addition, it is most probable that the carbonium ion produced in the rate-determining stage of the hydrolysis of alkoxymethyl esters is structurally similar to that postulated for the hydrolysis of acetals [8,11,17,18],

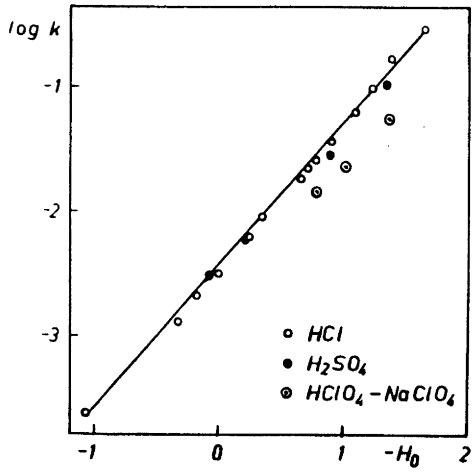


Fig. 1. Plot of log k against $-H_0$ for the hydrolysis of methoxymethyl acetate at 25°C.

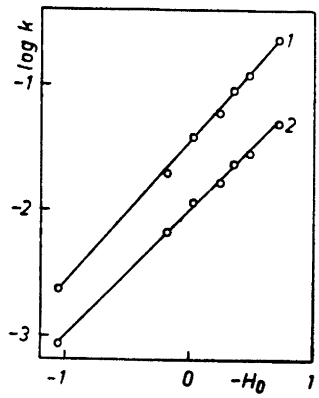


Fig. 2. 1. Plot of log $k+0.40$ against $-H_0$ for the hydrolysis of ethoxymethyl acetate. 2. Plot of log k against $-H_0$ for the hydrolysis of methoxymethyl formate. Hydrochloric acid solutions, 25°C.

i.e. the intermediate ion is a mesomeric alkoxymethyl cation. For that case, the rate-determining reaction stage which follows the preliminary proton uptake can be represented as follows:

$$RC(=O)-\overset{+}{O}H-CH_2OR' \xrightarrow[\text{slow}]{} RCOOH + CH_2=\overset{+}{O}R' \qquad \text{(II)}$$

Reaction (II) is then followed by the rapid subsequent reactions:

$$CH_2=\overset{+}{O}R' + H_2O \xrightarrow[\text{fast}]{} H^+ + HOCH_2OR' \xrightarrow[\text{fast}]{} H^+ + HCHO + HOR' \qquad \text{(III)}$$

which lead to the final products. In the present case, there are no structural factors to favour the formation of cations such as R^+, R'^+ or RCO^+ in the rate-determining reaction stage, whereas the production of an alkoxymethyl cation according to eqn. (II) is greatly facilitated by its mesomeric structure *cf.*[19-21]. The only alternative unimolecular mechanism, which were conceivable, would involve the formation of an acyloxymethyl cation in the rate-determining reaction stage:

$$RC(=O)-O-CH_2-\overset{+}{O}H-R' \xrightarrow[\text{slow}]{} RC(=\overset{+}{O})-O=CH_2 + HOR' \qquad \text{(IV)}$$

Also in this case, the formation of the cation is facilitated, although to a minor extent, by its possibility to resonate between different valence bond structures. Owing to the influence of the carbonyl group which is directly attached to the

ether oxygen atom, the resonance energy of this cation is materially reduced, and the conditions for its formation are thus less favourable. This is clearly illustrated by the results obtained for the solvolysis of chlorine in alkoxymethyl chlorides [19–21], $ROCH_2Cl$, when compared with those obtained for the corresponding reaction of acyloxymethyl chlorides, $RCOOCH_2Cl$, investigated by Euranto [22]. The former reaction takes place very rapidly with the unimolecular S_N1 mechanism involving the production of the alkoxymethyl cation in the rate-determining reaction stage, whereas the latter reaction is relatively slow and does not produce an intermediate carbonium cation, the reaction mechanism being S_N2. We must therefore conclude that the unimolecular hydrolysis of alkoxymethyl esters by aqueous acids takes place by the mechanism represented by eqns. (II) and (III). Our results thus provide an illustration for an acid-catalysed ester hydrolysis involving unimolecular alkyl-oxygen fission, designated $A_{AL}1$ by Ingold [23].

The application of the Hammett acidity function to relatively complicated reactions, where different points for initial rupture are conceivable as in the present case, does not give an information about the possible side mechanisms. Suppose, for instance, that a reaction in dilute acid solutions occurs by two simultaneous mechanisms, a unimolecular mechanism the rate of which follows the acidity function, and a bimolecular mechanism the rate of which depends primarily on the acid concentration. When passing to relatively concentrated acid solutions, the contribution of the latter reaction from the total reaction rate falls gradually off, and its presence cannot be clearly shown by the plot of log k against the acidity function. On view of the structural factors, discussed below, it is very probable that, at least in the case of methoxymethyl formate, the unimolecular reaction is at low acid concentrations accompanied to a certain extent by a bimolecular reaction, the mechanism of which is that of acid-catalysed ester hydrolysis involving bimolecular acyl-oxygen fission [23]. As shown by Bell, Dowling and Noble [10], the velocity of the latter type of reaction is more closely related to the acid concentration than to the acidity function of the solution.

The value of k_c (Table 3) determined for methoxymethyl formate in 0.1 N hydrochloric acid at 25°C, 0.00859 l mole^{-1}sec.$^{-1}$, is only 3.5-fold in comparison to the corresponding value for methyl formate, 0.00247 l mole^{-1}sec.$^{-1}$,determined by Salmi [4]. Owing to the fact that the rate of bimolecular acid-catalysed ester hydrolysis taking place with acyl-oxygen fission is but slightly influenced by changes in the alkyl part of the ester [23], it is reasonable to assume that the rate constant determined for methoxymethyl formate includes a contribution resulting from its hydrolysis by the acyl-oxygen fission mechanism, in addition to that which results from the unimolecular mechanism. Euranto [22] found that the rate constant for acid-catalysed ester hydrolysis at 25°C was reduced by a factor of about 3, when passing from methyl acetate to chloromethyl acetate, and a similar, although probably a smaller decrease is to be expected in the velocity of the bimolecular ester hydrolysis, when passing from methyl formate to methoxymethyl formate. On the contrary, in the cases of methoxymethyl acetate and ethoxymethyl acetate, the contribution from the bimolecular mechanism to the total hydrolysis rate is probably too small to be of practical importance. Tommila and Hella [24] determined for the rate constant

of methyl acetate in dilute aqueous acid at 25°C the value 0.000109 l mole^{-1} sec.$^{-1}$, whereas the corresponding values for methoxymethyl acetate and ethoxymethyl acetate (Tables 1 and 2) are considerably higher, 0.00237 l mole^{-1} sec.$^{-1}$ and 0.00871 l mole^{-1}sec.$^{-1}$, respectively. The smaller slope, 1.00, obtained for methoxymethyl formate by the plot of log k against $-H_0$, as compared with the slopes of 1.15 obtained for methoxymethyl acetate and ethoxymethyl acetate, is readily understood if it is assumed that in the former case the reaction rate involves a contribution from an accompanying bimolecular mechanism.

EXPERIMENTAL

Materials. Methoxymethyl acetate, $CH_3COOCH_2OCH_3$, and ethoxymethyl acetate, $CH_3COOCH_2OC_2H_5$, were prepared from the corresponding alkoxymethyl chlorides and potassium acetate according to Palomaa [1]. After fractionation, the products were found to be free from chlorine. The boiling points were: 118.6—118.8°C/766 mm Hg for methoxymethyl acetate, and 132.5—133.0°C/762 mm Hg for ethoxymethyl acetate. The purity of the products was controlled by hydrolysing weighed samples in dilute acid solutions and determining both the acetic acid and formaldehyde produced at the end of hydrolysis, the former by titrating against a standard sodium hydroxide solution, the latter using the modified bisulphite method described earlier by the author [19,25]. In the analysis, 59.9 mg of methoxymethyl acetate was found to be equivalent to 11.21 ml of 0.0519 N sodium hydroxide (*calc.* 11.09 ml), and to 16.64 ml of 0.0688 N iodine (*calc.* 16.73 ml). Ethoxymethyl acetate (78.3 mg) was equivalent to 12.58 ml of 0.0519 N sodium hydroxide (*calc.* 12.77 ml), and to 19.12 ml of 0.0688 N iodine (*calc.* 19.27 ml). Methoxymethyl formate, $HCOOCH_2OCH_3$, was prepared from methoxymethyl chloride and lead formate as described by Palomaa and Herna [2]. The boiling point was 103.6°C/762 mm Hg. In the analysis, 51.7 mg of the compound was equivalent to 11.24 ml of 0.0519 N sodium hydroxide (*calc.* 11.06 ml), and to 16.58 ml of 0.0688 N iodine (*calc.* 16.68 ml).

The acidic reaction solutions were prepared by diluting the corresponding concentrated acids, and their concentrations were determined by titrating against standard alkali solutions. Commercial acids of highest grade of purity were employed.

Kinetic measurements. The thermostat used in kinetic measurements and the technique of sampling were the same as described earlier [19,20]. The samples withdrawn from the reaction mixture at different time intervals were run into conical flasks, which contained 10 ml of the phosphate buffer solution (pH 7.3) which was employed for the formaldehyde determinations [19,25], and an amount of 0.5—5 N sodium hydroxide solution, which was calculated to neutralise the catalyst acid present in the sample. In the experiments, in which the concentration of the catalyst acid was relatively high, an amount of crushed ice was added, in order to avoid the considerable warming up of the mixture as a result of the heat of neutralisation. Particular experiments indicated that the velocities of alkaline hydrolysis of methoxymethyl acetate and ethoxymethyl acetate in the phosphate buffer were sufficiently small and did not cause an error in analysis. However, in the case of methoxymethyl formate it was established that an error in analysis resulted from a delayed analysis of the sample. The observed formaldehyde content increased slightly with time. The effect of this source of error was eliminated by performing the analysis immediately after taking the samples and by using a constant standing period (three minutes) for the bisulphite-formaldehyde addition reaction *cf.* [19]. In this case the small error resulting from the additional formaldehyde (estimated to be less than 5 % of the amount of remaining ester) did not affect the values of the rate constants as they were calculated by the first-order equation.

Zero time was the time of taking of the first sample. In addition, 6—8 samples were taken during the reaction. The concentration of formaldehyde formed after infinite time (over ten-fold period of the half-life) was checked by several parallel determinations. The initial concentration of the ester varied between 0.03—0.06 M. The volumes of the samples withdrawn from the reaction mixtures were 5 ml or 10 ml, and the concentration of the standard iodine solution used in the formaldehyde determinations was 0.06—0.07 N. The details for some typical runs are given in Tables 4, 5 and 6. In the tables, a denotes the

concentration of the ester at zero time, x the concentration of formaldehyde produced during time t, and k the first-order rate constant. The values of the rate constants were calculated by the usual equation for first-order reactions.

The author has received financial support for this study from the *Valtion Luonnontieteellinen Toimikunta*, which aid is gratefully acknowledged.

Table 4. Hydrolysis of methoxymethyl acetate in different acidic solutions at 25°C

A. 0.450 M hydrochloric acid. $a = 0.0348$.

t (in min.)	2	4	6	8	10	12	14
$10^2 \times (a-x)$	2.99	2.52	2.20	1.88	1.59	1.38	1.14
$10^3 \times k$	1.26	1.34	1.27	1.28	1.31	1.28	1.33

average $k = 0.00130$ sec.$^{-1}$

B. 1.99 M sulphuric acid. $a = 0.0278$.

t (in sec.)	15	30	45	60	75	90	105
$10^2 \times (a-x)$	2.09	1.60	1.23	0.92	0.72	0.54	0.46
$10^2 \times k$	1.90	1.84	1.81	1.84	1.80	1.82	1.71

average $k = 0.0182$ sec.$^{-1}$

C. 0.300 M perchloric acid, 5.700 M sodium perchlorate. $a = 0.0297$.

t (in sec.)	15	30	45	60	75	90	105
$10^2 \times (a-x)$	2.39	1.93	1.55	1.26	1.01	0.85	0.65
$10^2 \times k$	1.45	1.44	1.45	1.43	1.44	1.39	1.45

average $k = 0.0144$ sec.$^{-1}$

Table 5. Hydrolysis of ethoxymethyl acetate in 1.245 M hydrochloric acid at 25°C. $a = 0.0296$.

t (in sec.)	15	30	45	60	75	90
$10^2 \times (a-x)$	2.01	1.45	1.02	0.71	0.49	0.31
$10^2 \times k$	2.58	2.38	2.37	2.38	2.40	2.51

average $k = 0.0244$ sec.$^{-1}$

Table 6. Hydrolysis of methoxymethyl formate in 1.549 M hydrochloric acid at 25°C. $a = 0.0397$.

t (in sec.)	10	20	30	40	50	60	70
$10^2 \times (a-x)$	3.08	2.52	1.96	1.50	1.20	1.00	0.79
$10^2 \times k$	2.54	2.27	2.35	2.43	2.39	2.30	2.31

average $k = 0.0237$ sec.$^{-1}$

REFERENCES

1. Palomaa, M. H. *Ann. Acad. Sci. Fennicae, Ser.* **A IV** (1913) No. 2.
2. Palomaa, M. H. and Herna, T. O. *Ber.* **66** (1933) 305.
3. Palomaa, M. H. and Jaakkola, V. *Ber.* **67** (1934) 949.
4. Salmi, E. J. *Annales Universitatis Turkuensis, Ser.* **A III** (1932) No. 3.
5. Hammett, L. P. and Deyrup, A. J. *J. Am. Chem. Soc.* **54** (1932) 2721.
6. Hammett, L. P. and Paul, M. A. *J. Am. Chem. Soc.* **56** (1934) 827, 830.
7. Zucker, L. and Hammett, L. P. *J. Am. Chem. Soc.* **61** (1939) 2791.
8. McIntyre, D. and Long, F. A. *J. Am. Chem. Soc.* **76** (1954) 3240, 3243.
9. Long, F. A., Dunkle, F. B. and McDevit, W. F. *J. Phys. Chem.* **55** (1951) 829.
10. Bell, R. P., Dowling, A. L. and Noble, J. A. *J. Chem. Soc.* **1955** 3106.
11. Bell, R. P., Bascombe, K. N. and McCoubrey, J. C. *J. Chem. Soc.* **1956** 1286.

12. Ingold, C. K. *Structure and Mechanism in Organic Chemistry*, London 1953, pp. 310–313.
13. Harbottle, G. *J. Am. Chem. Soc.* **73** (1951) 4024.
14. Harned, H. S. and Ehlers, R. W. *J. Am. Chem. Soc.* **55** (1933) 2179.
15. *International Critical Tables*, New York 1928, Vol. III, p. 56.
16. Braude, E. A. *J. Chem. Soc.* **1948**, 1971.
17. O'Gorman, J. M. and Lucas, H. J. *J. Am. Chem. Soc.* **72** (1950) 5489.
18. Ingold, C. K. *Ref.* [12], pp. 333–335.
19. Salomaa, P. *Annales Universitatis Turkuensis, Ser.* **A XIV** (1953) No. 1.
20. Salomaa, P. *Acta Chem. Scand.* **8** (1954) 744.
21. Ballinger, P., de la Mare, P. B. D., Kohnstam, G. and Prestt, B. M. *J. Chem. Soc.* **1955** 3641.
22. Euranto, E. *Suomen Kemistilehti* **29 B** (1956) 144.
23. Ingold, C. K. *Ref.* [12], pp. 767–782.
24. Tommila, E. and Hella, A. *Ann. Acad. Sci. Fennicae, Ser.* **A II** (1954) No. 53.
25. Salomaa, P. *Suomen Kemistilehti* **27 B** (1954) 12.

Received October 1, 1956.

ACTA CHEMICA SCANDINAVICA 11 (1957) 141—150

The Acid-Catalysed Solvolysis of Alkoxymethyl Esters. Part II. Reaction Rates and Products in the Solvolysis of Methoxymethyl Esters in Methanol-Water Mixtures

PENTTI SALOMAA

Department of Chemistry, University of Turku, Turku, Finland

The acid-catalysed solvolysis reactions of methoxymethyl formate and methoxymethyl acetate have been investigated kinetically in methanol-water mixtures containing 30—65 moles per cent of methanol. A method has been developed to determine the reaction mechanisms which takes advantage of analysis of the different solvolysis products. The results indicate that the reactions of the esters take place involving two simultaneous mechanisms in the solvents under study. One mechanism is unimolecular and leads to the formation of methoxymethyl cation in the rate-determining stage. The second mechanism is bimolecular and takes place with an acyl-oxygen fission. The contribution of the bimolecular mechanism to the total solvolysis rate is more notable with methoxymethyl formate than with methoxymethyl acetate. Approximate calculations are made by Hammett's acidity function to elucidate the reaction mechanisms in pure water solution, the results suggesting that methoxymethyl acetate hydrolyses in this medium almost exclusively by the unimolecular mechanism, whereas in the case of methoxymethyl formate the unimolecular reaction is accompanied by a contribution from the bimolecular reaction.

In the first part of the present study [1] it was established that the acid-catalysed solvolysis of simple alkoxymethyl esters in water solution takes place predominantly according to a unimolecular mechanism involving the production of an intermediate alkoxymethyl cation. However, it was considered as being probable that, at least in the case of methoxymethyl formate, an alternative reaction mechanism of a normal type of acid-catalysed ester hydrolysis might play some role in the hydrolysis by dilute aqueous acids. The purpose of the present work is to furnish additional evidence for the reaction mechanisms suggested for the solvolysis of alkoxymethyl esters in hydroxylic media.

METHOD OF DETECTING THE MECHANISMS

In an earlier study [2] the author determined the values of Hammett's acidity function H_0 for solutions of hydrogen chloride in methanol-water mixtures and found the values to increase by 0.7—0.8 units when passing from water to media containing 30—65 moles per cent of methanol. The theory suggested *cf.* [1] that the logarithm of the rate constant for the unimolecular mechanism should decrease by an amount of nearly this order of magnitude when passing from water to the water-methanol mixtures, whereas such a decrease would not be probable for the postulated bimolecular mechanism. The change in solvent composition was thus expected to facilitate the detection of the possible bimolecular mechanism.

The investigation of reaction mechanisms in alcohol-water mixtures may be based on the following considerations. Let us assume that the alkoxyl group of the alkoxymethyl ester is the same as that of the alcohol in the water-alcohol mixture under study. Let it be at first presupposed that the reaction mechanism is unimolecular. The rate-determining stage which follows the initial proton uptake leads to the formation of an alkoxymethyl cation:

$$\mathrm{RC(=O)-O^{+}H-CH_2OR' \xrightarrow[\text{slow}]{} RCOOH + CH_2{=}\overset{+}{O}R'} \qquad \text{(I)}$$

The fast, product-forming reactions of the unstable cation are those given by eqns. (II):

$$\begin{aligned} &\mathrm{CH_2{=}\overset{+}{O}R' + H_2O \xrightarrow[\text{fast}]{} H^+ + HOCH_2OR' \xrightarrow[\text{fast}]{} H^+ + HCHO + HOR'} \\ &\mathrm{CH_2{=}\overset{+}{O}R' + R'OH \xrightarrow[\text{fast}]{} H^+ + CH_2(OR')_2} \end{aligned} \qquad \text{(II)}$$

The intermediate mesomeric ion is exactly the same, which is formed in the solvolysis reaction of the corresponding alkoxymethyl chloride. The latter reaction has been shown to take place by the S_N1 mechanism involving the ionisation reaction (III) as the rate-determining stage[3]:

$$\mathrm{ClCH_2OR' \xrightarrow[\text{slow}]{} Cl^- + CH_2{=}\overset{+}{O}R'} \qquad \text{(III)}$$

When the solvolysis of an alkoxymethyl ester in an alcohol-water mixture takes place exclusively by the mechanism represented by eqns. (I) and (II), that implies that the relative amounts of formaldehyde and formal produced at the end of reaction are the same as in the solvolysis reaction of the corresponding alkoxymethyl chloride under the same external conditions, because the product-forming reactions are identical in both cases.

Let us now suppose that the solvolysis occurs by a bimolecular mechanism, which involves an acyl-oxygen fission. In that case, the rate-determining, slow reactions which follow the preliminary proton uptake are those given by eqns. (IV) *cf.* [4]:

$$\begin{array}{l} \mathrm{RC(=O)—O^{+}(H)—CH_2OR' + H—OH \xrightarrow[\text{slow}]{} RCOOH_2^{+} + HOCH_2OR'} \\ \mathrm{RC(=O)—O^{+}(H)—CH_2OR' + H—OR' \xrightarrow[\text{slow}]{} RCOO^{+}(H)R' + HOCH_2OR'} \end{array} \qquad \text{(IV)}$$

Both of the possible reactions, the reaction with water and that with alcohol, give no formal, formaldehyde being one of the reaction products in both cases. Actually, the formaldehyde formed in the alcoholic media may be present, at least partly, in the form of semiacetal, but that is of no importance from the analytical viewpoint.

It thus appears that the relative amount of formaldehyde formed furnishes a criterion for the reaction mechanism. The unimolecular mechanism yields both formaldehyde and formal in a molar ratio, which is equal to that by the solvolysis of the corresponding alkoxymethyl chloride under the same conditions, whereas the bimolecular mechanism gives an amount of formaldehyde, which is equivalent to the amount of the ester initially present. It is seen that an assumption of alternative, less probable reaction mechanisms *cf.* [1] would not essentially alter the method of revealing the different mechanisms by the reaction products. If the mechanism (IV) were replaced by a unimolecular acyl-oxygen fission mechanism [4], the reaction would similarly produce quantitatively formaldehyde. The same situation prevails when the solvolysis would occur on the alkoxyl side of the ester molecule, the reaction with water giving formaldehyde and that with alcohol regenerating the ester, the observed net change thus being formaldehyde formation. Hence the contributions of these less probable mechanisms would be included in the observed net rate of formaldehyde production. The only alternative mechanism, which could produce formal in addition to formaldehyde, were bimolecular nucleophilic substitution at the carbon atom of the methylene group. This carbon atom is, however, much less electrophilic than that present in the carbonyl group, and actually, a bimolecular alkyl-oxygen fission mechanism has never been established in acid-catalysed ester hydrolysis [4].

The subsequent reactions, the esterification of the carboxylic acid formed and its reverse reaction, which followed the solvolysis of alkoxymethyl esters in methanol-water mixtures, did not affect our method as it took advantage only of the amounts of formaldehyde and methylal produced by the reactions. On the contrary, the rates of the subsequent acetalisation of formaldehyde and its reverse methylal hydrolysis were of such an order of magnitude, that these reactions must be taken into account in order to obtain reliable results.

METHOD OF CALCULATION

As shown experimentally, the acid-catalysed solvolysis of methoxymethyl esters in methanol-water mixtures under study proceeds to completion and yields both formaldehyde and methylal. The sum of the concentrations of

formaldehyde and methylal formed is equivalent to the amount of methoxymethyl ester reacted. Formaldehyde and methylal are converted to each other in a slow, subsequent equilibrium reaction. At a given acid concentration, all of these reactions are of the first order. Let the respective first-order rate constants be denoted as follows: k' for the formation of formaldehyde from the ester, k'' for the formation of methylal from the ester, k_a for the acetalisation of formaldehyde, and k_h for the hydrolysis of methylal. Independently of the reaction mechanisms involved, we thus have the following simplified reaction-scheme:

$$\begin{array}{l} \overset{k'}{\nearrow}\ \mathrm{HCHO} \\ \mathrm{RCOOCH_2OCH_3} \overset{k_a}{\underset{k_h}{\rightleftarrows}} \\ \underset{k''}{\searrow}\ \mathrm{CH_2(OCH_3)_2} \end{array} \qquad \text{(V)}$$

Making use of the known values of k_a and k_h which can be measured separately, we wish to calculate the values of k' and k'' from the experimental data.

If a denotes the initial ester concentration, and x and y are the concentrations of formaldehyde and methylal present at time t, respectively, we obtain eqns. (1) which express the rates of increase in formaldehyde and methylal concentrations:

$$\begin{aligned} \frac{\mathrm{d}x}{\mathrm{d}t} &= k'(a-x-y)-k_a x+k_h y \\ \frac{\mathrm{d}y}{\mathrm{d}t} &= k''(a-x-y)+k_a x-k_h y \end{aligned} \qquad (1)$$

By applying the initial conditions, $x = 0$ and $y = 0$, when $t = 0$, eqns. (1) may be integrated to give

$$\frac{x}{a} = \frac{k_h}{k_a+k_h}\left(1-\mathrm{e}^{-(k_a+k_h)t}\right) + \alpha\left(\mathrm{e}^{-(k_a+k_h)t} - \mathrm{e}^{-(k'+k'')t}\right) \qquad (2)$$

in which

$$\alpha = \frac{k'-k_h}{(k'+k'')-(k_a+k_h)} \qquad (3)$$

Taking advantage of the fact that the value of $(k'+k'')$ is large in comparison to that of (k_a+k_h), the last exponential of eqn. (2) can be neglected for large values of t, *i.e.* when practically all of the ester present initially has been converted to the final products, formaldehyde and methylal. We thus obtain from eqn. (2) the following expression which is valid for sufficiently long reaction times:

$$\alpha = \frac{x}{a}\,\mathrm{e}^{(k_a+k_h)t} - \frac{k_h}{k_a+k_h}\left(\mathrm{e}^{(k_a+k_h)t}-1\right) \qquad (4)$$

By this equation, the value of α can be calculated, and using the value found, values of $(k'+k'')$ can be calculated from the data referring to the earlier stages of the reaction by the following equation which is readily obtained from eqn. (2):

$$k'+k'' = \frac{1}{t}\ln\frac{\alpha a}{\alpha a\mathrm{e}^{-(k_a+k_h)t}-x+\dfrac{k_h a}{k_a+k_h}\left(1-\mathrm{e}^{-(k_a+k_h)t}\right)} \qquad (5)$$

From the known values of a, $(k'+k'')$, k_a and k_h, the values for k' and k'' can be calculated separately by eqn. (3).

The above calculation implies that the zero time is to be chosen at that time when no reaction has occurred. In actual measurements, some formaldehyde had been already formed at the time of taking of the first sample. The real zero time was hence determined by taking several samples with short time intervals at the initial phase of the reaction and by extrapolating to zero formaldehyde concentration. Table 1 shows a typical example of the individual experimental runs. Eqns. (3), (4) and (5) have been used in the calculations. The time interval passed from the time of taking of the first sample has been denoted by $(t—t_0)$, t being the actual reaction time which is found by a short extrapolation. As shown by the last column of the table, the values of $(k'+k'')$ remain practically constant at the different time intervals when the subsequent reactions have been taken into account. The effect of the subsequent reactions is clearly illustrated by the fact that the formaldehyde concentration which increases at first, reaches a maximum value, and then begins slowly to decrease, as shown by the values given in the second column of the table.

The solvolysis of methoxymethyl formate in methanol-water mixtures was so rapid in comparison to the subsequent reactions that their influence could be neglected, except in order to correct the final concentration of formaldehyde formed. In this case, the exponentials in eqn. (5) were practically unity, and the equation could be replaced by

$$k'+k'' = \frac{1}{t—t_0} \ln \frac{\alpha a—x_0}{\alpha a—x} \qquad (5\ a)$$

Table 1. The calculation of the constants k' and k'' for the solvolysis of methoxymethyl acetate in 47.2 moles per cent methanol at 25°C at 0.1182 N hydrogen chloride concentration. $a = 0.0658$. $k_a+k_h = 2.92 \times 10^{-6}$ sec.$^{-1}$, $k_h/(k_a+k_h) = 0.155$.

$t-t_0$ in min.	$10^2 \times x$	t in min.	a	$10^4 \times (k'+k'')$ in sec.$^{-1}$
0	0.03			
2	0.08			
4	0.11			
20	0.53	21.5		1.19
40	0.91	41.5		1.13
60	1.25	61.5		1.11
80	1.58	81.5		1.14
100	1.83	101.5		1.12
120	2.12	121.5		1.15
150	2.37	151.5		1.13
180	2.59	181.5		1.11
210	2.80	211.5		1.13
720	3.53	721.5	0.588	
1440	3.17	1 441.5	0.576	
1800	3.08	1 801.5	0.582	
2880	2.68	2 881.5	0.566	

Averages: $a = 0.578$, $k'+k'' = 0.000113$ sec.$^{-1}$
$k' = 0.000064$ sec.$^{-1}$
$k'' = 0.000049$ sec.$^{-1}$

Table 2. The calculation of the constants k' and k'' for the solvolysis of methoxymethyl formate in 64.2 moles per cent methanol at 25°C at 0.1182 N hydrogen chloride concentration. $a=0.0686$. $k_a+k_h = 3.32\times10^{-6}$sec.$^{-1}$, $k_h/(k_a+k_h) = 0.086$. The times are given in minutes, the rate constants in sec.$^{-1}$.

$t-t_0$	0	3	6	9	12	15	18	21	24	120	240	360	480
$10^2\times x$	0.83	1.87	2.68	3.39	3.89	4.30	4.67	4.82	5.13	6.08	5.99	5.77	5.66
a										0.906	0.912	0.897	0.899
$10^3\times(k'+k'')$		1.20	1.17	1.20	1.17	1.15	1.16	1.08	1.12				

Averages: $a = 0.904$, $k'+k'' = 0.00116$
$k' = 0.00105$, $k'' = 0.00011$

in which x_0 denotes the formaldehyde concentration present at the time (t_0) of taking of the first sample. Table 2 shows an example of experimental runs illustrating this case. The value of a has been calculated as above from the data referring to long reaction times, taking into account that for these times (t-t_0) becomes practically equal to t.

RESULTS AND DISCUSSION

Table 3 gives the experimental results for the solvolysis of methoxymethyl formate and methoxymethyl acetate in methanol-water mixtures. The rate constants for the subsequent reactions which were necessary for the calculation of the values of k' and k'' were estimated simultaneously by determining both the rate of formation of methylal from formaldehyde and the rate of methylal hydrolysis, as described in the experimental part which also contains the values observed. Although it was verified that the values of k' and k'' were proportional to the acid concentration when it was varied but slightly, all of the values included in Table 3 were determined at the same concentration, 0.1182 N, of hydrogen chloride.

Table 4 gives the average values determined for the molar ratios of formaldehyde and methylal formed in the solvolysis of methoxymethyl chloride in the methanol-water mixtures. Also in this case it was established that the

Table 3. The solvolysis of methoxymethyl esters in methanol-water mixtures at 25°C at 0.1182 N hydrogen chloride concentration. The values of k' and k'' are given in sec.$^{-1}$.

		Moles per cent of methanol		
		30.9	47.2	64.2
$HCOOCH_2OCH_3$	k'	0.000965	0.000919	0.00105
	k''	0.000065	0.000081	0.00011
$CH_3COOCH_2OCH_3$	k'	0.000098	0.000064	0.000054
	k''	0.000043	0.000049	0.000057

Table 4. The molar ratios of formaldehyde and methylal formed in the solvolysis of methoxymethyl chloride in methanol-water mixtures at 25°C at 0.1182 N initial hydrogen chloride concentration.

	Moles per cent of methanol		
	30.9	47.2	64.2
$[HCHO]/]CH_2(OCH_3)_2]$	1.538	0.681	0.348

product ratio was not affected by small variations in the initial hydrogen chloride concentration. The solvolysis of methoxymethyl chloride in these solvents took place much too rapidly to permit of kinetic measurements; still the composition of the final product could be easily determined. In this case, the slow, subsequent reactions of formaldehyde and methylal did not affect the results, the product analysis being performed almost immediately after mixing the components.

As shown above, the bimolecular solvolysis mechanism (IV) could produce no methylal, *i.e.* the value of k'' would be zero. This is not the case here, as indicated by the values determined for k'' (Table 3). On the other hand, the unimolecular mechanism which is presented by eqns. (I) and (II) would give formaldehyde and methylal in a molar ratio, which were exactly the same as in the solvolysis of methoxymethyl chloride under the same conditions, *i.e.* the value of the ratio k'/k'' would be identical with the molar ratio of formaldehyde and methylal, which is given in Table 4 for the solvent in question. A comparison between the values of Tables 3 and 4 shows that in all cases the values of k'/k'' are higher than the respective molar ratios of formaldehyde and methylal produced in the unimolecular solvolysis of methoxymethyl chloride. This indicates that the both reaction mechanisms occur simultaneously. The respective contributions of the mechanisms to the total rate of solvolysis may be evaluated as shown below.

Let k_1 denote the first-order rate constant for the solvolysis by the unimolecular mechanism. The first-order rate constants for the formation of formaldehyde and methylal by this mechanism are then given by *cf.* [3] $r\,k_1/(1+r)$ and $k_1/(1+r)$, respectively, in which r denotes the molar ratio of formaldehyde and methylal formed in the rapid, product-forming reactions (II) of the intermediate methoxymethyl cation. The values of r are identical with the ratios of formaldehyde and methylal concentrations, which are determined for the solvolysis of methoxymethyl chloride (Table 4). Let k_2 denote the first-order rate constant for the production of formaldehyde by the bimolecular mechanism (IV), the rate of methylal formation by this mechanism being zero. It is to be noted that in the case of bimolecular mechanism there are two different reactions, hydrolysis and alcoholysis, which both lead to the formation of formaldehyde, and k_2 thus represents the sum of the rate constants of these two reactions. Altogether, we obtain for the first-order rate constants of the formation of formaldehyde (k') and methylal (k'') the following expressions:

$$\begin{aligned} k' &= r\,k_1/(1+r)+k_2 \\ k'' &= k_1/(1+r) \end{aligned} \qquad (6)$$

by which, using the known values of k', k'' and r (Tables 3 and 4), the values of k_1 and k_2 can be readily calculated. The results of such calculations are given in Table 5 which also includes the values of the Hammett acidity function H_0 for the solutions under study [2].

A comparison between the values of k_1 and k_2 indicates that in the case of methoxymethyl formate, the contribution of the bimolecular mechanism is more pronounced than that of the unimolecular mechanism in the media under study, whereas the opposite situation prevails in the solvolysis of methoxy-

Table 5. The first-order rate constants (in sec.$^{-1}$) for the unimolecular (k_1) and bimolecular (k_2) solvolysis of methoxymethyl esters in methanol-water mixtures at 25°C at 0.1182 N hydrogen chloride concentration.

Moles % of MeOH		0	30.9	47.2	64.2
H_0		+0.91	+1.62	+1.69	+1.69
$HCOOCH_2OCH_3$	k_1		0.00016	0.00014	0.00015
	k_2		0.00087	0.00086	0.00101
	$\log k_1+H_0$		−2.18	−2.16	−2.13
$CH_3COOCH_2OCH_3$	k_1		0.000109	0.000082	0.000077
	k_2		0.000032	0.000031	0.000034
	$\log k_1+H_0$		−2.34	−2.40	−2.42

methyl acetate. This is in good accord with the previous results [1]. In addition, the values of the rate constants k_1 and k_2 are approximately of those orders of magnitude, which are to be expected in view of the reaction mechanisms involved (see below).

The unimolecular mechanism presupposes a linear relation between the logarithm of the first-order rate constant and $-H_0$ with a slope of close to unity. If the slope would be exactly unity, $\log k_1 + H_0$ would be constant for different media. In this case, the values of $\log k + H_0$ (k, the first-order rate constant in water solution) determined in water solution would be equal or higher in comparison to the respective values of $\log k_1 + H_0$ in methanol-water mixtures depending as the reaction mechanism in water solution were purely unimolecular or, if the unimolecular mechanism were accompanied by a contribution from the bimolecular mechanism. According to the previously determined values [1], the first-order rate constants for 0.1182 N aqueous hydrochloric acid at 25°C are: 0.00102 sec.$^{-1}$ for methoxymethyl formate, and 0.000281 sec.$^{-1}$ for methoxymethyl acetate; from these we obtain for the respective values of $\log k + H_0$ in water solution: −2.08 for methoxymethyl formate, and −2.64 for methoxymethyl acetate. The value for methoxymethyl formate is somewhat higher than the corresponding values of $\log k_1 + H_0$ determined in methanol-water mixtures (Table 5), whereas the opposite situation prevails in the case of methoxymethyl acetate. In view of the limitations involved in the calculation, this is in accord with the difference in mechanisms assumed for the hydrolysis of these compounds by aqueous acids [1]. The actual dependence of $\log k_1$ on H_0 in methanol-water mixtures remains obscure owing to the difficulties encountered in the determination of the values for k_1 in solvents of lower methanol content in which the changes in H_0 were more significant than in the present solvents [2]. In solvents of relatively low methanol content the determination of k_1 was found to be very inaccurate. This is also seen from the latter of eqns. (6) according to which the value of k_1 in water solution takes the indefinite form $0 \cdot \infty$.

The values of k_2 determined for methoxymethyl formate and methoxymethyl acetate in methanol-water mixtures (Table 5) are approximately threefold as compared with the respective rate constants for the hydrolysis of methyl formate and methyl acetate in aqueous acid (see *ref.* 1). This is in accord with the relatively small constitutional effect of the alkyl group of an ester,

which undergoes acid-catalysed solvolysis by the bimolecular acyl-oxygen fission mechanism [4], and to the relatively slight solvent influence. A comparison between the values determined by Salmi [5] and by Tommila and Hella [6] for the rate constants of acid-catalysed hydrolysis of methyl formate and methyl acetate in water, and the respective values for the hydrolysis in 50 moles per cent methanol, determined by Palomaa and Siitonen [7], shows the rate constants to decrease by 30—40 % when passing from water to the methanol solution. However, in the reactions of simple alkyl esters in alcoholic media, in which the alkyl group of the alcohol is the same as that present in the esters in question, the hydrolysis reactions of the esters and their reverse reactions are the only measurable processes, the reactions with alcohol molecules remaining obscure because they regenerate the esters present initially. Such a situation does not prevail in the solvolysis of methoxymethyl esters in methanol-water mixtures, the sum of the rates of the hydrolysis and alcoholysis reactions (IV) being that which is measured, and the somewhat higher values of k_2 as compared with the corresponding rate constants of the hydrolysis of alkyl esters may be primarily ascribed to the competing alcoholysis reactions.

EXPERIMENTAL

Materials. The methoxymethyl esters were prepared as described in the first part of the present study [1]. Methylal, which was used in the determination of the rates of its reversible hydrolysis reaction, was prepared from paraformaldehyde and methanol with hydrogen chloride as the catalyst. The raw product was refluxed over sodium and fractionated, b.p. 44°C/755 mm Hg. The degree of purity of the product was found to be over 99 % by formaldehyde analysis which followed the hydrolysis of a weighed sample by 2 N hydrochloric acid. Methanol, *pro analysi* from E. Merck, Darmstadt, was purified as described earlier [2]. The methanol-water mixtures employed for the kinetic measurements were prepared by weighing, after which carefully dried hydrogen chloride gas was passed in, and the solutions were diluted to give the hydrogen chloride concentration desired. All of the solutions were made up freshly before the experiments.

Kinetic measurements. The method of analysis used in following the solvolysis of methoxymethyl esters in methanol-water mixtures was essentially the same as in the first part of the present study [1]. In the kinetic experiments, a weighed sample of the ester which was sealed in a small glass bulb was brought into a measured volume of the reaction solvent, and after attainment of the thermostat temperature, the bulb was broken and the components were mixed by vigorous shaking to start the reaction. The value of the initial ester concentration was calculated from the amount of ester weighed, taking into account a small correction which was due to the deviation of the degree of purity of the ester from 100 % [1]. Particular experiments indicated that the solvolysis of the esters which produced both formaldehyde and methylal proceeded to completion, no methoxymethyl ester being present in the reaction mixture after sufficiently long reaction time. This was seen by running the samples into a large excess of 1 N sodium hydroxide solution, and after a standing period of 1 h, analysing the samples for formaldehyde. No increase in the formaldehyde content was observed during this time, which is sufficient to the quantitative hydrolysis of the methoxymethyl esters by the alkaline solution.

The method of determining the product composition for the solvolysis of methoxymethyl chloride in methanol-water mixtures was that described earlier by the author [3]. In all solvents investigated, several parallel determinations were conducted. In the solvolysis in 64.2 moles per cent methanol at 25°C, for instance, the following values were found for the molar percentage of formaldehyde in the product: 25.8, 26.6, 25.8, 25.4 and 25.6 (*average* 25.8). From the average value, the value 0.348 is obtained for the molar ratio of formaldehyde and methylal.

Table 6. The values of k_a and k_h (in sec.$^{-1}$) for the reversible acetalisation of formaldehyde in methanol-water mixtures at 25°C at 0.1182 N hydrogen chloride concentration. A. Measured by following the acetalisation of formaldehyde. B. Measured by following the hydrolysis of methylal.

Moles % of methanol		30.9	47.2	64.2
A	$10^6 \cdot (k_h+k_a)$	3.12	2.94	3.35
	$k_h/(k_h+k_a)$	0.264	0.155	0.084
B	$10^6 \cdot (k_h+k_a)$	3.16	2.91	3.28
	$k_h(k_h+k_a)$	0.276	0.156	0.088

Table 7. The determination of k_a and k_h by measuring the rate of the reversible acetalisation of formaldehyde in 30.9 moles per cent methanol at 25°C at 0.1182 N hydrogen chloride concentration.

t (in hours)	0	18	24	42	48	72	96	120	148	∞
$10^2 \cdot$ [HCHO]	5.34	4.61	4.38	3.86	3.64	3.22	2.75	2.44	2.21	1.41
$10^6 \cdot (k_h+k_a)$		3.17	3.24	3.12	3.28	2.99	3.11	3.10	2.99	

average $k_h+k_a = 0.00000312$ sec.$^{-1}$

$k_h/(k_h+k_a) = 1.41/5.34 = 0.264$

The determination of the rate constants for the hydrolysis of methylal (k_h) and the acetalisation of formaldehyde (k_a) took place by two different ways. In the first method, the acetalisation of formaldehyde was followed until the attainment of the equilibrium, in the second method the initial reactant was methylal. Both methods gave nearly identical results, as indicated by the values given in Table 6. Formaldehyde analysis was used for the rate measurements. In the second method, weighed samples of methylal were dissolved in measured volumes of the solvent, in order to calculate the initial concentration of methylal. In both methods, the first samples were taken almost immediately after mixing the components. Zero time was the time of taking of the first sample. Owing to the slowness of the reactions, practically no reaction had occurred at the zero time. The rate constants were calculated by the usual formulas for reversible first-order reactions [8]. Table 7 gives the details for one of the individual runs.

REFERENCES

1. Salomaa, P. *Acta Chem. Scand.* **11** (1957) 132.
2. Salomaa, P. *Acta Chem. Scand.* **11** (1957) 125.
3. Salomaa, P. *Annales Universitatis Turkuensis*, **Ser. A XIV** (1953) No. 1.
4. Ingold, C. K. *Structure and Mechanism in Organic Chemistry*, London 1953, pp. 767—782.
5. Salmi, E. J. *Annales Universitatis Turkuensis*, **Ser. A III** (1932), No. 3.
6. Tommila, E. and Hella, A. *Ann. Acad. Sci. Fennicae*, **Ser. A II** (1954), No. 53.
7. Palomaa, M. H. and Siitonen, T. A. *Ber.* **69** (1936) 1338.
8. Hammett, L. P. *Physical Organic Chemistry*, New York 1940, pp. 102—104.

Received October 1, 1956.

ACTA CHEMICA SCANDINAVICA 11 (1957) 151—165

Complexes of the 4d- and 5d-Groups

III. Absorption Spectra of Marcel Delépine's Rhodium(III) and Iridium(III) Complexes

CHR. KLIXBÜLL JØRGENSEN

Chemistry Department A, Technical University of Denmark, Copenhagen, Denmark

Professor M. Delépine has kindly furnished the octahedral complexes of rhodium(III) and iridium(III) with pyridine, oxalate, chloride, bromide, ammonia and water. In the *cis*-isomers of rhodium(III), the first transition to a singlet level is observed approximately at the position interpolated from the complexes with six equal ligands, while the first strong band is split into two bands of *trans*-isomers. However, it is difficult to describe this behaviour quantitatively by the ligand field theory for tetragonal symmetry without assuming interaction with higher $^1\Gamma_{t_5}$ levels. In iridium(III), the electron transfer bands of oxalate groups and the ultraviolet absorption of pyridine render the observation of singlet bands difficult, while the triplet bands are rather strong due to the intermediate coupling. The *trans*-isomer of Ir $py_2Cl_4^-$, but not of Ir $ox_2Cl_2^{-3}$, has the triplet band at a lower wavenumber than the *cis*-isomer. The acidity of water in iridium(III) complexes is remarkably low, thus $pK = 5.1$ of *trans*-Ir $py_2(NH_3)_3H_2O^{+3}$, 6.7 of *cis*-Ir $py_2Cl_3(H_2O)$ and ~10.1 of Ir $Cl_5(H_2O)^{--}$.

In the first paper of this series [1], the absorption spectra of several rhodium(III) and iridium(III) complexes were interpreted as transitions to one of the two triplet levels $^3\Gamma_4$ and $^3\Gamma_5$ and to the two singlet levels $^1\Gamma_4$ and $^1\Gamma_5$ of the excited configuration $\gamma_5^5\gamma_3$ while the groundstate is $^1\Gamma_1$ of γ_5^6. This notation [2] is only meaningful for complexes of perfect cubic symmetry, *e.g.* with six equal ligands in equal distances from the central ion. Most complexes MA_nB_{6-n} with two different ligands A and B arranged in a regular octahedron have tetragonal symmetry [3], of these *trans*-MA_4B_2 has a centre of inversion as also MA_6, while the other complexes have no centre of inversion. In some cases, the Jahn-Teller effect produces tetragonal symmetry by distortion of MA_6, *e.g.* copper(II)[4–7]. While these effects are conspicuous in the absorption spectra, the regular octahedral d^3-, d^8- and diamagnetic d^6-systems without Jahn-Teller effect [3,8,9] exhibit only small effects of tetragonal splitting with mixed sets of ligands, *e.g.* nickel(II) complexes [10–12]. Mr. C. E. Schäffer will later demonstrate that the absorption bands of chromium(III) complexes of tetra-

gonal symmetry generally are only slightly widened, but do not always exhibit the splitting, predicted from the ligand field theory by Hartmann and Kruse [13]; Linhard and Weigel [14] found that pentamine complexes of cobalt(III) in most cases exhibit a broadening or a splitting of the first singlet band, which is even more evident in *trans*-substituted cobalt(III) tetramine ions [15]. This led Orgel [16] to apply the ligand field theory on the case, and Basolo, Ballhausen and Bjerrum [17] have later given more evidence, while Yamada, Nakahara, Shimura and Tsuchida [18] investigated the dichroism* of *trans*-Co $en_2Cl_2^+$ and *trans*-Co $en_2Br_2^+$ in crystals.

Professor Marcel Delépine of Collège de France has kindly placed at my disposal samples of the highly robust *cis*- and *trans*-isomers of rhodium(III) and iridium(III) complexes, which allow a comparison with the behaviour of cobalt(III).

Table 1. Absorption bands of M. Delépine's rhodium(III) complexes. λ_n is the wavelength, σ_n the wavenumber, ε_n the molar extinction coefficient of each maximum. $\delta(-)$ is the halfwidth towards smaller and $\delta(+)$ towards larger wavenumbers. The ligand field quantum numbers of the excited levels are discussed in the text.

	λ_n mμ	σ_n K	ε_n	$\delta(-)$ K	$\delta(+)$ K
cis-Rh $ox_2Cl_2^{-3}$	435	23 000	190	1 900	—
	352	28 400	275	2 500	—
	285	35 100	1 900	1 900	—
trans-Rh $ox_2Cl_2^{-3}$	470	21 300	54	1 500	2 100
	398	25 100	38	—	—
	285	35 100	1 300	1 800	—
cis-Rh $py_2Cl_4^-$	448	22 400	91	1 800	—
	348	28 700	118	—	—
	270	37 000	8 300	1 100	—
	263.5	38 000	11 800	—	—
	257.0	38 900	14 500	—	—
	222	45 000	36 000	4 800	—
trans-Rh $py_2Cl_4^-$	500	20 000	39	1 600	—
	431	23 200	92	1 500	1 600
	269	37 200	11 600	1 200	—
	261	38 300	14 600	—	—
	256	39 100	14 400	—	—
	216	46 400	36 000	4 000	—
1,2,6-Rh py_3Cl_3	422	23 700	76	2 500	—
Rh $py_4Cl_2^+$	411	24 300	70	1 300	1 900
	268	37 300	7 700	500	—
	261.5	38 200	11 300	—	—
	255	39 200	12 100	—	—
	228	43 900	33 000	2 900	—

DICHLORO BIS(OXALATO)RHODIUM(III) IONS

Fig. 1 and Table 1 give the absorption spectra of *cis*- and *trans*-Rh $ox_2Cl_2^{---}$ prepared by Delépine [19]. The two bands of the *cis*-isomer are situated nearly as interpolated between the cubic Rh Cl_6^{---} and Rh ox_3^{---}, given in Ref. 1:

* Recently, Ballhausen and Moffitt [38] applied the selection rules for transitions, coupled with one quantum of odd vibration, to these dichroitic effects, supporting the identification of the first band as $^1\Gamma_{t_1} \rightarrow {}^1\Gamma_{t_2}$.

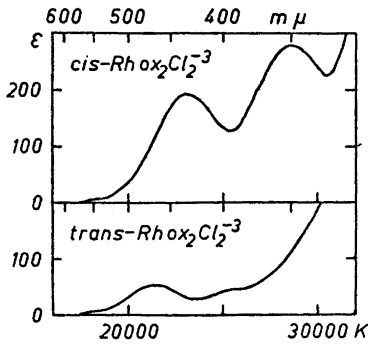


Fig. 1. Absorption spectra of rhodium(III) dichlorodioxalate complexes. 0.006 M *trans*-$K_3[Rhox_2Cl_2]$,$4H_2O$ and 0.005 M *cis*-$K_3[Rhox_2Cl_2]$, H_2O in aqueous solution.

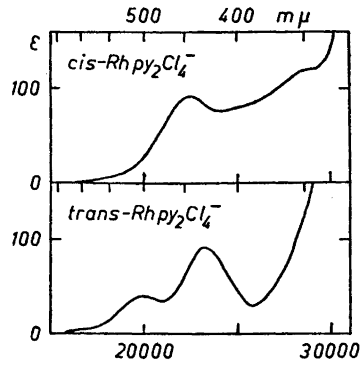


Fig. 2. Absorption spectra of rhodium(III) dipyridinotetrachloro complexes. 0.014 M *cis*-$K[Rhpy_2Cl_4]$, H_2O and 0.016 M *trans*-$K_3[Rhpy_2Cl_4]$, H_2O in aqueous solution.

	σ_1	σ_2
Rh Cl_6^{---}	19 300 K	24 300 K
Rh ox_3^{---}	25 100	30 000
cis-Rh $ox_2Cl_2^{---}$	23 000	28 400
$\frac{1}{3}\,\sigma_n(RhCl_6^{---}) + \frac{2}{3}\,\sigma_n(Rh\,ox_3^{---})$	23 170	28 100

In the place of σ_1, the *trans*-isomer gives two weak bands at 21 300 and 25 100 K. These bands [17] are caused by transitions to the levels $^1\Gamma_{t_5}$ and $^1\Gamma_{t_2}$, which have the degeneracy numbers 2 and 1, respectively. The weighted average of the two wavenumbers is then 22 600 K.

DIPYRIDINE TETRACHLORO RHODIUM(III) IONS

Fig. 2 and Table 1 give the absorption spectra of *cis*- and *trans*-Rh $py_2Cl_4^-$ studied by Delépine [20]. While *trans*-Rh $ox_2Cl_2^{---}$ is tetragonal in the same way as copper(II) complexes, *viz.* with less crystal field strength along one axis than along the two equivalent axes in a plane, *trans*-Rh $py_2Cl_2^-$ is »compressed« tetragonal [3], since the order in the spectrochemical series is:

$$Br^- < Cl^- < ox^{--} < H_2O < py < NH_3 < en.$$

The Rh py_6^{+++} is regrettably not known, but its first singlet band can be assumed [1] to be ~30 000 K. The cubic contribution [3] of Rh $py_2Cl_4^-$ is thus 22 900 K. *cis*-Rh $py_2Cl_4^-$ has the first singlet band at 22 400 K. In *trans*-Rh $py_2Cl_4^-$, two bands are observed at 20 000 and 23 200 K. In this case the second band is stronger than the first, agreeing with the degeneracy numbers 1 and 2. The weighted average is 22 200 K.

DICHLORO TETRAPYRIDINE RHODIUM(III) IONS

The pale yellow Rh $py_4Cl_2^+$ was first prepared by S. M. Jørgensen [21]. Recently, Delépine [22] discovered the strong catalytic influence of even 1 % of alcohols on the reaction between pyridine and a concentrated aqueous solution of Na_3RhCl_6, forming [Rh py_4Cl_2] Cl,6 H_2O.

The spectrum (Table 1) has a band at 24 400 K, which is so low a wavenumber that it presumably is due to ${}^1\Gamma_{t5}$ of a *trans*-complex, which here is analogous to copper(II). The *trans*-configuration is also supported by the formation [21] of [Rh py_4Cl_2]Cl,HCl, 2 H_2O analogous to the similar *trans*-[Co en_2Cl_2]Cl,HCl, 2 H_2O. Steric reasons seem to prevent pyridine from using the two perpendicular places.

When Rh $py_4Cl_2^+$ is boiled for some minutes with dilute Na_2CO_3, the band is shifted to 358 mμ (28 000 K) and by acidification with $HClO_4$, it is shifted to 384 mμ (26 000 K). This behaviour can be interpreted by the formation of hydroxo- and aquo-complexes, of which the spectra are analogous to Co $en_2(OH)_2^+$ and *trans*-Co $en_2(H_2O)_2^{+3}$ studied by Bjerrum and Rasmussen [23]. Analogously when *cis*-Rh $py_2Cl_4^-$ is boiled with water, or with Na_2CO_3 and subsequently with $HClO_4$, the first maximum is shifted to 421 mμ (23 700 K) corresponding to *cis*-Rh $py_2Cl_3(H_2O)$. If *trans*-Rh $py_2Cl_4^-$ is analogously treated, an orange precipitate [20], *trans*-Rh $py_2Cl_3(H_2O)$,H_2O is formed, which on heating polymerizes [20] to a completely insoluble pink product, Rh py_2Cl_3. Only one ligand field band has been observed of 1,2,6-Rh py_3Cl_3 (dissolved in $CHCl_3$) at 23 700 K. This seems somewhat less than the probable cubic contribution ~24 600 K and may be ascribed to rhombic splitting of ${}^1\Gamma_4$. However, the larger number of interactions possible between levels in low symmetry may systematically depress the wavenumber of the first band.

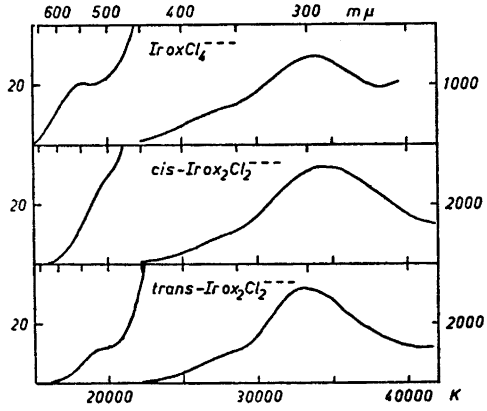


Fig. 3. Absorption spectra of iridium(III) chloro-oxalate complexes. 0.001 M to 0.014 M $K_3[Ir\,ox Cl_4]$, H_2O, 0.0006 M to 0.011 M *cis*-$K_3[Ir\,ox_2Cl_2]$, H_2O (racemic form), and 0.0006 M to 0.011 M *trans*-$K_3[Ir\,ox_2Cl_2]$,5 H_2O in aqueous solution.

Table 2. Absorption bands of M. Delépine's iridium(III) complexes. Notation as in Table 1. In the column "Excited level", triplet and singlet denote ligand field levels, Ir py the transition of an electron from the central ion to pyridine, redox the usual electron transfer spectra in the opposite direction, and py 0, py 1, . . . the vibrational structure of the pyridine band (py broad denotes the actual maximum, when this structure is blurred out), while "oxalate" denotes the ligand transition, polarized by the iridium ion.

	Excited level.	λ_n mμ	σ_n K	ε_n	$\delta(-)$ K
Ir $oxCl_4^{-3}$	triplet	550	18 200	21	1 700
	(singlet)	~375	26 600	500	—
	oxalate	298	33 600	1 450	4 400
cis-Ir $ox_2Cl_2^{-3}$	triplet	510	19 600	27	1 300
	(singlet)	~360	27 800	~1 100	—
	oxalate	294	34 000	3 100	4 200
trans-Ir $ox_2Cl_2^{-3}$	triplet	508	19 700	12	1 800
	(singlet)	~368	27 200	~800	—
	oxalate	303	33 000	3 200	3 100
$IrCl_5(H_2O)^{--}$	triplet	550	18 200	12	2 400
	singlet	405	24 700	110	2 200
	singlet	347	28 800	110	—
Ir $pyCl_5^{--}$	triplet	540	18 500	11	1 600
	(singlet)	~420	23 800	100	2 000
	Ir py	329.5	30 400	2 250	1 800
	py broad	279	35 800	5 100	1 900
cis-Ir $py_2Cl_4^-$	triplet	464	21 600	20	2 000
	Ir py	313	32 000	4 700	2 000
	(py 0)	267.5	37 400	9 600	—
	(py 1)	263	38 000	9 600	—
trans-Ir $py_2Cl_4^-$	triplet	515	19 400	8.8	1 600
	(singlet)	~395	25 300	~80	—
	Ir py	316	31 600	4 400	1 500
	py 0	273	36 600	8 700	—
	py 1	267	37 400	9 300	—
1,2,3-Ir py_3Cl_3	Ir py	326.5	30 600	—	1 700
	py 0	276	36 200	—	—
	py 1	265	37 700	—	—
1,2,6-Ir py_3Cl_3	triplet	432	23 100	53	2 000
	Ir py	319	31 400	1 600	2 800
	py broad	265	37 700	—	—
Ir $py_4Cl_2^+$	triplet	404	24 800	25	2 000
	Ir py	284	35 200	7 000	2 400
	py 0	271	36 900	11 400	—
	py 1	264.5	37 800	14 700	—
	py 2	257.5	38 900	16 400	—
	py 3	250	40 000	18 000	—
	py 4	245.5	40 800	—	—
cis-Ir $py_2Cl_3(H_2O)$	triplet	455	22 000	23	1 300
Sun-isomer	(singlet)	~378	26 500	~150	—
	Ir py	304.5	32 800	5 000	2 000
	py 0	265.5	37 700	9 700	—
	py 1	260	38 500	10 300	—
cis-Ir $py_2Cl_3OH^-$	Ir py	326	30 700	4 500	2 200
Sun-isomer	(py 0)	275	36 400	8 600	—
	py 1	267	37 400	9 100	—
cis-Ir $py_2Cl_3(H_2O)$	triplet	~445	22 500	28	2 800
autoclave-isomer	Ir py	304	32 900	5 600	2 000
	(py 0)	265	37 800	10 300	—
	py 1	259	38 600	11 700	—
cis-Ir $py_2Cl_3(OH)^-$	triplet	~475	21 000	38	—

autoclave-isomer	Ir py	317.5	31 500	5 300	2 700
	(py 0)	276	36 300	7 800	—
	py 1	268	37 300	8 100	—
trans-Ir $py_2Cl_3(H_2O)$	triplet	~475	21 000	17	—
	Ir py	307	32 600	4 900	1 800
	(py 0)	271	36 900	8 500	—
	py 1	265	37 800	10 300	—
	py 2	260	38 500	10 000	—
trans-Ir $py_2Cl_3(OH)^-$	triplet	~488	20 500	~18	—
	Ir py	329.5	30 400	3 900	2 400
	py broad	284.5	35 200	7 200	—
Ir $py(NH_3)_4$ Cl++	(triplet)	~365	27 400	30	1 100
	Ir py	290	34 500	2 040	2 000
	py 0	271	36 900	3 400	—
	py 1	265	37 800	3 870	—
	py 2	258.5	38 700	4 060	—
	py 3	251.5	39 800	4 230	—
	py 4	246	40 700	4 350	—
	py 5	239	41 900	4 410	—
Ir $py_2(NH_3)_3H_2O^{+3}$	(Ir py?)	282	35 400	5 700	1 400
	py 0	269.5	37 100	8 700	—
	py 1	263.5	38 000	9 700	—
	py 2	256.5	39 000	9 600	—
	py 3	251	39 900	8 700	—
	py 4	245	40 900	8 200	—
Ir $py_2(NH_3)_3OH$++	Ir py	304	32 900	4 500	2 600
	py 0	271	36 900	7 200	—
	py 1	263	38 000	8 800	—
	py 2	258	38 800	8 800	—
Ir $py_2(NH_3)_3Cl$++	(triplet)	~370	27 000	~24	700
	Ir py	285.5	35 000	6 600	2 400
	py 0	270.5	37 000	7 600	—
	py 1	264	37 900	9 600	—
	py 2	258	38 800	10 200	—
Ir $py_2(NH_3)_2Cl_2^+$	(triplet)	~380	26 300	38	1 300
	Ir py	295	33 900	6 200	2 000
	py 0	272	36 800	8 800	—
	py 1	265	37 700	10 500	—
	py 2	260	38 500	10 400	—
	py 3	254	39 400	8 900	—
$IrBr_6^{-3}$	triplet	645	15 500	12	—
	triplet	585	17 100	16	—
	singlet	442	22 600	175	1 900
	singlet	380	26 300	145	—
	redox	270	37 000	12 000	2 200
	redox	241	41 500	20 000	—
$IrBr_5(H_2O)^{--}$	redox	271	36 900	10 500	2 600
	redox	239.5	41 800	17 500	—
Ir $py_2Br_4^-$	triplet	515	19 400	17	1 400
	singlet	388	25 800	230	2 200
	Ir py	319	31 400	4 300	2 200
	py broad	270	37 000	11 500	2 700
	redox	~220	45 500	~25 000	—
1,2,3-Ir py_3Br_3	Ir py	335	29 800	~ 5 000	1 600
	py broad	284	35 200	~ 9 000	—
1,2,6-Ir py_3Br_3	triplet	471	21 200	36	1 900
	Ir py	321	31 200	~ 5 300	2 600
	py broad	269	37 200	~10 000	—

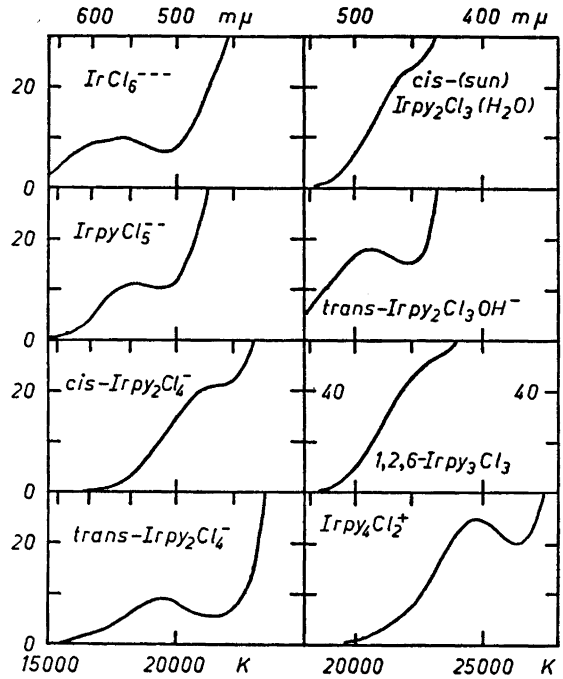


Fig. 4. The ligand field singlet → triplet bands of iridium(III) complexes.
0.01 M to 0.2 M K_3IrCl_6,3 H_2O in 1 M HCl and pure H_2O, immediately measured.
0.014 M $K_3[Ir\ pyCl_5]$,3 H_2O in H_2O, immediately measured.
0.009 M *cis*-$K[Ir\ py_2Cl_4]$, H_2O in H_2O
0.041 M *trans*-$K[Ir\ py_2Cl_3]$, H_2O in H_2O
0.011 M *cis*-$[Ir\ py_2Cl_3(H_2O)]$,2 H_2O (sun-isomer) in 0.1 M HCl.
0.005 M *trans*-Ir $py_2Cl_3OH^-$ from *trans*-$[Ir\ py_2Cl_3(H_2O)]$, H_2O in 1 M NH_3.
0.005 M 1,2,6-Ir py_3Cl_3 in $CHCl_3$.
0.005 M $[Ir\ py_4Cl_2]Cl$,6 H_2O in H_2O.

OXALATO- AND CHLORO-IRIDIUM(III) COMPLEXES

Vèzes and Duffour [24] studied the mixed chloro-oxalato complexes of iridium(III), and Delépine [25] later investigated the exact conditions for formation of Ir $oxCl_4^{-3}$, *cis*- and *trans*-Ir $ox_2Cl_2^{-3}$. In these complexes, the triplet band [1] of $IrCl_6^{-3}$ can be seen (Table 2 and Fig. 3) to be regularly shifted towards the higher wavenumbers with increasing number of oxalate groups, while the two singlet bands are hidden by the electron transfer band in the ultraviolet. This band has been found by Babaeva and Mosyagina [26] in all oxalate complexes. In iridium(III), the ε_n of the maximum is 1 600 per oxalate group.

In Ir ox_3^{---}, all the crystal field bands are hidden [1]. The differences between *cis*- and *trans*-Ir $ox_2Cl_2^{---}$ are the intensity of the triplet band (which have the same position in the two complexes) and 3 % different wavenumbers of the electron transfer band (which perhaps is an internal transition in the oxalate group, analogous to the acetylacetonate [7] absorption.)

PYRIDINE- AND CHLORO-IRIDIUM(III) COMPLEXES

Delépine [27] prepared the red-brown Ir $py Cl_5^{--}$, and [28] the pink *trans*-Ir $py_2Cl_2^-$ and orange *cis*-Ir $py_2Cl_4^-$, and the two yellow compounds [25] 1,2,3-Ir py_3Cl_3 and 1,2,6-Ir py_3Cl_3. Finally, Professor M. Delépine has sent me the chloride of Ir $py_4Cl_2^+$, which is not yet described in the literature, but is made by heating *cis*-Py H[Ir py_2Cl_4] with pyridine 1.5 h to 130°C.

As seen from Fig. 4 and Table 2, the triplet band is also here shifted from the place in $IrCl_6^{---}$ towards higher wavenumbers. But the triplet band of *trans*-Ir $py_2Cl_4^-$ is shifted 2 200 K towards the red and is less intense, compared to the band of the *cis*-form. It might be argued that the weak band observed in Ir $py_4Cl_2^+$ is the first singlet band as in the corresponding rhodium complex discussed above, but the extreme hypsochromy [1] of Mathieu's $Ir(NH_3)_5Cl^{++}$ and Ir en_3^{+++} makes the triplet assignment more probable.

The pyridine-complexes of iridium(III) all have a broad band in the range 30 000—34 000 cm^{-1} and a set of narrow bands, often four members of a vibrational structure 37 000—41 000 cm^{-1} (*cf.* Fig. 5). The latter bands are nearly equal in different complexes and can be ascribed to the π-electron system of the heterocyclic pyridine-ring. The broad band at lower wavenumber is not observed in free pyridine or pyridinium salts with a comparable intensity. Further, Rh $py_2Cl_4^-$ and Rh $py_4Cl_2^+$ do not either exhibit this band, which must be due to some electron transfer process in iridium(III) which is not observed in pyridine-free complexes [1].

In the fourth paper of the series, the latter band will be discussed. Its position is dependent on the other ligands and seems to follow the spectrochemical series. Actually, it has nearly the same wavenumber as predicted of the ligand field transition to the second singlet level $^1\Gamma_5$. However, it is not very likely that it is strongly intermixed with this Laporte-forbidden band, or that it is a triplet or weak singlet band elsewise known of pyridine: rather, it is probably due to transition of a γ_5-electron from iridium(III) to a π-antibonding orbital of pyridine.

THE THREE ISOMERS OF DIPYRIDINO TRICHLORO AQUO IRIDIUM(III)

Delépine [29,39] has prepared three isomers of Ir $py_2Cl_3(H_2O)$: one with the pyridines in *trans*-position, and the two possible monomers with pyridine in *cis*-position and the water in *trans*-position to either pyridine or chloride. The two latter isomers can be made from an aqueous solution of *cis*-Ir $py_2Cl_4^-$ by a photochemical reaction with sunlight, producing a relatively more water-soluble form, and by heating in an autoclave to 130°C, where polymerized by-products and a less soluble monomer is produced. The geometrical configuration of the "sun" and the "autoclave" isomer is not yet elucidated. *Cf.* the seven publications by Delépine [29].

It is seen in Table 2 that while the absorption spectra of the three isomers of Ir $py_2Cl_3(H_2O)$ are not very different, the alkaline solutions, forming Ir $py_2Cl_3(OH)^-$, have, *e.g.*, the iridium-pyridine band mentioned above at highly different wavenumbers. It is remarkable that the water group can be revers-

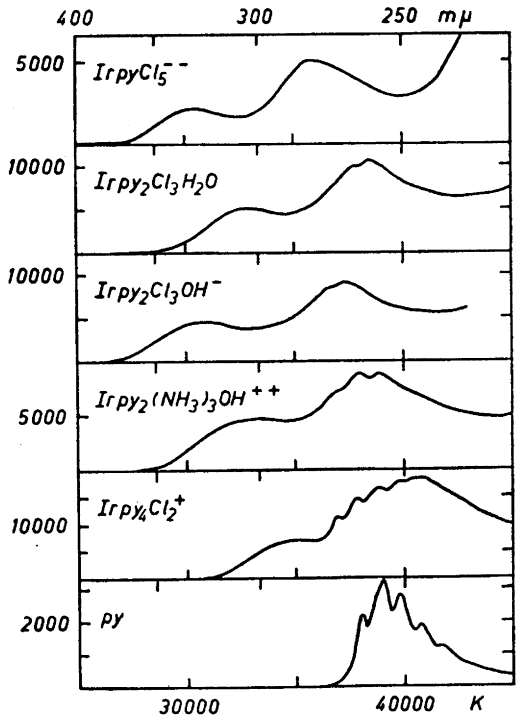


Fig. 5. The Ir-py and genuine pyridine bands of iridium(III) complexes.

0.0003 M K_2[Ir py Cl_5],3 H_2O in H_2O, immedately measured.
0.0002 M *cis*-[Ir $py_2Cl_3(H_2O)$],2 H_2O (sun-isomer) in 0.1 M HCl.
0.0002 M *cis*-Ir $py_2Cl_3OH^-$ from sun-isomer in 0.1 M Na_2CO_3.
0.0002 M Ir $py_2(NH_3)_3OH^{++}$ from [Ir $py_2(NH_3)_3H_2O]Cl_3$ (pyridine in *trans*-position) in 1 M NH_3.
0.0001 M [Ir py_4Cl_2]Cl $6H_2O$ in H_2O.
0.0005 M py in H_2O.

ibly titrated without appreciable loss of chloride in alkaline solution for many hours at room temperature. Even the least robust iridium(III) pyridine complex with the highest number of chloride groups, Ir $pyCl_5^{--}$, aquates during several days with the result that the Ir-py band shifts monotonously towards higher wavenumbers of the aquo forms and towards lower wavenumbers of the hydroxo forms, as discussed in the next paper. It is necessary to boil the alkaline solution of Ir $pyCl_5^{--}$ to efficiently destroy the binding between iridium and pyridine.

trans- and *cis*-(autoclave) Ir $py_2Cl_3(H_2O)$ are so weakly soluble in water that it is difficult to observe the ligand field triplet transition. Similar remarks apply to the 1,2,3-isomers of Ir py_3Cl_3 and Ir py_3Br_3, of which the best solvent known, chloroform, only dissolves a very small amount.

PYRIDINE-, AMMONIA-, CHLORO-, AQUO-COMPLEXES OF IRIDIUM(III)

Delépine [28] has prepared yellow Ir $py_2(NH_3)_2Cl_2^+$, pale yellow Ir $py_2(NH_3)_3Cl^{++}$, and white Ir $py_2(NH_3)_3H_2O^{+++}$, all with the pyridines in *trans*-position, and Delépine and Pineau [30] the pale yellow Ir $py(NH_3)_4Cl^{++}$. In the chloro complexes, there are very weak traces of a shoulder corresponding to the triplet band at 360 mμ of $Ir(NH_3)_5Cl^{++}$. The wavenumber of the broad and strong Ir-py band increases with a decreasing number of chloride groups, but seems still to subsist in Ir $py_2(NH_3)_3H_2O^{+++}$ superposed upon the narrow pyridine bands, while it is very evident in Ir $py_2(NH_3)_3OH^{++}$ (see Fig. 5).

THE ACIDITY OF WATER IN IRIDIUM(III) COMPLEXES

Reversible titration curves have been made with a glass electrode pH-meter of the following of Delépine's compounds:

cis-Ir $py_2Cl_3(H_2O)$ (sun) has $pK = 6.7$
trans-Ir $py_2(NH_3)_3H_2O^{+++}$ has $pK = 5.1$
Ir $Cl_5(H_2O)^{--}$ has $pK \sim 10.1$. however with some decomposition in alkaline solution.

Thus, the acidity of water increases with the positive external charge, but not to a larger extent than known of aquo complexes of cobalt(III) or chromium(III).

A sample of what was assumed to be Ir $py_2(NH_3)_3NH_2^{++}$ exhibited the same absorption spectrum as Ir $py_2(NH_3)_3OH^{++}$, and by titration of a sample of assumed Ir $py_2(NH_3)_4Cl_3$, 80 % of the calculated stoichiometric amount titrated with a fine one-proton curve, corresponding to $pK = 5.2$. Thus, the latter sample contains at most 20 % Ir $py_2(NH_3)_4^{+++}$, and its acidity cannot be ascribed to formation of amido complexes. This is not in disagreement with the analyses of Delépine [28], who determined only iridium and chloride but not nitrogen.

PYRIDINE- AND BROMO-IRIDIUM(III) COMPLEXES

Ir Br_6^{---} and Ir $Br_5(H_2O)^{--}$ have not very different spectra in aqueous solution, as seen from Table 2. The former ion aquates probably rather quickly in aqueous solution, explaining the slight deviation from the solution in HBr, described previously [1]. While most other iridium(III) complexes do not exhibit maxima of the electron transfer bands in the accessible range above 205 mμ Ir Br_6^{---} and Ir $Br_5(H_2O)^{--}$ have a double band with $\varepsilon_n \sim 11\,000$ and 20 000, resembling much the isoelectronic [32] Pt Br_6^{--}. The doublet structure and energy levels of halide complexes will be discussed in the fourth paper of this series.

In dilute solution, both $IrBr_6^{---}$ and $IrBr_5(H_2O)^{--}$ form the same $IrBr_6^{--}$ by addition of bromine:

$$IrBr_5(H_2O)^{--} + 1/2\ Br_2 = IrBr_6^{--} + H_2O$$

the total reaction thus being an addition of a bromine atom and not a simple electron transfer.

Madame Delépine-Tard [37] prepared dark red Ir $py_2Br_4^-$, which has the triplet at so high a wavenumber (compared to Ir $py_2Cl_4^-$) that the *cis*-structure is most probable. Besides the Ir-py and the py-bands, this ion exhibits also a genuine redox band at a much higher wavenumber than $IrBr_6^{---}$, as usually found for a decreasing number of halide ligands.

1,2,6-Ir py_3Br_3 is sufficiently soluble [29] in $CHCl_3$ to show the triplet band. The Ir-py band has a larger wavenumber in this isomer than in 1,2,3, as is also found for Ir py_3Cl_3.

Table 3. Absorption bands of iridium(IV) pyridine pentachloro complex.

	λ_n mμ	σ_n K	ε_n	$\delta(-)$ K	$\delta(+)$ K
Ir $pyCl_5^-$	625	16 000	400	900	—
	~503	19 900	2 450	1 300	—
	487	20 500	2 600	—	1 400
	405	24 700	1 500	1 700	2 000
	~344	29 100	~800	—	—
	~267	37 500	4 900	—	—

PYRIDINE- AND CHLORO-IRIDIUM(IV) COMPLEXES

Delépine [27,33] oxidized Ir $pyCl_5^{--}$, *cis*- and *trans*-Ir $py_2Cl_4^-$ to the corresponding iridium(IV) complexes Ir $pyCl_5^-$ and *cis*- and *trans*-Ir py_2Cl_4. The two latter neutral compounds are nearly insoluble in any solvent. Ir $pyCl_5^-$ and *trans*-Ir py_2Cl_4 are even stronger oxidizing agents than bromine [27]. Inamura and Kondo [34] have measured the spectrum of Ir $pyCl_5^-$, which is also given in Table 3 and can be compared with [32] Ir Cl_6^{--}. While the maximum in the blue-green is nearly identical except for a shoulder at 502 mμ of Ir $pyCl_5^-$, the double maximum at 431 and 414 mμ of $IrCl_6^{--}$ is here shifted to 405 mμ and is single. Further, Ir $pyCl_5^-$ has the first shoulder at 625 rather than at 575 mμ. Presumably, all the bands are mainly due to transfer of π-electrons [32]. If the band at 625 mμ of Ir $pyCl_5^-$ was a ligand field band, it would probably be shifted towards the blue; it has rather another, mainly even excited state.

Table 4. Absorption bands of pyridine and pyridinium ion in aqueous solution. Notation as in Table 1.

	Band No.	λ_n mμ	σ_n K	ε_n
py	0	262.8	38 050	2 100
	1	256.6	38 970	3 130
	2	250.7	39 890	2 780
	3	245.1	40 800	1 900
	4	~239	41 840	1 200
py H^+	0	262	38 170	3 600
	1	256	39 060	5 300
	2	251.5	39 760	4 700
	3	~245	40 820	2 900

Table 5. Absorption bands of S. M. Jørgensen's platinum(II) pyridine complexes. Notation as in Table 1.

	Band No.	λ_n mμ	σ_n K	ε_n
$Pt(NH_3)_3py^{++}$	0	267.5	37 380	1 930
	1	260.6	38 380	2 980
	2	254.2	39 340	3 320
	3	248.2	40 290	3 300
	4	~243.5	41 060	2 920
$Pt\,py_4^{++}$	0	267	37 450	8 700
	1	260.2	38 430	13 600
	2	253	39 530	15 300
	3	243 broad	41 150	19 800
$Pt(NH_3)_2py_2^{++}$	0	267.5	37 380	4 650
	1	260.3	38 410	7 800
	2	253.4	39 460	10 300
	3	249	40 160	10 100
trans-$Pt(NH_3)pyCl_2$	0	269.4	37 120	—
	1	262.2	38 140	—
	2	256.6	38 970	—

THE PYRIDINE BANDS AND S.M. JØRGENSEN'S PYRIDINO PLATINUM(II) COMPLEXES

Table 4 gives the absorption bands of pyridine, which are very narrow (δ = 300 K) and are nearly equidistant with σ_c = 920 K. This is evidently a vibrational structure, which is excited by a Franck-Condon mechanism. There is no sign of transitions from vibrationally excited levels of the electronic groundstate, and the bands can thus be numbered 0, 1, ... according to the vibrational quantum number of the excited electronic state. In aqueous solution, there is no sign of weaker bands at smaller wavenumbers than those of the vibrational structure. Thus, the values of ε are:

270	275	280	285	290	300 mμ
150	27	3	0.5	0.1	0.02

The pyridinium ion pyH^+ has bands at nearly the same wavenumbers as py, but they are blurred out ($\delta \sim 500$ K) and have ~70 % higher intensity. In rhodium(III) pyridine complexes, the bands have not much smaller wavenumbers than of py, and nearly the same intensity per pyridine molecule, as seen above. Some iridium(III) complexes have not very much larger bathochromic shifts of the py-bands, while other have very broad py-bands with vanishing vibrational structure at relatively low wavenumbers, σ ~4 000 K below the centre of the bands of py (*cf.* Fig. 5). The latter behaviour of iridium(III) is enhanced by the presence of many anions (Cl^-, Br^-, OH^-) among the ligands and a low number of pyridine molecules, suggesting an especially strong bonding of the pyridine with larger change of the π-electron system of this molecule than in most other complexes.

As discussed in the next paper, the electron transfer, producing the new Ir-py band may be expected to occur also in pyridine complexes of other metals with low oxidation states. Platinum(II) should have possibilities for exhibiting this effect, and therefore the absorption spectra were measured of

some of the pyridine complexes, prepared by S. M. Jørgensen [35]. As seen from Table 5, the py-bands are shifted towards lower wavenumbers to a remarkably low extent, and there is no sign of a Pt-py band in the complexes with neutral ligands, such as py and NH_3. In the chloro complex, there may be distinguished an increasing background, but no certain conclusion can be drawn.

LIGAND FIELD QUANTUM NUMBERS IN COMPLEXES OF TETRAGONAL SYMMETRY

Qualitatively, the order of tetragonal levels [3,16,17] are supported by the measurements of *cis*- and *trans*-isomers of Rh $ox_2Cl_2^{-3}$ and Rh $py_2Cl_4^-$:

$$^1\Gamma_5 \rightarrow {}^1\Gamma_{t_4},\ {}^1\Gamma_{t_5}$$
$$^1\Gamma_4 \nearrow\ {}^1\Gamma_{t_2}$$
$$\qquad\ \searrow\ {}^1\Gamma_{t_5}$$

"copper(II)-like" tetragonality

$$^1\Gamma_5 \rightarrow {}^1\Gamma_{t_4},\ {}^1\Gamma_{t_5}$$
$$^1\Gamma_4 \nearrow\ {}^1\Gamma_{t_5}$$
$$\qquad\ \searrow\ {}^1\Gamma_{t_2}$$

"compressed" tetragonality

The result, derived by Tanabe and Sugano [36] for an electrostatic ligand field acting on pure d^n-configurations, *viz.* that $^1\Gamma_4$ is lower than $^1\Gamma_5$ of $\gamma_5^5\gamma_3$, is highly supported, since $^1\Gamma_{t_4}$ could hardly [3] take the place of $^1\Gamma_{t_2}$ in the left-hand set of levels. But quantitatively, the results reported here cannot be explained without strong interactions between the electron configurations of tetragonal orbitals.

Thus, the ratio between the splitting of $^1\Gamma_{t_2}$ and $^1\Gamma_{t_5}$ and the differences of the cubic ligand field strength of the purely hexa-coordinated complexes should be a constant number [3]. However, this ratio is 0.65 for *trans*-Rh $ox_2Cl_2^{-3}$, but only 0.32 for *trans*-Rh $py_2Cl_4^-$. This is a more fundamental difficulty than the problem of the value [3] of B_2/B_4, which may be solved by use of other d-wavefunctions than the hydrogen-like ones, *e.g.* the Hartree model discussed by Linn Belford [7], and by consideration of the much stronger influence of charge distributions near to the surface of the central ion than the point charges and point dipoles assumed in early electrostatic theory [6]. According to calculations on strong tetragonal fields [3], it is an almost paradoxical fact that $^1\Gamma_{t_4}$ does not decrease much in energy, producing a larger splitting of the second band, if this is caused by $^1\Gamma_5$ (the energy difference between $^1\Gamma_4$ and $^1\Gamma_5$ is explained as the correlation energy between d-electrons expressed in the Racah parameters B and C). An interaction between the two $^1\Gamma_{t_5}$, useful for explaining a part of the splitting of the first band, will further increase the distance between $^1\Gamma_{t_4}$ and the second $^1\Gamma_{t_5}$, which actually have nearly the same energy. Among the tetragonal levels of $\gamma_5^4\gamma_3^2$, the lowest energy will probably be represented by $\gamma^3{}_{t_5}\gamma_{t_4}\gamma^2{}_{t_1}$ in *trans*-Rh $ox_2Cl_2^{-3}$ and $\gamma^3{}_{t_5}\gamma_{t_4}\gamma_{t_3}{}^2$ in *trans*-Rh $py_2Cl_4^-$, both composed of $^1\Gamma_{t_5}$ and $^3\Gamma_{t_5}$. Thus, the second $^1\Gamma_{t_5}$ may be held in place besides $^1\Gamma_{t_4}$ by the interaction from opposite directions. This can also explain, why the second cubic band in some few cases capriciously exhibits tetragonal splitting, *e.g.*[11] Co enta OH^{--}. It may be noticed that the non-diagonal elements of energy between the two $^1\Gamma_5$ of

$\gamma_5^4\gamma_3^2$ and the one $^1\Gamma_5$ of $\gamma_5^5\gamma_3$ are rather important [36], explaining the decrease of the distance between $^1\Gamma_4$ and $^1\Gamma_5$ from the asymptotical strong-field value 16 B to 10—12 B.

In the case of the first tetragonal level $^1\Gamma_{t5}$ the configurations $\gamma_{t5}^3\gamma_{t4}^2\gamma_{t1}$ and $\gamma_{t5}^3\gamma_{t4}^2\gamma_{t3}$ must be highly intermixed [3] at low values of the tetragonality. Actually, the intermixing does not need to produce a splitting, proportional to the tetragonality, but rather to the square. This would explain why the splitting of the first band of *cis*-complexes is not always half as large as in the corresponding *trans*-complex [3]. Figs. 1 and 2 show that the first band of *cis*-Rh $ox_2Cl_2^{-3}$ and *cis*-Rh $py_2Cl_4^-$ definitely do not exhibit splittings amounting to 1 900 and 1 600 K, respectively. Analogously, the first band [1] of $Rh(NH_3)_5I^{++}$ is only split 1 700 K, while the difference between the first band of $Rh(NH_3)_6^{+++}$ and the hypothetical RhI_6^{-3} must be over 15 000 K ($Rh(NH_3)_5I^{++}$ is remarkable by having a negative cubic contribution [3] of the iodide, since the wavenumber of the first band is less than 5/6 of that of $Rh(NH_3)_6^{+++}$). The tetragonality effect, calculated for *trans*-M A_4B_2 is thus only $\lesssim 0.22$ for $Rh(NH_3)_5I^{++}$ and 0.32 for *trans*-Rh $py_2Cl_4^-$ multiplied by the differences in cubic ligand field strengths, while most electrostatic models would have presumed this ratio near to or above 1.

EXPERIMENTAL

The absorption spectra were measured at 25°C on a Cary recording spectrophotometer 11 MS—50. Since many of the measured compounds are so rare, several samples were weighed and transferred to the 1 cm absorption cell, which by weighing was found to contain 3.1 ml. Subsequent dilutions were performed with A. Krogh's syringe-pipettes. The high absorption bands ($\varepsilon_n \sim 10\,000$) were redetermined with solutions of weighed portions ~5 mg in 50 ml or 250 ml measuring flasks.

The ligand field bands ($\varepsilon_n = 10-200$) were measured with solutions, 0.01—0.03 M. The aqueous solutions of chloro-complexes were measured twice within 10 min (as the other complexes) and one and four days later. Only during at least several days were aquation effects observed of complexes with at most four chloride ligands. The complexes Ir $py_2(NH_3)_2Cl_2^+$, Ir $py_2(NH_3)_2Cl^{++}$ and Ir $py(NH_3)_4Cl^{++}$ were measured in 2 M NH_3 without showing changes of spectra, which might be caused by acidity of the amine groups. The titration curves were measured on a Radiometer glass-electrode pH-meter M 22.

It was assumed that the crystalline compounds have the compositions, indicated by M. Delépine:

cis-$K_3[Rh\ ox_2Cl_2],H_2O$
trans-$K_3[Rh\ ox_2Cl_2],4H_2O$
cis-$K[Rh\ py_2Cl_4],H_2O$
trans-$K[Rh\ py_2Cl_4],H_2O$
1,2,6-$Rh\ py_3Cl_3$
$[Rh\ py_2Cl_4]Cl,6H_2O$
$K_3[Ir\ oxCl_4],H_2O$
cis-$K_3[Ir\ ox_2Cl_2],H_2O$ (racemic)
trans-$K_3[Ir\ ox_2Cl_2],6\ H_2O$
$K_3[Ir\ ox_3],4.5\ H_2O$ (racemic)
$K[Ir\ pyCl_5]$
$K_2[Ir\ pyCl_5],3\ H_2O$
cis-$K[Ir\ py_2Cl_4],H_2O$
trans-$K[Ir\ py_2Cl_4],H_2O$
1,2,3-$Ir\ py_3Cl_3$
1,2,6-$Ir\ py_3Cl_3$
$[Ir\ py_4Cl_2]Cl,6\ H_2O$
$Ir\ py_2Cl_3(H_2O),2\ H_2O$ (*cis*, sun)
$Ir\ py_2Cl_3(H_2O)$ (*cis*, autoclave)
$[Ir\ py_2Cl_3((H_2O)],H_2O$ (*trans*)
$[Ir\ py(NH_3)_4Cl]Cl_2,2\ H_2O$
$[Ir\ py_2(NH_3)_2H_2O]Cl_3$
$[Ir\ py_2(NH_3)_2Cl]Cl_2,4\ H_2O$
$[Ir\ py_2(NH_3)_2Cl_2]Cl,H_2O$
$Na_3[Ir\ Br_6],12\ H_2O$
$K_3[Ir\ Br_6],4\ H_2O$
$K_2\ [Ir\ Br_5(H_2O)],H_2O$
$NH_4[Ir\ py_2Br_4],H_2O$
1,2,3-$Ir\ py_3Br_3$
1,2,6-$Ir\ py_3Br_3$

Cf. also the review of the chemistry of iridium, written by Professor M. Delépine in Paul Pascal: *Traité de la Chimie Minerale*, Paris 1932, Vol. 11, p. 443—527.

Acknowledgements. I am very much indebted to Marcel Delépine, Professor of Collège de France for his generous present of the rhodium and iridium complexes, which he has investigated for so many years, and which are so valuable for theoretical reasons because of the robustness of their geometrical isomers. I express also my gratitude to Madame Madeleine Delépine-Tard for the bromo- and bromo-pyridine iridium(III) complexes. Finally, I thank Professor Jannik Bjerrum and Mr. Claus E. Schäffer for valuable discussions, and Mr. Kjeld Rasmussen for assistance with some of the measurements.

REFERENCES

1. Jørgensen, C. Klixbüll, *Acta Chem. Scand.* **10** (1956) 500.
2. Bethe, H. *Ann. Physik* [5] **3** (1929) 133.
3. Ballhausen, C. J. and Jørgensen C. Klixbüll, *Kgl. Danske Videnskab. Selskab, Mat.fys. Medd.* **29** (1955) No. 14.
4. Jordahl, O. M. *Phys. Rev.* **45** (1934) 87.
5. Bjerrum, J., Ballhausen, C. J. and Jørgensen, C. Klixbüll, *Acta Chem. Scand.* **8** (1954) 1275.
6. Ballhausen, C. J. *Kgl. Danske Videnskab. Selskab. Mat.fys. Medd.* **29** (1954) No. 4.
7. Belford, R. L. *Bonding and Spectra of Metal Chelates.* Thesis 1955. University of California (UCRL — 3051).
8. Jørgensen, C. Klixbüll, *Acta Chem. Scand.* **9** (1955) 405.
9. Bjerrum, J. and Jørgensen, C. Klixbüll, *Rec. trav. chim.* **75** (1956) 658.
10. Ballhausen, C. J. *Kgl. Danske Videnskab.Selskab. Mat.fys. Medd.* **29** (1955) No. 8.
11. Jørgensen, C. Klixbüll, *Acta Chem. Scand.* **9** (1955) 1362.
12. Jørgensen, C. Klixbüll, *Acta Chem. Scand.* **10** (1956) 887.
13. Hartmann, H. and Kruse, H. H. *Z. physik. Chem.* **5** (1955) 9.
14. Linhard, M. and Weigel, M. *Z. anorg. Chem.* **266** (1951) 49.
15. Linhard, M. and Weigel, M. *Z. anorg. Chem.* **264** (1951) 321.
16. Orgel, L. E. *J. Chem. Soc.* **1952** 4756.
17. Basolo, F., Ballhausen, C. J. and Bjerrum, J. *Acta Chem. Scand.* **9** (1955) 810.
18. Yamada, S., Nakahara, A., Shimura, Y. and Tsuchida, R. *Bull. Chem. Soc. Japan* **28** (1955) 222.
19. Delépine, M. *Bull. soc. chim. France* **29** (1921) 656.
20. Delépine, M. *Bull. soc. chim. France* **45** (1929) 235.
21. Jørgensen, S. M. *J. prakt. Chem.* **27** (1885) 478.
22. Delépine, M. *Compt. rend.* **236** (1953) 559.
23. Bjerrum, J. and Rasmussen, S. E. *Acta Chem. Scand.* **6** (1952) 1265.
24. Vèzes, M. and Duffour, A. *Bull. soc. chim. France* **5** (1909) 869, 872.
25. Delépine, M. *Ann. Chim.* [9] **19** (1923) 145.
26. Babaeva, A. V. and Mosyagina, M. A. *Doklady Akad. Nauk SSSR* **64** (1949) 823.
27. Delépine, M. *Ann. Chim.* [9] **19** (1923) 5.
28. Delépine, M. *Z. anorg. Chem.* **130** (1927) 222.
29. Delépine, M. *Compt. rend.* **233** (1951) 1156; **233** (1951) 1533; **234** (1952) 1721; **236** (1953) 1713; **238** (1954) 27; **240** (1955) 2468; **248** (1956) 27.
30. Delépine, M. and Pineau, J. *Bull. soc. chim. France* **45** (1929) 228.
31. Delépine, M. *Ann. Chim* [9] **7** (1917) 277, 320.
32. Jørgensen, C. Klixbüll, *Acta Chem. Scand.* **10** (1956) 518.
33. Delépine, M. *Bull. soc. chim. France* **9** (1911) 771.
34. Inamura, Y. and Kondo, Y. *J. Chem. Soc. Japan* **72** (1951) 787, 840.
35. Jørgensen, S. M. *J. prakt. Chem.* **33** (1886) 507, 531; *Z. anorg. Chem.* **25** (1900) 357.
36. Tanabe, Y. and Sugano, S. *J. Phys. Soc. Japan* **9** (1954) 753, 766.
37. Delépine-Tard, M. *Ann. Chim.* [11] **4** (1935) 283, 292.
38. Ballhausen, C. J. and Moffitt, W. *J. Inorg. Nucl. Chem.* **3** (1956) 178.
39. Delépine, M. *Ann. Chim.* [11] **4** (1935) 271.

Received October 12, 1956.

ACTA CHEMICA SCANDINAVICA 11 (1957) 166—178

Complexes of the 4d- and 5d-Groups

IV. Electron Transfer Bands with Special Application to M. Delépine's Complexes and a Transition from Iridium(III) to Pyridine, with some Remarks about Intermediate Coupling in Halide Complexes and the Uranyl Ion

CHR. KLIXBÜLL JØRGENSEN

Chemistry Department A, Technical University of Denmark, Copenhagen, Denmark

In addition to the narrow pyridine-bands, which are only moderately shifted towards lower wavenumbers in complexes, the twenty iridium(III) pyridine complexes prepared by M. Delépine exhibit a new, broad band in the range 29 000—35 000 K. The qualitative molecular orbital diagrams are related to energy levels of the complexes and it is suggested that the broad band is caused by an electron transfer from iridium(III) to the π^*-orbitals of pyridine. The "redox" bands, caused by electron transfer from reducing halide ions to the central ion are discussed. The doublet structure, which Scheibe and Katzin ascribe to the two possible values of J of a free halogen atom, is related to the energy levels of a single electron in a linear ligand field with intermediate coupling. The influence of non-diagonal elements of energy between two levels with the same Ω is emphasized, *e.g.* of a 5f-electron in a linear dioxo complex. Finally, the absorption spectra of α,α'-dipyridyl and o-phenanthroline complexes are investigated; the bands at low wavenumbers of complexes with low oxidation state of the central ion seem analogous to the Ir-py band.

The preceding paper [1] of this series considered the iridium(III) complexes, presented by Professor M. Delépine. In addition to the ligand field transitions (singlet → triplet bands with $\varepsilon \sim 10$ and singlet → singlet bands with $\varepsilon \sim 100$), and the narrow pyridine bands (which are part of a vibrational structure with $\sigma_c \sim 1\,000$ K and $\varepsilon_n \sim 4\,000$ per pyridine molecule), the pyridine complexes exhibit a broad band (with $\varepsilon_n \sim 2\,000$ per pyridine molecule) at lower wavenumber than the genuine pyridine bands. Since neither pyridine-free iridium complexes [2] such as $Ir(NH_3)_5Cl^{++}$ and Ir en_3^{+++}, nor rhodium(III) and platinum(II) pyridine complexes exhibit such a band, it may be denoted by the Ir-py band. Table 1 gives the wavenumbers in Kayser, K = cm^{-1}, of this band and the vibrational structure py 0, py 1, ... of the

Table 1. Wavenumbers of the iridium(III) pyridine electron transfer band Ir py and the pyridine bands py 0, py 1, etc. "b" denotes broad maximum without vibrational structure.

	Ir py	py 0	py 1	py 2	py 3
py	—	38 050	38 970	39 890	40 800
Ir py Cl_5^{--}	30 400	35 800 b	—	—	—
„ 1 day*	31 000	36 400 b	—	—	—
„ „ $+Na_2CO_3$	30 000	35 700 b	—	—	—
„ 3 days*	31 700	37 000 b	—	—	—
„ „ $+Na_2CO_3$	29 400	35 200 b	—	—	—
„ 14 days*	31 900	37 900 b	—	—	—
„ „ $+Na_2CO_3$	29 300	34 600 b	—	—	—
„ „ „ $+HClO_4$	32 500	39 200 b	—	—	—
Ir py $Cl_4(H_2O)^-$ (sun) **	31 500	37 000 b	—	—	—
Ir py Cl_4OH^{--} (sun) **	30 000	35 800 b	—	—	—
Ir py $Cl_4(H_2O)^-$ (warmed) **	31 300	36 900 b	—	—	—
Ir py Cl_4OH^{--} (warmed) **	30 000	36 000 b	—	—	—
cis-Ir $py_2Cl_4^-$	32 000	37 400	38 000	—	—
trans-Ir $py_2Cl_4^-$	31 600	36 600	37 400	—	—
1,2,3-Ir py_3Cl_3	30 600	36 200	37 700	—	—
1,2,6-Ir py_3Cl_3	31 400	37 700 b	—	—	—
Ir $py_4Cl_2^+$	35 200	36 900	37 800	38 900	40 000
cis-Ir $py_2Cl_3(H_2O)$ (sun) [1]	32 800	37 700	38 500	—	—
cis-Ir $py_2Cl_3OH^-$ (sun) [1]	30 700	36 400	37 400	—	—
cis-Ir $py_2Cl_3(H_2O)$ (autoclave) [1]	32 900	37 800	38 600	—	—
cis-Ir $py_2Cl_3OH^-$ (autoclave) [1]	31 500	36 300	37 300	—	—
trans-Ir $py_2Cl_3(H_2O)$	32 600	36 900	37 800	38 500	—
trans-Ir $py_2Cl_3OH^-$	30 400	35 200 b	—	—	—
Ir $py(NH_3)_4Cl^{++}$	34 500	36 900	37 800	38 700	39 800
Ir $py_2(NH_3)_3H_2O^{+3}$	(35 400)	37 100	38 000	39 000	39 900
Ir $py_2(NH_3)_3OH^{++}$	32 900	36 900	38 000	38 800	—
Ir $py_2(NH_3)_3Cl^{++}$	35 000	37 000	37 900	38 800	—
Ir $py_2(NH_3)_2Cl_2^+$	33 900	36 800	37 700	38 500	39 400
Ir $py_2Br_4^-$	31 400	37 000 b	—	—	—
1,2,3-Ir py_3Br_3	29 800	35 200 b	—	—	—
1,2,6-Ir py_3Br_3	31 200	37 200 b	—	—	—

* 0.0004 M $KIrpyCl_5$ in aqueous solution kept at ~25°C. After each measurement, the aquated ions were transformed into the hydroxo forms by making the solution 0.1 M in Na_2CO_3. The reversibility of the aquo-hydroxo equilibria were proven by addition of $HClO_4$, producing 0.2 M free H_3O^+. After 14 days, this reaction was not completely reversible.

** Recently, M. Delépine has sent me two different isomers of KIr py $Cl_4(H_2O)$, prepared from the action of sun-light and by warming of K_2Ir py Cl_5 in aqueous solution.

iridium(III) complexes and of py itself. In some cases of strong bathochromy, the vibrational structure is blurred out to a broad band, denoted by "b" in the Table.

It might be assumed that the Ir-py band is actually some feature of the absorption spectrum of pyridine itself, which has obtained better possibilities of observation in the complexes. Rush and Sponer [3] observed two excited electronic states in gaseous py with 0-vibrational levels at 34 769 K and 38 350 K. Stephenson [4] assumes that ~90 % of the oscillator strength (0.04) of the pyridine bands in a non-polar solvent such as *iso*-octane is due to the 38 350 K-state, but that ~10 % is concentrated in a weaker band towards lower wavenumbers nearer 34 769 K. The latter band is hidden by the higher band near 38 350 K in solvents such as ethanol [4]. This is also the case in

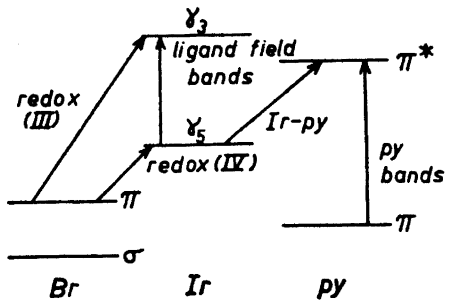


Fig. 1. Relative positions of molecular orbitals in an iridium complex with bromide and pyridine among the ligands. The disagreement of this qualitative picture with the observed energy differences is discussed p. 169. The four types of transitions are indicated:
1. Ligand field transitions within the d-shell (which is, however, intermixed with the orbitals of the ligands by partly covalent bonding).
2. Redox bands, caused by the transfer of an electron from the ligands to the central ion (having smaller wavenumbers in iridium(IV) than in iridium(III) complexes).
3. Ir-py bands, caused by the transfer of an electron from the d-shell to the empty π^*-orbitals of the ligands.
4. py bands, characteristic for the aromatic ligands, caused by internal transitions from π to π^*-orbitals.

aqueous solution [1]. The hypsochromic effect of polar solvents is explained by Stephenson [4] by the interpretation of the weak band as a transfer of a non-bonding electron mainly concentrated on the nitrogen atom, to the anti-bonding π^* orbitals of the heterocyclic ring. When hydrogen bonds stabilize the non-bonding electron, the wavenumber of the transition is increased. The influence of positive central ions will probably be much larger and thus, the Ir-py band can hardly be identified with this transition. Reid [5] has reported triplet levels of gaseous pyridine at 30 876 K (and also at 31 459 and 32 538 K) corresponding to $\varepsilon = 0.10$. The aqueous solution seem less absorbing at these wavenumbers [1]. Reid [5] reported also dubious bands with $\varepsilon \sim 10^{-4}$ of liquid py near 25 500, 26 490, and 27 500 K. However, the presence of other heterocyclic compounds *, overtones of infra-red bands etc. may explain this observation. It might be argued that the large extent of intermediate coupling in iridium(III) [2] ($k\zeta_{5d} = 2\,000$ K) may explain a high intensity of singlet-triplet transitions in pyridine by intermixing with the orbitals of the central ion. However, the present author believes that the observed effect is too strong for this type of explanation, and that its absence in platinum(II) complexes, where the intensity ratios in $PtCl_4^{--}$ and $PtBr_4^{--}$ also imply $k\zeta_{5d} = 2\,000$ K, is pertinent.

Thus, the Ir-py band must rather be ascribed to an electron transfer process. Since pyridine is not so reducing as Br^-, and since the "redox" bands of $IrBr_6^{-3}$ occur at 37 000 and 41 500 K and of $IrCl_6^{-3}$ at 48 500 K (see Table 2), while the Ir-py bands are situated in the range 29 000—35 000 K, it can be concluded

* Recently, Brealey [27] has demonstrated that the bands 29 000—33 000 K are caused by one part in 150 000 of pyrazine, and thus, no triplet levels are known of pyridine.

that the electron is transferred from the central ion to the pyridine ligand, the opposite direction of the usual redox bands. This might be visualized in a diagram of the relative energy of molecular orbitals such as Fig. 1. However, this diagram leads to a paradoxical contradiction, if applied to the energy difference between the ground level and the excited level of the Ir-py band. If a complex with pyridine and bromide among the ligands is considered with an energy difference Δ (also called $(E_1—E_2)$ or 10 Dq) between the γ_3- and γ_5-orbital of the 5d-shell equal to 25 000 K, it is concluded from the redox bands (Table 2) of both $IrBr_6^{--}$ (where the electron is excited to fill the γ_5-hole) and $IrBr_6^{-3}$ (where the electron is excited to the γ_3-orbital) that the highest orbital of Br^- is $\sim$ 15 000 K below γ_5. It is easily recognized that the highest filled π-orbital of py must have an energy at least 15 000 K below Br^- (*cf.* the redox spectrum [1] of Rh $py_2Cl_4^-$). Thus, the excited π^*-orbital of py, which is 38 000 K above the groundlevel, will be only $\sim$8 000 K above γ_5 of the central ion, *i.e.* the Ir-py band should have a wavenumber at least 20 000 K below the observed. This trend of thought leads generally to difficulties for all complexes of ligands, which have empty orbitals not much more than 50 000 K above their highest occupied orbital. While the high ultraviolet absorption [6] of most *o*-phenanthroline complexes undoubtedly represents a bathochromic shift of the aromatic absorption bands of the free ligand (*cf.* Table 1) the high band of Fe $phen_3^{++}$ at 19 600 K is perhaps analogous to the Ir-py band, as discussed in the last section. However, these cases do not seem very common; in contrast to $Fe(CN)_6^{-3}$, which may have redox bands [7] at 23 900 and 32 900 K, $Fe(CN)_6^{-4}$ does not exhibit such strong bands below 40 000 K. It may be questioned, if CN^- (which is itself practically non-absorbing [7] below 50 000 K) actually has π^*-orbitals at much lower energies than CO or N_2.

The failure of the qualitative diagram of molecular orbitals, Fig. 1, is of course that it does not take into account the change of equilibria positions of the ligands in the excited levels and the reciprocal influence of the energies of the molecular orbitals. Actually, only energy levels of the total system have physical significance; the distribution of the energy on the single orbitals is a matter of choice, if it cannot be assumed that the ionization potentials are a first order approximation to the negative orbital energies, *i.e.* that the other orbitals re-arrange but slightly during the ionization process. In the case of the Ir-py band, it must not be presumed that the energy of π^* in pyridine is independent of the existence of a hole in the elsewise filled π-orbitals. For this reason, the Ir-py band has higher wavenumber than implied from the energy levels of pyridine.

The former difficulty, the excitation according to the Franck-Condon principle [8] of vibrations, is probably even more important. Thus, an electron transfer process necessitates often supply of energy in both directions, which act as an activation energy to counteract the unfavourable interatomic distances of the excited system, compared to the vibrational groundstate of the excited system [9]. The reactions

$$Ir^{III}py\ Cl_5^{--} + 30\,400\ K \rightarrow Ir^{IV}py^*Cl_5^{--}$$
$$Ir^{IV}py\ Cl_5^{-} + 20\,000\ K \rightarrow Ir^{III}pyCl^*Cl_4^{-}$$

Table 2. "Redox" electron transfer bands of halide complexes. σ_n is the wavenumber in K (= cm^{-1}) and ε_n the molar extinction coefficient of each maximum and δ (—) the halfwidth towards smaller wavenumbers.

		σ_n	ε_n	$\delta(-)$
I_{aq}^-		44 200	13 100	2 200
	(Ref. 11)	52 000	—	—
$Cr(NH_3)_5I^{++}$	(Ref. 13)	34 400	4 000	—
	,,	45 000	10 000	—
$Co(NH_3)_5Cl^{++}$	,,	36 500	450	—
	,,	43 960	20 500	—
$Co(NH_3)_5Br^{++}$	,,	31 800	820	—
	,,	39 450	18 500	—
$Co(NH_3)_5I^{++}$	,,	26 110	2 700	—
	,,	34 930	16 500	—
$Rh(NH_3)_5Br^{++}$		40 600	950	—
		~50 000	15 000	—
$Rh(NH_3)_5I^{++}$		36 000	3 200	2 500
		44 300	20 000	2 300
$RhCl_6^{---}$		41 000	21 000	4 000
$RhBr_6^{---}$		28 600	4 000	1 900
		38 600	18 000	2 900
$IrCl_6^{---}$		48 500	28 000	4 100
$IrBr_6^{---}$	(Ref. 1)	37 000	12 000	2 200
	,,	41 500	20 000	—
$PtCl_6^{--}$	(Ref. 7)	38 200	24 500	2 700
$PtBr_6^{--}$	,,	27 500	7 400	2 200
	,,	32 200	17 800	2 800
PtI_6^{--}	,,	20 250	12 800	1 700
	,,	22 400	8 300	—
	,,	29 150	17 700	1 600
$IrCl_6^{--}$	,,	17 400	460	1 200
	,,	20 450	3 200	900
	,,	23 200	2 540	—
	,,	24 200	2 480	—
$IrBr_6^{--}$	,,	13 600	1 550	600
	,,	14 300	2 050	—
	,,	14 800	2 100	—
	,,	17 200	3 070	500
	,,	18 400	1 500	—
	,,	19 600	1 800	800

do not give any immediate evidence on the relative stability of the oxidation states +3 and +4 of iridium. They may suggest Franck-Condon activations of the order of magnitude 10 000 K.

REDOX BANDS OF METAL HALIDE COMPLEXES

Scheibe [10,11] assumed that the strong absorption bands in the far ultraviolet of Cl^-, Br^-, and I^- in aqueous solution is due to the photochemical reaction *e.g.*

$$Br_{aq}^- + 54\,000\ K \rightarrow Br_{aq} + e_{aq}^-$$

where the solvated electron of course is unstable towards formation of molecular hydrogen etc. Since the corresponding reaction *in vacuo* necessitates [12]

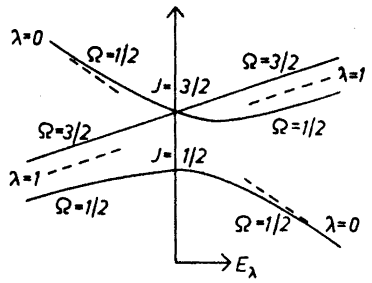


Fig. 2. The energy levels of a p-electron in a linear ligand field as function of the parameter E_λ. The intermediate coupling splits the levels with definite values of λ into two (for $\lambda > 0$) with different values of Ω (analogous to J of the gaseous ion). Levels with the same Ω interact, forming hyperbolic curves in the diagram.

only 3.56 eV, *i.e.* 27 700 K, Br^- must be stabilized considerably better by solvation than e^-.

If the halide ion is near a metal ion with larger electron affinity than water, it is natural to assume a smaller energy necessary for the transfer of an electron to the metal ion. Thus, the strong absorption will be shifted more towards lower wavenumbers, the more oxidizing the metal ion. This assumption was applied by Linhard and Weigel [13,14] to the halide pentammine cobalt(III) and chromium(III) complexes. If the electron shall penetrate the first coordination sphere, then the bathochromic shift of the electron transfer band will be smaller, as found for the ion pairs [15] of halide and $Co(NH_3)_6^{+++}$, even though the effect is stronger [16] in solid $Co(NH_3)_6I_3$, where the second ligand field band is masked.

Scheibe [10,11] found further that the absorption band of I^-_{aq} is double with maxima at 44 500 K and 52 000 K, while the splitting is smaller in Br^-_{aq} and not detectable in Cl^-_{aq}. This was ascribed to the two possible states $^2P_{3/2}$ of lowest and $^2P_{1/2}$ of higher energy of the free halogen atom with the outer electron configuration s^2p^5. This energy difference is for the gaseous atoms 881 K for Cl, 3 685 K for Br and 7 603 K for I, corresponding to increasing values of $3/2\ \zeta_{np}$ for n = 3, 4, 5. Katzin [17] has recently continued this study and found that a large number of iodide complexes have two absorption bands in the near ultraviolet with a wavenumber difference 6 000—8 000 K, while the similar values for bromide complexes are 3 000—7 000 K.

The present author does not doubt that most of these splitting effects* are caused by intermediate coupling. However, it is not very probable that the excited levels resemble the states with $J = 3/2$ and $1/2$ of the atomic spectroscopy very much. It is seen from Table 2 that only one broad redox band is observed of $IrCl_6^{-3}$ and $PtCl_6^{-2}$, while two bands are observed of $IrBr_6^{-3}$ and $PtBr_6^{-2}$ with the intensity ratio $\sim 1:2$, arranged according to increasing wavenumber. This is not quite expected in Scheibe's theory, since the de-

* However, most crystalline alkali metal halides [36] have from four to six absorption bands in the range 45—90 000 K and hence, the nature of the electronic states is not easily recognized.

generacy numbers of the levels are 4 and 2. Generally, the first band of bromide and iodide complexes is often remarkably weak.

However, it can be theoretically justified that the degeneracy numbers of the two first levels may be 2 and 2, while a third level, also with 2, may give rise to an even stronger absorption band at higher wavenumbers than usually observed. If the six halide ions are not very strongly perturbed by the central ion, they can be treated as independent of each other, placed in a linear ligand field from the positive central ion. If the ligand contains an electron with the angular momentum quantum number l, and if the effects of intermediate coupling are neglected, $l+1$ equidistant energy levels occur with the quantum number $\lambda = l, l-1, l-2, \ldots, 0$. The first-order effect of intermediate coupling will be to split all the levels with $\lambda > 0$ in two with the quantum number $\Omega = \lambda + \frac{1}{2}$ and $\lambda - \frac{1}{2}$ and with the energy difference $\lambda\zeta_{nl}$.

If we denote the energy difference between the levels $\lambda+1$ and λ by E_λ, E_λ will be positive when the linear field is caused by a positive charge and negative, when the linear field is supplied by negative ligands. For a p-electron with $l = 1$, this has a simple physical explanation: If the charge is placed on the z-axis of a Cartesian co-ordinate system, $\lambda = 0$ is represented by the p_z orbital (of which the potential energy is decreased by a positive charge) and $\lambda = 1$ is represented by the two equivalent orbitals p_x and p_y, concentrated in the plane perpendicular to the linear field. In a ligand field of tetragonal symmetry, supplied by four square-planar ligands, the opposite behaviour of p_z will occur.

If E_λ is not much larger than ζ_{nl}, the two levels with equal values of Ω (if less than $l + \frac{1}{2}$) will interact, forming a hyperbola in the energy diagram as function of E_λ. Fig. 2 gives the result for a p-electron and Fig. 3 for a f-electron. In the former case, the diagonal elements of energy, corresponding to the asymptotes of the hyperbolae, are:

$$\begin{aligned} &\lambda = 1,\ \Omega = 3/2: \quad 1/3\, E_\lambda + 1/2\zeta_{np} \\ &\lambda = 1,\ \Omega = 1/2: \quad 1/3\, E_\lambda - 1/2\zeta_{np} \\ &\lambda = 0,\ \Omega = 1/2: -2/3\, E_\lambda \end{aligned} \tag{1}$$

while the square of the non-diagonal element between the two latter levels is $1/2\ \zeta_{np}^2$. Thus the two levels with $\Omega = \frac{1}{2}$ cannot have a smaller distance than two times the non-diagonal element, *viz.* $\sqrt{2}\,\zeta_{np}$. In the general case, the diagonal elements of energy will be

$$\begin{aligned} &\Omega = \lambda + \tfrac{1}{2}: \left(\lambda - \frac{l(l+1)}{2l+1}\right) E_\lambda + \frac{\lambda}{2}\,\zeta_{nl} \\ &\Omega = \lambda - \tfrac{1}{2}: \left(\lambda - \frac{l(l+1)}{2l+1}\right) E_\lambda - \frac{\lambda}{2}\,\zeta_{nl} \end{aligned} \tag{2}$$

while the square of the non-diagonal element between two levels with the same Ω will be

$$\tfrac{1}{4}(l + \tfrac{1}{2} + \Omega)\ (l + \tfrac{1}{2} - \Omega)\ \zeta_{nl}^2 \tag{3}$$

The slopes of the lines in the energy diagram (Figs. 2 and 3) for $E_\lambda \to 0$ are a linear function of Ω. For the upper level with $J = l + \frac{1}{2}$ are the first-order splittings

$$E = \frac{2l}{2l+1}\left(\Omega - \frac{l+1}{2}\right) E_\lambda + \frac{l}{2}\zeta_{nl} \tag{4}$$

while for the lower atomic level with $J = l - \frac{1}{2}$, the first-order energies are

$$E = \frac{2l+2}{2l+1}\left(\Omega - \frac{l}{2}\right) E_\lambda - \frac{l+1}{2}\zeta_{nl} \tag{5}$$

In the case of an electron transfer, where a hole is created in a p-shell, and only one significant energy level occurs in the system which has accepted the electron, one would thus expect three absorption bands, arranged according to increasing wavenumbers:

$$(\lambda = 1, \Omega = 3/2) \quad (\lambda = 1, \Omega = \tfrac{1}{2}) \quad (\lambda = 0, \Omega = \tfrac{1}{2}).$$

The distance between the two first bands will be somewhat less than ζ_{nl}, while the distance between the two last bands will be slightly larger than $E_\lambda - \frac{1}{2}\zeta_{nl}$. The two first bands are due to transfer of π-electrons ($\lambda = 1$), if the intermixing of the two levels with $\Omega = \frac{1}{2}$ is neglected, and the last band is due to transfer of a σ-electron ($\lambda = 0$).

Orgel [9] assumes that the two bands, observed of halide pentammine cobalt(III) complexes [13,14], which have highly different intensities (*cf.* Table 2) are due to transfer of π- and σ-electrons, respectively. These bands are also observed of $Rh(NH_3)_5Br^{++}$ and $Rh(NH_3)_5I^{++}$ by the present author, but are perhaps a special feature of d^6-systems, since they seem to be absent in halide chromium(III) pentammines. The weak bands might be introduced by intermixing with ligand field bands by vibrational interaction with odd electron transfer states *. However, it is also possible that they actually represent the $\Omega = 3/2$ bands with accidentally low intensity. The similar problem has been treated by Mulliken [18,19] for halogen compounds and the halogen molecules [20]. Mulliken [19] found the distance between the two bands $^2\Pi_{3/2}$ and $^2\Pi_{1/2}$ (highest) equal to 5 570 K in HI, 4 915 K in CH_3I, 4 650 K in C_2H_5I, 3 457 K in HBr, and 3 070 K in CH_3Br. The intensity ratios were > 10 in the chlorides, ~4 in the bromides and ~2 in the iodides in favour of the second band, resembling the behaviour of halide pentammine-d^6-complexes. The partly σ-character of the second band might have been used as an argument for increased intensity, if it was higher for iodide than for chloride complexes.

* The effective value E_{af} of the non-diagonal element of energy between even and odd levels, to which the forbidden (with the oscillator strength P_f and wavenumber σ_f) and allowed (P_a,σ_a) transitions occur, can be defined:

$$\frac{P_f}{P_a} = \frac{\sigma_f}{\sigma_a} \cdot \frac{E_{af}^2}{(\sigma_f - \sigma_a)^2}.$$

For a large number of $3d^n$-, $4d^n$-, $5d^n$-, and $5f^n$-transitions, E_{af} is remarkably invariant in the range 1 500—2 500 K. The physical significance of E_{af} is the product of the amplitude of the odd vibrations in atomic units (~0.1) and an electrostatic interaction energy of the order of magnitude 20 000 K, as discussed for the case of benzene by Murrell and Pople [35].

The present author is not inclined to believe that the σ-band can occur at lower wavenumbers than the absorption band of the free halide ion in aqueous solution. Even though the strongest band of $Rh(NH_3)_5I^{++}$ has nearly the same wavenumber as the first band of I^- (Table 2), it cannot simply be argued that the transfer of electrons will occur to the solvent, if the metal ion has no larger electron affinity than water. The iodide ion must be stabilized by its bonding to the rhodium ion (even though the partial contribution to the ligand field strength is remarkably negative [1]) while the excited state, the free I, hardly can be so much stabilized. Thus, the anti-bonding character of the excited state will tend to increase the wavenumber of the σ-band in all cases.

From group-theoretical reasons, it is difficult to understand, why the redox spectra of hexahalide complexes do not contain much more than two bands. The 36 states of the resonance structure of five halide ions and one halogen atom (s^2p^5) might give 18 levels, if only one state is possible of the central ion + the added electron. If q states are possible in the latter system, 18 q levels are expected, if the Kramers' degeneracy does not allow 36 q levels (as is the case, if an even number of electrons occur in totality). Even though $ReCl_6^{--}$ exhibits [21,22] three bands and $ReBr_6^{--}$ six bands, such a complicated behaviour has never been reported. However, the "one-ligand excitation" model of the linear ligand field above seems to develop splittings for very large electron affinities of the central ion, *e.g.* the visible redox spectra of $IrCl_6^{--}$ and $IrBr_6^{--}$, which exhibit, respectively, four and six bands (Table 2) while in this case, q = 1 for the excited central ion configuration γ_5^6. If the symmetry of the complex is restricted to the cubic O_h, only four π-levels and three σ-levels are predicted [2]. If the Laporte-forbidden transitions to even levels are neglected, only two π- and one σ-absorption bands are expected of a d^5-system, while a d^6-system with q = 4 ($\gamma_5^6\gamma_3$) should exhibit the double number each of singlet and triplet levels. However, when intermediate coupling is considered, more bands are predicted. Thus, eight odd levels ($2\Gamma_6$, $2\Gamma_7$ and $4\Gamma_8$, of which the last four may be split by ligand fields of lower symmetry) occur, when a π-electron is transferred to the empty γ_3-shell of a d^6-system. It may be reasonable to conclude that the "one-ligand excitation" model seems satisfactory for redox spectra at not too low wavenumbers, *e.g.* of $IrBr_6^{-3}$ or $PtBr_6^{--}$, while systems with a large tendency of the electron transfer, *e.g.* PtI_6^{--}, may begin to exhibit some of the many bands predicted from group theory, *i.e.* the exchange integrals between different halide ligands begin to be important.

Table 3. The vibrational structures of the two weak uranyl band groups. Absorption spectra of 0.2 M down to 0.002 M $UO_2(ClO_4)_2$ in 0.1 M $HClO_4$.

Tentative $\Delta\nu$	λ_n mμ	σ_n K	ε_n	Tentative $\Delta\nu$	λ_n mμ	σ_n K	ε_n
−1	486.5	20 550	0.3	−1	(350.5)	28 530	4
0	468.5	21 340	1.1	0	342	29 240	8
1	454	22 030	1.6	1	335	29 850	16
2	440	22 730	3.2	2	326	30 670	32
3	425	23 530	5.9	3	318	31 450	43
4	413.5	24 180	7.2	4	(311)	32 150	50
5	403	24 810	6.4				
6	(390)	25 640	4.6				
7	(380)	26 320	2.7				

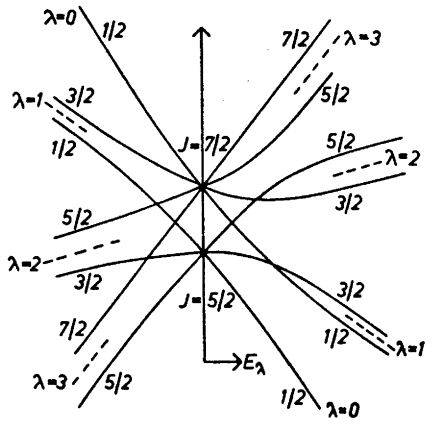


Fig. 3. The energy levels of a f-electron in a linear ligand field as function of the parameter E_λ. The numbers indicate the value of Ω for the individual levels. The oxygen atoms in dioxo actinide ions produce a negative value of E_λ.

THE DIOXO ACTINIDE IONS AND 5f-ELECTRONS IN LINEAR LIGAND FIELDS

The uranyl ion UO_2^{++} has no partly filled shell, and thus all electronic absorption bands must be due to electron transfer. Besides the well known group of bands in the range 20 500—26 300 K, a similar group with vibrational structure is observed in the range 28 500—32 200 K (see Table 3). The molar extinction coefficients ε_n of these bands are remarkably low, ~6 and ~10 (when corrected for the raising background). Besides the two band groups, there is only a monotoneously increasing absorption in the ultraviolet ($\varepsilon = 60$ at 300, 135 at 280, 300 at 260, 720 at 240 and 1 300 at 220 mμ).

The two band-groups are undoubtedly Laporte-forbidden and can be ascribed [23] to the transfer of an odd electron (*e.g.* with $\lambda = 1$, which is not σ-bonding as those with $\lambda = 0$) from the ligands to the empty 5f-shell of the central ion. Eisenstein and Pryce [24] investigate the dioxo actinide ions with one 5f-electron, *viz.* UO_2^{+} and NpO_2^{++}, and assume a large value of $E_\lambda \sim -15\,000$ K of eqn. 2. These authors did not discuss the influence of the non-diagonal elements of intermediate coupling (eqn. 3), which is rather conspicuous (*cf.* Fig. 3). While ζ_{5f} in trivalent and quadrivalent uranium [23] is ~1 600 K, it cannot easily be decided, if ζ_{5f} of UO_2^{++} has the value ~3 000 K expected [25] for gaseous U^{6+}, or if the partly covalent bonding [26] has decreased the value much.* Generally, it cannot be expected that the intermixing with the orbitals of the ligands conserves the equidistant splitting of the λ-levels, as expressed in eqn. 2. Rather, the distance between $\lambda = 0$ and $\lambda = 1$ may be much lar-

* Professor B. Weinstock, Argonne, has kindly informed me that NpF_6 exhibits a group of bands at 7 300—9 500 K and hence the ligand field splittings are small compared to $\zeta_{5f} \approx 2\,400$ K. Weinstock will later discuss the absorption spectrum of PuF_6, which has a sub-level $\Gamma_J = \Gamma_1$ as a rather isolated groundstate [27], corresponding to $^3H_4$ as weak field asymptote and γ_3^3 as strong field asymptote.

ger than between $\lambda = 2$ and $\lambda = 3$. In the latter case, Fig. 3 will be distorted (the left-hand side with negative E_λ applies to UO_2^{++}) such that the three lowest levels would have $\Omega = 5/2$, 3/2, and 7/2, with the subsequent distances $\sim 1/2$ and $\sim 5/2\ \zeta_{nf}$.

Since neither E_λ nor ζ_{5f} is known *a priori* for UO_2^{++}, Fig. 3 allows many possible explanations of the existence of the two electronic states with a distance ~7 900 K (Table 3). If E_λ is small, then the observed distance is simply the atomic splitting $\frac{7}{2}\ \zeta_{5f}$. This cannot be excluded, if 5f-electrons actually do not take any part in the covalent bonding.* However, it is more probable that E_λ is larger, and that the lowest level (which is fluorescent) is that with $\Omega = 5/2$. Then, the next electronic level might either have $\Omega = 7/2$ (with less than 3 ζ_{5f} higher energy) or $\Omega = 3/2$ (the energy difference then mainly being composed of E_λ).

Eisenstein and Pryce [24] assume that the weak bands of NpO_2^{++} with vibrational structure in the range 15 400—23 800 K are caused by an internal 5f-transition from $\Omega = 5/2$ to the two levels of $\lambda = 2$. However, the present author assumes as an alternative possibility that the weak vibrational bands of UO_2^{++}, NpO_2^{++}, PuO_2^{++}, and AmO_2^{++} (which must not be confused with the high, extremely narrow bands occurring in systems with at least two 5f-electrons in the groundstate [23]) have a common cause, *viz.* the transfer of an electron to the 5f-shell of the central ion. The wavenumbers decrease with increasing electron affinity of the central ion, analogous to the ordinary redox bands, and seem very high in the species MO_2^+.

ABSORPTION SPECTRA OF α,α'-DIPYRIDYL AND o-PHENANTHROLINE COMPLEXES

The complexes of α,α'-dipyridyl and o-phenanthroline have much more complicated absorption spectra than the pyridine iridium(III) complexes discussed above. Especially, low oxidation states of metals seem stabilized and form strongly coloured complexes with the heterocyclic diimines: red iron(II), red ruthenium(II), brown copper(I)[28], black vanadium(—I)[29], blue vanadium(0)[30], purple vanadium(I)[30], green vanadium(II)[30], blue chromium(I)[31] and purple chromium(II)[31].

Presumably, these strong absorption bands in the visible are caused by electron transfer from the central ion to the ligand, analogous to the Ir-py band studied here. The ground-state of the purplish red Fe dip_3^{++} and red-orange Fe $phen_3^{++}$ has been described [32] in terms of Pauling's directed valence bonds as a resonance of three π-bonds (in the direction towards the ligands) besides the usual d^2sp^3-hybridization. As discussed by Orgel [9], this is more adequately described by the molecular orbital theory, assuming increased

* Recently, Coulson and Lester [38] proposed that 6f-rather than 5f-electrons are involved in the partly covalent bonding of actinide complexes. Generally, the group-theoretical requirements of molecular orbitals (given for f-electrons by Eisenstein [39]) refer to the angular part of the wave-function only, while the radial function can be chosen rather arbitrarily. Hence, the partly covalent bonding can often be described by a complicated intermixing of empty and filled orbitals from the central ion and the ligands, resulting in the current reconciliation of ligand field and molecular orbital theory [40].

energy of the empty γ_3-sub-shell by formation of π-antibonding linear combinations with the empty orbitals of the ligands. Recently, Schläfer [33] has applied an electrostatic perturbation calculation to the energy levels of α,α'-dipyridyl, analogous to the considerations of Belford [34] for acetylacetonate. Even though it is interesting to note that a certain group of bands are identically shifted for all mono- and tris-dipyridyl complexes of divalent metal ions, Schläfer's theory [33] appears somewhat too simplified in the case of *o*-phenanthroline. These compounds have a very irregular vibrational structure of the bands, indicating strong coupling between electronic and vibrational states. Furthermore, while the pyridine complexes have only one conspicuous σ_c, several of the 60 characteristic frequencies seem to occur in *o*-phenanthroline, since no equidistant band groups can be observed.

The following bands are observed of some representative complexes in the range 12 500—50 000 K, with approximative values of ε_n, and shoulders in parenthesis.

dip		dip H^+		Fe dip_3^{++}		Ni dip_3^{++}	
(31 100)	1 000	33 200	15 700	19 100	8 600	24—30 000 increase	
35 600	12 800	(37 000)	4 000	(20 200)	7 800	32 400	40 000
42 900	10 700	41 600	8 000	(24 100)	2 400	33 800	42 000
				(25 800)	3 700	40 800	32 000
				28 500	6 500		
				33 500	70 000		
				(34 500)	60 000		
				40 500	32 000		
phen		phen H^+		Fe $phen_3^{++}$		Ni $phen_3^{++}$	
30 900	750	(33 300)	7 000	19 600	11 200	24—28 000 increase	
(32 300)	1 200	36 200	29 000	(21 000)	9 500	29 100	1 500
(34 600)	9 200	36 800	31 000	(22 800)	7 300	30 600	2 400]
37 800	28 000	45 500	36 000	31 200	3 300	(32 000)	3 300
44 000	40 000	48 700	38 000	(34 400)	20 000	34 000	28 000
				37 600	67 000	37 100	78 000
				44 400	64 000	44 000	93 000

The first five bands * of Fe dip_3^{++} and at least the three first bands of Fe $phen_3^{++}$ can thus be ascribed to a Laporte-allowed electron transfer from the γ_5-orbitals of iron(II) to the heterocyclic π^*-orbitals. They are very far removed from being internal d^n-transitions in the central ion, as also contradicted by the highly different band structure of the dip and the phen complex. The other bands can mainly be identified as bands of the free ligand, which are shifted and partly split during the influence of H^+, Fe^{++}, and Ni^{++}. However, many remarkable features are still unexplained: the slowly increasing absorption in the near ultraviolet of the nickel(II) complexes may be interpreted as a similar electron transfer or as a shift of the first shoulder of dip, not mentioned by Schläfer [33]. The narrow bands of moderate intensity of Ni $phen_3^{++}$ were found by Roberts and Field [6], who reported too many bands, because the absorption of an aqueous solution of 3 phen was subtracted from

* Busch and Bailar [32] prepared the diamagnetic tris (biacetylbismethylimine)iron(II) iodide $Fe(C_6H_{12}N_2)_3I_2$, which contains no heterocyclic rings. The bands reported at 17 600 K (ε=10 700) and 29 000 K (ε = 1 200) are undoubtedly of the Ir-py type, while the band at 44 000 K (E = 38 100) is under suspicion for being simply the iodide band.

that of Ni $phen_3^{++}$. They seem to be a general feature of all phen-complexes, comparable to the first, weak band of benzene [35]. The higher oxidation state iron(III) has in the blue Fe $phen_3^{++}$ (a band at 16 800 K, $\varepsilon = 750$) and Fe dip_3^{++} (16 300 K) much less colour. The broad band may be due to electron transfer from the ligands to the central ion, and may be compared to the relatively weak first band [7] of $IrCl_6^{--}$.

Acknowledgements. I am very much indebted to Professor Marcel Delépine of Collège de France for the valuable samples of iridium(III) and rhodium(III) complexes, which have made the observation of the Ir-py band possible. Further, I thank Professor Jannik Bjerrum for his kind interest in the work.

REFERENCES

1. Jørgensen, C. Klixbüll, *Acta Chem. Scand.* **11** (1957) 151.
2. Jørgensen, C. Klixbüll, *Acta Chem. Scand.* **10** (1956) 500.
3. Rush, J. H. and Sponer, H. *J. Chem. Phys.* **20** (1952) 1847.
4. Stephenson, H. P. *J. Chem. Phys.* **22** (1954) 1077.
5. Reid, C. *J. Chem. Phys.* **18** (1950) 1673.
6. Roberts, G. L. and Field, F. H. *J. Am. Chem. Soc.* **72** (1950) 4232.
7. Jørgensen, C. Klixbüll, *Acta Chem. Scand.* **10** (1956) 518.
8. Herzberg, G. *Spectra of Di-atomic Molecules.* 2. ed. 1950.
9. Orgel, L. E. *Reports on the Xth Solvay Conference*, Bruxelles, May 1956.
10. Franck, J. and Scheibe, G. *Z. physik. Chem.* **A139** (1928) 22.
11. Scheibe, G. *Z. physik. Chem.* **B5** (1929) 355.
12. Latimer, W. M. *Oxidation Potentials.* 2. ed. New York, 1952.
13. Linhard, M. and Weigel, M. *Z. anorg. Chem.* **266** (1951) 49.
14. Linhard, M., Siebert, H. and Weigel, M. *Z. anorg. Chem.* **278** (1955) 287.
15. Linhard, M. *Z. Elektrochem.* **50** (1944) 224.
16. Kondo, Y. *Bull. Chem. Soc. Japan* **28** (1955) 497.
17. Katzin, L. I. *J. Chem. Phys.* **23** (1955) 2055.
18. Mulliken, R. S. *J. Chem. Phys.* **8** (1940) 382.
19. Mulliken, R. S. *Phys. Rev.* **61** (1942) 277.
20. Mulliken, R. S. *Phys. Rev.* **57** (1940) 500.
21. Jørgensen, C. Klixbüll, *Acta Chem. Scand.* **9** (1955) 710.
22. Rulfs, C. L. and Meyer, R. J. *J. Am. Chem. Soc.* **77** (1955) 4505.
23. Jørgensen, C. Klixbüll, *Kgl. Danske Videnskab. Selskab Mat.fys.Medd.* **29** (1955) Nos. 7 and 11.
24. Eisenstein, J. C. and Pryce, M. H. L. *Proc. Roy. Soc. London* **A229** (1955) 20.
25. Jørgensen, C. Klixbüll, *J. Inorg. Nucl. Chem.* **1** (1955) 301.
26. Owen, J. *Proc. Roy. Soc. London* **A227** (1955) 183.
27. Brealey, G. J. *J. Chem. Phys.* **24** (1956) 571.
28. Pflaum, R. T. and Brandt, W. W. *J. Am. Chem. Soc.* **77** (1955) 2019.
29. Herzog, S. and Taube, R. *Naturwiss.* **43** (1956) 349.
30. Herzog, S. *Naturwiss.* **43** (1956) 35.
31. Hein, F. and Herzog, S. *Z. anorg. Chem.* **267** (1952) 337.
32. Busch, D. H. and Bailar, J. C. *J. Am. Chem. Soc.* **78** (1956) 1137.
33. Schläfer, H. L. *Z. physik. Chem.* **8** (1956) 373.
34. Belford, R. L. *Bonding and Spectra of Metal Chelates* Thesis 1955. University of California, UCRL-3051.
35. Murrell, J. N. and Pople, J. A. *Proc. Phys. Soc. London* **A69** (1956) 245.
36. Landolt-Börnstein. Tabelle . . . 6. Aufl., I. Band, 4. Teil. Kristalle. Springer Verlag, 1955.
37. Weinstock, B. and Malm, J. G. *J. Inorg. Nucl. Chem.* **2** (1956) 380.
38. Coulson, C. A. and Lester, G. R. *J. Chem. Soc.* **1956** 3650.
39. Eisenstein, J. C. *J. Chem. Phys.* **25** (1956) 142.
40. Jørgensen, C. Klixbüll, *Energy Levels of Complexes and Gaseous Ions.* Gjellerups Forlag, Copenhagen, 1957.

Received October 12, 1956.

ACTA CHEMICA SCANDINAVICA 11 (1957) 179—206

Short Communications

Ion Exchange of Quaternary Salts

A. BERGGREN and C. O. BJÖRLING

Laboratories of Pharmacia Ltd., Uppsala, Sweden

It is well known that organic ions of a high molecular weight are difficult to elute once they are taken up by a cation exchange resin containing a "normal" network. The ion exchange process seems not to be totally reversible (*e. g.* Refs.[1-4]). Lately, several authors have used cation exchange resins with a low percentage of crosslinking, (*e. g.* Refs.[5-7]). They could elute tertiary alkaloidal cations from the resins with alcoholic ammonia. Büchi and Furrer [5] also tried 10 % hydrochloric acid for the elution of quinine, but very large eluates were necessary.

We have repeated their experiments, using Dowex 50-X1, a cation exchange resin with 1 % crosslinking. 200—300 mg of quinine sulphate was applied to a column (10 × 150 mm). All the quinine was taken up and could be quantitatively eluted with 25 ml of 10 % ammonia in 60 % alcohol. However, a full recovery was also obtained with 75 ml of 2 N hydrochloric acid in 70 % alcohol.

On account of this very interesting result we tried to elute quaternary cations from Dowex 50-X1 with alcoholic media.

Method. Suitable quantities, usually 1—2 mg, of the compounds dissolved in water or alcohol of various strengths were run through a column, 4 × 30 mm, of Dowex 50-X1 (200—400 mesh) in its hydrogen form. The column was washed with the solvent. The bases were completely adsorbed. After elution, usually with 25 ml of the elutriant, the bases were determined by means of their ultraviolet spectra. Benzethonium chloride was titrated by Carkhuff and Boyd's method [8].

Results: 9-(4-Dimethylaminobenzylidene)-fluorene ethyltosylate. Aqueous mineral acids up to 2 N were without effect. 50 % alcoholic solution of mineral acids gave total yields if the acid was 1—2 N. Further, at this alcohol level there is a difference between perchloric, hydrochloric, and sulphuric acids as 0.2 N perchloric acid gave a full yield in contrast to hydrochloric which gave 60 % and sulphuric acid 20 % yields. 70 % alcoholic solution of mineral acids gave total yields if the acid was 0.5—2 N.

Experiments with aqueous and alcoholic potassium hydroxide were unsuccessful. 5 % sodium bromide in 70 % alcohol gave 95 % yield in 50 ml eluate.

Hyoscine methylnitrate. Of this alkaloid 10—15 mg was taken and was quantitatively eluted by 20 ml of 1 N hydrochloric acid in 50 % alcohol.

Codeine ethyliodide. The positive ion was eluted to 85—95 % by aqueous 1 N hydrochloric acid and totally by the same acid in 50 % alcohol. 0.5 N potassium hydroxide in 70 % alcohol gave 100 % recovery.

Papaverine ethyltosylate. 15—25 ml of 1 N hydrochloric acid in 50 % alcohol gave 100 % recovery.

Berberine sulphate. 1 N hydrochloric acid in 70 % alcohol gave a quantitative yield.

Strychnine ethyliodide. 1 N hydrochloric acid in water gave 75—80 %, in 50 % alcohol 85 %, and in 90 % alcohol 100 % recovery.

Benzethonium chloride. 100 % recovery was obtained with 10 ml of 1 N sulphuric acid in 90 % alcohol.

A full report will be given in a later publication.

Thanks are due to Mrs. Barbro Willman-Johnson who performed most of the experimental work.

1. Applezweig, N. *J. Am. Chem. Soc.* **66** (1944) 1950; *Ind. Eng. Chem.* **38** (1946) 576.
2. Sussman, S. and Mindler, A. B. *Chemistry & Industry* **57** (1945) 455.
3. Winters, J. and Kunin, R. *Ind. Eng. Chem.* **41** (1949) 460.
4. Hale, D. K., Packham, D. I. and Pepper, K. W. *J. Chem. Soc.* **1953** 844.

5. Büchi, J. and Furrer, F. *Arzneimittel-Forsch.* **3** (1953) 1.
6. Brochmann-Hanssen, E. *Medd. Norsk Farm. Selskap* **17** (1955) 76; *J. Am. Pharm. Assoc. Sci. Ed.* **45** (1956) 74.
7. van Etten, C. H., Earle, F. R., Mc Guire, T. A. and Senti, F. R. *Anal. Chem.* **28** (1956) 867.
8. Carkhuff, E. D. and Boyd, W. F. *J. Am. Pharm. Assoc. Sci Ed.* **43** (1954) 240.

Received December 3, 1956.

Mass Spectrometric Determination of the Structure of Phthiocerol

RAGNAR RYHAGE

Laboratory for Mass Spectrometry, Biochemical Institute, Karolinska Institutet, Stockholm

EINAR STENHAGEN

Department of Medical Biochemistry, Institute of Medical Chemistry, University of Uppsala, Uppsala

ERIK von SYDOW

Institute of Chemistry, University of Uppsala, Uppsala, Sweden

The position of the methoxyl group in phthiocerol previously inferred from mass-spectrometric and X-ray data [1] has now been confirmed by a mass-spectrometric study of synthetic 3-methoxy-4-methylheptene-6. The spectrum of this molecule, like that of phthiocerol, shows an intense peak at $m/e = 73$, arising from cleavage between carbon atoms 3 and 4.

A similar study of the parent hydrocarbon, phthiocerane [2], definitely settles the structure of this hydrocarbon in favour of 4-methyltetratriacontane and not 4-methyltritriacontane, which previously appeared more likely [3-5]. The mass-spectrum shows a small parent peak at $m/e = 492$ corresponding to $C^{35}H^{72}+$ (ionized unfragmented molecule), and very strong peaks at $m/e = 449$ and $m/e = 421$ corresponding to $C_{32}H_{65}+$ and $C_{30}H_{61}+$, respectively, arising from cleavage on both sides of the tertiary carbon atom in position 4.

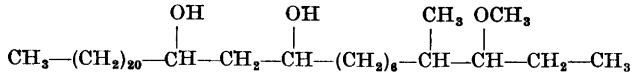
Parts of the mass-spectra of phthiocerol, 16,17-dihydroxydotriacontane, and 2,4-dihydroxyeicosane are shown in Fig. 1. A comparison between the spectrum of phthiocerol and those of the two synthetic glycols shows that phthiocerol is an 1,3-glycol as previously demonstrated by Demarteau-Ginsburg and Lederer [6] and excludes the possibility that phthiocerol is an 1,2-glycol. In the spectrum of 17,19-dihydroxyeicosane (2,4-dihydroxyeicosane) the C_{15}-alkene peaks $C_{15}H_{30}+$ and $C_{15}H_{28}+$ are considerably stronger than the corresponding peaks in the C_{14}- and C_{16}-groups. In the phthiocerol spectrum the $C_{20}H_{40}+$ and $C_{20}H_{38}+$ peaks are similarly increased, indicating the presence of a hydroxyl group in position 22. In phthiocerol the C_{27}- and C_{28}-groups of peaks are very weak, but a comparison with 17,19-dihydroxyeicosane is of course not possible as this molecule is too short. A comparison with the spectrum of 16,17-dihydroxydotriacontane, where the C_{20}- and C_{21}-groups of peaks are weak, does indicate, however, that phthiocerol has no hydroxyl group in position 25 or 26 from the normal chain end of the molecule.

Through the kind co-operation of Professor E. Lederer we have been able to make mass-spectrometric and monolayer studies of the acidic long-chain product obtained by Mme Demarteau-Ginsburg by oxidation of phthiocerol. The sample was found to consist of a mixture of about equal amounts of n-C_{22}- and n-C_{24}-acid together with smaller amounts of n-C_{21}- and n-C_{23}-acid. The presence of behenic acid supports the conclusion that phthiocerol has a hydroxyl group in position 22.

The presence of n-tetracosanoic acid appears more difficult to explain. This acid might arise from elimination of the hydroxyl group in position 22 before cleavage of the chain between the 24th and 25th carbon atom. It is hoped to settle this question by the study of oxidation products of a suitable synthetic 1,3-glycol.

Phthiocerol would thus have the empirical formula $C_{35}H_{69}(OH)_2OCH_3$ and be one of the sixteen theoretically possible stereoisomers of 3-methoxy-4-methyl-11,13-dihydroxytetratriacontane.

The mass-spectra of phthiocerol preparations from a virulent human strain of



5. Büchi, J. and Furrer, F. *Arzneimittel-Forsch.* **3** (1953) 1.
6. Brochmann-Hanssen, E. *Medd. Norsk Farm. Selskap* **17** (1955) 76; *J. Am. Pharm. Assoc. Sci. Ed.* **45** (1956) 74.
7. van Etten, C. H., Earle, F. R., Mc Guire, T. A. and Senti, F. R. *Anal. Chem.* **28** (1956) 867.
8. Carkhuff, E. D. and Boyd, W. F. *J. Am. Pharm. Assoc. Sci Ed.* **43** (1954) 240.

Received December 3, 1956.

Mass Spectrometric Determination of the Structure of Phthiocerol

RAGNAR RYHAGE

Laboratory for Mass Spectrometry, Biochemical Institute, Karolinska Institutet, Stockholm

EINAR STENHAGEN

Department of Medical Biochemistry, Institute of Medical Chemistry, University of Uppsala, Uppsala

ERIK von SYDOW

Institute of Chemistry, University of Uppsala, Uppsala, Sweden

The position of the methoxyl group in phthiocerol previously inferred from mass-spectrometric and X-ray data [1] has now been confirmed by a mass-spectrometric study of synthetic 3-methoxy-4-methylheptene-6. The spectrum of this molecule, like that of phthiocerol, shows an intense peak at $m/e = 73$, arising from cleavage between carbon atoms 3 and 4.

A similar study of the parent hydrocarbon, phthiocerane [2], definitely settles the structure of this hydrocarbon in favour of 4-methyltetratriacontane and not 4-methyltritriacontane, which previously appeared more likely [3-5]. The mass-spectrum shows a small parent peak at $m/e = 492$ corresponding to $C^{35}H^{72}+$ (ionized unfragmented molecule), and very strong peaks at $m/e = 449$ and $m/e = 421$ corresponding to $C_{32}H_{65}+$ and $C_{30}H_{61}+$, respectively, arising from cleavage on both sides of the tertiary carbon atom in position 4.

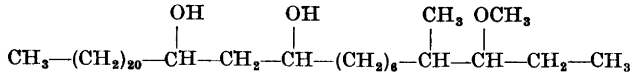
Parts of the mass-spectra of phthiocerol, 16,17-dihydroxydotriacontane, and 2,4-dihydroxyeicosane are shown in Fig. 1. A comparison between the spectrum of phthiocerol and those of the two synthetic glycols shows that phthiocerol is an 1,3-glycol as previously demonstrated by Demarteau-Ginsburg and Lederer [6] and excludes the possibility that phthiocerol is an 1,2-glycol. In the spectrum of 17,19-dihydroxyeicosane (2,4-dihydroxyeicosane) the C_{15}-alkene peaks $C_{15}H_{30}+$ and $C_{15}H_{28}+$ are considerably stronger than the corresponding peaks in the C_{14}- and C_{16}-groups. In the phthiocerol spectrum the $C_{20}H_{40}+$ and $C_{20}H_{38}+$ peaks are similarly increased, indicating the presence of a hydroxyl group in position 22. In phthiocerol the C_{27}- and C_{28}-groups of peaks are very weak, but a comparison with 17,19-dihydroxyeicosane is of course not possible as this molecule is too short. A comparison with the spectrum of 16,17-dihydroxydotriacontane, where the C_{20}- and C_{21}-groups of peaks are weak, does indicate, however, that phthiocerol has no hydroxyl group in position 25 or 26 from the normal chain end of the molecule.

Through the kind co-operation of Professor E. Lederer we have been able to make mass-spectrometric and monolayer studies of the acidic long-chain product obtained by Mme Demarteau-Ginsburg by oxidation of phthiocerol. The sample was found to consist of a mixture of about equal amounts of n-C_{22}- and n-C_{24}-acid together with smaller amounts of n-C_{21}- and n-C_{23}-acid. The presence of behenic acid supports the conclusion that phthiocerol has a hydroxyl group in position 22.

The presence of n-tetracosanoic acid appears more difficult to explain. This acid might arise from elimination of the hydroxyl group in position 22 before cleavage of the chain between the 24th and 25th carbon atom. It is hoped to settle this question by the study of oxidation products of a suitable synthetic 1,3-glycol.

Phthiocerol would thus have the empirical formula $C_{35}H_{69}(OH)_2OCH_3$ and be one of the sixteen theoretically possible stereoisomers of 3-methoxy-4-methyl-11,13-dihydroxytetratriacontane.

The mass-spectra of phthiocerol preparations from a virulent human strain of



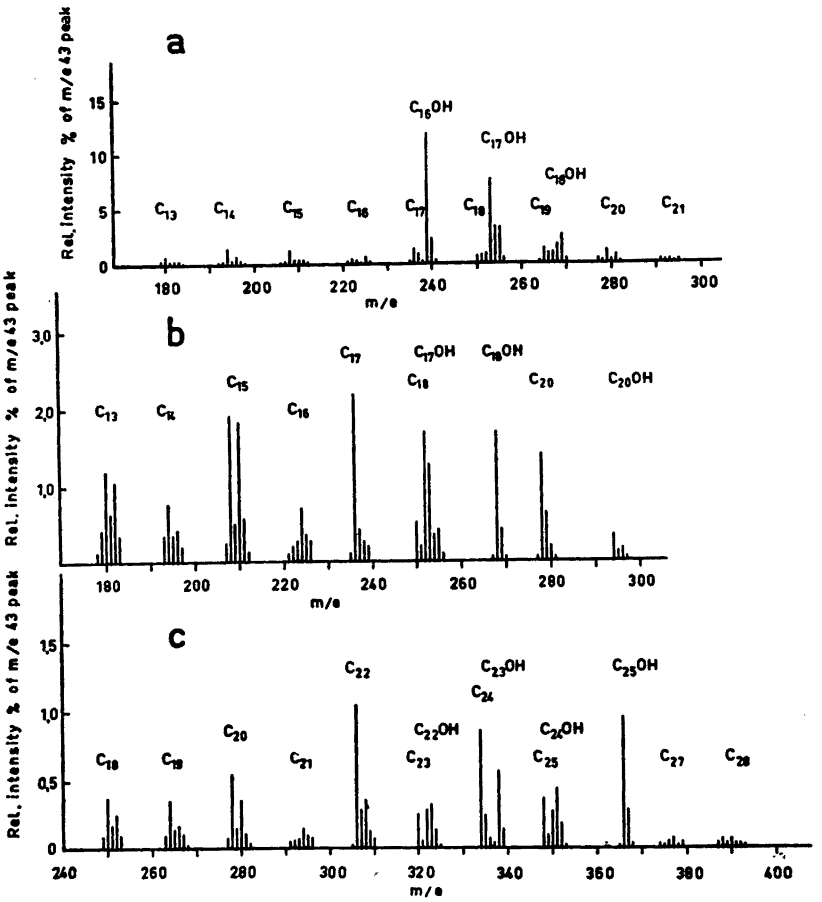


Fig. 1. Part of the mass-spectrum of a) 16,17-dihydroxydotriacontane b) 2,4-dihydroxyeicosane (17,19-dihydroxyeicosane). The two stereoisomers studied give closely similar spectra. c) phthiocerol from B.C.G.-strain of *M. tuberculosis*.

tubercle bacilli and from a B.C.G. strain were essentially similar.

We are indebted to Professor R. J. Anderson of Yale University and Professor E. Lederer of Institut de Biologie physico-chimique, Paris, for samples of phthiocerol. We wish to thank Mr. K. Serck-Hanssen for the synthetic 1,3-glycols and Mr. L. Ahlquist for assistance in the preparation of other synthetic material used for comparison. The expenses of this work have been defrayed in part by grants from the *Swedish Medical Research Council*.

Full details of this work will be published later.

1. Ryhage, R., Stenhagen, E. and von Sydow, E. *Acta Chem. Scand.* **10** (1956) 158.
2. Stodola, F. H. and Anderson, R. F. *J. Biol. Chem.* **114** (1936) 467.
3. Ställberg-Stenhagen, S., Stenhagen, E., Sheppard, N., Sutherland, G. B. B. M. and Walsh, A. *Nature* **160** (1947) 580.
4. Ställberg-Stenhagen, S. and Stenhagen, E. *J. Biol. Chem.* **173** (1948) 383.
5. Ställberg-Stenhagen, S. and Stenhagen, E. *J. Biol. Chem.* **183** (1950) 223.
6. Demarteau-Ginsburg, H. and Lederer, E. *Compt. rend.* **240** (1955) 815.

Received December 6, 1956.

Dihydroxyglutamic Acid in Plants

ARTTURI I. VIRTANEN and
TERTTU ETTALA

Laboratory of the Foundation for Chemical Research, Biochemical Institute, Helsinki, Finland

In an earlier paper [1] we reported the discovery of dihydroxyglutamic acid in the seeds of *Lepidium sativum* and in the green parts of *Rheum rhaponticum*.

On the two-dimensional paper chromatogram (solvents: butanol-acetic acid-water and phenol-water in NH_3-atmosphere) of 70 % ethanol extracts of the seeds of *Lepidium*, and of many plants later on, a spot could be detected after ninhydrin spraying which moved much slower than aspartic, γ- and β-hydroxyglutamic acids [2] in both solvents (Fig. 1). In butanol-acetic acid it moved somewhat slower than hydroxyaspartic acid. The colour of the spot was at first weak but turned stronger and violet later on. The substance was unaffected by mild (1 N HCl, 20 h, 108° C) as well as strong (6 N HCl, 20 h, 108° C) acid hydrolysis. The colour became even more intense when the ethanol extract was hydrolyzed before paper chromatography. When separating basic and neutral amino acids in an Amberlite IR-4B column the new amino acid remained in the fraction with acidic amino acids. In paper electrophoresis 2 000 V, 18 mA Na-acetate buffer, pH 3.2) it proved to be more strongly acid than any other known natural aminodicarboxylic acid.

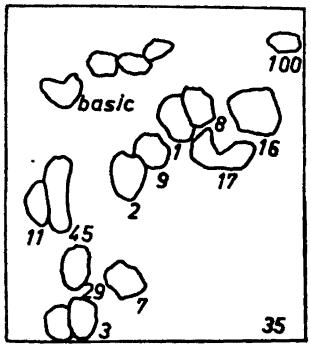


Fig. 1. Two-dimensional paper chromatogram of a 70 % ethanol extract (hydrolyzed with 6 N HCl) of the seeds of *Lepidium sativum*. Solvents: phenol-NH_3 and butanol-acetic acid. 100 = the new acidic amino acid (dihydroxyglutamic acid), 1 = gly, 2 = ala, 3 = val, 7 = tyr, 8 = ser, 9 = threo, 11 = pro, 16 = asp, 17 = glu, 29 = γ-aminobutyric acid, 45 = ethanolamine.

Isolation of the new amino acid from Rheum and the seeds of Lepidium. The amino acids in a 70 % ethanol extract were separated in an Amberlite IR-120 column. The eluate (1 N ammonia) was evaporated *in vacuo* and the extract hydrolyzed with 6 N HCl in order to split eventual peptides. Since the new amino acid moved slower in phenol than all other known natural amino acids, it was separated in a cellulose powder column using phenol as eluant. Before the run the cellulose powder column was washed with 1 % acetic acid and afterwards thoroughly with hot water. The fractions containing only the new amino acid were evaporated to dryness.

The structure of the new amino acid. The light coloured, slightly yellowish preparation obtained was on the basis of a two-dimensional paper chromatogram free from other amino acids. It did not contain sulphur or phosphorus. An aminodicarboxylic acid was thus obviously in question. An OH group in α-position to the NH_2 group was established with periodic acid and Nessler's reagent. On reduction with 66 % HI (d 1.96) and red phosphorus (4 mg substance + 18 μl HI + 3 mg P) at 140° C for 4 h mostly glutamic acid was found to be formed (Fig. 2). Small amounts of serine and glycine, and traces of threonine and alanine could also be found on the paper chromatogram. In some experiments a very faint spot was observed also in the position of β-hydroxyglutamic acid, but the substance could not be identified.

Using both phenol and butanol-acetic acid as solvents, the position of the new amino acid on the paper chromatogram (R_F values 0.05 and 0.04, respectively) showed that it was not β- or γ-hydroxyglutamic acid. Dihydroxyglutamic acid seemed thus probable. The amino acid contained 7.88 % N, calc. for dihydroxyglutamic acid $C_5H_9O_6N$, 7.85 % N.

Upon heating the amino acid at pH 3.3 at 125° C for 4 h the amino acid was transformed into the corresponding pyrroli-donecarboxylic acid to about 90 %. This compound was established by paper chromatography, treating the paper first with chlorine and then with a solution of 1 %

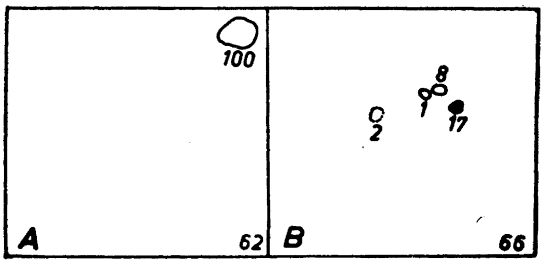


Fig. 2 A. Two-dimensional paper chromatogram of pure dihydroxyglutamic acid isolated from the seeds of *Lepidium sativum*. B. After reduction with HI and red P.

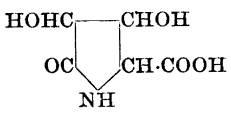
starch-KI, upon which the spot changed into bluish black [3]. The substance was isolated in a cellulose powder column using phenol-water as eluant. The fractions giving this colour reaction were evaporated to dryness *in vacuo* and extracted with ethyl-acetate, in which the pyrrolidonecarboxylic acid was difficult to dissolve. The substance was white, became darker upon heating at 235° C and decomposed at about 250° C. It contained 8.61 % N, calc. for $C_5H_7O_5N$, 8.70 % N.

The splitting of the carboxyl group as CO_2 by the effect of ninhydrin was determined according to Linko [4]. 0.269 mg of CO_2, or 26.4 %, were formed from 1.018 mg of the substance. Calc. for dihydroxypyrrolidonecarboxylic acid 27.3 %. Only little ammonia was formed, 27 % NH_3-N of total N. The determination, made for comparison, with pyrrolidonecarboxylic acid prepared from glutamic acid gave similar results: CO_2 formation 30.4 %, calc. 34.1 %, NH_3-N formation 22.1 % of total N.

The R_F value of the isolated dihydroxypyrrolidonecarboxylic acid was 0.33 in phenol-water. On hydrolysis with 6 N HCl the original aminodicarboxylic acid was re-formed.

The new amino acid had thus been established as dihydroxyglutamic acid,

The chromatographical and chemical properties of the new amino acid are compatible with the formula HOOC · CHOH · CHOH · $CHNH_2$ · COOH. The corresponding dihydroxypyrrolidonecarboxylic acid



seems not to be an artificial product only but also a very probable compound in fresh plants, because in the plant extract the amount of dihydroxyglutamic acid rises after strong acid hydrolysis. The increase is strongest in *Rheum* (pH of the sap 3.5—3.8) but can be noticed also in other plants (pH of the sap about 6.5).

The N-content of dihydroxyglutamic acid in the seeds of *Lepidium* is about 0.2 % of soluble N. On the whole the content of this amino acid is small in all the plants investigated. There is no experimental information yet about its biosynthesis. Hypothetically it can be assumed to be formed *via* transamination from the corresponding keto acid. The keto acid may be formed as an oxidation product of a ketopentose or also of γ-hydroxyglutamic acid.

Dihydroxyglutamic acid is comparatively common as a free amino acid in plants, and is to be found in all parts of the plants. By paper chromatography we have found it in the following plants: (The part of the plant in which the amino acid has been found is mentioned in parenthesis. Other parts have not been investigated. When both fruits and green parts have been investigated the amino acid has been found in both.)

Flowering plants. *Aesculus hippocastanum* (leaves and fruits), *Alchemilla vulgaris* (leaves and stem), *Angelica archangelica* (leaves), *Arctostaphylos uva-ursi* (leaves, stem and berries), *Brassica napa* (seeds), *Cornus alba* (berries), *Daucus carota* (stem and root), *Digitalis lanata* (leaves), *Lactuca sativa* (seeds), *Lepidium sativum* (seeds and sprouts), *Lilium bulbiferum* (leaves and stem), *Parthenocissus vitacea* (leaves), *Polygonum amphibium* (leaves and stem), *Polygonum aviculare* (leaves and stem), *Rheum rhaponticum* (leaves and stem), *Ribes alpinum*

(leaves), *Ribes grossularia* (leaves), *Ribes nigrum* (leaves and berries), *Ribes rubrum* (berries), *Spinacia oleracea* (leaves).

Ferns. *Struthiopteris filicastrum* (leaves).

Mosses. *Polytrichum commune.*

Mushrooms. *Amanita muscaria, Amanita virosa, Boletus luteus, Boletus versipellis.*

1. Virtanen, A. I. and Ettala, T. *Suomen Kemistilehti* **B 29** (1956) 107.
2. Virtanen, A. I. and Hietala, P. K. *Acta Chem. Scand.* **9** (1955) 175.
3. Ellfolk, N. and Synge, R. L. M. *Biochem. J. London* **59** (1955) 523.
4. Linko, P. *Suomen Kemistilehti* **B 28** (1955) 96.

Received December 1, 1956.

*iso*Thiocyanates XXIV*. (+)-, (—) and (±)-α-Methylbenzyl *iso*Thiocyanate

ANDERS KJÆR

Chemical Laboratory of the University of Copenhagen, Denmark

In connexion with other work in this laboratory pure specimens of the enantiomeric α-methylbenzyl *iso*thiocyanates became desirable. The racemic mustard oil has been described by Dyson and George [1] as a slightly yellow liquid, b.p. 240—244°, without presentation, however, of additional physical constants or analytical data. Recently, Luskin *et al.*[2] reported the preparation of (±)-α-methylbenzyl *iso*thiocyanate from α-methylstyrene and *iso*thiocyanic acid, as well as from α-methylbenzylamine by the customary decomposition of its dithiocarbamate.

In the present work the method of Schmidt *et al.*[3], involving hypochlorite oxidation of dithiocarbamates, was utilized for the synthesis of the racemic mustard oil, further characterized as its benzylthiourea-derivative. The pure, optically active α-methylbenzyl *iso*thiocyanates, (I) and (II), were produced on reaction of the corresponding amines with thiocarbonyl chloride by a slightly modified variation of the described procedure [1]. Again, the benzylthiourea-derivatives were synthesized for the purpose of characterization. Attempts to prepare the simple thioureas by reaction of the mustard oils with ammonia did not result in crystalline products.

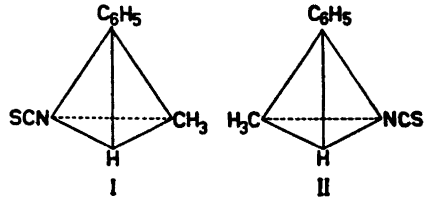


Fig. 1.

The symbols (I) and (II) are considered to represent the absolute configurations of (+)- and (—)-α-methylbenzyl *iso*thiocyanate, respectively. The former derives from (—)-α-methylbenzylamine, the transformation of which into (+)-alanine has been effected previously [4]. The configurational relationship of this amino acid with (—)-glyceraldehyde has been established by Wolfrom *et al.*[5] A unique three-dimensional representation of such molecules is required in consequence of the experimentally established absolute configuration of appropriate optically active molecules [6]. Adopting the recently proposed system for specification of absolute configuration [7] the sequence of transformations mentioned above is: *S*(—)-glyceraldehyde → *S*(+)-alanine → *S*(—)-α-methylbenzylamine → *S*(+)-α-methylbenzyl *iso*thiocyanate (I).

Experimental. Melting points are uncorrected and determined in capillary tubes in a slowly heated bath. Rotations are measured in a 1 dm tube.

S(+)-α-Methylbenzyl isothiocyanate (I). To (—)-α-methylbenzylamine (2.02 g, $[\alpha]_D^{24}$ —39.2° (neat)), dissolved in water, was added a chloroform solution of thiocarbonyl chloride (1.91 g). A total of 33.4 ml of 1 N NaOH was added in small portions to the vigorously stirred mixture. The organic layer was separated, the aqueous phase extracted twice with fresh portions of chloroform and the combined organic extracts dried over sodium sulphate. After removal of the solvent, the *iso*thiocyanate (1.12 g) distilled as a colourless oil, b.p. 126° at 16 mm, n_D^{25} 1.5802; $[\alpha]_D^{24}$ +17.5° (*c* 9.8, $CHCl_3$). (Found: C 66.50; H 5.52; N 8.91. Calc. for C_9H_9NS: C 66.24; H 5.56; N 8.59).

* Part XXIII of this series: *Acta Chem. Scand.* **10** (1956) 1358.

(leaves), *Ribes grossularia* (leaves), *Ribes nigrum* (leaves and berries), *Ribes rubrum* (berries), *Spinacia oleracea* (leaves).

Ferns. *Struthiopteris filicastrum* (leaves).

Mosses. *Polytrichum commune.*

Mushrooms. *Amanita muscaria, Amanita virosa, Boletus luteus, Boletus versipellis.*

1. Virtanen, A. I. and Ettala, T. *Suomen Kemistilehti* **B 29** (1956) 107.
2. Virtanen, A. I. and Hietala, P. K. *Acta Chem. Scand.* **9** (1955) 175.
3. Ellfolk, N. and Synge, R. L. M. *Biochem. J. London* **59** (1955) 523.
4. Linko, P. *Suomen Kemistilehti* **B 28** (1955) 96.

Received December 1, 1956.

*iso*Thiocyanates XXIV*. (+)-, (—) and (±)-α-Methylbenzyl *iso*Thiocyanate

ANDERS KJÆR

Chemical Laboratory of the University of Copenhagen, Denmark

In connexion with other work in this laboratory pure specimens of the enantiomeric α-methylbenzyl *iso*thiocyanates became desirable. The racemic mustard oil has been described by Dyson and George [1] as a slightly yellow liquid, b.p. 240—244°, without presentation, however, of additional physical constants or analytical data. Recently, Luskin *et al.*[2] reported the preparation of (±)-α-methylbenzyl *iso*thiocyanate from α-methylstyrene and *iso*thiocyanic acid, as well as from α-methylbenzylamine by the customary decomposition of its dithiocarbamate.

In the present work the method of Schmidt *et al.*[3], involving hypochlorite oxidation of dithiocarbamates, was utilized for the synthesis of the racemic mustard oil, further characterized as its benzylthiourea-derivative. The pure, optically active α-methylbenzyl *iso*thiocyanates, (I) and (II), were produced on reaction of the corresponding amines with thiocarbonyl chloride by a slightly modified variation of the described procedure [1]. Again, the benzylthiourea-derivatives were synthesized for the purpose of characterization. Attempts to prepare the simple thioureas by reaction of the mustard oils with ammonia did not result in crystalline products.

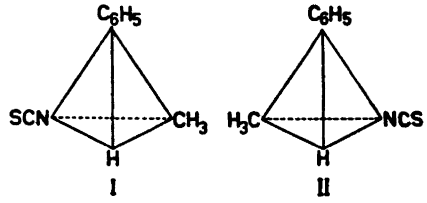


Fig. 1.

The symbols (I) and (II) are considered to represent the absolute configurations of (+)- and (—)-α-methylbenzyl *iso*thiocyanate, respectively. The former derives from (—)-α-methylbenzylamine, the transformation of which into (+)-alanine has been effected previously [4]. The configurational relationship of this amino acid with (—)-glyceraldehyde has been established by Wolfrom *et al.*[5] A unique three-dimensional representation of such molecules is required in consequence of the experimentally established absolute configuration of appropriate optically active molecules [6]. Adopting the recently proposed system for specification of absolute configuration [7] the sequence of transformations mentioned above is: *S*(—)-glyceraldehyde → *S*(+)-alanine → *S*(—)-α-methylbenzylamine → *S*(+)-α-methylbenzyl *iso*thiocyanate (I).

Experimental. Melting points are uncorrected and determined in capillary tubes in a slowly heated bath. Rotations are measured in a 1 dm tube.

S(+)-α-Methylbenzyl isothiocyanate (I). To (—)-α-methylbenzylamine (2.02 g, $[\alpha]_D^{24}$ —39.2° (neat)), dissolved in water, was added a chloroform solution of thiocarbonyl chloride (1.91 g). A total of 33.4 ml of 1 N NaOH was added in small portions to the vigorously stirred mixture. The organic layer was separated, the aqueous phase extracted twice with fresh portions of chloroform and the combined organic extracts dried over sodium sulphate. After removal of the solvent, the *iso*thiocyanate (1.12 g) distilled as a colourless oil, b.p. 126° at 16 mm, n_D^{25} 1.5802; $[\alpha]_D^{24}$ +17.5° (*c* 9.8, $CHCl_3$). (Found: C 66.50; H 5.52; N 8.91. Calc. for C_9H_9NS: C 66.24; H 5.56; N 8.59).

* Part XXIII of this series: *Acta Chem. Scand.* **10** (1956) 1358.

A solution of the *iso*thiocyanate (250 mg) and benzylamine (400 mg) in ether (5 ml) rapidly deposited the crystalline (*S*)-1-benzyl-3-(α-methylbenzyl)-thiourea. Two recrystallizations from aqueous ethanol afforded colourless needles (267 mg), m. p. 82.5°, $[\alpha]_D^{24}$ + 22.8° (*c* 2.4, 96 % EtOH). (Found: C 71.40; H 6.71; N 10.20. Calc. for $C_{16}H_{18}N_2S$: C 71.09; H 6.71; N 10.36). The UV-spectrum in ethanol displayed a maximum at 243 mμ (ε 14 800), a minimum at 238 mμ (ε 14 100), and strong end-absorption towards the short wave-length region.

R *(—)-α-Methylbenzyl* i*sothiocyanate* (II). This mustard oil was prepared from (+)-α-methylbenzylamine ($[\alpha]_D^{24}$ +38.9° (neat)) in exactly the same way, b. p. 121° at 10 mm, n_D^{25} 1.5801; $[\alpha]_D^{24}$ —17.3° (*c* 10.0, $CHCl_3$). (Found: C 66.15; H 5.44; N 8.68. Calc. for C_9H_9NS: C 66.24; H 5.56; N 8.59).

Upon reaction of the mustard oil with benzylamine the (*R*)-1-benzyl-3-(α-methylbenzyl)-thiourea was obtained, m. p. 82.5°, $[\alpha]_D^{24}$ —23.4° (*c* 2.3, 96 % EtOH). (Found: C 71.05; H 6.63; N 10.36. Calc. for $C_{16}H_{18}N_2S$: C 71.09; H 6.71; N 10.36).

(±)-α-Methylbenzyl i*sothiocyanate.* Racemic α-methylbenzylamine was transformed into the corresponding *iso*thiocyanate according to the directions given by Schmidt *et al.*[3] for the preparation of analogous compounds. The yield of pure mustard oil, b. p. 122—123° at 12 mm, was 55 %; n_D^{25} 1.5801. (Ref.[2]: b. p. 135-137°/23 mm, 133-134°/20 mm; n_D^{25} 1.5784, 1.5780).

The racemic 1-benzyl-3-(α-methylbenzyl)-thiourea separated in colourless needles from aqueous ethanol, m. p. 100°. (Found: C 71.35; H 6.62; N 9.98. Calc. for $C_{16}H_{18}N_2S$: C 71.09; H 6.71; N 10.36).

The oily thiourea, resulting from the reaction of the *iso*thiocyanate with ammonia, was subjected to paper chromatography in water-saturated chloroform according to our usual method [8]. An R_{Ph}-value of 1.15 was determined, *i. e.* the compound migrates at a rate definitely higher than that of control spots of benzyl- (R_{Ph} 0.93) and the isomeric β-phenylethyl-thiourea (R_{Ph} 1.08).

Microanalyses were made in this laboratory by Mr. P. Hansen. The experimental assistance of Mr. R. Boe Jensen is acknowledged. Dr. Egelund Pedersen of this laboratory kindly furnished the optically pure α-methylbenzylamines employed in the present work, which is part of investigations supported by *Statens Almindelige Videnskabsfond (The Danish State Research Foundation)* and *Carlsbergfondet (The Carlsberg Foundation)*.

1. Dyson, G. M. and George, H. J. *J. Chem. Soc.* **125** (1924) 1705.
2. Luskin, L. S., Gantert, G. E. and Craig, W. E. *J. Am. Chem. Soc.* **78** (1956) 4965.
3. Schmidt, E., Zaller, F., Moosmüller, F. and Kammerl, E. *Ann.* **585** (1954) 230.
4. Leithe, W. *Ber.* **64** (1931) 2827.
5. Wolfrom, M. L., Lemieux, R. U. and Olin, S. M. *J. Am. Chem. Soc.* **71** (1949) 2870.
6. Bijvoet, J. M., Peerdeman, A. F. and van Bommel, A. J. *Nature* **168** (1951) 271.
7. Cahn, R. S., Ingold, C. K. and Prelog, V. *Experientia* **12** (1956) 81.
8. Kjær, A. and Rubinstein, K. *Acta Chem. Scand.* **7** (1953) 528.

Received December 11, 1956.

A Rapid Method to Determine Sulphur

ROLF OTTOSSON and
OLLE SNELLMAN

Institute of Biochemistry, University of Uppsala, Uppsala, Sweden

In the method of determining sulphur in organic compounds used earlier here and described by Paulson [1], there were certain difficulties inherent in the combustion of the material. To facilitate the measurements and to obtain a better accuracy some modifications have been introduced in the measuring device and the oxidation of the material has been performed according to a modification of a method described by Schöniger [2]. With this method, sulphur determinations have been performed during the last year and the reproducibility has been very good. The method seems to be both rapid and accurate.

Apparatus. For burning the material a 500 ml bottle with a ground stopper is used. A platinum wire is sealed into the stopper. The wire is 10 cm long and has a diameter of 1 mm. A loop is made on the wire according to Fig. 1.

The same kind of measuring apparatus is used as described by Paulson. The milliam-

A solution of the *iso*thiocyanate (250 mg) and benzylamine (400 mg) in ether (5 ml) rapidly deposited the crystalline (*S*)-1-benzyl-3-(α-methylbenzyl)-thiourea. Two recrystallizations from aqueous ethanol afforded colourless needles (267 mg), m. p. 82.5°, $[\alpha]_D^{24}$ + 22.8° (*c* 2.4, 96 % EtOH). (Found: C 71.40; H 6.71; N 10.20. Calc. for $C_{16}H_{18}N_2S$: C 71.09; H 6.71; N 10.36). The UV-spectrum in ethanol displayed a maximum at 243 mμ (ε 14 800), a minimum at 238 mμ (ε 14 100), and strong end-absorption towards the short wave-length region.

R *(—)-α-Methylbenzyl* i*sothiocyanate* (II). This mustard oil was prepared from (+)-α-methylbenzylamine ($[\alpha]_D^{24}$ +38.9° (neat)) in exactly the same way, b. p. 121° at 10 mm, n_D^{25} 1.5801; $[\alpha]_D^{24}$ —17.3° (*c* 10.0, $CHCl_3$). (Found: C 66.15; H 5.44; N 8.68. Calc. for C_9H_9NS: C 66.24; H 5.56; N 8.59).

Upon reaction of the mustard oil with benzylamine the (*R*)-1-benzyl-3-(α-methylbenzyl)-thiourea was obtained, m. p. 82.5°, $[\alpha]_D^{24}$ —23.4° (*c* 2.3, 96 % EtOH). (Found: C 71.05; H 6.63; N 10.36. Calc. for $C_{16}H_{18}N_2S$: C 71.09; H 6.71; N 10.36).

(±)-α-Methylbenzyl i*sothiocyanate.* Racemic α-methylbenzylamine was transformed into the corresponding *iso*thiocyanate according to the directions given by Schmidt *et al.*[3] for the preparation of analogous compounds. The yield of pure mustard oil, b. p. 122—123° at 12 mm, was 55 %; n_D^{25} 1.5801. (Ref.[2]: b. p. 135-137°/23 mm, 133-134°/20 mm; n_D^{25} 1.5784, 1.5780).

The racemic 1-benzyl-3-(α-methylbenzyl)-thiourea separated in colourless needles from aqueous ethanol, m. p. 100°. (Found: C 71.35; H 6.62; N 9.98. Calc. for $C_{16}H_{18}N_2S$: C 71.09; H 6.71; N 10.36).

The oily thiourea, resulting from the reaction of the *iso*thiocyanate with ammonia, was subjected to paper chromatography in water-saturated chloroform according to our usual method [8]. An R_{Ph}-value of 1.15 was determined, *i. e.* the compound migrates at a rate definitely higher than that of control spots of benzyl- (R_{Ph} 0.93) and the isomeric β-phenylethyl-thiourea (R_{Ph} 1.08).

Microanalyses were made in this laboratory by Mr. P. Hansen. The experimental assistance of Mr. R. Boe Jensen is acknowledged. Dr. Egelund Pedersen of this laboratory kindly furnished the optically pure α-methylbenzylamines employed in the present work, which is part of investigations supported by *Statens Almindelige Videnskabsfond (The Danish State Research Foundation)* and *Carlsbergfondet (The Carlsberg Foundation)*.

1. Dyson, G. M. and George, H. J. *J. Chem. Soc.* **125** (1924) 1705.
2. Luskin, L. S., Gantert, G. E. and Craig, W. E. *J. Am. Chem. Soc.* **78** (1956) 4965.
3. Schmidt, E., Zaller, F., Moosmüller, F. and Kammerl, E. *Ann.* **585** (1954) 230.
4. Leithe, W. *Ber.* **64** (1931) 2827.
5. Wolfrom, M. L., Lemieux, R. U. and Olin, S. M. *J. Am. Chem. Soc.* **71** (1949) 2870.
6. Bijvoet, J. M., Peerdeman, A. F. and van Bommel, A. J. *Nature* **168** (1951) 271.
7. Cahn, R. S., Ingold, C. K. and Prelog, V. *Experientia* **12** (1956) 81.
8. Kjær, A. and Rubinstein, K. *Acta Chem. Scand.* **7** (1953) 528.

Received December 11, 1956.

A Rapid Method to Determine Sulphur

ROLF OTTOSSON and
OLLE SNELLMAN

Institute of Biochemistry, University of Uppsala, Uppsala, Sweden

In the method of determining sulphur in organic compounds used earlier here and described by Paulson [1], there were certain difficulties inherent in the combustion of the material. To facilitate the measurements and to obtain a better accuracy some modifications have been introduced in the measuring device and the oxidation of the material has been performed according to a modification of a method described by Schöniger [2]. With this method, sulphur determinations have been performed during the last year and the reproducibility has been very good. The method seems to be both rapid and accurate.

Apparatus. For burning the material a 500 ml bottle with a ground stopper is used. A platinum wire is sealed into the stopper. The wire is 10 cm long and has a diameter of 1 mm. A loop is made on the wire according to Fig. 1.

The same kind of measuring apparatus is used as described by Paulson. The milliam-

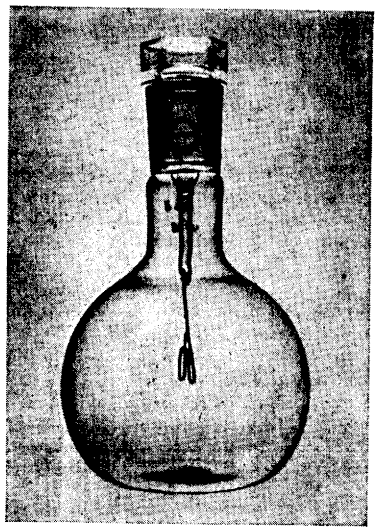


Fig. 1. The burning bottle.

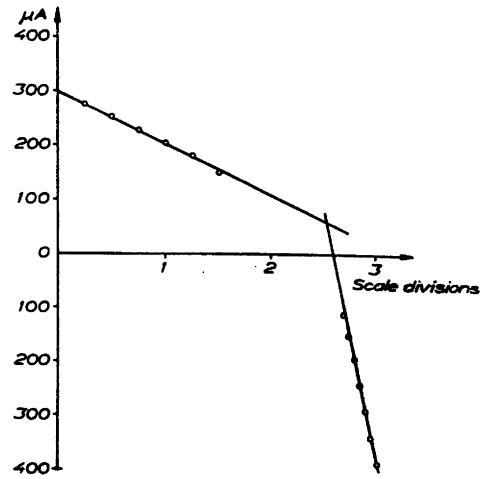


Fig. 2. Example of an analysis curve. The displacement of the micrometer screw is plotted as abscissa and the ammeter reading as ordinate.

meter (Philips mA) is used in such a range that a shift of about 40 Ω in the 1 000 Ω region on the bridge will cause a deflection of the whole scale on the ammeter (0—500 mA).

Method. The sample is burnt according to the method proposed by Schöniger [2], but without using the sodium hydroxide. 10 ml distilled water and 2 ml perhydrol are pipetted in the bottle. The last drop of the water in the pipette is used to make a wet zone around the ground stopper. Oxygen is let into the bottle from an oxygen cylinder for about 20 sec. The substance to be tested is wrapped in a filter paper strip and put into the loop in the platinum wire. The end of the strip is lighted and quickly put in the bottle where the substance is burnt in the oxygen. The bottle is left for 30 min. After this time, the ground surfaces are washed with the contents in the bottle, in case the drop on the stopper has absorbed any sulphur dioxide. Of the reaction mixture, 10 ml is transferred to the conductivity cell.

To the 10 ml reaction mixture in the conductivity cell, one drop of 20 % acetic acid and 1 ml of a barium sulphate suspension in distilled water are added. The content of the cell is then vigourously stirred with a rotating glass rod. It is important that the glass rod is not inserted between the platinum electrodes, as this causes variations in the conductivity and the capacitance of the circuit and hence the needle of the ammeter will not be stable. The apparatus is left for about 10 min for stabilization.

After this time, the apparatus is adjusted to zero deflection and then the resistance is lowered about 40 Ω. The barium chloride solution used for the titration is about 0.5 M. It is added in 0.002 ml portions and the readings after every addition are plotted against the total displacement of the micrometer screw.

The points on the steep line are taken after the zero point on the ammeter is passed and the same region of the scale is reached in which the first series of points was taken. The last points are plotted on the negative side of the diagram (Fig. 2). By these symmetric readings the non-linear sensitivity in the system is cancelled.

A calibration curve is given in Fig. 3, where the scission points of the lines are plotted against a known amount of sulphur. Using the same solution we have not detected any shift in the calibration curve over a period of six months. The substance used for calibration was sulfanilamide (Eastman Kodak).

Tests. Cystein hydrochloride (Merck) analytical reagent gave the following values

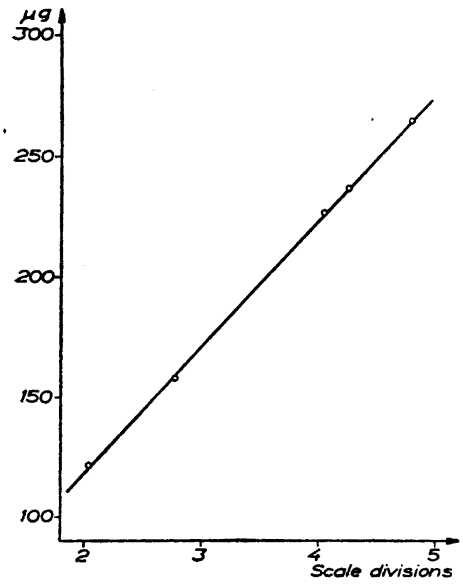


Fig. 3. Calibration curve in the region 100—250 µg. The displacement of the micrometer screw is plotted as abscissa and the sulphur amount as ordinate.

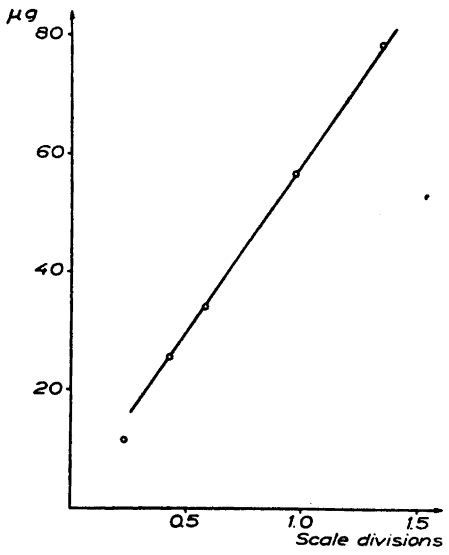


Fig. 4. Calibration curves in the region 20—80 µg. The same abscissa and ordinate as in Fig. 3. The lowest point on the line is not reliable.

Amount	5 per cent		
2.57 mg	18.11		
2.32	18.20		
2.52	18.00		
2.04	18.02		
	Mean 18.08	Calculated	18.32

Methionine (Merck)

Amount	5 per cent		
2.08	21.50		
1.57	21.80		
1.01	21.25		
	Mean 21.51	Calculated	21.48

The standard error is 0.4 %. In this error is included the error from the weighing of the sample. We used a balance which was graduated in 0.05 mg.

In the region 20—80 µg S, we got the calibration curve Fig. 4 by taking parts of the absorption fluid from different burnings, diluting to 6 ml in the conductivity cell and adding 1 drop 20 % acetic acid and ½ ml barium sulphate suspension. However, in this case it was very difficult to draw the lines in the diagram as one could get only few points in a narrow interval before the equivalence point was reached.

As the conductimetric titration takes about 5 min and the burning can be done in two bottles alternately, the method is not at all time consuming.

The investigation has been financially supported by a grant from Eli Lilly and Company, Indianapolis, U.S.A.

1. Paulson, S. *Acta Chem. Scand.* **7** (1953) 325.
2. Schöniger, W. *Mikrochemie ver. Microchim. Acta* **1955** 123.

Received December 17, 1956.

The Structure of Crystalline Cytidylic Acid b

E. ALVER and S. FURBERG

Chemical Institute, University of Bergen, Bergen, Norway

The crystal and molecular structure of cytidylic acid b is being investigated by X-ray diffraction methods. So far the main features of the structure have been established.

The crystal symmetry and the dimensions of the unit cell were derived from oscillation and Weissenberg photographs, taken with filtered copper radiation (λ = 1.542 Å). The crystals are orthorhombic, with space group $P2_12_12$, and unit cell dimensions [1]: a = 8.74 Å, b = 21.4 Å, c = 6.82 Å. The unit cell contains four molecules $C_9H_{14}N_3O_8P$. Weissenberg diagrams of the zones $hk0$-$hk4$ and $0kl$-$5kl$ were taken, and about 1 300 reflexes were recorded. The intensities were estimated visually.

Patterson projections along the two shortest axes indicated several possibilities for the position of the phosphorus atom. By the aid of three Harker sections and vector convergence maps [2] all of these except one were ruled out as improbable. The c-projection was very difficult to attack directly, as few unitary structure factors are larger than 0.15, and several attempts failed. It was then decided to try the a-projection, as the distribution of intensities in the $0kl$ zone seemed more favourable, though serious overlapping of atoms had to be expected.

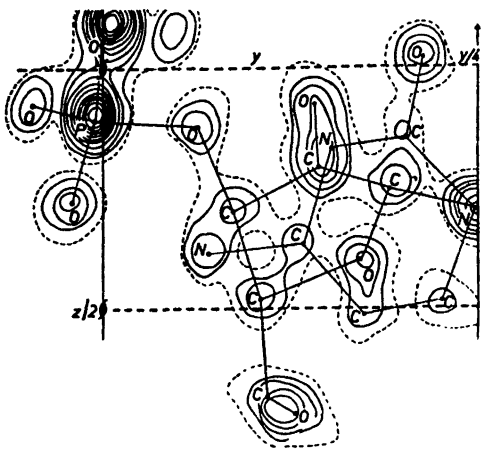


Fig. 1. Electron density projection along the a axis, showing one asymmetric unit. Plane group *pgm*. Contours at arbitrary but equal intervals.

It was found possible to derive the probable phases of four reflexes from an analysis of the distribution of vectors along the lines $x = 1/2$ and $z = 0$ in the two Patterson projections. From the distribution of positive and negative areas in the vector convergence map of the a-projection it could be concluded that the two largest structure factors should probably have opposite signs. One of these and one sign more could be chosen arbitrarily.

With these seven phases as a starting point a set of 22 probable phases was found by Harker-Kasper inequalities, using a high artificial temperature factor. The corresponding Fourier map was unclear, but indicated the positions of the oxygen atoms of the phosphate group. These were confirmed by the three-dimensional Patterson function. The rest of the molecule was then placed roughly by trial and error, and the structure refined by F_o and $(F_o - F_c)$ syntheses.

At the present stage the electron density map of the a-projection shows no false maxima, and the reliability index R is 0.30. We hope to be able to publish a full report on the work and a detailed discussion of the structure in the near future. So far it can only be said with a high degree of certainty that the phosphate group is bound to the ribose ring in the 3′ position, as should be expected [3].

We want to express our thanks to *Norges Almenvitenskapelige Forskningsråd*, whose financial support made this work possible.

1. Furberg, S. *Nature* **164** (1949) 22.
2. Beevers, C. A. and Robertson, J. H. *Acta Cryst.* **3** (1950) 164.
3. Fox, J. J., Cavalieri, L. F. and Chang, N. *J. Am. Chem. Soc.* **75** (1953) 4315.

Received December 15, 1956.

Structure of Formamidine Disulphide

OLAV FOSS and JONAS JOHNSEN

Chemical Institute, University of Bergen, Bergen, Norway

Salts of formamidine disulphide result on oxidation of thiourea with halogens or other oxidizing agents [1-3]. Although the disulphide nature of the salts appears to be fairly well established, *e. g.*, from the careful study by Preisler and Berger [4] of the oxidation-reduction potential of the reversible thiourea-formamidine disulphide system, it has been claimed [5] that they are not disulphides, but monomeric compounds containing one thiourea unit only in the molecule.

The crystal structure of the diiodide of formamidine disulphide has now been determined. The results indicate the presence of an S—S bond and the correctness of the formamidine disulphide structure.

Formamidine disulphide diiodide, $[(H_2N)_2CS]_2I_2 \cdot H_2O$, was prepared from iodine and thiourea as described by Marshall [2]. The colourless salt, which turned out to be a monohydrate, was obtained as plates {100}, or as flat prisms bounded by {100} and, less developed, {001}. The axial lengths are, $a = 5.15$ Å, $b = 16.52$ Å, $c = 13.39$ Å ($\pm$ 0.5 %). There are four formula units per unit cell; density, calc. 2.47, found 2.47 g/cm³. The space group, from systematic absences, is D_{2h}^{10}—*Pccn*, which has eightfold general positions, and centres of symmetry and twofold axes as special, fourfold positions.

Intensities of the 0*kl* and *hk*0 reflections were estimated visually from Weissenberg photographs taken with copper radiation, using crystals with cross-sections of 0.04 × 0.05 mm and 0.07 × 0.05 mm, respectively, in the case of the *a* and *c* axis photographs. Patterson, Fourier and Fourier difference projections along these axes, refined to reliability factors of $R = 8.8$ % and 9.7 %, respectively, for the 0*kl* and *hk*0 reflections, have led to the atomic coordinates given in Table 1.

Table 1. Atomic coordinates, in fractions of cell edges. Origin at a centre of symmetry.

	x	*y*	*z*
I	0.072	0.0783	—0.1453
S	0.578	0.2192	—0.008
C	0.665	0.141	0.071
N_1	0.481	0.080	0.076
N_2	0.850	0.142	0.136
H_2O	0.250	0.250	0.214

The data of Table 1 give a length of 2.04 Å for the S—S bond, across the twofold axis at ($\frac{1}{4}$, $\frac{1}{4}$, *z*). The C—S—S bond angles are 98°, and the C—S—S/S—S—C dihedral angle, 104°. The disulphide group has thus normal dimensions. The shortest I—I approaches are 4.60 Å and 4.73 Å, across a twofold screw axis and a centre of symmetry, respectively, and the shortest I—S approaches are 3.91 Å and 3.95 Å.

Details of the structure of the diiodide will be published later.

The crystal structure of the corresponding dibromide [1], $[(H_2N)_2CS]_2Br_2 \cdot H_2O$, is being studied [6]. This salt is monoclinic, with $a = 8.61$ Å, $b = 5.12$ Å, $c = 12.40$ Å, $\beta = 99\frac{1}{2}°$, and two formula units per unit cell. The probable space group is C_{2h}^4—*P*2/*c*.

1. Claus, A. *Ann.* **179** (1875) 112.
2. Marshall, H. *Proc. Roy. Soc. Edinburgh* **24 III** (1902) 233; *Chem. Zentralbl.* **1902 II** 1100.
3. Werner, E. A. *J. Chem. Soc.* **101** (1912) 2166.
4. Preisler, P. W. and Berger, L. *J. Am. Chem. Soc.* **69** (1947) 322.
5. Sahasrabudhey, R. H. *J. Indian Chem. Soc.* **28** (1951) 119, 309; **30** (1953) 64.
6. Foss, O. and Tvedten, O. *Work in progress.*

Received December 15, 1956.

Small-Angle Scattering of X-Rays in Aqueous Solutions of Sodium Salts of Conjugated and Unconjugated Bile Acids

PER EKWALL, KRISTER FONTELL and ARNE NORMAN*

Institute of Physical Chemistry, Åbo Akademi, Åbo, Finland

We have previously shown that aqueous sodium desoxycholate and cholate solutions produce a small angle X-ray pattern [1,2]. Using the same apparatus and technique we have now investigated solutions of sodium salts of a number of conjugated and unconjugated bile acids, which we have found to give rise to similar X-ray patterns. The salts studied are: sodium cholate, desoxycholate, chenodesoxycholate, dehydrocholate, taurocholate, taurodesoxycholate, taurochenodesoxycholate, glycocholate, glycodesoxycholate and glycochenodesoxycholate. The chenodesoxycholic acid and all the conjugated bile acids were synthesized by one of us (A.N.)[3]. The other acids were samples from Hoffmann-La Roche A. G., Basle, which were recrystallized several times before use. Their melting points were: cholic acid, 197° C, desoxycholic acid, 174—175° C, dehydrocholic acid 237° C.

The sodium dehydrocholate solutions (up to 0.4 molal) gave only a dark background; no intensity maximum was evident on the photometer curve. All the other bile salts, however, yielded pronounced intensity maxima, as seen in Figs. 1 and 2, where photometer recordings of the X-ray films obtained with 0.4 molal solutions of the salts are reproduced. It is immediately noted that the three cholates as a group and also the three desoxycholates and the three chenodesoxycholates exhibit closely similar X-ray patterns. Conjugation does not appear to have any greater influence on the location of the intensity maxima. Also the photometric curves for the desoxycholates and chenodesoxycholates are very similar, which indicates that the positions of the hydroxyl groups (3,12 and 3,7) do not exert any significant effect. The number of hydroxyl groups does, however, influence the scattering since marked differences are noted between the photometric curves of the cholate series (3 hydroxyl groups), on one hand, and those of the desoxy- and chenodesoxycholate series (2 hydroxyl groups), on the other.

* Present address: Department of Physiological Chemistry, University of Lund, Lund, Sweden.

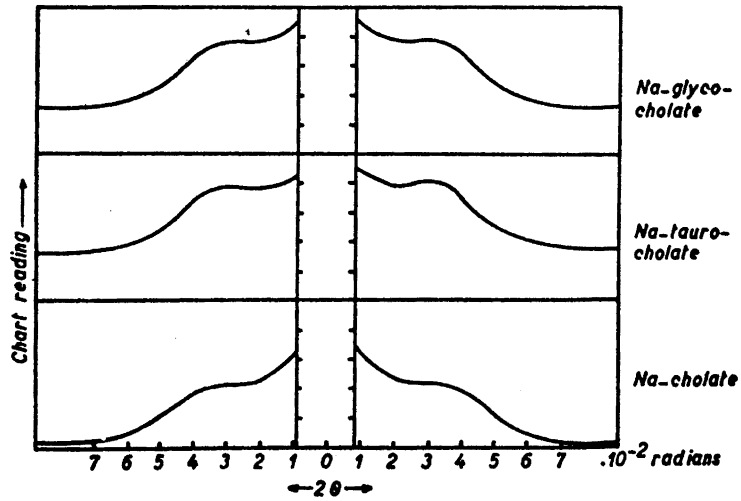


Fig. 1. Photometer recordings of the small angle scattering by 0.4 M aqueous solutions of sodium cholate, taurocholate and glycocholate.

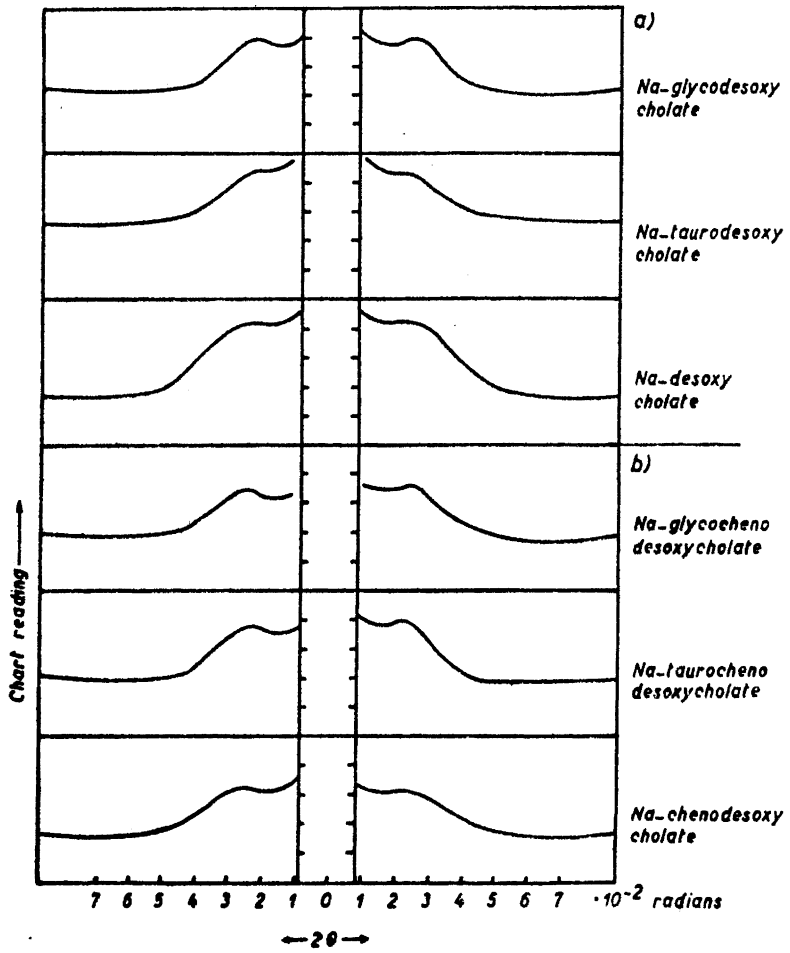


Fig. 2. Photometer recordings of the small angle scattering by 0.4 M aqueous solutions of

a) sodium desoxycholate, taurodesoxycholate and glycodesoxycholate.

b) sodium chenodesoxycholate, taurochenodesoxycholate and glycochenodesoxycholate.

The fact that the bile salt solutions yield small-angle X-ray scattering patterns shows that an association of the ions to colloidal aggregates, micelles, occurs in their solutions. This result is in agreement with earlier conclusions drawn on the basis of studies in which other methods have been employed [4,5]. Also the finding that conjugation does not greatly influence the micelle formation is in accordance with our previous experience [4,5]. The fact that sodium dehydrocholate solutions do not give rise to an intensity maximum in the small angle X-ray pattern agrees with the results of other physicochemical measurements which indicate that association in these solutions sets in only after a very high concentration, about 0.12 M, has been reached, *i. e.* the tendency of these anions to form micelles is weak [4].

1. Ekwall, P. and Fontell, K. *Acta Chem. Scand.* **10** (1956) 327.
2. Ekwall, P. and Fontell, K. *IX Nord. Kemistmötet, Aarhus, 1956.*
3. Norman, A. *Arkiv Kemi* **8** (1955) 331.
4. *Cf.* Refs. 1—8 in Ref. [1]
5. Ekwall, P. and coworkers. *Unpublished experiments.*

Received December 19, 1956.

Fractionation of Methyl Cellulose Hydrolysate

INGEMAR CROON and BENGT LINDBERG

Institutionen för Träkemi, Kungl. Tekniska Högskolan, Stockholm, Sweden

The distribution of substituents in cellulose derivatives has previously been studied by indirect analytical methods (*cf.* Ref.[1]), the results of which may be rather uncertain and open to some doubt. Spurlin [1] suggested that cellulose ethers should be studied by a different method, involving hydrolysis to glucose and glucose ethers and the fractionation of these by some chromatographic technique. The actual isolation and identification of these products would offer a more reliable basis for calculations. Several authors [2-5] have reported partial fractionations of the products obtained by hydrolysis of methyl cellulose, *e. g.* the fractionation of the three monomethylated glucoses or the fractionation of glucose, mono-, di- and trimethyl ethers. In the present paper the complete fractionation of the eight products in such a hydrolysate is reported. The fractionation was performed on a carbon column using the gradient elution technique. Lindberg and Wickberg[6] separated some methylated sugars by this method and we have recently reported a similar fractionation of the hydrolysate from a hydroxyethyl cellulose[7]. Two components, 6- and 3-*O*-methyl-D-glucose, did not separate by this method but were easily separated by paper chromatography. All components were obtained in a state of purity and identified by their behaviour in paper chromatography and paper electrophoresis, by comparison with authentic samples and by determination of m.p. and optical rotation. Some of them crystallised (see Table 1) and the values for their melting points and specific rotations were in good agreement with those previously recorded.

Experimental. The methyl cellulose investigated was prepared from cotton linters and had a D.S. of 0.90 (OCH_3 15.85, 15.91, 15.97). A sample (1.5 g) was treated with cold 72 % sulphuric acid (16.7 ml). After 30 min at 0° the sample had dissolved completely. It was then diluted with water to 150 ml and heated under nitrogen, first overnight at 60° and finally for 3 h at 100°. The sulphuric acid was neutralised with barium carbonate, the salts removed by filtration and the solution concentrated to dryness (1.460 g). No cellobiose could be detected in the hydrolysate. An aqueous solution of the hydrolysate (50 ml) was added to the top of a carbon column (43 × 3.5 cm) which was then eluted with the following solvents.

Water		1 000 ml
Aqueous ethanol	0 — 8 %	5 000 »
» »	8 — 25 »	2 500 »
» »	25 — 50 »	3 000 »

Fractions (26 ml) were collected and investigated by paper chromatography, paper electrophoresis and determination of the optical rotation (2 dm tube). The result of the fractionation is given in Fig. 1. The 6- and 3-*O*-methyl ethers did not separate well, the former is eluted very slightly faster, and they both contribute to the third peak in Fig. 1, which has a somewhat irregular shape. A small part of the 2-*O*-methyl-D-glucose (second peak) was mixed with the 6-*O*-methyl-D-glucose. Fractions containing s_0 (glucose), s_2(2-*O*-methyl-D-glucose), s_2+s_6, s_6+s_3, s_{26}, s_{36}, s_{23} and s_{236} respectively, were combined, taken to dryness and weighed. In the mixed fraction s_2+s_6, the rather small amount of s_2 was estimated from the shape of the curves. In the mixed fraction s_6+s_3, the proportion between the components was determined by paper chromatography, using methyl ethyl ketone-water (15:1) as solvent. An analytical determination, following the procedure of Hirst, Hough and Jones [8] and a preparative separation on thick filter paper, gave figures in reasonably good agreement, 2.32, 2.43 and 2.26:1, respectively. The yields of each component together with characterising data are given in Table 1.

In a preliminary experiment a larger amount (3.0 g) of methyl cellulose was hydrolysed in the same way and the components fractionated on the same column. A steeper gradient was

1. Ekwall, P. and Fontell, K. *Acta Chem. Scand.* **10** (1956) 327.
2. Ekwall, P. and Fontell, K. *IX Nord. Kemistmötet, Aarhus, 1956.*
3. Norman, A. *Arkiv Kemi* **8** (1955) 331.
4. *Cf.* Refs. 1—8 in Ref. [1]
5. Ekwall, P. and coworkers. *Unpublished experiments.*

Received December 19, 1956.

Fractionation of Methyl Cellulose Hydrolysate

INGEMAR CROON and BENGT LINDBERG

Institutionen för Träkemi, Kungl. Tekniska Högskolan, Stockholm, Sweden

The distribution of substituents in cellulose derivatives has previously been studied by indirect analytical methods (*cf.* Ref.[1]), the results of which may be rather uncertain and open to some doubt. Spurlin [1] suggested that cellulose ethers should be studied by a different method, involving hydrolysis to glucose and glucose ethers and the fractionation of these by some chromatographic technique. The actual isolation and identification of these products would offer a more reliable basis for calculations. Several authors [2-5] have reported partial fractionations of the products obtained by hydrolysis of methyl cellulose, *e. g.* the fractionation of the three monomethylated glucoses or the fractionation of glucose, mono-, di- and trimethyl ethers. In the present paper the complete fractionation of the eight products in such a hydrolysate is reported. The fractionation was performed on a carbon column using the gradient elution technique. Lindberg and Wickberg[6] separated some methylated sugars by this method and we have recently reported a similar fractionation of the hydrolysate from a hydroxyethyl cellulose[7]. Two components, 6- and 3-*O*-methyl-D-glucose, did not separate by this method but were easily separated by paper chromatography. All components were obtained in a state of purity and identified by their behaviour in paper chromatography and paper electrophoresis, by comparison with authentic samples and by determination of m.p. and optical rotation. Some of them crystallised (see Table 1) and the values for their melting points and specific rotations were in good agreement with those previously recorded.

Experimental. The methyl cellulose investigated was prepared from cotton linters and had a D.S. of 0.90 (OCH_3 15.85, 15.91, 15.97). A sample (1.5 g) was treated with cold 72 % sulphuric acid (16.7 ml). After 30 min at 0° the sample had dissolved completely. It was then diluted with water to 150 ml and heated under nitrogen, first overnight at 60° and finally for 3 h at 100°. The sulphuric acid was neutralised with barium carbonate, the salts removed by filtration and the solution concentrated to dryness (1.460 g). No cellobiose could be detected in the hydrolysate. An aqueous solution of the hydrolysate (50 ml) was added to the top of a carbon column (43 × 3.5 cm) which was then eluted with the following solvents.

Water		1 000 ml
Aqueous ethanol	0 — 8 %	5 000 »
» »	8 — 25 »	2 500 »
» »	25 — 50 »	3 000 »

Fractions (26 ml) were collected and investigated by paper chromatography, paper electrophoresis and determination of the optical rotation (2 dm tube). The result of the fractionation is given in Fig. 1. The 6- and 3-*O*-methyl ethers did not separate well, the former is eluted very slightly faster, and they both contribute to the third peak in Fig. 1, which has a somewhat irregular shape. A small part of the 2-*O*-methyl-D-glucose (second peak) was mixed with the 6-*O*-methyl-D-glucose. Fractions containing s_0 (glucose), s_2(2-*O*-methyl-D-glucose), s_2+s_6, s_6+s_3, s_{26}, s_{36}, s_{23} and s_{236} respectively, were combined, taken to dryness and weighed. In the mixed fraction s_2+s_6, the rather small amount of s_2 was estimated from the shape of the curves. In the mixed fraction s_6+s_3, the proportion between the components was determined by paper chromatography, using methyl ethyl ketone-water (15:1) as solvent. An analytical determination, following the procedure of Hirst, Hough and Jones [8] and a preparative separation on thick filter paper, gave figures in reasonably good agreement, 2.32, 2.43 and 2.26:1, respectively. The yields of each component together with characterising data are given in Table 1.

In a preliminary experiment a larger amount (3.0 g) of methyl cellulose was hydrolysed in the same way and the components fractionated on the same column. A steeper gradient was

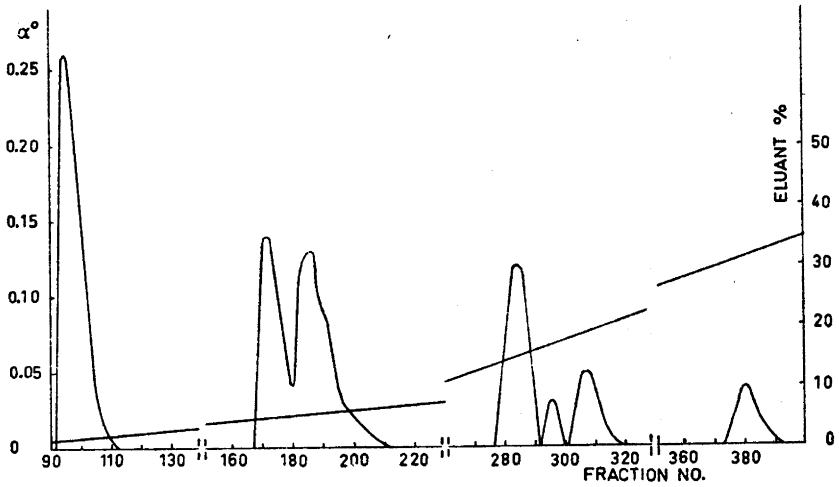


Fig. 1. Chromatographic fractionation of methyl cellulose hydrolysate.

Table 1. Yields and properties of the components from a methyl cellulose (1.5 g) hydrolysate. The components are listed in the order by which they were eluted from the carbon column.

Substance [a]	Yield mg	Mol %	R_G [b]	M_G [c]	M. p.	$[\alpha]_D^{20}$ [d]
s_0	540	40.1	1	1	145—146°	+54°
s_2	264	18.2	3.05	0.22	159—160°	+66°
s_6	191	13.2	2.85	0.84	145—147°	+59°
s_3	58	4.0	3.30	0.78	170—171°	+56°
s_{26}	180	11.5	10	0.04		
s_{36}	37	2.4	11	0.52		
s_{23}	85	5.5	14	0.14	115—118°	+52°
s_{236}	85	5.1	—	0.00	117—119°	+68°

a) s_{26} = 2,6-Di-*O*-methyl-D-glucose, a.s.o.
b) Solvent: Ethyl methyl ketone, saturated with water. R_G = 1 for glucose.
c) 0.2 M Borate buffer, pH 10. M_G = 1 for glucose.
d) In water, $c \simeq 2.0$.

used and practically no separation was obtained between the monomethyl ethers. The separation between the other components, however, was good and the agreement between the two experiments excellent. From both experiments the D.S. of the methyl cellulose could be calculated to 0.90, which is identical with the value calculated from the methoxyl analysis.

The results will be discussed in a forthcoming publication, where the investigation of different methyl celluloses with the present method will be reported.

1. Spurlin, H. M. in Ott, E. and Spurlin, H. M. *Cellulose and Cellulose Derivatives* II, New York 1954.
2. Rebenfeld, L. and Pacsu, E. *Textile Research J.* **24** (1954) 941.
3. Hess, K., Heumann, K. E. and Leipold, R. *Ann.* **594** (1955) 119.
4. Gibbons, G. C. *J. Textile Inst.* **47 : 10** (1956) T 511.
5. Lenz, R. W. and Holmberg, C. V. *Anal. Chem.* **28** (1956) 7.
6. Lindberg, B. and Wickberg, B. *Acta Chem. Scand.* **8** (1954) 569.
7. Croon, I. and Lindberg, B. *Svensk Papperstidn.* **59** (1956) 794.
8. Hirst, E. L., Hough, L. and Jones, J. K. N. *J. Chem. Soc.* **1949** 57.

Received December 21, 1956.

The Determination of N-terminal Amino Acids during the Conversion of Fibrinogen to Fibrin

BIRGER BLOMBACK and IKUO YAMASHINA

Chemistry Department II, Karolinska Institutet, Stockholm, Sweden

It has been suggested by earlier workers that the conversion of fibrinogen to fibrin is the result of a proteolytic reaction. Actually, in 1951, Lorand, Bettelheim and Bailey [1] showed by means of Sanger's method, differences in the N-terminal amino acids of fibrinogen and of fibrin. They also found "fibrinopeptides" in the supernatant of a fibrin clot produced by the action of thrombin [2-5]. However, due to the difficulties of determining the N-terminal amino acids quantitatively, no conclusive figures as to the number of polypeptide chains in either fibrinogen or in fibrin have been obtained [6]. Moreover, the doubtful purity of the fibrinogen preparations, used by earlier workers, might result in the release of contaminating substances from the fibrinogen preparation into the supernatant during the formation of fibrin.

Recently, a highly purified preparation of bovine fibrinogen has become available in our laboratory [7]. At least 99 % of the protein in this preparation is coagulable with thrombin, indicating that the fibrinopeptides make up only a very small part of fibrinogen. By applying Edman's method to this preparation, we reinvestigated the N-terminal amino acids both in fibrinogen and in fibrin. Determinations were also performed at different times during the conversion of fibrinogen to fibrin by thrombin.

The results show the presence of glutamine, glutamic acid and tyrosine as N-terminal amino acids in fibrinogen and the presence of glycine and tyrosine in fibrin. One glutamyl residue (amide plus acid) and one tyrosyl residue are present in about 1.7×10^5 g of fibrinogen and two glycyl residues and one tyrosyl residue in the corresponding amount of fibrin. Since the molecular weight of fibrinogen has been estimated to be $3.4 \times 100\,000$ [8,9], two glutamyl residues in the fibrinogen molecule seem to be replaced by four glycyl residues by the action of thrombin.

We have found that fibrin formed by means of papain or an enzyme extracted from snake venom has the same N-terminal amino acids as the normal fibrin. However, only two glycyl residues were found in those fibrins instead of four in the normal, thus indicating that there are differences in the mode of action among these three enzymes.

We have followed the proteolysis caused by thrombin in low concentration. The reaction was followed also by determining light-scattering [10]. During the action of thrombin on fibrinogen there is a time lag before polymerization and the subsequent coagulation occur. Glycine appeared as N-terminal amino acid immediately after the addition of thrombin to the fibrinogen solution, showing that there is a formation of an intermediary product, soluble fibrin, during this lag (Fig. 1). The amount of glycine released reaches a maximum value, about 40 % of the total, before any coagulation occurs.

During the coagulation the glycine in the supernatant decreases as shown in Fig. 2.

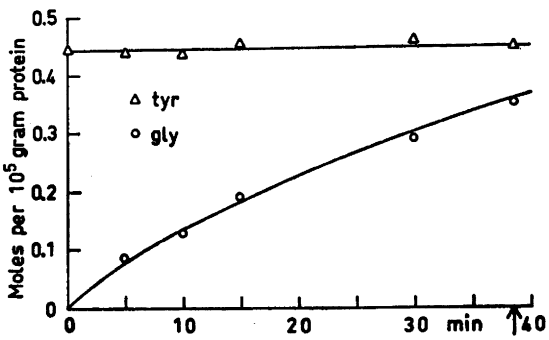


Fig. 1. The appearance of N-terminal glycine in the fibrinogen solution after addition of thrombin. The arrow indicates the coagulation-time.

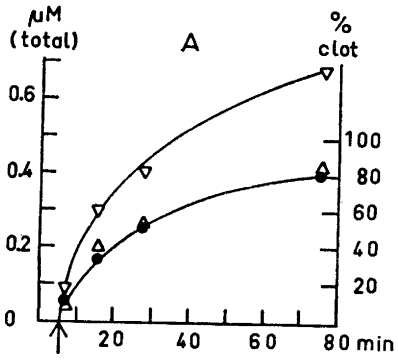
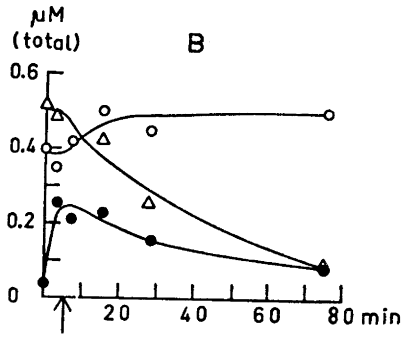


Fig. 2. A. N-Terminal amino acids and protein content of clots collected at different times. The arrow indicates the coagulation-time. ▽ gly; △ tyr; ● coagulated protein in per cent of total.



B. N-Terminal amino acids in the supernatant after removal of the clot. The arrow indicates the coagulation-time. △ tyr; ○ glu; ● gly.

Glutamic acid present originally as an N-terminal amino acid of fibrinogen remained in the supernatant throughout the reaction. The low figure found for glutamic acid in the early stage of the transformation is due to the lower yield of the phenylthiohydantoin amino acid in the presence of high concentrations of protein.

The total amount of tyrosine in fibrinogen and in fibrin was constant.

Judging from these experimental results, it is quite evident that the conversion of fibrinogen to fibrin includes the formation of soluble fibrin, and the subsequent polymerization of soluble fibrin to insoluble fibrin.

The complete paper will be published in Arkiv för Kemi in 1957.

1. Bailey, K., Bettelheim, F. R., Lorand, L. and Middlebrook, W. R. *Nature* **167** (1951) 233.
2. Lorand, L. and Middlebrook, W. R. *Biochem. J. London* **52** (1952) 196.
3. Lorand, L. *Biochem. J. London* **52** (1952) 200.
4. Bailey, K. and Bettelheim, F. R. *Biochim. et Biophys. Acta* **18** (1955) 495.
5. Bettelheim, F. R. *Biochim. et Biophys. Acta* **19** (1956) 121.
6. Bailey, K. and Bettelheim, F. R. *Brit. Med. Bull.* **11** (1955) 50.
7. Blombäck, M. and Blombäck, B. *Arkiv Kemi* **10** (1956) 415.
8. Katz, S., Gutfreund, K., Schulman, S. and Ferry, J. D. *J. Am. Chem. Soc.* **74** (1952) 5706.
9. Gaspary, E. A. and Kekwick, R. A. *Biochem. J. London* **56** (1953) xxxv.
10. Laurent, T. *et al. To be published.*

Received December 21, 1956.

Corrections to "Structure of the 1:1 Compound Pyridine — Iodo Monochloride"

O. HASSEL and CHR. RØMMING

Universitetets Kjemiske Institutt, Blindern-Oslo, Norway

In the paper[1] two corrections should be inserted: (1) The sign of the y parameter of the chlorine atom has to be changed from + to −, and (2) the distance quoted for the N-Cl separation (2.26) refers to the N-I bond distance.

1. Hassel, O. and Rømming, Chr. *Acta Chem. Scand.* **10** (1956) 696.

Received January 18, 1957.

Mass Spectrometric Studies of Long Chain Methyl Esters

A Determination of the Molecular Weight and Structure of Mycocerosic acid

JEAN ASSELINEAU*

Institute of Medical Biochemistry, University of Gothenburg, Gothenburg,

RAGNAR RYHAGE

Laboratory for Mass Spectrometry, Biochemical Institute, Karolinska Institutet, Stockholm, and

EINAR STENHAGEN

Department of Medical Biochemistry, Institute of Medical Chemistry, University of Uppsala, Uppsala, Sweden

Mass spectra of methyl esters of normal, long-chain fatty acids exhibit a series of peaks corresponding to ionized fragments of the general type $-(CH_2)_n-COOCH_3^+$ with intact methoxycarbonyl group.

The intensity distribution among this group of peaks in the case of methyl *n*-hexacosanoate is shown in Fig. 1 a. The spectrum also shows a large peak at $m/e = 74$, corresponding to an ionized molecule of methyl acetate formed by re-arrangement. This is analogous to the $m/e = 60$ peak found for *n*-carboxylic acids [1]. If the carbon atom in α-position to the methoxycarbonyl group carries one or two alkyl substituents these are included in the re-arranged fragment. A large peak thus appears at $m/e = 88$ for methyl 2-methylhexacosanoate (Fig. 1 b) and at $m/e = 116$ for methyl 2-methyl-2-ethyleicosanoate (Fig. 1 c).

Methyl 3-methyleicosanoate shows a large $m/e = 74$ peak, but the peak at $m/e = 87$ ($n = 2$) is comparatively low because the corresponding fragment can only be formed by the simultaneous breaking of two bonds and rearrangement of one hydrogen atom. On the other hand, $m/e = 101$ is large owing to easy cleavage of the bonds attached to the tertiary carbon atom in position 3.

Methyl 3,5-dimethyltricosanoate (Fig. 1 d) shows for $n = 1$—3 a behaviour very similar to that of the 3-methyl substituted ester just mentioned. The peak for $n = 4$ ($m/e = 129$) is small, as the corresponding fragment, like that of $m/e = 87$, can be formed only by the breaking of two bonds with simultaneous rearrangement.

Two stereo-isomers of methyl 3,4-dimethyldocosanoate have been studied. These give practically identical mass spectra, which show a strong $m/e = 74$ peak and a very large peak at $m/e = 101$. The latter corresponds to the fragment obtained by cleavage between the two tertiary carbon atoms in positions 3 and 4.

Methyl 2,4-dimethylheneicosanoate (Fig. 1 e) shows a weak peak at $m/e = 73$ and a strong one at $m/e = 88$, characteristic of a 2-methyl substituted ester. The peaks at $m/e = 101$ ($n = 3$) and 129 ($n = 5$) are strong, as they arise from cleavage of the bonds on both sides of the tertiary carbon atom in position 4. The peak at $m/e = 115$ is weak, as expected.

The methyl esters all give very strong parent peaks corresponding to the ionized unfragmented molecule. The mass-spectrum thus gives the exact molecular weight.

We have used the mass-spectrometric method to determine the molecular weight and structure of mycocerosic acid isolated from *M. tuberculosis* (human strain H-37) by Anderson and collaborators [2-4]. Ginger and Anderson [4] fractionated the methyl ester by distillation at low pressure. The highest-boiling fraction had m. p. 25°, $[\alpha]_D^{24}$—7.6° (chloroform), d_4^{30} 0.8541, n_D^{30} 1.4509. The analytical data for the acid agreed [4] best with $C_{30}H_{60}O_2$. Analogous or identical acids were later isolated by Chanley and Polgar [5] from a human strain of the bacillus, and by Asselineau [6] from the avirulent strain H 37 Ra. Polgar [7] subjected his compound, called mycoceranic acid, to stepwise degradation, and his results indicated the presence of methyl groups in positions 2, 4, and 6. The acid was considered probably to have 31 carbon atoms.

Cason and Fonken [8] have recently described a similar compound called C_{31}-mycosanoic acid. They report the following analytical data: C 79.89; H 13.50 %, equiv. wt. by titration 475. These data are, however, in better accord with the C_{32} formula (calc. for $C_{32}H_{64}O_2$: C 79.93; H 13.42 %; mol. wt. 480.8) than the C_{31} formula (calc. for $C_{31}H_{62}O_2$: C 79.76; H 13.39 %; mol. wt. 466.8).

The specimen of methyl mycocerosate used in the present work was prepared from a specimen of the acid obtained from Professor R. J. Anderson several years ago. A C-methyl

* Rockefeller Foundation Fellow, 1955—56. Present address: Institut de Biologie physico-chimique, Paris, France.

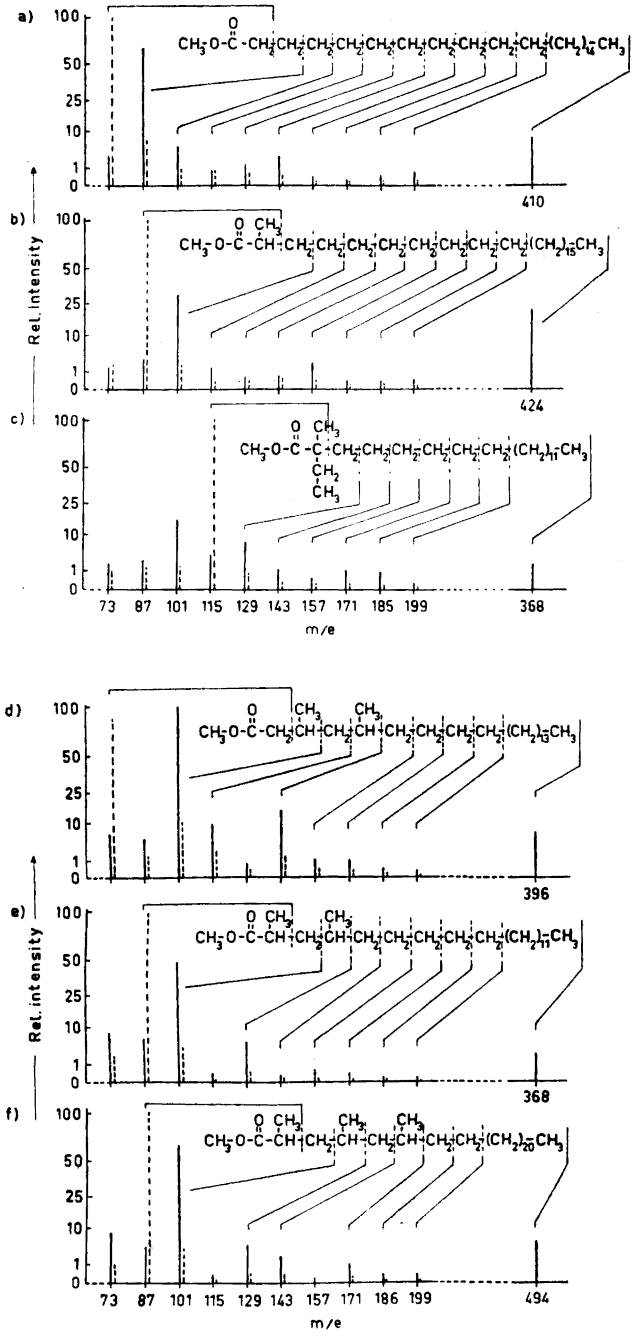


Fig. 1. Schematic diagram showing relative intensities of peaks corresponding to fragments containing an intact methoxycarbonyl group in mass-spectra of long-chain methyl esters. The heights of the vertical lines are proportional to the square root of the observed intensity, with the intensity of the strongest peak arbitrarily set at 100. Unbroken vertical lines represent normal fragments, and dotted lines re-arranged fragments in which the m/e is equal to m/e of the normal fragments plus one unit.
a) Methyl *n*-hexacosanoate b) Methyl 2-methylhexacosanoate c) Methyl 2-methyl-2-ethyleicosanoate d) Methyl 3,5-dimethyltricosanoate e) Methyl 2,4-dimethylheneicosanoate f) Methyl mycocerosate

group determination by a modified Kuhn-Roth method on the acid as received gave 3.33 equiv. of acetic acid, indicating the presence of four methyl groups [9]. The acid (887 mg) was converted into methyl ester by means of diazomethane, and the ester purified by chromatography on neutralized and slightly deactivated aluminium oxide. The ester fractions with the same refractive index (n_D^{25} 1.4520) were combined (589 mg), and distilled at 0.2 mm pressure: b. p. (air-bath temp.) 220—225°. The distilled methyl ester had m. p. 20.8—21.4°, $[\alpha]_D^{21.5}$ —7.8° (chloroform; *c*, 7.7); $n_D^{21.5}$ 1.4535; $d_4^{21.5}$ 0.8550.

The infra-red spectrum in the sodium chloride region was identical with that of methyl mycoceranate recently isolated by one of us (J.A.) from the *Test* strain of *M. tuberculosis* and with that of a specimen of methyl mycoceranate obtained from Dr. N. Polgar, Dyson Perrins Laboratory, Oxford, in 1953.

The purified methyl mycocerosate gave an excellent mass spectrum with a parent peak at $m/e = 494$ corresponding to the empirical formula $C_{33}H_{66}O_2$. There was no indication of the presence of homologous impurity. The empirical formula of the acid is thus $C_{32}H_{64}O_2$. In order to determine the nature and positions of the side chains the relevant parts of the mass spectrum were examined (Fig. 1 f). The low peak at $m/e = 74$ and strong peak at $m/e = 88$ show the presence of a methyl group in position 2. The low peak at $m/e = 115$ and the strong peaks at $m/e = 101$ and 129 indicate a further methyl side-chain in position 4 (*cf.* Fig. 1 e). Finally, the peak at $m/e = 157$ is very weak compared with those at $m/e = 143$ and 171, indicating the presence of a third methyl group in position 6. The methyl group positions derived for mycocerosic acid are thus the same as found for mycoceranic acid by Polgar [6].

A direct comparison with methyl mycoceranate from the *Test* strain was unfortunately not possible as the original sample had been converted into alcohol ("mycoceranol", m. p. 35.3—36.0°, $[\alpha]_D^{17}$ + 3.5° (chloroform)) before we had found that the methyl esters were especially suited to structure analysis. A mass-spectrometric study of the alcohol indicates the empirical formula $C_{32}H_{66}O$, and a comparison with the spectra of synthetic alcohols, including 2,4-dimethyleicosanol-1, shows that mycoceranol has methyl side-chains in positions 2, 4, and 6.

The results reported above make us believe that, apart from possible stereochemical differences (which cannot be studied by mass-spectrometric methods), mycocerosic, mycoceranic, and C_{31}-mycosanoic acids have the same structure, *viz.* that of 2,4,6-trimethylnonacosanoic acid.

We are indebted to Professor R. J. Anderson, Yale University, for the specimen of mycocerosic acid, and to Mrs. Stina Ställberg-Stenhagen for synthetic branched-chain acids. We also wish to thank Professor Einar Hammarsten for making possible the construction of a mass-spectrometer suitable for the study of structure problems in organic chemistry. Details of the instrument and details of the methyl ester and alcohol spectra will be given in forthcoming papers. The expenses of this work have been defrayed in part by grants from the *Swedish Medical Research Council.*

1. Happ, G. P. and Stewart, D. W. *J. Am. Chem. Soc.* **74** (1952) 4404.
2. Anderson, R. J. *J. Biol. Chem.* **97** (1932) 639.
3. Wieghard, C. W. and Anderson, R. J. *J. Biol. Chem.* **126** (1938) 505.
4. Ginger, L. G. and Anderson, R. J. *J. Biol. Chem.* **157** (1945) 203.
5. Chanley, J. D. and Polgar, N. *J. Chem. Soc.* **1954** 1003.
6. Asselineau, J. *Compt. rend.* **237** (1953) 1804.
7. Polgar, N. *J. Chem. Soc.* **1954** 1011.
8. Cason, J. and Fonken, G. J. *J. Biol. Chem.* **220** (1956) 391.
9. Kirsten, W. and Stenhagen, E. *Acta Chem. Scand.* **6** (1952) 682.

Received January 7, 1957.

Gradient Elution Analysis of Hop Bitter Substances

L. O. SPETSIG and MAJ STENINGER

Forskningslaboratoriet LKB, Äppelviken, Sweden

Studies in this laboratory [1] have shown recently that the humulones may be separated by reversed-phase partition chromatography with carbon tetrachloride as the stationary phase and 61 % (w/w) aqueous methanol as eluant. In the same manner the lupulones were resolved using 69 % (w/w) methanol as the moving phase.

Subsequent work has shown that both humulones and lupulones can be separated

group determination by a modified Kuhn-Roth method on the acid as received gave 3.33 equiv. of acetic acid, indicating the presence of four methyl groups [9]. The acid (887 mg) was converted into methyl ester by means of diazomethane, and the ester purified by chromatography on neutralized and slightly deactivated aluminium oxide. The ester fractions with the same refractive index (n_D^{25} 1.4520) were combined (589 mg), and distilled at 0.2 mm pressure: b. p. (air-bath temp.) 220—225°. The distilled methyl ester had m. p. 20.8—21.4°, $[\alpha]_D^{21.5}$ —7.8° (chloroform; *c*, 7.7); $n_D^{21.5}$ 1.4535; $d_4^{21.5}$ 0.8550.

The infra-red spectrum in the sodium chloride region was identical with that of methyl mycoceranate recently isolated by one of us (J.A.) from the *Test* strain of *M. tuberculosis* and with that of a specimen of methyl mycoceranate obtained from Dr. N. Polgar, Dyson Perrins Laboratory, Oxford, in 1953.

The purified methyl mycocerosate gave an excellent mass spectrum with a parent peak at $m/e = 494$ corresponding to the empirical formula $C_{33}H_{66}O_2$. There was no indication of the presence of homologous impurity. The empirical formula of the acid is thus $C_{32}H_{64}O_2$. In order to determine the nature and positions of the side chains the relevant parts of the mass spectrum were examined (Fig. 1 f). The low peak at $m/e = 74$ and strong peak at $m/e = 88$ show the presence of a methyl group in position 2. The low peak at $m/e = 115$ and the strong peaks at $m/e = 101$ and 129 indicate a further methyl side-chain in position 4 (*cf.* Fig. 1 e). Finally, the peak at $m/e = 157$ is very weak compared with those at $m/e = 143$ and 171, indicating the presence of a third methyl group in position 6. The methyl group positions derived for mycocerosic acid are thus the same as found for mycoceranic acid by Polgar [6].

A direct comparison with methyl mycoceranate from the *Test* strain was unfortunately not possible as the original sample had been converted into alcohol ("mycoceranol", m. p. 35.3—36.0°, $[\alpha]_D^{17}$ + 3.5° (chloroform)) before we had found that the methyl esters were especially suited to structure analysis. A mass-spectrometric study of the alcohol indicates the empirical formula $C_{32}H_{66}O$, and a comparison with the spectra of synthetic alcohols, including 2,4-dimethyleicosanol-1, shows that mycoceranol has methyl side-chains in positions 2, 4, and 6.

The results reported above make us believe that, apart from possible stereochemical differences (which cannot be studied by mass-spectrometric methods), mycocerosic, mycoceranic, and C_{31}-mycosanoic acids have the same structure, *viz.* that of 2,4,6-trimethylnonacosanoic acid.

We are indebted to Professor R. J. Anderson, Yale University, for the specimen of mycocerosic acid, and to Mrs. Stina Ställberg-Stenhagen for synthetic branched-chain acids. We also wish to thank Professor Einar Hammarsten for making possible the construction of a mass-spectrometer suitable for the study of structure problems in organic chemistry. Details of the instrument and details of the methyl ester and alcohol spectra will be given in forthcoming papers. The expenses of this work have been defrayed in part by grants from the *Swedish Medical Research Council.*

1. Happ, G. P. and Stewart, D. W. *J. Am. Chem. Soc.* **74** (1952) 4404.
2. Anderson, R. J. *J. Biol. Chem.* **97** (1932) 639.
3. Wieghard, C. W. and Anderson, R. J. *J. Biol. Chem.* **126** (1938) 505.
4. Ginger, L. G. and Anderson, R. J. *J. Biol. Chem.* **157** (1945) 203.
5. Chanley, J. D. and Polgar, N. *J. Chem. Soc.* **1954** 1003.
6. Asselineau, J. *Compt. rend.* **237** (1953) 1804.
7. Polgar, N. *J. Chem. Soc.* **1954** 1011.
8. Cason, J. and Fonken, G. J. *J. Biol. Chem.* **220** (1956) 391.
9. Kirsten, W. and Stenhagen, E. *Acta Chem. Scand.* **6** (1952) 682.

Received January 7, 1957.

Gradient Elution Analysis of Hop Bitter Substances

L. O. SPETSIG and MAJ STENINGER

Forskningslaboratoriet LKB, Äppelviken, Sweden

Studies in this laboratory [1] have shown recently that the humulones may be separated by reversed-phase partition chromatography with carbon tetrachloride as the stationary phase and 61 % (w/w) aqueous methanol as eluant. In the same manner the lupulones were resolved using 69 % (w/w) methanol as the moving phase.

Subsequent work has shown that both humulones and lupulones can be separated

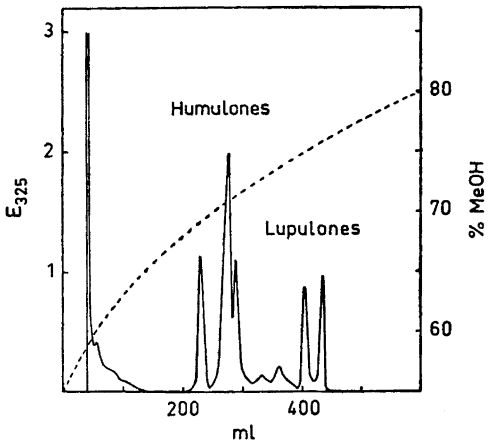


Fig. 1. Gradient elution analysis of humulones and lupulones from Hallertau hops. Column 800 × 8 mm.

in one single operation by means of gradient elution. If the analysis of the eluate is performed spectrophotometrically at 325 mμ, where the contributions from other hop substances is small, a solvent extract of hops can be used without purification. Fig. 1 shows the result of an analysis of the humulone and lupulone groups of Hallertau hops. The concentration gradient of the eluant was accomplished by letting 90 % (w/w) methanol flow into a constant volume mixing chamber loaded with 55 % (w/w) methanol, the effluent of which was fed to the column. The resolution was satisfactory but somewhat less complete than with normal elution. Thus lupulone and adlupulone were not separated.

In other experiments it has been possible to vary the methanol concentration over still wider ranges. Carbon tetrachloride extracts of hops have been shown to be very heterogeneous mixtures containing substances which may be eluted at methanol percentages varying from 0 to 85 % or still higher.

The collection of eluate fractions from a chromatographic column and the determination of the ultraviolet absorption of each fraction are inherently subject to systematic errors, which may be of a considerable magnitude, especially when working with substances which are unstable to air. The column effluent was therefore passed through a 5 mm absorption cell in a Hilger Uvispek spectrophotometer and the optical density at 280 or 325 mμ recorded automatically by a Brown recorder.

1. Spetsig, L. O. and Steninger, Maj, *J. Inst. Brewing* **62** (1956) 333.

Received January 14, 1957.

On the Production of Magnetic Centres in Glycine by X-Rays

A. EHRENBERG, L. EHRENBERG and K. G. ZIMMER

Biochemical Department, Nobel Medical Institute; Institute for Organic Chemistry and Biochemistry, University; and Genetics Department, Forest Research Institute, Stockholm, Sweden

The demonstration of the production of magnetic centres in a variety of chemicals by ionizing radiation might well lead to a better understanding of the mechanisms by which a relatively small amount of energy absorbed in the form of radiation causes marked biological effects [1-4]. The paramagnetic resonance spectra obtained have been tentatively explained by assuming that organic free radicals constitute the magnetic centres [5-8]. These results are of great interest to radiation biology when considered in relation to other evidence concerning aftereffects of irradiation and protection against radiation damage [9]. We thought it worth while to try and obtain data in order to evaluate, more quantitatively, the importance of the earlier observations for radiation biology. As a first step we investigated the relation between the dose of radiation administered and the number of magnetic centres produced in an amino acid, glycine.

For irradiation we used X-rays produced at 175 kV and filtered by 2 mm of aluminium (about 800 $r \cdot min^{-1}$). The dose was measured during the irradiation by means of a wavelength independent thimble chamber connected to a valve electrometer and integrating counter *(Duplex-Dosemeter)* carefully calibrated in Roentgens. The glycine, in amounts of about 150 mg, in the form of small crystals, was irradiated in evacuated and sealed quartz tubes, which were only half-filled. This en-

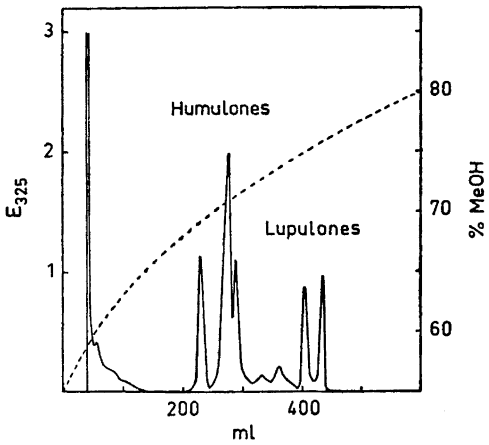


Fig. 1. Gradient elution analysis of humulones and lupulones from Hallertau hops. Column 800 × 8 mm.

in one single operation by means of gradient elution. If the analysis of the eluate is performed spectrophotometrically at 325 mμ, where the contributions from other hop substances is small, a solvent extract of hops can be used without purification. Fig. 1 shows the result of an analysis of the humulone and lupulone groups of Hallertau hops. The concentration gradient of the eluant was accomplished by letting 90 % (w/w) methanol flow into a constant volume mixing chamber loaded with 55 % (w/w) methanol, the effluent of which was fed to the column. The resolution was satisfactory but somewhat less complete than with normal elution. Thus lupulone and adlupulone were not separated.

In other experiments it has been possible to vary the methanol concentration over still wider ranges. Carbon tetrachloride extracts of hops have been shown to be very heterogeneous mixtures containing substances which may be eluted at methanol percentages varying from 0 to 85 % or still higher.

The collection of eluate fractions from a chromatographic column and the determination of the ultraviolet absorption of each fraction are inherently subject to systematic errors, which may be of a considerable magnitude, especially when working with substances which are unstable to air. The column effluent was therefore passed through a 5 mm absorption cell in a Hilger Uvispek spectrophotometer and the optical density at 280 or 325 mμ recorded automatically by a Brown recorder.

1. Spetsig, L. O. and Steninger, Maj, *J. Inst. Brewing* **62** (1956) 333.

Received January 14, 1957.

On the Production of Magnetic Centres in Glycine by X-Rays

A. EHRENBERG, L. EHRENBERG and K. G. ZIMMER

Biochemical Department, Nobel Medical Institute; Institute for Organic Chemistry and Biochemistry, University; and Genetics Department, Forest Research Institute, Stockholm, Sweden

The demonstration of the production of magnetic centres in a variety of chemicals by ionizing radiation might well lead to a better understanding of the mechanisms by which a relatively small amount of energy absorbed in the form of radiation causes marked biological effects [1-4]. The paramagnetic resonance spectra obtained have been tentatively explained by assuming that organic free radicals constitute the magnetic centres [5-8]. These results are of great interest to radiation biology when considered in relation to other evidence concerning aftereffects of irradiation and protection against radiation damage [9]. We thought it worth while to try and obtain data in order to evaluate, more quantitatively, the importance of the earlier observations for radiation biology. As a first step we investigated the relation between the dose of radiation administered and the number of magnetic centres produced in an amino acid, glycine.

For irradiation we used X-rays produced at 175 kV and filtered by 2 mm of aluminium (about 800 $r \cdot min^{-1}$). The dose was measured during the irradiation by means of a wavelength independent thimble chamber connected to a valve electrometer and integrating counter *(Duplex-Dosemeter)* carefully calibrated in Roentgens. The glycine, in amounts of about 150 mg, in the form of small crystals, was irradiated in evacuated and sealed quartz tubes, which were only half-filled. This en-

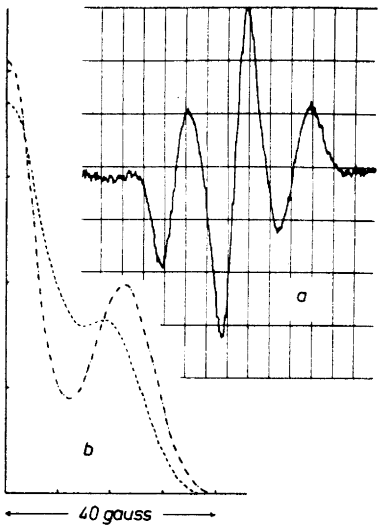


Fig. 1 a. Derivative of paramagnetic resonance spectrum of glycine, as recorded immediately after irradiation.
b. Paramagnetic resonance spectrum of glycine, —·— immediately and ····· 12 days after irradiation (integrated derivative curves).

abled one half of the tubes to be shielded from irradiation, and, after shaking the glycine into the unirradiated part of the tube, the measurement of paramagnetic resonance was conducted excluding completely the well known effects of radiation on quartz. The unirradiated quartz did not show any detectable signal. The spectrometer [10] used contained a simple microwave bridge operating at a frequency of 9 400 Mc. The signal reflected from the cavity could be recorded as an absorption curve on an oscillograph or as a derivative curve by means of a pen recorder. Irradiation and magnetic measurements were conducted at room temperature.

The spectra observed immediately after the irradiation (Fig. 1 a) showed a central peak at a g-value of 2.004 (± 0.001) and two satellites at ± 22.4 gauss. On keeping the material *in vacuo* and repeating the measurements the shape of the spectrum was found to change slowly (Fig. 1 b), though the area under the absorption curves remained essentially constant. This may be taken to indicate a constant number of magnetic centres. The decay, if any, is less than 1 % per day at about 20° C.

Spectra of identical shape could be recorded in the range from 2 kr to 350 kr, thus including much of the region of biological interest. Since the shape of the curves is independent of dosage, the linear rise in amplitude with dosage, shown in Fig. 2, indicates a corresponding increase in the number of magnetic centres.

Intensity, shape, and time dependence of the recorded spectra were not changed by the presence of air, neither during nor after irradiation, contrasting with results published for some other substances [5].

By comparing the areas under the absorption spectra of irradiated glycine and of a known amount of free radicals (diphenylpicryl hydrazyl) a rough estimate of the concentration of free radicals produced per unit dose in glycine could be obtained. The yield was found to be of the order of magnitude of 1 radical per 10 eV of radiation energy absorbed, *i. e.*, much higher than the values reported for plastics [11].

Another series of experiments was conducted with living material. Embryos cut from resting barley seeds yielded a resonance peak at a g-value characteristic of free radicals, when irradiated in air or in nitrogen. A more detailed account of these studies will appear elsewhere.

Acknowledgements. This work has been supported financially by the *Swedish Natural Science Research Council*, the *Magnus Bergvall Foundation* and the *Knut and Alice Wallen-*

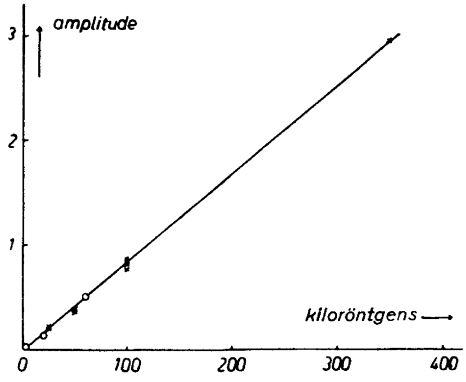


Fig. 2. Derivative amplitude (arbitrary units) of the paramagnetic absorption curve of glycine as a function of dose of irradiation by X-rays. × and O: two different series of experiments.

berg Foundation. Thanks are also due to Professor M. Siegbahn, Head of the Nobel Institute of Physics, for permission to use equipment of his institute. One of us (K.G.Z.) also wants to express his gratitude to the Max-Planck-Gesellschaft, Göttingen, for a maintenance and travelling grant.

1. Timoféeff-Ressovsky, N. W. and Zimmer, K. G. *Das Treffprinzip in der Biologie*, Leipzig 1947.
2. Zimmer, K. G. *Acta Radiol.* **46** (1956) 595.
3. Alper, T. *Radiation Research* **5** (1956) 573.
4. Gray, L. H. *Radiation Research* **1** (1954) 189.
5. Gordy, W., Ard, W. B. and Shields, H. *Proc. Natl. Acad. Sci. U.S.* **41** (1955) 983.
6. Gordy, W., Ard, W. B. and Shields, H. *Proc. Natl. Acad. Sci. U.S.* **41** (1955) 996.
7. Luck, C. F. and Gordy, W. *J. Am. Chem. Soc.* **78** (1956) 3240.
8. Gordy, W. and McCormick, C. G. *J. Am. Chem. Soc.* **78** (1956) 3243.
9. Ehrenberg, L. and Zimmer, K. G. *Hereditas* **42** (1956) 515.
10. Ehrenberg, A. and Hellström, B. *In preparation.*
11. Schneider, E. E. *Discussions Faraday Soc. No.* **19** (1955) 158.

Received January 15, 1957.

The Reduction of Plutonium by Tetravalent Uranium

JAN RYDBERG

Research Institute of National Defence, Dept. 1, Sundbyberg 4, Sweden

In the search for substances to reduce small amounts of plutonium of higher oxidation states to Pu(III) in the presence of large amounts of U(VI), U(IV) has been tested under a number of various conditions. The use of U(IV) for reducing plutonium does not seem not to have been described previously [1].

Tetravalent uranium at concentrations $\gtrsim 0.01$ M has been found to be stable in solutions of most acids for weeks or months if air is excluded. However, the stability in HNO_3 is poor, but increases with the U(IV) concentration. Maximum stability in HNO_3 seems to be obtained around 1 M HNO_3, where about 50 % of originally 0.1 M U(IV) is reduced in a little more than an hour at room temperature. Thus U(IV) can be used as a reducing agent even in HNO_3 solutions, provided the time of the experiments does not much exceed an hour.

In 1 M HNO_3, Pu(IV) and Pu(VI) are quantitatively (>99 %) reduced to Pu(III) by 0.1 M U(IV) within 5 min at room temperature. This effect can theoretically be used for separating uranium from plutonium in liquid-liquid extractions, if U(VI), U(IV), Pu(VI) and Pu(IV) prefer the organic phase and Pu(III) only prefers the aqueous phase [2]. The practical usefulness of this was tested in two sets of experiments.

In the first set of experiments two solutions were prepared. The organic solution consisted of methyl *iso*butyl ketone, which was 1.0 M in HNO_3 and contained Pu(IV) and Pu(VI); the aqueous solution was 0.7 M in HNO_3, 3 M in $Ca(NO_3)_2$ and contained a reductant. When these two phases are equilibrated with each other, the distribution ratio of the metals between the organic and the aqueous phases is for U(VI) 12, U(IV) $\sim$ 10, Pu(VI) 13, Pu(IV) 9, and Pu(III) $\lesssim 0.001$[3]; of these species thus only Pu(III) prefers the aqueous phase, and can easily be separated from the other metal ions. After the two phases had been shaken together, the amount of reduced plutonium (*i. e.* Pu(III)) was determined. Some of the results obtained with different reductants are given in the table for 5 min equilibration time.

Reducing agent	% Pu reduced
0.05 M $NH_2OH \cdot HCl$ + 0.005 M Fe^{2+}	65±8
0.05 M $H_4NOSO_2NH_2$ + 0.005 M Fe^{2+}	65±10
0.05 M U^{4+} in air	70±10
0.05 M U^{4+} in N_2	95±3

It is seen that U(IV) is equally or more effective than iron(II) plus hydroxylamine or sulfamate.

In the second set of experiments, the organic phase contained Pu(IV) as the uncharged TTA complex in 0.1 M TTA (thenoyltrifluoroacetone) in benzene, while the aqueous phase was 0.33 M in $HClO_4$ and contained U(IV). For 0.010 M U(IV), 14 % Pu had been reduced in 30 min, and 60 % in 20 h.

These experiments show the usefulness of U(IV) as a reducing agent for plutonium, either in aqueous solution or in two-phase

berg Foundation. Thanks are also due to Professor M. Siegbahn, Head of the Nobel Institute of Physics, for permission to use equipment of his institute. One of us (K.G.Z.) also wants to express his gratitude to the Max-Planck-Gesellschaft, Göttingen, for a maintenance and travelling grant.

1. Timoféeff-Ressovsky, N. W. and Zimmer, K. G. *Das Treffprinzip in der Biologie*, Leipzig 1947.
2. Zimmer, K. G. *Acta Radiol.* **46** (1956) 595.
3. Alper, T. *Radiation Research* **5** (1956) 573.
4. Gray, L. H. *Radiation Research* **1** (1954) 189.
5. Gordy, W., Ard, W. B. and Shields, H. *Proc. Natl. Acad. Sci. U.S.* **41** (1955) 983.
6. Gordy, W., Ard, W. B. and Shields, H. *Proc. Natl. Acad. Sci. U.S.* **41** (1955) 996.
7. Luck, C. F. and Gordy, W. *J. Am. Chem. Soc.* **78** (1956) 3240.
8. Gordy, W. and McCormick, C. G. *J. Am. Chem. Soc.* **78** (1956) 3243.
9. Ehrenberg, L. and Zimmer, K. G. *Hereditas* **42** (1956) 515.
10. Ehrenberg, A. and Hellström, B. *In preparation.*
11. Schneider, E. E. *Discussions Faraday Soc. No.* **19** (1955) 158.

Received January 15, 1957.

The Reduction of Plutonium by Tetravalent Uranium

JAN RYDBERG

Research Institute of National Defence, Dept. 1, Sundbyberg 4, Sweden

In the search for substances to reduce small amounts of plutonium of higher oxidation states to Pu(III) in the presence of large amounts of U(VI), U(IV) has been tested under a number of various conditions. The use of U(IV) for reducing plutonium does not seem not to have been described previously [1].

Tetravalent uranium at concentrations $\gtrsim 0.01$ M has been found to be stable in solutions of most acids for weeks or months if air is excluded. However, the stability in HNO_3 is poor, but increases with the U(IV) concentration. Maximum stability in HNO_3 seems to be obtained around 1 M HNO_3, where about 50 % of originally 0.1 M U(IV) is reduced in a little more than an hour at room temperature. Thus U(IV) can be used as a reducing agent even in HNO_3 solutions, provided the time of the experiments does not much exceed an hour.

In 1 M HNO_3, Pu(IV) and Pu(VI) are quantitatively (>99 %) reduced to Pu(III) by 0.1 M U(IV) within 5 min at room temperature. This effect can theoretically be used for separating uranium from plutonium in liquid-liquid extractions, if U(VI), U(IV), Pu(VI) and Pu(IV) prefer the organic phase and Pu(III) only prefers the aqueous phase [2]. The practical usefulness of this was tested in two sets of experiments.

In the first set of experiments two solutions were prepared. The organic solution consisted of methyl *iso*butyl ketone, which was 1.0 M in HNO_3 and contained Pu(IV) and Pu(VI); the aqueous solution was 0.7 M in HNO_3, 3 M in $Ca(NO_3)_2$ and contained a reductant. When these two phases are equilibrated with each other, the distribution ratio of the metals between the organic and the aqueous phases is for U(VI) 12, U(IV) $\sim$ 10, Pu(VI) 13, Pu(IV) 9, and Pu(III) $\lesssim 0.001$[3]; of these species thus only Pu(III) prefers the aqueous phase, and can easily be separated from the other metal ions. After the two phases had been shaken together, the amount of reduced plutonium (*i. e.* Pu(III)) was determined. Some of the results obtained with different reductants are given in the table for 5 min equilibration time.

Reducing agent	% Pu reduced
0.05 M $NH_2OH \cdot HCl$ + 0.005 M Fe^{2+}	65±8
0.05 M $H_4NOSO_2NH_2$ + 0.005 M Fe^{2+}	65±10
0.05 M U^{4+} in air	70±10
0.05 M U^{4+} in N_2	95±3

It is seen that U(IV) is equally or more effective than iron(II) plus hydroxylamine or sulfamate.

In the second set of experiments, the organic phase contained Pu(IV) as the uncharged TTA complex in 0.1 M TTA (thenoyltrifluoroacetone) in benzene, while the aqueous phase was 0.33 M in $HClO_4$ and contained U(IV). For 0.010 M U(IV), 14 % Pu had been reduced in 30 min, and 60 % in 20 h.

These experiments show the usefulness of U(IV) as a reducing agent for plutonium, either in aqueous solution or in two-phase

liquid-liquid extraction; however, in the presence of strong complexing agents for tetravalent actinides, the reduction is very slow. A more detailed account of the experiments will soon be given.

1. Connick, R. E. *Ch. 8 of "The Actinide Elements", National Nuclear Energy Series IV-14A*, McGraw-Hill Book Co, New York 1954.
2. Culler, F. L. § 5—2 of *"Process Chemistry, Vol. I", Progress in Nuclear Chemistry, Series III*, Pergamon Press Ltd, London 1956.
3. Rydberg, J. and Bernström, B. *Acta Chem. Scand.* **11** (1956) 86.

Received January 19, 1957.

Tritium Labelling of *p*-Aminosalicylic Acid (PAS)

ÅKE HANNGREN and JAN RYDBERG

Söderby Hospital, Uttran, and Pharm. Dept., Kgl. Veterinärhögskolan, Stockholm; Chem. Dept., Univ. of Stockholm, Stockholm, Sweden

For the study of the metabolic properties of the tuberculostatic agent *p*-aminosalicylic acid* (PAS) [1], it was of importance to obtain tritium labelled PAS. In order to avoid cumbersome syntheses, the possibility of using recoil tritons for the labelling [2] was investigated.

In this method the organic compound to be labelled is mixed with a lithium salt, and the mixture is irradiated with slow neutrons. From nuclear reactions between these neutrons and ^{6}Li, tritium atoms with a kinetic energy of 2.7 MeV** are produced. These fast tritons are successively slowed down by collisions with surrounding atoms, which cause heavy destruction along the path of the triton, until it is finally trapped in some molecule. Since the neutron irradiation usually is carried out in a nuclear reactor, considerable destruction of the organic compound is also caused by other high energy particles present (neutrons, γ-quanta, *etc.*). The irradiated mixture will therefore contain a number of decomposition products of the original compounds, which all may be labelled with tritons. As has been pointed out [3], the difficulty lies not in the labelling, but in the isolation of a pure product.

In our experiment, 6.0 g PAS was mixed with 0.6 g Li_2CO_3 and irradiated with a slow neutron flux of 1.4×10^{12} n/cm^2/sec for 120 h (temperature ~40° C) in the reactor at A. B. Atomenergi in Stockholm. The isolation of pure PAS from the product, which had slightly darkened during the irradiation, was made in the following manner.

The product was mixed with amyl alcohol, which dissolves PAS as well as some of the organic decomposition products but not the Li_2CO_3. After solid substances had been filtered off, the solution was shaken with an equal volume of 0.1 M $NaHCO_3$ in water.

The distribution ratio q of PAS between the two solvents is given by the equation

$$q = \frac{k_d}{1 + k_a [H^+]}$$

at pH > 3 (at lower pH another term has to be added in the denominator to correct for the amphoteric character of PAS). Since the dissociation constant [4] k_a of the carboxylic hydrogen in PAS is $10^{-4.08}$, and the distribution constant k_d of undissociated PAS between amyl alcohol and water was determined to be 36 ± 3, it is easily calculated that about 95 % of PAS goes down into the aqueous phase when this is 0.1 M in $NaHCO_3$ (pH ~ 7).

The aqueous solution thus obtained was washed five times with equal portions of amyl alcohol. Since the equation above is generally valid for monobasic acids, these washings with amyl alcohol remove all organic decomposition products with $k_a < 10^{-7}$ and $k_d > 1$ (including the probable decomposition product *m*-aminophenol (MAP) with [5] $k_a = 1.3 \times 10^{-10}$ and $k_d \sim 2$). The aqueous solution was then treated in two different ways.

In *procedure A*, 0.1 M HCl was added until pH 3.8 was reached. The solution was then shaken with an equal volume of amyl alcohol. From the equation above, it can be calculated that at pH 3.8 about 95 % of PAS will be obtained in the organic phase, while a number of organic impurities are left in the aqueous phase. By this procedure all substances are removed which do not have k_a and k_d close to that of PAS.

In *procedure B*, the aqueous phase was cooled in ice, and HCl was added until a

* Kindly supplied by A. B. Ferrosan, Malmö, Sweden.

** MeV = million electron volts.

liquid-liquid extraction; however, in the presence of strong complexing agents for tetravalent actinides, the reduction is very slow. A more detailed account of the experiments will soon be given.

1. Connick, R. E. *Ch. 8 of "The Actinide Elements", National Nuclear Energy Series IV-14A*, McGraw-Hill Book Co, New York 1954.
2. Culler, F. L. § 5—2 of *"Process Chemistry, Vol. I", Progress in Nuclear Chemistry, Series III*, Pergamon Press Ltd, London 1956.
3. Rydberg, J. and Bernström, B. *Acta Chem. Scand.* **11** (1956) 86.

Received January 19, 1957.

Tritium Labelling of *p*-Aminosalicylic Acid (PAS)

ÅKE HANNGREN and JAN RYDBERG

Söderby Hospital, Uttran, and Pharm. Dept., Kgl. Veterinärhögskolan, Stockholm; Chem. Dept., Univ. of Stockholm, Stockholm, Sweden

For the study of the metabolic properties of the tuberculostatic agent *p*-aminosalicylic acid* (PAS) [1], it was of importance to obtain tritium labelled PAS. In order to avoid cumbersome syntheses, the possibility of using recoil tritons for the labelling [2] was investigated.

In this method the organic compound to be labelled is mixed with a lithium salt, and the mixture is irradiated with slow neutrons. From nuclear reactions between these neutrons and ^{6}Li, tritium atoms with a kinetic energy of 2.7 MeV** are produced. These fast tritons are successively slowed down by collisions with surrounding atoms, which cause heavy destruction along the path of the triton, until it is finally trapped in some molecule. Since the neutron irradiation usually is carried out in a nuclear reactor, considerable destruction of the organic compound is also caused by other high energy particles present (neutrons, γ-quanta, *etc.*). The irradiated mixture will therefore contain a number of decomposition products of the original compounds, which all may be labelled with tritons. As has been pointed out [3], the difficulty lies not in the labelling, but in the isolation of a pure product.

In our experiment, 6.0 g PAS was mixed with 0.6 g Li_2CO_3 and irradiated with a slow neutron flux of 1.4×10^{12} n/cm^2/sec for 120 h (temperature ~40° C) in the reactor at A. B. Atomenergi in Stockholm. The isolation of pure PAS from the product, which had slightly darkened during the irradiation, was made in the following manner.

The product was mixed with amyl alcohol, which dissolves PAS as well as some of the organic decomposition products but not the Li_2CO_3. After solid substances had been filtered off, the solution was shaken with an equal volume of 0.1 M $NaHCO_3$ in water.

The distribution ratio q of PAS between the two solvents is given by the equation

$$q = \frac{k_d}{1 + k_a [H^+]}$$

at pH > 3 (at lower pH another term has to be added in the denominator to correct for the amphoteric character of PAS). Since the dissociation constant [4] k_a of the carboxylic hydrogen in PAS is $10^{-4.08}$, and the distribution constant k_d of undissociated PAS between amyl alcohol and water was determined to be 36 ± 3, it is easily calculated that about 95 % of PAS goes down into the aqueous phase when this is 0.1 M in $NaHCO_3$ (pH ~ 7).

The aqueous solution thus obtained was washed five times with equal portions of amyl alcohol. Since the equation above is generally valid for monobasic acids, these washings with amyl alcohol remove all organic decomposition products with $k_a < 10^{-7}$ and $k_d > 1$ (including the probable decomposition product *m*-aminophenol (MAP) with [5] $k_a = 1.3 \times 10^{-10}$ and $k_d \sim 2$). The aqueous solution was then treated in two different ways.

In *procedure A*, 0.1 M HCl was added until pH 3.8 was reached. The solution was then shaken with an equal volume of amyl alcohol. From the equation above, it can be calculated that at pH 3.8 about 95 % of PAS will be obtained in the organic phase, while a number of organic impurities are left in the aqueous phase. By this procedure all substances are removed which do not have k_a and k_d close to that of PAS.

In *procedure B*, the aqueous phase was cooled in ice, and HCl was added until a

* Kindly supplied by A. B. Ferrosan, Malmö, Sweden.

** MeV = million electron volts.

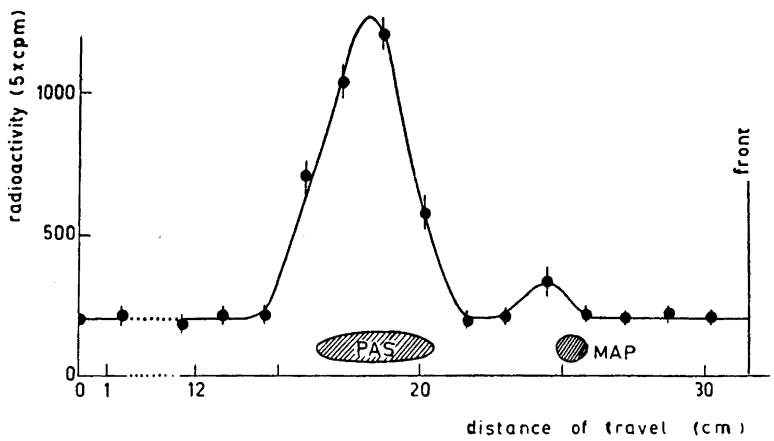


Fig. 1. Paper chromatogram of PAS purified according to method B. For comparison spots obtained with pure PAS and MAP are also shown.

pH around 3 was reached, when PAS precipitates. Now it is known that at this acidity PAS may decompose to MAP[6]; however, under the conditions used not more than a few percent was decomposed (see further below). The advantage of this procedure is that it leads to a solid PAS compound somewhat more rapidly than procedure A.

In both procedures tritium, which is unstably bound in the pH range 4—7 (as *e. g.* carboxylic hydrogen), is removed.

In order to test the purity of the products, paper chromatograms were run on Whatman No. 4 papers using a mixture of 40 % methyl alcohol, 20 % amyl alcohol, 20 % benzene, and 20 % water[7]. Due to the low energy of the β-radiation from tritium (0.018 MeV, corresponding to a maximum range of about 0.7 mg/cm^2), the radioactivity from tritium could not be measured directly on the paper chromatograms. These were therefore cut in pieces, and the activity eluted by several washings with the solvent mixture. The eluates were collected in aluminum dishes and evaporated, and the activity of the samples was measured in an internal proportional counter.

Fig. 1 shows the results obtained with PAS purified according to method B. As a comparison, parallel runs were made with ordinary PAS and MAP; these spots were determined either in ultraviolet light or developed with Ehrlich reagent. It is believed that the activity found is only due to tritium in PAS and MAP. The MAP may originate from the decomposition of some PAS at the high acidity used in the final step. By integrating the areas under the peaks in Fig. 1, after the back ground has been subtracted, it is found that 4 ± 2 % of the total tritium activity is due to tritium is bound in MAP; the rest of the activity to PAS.

The specific activity of the product was determined in the same counting arrangement, which had an efficiency of about 60 % for the β-radiation from tritium. This value includes geometry factors and back-scattering but excludes self-absorption. Since the self-absorption in the samples is very high, successive dilutions were made with ethyl alcohol, and the activity of aliquotes measured after each dilution. The following results were obtained:

μg PAS in sample	cpm	cpm/μg PAS
278	43 000	155
22.2	6 100	274
1.78	1 000$\pm$40	561
0.143	120$\pm$12	840
0.0114	11$\pm$5	970

The specific activity approaches a constant value, which is estimated to 1 500 ± 500 cpm/μg PAS. With this value and knowing the efficiency of the counter, the yield in the tritium labelling of PAS is calculated to 1.5 ± 0.5 mC/g PAS.

1. Hanngren, Å. *To be published.*
2. Wolfgang, R., Rowland, F. S. and Turton, C. N. *Science* **121** (1955) 715.
3. Rowland, F. S. and Wolfgang, R. *Nucleonics* **14** No. 8 (1956) 58.
4. Ågren, A. *Acta Chem. Scand.* **8** (1954) 1059.
5. Kuhn, R. and Wassermann, A. *Helv. Chim. Acta* **11** (1928) 23, 25.
6. Ågren, A. *Farmaceutisk Revy* **54** (1955) 225.
7. Ekman, B. *Acta Chem. Scand.* **2** (1948) 383.

Preparation of 2-Methyl[1-^{14}C]-octadecanoic Acid

GUNNEL WESTÖÖ

*Department of Physiological Chemistry *, University of Lund, Lund, Sweden*

2-Methyloctadecanoic acid has been prepared by several investigators, *e. g.* by Schneider and Spielman [1] from diethyl methylmalonate and hexadecyliodide and by Morgan and Holmes [2] from methylmagnesiumiodide and 2-bromooctadecanoic acid.

For the preparation of [carboxy-^{14}C] 2-methyloctadecanoic acid a Kolbe electrolysis of hexadecanoic acid and sodium 3-[^{14}C]cyanobutyrate and subsequent hydrolysis of the cyano group seemed more suitable and was found to be convenient. The cyanobutyrate (previously prepared in a different way by Widequist [3]) was easily obtained in comparatively good yield from ethyl crotonate and sodium [^{14}C]cyanide (*cf.* the preparation of methylsuccinic acid by Higginbotham and Lapworth [4]).

Experimental. Sodium 3-[^{14}C]cyanobutyrate (I). A solution of ethyl crotonate (0.91 g) in ethanol (3.6 ml) was mixed with 0.41 g of sodium [^{14}C]cyanide dissolved in 1.0 ml of water and the mixture refluxed on a water bath for 5 h. The solvents were removed by distillation and the residue extracted with boiling acetone. The insoluble fraction was filtered off. On cooling the filtrate, colourless crystals of I (0.72 g, 67 %) separated. They were dried at 0.4 mm Hg, 78°. (Found: C 44.0; H 4.7; N 10.1. Calc. for $C_5H_6NO_2Na$: C 44.4; H 4.5; N 10.4.)

2-Methyl[1-^{14}C]octadecanoic acid (III). A solution of I (0.64 g of crude product) and hexadecanoic acid (7.0 g) in methanol (75 ml) was electrolysed between platinum electrodes as described by Stenhagen [5]. The precipitate (triacontane and a small amount of 2-methyloctadecanenitrile, II) was filtered off at room temperature and dissolved in boiling methanol. The solution was cooled to 20° and the precipitate again removed by filtration. The combined methanol solutions were evaporated and the residue extracted with ether, saturated with water. After removal of free acids from the ether solution by the ion exchanger Amberlite IRA 400, the ether was evaporated and the product hydrolysed by refluxing with ethanolic potassium hydroxide solution. Water was added to the hydrolysate, and hydrocarbons were removed by extraction with ligroin. Acidification of the alcohol-water layer and extraction of the 2-methyl[1-^{14}C]octadecanoic acid with ether, yielded 0.65 g (46 %) of crude III. After recrystallization from methanol and ligroin, 0.36 g of pure acid, m.p. 54.5—55.0°, remained. Schneider and Spielman [1] give m.p. 54.5°, Cason, Wolfhagen, Tarpey and Adams [6] 54.6—55.1° and Morgan and Holmes 58°.

* Now Institute of Organic Chemistry.

$$CH_3CH{=}CHCOOC_2H_5 + Na^{14}CN + H_2O \rightarrow \underset{\text{I}}{CH_3CH(^{14}CN)CH_2COONa} + C_2H_5OH.$$

$$CH_3(CH_2)_{14}COOH + CH_3CH(^{14}CN)CH_2COONa \xrightarrow[\text{in } CH_3OH]{\text{electrolysis}}$$

$$CH_3(CH_2)_{15}CH(CH_3)^{14}CN \xrightarrow{\text{hydrolysis}} CH_3(CH_2)_{15}CH(CH_3)^{14}COOH.$$

II III

The specific activity approaches a constant value, which is estimated to 1 500 ± 500 cpm/μg PAS. With this value and knowing the efficiency of the counter, the yield in the tritium labelling of PAS is calculated to 1.5 ± 0.5 mC/g PAS.

1. Hanngren, Å. *To be published.*
2. Wolfgang, R., Rowland, F. S. and Turton, C. N. *Science* **121** (1955) 715.
3. Rowland, F. S. and Wolfgang, R. *Nucleonics* **14** No. 8 (1956) 58.
4. Ågren, A. *Acta Chem. Scand.* **8** (1954) 1059.
5. Kuhn, R. and Wassermann, A. *Helv. Chim. Acta* **11** (1928) 23, 25.
6. Ågren, A. *Farmaceutisk Revy* **54** (1955) 225.
7. Ekman, B. *Acta Chem. Scand.* **2** (1948) 383.

Preparation of 2-Methyl[1-^{14}C]-octadecanoic Acid

GUNNEL WESTÖÖ

*Department of Physiological Chemistry *, University of Lund, Lund, Sweden*

2-Methyloctadecanoic acid has been prepared by several investigators, *e. g.* by Schneider and Spielman [1] from diethyl methylmalonate and hexadecyliodide and by Morgan and Holmes [2] from methylmagnesiumiodide and 2-bromooctadecanoic acid.

For the preparation of [carboxy-^{14}C] 2-methyloctadecanoic acid a Kolbe electrolysis of hexadecanoic acid and sodium 3-[^{14}C]cyanobutyrate and subsequent hydrolysis of the cyano group seemed more suitable and was found to be convenient. The cyanobutyrate (previously prepared in a different way by Widequist [3]) was easily obtained in comparatively good yield from ethyl crotonate and sodium [^{14}C]cyanide (*cf.* the preparation of methylsuccinic acid by Higginbotham and Lapworth [4]).

Experimental. Sodium 3-[^{14}C]cyanobutyrate (I). A solution of ethyl crotonate (0.91 g) in ethanol (3.6 ml) was mixed with 0.41 g of sodium [^{14}C]cyanide dissolved in 1.0 ml of water and the mixture refluxed on a water bath for 5 h. The solvents were removed by distillation and the residue extracted with boiling acetone. The insoluble fraction was filtered off. On cooling the filtrate, colourless crystals of I (0.72 g, 67 %) separated. They were dried at 0.4 mm Hg, 78°. (Found: C 44.0; H 4.7; N 10.1. Calc. for $C_5H_6NO_2Na$: C 44.4; H 4.5; N 10.4.)

2-Methyl[1-^{14}C]octadecanoic acid (III). A solution of I (0.64 g of crude product) and hexadecanoic acid (7.0 g) in methanol (75 ml) was electrolysed between platinum electrodes as described by Stenhagen [5]. The precipitate (triacontane and a small amount of 2-methyloctadecanenitrile, II) was filtered off at room temperature and dissolved in boiling methanol. The solution was cooled to 20° and the precipitate again removed by filtration. The combined methanol solutions were evaporated and the residue extracted with ether, saturated with water. After removal of free acids from the ether solution by the ion exchanger Amberlite IRA 400, the ether was evaporated and the product hydrolysed by refluxing with ethanolic potassium hydroxide solution. Water was added to the hydrolysate, and hydrocarbons were removed by extraction with ligroin. Acidification of the alcohol-water layer and extraction of the 2-methyl[1-^{14}C]octadecanoic acid with ether, yielded 0.65 g (46 %) of crude III. After recrystallization from methanol and ligroin, 0.36 g of pure acid, m.p. 54.5—55.0°, remained. Schneider and Spielman [1] give m.p. 54.5°, Cason, Wolfhagen, Tarpey and Adams [6] 54.6—55.1° and Morgan and Holmes 58°.

* Now Institute of Organic Chemistry.

$$CH_3CH{=}CHCOOC_2H_5 + Na^{14}CN + H_2O \rightarrow \underset{\text{I}}{CH_3CH(^{14}CN)CH_2COONa} + C_2H_5OH.$$

$$CH_3(CH_2)_{14}COOH + CH_3CH(^{14}CN)CH_2COONa \xrightarrow[\text{in } CH_3OH]{\text{electrolysis}}$$

$$CH_3(CH_2)_{15}CH(CH_3)^{14}CN \xrightarrow{\text{hydrolysis}} CH_3(CH_2)_{15}CH(CH_3)^{14}COOH.$$

II III

The analyses were performed by Miss M. Westerdahl, Department of Analytical Chemistry, University of Lund.

The financial support of *Statens naturvetenskapliga forskningsråd* is gratefully acknowledged.

1. Schneider, A. K. and Spielman, M. A. *J. Biol. Chem.* **142** (1942) 345.
2. Morgan, G. T. and Holmes, E. *J. Soc. Chem. Ind.* **46** (1927) 152 (*Chem. Zentr.* 1927 II 1464).
3. Widequist, S. *Arkiv Kemi, Mineral. Geol.* **26** A (1949) No. 16.
4. Higginbotham, L. and Lapworth, A. *J. Chem. Soc.* **121** (1922) 49.
5. Ställberg-Stenhagen, S. *Arkiv Kemi* **2** (1951) 95.
6. Cason, J., Wolfhagen, H., Tarpey, W. and Adams, R. *J. Org. Chem.* **14** (1949) 147.

Received January 7, 1957.

The Paramagnetic Resonance Absorption of a Semiquinone of FMN

ANDERS EHRENBERG

Biochemical Department, Nobel Medical Institute, Stockholm, Sweden

Recently Beinert [1] has presented strong evidence for the existence of a semiquinoid compound appearing as an intermediate in the oxidation-reduction reactions of flavinmononucleotide (FMN). In collaboration with Gutowsky and Rutledge he succeeded in obtaining a paramagnetic resonance signal characteristic of a free radical from FMN reduced by Zn in an acid 50 % aqueous ethanol solution [1]. They failed to obtain any signal with a pure aqueous solution *, because of the high dielectric losses in liquid water. It is, however, of the greatest importance to be able to investigate the paramagnetic resonance of this and similar substances as the postulated semiquinones of FAD, DPN and TPN when they are dissolved in water, the milieu of the enzymatic reactions in which they are supposed to take part [2,3].

By freezing the samples, which diminishes the dielectric losses greatly, and working at liquid N_2 temperatures, which improved the sensitivity, it has now been possible to record intense resonance signals from the semiquinone of FMN in dilute solutions. The FMN was dissolved in 1 N HCl and reduced by metallic Zn, until the color was brownish. A 0.20 ml sample was transferred to a small quartz tube, which immediately was dipped into liquid N_2. The solution rapidly solidified and was cooled down to 80° K. The sample was then transferred into the precooled high-Q cavity of the spectrometer [4] operated at 9 400 Mc and the spectrum was recorded (Fig. 1). It did not change over a period of 30 min at liquid N_2 temperature. No signal could be obtained from FMN before adding Zn or after reoxidation in air, nor from a sample without FMN but reacted with Zn. The g-value of the resonance is practically identical with that of the free radical diphenylpicryl hydrazyl. No further signals could be seen in the region 2 600 to 3 900 gauss and no hyperfine structure has thus far been resolved.

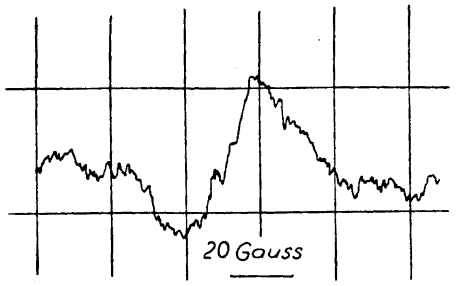


Fig. 1. Derivative of paramagnetic resonance absorption of 160 μM FMN in 1 N HCl after reduction by solid Zn for 8 min and subsequent rapid cooling to about 80° K.

Comparison of the surfaces under the absorption curve obtained by integration of Fig. 1 and that of a known amount of diphenylpicryl hydrazyl reveals that the concentration of free radicals is roughly half the initial concentration of FMN. This would appear to dispel any doubt that a semiquinone intermediate of FMN is really formed under the conditions described.

The technique used here will be of great value in cases when the intermediate is shortlived, since the low temperature will practically lock the reaction at a desired

* Personal communication.

The analyses were performed by Miss M. Westerdahl, Department of Analytical Chemistry, University of Lund.

The financial support of *Statens naturvetenskapliga forskningsråd* is gratefully acknowledged.

1. Schneider, A. K. and Spielman, M. A. *J. Biol. Chem.* **142** (1942) 345.
2. Morgan, G. T. and Holmes, E. *J. Soc. Chem. Ind.* **46** (1927) 152 (*Chem. Zentr.* 1927 II 1464).
3. Widequist, S. *Arkiv Kemi, Mineral. Geol.* **26** A (1949) No. 16.
4. Higginbotham, L. and Lapworth, A. *J. Chem. Soc.* **121** (1922) 49.
5. Ställberg-Stenhagen, S. *Arkiv Kemi* **2** (1951) 95.
6. Cason, J., Wolfhagen, H., Tarpey, W. and Adams, R. *J. Org. Chem.* **14** (1949) 147.

Received January 7, 1957.

The Paramagnetic Resonance Absorption of a Semiquinone of FMN

ANDERS EHRENBERG

Biochemical Department, Nobel Medical Institute, Stockholm, Sweden

Recently Beinert [1] has presented strong evidence for the existence of a semiquinoid compound appearing as an intermediate in the oxidation-reduction reactions of flavinmononucleotide (FMN). In collaboration with Gutowsky and Rutledge he succeeded in obtaining a paramagnetic resonance signal characteristic of a free radical from FMN reduced by Zn in an acid 50 % aqueous ethanol solution [1]. They failed to obtain any signal with a pure aqueous solution *, because of the high dielectric losses in liquid water. It is, however, of the greatest importance to be able to investigate the paramagnetic resonance of this and similar substances as the postulated semiquinones of FAD, DPN and TPN when they are dissolved in water, the milieu of the enzymatic reactions in which they are supposed to take part [2,3].

By freezing the samples, which diminishes the dielectric losses greatly, and working at liquid N_2 temperatures, which improved the sensitivity, it has now been possible to record intense resonance signals from the semiquinone of FMN in dilute solutions. The FMN was dissolved in 1 N HCl and reduced by metallic Zn, until the color was brownish. A 0.20 ml sample was transferred to a small quartz tube, which immediately was dipped into liquid N_2. The solution rapidly solidified and was cooled down to 80° K. The sample was then transferred into the precooled high-Q cavity of the spectrometer [4] operated at 9 400 Mc and the spectrum was recorded (Fig. 1). It did not change over a period of 30 min at liquid N_2 temperature. No signal could be obtained from FMN before adding Zn or after reoxidation in air, nor from a sample without FMN but reacted with Zn. The g-value of the resonance is practically identical with that of the free radical diphenylpicryl hydrazyl. No further signals could be seen in the region 2 600 to 3 900 gauss and no hyperfine structure has thus far been resolved.

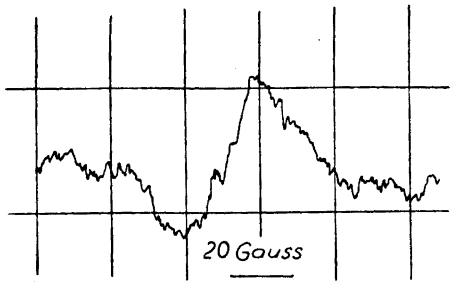


Fig. 1. Derivative of paramagnetic resonance absorption of 160 μM FMN in 1 N HCl after reduction by solid Zn for 8 min and subsequent rapid cooling to about 80° K.

Comparison of the surfaces under the absorption curve obtained by integration of Fig. 1 and that of a known amount of diphenylpicryl hydrazyl reveals that the concentration of free radicals is roughly half the initial concentration of FMN. This would appear to dispel any doubt that a semiquinone intermediate of FMN is really formed under the conditions described.

The technique used here will be of great value in cases when the intermediate is shortlived, since the low temperature will practically lock the reaction at a desired

* Personal communication.

stage. Work is in progress to correlate the amount of FMN-semiquinone to the absorption curves of the reaction mixture in the visible region under various conditions and to investigate whether the semiquinone can be formed from FMN, when it is bound to the apoprotein of the old yellow enzyme.

Acknowledgements. Thanks are due to the *Swedish Research Council of Natural Science* and the *Magnus Bergvall Foundation* for financial support and to Professor M. Siegbahn, Head of the Nobel Institute of Physics, for permission to use equipment of his institute.

1. Beinert, H. *J. Am. Chem. Soc.* **78** (1956) 5323.
2. Beinert, H. *Biochim. et Biophys. Acta* **20** (1956) 588.
3. Beinert, H. *In press.*
4. Ehrenberg, A. and Hellström, B. *In preparation.*

Received January 21, 1957.

ACTA CHEMICA SCANDINAVICA 11 (1957) 207—218

Electronic Structure of Metal Aromatic Complexes

A. D. LIEHR* and C. J. BALLHAUSEN**

Mallinckrodt Laboratory, Harvard University, Cambridge, Massachusetts, U.S.A.

A semi-quantitative theory of the electronic structure of aromatic complexes formed by the *cyclo*pentadienyl radical and by benzene is presented. The theory utilizes the wavefunctions given by the molecular-orbital theory, and on the basis of a simple scheme for evaluating the necessary integrals gives an internally consistent treatment of the bonding in metal aromatic complexes. The magnetic properties of these compounds are correlated by means of the given theory. A comparison between the treatment here presented and those of previous authors is given.

All of the theories of "sandwich" bonding thus far proposed have made use of the molecular orbital theory of valence.[1-4] The various treatments differ solely in the methods of determining the relative locations of the sundry molecular energy levels.

The most general mixing of the available *cyclo*pentadienyl radical and metal orbitals to form appropriate molecular orbitals has been performed by Jaffé [1] and by Ruch [4]. The approach of both of these authors is open to some criticism. Whereas Jaffé's treatment is too indefinite as to the relative positions of the molecular energy levels, Ruch's treatment is governed too much by a predisposition to obtain a rare gas configuration about the metal atom. Because of these objections neither Jaffé nor Ruch is able to give a satisfactory physical picture of the bonding in di-π-*cyclo*pentadienyl compounds.

The first physically appealing treatment of the problem was given by Dunitz and Orgel [2a]. These authors assumed that the *cyclo*pentadienyl orbital $\psi_{cp}(a_{1g})$ was too tightly bound to mix with any of the available metal orbitals of symmetry a_{1g}, such as $3d(a_{1g})$ and $4s(a_{1g})$. They likewise assumed that the empty 4p levels of the metal atom were too far removed energetically to interact with the filled *cyclo*pentadienyl orbitals $\psi_{cp}(a_{1u})$ and $\psi_{cp}(e_{1u})$. Further, they proposed that the bonding consisted mainly of two "covalent-ionic" bonds between the half-filled *cyclo*pentadienyl orbitals $\psi_{cp}(e_{1g})$ and the metal orbitals $3d(e_{1g})$. It was also supposed that the bonding could take place *via*

* National Science Foundation Post-doctoral Fellow, 1955—56. Now at Bell Telephone Laboratories, Murray Hill, New Jersey, U.S.A.

** On leave of absence from the Technical University of Denmark, Chemical Laboratory A, Copenhagen, Denmark.

two "donor" bonds formed by the mixing of the empty *cyclo*pentadienyl orbitals $\psi_{cp}(e_{2g})$ with the metal orbitals $3d(e_{2g})$.

However, as more experimental data became available, it was found that the bonding scheme as first proposed by Dunitz and Orgel was not adequate to explain the magnetic properties of all the newly prepared *cyclo*pentadienyl-metal compounds. This led Moffitt [3] to propose a modification of the Dunitz and Orgel model. He assumed that the large difference in energy between the $3d(e_{2g})$ and the $\psi_{cp}(e_{2g})$ orbitals precluded any interaction of these orbitals, and thus eliminated the "donor" bonds of Dunitz and Orgel. He also assumed that the $4s(a_{1g})$ and $3d(a_{1g})$ metal orbitals interact under the molecular force fields to produce one orbital lying in the vicinity of the 4p metal orbitals, and one in the vicinity of the $3d(e_{2g})$ orbitals. Moreover, he placed the antibonding orbital of symmetry e_{1g} above the 4p metal orbitals. This model will explain satisfactorily the magnetic properties of the di-π-*cyclo*pentadienyl compounds, but is admittedly of a qualitative nature.

The first and only other semi-quantitative treatment has been recently published by Dunitz and Orgel [2b]. They have retained the major portion of their own previous theory [2a], but have also included some of the modifications given by Moffitt. They differ from Moffitt in placing the antibonding levels of symmetry e_{1g} below the 4p levels of the metal. This calculation of Dunitz and Orgel is based on the heuristic principle which states that the interaction energy is proportional to the overlap, the overlap being computed according to the prescriptions of Craig, Maccoll, Nyholm, Orgel and Sutton [5]. This means of evaluating the molecular integrals seems to the present authors to be less satisfactory than that utilized in this paper.

1. ENERGY LEVELS FOR THE DI-π-*CYCLO*PENTADIENYL COMPOUNDS

The di-π-*cyclo*pentadienyl compounds have the structure depicted in Fig. 1[2a]. Thus, calling one *cyclo*pentadienyl ring CpA and the other CpB, we have the following wave functions for the *cyclo*pentadienyl ring systems [3],

$$\begin{aligned}
&\mathrm{Cp}S(a_2'') = (5)^{-\frac{1}{2}}\sum_r \varphi_r^{(s)} && (S = \mathrm{A, B}).\\
&\mathrm{Cp}S(e_{1\pm}'') = (5)^{-\frac{1}{2}}\sum_r (\omega^{\pm 1})^r \varphi_r^{(s)} && \omega = \exp(2\pi i/5)\\
&\mathrm{Cp}S(e_{2\pm}'') = (5)^{-\frac{1}{2}}\sum_r (\omega^{\pm 2})^r \varphi_r^{(s)}. && (1)
\end{aligned}$$

In eqn (1) we have given in parenthesis the symmetry designations of the wave functions CpS (S = A, B) in the point group D_{5h}. Combining the wave functions given in (1) to form molecular orbitals of symmetry D_{5d} we have

$$\begin{aligned}
\psi_{cp}(a_{1g}) &= (2)^{-\frac{1}{2}}\{\mathrm{CpA}(a_2'') - \mathrm{CpB}(a_2'')\}\\
\psi_{cp}(a_{1u}) &= (2)^{-\frac{1}{2}}\{\mathrm{CpA}(a_2'') + \mathrm{CpB}(a_2'')\}\\
\psi_{cp}(e_{1g}^{\pm}) &= (2)^{-\frac{1}{2}}\{\mathrm{CpA}(e_{1\pm}'') - \mathrm{CpB}(e_{1\pm}'')\}\\
\psi_{cp}(e_{1u}^{\pm}) &= (2)^{-\frac{1}{2}}\{\mathrm{CpA}(e_{1\pm}'') + \mathrm{CpB}(e_{1\pm}'')\}\\
\psi_{cp}(e_{2g}^{\pm}) &= (2)^{-\frac{1}{2}}\{\mathrm{CpA}(e_{2\pm}'') - \mathrm{CpB}(e_{2\pm}'')\}\\
\psi_{cp}(e_{2u}^{\pm}) &= (2)^{-\frac{1}{2}}\{\mathrm{CpA}(e_{2\pm}'') + \mathrm{CpB}(e_{2\pm}'')\} \quad . \qquad (2)
\end{aligned}$$

The wave functions of eqn. (2) represent the appropriate molecular orbitals for the di-π-*cyclo*pentadienyl ring system.

We must now construct wave functions for the metal atoms having the proper symmetry in D_{5d}. We shall assume that only the 3d and 4s orbitals of the metal are significantly involved in the bonding. In section 5 we shall discuss the validity of this assumption. Thus, the appropriate wave functions are *

$$\begin{aligned} \mathrm{s}(a_{1g}) &= R_{4s}(r)\Theta_{00}\,(2\pi)^{-\frac{1}{2}} \\ \mathrm{d}(a_{1g}) &= R_{3d}(r)\Theta_{20}\,(2\pi)^{-\frac{1}{2}} \\ \mathrm{d}(e^{\pm}_{1g}) &= R_{3d}(r)\Theta_{2\pm1}\,(2\pi)^{-\frac{1}{2}}\,\exp\,(\pm i\varphi) \\ \mathrm{d}(e^{\pm}_{2g}) &= R_{3d}(r)\Theta_{2\pm2}\,(2\pi)^{-\frac{1}{2}}\,\exp\,(\pm 2i\varphi) \end{aligned} \tag{3}$$

The molecular orbitals for the entire molecule are then formed by functions of the type

$$\chi(e^{\pm}_{1g}) = \sin\xi\cdot\psi_{cp}(e^{\pm}_{1g}) + \cos\xi\ \mathrm{d}\ (e^{\pm}_{1g}). \tag{4}$$

Following Moffitt [3], we shall assume that the bonding takes place primarily through the $e^{\pm}_{1g}$ orbitals, the remaining molecular orbitals being of the non-bonding variety. To determine the energies of these orbitals, we shall employ a new type of approximation scheme which combines the most appealing parts of the molecular orbital and crystal field theories of chemical valence.

Under the assumptions mentioned above, we may write the single electron *molecular orbitals* for the valence electrons as

$$\begin{aligned} \chi(e^{\pm}_{1g}) &= \sin\xi\cdot\psi_{cp}(e^{\pm}_{1g}) + \cos\xi\,\mathrm{d}(e^{\pm}_{1g}) \\ \check{\mathrm{d}}(a_{1g}) &= \cos\eta\ \mathrm{d}(a_{1g}) + \sin\eta\ \mathrm{s}(a_{1g}) \\ \check{\mathrm{s}}(a_{1g}) &= \sin\eta\ \mathrm{d}(a_{1g}) - \cos\eta\ \mathrm{s}(a_{1g}) \\ \check{\mathrm{d}}(e_{2g}) &= \mathrm{d}(e_{2g}) \end{aligned} \tag{5}$$

And, according to molecular orbital theory, we may determine the corresponding single electron energies as

$$\begin{aligned} \mathrm{h}(e_{1g})\chi(e^{\pm}_{1g}) &= E[\chi(e^{\pm}_{1g})]\chi(e^{\pm}_{1g}) \\ \mathrm{h}(a_{1g})\check{\mathrm{d}}(a_{1g}) &= E[\check{\mathrm{d}}(a_{1g})]\check{\mathrm{d}}(a_{1g}) \\ \mathrm{h}(a_{1g})\check{\mathrm{s}}(a_{1g}) &= E[\check{\mathrm{s}}(a_{1g})]\check{\mathrm{s}}(a_{1g}) \\ \mathrm{h}(e_{2g})\check{\mathrm{d}}(e^{\pm}_{2g}) &= E[\check{\mathrm{d}}(e^{\pm}_{2g})]\check{\mathrm{d}}(e^{\pm}_{2g})\ , \end{aligned} \tag{6}$$

where h is the appropriate single electron Hamiltonian.

Substituting eqns. (5) into eqns. (6), and performing the usual variational treatment, we obtain the following results:

* For the definition of $R_{3d}(r)$, $R_{4s}(r)$, and Θ_{lm} see Pauling, L. and Wilson, E. B. *Introduction to Quantum Mechanics*, McGraw-Hill, 1935, pp. 132–9.

$$E[\chi(e_{1g}^{\pm})] = \tfrac{1}{2}\{E[\psi_{cp}(e_{1g}^{\pm})] + E[d(e_{1g}^{\pm})]\} \pm \tfrac{1}{2}\{(E[\psi_{cp}(e_{1g}^{\pm})] - E[d(e_{1g}^{\pm})])^2 + 4(\mathrm{Rl.}\int \psi_{cp}^{*}(e_{1g}^{\pm})h(e_{1g})d(e_{1g}^{\pm}))^2\}^{\frac{1}{2}}$$

$$E[\tilde{d}(a_{1g})] = \tfrac{1}{2}\{E[d(a_{1g})] + E[s(a_{1g})]\} + \tfrac{1}{2}\{(E[d(a_{1g})] - E[s(a_{1g})])^2 + 4(\int d^{*}(a_{1g})h(a_{1g})s(a_{1g}))^2\}^{\frac{1}{2}}$$

$$E[\tilde{s}(a_{1g})] = \tfrac{1}{2}\{E[d(a_{1g})] + E[s(a_{1g})]\} - \tfrac{1}{2}\{(E[d(a_{1g})] - E[s(a_{1g})])^2 + 4(\int d^{*}(a_{1g})h(a_{1g})s(a_{1g}))^2\}^{\frac{1}{2}}$$

$$E[\tilde{d}(e_{2g})] = \int d^{*}(e_{2g}^{\pm})h(e_{2g})d(e_{2g}^{\pm})$$

$$\tan 2\xi = \frac{2\ \mathrm{Rl.}\{\int \psi_{cp}^{*}(e_{1g}^{\pm})h(e_{1g})d(e_{1g}^{\pm})\}}{E[d(e_{1g}^{\pm})] - E[\psi_{cp}(e_{1g}^{\pm})]}$$

$$\tan 2\eta = \frac{2\int d^{*}(a_{1g})h(a_{1g})s(a_{1g})}{E[d(a_{1g})] - E[s(a_{1g})]} \quad , \tag{7}$$

where Rl. = "real part of".
For convenience, we have set the overlap integral between the metal orbitals and the ring orbitals equal to zero in eqn. (7).

Since it is observed that the di-π-*cyclo*pentadienyl compounds are fairly stable, one would naturally wish to maximize the binding strength of the $\chi(e_{1g}^{\pm})$ orbitals. To accomplish this, we assume that the $\psi_{cp}(e_{1g}^{\pm})$ and $d(e_{1g}^{\pm})$ electrons have approximately the same energy. That is, we set

$$E[\psi_{cp}(e_{1g}^{\pm})] = E[d(e_{1g}^{\pm})]. \tag{8}$$

From (7) we see that the $\chi(e_{1g}^{\pm})$ energy is then given by (since this condition makes $2\xi = \pm\frac{\pi}{2}$)

$$E[\chi(e_{1g}^{\pm})] = E[d(e_{1g}^{\pm})] \pm \mathrm{Rl.}\{\int \psi_{cp}^{*}(e_{1g}^{\pm})h(e_{1g})d(e_{1g}^{\pm})\} \quad , \tag{9}$$

and the corresponding wave functions are

$$\chi_b(e_{1g}^{\pm}) = (2)^{-\frac{1}{2}}\{d(e_{1g}^{\pm}) + \psi_{cp}(e_{1g}^{\pm})\}$$
$$\chi_a(e_{1g}^{\pm}) = (2)^{-\frac{1}{2}}\{d(e_{1g}^{\pm}) - \psi_{cp}(e_{1g}^{\pm})\}. \tag{10}$$

In (9) and (10) the plus sign corresponds to the bonding orbital and the minus sign to the antibonding orbital.

We have yet to evaluate the integrals occurring in eqns. (7) and (9). In general, the evaluation of such integrals involves insuperable difficulties. However, there does exist a consistent approximation scheme for evaluating them. The procedure is the following:

For the electrons involved primarily in the bonding, the $e_{1g}^{\pm}$ electrons, we shall consider the effect of compound formation to be a strong attraction of the $d(e_{1g}^{\pm})$ electrons of the metal to the rings, with a similar attraction of the ring electrons to the metal atom. Thus, we *replace* the true expression for the energy of the $\chi_b(e_{1g}^{\pm})$ state, $E[\chi_b(e_{1g}^{\pm})]$, by an *estimate* obtained by considering the energy of attraction to be given by a set of *positive* point charges, $+qe_{1g}$,

situated on the carbon atoms of the two *cyclo*pentadienyl rings and interacting with the electrons, metal plus ring, which are moving in $d(e_{1g}^{\pm})$ orbitals. We hence assume that the energy of the *bonding* $e_{1g}^{\pm}$ orbitals is given by

$$E[\chi_b(e_{1g}^{\pm})] = E_d^0 + \int d(e_{1g}^{\pm})^* V_c(+ qe_{1g}) d(e_{1g}^{\pm}) \quad , \tag{11}$$

where E_d^0 is the energy of a d-electron in the normal atom and $V_c(+ qe_{1g})$ is the crystal field potential produced by the ten point charges $+ qe_{1g}$ of the two *cyclo*pentadienyl rings.

For the *antibonding* $\chi_a(e_{1g}^{\pm})$ electrons we replace the true $\chi_a(e_{1g}^{\pm})$ energy, $E[\chi_a(e_{1g}^{\pm})]$, by an estimate obtained by considering the energy of repulsion to be given by a set of *negative* point charges, $-qe_{1g}$, situated on the carbon atoms of the two *cyclo*pentadienyl rings and interacting with the electrons, metal plus ring, which are moving in $d(e_{1g}^{\pm})$ orbitals. That is,

$$E[\chi_a(e_{1g}^{\pm})] = E_d^0 + \int d(e_{1g}^{\pm})^* V_c(-qe_{1g}) d(e_{1g}^{\pm}) \tag{12}$$

For the *nonbonding* electrons, *i.e.*, those not primarily involved in the bonding, such as the $\tilde{d}(e_{2g}^{\pm})$, $\tilde{d}(a_{1g})$, and $\tilde{s}(a_{1g})$ electrons, the situation is conceptually simpler. Here we assume that the sole effect of compound formation is to *repel* these electrons from the region of the *cyclo*pentadienyl rings. We shall consider this repulsion to be represented by the effect of a set of ten negative point charges, $-qe_{2g}$ or $-qa_{1g}$, situated on the carbon atoms and interacting with the electrons moving in $d(a_{1g})$, $s(a_{1g})$, and $d(e_{2g}^{\pm})$ orbitals. Thus we can finally write

$$\begin{aligned}
&E[\chi_{(b)}^{(a)}(e_{1g}^{\pm})] \approx E_d^0 \pm \int d(e_{1g}^{\pm})^* V_c(qe_{1g})\, d(e_{1g}^{\pm}) \\
&E[\tilde{d}(e_{2g}^{\pm})] \approx E_d^0 + \int d(e_{2g}^{\pm})^* V_c(-qe_{2g}) d(e_{2g}^{\pm}) \\
&E[d(a_{1g})] \approx E_d^0 + \int d(a_{1g})^* V_c(-qa_{1g}) d(a_{1g}) \\
&E[s(a_{1g})] \approx E_s^0 + \int s(a_{1g})^* V_c(-qa_{1g}) s(a_{1g}) \\
&\int d(a_{1g})^* h(a_{1g}) s(a_{1g}) \approx \int d(a_{1g})^* V_c(-qa_{1g}) s(a_{1g})
\end{aligned} \tag{13}$$

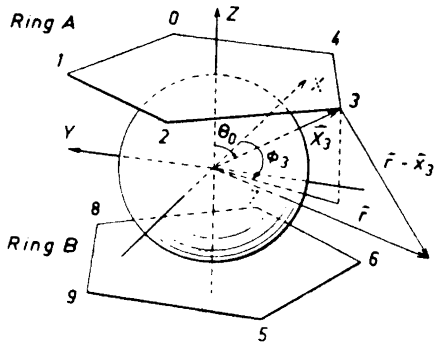


Fig. 1. Model of the compounds.

We next wish to consider the explicit evaluation of the integrals occurring in eqn. (13). Now by making use of Fig. 1, we see

$$V_c(\pm q) = \pm \frac{(-e)q}{a_0} \sum_{j=0}^{9} \frac{1}{|\vec{r}-\vec{x}_j|} \tag{14}$$

In eqn. (14) $\vec{r}$ and $\vec{x}_j$ are measured in units of the Bohr radius a_0. Expanding $|\vec{r}-\vec{x}_j|^{-1}$ in terms of the associated Legendre polynomials of the first kind and carrying out the sum over all the atoms occurring in (14) we obtain

$$V_c(\pm q) = \frac{\mp 10qe}{a_0 r_>} \sum_{l \geq 5m}^{\infty} \left(\frac{r_<}{r_>}\right)^l \sum_{5m=-l}^{l} \frac{(l-|m|)!}{(l+|m|)!} P_l^{|m|}(\cos\vartheta) P_l^{|m|}(\cos\vartheta_0) \exp.[5im(\varphi-\varphi_0)] \tag{15}$$

Substituting the wave functions of eqn. (3) together with the expansion of $V_c(\pm q)$ of eqn. (15) into eqn. (13) we have

$$\begin{aligned}
E[\chi_{(a)}^{(b)}(e_{1g}^{\pm})] &\approx E_d^0 \mp 10qe_{1g} \cdot e\{G_{0d} + \frac{1}{7} P_2(\cos\vartheta_0)\, G_{2d} - \frac{4}{21} P_4(\cos\vartheta_0)\, G_{4d}\} \\
E[\tilde{d}(e_{2g}^{\pm})] &\approx E_d^0 + 10qe_{1g} \cdot e\{G_{0d} - \frac{2}{7} P_2(\cos\vartheta_0) G_{2d} + \frac{1}{21} P_4(\cos\vartheta_0) G_{4d}\} \\
E[d(a_{1g})] &\approx E_d^0 + 10qa_{1g} \cdot e\{G_{0d} + \frac{2}{7} P_2(\cos\vartheta_0) G_{2d} + \frac{2}{7} P_4(\cos\vartheta_0) G_{4d}\} \\
E[s(a_{1g})] &\approx E_s^0 + 10qa_{1g} \cdot eG_{0s},
\end{aligned} \tag{16}$$

where

$$\begin{aligned}
G_{kd}(x) &= \frac{1}{a_0} \int_0^x \frac{r^k}{x^{k+1}} R_{3d}^2(r) r^2 dr + \frac{1}{a_0} \int_x^{\infty} \frac{x^k}{r^{k+1}} R_{3d}^2(r) r^2 dr \\
G_{ks}(x) &= \frac{1}{a_0} \int_0^x \frac{r^k}{x^{k+1}} R_{4s}^2(r) r^2 dr + \frac{1}{a_0} \int_x^{\infty} \frac{x^k}{r^{k+1}} R_{4s}^2(r) r^2 dr
\end{aligned} \tag{17}$$

Using [6-8] a carbon-carbon distance equal to 1.41 Å, a metal carbon distance of 2 Å, and the angle ϑ_0 equal to arc cos (0.80338) in the formulae given above we obtain the results tabulated in Tables 1 and 2. These results are also plotted

Table 1.

Z_{3d}	Units of $\frac{10}{a_0} qe_{1g} \cdot e$ $E[\tilde{d}(a_{1g})] - E_d^0$	Units of $\pm \frac{10}{a_0} qe_{1g} \cdot e$ $E(e_{1g}^{\pm}) - E_d^0$	Units of $\frac{10}{a_0} qe_{2g} \cdot e$ $E[\tilde{d}(e_{2g}^{\pm})] - E_d^0$
2.9780	0.25746	0.25834	0.22417
3.5736	0.26829	0.26853	0.23710
4.3677	0.27273	0.27196	0.24694
5.1618	0.27276	0.27130	0.25235
5.9560	0.27166	0.26993	0.25558
6.7501	0.27051	0.26875	0.25767
7.5442	0.26954	0.26788	0.25911

Energy Values

Table 2.

Z_{4s}	Units of $\frac{10}{a_0}$ $qa_{1g}e$ $E[\tilde{s}(a_{1g})]-E^0_{4s}$
1.58826	0.0807
2.11768	0.1039
2.64710	0.1260
2.91181	0.1360
3.17652	0.1455
3.70594	0.1630
4.23536	0.1801
4.76478	0.1970
5.29420	0.2131

Energy Values.

in Figure 2a. Since the computations for a wide range of values of Z_{3d} and Z_{4s} showed that the interaction integral, $\int d(a_{1g})^* h(a_{1g}) s(a_{1g})$, is only of the order of 10^{-2} times the diagonal terms $E[d(a_{1g})]$ and $E[s(a_{1g})]$, this term was neglected in computing the values given in Tables 1 and 2.

In the following section we shall use Tables 1 and 2 as well as Figures 2a and 2b to explain the magnetic properties of the di-π-*cyclo*pentadienyl compounds.

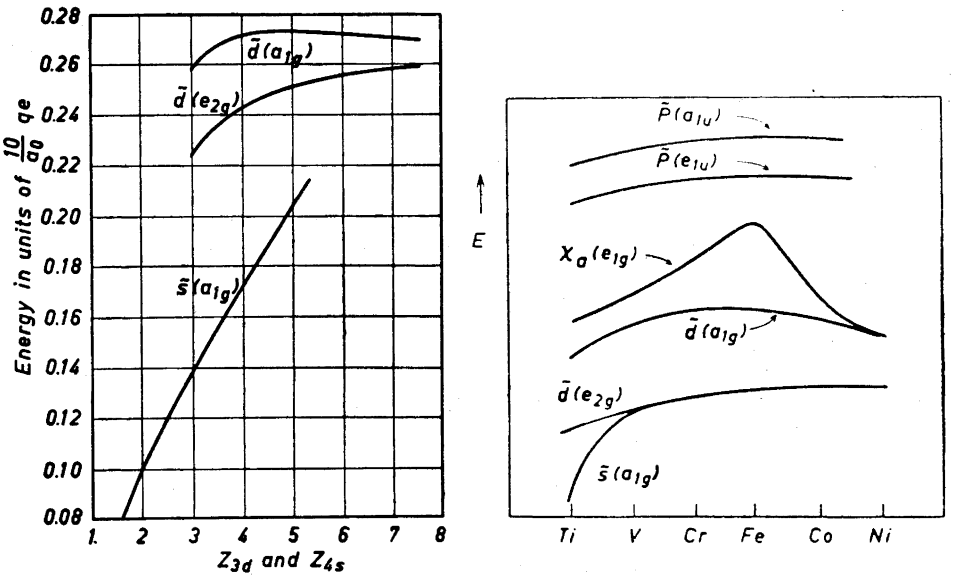


Fig. 2 a, b. A qualitative plot of the energy levels for the di-π-*cyclo*pentadienyl compounds of the first transition series. The energy spacings are distorted for illustrative clarity. Manganese is omitted from the plot for reasons stated in the text.

2. DISCUSSION OF THE MAGNETIC PROPERTIES OF THE DI-π-*CYCLO*-PENTADIENYL COMPOUNDS

Titanium. The compound $(C_5H_5)_2Ti$ is diamagnetic [9]. Hence, on our energy level diagram we must have the electronic structure * $[A]cp(a_{1g})^2cp(a_{1u})^2cp(e_{1u})^4 \chi_b(e_{1g})^4\tilde{s}(a_{1g})^2$. Since $E_s^0-E_d^0$ for Ti(II) is about $9\times10^{-2}\times\frac{10}{a_0}qa_{1g}e$, we see from Figure 2a that any value of $Z_{4s}\sim2.5$ and $Z_{3d}\sim4.5$ will ensure that the $\tilde{s}(a_{1g})$ level is well below the $\tilde{d}(e_{2g})$ level (if $qa_{1g}=1/5\ e$ it is $\sim16\ 000\ cm^{-1}$ below it) [10]. These values, in addition to yielding a diamagnetic molecule, are very reasonable physically for the $\tilde{s}(a_{1g})$ and $\tilde{d}(e_{2g})$ *molecular orbitals* of the *molecule* $(C_5H_5)_2Ti$. Ionization of the *molecule* to form $[(C_5H_5)_2Ti]^{+1}$ and $[(C_5H_5)_2Ti]^{+2}$ then takes place by the removal of first one and then the other $\tilde{s}(a_{1g})$ electron. This makes $[(C_5H_5)_2Ti]^{+1}$ paramagnetic with one unpaired electron and makes $[(C_5H_5)_2Ti]^{+2}$ diamagnetic.

Vanadium. The compound $(C_5H_5)_2V$ is paramagnetic with three unpaired electrons [11,12]. This implies that the $\tilde{s}(a_{1g})$ and $\tilde{d}(e_{2g})$ levels must be nearly degenerate. Thus the electronic structure is $[A]cp(a_{1g})^2cp(a_{1u})^2cp(e_{1u})^4 \chi_b(e_{1g})^4\tilde{s}(a_{1g})^1\tilde{d}(e_{2g})^2$. This will be the case if $Z_{4s}\sim3.3$ and $Z_{3d}\sim4.8$ for then the observed value of $E_s^0-E_d^0$ for V (II) will bring the $\tilde{s}(a_{1g})$ and $\tilde{d}(e_{2g})$ levels into near degeneracy (if $qa_{1g}=qe_{2g}\sim\frac{1}{5}e$ then $E_s^0-E_d^0=1\times10^{-1}\times\frac{10}{a_0}qa_{1g}e$). *The above choices of Z_{4s} and Z_{3d} are not critical. All that is required is that they be slightly higher than those occurring in $(C_5H_5)_2Ti$, as they must be on physical grounds.* Having determined the best values of Z to use for the $\tilde{s}(a_{1g})$ and $\tilde{d}(e_{2g})$ *molecular orbitals*, we would predict that $[(C_5H_5)_2V]^{+1}$ and $[(C_5H_5)_2V]^{+2}$ would be paramagnetic with two unpaired and one unpaired electrons, respectively.

Chromium. The additional electron introduced into the *cyclo*pentadienyl-metal electronic system upon replacement of vanadium by chromium will probably not introduce too great a change in the energy level scheme present in vanadium. Thus we might expect chromium to have the electronic structure:

$$[A]cp(a_{1g})^2cp(a_{1u})^2cp(e_{1u})^4\chi_b(e_{1g})^4[\tilde{s}(a_{1g})\tilde{d}(e_{2g})]^4.$$

This structure predicts that $(C_5H_5)_2Cr$ is paramagnetic with two unpaired electrons. The energy level scheme $(\tilde{d}(e_{2g}))^4(\tilde{s}(a_{1g}))^0$ is eliminated on the grounds that it would require larger values of Z_{4s} than are reasonable. We therefore have two possibilities: (a) The $\tilde{s}(a_{1g})$ and $\tilde{d}(e_{2g})$ levels are nearly degenerate as in vanadium, so that $[(C_5H_5)_2Cr]^{+1}$ and $[(C_5H_5)_2Cr]^{+2}$ are paramagnetic with three and two unpaired electrons, respectively; (b) the $\tilde{s}(a_{1g})$ level is lower than the $\tilde{d}(e_{2g})$ level as in titanium, so that $[(C_5H_5)_2Cr]^{+1}$ is paramagnetic with one unpaired electron and $[(C_5H_5)_2Cr)]^{+2}$ is diamagnetic. The investigations of the German school [13–15] indicate that $[(C_5H_5)_2Cr)^{+1}$ has three unpaired electrons

* The symbol [A] is used to designate the Argon core which is common to all of the metals of the first transition series.

and thus case (a) is the one actually occurring. The relative instability of $(C_5H_5)_2Cr$ indicates [16] that the binding parameter of qe_{1g} is not very large.

Manganese. The compound $(C_5H_5)_2Mn$ is known from experiment to be "ionic", and therefore has no $\chi_b(e_{1g})$ bonding orbital. In the crystal the ions $C_5H_5^-$ Mn^{++} $C_5H_5^-$ are probably arranged in a lattice having D_{5d} symmetry at the manganese sites.[16,17] Hence, the energy levels are given by a pure crystal field perturbation of the Mn^{+2} ion by the $C_5H_5^-$ rings. Since the ground state of Mn^{+2} is a ^6S state, which will not be split by a crystal field, the $(C_5H_5)_2Mn$ molecule will have five unpaired electrons [unless the crystal field is strong enough to depress one of the higher states, such as ^4G, ^4P, etc., below the ^6S state). Since it is observed that $(C_5H_5)_2Mn$ has five unpaired electrons [16], we see that the latter possibility is not realized.*

Iron. Here we have an extremely stable covalent compound having the formula $(C_5H_5)_2Fe$. Since iron has enough electrons to fill both the $\tilde{s}(a_{1g})$ and $\tilde{d}(e_{2g})$ shells, the relative location of these shells with respect to one another is immaterial from the magnetic viewpoint. Since the $\tilde{d}(a_{2g})$ level is significantly higher than the $\tilde{s}(a_{1g})$ and $\tilde{d}(e_{2g})$ levels, all possible assignments of the electrons will yield a diamagnetic $(C_5H_5)_2Fe$ molecule and a paramagnetic $[(C_5H_5)_2Fe]^{+1}$ ion having one unpaired electron. The degree of stability of this compound indicates a large positive value for qe_{1g}. The $\tilde{s}(a_{1g})$ and $\tilde{d}(e_{2g})$ levels are probably equi-energetic as in the case of vanadium.

Cobalt. It is likely that for $(C_5H_5)_2Co$, the $\tilde{s}(a_{1g})$ and $d(e_{2g})$ levels are, as in vanadium, nearly degenerate. The electrons are then placed in the molecule as $[A]cp(a_{1g})^2cp(a_{1u})^2cp(e_{1u})^4\chi_b(e_{1g})^4[\tilde{s}(a_{1g})\tilde{d}(e_{2g})]^6(\tilde{d}(a_{1g}))^1$, yielding a paramagnetic molecule with one unpaired electron. The cobalticinium ion, $[(C_5H_5)_2Co]^{+1}$, is then diamagnetic.

Nickel. This compound is relatively unstable thermally, in contrast to ferrocene.[18] Hence, we expect that qe_{1g} is not too large. This is further confirmed by the fact that the molecule is paramagnetic with two unpaired electrons. This paramagnetism implies that the antibonding orbital, $\chi_a(e_{1g})$, is nearly degenerate with the $\tilde{d}(a_{1g})$ nonbonding orbital. We see from Table 1 that the choice $q_{e_{1g}} = q_{a_{1g}}$ will bring about this degeneracy. Hence, we may assign to nickelocene the following electronic structure:

$$[A]cp(a_{1g})^2cp(a_{1u})^2cp(e_{1u})^4\chi_b(e_{1g})^4[\tilde{s}(a_{1g})\tilde{d}(e_{2g})]^6[\tilde{d}(a_{1g})\chi_a(e_{1g})]^2.$$

This structure gives nickelocene two unpaired electrons. We also see that this electronic assignment for $(C_5H_5)_2Ni$ implies that the nickelocinium ion is paramagnetic with one unpaired electron.

Miscellaneous Di-π-cyclopentadienyl Compounds. A number of other di-π-*cyclo*pentadienyl compounds have also been prepared, and a discussion of these follows much the same pattern as that given for the first transition series. For example, $[(C_5H_5)_2Zr]^{+2}$, $[(C_5H_5)_2Nb]^{+3}$, and $[(C_5H_5)_2Ta]^{+3}$ are formed exactly as is $[(C_5H_5)_2Ti]^{+2}$; $(C_5H_5)_2Ru$, $[(C_5H_5)_2Rh]^{+1}$, and $[(C_5H_5)_2Ir]^{+1}$ are similar to ferrocene; $[(C_5H_5)_2Ru]^{+1}$ is analogous to the ferricinium ion.

* In the solid state the five unpaired electrons interact to form an antiferromagnetic crystal. See Ref.[16]

The compounds $[(C_5H_5)_2Mo]^{+3}$ and $[(C_5H_5)_2W]^{+3}$ are completely analogous to the similar electronic systems $[(C_5H_5)_2V]^{+2}$ and $[(C_5H_5)_2Ti]^{+1}$. Preliminary investigations by Piper and Wilkinson [19] indicate that $(C_5H_5)_2Mo$ is analogous to $(C_5H_5)_2Cr$. However, $[(C_5H_5)_2Mo]^{+2}$ behaves quite differently from $[(C_5H_5)_2Cr]^{+2}$, being diamagnetic instead of paramagnetic [20]. Reference to the discussion of $(C_5H_5)_2Cr$ shows that for molybdenum we must thus have the $\tilde{s}(a_{1g})$ level below the $\tilde{d}(e_{2g})$ level. Hence, $[(C_5H_5)_2Mo]^{+2}$ resembles its neutral titanium analogue rather than its chromium and vanadium analogues.*

3. DISCUSSION OF THE MAGNETIC PROPERTIES OF THE *CYCLO*PENTADIENIDES OF THE GROUP III METALS AND THE ACTINIDES.

The group III metals form ionic compounds of the general formula $(C_5H_5)_3M$ (M = Sc, Y, and the rare earths).[21] Both the spectra and the magnetic properties are very similar to those of the normal triply ionized metals in solution. Thus, one is led to assume that, as in the case of manganese, the crystal field acting on the trivalent metal ions is of the same order of magnitude as that found in the normal salts of these metals. One then has the ordinary weak crystal field splitting of the trivalent ion which gives rise to the well-known magnetic properties of these ions [22].

Recently there have been reported [23] the stable ions $[(C_5H_5)_3U]^{+1}$ and $[(C_5H_5)_2Th]^{+2}$ (the latter ion has not as yet been fully characterized). The bonding in these ions would involve, in general, the low lying 5f, 6d, and 7s orbitals. A treatment similar to that given in sections 1 and 2 for the first series of transition elements could also be applied here. However, the uncertainty in geometry and the intrinsic complexity of the atomic systems involved makes a treatment of this sort impracticable.

4. DISCUSSION OF THE MAGNETIC PROPERTIES OF THE DI-π-BENZENE CHROMIUM COMPOUNDS

Fischer and Hafner [24] have recently reported the covalent diamagnetic compound $(C_6H_6)_2Cr$, and have, because of its great similarity to ferrocene, proposed a "sandwich" type bonding. ** They have also reported the stable ion $[(C_6H_6)_2Cr]^{+1}$ which they found to be chemically analogous to the ferricinium ion. As the theory of section 1 is completely general, it applies equally well to these di-π-benzene systems. To adapt section 2 to the di-π-benzene chromium compounds all one need to do is alter the geometrical parameters slightly and run all summations over twelve point charges rather than ten. Hence one would obtain exactly the same results for $(C_6H_6)_2Cr$ and $[(C_6H_6)_2Cr]^{+1}$ as were obtained for the isoelectronic systems $(C_5H_5)_2Fe$ and $[(C_5H_5)_2Fe]^{+1}$. These conclusions agree with the experimental findings [24].

---

* In an earlier paragraph we have shown that the hypothetical $[(C_5H_5)_2Cr]^{+2}$ ion must be paramagnetic.

** Previously Zeiss and Tsutsui had proposed a "sandwich" type bonding for several of the polyphenyl chromium compounds. See the review article by Cotton [25].

5. DISCUSSION

On the basis of a simple scheme for evaluating the necessary interaction integrals, we have been able to give an internally consistent semi-quantitative treatment of the bonding in metal aromatic complexes. This treatment has preserved those parts of the previous theories of Jaffé, Dunitz and Orgel, Moffitt, and Ruch which are most appealing physically. For example, we have followed Moffitt [3] in assuming that the only *cyclo*pentadienyl orbitals intimately involved in the bonding are the $\psi_{cp}(e_{1g})$ orbitals. However, as a calculation based on the *molecular orbital-crystal field* formalism employed in this paper shows that the p levels lie higher than the antibonding levels $\chi_a(e_{1g})$, we have followed Dunitz and Orgel [2b] rather than Moffitt in the ordering of these levels.

Of course, the explanation of the magnetic properties of the metal aromatic complexes is not alone sufficient proof of the validity of any given energy level scheme. A further test of the various theories concerning the electronic structure of these compounds could be obtained by a study of their absorption spectra. However, considerations of this kind have so far only been presented by Jaffé. In view of these facts, we plan next to apply the theory set forth in this paper to the problem of explaining the visible spectrum of the metal aromatic complexes.*

We wish to thank Professor G. Wilkinson for stimulating our interest in this problem and for many illuminating discussions. We also wish to express thanks to Drs. J. M. Birmingham, F. A. Cotton, and T. S. Piper and Mr. L. T. Reynolds for helpful discussions in connection with this work.

REFERENCES

1. Jaffé, H. H. *J. Chem. Phys.* **21** (1953) 156.
2. Dunitz, J. D. and Orgel, L. E. a) *Nature* **171** (1953) 121; b) *J. Chem. Phys* **23** (1955) 954.
3. Moffitt, W. E. *J. Am. Chem. Soc.* **76** (1954) 3386.
4. Ruch, E. *Sitz. ber. math. naturw. Abt. bayer. Akad. Wiss.* München **20** (1954) 347.
5. Craig, D. P., Maccoll, A., Nyholm, R. S., Orgel, L. E. and Sutton, L. E. *J. Chem. Soc.* **1954** 332.
6. Dunitz, J. D., Orgel, L. E. and Rich, A. *Acta Cryst.* **9** (1956) 373.
7. Eiland, P. F. and Pepinsky, R. *J. Am. Chem. Soc.* **74** (1952) 4971.
8. Seibold, E. A. and Sutton, L. E. *J. Chem. Phys.* **23** (1955) 1967.
9. Fischer, A. K. and Wilkinson, G. *J. Inorg. Nucl. Chem.* **2** (1956) 149.
10. Moore, C. E. *Atomic Energy Levels, National Bureau of Standards Circular* 467, Vol. I (1949), Vol. II (1952).
11. Schwab, G. M., Fischer, E. O. and Voitländer, J. *Naturwiss.* **41** (1954) 228.
12. Fischer, E. O. and Hafner, W. *Z. Naturforsch.* **9 B** (1954) 503.
13. Fischer, E. O. and Hafner, W. *Z. Naturforsch.* **10 B** (1955) 140.
14. Fischer, E. O. and Leipfinger, H. *Z. Naturforsch.* **10 B** (1955) 353.
15. Fischer, E. O., Hafner, W. and Stahl, H. O. *Z. anorg, allgem. Chem.* **282** (1956) 47.
16. Wilkinson, G., Cotton, F. A. and Birmingham, J. M. *J. Inorg. Nucl. Chem.* **2** (1956) 95.

* Note added in proof: M. Yamazaki has recently performed a simplified SCF-LCAO-MO computation for both the D_{5h} and D_{5d} structures of ferrocene, obtaining essentially the same electronic level ordering as all other workers in this field. Also, using the results of his calculations, he has presented an explanation of the absorption spectrum of ferrocene. See *J. Chem. Phys.* **24**, (1956) 1260.

17. Weiss, E. and Fischer, E. O. *Z. Naturforsch.* **10 B** (1955) 58.
18. Wilkinson, G., Pauson, P. L. and Cotton, F. A. *J. Am. Chem. Soc.* **76** (1954) 1970.
19. *Private Communication.*
20. Cotton, F. A. and Wilkinson, G. *Z. Naturforsch.* **9 B** (1954) 417.
21. Wilkinson, G. and Birmingham, J. M. *J. Am. Chem. Soc.* **76** (1954) 6210.
22. Van Vleck, J. H. *The Theory of Electric and Magnetic Susceptibilities*, Oxford 1932.
23. Reynolds, L. T. and Wilkinson, G. *J. Inorg. Nucl. Chem.* **2** (1956) 246.
24. Fischer, E. O. and Hafner, W. *Z. Naturforsch.* **10 B** (1955) 665.
25. Cotton, F. A. *Chem. Revs.* **55** (1955) 569.

Received September 29, 1956.

ACTA CHEMICA SCANDINAVICA 11 (1957) 219—229

On the Photo-transformation of Ergot Alkaloids

HANS HELLBERG

Chemical Department, State Pharmaceutical Laboratory, Stockholm, Sweden

The photo-catalyzed transformation of ergot alkaloids has been investigated. The results conform with the conclusion of Stoll and Schlientz that in aqueous solutions the reaction is an addition of water to the double bond of ring D. It is shown here that a prerequisite for the reaction is that the solution contains suitable, strongly polar constituents in sufficient quantities. In water solution hydrogen ions, primary phosphate ions and to a less extent acetate ions are highly active.

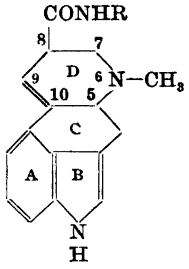
Paper chromatography is suggested as a new means for the assignment of configurational relationships within the lumialkaloids. The order of migration on paper is the reverse of that on alumina within every pair of lumialkaloids investigated. Theoretically, identification of the lumilysergic acid obtained on cleavage of a lumialkaloid should be the best way of establishing the connexions between lumi-derivatives from different alkaloid series. Such identifications have been approached here by paper chromatography of the products of alkaline hydrolysis of lumialkaloids and have led to certain conclusions. The spots can be tentatively assigned to the four possible lumilysergic acids.

The fact that the pK_a-values of the lumi-derivatives of ergometrine and ergometrinine are considerably higher than those of the dihydroalkaloids may be explained by axial conformation of the hydroxyl group at C_{10}.

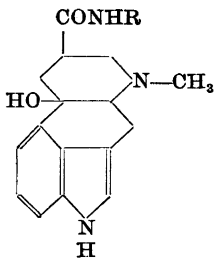
The preparation of lumi-derivatives of ergometrinine, ergocristine and ergocristinine is reported. Physical and chemical data of the new substances are given together with some supplementary findings on the lumi-derivatives of ergometrine, ergotamine and ergotaminine.

It is well known that ergot alkaloids are sensitive to light. This instability is of great importance in alkaloid chemistry and in pharmacy, but until recently it has not been studied in any detail. In this laboratory the subject had been treated for some time [1], when Stoll and Schlientz [2] gave an account of their work in that domain. They concluded that, on illuminating genuine ergot alkaloids in acid water solutions, a molecule of water is added to the double bond in ring D of the lysergic or *iso*lysergic acid, forming new series of alkaloids analogous to the dihydroalkaloids. They distinguished the new derivatives with the prefix lumi-, and in order to indicate the stereoisomeric connexions with corresponding dihydroalkaloids they added the figure I or

II to the names. The preparation of lumi-derivatives of ergometrine, ergotamine and ergotaminine, was described and the usual physical and chemical data of the substances were given.



Genuine alkaloid



Lumialkaloid

The results obtained in this laboratory confirm and enlarge the work of Stoll and Schlientz. Moreover, to some extent the problem has been attacked by us in another way.

I. ON THE EXTERNAL PREREQUISITES FOR THE TRANSFORMATION

Having noticed by chance that transformation occurred very easily in phosphate buffers we studied the influence of different electrolytes on the velocity of the transformation. The results are reported in Figs. 1—4. Practically no transformation occurs in water or in solutions of neutral salts, *e. g.* sodium chloride (Figs. 1 and 3). In acid solutions, however, transformation takes place, and its considerable rate increase in the series of tartaric, phosphoric, hydrochloric acid solutions (Fig. 1) and in the series of phosphate buffers with decreasing pH (Fig. 2) shows that the hydrogen ion activity has an important effect. This conclusion conforms with the extensively accepted theories on the addition to double bonds of for instance hydrogen halides directly or of water by acid catalysis. The electrophilic hydronium ions are thought to be able to attack the electron excess of the double bond [3].

However, certain anions, especially primary phosphate ions and to some extent acetate ions, promote the photo-transformation (Figs. 1, 2 and 4). On the other hand chloride, methanesulphonate and primary tartrate ions seem to have little or no effect. The rate variation in the series of phosphate buffers (Fig. 2) is interesting. The effect of the decreasing hydrogen ion concentration is compensated for by the increasing concentration of primary phosphate ions. Not until these begin to disappear above pH 6 does the transformation velocity diminish considerably. Moreover Fig. 3 shows that an increase of primary phosphate concentration enhances the transformation velocity appreciably. No satisfactory theoretical explanation of the influence of the anions has been found.

On irradiating glacial acetic acid solutions of ergot alkaloids we obtained rapid transformations with spectrophotometric characteristics similar to those in aqueous solutions. Judging from paper chromatography (see Section III A)

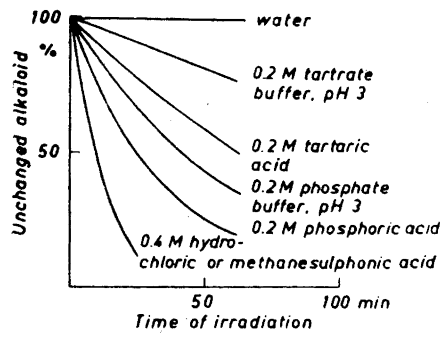


Fig. 1. Photo-transformation of ergotamine (tartrate) in water solutions of the composition stated in the figure. Irradiation with U.V.-light (max = 366 mμ) at standard distance. Room temperature. The content of unchanged alkaloid was followed spectrophotometrically at 315 mμ.

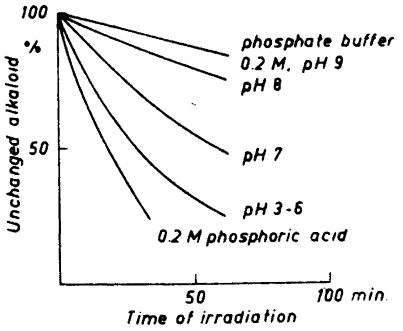


Fig. 2. Photo-transformation of ergometrine(maleate) in water solutions of the composition stated in the figure. Experimental conditions as in Fig. 1.

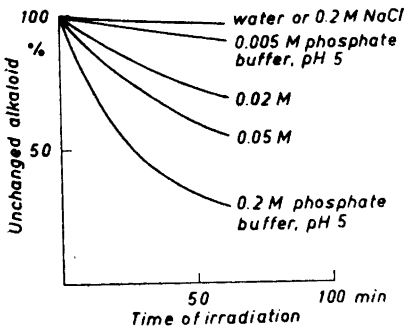


Fig. 3. Photo-transformation of ergometrine(maleate) in water solutions of the composition stated in the figure. Experimental conditions as in Fig. 1.

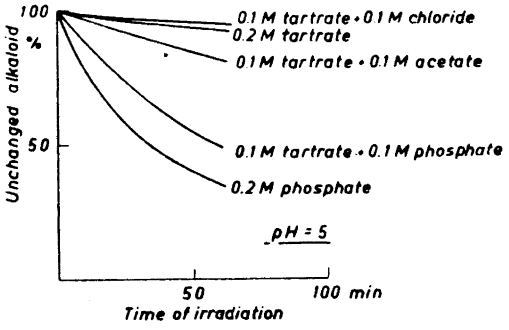


Fig. 4. Photo-transformation of ergometrine(maleate) in water solutions of the composition stated in the figure. Experimental conditions as in Fig. 1.

the transformation products were mainly the same as those obtained in water solutions *. Diluting the acetic acid with water or ether, respectively, we found that the transformation was much faster in the aqueous solution than in the ether solution.

From the above-mentioned facts it is possible to conclude that illumination is only one prerequisite for the transformation; another is that the solution contains suitable, strongly polar constituents in sufficient quantity. Thus in water solutions hydrogen ions, primary phosphate ions and to a less extent acetate ions are highly active.

* In the chromatographic process the transformation products came into contact with water.

II. ON THE PROPERTIES OF THE LUMIALKALOIDS

There are good theoretical and experimental reasons for the opinion that on the addition of water to the double bond of ring D the hydroxyl group goes to C_{10}, thus creating an asymmetric carbon atom. Like the dihydroalkaloids the lumialkaloids should exist in four series, deriving from four stereoisomeric lumilysergic acids, namely, according to Stoll's nomenclature, lumilysergic acid I, and II, lumi*iso*lysergic acid I and II. The derivatives of lysergic acid differ from those of *iso*lysergic acid by different configuration at C_8, and the substances designated I from those designated II by different configuration at C_{10}.

For the assignment of configurational relationships within the lumialkaloids as well as between the groups of dihydro- and lumialkaloids Stoll and Schlientz[2] used primarily the following indirect methods: 1) Comparison of the magnitude of the yields, 2) The order of adsorption on alumina, 3) Comparison of the specific optical rotations. In this work also paper chromatography of the lumialkaloids and of the lumilysergic acids obtained from them has been used for the same purposes.

From the beginning of our work we designated the lumialkaloids — regularly appearing in pairs — with the Greek letters α and β after their order of migration on paper chromatograms, the α-component moving more slowly than the β-component. This notation has been extensively used in this paper especially in the experimental part. However, the nomenclature of Stoll and Schlientz [2] seems more fundamental, and therefore later in this section a key will be given for the translation of our names into that nomenclature.

Already at the beginning of this work paper chromatography revealed that on illuminating a lysergic acid alkaloid only one transformation product appeared in quantities great enough to produce a spot while an *iso*lysergic acid alkaloid always caused two spots [1]. Working on a preparative scale with chromatography on alumina, however, new small fractions appeared as reported in the experimental section.

Comparing the R_F-values of Tables 2 and 3 with the order of migration on alumina (experimental part of this paper and Ref.[2]) it is found that the two lumi-derivatives of a certain alkaloid migrate on paper in an order which is the reverse of that on alumina. Paper chromatography seems to be an equally good method for classifying lumialkaloids as chromatography on alumina.

Experimental evidence obtained by Stoll and Schlientz supported the assumption that the substitution of the C_{10}-hydrogen of a pair of dihydroalkaloids for hydroxyl in the corresponding lumialkaloids did not affect the order of migration on alumina. It would have been interesting to investigate if this rule holds true also in paper chromatography but unfortunately the dihydroalkaloids necessary were not available. Stoll and his collaborators [4] used the different adsorbability on alumina as an argument for assigning definite conformations at C_8 to the different dihydroalkaloids. The paper chromatography of the lumialkaloids shows, however, the uncertainty of such conclusions.

As is well known, epimerization at C_8 takes place easily in the genuine alkaloids but much more slowly after saturation of the double bond of ring D.

It was therefore hoped that alkaline hydrolysis of the lumialkaloids would give the corresponding lumilysergic acids in fairly pure form, serving as a new means for the study of the mutual configurative connexions between the lumialkaloids. Paper chromatography of the lumilysergic acids obtained by alkaline hydrolysis of pure lumialkaloids (see Section III A) showed, however, that matters were not so simple. Thus double spots were obtained from all lumialkaloids tried. As is seen from Fig. 5 the chromatograms were of two different types, β-lumi-ins and α-lumi-inins giving type I (two spots near each other) α-lumi-ins and β-lumi-inins type II (two spots more widely separated). The most reasonable explanation of the two spots is that after all an epimerization at C_8 takes place, this reaction having several parallels in the chemistry of alkaloids [6,7]. This prompts to caution in the interpretation of experiments in preparing lumilysergic acids from lumialkaloids by alkaline hydrolysis. The results, however, constitute a proof that the α-lumi-ins and the β-lumi-inins have the same configuration at C_{10}, while β-lumi-ins and α-lumi-inins have the other. Desiring to relate these two groups to the configuration of dihydroalkaloids at C_{10} we established that the criteria magnitude of yields, and order of migration on alumina lead to the same conclusion within the lumiergometrine series and lumiergocristine series as Stoll and Schlientz [2] came to within the lumiergotamine series. Comparison of specific rotations lead to agreement with the other criteria in the ergocristine series, the ergometrine derivatives, however, giving inconsistant results; though of course this criterion is not to be trusted in the face of all other evidence.

The regularly recurring properties in each of the three series of lumialkaloids show the mutual connexions between the members, clearly reflected and confirmed also by the paper chromatograms, thus giving us a key to the configuration of the lumialkaloids hitherto investigated *.

α-lumi-in	= lumi-in II
β-lumi-in	= lumi-in I
α-lumi-inin	= lumi-inin I
β-lumi-inin	= lumi-inin II

In the light of this the paper chromatograms of the lumilysergic acids obtained on alkaline hydrolysis acquire renewed interest. In most cases the spots were unequal in magnitude, and if it is postulated that the bigger spot of a pair derives from the acid not rearranged at C_8 during hydrolysis it is possible to assign the spots to the four possible lumilysergic acids. This has been done at the bottom of Fig. 5, the perspicuousness of which is diminished by the fact that lumilysergic acid II and lumi*iso*lysergic acid I do not separate on the paper chromatograms. The interpretation in Fig. 5 is still to be considered as hypothetical but it is supported by the fact that irradiated lysergic acid gives practically only one spot, namely, the one assigned to lumilysergic acid I.

* The key is probably valid also for the lumialkaloids not yet investigated.

In the discussion of the configurations and conformations of ergot alkaloids the pK_a-values have played a certain rôle. Therefore an approach to these constants was made for the fairly watersoluble lumi-derivatives of ergometrine and ergometrinine. In the course of the potentiometric titrations of the equivalent weights (molecular weights), more closely described in the experimental part, we noted the pH's, at which the alkaloids were half-neutralized. These pH-values can be regarded as relative pK_a-values for the acid in the equation $HN^{+}CH_3 \rightleftharpoons H^+ + NCH_3$. The figures obtained are recorded in Table 1 together with some values for comparison, partly taken from literature [8,9].

Table 1. Estimated pK_a-values for ergometrine and derivatives. The figures obtained in this work refer to solutions containing 20 % ethanol.

	Obtained in this work	Obtained from literature	
Ergometrine	6.85	6.72 *	
Ergometrinine	7.40	7.26 **	7.38 **
Dihydroergometrine I		7.30 **	7.46 **
β-Lumiergometrine (I)	7.90		
α-Lumiergometrinine (I)	8.15		
β-Lumiergometrinine (II)	8.00		

* Ref.[9]; water solution.
** Ref.[8]; water solution.

Obviously the lumialkaloids are stronger bases than both genuine alkaloids and dihydroalkaloids. This is surprising at first sight because the inductive effect of an OH-group in C_{10} ought to be a weakening of the basicity of the nitrogen atom [3]. However, Stenlake [10] has emphasized the purely electrostatic effect, which negative substituents under favourable steric conditions can exert on the amino-nitrogen of lysergic acid. Stoll and collaborators [4], accepting this opinion, have shown that 6-methyl-8-*iso*hydroxyergoline I is a considerably stronger base than 6-methyl-8-hydroxyergoline I, concluding that the hydroxyl group is axial in the first-mentioned substance. C_8 and C_{10} are both equidistant from N_6 in ring D, and therefore the same substituent may have approximately the same influence on N_6, whether it is situated at C_8 or at C_{10}. Now according to the theories on the conformation of the dihydroalkaloids developed by Cookson [5] and by Stoll and his collaborators [4] the hydrogen of C_{10} is axial in relation to ring D. Probably the hydroxyl of the lumialkaloids takes the same position, and that explains the comparatively strong basicity of these substances.

III. EXPERIMENTAL

A. Paper chromatography

We used the descending technique, performed at 20—22° C in glass tanks of 22 × 32 × 61 cm with Whatman No. 1 paper in pieces of 54 × 23 cm. Papers with four applications each were kept over-night in the atmosphere of the water-rich phase. To

facilitate equilibration a filter paper moistened with the liquid was fixed in the middle of the container. The pre-treatment of the papers and the development of the chromatograms are described below for the different groups of substances. To visualize the spots after the evaporation of the solvent we used a reagent described by Berg [11], containing 0.5 g of *p*-dimetylaminobenzaldehyde in 5 ml of conc. HCl and 95 ml of ethanol. Fluorescent alkaloids could also be indicated by the U.V.-lamp.

Modifying the solvents suggested by Foster and collaborators [12] for the separation of ergometrine and ergometrinine, we used benzene, butanol, acetic acid and water in the proportions 2.5:2.5:1:4 for the lumi-derivatives of ergometrine, ergometrinine, lysergic and *iso*lysergic acid. At first considerable tailing was obtained. Shute [13] and Munier *et al.*[14], however, have suggested pretreatment of the papers with neutral salts. In our case a normalization of the spots was achieved by moistening the papers with 0.2 M NaCl and subsequent air-drying.

For paper chromatography of the peptide alkaloids of ergot many procedures have been suggested in recent years *e.g.* [11,12,15,16]. From our own investigations on counter current distribution [17,18] and from those of Berg on paper chromatography [11] it was known that benzene displays good separating properties on peptide alkaloids. Starting from this fact we found the following combination of solvents useful for the lumi-derivatives of ergotamine, ergotaminine, ergocristine and ergocristinine: benzene, butanol, acetic acid and water (9:1:2:8). The papers were impregnated with sodium chloride as above. Some precautions were necessary because of the great volatility of the solvents. Thus one of the papers in the tank was always run empty, starting 1.5 h before the real chromatogram in order to keep the atmosphere saturated with the solvents.

In Tables 2 and 3 the results of the paper chromatography have been summarized and given as average R_F-values. The R_F-values were not very well reproducible probably because of the high volatility of the solvents. This disadvantage could as usual be overcome by running standard substances for comparison parallel to the test substances.

Alkaline hydrolysis of lumialkaloids was performed on the pattern given in Ref.[6]. Protected from light about 1 mg of the substance was refluxed for 2 h with 1 ml of a 20 % solution of KOH in 50 % ethanol. After saturation with CO_2 (pH < 7) the solution was quickly evaporated to dryness on the water bath and the residue extracted with a few small portions of absolute ethanol. The filtered ethanol solution was directly applied to the chromatographic paper.

The chromatographic procedure was the same as for the lumiergometrins. Average R_F-values for the lumilysergic acids are given in Fig. 5.

B. The preparation of some lumialkaloids; their physical and chemical properties

For the preparation of lumialkaloids we had comparatively small quantities of genuine alkaloids at our disposal, and therefore some derivatives forming only in minor quantities have not been characterized completely.

Owing to experiences in the transformation velocity, reported in Section I of this paper, the alkaloids were illuminated in water solutions containing a strong acid (hydrochloric or methanesulphonic). For the separation of the reaction mixtures we applied chromatography on alumina, this method having been extensively used by Stoll and his collaborators [2,6].

The elementary analyses have been performed under the direction of Dr. K. J. Karrman in the Analytical Department of the Chemical Institute, University of Lund. The paper chromatographic methods have been described in Section III A of this paper.

Transformation products of ergometrine

A solution of 0.25 g of ergometrine maleate in 10 ml of M/10 HCl was irradiated in a quartz flask under N_2 atmosphere, until the transformation had almost ceased as judged from spectrophotometric measurements of samples drawn; time: *ca.* 8 h; light-source: "Mineralight" U.V.-lamp, the radiation of which was limited to the region of 366 mμ. Some sodium phosphate and 2.5 g of NaCl were added to the liquid, and after adjusting

Table 2. R_F-values for ergometrine alkaloids and lumi-derivatives. The chromatographic procedure is described in the text (Section III A).

Ergometrine	0.57	Ergometrinine	0.68
α-Lumiergometrine	0.29	α-Lumiergometrinine	0.37
β-Lumiergometrine	0.36	β-Lumiergometrinine	0.54

Table 3. R_F-values for ergotamine and ergocristine alkaloids and lumi-derivatives. The chromatographic procedure is described in the text (Section III A).

Ergotamine	0.85	Ergocristine	>0.90
α-Lumiergotamine	0.25	α-Lumiergocristine	0.59
β-Lumiergotamine	0.54	β-Lumiergocristine	0.79
Ergotaminine	0.69	Ergocristinine	0.89
α-Lumiergotaminine	0.23	α-Lumiergocristinine	0.49
β-Lumiergotaminine	0.68	β-Lumiergocristinine	0.88

the pH to 9 it was extracted with 3 × 20 ml of a mixture of ethanol and ether (1:2). The extract was evaporated to dryness in a vacuum (N_2 atmosphere). The residue, dissolved in 1 ml of ethanol and 100 ml of absolute chloroform, was transferred to the top of a column of alumina (10—20 g), and gradually eluted with chloroform (*ca.* 500 ml) containing increasing amounts of ethanol (1—7 %). First a small fraction of unchanged ergometrine was obtained and then two fractions of transformed alkaloid, the first one very small, the second one strongly dominating. Their paper chromatographic properties showed them to be α-lumiergometrine and β-lumiergometrine, respectively.

α-Lumiergometrine was obtained in a quantity of only a few mg of raw product, which showed, however, a pure lumialkaloid absorption spectrum and gave a single spot on the paper chromatogram (Table 2).

β-Lumiergometrine. The dominating second fraction was dissolved in some absolute methanol and diluted with 5—7 volumes of ether. On scratching the walls of the vessel needle-shaped crystals were formed. Yield: 90 mg (air-dry). On the Kofler block the crystals gave off their solvent of crystallization at about 110° C, transforming into an apparently amorphous modification with a very diffuse melting point (about 146°—150° C). The material was uniform on paper chromatograms (Table 2).

After drying the substance in a high vacuum at 130° C the following constants were obtained: *Light absorption:* E (1 %, 1 cm) = 196 at 283 mμ (max.) in M/10 HCl. *Optical rotation:* $[\alpha]_D^{20°} = -27°$ (pyridine, $c = 1$). *Molecular weight:* acidimetric equiv.wt. = 347* (calc. for ergometrine + 1 H_2O : 343). *Elementary analysis:* Found: C 64.9; H 7.40; O 14.3; N 12.9. Calc. for $C_{19}H_{25}O_3N_3$ (343.4): C 66.45; H 7.34; O 13.98; N 12.24.

The properties of β-lumiergometrine are chiefly the same as reported by Stoll and Schlientz [3] for lumiergobasine.

Transformation products of ergometrinine

The same preparation procedure was used as for ergometrine. We obtained three fractions of non-fluorescent alkaloid, all with a maximum of light absorption at 283 mμ. The first and the last of these were the main fractions and according to their paper-chromatographic properties they were called α-lumiergometrinine and β-lumiergometrinine, respectively. The very small intermediate fraction, which differed from the other two even paper chromatographically, was not examined any more.

α-Lumiergometrinine crystallized from absolute methanol as needles. Yield: 30 mg of air-dry crystals from 150 mg of ergometrinine. On the Kofler block the crystals were transformed into an apparently amorphous modification at about 135° C and melted diffusely and under decomposition at 193°—197° C. The material was uniform on the paper chromatogram (Table 2).

* Obtained by titrating potentiometrically *ca.* 2 mg of substance, dissolved in 0.15 ml of ethanol and 0.50 ml of water, with 0.02 N HCl.

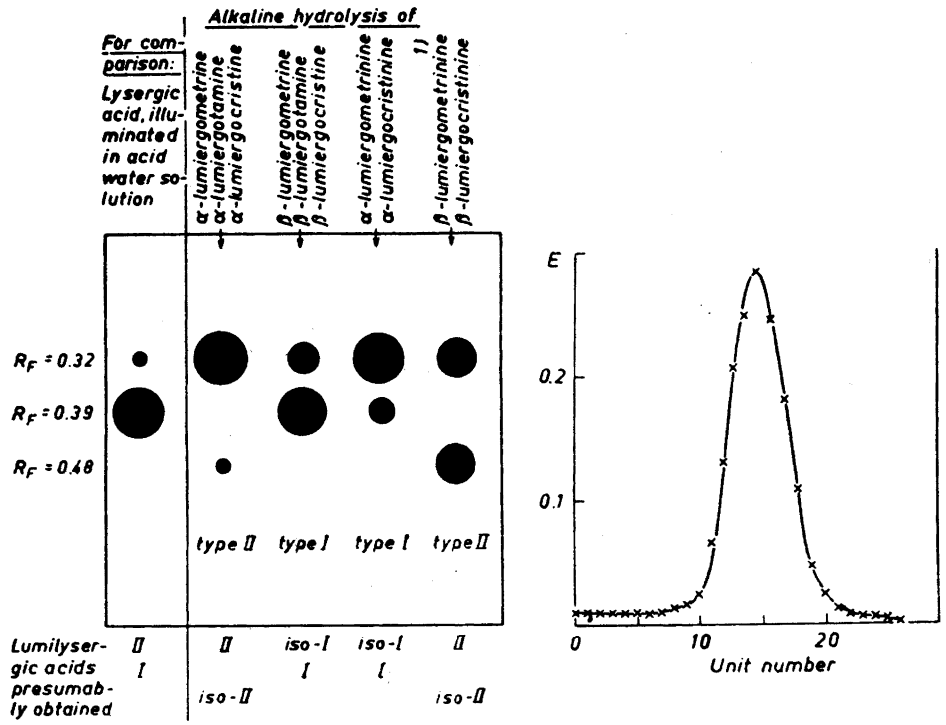


Fig. 5. Paper chromatography of lumilysergic acids obtained by alkaline hydrolysis of lumialkaloids (idealized picture).

Fig. 6. Counter current distribution of β-lumiergocristinine. Benzene/0.2 M phosphate buffer pH 5.9 (Photometric determination by *p*-dimethylaminobenzaldehyde).

After drying in a high vacuum at 130° C the substance showed the following properties: *Light absorption:* E (1 %, 1 cm) = 193 at 283 mμ (max.) in M/10 HCl. *Optical rotation:* $[\alpha]_D^{20°}$ = + 24° (pyridine, c = 1). *Molecular weight:* acidimetric equiv.wt. = **341** (calc. for ergometrinine + 1 H_2O: 343). *Elementary analysis:* Found: C 66.5; H 7.57; O 14.1; N 11.7. Calc. for $C_{19}H_{25}O_3N_3$ (343.4): C 66.45; H 7.34; O 13.98; N 12.24.

β-Lumiergometrinine crystallized on evaporation of a solution in little ethanol and much chloroform. Yield: 55 mg of air-dry crystals from 150 mg of ergometrinine. All attempts failed to crystallize the substance from solvents usually applied to ergot alkaloids as methanol, ethyl acetate or acetone. From warm benzene solutions it was precipitated as an apparently amorphous modification. On the Kofler block the crystalline β-lumiergometrinine at 105° C gave off its solvent of crystallization, changing into an apparently amorphous modification, the melting point of which (*ca.* 125° – 135° C) was very difficult to observe. The product was uniform on paper chromatogram (Table 2).

After drying the substance in a high vacuum at 120° C we obtained the following constants: *Light absorption:* E (1 %, 1 cm) = 188 at 283 mμ (max.) in M/10 HCl. *Optical rotation:** $[\alpha]_D^{30°}$ = + 18° (pyridine, c = 1). *Molecular weight:* acidimetric equiv.wt. = 356

* Based on one single experiment.

(calc. for ergometrinine + 1 H_2O: 343). *Elementary analysis:* Found: C ...; H 7.30; O 14.2; N 12.0. Calc. for $C_{19}H_{25}O_3N_3$ (343.4): C 66.45; H 7.34; O 13.98; N 12.24.

Transformation products of ergocristine

0.25 g of ergocristine was dissolved in 50 ml of M/10 methanesulphonic acid. In order to give the same effect on the peptide alkaloids as on ergometrine the irradiation had to be more powerful and therefore a strong mercury-lamp without a filter was used in this case, completing the transformation in 1—2 h. The products were extracted with absolute chloroform after alkalinizing the reaction mixture with ammonia. The chloroform extract was dried over anhydrous sodium sulphate and poured onto a column of alumina (20—40 g). The elution was made step by step, first with chloroform containing 1 % ethanol until the small fraction of α-lumiergocristine had been obtained and then with chloroform containing 3 % ethanol until the dominating fraction of β-lumiergocristine had come out. The fractions were as soon as possible evaporated in a vacuum to dryness.

α-Lumiergocristine was formed only in minor quantities. The top fractions from several preparations — strongly contaminated with coloured substance — were collected and distributed between a large quantity of diluted hydrochloric acid (about M/20) and a small quantity of chloroform. The nearly colourless aqueous solution was alkalinized with ammonia and extracted with chloroform. From this solution a small quantity of substance (*ca.* 10 mg) could be obtained but we did not succeed in crystallizing it. However, it was uniform on paper chromatogram (Table 3).

β-Lumiergocristine was purified from colouring matter in the same way as the α-product and could be crystallized from methanol in short, thick prisms. Yield: 90 mg of air-dry crystals from 200 mg of ergocristine. Melt.p. on the Kofler block: 179°—181° (decomp.). It was uniform on the paper chromatogram (Table 3).

After drying in a high vacuum at 130° C the substance showed the following properties: *Light absorption:* E (1 %, 1 cm) = 109 at 283 mμ (max.) in M/10 HCl. *Optical rotation:* $[\alpha]_D^{20°}$ = + 17° (pyridine; c = 1). *Molecular weight:* acidimetric equiv.wt.: 641 * (calc. for ergocristine + 1 H_2O: 628). *Elementary analysis:* Found: C 65.6; H 6.62; O 15.4; N 10.9. Calc. for $C_{35}H_{41}O_6N_5$ (627.7); C 66.96; H 6.58; O 15.29; N 11.16.

Transformation products of ergocristinine

The ergocristinine had to be dissolved in glacial acetic acid, the solution diluted with water to the strength of about 5 % acetic acid and finally made M/10 in respect of methanesulphonic acid. The irradiation and the extraction were made as described for ergocristine. For the separation gradient elution was used again. The transformation products were very sensitive to the ethanol percentage of the elutrient and therefore this was allowed to increase only slowly (0—1 % in 500 ml of elutrient). The main products were the α-lumiergocristinine and the β-lumiergocristinine. Between them small fractions with variable paper chromatographic properties appeared. These were not further examined.

α-Lumiergocristinine crystallized from methanol as needles. The yield was remarkably small. From 300 mg of ergocristinine only 33 mg of air-dried crystals were obtained. M.p. on the Kofler block: 234—236° C. It was uniform on paper chromatogram (Table 3).

Dried in a high vacuum at 130° C the α-lumiergocristinine showed the following properties. *Light absorption:* E (1 %, 1 cm) = 107 at 283 mμ (max.) in M/10 Hcl. *Optical rotation* **: $[\alpha]_D^{20°}$ = +116° (pyridine, c = 0.6). *Molecular weight:* acidimetric equiv.wt.: 638 (calc. for ergocristinine + 1 H_2O: 628). *Elementary analysis:* Found: C 66.6; H 6.71; O 15.7; N 11.0. Calc. for $C_{35}H_{41}O_6N_5$ (627.7): C 66.96; H 6.58; O 15.29; N 11.16.

β-Lumiergocristinine. The raw product was purified from most of the coloured material as described for α-lumiergocristine. It was dissolved in much boiling benzene from which it precipitated on cooling in an apparently non-crystalline form. The yield of this product

* Obtained for the petide alkaloids by titrating potentiometrically *ca.* 3 mg of substance, dissolved in 0.50 ml of glacial acetic acid, with 0.02 N perchloric acid.

** Based on one single experiment.

was 150—200 mg from 300 mg of ergocristinine. The material could not be brought to crystallization even after further chromatographic purifications. However, the substance obtained was uniform on paper chromatogram and gave a single top on counter current distribution (Fig. 6). On the Kofler block it had a reproducible and comparatively good melting point at 171—172° C (decomp.). Thus there are good reasons to believe that the substance was pure.

After drying in a high vacuum at 130° C the substance showed the following properties: *Light absorption:* E (1 %, 1 cm) = 107 at 283 mμ (max.) in M/10 HCl. *Optical rotation:* $[\alpha]_D^{20°} = \pm 0°$ (pyridine, $c = 1$). *Molecular weight:* acidimetric equiv.wt.: 650 (calc. for ergocristinine + 1 H_2O: 628). *Elementary analysis:* Found: C 66.5; H 6.57; O 15.6; N 11.0. Calc. for $C_{35}H_{41}O_6N_5$ (627.7): C 66.96; H 6.58; O 15.29; N 11.16.

Transformation products of ergotamine and ergotaminine

The lumi-derivatives from these alkaloids have been prepared and described by Stoll and Schlientz [2]. The β-lumiergotamine had been made by us before we were aware of the Swiss paper. The main properties of our product were the following: It crystallized from methanol in short, thick prisms. M.p. on the Kofler block: 248° C (decomp.); $[\alpha]_D^{20°} = +12°$ (pyridine; $c = 1$) E (1 %, 1 cm) = 115 at 283 mμ (max.) in M/10 HCl. Acidimetric equiv. wt. (mol. wt.) = 605 (calc. for ergotamine + 1 H_2O: 600). Found: C 66.1; H 6.38; O 16.15; N 11.55. Calc. for $C_{33}H_{37}O_6N_5$ (599.7): C 66.09; H 6.22; O 16.01; N 11.68.

β-Lumiergotamine gave a slightly soluble hydrochloride and could be almost totally precipitated from its aqueous solution by an excess of hydrochloric acid. The paper chromatographic properties of the lumiergotamines and lumiergotaminines are reported in section III A of this paper (Table 3, Fig. 5).

Acknowledgements. I wish to thank Dr. K. J. Karrman of the University of Lund for the elementary analyses and Mrs. Ingegerd Dinnetz of this laboratory for technical assistance. My thanks are also due to Mrs. M. Spilsbury, who revised the English.

REFERENCES

1. Hellberg, H. *Pharm. Ztg.* **91** (1955) 1227.
2. Stoll, A. and Schlientz, W. *Helv. Chim. Acta* **38** (1955) 585.
3. Dewar, M. J. S. *The Electronic Theory of Organic Chemistry*, Oxford 1949.
4. Stoll, A., Petrzilka, Th., Rutschmann, J., Hofmann, A. and Günthard, Hs. H. *Helv. Chim. Acta* **37** (1954) 2039.
5. Cookson, R. C. *Chemistry & Industry* **1953** 337.
6. Stoll, A., Hofmann, A. and Petrzilka, Th. *Helv. Chim. Acta* **29** (1946) 635.
7. Janot, M. M. and Goutarel, R. *Bull. soc. chim. France*, **1949** 509.
8. Craig, L. C., Shedlovsky, Th., Gould, R. S. and Jacobs, W. A. *J. Biol. Chem.* **125** (1938) 289.
9. Reimers, F. *Dansk Tidskr. Farm.* **12** (1938) 191.
10. Stenlake, J. B. *Chemistry & Industry* **1953** 1089.
11. Berg, A. M. *Diss.* Utrecht 1953.
12. Foster, G. E., Macdonald, J. and Jones, T. S. G. *J. Pharm. Pharmacol.* **2** (1951) 802.
13. Shute, J. B. *Diss.* Leiden 1953.
14. Munier, R., Macheboeuf, M. and Cherrier, N. *Bull. soc. chim. biol.* **34** (1952) 204.
15. Brindle, H., Carless, J. E. and Woodhead, H. B. *J. Pharm. Pharmacol.* **3** (1951) 793.
16. Stoll, A. and Rüegger, A. *Helv. Chim. Acta* **37** (1954) 1725.
17. Hellberg, H. *Farm. Revy* **50** (1951) 17.
18. Hellberg, H. *Farm. Revy* **52** (1953) 535.

Received October 20, 1956.

ACTA CHEMICA SCANDINAVICA 11 (1957) 230—234

The Effect of Volatile Substances on the Chemical Activity of Ultrasonic Cavitation

NILS ELLFOLK and ARTTURI I. VIRTANEN

Laboratory of the Foundation for Chemical Research, Biochemical Institute, Helsinki, Finland

The effect of volatile substances on the reactions in ultrasonic-treated water was investigated. It was found that butanol, propanol *etc.* are able to inhibit practically all reactions, the oxidation of luminol being, however, unchanged. The sonoluminescence of pure distilled water could not be observed in the presence of these substances.

In an earlier paper [1] we reported that different volatile substances such as fatty acids, alcohols, *etc.* are able to inhibit nitrogen fixation in water treated with ultrasonics In the homologous series the inhibition was observed to increase with the length of the carbon chain. When trying to explain this inhibition it seemed at least apparent that the vapour pressure of the substances was not the cause of the inhibitory effect. Since the inhibition generally increased with the length of the carbon chain it seemed reasonable to suppose that the substances caused the inhibition of the reactions by lowering the surface tension of the solution. It is, however, to be observed that other properties also change with the lengthening of the carbon chain.

In the present work attempts were made to elucidate this problem by observing the effect of volatile substances on the oxidation of compounds like luminol during the ultrasonic treatment of distilled water.

EXPERIMENTAL

Ultrasonic vibrations were produced as described previously [1]. A sensitive photometer was used for the measuring of the luminescence produced by ultrasonics in distilled water with or without the addition of luminol. The photoelectric cell (RCA 931 A) and the amplifying system were enclosed in a light-tight metal box with a window for the light to be measured. Fig. 1 shows a schematic diagram of the complete electronic circuit [2]. The weak electric current was measured with a sensitive galvanometer (Lange) having a current sensitivity of 3.5×10^{-9} amp/mm.

In the experiments with luminol the following solution was used: 100 ml of the test solution, 0.01 % luminol (5-amino-2,3-dihydro-1,4-phthalazinedione) in 0.05 % Na_2CO_3. The light emitted was measured after it had reached its maximum. Table 1 shows the influence of different substances on the chemiluminescence of luminol.

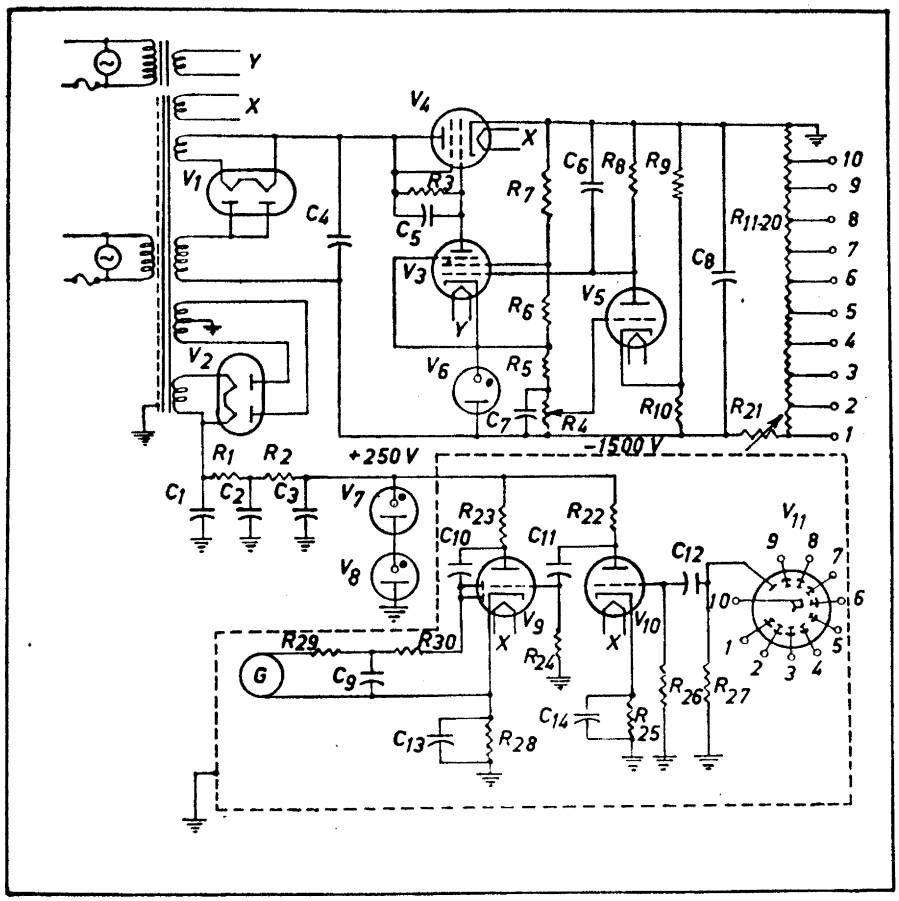


Fig. 1. Circuit of the a—c amplifier and voltage regulated power supply for the phototube.

R_1 = 5.6 kΩ
R_2 = 4 kΩ
$R_{3,22,23}$ = 0.5 MΩ
R_4 = 50 kΩ pot.m (wire wound)
R_5 = 0.25 MΩ
R_6 = 25 kΩ
R_7 = 75 kΩ
R_8 = 25 MΩ
R_9 = 0.34 MΩ
R_{10} = 3.4 kΩ
R_{11-20} = 0.1 MΩ
R_{21} = 0.2 MΩ pot.m (wire wound)
$R_{24,26,27,30}$ = 1 MΩ
R_{25} = 7 kΩ
R_{28} = 8 8Ω
R_{29} = 50 kΩ

G = 0—70 μA

C_1 = 0.1 μF
C_2 = 8 μF el.kond.
C_3 = 4 μF »
C_4 = 16 μF » 1 500 v (oil filled)
$C_{5-7,13,14}$ = 1 μF
C_8 = 2 μF el.kond. 1 500 v (oil filled)
C_9 = 10 μF
C_{10-12} = 0.06 μF

V_1 = 5R4G
V_2 = 5Y4
V_3 = 6AC7
V_4 = 6L6
$V_{5,10}$ = 6SF5
V_{6-8} = VR150
V_9 = 6SQ7
V_{11} = 931-A (phototube)

Table 1. Effect of volatile substances on the chemiluminescence of luminol.

Substance	Added in %	Galvanometer reading in mm $n-n_0$
No addition	—	700
Ether	0.2	0
iso-Amylalcohol	0.2	700
n-Butanol	1	700
Propanol	1	680
Ethanol	2	700
Benzene	0.2	20
Xylene	0.2	450
Toluene	0.2	150

These experiments show that alcohols are hardly competing for oxygen with nitrogen because practically no decrease in light intensity can be observed in the presence of luminol. On the other hand we have previously found that nitrogen fixation does not take place in the presence of alcohol [1]. This question will be reverted to below.

To elucidate the interrelationship between the chemiluminescence of luminol and the luminescence of distilled water, treated with ultrasonics, experiments were made with pure distilled water in the same way as with luminol, *i. e.* measuring luminescence after the maximum had been developed. Table 2 shows the influence of different substances on luminescence.

Table 2. Luminescence of water with volatile substances without luminol.

Substance	Added in %	Galvanometer reading in mm $n-n_0$
No addition	—	30
Ether	0.2	0
Butyric acid	1	0
n-Butanol	1	0
Propanol	1	0

A KI solution was treated in the ultrasonic field (100 ml of a solution made up of 50 ml of 1 % KI, 45 ml of 1 % H_2SO_4, and 5 ml of 0.1 % starch solution). The liberated iodine was titrated with thiosulphate. It can be seen in Fig. 2 that no oxidizing substances are produced in the solution in presence of *n*-butanol.

When 1 ml of chloroform is added to this solution some oxidizing substances are still produced in the presence of *n*-butanol as can be seen from the liberation of iodine (Fig. 3). An experiment was made to find out if a change in the physical structure of water possibly causes changes in the chemical activity of cavitation. No effect was observed in 1 M NaCl solution.

DISCUSSION

If oxygen containing water with or without luminol is treated with ultrasonics, molecular nitrogen is fixed under the formation of nitrite, but if for instance 1 % butanol is added nitrogen fixation is completely inhibited. So is also the formation of hydrogen peroxide. Butanol does not, however, notably decrease the chemiluminescence of luminol, a fact which shows that easier

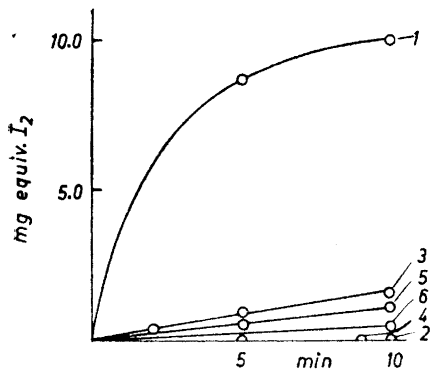


Fig. 2. Inhibitory effect of volatile substances on liberation of iodine from KI. 1) Control without *n*-butanol addition, 2) addition of 1 % *n*-butanol, 3) 1 % butyric acid, 4) 0.2 % toluene, 5) 0.25 % caproic acid, 6) 0.5 % *iso*-amylalcohol.

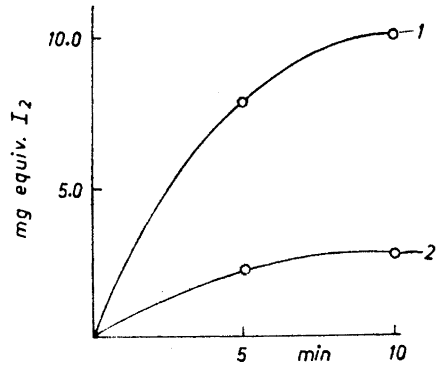


Fig. 3. 1) Control without butanol addition, 2) addition of 1 % *n*-butanol.

occurring oxidation reactions still take place and that cavitation occurs in the presence of this alcohol, since substances with a high vapour pressure such as ether *etc.* completely extinguish the light given by luminol. Due to the addition of alcohol, however, radical changes have taken place in the system. The hypothesis that alcohols should act as acceptors for oxidizing agents is not well-founded because no liberation of iodine from KI was observed in a 1 % butanol solution. Since the changes caused by alcohol cannot be due to the ability of the substances to compete for oxygen with nitrogen, nor to the destruction of cavitation because of the vapour pressure, it seems reasonable to suppose that the substances which lower the surface tension decrease the energetic state of cavitation, so that for merely energetic reasons some reactions do not take place. As to the mechanism of the decrease of the energy level at least two possible ways had to be observed.

In the first case the mechanism of the lowering of the energy level is assumed to be connected with the mechanism of cavity formation. According to Lindström [3] cavitation is preceded by the nucleation process during which separate gas bubbles dissolved in the liquid combine, and a germ consisting of six gas molecules is built up. Through the formation of this germ, or box, the great cohesive forces in water are overcome and cavitation is initiated. Earlier we assumed it hardly likely that surface active substances should accumulate on the inside surface of the cavitation bubble because of its short duration, but if the nucleation process precedes cavitation it may be assumed that during this lag period surface active substances are mobilized in the vicinity of the box. On this account it can perhaps be understood why there is a difference in regard to inhibition between dissociated and undissociated fatty acids. The dissociated carboxyl group is surrounded by such a large amount of water molecules that, contrary to the undissociated group, its

mobility is hampered. From this the observed difference between neutralized and unneutralized valeric acid arises, *i. e.* the former is able to inhibit nitrogen fixation by only 30 or 40 % whereas the latter inhibits it completely.

Lindström assumes further that the chemical reactions in cavitation are due to the fact that the water surface around a gas bubble is negatively charged, the surface charge acquiring rather high values (0.08 e.s.u./cm^2). When the surface of the cavity is formed the surface charge must be established by transport of electricity, by which process the gas molecules in the cavity will be ionized. In such a case it is evident that if surface active substances have been accumulated in the surface of the gas bubble the surface charge per cm^2 should be lower than in a solution without surface active substances for the very reason that the number of water molecules per cm^2 of the surface of the bubble has decreased.

In this case the explanation of the changes in the chemical activity of cavitation is assumed to be connected with the drastic changes in the physical structure of water caused by addition of different alcohols.

According to Bernal and Fowler [4] water may be regarded as a partially broken down ice structure, tridymite-like, with each oxygen atom surrounded tetrahedrally by four other oxygen atoms, the structure being held together by hydrogen bonds. When a molecule of solute is introduced into the water structure a cavity can first be formed in this by taking away a given number of water molecules. Hereby a number of hydrogen bonds have to be broken proportional to the size of the molecule. This breaking of hydrogen bonds is reflected in changes in compressibility, viscosity and surface tension. A decrease in compressibility means a closer packing of the water molecules with increased cohesive forces. It could therefore be assumed that the formation of cavity is prevented because of the depolymerization of the association of water.

It should, however, be observed that no inhibition of nitrogen fixation was observed in a solution in which a depolymerization of water had been produced by sodium chloride. It is therefore suggested that changes in the physical structure of water is not responsible for changes in the chemical activity of the cavitation.

REFERENCES

1. Virtanen, A. I. and Ellfolk, N. *Acta Chem. Scand.* **6** (1952) 660.
2. Bennett, G. F. and Free, A. L. *Electronics* **19** (1946) 116.
3. Lindström, O. *J. Acoust. Soc. Amer.* **27** (1955) 654.
4. Bernal, J. D. and Fowler, R. H. *J. Chem. Phys.* **1** (1933) 515.

Received April 23, 1956.

ACTA CHEMICA SCANDINAVICA 11 (1957) 235—238

The Acid-Catalysed Solvolysis of Alkoxymethyl Esters. Part III. Reaction Rates and Products in the Solvolysis of Ethoxymethyl Acetate in Ethanol-Water Mixtures

PENTTI SALOMAA

Department of Chemistry, University of Turku, Turku, Finland

The kinetics of the acid-catalysed solvolysis of ethoxymethyl acetate have been investigated in six ethanol-water mixtures containing 35—78 moles per cent of ethanol. By the composition of the solvolysis product it has been established that the reaction takes place in these media by two simultaneously occurring mechanisms: a unimolecular mechanism which involves an intermediate formation of ethoxymethyl cation, and a bimolecular mechanism which is identical with the acyl-oxygen fission mechanism of the acid-catalysed solvolysis of simple alkyl esters. The contribution of the unimolecular mechanism has been found to be more marked than that of the bimolecular mechanism in the solvents investigated. The results have been discussed and compared to earlier observations made on the hydrolysis of ethoxymethyl acetate in water solution.

In extension of the earlier study on the mechanisms of acid-catalysed solvolysis reactions of alkoxymethyl esters [1,2], the present paper deals with results obtained for the solvolysis of ethoxymethyl acetate in ethanol-water mixtures of a sufficiently low proton-availability, in which an experimental distinction could be made between the two different mechanisms of the solvolysis.

Table 1. The first-order rate constants (in sec.$^{-1}$) for the formation of formaldehyde (k') and ethylal (k'') from ethoxymethyl acetate in ethanol-water mixtures at 25° C at 0.1 N hydrogen chloride concentration.

Moles % of EtOH	0	34.9	43.8	51.2	60.9	69.3	78.1
H_0	+ 1.01	+ 2.07	+ 2.19	+ 2.23	+ 2.24	+ 2.23	+ 2.16
$10^5 \times k'$	87.1	8.38	6.57	6.05	5.29	4.78	4.48
$10^5 \times k''$	—	4.12	3.43	3.30	3.54	4.70	6.12

Table 2. The molar ratios of formaldehyde and ethylal formed by the solvolysis of ethoxymethyl chloride in ethanol-water mixtures at 25° C at 0.1 N initial hydrogen chloride concentration.

Moles % of EtOH	34.9	43.8	51.2	60.9	69.3	78.1
[HCHO] / [$CH_2(OEt)_2$]	1.430	1.008	0.766	0.534	0.394	0.280

Table 3. The values of first-order rate constants (in $sec.^{-1}$) calculated for the unimolecular (k_1) and bimolecular (k_2) solvolysis of ethoxymethyl acetate in ethanol-water mixtures at 25° C at 0.1 N hydrogen chloride concentration.

Moles % of EtOH	34.9	43.8	51.2	60.9	69.3	78.1
$10^5 \times k_1$	10.0	6.9	5.8	5.4	6.6	7.8
$10^5 \times k_2$	2.5	3.1	3.5	3.4	2.9	2.8
$\log k_1 + H_0$	−1.93	−1.97	−2.01	−2.03	−1.95	−1.95

The method of measuring the rates of the solvolysis reactions and that of estimating the rate constants referring to the different mechanisms were those described in the second part of the present study [2]. The results are given in Tables 1, 2 and 3, the meaning of the symbols being the same as before. Table 1 also includes the value of k' in water solution which has been taken from the results of the previous measurements [1], and the values of the Hammett acidity function H_0 for the reaction solutions employed. The latter values have been obtained by interpolation from the data given by Braude and Stern [3] for ethanol-water mixtures. The rate constants of the slow, subsequent reactions, the hydrolysis of ethylal and its reverse reaction, which were used for the calculation of the values of k' and k'' are given in the experimental part.

The results of the present study show a close similarity to the corresponding values determined for the solvolysis of methoxymethyl acetate in methanol-water mixtures [2]. As indicated by the values of Table 3, the contribution of the unimolecular mechanism is about 60—80 % of the total rate of solvolysis in the media investigated. Although the resolution of the solvolysis rate into the two parts which correspond to the different mechanisms is remarkably susceptible to the influence of experimental errors, the values of k_1 are seen, as expected by the theory, to pass through a minimum at approximately the same alcohol contents of the solvent at which the solutions have their lowest proton-availabilities, as measured by the Hammett acidity function.

The value of H_0 decreases by about one unit, when passing from a solution containing 34.9 moles per cent of ethanol to water solution. The theory suggests that the rate constant of the unimolecular reaction will be increased by a factor of about 10 by this change of medium, whereas a decrease of the value of k_2 is to be expected, *cf.* Ref.[2] Thus the fact that in 34.9 moles per cent ethanol approximately 80 % of the total solvolysis reaction does occur by the unimolecular mechanism furnishes an additional evidence for the suggestion made [1], according to which the hydrolysis of ethoxymethyl acetate by aqueous acid takes place almost exclusively by the unimolecular mechanism.

Table 4. The values of k_a and k_h (in sec.$^{-1}$) determined for the reversible acetalisation of formaldehyde in ethanol-water mixtures at 25° C at 0.1 N hydrogen chloride concentration.

Moles % of EtOH	34.9	43.8	51.2	60.9	69.3	78.1
$10^6 . (k_a + k_h)$	4.38	3.53	3.50	3.69	4.40	6.20
$k_h / (k_a + k_h)$	0.301	0.244	0.200	0.160	0.125	0.087

Table 5. The determination of the constants k_a and k_h for the reversible acetalisation of formaldehyde in 69.3 moles per cent ethanol at 25° C at 0.1 N hydrogen chloride concentration.

t (in minutes)	0	600	900	1 200	1 525	1 900	2 100	2 400	7 250	∞
$10^3 . [HCHO]$	9.25	8.10	7.51	7.05	6.54	6.03	5.80	5.49	2.36	1.16
$10^6 . (k_a + k_h)$		4.26	4.48	4.40	4.46	4.46	4.42	4.34	4.38	

Average $k_a + k_h = 0.00000440$ sec.$^{-1}$; $k_h / (k_a + k_h) = 0.125$

Table 6. The determination of the first-order rate constants for the formation of formaldehyde (k') and ethylal (k'') by the solvolysis of ethoxymethyl acetate in 60.9 moles per cent ethanol at 25° C at 0.1 N hydrogen chloride concentration. Eqns. 3, 4 and 5 (Ref.[2]) have been used for the calculations. $k_a + k_h = 0.00000369$ sec.$^{-1}$, $k_h / (k_a + k_h) = 0.160$, $a = 0.0613$.

$t-t_0$ in minutes	[HCHO]	t in minutes	a	$k' + k''$ in sec.$^{-1}$
0	0.0002			
1	0.0004			
2	0.0007			
30	0.0057	31		0.0000908
50	0.0085	51		0.0000865
70	0.0116	71		0.0000897
90	0.0141	91		0.0000896
125	0.0177	126		0.0000884
155	0.0202	156		0.0000873
275	0.0271	276		0.0000860
1 505	0.0296	1 506	0.611	
2 030	0.0279	2 031	0.623	
2 210	0.0271	2 211	0.620	

Averages: $a = 0.618$, $k' + k'' = 0.0000883$ sec.$^{-1}$
$k' = 0.0000529$ sec.$^{-1}$, $k'' = 0.0000354$ sec.$^{-1}$

The values of k_1 determined in ethanol-water mixtures (Table 3) are nearly of that order of magnitude which is to be expected for the unimolecular mechanism. From the first-order rate constant of the hydrolysis of ethoxymethyl acetate in water at 25° C at 0.1 N hydrogen chloride concentration, 0.000871 sec.$^{-1}$, and from the corresponding value of the acidity function, +1.01, it is obtained: $\log k + H_0 = -2.05$. This value shows a satisfactory agreement with the values calculated for $\log k_1 + H_0$ for ethanol-water mixtures (Table 3), in view of the difficulties encountered in revealing the actual dependence of $\log k_1$ on the acidity function in ethanol-water mixtures, *cf.* Ref.[2]

EXPERIMENTAL

The methods of preparing and purifying the materials used were those described earlier [1,4]. The technique of the kinetic measurements and the methods of calculation were the same as those applied to the solvolysis of methoxymethyl esters in methanol-water mixtures [2]. Table 4 gives the rate constants measured for the hydrolysis of ethylal and its reverse reaction, the acetalisation of formaldehyde, Table 5 illustrating one of the individual measurements. Table 6 gives the details for a typical example of the experimental runs in which the solvolysis of ethoxymethyl acetate was investigated. The meaning of the symbols is the same as previously [2].

REFERENCES

1. Salomaa, P. *Acta Chem. Scand.* **11** (1957) 132.
2. Salomaa, P. *Acta Chem. Scand.* **11** (1957) 141.
3. Braude, E. A. and Stern, E. S. *J. Chem. Soc.* **1948** 1976.
4. Salomaa, P. *Ann. Univ. Turkuensis*, **Ser. A XIV** (1953) No. 1.

Received October 23, 1956.

ACTA CHEMICA SCANDINAVICA 11 (1957) 239—246

The Acid-Catalysed Solvolysis of Alkoxymethyl Esters. Part IV. The Temperature Dependence of the Hydrolysis Rate

PENTTI SALOMAA

Department of Chemistry, University of Turku, Turku, Finland

The kinetics of the hydrolysis of methoxymethyl acetate, ethoxymethyl acetate and methoxymethyl formate by dilute hydrochloric acid have been investigated over a temperature range from 0°C to 60°C. The reactions of the two former compounds show a linear relationship between the logarithm of the rate constant and $1/T$, in a satisfactory agreement with the Arrhenius equation, over the whole temperature range investigated. By methoxymethyl formate, on the contrary, an apparent deviation from the Arrhenius equation is notable especially at relatively low temperatures, the logarithm of the rate constant increasing more rapidly than as proportional to $-1/T$. This deviation can be interpreted in terms of the previous observations according to which the hydrolysis of this compound by dilute aqueous acid occurs by two simultaneous mechanisms, a unimolecular and a bimolecular mechanism, the unimolecular mechanism involving a considerably higher activation energy. By assuming the Arrhenius equation to be well obeyed by the two reactions involving the different mechanisms, the respective activation energies and frequency factors have been estimated from the experimental rate constants and found to be in agreement with the mechanisms suggested. The factors determining the mechanism of the acid-catalysed solvolysis of alkoxymethyl esters have been generally discussed.

In the previous kinetic study on the acid-catalysed solvolysis of alkoxymethyl esters in water [1] and in water-alcohol mixtures [2,3] it was established that these reactions can take place by two different mechanisms. The former mechanism involves a unimolecular formation of an alkoxymethyl cation in the rate-determining reaction stage, whereas the latter mechanism is bimolecular and consists of an acyl-oxygen bond fission. In the solvolysis by dilute aqueous acids at 25°C, it was found that the bimolecular mechanism is insignificant except the reaction of methoxymethyl formate.

In view of the relatively large differences between the activation energies involved in the two different reaction mechanisms, it was expected that these differences might be revealed by deviations from the Arrhenius equation, thus furnishing an additional criterion for the simultaneous occurrence of the two mechanisms. The present paper gives the results obtained for the hydrolysis of methoxymethyl acetate, ethoxymethyl acetate and methoxymethyl formate by dilute hydrochloric acid solutions over a wide temperature range. The kinetics of the hydrolysis of these compounds have been previously investigated by Palomaa and co-workers [4,5] at three temperatures from 15°C to 35°C, but this temperature range is too limited to allow a reliable experimental verification as to the validity of the Arrhenius equation for the reactions investigated.

RESULTS AND DISCUSSION

At relatively low acid concentrations the first-order rate constants of the hydrolysis of alkoxymethyl esters are directly proportional to the concentration of the catalyst acid, the values of pH and the acidity function H_0 becoming practically identical, *cf.* Refs.[1,6]. For these solutions the second-order rate constant which is obtained by dividing the experimental first-order constant by the catalyst concentration is thus independent of the latter. The concentration of the catalyst hydrochloric acid used in the present study was about 0.1 N, except in the measurements carried out at 45°C and at 60°C, at which temperatures, owing to the rapidity of the reactions, lower catalyst concentrations, *viz.* about 0.025 N, were chosen. The results obtained in the rate measurements are given in Table 1. In the table, k denotes the second-order rate constant.

Table 1. The values of the second-order rate constants (in l mole^{-1} sec.$^{-1}$) for the hydrolysis of alkoxymethyl esters in dilute aqueous hydrochloric acid at various temperatures.

°C	$10^4 \times k$		
	$CH_3COOCH_2OCH_3$	$CH_3COOCH_2OC_2H_5$	$HCOOCH_2OCH_3$
0	0.746	2.82	5.09
6			9.80
12	4.26	15.7	20.0
18			40.6
25	24.5	88.6	85.8
35	83.3	302	254
45	270	954	794
60	1 360	4 300	3 480

As shown by the values of Table 1, the effect of structure on the velocity of hydrolysis is notably dependent on the temperature. At relatively low temperatures methoxymethyl formate is hydrolysed more rapidly than methoxymethyl acetate and ethoxymethyl acetate, whereas at higher temperatures its hydrolysis rate is between those of the two latter compounds.

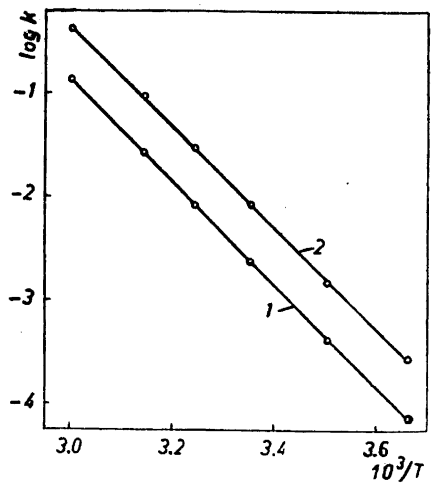


Fig. 1. The plot of log k against $1/T$ for the hydrolysis of methoxymethyl acetate (1) and ethoxymethyl acetate (2).

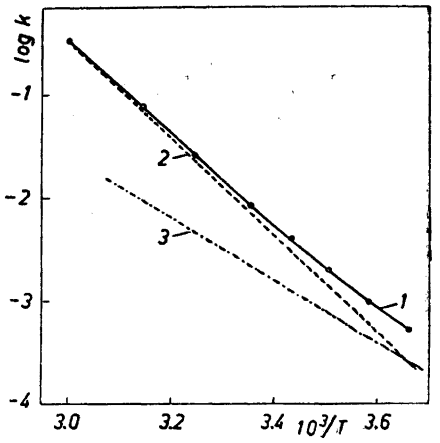


Fig. 2. The plot of log k against $1/T$ for the hydrolysis of methoxymethyl formate. 1. The experimental values. 2. The values calculated for the unimolecular mechanism. 3. The values calculated for the bimolecular mechanism.

In Figs. 1 and 2 the values of log k are plotted against $1/T$ for the hydrolysis of the different alkoxymethyl esters investigated. By methoxymethyl acetate and by ethoxymethyl acetate the plots show a linear course over the whole temperature range investigated, in accord with the Arrhenius equation. In the case of methoxymethyl formate, on the contrary, the logarithm of the rate constant decreases somewhat less rapidly than as directly proportional to $1/T$. This apparent deviation from the Arrhenius equation is most material at relatively low temperatures. The difference in the temperature dependence of the hydrolysis rates of the different alkoxymethyl esters is also seen, although to a more limited extent, from the values determined by Palomaa and co-workers [4,5]; the relative increases in the rate constants of methoxymethyl acetate and ethoxymethyl acetate are seen to be slightly higher, when passing from 15°C to 25°C, than when passing from 25°C to 35°C, in accordance with the Arrhenius equation, whereas the opposite situation is found to prevail in the hydrolysis of methoxymethyl formate.

From the plots of Fig. 1, the following values can be calculated for the parameters of the Arrhenius equation: log $A = 13.97$, $E = 22\,600$ cal/mole for methoxymethyl acetate, and log $A = 14.19$, $E = 22\,150$ cal/mole for ethoxymethyl acetate, respectively. Thus the frequency factor of the former compound is slightly lower than that of the latter, the activation energy of the former compound being somewhat higher. Both of these factors act in the same direction and increase the hydrolysis rate, when passing from the methoxymethyl ester to the corresponding ethoxymethyl ester.

In the case of methoxymethyl formate, a calculation of the parameters of the Arrhenius equation by a similar method is not possible over the whole temperature range. However, the satisfactory validity of the Arrhenius equation for the acetates, and the previous results [1,2], allow it to be presumed that the apparent deviation is in the present case due to two simultaneously occurring reaction mechanisms. The Arrhenius parameters for both the reactions concerned can be, at least approximately, evaluated from the experimental data by the method described below.

Let A_1 and E_1 denote the frequency factor and the activation energy of the one reaction, and A_2 and E_2 the corresponding parameters of the other reaction, respectively. If the Arrhenius equation can be assumed to be obeyed by both the reactions separately, and if the respective rate constants are denoted by k_1 and k_2, we have the following expression for the experimentally determined rate constant k:

$$k = k_1 + k_2 = A_1 \, e^{-E_1/RT} + A_2 \, e^{-E_2/RT}$$

The values of E_1 and E_2 must necessarily differ essentially, in order to give rise to such an apparent deviation from the Arrhenius equation, that can be experimentally detected at the temperatures investigated. Let the value of E_1 be higher than that of E_2. That implies that the relative contribution of k_1 to the experimentally measured rate constant k increases with temperature, and if the rate determinations have been extended up to sufficiently high temperatures the total reaction rate is practically determined by the values of k_1. In this case the plot of log k against $1/T$ at high temperatures gives the parameters A_1 and E_1 as a first approximation. From these values the values of k_1 can be calculated for the lowest temperatures, and the values of $k-k_1$ thus give the first approximations for the values of k_2 at these temperatures. A plot of the values of log k_2 thus found against $1/T$ gives approximations for the values of A_2 and E_2 from which, in turn, the values of k_2 and $k_1 = k - k_2$ can be calculated for the higher temperatures. From the values of log k_1 thus obtained, the second approximations for E_1 and A_1 can be determined. Similar successive approximations are reiterated until both the sets of values for the parameters of the Arrhenius equation remain practically constant over the whole temperature range investigated.

The application of the above method of successive approximations to the rate constants of the hydrolysis of methoxymethyl formate at various temperatures (Table 1) gave the following values for the parameters of the Arrhenius equation: log $A_1 = 13.82$, $E_1 = 21\,790$ cal/mole, and log $A_2 = 7.6$, $E_2 = 14\,000$ cal/mole, respectively. It is to be noted that the above values are influenced by experimental errors much more significantly than such, in which only one reaction is involved, because the errors are here absorbed into four parameters instead of two. In addition, small genuine deviations from the Arrhenius equation which are conceivable, will be included in the values calculated for the two sets of parameters. However, owing to the fact that the hydrolysis rates of methoxymethyl and ethoxymethyl acetates are satisfactorily expressed in terms of the Arrhenius equation, we have no reason to assume that this would not be the case for that reaction of methoxymethyl formate, the values of which have been denoted by the subscript 1, these values being similar to those determined for the acetates, and thus obviously referring to the same reaction mechanism. Because this reaction of methoxymethyl formate was the dominating over nearly the whole temperature range investigated, its Arrhenius parameters could be calculated relatively accurately, whereas the corresponding values for that reaction, the constants of which have been denoted by the subscript 2, were found to be relatively inaccurate (*e. g.* it could

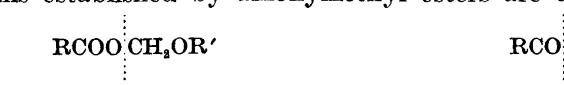
be estimated that the value of E_2 is accurate only within ± 2 000 cal/mole). Table 2 gives the values of k_1 and k_2 for the hydrolysis of methoxymethyl formate at various temperatures which have been calculated from the above values for the respective activation energies and frequency factors. It is seen that the contributions of both the reactions are nearly equal at 0°C, but at higher temperatures the contribution of k_2 to the total hydrolysis rate is rapidly decreased with temperature. Thus a more accurate determination of the parameters of the Arrhenius equation for the latter reaction would necessarily involve an extension of the rate measurements down to very low temperatures. The contributions estimated for the two different reactions are also illustrated by the straight lines drawn in Fig. 2.

Table 2. The values of k_1 and k_2 (in l mole^{-1} sec.$^{-1}$) for the hydrolysis of methoxymethyl formate at various temperatures.

°C	0	6	12	18	25	35	45	60
$10^3 . k_1$	0.238	0.564	1.29	2.85	6.90	22.8	69.7	329
$10^3 . k_2$	0.25	0.43	0.73	1.2	2.1	4.6	9.5	26

The values of log A_1 and E_1 calculated for methoxymethyl formate which are close to the corresponding values of log A and E determined for methoxymethyl and ethoxymethyl acetates are in good agreement with the assumption that all of the respective reactions take place by the same mechanism, *i. e.* by the unimolecular mechanism involving an alkoxymethyl cation as a reaction intermediate [1–3]. On the other hand, those values for methoxymethyl formate which have been denoted by the subscript 2, show, in spite of the approximativeness of their determination, a close similarity to the corresponding values of the acid-catalysed hydrolysis of simple alkyl formates. The value of k_2 estimated for methoxymethyl formate at 25°C, 0.0021 l mole^{-1} sec.$^{-1}$, is of the same order of magnitude as the corresponding values for methyl formate and ethyl formate, 0.00247 l mole^{-1}sec.$^{-1}$ and 0.00307 l mole^{-1}sec.$^{-1}$, determined by Salmi [7] and by Tommila and Hella [8], respectively. The activation energies calculated for the hydrolysis of methyl and ethyl formates are 14 500 and 15 770 cal/mole correspondingly, which are of that order of magnitude than the approximate value of E_2, 14 000 cal/mole, estimated for methoxymethyl formate.

Although the experimental material presented in this and in the three preceding papers [1–3] has so far been confined to the acid-catalysed solvolysis reactions of relatively few, constitutionally simple alkoxymethyl esters, some characteristic features of the different solvolysis mechanisms of these compounds may be presented, in accordance with the general theory on the acid-catalysed ester hydrolysis, extensively discussed by Ingold [9]. The two mechanisms established by alkoxymethyl esters are the following:



Unimolecular alkyl-oxygen fission $A_{AL}1$

Bimolecular acyl-oxygen fission $A_{AC}2$

In the first place, the above mechanisms are differently influenced by the external conditions, the reaction medium and temperature. The unimolecular mechanism is much more dependent on the proton-availability of the reaction solution than is the bimolecular mechanism. Thus the contribution of the bimolecular mechanism becomes more significant in solutions of low proton-donating power, whereas the unimolecular mechanism is greatly favoured by solvents of high proton-availability, in particular by concentrated, strong aqueous acids. As to the effect of temperature, the bimolecular mechanism involving a lower activation energy is more favoured by low temperatures.

From the constitutional point, the bimolecular mechanism is more notably dependent on the structure of the acyl group of the ester than is the unimolecular mechanism. In the case of the latter mechanism, changes of the acyl part of the ester do not materially influence the reaction velocity, as shown by the rate constants of the solvolysis of methoxymethyl formate and methoxymethyl acetate, the values for the former compound being only about 1.5—3 times larger than those of the latter compound in the solvolysis in water and in methanol-water mixtures. In the case of the bimolecular mechanism, the effect of the structure of the acyl group is much more significant. Alkyl formates are hydrolysed much more rapidly than the corresponding acetates by the bimolecular acyl-oxygen fission mechanism. The same structural effect is clearly illustrated also by alkoxymethyl esters. In water-methanol mixtures, the solvolysis rate constants of methoxymethyl formate which referred to the bimolecular mechanism, were observed to be about 30 times higher than the corresponding values for methoxymethyl acetate [2]. The fact that in the hydrolysis in water, the bimolecular mechanism has a significant contribution only for methoxymethyl formate, but not for methoxymethyl and ethoxymethyl acetates, is also well understood in terms of these structural effects.

In addition, the polar effects in the alkoxyl group of the ester are much more significant for the unimolecular mechanism which involves a production of an alkoxymethyl cation in the rate-determining reaction stage. Electron-releasing substituents are able greatly to stabilise the mesomeric cation, and thus favour the unimolecular mechanism, whereas electron-attracting substituents effect a material decrease of the velocity of the unimolecular reaction, thus favouring the bimolecular mechanism. The extent of this influence of a substituent depends primarily on the distance between the substituent and the point of the reaction, *i. e.* the carbon atom of the methylene group which acquires a positive charge on the attainment of the transition state. The retarding influence of an electron-attracting substituent on the velocity of the unimolecular reaction is clearly illustrated by the rate constants, determined by Palomaa and Herna [4] for the hydrolysis of 2-chloro-ethoxymethyl formate, $HCOOCH_2OCH_2CH_2Cl$. The value of the rate constant at 25°C, 0.00187 l mole^{-1}sec.$^{-1}$, as well as the value for the activation energy, 15 200 cal/mole, which can be calculated from the rate constants given by these authors for different temperatures, show such a close similarity to the corresponding values for simple alkyl formates (see above) that one can rather safely presume that in this case, the rate of the unimolecular reaction is effectively suppressed by the negative chlorine as a substituent, and hence the bimolecular mechanism is the dominating. Palomaa and Herna also

suggested that the hydrolysis mechanism of this compound will resemble most closely that of simple alkyl formates, thus differing from the behaviour of the other alkoxymethyl esters investigated, although the actual nature of the different mechanisms could not be elucidated by the observations thus far made.

EXPERIMENTAL

The preparation and purification of the materials used and the technique of kinetic measurements have been described in the first part of the present study [1]. The thermostat which was employed for measurements below room temperature, was situated in a room the temperature of which was refrigerated to −2°C, and the thermostat was filled with sodium chloride solution to allow the measurements at 0°C. The electrical heating and controlling system of this thermostat was the same as that used for measurements at the higher temperatures.

The concentration of the catalyst hydrochloric acid in the reaction solutions was 0.1 N or 0.025 N, measured at 20°C. The corresponding concentrations at the temperatures of the rate measurements were calculated from the values of the density of water at different temperatures, using the data given in the *International Critical Tables* [10]. Tables 3, 4 and 5 give the details for three typical individual runs. In the tables, a denotes the ester concentration at zero time (at the time of taking of the first sample), $a-x$ the ester concentration remaining after time t, and $\bar{k}$ the first-order rate constant.

Table 3. The hydrolysis of methoxymethyl acetate at 60°C. [HCl] = 0.02464, a = 0.0838.

t (in minutes)	1	2	3	4	5	6	7	8
$10^2 \cdot (a-x)$	6.89	5.58	4.60	3.78	3.13	2.47	1.93	1.62
$10^3 \cdot \bar{k}$	3.26	3.39	3.33	3.32	3.28	3.39	3.49	3.42

Average $k = 0.00\bar{3}36$ sec.$^{-1}$

Table 4. The hydrolysis of ethoxymethyl acetate at 12°C. [HCl] = 0.1001, a = 0.0601.

t (in minutes)	20	40	60	80	100	120	140	160
$10^2 \cdot (a-x)$	4.96	4.15	3.42	2.76	2.41	1.93	1.59	1.36
$10^4 \cdot \bar{k}$	1.60	1.54	1.57	1.62	1.52	1.58	1.58	1.55

Average $\bar{k} = 0.000157$ sec.$^{-1}$

Table 5. The hydrolysis of methoxymethyl formate at 35°C. [HCl] = 0.0996, a = 0.0776.

t (in minutes)	1	2	3	4	5	6	8	10
$10^2 \cdot (a-x)$	6.71	5.65	4.95	4.21	3.66	3.09	2.31	1.72
$10^3 \cdot \bar{k}$	2.42	2.65	2.50	2.55	2.50	2.56	2.52	2.51

Average $\bar{k} = 0.00253$ sec.$^{-1}$

REFERENCES

1. Salomaa, P. *Acta Chem. Scand.* **11** (1957) 132.
2. Salomaa, P. *Acta Chem. Scand.* **11** (1957) 141.
3. Salomaa, P. *Acta Chem. Scand.* **11** (1957) 235.
4. Palomaa, M. H. and Herna, T. O. *Ber.* **66** (1933) 305.
5. Palomaa, M. H. and Jaakkola, V. *Ber.* **67** (1934) 949.
6. Hammett, L. P. *Physical Organic Chemistry*, New York 1940, p. 269.
7. Salmi, E. J. *Ann. Univ. Turkuensis, Ser.* **A** III (1932), No. 3.
8. Tommila, E. and Hella, A. *Ann. Acad. Sci. Fennicae, Ser.* **A** II (1954), No. 53.
9. Ingold, C. K. *Structure and Mechanism in Organic Chemistry*, London 1953, pp. 767–782.
10. *International Critical Tables*, New York 1928, Vol. III, pp. 24–26.

Received October 23, 1956.

ACTA CHEMICA SCANDINAVICA 11 (1957) 247—252

The Hydrolysis of Methylene Diacetate and Ethylidene Diacetate in Concentrated Hydrochloric Acid Solutions

PENTTI SALOMAA

Department of Chemistry, University of Turku, Turku, Finland

Kinetic measurements have been made of the hydrolysis of methylene diacetate and ethylidene diacetate at 25°C in aqueous hydrochloric acid solutions at acid concentrations varying from 0.1 N up to 8 N. The results show that the velocity of the hydrolysis is more closely related to the acid concentration than to the acidity function of the reaction solution, thus indicating, in accord with the constitutional effects observed, that the hydrolysis of these esters takes place by a bimolecular mechanism, the transition state of which contains a water molecule in addition to the conjugate acid of the ester. No change of the reaction mechanism was observed even at the highest acid concentrations investigated.

In the previous study [1–4] the author established that the hydrolysis of simple alkoxymethyl esters, $RCOOCH_2OR'$, in aqueous acids takes place preferably by a unimolecular mechanism involving an intermediate formation of an alkoxymethyl cation, although under certain conditions a bimolecular mechanism which was considered to be essentially the same as that of simple alkyl esters, was also found to contribute to the reaction rate. The present paper gives the results of a kinetic study on the hydrolysis of constitutionally closely related compounds, methylene diacetate and ethylidene diacetate. Hammett's acidity function has been applied as a kinetic criterion of the molecularity of the rate-determining stage of the reaction, and for this the rate measurements have been extended up to high acid concentrations. The kinetics of the hydrolysis of these compounds by dilute aqueous acid solutions have been previously investigated by Skrabal and Schiffrer [5] and by Salmi [6].

RESULTS AND DISCUSSION

The method of following the rates of the hydrolysis reactions (R = H, Me)

$$(CH_3COO)_2CHR + H_2O \xrightarrow{H^+} RCHO + 2\ CH_3COOH$$

at various acid concentrations was based on the determination of formaldehyde or acetaldehyde produced during different reaction times. By this method it

was possible to extend the rate measurements up to about 8 N hydrochloric acid concentration. The results of the kinetic measurements are given in Tables 1 and 2. In the tables the values of $\bar{k}$ denote the first-order rate constants directly measured, the values of k giving the second-order rate constants which have been obtained by dividing the first-order rate constants by the concentrations of the catalyst hydrochloric acid. The tables also include the values of the Hammett acidity function H_0 for the solutions employed. These values have been obtained by interpolation from the data given by Hammett and Deyrup [7] and by Bell, Dowling and Noble [8].

The values obtained for the rate constants at relatively low acid concentrations are in good agreement with the corresponding values determined earlier by Skrabal and Schiffrer [5] and by Salmi [6]. The first authors found for the second-order rate constants at 25°C the following values: 0.000134 l mole^{-1}

Table 1. The hydrolysis of methylene diacetate by aqueous hydrochloric acid at 25 °C.

[HCl]	$10^4 \cdot \bar{k}$ sec.$^{-1}$	$10^4 \cdot k$ l mole^{-1}sec.$^{-1}$	H_0
0.1020	0.140	1.37	+ 1.06
0.396	0.550	1.39	+ 0.36
0.792	1.13	1.43	+ 0.02
1.188	1.80	1.52	− 0.19
1.584	2.56	1.62	− 0.36
1.980	3.29	1.66	− 0.53
2.376	4.22	1.78	− 0.68
3.168	6.18	1.95	− 0.98
3.96	8.23	2.08	− 1.28
4.75	11.9	2.50	− 1.57
5.94	18.2	3.06	− 1.98
7.13	27.1	3.80	− 2.47
7.92	33.2	4.19	− 2.84

Table 2. The hydrolysis of ethylidene diacetate by aqueous hydrochloric acid at 25°C.

[HCl]	$10^4 \cdot \bar{k}$ sec.$^{-1}$	$10^4 \cdot k$ l mole^{-1}sec.$^{-1}$	H_0
0.1020	0.114	1.12	+ 1.06
0.396	0.444	1.12	+ 0.36
0.792	0.920	1.16	+ 0.02
1.188	1.41	1.19	− 0.19
1.584	2.01	1.27	− 0.36
1.980	2.58	1.30	− 0.53
2.376	3.22	1.36	− 0.68
3.168	5.04	1.59	− 0.98
3.96	6.92	1.75	− 1.28
4.75	9.70	2.04	− 1.57
5.94	14.6	2.46	− 1.98
7.13	22.0	3.09	− 2.47
7.92	27.6	3.48	− 2.84

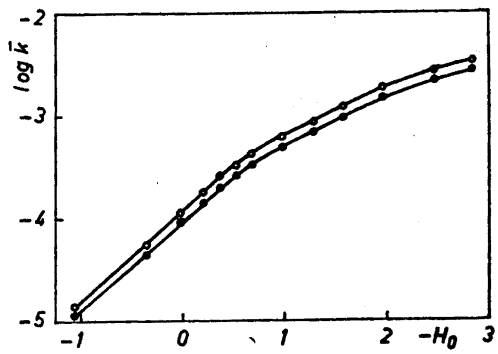


Fig. 1. The plots of the logarithms of the first-order rate constants against $-H_0$. Aqueous hydrochloric acid, 25°C. Upper curve, the hydrolysis of methylene diacetate; lower curve, the hydrolysis of ethylidene diacetate.

sec.$^{-1}$ for methylene diacetate, and 0.000108 l mole^{-1}sec.$^{-1}$ for ethylidene diacetate, respectively. Salmi determined the value 0.000144 l mole^{-1}sec.$^{-1}$ for the hydrolysis of methylene diacetate at 25°C.

A comparison between the values of Tables 1 and 2 shows that the hydrolysis rates of methylene diacetate and ethylidene diacetate are similarly influenced by the acid concentration of the solution, the rate constants of the former compound being slightly higher than those of the latter at the same acid concentrations. In both cases the second-order rate constants increase slightly when passing over to higher acid concentrations, the relative increases being, however, of a much lower order of magnitude than those observed by alkoxymethyl esters [1].

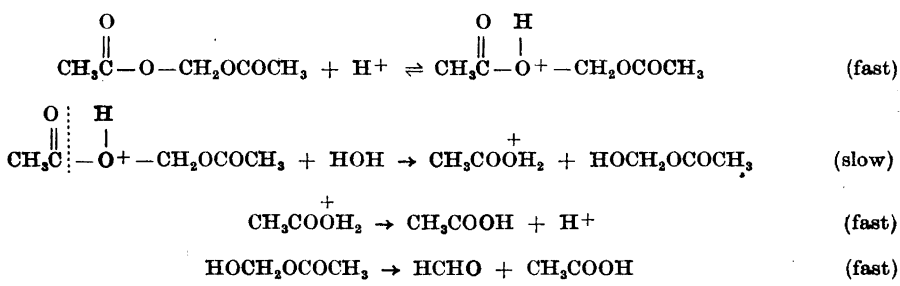
Fig. 1 gives the plots of the logarithms of the first-order rate constants against the Hammett acidity function. The plots show that the values of log $\bar{k}$ increase much less rapidly than the values of $-H_0$, when passing up to higher acid concentrations, thus considerably differing from the behaviour observed by alkoxymethyl esters [1]. *E. g.*, in the case of methylene diacetate, a linear relation between log $\bar{k}$ and $-H_0$ with a slope of unity would imply an about 8 000-fold increase in the first-order rate constant, when passing from 0.1020 N up to 7.92 N hydrochloric acid, and even a larger increase were to be expected, if the dependence of log $\bar{k}$ on the acidity function were similar to that observed by methoxymethyl and ethoxymethyl acetates. The actual increase in the value of $\bar{k}$ is, however, much lower in magnitude, *viz.* 240-fold (Table 1).

On the contrary, the results for the diacetates show a close similarity to the observations made by Bell, Dowling and Noble [8] of the hydrolysis of methyl formate and ethyl acetate by concentrated hydrochloric acid solutions. These authors found the first-order rate constants to increase slightly more rapidly than the acid concentration of the solution. The increase was, however, too small to be interpreted in terms of the acidity function of the solution. It was considered that the results are in a satisfactory agreement

with the bimolecular mechanism of the acid-catalysed ester hydrolysis, in view of the fact that there is no reason to assume that the hydrolysis velocity would remain strictly proportional to the acid concentration, when going up to relatively high acid concentrations.

The fact that the esters investigated here are affected by the acid concentration of the reaction solution similarly as the simple alkyl esters indicates that both the reactions take place by an essentially similar mechanism. As the hydrolysis velocity of the diacetates is also more closely related to the acid concentration than to the value of H_0 of the reaction solution, it implies that the reaction is bimolecular, *i. e.* the critical complex contains a water molecule which is undergoing a change of covalency, in addition to the conjugate acid of the substrate, *cf.* Ref.[1]

Although the rate measurements at high acid concentrations furnish only a criterion of molecularity of the rate-determining reaction stage, and do not allow a distinction as to the point of the initial bond rupture, there are no reasons to support an assumption that this point would not be the same here as in the acid-catalysed hydrolysis of simple alkyl esters, *i. e.* the acyl-oxygen bond [9]. Owing to the less electrophilic character of the carbon atom of the methylene or ethylidene group, in comparison to that of the carbonyl group, a bimolecular alkyl-oxygen fission mechanism would be less probable, as also shown by the fact that this type of mechanism has never been established in acid-catalysed ester hydrolysis. The bimolecular acyl-oxygen fission mechanism [9], as particularised to the hydrolysis of methylene diacetate



is also in accord with the constitutional effects. The values of k determined for the hydrolysis of methylene diacetate and ethylidene diacetate at relatively low acid concentrations at 25°C (Tables 1 and 2) are of the same order of magnitude as the corresponding value for methyl acetate, 0.000109 l mole^{-1}sec.$^{-1}$, determined by Tommila and Hella [10]. This is well understood in view of the fact that the velocity of the acid-catalysed ester hydrolysis by the bimolecular mechanism is but slightly influenced by substituents on the alkyl group of the ester.

It might be suggested that the small increase in the values of the second-order rate constants with acid concentration (Tables 1 and 2) is due, at least partly, to a simultaneous unimolecular mechanism which is greatly favoured by the high proton-availability of the concentrated acid solutions, *cf.* Ref.[4] This assumption is, however, rendered doubtful by the following reasons. The

cation formed in the rate-determining unimolecular reaction stage could be presented as (*cf.* Ref.[1]) $CH_3COO\overset{+}{C}HR$ (R = H, Me). The unimolecular reaction would be greatly accelerated by an electron-releasing substituent directly attached to the site of reaction, *i. e.* that carbon atom, which acquires a positive charge on the attainment of the transition state. The influence of this effect is illustrated, for instance, by the unimolecular solvolysis of 1-chloroethers where it was established [11] that the rate-determining formation of the cation $CH_3O\overset{+}{C}HCH_3$ is greatly more rapid than that of the cation $CH_3O\overset{+}{C}H_2$. Thus the conditions for the unimolecular mechanism are much more favourable in the hydrolysis of ethylidene diacetate than in that of methylene diacetate, and hence a change of the reaction mechanism, when passing up to higher acid concentrations, would occur by the former compound earlier than by the latter. If such a change of mechanism were actually present here, the values of the rate constants of ethylidene diacetate would increase in comparison to the corresponding values of methylene diacetate, when higher acid concentrations are approached. As shown by Fig. 1, however, the relative hydrolysis velocities of both the diacetates remain practically unaffected by the acid concentration of the reaction solution, thus indicating that the reaction mechanisms remain bimolecular even at the highest acid concentrations investigated.

EXPERIMENTAL

Materials. Methylene diacetate, $(CH_3COO)_2CH_2$, and ethylidene diacetate, $(CH_3COO)_2CHCH_3$, were prepared by the method described by Knoevenagel [12]. The raw products were purified by repeated fractional distillations. The boiling points were: 88.5°C/40 mm Hg for methylene diacetate, and 166.5–167.0°C/752 mm Hg for ethylidene diacetate, respectively. The purity of the products was controlled by hydrolysing weighed samples by alkali (one minute was found to be sufficient for a quantitative hydrolysis of the esters by a large excess of 0.25 N sodium hydroxide solution), and after neutralisation, by determining the aldehyde formed using the previous method [11,13]. The standard iodine solution used for the aldehyde determinations was 0.0688 N. In the analysis of formaldehyde formed by the hydrolysis of methylene diacetate, a sample of 45.6 mg of the ester was equivalent to 10.17 ml of the standard iodine solution (calc. 10.03 ml), and a sample of 66.2 mg was equivalent to 14.70 ml of the iodine solution (calc. 14.57 ml). In the analysis of acetaldehyde formed by the hydrolysis of weighed samples of ethylidene diacetate, respectively, 43.5 mg of the ester was equivalent to 8.76 ml of the standard iodine solution (calc. 8.65 ml), and 60.7 mg was equivalent to 12.16 ml of the standard solution (calc. 12.07 ml).

Kinetic measurements. The preparation of the reaction solutions and the method of kinetic measurements were similar to those described in connection with the earlier work on the hydrolysis of alkoxymethyl esters [1]. In all cases the first-order kinetics were well obeyed. Tables 3 and 4 give the details for two typical examples of the individual rate

Table 3. The hydrolysis of methylene diacetate in 7.92 N hydrochloric acid at 25°C. $a = 0.0440$.

t (in minutes)	1	2	3	4	5	6	8	10
$10^2\ (a-x)$	3.59	2.97	2.42	2.04	1.65	1.31	0.87	0.60
$10^3 \cdot \bar{k}$	3.39	3.27	3.32	3.20	3.27	3.37	3.38	3.32

Average $\bar{k} = 0.00332$ sec.$^{-1}$

Table 4. The hydrolysis of ethylidene diacetate in 5.94 N hydrochloric acid at 25°C.

$a = 0.0503$.

t (in minutes)	2	4	6	8	10	12	14	16
$10^2\ (a-x)$	4.25	3.53	2.94	2.54	2.10	1.75	1.48	1.24
$10^3 \cdot \bar{k}$	1.40	1.48	1.49	1.42	1.46	1.47	1.46	1.46

Average $\bar{k} = 0.00146$ sec.$^{-1}$

measurements. In the tables, a denotes the ester concentration at zero time (at the time of taking the first sample), $(a-x)$ the ester concentration remaining at time t, and $\bar{k}$ the first-order rate constant, respectively.

REFERENCES

1. Salomaa, P. *Acta Chem. Scand.* **11** (1957) 132.
2. Salomaa, P. *Acta Chem. Scand.* **11** (1957) 141.
3. Salomaa, P. *Acta Chem. Scand.* **11** (1957) 235.
4. Salomaa, P. *Acta Chem. Scand.* **11** (1957) 239.
5. Skrabal, A. and Schiffrer, A. *Z. physik. Chem.* **99 B** (1921) 290.
6. Salmi, E. J. *Annales Universitatis Turkuensis, Ser.* **A III** (1932) No. 3.
7. Hammett, L. P. and Deyrup, A. J. *J. Am. Chem. Soc.* **54** (1932) 2721.
8. Bell, R. P., Dowling, A. L. and Noble, J. A. *J. Chem. Soc.* **1955** 3106.
9. Ingold, C. K. *Structure and Mechanism in Organic Chemistry*, London 1953, pp. 752–782.
10. Tommila, E. and Hella, A. *Ann. Acad. Sci. Fennicae, Ser.* **A II** (1954) No. 53.
11. Salomaa, P. *Ann. Univ. Turkuensis, Ser.* **A** XIV (1953) No. 1.
12. Knoevenagel, E. *Ann.* **402** (1914) 127.
13. Salomaa, P. *Suomen Kemistilehti* **27 B** (1954) 12.

Received October 23, 1956.

ACTA CHEMICA SCANDINAVICA 11 (1957) 253—260

Kinetics of the Alcoholysis of Hydroxymethylacetamide and Proton Transfer Equilibria in Methanol, Ethanol and *iso*Propanol

JOUKO KOSKIKALLIO

Institute of Chemistry, University of Helsinki, Helsinki, Finland

In a previous study [1] the kinetics of formation and hydrolysis of hydroxymethylacetamide were studied in alkaline aqueous solutions. The analogous alcoholysis reactions in a number of alcohols have now been investigated. In the alcoholysis of hydroxymethylacetamide in methanol, ethanol and *iso*propanol, similarly as in the hydrolysis, the role of a base is to produce the hydroxymethylacetamide anion which reacts with the solvent molecule to give acetamide and monoformal anion. The rate constant for the reaction between hydroxymethylacetamide anion and the solvent has been calculated in each case from the kinetic data obtained by varying the concentration of alcoholate. Also the equilibrium constants of the alcoholysis reactions were determined. The equilibrium is shifted further towards hydroxymethylacetamide in different alcohols in the following order: methanol, ethanol, *iso*propanol and *tert.*-butanol. Values of the equilibrium constants for the proton transfer between alcoholate ions and hydroxymethylacetamide were also derived from the kinetic data. The acidities of the various alcohols relative to that of the hydroxymethylacetamide anion were found to decrease in the order: methanol, ethanol, *iso*propanol. The heat of the proton transfer reaction was found to vary considerably in the different alcohols.

Similarly as the hydrolysis [1], the alcoholysis of hydroxymethylacetamide is a three-step process:

$$CH_3CONHCH_2OH + RO^- \rightleftharpoons CH_3CONHCH_2O^- + ROH \quad (1)$$
$$CH_3CONHCH_2O^- + ROH \rightleftharpoons CH_3CONH_2 + ROCH_2O^- \quad (2)$$
$$ROCH_2O^- + ROH \rightleftharpoons ROCH_2OH + RO^- \quad (3)$$

The proton transfer reactions (1) and (3) are fast, the alcoholysis reaction (2) being the slow, rate-determining step. The reaction product monoformal is believed to be stable in the alcohol solutions used, but if free formaldehyde (CH_2O) is formed, it will influence only the calculation of the equilibrium constant of reaction (3).

Fortunately the acidity of hydroxymethylacetamide does not differ very much from the acidities of the alcohols used as solvents, so that by varying the concentration of alcoholate ion (RO^-) the amount of ionized hydroxymethylacetamide can be altered, this will effect a change in the reaction rate

$$-\frac{dc_{CH_3CONHCH_2O^-}}{dt} = k_1\ c_{CH_3CONHCH_2O^-} - k_2\ c_{CH_3CONH_2}\ c_{ROCH_2O^-} \qquad (4)$$

where k_1 is the first-order rate constant of the alcoholysis reaction and k_2 the second-order rate constant of the reverse reaction 2.

EXPERIMENTAL

Materials. Methanol, ethanol and *iso*propanol, all of the highest purity obtainable, were dried by adding the corresponding aluminium alcoholate [2] and distilling. Usually only about 0.1 g of water per liter was found to be present in the dried alcohols by the Fischer titration. *Tert.*-butanol was purified by crystallisation. The other compounds were prepared as described earlier [1].

Analytical. The kinetic measurements were performed as described in the previous paper [1]. The amount of formaldehyde liberated during the reaction was analysed by the sulphite method [1] used previously except that phosphate buffer solution (0.5 M NaH_2PO_4, 0.125 M K_2HPO_4) was added to the sample in order to reduce the standing period required after the addition of bisulphite solution [3], since the reaction between bisulphite and formaldehyde is retarded by alcohols.

Calculations. The alcoholysis of hydroxymethylacetamide did not go to completion in the solvents studied. The rate eqn. (4) yields on integration

$$k_1 = \frac{2.303}{t} \cdot \frac{A_{eq} \cdot F_{eq}}{(M_0+A)\,(M_0+F_0)} \log \left[\frac{M_0 - M_{eq}}{M_t - M_{eq}} \cdot \frac{(M_0+A_0)\ (M_0+F_0) - M_tM_{eq}}{(M_0+A_0)\ (M_0+A_0) - M_0M_{eq}} \right] \qquad (5)$$

Table 1. Rate constants for the ethanolysis of hydroxymethylacetamide at 20° (eqn. (5). Initial concentrations: hydroxymethylacetamide 0.0196 mole/l (which corresponds to 9.57 ml of 0.0246 N iodine solution), acetamide 0.200 mole/l and sodium ethylate 0.0482 mole/l.

Time min	0.0246 N iodine consumed ml	% reacted	$10^3 \times k_1$ $sec.^{-1}$
0	0.12	0	
0.5	0.71	9.7	2.18
1	1.20	17.7	2.11
1.5	1.61	24.5	2.00
2	1.99	30.7	1.98
3	2.68	42.1	1.96
4	3.25	51.5	1.94
5	3.70	58.9	1.91
6	4.13	65.9	1.92
7	4.42	70.7	1.88
12	5.48	88.2	1.89
17	5.93	95.5	1.95
20	6.06	97.7	2.04
100	6.20	100	mean 1.96

Table 2. Equilibrium and first-order rate constants and activation energies for the alcoholysis of hydroxymethylacetamide in methanol.

$t°$	Concentrations mole/l initial			at equilibrium			$K = \frac{c_M}{c_A c_F}$ l/mole	$10^3 \times k_1$ sec.$^{-1}$		$E_{0°-40°}$ kcal
	c_{RO^-}	c_M	c_A	c_M	c_A	c_F		exptl.	calc.*	
0	0.0499	0.0091						0.00308	0.00315	
	0.201	0.0085						0.0126	0.0125	
	1.005	0.0097						0.0575	0.0568	
	0.975	0.0776	0.600	0.0370	0.641	0.0406	1.42			
	∞								0.5	
20	0.0097	0.0088						0.0196	0.0189	
	0.0496	0.0091						0.098	0.093	27.5
	0.202	0.0087						0.367	0.359	
	0.202	0.044						0.336	).356	
	0.202	0.036	0.300	0.0268	0.327	0.0091	1.05	0.338	0.356	27.1
	0.99	0.0094						1.46	1.42	
	1.00	0.044						1.36	1.42	26.1
	0.975	0.0776	0.600	0.0305	0.647	0.0471	1.00			
	∞								6	21.1
40	0.0499	0.0091						1.98	2.00	
	0.201	0.0085						7.34	7.43	
	1.00	0.0096						26.5	26.2	
	0.975	0.0776	0.600	0.0247	0.653	0.0529	0.72			
	∞								70	

* Calculated using eqns. (7) and (8) with $K_1 = 7.84$, 3.16 and 1.68 at 0°, 20° and 40°, respectively.

where M, A and F denote the concentrations of hydroxymethylacetamide, acetamide and formaldehyde, respectively, and subscripts o, t and eq referring to times $t = 0$, t and infinity, and k_1 is the first-order rate constant of the alcoholysis reaction. The rate constant of the reverse reaction is computed in the usual way from $k_2 = k_1 K$, where K is the equilibrium constant of the reaction 2

$$K = \frac{M_{eq}}{F_{eq}\ A_{eq}} = \frac{k_2}{k_1} \tag{6}$$

The rate constants were usually calculated from data for 15–90 % reaction. The first-order rate constant showed a slight tendency to decrease as the reaction proceeded. A typical run is shown in Table 1. The variation in the rate constant may be due to the incorrect substitution of total concentrations of hydroxymethylacetamide and formaldehyde for the concentrations of the respective ions in eqn. (5). The concentrations of the ionic forms could be obtained from eqns. (7) if the respective equilibrium constants of the proton transfer reactions (1) and (3), K_1 and K_3, were known.

$$K_1 = \frac{c_{MH}\ c_{RO^-}}{c_{M^-}} \text{ and } K_3 = \frac{c_{FH}\ c_{RO^-}}{c_{F^-}} \tag{7}$$

MH and M^- denote hydroxymethylacetamide and its anion, FH and F^- monoformal and its anion and RO^- the alcoholate anion. Because the values of K_1 and K_3 were not known, it was assumed that the decrease of the alcoholate ion concentration in reactions (1) and (3) can be neglected, *i. e.* $c_{RO^-} \gg c_{M^-}$ and c_{F^-}. This assumption proved to be a good approximation for methanol and ethanol but only approximately valid for *iso*propanol. The error can be diminished further by extrapolating rate constants obtained at a con-

Table 3. Equilibrium and first-order rate constants and activation energies for the alcoholysis of hydroxymethylacetamide in ethanol.

$t°$	Concentrations mole/l initial			at equilibrium			$K_2 = \frac{c_M}{c_A c_F}$		$10^3 \times k_1$ sec.$^{-1}$		$E_{0°-40°}$ kcal
	c_{RO^-}	c_M	c_A	c_M	c_A	c_F	exptl.	calc.**	exptl.	calc.*	
0	0.0207	0.0202	0.200	0.0091	0.211	0.0111	3.88	4.76	0.0375	0.0395	
	0.0505	0.0198	0.200	0.0085	0.211	0.0112	3.60	4.25	0.0832	0.0810	
	0.104	0.0204	0.200	0.0095	0.211	0.0109	4.45	5.05	0.122	0.128	
	0.201	0.0200	0.201	0.0097	0.212	0.0107	4.29	4.69	0.183	0.177	
	0.504	0.0204	0.199	0.0098	0.210	0.0106	4.41	4.62	0.240	0.222	
	∞						mean	4.67		0.27	
20	0.0105	0.0198	0.200	0.0070	0.218	0.0127	2.54	3.46	0.573	0.547	
	0.0204	0.0194	0.200	0.0071	0.212	0.0123	2.72	3.60	0.952	0.990	24.6
	0.0482	0.0196	0.200	0.0069	0.213	0.0127	2.55	3.18	1.96	1.91	23.7
	0.0485	0.0192	0	0.0010	0.018	0.0182	2.95	3.64	1.97	1.92	
	0.103	0.0194	0.200	0.0077	0.212	0.0117	3.11	3.64	2.90	2.96	23.0
	0.207	0.0194	0.200	0.0076	0.212	0.0117	3.08	3.41	3.59	3.83	23.2
	0.512	0.0194	0.200	0.0083	0.211	0.0110	3.57	3.75	5.27		
	1.04	0.0198	0.200	0.0075	0.212	0.0122	2.80	2.88			
	∞						mean	3.43		5.26	22.3
40	0.0207	0.0202	0.200	0.0091	0.211	0.0111	2.07	2.96	12.4	12.0	
	0.0505	0.0198	0.200	0.0061	0.214	0.0137	2.09	2.72	22.8	22.8	
	0.104	0.0204	0.200	0.0077	0.213	0.0127	2.85	3.44	31.5	32.9	
	0.201	0.0200	0.201	0.0067	0.214	0.0133	2.35	2.64	43.4	41.1	
	0.504	0.0204	0.199				2.57	2.72			
	∞						mean	2.76		52.6	

* Calculated using eqns. (7) and (8) with $K_1 = 0.104$, 0.072 and 0.054 at 0°, 20° and 40°, respectively.

** Calculated using eqn. (9) with $K_3 = 0.132$, 0.102 and 0.086 at 0°, 20° and 40°, respectively.

stant alcoholate concentration to zero hydroxymethylacetamide concentration. The rate constant k_1 is obtained by extrapolating the experimental k_1' values to infinite alcoholate concentration by the method described in the previous paper [1]. Using the extrapolated value k_1 together with the different k_1' values c_{M^-} is calculated from

$$c_{M^-} = \frac{k_1'}{k_1} \cdot c_{M_{total}} \qquad (8)$$

and K_1 from eqn. (7). The constancy of the K_1 values gives evidence for the validity of the assumptions made in the calculations. The mean value of K_1 was used to recalculate k_1, but the latter was not found to be altered. Tables 2, 3 and 4 give the experimental first-order rate constants, the extrapolated values of the first-order rate constants, and the rate constants calculated using the values of k_1 and K_1 obtained by extrapolation (eqns. (7) and (8)). The agreement between the experimental and calculated values are satisfactory in methanol and ethanol, but in *iso*propanol only when the alcoholate concentration is greater than the concentration of hydroxymethylacetamide.

When total concentrations of hydroxymethylacetamide and formaldehyde are used in the calculations of the equilibrium constant K of reaction 2 (eqn. (6)), a considerable change in the values of K are obtained as the alcoholate concentration is altered. This

Table 4. Equilibrium and first-order rate constants and activation energies for the alcoholysis of hydroxymethylacetamide in *iso*propanol.

$t°$	Concentrations mole/l initial			Concentrations mole/l at equilibrium			$K = \frac{c_M}{c_A c_F}$		$10^3 \times k_1$ sec^{-1}		$E_{0°-40°}$ kcal
	c_{RO^-}	c_M	c_A	c_M	c_A	c_R	exptl.	calc.**	exptl.	calc.*	
0	0.0023	0.0180	0.100	0.0114	0.1066	0.0066	16.1	25.9	0.165	0.120	22.1
	0.0092	0.0089	0.0015	0.0015	0.0089	0.0074	23.4	31.3	0.577	0.535	22.8
	0.0100	0.0180	0.0030	0.0046	0.0164	0.0134	21.2	28.4	0.456	0.422	23.0
	0.0393	0.0090	0.0015	0.0016	0.0089	0.0074	23.9	26.5	0.920	0.975	23.2
	0.0394	0.0164	0.0027	0.0044	0.0150	0.0120	24.4	27.1	0.850	0.960	23.1
	0.0393	0.0360	0.0060	0.0153	0.0267	0.0207	27.7	30.7	0.682	0.810	23.6
	0.0735	0.0180	0.100	0.0133	0.1047	0.0047	27.4	29.2	1.315		
	0.0895	0.0180	0.0030	0.0053	0.0157	0.0127	26.7	28.1	0.950	1.07	23.7
	∞						mean	28.4		1.16	23.2
20	0.0023	0.0180	0.100	0.0094	0.1086	0.0086	10.1	15.3	2.66	1.97	
	0.0092	0.0089	0.0015	0.0009	0.0094	0.0080	12.5	16.0	10.4	9.85	
	0.0100	0.0180	0.0030	0.0029	0.0181	0.0150	10.8	13.7	8.25	8.10	
	0.0195	0.0180	0.0030	0.0035	0.0175	0.0145	13.8	16.0	12.7	12.7	
	0.0393	0.0090	0.0015	0.0009	0.0095	0.0080	12.3	13.5	17.4	18.0	
	0.0394	0.0164	0.0027	0.0031	0.0160	0.0133	14.1	15.4	15.7	17.4	
	0.0393	0.0360	0.0060	0.0111	0.0309	0.0249	14.4	15.7	13.1	15.8	
	0.0895	0.0180	0.0030	0.0038	0.0172	0.0142	15.5	16.1	18.5	19.8	
	0.120	0.0180	0.103				15.0	15.5	20.2	20.3	
	∞						mean	15.2		21.5	

* Calculated using eqns. (7) and (8) with $K_1 = 0.006$ at 0° and 20°.
** Calculated using eqn. (9) with $K_2 = 0.0103$ and 0.0111 at 0° and 20°, respectively.

implies that $K_1 \neq K_2$. By making the simplifying assumption, $c_{RO^-} \gg c_{M^-}$ and c_{F^-}, which was previously found to be a good approximation, the equation

$$K_2 = K_{tot} \frac{K_1 + c_{RO^-}}{K_1 + c_{RO^-}} \qquad (9)$$

used previously [1] is obtained. K_2 is the equilibrium constant for reaction (2) and K_{tot} the equilibrium constant for the same reaction when total concentrations of hydroxymethylacetamide and formaldehyde are substituted in eqn. (6). K_2 and K_3 both can be determined, as K_1 is previously known from kinetic experiments, from the slope and intercept of the straight line plotting $K_{tot} / (K_1 + c_{RO^-})$ *versus* $K_{tot} c_{RO^-} / K_1 + c_{RO^-})$. The values of K_{tot} and K_2 are given in Tables 2, 3 and 4. The constancy of calculated K_2 values illustrate the validity of the approximations made in the calculations.

RESULTS AND DISCUSSION

The values of the rate and equilibrium constants of reaction (2) and the equilibrium constants of the proton transfer reactions (1) and (3) calculated from the kinetic experiments by the methods described are summarized in Tables 5 and 6. For comparison, also values obtained previously [1] are included. Because of the poor reproducibility of the experiments made in *tert.*-butanol due to the high rate of the reaction and to the great sensitivity of the alcoholate

Table 5. Rate constants (k_1 and k_2), equilibrium constant (K), heats of reaction (ΔH) and the Arrhenius parameters (E and A) for reaction (2) in water, methanol, ethanol, *iso*propanol and *tert.*-butanol.

Solvent	$10^3 \times k_1$ sec^{-1}			$10^3 \times k_2 = k_1 K$	$K = \frac{c_{M^-}}{c_A \, c_{F^-}}$			E_1	E_2	ΔH	log A_1	log A_2
	0°	20°	40°	20°	0°	20°	40°	kcal	kcal	kcal		
H_2O	0.264	3.72	44.1	80	41.4	21.4	14.8	21.8	17.5	−4.3	13.8	12.0
MeOH	0.5	6	70	6	1.42*	1.05*	0.72*	21.1	18.0	−3.1	13.5	11.2
EtOH	0.27	5.3	53	18	4.67	3.43	2.76	22.3	19.8	−2.1	14.3	13.0
i-PrOH		21.5		327	28.4	15.2		23.2	18.3	−4.9	15.7	13.2
t-BuOH		~200		~20.000		~100						

* measured with $c_{RO^-} = 0.975$ M.

solution to traces of water, only approximate values were obtained; these are included in Table 5 to illustrate the order of magnitude.

The values obtained for the proton transfer constants K_1 and K_3 given in Table 6 show that the acidities of the hydroxylic solvents decrease in the order methanol, water, ethanol, *iso*propanol. Similar results were obtained by Koivisto [4], Calding [5], and Hine [6]. Formaldehyde is known to exist practically entirely in the hydrated form $HOCH_2OH$ in dilute aqueous solutions and thus contains two hydroxyl groups (for references see Ref.[1]) whereas the monoformal $ROCH_2OH$ present in alcohol solutions contains only one hydroxyl. In order to get comparable values, the value of K_3 obtained in water should be multiplied by two; for example at 20° $K_3 = 2 \times 0.11 = 0.22$. After this correction, the formaldehyde-solvent addition product is found to be an about 1.5 times stronger acid than hydroxymethylacetamide in all the solvents studied. Compared with the solvents, hydroxymethylacetamide and formaldehyde monoformals at first seem to be of the same order of strength as acids, but according to the reaction $FH + RO^- = F^- + ROH$, the concentrations of the solvent molecules should be included in eqns. (7). Thus the hyd-

Table 6. Equilibrium constants and heats of the proton transfer equilibria between hydroxymethylacetamide (K_1) and formaldehyde hydrate and monoformal (K_3) and the solvent anions (HO^-, MeO^-, EtO^-, *iso*PrO^-) in the respective solvents.

Solvent	$K_1 = \frac{c_{MH} \cdot c_{RO^-}}{c_{M^-}}$			$K_3 = \frac{c_{FH} \cdot c_{RO^-}}{c_{F^-}}$			ΔH_1	ΔH_3
	0°	20°	40°	0°	20°	40°	kcal	kcal
H_2O	0.14	0.16	0.19	0.09	0.11	0.13	1.3	1.4
MeOH	7.8	3.2	1.7				−6.5	
EtOH	0.10	0.07	0.05	0.13	0.10	0.08	−2.1	−1.8
i-PrOH	0.006	0.006		0.010	0.011		0	0.5

roxymethylacetamide and formaldehyde monoformals are much stronger acids than the alcohols used as solvents.

Great differences were found in the heats of proton transfer reactions (1) and (3) in the solvents studied. Although the values obtained by extrapolation in methanol are not very accurate, the values of ΔH of proton transfer equilibria in methanol and water were found to differ by about 7.8 kcal. It is of the same order of magnitude as found by other methods. Koivisto [4] found calorimetrically when neutralizing phenol or acetic acid with sodium alcoholate in methanol and sodium hydroxide in water, a difference $\Delta H_w - \Delta H_m = 7.2$ kcal. In ethanol and *iso*propanol the values of ΔH are 3.4 and 1.3 kcal. greater than the value of ΔH in water for the proton transfer reaction (1), whereas the calorimetric values obtained by Koivisto using carboxylic acids and phenol gave a difference of about 6 and 4 kcal in ΔH in the corresponding solvents.

At low alcoholate concentrations the experimental rate constant k_1' is approximately proportional to the alcoholate concentration. When $c_{RO^-} \gg c_{M^-}$ and $c_{MH} \gg c_{M^-}$, $k' = k_1 c_{RO^-} / K_1$ (eqns. (7) and (8).

The experimental activation energy should approach the value $E' = E - \Delta H_1$ at low alcoholate concentrations. From the last column in Tables 2, 3 and 4 it will be seen that the change in the calculated activation energy is of the same order of magnitude as ΔH_1 in Table 6, which gives further evidence that the method of extrapolation used gives correct values.

When comparing the rate constants of reaction 2 (Table 5), it must be remembered that as the group R in the reactant is altered, also the solvent is changed. Thus both the solvent and substituent effects are superimposed in the change in the reaction rate. The rates of solvolysis of hydroxymethylacetamide anion in water, methanol and ethanol are approximately equal. It seems that the solvent effects are of minor importance as the rate is not much altered in spite of a considerable change in the nature of the solvent. The observed difference in the reaction rates in *iso*propanol and *tert.*-butanol is evidently mainly due to substituent effects. For the two reactions:

	Values of ΔH (kcal) when R is H	CH_3	CH_3CH_2	$(CH_3)_2C$	
$ROH + CH_3CONHCH_2O^- \rightarrow RO^- + CH_3CONHCH_2OH$	−1.3	6.5	2.1	0	(10)
$ROH + CH_3CONHCH_2O^- \rightarrow ROCH_2O^- + CH_3CONH_2$	−4.3	−3.1	−2.1	−4.9	(11)

the heats of the proton transfer and solvolysis reactions change in the same direction when R is altered. The equilibria of both reactions (10) and (11) are shifted towards the left in the series R = CH_3, CH_3CH_2, $(CH_3)_2CH$, the equilibrium values found in water (R = H) being exceptional in that they are intermediate between those in methanol and ethanol for reaction (10) and between those in ethanol and *iso*propanol for reaction (11). Both reactions involve a proton transfer. A proton is donated by ROH to an oxygen atom in reaction (10) and to a nitrogen atom of the amide in reaction (11). In the latter reaction there occurs in addition a breaking-up of the formaldehyde-amide bond and the formation of the formaldehyde-alcohol bond. These latter changes are the reason for the smaller changes observed in the heats and rates

of reaction as compared with those of the proton exchange. In accordance with the above discussion, the following mechanism is proposed for reaction (2):

$$CH_3CONHCH_2O^- + ROH \rightleftharpoons \begin{matrix} CH_3CONH...CH_2O^- \\ \vdots \quad \vdots \\ H...OR \end{matrix} \rightleftharpoons CH_3CONH_2 + ROCH_2O^- \qquad (12)$$

The hydrogen of ROH can become bonded ("hydrogen bond") to the nitrogen of hydroxymethylacetamide before the molecule reaches the energy level necessary for reaction and only a part of the energy of proton transfer is included in the activation energy. The formation of two bonds and the breaking of two other bonds in the transition complex probably occurs in one step simply by a simultaneous shift of the electron pairs forming the four reacting bonds.

Acknowledgement. The author wishes to record his indebtedness to the *Alfr. Kordelin Foundation* for supporting this work by a grant.

REFERENCES

1. Koskikallio, J. *Acta Chem. Scand.* **10** (1956) 1267.
2. Walden, P. *Z. physik. Chem.* **114** (1925) 181.
3. Salomaa, P. *Ann. Acad. Turkuensis* **A 14** (1953).
4. Koivisto, A. *Acta Chem. Scand.* **9** (1955) 166; **8** (1955) 1218, 1223, 1229.
5. Calding, E. F. and Lond, G. *J. Chem. Soc.* **1954** 3737.
6. Hine, J. and Hine, M. *J. Am. Chem. Soc.* **74** (1952) 5266.

Received October 29, 1956.

ACTA CHEMICA SCANDINAVICA 11 (1957) 261—264

Note on the Chloride Content of the Mineral Constituents of the Skeleton

G. HEVESY

Institute of Organic Chemistry and Biochemistry, University, Stockholm, Sweden

By adding ^{36}Cl to the diet of pregnant mice and to their offspring until they are outgrown uniformly labelled animals are obtained. Prior to administering non-labelled diet to the outgrown labelled mice the total activity of the body of one member of the litter is determined. All ^{36}Cl with the exception of that sequestered in the skeleton is then removed by keeping the mice for 6 months on non-radioactive diet. After that date the skeleton is found to contain 0.73 % of the total activity which the sister mouse had prior to removal of the radioactive diet. From this figure and the chloride content of the mouse the chloride sequestered in the skeleton of a 35 g mouse is calculated to amount to 0.35 mg. While almost 90 % of the bone sodium is excess sodium, the corresponding figure for chloride is about 10 only.

In view of the only slightly differing size of the hydroxyl and fluoride ion, the hydroxyl ions of the bone apatite can be replaced by fluoride ions. Furthermore some of the fluoride may be present in the bone mineral as calcium fluoride.

The fluoride content of the bone apatite is determined by that of the plasma, which in turn depends on the fluoride content of the food. The fluoride content of the earth's crust is much lower than that of the seawater, the mineral constituents of the skeleton of mammals living in the sea is, correspondingly, very much, about eleven times, larger than that of mammals living on land, which contain 0.05 % fluoride only. The skeleton of fish living in the Baltic, which has a low fluoride content, have a much lower fluoride percentage (0,06 %) than the skeleton of fish living in the Atlantic (0.43 %). Incorporation of fluoride into the mineral constituents of the bone was in recent years much investigated, mainly in connection with the observation that the presence of fluoride in the mineral constituents of teeth increases their resistance to caries.

The radius of the chloride ion is much larger (1.81 Å) than that of the fluoride ion (1.33 Å) and calcium chloride being very soluble we can expect to find slight amounts of chloride in the mineral constituents of the bone. While the

X-ray diagram of fluoroapatite is almost identical with that of hydroxyapatite that is far from being the case for chloroapatite[9]. The fluids circulating in the bone tissue having a high chloride content (about 300 mg/100 ml); this has to be quantitatively removed prior to the determination of the amount of chloride incorporated into the mineral constituents. Such removal by chemical treatment of the bone encounters great difficulties. However, when labelling the skeleton all through with radiochloride and then placing the animal, *e. g.* the mouse, on diet containing non-radioactive chloride for several months, all exchangeable radiochloride will be removed and excreted, the radiochloride fixed in the mineral constituents alone remaining in the skeleton.

In the human half of the exchangeable chloride is removed in the course of 14 days [1] and replaced by chloride of the food and after 6 months, *i. e.* after 12 periods, all exchangeable chloride initially present will be practically absent. In the mouse, with its high metabolic rate, the removal rate of chloride can be expected to be still higher than in man. The removal can be accelerated by increased chloride feeding. Besides the chloride present in the standard biscuits fed we added 0.2 % NaCl to the water the mice were drinking after they were put on non-radioactive diet. To the water administered to the mice in the first phase of the experiment ^{36}Cl of 0.67 μ C activity per liter was added as sodium chloride weighing 9.3 mg. The labelled chloride was administered to pregnant mice about 2 weeks prior to gestation. After gestation the administration of labelled chloride was continued for 4 months when the animals were fully grown. One member of each litter was then killed and its total ^{36}Cl content and that of its skeleton determined. The remaining members of the litters were investigated 6 months later.

The bone was ashed in the presence of sodium carbonate. The activity of 100 mg, thus of an infinite thick layer of the samples obtained was determined, the counts registered being multiplied by the total weight of the ash-sodium carbonate mixture.

The total ash of the first member of the litter of the mice investigated had a total activity of 2 780 counts per min, mean value 2 910 $\pm$ 452 counts, that of the mineral constituents of the skeleton of the first investigated offspring 56.6 counts. This was prior to biological removal of all exchangeable chloride from the skeleton but after the removal of some of the latter in the course of the isolation of the mineral constituents.

By keeping the mice on an activity-free diet for 6 months the activity of the mineral constituents declined in the average to 21.2 counts (*cf.* Table 1).

The total chloride content of a 35 g mouse taken to be 48 mg, the activity of 1 mg of the body chloride prior to removal of the active food was 60.6 counts per min. As the total skeleton after biological removal of all exchangeable chloride had an activity of 21.2 counts per min the sequestered chloride content of the bone mineral amounted to 0.35 mg or 0.73 % of the total body chloride.

The sequestered fraction of the bone calcium of the mouse, that non-replaceable by circulating calcium, was found [2] to be 67.2 $\pm$ 7.9 %. The corresponding figure for bone sodium is stated to be 60—70 [3], 65 [4], 60 [5] and 69 [6]

Table 1. Counts per min. ^{36}Cl activity of the skeleton of 33—36 g mice after keeping on non-active diet, thus after biological removal of exchangeable radiochloride, for 6 months

18.2
24.6
25.1
28.6
25.1
26.6
25.5
16.4
19.4
12.1
211.6 : 10 = 21.2 ± 2.08
m.e.v. = ± 0.208

by different authors. Thus about a similar percentage of excess sodium and of excess calcium is prevented from interchanging with their circulating atoms. The sequestration of bone constituents is presumably due to the fact that a contact between these constituents and the circulating body fluids is obstructed. To arrive at the total excess chloride content of the bone of the mouse we correspondingly have to multiply the figure of 0.35 mg found for the non-exchangeable bone chloride by about 1.5, thus arriving at the result that the total excess bone chloride content of our 35 g mice amounts to about 0.53 mg.

In contrast to the bone sodium which is to a large extent present as excess sodium in the skeleton it can be shown that the chloride present as excess chloride makes out 1/10 only of the total bone chloride.

From 234 meqiv sodium present in 1 kg of dry human bone 84.9 %, thus 46 g, was found by Edelman *et al.*[5] to be excess sodium in a 70 kg man. For the dog Edelman and associates found 89.5 % of the bone sodium to be excess sodium and a similar figure is stated by Miller and associates [7]. 1 kg of rat bone was found to contain 125 meqiv excess sodium [8]. As to the total chloride content of 1 kg fat free bone this was found to amount to 19 meqiv only [5], thus to less than the extracellular bone sodium which makes out 25 meqiv. While excess bone sodium is to a marked extent responsible for the difference between total and extracellular body sodium, for chloride this difference is almost entirely due to the presence of intracellular chloride in the soft tissues.

The author's thanks are due to Miss Jutta Schliack for her very effective assistance and to *Statens Naturvetenskapliga Forskningsråd* for the support of this investigation.

REFERENCES

1. Ray, C. T., Burch, G. E. and Threfoot, S. A. *J. Lab. Clin. Med.* **39** (1952) 673.
2. Hevesy, G. *Kgl. Danske Videnskab. Selskab Biol. Medd.* **22** (1955) No 9.
3. Bauer, G. C. H. *Acta Physiol. Scand.* **31** (1954) 334.
4. Davies, R. E., Kornberg, H. L. and Wilsons, G. M. *Biochim. et Biophys. Acta* **9** (1952) 403.

5. Edelman, J. S., James, A. H., Baden, H. and Moore, F. D. *J. Clin. Invest.* **33** (1954) 122.
6. Bergström, W. H. *J. Clin. Invest.* **34** (1955) 997.
7. Miller, H., Munro, D. S., Renschler, E. and Wilson, G. M. *Radioisotope Conference*, Oxford, Vol. I, p. 138.
8. Bergstrom, W. H. and Wallace, W. M. *J. Clin. Invest.* **33** (1954) 867.
9. Wallacys, R. and Chandron, G. *Comt. rend.* **230** (1950) 1867.

Received November 7, 1956.

ACTA CHEMICA SCANDINAVICA 11 (1957) 265—274

The Free-Electron Model, "Overtone" Bands, and Vibrational Structure in Absorption Spectra of Polyenes and Polyenynes

JOHANNES DALE

Forsvarets Forskningsinstitutt, Kjeller, Norway

An analysis of the free-electron model for polyenes has provided theoretical justification for the empirical spectral rule correlating electronic "overtone" bands with the main band of shorter polyenes of lengths equal to integral fractions of the polyene considered. It is further shown how the vibrational structure of the various bands of polyenynes can be predicted by considering the detailed π-electron density displacement pattern along the chain during the transition. The relative intensities of the short wave length bands of polyenynes, in particular of dehydro-carotenoids, indicate that these bands are never due to independent partial chromophores, but must be regarded as overtone transitions. It is also concluded that the most stable configuration around an acetylenic (or odd-cumulenic) link in a polyene chain must be the planar *trans*-configuration.

In an earlier paper [1] it was shown that the minor bands, or "overtone" bands, of polyenes with n conjugated double bonds correspond in wave length location to the main band of polyenes with n/s conjugated bonds, where s is the band order (= 1 for the main band, 2 for the first overtone, and so on). The experimental data available at that time, and, in addition, numerous recently published spectra, fully confirmed the general validity of this rule. However, no theoretical interpretation was attempted.

The success of the free-electron gas model in making spectral predictions for conjugated systems would indicate that it might be of promise when trying to put the rule on a theoretical basis. A comparison of absolute transition energies is of little interest, since Bayliss [2], and Kuhn [3], have shown that simple quantum mechanical calculations based on this crude model, with the assumption of a uniform potential well with infinitely high walls, give fair results only for the main band of short polyenes. For longer chains, and quite generally for overtone bands, the agreement is very poor. However, as Bayliss has emphasized [4], it is the number and position of the orbital nodes of π-electrons confined to a given space, and not the detailed shape of the force field that

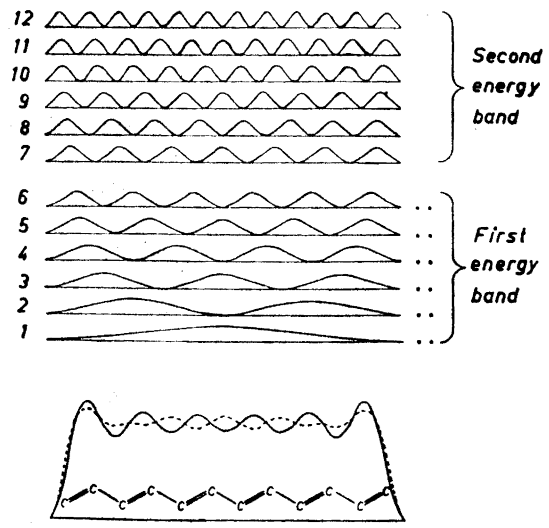


Fig. 1. Top: π-electron density (φ_n^2) along the chain for free-electron orbitals (φ_n) of the hexaene chromophore. Energy scale is arbitrary.
Bottom: Total π-electron density for the ground state (full line) and the first excited state (dashed line). (*Cf.* Bayliss [4].)

keeps the electrons within that space, which are of prime importance in determining the character (polarization, selection rules, intensities, *etc.*) of the electronic transitions as well as the distribution of π-electron charge density, and in this respect the free-electron model, even in its crude shape, is a good approximation.

A qualitative examination of this simple model leads to results in accordance with the observed empirical rule, but it also raises an important question.

As an illustration the hexaene chromophore has been chosen to enable a direct comparison of its first two overtones with the main bands of the triene and diene chromophores. In Fig. 1 the 12 lowest free-electron molecular orbitals (corresponding to all the possible LCAO molecular orbitals) have been represented in their squared form, which is a measure of the π-electron density along the chain. The energy of each orbital is given by $E = \frac{h^2 n^2}{8 m L^2} = k \frac{n^2}{L^2}$ where n is now the quantum number. The length L of the potential well has for simplicity been set equal to 12 times the average C—C distance since there is no more theoretical justification for other choices made by Bayliss and by Kuhn. The orbitals have been split into two groups, or energy bands, corresponding to the introduction of a Kuhn's periodic potential with minima at each formal double bond [3]. In the ground state the lowest energy band is completely filled by the 12 electrons. Summation gives the total electron density distribution given in Fig. 1 (full line) which is seen to correspond roughly

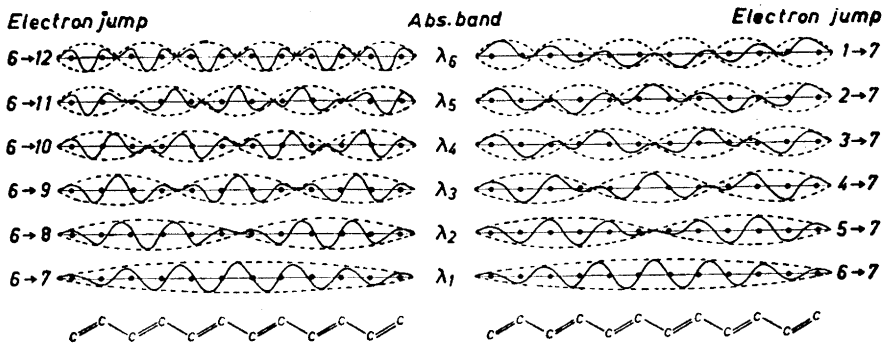


Fig. 2. Differential curves illustrating the displacement of electron density during transitions from the highest filled orbital (left), and similar transitions to the lowest vacant orbital (right). Electronic charge moves from regions where the curve is below the zero line to regions where it is above.

to the classical chemical formula [4,5]. Transfer of one electron from level 6 to level 7 ($\Delta n = s = 1$) gives the first excited state (dashed line) which is seen to correspond to a tendency towards the classical structures

$$\overset{\pm}{\mathrm{C}}-\mathrm{C}=\mathrm{C}-\mathrm{C}=\mathrm{C}-\mathrm{C}=\mathrm{C}-\mathrm{C}=\mathrm{C}-\mathrm{C}=\mathrm{C}-\overset{\mp}{\mathrm{C}}.$$

The displacement of electron density that takes place during a transition is more conveniently represented by the differential curves shown in Fig. 2. It is clearly seen that for the 6—7 transition, or in general: *f*—*g* transition according to Platt's notation [6], most of the excitation resides in the middle of the chain (*cf.* results from LCAO calculations for stilbene by Coulson and Jacobs [7]), the envelope of the displacement curve ("beat" curve) resembling the fundamental tone of a vibrating string.

OVERTONE BANDS

When the quantum number changes by more than one unit, there will, for a certain change *s*, be *s* different transitions; for example, *f*—*h* and *e*—*g* for $s = 2$; *f*—*i*, *e*—*h* and *d*—*g* for $s = 3$; and so on. Now the experimental data indicate that we have to do in each case with only one electronic transition. Thus, overtone bands show just as distinct vibrational structure as the main band of other polyenes that fall in the same wave length region. That all quasi-degenerate transitions within a group should coincide so perfectly, would only be possible if the energy levels were equidistant (with the exception of the *f*—*g* interval), and this possibility can be safely excluded since it conflicts with the convergence of the overtone bands, presumably towards an ionization limit, that is observed in all known spectra. The two remaining possibilities would then be that the transitions are either all from the highest occupied energy level or they are all to the lowest empty level. The pertinent differential curves are given in Fig. 2.

It is at once seen that the envelope of the displacement curves for overtone transitions are identical in both series and resemble the corresponding overtones of a vibrating string. However, the detailed displacement patterns differ more and more with increasing s. For transitions from the highest filled level they are in good accordance with chemical intuition; thus, the structures given below for various values of s are good representations for the corresponding excited states:

$s = 2$ $\overset{\pm}{C}-C=C-C=C-\overset{\mp}{C}-\overset{\mp}{C}-C=C-C=C-\overset{\pm}{C}$

$s = 3$ $\overset{\pm}{C}-C=C-\overset{\mp}{C}-\overset{\mp}{C}-C=C-\overset{\pm}{C}-\overset{\pm}{C}-C=C-\overset{\mp}{C}$

$s = 4$ $\overset{\pm}{C}-\overset{\mp}{C}-C=C-\overset{\mp}{C}-\overset{\pm}{C}-\overset{\pm}{C}-\overset{\mp}{C}-C=C-\overset{\mp}{C}-\overset{\pm}{C}$

$s = 5$ $\overset{\pm}{C}-\overset{\mp}{C}-\overset{\mp}{C}-\overset{\pm}{C}-\overset{\pm}{C}-C=C-\overset{\mp}{C}-\overset{\mp}{C}-\overset{\pm}{C}-\overset{\pm}{C}-\overset{\mp}{C}$

$s = 6$ $\overset{\pm}{C}-\overset{\mp}{C}-\overset{\mp}{C}-\overset{\pm}{C}-\overset{\pm}{C}-\overset{\mp}{C}-\overset{\mp}{C}-\overset{\pm}{C}-\overset{\pm}{C}-\overset{\mp}{C}-\overset{\mp}{C}-\overset{\pm}{C}$

We see from the left side of Fig. 2 that the electrons are mainly displaced from regions with high density ("double bonds") to regions with low density ("single bonds"). In contrast, overtone transitions to the lowest vacant level (right side of Fig. 2) must also involve displacement of electrons from regions with low density to regions with high density.

Furthermore, only transitions from the highest filled level will give the same displacement pattern for each half of the hexaene chromophore when $s = 2$ as for the triene chromophore when $s = 1$, and for each third of the hexaene chromophore when $s = 3$ as for the diene chromophore when $s = 1$, etc., which might be expected from the empirical rule.

It has also been empirically established [1] that steric prevention of coplanarity at certain points, as with *cis*-bonds, both "hindered" and "unhindered", decreases the intensity of bands for which the excitation, as deduced from Fig. 2, is considerable in the part of the molecule where the hindrance is located, but enhances the intensity of bands for which the displacement curve envelope (Fig. 2) is zero at the hindrance. It might therefore be expected that electronic charge transfer is negligible through these zero points, or nodes of the "beat" curve. From Fig. 2 it will be seen that transitions from the highest filled level satisfy this requirement, whereas for overtone transitions to the lowest vacant level electronic charge will have to be transferred through the "nodes". The extreme case is the 1—7 transition where the charge has moved from the double bonds in the middle to the double bonds at both ends.

It is also interesting to observe that if the free-electron expression for the excitation energies [2,3] is developed in a more general form to include also overtones, the following expression is obtained for transitions from the highest filled level:

$$\Delta E_{\frac{N}{2} \rightarrow \frac{N}{2}+s} = \frac{h^2}{2\,m\,a_0^2}\left[\frac{s}{N} + \frac{s^2}{N^2}\right]$$

Here N is the number of π-electrons in a polyene with $N/2$ double bonds, and s the change in quantum number ($\Delta\, n$) (which is equal to the band order). The length of the chromophore has been set equal to $\frac{N}{2} \cdot a_0$, where a_0 is the length of one single bond plus one

double bond. The only variables are N and s which occur here as the ratio s/N as would be required in order to satisfy the empirical rule. In contrast, the analogous general expression for transitions to the lowest unfilled orbital

$$\Delta E_{\frac{N}{2}+1-s \rightarrow \frac{N}{2}+1} = \frac{h^2}{2\,m\,a_0^2}\left[\frac{s}{N} + \frac{s(2-s)}{N^2}\right]$$

also contains the variables in the ratio $(2-s)/N$ in conflict with the requirements.

If Kuhn's sine curve potential [3] is introduced we get in both cases the additional energy term $V_0(1-\frac{s}{N})$, where V_0 is the amplitude of the potential energy variation along the chain (period $= a_0$). This term contains the variables only as the ratio s/N.

It is not easy to explain theoretically why only electrons of the outermost π-electron shell should be excited by light. Neither the LCAO nor the free-electron approximation lead to any such selection rule *.

VIBRATIONAL STRUCTURE IN POLYENE SPECTRA

From Fig. 2 we have seen that the excitation responsible for the main band in polyene spectra is concentrated mainly in the middle of the chain. Now from the Franck-Condon principle one should expect that the stretching frequency of the bonds that receive the greatest change in bond order should be coupled most strongly with the electronic transition and thus contribute most to the vibrational structure of the absorption band. It is therefore not surprising that even in α,ω-diphenylpolyenes [8] it is the polyene frequencies 1 570 cm^{-1} and 1 230 cm^{-1} (in average about 1 400 cm^{-1}) that build up the structure, not only for the long chains, but also in stilbene.

As to the distribution of intensity among the vibrational peaks in the absorption bands of polyenes it is clear that as the number of conjugated double bonds increases, a one-electron jump from a bonding π-orbital to an antibonding π-orbital will have proportionately less and less effect on the binding force, so that the change in bond order decreases and the first peak (vibrationless transition) will have to gain intensity. This is in accord with observations in the unsubstituted polyene series [9] as well as in the diphenylpolyene series [8]. However, with increasing length *cis*-isomerization will often complicate this behaviour of the main band. It may therefore be more illustrating to compare bands in the same wave length region, that is, overtones of long polyenes with main bands of short polyenes. Numerous examples can be found where the first peak is the strongest in the λ_2-band, although λ_1-bands of comparable chromophores with half the length usually have the second peak the strongest. In the λ_3-band of very long chromophores practically all the intensity may be concentrated in the first peak, as can be seen in the spectrum of lycopene [10]. That the vibrationless transition is by far the strongest in the main band of the spectra of similar ionic compounds, such as the cya-

* A solution of this problem has been proposed to the writer by Prof. J. R. Platt, who thinks that the observed "selection rule" is only apparent and that the s quasi-degenerate transitions of a group mix to give one with strong transition moment and $s-1$ transitions with zero moment (*cf.* his recent paper on configuration interaction [42]).

nine dyes [11], can also be explained by using the free electron model, from which it is seen that very little change of bond order will occur during excitation, since bonds have now taken the positions occupied by the atoms of polyenes, and *vice versa* [4]. The same deduction has also been made by Platt in his recent paper [42].

VIBRATIONAL STRUCTURE IN POLYENYNE SPECTRA

Since the excitation for the various bands in polyene spectra is located in different parts of the chromophore, it should be possible to predict the vibrational structure of these absorption bands if some of the ethylenic bonds are exchanged with acetylenic bonds. Thus, one acetylenic bond in the middle of a polyene chain should be sufficient to give the λ_1-band acetylenic spacing ($\sim$ 2 000 cm^{-1}) if the chain is very short, as in divinylacetylene [12]. In longer chains both acetylenic and ethylenic spacings should occur and the result may be a smearing out of the structure, especially on the short wave length side of the band, since the number of possible combinations of the vibrational quanta will increase rapidly as more quanta are excited. A greater number of acetylenic bonds are therefore needed to give the band clear acetylenic spacing. However, the λ_2-band should be unaffected and show ethylenic spacing ($\sim$ 1 400 cm^{-1}).

If now the acetylenic bonds are instead at the end, the λ_1-band will remain ethylenic, but it will probably be necessary to have acetylenic bonds located in both halves in order to give clear acetylenic structure to the λ_2-band.

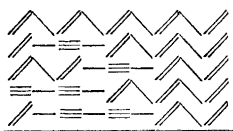
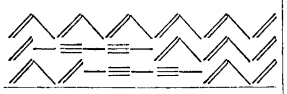
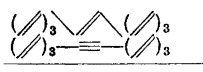
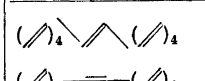
Available experimental data for polyenynes and corresponding polyenes have been compiled in Table 1. It is seen that to the extent that the vibrational structure is resolved, the observed spacings agree well with the spacings that would be expected from the geometry of the chromophores. Compounds in which the acetylenic portion constitutes more than half the chromophore have not been included, since they show the spectral anomalies typical for polyacetylenes. Unfortunately, no examples of chromophores consisting of a polyacetylene chain with a few ethylenic bonds in the middle are known.*

WAVELENGTH SHIFTS AND INTENSITY RELATIONSHIPS IN POLYENYNE SPECTRA

In Table 1 the substitution patterns on the chromophores have not been included. But when substances with equal substitution are compared, it is always found that there is an intensity reduction and a blue-shift of the λ_1-band as compared with polyenes (*cf.* Inhoffen and Bohlmann [13]). This may be connected with the stronger binding of π-electrons to *sp*-hybridized carbon

* *Note added in proof:* Very recently Bohlmann and Politt (*Chem. Ber.* **90**(1957)130) have synthesized compounds with the following chromophores: ≡–≡–⟋⟍⟋⟍≡, ≡–≡–⟋⟍⟋≡–≡, and ≡–≡–⟋⟍⟋⟍≡–≡–⟋⟍⟋⟍≡–≡. The main bands show the vibrational spacings which can be predicted from the arguments given above. As expected, the overtone bands of the second compound have acetylenic structure, but position and intensity are apparently complicated by interaction between the two short π-electron components of the acetylenic portions and the polyene-like "hexaene" component. The overtone bands of the last compound do not show resolved structure.

Table 1. Predicted and observed vibrational structure in spectra of polyenynes (and corresponding polyenes).

Chromophore (substitution not indicated)	λ_1-band			λ_2-band			Ref.
	Wavelength of first peak in mμ	Predicted spacings	Observed spacings in cm^{-1}	Wavelength of first peak in mμ	Predicted spacings	Observed spacings in cm^{-1}	
	310	eth.	1 500; 1 400	212w	eth.		33
	306	eth.	1 500; 1 200	230w	mixed		34
	308	mixed	1 900; 1 300	224s	mixed		35
	311	acet.	2 000; 2 100	244s	mixed	1 500; 1 000	36
	341	eth.	1 500; 1 400	236w	eth.		33
	345	eth.	1 500; 1 500	251m	mixed	1 200	26
	341	mixed	1 700; (2 300)	228m	eth.		37
	335	eth.	1 500; (1 600)	253m	mixed	1 600	38
	336	acet.	2 000; 2 100	266s	mixed	2 100; (2 400)	38,39
	370*	eth.	1 500; 1 400		eth.		33
	354	mixed	2 100; 2 000	277s	mixed	1 700	40
	364	acet.	2 100; 1 800	279m	mixed	2 600; (1 600)	39
	390	eth.	1 500; 1 400	274w	eth.	1 400; 1 300	9
	392	mixed	1 900	280m	eth.	1 300	37
	420	eth.	1 500, 1 400, 1 300	296w	eth.	1 200	41
	403	acet.	2 000; 1 500; 600	308m	eth.	1 400; 1 100	34,41
	441	eth.	1 500; 1 400; 1 300	313w	eth.	1 300	41
	425	mixed	1 500	314m	eth.	1 300	41
	463*	eth.	1 500; 1 400	331*w	eth.	1 400	41
	435	mixed	2 000; 1 400	342m	eth.	1 500	41

* Data in benzene corrected for solvent shift.
Intensities: w = weak, m = medium, s = strong.

atoms [14]. The effect should be particularly pronounced when the acetylenic bonds are in the middle of the chain where most of the excitation occurs. The λ_2-band may then be wholly unaffected and even undergo a red-shift since the excitation is made easier by the attraction of π-electrons by *sp*-carbons. Similar observations have been made on replacement of carbon by nitrogen, in a comparison of diphenylpolyenes with diphenylpolyenalazines [1]. Alternatively, these phenomena can be discussed in terms of energy changes of the orbitals

involved as Kuhn has shown for polymethine dyes in which carbon has been replaced by nitrogen [5].

Most of the published spectra of polyenynes show rather weak λ_2-bands except when the acetylenic section is not centrally located. If there were free rotation around the acetylenic bonds one should expect strong λ_2-bands in all cases, so that one is led to conclude that the planar *trans*-configuration, for which λ_2-transitions are forbidden, must be the most stable one. For the very few symmetrical polyenynes which show strong λ_2-bands, the explanation may be that some of the double bonds have a *cis*-configuration or that geometrical isomerism occurs around the acetylene system, so that there can exist also a planar "*cis*-isomer", if both ethylenic π-electron systems remain conjugated with the same component of the acetylenic π-electron system, and a non-planar isomer if they do not conjugate with the same component. According to calculations by Dunitz and Orgel [15] energy differences between such isomers would be small and are further decreased with increasing length of the acetylenic system.

Another effect, which has been observed for *cis*-polyenes, is also encountered in polyenynes. Like *cis*-bonds, acetylenic and cumulenic bonds apparently have a blocking effect for transitions for which there will be excitation in these bonds, but enhance the intensity of transitions for which the bonds are in regions where no excitation occurs ("nodes" of the "beat curve"). Thus, some bisdehydro-lycopenes [16], in which the acetylenic or cumulenic hindrances have divided the chromophore into three roughly equal sections, show degraded λ_1-bands and only weak λ_2-bands, since the chain is essentially straight, but the λ_3-bands at about 300 mμ, the same location as λ_3-bands in the corresponding hindered di-*cis*-lycopenes, have become exceptionally intense, since they have to take over the intensity of the hindered transitions. Even more illustrative material is afforded by the closely related lycopene analogues bis-dehydro-diphenyl-tetramethyl-octadecanonaenes (Fig. 3) synthesized by Karrer and coworkers [17]. It is evident from the spectra that the cumulene system $\rangle C{=}C{=}C{=}C\langle$ represents a more severe hindrance in a polyene chain than the $-C{\equiv}C-$ system. Thus, the dicumulene has a much more degraded λ_1-band and a correspondingly stronger λ_3-band than the diacetylene. The acetylene-cumulene has an intermediate λ_1-band, but the λ_3-band is lower, since because of the unsymmetry (Fig. 3) the λ_2-band (at 360 mμ) and the λ_4-band (at 265 mμ) become allowed and take over much of the intensity. The λ_5-band (at 240 mμ) is also quite distinct in these compounds and its intensity variation can likewise be predicted.

The corresponding unsymmetric monocumulene and monoacetylene have also been obtained [18], and their spectra can be interpreted by similar considerations. The λ_2-bands are here relatively weak since the chains are approximately linear. It is then very interesting to observe that upon *cis*-isomerization of the ethylenic bonds, the λ_2-, λ_4-, and λ_5-bands increase in intensity, while the λ_1- and λ_3-bands decrease correspondingly.

An analogous diacetylenic bisdehydro-methylbixin has been prepared [19]. It shows no λ_2-band but a very strong λ_3-band.

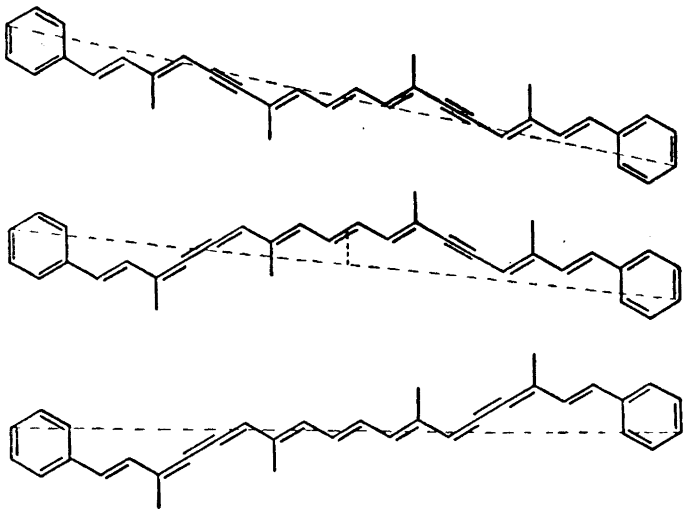


Fig. 3. Skeleton models of bisdehydro-diphenyl-tetramethyl-octadecanonaenes. Planar *trans*-configuration around the linear C_4-sections has to be assumed to account for the absorption spectra. Top, diacetylene; middle, acetylene-cumulene; and bottom, dicumulene.

That the spectra of the numerous dehydro-carotenoids with one (or two) centrally located acetylenic bonds prepared by Inhoffen and coworkers [13,20-25] show no correspondingly intense band in the λ_2-band region (forbidden by symmetry), and only moderate λ_3-bands, is a very strong support for the idea that in polyenynes, as well as in polyenes, the minor bands are always to be regarded as overtones and never as due to independent partial chromophores as has been suggested by Oroshnik and Mebane [26] for these polyenynes, and earlier by Heilbron *et al.*[27] for polyenynes containing the diacetylene grouping. The present interpretation implies that the planar *trans*-configuration is the most stable one around an acetylenic (or odd-cumulenic) link. The same configuration has been established earlier for a few compounds in the crystalline state by X-ray diffraction [28-32], but these results have not, of course, allowed any conclusion to be drawn as to the configuration of free molecules, since packing effects may come into play in the crystal lattice.

REFERENCES

1. Dale, J. *Acta Chem. Scand.* **8** (1954) 1235.
2. Bayliss, N. S. *J. Chem. Phys.* **16** (1948) 287.
3. Kuhn, H. *J. Chem. Phys.* **17** (1949) 1198.
4. Bayliss, N. S. *Quart. Revs.* **6** (1952) 319.
5. Kuhn, H. *Chimia* **4** (1950) 203.
6. Platt, J. R. *Radiation Biology* McGraw-Hill N.Y., 1956, Vol. 3, Chapter 2, p. 71.
7. Coulson, C. A. and Jacobs, J. *J. Chem. Soc.* **1949** 1983.
8. Hausser, K. W., Kuhn, R. and Seitz, G. *Z. physik. Chem.* **B29** (1935) 391.

9. Mebane, A. D. *J. Am. Chem. Soc.* **74** (1952) 5227.
10. Zechmeister, L., LeRosen, A. L., Schroeder, W. A., Polgár, A. and Pauling, L. *J. Am. Chem. Soc.* **65** (1943) 1940.
11. Brooker, L. G. S., Sprague, R. H., Smyth, C. P. and Lewis, G. L. *J. Am. Chem. Soc.* **62** (1940) 1116.
12. Price, W. C. and Walsh, A. D. *Proc. Roy. Soc. London* **A185** (1946) 182.
13. Inhoffen, H. H. and Bohlmann, F. *Ann.* **565** (1949) 41.
14. Walsh, A. D. *Quart. Revs.* **2** (1948) 73.
15. Dunitz, J. D. and Orgel, L. E. *J. Chem. Phys.* **20** (1952) 1328.
16. Garbers, C. F. and Karrer, P. *Helv. Chim. Acta* **36** (1953) 828.
17. Garbers, C. F., Eugster, C. H. and Karrer, P. *Helv. Chim. Acta* **35** (1952) 1850.
18. Garbers, C. F., Eugster, C. H. and Karrer, P. *Helv. Chim. Acta* **36** (1953) 562.
19. Ahmad, R. and Weedon, B. C. L. *J. Chem. Soc.* **1953** 3286.
20. Inhoffen, H. H., Bohlmann, F. and Rummert, G. *Ann.* **569** (1950) 226.
21. Inhoffen, H. H., Bohlmann, F., Bartram, K., Rummert, G. and Pommer, H. *Ann.* **570** (1950) 54.
22. Inhoffen, H. H., Bohlmann, F., Aldag, H.-J., Bork, S. and Leibner, G. *Ann.* **573** (1951) 1.
23. Inhoffen, H. H., Isler, O., Bey, G. v.d., Raspé, G., Zeller, P. and Ahrens, R. *Ann.* **580** (1953) 7.
24. Inhoffen, H. H. and Raspé, G. *Ann.* **592** (1955) 214.
25. Inhoffen, H. H. and Raspé, G. *Ann.* **594** (1955) 165.
26. Oroshnik, W. and Mebane, A. D. *J. Am. Chem. Soc.* **76** (1954) 5719.
27. Heilbron, I., Jones, E. R. H. and Sondheimer, F. *J. Chem. Soc.* **1947** 1586.
28. Robertson, J. M. and Woodward, I. *Proc. Roy. Soc. London* **A164** (1938) 436.
29. Wiebenga, E. H. *Z. Krist.* **102** (1940) 193.
30. Dunitz, J. D. and Robertson, J. M. *J. Chem. Soc.* **1947** 148.
31. Rollet, J. S. *Acta Cryst.* **8** (1955) 487.
32. Sly, W. G. *Acta Cryst.* **8** (1955) 115.
33. Nayler, P. and Whiting, M. C. *J. Chem. Soc.* **1955** 3037.
34. Bohlmann, F. and Viehe, H.-G. *Chem. Ber.* **88** (1955) 1347.
35. Heilbron, I., Jones, E. R. H., Lewis, D. G. and Weedon, B. C. L. *J. Chem. Soc.* **1949** 2023.
36. Jones, E. R. H., Whiting, M. C., Armitage, J. B., Cook, C. L. and Entwistle, N. *Nature* **168** (1951) 900.
37. Heilbron, I. M., Jones, E. R. H. and Raphael, R. A. *J. Chem. Soc.* **1944** 136.
38. Anet, E. F. L. J., Lythgoe, B., Silk, M. H. and Trippett, S. *J. Chem. Soc.* **1953** 309.
39. Bohlmann, F. and Viehe, H.-G. *Chem. Ber.* **88** (1955) 1245.
40. Sörensen, J. S. and Sörensen, N. A. *Acta Chem. Scand.* **8** (1954) 1741.
41. Bohlmann, F. and Mannhardt, H.-J. *Chem. Ber.* **89** (1956) 1307.
42. Platt, J. R. *J. Chem. Phys.* **25** (1956) 80.

Received October 23, 1956.

ACTA CHEMICA SCANDINAVICA 11 (1957) 275—282

The Biochemical Evaluation of Paper Chromatograms of Parathion, its Isomers and Analogues

KLAS-BERTIL AUGUSTINSSON and GUNNEL JONSSON

Institute of Organic Chemistry and Biochemistry, University, Stockholm, Sweden

Parathion, its analogues and isomers were separated from mixtures by paper chromatography. The chromatograms were evaluated biochemically by dividing the chromatogram into sections, the cholinesterase inhibiting effects of which were measured against a system of acetylcholine and purified enzyme. The enzyme inhibiting power of several pure *p*-nitrophenyl esters of phosphoric and thiophosphoric acids was determined and the biochemical evaluation of the chromatograms was carried out with four samples (pure compound, heterogeneous technical grade compound, 96.5 % technical grade parathion, and a commercial formulation for insecticidal use). The various derivatives formed by heating parathion and methyl-parathion, can be demonstrated with the new technique.

In connection with the testing of various methods for the chemical assay of parathion, including the chromatographic separation on paper of the different constituents present in technical grade preparations [1], certain biochemical studies were made, and these results are the basis of the present paper.

Methods for paper chromatography of parathion (O,O-diethyl-O-*p*-nitrophenyl thiophosphate) and related compounds have been described in recent publications. A variety of solvents and stationary phases have been tested but the most convenient technique reported so far is that described by Metcalf and March [2]. This method gives the best results according to the experience of our laboratory and has therefore been used, partly modified throughout the present investigation. Other methods use ethanol-ammonia-water [3,4] as solvent or ethyl ether in water-saturated petroleum ether [5]. The detection of parathion and its degradation product (*p*-nitrophenol) in these methods is based either upon ultraviolet absorption [3,5] or upon spraying with Millon's reagent [4].

In the biochemical analysis of paper chromatograms such as that described below, the enzyme (cholinesterase) inhibition by various sections or spots of the chromatograms was measured. The technique used is suggested as a valuable complement for the evaluation of paper chromatograms of organophosphorus compounds.

METHODS AND MATERIAL

Paper chromatography. Filter paper (Munktell OB) was impregnated with silicone (MS 550) from a 5 % hexane solution and air dried. The phosphate esters (ethanol solutions) were applied to the paper and chromatographed using the ascending technique. The solvent used was the upper phase from a mixture containing water-ethanol-chloroform (6 : 10 : 10). The paper was afterwards dried in an air stream, sprayed with 5 % alcoholic potassium hydroxide solution, and finally kept for some minutes in steam over boiling water. The various components were visible as yellow spots (*p*-nitrophenolate).

Measurement of enzyme inhibition. Undeveloped chromatograms, *i. e.*, those not treated with alcoholic potassium hydroxide solution, were used to study the cholinesterase inhibition by separated phosphate and thiophosphate esters. The chromatogram was cut into sections of the same size, usually 20 sections from the starting point to the solvent front and extracts of each section were made in a bicarbonate buffer solution. Cholinesterase inhibition by these extracts was assayed, using a technique described previously [6], with acetylcholine chloride as substrate and a purified preparation from human blood serum as enzyme source. Before the addition of substrate the enzyme was incubated for 50 min with the extract. The location of the active constituents thus obtained, evaluated as per cent enzyme inhibition, was compared with a chromatogram developed with the technique described above.

Phosphate and thiophosphate esters. Most compounds (see Table 1) used in the present study were kindly supplied by Dr. Gerhard Schrader [7]. Gifts of pure parathion were made by Plant Protection (England) and the American Cyanamid Co. (USA).

RESULTS

Paper chromatograms. The results obtained on analysing the various phosphate and thiophosphate esters by the paper chromatographic technique are summarised in Table 1. It gives the R_F values of all the pure grade compounds tested and, in addition, the values for three unknown constituents which were traced in a parathion preparation heated for 40 h at 140° C. Some of these unknown compounds were also found in some technical preparations. The *o*- and *m*-nitrophenyl esters had the same R_F values as the corresponding *p*-nitrophenyl ester, as demonstrated with the S-phenyl isomers of parathion and methyl-parathion.

Cholinesterase inhibiting effect. The I_{50} values (*i. e.*, molar inhibitor concentration giving 50 % enzyme inhibition) are recorded in Table 1. These values were obtained by incubating a cholinesterase preparation for 50 min at 25° C with various concentrations of the inhibitor prior to the addition of substrate (acetylcholine). The most active inhibitor of cholinesterase was found to be the S-phenyl isomer of parathion, confirming a recent observation made by Hecht and Wirth [9] with horse serum as an enzyme source. The bis-(*p*-nitrophenyl) ethyl ester of phosphoric acid came next, and then paraoxon and methyl-paraoxon. The inhibiting power of parathion was relatively low. The least active inhibitors in this series were methyl-parathion and bis-(*p*-nitrophenyl) ethyl thiophosphate. Amongst the three unknown compounds traced on the chromatograms, the two slow running esters had no measurable inhibiting effect on cholinesterase activity. The compound with R_F 0.90, on the other hand, did inhibit the enzyme, but its nature could not be determined. Double spotting cannot be excluded, however, in these cases.

Table 1. R_F values and cholinesterase inhibiting power of various *p*-nitrophenyl esters of phosphoric and thiophosphoric acids. pI_{50} = negative logarithm of molar inhibitor concentration (during enzyme incubation) giving 50 % inhibition.

R_F at 22° C	Formula	Code name	pI_{50}
0.01	$(C_2H_5O)_2P(S)-O-C_6H_4-NO_2$	Bis-nitrophenyl thioester *	<2.3
0.03	$(C_2H_5O)_2P(S)-O-C_6H_4-NO_2$	Parathion, E 605	< 4
0.06	$(CH_3O)_2P(S)-O-C_6H_3-NO_2Cl(m)$	Chlorthion	— **
0.11	$(CH_3O)_2P(S)-O-C_6H_4-NO_2$	Methyl-parathion	< 2
0.12	Unknown	—	No inhibitor
0.17	Unknown	—	No inhibitor
0.22	$(C_2H_5O)_2P(O)-O-C_6H_4-NO_2$	Bis-nitrophenyl ester *	8.2
0.40	$C_2H_5O(C_2H_5S)P(O)-O-C_6H_4-NO_2$	S-ethyl isomer	~ 6
0.51	$(C_2H_5O)_2P-S-C_6H_4-NO_2$	S-phenyl isomer of parathion	8.55
0.60	$CH_3O(CH_3S)P(O)-O-C_6H_4-NO_2$	S-methyl isomer	— **
0.70	$(C_2H_5O)_2P(O)-O-C_6H_4-NO_2$	Paraoxon, E 600	8.18
0.72	$(CH_3O)_2P-S-C_6H_4-NO_2$	S-phenyl isomer of methyl-parathion	6.5
0.79	$HO-C_6H_4-NO_2$	pNP	No inhibitor
0.84	$(CH_3O)_2P(O)-O-C_6H_4-NO_2$	Methyl-paraoxon	6.0
0.90	Unknown	—	Inhibitor

* The corresponding methyl ester probably has an R_F close to this.

** Pure compound not available. DuBois *et al.*[8] give for chlorthion a pI_{50} of 4.4 (rat serum; compound "more than 95 % pure"), Hecht and Wirth [9] for the S-methyl isomer a pI_{50} of 5.55 (horse serum).

The I_{50} values, as shown in Table 1, do not always give the correct measure of the inhibitory effects of a compound. This is especially true for parathion and its analogues because they are mostly very difficult to obtain in a pure state and the presence of an impurity may not be detected in a simple determination of the 50 % inhibition concentration (I_{50}). A better technique was introduced by Aldridge and Davison [10], who used bimolecular rate constants (for reaction of inhibitor with cholinesterase) instead of I_{50}. Despite this criticism of a comparison of the inhibitory power based upon I_{50} values, we believe the values of Table 1 to be of value for the technique described in the present paper. In fact, the 50 % inhibition concentration is a useful property of a preparation, pure or not, in deciding the amount to be applied to the filter paper for chromatography with subsequent enzymic evaluation.

The effect of solvent and silicone treated filter paper on the inhibitory effect. Before measuring the cholinesterase inhibition by various sections of paper chromatograms, the effects on enzyme inhibition by the solvent and the silicone treated paper were studied. There is a possibility that a compound may

Table 2. Change of cholinesterase inhibiting power of parathion and methyl-parathion applied on filter paper. Samples kept at room temperature for various periods of time before testing.

Compound	Days	% Inhibition		
		Untreated paper	Paper treated with silicone	Paper treated with silicone + solvent
Parathion	0	29	14.5	15
	1	64.5	32	39.5
	10	87	81	91.5
Methyl-parathion	0	13.5	3.5	9
	1	25.5	8.5	9.5
	8	28	13.5	17.5
	15	32.5	16	17.5

undergo isomerisation or oxidation during chromatography or spontaneous reactions may take place on a chromatogram kept for some time before biochemical evaluation.

The following experiments were made. Ethanol solutions of parathion and methyl-parathion respectively were placed on chromatographic paper

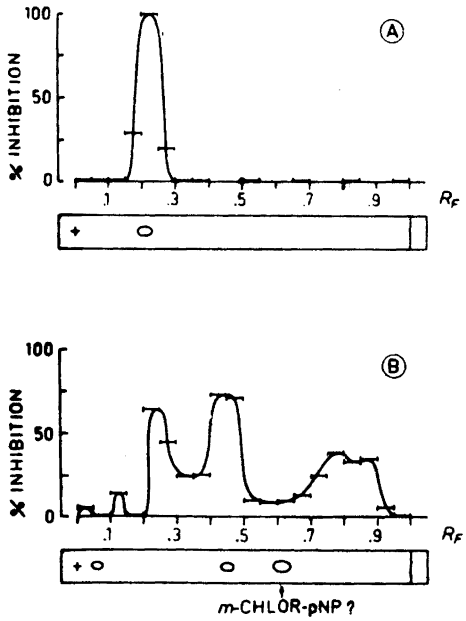


Fig. 1. Inhibition of cholinesterase by various sections of the paper chromatograms of bis- (*p*-nitrophenyl) ethyl phosphate (A), and a chlorthion preparation ("Chlorthion-Forte, Bayer") (B).

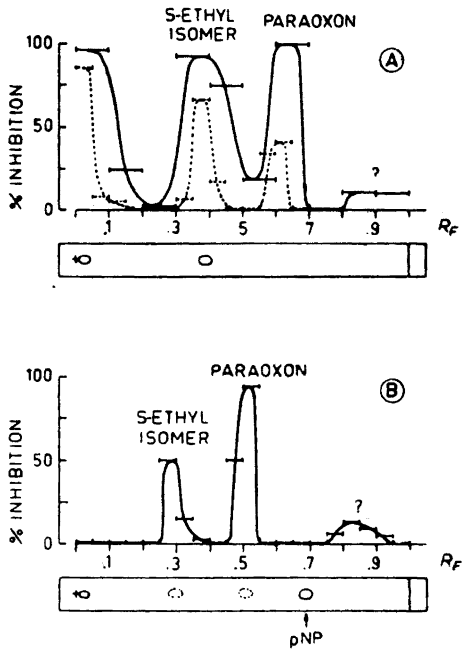


Fig. 2. Inhibition of cholinesterase by various sections of the paper chromatograms of a 96.5 % parathion preparation (American Cyanamid Co.) (A) (two separate experiments with various amounts applied on the paper), and a commercial formulation ("Ara-Parathion 35") for insecticidal use containing 35 % parathion (B).

(untreated, treated with silicone, and with silicone + solvent). After varying times, extracts of the spots were made in bicarbonate buffer and the cholinesterase inhibitory effect tested in the usual way. Table 2, recording the results, shows that both compounds studied underwent transformations to more active cholinesterase inhibitors, parathion more rapidly than its methyl analogue. It will be noted that the inhibitory effect of the samples on the silicone treated paper was about 50 % lower than the effect shown by the samples on untreated paper, except for very high inhibition values. The derivatives produced in these reactions are most probably the oxygen analogues (paraoxon and methyl-paraoxon) and the S-ethyl and S-methyl isomers which are known to be formed rather easily under a variety of experimental conditions. It is therefore to be expected that the section of a chromatogram containing parathion will show enzyme inhibition if it is not tested immediately after chromatographic separation, although parathion itself should not show this property (*cf.* Table 1). This is in accord with the experimental results (see Fig. 2 A).

The biochemical evaluation of chromatograms of pure and "pseudo pure" compounds. The results obtained in the biochemical evaluation of paper chromatograms are exemplified by four analyses. Fig. 1 A illustrates the

results obtained with bis-(*p*-nitrophenyl) ethyl phosphate. This highly active cholinesterase inhibitor gave only a single spot on the developed chromatogram and the biochemical results confirmed the purity of the preparation used. Fig. 1 B illustrates the chromatographic and biochemical results obtained with a technical grade preparation of chlorthion. Pure chlorthion is probably a weak enzyme inhibitor and it would therefore be expected that biochemical means would not be able to detect it on the chromatogram. The heterogeneity of the preparation used in this case was clear from the developed chromatogram but was still more pronounced when the various sections of the chromatogram were tested against a cholinesterase preparation. No efforts were made in the present investigation to identify the various constituents shown in the diagram, because pure preparations of chlorthion, its isomers and analogues were not available.

The chromatogram (Fig. 2 A) of a 96.5 % parathion preparation showed, in addition to the parathion area, an area of R_F 0.40 represented by the S-ethyl isomer. The biochemical results demonstrated the presence of a third constituent identified as the oxygen analogue of parathion (paraoxon). The results shown are from two separate experiments in which various amounts of the preparation were applied on the filter paper. The weak inhibitory effect of the area with R_F 0.9 was due to an unknown constituent demonstrated in several other parathion preparations analysed. It will be noted that the parathion section inhibited cholinesterase, an effect which would not be expected from the known weak inhibiting effect of this compound. The chromatograms in this case were kept for several days at room temperature before being analysed biochemically and during this period more active enzyme inhibitors (S-ethyl isomer and paraoxon) had been produced by spontaneous reactions (see above for proof of this explanation).

The next example is given in Fig. 2 B which illustrates the results obtained with a commercial parathion formulation. The lower R_F values obtained for the four visible constituents on the chromatogram (parathion, S-ethyl isomer, paraoxon, and *p*-nitrophenol) were most probably due to the disturbing effects of other unknown constituents (65 %) in this mixture. The biochemical analysis confirmed the presence of the S-ethyl isomer and paraoxon; in addition, the typical (for many technical grade parathion preparations) but unknown derivative with R_F 0.9 was present.

Isomerisation of parathion and methyl-parathion at high temperature. It is known from previous investigations [7,11,12] that parathion isomerises on heating, one of the products being the S-ethyl isomer. The strong cholinesterase inhibitor derived from parathion *in vivo*, on the other hand, is paraoxon [13]. After heating pure parathion for 40 h in a sealed tube at 140° C, chromatographic analysis of the mixture revealed the presence of eight constituents (Fig. 3 B). Four of these could be seen without difficulty on the developed chromatogram, *i. e.*, the bis-nitrophenyl ester, the S-ethyl isomer, paraoxon and *p*-nitrophenol. The other four (parathion and the three unknown constituents with R_F 0.12, 0.17 and 0.90) were visible when a greater amount of the heated mixture was chromatographed. Amongst these eight constituents, four were known to be highly active cholinesterase inhibitors and they were demonstrated clearly in the biochemical analysis (Fig. 3 B).

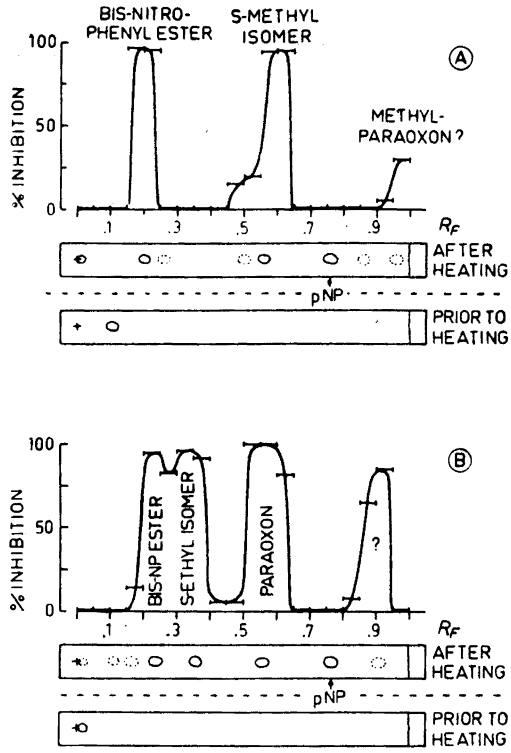


Fig. 3. Inhibition of cholinesterase by various sections of the paper chromatograms of methyl-parathion (A) and parathion (B); both preparations heated at 140° C for 40 hours.

The various constituents present in a methyl-parathion preparation heated in the same way were not as easily identified (Fig. 3 A). Eight constituents were present in this mixture also, some of which were traced from known R_F values. The slow running compound (R_F 0.02) was probably bis-(*p*-nitrophenyl) methyl thiophosphate. Two constituents were found to be strong cholinesterase inhibitors and they were almost certainly identical with bis-(*p*-nitrophenyl) methyl phosphate (R_F 0.20) and the S-methyl isomer (R_F 0.60), respectively. Except for *p*-nitrophenol the remaining constituents were unknown; one of the two fast running constituents was presumably identical with methyl-paraoxon.

DISCUSSION

Paper chromatography has been a valuable tool in analysing organophosphorus insecticides, especially technical grade parathion preparations [1]. It is proposed that this technique should be combined with a biochemical evaluation of the chromatograms as described in the present paper. Many parathion

preparations are more or less heterogeneous. The toxicity of these preparations is greatly dependent on the amounts of S-ethyl isomer, bis-(*p*-nitrophenyl) ethyl phosphate, and paraoxon present. These derivatives, especially in small amounts, are difficult to assay by available chemical methods. Paper chromatography alone is not sufficient in many cases, as its sensitivity is not high enough. A knowledge of the presence of these highly active constituents is important since otherwise misleading values may be obtained for toxicity, cholinesterase inhibitory power, hydrolysis rates, and insecticidal usefulness. These highly toxic isomers and analogues of parathion are formed spontaneously under various conditions and are especially important in the case of preparations which have been stored under uncontrolled conditions.

The technique described should be valuable in studying the metabolism of parathion, methyl-parathion, *etc.* in animals and plants as well as the mode of action of such compounds in mammals and insects and its usefulness may be extended to other organophosphorus compounds, many of which are highly active cholinesterase inhibitors. For parathion, and several related compounds, the toxicity and other properties are dependent on the presence of trace amounts of isomers or analogues which may give misleading results in pharmacological, biochemical and chemical studies. The homogeneity of preparations under examination can be tested easily by the technique as described in the present paper for a few compounds, the biochemical properties of which are characteristic of a larger group of toxic agents.

This investigation has been supported by grants from *Jordbrukets Forskningsråd (Swedish Agricultural Research Council)* and *Statens Institut för Folkhälsan (National Institute for Public Health*, Sweden). The kind interest shown by Professor Ernst Abramson is gratefully acknowledged.

I wish to express my sincere gratitude to Dr. Gerhard Schrader, Farbenfabriken Bayer, Wupperthal-Elberfeld (Germany) for his generous gift of the pure grade phosphorus compounds.

REFERENCES

1. Augustinsson, K.-B. *Acta Agr. Scand.* **7** (1957) 165.
2. Metcalf, R. L. and March, R. B. *Science* **117** (1953) 527.
3. Pfeil, E. and Goldbach, H. J. *Klin. Wochschr.* **31** (1953) 1011.
4. Kaiser, H. and Haag, T. *Arch. Pharm.* **9/10** (1954) 143.
5. Fiori, A. *Nature* **178** (1956) 423.
6. Augustinsson, K.-B. *Methods of biochemical analysis* (ed. D. Glick) **5** (1957) 1.
7. Schrader, G. *Die Entwicklung neuer Insektizide auf Grundlage organischer Fluor- und Phosphor-Verbindungen*, 2. Aufl., Verlag Chemie, Weinheim/Bergstr. 1952.
8. DuBois, K. P., Doull, J., Deroin, J. and Cummings, O. K. *Arch. Ind. Hyg. and Occupational Med.* **8** (1953) 350.
9. Hecht, G. and Wirth, W. *Arch. exptl. Pathol. Pharmakol., Naunyn-Schmiedeberg's* **211** (1950) 264.
10. Aldridge, W. H. and Davison, A. N. *Biochem. J.* **52** (1952) 663.
11. Morrill, H. L. *U.S. Pat.* 2,601,219 (June 17, 1952); abstracted in *Chem. Abstr.* **46** (1952) 8322.
12. Metcalf, R. L. and March, R. B. *J. Econ. Entomol.* **46** (1953) 288.
13. Gage, J. C. *Biochem. J.* **54** (1953) 426.

Received October 31, 1956.

ACTA CHEMICA SCANDINAVICA 11 (1957) 283—290

Electroorganic Preparations 1. Reduction of Steroid Ketones

HENNING LUND

Leo Pharmaceutical Products, Copenhagen, Denmark

It is shown that Δ^4-keto-3-steroids and $\Delta^{1,4}$-keto-3-steroids can be reduced at a mercury cathode at controlled cathode potential to pinacols, whereas saturated keto groups are not reduced at the potential used. The stereochemistry of the pinacols is discussed. The formation and a subsequent oxidation of the pinacols with a 1,2-glycol splitting reagent as lead tetraacetate or periodic acid is proposed as a method for protection of the reactive unsaturated keto group in the presence of saturated keto groups.

Δ^4-Unsaturated steroid ketones are known to be reducible at the dropping mercury electrode [1–4], but no conclusive evidence of the electrode reaction has been presented. The purpose of the present work is to examine the electrode reaction and its use in preparative chemistry. The investigation consists of a polarographic examination of the compounds under different conditions and controlled potential electrolysis under similar conditions.

POLAROGRAPHIC INVESTIGATIONS

The half-wave potentials of progesterone and androsta-1,4-diene-17β-ol-3-one in 75 % methanol—25 % water containing 0.5 M LiCl and 0.05 M buffer are listed in Table 1. The compounds showed only one wave when the solutions had been deaerated for half an hour. The slope of $E_{\frac{1}{2}}$ *vs* pH is near the value 0.059 required for reversible reactions [5].

The height of the wave varies only slightly with pH indicating that the same number of electrons participate in the electrode reaction in acid and alkaline solution. The reduction of an $\alpha,\beta,\alpha',\beta'$-unsaturated ketone must take place at the carbonyl group as the reduction of a double bond would yield an α,β-unsaturated ketone that would show a reduction wave.

The diffusion coefficients D are calculated from the diffusion currents by means of the Ilkovic equation [5]. As the product of D and the molecular weight M is the same for the two compounds it is likely that they use the same number of electrons in the electrode reaction.

The pH-values are measured with a glass electrode, but it was felt necessary to control the found values in the medium used by measuring the half-

wave potentials of anthraquinone-2-sulfonate in the same solutions. By assuming a linear connection between $E_{\frac{1}{2}}$ for anthraquinone-2-sulfonate and pH, the pH of the solution used was found as the abscissa-value corresponding to the measured $E_{\frac{1}{2}}$-ordinate. The two methods gave identical results from pH 1 to pH 11.

The polarographic results can be accounted for by the following assumptions. The potential determining step of the electrode reaction is reversible in the examined pH-interval. The number of electrons in the electrode reactions for α,β-unsaturated and $\alpha,\beta,\alpha',\beta'$-unsaturated steroid ketones is the same and probably one from pH 1 to 11. The similarity of the polarographic behaviour of an α,β- and an $\alpha,\beta,\alpha',\beta'$-unsaturated steroid ketone makes it likely that an α,β-unsaturated steroid ketone also is reduced at the carbonyl group. The polarographic behaviour of an α,β-unsaturated steroid ketone is thus different from that of the simple α,β-unsaturated ketones [6].

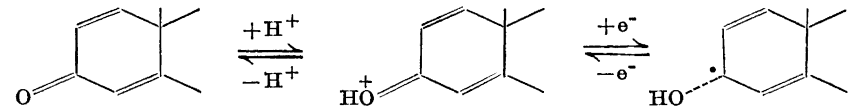
Table 1. **Half-wave potential (*vs.* saturated silver/silver chloride electrode) and diffusion current at different pH's for progesterone and androsta-1,4-diene-17β-ol-3-one. Drop time t measured at $E_{\frac{1}{2}}$.**

	Progesterone			Androstadieneolone		
Concentration	1.85×10^{-3} M			2.32×10^{-3} M		
D	7.0×10^{-6} cm²/sec			7.6×10^{-6} cm²/sec		
$D \times M$	2.18×10^{-3}			2.18×10^{-3}		
pH	$-E_{\frac{1}{2}}$ V	i_d μA	t sec	$-E_{\frac{1}{2}}$ V	i_d μA	t sec
1.05	1.01_3	5.00	3.08	0.87_5	6.60	3.15
4.00	1.18	4.95	3.05	1.06	6.60	3.14
5.08	1.24_7	4.94	3.00	1.11_3	6.45	3.11
9.80	1.56_3	4.75	2.70	1.41_2	6.25	2.84
10.16	1.58_3	4.75	2.62	1.42_5	6.25	2.83
11.0	1.67	4.70	2.43	1.48_5	6.20	2.73

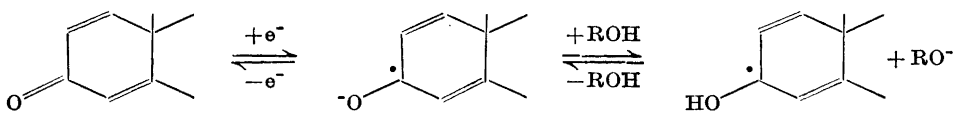
PREPARATIVE REDUCTIONS

The controlled potential electrolysis showed that α,β-unsaturated and $\alpha,\beta,\alpha',\beta'$-unsaturated steroid ketones yielded pinacols both in acid and alkaline solution and are thus different from the simple α,β-unsaturated ketones which dimerise at the β-carbon atom [6]. The reaction path of the reduction of an $\alpha,\beta,\alpha',\beta'$-unsaturated steroid ketone may be formulated as follows:

Acid solution:



Alkaline solution:



The radical formed dimerises slowly and irreversibly thus forming a pinacol. The products were proved to be pinacols by their ability to form the original ketones on oxidation with lead tetraacetate. The dimerisation takes place at carbon atom number 3 rather than at 1 or 5, as a dimerisation at one of the latter carbon atoms would be subject to severe steric hindrance.

The polarographic reduction is not the only reduction in which the α,β-unsaturated steroid ketones behave in another way than the simple unsaturated ketones. Windaus [7] found that cholestenone yielded a pinacol by reduction with sodium amalgam, and as he expected to get a saturated dimerised ketone from an α,β-unsaturated ketone he concluded that cholestenone was not an α,β-unsaturated ketone.

The reduction of a Δ^4-3-keto-steroid to a pinacol gives rise to the formation of two asymmetric carbon atoms and there is thus the possibility of formation of three compounds, one with both hydroxyl groups α, one with both hydroxyl groups β and one with one α and one β hydroxyl group.

An investigation of a model shows that in the compound where both hydroxyl groups are α the ring A will be in the 'half-chair' conformation and the bonding between the two dimerised radicals 'quasi-equatorial'. When the hydroxyl groups are β it is likely that the ring A adopts the 'half-boat' conformation and the hydroxyl groups are thus 'quasi-flagpole' and the carbon-carbon bond 'quasi-bowsprit'. In that case there will be free rotation of the carbon-carbon bond and the hydroxyl groups would then have the possibility of being *cis* which would facilitate the oxidation of the glycol with lead tetraacetate.

The relative amounts of the possible isomers depend among other things upon pH. Thus androsta-1,4-diene-17β-ol-3-one yields at pH 5 almost exclusively a pinacol with the rotation $[\alpha]_D^{23} = +277°$, whereas it in alkaline solution nearly quantitatively yields a pinacol with the rotation $[\alpha]_D^{23} = +8°$. The pinacol formed in acid solution dehydrates very easily by treatment with acid, whereas the one formed in alkaline solution requires more drastic conditions for the dehydration.

It is tempting to explain this by assuming that in acid solution it is the protonated ketone which is reduced, whereas the free ketone is reduced in alkaline solution. The most likely way for a steroid molecule to get the con-

jugated ketone system in contact with the cathode is by approaching the cathode with the methyl groups in the positions 10 and 13 pointing away from the electrode. In acid solution the positive protonated carbonyl oxygen would be attracted by the negative cathode, and the formed pinacol would thus have the hydroxyl group α. In alkaline solution the negative carbonyl oxygen would be repulsed from the cathode to the β configuration, where it also has the best chance of extracting a proton from a solvent molecule.

The proposed configurations are consistent with the difference found in the rate of dehydration. It has been shown [8] that divinyl carbinols very easily by an allylic rearrangement form a carbinol with the double bonds conjugated. According to Stork and White [9] there is a *cis* relation between the departing and the entering group in a S_N2' allylic rearrangement. A S_N1' mechanism must be rejected as it does not distinguish between the two isomers. The α-hydroxyl pinacol would thus yield a 5-α-carbinol, where the hydroxyl group is axial. As the 6-β-hydrogen is axial too, the 5-α-carbinol would dehydrate smoothly on treatment with acid. The β-hydroxyl pinacol would not have the same chance for dehydration as there is less tendency to form a 5-β-carbinol and no axial α-hydrogen in position 6 or 10.

It has furthermore been pointed out [10] that there is a difference in rotation from 200° to 300° between the α-hydroxy and the β-hydroxy isomer of unsaturated 3-hydroxy steroids as Δ^4-cholestenol ($\alpha-\beta = +297°$) and cholesta-4,7-dien-3-ol ($\alpha-\beta = +269°$). The difference in rotation between the proposed α-hydroxyl pinacol and the β-hydroxyl pinacol is $+269°$.

For the Δ^4-steroid ketones the difference in the composition of the mixture of pinacol isomers formed in acid and alkaline solution is not as pronounced as in the case of $\Delta^{1,4}$-steroid ketones. This is probably due to the fact that whereas in the latter the ring A is planar or nearly planar the former has the possibility of existing in a 'half-chair' or a 'half-boat' conformation. Etiocholane-3,17-dione exists partly with ring A in the boat form [11] and if it is assumed that the same is the case for the unsaturated 3-ketones, this explains the formation of a mixture of the pinacol isomers, as the reduction of the 'half-chair' and the 'half-boat' may result in the formation of different isomers. The isomer with the hydroxyl groups in the β-configuration probably has the ring A in the 'half-boat' conformation and it may, therefore, be impossible to deduce anything concerning the configuration from the rotations.

Like other 1,2-glycols the pinacols are quantitatively oxidized at room temperature by lead tetraacetate to carbonyl compounds the carbon-carbon bond being cleaved, thus forming the original α,β-unsaturated ketones. This reaction has been used to prove the reduction products to be 1,2-glycols.

The reduction of an α,β-unsaturated keto group to a pinacol and the subsequent oxidation of the pinacol to an α,β-unsaturated carbonyl group may be used to protect the more reactive conjugated carbonyl group, while the less reactive saturated keto group is brought to reaction with some other reagent, which does not attack the pinacol system. After the reactions the pinacol is oxidized with lead tetraacetate or periodic acid to the α,β-unsaturated carbonyl group.

The pinacols are slowly, but well crystallizing compounds which mostly are less soluble than the ketones from which they are formed. Sometimes a

pinacol crystallizes in two forms with different solubilities and it is not always easy to get the more soluble form to crystallize in the less soluble form [12]. The solubilities of the isomers are qualitatively the same but quantitatively there may be quite a difference. They are all soluble in tetrahydrofuran, soluble or recrystallizable from amyl acetate, toluene and ethyl alcohol and slightly soluble in water and hexane. The pinacols are stable in alkaline solution, whereas in acid solution they more or less rapidly lose water thus forming a compound with four (for the diene six) conjugated double bonds [13]. Dilute acetic acid affects the pinacols very slowly, whereas hydrochloric acid acts very quickly as dehydrating agent. Even the small amount of hydrochloric acid present in ordinary chloroform makes it impossible to use chloroform as a solvent for the pinacols for more than a short period. That is the reason why tetrahydrofuran has been used as solvent in the measurements of the rotation of the compounds. The pinacols themselves are also dehydrated at elevated temperatures, a fact which makes the melting point of minor importance as a physical constant of the compound.

EXPERIMENTAL

Apparatus. To the polarographic investigation were used a Sargent-Heyrovsky Model XII photographically recording polarograph and a recording polarograph Radiometer Type PO 3 a; the reported results are obtained with the latter. The capillary delivered 2.346 mg of mercury per second at an effective column height of 48 cm. The drop times reported were measured in the test solutions at the half-wave potential of the reducible compound.

All potentials are measured against a silver/silver chloride electrode in an aqueous saturated potassium chloride solution separated from the test solution with an agar plug and fritted glass diaphragm.

The potentiostat was a Lingane-Jones potentiostat [14]. For manual control a circuit adapted from Lingane [15] was used, in which the D.C. source was a 12 volts accumulator, the voltage adjuster a variable resistance (50 Ω) and the potential measuring device a "Polymeter" manufactured by Radiometer, Copenhagen, which had a resistance of 12×10^6 Ω.

The cell for the preparative reduction is adapted from Pasternak [6]. It consists of two conical 200 ml flasks which are connected through two fritted glass diaphragms 30 mm in diameter. In the cathode chamber is placed the mercury cathode (34 cm^2) which is connected through a platinum wire through the bottom of the flask to the outer circuit, the silver/silver chloride reference electrode, which has the fritted glass diaphragm just above the cathode, and a dropping mercury electrode. Further there are a stirrer (a uniform stirring is important) and an inlet for purified [16] nitrogen. Between the diaphragms agar containing potassium chloride or some other suitable salt is placed, and in the anode chamber is the platinum anode (15 cm^2). When the cell contains a 2 M salt solution the resistance is about 10 Ω.

Materials. The buffer solutions were made according to Ref.[17]. The materials were analytical grade. The steroids were recrystallized to constant properties.

Procedure. The controlled-potential electrolysis were performed in the following way. In the cathode chamber is placed 150 ml of the reaction medium (aqueous buffer solution and methanolic lithium chloride solution) and the anode chamber is filled with aqueous, alkaline sodium nitrite. The cathode chamber is deaerated with purified nitrogen [16] and reducible impurities are removed by electrolysis by keeping the cathode potential 0.3—0.4 volts more negative than the half-wave potential of the compound to be reduced. When the current has reached a stationary value, the reducible compound is added. By use of a potentiostat or by manual control the cathode potential is kept 0.1—0.2 volt more negative than the half-wave potential of the compound in the medium used. The current

drops from an initial value of 0.5—0.3 A to about 5 mA during 3—4 h. The reduction is followed polarographically with the dropping mercury electrode in the reaction medium whereby it is ensured that the reduction is undertaken at the right potential and the progress of the reduction can be followed. When the polarogram shows that the reduction is complete, the process is discontinued.

ISOLATION OF THE PINACOLS

The cathode chamber is emptied, the reaction medium is diluted with 200 ml water and made alkaline, if that does not affect the side chain of the steroid. The pinacols are extracted with a mixture of tetrahydrofuran and ether. After washing the organic layer with a bicarbonate solution and water, the solvents are evaporated at temperatures not exceeding 40°.

Androstenedione pinacol (1). 1.00 g of androstenedione was reduced at pH = 5 at —1.30 V. The pinacol residue was refluxed half an hour with 20 ml ethanol until a uniform suspension was obtained. After cooling for two days 690 mg (compound A) were filtered off, which after recrystallization from 25 ml toluene yielded 600 mg. $[\alpha]_D^{23} = +153° \pm 2°$ (tetrahydrofuran, $c = 0.438$, $a = 1.34°$, $l = 2$ dm). The compound dehydrates before melting. The dehydrated compound decomposes at about 305°. (Found: C 79.45; H 9.45. Calc. for $C_{38}H_{54}O_4$: C 79.47; H 9.47). The infra-red and ultra-violet spectrum and polarographic data show that no conjugated carbonyl group is present and the ability to form a semicarbazone and the infra-red spectrum show the presence of a keto group. The compound yields a yellow compound on treatment with acid and it yields quantitatively androstenedione by oxidation with lead tetraacetate in dry benzene at room temperature. From these pieces of evidence it is concluded that the compound A is one of the possible isomers of androstenedione pinacol.

The mother liquor was evaporated and the residue recrystallized from 3 ml ethanol. There was obtained 80 mg of compound A identified by its rotation and its ability to form androstenedione by oxidation with lead tetraacetate.

Androstenedione pinacol (2). 1.00 g of androstenedione was reduced at pH about 12.5 at —1.70 V. The pinacol residue was boiled with 20 ml 96 % ethanol until a uniform suspension was obtained. After cooling for two days 420 mg was filtered off, which after recrystallization from 15 ml toluene (360 mg) had a rotation of $[\alpha]_D^{23} = +152° \pm 2°$ (tetrahydrofuran, $c = 0.558$, $a = 1.70°$, $l = 2$ dm) (Found: C 79.43; H 9.40. Calc. for $C_{38}H_{54}O_4$: C 79.47; H 9.47). As all the chemical and physical data are indistinguishable from those of androstenedione pinacol A it was concluded that the isolated compound was the same isomer of androstenedione pinacol. The mother liquor was evaporated and the residue dissolved in benzene. On addition of hexane a component is obtained (410 mg) which after recrystallization from alcohol-water (340 mg) has a rotation of $[\alpha]_D^{23} = +174° \pm 2°$ (tetrahydrofuran, $c = 0.705$, $a = 2.45°$, $l = 2$ dm). The compound shrinks about 160° and dehydrates. The dehydrated compound decomposes at about 300°. (Found: C 79.45; H 9.48. Calc. for $C_{38}H_{54}O_4$: C 79.47; H 9.47). This compound had an infra-red spectrum very similar to that of compound A, and as it yielded androstenedione by oxidation with lead tetraacetate it was concluded, that this compound B was another isomer of androstenedione pinacol.

Progesterone pinacol (1). 1.00 g of progesterone was reduced at pH = 5 at —1.30 V. The pinacol residue was boiled with 20 ml ethanol until a uniform suspension was obtained. After cooling for two days 650 mg (compound PA) were filtered off. It was recrystallized from 20 ml acid-free amyl acetate. Rotation $[\alpha]_D^{23} = +162° \pm 2°$ (tetrahydrofuran, $c = 1.27$, $a = 4.10°$, $l = 2$ dm). The compound dehydrates before melting. The dehydrated product decomposes at about 290°. (Found: C 79.68; H 10.05. Calc. for $C_{42}H_{62}O_4$: C 79.94; H 9.91). The compound is soluble in tetrahydrofuran, less soluble in ethanol and benzene and insoluble in water and hexane. The infra-red spectrum shows the presence of an unconjugated carbonyl group and the absence of a conjugated ketone. This is confirmed by polarographic data and ability to form a semicarbazone. The compound PA yields a yellow compound on treatment with acid or heating to about 190°. It gives by oxidation with lead tetraacetate at room temperature in dry benzene quanti-

tatively progesterone. It is, therefore, concluded that the compound PA is one of the possible isomers of progesterone pinacol.

The mother liquor was evaporated and the residue dissolved in 4 ml ethanol. On standing was obtained 65 mg of a compound which was identified as compound PA by its rotation and ability to form progesterone by oxidation with lead tetraacetate.

Progesterone pinacol (2). 1.00 g of progesterone was reduced at pH 12.5 at −1.70 V. The pinacol residue was refluxed with 20 ml ethanol for half an hour. After cooling for two days a compound (560 mg) was filtered off. The rotation was not changed by recrystallization from amyl acetate. $[\alpha]_D^{23} = +163° \pm 2°$ (tetrahydrofuran, $c = 0.675$, $a = 2.20°$, $l = 2$ dm). M. p. (after dehydration) 285−290° (decomp.) (Found: C 79.80; H 9.79. Calc. for $C_{42}H_{62}O_4$: C 79.94; H 9.91). As all the physical and chemical data for the compound are indistinguishable from those of progesterone pinacol PA it was concluded that the isolated compound was the same isomer of progesterone pinacol.

The filtrate from compound PA was evaporated and the residue dissolved in hot benzene. On addition of hexane a compound is obtained (280 mg) which after recrystallization from ethanol-water yields 190 mg. $[\alpha]_D^{23} = +186° \pm 2°$ (tetrahydrofuran, $c = 0.536$, $a = 1.99°$, $l = 2$ dm). M. p. 165°. On further heating it dehydrates and solidifies at about 180° and the dehydrated compound decomposes at about 285°. (Found: C 79.43; H 9.84. Calc. for $C_{42}H_{62}O_4$: C 79.94; H 9.91). The compound has an infra-red spectrum very similar to that of compound PA and as it yielded progesterone by oxidation with lead tetraacetate it was concluded that the compound PB was an isomer of progesterone pinacol.

Androstadieneolone pinacol (1). 1.00 g of androsta-1,4-diene-17β-ol-3-one was reduced at pH=5 at −1.20 V. The pinacol residue was dissolved in benzene. On addition of hexane a compound is obtained (850 mg) with a rotation of $[\alpha]_D^{23} = +277° \pm 2°$ (tetrahydrofuran, $c = 0.542$, $a = 3.11°$, $l = 2$ dm). M. p. after dehydration 208−211° (decomp.). (Found: C 79.10; H 9.49. Calc. for $C_{38}H_{54}O_4$: C 79.47; H 9.47). The compound is very easily dehydrated under influence of acid, light or heat and yields a yellow compound. The infra-red spectrum shows absence of a carbonyl group. By oxidation with lead tetraacetate in dry benzene androstadieneolone is the main product, but a minor part of the compound is dehydrated by the acetic acid. All the data are consistent with the assumption that the isolated compound is one of the isomers of androstadieneolone pinacol.

The mother liquor was evaporated and evidence of a compound with lower rotation was found, but the compound was not isolated.

Androstadieneolone pinacol (2). 0.620 g of androstadieneolone was reduced at pH = 12.5 at −1.60 V. The pinacol residue was recrystallized from benzene yielding 510 mg of a compound with a rotation of $[\alpha]_D^{23} = +8° \pm 2°$ (tetrahydrofuran, $c = 0.683$, $a = 0.11°$, $l = 2$ dm). M. p. 180−182° (decomp.). (Found: C 79.63; H 9.30. Calc. for $C_{38}H_{54}O_4$: C 79.47; H 9.47). This compound is not dehydrated as easily as the above mentioned isomer of androstadieneolone pinacol, but can be dehydrated by heating to about 200° or by treatment with hydrochloric acid. It is quantitatively oxidized by lead tetraacetate at room temperature to androstadieneolone. It contains no carbonyl absorption in the infra-red spectrum. From the evidence it is concluded that the compound is a second isomer of androstadieneolone pinacol.

The mother liquor was evaporated and evidence of a compound with higher rotation was found, but the compound was not isolated.

Cholestenone pinacol. 1.00 g of cholestenone was reduced at pH = 5 at −1.30 V. The pinacol residue was refluxed with 25 ml ethanol for two hours. After cooling a compound (850 mg) was obtained, which after recrystallization from amyl acetate has a rotation of $[\alpha]_D^{23} = +92° \pm 2°$ (tetrahydrofuran, $c = 3.052$, $a = 5.65°$, $l = 2$ dm). Dolou *et al.*[13] report $[\alpha]_D^{23} = 85°$, but a recalculation of their data gives 92°. (Found: C 84.12; H 11.72. Calc. for $C_{54}H_{90}O_2$: C 84.08; H 11.77). The compound has physical and chemical data consistent with the data reported [12,13] for cholestenone pinacol. The compound yields quantitatively cholestenone by oxidation with lead tetraacetate.

Testosterone propionate pinacol. 1.00 g of testosterone propionate was reduced at pH = 5 at −1.30 V. The pinacol residue was recrystallized from ethanol giving 700 mg of a compound with a rotation of $[\alpha]_D^{23} = +76° \pm 2°$ (tetrahydrofuran, $c = 0.586$,

$a = 0.90°$, $l = 2$ dm). (Found: C 76.68; H 9.46. Calc. for $C_{44}H_{66}O_6$: C 76.46; H 9.63). The found data are consistent with the data reported [12] for testosterone propionate pinacol. It possesses no androgenic activity.

Part of this investigation was carried out at the Chemistry Department of Harvard University 1954—1955. The author wishes to express his thanks to Dr. L. F. Fieser and Dr. J. J. Lingane for their kind interest and for many facilities which have been put at his disposal.

REFERENCES

1. Eisenbrand, J. H. and Picher, H. *Hoppe-Seylers Z. Physiol. Chem.* **260** (1939) 83.
2. Wolfe, J. K., Hershberg, F. B. and Fieser, L. F. *J. Biol. Chem.* **136** (1940) 653.
3. Zuman, P., Tenygl, J. and Brezina, M. *Collection Czechslov. Chem. Communs.* **19** (1954) 46.
4. Kabasakalian, P. and McGlotten, J. *J. Am. Chem. Soc.* **78** (1956) 5032.
5. Kolthoff, I. M. and Lingane, J. J. *Polarography*, Interscience Publishers, New York, London 1952.
6. Pasternak, R. *Helv. Chim. Acta* **31** (1948) 753.
7. Windaus, A. *Ber.* **39** (1906) 518.
8. Heilbron, I. M., Jones, E. R. H., McCombie, J. T. and Weedon, B. C. L. *J. Chem. Soc.* **1945** 85.
9. Stork, G. and White, W. N. *J. Am. Chem. Soc.* **75** (1953) 4119.
10. Mills, J. A. *J. Chem. Soc.* **1952** 4976.
11. Nace, H. R. and Turner, R. B. *J. Am. Chem. Soc.* **75** (1953) 4063.
12. Butenandt, A. and Poschmann, L. *Ber.* **73** (1940) 893.
13. Dolou, R., Chopin, J. and Raoul, Y. *Bull. soc. chim.* **18** (1951) 646.
14. Lingane, J. J. and Jones, S. L. *Anal. Chem.* **22** (1950) 1169.
15. Lingane, J. J. *Electroanalytical Chemistry*, Interscience Publishers, New York, London 1953, p. 202.
16. Meites, L. and Meites, T. *Anal. Chem.* **20** (1948) 984.
17. *Pharmacopoea Danica* 1948 I, p. 222.

Received November 13, 1956.

ACTA CHEMICA SCANDINAVICA 11 (1957) 291—298

Insulin Crystals

III. Determination of the Rhombohedral Zinc-Insulin Unit-Cell by Combined Microscopical and Chemical Examinations

JØRGEN SCHLICHTKRULL

NOVO Terapeutisk Laboratorium, Copenhagen, Denmark

Cattle insulin is recrystallized by a method yielding perfectly shaped rhombohedral zinc-insulin crystals. During crystallization, samples are taken in which the process of crystallization is arrested by adding zinc ions.

The crystalline fractions in the samples are separated from non-crystalline insulin and determined quantitatively.

The volumes of insulin crystals in the stabilized suspensions as well as the size distributions are determined by a special microscopical counting procedure. Ordinary microscope equipment is used.

From the ratio between the volume of crystals and their content of nitrogen, the dimensions of the unit-cell are calculated to be $a = 50.7 \pm 0.7$ Å ($P = 0.95$). The volume of crystals containing 1 g of protein (water and salt-free) is calculated to be 1.35 ml. The possible causes of the significant difference between the estimate $a = 50.7$ Å and the X-ray estimate $a = 49.4$ Å are discussed.

Crowfoot and Riley [1] in 1939, by means of X-ray analyses, measured the dimensions of the unit-cell of wet zinc-insulin crystals lying in their mother-liquid. The length of the edge of the unit-cell rhombohedron is called a and the obtuse angle of the rhomb is α. They found that $a = 49.4$ Å (with 0.5 % accuracy) and $\alpha = 114° 16'$.

On a 1.3 mm large perfect zinc-insulin crystal the angle, α, has already been estimated by goniometric measurement [2] as $\alpha = 114° 22'$. The purpose of the present investigation is to determine the dimension a by a combined chemical and microscopical examination.

THE PRINCIPLE OF INVESTIGATION

It is assumed that the unit-cell contains 6 of the smallest molecular units, the structure of which was established by Sanger and coworkers [3]. Thus, the insulin content of the unit-cell is M = 34 400 and the nitrogen content is $6 \times 65 = 390$ atoms.

The number of unit-cells, n, present in the rhombohedral crystal is proportional to the volume and hence to the cubes of the edges, l_a (Å), *i. e.*

$$l_a^3 = n \cdot a^3.$$

Thus the nitrogen content, m_N, of a crystal is

$$m_N = \frac{n}{N} \times 390 \times 14.008 \text{ g, where } N = 6.02 \times 10^{23}.$$

Hence,

$$a = 2.086 \times 10^{-7} \left(\frac{l_a^3}{m_N}\right)^{\frac{1}{3}} \text{ Å}.$$

When a drop of an insulin crystal suspension is placed on a slide on the microscope stage, the crystals settle down on their faces. Therefore the greatest diagonal, l, in the crystal projection on the horizontal plane is used as a convenient measure of the crystal size. It follows that

$$l = l_a \times \sec \frac{\alpha}{2}$$

and

$$a = 1.130 \times 10^{-7} \left(\frac{l^3}{m_N}\right)^{\frac{1}{3}} \text{ Å}$$

Consider a suspension of insulin crystals containing c_N g/ml nitrogen belonging to the crystals. The cumulative distribution of crystal sizes, $P(l)$, *i. e.* the number of crystals per ml greater than l, is determined in a counting chamber using a calibrated eye-piece scale for measuring l. Using the volume of a rhombohedron with $l = 1$ Å as volume unit for the crystals, the volume, V, of crystals per ml of suspension is

$$V = \int_0^{l_{max}} p(l) l^3 \, dl$$

where

$$p(l) = -\frac{dP(l)}{dl}$$

thence,

$$a = 1.130 \times 10^{-7} \left(\frac{V}{c_N}\right)^{\frac{1}{3}} \text{ Å} \qquad (1)$$

When V and c_N are known, a can be calculated from eqn. (1). In the following the methods used for the determination of V and c_N are described.

METHODS

The perfect rhombohedral shape which is essential for the investigation is ensured by adding halogen ions to the medium of crystallization [2]. In order to get several estimates of a, samples are taken at different times during the crystallization. The crystallization process in the samples is immediately arrested

by diluting with a zinc salt solution. The crystals in the stabilized suspension are measured and counted, and the amount of nitrogen in the crystals is determined by Kjeldahl analyses on the isolated crystals.

Determination of V

About 0.1 ml of the stabilized suspension is drawn up into a narrow pipette and let out into the chamber (Fuchs-Rosenthal) which is 0.200 mm deep. (Verified by check-up). The 2 great squares (4 × 4 mm each) are both divided into 256 small squares each corresponding to c ml of the crystallization mixture, $c = 1.25 \times 10^{-6}$ ml. The crystals are measured and classified. Class limits $l_1 = 0$, l_2, l_3, *etc.* are devised, $l_i - l_{i-1} = 3-6$ μ. The inspection may begin in one corner and proceed as when reading a page. In A_i small squares, n_i crystals are found to be greater than l_i. A_i and n_i are counted simultaneously. The areas inspected within the large squares are not chosen at random as this process is very time consuming. As no significant differences have been observed when changing the system of inspection, it is believed that systematic errors are unimportant. About 30 crystals are counted per class limit, but not more than one large square is generally inspected per class. When the area is insufficient, the chamber is refilled. Two determinations of V are made for each suspension.

The number of crystals per square unit, n_i', belonging to the class $l_i < l < l_{i+1}$ is

$$n_i' = \frac{n_i}{A_i} - \frac{n_{i+1}}{A_{i+1}}$$

The volume V_i of these crystals is calculated from the assumption that $p(l_i)$ is constant in the intervals.

It follows that

$$V_i = \int_{l_i}^{l_{i+1}} p(l) l^3 \, dl = p(l) \, (l_{i+1} - l_i) \, \frac{l^4_{i+1} - l_i^4}{4(l_{i+1} - l_i)} \qquad (2)$$

Since

$$p(l) \, (l_{i+1} - l_i) = n_i'/c$$

then, estimates of V_i may be obtained from

$$V_i = f_i \, n_i'; \; f_i = \frac{m_i^3 + m_i d_i^2}{8c} \qquad (3)$$

where

$$m_i = l_{i+1} + l_i; \; d_i = l_{i+1} - l_i.$$

The distribution of particles according to weight may be obtained from eqn. (3). The volume per ml of all the crystals is then obtained by summation of V_i,

$$V = \sum_{i=1}^{i=i_{max}} V_i$$

The limit i_{max} is the smallest limit above which no crystals are found.

Error: As $p(l)$ is not strictly constant within the classes, a systematical error is introduced by eqn. (2). The error is estimated from an examination of the size distributions. It can be shown that

$$P(l) = c_1 \cdot \exp.\ (-\ c_2 l);\ c_1,\ c_2 > 0;\ l_i < l < l_{i+1}$$

or

$$p(l) = c_1 \cdot c_2 \cdot \exp.\ (-\ c_2 l).$$

This relation is observed when the logarithms of the numbers in column (4) are plotted against the class limits (1) in Table 1. Deviations which are insignificant in this connection occur in the outer regions of the distributions [5].

Hence, the actual volume of crystals within the size interval $(l_i,\ l_{i+1})$ is

$$V_i = c_1 \cdot c_2 \int_{l_i}^{l_{i+1}} l^3 \exp.\ (-c_2 l)\mathrm{d}l = c_1\ [\mathrm{F}(l_i) - \mathrm{F}(l_{i+1})] \qquad (4)$$

where

$$\mathrm{F}(l) = (l^3 + 3l^2 c_2^{-1} + 6l c_2^{-2} + 6c_2^{-3}) \exp.\ (-c_2 l)$$

Table 1. Determination of crystal volume (V) by the counting procedure.

i:	(1)	(2)	(3)	(4)	(5)	(6)	(7)	(8)
1	0.0	53	2	27	12	0.003	0.0	0.0
2	2.5	30	2	15	0	0.046	0.0	0.0
3	5.0	30	2	15	2	0.203	0.4	0.0
4	7.5	26	2	13	3	0.547	1.6	2.2
5	10.0	31	3	10	0	1.15	0.0	5.6
6	12.5	29	3	10	2.5	2.10	5.3	18.6
7	15.0	30	4	7.5	4.1	3.45	14.1	30.6
8	17.5	37	11	3.4	0.7	5.30	3.7	12.2
9	20.0	32	12	2.7	0.4	7.70	3.1	19.5
10	22.5	27	12	2.3	1.41	10.7	15.1	32.7
11	25.0	25	28	0.89	0.22	14.4	3.2	10.3
12	27.4	32	48	0.67	0.38	20.3	7.7	8.6
13	31.3	28	96	0.29	0.12	29.5	3.5	3.9
14	35.3	27	160	0.17	0.10	41.4	4.1	2.7
15	39.2	27	384	0.070	0.035	57	2.0	0.8
16	43.6	9	256	0.035	0.023	81	1.9	1.4
17	49.4	3	256	0.012	0.012	116	1.4	0.9
18	55.6	0	256	0.000	0.000	162	0.0	0.0
						Total:	67	150

(1) $10^{-4} \cdot l_i$ (l_i in Å)
(2) n_i (number of crystals greater than l_i)
(3) A_i (number of squares in which n_i are counted)
(4) n_i/A_i
(5) $n_i' = n_i/A_i - n_{i+1} / A_{i+1}$
(6) $10^{-21} \times f_i$; $f_i = (m_i^3 + m_i d_i^2) / 8c$; $c = 1.25 \times 10^{-6}$ ml
(7) $10^{-21} \times f_i n_i'$
(8) $10^{-42} \times n_i\ (f_i^2 + f_{i-1}^2) / A_i^2$

$V = 67 \times 10^{21}$; $\sigma_V^2 = 150 \times 10^{42}$

The volume calculated from eqn. (3) is

$$V_i = \frac{m_i^3 + m_i d_i^2}{8c} [P(l_i) - P(l_{i+1})] \cdot c$$

or

$$V_i = \frac{m_i^3 + m_i d_i^2}{8} \cdot c_1 [\text{exp. } (-c_2 l_i) - \text{exp. } (-c_2 l_{i+1})]$$

Hence, the ratio between this volume and that from eqn. (4) is

$$r = \frac{[\text{exp. } (-c_2 l_i) - \text{exp. } (-c_2 l_{i+1})] (m_i^3 + m_i d_i^2)}{8 [F(l_i) - F(l_{i+1})]} \quad (5)$$

It is found that $r = 1.00—1.02$ so that this error can be neglected.

The variance of V is the sum of the variances of V_i.

$$\sigma_V^2 = \sum_{i=1}^{i=i_{max}} \sigma_{V_i}^2$$

where

$$\sigma_{V_i}^2 = f_i^2 \sigma_{n_i'}^2$$

The error of A_i is considered negligible, then

$$\sigma_{n_i'}^2 \approx \frac{\sigma_{n_i}^2}{A_i^2} + \frac{\sigma_{n_{i+1}}^2}{A_{i+1}^2}$$

If it is further assumed that the crystals are classified without error and that they are distributed in the chamber according to the Poisson distribution, it follows that

$$\sigma_{n_i}^2 \approx n_i$$

and

$$\sigma_V^2 \approx \sum_{i=1}^{i=i_{max}} n_i \cdot \frac{f_{i-1}^2 + f_i^2}{A_i^2}, \quad (f_0 = 0) \quad (6)$$

In order to keep σ_V^2 within reasonable limits, the terms in the last equation must not be allowed to increase too much with l_i. Aiming at constant terms it follows from eqn. (6) that the area of inspection shall be

$$A_i = \text{const.} \cdot P(l_i) \cdot l_i^6$$

The specific feature of this counting method is that both the particles and the squares are counted; the latter increase with the particle size.

Determination of c_N

The isolation of insulin crystals from the stabilized suspensions is achieved by extracting the amorphous particles.

Solvent:
8.15 g CH_3COONa, $3H_2O$
42.0 g NaCl
150 ml acetone
+ water to make 500 ml.

15 ml of the stabilized suspension are centrifuged and the supernatant liquid is discarded. The precipitate is resuspended in 5 ml of distilled water, 10 ml of the solvent are added and mixed with the suspension. The suspension is centrifuged and the supernatant liquid containing the dissolved amorphous fraction is discarded. The crystals are suspended in 10 ml of 60 % (v/v) acetone, centrifuged and the acetone is discarded. The nitrogen content of the remaining crystals is determined by semi-micro Kjeldahl analysis. The result is expressed in g of nitrogen per ml of the original crystallization medium. The test has been included in the British Pharmacopoeia [6].

Error: Mixed suspensions containing amorphous and crystalline insulin in different proportions have been analyzed. The results of analyses were in agreement with the values of c_N predicted from analyses of the original suspensions used for the mixing. A small systematical error is caused by the fact that a part of the amorphous particles is denatured and heavily soluble, which causes overestimation of the crystal fraction. This error which amounts to 2—3 % of the total insulin-nitrogen, is corrected by making analyses of the crystallization mixture before crystals are formed.

The standard deviation of a single determination has been estimated from double analyses as 1.0×10^{-5} g N/ml.

EXPERIMENTAL

Composition of crystallization mixture: 2.42 mg/ml insulin-nitrogen (equiv. to 1.7 % insulin)
155 µg/ml Zn++, as chloride (including the Zn++ from the insulin)
7 % NaCl
0.1 M CH_3COONa
+ HCl to pH = 5.45—5.55.

Solutions: (I). 68 g recrystallized insulin from beef pancreas, containing 9.68 g insulin-nitrogen were dissolved in water containing 80 ml 1 N HCl and so much $ZnCl_2$ that the final solution contained a total of 0.62 g Zn++. The solution was sterilized by filtering through an asbestos filter previously rinsed with diluted HCl. The filtered solution was diluted with water to 3 000 ml.

(II). 54.4 g CH_3COONa, $3H_2O$ + 280 g NaCl + 44 ml 1 N NaOH + water to make 1 000 ml.

The crystallization: The solutions (I) and (II) were poured simultaneously into an 8-litre glass beaker placed in a water thermostat at 25° C. The beaker was covered with a glass lid. Slow, continuous stirring was provided with a glass propeller through a hole in the lid.

Initially about 95 % of the insulin was precipitated as amorphous particles. During the first 30 min between one fourth and one third of the amorphous insulin was dissolved but only a few crystals were formed. After a further 30 min the crystallization became

rapid, but soon slowed down again and was practically finished within 12 h. At that time approximately 92 % of the insulin was crystalline, 3 % was still in solution and the rest was in the amorphous state.

The stabilized samples: The process of crystallization was arrested by combining the insulin with zinc ions at neutral reaction [4]. A 10 ml sample was added to 90 ml of a neutral solution of zinc chloride containing 7.2 mg Zn^{++}, 100 mg methyl-*p*-hydroxybenzoate and 2.75 ml 0.1 N NaOH. The total volume was adjusted to 100 ml. The insulin thereby immediately combined with some of the zinc ions. The crystals and the amorphous particles were not visibly altered, whereas the dissolved insulin from the samples was precipitated as stable amorphous particles.

RESULTS

Two crystallizations were made and analyzed with an interval of 19 months. Fourteen samples were taken during the first crystallization and seventeen in the second experiment. Each sample was subjected to counts twice. The results of the 62 countings are too numerous to be compiled in a table, but for the purpose of illustration the result from one of them is presented in Table 1. The volume V is estimated from this counting to be 67×10^{21}. The systematical error is calculated by means of eqn. (5) using $c_2 = 0.18$. When $l_i = 50$ and $l_{i+1} = 55$, it is found that $r = 1.021$ and likewise for $l_i = 22$, $l_{i+1} = 25$, $r = 1.017$. This error is considered insignificant. The standard deviation of the V estimate is calculated by means of eqn. (6) and found to be 12×10^{21}.

Table 2 contains all the condensed data. The two rectangular parts correspond to the two crystallizations and each row represents a sample. As crystallization proceeds, both V and c_N increase, while a remains constant except for casual variations. The systematical error of V has been calculated for the samples in Table 2. In the first crystallization it is found to be 2 % or less and in the second where $c_2 = 0.07$ it is less than 1 %. Hence, this error is neglected. The standard deviation of the V estimate from a counting has been calculated from eqn. (6) to be 12×10^{21} (Table 1). As two countings are made on each of the samples it is also possible to calculate s_V from the double determinations. However, as V increases, s_V increases also as seen from the ranges in column (3), but in spite of this a pooled estimate of the standard deviation has been calculated in the usual way. It is found that $s_V = 13 \times 10^{21}$, with 14 and 17 d.f. from each of the two experiments, in close agreement with the result, 12×10^{21}, from Table 1.

The standard deviation of a is calculated from the variation of a between the 14 resp. 17 samples taken during each of the two crystallizations.

The estimates of a from I and II are pooled as their difference is insignificant. $a = 50.7$ Å with confidence limits $\pm$ 0.7 Å (P = 0.95). The volume of the unit-cell is calculated from the values $a = 50.7$ Å and $\alpha = 114° 22'$ using the formula

$$\text{Volume} = 2 \cdot \sin^2\left(\frac{\alpha}{2}\right) \cdot \sqrt{1 + 2\cos\alpha} \cdot a^3$$

The volume is $0.591 \times 50.7^3 = 7.70 \times 10^4$ Å^3. The weight of insulin within the unit-cell is $6 \times 5\,734 / 6{,}02 \times 10^{23} = 5.71 \times 10^{-20}$ g. Hence the volume of crystals containing 1 g of insulin is 1.35 ml.

Table 2. Results of analyses of two crystallizations.

I. (March 1954)						II. (November 1955)					
(1)	(2)	(3)	(4)	(5)	(6)	(1)	(2)	(3)	(4)	(5)	(6)
27	35	8	31	37	49.5	21	16	5	10	23	49.3
67	66	1	66	70	51.4	33	34	1	34	35	52.0
78	78	0	78	85	51.0	25	45	10	35	49	46.9
95	96	1	96	97	52.3	48	45	3	47	64	47.3
111	86	25	99	114	50.1	83	74	9	79	81	52.0
152	145	7	149	149	52.4	71	74	3	73	97	47.7
156	141	15	148	175	49.6	101	86	5	94	108	50.1
167	227	60	197	189	53.2	99	118	19	109	121	50.6
187	149	38	168	197	49.7	104	115	11	110	142	48.1
204	189	15	197	202	52.0	179	130	49	155	147	53.3
188	215	27	202	204	52.3	165	162	3	164	165	52.3
184	178	6	181	209	49.9	164	178	13	171	172	52.3
197	183	14	190	214	50.4	179	190	11	185	190	52.0
167	151	16	159	216	47.3	179	175	4	177	220	48.8
						239	239	0	239	221	53.8
						221	208	13	215	227	51.5
						242	203	39	223	226	52.2

(1) $10^{-21} \times V$ from first counting;
(2) $10^{-21} \times V$ from a second counting;
(3) The range between (1) and (2);
(4) The average of (1) and (2);
(5) $10^5 \times c_N$;
(6) $a = 1.130 \times 10^{-7}\left(\frac{V}{c_N}\right)^{\frac{1}{3}}$ Å.

I. $s_V = 13 \times 10^{21}$ with 14 d.f. II. $s_V = 13 \times 10^{21}$ with 17 d.f.
$a = 50.8 \pm 0.4$ Å (S.E.) $a = 50.6 \pm 0.5$ Å (S.E.)
$a_{I,II} = 50.7 \pm 0.7$ Å (confidence limits, P = 0.95)

DISCUSSION

The estimate $a = 50.7$ Å differs significantly from the X-ray value $a = 49.4$ Å and it may be due to an overestimate of V by 8 %. In that case a systematical error is present in the counting method, but this possibility cannot be verified from the present data. However, the crystals examined by X-ray were lying in their mother-liquid of crystallization while in the present investigation the crystals were actually insulin-zinc crystals containing approximately 2.3 % zinc calculated on dry weight [4]. It appears possible that the stabilization with zinc causes the lattice to expand, just as drying causes it to shrink. Thus experimental conditions may be responsible for the difference observed in a.

REFERENCES

1. Crowfoot, D. and Riley, D. *Nature* **144** (1939) 1011.
2. Schlichtkrull, J. *Acta Chem. Scand.* **10** (1956) 1459.
3. Brown, H., Sanger, F. and Kitai, R. *Biochem. J. London* **60** (1955) 556.
4. Hallas-Møller, K., Petersen, K. and Schlichtkrull, J. *Science* **116** (1952) 394.
5. Schlichtkrull, J. *Acta Chem. Scand.* **11** (1957) *In press.*
6. *Addendum 1955 to the British Pharmacopoeia 1953*, p. 39.

Received October 24, 1956.

ACTA CHEMICA SCANDINAVICA 11 (1957) 299—302

Insulin Crystals

IV. The Preparation of Nuclei, Seeds and Monodisperse Insulin Crystal Suspensions

JØRGEN SCHLICHTKRULL

Novo Terapeutisk Laboratorium, Copenhagen, Denmark

Nuclei were formed by freeze-drying a crystallization mixture containing dissolved insulin. The freeze-dried insulin was suspended in a buffered insulin solution whereupon the nuclei grew up to 1—2 μ crystals which were used as seeds for the preparation of monodisperse insulin crystal suspensions with different crystal sizes (5, 25 and 40 μ)

It is the purpose of the present investigation to demonstrate the effect of seeding with a large number of small seed crystals on insulin crystallization.

The size of a rhombohedral insulin crystal has been defined [1] as the greatest diagonal in the projection of the crystal on a plane through a face. An amount of seed-crystals weighing w_s g contains n seeds of almost uniform size, l_s μ. Hence,

$$w_s = knl_s^3$$

where k is a constant. The total weight of insulin gained as crystals after seeding is w_i. Assuming that the crystals grow with identical rates of linear growth, it follows that

$$\alpha w_i = knl^3$$

where (1—α) is the fraction of spontaneously formed crystals, and l is the size of the grown up seeds. Hence,

$$l = l_s \sqrt[3]{\frac{\alpha}{r}} \tag{1}$$

or

$$\alpha = r\left(\frac{l}{l_s}\right)^3 \tag{2}$$

where r is the ratio w_s/w_i between weight of seeds and total insulin gained as crystals. The fraction, α, of uniform crystals depends on the conditions of crystallization as well as on l_s and r. When the conditions and the size of seeds are fixed, a decrease in r causes α to decrease.

When seeding is employed immediately after mixing the components for crystallization, it follows from the assumption and eqn. (1) that the upper limit of crystal size is

$$l_u = l_s \sqrt[3]{\frac{1}{r}}$$

PREPARATION OF SEED-CRYSTALS

Solutions: (1). 5 g beef insulin, recrystallized from a citrate buffer [2] + 42.5 ml 0.1 N HCl + water to make 500 ml; (2). 500 mg citric acid + 20 mg Zn^{++} (as chloride) + 800 mg methyl-*p*-hydroxybenzoate + 11.2 ml 1 N NaOH + water to make 500 ml.

Freeze-drying: To 100 ml of sol. (1) were added 100 ml (2) and 1 N NaOH to pH = 6.7. The solution was frozen at once and freeze-dried.

Crystallization: The freeze-dried insulin was suspended in 400 ml of the alkaline (pH 8.5) solution (2) and immediately thereafter 400 ml of sol. (1) were added. The mixture (pH = 6.2—6.5) was shaken over night at room temperature. The crystals which developed were 1 μ large.

CRYSTALLIZATION WITH AND WITHOUT SEEDS

The first experiment is a comparison between crystallizations with and without seeding.

The crystallization mixture had the following composition [3]:

1.7 % beef insulin, 155 μg/ml Zn^{++} (as chloride, including the zinc from the insulin), 7 % NaCl, 0.1 M CH_3COONa + HCl to pH = 5.45 to 5.55.

One ml of the 1 μ-seed crystal suspension containing 6 mg insulin was diluted with water to 20 ml and added to 4 litres of crystallization mixture containing 68 g insulin. The final distribution of crystal sizes was determined by the technique described earlier [1]. The cumulative distribution of insulin units was calculated and presented in a graph, Fig. 1, in which can be seen that 90 % of the weight was concentrated in the size range 20—30 μ.

In the control, which was not seeded, 90 % of the insulin was found in the much greater interval 25—100 μ. It is concluded that seed crystals grow with identical rates of linear growth in accordance with the assumption for eqn. (1).

VARIATION OF THE AMOUNT OF SEED-CRYSTALS

The dependence of α on r is illustrated by an experiment in which the conditions of crystallization remain as in the previous experiment while r is varied. The size of seeds was 2—3 μ. The resulting cumulative distributions of units (or weight) on crystal size are shown in Fig. 2. The median size is taken as

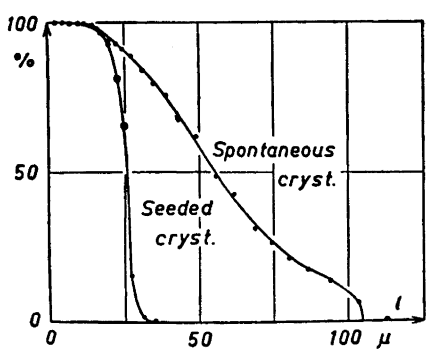


Fig. 1. Cumulative distribution of insulin units.

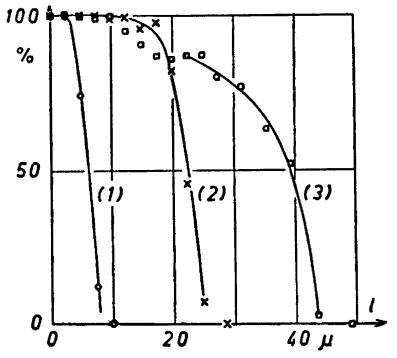


Fig. 2. Cumulative distribution of insulin units. The suspensions were prepared with different amounts of seeds (see Table 1).

representative of l, the size of grown up seeds. The results from 3 crystallizations are presented in Table 1. It is assumed that spontaneous crystallization is negligible ($\alpha = 1$) in the first case where r is relatively large. Hence, by inserting l_{50}, r and $\alpha = 1$ in eqn. (1) it is calculated that $l_s = 3.0\ \mu$. When eqn. (2) is employed in case 2 and case 3, α is found to be 0.9 and 0.7, respectively. These values of α are confirmed by Fig. 2 as they are found to be the ordinates corresponding to deflections of the curves. These points presumably divide the distributions in the two parts containing, respectively, spontaneously formed crystals and grown up seeds.

Table 1. Variation of the amount of seed-crystals.

No.	r	l_{50}	$\alpha = r\left(\frac{l}{3}\right)^3$
(1)	12×10^{-2}	6 μ	1.0
(2)	21×10^{-4}	23 μ	0.9
(3)	30×10^{-5}	39 μ	0.7

Legend: r, The ratio between weight of seed-insulin and total insulin.
l_{50}, The median size in the distribution of insulin units.
α, The weight of spontaneously formed crystals is $(1-\alpha)w_i$, where w_i is the total weight of insulin gained as crystals.

DISCUSSION

The freeze-drying method originated from the incidental observation that crystallization yielded smaller crystals when using glass apparatus which had not been cleansed after a previous crystallization process. The small amounts of dried-in insulin on the propeller rod and in the beaker were apparently responsible. The number of crystals was further increased hundredfold when freeze-dried insulin was added.

When suspended in the alkaline (pH = 8.5) solution (2), the freeze-dried insulin is partially dissolved. The pH may even be increased to 11 (glass-electrode). In this case the insulin disappears into solution, apart from a great number of particles which are visible in the dark field microscope. The seeding properties of the colloidal solution vanish within one hour together with the small particles.

The faces of the seed-crystals do not grow with equal growth rate upon seeding. Thus the seed-bodies from 3—5 μ seeds are finally found in the obtuse vertices of the crystals. Smaller seeds are barely or not at all visible in the final crystal suspension.

REFERENCES

1. Schlichtkrull, J. *Acta Chem. Scand.* **11** (1957) 291.
2. Schlichtkrull, J. *Acta Chem. Scand.* **10** (1956) 1455.
3. Schlichtkrull, J. *Acta Chem. Scand.* **10** (1956) 1459.

Received October 24, 1956.

ACTA CHEMICA SCANDINAVICA 11 (1957) 303—314

Die Verteilung von Äthylalkohol und Wasser bei Ionenaustauschern auf Harzbasis

HEINZ RÜCKERT und OLOF SAMUELSON

Institut für Technische Chemie, Chalmers Technische Hochschule, Göteborg, Schweden

Die Verteilung von Äthylalkohol und Wasser wurde für Kationenaustauscher und Anionenaustauscher in verschiedenen Ionenformen bestimmt. Die Alkoholkonzentration der Harzphase ist im allgemeinen kleiner als in der Aussenlösung (Aussalzen). Je höher die Ionenkonzentration der Austauscherphase ist (kleine Quellung), umso mehr wird der Alkohol ausgesalzt. Unter gewissen Umständen kann man aber auch ein Einsalzen erhalten. Die Quellung der Austauscher nimmt, je nach Beladungszustand und Vernetzungsgrad, entweder mit steigender Alkoholkonzentration kontinuierlich ab oder durchläuft ein Maximum.

Es ist bekannt, dass sich organische Moleküle in wässeriger Lösung ungleichmässig zwischen einem Ionenaustauscher und der ihn umgebenden Lösung (Aussenlösung) verteilen. Das System Äthylalkohol-Wasser ist früher von Gregor und Mitarbeitern [1] untersucht worden und diese Untersuchungen zeigten, dass der Alkoholgehalt der Harzphase (Innenlösung) niedriger ist als in der Aussenlösung.

In einer früheren Arbeit [2] wurde gezeigt, dass Ionenaustauscher zur Adsorption von Zuckerarten aus Mischungen von Wasser und Alkohol verwendet werden können und dass diese Adsorption von der Art der Gegenionen stark abhängig ist. Um die Grundlagen einer Diskussion über die Zuckeradsorption zu schaffen, wird in der vorliegenden Arbeit über die Verteilung von Wasser und Äthylalkohol berichtet und zwar für Austauscher in denselben Ionenformen, wie sie bei den Zuckeruntersuchungen verwendet wurden.

EXPERIMENTELLER TEIL

Prinzip der Versuche. Um die Verteilung von Alkohol und Wasser zwischen den beiden Phasen zu studieren, wird eine bestimmte Austauschermenge mit einer Alkohol-Wasserlösung bis zur Erreichung des Gleichgewichtes geschüttelt. Die Zusammensetzung der Innenlösung kann auf zwei verschiedene Arten bestimmt werden. Entweder berechnet man aus der Konzentrationsänderung der Aussenlösung die Zusammensetzung der Innenlösung, oder jede Phase wird für sich analysiert. Die erste Methode führt schneller zum

Resultat, jedoch auf Kosten der Genauigkeit und bei sehr kleinen Konzentrationsänderungen ist diese Methode unbrauchbar. Daher wurde bei allen Versuchen sowohl die Innenlösung als auch die Aussenlösung auf ihre Zusammensetzung analysiert. Die beiden Phasen wurden durch Abzentrifugieren der Aussenlösung von einander getrennt. Diese Methode ist für wässerige Lösungen von Gregor [3] und Pepper [4] eingehend studiert worden. Durch das Zentrifugieren erhielt man das feuchte Gewicht des Austauschers. Das Gewicht der Innenlösung konnte somit durch Subtrahieren des Trockengewichtes ermittelt werden. Um die Zusammensetzung der Innenlösung festzustellen, wurde diese entweder mit Wasser oder Methylalkohol verdrängt. Der Wassergehalt wurde im allgemeinen aus der Differenz zwischen dem Gewicht der Innenlösung und dem titrimetrisch bestimmten Gewicht des Alkohols berechnet. Bei Alkoholgehalten von über 50 Mol % liess sich die Zusammensetzung der Innenlösung genauer durch Bestimmung des Wassergehaltes ermitteln. Für den Kationenaustauscher ergaben beide Methoden übereinstimmende Werte. Beim Anionenaustauscher hingegen erhielt man mit der Wasserbestimmungsmethode stets einen höheren Alkoholgehalt in der Innenlösung als bei jenen Versuchen, wo der Alkohol direkt bestimmt wurde. In den Tabellen ist das arithmetische Mittel von den nach beiden Methoden bestimmten Werten angegeben.

Die verwendeten Ionenaustauscher. Als Ionenaustauscher dienten der Kationenaustauscher Dowex 50 und der Anionenaustauscher Dowex 2. Aus den handelsüblichen Produkten wurde im lufttrockenen Zustand eine Fraktion von 0,2—0,4 mm Korndurchmesser herausgesiebt. Für die Untersuchungen mit schwach vernetzten Austauschern (1 % Divinylbenzen) wurden die vom Hersteller mit 0,15—0,30 mm Korndurchmesser gelieferten Austauscher Dowex 50 X1 und Dowex 2 X1 ohne weiteres Sieben verwendet. Alle Austauscher wurden in der üblichen Weise konditioniert [5] und in die entsprechenden Ionenformen übergeführt, an der Luft bei Zimmertemperatur getrocknet, und in diesem Zustand in dicht verschlossenen Gefässen verwahrt. Die Feuchtigkeit wurde durch Trocknen im Vakuum über Magnesiumperchlorat bei 50—60° C ermittelt. Konstantes Gewicht stellte sich nach drei bis vier Tagen ein. Die Kapazität der Austauscher wurde auf folgende Weise bestimmt. 1 g des Austauschers wurde in Wasser gequollen und in eine Austauschersäule von etwa 4 ml gefüllt. Durch 50 ml 3 M Salzsäure (für ClO_4^- - Anionenaustauscher 100 ml) wurde der Austauscher in die H^+- bzw. Cl^--Form übergeführt. Nach Auswaschen mit entionisiertem Wasser wurden die Wasserstoffionen des Kationenaustauschers mit 25 ml 1 M Natriumchloridlösung aus der Säule verdrängt und das Eluat mit 0,1 N Natronlauge titriert. Der in die Chloridform übergeführte Anionenaustauscher wurde mittels 3 M Natronlauge mit Hydroxylionen beladen und die letzteren nach Auswaschen mit entionisiertem Wasser mit einem Überschuss an 0,1 N Salzsäure aus der Säule verdrängt. Der Säureüberschuss im Eluat wurde dann mit 0,1 N Natronlauge zurücktitriert. In Tabelle 1 sind die gefundenen Werte für die Kapazität zusammengestellt, ausgedrückt in Milliäq. pro g Trockensubstanz in der entsprechenden Ionenform.

Tabelle 1. Kapazität der verwendeten Ionenaustauscher.

Austauscherharz	Kapazität Milliäq. / g Trockensubstanz
Dowex 50 Li^+	4,91
Na^+	4,50
K^+	4,34
Dowex 50 X1 Li^+	5,00
K^+	4,41
Dowex 2 ClO_4^-	2,27
Cl^-	2,71
SO_4^{2-}	2,60
Dowex 2 X1 ClO_4^-	3,03
SO_4^{2-}	3,58

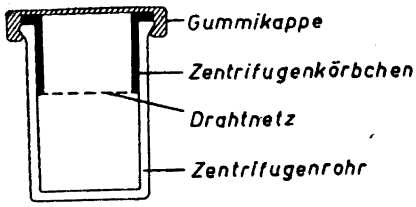


Abb. 1. Zentrifugenkörbchen im Zentrifugenrohr.

Einstellung des Gleichgewichtes. Etwa 1 g des an der Luft getrockneten Austauscherharzes samt 40 ml der alkoholischen Lösung wurden in ein 50 ml Reagenzglas eingeführt. Das Reagenzglas wurde dann mit einem Glasstopfen verschlossen und an einer sich langsam drehenden Scheibe befestigt. Ein Luftthermostat sorgte für die Konstanthaltung der Temperatur auf 25 ± 0,1° C. Alle Verteilungsversuche liefen mindestens 3 Tage. Innerhalb dieser Zeit stellte sich für alle Alkoholkonzentrationen das Gleichgewicht ein.

Die Abtrennung des Austauschers. Nach Einstellung des Gleichgewichts wurde das Reagenzglas von der Scheibe abgenommen und das Austauscherharz durch ein siebartiges Zentrifugenkörbchen aus rostfreiem Stahl (Abb. 1) von der Aussenlösung abfiltriert. Das Zentrifugenkörbchen befand sich dabei in einem kleinen Trichter, durch den die Aussenlösung in einen verschliessbaren Messkolben rann. Die Entleerung des Reagenzglases geschah mit einer besonderen Vorrichtung, um Konzentrationsänderungen wegen der Hygroskopizität bzw. Flüchtigkeit des Alkohols möglichst zu vermeiden. Das eine Ansatzrohr eines grossen Einweghahnes war mit einem Normalschliff versehen, sodass der Hahn anstelle des Glasstopfens auf das Reagenzglas aufgesetzt werden konnte. Der Innendurchmesser der Ansatzrohre betrug 1 cm. Das Reagenzglas mit aufgesetztem Hahn wurde nun umgedreht und senkrecht mit dem freien Ansatzrohr in das Zentrifugenkörbchen hineingehalten und der Hahn geöffnet. Auf diese Weise konnte der Austauscher in kürzester Zeit und beinahe quantitativ im Zentrifugenkörbchen aufgesammelt werden.

Als nächstes wurde die am Austauscher haftende Aussenlösung bei einer Umdrehungszahl entsprechend 600 g während 40 Min. abzentrifugiert. Abb. 1 zeigt das Körbchen im Zentrifugenrohr. Eine dichtschliessende Gummikappe verhinderte das Verdunsten des Alkohols. Um das Erwärmen der Zentrifuge zu vermeiden, blieb der Deckel während des Zentrifugierens offen. Die Temperaturerhöhung betrug dadurch nur 1° C. Nach dem Zentrifugieren wurde das Körbchen zum Wiegen in ein Wägeglas mit eingeschliffenem Stopfen gestellt. Der vom Austauscher verdunstende Alkohol kondensierte an den Glaswänden des Wägeglases und konnte nachher abgespült werden und ging somit der Analyse nicht verloren.

Die Reproduzierbarkeit der erhaltenen Werte für das Gewicht der Austauscherphase war zufriedenstellend. Bei 4 parallelen Zentrifugierungen betrug der mittlere Fehler 0,4 %.

In Vorversuchen wurde der Einfluss der Zentrifugierungszeit und der Umdrehungsgeschwindigkeit studiert. Ein in 73 Mol% Äthylalkohol gequollener Austauscher wurde verschieden lange bei bestimmten Umdrehungsgeschwindigkeiten zentrifugiert. Bei allen Umdrehungsgeschwindigkeiten fiel das Gewicht der Austauscherphase innerhalb der ersten 5 Min. stark ab. Bis zu 40 Min. wurde die Abnahme schwächer und über 40 Min. war diese proportional der Zentrifugierungszeit (1 % für die darauffolgende Stunde). Die letzte Gewichtsabnahme kann auf der langsamen Erwärmung der Zentrifuge beruhen. Als Zentrifugierungszeit wurden daher 40 Min. gewählt. Die Änderung der Umdrehungsgeschwindigkeit zeigte, dass das Gewicht der Innenlösung innerhalb des untersuchten Umdrehungsbereiches (300—1 000 g) mit der relativen Zentrifugalkraft linear abnahm. Die Gewichtsabnahme der Austauscherphase betrug 1 % zwischen 600 und 800 g.

Bestimmung des Äthylalkohols in der Innenlösung. Zur Bestimmung des Alkohols in der Innenlösung wurde der Austauscher mit destilliertem Wasser aus dem Zentrifugenkörbchen in einen Messkolben hineingespült und bis zur Marke aufgefüllt. Das Volumen des Messkolbens richtete sich nach der aufgenommenen Alkoholmenge und variierte zwischen 100 und 5 000 ml. Eine Verdünnung der Aussenlösung auf 100 ml kann schon

als genügend betrachtet werden. Unter diesen Bedingungen ist der Fehler, der von der ungleichmässigen Verteilung des Alkohols herrührt, sehr klein.

In dieser Lösung wurde der Äthylalkohol durch Oxydation mit schwefelsaurer Bichromatlösung bestimmt. Danach wurde das Austauscherharz quantitativ in einen gewogenen Glasfiltertiegel übergeführt und im Vakuum bei 50—60° C über Magnesiumperchlorat bis zum konstanten Gewicht getrocknet. Die Oxydation wurde nach den Methoden von Neish [6] und Nogare [7] mit kleinen Änderungen ausgeführt. In einen 200 ml Erlenmeyerkolben wurden 20 ml 0,04 N $K_2Cr_2O_7$, gelöst in 18 N H_2SO_4, und 10 ml der Probelösung eingeführt. Der Kolben wurde mit einem Gummistopfen schnell verschlossen und mehrere Male kräftig geschüttelt. Die Oxydation war nach 30 Min. beendet und der Inhalt des Kolbens wurde mit 100 ml destilliertem Wasser und 10 ml Kaliumjodidlösung (300 g/l) versetzt und schliesslich mit 0,05 N $Na_2S_2O_3$ aus einer 10 ml Bürette, die durch eine aufgeschmolzene 10 ml Pipette verlängert war, titriert. Ein Blindversuch unter denselben Bedingungen nur mit Wasser anstelle der Probelösung wurde ausgeführt. Aus der Differenz des Thiosulfatverbrauches errechnete sich der Alkoholgehalt unter Berücksichtigung, dass einem Mol Äthylalkohol vier Äquivalente $K_2Cr_2O_7$ entsprechen.

Bestimmung des Wassers. Die Bestimmung des Wassergehaltes der Aussenlösung erfolgte mit dem Reagenz nach Karl Fischer. In einem 25 ml Messkolben wurde eine bestimmte Menge der Aussenlösung entsprechend 75—150 mg Wasser eingewogen und mit wasserfreiem Methylalkohol bis zur Marke aufgefüllt. Davon gelangten 5 ml zu der von Johansson [8] modifizierten Wassergehaltsbestimmung.

Wie schon oben erwähnt, wurde bei hohen Alkoholgehalten die Innenlösung auf ihren Wassergehalt analysiert. Zu diesem Zwecke wurde nach dem Zentrifugieren das Zentrifugenkörbchen in einen besonders konstruierten Extraktor gestellt, der Austauscher unter Ausschluss der Luftfeuchtigkeit mit 25 ml wasserfreiem Methylalkohol eine Stunde extrahiert und darin das Wasser nach obiger Methode bestimmt.

RESULTATE UND DISKUSSION

Das ganze Versuchsmaterial ist in Tabelle 2 und Tabelle 3 zusammengestellt. Für jede Alkoholkonzentration der Aussenlösung, ausgedrückt durch den Molenbruch (x), sind die entsprechenden Werte der Innenlösung angegeben. Bei der Berechnung des Molenbruches der Innenlösung (x_r) wurde der Austauscher nicht berücksichtigt sondern nur Wasser und Alkohol. Ferner sind in den Tabellen die Quellung der Austauscher, ausgedrückt in g Innenlösung pro Äquivalent Austauscher, und die absoluten Mengen an Wasser bzw. Äthylalkohol in der Innenlösung, ausgedrückt in Mol pro Äquivalent Austauscher, wiedergegeben.

Die Quellung der Austauscher kann sowohl als Funktion der Alkoholkonzentration der Aussenlösung als auch der Innenlösung studiert werden. Um Zusammenhänge zwischen der Alkoholkonzentration und der Quellung näher zu betrachten, ist es zweckmässiger, die Alkoholkonzentration der Innenlösung als Vergleichsbasis zu wählen. Dies ermöglicht einen leichten Vergleich der Quellung bei verschiedenen Gegenionen, denn das Volumen der Innenlösung ist bei gleicher Alkoholkonzentration dem Gewicht proportional, wenn man von etwaigen Änderungen der partiellen Molvolumina durch die Gegenwart der betreffenden Ionen absieht.

Wie man aus Tabelle 2 sieht, nimmt für den normal vernetzten Kationenaustauscher das Gewicht der Innenlösung mit steigender Alkoholkonzentration ab. Die individuellen Eigenschaften der Gegenionen haben einen starken Einfluss auf die Quellung. Unabhängig davon, ob man die Quellung durch das Gewicht oder Volumen ausdrückt, nimmt diese mit dem Gegenion nach folgender Reihe ab: $Li^+ > Na^+ > K^+$.

Tabelle 2. Alkohol-Wasserverteilung und Quellung bei dem Kationenaustauscher Dowex 50.

Austauscherharz	x	x_r	Quellung Gramm / Äq. Austauscher	Mol H_2O / Äq. Austauscher	Mol C_2H_5OH / Äq. Austauscher
Dowex 50 Li^+	0,000	0,000	213	11,82	0,00
	0,0152	0,0135	210	11,27	0,15
	0,320	0,145	191	7,41	1,25
	0,483	0,191	177	6,12	1,44
	0,642	0,265	157	4,51	1,63
	0,732	0,347	140	3,29	1,75
	0,842	0,506	127	1,94	1,99
	0,901	0,640	122	1,23	2,19
	0,977	0,905	123	0,27	2,56
Dowex 50 Na^+	0,000	0,000	196	10,86	0,00
	0,0152	0,0110	191	10,33	0,12
	0,333	0,123	157	6,40	0,90
	0,557	0,174	122	4,40	0,92
	0,730	0,259	90	2,63	0,92
	0,841	0,384	74	1,58	0,99
Dowex 50 K^+	0,000	0,000	163	9,05	0,00
	0,0152	0,0109	161	8,70	0,10
	0,317	0,130	122	4,92	0,73
	0,481	0,165	103	3,80	0,75
	0,639	0,221	82	2,64	0,75
	0,731	0,273	74	2,09	0,78
	0,841	0,385	63	1,34	0,84
	0,904	0,495	59	0,93	0,91
	0,983	0,740	49	0,33	0,93

Die Quellung des normal vernetzten Anionenaustauschers weist für alle untersuchten Ionenformen ein Maximum auf (vgl.[1]). Dies ist besonders auffallend für die ClO_4^--Form, die auch, verglichen mit anderen Ionenformen, sehr wenig Lösung absorbiert. Bei niedriger Alkoholkonzentration ist die Quellung für die SO_4^{2-}-Form grösser als für die Cl^--Form. Bei höherer Alkoholkonzentration ergeben die Gegenionen bezüglich der Quellung folgende Reihe: $Cl^- > SO_4^{2-} > ClO_4^-$.

Für den Anionenaustauscher mit geringem Vernetzungsgrad zeigt die ClO_4^--Form sowohl in Wasser als auch in Alkohol eine geringere Quellung. Bei steigender Alkoholkonzentration durchläuft die Quellungskurve ebenfalls ein Maximum. Die SO_4^{2-}-Form desselben Austauschers quillt in Wasser mehr als der normal vernetzte. Mit steigender Alkoholkonzentration gleicht sich für Sulfat die Verschiedenheit in der Quellung aus, und bei höherer Alkoholkonzentration ist die Quellung auch hier kleiner als beim Anionenaustauscher mit normaler Vernetzung.

Als allgemeine Regel hat man bekanntlich gefunden, dass schwach vernetzte Austauscher mehr quellen als Austauscher mit dichterer Vernetzung [5]. Dies wurde dadurch erklärt, dass die Querbindungen die fortschreitende Quellung hindern. Aus den Versuchen mit Anionenaustauschern geht hervor,

Tabelle 3. Alkohol-Wasserverteilung und Quellung bei den Anionenaustauschern Dowex 2 und Dowex 2 X1

Austauscherharz	x	x_r	Quellung Gramm / Äq. Austauscher	Mol H_2O / Äq. Austauscher	Mol C_2H_5OH / Äq. Austauscher
Dowex 2 ClO_4^-	0,000	0,000	92	5,10	0,00
	0,0152	0,0331	100	5,12	0,18
	0,171	0,222	125	4,02	1,15
	0,314	0,309	131	3,39	1,52
	0,477	0,396	123	2,55	1,67
	0,547	0,430	120	2,28	1,71
	0,636	0,478	112	1,87	1,71
	0,729	0,542	103	1,42	1,68
	0,844	0,684	93	0,79	1,71
	0,987	0,952	85	0,088	1,80
Dowex 2 Cl^-	0,000	0,000	239	13,26	0,00
	0,0152	0,0218	246	12,90	0,29
	0,097	0,105	260	11,10	1,30
	0,189	0,176	273	9,81	2,09
	0,331	0,239	260	8,01	2,52
	0,556	0,336	232	5,62	2,84
	0,731	0,460	198	3,46	2,94
	0,844	0,600	180	2,06	3,09
Dowex 2 SO_4^{2-}	0,000	0,000	273	15,15	0,00
	0,0152	0,0177	276	14,62	0,26
	0,097	0,084	275	12,36	1,13
	0,192	0,144	271	10,50	1,77
	0,314	0,196	265	9,07	2,21
	0,481	0,251	244	7,29	2,44
	0,637	0,315	211	5,38	2,48
	0,729	0,377	193	4,20	2,54
	0,842	0,531	168	2,39	2,71
	0,901	0,680	161	1,39	2,96
	0,980	0,922	157	0,28	3,29
Dowex 2 X1 ClO_4^-	0,000	0,000	77	4,30	0,00
	0,082	0,095	94	4,13	0,44
	0,174	0,185	121	4,23	0,96
	0,318	0,262	129	3,76	1,33
	0,552	0,356	93	2,15	1,18
	0,729	0,428	70	1,33	1,00
	0,839	0,540	55	0,77	0,90
Dowex 2 X1 SO_4^{2-}	0,000	0,000	427	23,67	0,00
	0,084	0,064	360	16,99	1,16
	0,172	0,110	308	12,99	1,61
	0,320	0,144	271	10,53	1,77
	0,555	0,197	203	6,93	1,70
	0,729	0,279	154	4,28	1,66
	0,837	0,382	129	2,77	1,71

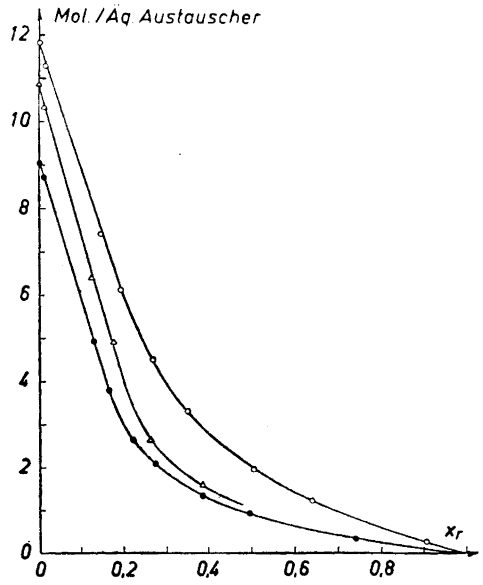


Abb. 2. Aufgenommene Wassermengen in Mol/Äq. Austauscher als Funktion des Molenbruches für Äthylalkohol der Innenlösung x_r für Dowex 50 in verschiedenen Ionenformen.
Ionenform: ○ Li^+ △ Na^+ ● K^+

dass bei der ClO_4^--Form entgegengesetzte Verhältnisse herrschen sowohl in Wasser als auch in Alkohol-Wasserlösungen. Auch die SO_4^{2-}-Form nimmt eine Ausnahmestellung ein, aber nur bei höherer Alkoholkonzentration. In Systemen, bei denen das Quellungsvermögen niedrig ist, können die Querbindungen im Harzskelett das Schrumpfen behindern. Den Molekülketten wird es somit erschwert, sich so dicht wie möglich zu packen. Weitere Versuche mit gut

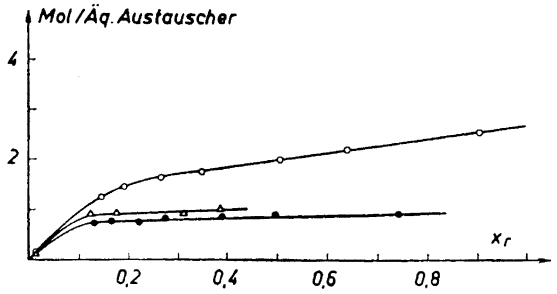


Abb. 3. Aufgenommene Äthylalkoholmengen in Mol/Äq. Austauscher als Funktion des Molenbruches für Äthylalkohol der Innenlösung x_r für Dowex 50 in verschiedenen Ionenformen.
Ionenform: ○ Li^+ △ Na^+ ● K^+

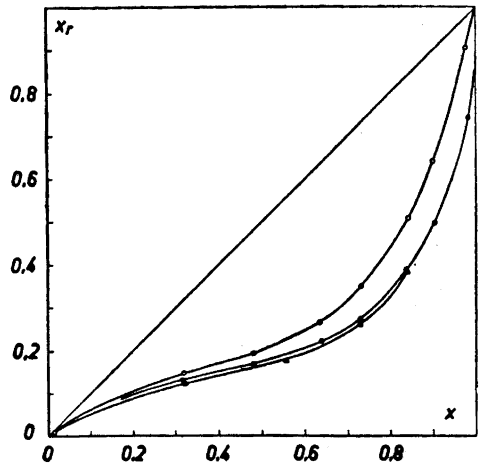


Abb. 4. Äthylalkohol-Wasserverteilungskurven für Dowex 50 in verschiedenen Ionenformen. Molenbruch des Äthylalkohols der Innenlösung x_r als Funktion des Molenbruches für Äthylalkohol der Aussenlösung x.
Ionenform: O Li^+ △ Na^+ ● K^+

definierten Ionenaustauschern und mit anderen Lösungsmittelsystemen sind wünschenswert, um die hierher gehörenden interessanten Erscheinungen näher zu klären.

In Abb. 2 und Abb. 3 sind die absoluten Mengen an Wasser bzw. Alkohol der Innenlösung, ausgedrückt in Mol pro Äquivalent Austauscher, gegen den Molenbruch des Alkohols der Innenlösung aufgetragen. Man erhält für jede Ionenform Kurven gleicher Art, wie es hier für den Kationenaustauscher gezeigt ist. Die Kurven für die Wassermengen fallen erst linear mit der Alkoholkonzentration ab, um dann langsam gegen Null abzuflachen. Für den Alkohol zeigen die Kurven einen umgekehrten Verlauf. Für die vom Austauscher aufgenommenen Wassermengen ergibt sich eine offensichtliche Parallelität mit der Hydratation der Gegenionen. Bei den Systemen Azeton-Wasser und Dioxan-Wasser erhielten Davies und Owen [9] den gleichen Kurventypus für die absorbierten Wassermengen. Es sei aber darauf aufmerksam gemacht, dass bei diesen Systemen die Kurve einen markanten Knick aufweist, während bei Äthylalkohol-Wasser die beiden Kurventeile allmählich ineinander übergehen. Die erwähnte Parallelität zwischen der Hydratation und der Wasserabsorption scheint daher nicht für eine quantitative Bestimmung der Hydratation geeignet zu sein.

Die ungleichmässige Verteilung des Alkohols zwischen Harzphase und Aussenlösung kommt am besten zum Ausdruck, wenn man die Versuchsresultate in Form von Verteilungskurven wiedergibt. Abb. 4 zeigt solche Verteilungskurven für den Kationenaustauscher in verschiedenen Ionenformen. Die Zusammensetzung ist durch den Molenbruch Äthylalkohol sowohl für die Aussenlösung (x) als auch für die Innenlösung (x_r) angegeben. Alle Kurven zeigen einen S-förmigen Verlauf und in allen Fällen ist der Alkoholgehalt in

der Harzphase kleiner als in der Aussenlösung. Die verschiedenen Gegenionen im Austauscher beeinflussen die Verteilung mehr oder weniger stark. Qualitativ können die erhaltenen Effekte durch einen Aussalzeffekt erklärt werden, d.h. die Ionen des Austauschers wirken auf den Alkohol aussalzend. Beim Kationenaustauscher nimmt der Aussalzeffekt in der Reihenfolge $Li^+ < K^+ < Na^+$ zu. Es sei darauf aufmerksam gemacht, dass sich ein grösserer Aussalzeffekt beim Natriumion bemerkbar macht im Vergleich zum Kaliumion, obwohl der Austauscher in der Na^+-Form mehr quillt als in der K^+-Form, oder mit anderen Worten, dass die Natriumionenkonzentration in der Harzphase kleiner ist. Zu dem geringen Aussalzeffekt bei Lithium trägt wahrscheinlich die Tatsache dazu bei, dass die Quellung hier grösser ist als bei Natrium und Kalium.

Versuche wurden auch ausgeführt mit dem schwach vernetzten Kationenaustauscher (Dowex 50 X1) in Li^+- und K^+-Form. Die Quellung war hier grösser als bei normalem Vernetzungsgrad und es zeigte sich auch eindeutig, dass der Aussalzeffekt kleiner war, was durch die niedrigere Ionenkonzentration in der Innenlösung erklärt werden kann. Da es sich als sehr schwierig erwies bei dem schwach vernetzten Kationenaustauscher reproduzierbare Resultate zu erhalten, wurden diese in den Tabellen nicht wiedergegeben.

Ein eindeutiger Zusammenhang zwischen dem Aussalzeffekt bei den verschiedenen Kationen und der Hydratation liegt in diesem Falle nicht vor. Von anderen Systemen ist es jedoch auch bekannt, dass das Lithiumion eine Ausnahme von den Alkalimetallen macht und dass die Salzeffekte in derselben Reihenfolge zunehmen, wie sie hier beim Kationenaustauscher beobachtet wurden [10].

In Abb. 5 sind die entsprechenden Kurven für den Anionenaustauscher in verschiedenen Ionenformen wiedergegeben. Die Kurven sind symmetrischer

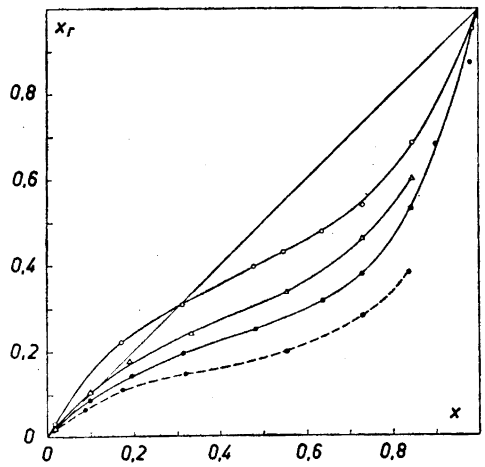


Abb. 5. Äthylalkohol-Wasserverteilungskurven für Dowex 2 (————) und Dowex 2 X1 (– – – –) in verschiedenen Ionenformen. Molenbruch für Äthylalkohol der Innenlösung x_r als Funktion des Molenbruches für Äthylalkohol der Aussenlösung x. Ionenform: O ClO_4^- △ Cl^- ● SO_4^{2-}

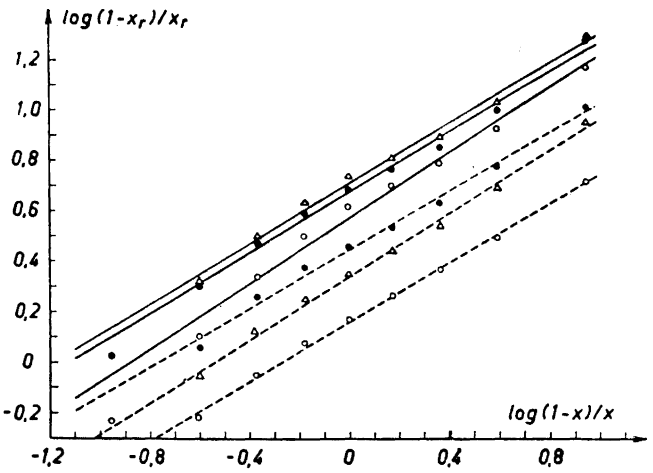


Abb. 6. log $(1-x_r)/x_r$ als Funktion von log $(1-x)/x$ für Dowex 50 (– – – –) und Dowex 2 (————) in verschiedenen Ionenformen.
Ionenform: ○ Li^+ ○ ClO_4^-
△ Na^+ △ Cl^-
● K^+ ● SO_4^{2-}

als beim Kationenaustauscher und unterscheiden sich in einer wichtigen Beziehung von den Kurven des Kationenaustauschers. Bei niedrigen Alkoholkonzentrationen schneiden nämlich die Kurven die Diagonale. Dies bedeutet, dass man bei niedrigen Alkoholkonzentrationen ein Einsalzen des Alkohols erhält, d.h., der Alkoholgehalt in der Innenlösung ist grösser als in der Aussenlösung. Besonders deutlich tritt diese Erscheinung bei der ClO_4^--Form zu Tage. Die Kurven für die verschiedenen Ionenformen schneiden einander nicht. Der Alkoholgehalt der Innenlösung nimmt im ganzen Konzentrationsbereich nach folgender Reihe ab: $ClO_4^- > Cl^- > SO_4^{2-}$. Innerhalb des Bereiches, wo ein Aussalzen stattfindet, steigt dieses also in der Reihenfolge $ClO_4^- < Cl^- < SO_4^{2-}$ an. In diesem Falle herrscht eine Parallelität zwischen der Alkohol-Wasserverteilung und der Hydratation der Ionen dahingehend, dass eine zunehmende Hydratation zu einer steigenden Wasserabsorption beiträgt (steigender Aussalzeffekt). Dies ist im allgemeinen der Fall, wenn es sich um das Aussalzen von Nichtelektrolyten handelt [10], aber, wie schon oben erwähnt, gibt es auch Ausnahmen von dieser Regel.

Wenn die Ionenkonzentration in der Harzphase geändert wird, ergibt sich für den Anionenaustauscher eine analoge Änderung des Aussalzeffektes wie beim Kationenaustauscher. Dies zeigen die Versuche mit der ClO_4^-- und SO_4^{2-}-Form. Da schwach vernetzte Anionenaustauscher bei höherer Alkoholkonzentration weniger quellen als die normal vernetzten und folgedessen die Ionenkonzentration grösser ist, wirken schwach vernetzte Anionenaustauscher auch stärker aussalzend für Äthylalkohol.

Bei den Versuchen, wo die Alkohol-Wasserverteilungskurven die Diagonale schneiden, haben die Austauscher ihr Quellungsmaximum bei der gleichen Alkoholkonzentration. Diese Erscheinung kann mit der azeotropen Destillation verglichen werden.

Es wurde versucht, eine einfache empirische Gleichung zu finden, die die erhaltenen Resultate bezüglich der Verteilung von Alkohol und Wasser wiedergeben kann. Zu diesem Zwecke wurden aus den in Abb. 4 und Abb. 5 wiedergegebenen Verteilungskurven für bestimmte x-Werte die entsprechenden x_r-Werte entnommen. In Abb. 6 sind $\log (1-x_r) / x_r$ gegen $\log (1-x) / x$ aufgetragen. Man erhält bis zu $x = 0{,}8$ eine lineare Beziehung. Somit gilt die Gleichung

$$\frac{1-x_r}{x_r} = k \left(\frac{1-x}{x} \right)^p \qquad (1)$$

in der k und p Parameter bedeuten.

Die beste Gerade innerhalb dieses Konzentrationsbereiches wurde nach der Methode der kleinsten Quadrate errechnet. In Tabelle 4 sind die gefundenen Parameter p und k zusammengestellt. Der Parameter p besitzt für alle Ionen fast den gleichen Wert. Als Mittelwert erhält man $p = 0{,}6$, welcher als charakteristischer Wert für das hier untersuchte System Äthylalkohol-Wasser angesehen werden kann. Daher wurde durch die aus den Verteilungskurven entnommenen Punkten für jede Ionenform die beste Gerade mit dem Winkelkoeffizienten 0,6 gelegt und der Parameter k berechnet. In Tabelle 4 sind auch die gefundenen Werte für k mit $p = 0{,}6$ zusammengestellt. Mit Hilfe obiger empirischer Gleichung und den zuletztgenannten Parametern wurden die Äthylalkohol-Wasserverteilungskurven berechnet und mit den experimentellen erhaltenen Kurven verglichen. Es zeigte sich, dass bis zu einem Molenbruch von 0,8 Äthylalkohol in der Aussenlösung die experimentellen und berechneten Kurven sehr gut übereinstimmen. Auf Grund der hier gemachten Beobachtungen, dürfte also Gleichung (1) dazu geeignet sein, die ganze Alkohol-Wasserverteilungskurve aus wenigen experimentellen Punkten berechnen zu können. Will man nur durch einen einzigen Versuch die Verteilungskurve bestimmen, so nimmt man $p = 0{,}6$ und für die Ermittlung des Parameters k wählt man am besten als Alkoholkonzentration der Aussenlösung $x = 0{,}5$.

Tabelle 4. Parameter für die Gleichung (1).

Austauscher	p	k	k für $p = 0{,}6$
Dowex 50 Li^+	0,647	3,68	3,89
Na^+	0,596	5,08	5,20
K^+	0,594	4,67	4,73
Dowex 2 ClO_4^-	0,582	1,44	1,44
Cl^-	0,621	2,18	2,24
SO_4^{2-}	0,578	2,78	2,82

In diesem Punkte gibt dann der Bruch $1-x_r / x_r$ direkt den Parameter k an. Gleichung (1) ist vom gleichen Typus, wie die Gleichung von Rothmund und Kornfeld [11], die sich als sehr verwendungsfähig erwies, um Ionenaustauschergleichgewichte quantitativ wiederzugeben. Es sei jedoch an dieser Stelle hervorgehoben, dass der Austausch von Ionen in äquivalenten Mengen erfolgt, während dies bei der Verteilung von Nichtelektrolyten nicht der Fall ist.

Wir danken dem *Schwedischen Technischen Forschungsrat* für die Bereitstellung von Mitteln.

LITERATURVERZEICHNIS

1. Gregor, H. P., Nobel, D. und Gottlieb, M. H. *J. Phys. Chem.* **59** (1955) 10.
2. Rückert, H. und Samuelson, O. *Svensk Kem. Tidskr.* **66** (1954) 337.
3. Gregor, H. P., Held, K. M. und Bellin, J. *Anal. Chem.* **23** (1951) 620.
4. Pepper, K. W., Reichenberg, D. und Hale, D. K. *J. Chem. Soc.* **1952** 3129.
5. Samuelson, O. *Ion Exchangers in Analytical Chemistry*, Stockholm 1952 und New York 1953.
6. Neish, A. C. *Can. J. Chem.* **29** (1951) 552.
7. Nogare, S. D. *Anal. Chem.* **25** (1953) 1874.
8. Johansson, A. *Svensk Papperstidn.* **50** (1947) 124.
9. Davies, C. W. und Owen, B. D. R. *J. Chem. Soc.* **1956** 1676.
10. Long, F. A. und McDevit, W. F. *Chem. Revs.* **51** (1952) 119.
11. Rothmund, V. und Kornfeld, G. *Z. anorg. u. allgem. Chem.* **103** (1918) 129.

Eingegangen am 6. November 1956.

ACTA CHEMICA SCANDINAVICA 11 (1957) 315—323

Die Verteilung von Glukose bei Ionenaustauschern auf Harzbasis in Äthylalkohol-Wassergemischen

HEINZ RÜCKERT und OLOF SAMUELSON

Institut für Technische Chemie, Chalmers Technische Hochschule, Göteborg, Schweden

Die Sorption von Glukose an Ionenaustauscher aus Äthylalkohol-Wasserlösungen wurde für Kationenaustauscher und Anionenaustauscher studiert. Die vom Austauscher aufgenommene Glukosemenge ist sowohl von der Ionenform als auch der Alkoholkonzentration abhängig. Eine gewisse Parallelität zwischen der Verteilung von Äthylalkohol und Wasser und der Glukosesorption wurde festgestellt dahingehend, dass eine hohe Wasserkonzentration in der Austauscherphase eine hohe Glukosesorption begünstigt. Der direkte Salzeffekt der Ionen auf die Glukosemoleküle kann jedoch nicht vernachlässigt werden.

In einer früheren Arbeit [1] wurde gezeigt, dass Ionenaustauscher zur Sorption von Zuckerarten befähigt sind, wenn man als Lösungsmittel Äthylalkohol-Wassergemische verwendet. Die vom Austauscher aufgenommene Zuckermenge kann sehr beträchtlich sein. So werden z.B. von einem Kationenaustauscher in K^+-Form etwa 200 mg Glukose pro Gramm Austauscher aus 73 mol %iger Alkohollösung bei einer Gleichgewichtskonzentration von 10 g Glukose pro Liter aufgenommen. Diese ungleichmässige Verteilung ist in hohem Grade von der Kapazität des Austauschers und der Art der Gegenionen abhängig. Es konnte somit gezeigt werden, dass die Ionen direkt oder indirekt für die Zuckersorption verantwortlich sind. In der vorliegenden Arbeit wurden die Versuche mit Glukose auf andere Alkoholkonzentrationen ausgedehnt, um die Ursachen der Glukoseverteilung näher zu studieren.

EXPERIMENTELLER TEIL

Bezüglich der verwendeten Austauscherharze und des Arbeitsganges für die Bestimmung der Alkoholsorption sei auf eine Arbeit über die Verteilung von Wasser und Äthylalkohol bei Ionenaustauschern auf Harzbasis verwiesen [2]. Hier werden im folgenden nur die fehlenden und geänderten Bestimmungsmethoden, bedingt durch die Gegenwart der Glukose, behandelt. In der früheren Arbeit über die Zuckersorption wurde die vom Austauscher aufgenommene Zuckermenge durch die Konzentrationsänderung der Aussenlösung bestimmt. Bei den hier beschriebenen Versuchen sollte aber neben der Glukose

auch gleichzeitig der Alkohol in der Innenlösung bestimmt werden, was sich nur dann durchführen lässt, wenn sowohl die Aussenlösung als auch die Innenlösung für sich auf ihre Zusammensetzung analysiert werden. Aus diesem Grunde wurden die beiden Phasen durch Zentrifugieren von einander abgetrennt.

Bestimmung des Äthylalkohols in der Austauscherphase. Da bei der Alkoholbestimmung durch Oxydation mit schwefelsaurer Bichromatlösung auch Glukose oxydiert wird, musste der Alkohol durch Destillation von der Glukose getrennt werden. Zu diesem Zwecke wurde nach der Extraktion des Austauscherharzes mit Wasser 50 ml von dieser Lösung destilliert und das Destillat in einem 100 ml Messkolben aufgefangen. Die Destillationsapparatur wurde im Hinblick auf die geringen Alkoholmengen so klein wie möglich gehalten und bestand aus Normalschliffteilen. Bei allen Versuchen wurden 30 ml Destillat gesammelt, der Messkolben bis zur Marke mit Wasser aufgefüllt und der Alkohol darin bestimmt.

Bestimmung der Glukose in der Austauscherphase. Nach der Extraktion des Austauschers mit Wasser wurde die Glukose mit dem Anthronreagenz [3] colorimetrisch bestimmt.

Bestimmung der Glukose in der Aussenlösung. Eine gewogene Menge der Aussenlösung entsprechend 25—60 mg Glukose wurde auf dem Wasserbad eingedampft und der Rückstand in 20 ml destilliertem Wasser gelöst. Davon gelangten 10 ml zur Glukosebestimmung nach Schoorl [4]. Bei der hier verwendeten modifizierten Methode hat es sich als vorteilhaft erwiesen, zur jodometrischen Titration des Kupferüberschusses eine erheblich grössere Menge an Kaliumjodid zu nehmen, als die CCA-Methode vorschreibt. Der Endpunkt der Titration konnte wesentlich leichter erfasst werden, wenn für jede Titration etwa 10 g Kaliumjodid zugesetzt wurden [5]. Das Eindampfen der alkoholischen Glukoselösung war aus dem Grunde erforderlich, weil der Alkohol den Siedepunkt bei der Reduktion herabsetzte und somit die empirischen Umrechnungsfaktoren ungültig wurden. Ein separater Versuch zeigte, dass sich die Glukose durch das Eindampfen nicht zersetzte.

Einstellung des Gleichgewichtes. Die Einstellung des Gleichgewichtes für die Glukosesorption war sowohl von der Äthylalkoholkonzentration als auch von der Ionenform des Austauschers abhängig. Separate Untersuchungen haben ergeben, dass sich beim Lithiumion das Gleichgewicht bei allen Alkoholkonzentrationen schon innerhalb 50—100 Std. eingestellt hatte und ebenso für den Anionenaustauscher in den untersuchten Ionenformen. Beim Kaliumion hingegen wurde das Gleichgewicht bei 73 Mol % Äthylalkohol nach etwa 200 Std. erreicht. Alle Glukosesorptionsversuche liefen zur Sicherheit 500—1 000 Std.

RESULTATE UND DISKUSSION

Die Resultate der Glukoseverteilung bei verschiedenen Alkoholkonzentrationen sind in Tabelle 1 für den Kationenaustauscher und in Tabelle 2 für den Anionenaustauscher zusammengestellt. Für jede Alkoholkonzentration der Aussenlösung (x) sind die entsprechenden Werte für die Alkoholkonzentrationen der Innenlösung (x_r) angegeben. In die Berechnung des Molenbruches (x_r) wurden nur Alkohol, Wasser und Glukose einbezogen. Die Änderung von x_r mit der Glukosekonzentration lag innerhalb des experimentellen Fehlers. Daher ist für x_r nur jeweils der Mittelwert angegeben. Für jede Alkoholkonzentration wurde die Glukoseverteilung für mindestens zwei verschiedene Glukosekonzentrationen bestimmt. Die Glukosekonzentrationen der Aussen- und Innenlösung sind ebenfalls durch den Molenbruch (x_G bzw. x_{G_r}) ausgedrückt. Da der Molenbruch nur ein relatives Mass darstellt, eignet sich dieser sehr gut dafür, die Konzentration der Innenlösung unabhängig von der Quellung des Austauschers auszudrücken. Vom praktischen Standpunkt aus kann es jedoch von grösserem Interesse sein, ein absolutes Mass für die vom Austauscher aufgenommenen Glukosemengen zu haben. Daher sind auch die Werte für die pro Äquivalent Austauscher absorbierte Anzahl Mol Glukose tabelliert.

Tabelle 1. Glukoseverteilung bei dem Kationenaustauscher Dowex 50.

Austauscher	x	x_r	x_G	x_{G_r}	Mol Glukose / Äq. Austauscher	K^*
Dowex 50 Li+	0,00	0,00	0,00103	0,000323	0,0038	0,31
			0,00254	0,000796	0,0094	
	0,32	0,15	0,00099	0,00091	0,0077	0,89
			0,00243	0,00216	0,0184	
	0,55	0,22	0,00095	0,00254	0,0172	2,67
			0,00237	0,00631	0,0424	
	0,73	0,32	0,00171	0,0115	0,059	7,2
			0,00307	0,0235	0,121	
	0,84	0,51	0,00077	0,0124	0,045	16,1
			0,00191	0,0310	0,110	
	0,90	0,68	0,00072	0,0176	0,052	23,7
			0,00171	0,0398	0,115	
Dowex 50 Na+	0,00	0,00	0,00102	0,00044	0,0047	0,42
			0,00256	0,00107	0,0116	
	0,33	0,12	0,00098	0,00182	0,0133	1,85
			0,00240	0,00440	0,0319	
	0,56	0,18	0,00089	0,0060	0,0323	6,8
			0,00224	0,0152	0,0803	
	0,73	0,24	0,00093	0,0262	0,091	28,2
			0,00248	0,0529	0,189	21,3
	0,84	0,34	0,00050	0,0489	0,117	98
			0,00129	0,0783	0,196	61
Dowex 50 K+	0,00	0,00	0,00102	0,00065	0,0059	0,64
			0,00254	0,00161	0,0147	
	0,32	0,13	0,00097	0,00329	0,0178	3,3
			0,00236	0,00780	0,0427	
	0,55	0,19	0,00083	0,0115	0,045	13,9
			0,00214	0,0260	0,101	12,1
	0,73	0,25	0,00081	0,0434	0,115	54
			0,00226	0,0839	0,223	37
Dowex 50 X1 Li+			0,00059	0,0018	0,033	
	0,73	0,57	0,00118	0,0039	0,069	3,4
			0,00230	0,0079	0,132	
			0,00288	0,0109	0,172	
Dowex 50 X1 K+			0,00064	0,0229	0,094	
	0,73	0,34	0,00119	0,0435	0,146	36
			0,00140	0,0510	0,169	

Tabelle 2. Glukoseverteilung bei dem Anionenaustauscher Dowex 2.

Austauscher	x	x_r	x_G	x_{G_r}	Mol Glukose / Äq. Austauscher	K^*
Dowex 2 ClO_4^-	0,00	0,00	0,00100	0,00042	0,0024	0,42
			0,00256	0,00110	0,0061	
	0,73	0,53	0,00127	0,00140	0,0076	
			0,00186	0,00202	0,0109	1,1
			0,00306	0,00342	0,0185	
			0,00353	0,00426	0,0228	
Dowex 2 Cl^-	0,00	0,00	0,00101	0,00059	0,0078	0,57
			0,00258	0,00145	0,0198	
	0,73	0,44	0,00112	0,0091	0,056	8,2
			0,00262	0,0219	0,143	
Dowex 2 SO_4^{2-}	0,00	0,00	0,00100	0,00073	0,0110	0,73
			0,00256	0,00188	0,0276	
	0,73	0,35	0,00086	0,0279	0,181	32,4
			0,00131	0,0384	0,252	29,3
			0,00232	0,0571	0,361	24,6
			0,00283	0,0628	0,406	22,2
Dowex 2 X1 ClO_4^-	0,73	0,43	0,00137	0,00173	0,0052	
			0,00195	0,00265	0,0080	1,3
			0,00263	0,00312	0,0110	
			0,00326	0,00426	0,0134	
Dowex 2 X1 SO_4^{2-}	0,73	0,25	0,00050	0,0270	0,189	54,0
			0,00080	0,0397	0,273	49,6
			0,00116	0,0501	0,349	43,2
			0,00150	0,0609	0,425	40,6

In Abb. 1 sind die von dem normal vernetzten Kationenaustauscher Dowex 50 in Li^+-Form aufgenommenen Glukosemengen gegen die Glukosekonzentration der Aussenlösung aufgetragen. Die einzelnen Geraden entsprechen verschiedenen Alkoholkonzentrationen der Aussenlösung. Man sieht, wie die Glukosesorption mit der Alkoholkonzentration kräftig ansteigt. Aus 90 mol %igem Äthylalkohol nimmt dieser Austauscher ungefähr das 20-fache an Glukose auf als aus wässeriger Lösung. Zum Vergleich sind die entsprechenden Kurven für die K^+-Form desselben Austauschers in Abb. 2 wiedergegeben. Auch hier findet man eine mit der Alkoholkonzentration steigende Glukosesorption, die bei allen Alkoholkonzentrationen grösser ist als für Lithium. Bei niedriger Alkoholkonzentration ist die aufgenommene Glukosemenge der Glukosekonzentration der Aussenlösung proportional, bei höheren Alkoholkonzentrationen sind die Kurven gebogen.

Über die Abhängigkeit der Glukosesorption sowohl von der Alkoholkonzentration als auch von der Ionenform des Austauschers gibt am besten der Verteilungskoeffizient K^* Auskunft. Der Verteilungskoeffizient ist durch die

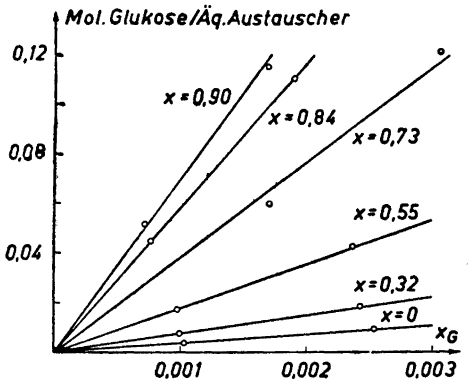


Abb. 1. Aufgenommene Glukosemenge in Mol Glukose/Äq. Austauscher als Funktion des Molenbruches für Glukose der Aussenlösung x_G bei verschiedenen Äthylalkoholkonzentrationen für Dowex 50 Li^+. Die Äthylalkoholkonzentration der Aussenlösung ist durch den Molenbruch x ausgedrückt.

Gleichung $K^* = x_{G_r}/x_G$ definiert. Innerhalb des untersuchten Konzentrationsbereiches ($x_G = 0 - 0{,}0025$) sind in den Fällen, wo die Sorption niedrig ist, die K^*-Werte von der Glukosekonzentration unabhängig. Bei hoher Sorption nehmen die K^*-Werte mit der Glukosekonzentration ab. Für die Versuchsreihen, bei denen K^* innerhalb der Grenzen des experimentellen Fehlers konstant ist, sind in den Tabellen die Mittelwerte für K^* angegeben, anderenfalls für jede Glukosekonzentration der entsprechende K^*-Wert.

Wie man aus den Tabellen ersieht, steigen die K^*-Werte mit der Alkoholkonzentration. Die Gegenionen lassen sich bezüglich ihres Einflusses auf den Verteilungskoeffizienten bei allen Alkoholkonzentrationen und jedem Austauscher in folgende Reihe für steigendes K^* einordnen: $Li^+ < Na^+ < K^+$ bzw. $ClO_4^- < Cl^- < SO_4^{2-}$. Es wurde versucht, K^* als Funktion der Alkoholkonzentration der Aussenlösung durch die empirische Gleichung

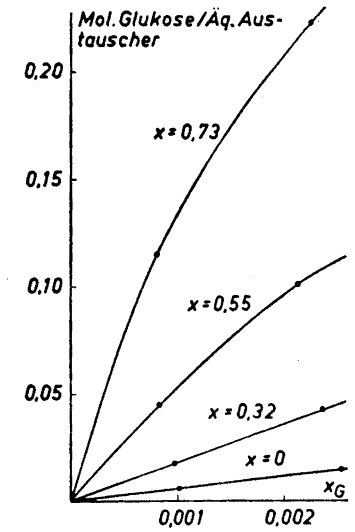


Abb. 2. Aufgenommene Glukosemenge in Mol Glukose/Äq. Austauscher als Funktion des Molenbruches für Glukose der Aussenlösung x_G bei verschiedenen Äthylalkoholkonzentrationen für Dowex 50 K^+. Die Äthylalkoholkonzentration der Aussenlösung ist durch den Molenbruch x ausgedrückt.

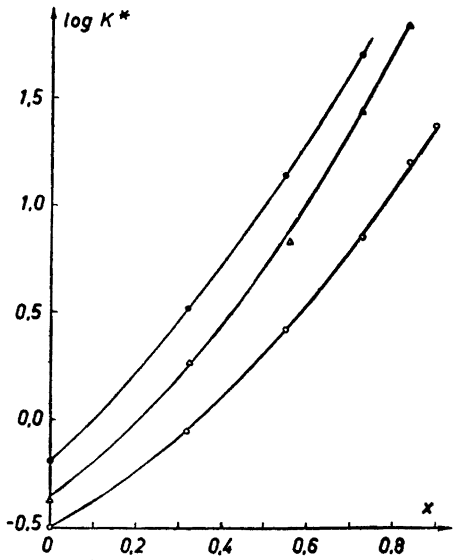


Abb. 3. log K^* als Funktion des Molenbruches für Äthylalkohol der Aussenlösung x für Dowex 50 in verschiedenen Ionenformen.
Ionenform: ○ Li^+, △ Na^+, ● K^+.

$$\log K^* = \log K^*_W + ax + bx^2$$

auszudrücken. In dieser Gleichung sind a und b empirische Konstante und K^*_W bedeutet die Verteilungskonstante in wässeriger Lösung. In Tabelle 3 sind die nach der Methode der kleinsten Quadrate berechneten Konstanten für den normal vernetzten Kationenaustauscher in Li^+-, Na^+- und K^+-Form zusammengestellt. Da, wie schon erwähnt, K^* auch von der Glukosekonzentration abhängig sein kann, wurden die Berechnungen für eine Glukosekonzentration der Aussenlösung von $x_G = 0{,}001$ durchgeführt. Abb. 3 zeigt den empirisch gefundenen Zusammenhang zwischen log K^* und x entsprechend obiger Gleichung mit den Konstanten aus Tabelle 3. Zum Vergleich sind auch in demselben Diagramm die experimentellen Punkte eingezeichnet.

In der Praxis wird man im allgemeinen daran interessiert sein, die pro Austauschereinheit aufgenommenen Glukosemengen berechnen zu können. Da diese auch von der Quellung des Austauschers abhängen, eignet sich obige empirische Gleichung nicht unmittelbar für so eine Berechnung. Die Quellung des Austauschers in Alkohol-Wassergemischen wurde in einer früheren Arbeit [2] behandelt, aus der die Summe der pro Äquivalent Austauscher aufgenommenen Mole Wasser und Alkohol zu entnehmen ist. Wenn zu der Innenlösung auch

Tabelle 3. Konstanten der Gleichung log $K^* = \log K^*_W + ax + bx^2$.

Austauscher	log K^*_W	a	b
Dowex 50 Li^+	−0,501	1,08	1,09
Na^+	−0,356	1,42	1,45
K^+	−0,196	1,91	0,96

die sorbierte Glukose hinzukommt, zeigte es sich, dass diese Summe innerhalb der Grenzen des experimentellen Fehlers unverändert blieb. Man kann also für die Glukosesorption mit hinreichender Genauigkeit die gleichen Quellungswerte wie für das System Äthylalkohol-Wasser verwenden. Mit Hilfe der K^*- und Quellungswerte lassen sich dann auch für jede Alkoholkonzentration die pro Austauschereinheit aufgenommenen Glukosemengen berechnen.

Bei hohen Alkoholkonzentrationen ($x = 0{,}84$ und $x = 0{,}90$) wurde für die K^+-Form das Gleichgewicht noch nicht nach 2 000 Std. erreicht und dasselbe ergab sich für die Na^+-Form bei $x = 0{,}90$. Diese Versuche sind daher auch nicht in den Tabellen verzeichnet. Die lange Dauer für die Einstellung des Gleichgewichtes bei hohen Alkoholkonzentrationen kann in der Schrumpfung des Austauschers seine Erklärung finden. Wenn der Austauscher mit zunehmendem Alkoholgehalt schrumpft, kann bei einer bestimmten Alkoholkonzentration die Maschenweite des Harzskelettes so eng werden, dass die im Verhältnis zu Alkohol und Wasser grossen Glukosemoleküle nur mehr schwer in den Austauscher eindringen können. Dieser beginnende Sperreffekt für Glukosemoleküle tritt für die K^+-Form bei einer Alkoholkonzentration in der Aussenlösung zwischen $x = 0{,}73$ und $x = 0{,}84$ ein. Untersuchungen über die Quellung in Äthylalkohol-Wassergemischen [2] zeigten, dass das Volumen der Na^+-Form bei $x = 0{,}9$ kleiner ist als das der K^+-Form bei $x = 0{,}73$. Der Sperreffekt ist also für die Na^+-Form bei etwa $x = 0{,}9$ zu erwarten, während die Li^+-Form auf Grund der grösseren Quellung bei allen Alkoholkonzentrationen zur ungehinderten Glukosesorption befähigt sein müsste.

Die ungleichmässige Verteilung von Alkohol und Wasser wurde qualitativ durch einen Aussalzeffekt bzw. Einsalzeffekt erklärt [2]. Die Verhältnisse bei der Glukoseverteilung werden dadurch noch komplizierter, weil hier nicht nur die Ionen sondern auch die Alkoholkonzentration die Verteilung beeinflussen. Man könnte sich als Grenzfall denken, dass die Ionen auf die Glukosemoleküle gar nicht einwirken und dass die Glukosesorption eine direkte Folge der ungleichmässigen Verteilung von Wasser und Alkohol zwischen der Aussen- und Innenlösung wäre. Da die Alkoholkonzentration in der Austauscherphase meistens kleiner ist als in der Aussenlösung und die Löslichkeit der Glukose mit steigender Alkoholkonzentration abnimmt, könnte man die Glukosesorption qualitativ als eine Verteilung zwischen zwei Phasen mit verschiedenen Lösungsmitteln erklären, d.h., die Glukose dringt vorzugsweise in die Phase mit dem besseren Lösungsmittel ein, also in die wasserreichere Innenlösung.

Auf Grund von Löslichkeitsbestimmungen für Glukose in Alkohol-Wassergemischen und der Verteilung von Alkohol und Wasser kann eine theoretische Glukoseverteilung berechnet werden. Hierbei wird also angenommen, dass die direkte Einwirkung der Ionen auf die Glukosemoleküle vernachlässigt werden kann. Ein Vergleich dieser berechneten Verteilung mit der experimentell gefundenen zeigte, dass eine solche Approximation unzulässig ist. Bedeutende Abweichungen ergaben sich und zwar in der Richtung, dass man bei niedriger Alkoholkonzentration einen deutlichen Aussalzeffekt für Glukose erhält und bei höherer Alkoholkonzentration statt dessen einen Einsalzeffekt. Der Aussalzeffekt im niedrigen Konzentrationsbereich kann übrigens direkt aus den Tabellen entnommen werden. Die Tatsache, dass in wässeriger Lösung Glukose ausgesalzt wird, ist schon früher bekannt [6].

Tabelle 4. Vergleich des Verteilungskoeffizienten für Glukose K^* mit der Alkoholkonzentration der Innenlösung x_r.

Austauscher	x_r	K^* bei $x = 0{,}73$ und $x_G = 0{,}001$
Dowex 50 Li^+	0,32	7,2
Na^+	0,24	27,5
K^+	0,25	50,8
Dowex 50 X1 Li^+	0,57	3,4
K^+	0,34	36,3
Dowex 2 ClO_4^-	0,53	1,1
Cl^-	0,44	8,2
SO_4^{2-}	0,35	31,2
Dowex 2 X1 ClO_4^-	0,43	1,3
SO_4^{2-}	0,25	46,3

Ohne irgend welche anderen theoretischen Berechnungen heranziehen zu müssen, kann man mit dem hier gesammelten experimentellen Material zeigen, dass die Wechselwirkung zwischen den Ionen und Glukosemolekülen nicht vernachlässigt werden kann. In Tabelle 4 sind die K^*-Werte für die untersuchten Austauscher bei einer konstanten Zusammensetzung der Aussenlösung [$x = 0{,}73$ und $x_G = 0{,}001$] zusammengestellt. Die Alkoholkonzentration der Innenlösung x_r ist dann für jeden Austauscher verschieden und ebenfalls in der Tabelle verzeichnet. Es soll nun die Alkoholkonzentration der Innenlösung mit K^* verglichen werden. Beim normal vernetzten Anionenaustauscher Dowex 2 findet man eine Parallelität zwischen dem Verteilungskoeffizienten und der Alkoholkonzentration. Wie erwartet steigt die Glukosesorption, wenn die Alkoholkonzentration der Innenlösung abnimmt, d.h. wenn das Lösungsmittel in der Harzphase für Glukose besser wird. Dasselbe ergibt sich für den schwach vernetzten Anionenaustauscher Dowex 2 X1. Vergleicht man diesen bei gleichem Gegenion mit dem normal vernetzten Anionenaustauscher, so nimmt hier auch die Glukosesorption mit fallendem Alkoholgehalt der Innenlösung zu. Für den Kationenaustauscher findet man ebenfalls eine gewisse Parallelität aber auch das Gegenteil. Die Alkoholkonzentration der Na^+-Form des normal vernetzten Kationenaustauschers ist z.B. niedriger als die der K^+-Form. Trotzdem wird von der Na^+-Form viel weniger Glukose aufgenommen als von der K^+-Form. Überhaupt lässt sich eine allgemeine Parallelität zwischen der Alkohol-Wasserverteilung und der Glukosesorption nicht aufstellen. Wenn diese Parallelität vorhanden wäre, müssten alle in Tabelle 4 angeführten Alkoholkonzentrationen die gleiche Reihenfolge für die entsprechenden Verteilungskonstanten geben, was aber nicht zutrifft. Dies zeigt deutlich, dass die Verschiedenheit der Alkoholkonzentration der Innen- und Aussenlösung eine zufriedenstellende Erklärung für die Glukosesorption nicht gibt, sondern dass man ebenfalls auf den Salzeffekt Rücksicht nehmen muss, der auf die Glukosemoleküle ausgeübt wird.

Wir danken dem *Schwedischen Naturwissenschaftlichen Forschungsrat* für die Bereitstellung von Mitteln.

LITERATURVERZEICHNIS

1. Rückert, H. und Samuelson, O. *Svensk Kem. Tidskr.* **66** (1954) 337.
2. Rückert, H. und Samuelson, O. *Acta Chem. Scand.* **11** (1957) 303.
3. Scott, T. A., Jr. und Melvin, E. H. *Anal. Chem.* **25** (1953) 1656.
4. *Svenska Pappers- och Cellulosaingenjörsföreningens tekniska meddelanden*, CCA 11 (1942).
5. Du Rietz, C. *Diss.* Tekniska Högskolan, Stockholm, 1938.
6. Wheaton, R. M. und Bauman, W. C. *Ann. N. Y. Acad. Sci.* **57** (1953) 159.

Eingegangen am 6. November 1956.

ACTA CHEMICA SCANDINAVICA 11 (1957) 324—328

Thermodynamic Dissociation Constants of 2,4-Dichlorophenoxyacetic Acid (2,4-D) and Some Related Plant Growth Regulators

MAGNUS MATELL* and SVEN LINDENFORS

Institute of Organic Chemistry, Royal Agricultural College, Uppsala, and Department of Organic Chemistry, University of Uppsala, Sweden

The dissociation constants of four substituted aryloxyacetic acids in water at 25° C have been determined by the conductivity method. The acids belong to the group of plant growth regulators.

The biological activity of weak acids and bases is strongly influenced by the pH of the medium in which the activity is measured. In many cases it has been found that the activity of weak acids is independent of the acidity at pH levels below pK but decreases rapidly when the pH is raised above pK [1]. The aryloxyacetic acids, to which 2,4-D, 2,4,5-T and MCPA belong, is an important type of biologically active, weak acids for which similar relations have been found. It has been assumed that only the undissociated molecule is active in bringing about a physiological response [2]. This view is supported by the fact that undissociated organic acids appear to penetrate the plasma membranes more easily than their anions [3]. In contrast to this some cases have been reported where the physiological response appeared to be determined by the concentration of the anion [4,5].

In spite of these conflicting conclusions it is obvious that the degree of dissociation is of great importance for the growth regulating properties of weak acids. For a quantitative discussion of the influence of pH on the activity of 2,4-D and related growth regulators, the dissociation constants must be known with some accuracy. An examination of the literature has displayed that several determinations of dissociation constants of these compounds have been carried out (Table 1). Most of these refer to classical dissociation constants calculated from the pH of aqueous solutions of the acids, free or neutralized to 50 %. Such methods are only approximate, especially when the solubility of the acid investigated is small. Thus the discrepancies between values given by different authors are not surprising.

* Present address: Research Laboratory, Mo & Domsjö AB, Örnsköldsvik, Sweden.

Because of this need for more dependable data we have calculated thermodynamic dissociation constants from conductivity measurements of the phenoxyacetic acids recorded in Table 1.

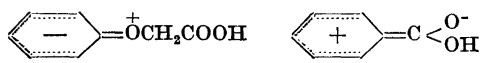
Table 1.

Acid	10^4 K	10^4 K_0	Method	Reference
4-Chlorophenoxyacetic	9.62		Conductivity	6
		7.89	E. m. f.	7
		9.79	Conductivity	This investig.
2,4-Dichlorophenoxy-acetic (2,4-D)	5.3		—	8
	15.5		pH	2
	10.9		pH	9
	10		pH	10
		12.7	Conductivity	This investig.
2-Methyl-4-chloro-phenoxyacetic (MCPA)	3.2		—	11
	8.9		pH	10
		7.81	Conductivity	This investig.
2,4,5-Trichlorophenoxy-acetic (2,4,5-T)	26.6		pH	2
		14.7	Conductivity	This investig.
2-Chlorobenzoic	12.8—13.0		Conductivity	12
		11.4	»	13
		12.0	»	14
	12.8—13.2	12.6	»	This investig.

The measurements were performed with a conductivity bridge, built according to the principles of Jones and Josephs [15]. The acids examined are rather strong and therefore the limiting conductivity at infinite dilution was not determined by the sodium salt method but from the conductivity of the aqueous acid solutions by the extrapolation method of Fuoss [16].

In order to test the bridge and the procedure, the dissociation constant of 2-chlorobenzoic acid was determined too. As seen from Table 1 the result is in fairly good agreement with data obtained from the literature.

The phenoxyacetic acids now studied, are rather strong, and their dissociation constants do not differ very much. This is a general feature of substituted phenoxyacetic acids as pointed out by Hayes and Branch [7]. The unusual strength is probably due to resonance structures of type I. In the phenoxyacetic acids there is no conjugation between the carboxylic group and the aromatic nucleus. Consequently, substituents will not affect the carboxyl group to the same extent as in the benzoic acids with resonance structures of type II.



I II

It was found by Hayes and Branch that the strength of phenoxyacetic acid was decreased by a methyl group in the nucleus but increased by a chlorine

atom [7]. These rules were derived for monosubstituted acids but they seem to be valid also for the acids investigated here. However, the material is too small to permit a general statement.

EXPERIMENTAL

Materials. 2-Chlorobenzoic acid, recrystallized three times from conductivity water, m. p. 140—141°.

4-Chlorophenoxyacetic acid, recrystallized twice from conductivity water, m. p. 157.2 —157.9°.

2-Methyl-4-chlorophenoxyacetic acid, recrystallized three times from toluene, m. p. 119.0—119.8°.

2,4-Dichlorophenoxyacetic acid, recrystallized once from formic acid and twice from toluene, m. p. 139.0—139.8°.

2,4,5-Trichlorophenoxyacetic acid, recrystallized once from formic acid, once from toluene and twice from benzene, m. p. 155.0—155.8°.

Potassium chloride (p. a.), recrystallized twice from conductivity water and fused in a platinum dish.

Melting points (corrected) were determined with a hot stage microscope. The conductivity water, which had a specific conductance of $0.8—0.9 \times 10^{-6}$ ohm^{-1} cm^{-1}, was obtained by aeration of the distillate from a two-stage, all quartz still.

Conductivity measurements. The bridge network was based essentially on the bridge described by Jones and Josephs [15]. The ratio arms of the bridge were two equal, 1 000 Ω, low-inductance resistances. The variable resistance was a calibrated, low-inductance, five-decade box of total resistance 11 111 Ω, with a variable resistance, adjustable to 0.001 Ω (Leeds and Northrup, Cat. No. 43 256). The capacitances in the bridge were as follows: a variable capacitance (0—500 pF) across earth and either end of the bridge, a capacitance (200 pF) across the conductivity cell, two capacitances (500 pF, 1 000 pF) and a variable capacitance (0—500 pF) across the decade box. The detector was a high-resistance (2 000 ohms) telephone without amplifier. The earphone was covered with sheetmetal, connected to earth. The oscillator was an audion tube oscillator giving 4 V at 1 000 cycles per sec (Philips type GM 4260). The conductivity cells, of the type described by Jones *et al.*[17], had greyed platinum electrodes. During measurements the cells were immersed in a thermostat filled with oil and controlled within 0.005 °C. The whole assembly was placed in a constant temperature room at 20.0 ± 0.1 °C.

One of the conductivity cells was directly calibrated against M/100 potassium chloride solution, using the conductance data of Jones and Bradshaw [18]. This cell (constant 1.315) was used for calibration of the other (constant 0.3483).

The conductance at 25 °C of the pure acids dissolved in conductivity water was measured at different concentrations in the range 0.0003—0.003 M. The conductance of the acid solutions was not corrected for water conductance. All solutions were prepared by weighing and the weighings were corrected to *vacuo*.

The results of the conductivity measurements are found in Tables 2—6. The following symbols are used.

C	total concentration of acid
Λ_0	equivalent conductance at infinite dilution
Λc	equivalent conductance at concentration C
K_0	thermodynamic dissociation constant
K	classical dissociation constant.

Table 2. 2-Chlorobenzoic acid $\Lambda_0 = 373.4$.

$10^3\,C$	Λ_c	$10^4\,K$	$10^4\,K_0$	
2.954	180.0	13.25	12.67	
2.459	190.6	13.08	12.56	
1.843	208.3	12.97	12.54	$K_0 = (12.6 \pm 0.1)\ 10^{-4}$
1.288	231.2	12.96	12.65	
0.686	269.3	12.80	12.65	

Table 3. 4-Chlorophenoxyacetic acid. $\Lambda_0 = 370.8$.

$10^3\,C$	Λ_c	$10^4\,K$	$10^4\,K_0$	
2.830	166.0	10.27	9.83	
2.308	177.6	10.16	9.76	
1.817	191.9	10.09	9.74	$K_0 = (9.79 \pm 0.04)\ 10^{-4}$
1.416	207.6	10.10	9.80	
1.013	228.5	10.03	9.80	
0.6352	257.0	9.95	9.82	

Table 4. 2-Methyl-4-chlorophenoxyacetic acid $\Lambda_0 = 374.0$.

$10^3\,C$	Λ_c	$10^4\,K$	$10^4\,K_0$	
2.616	158.4	8.14	7.80	
2.202	168.6	8.15	7.84	
1.788	180.8	8.08	7.80	$K_0 = (7.81 \pm 0.03)\ 10^{-4}$
1.361	197.5	8.04	7.80	
0.9332	221.0	7.96	7.78	
0.5223	257.5	7.95	7.85	

Table 5. 2,4-Dichlorophenoxyacetic acid $\Lambda_0 = 361.1$.

$10^3\,C$	Λ_c	$10^4\,K$	$10^4\,K_0$	
1.503	215.0	13.17	12.80	
1.265	225.0	13.04	12.71	
1.002	238.7	12.91	12.66	$K_0 = (12.7 \pm 0.1)\ 10^{-4}$
0.7480	256.0	12.93	12.76	
0.5021	277.4	12.79	12.73	
0.3370	296.5	12.69	12.75	

Table 6. 2,4,5-Trichlorophenoxyacetic acid $\Lambda_0 = 362.7$.

$10^3\,C$	Λ_c	$10^4\,K$	$10^4\,K_0$	
0.9860	249.5	14.95	14.69	
0.7822	262.9	14.95	14.77	
0.5171	284.4	14.75	14.72	$K_0 = (14.7 \pm 0.1)\ 10^{-4}$
0.2592	314.0	14.46	14.69	

This investigation was carried out at the Institute of Organic Chemistry, Royal Agricultural College, Uppsala. The authors are much indebted to the head of the institute, Professor Nils Hellström, for all facilities put at our disposal. This work has been financially supported by a grant from the *Swedish Natural Science Research Council*, which is gratefully acknowledged.

REFERENCES

1. Simon, E. W. and Beevers, H. *New Phytologist* **51** (1952) 163.
2. van Overbeek, J., Blondeau, R. and Horne, V. *Plant Physiol.* **26** (1951) 687.
3. Davson, H. and Danielli, J. F. *The Permeability of Natural Membranes*, New York 1943.
4. Lundegårdh, H. *Arkiv Botanik* **1** (1949) 289.
5. Burström, H. *Physiol. Plantarum* **4** (1951) 470.
6. Behaghel, O. *J. prakt. Chem.* **114** (1926) 287.

7. Hayes, N. and Branch, G. *J. Am. Chem. Soc.* **65** (1943) 1555.
8. Audus, L. J. *New Phytologist* **48** (1949) 97.
9. Wedding, R. T., Erickson, L. C. and Brannaman, B. L. *Plant Physiol.* **29** (1954) 64.
10. Burström, H., Sjöberg, B. and Hansen, B. *Acta Agr. Scand.* **6** (1956) 155.
11. Brian, R. C. and Rideal, E. K. *Biochim. et Biophys. Acta* **9** (1952) 1.
12. Kendall, J. *J. Chem. Soc.* **101** (1912) 1275.
13. Dippy, F., Williams, F. and Lewis, R. *J. Chem. Soc.* **1935** 343.
14. Saxton, B. and Meier, H. F. *J. Am. Chem. Soc.* **56** (1934) 1918.
15. Jones, G. and Josephs, R. *J. Am. Chem. Soc.* **50** (1928) 1067.
16. Fuoss, R. M. *J. Am. Chem. Soc.* **57** (1935) 488.
17. Jones, G. and Bollinger, G. *J. Am. Chem. Soc.* **53** (1931) 411.
18. Jones, G. and Bradshaw, B. C. *J. Am. Chem. Soc.* **55** (1933) 1780.

Received December 5, 1956.

ACTA CHEMICA SCANDINAVICA 11 (1957) 329—339

Mercury(II) Halide Mixed Complexes in Solution

I. The Experimental Method and the Distribution of the Neutral Complex

Y. MARCUS*

Department of Inorganic Chemistry, Royal Institute of Technology, Stockholm 70, Sweden

Experimental details are described for a study of the formation of mixed mercury(II) halide complexes. The distribution coefficients log λ° of HgX_2 between benzene and water, obtained both directly and from the solubilities, are: $HgCl_2$ — 1.06 ± 0.01; $HgBr_2$ 0.05±0.01; HgI_2 1.66 ± 0.01. The coefficients for benzene — 0.5 M perchlorate ionic medium were also obtained. The solubilities of HgX_2 in benzene are: $HgCl_2$ (1.92±0.01) × 10^{-2} M; $HgBr_2$ (1.90 ± 0.01) × 10^{-3} M; HgI_2 (4.78 ± 0.05) × 10^{-3} M. Literature values for the solubilities and the distribution coefficients are reviewed. The salting-out effect of up to 2 M $NaClO_4$ on HgX_2 was studied, and the same salting-out coefficient k_c = 0.14 was found for all three halides. This value agrees with McDevit and Long's compression theory, although equations of other authors also fit the data.

1. INTRODUCTION

The careful study of metal complex formation in solution has mainly been confined, until recently, to systems of one metal and one ligand, which we shall call binary systems. Although practically no systematic investigation of complex systems between a metal and two ligands — which might be called ternary systems — has taken place, such cases have already been mentioned in passing, and sometimes complexity constants have been assigned to them. For instance Lister and Rivington [1] report the species $FeClCNS^+$, $FeBrCNS^+$, $FeCl_2CNS$ and $FeSO_4CNS$, while Newman [2] in his recent thesis studied complexes of the type $BiCl_nBr_{5-n}^{2-}$.

It was felt that a more systematic work on ternary systems was desirable, in particular in order to find whether their formation obeys the statistical rules or is favoured or obstructed by the intra-molecular forces.

A convenient system to study was found in the mercury(II) halide complexes. These have been thoroughly studied before [3], and accurate constants for the binary complexes are available. Furthermore, a convenient method of

* Permanent address: Israel Atomic Energy Commission, Hakiryah, Tel-Aviv, Israel.

solvent distribution can be applied to the system, which has the advantage that the distribution of one of the mixed complexes, the neutral one, may be studied almost directly (part III).

a) Plan of work

The experimental study of mixed halide complexes of mercury included also a restudy of the binary complexes, the data for which are important in subsequent calculations. First the distribution of the neutral complex (*e. g.* $HgCl_2$) was studied, in the range of concentrations where it is stable, and its distribution coefficient was determined for all the halide ligands as a function of the ionic medium concentration (part I). The stepwise complexity constants of the binary complexes were then studied under the same conditions as formerly applied [3], in order to check the constants against the earlier potentiometric values (part II). Later, mixed complexes were considered, where the ligand number is two, *i. e.* only the neutral species exist. Two such binary complexes (*e. g.* $HgCl_2$ and $HgBr_2$) may interact to give a ternary one ($HgClBr$) (part III). In the next paper the system mercury(II)-bromide-iodide is completely worked out, by both central group (Hg) and ligand (I) solvent distribution methods. The latter, incidentally, does not seem to have been used before (part IV). Finally, a literature survey of mixed complex formation is presented and commented on, and the question of ternary complex formation is discussed against the background of complex formation in general (part V).

b) Symbols

The following symbols apply in all the papers of this series:

A, B	two different ligands, for instance two halide ions, where B applies to the heavier of the two.
A, B	analytical (total) concentrations of A and B present in both the phases.
a, b	concentrations of free A and B in the aqueous phase.
D	gross distribution of M between the organic solvent and the aqueous solution, *i. e.* the ratio of concentrations, organic to aqueous, for equal volumes of the phases. (In part IV it denotes also distribution of B in the section devoted to it.)
i, j	indices, integers or zero (for mercury always $i + j \leq 4$). i usually applies to A, j to B.
K	disproportionation constant, for $M + MX_2 \rightleftharpoons 2\ MX$ in part II, and for $MA_2 + MB_2 \rightleftharpoons 2\ MAB$ in part III.
k_n	successive equilibrium constant for $MX_{n-1} + X \rightleftharpoons MX_n$.
$k_{i,j}$	equilibrium constant for $MA_{i-1}B_j + A \rightleftharpoons MA_iB_j$.
$k_{i',j}$	equilibrium constant for $M_iAB_{j-1} + B \rightleftharpoons MA_iB_j$.
M	complex-forming central group, for instance Hg^{2+}.
M	analytical (total) concentration of M present in both phases.
m	concentration of free M in the aqueous phase.
$\bar{n}$	ligand number for the binary complexes M—X.
$\bar{n}_{A,B}$	total ligand number for the ternary system M—A—B (*i. e.* the sum $\bar{n}_A + \bar{n}_B$).
$)_{or}$	subscript, the organic solvent phase (no subscript — the aqueous phase).
R	ratio B/A.
r	ratio b/a.
$s_{solvent}$	molar solubility in solvent stated.
u	concentration $[MA_2]$ in part IV.
X	general ligand, for instance halide.
X	analytical (total) concentration of X in both phases.

x concentration of free X in the aqueous phase.
$\beta_{i,j}$ overall complexity constant for $M + iA + jB \rightleftharpoons MA_iB_j$.
β_n overall complexity constant for $M + nX \rightleftharpoons MX_n$.
λ distribution coefficient of MX_2 between organic solvent and aqueous solution.
λ^0 distribution coefficient at zero ionic medium concentration (*i. e.* distribution benzene — pure water).
$\lambda_{i,j}$ distribution coefficient of MA_iB_j $(i + j = 2)$.
[ ] molar concentration of the species within the brackets.

Further symbols may be introduced and defined for occasional use in the appropriate places.

Charges are omitted in the mathematical equations and in reactions generally.

Concentrations and constants are given on the molar (moles per liter solution) scale, denoted by M.

2. EXPERIMENTAL METHOD

The description in this section applies to all the papers in this series (parts I—V).

a) Conditions of study

The complexes were studied in aqueous solutions of 0.50 M (ClO_4^- + X^-) *ionic medium*, which was made up from 0.010 M hydrogen ions, M M mercury(II) ions, 0.490—2M M sodium ions, $A + B$ M halide and 0.500—$(A+B)$ M perchlorate. The function of the hydrogen ions was to repress hydrolysis, although this was actually unnecessary, since the complexing by halide is very strong. Nevertheless, this acidity was retained so that the conditions would be the same as in the earlier potentiometric study [3].

The *temperature* of equilibration was kept fixed at 25.0 ± 0.2 °C, again the same as in the earlier study. This was achieved by equilibrating the solutions in a thermostated room.

The *method* of study consisted of measuring the gross distribution of the central group (mercury), or of a ligand (iodine), between an organic solvent phase (benzene) and the immiscible aqueous solution described above, by measuring the distribution of the radioactivity of ^{203}Hg or ^{131}I. The amount of benzene introduced into the ionic medium (0.036 mole %, calculated from McDevit and Long's data [4]) is quite negligible.

b) Materials

The *sodium perchlorate* used for the ionic medium was made by neutralizing perchloric acid with sodium carbonate to the extent of 98 %, boiling off the carbon dioxide, and making up to volume with distilled water. Sometimes a slight adjustment of acidity to exactly 0.010 ± 0.001 M was made after titration. The perchlorate concentration was checked by passing the solution through a cation exchange column in the hydrogen form and titrating the total acid. It always corresponded to 0.500 ± 0.005 M. The solution was checked from time to time for presence of halide, but always with negative results.

Stock solutions of *sodium halides* were prepared, about 0.49 M in halide and 0.010 M in perchloric acid, except the iodide, which was kept neutral in concentrated solutions, and was acidified only when [I] was below 0.001 M. The halide concentration was measured by Volhard titration of the stock solutions.

A 0.0440 M *mercury(II) perchlorate* stock solution was prepared by dissolving mercury(II) oxide in a calculated amount of perchloric acid, so that after dilution by sodium perchlorate solution and water the final acidity would be 0.010 M, and the final perchlorate concentration 0.50 M. The mercury(II) oxide, in its turn, was prepared by precipitation

from mercury(II) sulphate solution by sodium hydroxide, filtration and thorough washing. The mercury concentration was measured by titration with standard thiocyanate.

Benzene was equilibrated with sodium perchlorate ionic medium prior to use. The benzene then contained 0.26 mole % water [5], but only 0.01 % material not volatile at 5° C. Apart from the water, the only species which benzene extracts from the aqueous solutions seems to be the neutral mercury halides.

Radioactive mercury(II) oxide, containing the ^{203}Hg isotope (half-life 47.9 days, the characteristic radiation being 0.21 MeV β-rays and 0.28 MeV γ-rays) was obtained from A.E.R.E., Harwell, England, and was used after the decay of the 65 hour ^{197}Hg produced together with it. It was "specpure" and had an activity of about 26 mC/g. A weighed amount of it was dissolved in the minimum amount of 1.0 M perchloric acid and diluted with sodium perchlorate solution to a known volume. The stock solution was 0.00117 M in mercury.

A *radioactive* carrier-free *iodide* solution containing the ^{131}I isotope (half-life 8.0 days, characteristic radiation 0.61 MeV β-rays and 0.36 MeV γ-rays) was obtained from J.E.N. E.R., Kjeller, Norway. Its activity was initially 2 mC/ml, it contained less than 1 μg/ml iodide and less than 0.05 M reducing substances. It was added to known amounts of iodide solution before use, giving a negligible contribution to the total iodine concentration, and diluting the solutions by no more than 1 %, for which, however, no correction was made.

All the *reagents* used were of analytical quality grade, in particular the benzene was thiophene-free, according to the A.C.S. standard.

c) Equilibration and radioactive assay

Equilibration of the phases was effected by shaking together equal volumes (10.00 $\pm$ 0.05 ml) of aqueous solution and benzene in 40 ml glass stoppered bottles by a mechanical shaker rotating at 24 r.p.m.

The time of contact was in the large majority of cases 17 $\pm$ 1 h (overnight). In a few instances it was as short as 5 $\pm$ 1 h or as long as 43 $\pm$ 1 h. A number of experiments were made to determine the time needed for equilibrium to be reached. A small difference was sometimes found between the distribution values for 0.5 h and 1.5 h, but the latter value agreed with those for 5, 17 and 42 h, within the experimental errors.

When the shaking ended the phases separated cleanly, and were pipetted each in its turn up to a fixed height into the G.-M. tube. This was a "20th Century Electronics" M6 concentric-tubes liquid counter, containing about 9.5 ml. All measurements of radioactivity were relative, *i. e.* only ratios were obtained (usually between the activities in the two phases, in part III also between stock solutions of mercury(II) halides in benzene). Moreover, the activities making up the ratio were measured on the same day, so that no correction for decay was necessary.

Since there is a difference between the absorption of radioactive rays in the benzene and aqueous solutions, a correction must be applied. From radioactivity balance it was found that the value for the activity of Hg in benzene must be multiplied by 0.89 and that of I by 0.85 to make them comparable with those in aqueous solutions. In practice, 0.050 log units were subtracted from the log D values for radioactive Hg, and 0.070 log units for I.

d) Representation of results and errors

Primary data will usually appear as graphs of log D *vs* a suitable variable. Sometimes, however, they will appear in tabular form.

The experimental errors may be divided into two groups: analytical and volumetric errors on the one hand and counting errors on the other. Results of titrations are usually accurate to within $\pm$0.7 %. The error in the relative volumes of the phases might have come to $\pm$1.0 %. The errors in the counting varied, as it was necessary sometimes to count values not much above the

background. Usually the statistical error was within ±1.5 %, and thus the total error of an individual determination was about ±2.5 % or 0.010 log units in log *D*. The reproducibility was quite good, even experiments made several months apart with different stock solutions usually showed results not deviating by more than the sum of the experimental errors.

In the calculation of the equilibrium constants from the data, such limits of error were assigned to them, that at least 90 % of the experimental points fell between curves calculated with the extreme values of the constants.

3. THE DISTRIBUTION COEFFICIENTS

a) Experimental results

The distribution of mercury(II) halides between an organic and an aqueous phase was studied by two approaches. One was to measure the distribution directly, at very low mercury concentrations — of the order of 10^{-5} M—using radioactive mercury. The other approach was to measure the solubility of the mercury halide in each phase separately, and to take the ratio as representing the distribution coefficient, according to Nernst's law. This is permissible, provided there is only negligible intersolubility of the phases and no association, dissociation or solvation of the solute occurs. This seems to be the case with the mercury(II) halides (except for $HgCl_2$, see discusssion below).

The solubility of HgX_2 in water saturated benzene was measured by shaking excess HgX_2 with the benzene in a thermostated room at 25.0 ± 0.2°C for 42 h, allowing the solid to settle for half an hour, taking an aliquot with a calibrated pipette from the clear supernatant liquid, evaporating the benzene at room temperature in a current of air and weighing the residue. In separate experiments it was checked that no HgX_2 volatilized with the benzene by the above procedure.

The values of the benzene solubility of the mercury(II) halides $s_{C_6H_6}$ are given in Table 1 and also in Table 2.

Distribution coefficients were calculated as the ratio of the benzene solubility to the aqueous solubility, using the average of the values that are not in parenthesis in Table 2. (Column "Solubility" in Table 1).

Table 1. Experimental distribution coefficients of mercury(II) halides, log λ.

Molar Solubility $s_{C_6H_6}$	"Solubility" log λ°	Distribution coefficients "Direct determination" log λ°	"Direct determination" log λ	"Extrapolation" log λ
$HgCl_2$ $(1.92\pm0.01)10^{-2}$	$\left\{\begin{matrix}(-1.142\ \ )\text{a)}\\ -1.084\pm0.003\end{matrix}\right\}$	-1.057 ± 0.007	-0.965 ± 0.010	-0.960 ± 0.015
$HgBr_2$ $(1.90\pm0.01)10^{-2}$	0.049 ± 0.004	0.040 ± 0.007	0.150 ± 0.005	0.155 ± 0.010
HgI_2 $(4.78\pm0.05)10^{-3}$	$1.68\ \pm0.02$	1.658 ± 0.010	1.782 ± 0.010	1.760 ± 0.015
$Hg(CNS)_2(8\pm2)10^{-6}$	$-2.5\ \ \pm0.1$		$-2.2\ \ \pm0.1$	

a) See discussion, p. 336.

Table 2. The molar solubilities in water, benzene and toluene, and the distribution coefficients of mercury(II) halides at 25°C.

Author	Ref.	log s_{H_2O}	log $s_{C_6H_6}$	log $\lambda°_{C_6H_6}$	log $s_{C_7H_8}$	log $\lambda°_{C_7H_8}$
			a) Mercury (II) chloride, $HgCl_2$			
Linhart	6		−1.680	−1.08 [a]		−1.02 [a]
Sherrill	7	(−0.580)	−1.705	(−1.12 [b])		
Laszcynski	8		−1.74 [c]			
Dukelski	9					
Marden	10		−1.674			
Flöttmann	11	−0.577				
Herz	12	−0.577				
Eddy	13	−0.577				
Thomas	14	−0.573				
Moles	15	(−0.61) [d]				
Morse	16	(−0.582)				−1.00
Brown g	17	(−0.61)			−1.71	−1.10
Drucker	18					−1.04
Hanzsch	19					−1.03
Krishtalik	20		−1.739			
This work			−1.717±0.007	−1.057±0.007		
			b) Mercury (II) bromide, $HgBr_2$			
Krishtalik	20		−1.740			
Sherrill	7	−1.770	−1.712	0.050 ± 0.005		
Herz	12	−1.77				
Moles	15	−1.770				
Garrett	21	−1.770				
Morse	16					0.01
Tyrrell	22	−1.768				
This work			−1.721 ± 0.002	0.047 ± 0.007		
			c) Mercury (II) iodide, HgI_2			log $\lambda_{0.5\ M\ NaClO_4}$
Sherrill	7		−2.307	(1.58) [b]		
Laszcynski	8		−2.31 [e]			
Gautier	23					
Beckmann	24					
Morse	16	(−3.89)				
Tananaev	25	(−4.12) [j]				
DeBruijn	26	−4.01				
Sillén	27	−3.98				1.81 ± 0.03
This work			−2.321 ± 0.005	1.66 ± 0.01		1.77 ± 0.01
			d) Mercury (II) thiocyanate, $Hg(CNS)_2$			
Grossmann	28	−2.661 [h]				
Mason	29	−2.7 [i]				
Sherrill	30	−2.66				
This work		−2.658±0.006	−5.1±0.1	−2.5 ± 0.1		−2.2 ± 0.1

Table 2 (Contd.)

a) Extrapolated to zero concentration.
b) From ratio of solubilities.
c) Interpolated, though with little accuracy, from values at several temperatures between 6.5° and 54°.
d) Additional, less reliable, values are: Benrath [31] −0.59, and Benrath and Ammer [32] −0.58.
e) Extrapolated linearily from values at 15°: −2.37 and at 23°: −2.32.
f) The authors give a critical discussion on the solubility of HgI_2 in water, and also a value for the solubility in the 0.50 M $NaClO_4$ ionic medium: -4.13 ± 0.02.
g) Brown's values apply to 24°.
h) Author gives solubility as 0.00218 n, but, apparently this should read M.
i) A misquotation, *via* Comey and Hahn's "Dictionary" [33] value of 0.0063 g/100 g solution, which is Grossmann's value.
j) This is the value obtained experimentally by Tananaev and Pilipenko, but with only 10 minutes' shaking. Garrett [21] misquoted them, the value he reports in their name is what they think is Sherrill's figure, and actually is Morse's.

The column "Direct determination" in Table 1 gives the values found by determination of the distribution of HgX_2 between benzene and water (λ^0), and between benzene and 0.50 M sodium perchlorate ionic medium λ, starting with a benzene solution of HgX_2 to ensure having only the neutral complex.

Finally, the column "Extrapolation" gives the values found by extrapolation of distribution data of HgX_2 between benzene and excess halide X^- in the ionic medium (described in detail in part II) to zero excess halide.

In addition, a few experiments were made to see if $Hg(CNS)_2$ could also be extracted by benzene. Owing to the extremely small solubility in benzene, the distribution coefficient between benzene and the ionic medium could be obtained only very roughly. The best estimates are $\log \lambda = -2.2 \pm 0.1$. The values for solutions where excess thiocyanate was present also extrapolate roughly to the same value:

$[CNS^-]$ M:	0.015	0.019	0.027
log D:	-2.4 ± 0.2	-2.4 ± 0.2	-2.5 ± 0.3

The aqueous solubility of $Hg(CNS)_2$ does not seem to have been determined since 1905 (see Table 2), and no experimental details were given for the reported figures. The solubility was therefore determined anew. Mercury(II) thiocyanate was precipitated from a solution of radioactive mercury, and the precipitate washed well with water and dried. A portion of 0.360 g was weighed out and dissolved in 25.00 ml 0.1 M NaCNS solution, which became thus 0.00454 M in mercury, and its activity a_0 was counted. Water and 0.50 M $NaClO_4$ ionic medium were then shaken for 72 h at 25° with excess radioactive mercury(II) thiocyanate, and the activities a_w and a_m of the filtered solutions determined. The concentrations (*i. e.* solubilities) are then $a_w a_0^{-1}$ 0.00454 and $a_m a_0^{-1}$ 0.00454 M, respectively. The averages of two determinations are:

water solubility:	$(2.20 \pm 0.03)10^{-3}$ M and
ionic medium solubility:	$(1.34 \pm 0.03)10^{-3}$ M.

From the ionic medium solubility and the coefficient log $\lambda = -2.2 \pm 0.1$, the benzene solubility log $s_{C_6H_6} = -5.1 \pm 0.1$ was calculated, and from the latter and the water solubility, the coefficient log $\lambda^\circ = -2.5 \pm 0.1$ was obtained.

b) Previous results

Literature values, which are mostly rather old and sometimes conflicting, are summarized in Table 2.

c) Discussion

Table 1 shows very good agreement between log λ and log λ° values found by two different methods. Of the two values of log λ° reported for $HgCl_2$ in column 3, —1.142 is the value obtained directly from the solubilities. This value must be corrected for dimerization. According to Linhart [6a] $[Hg_2Cl_4] = 0.3\,[HgCl_2]^2$. If this is correct, then in a saturated solution (total concentration of mercury chloride 0.265 M), there is 0.233 M free $HgCl_2$ and 0.016 M Hg_2Cl_4. The same equilibrium constant applies also to the benzene phase, according to Linhart, but because of the low solubility the necessary correction is negligible. If now the corrected water solubility of $HgCl_2$ is used, the value log $\lambda^\circ = -1.084$ is obtained, which is nearer to the value obtained from the distribution. Moreover, as will be shown below, the salting out effect on the distribution is independent of the particular halide used, so that there is a constant difference of (approximately) 0.11 log units between log λ for 0.50 M $NaClO_4$ ionic medium and log λ° (this may be seen also in Table 1). If 0.11 is subtracted from the average log λ for $HgCl_2$ in Table 1, the value —1.07 is obtained, agreeing with the value obtained from the distribution and the corrected solubility.

The values found in this work may now be compared with those reported in literature (Table 2). Regarding the aqueous solubility of $HgCl_2$, an average value of the more modern figures, log $s_{H_2O} = -0.575 \pm 0.002$ might be a fair approximation to the truth. Very good agreement is observed among the various determinations of the aqueous solubility of $HgBr_2$. Of the two groups of values for the aqueous solubility of HgI_2, the more recent one (DeBruijn and Sillén and Biedermann), combined with the benzene solubility gives a distribution coefficient log λ° about 1.68, in agreement with the directly determined value 1.66, and therefore seems to be better than the older one, yielding a coefficient of only 1.58. The aqueous solubility of $Hg(CNS)_2$ is seen to be in very good agreement with the previously reported values.

Considering the benzene solubilities, there seems to be good agreement with the few reported values, apart from $HgCl_2$, where the reported data are conflicting. The directly determined distribution coefficients of $HgCl_2$ (Linhart [6]) and $HgBr_2$ (Sherrill [7]) are quite near those obtained in this work. The salting-out of HgI_2 by 0.50 M $NaClO_4$ observed by Sillén and Biedermann [27] — a difference of 0.15 ± 0.03 log units in the solubilities — is quite near the value obtained here, 0.11 ± 0.01 log units.

4. EFFECT OF IONIC MEDIUM CONCENTRATION

a) Experimental results

The effect of the sodium perchlorate ionic medium on the distribution was studied further. Experiments were made where the distribution was measured as function of the ionic medium concentration, called C below, up to 2 M. All solutions more concentrated than 0.01 M contained 0.01 M perchloric acid, the remainder being sodium perchlorate, while more dilute solutions contained only perchloric acid. The data are summarized in Fig. 1 as plots of log λ—log λ° *vs* C.

As may be seen in Fig. 1, the values for all three halides lie on a single curve, with only slight random deviations.

b) Discussion

Many approaches have been proposed to describe and explain the salting-out effect, but none has found complete quantitative success. (See Ref.[34] for a modern review.) Empirically, salting-out data may be described by the Setchenov equation:

$$\log \lambda - \log \lambda^\circ = \log f_c = k_c C \qquad (1)$$

where f_c is the activity coefficient of the non-electrolyte in the ionic medium of concentration C and k_c is the salting-out constant, and where all the symbols refer to a very dilute solution of the non-electrolyte.

When eqn. (1) is applied to the data in Fig. 1, it is seen that it described them well at the lower concentrations, with the parameter $k_c = 0.14$. However, at concentrations C above about 1.5 M a curvature upwards occurs.

Various non-linear equations have been proposed to account for this. The simplest empirical one is due to Morrison [35]:

$$\log \lambda - \log \lambda^\circ = \log f_c = k_c C^{k_p} \qquad (2)$$

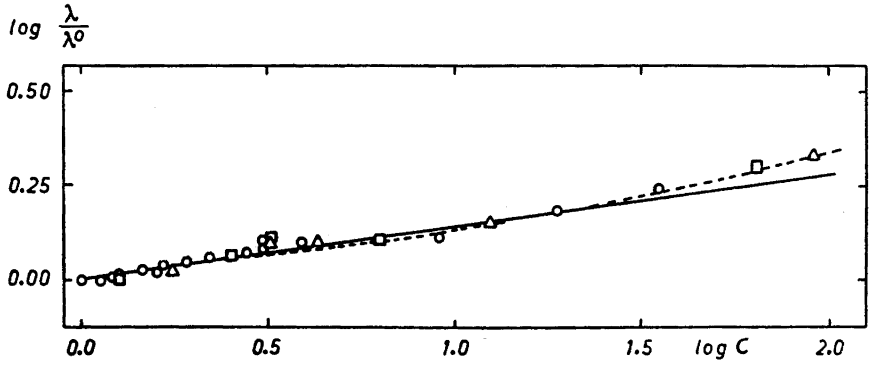


Fig. 1. Salting-out mercury(II) halides as function of ionic medium concentration. ○ Hg(II) chloride, □ Hg(II) bromide, △ Hg(II) iodide. ——— equation (1), $k_c = 0.14$, ····· equations (2), (3) and (4).

where k_p is an empirical constant. A curve with $k_c = 0.14$ and $k_p = 1.3$ expresses the data fairly well.

Of the more fundamental approaches, Debye's electrostatic theory [36] has won recognition as being able to explain the effects at least qualitatively for an electrolyte of the type of sodium perchlorate. It should be possible, in principle, to calculate the parameter J in eqn. (3) below for any pair of electrolyte- non-electrolyte, provided the ionic radii of the ions and the dielectric decrement of the non-electrolyte solutions are known.

$$\log \lambda - \log \lambda^\circ = \log f_c = -\log (1-JC) \qquad (3)$$

Eqn. (3) fits the data quite well with the parameter $J = 0.27$.

Finally, a recent equation proposed by Nakajima [37] can be rewritten in the form:

$$\log \lambda - \log \lambda^\circ = \log f_c = -\log (1-\mu C(1+\nu\sqrt{C})\ (1+0.707\sqrt{C})^{-1}) \qquad (4)$$

which is, again, a two parameter equation, and gives with $\mu = 0.18$ and $\nu = \sqrt{2}$ a very good fit with the data.

Eqns. (2), (3) and (4) give such similar results that they are incorporated into one curve in Fig. 1.

Although the one-parameter eqn. (1) fails at higher concentrations, it is possible to calculate the expected k_c from compressibility and volume data. According to McDevit and Long [4] k_c is given by:

$$k_c = \lim_{C \to 0} \mathrm{d}(\log \lambda - \log \lambda^\circ) / \mathrm{d}C = \overline{V}_n^\circ\ (V_e - \overline{V}_e^\circ)\ (2.3\beta_0 RT)^{-1} \qquad (5)$$

where $\overline{V}_n^\circ$ is the partial molar volume of the non-electrolyte, $\overline{V}_e^\circ$ that of the electrolyte — both at infinite dilution — and β_0 is the compressibility of water. Inserting the values $\beta_0 = 4.56.10^{-5}$ bar $^{-1}$, R = gas constant = 83.11 ml bar deg^{-1} mole^{-1}, $T = 298$ deg, $\overline{V}_n^\circ = 49$ ml mole^{-1} (given by Linhart [6a], p. 273) for $HgCl_2$, $(V_e - \overline{V}_e^\circ) = 7.5$ ml^{-1} mole (Mc Devit and Long [4]), the value $k_c = 0.141$ is obtained, in very good agreement with the observed value.

This good agreement might, however, be only fortuitious. For instance, the theory assumes that the radius of the non-electrolyte molecules is much smaller than the radii of the ions, whereas they are really comparable. Moreover, the variability of $\overline{V}_n^\circ$ with the various halides was neglected here.

The author wishes to thank the Israel Atomic Energy Commission for a research grant abroad, Professor Lars Gunnar Sillén for the facilities provided, and particularly for his advice, comments and criticism, and Dr. Helen S. Dunsmore for improving the English presentation.

REFERENCES

1. Lister, M. W. and Rivington, D. E. *Canad. J. Chem.* **33** (1955) 1591, 1603.
2. Newman, L. *Thesis* M.I.T., Cambridge, Mass. 1956.
3. Sillén, L. G. *Acta Chem. Scand.* **3** (1949) 515.
4. McDevit, W. F. and Long, F. A. *J. Am. Chem. Soc.* **74** (1952) 1733.

5. Seidell, A. *Solubilities of Organic Compounds* D. Van Nostrand, N. Y. 1941, 3rd Ed., Vol. II, p. 368.
6. Linhart, G. A. a) *J. Am. Chem. Soc.* **37** (1915) 258; b) *J. Am. Chem. Soc.* **38** (1916) 1272.
7. Sherrill, M. S. *Z. physik. Chem.* **43** (1902) 705.
8. Laszcynski, v. St. *Ber.* **27** (1894) 2285.
9. Dukelski, M. P. *J. Russ. Phys. Chem. Soc.* **39** (1907) 975.
10. Marden, J. W. and Dover, M. V. *J. Am. Chem. Soc.* **39** (1917) 4.
11. Flöttmann, F. *Z. anal. Chem.* **73** (1928) 1.
12. Herz, W. and Paul, W. *Z. anorg. Chem.* **82** (1913) 431.
13. Eddy, R. D. and Menzies A. W. C. *J. Phys. Chem.* **44** (1940) 207.
14. Thomas, H. C. *J. Am. Chem. Soc.* **61** (1939) 902.
15. Moles, E. and Marquina, M. *Ann. Soc. Espan. Fis. Quim.* **22** (1924) 551.
16. Morse, H. *Z. physik. Chem.* **41** (1920) 709.
17. Brown, O. W. *J. Phys. Chem.* **2** (1898) 51.
18. Drucker, K. *Z. Elektrochem.* **18** (1912) 246.
19. Hantzsch, A. and Vagt, A. *Z. physik. Chem.* **38** (1901) 735.
20. Krishtalik, L. I. *Izvest. Sektora Fiz. Khim. Anal. Akad. Nauk. SSSR* **20** (1950) 380.
21. Garrett, A. B. *J. Am. Chem. Soc.* **61** (1939) 2744.
22. Tyrrell, W. P. and Richards, J. *J. Chem. Soc.* **1953** 3812.
23. Gautier, H. and Charpy, G. *Compt. rend.* **111** (1890) 645.
24. Beckmann, E. and Stock, A. *Z. physik. Chem.* **17** (1895) 130.
25. Tananaev, N. A. and Pilipenko, A. T. *J. Appl. Chem. USSR* **10** (1937) 549.
26. DeBruijn, J. A. Jr. *Rec. trav. chim.* **160** (1941) 309.
27. Sillén, L. G. and Biedermann, G. *Svensk Kem. Tidskr.* **61** (1949) 63.
28. Grossmann, H. *Z. anorg. Chem.* **43** (1905) 358.
29. Mason, C. W. and Forgeng, W. D. *J. Phys. Chem.* **35** (1931) 1123.
30. Sherrill, M. S. and Skowronski, S. *J. Am. Chem. Soc.* **27** (1905) 30.
31. Benrath, A. *Z. anorg. u. allgem. Chem.* **163** (1927) 396.
32. Benrath, A. and Ammer, G. *Z. anorg. u. allgem. Chem.* **177** (1929) 129.
33. Comey, A. M. and Hahn, D. A. *Dictionary of Chemical Solubilities* 2nd Ed. McMillan, N.Y. 1921, p. 882.
34. McDevit, W. F. and Long, F. A. *Chem. Revs.* **51** (1952) 119.
35. Morrisson, T. J. *Trans. Faraday Soc.* **48** (1944) 43.
36. Debye, P. *Z. physik. Chem.* **130** (1927) 56.
37. Nakajima, M. *J. Electrochem. Soc. Japan* **21** (1953) 166.

Received November 27, 1956.

ACTA CHEMICA SCANDINAVICA 11 (1957) 340—359

Diffusion from a Bottom Layer; Diffusion with Moving Boundaries

STIG LJUNGGREN and OLE LAMM

The Royal Institute of Technology, Division of Physical Chemistry, Stockholm 70, Sweden

A new method of carrying out diffusion experiments is outlined, the initial condition being that the whole quantity of diffusing substance is concentrated in a thin layer at the bottom of the cell at zero time. Ideal equations are derived for uniform and non-uniform substances and a normalization procedure is described. The diffusion curves theoretically calculated for various binary mixtures of solutes are discussed and it is pointed out that in this type of diffusion the distortion of the curves due to non-uniformity is usually greater than that which occurs in ordinary diffusion. The apparatus and mode of operation are described in detail and a few experiments with uniform and non-uniform substances are related. In particular, mixtures of partially hydrolyzed dextran and sodium chloride were investigated.

I. INTRODUCTION

If pure solvent or a dilute solution of a single substance is levelled above a more concentrated solution of the same substance, so that the initial concentration difference equals Δc° (Fig. 1), the resulting one-dimensional diffusion process will under ideal conditions be governed by the following equation [2,3]

$$\frac{\partial c}{\partial x} = \frac{\Delta c^\circ}{2\sqrt{\pi D t}} e^{-x^2/4Dt},$$

where x denotes the position coordinate with reference to the original boundary surface, D the diffusion coefficient and t the diffusion time. If a linear relation is assumed between the concentration and the refractive index of the solution (which holds fairly accurately in most cases), the concentration gradient can be measured, using, *e. g.*, the scale method.

For non-uniform diffusion, *i. e.* if there are two or more components with different diffusion coefficients present, this equation is not valid. This fact may be utilized as an indication of non-uniformity. Thus it was shown by Lamm [1] that in normal coordinates the curve of a non-uniform diffusion

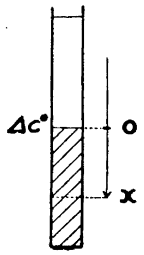


Fig. 1. Principle of "ordinary" diffusion.

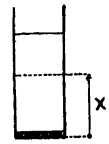


Fig. 2. Principle of bottom layer diffusion.

process will always have a positive excess at the axis of symmetry as compared to the curve of uniform diffusion. Theoretically the shape of an experimentally obtained curve would even permit the distribution function of diffusion coefficients to be calculated using numerical methods, although the experimental accuracy is as a rule too low for this to be practical.

It was pointed out by Lamm [2] that ordinary diffusion is by no means the ideal process for indicating non-uniformity. The uniform diffusion curves of the single components, which combine to give the resulting compound curve, will all have a mutual axis of symmetry at the position of the original boundary. This results in rather a close amalgamation of the curves.

It seems, therefore, that if the diffusion could be arranged with a different initial condition so that the resulting uniform diffusion curve was non-symmetrical, non-uniformity would be more clearly displayed. Such a possibility is offered by diffusion from a bottom layer, where the diffusion starts out from a very thin layer of relatively concentrated solution at the bottom of the cell, levelled below pure solvent (Fig. 2). If the bottom layer is infinitely thin and if the influence of the concentration on the diffusion coefficient is neglected, the equation of uniform diffusion from bottom layer can be written [3]

$$\frac{\partial c}{\partial x} = -\frac{Ax}{2\sqrt{\pi}\, D^{3/2} t^{3/2}} e^{-x^2/4Dt}$$

where x is the height above the bottom of the cell. This function is the first derivative with respect to x of the above function for "ordinary" diffusion and it is non-symmetrical, as is seen from Fig. 3. Further it is easily seen that the abscissa of the maximum point depends on D and t. Some elementary properties of the function will be given for convenience in the theoretical section below. In cases, however, where non-uniformity is not very pronounced, a direct comparison with the ideal curve suggests itself. In order that this be possible, the curve must be plotted in normal coordinates independent of time and other general experimental conditions. The normalization procedure, analogous to that applied in connection with "ordinary" diffusion, rests on the calculation of moments and it will be shown that the first moment can advantageously be used for the normalization.

In this connection it may be worth mentioning that the first "absolute" moment can also be used for the normalization of "ordinary" diffusion curves in place of the second moment ordinarily used.

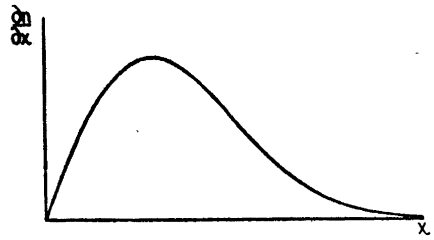


Fig. 3. Ideal curve for uniform bottom layer diffusion, according to eqn. (4).

II. THEORETICAL

a) Elementary properties of the uniform curve

If A moles per cm² are concentrated to $x = 0$ at the time $t = 0$ (Fig. 2), the following equation will now hold for the concentration (compare above)

$$\bar{c} = \frac{A}{\sqrt{\pi Dt}} e^{-x^2/4Dt} \tag{1}$$

The bar above c denotes that we are dealing with a uniform case. This mode of notation will be generally adopted in the subsequent discussion. Derivation with respect to x yields

$$\frac{\partial \bar{c}}{\partial x} = -\frac{Ax}{2\sqrt{\pi} D^{3/2} t^{3/2}} e^{-x^2/4Dt} \tag{2}$$

If a linear relation is assumed between refractive index and concentration [4],

$$n = n^0 + Rc \tag{3}$$

we obtain for the refractive index gradient

$$-X = \frac{\partial \bar{n}}{\partial x} = -\frac{RAx}{2\sqrt{\pi} D^{3/2} t^{3/2}} e^{-x^2/4Dt} \tag{4}$$

For the abscissa of the maximum point we get

$$\bar{x}_m^2 = 2Dt \tag{5}$$

and for the abscissa of the point of inflexion

$$\bar{x}_i^2 = 6Dt \tag{6}$$

Thus

$$\bar{x}_i/\bar{x}_m = \sqrt{3} \tag{7}$$

The area of the curve is

$$\Phi = -\int_0^\infty \frac{\partial \bar{n}}{\partial x} dx = \int_0^\infty \bar{X} dx = \frac{RA}{\sqrt{\pi Dt}} \tag{8}$$

and the maximum ordinate is obtained if x_m is inserted into (4):

$$\bar{X}_m = \frac{RA}{\sqrt{2\pi e Dt}} \tag{9}$$

Hence

$$\frac{\Phi^2}{\bar{X}_m^2} = 2eDt \tag{10}$$

The ordinate of the point of inflexion is

$$\bar{X}_i = \frac{RA\sqrt{6}}{2e\sqrt{\pi eDt}} \tag{11}$$

Thus

$$\frac{\bar{X}_i}{\bar{X}_m} = \frac{\sqrt{3}}{e} \tag{12}$$

The slope of the curve at the point of inflexion is

$$\left(\frac{\partial \bar{X}}{\partial x}\right)_i = \frac{-RA}{\sqrt{\pi e^3 D^3 t^3}} \tag{13}$$

But the slope at $x = 0$ is

$$\left(\frac{\partial \bar{X}}{\partial x}\right)_{x=0} = \frac{RA}{2\sqrt{\pi D^3 t^3}} \tag{14}$$

Hence

$$\left(\frac{\partial \bar{X}}{\partial x}\right)_{x=0} = -\frac{e^{3/2}}{2}\left(\frac{\partial \bar{X}}{\partial x}\right)_i$$

The slope of a line combining the maximum point with the origin is

$$\frac{\bar{X}_m}{x_m} = \frac{RA}{2\sqrt{\pi eD^3 t^3}} \tag{15}$$

Thus

$$\frac{\bar{X}_m}{x_m} = \frac{1}{\sqrt{e}}\left(\frac{\partial \bar{X}}{\partial x}\right)_{x=0} = -\frac{e}{2}\left(\frac{\partial \bar{X}}{\partial x}\right)_i \qquad \text{(Fig. 5)} \tag{16}$$

A combination of some of the foregoing expressions yields

$$\frac{\bar{x}_i \bar{X}_m}{\left(\frac{\partial \bar{X}}{\partial x}\right)_i} = Dt\ e\sqrt{3} \tag{17}$$

In case it should be difficult to find the exact position of the origin, the width of the curve, δ, at the ordinate of the inflexion point (Fig. 4) may be used. By the use of the tables of Jahnke and Emde it is found that

$$\delta \approx 1.852\sqrt{Dt} \tag{18}$$

Hence

$$Dt \approx \frac{\delta^2}{3.43} \tag{19}$$

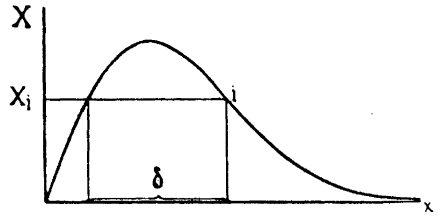


Fig. 4. "Width" of ideal curve.

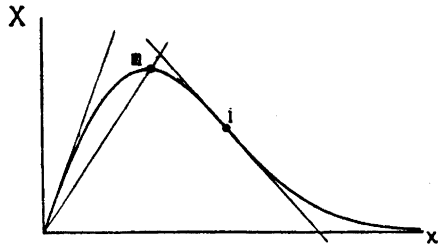


Fig. 5. Elementary properties of bottom layer diffusion curves.

For the calculation of the diffusion coefficient, relations (5), (6), (10), (17) and (19) may be used.

b) Relations for non-uniform curves

We will now assume that there are several components present, each of which diffuses independently of the others, *i. e.* the Arrhenius-Thovert effect is neglected. Then

$$-X = \frac{\partial n}{\partial x} = \sum_{i=1}^{q} \frac{\partial n_i}{\partial x} = -\sum_{i=1}^{q} \frac{R_i A_i x}{2\sqrt{\pi}\, D_i^{3/2} t^{3/2}}\, e^{-x^2/4D_i t} \qquad (20)$$

owing to the additive property of the refractive index contributions. If the number of substances were increased infinitely, the sum of eqn. (20) would go over into an integral. For the sake of generality we define a distribution function, $f(D)$, such that

$$d(RA) = f(D)\, dD$$

The expression equivalent to eqn. (20) will then be

$$-X = \frac{\partial n}{\partial x} = -\frac{1}{2\sqrt{\pi}} \int_0^\infty \frac{x}{D^{3/2} t^{3/2}}\, e^{-x^2/4Dt}\, f(D)\, dD \qquad (21)$$

A discontinuous distribution case cannot be described exactly by eqn. (21) but it can be approximated with any desired degree of accuracy. The calculation of the maximum and inflexion point coordinates of a non-uniform curve does not give any simple explicit result. From a practical point of view, however, it is obvious that at least in cases of pronounced non-uniformity there will be a deviation from the conditions of eqn. (16).

c) Moment expressions

The r:th moment of the refractive index gradient curve is defined in the following way

$$m_r = \int_0^\infty x^r X dx = -\int_0^\infty x^r \frac{\partial n}{\partial x}\, dx \qquad (22)$$

Obviously the moment of order zero is identical with the area of the curve, previously denoted by Φ:

$$m_0 = \Phi$$

Substituting for X the expression of eqn. (21) we obtain

$$m_r = \frac{1}{2\sqrt{\pi}} \int_0^\infty x^r \mathrm{d}x \int_0^\infty \frac{x}{D^{3/2} t^{3/2}} \mathrm{e}^{-x^2/4Dt} f(D)\, dD \tag{23}$$

By the substitution

$$\zeta = x / 2\sqrt{Dt}$$

(23) is transformed into

$$m_r = \frac{2^{r+1} t^{(r-1)/2}}{\sqrt{\pi}} \int_0^\infty f(D)\, D^{(r-1)/2}\, \mathrm{d}D \int_0^\infty \zeta^{r+1} \mathrm{e}^{-\zeta^2} \mathrm{d}\zeta$$

We will abbreviate

$$\mu_r = \int_0^\infty f(D)\, D^{(r-1)/2}\, \mathrm{d}D \tag{24}$$

Hence

$$m_r = \frac{2^r t^{(r-1)/2}}{\sqrt{\pi}} \Gamma\left(\frac{r+2}{2}\right) \mu_r = \alpha \cdot \mu_r \tag{25}$$

since

$$\int_0^\infty \zeta^{r+1} \mathrm{e}^{-\zeta^2} \mathrm{d}\zeta = \frac{1}{2} \Gamma\left(\frac{r+2}{2}\right)$$

provided that $r + 2 > 0$, or $r > -2$.

For convenience the factor, $\alpha = \frac{1}{\sqrt{\pi}} 2^r t^{(r-1)/2} \Gamma\left(\frac{r+2}{2}\right)$, is listed in Table 1 for some values of r.

Table 1.

r	α
0	$1/\sqrt{\pi t}$
1	1
2	$4\sqrt{t}/\sqrt{\pi}$
3	$6t$
4	$32t^{3/2}/\sqrt{\pi}$

The reduced moments of the distribution function are defined as follows:

$$\mathcal{D}_{rm}^{r/2} = \frac{\mu_r}{\mu_0}; \qquad \mathcal{D}_{rm} = \left(\frac{\mu_r}{\mu_0}\right)^{2/r} \tag{26}$$

In the uniform case, (24) reduces to

$$\bar{\mu}_r = RAD^{(r-1):2} \tag{27}$$

Hence

$$\bar{\mathcal{D}}_{rm} = D \tag{28}$$

Relation (28) provides a method for obtaining the diffusion coefficient from an experimental curve. For the calculation of moments the use of Simpson's formula is recommended.

If the error in a moment computed from an experimental curve is $\delta\, m_r$, then the error in the reduced moment calculated according to eqn. (26) will be

$$\left| \frac{\delta\, \mathcal{D}_{rm}}{\mathcal{D}_{rm}} \right| = \left| \delta \ln \mathcal{D}_{rm} \right| = \frac{2}{r} \cdot \left| \delta \ln \frac{\mu_r}{\mu_0} \right|$$

or

$$\frac{\delta\, \mathcal{D}_{rm}}{\mathcal{D}_{rm}} = \frac{2}{r} \left| \frac{\delta\, m_r}{m_r} \right| + \frac{2}{r} \left| \frac{\delta\, m_0}{m_0} \right| \tag{29}$$

Since the error in a moment calculated from an experimental curve increases greatly with increasing r, it should be possible to find an optimum value of r, depending on the experimental degree of accuracy, which gives $|\delta\, \mathcal{D}_{rm} / \mathcal{D}_{rm}|$ a minimum value. For practical purposes it seems reasonable to use the first moment.

d. Normalization

By the linear transformations

$$\Xi = -\frac{\sqrt{\mathcal{D}_{rm} t}}{m_0} \frac{\partial\, n}{\partial\, x} \tag{30}$$

$$\xi = x/2\sqrt{\mathcal{D}_{rm} t}$$

the equation of uniform diffusion is transformed into

$$\Xi = \xi \cdot e^{-\xi^2} \tag{31}$$

since, in the uniform case,

$$\bar{m}_0 = RA/\sqrt{\pi D t}$$

$$\bar{\mathcal{D}}_{rm} = D$$

The normalized curve is independent of time. In the discussion below it will be assumed that $\mathcal{D}_{1m}$ has been used for the normalization. In non-uniform cases, the normalized curve will deviate from the curve of eqn. (31). The applied mode of normalization implies that the first and zero moments will always be identical with those of the ideal curve, *i. e.* the area and the ξ-coordinate of the point of gravity of all normalized curves will have fixed values.

e. Recognition of non-uniformity

From the foregoing we recall that

$$\mu_r = \int_0^\infty f(D)\ D^{(r-1)/2}\ \mathrm{d}D \tag{24}$$

and

$$\bar{\mu}_r = RAD^{(r-1)/2} \tag{27}$$

Hence

$$\bar{\mu}_p = \bar{\mu}_r^\alpha \bar{\mu}_s^\beta \tag{32}$$

if

$$p = \alpha r + \beta s; \quad \alpha + \beta = 1$$

By a simple application of the Hölder inequality it can be shown that

$$\mu_p < \mu_r^\alpha \mu_s^\beta \tag{33}$$

if $p = \alpha r + \beta s$, $\alpha,\beta > 0$, $\alpha + \beta = 1$
From (32) and (33) it follows that for $\mu_r = \bar{\mu}_r$ and $\mu_s = \bar{\mu}_s$

$$\mu_p < \bar{\mu}_p \tag{34}$$

if

$$r < p < s$$

In a similar manner we find that

$$\mu_p > \bar{\mu}_p \tag{35}$$

if

$$p < r \text{ or } p > s,\ r < s$$

These relations can be applied to show that the slope at $\xi = 0$ of a non-uniform curve in normal coordinates is always greater than that of the uniform curve.

Other elementary methods for recognizing non-uniformity rest on a comparison of the values of the diffusion coefficient obtained by different methods (5), (6), (10), (17) and (19). As already mentioned, there will also be a deviation from eqn. (16) in non-uniform cases. Depending on the nature and degree of non-uniformity present, the eye will be more or less sensitive to the deviation from the shape of the ideal curve.

f. Non-uniformity in two-component cases

The simplest non-uniform cases are those where there are only two diffusing components present, denoted by the respective indices 1 and 2. If the following two parameters are introduced

$$\beta = R_1A_1 / R_2A_2 \tag{36}$$

$$\gamma = \sqrt{D_1 / D_2}$$

the compound curve in its normalized form can be written

$$\Xi = \Xi_1 + \Xi_2 \tag{37}$$

where

$$\Xi_1 = \frac{\beta(\beta+1)}{(\beta+\gamma)^2} e^{-\xi_1} \xi_1; \quad \xi_1 = \frac{\beta+1}{\beta+\gamma} \xi \tag{38}$$

$$\Xi_2 = \frac{\gamma^2(\beta+1)}{(\beta+\gamma)^2} e^{-\xi_2} \xi_2, \quad \xi_2 = \frac{\gamma(\beta+1)}{\beta+\gamma} \xi \tag{39}$$

Here Ξ_1 and Ξ_2 are the respective contributions from the two components. In the case of "ordinary" diffusion, the corresponding equations are

$$\Xi_1 = \frac{2}{\sqrt{\pi}} \frac{\beta(\beta\gamma+1)}{\gamma(\beta+1)^2} e^{-\xi_1}; \quad \xi_1 = \frac{\beta\gamma+1}{\gamma(\beta+1)} \xi \tag{40}$$

$$\Xi_2 = \frac{2}{\sqrt{\pi}} \frac{\beta\gamma+1}{(\beta+1)^2} e^{-\xi_2}; \quad \xi_2 = \frac{\beta\gamma+1}{\beta+1} \xi \tag{41}$$

For a comparison between the two methods, the following six cases are reproduced in normal coordinates along with the uniform curve, denoted by index zero

Curve No.	β	γ
1	5	2
2	1	2
3	10	4
4	1	4
5	100	4
6	1/100	4

in Figs 6, 7 and 8 for diffusion from a bottom layer and in Figs 9, 10 and 11 for "ordinary" diffusion. Especially important from the point of view of judging the relative merits of the two methods are cases 5 and 6, where one of the components is present only in minute amounts, *i. e.* may be regarded as a

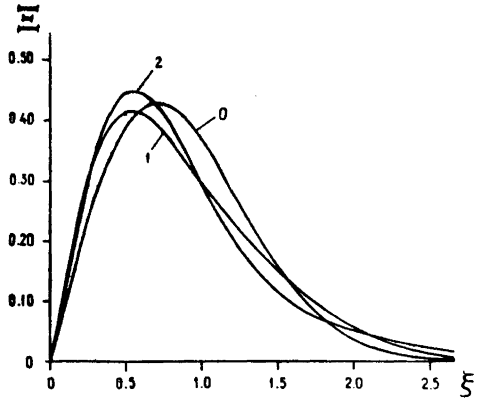


Fig. 6. Normalized curves for two-component cases. Bottom layer diffusion. 0, Ideal curve; 1, $\beta = 5$, $\gamma = 2$; 2, $\beta = 1$, $\gamma = 2$.

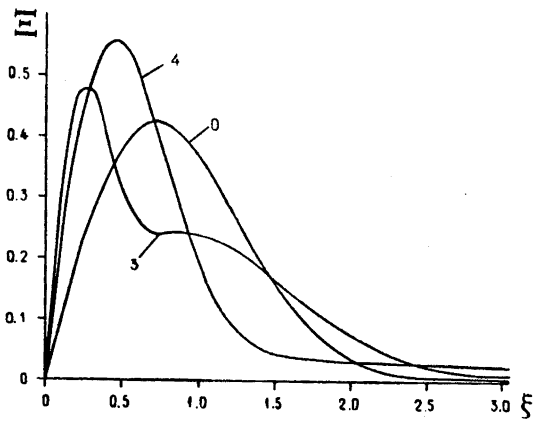


Fig. 7. Normalized curves for two-component cases. Bottom layer diffusion. 0, Ideal curve; 3, $\beta = 10$, $\gamma = 4$; 4, $\beta = 1$, $\gamma = 4$.

contamination. As appears from the figures, the assymmetrical character of the curves for bottom layer diffusion will generally cause a considerable deviation from the ideal curve to occur over a greater range of abscissa values. Further it is seen that the bottom layer method is particularly favourable when the "contamination" has a lower diffusion coefficient than the main component (Fig. 8). From the equations above, it is found that if

$$\eta = \frac{(\Xi \text{ contaminant})_{max}}{(\Xi \text{ main.comp.})_{max}}; \qquad \gamma > 1 \tag{42}$$

then

$$\text{for } \beta > 1;\ \eta' = \frac{(\Xi_2)_{max}}{(\Xi_1)_{max}} = \frac{\gamma^2}{\beta} \tag{43}$$

and

$$\text{for } \beta < 1;\ \eta'' = \frac{(\Xi_1)_{max}}{(\Xi_2)_{max}} = \frac{\beta}{\gamma^2} \tag{44}$$

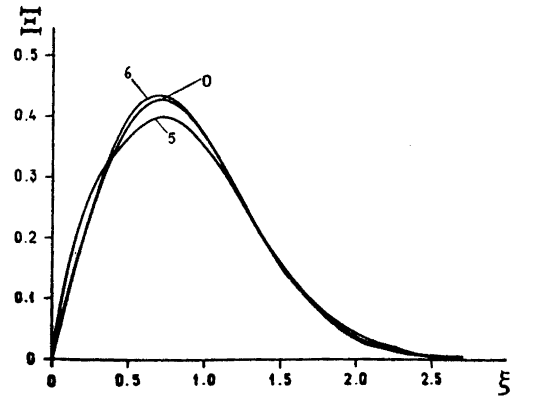


Fig. 8. Normalized curves for two-component cases. Bottom layer diffusion. 0, Ideal curve; 5, $\beta = 100$, $\gamma = 4$; 6, $\beta = 1/100$, $\gamma = 4$.

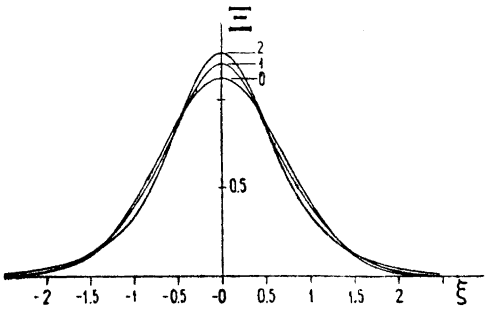


Fig. 9. Normalized curves for two-component cases. "Ordinary" diffusion. 0, Ideal curve; 1, $\beta = 5$, $\gamma = 2$; 2, $\beta = 1$, $\gamma = 2$.

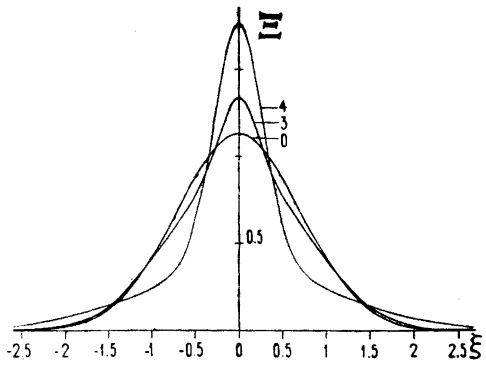


Fig. 10. Normalized curves for two-component cases. "Ordinary" diffusion. 0, Ideal curve; 3, $\beta = 10$, $\gamma = 4$; 4, $\beta = 1$, $\gamma = 4$.

Thus

$$\eta' / \eta'' = \gamma^4 \tag{45}$$

i. e. the former case is greatly favoured. For "ordinary" diffusion we have

$$\eta' = \frac{\gamma}{\beta}, \quad \eta'' = \frac{\beta}{\gamma} \tag{46}$$

Hence

$$\eta' / \eta'' = \gamma^2 \tag{47}$$

Further it can be shown that the excess,

$$\Delta = \Xi_{max} - \bar{\Xi}_{max} = \frac{\beta}{\gamma} \frac{(\gamma - 1)^2}{(\beta + 1)^2} \tag{48}$$

Thus

$$\Delta(\beta) = \Delta(1 / \beta) \tag{49}$$

i. e. the excess is independent of whether the "contamination" has a greater or smaller diffusion coefficient than the main component, although in the former case the excess will occur over a greater range of abscissa values.

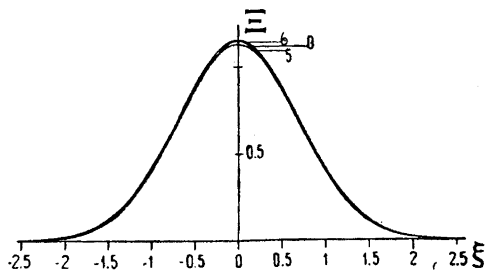


Fig. 11. Normalized curves for two-component cases. -'Ordinary" diffusion. 0, Ideal curve; 5, $\beta - 100$, $\gamma - 4$; 6, $\beta - 1/100$, $\gamma - 4$.

From the above arguments it is concluded that in cases of very low β and large γ, the "ordinary" diffusion method would be favoured in comparison with diffusion from bottom layer from the point of view of recognizing non-uniformity. This is evidently true, but rather extreme conditions are probably required to outweigh the advantages of the bottom layer method. As is seen in case 6, the two methods are practically equal even for $\beta = \frac{1}{100}$, $\gamma = 4$. Thus it is concluded that, for most practical purposes, diffusion from a bottom layer is a more sensitive means of detecting non-uniformity.

Note: In eqns. (38), (39) and (40), (41) the "ordinary" diffusion curves are assumed to have been normalized using the first absolute moment. Some words on this method may therefore be apposite.

If the moments are defined in the usual way

$$m_r = \int_{-\infty}^{+\infty} x^r X \mathrm{d}x \tag{50}$$

it is obvious that all moments of odd order will disappear, due to the symmetrical shape of the curves. This fact may even be utilized to find the position of the axis of symmetry. For this reason, the second moment has usually been employed for the normalization.

If we instead introduce the "absolute" moments

$$M_r = \int_{-\infty}^{+\infty} |x|^r X \mathrm{d}x \tag{51}$$

which can be readily calculated from an experimental curve, it can be shown that

$$M_r = \alpha' \mu_{r+1} \tag{52}$$

where u_{r+1} is defined according to eqn. (24) and

$$\alpha' = \frac{1}{\sqrt{\pi}} 2^r t'^{/2} \Gamma\left(\frac{r+1}{2}\right) \tag{53}$$

The reduced moments are then defined by

$$\mathscr{D}_{rM} = \left(\frac{\mu_{r+1}}{\mu_1}\right)^{2/r} \tag{54}$$

and normalization is effected by the transformations

$$\Xi = \frac{4\sqrt{\mathscr{D}_{rM} t}}{M_0} X \tag{55}$$

$$\xi = x / 2\sqrt{\mathscr{D}_{rM} t}$$

III. EQUIPMENT AND OPERATION

a. *The thermostat.* The thermostat, shown in Fig. 12, had the outside dimensions, 31 × 36 × 33 cm. It was insulated by 3 cm thick insulating cork, C, painted black, and protected from radiation losses by aluminium foil. The distilled water serving as thermostat liquid was stirred by a propeller stirrer driven by an almost vibrationless electric motor, B. The temperature control system was the usual one, including a contact thermometer, D, a relay and a dip-heater, E. A precision thermometer F enabled temperature fluctuations of 0.002 °C to be measured. The cell was placed between two brass blocks in position A. Slits in the brass blocks and a tube passing through the thermostat gave free passage to the light beam. The thermostat was mounted on a rider of a very stable (lathe type) optical bench, which in turn rested on a solid foundation.

The temperature fluctuations of the thermostat liquid never exceeded ± 0.002° C during the experiments.

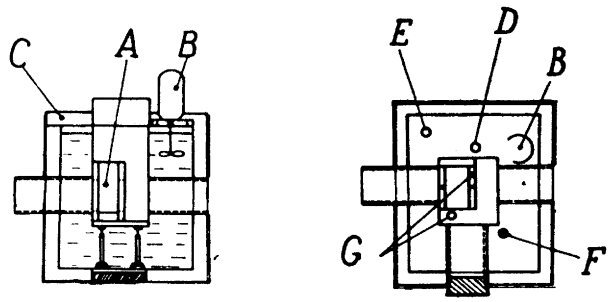


Fig. 12. Thermostat. A, cell position; B, electric stirrer motor; C, cork insolation; D, position for contact thermometer; E, Immersion heater; F, position for precision thermometer; G, position for thermometers for air and brass-block temperatures.

b. *The diffusion cell.* In the construction of the cell and the levelling arrangement the greatest possible simplicity was aimed at, simultaneously as the risk of convection and leakage had to be duly considered.

The cell was composed of plane parallel glass plates as shown in Fig. 13, the inner dimensions being: height 7.9 cm, bottom area 3 × 3 cm^2. At the center of the bottom plate there was a small hole filled with mercury into which the cannula of a tuberculine syringe dipped. The mercury served the double purpose of preventing the syringe leaking and of preventing cascade formation on injection of the bottom layer. The plexi-glas cover of the cell was provided with two holes, one for the cannula and one for the introduction of the solvent. To enable a slow and vibrationless operation of the syringe, a simple device was constructed, which included a micrometer screw acting directly upon the piston, Fig. 14. One turn of the screw corresponded to an injected volume of 0.008 ml.

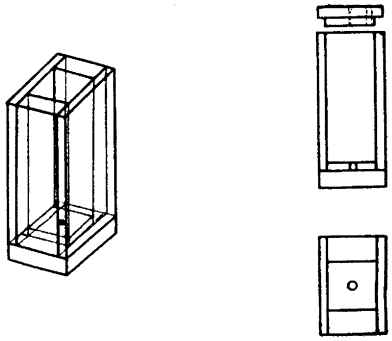


Fig. 13. Diffusion cell with plexi-glas cover.

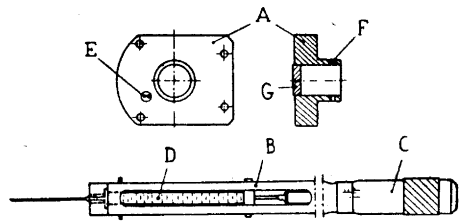


Fig. 14. Injection device. A, holder; B, syringe holder; C, micrometer screw, D, syringe; E, hole for the introduction of solvent; F, socket for B; G, rubber washer.

The cell fitted precisely into the space between two brass blocks in the thermostat, A, Fig. 12, and the holder of the injection device was screwed fast to the brass blocks. Fig. 15 shows the final arrangement with the cell in position in the thermostat.

c. *The optical arrangement.* The optical arrangement, schematically shown in Fig. 16, was based on the Svensson short focus modification of the scale method [5]. As suggested by Lamm [6], the diffusion cell was placed on the "plate" side of the lens system. The Svensson modification claims the advantage of reducing the length of optical bench required, without neglecting the

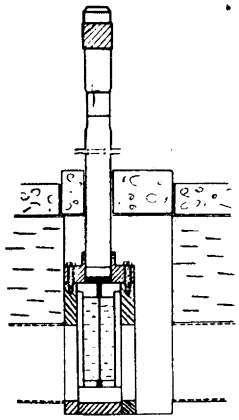


Fig. 15. Cell in position in the thermostat.

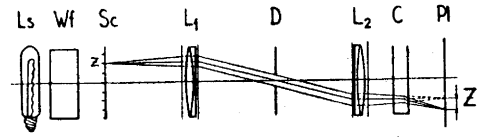


Fig. 16. Schematic outline of optical arrangement. Ls, light source; Wf, water filter; Sc, original scale; L_1 and L_2, astronomical objectives; D, diaphragm; C, diffusion cell; Pl, photographic plate; z, scale line number; Z, scale line displacement.

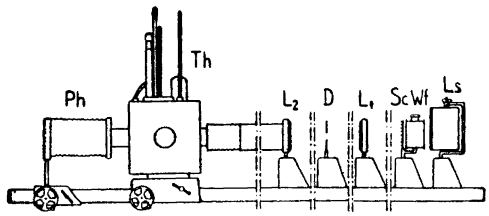


Fig. 17. Experimental set up. Ph, plate holder; Th, thermostat; L_1 and L_2, objectives; D, diaphragm; Sc, glass scale; Wf, water filter; Ls, light source.

demand for parallel or nearly parallel light through the cell. The condition is, however, that the focal distances of the lenses chosen should be sufficiently small. With focal distances of around 120 cm as used in our experiments, the necessity of using the Svensson method is debatable; it also limits the non-distorted part of the image. The diaphragm diameter used was 1.4 cm, which corresponds to an aperture of approx. 1 : 86. A precision glass scale with a scale constant of 0.399 mm was used. Fig. 17 shows the actual arrangement. During the experiments, however, the injection device was insulated by a tube of aluminium foil, lined with cotton.

The adjustment of the optical system was carried out by means of a telescope provided with cross-hairs adjusted for infinity. An illuminated scale was observed through the telescope and one of the lenses of the optical system and the position of the scale adjusted until no parallax between the cross-hairs and the scale remained. The scale was then assumed to be in the focal plane of the lens.

d. *Mode of operation.* The carefully cleaned and dried cell was then inserted in the thermostat. The syringe was filled with the solution to be injected and the top of the piston was greased to prevent vibrations while the micrometer screw was being turned. The syringe was placed in its holder, and the cannula carefully wiped. The injection device was then placed in position in the thermostat and screwed fast. Through the hole in the glass and plexi-glas covers, 50 ml of freshly boiled distilled water of a temperature slightly exceeding that of the thermostat was introduced by means of a cannula, connected with a separatory funnel by a polythene tube. After the introduction of the water the hole was plugged with cotton wool and the cork cover of the thermostat was put on. The thermostat was left for temperature equilibration, the mercury preventing the syringe from leaking. The bottom layer was then injected by slowly turning the micrometer screw at a uniform rate. The process could be followed on the ground glass plate. The time required for injection was 3—4 min, which, of course, introduces a small time-dependent non-uniformity since the diffusion constant always appears in eqn. (4) in connection with the time. The height of the injected layer was approx. 0.4 mm. Obviously it is desirable that the height of the bottom layer should be as small as possible, if the simple eqn. (4) is to be valid. This, however, requires that the bottom of the cell should be nearly perfectly horizontal.

The scale pictures were recorded on 6 × 9 process plates with one exposure per hour during the first 6 h of the experiment. The best exposures were obtain-

ed several hours (3 or 4 h with KCl) after the experiment had been started. During the first few hours, while the concentration gradient was still very high, the effective part of the scale was considerably blurred, owing to the defocussing effect of the gradient. This is, however, not serious for the accuracy of the measurement [1].

IV. EXPERIMENTS

A. Experiments with uniform substances

Experiment 1. In order to test the method, experiments with uniform substances were first conducted. 0.4 ml of 0.5 N KCl (analytical reagent) was injected. The thermostat temperature was 24.78 °C. Exposures were taken before the beginning of the levelling and after 2, 3, 4, 5 and 6 h. The scale photographs were comparated in the usual manner and the corresponding curves drawn, Fig. 18. The parts of the scales corresponding to low values of x were rather diffuse, due to the cutting-off effect of the cell bottom. For this reason it was difficult to find the exact Z-value corresponding to $x = 0$. By a consideration of various elementary properties of shape (rel. (20)), however, the position of the origin was estimated.

The curve taken after 4 h was normalized in the way described above and the ideal curve was drawn for comparison, Fig. 19. As appears from the diagram, the experimental difficulties have not yet been overcome. At present, however, it is difficult to judge whether the deviation is due to the systematic short-comings of the method of levelling or to other experimental circumstances.

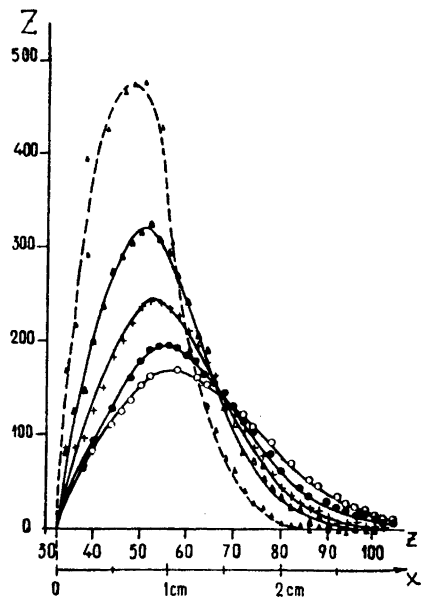


Fig. 18. Experimental (z, Z)-curves for the diffusion of potassium chloride in water at 24.78°C. Expt. 1.

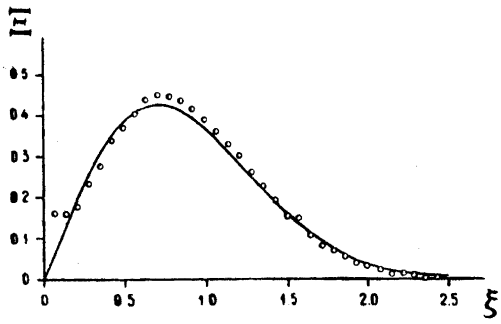


Fig. 19. Points of normalized 4-h curve of expt. 1 together with normal ideal curve.

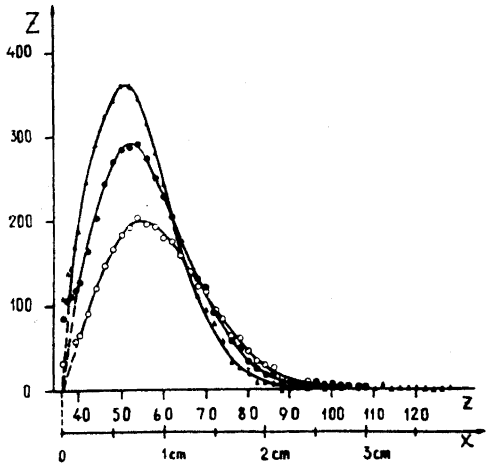


Fig. 20. Experimental curves from expt. 2. NaCl in water at 24.77°C. Filled triangles, 3-h curve; filled circles, 4-h curve; empty circles, 5-h curve. The deviation from the ideal shape of the curve for low values of x is probably due to minute amounts of high-molecular impurities.

Experiment 2. 0.4 ml of a 3 % NaCl solution was injected. Curves analogous to those for KCl were obtained.

In expt. 2 as in expt. 1, it was noted that the deviation from the ideal shape of curve for low x is not altogether irregular but exhibits a positive tendency. This is probably due to the presence of quite minute amounts of high-molecular impurities, which will cause, even at very low concentrations, an appreciable deviation from the ideal curve (compare Fig. 8).

The diffusion coefficient was calculated according to the maximum point, the inflexion point and the "width" methods, Table 2 and Figs. 21, 22 and 23.

Table 2.

t	x_m	x_i	δ
3	0.599	1.002	0.794
4	0.656	1.107	0.840
5	0.761	1.286	0.938

The diffusion coefficient was recalculated for 25 °C using the viscosity ratio, giving the following result.

Inflexion point method:

$$D_{25°} = 1.29 \text{ cm}^2/\text{day}$$

"Width" method:

$$D_{25°} = 1.30 \text{ cm}^2/\text{day}$$

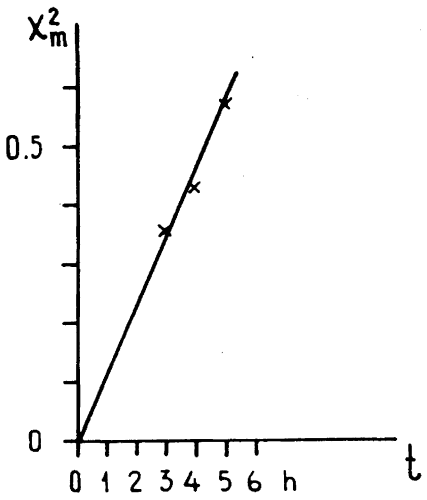


Fig. 21. Maximum point method for the determination of the diffusion coefficient of NaCl. Expt. 2.

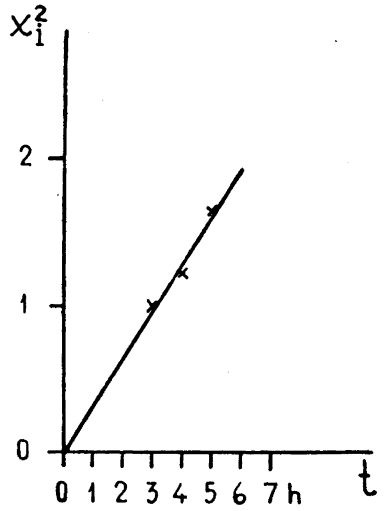


Fig. 22. Inflexion point method. Expt. 2.

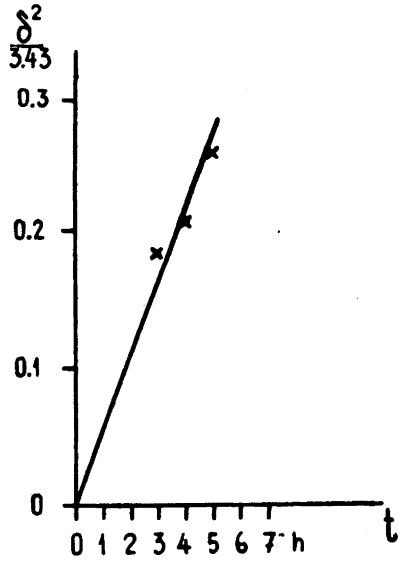


Fig. 23. "Width" method. Expt. 2.

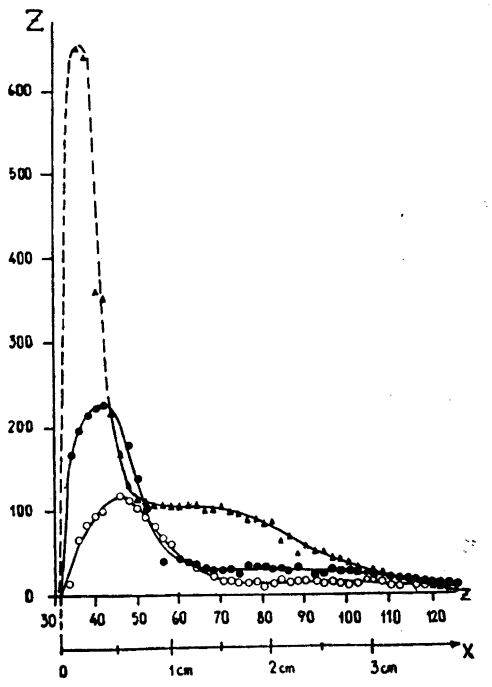


Fig. 24. Expt. 3. 0.6 % dextran + 2.4 % NaCl at 24.77°. Filled triangles, 12-h curve; filled circles, 35.3-h curve; empty circles, 71-h curve.

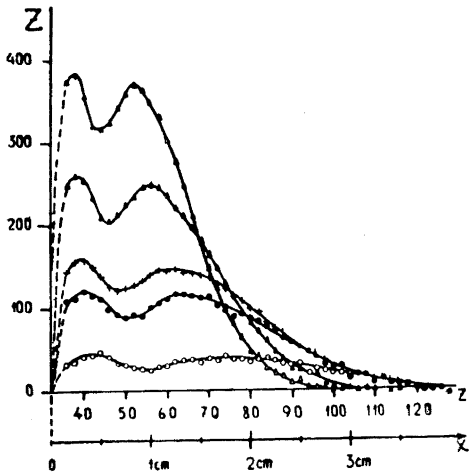


Fig. 25. Expt. 4. 0.1 % dextran + 2.9 % NaCl at 24.77°. Empty triangles, 4-h curve; filled triangles, 6-h curve; crosses, 10-h curve; filled circles, 12-h curve; empty circles, 24.5-h curve.

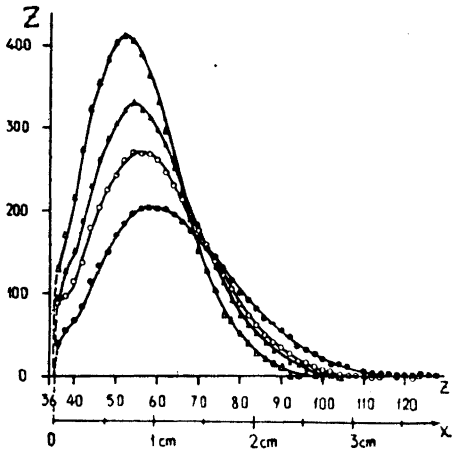


Fig. 26. Expt. 5. 0.03 % dextran + 3 % NaCl at 24.78°. Empty triangles, 4-h curve; filled triangles, 5-h curve; empty circles, 6-h curve; filled circles, 8-h curve.

Maximum point method:

$$D_{25°} = 1.38 \text{ cm}^2/\text{day}$$

illustrative of the fact that the maximum point abscissae are less accurately read from the curve diagram than the widths and the influxion point abscissae.

These values can be compared with the following values given by Kortüm and Bockris, *Textbook of Electrochemistry* for the diffusion coefficient of NaCl:

at $c = 0$ $D_{25°} = 1.39$ cm²/day

$c = 0.5$ $D_{25°} = 1.27$ cm²/day

in fair agreement with the above results. It should, however, be mentioned that the precision determinations of diffusion coefficients approach or attain an accuracy of 0.1 %.

B. Experiments with non-uniform substances

Native dextran as produced by *Leuconostoc mesenterioides* is a polydisperse polysaccharide with molecular weight ranging from 14 000 to 40 000 000. A partially hydrolyzed form with molecular weight of 20 000—200 000 has gained use as a plasma substitute. A commercial preparation, "Macrodex", manufactured by the Pharmacia company, Uppsala, Sweden, contains 6 % partially hydrolyzed dextran and 0.9 % NaCl. The solutions used in the experiments described below were prepared by diluting "Macrodex" and adding the required amount of sodium chloride.

Experiment 3. 0.4 ml of a solution containing 0.6 % dextran and 2.4 % NaCl was injected. The diffusion curves obtained are reproduced in Fig. 24. In this case the dextran gives by far the greatest contribution to the refractive index gradient, which illustrates the facts already pointed out in the theoretical section.

Experiment 4. 0.4 ml of a solution of 0.1 % dextran and 2.9 % NaCl was injected. The diffusion curves are reproduced in Fig. 25. If we assume $R_1 = R_2$ we get

$$\beta = A_1 / A_2 = 2.9/0.1 = 29$$

It is remarkable, and in conformity with the foregoing discussion, how much this small amount of dextran contributes to the refractive index gradient. In fact two distinct peaks in the curve are obtained, the relative positions of which agree fairly well with the relation between the diffusion coefficients.

Experiment 5. 0.4 ml of 0.03 % dextran and 3 % NaCl was injected. The diffusion curves are reproduced in Fig. 26. If $R_1 = R_2$ we have $\beta = A_1/A_2 = 100$. A definite deviation from the curve for pure sodium chloride is seen to occur for low values of x. However, this probably represents the limiting case unless high-molecular impurities can be wholly avoided. In fact, the quantity of dextran injected in this case is only $0.4 \times 0.03 \times 10^{-2}$ g $= 0.12$ mg.

Acknowledgements. Preliminary experimental work was performed by Marianne Lindelöf in co-operation with one of us. Part of the work has been supported by the *Swedish National Research Council.*

REFERENCES

1. Lamm, O. *Diss.* Uppsala 1937, p. 38.
2. Lamm, O. *Diss.* Uppsala 1937, p. 35.
3. Fürth, R. *Hdb. der phys. u. tech. Mechanik,* vol. VII.
4. Lamm, O. *Diss.* Uppsala 1937, p. 64.
5. Svensson, H. *Nature* **161** (1948) 234.
6. Lamm, O. *Acta Chem. Scand.* **9** (1955) 546.
7. Lamm, O. *Diss.* Uppsala 1937, p. 71.

Received December 3, 1956.

ACTA CHEMICA SCANDINACIVA 11 (1957) 360—361

An Analytical Treatment of a Reference Coordinate for the Diffusion and Sedimentation Processes

OLE LAMM

The Royal Institute of Technology, Division of Physical Chemistry, Stockholm 70, Sweden

In order to ensure a clear significance of a reference equation, which is used in certain theories of the diffusion and sedimentation processes, a general derivation and discussion of this equation is developed.

At least in fluid systems, the diffusion and sedimentation processes are generally studied under such conditions that there is no, or only a negligibly small, "bulk displacement" or flow of the mixture as a whole. Here, we will stick to the typical case of a mixture in which the *partial volumes* of the different components are practically independent of the time and the distance coordinates, either owing to very small concentration differences (differential diffusion) or due to the use of nearly ideal mixtures. Absence of flow then simply means that the system is enclosed in a diffusion or sedimentation cell.

The fundamental equations in the diffusion and sedimentation theories (*cf.* Refs.[1–3]) need a complementary equation which defines a reference frame for the flows. In this respect, an equation proposed by Onsager [4]

$$\sum \bar{v}_i J_i = \sum \bar{v}_i C_i c_i = 0 \qquad (1)$$

has been used. J is the flow in moles/cm^2 sec, C the linear velocity of the component, c mole/cm^3 the concentration of the component and $\bar{v}$ its partial molar volume. The sums in these equations have the dimension of velocity and represent the flow in bulk of the mixture. Eqn. (1) has never been deduced analytically and the underlying facts have been explained only for *two* components [5,6]. It is felt that this is disadvantageous at least from an elementary point of view, especially in a case like the sedimentation diffusion process in a centrifugal field. This proceeds in a cell of sector shape and there should be no doubt as to the applicability of eqn. (1) also in this case.

The procedure is to combine the equation of continuity with the general expression $\sum \bar{v}_i dc_i = 0$, known from the treatment of partial quantities in thermodynamics. The former gives for the (trivial) case of parallel flow

$$\frac{\partial c_i}{\partial t} = -\frac{\partial J_i}{\partial x} \tag{2a}$$

and for the cylindrical flow in a parallel-walled cell of sector shape

$$\frac{\partial c_i}{\partial t} = -\frac{1}{x}\frac{\partial xJ_i}{\partial x} \tag{3a}$$

Combining these equations with $\sum \bar{v} \frac{\partial c_i}{\partial t} = 0$ gives

$$\sum \bar{v}_i \partial J_i = 0 \tag{2b}$$

and

$$\sum \bar{v}_i \partial J_i / \sum \bar{v}_i J_i = -\partial x/x \tag{3b}$$

or by integration

$$\sum \bar{v}_i J_i = C' \tag{2c}$$

and

$$\sum \bar{v}_i J_i = \frac{D'}{x} \tag{3c}$$

Owing to $\sum \bar{v}_i (C_i + C)c_i = \sum \bar{v}_i C_i c_i + C$, to give a certain value to the integration contants C' or D' is to define a coordinate for the velocities which is common to all the components. In eqn. (1) these constants are put equal to zero.

In order to see that $C' = 0$ and $D' = 0$ correspond to the case of a closed cell, *i. e.* absence of flow in bulk, we simply have to consider the volume change caused by the transports of ∂n_i mole in the time ∂t per cm² through a certain x-level. This is $\partial V = \sum \bar{v}_i \partial n_i = \sum \bar{v}_i J_i \partial t = \partial t \sum \bar{v}_i J_i$. Hence, $\partial V = 0$ corresponds to the validity of eqn. (1) and *vice versa*.

That $\sum \bar{v}_i J_i$ represents the velocity of the flow in bulk of the mixture is illustrated by eqn. (3c) since, in the sector shaped cell, the velocity of a flow in bulk is inversely proportional to the radius x. It is seen that $D' = 0$ is the only assumption which gives a *fixed* coordinate for the diffusion sedimentation process in a sector-shaped cell. Any other assumption defines a *local* frame, varying with x. This fixed coordinate evidently also holds for the cell itself and the measuring arrangement as a whole.

REFERENCES

1. Onsager, L. *Ann. N. Y. Acad. Sci.* **46** (1945) 241.
2. Lamm, O. *Arkiv Kemi, Mineral. Geol.* **18A** (1944) No. 2.
3. Lamm, O. *Acta Chem. Scand.* **7** (1953) 173; **8** (1954) 1120.
4. Onsager, L. and Fuoss, R. M. *J. Phys. Chem.* **36** *: 2* (1932) 2689.
5. Hartley, G. S. and Crank, *J. Trans. Faraday Soc.* **45** (1949) 801.
6. Lamm, O. *Arkiv Kemi, Mineral. Geol.* **17A** (1943) No. 9.

Received December 3, 1956.

ACTA CHEMICA SCANDINAVICA 11 (1957) 362—364

The Force and Friction Conception in the Diffusion of Multicomponent Systems

OLE LAMM

The Royal Institute of Technology, Division of Physical Chemistry, Stockholm 70, Sweden

The reciprocal relations of irreversible thermodynamics have been examined from the standpoint of the force and friction theory of pure diffusion. In cases where this theory is practicable, it gives a complete description in the sense that the reciprocal relations are dispensable. These latter are shown to be valid for relative flows, whereas the introduction of a special reference frame for the flows gives equations for which the reciprocal relations are not valid. — The force and friction theory contains throughout magnitudes of a direct physical significance, *e.g.* frictional coefficients of a uniform character. The latter coefficients are compared with those occurring in Onsagers theory of diffusion.

According to the force and friction conception, the dynamics [1] of pure diffusion in multicomponent systems is described by [2,8]

$$-c_i \frac{\partial \mu_i}{\partial x} = \sum_{j=1}^{k} (C_i - C_j) \varphi_{ij} \qquad (i = 1 \ldots . k) \tag{1}$$

These equations equalize, for each component i, the forces per unit volume; on the left hand side we have the driving force and on the right hand side the frictional forces for component i. The equations are written here for one-dimensional diffusion (in the x direction); c is the concentration in mole/cm^3, μ the chemical potential, C the component velocity (the flow J_i divided by c_i), φ the friction/cm^3 and k the number of components. The equations refer to the conditions in a volume element (dx).

In Onsagers system of description, the flows are written [3]

$$J_i = - \sum_{j=1}^{k} D_{ij} \frac{\partial c_i}{\partial x} \tag{2}$$

In addition to this we have [2] (*cf.* Refs.[4,5])

$$J_i = - \sum_{j=1}^{k} \Omega_{ij} \frac{\partial \mu_i}{\partial x} \tag{3}$$

According to eqn. (1), the coefficients of eqn. (2) may be expressed in terms of frictions, thermodynamic factors, and concentrations. This will be treated in detail elsewhere [7]. We are, for the present, more interested in eqn. (3), in order to study the reciprocal relations $\Omega_{ij} = \Omega_{ji}$. The coefficients Ω may, according to eqn. (1) be expressed in terms of concentrations and frictions. For this purpose we must, however, have an additional condition for the flows, since otherwise the coefficients Ω are indeterminate. We may define the flows relative to a certain component (= the solvent as "macro-component" in Refs. [4,5]), say component l, by the condition $J_l = 0$. It is, then, an easy matrix calculation to show that, if (as is physically self-evident) $\varphi_{ij} = \varphi_{ji}$, we must also have $\Omega_{ij} = \Omega_{ji}$ and *vice versa*. In view of this, it is difficult to see that the reciprocal relations of pure diffusion are, on principle, capable of giving any new information regarding the process.

The process is completely described in terms of concentrations, frictions and thermodynamic factors, and it can be stated *a priori* that the reciprocal relations can only, at most, yield relations between these magnitudes which are already known.

If, instead of reckoning the flows relative to a component l (see above), we prefer to define a reference frame for the flows [3] by means of the equation $\Sigma J\bar{v}_i = 0$ ($\bar{v}$ = partial molar volume), which has proved very useful in other connections, the coefficients no longer fulfil the condition $\Omega_{ij} = \Omega_{ji}$. Thus it seems that the conditions for a proper choice of fluxes and forces in Onsagers theory have to contain some restrictions regarding the reference frame for the fluxes, especially as the coefficients Ω are always indeterminate (0/0) if *no* additional condition for the flows is introduced.

It should be pointed out that if the force and friction conception is not used and the interpretation (as in the current treatment of the diffusion of gases) is directly concerned with the diffusion coefficients, the reciprocal relations are profitable in giving connections between these coefficients, see Ref.[6].

In addition to eqn. (2), Onsagers system also contains the equations [3].

$$\frac{\partial \mu_i}{\partial x} = -\sum_j R_{ij} J_j \qquad (i = 1 \ldots . k) \tag{4}$$

If $c_i R_{ij}$ are denoted by Φ_{ij}, eqn. (4) may be written

$$\frac{\partial \mu_i}{\partial x} = -\sum_j \Phi_{ij} C_j \tag{5}$$

It is of interest to compare this with eqn. (1), now in the form

$$\frac{\partial \mu_i}{\partial x} = -\sum_j (C_i - C_j) \Phi_{i(j)} \tag{6}$$

where $\Phi_{i(j)}$ is the coefficient of *molar* friction of component i in relation to component j, *i. e.* the friction between the components i and j in a volume, containing one mole of i. It is seen that the two equations, (5) and (6), are identical if

$$\text{a) } \Phi_{ii} = \sum_{\substack{j \\ j \neq i}} \Phi_{i(j)} \quad \text{and b) } \Phi_{ij} = -\Phi_{i(j)} \qquad (j \neq i) \tag{7}$$

Owing to $c_i c_j R_{ij} = -\varphi_{ij}$ $(j \neq i)$, the symmetry of φ_{ij} automatically also leads to symmetry of the R_{ij} coefficients. Whereas the $\Phi_{i(i)}$ evidently do not exist, $\Phi_{ii} = 0$ or $R_{ii} = 0$ are physically unallowable assumptions.

The final aim for the diffusion measurements is to determine the φ-values of eqn. (1) through a solution of the corresponding differential equations [7]. — As the diffusion theory can be outlined in different ways, it is appropriate to make reference also to the well-known work of de Groot [8] for other sides of the problem.

The author's thanks are due to Mr. O. Persson, Civ.Eng., of the Institute of Applied Mathematics (Professor C. G. Esseen), for very valuable help with the matrix calculations, the routine character of which made their reproduction unnecessary.

REFERENCES

1. Lamm, O. *J. Phys. Chem.* **59** (1955) 1149.
2. Lamm, O. *Acta Chem. Scand.* **8** (1954) 1120.
3. Onsager, L. *Ann. N. Y. Acad. Sci.* **46** (1945) 241.
4. Onsager, L. and Fuoss, R. M. *J. Phys. Chem.* **36** (1932) 2689.
5. Harned, H. S. and Owen, B. B. *The Physical Chemistry of Electrolytic Solutions*, N. Y. 1943, p. 87.
6. Hirschfelder, Curtiss and Bird, *Molecular Theory of Gases and Liquids*, N. Y. and London 1954.
7. Lamm, O. *J. Phys. Chem. In print.*
8. de Groot, S. R. *Thermodynamics of irreversible processes*, Amsterdam 1952.

Received December 3, 1956.

ACTA CHEMICA SCANDINAVICA 11 (1957) 365—372

Investigations on σ-FeCrSi

BERTIL ARONSSON and TORSTEN LUNDSTRÖM

Institute of Chemistry, University of Uppsala, Uppsala, Sweden

The solubility of Si in σ-FeCr at 690° and the lattice dimensions of the sigma-phase as functions of the Si-content have been determined.

The distribution of the Si-atoms in σ-FeCrSi is discussed in comparison with some common transition metal silicide structures.

The brittle non-magnetic FeCr sigma phase was first reported by Bain and Griffiths [1] and Chevenard [2] in 1927. In the following years it was discussed whether this phase existed in the *pure* binary system or not. That the sigma phase did exist also when only very small amounts of impurities were present, was shown in 1936 by Jette and Foote [3], who pointed out the accelerating effect of Si and of cold work on sigma phase formation. In the same year, Andersen and Jette [4] investigated the Fe-Cr-Si system (mainly the Fe-rich corner). These authors found that considerable amounts of Si were dissolved in the sigma phase and they outlined the sigma phase region in the ternary system.

In connection with studies of transition metal silicides at this institute we decided to investigate more closely the solubility of Si in the sigma phase. The investigation was limited to the FeCr-Si section of the ternary system. Our results are presented in two parts — the first dealing with the lattice dimensions and the determination of the solubility limit, and the second dealing with our ideas of the distribution of Si-atoms in σ-FeCrSi. In the latter part, some aspects on the relation between the sigma phase structure and some common silicide structures are given.

I. THE SOLUBILITY OF Si IN σ-FeCr

(T. Lundström and B. Aronsson)

Experimental

Electrolytic Cr-powder and Baker's Fe (> 99.8 %) were used. The silicon was analysed and found to contain 98.92 % Si with iron as main impurity. The alloys were prepared by melting in an arc furnace. After annealing at the relevant temperature in evacuated silica tubes they were quenched in oil. The following annealing times were used: 690°,

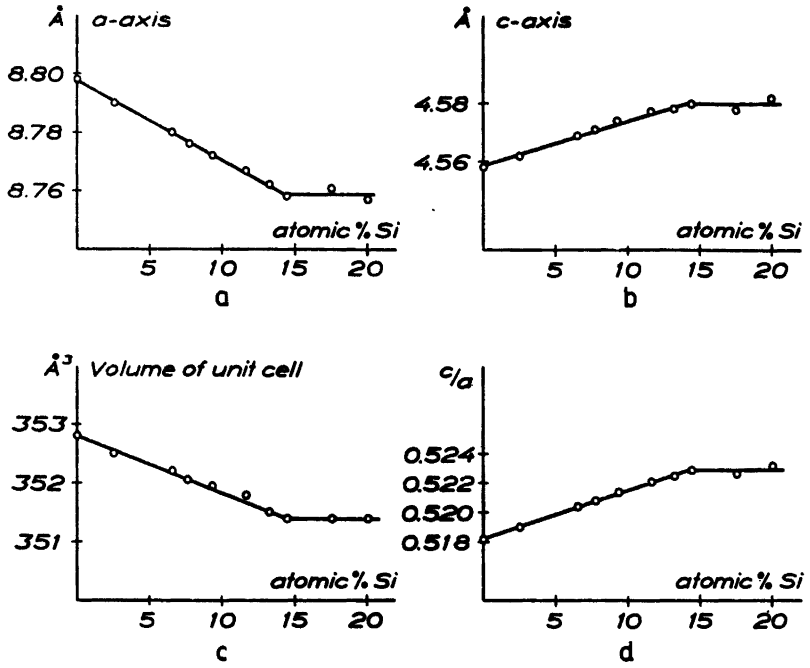


Fig. 1. Lattice parameters of σ-FeCrSi as functions of Si-content at 690°.

22—26 days; 950°, 7 days; 1 200°, 48 hours. All alloys containing less than 15 atomic % Si were analysed for Si and some alloys also for Fe and Cr. It was found that the atomic quotient Fe/Cr was constant = 1.01 with variations less than one per cent. This variation should not affect the lattice parameters more than within the experimental errors. Powder photographs were obtained in a Guinier type focusing camera, using Cr*Ka*-radiation. All specimens were mixed with some NaCl before the exposure and the camera constant was evaluated for each film, assuming the cube edge of NaCl to be 5.6394 Å (18° C) [5]. The agreement between observed and calculated $\sin^2\Theta$-values was ± 0.03 % and the lattice parameters were considered to be accurate to about 0.02 %. Because of the impurities present and a possible error in a_{NaCl}, all values may be subject to a small systematic error. These sources of error are, however, not likely to influence the changes of the lattice parameters.

Results

Alloys, annealed at 690°, showed only the sigma phase lines up to 14.4 atomic % Si. In the 17 % alloy the *110*-line of the α-phase could be observed. The changes of the lattice dimensions with Si-concentration are given in Fig. 1. The figure shows that σ-FeCr dissolves 14.2 % Si at 690° (estimated error about ± 0.5 %). Annealing of the 20 % alloy at 950° and 1 175° has shown that the upper solubility limit varies little with temperature (Fig. 2). At the lower solubility limit no two-phase range was observed between σ and α and for this reason the lower limit, outlined in Fig. 2, is only very approximate. In alloys, containing about 10 atomic % Si, the sigma phase is evidently

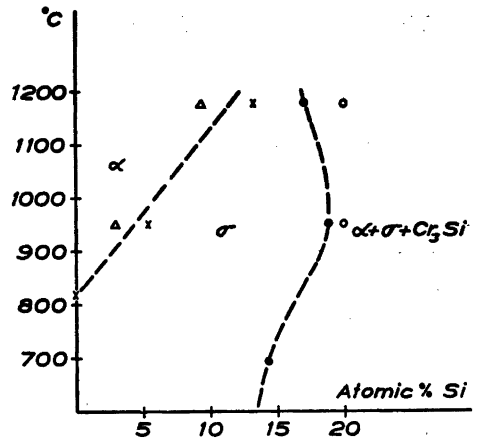


Fig. 2. Sigma region in the section FeCr-Si of the Fe-Cr-Si system.

△ Powder photographs showing α-phase
× » ——— » ——— » σ-phase
○ » ——— » ——— » α+σ+Cr_3Si
● Solubility limit of sigma phase, determined from lattice dimensions.

stable up to near the melting point, since around this composition, this phase is the only one found even in the unannealed melts.

The changes of the lattice parameters with variation of the Si-concentration are small (Fig. 1 c). The unit cell volume decreases only 0.03 % per atomic % Si, which is about half the decrease when small amounts of Si (< 10 atomic %) are dissolved in iron [6]. The axial ratio increases from 0.5181 to 0.5229 (Fig. 1 d) when the Si concentration is increased from 0 to 14 atomic % and the highest value of c/a which we have observed is 0.5246 (in an alloy annealed at 950°). The axial ratio is evidently very critical for the sigma structure. It is almost the same for all known sigma phases [7,7a] and the highest value hitherto reported is 0.5237 for σ-MoFe [8] which is only stable in a small temperature interval. It seems probable that when c/a exceeds 0.524 the sigma phase structure becomes energetically unfavourable and is not likely to be formed.

The influence of Si on FeCr-sigma phase formation is quite different from that of carbon [9] and nitrogen [10]. (Recent investigations at this institute indicate that boron behaves similarly to these elements.) When these small non-metals are present, Cr-rich carbides and nitrides are formed, thereby lowering the amount of Cr, available for sigma formation. Silicon, on the other hand, is dissolved in the sigma phase and expands its region of existence appreciably. When the solubility limit is exceeded we have found — confirming the results of Andersen and Jette [4] — that Cr-rich Cr_3Si and Fe-rich α-phase with about the same Si-content are formed. Thus, the equilibria in this part of the Fe-Cr-Si system indicate that Fe and Cr have about the same "affinity" towards Si.

The stabilizing effect of Si on the sigma phase is also revealed in the Cr-Ni-Si system, where this phase is easily formed when small amounts of Si are present but has not been found in the binary Cr-Ni system.

II. THE STRUCTURE OF σ-FeCrSi AND ITS RELATION TO SOME SILICIDE STRUCTURES

(B. Aronsson)

The crystal structure of the sigma phase has been determined by Bergman and Shoemaker [8] and by Dickins, Douglas and Taylor [11]. The unit cell is tetragonal and the space group is D_{4h}^{14}—$P4/m\,n\,m$. The atomic parameters of FeCr, according to B. and S., are given in Table 1 together with the coordination numbers (C.N.) and the number of electrons which these authors have found in the different maxima of the electron density function. As pointed out in Refs.[8,11] the structure resembles that of β—U [12]. (The details of this structure are still under discussion [13].)

Following the nomenclature of Tucker [12], the structure can be described as built up of *main layers*, pseudohexagonal layers from which some atoms have dropped out. Between these are the *subsidiary layers*, the atoms of which are placed above and beneath the holes of the main layers. Atoms of successive subsidiary layers have close contact with each other and form straight rows, perpendicular to the layers.

The ordering in the sigma phase has been discussed in Refs.[8,11]. More definite results on this point have been obtained by Kasper and Waterstrat [14], who investigated the sigma phases, appearing in the Ni-V, Fe-V and Cr-Mn systems, using neutron diffraction. The conclusions of the latter authors are, that V, Cr and Mo (A metals) prefer the positions with the highest C. N. (II, III and V), while Fe, Co and Ni (B metals) prefer the positions with the lowest C. N. (I and IV). Mn can behave both as an A- and a B-metal. The sigma phase appears at different compositions in different systems. Of course, this affects the distribution of the atoms so that III and V may be more or less mixed positions. We have tried to determine if Si behaves as an A-metal, as a B-metal or as Mn.

Experimental

Powder photographs of alloys containing 0, 9.3 and 14.4 atomic % Si were microphotometered and the intensities determined. It was found that the intensity of the *002* powder line of the sigma phase decreased 33 ($\sim \pm 10$) % when its Si concentration increased from 0 to 14.4 %. This shows that the Si-atoms chiefly substitute atoms in the main layers. This is also to be expected from the lattice spacing relations. In order to get some information of the substitution within the main layers a single crystal investigation was undertaken.

A small crystal fragment was picked out of the 11.6 % alloy. When a narrow collimator was used the spots were split into triplets at high glancing angles. This did not affect the intensity measurements appreciably but made an accurate determination of the composition from its lattice parameters difficult. With a method described by Weisz, Cochran and Cole [15] (Θ-method) the a-axis of the crystal was found to be 8.758 Å ($\sim \pm 0.010$ Å), corresponding to a composition of 12—14 atomic % Si or 3.5—4 Si-atoms per unit cell. In this determination Cu$K\alpha$-radiation and the reflexion *11, 1, 0* were used. Efforts to get a better crystal were unsuccessful.

Weissenberg photographs were taken around the c-axis, using Mo$K\alpha$-radiation. The layer lines 0—4 were recorded. The multiple film method was used and the intensities of 110 nonequivalent reflexions were visually estimated. No deviation in the linear dependence of $\log \frac{I_{obs}}{I_{calc}}$ on $\left(\frac{\sin\Theta}{\lambda}\right)^2$ was observed. The temperature constant B was found to be

0.77 Å². Using the structure of Bergman and Shoemaker [8], the observed F-values were put on an absolute scale. The temperature factors were divided out and a threedimensional Fourier-synthesis $\left(\frac{x}{60}\frac{y}{60}\frac{z}{24}\right)$ was made with the aid of the Hägg-Laurent [16] machine. The number of electrons in the different maxima of the electron density function were summed. With these atomic numbers and the parameters of Bergman and Shoemaker a three-dimensional $F_o - F_c$ synthesis was worked out in the section $xy0$. Small maxima of nearly the same height were found at the assumed atomic positions — confirming that the result of the electron counts fitted well to the intensity data. The atomic coordinates, determined from the difference synthesis, were not significantly different from those of Bergman and Shoemaker. The background indicated that a standard deviation in number of electrons of 0.5 e for the atoms II, III and IV and of 1.0 e for the atom I was reasonable. The same value was obtained with a formula given by Cruickshank [17].

The distribution of Si-atoms may, of course, vary with annealing temperature and Si-content. It should be emphasized that the results of this investigation have been obtained from a 12 % alloy, annealed 22 days at 690°.

Results and discussion

The result of the electron counts is given in Table 1, column 5. The number of electrons found in position IV is about 10 % lower than the numbers found in the other positions. The considerations of the preceding paragraph indicate that this difference is significant. Certainly there are many factors which may influence the result of electron counts, but the most reasonable interpretation

Table 1.

	Position [8]	Parameters [8]	C.N. [8]	Atomic number in σ-FeCr [8]	Atomic number in σ-FeCrSi$_{0.25}$
I	2(*a*)		12	28.1	26.0
II	4(*f*)	$x = 0.3981$	15	23.8	23.8
III	8(*i*)	$x = 0.4632$, $y = 0.1316$	14	25.8	24.2
IV	8(*i*)	$x = 0.7376$, $y = 0.0653$	12	25.8	21.6
V	8(*j*)	$x = 0.1823$, $z = 0.2524$	14	23.3	24.1

of the above mentioned result is that the Si-atoms mainly occupy IV-positions. That is, Si behaves as a B metal. If the metal atoms are ordered as Kasper and Waterstrat [14] suggest, the approximate distribution of atoms in σ-FeCrSi— should be: mainly Fe in I, mainly Cr in II, about 3 Si- and 5 Fe-atoms in IV and a mixture of Fe and Cr (and perhaps a little Si) in the III- and V-positions.

That silicon behaves as a B-metal in σ-FeCr is in accordance with the facts that the solubility of Si is greater in Fe (26 atomic %)[6] than in Cr (< 14 %) [18] and that the highest coordination number of Si in any known silicide structure is 12. At first glance, it seems curious that no Si-atoms are found in I-positions. Inspecting Fig. 3 a more closely we see, however, that if more than two Si atoms shall be placed in the unit cell the IV-positions alone permit a more even distribution of the Si-atoms in the structure, than does a combination of I- and IV-positions. If Si-Si contacts are to be avoided, a maximum of four Si-atoms per unit cell can occupy the positions, having 12 coordination, and this can only be achieved if IV-positions alone are occupied. It must be mentioned that the solubility limit corresponds to about four Si-atoms per unit cell.

There are some interesting common features in the sigma- and the cubic *A* 15-(or W_3O-[19]) structures in both of which straight rows of metal atoms with close contact are found. Inspecting Figs. 3 a and 3 d and Table 2, we see that the III-atoms of the sigma phase have two close and eight remote A-metal neighbours as well as four B-metal neighbours at "normal" distances, while the Cr-atoms of Cr_3Si [18] (W_3O-type) are surrounded by 2 + 8 Cr-atoms and 4 Si-atoms at similar distances. The figures further show that the spatial arrangements of atoms around the III- and V-atoms are roughly the same as around the Cr-atoms of Cr_3Si. On the other hand, the I- and IV-atoms have environments, similar to that of the Si-atom of Cr_3Si. These similarities are only qualitative, but it is interesting to note that — following the nomenclature of Kasper and Waterstrat [14] — all the hitherto reported phase of W_3O-type [20,20a,20b,31] can be written A_3B, where we have to add Ti, Zr, Nb, Ta and W to the A-metals and Ru, Rh, Os, Ir, Pt, Au, Hg, Ga, Sn, Si, As and

Table 2. Interatomic distances (in Å units).

Sigma-structure [8]									Cr_3Si [18]		
I—IV	2.380	(4)	2.51	IV—I	2.380	(1)	2.53		Si—Cr 2.55		(12)
—V	2.542	(4)		—IV	2.453	(1)					
—II	2.603	(4)		—III	2.470	(2)					
				—III	2.476	(1)					
				—III	2.483	(1)					
				—V	2.538	(2)					
				—V	2.562	(2)					
				—II	2.695	(2)					
III—III	2.404	(1)	2.41	V—V	2.253	(1)	2.27		Cr—Cr 2.28		(2)
—II	2.414	(1)		—V	2.294	(1)					
—IV	2.470	(2)	2.48	—IV	2.538	(2)	2.55		Cr—Si 2.55		(4)
—IV	2.476	(1)		—I	2.542	(1)					
—IV	2.483	(1)		—IV	2.562	(2)					
—V	2.763	(2)	2.80	—III	2.763	(2)	2.81		Cr—Cr 2.79		(8)
—V	2.768	(2)		—III	2.768	(2)					
—III	2.838	(4)		—II	2.833	(2)					
				—II	2.920	(1)					

Sb to the B-metals given by these authors. Perhaps, some general principle accounts for the structural similarities between V_3Ni [21] (W_3O-type) and σ-NiV [14] as well as between Cr_3Si and σ-FeCrSi.

As seen from Figs. 3 b and 3 e, the concepts of main and subsidiary layers are also very suitable for the description of two other silicide structures, namely the W_5Si_3—[22,23] ($T1$-) [24] and $D8_8$[25]-structures. The main layers are more irregular than in the sigma phase, but the short distances between atoms of successive subsidiary layers and the characteristic 14-coordination around these atoms are also found here. In W_5Si_3, the structure of which can be described as a combination of the sigma- and the $CuAl_2$-structures, both Me- and Si-rows are found. In order to be stable such a structure probably demands shorter distances in the rows than do structures which contain only Me-rows (*e. g.*, $D8_8$). The discussion of the sigma- and W_3O-structures has shown that rows with the closest interatomic contact are most easily formed by the metals

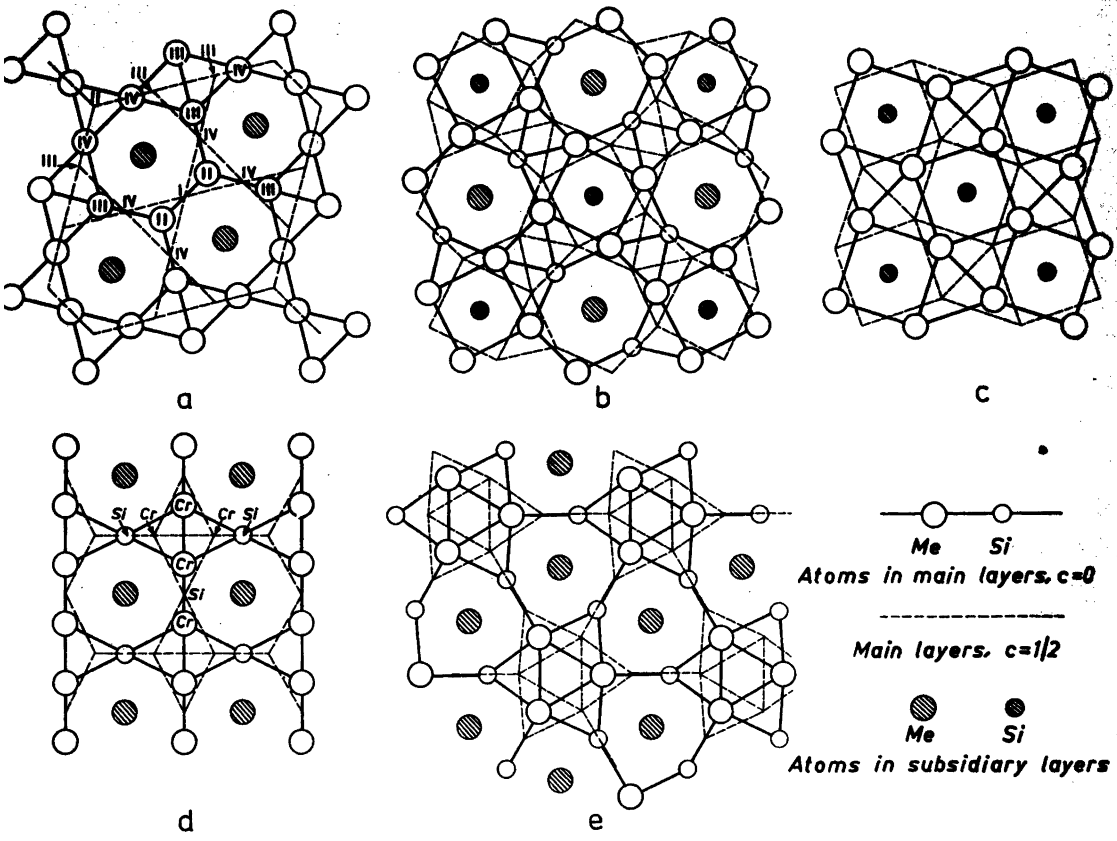


Fig. 3. The sigma structure and some silicide structures. a. σ -FeCr [8]. b. W_5Si_3 [22,23]. c. Ta_2Si [30] ($CuAl_2$-type). d. Cr_3Si [18]. e. Mn_5Si_3 [25]. The layers are parallel to the plane of the paper. (In $D8_8$ the main layers are found in the planes $c = 1/4$ and $c = 3/4$.)

of the Va and VIa groups. This may be part of the explanation of the curious morphotropy among the Me_5Si_3-phases: Ti_5Si_3 [26] ($D8_8$), V_5Si_3 [27] ($T1$), Cr_5Si_3 [22] ($T1$), Mn_5Si_3 [25] ($D8_8$) and Fe_5Si_3 [6] ($D8_8$) with the following interatomic distances in the metal rows: 2.58 Å, 2.37 Å, 2.30 Å, 2.40 Å and 2.36 Å. Recently these phases have been comprehensively discussed by Nowotny and his school [24,28].

As pointed out by Bergman and Shoemaker [8], Fe_7W_6 is structurally related to the sigma phases. In the rhombohedral Fe_7W_6 [25]-structure, groups of four W-atoms are found on the trigonal axis. The distances between adjacent atoms of such a group are less than in elementary W.

The most conspicuous structural feature of all these metallic phases are the straight rows of atoms with close contact. These rows are most easily formed by the transition metals of the Va- and VIa-groups. They are found in a number of common silicide structures, which indicates that silicon has

some beneficial effect on the stability of these rows. As long as so little is known about the electronic structures of the transition elements, it is probably meaningless to try to give a more fundamental explanation of the mentioned facts.

Acknowledgements. We want to express our gratitude to Professor G. Hägg and Dr. I. Lindqvist for their kind interest in this work and for all the facilities they have put at our disposal.

The chemical analyses were carried out at the analytical department of this institute. We wish to thank the Head of this department, Dr. F. Nydahl, as well as Dr. Lilly Gustafsson and Mr. L. Bergin for their excellent assistance.

Thanks are also due to Mrs. B. Flemström, who has prepared the manuscript and to Mr. S. Wahlgren and J. Åselius for technical assistance.

This investigation has been supported by the *Swedish State Council for Technical Research*, whose aid is gratefully acknowledged.

REFERENCES

1. Bain, E. C. and Griffiths, W. E. *Trans Am. Inst. Mining Met. Eng.* **75** (1927) 166.
2. Chevenard, P. *Travaux et Mémoires du Bureau International des Poids et Mesures* **17** (1927) 60.
3. Jette, E. R. and Foote, F. *Metals & Alloys* **7** (1936) 207.
4. Andersen, A. G. H. and Jette, E. R. *Trans. Am. Soc. Metals* **24** (1936) 375.
5. Parrish, W. *Philips Laboratories Inc. Tech. Rept.* No. 17, Febr. 14, 1948.
6. Farquhar, C. M., Lipson, H. and Weill, A. R. *J. Iron Steel Inst.* **152** (1945) 457.
7. Pearson, W. B., Christian, J. W. and Hume-Rothery, W. *Nature* **167** (1951) 110.
7a. Duwez, P. and Baen, S. E. *ASTM Symposium on the Nature, Occurence and Effects of the Sigma phase* 1950, p. 48.
8. Bergman, G. and Shoemaker, D. P. *Acta Cryst.* **7** (1954) 857.
9. Shortsleave, F. J. and Nicholson, M. E. *Trans. Am. Soc. Metals* **43** (1951) 142.
10. Tisinai, G. F., Stanley, J. K. and Samans, C. H. *Trans. Am. Inst. Mining Met. Eng.* **200** (1954) 1259.
11. Dickins, G. J., Douglas, A. M. B. and Taylor, W. H. *Acta Cryst.* **9** (1956) 297.
12. Tucker, C. W. and Senio, P. *Acta Cryst.* **6** (1953) 753.
13. Tucker, C. W., Senio, P., Thewlis, J. and Steeple, H. *Acta Cryst.* **9** (1956) 472.
14. Kasper, J. S. and Waterstrat, R. M. *Acta Cryst.* **9** (1956) 289.
15. Weisz, O., Cochran, W. and Cole, W. F. *Acta Cryst.* **1** (1948) 83.
16. Hägg, G. and Laurent, T. *J. Sci. Instr.* **23** (1946) 155.
17. Cruickshank, D. W. J. *Acta Cryst.* **2** (1949) 65.
18. Borén, B. *Arkiv Kemi, Mineral, Geol.* **11 A** (1933) No. 10.
19. Hägg, G. and Schönberg, N. *Acta Cryst.* **7** (1954) 351.
20. Geller, S., Matthias, B. T. and Goldstein, R. *J. Am. Chem. Soc.* **77** (1955) 1502.
20a. Raub, E. and Mahler, W. *Z. Metallkunde* **46** (1955) 210.
20b. Greenfield, P. and Beck, P. A. *Trans. Am. Inst. Mining Met. Eng.* **206** (1956) 265.
21. Rostoker, W. and Yamamoto, A. *Trans. Am. Soc. Metals* **46** (1954) 1136.
22. Dauben, C. H., Templeton, D. H. and Myers, C. E. *J. Phys. Chem.* **60** (1956) 443.
23. Aronsson, B. *Acta Chem. Scand.* **9** (1955) 1107.
24. Parthé, E., Lux, B. and Nowotny, H. *Monatsh.* **86** (1955) 859.
25. Åmark, K., Borén, B. and Westgren, A. *Metallwirtschaft* **15** (1936) 835.
26. Pietrokowsky, P. and Duwez, P. *J. Metals* **3** (1951) 772.
27. Parthé, E., Nowotny, H. and Schmid, H. *Monatsh.* **86** (1955) 385.
28. Nowotny, H., Kudielka, H. and Parthé, E. *2. Plansee Seminar* 1956, Springer-Verlag, p. 166.
29. Arnfelt, H. and Westgren, A. *Jernkontorets Ann.* **119** (1935) 185.
30. Nowotny, H. Schachner, H., Kiefer, R. and Benesovsky, F. *Monatsh.* **84** (1953) 1.
31. Geller, S. *Acta Cryst.* **9** (1956) 885.

Received December 3, 1956.

ACTA CHEMICA SCANDINAVICA 11 (1957) 373—381

On the Hydrolysis of Trialkylphenoxysilanes. II

EVERT ÅKERMAN

Department of Organic Chemistry, University of Lund, Lund, Sweden

The hydrolysis of twelve substituted triethylphenoxysilanes in aqueous ethanol has been studied spectrophotometrically. The reaction is catalysed by both acid and alkali. The catalytic constants for the *meta*- and *para*-substituted compounds agree well with the Hammet equation. Dimethyl-*t*-butylphenoxysilane has been prepared and its hydrolysis studied. The mechanisms of the reactions are discussed and the ultraviolet spectra are described.

In a previous paper [1] the preparation and hydrolysis of five trialkylphenoxysilanes was described, the alkyl groups being methyl, ethyl, *n*-propyl, *n*-butyl and *n*-amyl. The specific rate of the reaction was found to be proportional to the hydrogen ion concentration in acid solution and the sum of hydroxide and ethoxide ion concentrations in alkaline solution and to diminish with increasing length of the alkyl groups. The investigation has now been extended to phenoxysilanes with substituents in the phenoxy group in order to acquire better knowledge of the mechanism of the reactions and, if possible, to obtain a quantitative relationship between rate constants and substituents according to Hammet's equation [2]. Some reactions of substituted aryl- and benzylsilanes have been reported, where the rate constants satisfy the Hammet equation. Gilman and Dunn [3] investigated the hydrolysis of six triarylsilanes in wet piperidine and found a reaction constant $\varrho = 3.09$, but the rate constant for one of the substituents, the *para*-dimethylamino group, did not satisfy the equation when the σ-value from Hammet's table was used. Eaborn and Parker [4] studied spectrophotometrically the alkali-catalysed cleavage of seventeen substituted benzyltrimethylsilanes in aqueous methanol. They found the substituent effects to agree well with Hammet's σ constants and they calculated a reaction constant $\varrho = 4.88$.

The reaction now examined is described by the over-all reaction formula

$$(C_2H_5)_3SiOC_6H_4R + H_2O \longrightarrow (C_2H_5)_3SiOH + HOC_6H_4R$$

From the five trialkylphenoxysilanes previously measured triethylphenoxysilane was chosen as the unsubstituted compound, as it has the most convenient rate of reaction. The corresponding trimethyl compound was not chosen, as its rate constants are much too great to be measured with accuracy. The

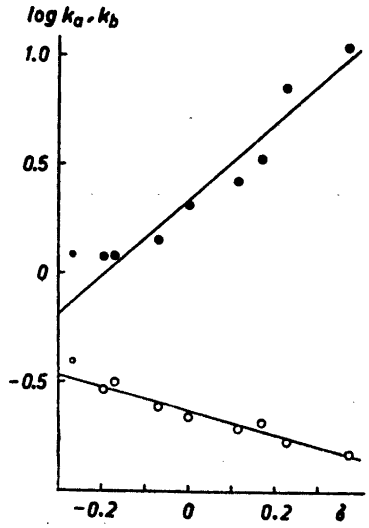


Fig. 1. Catalytic constants *versus* Hammet's σ-constants.
● Alkaline hydrolysis of triethylphenoxysilanes.
O Acid » » »

following twelve substituents have been introduced in the phenoxy group: *o*-CH_3, *m*-CH_3, *p*-CH_3, *p*-*t*-C_4H_9, *o*-CH_3O, *m*-CH_3O, *p*-CH_3O, *o*-Cl, *m*-Cl, *p*-Cl, 1,3$(CH)_4$ (*α*-naphthyl) and 2,4$(CH)_4$ (*β*-naphthyl). The rate constants k were determined for at least five different concentrations of hydrogen ions and five concentrations of hydroxyl ions. The catalytic constants $k_a = k/[\text{acid}]$ and $k_b = k/[\text{base}]$ were calculated and were found to be reasonably constant for each compound. Consequently none of the compounds have any spontaneous hydrolysis rapid enough to be noticed at the actual concentrations. These results are collected in Table 1.

According to Hammet [2] the quantitative relationship between the rate constants k' for the reaction of a *meta*- or *para*-substituted benzene derivative and the so called substituent constant σ is expressed by the formula

$$\log k' - \log k_0' = \varrho\,\sigma$$

where k'_0 is the rate constant of the unsubstituted compound, ϱ is a constant, the reaction constant, and σ is defined from the equation

$$\sigma = \log K - \log K_0$$

K and K_0 being the dissociation constants of the benzoic acid with the same substituent and that of unsubstituted benzoic acid, respectively. A plot of the catalytic constants k_a and k_b of the *meta*- and *para*-substituted phenoxysilanes in Table 1 against σ is shown in Fig. 1. (The two small circles at $\sigma = -0.27$ refer to the *para*-methoxy group, *cf* below). The σ values are taken from Jaffé's review on the Hammet equation[5]. The plot shows that the expected

Table 1. Acid and alkaline hydrolysis of $Et_3SiOC_6H_4R$.

R	10^4[H+] M	10^4 k sec^{-1}	k_a $M^{-1}sec^{-1}$	$k_a$mean $M^{-1}sec^{-1}$	10^4[OH⁻] M	10^4 k sec^{-1}	k_b $M^{-1}sec^{-1}$	k_b mean $M^{-1}sec^{-1}$
o-CH_3	20.0	1.85	0.0925	0.0906	2.94	1.80	0.612	0.633
	30.0	2.65	.0883		6.22	3.98	.640	
	80.0	7.18	.0898		10.3	6.55	.636	
	120	11.0	.0916		15.9	10.3	.648	
	200	18.1	.0907		31.9	20.0	.627	
m-CH_3	10.0	2.34	0.234	0.244	2.98	4.41	1.48	1.43
	20.0	4.90	.245		6.27	9.00	1.44	
	30.0	7.27	.242		9.96	13.5	1.36	
	50.0	12.9	.258		18.0	25.8	1.43	
	80.0	19.9	.249		24.6	35.7	1.45	
	120	28.5	.237					
p-CH_3	10.2	3.17	0.311	0.317	2.87	3.50	1.22	1.20
	20.0	6.24	.312		6.19	7.15	1.16	
	50.0	16.0	.320		8.43	10.2	1.21	
	80.0	26.1	.326		29.9	35.5	1.19	
	120	37.8	.315		51.6	62.4	1.21	
p-*t*-C_4H_9	9.77	2.78	0.284	0.290	2.86	3.35	1.17	1.19
	18.2	5.33	.293		6.37	7.43	1.17	
	50.3	14.8	.293		8.95	10.9	1.22	
	80.0	23.1	.289		16.4	19.4	1.18	
	120	34.7	.289		29.6	35.7	1.21	
o-CH_3O	9.57	1.84	0.192	0.207	2.79	2.06	0.737	0.729
	19.8	4.24	.214		6.31	4.49	.712	
	49.2	10.5	.214		10.0	7.38	.738	
	120	23.9	.199		15.1	11.0	.728	
	200	43.0	.215		30.1	22.0	.732	
m-CH_3O	9.57	1.97	0.206	0.196	1.30	3.61	2.79	2.67
	19.5	3.79	.194		2.66	7.38	2.78	
	29.4	5.80	.197		5.96	16.1	2.69	
	50.0	9.55	.191		9.93	25.1	2.53	
	80.0	15.8	.197		14.1	36.1	2.56	
	120	23.2	.193					
p-CH_3O	4.66	1.89	0.405	0.396	3.03	3.66	1.21	1.22
	19.1	7.87	.412		6.17	7.48	1.21	
	29.9	11.4	.382		9.12	11.1	1.22	
	50.1	19.3	.386		28.2	33.0	1.21	
	80.0	31.7	.396		50.0	64.7	1.25	
o-Cl	19.5	1.44	0.0738	0.0734	0.321	2.27	6.81	6.86
	50.0	3.65	.0730		0.767	5.33	6.95	
	80.0	5.92	.0739		1.50	10.2	6.80	
	120	8.78	.0732		3.06	20.6	6.73	
	200	14.6	.0730		6.25	43.7	6.99	
m-Cl	19.3	2.83	0.147	0.150	0.308	3.51	11.4	11.0
	28.9	4.30	.149		0.792	8.88	11.2	
	50.0	7.71	.154		1.23	13.9	11.3	
	120	17.7	.148		2.72	29.7	10.9	
	200	30.0	.150		6.21	64.8	10.4	

Table 1 continued.

p-Cl	10.0	1.73	0.173	0.170	0.296	2.12	7.15	7.17
	19.5	3.38	.173		0.762	5.57	7.30	
	50.0	8.40	.168		1.49	10.7	7.20	
	80.0	13.5	.169		2.82	20.0	7.09	
	120	20.2	.168		6.33	45.1	7.12	
1,3(CH)$_4$[a]	19.5	1.27	0.0649	0.0648	1.32	2.95	2.23	2.18
	30.0	1.95	.0648		2.78	6.13	2.22	
	80.0	5.23	.0654		6.28	13.1	2.09	
	120	7.77	.0647		10.3	21.8	2.12	
	200	12.8	.0640		16.3	36.2	2.22	
2,4(CH)$_4$[b]	10.0	2.13	0.213	0.209	1.24	4.14	3.34	3.39
	20.0	4.31	.215		2.68	9.35	3.49	
	49.8	10.4	.209		5.72	19.3	3.38	
	80.0	16.4	.206		9.68	32.5	3.36	
	120	24.9	.207		15.0	50.7	3.38	
	200	40.3	.202					
H[c]				0.219				2.05

a α-naphthyl, b β-naphthyl, c from Ref[1].

linear relationship between log k and σ is rather well satisfied. One of the points, *viz* that for the *para*-methoxy group, has an obviously greater deviation than the others from the best straight line. This is, however, not uncommon (*cf* Ref. 5. p. 230), and so it seems reasonable to exclude this point when calculating the reaction constant. This constant ϱ and the calculated catalytic constant for the unsubstituted compound k_0 were obtained according to the method of least squares. The results together with the standard deviation s and the correlation coefficient r (calculated in the same way as in Jaffé's review [5]) are given in Table 2. The figures in parenthesis are the values obtained when the rate constants for the *para*-methoxy group are included.

Attempts have been made to extend the Hammet equation to other reactions than those of *meta*- and *para*-substituted benzene derivatives. Thus Taft [6–8] succeeded in modifying the equation by introducing a steric term E_s in such a way that the equation became valid also for *ortho* substituents:

$$\log k - \log k_0 = \varrho\sigma^* + E_s \qquad (1)$$

Table 2. Reaction constant ϱ, log k_0, standard deviation s and correlation coefficient r for the acid and base catalysed hydrolysis of triethylphenoxysilanes.

Catalysis	ϱ	log k_0	s	r
Acid	−0.533 (−0.600)	−0.632 (−0.621)	0.030 (0.038)	0.968 (0.964)
Base	1.742 (1.575)	0.337 (0.364)	0.094 (0.109)	0.970 (0.958)

The polar substituent in this equation was originally indicated by E_σ, but this was later [7] changed to σ^*. The substituent constants are evaluated by assuming that ϱ has the same value as for *meta-para*-substituted derivatives and that E_s has the same value in alkaline as in acid hydrolysis. The agreement between Taft's values and those that can be calculated from the rate constants in Table 1 are, however, only qualitative. This is not unexpected as the validity of eqn. (1) is much more limited than that of the Hammet equation. Thus all the reactions investigated by Taft are of one single type, *viz.* esterification and ester hydrolysis.

It is still less probable that the hydrolysis of trialkylphenoxysilanes with different alkyl groups should fit eqn. (1). It is possible in the case of substituted acetates as shown by Taft [6-8], but here only *one* substituent is changed and in the compounds described in Part I [1] of this work *three* substituents are changed. Even if polar effects might be additive as in the case of *meta-para*-substituted benzene derivatives, this is probably not true for steric effects.

In addition to the five compounds previously described, dimethyl-*t*-butylphenoxysilane has been prepared and its hydrolysis studied (Table 3). The rate constants of these six compounds cannot - as expected - be correlated with Taft's σ^* and E_s constants according to eqn. (1). It is interesting, however, to compare the specific rate constants of dimethyl-*t*-butylphenoxysilane with those of triethylphenoxysilane ($k_a = 0.219$, $k_b = 2.05$) and trimethylphenoxysilane ($k_a = 10.4$, $k_b \approx 330$). The substitution of a *t*-butyl group for a methyl group lowers the catalytic constants by a factor of 10^{-5}. But even in comparison with triethylphenoxysilane, dimethyl-*t*-butylphenoxysilane is hydrolysed very slowly, the ratio between the catalytic constants being less than 10^{-2}. If the polar effects in these two compounds are assumed to be of the same order of magnitude (the numbers of carbon atoms in α- and β-position to the silicon atom are the same, and according to Taft [7], σ^* for three ethyl groups is —0.72, σ^* for two methyl groups plus one *t*-butyl group is —0.84), the low rate constants can at least to a large extent be ascribed to the steric influence of the *t*-butyl group.

From these facts several mechanisms of the reactions can be formulated. As the reaction constant for the alkaline hydrolysis has a rather high positive value, this reaction is obviously facilitated by a low electron density at the

Table 3. Acid and alkaline hydrolysis of Me_2-*t*-BuSiOC$_6$H$_5$.

[H+] mM	$10^6\,k$ sec^{-1}	$10^4\,k_a$ M^{-1} sec^{-1}	$10^4\,k_a$ mean M^{-1}sec^{-1}	[OH$^-$] mM	$10^5\,k$ sec^{-1}	$10^2\,k_b$ M^{-1}sec^{-1}	$10^2\,k_b$ mean M^{-1}sec^{-1}
12.0	7.23	6.03	5.91	5.00	8.52	1.70	1.72
20.0	11.4	5.70		8.00	13.8	1.73	
25.0	14.7	5.88		12.0	20.4	1.70	
40.0	23.8	5.95		20.0	34.7	1.73	
50.0	30.0	6.00		30.0	52.2	1.74	

reaction centre. The simplest mechanism consistent with this is an S_N2 mechanism:

$$RO^- + Et_3SiOC_6H_4R' \rightarrow \overset{\delta^-}{RO} \ldots Et_3Si \ldots \overset{\delta^-}{OC_6H_4R'} \rightarrow ROSiEt_3 + {}^-OC_6H_4R'$$

followed by the equilibrium

$$R'C_6H_4O^- + ROH \rightleftharpoons R'C_6H_4OH + RO^-$$

where R is H or Et.

The acid hydrolysis has a negative value of the reaction constant, so it must be facilitated by a high electron density at the reaction centre. A simple mechanism involves a fast proton transfer and a slow reaction between a charged complex and a solvent molecule:

$$ROH_2^+ + Et_3SiOC_6H_4R' \rightarrow ROH + Et_3\overset{H}{\underset{+}{Si}}OC_6H_4R'$$

$$Et_3\overset{H}{\underset{+}{Si}}OC_6H_4R' + ROH \rightarrow Et_3\overset{H}{\underset{+}{Si}}OR + HOC_6H_4R'$$

$$Et_3\overset{H}{\underset{+}{Si}}OR + ROH \rightarrow Et_3SiOR + ROH_2^+$$

However, the first step can also be rate determining and the second one rapid. R is also here H or Et.

In either case it is possible to formulate a mechanism involving a pentacovalent silicon atom. Eaborn and Parker [4] did not exclude this possibility in the alkaline hydrolysis of benzyltrimethylsilanes, and Swain, Esteve and Jones [9] made such an intermediate probable in the reaction between water and triphenylsilylfluoride. According to this mechanism the alkaline hydrolysis could be represented by the formula

$$RO^- + Et_3SiOC_6H_4R' \overset{\text{fast}}{\rightleftharpoons} Et_3(RO)\overset{-}{Si}OC_6H_4R' \overset{\text{slow}}{\rightarrow} Et_3SiOR + R'C_6H_4O^-$$

if the last step is assumed to be rate determining as in the hydrolysis of triphenylsilylfluoride. A similar mechanism - with a positive intermediate - can be formulated for the acid hydrolysis.

In addition to these mechanisms there are also other possibilities where the carbon-oxygen bond is broken, but there is some indication that the cleavage of silicon-oxygen bond is favoured at least in the case of alkoxysilanes [10]. The stability of aryl ethers against hydrolysis at room temperature also indicates a cleavage of the silicon-oxygen bond. It is true that *t*-butyl phenyl ether - the carbon analogue of trimethylphenoxysilane - is less stable than *n*-alkyl phenyl ethers, but the ease with which it is cleaved by mineral acids depends on the formation of *i*-butylene and phenol [11].

EXPERIMENTAL

The phenoxysilanes were prepared from triethylchlorosilane and the corresponding phenol according to the formula

$$(C_2H_5)_3SiCl + HOC_6H_4R \rightarrow (C_2H_5)_3SiOC_6H_4R + HCl$$

Table 5. Extinction coefficient ε and wavelength λ for the absorption maxima of $Et_3SiOC_6H_4R$.

Substituent	Absolute maximum		Secondary maximum		Measuring Wavelength	
	ε	λ	ε	λ	acid	alkaline
H	267.5	1 050			280	280
o-CH_3	270	1 200	275.5	1 080	280	285
m-CH_3	270	1 000	275	910	280	285
p-CH_3	274	1 240			285	290
o-CH_3O	274.5	2 380			285	285
m-CH_3O	273	1 960	280	1 660	284	285
p-CH_3O	286	2 350			300	302.5
p-*t*-C_4H_9	272	1 200			285	285
o-Cl	272.5	1 440	278.5	1 320	285	290
m-Cl	274	1 250	278	1 120	285	290
p-Cl	278	1 230			290	292

Table 4. Physical constants and analyses of $Et_3SiOC_6H_4R$.

R	B.p. °C	Pressure mm Hg	n_D^{20}	d^{20}	MR_D		% Si		% C		% H	
					found	calc.	found	calc.	found	calc.	found	calc.
o-CH_3	126	13	1.4913	0.9292	69.37	69.25	12.7	12.6	69.9	70.2	9.9	10.0
m-CH_3	125	13	1.4893	0.9240	69.50	69.25	12.8	12.6	70.1	70.2	10.0	10.0
p-CH_3	128—9	13	1.4891	0.9240	69.50	69.25	12.8	12.6	70.0	70.2	9.8	10.0
o-CH_3O	133	12	1.4949	0.9736	71.38	71.02	11.7	11.8	65.5	65.5	9.2	9.3
m-CH_3O	138—9	10	1.4962	0.9762	71.36	71.02	11.8	11.8	65.6	65.5	9.4	9.3
p-CH_3O	150—1	13	1.4955	0.9772	71.20	71.02	11.6	11.8	65.2	65.5	9.3	9.3
p-*t*-C_4H_9	150	11	1.4885	0.9127	83.58	83.42	10.7	10.6	72.4	72.7	10.6	10.7
o-Cl[a]	134—5	12	1.5035	1.0334	69.51	69.42	11.6	11.6	59.5	59.4	8.0	7.9
m-Cl[a]	137—8	14	1.5017	1.0268	69.75	69.42	11.6	11.6	59.4	59.4	8.0	7.9
p-Cl[b]	140	13	1.5021	1.0288	69.66	69.42	11.6	11.6	59.3	59.4	7.9	7.9
1,3$(CH)_4$	168—9	10	1.5550	1.0017	82.82	—	10.9	10.9	74.1	74.4	8.6	8.6
2,4$(CH)_4$	172	10	1.5537	0.9962	83.08	—	10.9	10.9	74.3	74.4	8.7	8.6

[a] % Cl found 14.6; calc. 14.6.
[b] » » » 14.7; » 14.6.

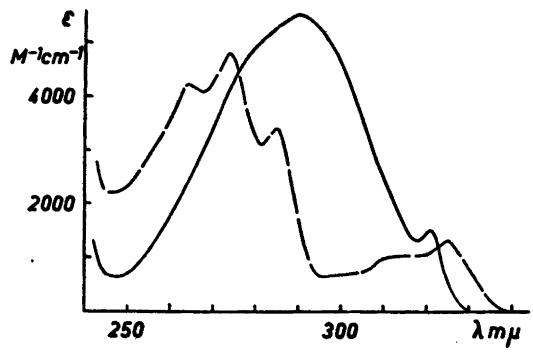


Fig. 2. Ultraviolet spectra of triethylnaphthoxysilane in 51.4 weight-% ethanol. ———— the α-compound, — — — — the β-compound.

as previously described [1]. If the evolution of hydrochloric acid was very slow, as in the case of dimethyl-*t*-butylphenoxysilane, the reaction was carried out in pyridine.

Dimethyl-t-butylphenoxysilane. To 6.6 g (0.07 mole) of phenol in 5 g of pyridine were added 10.6 g (0.07 mole) of dimethyl-*t*-butylchlorosilane prepared according to Sommer and Tyler [12] dissolved in 15 g of pyridine, and the mixture was refluxed for half an hour. The precipitated pyridine hydrochloride (6.0 g, calc. 8.1 g) was filtered off and washed with dry ether. The ether and pyridine was distilled off and the residue distilled *in vacuo*. 3.0 g = 45 % of phenol were recovered and the yield of the silane was 6.8 g = 48 %. B. p. 100–101°/15 mm, $n_D^{20} = 1.4812$, $d^{20} = 0.9127$, $MR_D = 64.97$. (Found: C 69.3; H 9.7; Si 13.6; Calc. for $C_{12}H_{20}OSi$: C 69.2; H 9.7; Si 13.5). Analyses and physical constants for the other compounds are found in Table 4. The agreement between the found and calculated molecular refractivity is not very good, the found value being on the average 0.2 ml too high, but it is known that the phenoxy group attached to silicon has no constant group refractivity as shown by Smith [13] in the case of mixed alkoxy-phenoxysilanes.

The rate constants were determined as in Ref.[1] and thus the temperature was 25.0°C, the ionic strength 0.05 M and the solvent 51.4 wt-% ethanol. As examples of buffers used in the alkaline hydrolysis at low hydroxyl ion concentrations can be mentioned: in 0.013 M glycinate + 0.003 M glycine [OH^-] is equal to 3×10^{-5} M, in 0.012 M $NaHCO_3$ + 0.006 M Na_2CO_3 [OH^-] is equal to 3×10^{-4} and in 0.005 M $NaHCO_3$ + 0.010 M Na_2CO_3 [OH^-] is equal to 10^{-3} M.

The ultraviolet spectra were determined and are generally similar to those of unsubstituted phenoxysilane in having only one maximum in the region 250–320 mμ, but five of the compounds have a secondary maximum. The wavelengths and extinction coefficients of these maxima are given in Table 5 together with the wavelengths used for the kinetics. The spectra of the naphthoxysilanes are more complicated (Fig. 2). The rate of hydrolysis for the α-naphthoxycompound was determined at 325 mμ and that for the β-naphthoxycompound at 335 mμ in acid and 340 mμ in alkaline solution.

The author is indebted to Professor Erik Larsson for his kind interest in this work.

REFERENCES

1. Åkerman, E. *Acta Chem. Scand.* **10** (1956) 298.
2. Hammet, L. P. *Physical Organic Chemistry*, McGraw-Hill Book Company, Inc., New York 1940, Chapter VII.
3. Gilman, H. and Dunn, G. E. *J. Am. Chem. Soc.* **73** (1951) 3404.
4. Eaborn, C. and Parker, S. H. *J. Chem. Soc.* **1955**, 126.

5. Jaffé, H. H. *Chem. Revs.* **53** (1953) 191.
6. Taft, Jr., R. W. *J. Am. Chem. Soc.* **74** (1952) 2729.
7. Taft, Jr., R. W. *J. Am. Chem. Soc.* **74** (1952) 3120.
8. Taft, Jr., R. W. *J. Am. Chem. Soc.* **75** (1953) 4231.
9. Swain, G., Esteve, R. M. and Jones, R. H. *J. Am. Chem. Soc.* **71** (1949) 965.
10. Krieble, R. H. and Burkhard, C. A. *J. Am. Chem. Soc.* **69** (1947) 2689.
11. Evans, T. W. and Edlund, K. R. *Ind. Eng. Chem.* **28** (1936) 1186.
12. Sommer, L. H. and Tyler, L. J. *J. Am. Chem. Soc.* **76** (1954) 1030.
13. Smith, B. *Acta Chem. Scand.* **9** (1955) 1337.

Received November 15, 1956.

ACTA CHEMICA SCANDINAVICA 11 (1957) 382—390

Recommendations by the Commission on Physico-Chemical Symbols and Terminology under the International Union of Pure and Applied Chemistry (IUPAC), 1955

The following pages contain a reprinted edition of the recommendations by the above mentioned Commission from its meeting in Zürich 1955. It has been submitted to this journal by its chairman J. A. Christiansen, who has also read the proofs.

RECOMMENDATIONS ON MATTERS OF DETAIL

The recommendations on the following pages are mainly those agreed upon in Amsterdam (1949), with modifications which subsequent discussions in the commission have made desirable. The commission refers to the report of 1949 concerning the history and concerning the agreement with recommendations from related bodies, especially the S. U. N. commission of I. U. P. A. P.

Referring to section III below the commission has found it desirable however to quote two paragraphs from the introduction to the report of 1949.

"It is recognised that recommendations by an international body must involve compromises and will sometimes have to include alternative usages for particular quantities from which the various national organisations can select those most closely in accord with their established practices. The proposals now made are not therefore intended to prescribe rigidly usages that should be universally adopted, but to give guidance in seeking a wider measure of international agreement and warning of instances where existing diversities may cause misunderstandings."

"Even among chemists in different countries, or belonging to different schools, complete agreement has not been attained on the use of symbols for certain quantities and in a few instances it may be necessary, at least temporarily, to agree to disagree and to say so."

I. NUMBERS AND MATHEMATICAL OPERATIONS

Numbers should be printed in upright figures, using a comma or point only to separate whole numbers from the decimals. To facilitate reading of long numbers the figures may be grouped together in threes without using commas or points to separate the groups.

Symbols for mathematical operations should be printed in roman (upright) type.

II. ABBREVIATIONS FOR WORDS

To be printed in upright type.

A. ABBREVIATIONS FOR THE NAMES OF UNITS

Abbreviations for units named after persons begin with a capital letter. Single capital letters used as abbreviations may be printed in smaller type than is used in the body of the text, but practice in this varies and no recommendation is made.

metre	m	degree Celsius (1)	°C
micron	μ	degree Fahrenheit (1)	°F
ångström	Å	degree Kelvin (1)	°K
litre	l	lumen	lm
second	s	lux	lx
minute	min	stilb	sb
hour	h	candela	cd
hertz	Hz	coulomb	C
gramme	g	ampère	A
tonne	t	volt	V
dyne	dyn	ohm	Ω
newton	N	farad	F
bar	b	henry	H
poise	P	molal (concentration) (2)	m
joule	J	molar (concentration) (2)	M
watt	W	normal (concentration) (2)	N
calorie	cal	formal (concentration) (2)	F

Prefixes to abbreviations for the names of units indicating:

Multiples			Sub-multiples		
tera	10^{12}	T	deci	10^{-1}	d
giga	10^{9}	G	centi	10^{-2}	c
mega	10^{6}	M	milli	10^{-3}	m
kilo	10^{3}	k	micro	10^{-6}	μ
			nano	10^{-9}	n
			pico	10^{-12}	p

(1) The °sign and the letter following form *one symbol* and there should be no space between them *e. g.* 25 °C or 25°C but *not* 25° C.

(2) Used only when preceded by numerals to indicate the magnitude of a concentration in the specified terms and not as symbols for concentrations in equations.

B. ABBREVIATIONS FOR OTHER WORDS

These will vary with the language used and no attempt is therefore made to secure uniformity of practice at an international level.

A full point is sometimes used after abbreviations but this practice is not recommended except when required to avoid confusion.

III. SYMBOLS FOR PHYSICAL AND CHEMICAL QUANTITIES

Symbols for physical and chemical quantities, in contrast to abbreviations for units, should be printed in sloping (italic) type whenever these symbols are letters of the latin alphabet and if practicable when they are letters of the greek alphabet. A bold face italic type may be used to represent certain specified physical constants or conversion factors.

Symbols separated by commas represent equivalent recommendations.

Symbols preceded by three dots are alternatives to be used only when there is some reason for not using a symbol before the three dots.

Space, time, mass and related quantities

	Quantity	Symbol
1	length	l
2	height	h
3	radius	r
4	diameter	d
5	path, length of arc	s
6	plane angle	$\alpha, \beta, \gamma, \vartheta, \varphi, \psi$
7	solid angle	ω
8	area	A, S
9	volume	$V \ldots v$
10	specific volume	v
11	wave length	λ
12	wave number	σ, ν
13	time	t
14	period or other characteristic time interval	T, τ
15	frequency	ν, f
16	angular frequency ($2 \pi \nu$)	ω
17	velocity	$v \ldots u, w$
18	angular velocity	ω
19	acceleration	a
20	» of free fall	g
21	mass	m
22	moment of inertia	I
23	density	ϱ
24	relative density	d

Molecular and related quantities

	Quantity	Symbol
101	molecular mass	m
102	molar mass	M
103	Avogadro's number	N_0, L, N
104	number of molecules	N
105	number of moles	n
106	mole fraction	$x \ldots X$, y
107	molality	m
108	concentration	c
109	molar concentration of substance B	c_B, [B], c(B)
110	molecular concentration	C
111	partition function	Q
112	statistical weight	$g \ldots p$
113	symmetry number	σ
114	characteristic temperature	Θ
115	diameter of molecule	$\sigma \ldots D$
116	mean free path	l
117	diffusion coefficient	D
118	osmotic pressure	Π
119	surface concentration	Γ

Mechanical and related quantities

	Quantity	Symbol
201	force	F
202	force due to gravity (weight)	$G \ldots W$
203	moment of force	M
204	power	P
205	pressure	p, P
206	traction	σ
207	shear stress	τ
208	modulus of elasticity	E
209	shear modulus	G
210	compressibility	$\varkappa$
211	compression modulus ($1/\varkappa$)	K
212	viscosity	η
213	fluidity	φ
214	kinematic viscosity	ν
215	friction coefficient	f
216	surface tension	$\gamma \ldots \sigma$
217	angle of contact	ϑ

Thermodynamic and related quantities

	Quantity	Symbol	
		(1)	(2)
301	temperature	$\vartheta \ldots t$	
302	temperature, absolute	T	
303	gas constant	R, R	
304	Boltzmann constant	k, k	
305	heat	q, Q	
306	work	w, A	
307	energy (Gibbs' ε)	$U \ldots E$	$E \ldots U$
308	entropy (Gibbs' η)	S	S
309	Helmholtz' free energy (Gibbs' ψ)	F	A
310	enthalpy (Gibbs' χ)	H	H
311	Gibbs' function (ζ)	G	$F \ldots G$
312	heat capacity	C	
313	specific heats	c_p, c_v	
314	ratio c_p/c_v	$\gamma, \varkappa$	
315	chemical potential	μ	
316	activity, absolute	λ	
317	activity (relative)	a	
318	activity coefficient	f, γ	
319	osmotic coefficient	g, φ	
320	thermal conductivity	λ	
321	Joule-Thomson coefficient	μ	

Recommended by IUPAP (without... E)	(1)
European practice	(1)
American practice	(2)

Chemical Reactions

	Quantity	Symbol
401	stoichiometric number of molecules (negative for reactants, positive for products)	ν
402	standard equation of chemical reaction	$\Sigma \nu_B B = 0$
403	affinity ($-\Sigma \nu_B \mu_B$) of a reaction	A
404	equilibrium constant	K
405	equilibrium quotient or equilibrium product (of molalities)	Q
406	extent of reaction ($dn_B = \nu_B d\xi$)	ξ
407	degree of reaction (*e.g.* degree of dissociation)	α
408	rate constant	k
409	collision number (collisions per unit volume and unit time)	Z

Light

	Quantity	Symbol
501	Planck's constant	h, $\boldsymbol{h}$
502	» » divided by 2π	$\frac{1}{2}\boldsymbol{h}$
503	quantity of light	Q
504	radiant power, flux of light ($\mathrm{d}Q/\mathrm{d}t$)	Φ
505	luminous intensity ($\mathrm{d}\Phi/\mathrm{d}\omega$)	I
506	illumination ($\mathrm{d}\Phi/\mathrm{d}S$)	E
507	luminance	L, B
508	luminous emittance	H
509	absorption factor (fraction of incident radiant power which is absorbed)	α
510	reflection factor (fraction of incident radiant power which is reflected)	ϱ
511	transmission factor (fraction of incident radiant power which is transmitted)	τ
512	transmittance ($T = I/I_0$)	T
513	absorption (extinction) coefficient ($\varkappa lc = \ln(1/T)$	$\varkappa$
514	absorbance (extinction) ($A = \log_{10}(1/T)$)	$A...E$
515	absorptivity (specific absorbance) (decadic absorption or extinction coefficient)	a
516	molar absorptivity (molar decadic absorption or extinction coefficient) ($\varepsilon lc = A$)	ε
517	refraction index	n
518	refractivity	r
519	angle of optical rotation	α

Electricity and magnetism

	Quantity	Symbol
601	elementary charge	e, $\boldsymbol{e}$
602	quantity of electricity	Q
603	charge density	ϱ
604	surface charge density	σ
605	electric current	$I...i$
606	electric current density	J
607	electric potential	V
608	electric field strength	E
609	electric displacement	D
610	electrokinetic potential	ζ
611	capacity	C
612	permittivity (dielectric constant)	ε
613	dielectric polarisation	P
614	dipole moment	μ
615	electric polarisability of a molecule	α, γ
616	magnetic field strength	H
617	magnetic induction	B

618	magnetic permeability	μ
619	magnetisation	M
620	magnetic susceptibility	χ
621	resistance	R
622	resistivity	ϱ
623	self inductance	L
624	mutual inductance	M, L_{12}
625	reactance	X
626	impedance	Z
627	admittance	Y

Electrochemistry

	Quantity	Symbol
701	Faraday's constant (the faraday)	F, F
702	charge number of an ion, plus or minus	z
703	degree of electrolytic dissociation	α
704	ionic strength	$I...\mu$
705	electrolytic conductivity (specific conductance)	$\varkappa$
706	equivalent or molar conductance of electrolyte or ion	Λ
707	transport number	t, T
708	electromotive force	E
709	overpotential	η

SYMBOLS FOR SUBSIDIARY QUANTITIES

It is much more difficult to make detailed recommendations on symbols for subsidiary quantities than on symbols for the principal quantities. The reason is the incompatibility between the need for specifying numerous details and the need for keeping the printing reasonably simple. Among the most awkward things to print are superscripts to subscripts and subscripts to subscripts. Examples of symbols to be avoided are

$$\Lambda_{NO_3^-} \text{ and } H_{25°C}$$

The problem is vastly reduced if it is recognized that two different kinds of notation are required for two different purposes. In the formulations of general fundamental relations the most important requirement is a notation easy to understand and easy to remember. In applications to particular cases, in quoting numerical values and in tabulation the most important requirement is complete elimination of any possible ambiguity even at the cost of an elaborate notation.

The advantage of a dual notation is already to some extent accepted in the case of concentration. The best notation for formulating the laws of homogeneous chemical equilibrium is something such as

$$\mathrm{A} + ... \rightleftharpoons \mathrm{L} + ...$$

$$\frac{c_{\mathrm{L}...}}{c_{\mathrm{A}...}} = K_c$$

$$\frac{m_{\mathrm{L}...}}{m_{\mathrm{A}...}} = K_m$$

but when we turn to a particular example it is better to use a notation such as

$$Br_2 + H_2O \rightleftharpoons HOBr + H^+ + Br^-$$
$$\frac{[HOBr]\,[H^+]\,[Br^-]}{[Br_2]} = K_c$$
$$K_c(25\,^\circ C) = 6 \times 10^{-9}\ \text{mole}^2\,\text{l}^{-2}$$

Once the principle of dual notation is accepted, its adaptibility and usefulness become manifest in all fields of physical chemistry. It will here be illustrated by just a few examples.

The general relation between the equivalent conductance of an electrolyte and the equivalent conductance of the two ions is written most simply and most clearly as

$$\Lambda = \Lambda^+ + \Lambda^-$$

but when it comes to giving values in particular cases a much more appropriate notation is

$$\begin{aligned}
\Lambda(\tfrac{1}{2}\,Mg^{++}) &= 53\ \Omega^{-1}\,\text{cm}^2\,\text{equiv}^{-1}\ \text{at}\ 25\,^\circ C\\
\Lambda(Cl^-) &= 76\ \Omega^{-1}\,\text{cm}^2\,\text{equiv}^{-1}\ \text{at}\ 25\,^\circ C\\
\Lambda(\tfrac{1}{2}\,MgCl_2) &= 129\ \Omega^{-1}\,\text{cm}^2\,\text{equiv}^{-1}\ \text{at}\ 25\,^\circ C\\
\Lambda(MgCl_2) &= 258\ \Omega^{-1}\,\text{cm}^2\,\text{mole}^{-1}\ \text{at}\ 25\,^\circ C
\end{aligned}$$

In both notations the meaning of the symbols is so obvious and so well suited to the purpose that it is hardly necessary even to define them.

Again partial quantities are most simply denoted by the use of a subscript, for example V for partial volume and the general relation between the partial volumes of the two components of a binary system is written most simply

$$n_1 \mathrm{d}V_1 + n_2 \mathrm{d}V_2 = 0 \qquad (T,\ P\ \text{const.})$$

and this relation holds whether the partial volumes V_1, V_2 are expressed per mole or per gram or per kilogram according as the quantities n_1, n_2 are measured in moles or grams or kilograms. When it is desired to emphasize the contrast between partial quantities, which are intensive, and the extensive properties from which they are derived, this may be achieved either by use of a bar over the symbol or by use of the corresponding lower case letter. Thus in these notations

$$n_1 \mathrm{d}\overline{V}_1 + n_2 \mathrm{d}\overline{V}_2 = 0 \qquad (T,\ P\ \text{const.})$$
$$n_1 \mathrm{d}v_1 + n_2 \mathrm{d}v_2 = 0 \qquad (T,\ P\ \text{const.})$$

But when it comes to specifying values a completely different notation is called for such as

$$\begin{aligned}
V\,(K_2SO_4,\ \text{aq.},\ 0.1\ \text{M},\ 25\,^\circ C) &= 48\ \text{ml mole}^{-1}\\
&= 24\ \text{ml equiv}^{-1}\\
&= 0.27\ \text{ml g}^{-1}
\end{aligned}$$

Each kind of notation is appropriate to its purpose.

Incidentally the notation for extensive and partial quantities need not be restricted to purely thermodynamic quantities but is also appropriate to such quantities as refractions. Thus if we define the refraction R (an extensive property) by

$$R = \frac{n^2-1}{n^2+2} V$$

then it becomes natural to denote the derived partial refractivity by R_i or $\overline{R}_i$ or r_i.*

Acknowledgement. The editors of Acta Chemica Scandinavica express their gratitude to IUPAC for permission to reprint the above pages from the union's Comptes-rendus de la dix-huitième Conférence, Zürich 1955, pp. 92–98.

* This paragraph has been approved in principle but not in detail by the Commission.

ACTA CHEMICA SCANDINAVICA 11 (1957) 391—408

Short Communications

Δ^3-Carene and (+)-Limonene Mixtures

GUNNAR WIDMARK

Institute of Organic Chemistry and Biochemistry, University of Stockholm, Sweden

In a previous communication, Widmark and Blohm [1] have demonstrated the usefulness of an analytical micro-sorption method devised by Blohm [2], when studying terpene mixtures. In the above mentioned paper [1] it was shown that the refractive indices of Δ^3-carene and (+)-limonene, n_D^{25} = 1.4700 and 1.4703, respectively, were too close to allow good readings of the sorptograms of mixtures of these two pure terpenes.

This paper demonstrates that this limitation of the sorption method can be overcome by measuring in a microtube the optical rotations of 0.4 ml ethanolic solutions made up from the 5 μl fractions obtained from the sorption. This method is of course limited to compounds possessing marked differences in their optical activities, *e.g.* (+)-limonene, $[\alpha]_D^{25}$ = +123, and Δ-carene, $[\alpha]_D^{25}$ = +17, and is found to be less accurate and much more laborious than the ordinary way of reading the refractive indices.

Experimental part. The Δ^3-carene and (+)-limonene were purified to index homogeneity according to Widmark [3,4]. The mixtures were prepared by weighing *ca.* 0.4 g samples to form five solutions containing 5, 10, 50, 75 and 90 % (+)-limonene in Δ^3-carene. 40 μl lots of these solutions were pipetted into the top of a 250 mm high column (i Ø 1.4 mm) of activated silica gel [2]. The samples were displaced with ethanol at 1 atm. pressure in the ordinary way [2,1] and eight 5.0 μl fractions were collected in capillaries. The fractions were transferred to 0.40 ml quantities of ethanol in small test tubes. The capillaries were rinsed by sucking the solutions up and down several times. The optical rotations of the solutions were measured in a 5 cm microtube (Hilger Co., M 289, volume 0.35 ml) and the mean value of 10 readings was taken. The results are given in Fig. 1.

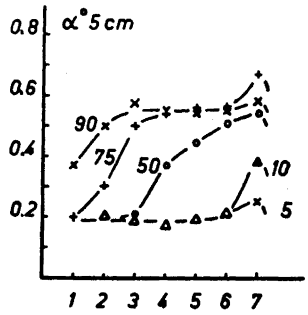


Fig. 1. Sorptograms of Δ^3-carene — (+)-limonene mixtures indicated by optical rotation. Percent(+)-limonene is given.

1. Widmark, G. and Blohm, S.-G. *Acta Chem. Scand.* **9** (1955) 1296.
2. Blohm, S.-G. *Arkiv Kemi* **6** (1954) 317.
3. Widmark, G. *Acta Chem. Scand.* **9** (1955) 925.
4. Widmark, G. *Acta Chem. Scand.* **9** (1955) 938.

Received February 1, 1957.

A Comparative Study of the Autoxidation of Δ^3-Carene, α-Pinene, β-Pinene and (+)-Limonene

GUNNAR WIDMARK and
SVEN-GÖSTA BLOHM

Institute of Organic Chemistry and Biochemistry, University of Stockholm, and Department of Dermatology, Karolinska Institutet, Stockholm, Sweden

A comparison of the rates of autoxidation of the four most commonly occurring terpenes in technical turpentine is a question of technical interest, but as oxidized turpentine is aggressive to sensitive human skin [1], the oxidation rates are of importance for dermatological research. In a preceding series of communications, the present authors have given the experimental conditions for this investigation. These necessitate having a method to investigate the homogeneity [2,3] and a way to purify [4,5] the individual terpenes. However, the inhibiting or accelerating influence of minimum impurities, which cannot be detected by the sorption method has not of course been taken into consideration.

The four terpenes, freshly distilled, were prepared in a state of index homogeneity giving the sorptograms; Δ^3-carene $n_D^{25} =$ 1.4700US, 1–7, α-pinene 1.4632US, 1–7, β-pinene 1.4762US, 1–7 and (+)-limonene 1.4703US, 1–7. Twenty-gram samples were added to four oxidation apparatus assembled side by side on a wooden stand (*cf.* Blohm and Widmark [6]) which were kept at room temperature (22±2°C) and in diffuse daylight *. The consumption of oxygen was measured daily, and at the same time the oxidation vessels were removed and weighed. The samples were analysed by sorption and iodine titration, and the viscosity,

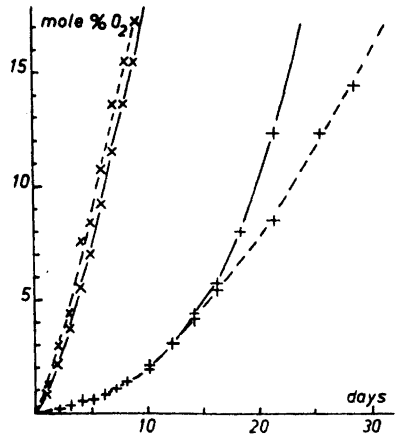


Fig. 1. Rates of oxidation of Δ^3-carene (×) and (+)-limonene (+) and peroxide content from iodine titration (broken lines).

the density and the optical rotation were determined. (In order to save material, these determinations were not made every day.) A small sample was saved for medical investigations. After the determinations, the liquids were replaced in the oxidation vessels which were reweighed, usually indicating a loss of 0.1 g *. The vessels were reconnected to the oxidation apparatus which were totally refilled with oxygen, *cf.* Lombard [7]. Care was taken to prevent contaminations within the four terpenes and separate sets of glass apparatus were used for analysis.

The results of the oxidation series are given in Figs. 1–5 and by the sorptograms, Figs 6–8. Sorptograms of oxidized Δ^3-carene have been published earlier [6] and therefore have been excluded here. It is seen that Δ^3-carene is by far the most easily oxidized, α-pinene and (+)-limonene follow, with very similar behaviour, whereas β-pinene is very slowly oxidized and remains an easily flowing liquid when the others have become yellow resins. There is a relationship between the sorptograms due to degree of oxidation. The medical investigations show that the der-

* The oxidation series was performed in the period February to March, whereas the earlier reported [6] oxidation of Δ^3-carene was made during June and July. It is very likely that the slower rate in the present oxidation experiments is explained by the difference in illumination.

* The rate of oxidation has been corrected for this loss and the mole percent oxygen consumed has been calculated on the hydrocarbon remaining, assuming a monoreaction.

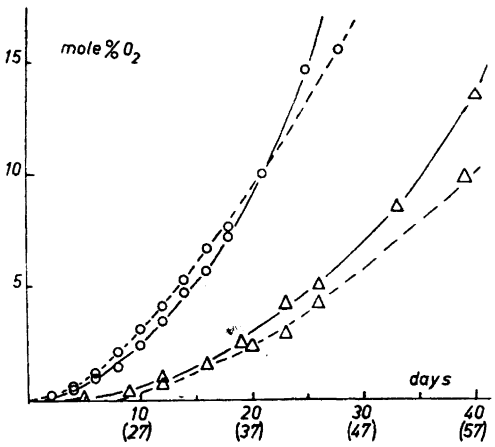


Fig. 2. Rates of oxidation of α-pinene (O) and β-pinene (△) and peroxide content. (β-pinene 18 to 50 days.)

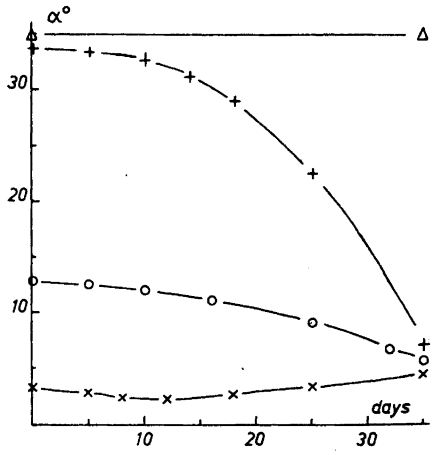


Fig. 4. Changes in optical rotations ($\alpha_{10\ cm}$); Δ^3-carene (pure) 15.°2, after 32 days 16.°4; α-pinene 29.°4 and 22.°8; β-pinene −18.°5 and −18.°5; (+)-limonene 102° and 70°, resp.

matologically active compounds are enriched in the "peaks" of the sorptograms. In the case of (+)-limonene a lift of the "plateau" in a sorptogram is observed.

This paper reports only the figures from the consumption of up to 20 mole percent of oxygen which from a dermatological and chemical point of view is the most interesting part. For the higher stages, the measurements become less accurate due to the marked increase in viscosity, and the curves are similar to that of Δ^3-carene previously reported by the present authors [6]. Furthermore, a detailed report together with the results of the medical investigation will be given elsewhere [8].

Experimental. The oxidation apparatus and the sorption equipment are similar to the ones used previously [6], but the surfaces of the oxidation vessels were made larger = 8.7—9.2 cm².

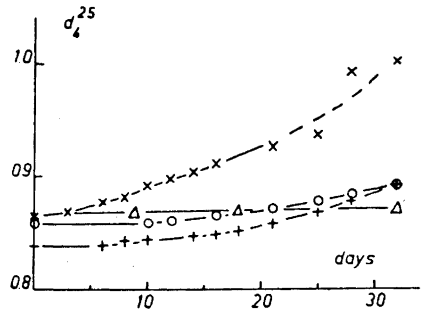


Fig. 3. Changes in densities during the oxidation. × = Δ^3-carene. O = α-pinene. △ = β-pinene. + = (+)-limonene. (The same marks are valid for Figs. 1—5.)

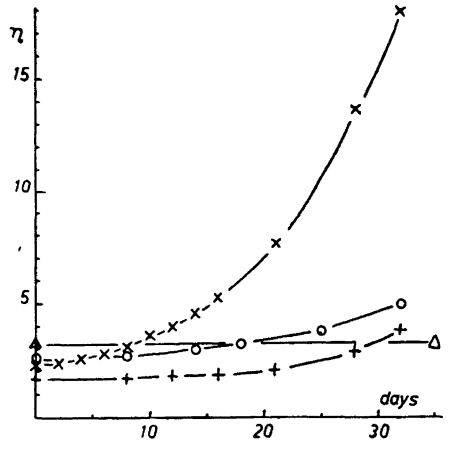


Fig. 5. Changes in viscosities, centipoises.

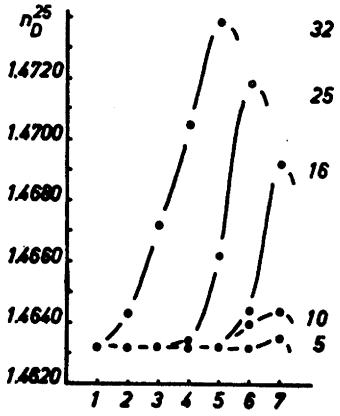


Fig. 6. Sorptograms of oxidized α-pinene. The number of days of reaction is given to the right.

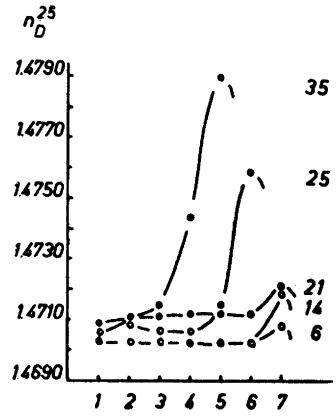


Fig. 8. Sorptograms of oxidized(+)-limonene.

The four viscometers, type Ostwald, volumes 3 ml, had the flow times for water at 25°C 16.9, 18.0, 15.3 and 15.2 sec. and the flow times of the pure terpenes (in the order given in the title) 24.1, 29.8, 30.6 and 16.4 sec., which gave 2.34, 2.66, 3.22 and 1.71 centipoises, respectively. The optical rotations were measured in four 10 cm tubes (volume 6 ml) which also have been used as containers when determining the densities by the aid of a Mohr's balance. In this case, a fall in the temperature of one degree was unavoidable. The iodine titrations were performed as before [6], but the time was increased to 12 min.

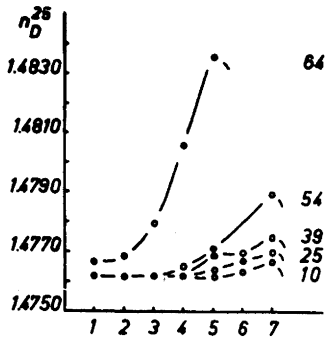


Fig. 7. Sorptograms of oxidized β-pinene.

1. Hellerström, S., Thyreson, N., Blohm, S.-G. and Widmark, G. *Acta Dermato-Venereol.* **33** (1953) 51; *J. Invest. Dermatol.* **24** (1955) 217.
2. Blohm, S.-G. *Arkiv Kemi* **6** (1954) 317.
3. Widmark, G. and Blohm, S.-G. *Acta Chem. Scand.* **9** (1955) 1296.
4. Widmark, G. *Acta Chem. Scand.* **9** (1955) 925.
5. Widmark, G. *Acta Chem. Scand.* **9** (1955) 938.
6. Blohm, S.-G. and Widmark, G. *Acta Chem. Scand.* **9** (1955) 920.
7. Lombard, R. and Kohler, A. *Bull. soc. chim. France* **1954** 639.
8. Hellerström, S., Thyreson, N., Blohm, S.-G. and Widmark, G. *To be published in Acta Dermato-Venereol.*

Received February 1, 1957.

On Anti-Fungal Factors in Potato Leaves

EERO VALLE

Laboratory of the Foundation for Chemical Research, Biochemical Institute, Helsinki, Finland

There are considerable varietal differences in the damage of potato (*Solanum tuberosum*) leaves caused by late blight (*Phytophora infestans* de By). Anti-fungal factors have been demonstrated in all cultivated plants so far investigated in this laboratory [1] and new light has thus been thrown on the nature of the resistance of these plants to pathogenic fungi. Attention was also paid to corresponding factors against *Phytophthora infestans* in potato leaves. *Phytophthora infestans* and *Fusarium nivale* have been used as test organisms in these experiments. The latter fungus was used because its cultivation on an entirely synthetic medium was easy and results were soon obtained. *Phytophthora infestans* was cultivated on pea-agar, on which its growth was good.

The leaf material used in the experiments was taken at various stages of development from potato plants grown under natural conditions in the field. A highly active extract was obtained when the leaves were macerated in 96 % ethanol for 5 min. The leaf material was taken from Aquila, a variety highly resistant to late blight. Ethanol was evaporated before biological activity estimations. The ethanol residue of 0.5 g fresh leaf material in 1 ml synthetic medium totally inhibited the mycelial growth of *Fusarium nivale*. On pea-agar the inhibition limit was 0.7 g fresh wt/1 ml medium. The growth of *Phytophthora infestans* on pea-agar was inhibited when the concentration exceeded 1 g fresh wt/1 ml medium. An anti-fungal effect was also observed in an extremely late blight-susceptible variety, Sieglinde, but the inhibition limits were considerably higher.

For the investigation of the active factor, 3.8 kg of sound leaves of Aquila were taken on August 30, and homogenised by grinding. 96 % ethanol was added immediately, until there was 70 % alcohol in the whole homogenate. The homogenate was kept for 2 days at +5°C and then filtered under pressure through filter paper. No activity was observed in the compact residue. The filtrate was concentrated *in vacuo* at 30°C to 350 ml; the pH of this press juice was 4.7. It was extracted with equal amounts of ether ten times. From each fraction both a biological activity determination and a one-dimensional paper chromatogram using acetic acid-water (15:85) as solvent was made. The highest activity was found in fractions 1 and 2. In fractions 3—10 an activity, though considerably weaker than in the first two fractions, was still observed.

Three fluorescent spots with the R_F-values ~0.02, ~0.50, and ~0.70 were found in fractions 1 and 2 in chromatograms exposed to ultraviolet radiation. In fractions 3—10 only the last spot was found. The blue fluorescence of the first two spots was unchanged in NH_3 vapour, the light blue fluorescence of the last changed into yellowgreen. The spots with R_F ~0.50 and 0.70 were eluted with 96 % ethanol and the ultraviolet absorption spectrum of the two solutions was determined. The spectra were much alike, the spot with R_F ~0.70 having a maximum at 245 and 330 mμ and a minimum at 266 mμ, the spot with R_F ~0.50 a maximum at 237 and 325 mμ and a minimum at 264 mμ in ethanol. (Fig. 1.) These results suggested chlorogenic and caffeic acids. The spectra and the corresponding fluorescence of the pure preparations of these acids supported this view. Chromatograms of a mixture of caffeic acid and the spot with R_F ~0.50 gave only one spot when different solvents were used and this was also the case with a mixture of chlorogenic acid and the spot with R_F ~0.70. The following solvent-systems were used: methanol-water (1:2), *iso*propanol-ammonia (25 %)-water (8:1:1), butanol-acetic acid-water (6.3:2.7:1) and (5:4:1), butanol saturated with water, benzene, chloroform, dist. water.

A very strong blue fluorescence was still found in the press juice of Aquila after the ether extractions. The pH of the juice was lowered with phosphoric acid to 3 and immediately extracted with ether. The ether extract was active, the extract from 5 g fresh wt in 1 ml medium totally inhibiting the growth of *Fusarium nivale*. The spectrum of this fraction, measured in ethanol, was exactly the same as that of pure chlorogenic acid. The calculated content of chlorogenic acid ($E^{1\%}_{1cm}$ = 526)[2] in this fraction was 480 μg fresh wt.

The pH of the press juice was further lowered to 1 and the juice extracted with ether. A weak activity was found in the ether extract, 10 g fresh wt/1 ml medium had a clearly inhibiting effect on the growth of *Fusarium nivale*. A light blue fluorescence was found in the chromato-

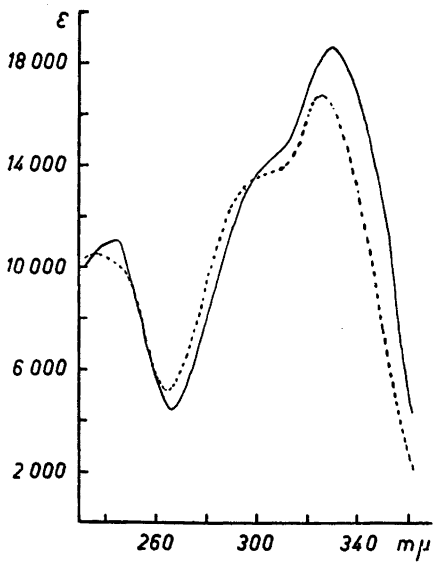


Fig. 1. The molar absorption spectra of chlorogenic (———) and caffeic (·····)acids.

gram from the starting point to the liquid front, the strongest fluorescence, however, in the region of chlorogenic acid (R_F 0.65—0.75). The calculated content of chlorogenic acid amounted to 60 μg/g fresh wt. The press juice, which had now lost its fluorescence, was allowed to stand at —10°C for 7 days and was then extracted with ether. Even this extract had a weak activity and the chromatogram of the extract was about the same as above. It is probable that chlorogenic acid was slowly liberated through hydrolysis at pH 1. On stronger hydrolysis (2 h at 100°C in bomb in 1 % HCl) a very weak light blue fluorescence all over the chromatogram was obtained from the press juice. After hydrolysis the spectrum of the juice was very uncharacthristic, bearing no relation to those of the above-mentioned acids.

The author tried to isolate chlorogenic acid from the ether fraction, which was obtained after lowering the pH to 3. The ether was evaporated *in vacuo* and the residue carefully washed with chloroform and small amounts of cold dist. water. The residue was dissolved in 50 % ethanol and kept at room temperature until crystals began to form. Ethanol was added and the solution cooled to —10°C. The crystals were washed with 50 % ethanol and dried in a vacuum desiccator above P_2O_5 at room temperature. The m.p. of the crystals obtained was 207—209°C, which is in agreement with that given for chlorogenic acid [2]. The mixed m.p. with pure chlorogenic acid was 206—209°C.

For biological activity tests with pure substances, a preparation of chlorogenic acid (m.p. 206—209°C) was obtained from the Laboratory of Biochemistry, University of Helsinki. A commercial product of caffeic acid (Light & Co.) was used. Because chlorogenic acid is composed of one caffeic and one quinic acid molecule [3], the activity of quinic acid was also investigated. On a synthetic medium, chlorogenic acid totally inhibited the growth of *Fusarium nivale* in a concentration of ~1 mg/ml medium, on pea-agar in a concentration of ~1.5 mg/ml.

The anti-fungal effect of caffeic acid was considerably higher, the corresponding inhibition limits being ~0.5 mg/ml and ~0.8 mg/ml. The very weak solubility of caffeic acid in water made the determination of the inhibition limit more difficult. Quinic acid had no inhibiting effect on the growth of *Fusarium nivale* in corresponding concentrations. The growth of *Phytophthora infestans* was inhibited on pea-agar when the amount of caffeic acid exceeded 1 mg/ml and that of chlorogenic acid 2 mg/ml. Quinic acid had no effect.

The quantitative determinations of chlorogenic and caffeic acids in potato leaves show that the amount of free chlorogenic acid is often sufficient to inhibit the mycelial growth of various fungi, since determinations with various potato varieties indicated 0.5—4 mg free chlorogenic acid in one g fresh leaves. Because it is evident that considerable amounts of chlorogenic acid may be bound in complex form, the anti-fungal effect of leaves improves when the complex is disorganized. It is possible that such a defence mechanism begins to function chiefly after infection. The amount of free caffeic acid in potato leaves is so insignificant that only a minor part of the plant's resistance can be due to it.

Among the above mentioned fluorescent spots on the paper chromatogram, of which the spot with R_F ~0.70 contained chlorogenic acid, the spot with R_F ~0.02 was also found to have an anti-fungal effect. The substance has absorption maxima at 272 and 310 mμ in ethanol and it appears to be comparatively unstable. Its chemical nature is not established yet. The substance is found both in leaves, stems and tubers although in so small amounts that

its effect is of no importance. Chlorogenic and caffeic acids are thus not the only anti-fungal factors in the potato plant.

Acknowledgments. The author is deeply indebted to Professor A. I. Virtanen for his valuable advice and for the facilities put at the author's disposal. Thanks are also due to the Laboratory of Biochemistry, University of Helsinki, for the supply of chlorogenic acid. A grant from the *Finnish Cultural Fund*, which has made possible this investigation, is gratefully acknowledged.

1. Virtanen, A. I., Hietala, P. K., Valle, E. and Salakivi, V. *Suomen Kemistilehti B* **29** (1956) 108.
2. Moores, R. G., McDermott, Dorothy L. and Wood, T. R. *Anal. Chem.* **20** (1948) 620.
3. Rudkin, G. O. and Nelson, J. M. *J. Am. Chem. Soc.* **69** (1947) 1470.

Received January 12, 1957.

The Assay and Specific Activity of Crystalline Alcohol Dehydrogenase of Horse Liver

KEITH DALZIEL *

Biochemical Department, Nobel Medical Institute, Stockholm, Sweden

Crystalline alcohol dehydrogenase was first prepared from horse liver by Bonnichsen and Wassén [1]. Modifications of the procedure were reported by Bonnichsen [2] and Bonnichsen and Brink [3]. Assay of the enzyme, based on spectrophotometric measurements of the reduction of diphosphopyridine nucleotide (DPN) coenzyme by excess ethanol substrate at alkaline pH, was described by Theorell and Bonnichsen [4,3]. A modification of this assay method is described below.

Reagents. 0.1 M glycine-NaOH buffer, pH 10.0. DPN solution 0.83 mg/ml (1 mg/ml »cozymase 90», Sigma Chemical Co.). Ethanol solution, 1 ml 96 % to 100 ml with water.

Procedure. The reagents and the cell compartment of the spectrophotometer are kept at 23.0°. 1.85 ml buffer, 1.0 ml DPN solution and 0.15 ml ethanol solution are mixed in a cuvette of 1 cm optical depth, and the extinction at 340 mμ (E_{340}) is measured. A small volume (1 to 10 μl) of enzyme solution is introduced into the reaction mixture on a stirrer, and the time ($t_{0.2}$) required for an increase of 0.200 in E_{340} (λ_{max}DPNH) is measured.

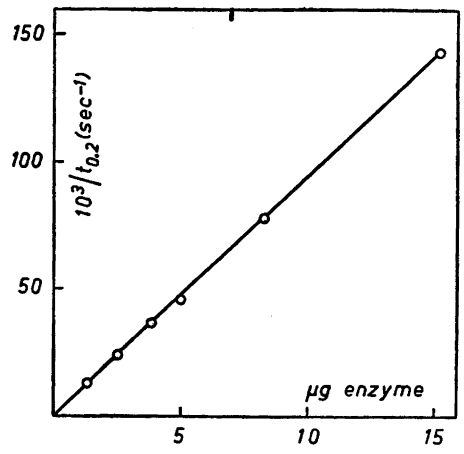


Fig. 1.

Theoretically, the enzyme concentration should be more closely proportional to the reciprocal of $t_{0.2}$, the time required for the reduction of a definite fraction of the DPN, than to the amount of DPN reduced in a fixed time (E_{340} in 3 min) measured in the earlier method [3], provided that the enzyme is stable in the test mixture [5]. This was found to be the case, as shown in Fig. 1 by a plot of measured values of $1/t_{0.2}$ against the weight of enzyme used in the test, obtained by adding different volumes (0.9 to 10 μl) of the same enzyme solution. The plot is a satisfactory straight line passing through the origin, *i.e.* the product, $t_{0.2} \times$ amount of enzyme, is constant to within 2 %. The method has proved consistently reproducible to this extent.

The ethanol concentration (9 mM) is the optimum value [6]; the concentration of 300 mM used originally causes considerable inhibition. Neither the ethanol nor the DPN concentration (0.42 mM) is critical, variations of 50 % in either causing only 10 % variation in the results. Semicarbazide has no effect, as at pH 10.0 the reduction of DPN goes practically to completion with these reactant concentrations [4].

Specific Activity. The enzyme used for the assays of Fig. 1 had been recrystallized with ethanol to constant activity/E_{280} ratio. The enzyme was prepared as described by Bonnichsen and Brink [3]; after removal of the haemoglobin, the enzyme

* Rockefeller Fellow, 1955—7.

its effect is of no importance. Chlorogenic and caffeic acids are thus not the only anti-fungal factors in the potato plant.

Acknowledgments. The author is deeply indebted to Professor A. I. Virtanen for his valuable advice and for the facilities put at the author's disposal. Thanks are also due to the Laboratory of Biochemistry, University of Helsinki, for the supply of chlorogenic acid. A grant from the *Finnish Cultural Fund*, which has made possible this investigation, is gratefully acknowledged.

1. Virtanen, A. I., Hietala, P. K., Valle, E. and Salakivi, V. *Suomen Kemistilehti B* **29** (1956) 108.
2. Moores, R. G., McDermott, Dorothy L. and Wood, T. R. *Anal. Chem.* **20** (1948) 620.
3. Rudkin, G. O. and Nelson, J. M. *J. Am. Chem. Soc.* **69** (1947) 1470.

Received January 12, 1957.

The Assay and Specific Activity of Crystalline Alcohol Dehydrogenase of Horse Liver

KEITH DALZIEL *

Biochemical Department, Nobel Medical Institute, Stockholm, Sweden

Crystalline alcohol dehydrogenase was first prepared from horse liver by Bonnichsen and Wassén [1]. Modifications of the procedure were reported by Bonnichsen [2] and Bonnichsen and Brink [3]. Assay of the enzyme, based on spectrophotometric measurements of the reduction of diphosphopyridine nucleotide (DPN) coenzyme by excess ethanol substrate at alkaline pH, was described by Theorell and Bonnichsen [4,3]. A modification of this assay method is described below.

Reagents. 0.1 M glycine-NaOH buffer, pH 10.0. DPN solution 0.83 mg/ml (1 mg/ml »cozymase 90», Sigma Chemical Co.). Ethanol solution, 1 ml 96 % to 100 ml with water.

Procedure. The reagents and the cell compartment of the spectrophotometer are kept at 23.0°. 1.85 ml buffer, 1.0 ml DPN solution and 0.15 ml ethanol solution are mixed in a cuvette of 1 cm optical depth, and the extinction at 340 mμ (E_{340}) is measured. A small volume (1 to 10 μl) of enzyme solution is introduced into the reaction mixture on a stirrer, and the time ($t_{0.2}$) required for an increase of 0.200 in E_{340} (λ_{max}DPNH) is measured.

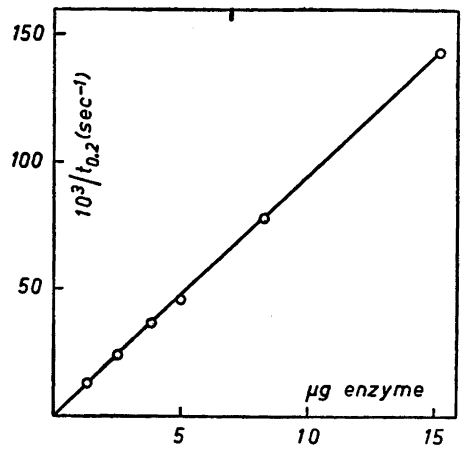


Fig. 1.

Theoretically, the enzyme concentration should be more closely proportional to the reciprocal of $t_{0.2}$, the time required for the reduction of a definite fraction of the DPN, than to the amount of DPN reduced in a fixed time (E_{340} in 3 min) measured in the earlier method [3], provided that the enzyme is stable in the test mixture [5]. This was found to be the case, as shown in Fig. 1 by a plot of measured values of $1/t_{0.2}$ against the weight of enzyme used in the test, obtained by adding different volumes (0.9 to 10 μl) of the same enzyme solution. The plot is a satisfactory straight line passing through the origin, *i.e.* the product, $t_{0.2} \times$ amount of enzyme, is constant to within 2 %. The method has proved consistently reproducible to this extent.

The ethanol concentration (9 mM) is the optimum value [6]; the concentration of 300 mM used originally causes considerable inhibition. Neither the ethanol nor the DPN concentration (0.42 mM) is critical, variations of 50 % in either causing only 10 % variation in the results. Semicarbazide has no effect, as at pH 10.0 the reduction of DPN goes practically to completion with these reactant concentrations [4].

Specific Activity. The enzyme used for the assays of Fig. 1 had been recrystallized with ethanol to constant activity/E_{280} ratio. The enzyme was prepared as described by Bonnichsen and Brink [3]; after removal of the haemoglobin, the enzyme

* Rockefeller Fellow, 1955—7.

was precipitated twice with 30 % (v/v) ethanol and then recrystallized 5 times with 7—10 % ethanol. The relative values of the activity/E_{280} ratio obtained for the 5 crystalline products were, successively, 0.80, 0.89, 0.97, 1.00, 0.98 and 0.99.

A solution of the final product, after thorough dialysis against 0.01 M phosphate, pH 7.3, was found by dry weight to contain 15.5 mg protein/ml, and was diluted 10 fold for activity and E_{280} measurements. From the latter a value of 0.450 was obtained for the extinction of 1 mg/ml in 1 cm optical depth, in good agreement with Bonnichsen's [2,3] value of 0.455. From the activity measurements (Fig. 1) the relationship between the volume in ml (v) of an enzyme solution used in the assay, the value of $t_{0.2}$ in seconds, and the concentration of the enzyme solution is mg/ml $= 1.05/(t_{0.2} \times v)$. If E_{280} is measured on the same solution in 1 cm optical depth, the % purity of the sample relative to the above preparation will be $0.47/(E_{280} \times t_{0.2} \times v)$. These data have been reproduced to within a few per cent with many other crystalline preparations.

In the activity test of Theorell and Bonnichsen [4], our enzyme preparations gave an increase of E_{340} of 0.058 in 3 min per μg enzyme per ml, which is significantly higher than values previously reported (0.036[4], 0.045[5]). The corresponding value of the maximum initial rate of the reaction of ethanol and DPN at pH 10.0 was $k_2 = 8.0$ sec^{-1}, compared with 5.5 sec^{-1} obtained by Theorell and Bonnichsen [4]. In spite of the high activity, evidence of inhomogeneity in the present preparations was obtained in prolonged electrophoresis, indicating the presence of about 10 % of a second component. Further work on the preparation and properties of the enzyme is in progress.

The author is grateful to Professor Hugo Theorell and Dr. Roger Bonnichsen for guidance and helpful criticism.

1. Bonnichsen, R. K. and Wassén, A. M. *Arch. Biochem.* **18** (1948) 361.
2. Bonnichsen, R. K. *Acta Chem. Scand.* **4** (1950) 715.
3. Bonnichsen, R. K. and Brink. B. G. in *Methods in Enzymology*, ed. Colowick, S. P. and Kaplan, N. O., Vol. **I**, p. 495, Academic Press, New York 1955.
4. Theorell, H. and Bonnichsen, R. K. *Acta Chem. Scand.* **5** (1951) 1105.
5. Van Slyke, D. D. *Advances in Enzymol.* **2** (1942) 33.
6. Theorell, H., Nygaard, A. P. and Bonnichsen, R. K. *Acta Chem. Scand.* **9** (1955) 1148.

Received January 22, 1957.

The Sedimentation Constant of Crystalline Horse Liver Alcohol Dehydrogenase

ANDERS EHRENBERG and KEITH DALZIEL*

Biochemical Department, Nobel Medical Institute, Stockholm, Sweden

The sedimentation constant of crystalline alcohol dehydrogenase (ADH) prepared from horse liver [1,2] was found by Pedersen to be $S^0_{20} = 4.9$ S as the mean of two runs in the oil driven ultracentrifuge at Uppsala, with *ca.* 10 mg protein/ml at pH 7.8 [3]. This gives 4.5 S after correction as suggested by Pedersen [4]. In connection with the interpretation of marked effects of pH and chloride ion concentration on the kinetics of the enzyme reaction, DPNH + acetaldehyde + H$^+$ $\rightleftharpoons$ DPN + ethanol, reported by Theorell and his collaborators [3,5], it is of interest to test the possibility that the enzyme itself undergoes some change, such as dissociation or polymerisation, with change of ionic milieu. Such changes might be revealed by variations of the sedimentation constant.

Table 1. Sedimentation constants of liver alcohol dehydrogenase.

ADH mg/ml	NaCl M	Buffer (ionic strength = 0.1)	pH	S^0_{20} Svedberg units
7.8	0.075	phosphate	7.15	4.91
7.8	0.15	phosphate	7.15	4.90
7.8	0.30	phosphate	7.15	4.85
13.3	0.075	phosphate	7.15	4.69
13.3	0.30	phosphate	7.15	4.71
7.8	0.15	phosphate	5.85	4.93
7.8	0.15	glycine	9.9	4.82

* Rockefeller Fellow, 1955—7.

was precipitated twice with 30 % (v/v) ethanol and then recrystallized 5 times with 7—10 % ethanol. The relative values of the activity/E_{280} ratio obtained for the 5 crystalline products were, successively, 0.80, 0.89, 0.97, 1.00, 0.98 and 0.99.

A solution of the final product, after thorough dialysis against 0.01 M phosphate, pH 7.3, was found by dry weight to contain 15.5 mg protein/ml, and was diluted 10 fold for activity and E_{280} measurements. From the latter a value of 0.450 was obtained for the extinction of 1 mg/ml in 1 cm optical depth, in good agreement with Bonnichsen's [2,3] value of 0.455. From the activity measurements (Fig. 1) the relationship between the volume in ml (v) of an enzyme solution used in the assay, the value of $t_{0.2}$ in seconds, and the concentration of the enzyme solution is mg/ml $= 1.05/(t_{0.2} \times v)$. If E_{280} is measured on the same solution in 1 cm optical depth, the % purity of the sample relative to the above preparation will be $0.47/(E_{280} \times t_{0.2} \times v)$. These data have been reproduced to within a few per cent with many other crystalline preparations.

In the activity test of Theorell and Bonnichsen [4], our enzyme preparations gave an increase of E_{340} of 0.058 in 3 min per μg enzyme per ml, which is significantly higher than values previously reported (0.036[4], 0.045[5]). The corresponding value of the maximum initial rate of the reaction of ethanol and DPN at pH 10.0 was $k_2 = 8.0$ sec^{-1}, compared with 5.5 sec^{-1} obtained by Theorell and Bonnichsen [4]. In spite of the high activity, evidence of inhomogeneity in the present preparations was obtained in prolonged electrophoresis, indicating the presence of about 10 % of a second component. Further work on the preparation and properties of the enzyme is in progress.

The author is grateful to Professor Hugo Theorell and Dr. Roger Bonnichsen for guidance and helpful criticism.

1. Bonnichsen, R. K. and Wassén, A. M. *Arch. Biochem.* **18** (1948) 361.
2. Bonnichsen, R. K. *Acta Chem. Scand.* **4** (1950) 715.
3. Bonnichsen, R. K. and Brink. B. G. in *Methods in Enzymology*, ed. Colowick, S. P. and Kaplan, N. O., Vol. **I**, p. 495, Academic Press, New York 1955.
4. Theorell, H. and Bonnichsen, R. K. *Acta Chem. Scand.* **5** (1951) 1105.
5. Van Slyke, D. D. *Advances in Enzymol.* **2** (1942) 33.
6. Theorell, H., Nygaard, A. P. and Bonnichsen, R. K. *Acta Chem. Scand.* **9** (1955) 1148.

Received January 22, 1957.

The Sedimentation Constant of Crystalline Horse Liver Alcohol Dehydrogenase

ANDERS EHRENBERG and KEITH DALZIEL*

Biochemical Department, Nobel Medical Institute, Stockholm, Sweden

The sedimentation constant of crystalline alcohol dehydrogenase (ADH) prepared from horse liver [1,2] was found by Pedersen to be $S^0_{20} = 4.9$ S as the mean of two runs in the oil driven ultracentrifuge at Uppsala, with *ca.* 10 mg protein/ml at pH 7.8 [3]. This gives 4.5 S after correction as suggested by Pedersen [4]. In connection with the interpretation of marked effects of pH and chloride ion concentration on the kinetics of the enzyme reaction, DPNH + acetaldehyde + H$^+$ $\rightleftharpoons$ DPN + ethanol, reported by Theorell and his collaborators [3,5], it is of interest to test the possibility that the enzyme itself undergoes some change, such as dissociation or polymerisation, with change of ionic milieu. Such changes might be revealed by variations of the sedimentation constant.

Table 1. Sedimentation constants of liver alcohol dehydrogenase.

ADH mg/ml	NaCl M	Buffer (ionic strength = 0.1)	pH	S^0_{20} Svedberg units
7.8	0.075	phosphate	7.15	4.91
7.8	0.15	phosphate	7.15	4.90
7.8	0.30	phosphate	7.15	4.85
13.3	0.075	phosphate	7.15	4.69
13.3	0.30	phosphate	7.15	4.71
7.8	0.15	phosphate	5.85	4.93
7.8	0.15	glycine	9.9	4.82

* Rockefeller Fellow, 1955—7.

Alcohol dehydrogenase was prepared by the method of Bonnichsen and Brink [6] and recrystallized 5 times to constant activity/protein ratio, as described earlier [7]. The sedimentation constant was measured in the Spinco ultracentrifuge at 59 780 r.p.m. and 20°C with various protein, chloride and hydrogen ion concentrations. The results are shown in Table. 1. There is no evidence of any significant effect of chloride or hydrogen ion concentration on the sedimentation constant. Extrapolation to infinite dilution of the protein gives $S^0_{20} = 5.1\ S$.

These data give a value of 4.8 S at a protein concentration of 10 mg/ml, slightly greater than Pedersen's value. The difference is probably to be ascribed to the greater purity of our material indicated by higher specific activity [7]. More complete data on the molecular weight will be reported shortly.

1. Bonnichsen, R. K. and Wassén, A. M. *Arch. Biochem.* **18** (1948) 361.
2. Bonnichsen, R. K. *Acta Chem. Scand.* **4** (1950) 715.
3. Theorell, H. and Bonnichsen, R. K. *Acta Chem. Scand.* **5** (1951) 1105.
4. Pedersen, K. O. n *Les Protéines, Neuvième Conseil de Chimie Solvay, Bruxelles* 1953, p. 35.
5. Theorell, H., Nygaard, A. P. and Bonnichsen, R. K., *Acta Chem. Scand.* **9** (1955) 1148.
6. Bonnichsen, R. K. and Brink. N. G. in *Method in Enzymology*, ed .Colwick, S. P. and Kaplan, N. O., Vol. I, p. 495, Academic Press, New York, 1955.
7. Dalziel, K. *Acta Chem. Scand.* **11** (1957) 397.

Received January 22, 1957.

The Equilibrium Between Yellow and Blue Nickel(II) Triethylenetetramine Ions in Strong Salt Solutions

CHR. KLIXBÜLL JØRGENSEN

Chemistry Department A, Technical University of Denmark, Copenhagen, Denmark

Lifschitz *et al.*[1,2] prepared solid nickel(II)bis(stilbenediamine) complexes in two isomers, one yellow, diamagnetic, and one blue, paramagnetic. The equilibrium between two such forms in solution has not yet been studied by means of the absorption spectra. Jonassen and Douglas [3] investigated nickel(II) complexes of triethylenetetramine (= trien) and prepared solid salts of $Ni_2trien_3^{+3}$, but not of Ni trien++. The latter violet-blue ion turns brownish yellow in strong salt solutions. Fig. 1 gives the absorption spectra at 19°C in different concentrations of sodium perchlorate. The absorption band at 443 mμ, which increases in the yellow solutions, corresponds to the planar, diamagnetic complex. Basolo *et al.*[4] prepared the yellow Nitemeen$_2$++ (temeen = C, C, C′, C′ tetramethyl-ethylenediamine) which has a Gaussian shaped band at 433 mμ with $\varepsilon = 67$. It is interesting that Ni temeen$_2$++ does not exhibit other spin-allowed, Laporte-forbidden ligand field bands below the ultra-violet absorption limit ($\varepsilon = 8$ at 260 mμ), since the ligand field theory [5] would predict three transitions at not very different wavenumbers (the analogous difficulty * occurs in Cu en$_2$++). The two

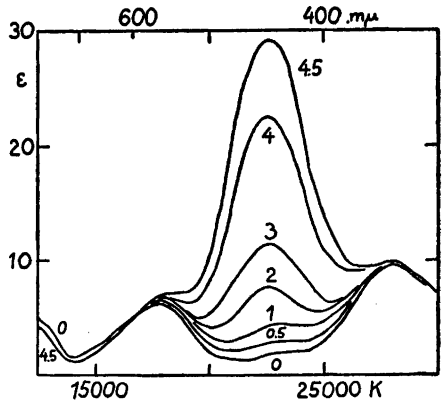


Fig. 1. The absorption spectra of 0.1 M Ni trien$(NO_3)_2$ in water and aqueous solutions of sodium perchlorate. The numbers on the curves indicate the molarity of $NaClO_4$. The spectra were measured at 19°C on a Cary spectrophotometer.

* However, the band at 422 mμ of Ni(II) in ethanolic sodio-succinimide has a shoulder at 470 mμ, and the band at 440 mμ of Ni(II) in 1 M NaOH with caseine has a shoulder at 510 mμ. These orange solutions do not seem to contain paramagnetic nickel, according to the spectra. Sodium caseinate is very effective for formation of tetragonal complexes; its biuret reaction with Cu(II) has the band maximum at 547 mμ.

Alcohol dehydrogenase was prepared by the method of Bonnichsen and Brink [6] and recrystallized 5 times to constant activity/protein ratio, as described earlier [7]. The sedimentation constant was measured in the Spinco ultracentrifuge at 59 780 r.p.m. and 20°C with various protein, chloride and hydrogen ion concentrations. The results are shown in Table. 1. There is no evidence of any significant effect of chloride or hydrogen ion concentration on the sedimentation constant. Extrapolation to infinite dilution of the protein gives $S^0_{20} = 5.1\ S$.

These data give a value of 4.8 S at a protein concentration of 10 mg/ml, slightly greater than Pedersen's value. The difference is probably to be ascribed to the greater purity of our material indicated by higher specific activity [7]. More complete data on the molecular weight will be reported shortly.

1. Bonnichsen, R. K. and Wassén, A. M. *Arch. Biochem.* **18** (1948) 361.
2. Bonnichsen, R. K. *Acta Chem. Scand.* **4** (1950) 715.
3. Theorell, H. and Bonnichsen, R. K. *Acta Chem. Scand.* **5** (1951) 1105.
4. Pedersen, K. O. n *Les Protéines, Neuvième Conseil de Chimie Solvay, Bruxelles* 1953, p. 35.
5. Theorell, H., Nygaard, A. P. and Bonnichsen, R. K., *Acta Chem. Scand.* **9** (1955) 1148.
6. Bonnichsen, R. K. and Brink. N. G. in *Method in Enzymology*, ed .Colwick, S. P. and Kaplan, N. O., Vol. I, p. 495, Academic Press, New York, 1955.
7. Dalziel, K. *Acta Chem. Scand.* **11** (1957) 397.

Received January 22, 1957.

The Equilibrium Between Yellow and Blue Nickel(II) Triethylenetetramine Ions in Strong Salt Solutions

CHR. KLIXBÜLL JØRGENSEN

Chemistry Department A, Technical University of Denmark, Copenhagen, Denmark

Lifschitz *et al.*[1,2] prepared solid nickel(II)bis(stilbenediamine) complexes in two isomers, one yellow, diamagnetic, and one blue, paramagnetic. The equilibrium between two such forms in solution has not yet been studied by means of the absorption spectra. Jonassen and Douglas [3] investigated nickel(II) complexes of triethylenetetramine (= trien) and prepared solid salts of $Ni_2trien_3^{+3}$, but not of Ni trien++. The latter violet-blue ion turns brownish yellow in strong salt solutions. Fig. 1 gives the absorption spectra at 19°C in different concentrations of sodium perchlorate. The absorption band at 443 mμ, which increases in the yellow solutions, corresponds to the planar, diamagnetic complex. Basolo *et al.*[4] prepared the yellow Nitemeen$_2$++ (temeen = C, C, C′, C′ tetramethyl-ethylenediamine) which has a Gaussian shaped band at 433 mμ with $\varepsilon = 67$. It is interesting that Ni temeen$_2$++ does not exhibit other spin-allowed, Laporte-forbidden ligand field bands below the ultra-violet absorption limit ($\varepsilon = 8$ at 260 mμ), since the ligand field theory [5] would predict three transitions at not very different wavenumbers (the analogous difficulty * occurs in Cu en$_2$++). The two

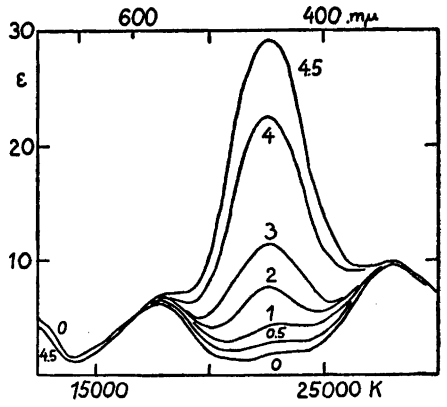


Fig. 1. The absorption spectra of 0.1 M Ni trien$(NO_3)_2$ in water and aqueous solutions of sodium perchlorate. The numbers on the curves indicate the molarity of $NaClO_4$. The spectra were measured at 19°C on a Cary spectrophotometer.

* However, the band at 422 mμ of Ni(II) in ethanolic sodio-succinimide has a shoulder at 470 mμ, and the band at 440 mμ of Ni(II) in 1 M NaOH with caseine has a shoulder at 510 mμ. These orange solutions do not seem to contain paramagnetic nickel, according to the spectra. Sodium caseinate is very effective for formation of tetragonal complexes; its biuret reaction with Cu(II) has the band maximum at 547 mμ.

equally strong bands of $PtCl_4^{--}$ may be caused by effects of intermediate coupling [6].

However, the height of the new band of yellow Nitrien++ cannot be implied with certainty from the Figure, since the decrease of the concentration of the blue form cannot be determined, due to salt effects. However, ε seems to be between 50 and 80, as expected. The formation of the yellow isomer is endothermic; a boiling solution of 0.1 M Ni trien$(NO_3)_2$ alone turns reversibly yellowish. Some salt solutions, such as nine-tenths-saturated $CaCl_2$ ($\varepsilon = 27$ at 443 mμ and the same shape of the band as in 4.5 M $NaClO_4$) and molten $Mg(NO_3)_2$, 6 H_2O, are equally effective for forming the yellow colour, while saturated NaBr and molten Na_2SO_4, 10 H_2O produce only a brownish purple mixture. Since Ni temeen$_2$++ neither solvates nor takes up chloride ions [7], it is not believed that ClO_4^- or Cl^- directly participate in the first coordination sphere of the yellow Ni trien++, even though a general effect of ion-pair formation cannot be excluded. However, a special de-hydration effect does not seem to occur in aqueous ethanol, compared to an aqueous solution with identical salt content. Actually, Lifschitz *et al.*[1] observed blue solutions in chloroform and other non-polar solvents of salts, which are yellow in aqueous solution. Thus an equilibrium may be postulated between blue *cis*-NiA_4X_2, blue *trans*-NiA_4X_2 and yellow *trans*-NiA_4, where X are water, alcohol, anions, etc., which are more strongly bound in solutions with low dielectric constant than in water. It is a necessary condition [5] for diamagnetism in d^8-systems to have a much weaker ligand field along the tetragonal axis than in the plane of the four strongly bound ligands.

The blue isomer is not tetrahedrally coordinated, but is rather *cis*-octahedral. Thus, the water can be exchanged by other ligands, and the absorption spectra greatly resemble those of the corresponding tren- (= β, β', β'' tris(ethylamino)amine)nickel (II) complexes [7]. The spin-allowed transitions from $^3\Gamma_2$ (F) to $^3\Gamma_4$ (F) and $^3\Gamma_4$ (P) are situated at:

Ni trien $(H_2O)_2$++	564 mμ	358 mμ
Ni_2 trien$_3$+4	539	346
Ni trien $(NH_3)_2$++	546	350
Ni trien en++	538	344
Ni trien gly+	550	352

The last glycinate complex resembles more Ni en$_2$gly+ than Ni tren gly+, which [7] has the bands at 532 and 354 mμ. It is not easily decided whether *trans*-Ni trien++ also exists as a blue diaquo complex in equilibrium with the anhydrous yellow form. At most 2 % of the yellow form occurs in the most dilute solution of the Figure (a spin-forbidden band may be the cause of the weak shoulder ~443 mμ). If all the *trans*-isomer is diamagnetic, this would correspond to a similar deviation from the statistical *cis*/*trans* equilibrium constant [8] as in the case of Coen$_2(H_2O)_2$+++. J. Bjerrum and Poulsen [9] have reported yellow Nien$_2$++ as an intermediate by low-temperature kinetic studies. Even though Cutrien++ has mainly the *trans*-configuration, it has only been possible [10] to prepare *cis*-Co trienCl_2+. Mr. Kjeld Rasmussen and the present author will later discuss a possible blue *trans*-isomer of the latter ion.

Analogous [5] to the behaviour of Nien$_2$++, it is possible to precipitate yellowish pink [Ni trien] $[AgBrI]_2$. Most other salts of Ni trien++ seem to be paramagnetic. Thus, thiocyanates produce a copious precipitate of pale blue Ni trien$(SCN)_2$, which is soluble in excess of trien. If a solution of $NiBr_2$ and trien is evaporated to dryness, a dark purple salt results, which deliquesces to a brown solution. $Ni(ClO_4)_2$ and trien produces a sticky reddish brown syrup. On inflaming some mg of this material, it explodes violently. Yellow colour of the commercial trien can be removed by treating the 1 M aqueous solution with norite carbon for several weeks.

1. Lifschitz, I., Bos, J. G. and Dijkema, K. M. *Z. anorg. Chem.* **242** (1939) 97.
2. Lifschitz, I. and Schouteden, F. L. M. *Rec. trav. chim.* **58** (1939) 411.
3. Jonassen, H. B. and Douglas, B. E. *J. Am. Chem. Soc.* **71** (1949) 4094.
4. Basolo, F., Chen, Y. T. and Murmann, R. K. *J. Am. Chem. Soc.* **76** (1954) 956.
5. Ballhausen, C. J. and Jørgensen, C. Klixbüll *Kgl. Danske Videnskab. Selskab, Mat.-fys. Medd.* **29** (1955) No. 14.
6. Jørgensen, C. Klixbüll *Reports to the Xth Solvay Conference.* Bruxelles, May 1956.
7. Jørgensen, C. Klixbüll *Acta Chem. Scand.* **10** (1956) 887.
8. Bjerrum, J. and Rasmussen, S. E. *Acta Chem. Scand.* **6** (1952) 1265.
9. Bjerrum, J., Poulsen, K. G. and Poulsen, I. *Symposium on Co-ordination Chemistry.* Copenhagen 1953.
10. Basolo, F. *J. Am. Chem. Soc.* **70** (1948) 2634.

Received December 21, 1956.

The Infrared Absorption of Rosin Acids in Tall Oil Rosin

HENRIK H. BRUUN and PENTTI JALAVA

Department of Medical Biochemistry, Institute of Medical Chemistry, University of Uppsala, Uppsala, Sweden, and The Institute of Wood Chemistry, Åbo Akademi, Åbo, Finland

The tall oil rosin produced in Northern Europe is composed of 90—95 % rosin acids, 5—10 % fatty acids and 0.3—2 % unsaponifiables [1,2]. Sandermann [3] studied the rosin acid fraction of tall oil rosin using chemical methods and found it to contain about 50 % abietic acid, up to 25 % dextropimaric acid, and up to 25 % pyroabietic acids which represent a mixture of dehydro-, dihydro- and tetrahydroabietic acids [4]. Later spectrophotometric studies [5,6] of the rosin acids of tall oil rosin have shown the abietic acid content to vary from 23 to 52 % and that of dehydroabietic acid [5] from 30 to 45 %.

The present paper deals with an investigation of the infrared absorption of two samples of the rosin acid fraction of tall oil rosin. The purpose of the study was to utilize previously recorded infrared absorption spectra for individual rosin acids [7,8] to obtain information about the composition of the rosin acid fraction in tall oil rosin. The isolation of the rosin acids from tall oil rosin which was a crystalline, batch-distilled quality (a commercial product of Enso-Gutzeit Oy, Kotka, Finland) was in one case performed using the customary method of extracting the esterified fatty acids and unsaponifiables and in the other by precipitating the rosin acids with *cyclo*hexylamine from the solution of tall oil rosin in acetone [9]. Both rosin acid fractions were recrystallized from methanol and acetone.

The infrared absorption curves recorded for the two samples are reproduced in Figs. 1 and 2, respectively. The curves are seen to be identical. All the bands in one can be distinguished in the other and corresponding bands are almost equal in height. (Absorption curves similar to these were also recorded for rosin acid samples isolated by *cyclo*hexylamine preci-

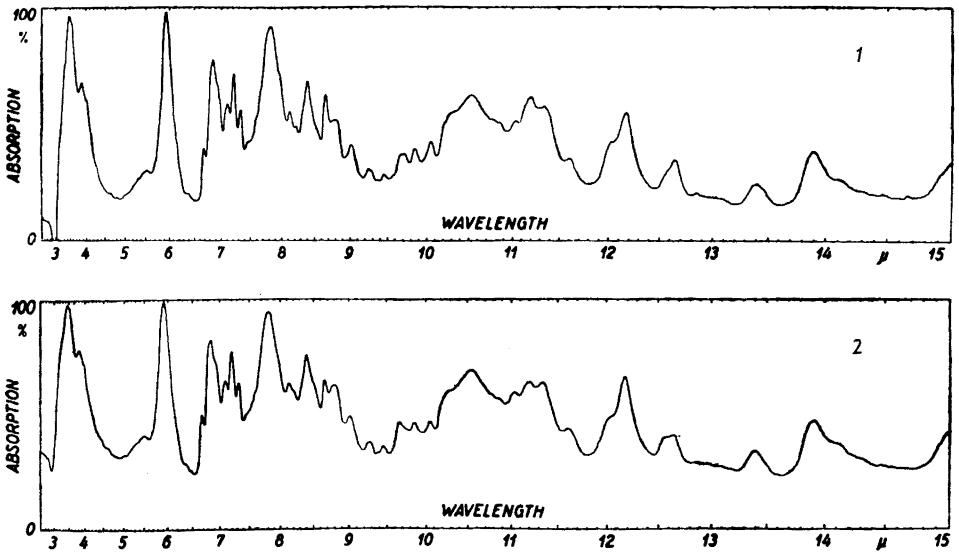


Fig. 1 and *Fig. 2.* Infrared absorption spectra of the rosin acid fraction of tall oil rosin: 1) Rosin acid fraction isolated from tall oil rosin by removing esterified fatty acids and unsaponifiables by solvent extraction. 2) Fraction isolated by precipitating the rosin acids with *cyclo*hexylamine.

pitation from amorphous tall oil rosin (also a product of the above-mentioned company) and from a crystalline, continuously distilled product of Oulu Oy, Oulu). Bands typical of abietic acid occur at 8.66, 11.21, 12.65 and 13.87 μ and bands typical of dehydroabietic acid at 6.68, 8.82, 9.65, 12.20 and 13.89 μ. No bands are observed which would indicate the presence of tetrahydroabietic acid (characteristic bands at 8.47, 8.61 and 14.27 μ), dihydroabietic acid (bands at 11.53 + 11.68 and 14.12 μ; the shoulder at 14.12 μ results from the combined medium strong absorptions of abietic and dehydroabietic acids), dextropimaric acid (bands at 6.97, 11.75, 14.00 and 14.61 μ), and *iso*dextropimaric acid (bands at 8.00, 8.68 + 8.75, 11.00, 13.67 and 13.99 μ). The rosin acid mixture isolated from tall oil rosin thus seems to consist solely of abietic and dehydroabietic acids. No signs indicating the presence of other acids of the abietic series or of pimaric acids are evident (if these do exist in the mixture, their contents amount to a few per cent at the most).

Absorption spectra * recorded for binary mixtures of abietic and dehydroabietic acid suggested that the batch-distilled rosin acid samples studied contained about 55 % abietic acid and about 45 % dehydroabietic acid.

Absorption spectra * recorded for rosin acid mixtures isolated by *cyclo*hexylamine precipitation from crystalline tall oil rosin samples which were heated at 300°C for periods of different length revealed that the content of dehydroabietic acid in the mixtures increased with the time of heating. The rosin acid mixture precipitated with *cyclo*hexylamine from a tall oil rosin sample that had been heated three hours at 300°C was found to consist almost solely of dehydroabietic acid. A similar observation concerning American tall oil rosin has been previously reported by Hasselström [10].

The observation that the rosin acid mixture isolated from tall oil rosin does not contain pimaric acids is somewhat surprising and does not conform with the analytical data of Sandermann or with the general opinion of the composition of the rosin acid fraction of tall oil rosin. However, the somewhat erroneous conclusions that were drawn on the basis of the very extensive work that was done after the turn of the century to determine the structure of pinabietic acid is now easily understood when one realizes that this rosin acid mixture primarily consisted of only two abietic acids.

We wish to express our sincere gratitude to Dr. Ingrid Fischmeister of the Department of Medical Biochemistry for the spectrophotometric measurements. One of us (H.H.B.) is indebted to Professor Einar Stenhagen for placing the facilities of the Department at his disposal and to the *Natural Science Council of Finland* for a grant which made possible a study visit to Uppsala.

1. Juvonen, V.-V. *Finnish Paper Timber J.* **28** (1946) 8.
2. Johanson, S. *Svensk Papperstidn.* **53** (1950) 258.
3. Sandermann, W. *Fette und Seife* **49** (1942) 578.
4. Fleck, E. E. and Palkin, S. *J. Am. Chem. Soc.* **60** (1938) 921.
5. Mo och Domsjö Ab, Research Laboratory; *cf.* Johanson [2].
6. Harva, O. *Paper and Timber, Finland* **34** (1952) 31.
7. Bruun, H. H. *Paper and Timber, Finland* **38** (1956) 577.
8. Bruun, H. H. *Paper and Timber, Finland* **39** (1957) No. 4.
9. Harris, G. C. and Sanderson, T. *J. Am. Chem. Soc.* **70** (1948) 334.
10. Hasselström, T. *Paper Trade J.* **118** (1944), TAPPI Sect., p. 134.

Received January 15, 1957.

* To be reproduced in the same series of papers as Refs.[7,8]

Association of Crystallized Bovine Plasma Albumin

J. A. CHRISTIANSEN, C. E. JENSEN and K. MARCKER

Universitetets fysisk-kemiske institut, Copenhagen, Denmark

Many investigators have found that the molecular weight of bovine plasma albumin (B.P.A.) is about 70×10^3. This figure has been obtained from osmotic measurements (see, *e. g.*, Scatchard

pitation from amorphous tall oil rosin (also a product of the above-mentioned company) and from a crystalline, continuously distilled product of Oulu Oy, Oulu). Bands typical of abietic acid occur at 8.66, 11.21, 12.65 and 13.87 μ and bands typical of dehydroabietic acid at 6.68, 8.82, 9.65, 12.20 and 13.89 μ. No bands are observed which would indicate the presence of tetrahydroabietic acid (characteristic bands at 8.47, 8.61 and 14.27 μ), dihydroabietic acid (bands at 11.53 + 11.68 and 14.12 μ; the shoulder at 14.12 μ results from the combined medium strong absorptions of abietic and dehydroabietic acids), dextropimaric acid (bands at 6.97, 11.75, 14.00 and 14.61 μ), and *iso*dextropimaric acid (bands at 8.00, 8.68 + 8.75, 11.00, 13.67 and 13.99 μ). The rosin acid mixture isolated from tall oil rosin thus seems to consist solely of abietic and dehydroabietic acids. No signs indicating the presence of other acids of the abietic series or of pimaric acids are evident (if these do exist in the mixture, their contents amount to a few per cent at the most).

Absorption spectra * recorded for binary mixtures of abietic and dehydroabietic acid suggested that the batch-distilled rosin acid samples studied contained about 55 % abietic acid and about 45 % dehydroabietic acid.

Absorption spectra * recorded for rosin acid mixtures isolated by *cyclo*hexylamine precipitation from crystalline tall oil rosin samples which were heated at 300°C for periods of different length revealed that the content of dehydroabietic acid in the mixtures increased with the time of heating. The rosin acid mixture precipitated with *cyclo*hexylamine from a tall oil rosin sample that had been heated three hours at 300°C was found to consist almost solely of dehydroabietic acid. A similar observation concerning American tall oil rosin has been previously reported by Hasselström [10].

The observation that the rosin acid mixture isolated from tall oil rosin does not contain pimaric acids is somewhat surprising and does not conform with the analytical data of Sandermann or with the general opinion of the composition of the rosin acid fraction of tall oil rosin. However, the somewhat erroneous conclusions that were drawn on the basis of the very extensive work that was done after the turn of the century to determine the structure of pinabietic acid is now easily understood when one realizes that this rosin acid mixture primarily consisted of only two abietic acids.

We wish to express our sincere gratitude to Dr. Ingrid Fischmeister of the Department of Medical Biochemistry for the spectrophotometric measurements. One of us (H.H.B.) is indebted to Professor Einar Stenhagen for placing the facilities of the Department at his disposal and to the *Natural Science Council of Finland* for a grant which made possible a study visit to Uppsala.

1. Juvonen, V.-V. *Finnish Paper Timber J.* **28** (1946) 8.
2. Johanson, S. *Svensk Papperstidn.* **53** (1950) 258.
3. Sandermann, W. *Fette und Seife* **49** (1942) 578.
4. Fleck, E. E. and Palkin, S. *J. Am. Chem. Soc.* **60** (1938) 921.
5. Mo och Domsjö Ab, Research Laboratory; *cf.* Johanson [2].
6. Harva, O. *Paper and Timber, Finland* **34** (1952) 31.
7. Bruun, H. H. *Paper and Timber, Finland* **38** (1956) 577.
8. Bruun, H. H. *Paper and Timber, Finland* **39** (1957) No. 4.
9. Harris, G. C. and Sanderson, T. *J. Am. Chem. Soc.* **70** (1948) 334.
10. Hasselström, T. *Paper Trade J.* **118** (1944), TAPPI Sect., p. 134.

Received January 15, 1957.

* To be reproduced in the same series of papers as Refs.[7,8]

Association of Crystallized Bovine Plasma Albumin

J. A. CHRISTIANSEN, C. E. JENSEN and K. MARCKER

Universitetets fysisk-kemiske institut, Copenhagen, Denmark

Many investigators have found that the molecular weight of bovine plasma albumin (B.P.A.) is about 70×10^3. This figure has been obtained from osmotic measurements (see, *e. g.*, Scatchard

et al.[1], and Adair and Robinson [2]). We have tried to reproduce these results by means of the osmometer described previously by two of the present authors [3]. By means of this apparatus it is possible to measure the osmotic pressure of the solution about one hour after it has been placed in the osmotic cell.

The preparation used was Armour crystallized B.P.A. The substance was dissolved in acetate buffer (M = 0.2; pH = 4.64, the isoelectric point of B.P.A.) and put into the osmometer immediately after dissolution. Under these conditions we observed that solutions of B.P.A. showed an osmotic pressure corresponding to a molecular weight of 270×10^3. This result may be interpreted as an aggregation of four molecules of B.P.A.

In order to explain the disagreement between our results and those obtained by other workers it should be noticed that the experiments described by other investigators have been performed on stock solutions or by means of static-elevation cells, which require several days for the attainment of equilibrium. We suspected therefore that the disagreement was due to a gradual depolymerization of a tetramer. To verify this assumption the following experiments were performed. Two stock solutions of B.P.A. were prepared and placed at 20° C and 30° C, respectively. At certain intervals of time aliquots were withdrawn and their osmotic pressures determined at 20° C. The aliquot at 30° C was first cooled to 0° C to delay the reaction before the measurement. The results are in Fig. 1. It is seen that the molecular weight decreases with time, and that the rate of the decrease increases with temperature. These facts strongly indicate a gradual depolymerization.

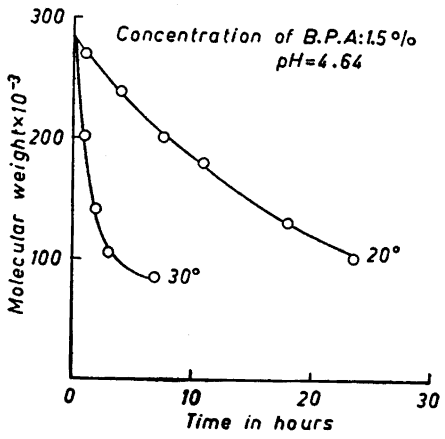


Fig. 1. Decrease in molecular weight with time at 20° C and 30° C.

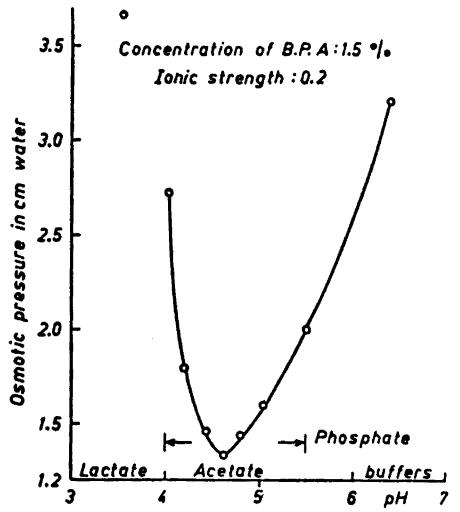


Fig. 2. Relation between osmotic pressure and pH.

Experiments have been carried out which show that the osmotic pressure, measured one hour after dissolution, is dependent on the pH. A minimum is found at the isoelectric point (Fig. 2).

It was further observed that the acidity of unbuffered solutions of B.P.A. increased with time. This phenomenon has been found previously by Tanford [4].

One of us (C.E.J.) wishes to thank *Købmand i Odense Johann og Hanne Weimann født Seedorffs legat* for financial support.

We are grateful to mag.scient. Mogens Lassen of this institute for valuable discussions.

1. Scatchard, G., Batchelder, A. C. and Brown, A. *J. Am. Chem. Soc.* **68** (1946) 2320.
2. Adair, G. S. and Robinson, H. E. *Biochem. J. London* **24** (1930) 1864.
3. Christiansen, J. A. and Jensen, C. E. *Acta Chem. Scand.* **7** (1953) 1247.
4. Tanford, C. *J. Am. Chem. Soc.* **72** (1950) 441.

Received February 4, 1957.

Darstellung langkettiger Alkylborsäuren

KURT TORSSELL und ERIK N. V. LARSSON

Institut für organische Chemie und Biochemie der Universität, Stockholm, Schweden

Im Verhältnis zu den Arylborsäuren sind die Alkylborsäuren viel unbeständiger. Sie zersetzen sich langsam an der Luft unter Bildung von Borsäure und Alkohol [1]. In feuchtem Zustand sind sie stabiler und beim Aufbewahren unter Stickstoff sind sie unbegrenzt haltbar. Veresterung mit Diäthanolamin hat sich auch gut bewährt um die Säuren in stabile und handliche Derivate zu überführen [2]. Bis jetzt sind nur die niedrigeren Glieder der Alkylborsäuren — Methyl- bis Hexylborsäure — dargestellt worden [1,3]. Es wäre aber denkbar, dass die langkettigeren Alkylborsäuren eine höhere Stabilität besitzen, da die Umhüllung der B—C-Bindung mit einem grösseren Alkylrest eine Schutzwirkung bedingen könnte. Dies scheint auch tatsächlich der Fall zu sein. Die Stabilität erlaubt jedoch kein unbegrenztes Aufbewahren an der Luft. Nach einiger Zeit bemerkt man den Geruch des Alkohols, und die Verbindung, die zuerst in unpolaren Lösungsmitteln, z.B. in Benzol leicht löslich ist, ergibt eine schwache Trübung von freigesetzter Borsäure.

Die langkettigen Alkylborsäuren bilden farblose, niedrig (bei etwa 70—80°) schmelzende und in reinem Zustand geruchlose Substanzen, die in den gebräuchlichsten organischen Lösungsmitteln löslich, in Wasser aber fast unlöslich sind. Infolge weitgehender Hydrolyse lösen sie sich auch nicht in Lauge:

$$RB(OH)_3^- K^+ \overset{H_2O}{\rightleftharpoons} RB(OH)_2 + KOH$$

Es ist zu erwarten, dass langkettige Verbindungen dieser Art oberflächenaktiv sind. Wegen ihrer Schwerlöslichkeit und geringen Beständigkeit besitzen sie jedoch kein Interesse in diesem Zusammenhang.

Alkylborsäuren mit einer geraden Anzahl von Kohlenstoffatomen, C_8 bis C_{18}, sind durch Umsetzung der Grignardverbindungen mit Tributylborat dargestellt worden. Bei der Darstellung von den langkettigeren *n*-Alkylmagnesiumverbindungen entstanden beträchtliche Mengen von Kohlenwasserstoffen (Paraffinen), die schwierig von den Alkylborsäuren zu trennen waren.

$$2\ RX + Mg \rightarrow R—R + MgX_2$$

Diese Nebenreaktion konnte durch vorsichtiges Zusammenbringen der Reaktionspartner teilweise unterdrückt werden. Nach dem Zusatz des Alkylhalogenids wurde die Ätherlösung auf dem Wasserbad unter Rückfluss 5 Min. gekocht, wonach die Grignardlösung sofort verwendet wurde. Die höheren Kohlenwasserstoffe, die in Äther ziemlich schwerlöslich waren, fielen bei der Reaktion in Form von blättrigen Kristallen aus.

Die C—H-Analysen zeigten besonders bei den langkettigeren Alkylborsäuren einen etwas zu hohen C-Wert, was auf eine geringe Verunreinigung mit Kohlenwasserstoff hindeutete.

Experimenteller Teil. n-*Oktylborsäure.* Die Grignardlösung, aus 10 g *n*-Oktylchlorid und 1,9 g Magnesium in 80 ml Äther dargestellt, wurde tropfenweise unter Stickstoff und Umrühren zu einer auf —70° gekühlten Lösung von 18,4 g Tri-*n*-butylborat in 30 ml Äther zugegeben. Die Reaktionstemperatur wurde während der Umsetzung bei —65 bis —70° gehalten. Die Lösung durfte dann langsam Zimmertemperatur erreichen und wurde in einem Scheidetrichter in 100 ml Eiswasser + 5 ml konz. Schwefelsäure hydrolysiert. Die wässrige Schicht wurde von der ätherischen getrennt und zweimal mit je 30 ml Äther extrahiert. Von den vereinigten Ätherlösungen wurde die Hauptmenge des Äthers bei gewöhnlichem Druck abdestilliert. Der Rückstand wurde stark alkalisch gemacht worauf das Butanol-Wasser-Gemisch im Vakuum abgetrieben wurde. Wasser wurde gelegentlich während der Destillation zugesetzt um die Wassermenge einigermassen konstant zu halten ($\sim$ 100 ml). Inzwischen hatte sich ein weisser Niederschlag gebildet, der abgenutscht, auf dem Filter mit einem Glasstopfen zusammengepresst, mit Wasser gewaschen und an der Luft getrocknet wurde. Das Filtrat enthielt ein Öl, das zum grössten Teil aus Hexakosan bestand. Oktylborsäure lässt sich aus Nitromethan oder Toluol umkristallisieren; Rohausbeute 6,3 g oder 59 %. Sintert leicht bei 70°. Zersp. 77—78°. Sie zerfällt langsam an der Luft unter Bildung von Borsäure und Oktylalkohol. Wenig löslich in Wasser, löslich in Lauge ($C_8H_{19}O_2B$ (158,1): Ber. C 60,77; H 12,11. Gef. C 60,09; H 12,57).

n-*Heptylborsäure* und n-*Decylborsäure* wurden in ähnlicher Weise dargestellt. Die beiden Substanzen zersetzen sich langsam an der Luft. *Heptylborsäure* ist schwerlöslich in Wasser.

Sie lässt sich aus Nitromethan oder Toluol umkristallisieren. Zersp. 81—83°. Sintert bei etwa 70°. Rohausbeute 43 %. *Decylborsäure* ist fast unlöslich in Wasser und Lauge. Sie wurde aus Nitromethan-Äthylacetat (1:1) umkristallisiert. Zersp. 76—78°. Ausbeute 44 %. ($C_{10}H_{23}O_2B$ (186,1): Ber. C 64,54; H 12,46. Gef. C 64,82; H 13,07).

Bei der Darstellung der *Lauryl-*, *Myristyl-*, *Cetyl-* und *Stearyl*-borsäuren wurden den Vorschriften für *Oktylborsäure* bis auf die Aufarbeitung des Reaktionsguts gefolgt. Wegen der Schwerlöslichkeit der Produkte in Wasser ist es nicht notwendig die wässrige Schicht mit Äther zu extrahieren.

Laurylborsäure. Die bei der Aufarbeitung erhaltene ätherische Schicht wurde einige Stunden in den Kühlschrank gestellt, um den gebildeten Kohlenwasserstoff möglichst zum Ausfällen zu bringen, wonach dieser abfiltriert wurde. Diese Fraktion bestand aus fast reinem Tetrakosan. Schmp. 56,0—56,5°. ($C_{24}H_{50}$(338,6) Ber. C 85,12; H 14,88. Gef. C 84,70; H 15,23). Die Ätherlösung wurde dann wie oben eingedampft. Der Niederschlag wurde wiederholt aus Toluol umkristallisiert, wobei die Lösung nur auf Zimmertemperatur gekühlt wurde, um Mitfällung von Kohlenwasserstoff zu vermeiden. Zersp. 70—75°. ($C_{12}H_{27}O_2B$(214,2): Ber. C 67,30; H 12,71. Gef.C 68,03; H 12,54). Die Ausbeute war gering.

Myristylborsäure wurde ähnlich wie Laurylborsäure dargestellt. Ausbeute 24 %. Zersp. 74—76°. ($C_{14}H_{31}O_2B$ (242,2): Ber. C 69,41; H 12,90. Gef. C 70,38; H 12,89).

Cetylborsäure. Es wurde von 20 g Cetylbromid + 1,9 g Magnesium in 90 ml Äther und 18 g Tributylborat in 40 ml Äther ausgegangen. Die bei der Hydrolyse gewonnene Ätherlösung wurde über Nacht sich selbst überlassen. Nach Abfiltrieren des Niederschlags (Dotriakontan) wurde die Lösung einige Stunden auf —10° abgekühlt. Die gebildeten Kristalle, 3 g, die etwas mit Kohlenwasserstoff verunreinigt waren, wurden wiederholt aus Toluol umkristallisiert. Beim Eindampfen der Ätherlösung konnte noch etwas von der Substanz erhalten werden. Zersp. 78—79°. ($C_{16}H_{35}O_2B$ (270,3): Ber. C 71,08; H 13,06. Gef. C 72,52; H 13,38).

Stearylborsäure wurde aus Stearylmagnesiumbromid und Tributylborat nach den Vorschriften für Oktyl- und Cetylborsäure dargestellt. Ausbeute 33 %. Zersp. 82—84°. ($C_{18}H_{39}O_2B$ (298,3): Ber. C 72,51; H 13,18. Gef. C 73,45; H 13,41).

Für die ökonomische Unterstützung dieser Arbeit danken wir *Statens Naturvetenskapliga Forskningsråd.*

1. Snyder, H. R., Kuck, J. A. und Johnson, J. R. *J. Am. Chem. Soc.* **60** (1938) 105.
2. Lawesson, S.-O. *Arkiv Kemi* **10** (1956) 171.
3. Krause, E. und von Grosse, A. *Die Chemie der metallorganischen Verbindungen.* Berlin 1937, S. 200.

Eingegangen am 4. Februar 1957.

Synthesis of the *cis*- and *trans*-Isomers of Methyl 2,4L,21,21-tetramethyl- L$\Delta^{2:3}$-docosenoate

INGRID HEDLUND-STOLTZ and EINAR STENHAGEN

Department of Medical Biochemistry, Institute of Medical Chemistry, University of Uppsala, Uppsala, Sweden

In the course of work on the synthesis of compounds structurally related to C_{27}-phthienoic acid from virulent tubercle bacilli [1], Ställberg-Stenhagen [2] prepared the *trans*-isomer of 2,4D-dimethyl-$\Delta^{2:3}$-heneicosenoic acid. This acid and its ethyl ester were strongly laevorotatory. The corresponding *cis*-compound and the isomer with α-methylene structure were not isolated in pure form, but both appeared to be dextrorotatory.

The *cis*- and *trans*-isomers of methyl 2,4L,21,21-tetramethyl-$\Delta^{2:3}$-docosenoate have now been prepared in order to study the biological properties of fatty acids related to the phthienoic acid type but possessing a neopentyl group in ω-position, the presence of which renders biological ω-oxidation difficult. The *trans*-ester is strongly dextrorotatory, whereas the *cis*-ester is laevorotatory, the molecular rotations being +69° and −40°, respectively. The geometrical arrangement of the substituent groups attached to the carbon atoms forming the α,β-double bond has thus a very marked effect on the optical rotation of the asymmetric carbon atom in γ-position.

The synthesis follows that of racemic methyl phthienoate described by Asselineau *et al.*[3]

Experimental. Methyl 17,17-dimethyloctadecanoate was prepared from *tert*-butylacetic acid and methyl hydrogen tetradecane-1,14-dioate *via* the Kolbe reaction. Hydrolysis gave

Sie lässt sich aus Nitromethan oder Toluol umkristallisieren. Zersp. 81—83°. Sintert bei etwa 70°. Rohausbeute 43 %. *Decylborsäure* ist fast unlöslich in Wasser und Lauge. Sie wurde aus Nitromethan-Äthylacetat (1:1) umkristallisiert. Zersp. 76—78°. Ausbeute 44 %. ($C_{10}H_{23}O_2B$ (186,1): Ber. C 64,54; H 12,46. Gef. C 64,82; H 13,07).

Bei der Darstellung der *Lauryl-*, *Myristyl-*, *Cetyl-* und *Stearyl*-borsäuren wurden den Vorschriften für *Oktylborsäure* bis auf die Aufarbeitung des Reaktionsguts gefolgt. Wegen der Schwerlöslichkeit der Produkte in Wasser ist es nicht notwendig die wässrige Schicht mit Äther zu extrahieren.

Laurylborsäure. Die bei der Aufarbeitung erhaltene ätherische Schicht wurde einige Stunden in den Kühlschrank gestellt, um den gebildeten Kohlenwasserstoff möglichst zum Ausfällen zu bringen, wonach dieser abfiltriert wurde. Diese Fraktion bestand aus fast reinem Tetrakosan. Schmp. 56,0—56,5°. ($C_{24}H_{50}$(338,6) Ber. C 85,12; H 14,88. Gef. C 84,70; H 15,23). Die Ätherlösung wurde dann wie oben eingedampft. Der Niederschlag wurde wiederholt aus Toluol umkristallisiert, wobei die Lösung nur auf Zimmertemperatur gekühlt wurde, um Mitfällung von Kohlenwasserstoff zu vermeiden. Zersp. 70—75°. ($C_{12}H_{27}O_2B$(214,2): Ber. C 67,30; H 12,71. Gef.C 68,03; H 12,54). Die Ausbeute war gering.

Myristylborsäure wurde ähnlich wie Laurylborsäure dargestellt. Ausbeute 24 %. Zersp. 74—76°. ($C_{14}H_{31}O_2B$ (242,2): Ber. C 69,41; H 12,90. Gef. C 70,38; H 12,89).

Cetylborsäure. Es wurde von 20 g Cetylbromid + 1,9 g Magnesium in 90 ml Äther und 18 g Tributylborat in 40 ml Äther ausgegangen. Die bei der Hydrolyse gewonnene Ätherlösung wurde über Nacht sich selbst überlassen. Nach Abfiltrieren des Niederschlags (Dotriakontan) wurde die Lösung einige Stunden auf —10° abgekühlt. Die gebildeten Kristalle, 3 g, die etwas mit Kohlenwasserstoff verunreinigt waren, wurden wiederholt aus Toluol umkristallisiert. Beim Eindampfen der Ätherlösung konnte noch etwas von der Substanz erhalten werden. Zersp. 78—79°. ($C_{16}H_{35}O_2B$ (270,3): Ber. C 71,08; H 13,06. Gef. C 72,52; H 13,38).

Stearylborsäure wurde aus Stearylmagnesiumbromid und Tributylborat nach den Vorschriften für Oktyl- und Cetylborsäure dargestellt. Ausbeute 33 %. Zersp. 82—84°. ($C_{18}H_{39}O_2B$ (298,3): Ber. C 72,51; H 13,18. Gef. C 73,45; H 13,41).

Für die ökonomische Unterstützung dieser Arbeit danken wir *Statens Naturvetenskapliga Forskningsråd.*

1. Snyder, H. R., Kuck, J. A. und Johnson, J. R. *J. Am. Chem. Soc.* **60** (1938) 105.
2. Lawesson, S.-O. *Arkiv Kemi* **10** (1956) 171.
3. Krause, E. und von Grosse, A. *Die Chemie der metallorganischen Verbindungen.* Berlin 1937, S. 200.

Eingegangen am 4. Februar 1957.

Synthesis of the *cis*- and *trans*-Isomers of Methyl 2,4L,21,21-tetramethyl- L$\Delta^{2:3}$-docosenoate

INGRID HEDLUND-STOLTZ and EINAR STENHAGEN

Department of Medical Biochemistry, Institute of Medical Chemistry, University of Uppsala, Uppsala, Sweden

In the course of work on the synthesis of compounds structurally related to C_{27}-phthienoic acid from virulent tubercle bacilli [1], Ställberg-Stenhagen [2] prepared the *trans*-isomer of 2,4D-dimethyl-$\Delta^{2:3}$-heneicosenoic acid. This acid and its ethyl ester were strongly laevorotatory. The corresponding *cis*-compound and the isomer with α-methylene structure were not isolated in pure form, but both appeared to be dextrorotatory.

The *cis*- and *trans*-isomers of methyl 2,4L,21,21-tetramethyl-$\Delta^{2:3}$-docosenoate have now been prepared in order to study the biological properties of fatty acids related to the phthienoic acid type but possessing a neopentyl group in ω-position, the presence of which renders biological ω-oxidation difficult. The *trans*-ester is strongly dextrorotatory, whereas the *cis*-ester is laevorotatory, the molecular rotations being +69° and −40°, respectively. The geometrical arrangement of the substituent groups attached to the carbon atoms forming the α,β-double bond has thus a very marked effect on the optical rotation of the asymmetric carbon atom in γ-position.

The synthesis follows that of racemic methyl phthienoate described by Asselineau *et al.*[3]

Experimental. Methyl 17,17-dimethyloctadecanoate was prepared from *tert*-butylacetic acid and methyl hydrogen tetradecane-1,14-dioate *via* the Kolbe reaction. Hydrolysis gave

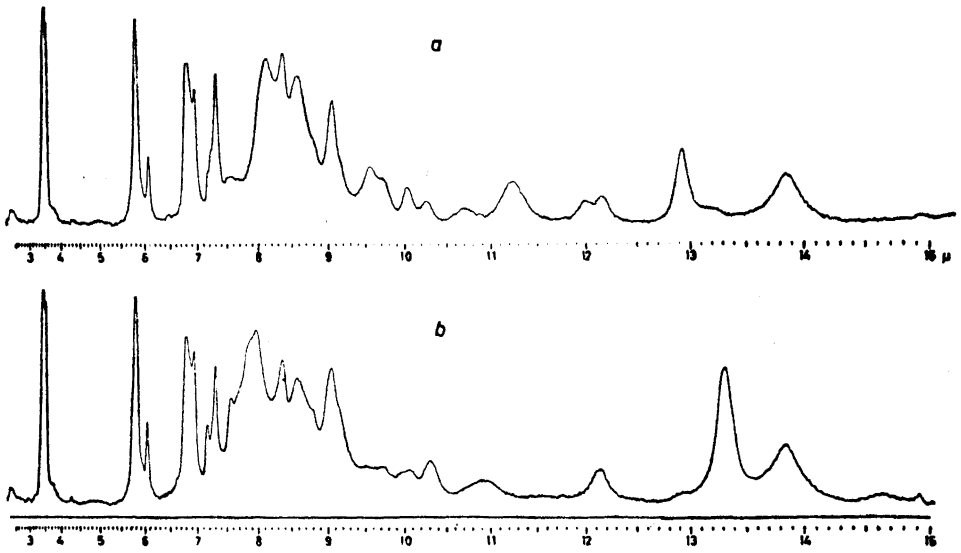


Fig. 1. Infra-red absorption spectra in the liquid state: a) (—)-methyl *cis*-2,4L,21,21 tetramethyl-$\Delta^{2:3}$-docosenoate; b) (+)-methyl *trans*-2,4L,21,21-tetramethyl-$\Delta^{2:3}$-docosenoate Cell thickness 0.02 mm.

17,17-dimethyloctadecanoic acid of m. p. 56.7 —57.2° (Sobotka and Stynler [4] give m. p. 57.2 —57.7°), which, *via* a second mixed Kolbe reaction with (—)-methyl hydrogen β-methylglutarate [5], followed by hydrolysis, gave (—)-3L, 20,20-trimethylheneicosanoic acid (m. p. 43.5—43.9°, $[M]_D^{27}$ — 12.6° (chloroform; *c*, 14.5), amide m. p. 91.7—91.9°). Reaction of the acid chloride of this acid with methyl cadmium [6] gave (—)-2-oxo-4L, 21,21-trimethyldocosane. After purification by chromatography on aluminium oxide the ketone had n_D^{30} 1.4477, $[\alpha]_D^{22}$ — 4.6° (chloroform, *c*, 10.4). It was converted into cyanhydrin by means of hydrogen cyanide, and the crude cyanhydrin was hydrolysed by hydrochloric acid in glacial acetic acid to a mixture of stereoisomeric hydroxy-acids melting at 83.8—85.1°. This mixture was pyrolysed by heating to 206° for one hour, followed by half an hour at 215°. After treatment with diazomethane in ether solution the resulting mixture of methyl esters was separated by chromatography on aluminium oxide. (—)-Methyl *cis*-2,4L,21,21-tetramethyl-$\Delta^{2:3}$-docosenoate, m.p. 25.5—25.8°; n_D^{25} 1.4572; $d_4^{24.5}$ 0.869; $[\alpha]_D^{24.5}$ —9.87° ± 0.27° (chloroform; *c*, 7.6); $[M]_D^{24.5}$ —40°, was followed by (+)-methyl *trans*-2,4L, 21,21-tetramethyl- $\Delta^{2:3}$ -decosenoate, m. p. 27.1—27.5°, n_D^{25} 1.4588 (supercooled liquid); $[\alpha]_D^{26}$ + 16.9° ± 1.0° (chloroform; *c*, 1.95); $[M]_D^{26}$ + 69°. Ultra-violet spectrum: *cis*-isomer λ_{max} 216 mμ, ε = 10.200; *trans*-isomer λ_{max} 215 mμ, ε = 13.500 (hexane).

The infra-red spectra are shown in Fig. 1. The strong absorption band at 750 cm^{-1} (13.33 μ) of the *trans*-isomer is observed also in the spectra of racemic methyl phthienoate [2] and methyl *trans*-2,4D-dimethyl-$\Delta^{2:3}$-heneicosenoate [2], and thus appears characteristic for methyl esters of acids having the 2,4-diMe-2-enoic structure. In methyl *trans*-2,5D-dimethyl-$\Delta^{2:3}$-heneicosenoate the frequency is shifted to 740 cm^{-1} (13.51 μ).

In the spectra of *cis*-forms of the 2,4-diMe-2-enoate structure, represented by the *cis*-ester now described and by the *cis*-isomer of racemic methyl phthienoate, a corresponding absorption occurs at 773 cm^{-1} (12.93 μ).

Details of this work will be published later.

Acknowledgements. We wish to thank Professor Arne Fredga for his interest in the work, and Dr. Ingrid Fischmeister for the infra-red absorption spectra. The financial support of the *Swedish Medical Research Council* is gratefully acknowledged.

1. *Cf.* Cason, J., Allen, C. F., DeAcetis, W. and Fonken, G. J. *J. Biol. Chem.* **220** (1956) 893.
2. Ställberg-Stenhagen, S. *Arkiv Kemi* **6** (1954) 537.
3. Asselineau, C., Asselineau, J., Ställberg-Stenhagen, S. and Stenhagen, E. *Acta Chem. Scand.* **10** (1956) 478.
4. Sobotka, H. and Stynler, F. E. *J. Am. Chem. Soc.* **72** (1950) 5139.
5. Ställberg-Stenhagen, S. *Arkiv Kemi, Mineral. Geol.* **25A** (1947) No. 10.
6. Cason, J. *Chem. Revs.* **40** (1947) 15.

Received February 9, 1957.

On the Effect of Organic Mercury Compounds and Copper Salts on Catalase Cyanide

BO SÖRBO

Research Institute of National Defence, Dept. 1, Sundbyberg 4, and Medicinska Nobelinstitutet, Biokemiska avdelningen, Stockholm, Sweden

In connection with studies of different antidotes in cyanide poisoning it became of interest to investigate the action of certain heavy metal compounds on cyanide inhibited heme enzymes. The toxicity of cyanide is attributed to its inhibitory action on cytochrome oxidase, but another heme enzyme, catalase, was used as a model enzyme in these studies, as it in contrast to cytochrome oxidase can be obtained in a pure state. It is of importance in this connection that catalase qualitatively behaves as cytochrome oxidase in its reaction with cyanide, as both the association and dissociation velocity constants are high [1]. It has previously been demonstrated by Chance [1] that silver ions generate free catalase from the catalase cyanide complex, due to the fact that silver ions combine with the free cyanide in equilibrium with catalase cyanide. The high toxicity of silver salts, however, apparently prevents their use as antidotes in cyanide poisoning. Incidentally we observed that organic mercury compounds had a high affinity for cyanide and could completely reactivate cyanide inhibited catalase. This suggested that these compounds may have an antidotal effect in cyanide poisoning. Of special interest were those organic mercury compounds which are used as diuretics, as they might be easily available for use as antidotes. The complete reactivation of cyanide inhibited catalase by one of these diuretics, Mersalyl (Salyrgan), is shown in Fig. 1. Experiments on rabbits [2] demonstrated, however, that Mersalyl had no antidotal effect in cyanide poisoning. Presumably the mercury compound was bound to sulfhydryl groups in the body before it could react with cyanide. (The mercurials have a very high affinity for sulfhydryl groups and their diuretic action is in fact attributed to an inhibition of sulfhydryl enzymes in the kidney.)

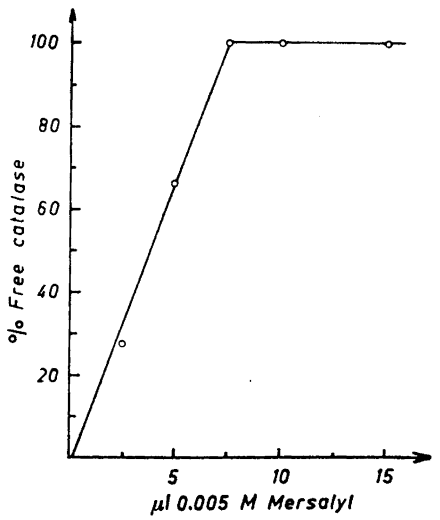


Fig. 1. Effect of Mersalyl on catalase cyanide. Horse blood catalase 0.8×10^{-6} M, cyanide 1×10^{-5} M, phosphate buffer 0.025 M of pH 7.4, final volume 3.0 ml. Indicated amounts of the mercurial added and the free catalase formed was determined spectrophotometrically from the decrease in absorbancy at 425 mµ.

Agner [3] reported that cupric salts could be used as antidotes in cyanide poisoning. This was disputed by Walther and Meyer [4] but Agner's results have been confirmed in connection with the present work [5]. However, when the effect of cupric chloride on catalase cyanide was studied, it was found that even a considerable excess of cupric

1. *Cf.* Cason, J., Allen, C. F., DeAcetis, W. and Fonken, G. J. *J. Biol. Chem.* **220** (1956) 893.
2. Ställberg-Stenhagen, S. *Arkiv Kemi* **6** (1954) 537.
3. Asselineau, C., Asselineau, J., Ställberg-Stenhagen, S. and Stenhagen, E. *Acta Chem. Scand.* **10** (1956) 478.
4. Sobotka, H. and Stynler, F. E. *J. Am. Chem. Soc.* **72** (1950) 5139.
5. Ställberg-Stenhagen, S. *Arkiv Kemi, Mineral. Geol.* **25A** (1947) No. 10.
6. Cason, J. *Chem. Revs.* **40** (1947) 15.

Received February 9, 1957.

On the Effect of Organic Mercury Compounds and Copper Salts on Catalase Cyanide

BO SÖRBO

Research Institute of National Defence, Dept. 1, Sundbyberg 4, and Medicinska Nobelinstitutet, Biokemiska avdelningen, Stockholm, Sweden

In connection with studies of different antidotes in cyanide poisoning it became of interest to investigate the action of certain heavy metal compounds on cyanide inhibited heme enzymes. The toxicity of cyanide is attributed to its inhibitory action on cytochrome oxidase, but another heme enzyme, catalase, was used as a model enzyme in these studies, as it in contrast to cytochrome oxidase can be obtained in a pure state. It is of importance in this connection that catalase qualitatively behaves as cytochrome oxidase in its reaction with cyanide, as both the association and dissociation velocity constants are high [1]. It has previously been demonstrated by Chance [1] that silver ions generate free catalase from the catalase cyanide complex, due to the fact that silver ions combine with the free cyanide in equilibrium with catalase cyanide. The high toxicity of silver salts, however, apparently prevents their use as antidotes in cyanide poisoning. Incidentally we observed that organic mercury compounds had a high affinity for cyanide and could completely reactivate cyanide inhibited catalase. This suggested that these compounds may have an antidotal effect in cyanide poisoning. Of special interest were those organic mercury compounds which are used as diuretics, as they might be easily available for use as antidotes. The complete reactivation of cyanide inhibited catalase by one of these diuretics, Mersalyl (Salyrgan), is shown in Fig. 1. Experiments on rabbits [2] demonstrated, however, that Mersalyl had no antidotal effect in cyanide poisoning. Presumably the mercury compound was bound to sulfhydryl groups in the body before it could react with cyanide. (The mercurials have a very high affinity for sulfhydryl groups and their diuretic action is in fact attributed to an inhibition of sulfhydryl enzymes in the kidney.)

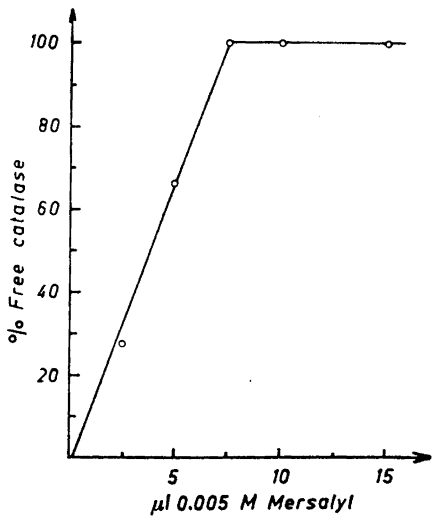


Fig. 1. Effect of Mersalyl on catalase cyanide. Horse blood catalase 0.8×10^{-6} M, cyanide 1×10^{-5} M, phosphate buffer 0.025 M of pH 7.4, final volume 3.0 ml. Indicated amounts of the mercurial added and the free catalase formed was determined spectrophotometrically from the decrease in absorbancy at 425 mµ.

Agner [3] reported that cupric salts could be used as antidotes in cyanide poisoning. This was disputed by Walther and Meyer [4] but Agner's results have been confirmed in connection with the present work [5]. However, when the effect of cupric chloride on catalase cyanide was studied, it was found that even a considerable excess of cupric

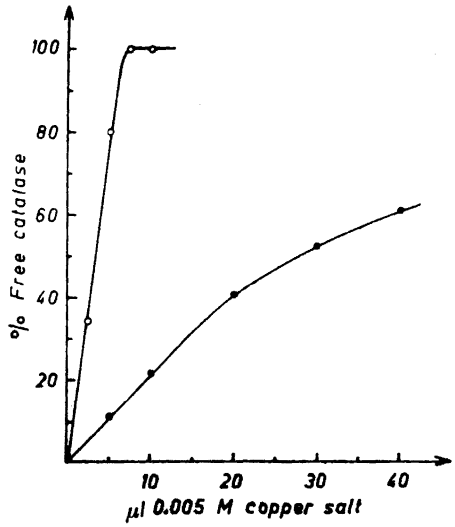


Fig. 2. Effect of cupric and cuprous ions on catalase cyanide. Conditions as in Fig. 1. O O O $CuCl_2$. ● ● ● CuCl. The latter prepared immediately before use by dissolving the salt (a colorless preparation from Schering-Kahlbaum) in 5 % KCl under nitrogen.

ions could not completely reactivate cyanide inhibited catalase, Fig. 2. Cupric chloride was thus inferior to Mersalyl in this respect, although it was effective as an antidote, whereas Mersalyl was not. This discrepancy could be explained when further experiments demonstrated that cuprous ions in contrast to the cupric ions very effectively liberated catalase from catalase cyanide; see Fig. 2. (The antidotal effect of cuprous chloride was not determined, as this compound is only sparingly soluble and is rapidly oxidized to cupric chloride in the presence of air). If cupric ions could be reduced to the cuprous state in the vicinity of the cyanide inhibited cytochrome oxidase, an efficient reactivation of the latter could be expected. Cupric ions are in fact reduced by ferrocytochrome c[5] and as cytochrome c is mainly present in the reduced form in cyanide poisoned cells, good possibilities exist for an intracellular reduction of the cupric ions. It is relevant that cupric ions have much less affinity for sulfhydryl groups than cuprous ions or organic mercury compounds [6,7]. (The reaction between mercaptans and cupric ions involves a reduction of the latter to the cuprous state.) This suggests that cupric ions are not so rapidly bound to sulfhydryl groups in the body as the mercurials and could then better reach the cyanide inhibited cytochrome oxidase in the central nervous system.

The crystalline horse blood catalase used in these experiments was a generous gift from Dr. R. K. Bonnichsen. The author is also grateful to Miss A.-M. Sjödén and Mr. O. Eriksson for valuable technical assistance.

1. Chance, B. *J. Biol. Chem.* **179** (1949) 1279.
2. Clemedson, C. J., Hultman, H. I:son and Sörbo, B. *Unpublished results.*
3. Agner, K. *Naturwiss.* **27** (1939) 31.
4. Walther, R. and Beyer, K. *Biochem. Z.* **301** (1939) 315.
5. Keilin, D. *Proc. Roy. Soc. London B* **104** (1929) 206.
6. Mapson, L. W. *Biochem. J. London* **40** (1946) 240.
7. Slater, E. C. *Biochem. J. London* **45** (1949) 130.

Received February 14, 1957.

ACTA CHEMICA SCANDINAVICA 11 (1957) 409—413

On the Metabolism of 3α, 7α, 12α-Trihydroxycoprostanic Acid in the Rat *

Bile Acids and Steroids 44

R. J. BRIDGWATER

Department of Biochemistry and Chemistry, Guy's Hospital Medical School, London, S.E.1,

and

S. LINDSTEDT

Department of Physiological Chemistry, University of Lund, Lund, Sweden

Tritium labelled D- and L-3α,7α,12α-trihydroxycoprostanic acids have been prepared. They have been found to be rapidly degraded to cholic acid in the rat liver, only a minor amount appearing in the bile as the taurine conjugate of the injected acid.

Bile acids with 27 carbon atoms have been found in various animals. (For a review see Haslewood [1]) 3α, 7α, 12α-25-L-trihydroxycoprostanic acid (II) has been isolated from the bile of *Alligator mississippiensis* [2] and also from the bile of *Rana nigromaculata nigromaculata* [3]. From the bile of this latter species the isomeric 3α, 7α, 12α-25-D-trihydroxy-coprostanic acid has also been isolated [3]. Both isomers have also been isolated previously from the bile of *Rana catesbiana* [4,5].

Tetrahydroxybinorsterocholanic acid (27 carbon atoms) has also been isolated from the bile of the domestic chicken [6].

Both the 25-D- and the 25-L-3α, 7α, 12α-trihydroxycoprostanic acids have been prepared by partial synthesis [7]. Haslewood has put forward the theory that the C-27 bile acids represent a primitive stage in the evolutionary chain leading up to the C-24 acids of many animals.

As the bile acids of mammals are end products of cholesterol metabolism one could expect a hydroxylated coprostanic acid to be an intermediate in the

* A preliminary report of this work was read at the Meeting of the Norwegian Biochemical Society in June, 1956 [18].

conversion of cholesterol into bile acids. This would also be in accord with the view that hydroxylations in the steroid nucleus might precede the total degradation of the side chain [8].

EXPERIMENTAL

L- and D-Trihydroxycoprostanic acids were prepared by anodic coupling of cholic acid with D- and L-methylhydrogen-α-methyl glutarate, respectively, followed by degradation of the resulting acids by the Barbier-Wieland procedure.

The sodium salts of the acids were tritiated by a platinum-catalyzed exchange with tritium water at 120° for four days [6]. The acids were then purified by chromatography with phase system F (see below) and crystallized. The L-trihydroxycoprostanic acid melted at 194—196° and had a specific activity of 2.2×10^5 c.p.m. when counted in an "infinitely thin" layer in a Tracerlab gas-flow counter. The D-form melted at 185° and had a specific activity of 5×10^5 c.p.m.

Bile fistulas were made on white rats weighing about 200 g. The bile was collected in 50 % ethanol. The conjugated bile acids were extracted with *n*-butanol after acidification to pH 1. Saponifications were carried out in sealed glass tubes in 2 N sodium hydroxide at 120° for 12 h, and the free acids extracted with ether after acidification.

The reversed-phase chromatographic technique worked out by Bergström, Sjövall and Norman [10-12] was used for separation of the bile acids. The following solvent systems were used.

System	Moving phase	Stationary phase
C (Ref.[12])	methanol / water 50/50	chloroform / "*iso*octanol" 50/50
D (Ref.[12])	water	butanol
F (Ref.[11])	methanol / water 55/45	chloroform / heptane 90/10

Each fraction from the chromatogram was titrated with 0.02 N sodium hydroxide, and an aliquot plated in an "infinitely thin" layer on an aluminium or copper planchet. These were then counted in a Tracerlab gas-flow counter. The specific activity of the isolated cholic acid was determined after combustion and conversion into tritiobutane by the methods of Glascock [13].

RESULTS

Excretion and conjugation. L-Trihydroxycoprostanic acid (1—3 mg) was neutralized with sodium hydroxide and injected intraperitoneally into a rat with a bile fistula. About 70 % of the administered activity was excreted within 24 h. The bile acids were extracted and chromatographed with phase system D. The resulting chromatogram is seen in Fig. 1. The first activity peak coincides with the titration peak caused by taurocholic acid at 10—20 ml. The second activity peak at 25—35 ml appears at the position of taurochenodeoxy acid. In this system, however, taurine-conjugated trihydroxycoprostanic acid moves as a taurine-conjugated dihydroxycholanic acid. Any free trihydroxycoprostanic acid that might occur would have remained in the stationary phase. The column was eluted and the material rerun with phase system F. No sign of free trihydroxycoprostanic acid was found. The second peak in Fig. 1 was saponified and rerun with unlabelled trihydroxycoprostanic acid with phase system F. The titration and activity peaks coincided.

Identification of cholic acid. A bile sample from a rat that had received L-trihydroxycoprostanic acid was saponified and run on a chromatogram with phase system C. An activity peak coinciding with the titration peak caused

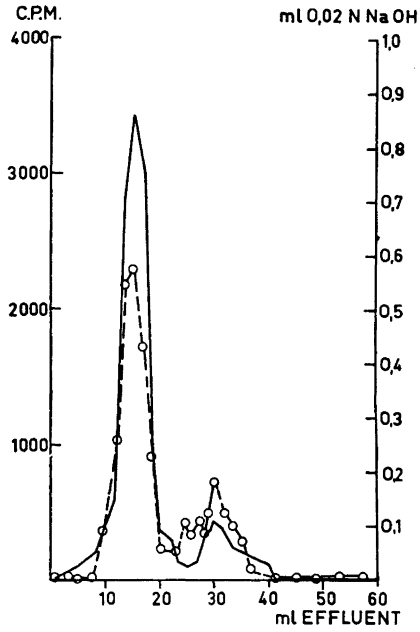


Fig. 1. Chromatogram of conjugated bile acids after administration of tritium-labelled L-trihydroxycoprostanic acid. Column: 4.5 g of hydrophobic kieselguhr. Phase system D. Solid line: titration values. Broken line: isotope determinations.

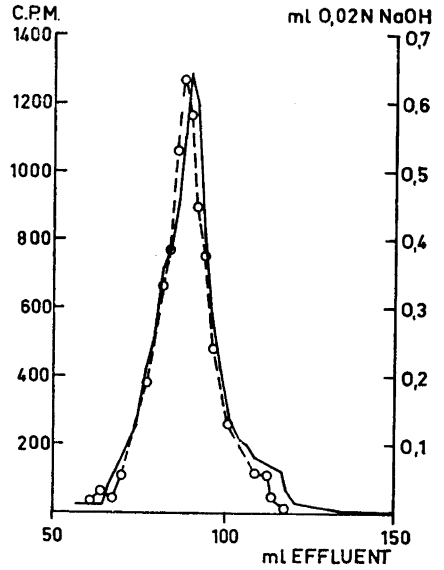


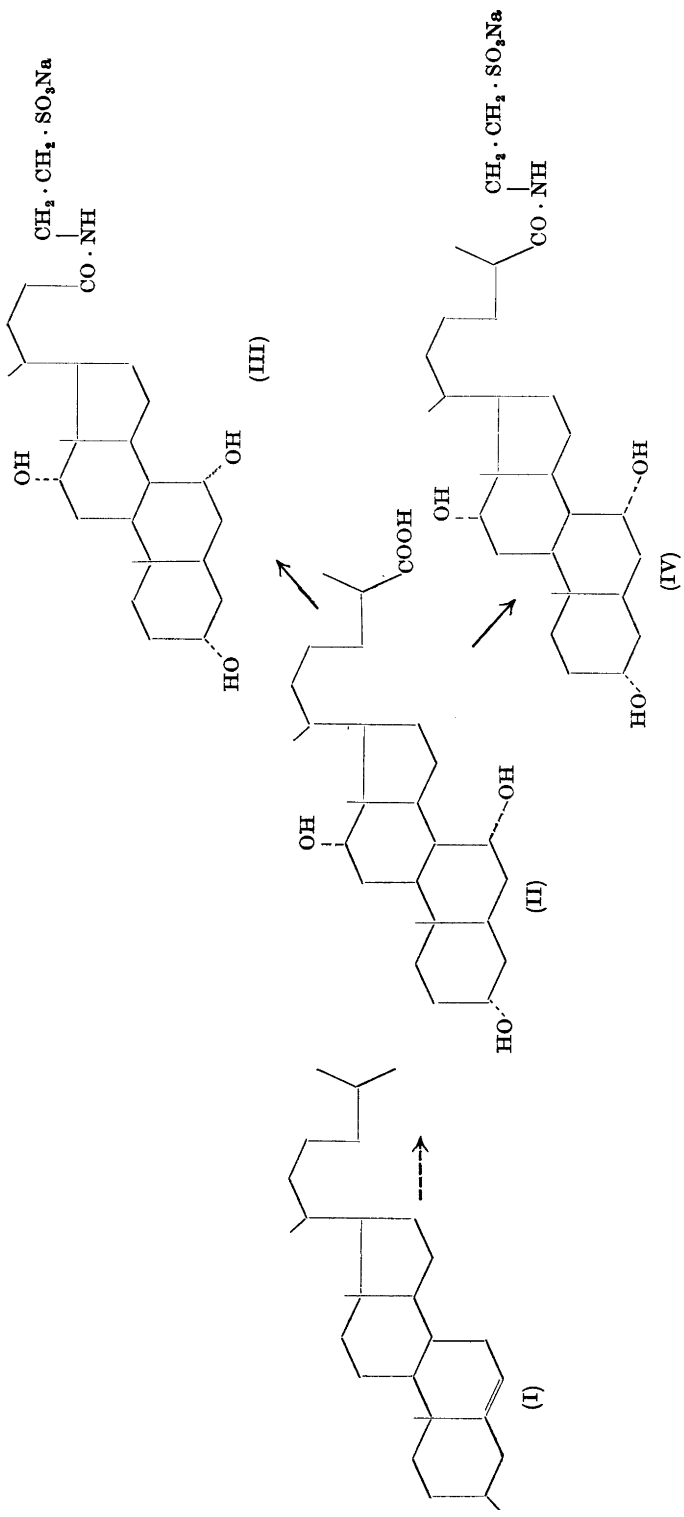
Fig. 2. Chromatogram of cholic acid after administration of tritium-labelled L-trihydroxycoprostanic acid. Column: 4.5 g of hydrophobic kieselguhr. Phase system C. Solid line: titration values. Broken line: isotope determinations.

by cholic acid was found (Fig. 2). The acid isolated from the combined fractions (60—120 ml effluent, *cf.* Fig. 2) was diluted with carrier cholic acid and the material recrystallized five times from different solvents (EtOH/aq, acetone/aq, EtOAc). Duplicate determinations of specific activity were carried out on material from the last four crystallizations. This specific activity was found to remain constant.

D-*Trihydroxycoprostanic acid.* When the D-form was given to a rat with a bile fistula and the bile acids fractionated, results identical with those described for the L-form were obtained.

DISCUSSION

As a result of earlier investigations it would appear probable that the first steps in the conversion of cholesterol into bile acids in mammals are hydroxylations in the steroid nucleus, which are then followed by the degradation of the side chain, the latter proceeding at a rapid rate. It has thus been shown that both 3α, 7α, 12α-trihydroxycoprostane, 3α,12α-dihydroxycoprostane and 3α,


(I)
(II)
(III)
(IV)
COOH
OH
HO
CH₂ · CH₂ · SO₃Na
CO · NH

7α-dihydroxycoprostane give rise to bile acids more rapidly than cholesterol itself [14–16].

It is assumed that the degradation of the side chain starts with a methyl-oxidation followed by a β-oxidation. This latter oxidation is known to be unhindered by the presence of a methyl group in the α-position (*cf.* Tryding and Westöö [17]). The present investigation clearly shows the rapid rate of the β-oxidation. It is also evident that the oxidation does not proceed beyond the cholic acid stage, the enzymatic reaction probably being blocked by the bulky steroid nucleus. It is of interest to note that the steric configuration at carbon atom 25 is of no importance, both stereoisomers being attacked to approximately the same extent.

Although no C-27 bile acids have been found in mammals they may appear as short-lived intermediates in the conversion of cholesterol(I) into bile acids.

The trihydroxycoprostanic acid (II) that was not degraded to cholic acid (III) appeared as a taurine-conjugate (IV), no trace of glycine-conjugate or free acid being found. Since both the conjugation [19,20] and the β-oxidation presumably proceed *via* a CoA-compound there is apparently a competition between the dehydrogenation and the conjugation resulting in a preponderance of the products of the former reaction.

We wish to thank Professor S. Bergström, who suggested the problem, for advice and encouragement. One of us (R.J.B.) expresses his gratitude for financial assistance from the *Clinical Research Committee of Guy's Hospital Medical School* and for facilities provided at the University of Lund. The work is part of a program supported by *Knut och Alice Wallenbergs Stiftelse* and the *Medical Faculty of Lund.*

Skilful technical assistance was given by Mr. Bengt Åkesson.

REFERENCES

1. Haslewood, G. A. D. *Physiol. Rev.* **35** (1955) 178.
2. Haslewood, G. A. D. *Biochem. J. London* **52** (1952) 583.
3. Komatsubara, T. Proc. *Japan Acad.* **30** (1954) 618.
4. Kurauti, Y. and Kazuno, T. *Hoppe-Seylers Z. physiol. Chem.* **262** (1939) 53.
5. Mabuti, H. *J. Biochem. Japan* **33** (1941) 131.
6. Yamasaki, D. *J. Biochem. Japan* **38** (1951) 93.
7. Bridgwater, R. J. *Biochem. J. London* **64** (1956) 593.
8. Bergström, S. *Record Chem. Progr. Kresge-Hooker Sci. Lib.* **16** (1955) 63.
9. Trenner, N. R., Pfluger, H. L., Newstead, E. G., Jones, S. L. and Sutton, C. T. *J. Am. Chem. Soc.* **76** (1954) 1196.
10. Bergström, S. and Sjövall, J. *Acta Chem. Scand.* **5** (1951) 1267.
11. Sjövall, J. *Acta Physiol. Scand.* **29** (1953) 232.
12. Norman, A. *Acta Chem. Scand.* **7** (1953) 1413.
13. Glascock, R. *Isotopic Gas Analysis for Biochemists.* Academic Press N.Y. 1954.
14. Bergström, S., Pääbo, K. and Rumpf, J. A. *Acta Chem. Scand.* **8** (1954) 1109.
15. Lindstedt, S. *To be published.*
16. Bergström, S. and Lindstedt, S. *Biochim. et Biophys. Acta* **19** (1956) 556.
17. Tryding, N. and Westöö, G. *Acta Chem. Scand.* **11** (1957) 427.
18. Bergström, S. and Lindstedt, S. *Acta Chem. Scand.* **6** (1956) 1049.
19. Elliot, W. H. *Biochem. J. London* **62** (1956) 427.
20. Bremer, J. *Acta Chem. Scand.* **9** (1955) 1036.

Received February 1, 1957.

ACTA CHEMICA SCANDINAVICA 11 (1957) 414—416

On the Metabolism of Taurine Conjugated 3α, 7α, 12α-Trihydroxycoprostanic Acid in the Rat

Bile Acids and Steroids 45

SVEN LINDSTEDT and ARNE NORMAN

Department of Physiological Chemistry, University of Lund, Lund, Sweden

The taurine conjugate of tritium labelled 3α,7α,12α-trihydroxycoprostanic acid has been prepared. In experiments on rats it was found that no splitting of the conjugate occurs in the liver but that it is split to a small extent in the intestine.

It has been shown that all bile acids naturally occurring in the rat bile are conjugated with taurine, only traces of glycine conjugates being found [1]. When the bile acids in the feces are examined by chromatography one finds only a small amount of conjugated acids [2]. When, however, the bacterial flora in the intestine has been depressed with chemoterapeutics practically all the bile acids in the feces are in the conjugated form [3]. This has led to the view that the microbial enzymes are mainly responsible for the normally occurring hydrolysis, an opinion which is further supported by the observation that certain anaerobic bacteria have a high capacity of splitting conjugated bile acids [4].

It has not, however, been definitely settled whether the digestive enzymes or enzymes in the liver are capable of splitting bile acid conjugates. Portman and Mann [5] have fed ^{35}S-labelled taurocholic acid to bile fistula rats and found 2—18 % of the radiosulfur in the urine. The hydrolysis in this case may well have been caused by bacterial enzymes attacking bile salts. Norman [6] has injected glycocholic acid-24-^{14}C intraperitoneally into bile fistula rats and into rats on which the bile fistula was made 6 h after injection. In the first case no taurocholic acid was found in the bile while in the latter about 50 % of the given amount appeared as taurocholic acid. The results indicated that no hydrolysis of the glycocholic acid occurs in the liver.

We have made similar experiments with tauro-trihydroxycoprostanic acid. The free trihydroxycoprostanic acid is known to be rapidly degraded to cholic acid in the liver [7]. If any hydrolysis of the taurine conjugates occurs in the liver one would thus expect to find activity in the cholic acid excreted in the bile.

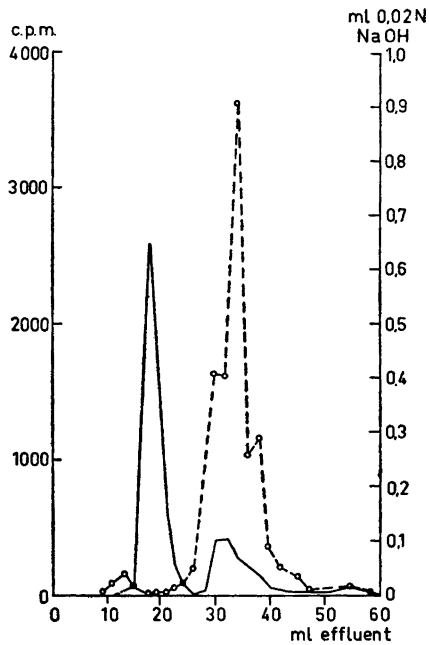


Fig. 1. Chromatography of conjugated bile acids excreted in a bile fistula rat after intraperitoneal injection of tritium labelled taurotrihydroxycoprostanic acid. Phase system D. Moving phase: water. Stationary phase: butanol. Solid line: Titration. Broken line: Radioactivity.

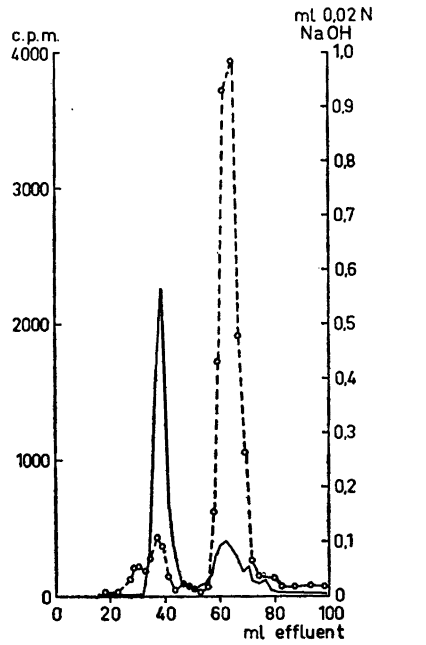


Fig. 2. Chromatography of conjugated bile acids in the bile fistula of a rat that had received an intraperitoneal injection of tritium labelled tauro-trihydroxycoprostanic acid 6 hours prior to operation. Phase system D. Solid line: Titration. Broken line: Radioactivity.

EXPERIMENTAL

Tritium-labelled 3*a*,7*a*,12*a*-25-L-trihydroxycoprostanic acid prepared by Bridgwater and Lindstedt [7] was coupled to taurine by the micromethods described by Norman [8]. The acid was purified by chromatography with phase system D (*cf.* Ref.[7]). It had a specific activity of about 250 000 c.p.m. per mg when counted in an "infinitely thin" layer in a Tracerlab gas-flow counter.

One mg of the sodium salt of the taurine-conjugated acid was administered intraperitoneally to bile fistula rats or normal rats on which a bile fistula was made 6 h after the administration. For details of the fractionation procedure see the preceding paper [7].

RESULTS AND DISCUSSION

Fig. 1 shows a chromatogram of an unhydrolyzed butanol extract of the bile excreted during a 24 h period after intraperitoneal administration of taurotrihydroxycoprostanic acid. The titration peaks at 15—25 ml and 30—40 ml are caused by taurocholic and taurochenodesoxycholic acid, respectively. No activity is present at the place of taurocholic acid, all of it being confined to a peak immediately after taurochenodesoxycholic acid at the place where tauro-

trihydroxycoprostanic acid is known to appear. For further identification the fractions containing the labelled material were hydrolyzed and rerun with phase system F (*cf.* Ref.[7]). The labelled compound now appeared at the place of free trihydroxycoprostanic acid added as carrier.

In Fig. 2 a chromatogram is shown of the bile acids excreated in a bile fistula made 6 h after injection of tauro-trihydroxycoprostanic acid. In this case about 10 % of the activity appears at the place of taurocholic acid and the rest at that of tauro-trihydroxycoprostanic acid. After hydrolysis the free bile acids were identified as cholic and trihydroxycoprostanic acid.

The results show that taurotrihydroxycoprostanic acid is excreted unchanged by the liver and indicate that the conjugating reaction in general is to no noticeable extent reversible. A slight hydrolysis of a minimum of 10 % must have occurred when the injected taurotrihydroxycoprostanic acid had taken part in the enterohepatic circulation for 6 h as this percentage of the tauro-conjugated C_{27}-acid was then recovered as the C_{24} cholic acid that was excreted as its taurine conjugate.

This work is part of investigations supported by *Statens medicinska forskningsråd* and *Knut och Alice Wallenbergs Stiftelse.*

REFERENCES

1. Norman, A. *Acta Physiol. Scand.* **32** (1954) 1.
2. Lindstedt, S. and Norman, A. *Acta Physiol. Scand.* **34** (1955) 1.
3. Norman, A. *Acta Physiol. Scand.* **33** (1955) 99.
4. Norman, A. and Grubb, R. *Acta Pathol. et Microbiol. Scand.* **36** (1955) 537.
5. Portman, O. W. and Mann, G. V. *J. Biol. Chem.* **213** (1955) 733.
6. Norman, A. *Proc. Roy. Physiograph. Soc. Lund* **25** (1955) No. 2.
7. Bridgwater, R. J. and Lindstedt, S. *Acta Chem. Scand.* **11** (1957) 409.
8. Norman, A. *Arkiv Kemi* **8** (1955) 331.

Received February 1, 1957.

ACTA CHEMICA SCANDINAVICA 11 (1957) 417—420

The Formation of Bile Acids from 7 α-Hydroxycholesterol in the Rat *

Bile Acids and Steroids 47

SVEN LINDSTEDT

Department of Physiological Chemistry, University of Lund, Lund, Sweden

Tritium labelled 7α-hydroxycholesterol has been prepared. It has been injected intraperitoneally into bile fistula rats and cholic and chenodeoxycholic acid identified as acid metabolities. The mechanism of the degradation of cholesterol is discussed.

In the autoxidation of cholesterol the two epimeric 7-hydroxycholesterols are formed [2,3]. They have also been reported to occur in small amounts in the unsaponifiable fraction in various organ lipids [4-7]. The possibility of their formation by autoxidation during the isolation procedure has, however, not been rigorously excluded.

It has been suggested that a 7-hydroxycholesterol may appear as an intermediate in the *in vivo* degradation of cholesterol [2,8].

In this work the formation of bile acids from 7α-hydroxycholesterol is demonstrated.

EXPERIMENTAL

7α-Hydroxycholesterol was prepared essentially according to Henbest *et al.* [9,10]. 2 g of sodium formiate dissolved in 20 ml of formic acid was added to a solution of 2 g of 7α-bromocholesterylbenzoate in 20 ml of ether. After 24 h water was added and the steroid extracted with ether. The material was dissolved in 2 ml of benzene and 15 ml of methanol added. After 8 h at room temperature 1.35 g of crystals melting at 115—144° were obtained. This material was brought onto a 20 g alumina column and eluted with increasing concentration of benzene in light petroleum. The material eluted with 0—30 % of benzene in light petroleum was crystallized from benzene/methanol and yielded 0.91 g of 7α-formoxycholesterolbenzoate m. p. 150—152°. Saponification with alcoholic potassium hydroxide gave 7α-hydroxycholesterol m. p. 150°.

Tritium-labelled 7α-hydroxycholesterol. Attempts to label 7α-hydroxycholesterol by platinum catalyzed exchange in tritiated water/acetic acid or tritiated water-ethanol/

* For a discussion of the steric configuration at the 7-position see Ref.[1]. A preliminary report of this work was read at the meeting of the Norwegian Biochemical Society, June 1956 [20].

sodium hydroxide were not successful and led to extensive destruction. The labelled 7α-hydroxycholesterol was therefore synthesized by the above procedure from tritium-labelled cholesterol prepared according to Bloch [11]. To ensure the absence of radioactive contaminants it was chromatographed according to Danielsson [12] on hydrophobic kieselguhr with 50 % (v/v) aqueous *iso*propanol as moving phase and 20 % (v/v) chloroform in heptane as stationary phase. The tritium labelled 7α-hydroxycholesterol had a specific activity of 4.3×10^5 c.p.m. when counted in an "infinitely thin" layer in a gas-flow counter.

Chromatographic separations of the bile acids were performed according to Sjövall and Norman [13,14]. The following two systems were used:

Phase system	moving phase	stationary phase
C(Ref.[14])	methanol/water 50/50	*iso*octanol/chloroform 1/1
F(Ref.[13])	methanol/water 55/10	chloroform/heptane 9/1

Each fraction was titrated with 0.02 N sodium hydroxide and an aliquot plated on a copper planchet for counting in a gas-flow counter. Accurate determinations of specific activity were performed by the gas-phase counting technique of Glascock [15].

RESULTS

2—3 mg of tritium-labelled 7α-hydroxycholesterol was dissolved in 0.2 ml of ethanol and brought into a colloidal suspension by the addition of 2 ml of 0.9 % sodium chloride containing 2 mg of sodium oleate. It was injected intraperitoneally into white rats with a bile fistula, and the bile collected.

After hydrolysis in 2 N sodium hydroxide in a sealed glass tube at 120° for 8 h the bile acids were extracted and isolated by chromatography with phase system C.

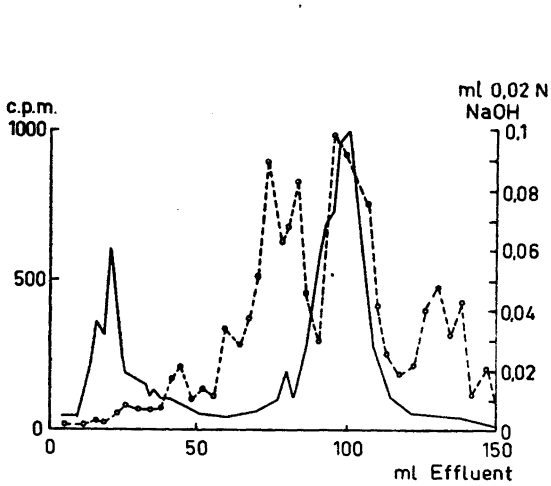


Fig. 1. Chromatogram of hydrolyzed bile after intraperitoneal injection of tritium-labelled 7α-hydroxycholesterol. Phase system C. Broken line: isotope determination. Solid line: titration values.

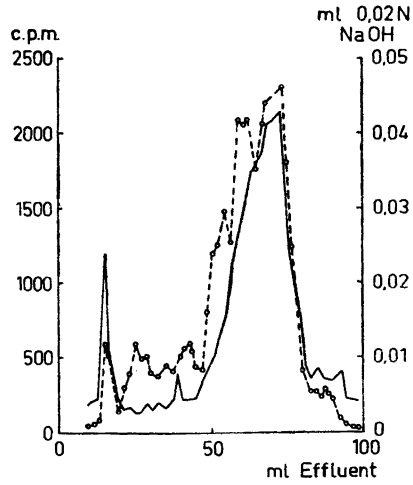


Fig. 2. Chromatogram of dihydroxy-acids after intraperitoneal administration of tritium-labelled 7α-hydroxycholesterol. Phase system F. Broken line: isotope determination. Solid line: titration values.

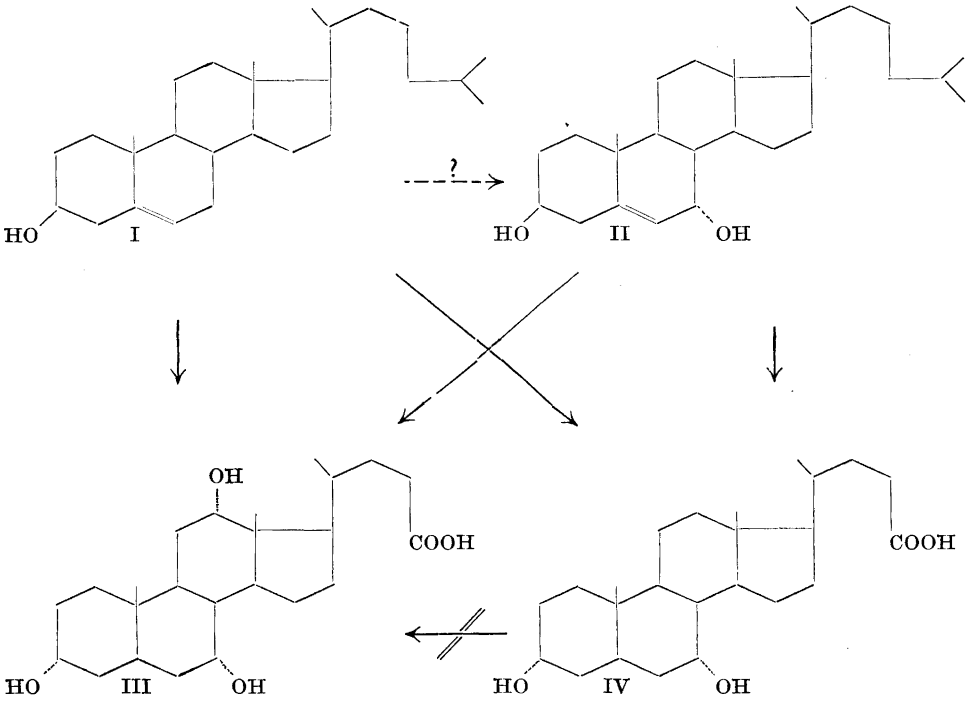


Fig. 3.

Fig. 1 shows a chromatogram where the titration peak of cholic acid appears at 80—120 ml. At the same position a peak of radioactivity is seen. This material was collected, rerun with the same chromatographic system, diluted with carrier cholic acid and recrystallized from different solvents. From each crystallization material was taken for determination of the specific activity by the gas-phase counting method [15]. It remained constant throughout five recrystallizations (EtOH, EtOAc, acetone/water) and the identity of the material with cholic acid seems established.

The material remaining in the column was eluted and rechromatographed on system F suitable for the separation of dihydroxycholanic acids. The chromatogram which is seen in Fig. 2 shows a titration peak at 50—80 ml caused by chenodeoxycholic acid in the bile. The identity of the labelled compound eluted at this position with chenodeoxycholic acid was established by recrystallization with carrier and determination of specific activity as for cholic acid.

In Fig. 1 labelled material is eluted before and after the cholic acid peak. When labelled chenodeoxycholic acid is administered to rats labelled metabolites appear at these locations [16,21] and in this experiment they probably also represent metabolites of the chenodeoxycholic acid.

DISCUSSION

In the rat cholesterol (I) gives rise to cholic acid (III) and chenodeoxycholic acid (IV) [16,17]. Work by Bergström and Sjövall [16] has, however, established that cholic acid is not formed by a 12α-hydroxylation of chenodeoxycholic acid. This type of reaction has been shown to take place when 3α,7α-dihydroxycoprostane is administered leading to the formation of cholic acid as well as of chenodeoxycholic acid [18]. This has brought further support to the view that in the formation of bile acids from cholesterol hydroxylations in the steroid nucleus precede the total degradation of the side chain [19].

Although the *in vivo* formation of 7α-hydroxycholesterol (II) from cholesterol has never been demonstrated, the results suggest the possibility that one of the primary steps in the degradation of cholesterol in the rat is a 7-hydroxylation.

A summary of some of the reactions studied in the rat is given in Fig. 3.

REFERENCES

1. Heymann, H. and Fieser, L. F. *Helv. Chim. Acta* **35** (1952) 631.
2. Bergström, S. and Wintersteiner, O. *J. Biol. Chem.* **141** (1951) 597.
3. Bergström, S. *Arkiv Kemi Mineral. Geol.* **16** A (1943) No. 10.
4. Haslewood, G. A. D. *Biochem. J. London* **33** (1939) 709.
5. Wintersteiner, O. and Ritzmann, J. R. *J. Biol. Chem.* **136** (1940) 697.
6. Hardegger, E., Ruzicka, L. and Tagmann, E. *Helv. Chim. Acta* **26** (1943) 2205.
7. Prelog, V., Ruzicka, L. and Stein, P. *Helv. Chim. Acta* **26** (1943) 2222.
8. Haslewood, G. A. D. *Biochem. J. London* **36** (1942) 389.
9. Bide, A. E., Henbest, H. B., Jones, E. R. H., Peevers, R. W. and Wilkinson, P. A. *J. Chem. Soc.* **1948** 1783.
10. Henbest, H. B. and Jones, E. R. H. *J. Chem. Soc.* **1948** 1792.
11. Danielsson, H. *Acta Chem. Scand. In press.*
12. Bloch, K. and Rittenberg, D. *J. Biol. Chem.* **149** (1943) 505.
13. Sjövall, J. *Acta Physiol. Scand.* **29** (1953) 232.
14. Norman, A. *Acta Chem. Scand.* **7** (1953) 1413.
15. Glascock, R. F. *Isotopic Gas Analysis for Biochemists*, Academic Press Inc., New York 1954.
16. Bergström, S. and Sjövall, J. *Acta Chem. Scand.* **8** (1954) 611.
17. Bergström, S. *Proc. Roy. Physiograph. Soc. Lund.* **22** (1952) No. 16.
18. Bergström, S. and Lindstedt, S. *Biochim. et Biophys. Acta* **19** (1956) 556.
19. Bergström, S. *Record Chem. Progr. Kresge-Hooker Sci. Lib.* **16** (1955) 63.
20. Bergström, S. and Lindstedt, S. *Acta Chem. Scand.* **10** (1956) 1044.
21. Mahowald, T. A., Elliott, W. W. and Thayer, S. A. *Federation Proc.* **14** (1950) 250.

Received February 2, 1957.

ACTA CHEMICA SCANDINAVICA 11 (1957) 421—426

On the Formation of Deoxycholic Acid from Cholic Acid in the Rabbit

Bile Acids and Steroids 48

SVEN LINDSTEDT and JAN SJÖVALL

Department of Physiological Chemistry, University of Lund, Lund, Sweden

The excretion of glycocholic acid and glycodeoxycholic acids in rabbits with a bile fistula has been studied. 30—40 h after operation glycodeoxycholic acid has almost disappeared. In rabbits with a bile fistula administered cholic acid-24-^{14}C is excreted unchanged in the fistula. In "whole" animals labelled cholic acid gives rise to labelled deoxycholic acid probably through the action of intestinal micro-organisms.

The main bile acids in rabbit bile are glycocholic and glycodeoxycholic acids [1-4]. When rabbit fistula bile collected immediately after surgery was fractionated by chromatography the amount of glycodeoxycholic acid was about ten times that of glycocholic acid [4]. On the other hand Okamura and Okamura were not able to isolate deoxycholic acid from a large amount of fistula bile [1].

In normal human bile, collected by duodenal tubage, cholic and deoxycholic acids are regularly present together with chenodeoxycholic acid [5]. The acids occur conjugated with glycin or taurin. When human bile from post-operative choledochal drainage was examined by paper chromatography no deoxycholic acid could be detected [6], nor could it be found in the duodenal contents of newborn babies [7].

The absence of deoxycholic acid from bile that has not been subjected to the action of intestinal microorganisms suggested the possibility that this acid is not primarily formed in the liver but arises from the attack of the microorganisms on some other bile acid, *e. g.* cholic acid. It has been found, that when ^{14}C-labelled cholic acid is administered to normal human subjects, and the bile acids fractionated a few days later, significant label is found in the dihydroxycholanic acid fraction [8].

In the present work the relationship between cholic and deoxycholic acids in the rabbit has been studied.

EXPERIMENTAL

Cholic acid-24-^{14}C had been prepared according to Bergström, Rottenberg and Voltz [9].

Bile fistula rabbits. Animals weighing 2—3 kg were anesthetized with ether and cannulation of the common bile duct was performed with a polythene tube just above the entrance of the common duct into the duodenum. No attempt was made to remove the gall-bladder. After operation the rabbits were given a subcutaneous infusion of 0.9 % sodium chloride at a rate of 10—20 ml per hour. This was found to be necessary as the animals otherwise died. The rabbits started eating after about one day and were fed on cabbage, carrots and oats and had access to 0.9 % sodium chloride as drinking water. When the rabbits were found to eat normally the infusion was no longer necessary. They were kept in cages that somewhat restricted their movements and could be kept in seemingly good condition for at least two weeks.

Chromatographic separation of the bile acids was carried out with reversed phase column chromatography [10] and by paper chromatography, by which technique the quantitative composition could also be determined [11,12]. Glycocholic and glycodeoxycholic acids were separated with ascending chromatography of the bile using ethylene chloride/heptane 70/30 (v/v) saturated with 70 % acetic acid as moving phase. After localization the acids were eluted and the amounts calculated from the absorbancy in 65 % sulfuric acid [13]. For identification purposes sulfuric acid absorption spectra were recorded with a self-recording spectrophotometer (Perkin-Elmer Spectracord 4 000).

RESULTS

Excretion of glycocholic and glycodeoxycholic acids in bile fistulas. The concentration of glycocholic and glycodeoxycholic acids in bile was followed in three animals. The values are given in Table 1 and show a marked decrease in the quotient between glycodeoxycholic and glycocholic acids.

A more detailed analysis of the course of the excretion was performed in animal No. 3 from which bile was collected in 2-h fractions with a fraction collector for the first 42 h following the operation and the bile acid concentration was determined in each fraction. These data have been used for con-

Table 1. Concentration of glycocholic and glycodeoxycholic acids in small samples of fistula bile collected at different times after operation.

Animal	Hours after operation	Glycocholic acid (GC) mg/100 ml	Glycodeoxycholic acid (GD) mg/100 ml	GD/GC
1.	0	33	655	19.9
	24	162	14	0.09
	72	407	8	0.02
2.	0	24	192	8.0
	12	8	30	3.8
	24	62	55	0.9
3.	0	30	420	14.0
	12	19	56	2.9
	24	186	65	0.35
	36	223	16	0.07

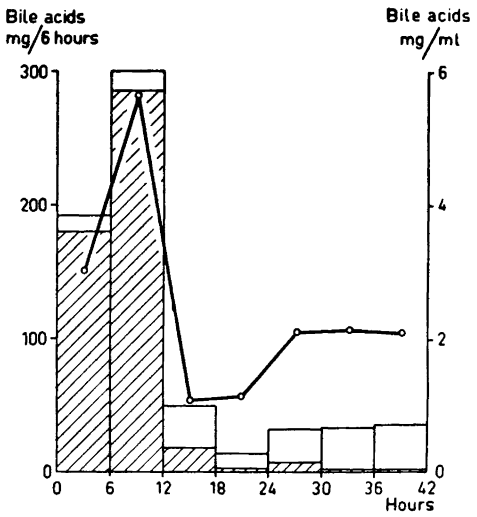


Fig. 1. Excretion of bile acids in a bile fistula rabbit. ▭ glycodeoxycholic acid □ glycocholic acid. O····· O glycocholic + glycodeoxycholic acid mg/ml.

structing Fig. 1 which shows the amounts of glycocholic and glycodeoxycholic acids excreted during each 6-h interval and also the mean bile acid concentration in these periods. A gradual shift in the proportion between the excreted amounts of glycocholic and glycodeoxycholic acids is obvious. Thus during the first periods glycodeoxycholic acid constitutes more than 90 % of the total bile acids excreted, while glycocholic acid is by far dominating in the later periods. The quotient between the amount of glycodeoxycholic acid and glycocholic acids excreted in different periods reached a maximum of 35 at 6—8 h after operation — in this period highly concentrated bile probably originating from the gall-bladder was obtained — and then decreased attaining a plateau level of 0.05 from 32 h onwards. The absorption spectra in 65 % sulfuric acid of material eluted from the glycodeoxycholic acid spot and of authentic glycodeoxycholic acid were recorded. The two spectra showed a good agreement in the first periods, while in the later a discrepancy was noted. Recordings from the first and the last 2-h intervals are shown in Figs. 2 and 3. Descending paper chromatograms in a medium suitable for the separation of glycodeoxycholic and glycochenodeoxycholic acids were run and showed that most of the acid excreted in small amount at the end of the experiment was not identical with glycodeoxycholic acid.

Fig. 1 further shows that the excreted amount of bile acids as well as their concentration fell during the experimental period. In the first 18 h a total of 550 mg of glycine conjugated bile acids was excreted. Most of this amount probably represents bile salts taking part in the enterohepatic circulation at the time of the operation.

Administration of cholic acid-24-^{14}C to rabbits with a bile fistula. Bile fistulas were made on two rabbits and cholic acid-24-^{14}C injected intraperitoneally 6 h and 36 h after the operation, respectively. The bile was collected for 3 h after the injection and hydrolyzed for 8 h at 120° C in a sealed glass tube.

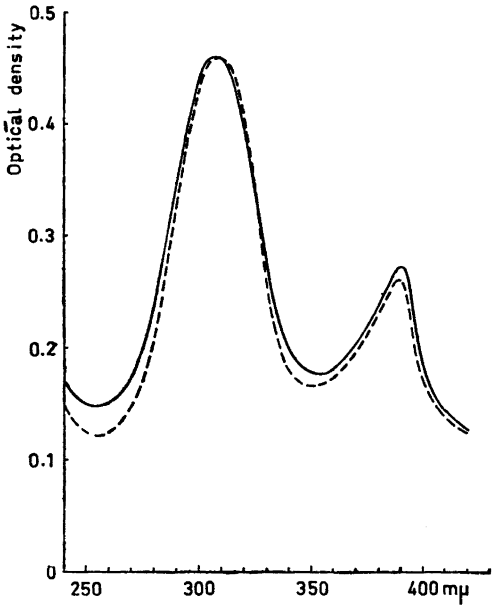


Fig. 2. Absorption spectra of glycodeoxycholic acid (——) and material from the glycodeoxycholic acid spot (0—2 hours) (- - -). Samples heated simultaneously for 10 minutes at 60° C in 65 per cent sulfuric acid.

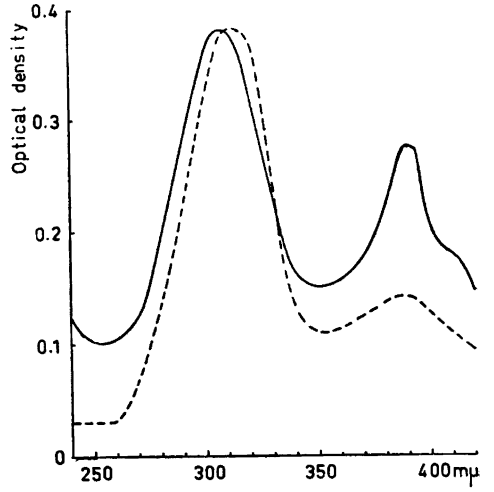


Fig. 3. Absorption spectra of glycodeoxycholic acid (——) and material from the glycodeoxycholic acid spot (40—42 hours) (- - -). Samples heated as in Fig. 2. The difference between the spectra of authentic glycodeoxycholic acid in Fig. 2 and Fig. 3 is due to minor variations in the concentration of the sulfuric acid.

A chromatogram of the free acids from the first rabbit is shown in Fig. 4. One titration peak is seen at 15—30 ml caused by cholic acid and one at 50—80 ml due to deoxycholic acid. All the activity is confined to the cholic acid peak whereas none is present in the deoxycholic acid. In the second rabbit the same result was obtained except for the almost complete absence of a titration peak at the position of deoxycholic acid.

Administration of cholic acid-24-^{14}C to "whole" animals. Two rabbits were injected intraperitoneally with labelled cholic acid. Three days later a bile fistula was made on the animals. The bile was collected, hydrolyzed and subjected to chromatography as above. The results from one of the rabbits is shown in Fig. 5. Only traces of radioactivity remain at the position of cholic acid, whereas practically all of it is found in the deoxycholic acid band. A minor amount appeared as a less hydrophilic compound. The deoxycholic acid was crystallized from acetic acid/water and gave 30 mg of crystals, m. p. 169—70 °C and a specific activity of 1 200 c.p.m. which was found to remain unchanged on further recrystallization from different solvents. The less hydrophilic compound has not been further investigated.

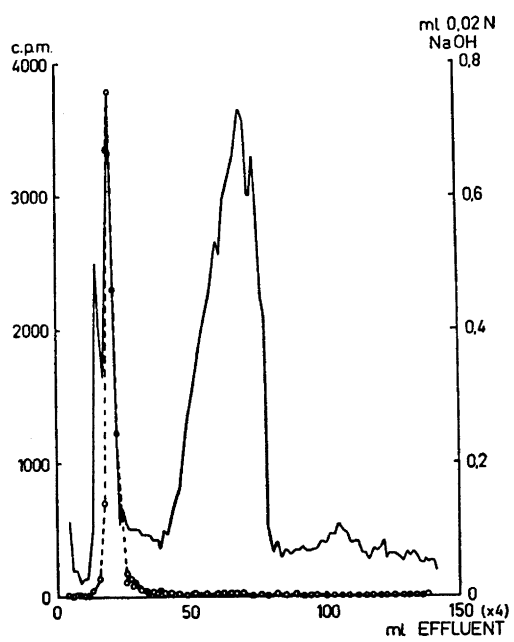


Fig. 4. Chromatography of hydrolyzed bile from a bile fistula rabbit injected intraperitoneally with cholic acid-24-^{14}C 6 hours after operation. Phase system: Moving phase: methanol/water 55/45. Stationary phase: chloroform/heptane 9/1. Solid line: titration values. Broken line: radioactivity.

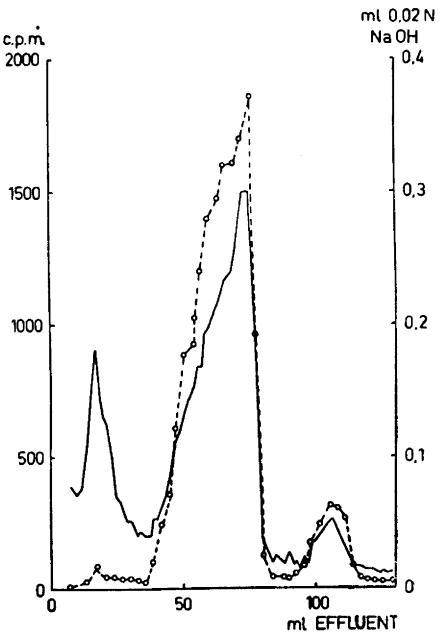


Fig. 5. Chromatography of hydrolyzed bile from a bile fistula rabbit, injected intraperitoneally with cholic acid-24-^{14}C 3 days before operation. Phase system: same as in Fig. 4. Solid line: titration values. Broken line: radioactivity.

DISCUSSION

The transformation of cholic acid into deoxycholic acid has been postulated by Japanese workers. Their conclusions, however, are mainly based on experiments in which as much as 30 g of the bile acid was fed and small amounts of the metabolites isolated from the urine (for a summary see Refs.[14,15]).

The disappearance of deoxycholic acid from bile fistula bile in 30—40 h clearly suggests that this acid is not an excretory metabolic product of the rabbit liver. The possibility remains, however, that a change in the proportion between the bile acids formed in the liver is induced by the continuous withdrawal of the bile. The very rapid disappearance of the deoxycholic acid makes this assumption less likely as do also experiments with rats where the proportion between cholic and chenodeoxycholic acid remains mainly unchanged when a bile fistula is made [16].

When labelled cholic acid is administered intraperitoneally into a rabbit with a bile fistula it is absorbed from the peritoneal cavity into the portal circulation passing through the liver into the bile fistula. If the liver was able to transform cholic acid into deoxycholic acid one would expect the label to

appear in the deoxycholic acid, even though only one passage through the liver has taken place. In the rat, *e. g.*, where certain transformations of the bile acids have been studied (*e. g.* deoxycholic acid → cholic acid; chenodeoxycholic acid → hydroxylated metabolites; *cf.* Ref.[17]) one passage through the liver suffices to give a high percentage of conversion.

When cholic acid is given to whole animals the acid will take part in the enterohepatic circulation and thus be subjected to the action of the intestinal microorganisms. It is well known that they effectively attack bile acid molecules resulting in the formation of various metabolites (*cf.* Refs.[18,19]). They may therefore be responsible for the conversion of cholic acid into deoxycholic acid or into some intermediate which is then converted to cholic acid in the liver. This is made very probable by the experiments in which labelled cholic acid was allowed to circulate for three days in the intact animal. Practically all of the recovered activity was then found in the deoxycholic acid.

The results of this work once more show the necessity of considering the influence of intestinal microorganisms in studies of cholesterol and bile acid metabolism.

This work has been supported by grants from *Knut och Alice Wallenbergs Stiftelse* and the *Medical Faculty, Lund.*

The technical assistance of Miss Irene Lindell is gratefully acknowledged.

REFERENCES

1. Okamura, T. and Okamura, T. *Hoppe-Seylers Z. physiol. Chem.* **199** (1930) 11.
2. Kishi, S. *Ibid.* **238** (1936) 210.
3. Sekitoo, T. *Ibid.* **199** (1931) 225.
4. Ekdahl, P. H. and Sjövall, J. *Acta Physiol. Scand.* **34** (1955) 287.
5. Sjövall, J. *To be published.*
6. Ekdahl, P. H. and Sjövall, J. *To be published.*
7. Enkrantz, J. C. and Sjövall, J. *To be published.*
8. Lindstedt, S. *To be published.*
9. Bergström, S., Rottenberg, M. and Voltz, J. *Acta Chem. Scand.* **7** (1953) 481.
10. Sjövall, J. *Acta Physiol. Scand.* **29** (1953) 232.
11. Sjövall, J. *Arkiv Kemi* **8** (1955) 317.
12. Sjövall, J. *Acta Chem. Scand.* **10** (1956) 1051.
13. Eriksson, S. and Sjövall, J. *Arkiv Kemi* **8** (1955) 311.
14. Haslewood, G. A. D. *Physiol. Rev.* **35** (1955) 178.
15. Tayeau, F. *Exposés ann. biochim. méd.* **10** (1949) 251.
16. Eriksson, S. *Acta Chem. Scand.* **10** (1956) 156.
17. Bergström, S. *Record Chem. Progr. Kresge-Hooker Sci. Lib.* **16** (1955) 63.
18. Lindstedt, S. and Norman, A. *Acta Physiol. Scand.* **34** (1955) 1.
19. Ekdahl, P. H. and Sjövall, J. *Ibid.* **34** (1955) 329.

Received February 1, 1957.

ACTA CHEMICA SCANDINAVICA 11 (1957) 427—438

Metabolism of 2-Methylstearic Acid in the Rat

N. TRYDING and G. WESTÖÖ

Department of Physiological Chemistry and Institute of Organic Chemistry, University of Lund, Lund, Sweden

The intestinal absorption and the metabolism of 2-methyl[1-^{14}C]-octadecanoic acid were found to be very similar to those of the ordinary, long, straight chain fatty acids. For the first time, however, a small amount of metabolites from 2-methylstearic acid could be isolated from the urine and identified as 2-methyladipic (1.1 %) and 2-methylsuccinic acid (0.6 %).

In extensive studies on dogs Weitzel [1] investigated the effect on metabolism of monoalkylsubstitution in the α-position of long chain fatty acids. He found that 2-ethylstearic acid was excreted in the urine to 1.2 % as 2-ethyladipic acid. Analogously he showed that 2-propylstearic acid and 2-butylstearic acid gave rise to 2-propyladipic acid (5.2 %) and 2-butyladipic acid (6.5 %), respectively. With the methods used Weitzel found that, in contrast to these higher fatty acids with comparatively large α-substituents, α-methyl-substituted acids (fed in the ester form) did not produce any short dicarboxylic acids in the urine [2,3].

Continuing the investigation on the metabolism of long, branched chain fatty acids started with 2,2-dimethylstearic acid [4] and 2,2-dimethylnonadecanoic acid [5], we have now studied 2-methyl[1-^{14}C]stearic acid. It was given *per os* to intact rats or rats with thoracic duct fistulas. The isotopic distribution in the neutral fat, phospholipids and unesterified fatty acids of the lymph has been investigated. In addition the isotope excretion has been followed in the expired carbon dioxide, the feces and the urine. The metabolites were isolated by partition chromatography and identified by repeated recrystallizations with inactive, synthetic material.

When the 2-methyl[1-^{14}C]stearic acid was fed to unanesthetized rats with lymph fistulas [6], about 60 % of the absorbed activity was recovered in the lymph lipids. This is about the same figure as those found in similar experiments with other, long chain, branched or unbranched fatty acids. The main transport form of the 2-methyl[1-^{14}C]stearic acid was as glycerides (89—96 % of the total lymph fat activity). Only small amounts of cholesterol esters were present, and just a few per cent of the acid (Table 2) was found to be in unesterified form (3.7 %) or incorporated into phospholipids (4.0 %).

The specific activities of the unesterified fatty acids were in three experiments with 2-methyl[1-^{14}C]stearic acid 75, 36 and 14 % of the specific activities of the neutral fat fatty acids (Table 2). These figures were always found to be less than 100 % for ordinary straight chain fatty acids, whereas the corresponding values for the 2,2-dimethyl[1-^{14}C]nonadecanoic acid were 200—300 %. Thus the distribution of the lymph activity between neutral fat and unesterified fatty acids was the same as for ordinary straight chain fatty acids [7] or 15,15-dimethylpalmitic acid *, and it differs from fatty acids with two methyl groups in the α-position (*i. e.*, 2,2-dimethylstearic acid [4], 2,2-dimethylnonadecanoic acid [5] and 2,2,17,17-tetramethylstearic acid [8]).

The feces were collected daily from each rat and their isotope contents determined after saponification and extraction of the acids with ether. In thirteen experiments between 3 and 31 % (mean 13 %) of the fed activity could be recovered in the feces during four days after the administration of 2-methyl[1-^{14}C]stearic acid.

Almost all the active material in the feces was identified as the 2-methylstearic acid. Consequently, throughout this investigation, the absorbed activity has been calculated as the difference between the fed activity and the activity recovered in the feces. — However, a small amount of the fecal activity (in one experiment less than 0.2 %) chromatographically appeared as 2-methylsuccinic and 2-methyladipic acid, identical with the urinary metabolites of 2-methyl stearic acid (see below). Earlier, 2,2-dimethylnonadecanoic acid has been shown to produce dicarboxylic acids in the feces as well as in the urine [5].

After feeding carboxyl-labelled 2-methylstearic acid to a rat, about 25 % of the absorbed activity was found in the expired carbon dioxide in two days. The same value was found in a parallel experiment with [1-^{14}C]stearic acid. From these data one methyl group in the α-position does not seem to hinder the oxidation of the higher fatty acids. In contrast, after administration of 2,2-dimethyl[1-^{14}C]stearic acid [4] and 2,2,17,17-tetramethyl[1-^{14}C]stearic acid [8], less than 3 % of the absorbed activity was excreted as carbon dioxide. The β-oxidation from the carboxyl end of the molecule is not possible, because the two hydrogen atoms on the α-carbon atom are substituted with methyl radicals. The different metabolism of 2-methylstearic acid and 2,2-dimethylstearic acid is also strongly reflected in the isotope recoveries in the urine.

The urine from rats fed 2-methyl[1-^{14}C]stearic acid has been found to contain 1.6—3.5 % of the absorbed activity (Table 6). (After feeding [1-^{14}C]-palmitic acid to rats less than 0.5 % of the activity can be recovered from the urine [9]). By partition chromatography and repeated recrystallizations with synthetic unlabelled compound, two of the active substances have been identified as 2-methyladipic acid (0.8—1.7 % of the absorbed activity) and 2-methylsuccinic acid (0.4—0.9 %). They were excreted partly in conjugated form. The methyl side chain of 2-methylstearic acid thus has some, although a minor effect in impeding the β-oxidation from the carboxyl end.

* To be published.

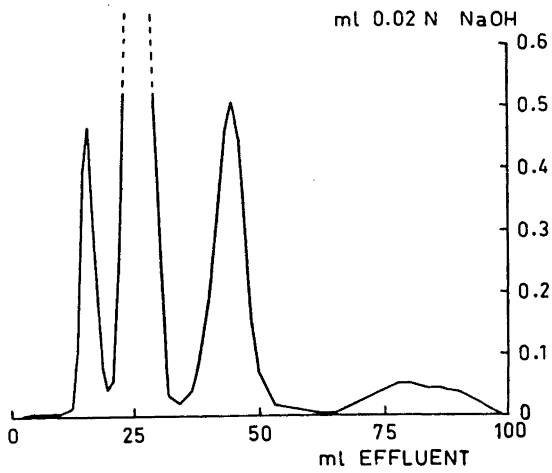


Fig. 1. Partition chromatography of part (39 mg) of an acid mixture obtained after Kolbe electrolysis of methyl hydrogen succinate and sodium 3-cyanobutyrate. Phase system C. Supporting medium: 4.5 g of hydrophobic kieselguhr.

SYNTHESES

2-Methyl[1-^{14}C]octadecanoic acid. Two different methods were used for the preparation of the labelled 2-methyloctadecanoic acids. The comparatively weakly radioactive product (0.13 μC/mg) was prepared by a Kolbe electrolysis of palmitic acid and sodium 3-[^{14}C]cyanobutyrate according to Westöö [10], the strongly active one (6.5 μC/mg) was made from inactive 2-methyloctadecanoic acid (prepared by the above method) by exchange of the carboxyl group for bromine by degradation of the silver salt (Rottenberg [11]) and reaction of the 2-bromooctadecane formed with K^{14}CN.

Silver 2-methyloctadecanoate (0.50 g) and silver acetate (0.20 g) were thoroughly mixed, pulverized and dried at 0.1 mm Hg over P_2O_5. Dry ethyl bromide (4 ml) was added and into the boiling mixture 0.13 ml of dry bromine was dropped. The boiling was continued for half an hour. Part of the ethyl bromide was distilled off, the mixture was filtered, and the filtrate was shaken with potassium iodide solution, water, sodium thiosulphate solution, and water again. It was dried over anhydrous sodium sulphate and filtered. After removal of the solvent, the residue was dissolved in light petroleum and chromatographed on 2.5 g of alumina. The front band (0.35 g) contained the 2-bromooctadecane.

Crude 2-bromooctadecane (0.11 g) was heated with K^{14}CN (0.017 mg, 0.50 mC), ethanol (2.5 ml) and water (0.7 ml) in a sealed glass tube at 95° for 24 h. The nitrile formed was hydrolyzed by heating with an excess of 10 % potassium hydroxide solution (ethanol-water, 4:1) in an autoclave at 130° for 4 h. Part of the ethanol was removed by distillation, and the rest of the solution was acidified with dilute hydrochloric acid and extracted with ether. The ether solution was washed with water, dried with sodium sulphate and evaporated to dryness. The product obtained was chromatographed according to system A (Table 1).

2-Methyladipic acid. Methyl hydrogen succinate (10.5 g) and sodium 3-cyanobutyrate (1.0 g) were electrolyzed in methanol (400 ml). The electrolysis was carried out as described earlier [5]. The slightly alkaline solution (pH 8) was evaporated to 50 ml. The products of the electrolysis were hydrolyzed in 2 N alcoholic potassium hydroxide for 2 h. The methanol was evaporated and after acidification the hydrolysate was extracted with ether. The acids obtained (4.4 g) were chromatographed three times according to system

C (Table 1). They were eluted in the following order: succinic and 2-methylsuccinic acid (in the front band), adipic, 2-methyladipic acid and 2,5-dimethyladipic acid (*cf.* Fig. 1). The 2-methyladipic acid (0.36 g) was recrystallized repeatedly from water and from benzene-light petroleum; m. p. 61° (equiv. wt. 80.1).

CHROMATOGRAPHIC SYSTEMS

The chromatographic systems used in this investigation are summarized in Table 1. System A was used for the isolation and identification of 2-methylstearic acid. Phase system B was found suitable for the separation of dicarboxylic acids with five to nine carbon atoms. The phases used in system C are more polar than those of system B, which enables also C_4-dicarboxylic acids to be chromatographed. The ordinary partition chromatography (with phase system D) was used as an alternative to the reversed phase system C.

Table 1. Chromatographic systems.

System	According to	Supporting medium	Stationary phase	Moving phase
A	Howard and Martin [12]	Hydrophobic kieselguhr (Hyflo supercel treated with dimethyldichlorosilane)	Paraffin oil (25 ml)	Acetone: water 7:3, v/v (210 ml: 90 ml)
B	Bergström and Sjövall [13] for the separation of free bile acids. Also used by Bergström, Borgström, Tryding and Westöö[4] for the separation of dicarboxylic acids	see above	*iso*-octanol (2-ethylhexanol)-chloroform 1:1,v/v (25 ml: 25 ml)	methanol: water 1:3, v/v (75 ml: 225 ml) (modified from 2:3, v/v)
C	Norman [14] for the separation of conjugated bile acids	see above	*n*-butanol (100 ml)	distilled water (300 ml)
D	Isherwood [15]	silica gel prepared according to Nijkamp [16]	0.5 N sulfuric acid (50 ml)	butanol : chloroform 1:9, v/v (30 ml: 270 ml)

The volumes of solvents given in Table 1 for each system were mixed in a separatory funnel and equilibrated at room temperature (23° C) before use. Four ml of the stationary phase were used per 4.5 g of supporting medium. Generally 9 g columns were made with solvent systems B and C, while all the chromatograms with phase system A and D were run on 4.5 g columns. The internal diameter of the chromatographic tubes used was 12 mm. The techniques of fraction collection, titration and determination of ^{14}C-activity have been described earlier [4].

METABOLIC EXPERIMENTS

A 3.6 % stock solution (I) of 2-methyl[1-^{14}C]stearic acid (specific activity 110 000 cpm/mg) in olive oil was prepared and found to have a specific activity of 3 900 cpm/mg.

Another olive oil solution (II) contained 0.045 % of the strongly active 2-methyl-[1-^{14}C]stearic acid (s. a. 5 400 000 cpm/mg). The specific activity of this solution was 2 400 cpm/mg. No differences were found in the absorption or metabolism of the two stock solutions.

Radioactivity determinations were performed with a gas flow counter (background effect 30 cpm) generally after direct plating of the samples on aluminium planchets.

The animals used in these investigations were white, adult, male rats weighing about 250 grams.

Administration of 2-methylstearic acid to rats with lymph fistula

Unanesthetized rats provided with a thoracic duct fistula [6] were fed 1 ml of the olive oil solution containing 2-methylstearic acid (stock solution I). The general procedure for the collection, extraction and separation of the lymph lipids has been reported earlier from this institute [6,7]. From Table 2 it is seen that the absorption of 2-methyl[1-^{14}C]-stearic acid varied from 69 to 96 % of the fed amount. However, the percentage of absorbed activity recovered in the lymph was relatively constant, about 60 % in three rats out of four. Almost all the lymph activity (96 % for rat No. 1, Table 2) could be recovered during the first 12 h after the administration, but the values given in the table were determined on 24-h-specimens.

Table 2. Recovery of activity in lymph fatty acids after oral administration of 2-methyl-[1-^{14}C]stearic acid to rats.

Rat No.	Per cent of administered activity absorbed	Per cent of absorbed activity recovered in lymph fatty acids	Per cent of lymph fat activity found as		
			unesterified fatty acids	neutral fat	phospholipids
1	85.3	61.2	96.5		3.5
2	69.3	62.5	5.0	88.7	6.3
3	95.7	63.2	2.4	95.6	2.0
4	91.9	45.1	3.7	92.1	4.2

Two of the experiments (Rats No. 3 and 4) complete an investigation by Borgström and Tryding on the free fatty acid content of rat thoracic duct lymph [7]. Table 3 summarizes the results of these two experiments. — Cholesterol esters could be present only in very small amounts, as only traces of the lymph fat activity could be eluted with light petroleum from a silicic acid column [17].

Table 3. Weight of different lymph fat fractions and specific activity of their fatty acids.

Rat No.	Neutral fat		Free fatty acids		s.a. of free fatty acids in % of s.a. of neutral fat fatty acids
	Weight mg	Spec. activity	Weight mg	Spec. activity	
3	690	70	48.4	25	36
4	784	50	22.6	7	14

Isotope recovery in feces after feeding 2-methyl-[1-^{14}C]stearic acid to rats

The feces from the rats were collected daily during at least four days after the oral administration of the labelled acid. After homogenization they were hydrolyzed with 5 N alcoholic potassium hydroxide. The alcohol was evaporated and the acidified mixture was extracted three times with three volumes of peroxide-free ether. In the feces from twelve animals between 3 and 31 % of the fed activity was recovered (*cf.* Tables 2 and 4).

Table 4. Isotope recovery in the urine from rats fed 2-methyl[1-^{14}C]stearic acid.

Rat No.	Per cent of administered activity absorbed	Per cent of absorbed activity recovered in the urine		
		total	chromatographically identified as	
			2-methylsuccinic acid	2-methyladipic acid
5	89.5	1.9		
6	73.3	1.6	0.5	0.9
7	94.2	2.7	0.8	1.1
8	91.1	3.1	0.8	1.5
9	84.8	3.5	0.9	1.7
10	93.2	2.3	0.4	1.0
11	80.9	2.2	0.5	0.8
12	97.0	2.3	0.6	1.1

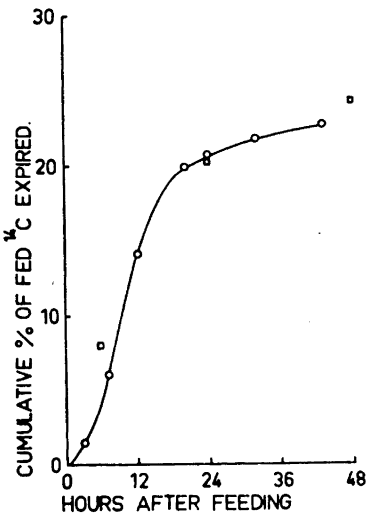


Fig. 2. Recovery of ^{14}C in expired carbon dioxide after feeding 2 methyl-[1-^{14}C]stearic acid (circles) and [1-^{14}C]stearic acid (squares) to rats.

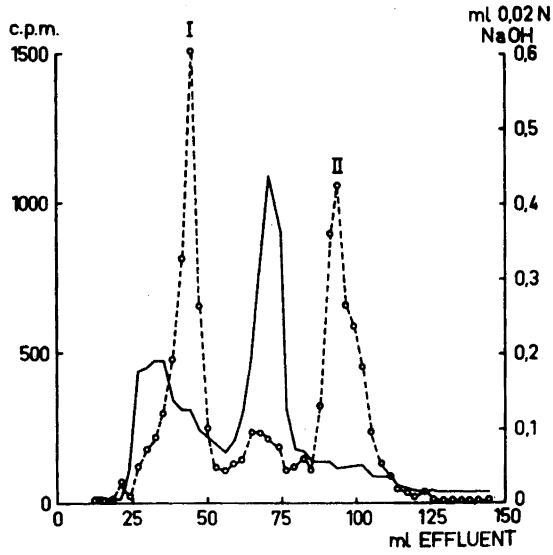


Fig. 3. Chromatography of part of an ether extract of urine from Rat No. 11. The titration peaks are caused by ordinary urine metabolites, as no carrier substances were added. Phase system B. Supporting medium: 9 g of hydrophobic kieselguhr; ——— titration curve, — — — c.p.m./fraction. Band I contains α-methylsuccinic acid and conjugated products.

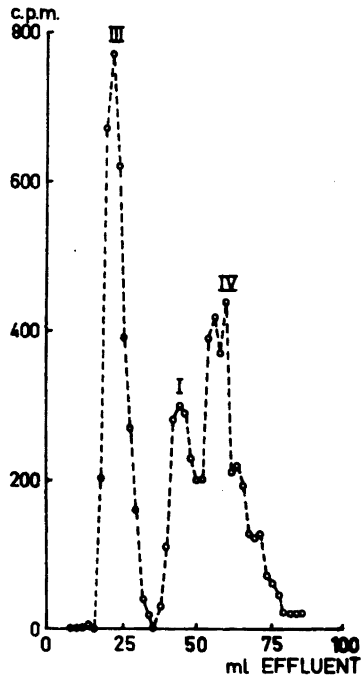


Fig. 4. Rechromatography of band I, Fig. 3. Phase system D. Supporting medium: 4.5 g of silica gel. Band I represents α-methylsuccinic acid. Band III and IV contain conjugated metabolites.

In one additional experiment the isotope contents of the feces were determined during 15 days after the administration of 1 ml of the olive oil solution (I) containing 3.6 % of 2-methyl[1-^{14}C]stearic acid. The feces from the first day after the feeding contained 8 % of the fed activity. During the second, third and fourth day 4.3, 3.4 and 1.3 % respectively appeared in the feces. In ten days the total isotope recovery was 21 %. In the next five days only 0.8 % of the fed activity was found in the feces.

The feces excreted by a rat during the first day after the administration of 2-methylstearic acid was saponified and extracted as described above. The ether extract contained 5.7 % of the fed activity. When half of this extract was chromatographed according to system A, 95 % of the activity was found unchanged in the band of 2-methylstearic acid, which appeared at 60 ml on a 4.5 g column. The other half of the ether extract was subjected to partition chromatography according to system C.

A small amount (less than 0.2 %) of the activity was found at the positions of 2-methylsuccinic and 2-methyladipic acid.

Isotope recovery in expired carbon dioxide after oral administration of carboxyl-labelled 2-methylstearic and stearic acids

A male rat weighing 250 g (Rat No. 5, Table 4) was given through a stomach tube 1 ml of the olive oil solution (I), corresponding to 0.3 ml per dm^2 of body surface (Lee [18]).

The isotope content of the expired carbon dioxide was determined with the technique described earlier [4]. The accumulation curve is shown in Fig. 2.

Another 250 g rat from the same litter was fed 1 ml of an olive oil solution of [1-^{14}C]-stearic acid with a specific acvitity of 130 000 cpm/mg *.

* Kindly placed at our disposal by Professor S. Bergström.

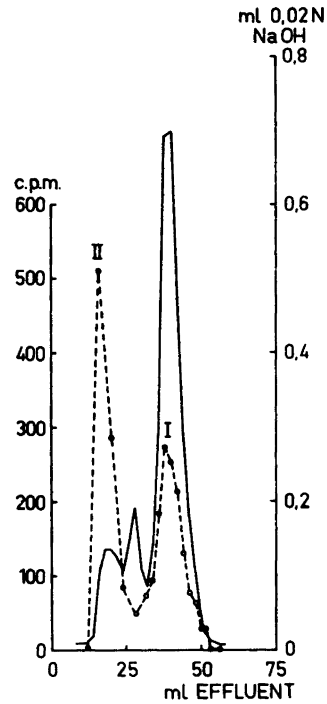


Fig. 5 *. Partition chromatography of metabolites in hydrolyzed urine together with unlabelled 2-methylsuccinic acid (5.4 mg). Phase system D. Supporting medium: 4.5 g of silica gel. ——— titration curve, — — — c.p.m./fraction.

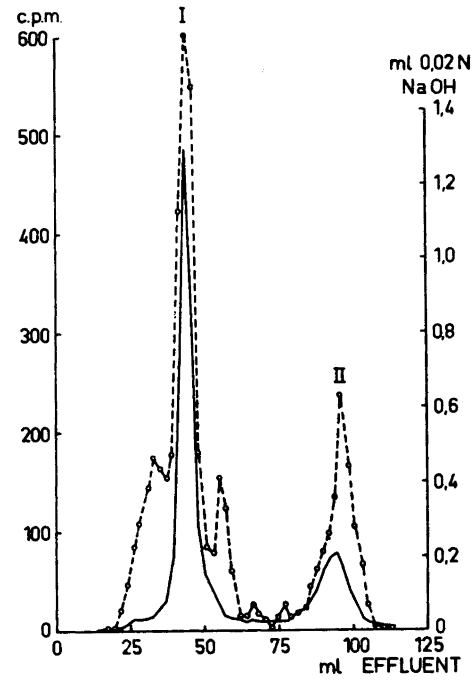


Fig. 6 *. Rechromatography of the material from the chromatogram shown in Fig. 5 and a parallel chromatogram together with synthetic 2-methyladipic acid (2.4 mg). Phase system C. Supporting medium: 9 g of hydrophobic kieselguhr; ——— titration curve, — — — c.p.m./fraction.

In four days 31.8 % of the fed activity was recovered in the feces. The CO_2 of the expired air was collected during six, twenty-four and forty-eight hours after the administration of the acid. From Fig. 2 it is seen that the $^{14}CO_2$-excretion in per cent of the absorbed activity was about the same for the two acids.

Isotope recovery in urine and identification of isotopic urinary compounds after the administration of 2-methyl[1-^{14}C]stearic acid

In order to obtain the urine completely free from fecal radioactive impurities a plastic funnel was sewn on to the cutis around the penis of the rat. The urine was collected into a flask with toluene. The activities recovered in the urine collected for 3 days after the administration of 2-methyl[1-^{14}C]stearic acid are given in Table 4. More than 75 % of the total urinary activity was excreted during the first day. The urine was acidified with hydrochloric acid and extracted three times with two volumes of peroxide-free ether. After that the urine was either extracted with butanol or continuously with ether for 24 h.

* See footnote p. 436.

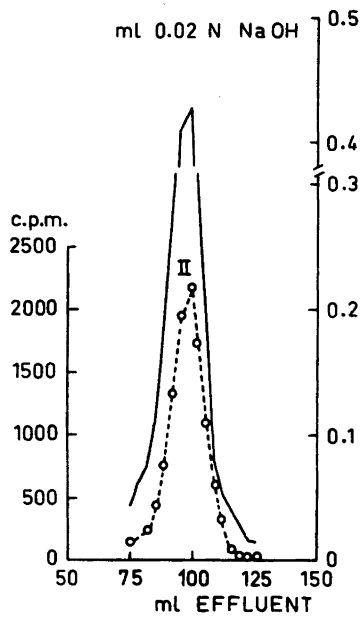


Fig. 7 *. Chromatography of an ether extract of hydrolyzed urine from Rat No. 10 together with unlabelled 2-methyladipic acid (4.0 mg). Phase system C. Supporting medium: 9 g of hydrophobic kieselguhr; ——— titration curve, — — — c.p.m./fraction.

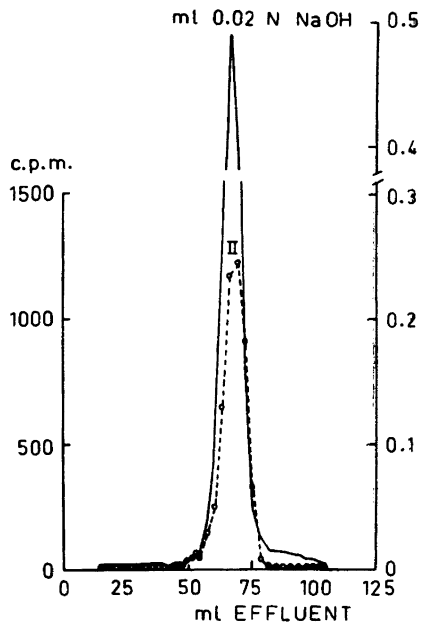


Fig. 8 *. Rechromatography of material from the active band II in a chromatogram with phase system C together with synthetic 2-methyladipic acid (2.9 mg). Phase system B. Supporting medium: 9 g of hydrophobic kieselguhr; ——— titration curve, — — — c.p.m./fraction.

The urine from Rat No. 11 was divided into two equal parts. One of these was extracted three times with two volumes of ether. The extract (17.6 mg) contained 0.8 % of the absorbed activity. Part of the ether extract was chromatographed according to system C as shown in Fig. 3. Two distinct active bands were found containing about the same amount of activity.

The other half of the urine was hydrolyzed with 2 N potassium hydroxide before acidification and analogous ether extraction.

The ether extract of the hydrolyzed urine contained 30 % more activity than the corresponding extract of unhydrolyzed urine. This finding indicates the existence of conjugated active products. The chromatogram showed two main active peaks as for the unhydrolyzed urine. However, the relation between the active bands Nos. I and II (Fig. 3) was changed. In the chromatogram of the hydrolyzed urine the second active

* The isotope and titration curves do not coincide exactly in the chromatograms of this investigation (see Figs. 5—8). The ^{14}C-labelled dicarboxylic acids seem to be somewhat less polar than the corresponding unlabelled compounds. Thus the ^{14}C-labelled acids are inclined to come out a little more slowly from the 9 g columns with the reversed phase systems B and C than does the unlabelled material (Figs. 6—8). In the ordinary partition chromatographic system (D) the 2-methyl[1-^{14}C]succinic acid tends to move more rapidly than the added unlabelled carrier (Fig. 5). These findings are in good agreement with the recent reports by Piez and Engle [19,20] on the ^{14}C-effect in amino acids, as demonstrated on the ion-exchange resin Dowex 50. An isotope effect has earlier been noticed for tritium-labelled organic acids with partition chromatography [21].

band contained 7 520 cpm (0.42 % of the absorbed amount) while 4 720 cpm (0.26 %) were found in the first band.

The first day urine from Rat No. 12 was extracted continuously with ether. The extract containing 51 000 cpm, *i. e.*, 1.9 % of the absorbed activity, was chromatographed on a 9 g column with phase system C. The two main peaks (23 000 cpm each) appeared as in Fig. 3, but in addition there was a front peak (4 000 cpm). This active material, which we have not yet identified, was found to be present also in hydrolyzed urine. After the continuous ether extraction of the first day urine, 5 600 cpm remained in the water phase. After alkaline hydrolysis, however, one half of this activity could be extracted with ether.

When the first band of the unhydrolyzed urine was rechromatographed according to system D, it was found to be heterogeneous, as it was split into three active peaks (Fig. 4). After hydrolysis, however, only two active bands remained (*cf.* Fig. 5). One of them (I) was found at the position of the titration peak of added, unlabelled 2-methylsuccinic acid (5.3 mg), the other one (II) was moving with the front.

When the material of this and a parallel chromatogram was rechromatographed with the reversed phase system C together with 2.4 mg of synthetic unlabelled 2-methyladipic acid, the titration peaks of 2-methylsuccinic acid (I) and 2-methyladipic acid (II) were found at the same positions as the two main active peaks (Fig. 6).

The ether extract of the hydrolyzed urine from Rat No. 10 was chromatographed on a 9 g column with phase system C together with 4 mg of unlabelled 2-methyladipic acid. The titration peak of this acid corresponded to the active peak II_1 (Fig. 7). Also in a chromatogram with phase system B the titration curve of synthetic 2-methyladipic acid (2.9 mg) was found at the same position as the active band II from the urine of Rat No. 7 (Fig. 8).

The ether extracts of the hydrolyzed urine from Rats No. 8 and 9 were chromatographed separately according to system B. The material from the second active bands (*cf.* Fig. 3) was rechromatographed together with 19.8 mg of inactive 2-methyladipic acid on a 9 g column of hydrophobic kieselguhr with phase system C. After addition of 132.7 mg of inactive synthetic 2-methyladipic acid, the material of the single active band was crystallized twice from water and twice from benzene-light petroleum alternately (Table 5). The specific activity was shown to remain constant. Consequently one of the metabolites of 2-methylstearic acid was 2-methyladipic acid.

Analogously the first active bands from two chromatograms with phase system C were rechromatographed according to system D before crystallization together with unlabelled 2-methylsuccinic acid (125.0 mg). The specific activity remained constant during four crystallizations from hydrochloric acid and from ether-benzene alternately

Table 5. Identification of 2-methyladipic acid in the urine of rats fed 2-methylstearic acid. Specific activity of material from the active band II of chromatogram of urinary extracts with phase system B, after rechromatography in system C recrystallized with inactive 2-methyladipic acid.

Recrystallization from	Crystal weight, mg	Counts/min/mg
water	101.2	390
benzene-light petroleum	76.0	375
water	50.3	355
benzene-light petroleum	35.4	361

Table 6. Identification of 2-methylsuccinic acid in the urine of rats fed 2-methylstearic acid. Specific activity of material from the active band I of chromatograms of urinary extracts with phase system C, after rechromatography in system D recrystallized with inactive 2-methylsuccinic acid.

Recrystallization from	Crystal weight, mg	Counts/min/mg
hydrochloric acid	98.4	154
ethyl ether-benzene	60.0	145
hydrochloric acid	41.0	150
ethyl ether-benzene	20.3	150

(Table 6). Thus 2-methylsuccinic acid was another urinary metabolite of 2-methylstearic acid. The amounts of activity which were extracted from the urine of the different rats and chromatographically identified as 2-methylsuccinic acid or 2-methyladipic acid are given in Table 4 in per cent of the absorbed activity.

We are indebted to Miss Kerstin Sjöström for valuable technical assistance. The financial support of *Statens naturvetenskapliga forskningsråd, Knut och Alice Wallenbergs Stiftelse* and the *Medical Faculty of the University of Lund* is gratefully acknowledged.

REFERENCES

1. Weitzel, G. *Hoppe-Seylers Z. physiol. Chem.* **287** (1951) 254.
2. Weitzel, G., Fretzdorff, A. M., Wojahn, J., Savelsberg, W. and Thomas, K. *Nature* **163** (1949) 406.
3. Weitzel, G., Fretzdorff, A. M. and Wojahn, J. *Naturwiss.* **37** (1950) 68.
4. Bergström, S., Borgström, B., Tryding, N. and Westöö, G. *Biochem. J. London* **58** (1954) 604.
5. Tryding, N. and Westöö, G. *Acta Chem. Scand.* **10** (1956) 1234.
6. Bergström, S., Blomstrand, R. and Borgström, B. *Biochem. J. London* **58** (1954) 600.
7. Borgström, B. and Tryding, N. *Acta Physiol. Scand.* **37** (1956) 127.
8. Tryding, N. and Westöö, G. *Arkiv kemi* **11** (1957) 291.
9. Tryding, N. *To be published.*
10. Westöö, G. *Acta Chem. Scand.* **11** (1957) 204.
11. Rottenberg, M. *Helv. Chim. Acta* **35** (1952) 1286.
12. Howard, G. A. and Martin, A. J. P. *Biochem. J. London* **46** (1950) 532.
13. Bergström, S. and Sjövall, J. *Acta Chem. Scand.* **5** (1951) 1267.
14. Norman, A. *Acta Chem. Scand.* **7** (1953) 1413.
15. Isherwood, F. A. *Biochem. J. London* **40** (1946) 688.
16. Nijkamp, H. J. *Anal. Chim. Acta* **5** (1951) 325.
17. Borgström, B. *Acta Physiol. Scand.* **25** (1952) 111.
18. Lee, M. O. *Am. J. Physiol.* **89** (1929) 24.
19. Piez, K. A. and Eagle, H. *Science* **122** (1955) 968.
20. Piez, K. A. and Eagle, H. *J. Am. Chem. Soc.* **78** (1956) 5284.
21. Van Dyken, A. R. *Abstracts of the 128th Meeting of the American Chemical Society, Minneapolis* 1955, p. 28.

Received February 4, 1957.

ACTA CHEMICA SCANDINAVICA 11 (1957) 439—460

Insulin Crystals

V. The Nucleation and Growth of Insulin Crystals

JØRGEN SCHLICHTKRULL

Novo Terapeutisk Laboratorium, Copenhagen, Denmark

Beef-insulin is crystallized from a buffered solution of sodium chloride as geometrically similar rhombohedrons. During the process of crystallization running determinations of the concentration, c_s, of dissolved insulin are made. Simultaneously, samples are taken in which the crystallization is immediately arrested by diluting with a solution of zinc chloride. The concentrations of crystalline insulin, C, are determined by analyses of the stabilized samples. The total volumes and surfaces of the crystals, as well as the cumulative distributions of sizes are also determined in these samples by a special counting technique.

The total number (N), length (L), surface (S) and volume (V) of crystals are found to be mutually proportional during crystallization, except for the short initial stage.

The rate of linear crystal growth, $\dot{g}$, is found to be independent of crystal size and proportional to $(c_s-c)^2$, where c is the final concentration of dissolved insulin.

The rate of nucleation is found to be proportional to the product of g and N, L, S and V, respectively, except for the short initial stage of crystallization.

The experimental results are predicted from the simple concept that nuclei are mainly formed on the surface of the crystals. This self-reproduction of crystals was not observed when the insulin was crystallized in the twin-like distorted shape.

The outer surface of the system, exposed to glass and air, is of prime importance to the process of nucleation. Nucleation is diminished when the crystallization is carried out in a paraffin enclosure or when Tween 80 is added, and it is considerably enhanced by foam or other increase in surface.

The purpose of the present paper is to investigate the rate of nucleation and growth of insulin crystals as functions of the concentration of insulin in the crystallization mixture. In earlier papers [1,2] a crystallization method was described which yielded perfectly shaped rhombohedral zinc-insulin crystals irrespective of the species of insulin. This method is suitable for a study of the kinetics of insulin crystallization for several reasons:

1) During the process of crystallization, which is not too rapid for study, samples can be taken in which the process of crystallization can be immediately arrested with zinc ions [2].

2) The fraction of crystalline insulin in the stabilized samples can be determined accurately [2].

3) The dimensions of a crystal are completely defined by one parameter, *e. g.* the largest diagonal, l, in the crystal projection on a plane through the microscope stage [2].

4) The distributions of crystal sizes in the stabilized suspensions can be determined by a counting procedure [2].

SYMBOLS*

c_s = The concentration of dissolved insulin in per cent of the total insulin concentration which is 1.7 % or 2.42 mg/ml insulin nitrogen.

C = The concentration of crystalline insulin in per cent of the total insulin concentration.

t = The time in min from the moment buffer is added to the acid insulin solution.

t_n = A moment of nucleation.

t_* = The time when crystallization is finished.

l = The size of crystals, *i. e.* the largest diagonal in the crystal projection on a plane through one of the faces. As the crystals lie on their faces, the plane is parallel to the slide on the microscope stage. l is measured in μ.

$\mathfrak{P}(l,t)$ = The cumulative distribution of crystal sizes at the moment t, *i. e.* the number per ml of suspension of crystals which are greater than l at the moment t.

$\mathfrak{p}(l,t) = -\frac{\delta \mathfrak{P}(l,t)}{\delta l}$, *i. e.* the distribution of sizes at the moment t.

$\dot{g} = \frac{\delta l(\mathfrak{P},t)}{\delta t}$, *i. e.* the rate of linear crystal growth which is supposed to be independent of the crystal size.

$g = \int_0^t \dot{g}\,dt$ is called the growth function.

$l_{max}(t) = g(t)$ as it is supposed that nucleation occurs already at $t = 0$.

$\mathfrak{N} = N = \int_0^g \mathfrak{p}(l,t)dl$ is the number of crystals per ml of suspension.

$\mathfrak{L} = L = \int_0^g l \cdot \mathfrak{p}(l,t)dl$ is the total length of crystals per ml of suspension.

$\mathfrak{S} = S = \int_0^g l^2 \cdot \mathfrak{p}(l,t)\,dl$ is the total surface of crystals per ml of suspension, the unit of area being the area of a rhombohedron with size $l = 1\ \mu$.

* P, p, h, N, L, S and V are typed in gothics when the independent variable is t and in italics when it is g.

$\mathfrak{V} = V = \int_0^g l^3 \cdot \mathfrak{p}\,(l, t)\,\mathrm{d}l$ is the total volume of crystals per ml of suspension, the unit of volume being that of the rhombohedron with size $l = 1\ \mu$.

$\bar{l}$ = L/N, *i. e.* the average crystal size.

m_i = $l_{i+1} + l_i$, where l_i are class limits in the counting scheme.

d_i = $l_{i+1} - l_i$.

n_i' = The number of crystals in 1 small square in the counting chamber belonging to the size interval $l_i < l < l_{i+1}$.

c = The volume in ml of crystallization mixture corresponding to 1 small square in the chamber.

S_i = $f_{si} \cdot n_i'$ is the surface per ml of suspension of crystals belonging to the size range $l_i < l < l_{i+1}$, the unit of area being the area of a rhombohedron with size $l = 1\ \mu$.

$\mathfrak{h}$ = $\frac{\mathrm{d}\mathfrak{N}}{\mathrm{d}t}$ is the rate of nucleation, as it is assumed that nuclei are immediately transformed into crystals.

h_s = $\mathfrak{h}/\dot{g}$ is called the specific rate of nucleation.

r and u are positive constants in the eqn (40), $S = rV^u$.

m is the concentration of a crystallizing substance present as monomer dissolved particles.

p and q are positive powers.

a, a_1, a_2, a_3, a_4 = constants.

b_1, b_2, b_3, b_4 = constants.

c_1, c_2, c_3, c_4, c_5, c_6, c_7 = constants.

α = const. $\times\ g$.

$\beta = \frac{\sqrt{3}}{2} \cdot \alpha$.

METHODS

1. *Crystallization.* The method of crystallization has been described recently [1,2]. The volume of crystallization mixture used was 4 litres, and the concentration of insulin was 1.7 %, *i. e.* 2.42 mg insulin-nitrogen per ml. Any foam that formed was removed.

2. *Determination of the insulin in solution,* c_s. 80—90 ml of the crystallizing suspension are filtered through filter paper covered with kieselguhr. Pressure is applied in order to keep down the filtration time to within 1 min. The filtrate is acidified with 1 N HCl in order to avoid crystallization on the walls of the flask. The concentration of insulin in solution, c_s, is determined by the semi-micro Kjeldahl analysis and expressed in per cent of the total concentration of insulin in the suspensions.

3. *Determination of the crystalline fraction, C.* A 10 ml sample is stabilized with zinc, the amorphous precipitate is dissolved, and the amount of crystalline insulin determined by semi-micro Kjeldahl analysis. The procedure has been described earlier [2]. The concentration of insulin in the crystalline state, C, is expressed in per cent of the total concentration of insulin in the suspension.

4. *Determination of the total volume ($\mathfrak{V}$) and surface ($\mathfrak{S}$) of crystals, and the cumulative distribution of crystal sizes ($\mathfrak{P}$).**

The cumulative distributions of crystal sizes are $\mathfrak{P}(l, t)$. At the time t, $\mathfrak{P}$ crystals per ml are bigger than l. Hence, the distribution of crystal sizes is

$$\mathfrak{p}(l,t) = -\frac{\delta \mathfrak{P}(l,t)}{\delta l} \tag{1}$$

The total number, length, surface and volume of crystals per ml of suspension are defined by

$$\mathfrak{N}(t) = \int_0^{l_{max}} \mathfrak{p}\ (l,t)\ \mathrm{d}l \tag{2}$$

$$\mathfrak{L}(t) = \int_0^{l_{max}} l\ \mathfrak{p}\ (l,t)\ \mathrm{d}l \tag{3}$$

$$\mathfrak{S}(t) = \int_0^{l_{max}} l^2\ \mathfrak{p}\ (l,t)\ \mathrm{d}l \tag{4}$$

$$\mathfrak{V}(t) = \int_0^{l_{max}} l^3\ \mathfrak{p}\ (l,t)\ \mathrm{d}l \tag{5}$$

Thus, an insulin rhombohedron with size $l = 1\ \mu$ has unit size, unit surface and unit volume.

The $\mathfrak{N}(t)$ values are not estimated directly from countings, as it is difficult to count very small crystals. The surface areas and the volumes are calculated from the $\mathfrak{P}(l, t)$ estimates obtained by the counting technique described earlier [2]. In analogy with the previous [2] formula for V_i

$$S_i = f_{si} \cdot n_i' \tag{6}$$

where

$$f_{si} = \frac{3m_i^2 + d_i^2}{12\ c} \tag{7}$$

THEORY

1. The growth of crystals.

The time, t, is counted in min from the moment buffer is added to the insulin solution. It is assumed that crystals are formed so early that

$$\dot{\mathfrak{N}}\ (0) > 0 \tag{8}$$

where the dot symbolizes differentiation with respect to time. The number of crystals per ml of suspension increases with time as shown by the fictitious curve in Fig. 1.

* These symbols are typed in gothics when the independent variable is t and in italics when it is g.

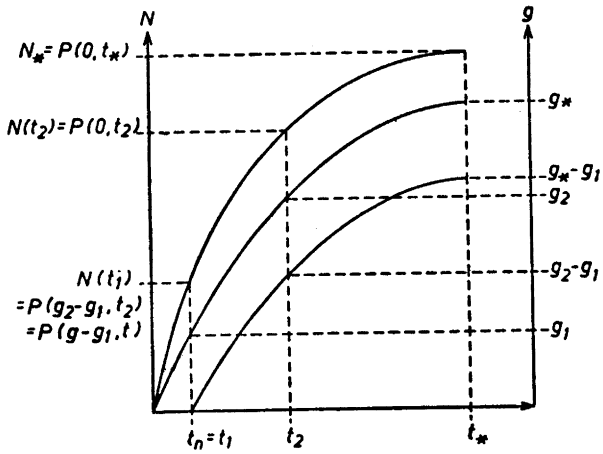


Fig. 1.

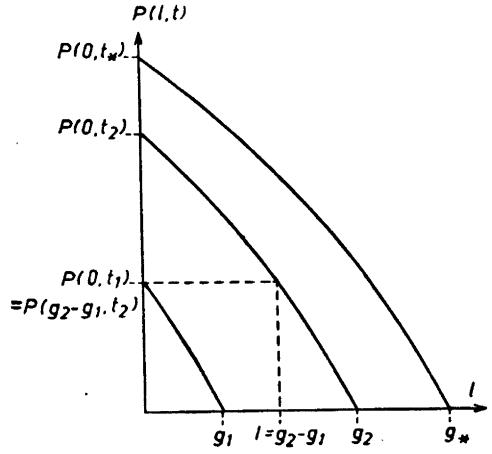


Fig. 2.

The crystallization is finished at the time t_* defined by

$$\dot{C}(t_*) = 0 \tag{9}$$

At that time the crystals are not further increasing in number, *i. e.*

$$\dot{\mathfrak{N}}(t_*) = 0 \tag{10}$$

Strictly speaking $t_* = \infty$, but in an actual experiment any t value above a certain limit may be symbolized through t_*.

The growth of a crystal proceeds as insulin is deposited on the faces which thereby move outwards in directions perpendicular to the faces. The rhombohedral shape is maintained, and the three faces meeting in an obtuse vertex move with identical rates. It is of course possible that the three opposite faces move at another rate, or even not at all. It is now assumed that the rate of movement of a face does not at any time vary between crystals having the same or different sizes. As the dimensions of a crystal are completely defined by the size, l, it follows from this assumption that at the time t all crystals grow with the same linear rate of growth, $\dot{l}(t)$. In order to distinguish between size and growth, $\dot{l}$ is denoted by the symbol $\dot{g}$. It is seen that $\dot{g}$ is a function of one parameter only, *e. g.* the time.

The maximum crystal size

$$l_{\max}\ (t) = \int_0^t \dot{g}(t)\mathrm{d}t = g(t) \tag{11}$$

is shown by the middle fictitious curve in Fig. 1. While this $g(t)$ curve indicates the size of crystals formed at $t = 0$, the curve below indicates the size of crystals formed at the arbitrary moment $t = t_n$. The moment t_n is called the moment of nucleation of these crystals. As all crystals grow with identical rates of linear growth, it follows that the size of these crystals is always $g(t)$—$g(t_n)$.

The cumulative distributions, $\mathfrak{P}(l,\ t)$, can be expressed in terms of $\mathfrak{N}(t)$ and $g(t)$. The $\mathfrak{P}$ function is considered at the arbitrary moment $t = t_2$ (Fig. 2). The total number of crystals is

$$\mathfrak{P}(0,\ t_2) = \mathfrak{N}(t_2) \tag{12}$$

At the moment t_2 no crystals are bigger than the maximum size, $g_2 = g(t_2)$, and consequently

$$\mathfrak{P}(g_2,\ t_2) = 0 \tag{13}$$

The crystals of the size l were formed at the moment t when the biggest crystals had the size g_2—l. At that moment $\mathfrak{N}(t)$ crystals were present. These are consequently the crystals which at the time t_2 are bigger than l. Hence,

$$\mathfrak{P}(l,\ t_2) = \mathfrak{N}(t) \tag{14}$$

where t is derived from

$$g(t) = g_2 - l \tag{15}$$

Inversely,

$$\mathfrak{N}(t) = \mathfrak{P}(g_2—g(t),\ t_2) \tag{16}$$

or with g as sole parameter,

$$N(g) = P(g_2—g,\ g_2) = P(g_3—g,\ g_3),\ \textit{etc.} \tag{17}$$

Thus, the number of crystals can be calculated from determinations of P and g.

As shown graphically in Fig. 2, eqn. (17) reveals the relationship between the P-functions at different g (or t) values. The horizontal distance between two $P(l)$ curves is constant, since it follows from eqn. (17) that

$$P(l,\ g_1) = P(l+g_2—g_1,\ g_2) \tag{18}$$

The same horizontal displacement of the distributions, eqn. (1), is observed by differentiation of eqn. (18) which thereby becomes

$$p(l,\ g_1) = p(l+g_2—g_1,\ g_2) \tag{19}$$

2. The nucleation

It is assumed that nuclei are immediately transformed into crystals. Hence, the rate of nucleation is

$$\mathfrak{h}(t) = \dot{\mathfrak{N}}(t) \tag{20}$$

It follows from this definition and eqn. (16) that

$$\mathfrak{h}(t) = p(g_2—g(t),\ g_2) \cdot \dot{g}(t) \tag{21}$$

Thus, the rate of nucleation at the moment t is the product of a value in the distributions of crystal sizes and the growth rate. The physical meaning of this equation can be made clear from Fig. 2 by moving one of the curves the distance $\mathrm{d}g$ to the right in the time $\mathrm{d}t$. The point of interception between curve and P-axis thereby moves $\mathrm{d}N$ upwards.

The derivative of N with respect to g

$$h_s(g) = p(g_2—g(t),\ g_2) \tag{22}$$

is obtained from eqn. (21). It is called the specific rate of nucleation and is simply a value in the distributions of crystal sizes. When the function $h_s(g)$ is known, it follows from eqn. (22) that the crystals are completely defined for every value (g_2) of the growth function. Hence, not only the size distributions but also the total volume, V, surface, S, and length, L, are defined by $h_s(g)$ and the g-value. Inversely, as will be demonstrated, inferences about $h_s(g)$ can be drawn from $V(g)$, $S(g)$ and $L(g)$.

The volume is given by eqn. (5). According to eqn. (22)

$$p(l,\ g) = h_s(x) \tag{23}$$

where

$$l = g — x \tag{24}$$

from which

$$V(g) = \int_0^g (g—x)^3 h_s(x)\mathrm{d}x \tag{25}$$

or

$$V(g) = g^3N(g) — 3g^2\int_0^g x h_s(x)\mathrm{d}x + 3g\int_0^g x^2 h_s(x)\mathrm{d}x — \int_0^g x^3 h_s(x)\mathrm{d}x \tag{26}$$

The surface, S, and the length, L, may be written in a quite analogous way, *viz.*

$$S(g) = g^2N(g) — 2g\int_0^g x h_s(x)\mathrm{d}x + \int_0^g x^2 h_s(x)\mathrm{d}x \tag{27}$$

and

$$L(g) = gN(g) - \int_0^g x h_s(x)\mathrm{d}x \tag{28}$$

By differentiation of the eqns. (26), (27) and (28) with respect to g the following is found:

$$\begin{array}{llllll} V' = 3S & S' = 2L & L' = N & N' = h_s(g) \\ V'' = 6L & S'' = 2N & L'' = N' & \\ V''' = 6N & S''' = 2N' & & \\ V'''' = 6N' & & & \end{array} \tag{29}$$

from which can be read that

$$h_s(g) = N'(g) = L''(g) = \frac{1}{2}S'''(g) = \frac{1}{6}V''''(g) \tag{30}$$

3. Volume and surface relations

From determinations of S and V in the course of crystallization, inferences can be drawn about the rates of growth and nucleation. The surface

$$S = f(V) \text{ or } \mathcal{S} = f(\mathcal{V}) \tag{31}$$

is expressed as a function of the volume. As according to eqn. (29)

$$\dot{\mathcal{V}} = 3\mathcal{S}\dot{g} \tag{32}$$

it follows that

$$\dot{g} = \dot{\mathcal{V}}/3f(\mathcal{V}) \tag{33}$$

The specific rate of nucleation is obtained from eqn. (30). The eqn. (31) is differentiated

$$S' = f'(V) \cdot V' \tag{34}$$

with respect to g. As according to eqn. (29)

$$V' = 3S \tag{35}$$

it follows that

$$S' = 3f'(V) \cdot S \tag{36}$$

and by inserting eqn. (31)

$$S' = 3f' \cdot f \tag{37}$$

When differentiation is repeated twice more, it is found that

$$h_s(g) = \frac{27}{2}\,(f^3\, f''' + 4f^2 f' f'' + f(f')^3) \tag{38}$$

and when eqn. (33) is inserted

$$h(t) = \frac{27}{6}\,\dot{\mathcal{V}}(f^2 f''' + 4ff' f'' + (f')^3) \tag{39}$$

As an example, let it be possible to express S by

$$S = r \cdot V^u \qquad g(t_1) < g < (t_2) \tag{40}$$

where r and u are positive constants. The eqn. (38) then becomes

$$h_s(g) = 81r^4u\left(u-\frac{1}{2}\right)\left(u-\frac{2}{3}\right)V^{4u-3} \qquad g(t_1) < g < g(t_2) \tag{41}$$

A few special cases of eqn. (40) will now be considered.

Case 1, $u = 2/3$. From eqn. (41) it is seen that

$$h_s(g) = 0 \qquad g(t_1) < g < g(t_2) \tag{42}$$

which means that crystallization proceeds without nucleation. The inverse inference — that equation (40) is valid with $u = 2/3$ when $h_s = 0$ — is generally false as can be understood from the eqns. (26) and (27). It is, however, true when the crystal suspension is known to be monodisperse at $t = t_1$ as may happen, *e. g.*, from a previous seeding.

Case 2, $u = 3/4$. This case is compatible with the observations made during the initial stage of the insulin crystallization. The specific rate of nucleation is calculated from eqn. (41) to be

$$h_s(g) = \frac{3^4}{2^6}\,\mathrm{r}^4 \qquad g(t_1) < g < g(t_2) \tag{43}$$

Thus, the rate of nucleation is proportional to the rate of linear growth. As the distributions of crystal sizes are identical with $h_s(g)$, all sizes of crystals formed in the time interval occur with equal frequency, *i. e.*

$$\mathrm{p}(l,\ t) = \frac{3^4}{2^6}\,\mathrm{r}^4 \qquad (t_1 < t < t_2) \tag{44}$$

when

$$l < g(t) - g(t_1)$$

Case 3, $u = 1$. This is the case actually observed except for the initial period of crystallization. The eqn. (41) shows that

$$h_s(g) = \frac{27}{2}\,r^4V \qquad g(t_1) < g < g(t_2) \tag{45}$$

which by means of eqn. (40) is changed into

$$h_s(g) = \frac{27}{2}\,r^3S \qquad g(t_1) < g < g(t_2) \tag{46}$$

From the eqns. (29) and (40) it follows further that

$$h_s(g) = 9r^2L \qquad g(t_1) < g < g(t_2) \tag{47}$$

and

$$h_s(g) = 3rN \qquad g(t_1) < g < g(t_2) \tag{48}$$

Thus, in the time interval, $t_1 < t < t_2$, the specific rate of nucleation is proportional to the number of crystals present, their total length, surface or volume. The constant mutual ratios are

$$N = 3rL = \frac{9}{2} r^2 S = \frac{9}{2} r^3 V \qquad g(t_1) < g < g(t_2) \tag{49}$$

This equation shows further that the average crystal size, L/N, is constantly

$$\bar{l} = 1/3r \qquad (t_1 < t < t_2) \tag{50}$$

The distribution of crystal sizes is obtained from eqns. (16), (22) and (48) which give

$$\mathfrak{p}(l,\ t) = 3r\mathfrak{P}(l,\ t) \qquad (t_1 < t < t_2) \tag{51}$$

when

$$l < g(t) - g(t_1)$$

From eqns. (1) and (51) it follows that

$$\mathfrak{p}(l,\ t) = f(t)\ \mathrm{e}^{-3rl} \qquad (t_1 < t < t_2 \text{ and } l < g(t)—g(t_1)) \tag{52}$$

where $f(t)$ is a function of time only.

The cumulative distribution of crystal sizes is obtained by means of eqn. (51) from which

$$\mathrm{d}\ln\mathfrak{P}(l,\ t) = —3r\mathrm{d}l \tag{53}$$

and

$$\ln\mathfrak{P}(l,\ t) = —3rl + \ln\mathfrak{N}(t) \tag{54}$$

in which

$$t_1 < t < t_2 \qquad \text{and} \qquad l < g(t) - g(t_1) \tag{55}$$

Thus in the interval (55) the logarithms of the cumulative distributions are graphically represented by the straight lines, eqn. (54). As the slopes of these lines are identical, the lines may be moved in a graph to cover each other. At $t = t_2$, eqn. (54) gives

$$\ln\mathfrak{P}(g(t_2) - g(t),\ t_2) = — 3r(g(t_2) — g(t)) + \ln\mathfrak{N}(t_2) \tag{56}$$

Using eqn. (16), the addition of the eqns. (54) and (56) shows that

$$\ln\mathfrak{P}(l,\ t) = — 3rx + \ln\mathfrak{N}(t_2) \tag{57}$$

where

$$x = l + g(t_2) — g(t) \tag{58}$$

Thus, all $\mathfrak{P}$-values observed in the time interval $t_1 < t < t_2$ will lie on the straight line, eqn. (57), provided the l-values are smaller than $g(t)—g(t_1)$.

4. The origin of nuclei

A fundamental theory of nucleation and crystal growth has been developed by Christiansen [3]. According to this theory

$$\dot{\mathfrak{N}} = \text{const. } m^p \tag{59}$$

where m is the concentration of substance present as monomer dissolved particles and p is a positive integer. This relation was demonstrated by the same author to be valid for the precipitation of barium sulphate ($p = 8$). The rate of linear growth of barium sulphate was found to be

$$\dot{g} = \text{const. } m^q \tag{60}$$

where q is positive ($q = 4$). The power q was also explained by the theory.

When the eqns. (59) and (60) are applied to the present case of insulin crystallization, the specific rate of nucleation is found to be

$$h_s(g) = \text{const. } \dot{g}^{(\frac{p}{q}-1)} \tag{61}$$

This equation is compatible with the observations in the initial stage of insulin crystallization, although as already mentioned,

$$h_s(g) = \text{const. } (V,\ S,\ L \text{ or } N) \tag{62}$$

in the main part of crystallization. Hence, the hypothesis is set up that the insulin nuclei have different origins. It is assumed that some of the insulin nuclei are formed spontaneously according to eqn. (61), and further that other insulin nuclei are formed by interaction of the solution with the faces, edges or vertices of the crystals. Thus, in the initial stage of crystallization, where crystals are few and interaction therefore insignificant, nucleation may proceed according to eqn. (61). Later the interaction becomes of overwhelming significance and thereby masks the process, eqn. (61), so much that the specific rate of nucleation follows eqn. (62).

ANALYSIS OF DATA FROM THE CRYSTALLIZATION EXPERIMENT

1. Changes with time in the concentrations of dissolved and crystalline insulin

At $t = 0$ the insulin is almost altogether (94 %) precipitated as amorphous particles. In the course of the following 50 min, 26 % of the insulin is gradually dissolved. At $t = 50$, the crystalline fraction appears in chemically measurable quantities. It increases first rapidly and later more slowly as seen in Fig. 3 and Table 1. At the same time the concentration of dissolved insulin decreases. The drop in c_s indicates that crystals grow from dissolved insulin.

2. The linear growth rate

As the crystals apparently grow from dissolved insulin being deposited on the faces, it is of prime interest to determine the functional relationship between the linear growth rate and the concentration of dissolved insulin. The $C(t)$ and $c_s(t)$ data will be used first in connection with eqn. (33). In the next paragraph it will be demonstrated that

$$G = rv \qquad (t > 60) \tag{63}$$

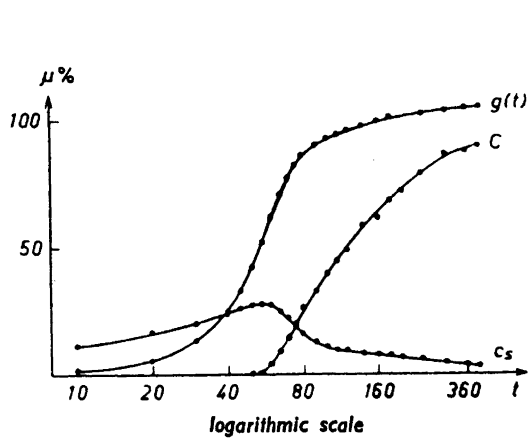


Fig. 3.

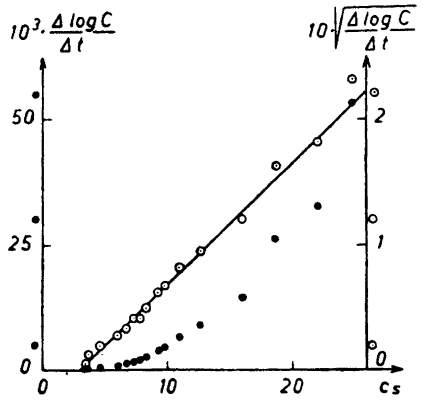


Fig. 4.

where r is a constant. Hence,

$$\dot{g} = \frac{(\dot{\ln v})}{3r} \qquad (t > 60) \tag{64}$$

and

$$\dot{g} = \frac{(\dot{\log C})}{3rM} \qquad (t > 60),\ (M = 0.4343) \tag{65}$$

Estimates of the growth rate can be obtained from

$$\dot{g}_i \approx \frac{1}{3rM} \cdot \frac{\log C_{i+1} - \log C_{i-1}}{t_{i+1} - t_{i-1}} \qquad (t > 60) \tag{66}$$

in which i is the sample number. The fractions on the right side of the equation are calculated and plotted against c_s in Fig. 4.

The configuration of the points in the graph suggests a power relation, and when the square roots of the fractions are tentatively plotted against c_s, it appears that

$$\dot{g}(t) = c_7(c_s(t) - 3)^2 \qquad (t > 60) \tag{67}$$

where c_7 is a constant. Assuming this equation to be valid for $t < 60$ also, it follows that

$$g(t) = c_7 \cdot \int_0^t (c_s - 3)^2 \, dt \tag{68}$$

The value of the integral corresponding to each sample is calculated by the approximative formula

$$\int_0^{t_x} (c_s - 3)^2 \, dt \approx \frac{1}{2} \sum_{i=1}^{i=x} (t_i - t_{i-1}) \left[(c_{s_i} - 3)^2 + (c_{s_{i-1}} - 3)^2\right] \tag{69}$$

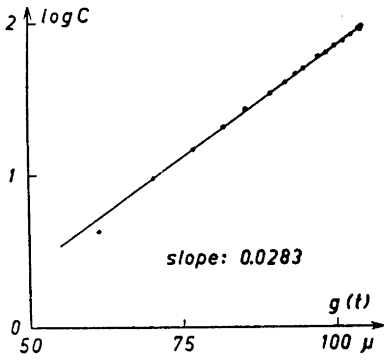


Fig. 5.

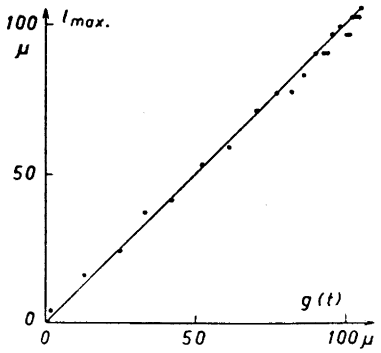


Fig. 6.

where i = 1 when $t = 0$. When crystallization was finished, the biggest crystals found were $g_* = 105\ \mu$. The value of the integral at the same time, t_*, is calculated as 3.20×10^4. Hence,

$$c_7 = \frac{105}{3.20} \times 10^{-4} = 3.28 \times 10^{-3} \tag{70}$$

which is used in eqn. (68) to calculate a $g(t)$ estimate for each sample. These estimates are now plotted against $\log C$ in Fig. 5.

The slope of the straight line is 0.0283. As from eqn. (65)

$$g(t) = \frac{\log C(t)}{3rM} + \text{const.} \quad (t > 60) \tag{71}$$

it follows that

$$r = \frac{0.0283}{3M} = 0.022 \tag{72}$$

In order to compare the $g(t)$ estimates with the size of crystals actually found, $g(t)$ is plotted (Fig. 6) against the maximum size, l_{max}, of crystals observed in all samples including those from $t < 60$. The calculated and observed maximum sizes are in agreement, also for $t < 60$.

Finally the $g(t)$ values are plotted against different quantiles in the cumulative distributions of crystal sizes (Fig. 7). The quantiles are derived from the countings by picking out of the counting tables the crystal sizes corresponding to the ϱ-value in question. The theoretical lines inserted in the figure were calculated from eqns. (68) and (88). It appears from Fig. 7 that crystals of different sizes grow with identical rates of growth and further that this rate of growth is $\dot{g}$ as calculated by means of eqn. (67). Thus, the linear growth rate is proportional to the square of $(c_s - 3)$, which may be the supersaturation but presumably is not. When the crystal suspension is left for several days, the c_s value drops below 2 %. Further, when the crystals are filtered off and resuspended in a fresh insulin-free medium of the same small molecular

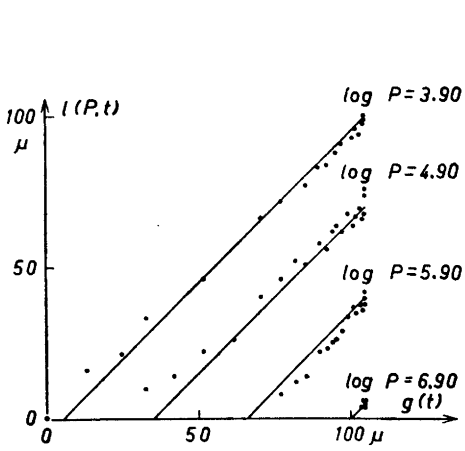


Fig. 7.

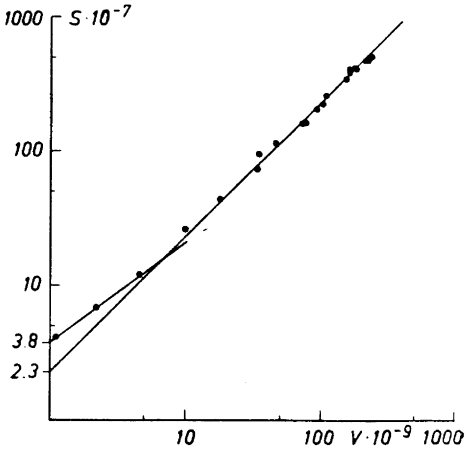


Fig. 8.

composition, c_s is found to be only 0.5 % after equilibration for two days. These supplementary findings must be considered in the chemical interpretation of eqn. (67).

3. The rate of nucleation

In the present case of crystallization the functional relationship between the total volume and surface of crystals is so simple that inferences can be drawn about the specific rate of nucleation. The V and S means from two, and sometimes more countings are plotted against each other on double logarithmic paper in Fig. 8.

The crystallization is divided into two periods, A and B, by the two straight lines with slopes 3/4 and 1. In the first initial stage

$$\text{(A)} \qquad S \approx 3.8 \times 10^{\frac{1}{4}} \times V^{\frac{3}{4}} \qquad (10^9 < V < 10^{10}) \tag{73}$$

and in the second main part of the crystallization

$$\text{(B)} \qquad S \approx 0.023 \times V^1 \qquad (10^{10} < V < V_*) \tag{74}$$

The value (0.023) of the constant in the last equation is in agreement with the former value (0.022) from the preceding paragraph.

From eqns. (73) and (43) it is calculated that

$$\text{(A)} \qquad h_s \approx \frac{3^4}{2^6} \times 3.8^4 \times 10^1 = 2 \times 10^3 \tag{75}$$

and from eqns. (74) and (48) it follows that

$$\text{(B)} \qquad h_s \approx 0.07 \times N \tag{76}$$

The eqn. (75) is a special case of eqn. (61), *viz.* the case where $p = q$. The assumption is now made, that during the whole period of crystallization nucleation proceeds according to eqn. (61) in which $p = q$. There is no incompatibility between this assumption and the eqn. (76) when it is further assumed that a second nucleation process takes place on the crystals. When N exceeds 10^5 this second process becomes dominating and especially as N increases to 10^7, the final value.

It follows from these assumptions that

$$h_s = a + b_1N + b_2L + b_3S \tag{77}$$

in which a is the constant specific rate of spontaneous nucleation, b_1N is the specific rate of nucleation from the vertices, b_2L at the edges and b_3S on the faces. As N, L, S and V become mutually proportional when about 1 % of the final crystals are formed, it is not possible to infer from the data whether or not the surface nucleation occurs on the faces or rather at the edges or vertices. However, the agreement of the data with

$$h_s = a_1 + b_1N \quad \text{(vertices)} \tag{78}$$
$$h_s = a_2 + b_2L \quad \text{(edges)} \tag{79}$$
$$h_s = a_3 + b_3S \quad \text{(faces)} \tag{80}$$
$$h_s = a_4 + b_4V \quad \text{(eqn. 45)} \tag{81}$$

will be investigated. When these four equations are differentiated by means of eqn. (29) they become ordinary differential equations

$$N'(g) = a_1 + b_1N(g) \tag{82}$$
$$N''(g) = b_2N(g) \tag{83}$$
$$N'''(g) = 2b_3N(g) \tag{84}$$
$$N''''(g) = 6b_4N(g) \tag{85}$$

having the solutions

$$N(g) = c_1\ e^{\alpha}\ (1—e^{-\alpha});\ c_1 = \frac{a_1}{b_1}\ ;\ \alpha = b_1g \tag{86}$$

$$N(g) = c_2\ \sinh\alpha;\ c_2 = \frac{a_2}{\sqrt{b_2}}\ ;\ \alpha = \sqrt{b_2}\cdot g \tag{87}$$

$$N(g) = c_3\ e^{\alpha}[1 + e^{-\frac{3}{2}\alpha}\ (\sqrt{3}\cdot\sin\beta - \cos\beta)];\ c_3 = \frac{a_3}{3c_4}\ ;\ c_4 = \sqrt[3]{2b_3}\ ; \tag{88}$$

$$\alpha = c_4g;\ \beta = \frac{\sqrt{3}}{2}\ \alpha$$

$$N(g) = c_5\ (\sinh\alpha + \sin\alpha);\ c_5 = \frac{a_4}{2c_6}\ ;\ c_6 = \sqrt[4]{6b_4}\ ;\ \alpha = c_6\ g \tag{89}$$

It follows from eqn. (48) that

$$\frac{d\ln N}{dg} = 3r \tag{90}$$

in the second period of crystallization. Hence,

$$a = 3rg = \frac{0.0283}{0.4343}\, g = 0.0652\, g \tag{91}$$

or

$$b_1 = \sqrt{b_2} = \sqrt[3]{2b_3} = \sqrt[4]{6b_4} = 0.0652 \tag{92}$$

When crystallization is finished the growth function has reached the value $g_* = 105\ \mu$ and, as will be explained later, the number of crystals is 1.02×10^7 per ml. Hence,

$$c_1 = \frac{1}{2}\, c_2 = c_3 = \frac{1}{2}\, c_5 = 1.02 \times 10^7/\text{exp.}\ (0.0652 \times 105) = 1.1 \times 10^4 \tag{93}$$

The numerical values of the constants, eqns. (92) and (93), are introduced into the eqns. (86)—(89), which are then used to calculate sets of $N(g)$ values to be compared with P-values from the observed cumulative distributions of crystal sizes.

The cumulative distribution of sizes when crystallization is finished (asterisk) can be expressed by these equations, as from eqns. (14) and (15)

$$\mathrm{P}_*(l) = N(g) \tag{94}$$

where

$$g = g_* - l \tag{95}$$

The curves in Fig. 9 represent the logarithms of $N(g)$ from eqns. (86), (87), (88), (89), (92) and (93) against l, where l is connected to g by eqn. (95). The dots represent the almost coinciding observation data gained from the three last samples. The data fit best to the curves calculated according to eqns. (87) and (88) corresponding to nucleation at edges and faces, respectively.

In order to utilize the information gathered from all the countings, their data are compiled in one graph (Fig. 10). Let the crystal sizes at $t = t_*$ be denoted by x, then it follows from eqn. (18) that

$$\mathrm{P}_*(x) = \mathrm{P}(l,\ t) \tag{96}$$

where

$$x = l + g_* - g(t) \tag{97}$$

The substitution, eqn. (97), is used in the presentation of all the $\mathrm{P}(l, t)$ values observed (Fig. 10). The scattering of the dots increases towards the lower region of the graph where the P-values are based upon counts of a few crystals only. The trend of the dots is in agreement with Fig. 9 and with the theoretical curves although too many points are below the curve in the interval $20 < x < 40$. The eqns. (87) and (88) fit best to the observations depicted in this figure also.

When the method of least squares is used (Fig. 10) on $\log \mathrm{P}_*(x)$ where $\log \mathrm{P}_*(x) > 4.4$, the slope is found to be —0.0283. A straight line with this slope was already expected in accordance with eqn. (57) and Fig. 5. The line intercepts the $\log \mathrm{P}_*(x)$ axis at 7.01. Hence, the final number of crystals is estimated as 1.02×10^7 per ml.

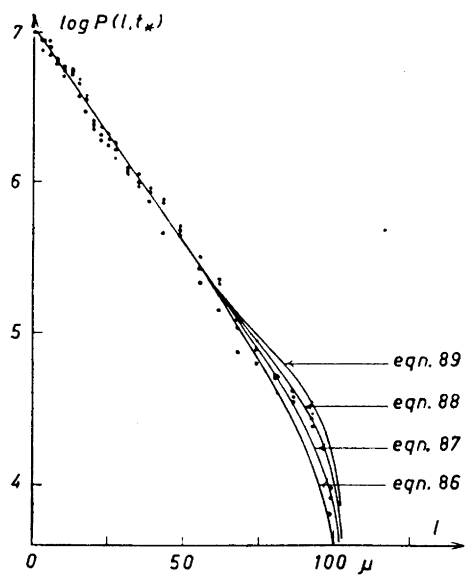


Fig. 9.

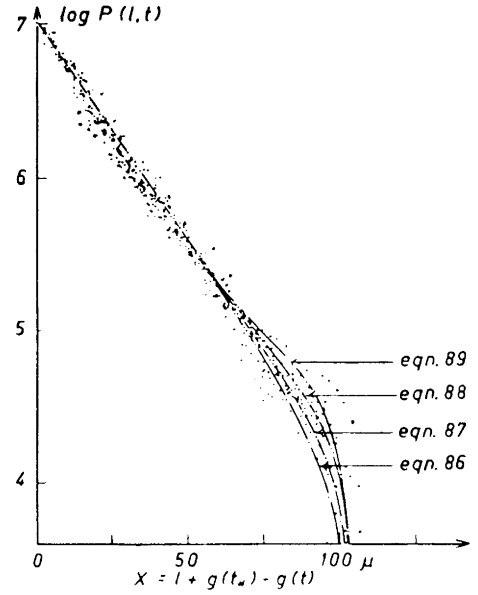


Fig. 10.

The total volumes and surfaces expected in accordance with eqns. (68), (88), (92) and (93) have been calculated and presented in Table 1 and as a curve in Fig. 11 in comparison with the observed values. The eqn. (80) is written

$$h_s = a_3 + \frac{b_3}{3} \cdot V' \tag{98}$$

which by integration becomes

$$V(g) = \frac{3}{b_3} [N(g) - a_3 g] \tag{99}$$

from which $V(g)$ can be calculated by inserting g from eqn. (68) and $N(g)$ from eqn. (88). It follows from eqn. (99) that the number of insulin crystals is proportional to the weight or volume of crystallized insulin, provided a_3 is relatively small. The surface was calculated from eqn. (80)

$$S = \frac{1}{b_3} [N'(g) - a_3] \tag{100}$$

in which

$$N'(g) = \frac{1}{3} a_3 \, (e^{a} + 2e^{-\frac{1}{2}a} \cos\beta) \tag{101}$$

is obtained by differentiating eqn. (88). There is a reasonable agreement between the calculated and observed values.

Table 1. Data relating to the crystallization experiment.

(1)	(2)	(3)	(4)	(5)	(6)	(7)	(8)	(9)	(10)	(11)	(12)
1	2	6.1	0.0	0.0	—	—	—	—	3	2	0.1
2	10	11.0	0.4	1.3	—	—	—	—	21	2	0.4
3	20	16.7	0.0	5.2	—	—	—	—	62	2	1.3
4	30	19.8	0.0	13.1	0.1	0.0	0.5	0.2	93	2	2
5	40	24.1	0.0	24.9	0.3	0.2	1.4	1.1	146	4	5
6	45	25.9	0.0	32.8	1.1	0.7	4.1	2.7	172	6	10
7	50	27.3	0.4	42.0	2.2	1.9	6.8	6.2	178	11	19
8	55	27.4	0.8	51.5	4.6	4.5	12	13	180	20	36
9	60	27.3	4.2	61.3	10	10	26	26	178	38	68
10	65	24.9	9.4	70.2	18	20	43	47	157	68	107
11	70	22.1	14.3	77.1	34	33	73	76	120	106	127
12	75	18.8	20.0	82.0	35	47	96	105	82	147	120
13	80	16.0	26.2	85.6	47	59	115	132	55	185	102
14	90	12.6	32.9	89.9	78	80	168	175	30	245	74
15	100	11.0	39.8	92.5	72	95	162	208	21	291	61
16	110	9.8	44.6	94.1	94	107	210	232	15	323	49
17	120	9.3	48.8	95.4	104	116	231	252	13	351	46
18	140	8.3	58.4	97.7	109	135	261	293	9	408	38
19	160	7.9	61.2	99.4	155	150	355	327	8	456	36
20	180	7.3	68.1	101.0	164	165	406	365	6	506	31
21	200	6.7	72.0	102.0	165	179	388	388	5	540	24
22	240	6.0	78.8	103.3	181	196	418	425	3	588	18
23	300	4.6	86.5	104.6	177	212	426	461	1	640	5
24	360	3.7	87.6	105.0	239	219	517	474	0	657	1
25	400	3.4	89.6	105.0	214	219	483	474	0	657	0.7
26	1 400	2.3	92.7	105.0	222	219	485	474	0	657	0.0

Legend to table:
(1) i, sample number.
(2) t, time in minutes from the moment of mixing.
(3) c_S, the percentage of insulin in solution.
(4) C, the percentage of insulin in the crystalline state.
(5) $g(t) = 3.28 \times 10^{-3} \int_0^t (c_S - 3.0)^2 \, dt$.
(6) $V \times 10^{-9}$, calculated from the distributions of crystal sizes observed. See eqns. (1) and (5).
(7) $V \times 10^{-9}$, predicted values from eqn. (99) in which $a_3 = 2\,094$, $b_3 = 1.385 \times 10^{-4}$ and $N(g)$ is calculated from eqn. (88) where $g = g(t)$ from column (5).
(8) $S \times 10^{-7}$, calculated from the distributions of crystal sizes observed. See eqns. (1), (4), (6) and (7).
(9) $S \times 10^{-7}$, predicted values from eqns. (100) and (101) in which $a_3 = 2\,094$, $b_3 = 1.385 \times 10^{-4}$ and $g = g(t)$ from column (5).
(10) $\dot{g} \times 10^2 = 0.328 \, (c_S - 3.0)^2$
(11) $h_S \times 10^{-3} = 10^{-3} \, N'(g)$. $N'(g)$ is calculated from eqn. (101), $g = g(t)$ from column (5).
(12) $\dot{h} \times 10^{-3} = 10^{-3} \times \dot{g} \times h_S$.

4. The microscopic appearance

The photomicrograph (Fig. 12) shows the appearance of the crystals upon completion of crystallization. The crystals are apparently not distributed in space at random. The number of crystals smaller than 4 μ (175 × magnified) was counted in the photomicrograph and estimated as 41. Out of these, 15 were free, 10 occurred in pairs, 14 were found at the edges or vertices of

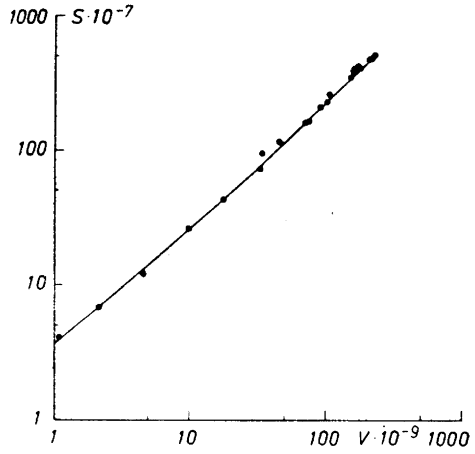


Fig. 11.

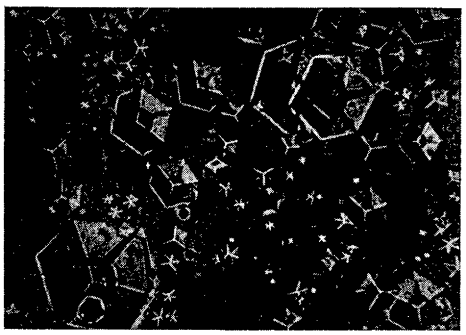


Fig. 12.

bigger crystals, and 2 on the crystal faces. It is concluded that either small new crystals wander about and become attracted and held fast by other crystals, or they originate on them.

OTHER EXPERIMENTS

1. *Crystallization of pig insulin from a clear solution.* The eqns. (78), (79), (80) and (81) which were formed on the hypotheses set up to explain the $\varrho(l, t)$ function contain some remarkable consequences. The specific rate of nucleation, being a function of g, is seen to be independent of $\dot{g}$ and of the concentration of dissolved insulin. However, in a single experiment $\dot{g}$ is certainly a function of g and it is therefore possible to express h_s and $\mathfrak{h}$ by means of $\dot{g}$. It turns out that $h_s(\dot{g})$ and $\mathfrak{h}(\dot{g})$ are complicated functions which seem to have no underlying pattern from the point of view of chemical interpretation. Thus, up to the present it has not been possible to find any explanation except for the simple hypothesis of nucleation by crystal self-reproduction. In order to test experimentally whether h_s is chemically independent of $\dot{g}$, crystallizations were made in which the concentration of dissolved insulin, and hence $\dot{g}$, varies with g in a different pattern, *i. e.* by crystallizing from a clear solution.

The composition was: 1 % pig insulin, 0.04 % Zn^{++}, 0.05 M sodium citrate, 15 % (v/v) acetone, pH = 6.2. Volume 1 l. The crystallizations were carried out in ordinary glass beakers equipped with a mechanical glass stirrer. The acetone prevented any foam formation. In one of the two experiments the glass was covered with a paraffin layer and the surface was covered with paraffin oil. The resulting cumulative distributions of crystal sizes are shown in Fig. 13.

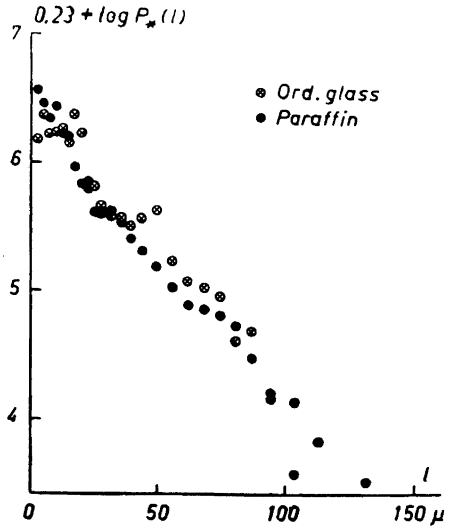


Fig. 13.

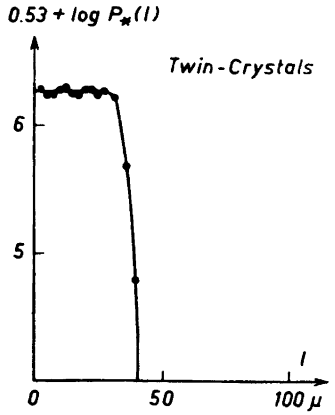


Fig. 14.

To all log ρ_* values are added log $\frac{1.7}{1} = 0.23$ so as to render direct comparison with previous figures possible. It is seen that the change of the $\dot{g}(g)$ function together with the elimination of the amorphous phase did not abolish the straight line relationship expected in accordance with the hypothesis of crystal reproduction.

2. *Crystallization of beef insulin from a clear solution.* An experiment was made using the same composition as in the case of pig insulin crystallization except for the insulin concentration which was 0.5 % and pH which was 6.7. The crystals were as expected more or less distorted apparently by twin formation [1]. The resulting cumulative distribution of crystal sizes is shown in Fig. 14. The shape of the curve is inconsistent with the eqns. (86)—(89) derived from the hypothesis of crystal reproduction. Furthermore the distribution of sizes shows a maximum at about 35 μ corresponding to a rather monodisperse suspension. It means that h_s drops sharply when the concentration of dissolved insulin decreases. Assuming that the nucleation occurs spontaneously within the solution and further that eqn. (61) can be employed in the present case, it follows that $p > q$ as in the case of barium sulphate. Thus, the mechanism of nucleation in the citrate-acetone buffer appears to depend on the species of insulin. In the sodium chloride medium, however, there is no such dependence as illustrated by the 4-litre experiment for which beef insulin was used.

It is concluded that the observed pattern of nucleation is in accordance with the fundamental concepts of spontaneous nucleation, eqn. (61), when the crystals are of the usual distorted twin-like type. The data of crystallization of plain single rhombohedrons are also in agreement with the fundamental con-

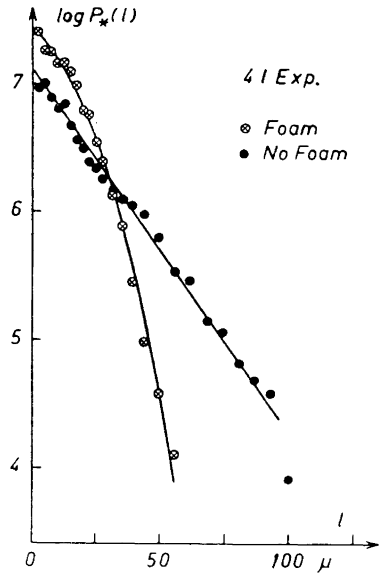


Fig. 15.

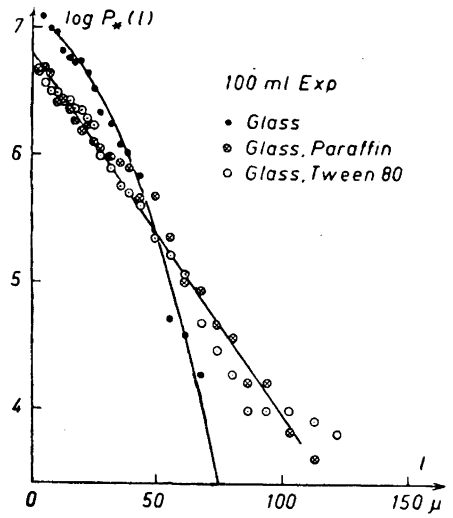


Fig. 16.

cepts when it is accepted that a second population of nuclei originates on the existing crystals. In this latter case it was estimated that $p = q$ in eqn. (61), but the masking effect of the apparent self-reproduction makes this estimate somewhat uncertain.

3. *The outer surface.* The investigation of the nucleation process is complicated by an apparent nucleation process taking place in the outer surface of the suspension.

When insulin crystallizes slowly from a calm solution, it is observed that crystals are primarily formed in the glass surface, in the surface exposed to air and on foreign bodies (*e. g.* a hair fiber) if such are suspended in the solution. In the 4-litre experiment some foam is formed on the surface. If the foam is not quantitatively removed, the crystallization yields a larger number of crystals, the maximum size becomes smaller and the graphical picture of $\log \varrho_*(l)$ becomes curved as shown in Fig. 15.

In another experiment the surface was increased (without perceptible foam) by reducing the volume of the crystallizing suspension to 100 ml. The resulting cumulative distribution of sizes (Fig. 16) resembles that of the 4-litre experiment with foam. Thus, it seems that nucleation may occur in the surface to such an extent as to cause a significant change in the distribution of sizes.

Inversely, it has been demonstrated by experiment, that the apparent excess nucleation from the surface can be reduced or eliminated. The 4-litre experiment was repeated on a 100 ml scale in 3 experiments carried out in identical apparatus. The one experiment served as the control for the case with relatively large surface. Number two beaker was covered with paraffin

and the surface of the suspension was covered with paraffin oil. The third suspension contained 0.05 % of the surface active agent Tween 80. It is seen from Fig. 16 that the paraffin cover as well as the Tween 80 causes a bigger maximum size of crystals, a smaller crystal number, and the reappearance of the straight line relationship characteristic of the 4-litre experiment when foam is absent.

DISCUSSION

Nucleation may occur within the solution, in the interfaces between solution and glass or air and on the surface of the crystals. The great changes in nucleation produced by foam or other increases in the surface, by the paraffin coating, and by Tween 80 indicate that the rate of nucleation increases towards the surface. The hypothesis of surface nucleation on the crystals provides a simple explanation of the size distributions observed. It has not been possible to determine whether this nucleation is located on the faces or rather at the edges or vertices. It is interesting that this type of nucleation is apparently wholly or partially absent when the insulin crystallizes in the twin-like distorted shape. One can imagine that the crystal reproduction may be the repeated development and disengagement of twins.

REFERENCES

1. Schlichtkrull, J. *Acta Chem. Scand.* **11** (1956) 1459.
2. Schlichtkrull, J. *Acta Chem. Scand.* **11** (1957) 291.
3. Christiansen, J. A. *Fysisk Tidsskrift* **2** (1955) 200.

Received October 24, 1956.

ACTA CHEMICA SCANDINAVICA 11 (1957) 461—467

The Kinetics of the Acid-Catalysed Solvolysis of Ethylal in Water-Ethanol Mixtures

PENTTI SALOMAA

Department of Chemistry, University of Turku, Turku, Finland

The kinetics of the reversible, acid-catalysed hydrolysis of ethylal have been investigated in water-ethanol mixtures. By the stationary state principle, it has been shown that the results are in accord with a unimolecular solvolysis mechanism. The velocity of the overall solvolysis of ethylal can be measured by a refined kinetic method which makes use of determining the relative rates of the fast, product-forming hydrolysis and alcoholysis reactions of the unstable ethoxymethyl cation which is formed in the rate-determining, unimolecular reaction stage. The solvolysis rate constants are found to be closely related to the Hammett acidity function of the reaction solution, in accord with the unimolecular mechanism suggested.

The dependence of the solvolysis rate on the acidity function and on the dielectric properties of the medium have been discussed. By electrostatic theories on solvent influence on relative base strengths, an equation has been derived for the effect of medium on the velocity of a unimolecular, acid-catalysed reaction.

In several recent publications [1–4] evidence has been furnished to support the assumption that the hydrolysis of acetals takes place by a unimolecular mechanism, which in the rate-determining stage of reaction involves a formation of a positively charged carbonium ion from the conjugate acid of the acetal. In two cases, in the hydrolysis reactions of methylal [3] and trioxan [4] in concentrated aqueous acids, Hammett's acidity function was applied as a criterion of molecularity of the rate-determining reaction step.

In connection with the earlier study on the mechanisms of solvolytic reactions of ethoxymethyl acetate [5], the author also determined the rate constants for the reversible hydrolysis of ethylal

$$EtOCH_2OEt + H_2O \underset{k_a}{\overset{k_h}{\rightleftharpoons}} HCHO + 2\ EtOH\ (H^+ \text{ as catalyst}) \qquad (I)$$

in a number of water-ethanol mixtures. As the main applications hitherto made of the Hammett acidity function are to hydrolysis reactions in concentrated acids, it seemed of interest to study whether the general theory could also

be applied to the solvolysis of ethylal by dilute acid solutions, if the solvent is varied. In the present work, the earlier data on the reaction of ethylal have been extended by complementary experimental measurements, which were necessary for the kinetic applications.

RESULTS AND THEORY

Table 1 contains the values of the first-order rate constants k_h, determined for the hydrolysis of ethylal in water and in various water-ethanol mixtures at 25°C at 0.1 N hydrogen chloride concentration. The table also includes the values of the Hammett acidity function H_0 for the reaction solutions employed. These have been obtained by interpolation from the data given by Braude and Stern [6]. It is seen from the table that the values of k_h decrease continuously with increasing alcohol content of the solvent, whereas the values of H_0 pass through a maximum, *i. e.* the proton-availability of the solutions reaches a minimum, in solutions containing 50—70 moles per cent of ethanol. According to the theory (*cf.* Ref.[7]), the velocity of a mechanistically unimolecular, acid-catalysed solvolysis reaction should depend primarily on the acidity function of the reaction solution. As shown below, the requirements of the theory are satisfactorily fulfilled here, in spite of the continuously decreasing values of k_h with increasing alcohol content, depending on the fact that the values of k_h do not directly measure the velocity of a solvolysis reaction, which is assumed to be unimolecular.

Table 1. The solvolysis of ethylal in ethanol-water mixtures at 25° C at 0.1 N hydrogen chloride concentration. k_h = the first-order rate constant (in sec.$^{-1}$) for the formation of formaldehyde from ethylal. r = the molar ratio of formaldehyde and ethylal formed by the solvolysis of ethoxymethyl chloride. k_1 = the first-order rate constant (in sec.$^{-1}$) calculated for the overall solvolysis reaction of ethylal.

Mols. % EtOH	H_0	$10^6 \cdot k_h$	r	$10^6 \cdot k_1$
0	+ 1.01	16.4	∞	16.4
7.5	+ 1.20	10.3	89.0	10.4
18.2	+ 1.69	4.21	32.9	4.34
26.6	+ 1.91	2.64	20.6	2.77
34.9	+ 2.07	1.32	1.430	2.24
43.8	+ 2.19	0.861	1.008	1.72
51.2	+ 2.23	0.700	0.766	1.61
60.9	+ 2.24	0.590	0.534	1.69
69.3	+ 2.23	0.550	0.394	1.95
78.1	+ 2.16	0.539	0.280	2.46

For the sake of simplicity, let us neglect the reverse reaction, the acetalisation of formaldehyde, because this reaction does not affect the values of k_h (quite similar considerations apply to the case, in which the reverse reaction is taken into account). The unimolecular mechanism of acetal hydrolysis [2], as particularised to the hydrolysis of ethylal, is the following:

$$EtOCH_2OEt + H^+ \underset{\text{fast}}{\rightleftharpoons} EtOCH_2\overset{H}{\overset{|}{O}}{}^+Et \xrightarrow[\text{slow}]{} Et\overset{+}{O}{=}CH_2 + HOEt \quad (II)$$

$$Et\overset{+}{O}{=}CH_2 + H_2O \xrightarrow[\text{fast}]{} EtOH + H^+ + HCHO \quad (III)$$

The intermediate, unstable cation which is formed in the slow, rate-determining stage has a mesomeric structure, which is a hybridised form of the carbonium ion and oxonium ion structures. Supposing that the rate measurements are made at a fixed acid concentration, and denoting by $1/K$ the ratio of the concentration of ethylal to its conjugate acid at this acid concentration, and by k the rate constant of the unimolecular rate-determining reaction stage, respectively, it is found that the product $kK = k_1$ represents the experimental first-order rate constant of the reaction taking place at the acid concentration in question. Supposing that the reaction occurs in water, the value of k_1 is identical with the value of k_h, because only minute quantities of ethanol, formed by the hydrolysis, are present, and therefore practically all of the mesomeric cations, once having been formed, react with water molecules to give formaldehyde. Such a situation does not prevail in solvents of a moderate ethanol content. In these solvents, reaction (IV) which is the reversal of the rate-determining reaction stage competes significantly with reaction (III) for the unstable, intermediate cation:

$$Et\overset{+}{O}{=}CH_2 + EtOH \xrightarrow[\text{fast}]{} EtOCH_2\overset{H}{\overset{|}{O}}{}^+Et \quad (IV)$$

The relative contribution of this competing reaction increases with the alcohol content of the solvent, and thus the values of k_h which measure the rate of formaldehyde formation no longer represent the rate constants of the overall solvolysis reaction, k_1, which depend partly on the velocity of the rate-determining stage, partly on the pre-equilibrium of the proton uptake. In solutions containing ethanol, the other of the two rapid, product-forming reactions remains obscure, because it leads back to the initial reactant, ethylal. However, in this particular case, the relative contributions of the product-forming reactions are adapted to permit of measurements, and the values of k_1 can be determined, as shown below.

In view that both the substituting agents, water and alcohol, are the main constituents of the reaction solutions, the reactions of ethoxymethyl cation with water and alcohol molecules can be considered as first-order reactions, irrespective of their actual molecularities. Let k_{H_2O} and k_{EtOH} denote the first-order rate constants for these reactions, respectively. By the stationary state principle, it is found that

$$\frac{d[Et\overset{+}{O}{=}CH_2]}{dt} = k_1[EtOCH_2OEt] - (k_{H_2O} + k_{EtOH})\,[Et\overset{+}{O}{=}CH_2] = 0 \quad (1)$$

From eqn. (1) it follows that the rate of formaldehyde formation is given by

$$\frac{d[HCHO]}{dt} = k_{H_2O}[Et\overset{+}{O}{=}CH_2] = \frac{rk_1}{1+r}\,[EtOCH_2OEt] \quad (2)$$

in which the relative rates of the hydrolysis and alcoholysis reactions of the intermediate cation have been denoted by r:

$$r = k_{H_2O} / k_{EtOH} \tag{3}$$

On the other hand, the rate of formation of formaldehyde is given by

$$\frac{d[HCHO]}{dt} = k_h[EtOCH_2OEt] \tag{4}$$

in which k_h is the experimental rate constant for the hydrolysis reaction (I). A comparison of eqns. (2) and (4) shows that

$$k_1 = \frac{1 + r}{r} k_h \tag{5}$$

Eqn. (5), derived above, is consistent with the typical kinetic form of a unimolecular nucleophilic substitution [8].

From eqn. (5) it follows that, once we know the ratio of the rates of the rapid, product-forming reactions of the intermediate cation, the values of k_1 for the overall solvolysis reaction can be readily calculated from the values of k_h. In the present case, the values of r can be easily determined from the solvolysis products of ethoxymethyl chloride, $EtOCH_2Cl$, in the same media [5,9,10]. As the product-forming reactions involved in the unimolecular solvolysis of this compound are identical with those of the unimolecular mechanism suggested for the solvolysis of ethylal, the relative amounts of formaldehyde and ethylal formed by the solvolysis of ethoxymethyl chloride directly measure the values of r which can be also applied to the solvolysis of ethylal under the same conditions. Table 1 includes the values thus determined for r which have been taken partly from the data given in connection with the solvolysis of ethoxymethyl acetate [5], partly from the results of complementary measurements. Table 1 also gives the values calculated for k_1 by eqn. (5). It is seen from the table that the rate constants of the overall solvolysis reaction are closely related to the acidity function of the reaction solution, and pass through a minimum at approximately the same alcohol contents of the solvent, at which the proton-donating power of the acid solutions is least pronounced. This is in excellent agreement with the unimolecular mechanism suggested.

As the present method allowed the determination of the rate constants k_1 in alcohol-water mixtures of relatively widely varying values of the acidity function, thus differing from measurements on the solvolysis of alkoxymethyl esters [5,9], the dependence of log k_1 on the acidity function may be discussed in more detail. The theory in its original form suggests that a plot of log k_1 against $-H_0$ should give a straight line with a slope of unity (for references, see Ref.[7]). This relation has been found to be satisfactorily obeyed by several unimolecular hydrolysis reactions in concentrated aqueous acids. Table 2 which gives the values of log $k_1 + H_0$ for the solvolysis of ethylal in water-ethanol mixtures shows that the values increase with the alcohol content of the solvent. When the values of log k_1 are plotted against $-H_0$, it is found that the slope is somewhat less than unity, and decreases slightly, when passing to solutions of higher ethanol content. As shown below, these deviations

Table 2. The dependence of log k_1 on the acidity function and on the dielectric constant of the medium in the solvolysis of ethylal in water-ethanol mixtures at 25° C at 0.1 N hydrogen chloride concentration.

Mols. % EtOH	D	log $k_1 + H_0$	log $k_1 + H_0 - \frac{14.8}{D}$
0	78.5	− 3.78	− 3.97
7.5	68.6	− 3.78	− 4.00
18.2	57.3	− 3.67	− 3.93
26.6	50.0	− 3.65	− 3.95
34.9	44.5	− 3.58	− 3.91
43.8	39.8	− 3.57	− 3.94
51.2	36.5	− 3.56	− 3.97
60.9	32.8	− 3.53	− 3.98
69.3	30.5	− 3.48	− 3.97
78.1	28.0	− 3.45	− 3.98

from the slope of unity can be interpreted in terms of changes in the relation between the solvolysis rate and the acidity function, which may be expected to occur, when passing from water to solvents of lower dielectric constants.

Supposing the reaction mechanism to be unimolecular, the dependence of log k_1 on the acidity function is given by the equation:

$$\log k_1 = constant - H_0 + \log \frac{f_S f_{IH^+}}{f_{X^+} f_I} \qquad (6)$$

which is derived from the definition of H_0 by the Brönsted rate equation. In this equation, f's are the respective activity coefficients of the substrate S, the critical complex X^+, and the uncharged indicator base I and its conjugate acid IH^+, which have been used for the colorimetric determination of the values of H_0. As the critical complex contains only a proton, in addition to the substrate molecule, its activity coefficient is similarly affected by changes in medium as that of the conjugate acid of the substrate. Therefore, a slope of unity in the plot of log k_1 against $-H_0$ implies merely that the activity coefficient ratios of different bases to their conjugate acids are influenced by medium in a similar way, *i. e.* the relative base strengths of the different bases remain unchanged. However, such a relation is not to be expected to be valid when passing from water to solvents of lower dielectric constants.

Minnick and Kilpatrick [11] measured the relative acid strengths of a number of organic acids in water, methanol, ethanol and in water-dioxan mixtures, by determining the equilibrium constants for reactions:

$$H_1A + A_2^- \rightleftharpoons A_1^- + HA_2 \qquad (V)$$

Here, HA_1 and HA_2 are the acids, and A_1^- and A_2^- their anions, respectively. It was found that the values of the logarithms of the equilibrium constants were in all cases satisfactorily represented by functions of the form: $a+b/D$; a and b are constants for a given pair of acids, and D denotes the dielectric constant of the medium. This form of relation between the equilibrium constant and the dielectric constant is that expected by electrostatics (*cf.* Ref.[12]).

In this particular case, the success of the electrostatic theory, which has been found to fail for many other applications to solvent effects, is presumably due to the circumstance that the influence of solvent effects other than electrostatic becomes effectively masked, when changes of relative acid strengths are measured. As the electrostatic relation holds for reactions of type (V), it can be assumed that a similar relationship is valid for equilibria

$$B_1 + B_2H^+ \rightleftharpoons B_1H^+ + B_2 \qquad \text{(VI)}$$

which measure the relative strengths of a pair of uncharged bases, B_1 and B_2. It may be written

$$\log \frac{[B_1H^+][B_2]}{[B_1][B_2H^+]} = a + \frac{b}{D} \qquad (7)$$

in which a and b are constants. Taking into account that

$$\frac{[B_1H^+][B_2]}{[B_1][B_2H^+]} = \frac{f_{B_1}f_{B_2H^+}}{f_{B_1H^+}f_{B_2}} K_0 \qquad (8)$$

in which K_0 is the thermodynamic equilibrium constant, and f's are the activity coefficients, eqn. (7) implies that

$$\log \frac{f_{B_1}f_{B_2H^+}}{f_{B_1H^+}f_{B_2}} = a' + \frac{b}{D} \qquad (9)$$

in which a' is a constant, which is obtained by subtracting $\log K_0$ from a. Let B_2 denote the indicator base, which is used for the determination of the values of H_0, and let B_1 mean the basic substrate, which is undergoing an acid-catalysed, unimolecular solvolysis reaction the critical complex of which resembles closely the conjugate acid of the substrate. From eqns. (6) and (9), it then follows that

$$\log k_1 = constant - H_0 + \frac{b}{D} \qquad (10)$$

which equation represents the dependence of the velocity of the unimolecular reaction on the acidity function and on the dielectric constant of the reaction solution.

Table 2 contains the values of the dielectric constants for the water-ethanol mixtures employed. These values have been interpolated from the data of Åkerlöf [13]. A plot of $\log k_1 + H_0$ against $1/D$ for the solvolysis of ethylal in ethanol-water mixtures is found to give, within the limits of experimental accuracy, a straight line with a slope of 14.8. From the last column of Table 2, it is seen that the deviations from eqn. (10) are not larger than those, which may be ascribed to the sum of experimental errors involved in the determination of the values of $\log k_1$ and H_0.

The electrostatic theory suggests that the value of b, 14.8, found for ethylal solvolysis should be roughly of a similar order of magnitude as the values obtained by Minnick and Kilpatrick [11], when comparing the relative acid strengths of organic acids. Actually, the corresponding slopes measured for

different acid pairs varied between 5.5 and 21.0, when their signs were not taken into account. Moreover, the positive sign of b which indicates that the activity coefficient ratio of eqn. (6) decreases with increasing dielectric constant of the medium is not unexpected here. As the changes of activity coefficients of charged species with the dielectric constant are generally more significant than those of uncharged species, the decrease of the value of the activity coefficient ratio of eqn. (6) with increasing dielectric constant may be ascribed as being primarily due to a decrease in the value of f_{IH^+} / f_{X^+}. Here, IH^+ is the conjugate acid of *p*-nitroaniline or *m*-nitroaniline, which were used by Braude and Stern [6] for the determination of the values of H_0. These protonated bases have probably a more intensive charge distribution than that in the critical complex of the solvolysis of ethylal. According to eqn. (II), the rate-determining stage of the ethylal solvolysis involves a relatively large dispersal of charge. On the attainment of the transition state, the positive charge is being partly removed from the oxygen atom to a nascent mesomeric system, in which the charge is shared between a carbon atom and another oxygen atom. In addition, that carbon-oxygen bond which is broken in the rate-determining reaction step, is lengthened. In view of the less intensive electrical field around the critical complex of the ethylal solvolysis, in comparison to the fields of the conjugate acids of the nitroanilines, the activity coefficient of the critical complex is less reduced by increases in the dielectric constant of medium, as a result of which the value of f_{IH^+} / f_{X^+} decreases, when passing over to solvents of higher water content.

REFERENCES

1. O'Gorman, J. M. and Lucas, H. J. *J. Am. Chem. Soc.* **72** (1950) 5489.
2. Ingold, C. K. *Structure and Mechanism in Organic Chemistry*, London 1953, pp. 334–335.
3. McIntyre, D. and Long, F. A. *J. Am. Chem. Soc.* **76** (1954) 3240, 3243.
4. Bell, R. P., Bascombe, K. N. and McCoubrey, J. C. *J. Chem. Soc.* **1956** 1286.
5. Salomaa, P. *Acta Chem. Scand.* **11** (1957) 235.
6. Braude, E. A. and Stern, E. S. *J. Chem. Soc.* **1948** 1976.
7. Salomaa, P. *Acta Chem. Scand.* **11** (1957) 132.
8. Ingold, C. K. *Structure and Mechanism in Organic Chemistry*, London 1953, p. 313.
9. Salomaa, P. *Acta Chem. Scand.* **11** (1957) 141.
10. Salomaa, P. *Ann. Univ. Turkuensis, Ser.* **A XIV** (1953) No.1.
11. Minnick, L. J. and Kilpatrick, M. *J. Phys. Chem.* **43** (1939) 259.
12. Hammett, L. P. *Physical Organic Chemistry*, New York 1940, pp. 80–83.
13. Åkerlöf, G. *J. Am. Chem. Soc.* **54** (1932) 4125.

Received November 22, 1956.

ACTA CHEMICA SCANDINAVICA 11 (1957) 468—472

Activation in the Solvolytic Substitution Reactions of Unstable Alkoxymethyl Cations

PENTTI SALOMAA

Department of Chemistry, University of Turku, Turku, Finland

Measurements have been made of the reaction product composition in the unimolecular solvolysis of methoxymethyl chloride and ethoxymethyl chloride in water-ethanol mixtures at temperatures varying between 0°C and 75°C. In all cases, it was found that the relative amount of formal formed by the solvolysis, as compared with that of formaldehyde, increases with temperature. By the plots of log ([formal] / [formaldehyde]) against $1/T$, it was shown that the cation-ethanol reactions have activation energies of about 2 kilocalories per mole higher than the simultaneously occurring cation-water reactions.

The kinetic features of the fast, product-forming stages of unimolecular nucleophilic substitution reactions have been extensively discussed by Ingold, Hughes and co-workers [1–3]. In one particular case, for the reaction of di-*p*-tolylmethyl chloride in aqueous acetone containing added azide ions [3], these authors showed that the relative rate of formation of di-*p*-tolylmethyl azide, in comparison to that of di-*p*-tolylmethyl alcohol, increases with temperature by an amount which indicates that the cation-azide ion reaction has an activation energy of about 4 kilocalories per mole higher than the cation-solvent reaction, and therefore, at least the former process must be activated. On the other hand, there was no experimental evidence as to whether or not the fast cation-solvent reactions of unimolecular substitutions are activated. The theory on unimolecular solvolytic substitutions, developed by Ingold and Hughes, did not include, but did not require, an activation in these reactions.

An illustration of competing unimolecular, purely solvolytic substitution reactions, for which the relative contributions of the simultaneously occurring reactions can be easily measured at different temperatures, is furnished by the solvolysis of alkoxymethyl chlorides in water-ethanol mixtures. According to the earlier study [4], these reactions take place by the S_N1 mechanism:

$$ROCH_2Cl \xrightarrow[\text{slow}]{} R\overset{+}{O}{=}CH_2 + Cl^- \qquad (I)$$

$$R\overset{+}{O}{=}CH_2 + H_2O \xrightarrow[\text{fast}]{} HCHO + ROH + H^+; \qquad (II)$$

$$R\overset{+}{O}{=}CH_2 + EtOH \xrightarrow[\text{fast}]{} ROCH_2OEt + H^+$$

The present paper gives the results of a study, in which the solvolysis products of methoxymethyl chloride and ethoxymethyl chloride were determined at various temperatures.

The procedure used to investigate the product-forming reactions (II) was to determine the composition of the solvolysis product, this composition giving a direct measure of the relative rates of reactions (II). This method necessarily involved a performance of measurements in water-ethanol mixtures of such a composition, that the molar percentages of formaldehyde and formal formed by the solvolysis were of a similar order of magnitude, because only in such solvents the relative contributions of reactions (II) could be determined accurately enough. Although in the water-ethanol mixtures employed even the rate-determining reactions (I) were much too rapid to permit of kinetic measurements, still the compositions of the final products could be analysed. The results are collected in Tables 1 and 2. The molar percentage of formaldehyde

Table 1. Molar percentages of formaldehyde formed by the solvolysis of methoxymethyl chloride in water-ethanol mixtures at various temperatures.

43.8 mole % EtOH		60.9 mole % EtOH		78.1 mole % EtOH	
°C	mole % HCHO	°C	mole % HCHO	°C	mole % HCHO
0	60.9	0	47.0	0	29.8
10	58.9	10	44.7	10	28.2
20	54.7	20	42.3	20	23.7
30	51.3	30	38.8	30	22.8
40	50.2	40	37.0	40	22.6
50	47.2	50	34.5	50	22.3
60	45.3	60	31.2	60	20.0
70	43.9	70	30.5	70	18.5

Table 2. Molar percentages of formaldehyde formed by the solvolysis of ethoxymethyl chloride in water-ethanol mixtures at various temperatures.

43.8 mole % EtOH		60.9 mole % EtOH		78.1 mole % EtOH	
°C	mole % HCHO	°C	mole % HCHO	°C	mole % HCHO
0	58.6	0	41.9	0	28.4
		5	39.2		
12	53.5	10	38.8	12	23.6
		15	37.5		
25	50.2	20	35.9	25	21.9
		25	34.8		
38	46.5	30	34.6	38	20.2
		35	32.4		
50	44.6	40	30.7	50	17.5
		45	31.1		
62	41.3	50	27.9	75	14.0
		55	28.5		
75	39.6	60	26.4		
		65	26.1		
		70	25.0		

formed was found to be substantially unaffected by the initial concentration of alkoxymethyl chloride.

The tables show that the composition of the final product of solvolysis is dependent on temperature. In all cases the molar percentages of formaldehyde formed decrease with temperature. This indicates that the relative contribution of the latter reaction (II) increases with temperature, *i. e.* the latter reaction involves a higher energy of activation. Therefore, at least the cation-ethanol reaction must be activated. On the other hand, in view of the fact that both the reactions (II) are apparently of a similar type, there is no reason to assume that the cation-water reaction would not be activated.

Although the actual molecularities of reactions (II) cannot be determined by the available methods, these reactions can be considered as being of the first order, in view of the large excesses of water and ethanol molecules present in the reaction solvents. Supposing the Arrhenius equation to be valid for both the reactions, and denoting their respective Arrhenius parameters by A_{H_2O}, E_{H_2O}, A_{EtOH} and E_{EtOH}, and denoting by α the molar ratio of formal to formaldehyde present in the final product, it is seen that

$$\log \alpha = \log (A_{EtOH} / A_{H_2O}) - \Delta E / 2.303 RT \quad (1)$$

in which

$$\Delta E = E_{EtOH} - E_{H_2O} \quad (2)$$

According to eqn. (1), a plot of the values of log α against $1/T$ should give a straight line. Such plots are made in Figs. 1 and 2. Although there is some scattering of the values, the deviations from eqn. (1) do not exceed the experimental errors in magnitude. The slopes of the lines are seen to be of nearly the same magnitude, *viz.* —400, independently on the halide and solvent mixture used. The average value of the slopes indicates that the activation energy of the cation-ethanol reaction exceeds that of the cation-water reaction by about 1 800 calories per mole.

The theory on unimolecular solvolytic substitution, developed by Ingold and Hughes [1-3], suggests that the fast, product-forming reaction stage is an internal collapse of the solvation shell of the intermediate cation. If the theory is applied to the present case, it can be assumed that the inner solvation shell of the alkoxymethyl ion in water-ethanol mixtures consists of a number of water and ethanol molecules. When one of these molecules attains a certain, critical distance from the point of reaction, a destruction of the solvation shell occurs, and the reaction follows. One of the factors involved in the activation energies of reactions (II) may be merely due to the spatial conditions prevailing in the solvation shell. The water or ethanol molecule, which converts the solvated cation to the final product, must be able to overcome a certain amount of steric strain exerted by the neighbouring molecules present in the solvation shell, before the critical separation, which is necessary for the reaction to occur, can be attained. This may be one of the factors which give rise to a higher activation energy for the cation-ethanol reaction, in comparison to that of the cation-water reaction. As the size of ethanol molecules is larger than that of water molecules, the approach of an ethanol molecule to the critical distance of reaction is accompanied by a higher degree of destruction of the solvation shell.

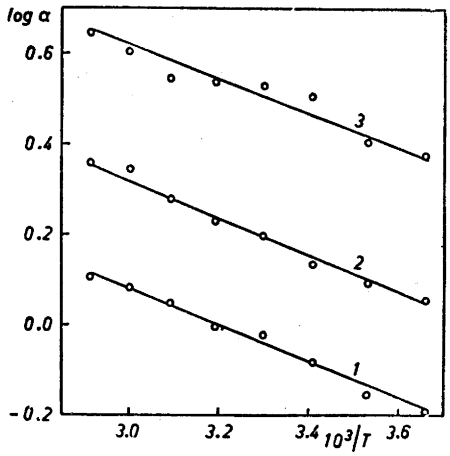


Fig. 1. Plot of log a against $1/T$ for the solvolysis of methoxymethyl chloride.

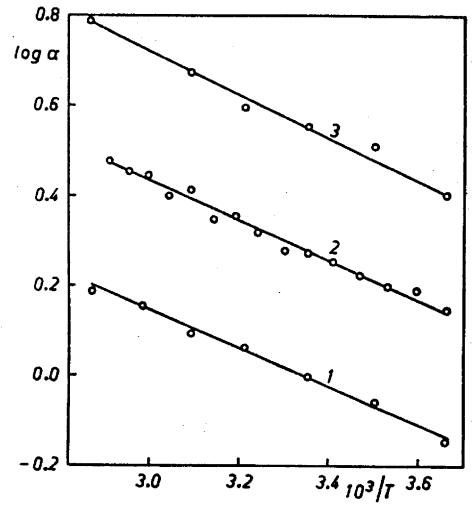


Fig. 2. Plot of log a against $1/T$ for the solvolysis of ethoxymethyl chloride.

1. 43.8 mole% EtOH. 2. 60.9 mole% EtOH. 3. 78.1 mole% EtOH.

Although reactions (II) have a certain amount of activation energy, their enormous rapidity is, however, understood by the activation entropies involved in such processes. The destructions of the solvation shells are accompanied by great decreases in order, *i. e.* the activation entropies must have large positive values, and hence the frequency factors are probably very large.

EXPERIMENTAL

The methods of preparing the materials, and those used for analysing the reaction product compositions were essentially those described earlier [4]. Owing to the great rapidity of the reactions, the product analysis could be performed almost immediately after mixing the reaction components. At relatively high temperatures, *viz.* at 50°C and above this temperature, the method of sealed bulbs was used, in order to eliminate volatility errors. In these experiments, a small, thin-walled glass ampoule containing the alkoxymethyl chloride was sealed together with small pieces of stone into a larger glass bulb which contained the reaction solvent. After the bulb, when immersed in a thermostat, had attained the thermostat temperature, the reaction components were brought together by vigorous shaking by which the small ampoule was broken. As it was verified that the subsequent reactions, the hydrolysis of formal and its reversal, were at relatively high temperatures rapid enough to effect an error in analysis, if the bulbs were kept a prolonged period of time at these temperatures, the bulbs were immersed in an ice-water mixture immediately after mixing the reaction components. After cooling, the bulbs were broken and the reaction product was analysed. By this method reproducible values were obtained even at the highest temperatures used.

Table 3 shows an example of experiments, in which the effect of initial alkoxymethyl chloride concentration on the composition of the final product was investigated. It is seen that the molar percentage of formaldehyde increases with decreasing alkoxymethyl chloride concentration. However, the increase is not material. In order to eliminate the

error due to differences in initial concentrations, all of the determinations, the results of which are included in Tables 1 and 2, were performed using approximately the same initial concentrations of the alkoxymethyl chlorides, *viz.* about 0.1 M.

Table 3. The solvolysis of ethoxymethyl chloride in 60.9 moles per cent ethanol at 25°C. The influence of the initial concentration on the composition of solvolysis product.

[$EtOCH_2Cl$] initially	0.3050	0.2273	0.1015	0.0627	0.0247
mole % HCHO in the product	32.0	33.9	34.8	35.9	35.2

REFERENCES

1. Bateman, L. C., Church, M. G., Hughes, E. D., Ingold, C. K. and Taher, N. A. *J. Chem. Soc.* **1940** 979.
2. Benfey, O. T., Hughes, E. D. and Ingold, C. K. *J. Chem. Soc.* **1952** 2488, 2494.
3. Hawdon, A. R., Hughes, E. D. and Ingold, C. K. *J. Chem. Soc.* **1952** 2499.
4. Salomaa, P. *Ann. Univ. Turkuensis, Ser.* **A XIV** (1953).

Received November 22, 1956.

ACTA CHEMICA SCANDINAVICA 11 (1957) 473—478

Preparation of Infinitely Thin Plutonium Sources by Adsorption

M. A. EL GUEBELY and T. SIKKELAND

Chemistry Department, Joint Establishment for Nuclear Energy Research, Kjeller, Norway

Infinitely thin sources have been prepared by adsorption of ^{239}Pu from hydrochloric acid solutions onto glass, aluminium and platinum surfaces. The validity of the method was studied by autoradiography. Results show that glass and aluminium are the best surfaces for such sources. The same method has been applied for the preparation of sources of ^{233}U on glass. Segregation of Pu and U has been observed on glass as well as on metallic surfaces.

Different methods exist for the preparation of α sources as described elsewhere [1]. King has studied the adsorption of Pu(IV) at trace concentration on the internal surface of a glass pipet [2]. He found that adsorption increases as the hydrogen-ion concentration is decreased. The purpose of the present work was to examine the possibility of using adsorption of Pu on glass and different metal surfaces as a method for the preparation of infinitely thin sources of α emitters as well as to determine the best conditions in which such preparation is to be carried out.

Haissinsky *et al.*[3] have developed an autoradiographic method for the study of metallic surfaces by examining the distribution of ranges of α-particles of Po deposited spontaneously or electrolytically on these surfaces. They found that in all cases there is an apparent shortening of a certain number of ranges in the gelatine. This was explained by the penetration of a certain number of Po-atoms inside the metallic surface. This apparent shortening would be a disadvantage for the preparation of sources of α-emitters and may lead to wrong interpretations of the α-spectrum [3].

In the present work we have applied the same method for the study of the adsorbed activity.

EXPERIMENTAL

The plutonium used in our experiments was separated from irradiated uranium by ion exchange technique [4]. Pu(IV) was prepared by dissolving a Pu-residue in 9 M hydrochloric acid containing 1 drop conc. nitric acid per ml [5].

^{233}U was prepared by extraction from neutron irradiated ^{232}Th. The reagents used were of analytical grade and the water was bidistilled. The adsorption of the activity was performed by simple rotation of the glass or metal slide in the solution. The glass slides, before adsorption, were washed in *aqua regia*, sodium carbonate and finally in water. Two types of glass were used: ordinary soda-objectiveglass (0.15 mm thick) and pyrex-glass.

The aluminium plates were either rolled or electropolished and 0.1 mm thick. Before use they were washed with acetone and water.

The platinum (0.2 mm thick) was electropolished and before adsorption the slide was washed with boiling conc. nitric acid and finally in water. The different slides were, after adsorption, washed twice in water and dried by rotating in air.

The surface of the slide was then, for a certain time, brought into good contact with an α-nuclear plate, Ilford E. 1, 50 μ thick. The aluminium plates had to be kept in a desiccator with P_2O_5 during exposure to depress the chemical attack on aluminium by the photographic emulsion. The plates were developed by a conventional photographic technique [6]. Rubbing of the plates was avoided in order not to reduce the lengths of the α tracks.

The lengths of the α-tracks were measured with a microscope (type Laborlux III, Ernst Leitz). The magnification was 570: and 400 horizontal tracks for each plate were investigated (those which had an angle of less than 10° with the plane of the emulsion) [3]. In all cases corrections for the background of the slides used were applied.

RESULTS

In Table 1 are given the conditions under which the experiments were performed. The experiment with the pyrex glass gave results similar to those obtained with soda-objective glass, and is not therefore indicated here.

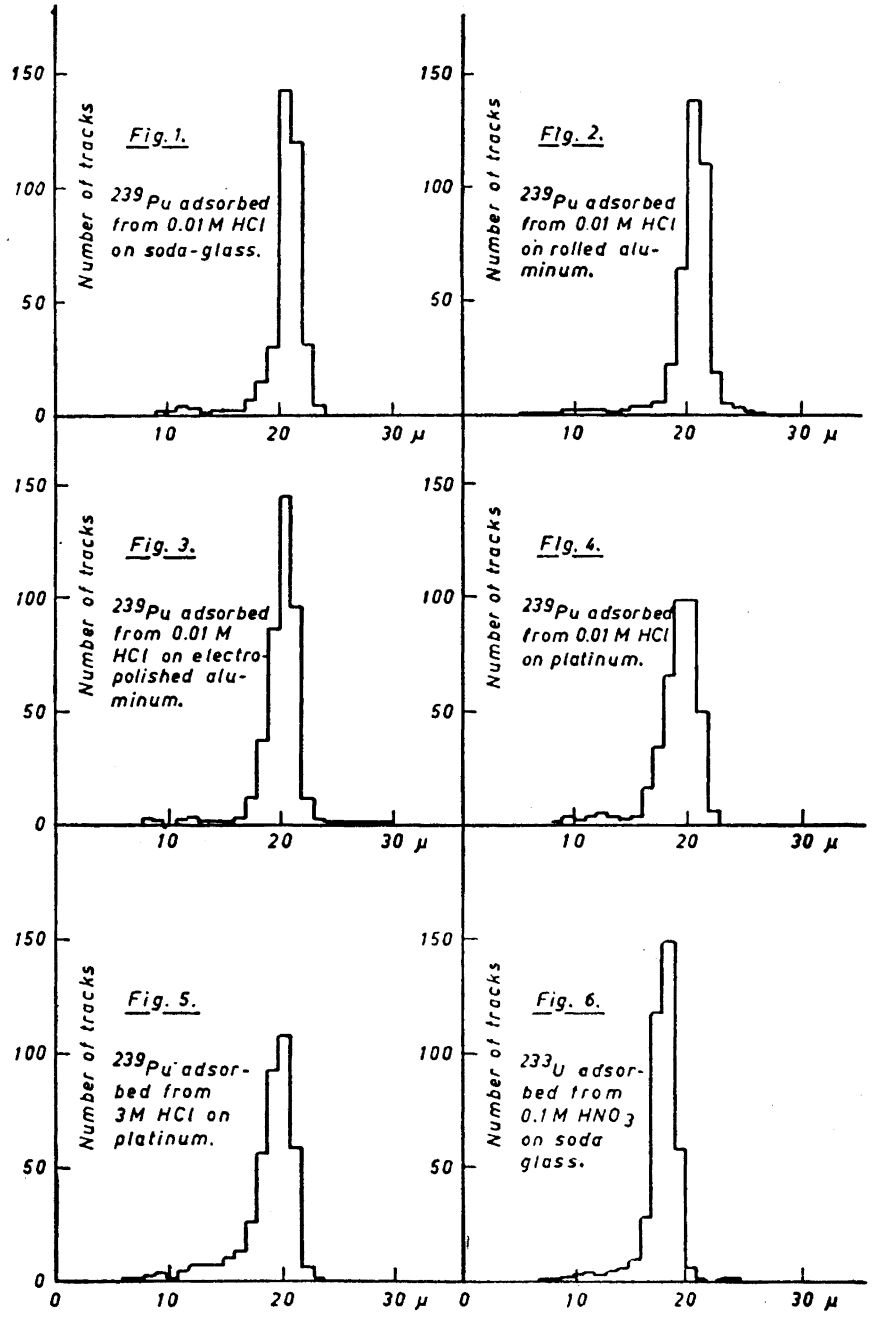
Table 1. Experimental conditions.

No.	Type of Slide	Acidity	Conc. in μg/ml	Ox. state added	Adsorption time in h.	Exposure time in h.
1.	Na-glass	0.01 M HCl	0.10	Pu(IV)	22	19
2.	Al-rolled	0.01 M HCl	0.10	Pu(IV)	4	42
3.	Electro-polished Al	0.01 M HCl	0.05	Pu(IV)	4	43
4.	Electro-polished Pt	3 M HCl	1.6	Pu(III) Pu(IV)	22	48
5.	»	0.01 M HCl	0.10	Pu(IV)	22	42
6.	Na-glass	0.1 M HNO_3	4.0	U(VI)	20	46

In Figs. 1—5 are plotted the histograms for ^{239}Pu of the number of α-tracks against their length, corresponding respectively to the experimental conditions indicated 1—5 in Table 1. Experiments were repeated several times, specially on glass (acidities from 0.01 to 3 M) and results were highly reproducible.

In Fig. 6 is given the histogram of the α-tracks of ^{233}U adsorbed onto glass (conditions 6 in Table 1).

Other experiments on Pu have shown that the shape of the histograms is independent of the lapse of time between the end of adsorption and the beginning of exposure, at least for 12 days. Again changing of acidity from 3 M hydrochloric acid (ionic species of Pu) to 0.01 M hydrochloric acid (colloidal Pu) similarly had no influence on the form of the range distribution curve.



Figs. 1—6. Histograms of number of tracks *vs.* length.

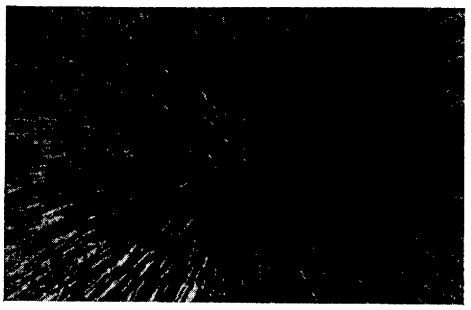


Fig. 7. Segregate on aluminium.

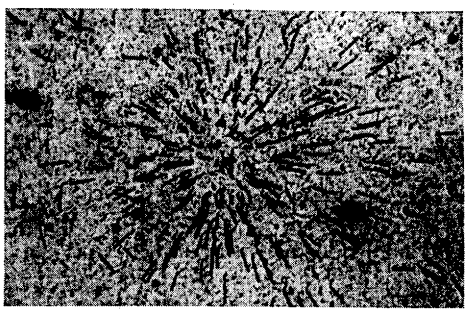


Fig. 8. Segregate on glass.



Fig. 9. Random distribution of tracks.

In all the plates examined segregates of ^{239}Pu or ^{233}U were observed on certain points. In Figs. 7 and 8 are given photographs of segregates of ^{239}Pu on aluminium and on glass, respectively, and in Fig. 9 a photograph from a region with random distribution of α-tracks.

DISCUSSION

The experiments show that the most probable range of the α-particles of ^{239}Pu (α: 5.10, 5.15, 5.17 MeV) in the Ilford E. 1 plate is 21 ± 1 μ which is in good agreement with the α-energy-range curve [7]. For that of ^{233}U (α: 4.80 MeV) we found 18.5 ± 1 μ.

Apparent shortening has been observed in the case of platinum (14 tracks per 100 have ranges shorter than 18 μ). This phenomenon is far less pronounced on aluminium and glass (only 3 tracks per 100 have ranges shorter than 18 μ).

Apparent shortening may be due to:

a) the penetration of plutonium atoms into the surface, phenomenon comparable to that found previously for polonium [3].
b) possible backscattering of the α-particles from the sample plate.

The backscattering of ^{239}Pu α-particles from platinum has been studied by Cunningham *et al*[8]. They found that identical quantities of essentially weight-

less samples of ^{239}Pu show a 3 % lower counting rate when mounted on quartz in a 50 % geometry counter than similar samples mounted on platinum and concluded that this difference is possibly due to small angle scattering in the latter case. This backscattering would be more manifest for the horizontal or nearly horizontal tracks on which we concentrated our studies. Backscattering would lead to a loss of a part of the energy of the scattered particles and hence to shorter ranges in the gelatin. In fact our experiments show that the histograms for electropolished and rolled aluminium are similar, in spite of the relatively rougher surface of the latter. This could be understood if we assume that backscattering plays an appreciable role for apparent shortening. Due to the low atomic number of aluminium, backscattering from it should be far less pronounced than from platinum. Therefore the absence practically of apparent shortening on glass and aluminium may be explained by the highly plane surface of glass objective slides and negligible backscattering from both materials. The presence of a certain number of shorter ranges for ^{233}U on glass is probably due to a trace of thorium impurity.

The study of the adsorbed phase represented certain peculiarities. In all conditions using ^{239}Pu or ^{233}U on glass or metallic surfaces, and irrespective of the acidity, part of the adsorbed atoms was distributed at random while the rest was in the form of segregates. The measurements of the length of the tracks originating from the segregates were often very difficult, due to the high activity in these regions. No conclusions regarding shortening may then be drawn from these cases. The numbers of Pu atoms accumulated in the segregate may be calculated from the number of tracks emanating from it. Assuming 2 π-geometry the number of ^{239}Pu atoms, N, corresponding to n tracks in the emulsion after d days exposure is:

$$N = \frac{24\,300 \cdot 2\ n \cdot 365}{0.69 \cdot d} = (2.57\ n/d) \times 10^7 \text{ atoms} \qquad (1)$$

Using this formula we have found segregates with 10^8 up to $\gg 10^{10}$ atoms. The number of atoms in the biggest segregates, as for example that of Fig. 7, was impossible to calculate due to the high density of tracks in their regions.

The maximum activity in 2 α-geometry of the adsorbed ^{239}Pu was 135 c/m/cm^2 which corresponds to 5×10^{12} atoms/cm^2. Assuming a homogeneous surface and taking the value of 1 Å for the radius of the Pu atom, the maximum covering of the surface in our experiments did not exceed 0.2 % of a "monoatomic" layer. Under such conditions the distribution of the energy of adsorption on the surface should play an important role in the distribution of the adsorbed atoms. The segregation phenomenon may be attributed to the presence of particularly privileged microscopic regions of the surface possessing a high energy of adsorption. Further study of this phenomenon is necessary to elucidate clearly its nature.

CONCLUSION

The experiments show that the adsorption method can be used for the preparation of extremely thin sources of plutonium. Glass and aluminium offer particularly good conditions. A relatively high pH would be preferable owing

to the higher adsorbability, probably due to the formation of radiocolloids. The adsorption method presents the advantages of simplicity and the possibility of having sources without self-absorption. The limit of the method is that a relatively high specific activity of the α-emitter is to be accounted for, but the method could be applied with good results even for ^{233}U ($T_{1/2} = 1.6 \times 10^5$y).

Acknowledgement. We are indebted to Dr. E. Sæland, Director of Isotopes, who kindly provided us with ^{233}U and to Dr. Younis for valuable help in connection with the autoradiographic technique.

One of us, M. El Guebely, wishes to express his deepest thanks to Dr. G. Randers, Director of JENER and to Dr. T. J. Barendregt, Director of Chemistry, JENER, for the hospitality and the possibility they provided him to work in the institute.

REFERENCES

1. Hufford, D. L. and Scott, B. F. Paper 16.1 *The Transuranium Elements, National Nuclear Energy Series IV 14B.*
2. King, E. L. Paper 4.11 *The Transuranium Elements, National Nuclear Energy Series* IV 14B.
3. Coche, M. A., Faraggi, H., Avignon, P. and Haissinsky, M. *J. phys. radium,* Serie VIII, Tome X (1949) 312.
4. Sikkeland, T. *JENER Report* No. 38.
5. Grouch, E. A. C. and Cook, G. B. *J. Inorg. Nuclear Chem.* 2 (1956) 223.
6. Yagoda, H. *Radioactive Measurements with Nuclear Emulsions,* John Wiley, N.Y. 1949
7. Lattes, C. M. G., Fowler, P. H. and Cuer, P. *Nature* 159 (1947) 301.
8. Cunningham, B. B., Ghiorso, A. and Hindman, J. C. Paper 16.3 *The Transuranium Elements, National Nuclear Energy Series IV 14B.*

Received September 22, 1956.

ACTA CHEMICA SCANDINAVICA 11 (1957) 479—483

The Diamagnetic Susceptibility and the High-Frequency Term in Co(III)- and Rh(III)-Complexes

C. J. BALLHAUSEN and R. W. ASMUSSEN

Chemistry Departments A and B, Technical University of Denmark, Copenhagen, Denmark

A number of diamagnetic Co(III)- and Rh(III)-complexes are discussed on the basis of Van Vleck's formula for the magnetic susceptibility. It seems possible to correlate the measured magnetic susceptibility with the tendency for forming "covalent" complexes by means of a calculation of the high-frequency term in this formula. As to be expected it is found that the "degree of covalency" for different ligands follows the spectrochemical series closely. The theory gives an interpretation of the variation of the magnetic susceptibilities in the series of complex ions $Co(NO_2)_n\ (NH_6)_{6-n}$.

In this note the measured magnetic susceptibilities of various diamagnetic Co(III)- and Rh(III)-complexes will briefly be considered for the purpose of studying the bonding in these compounds. Diamagnetism of a complex has in the past generally been taken as an indication of "covalency" if spin magnetism could be attributed to the gaseous central ion [1]. This criterium, however, can no longer be considered to be valid, as it has been shown [2] that an "ionic" model of the same complex certainly also could lead to diamagnetism. The actual bonding in the compounds is therefore likely to be one in between these two extremes.

We will try to show that it seems possible to indicate the "degree of covalency" for a number of diamagnetic hexacoordinated Co(III)- and Rh(III)-compounds. Further, the qualitative explanation of the variation in the measured susceptibilities in the series of Co(III)-nitroammines suggested by Asmussen [3] is in accordance with the present theory. The experimental results have all been taken from the long series of measurements on Co(III)- and Rh(III)-complexes earlier carried out by one of us [3,4].

THEORY

Van Vleck [5] has shown that for a diamagnetic substance the following formula holds for the measured molar susceptibility χ_M:

$$\chi_M = \frac{2}{3} N \left(\frac{e}{2mc}\right)^2 \sum_n \frac{|(n^*|\vec{L}|o)|^2}{E_n - E_0} - \frac{Ne^2}{6mc^2} \sum_q \overline{r_q^2}$$

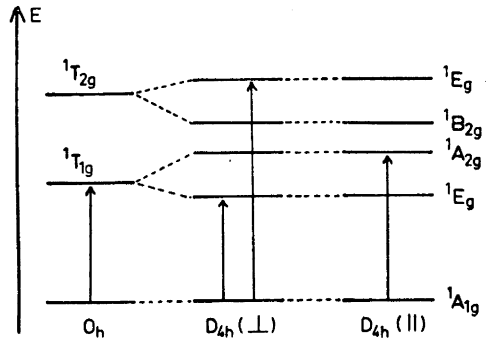


Fig. 1. The various levels and allowed magnetic dipole transitions for diamagnetic Co(III) and Rh(III) complexes.

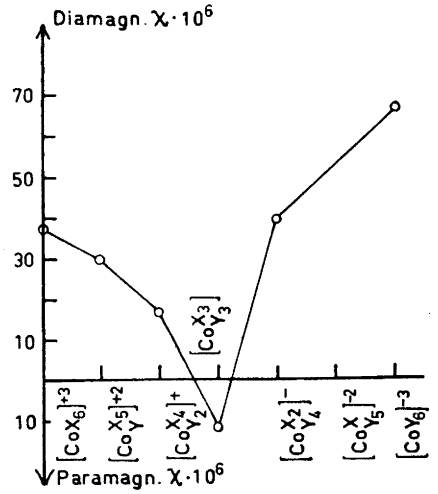


Fig. 2. The variation of the "paramagnetic increment" by substitution. The compounds are CoX_nY_{6-n} with $X = NH_3$ and $Y = NO_2^-$. The figure is taken from Ref.[3]

Here N is Avogadro's number, E_n and E_0 the energy of the upper and the lower state, e and m the electronic charge and mass, c the velocity of light and $\overline{r_q^2}$ the mean square radius for electron number q. $M^2 = |(n^*|\vec{L}|o)|^2$ is the square of the operator representing the angular momenta (unit $\hbar$) as taken between the ground and the upper state. The first term in the equation gives rise to a temperature independent paramagnetism if L is able to couple ψ_n with ψ_0; the second term is a purely diamagnetic term.

Let us assume that the crystal field approximation is valid when dealing with complexes of the transition metals. By means of the wave-functions thus obtained it is easy to calculate the high-frequency term in Van Vleck's equation. Furthermore we would expect the results to be a good approximation at least for cubic and pseudocubic complexes. However, it is perhaps instructive to see what information can be obtained by means of symmetry arguments before we give the results of such a calculation.

In complexes of symmetry O_h the angular momenta $\vec{L}$ transforms under T_{1g}. As the groundstate of a diamagnetic Co(III)- and Rh(III)-complex always transforms under A_{1g} in any symmetry, it follows that, in O_h, $\vec{L}$ can only couple the ground state to an upper state of symmetry T_{1g}. Crystal field considerations [6-7] show that such a state is found as the first excited level in diamagnetic d^6 systems, the next excited level being a T_{2g} state. Both are derived by exciting *one* electron from the groundstate, and as we are operating with determinental one-electron wavefunctions, these are thus the only excited states we need to consider in the strong field approximation.

Table 1. Variation of the diamagnetic term with various ligands. All the measured magnetic susceptibilities are from Refs.[3,4] except that of the Zn(II) complex, which was measured for this investigation by J. Potts Jensen. Details to be published later.

Compound	χ_M of naked metal ion $\times 10^6$	Calculated high term $\times 10^6$	Calculated diamagn. term $\times 10^6$
$Co(ox_3)^{-3}$	−42	250	292
$Co(NH_3)_6^{+3}$	52	198	146
$Co(en_3)^{+3}$	59	196	137
$Co(CN)_6^{-3}$	32	130	98
trans $Co(en)_2Cl_2^+$	69	235	166
trans $Co(NH_3)_4(H_2O)_2^{+3}$	67	214	147
$Rh(NH_3)_5Cl^{+2}$	10	143	133
$Rh(NH_3)_5NO_2^{+2}$	20	122	102
$Rh(NH_3)_6^{+3}$	65	127	62
$Zn(en)_3^{+2}$	−14	0	14

If the system under consideration has tetragonal symmetry D_{4h}, the magnetic moment transforms under E_g (perpendicular to the four-fold axis) and under A_{2g} (parallel to the four-fold axis). On going from O_h to D_{4h} symmetry the degeneracy of the excited states is partially removed: $T_{2g} \rightarrow B_{2g} + E_g$ and $T_{1g} \rightarrow A_{2g} + E_g$. Therefore the magnetic moment can couple the groundstate to three of the four states; A_{2g} ($\parallel$) and the two E_g ($\perp$) (*cf.* Fig. 1). Because of the different selection rules we would predict the magnetic susceptibility in diamagnetic Co(III) and Rh(III) complexes having tetragonal symmetry to be rather anisotropic.

The actual calculation gives[9] that in O_h symmetry $M^2 = 24\ \hbar^2$ for the $^1A_{1g}$ to $^1T_{1g}$ transition. With no account taken of the interaction between the two E_g states, and with the wavefunctions given by Ballhausen and Moffitt [10] we obtain for D_{4h}: $M^2 = 16\ \hbar^2$ for the transition $^1A_{1g}$ to $^1E_g(T_{1g})$, $M^2 = 8\ \hbar^2$ for $^1A_{1g}$ to $^1A_{2g}(T_{1g})$ and $M^2 = 0\ \hbar^2$ for $^1A_{1g}$ to $^1E_g(T_{2g})$. The energy differences are taken from the absorption spectra [11,12] and hence we can calculate the high-frequency term in the formula. It is interesting to notice that in D_{4h} symmetry the value of the "parallel" high-frequency term is exactly one third of the value for the high-frequency term in O_h symmetry; the denominater in the expression is namely equal for these two transitions [10].

We are interested in the diamagnetic term which can be obtained if the calculated high-frequency term is subtracted from the measured molar susceptibility of the *gaseous* metal-ion. The results are given in Table 1. The measured molar susceptibilities are all taken from Refs. [3,4] and corrected according to the prescriptions given there.

CONCLUSIONS AND DISCUSSION

It is seen from the table that the pure diamagnetic term is highly dependent upon the nature of the various ligands, having a maximum with oxalate and a minimum with cyanide as ligands. This sequence follows the spectrochemical series very closely. According to the crystal field theory we would

expect the diamagnetic term to be nearly independent of the nature of the different ligands. As this is not the case we must conclude that the complexes under consideration have at least partially "covalent" bonds. This result must then of course be taken into consideration in a recalculation of the high-frequency term. However, this is estimated to produce only a small correction of the previous calculated numbers, which is unable to change these to any considerable extent.

A reasonable explanation of the table seems thus to be that more and more electrons are donated from the ligands to the metal ion when going from oxalate towards cyanide. Ultimately a closed shell of e_g-electrons may be obtained, having the effect of lowering the diamagnetic term of the gaseous ion. This explanation is confirmed by the value of the diamagnetic term for Zn(II) complexes. Zn complexes have a filled d-shell with virtually no high-frequency term, and these compounds are seen to have a very small diamagnetic term.

Given a hexacoordinated diamagnetic Co(III)- or Rh(III)-complex with two different kinds of ligands, X and Y, placed in this sequence in the spectrochemical series. Then it seems qualitatively possible to explain the found variation [3] of the "paramagnetic increment" with substitution (*cf.* Fig. 2). As the symmetry is lowered from CoX_6 to CoX_4Y_2 and further to CoX_3Y_3 the high-frequency term in Van Vleck's formula must increase, firstly because all the higher levels can be coupled *via L* to the groundstate in the resulting low symmetry and secondly because of the depression in energy of some of the levels. By again increasing the symmetry to CoX_2Y_4 and further to CoY_6 the high-frequency term decreases again. This behaviour is just found for the measured values of the molar susceptibilities of the Co(III) nitro-ammines (Fig. 2). Both NH_3 and NO_2^- have the same value for their diamagnetic corrections so by a comparison of the different compounds this correction does not disturb. Finally we have a higher value of the molar diamagnetic susceptibility in $Co(NO_2)_6^{-3}$ than in $Co(NH_3)_6^{+3}$ because $E_n - E_0$ is greater in the former than in the latter case.

Thus there seems to be a close correspondence between the measured diamagnetism and the amount of electrons donated to the transition metal central ion. The closer the magnetism of the compounds is to that of the corresponding Zn(II) complexes, the more "covalent" they seem to be.

In this note we have followed the usual convention in assuming the diamagnetic susceptibilities of the ligands to remain unaltered by complex formation. This is probably not a very good assumption as the final analysis depends upon differences between numbers of nearly the same order of magnitude. Nevertheless, we feel that the tendency, being also what one would expect from chemical considerations, is too pronounced to be purely accidental.

REFERENCES

1. Pauling, L. *Nature of the Chemical Bond.* Cornell University Press, 1939.
2. Van Vleck, J. H. *J. Chem. Phys.* 3 (1935) 807.
3. Asmussen, R. W. *Studies in the Magnetochemistry of Inorganic Complex Compounds* (Thesis in Danish). København, 1944.

4. Christiansen, J. A. and Asmussen, R. W. *Kgl. Danske Videnskab. Selskab, Mat.-Fys. Medd.* **12** (1934) No. 10.
5. Van Vleck, J. H. *Theory of Electric and Magnetic Susceptibilities.* Oxford University Press, 1932.
6. Orgel, L. E. *J. Chem. Soc.* **1952** 4756.
7. Tanabe, Y. and Sugano, S. *J. Phys. Soc. Japan* **9** (1954) 753.
8. Moffitt, W. and Ballhausen, C. J. *Ann. Rev. Phys. Chem.* **7** (1956) 107.
9. Moffitt, W. *J. Chem. Phys.* **25** (1956) 1189.
10. Ballhausen, C. J. and Moffitt, W. *J. Inorg. Nucl. Chem.* **3** (1956) 178.
11. Basolo, F., Ballhausen, C. J. and Bjerrum, J. *Acta Chem. Scand.* **9** (1955) 810.
12. Jørgensen, C. Klixbüll *Acta Chem. Scand.* **10** (1956) 500.

Received November 17, 1956.

ACTA CHEMICA SCANDINAVICA 11 (1957) 484—486

Insulin Crystals

VI. The Anisotropic Growth of Insulin Crystals

JØRGEN SCHLICHTKRULL

Novo Terapeutisk Laboratorium, Copenhagen, Denmark

Rhombohedral pig insulin crystals are formed in a medium containing Indian ink. Growth of the isolated black crystals is continued in a non-coloured medium. It is observed that insulin is not deposited on three of the faces meeting in one of the obtuse vertices, whereas the three opposite faces move outwards with equal rates of growth. The rate is proportional to $(c_s - c)^2$ where c_s is the actual and c the final insulin concentration of the medium. This anisotropy of growth indicates asymmetry of the atomic configuration within the unit-cell.

The purpose of the present investigation is to examine the linear rates of deposition of insulin on the faces during crystallization. Perfect rhombohedral single crystals are obtained when pure pig insulin is crystallized from a citrate buffer and when beef insulin is crystallized from a buffered solution of sodium chloride [1]. The crystals are geometrically similar, as the faces of a growing crystal remain equal in size. Hence, the dimensions of a crystal may be defined by one parameter only, *e. g.* by the largest diagonal, l, in the crystal projection on a plane through one of the faces [2]. Previous experiments demonstrate that during crystallization in a 7 % saline

$$\frac{dl}{dt} = \text{const.}\ (c_s - c)^2 \qquad (1)$$

where c_s is the actual and c the final concentration of dissolved insulin [3]. The linear rate of growth, dl/dt, was found to be independent of the crystal size.

THEORY

The three faces meeting in one of the obtuse vertices are called A, B and C, and the opposite faces A_0, B_0 and C_0 where A is parallel to A_0, etc. The growth of a crystal proceeds as insulin is deposited on the faces which thereby move outwards in directions perpendicular to the faces. The rates of movement

caused by deposition are h_A, h_{A_0}, etc. Let the distances between parallel faces be a, b and c, respectively. Then the rates of increase of these distances are

$$\frac{da}{dt} = h_a = h_A + h_{A_0} \tag{2a}$$

$$\frac{db}{dt} = h_b = h_B + h_{B_0} \tag{2b}$$

$$\frac{dc}{dt} = h_c = h_C + h_{C_0} \tag{2c}$$

As during growth

$$a = b = c \tag{3}$$

it follows that

$$h_a = h_b = h_c = h = \text{const.} \frac{dl}{dt} \tag{4}$$

where h symbolizes the common rate of increase of the distances between parallel faces. The trigonal symmetry implicates that the atomic structure of the three faces is identical. Hence, it is assumed that

$$h_A = h_B = h_C = H \tag{5}$$

and

$$h_{A_0} = h_{B_0} = h_{C_0} = H_0 \tag{6}$$

It follows from eqns. (2), (4), (5) and (6) that

$$h = H + H_0. \tag{7}$$

EXPERIMENTAL

It has been observed that when small (5 μ) seed crystals are allowed to grow into bigger (30μ) crystals the seed particles remain in one of the obtuse vertices of the growing crystal [4]. If the rate of deposition of insulin is the same on all six faces then the seeds are expected to be enclosed in the center of the crystal. The observation reveals that insulin is not deposited on the three faces meeting in one of the obtuse vertices. This peculiarity of growth has now been substantiated by staining crystals during the first period of their growth. Indian ink is suitable for the purpose as it does not diffuse within the crystal body.

Pork insulin was recrystallized from a medium containing 0.5 % insulin, 0.08 % $ZnCl_2$, 0.05 M sodium citrate, 15 % (v/v) acetone and 1 % (v/v) Indian ink (Pelikan No. 541), pH = 6.3. The clear solution was stirred slowly mechanically. During crystal growth particles of Indian ink became enclosed in the crystal bodies and stained them. The crystals were filtered off and one part allowed to continue growing in a medium of the original composition but without Indian ink. The other part was grown in a crystallization medium containing 1.7 % insulin, 0.014 % Zn^{++} (total Zn), 0.1 M sodium acetate, 7 % NaCl, pH = 5.5. In both cases the weight of stained crystals was 10 % of the weight of insulin present.

Finally, the two crystal suspensions were fixed in gelatine in order to prevent sedimentation of all the crystals on their faces during the microscopical inspection. This revealed that the original black part of the crystal is lying in one of the obtuse vertices of the large crystal and not in the center (Fig. 1).

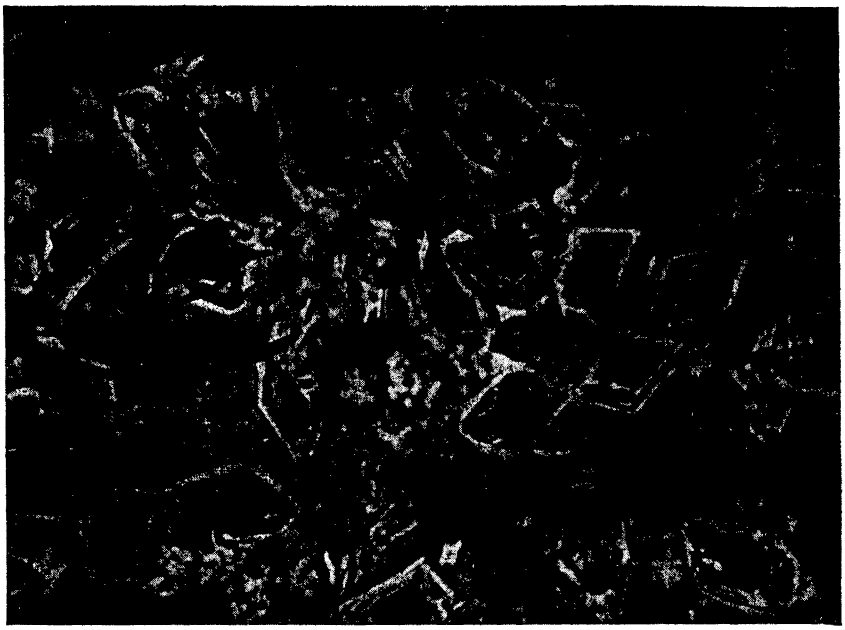


Fig. 1. Stained crystals after growth in saline medium (300 ×).

CONCLUSION

These experiments demonstrate that insulin is only deposited on the three faces meeting in one of the obtuse vertices of the crystal. The linear rate of deposition does not vary between these faces. Thus, in eqn. (7) either H or H_0 is zero. It is concluded that the atomic structure of the three moving faces is different to that of the immobile faces. The structural difference also pertains to the unit-cells as they are all identically orientated within the crystal. In other words, when the unit-cell is turned upside down so as to invert the trigonal axis, it is impossible to obtain the original atomic configuration by rotating about this axis.

REFERENCES

1. Schlichtkrull, J. *Acta Chem. Scand.* **10** (1956) 1459.
2. Schlichtkrull, J. *Acta Chem. Scand.* **11** (1957) 291.
3. Schlichtkrull, J. *Acta Chem. Scand.* **11** (1957) 439.
4. Schlichtkrull, J. *Acta Chem. Scand.* **11** (1957) 299.

Received December 19, 1956.

ACTA CHEMICA SCANDINAVICA 11 (1957) 487—490

Acetic, Propionic and Butyric Esters of 2-Dimethylaminoethanol, 2-Dimethylaminoethanthiol and 2-Dimethylamino-1-methylethanol

L.-E. TAMMELIN

Research Institute of National Defence, Dept. 1, Sundbyberg 4, Sweden

The nine esters corresponding to 2-dimethylamino-ethanol, 2-dimethylamino-ethanthiol, 2-dimethyl-1-methyl-ethanol and acetic, propionic and butyric acid have been prepared and described as ammonium bromides and free amines. The corresponding acid-base pairs have been used for the determination of pK_a.

Esters of dimethylaminoethanol and related compounds are of interest as precursors of the choline esters in preparative work. In synthesis of the choline esters the corresponding tertiary amines are not necessarily prepared in pure form [1]. Some interest has been shown, however, in comparative studies of the tertiary and quaternary compounds in relation to cholinesterase [2,3]. Moreover, the action on the central nervous system of compounds related to the cholinesters but of the tertiary type has received attention. Some modifications of an earlier method for the preparation of choline esters [1] are therefore presented which enable the tertiary amino esters to be prepared.

It has been shown by Wilson [2,5] that the ammonium ester is more easily hydrolyzed by cholinesterases than is the amino ester in the case of dimethylaminoethyl acetate. In a system with a given pH and ionic strength, *e. g.* body fluids, the pK_a governs the quotient (amine) / (ammonium). In view of the probable pharmacodynamic disparity of the amino and ammonium forms, due, *e. g.*, to their different affinities for cholinesterase, the degree of protolysis is obviously of interest. It was therefore decided to determine the pK_a of the esters synthesized.

METHODS

The mode of synthesis followed is esterification of the ethanol or thiol by means of acid anhydride, preliminary purification by distillation and precipita-

Table 1. Boiling points of the crude distillates from the esterification.

Alcohol	Acetic ester	Propionic ester	Butyric ester
2-Dimethylaminoethanol	68°/8 mm	70°/8 mm	81°/8 mm
2-Dimethylaminoethanthiol	182°	190°	205°
2-Dimethylamino-1-methyl-ethanol	152°	165°	185°

tion of the amino ester by hydrogen bromide, recrystallisation or liberation of the free amine and redistillation.

Esterification. One mole of the ethanol or thiol (the thiols were prepared *ad modum* Hansen [4]) derivative is heated on a water bath with 1 mole of acid anhydride overnight. The reaction mixture is distilled. All fractions are collected, up to and including the one at the temperature given in Table 1.

Dimethylammonium ester bromides. The crude distillate from the esterification is diluted six times with anhydrous ether. Hydrogen bromide is bubbled through the solu-

Table 2.

Dimethylamino-ethanol	Amines							Ammonium bromides							
		n_D^{25}	d_{25}	R_D calc.	R_D found	B. p. °C/mm	M	M	M.p. °C	% Br calc.	% Br found	% C calc.	% C found	% H calc.	% H found
acetate	$C_6H_{13}O_2N$	1.4158	0.932	35.2	35.2	44/8	131.2	212.1	84	37.7	37.4	33.9	33.4	6.7	6.6
propionate	$C_7H_{15}O_2N$	1.4193	0.916	39.8	39.8	59/10	145.2	226.1	112	35.3	35.3	37.2	37.2	7.1	7.0
butyrate	$C_8H_{17}O_2N$	1.4233	0.909	44.5	44.8	65/8	159.2	240.1	111	33.3	33.4	40.0	39.9	7.6	7.4
Dimethylamino-ethanthiol										% N calc.	% N found				
acetate	$C_6H_{13}ONS$	1.4763	0.981	41.7	41.6	78/14	147.3	228.2	96	6.14	6.10	31.6	31.3	6.1	6.1
propionate	$C_7H_{15}ONS$	1.4762	0.964	46.4	46.6	89/8	161.3	242.2	88	5.79	5.76	34.7	34.2	6.2	6.1
butyrate	$C_8H_{17}ONS$	1.4693	0.948	50.8	51.2	101/8	175.3	256.2	80	5.48	5.43	37.5	37.2	6.7	6.9
Dimethylamino-methylethanol										% Br calc.	% Br found				
acetate	$C_7H_{15}O_2N$	1.4132	0.907	39.8	39.9	53/13	145.2	226.1	121	35.3	35.3	37.2	37.3	7.1	7.2
propionate	$C_8H_{17}O_2N$	1.4150	0.893	44.5	44.5	62/8	159.2	240.1	123	33.3	33.2	40.0	39.8	7.6	7.4
butyrate	$C_9H_{19}O_2N$	1.4191	0.886	49.1	49.2	71/12	173.3	254.2	129	31.4	31.3	42.5	42.3	7.9	7.9

tion until all amine has precipitated. The crude precipitate is recrystallized from dioxan. Thus, a pure preparation is obtained in a yield of about 65 % calculated from the alcohol or thiol. For analytical data see Table 2.

Dimethylamino esters. Sodium hydroxide in water solution is used for liberation of the free amine. Rapid ether extraction, drying of the ether solution with sodium sulfate and distillation under reduced pressure give pure preparations of the amino esters. The yield is about 70 %, calculated from the crude ammonium ester bromide.

Physical data. Densities, refractive indices, boiling points and molar refractions are shown in Table 2. The densities were determined by means of a pycnometer and the refractive index in an Abbe refractometer. Melting points were determined on a "Kofler Heizbank". Molar refractions were calculated from group and atomic refractions given by Vogel [5].

Determinations of pK_a

Due to hydrolysis of the esters, time-consuming methods such as titrations had to be avoided in the pK_a determinations. Determinations of pH in solutions of known ionic strength and concentrations of acid and base were considered to be the best method, especially as both amines and corresponding ammonium bromides had been prepared.

For every compound three solutions were prepared, each about 10^{-3} M with regard to the acid and 0.5×10^{-3} M, 10^{-3} M and 2×10^{-3} M with regard to the base. The solutions were prepared by weighing the compounds and dissolution in deionized water of a known volume. The pH determinations were performed immediately after the dissolution.

The pH meter was a PHM3 Radiometer, Copenhagen, and the electrodes (glass/calomel) were checked against a standard buffer solution of potassium hydrogen phthalate (pH 4.01). Temperature was kept at 25° C.

For calculation of pK_a, the following formula was used:

$$pK_a = pH + \log \frac{(\text{ammonium ion})}{(\text{amine})} + \log f+$$

log $f+$ is defined after Debye-Hückel, and was found to be -0.013.

RESULTS

The ammonium ester bromides are all colorless, water-soluble crystalline compounds. In the case of dimethylaminoethyl thioacetate as ammonium bromide, a faint red discoloration has frequently been observed, the origin of which is unknown. The bromides are more or less hygroscopic, but since this

Table 3.

Alcohol	pK_a		
	Acetic ester	Propionic ester	Butyric ester
Dimethylaminoethanol	8.35 ± 0.01	8.29 ± 0.01	8.31 ± 0.02
Dimethylaminoethanthiol	8.27 ± 0.02	8.28 ± 0.03	8.32 ± 0.03
Dimethylamino-methyl-ethanol	8.32 ± 0.02	8.26 ± 0.01	8.27 ± 0.01

form is fairly easy to handle, it is recommended as the normal one for laboratory work with these compounds. The amino esters are colorless, hygroscopic, water-soluble oils with very characteristic odors. Dimethylaminoethanthiol butyrate, for instance, develops odors combining the impressions of amines, thiols and butyric acid in a most disagreeable way. A hood is recommended while handling these compounds, not only because of the odors but also in view of their toxic effects.

Water solutions of the amino esters show gradual changes in pH due to hydrolysis. Ether solutions react rapidly with methyl iodide and give choline esters in a yield close to 100 %[1,4].

A list of the compounds synthesized, with analytical and physical data, is given in Table 2.

The results of the pK_a determinations are summarized in Table 3. Accuracy is indicated by means of maximum deviations in each group of three determinations.

My sincere thanks are due to Professor G. Ljunggren, Director of this Institute, for his kind interest in this work.

REFERENCES

1. Tammelin, L.-E. *Acta Chem. Scand.* **10** (1956) 145.
2. Wilson, I. B. *J. Biol. Chem.* **197** (1952) 215.
3. Wilson, I. B. *J. Biol. Chem.* **208** (1954) 123.
4. Hansen, B. *Acta Chem. Scand.* **11** (1957) 537.
5. Vogel, A. I. *J. Chem. Soc.* **1948** 1833.

Received December 15, 1956.

ACTA CHEMICA SCANDINAVICA 11 (1957) 491—498

Electroorganic Preparations II. Oxidation of Carbinols

HENNING LUND

Leo Pharmaceutical Products, Copenhagen, Denmark

An anodic voltammetric investigation of about thirty carbinols with a vibrating platinum electrode in acetonitrile containing sodium perchlorate is carried out. The electrode reaction corresponding to the first wave of anisyl alcohol is shown by controlled potential electrolysis to be an oxidation of anisyl alcohol to anisaldehyde.

Organic electrolytic oxidations have not been investigated as much as reductions, and no controlled potential electrolysis of irreversibly oxidizable compounds seems to have been reported, although it is still more important to control the potential in anodic than in cathodic processes in order to get a well defined product.

In this investigation the purpose was to find, from a current-potential curve of a micro electrode, conditions under which carbinols could be oxidized to carbonyl compounds. As the potential of a given electrode reaction found by means of an indicator micro electrode depends upon the electrode material and the medium the first aim was to find a suitable electrode material and reaction medium.

Electrode material. The ideal micro electrode must be unattackable in the potential range used and should be independent of its 'history'. It should be easy to make with a well defined shape and area and should possess a certain mechanical strength, because it is necessary to vibrate or rotate the electrode during the measurements [1].

As cathode the dropping mercury electrode comes very near the requirements, but as mercury is oxidized at a rather low potential its use as an anode is very restricted. It was, therefore, necessary to use a solid micro electrode and the greatest advantage of the mercury electrode — the continual renewal of the surface — is thus lost.

As material for micro electrodes have been described platinum [1,2], gold [2], silver [3], copper [3] and amalgams of these, carbon [2,4], and lead dioxide [2]. Of these lead dioxide, carbon and platinum have been tried in the present investigation.

The lead dioxide electrode was made according to Lord and Rogers [2] and their results that this electrode could only be used within a narrow potential range was confirmed.

The graphite electrodes were made according to Lord and Rogers [2] and Gaylor *et al.*[4] Lord and Rogers coat the graphite electrode with Apiezon W carefully avoiding the Apiezon getting into the pores of the graphite, whereas Gaylor *et al.* impregnate the electrode with wax in such a way that the pores are filled with wax. One advantage of the carbon electrode is that a new surface can easily be produced by breaking off the tip of the electrode. Probably due to insufficient technique in preparing the electrodes the

carbon anodes gave in our hands too high residual currents and this together with the lack of mechanical strength caused us to abandon the carbon electrode as indicator electrode.

Preliminary investigations showed that platinized platinum did not possess advantages in preference to bright platinum so all further experiments were made with a bright platinum micro electrode. It had the required features, except that the surface could not easily be renewed, but as the main purpose was not analytical but to find the potential at which the electrode reaction took place this shortcoming was not deemed serious. In some cases it could even be an advantage as the electrode showed deformed curves in the cases, where the reaction products were ill-defined and tar-like.

Solvent. The solvent must not be oxidized in the potential range used, should have a high dielectric constant to diminish the resistance of the cell, be able to dissolve organic molecules as well as inorganic salts, and to take up and give off protons readily. It should be easily purified and not too expensive. The following solvents were tried: water, *t*-butanol, acetone, nitromethane, ethyleneglycol dimethylether, and acetonitrile.

Water evolves oxygen at the anode at too low potentials and this is also the case in mixtures with dioxan. *t*-Butanol has a rather low dielectric constant and its ability to dissolve inorganic salts is very limited. Nitromethane has a high dielectric constant, but a poor dissolving power for inorganic salts.

Acetone has some advantages, but as it is rather difficult to remove water and methanol to the required extent and as the current-potential curves were somewhat deformed in acetone this solvent was abandoned. Ethyleneglycol dimethylether was not found suitable as it was difficult to remove the monomethyl ether to a satisfactory degree.

Acetonitrile which was chosen as the solvent has a high dielectric constant, a good dissolving power for organic compounds and for some inorganic salts and is usable within a wide potential range. Its most serious shortcoming is its poor protolytic properties which make a buffering of the system difficult. The low protolytic capacity is not felt as much in the voltammetric investigations, where the number of reacting molecules is rather low, as in the preparative oxidations, where it is necessary to add a proton acceptor.

Supporting electrolyte. An indifferent supporting electrolyte is required to conduct the current in the solvent. Iodide, bromide, and chloride ions are oxidized at rather low potentials, nitrate a little higher, but only perchlorates were found satisfactory. Silver perchlorate and sodium perchlorate, for instance, are very soluble in acetonitrile giving solutions with a low resistance, and anhydrous sodium perchlorate in anhydrous acetonitrile is not attacked anodically until a potential at about 2.2 V *vs* the silver ion/silver electrode.

Reference electrode. The silver/silver chloride electrode in acetonitrile has been investigated by Ulich and Spiegel [5,6] who found it reproducible within 0.1 mV. The silver ion/silver electrode was found by Pleskow [7] to be reproducible within 0.1 mV. Although both electrodes were found satisfactory the latter was preferred, because it was necessary to keep the former in a separate compartment, as the chloride ions were oxidized at a too low potential. The silver ions were only in special cases undesirable in the anode compartment.

RESULTS

In Table 1 are given the half-wave potentials of a number of aromatic alcohols and one aldehyde. For the compounds giving deformed waves is given the 'half-peak' potential. All the potentials are measured against the 0.1 N silver ion/silver electrode and the half-wave potentials are corrected for iR drop in the solution. The potentials are measured in solutions containing the oxidizable compound in concentrations 10^{-4}—10^{-3} M with a voltage scanning rate of about 200 mV/min.

In the first column is given the compound, in the second one the half-wave potential and in the third one the shape of the current-voltage curve. 'Normal' means that the curve is S-shaped without peak, whereas 'deformed' indicates the appearance of a peak on the curve. Curves taken successively in

Table 1. Half-wave potentials of the investigated compounds in unbuffered acetonitrile containing 0.5 M sodium perchlorate measured against the 0.1 N silver ion/silver electrode in acetonitrile.

		1. wave $E_{\frac{1}{2}}$	shape	2. wave $E_{\frac{1}{2}}$	shape
I	*p*-Methoxybenzyl alcohol	1.22	normal	1.64	normal
IA	Anisaldehyde	1.63	normal		
II	*m*-Methoxybenzyl alcohol	1.28	normal		
III	*o*-Methoxybenzyl alcohol	1.25	normal		
IV	*α*-Naphthyl carbinol	1.25	normal	1.63	normal
V	*β*-Naphthyl carbinol	1.25	nearly normal		
VI	*p*-Chlorobenzyl alcohol	1.79	normal		
VII	*m*-Chlorobenzyl alcohol	1.85	normal		
VIII	*o*-Chlorobenzyl alcohol	1.84	normal		
IX	*p*-Bromobenzyl alcohol	1.75	normal		
X	*p*-Iodobenzyl alcohol	1.58	normal	1.91	normal
XI	*p*-Methylbenzyl alcohol	1.59	normal		
XII	Furfuryl alcohol	1.33	normal	1.82	normal
XIII	Cinnamyl alcohol	1.36	normal	1.77	normal
XIV	*p*-Nitrocinnamyl alcohol	1.72	normal		
XV	Methyl *p*-methoxyphenyl carbinol	1.24	normal		
XVI	Methyl *p*-chlorophenyl carbinol	1.80	normal		
XVII	Methyl *p*-iodophenyl carbinol	1.58	normal		
XVIII	Methyl *β*-naphthyl carbinol	1.29	normal		
XIX	Fluorenol	1.31	deformed		
XX	2,7-Dichlorofluorenol	1.32	deformed		
XXI	4-Methoxybenzhydrol	1.23	normal		
XXII	4,4′-Dimethoxybenzhydrol	1.22	normal		
XXIII	Phenyl *α*-naphthyl carbinol	1.27	deformed		
XXIV	4,4′-Dichlorobenzhydrol	1.77	deformed		
XXV	Benzhydrol	> 2.0			
XXVI	Methyl phenyl carbinol	> 2.0			
XXVII	Benzyl alcohol	> 2.0			
XXVIII	*o*-Nitrobenzyl alcohol	> 2.0			
XXIX	*p*-Bromophenacyl alcohol	> 2.0			
XXX	*p*-Bromophenyl ethylene glycole	1.62	normal		
XXXI	*Cyclo*hexanol	> 2.0			
XXXII	Allyl alcohol	> 2.0			

the same solution of a compound giving deformed curves are not identical, unless the electrode is cleaned in between. The fourth column gives the half-wave potential of a second wave and the fifth one the shape of this wave.

DISCUSSION

In comparing the half-wave potentials of different compounds it must be remembered that empirical rules of any significance can only be expected when the reaction mechanisms are the same and when factors as energy of activation vary only slightly. As the half-wave potentials of the carbinols are closely related to those of the parent compounds a discussion of the half-wave potentials will be postponed to a later communication.

It is seen from Table 1 that the investigated compounds can be divided into three groups, the first one containing alcohols giving a normal voltammetric curve, the second group carbinols giving deformed waves and the third one not participating in any electrode reaction in the experimentally accessible potential range.

Primary alcohols of the first group show two waves unless the first wave occurs at a potential so positive that a possible second wave would be expected to occur outside the accessible potential range. It seems natural to assume that the electrode reaction corresponding to the first wave is a two electron oxidation of the carbinol to a carbonyl compound, and that the electrode reaction corresponding to the second wave is a two electron oxidation of the aldehyde to the oxidation state of a carboxyl compound.

This assumption is confirmed by the following facts. Hydroquinone and *p*-methoxybenzyl alcohol give nearly the same wave height in the same molar concentration. The molecular weight and thus the diffusion coefficient are nearly the same for both compounds, and as hydroquinone is oxidized in a two electron electrode reaction it is very likely that the same is true for anisyl alcohol. That the wave height of anisyl alcohol is diffusion-controlled is qualitatively shown by the fact that the wave height increases when the amplitude of the vibration increases. Furthermore, anisaldehyde gives a wave with very nearly the same half-wave potential as the second wave of anisyl alcohol.

Although these facts are suggestive a proof of the course of the electrode reaction can only be obtained from a preparative oxidation at a suitable potential and, as will be mentioned later, the preparative oxidation showed that the electrode reaction corresponding to the first wave was indeed an oxidation of the carbinol to a carbonyl compound.

No preparative oxidations have been performed at potentials more positive than the half-wave potential of the second wave and no conclusive evidence of the course of the reaction can be given here. From the height of the wave it is known that it is a two electron oxidation, but as no oxygen is present in the deaerated solution except in the perchlorate ions the formation of a carboxyl group is dubious.

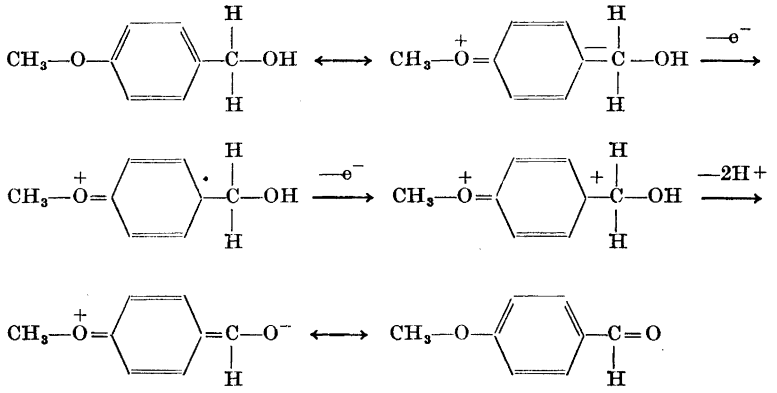
Addition of anhydrous perchloric acid in acetonitrile (from 100 % H_2SO_4 and $Ba(ClO_4)_2$) does not affect the half-wave potential of anisyl alcohol, whereas addition of pyridine lowers the half-wave potential from 0.05 to 0.1 V. The second wave of anisyl alcohol (and that of anisaldehyde) disappears on addition of pyridine.

Carbinols giving waves with half-wave potentials below + 1.65 V are not affected by the presence of silver ions, whereas carbinols having half-wave potentials at higher potentials or not producing any wave in the accessible potential range in the presence of silver ions produce a wave about + 1.69 V. The nature of this wave is not known.

The carbinols giving deformed waves with peaks are not oxidized to the carbonyl compounds, but yield unidentified products which cover the electrode with a visible, black layer. The electrode is thereby insulated from the solution and as the current is inversely proportional to the resistance of the cell it drops, giving the current-voltage curve its characteristic peak. At low concentrations the curves are more normal because the electrode is not covered com-

pletely with the reaction product during the voltammetric measurement. More often than not the electrode could be cleaned by wiping off the black layer, but in some cases it was necessary to burn it off.

As will be shown in later communications on electrolytic oxidation of hydrocarbons, heterocyclic compounds, phenols, and amines, it is likely that the primary step in the electrode reaction is a loss of an electron from the aromatic system. The radical formed is stabilized by the removal of a second electron and two protons after the following outline which gives a possible route for the oxidation of anisyl alcohol. Not all the resonance possibilities of the radicals are given.



It is essential for the formation of an aldehyde that the radical is stable long enough for the removal of two protons from the carbinol carbon atom and that seems to require that the electron deficiency is localized during a considerable time at the carbon atom next to the carbinol carbon atom.

This is illustrated strikingly in the cases of α- and β-naphthyl carbinol, p- and m-methoxybenzyl alcohol and fluorenol. Whereas α-naphthyl carbinol produces two normal waves β-naphthyl carbinol gives only one slightly deformed wave. The methoxybenzyl alcohols give the same picture. The p-isomer gives two normal waves, the o-isomer one normal and one with a smaller wave height than corresponding to a two-electron oxidation and the m-isomer produces only one normal wave. Fluorenol gives a very pronounced peak.

The difference between α- and β-naphthyl carbinol is, according to the explanation given above, due to the wellknown fact that there are more resonance possibilities where the electron deficiency is in the α-position than in the β-position, but as the difference in resonance possibilities between the α- and the β-position is not great, the tendency of the β-naphthyl carbinol to produce a deformed wave is not pronounced. In fluorenol, however, where the probability of an electron deficiency at the carbon atoms neighbouring the 9-position is very low, the chances of getting the carbinol oxidized to a carbonyl compound are few. The oxidation takes place in some other part of the molecule (probably in the 2 and 7 positions) and it seems likely that the polymerization product thus formed would be ill-defined and tar-like, thus explaining the great tendency of fluorenol to produce deformed curves.

PREPARATIVE OXIDATIONS

The controlled potential anodic electrolysis was undertaken in order to prove the course of the electrode reaction corresponding to the first wave in the voltammetric diagram. As representative for the first group was chosen anisyl alcohol, for the second group giving deformed voltammetric curves fluorenol and as a compound between the first and the second group β-naphthyl carbinol.

When anisyl alcohol was oxidized in a medium of 0.5 M sodium perchlorate in acetonitrile at an anode potential about + 1.35 V only about 5 % of the theoretical amount of electricity was consumed and no carbonyl compounds could be detected in the reaction medium. When the same medium, however, contained a proton acceptor as pyridine in a concentration sufficiently high to combine with all the protons formed in the electrode reaction the consumption of electricity was nearly theoretical and anisaldehyde could be isolated in a yield of 72 % as its 2,4-dinitrophenyl hydrazone. As proton acceptor pyridines or quinolines could be used, but not aliphatic or aromatic amines, as they themselves gave off electrons at a potential lower than the half-wave potential of anisyl alcohol.

Oxidation of fluorenol in acetonitrile yielded both in the absence and presence of pyridine a black, insoluble tar which covered the electrode in a very short time. No fluorenone could be detected in the tar or in the solution.

Neither did β-naphthyl carbinol yield its aldehyde on electrolytic oxidation at +1.40 V, but the covering of the electrode was slower than in the case of fluorenol.

EXPERIMENTAL

Apparatus. For the voltammetric investigation a Sargent-Heyrovsky photographic recording polarograph Model XII was used. The electrode potential was controlled by a Lingane-Jones potentiostat [8]. The coulometer used was an electromechanical current integrator [9].

The construction of the platinum micro electrode is shown in Fig. 1. The electrode tip is a platinum wire 4.0 mm long with a diameter of 0.5 mm. The vibrator was manufactured by Fisher Scientific Company, Switzerland. The advantages of this electrode are its simplicity in construction and absence of rotating parts, which makes the exclusion of oxygen easy. It has the disadvantage that the amplitude of the vibration is difficult to measure exactly, and for analytical purposes the rotating electrode is more appropriate.

The electrolysis cell was similar to that used in Part I [10]. The reference electrode was a silver wire in a 0.1 M silver perchlorate and 0.5 M sodium perchlorate solution in acetonitrile separated from the test solution by a fritted glass diaphragm.

Materials. The *acetonitrile* (Eastman, white label) was purified according to Walden and Birr [11]. The acetonitrile purified in this manner shows less infra-red absorption than Eastman's 'Spectro grade' acetonitrile. The pure acetonitrile is only slightly hygroscopic and can be stored for a month in a flask equipped with an effective drying tube.

The *acetone* was purified according to Livingstone [12].

Sodium perchlorate (Riedel-de-Haën, p.a.) was dried without further purification at 145°—150° for 24 h and finally in vacuum over P_2O_5 at 150°. As the dry product is very hygroscopic it was stored over P_2O_5.

Silver perchlorate. To a stirred solution of 24.5 g dry sodium perchlorate in 100 ml acetonitrile is added drop by drop a solution of 34 g silver nitrate in 100 ml acetonitrile. The precipitate of sodium nitrate is filtered off, the solution evaporated to 50 ml and

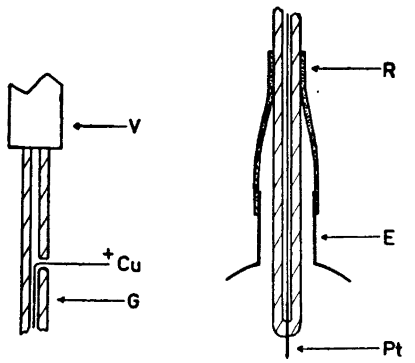


Fig. 1. Vibrating platinum electrode. V is a vibrator, Cu a copper wire soldered to the platinum wire Pt. G is a glass capillary tube, R a rubber tube, and E the electrode chamber.

traces of sodium nitrate are removed by centrifuging. On addition of dry ether the silver perchlorate is brought to crystallization. The crystals are washed with a mixture of ether and acetonitrile, 1:1, and dried in vacuum. The composition of the crystals correspond to $AgClO_4$, 3 CH_3CN (found: Ag 31.5, Calc. for $C_6H_9N_3AgClO_4$: Ag 32.6). On heating, the crystals dissolve in their acetonitrile. If this acetonitrile is evaporated at elevated temperature a solid cake of silver perchlorate remains, which is known [13] to be explosive. The crystals containing acetonitrile were, therefore, used and the solutions were made up according to the silver analysis.

The following carbinols were prepared *from the corresponding acids or acid derivatives* by reduction with $LiAlH_4$: IV, m.p. 61° (59.5°—60° [14]); V, m.p. 81° (80.5° [15]); X, m.p. 72° (72°—73° [16]). *From the carbonyl compounds* by reduction with $LiAlH_4$: XIX, m.p. 154° (155°—56° [17]); XXIII, m.p. 85° (84°—86° [18]); XXV, m.p. 68° (68° [20]). From the carbonyl compounds by reduction with aluminium isopropoxide: VI, m.p. 71.5° (71°—72.5° [20]); VII, b.p. 128°—30°/10 mm (242° [21]); VIII, m.p. 69.5° (70° [21]); IX, m.p. 76° (76°—76.5° [20]); XVIII, m.p. 71° (71° [22]); methyl *p*-iodophenyl carbinol, m.p. 52°—52.5°, has not been described before. It was recrystallized from heptane. (Found: C 38.71; H 3.79; I 51.00. Calc. for C_8H_9OI: C 38.76; H 3.66; I 51.13); XX, m.p. 161° (161°—62° [23]).

From a carbonyl compound and a Grignard compound: XVI, b.p. 84°—88°/1 mm (87°—89°/2 mm [24]); XV, b.p. 105°—10°/10 mm (95°/1 mm [25]); XXI, m.p. 66° (65°—66° [26]).

XI, m.p. 59° was made according to Ref.[27]; XXIX, m.p. 136° according to Ref.[28]; XXX, m.p. 102° according to Ref.[29].

Electrolytical oxidation of anisyl alcohol. 35 ml 0.5 N sodium perchlorate in acetonitrile were deaerated with purified nitrogen [30] and oxidizable impurities were removed by electrolysis at an anode potential of +1.50 V. When the current had reached a stationary value (residual current) 59.3 mg (0.43 mMole) of anisyl alcohol and 106.5 mg (1.35 mMole) of pyridine were added and the carbinol was oxidized at an anode potential of +1.35 V *vs.* the 0.1 N silver ion/silver electrode. The platinum anode had an area of 10 cm^2; the initial current was 60 mA and decreased in the course of 5 h to about 1 mA. The amount of electricity used was, after correction for residual current, 81 coulombs (theoretically 82 coulombs for 100 % oxidation).

4 ml of the anode chamber solution was evaporated and the residue extracted with carbon tetrachloride. An infra-red spectrum of this solution was identical with that of actual anisaldehyde in carbon tetrachloride. The rest of the anode solution was evaporated through a small column and the residue dissolved in ethyl alcohol. The carbonyl compound was precipitated as its 2,4-dinitrophenyl hydrazone. After recrystallization from xylene were obtained 89 mg (m.p. 249°—51° (253°—54° [31]). The 89 mg (plus those from the test) correspond to a yield of 72 % of anisaldehyde, but the actual yield may have been somewhat higher.

This investigation was carried out at the Chemistry Department of Harvard University, Cambridge 38, Mass. 1954—1955. The author wishes to express his thanks to Dr. L. F. Fieser and Dr. J. J. Lingane for their kind interest and for many facilities which have been put at his disposal.

REFERENCES

1. Laitinen, H. A. and Kolthoff, I. M. *J. Phys. Chem.* **45** (1941) 1079.
2. Lord, S. S. and Rogers, L. B. *Anal. Chem.* **26** (1954) 284.
3. Lydersen, D. *Acta Chem. Scand.* **3** (1949) 259.
4. Gaylor, V. F., Conrad, A. L. and Landerl, J. H. *Anal. Chem.* **27** (1955) 310.
5. Ulich, H. and Spiegel, G. *Z. physik. Chem.* **177** (1936) 103.
6. Spiegel, G. and Ulich, H. *Z. physik. Chem.* **178** (1937) 187.
7. Pleskow, W. A. *J. phys. Chem. (U.S.S.R.)* **22** (1948) 351.
8. Lingane, J. J. and Jones, S. L. *Anal. Chem.* **22** (1950) 1169.
9. Lingane, J. J. and Jones, S. L. *Anal. Chem.* **22** (1950) 1220.
10. Lund, H. *Acta Chem. Scand.* **11** (1957) 283.
11. Walden, P. and Birr, E. J. *Z. physik. Chem.* **144** (1929) 269.
12. Livingstone, R. *J. Am. Chem. Soc.* **69** (1947) 1220.
13. Brinkley, S. R. *J. Am. Chem. Soc.* **62** (1940) 3524.
14. Bamberger, E. and Lodter, W. *Ber.* **21** (1888) 256.
15. Bamberger, E. and Boekmann, O. *Ber.* **20** (1887) 1115.
16. Olivier, S. J. C. *Rec. trav. chim.* **42** (1923) 516.
17. Baker, R. H. and Adkins, H. *J. Am. Chem. Soc.* **62** (1940) 3305.
18. Blicke, F. F. and Powers, L. D. *J. Am. Chem. Soc.* **51** (1929) 3378.
19. *Org. Synth. Coll. Vol.* **1** (1941) 90.
20. Carothers, W. H. and Adams, R. *J. Am. Chem. Soc.* **46** (1924) 1675.
21. Shoesmith, J. B. and Slater, R. H. *J. Chem. Soc.* **1926** 214.
22. Lund, Hakon *Ber.* **70** (1937) 1520.
23. Adkins, H., Elofson, R. M., Rossow, A. G. and Robinson, C. C. *J. Am. Chem. Soc.* **71** (1949) 3622.
24. Brooks, L. A. *J. Am. Chem. Soc.* **66** (1944) 1295.
25. Winstein, S., Lindegren, C. R., Marshall, H. and Ingraham, L. L. *J. Am. Chem. Soc.* **75** (1953) 147.
26. Tietz, R. F. and McEwen, W. E. *J. Am. Chem. Soc.* **77** (1955) 4007.
27. *Org. Synth. Coll. Vol.* **2** (1943) 590.
28. Judefind, W. L. and Reid, E. E. *J. Am. Chem. Soc.* **42** (1920) 1043.
29. Bergkvist, T. *Svensk Kem. Tidskr.* **59** (1947) 205.
30. Meites, L. and Meites, T. *Anal. Chem.* **20** (1948) 984.
31. Johnson, G. D. *J. Am. Chem. Soc.* **75** (1953) 2720.

Received December 15, 1956.

ACTA CHEMICA SCANDINAVICA 11 (1957) 499—505

Studies on Carbamates

XII. The Carbamates of the Butylamines

MOGENS BALLUND JENSEN

The Royal Danish School of Pharmacy, Copenhagen, Denmark

The velocity constants for the reaction "amine + CO_2 → carbamic acid" and the equilibrium constants for the equilibrium "carbamate$^-$ + + $H_2O \rightleftharpoons HCO_3^-$ + amine" have been determined for *n*-, *sec.*-, *iso*-, *tert.*-, di-*n*- and di-*iso*-butylamine. Di-*sec.*-butylamine and carbon dioxide form no carbamate in aqueous solution. Di-*tert.*-butylamine could not be prepared.

1. The velocity constant for the reaction "amine + CO_2 = carbamic acid" and the equilibrium constant for the reaction "carbamate$^-$ + H_2O = HCO_3^- + amine" have been determined for the following amines:

1) $CH_3 \cdot CH_2 \cdot CH_2 \cdot CH_2 \cdot NH_2$	*n*-butylamine
2) $CH_3 \cdot CH_2 \cdot CHCH_3 \cdot NH_2$	*sec.*-butylamine
3) $(CH_3)_2CH \cdot CH_2 \cdot NH_2$	*iso*-butylamine
4) $(CH_3)_3C \cdot NH_2$	*tert.*-butylamine
5) $(CH_3 \cdot CH_2 \cdot CH_2 \cdot CH_2)_2NH$	di-*n*-butylamine
6) $(CH_3 \cdot CH_2 \cdot CHCH_3)_2NH$	di-*sec.*-butylamine
7) $((CH_3)_2CH \cdot CH_2)_2NH$	di-*iso*-butylamine

but not for

8) $((CH_3)_3C)_2NH$	di-*tert.*-butylamine

the synthesis of which failed although several attempts were made.

The experimental and theoretical conditions are analogous to those of the carbamates previously investigated. Detailed information concerning the method of analysis, theory, significance of constants *etc.* is to be found in previous papers [1].

2. The butylamines were purified by distillation through wire gauze columns. The fractions employed for the experiments had the following boiling points: No. 1 (commercial product): 77.4° C (764 mm Hg); No. 2 (prepared by the author): 63.4—63.8° C (768 mm Hg); No. 3 (Eastman Organic Chemicals): 67.6° C (755 mm Hg); No. 4 (Light and Co. Ltd.): 43.8—44.1° C

(749 mm Hg); No. 5 (commercial product): 159.8—160.3° C (765 mm Hg); No. 6 (Light and Co. Ltd.): 136.0—136.8° C (760 mm Hg) and No. 7 (FLUKA AG.): 140.5—140.6° C (765 mm Hg).

Sec.-butylamine was prepared from methyl ethyl ketoxime by reduction with metallic sodium. The oxime was prepared from hydroxylamine hydrochloride and methyl ethyl ketone [2].

3. An attempt to prepare the carbamate of amine No. 6, *i. e.* di-*sec.*-butylamine, was unsuccessful whereas the carbamates of the other six amines were prepared not only in solution but also as solids in the following manner:

A small portion, *viz.* about 2 ml of butylamine was distributed on the inner surface of a 300 ml Erlenmeyer-flask and carbon dioxide was lead into the flask whereby a white compound was formed; a little more amine was added followed by further carbon dioxide *etc.*

The content of amine in the compounds was determined by acidimetric titration. The content of carbon dioxide was determined by acidimetric titration of the barium carbonate formed when the carbamate was dissolved in a solution of sodium hydroxide and barium chloride and then heated.

The analysis gave the following results. In the case of the four primary amines, *i. e.* Nos. 1, 2, 3 and 4, a content of 76.7 %, 75.0 %, 76.6 % and 76.7 % amine, respectively, was found; the content of carbon dioxide was found to be 23.8 %, 22.0 %, 22.9 % and 23.0 %, respectively. These results correspond to the formula $C_4H_9NHCOOH_3NC_4H_9$ (theoretical values: 76.9 % amine and 23.1 % carbon dioxide).

In the case of di-*n*-butylamine, *i. e.* No. 5, a content of 85.4 % of amine and 14.0 % of carbon dioxide was found. This corresponds to a formula analogous to the above, *viz.* $(C_4H_9)_2NCOOH_2N(C_4H_9)_2$ (theoretical values: 85.4 % amine and 14.6 % carbon dioxide).

In the case of di-*iso*-butylamine, *i. e.* No. 7, a content of 81.2 % amine and 18.5 % carbon dioxide was found. This would be in accordance with the formula $(C_4H_9)_2NCOOH_2N(C_4H_9)_2$, $(C_4H_9)_2NCOOH$ (theoretical values: 81.5 % amine and 18.5 % carbon dioxide).

The solutions of the aminium carbonate, $(AmH)_2CO_3$, were prepared by mixing equivalent amounts of solutions of aminium chloride and sodium carbonate.

4. All the experiments were carried out at 18° C, and the velocity constants were calculated by means of Briggs' logarithms, the unit of time being the minute. As in previous investigations, the activity coefficient f for a monovalent ion was calculated from Bjerrum's expression $-\log f = 0.3 \sqrt{c_{ion}}$. The data presented in the later tables are corrected for blank values, *viz.* 1—5 units of the percentage.

5. Hall and Sprinkle [3] have found the dissociation constants for *n*-butylaminiumion and di-*n*-butylaminiumion at 18° C to be $10^{-10.76}$ and $10^{-11.46}$, respectively. Bredig's [4] corrected values for the dissociation constants for *sec.*-butylamine, *iso*-butylamine, *tert.*-butylamine and di-*iso*-butylamine at 25° C are $10^{-3.44}$, $10^{-3.58}$, $10^{-3.55}$, and $10^{-3.41}$, respectively. As the heat effect of the reactions is very slight, these values may also be used for 18° C. The value of K_{H_2O} was fixed at $10^{-14.22}$.

Table 1. Carbon dioxide in amine + NaOH. 18°.

Amine No.	Initial solution		Absorb. CO_2 mole/litre	% carbamate	Final solution		Mean		$k_{CO_2 \cdot Am}$	
	c_{NaOH}	c_{Am}			c_{NaOH}	c_{Am}	c_{NaOH}	c_{Am}		Mean
1 *n*-	0.20	0.10	0.0200	49	0.17	0.09	0.19	0.10	$10^{5.29}$	$10^{5.29}$
	0.10	0.10	0.0224	66	0.07	0.09	0.09	0.09	$10^{5.28}$	
2 *sec.*-	0.10	0.10	0.0189	42	0.07	0.09	0.09	0.09	$10^{4.85}$	$10^{4.85}$
	0.08	0.10	0.0180	48	0.05	0.09	0.07	0.09	$10^{4.84}$	
3 *iso*-	0.10	0.10	0.0198	61	0.08	0.09	0.09	0.09	$10^{5.20}$	$10^{5.20}$
	0.20	0.10	0.0191	43	0.18	0.09	0.19	0.10	$10^{5.19}$	
4 *tert.*-	0.10	0.20	0.0191	31 *	0.07	0.20	0.08	0.20	$10^{4.30}$	$10^{4.28}$
	0.10	0.40	0.0196	45 *	0.07	0.40	0.08	0.40	$10^{4.26}$	
5 di-*n*-	0.10	0.022	0.0152	39	0.08	0.016	0.09	0.019	$10^{5.51}$	$10^{5.49}$
	0.10	0.026	0.0140	42	0.08	0.020	0.09	0.023	$10^{5.47}$	
6 di-*sec.*-	0.10	0.04	0.0195	0	0.06	0.04	0.08	0.04		
7 di-*iso*-	0.10	0.014	0.0199	16	0.06	0.011	0.08	0.013	$10^{5.13}$	$10^{5.12}$
	0.05	0.014	0.0185	28	0.02	0.011	0.04	0.013	$10^{5.11}$	

* Found by analysis: 29 and 43 %, respectively. The listed values are corrected to zero time.

On the reaction 'amine + carbon dioxide → carbamic acid'

500 ml of an aqueous solution containing both amine and sodium hydroxide were placed in a 2 litre flask. Approximately 250 ml of carbon dioxide were substituted for an equal amount of atmospheric air in the gas phase above this solution, and the flask was shaken vigorously for about 2 min to obtain absorption of the carbon dioxide.

The experimental results for the addition of carbon dioxide to the amines together with the calculated velocity constants are listed in Table 1. Since the carbamate of *tert.*-butylamine is very rapidly decomposed it was found necessary to delay the conversion to carbonate by the addition of dimethylamine immediately after the shaking with carbon dioxide. If the solution is made 0.5—1 M with regard to dimethylamine, about 98 % of the carbon dioxide dissociated from the carbamate of *tert.*-butylamine is converted into the carbamate of dimethylamine, which decomposes very slowly into carbonate [5]. Nevertheless, some decomposition takes place during the 1—2 min which elapse between the shaking with carbon dioxide and the addition of dimethyl-

Table 2. The solution carbonate-carbamate in equilibrium. 18°.

Amino No.	Initial solution				% carbamate	Equilibrium				K_{Eq}	
	c_{Am}	c_{AmH^+}	$c_{(AmH)_2CO_3}$	$c_{AmH\ carbamate}$		c_{AmH^+}	c_{Am}	$c_{carbamate}$	$c_{HCO_3^-}$		Mean
1 *n*-	0.11	0.10		0.0152	53	0.12	0.11	0.00809	0.00117	$10^{-1.80}$	$10^{-1.79}$
	0.10	0.10	0.0202		51	0.13	0.10	0.0103	0.00167	$10^{-1.78}$	
2 *sec.*-	0.05	0.13		0.0185	25	0.16	0.058	0.00456	0.00413	$10^{-1.28}$	$10^{-1.31}$
	0.05	0.10	0.0203		25	0.13	0.058	0.00499	0.00396	$10^{-1.34}$	
3 *iso*-	0.10	0.10	0.0203		68	0.12	0.10	0.0138	0.00135	$10^{-2.00}$	$10^{-1.99}$
	0.062	0.14		0.0169	69	0.16	0.058	0.0116	0.00179	$10^{-1.98}$	
4 *tert.*-	0.10		0.10[a]		<0.1	0.23	0.07		0.07		$10^{-0.86}$ b
	0.20	0.20		0.02	<1	0.23	0.21		0.003		
5 di-*n*-	0.020	0.20	0.0203		4.4	0.24	0.024	0.0009	0.0043		$10^{-0.71}$ b
	0.020	0.20	0.0195		4.8	0.24	0.024	0.0009	0.0041		
6 di-*sec.*-	0.03	0.20	0.0200		0						
7 di-*iso*-		0.16	0.0203		6.4	0.19	0.013	0.00129	0.0126	$10^{-0.91}$	$10^{-0.92}$
	0.015	0.16	0.0081[c]		7.0	0.18	0.015	0.00142	0.0115	$10^{-0.92}$	

[a] The solution was 0.1 M with regard to $NaHCO_3$ corresponding to $c_{HCO_3^-} = 0.10$.
[b] Calculated from the data on the decomposition of the carbamate, see Table 3.
[c] The solution was 0.012 M with regard to $NaHCO_3$ corresponding to $c_{HCO_3^-} = 0.012$.

amine; the listed values are corrected to zero time on the basis of the velocity constants determined in section IV.

It is seen from Table 1 that no carbamate was found in the case of di-*sec.*-butylamine, nor was it found in another experiment where a solution containing only the amine (0.04 M), but no sodium hydroxide, was shaken with carbon dioxide. In connection with this it should be mentioned that di-*iso*-propylamine does not react with carbon dioxide in aqueous solution either [6].

The low value of $k_{CO_2 \cdot Am}$ for *tert.*-butylamine compared to that of other primary alifatic amines should also be noted.

No experiments as already mentioned, were carried out with di-*tert.*-butylamine, but since neither di-*iso*-propylamine nor di-*sec.*-butylamine form carbamates in aqueous solution a similar passivity towards carbon dioxide is to be expected in the case of di-*tert.*-butylamine.

The equilibrium 'carbamate ⇌ carbonate'

In some cases experiments have been carried out from the carbamate side and from the carbonate side, in other cases from the carbonate side only.

Table 3. Velocity constants for the process "carbamate → carbonate". p_{aH} = approx. 13. 18°.

Amine No.	Initial solution			Min.	% carbamate left	k_{amate}	
	$c_{carbamate}$	c_{NaOH}	c_{Am}			exptl.	calc.
1 *n*-	0.018	0.10	0.12	1 122	76.1	0.000106	
				1 754	65.8	0.000104	
				2 751	52.7	0.000101	
				4 285	36.7	0.000102	
				7 081	19.5	0.000100	
						Mean: 0.000103	0.000190
	0.020	0.18	0.12	1 207	81.0	0.0000759	
				1 845	73.1	0.0000738	
				3 008	59.7	0.0000745	
				5 778	37.3	0.0000741	
						Mean: 0.0000746	0.000157
2 *sec.*-	0.018	0.16	0.08	408	82.3	0.000207	
				645	72.0	0.000221	
				1 528	49.1	0.000202	
				2 090	37.0	0.000207	
						Mean: 0.000209	0.000325
3 *iso*-	0.011	0.11	0.13	1 413	79.0	0.0000726	
				1 853	70.9	0.0000806	
				2 906	60.5	0.0000748	
				4 306	46.9	0.0000764	
						Mean: 0.0000761	0.000104
4 *tert.*-	0.020	0.066	0.20	3.0	83.7	0.0257	
				8.0	60.2	0.0276	
				13.0	43.9	0.0275	
				18.0	31.1	0.0282	
						Mean: 0.0273	—
	0.020	0.20	0.20	3.0	91.5	0.0129	
				13.0	71.8	0.0112	
				28.0	47.7	0.0115	
				48.0	27.3	0.0120	
						Mean: 0.0119	—
5 di-*n*-	0.010	0.10	0.02	15	78.4	0.00710	
				39	52.8	0.00712	
				113	18.8	0.00644	
						Mean: 0.00698	—
	0.006	0.08	0.02	27	57.5	0.00893	
				51	37.7	0.00831	
				114	10.0	0.00882	
						Mean: 0.00872	—

This Table is continued

Table 3 continued.

7	0.009	0.09	0.009	6 22 42 77 110 169	96.2 86.0 75.9 59.0 48.5 33.1	0.00283 0.00297 0.00286 0.00298 0.00286 0.00284	
di-*iso*-						Mean: 0.00289	0.00332
	0.006	0.11	0.011	6 27 56 135 190	96.6 85.3 72.4 45.7 34.0	0.00251 0.00256 0.00252 0.00252 0.00246	
						Mean: 0.00251	0.00254

Table 2 shows the composition of the equilibrium solutions and the equilibrium constant, K_{Eq}, for the reaction 'carbamate$^-$+H_2O=HCO_3^-+amine'.

It is seen from Table 2 that measurable amounts of carbamate are formed in the experiments with *n*-butylamine, *sec.*-butylamine, *iso*-butylamine, and di-*iso*-butylamine while only small amounts are formed in the case of *tert.*-butylamine. No detectible amounts of carbamate were found in the experiment with di-*sec.*-butylamine.

In the experiments with di-*n*-butylamine it was not possible to obtain more than a few per cent of carbamate, the amine being slightly soluble in water, *i. e.* the solution was only about 0.02 M with regard to amine.

In the case of *tert.*-butylamine and di-*n*-butylamine the value of K_{Eq} was not calculated from the experiments on equilibrium but this value was obtained in another way, *viz.* indirectly from the data on the velocity of the decomposition of the carbamates in strong alkaline solution, see next section.

The velocity of the conversion 'carbamate → carbonate'

The decomposition, in alkaline medium, of the carbamates of the amines previously investigated may be explained by assuming that the decomposition is a two-stage reaction, *viz.*

$$\text{carbamate} = \text{amine} + \text{carbon dioxide}$$
$$\text{carbon dioxide} = \text{carbonate}$$

and the velocity constants may be calculated from the expression

$$k_{\text{amate}} = \frac{k_{CO_2 \cdot Am} \cdot K_{Eq} \cdot K_{H_2O} \cdot \frac{1}{K_{CO_2}}}{c_{OH^-} + \frac{k_{CO_2 \cdot Am}}{k_{CO_2 \cdot OH}} \cdot c_{Am}}$$

On the assumption that there is the same two-stage reaction for the decomposition of the carbamates of the butylamines it is possible to calculate, in advance, the velocity constants in the case of *n*-butylamine, *sec.*-butylamine, *iso*-butylamine and di-*iso*-butylamine. The experiments on the decomposition of the carbamates in alkaline medium together with the calculated values of k_{amate} are listed in Table 3. Considering the nature of the experimental conditions the agreement may be described as rather satisfactory.

In the case of *tert.*-butylamine and di-*n*-butylamine the value of K_{Eq} was then calculated from the experimental value of k_{amate} by means of the above expression. The values of K_{Eq} determined in this way correspond to a theoretical content of less than 1 % and 2.6 % carbamate, respectively, in the experiments on equilibrium with *tert.*-butylamine and di-*n*-butylamine (Table 2).

As seen from Table 3 the carbamate of *tert.*-butylamine is rapidly decomposed. The experiments were carried out in such a way that 100 ml of the solution under investigation were quickly adjusted to 0.5—1 M with regard to dimetylamine and the time was noted; on addition of dimethylamine the conversion of carbamate to carbonate was brought to a standstill.

The author wishes to express his sincere thanks to Professor, dr.phil. Carl Faurholt, Head of the Department of Inorganic Chemistry, for his very kind interest in this work.

REFERENCES

1. Jensen, A. and Faurholt, C. *Acta Chem. Scand.* **6** (1952) 385.
2. Blatt, A. H. *Organic Synthesis*, John Wiley and Sons, Inc., New York, London, Coll. Vol. 2 (1943) 318.
3. Hall, N. F. and Sprinkle, M. R. *J. Am. Chem. Soc.* **54** (1932) 3469.
4. Breding, G. *Z. physik. Chem.* **13** (1894) 289 as corrected in '*International Critical Tables*'.
5. Faurholt, C. *J. Chem. phys.* **22** (1925) 1.
6. Jensen, A., Jensen, M. B. and Faurholt, C. *Acta Chem. Scand.* **8** (1954) 1129.

Received December 18, 1956.

ACTA CHEMICA SCANDINAVICA 11 (1957) 506—511

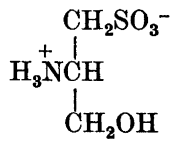
Isolation of 2-L-Amino-3-hydroxy-1-propane Sulphonic Acid from *Polysiphonia fastigiata*

BÖRJE WICKBERG

Organisk-kemiska Institutionen, Kungl. Tekniska Högskolan, Stockholm, Sweden

The low-molecular weight internal salts and carbohydrates from the red alga *Polysiphonia fastigiata* have been investigated. A new internal salt, shown to be 2-L-amino-3-hydroxy-1-propane sulphonic acid, and in addition mytilitol, laminitol, mannitol and a glycosidic compound were isolated.

It has recently been shown that taurine and certain N-substituted taurine derivatives [1,2] seem to be common constituents of the red algae. The red alga *Polysiphonia fastigiata*, *Florideae*, order *Ceramiales*, from which dimethyl-β-propiothetin chloride [3] and 2-D-glyceric acid α-D-mannopyranoside [4,5] have previously been isolated, has now been found to contain an internal salt, 2-L-amino-3-hydroxy-1-propane sulphonic acid (I), together with scyllitol, mytilitol, laminitol, mannitol and a new glycoside which is non-reducing and has the chromatographic properties of a disaccharide.



I

While scyllitol occurred only in very small quantities the amount of mytilitol found makes it most probable that this compound originates from the alga itself. The red algae *Gelidium cartilagineum* [1] and *Gigartina leptorhynchos* [2] gave mytilitol in very small quantities only and since it has been isolated from the blue mussel *Mytilus edulis* it was supposed that it might come from contaminating invertebrates in the samples extracted.

The isolation of laminitol and mannitol support earlier findings [6] that these substances are common in the red as well as in the brown algae.

The mannitol mother liquors, which contained mannitol and compounds with lower R_F-values, were hydrolysed yielding a mixture containing only traces of reducing sugar. The hydrolysate was acetylated and the acetates subjected to paper chromatography in a methyl sulphoxide-petroleum ether system [7]. The presence of mannitol, laminitol and mytilitol was indicated but only traces of sorbitol and no dulcitol.

The new internal salt can formally be derived from D-cysteic acid by reduction of the carboxyl group and therefore the name D-cysteinolic acid is suggested for the compound. It seemed to travel a little slower than taurine both on a carbon column and on paper chromatograms run in ethyl acetate-acetic acid-water (3:1:1). The compound could be detected on paper chromatograms by spraying with ninhydrin reagent but rather strong heating was required to produce the colour. When the silver nitrate-sodium ethoxide reagent was used the substance first appeared as a lighter spot which darkened only after several hours.

After purification by adsorption on Amberlite resin IR 400 in the OH-state and subsequent elution with dilute acetic acid and recrystallisation, the compound had m. p. 279—282° (decomp.), $[\alpha]_D^{23} + 7°$ (water) and gave an analysis which agreed fairly well with the composition $C_3H_9NO_4S$. A sample was oxidised with sodium periodate in aqueous solution. The mixture was buffered with sodium bicarbonate; potassium iodide and sodium arsenite solutions were added, and the excess arsenite titrated with iodine solution. No sharp endpoint could be detected, indicating that some reaction between iodine and the oxidised compound was occurring. Instead the periodate consumed was determined by the addition of potassium iodide and hydrochloric acid to the oxidation mixture and titration with sodium thiosulphate. A periodate consumption of 1 mole was indicated. One mole of formaldehyde determined as the dimedon complex was liberated.

These facts are in accordance with the formulation of the internal salt as 2,3-(amino-hydroxy-)-1-propane sulphonic acid, which upon periodate oxidation should give formylmethane sulphonic acid; this would be expected to undergo further oxidation. By analogy with the naturally occurring L-cysteine and L-cysteic acid the structure 2-D-amino-3-hydroxy-1-propane sulphonic acid seemed to be the most probable for the compound, and L-cysteinolic acid was therefore synthesised from L-cysteine. The latter was benzylated, the S-benzyl cysteine esterified with ethanol and the ethyl ester reduced to S-benzyl cysteinol. After removal of the benzyl group the cysteinol was oxidised with bromine in acid aqueous solution. From the reaction product a compound was isolated in 24 % yield based upon S-benzyl-L-cysteine, which was the only crystalline intermediate. It had the same melting point (279—281°) and chromatographic behaviour as the internal salt from the alga, but the opposite optical rotation, $[\alpha]_D^{23} -6°$ (water); the mixed melting point of the two compounds showed a strong depression. As the X-ray diffraction patterns of the natural and synthetic materials were identical it follows that the internal salt from the alga is D-cysteinolic acid and thus configurationally related to the rare D-amino acids. It is also of interest that neither taurine nor its derivatives have been found in amounts sufficient to permit their isolation.

EXPERIMENTAL *

The alga (360 g) was extracted continuously with ether for 3 days and then with methanol for 14 days. The methanol extract was concentrated *in vacuo*, the residual syrup stirred with water and the aqueous solution after filtration passed through Amberlite IR 120 and IR 4B and then concentrated to dryness yielding a syrup (9.9 g). After standing for two months the syrup was dissolved in ethanol-water (50 %) depositing crystals which were removed (Fraction 1). The filtrate was passed through a layer of decolorising carbon, concentrated to dryness, the residue dissolved in water (150 ml) and this solution added to the top of a carbon-Celite column (1:1, 35 × 4.5 cm). The column was first eluted with water (2 000 ml) and then with dilute ethanol the concentration of which was linearly increased (0—30 %, 4 000 ml). Fractions were collected automatically and investigated by paper chromatography using as solvent ethyl acetate-acetic acid-water (3:1:1). As it turned out that the sample had not been completely deionised before being put on the column, the appropriate fractions were combined and filtered through Amberlite IR 120 and IR 4B.

Fraction No. 1 contained a mixture of cyclitols.

Fraction No. 2 contained D-cysteinolic acid in addition to traces of compounds with the R_F-values of glycerol, volemitol and scyllitol.

Fraction No. 3 contained D-cysteinolic acid and mytilitol.

Fraction No. 4 contained laminitol and traces of D-cysteinolic acid.

Fraction No. 5 contained small amounts of mannitol and traces of laminitol.

Fraction No. 6 contained mannitol.

Fraction No. 7 contained mannitol and traces of compounds with lower R_F-values.

The next fractions contained small amounts of several compounds with the chromatographic characteristics of non-reducing disaccharides. Hydrolysis yielded mixtures which on paper chromatograms gave spots for galactose, glucose and glycerol. The following fractions were more closely examined:

Fraction No. 8 gave one principal spot with the R_F-value of α,α-trehalose. A hydrolysed sample gave one strong spot for glucose and two faint spots for galactose and glycerol in a butanol-pyridine-water (3:1:1.5) solvent.

Fraction No. 9 contained several components one of which, with a low R_F-value, predominated. After hydrolysis, a sample run in the butanol solvent gave spots with the R_F-values of galactose and glycerol.

As only traces of reducing sugars could be present, the above fractions were further purified by treatment with Amberlite IR 400 in the OH-state to remove internal salts. These were recovered by elution of the ion exchanger with 5 % acetic acid.

Carbohydrates. After combining the appropriate fractions, purification by chromatography on carbon and recrystallisation gave the following carbohydrate compounds:

Scyllitol (9 mg) from fractions 1 and 2, m. p. 300° (decomp.), acetate m. p. 275—280°;

Mytilitol (150 mg) from fractions 1, 3 and 4, m. p. 266—269°, acetate m. p. 186—188°, undepressed on admixture with mytilitol hexaacetate;

Laminitol (213 mg) from fraction 1 and 4, m. p. 270—274°, acetate m. p. 155—157°, alone or admixed with authentic laminitol;

Mannitol (108 mg) from fractions 5, 6 and 7, m. p. 160—162° alone or admixed with an authentic sample of D-mannitol;

Unknown compound (60 mg) from fraction 8. It was chromatographically similar to α,α-trehalose and gave a strong glucose spot after hydrolysis. After standing for several months the syrup has started to crystallise.

Unknown compound (200 mg) from fraction No 9, m. p. 196—198°, $[\alpha]_D^{23}$ +88° (water, $c = 1.8$). After a sample had been hydrolysed in 0.2 N HCl at 108° for 14 h a strong spot, indistinguishable from that of galactose, and a rather faint spot with the R_F-value of glycerol were obtained on chromatograms run in butanol-pyridine-water (3:1:1.5). This substance will be further investigated.

The mannitol mother liquors from fractions Nos. 6 and 7 could also contain other hexitols as well as mannitol and on paper chromatograms they gave additional spots with

* All melting points are corrected.

lower R_F-values. They were hydrolysed in 0.2 N HCl at 100° over night. Paper chromatograms of the hydrolysate showed 2 strong spots with the R_F-values of a hexitol and a C-methyl cyclitol, while only traces of reducing sugars were detectable. A sample of the mixture was acetylated, and the acetates subjected to paper chromatography on Whatman No. 1 filter paper impregnated with methyl sulphoxide, using petroleum ether (b. p. 65—75°) or petroleum ether-*iso*propyl ether (1:2) as the mobile phase. The chromatograms were afterwards soaked with dilute silver nitrate solution (saturated solution-water 1:100), dried and sprayed with 1 N NaOH in ethanol. Mannitol and laminitol were indicated together with traces of sorbitol but no dulcitol.

Internal salts

From fractions Nos. 2, 3 and 4 only, an internal salt was obtained in appreciable amounts (325 mg), m. p. 270—275°. After adsorption on Amberlite IR 400 in the OH-state, elution with 5 % acetic acid and recrystallisation from dilute ethanol it had m. p. 279—282° (decomp.) and $[\alpha]_D^{23}$ + 7° (water, c = 2.0). (Found: C 23.6; H 5.88; N 8.27; S 18.0. Calc. for $C_3H_9NO_4S$: C 23.2; H 5.85; N 9.03; S 20.7.)

Of the combined mother liquors from fractions Nos. 2, 3 and 4, a sample (*ca.* 10 % of the total amount) was oxidised with excess periodate to decompose any D-cysteinolic acid. After de-ionising and evaporating, less than 1 mg of material was obtained. On paper chromatograms several ninhydrin-positive components were detected, none of which, however, could be taurine or N-methyltaurine.

The periodate consumption of the internal salt from fractions Nos. 2, 3 and 4 could not be determined as described previously [2] since the products of oxidation interfered with the titration of excess arsenite with iodine in a sodium bicarbonate buffer. Instead the sample (*ca.* 1 mg) in water (0.5 ml) was oxidised with 0.03 M sodium periodate (1 ml). At intervals potassium iodide solution (20 % in water, 0.5 ml) and 2 N hydrochloric acid (2 ml) were added and the liberated iodine titrated with 0.05 N sodium thiosulphate. After about 20 min the periodate consumed was 1.0 mole and this value rose to about 1.2 in 3 h.

The formation of formaldehyde upon periodate oxidation was 0.9 mole as determined by the method of Reeves [8]. Dimedone compound m.p. 191—193,5° alone or admixed with an authentic sample.

Synthesis of L-cysteinolic acid

S-Benzyl-L-cysteine was prepared following the directions of Hegedüs [9]. In a three-necked 500 ml flask equipped with a stirrer, dry L-cysteine hydrochloride (13 g) was added in portions to liquid ammonia (200 ml) and then sodium was added until a stable blue colour was produced. After the excess of sodium had been removed by the addition of small amounts of ammonium chloride, freshly distilled benzyl chloride (10.5 ml) was added. The ammonia was allowed to evaporate and the flask was evacuated and heated to 50° for 30 min. The residue was extracted with water, the solution filtered and the filtrate after extraction with ether brought to pH 5—6 with hydrochloric acid. After standing in a refrigerator overnight, the S-benzyl-L-cysteine was filtered off and washed with water. Yield 14.9 g (85 % of theory), m. p. 203—206° (decomp.).

S-Benzyl-L-cysteine ethyl ester. S-Benzyl-L-cysteine (14.9 g) was refluxed for 3 h in dry ethanol (300 ml) containing sulphuric acid (10 ml). After cooling on ice and neutralisation with a cooled solution of potassium carbonate (15 g) in water (20 ml) the mixture was filtered with Celite and the filtrate concentrated to dryness. The residue was covered with ether and 2 N sodium hydroxide solution (100 ml) added with cooling and shaking. The ether extract was dried over potassium carbonate and after filtration evaporated to dryness yielding an oil (9.6 g).

From the aqueous alkaline solution benzyl cysteine (4.2 g) was recovered by neutralisation with hydrochloric acid.

S-Benzyl-L-cysteinol was prepared by a method analogous to that used by Karrer and Aman [10] for the synthesis of S-propyl-L-cysteinol. A solution of S-benzyl-L-cysteine ethyl ester (9.6 g) in dry ether (80 ml) was slowly added to a solution of lithium aluminium

hydride (3 g) in dry ether (150 ml) contained in a three-necked flask with a stirrer and a condenser. After the mixture had been stirred for an additional 30 min, excess hydride was decomposed by the addition of ethyl acetate (20 ml) in ether (20 ml) and a mixture of water (6 ml), ethanol (10 ml) and ether (20 ml). After standing overnight the ether solution was filtered by suction from the precipitate, dried over potassium carbonate and concentrated to dryness. Crude S-benzyl-L-cysteinol was obtained as an oil (8.1 g).

L-Cysteinol. The debenzylation of S-benzyl-L-cysteinol was carried out by the method of du Vigneaud. Sodium was added to a solution of crude S-benzyl-L-cysteinol (8.1 g) in liquid ammonia (*ca.* 200 ml) until a stable blue colour appeared. The mixture was allowed to stand for 30 min and then neutralised by the addition of ammonium sulphate (7 g). After most of the ammonia had evaporated the flask was evacuated and kept at 50° for 15 min. The residue was extracted with dry ethanol (150 ml), the solution was filtered and the filtrate concentrated. The residual syrup was dissolved in water (100 ml) and the solution after extraction with ether concentrated under reduced pressure yielding a syrup (5.5 g). This amount exceeds the theoretical yield by 1.1 g, probably due to insufficient drying. Paper chromatograms of the product run in ethyl acetate-acetic acid-water (3:1:1) gave only one strong and a few very faint spot when sprayed with ninhydrin reagent.

L-Cysteinolic acid. While the oxidation of cystine to cysteic acid with bromine in hydrochloric acid solution [11] proceeds smoothly (80–90 % yield), the oxidation of L-cysteinol under the same conditions gave an inferior result. Preliminary experiments which were followed by paper chromatography indicated that the oxidation took several different routes, yielding mainly two compounds behaving as internal salts, one of which proved to be the enantiomorph of the internal salt from the alga. The other component did not crystallise readily and seemed to be unstable upon prolonged storage. It was not further investigated.

Probably hydrolytic reactions took place also, since if the solution after saturation with bromine at 35° was heated to boiling for a short time and cooled, more bromine was then rapidly absorbed.

To a solution of crude L-cysteinol (2.7 g) in 1 N hydrochloric acid (50 ml) bromine was added, with stirring, at such a rate that it was immediately consumed and the temperature did not rise above 35°. After 8.8 g of bromine had been added the uptake of bromine was very slow and the mixture was left over night at room temperature. More bromine

Table 1. Spacing values.

Internal salt from the alga (D-cysteinolic acid)		Synthetic L-cysteinolic acid	
d (Å)	I/I_1	d (Å)	I/I_1
9.35	100	9.27	100
5.07	5	5.06	10
4.69	70	4.69	85
4.22	10	4.23	15
4.13	50	4.13	70
3.91	35	3.90	50
3.65	25	3.65	35
3.35	15	3.35	15
3.26	10	3.26	10
3.16	70	3.16	30
3.13	15	3.13	25
2.73	35	2.73	35
2.51	5	2.51	10
2.31	10	2.31	10
2.25	5	2.25	10
1.95	5	1.95	10
1.88	5	1.88	10

(0.25 g) was then quickly consumed. After the reaction mixture had been heated to boiling for a few minutes and cooled to room temperature, bromine (0.5 g) was added until no more was absorbed.

After concentration *in vacuo*, dilution with water and de-ionisation with Amberlite IR 120 and IR 4B the reaction mixture was taken to dryness yielding an amorphous mixture (2.7 g). This was separated on a carbon-Celite column (1:1; 35 × 4.5 cm) using water as eluant. A fraction was obtained which on paper chromatograms gave a spot indistinguishable from that of the internal salt from the alga. Concentration and crystallisation from dilute ethanol gave a product with m. p. 265—275° (decomp.). The yield was 1.16 g or 24 % calculated from the S-benzyl-L-cysteine utilised. Further recrystallisation yielded a pure product m. p. 279—281° (decomp.), $[\alpha]_D^{23}$ −6° (water, c = 2.0). Mixed m. p. with the internal salt from the alga (m. p. 279—282°) 245—260°.

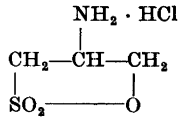
X-Ray diffraction. The X-ray diffraction patterns for the cysteinolic acid from the alga and for synthetic L-cysteinolic acid (Table 1) were determined on a "Norelco X-ray Diffraction Apparatus with High Angle Goniometer" (Philips Co).

(Cu K_α) = 1.5418 Å. The samples for examination were finely ground, suspended in ethanol and spread in a thin layer on glass plates and the ethanol allowed to evaporate.

The discrepancies between the relative intensities (I/I_1) obtained from the two samples may be due to slightly different orientation of the crystals.

Acknowledgement. The author is indebted to *Statens Naturvetenskapliga Forskningsråd* for financial support, to *Norsk Institutt for Tang- og Tare-forskning, Trondheim*, for a generous gift of the alga, to Tekn.lic. S. T. Lundin, Stockholm, for the X-ray diffraction investigations and to Ing. L. Mikiver and Ing. Gurli Hammarberg for their skilful assistance.

Added in proof: Recently the synthesis and oxidation of cysteinol has been described by J. C. Crawhall, D. F. Elliott and K. C. Hooper (*J. Chem. Soc.* **1956** 4066). These authors have found that oxidation of cysteinol hydrochloride with bromine water yields cysteic acid and occasionally the sultone II. No cysteinolic acid was produced.



II.

With a view to these findings, L-cysteic and L-cysteinolic acid were compared. A sample of L-cysteic acid decomposed at ca 275° on rapid heating, whereas L-cysteinolic acid melted at 279—281° before any considerable decomposition took place. The mixed samples rapidly decomposed at 260—270°. On a paper chromatogram run in a butanol-pyridine-water mixture (2:3:1.5) mixture the R_F values were 0.17 and 0.35 for L-cysteic and L-cysteinolic acid respectively.

REFERENCES

1. Lindberg, B. *Acta Chem. Scand.* **9** (1955) 1323.
2. Wickberg, B. *Acta Chem. Scand.* **10** (1956) 1097.
3. Challenger, F. and Simpson, Margaret I. *J. Chem. Soc.* **1948** 1591.
4. Colin, H. and Augier, J. *Compt. rend.* **209** (1939) 1450.
5. Bouveng, H., Lindberg, B. and Wickberg, B. *Acta Chem. Scand.* **9** (1955) 807.
6. Lindberg, B. *Acta Chem. Scand.* **9** (1955) 1097.
7. *To be published.*
8. Reeves, R. E. *J. Am. Chem. Soc.* **63** (1941) 1476.
9. Hegedüs, B. *Helv. Chim. Acta* **31** (1948) 737.
10. Karrer, P. and Aman, G. *Helv. Chim. Acta* **33** (1950) 305.
11. *Org. Synthesis* Coll. Vol. **3** (1955) 226.

Received January 2, 1957.

ACTA CHEMICA SCANDINAVICA 11 (1957) 512—522

Fractionation of the Phosphorus-Containing Proteins of Rat Liver Cell Supernatant

JOHN GLOMSET

Institute of Medical Chemistry, University of Uppsala, Sweden

Rat liver supernatant proteins have been fractionated by ammonium sulfate precipitation, zone electrophoresis and ion exchange chromatography with special reference to phosphoserine and phosphothreonine-containing proteins. Several phosphorus-containing fractions have been obtained which together account for most of the protein-bound phosphoserine and phosphothreonine present.

In earlier publications from this laboratory [1,2] direct evidence was presented concerning the nature of a type of phosphoprotein present in liver. Methods were described by which crystalline phosphoserine and phosphothreonine could be isolated from partial hydrolysates of cell protein. And it was observed that these two phosphorylated amino acids could be prepared from each of the cell fractions obtained by the differential centrifugation method of Hogeboom and Schneider [3]. Moreover, experiments were described which indicated that protein-bound phosphorus might possibly play an active role in the metabolism of the cell. Recently, this possibility has been considerably strengthened by the work of Sutherland [4,5] and of Ågren and Engström [6,7] The former found that liver phosphorylase, a phosphoprotein, is inactivated by dephosphorylation and becomes active again after rephosphorylation. The latter authors presented evidence to show that an exchange of the phosphorus of a muscle phosphorylase and yeast hexokinase preparation occurred during the reactions catalyzed by these enzymes.

In the present paper a separation of the soluble phosphorus-containing proteins of rat liver has been attempted in order to provide a basis for subsequent studies of their structure and function. Both conventional precipitation methods and the more recent methods of ion exchange chromatography and zone electrophoresis have been employed. Several phosphorus-containing peaks have been obtained by zone electrophoresis and phospho-protein fractions corresponding to two of these and containing a considerable part of the protein-bound phosphoserine of the cell sap have been isolated. A preliminary report of some of this work has been published [8]. Some preliminary metabolic experiments have also been performed.

EXPERIMENTAL

Three month old male Wistar rats from the departmental colony were employed as experimental animals. They averaged about 300 g in weight and had not been fasted previously. Generally, they were injected intraperitoneally with 1—2 mC carrier-free radioactive phosphate 1—2 h previous to each experiment. The rats were killed by cervical dislocation and their livers quickly perfused *via* the hepatic portal vein, first with ice-cold isotonic NaCl and then with ice-cold 0.25 M sucrose solution, both solutions having been made up with glass-distilled water and adjusted to a pH of 7.4 with KOH. The perfusion was performed *in situ* using a long plastic tube connected to a syringe. After the plastic cannula had been inserted into the vein and securely tied in place, a few ml of saline were forced into the liver and then the abdominal and thoracic *vena cava* were cut to allow the free flow of blood from the liver. During perfusion the liver was cooled with ice-cold sucrose. The perfused livers were minced with a scissors and homogenized in 9 vol. of 0.25 M sucrose for 2 min in a homogenizer of the Potter & Elvehjem type consisting of a smooth-walled glass tube fitted with a teflon pestle (manufactured by Arthur H. Thomas Co., Philadelphia). The liver supernatant was then prepared essentially according to Hogeboom [9]; the microsomes, however, were spun down at 30 000 R.P.M. for one hour in rotor No. 40 of the Spinco model L preparative centrifuge. All centrifugations and manipulations were carried out at 0°—2°C. Furthermore, all solutions were made up with glass-distilled water using analytical grade reagents and were adjusted to pH 7.4 with KOH unless otherwise noted. All glass-ware and instruments were rinsed with glass-distilled water before use.

Precipitation with ammonium sulfate. Fractions were obtained by adding to the supernatant a saturated aqueous solution of ammonium sulfate, the pH of which had been adjusted so that it was 7.0 after ten-fold dilution. Fraction "AS 50" was obtained by adding 1 vol. of saturated ammonium sulfate. The resulting precipitate was then washed three times with 50 % saturated ammonium sulfate. The first washing having been combined with the original supernatant, fraction "AS 85" was obtained by adding additional saturated ammonium sulfate solution to 85 % saturation. This fraction was also washed three times. The two precipitates were then dissolved in 0.06 M tris(hydroxymethyl)aminomethane buffer, pH 7.8 (unless otherwise noted) and then dialyzed for 2 h before application to the zone electrophoresis columns. In all the ammonium sulfate fractionation experiments, the sucrose used in preparing the cell sap contained 0.01 M versene.

Zone electrophoresis was performed according to Porath [10] on 150 × 3 cm columns. Generally "tris" buffers were employed at a pH of 7—8 and a concentration of 0.03—0.1 M. The electrophoresis required from 36—48 h and was always performed in the cold.

Ion exchange chromatography. Triethylaminoethyl cellulose columns and sulfomethyl cellulose columns prepared according to Porath [11] and ECTEOLA columns prepared at room temperature according to Peterson and Sober [12] (however, using cellulose linters instead of solka floc) were employed for the protein fractionation experiments. The columns were of varying dimensions, but the exchanger was always supported by cellulose discs at the lower end of the column. The chromatography was always carried out in the cold.

The chromatographic and electrophoretic fractionations were followed spectrophotometrically at 260 and 280 mμ. Cold precautions were taken at all possible points. ^{32}P determinations were made on aliquots of the fractions and counted on an automatic scaler. For a more specific determination of the phosphoserine and phosphothreonine-containing proteins, the two amino acids were isolated from partial hydrolysates of the protein fractions as described previously [1,2]. For a crude estimation of the relative amounts of radioactive phosphoserine and phosphothreonine present in the fractions the total activity of the two phosphorus-containing amino acids was determined. For concentration of the protein fractions the ultrafiltration apparatus described by Aronsson [13] was employed. Phosphorus determinations were performed as described previously [2]. The following abbreviations have been used: "tris" = tris(hydroxymethyl)-aminomethane; RNA = ribonucleic acid; PCA = perchloric acid; TEAE = triethylaminoethyl cellulose; ATP = adenosine triphosphate.

RESULTS

The first step of the fractionation procedure was initially planned to comprise a precipitation method in order to concentrate the supernatant (initial volume 140 ml), remove organic phosphorus compounds of low molecular weight and obtain a preliminary fractionation of the proteins.

In preliminary experiments [8] ethanolic fractionation by the method of Cohn *et al.*[14] was attempted. Fractions containing relatively increased amounts of phosphoserine and phosphothreonine proteins could be obtained, but it was difficult to obtain satisfactory reproducibility from experiment to experiment (on the basis of radioactive phosphoserine determinations and the relative number and amount of peaks present when the fractions were subjected to zone electrophoresis) although adequate reproducibility could be obtained with aliquots of the same supernatant preparation. Moreover, similar difficulties were encountered in fractionating solubilized proteins from mitochondria (unpublished results). It was also noted that even when the method was slightly modified so that the first precipitation was performed at a lower ethanol concentration (10 % by volume) some apparent denaturation of a nucleoprotein, phosphoprotein fraction was obtained under such mild conditions as pH 5.8, 10 % ethanol, —3°C, 45 min. Thus, in every experiment a residue remained after the first precipitation step which could not be redissolved although several different solvent systems were tried.

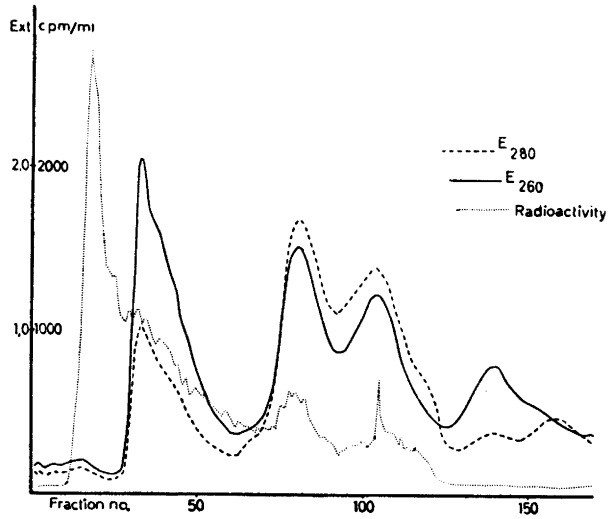


Fig. 1. Electropherogram of liver cell supernatant, fraction "AS 50". 2 rats injected with 1 mC ^{32}P 1 h previous to liver perfusion. Supernatant prepared with 0.25 M sucrose — 0.01 M versene, pH 7.4. 1 vol. saturated ammonium sulfate added: precipitate washed thrice, dialyzed 2 h; insoluble material removed by centrifugation. Clear solution displaced into the zone electrophoresis column with 50 ml buffer (0.06 M tris, pH 7.8). Electrophoresis for 45 h at 40 mA (1 300 V). Fractions of approximately 5 ml collected. Each measured at 260 mμ and 280 mμ; 1 ml aliquots taken for ^{32}P determination.

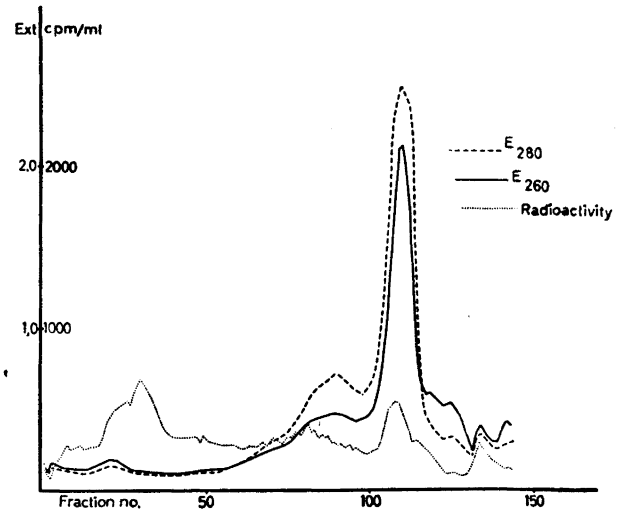


Fig. 2. Electropherogram of liver cell supernatant, fraction "AS 85". Same experiment as shown in Fig. 1. Precipitate obtained with 85 % saturated ammonium sulfate. Treated in same manner as fraction "AS 50".

Ammonium sulfate precipitation. In view of the difficulties encountered in the ethanolic fractionation experiments, a cruder separation into only 2 fractions was attempted, using ammonium sulfate precipitation. Subsequently, the precipitates were further fractionated using a more selective method (zone electrophoresis). In preliminary experiments it was found that approximately 80 % of the phosphoserine protein fraction of the supernatant fraction (and a nearly proportionate amount of the total RNA as estimated by measuring the total quantity of 260 mμ adsorbing material released by warm PCA extraction) could be precipitated by adding 1 vol. saturated ammonium sulfate solution to the cell sap, the resulting precipitate corresponding to 30—40 % of the total cell sap protein by weight. Further, it was found that little or no enzymatic dephosphorylation could be demonstrated after the phosphoserine protein-containing fractions had been allowed to stand in the cold for a period of 48 h (the maximum time usually employed for the zone electrophoresis).

The results of a typical experiment where ammonium sulfate fractionation was followed by a further separation of the fractions by zone electrophoresis are shown in Figs. 1 and 2.

As is apparent, both the ammonium sulfate precipitation and the electrophoresis yield a rather sharp separation of the cell sap proteins. Moreover, this two step separation is reproducible, although it must be mentioned that the ammonium sulfate fractionation at this pH causes the irreversible precipitation of a small amount of protein when the ammonium sulfate concentration approaches 35 % saturation so that this protein does not appear on the zone electrophoresis diagram.

Another point to be mentioned is that some of the protein migrating toward the cathode has not been included in the electrophoresis diagram, it having moved into the unstabilized buffer region.

The fractions which have been of the greatest interest in the present investigation are those which contain radioactive phosphorus. As may be seen there are a number of radioactive peaks. The first radioactive peak of the "AS 50" fraction remained soluble after cold PCA had been added to a final concentration of 0.6 N and was found to consist mainly of inorganic phosphate. The second peak was found to contain RNA. Radioactive phosphoserine and phosphothreonine were isolated in relatively large amounts from the third and fourth radioactive peaks and also from the main peak of fraction "AS 85". The identity of the remaining peaks is under investigation. The adsorption properties of the most slowly moving fractions suggest the presence of relatively large amounts of bound nucleotide. Most of the 260 mμ-adsorbing material of these fractions could be released from the protein by treatment with cold 0.6 N perchloric acid.

Ion exchange chromatography. In a series of experiments acidic and basic cellulose derivatives were substituted for the precipitation with ammonium sulfate as the first step in the procedure. It was found that when the supernatant was passed through the acidic exchanger, sulfomethyl cellulose, at pH 6.0 almost no phosphoprotein was adsorbed and most of the additional cell sap protein also passed through the column. Moreover, when the cation exchanger was used in an attempt to fractionate an already purified phosphoprotein fraction some denaturation apparently occurred.

The basic exchangers used were triethylaminoethyl cellulose and ECTEOLA cellulose. The former is rather similar in its properties to the DEAE cellulose described by Sober and Peterson (see Porath [10]) and affords a similar separation of serum proteins (unpublished experiments). Columns 10 cm in length and 3 cm in diameter were usually employed. The fresh cell sap (usually of a pH of 6.8—7.0) was allowed to pass through the column in the cold room, the column having previously been equilibrated with 0.005 N or 0.01 N tris buffer, pH 7.4. The column was then washed with 0.01 N buffer and subsequent fractions were displaced from the column by successively higher concentrations of Cl^- ion obtained by increasing the concentrations of the buffer solution or by adding NaCl. Fig. 3 shows the type of separation obtained.

Fraction I (not included in the curve) consists of those cell sap components which have not been adsorbed by the ion exchanger under these experimental conditions and comprises about 30 % of the total cell sap protein by weight. This fraction contains only a very small amount of the total radioactive phosphoserine protein and 4 % or less ot the total material yielding 260 mμ adsorbing substances when extracted with warm PCA. In most preparative experiments fractions II—V were combined. The combined fraction then amounted to about 30 % of the total cell sap protein, roughly 20 % of the radioactive phosphoserine protein and about 12 % of the total "RNA". Also, for cruder, initial separations VI—IX were combined corresponding to about 20 % of the total protein but more than 60 % of the total radioactive phosphoserine protein and RNA. Reducing the pH of the displacing buffer (to pH 6 or 5) did not cause the displacement of any additional protein from the column.

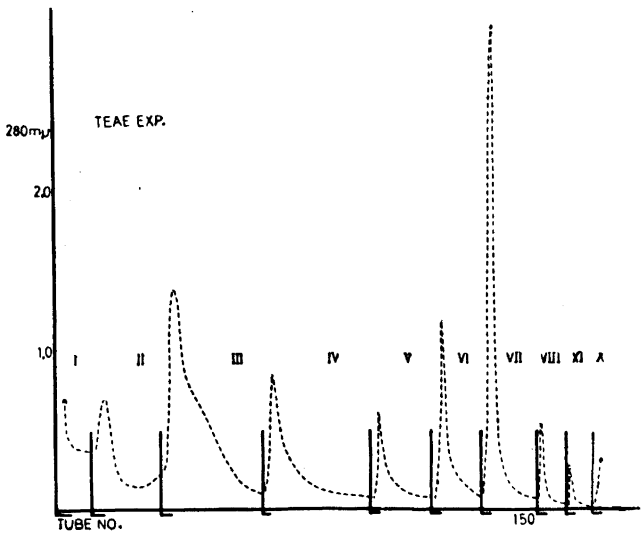


Fig. 3. Fresh supernatant prepared with 0.25 M sucrose from 2 rats, chromatographed on a 3 × 10 cm TEAE column, previously equilibrated with 0.005 M "tris", pH 7.4, subsequently washed with 0.005 M "tris", pH 7.4 to obtain fraction 1. Stepwise elution at same pH with 0.01 M "tris", 0.05 M "tris" + 0.05 M NaCl, 0.05 M "tris" + 0.1 M NaCl, 0.05 M "tris" + 0.2 M NaCl, 0.05 M "tris" + 0.5 M NaCl, 0.1 M "tris" + 0.9 M NaCl, 0.1 M "tris" + 1.5 M NaCl to obtain fractions II—IX, respectively. Remaining adsorbed material eluted with 2 % NaOH. Approximately 15 ml fractions taken, measured at 280 mμ.

However, an additional fraction (not shown in the curve) which corresponded to about 10 % of the total protein was displaced from the column by 2 % NaOH. This apparently corresponds to protein, denatured during the chromatographic procedure (however, see discussion) and in several experiments was found to contain between 20 and 30 % of the total radioactive phosphoserine protein as well as a considerable amount of RNA. Experiments in which the initial pH of the ion exchange column was lower (6.2) (that of the cell sap had also been reduced) yielded no reduction in the amount of "denatured" phosphoprotein. Nor did increasing the initial chloride concentrations of the cell sap and column have a favorable effect.

When TEAE fractions II—V were combined, ultrafiltered, dialyzed and subjected to zone electrophoresis the electropherogram shown in Fig. 4 was obtained. The main peak appears to correspond to the last radioactive peak in Fig. 1. Moreover, when in another experiment, material corresponding to the latter peak was chromatographed on a TEAE column it was found to be eluted with Cl-concentrations corresponding to fractions II—V. TEAE fractions VI—IX yielded the electropherogram shown in Fig. 5. The main peak resembles the third radioactive peak in Fig. 1. The identity of the two peaks was confirmed by chromatography of peak 3, Fig. 1, on a TEAE column. It should be noted that the most slowly moving peaks in Fig. 1 are contained

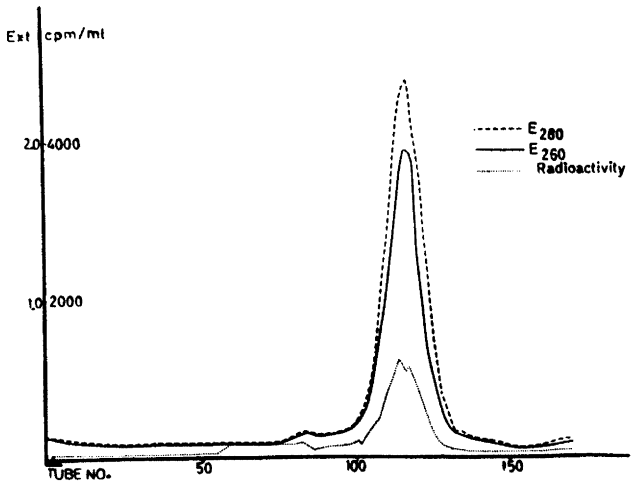


Fig. 4. Same experiment as in Fig. 3. Electropherogram of TEAE fraction corresponding to fractions III—V, Fig. 3. After ultrafiltration and dialysis, electrophoresis and elution as in Fig. 5.

in TEAE fractions VI—IX which otherwise contains only the faster moving electrophoretic components. As may be seen in both Figs. 1 and 5 the slower moving components appear to contain bound nucleotide material, which

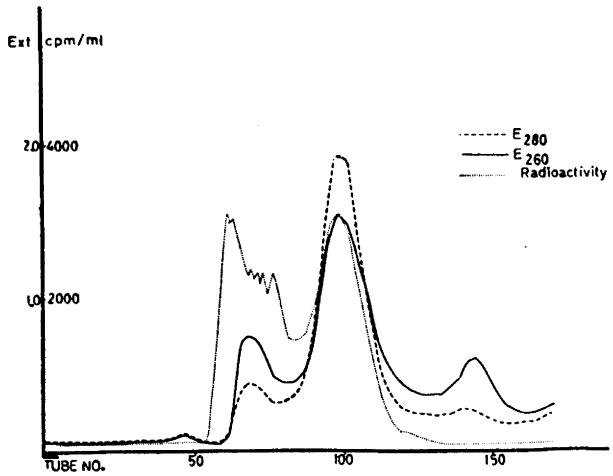


Fig. 5. Electropherogram of TEAE fraction corresponding to fractions VI—VIII, Fig. 3. 4 rats injected with 1.5 mC ^{32}P each, 2 h previous to perfusion. Supernatant prepared with 0.25 M sucrose, pH 7.4, chromatographed on 3 × 10 cm TEAE column. Fraction corresponding to fractions VI—VIII, Fig. 3, ultrafiltered and applied to electrophoresis column. Electrophoresis in 0.1 M "tris", pH 7.8 for 46 h, 45 mA (900 V). Fractions collected and measured as in Fig. 1.

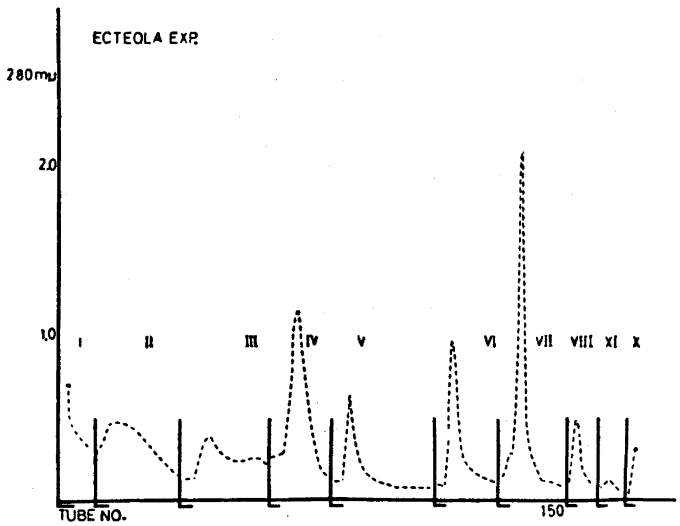


Fig. 6. Fresh supernatant prepared with 0.25 M sucrose from 2 rats, chromatographed on a 3 × 10 cm ECTEOLA column under conditions identical to those in the TEAE experiment shown in Fig. 3.

although released for the most part by cold perchloric acid, does not appear to contain phosphorus which has exchanged with other nucleotide compounds of the cell.

ECTEOLA columns were also found to be useful for the fractionation of the acidic cell sap proteins. While a large part of the total cell sap protein passes through the column with 0.005 N tris, pH 7.4, the phosphoserine and phosphothreonine proteins are retained and may be displaced to yield a fractionation pattern which is quite similar to that of the TEAE columns. Moreover, electropherograms of the ECTEOLA fractions were similar to those obtained with the corresponding TEAE fractions. As is the case with the TEAE columns some of the phosphoprotein is retained by the column in such a way that it can only be displaced by weak NaOH. An elution curve is reproduced in Fig. 6 for purposes of comparison.

Incubation experiments. Some preliminary incubation experiments have been carried out with the whole rat liver supernatant fraction. When a mixture of ^{32}P-containing nucleotides fortified with highly radioactive $AT^{32}P$ was added to fresh non-radioactive supernatant from two rat liver homogenates incorporation of ^{32}P into not only the phosphoserine but also the phosphothreonine of the protein could be demonstrated. Moreover, incorporation of the isotope could also be demonstrated in an experiment in which 1 mC inorganic ^{32}P was added to fresh rat liver supernatant and the mixture shaken at 20—21° C for 15 min. While under these conditions no exchange of RNA phosphorus occurred, the phosphoserine and phosphothreonine isolated from hydrolysates of the protein both contained ^{32}P.

DISCUSSION

Determination of phosphoproteins. Although phosphorus conceivably may be bound to protein in a number of ways, the experiments described in the present paper have mainly concerned those proteins of rat liver cell sap which contain phosphoserine and phosphothreonine. As yet these are the only two phosphorylated amino acids which have been isolated from liver protein. These amino acid derivatives may be qualitatively determined as described previously [1,2], but, unfortunately, there is still no satisfactory method for their quantitative determination in protein linkage. The methods which have hitherto been employed for the determination of protein phosphorus have been based on the old observation by Plimmer [15] that the phosphorus of casein is relatively alkali labile. Thus, Schmidt and Thannhauser [16] and Johnson and Albert [17] among others have subjected organ protein to partial alkaline hydrolysis and designated the liberated inorganic phosphorus as "phosphoprotein phosphorus". The reliability of this type of method for the determination of phosphoserine and phosphothreonine proteins has been questioned earlier [1]. Moreover, since then Crosby *et al.*[18] have reported that the alkaline hydrolysis method used by them to obtain RNA nucleotides from rat liver does not hydrolyze all of the phosphoserine present, and this has been confirmed by the author, under more vigorous alkaline hydrolysis conditions (unpublished experiments). Thus, the alkaline hydrolysis method would definitely seem inadequate when applied to liver phosphoprotein determination.

In the experiments described in this paper the protein separations have been followed by (1) measuring the radioactivity of the protein fractions eluted from the columns and (2) measuring the total ^{32}P-activity of the phosphoserine and phosphothreonine fractions isolated from partial hydrolysates of the fractionated proteins using Dowex 50. The determinations have thus necessarily been only approximate and have not included phosphoproteins in which there is a negligible uptake of radioactive phosphate under the conditions of these experiments. Yet they have been of value here since the phosphoproteins which have been of greatest interest have been those in which the phosphorus itself is metabolically active, with extent and rapidity of uptake of radioactive phosphate being taken as a provisional measure of metabolic activity.

Fractionation methods. It seems likely that the difficulty in obtaining reproducible precipitation of the cell sap phosphoproteins using the method of Cohn may be the result of the very factor, *viz.* co-precipitation, which has made the method so selective when used for the fractionation of serum proteins in the hands of Cohn and collaborators. Thus, small differences in the protein and inorganic cation concentrations of the cell sap caused by irregular perfusion or an altered adsorption of soluble proteins onto the intracellular particles as result of changes in the pH of the cell sap during the preparation could conceivably result in significant changes in the fractionation pattern. This would be especially true for the more highly charged proteins which would normally show a strong tendency to form co-precipitates. To reduce these effects in the subsequent ammonium sulfate fractionation experiments the following steps were taken. 0.01 M versene was included in the homogenization medium (and perfusion media). The precipitation was carried out at

pH 7.0 and only a few fractions were taken to facilitate the subsequent zone electrophoresis.

In the experiments with the strongly basic ion exchangers it was found that a considerable amount of phosphoprotein + nucleoprotein material ostensibly became strongly bound to the column (the fractions eluted with NaOH). Experiments designed to prevent this effect were not successful. It seems possible that denaturation of the proteins has occurred here. To further investigate this possibility experiments with more weakly basic ion exchange columns would be of value. Another possibility is that all or a major part of the strongly "adsorbed" material is in fact submicroscopic particulate matter [19] which has not been sedimented in the centrifugal fields employed here. It is perhaps significant that roughly proportional amounts of phosphoprotein + nucleoprotein material is "denatured" or rendered insoluble by (1) treatment with low concentrations of ethanol, (2) passage through ion exchange columns, (3) precipitation with low concentrations of $MgCl_2$ (unpublished experiments).

The ion exchange experiments described here have been of a preparative nature, and no attempt has been made to obtain a finer separation of the less strongly bound, non phosphothreonine or phosphoserine-containing proteins. Some experiments have been carried out where the purified phosphoamino acid-containing fractions were rechromatographed on TEAE columns with gradient elution but so far neither these nor re-electrophoresis experiments have yielded a subfractionation of the main phosphorus-containing peaks shown in Figs. 4 and 5. However, additional attempts to purify the phosphoprotein fractions are in progress as well as incubation experiments with the purified fractions. These experiments will be reported in a later paper.

Acknowledgments. This investigation was supported by grants from the *Medical Faculty of the University of Uppsala.* The author wishes to thank Prof. Gunnar Ågren for the privilege of working in his laboratory. He is also indebted to Dr. Jerker Porath for generous gifts of TEAE-cellulose and for many valuable discussions. Thanks are also due to Mrs Margot Persson for faithful technical assistance.

REFERENCES

1. Ågren, G., de Verdier, C.-H. and Glomset, J. *Acta Chem. Scand.* **8** (1954) 503.
2. Ågren, G., de Verdier, C.-H. and Glomset, J. *Acta Chem. Scand.* **8** (1954) 1570.
3. Schneider, W. C. and Hogeboom, G. H. *J. Biol. Chem.* **183** (1950) 123.
4. Wosilait, W. D. and Sutherland, E. W. *J. Biol. Chem.* **218** (1956) 469.
5. Rall, T. W., Sutherland, E. W. and Wosilait, W. D. *J. Biol. Chem.* **218** (1956) 483.
6. Ågren, G. and Engström, L. *Acta Chem. Scand.* **10** (1956) 489.
7. Engström, L. and Ågren, G. *Acta Chem. Scand.* **10** (1956) 877.
8. Glomset, J. *Acta Chem. Scand.* **10** (1956) 1045.
9. Hogeboom, G. H. in *Methods in Enzymology*, Vol. I. Academic Press Inc. Publishers, New York 1955, p. 16.
10. Porath, J. *Biochim. et Biophys. Acta* **22** (1956) 151.
11. Porath, J. *Arkiv Kemi (In press).*
12. Peterson, E. A. and Sober, H. A. *J. Am. Chem. Soc.* **78** (1956) 751.
13. Aronsson, T. *Scand. J. Clin. & Lab. Invest. (In press).*

14. Cohn, E. J., Gurd, F. R. N., Surgenor, D. M., Barnes, B. A., Brown, R. K., Deronaux G., Gillespie, J. M., Kahnt, F. W., Lever, W. F., Lin, C. H., Mittelman, P., Mouton, R. F., Schmid, K. and Uroma, E. *J. Am. Chem. Soc.* **72** (1950) 465.
15. Plimmer, R. H. A. and Baylis, W. M. *J. Physiol.* **33** (1906) 439.
16. Schmidt, G. and Thannhauser, S. J. *J. Biol. Chem.* **161** (1945) 83.
17. Johnson, R. M. and Albert, S. J. *J. Biol. Chem.* **200** (1953) 335.
18. Crosbie, G. W., Hutchison, W. C., Mc Indoe, W. M., Childs, M. and Davidson, J. N. *Biochim. et Biophys. Acta* **14** (1954) 580.
19. Newburgh, R. W. and Cheldelin, V. H. *J. Biol. Chem.* **218** (1956) 89.

Received January 8, 1957.

ACTA CHEMICA SCANDINAVICA 11 (1957) 523—536

Ornithine Carbamyl Transferase from Rat Liver

PETER REICHARD

Biochemical Department, Karolinska Institutet, Stockholm, Sweden

An enzyme (ornithine carbamyl transferase) has been purified from rat liver which catalyzes the formation of citrulline according to: L-ornithine + carbamyl phosphate ⇌ L-citrulline + phosphate. The enzyme moved as a single compound during paper electrophoresis between pH 5.0 and 8.5 with an isoelectric point around 8.1. A minor impurity amounting to *ca.* 5—8 % was found during ultracentrifugation.

The reaction greatly favoured citrulline synthesis, the equilibrium constant being *ca.* 10^6. Out of 26 amino acids tested only L-ornithine was able to accept the carbamyl group of carbamyl phosphate. Inhibition by SH-reagents was observed and partial protection from inhibition could be obtained with each of the substrates, tentatively indicating binding of both substrates to SH groups of the enzyme. Isotope exchange experiments indicated that the transfer reaction was of the single displacement type.

The citrulline phosphorylase of Krebs *et al.*[8] has been found to be identical with ornithine carbamyl transferase.

By coupling ornithine carbamyl transferase with aspartate carbamyl transferase [5] synthesis of carbamyl aspartate was obtained from citrulline + aspartate in the presence of phosphate.

The work of Grisolia and Cohen [1] has demonstrated that citrulline is formed enzymically in mammalian liver through a transfer of the carbamyl group of an active carbamyl compound to ornithine. Jones *et al.*[2] recently synthesized carbamyl phosphate and demonstrated its identity with the active carbamyl compound.

Our interest in carbamyl transfer reactions originated from investigations of the enzymic formation of carbamyl aspartate, an intermediate in pyrimidine biosynthesis. We found that this substance was formed from aspartate, CO_2 and NH_3 in the presence of ATP and acetylglutamate and that carbamyl phosphate (CAP*) was an intermediate in the reaction [3-5]. An enzyme (aspartate carbamyl transferase) which catalyzed the transfer of the carbamyl

* The following abbreviations are used in this paper: CA = carbamyl, CAP = carbamyl phosphate, P_i = inorganic phosphate, ATP = adenosine triphosphate, PCA = perchloric acid, tris = tris(hydroxymethyl)amino methane, CMBA = *p*-chloromercuribenzoic acid, EDTA = ethylenediamine tetraacetic acid.

group was purified a hundredfold from *E. coli* [5] and a study of the mechanism of its action was made. The limited supply of the starting material and the relative instability of the purified enzyme made further purification difficult.

The present investigation was started with a twofold purpose. First it was intended to study a carbamyl transfer reaction with an essentially pure enzyme. Second it was of interest to investigate whether the citrulline forming enzyme by a reversal of its action could form carbamyl phosphate which then together with aspartate would give rise to carbamyl aspartate. Such a reaction would represent a second mechanism for the utilization of the carbamyl group of citrulline for pyrimidine synthesis [6], the first being the transfer of the carbamyl group of citrulline to a phosphate group of ATP with the formation of CAP [7]. In this connection it was also of interest to determine whether citrulline phosphorylase as described by Krebs *et al.*[8] was identical with the citrulline forming enzyme.

After purification of the enzyme from rat liver the following stoichiometric reaction could be demonstrated:

$$\text{Carbamyl phosphate} + \text{L-ornithine} \rightleftharpoons \text{L-citrulline} + \text{phosphate} \quad (1)$$

The name ornithine carbamyl transferase is proposed for this enzyme.

MATERIALS AND METHODS

L-*Citrulline-carbamyl-*^{14}C was synthesized according to Smith [9]. In spite of repeated crystallizations the compound contained a small amount (*ca.* 1 %) of ornithine. For the determination of the equilibrium constant this amino acid was removed by paper electrophoresis (1 h, 12.5 V/cm) in 0.1 M acetic acid. Using acid washed Whatman filter paper (No. 3) 300 μmoles of citrulline could be run on one sheet. A small strip was sprayed with ninhydrin to locate the amino acids. The main amount of citrulline was then eluted with water from the paper. After evaporation to dryness it was redissolved in a small amount of water and used directly. On paper chromatography (phenol:water, 9:1) no ornithine could be detected.

^{14}*CA-aspartate* was synthesized according to Nyc and Mitchell [10], *CAP* according to Jones *et al.*[2] DL-*Ornithine*, L-*ornithine* and DL-*ornithine-2-*^{14}C were commercial samples (Schwarz laboratories, Inc. and California Foundation for Biochemical Research).

Protein determinations were made by the method of Bücher [11]. When checked by nitrogen analysis of PCA precipitates at different points during the preparation good relative agreement was obtained. During zone electrophoresis and chromatography protein was measured by light absorption at 280 mμ.

Determination of enzyme activity. Forward reaction. The enzyme was incubated for 15 min at 37° with 30 μmoles of CAP, 100 μmoles of DL-ornithine and 100 μmoles of tris buffer, pH 7.3—7.4, in a final volume of 1.0 ml. The tubes were then immediately immersed in an ice bath and the amount of inorganic phosphate present was determined directly on 0.02 ml aliquots by the Lowry-Lopez [12] method. Readings were made after 5 min. A blank without enzyme was treated in the same manner.

Under those conditions the difference between the amount of inorganic phosphate formed in the sample containing enzyme and the blank was proportional to the amount of enzyme added (Fig. 1) up to a value of *ca.* 6—8 μmoles.

One unit of enzyme activity was defined as a difference of 1 μmole of P_i formed under the above conditions. The specific activity of the enzyme was defined as units/mg protein.

Sometimes the amount of citrulline formed was determined rather than P_i. In this case the enzyme reaction was stopped by the addition of 0.1 ml of 4.4 M PCA and citrulline [13] determined directly on aliquots. This method was more time consuming but was used whenever high accuracy was desired or when substances were present which inter-

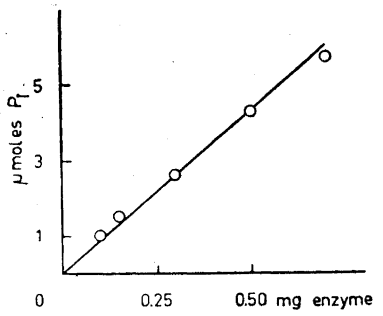


Fig. 1. Enzymic formation of P_i from CAP. Standard conditions as described in text.

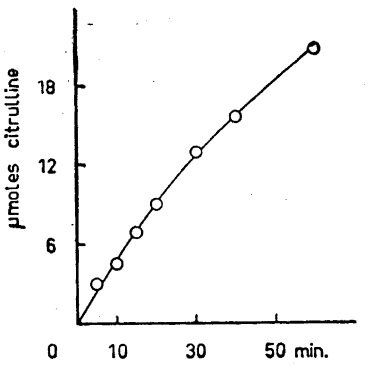


Fig. 2. Time curve of transferase action. Standard conditions with citrulline determination.

fered with phosphate analysis. Identical results were obtained with both methods. A *time curve* of the enzyme reaction is demonstrated in Fig. 2 (citrulline determinations).

Back reaction: It could be demonstrated that the arsenolysis of citrulline [8] is carried out by ornithine carbamyl transferase. The rate of the back reaction was measured by the formation of $^{14}CO_2$ from citrulline-carbamyl-^{14}C in the presence of arsenate. In principle the method was the same as the one used earlier for the determination of CAP formation from citrulline [7]. The enzyme was incubated with 6 µmoles of citrulline-^{14}C (130 000 ct/min/µmole) and 100 µmoles of arsenate buffer, pH 6.7, for 15 min at 37° in a stoppered Warburg vessel, containing 4 N NaOH in the center well and 9 N H_2SO_4 in the side arm. The vessel was cooled on ice, 100 µmoles of $NaHCO_3$ were added and the acid tipped into the main compartment. After shaking for 30 min at 37° the alkali from the center well was precipitated with barium hydroxide, the formed $BaCO_3$ was washed with hot water, filtered on to a paper disk of standard size, and counted as an infinitely thick sample in an end window Geiger-Müller counter. The number of µmoles $^{14}CO_2$ formed could then be calculated from an experimentally determined conversion factor.

One unit of enzyme activity for the back reaction was defined as the amount of enzyme which under the above conditions formed 0.1 µmoles of CO_2.

The same general technique was used during the determination of the equilibrium constant, with the exception that phosphate buffer was used instead of arsenate. In this case the purified (paper electrophoresis) citrulline was used.

Ion exchange chromatographies. The chromatographic separation of CAP from P_i was performed as described earlier [5]. CA-aspartate was separated from citrulline by gradient elution chromatography on Dowex-2-formate (diam. 0.9 cm, length 11 cm) with a 250 ml mixing flask receiving 4 N formic acid. Citrulline was eluted with water, while CA-aspartate appeared after 7—8 column volumes.

RESULTS AND DISCUSSION

Purification of the enzyme

The work of Grisolia and Cohen [1] has demonstrated the localization of the enzyme in the particulate fraction of rat liver. In conformity with these authors the starting material for our enzyme preparation was an acetone powder of "rat liver residue". Essentially no activity was found in the supernatant fraction.

Preliminary experiments were carried out with rat, rabbit and beef liver. By far the highest activity was observed in crude extracts of rat liver and it was also found that fractionation with ammonium sulfate gave better results in this case. Further work was therefore carried out with rat liver.

Preparation of the acetone powder. All work was performed in a cold room at +2°. The livers (500—600 g) from 80 rats were homogenized in a Waring blendor (low speed) in 3 liters of 1.15 % KCl. The solution was poured through a double layer of cheese cloth and then centrifuged in a Sharples centrifuge (rotor size 200 ml) at 25 000 r.p.m. The flow through the rotor was adjusted to a rate of 50—60 ml/min.

The sediment was removed from the rotor and suspended in a minimum amount of 0.05 M phosphate buffer, pH 7.4. Liver residues from six centrifugations may be conveniently pooled at this point.

The suspension was mixed in a Waring blendor with a five to ten fold excess of acetone (—15°). After filtration the residue was once more treated with cold acetone, filtered again and dried in a desiccator.

The livers from 100 rats corresponded roughly to 40—50 g powder.

Extraction of the acetone powder was carried out with 0.05 M tris buffer, pH 7.4, containing 0.001 M EDTA *. It was found that the enzyme was not appreciably inactivated by heating at 52° for 1 h (*cf.* Ref.[1]). The extraction was therefore directly carried out at this temperature.

The acetone powder (205 g) was ground in a mortar with 2 050 ml of buffer. The suspension was immersed in a water bath of 55° and stirred continuously. When the temperature inside had reached 52° the outside temperature was lowered to the same value and heating was continued for one hour. The solution was then cooled in ice water. From this point all operations were performed at 0—4°.

The suspension was centrifuged in the No. 21 head of a Spinco centrifuge (15 min at 12 000 r.p.m.). The residue was washed with 600 ml of buffer. By addition of more buffer the protein concentration was adjusted to 1 %. Volume 3 150 ml.

Solid *ammonium sulfate* (880 g) was added slowly and under stirring. The solution was allowed to stand overnight and the clear supernatant was decanted. The cloudy bottom layer was centrifuged and the precipitate was discarded. To the combined supernatants (3 500 ml) was added 585 g of solid ammonium sulfate and precipitation allowed to take place overnight. The precipitate was centrifuged in the Spinco centrifuge (12 000 r.p.m. at 15 min), and dissolved in 0.05 M tris buffer, pH 7.4, final volume 210 ml. The clear solution was dialyzed against a total of 9 liters of 0.01 M tris buffer for 16 h.

Alcohol precipitation. The volume of the dialyzed solution was adjusted to 1 120 ml with 0.01 M buffer, giving a final protein concentration of 1 %, and 28 ml of 2 M KCl was added.

The solution was placed in a cooling bath and 50 % ethanol (360 ml) was added slowly under constant stirring. During the operation the temperature of the bath was lowered to —3°. After standing for 1 h the formed precipitate was centrifuged and discarded.

* All solutions throughout the whole preparation contained 0.001 M EDTA.

To the clear supernatant more 50 % ethanol (560 ml) was added slowly while the temperature of the cooling bath was lowered to —5°. After standing for 1 h the precipitate was centrifuged (P_2). A third precipitate (P_3) was obtained after addition of 250 ml of 50 % ethanol and standing for 3 h at —10°. To the supernatant after centrifugation was added 100 ml of 50 % ethanol and the solution was allowed to stand at —10° overnight, yielding a fourth precipitate (P_4). The clear supernatant after centrifugation always contained very little activity. Each precipitate (P_2, P_3 and P_4) was dissolved separately in *ca.* 150 ml of 0.01 M tris buffer, and all solutions were assayed for protein and enzyme activity. The bulk of activity was located in P_2 and P_3*.

Second ammonium sulfate fractionation. P_2 and P_3 were combined (290 ml) and 5 ml of M tris buffer, pH 8.5, was added. A saturated solution of ammonium sulfate (pH 8.0, 320 ml) was added dropwise under constant stirring. After 30 min the solution was centrifuged and the precipitate discarded. Solid ammonium sulfate (54 g) was added to the supernatant and precipitation allowed to take place overnight.

After centrifugation the resulting precipitate was dissolved in 0.01 M tris buffer, pH 7.4, and dialyzed against a total of 6 liters of the same buffer for 24 h.

DEAE adsorption. Attempts to chromatograph the enzyme on DEAE cellulose columns [14] were unsuccessful. It was difficult to obtain complete adsorption of the enzyme, a large amount of activity disappeared during the procedure and the results were not very reproducible. By batchwise treatment with DEAE cellulose in the presence of phosphate buffer it was possible, however, to remove acidic impurities from the enzyme and to obtain further purification.

Five g of the cellulose powder prepared according to Peterson and Sober [14] was washed first with 500 ml of M phosphate buffer, pH 7.4 in a chromatographic column, and then with three 20 ml portions of 0.01 M phosphate buffer, pH 7.4. The cellulose was then suspended in an equal volume of 0.01 M phosphate buffer (90 mg of dry cellulose per ml).

One ml of 0.1 M phosphate buffer, pH 7.2, and 28 ml of the cellulose suspension were added to the dialyzed solution (70 ml) from the second ammonium sulfate precipitation step. After 10 min the cellulose was filtered off by suction and washed twice with 10 ml of 0.01 M phosphate buffer.

Saturated ammonium sulfate (102 ml), pH 8.0, was added to the filtrate (102 ml) and the resulting precipitate was discarded after centrifugation. Solid ammonium sulfate (21 g) was added to the supernatant and precipitation allowed to take place overnight.

The precipitate was centrifuged and dissolved in the smallest possible amount of 0.05 M tris buffer, pH 7.4. It was dialyzed for 18 h against a total of 4 liters 0.03 M tris buffer, pH 8.5.

Zone electrophoresis. After the previous step the solution was deep red. Paper electrophoresis demonstrated that at pH 8.5 the enzyme could be

* In some preparations P_4 was also used for the further purification. In one preparation practically all activity was contained in P_2.

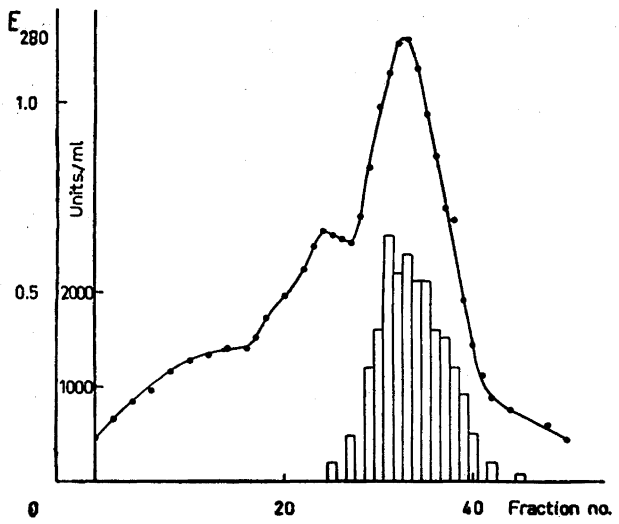


Fig. 3. Zone electrophoresis of ornithine carbamyl transferase. Continuous curve = E_{280}; stepped curve = enzyme activity.

separated from the coloured components. At this pH the enzyme moved very slowly towards the anode, while the coloured components moved faster in the same direction. Separation on the preparative scale was therefore carried out by electrophoresis on a cellulose column according to Porath [15].

The size of the cellulose column was 7.1 $cm^2 \times 52$ cm. Tris buffer (pH 8.5, 0.03 M) was used for the electrophoresis. The enzyme (240 mg of protein, volume = 5 ml) was applied to the top of the column. It was displaced 10 cm downward on the column by buffer. A current of 30 mA at a voltage of 5.5 V/cm was applied for 20 h. Ice water was circulated through the cooling jacket of the column during the electrophoresis.

The proteins were eluted from the column with buffer. Fifteen minute fractions (5—7 ml) were collected and analyzed for protein (light absorption at 280 mμ) and enzyme activity (Fig. 3). The enzyme started to appear after 160 ml. The first 39 ml containing enzyme were discarded, since the specific activity was lower than in the following fractions. Between 200 and 250 ml the specific activity of the protein was constant. These fractions were pooled and the volume of the solution concentrated by ultra filtration. During this process the filtration sac was suspended in 0.01 M tris buffer, pH 7.4, to avoid precipitation of salts on the outside of the membrane *.

A summary of the purification procedure is given in Table 1. The specific activities of an extract of whole liver acetone powder and of a 0° extract of

* The total recovery of enzyme and protein after zone electrophoresis was always low and never exceeded 60 %, probably because of adsorption of proteins to the ethanolyzed cellulose.

I am much indebted to Dr. J. Porath and Mr. J. Glomset for advice in connection with the zone electrophoresis prior to publication of Dr. Porath's paper [15].

Table 1. Purification of ornithine carbamyl transferase from rat liver.

	mg protein	Enzyme units × 10^6	Spec. activ.	Yield %
52° extract, liver resid. powder	31 500	3.44	110	100
First ammonium sulfate precip.	11 200	2.68	240	77
Alcohol fractionation	2 600	1.89	730	55
Second ammonium sulfate precip.	700	1.10	1 570	32
DEAE-cellulose treatment	310	0.67	2 160	19
Zone electrophoresis	68	0.21	3 050	6
0° extract, liver resid. powder			32	
0° extract, whole liver powder			11	

acetone powder from liver residue are also included in the table for comparison.

Properties of the enzyme. The concentrated enzyme solution (1—3 % protein) had a slightly yellowish colour. It was kept at 0° and lost little activity over a period of 4 months. After freezing in buffer solution some precipitation and denaturation sometimes occurred.

Because of the scarcity of the material no free electrophoresis was carried out. On paper electrophoresis between pH 5.0 and 8.5 the protein migrated as a single component. The isoelectric point was around 8.1. On ultra centrifugation * (protein concentration 0.4 % in 1 % NaCl and 0.01 M tris buffer, pH 7.4) two peaks were observed. The main component had a sedimentation constant ($s_{w,20}$) of 5.5 *S*, while a minor component amounting to *ca.* 5—8 % of the main peak had a sedimentation constant of *ca.* 8 *S*.

Properties of the transferase reaction

The *stoichiometry* of reaction (1) is demonstrated in Table 2. The slightly larger formation of P_i than citrulline is fully explained by the non-enzymic decomposition of CAP during the incubation.

Isolation of L-*citrulline.* In a large scale experiment 1 600 μmoles of L-ornithine, 2 000 μmoles of CAP and 5 000 units of transferase were incubated for 15 min at 37°. The solution was then put in a boiling water bath for 1 min

Table 2. Stoichiometry of transferase reaction.

	L-Ornithine	CAP	Citrulline	Phosphate
		μmoles		
Initial	40.0	40.7	0	2.1
Final	21.2	20.5	18.6	22.9
Δ	18.8	20.2	18.6	20.8

Incubation for 5 min at 37° with 60 units of transferase, vol. 1 ml.
Ornithine was determined by ion exchange chromatography. CAP was determined by phosphate analysis [12] (phosphate after 5 min at 100° minus P_i).

* I am indebted to civ.ing. A. Ehrenberg for performing the ultra centrifugation.

and thereafter poured through a Dowex-2-formate column (diam. 0.9, length 15 cm). The column was washed with 20 ml of water and the washing evaporated to a small volume *in vacuo*. $CuCl_2$ (800 μmoles) was added and the solution allowed to crystallize in the refrigerator overnight.

The crystals were filtered by suction and washed carefully with cold water. They were then suspended in 20 ml of boiling water and decomposed with H_2S for 2 h. The CuS was removed by filtration and the solution evaporated to dryness *in vacuo*. The residue was crystallized twice from 95 % alcohol. The product (145 mg) melted with decomposition at 232—235° (uncorr.). A mixed melting point with authentic citrulline gave the same value. It showed $[\alpha]_D^{25} = +24°$ in 6 N HCl as compared to a value of 26° for authentic L-citrulline.

Dependence on substrate concentration. The Lineweaver-Burk plots in Fig. 4 demonstrate the dependence of the reaction rate on the concentrations of CAP and ornithine, respectively. No inhibition was observed at substrate concentrations up to 0.05 M. When DL-ornithine was used but the substrate concentration was calculated only from the amount of L-ornithine present (triangles in Fig. 2) identical results were obtained as with pure L-ornithine. This demonstrates that (a) only the L-isomer was participating in the reaction, (b) D-citrulline did not influence the reaction rate when present in equimolar concentration with the L-isomer.

From the two curves Michaelis constants of 1.4×10^{-3} and 4.1×10^{-4} can be calculated for L-ornithine and CAP, respectively.

The *pH optimum* (7.3) of the reaction is demonstrated by Fig. 5.

Specificity of the reaction. The following amino acids (60 μmoles of L-isomer, 120 μmoles of DL-isomer) were incubated with 12 μmoles of CAP, 200 μmoles of tris buffer, pH 7.4, and 90 units of transferase: L-α-alanine, β-alanine, DL-α-aminoadipic acid, L-arginine, L-asparagine, L-aspartic acid, L-citrulline, L-cysteic acid, L-glutamic acid, L-glutamine, glycine, L-histidine, DL-homoserine, L-hydroxylysine, L-*iso*leucine, L-leucine, L-lysine, L-methionine, L-norleucine, L-phenylalanine, L-serine, L-threonine, L-tryptophane, L-tyrosine and L-valine.

None of these substances had the ability to bring about the enzymic dephosphorylation of CAP *.

Inhibition of transferase activity. The effect of several different enzyme inhibitors is demonstrated in Table 3. The inhibition by phosphate and arsenate is explained by the fact that phosphate is one of the products of the reaction. Inhibition was also observed with the SH-inhibitors iodosobenzoate and *p*-chloromercuribenzoate and could be partially reversed by glutathione. Of interest was also the observation that both substrates had the capacity to protect the enzyme to some degree from inhibition. Thus the inhibition was higher if CMBA (10^{-7} M) was added to the buffered enzyme solution before either of the two substrates than if one substrate was added before the inhibitor.

* J. M. Lowenstein and P. P. Cohen (*J. Biol. Chem.* **220** (1956) 227) have found that a low speed supernatant solution of rat liver was able to form a small amount of homocitrulline from lysine + CAP. Our experimental conditions would not allow a demonstration of enzyme activity with lysine which amounts to less than 0.5 % of the activity with ornithine.

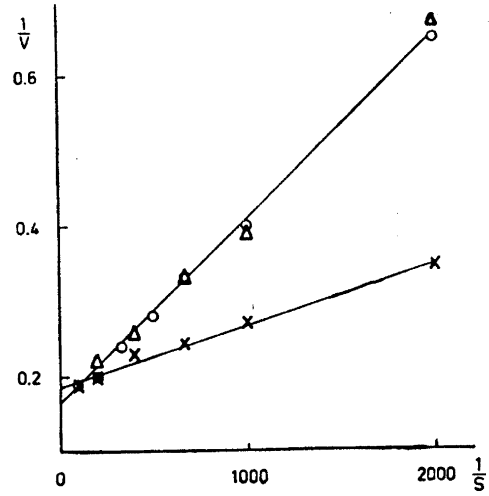


Fig. 4. Dependence of transferase action on CAP (×), L-ornithine (○) and DL-ornithine (△). In the last case the substrate concentration was calculated from the amount L-ornithine in the DL-isomer. Standard conditions except for substance under investigation. Citrulline determination.

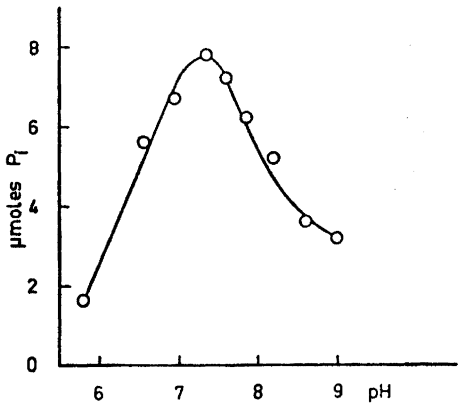


Fig. 5. pH curve of transferase action. Standard conditions but with tris and imidazol buffers at pH values indicated. Phosphate determination.

This demonstration is similar to results obtained earlier with aspartate carbamyl transferase. In this case the presence of both substrates was necessary for protection from CMBA.

A tentative interpretation for both transferases is that SH-groups are involved during the enzyme reaction and that both substrates are bound to these groups during the reaction.

Reversibility and equilibrium of transferase reaction. The equilibrium of the reaction greatly favoured citrulline synthesis but reversibility could be readily demonstrated and the equilibrium position measured from the back reaction with the aid of isotopic compounds.

The qualitative formation of radioactive CAP from $^{32}P_i$ and L-citrulline in the presence of transferase could be demonstrated by paper chromatography and ion exchange chromatography [5].

The quantitative measurement of the amount of CAP formed under different experimental conditions was carried out by using citrulline-carbamyl-^{14}C as substrate. Radioactive CAP was formed only in the presence of both enzyme and phosphate. CAP was decomposed with acid and the radioactive CO_2 formed was measured as described in the experimental part for the back reaction. Time curves of CAP formation with different amounts of substrates and large amounts of enzyme are demonstrated in Fig. 6.

All curves show at first a very rapid formation of CAP followed by a much slower linear increase. The curves are interpreted in the following way: The

Table 3. Inhibition of transferase reaction.

	Conc. of inhibitor (M)	% inhibition
Phosphate, pH 7.4	0.1	51
Arsenate, pH 7.4	0.1	12
EDTA	0.01	0
NaCN	0.01	0
NaCl	1	20
$(NH_4)_2SO_4$	1	50
Semicarbazide	0.01	0
Phenylhydrazine	0.01	0
Arsenite	0.01	0
Iodoacetate	0.01	0
Iodosobenzoate	0.001	46
CMBA	5×10^{-7}	82
CMBA + glutathione (10^{-4} M)	5×10^{-7}	45
CMBA	10^{-7}	56
CAP + CMBA	10^{-7}	15
Ornithine + CMBA	10^{-7}	15
CAP + ornithine + CMBA	10^{-7}	13

Incubation under standard conditions with 5 units of transferase. In the last three experiments the indicated substrates were added to the enzyme before the inhibitor. In all other experiments the inhibitor was first added to the buffered enzyme solution (0°) and CAP + ornithine was added afterwards in a small volume.

rapid phase represents the attainment of the equilibrium. The formed CAP undergoes, however, a slow non-enzymic decomposition and disappears from the reaction. This in turn pulls the reaction towards more formation of CAP which results in the second slow phase of the curve. By extrapolation to zero time a correction can be obtained for this non-enzymic decomposition.

The equilibrium constant

$$K_{eq} = \frac{[\text{citrulline}]\ [\text{phosphate}]}{[\text{ornithine}]\ [\text{CAP}]}$$

was calculated from the three experiments of Fig. 6 and values of 89 000, 103 000 and 114 000 were obtained, giving an average value of 10.2×10^4. The reasonable conformity between the three values is good support for the correctness of the applied method.

Identity of citrulline phosphorylase and ornithine carbamyl transferase. Krebs *et al.*[8] described an enzyme from mammalian liver which formed CO_2, NH_3 and ornithine from citrulline in the presence of phosphate or arsenate. These authors could not demonstrate the formation of a phosphorylated intermediate. It seemed nevertheless rather probable that their enzyme was identical with ornithine carbamyl transferase and that their inability to demonstrate the formation of carbamyl phosphate was dependent on the equilibrium position of the reaction and on the fact that carbamyl phosphate at that time had not been described in the literature.

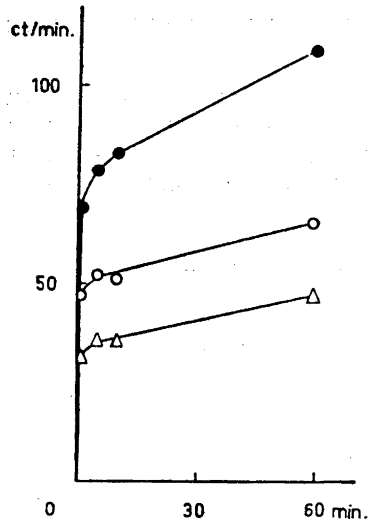


Fig. 6. Formation of ^{14}CAP from citrulline-carbamyl-^{14}C (see text). Experimental conditions (for one point): 40 units of transferase, vol. 1 ml, temperature 37° in all experiments. *Upper curve:* 94 μmoles of phosphate (pH 7.4), 28 μmoles of citrulline. *Middle curve:* 47 μmoles of phosphate, 28 μmoles of citrulline. *Lower curve:* 47 μmoles of phosphate, 14 μmoles of citrulline.

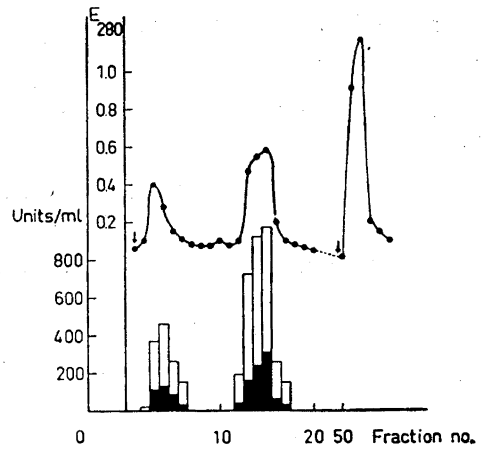


Fig. 7. Identity of citrulline phosphorylase with ornithine carbamyl transferase. 20 mg of transferase (specific activity = 1 500) was adsorbed to a column (0.61 cm² × 14 cm) of DEAE cellulose which had been washed with 0.02 M phosphate buffer, pH 7.4. Elution (4 ml fractions / h) was started with 0.01 M phosphate, pH 7.2, at the first arrow, changed to M KH_2PO_4 at the second arrow. Each fraction was analyzed for protein (E_{280}, continuous curve) transferase activity (upper stepped curve) and arsenolysis of citrulline (shaded stepped curve).

The arsenolysis of citrulline could be readily demonstrated with the pure transferase preparation. It was also found that the ratio between the rate of arsenolysis of citrulline and the rate of citrulline formation from ornithine and CAP was the same in a crude liver extract and with the enzyme after final purification. Further proof was obtained when the enzyme was chromatographed on a column of DEAE cellulose after the second ammonium sulfate precipitation step. In each chromatographic fraction the amount of protein, citrulline formation from ornithine, and arsenolysis of citrulline was determined (Fig. 7). It is evident that the rates of the two enzyme reactions follow each other closely in all fractions.

It should be mentioned that the two peaks with enzyme activity in Fig. 7 do not represent two transferases. The first peak merely represents a break through of non adsorbed protein. The total amount of protein and of enzyme in this peak depended on the load of the column.

Coupling of ornithine carbamyl transferase with carbamyl transferase

In previous investigations we were interested in the formation of carbamyl aspartate from citrulline [7]. We found that CAP could be formed from citrulline and ATP in the presence of acetyl glutamate (reaction 2 below). CA-aspartate could then be formed from CAP + aspartate through the action of aspartate carbamyl transferase (3):

$$\text{Citrulline} + \text{ATP} \xrightarrow[\text{glutamate}]{\text{acetyl}} \text{CAP} + \text{ornithine} + (\text{ADP}) \qquad (2)$$

$$\text{CAP} + \text{aspartate} \longrightarrow \text{CA-aspartate} + \text{phosphate} \qquad (3)$$

The equilibrium of reaction (3) is very favourable for CA-aspartate formation [5]. This together with the formation of CAP by the reversal of the citrulline forming reaction as demonstrated above made it very likely that an alternative formation of CA-aspartate from citrulline might take place through the participation of the two carbamyl transferases:

$$\begin{aligned} \text{Citrulline} + P_i &\longrightarrow \text{CAP} + \text{ornithine} \qquad (4) \\ \text{CAP} + \text{aspartate} &\longrightarrow \text{CA-aspartate} + P_i \qquad (3) \end{aligned}$$

To test this possibility the following experiment was carried out: Two μmoles of citrulline-carbamyl-^{14}C (130 000 ct/min/μmole) + 100 μmoles of L-aspartate + 500 μmoles of phosphate, pH 7.4, were incubated with 800 units of ornithine carbamyl transferase and 250 units of aspartate carbamyl transferase for 15 min at 37°. The reaction was stopped by the addition of 0.2 ml of 4.4 M PCA and, after neutralization with KOH, CA-aspartate (0.52 μmoles calc. from total ^{14}C) was obtained by ion exchange chromatography *.

In a corresponding experiment with ^{14}CA-aspartate + ornithine + phosphate only trace amounts of radioactivity in the citrulline fractions could be demonstrated **.

It is thus clear that two enzymic ways exist for the transfer of the carbamyl group of citrulline to aspartate. Both involve the intermediate formation of CAP and the formation of CA-aspartate from CAP + aspartate. The relative importance of the two pathways is dependent on the availability of ATP and phosphate in the cell. Both reactions are strongly inhibited by

* The fractions containing CA-aspartate were pooled and evaporated to dryness *in vacuo*. The residue was dissolved in 2 ml of hot water and 100 μmoles of carrier non-labeled CA-aspartate was added. CA-aspartate was recrystallized and its specific activity determined. From this value and the specific activity in the citrulline-carbamyl-^{14}C the amount of CA-aspartate formed during the enzyme experiment could be calculated by the isotope dilution method (*cf.* Ref[3]). A value of 0.46 μmoles was obtained.

** It has not been possible to determine the equilibrium constant for aspartate carbamyl transferase, since only very small amounts of $^{14}CO_2$ were formed from ^{14}CA-aspartate + phosphate. The absence of inhibition by phosphate or arsenate [5] and the fact that practically no citrulline could be obtained from ^{14}CA-aspartate in the presence of phosphate by the combined action of the two carbamyl transferases indicate that the equilibrium position is still more favourable for the synthesis of the carbamylamino acid than in the case of ornithine carbamyl transferase.

Table 4. Isotope exchange experiments with $^{32}P_i$.

	Reisolated P_i		Reisolated CAP	
	μmoles	ct/min/μmole	μmoles	ct/min/μmole
Complete	61.0	0.62×10^6	9.8	3.61×10^3
No ornithine	44.7	0.90×10^6	21.3	1.94×10^3
No enzyme	45.8	0.89×10^6	20.7	1.89×10^3
No enzyme and ornithine	44.7	0.98×10^6	20.5	1.78×10^3

Complete experiment: 40 μmoles of CAP and $^{32}P_i$ (1.02×10^6 ct/μmole), 100 μmoles of DL-ornithine and 15 units of enzyme. Incubation 15 min at 37°, vol. 1 ml.

ornithine and are of minor significance as compared to the *de novo* formation of the carbamyl group of CAP from CO_2, NH_3 and ATP in the presence of acetyl glutamate [1].

We have also tested the ability of the purified ornithine carbamyl transferase to form CAP from citrulline + ATP in the presence of acetylglutamate and absence of phosphate [7] (reaction (2) above). No such activity could be demonstrated.

The mechanism of the reaction

Enzymic citrulline formation might be imagined to involve the intermediate formation of a carbamyl enzyme:

$$\text{CAP} + \text{Enzyme} \rightleftharpoons \text{CA-Enzyme} + P_i \quad (5)$$

$$\text{CA-Enzyme} + \text{L-Ornithine} \rightleftharpoons \text{L-Citrulline} + \text{Enzyme} \quad (6)$$

This possibility was tested by isotope exchange experiments. The reversible reaction (5) was excluded by the absence of enzymic exchange of isotope between $^{32}P_i$ and CAP (Table 4). In the presence of ornithine, however, such an exchange did take place. This again demonstrates the reversibility of the over all reaction (1).

When ornithine-^{14}C was incubated together with nonlabeled citrulline and enzyme no enzymic isotope exchange took place in the absence of phosphate

Table 5. Isotope exchange experiment with ornithine-^{14}C.

	^{14}C (ct/min) in	
	Citrulline	Ornithine
Phosphate buffer	6 000	42 000
Tris buffer	0	40 500

Experimental conditions: 2 μmoles of DL-ornithine-2-^{14}C (6.1×10^5 ct/μmole), 1 μmole of L-citrulline, 100 μmoles of phosphate buffer or 5 μmoles of tris buffer, pH 7.4, 80 units of enzyme. Vol. 0.14 ml, incubation 15 min at 37°.

Inactivation with 0.02 ml 4.4 M PCA. After centrifugation aliquots were directly subjected to paper electrophoresis (2 h, 5 V/cm) in 0.1 M ammonium acetate buffer, pH 5.0 (see experimental part). The areas corresponding to citrulline and orn thine were eluted with 10 ml of water and counted.

(Table 5) while one eighth of the isotope was transferred from ornithine to citrulline in the presence of phosphate.

As in the case of aspartate carbamyl transferase the isotope exchange experiments speak against the formation of a carbamylated enzyme. The mechanism for both carbamyl transferases seems to involve instead a single displacement [16] reaction during which both CAP and ornithine are attached to the enzyme. The carbon-oxygen bond of CAP is then broken simultaneously with the formation of the new carbon-nitrogen bond.

The participation of SH groups during the reaction is indicated from inhibition experiments for both carbamyl transferases. The partial protection from inhibition by both CAP and ornithine tentatively indicates that these substances are bound to SH groups of the enzyme during the displacement reaction.

REFERENCES

1. Grisolia, S. and Cohen, P. P. *J. Biol. Chem.* **198** (1952) 561.
2. Jones, M. E., Spector, L. and Lipmann, F. *J. Am. Chem. Soc.* **77** (1955) 819.
3. Reichard, P. *Acta Chem. Scand.* **8** (1954) 795.
4. Reichard, P. and Hanshoff, G. *Acta Chem. Scand.* **9** (1955) 519.
5. Reichard, P. and Hanshoff, G. *Acta Chem. Scand.* **10** (1956) 548.
6. Schulman, M. P. and Badger, S. J. *Federation Proc.* **13** (1954) 292.
7. Smith, L. H. Jr. and Reichard, P. *Acta Chem. Scand.* **10** (1956) 1024.
8. Krebs, H. A., Eggleston, L. V. and Knivett, V. A. *Biochem. J. London* **59** (1955) 185.
9. Smith, L. H. Jr. *J. Am. Chem. Soc.* **77** (1955) 6691.
10. Nyc, J. F. and Mitchell, H. K. *J. Am. Chem. Soc.* **69** (1947) 1382.
11. Bücher, T. *Biochim. et Biophys Acta* **1** (1947) 292.
12. Lowry, O. H. and Lopez, J. A. *J. Biol. Chem.* **162** (1946) 421.
13. Koritz, S. B. and Cohen, P. P. *J. Biol. Chem.* **209** (1954) 145.
14. Peterson, E. A. and Sober, H. A. *J. Am. Chem. Soc.* **78** (1956) 751.
15. Porath, J. *Biochim. et Biophys Acta* **22** (1956) 151.
16. Koshland, D. E. Jr. in Mc Elroy, W. D. and Glass, B. *The Mechanism of Enzyme Action*, John Hopkins Press, Baltimore 1954, p. 608.

Received November 26, 1956.

ACTA CHEMICA SCANDINAVICA 11 (1957) 537—540

The Preparation of Thiocholine Esters

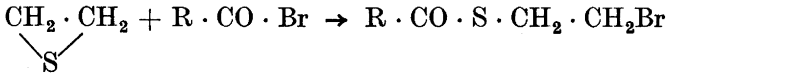
BERTIL HANSEN

Research Institute of National Defence, Dept. 1, Sundbyberg 4, Sweden

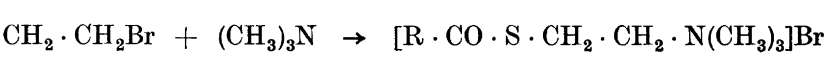
Ethylene sulphide has been prepared. From this the thiocholine esters of acetic, propionic, *n*-butyric, *n*-valeric, and benzoic acids have been synthesized in two ways. According to the first method, ethylene sulphide was treated with acyl bromides, and the 1-bromoethanethiol-(2) esters formed were transformed to thiocholine esters by trimethylamine. By the second method, dimethylamine and ethylene sulphide gave 1-dimethylaminoethanethiol-(2), which was esterified with acid anhydrides and then quaternized with methyl iodide. The methods are discussed, and the second one recommended for use.

Esters of thiocholine have, during the last years, attracted much interest within biochemistry because of their relationship to choline esters [1], and in histochemistry as a means for localizing choline esterases in tissues [2]. It thus seemed reasonable to study the preparation of thiocholine esters.

Several methods for the synthesis of acetyl thiocholine have been described in the literature [3–5]. Of these methods, the one according to Ivin [5] (Method A) seemed to be the most convenient and thus was used with some modifications.

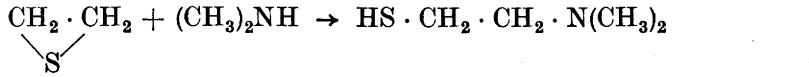


$$\mathrm{CH_2 \cdot CH_2} + \mathrm{R \cdot CO \cdot Br} \rightarrow \mathrm{R \cdot CO \cdot S \cdot CH_2 \cdot CH_2Br}$$

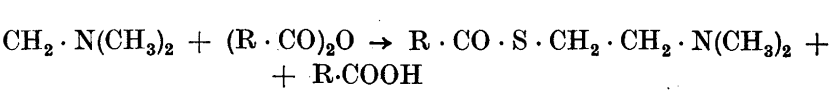


$$\mathrm{R \cdot CO \cdot S \cdot CH_2 \cdot CH_2Br} + \mathrm{(CH_3)_3N} \rightarrow \mathrm{[R \cdot CO \cdot S \cdot CH_2 \cdot CH_2 \cdot N(CH_3)_3]Br}$$

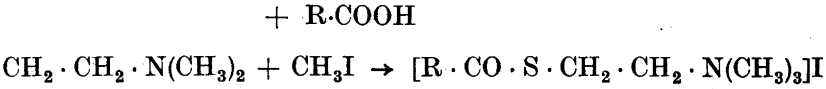
Moreover, a new method (Method B) using acylation of 1-dimethylaminoethanethiol-(2) with acid anhydride and subsequent quaternization with methyl iodide was tested.



$$\mathrm{CH_2 \cdot CH_2} + \mathrm{(CH_3)_2NH} \rightarrow \mathrm{HS \cdot CH_2 \cdot CH_2 \cdot N(CH_3)_2}$$



$$\mathrm{HS \cdot CH_2 \cdot CH_2 \cdot N(CH_3)_2} + \mathrm{(R \cdot CO)_2O} \rightarrow \mathrm{R \cdot CO \cdot S \cdot CH_2 \cdot CH_2 \cdot N(CH_3)_2} + \mathrm{R \cdot COOH}$$



$$\mathrm{R \cdot CO \cdot S \cdot CH_2 \cdot CH_2 \cdot N(CH_3)_2} + \mathrm{CH_3I} \rightarrow \mathrm{[R \cdot CO \cdot S \cdot CH_2 \cdot CH_2 \cdot N(CH_3)_3]I}$$

The reaction between alkene sulphide and amines other than dimethylamine has been discussed in two earlier papers [6,7]. The last two steps are analogous to those used by Tammelin [8] for the preparation of choline esters.

The ethylene sulphide required for the two methods was synthesized by modifying a method used by Bordwell and Andersen [9] for the preparation of propylene sulphide.

EXPERIMENTAL

Ethylene sulphide. To a mixture of 80 g (1.05 mole) of thiourea, 250 ml of water and 30 ml (0.55 mole) of concentrated sulphuric acid, a solution of 49 ml (1.00 mole) of ethylene oxide in 125 ml of xylene was added. The mixture was continuously stirred and the temperature was kept below +10°. A solution of 106 g (1.00 mole) of anhydrous sodium carbonate in 500 ml of water was added during 3 h without external cooling. After a further half-hour's stirring, the organic phase was separated, dried with calcium chloride and filtered. Distillation through a 25 cm glass spiral column gave 29 g (0.48 mole) of ethylene sulphide at 55—56°. Yield 48 %.

The experiments had to be performed in a well ventilated fume-hood because of the odours evolved.

Method A

Esters of 1-bromoethanethiol-(2). 59 ml (1.00 mole) of ethylene sulphide was dissolved in 300 ml of dry carbontetrachloride, and 1.00 mole of acid bromide was added. The temperature of the reaction mixture increased to about 40°. The small precipitate formed was removed. The carbontetrachloride was distilled off at ordinary pressure. The residue gave a colourless product when distilled at reduced pressure. The results are given in Table 1.

Table 1. Esters of 1-bromoethanethiol-(2).

Acid	Formula	Mol.wt.	B. p./mm Hg	Yield in g from 1 mole of ethylene sulphide
Acetic	C_4H_7BrOS	183.1	66—8°/6	123
Propionic	C_5H_9BrOS	197.1	78—80°/6	138
n-Butyric	$C_6H_{11}BrOS$	211.1	96—7°/8	114
n-Valeric	$C_7H_{13}BrOS$	225.1	75.5°/0.9	157
Benzoic	C_9H_9BrOS	245.1	113—8°/0.4—0.5	220

Esters of thiocholine bromide. 90 ml (1.20 mole) of anhydrous trimethylamine were added to a mixture of 1.00 mole of ester of 1-bromoethanethiol-(2) and 1 l of dry acetone, cooled to —10°. White crystals were as a rule formed within a quarter of an hour. After a week at room temperature, 1 l of dry ether was added to precipitate the ester of thiocholine bromide still in solution. The precipitate was filtered off and recrystallized for analyses as follows: the acetic, propionic and benzoic derivatives from ligroin/absolute ethanol (1:1), the butyric derivative from dry acetone and the valeric derivative from dry acetone/ligroin (2:1). After drying in a vacuum desiccator the melting-points and analyses, given in Table 2, were obtained.

Method B

1-Dimethylaminoethanethiol-(2). 59 ml (1 mole) of ethylene sulphide, dissolved in 100 ml of dry ether, were cooled to —10° and 88 ml (1.33 mole) of anhydrous dimethylamine were added. The mixture was allowed to stand at room temperature for 4 days.

Table 2. Esters of thiocholine bromide.

Acid	Formula	Mol. wt.	M.p. *	C		H		Br		Yield in %
				calc.	found	calc.	found	calc.	found	
Acetic	$C_7H_{16}BrNOS$	242.2	227°	34.7	35.0	6.7	6.7	33.0	32.9	65
Propionic	$C_8H_{18}BrNOS$	256.2	196°	37.5	37.6	7.1	7.0	31.2	31.2	96
n-Butyric	$C_9H_{20}BrNOS$	270.2	150°	40.0	40.2	7.5	7.4	29.6	29.6	94
n-Valeric	$C_{10}H_{22}BrNOS$	284.3	114°	42.3	42.3	7.8	7.8	28.1	28.4	94
Benzoic	$C_{12}H_{18}BrNOS$	304.3	239°	47.4	47.2	6.0	6.0	26.3	26.3	94

* Determined with a "Kofler Heizbank".

The small precipitate formed was removed. The dimethylamine and the ether were distilled off at ordinary pressure. The residue was fractionated through a 25 cm glass spiral column under reduced pressure. The fraction collected at 58—59°/63 mm contained 73 g (0.70 mole) 1-dimethylaminoethanethiol-(2). In the distillation flask a few ml of a high boiling liquid remained. $n_D^{25} = 1.4630$; $d^{25} = 0.8943$ g/cm³. (Found: C 46.0; H 10.6. Calc. for $C_4H_{11}NS$ (105.2): C 45.7; H 10.5).

Esterification of 1-dimethylaminoethanethiol-(2). 117 ml (1.00 mole) of 1-dimethylaminoethanethiol-(2) and 1.05 mole of acid anhydride were mixed. The temperature at once rose to 70—100°, except in the reaction with benzoic anhydride when it rose to only about 40°. The mixture was distilled under reduced pressure until the temperature exceeded the values given in Table 3. Almost no residue remained in the distillation flask. The distillates were colourless and evil-smelling. The viscosity of the benzoic derivative was very high.

Table 3. Esters of 1-dimethylaminoethanethiol-(2).

Acid	Acetic	Propionic	*n*-Butyric	*n*-Valeric	Benzoic
Final b.p./mm Hg	70°/8	80°/8	93°/8	109°/9	104°/0.01

Esters of thiocholine iodide. The distillate from the esterification of 1.00 mole of 1-dimethylaminoethanethiol-(2) was dissolved in 750 ml of dry ether and 100 ml (1.60 mole) of methyl iodide were added. A white precipitate was formed at once. After three days at room temperature it was filtered off and dried in a vacuum desiccator. Recrystallization did not change the melting-points or analyses given in Table 4.

Table 4. Esters of thiocholine iodide.

Acid	Formula	Mol. wt.	M. p. *	C		H		I	
				calc.	found	calc.	found	calc.	found
Acetic	$C_7H_{16}INOS$	289.2	204°**	29.1	29.2	5.6	5.7	43.9	44.0
Propionic	$C_8H_{18}INOS$	303.2	208°	31.7	31.8	6.0	6.3	41.9	41.8
n-Butyric	$C_9H_{20}INOS$	317.2	173°	34.1	34.0	6.4	6.5	40.0	40.1
n-Valeric	$C_{10}H_{22}INOS$	331.3	146°	36.3	36.3	6.7	6.5	38.3	37.9
Benzoic	$C_{12}H_{18}INOS$	351.3	>250°***	41.0	41.2	5.2	5.1	36.1	—

* Determined with a "Kofler Heizbank".
** Renshaw *et al.* observed 203—4°.
*** » » » » 257°.

DISCUSSION

In method A no analyses have been made of the esters of 1-bromoethanethiol-(2), because of their partial decomposition during the distillation. If they were allowed to stand for a few weeks, a red-violet colour appeared, probably caused by the oxygen in the air. The addition of trimethylamine to the bromo esters was found to proceed much faster in acetone than in ether.

The 1-dimethylaminoethanethiol-(2) prepared in method B can also be obtained from 1-dimethylamino-2-chloroethane hydrochloride [4,10,11], but in that case a great part of the thiol is oxidized to the corresponding disulphide. The reactions between acid anhydrides and the thiol start at room temperature and are very exothermic because of the heat of neutralization evolved during the formation of the ammonium salt instead of the free acid and aminoester. This shows that it is impossible to separate the esters of the 1-dimethylaminoethanethiol-(2) from the acids by directly applied distillation. However, the acid impurities do not seem to have a bad effect on the subsequent quaternization. The tertiary esters can be prepared from their hydrobromides [12].

Of the two methods used for the preparation of thiocholine esters, method B is to be preferred. It gives iodides which are less hygroscopic than the bromides obtained according to method A and the products formed give correct analyses without recrystallization. The only disadvantage is that method B is restricted to mono esters.

My thanks are due to the Head of this Institute, Professor G. Ljunggren, for his kind interest in this work.

REFERENCES

1. Meyer, A. and Wilbrandt, W. *Helv. Physiol. et Pharmacol. Acta* **12** (1954) 206.
2. Koelle, G. B. *J. Pharmacol. Exptl. Therap.* **100** (1950) 158.
3. Renshaw, R. R., Dreisbach, P. F., Ziff, M. and Green, D. *J. Am. Chem. Soc.* **60** (1938) 1765.
4. Suzuki, T., Kubota, M. and Tagaki, H. *Japan. J. Pharm. & Chem.* **22** (1950) 464.
5. Ivin, S. Z. *Zhur. Obscheĭ Khim. (J. Gen. Chem.)* **22** (1952) 267.
6. Rappe, W. and Nicolai, F. *German Patent* 631,016 (1936).
7. Snyder, H. R., Stewart, J. M. and Ziegler, J. B. *J. Am. Chem. Soc.* **69** (1947) 2672.
8. Tammelin, L.-E. *Acta Chem. Scand.* **10** (1956) 145.
9. Bordwell, F. G. and Andersen, H. M. *J. Am. Chem. Soc.* **75** (1953) 4959.
10. Clinton, R. O., Salvador, U. J., Laskowski, S. C. and Suter, C. M. *J. Am. Chem. Soc.* **70** (1948) 950.
11. Merck & Co., Inc. *Brit. Patent* 688,726 (1953).
12. Tammelin, L.-E. *Acta Chem. Scand.* **11** (1957) 487.

Received January 8, 1957.

ACTA CHEMICA SCANDINAVICA 11 (1957) 541—544

The Effect of Salicylic Acid, Benzoic Acid and some of their Derivatives on Oxidative Phosphorylation

INGMAR BOSUND

The Wenner-Gren Institute for Experimental Biology, University of Stockholm, and Swedish Institute for Food Preservation Research, Gothenburg, Sweden

Salicylic acid (10^{-2} M) and benzoic acid (10^{-1} M) cause an uncoupling of oxidative phosphorylation from respiration in isolated rat liver mitochondria. Similar results are obtained with 5-nitro-salicylic acid and with methyl benzoate.

The growth inhibiting effect of salicylic and benzoic acids on microorganisms has been the subject of many studies with the purpose of elucidating the mode of action of these compounds. In recent years investigations have been published which call attention to the possibility that the growth inhibiting effect might originate, at least to some extent, in an inhibition of the formation or utilization of high energy compounds [1-5]. In order to obtain further evidence, the effect of salicylic and benzoic acids and some of their derivatives on the oxidative phosphorylation in isolated rat liver mitochondria was studied in this work.

EXPERIMENTAL

Preparation of mitochondria. The preparation of mitochondria was carried out according to the method of Schneider and Hogeboom [6]. The rats were killed by decapitation and the livers put in 0.25 M ice-cold sucrose as fast as possible. In this solution the liver was cut into small pieces and rinsed several times with sucrose solution. The homogenization was carried out in a Potter-Elvehjem homogenizer. The homogenate was diluted to *ca.* 100 ml with 0.25 M sucrose and centrifuged at 1 600 *g* for 10 minutes. The supernatant was decanted and recentrifuged at 4 100 g for 20 min. The mitochondria were washed twice with *ca.* 100 ml sucrose each time.

Materials. Yeast hexokinase was used as a stock solution which had been prepared according to Berger *et al.*[7] with minor modifications [8]. ATP, as the crystalline disodium trihydrate, had been furnished by the Sigma Chemical Company, St. Louis, Mo., U.S.A., and $H_3{}^{32}PO_4$ by the Radiochemical Centre, Amersham, England. All solutions were prepared in glass-distilled deionized water.

Incubation procedure. Mitochondria from one liver were suspended in 13.3 ml 0.25 M sucrose containing 116 mg $K_2H^{32}PO_4$, 144 mg glucose and 12 mg ATP. The pH was adjusted to 7.5 by means of glass electrode. To this suspension 1.3 ml 0.1 M $MgCl_2$ was added and the suspension was diluted to 20 ml with 0.25 M sucrose. In all experiments 1.5 ml of this suspension was added to each vessel.

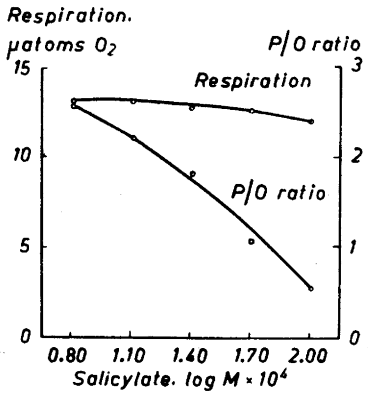


Fig. 1. The effect of increasing concentrations of salicylate on oxidative phosphorylation. Each vessel contained besides the suspension described in the experimental part 30 μmoles potassium α-ketoglutarate as substrate and potassium salicylate in the concentrations indicated in the figure. Experimental conditions: gas phase, air; temp., 30°C; time of incubation, 20 min.

Analytical procedures. Oxygen consumption was measured by the conventional Warburg technique. The described suspension and neutralized solutions of the different inhibitors were added to the main compartments of the Warburg vessels, substrates and hexokinase (0.1 ml of the stock solution) to the sidearms. The centre wells contained 0.2 ml 2 M KOH, absorbed on a roll of filter paper. The final volume of solution in the vessels was adjusted to 2 ml with 1.15 % KCl. Manometer readings were made at 5 min invervals, starting 5 min after the addition of substrate and hexokinase from the sidearms. Oxygen consumption for the period 0—5 min was calculated by extrapolation. At the end of the experiments, enzymatic activity was terminated by the addition of 0.2 ml 5 M H_2SO_4. Phosphate uptake was determined as the ratio of organic phosphate formed to inorganic phosphate added by the isotope distribution method described by Lindberg and Ernster [9].

RESULTS

The effect of increasing concentrations of salicylate on oxidative phosphorylation and oxygen consumption with α-ketoglutarate as substrate is illustrated by Fig. 1.

The figure shows that salicylate at a concentration of about 1×10^{-2} M almost completely inhibits phosphorylation, while the inhibition of oxygen consumption is negligible. Similar results are obtained if α-ketoglutarate is replaced by pyruvate + malate, succinate, or glutamate.

Table 1. The effect of salicylate on oxidative phosphorylation.

Additions	Without hexokinase	With hexokinase	
	Oxygen μatoms	Oxygen μatoms	P/O ratio
None	4.6	11.2	2.5
DPN + cytochrome c	5.3	11.7	2.3
Salicylate	9.4	8.5	0.6
Salicylate + DPN + cytochrome c	10.3	9.6	0.5

The final concentrations of the substances added to the suspension of the mitochondria were as follows: DPN, 6.8×10^{-4} M; cytochrome c, 10^{-5} M; potassium salicylate, 10^{-2} M, Each vessel contained 30 μmoles potassium α-ketoglutarate as substrate. Experimental conditions as in Fig. 1.

Table 1 exemplifies an experiment which shows that salicylate, at the concentration mentioned above, is able to induce an almost maximum level of respiration in the absence of hexokinase. This is a further indication that salicylate uncouples phosphorylation from respiration, since, in this case, respiration proceeds in the absence of a terminal phosphate acceptor.

Experiments with benzoate showed that this substance had a similar effect, which, however, became noticeable only at still higher concentrations than those which were necessary in the case of salicylate. The results of a typical experiment with benzoate are shown in Table 2. The relatively high concentrations of benzoate caused a partial inhibition of respiration along with the effect on phosphorylation. It was possible to bring up the respiration to the original level by the addition of DPN and cytochrome c, without, however, a simultaneous recovery of the phosphorylation. This indicates that the inhibition of respiration is a secondary effect, due to a release of DPN and cytochrome c from the mitochondria.

Similar pictures are obtained if glutamate is replaced by other substrates such as succinate and α-ketoglutarate.

Table 2. The effect of benzoate on oxidative phosphorylation.

Additions	Without hexokinase	With hexokinase	
	Oxygen μatoms	Oxygen μatoms	P/O ratio
None	3.5	12.3	2.1
DPN + cytochrome c	6.7	12.2	2.0
Benzoate	8.2	10.7	1.0
Benzoate + DPN + cytochrome c	8.7	12.1	0.9

Experimental conditions as in Fig. 1. Each vessel contained 30 μmoles potassium glutamate. DPN and cytochrome c were added at the same concentrations as in Table 1. The benzoate concentration was 8×10^{-2} M.

In order to further elucidate the mode of action of salicylate and benzoate on oxidative phosphorylation, the effect of some related substances was investigated. Of these compounds 5-nitro-salicylic acid (which differs from 2,4-dinitrophenol only by the replacement of one of the nitro groups by a

Table 3. The effect of 5-nitro-salicylic acid on oxidative phosphorylation.

Substrate	Without 5-nitro-salicylic acid		With 10^{-3} M 5-nitro-salicylic acid		With 10^{-2} M 5-nitro-salicylic acid	
	Oxygen μatoms	P/O ratio	Oxygen μatoms	P/O ratio	Oxygen μatoms	P/O ratio
Glutamate	13.4	2.3	12.8	1.8	11.1	0.14
Succinate	13.8	1.5	13.9	1.2	4.8	0.15

Each vessel contained 30 μmoles substrate. Experimental conditions as in Fig. 1.

carboxyl group) and methyl benzoate inhibited phosphorylation to about the same extent as did salicylic acid, while 4-hydroxy-salicylic, 5-hydroxy-salicylic and 4-amino-salicylic acids (PAS) were without effect. Table 3 shows the results of an experiment with 5-nitro-salicylic acid.

DISCUSSION

It is evident from the results described in this paper that salicylic and benzoic acids produce an effect on oxidative phosphorylation, which is reminiscent of that obtained with 2,4-dinitrophenol. The concentrations required to obtain a marked effect are of the same magnitude as those required for a complete suppression of bacterial growth at the pH in question (7.5). As is well known, however, the growth inhibiting effect of salicylic and benzoic acids increases as the pH is lowered. This is probably due to the fact that the undissociated molecules of these acids are more lipophilic than the respective anions and, thus, more easily taken up by the bacteria. Such a correlation is well conceivable to prevail even in the present case, where an increasing lipid solubility might facilitate the penetration of these inhibitors into the mitochondrial structure. This point is, however, hard to test in experiments with isolated mitochondria, which lack the mechanism by which bacterial cells can make themselves independent at least to some extent of the pH of the environment. A lowering of the pH in such experiments may thus render oxidative phosphorylation impossible.

This work is part of an investigation supported by *Statens Naturvetenskapliga Forskningsråd* and *Statens Tekniska Forskningsråd*.

I wish to express my sincere gratitude to Professor Olov Lindberg for allowing me to perform these experiments at his Institute and to Dr. Lars Ernster for indispensable advice and valuable discussions throughout the work. I also wish to thank Professor Gösta Ehrensvärd for providing me with samples of some of the inhibitors and for stimulating discussions.

REFERENCES

1. Bernheim, F. and DeTurk, W. E. *J. Pharmacol. Exptl. Therap.* **103** (1951) 107.
2. Meade, B. W. *Ann. Rheum. Dis.* **13** (1954) 60.
3. Smith, M. J. H. and Jeffrey, S. W. *Biochem. J. London* **63** (1956) 524.
4. Smith, M. J. H. and Jeffrey, S. W. *Biochem. J. London* **64** (1956) 589.
5. Bosund, I. *(To be published in this journal).*
6. Schneider, W. C. and Hogeboom, G. H. *J. Biol. Chem.* **183** (1950) 123.
7. Berger, L., Slein, M., Colowick, S. P. and Cori, C. F. *J. Gen. Physiol.* **29** (1946) 379.
8. Ernster, L. and Löw, H. *Exptl. Cell Research, Suppl.* **3** (1955) 133.
9. Lindberg, O. and Ernster, L. *Methods of Biochemical Analysis* (D. Glick, Ed., Interscience, New York). **III** (1956) 1.

Received January 12, 1957.

ACTA CHEMICA SCANDINAVICA 11 (1957) 545—550

Crystallographic Studies of Calcium and Strontium Hydroxyapatites

CURT LAGERGREN and DIEGO CARLSTRÖM

Department of Medical Physics, Karolinska Institutet, Stockholm, Sweden

From X-ray crystallographic investigations on apatites in the system $Ca_{10}(PO_4)_6(OH)_2-Sr_{10}(PO_4)_6(OH)_2$ it was found that no solid solutions could be formed in the region $Ca_3Sr_7(PO_4)_6(OH)_2$ to $Ca_7Sr_3(PO_4)_6(OH)_2$. The mixed apatite $Ca_5Sr_5(PO_4)(OH)_2$, however, was shown to have a very well ordered lattice. In the light of these experimental findings, it is concluded that strontium ions in the inorganic crystalline phase of bone are probably bound rather firmly to the surface of the extremely small apatite crystallites.

The localization and metabolic control of many trace elements by the skeleton has been known for a number of years. Recently, the number of cationic radioactive emitters found to be preferentially incorporated in bone has increased and of these, strontium, because it has many atomic characteristics and chemical properties similar to calcium and is probably metabolized and incorporated in the same fashion, has received particular attention [4,5,15].

This study was undertaken in order to determine the manner in which strontium is incorporated into the inorganic crystal phase of bone. Although the exact molecular structure of the inorganic bone crystals has not been definitely agreed on by workers in the field, there is general agreement that it differs but little from calcium hydroxyapatite ($Ca_{10}(PO_4)_6(OH)_2$). In the apatite structure several isomorphic substitutions are known to occur and in some cases a continuous series of solid solutions have been demonstrated to exist. For example the mixed apatites in the system $Ca_{10}(PO_4)_6(OH)_2$—$Ca_{10}(PO_4)_6F_2$—$Ca_{10}(PO_4)_6Cl_2$ have been thoroughly investigated by means of X-ray diffraction [16,17] and the calcium-lead-hydroxyapatites have also been shown to form solid solutions [10]. However, relatively little is known about the strontium apatites. Pure strontium hydroxyapatite ($Sr_{10}(PO_4)_6(OH)_2$) has been synthesized in several ways [8,12] and natural mineral fluorapatite containing less amounts of strontium has been described [9], but investigations have not been carried out on the mixed calcium-strontium apatites.

There are three possible ways by which the Sr ion could be incorporated into the inorganic crystalline structure of bone. Because of the extremely

small size (approx. 220 Å × 50 Å) of the Ca apatite crystallites in bone [3,6], there is consequently a large surface area available to which the Sr ion could be bound. This mode of incorporation has been shown to exist for many other ions. Sr could also be incorporated as part of the apatite lattice as an isomorphic substitution for calcium, or a combination of both isomorphic substitution and surface binding could occur.

Because Sr^{++} has a larger ionic radius than Ca^{++} (1.13 *versus* 0.99 Å) isomorphic substitution of Sr^{++} for Ca^{++} will result in an enlargement of the unit cell dimensions. This difference in the lengths of the axes of the unit cell can be detected by X-ray diffraction and it should therefore be possible to correlate the degree of expansion of the lattice with the amount of isomorphic substitution of Sr^{++} for Ca^{++} that occurs.

EXPERIMENTAL

Material. Pure calcium and strontium hydroxyapatites, (in the following abbreviated to CaHA and SrHA) were synthesized in aqueous solutions at a pH of about 9 by adding a dilute solution of Na_2HPO_4 to solutions of Ca and Sr nitrate. The precipitates formed were thoroughly washed with water and samples were heated at 900°C for 2 h after which crystallographic homogeneity was determined by X-ray diffraction. No diffraction lines other than those of pure apatite could be detected. In addition, as a control, a commercial strontium phosphate was similarly heated and this sample showed almost pure SrHA containing only small amounts of $Sr_3(PO_4)_2$. Since it was not found possible to synthesize the desired mixed apatites in aqueous solutions, these mixed apatites were made in the solid state. Several different methods were tried but the most satisfactory results were obtained by heating mixtures of the respective apatites to high temperatures. After the non-constituent water of the pure CaHA and SrHA were accurately determined a series of mixtures with known mole fractions of Ca and Sr were prepared and these mixtures were heated for 4 h at 1 300° ± 15°C. It was found that at lower temperatures and/or shorter durations the reactions did not proceed to completion and that the original apatites could occasionally be detected by X-ray diffraction.

Methods. A Philips diffractometer unit with nickel-filtered copper radiation was used. In order to get the highest possible precision and to avoid errors depending on the varying absorption in the specimens, a standard substance (silicon) with an accurately known lattice constant (a = 5.4306 Å) was mixed with all samples. As it was evident that several of the solid solutions gave badly defined diffraction lines only the strongest reflections could be used for measurements. However, as the (00 * 4) — reflection was superimposed on the (40 * 2—04 * 2)-reflection when the specimens contained large amounts of strontium the c-axis could not be determined with sufficient accuracy in all cases and it was therefore decided to determine only the a-axis by measuring the (14 * 0—41 * 0)-line. For the pure CaHA and SrHA which gave well defined diffraction patterns it was possible to determine both axes with high precision by measuring reflections in the region 60°—70° Θ.

RESULTS

The lattice constants for pure CaHA and SrHA were found to have the following values:

$Ca_{10}(PO_4)_6(OH)_2$	$a = 9.42_3$ Å	$c = 6.88_4$ Å	$c/a = 0.7306$
$Sr_{10}(PO_4)_6(OH)_2$	$a = 9.76_1$ Å	$c = 7.27_7$ Å	$c/a = 0.7455$

The axes dimensions of CaHA are in very good agreement with earlier published precision measurements [1,3,11,13] whereas those for SrHA showed a much larger deviation from the only other measurements in the literature

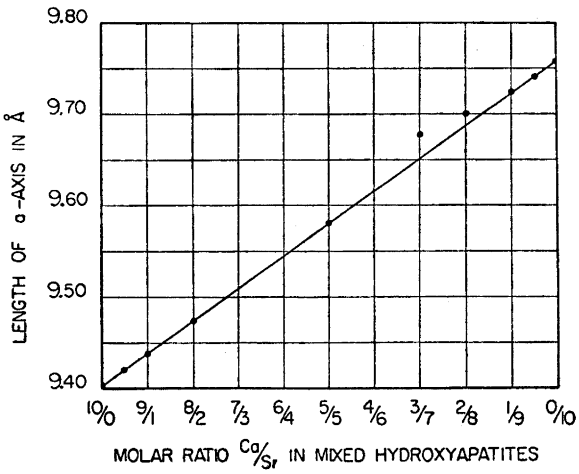


Fig. 1. Graph showing the relationship between the length of the *a*-axis and the degree of substitution in mixed Ca-Sr-hydroxyapatites.

($a = 9.74$; $c = 7.20$ kX) [8]. The change in the c/a ratio causes the general appearance of the diffraction pattern of SrHA to differ considerably from that of CaHA.

The diffraction patterns of the mixed Ca-Sr-HA were of a varying character. The diffraction lines showed a noticeable broadening when one Sr^{++} was introduced in the CaHA-unit cell, and with two Sr^{++} ions in the lattice the reflections were almost impossible to measure. The solid solutions, Ca_7Sr_3HA and Ca_6Sr_4HA, gave no recognizable patterns at all. On the other hand the compound Ca_5Sr_5HA appeared to have an almost perfect lattice and the diffraction lines were as well defined as in the pure Ca or SrHA. The next member in the series, Ca_4Sr_6HA, again gave an extremely bad diffraction pattern without identifiable reflections. With increasing amounts of Sr in the lattice the diffraction patterns became better and better and that of Ca_1Sr_9HA was almost as good as that of pure SrHA. The lengths of the *a*-axis for the mixed apatites in the Ca-SrHA-system have been plotted in Fig. 1. In order to compare the pure members (CaHA, SrHA) with the mixed ones in this series under comparable conditions, pure CaHA, and SrHA were also heated to 1 300° C. This resulted in a decrease of the *a*-axis of 0.02 Å. In order to find at what temperature ranges this effect occurred, 6 different samples of CaHA were heated for 4 h at temperatures between 900° and 1 300°C. The result is shown in Fig. 2.

DISCUSSION AND CONCLUSIONS

From Fig. 1 it is evident that the alteration in the *a*-axis dimension is directly proportional to the degree of substitution as long as the amount of substitution is low. The well crystallized apatite, Ca_5Sr_5HA, also shows an

a-axis dimension midway between the pure CaHA and pure SrHA. However, the *a*-axis dimension of the strontium apatites deviates more and more from the straight line as their content of calcium increases and the *a*-axis of Ca_3Sr_7HA corresponds in reality to the one expected for Ca_2Sr_8HA. Since, as already has been pointed out, the diffraction patterns of these compounds were very poorly defined, it was impossible to measure the position of the reflections with accuracy, or to judge whether these solid solutions were pure, or if they were instead made up of several badly crystallized products. Thus, it seems most possible that the apatite which is indicated in the diagram in the position of Ca_3Sr_7HA was not formed during the heating but rather it was mainly composed of the solid solution Ca_2Sr_8HA. With the exception of the intermediate apatite Ca_5Sr_5HA, it is evident that only about two Sr ions or two Ca ions can be forced into the respective CaHA and SrHA lattices without a total collapse of the structure. But even at this moderate degree of substitution the lattice is badly distorted and evidently no solid solutions can be formed in the range Ca_3Sr_7HA to Ca_7Sr_3HA. This conclusion was very surprising in the light of the statement [10] that a continuous series of solid solutions could be formed in the system $Ca_{10}(PO_4)_6(OH)_2$—$Pb_{10}(PO_4)_6(OH)_2$, as it seemed by all means that Sr^{++} should be easier to introduce into the lattice than the larger Pb^{++}. However, on careful examination of the paper by Müller [10] on the calcium-lead apatites, it appears that he did not synthesize or investigate the solid solutions between Ca_7Pb_3HA and Ca_2Pb_8HA with exception of the intermediate apatite Ca_5Pb_5HA. From this work it is also evident that in spite of heat treatment Ca_7Pb_3HA was so badly crystallized that only the strongest reflections in the X-ray diffraction pattern could be measured. For these reasons it seems most likely that the conclusions reached above regarding the Ca—Sr apatites also apply to the Ca—Pb apatites, and that both Sr^{++} and Pb^{++} deviate too much in size from Ca^{++} to be able to form continuous series of solid solutions. It is interesting to note that the intermediate Ca_5Sr_5HA and Ca_5Pb_5HA both exist, and apparently these mixed, apatites are not solid solutions but have a more or less ordered structure possibly forming a superlattice.

The contraction of the *a*-axis of CaHA at temperatures above 1 000°C (see Fig. 2) has not been described before. It has long been known that a total loss of the constitutional water of CaHA is inconsistent with the apatite structure and that a pure oxyapatite ($Ca_{10}(PO_4)_6O_2$) does not exist, but it has been shown [2] that a partial loss of the water can occur without the destruction of the apatite lattice. As no special efforts were made to measure the loss of water or to work in an absolutely water-free atomsphere (CaHA can be synthesized from perfectly dry components in the presence of water vapour even at 1 000°C [7,14],) no definite explanation can be given to the shrinkage of the *a*-axis, but it seems most reasonable that this phenomenon is due to a partial loss of the constitutional water.

From the work by Müller on Ca-Pb apatites [10] it is clear that the precipitates of mixed apatites which he prepared were very badly crystallized. The same almost noncrystalline state was found in the precipitates of Ca-Sr-apatites. In several cases in which the precipitates were heated in order to increase their crystallinity, additional lines were obtained in the diffraction

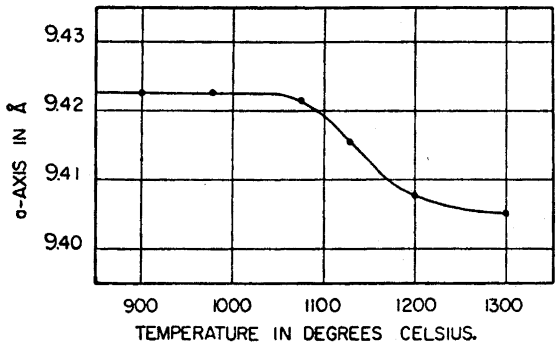


Fig. 2. Plot of the change in the *a*-axis dimension of calcium hydroxyapatite ($Ca_{10}(PO_4)_6(OH)_2$) *versus* temperature.

patterns, resulting from the presence of triphosphate compounds. For that reason we abandoned the latter method of preparing the mixed apatites. However, as the heating of an apatite precipitate above 500—600°C not only causes a growth of the crystallites but also implies a total reorganization of the lattice, with the introduction into the lattice of ions previously adsorbed to the surface of the crystallites, or even creation of compounds other than those originally present, it is impossible to judge if the badly crystallized original precipitate consisted of one or several phases with or without adsorbed or surface bound ions. Thus, no direct conclusions can be drawn regarding the nature of the precipitates formed in solutions containing both Ca and Sr ions, but it is clear that even small amounts of strontium in a solution containing calcium and phosphate ions considerably inhibits the orderly crystallization of an apatite. This is a further indication that strontium ions do not easily replace Ca^{++} in the CaHA lattice.

It thus appears that because of its size the Sr ion is not well suited for any great amount of isomorphic ion exchange with calcium for positions in the lattice, particularly in the formation of the apatite lattice from dilute solutions comparable to those occurring in the body fluids. We are thus inclined to conclude that Sr^{++} introduced in the body will be bound mainly to the surface of the extremely small apatite crystallites of bone, the surface area of which has been shown to have very great binding properties for ions of various kinds [3]. The similarity in the metabolism of Ca^{++} and Sr^{++}, demonstrated in experiments with radioactive isotopes, suggests that Sr ions on the surface of the bone crystallites may be as tightly bound as Ca ions in surface positions.

This work was supported by a grant from *Air Research and Development Command, U. S. Air Force*, through its European Office, under Contract No. AF 61 (514)-861, to the Department of Medical Physics, Karolinska Institutet.

REFERENCES

1. Brasseur, H. *Proc. Intern. Reactiv. Solids, Gothenburg*, **1952** 363.
2. Bredig, M. A., Franck, H. H. and Füldner, H. *Z. Electrochem.* **39** (1933) 959.
3. Carlström, D. *Acta Radiol.* Suppl. **121** (1955).
4. Engfeldt, B., Björnerstedt, R., Clemedson, C.-J. and Engström, A. *Acta Orthopaed. Scand.* **24** (1954) 101.
5. Engfeldt, B. and Hjertquist, S.-O. *Acta Pathol. Microbiol. Scand.* **35** (1954) 205.
6. Finean, J. B. and Engström, A. *Biochim. et Biophys. Acta* **11** (1953) 178.
7. Hayek, E., Müllner, F. and Koller, K. *Monatsh.* **82** (1951) 959.
8. Klement, R. *Z. anorg. u. allgem. Chem.* **242** (1939) 215.
9. Larsen, E. S. Jr., Fletcher, M. H. and Cisney, E. A. *Am. Mineralogist* **37** (1952) 656.
10. Müller, M. *Helv. Chim. Acta* **30** (1947) 2069.
11. Perdok, W. G. *Schweiz. Monatschr. f. Zahnheilk.* **62** (1952) 269.
12. Rathje, W. *Ber.* **74 B** (1941) 342.
13. Trautz, O. R. *Ann. N. Y. Acad. Sci.* **60** (1955) 696.
14. Trömel, G. *Mitt. Kaiser-Wilhelm-Inst. Eisenforsch. Düsseldorf*, **14** (1932) 25.
15. Vaughan, J. M. Chapter 23 in Bourne, G. H. *The biochemistry and physiology of bone.* Academic Press, New York 1956.
16. Wallaeys, R. and Chaudron, G. *Compt. rend.* **230** (1950) 1867.
17. Wallaeys, R. and Chaudron, G. *Compt. rend.* **231** (1950) 355.

Received January 16, 1957.

ACTA CHEMICA SCANDINAVICA 11 (1957) 551—554

The Ethylenediaminetetraacetate Complexes of Vanadium(V)

ANDERS RINGBOM, SOINI SIITONEN and BENGT SKRIFVARS

Institutet för analytisk och oorganisk kemi, Åbo Akademi, Åbo, Finland

Pentavalent vanadium forms with ethylenediaminetetraacetic acid (H_4Y) a complex compound VO_2Y^{3-} with a stability constant log $K = 18.05$. At pH values below about 3.5 the complex VO_2HY^{2-} is formed; the acidic dissociation constant of this compound is $pk = 3.60$. In alkaline solutions vanadates are formed.

The complexes of divalent, trivalent and tetravalent vanadium with ethylenediaminetetraacetic acid (EDTA) have been investigated by Schwarzenbach [1], but about the complexes of pentavalent vanadium little is known. Polarographic investigations of Pecsok and Juvet [2] and of Micka and Tockstein [3] point to the formation of some complexes. However, there seems to be no information in the literature about the composition and the stability of these compounds. In the following the results of some investigations made in order to clear up these questions will be reported.

It seems likely that in a weak acid solution a compound VO_2Y^{3-} is formed. This assumption is made on the basis of the fact that when a solution of ammonium metavanadate is titrated with the disodium salt of EDTA the acidity remains constant (pH $\sim$ 6.5) until the equivalence point is reached, which points to the reaction

$$VO_3^- + H_2Y^{2-} = VO_2Y^{3-} + H_2O$$

A compound of this formula is also in accordance with the results recently obtained by Rossotti and Rossotti [4] in an investigation on the hydrolysis products of pentavalent vanadium.

When the solution is made more acid — at pH values below 3 — another complex is formed. Equilibrium measurements showed that this reaction involves the addition of one hydrogen ion. In other words, Y^{4-} is replaced by HY^{3-} according to

$$VO_2Y^{3-} + H^+ = VO_2HY^{2-}$$

A change of the shade of the greenish yellow colour is connected with this reaction.

It is possible to determine photometrically the stability constants of the complexes on the basis of the colours of the various compounds. The stability ranges of these complexes will be clear from Fig. 1 giving the absorbance index of vanadium as a function of pH.

Tables 1 and 2 illustrate the way of calculating the equilibrium constants.

Table 1. Determination of the stability constant $K_{VO_2HY^{2-}} = \frac{[VO_2HY^{2-}]}{[VO_2^+][HY^{3-}]}$

$C_V = C_{EDTA}$ M	pH	$\log \beta_{HY}$	$A^{340}_{VO_2HY}$	$A^{340}_{VO_2}$	A^{340}	$\alpha = \frac{A_{VO_2HY} - A}{A_{VO_2HY} - A_{VO_2}}$	$\log K_{VO_2HY} = \log \frac{(1-\alpha)}{\alpha^2 \beta_{HY} C}$
1×10^{-3}	0.85	−8.38	0.400	0.190	0.272	0.610	11.40
1×10^{-3}	1.25	−7.22	0.400	0.190	0.357	0.204	11.50
1×10^{-3}	1.45	−6.66	0.400	0.190	0.367	0.157	11.20
1×10^{-3}	1.75	−5.86	0.400	0.190	0.388	0.057	11.32
			$A^{320}_{VO_2HY}$	$A^{320}_{VO_2}$	A^{320}		
2×10^{-4}	1.40	−6.80	0.148	0.062	0.122	0.302	11.38
2×10^{-4}	1.65	−6.12	0.148	0.062	0.137	0.127	11.55
1×10^{-4}	1.20	−7.37	0.074	0.031	0.051	0.535	11.58
1×10^{-4}	1.40	−6.80	0.074	0.031	0.056	0.419	11.32
1×10^{-4}	1.60	−6.26	0.074	0.031	0.063	0.256	11.31
1×10^{-4}	1.95	−5.36	0.074	0.031	0.070	0.093	11.38

Average: 11.39

Table 2. Determination of the dissociation constant $k_{VO_2HY^{2-}} = \frac{[H^+][VO_2Y^{3-}]}{[VO_2HY^{2-}]}$

C_V	C_{EDTA}	pH	$A^{360}_{VO_2Y}$	$A^{360}_{VO_2HY}$	A^{360}	$\alpha = \frac{A_{VO_2Y} - A}{A_{VO_2Y} - A_{VO_2HY}}$	$-\log k_{VO_2HY^{2-}} = -\log \frac{[H^+](1-\alpha)}{\alpha}$
1×10^{-4}	5×10^{-3}	2.75	0.210	0.148	0.156	0.872	3.58
1×10^{-4}	5×10^{-3}	2.90	0.210	0.148	0.158	0.839	3.62
1×10^{-4}	5×10^{-3}	3.10	0.210	0.148	0.165	0.726	3.52
1×10^{-4}	5×10^{-3}	3.60	0.210	0.148	0.183	0.435	3.49
1×10^{-4}	5×10^{-3}	3.95	0.210	0.148	0.190	0.322	3.63
1×10^{-4}	5×10^{-3}	4.25	0.210	0.148	0.197	0.210	3.67
1×10^{-4}	5×10^{-3}	4.40	0.210	0.148	0.201	0.145	3.63
			$A^{360}_{VO_2Y}$	$A^{360}_{VO_2HY}$	A^{360}		
5×10^{-3}	4×10^{-2}	3.00	0.740	0.625	0.656	0.730	3.43
5×10^{-3}	4×10^{-2}	3.40	0.740	0.625	0.663	0.670	3.71
5×10^{-3}	4×10^{-2}	3.60	0.740	0.625	0.674	0.574	3.73
5×10^{-3}	4×10^{-2}	4.05	0.740	0.625	0.708	0.278	3.64
5×10^{-3}	4×10^{-2}	4.35	0.740	0.625	0.723	0.148	3.59

Average: 3.60

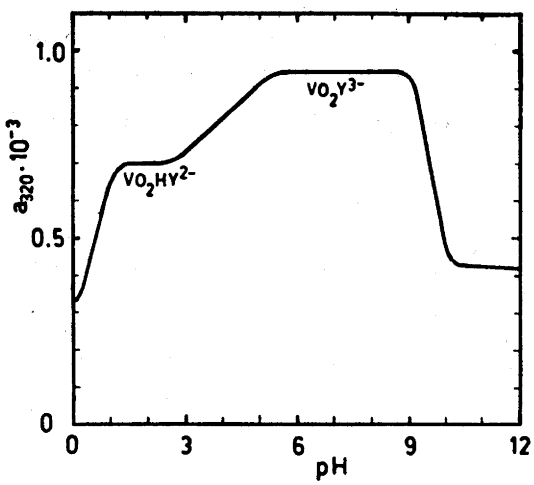


Fig. 1. Absorbance index of vanadium at an excess of EDTA as a function of pH. $C_V = 10^{-3}$, $C_{EDTA} = 5 \times 10^{-3}$.

The absorbances are designed by A. β_{HY} is the fraction of EDTA not bound to vanadium that appears as HY^{-3} ions. Usually β_{HY} is calculated from the equation

$$\beta_{HY} = \frac{[H^+]\beta_Y}{k_4}$$

β_Y can be determined graphically [5] or from the equation

$$\beta_Y = \frac{[H^+]^4}{k_1k_2k_3k_4} + \frac{[H^+]^3}{k_2k_3k_4} + \frac{[H^+]^2}{k_3k_4} + \frac{[H^+]}{k^4} + 1$$

The following values of the dissociation constants of EDTA were used: $pk_1 = 2.0$; $pk_2 = 2.76$; $pk_3 = 6.16$; $pk_4 = 10.26$. α is the fraction of vanadium present in the less coloured form (VO_2^+ in Table 1, VO_2HY^{2-} in Table 2).

Perchloric acid was used for the regulation of the acidity. The ionic strength was kept at approximately 0.1 by the addition of sodium perchlorate. The temperature was *ca.* 20°.

By combining the constants obtained above it is possible to calculate in addition the following constant

$$K_{VO_2Y} = \frac{[VO_2Y^{3-}]}{[VO_2^+]\,[Y^{4-}]} = \frac{K_{VO_2HY}\,k_{VO_2HY}}{k_4} = 10^{18.05}$$

The vanadium(V)-EDTA complex is thus almost as strong as the corresponding copper complex.

Fig. 1 points to the formation of vanadates in alkaline solution. It is likely that the compound stable at the pH range 10—12 is a pyrovanadate [6] and that in a still more alkaline solution orthovanadate VO_4^{3-} is formed.

This investigation has been supported by grants from *Statens Naturvetenskapliga Kommission*, Finland.

REFERENCES

1. Schwarzenbach, G. and Sandera, J. *Helv. Chim. Acta* **36** (1953) 1089.
2. Pecsok, R. L. and Juvet, R. S. *J. Am. Chem. Soc.* **75** (1953) 1202.
3. Micka, K. and Tockstein, A. *Chem. Listy* **48** (1954) 648; *cf. Chem. Abstr.* **48** (1954) 9835.
4. Rossotti, F. J. C. and Rossotti, H. *Acta Chem. Scand.* **10** (1956) 957.
5. Ringbom, A. and Wänninen, E. *Anal. Chim. Acta* **11** (1954) 155.
6. Hazel, J. F., Mc Nabb, W. M. and Santini, R. *J. Phys. Chem.* **57** (1953) 681.

Received January 12, 1957.

ACTA CHEMICA SCANDINAVICA 11 (1957) 555—557

3-Hydroxyphthalic Acid, a Metabolite in *Penicillium islandicum* Sopp

STEN GATENBECK

Department of Physiological Chemistry, Wenner-Gren Institute, University of Stockholm, Sweden

In an investigation of *Penicillium islandicum* Sopp 3-hydroxyphthalic acid was isolated from the culture medium. The structure was proved by paper chromatography and degradation to *m*-hydroxybenzoic acid.

It has been shown previously [1-3] that the mycelium of *Penicillium islandicum* Sopp, when grown on a synthetic medium containing glucose as the sole source of carbon, contains large amounts of red pigments consisting of a mixture of islandicin, iridoskyrin, skyrin, rubroskyrin and erythroskyrine. Of these pigments islandicin is 1,4,5-trihydroxy-2-methylanthraquinone, iridoskyrin a dimeric derivative of islandicin and skyrin a dimeric derivative of *Frangula* emodin (4,5,7-trihydroxy-2-methylanthraquinone). The structures of rubroskyrin and erythroskyrine are unknown.

During the studies of the biological formation of islandicin, the culture medium of *P. islandicum* Sopp has been examined for aromatic substances. The examination has been made by paper chromatographical methods with a technique elaborated at this laboratory by Ehrensvärd and his group [4].

The ether extract of the acidified culture medium contains very small amounts of aromatic compounds detectable with the reagents used. 3 or 4 different aromatic substances could be detected. One of them has been identified as 3-hydroxyphthalic acid which has not previously been obtained from any natural source.

3-Hydroxyphthalic acid was identified after isolation by fractionation on a silica gel column. The crude fraction was extracted in a countercurrent distribution apparatus. The amount of natural 3-hydroxyphthalic acid was estimated to be 1—2 mg per litre culture medium by comparing the fluoroscence in UV light of a solution of the natural product with a standard solution of synthetic 3-hydroxyphthalic acid [5] in ether. Owing to the difficulty in getting the acid in a pure, crystalline form the identification was made by comparing its color reactions and R_F values in 6 different solvents with those of pure,

synthetic 3-hydroxyphthalic acid. Furthermore, the natural product was decarboxylated to *m*-hydroxybenzoic acid which was identified in the same way by comparison with synthetic *m*-hydroxybenzoic acid.

3-Hydroxyphthalic acid has a very close structural relationship to 3,5-dihydroxyphthalic acid which occurs in *Penicillium brevi-compactum* [6]. According to Oxford and Raistrick [7,8] dihydroxyphthalic acid appears to be an oxidation product of the different propyl derivatives of β-resorcylic acid which accompany 3,5-dihydroxyphthalic acid in *P. brevi-compactum*. The biological formation of 3-hydroxyphthalic acid in *P. islandicum* does not seem to follow the same route because the corresponding methyl- and propyl derivatives of salicylic acid cannot be detected in the culture medium. Nor can the 3-hydroxyphthalic acid in the culture medium be looked upon as a degradation product of islandicin or any other pigment because the acid is formed at an early stage during growth at a time when there is hardly any pigment production. The question whether 3-hydroxyphthalic acid is a metabolite in a reaction series leading to the formation of islandicin or represents a by-product in this chain will be a subject for further investigations.

EXPERIMENTAL

Culture conditions. Culture medium: Czapek-Dox solution: Glucose, 50.0 g; $NaNO_3$, 2.0 g; KH_2PO_4, 1.0 g; KCl, 0.5 g; $MgSO_4 \cdot 7H_2O$, 0.5 g; $FeSO_4 \cdot 7H_2O$, 0.01 g; distilled water 1 l.

Ten 1-litre flat-bottomed culture flasks plugged with cotton wool each containing 500 ml of Czapek-Dox solution were sterilized. Small inoculates of *P. islandicum*, strain N.R.R.L. 1036, were placed in the flasks. The cultures were incubated in the dark at 24°C and were harvested after 20 days' incubation.

Isolation of 3-hydroxyphthalic acid. The orange-yellow culture medium was separated by filtration from the mold mycelium which was washed with distilled water. The acid medium, pH 4, was neutralized with 33 % aqueous NaOH and evaporated at reduced pressure on a water bath to about 500 ml. The concentrated solution was acidified with conc. HCl and extracted 6 times with a total amount of 2 l of ether. The ether solution was dried over anhydrous Na_2SO_4 and then evaporated to about 100 ml. The evaporation was continued in an air stream under a heating lamp to almost dryness. The last trace of solvent was removed in a vacuum-desiccator over silica gel. The residue was dissolved in 4—5 ml of acetone and the solution added to a silica gel column (45 × 2.5 cm). The 3-hydroxyphthalic acid was eluted with a mixture of acetone:chloroform (1:3). The column was illuminated with UV light and the band with the light blue fluorescence of 3-hydroxyphthalic acid was collected. This fraction, intensively red colored, was evaporated to dryness. The residue was fractionated in an ordinary manual Craig distribution apparatus consisting of 50 transfer tubes, each tube holding 20 ml. An aqueous solution of 3 % formic acid was used as stationary phase and the mobile phase consisted of methyl *iso*butyl ketone equilibrated with the stationary phase. The residue was dissolved in 10 ml of the mobile phase and placed in the first transfer tube together with 10 ml of the stationary phase. The colored substances run in the front and after 40 transfers the 3-hydroxyphthalic acid could be localized to the tubes 25—34 by illumination with UV light. The solutions in these tubes were collected and the methyl *iso*-butyl ketone was removed by distillation at reduced pressure. The remaining aqueous solution was extracted several times with ether. The collected ether phases were evaporated in an air stream under a heating lamp. The residue that had a faint yellow color was dissolved in about 1.5 ml of boiling water. The solution was treated with a little active carbon and filtered hot, leaving a colorless filtrate.

Identification of 3-hydroxyphthalic acid. The filtrate was cooled in a refrigerator overnight. A very small precipitate was formed. The mixture was shaken with an equal volume of ether. Paper chromatograms were run from the ether solution on Whatman

filter paper No. 1 in 6 different solvents at 22°C. The composition of the solvents has been elaborated at this laboratory and they have been extensively used for identification of organic substances in the *Penicillium* series. The solvents are [4]:

A. methyl *iso*butyl ketone/4 % aqueous formic acid
B. chloroform/methanol, 2 % aqueous formic acid
C. benzene, methyl ethyl ketone/2 % aqueous formic acid
D. benzene/2 % aqueous formic acid
E. water, methyl ethyl ketone, diethylamine
F. methyl ethyl ketone, acetone, aqueous formic acid

On each paper chromatogram were placed: I, natural product; II, pure, synthetic 3-hydroxyphthalic acid; III, a mixture of I and II. The chromatograms were analyzed with a) UV light, b) *p*-nitrobenzenediazoniumfluoborate in 50 % aqueous ethanol + ammonia, c) aqueous ferric chloride. I, II and III had the same R_F values and gave spots indistinguishable from each other with all the reagents used; a) gave a light blue fluorescence, b) an orange color, c) a violet color.

The following R_F values were obtained:

Solvent	A	B	C	D	E	F
R_F value	0.60	0.08	0.05	0.00	0.00	0.83

The water-ether solution of natural 3-hydroxyphthalic acid was heated on a water bath until the ether had evaporated. An equal volume of conc. H_2SO_4 was added to the remaining aqueous solution and the mixture was refluxed for 2 h at 125°C. A corresponding amount of synthetic 3-hydroxyphthalic acid was treated in the same way. The solutions were cooled to room temperature and extracted with ether. The ether solutions were tested paper-chromatographically in the same solvents as above. On each chromatogram were placed: 1. H_2SO_4-treated natural product, 2. H_2SO_4-treated synthetic 3-hydroxyphthalic acid. 3. synthetic *m*-hydroxybenzoic acid. The chromatograms were analyzed with d) *p*-nitrobenzenediazoniumfluoborate in 50 % aqueous ethanol + ammonia, e) 2,6-dibromoquinonechlorimide in dioxan + ammonia. 1, 2 and 3 gave identical spots with the same R_F values and the same color reactions, *i. e.* with d) a reddish brown color, e) a blue color.

Solvent	A	B	C	D	E	F
R_F value	0.86	0.45	0.35	0.01	0.09	0.91

No 3-hydroxyphthalic acid could be detected.

Acknowledgment. The author is indebted to Professor G. Ehrensvärd for his stimulating interest in this work.

REFERENCES

1. Howard, B. H. and Raistrick, H. *Biochem. J. London* **44** (1949) 227.
2. Howard, B. H. and Raistrick, H. *Biochem. J. London* **56** (1954) 56.
3. Howard, B. H. and Raistrick, H. *Biochem. J. London* **57** (1954) 212.
4. Ehrensvärd, G. *et al. To be published.*
5. Amstutz, E. D., Fehnel, E. A., Neumoyer, C. R. *J. Am. Chem. Soc.* **68** (1946) 352.
6. Clutterbuck, P. W., Oxford, A. E., Raistrick, H. and Smith, G. *Biochem. J. London* (1932) 1441, 1902.
7. Oxford, A. E. and Raistrick, H. *Biochem. J. London* **26** (1932) 1441, 1902.
8. Oxford, A. E. and Raistrick, H. *Biochem. J. London* **27** (1933) 634, 1473.

Received January 21, 1957.

ACTA CHEMICA SCANDINAVICA 11 (1957) 558—564

Quantitative Analysis of Aryloxysilanes

BENGT SMITH

Institutionen för Organisk Kemi, Chalmers Tekniska Högskola, Göteborg, Sweden

Two new methods for the quantitative analysis of aryloxysilanes have been developed. The first one involved bromide-bromate titration in glacial acetic acid, the second titration with potassium methoxide in anhydrous ethylenediamine using *o*-nitroaniline as an indicator. The scope and limitations of the methods have been discussed. The first method was also applicable to phenyl orthoesters of carboxylic acids.

The investigation of silanes, especially of those containing aryloxy, alkoxy, alkyl and aryl groups in different combinations bonded to a silicon atom has for a long time been hampered by the lack of convenient rapid methods for their quantitative analysis. To ascertain their purity it has been necessary generally to determine the silicon, carbon and hydrogen content which is, as a rule, a time consuming procedure. The present investigation was undertaken in an attempt to improve this situation.

BROMIDE-BROMATE TITRATION

Recently it was shown by the present author [1] that many phenols can be titrated directly in glacial acetic acid using bromide-bromate solution. In view of the ease with which aryloxy groups bonded to silicon are split off by hydrolysis it seemed justified also to investigate whether the method was applicable to aryloxysilanes. This proved to be the case for such aryloxysilanes in which the corresponding free phenol was directly titratable (see Ref.[1]). Thus phenoxy-, *o*-cresoxy-, *m*-cresoxy-, *p*-cresoxy- and 2,6-xylenoxysilanes could be accurately analyzed. Judging from the amount of bromine consumed, the bromine atoms entered the vacant *ortho* and *para* positions *. The bromide-, bromate method was applicable to all aryloxysilanes investigated, with the above-mentioned aryloxy groups, except those where tertiary butoxy groups

* No investigation has been made of the mechanism of the reaction or of the products formed. Thus it is unknown whether hydrolysis takes place prior to the reaction with bromine or if the aryloxysilane is brominated as such.

also were linked to the silicon atom. A decreased reactivity of tertiary alkoxysilanes in various reactions has been observed previously [2,3]. In the present case the inactivation is most likely due to shielding of the silicon atom and the *ortho* positions of the aryloxy group (see also p. 560). Although the "direct" titration method failed, the *tert.*-alkoxyaryloxysilanes could be analyzed by hydrolyzing the silanes in a mixture of glacial acetic acid and conc. hydrochloric acid and then titrating the mixture with bromide-bromate solution. The accuracy is, however, somewhat less than that of the "direct" titration method.

As might be expected the "direct" titration method failed for those aryloxysilanes where the corresponding phenol had to be analyzed by the excess method (see Ref.[1]). Thus, the bromine consumption of thymoxytriethoxysilane and the corresponding carvacryloxysilane was too low. Application of the "excess" bromination method under the conditions used for the determination of the free phenols (*cf.* Ref.[1]) resulted in a too high bromine consumption. Under the prevailing conditions bromine obviously reacts with the ethoxy groups or the ethyl alcohol formed by hydrolysis.

The direct titration method was also suitable for the quantitative determination of phenyl orthoesters of carboxylic acids as demonstrated by the analysis of phenyl diethyl orthoformate and the corresponding orthoacetate.

PROCEDURE

About 1.5 mequiv.* of the aryloxysilane were dissolved in the prescribed amount of glacial acetic acid (see Table 1 and below) and 5 ml of conc. hydrochloric acid added. Sixteen ml of a 0.1 N potassium bromide-bromate solution were then dropped into the solution as fast as the bromine was consumed. After addition of 5 ml of a 10 % solution of potassium iodide the liberated iodine was titrated with 0.1 N thiosulfate using starch as an indicator.

Ir the case of aryloxysilanes with tertiary butoxy groups the solution was heated on a boiling water bath for half an hour after the addition of the conc. hydrochloric acid and then treated as above.

All of the phenoxysilanes as well as the phenyl orthoesters were titrated in 5 ml of glacial acetic acid, the rest of the aryloxysilanes in 20 ml of the same solvent. For accurate results it is recommended not to deviate too much from these volumes.

TITRATION WITH POTASSIUM METHOXIDE IN ETHYLENEDIAMINE

Day *et al.*[4,5] have investigated the reaction between esters of carboxylic acids and ammonia or amines. Among the most reactive participants in this reaction were phenolic esters and ethylenediamine. This circumstance was utilized by Glenn and Peake [6] for the quantitative determination of phenolic esters of carboxylic acids. These compounds undergo aminolysis in excess ethylenediamine at room temperature to form phenols and amides of ethylenediamine. The resulting phenols were titrated using potassium methoxide in benzene-methanol.

The postulated mechanism of the reaction involves a nucleophilic attack by the amine on the carbonyl carbon atom of the ester followed by the libera-

* It is assumed that each vacant *ortho* or *para* position consumes 2 equiv. of bromine.

tion of the phenol. This mechanism is also supported by the finding in this work that no reaction takes place between the phenyl orthoesters in Table 1 and ethylenediamine. On the other hand, nucleophilic attack by amines would be possible in the aryloxysilanes. These compounds have been shown to undergo exchange reactions, which are assumed to proceed through a nucleophilic mechanism with intermediate addition compounds [7].

The necessary qualifications for a ready reaction between ethylenediamine and an aryloxysilane thus seemed to be met, and this suggested the possibility of a quantitative determination of the aryloxysilanes. The result of the application of the Glenn and Peake method to the aryloxysilanes, however, was not that expected. The consumption of potassium methoxide was invariably too high (see Table 1). Thus, while the tetraaryloxysilanes should consume 4 equiv. of potassium methoxide per mole, values between 4.85 and 4.96 equiv. per mole were obtained. The aryloxytrialkoxysilanes should consume 1 equiv. of potassium methoxide according to theory, but the experimental values were 1.81 to 1.87. For the diaryloxydialkoxysilanes the corresponding values were 2.80 to 2.88 instead of 2 and the only triaryloxyalkoxysilane tested, triphenoxymethoxysilane, consumed 3.80 equiv. instead of 3. A small number of alkylphenoxysilanes were also titrated. It was found, that the excess consumption of potassium methoxide decreased as alkyl groups were substituted for phenoxy groups on the silicon atom.

From the above it is evident that the excess consumption of potassium methoxide is related to the structure of the organosilicon compound but independent of the number of aryloxy groups linked to the silicon atom. The reason of the high values is evidently to be sought in the organosilicon compounds present in the solution after the aminolysis of the aryloxysilanes. By analogy to the reaction between phenolic esters of carboxylic acids and ethylenediamine it can be assumed that phenols and aminosilanes are formed in the aminolysis of aryloxysilanes. An aminolysis of alkoxy groups, if such are present, might also take place. Thus in the case of the tetraaryloxysilanes the end products should contain silanes in which the silicon atom is linked to four nitrogen atoms. In the case of the alkoxyaryloxysilanes the same type of compounds might be formed as well as structures in which the silicon atom is linked to both oxygen and nitrogen. The carbon-silicon bonds in the alkylaryloxysilanes can be assumed to be unchanged after the aminolysis which thus results in structures with carbon and nitrogen atoms linked to the silicon atom. Finally, during the titration the methyl alcohol which is present in the reaction medium might react with the aminosilanes resulting in an exchange of methoxy groups for amino groups. Obviously, it is impossible to predict with any certainty the exact structure of the compounds formed.

We will now consider the question as to why these compounds consume potassium methoxide. The ability of certain organosilicon compounds to add reagents with electron-donor atoms with the formation of penta- and hexacovalent compounds is well known *. While it has been possible to isolate addition compounds between halogenosilanes and amines or amides [9-12], no similar adducts between organosilicon compounds and oxygen bases have

* For a detailed discussion of these types of compounds see Stone and Seyferth [8].

been recorded so far (see, however, Ref.[13]). However, they have been assumed to occur as intermediates in several reactions. In the base-catalyzed rearrangement of organopolysiloxanes, bases, such as potassium methoxide, were found to be effective [14]. It was postulated that the first step in the base-catalyzed reaction is the coordination of the oxygen atom in the base to a silicon atom in the siloxane. The alcoholysis of alkoxysilanes in the presence of sodium alkoxides has been assumed to proceed *via* pentacovalent silicon intermediates formed from the alkoxysilane and alkoxide ion [15]. In a study of the hydrolysis of triphenylsilyl fluoride Swain *et al.*[16] obtained kinetic evidence of the formation of intermediate adducts between this compound and water. Other similar examples exist [17,18].

The obvious conclusion to be drawn from this discussion is that the "excess" potassium methoxide is used up by addition to the silicon atom. We may consider the organosilicon compounds in question as Lewis acids which are neutralized by the base present. This assumption is in accordance with the decrease in excess base consumption in the series $(CH_3)_nSi(OC_6H_5)_{4-n}$ when n increases from 0 to 3. Replacement of a phenoxy group by a methyl group should cause a decrease in *L*-acidity from inductive as well as steric reasons *.

Not only aryloxysilanes can be titrated with potassium methoxide in ethylenediamine. This method was also found applicable to alkoxysilanes. Thus tetraethoxysilane in two runs used up 0.98 and 1.00 equiv. of potassium methoxide per mole and methyltriethoxysilane 0.72 and 0.73 equiv. per mole. Trimethylethoxysilane consumed less than 0.01 equiv. per mole and tetraethylsilane did not react at all with potassium methoxide **. Here only *L*-acidity is present while in the case of the aryloxysilanes the sum of the *H*-acidity and *L*-acidity is obtained. It is unsettled whether the alkoxysilanes remain unchanged or an aminolysis of the alkoxy groups takes place. A sharp decrease in acidity as ethoxy groups are replaced by methyl groups is clearly shown. It was not the purpose of this paper to investigate the reaction between alkoxysilanes and potassium methoxide in ethylenediamine. The few results presented here are, however, promising from a practical as well as a theoretical point of view. This reaction might find valuable application for identification and quantitative analysis of organosilicon compounds and also for studying the relationship between the structure of the latter and their ability to react with electron donating compounds.

The results of the analysis of 19 aryloxysilanes are summarized in Table 1. It is seen that compounds for which the bromination method failed, as thymoxytriethoxy- and carvacryloxytriethoxysilane, can be titrated readily (Nos. 17 and 18). On the other hand the method failed for aryloxysilanes with a tertiary butoxy group linked to the silicon atom (Nos. 8 and 10). For these compounds the modified bromination procedure was applicable. The two methods thus complement each other. The variation of the excess base consumption (due to the *L*-acidity of the organosilicon compounds) makes the

* As pointed out previously it is not the *L*-acidity of the phenoxysilane that is measured but of a reaction product the exact structure of which is unknown.

** This is in accordance with the fact that the coordination number of silicon rises above four only when it is bonded to highly electronegative elements [8].

Table 1. Quantitative analysis of aryloxysilanes and phenyl orthoesters.

No.	Compound	Bromide-bromate titration					Potassium methoxide titration					
		Ml of glacial acetic acid	Equiv. weight				Equiv. weight			Base consumption equiv. per mole of silane		
			Found	Mean value	Calc.	% Error	Calc.	Found	Mean value	Total	Due to *H*-acidity	Due to *L*-acidity
1	Tetraphenoxysilane	5	16.68 16.70	16.69	16.69	0	100.1	82.7 82.7	82.7	4.84	4.00	0.84
2	Tetra-*o*-cresoxysilane	20	28.46 28.56	28.51	28.54	0.1	114.1	92.0 92.0	92.0	4.96	4.00	0.96
3	Tetra-*m*-cresoxysilane	20	19.14 19.07	19.11	19.02	0.5	114.1	92.7 92.9	92.8	4.92	4.00	0.92
4	Tetra-*p*-cresoxysilane	20	28.53 28.61	28.57	28.54	0.1	114.1	93.9 94.2	94.1	4.85	4.00	0.85
5	Triphenoxymethoxy-silane	5	18.57 18.60	18.59	18.80	1.1	112.8	88.8 89.4	89.1	3.80	3.00	0.80
6	Diphenoxydimethoxy-silane	5	23.03 23.04	23.04	23.03	0	138.2	98.9 98.4	98.7	2.80	2.00	0.80
7	Diphenoxydiethoxy-silane	5	25.36 25.32	25.34	25.37	0.1	152.2	106.3 106.3	106.3	2.86	2.00	0.86
8	Diphenoxydi-*tert*.but-oxysilane	5	30.31 30.42	30.32	30.04	0.9	—	—	—	—	—	—
9	Di-*o*-cresoxydiethoxy-silane	20	41.30 41.31	41.31	41.56	0.6	166.2	115.6 116.1	115.9	2.87	2.00	0.87
10	Di-*o*-cresoxy-di-*tert*. butoxysilane	20	48.18 48.66	48.42	48.57	0.3	—	—	—	—	—	—
11	2,6-Xylenoxytrieth-oxysilane	20	140.6 140.8	140.7	142.21	1.1	284.4	152.4 152.3	152.4	1.87	1.00	0.87
12	Di-2,6-xylenoxydietho-xysilane	20	90.32 90.27	90.30	90.13	0.2	Not analyzed					
13	Phenoxytrimethoxy-silane	5	35.75 35.71	35.73	35.72	0	214.3	116.4 116.5	116.5	1.84	1.00	0.84
14	Phenoxytriethoxy-silane	5	42.72 42.77	42.75	42.73	0.1	256.4	137.8 137.6	137.7	1.86	1.00	0.86
15	*o*-Cresoxytriethoxy-silane	20	67.70 67.61	67.66	67.60	0.1	270.4	144.2 144.3	144.3	1.87	1.00	0.87
16	*p*-Cresoxytriethoxy-silane	20	67.59 67.47	67.53	67.60	0.1	270.4	148.4 149.0	148.7	1.82	1.00	0.82

Table 1. Continued.

17	Thymoxytriethoxy-silane	—	—	—	—	—	312.5	168.2 168.2	168.2	1.86	1.00	0.86
18	Carvacryloxytrieth-silane	—	—	—	—	—	312.5	166.8 167.2	167.0	1.87	1.00	0.87
19	Methyltriphenoxy-silane	5	17.92 17.97	17.95	17.91	0.2	107.5	87.6 88.0	87.8	3.67	3.00	0.67
20	Dimethyldiphenoxy-silane	5	20.43 20.49	20.46	20.36	0.5	122.2	103.1 103.2	103.2	2.37	2.00	0.37
21	Trimethylphenoxy-silane	5	27.79 27.81	27.80	27.72	0.3	166.3	155.5 157.5	156.5	1.06	1.00	0.06
22	Triethylphenoxysilane	5	34.92 34.99	34.96	34.73	0.7	208.4	201.0 203.0	202.0	1.03	1.00	0.03
23	Phenyl diethyl ortho-formate	5	32.85 32.91	32.88	32.71	0.5	—	—	—	—	—	—
24	Phenyl diethyl ortho-acetate	5	35.10 35.16	35.13	35.04	0.3	—	—	—	—	—	—

potassium methoxide method less accurate than the bromination method. However, the reproducibility for one and the same compound is generally very good under identical conditions *. It is possible that a separate measurement of the *H*-acidity and *L*-acidity can be attained potentiometrically, thus increasing the accuracy of the method.

PROCEDURE, REAGENTS AND SOLUTIONS

The aryloxysilanes were prepared in this laboratory. The synthesis of some of them was previously described [7].

Potassium methoxide, 0.1 N. The procedure of Fritz and Keen [19] was used in the preparation of the potassium methoxide solution. About 4 g of potassium were dissolved in 20 ml of absolute methanol and 50 ml of benzene in a loosely stoppered flask. Methanol was added until the solution became homogeneous, then benzene until the solution became cloudy, then it was cleared again with methanol and so on until 1 liter of clear solution was obtained. It was standardized using phenol or one of the cresols.

Indicator. *o*-Nitroaniline, 1.5 g, was dissolved in 100 ml of benzene.

Titration procedure. About 0.5 mequiv.** of the sample was weighed into a small glass tube. To 25 ml of anhydrous ethylenediamine in a 100 ml Erlenmeyer flask were added 2 drops of indicator solution. The flask was stoppered with a cork with a hole fitting the tip of a 10 ml burette. Potassium methoxide solution was added until the yellow colour changed to orange-red. Then the tube with the sample was added and the titration continued to the reappearance of the orange-red colour. During the titration the solution was rapidly stirred using a magnetic stirrer. To obtain reproducible results it was necessary to use a colour standard. A recommended procedure is to add the theore-

* The quality of the ethylenediamine seems to be of some significance for the results.

** On the basis of the aryloxy groups present.

tical amount of titrant to a phenol sample and use this solution as a colour standard. However, the colour fades rather rapidly. It is better to prepare a second standard of the same colour intensity as the first using methyl orange and the appropriate amounts of acid and alkaline water solutions. This standard is stable for months.

REFERENCES

1. Smith, B. *Acta Chem. Scand.* **10** (1956) 1589.
2. Miner Jr., C. S., Bryan, L. A., Holysz Jr., R. P. and Pedlow Jr., G. W. *Ind. Eng. Chem.* **39** (1947) 368.
3. Larsson, E. and Smith, B. *Svensk Kem. Tidskr.* **62** (1950) 141.
4. Gordon, M., Miller, J. G. and Day, A. R. *J. Am. Chem. Soc.* **70** (1948) 1946; **71** (1949) 1245.
5. McC. Arnett, E., Miller, J. G. and Day, A. R. *J. Am. Chem. Soc.* **72** (1950) 5635.
6. Glenn, A. R. and Peake, J. T. *Anal. Chem.* **27** (1955) 205.
7. Smith, B. *Acta Chem. Scand.* **9** (1955) 1337.
8. Stone, F. G. A. and Seyferth, D. *J. Inorg. Nuclear Chem.* **1** (1955) 112.
9. Trost, W. R. *Can. J. Chem.* **29** (1951) 877; **30** (1952) 835, 842.
10. Burg, A. B. *J. Am. Chem. Soc.* **76** (1954) 2674.
11. Gingold, K. and Rochow, E. G. *J. Am. Chem. Soc.* **76** (1954) 288.
12. Piper, T. S. and Rochow, E. G. *J. Am. Chem. Soc.* **76** (1954) 4318.
13. Sisler, H. H., Wilson, W. J., Gibbins, B. J., Batey, H. H., Pfahler, B. and Mattair, R. *J. Am. Chem. Soc.* **70** (1948) 3818.
14. Hurd, D. T., Osthoff, R. C. and Corrin, M. L. *J. Am. Chem. Soc.* **76** (1954) 249.
15. Helferich, B. and Reimann, W. *Chem. Ber.* **80** (1947) 163.
16. Swain, C. G., Esteve Jr., R. M. and Jones, R. H. *J. Am. Chem. Soc.* **71** (1949) 965.
17. Grubb, W. T. *J. Am. Chem. Soc.* **76** (1954) 3408.
18. Aelion, R., Loebel, A. and Eirich, F. *J. Am. Chem. Soc.* **72** (1950) 5705.
19. Fritz, J. S. and Keen, R. T. *Anal. Chem.* **25** (1953) 179.

Received January 24, 1957.

ACTA CHEMICA SCANDINAVICA 11 (1957) 565—567

The Structure of the High Temperature Modification of Lithium Sulfate *

T. FORLAND and J. KROGH-MOE

The Pennsylvania State University, Department of Ceramic Technology, College of Mineral Industries, University Park, Pennsylvania, U.S.A.

The high temperature modification of lithium sulfate has been found to be cubic with a unit cell length of 7.07 Å. The sulfate groups are arranged in a face centered lattice, and the cations can probably exchange between tetrahedral and octahedral positions.

The monoclinic, room-temperature modification of anhydrous lithium sulfate has been studied by Albright [1]. At 575 °C a transition takes place. Wyrouboff observed that the birefringence disappeared at the transition point and concluded that the high temperature modification was cubic [2]. A cubic symmetry is indicated by the present X-ray investigation.

Table 1 gives observed lines and their relative intensities for lithium sulfate determined from a powder pattern taken at 610 °C with filtered Cu$K\alpha$ radiation. It was noted that the relative X-ray intensities from a sample of the low temperature modification were different before and after being heated above the transition point. Preferred orientation is therefore taking place, and the intensities given in Table 1 cannot be regarded as reliable. Hence no effort was made to use these intensity values for a structure determination.

The observed lines can be indexed by means of a face centered cubic lattice with an edge length:

$$a = 7.07 \text{ Å}$$

A density of 2.07 corresponds to 4 formula units in the unit cell. The monoclinic modification has a density of 2.22 at room temperature.

From conventional space group considerations a structure of the high temperature lithium sulfate modification can be derived. This structure will

* Office of Naval Research Technical Report No. 72 under Contract N6 onr 269 Task Order 8, NR 032—264, The Pennsylvania State University, University Park, Pennsylvania. Mineral Industries Contribution No. 56—17. Reproduction in whole or in part is permitted for any purpose of the United States Government.

Table 1. Scattering angles and intensities observed for lithium sulfate at 610° C with CuK_α radiation.

2θ	$\frac{4 \sin^2\theta}{\lambda}$	Int.
21.8	0.0600	24
25.2	0.0803	7
35.9	0.1600	7
42.4	0.2202	7
44.4	0.2404	2
58.4	0.4000	1

be shown to be not quite satisfactory, however, since it does not account for rotation or oscillations of the sulfate groups. By assuming that equivalent atoms take equivalent fixed crystallographic positions, all but two space groups can be ruled out. Only the space groups $F23$ and $F\bar{4}3m$ will simultaneously take 4 sulfur, 8 lithium, and 16 oxygen atoms in one unit cell. With either of these space groups the following coordinates can be assigned to the atoms:

S 0, 0, 0.
O $u, u, u;\ u, \bar{u}, \bar{u};\ u, u, \bar{u};\ \bar{u}, \bar{u}, u.$
Li two of the following three coordinates:
1/4, 1/4, 1/4; 3/4, 3/4, 3/4; 1/2, 1/2, 1/2.

If it is assumed that the tetrahedral sulfate group has the usual sulfur-oxygen distance of about 1.50 Å, the parameter u will have the value 0.12. Of the possible lithium positions, those given by the coordinates 1/4, 1/4, 1/4 and 3/4, 3/4, 3/4 correspond to a tetrahedral coordination with respect to sulfate groups, though the former gives the cation a 4 coordination and the latter a 12 coordination with respect to oxygen. In the following, however, both these positions shall be referred to as tetrahedral. The position 1/2, 1/2, 1/2 is 6 coordinated by sulfate groups, and will hence be referred to as octahedral though the coordination number with respect to oxygen is 12.

Except for the positions and numbers of the cations this structure of lithium sulfate appears identical with the structures derived for the high temperature modifications of sodium and potassium perchlorates [3,4] and borofluorides [5]. The sodium and potassium ions in these structures will occupy the spacious octahedral 1/2, 1/2, 1/2 positions. This position provides a lithium ion with a too large space. In accordance with this, no analogous cubic high temperature modification has been found for lithium perchlorate and borofluoride.

The structures discussed above lead to some improbable interatomic distances. In lithium sulfate the closest approach of two oxygens belonging to different sulfate groups will be 2.56 Å. Lithium ions in the 1/4, 1/4, 1/4 positions would be surrounded by oxygen at a lithium-oxygen distance of 1.56 Å. Thus the 1/4, 1/4, 1/4 lattice sites provide the lithium ions with a too small space. On the other hand, both the 1/2, 1/2, 1/2 and the 3/4, 3/4, 3/4 lattice sites provide the lithium ions with a too large space. A rotation of the sulfate

groups through 45° around one axis, however, will increase the previously too short oxygen-oxygen distance of 2.56 Å. The closest distance between oxygens in neighboring sulfate groups will now be 3.18 Å. Now all the lithium ions can occupy tetrahedral positions, four coordinated by oxygen and with a reasonable lithium-oxygen distance of 2.06 Å. Since strong rotational oscillations must be expected for the sulfate groups, the lithium ions most probably can exchange between tetrahedral and octahedral lattice positions. With this high degree of disorder, the given space group can at most be approximately correct. It is even conceivable that the compound has a pseudocubic structure, but any weak reflections which could indicate this would only be noticeable in single crystal exposures.

X-Ray intensities observed for the perchlorates and the borofluorides do not in all cases agree with a reasonable size of the anion group. Finbak and Hassel obtained a better fit of the intensity data by assuming a rotation of the anion group [5,6]. As in the lithium sulfate, anion groups of acceptable sizes will approach each other too closely when the atoms are in positions prescribed by the adopted space group. Hence a steric hindrance to free rotation is provided. Coupled rotation or strong rotational oscillations must occur, however. In agreement with this, a fairly strong continuous background scattering is observed in lithium sulfate. The scattering has a maximum at $2\Theta = 36°$ for the Cu$K\alpha$ radiation employed. This background did not change appreciably in intensity on passing the transition point indicating strong rotational oscillation of the sulfate groups already below the transition point.

Acknowledgement. Thanks are expressed to the *Office of Naval Research* and the *International Corporation Administration* for their financial support. The authors also want to give acknowledgment to Dr. H. A. McKinstry for his assistance in obtaining the high temperature X-ray pattern.

REFERENCES

1. Albright, J. G. *Z. Krist* **84** (1932) 150.
2. Wyrouboff, G *Bull. soc. franc. minéral.* **14** (1890) 316.
3. Herrmann, K. and Ilge, W. *Z. Krist* **75** (1930) 41.
4. Braekken, H. and Harang, L. *Z. Krist* **75** (1930) 538.
5. Finbak, C. and Hassel, O. *Z. physik. Chem.* **B32** (1936) 433.
6. Finbak, C. and Hassel, O. *Z. physik. Chem.* **B32** (1936) 130.

Received December 16, 1956.

ACTA CHEMICA SCANDINAVICA 11 (1957) 568—584

Short Communications

Small-angle Scattering of X-Rays in Aqueous Sodium Desoxycholate Solutions Containing Decanol-1

PER EKWALL and KRISTER FONTELL

Institute of Physical Chemistry, Åbo Akademi, Åbo, Finland

Aqueous bile salt solutions are able to dissolve both hydrocarbons and polar lipophilic compounds. Appreciable amounts of long-chain alcohols, decanol-1 for instance, are solubilized by these solutions. For example, a 0.20 M sodium cholate solution dissolves about 28 ml of decanol per litre of solution at 40°C. A 0.20 m sodium desoxycholate solution dissolves about 55 ml of decanol per 1 000 g solution at 25°C, a 0.35 m solution about 105 ml and a 0.53 m solution about 200 ml[1]. The solubilization process involves two stages, as shown by the fact that when small amounts of decanol are added to cholate solutions, the ability of the latter to solubilize *p*-xylene is not appreciably altered, whereas the solubility of the hydrocarbon rapidly decreases when the molar ratio of decanol to cholate exceeds a certain value [2]. The same has been found to apply also in the case of desoxycholate solutions. This variation of the solubility of *p*-xylene with increasing additions of decanol to a 0.35 m sodium desoxycholate solution is shown in Fig. 1 a; the solubility of *p*-xylene remains almost unaltered as the decanol content increases to 50 ml per 1 000 g of solution, but then falls off rapidly as more decanol is added.

The mentioned variation in the solubility of *p*-xylene is accompanied by changes in the small-angle X-ray scattering by the solutions [3]. The X-ray scattering has been investigated with the same apparatus and technique we have used in our earlier investigations [4]. Fig. 2 shows photometer recordings of the X-ray films obtained with 0.35 m sodium desoxycholate solutions containing different amounts of decanol. As long as the decanol content is below about 40 ml per 1 000 g of solution, the small-angle X-ray pattern remains largely unaltered. As larger amounts of decanol are dissolved the pattern becomes

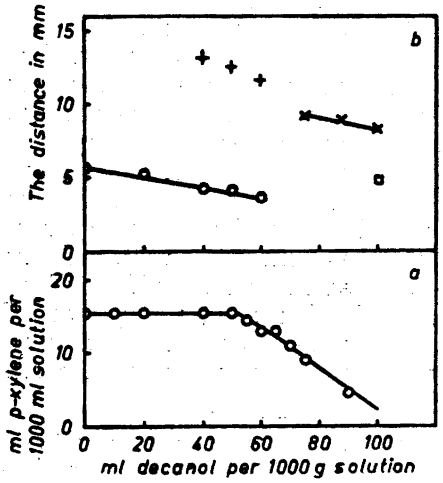


Fig. 1. a) The maximum solubility of *p*-xylene in 0.35 molal sodium desoxycholate solutions containing different amounts of decanol-1. b) The distance of the intensity maxima from the incident beam in the small-angle X-ray patterns of 0.35 m sodium desoxycholate solutions containing different amounts of decanol-1. The inner maximum. Points marked O and □. The outer maximum. Points marked × and +. The intensity maxima + are very vague and blurred.

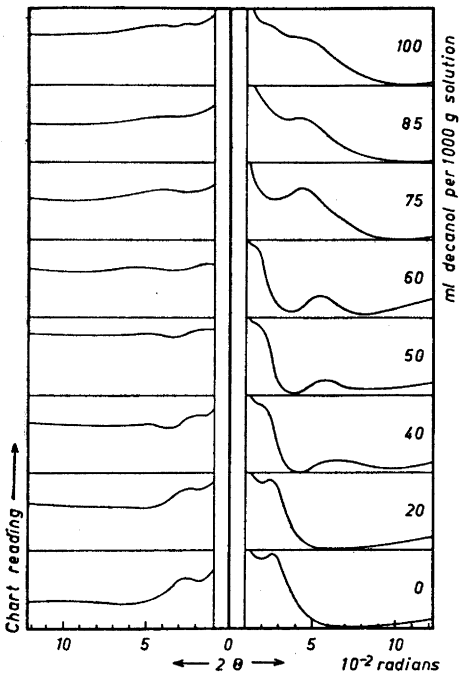


Fig. 2. Photometer recordings of the small-angle scattering by 0.35 M sodium desoxycholate solutions containing different amounts of decanol-1. a) Left side. Recordings obtained with the same photometer sensitivity for all films and with the photometer set to zero for unexposed areas of the films. b) Right side. Recordings obtained when the full-scale reading was set equal to the difference in maximum blackening and background for each film separately.

less and less distinct until it finally fades into the background. At the same time a new very diffuse ring which is located farther from the incident beam gradually becomes evident. When the decanol content is increased further to a high value close to saturation a second inner ring appears at a distance from the incident beam which almost coincides with that of the ring for the original desoxycholate solution or at a somewhat smaller distance. The curves in Fig. 1b show the shift of the intensity maxima with increasing decanol content. — We have found the same phenomenon to occur also with 0.53 m and 0.20 m sodium desoxycholate solutions containing decanol.

Exposures made with an ordinary X-ray powder camera have indicated the occurrence of a similar phenomenon to that described above. At low decanol contents the same pattern is obtained as for pure sodium desoxycholate solutions with Bragg spacings at 2.7—3.3 Å and 6.0—6.2 Å. At higher decanol contents, about 100 ml of alcohol per 1 000 g of a 0.53 m sodium desoxycholate solution, a new ring with a Bragg spacing of 4.5—5.0 Å appears. This spacing corresponds to that of pure decanol; in these quite clear solutions there is no separated decanol and practically all the dissolved decanol is in the solubilized state.

The observation that the original small-angle X-ray pattern for desoxycholate solutions disappears gradually and is replaced by another pattern indicates that decanol effects a radical rearrangement of the micelle structure. It is obvious that desoxycholate micelles are able to incorporate only a limited amount of decanol before their structure undergoes a change. When this critical molar ratio of decanol to desoxycholate is exceeded, the original micelles break down and a new type of mixed micelle composed of bile salt and decanol is formed. These new micelles are not able to solubilize *p*-xylene. It seems probable that the long paraffin chains of the alcohol molecules (alcohol is present in these solutions in molar ratios of decanol to desoxycholate from 1:1 to 2:1) primarily determine the structure of the new micelle. The appearance of a new short spacing at 4.5—5.0 Å possibly indicates the occurrence of parallel-oriented paraffin chains, obviously an arrangement resembling that in micelles of association colloids of the paraffin-chain type.

1. Ekwall, P., Fontell, K. and Sten, A. *Unpubl. results.*
2. Ekwall, P., Sten, A. and Norman, A. *Acta Chem. Scand.* **10** (1956) 681.
3. Ekwall, P. and Fontell, K. *IX Nord. Kemistmötet,* Aarhus 1956.
4. Ekwall, P. and Fontell, K. *Acta Chem. Scand.* **10** (1956) 327.

Received January 21, 1957.

Study of the Relation between Brightness Reversion and Carbonyl Content in Cellulose Pulp

INGVAR JULLANDER and KURT BRUNE

Research Laboratory, Mo och Domsjö AB, Örnsköldsvik, Sweden

Giertz [1] in a study of the brightness reversion of pulp upon heating, found for sulfite pulps a reasonably good correlation between the brightness reversion during heating and carbonyl content (copper number) as well as carboxyl content.

The discovery and subsequent commercial manufacture of the strong reducing agent sodium borohydride has given the cellulose chemist means to reduce the carbonyl groups in carbohydrates to alcohol groups. Treatment of pulp with sodium borohydride results in improved hot alkali stability and sometimes slightly increased viscosity [2,3]. Recently Giertz and McPherson [4] in connection with a study of the coloring matter formed when pulp is heated, also reported an experiment where partial borohydride reduction of an overbleached sulfite pulp resulted in reduced brightness reversion.

The aim of the present work was to investigate further the connection between carbonyl content (measured as copper number) and brightness reversion. Even a complete reduction of pulp can be made under mild experimental conditions. It is therefore unlikely that any other undesirable changes take place in the pulp.

Air-dried pulp was defibrated with a mechanical stirrer in water into which sodium borohydride had been dissolved in amounts corresponding to 0.1—10 % calculated on the pulp. Pulp concentration 2 %. The mixture was kept at 50°C for 3 h. The slightly alkaline solution was then sucked off on a Büchner funnel, the cellulose pulp washed several times with water, then acidified with acetic acid and finally washed again with water to a pH of around 6.5. Drying in air at room temperature.

Copper number was determined according to Braidy [5]. Pulp sheets were formed and brightness measurements performed in an Elrepho instrument. The brightness reversion was calculated by means of the Kubelka and Munk theory as recommended by Tongren [6], Mc Intyre [7] and Giertz [1] and by the last author expressed as "post-color" value (pc-value). The pc-value can be regarded as a relative measure of the amount of coloring substance formed during the heat treatment.

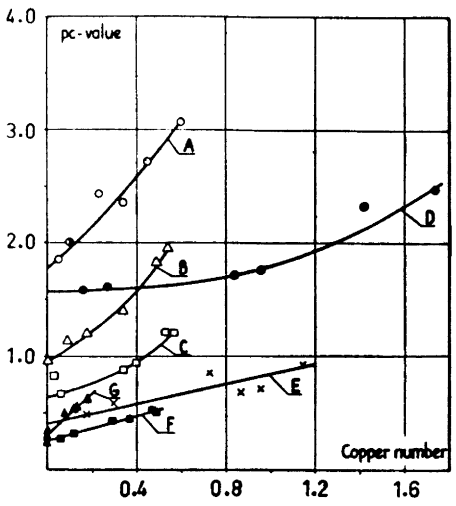


Fig. 1. Brightness reversion (pc-value) as a function of copper number for different types of pulp.

A, B and C — bleached sulfate paper pulps from pine.
D — bleached sulfite paper pulp from spruce.
E — bleached sulfite pulp from spruce, dissolving grade.
F — bleached, cold-alkaline treated sulfite pulp from spruce.
G — bleached cotton linters.

On each curve in Fig. 1 the point with the highest copper number corresponds to pulp treated only with water in blank experiments. The carbonyl content was then reduced by increasing amounts of sodium borohydride down to such low values as to allow an extrapolation to copper number zero.

It can be seen that the carbonyl groups on an average are responsible for approximately half the brightness reversion. In the cases studied so far, the slope of the curves seems to be higher for sulfate pulps and linters than for sulfite pulps, but the experimental material is too scanty to

allow a conclusion that this applies to all types of sulfite and sulfate pulps. Highly refined sulfite pulp is at least as good as linters as far as brightness stability is concerned, in spite of the higher copper number.

1. Giertz, H. W. *Svensk Papperstidn.* **48** (1945) 317.
2. Meller, A. *Tappi* **38** (1955) 682.
3. Head, F. S. H. *J. Textile Inst.* **46** (1955) T 400, T 584.
4. Giertz, H. W. and McPherson, J. *Svensk Papperstidn.* **59** (1956) 93.
5. *Swedish Association of Pulp and Paper Engineers, Technical Communications,* CCA 3.
6. Tongren, J. C. *Paper Trade J.* **107** (1938) TAPPI Section 76.
7. Mc Intyre, J. W. *Paper Trade J.* **109** (1939) TAPPI Section 317.

Received February 15, 1957.

Aliphatic Ditellurides

GÖRAN BERGSON

Chemical Institute, University of Uppsala, Sweden

Only two aliphatic ditellurides are described in literature; ditellurium-diacetic acid ($HOOCCH_2TeTeCH_2COOH$) and ditellurium-α-dipropionic acid [1,2]. These substances have been prepared by reduction of the trichlorotellurium compounds obtained by the interaction of tellurium tetrachloride with the corresponding acid anhydrides. This method seems to be suited only for the introduction of the tellurium function in the α-position relative the carboxylic group.

The author has started an investigation of synthetic methods for aliphatic ditellurides in general. This paper gives a preliminary report of the reaction between aliphatic halogen compounds and the Te_2^{2-} ion. The first electronic excitation band for di-*n*-butylditelluride and ditellurium-diacetic acid has been determined and compared with that for disulfides and diselenides extensively studied by Schotte [3,4] and Bergson [5,6]. An infra-red investigation of the ditellurides is being prepared. A polarographic investigation of ditellurium-diacetic acid has been started by Nygård [7].

A sodium ditelluride solution was prepared by dissolving finely powdered tellurium in an alkaline solution of sodium formaldehyde sulphoxylate (Rongalite C). When excess Rongalite C is used for the preparation of sodium telluride solution the tellurium is readily dissolved [8], but in the preparation of sodium ditelluride the molar ratio between tellurium and Rongalite C must be 2:1, and it is then necessary to reflux and to stir the mixture for several hours. The sodium ditelluride solution (which certainly contains also some telluride and polytelluride) reacts readily with *n*-butyl bromide. An attempt to prepare ditellurium-diacetic acid in this way from chloroacetic acid failed, because this acid oxidized the ditelluride ion to elementary tellurium, and from the reaction mixture acetic acid was isolated. Sodium telluride reacts in the same way with chloroacetic acid. Here we have a difference between tellurium, selenium and sulfur, because disulfide-, sulfide-, diselenide- and selenide ions react in the normal way with α-haloacids. These facts should be compared with the oxidative action of *vic*-dihalides on selenoles [9,10] contrary to their behavior towards thiols, and with the oxidation of sodium disulfide by bromomalonic ester [11].

Di-*n*-butylditelluride has an absorption band with maximum at 3 990 Å as can be seen from Fig. 1. The author has shown that the lowest electronic excitation energy for disulfides and diselenides can be expressed by an empirical formula with the parameters α and β:

$$E = \alpha\sqrt{k} + \beta$$

with $\alpha_S = \alpha_{Se}$, where k is the number of hydrogen atoms joined to the α-carbon atom [6]. The author hopes to be able to test the validity of this relation for ditellurides. An increase in excitation energy is found when the molecule contains a carboxylic group close to the S—S or Se—Se group. For diselenium-diacetic acid ($HOOCCH_2SeSeCH_2COOH$) the band is overlapped by a high intensity band (λ_{max} = 2 290 Å) and is only detectable [5] as an inflexion at 2 930 Å. The same behavior has been found for ditellurium-diacetic acid (inflexion at 3 600 Å). The 2 290 Å band of the selenium compound has its correspondence in a band with λ_{max} = 2 730 Å.

allow a conclusion that this applies to all types of sulfite and sulfate pulps. Highly refined sulfite pulp is at least as good as linters as far as brightness stability is concerned, in spite of the higher copper number.

1. Giertz, H. W. *Svensk Papperstidn.* **48** (1945) 317.
2. Meller, A. *Tappi* **38** (1955) 682.
3. Head, F. S. H. *J. Textile Inst.* **46** (1955) T 400, T 584.
4. Giertz, H. W. and McPherson, J. *Svensk Papperstidn.* **59** (1956) 93.
5. *Swedish Association of Pulp and Paper Engineers, Technical Communications,* CCA 3.
6. Tongren, J. C. *Paper Trade J.* **107** (1938) TAPPI Section 76.
7. Mc Intyre, J. W. *Paper Trade J.* **109** (1939) TAPPI Section 317.

Received February 15, 1957.

Aliphatic Ditellurides

GÖRAN BERGSON

Chemical Institute, University of Uppsala, Sweden

Only two aliphatic ditellurides are described in literature; ditellurium-diacetic acid ($HOOCCH_2TeTeCH_2COOH$) and ditellurium-α-dipropionic acid [1,2]. These substances have been prepared by reduction of the trichlorotellurium compounds obtained by the interaction of tellurium tetrachloride with the corresponding acid anhydrides. This method seems to be suited only for the introduction of the tellurium function in the α-position relative the carboxylic group.

The author has started an investigation of synthetic methods for aliphatic ditellurides in general. This paper gives a preliminary report of the reaction between aliphatic halogen compounds and the Te_2^{2-} ion. The first electronic excitation band for di-*n*-butylditelluride and ditellurium-diacetic acid has been determined and compared with that for disulfides and diselenides extensively studied by Schotte [3,4] and Bergson [5,6]. An infra-red investigation of the ditellurides is being prepared. A polarographic investigation of ditellurium-diacetic acid has been started by Nygård [7].

A sodium ditelluride solution was prepared by dissolving finely powdered tellurium in an alkaline solution of sodium formaldehyde sulphoxylate (Rongalite C). When excess Rongalite C is used for the preparation of sodium telluride solution the tellurium is readily dissolved [8], but in the preparation of sodium ditelluride the molar ratio between tellurium and Rongalite C must be 2:1, and it is then necessary to reflux and to stir the mixture for several hours. The sodium ditelluride solution (which certainly contains also some telluride and polytelluride) reacts readily with *n*-butyl bromide. An attempt to prepare ditellurium-diacetic acid in this way from chloroacetic acid failed, because this acid oxidized the ditelluride ion to elementary tellurium, and from the reaction mixture acetic acid was isolated. Sodium telluride reacts in the same way with chloroacetic acid. Here we have a difference between tellurium, selenium and sulfur, because disulfide-, sulfide-, diselenide- and selenide ions react in the normal way with α-haloacids. These facts should be compared with the oxidative action of *vic*-dihalides on selenoles [9,10] contrary to their behavior towards thiols, and with the oxidation of sodium disulfide by bromomalonic ester [11].

Di-*n*-butylditelluride has an absorption band with maximum at 3 990 Å as can be seen from Fig. 1. The author has shown that the lowest electronic excitation energy for disulfides and diselenides can be expressed by an empirical formula with the parameters α and β:

$$E = \alpha\sqrt{k} + \beta$$

with $\alpha_S = \alpha_{Se}$, where k is the number of hydrogen atoms joined to the α-carbon atom [6]. The author hopes to be able to test the validity of this relation for ditellurides. An increase in excitation energy is found when the molecule contains a carboxylic group close to the S—S or Se—Se group. For diselenium-diacetic acid ($HOOCCH_2SeSeCH_2COOH$) the band is overlapped by a high intensity band (λ_{max} = 2 290 Å) and is only detectable [5] as an inflexion at 2 930 Å. The same behavior has been found for ditellurium-diacetic acid (inflexion at 3 600 Å). The 2 290 Å band of the selenium compound has its correspondence in a band with λ_{max} = 2 730 Å.

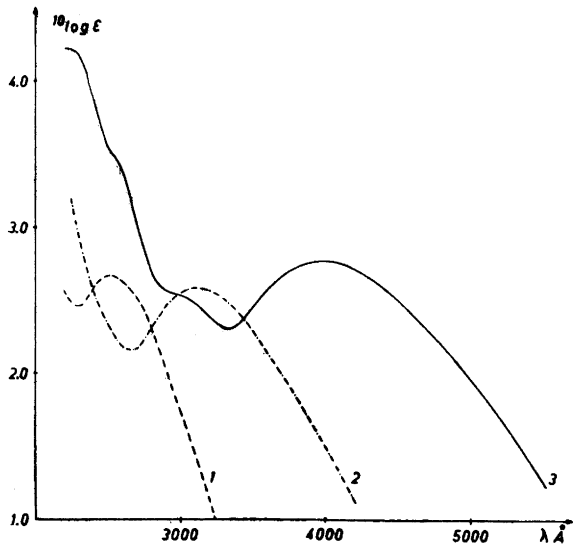


Fig. 1. Ultraviolet absorption of:
1. Di-*n*-propyldisulfide [13].
2. Di-*n*-butyldiselenide [5].
3. Di-*n*-butylditelluride, in (*cyclo*hexane).

Experimental: Di-n-butylditelluride. In a 500 ml three necked flask 9.24 g Rongalite C and 9.0 g sodium hydroxide are dissolved in 200 ml water. The flask is flushed out with nitrogen, and 15.32 g finely powdered tellurium is added. The mixture is vigorously stirred under reflux for 5 h. After that time 16.4 g *n*-butyl bromide is added dropwise, the mixture is allowed to cool, and the stirring continued for 30 min. The content of the flask is extracted with 2 × 150 ml ether, the extract dried with $CaCl_2$, and the ether distilled off in a nitrogen atmosphere. The residue is distilled in vacuum (nitrogen) and the fraction boiling between 112—115°/1.5 mm Hg is collected. The ditelluride is a dark red oil with a pungent smell. Yield 23 %. (58.70 mg subst. gives 40.91 mg Te. Found: Te 69.7. Calc. Te 69.1). The analysis was carried out according to Drew and Porter [12].

Ditellurium-diacetic acid was prepared according to Morgan and Drew [1]. The spectra were determined with a Beckman model DU (2 200—4 000 Å) and a Beckman model B (4 000—5 500 Å) photoelectric spectrophotometer.

The author is indebted to Professor Arne Fredga for suggesting the investigation. A grant from the *Swedish Natural Science Research Council* is gratefully acknowledged.

1. Morgan, G. T. and Drew, H. D. K. *J. Chem. Soc.* **127** (1925) 531.
2. Morgan, G. T. and Kellett, R. E. *J. Chem. Soc.* **1926** 1080.
3. Schotte, L. *Arkiv Kemi* **8** (1956) 579.
4. Schotte, L. *Arkiv Kemi* **9** (1956) 441.
5. Bergson, G. *Arkiv Kemi* **9** (1956) 121.
6. Bergson, G. *9. Nordiske Kemikermøde i Aarhus* 1956, p. 47.
7. Nygård, B. *Private communication.*
8. Farrar, W. V. and Gulland, J. M. *J. Chem. Soc.* **1945** 13.
9. Tschugaeff, L. *Ber.* **42** (1909) 49.
10. Fredga, A. *Svensk Kem. Tidskr.* **48** (1936) 92.
11. Schotte, L. *Private communication.*
12. Drew, H. D. K. and Porter, C. R. *J. Chem. Soc.* **1929** 2091.
13. Barltrop, J. A., Hayes, P. M. and Calvin, M. *J. Am. Chem. Soc.* **76** (1954) 4349.

Received February 25, 1957.

Anion Exchanging Polymers from Sodium Cellulose Xanthate and Polyethylenimine

SVEN SONNERSKOG

A-B Svenskt Konstsilke, Borås, Sweden

Alkaline solutions of sodium cellulose xanthate react with polyethylenimine at room temperature. If an excess (weight by weight) of the latter polymer is present, solidification gradually takes place, accompanied by a strong syneresis. The final, transparent gel shows all distinctive features of rubber elasticity in a qualitative sense. Another striking change is established at a subsequent purification of the gel in water. The specimen keeps its geometric shape and degree of swelling virtually unchanged. Furthermore, this purified gel is insoluble in cuprammonium solution.

The time required for complete gelation is highly dependent on the composition and physical state of the viscose. At a given salt index a technical grade of viscose reacts faster than a corresponding one, from which anions such as trithiocarbonate have been removed by ion exchange. Such a solution shows a slightly greenish yellow colour even after complete gelation, which would imply that a reformation of trithiocarbonate ions is suppressed. Appreciable amounts of sulphide ions are formed, however, as can be seen by successive tests with standard reagents. It is apparent that a reaction takes place between cellulose xanthate ions and polyethylenimine, carbon disulphide acting as an interlinking agent. As is known, there is always a small amount of free carbon disulphide present in every viscose [1] at equilibrium. In the actual case the *added* polymer acts as an acceptor of CS_2, thus also causing a gradual dexanthation of the cellulose, but this circumstance alone does not explain the observed insolubility in cuprammonium.

The rates of gelation of technical viscoses are shown in Fig. 1. At a high salt index the gel point is reached within two hours, to judge from the viscosity increments in a Cochius tube. At a low salt index gelation is very slow. The change of viscosity during the same time is insignificant, but gelation is complete within 20—24 h. The same statement is valid for all viscoses, purified by anion exchange before the addition of coreactant. Their flow diagrams are not included here due to this circumstance.

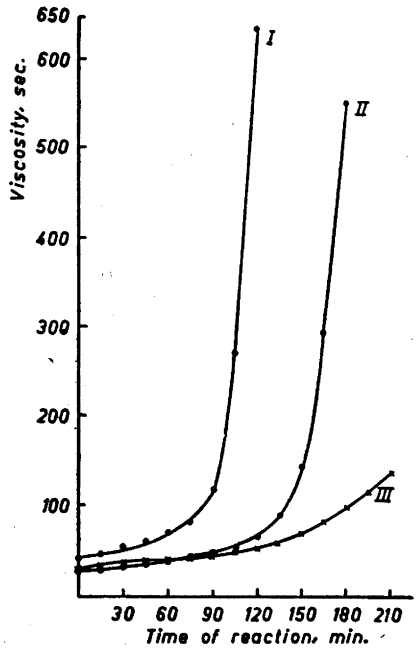


Fig. 1. Diagram, showing the viscosity increments in a Cochius tube at the gelation of technical viscoses, containing an excess (w/w) of polyethylenimine). Weight ratio polyethylenimine / cellulose = 3. Content of polymers in solution = 16 %. Type of Cochius tube: length = 195 mm, diam. = 18 mm, length of air bubble = 20 mm (approx). Temperature of solution 19.0° C.

Curve I: Low degree of ripeness, high salt index. (Index = 21).
Curve II: Medium degree of ripeness, salt index = 10.
Curve III. High degree of ripeness, low salt index. (Index = 2).

Purification of the final crude reaction mixture is simple in principle but tedious in practice. The following description is valid for the specimen obtained in accordance with curve II in Fig. 1. The jelly was cut into chips, soaked in running distilled water for several days, until tests for sulphide ions were negative. This operation was repeated after swelling in dilute sodium hydroxide solution (strength 4 % b.w., temperature 70°C, time of

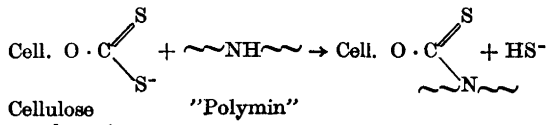
swelling 60 min.). For complete regeneration the wet chips were immersed in cold 1 N hydrochloric acid for 24 h, followed by washing in distilled water, soaking in sodium hydroxide solution and a final washing with hot distilled water until the excess of inorganic base has been removed.

The highly swollen, transparent chips show an average water content of 92 %. Drying at 70—80°C reduces the volume at least a tenfold. The dry polymer is a brittle, light yellow or amber, transparent resin, which cracks into flakes on rewetting. Polymer, prepared from viscose of medium degree of ripeness, showed a nitrogen content of 13.6 % (Kjeldahl) and a sulphur content of 2.1 % (Grote-Krekeler).

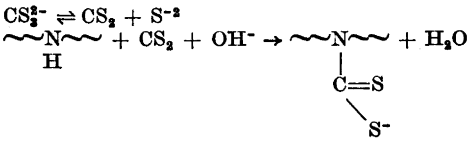
The wet polymer (primary gel or reswollen resin) acts as an anion exchanger. Chloride ions are adsorbed at the regeneration step in hydrochloric acid. This is easily seen at the addition of dilute nitric acid to a washed sample; chloride ions immediately reappear in the aqueous phase, as indicated by silver nitrate. Ion exchange in sodium hydroxide solution operates in an analogous manner and was used for determination of exchange capacity. A direct titration of chloride ions liberated by 1 N sodium hydroxide showed a value of 4.15 mequiv./g dry polymer. An alternative test, carried out by passing the aqueous phase through a hydrogen saturated cation exchanger, followed by alkalimetric titration, showed a capacity of 4.40 mequiv./g dry polymer.

It is apparent that a considerable amount of polyethylenimine has been linked to the cellulose molecules. As the interaction between the two components ends in non-solubility in cuprammonium, the formation of infinite networks by a chemical reaction between the two polymer species seems most probable. The polyelectrolyte (cellulose xanthate), as well as polyethylenimine possesses abundant degree of functionality for a cross-linking reaction. Available information from analogous cases [2] indicates a reaction scheme as follows:

1. Formation of N-substituted thiourethans:

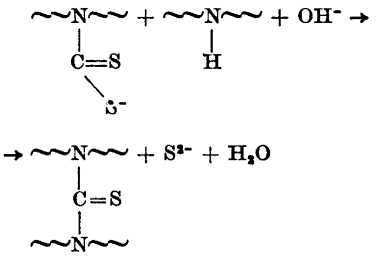


2. Formation of a derivative from dithiocarbamic acid. This may occur at random along chain molecules:

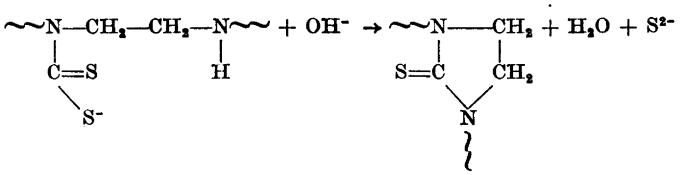


possibly accompanied by a minor formation of thiourea groupings, low enough to prevent insolubilization. (Alkaline solutions of polyethylenimine do not change their solubility characteristics when saturated with carbon disulphide at room temperature):

Interlinking:



Intralinking:



At the purification of the crude reaction mixture components according to (2) are removed. All essential features of the reaction seem to be satisfactorily explained by the two cases in combination, *e. g.*

a. The formation of sulphide ions during the reaction.

b. The decreased rate of gelation when trithiocarbonate ions are removed by ion exchanger.

c. The regular formation of trithiocarbonate ions in viscose is suppressed by polyethylenimine.

d. The presence of sulphur and nitrogen in the purified polymer.

The analytical data permit an estimation of an average structural unit of the infinite network. This building unit may be preferably expressed by telling the numbers of anhydroglucose units and ethylenimine units statistically shared to a single interlinking unit:

$$\frac{b \text{ units of ethylenimine} \mid \text{interlinking unit } (> C{=}S)}{a \text{ anhydroglucose units}}$$

Weight of building unit $= 162a-1+44+43b-1 = 162a+43b+42 = M_w$

Two equations are obtained from analytical data:

$14b/M_w = 13.6/100$, $32/M_w = 2.1/100$

with approximative solution (whole numbers) $a = 5$, $b = 15$, $M_w = 1\,500$.

$\%\,N_{calc} = 14.0$, $\%\,S_{calc} = 2.1$

The calculated building unit M_w contains 14 centres where anion exchange is possible. The maximum exchange capacity would thus be $14\,000/1\,500 = 9.3$ mequiv./g dry polymer, which should be compared with 4.4 mequiv./g, found in the actual case. Such a relation seems in no way unreasonable.

1. Hermans, P. H. *Physics and Chemistry of Cellulose Fibres*, Elsevier Publishing Co., Amsterdam 1949, p. 337.
2. Kline, E., in Ott, E. *Cellulose and Cellulose Derivatives*, Interscience Publishing Inc., New York 1943, p. 849.

Received February 26, 1957.

The Ultraviolet Spectrum of Vitamin A_2

GEORG LAMBERTSEN and OLAF R. BRÆKKAN

Governmental Vitamin Laboratory, Norwegian Fisheries Research Institute, Bergen, Norway

The spetroscopic properties of vitamin A_2 have been investigated by several workers [1-3]. The most complete data up till now have been given by Cama and Morton [3] who made vitamin A_2 by reducing retinene$_2$ with lithium aluminium hydride. We have previously reported a method for the determination of vitamin A_2 based on a calculation of the data obtained from the ultraviolet absorption curve after careful chromatography of the unsaponifiable matter [4]. The method was extensively compared with the hitherto used method for the determination of vitamin A_2 based

Table 1. Relative extinction values for vitamin A_2-alcohol in abs. ethanol.

Wavelength	E/E_{max}	Wavelength	E/E_{max}
230	0.206	304	0.376
235	0.195	305	0.390
240	0.167	310	0.475
245	0.150	315	0.552
250	0.160	320	0.640
255	0.189	325	0.730
260	0.210	330	0.820
265	0.250	335	0.890
270	0.303	340	0.940
272	0.351	345	0.979
274	0.395	348	0.993
275	0.407	350	0.996
276	0.416	351	1.000
277	0.416	352	0.999
278	0.409	354	0.995
280	0.400	355	0.992
282	0.426	356	0.984
284	0.473	360	0.958
285	0.495	365	0.908
286	0.510	370	0.855
288	0.498	375	0.761
290	0.441	380	0.637
292	0.374	385	0.523
294	0.338	390	0.449
295	0.324	395	0.362
296	0.320	400	0.249
298	0.324	410	0.078
300	0.388	420	0.025
302	0.355		

At the purification of the crude reaction mixture components according to (2) are removed. All essential features of the reaction seem to be satisfactorily explained by the two cases in combination, *e. g.*

a. The formation of sulphide ions during the reaction.

b. The decreased rate of gelation when trithiocarbonate ions are removed by ion exchanger.

c. The regular formation of trithiocarbonate ions in viscose is suppressed by polyethylenimine.

d. The presence of sulphur and nitrogen in the purified polymer.

The analytical data permit an estimation of an average structural unit of the infinite network. This building unit may be preferably expressed by telling the numbers of anhydroglucose units and ethylenimine units statistically shared to a single interlinking unit:

$$\frac{b \text{ units of ethylenimine} \mid \text{interlinking unit } (> C{=}S)}{a \text{ anhydroglucose units}}$$

Weight of building unit $= 162a-1+44+43b-1 = 162a+43b+42 = M_w$

Two equations are obtained from analytical data:

$14b/M_w = 13.6/100$, $32/M_w = 2.1/100$

with approximative solution (whole numbers) $a = 5$, $b = 15$, $M_w = 1\,500$.

$\%\,N_{calc} = 14.0$, $\%\,S_{calc} = 2.1$

The calculated building unit M_w contains 14 centres where anion exchange is possible. The maximum exchange capacity would thus be $14\,000/1\,500 = 9.3$ mequiv./g dry polymer, which should be compared with 4.4 mequiv./g, found in the actual case. Such a relation seems in no way unreasonable.

1. Hermans, P. H. *Physics and Chemistry of Cellulose Fibres*, Elsevier Publishing Co., Amsterdam 1949, p. 337.
2. Kline, E., in Ott, E. *Cellulose and Cellulose Derivatives*, Interscience Publishing Inc., New York 1943, p. 849.

Received February 26, 1957.

The Ultraviolet Spectrum of Vitamin A_2

GEORG LAMBERTSEN and OLAF R. BRÆKKAN

Governmental Vitamin Laboratory, Norwegian Fisheries Research Institute, Bergen, Norway

The spetroscopic properties of vitamin A_2 have been investigated by several workers [1-3]. The most complete data up till now have been given by Cama and Morton [3] who made vitamin A_2 by reducing retinene$_2$ with lithium aluminium hydride. We have previously reported a method for the determination of vitamin A_2 based on a calculation of the data obtained from the ultraviolet absorption curve after careful chromatography of the unsaponifiable matter [4]. The method was extensively compared with the hitherto used method for the determination of vitamin A_2 based

Table 1. Relative extinction values for vitamin A_2-alcohol in abs. ethanol.

Wavelength	E/E_{max}	Wavelength	E/E_{max}
230	0.206	304	0.376
235	0.195	305	0.390
240	0.167	310	0.475
245	0.150	315	0.552
250	0.160	320	0.640
255	0.189	325	0.730
260	0.210	330	0.820
265	0.250	335	0.890
270	0.303	340	0.940
272	0.351	345	0.979
274	0.395	348	0.993
275	0.407	350	0.996
276	0.416	351	1.000
277	0.416	352	0.999
278	0.409	354	0.995
280	0.400	355	0.992
282	0.426	356	0.984
284	0.473	360	0.958
285	0.495	365	0.908
286	0.510	370	0.855
288	0.498	375	0.761
290	0.441	380	0.637
292	0.374	385	0.523
294	0.338	390	0.449
295	0.324	395	0.362
296	0.320	400	0.249
298	0.324	410	0.078
300	0.388	420	0.025
302	0.355		

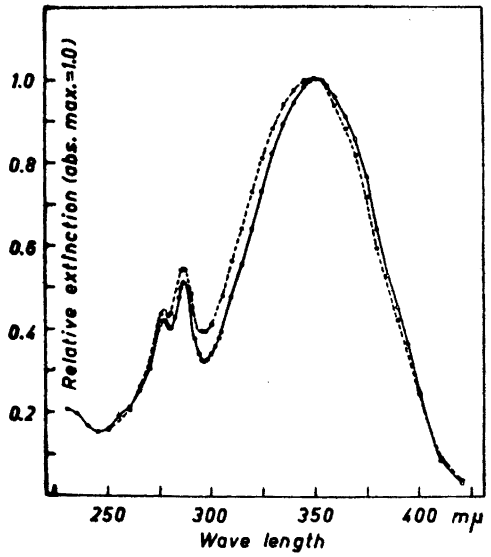


Fig. 1. Relative extinction values for vitamin A_2.
● from retinine$_2$ (Cama and Morton [3]).
○ from perch liver (present investigation).

on the ratio of the E-values at 693 mμ and 620 mμ of the antimony trichloride reaction, and a good agreement was found. The formula for the calculation of vitamin A_2 in our method has been derived from the absorption data reported for all-*trans* vitamin A_1 by Cama, Collins and Morton [5] and for vitamin A_2 by Cama and Morton [3].

In the spectrophotometric methods used at present for the determination of vitamin A, the exact absorption data of the pure substance are indispensible for the correct calculation of the results. This also applies to the proposed [4] joint ultra-violet-spectrophotometric determination of vitamin A_1 and A_2. From the investigation of Abdullah *et al.*[6] and recently Barnholdt and Hjarde [7], the expected existence of isomeric forms of vitamin A_2 has been demonstrated. During our extensive study of vitamin A components in fish liver and liver oils, we have found reason to conclude that the vitamins A are stored *in vivo* as the all-*trans* isomers. During our routine investigations of fish livers, samples of perch liver were found to be devoid of vitamin A_1 and *cis* isomers (maleic anhydride reaction). This made it of interest to examine more carefully and in detail the U.V.-absorption curve. The measurements were carried out with a Beckman Spectrophotometer Model DU. The results are reported in Table 1, and compared with the values of Cama and Morton [3] in Fig. 1. As may be noted, the absorption maximum in ethanol of vitamin A_2-alcohol was found at 351 mμ, with a second peak at 286 mμ, in agreement with the previous findings. The ratio $E_{286} / E_{351} = 0.320$ is lower, however, than the value 0.393 reported by Cama and Morton [3], indicating a higher degree of purity. It may further be noted that a small but distinct peak was observed at 277 mμ ($E_{277} / E_{351} = 0.417$). Actually, this peak was indicated already when the observations of Cama and Morton [3] were plotted graphically.

The results presented make a revised value of the absorption maximum of a purified (crystalline) all-*trans* vitamin A_2 of importance for further studies of this vitamin.

1. Schantz, E. M. *Science* **108** (1948) 417.
2. Farrar, K. R., Hamlet, J. C., Henbest, H. B. and Jones, E. R. H. *Chemistry & Industry* **1951** 49.
3. Cama, H. R. and Morton, R. A. *Analyst* **78** (1953) 74.
4. Lambertsen, G. and Brœkkan, O. R. *Proc. 2. Int. Conf. Biochem. Probl. Lipids, Ghent* **1955**, p. 56.
5. Cama, H. R., Collins, F. D. and Morton, R. A. *Biochem. J. London* **50** (1951) 48.
6. Abdullah, M. M., Morcos, S. R. and Salah, M. K. *Biochem. J. London* **56** (1954) 569.
7. Barnholdt, B. and Hjarde, W. *Acta Chem. Scand.* **10** (1956) 1635.

Received February 21, 1957.

Corrections to "Tritium Labelling of *p*-Aminosalicylic Acid (PAS)"

ÅKE HANNGREN and JAN RYDBERG

Söderby Hospital, Uttran, and Pharm.Dept., Kgl. Veterinärhögskolan, Stockholm; Chem. Dept., Univ. of Stockholm, Stockholm, Sweden

In our paper [1] the equation shall read:

$$q = \frac{k_d}{1 + k_a [H^+]^{-1}}$$

1. Hanngren, Å. and Rydberg, J. *Acta Chem.* **11** (1957) 202.

*iso*Thiocyanates XXV *. Methyl 4-*iso*Thiocyanatobutyrate, a New Mustard Oil Present as a Glucoside (Glucoerypestrin) in *Erysimum* Species

ANDERS KJÆR and ROLF GMELIN

Chemical Laboratory of the University of Copenhagen, Denmark

A few years ago it was noticed in this laboratory [1] that seeds of various species of the genus *Erysimum (Cruciferae)* contain a mustard oil glucoside which is different from those formerly recognized in Nature. A substantial seed sample of *Erysimum rupestre* DC., procured by cultivation of the plant on a larger scale **, has now made it possible to characterize and identify the new glucoside for which we wish to introduce the name *glucoerypestrin* ***.

According to paperchromatographic analysis, glucoerypestrin is accompanied by minor amounts of glucocheirolin in seed extracts of *E. rupestre*. The partly purified, glassy glucoside fraction yielded a crystalline product on acetylation. Fractional crystallization of this from 90 % ethanol afforded a homogeneous specimen of *glucoerypestrin tetraacetate monohydrate*, decomposing at 188–190° (uncorr.) †; $[\alpha]_D^{23}$ −18.0° (H_2O, c = 1.7). (Found ††: C 37.40; H 4.85; N 2.05; K 6.19. Calc. for $C_{20}H_{28}O_{15}NS_2K, H_2O$ (643.7): C 37.32; H 4.70; N 2.18; K 6.07). The infra-red spectrum was of the usual type [3,4] and did not provide much information as to structural details.

Deacetylation with 1.5 N methanolic ammonia, under carefully controlled conditions, furnished the alkali-labile, paperchromatographically homogeneous glucoerypestrin which, in turn, was subjected to enzymic hydrolysis with myrosinase at pH 6.7. The resulting mustard oil, isolated by ether extraction or distillation at diminished pressure, yielded a crystalline, optically inactive *thiourea* (IIa), $C_6H_{12}O_2N_2S$, m.p. 93° (uncorr.) (Found: C 40.85; H 6.83; N 15.65; S 18.60; OCH_3 17.58. Calc.: C 40.90; H 6.87; N 15.90; S 18.20; OCH_3 17.61), on treatment with methanolic ammonia, again under strictly controlled conditions. The ultra-violet spectrum of the thiourea (in EtOH) was of the usual type (λ_{max} 243 mμ (ε 12 600), λ_{min} 223 mμ (ε 1 500). A very strong band at 1 728 cm^{-1} in the infra-red spectrum (in KBr) was suggestive of the presence of an ester grouping in the thiourea. On paper chromatography in water-saturated chloroform, the new thiourea travelled at a rate corresponding to an R_{Ph}-value of 0.65 [5].

Reaction of the *iso*thiocyanate with aniline and 1-naphthylamine in methanolic solutions afforded the nicely crystalline *phenylthiourea* (IIb), $C_{12}H_{16}O_2N_2S$, m. p. 91° (uncorr.) (Found: C 57.00; H 6.39; N 11.01. Calc.: C 57.12; H 6.39; N 11.11), and *(1-naphthyl)-thiourea* (IIc), $C_{16}H_{18}O_2N_2S$, m. p. 132° (uncorr.) (Found: C 63.70; H 5.85; N 9.03. Calc.: C 63.56; H 6.00; N 9.27), respectively.

$$SCNCH_2CH_2CH_2COOCH_3$$
I

$$R—NHCSNHCH_2CH_2CH_2COOCH_3$$
IIa : R = H
IIb : R = C_6H_5
IIc : R = 1-$C_{10}H_7$

The cumulate data suggested that the new mustard oil was *methyl 4-isothiocynatobutyrate* (I), an assumption fully verified through the following synthesis.

* Part XXIV of this series: *Acta Chem. Scand.* **11** (1957) 184.

** We are much indebted to the *Botanical Garden of the University of Copenhagen* for the cultivation of this and other biennial *Erysimum* species.

*** This name has been preferred to the more consistent designation "glucoerysimin" in order to avoid confusion with the cardiac glycoside erisimin of similar provenance (*cf.* Ref.[2]).

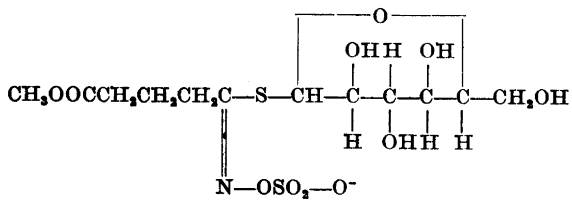
† It has been observed in this laboratory that the decomposition temperature of most acetylated *iso*thiocyanate glucosides is very dependent on the rate of heating. The present value was determined in capillary tubes by inserting the sample at 140° and raising the temperature at a rate of 8° per min.

Polymorphism may also in some cases contribute to the widely varying values observed (M. G. Ettlinger, private communication).

†† A Karl Fischer titration gave: 2.85 % H_2O. Calc. for the monohydrate: 2.80 %.

Treatment of 4-aminobutyric acid with hydrogen chloride in anhydrous methanol gave a quantitative yield of *methyl 4-aminobutyrate hydrochloride* * as hygroscopic needles, m. p. 96—99° (uncorr.) (Found: C 38.70; H 7.69; Cl 22.71. Calc. for $C_5H_{12}O_2NCl$ (153.6): C 39.09; H 7.88; Cl 23.08). Equimolecular amounts of thiocarbonyl chloride in chloroform, and the hydrochloride, dissolved in water containing excess sodium carbonate, reacted to give the mustard oil (I) as an almost colourless oil, b. p. 70° at 0.2 mm, n_D^{25} 1.5066. (Found: C 45.40; H 5.82; N 8.77; S 20.22. Calc. for $C_6H_9O_2NS$ (159.2): C 45.26; H 5.70; N 8.80; S 20.14). Upon reaction with ammonia, aniline and 1-naphthylamine, respectively, the synthetic mustard oil yielded thioureas (IIa, b, c) identical with those obtained from the natural *iso*thiocyanate, as apparent from mixed melting point determinations and coinciding infra-red spectra.

The presence in glucoerypestrin of glucose and sulphate has been unequivocally established by paper chromatography subsequent to enzymic hydrolysis. In accord with the notable discovery of Ettlinger and Lundeen [7], leading to a revised general structure for the mustard oil glucosides, glucoerypestrin splits off hydroxylamine on hydrolysis with strong acids. Hence, the formula (III) is considered likely to be a correct expression for the glucoerypestrin anion **.



III

Of several *Erysimum* species investigated thus far in this laboratory, seeds of *E. ochroleucum* DC. and *E. pumilum* DC. exhibited the same glucoside pattern as *E. rupestre* DC. In a recent survey of paperchromatographic analyses of a considerable number of plants, Schultz and Wagner [8] list the R_B-values 0.65 and 0.68 in *n*-butanol : acetic acid : water (4:1:3) and *n*-butanol : pyridine : water (6:4:3), respectively, for a glucoside present in *E. pumilum* DC. and *E. rupestre* DC. *f. aurantiacum*. There can be little doubt that this glucoside is glucoerypestrin.

A detailed account of the present work, together with some biogenetic considerations, will form the subject of a forthcoming publication.

Microanalyses were performed in this laboratory by Mr. P. Hansen. The work is part of investigations supported by *Statens Almindelige Videnskabsfond (The Danish State Research Foundation)* and *Carlsbergfondet (The Carlsberg Foundation)*. A special grant from *Kai Hansens Fond* is gratefully acknowledged.

1. Kjær, A. and Gmelin, R. *Unpublished results.*
2. Nagata, W., Tamm, C. and Reichstein, T. *Helv. Chim. Acta* **40** (1957) 41.
3. Kjær, A., Gmelin, R. and Boe Jensen, R. *Acta Chem. Scand.* **10** (1956) 432.
4. Schultz, O.-E. and Wagner, W. *Arzneimittel-Forsch.* **6** (1956) 647.
5. Kjær, A. and Rubinstein, K. *Acta Chem. Scand.* **7** (1953) 528.
6. Späth, E., Kuffner, F. and Platzer, N. *Ber* **68** (1935) 497.
7. Ettlinger, M. G. and Lundeen, A. J. *J. Am. Chem. Soc.* **78** (1956) 4172.
8. Schultz, O.-E. and Wagner, W. *Z. Naturforsch.* **11b** (1956) 73.

* No physical constants or analyses of this salt can be found in the literature, although it appears that Späth *et al.*[6] have employed the compound for further syntheses.

** The stereochemistry of the oxime linkage has not yet been definitely established.

Received February 27, 1957.

Silicon Determination in Low-Boiling Organosilicon Compounds by Acid Digestion

BENGT SMITH

Institutionen för Organisk Kemi, Chalmers Tekniska Högskola, Göteborg, Sweden

Several methods have been proposed for the quantitative determination of silicon in organosilicon compounds *. The best analytical method from the standpoint of accuracy is considered to be the acid digestion method [1]. The compound is oxidized generally by fuming sulphuric acid alone or mixed with fuming nitric acid and the residual silicon dioxide weighed. It is usual to carry out the oxidation either in a Kjeldahl flask with the mouth closed by a glass balloon or in a crucible [2]. The former technique is applicable to compounds with boiling points even below 100° C (*cf.* Ref.[2] pp. 54 and 143). The latter method is best suited to high-boiling compounds or resinous polymers, because of the losses of material which can easily take place during the initial oxidation period. This limitation to the crucible method is regrettable since from the standpoint of speed and simplicity it is superior to the Kjeldahl method. The present paper is a description of an adaption of the crucible method to the analysis of low-boiling organosilicon compounds.

The new method might be called "the double crucible method" since two transparent quarts crucibles, volumes 10 and 50 ml, respectively, are used (Fig. 1). The empty crucibles are heated over a Meker burner for 15 min and then weighed. The inner crucible is filled with a mixture of 2 ml of 60 % fuming sulphuric acid and 2 ml of fuming nitric acid (d = 1.50) and cooled in iced water. The substance (calculated to give about 0.05 g of silicon dioxide) is weighed in a sealed glass ampoule. The tip of the ampoule is broken and the ampoule immediately placed in the acide-filled crucible as shown by Fig. 1. The substance is slowly driven out of the ampoule by heating the top with a small flame. The comparatively large depth reduces the risk of any material escaping through the layer of acid. As soon as the ampoule is empty the heating of the crucibles is begun using a low flame. The heating must be done carefully until the sample has frothed. Most types of organosilicon compounds froth violently on digestion with a mixture of sulphuric and nitric acid, and the flame must be removed until the frothing has subsided. This tendency to froth has led to the use of the outer larger crucible which catches any overflow from the small crucible. The heating is continued until the crucibles are dry and they are heated finally over a Meker burner to constant weight. Half an hour is generally enough. Residual silicon dioxide is calculated back to silicon in the original sample.

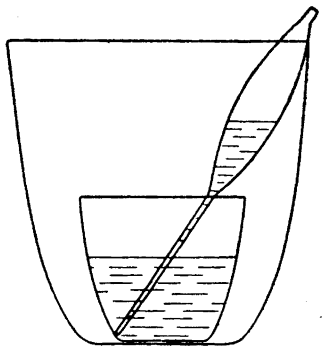


Fig. 1. Arrangement for acid digestion.

This method is also suited to the analysis of organosilicon compounds which react violently with the acid digestion mixture *e. g.* certain aminosilanes and silazanes. Table 1 contains analytical values for trimethylethoxysilane and hexamethyldisiloxane which cannot be analysed using the ordinary crucible method (*cf.* Ref. [1]).

Table 1. Analysis values, using the "double crucible method".

Compound	B. p. °C (760 mm)	% Si	
		Found	Calc.
Hexamethyldisiloxane	100	34.56 34.41	34.60
Trimethylethoxysilane	75	23.83 23.88	23.75

* A review has been given by McHard *et al.*[1]

The success of the present method depends on the following conditions which differ from those in the ordinary crucible method. The substance is weighed in an ampoule, a stronger oxidising acid mixture is used, which is cooled at the start of the reaction, a comparatively thick layer of acid hinders material from escaping, and the large outer crucible diminishes the risk of spoiling the analysis by the frothing of the mixture. As the volume of the acid mixture is kept small by the use of the inner crucible the time required for the expulsion of the acid fumes is shortened too.

1. McHard, J. A., Servais, P. C. and Clark, N. A. *Anal. Chem.* **20** (1948) 325.
2. Smith, B. *Kiselorganiska Studier* (Diss.) Gothenburg 1951.

Received March 19, 1957.

A New Synthesis of Selenanthren-5,10-dioxide

GÖRAN BERGSON

Chemical Institute, University of Uppsala, Sweden

Selenanthren-5,10-dioxide (IV) is of considerable theoretical interest because it might exist in a *cis-* and a *trans*-form if there is a pyramidal configuration at the selenium atom. Neither optical nor geometrical isomerism has been demonstrated for selenoxides in spite of several attempts[1]. Recently Gould and McCullough [2] suggested that *cis-trans* isomerism was to be expected for 1,4-di-selenane-1,4-dioxide. Owing to the great difficulties in the synthesis of 1,4-diselenane its oxidation products were never prepared. Following a suggestion of professor Arne Fredga the present author started an investigation of the oxides of selenanthren (I). Since then Gould and Burlant [3] have reported very promising results of a study of 1,4-diselenane. They have prepared a 1,4-dioxide and will determine its structure by X-ray methods.

The present paper describes a new synthesis of selenanthren-5,10-dioxide. A detailed report of the studies of selenanthren oxides and thianthren oxides will be published elsewhere.

Selenanthren-5,10-dioxide was first prepared by Krafft and Kaschau [4] by the oxidation of selenanthren with nitric acid. In 1951 Cullinane [5] reported a modification of the same method, and established the melting point to be 265°. He also characterized a hydrate and a dihydrochloride of IV. The present author has prepared selenanthren-5,10-dioxide in a way represented by the reaction scheme below.

The dioxide obtained by this method is identical with the product of Cullinane, as has been shown by IR-spectra (Fig. 1) and mixed melting points. The peak at 13.05 μ is due to out-of-plane vibration of the hydrogen atoms in the benzene nucleus,

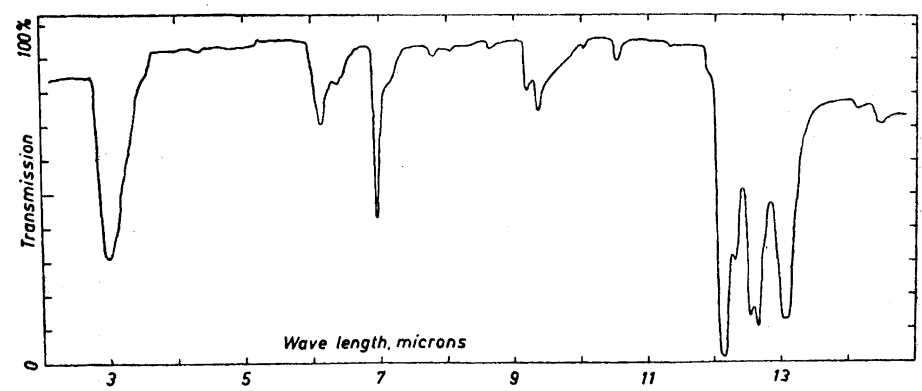


Fig. 1. Infrared absorption spectrum of selenanthren-5,10-dioxide in pressed KBr. Perkin Elmer model 21 spectrometer with NaCl prism.

The success of the present method depends on the following conditions which differ from those in the ordinary crucible method. The substance is weighed in an ampoule, a stronger oxidising acid mixture is used, which is cooled at the start of the reaction, a comparatively thick layer of acid hinders material from escaping, and the large outer crucible diminishes the risk of spoiling the analysis by the frothing of the mixture. As the volume of the acid mixture is kept small by the use of the inner crucible the time required for the expulsion of the acid fumes is shortened too.

1. McHard, J. A., Servais, P. C. and Clark, N. A. *Anal. Chem.* **20** (1948) 325.
2. Smith, B. *Kiselorganiska Studier* (Diss.) Gothenburg 1951.

Received March 19, 1957.

A New Synthesis of Selenanthren-5,10-dioxide

GÖRAN BERGSON

Chemical Institute, University of Uppsala, Sweden

Selenanthren-5,10-dioxide (IV) is of considerable theoretical interest because it might exist in a *cis-* and a *trans*-form if there is a pyramidal configuration at the selenium atom. Neither optical nor geometrical isomerism has been demonstrated for selenoxides in spite of several attempts[1]. Recently Gould and McCullough [2] suggested that *cis-trans* isomerism was to be expected for 1,4-di-selenane-1,4-dioxide. Owing to the great difficulties in the synthesis of 1,4-diselenane its oxidation products were never prepared. Following a suggestion of professor Arne Fredga the present author started an investigation of the oxides of selenanthren (I). Since then Gould and Burlant [3] have reported very promising results of a study of 1,4-diselenane. They have prepared a 1,4-dioxide and will determine its structure by X-ray methods.

The present paper describes a new synthesis of selenanthren-5,10-dioxide. A detailed report of the studies of selenanthren oxides and thianthren oxides will be published elsewhere.

Selenanthren-5,10-dioxide was first prepared by Krafft and Kaschau [4] by the oxidation of selenanthren with nitric acid. In 1951 Cullinane [5] reported a modification of the same method, and established the melting point to be 265°. He also characterized a hydrate and a dihydrochloride of IV. The present author has prepared selenanthren-5,10-dioxide in a way represented by the reaction scheme below.

The dioxide obtained by this method is identical with the product of Cullinane, as has been shown by IR-spectra (Fig. 1) and mixed melting points. The peak at 13.05 μ is due to out-of-plane vibration of the hydrogen atoms in the benzene nucleus,

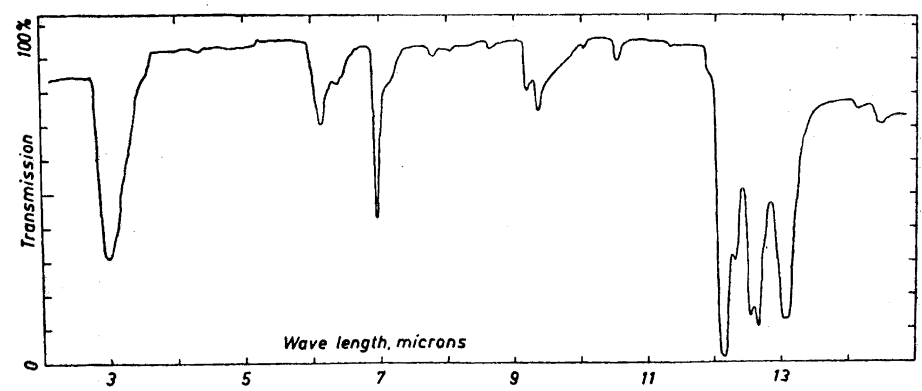
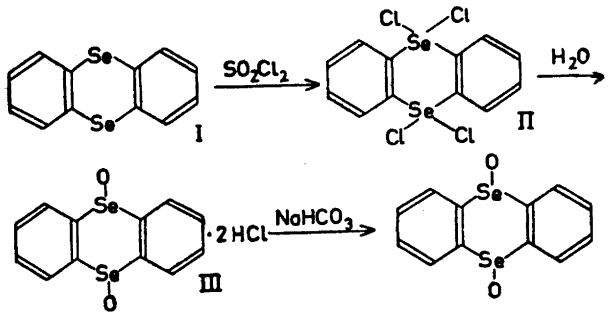


Fig. 1. Infrared absorption spectrum of selenanthren-5,10-dioxide in pressed KBr. Perkin Elmer model 21 spectrometer with NaCl prism.



and the peaks at 12.15, 12.32, 12.55 and 12.65 μ must be due to the presence of the Se-O groups. (IR-spectra of selenoxides have not been described in the literature.) A comparison of this peak system with the characteristic absorption peaks for S—O in the *trans-* and *cis*-form of thianthren-5, 10-dioxide suggests that the selenoxide is not a pure *trans-* form but rather a *cis*-form or a mixture of both or perhaps a dioxide with planar configuration [6].

Experimental: Selenanthren-5,5-10,10-tetrachloride (II). To a solution of 1.55 g of selenanthren in 100 ml of dry benzene, 5.0 g (excess) of SO_2Cl_2 in 50 ml of benzene was added. The mixture was boiled under reflux for 30 min. The tetrachloride separated as a yellow fine crystalline solid. About 70 ml of benzene was then removed by distillation, and from the cooled reaction mixture the tetrachloride was obtained by filtration. It was washed with dry benzene and then dried in vacuum, m. p. 208—209.5° (decomp.). Yield 2.10 g (89 %). (Found: Se 34.3; 34.7; Cl 31.3. Calc. for $C_{12}H_8Se_2Cl_4$: Se 34.9; Cl 31.4).

Selenanthren - 5,10 - dioxide dihydrochloride (III). 2.00 g of selenanthren tetrachloride was hydrolysed with 100 ml of boiling water. After filtration and evaporation the dihydrochloride was obtained as a white solid in quantitative yield, m. p. 228—229° (decomp.). (Found: Se 38.1; Cl 17.1. Calc. for $C_{12}H_8O_2Se_4 \cdot 2HCl$: Se 38.4; Cl 17.1).

Selenanthren-5,10-dioxide (IV). 1.25 g of selenanthren-5,10-dioxide dihydrochloride was dissolved in 100 ml of water. 0.56 g of $NaHCO_3$ was added and the solution evaporated on a water bath. The residue was extracted with 100 ml of boiling chloroform and after evaporation the crude dioxide (m. p. 256—258°) was obtained in quantitative yield. This product was washed with 50 ml of ether and 15 ml of water and then recrystallized from water. The dioxide separated on cooling as a hydrate which was dried to constant weight at 120°. In this way selenanthren-5,10-dioxide with m. p. 264—265° (decomp.) was obtained. Yield 0.68 g (66 %). (Found: Se 46.3. Calc. for $C_{12}H_8O_2Se_4$: Se 46.2). The selenium analyses have been carried out according to Fredga [7].

Thanks are due to Mr. Stig Bergwall for technical assistance with the IR-spectra. A grant from the *Swedish Natural Science Rese-Research Council* is gratefully acknowledged.

1. Campbell, T. W., Walker, H. G. and Coppinger, G. M. *Chem. Revs.* **50** (1952) 335.
2. Gould, E. S. and McCullough, J. D. *J. Am. Chem. Soc.* **73** (1951) 1105.
3. Gould, E. S. and Burlant, Wm. *J. Am. Chem. Soc.* **78** (1956) 5825.
4. Krafft, F. and Kaschau, A. *Ber.* **29** (1896) 443.
5. Cullinane, N. M. *J. Chem. Soc.* **1951** 237.
6. Bergson, G. *To be published.*
7. Fredga, A. *Diss. Uppsala Universitets Årsskrift* 1935:5, p. 16.

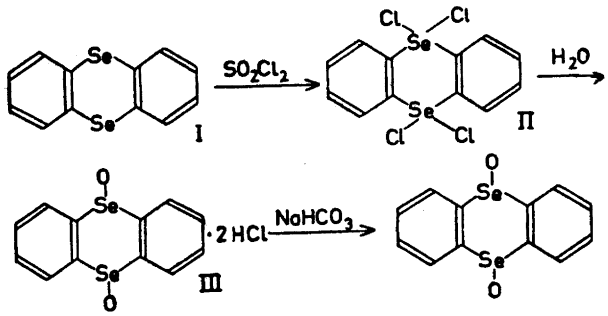
Received March 20, 1957.

Preparation of Lithium Azide

NIELS HOFMAN-BANG

Chemistry Department A, Technical University of Denmark, Copenhagen, Denmark

The most common methods for the preparation of lithium azide, LiN_3, are interaction of lithium sulfate and barium azide, and, especially, neutralization of aqueous hydrazoic acid with lithium hydroxide. Considering that preparation and handling of hydrazoic acid require care, it occurred to me that sodium azide and



and the peaks at 12.15, 12.32, 12.55 and 12.65 μ must be due to the presence of the Se-O groups. (IR-spectra of selenoxides have not been described in the literature.) A comparison of this peak system with the characteristic absorption peaks for S—O in the *trans-* and *cis*-form of thianthren-5, 10-dioxide suggests that the selenoxide is not a pure *trans-* form but rather a *cis*-form or a mixture of both or perhaps a dioxide with planar configuration [6].

Experimental: Selenanthren-5,5-10,10-tetrachloride (II). To a solution of 1.55 g of selenanthren in 100 ml of dry benzene, 5.0 g (excess) of SO_2Cl_2 in 50 ml of benzene was added. The mixture was boiled under reflux for 30 min. The tetrachloride separated as a yellow fine crystalline solid. About 70 ml of benzene was then removed by distillation, and from the cooled reaction mixture the tetrachloride was obtained by filtration. It was washed with dry benzene and then dried in vacuum, m. p. 208—209.5° (decomp.). Yield 2.10 g (89 %). (Found: Se 34.3; 34.7; Cl 31.3. Calc. for $C_{12}H_8Se_2Cl_4$: Se 34.9; Cl 31.4).

Selenanthren - 5,10 - dioxide dihydrochloride (III). 2.00 g of selenanthren tetrachloride was hydrolysed with 100 ml of boiling water. After filtration and evaporation the dihydrochloride was obtained as a white solid in quantitative yield, m. p. 228—229° (decomp.). (Found: Se 38.1; Cl 17.1. Calc. for $C_{12}H_8O_2Se_4 \cdot 2HCl$: Se 38.4; Cl 17.1).

Selenanthren-5,10-dioxide (IV). 1.25 g of selenanthren-5,10-dioxide dihydrochloride was dissolved in 100 ml of water. 0.56 g of $NaHCO_3$ was added and the solution evaporated on a water bath. The residue was extracted with 100 ml of boiling chloroform and after evaporation the crude dioxide (m. p. 256—258°) was obtained in quantitative yield. This product was washed with 50 ml of ether and 15 ml of water and then recrystallized from water. The dioxide separated on cooling as a hydrate which was dried to constant weight at 120°. In this way selenanthren-5,10-dioxide with m. p. 264—265° (decomp.) was obtained. Yield 0.68 g (66 %). (Found: Se 46.3. Calc. for $C_{12}H_8O_2Se_4$: Se 46.2). The selenium analyses have been carried out according to Fredga [7].

Thanks are due to Mr. Stig Bergwall for technical assistance with the IR-spectra. A grant from the *Swedish Natural Science Rese-Research Council* is gratefully acknowledged.

1. Campbell, T. W., Walker, H. G. and Coppinger, G. M. *Chem. Revs.* **50** (1952) 335.
2. Gould, E. S. and McCullough, J. D. *J. Am. Chem. Soc.* **73** (1951) 1105.
3. Gould, E. S. and Burlant, Wm. *J. Am. Chem. Soc.* **78** (1956) 5825.
4. Krafft, F. and Kaschau, A. *Ber.* **29** (1896) 443.
5. Cullinane, N. M. *J. Chem. Soc.* **1951** 237.
6. Bergson, G. *To be published.*
7. Fredga, A. *Diss. Uppsala Universitets Årsskrift* 1935:5, p. 16.

Received March 20, 1957.

Preparation of Lithium Azide

NIELS HOFMAN-BANG

Chemistry Department A, Technical University of Denmark, Copenhagen, Denmark

The most common methods for the preparation of lithium azide, LiN_3, are interaction of lithium sulfate and barium azide, and, especially, neutralization of aqueous hydrazoic acid with lithium hydroxide. Considering that preparation and handling of hydrazoic acid require care, it occurred to me that sodium azide and

lithium sulfate, which is generally kept on stock in a laboratory, might interact to give lithium azide and sodium sulfate.

The four salts in question are all soluble in water. Lithium azide is soluble and sodium azide is sparingly soluble in ethanol (0.22 g NaN_3 per 100 g at 0 °C), while lithium and sodium sulfate are insoluble. Even in 75—80 % ethanol the solubilities of lithium and sodium sulfate are very small. Based on these facts the following method of preparation has been worked out:

1.30 g of sodium azide and 1.41 g of lithium sulfate, Li_2SO_4, H_2O, which is 10 % in excess, are dissolved in 7 ml of water by shaking and gentle heating. 35 ml of ordinary 96 % ethyl alcohol are now added in a thin stream, while stirring with a spatula. After 10 min (it has been ascertained that a longer time is of no effect) the mixture is filtered. The precipitate, which consists of sodium and lithium sulfate, is washed with a few ml of ethanol, and the filtrate plus the washing liquid is evaporated on a water bath to near dryness. Finally, it is dried at 80 °C in a drying oven. The theoretical yield of lithium azide is 0.98 g, while actually 1.02—1.04 g is obtained. This raw product contains no sulfate but a few per cent of sodium. It can be purified by 2 min digestion with 10 ml 96 % ethanol at about 35 °C, filtering the undissolved sodium azide, and evaporating and drying as above. The yield is usually *ca.* 0.6 g lithium azide of a purity not less than 99.5 %. It contains a slight trace of organic material due to the use of ethyl alcohol.

The purified lithium azide has been analyzed by two methods. The content of azide has been determined according to Martin [1] by oxidation with Ce(IV). Analysis of two products of lithium azide gave 99.5 % and 99.5 %. The same two products were analyzed by conversion to lithium sulfate and weighing [2]. The results were 100.2 % and 99.7 % lithium azide, respectively. Thus it seems that the prepared lithium azide is slightly "basic" due to loss of hydrazoic azid when evaporating.

1. Martin, J. *J. Am. Chem. Soc.* **49** (1927) 2133.
2. Fresenius, R. and Jander, G. *Handbuch der analytischen Chemie III, Ia*, Springer, Berlin 1940, p. 3.

Received March 20, 1957.

The Rearrangement of *cis*-2-en-4:6-diyn-oic Acids to $\alpha\beta$-Unsaturated γ-Lactones

PER KOCH CHRISTENSEN

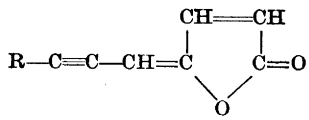
Sintef, Norges Tekniske Høgskole, Trondheim, Norway

The so called "Composit-Cumulene I" originally reported by Sørensen and Stavholt [1] was given the structural formula I

$$CH_3—CH_2—CH_2—CH_3—CH_2—CH=C=C=CH—COOCH_3 \qquad I$$

based on the UV-absorption and the hydrogenation to a hexahydro derivative with an odour of strawberry like methyl caprate.

A reinvestigation of this compound isolated from scentless mayweed *(Matricaria inodora* L.) showed that the substance contained a disubstituted acetylenic bond (2 190 cm^{-1}) and the carbonyl frequency (1 793 and 1 765 cm^{-1}) indicated a five-ring lactone. Hydrogenation with $Pd/BaSO_4$ showed a consumption of 5 moles of hydrogen and the product was a saturated five-ring lactone with carbonyl frequency at 1 786 cm^{-1}. The formula accordingly had to be revised [2,3] and the substance was found to be the lactone II (R = *cis* $CH_3—CH=CH—$)



II

The formation of this type of lactone from the free 2-*cis*-acid III was first observed when III ($R=CH_3C\equiv C-C\equiv C-$) was treated with dilute sodium hydrogencarbonate [3]

$$R—C\equiv C—CH=CH—COOH \qquad III$$

On measuring the ultra-violet absorption of an alcoholic solution of *cis*:*cis* matricaria acid III ($R=CH_3CH=CH-C\equiv C-$) in a UV-recorder (Beckman DK) it was noticed that on scanning the spectrum of two solutions with different concentrations, the absorption curve was markedly different the second time. The long wave-

lithium sulfate, which is generally kept on stock in a laboratory, might interact to give lithium azide and sodium sulfate.

The four salts in question are all soluble in water. Lithium azide is soluble and sodium azide is sparingly soluble in ethanol (0.22 g NaN_3 per 100 g at 0 °C), while lithium and sodium sulfate are insoluble. Even in 75—80 % ethanol the solubilities of lithium and sodium sulfate are very small. Based on these facts the following method of preparation has been worked out:

1.30 g of sodium azide and 1.41 g of lithium sulfate, Li_2SO_4, H_2O, which is 10 % in excess, are dissolved in 7 ml of water by shaking and gentle heating. 35 ml of ordinary 96 % ethyl alcohol are now added in a thin stream, while stirring with a spatula. After 10 min (it has been ascertained that a longer time is of no effect) the mixture is filtered. The precipitate, which consists of sodium and lithium sulfate, is washed with a few ml of ethanol, and the filtrate plus the washing liquid is evaporated on a water bath to near dryness. Finally, it is dried at 80 °C in a drying oven. The theoretical yield of lithium azide is 0.98 g, while actually 1.02—1.04 g is obtained. This raw product contains no sulfate but a few per cent of sodium. It can be purified by 2 min digestion with 10 ml 96 % ethanol at about 35 °C, filtering the undissolved sodium azide, and evaporating and drying as above. The yield is usually *ca.* 0.6 g lithium azide of a purity not less than 99.5 %. It contains a slight trace of organic material due to the use of ethyl alcohol.

The purified lithium azide has been analyzed by two methods. The content of azide has been determined according to Martin [1] by oxidation with Ce(IV). Analysis of two products of lithium azide gave 99.5 % and 99.5 %. The same two products were analyzed by conversion to lithium sulfate and weighing [2]. The results were 100.2 % and 99.7 % lithium azide, respectively. Thus it seems that the prepared lithium azide is slightly "basic" due to loss of hydrazoic azid when evaporating.

1. Martin, J. *J. Am. Chem. Soc.* **49** (1927) 2133.
2. Fresenius, R. and Jander, G. *Handbuch der analytischen Chemie III, Ia*, Springer, Berlin 1940, p. 3.

Received March 20, 1957.

The Rearrangement of *cis*-2-en-4:6-diyn-oic Acids to $\alpha\beta$-Unsaturated γ-Lactones

PER KOCH CHRISTENSEN

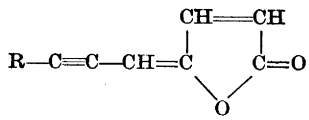
Sintef, Norges Tekniske Høgskole, Trondheim, Norway

The so called "Composit-Cumulene I" originally reported by Sørensen and Stavholt [1] was given the structural formula I

$$CH_3—CH_2—CH_2—CH_3—CH_2—CH=C=C=CH—COOCH_3 \qquad I$$

based on the UV-absorption and the hydrogenation to a hexahydro derivative with an odour of strawberry like methyl caprate.

A reinvestigation of this compound isolated from scentless mayweed *(Matricaria inodora* L.) showed that the substance contained a disubstituted acetylenic bond (2 190 cm^{-1}) and the carbonyl frequency (1 793 and 1 765 cm^{-1}) indicated a five-ring lactone. Hydrogenation with $Pd/BaSO_4$ showed a consumption of 5 moles of hydrogen and the product was a saturated five-ring lactone with carbonyl frequency at 1 786 cm^{-1}. The formula accordingly had to be revised [2,3] and the substance was found to be the lactone II (R = *cis* $CH_3—CH=CH—$)



II

The formation of this type of lactone from the free 2-*cis*-acid III was first observed when III ($R=CH_3C\equiv C-C\equiv C-$) was treated with dilute sodium hydrogencarbonate [3]

$$R—C\equiv C—CH=CH—COOH \qquad III$$

On measuring the ultra-violet absorption of an alcoholic solution of *cis*:*cis* matricaria acid III ($R=CH_3CH=CH-C\equiv C-$) in a UV-recorder (Beckman DK) it was noticed that on scanning the spectrum of two solutions with different concentrations, the absorption curve was markedly different the second time. The long wave-

length absorption had shifted to longer wave-lengths with stronger intensity while the short wave-length absorption (~ 2 570 Å) had undergone a hypsochromic shift with lower intensity. This phenomenon was further investigated, and it turned out that on dissolving *cis:cis* matricaria acid in a solvent containing water, in this case 95 % ethanol, the rearrangement free acid → lactone took place spontaneously. In absolute ethanol (~ 99.8 %) the speed of reaction was very much slower.

A solution of the free acid in dry tetrahydrofuran was stable and the UV-absorption was quite similar to a solution in hexane. Addition of distilled water to the tetrahydrofuran immediately caused rearrangement to the lactone.

Working in a mixture of tetrahydrofuran and buffers (1:1) the reaction took place with a measurable speed in the interval pH ~ 4.5 – 11. Above pH ~ 11 also other reactions occurred and the product was no longer pure. Measurement of reaction velocities by means of UV-absorption was impossible.

In the interval pH ~ 6 – 11 the rate of reaction was approximately constant. The reaction appeared to be of first order with half-times of ~3.5 min at 30 °C and ~ 11 min at 20 °C. Below pH ~ 6 the rate decreased rapidly.

The same rearrangement in water-containing solvents has been followed starting

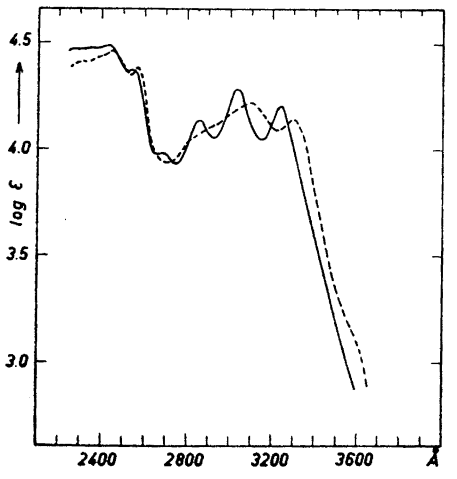


Fig. 1. 2-*trans* Matricaria acid, — — — in dry tetrahydrofuran; ——— in tetrahydrofuran-water (10:1).

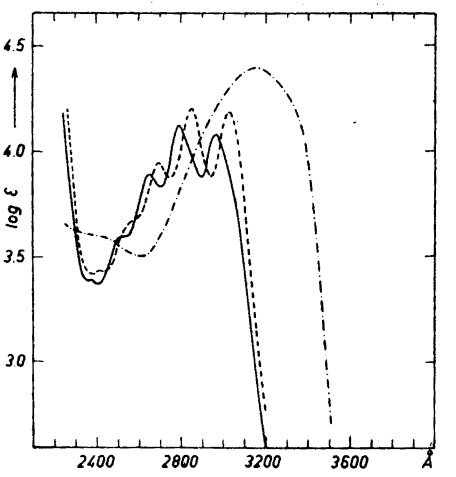
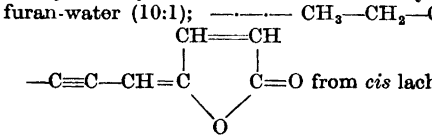


Fig. 2. trans Lachnophyllum acid, — — — in dry tetrahydrofuran; ——— in tetrahydrofuran-water (10:1); —·—·— $CH_3—CH_2—CH_2$



from *cis* lachnophyllum acid.

with *cis* lachnophyllum acid (III, R = $CH_3—CH_2—CH_2—C≡C—$). According to Ref.[3] it also takes place with *cis* dehydro matricaria acid (III, R = $CH_3—C≡C—C≡C—$) at pH = 8.4. Other substances have not yet been tried.

When the rearrangement was followed in the UV-recorder with rapid successive scannings of the spectrum, it turned out that with the *cis:cis* matricaria acid no direct transformation from the free acid spectrum to the lactone spectrum took place, but some intermediate absorption with more pronounced fine structure (Fig. 3, curve 1) was observed. The transformation from the normal free acid spectrum to this spectrum took place in less than 0.5 min.

In order to be able to make a reasonable guess as to the origin of the absorption of this compound, some 2-*trans* matricaria acid was dissolved in tetrahydrofuran with water. This acid is incapable of forming a lactone for steric reasons and gave immediately after having been dissolved (< 0.5 min) a spectrum entirely different

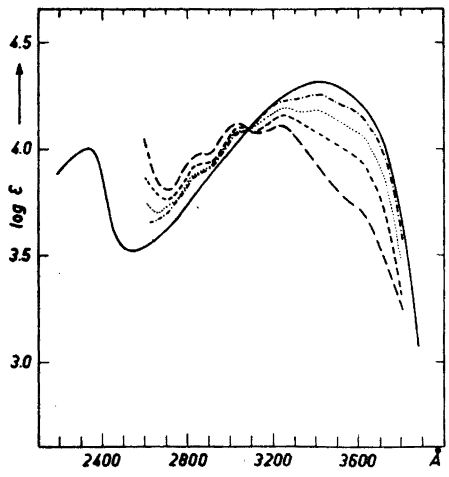


Fig. 3. Rearrangement of di *cis* matricaria acid in 95 % ethanol. *Curve 1:* – – – 0.5—3.5 min after dissolving the acid, start at long wavelengths. *Curve 2:* ——— 80 min after dissolving the acid, total lactone formation. Other curves measured at intermediate times.

from that of the acid dissolved in hexane or dry tetrahydrofuran. In these two solvents the spectrum of the 2-*trans* acid (Fig. 1) was very similar to the spectrum of both the 2-*trans* and the 2-*cis*-ester with no marked fine structure in the long wavelength area (2 800—3 400 Å). When dissolved in tetrahydrofuran with water (10:1) a marked fine-structure developed with bands at 2 850, 3 035 and 3 240 Å (Fig. 1). The 2-*trans* lachnophyllum acid gave the same overall picture with a shift from 2 690, 2 850 and 3 025 Å in dry tetrahydrofuran to 2 645, 2 790 and 2 965 Å in tetrahydrofuran-water (10:1) (Fig. 2).

The substances *trans* ($HC{\equiv}C-CH=CH-COOH$ and *trans* $(-C{\equiv}C-CH=CH-COOH)_2$ gave the same shift to shorter wavelengths, although less pronounced.

When 2-*cis*-matricaria acid is dissolved in 0.01 N ethanolic H_2SO_4, there is no formation of the fine-structure spectrum.

If samples are withdrawn at certain time intervals from a solution of the *cis*-acid in 95 % ethanol the reaction can be stopped with acid. Analysis of these samples in UV now gives as result a set of curves where the intermediate curves between pure acid and pure lactone are mixtures of the normal acid spectrum and the lactone spectrum.

At present it is not possible to give a detailed reaction mechanism, but from the spectral studies two general routes are possible:

A: Fine-structure complex ⇌ free acid → lactone

B: Free acid ⇌ fine-structure complex → lactone

The choice between the two must await more detailed studies, the most probable is apparently B. If, in B, the equilibrium acid ⇌ complex is over to the right, there would be an apparent isosbestic point [4] in the UV-curves from the reaction fine-structure complex → lactone. (Fig. 3).

Holman and Sørensen [5] reported in 1950 some spectral and oxidation studies on matricaria ester and the free acid. Their curve for the UV-absorption of the acid in ethanol can now be interpreted as being the curve for a mixture of the free acid and the lactone formed from it. The sharp maximum at ~ 2 580 Å in the pure free acid been reduced and indicates a fairly large amount of lactone formation. The maximum at 3 250 Å corresponds to the rapidly developed maximum in solvents containing water.

This work is in progress and further results will be published elsewhere.

The author thanks Prof. N. A. Sørensen for his interest and *Norges Teknisk-Naturvitenskaplige Forskningsråd* for financial support.

1. Sørensen, N. A. and Stavholt, K. *Acta Chem. Scand.* **4** (1950) 1080.
2. Christensen, P. K. *Det 9. Nordiske Kemikermøde*, Aarhus 1956.
3. Christensen, P. K., Sørensen, N. A., Bell, I., Jones, E. R. H. and Whiting, M. C. *Festschrift Prof. Dr. Arthur Stoll*, Basel 1957, p. 545.
4. Schläfer, H. L. and Kling, O. *Angew. Chem.* **68** (1956) 667.
5. Holman, R. T. and Sørensen, N. A. *Acta Chem. Scand.* **4** (1950) 416.

Received March 12, 1957.

ACTA CHEMICA SCANDINAVICA 11 (1957) 585—589

Autoradiographic Studies on the Effect of Cathodic Prepolarization on Metallic Surfaces

M. A. EL GUEBELY*

Curie Laboratory, Paris, France

The effect of cathodic prepolarization of platinum, gold and silver electrodes has been studied. It has been found in all cases that the velocity of the spontaneous deposition of Po is greater on a prepolarized than on a non-polarized electrode. Studies of the histograms of the α-particles of Po showed a relative increase of the apparently shortened trajectories in case of the previously polarized electrodes.

The effect of prepolarization on the process of electro-deposition of radio-elements was noticed by Haissinsky [1] in a study of the cathodic deposition of ThC on a gold electrode. The curve representing the quantity deposited in function of time manifested a maximum which indicated the possibility of a change of the state of the cathodic surface during electrolysis. In fact he noticed moreover that if the electrolysis is carried out under the same conditions, using a fresh electrode in a solution exempt from the radio-element, and then the radio-element is added while continuing the electrolysis, the maximum disappears and the deposition curve has a normal form. Since then the same author and his collaborators studied different aspects of this interesting phenomenon. Danon and Haissinsky [2] have indicated that the Nernst law is not applicable to the deposit of RaE (10^{-16} M) on a gold cathode in nitric acid solution except after prepolarization of the electrode. Haissinsky and Coche [3] have found, in the case of the cathodic deposition of Po on tantalum, a modification in the form of the deposition curve as well as a displacement of the critical deposition potential towards more positive values as a result of the prepolarization of the electrodes. Ferradini [4] has observed a spontaneous deposit of Pa on platinised platinum which was prepolarized anodically. Finally our recent studies [5] on Rd-Ru have shown that prepolarization of the cathode plays a decisive role on the electro-deposition of this radio-element. In all cases studied, except for platinised platinum, there is practically no

* Present address: Egyptian Atomic Energy Commission, El-Dokky, Cairo.

deposit at ordinary temperature without prepolarization, while after prepolarization under favourable conditions practically quantitative deposits can be obtained.

The object of this study is to provide a direct evidence of the modification of the metallic surface produced by the cathodic prepolarization of metallic electrodes.

EXPERIMENTAL

In the present work we have used the autoradiographic method which has been previously utilized by Haissinsky *et al.*[6] in their studies of the metallic surfaces.

In our experiments we have studied the spontaneous deposit of Po on prepolarized and non-polarized platinum, gold and silver electrodes. All the electrodes were pure and electro-polished thin metallic foils. They were further purified chemically. Platinum electrodes were ignited in an oxidising flame and then boiled with concentrated nitric acid while gold electrodes received the nitric acid treatment only. Silver electrodes were purified by introducing them rapidly for a few times in 50 % HNO_3. The water used for washings and preparation of solutions was bidistilled and different reagents were of analytical purity.

Prepolarization was effected by electrolysing 10 ml of N H_2SO_4 using these electrodes as cathodes while separating the cathodic from the anodic compartments by an appropriate electrolytic bridge. The anode was a thin platinum wire. Concerning conditions of prepolarization, *cf.* Table 1.

Table 1. Conditions of prepolarization.

Metal	Current density (in mA/cm²)	Time, h	Temperature, °C	Approximate cathode potential, V
Pt	500	5	85	−2
Au	2.7−1.3	48	ordinary	−0.6
Ag	2−1	48	ordinary	−0.7

Each polarized electrode was washed and introduced together with a non-polarized foil into 10 ml of a normal sulphuric acid, 10^{-12} N in Po, for 20 h. The solution was stirred mechanically while the two foils were kept at equal distance from the stirrer. Each foil was washed and dried and an α-nuclear plate, Ilford C_2 50 microns then applied for an hour to the surface that was opposite to the stirrer. The plates were then developed by the appropriate photographic technique [7] and then examined under a microscope.

RESULTS

The microscopic examination of the nuclear plates consisted of establishing the topographic distribution of the trajectories of the α-rays on the metallic surface, by counting their number per field of vision of the microscope (150 fields studied for each plate) and by measuring the ranges of the α-particles in the gelatine (300 per plate). In these studies we have limited our measurements of ranges to the horizontal tracks, *i. e.* those for which practically the total length is visible for the same focussing.



Fig. 1. Prepolarized Pt foil.

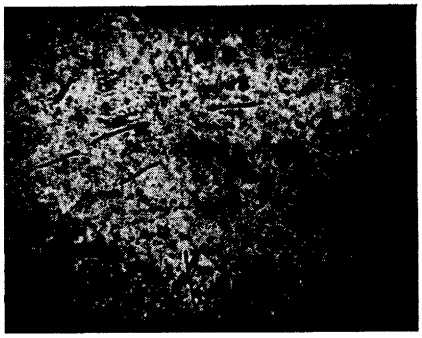


Fig. 2. Non-polarized Pt-foil.

Our results show that:

a) The tracks are distributed in all cases at random. No priviliged accumulation of the deposited Po atoms was found at certain points of the surface, as was found [6] in case of Po in HNO_3 and ^{239}Pu and ^{235}U in hydrochloric and nitric acids, respectively [8].

b) The velocity of the spontaneous deposition of Po is always greater on a prepolarized than on a non-polarized foil, the ratio between the two velocities being 2 for Pt, 1.64 for Au and 1.75 for Ag.

Figs. 1 and 2 represent, for example, two fields of vision, the first for a prepolarized Pt foil and the other for a non-polarized one.

c) The curves A and B of Figs. 3, 4 and 5 represent the distribution of the ranges of the α-particles of the spontaneously deposited Po atoms on Pt, Au and Ag foils, respectively; A for the non-polarized foils and B for the prepolarized ones.

DISCUSSION

The results obtained indicate that the most probable range of the α-particles of Po in Ilford C_2 plates is 21 ± 1 μ which is in good agreement with the value found previously [6].

The study of the histograms in Figs. 3, 4 and 5 representing the distribution of the ranges of the α-particles of Po shows that the curves are deformed in the case of the prepolarized foils. This deformation corresponds to a relative increase of the apparently shortened ranges. Apparent shortening of the ranges of the α-particles of Po spontaneously or electrolytically deposited on metallic surfaces has been attributed by Haissinsky *et al.*[6] to penetration of a certain number of Po atoms into the surface. In a recent work [8] on the adsorption of Pu on glass and metallic surfaces we admitted that back-scattering of the α-particles from the carrying surface may, together with the penetration factor,

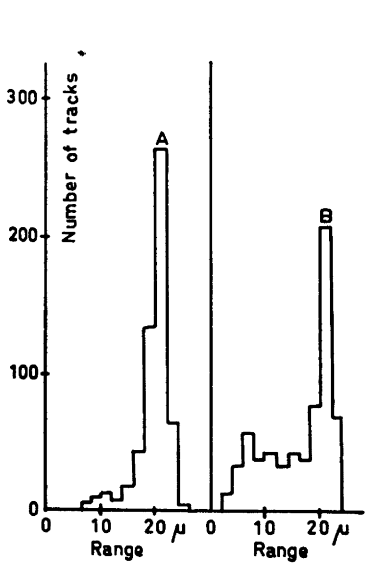


Fig. 3. Histograms of α-particles of Po on platinum foils.

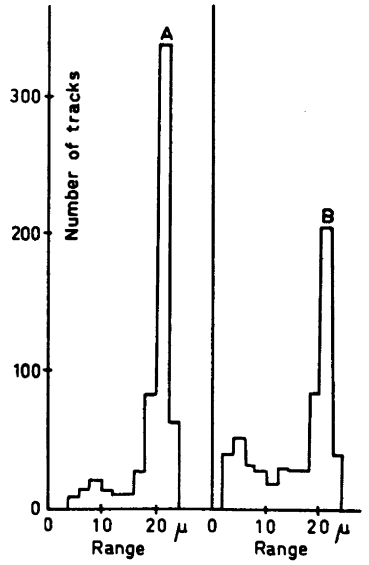


Fig. 4. Histograms of α-particles of Po on gold foils.

play a role in the phenomenon of apparent shortening. However, the observed increase in the apparent shortening in case of prepolarized electrodes cannot possibly be due to an increase in back-scattering since the only possible chemical change of the metallic surface in our experimental conditions would be the inclusion of hydrogen under one form or another. It seems therefore more plausible to suppose that cathodic prepolarization leads to a micro-deformation of the metallic surface connected with the formation of ultramicro pores or lacunae which would facilitate the penetration of a further number of the deposited atoms into the surface. Such deformation may be due to adsorption and desorption of hydrogen, or to the possible formation of a trace of a hydride which may be hydrolysable as in the case of Pt and Pd, or volatile as in the case of Pb and which would as such separate from the surface.

The increased heterogeneity of the metallic surface connected with a more favourable distribution of "active centres" would in general explain the observed effects of prepolarization on the spontaneous and electro-deposition of radio-elements. The higher velocity of spontaneous deposition of Po on prepolarized electrodes may thus be attributed to the increased number of "active centres". A similar explanation might account for the more positive critical deposition potential of Po on prepolarized tantalum. However, in certain particular cases, the chemical changes of the surface have to be taken into consideration together with the physical changes. Such is for example the case of the spontaneous deposition of Pa on anodically prepolarized platinised platinum where atomic oxygen is supposed to play a role [4]. It is again equally important, for the explanation of the induction period in the cathodic

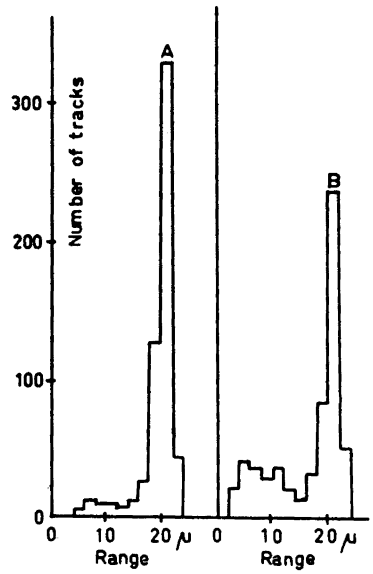


Fig. 5. Histograms of the α-particles of Po on silver foils.

deposition of Rd-Ru, to consider the possible accumulation on the cathodic surface of atomic hydrogen which would effect the reduction of the strong Ru complexes to more easily reducible forms [5].

Finally segregation of Po in HNO_3, as well as of Pu in HCl and U in HNO_3 solution, on metallic and / or glass surfaces was attributed to the possibility of existence of particularly priviliged regions having a relatively high energy of adsorption [8]. However, the absence of the segregation phenomenon in case of Po in N H_2SO_4 solution, as has been indicated in the present work, seems to suggest that, in addition to the distribution of the energy of adsorption on the metallic surface, one has to consider the role of the solvent and probably also the nature of the deposited atoms.

Acknowledgement. I should like to express my deepest thanks to Professor M. Haissinsky for his continuous advice and encouragement, and to Mademoiselle Albouiy for her help concerning the autoradiographic technique.

REFERENCES

1. Haissinsky, M. *J. Chim. Phys.* **32** (1935) 119.
2. Danon, J. and Haissinsky, M. *J. Chim. Phys.* **49** (1952) C 123.
3. Coche, A. and Haissinsky, M. *Compt. rend.* **222** (1946) 1284.
4. Ferradini, C. *Thesis*, Institut du Radium, Paris (1955).
5. Haissinsky, M. and El Guebely, M. A. *J. Chim. Phys.* **81** (1956) 744.
6. Haissinsky, M. *et al. J. Phys. et Radium* **8** (1949) 213.
7. Yagoda, H. *Radioactive Measurements with Nuclear Emulsions*, John Wiley, New York 1949.
8. El Guebely, M. A. and Sikkeland, T. *Acta Chem. Scand.* **11** (1957) 473.

Received December 18, 1956.

ACTA CHEMICA SCANDINAVICA 11 (1957) 590—598

Studies on Bile Acid Salt Solutions

I. The Dissociation Constants of the Cholic and Desoxycholic Acids

PER EKWALL, TORSTEN ROSENDAHL and NILS LÖFMAN

Institute of Physical Chemistry, Åbo Akademi, Åbo, Finland

The dissociation constants of cholic and desoxycholic acids have been evaluated from data obtained by potentiometric titration of aqueous solutions of their sodium salts with hydrochloric acid at 20 °C. The values obtained are: cholic acid, $pK_A = 4.98 \pm 0.05$, $K_A = 1.05 \times 10^{-5}$; desoxycholic acid $pK_A = 5.17 \pm 0.04$; $K_A = 6.76 \times 10^{-6}$.

Sodium cholate behaves as a normal uni-univalent electrolyte up to a concentration of 0.014—0.015 M; for sodium desoxycholate, the corresponding concentration limit is 0.0045—0.0055 M. Above these concentration limits, deviations occur which are due to micelle formation. After a transition region which for sodium cholate extends to a concentration of approximately 0.05 M and for sodium desoxycholate to about 0.01 M, a concentration range is reached in which the micelle formation is fully developed and which is characterized by a high, nearly constant ratio of the activities of the bile acid and its anion.

Many attempts have been made to determine the dissociation constants of the bile acids. Bondi [1] used conductance values to calculate the dissociation constant of glycocholic acid, Hammarsten [2] determined the constants of tauro- and glycocholic acids by potentiometric titration, whereas Henriques [3] utilized colorimetric pH-determinations to obtain the dissociation constants of several bile acids. Josephson [4] calculated the dissociation constants of a number of bile acids from potentiometrically determined pH values of aqueous solutions of the sodium salts to which different amounts of hydrogen chloride had been added. With the aid of glass electrode measurements, Kumler and Halverstadt [5] determined the dissociation constants of six bile acids in 50—67 % ethanol-water solutions and from these values they calculated the approximate values of the constants in water by assuming that the constants of all the acids in pure water are 17 times greater than in 50 % ethanol-water. They emphasized, however, that the difference is not constant for different acids and hence "an exact calculation of K_A values in one solvent cannot be made from those in another solvent" [5].

The values reported by the above-mentioned authors are collected in Table 1. The values are seen to deviate considerably from each other.

Table 1. The dissociation constants of bile acids.

Acid	Bondi	Hammarsten	Henriques	Josephson	Kumler and Halverstadt
Glycocholic acid	$1.32 \cdot 10^{-4}$	$4.0 \cdot 10^{-5}$	$1.66 \cdot 10^{-3}$	$3.55 \cdot 10^{-5}$	
Taurocholic »		$6.77 \cdot 10^{-2}$	$5.89 \cdot 10^{-4}$	$2.75 \cdot 10^{-2}$	
Glycodesoxycholic »			$3.47 \cdot 10^{-3}$	$10.49 \cdot 10^{-5}$	
Taurodesoxycholic »			$1.18 \cdot 10^{-3}$	$1.23 \cdot 10^{-2}$	
Cholic »				$6.46 \cdot 10^{-6}$	$1.12 \cdot 10^{-5}$
Desoxycholic »				$3.8 \cdot 10^{-7}$	$1.08 \cdot 10^{-5}$
Apocholic »					$1.09 \cdot 10^{-5}$
Lithocholic »					$1.02 \cdot 10^{-5}$
Dehydrocholic »					$1.22 \cdot 10^{-5}$
Dehydrodes-oxycholic »					$1.24 \cdot 10^{-5}$

At the time these determinations were carried out, very little was known about the colloidal properties of the bile acid salts; these properties may have affected many of the results. It occurred to us that the values of the dissociation constants should be checked. We have therefore carried out a redetermination of the dissociation constants of cholic and desoxycholic acids [11–13].

EXPERIMENTAL

Cholic acid (Hoffman-La Roche, Basel) was recrystallized several times from 96 % ethanol. The sample used in the measurements had after drying a m. p. of 197 °C.

Desoxycholic acid (Hoffman-La Roche, Basel) was recrystallized three times from glacial acetic acid, dissolved in ethanol and precipitated with ether two times, and boiled in water for 3 h. After drying the sample had a m. p. of 172–173 °C.

The sodium salts of both acids were prepared by dissolving the corresponding acids in absolute ethanol and neutralizing the warmed solutions with equivalent amounts of sodium ethylate in absolute ethanol. The salts crystallizing from the solutions on cooling were dried *in vacuo* over phosphorus pentoxide at an elevated temperature.

The determination of the dissociation constants involved potentiometric titration of aqueous solutions of the bile acid sodium salts with dilute hydrochloric acid. The pH values were determined with a valve potentiometer (Radiometer PHM3, Copenhagen) fitted with a glass electrode and a saturated calomel electrode as reference electrode. The titrations were conducted in a nitrogen atmosphere and were performed so that the method of Back and Steenberg [6] for the determination of the solubilities and solubility products of the acids could be utilized. Before the titration a slight excess of sodium hydroxide solution was added to the bile acid salt solution and the titration was continued over the equilibrium point until the bile acid began to precipitate.

RESULTS

Figs. 1 and 2 show two typical titration curves. The first parts of the curves are quite normal. The liberated acid, particularly cholic acid, has, however, a tendency to remain in solution, whereupon a supersaturated solution is produced. When precipitation finally occurs, the pH of the solution increases abruptly to the equilibrium value of the solution saturated with acid.

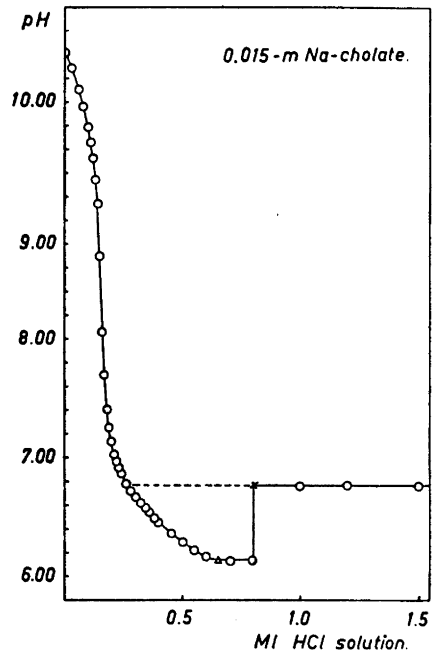


Fig. 1. Potentiometric titration of sodium cholate with HCl. 20 ml 0.0150 M sodium cholate solution + NaOH. Titrant: 0.0500 M HCl. △ The solution became turbid. × Precipitation occurred.

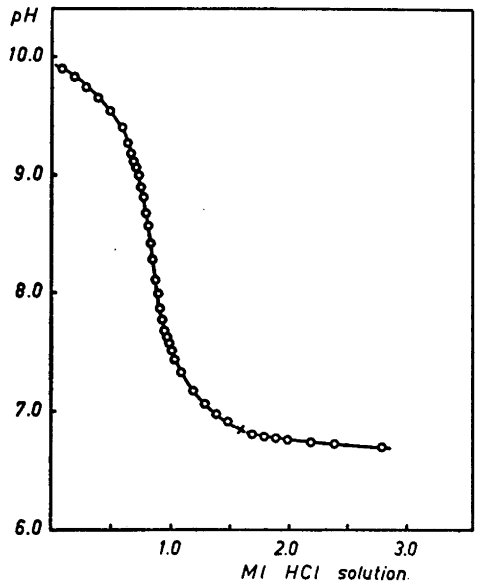


Fig. 2. Potentiometric titration of sodium desoxycholate with HCl. 40 ml 0.0050 M sodium desoxycholate solution + NaOH. Titrant: 0.0050 M HCl. × Precipitation occurred.

The calculation of the dissociation constants was based on the assumption that the ordinary dissociation equilibrium of weak acids is valid:

1. $$\frac{a_{H_3O^+} \cdot a_{A^-}}{a_{HA}} = K_A$$

Only the first parts of the titration curves which were unaffected by precipitation of acid or supersaturation were used in the calculations which were based on eqn. 2 [6].

Table 2. The dissociation constant of cholic acid at 20° C.

Initial sodium cholate concentration Moles per litre	pK_A	Mean value of pK_A
0.00300	5.03 4.99 5.00 4.94	4.98 ± 0.05
0.00600	4.96 4.94	
0.00800	4.95 4.96	
0.0100	4.98 4.96 5.01	
0.0120	4.95	
0.0140	4.99 5.02	
0.0150	5.07	5.07
0.0160	5.07	5.07
0.0180	5.13 5.14	5.13
0.0200	5.17 5.22	5.19
0.0220	5.23	5.23
0.0250	5.25 5.27	5.26
0.0300	5.35	5.35
0.0400	5.44	5.44
0.0500	5.48	5.48 ± 0.01
0.0700	5.49	
0.100	5.49	
0.125	5.48	
0.150	5.49	
0.175	5.48	
0.200	5.48	

Table 3. The dissociation constant of desoxycholic acid at 20° C.

Initial sodium desoxycholate concentration Moles per litre	pK_A	Mean value of pK_A
0.00100	5.21 5.17	5.15 ± 0.04
0.00200	5.15 5.15	
0.00300	5.16 5.20 5.17	
0.00400	5.20 5.17 5.16	
0.00500	5.17 5.15 5.14 5.15	
0.00550	5.24	5.24
0.00600	5.30 5.28 5.30	5.30
0.00650	5.45	5.45
0.00700	5.44 5.48	5.46
0.00800	5.58 5.56	5.57
0.00900	5.82 5.71	5.76
0.0100	5.79	5.79
0.0110	5.89	5.89
0.0120	5.89	5.89
0.0130	5.96	5.96
0.0150	6.04 6.12	6.08
0.0170	6.18	6.18
0.0200	6.17	6.17
0.0300	6.23	6.23
0.0500	6.35	6.35
0.0750	(6.21)	

2. $$pK_A = pH_x + \log \frac{C_s + C_{OH^-} - C_{H_3O^+}}{C_{tot} - C_s - C_{OH^-} + C_{H_3O^+}} + \frac{0.5\sqrt{\mu}}{1+\sqrt{\mu}}$$

where

$$(C_s + C_{OH^-} - C_{H_3O^+}) \cdot f_{HA} = a_{HA}$$

and

$$(C_{tot} - C_s - C_{OH^-} + C_{H_3O^+}) \cdot f_{A^-} = a_{A^-}$$

(pH_x is a recorded pH value; C_s is the corresponding concentration of hydrogen chloride added after the equivalence point and C_{OH^-} and $C_{H_3O^+}$ the corresponding hydroxyl and hydroxonium ion concentrations; C_{tot} is the original concentration of bile acid salt recalculated to the conditions at the point x; a_{HA} and a_{A^-} are the activities of the undissociated bile acid and its anion, respectively, and f_{HA} and f_{A^-} the corresponding activity coefficients; μ is the ionic strength of the solution).

In the calculation of pK_A, we have used 10—20 titration points after the equivalence point which yielded conforming values for the constant. The results of the calculations are given in Tables 2 and 3.

The titrations of dilute cholate solutions up to 0.014 M give a constant value of the dissociation constant of cholic acid: $pK_A = 4.98 \pm 0.05$ (Fig. 3). In the range from 0.015 to 0.040 M, the pK_A values increase with cholate concentration. Beginning with the 0.05 M and up to 0.20 M cholate solution, the

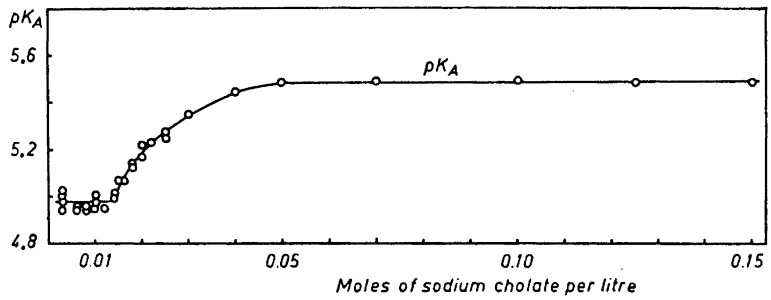


Fig. 3. The dissociation constant of cholic acid determined by potentiometric titration of sodium cholate solutions of different concentration with HCl.

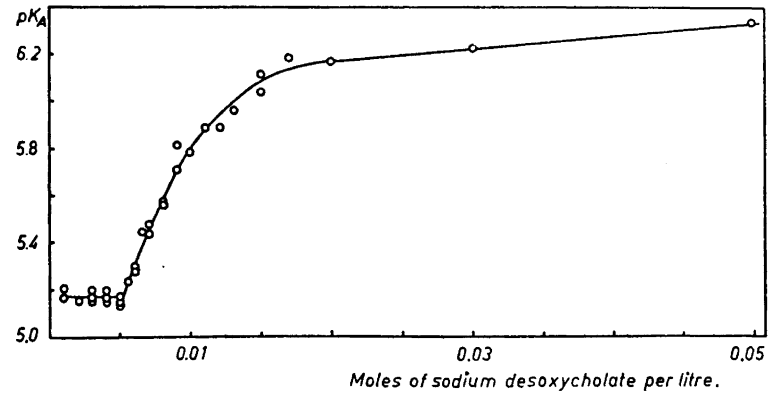


Fig. 4. The dissociation constant of desoxycholic acid determined by potentiometric titration of sodium desoxycholate solutions of different concentration with HCl.

titrations again give a constant pK_A value, $pK_A = 5.48 \pm 0.01$, which is considerably higher than the value obtained for the dilute cholate solutions.

The results for desoxycholic acid are similar (Fig. 4). At high desoxycholate dilutions, up to 0.005 M, the dissociation constant is constant, $pK_A = 5.17 \pm 0.04$. The value of the constant then increases rapidly in the concentration range from 0.006 to 0.010 M, but more slowly above the latter concentration. The highest value of pK_A obtained was 6.35. Values relating to concentrations higher than 0.05 M are uncertain.

DISCUSSION

Many earlier studies have shown that sodium cholate and desoxycholate behave as normal uni-univalent electrolytes only in relatively dilute solutions [7-13]. The deviations from the normal behaviour that occur at higher concentrations are due to micelle formation. One of us has previously established that the power to solubilize hydrocarbons is first observed when the concentration of the solution exceeds 0.015 M in the case of cholate and 0.005 M in the case of the desoxycholate [9-13]. This indicates that micelle formation sets in approximately at these concentrations. The micelle formation influences many of the other properties of the solutions.

The method we have used to calculate values of dissociation constants assumes that micelle formation does not take place and gives correct values only if this condition is fulfilled. Consequently only those values are reliable that apply to dilute solutions whose concentrations are below the limits given above. Accordingly, the following values are presented for the dissociation constants of the two bile acids:

Cholic acid: $pK_A = 4.98 \pm 0.05$; $K_A = 1.05 \times 10^{-5}$ (20 °C)
Desoxycholic acid: $pK_A = 5.17 \pm 0.04$; $K_A = 6.76 \times 10^{-6}$ (20 °C)

These dissociation constants are definitely higher than those reported by Josephson [4]. The value for cholic acid agrees very well with that calculated by Kumler and Halverstadt [5], but our value for desoxycholic acid is lower than their value.

Kumler and Halverstadt [5] remarked that the dissociation constants of the unconjugated bile acids should be of the same order as the constants of the higher aliphatic carboxylic acids, *i. e.* $1.0—1.4 \times 10^{-5}$, since the bile acids can be considered derivatives of valeric acid with a sterol group in the γ position. They presumed that the introduction of an unsubstituted sterol nucleus should lead to a decrease in the acid strength; hydroxyl and ketonic groups substituted on the sterol nucleus should strengthen the acid properties, but owing to the distance separating them from the carboxyl group, their effect can only be very slight. Kumler and Halverstadt thus came to the conclusion that the dissociation constants of cholic and desoxycholic acids should be almost equal, since the only structural difference between them is the presence of a hydroxyl group in position 7 in cholic acid which is separated from the carboxyl group by seven carbon atoms and that both acids should be approximately equal in strength to caproic acid ($K_A = 1.32 \times 10^{-5}$). Their own measurements of the dissociation constants in ethanol-water solutions and also the calculated values for water solutions seemed to verify these assumptions. Josephson's value for

the dissociation constant of cholic acid was, however, seventeen times as great as the value obtained for desoxycholic acid, and both acids, especially the latter, seemed to be much weaker than caproic acid. Our results verify the assumption of Kumler and Halverstadt that the dissociation constants of both acids are of the same magnitude as but slightly lower than that of caproic acid. The presence of one hydroxyl group more in cholic acid than in desoxycholic acid molecule seems, however, to influence the acid strength in water more than Kumler and Halverstadt presumed.

The reason for the very low value of desoxycholic acid obtained by Josephson is evident from our study. When the calculation of the value of the dissociation constant is based on pH measurements in 0.01—0.015 M solutions and the presence of micelles in these solutions is not taken into account, the values obtained are approximately $16—8 \times 10^{-7}$. Josephson's calculations were based on measurements of solutions whose concentrations were 0.01 M. Furthermore, many of the measurements were carried out on solutions supersaturated with bile acid.

From the data we have presented, also the concentrations at which the properties of the solutions begin to deviate from those typical of solutions of uni-univalent electrolytes become clearly evident. These deviations are indicated by the increased values of the dissociation constant when the concentration exceeds 0.013—0.015 M for sodium cholate and 0.0045—0.0055 M for sodium desoxycholate. At these concentrations, micelle formation by bile acid anions evidently begins, which is in accordance with the results of other measurements carried out in this laboratory [9-13].

If it is assumed that the equilibrium is correctly represented by eqn. 1 in all concentration ranges and that the values of K_A are those given above, it is obviously possible to determine from the experimental data the ratio of the activities of the bile acid and its anion at different concentrations and at different stages of the titrations. We shall only draw attention to the variation of this activity ratio with the concentration of the bile acid salt. The pH values at the equivalence points have been employed to determine this relationship. It is seen from Fig. 5 that the activity ratio remains constant in cholate solutions above 0.05 M and nearly constant in desoxycholate solutions above 0.010 M. This provides an explanation for the observation that the apparent dissociation constants calculated from the experimental data for the more concentrated bile acid salt solutions remain practically constant at values higher than the correct value. In solutions above 0.015 M in cholate and above 0.005 M in desoxycholate the bile acid anions associate to micelles in increasing proportion [9, 11-13], as a result of which the activities of the free anions are lowered. On the other hand, solubility measurements conducted in this laboratory have shown that a part of the bile acid molecules are solubilized by the micelles [11, 14] and as a consequence the activity of the bile acid molecules is lower than would otherwise be the case. Micelle formation and solubilization thus tend to maintain the ratio of the activities of bile acid molecules and bile acid anions nearly constant at higher concentrations.

Our study shows that sodium cholate behaves as a normal uni-univalent electrolyte only up to a concentration of about 0.014 M and that micelle formation obviously is fully developed when the concentration exceeds 0.05 M. In

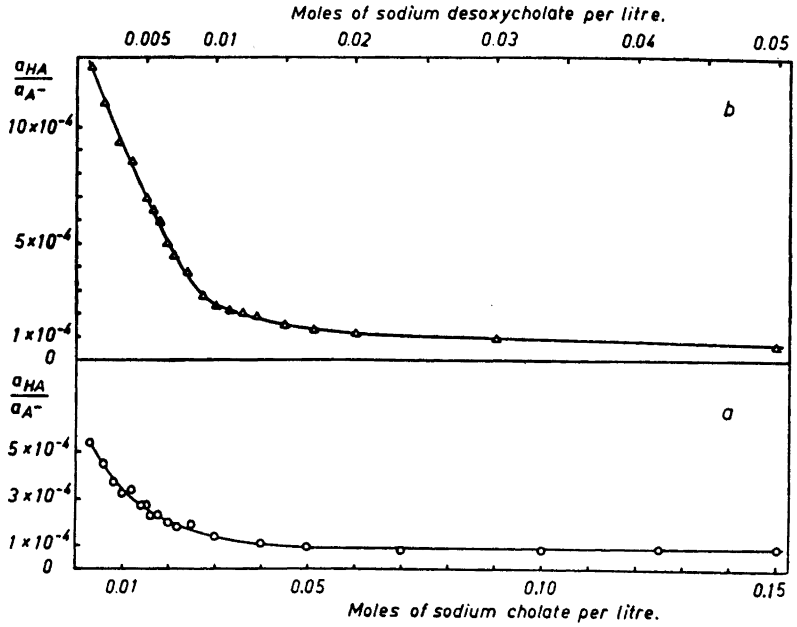


Fig. 5. The ratio of the activities of bile acid and its anions in sodium cholate and desoxycholate solutions.
a) Sodium cholate solutions.
b) Sodium desoxycholate solutions.

the concentration range between these two limits, evidently only a part of the cholate anions have undergone micelle formation. — Sodium desoxycholate behaves normally up to a concentration of about 0.0045 M and micelle formation is obviously fully developed in solutions above 0.01 M; between these two limits there is a transition region.

REFERENCES

1. Bondi, *Hoppe-Seylers Z. physiolog. Chem.* **53** (1907) 8.
2. Hammarsten, H. *Biochem. Z.* **147** (1924) 481.
3. Henriques, O. M. *Acta Pathol. Microbiol. Scand. Suppl.* **3** (1930) 141.
4. Josephson, B. A. *Biochem. Z.* **263** (1933) 428.
5. Kumler, W. D. and Halverstadt, J. F. *J. Biochem.* **137** (1941) 765.
6. Back, E. and Steenberg, B. *Acta Chem. Scand.* **4** (1950) 810.
7. Merrill, C. R. and McBain, J. W. *J. Phys. Chem.* **46** (1942) 10.
8. Johnston, S. A. and McBain, J. W. *Proc. Roy. Soc. London* **181** (1943) 119.
9. Ekwall, P. *Acta Acad. Aboensis, Math. et Phys.* **XVII** (1951) 8.
10. Ekwall, P. *Svensk Kem. Tidskr.* **63** (1951) 277.
11. Ekwall, P. *Koninkl. Vlaamse Acad. v. Wetenschap. v. België, Intern. Conference on Biochemical Problems of Lipids,* Brüssel 1953, p. 103.
12. Ekwall, P. *J. Colloid Sci. Suppl.* **1.** (1954) 66.
13. Ekwall, P. *Kolloid-Z.* **136** (1954) 37.
14. Ekwall, P., Sten, A. and Rosendahl, T. *Unpublished experiments.*

Received December 14, 1956.

ACTA CHEMICA SCANDINAVICA 11 (1957) 599—609

Mercury(II) Halide Mixed Complexes in Solution

II. Complexity Constants of the Binary Complexes

Y. MARCUS*

Department of Inorganic Chemistry, Royal Institute of Technology, Stockholm 70, Sweden

Complexity constants for mercury(II) halide complexes were determined by solvent (benzene) distribution for 0.50 M $NaClO_4$ ionic medium and 25°. The constants found are:

Reaction	Constant	Chloride	Bromide	Iodide
$Hg^{2+} + HgX_2 \rightleftharpoons 2HgX^+$	log K	0.26 ± 0.03	0.94 ± 0.06	1.91 ± 0.07
$HgX^+ + X^- \rightleftharpoons HgX_2$	log k_2	6.3 ± 0.2	8.3 ± 0.3	
$HgX_2 + X^- \rightleftharpoons HgX_3^-$	log k_3	0.95 ± 0.03	2.27 ± 0.02	3.67 ± 0.02
$HgX_2 + 2X^- \rightleftharpoons HgX_4^{2-}$	log k_3k_4	2.00 ± 0.05	4.02 ± 0.02	6.04 ± 0.02

These values agree with published potentiometric values, except for bromide, but the solvent distribution value of log K agrees with a redetermined potentiometric value of log $K = 0.94 \pm 0.03$. The constants found here will be taken to apply in the solvent distribution work on the mixed complexes.

In order to study the relative stability of the mixed mercury(II) halide complexes, the complexity constants of the binary complexes were measured, using the same ionic medium and temperature, and the same method (solvent distribution), as later on for the ternary systems. The binary constants have previously [2] been determined by potentiometric methods for these same conditions, namely 25° and 0.50 M (perchlorate + halide) ionic medium. As a check on the assumption that benzene has no effect on the aqueous equilibria, some potentiometric measurements were made on comparable solutions with and without benzene.

Symbols. The symbols used here are defined in part I[1] p. 330.

EXPERIMENTAL

The experimental details of the solvent distribution experiments are described in part I[1] p. 331. The potentiometric measurements followed the procedure of Sillén and Infeldt [3].

* Permanent address: Israel Atomic Energy Commission, Hakiryah, Tel-Aviv, Israel.

The titrations consisted of adding (Hg^{2+} + Br^-) titrant to 100.0 ml (Hg^{2+} + Hg_2^{2+}) solution in the titration vessel. The 0.2 M bromide stock solution was tested for iodide, but no coloration by iodine could be detected by the nitrite-starch test, whereas adding I^- to a ratio $(I^-)/(Br^-) = 5 \times 10^{-5}$ gave an observable coloration. The titrations were performed in a thermostated bath at 25.0 ± 0.1° and N_2, free from O_2, was bubbled through the solution during the titration. The reference electrode was Ag, AgCl/10 mM Ag^+, 10 mM H^+ 480 mM Na^+ 500 mM ClO_4^-// and two Pt electrodes, compared against it, usually agreed to within 0.05 mV. Steady potentials were obtained 5 min after the addition of titrant, and the potentials usually deviated no more than 0.03 mV from values obtained 25 min later.

DETERMINATION OF K, THE EQUILIBRIUM CONSTANT FOR $Hg^{2+} + HgX_2 \rightleftharpoons 2\ HgX^+$

Derivation of equations, solvent distribution

In solutions of mercury and halide, where the stoichiometric ratio X/M is 2.00 or less, the only species occurring will be M^{++}, MX^+ and MX_2, provided the solutions are not so dilute that X^- also appears (see below, p. 603). The pertinent equilibrium reaction will then be

$$M^{++} + MX_2 \rightleftharpoons 2\ MX^+;\ K \tag{1}$$

The mass balances of mercury and halide will be

$$M = [M] + [MX] + [MX_2] + [MX_2]_{or} \text{ and} \tag{2}$$

$$X = M\bar{n} = [MX] + 2[MX_2] + 2\ [MX_2]_{or} \tag{3}$$

The equilibrium constant of (1) will give

$$[MX]^2 = K\ [M]\ [MX_2] \tag{4}$$

When such an aqueous solution is equilibrated with benzene,

$$[MX_2]_{or} = \lambda\ [MX_2] \tag{5}$$

and the distribution ratio of mercury will be

$$D = [MX_2]_{or}\ ([M] + [MX] + [MX_2])^{-1} \tag{6}$$

Eliminating all concentrations from (2), (3), (4), (5) and (6), the following expression for K is obtained:

$$K = \frac{[\bar{n}(1 + D)\ \lambda - 2D\ (1 + \lambda)]^2}{D[(1-\bar{n})\ (1 + D)\lambda + D(1 + \lambda)]} \tag{7}$$

For the special case $\bar{n} = 1.00$ this reduces to:

$$K_{\bar{n}=1.00} = [\lambda - D(2 + \lambda)]^2\ D^{-2}\ (1 + \lambda)^{-1} \tag{7a}$$

Although eqn. (7) is valid for all values of $\bar{n}$ less than 2.00, the best accuracy is obtained with $\bar{n}$ around unity.

Experimental results, solvent distribution

Table 1 gives the results for the three halides, as log D ($\bar{n}$). The M values are also given, although they do not enter the calculations. The values of log

K were obtained by solving numerically (7) — or (7a) in the case of bromide — and are averaged at the end of each section. The values of λ, obtained from part I[1], are given at the top of each section.

Table 1. The constant K of the equilibrium $Hg^{2+} + HgX_2 \rightleftharpoons 2\ HgX^+$

Chloride, log λ = −0.963				Bromide, log λ = 0.152				Iodide, log λ = 1.77			
$\bar{n}$	−log M	−log D	log K	$\bar{n}$	−log M	−log D	log K	$\bar{n}$	−log M	−log D	log K
0.20	3.37	1.07	0.23	1.00	3.15	0.75	0.93	0.64	3.33	0.73	1.85
0.20	3.15	1.04	0.25	1.00	3.02	0.74	0.88	0.86	3.33	0.48	1.84
0.20	3.07	1.04	0.25	1.00	2.85	0.74	0.88	0.88	4.00	0.42	1.89
0.20	2.85	1.01	0.27	1.00	2.72	0.77	1.00	1.00	4.00	0.36	1.92
0.20	2.73	0.99	0.28	1.00	2.55	0.74	0.88	1.08	3.33	0.29	2.02
0.20	2.55	1.04	0.25	1.00	2.42	0.74	0.88	1.28	3.33	0.08	1.92
0.20	2.47	1.01	0.27	1.00	2.25	0.77	1.00				
0.20	2.25	1.03	0.26	1.00	2.11	0.77	1.00				
0.20	2.17	1.05	0.24	1.00	1.95	0.76	0.97				
0.20	1.95	1.03	0.26								
0.94	1.75	1.55	0.26								
1.09	1.75	1.45	0.29								
1.17	1.75	1.39	0.24								
log K_{av} = 0.26 ± 0.03				log K_{av} = 0.94 ± 0.06				log K_{av} = 1.91 ± 0.07			
log K_{pot} = 0.26 ± 0.03				log K_{pot} = 0.77 ± 0.05				log K_{pot} = 1.92 ± 0.05			

Potentiometry

The value of K for bromide from the solvent distribution experiments differs sufficiently from the earlier potentiometric value to warrant being checked. The method of Sillén and Infeldt [3] used in the earlier potentiometric work was followed. These authors showed that if v ml titrant (X M Br^- + M M Hg^{2+}) is added to 100.0 ml solution (M M Hg^{2+} + some Hg_2^{2+}), the potential of a Pt electrode against a suitable reference electrode at 25° will be

$$E_v = E_0 - 29.58 \log (1 + v/100) + 59.16 \log mM^{-1} \quad (8)$$

where E_0 is the potential before the addition of any titrant. The ligand number will be

$$\bar{n} = Xv\ (100 + v)^{-1}\ M^{-1} \quad (9)$$

and combined with mM^{-1} obtained from (8) this gives

$$K = (2 - 2mM^{-1} - \bar{n})^2\ (mM^{-1})^{-1}\ (mM^{-1} + \bar{n} - 1)^{-1} \quad (10)$$

Table 2 gives the values of K (numerical averages from the values at individual points) obtained for several experiments with solutions at different con-

Table 2. Potentiometric titrations for K for $Hg^{2+} + HgBr_2 \rightleftharpoons 2\ HgBr^+$.

Benzene	M (in mM)	X (in mM)	log K	Symbol in Fig. 1
—	2.7	24.1	0.96 ± 0.03	○
Present	2.7	24.1	0.95 ± 0.02	●
—	5.3	24.1	0.96 ± 0.03	□
Present	5.3	24.1	0.94 ± 0.04	■
—	10.7	48.3	0.93 ± 0.05	△
—	10.7	48.3	0.91 ± 0.03	△
Present	10.7	48.3	0.95 ± 0.04	▲
—	21.3	48.3	0.92 ± 0.02	×
		Grand average	0.94 ± 0.03	

centrations, with benzene present in some of them. (The solutions were saturated with benzene by passing the N_2 through benzene before bubbling it through the solution in the titration vessel for a sufficient time.)

From Tables 1 and 2 the new potentiometric value of K is seen to agree very well with the solvent distribution value. Also, the presence of benzene

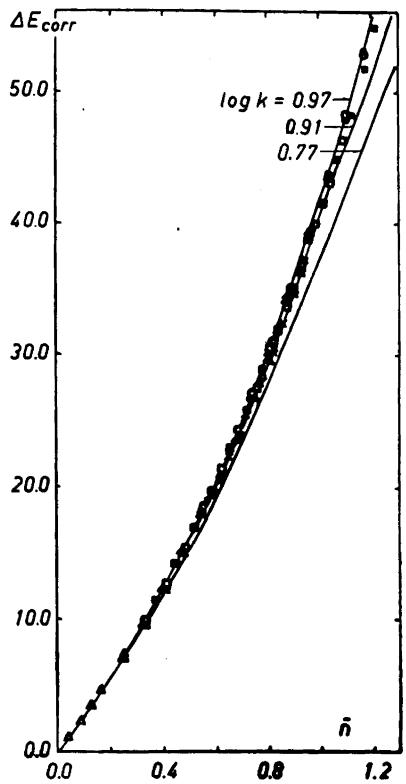


Fig. 1. The dilution corrected potential difference $E_v - E_0 + 29.58 \log (1 + v/100)$ as function of the ligand number $\bar{n}$, for the reaction $Hg^{2+} + HgBr_2 \rightleftharpoons 2\ HgBr^+$. The symbols refer to Table 2. The curves were calculated with the indicated constants.

does not seem to affect the equilibrium in the aqueous phase. The results of the experiments are also shown in Fig. 1, where the data $E_v—E_0 + 29.58 \log (1 + v/100)$ as function of $\bar{n}$ are compared with curves calculated with various constants K. The best fit is evidently with $\log K = 0.94 + 0.03$, while the former potentiometric value of Sillén and Infeldt [3] $\log K = 0.77$ does not fit the present data *.

DETERMINATION OF k_2, THE EQUILIBRIUM CONSTANT OF $HgX^+ + X^- \rightleftharpoons HgX_2$

Derivation of equations

If a solution of MX_2 is sufficiently diluted, the dissociation $MX_2 \rightleftharpoons MX^+ + X^-$ will become appreciable, and the D values will deviate from λ. The concentration should, however, not be so low that the further dissociation of $HgX^+ \rightleftharpoons Hg^{++} + X^-$ becomes noticeable. If, then, the mass balance is $M = [MX] + [MX_2] + [MX_2]_{or}$, the charge balance is $x = [MX]$ and the ratio $\bar{n} = 2.00$, eqn. (11) may be derived:

$$k_2 = D\ \lambda\ (1 + D)\ (\lambda—D)^{-2}\ M^{-1} \qquad (11)$$

The value obtained for k_2, combined with that of K found above, yield the value of k_1.

It may be mentioned in passing that the disproportionation $2\,HgX_2 \rightleftharpoons HgX^+ + HgX_3^-$, equilibrium constant k_3/k_2, was neglected in this work. Strictly speaking the distribution expression in HgX_2 solutions should be $\lambda = \lambda'(1+2\sqrt{k_3/k_2})^{-1}$, where λ' is the true distribution coefficient of the species MX_2. Inserting the values of k_3/k_2 one finds $\log \lambda \approx \log \lambda' + 0.0008$, so that the difference between λ and λ' is much smaller than the experimental error.

Experimental results

As is seen from equation (11), the constant k_2 is inversely proportional to M, and as k_2 is of the order of 10^6 for chloride, and larger still for the other halides, this means that very low M values are necessary. If, moreover, the value of $(\lambda—D)$ should be larger than 10 % λ, in order that the values do not become too uncertain, the upper limits for $\log M$ are: chloride —4.5, bromide —5.8, and iodide —7.2. The specific activity of the mercury available was, however, too low to permit a sufficient dilution of the solutions, so that no value of k_2 for iodide, and only rough estimates for chloride and bromide could be obtained. Results are shown in Table 3. The constants were calculated only from the experiments indicated, since for the others the results were too uncertain.

* It is very remarkable that such a large difference has been found between the potentiometric values of K determined in 1943 and now. Gunnar Infeldt was a very careful worker and a good analyst, and in general his values have been well confirmed, when they have later on been checked by others. One possible explanation is that there was some impurity in the bromide used by Infeldt, although it is hard to see what this could have been. Since Gunnar Infeldt has passed away in the meantime, and no samples of the old solutions are left, it is impossible to make sure.
Lars Gunnar Sillén

Table 3. The constants k_2, k_1 and β_2 for chloride and bromide.

	log M	log D	log k_1	log k_2	log β_2
Chloride	−4.83 ± 0.03	−1.05 ± 0.05			
	−5.13 ± 0.03	−1.09 ± 0.06			
	−5.43 ± 0.03	−1.13 ± 0.06	6.3 ± 0.2	6.6 ± 0.2	12.9 ± 0.3
Bromide	−5.46 ± 0.02	0.126 ± 0.010	8.3 ± 0.3	9.2 ± 0.3	17.5 ± 0.5
	−5.76 ± 0.05	0.09 ± 0.06			
	−6.06 ± 0.08	−0.17 ± 0.12			

DETERMINATION OF k_3 AND k_3k_4, THE EQUILIBRIUM CONSTANTS OF $HgX_2 + X^- \rightleftharpoons HgX_3^-$ AND $HgX_2 + 2X^- \rightleftharpoons HgX_4^{2-}$

When there is an excess of free halide, *i. e.* when $\bar{n} > 2.00$, the complexes HgX_3^- and $HgX_4^{=}$ are gradually formed, whereas species with $\bar{n} < 2$ may be completely neglected. The solvent distribution will then follow the expression:

$$D = [MX_2]_{or}\,([MX_2] + [MX_3] + [MX_4])^{-1} = \lambda\,(1 + k_3x + k_3k_4x^2)^{-1} \quad (12)$$

The constants k_3 and k_3k_4 may be found by the following methods.

Curve fitting

For applying the curve fitting method [4], the normalized variables Y and Z are introduced:

$$Y = \log \lambda - \log D = \log (1 + v + pv^2) \qquad Z = \log v \qquad (13a)$$
$$v = k_3x \text{ and } p = k_4/k_3$$

or, alternatively:

$$Y' = \log \lambda - \log D = \log (1 + p'v' + v'^2) \qquad Z' = \log v' \qquad (13b)$$
$$v' = (k_3k_4)^{1/2}\,x \text{ and } p' = (k_3/k_4)^{1/2}.$$

The data in the form log D (log x) are plotted, and compared with families of curves $Y(Z)_p$ or $Y'(Z')_{p'}$, whence the values of:

$$\log D\ (Y = 0) = \log D\ (Y' = 0) = \log \lambda$$
$$\log x\ (Z = 0) = -\log k_3$$
$$\log p = \log k_4 - \log k_3$$
$$\log x\ (Z' = 0) = -1/2 \log k_3k_4$$
$$\log p' = 1/2 \log k_3/k_4$$

are obtained. In practice, the best values of log k_3 are obtained from the Y, Z, v, p family, while those of log k_3k_4 are best obtained from the Y', Z', v', p' family.

Linear plots

An alternative method is to transform eqn. (12) so that its plot will be a straight line from which k_3 and k_3k_4 are obtained as intercept and slope:

$$(\lambda\ D^{-1} - 1)\ x^{-1} = k_3 + k_3k_4x \qquad (14a)$$

or, alternatively:

$$(\lambda\ D^{-1} - 1)\ x^{-2} = k_3x^{-1} + k_3k_4. \qquad (14b)$$

In practice it is found that k_3 is best obtained as the slope when the left term of (14b) is plotted *vs* x^{-1}, and k_3k_4 is best obtained when the left term of (14a) is plotted *vs* x.

Experimental results

Experimental data log D(log x) were obtained in the following ranges of concentrations:

$-4.1 < \log [Cl^-] < -0.7$; $-4.0 < \log [Br^-] < -1.0$; $-5.3 < \log [I^-] < -2.1$

In every case $X > 100\ M$ (except for the lowest [I], where $X > 10\ M$), so that x may be safely put equal to X. Plots of the data are shown in Figs. 2, 3 and 4 for chloride, bromide and iodide. The data for bromide are also given in Table 4.

Table 4. The distribution of $HgBr_2$ as function of excess bromide concentration.

$-\log x$	$-\log M$	$\log D$	$-\log x$	$-\log M$	$\log D$
4.01 ± 0.03	5.0	0.150 ± 0.030	2.01	4.6	−0.400 ± 0.007
3.71 ± 0.02	5.0	0.145 ± 0.015	1.86	4.6	−0.590 ± 0.010
3.41 ± 0.02	5.0	0.135 ± 0.015	1.71	4.6	−0.775 ± 0.010
3.23 ± 0.01	5.0	0.115 ± 0.015	1.63	4.6	−0.850 ± 0.010
3.01	4.6	0.060 ± 0.010	1.53	4.6	−1.055 ± 0.010
2.86	4.6	0.030 ± 0.010	1.41	4.6	−1.230 ± 0.015
2.71	4.6	0.005 ± 0.015	1.23	4.6	−1.540 ± 0.035
2.60	4.6	−0.020 ± 0.010	1.11	4.6	−1.740 ± 0.045
2.50	4.6	−0.060 ± 0.010	1.10	4.0	−1.830 ± 0.010
2.41	4.6	−0.120 ± 0.007	1.01	4.0	−1.930 ± 0.010
2.23	4.6	−0.230 ± 0.007			

Values of log x are ±0.005 when not otherwise indicated. Values of log M are ±0.05.

The curve fitting technique outlined above was applied to the data, as also was the alternative method of linear plots, first transforming the data to the forms of eqns. (14a) and (14b). The results are shown in Table 5. Curves calculated from the average constants of Table 5 appear as solid lines in Figs. 2, 3 and 4. The less accurately obtained constants (in parenthesis) were not included in the average.

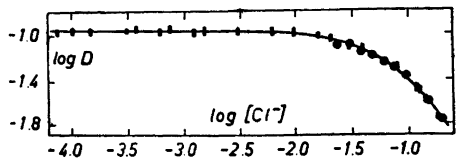


Fig. 2. Log D for $HgCl_2$-benzene-ionic medium as function of log x, excess chloride concentration. ● $M = 5.10^{-4}$ M, ■ $M = 2.10^{-5}$ M, ———— calculated with log $k_3 = 0.95$ and log $k_3k_4 = 2.00$.

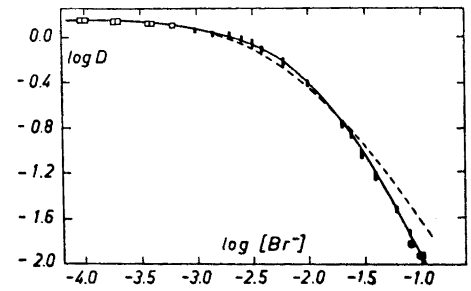


Fig. 3. Log D for $HgBr_2$-benzene-ionic medium as function of log x, excess bromide concentration. ● $M = 1.10^{-4}$ M, ■ $M = 2.5 \cdot 10^{-5}$ M, □ $M = 1.10^{-5}$ M, ———— calculated with log $k_3 = 2.27$ and log $k_3k_4 = 4.02$, - - - - - - - - calculated with log $k_3 = 2.41$ and log $k_3k_4 = 3.67$.

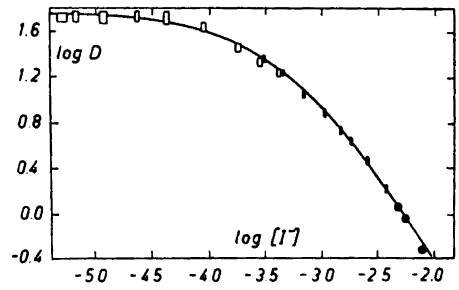


Fig. 4. Log D for HgI_2-benzene-ionic medium as function of log x, excess iodide concentration. ● $M = 8.10^{-5}$ M, ■ $M = 4.10^{-5}$ M, □ $M = 2.10^{-5}$ M, ———— calculated with log $k_3 = 3.67$ and log $k_3k_4 = 6.04$.

It may also be stated in passing that experiments with various M's showed no formation of polynuclear complexes, as all points were on the same curve (see Figs. 2, 3 and 4). This is not surprising at the low concentrations of mercury(II) employed.

PREVIOUS WORK

The constants obtained in this work are compared with those obtained in the careful and systematic potentiometric study of Sillén *et al.* (Ref.[2] summarizing their results) at the bottom of Tables 1 and 5. Agreement between the two sets of constants is quite good for the chloride and the iodide, within the stated limits of error, but much less so for the bromide. In the latter case, curves calculated with the earlier constants do not fit the present data (Figs. 1 and 3).

Table 5. The constants k_3 and k_3k_4 for the equilibria $HgX_2 + X^- \rightleftharpoons HgX_3^-$ and $HgX_2 + 2X^- \rightleftharpoons HgX_4^{2-}$ respectively.

	Chloride	Bromide	Iodide
Curve fitting			
log λ	−0.960 ± 0.015	0.155 ± 0.010	1.760 ± 0.015
log p	0.20 ± 0.10	−0.52 ± 0.07	−1.30 ± 0.06
log x (Z = O)	−0.95 ± 0.02	−2.27 ± 0.02	−3.67 ± 0.02
log p'	−0.1 ± 0.1	0.23 ± 0.07	0.65 ± 0.06
log x (Z' = O)	−1.00 ± 0.02	−2.01 ± 0.02	−3.02 ± 0.02
log k_3 (from p, Z)	0.95 ± 0.02	2.27 ± 0.02	3.67 ± 0.02
log k_4 (from p, Z)	(1.15 ± 0.10)	(1.75 ± 0.07)	(2.37 ± 0.06)
log k_3k_4 (from p', Z')	2.00 ± 0.04	4.02 ± 0.04	6.04 ± 0.04
log k_3 (from p', Z')	(0.90 ± 0.10)	(2.24 ± 0.07)	(3.67 ± 0.06)
Linear plots			
log k_3 (eqn. 14a)	(1.00 ± 0.12)	(2.28 ± 0.06)	(3.68 ± 0.04)
log k_3k_4 (eqn. 14a)	2.02 ± 0.06	4.02 ± 0.02	6.05 ± 0.02
log k_3 (eqn. 14b)	0.95 ± 0.06	2.26 ± 0.03	3.66 ± 0.03
log k_3k_4 (eqn. 14b)	(2.00 ± 0.12)	(4.04 ± 0.05)	(6.02 ± 0.05)
Average constants			
log k_3	0.95 ± 0.03	2.27 ± 0.02	3.67 ± 0.02
log k_3k_4	2.00 ± 0.05	4.02 ± 0.04	6.04 ± 0.04
log k_4 (difference)	1.05 ± 0.06	1.75 ± 0.05	2.37 ± 0.05
Previous results [2]			
log k_3	0.85 ± 0.15	2.41 ± 0.11	3.78 ± 0.14
log k_3k_4	1.85 ± 0.06	3.67 ± 0.05	6.01 ± 0.04

The values of K were obtained by the solvent distribution and the potentiometric methods with about the same accuracy, and agreement for chloride and iodide is excellent, but although the solvent distribution value for bromide agrees well with the new potentiometric value, both are 0.17 ± 0.08 log units higher than the previous potentiometric value. The solvent distribution method gives much more accurate values of k_3 than the potentiometric method, and the values obtained here all lie within the (wide) limits of error given for the potentiometric constants. The values of k_3k_4 are of comparable accuracy, agreeing very well for iodide, fairly well for chloride but not at all for bromide.

One reason for the discrepancy may, perhaps, be the fact that the potentiometric value of k_3k_4 was obtained in a region of concentration (0.15—0.40 M) where the bromide is a very high fraction of the total ionic medium, so that the assumption of constant activity factors may no longer be valid. In the present study, concentrations ranged at most to 20 % exchange of bromide for perchlorate.

Moreover, it is felt that the potentiometric values of k_3 and k_3k_4 were obtained in rather a round-about way, by directly determining β_3 and β_4, while β_2 was obtained by a method depending on the experimentally difficult "maximum potential titration". The difference in β_2 which would bring k_3k_4 into agreement with the present value corresponds to a difference of about 9 mV in the potential. Of this, 3 mV is due to the different K values used.

The remaining 6 mV and the difference in K are difficult to explain; perhaps they are due to an impurity in the bromide solutions used previously (see foot-note p. 603).

The work done previously to 1946—1948, was fully discussed by Sillén *et al.* (Refs.[3] p. 61; [5] p. 52; [6] p. 482; 487; [7] p.505; [8] p. 828) and since then, few determinations of the pertinent equilibrium constants have been undertaken. The authors not mentioned in the above references usually did not use a constant ionic medium, so that their results are not comparable with the above. Tourneux's [9] values obtained from the solubility of KCl in $HgCl_2$ solutions extrapolate to log $k_3k_4 = 2.0$ at 25°, while Grinberg and Nikolskaya [10] quote a similar value. They also give log β_4 as 16.23 21.64 and 30.28 for $HgCl_4^=$ $HgBr_4^=$ and $HgI_4^=$. Peschanski [11] found for $HgCl_3^-$ log $k_3 = 0.52$ at 18° and ionic strength 0.5, while for $Hg^{2+} + HgCl_2 \rightleftharpoons 2\ HgCl^+$ she found log $K = 0.40$ at 17°, the first being lower, the second higher than the present values for 25°. The method she employed — continuous variation for UV light absorption — is, however, open to much criticism. Strocchi [12] states that species MX_3^- and $MX_4^=$ are formed, without giving formation constants, Yatsimirskii [13] gives log $k_1 = 12.36$ for HgI^+, while a year later Yatsimirskii and Shutov [14] revised this to log $k_1 = 13.15$. Finally, Golub [15] gives log $\beta_4 = 30.18$ for $HgI_4^=$ at "constant ionic strength", and Damm and Weiss [16] give for unspecified conditions log $k_1 = 6.80$, log $\beta_2 = 13.60$, log $k_3 = 0.57$ and log $k_3k_4 = 2.03$.

DISCUSSION

The constants k_3 and k_3k_4 together with the distribution coefficient are adequate for describing the behaviour of mercury halide complexes at $n \geq 2$, *i. e.* the region important to mixed-complex formation. The values of λ for the 0.5 M perchlorate ionic medium obtained here (Table 5) have already been compared with values obtained otherwise in part I[1]. To complete the picture, values of β_2 are also necessary. The values found here for k_2 give only the orders of magnitude of the constants (see p. 603):

Chloride, solvent distribution	log $\beta_1 \sim 6.6 \pm 0.2$	log $\beta_2 \sim 12.9 \pm 0.3$
potentiometry	$= 6.74 \pm 0.02$	$= 13.22 \pm 0.02$
Bromide, solvent distribution	$\sim 9.2 \pm 0.3$	$\sim 17.5 \pm 0.5$
potentiometry	$= 9.05 \pm 0.03$	$= 17.33 \pm 0.04$

Work on mixed bromide-iodide complexes, to be described in part IV, led to a value for log $\beta_2(HgI_2) - \log \beta_2(HgBr_2) = 6.94 \pm 0.03$. Accepting the potentiometric value of log $\beta_2(HgI_2) = 23.82 \pm 0.04$, this yields a value for log $\beta_2(HgBr_2) = 16.88 \pm 0.06$, in closer agreement with 16.98 ± 0.04, the value obtained from the directly determined log $\beta_4(HgBr_4^=) = 21.00 \pm 0.03$ [8] and the solvent distribution value log $k_3k_4 = 4.02 \pm 0.02$, than is 17.33, the potentiometric value of β_2. To have a consistent set of equilibrium constants, the values log β_2 13.22 ± 0.02 for $HgCl_2$ and 23.82 ± 0.04 for HgI_2 are borrowed from the potentiometric investigation, 16.88 ± 0.06 for $HgBr_2$ is obtained from part IV, and the values of K, k_3 and k_3k_4 are taken from the solvent distribution work described above. The resulting constants are tabulated in Table 6.

The author wishes to thank the *Israel Atomic Energy Commission* for a research grant abroad, Professor Lars Gunnar Sillén for the facilities provided, and particularly for his advice, comments and criticism, and Dr. Helen S. Dunsmore for improving the English presentation.

Table 6. Equilibrium constants for 0.5 M $NaClO_4$ ionic medium and 25°, applicable to the solvent distribution study of mercury(II) halide complexes.

Reaction	Constant	Chloride	Bromide	Iodide
$Hg^{2+} + X^- \rightleftharpoons HgX^+$	$\log \beta_1$	6.74 ± 0.03	8.94 ± 0.07	12.87 ± 0.06
$Hg^{2+} + 2X^- \rightleftharpoons HgX_2$	$\log \beta_2$	13.22 ± 0.02	16.88 ± 0.06	23.82 ± 0.04
$Hg^{2+} + 3X^- \rightleftharpoons HgX_3^-$	$\log \beta_3$	14.17 ± 0.04	19.15 ± 0.06	27.49 ± 0.04
$Hg^{2+} + 4X^- \rightleftharpoons HgX_4^{2-}$	$\log \beta_4$	15.22 ± 0.05	20.90 ± 0.06	29.86 ± 0.04

REFERENCES

1. Marcus, Y. *Acta Chem. Scand.* **11** (1957) 329, part I.
2. Sillén, L. G. *Acta Chem. Scand.* **3** (1949) 539.
3. Sillén, L. G. and Infeldt, G. *Svensk Kem. Tidskr.* **58** (1946) 61.
4. Sillén, L. G. *Acta Chem. Scand.* **10** (1956) 186.
5. Sillén, L. G. *Svensk Kem. Tidskr.* **58** (1946) 52.
6. Lindgren, B., Jonsson, A. and Sillén, L. G. *Acta Chem. Scand.* **1** (1947) 479.
7. Qvarfort, I. and Sillén, L. G. *Acta Chem. Scand.* **3** (1949) 505.
8. Bethge, P. O., Jonevall-Westöö, I. and Sillén, L. G. *Acta Chem. Scand.* **2** (1948) 828.
9. Tourneux, C. *Bull. soc. chim. France* **1934** 1043.
10. Grinberg, A. A. and Nikolskaya, L. E. *Zhur. Priklad. Khim.* **24** (1951) 893.
11. Peschanski, D. *J. Chim. Phys.* **50** (1953) 640.
12. Strocchi, P. *Gazz. chim. ital.* **79** (1949) 47, 270.
13. Yatsimirskii, K. B. *Doklady Akad. Nauk SSSR* **77** (1951) 819.
14. Yatsimirskii, K. B. and Shutov, A. A. *Zhur. Fiz. Khim.* **26** (1952) 842.
15. Golub, A. M. *Ukrain. Khim. Zhur.* **19** (1953) 467.
16. Damm, K. and Weiss, A. *Z. Naturforsch.* **10B** (1955) 534.

Received January 23, 1957.

ACTA CHEMICA SCANDINAVICA 11 (1957) 610—618

Mercury(II) Halide Mixed Complexes in Solution

III.[1] The Uncharged Mixed Complexes

Y. MARCUS*

Department of Inorganic Chemistry, Royal Institute of Technology, Stockholm 70, Sweden

The equilibrium constant K of the reaction $HgA_2 + HgB_2 \rightleftharpoons 2HgAB$ was determined by studying the distribution of mercury between benzene and an aqueous solution. The distribution coefficient λ_{11} of HgAB was obtained from the extreme parts of the log distribution ratio *vs* log total B/total A curve, while K was obtained from the middle part of the curve. The values (log λ_{11}, log K) are: HgClBr (-0.42 ± 0.04, 2.0 ± 0.5), HgClI (0.28 ± 0.02, 1.75 ± 0.20), HgBrI (0.79 ± 0.04, 1.10 ± 0.20). The "stabilization constant", *i. e.* the ratio of the experimental to the statistical value ($= 4$), is larger than unity for these complexes, more so for the aqueous phase than for the organic phase.

A mixture of MA_2 and MB_2 will contain also MAB, according to the equilibrium reaction

$$MA_2 + MB_2 \rightleftharpoons 2MAB; \quad K = [MAB]^2\,[MA_2]^{-1}\,[MB_2]^{-1} \qquad (1)$$

Owing to the extraordinary stability of the uncharged mercury (II) halide complexes, all species other than MA_2, MAB and MB_2 may be neglected. The above reaction was studied by measuring the mercury distribution between benzene and an aqueous ionic medium, for the pairs A—B: Cl—Br, Cl—I and Br—I.

Symbols. The symbols used here were defined in part I [2].

Experimental. The experiments were in the main carried out as described in part I[2]. Benzene solutions of MA_2 and MB_2 were mixed and shaken at 25° with an equal volume of the aqueous ionic medium, 0.490 M $NaClO_4$ + 0.010 M $HClO_4$, in this way ensuring that $\bar{n}_{A,B} = 2.00$ for all the solutions. The mercury concentration was about 10^{-4} to 10^{-5} M, so that no dissociation $MX_2 \rightleftharpoons MX^+ + X^-$ had to be feared (see part II[1]). R, the ratio of the reactants A/B, was obtained from the volume ratio of the benzene solutions of MA_2 and MB_2, the relative concentration of which was determined by the ratio of their radioactivities. By choosing suitable volume and activity ratios it was possible to cover and measure accurately a range of 4 to 5 powers of ten in R.

* Permanent address: Israel Atomic Energy Commission, Hakiryah, Tel-Aviv, Israel.

DERIVATION OF EQUATIONS

Let a benzene solution of MA_2 be mixed with one of MB_2 and the mixture be shaken with an equal volume of the ionic medium. The general equations governing the distribution will be (in addition to (1) above):

$$MA_{2\,or} + MB_{2\,or} \rightleftharpoons 2MAB_{or}; \quad K_{or} = K\lambda_{11}^2\,\lambda_{20}^{-1}\,\lambda_{02}^{-1} \tag{1a}$$

$$[MA_2]_{or} = \lambda_{20}[MA_2]; \quad [MB_2]_{or} = \lambda_{02}\,[MB_2]; \quad [MAB]_{or} = \lambda_{11}\,[MAB] \tag{2}$$

The ratio R will be given by

$$R = \frac{2[MB_2]\,(1 + \lambda_{02}) + [MAB]\,(1 + \lambda_{11})}{2[MA_2]\,(1 + \lambda_{20}) + [MAB]\,(1 + \lambda_{11})} \tag{3}$$

and the distribution ratio D by

$$D = \frac{\lambda_{20}\,[MA_2] + \lambda_{11}\,[MAB] + \lambda_{02}\,[MB_2]}{[MA_2] + [MAB] + [MB_2]} \tag{4}$$

Determination of λ_{11}. Consider now the gradual addition of MB_2 to a large excess of MA_2. As a first approximation this will result in the gradual formation of MAB by reactions (1) and (1a), while the concentration $[MB_2]$ will remain negligible, provided that R remains small. If $[MA_2]$ and [MAB] are eliminated from (3) and (4) — and $[MB_2]$ neglected — the following expression is obtained

$$D = \frac{\lambda_{20}\,(1 + \lambda_{11})\,(1-R) + 2\lambda_{11}\,R\,(1 + \lambda_{20})}{(1 + \lambda_{11})\,(1-R) + 2\,R\,(1 + \lambda_{20})} \tag{5}$$

From this the linear expression for λ_{11}

$$2(1 + \lambda_{20})\,RD + (D-\lambda_{20})\,(1-R) = (2(1 + \lambda_{20})R - (D-\lambda_{20})\,(1-R))\lambda_{11} \tag{6}$$

is obtained, where λ_{11} is the slope when the left term is plotted *vs* the term in brackets on the right.

The ratio R must not be decreased too much, if λ_{11} is to be obtained accurately from (6), as otherwise there will be too large a spread in the points. On the other hand, as R is increased towards unity, the assumption $[MB_2] \approx 0$ is no longer valid if $K \neq \infty$, so that a plot of (6) will be curved, and λ_{11} will be the limiting slope at $R = 0$. Actually, as will be seen below, K is large and the plot of (6) is linear, within experimental errors, up to about $R = 0.40$.

The same arguments can be applied to the opposite case, *i. e.* when MA_2 is added to a large excess of MB_2, and R is very large. Then:

$$D = \frac{\lambda_{02}\,(1 + \lambda_{11})\,(R-1) + 2\lambda_{11}\,(1+\lambda_{02})}{(1+\lambda_{11})\,(R-1) + 2\,(1 + \lambda_{02})}\ \text{,and} \tag{7}$$

$$2(1 + \lambda_{02})\,D + (\lambda_{02}-D)\,(R-1) = (2(1 + \lambda_{02}) + (\lambda_{02}-D)\,(R-1))\lambda_{11}, \tag{8}$$

so that λ_{11} may be obtained also from plotting eqn. (8).

The distribution coefficient of MAB, λ_{11}, is thus obtained independently from the two ranges where R is small and where it is large.

Determination of K. It remains now to consider the intermediate region where $R \sim 1$ and it is no longer permissible to neglect any of the species MA_2, MAB and MB_2. If, then, the concentrations of these species are eliminated from (1), (3) and (4), and the equations solved for K, the following is obtained:

$$K = 4[(\lambda_{02}-D)(1+\lambda_{20})R-(D-\lambda_{02})(1+\lambda_{02})]^2[2(1+\lambda_{02})(D-\lambda_{11})+(1+\lambda_{11})(R-1)(D-\lambda_{02}]^{-1}[2(1+\lambda_{20})(D-\lambda_{11})R-(D-\lambda_{20})(1+\lambda_{11})(R-1)]^{-1} \quad (9)$$

which simplifies in the case of $R = 1.00$ to

$$K = \frac{((\lambda_{02}-D)(1+\lambda_{20})-(D-\lambda_{20})(1+\lambda_{02}))^2}{(1+\lambda_{20})(1+\lambda_{02})(D-\lambda_{11})^2} \quad (9a)$$

In this way K is obtained from the distribution at $R \sim 1$ combined with the value of λ_{11} obtained above. To test its validity, it is inserted into the general equations (3) and (4). Introducing the parameter $y = [MB_2]^{\frac{1}{2}}[MA_2]^{-\frac{1}{2}}$, the expressions:

$$R = \frac{2y^2(1+\lambda_{02}) + K^{\frac{1}{2}}y(1+\lambda_{11})}{2(1+\lambda_{20}) + K^{\frac{1}{2}}y(1+\lambda_{11})} \quad (10)$$

and

$$D = \frac{\lambda_{20} + \lambda_{11}K^{\frac{1}{2}}y + \lambda_{02}y^2}{1 + K^{\frac{1}{2}}y + y^2} \quad (11)$$

are obtained, and a plot of log D *vs* log R, calculated with y as auxiliary variable, may then be compared with experimental values.

Table 1. Distribution data for the Hg—Br—I neutral complexes.

log R	log M	log D	log R	log M	log D
−2.40	−4.6	0.160 ± 0.010	0.30	−4.5	0.900 ± 0.010
−1.90	−4.1	0.170 ± 0.008	0.40	−4.3	0.975 ± 0.010
−1.70	−4.8	0.175 ± 0.015	0.46	−5.0	1.020 ± 0.015
−1.50	−4.6	0.180 ± 0.010	0.52	−4.5	1.050 ± 0.010
−1.30	−4.6	0.195 ± 0.010	0.70	−4.5	1.185 ± 0.010
−1.10	−5.1	0.225 ± 0.015	0.73	−4.3	1.230 ± 0.008
−0.90	−4.1	0.270 ± 0.008	0.90	−4.3	1.290 ± 0.010
−0.70	−4.3	0.330 ± 0.008	0.92	−5.0	1.335 ± 0.015
−0.50	−4.1	0.420 ± 0.008	1.20	−4.3	1.485 ± 0.008
−0.30	−4.9	0.480 ± 0.015	1.30	−4.9	1.515 ± 0.015
−0.20	−4.6	0.555 ± 0.010	1.35	−4.5	1.545 ± 0.010
−0.10	−4.1	0.600 ± 0.008	1.36	−4.5	1.530 ± 0.010
0.00	−4.3	0.675 ± 0.008	1.60	−5.0	1.590 ± 0.015
0.05	−5.0	0.720 ± 0.015	2.00	−4.5	1.665 ± 0.010
0.20	−5.1	0.795 ± 0.015	2.70	−5.0	1.740 ± 0.015

All values of log R are ±0.01, all values of log M are ±0.1. Symbols in Fig. 3 are: log M −4.1 to −4.3 ●, log M −4.5 to −4.6 ■, and log M −4.8 to −5.1 ▲.

EXPERIMENTAL RESULTS

The distribution values obtained for the pair of ligands Br—I are given in Table 1, while for all three pairs Cl—Br, Cl—I and Br—I the data are given as log D (log R) curves in Figs. 1, 2 and 3.

In order to obtain λ_{11}, plots were made (Fig. 4) of eqns. (6) — squares — and (8) — circles — for the ranges of low R and high R, for the above three pairs of ligands, using the values of λ_{20} and λ_{02} found previously (part I[2]): log $\lambda(HgCl_2) = -0.963$, log $\lambda(HgBr_2) = 0.152$, log $\lambda(HgI_2) = 1.77$, in conjunc tion with the present data.

Fig. 4 shows that the plots are linear in the regions used, $R < 0.40$ and $R > 2.5$, and shows also very good agreement of the slopes in these regions with each other, so that the value of λ_{11} obtained expresses the data well.

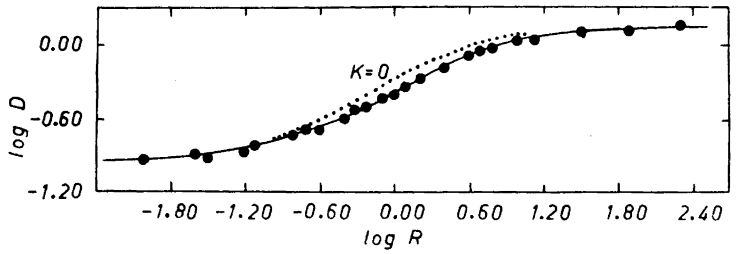


Fig. 1. The distribution ratio D of mercury between benzene and aqueous solutions in system Hg-Cl-Br, as function of the ratio R of $HgBr_{2\ tot}$ / $HgCl_{2\ tot}$ ● experimental points, ——— calculated with log $\lambda_{11} = -0.42$ and log $K = 2.0$, ... calculated with $K = 0$.

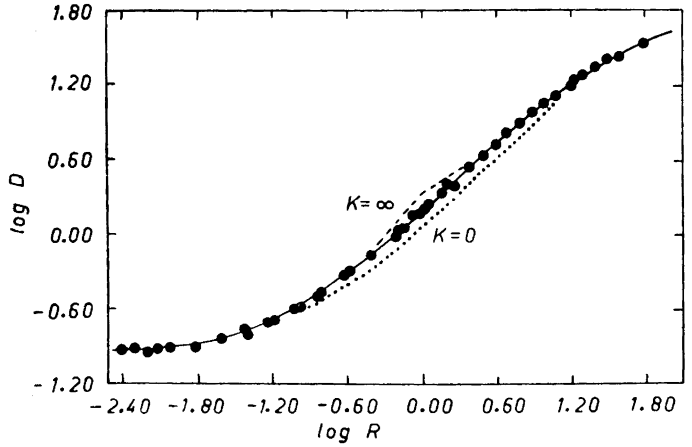


Fig. 2. The distribution ratio D of mercury between benzene and aqueous solutions in system Hg-Cl-I, as function of the ratio R of $HgI_{2\ tot}$ / $HgCl_{2\ tot}$ ● experimental points, ——— calculated with log $\lambda_{11} = 0.28$ and log $K = 1.75$, ... calculated with $K = 0$, — — — — calculated with $K = \infty$.

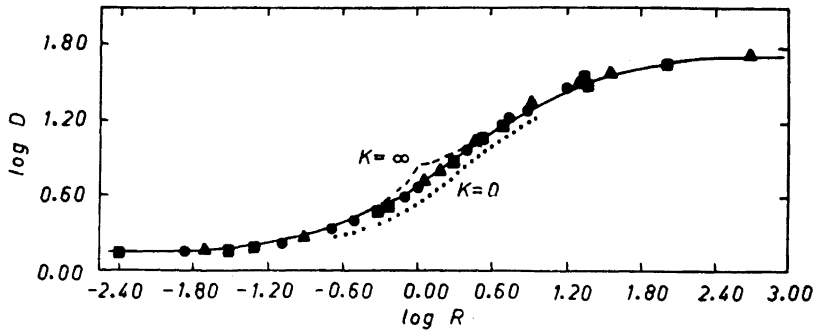


Fig. 3. The distribution ratio D of mercury between benzene and aqueous solutions in system Hg-Br-I, as function of ratio R of $HgI_{2\ tot}$ / $HgBr_{2\ tot}$. ●, ■, and ▲ experimental points explained in Table 1, ——— calculated with $\log \lambda_{11} = 0.79$ and $\log K = 1.10$, ... calculated with $K = 0$, — — — calculated with $K = \infty$.

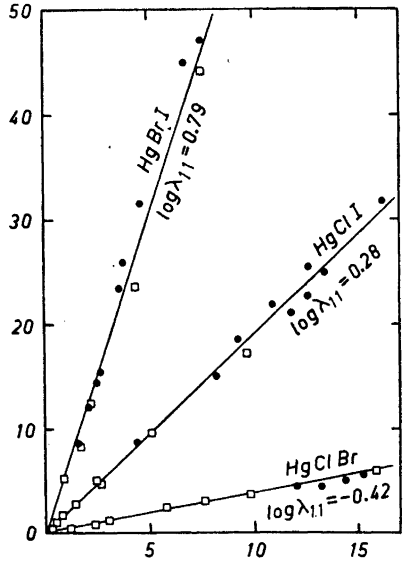


Fig. 4. Plots of eqns. (6) and (8) (□ and ●, respectively), where both sides of the equations were multiplied by the same arbitrary constant to bring them down to the same scale. The best straight lines drawn have slopes equal to the λ_{11} values given in the text.

Ordinate: □ $\text{const}_1(2(1+\lambda_{20})\ R\ D+(D-\lambda_{20})\ (1-R))$
● $\text{const}_2(2(1+\lambda_{02})D+(\lambda_{02}-D)(R-1))$

Abscissa: □ $\text{const}_1(2(1+\lambda_{20})R-(D-\lambda_{20})(1-R))$
● $\text{const}_2(2(1+\lambda_{02})+(\lambda_{02}-D)(R-1))$

The values of λ_{11} obtained are:

$\log \lambda(\mathrm{HgClBr}) = -0.42 \pm 0.04$ $\log \lambda(\mathrm{HgClI}) = 0.28 \pm 0.02$
$\log \lambda(\mathrm{HgBrI}) = 0.79 \pm 0.04$

For the range $-0.4 < \log R < 0.4$, the experimental values of R and D, together with the binary and ternary distribution coefficients listed above, were inserted into eqn. (9) to calculate K. The values obtained (numerical averages) are:

$\log K(\mathrm{HgClBr}) = 2.0 \pm 0.5$ $\log K(\mathrm{HgClI}) = 1.75 \pm 0.20$
$\log K(\mathrm{HgBrI}) = 1.10 \pm 0.20$

The values of λ_{11} and K were inserted into eqns. (5), (7) and (11) and the calculated distribution plotted in Figs. 1, 2 and 3 (dashed curves for (5) and (7) in the range $-0.4 < \log R < 0.4$, otherwise solid curves), agreeing well with the data.

Had no mixed complexes been formed, *i. e.* $K = 0$, the dotted curves in Figs. 1, 2 and 3 would have been obtained. These, however, do not agree with the experimental data, so that the formation of the ternary complexes in solution might be considered proved.

DISCUSSION

The equilibrium in the aqueous phase. The significance of the constants obtained above may be seen in Fig. 5. In it is plotted the mole percentage of the three species MA_2, MAB and MB_2 as function of $\log R$. The continuous curves were calculated with the experimental value $K = 56$ for Hg—Cl—I, but they express also approximately the cases of Hg—Cl—Br and Hg—Br—I, since the K values possess wide limits of error, and since the curves are not too sensitive to the exact value of K, provided it is "large". It is seen that MAB is an important species in the range of about $-1.2 < \log R < 1.2$. Moreover, it is seen that $[MB_2]$ is negligibly small up to $\log R = -0.4$ and that $[MA_2]$ is so above $\log R = 0.4$ as assumed in the calculations.

If K were equal to infinity, MAB would be completely stable at $R = 1$, and $[MA_2]$ and $[MB_2]$ would remain negligible respectively right up to and above $R = 1$. This is shown by the long-dashed curves in Fig. 5.

Had the mixed complex formation proceeded statistically, there would have been at equilibrium 25 mole % MA_2, 25 mole % MB_2 and 50 mole % MAB when $R = 1$. The equilibrium constant would then have been $(0.50)^2 (0.25)^{-1} (0.25)^{-1} = 4$. Fig. 5 shows this case by a pair of short-dashed curves. The area enclosed between them is smaller than that corresponding to the observed K, or in other words, the mixed complexes are more stable than statistically expected. The difference $\log K - \log K_{\mathrm{stat.}} = \log K - 0.60$ may be called the stabilization constant, $\log K_{\mathrm{stab.}}$:

$\log K_{\mathrm{stab.}}(\mathrm{HgClBr}) = 1.4 \pm 0.5$ $\log K_{\mathrm{stab.}}(\mathrm{HgClI}) = 1.15 \pm 0.20$
$\log K_{\mathrm{stab.}}(\mathrm{HgBrI}) = 0.5 \pm 0.2$

More will be said about this in part V of this series.

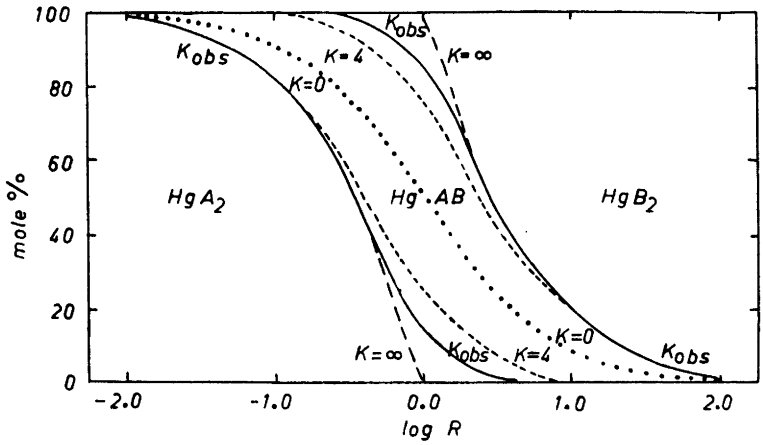


Fig. 5. The mole percentage of the species MA_2, MAB and MB_2 as function of the ratio R of $MB_{2\ tot}$ / $MA_{2\ tot}$. ——— calculated with observed value of K (for HgClI), — — — calculated with $K = \infty$, - - - - - - calculated with $K_{stat.} = 4$, ... calculated with $K = 0$.

Finally, had there been no mixed-complex formation, $K = 0$, then, of course, the area of MAB would have vanished, and the single dotted curve in Fig. 5 would have described the system MA_2—MB_2.

The equilibrium in the organic phase. Equilibrium and stabilization constants may also be calculated for the organic phase according to eqn. (1a):

HgClBr	$\log K_{or} = 2.0 \pm 0.5$	$\log K_{or\ stab.} = 1.4 \pm 0.5$
HgClI	$= 1.51 \pm 0.20$	$= 0.91 \pm 0.20$
HgBrI	$= 0.76 \pm 0.20$	$= 0.16 \pm 0.20$

The statistical value for the distribution coefficient of the ternary complexes is the geometrical mean of the coefficients of the binary complexes, and is compared below with the observed values:

HgClBr	$\log \lambda_{11}$ observed $= -0.42 \pm 0.04$	$\log \lambda_{11}$ statis. $= -0.40 \pm 0.02$
HgClI	$= 0.28 \pm 0.02$	$= 0.40 \pm 0.02$
HgBrI	$= 0.79 \pm 0.04$	$= 0.96 \pm 0.02$

It is seen that the distribution coefficient is significantly smaller, at least for HgClI and HgBrI, than the statistically calculated value. This means that the ternary complex is more favoured in the aqueous than in the benzene phase, as may also be seen by comparing the respective stabilization constants in the two phases.

Previous work. Previous reports of mercury(II) mixed halides are quite numerous. Although Pelt and Boes [3] could not find an indication for HgClBr formation from solubility measurements on mixtures of $HgCl_2$ and $HgBr_2$,

Losana [5] and later Scholter and Bijvoet [4] found a solid, so called B-phase, made up of linear HgClBr molecules. However, with solids, mixed compound formation might be confused with mixed crystal (solid solution) formation. Mixed $Hg(Cl_2, Br_2)$ crystals have thus been found formed from melts [6] or solutions [7]. Oppenheim [8] claimed almost 90 years ago that HgBrI precipitates (and may be sublimed unchanged) if an alkyl iodide is added to an acetone solution of $HgBr_2$. Köhler [9] ten years later gave a method to prepare what he stated to be HgClI. Vournazos [10] concluded that a mixed bromide-iodide compound of mercury, which he claimed contains the ion $Hg_2Br_4I^-$, is formed when water insoluble iodides dissolve in acetone solutions of $HgBr_2$.

All the above is evidence (though sometimes disputed) for the formation of solid ternary complexes, but there is also evidence for their formation in solution. Delwaulle and Francois, in a number of papers [11], reported that ethanolic, methanolic and aqueous solutions of mixtures of mercury(II) halides show Raman lines which could not be ascribed to either of the binary components, but must be due to a ternary compound. Moreover, they state [11d] that the intensity of the Raman lines is proportional to the concentration, so that in principle it should have been possible to calculate the equilibrium constants. Unfortunately, the authors generally neither calculated the constants, nor reported their primary data, so that their results are only qualitative.

The one exception to this is the constant $K = 2{,}0 \pm 0{,}2$ reported for the reaction $HgCl_2 + HgBr_2 = 2\ HgClBr$ in methanol [11c]. This constant is smaller than the statistical value, but the reliability of the constant seems to be less than its reported precision indicates, because of larger possible errors in the quantities entering its calculation.

Even in the vapour phase the ternary compounds seem to be rather stable. Although Hintz and Jellinek [12] found that the vapour phase above a $HgCl_2$—$HgBr_2$ mixture is an ideal mixture, Wehrli and Milazzo [13] found stable HgClBr and HgBrI vapours that dissociate only under UV radiation. Müller [14] measured the spectra of MAB vapours already at temperatures as low as 50° C. He prepared HgBrI according to Oppenheim's procedure [8] and HgClI and HgClBr according to Köhler's [9]. The special "mixed" bands he observed in the spectra were most intense for HgClI. He explained this effect by pointing out that HgClI has the most unsymmetrical weight distribution among the three ternary compounds.

Although the authors cited above indicate qualitatively the formation of mixed halide compounds HgAB, no values of the equilibrium constants for aqueous solutions seem to have been hitherto reported.

The author wishes to thank the *Israel Atomic Energy Commission* for a research grant abroad, Professor Lars Gunnar Sillén for the facilities provided, and particularly for his advice, comments and criticism, and Dr. Helen S. Dunsmore for improving the English presentation.

REFERENCES

1. Marcus, Y. *Acta Chem. Scand.* **11** (1957) 599. Part II.
2. Marcus, Y. *Acta Chem. Scand.* **11** (1957) 329. Part I.
3. van Pelt, A. J. and de Boes F. *Z. physik. Chem.* **170 A** (1934) 256.
4. Scholter, W. and Bijvoet, J. M. *Z. Krist.* **A 103** (1941) 415.

5. Losana, L. *Gazz. chim. ital.* **56** (1926) 301.
6. Reinders, W. *Z. physik. Chem.* **32** (1900) 494.
7. Vegard, L. *Skrifter Norske Videnskaps-Akad. Oslo I. Mat. Naturv. Kl.* **1947** No. 2, p. 9.
8. Oppenheim, A. *Ber.* **2** (1869) 571.
9. Köhler, H. *Ber.* **12** (1879) 1187.
10. Vournazos, A. C. *J. prakt. Chem.* **136** (1933) 41.
11. a. Delwaulle, M. I. *Compt. rend.* **206** (1938) 1965.
    b. Francois, F. *Compt. rend.* **207** (1938) 425.
    c. Delwaulle, M. and Francois, F. *Compt. rend.* **208** (1939) 999, 1002.
    d. Delwaulle, M. and Francois, F. *Bull. soc. chim. France* **1940** 359.
    e. Delwaulle, M. *Bull. soc. chim. France* **1955** 1294.
12. Hintz, H. and Jellinek, K. *Z. Elektrochem.* **42** (1936) 187.
13. Wehrli, M. and Milazzo, G. *Helv. Chim. Acta* **26** (1943) 1025.
14. Müller, P. *Helv. Phys. Acta* **15** (1952) 233.

Received January 4, 1957.

ACTA CHEMICA SCANDINAVICA 11 (1957) 619—627

The Anion Exchange of Metal Complexes

The Silver — Thiosulphate System

Y. MARCUS

Israel Atomic Energy Commission Research Establishment and Royal Institute of Technology, Department for Inorganic Chemistry, Stockholm 70, Sweden

The silver thiosulphate system has been studied by an anion exchange method. Batch equilibrations and column elutions gave silver distribution data between Dowex-1-thiosulphate resin and solutions of $Na_2S_2O_3$ in the concentration range 0.01—4 M. The thiosulphate concentrations in the resin in excess over its capacity were measured, and the activity of thiosulphate ion in the resin calculated. This together with the distribution data yielded the "ideal" distribution curve, whence it appears that if the resin species is $RAgS_2O_3$, then $Ag(S_2O_3)_3^{5-}$ will predominate in the solution. For the reaction $Ag(S_2O_3)_2^{3-} + S_2O_3^{2-} \rightleftharpoons Ag(S_2O_3)_3^{5-}$ the concentration quotient at 1—2 M ionic strength is $k' = 2.5 \pm 0.5$, while for $Ag(S_2O_3)_3^{5-} + 1/2\ R_2S_2O_3 \rightleftharpoons RAgS_2O_3 + 5/2\ S_2O_3^{2-}$ the constant is $K'' = 5$.

The complex systems previously studied in this laboratory were of the type in which a neutral complex could form. The anion exchange method developed for studying complex systems may, however, also be applied to systems in which neutral complexes are unable to form. This has already been demonstrated by the calcium citrate system [1], for which, however, the data are rather scant. It was thought, therefore, that it would be of interest to work out a similar system in detail.

The silver thiosulphate system was chosen, as it has already been studied by a number of authors [2-4], and complexity constants are available for comparison. The system has been shown to be mononuclear, so that in the sequence of species: Ag^+, $Ag(S_2O_3)^-$, $Ag(S_2O_3)_2^{3-}$ ... no neutral species appears.

Apart from the general interest in the silver-thiosulphate system (for photography), there is also a specific interest in its anion-exchange behaviour, in connection with the separation of silver from other metals or its recovery from spent photographic solutions. Lure and Perenyslova [5] have applied the resin *m*-phenylenediamine sulphate to silver-thiosulphate solutions. The silver was absorbed (as $Ag(S_2O_3)_2^{3-}$ according to the authors), but was rapidly reduced to Ag_2S, the resin functioning as catalyst.

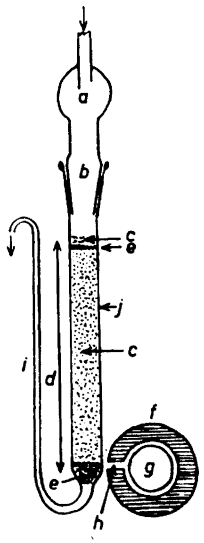


Fig. 1. The column for elution experiments. a: dropping rate counter; b: standard taper 14/35 ground joint; c: Dowex-1-X10 thiosulphate resin; d: distance between top and bottom of column $d = 8.0 \pm 0.2$ cm; e: glass wool plugs; f: lead shield; g: G.-M. cylindrical counter; h: 3 mm diameter hole in shield; i: 1 mm diameter capillary tube; j: 4.8 mm inner diameter glass column.

In order to apply the anion exchange distribution data quantitatively to complexity calculations, it is necessary, as has been pointed out before, to know the activity of the ligand in the resin. This could not be found in the literature, and had to be determined in addition to the silver distribution.

EXPERIMENTAL

Materials. A known weight of > 99.9 % pure silver wire, irradiated by A. E. R. E. Harwell, England, to produce ^{110}Ag (half life = 9 months), was dissolved in moderately concentrated nitric acid. The solution was then neutralized with ammonia and diluted with water to 1.00×10^{-4} M in silver and about 0.01 M in nitrate.

Sodium thiosulphate pentahydrate was dissolved in water to saturation (about 4 M), and from this stock solution others were prepared by dilution. No mould growth was observed in the concentrated solution during more than a month.

Dowex-1 resin, 10 % cross-linked and 100—200 mesh, was converted from the chloride to the thiosulphate state by passing a tenfold excess of 2 M sodium thiosulphate through a column of the resin. Finally, after destruction of the thiosulphate in the effluent by adding 1 M sulphuric acid, heating to coagulate the sulphur and centrifuging it off, no more chloride could be detected. The resin was then thoroughly washed with water, and a portion shaken with 1 M ammonium nitrate showed no remaining chloride.

Pyrex glass was ground to a powder of 100—200 mesh, washed with dilute nitric acid and water and dried.

All other reagents were of analytical grade.

Procedure. The column for the elution studies consisted of a narrow glass tube (Fig. 1), of inner diameter 0.48 cm (cross section $A = 0.180 \pm 0.003$ cm^2). It contained a weight $w = 0.725 \pm 0.002$ g of air dried resin to a height $d = 8.0 \pm 0.2$ cm above a glass wool plug. A G.-M. counter surrounded by a thick lead shield was mounted with a window in the shield opposite the bottom of the resin column. On top of the resin was another, narrow, glass wool plug, on top of which was placed a small portion of resin (50.0 ± 1.0 mg), previously saturated with radioactive silver (absorbed from 0.05 M sodium thiosulphate). Thiosulphate solutions were passed through the column to elute the silver.

The active zone passed the distance d cm from the top of the column to the counter at the bottom at a known volume of eluant, V ml, obtained from the maximum in a plot of counting rate *vs.* volume. Similar arrangements are described by Forsling [6] and Kraus and Moore [7].

Batch experiments were made by shaking resin with solution for 16—20 h, which was shown to be two to three times in excess of that needed for equilibration. The dipping G.-M. tube used for radioassay counted only the gamma rays owing to its rather thick walls.

For measuring the excess thiosulphate in the resin, portions of resin or glass were shaken for 2 h with aliquots of thiosulphate solutions. The solid was then quantitatively filtered off, and thiosulphate was determined in the filtrate by titration with iodine solutions standardized against pure solid arsenic(III) oxide. The powder on the filter was washed thoroughly with water, then shaken for 2 h with a hundred times excess, on an equivalent basis, of 5 % sodium chloride. The selectivity coefficient value of Wheaton and Bauman [21] for the sulphate-chloride exchange was taken as indicative of that of the thiosulphate-chloride exchange. On this basis it was calculated that at equilibrium with the 5 % sodium chloride (0.85 M), no more than 0.2 % of the thiosulphate will remain on the resin. The sodium chloride solution was filtered away and the powder was again washed. In the combined filtrate and washing, thiosulphate was determined. In this way both the solution and the resin thiosulphate concentration were known for equilibrium.

All experiments were repeated and agreed within ± 1.5 %. They were made at room temperature, about 25—30 °C.

RESULTS

No significant influence of silver concentration on the anion exchange distribution in the silver concentration range 2×10^{-6} to 2×10^{-4} M with a thiosulphate concentration of 0.64 M could be found. The value of the distribution obtained from eight measurements was $D = 180 \pm 15$. The formation of polynuclear complexes in the solutions is thus very unlikely.

Batch equilibrations, using 4×10^{-3} to 1.28 M thiosulphate solutions, with equilibrium concentration of silver less than 5×10^{-6} M and loading less than 1 % of the capacity, gave the distribution values D in Table 1.

Elution experiments using 0.10 to 4.24 M thiosulphate solutions gave the distribution values appearing in Table 2. They were calculated in the following way, based on the method of Kraus and Moore [7].

Table 1. Anion exchange distribution of silver as function of thiosulphate concentration; batch method.

Thiosulphate concentration M	$-\log a_{Na_2S_2O_3}$	log D (ml/g)	Thiosulphate concentration M	$-\log a_{Na_2S_2O_3}$	log D (ml/g)
0.004	2.43	$\geqslant 5.15$	0.080	1.45	3.90 ± 0.20
0.008	2.20	$\geqslant 5.15$	0.128	1.29	3.36 ± 0.02
0.016	1.98	4.64 ± 0.10	0.16	1.22	3.23 ± 0.05
0.032	1.75	4.48 ± 0.08	0.32	0.99	2.71 ± 0.05
0.040	1.67	4.10 ± 0.25	0.64	0.76	2.25 ± 0.02
0.064	1.51	3.79 ± 0.05	1.28	0.53	1.49 ± 0.02

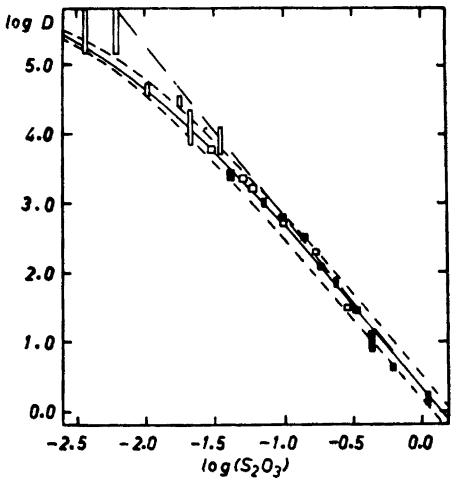


Fig. 2. The distribution of silver as function of thiosulphate activity. ■ and □ experimental points with margins of error for column and batch, methods. ═══ Curves calculated with the constants log $K = 2.1 \pm 0.1$ and log $k_3 = 1.7 \pm 0.2$. — — — — Straight line with slope −5/2.

An elution constant E is defined by eqn. (1)

$$E = d \cdot A \cdot V^{-1} \tag{1}$$

where d, A and V are the quantities defined above. E is related to the volume distribution coefficient D_v by eqn. (2)

$$E = (D_v + i)^{-1} \tag{2}$$

where i is the fractional interstitial volume, having the value 0.45 (this, however, need not be known accurately for large enough distributions). The mass distribution coefficient D is related to D_v by the specific volume of the resin $d \cdot A \cdot w^{-1}$ where w is the weight of the resin in g in the d cm long column:

$$D = d \cdot A \cdot w^{-1} \cdot D_v = w^{-1} \cdot V - (i \cdot d \cdot A \cdot w^{-1}) \tag{3}$$

Inserting the particular values for the column amployed, D is obtained in terms of V directly as

$$D = 1.38\ V - 0.9 \text{ ml/g} \tag{4}$$

Table 2. Anion exchange distribution of silver as function of thiosulphate concentration; column method.

Thiosulphate concentration M	$-\log a_{Na_2S_2O_3}$	log D (ml/g)	Thiosulphate concentration M	$-\log a_{Na_2S_2O_3}$	log D (ml/g)
0.10	1.37	3.45 ± 0.05	0.96	0.62	1.81 ± 0.05
0.20	1.14	2.99 ± 0.07	1.49	0.47	1.43 ± 0.06
0.30	1.00	2.79 ± 0.05	2.00	0.36	0.94 ± 0.20
0.50	0.84	2.49 ± 0.05	2.96	0.21	0.60 ± 0.06
0.72	0.72	2.08 ± 0.05	4.24	−0.05	0.16 ± 0.10
0.96	0.62	1.88 ± 0.05			

Values of the activity coefficients of thiosulphate solutions were taken from Stokes [8] and converted from the molal to the molar scale.

A log D(log $a_{Na_2S_2O_3}$) plot is shown in Fig. 2 for values of both Tables 1 and 2.

The thiosulphate capacity of the resin was determined to be 1.255 ± 0.003 mmole/g. The chloride displaced from the resin amounted to 2.55 mequiv/g, which means that the thiosulphate occupies 2.55/1.255 = 2.0 sites on the resin, as would be expected from its charge.

The water content of air-dried resin was determined in a "drying pistol" at 78° C, and was found to be 29.5 ± 0.3 % W/W.

The concentration of thiosulphate in a resin in equilibrium with a thiosulphate solution is made up of three parts: the fixed capacity, the invading electrolyte, and the surface-sorbed material, *i. e.* the part contained in a mechanically-held film on the surface, of the same concentration as the bulk of the solution, and assumed to be equal to the amount sorbed on a similar glass powder surface. Table 3 gives the thiosulphate concentrations in these three categories as functions of solution concentration in the range 0.01 to 2 M.

In cases where the excess electrolyte is small, and at low thiosulphate concentrations, the combined amounts "excess electrolyte" + "glass" were obtained directly from the difference between initial and final thiosulphate concentration in the solution. At high thiosulphate concentrations, when this becomes inexact, the thiosulphate displaced from the resin by 5 % sodium chloride, *i. e.* the "total resin" concentration was the directly measured quantity.

Table 3. Thiosulphate concentration on resin and glass as function of solution concentration.

Solution M	Total resin mmole/g	Glass mmole/g	Net resin mmole/g	Excess electrolyte mmole/g
0.010	1.265	0.005	1.260 ± 0.005	0.005 ± 0.005
0.020	1.270	0.005	1.265 ± 0.005	0.010 ± 0.005
0.050	1.290	0.005	1.285 ± 0.005	0.030 ± 0.005
0.100	1.310	0.005	1.305 ± 0.005	0.05 ± 0.01
0.300	1.375 ± 0.005	0.010	1.365 ± 0.005	0.11 ± 0.01
0.706	1.55 ± 0.01	0.010	1.530 ± 0.005	0.28 ± 0.01
1.00	1.67 ± 0.01	0.047	1.62 ± 0.01	0.37 ± 0.01
2.02	2.48 ± 0.01	0.098	2.38 ± 0.01	1.13 ± 0.01

CALCULATIONS

The resin thiosulphate activity was calculated by the method used by Kraus and Moore [9] and by Gottlieb and Gregor [10]. At equilibrium the activities of sodium thiosulphate are equal in both phases:

$$(Na)^2(S_2O_3) = 4[S_2O_3]^3 f_{\pm}^3 = (Na)_r^2(S_2O_3)_r = [Na]_r^2[S_2O_3]_r f_{\pm r}^3 \qquad (5)$$

where parentheses denote activities, square brackets — concentrations, suffix r — resin phase, no suffix — solution phase and $f_{\pm}$ the average activity coefficients.

In order to compare the two phases, resin concentrations were converted to mole/liter by the factor 3.40 kg/l, obtained from the water content of the air-dried resin. This factor was assumed to be independent of the thiosulphate concentrations because no expansion or contraction of the resin could be observed when the concentration of the eluant was changed in the column experiments.

The term $[Na]_r$ is equal to twice the "excess electrolyte" in Table 3, as this is the only sodium ion source in the resin. The term $[S_2O_3]_r$ is equal to "net resin" in Table 3. Rearranging eqn. (5), the ligand activity in the resin is obtained

$$\log (S_2O_3)_r = \log [S_2O_3]_r f_{\pm r} = 2/3 \log \text{"net resin"} + \log [S_2O_3] + \quad (6)$$
$$+ \log f_{\pm} - 2/3 \log \text{"excess electrolyte"} - \log 3.40$$

Eqn. (6) introduces the activity of a single ion — $S_2O_3^{2-}$ — which necessitates an extrathermodynamic assumption. As the resin phase is a concentrated aqueous solution, at least 2.5 equiv. per 295 g water, *i. e.* 8.5 N, it is felt that this is a region where the Debye-Hückel term of the activity coefficient plays a minor role compared with the hydration term. Thus $f^r_{S_2O_3^{2-}}$ was assumed equal to $f_{\pm r}$. As regards the aqueous solutions, although their concentration range was mainly much lower than that of the resin, the same assumption was made, as the alternate extreme assumption: $\log f_{S_2O_3^{2-}} = 4 \log f_{Na^+}$ led to a curve concave upwards, *i. e.* representing a decreasing formation function $\bar{n}$ with increasing concentration, and this is untenable.

Values of the ligand activity calculated from eqn. (6) are given in Table 4.

Table 4. Resin ligand activity as function of solution activity.

$[Na_2S_2O_3]$ M	0.010	0.020	0.050	0.100	0.300	0.706	1.00	2.02
$-\log (S_2O_3)$	2.14	1.97	1.60	1.35	1.00	0.72	0.62	0.36
$-\log (S_2O_3)_r$	1.2	1.1	1.02	0.94	0.81	0.75	0.73	0.67

An arbitrary standard state will be defined as that corresponding to unit solution activity, and from extrapolation of the values of Table 4 — which, incidentally gives a linear plot — the value $\log (S_2O_3)^0_r = -0.56$ was obtained from eqn. (7)

$$\log (S_2O_3)_r = \log (S_2O_3)^0_r + F(\log (S_2O_3)) \quad (7)$$

The main reaction of absorption of silver by the resin may be formulated as

$$Ag(S_2O_3)_p^{1-2p} + (p - 1/2)R_2S_2O_3 \rightleftharpoons R_{2p-1}Ag(S_2O_3)_p + (p - 1/2)S_2O_3^{2-} \quad (8)$$

where p might be 1,2,... and R is one equivalent of resin cation. The range of variation of the resin ligand activity is not very large, so it may be assumed that only one value of p must be considered, and the total concentration of silver on the resin is $[Ag(S_2O_3)_p]_r$.

The equilibrium constant of reaction (8) will have the resin ligand activity to the $(p - 1/2)$ power. It has been shown before [1] that this means that the ideal distribution D_0 is obtained from the measured D from the relationship

$$\log D_0 = \log D - (p - 1/2) \cdot F(\log (S_2O_3)) \quad (9)$$

As in the thiosulphate range employed the function F has negative values ($\log (S_2O_3)^0_r$ greater than any value of $\log (S_2O_3)_r$), the actual "invasion" correction will give a curve $\log D_0$ ($\log (S_2O_3)_r$), above the $\log D$ curve, and with a steeper slope.

The values $p = 1$, 2 and 3 were tried and found to yield $\log D_0$ curves with limiting slopes of —2.5, —2.9 and —3.3, respectively. However, only the value of $p = 1$, giving a slope of —2.5, is consistent with the presence of $Ag(S_2O_3)^{3-}_2$ and $Ag(S_2O_3)^{5-}_3$ in the solutions under consideration, to which the evidence points [2-4,17,18,20]. That this is so may be seen from the expression for D_0 which may easily be derived (see also Ref.[1]).

$$D_0 = k_\alpha \beta_p (S_2O_3)^{0p-1/2}_r (S_2O_3)^{1/2} / (\beta_2 (S_2O_3)^2 + \beta_3 (S_2O_3)^3) =$$
$$= K \ (S_2O_3)^{-3/2} (1 + k_3 (S_2O_3))^{-1} \quad (10)$$

where $K = k_\alpha \beta_p \beta_2^{-1} (S_2O_3)^{0p-1/2}_r$, and k_α is the equilibrium constant of (8).

Combining eqns. (9) and (10), $\log D$ is obtained in terms of $\log (S_2O_3)$

$$\log D = (p - 1/2) \cdot F(\log (S_2O_3)) + \log K - 3/2 \log (S_2O_3) - \quad (11)$$
$$- \log (1 + k_3 (S_2O_3)$$

Using $p = 1$ and the values $\log K = 2.1 \pm 0.1$ and $\log k_3 = 1.7 \pm 0.2$, the calculated solid curve in Fig. 2 is obtained, and is considered as giving the best fit with the experimental data. However, owing to the relatively large random errors in the data, especially in the low concentration range, the curvature of the plot in this range, indicating the presence of $Ag(S_2O_3)^{3-}_2$ in the most dilute solutions, may not be real. The data could also be fitted by a curve $\log D = 1/2$ F($\log (S_2O_3)$) + $\log K$ — 5/2 $\log (S_2O_3)$ (and even by a straight line of slope —5/2, which neglects the invasion correction), but these curves would mean that no $Ag(S_2O_3)^{3-}_2$ is present in this concentration range. The fit of these latter two curves is poorer than the fit obtained when unity is not neglected in comparison with $k_3(S_2O_3)$ in this range (eqn. (11)). The value found for k_3 may be considered as the lower limit of the equilibrium constant.

DISCUSSION

The value of the complexity constant found, k_3, is not immediately comparable with reported values, as the latter are all concentration constants, while the former is valid for zero ionic strength. However, by replotting the D_0 distribution curve against the thiosulphate concentration, instead of against its activity, a concentration quotient $k'_3 = 2.5 \pm 0.5$ is obtained, which is consistent with the experimental data. The main effect of the transition of $Ag(S_2O_3)^{3-}_2$ to $Ag(S_2O_3)^{5-}_3$ occurs in the range 0.3 to 0.7 M thiosulphate, therefore this value of k'_3 should be valid around ionic strengths of one to two.

Bodländer's values [2] may be regarded only as approximate, but they are of the correct order of magnitude: $\beta_2 = 10^{13}$ and $\beta_3 = 3.5 \times 10^{13}$, *i. e.* $k_3' = 3.5$. Concentration quotients valid at 2 M ionic strength were obtained by Ölander and Adelson [3], using a potentiometric method, at 25° C. They obtained $\beta_2 = 6.0 \times 10^{12}$ and $\beta_3 = 1.15 \times 10^{13}$, *i. e.* $k_3' = 1.9$. Chateau and Pouradier [4] assume that the activity coefficient of $Ag(S_2O_3)_2^{3-}$ is equal to that of $S_2O_3^{2-}$ (obtaining $\beta_2 = 2.8 \times 10^{13}$), but that the coefficient of $Ag(S_2O_3)_3^{5-}$ is different, obtaining β_3 values in the range 1.5×10^{14} to 5.0×10^{14}, or, extrapolated to zero thiosulphate concentration, 1.4×10^{14}, *i. e.* $k_3 = 4.8$. They worked at 20° C, also employing a potentiometric method. No other determinations of k_3 are reported.

Determination of other constants in the silver-thiosulphate system were also made. Pawelka [11] found $\beta_2 = 2.4 \times 10^{13}$, while Ferrell and coworkers [12] obtained only an approximate estimate of 4×10^{14} for this constant. Carriere [13] found by a conductivity method $\beta_1 = 7.4 \times 10^8$, and Chateau and Pouradier [14], working at 70° C with a potentiometric method found it to be 2.75×10^7.

The assumption of the presence of both $Ag(S_2O_3)_2^{3-}$ and $Ag(S_2O_3)_3^{5-}$ in thiosulphate solutions of moderate concentrations is supported by much additional, though qualitative, evidence. Conductivity measurements of Ryabchikov and Silnichenko [15] and of Saxena and Jain [16] indicate the presence of $Ag(S_2O_3)^-$ and $Ag(S_2O_3)_2^{3-}$ in dilute solutions. Potentiometric determinations of Ashihara and Matsuda [17], Schmitz-Dumont and Schmitz [18], Brehmer [19] and Spacu and Murgulescu [20] indicate the presence of $Ag(S_2O_3)_2^{3-}$ and $Ag(S_2O_3)_3^{5-}$ in more concentrated solutions. It appears that, except when the silver concentration is high (when $Ag(S_2O_3)^-$ and possibly even polynuclear complexes form), $Ag(S_2O_3)_2^{3-}$ and $Ag(S_2O_3)_3^{5-}$ are the complex silver species present in thiosulphate solutions.

Using the constant K in eqn. (10), it is possible to state the main reaction with the resin not in terms of eqn. (8), which considers the exchange of the first anionic complex $Ag(S_2O_3)^-$, but in terms of the complexes actually present in the solutions. At low concentrations:

$$Ag(S_2O_3)_2^{3-} + 1/2\ R_2S_2O_3 = RAgS_2O_3 + 3/2\ S_2O_3^{2-} \qquad (12)$$

$$\log K' = \log K - 3/2\ \log (S_2O_3)_r^0 = 2.38 \pm 0.10$$

and at high concentrations:

$$Ag(S_2O_3)_3^{5-} + 1/2\ R_2S_2O_3 = RAgS_2O_3 + 5/2\ S_2O_3^{2-} \qquad (13)$$

$$\log K'' = \log K' - \log k_3 = 0.7 \pm 0.2$$

Whichever of these reactions is used, it is important to realize that silver is absorbed quite strongly from dilute solutions but only weakly from concentrated ones, there being a span of five powers of ten in the distribution coefficients. Anion exchange separation from metals not absorbed from dilute thiosulphate solutions is thus possible, with subsequent elution of the silver with a concentrated thiosulphate solution.

Acknowledgement. Thanks are due to Dr. I Dostrovsky, Scientific Director, Israel Atomic Energy Commission Research Establishment, under whose direction the experimental part of this work was carried out, for his help and encouragement, and to Mr. A. Citron for his assistance in the elution experiments. Thanks are also due to Prof.

L. G. Sillén, the Royal Institute of Technology, Stockholm, in whose laboratory the manuscript was prepared, for its critical discussion. The help of Dr. H. S. Dunsmore and of Miss Myra Ockrant in improving the English presentation is also acknowledged.

REFERENCES

1. Marcus, Y. *Thesis, The soluble complexes of uranium in phosphoric acid*, Jerusalem, 1955.
2. Bodländer, G. *Ber.* **36** (1903) 3933.
3. Ölander A. and Adelson O. *Svensk Kem. Tidskr.* **58** (1946) 33.
4. Chateau, A. and Pouradier, J. *Science et Inds. Phot.* **24** (1953) 129.
5. Lure, Y. Y. and Perenyslova, E. S. *Zhur. Priklad. Khim.* **27** (1954) 1207.
6. Forsling, W. *Arkiv Kemi* **5** (1953) 507.
7. Kraus, K. A. and Moore, G. E. *J. Am. Chem. Soc.* **73** (1951) 9.
8. Stokes, R. H. *Trans. Faraday Soc.* **44** (1948) 295.
9. Kraus, K. A. and Moore, G. E. *J. Am. Chem. Soc.* **75** (1953) 1457.
10. Gottlieb, M. H. and Gregor, H. P. *J. Am. Chem. Soc.* **76** (1954) 4639.
11. Pawelka, F. G. *Z. Elektrochem.* **30** (1924) 180.
12. Ferrell, E., Ridgion, J. M. and Riley, H. *J. Chem. Soc.* **1936** 1121.
13. Carrière, E. and Raulet, M. *Compt. rend.* **192** (1931) 423.
14. Chateau, H. and Pouradier, J. *Compt. rend.* **240** (1955) 1882.
15. Ryabchikov, D. I. and Silnichenko, V. G. *Izvest. Akad. Nauk SSSR Otdel. Khim. Nauk* **1949** 364.
16. Saxena, R. S. and Jain, N. L. *J. Indian Chem. Soc.* **31** (1954) 319.
17. Ashihata, S. and Matsuda, Y. *J. Soc. Ind. Photogr. (Japan)* **14** (1952) 125.
18. Schmitz-Dumont, O. and Schmitz, E. *Z. anorg. Chem.* **247** (1941) 35.
19. Brehmer, I. E. *Finska Kemistsamfundets Medd.* **58** (1949) 79.
20. Spacu, G. and Murgulescu, J. G. *Z. anorg. u. allgem. Chem.* **207** (1932) 150.
21. Wheaton, R. N. and Bauman, W. C. *Ind. Eng. Chem.* **43** (1951) 1088.

Received January 8, 1957.

ACTA CHEMICA SCANDINAVICA 11 (1957) 628—633

Sulfite and Complex-bound Cyanide as Sulfur Acceptors for Rhodanese

BO SÖRBO

Research Institute of National Defence, Dept. 1, Sundbyberg 4, and Medicinska Nobelinstitutet, Biokemiska avdelningen, Stockholm, Sweden

The catalytic effect of rhodanese on the reaction between thiosulfonates and sulfite has been demonstrated. Rhodanese, combined with thiosulfate, can in part reactivate cyanide inhibited cytochrome oxidase. A similar effect on the cyanide compounds of catalase and methemoglobin was also demonstrated. Vitamin B_{12} (cyanocobalamin) was not converted to the corresponding thiocyanate compound by the action of rhodanese and thiosulfate. A possible function of cobalamins in thiocyanate metabolism is suggested.

Previous studies of the substrate specificity of rhodanese [1,2] have demonstrated that thiosulfonates could replace thiosulfate as sulfur donor in the enzyme catalyzed reaction. Up to this time cyanide was the only known sulfur acceptor in the system. The present paper reports that sulfite can replace cyanide as acceptor; the reaction products being in this case thiosulfate and the corresponding sulfinate. The effect of rhodanese and thiosulfate on certain cyanide complexes of biological importance have also been investigated.

EXPERIMENTAL

Materials. Rhodanese was a twice crystallized preparation from beef liver [3]. The thiosulfonates were prepared as previously described [2]. Catalase was a recrystallized preparation from beef liver and methemoglobin was prepared by oxidizing a rabbit blood hemolysate with ferricyanide, followed by dialysis in order to remove excess ferricyanide. Cytochrome oxidase was a 10 % rabbit brain homogenate in 0.01 M phosphate buffer of pH 7.4. Ferrocytochrome c was a commercial beef heart preparation, reduced with hydrogen in the presence of platinum asbestos.

Methods. The formation of thiosulfate from a mixture of a thiosulfonate and sulfite was followed with the iodometric titration method given by Foss [4]. A correction for "induced oxidation" was obtained by titrating standard amounts of thiosulfate in the presence of the thiosulfonate and sulfite. The disappearance of the cyanide complexes of catalase and methemoglobin was followed spectrophotometrically at 425 and 630 mμ, respectively. Cytochrome oxidase activity was assayed spectrophotometrically by following the oxidation of ferrocytochrome c at 550 mμ[5]. A test for the formation of thiocyanate from vitamin B_{12} was developed on the base of the copper-pyridine-reaction [6]. For this

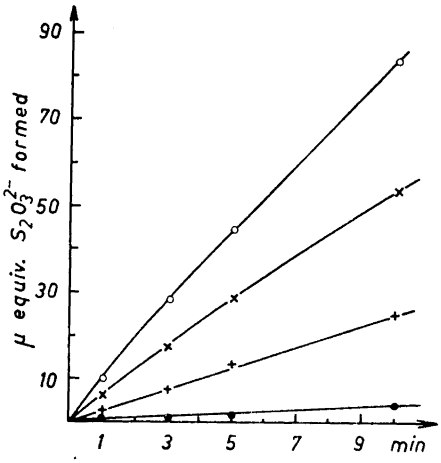


Fig. 1. Reaction between thiosulfonates and sulfite.
●●● Ethanethiosulfonate, spontaneous reaction.
○○○ In the presence of 6.8 μg rhodanese.
+ + + Toluenethiosulfonate, spontaneous reaction.
× × × In the presence of 13.5 μg rhodanese.
Test conditions: Final volume 5 ml, pH 7.4, phosphate concentration 0.1 M, thiosulfonate and sulfite 0.05 M, bovine serum albumin 0.005 %, temp. 20 °C. Reaction stopped at indicated time by the addition of 0.5 ml formaldehyde followed by 10 ml 10 % KI and 2.5 ml 10 % acetic acid. Titrated with 0.01 N iodine with starch as indicator.

test, 0.5 ml of reaction mixture, containing 0.005 M vitamin B_{12} and 0.01 M thiosulfate in 0.1 M phosphate buffer pH 7.4 was incubated with rhodanese and the enzyme, then destroyed by heating the sample in boiling water for 2 min. The sample was cooled and 0.05 ml 0.1 M KCN was added, in order to liberate thiocyanate from any thiocyanatecobalamin formed, followed by 4.5 ml water, 1 ml pyridine and 1 ml 10 % $CuSO_4$, $5H_2O$. Any copper-pyridinethiocyanate complex formed was then extracted with 2 + 1 + 1 ml bromobenzene and the optical density of the latter determined at 410 mμ. Vitamin B_{12} is not extracted by bromobenzene, but appropriate blank determinations had to be carried out, as both cyanide and thiosulfate interfered with the determinations. Recovery experiments demonstrated that a conversion of 5 % of the cyanide of vitamin B_{12} could be safely detected by this method.

RESULTS

The rhodanese catalyzed reactions between two thiosulfonates and sulfite and the corresponding spontaneous reactions are shown in Fig. 1. In agreement with Foss [4] it was found that the spontaneous reaction between toluenethiosulfonate and sulfite was more rapid than the corresponding reaction with ethanethiosulfonate. The rhodanese catalyzed reaction was on the contrary more rapid with ethanethiosulfonate. A similar behaviour of the thiosulfonates was previously [2] noticed in their reactions with cyanide. A comparison between the two sets of data demonstrates that sulfite is inferior to cyanide as sulfur acceptor in the rhodanese reaction. With ethanethiosulfonate as

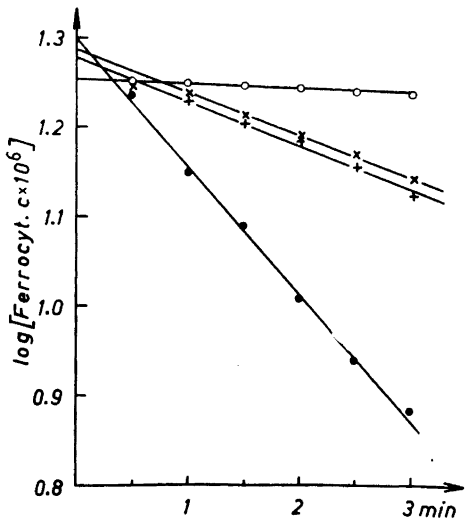


Fig. 2. Reactivation of cyanide inhibited cytochrome oxidase by rhodanese.

●●● Cytochrome oxidase alone ($k = 5.4 \times 10^{-3}$ sec^{-1})
○○○ Cytochrome oxidase + 0.001 M cyanide ($k = 0.18 \times 10^{-3}$sec^{-1}).
× × × Cytochrome oxidase + 0.001 M cyanide + 0.05 M thiosulfate + 36 μg rhodanese/ml added in the indicated order. Tested immediately after the rhodanese addition ($k = 1.8 \times 10^{3-}$ sec^{1-}).
+ + + The same tested 15 min. later ($k = 1.8 \times 10^{-3}$sec^{-1}).

The oxidase activity assayed by adding 0.04 ml of the reaction mixtures to 4.0 ml of ferrocytochrome c (appr. 2×10^{-5} M) and following the reaction at 550 mμ. Figures in brackets indicate the first order reaction constant.

donor and sulfite as acceptor, 1 μg of rhodanese gave 6.4 μ-equiv. of thiosulfate in 5 min, whereas with cyanide as acceptor 10 μ-equiv. of thiocyanate were formed. With *p*-toluenethiosulfonate as donor and sulfite as acceptor 1 μg of rhodanese formed in 5 min 1.1 μ-equiv. of thiosulfate and the corresponding value with cyanide was 3.8 μ-equiv. of thiocyanate. (These values have been corrected for the effect of the spontaneous reaction.)

In connection with a study of the antidote effect of rhodanese in cyanide poisoning it became of interest to study the activity of rhodanese to transform complex-bound cyanide into thiocyanate. As the toxic properties of cyanide is attributed to its strong inhibitory action on cytochrome oxidase, the established antidote effect of rhodanese combined with thiosulfate [7] suggests, that this combination can reactivate cyanide inhibited cytochrome oxidase. Albaum *et al.*[8] have previously demonstrated that another cyanide antidote, methemoglobin, in part reactivates cytochrome oxidase. When rhodanese + thiosulfate was added to cyanide inhibited cytochrome oxidase (Fig. 2), a rapid reactivation was in fact obtained, but it was incomplete. As thiosulfate, thiocyanate and sulfite at the actual concentrations did not affect the oxidase, it must be concluded also that the conversion of cyanide to thiocyanate was

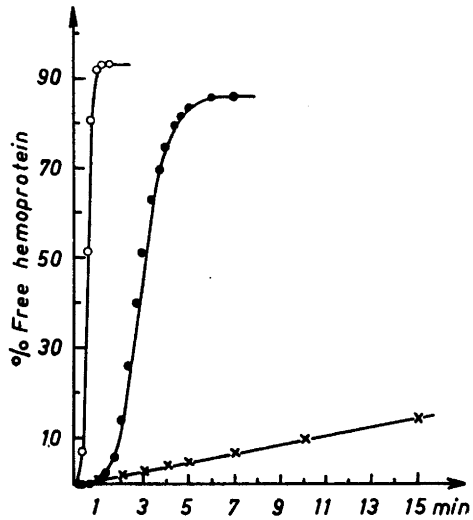


Fig. 3. Action of rhodanese on cyanide compounds of catalase and methemoglobin.

●●● 2.8×10^{-6} M catalase + 3.10^{-4} M cyanide + 0.05 M thiosulfate in 0.025 M phosphate buffer pH 7.4. At zero time rhodanese (8.6 μg/ml) added.

○○○ As the preceding with 39 μg rhodanese/ml.

××× 1.3×10^{-4} M methemoglobin + 3×10^{-4} M cyanide in 0.025 M phosphate buffer pH 7.4. After 5 minutes incubation thiosulfate (to 0.05 M concentration) and rhodanese (36 μg/ml) were added.

The lag period observed in the two curves with catalase corresponds to the time necessary for converting the excess of cyanide into thiocyanate.

incomplete, although rather high concentrations of rhodanese and thiosulfate were used. Thiosulfate alone had no reactivating effect on the inhibited cytochrome oxidase, as the rhodanese activity of brain homogenates is low. The behaviour of the cyanide complexes of two other heme proteins was then investigated. Catalase cyanide was rapidly reactivated by the action of rhodanese and thiosulfate, whereas methemoglobin cyanide reacted much more slowly (Fig. 3). These results are explained, if rhodanese does not react with the heme-bound cyanide but only with the free cyanide (hydrocyanic acid), which is in equilibrium with the heme-cyanide complex. The dissociation velocity constant for catalase cyanide is about 3 000-fold greater than that for methemoglobin cyanide [9,10], which explains the much more rapid reaction with the catalase compound. The reaction with catalase cyanide like that with cytochrome oxidase cyanide was incomplete even in the presence of high concentrations of rhodanese. However, 93 % of the catalase cyanide was converted to free catalase as compared with 33 % of cytochrome oxidase cyanide under similar conditions *. When the rhodanese concentration was reduced

* The maximum conversion, obtainable with methemoglobin cyanide, could not be determined, as the reaction was so slow, that about 24 h were required for equilibrium, and free methemoglobin was not completely stable under these conditions.

5-fold, the maximum conversion of catalase cyanide was reduced to 86 %, indicating that the concentration of rhodanese also influences the extent of conversion. From the known values for the dissociation constants of catalase cyanide [9] (K: 4×10^{-6}) and cytochrome oxidase cyanide [5] (K: 7×10^{-7}) it was possible to calculate the concentration of free cyanide (hydrocyanic acid), which would give the final value of inhibited heme-enzyme. This calculation gives 1.2×10^{-6} M cyanide in the cytochrome oxidase experiment and 3×10^{-7} M cyanide in the corresponding catalase experiment. This discrepancy, observed in repeated experiments, is yet unexplained.

Vitamin B_{12} (cyanocobalamin) is a cyanide complex of biological importance. Furthermore, it was of interest to test cyanocobalamin as a substrate for rhodanese. When cyanocobalamin (0.004 M) and thiosulfate (0.01 M) were incubated for 30 min at pH 7.4 and 20 °C in the presence of high concentrations of rhodanese (39 μg/ml) no conversion of cyanocobalamin to thiocyanatocobalamin was detected. In the light of the previous results this was not unexpected, as the cyanide is very tightly bound to the cobalt in vitamin B_{12} and thus no free cyanide is accessible to rhodanese.

DISCUSSION

The formation of thiosulfate from a thiosulfonate and sulfite by the action of rhodanese may occur in the body as both thiosulfonates [11] and sulfite can be formed by enzymatic mechanisms. The precursors to thiosulfonates are, however, a sulfinic acid and β-mercaptopyruvic acid, and as the latter gives thiosulfate directly with sulfite in an enzymatic reaction [11], this latter reaction is probably of greater importance.

As cyanide, vitamin B_{12} and thiocyanate are in a dynamic equilibrium *in vivo* (demonstrated by isotope experiments [13]) the failure of vitamin B_{12} to react with rhodanese is of certain interest. It is possible that the cyanide of vitamin B_{12} is first released from the cobalt atom by specific mechanisms before being converted to thiocyanate by the rhodanese system. It is also possible that this conversion occurs through other enzyme systems. In this connection an interesting metabolic function of vitamin B_{12} may be considered. Vitamin B_{12} is in part present in liver not only as cyanocobalamin but also as hydroxycobalamin (vitamin B_{12}a) [13]. The latter has a very high affinity for cyanide and it is possible that the presence of hydroxycobalamin may change the overall equilibrium of certain enzyme systems, so that thiocyanate may be converted to cyanide (bound in vitamin B_{12}) and a sulfur compound, even though the equilibrium constant of these enzyme systems are in favour of the formation of thiocyanate from cyanide. Thiocyanate could thus be converted to thiosulfate by rhodanese, or more interesting, thiocyanate and pyruvic acid may yield mercaptopyruvic acid by the action of an enzyme, which catalyses the formation of thiocyanate from mercaptopyruvic acid and cyanide [14]. A subsequent transamination of mercaptopyruvic acid would then give cysteine and the net result would be a synthesis of cysteine with thiocyanate as the sulfur source. Wokes and Picard [15] have also recently proposed a mechanism, although different from that outlined above, by which the sulfur of thiocyanate could be converted into the sulfur containing amino acids by the action of

vitamin B_{12}. It must be added that no experimental evidence for the formation of cysteine from thiocyanate has as yet been obtained, but experiments designed to test this hypothesis, using sulfur labeled thiocyanate, are now planned in this laboratory.

The author is very grateful to Miss A. M. Sjödén for her valuable technical assistance.

REFERENCES

1. Sörbo, B. H. *Acta Chem. Scand.* **7** (1953) 32.
2. Sörbo, B. H. *Acta Chem. Scand.* **7** (1953) 1137.
3. Sörbo, B. H. *Acta Chem. Scand.* **7** (1953) 1129.
4. Foss, O. *Kgl. Norske Videnskab. Selskab. Skrifter* **1945** No. 2, p. 98.
5. Horecker, B. L. and Stannard, J. N. *J. Biol. Chem.* **172** (1948) 599.
6. Lang, K. *Biochem. Z.* **262** (1933) 14.
7. Clemedson, C-J., Hultman, H. I:son and Sörbo, B. *Acta Physiol. Scand.* **32** (1954) 245.
8. Albaum, H. G., Tapperman, J. and Bodansky, O. *J. Biol. Chem.* **163** (1946) 641.
9. Chance, B. *J. Biol. Chem.* **179** (1949) 1299.
10. Chance, B. *J. Biol. Chem.* **194** (1952) 483.
11. Sörbo, B. *Biochim. et Biophys. Acta* **21** (1956) 393.
12. Fromageot, Cl. and Chatagner, F. *Compt. rend.* **224** (1947) 367.
13. Boxer, G. E. and Richard, J. C. *Arch. Biochem. and Biophys.* **39** (1952) 7.
14. Sörbo, B. *Acta Chem. Scand.* **8** (1954) 694.
15. Wokes, F. and Picard, C. W. *Am. J. Clin. Nutrition* **3** (1955) 383.

Received January 16, 1957.

ACTA CHEMICA SCANDINAVICA 11 (1957) 634—639

Constituents of Pollen

II.* Long-chain Hydrocarbons and Alcohols

MARTIN NILSSON, RAGNAR RYHAGE and ERIK von SYDOW

Organisk-kemiska Institutionen, Kungl. Tekniska Högskolan, Stockholm; Kemiska Institutionen, Karolinska Institutet, Stockholm; Kemiska Institutionen, Uppsala Universitet, Uppsala, Sweden

Some waxy, crystalline fractions isolated from pollen have been investigated by mass spectrometry. This method has proved to be most convenient for the investigation of these mixtures of long-chain natural products.

Pollen from *Pinus montana* contains *n*-tetracosanol-1, *n*-hexacosanol-1 and *n*-octacosanol-1, while pollens from *Zea mays* and *Alnus glutinosa* have been found to contain paraffins; maize *n*-pentacosane and *n*-heptacosane, alder mainly *n*-heptacosane and *n*-nonacosane.

For the investigation of pollen constituents carried out at the Royal Institute of Technology, Stockholm, some representative plants have been chosen; the gymnosperm *Pinus montana*, Mill. and the angiosperms *Zea mays*, L. and *Alnus glutinosa*, Gaertn., representing mono- and dicotyledons respectively [1].

The present paper deals with the ether-extractable material from these pollens. The amount of ether-extract was approximately the same in pine and alder pollen (around 9 %), but rather small (2 %) in maize pollen. This difference is, however, not so significant as the amount of ether-extract in the maize pollen apparently varies widely from year to year [1]. The extracts were divided into acid and neutral fractions; the neutral fractions were semisolid and crystalline material deposited when the hot solutions in acetone (ethanol) were left to cool. These crystalline products had a waxy consistency and appeared to consist of long-chain aliphatic compounds.

X-Ray powder photographs of the different long-chain mixtures were taken in a Guinier camera using Cu-$K\alpha$ radiation. They were all very similar and one of them is shown in Fig. 1. The appearance and distribution of the strong diffraction lines indicate that the mixtures consist of long straight-chain hydrocarbons with no substituents or only smaller ones (*e. g.* paraffins and alcohols). The chains are packed in the common *ortho*-rhombic structure [2-4] with the chain-plane of each molecule approximately perpendicular to that of the next.

* Part I. *Acta Chem. Scand.* **10** (1956) 413.

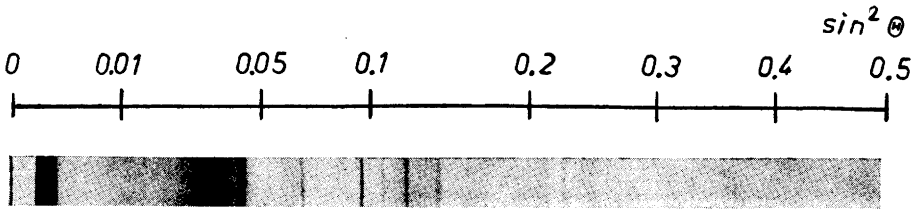


Fig. 1. Guinier X-ray powder photograph of the crude long-chain mixture from *Alnus glutinosa* pollen. Cu-*Kα*-radiation. Exposure 4 h.

To show the nature of the long-chain mixtures they were investigated using the mass spectrometer described by Ryhage [5], which has been used in structural research on long-chain compounds and mixtures [6,7].

Mountain pine gave a large amount (1 %) of a material, m. p. 70—74°, which when treated with urea in methanol formed a complex [8]. Purification by recrystallisation and by complex formation did not raise the melting point appreciably (72—74°). The elementary analysis was consistent with the composition $C_{24}H_{50}O$ and hence the product was presumed to be a mixture of straight chain alcohols in the C_{24}—C_{26}-region.

Similar fractions have frequently been isolated from plants. On careful fractionation and X-ray investigation they have generally proved to be mixtures of closely related alcohols, sometimes contaminated with hydrocarbons [9,10]. The mass spectrometric investigation, discussed in detail in a later section, showed that the product from *P. montana* contained *n*-tetracosanol-1, *n*-hexacosanol-1 and *n*-octacosanol-1. The mass spectrum of the crude product was easily interpreted and the investigation of the purified material merely served to confirmed the result.

The crude materials from maize and alder pollen were therefore investigated directly although their melting point intervals were very broad. The mass spectra showed them to consist largely of paraffins and also revealed the presence of other compounds so they were purified by filtration through alumina and the preliminary results confirmed by an additional mass spectrometric analysis. The maize pollen contained *n*-pentacosane and *n*-heptacosane and the alder pollen *n*-heptacosane, *n*-nonacosane and smaller amounts of *n*-tricosane and *n*-pentacosane.

DISCUSSION

The investigation has revealed a marked difference between the gymnosperm pollen, which contains large quantities of longchain alcohols and the angiosperm pollens, which contain smaller amounts of paraffins.

Paraffins have been found in angiosperm pollen earlier; "tricosane" in hazel pollen [11], "heptacosane" in pollen from sugar beet [12] and as a mixture in maize pollen [10,13]. A fraction closely related to "ceryl alcohol" has been found in pollen from a pine [12] and in an investigation of *Pinus silvestris* pollen a waxy substance, m. p. 80°, has been obtained [14], which can now be supposed to be a wax alcohol mixture.

If the ether-extracted pollens were extracted with alcohol a further quantity of lipid material was obtained, which was obviously retained by the pollen membrane during the ether extraction (*c. f.* Ref.[15]). It may be presumed that the waxes dealt with in this paper are located on or near the surface of the pollen grains in the same way as plant waxes in general are located in the outer layer of the tissues [16]. The function of the pollen waxes is apparently the same as that of plant waxes in general — a barrier against loss of water — as shown by the striking parallel between the waxy conifer-needles [17] and the heavily wax-impregnated pine pollen.

The gymnosperms are wind-pollinated whereas the angiosperms are generally pollinated by insects and this might have some connection with the differences between the long-chain compounds in the gymnosperm and the angiosperm pollen.

EXPERIMENTAL

Extraction, isolation and purification

The melting points were determined on a Kofler block. The pollen samples were collected in 1954 by *A. B. Cemille*, Vegeholm, Sweden, and contained at least 99 % of the right pollen [1].

Air-dried pollen (500 g) was exhaustively extracted with ether in a Soxhlet apparatus (*ca.* 2 weeks); the extraction temperature was *ca.* 25°. The ether was evaporated, the residue dissolved in chloroform and extracted with 2 M potassium hydroxide. After appropriate back extractions an acid fraction and a neutral fraction were obtained. The neutral fractions were dissolved in a minimum amount of hot acetone (for maize ethanol) and the crystalline precipitate obtained after cooling collected.

Pinus montana gave 8.0 % ether-extract giving 3.6 % neutral material, from which 1.0 % crystalline material, m. p. 70—74°, was obtained. The corresponding figures for *Zea mays* were 2.0, 1.1, 0.2 %, m. p. 48—58° and for *Alnus glutinosa* 10.0, 8.5, 0.6 % and m. p. 57—64°, all percentages being calculated on an air-dried pollen basis.

The crude product from *P. montana* was recrystallised from acetone and dissolved in a hot solution of urea in methanol (160 g/l). On cooling long needles separated. The urea complex was collected and decomposed with chloroform and dilute hydrochloric acid, the chloroform layer was separated, evaporated and the product recrystallised from acetone, m. p. 72—74°. (Found: C 81.4; H 13.8. Calc. for $C_{24}H_{50}O$: C 81.4; H 14.1.)

For purification of the maize and alder products, samples (*ca.* 1 g) were dissolved in methyl *cyclo*hexane (50 ml), passed through a column of alumina (10 × 1.5 cm, 20 g) and the column was washed with the same solvent (150 ml). On evaporation colourless waxes were obtained; from maize 65 % of input with a melting point range of 45—60°, from alder 55 %, m. p. 55—70°. Elution with benzene (200 ml) gave 10 and 15 %, m. p. 45—55° and 60—75°, respectively, of pale yellow waxy material. Further elution with ethyl acetate and methanol gave discoloured, heterogeneous material. The methyl *cyclo*hexane fractions are referred to in the next section as purified products, the benzene fractions were investigated with the mass spectrometer but the spectra were too complicated for interpretation presently. The other fractions were not further investigated.

Mass spectrometric study

The mass spectrometer used is that described by Ryhage [5]. For typographic reasons only the high mass regions of the mass spectra are shown in the figures. The mass spectrum of the crude product from *Pinus montana* is shown in Fig. 2. This is a spectrum typical of long-chain compounds. In the C_{28}-, C_{26}- and C_{24}-alkyl groups of peaks there are two comparatively strong peaks corresponding to $C_nH_{2n}^+$ and $C_nH_{2n-2}^+$, which is typical of a long-chain alcohol with n carbon atoms [6]. Such an alcohol gives, however, also

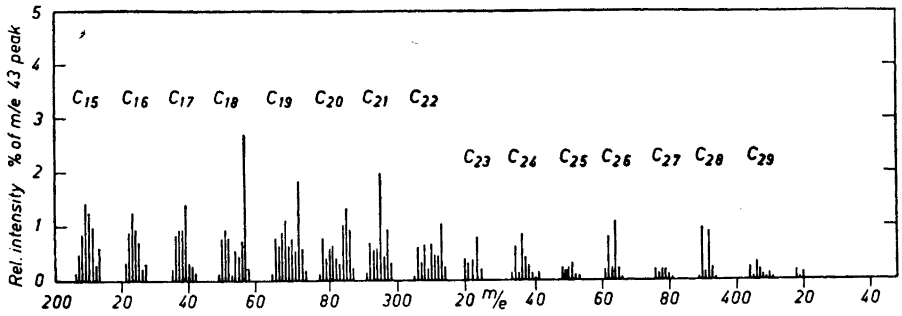


Fig. 2. Mass spectrum of the crude long-chain mixture from *Pinus montana.*

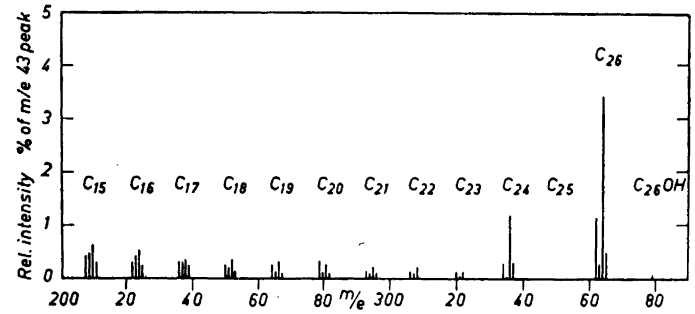


Fig. 3. Mass spectrum of pure *n*-hexacosanol-1.

peaks at *m/e* corresponding to $C_{n-2}H_{2n-4}^+$ and $C_{n-2}H_{2n-6}^+$ but these are much lower. For comparison the spectrum of pure *n*-hexacosanol is shown in Fig. 3. In the case of *P. montana* there are peaks at *m/e* = 392 ($C_{28}H_{56}^+$) and *m/e* = 390 ($C_{28}H_{54}^+$) indicating the presence of *n*-octacosanol-1. There are also peaks at *m/e* = 364 ($C_{26}H_{52}^+$) and 362 ($C_{26}H_{50}^+$) which to a small part are due to fragmentation of *n*-octacosanol-1 and to a larger extent to fragments from *n*-hexacosanol-1. The same thing is valid for the peaks in the C_{24}-group, which indicate smaller amounts of *n*-tetracosanol-1, as the peaks in the C_{22}-group are lower. There are no obvious signs of any other long-chain compounds. The purified mixture from *P. montana* was also analysed and found to contain more *n*-octacosanol-1 and less *n*-tetracosanol-1 than the crude product, which is of course consistent with the larger solubility of the shorter alcohols.

The mass spectra of the products from *Zea mays* and *Alnus glutinosa* are also typical of long chain compounds, but in this case of *n*-hydrocarbons. The mass spectrum of the purified product from *Zea mays* is shown in Fig. 4 and that of the crude product from *Alnus glutinosa* in Fig. 5. Mass spectra of heavy normal and branched chain hydrocarbons have been extensively studied by O'Neal and Wier [18]. A normal chain hydrocarbon spectrum always contains a strong parent peak corresponding to the unfragmented molecule and a series of peaks corresponding to $C_nH_{2n+1}^+$ with *n* up to the number of carbon atoms in the molecule.

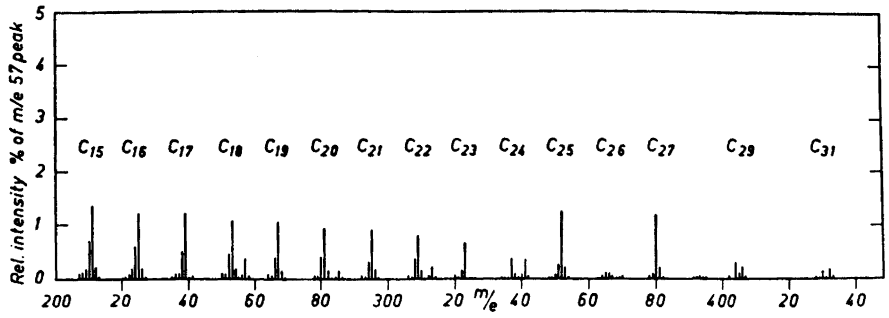


Fig. 4. Mass spectrum of the purified product from *Zea mays*.

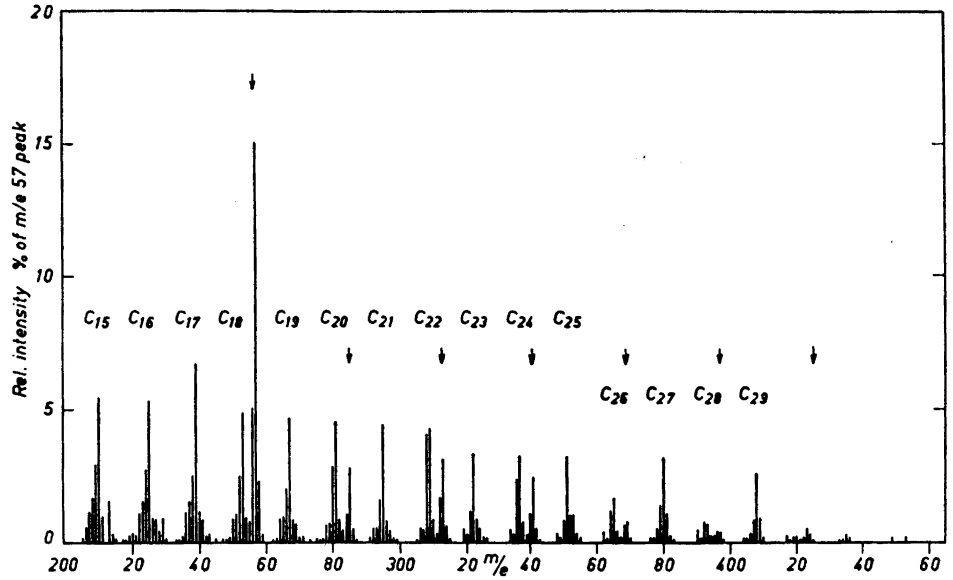


Fig. 5. Mass spectrum of the crude product from *Alnus glutinosa*.

It can be seen that the spectra of the mixtures from *Zea mays* and *Alnus glutinosa* (Fig. 4 and 5) are characteristic for hydrocarbons. The first one contains only *n*-pentacosane and *n*-heptacosane while the last one contains *n*-heptacosane, *n*-nonacosane and traces of *n*-tricosane and *n*-pentacosane. There are peaks in both spectra, which cannot be referred to fragments of these hydrocarbons, but which indicate the presence of other compounds. Thus the spectrum of the crude product from *A. glutinosa*, which had a faint yellow colour, had strong peaks at $m/e = 257 + n \times 28 = 285, 313, 341$ .... (marked with arrows in Fig. 5). This might indicate some sort of conjugated system attached to a fragment with a molecular weight approximately equal to 257. The same series of peaks was also recognised in the spectrum of *P. montana* although the intensities were lower.

The weak peaks in the C_{29}-and C_{31}-regions of the maize spectrum cannot be due to saturated hydrocarbons or alcohols but possibly to unsaturated hydrocarbons. In lack of reference substances no conclusions should be drawn however. In the crude products from maize and alder there are also smaller amounts of other compounds, probably containing oxygen. The investigation of the purified mixture from alder gave no further information.

Acknowledgements. We are indebted to *A. B. Kabi* for generous gifts of pollen, to Prof. E. Stenhagen for a sample of pure *n*-hexacosanol-1, which he had obtained from Prof. A. C. Chibnall, and one of us (M. N.) to *Statens Tekniska Forskningsråd* for a fellowship.

REFERENCES

1. Nielsen, N., Grömmer, J. and Lundén, R. *Acta Chem. Scand.* **9** (1955) 1100.
2. Bunn, C. W. *Trans. Faraday Soc.* **35** (1939) 482.
3. Vainshtein, B. K. and Pinsker, Z. G. *Doklady Akad. Nauk S.S.S.R.* **72** (1950) 53.
4. von Sydow, E. *Arkiv Kemi* **9** (1956) 231.
5. Ryhage, R. *To be published.*
6. Bergström, H., Ryhage, R. and Stenhagen, E. *Svensk Papperstidn.* **59** (1956) 593.
7. Ryhage, R., Stenhagen, E. and von Sydow, E. *Acta Chem. Scand.* **11** (1957) 180.
8. Schlenk Jr., W. *Ann.* **565** (1949) 204.
9. Pollard, A., Chibnall, A. C. and Piper, S. H. *Biochem. J. London* **25** (1931) 2111.
10. Chibnall, A. C., Piper, S. H., Pollard, A., Williams, E. F. and Sahai, P. N. *Biochem. J. London* **28** (1934) 2189.
11. Sosa, A. and Sosa-Bourduil, C. *Compt. rend.* **237** (1952) 971.
12. Kiesel, A. and Rubin, B. *Hoppe-Seylers's Z. physiol. Chem.* **182** (1929) 241.
13. Anderson, R. J. *J. Biol. Chem.* **55** (1923) 611.
14. von Planta, A. *Lantwirtsch. Vers. Sta.* **32** (1886) 215.
15. Anderson, R. J. und Kulp, W. L. *J. Biol. Chem.* **50** (1922) 433.
16. van Overbeek, J. *Ann. Rev. Plant Physiol.* **7** (1956) 355.
17. Watanabe, H. *J. Pharm. Soc. Japan* **73** (1953) 176. *Cf. Chem. Abstr.* **47** (1953) 4634e.
18. O'Neal, M. J. and Wier, T. P. *Anal. Chem.* **23** (1951) 830.

Received January 18, 1957.

ACTA CHEMICA SCANDINAVICA 11 (1957) 640—649

Infrared Absorption Spectra of *ortho*- and *para*-Linked Polyphenyls

JOHANNES DALE

Forsvarets Forskningsinstitutt, Kjeller, Norway

The absorption spectra of biphenyl, *o*- and *p*-terphenyl, *o,o'*-, *o,p'*- and *p,p'*-quaterphenyl have been recorded from 2 to 25 μ both in solution and in the solid state. Oriented crystallization takes place when melts of the linear compounds solidify between salt plates. Some of the bands observed in the spectra obtained by the KBr technique are lacking in the oriented crystal spectra; they must be due to vibrations polarized parallel to the long molecular axis. Most of the vibrations seem to occur independently within each ring of the chain, and assignments can be made on the basis of the assignments for methylbenzenes given by Pitzer and Scott [12]. For the linear compounds the intensity variation of the bands classified as due to in-plane skeletal deformation modes suggests that these vibrations are coupled together, the selection rules being determined by the symmetry of the whole molecule, and that the molecules are planar in the crystalline state, but non-planar in solution.

The synthesis of *o,p'*-quaterphenyl is described.

In connection with a study of the ultraviolet spectra of through-conjugated polyphenyls in the solid state and in solution (*cf.* the following paper [1]), it was of great interest to know whether any change of conformation would occur in going from one state to the other, since such changes would be expected to affect the degree of interaction between the π-electron systems of the linked benzene nuclei. In particular it was of importance to ascertain whether the *p*-polyphenyl molecules are planar in solution as they are known to be in the crystal [2–5], or non-planar, as has been established for biphenyl in the gaseous state [6]. For one of the non-linear compounds, *o,o'*-quaterphenyl, one might even anticipate, as a result of the tendency towards coplanarity, the existence of *cis*- and *trans*-like conformations, for which the electronic absorption spectra would be expected to differ.

Biphenyl and all the possible *o*- and *p*-linked terphenyls and quaterphenyls were studied. Of these, *o,p'*-quaterphenyl has not been described before, and a method for its synthesis is given in the experimental part.

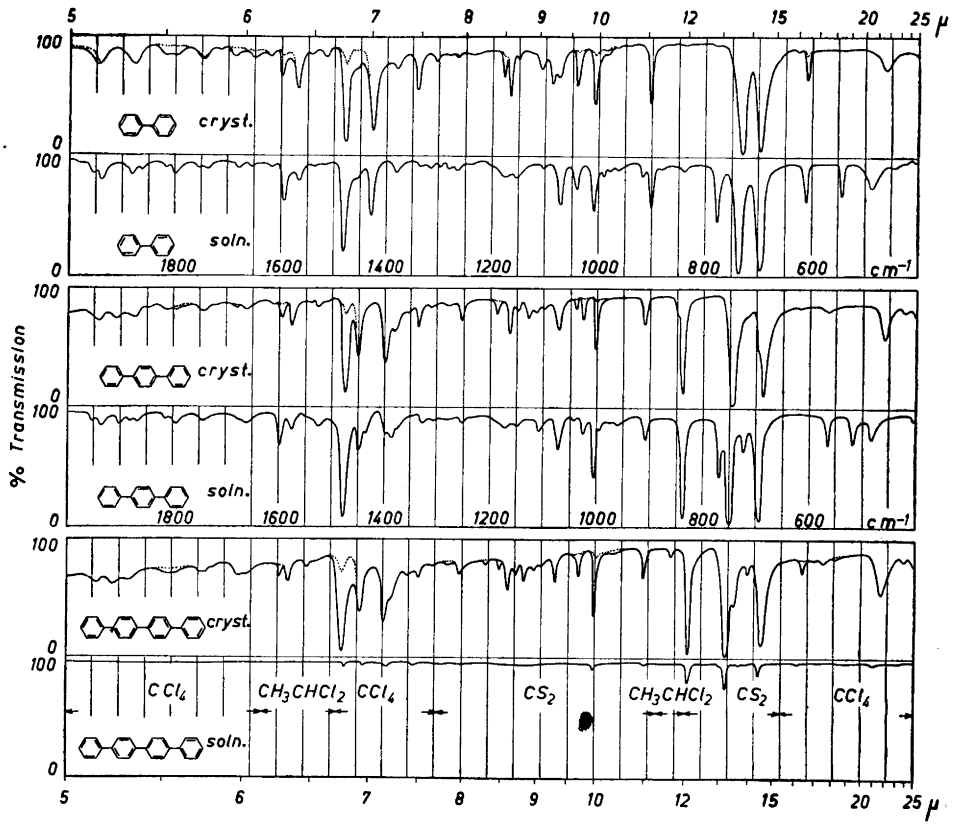


Fig. 1. Infrared spectra of linear polyphenyls in solution (1 % or saturated, 1 mm cell thickness) and in the solid, crystalline state. The dotted curves represent spectra of melts solidified between salt plates (0.01 mm layer thickness) in regions where these differ from the spectra of pressed KBr disks (full line). The solvents used in the various regions have been indicated in the lower part of the figure.

Infrared spectra of some of these compounds have been reported earlier [7–11], but these spectra are partly of poor quality, especially for solids prepared as mineral oil mulls [10]; they are mostly not available for both solid state and solution; and they cover only the NaCl-region, or part of it [7]. Since the skeletal deformation vibrations would be expected to be most sensitive to changes of molecular shape, it was considered especially important for the present purpose to include the long-wave region from 15 to 25 μ (KBr-prism).

The infrared spectra are given in Figs. 1 and 2. Below 5 μ they are very similar, the absorption due to the various CH-stretching modes appearing as an unresolved band at 3 040—3 060 cm^{-1} for all members. This region has not therefore been reproduced in the figures and will not be further discussed. The solid state spectra were taken both of solidified melts and of pressed KBr-

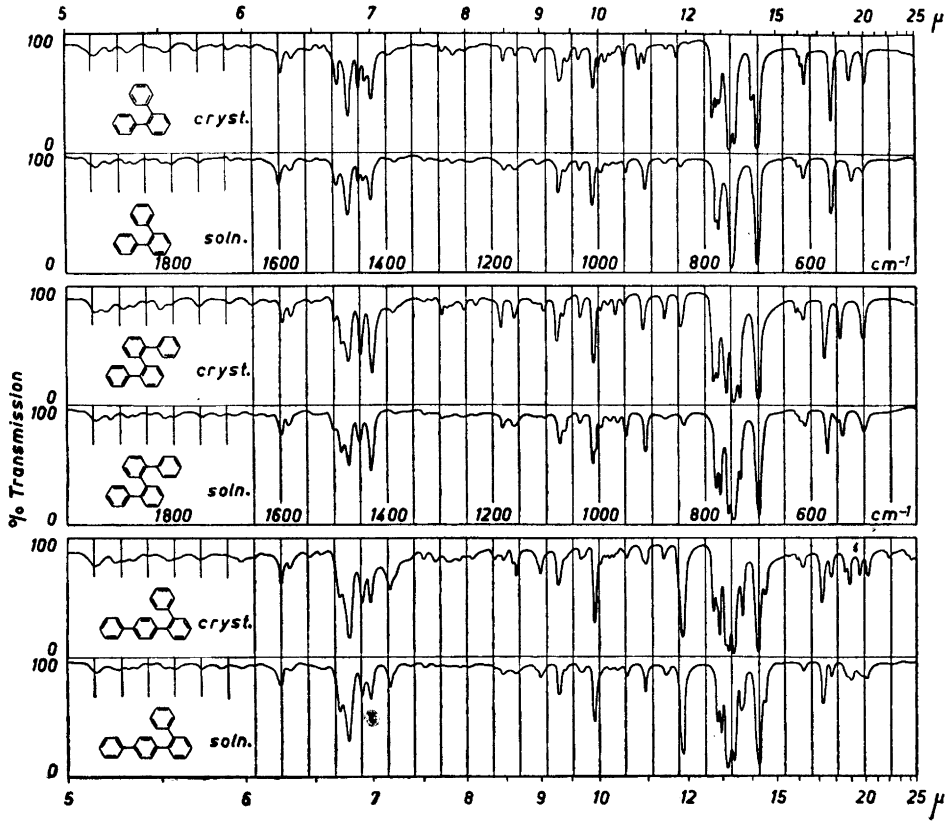


Fig. 2. Infrared spectra of non-linear polyphenyls in solution (1 %, 1 mm cell thickness) and in the solid, crystalline state. Pressed KBr disks and solidified melts give indistinguishable spectra. The solvents used in the various regions have been indicated in Fig. 1.

disks. While these were identical for the non-linear compounds, it was observed that for the linear compounds some of the bands present in the KBr-disk spectra were missing or of very low intensity in the spectra of the solidified melts. Evidently, oriented crystallization between the salt plates must be responsible for this effect *, since just these compounds tend to crystallize in very thin leaflets. It was also observed that if the linear polyphenyls are sublimed on to a salt plate, the same bands are absent in the spectra. It is easy to understand that in this case the leaflets that are oriented parallel to the salt plate must make by far the largest contribution to the absorbing area. Now it is known from X-ray diffraction that these molecules have their long axis perpendicular to the main plane of the crystal leaflets [2-5]. The bands that are

* From a spectrum of biphenyl, published by Richards and Thompson [6], it may be seen that they have also had a strongly oriented sample, apparently without being aware of it.

absent in the oriented samples must therefore be due to those vibrations which are polarized parallel to the long axis, and we have thus a means of sorting out vibrations of this symmetry type.

It was further found that when the solution spectra were compared with the solid state spectra, there are practically no differences in the non-linear compounds (Fig. 2), whereas for the linear compounds (Fig. 1) some bands present in the solution spectra disappear completely in the spectra of the solid, crystalline state *. For this latter case one is thus at once forced to conclude that the molecules, which are planar in the solid state, become non-planar in solution, since by such a change the symmetry of the molecule will be altered (loss of symmetry center) and the selection rules will change. However, this concerns only a few bands below 800 cm^{-1}; the remaining bands seem to behave as if they belonged to separate rings with the same substitution, as has already been noted by Cannon and Sutherland [10].

BANDS CHARACTERISTIC OF MONO-SUBSTITUTED BENZENES.

A complete assignment of the main bands below 1 600 cm^{-1} in the biphenyl spectrum, and most of the bands in the other spectra, could be made on the basis of the assignment given by Pitzer and Scott for methylbenzenes [12], because of the fortunate circumstance that most of the vibrations seem to occur independently within each nucleus. Since there are no disturbing bands due to methyl groups, and the vibrations of symmetry class A_1 can be identified with certainty, as shown above, it is believed that the present assignments for biphenyl (Table 1) are quite reliable, and may be of value in the revision of Pitzer and Scott's data which Plyler considers necessary [13]. To be specific, vibrations 6a and 6b (using Wilson's numbering scheme [14]) had to be interchanged, although good arguments have been advanced for their classification in monosubstituted benzenes based on the mass sensitivity of the lower frequency band and constancy of the higher one [13]. Furthermore, vibrations 19b, 3 and 5 had to be shifted to much higher frequencies; for vibration 5 the new position is in good agreement with calculations by Cole and Thompson [15].

By comparing the classification according to main vibrational type in Table 1 with the spectrum of biphenyl in Fig. 1 it is seen that the bands due to CC-stretching modes (ν CC in Table 1) are rather similar in solution and in the solid state, except that for the pair just below 1 600 cm^{-1}, 8a is more intense than 8b in solution, while 8b is the stronger band in the solid. Their assignment is strongly supported by the appearance of intense Raman lines [16] at 1 600 and 1 584 cm^{-1}. The bands attributed to CH-in-plane-deformation modes (δ CH) are characterized by being sharp in the solid, but broad and diffuse, even weak, in solution. This broadening may perhaps be due to interaction between the hydrogen atoms and the solvent, or to oscillations of the rings about some interplanar equilibrium angle. The bands which represent CH-

* The spectrum of biphenyl as mineral oil mull, given by Burton and Richards [9], reveals that it is actually a mixture of solid and solution; the substance must have been partly dissolved by the oil.

Table 1. Tentative assignments of the main absorption bands of monosubstituted benzene rings in polyphenyl chains.

ain ra- nal pe	Num- bering acc. to Wilson	Sym- metry type	Biphenyl		*p*-Terphenyl		*p,p'*-Qua- terphenyl		*o*-Terphenyl		*o,o'*-Qua- terphenyl		*o,p'*-Qua- terphenyl	
			cryst.	soln.	cryst.	soln.	cryst.	soln.	cryst.	soln.	cryst.	soln.	cryst.	soln.
C	8a	A_1	1 595	1 593	1 593	1 596	1 596		1 594	1 597	1 592	1 594	1 594	1 59
C	8b	B_1	1 568	1 563	1 574	1 575	1 578		1 572	1 574	1 575	1 575	1 575	~1 57
C	19a	A_1	1 478	1 480	1 478	1 479	1 479	~1 480	1 470	1 472	1 470	1 470	1 471	1 47
C	19b	B_1	1 428	1 429	1 454	1 449	1 445	~1 440	1 428	1 429	1 426	1 429	1 429	1 43
C	1	A_1	1 007	1 008	1 002	1 006	1 002	1 004	1 007	1 008	1 007	1 008	1 005	1 00
H	3	B_1	1 342	~1 333	1 337	~1 330	1 334							
H	9a	A_1	1 179	~1 172	1 188	~1 174	1 208 1 182		1 177	~1 178	1 182	1 177	1 177	~1 17
H	9b	B_1	1 167	~1 153	1 166	~1 152	1 167		1 152	~1 154	1 156	~1 155	1 153	~1 15
H	15	B_1	1 109	~1 104	1 117	1 110	1 117		1 116	~1 112	1 100	~1 099	1 109	1 10
H	18a	A_1	1 041	1 042	1 041	~1 042	1 033		1 033	1 033	1 032	1 033	~1 031	~1 02
H	5	B_2	1 076	1 072	1 073	1 072	1 076		1 070	1 071	1 075	1 072	1 074	1 07
H	17b	B_2	903	902	909	909	909	~908	920 909	910	914	910	~910	91
H	10a	A_2*	~840	~842	~850		858							
H	10b	B_2	730	735	745	750	753	757	740	746	741	742	743	74
C	12	A_1		778		769			775 769	772	773	769	770	76
C	6a	A_1	610	609			610		612	611	612	611	612	61
C	6b	B_1		544		518			524	521	542	539	531 524	~53 52
C	4	B_2	696	697	687	693	687	693	694	698	697	695	698	69
C	16b	B_2	461	~488	460	~483	462	~475	495	~500	498	~499	506 490	~50 49

Symmetry type" refers to the symmetry of the separate ring; not of the whole molecule. An asterisk denot the vibration is strictly infrared inactive, but occurs in violation of the selection rules.

and CC-out-of-plane-deformation modes (γ CH and γ CC) * are very similar in both states, except that the 16b vibration is displaced to higher frequency in solution.

The remaining three bands due to the CC-in-plane-deformation modes (δ CC), illustrated for benzene in Fig. 3, are the most important ones, since two of these bands, 12 ** and 6b, are just those which do not appear in the solid; the third one, 6a, disappears on lengthening the chain (*p*-terphenyl) and reappears on further lengthening (*p,p'*-quaterphenyl). It would seem reason-

* It should be emphasized at this point that of the two bands 10b and 4, which are very strong and characteristic in monosubstituted benzenes, 10b is chiefly a γ CH-vibration, while 4 is chiefly a γ CC-vibration. They are both commonly and confusingly referred to in the literature as γ CH-vibrations [11,17].

** This vibration has been assigned by Frühling [16] to a strong Raman line at 1 028 cm^{-1}, close to its frequency in benzene, but this line is rather due to the 18a vibration which in the infrared gives rise to a band at 1 042 cm^{-1}.

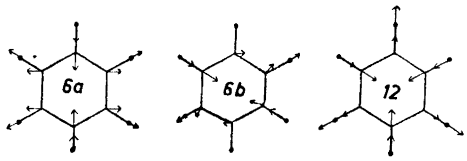


Fig. 3. The three normal modes of in-plane-deformation vibration of benzene according to Pitzer and Scott [12].

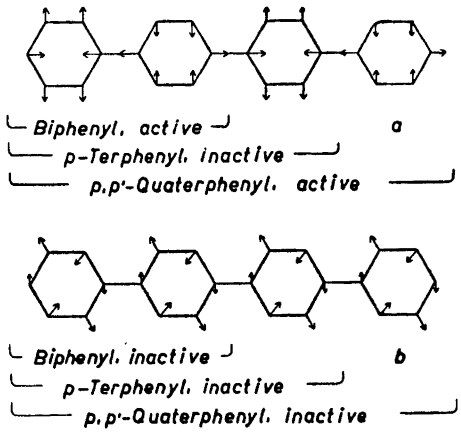


Fig. 4. "Whole-molecular" vibrations obtained by coupling in-plane-deformation modes of the rings in the manner suggested by the intensity variations of the corresponding bands; a) vibration 6a; b) vibration 6b.

able to expect that skeletal deformation vibrations in the plane should be coupled most strongly through the whole molecule, more so than skeletal deformation vibrations perpendicular to the molecular plane. But although the selection rules seem to be determined by the symmetry of the whole molecule, the frequencies are apparently not much affected; thus, Raman lines are observed in solid biphenyl at the same frequencies as for the infrared bands 12 and 6b in solution [16].

Let us now consider the 6a vibration. If it is coupled together as shown in Fig. 4a (the other possible manner would lead to stretching of the bond connecting the rings), it is easy to see that this will explain why the vibration should be allowed in the infrared for biphenyl, *p,p'*-quaterphenyl, etc., but forbidden for *p*-terphenyl, *p*-quinquiphenyl, etc., and why it is unaffected by rotation of the rings relative to each other about the connecting bonds or "pivot bonds" upon dissolution.

The 6b vibration can be coupled together in the manner shown in Fig. 4b. This coupled vibration would give rise to no absorption in planar molecules irrespective of the length, in agreement with the spectral evidence (Fig. 1). In non-planar molecules of any length it will become allowed, and the intensity

will depend on the interplanar angle. The forbidden 6b vibration of the *p*-disubstituted ring (Table 2) which "transmits" the coupled vibration through the longer chains, is apparently so mixed with the 6b vibration of the monosubstituted rings that two bands appear, subject to the same "molecular" selection rules (*cf.* the terphenyl spectrum). Their classification is obviously only tentative.

The 12 vibration is more difficult to interpret. If it is coupled together in a manner analogous to the coupling of 6a above, one should expect absorption both for planar and non-planar molecules irrespective of the number of nuclei in the chain. Instead, a band appears only in the solution spectra. There are other ways in which this vibration may be coupled to fit the observations, but since additional assumptions are needed, further discussion does not seem justified.

However, the important fact is that the three vibrations which do not obey the selection rules of separated rings, all belong to the skeletal in-plane-deformation modes. The only obvious conclusion from the behaviour of these bands is that the linear polyphenyl molecules are planar in the solid crystalline state, and non-planar in solution. Nothing definite can be said about the magnitude of the interplanar angle, but since Frühling [16] has concluded from polarization measurements of the Raman lines of liquid biphenyl, that the molecules have a center of symmetry, the interplanar angle may be quite small.

It remains to be mentioned that a band corresponding to the 7a vibration, which in toluene represents stretching of the CC-bond between the methyl group and the ring [12], is not found in the biphenyl spectrum, since it would here correspond to the pivot-bond stretching, which, even with less symmetric substitution than in biphenyl, would be expected to be inactive in the infrared, but give a very strong, polarized Raman line. In fact, the strongest line observed in the Raman spectrum of biphenyl [16, 18] as well as the terphenyls [18, 19], is at around 1 280 cm^{-1} and has been attributed to this stretching mode [18]. The absence of this band in the infrared spectrum strongly confirms this assignment. A very weak band at 1 275 cm^{-1} in the infrared spectrum of *p,p'*-quaterphenyl might be due to stretching of the two unsymmetrically substituted pivot bonds, since it is polarized parallel to the long axis of the molecule.

A strong band is present at 1 089 cm^{-1} in solid biphenyl but absent in solution and in all the other compounds. Its origin is uncertain. On the other hand, a few of the weak bands can be interpreted. Thus, the inactive 10a vibration can be detected at 840 cm^{-1} in biphenyl. It may be significant that it belongs to the γ CH-vibrations which are generally the strongest bands of aromatics. The weak band at 1 377 cm^{-1} is probably the first overtone of vibration 4 at 696 cm^{-1}.

Of the normal vibrations still not accounted for, there are five CH-stretching modes: 2, 7b, 13, 20a, and 20b; and one CC-stretching mode: 14. Then there is one CH-out-of-plane deformation mode, 17a, which is only Raman active, and one CC-out-of-plane deformation, 16a, active in the Raman [16] at 402 cm^{-1}. Vibrations 18b and 11, which are CH-in-plane and out-of-plane deformations respectively in benzene, would in biphenyl correspond to bending vibrations of the rings against each other and should occur below 400 cm^{-1}.

In the spectra of the remaining polyphenyls it is possible to trace most of the bands due to vibrations in monosubstituted rings through the whole series (Table 1). The very constant frequency of many of them is noteworthy. In *o*-terphenyl a few bands split in the solid, possibly because of non-equivalence of the two mono-substituted rings caused by packing effects in the crystal lattice. In *o,p'*-quaterphenyl doubling of some bands persists even in solution, since the two rings are unequally substituted.

BANDS CHARACTERISTIC OF DISUBSTITUTED BENZENE RINGS

The bands that are left over must then be due to vibrations within *para*- and *ortho*-disubstituted benzene rings, respectively. The most characteristic of these bands have been tentatively classified on the basis of Pitzer and Scott's work [12], and are given in Tables 2 and 3. Of course, other bands due to the disubstituted rings may be hidden by bands already assigned to monosubstituted rings. In particular, the bands are so numerous below 800 cm^{-1} for the more complex molecules, that their classification is rather uncertain.

For *p*-disubstituted rings (Table 2) the most characteristic bands are the CC-stretching 19b at 1 400 cm^{-1} and the CH-out-of-plane-deformation 17b at 830—840 cm^{-1}. It should be noted that a few vibrations give infrared bands in violation of the selection rules.

Table 2. Tentative assignments of some characteristic absorption bands of *para*-disubstituted benzene rings in polyphenyl chains (see Footnote to Table 1).

Main vibrational type	Numbering acc. to Wilson	Symmetry type	*p*-Terphenyl		*p,p'*-Quaterphenyl		*o,p'*-Quaterphenyl	
			cryst.	soln.	cryst.	soln.	cryst.	soln.
ν CC	19b	B_{2u}	1 401	~1 400	1 399	~1 395	1 392	1 393
δ CH	3	B_{3g}*	1 256	~1 254	1 256			
	18a	B_{1u}	1 027	1 026				
γ CH	17b	B_{3u}	838	840	826	825	839	832
δ CC	12	B_{1u}		723			728	728
	6b	B_{3g}*	~ 565	565	570		558	558

For *o*-disubstituted rings (Table 3) the bands are more numerous, but less characteristic. In *o,o'*-quaterphenyl there is a doubling of the CC-stretching 19b, but since the two rings are identical, the reason may be strong coupling between them for this stretching mode. It will be noticed that the γ CH-vibration 10a has been correlated with a band at 750 cm^{-1}. This is in agreement with calculations by Cole and Thompson [15], although Pitzer and Scott did not assign the strong band at 740 cm^{-1} of *o*-xylene to this mode [12]. Two other γ CH-vibrations, 5 and 17a, give rise to bands in violation of the selection rules.

Table 3. Tentative assignments of some characteristic absorption bands of *ortho*-disubstituted benzene rings in polyphenyl chains (see Footnote to Table 1).

Main vibrational type	Numbering acc. to Wilson	Symmetry type	*o*-Terphenyl		*o,o'*-Quaterphenyl		*o,p'*-Quaterphenyl	
			cryst.	soln.	cryst.	soln.	cryst.	soln.
ν CC	19b	A_1	1 493	1 495	1 497 ~1 484	~1 497 1 485	1 486	1 488
	19a	B_1	1 451	1 453	1 447	1 449	1 444	1 444
γ CH	17b	B_2	949	947	946	~ 950	943	945
	5	A_2*	867	~ 873	874	~ 870	875	870
	17a	A_2*	849	~ 842	843	~ 839	(~845)	
	10a	B_2	749	(746)	756	753	752	753
δ CC	12	B_1	781	~ 776	780	776	781	775
	6a	A_1	558	558	570	567	576	575

They are weak in *o*-terphenyl, but stronger in *o,o'*-quaterphenyl where the selection rules are not strictly valid because the two substituents on each ring are unequal.

The great similarity between the solid state and the solution spectra of the non-linear polyphenyls even below 800 cm^{-1} would indicate that there are no great conformational differences between these two states. However, a small increase in interplanar angles upon dissolution would not lead to a change in symmetry and selection rules as it does in the linear series, and such widening of interplanar angles might well take place. Whether a mixture of *cis*- and *trans*-like conformations of *o,o'*-quaterphenyl exists in solution, or the *trans*-like conformation is alone present in both solution and solid, cannot be decided with certainty, but the spectra are so similar that the latter alternative appears most likely.

EXPERIMENTAL

The *spectra* were recorded in a Perkin-Elmer double-beam instrument, Model 21, using a NaCl prism from 2 to 15 μ and a KBr-prism from 15 to 25 μ. 1 % solutions in a 1 mm cell were used, except for *p*-terphenyl and *p,p'*-quaterphenyl which were measured as saturated solutions. In addition to CCl_4 and CS_2 it was found necessary with this cell thickness to use ethylidene chloride to get reliable readings in a few wavelength regions (Fig. 1).

Biphenyl and p-*terphenyl* (1,4-diphenylbenzene) were commercial samples purified by sublimation.

p,p'-*Quaterphenyl* (4,4'-diphenylbiphenyl) was prepared according to Bowden [20], recrystallized from benzene, and sublimed *in vacuo*.

o-*Terphenyl* (1,2-diphenylbenzene) and o,o'-*quaterphenyl* (2,2'-diphenylbiphenyl) were prepared as described by Bachmann and Clarke [21]. *o*-Terphenyl was recrystallized from methanol; *o,o'*-quaterphenyl first from ethanol, and then several times from acetone.

o,p'-*Quaterphenyl* (2,4'-diphenylbiphenyl) was prepared in the following manner: A mixture of *o*-iodobiphenyl (4 g), *p*-iodobiphenyl (4 g), and 10 g of finely ground copper powder (commercially available as "copper bronze" pigment) was heated to 260° C for 30 min, then cooled and extracted with benzene. The extract was purified by running it

through an alumina column. Some of the *p,p'*-quaterphenyl that is formed in the reaction had entered the extract, but separated out on evaporation. Formed biphenyl could be removed either by distillation or by chromatography from petrol ether on alumina, but it was not possible to separate *o,p'*-quaterphenyl from formed *o,o'*-quaterphenyl by either method, nor by fractional crystallization. However, when the mixture was very slowly crystallized from ethanol, the *o,o'*-compound formed large bipyramids, while the *o,p'*-compound crystallized as long, thin needles. By decanting off the stirred mixture, only the fine needles followed the liquid. The needles were allowed to settle, and the mother liquor decanted back. By repeating this procedure about 20 times, a quantitative separation could be effected. Yield: 0.9 g *o,p'*-quaterphenyl or 20 % of the theoretically possible total yield of quaterphenyls. Since the yield of *o,o'*-quaterphenyl is 1.1 g or 25 %, it is probable that the yield of *o,p'*-quaterphenyl may be increased by using more *p*-iodobiphenyl than *o*-iodobiphenyl.

The needles were recrystallized several times from acetone, giving large beautiful monoclinic crystals melting at 117.5—118 °C (as compared with 118.5 °C for the *o,o'*-compound). C and H content, as well as molecular weight, were in good agreement with calculated values.

REFERENCES

1. Dale, J. *Acta Chem. Scand.* **11** (1957) 650.
2. Dhar, J. *Indian J. Phys.* **7** (1932) 43.
3. Clark, G. L. and Pickett, L. W. *J. Am. Chem. Soc.* **53** (1931) 167.
4. Pickett, L. W. *Proc. Roy. Soc.* **A142** (1933) 333.
5. Pickett, L. W. *J. Am. Chem. Soc.* **58** (1936) 2299.
6. Bastiansen, O. *Acta Chem. Scand.* **3** (1949) 408.
7. Barnes, R. B., Liddel, U. and Williams, V. Z. *Ind. Eng. Chem. (Anal. Ed.)* **15** (1943) 659.
8. Richards, R. E. and Thompson, H. W. *Proc. Roy. Soc.* **A195** (1949) 1.
9. Burton, W. R. and Richards, R. E. *J. Chem. Soc.* **1950** 1316.
10. Cannon, C. G. and Sutherland, G. B. B. M. *Spectrochim. Acta* **4** (1951) 373.
11. Lunde, K. and Zechmeister, L. *Acta Chem. Scand.* **8** (1954) 1421.
12. Pitzer, K. S. and Scott, D. W. *J. Am. Chem. Soc.* **65** (1943) 803.
13. Plyler, E. K. *Discussions Faraday Soc.* **9** (1950) 100.
14. Wilson, E. B. *Phys. Rev.* **45** (1934) 706.
15. Cole, A. R. H. and Thompson, H. W. *Trans. Faraday Soc.* **46** (1950) 103.
16. Frühling, A. *Ann. phys.* **6** (1951) 401.
17. Dannenberg, H., Schiedt, U. and Steidle, W. *Z. Naturforsch.* **8b** (1953) 269.
18. Mukerji, S. K. and Aziz, S. A. *Phil. Mag.* **31** (1941) 234.
19. Mukerji, S. K. and Singh, L. *Phil. Mag.* **37** (1946) 874.
20. Bowden, S. T. *J. Chem. Soc.* **1931** 1111.
21. Bachmann, W. E. and Clarke, H. T. *J. Am. Chem. Soc.* **49** (1927) 2089.

Received January 12, 1957.

ACTA CHEMICA SCANDINAVICA 11 (1957) 650—659

Ultraviolet Absorption Spectra of *ortho*- and *para*-Linked Polyphenyls

JOHANNES DALE

Forsvarets Forskningsinstitutt, Kjeller, Norway

The electronic absorption spectra of biphenyl, *o*- and *p*-terphenyl, *o,o'*-, *o,p'*- and *p,p'*-quaterphenyl have been measured in solution down to 195 mμ. By adapting the pressed disk technique, good solid state spectra could be obtained with KCl down to 210 mμ. They are very similar to the solution spectra; the bands are broad and without structure. In oriented samples of the linear polyphenyls the "conjugation band" in the region 250—300 mμ is so reduced that a weak hidden transition at 275 mμ is revealed; this band does not move with chain length and shows vibrational structure. The strongest band in all spectra is found at about 205 mμ.

The observed bands have been tentatively interpreted, and factors of importance for the development of vibrational structure briefly discussed.

Interplanar angles in the solid state have been considered in relation to intermolecular forces which seem to favour mutually perpendicular orientation of ring planes in adjacent molecules.

An earlier study of the electronic absorption spectra of polyenes [1] led to the conclusion that all minor bands had to be interpreted as overtone transitions of the total chromophore and could hardly be due to independent partial chromophores, as had been suggested in some cases. It could also be shown that the minor bands correspond in wave length location with the main band of shorter chromophores of lengths equal to integral fractions of the chromophore considered, and that stereochemical factors determine the distribution of extinction value among the bands.

The principle was found to be valid even in more complicated systems. However, in the series of "through-conjugated" polyphenyls, which consist of chains of *ortho*- or *para*-linked benzene nuclei, the experimental material was rather meagre, since only the spectrum of biphenyl [2] was known below 210 mμ. For the terphenyls the spectra were complete above 210 mμ [3–5], but for *o,o'*- and *p,p'*-quaterphenyl only incomplete spectra have been reported [6,7]. For all these compounds, as well as for *o,p'*-quaterphenyl, the preparation of which

has been described in the preceding paper [8], the spectra have now been extended down to 195 mμ in solution and have been given as full curves in Fig. 1.

Since biphenyl and the *p*-polyphenyl molecules have been shown to be planar in the solid, crystalline state [9-12], and infrared spectroscopic evidence has been given in the preceding paper indicating that they are non-planar in solution [8], it was of interest to record also the spectra of the solids, as it would be expected that the degree of interaction between the π-electron systems of

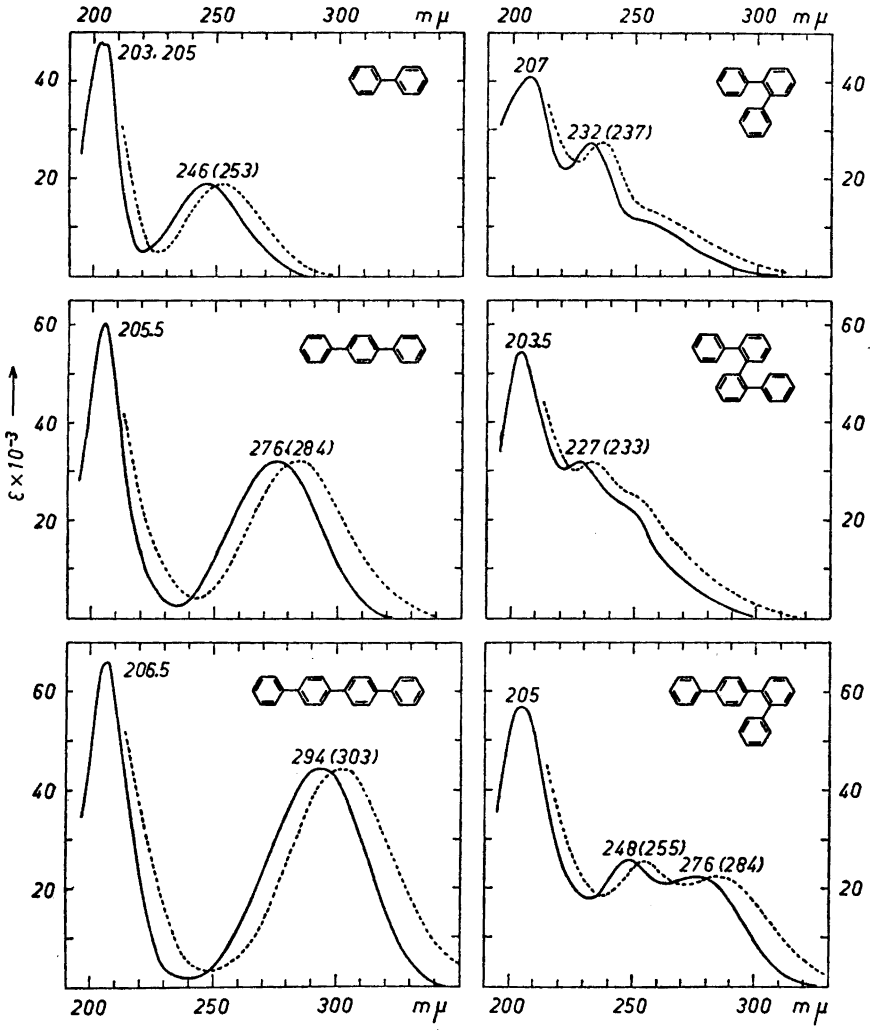


Fig. 1. Ultraviolet spectra of polyphenyls in hexane solution (full lines) and as pressed KCl-disks (dashed lines). The extinction scale of the latter curves is arbitrary.

the rings might be different and manifest itself as a spectral change. By adapting the well known KBr pressed disk technique developed for infrared spectroscopy [13], but using KCl instead of KBr, good qualitative spectra could be obtained down to 210 mμ, and have been given as dashed curves in Fig. 1. Unfortunately, reliable absolute extinction values could not be obtained, and the extinction of the main band has been arbitrarily set equal to its extinction in solution.

The most surprising feature of Fig. 1 is that there are no significant differences between solution and solid state spectra; just a normal, or slightly larger than normal, red-shift which increases with wave length in the same way as the red-shift observed with compounds like naphthalene and anthracene (see Experimental part), which obviously cannot assume other conformations in solution than in the crystal lattice.

VIBRATIONAL STRUCTURE

Another interesting result is that there is no indication of vibrational structure in the solid state spectra of the linear polyphenyls. It has been suggested by Merkel and Wiegand [14] that the lack of structure in the solution spectrum of biphenyl etc. is due to the non-planarity of the molecules, which would imply that vibrational structure should appear in the solid state if the molecules are then planar. The presence of vibrational structure is, however, a very doubtful criterion of coplanarity, as it is well recognized that when voluminous substituents occupy all four *ortho*-positions of biphenyl, the pronounced structure of the low intensity band of the unconjugated benzenoid chromophore is rather an indication that the rings are not coplanar [3,15], although each isolated chromophore is of course strictly planar. Since the broad, structureless appearance of the conjugation bands of the linear polyphenyls persists in the planar molecules of the crystal, whereas condensed aromatics show sharp structure both in solution and in the crystal, the explanation proposed by Kortüm and Dreesen [16] receives considerable support; these authors have emphasized that the appearance of vibrational structure is more a question of rigidity than of coplanarity of the molecules. In biphenyl the lack of structure was assumed to be connected with the possibility of low-frequency torsional oscillations of the rings against each other. This possibility is still present when the interplanar equilibrium angle is zero, since the double bond character of the "pivot bond" is rather small ($\sim$10 %), and this bond is therefore not very stiff even when the rings are coplanar. In polyenes the "single" bonds are much stiffer; hence, structure develops.

On the other hand, the great increase in vibrational structure of the main absorption band through the series *p*-polyphenyls → polyenes → polyynes might be explained alternatively by the rapidly decreasing number of normal vibrations of the right symmetry type that according to the Franck-Condon principle can be coupled with the electronic transition. For instance, quinoid polarization of a benzene ring would already be expected to excite three E_{2g} vibrations, which all involve appreciable percentages of CC-stretching [17] but have so different frequencies (1 595, 1 178, and 606 cm^{-1} in the ground state, and somewhat lower in the excited state) that the peaks may overlap each other

and the structure become blurred. In the transition responsible for the conjugation band of biphenyl and the *p*-polyphenyls the situation will of course be very much more complicated, since the electronic transition depends on the symmetry of the chromophore, that is, the whole molecule, whereas most of the vibrations are related to the symmetry of the separated ring in which they occur [8]. A very large number of different vibrations will therefore be coexcited.

The strongest transition of a polyene should mainly arouse one or several symmetrical C=C stretching modes, with frequencies just above 1 600 cm^{-1} in the ground state, since calculations by Kynch and Penney [18] show that the length of the "single bonds" remains almost unchanged during the transition, whereas the "double bonds" increase in length, especially the central ones. But also other modes of the same symmetry, classified as mainly CH-in-plane-deformations and with frequencies in the region 1 300—1 400 cm^{-1} [19], will probably involve much CC-stretching. The spacings 1 570 cm^{-1} and 1 230 cm^{-1} observed at low temperatures [20] agree well with these expectations, and are so close that peaks spaced at the average value of about 1 400 cm^{-1} are quite distinct under ordinary conditions.

In polyynes one or several symmetrical C≡C stretching frequencies at about 2 000 cm^{-1} will be the only ones that can be excited in an electronic transition which preserves the linear shape of the molecule. This explains the enormously sharp peaks in these spectra [21].

The above statements are not contradicted by the very sharp structure of the well known and weak 260 mμ band of benzene, because this forbidden transition, $^1A_{1g} \rightarrow {}^1B_{2u}$, is of a symmetry type [22] which will arouse strongly only the breathing frequency at 923 cm^{-1} in the excited state, neglecting the single quantum of the E_{2g} vibration at 520 cm^{-1} which is necessary to deform the skeleton and make the transition possible.

However, it is most likely that for the development of structure both these factors must be considered of importance: a rigid structure; and relatively few vibrations, or several with close-lying frequencies, that can couple with the electronic transition. This is equivalent to saying that the normal vibrations should depend on the symmetry of the whole chromophore.

REVELATION OF HIDDEN TRANSITIONS

The lack of structure in the spectrum of solid biphenyl as pressed KCl-disk would seem to be in conflict with the qualitative statement by Merkel and Wiegand [14] that sharp peaks appear in the spectrum of biphenyl crystals*. However, in view of the marked orientation effects observed with the linear polyphenyls in the infrared (*cf.* preceding paper [8]), one should expect that, also in the ultraviolet, bands that are due to transitions with dipole moment along the long molecular axis, such as the strong conjugation band, would disappear in the spectra of thin layers of solidified melts or sublimed crystals, so that weak bands which are transversely polarized, and normally hidden

* The banded absorption at 300—330 mμ, observed in thin crystal plates of biphenyl [23], is so extremely weak that it must be due to some singlet-triplet transition, and is of little interest in this connection.

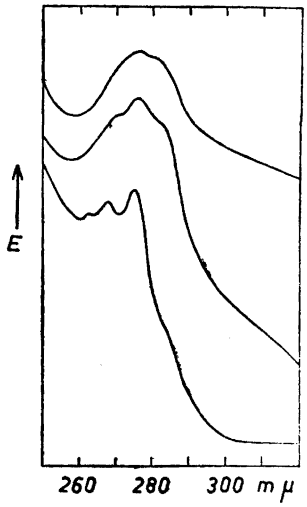


Fig. 2. Ultraviolet spectra of oriented solid samples of linear polyphenyls; bottom, biphenyl; middle, *p*-terphenyl; and top, *p,p'*-quaterphenyl. Incident radiation is parallel to the long axis of the molecules.

by the stronger band, may be detected. This could be confirmed experimentally, either by letting an extremely thin film of melted substance ($< 1\ \mu$) solidify between silica plates; by evaporation of a thin layer of solution; or by sublimation on to a silica window. The absorption curves of oriented samples of biphenyl and the linear polyphenyls are shown in Fig. 2 and reveal that there is a band showing structure with a maximum at about 275 mμ for all compounds. Although the extinction coefficients could not be determined exactly, they may be very roughly estimated to about 1 000—2 000. These values are reasonable, since appreciably lower values would not be sufficient to let this band protrude from the rudiments of the strong band, which, at least for longitudinally polarized bands in the infrared, amounts to about 5 % of the full value [8]. The extinction coefficient, which for biphenyl is 19 000, would thus be reduced to about 1 000.

The 275 mμ band can scarcely be due to the forbidden transition, discussed by Platt [2], between a localized π-orbital with a longitudinal node and a polyene-like orbital (see below). This transition has been assumed by Platt to be hidden by the conjugation band and predicted to move towards the red about half as fast upon lengthening of the system, whereas the 275 mμ band remains stationary throughout the series. Rather, it may be related to the forbidden 260 mμ transition in benzene, as already suggested by Wenzel [24] for the hidden transition in biphenyl, and for which she deduced, from a comparison with substituted biphenyls, position and intensity in good agreement with the present findings. Correcting for the "normal red-shift", the location of the peaks of biphenyl corresponds very well with the peaks of a mono-substituted benzene ring like toluene [5]. The less resolved structure and very slight red-shift in *p*-terphenyl and *p,p'*-quaterphenyl is presumably due to overlapping of similar bands arising from *p*-disubstituted rings, since the peaks in the *p*-xylene spectrum [5] are shifted to the red as compared with toluene. According to the ideas outlined above, the presence of structure in

this band can also be taken as an indication that the transitions occur within each isolated rigid ring, rather than as an indication of coplanarity of the rings.

The conjugation band can also be weakened, and shifted to shorter wave lengths, by providing large deviations from coplanarity, so that the weak hidden transition in each ring may be revealed. The well-known effect of large alkyl-substituents in the *ortho*-positions of biphenyl is an example of this [3]. Furthermore, in the vapour phase [25] the angle of twist is as large as 45°, and the hidden transition is probably identical with the structureless absorption tail that appears in the gas spectrum [26] at around 270 mμ. The lack of structure, the broadening towards the red, and the increase in intensity with temperature (170—520° C), may be explained by the increased population of vibrational levels in the ground state. Some of the vibrations destroy the hexagonal symmetry of each ring so that the electronic transition becomes allowed.

INTERPLANAR ANGLES

The displacement towards the ultraviolet and the weakening of the conjugation band must be related to the reduced electronic interaction when the interplanar angle is increased. According to calculations by Guy [27] this angle of twist may become as large as 22° before the resonance energy is appreciably reduced, and somewhere between 45 and 68° before it reaches zero. Since the spectra of solids and solutions are so similar, one should therefore expect that the interplanar angle of biphenyl in solution would not exceed much the value of 22°. The values of +34°, —27° and +24° reported for solid 1,3,5-triphenylbenzene [28] are surprisingly large, since the steric repulsion between *ortho*-hydrogen atoms should be the same as in biphenyl. Moreover, both molecules have angles of twist near 45° in the vapour phase [25, 29]. The planar structure of solid biphenyl and the *p*-polyphenyls is not immediately understandable as being necessary to obtain the most favourable packing, because the molecules are in fact rather loosely packed, having their planes not parallel, which would give the densest packing, but mutually inclined at an angle of approximately 66° [9, 11]. On the other hand, the molecules of solid 1,3,5-triphenylbenzene form an approximately layer arrangement [28], and in this case planar molecules would obviously have been able to pack more densely.

A simple explanation can be arrived at by assuming that intermolecular forces operate in such a way that aromatic hydrocarbon molecules tend to avoid being stacked with their planes parallel, and instead prefer mutually perpendicular orientation. Whether these forces are simply repulsive forces between filled π-orbitals, or some sort of bonding forces between hydrogen atoms and π-electrons, is irrelevant for the present discussion. The crystal structure of benzene [30] most strikingly demonstrates this feature; adjacent molecules have their planes mutually perpendicular and form a loosely knit structure. More elongated molecules like naphthalene and anthracene also have their planes tilted away from each other, but at somewhat smaller angles [31]. It will now be easily realized that the planar conformation of *p*-polyphenyl molecules is best suited to obtain a relatively large inclination angle between the ring planes of adjacent molecules with a minimum of empty space between the molecules.

The larger disk-like molecules, like coronene and ovalene [31], cannot be packed in this manner, because too large voids would result. Instead, they are stacked in columns, but the molecules of adjacent columns still have their planes perpendicular to each other. In 1,3,5-triphenylbenzene, packing of mutually perpendicular molecules would be very awkward and lead to an excessively loose structure. The molecules therefore have to form roughly planar layers [28], but phenyl groups of each layer can be twisted about the pivot bond to make fairly large angles with the planes of phenyl groups in the next molecular layer twisted in the opposite sense. In this way the curious crystal structure, the large and dissimilar angles of twist, and the lack of perfect cleavage parallel to the molecular layer planes can be understood. The apparent strength of the intermolecular forces in the crystal suggests that the angles of twist may even be smaller in solution than in the solid for this compound.

In *o*-terphenyl the angle between adjacent ring-planes is 45—50° in the solid [32], and increases to very roughly 90° in the vapour phase [33]. Considering the spectral similarity, the angle at *ortho*-links in solution most likely is not much larger than in the solid. However, this conclusion concerning one state, the ground state, based entirely on the ultraviolet spectrum, which involves two states, is presented with much reserve.

EMPIRICAL CLASSIFICATION OF THE BANDS

Several authors have calculated the energy levels of biphenyl and the *p*-polyphenyls [34–38], but their results will not be discussed here. The present approach will instead be limited to correlations of a more qualitative nature.

The strongest band in the spectra of all the polyphenyls investigated appears at around 205 mμ. According to Platt [2], transitions between localized π-orbitals within each mono- and *p*-disubstituted benzene ring, that is, orbitals which have a longitudinal node and thus cannot conjugate with adjacent rings to form polyene-like whole-molecular orbitals, would be expected to give rise to intense absorption in this region. This is then a band for which the term "partial" is certainly justified.

The long-wave absorption bands, except weak bands like the hidden transition in biphenyl, which will not be further considered, should originate from transitions between whole-molecular, polyenelike π-orbitals made up from ring orbitals with no longitudinal node [2], and are the bands to be considered when testing the validity of the empirical rule established for polyene spectra [1]. At *ortho*-links the molecular orbital picture will not be so simple, and, of course, there will be a great steric hindrance preventing coplanarity, so that the electronic interaction will be reduced, and a blue shift of all bands might be expected.

When trying to correlate the bands, the wave length position of the main band of the linear polyphenyls must be plotted against number of linked chain nuclei. The question then arises which value should be used for benzene. The strongest band of benzene is at 185 mμ [5], but there are reasons for using a value of about 205 mμ; on the one hand, because this medium intensity band in benzene fits best with the value obtained from extrapolation of wave length

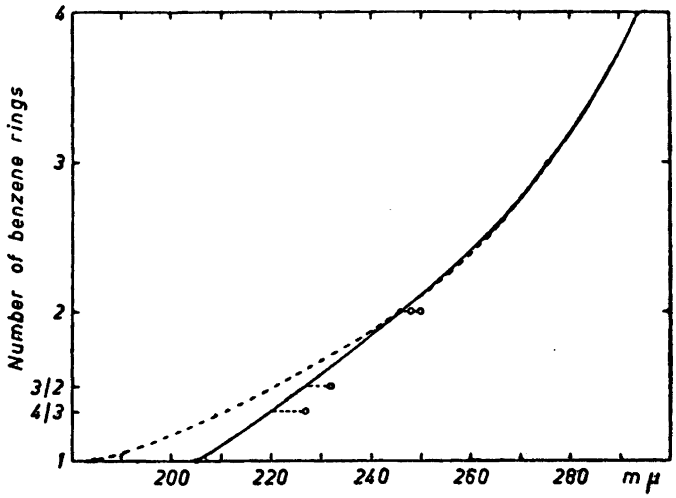


Fig. 3. Wave length position of the "conjugation band" of linear polyphenyls plotted against number of benzene rings. Dashed curve is obtained by using an alternative value for benzene. Positions of assumed overtone bands of non-linear polyphenyls have been indicated as circles; horizontal lines give the deviation from estimated values.

position and intensity of the conjugation band of *p*-polyphenyls [24]; on the other hand, because it happens to be the center of gravity of the four one-quantum transitions which are assumed to arise from strong splitting due to the high symmetry of benzene [39]. In Fig. 3 both values have been used in drawing the lines used for calculation. Experimentally observed wave lengths for assumed overtone bands have been given as circles, and are seen to come closest to the 205 mμ curve.

Considering the linear polyphenyls first, it is seen that there are here no overtones, and none would be expected either in such a strictly linear chain, except possibly a weak λ_3-band in *p,p'*-quaterphenyl. The band at 205 mμ may in part be due to the overtone transition corresponding to one benzene ring in all compounds, that is, λ_2 for biphenyl, λ_3 for terphenyl, and λ_4 for quaterphenyl; it may be of special preference, since there would be no displacement of electron density from one ring to the other during excitation [1, 40].

In *o*-terphenyl the step-out at around 260 mμ may be regarded as a λ_1-band which is reduced in intensity and shifted to shorter wave lengths because of the bent shape and steric hindrance. The λ_2-band at 232 mμ is correspondingly stronger since it is allowed in this bent molecule and takes over much of the intensity.

In *o,p'*-quaterphenyl the bands at 276 and 248 mμ are similarly interpreted as λ_1- and λ_2-bands, respectively. A λ_3-band should be of no special preference, and is not observed.

In *o,o'*-quaterphenyl it is necessary to assume that the λ_1-band is so degraded because of the many sterically hindered links and the kinked shape, that it is represented by the absorption tail in the 270—290 mμ region. In a hypo-

thetical coplanar *trans*-conformation the λ_2-band would be forbidden, but as the molecule cannot become planar, it will be weakly allowed. The observed shoulder at 250 mμ is in good agreement with this expectation. A *cis*-like conformation would require a strong λ_2-band, so it is believed that the molecule has a *trans*-conformation both in solution and in the solid phase. This conclusion is supported by the lack of significant differences between the two states both in the ultraviolet and the infrared [8] absorption spectra. The λ_3-band would be strongly allowed, and would also have to take over intensity from the hindered transitions; it fits well with the strong band at 227 mμ.

Also for the non-linear polyphenyls one would expect an overtone band to coincide with the partial band at 205 mμ.

Admittedly, the agreement between the graphically estimated and the observed wavelength maxima is only qualitative, but certainly better than might be expected considering the complexity of these branched π-electron systems. However, one should be cautious and not attach too much theoretical significance to this result, but consider it only as an empirical classification. It is noteworthy that the spectra might in this way be interpreted in a more satisfactory manner than by postulating partial chromophores consisting of 1, 2 or 3 benzene rings. Much more convincing material, illustrating the success of the "overtone" interpretation and the failure of the "partial chromophore" concept, will be presented in a later paper on the spectra of conjugated chains consisting of alternating ethylenic bonds and benzene nuclei (stilbene homologs).

EXPERIMENTAL

The preparation or origin of the compounds studied has been given in the preceding paper [8].

The *solution spectra* were recorded in a Beckman DK-1 instrument using hexane as a solvent. In the lowest wave length region 2 mm silica cells were used.

The *solid state spectra* were measured in a Beckman DU instrument. The disks were pressed under vacuum in the usual manner, but were of only half the ordinary thickness. Since KBr starts to absorb appreciably below 240 mμ, KCl was tried and found useful throughout the whole range of the instrument. Disks of 0.55 mm thickness made from 150 mg KCl (Merck, *p. a.*), which had been precipitated from water solution with hydrochloric acid to obtain small particle size [41], showed a transmission of around 75 % at 400 mμ, 65 % at 300 mμ, 55 % at 250 mμ, 40 % at 220 mμ, and 25 % at 205 mμ. Using KCl which had been melted and rapidly cooled [42], the transmission was still better, namely 80 %, 75 %, 65 %, 55 %, and 40 %, respectively, at the corresponding wave lengths (*cf.* Ford and Wilkinson [43]). However, it was easier to get the organic substance evenly dispersed in the precipitated salt, so that the loss by scattering was much smaller, and this grade was used throughout. Usually, about 1 mg of the substance was thoroughly ground in a mortar with 200 mg KCl, preferably with a small amount of a volatile solvent. 1 mg of the dry mixture was then ground with 150 mg of new KCl, and pressed into a disk. Unfortunately, the extinction values were not reproducible. The loss of the more volatile compounds like biphenyl, and even the terphenyls, during grinding and evacuation of the press, was so great that a considerable excess of substance had to be weighed in. However, the wave length position of the extinction maxima could be reproduced as long as the disks looked clear to the eye. The spectra of disks which became slightly milky because of imperfect dispersion of the substance, showed distortion of the bands with a slight shift of the maxima (Christiansen effect) like what is very often observed in the infrared with non-transparent disks and, particularly, with mineral oil mulls [43,44].

The *normal red-shift* of rigid molecules, from hexane solution to the solid state, was determined by measuring the solid state spectra of naphthalene and anthracene (wave lengths are in mμ; values in parentheses refer to hexane solutions):

Naphthalene: 292(285), 281(275), 272(267), 223(221).

Anthracene: 394(376), 373(357), 353(339), 336(324), 318(309), 256(252), 249(246).

When the differences are plotted against wave length, the red-shift is seen to increase regularly from about 2 mμ at 220 mμ to 8 mμ at 300 mμ, and to 19 mμ at 400 mμ.

REFERENCES

1. Dale, J. *Acta Chem. Scand.* **8** (1954) 1235.
2. Platt, J. R. *J. Chem. Phys.* **19** (1951) 101.
3. Pickett, L. W., Walter, G. F. and France, H. *J. Am. Chem. Soc.* **58** (1936) 2296.
4. Mueller, G. P. and Pickens, D. *J. Am. Chem. Soc.* **72** (1950) 3626.
5. *A. P. I. Research Project 44. Ultraviolet Spectral Data.*
6. Rapson, W. S., Schwartz, H. M. and Stewart, E. T. *J. Chem. Soc.* **1944** 73.
7. Gillam, A. E. and Hey, D. H. *J. Chem. Soc.* **1939** 1170.
8. Dale, J. *Acta Chem. Scand.* **11** (1957) 640.
9. Dhar, J. *Indian J. Phys.* **7** (1932) 43.
10. Clark, G. L. and Pickett, L. W. *J. Am. Chem. Soc.* **53** (1931) 167.
11. Pickett, L. W. *Proc. Roy. Soc.* **A142** (1933) 333.
12. Pickett, L. W. *J. Am. Chem. Soc.* **58** (1936) 2299.
13. Schiedt, U. and Reinwein, H. *Z. Naturforsch.* **7b** (1952) 270.
14. Merkel, E. and Wiegand, C. *Z. Naturforsch.* **3b** (1948) 93.
15. Beaven, G. H., Hall, D. M., Lesslie, M. S. and Turner, E. E. *J. Chem. Soc.* **1952** 854.
16. Kortüm, G. and Dreesen, G. *Chem. Ber.* **84** (1951) 182.
17. Whiffen, D. H. *Phil. Trans.* **A248** (1955) 131.
18. Kynch, G. J. and Penney, W. G. *Proc. Roy. Soc.* **A179** (1941) 214.
19. Richards, C. M. and Rud Nielsen, J. *J. Opt. Soc. Amer.* **40** (1950) 438.
20. Hausser, K. W., Kuhn, R. and Seitz, G. *Z. physik. Chem.* **B29** (1935) 391.
21. Bohlmann, F. *Chem. Ber.* **86** (1953) 657.
22. Sponer, H., Nordheim, G., Sklar, A. L. and Teller, E. *J. Chem. Phys.* **7** (1939) 207.
23. Kortüm, G. and Haug, P. *Z. Naturforsch.* **8a** (1953) 372.
24. Wenzel, A. *J. Chem. Phys.* **21** (1953) 403.
25. Bastiansen, O. *Acta Chem. Scand.* **3** (1949) 408.
26. Almasy, F. and Laemmel, H. *Helv. Chim. Acta* **33** (1950) 2092.
27. Guy, J. *J. chim. phys.* **46** (1949) 469.
28. Farag, M. S. *Acta Cryst.* **7** (1954) 117.
29. Bastiansen, O. *Acta Chem. Scand.* **6** (1952) 205.
30. Cox, E. G. *Proc. Roy. Soc.* **A135** (1932) 491.
31. Robertson, J. M. *Proc. Roy. Soc.* **A207** (1951) 101.
32. Clews, C. J. B. and Lonsdale, K. *Proc. Roy. Soc.* **A161** (1937) 493.
33. Karle, I. L. and Brockway, L. O. *J. Am. Chem. Soc.* **66** (1944) 1974.
34. London, A. *J. Chem. Phys.* **13** (1945) 396.
35. Davydov, A. S. *Zhur. Eksptl. Teort. Fiz.* **18** (1948) 201, 515.
36. Dewar, M. J. S. *J. Chem. Soc.* **1952** 3544.
37. Nakajima, T. *Science Repts. Research Insts., Tôhoku Univ.* **5A** (1953) 98.
38. Murrell, J. N. and Longuet-Higgins, H. C. *J. Chem. Soc.* **1955** 2552.
39. Platt, J. R. *J. Chem. Phys.* **18** (1950) 1168.
40. Dale, J. *Acta Chem. Scand.* **11** (1957) 265.
41. Hales, J. L. and Kynaston, W. *Analyst* **79** (1954) 702.
42. Dietrich, H. v. *Z. Naturforsch.* **11b** (1956) 175.
43. Ford, M. A. and Wilkinson, G. R. *J. Sci. Instr.* **31** (1954) 338.
44. Price, W. C. and Tetlow, K. S. *J. Chem. Phys.* **16** (1948) 1157.

Received January 12, 1957.

ACTA CHEMICA SCANDINAVICA 11 (1957) 660—662

An Addendum to the Henri-Michaelis Mechanism

J. A. CHRISTIANSEN

Institute of Physical Chemistry, University of Copenhagen, Denmark

It is shown that in an enzymic reaction obeying the Henri-Michaelis law the existence of an inactive form with low energy content of the enzyme-substrate complex must exist besides the active, energy-rich form.

The Henri-Michaelis mechanism [1-3] can be written in the form

$$A + X_1 \rightleftharpoons X_2 \quad (\pm 1)$$
$$X_2 \rightarrow X_1 + B \quad (2)$$

where the stoichiometric equation of the overall reaction is A = B.

As pointed out by Haldane and Briggs [4], Michaelis in his original treatment of the reaction makes the error of assuming equilibrium as regard to (±1) which is obviously untrue, if the rate of reaction is not zero.

Application of the steady-state method yields, with s for steady state rate, X_1 for $[X_1]$, x_2 for $[X_2]$ and w_i for the probability of reaction i in unit time:

$$x_1/s = 1/w_1 + w_{-1}/w_1w_2 \quad (3)$$
$$x_2/s = 1/w_2 \quad (4)$$

or as $x_1 + x_2$ = total enzyme concentration = E,

$$E/s = (1 + w_{-1}/w_2)/w_1 + 1/w_2 \quad (5)$$

According to the mechanism $w_1 = k_1(a—x)$; $w_{-1} = k_{-1}$; $w_2 = k_2$, where $a—x = [A]$ at time t.

$$E/s = 1/k_2 + (1+k_{-1}/k_2)/k_1(a—x) \quad (6)$$

which of course agrees exactly with Haldane and Briggs' result.

Replacing $1/k_2$ by A_0 and $(1+k_{-1}/k_2)/k_1$ by A_1 and $1/s$ by dt/dx we get by integration

$$Et = A_0x + A_1 \ln a/(a—x) \quad (7)$$

where $A_1/A_0 = K_m$, the Michaelis constant. (The symbol K_m is due to Henri). Obviously

$$(k_2 + k_{-1})/k_1 = K_m \quad (8)$$

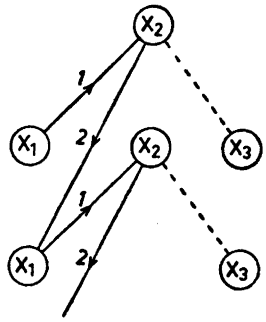


Fig. 1.

A number of enzymic reactions but by no means all yield experimentally an expression of the type (7). (It is convenient to denote the function on the right hand side of (7) by the name a chronometric integral.) Therefore a A_0 and A_1 must in these cases be of the same order of magnitude. This however is impossible if the reaction has an activation-energy. In that case the diagram of the reaction must be qualitatively as in Fig. 1.

The encircled symbols represent the "states" of the enzyme. The system proceeds along the path indicated by arrows. Vertical distances indicate qualitatively energy differences. Particularly the vertical distance between two consecutive X_1's indicates the loss of (free) energy during the reaction. Now from a well known theorem a reaction proceeding from a lower to a higher energy level has an activation energy while its reverse has none.

Further unimolecular and bimolecular rate-constants are known to be, within a few powers of ten, $10^{12} \times \exp(-Q/RT)$ sec^{-1} and $10^{11}\exp(-Q/RT)$ litre $mole^{-1}$ sec^{-1}, respectively. Therefore $1 + k_{-1}/k_2 \simeq 1$ and $k_1 a \simeq 10^9 \exp(-Q/RT)$ if $a \simeq 10^{-2}$ mole/litre. Consequently $A_1/a \simeq 10^{-9} \times \exp(Q/RT)$ sec and $A_0 \simeq 10^{-12}$ sec, that is A_0 is disappearingly small as compared to A_1/a or the reaction must be expected to be purely of the first order. If in the diagram X_2 were placed below the lower X_1 the result would be a reaction of the zeroth order.

To make $A_0 a$ and A_1 comparable it is necessary to add a reaction of the type indicated in Fig. 1 by dotted lines

$$X_2 \rightleftharpoons X_3 \qquad (\pm 3)$$

whose steady state rate is zero. (± 3) means that we assume the existence of an isomer X_3 of X_2 with a low energy-content. We now have

$$x_1 + x_2 + x_3 = E \tag{9}$$

and $x_3 = K_3 x_2$, where K_3 is large ($\simeq \exp Q_3/RT$)

$$x_1 + x_2 (1 + K_3) = E \tag{10}$$

Using (3) and (4) we thus get instead of (5)

$$E/s = (1 + w_{-1}/w_2)/w_1 + (1+K_3)/w_2 \qquad (11)$$

or

$$A_0 = (1 + K_3)/k_2;\ A_1 = (1 + k_{-1}/k_2)/k_1 \qquad (12)$$

where evidently K_3/k_2 may very well be of the same order of magnitude as $1/k_1a$.

This extension of the original picture is new but it has probably existed implicitly in the minds of the originators of the theory. It means simply that the greater part of the enzyme-substrate complex does exist in appreciable amounts in the solution but that only a minute fraction of it is active in reaction (2).

It should be added, that Huennekens [5] (p. 606) discusses a mechanism in which three forms of the enzyme-substrate complex are assumed. But these are connected in series, while in our case one of the two forms is branched off from the main closed sequence. The two assumptions (a reaction in series *versus* a branched sequence) lead to quite different kinetic expressions and only the latter one to a natural explanation of the actual occurrence of reactions of the Michaelis-type.

Gibson [6] assumes four different forms, two with high energy content and two with low but a discussion even of this rather complicated case along the lines indicated above and in former papers [3,7] by the present author again shows that K_m/a in cases where the rate depends strongly on temperature will be either very large in which case the reaction is of the first order, or very small in which case the reaction is of the zero'th order. Incidentally, the present author completely agrees with Gibson in his statement, that activation energies calculated from rate-data for reactions whose mechanism has not been unravelled have no physical significance, compare for example Ref.[8].

Thus again in contrast to the assumption that energetically different forms of the enzyme-substrate complex are inserted in series, the assumption that one (or several) of the forms is branched off from the main closed sequence leads to a natural explanation of the frequent occurrence of reactions obeying the Michaelis law.

REFERENCES

1. Henri, V. *Lois générales de l'Action des Diastases.* Paris 1903.
2. Michaelis, L. and Menten, M. L. *Biochem. Z.* **49** (1913) 333.
3. Christiansen, J. A. *Acta Chem. Scand.* **3** (1949) 493.
4. Briggs, G. E. and Haldane, J. B. S. *Biochem. J. London* **19** (1925) 308.
5. Huennekens, Frank M. *Technique of Organic Chemistry* **8** (1953) 535.
6. Gibson, K. D. *Biochim. et Biophys. Acta* **10** (1953) 221.
7. Christiansen, J. A. *Advances in Catalysis* **5** (1953) 311.
8. Christiansen, J. A. *J. Colloid Sci.* **6** (1951) 213.

Received January 30, 1957.

ACTA CHEMICA SCANDINAVICA 11 (1957) 663—667

Alkaline Hydrolysis of Glycosidic Linkages

II.* Investigation of Cellobitol, Lactitol and Maltitol

ELISABETH DRYSELIUS, BENGT LINDBERG and OLOF THEANDER

Träkemiska avdelningen, Svenska Träforskningsinstitutet, Stockholm, Sweden

The hydrolysis of cellobitol, lactitol and maltitol in alkaline, aqueous solutions at 170° has been studied as part of an investigation of the decomposition of carbohydrates during alkaline pulping. All substances were hydrolysed at roughly comparable rates. D-Glucitol, 1,4-anhydro-D-glucitol and levoglucosan were formed from cellobitol, the first two together with 1,6-anhydro-D-galactose were formed from lactitol. Another, isomeric glucitol β-glucoside was formed from cellobitol and an analogous β-galactoside from lactitol.

It was briefly reported in Part I * that some glycosides, such as methyl β-glucoside and cellobitol, although generally considered to be stable to alkali, were decomposed under the conditions of sulphate or soda cooking, *e. g.* in alkaline solution at 170°. In the present paper a more detailed investigation of some glucitol glycosides is reported.

Cellobitol, lactitol and maltitol were prepared from the corresponding disaccharides by reduction with sodium borohydride [1]. Cellobitol was obtained in a crystalline state, anhydrous, m. p. 149—150°, $[\alpha]_D^{20}$ + 8°, and with one mole of water of crystallisation, m. p. 107—108°. The previously recorded m. p. is 133° [2], which might indicate that the sample investigated consisted of a mixture of the two forms above. Lactitol and maltitol were obtained as syrups.

The glycosides were dissolved in 10 % aqueous sodium hydroxide and heated in stainless steel autoclaves at 170° for various times. The alkali, together with the acids formed during the reaction, was removed by ion exchange and the yield of non-ionic material, a mixture of starting material and the products of reaction, was determined. The yields are given in Table 1. If the glucitol glycosides were completely degraded into glucitol and acidic products, the final yield should be 53 %.

* Part I, *Svensk Papperstidn.* **59** (1956) 531.

Table 1. Yield of non-ionic material, in percentage of starting material, after treatment of cellobitol, lactitol and maltitol with 10 % sodium hydroxide at 170°.

Time, h	Cellobitol, yield	Lactitol, yield	Maltitol, yield
5	73	86, 92	85, 93
24	65	61	60
48	49	53	45

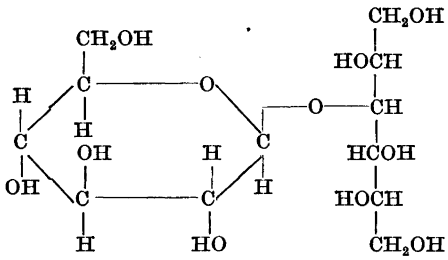
Due to mechanical losses, difficulties in drying the amorphous starting materials and products and to imperfect temperature control, the values in Table 1 are not very accurate, but they show that all the substances have been degraded to a considerable extent and at rates that are of the same order of magnitude.

A chromatographic investigation of the products from the cellobitol (I) revealed the presence of unchanged starting material, a substance with the same R_F-value as glucitol and of two substances with higher R_F-values. The product was fractionated on a cellulose column and the pure components were isolated. The substance with the highest R_F-value was identified as levoglucosan (II), the next as 1,4-anhydro-D-glucitol (arlitan) (III); both substances were identical with authentic specimens. The D-glucitol and cellobitol were also characterised. A small amount of material with an R_F-value slightly faster than that of cellobitol was also obtained.

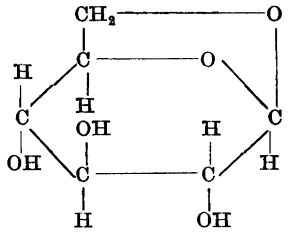
Analogous or identical substances were obtained from lactitol, that is 1,6-anhydro-D-galactose, 1,4-anhydro-D-glucitol, D-glucitol, unknown material and unchanged starting material. The presence of glucitol and 1,4-anhydro-D-glucitol in the products obtained from the maltitol was demonstrated by paper chromatography.

The stability to alkali of the substances formed was investigated. Faint traces of 1,4-anhydro-D-glucitol and another substance with somewhat lower R_F-value, possibly 1,5-anhydro-D-glucitol (polygalitol) could be observed after treatment of D-glucitol with 10 % sodium hydroxide at 170° for 24 h. Some D-glucitol was also formed when 1,4-anhydro-D-glucitol was given an analogous treatment. Levoglucosan and 1,6-anhydro-D-galactose were more labile. The yield of non-ionic material, in this case consisting of pure starting material, decreased rapidly with the time of treatment in alkali. The percentages of unchanged levoglucosan after 1, 3 and 5 h in 10 % sodium hydroxide at 170° were 58, 35 and 25, respectively. The corresponding figures for 1,6-anhydro-D-galactose were 85, 69 and 53 % after 2, 4 and 6 h, respectively. Thus these anhydrides are considerably more labile than the glucitol glycosides and the percentage present in the reaction mixtures should consequently be quite low. As levoglucosan is the most labile of the two, it should be present in the lowest concentration, as was the case.

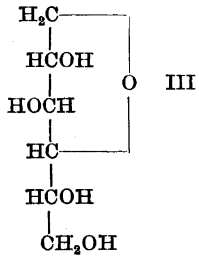
Levoglucosan and 1,6-anhydrogalactose are also formed by the alkaline hydrolysis of phenyl β-glucosides and β-galactosides, respectively. These reactions involve the intermediate formation of a 1,2-anhydrosugar (*cp.* Ref.[3]),



I



II



III

and it is possible that the alkaline hydrolysis of cellobitol and lactitol follows a similar route. As 1,4-anhydro-D-glucitol is formed in a higher yield in these reactions than in the analogous alkaline treatment of D-glucitol, it is evident that this is not the only mechanism by which the glycosidic linkage is cleaved. A reasonable assumption is that the 1,4-anhydro-D-glucitol is formed by a nucleophilic attack on $C_{(4)}$ of the primary hydroxyl at $C_{(1)}$ (as alkoxide) in the glucitol unit. This reaction may be preceded by the formation of an ethylene oxide ring either between $C_{(4)}$ and $C_{(5)}$ or between $C_{(3)}$ and $C_{(4)}$; of these alternatives the former appears to be the more plausible.

Fission between the glycosidic oxygen and $C_{(1)}$ in the glucose unit should therefore yield 1,6-anhydrosugar and glucitol, fission between this oxygen atom and C_4 in the glucitol unit, on the other hand, should yield glucose and 1,4-anhydro-D-glucitol. A direct attack of hydroxyl ion, either on $C_{(1)}$ in the glucose unit or on $C_{(4)}$ in the glucitol unit, should give glucose and glucitol. The glucose, of course, is rapidly decomposed into acidic products under the experimental conditions. No formation of levoglucosan from maltitol was observed, which is in agreement with the mechanism postulated; however, a small amount of this substance could easily have escaped detection.

As mentioned above, a substance moving only slightly faster on the paper chromatogram than the starting material was obtained in a low yield both from cellobitol and lactitol. The substance from cellobitol was obtained chromatographically pure and on hydrolysis yielded glucose and glucitol, identified by paper chromatography in various solvent. The specific rotation was low, $+20°$, indicating a β-glucosidic structure. The substance therefore should be a D-glucitol β-D-glucoside, isomeric with cellobitol. Analytical periodate oxidations did not give further information about its structure, as the substance

was obviously not pure. The substance from the lactitol cook was obtained chromatographically pure and on hydrolysis yielded galactose and glucitol, identified chromatographically. The formation of these substances is of considerable interest and demonstrates the possibility of transglycosidation reactions during alkaline pulping. Transglycosidations during alkaline treatment of phenyl glycosides are known [3] and have recently been further illustrated [4]; they most probably proceed *via* the 1,2-anhydrosugar. The present case seems, however, to be the first observation of a reaction of this type, starting from an alkyl glycoside.

EXPERIMENTAL.

All melting points are corrected. All evaporations were carried out under reduced pressure. Optical rotations were determined in aqueous solutions, $c \simeq 2$.

Chromatography. Whatman No. 1 and 3 MM filter papers and Whatman ashless cellulose powder, standard grade, were used.
Solvent systems: A. Methyl ethyl ketone, saturated with water.
B. Ethyl acetate-acetic acid-water, 3:1:1.
Developers: Silver nitrate-sodium hydroxide and, for the reducing sugars, anisidine hydrogen chloride.

Preparation of the glucitol glycosides. Cellobitol, lactitol and maltitol were prepared from the corresponding disaccharides by reduction with sodium borohydride following the procedure of Abdel-Aker *et al.*[1]. After deionisation, the boric acid was removed by repeated distillations with methanol. Lactitol and maltitol were obtained as syrups. Crystallisation of cellobitol from methanol yielded the anhydrous substance, m. p. 149–150° $[\alpha]_D^{20}$ +8°. By crystallisation from aqueous ethanol it was obtained with water of crystallisation, m. p. 106–108°. After drying in a vacuum at 75° over phosphorus pentoxide, the loss in weight corresponded to 1 mole water per mole cellobitol.

Alkaline treatment, procedure. A known amount of substance was dissolved in 7–10 parts of 10 % aqueous sodium hydroxide and transferred into a stainless steel autoclave. The air was replaced with nitrogen and the autoclave heated at 170° for various times. The heating was performed either in a gas-heated oil bath (shorter reaction times) or in an electrically heated oven. The cooled solution was then filtered through a column, prepared from equal parts of the ion exchange resins Amberlite IR 120 and Dowex 2, in the hydrogen and hydroxyl state, respectively. The eluate and washings were concentrated to dryness and weighed. The yields of non-ionic products which were obtained from cellobitol, lactitol, maltitol, levoglucosan and 1,6-anhydro-D-galactose after alkaline treatment for various times are given in the account above.

Products from the alkaline treatment of cellobitol. Anhydrous cellobitol (8.56 g) was dissolved in 10 % aqueous sodium hydroxide (50 ml), kept at 170° for five hours and worked up as described above. The yield of non-ionic material was 6.24 g. Unchanged starting material (5.1 g) was recovered by crystallisation from 90 % aqueous ethanol. The material from the mother liquors (1.00 g) was fractionated on a cellulose column (20 × 4.5 cm), using solvent system B as eluant. The following fractions, listed in the order in which they eluted from the column, were obtained.

a. Levoglucosan, 33 mg. Recrystallisation from ethanol yielded the pure substance, m. p. 178–180°, undepressed on admixture with authentic material.

b. 1,4-Anhydro-D-glucitol, 475 mg. The substance was further purified by recrystallisation from ethanol. M. p. 116–117°. $[\alpha]_D^{20}$ −22°. The substance was indistinguishable from an authentic sample, prepared according to Soltzberg, Goepp and Freudenberg [5].

c. D-Glucitol, 209 mg. M. p. after recrystallisation from ethanol, 96–97°. The acetate was also prepared, m. p. 101–102°, undepressed on admixture with an authentic sample.

d. Unknown + cellobitol, 76 mg.

e. Cellobitol, 277 mg.

The unknown substance in fraction *d* was further purified by chromatography on thick filter paper, using solvent system B. It had an R_F-value slightly higher than that of cellobitol. The chromatographically pure substance (25 mg) on hydrolysis yielded glucose and glucitol, as identified by paper chromatography. The amorphous product had $[\alpha]_D^{20}$ + 20° and on periodate oxidation with 0.03 N sodium metaperiodate solution rapidly consumed about 7.1 moles of periodate with the formation of 2.7 moles of formic acid. These results would not be expected from a pure hexitol glycoside and indicate that the substance was not pure.

Products from the alkaline treatment of lactitol. Lactitol (2.80 g) was treated with 10 % aqueous sodium hydroxide at 170° for 5 h and worked up as described above. The non-ionic products (2.37 g) were fractionated on a cellulose column, (27 × 4.5 cm), using solvent system A as eluant. The following fractions, listed in the order in which they were eluted from the column, were obtained.

a) 1,6-Anhydro-D-galactose, 0.18 g. The substance was purified by recrystallisation from ethanol. $[\alpha]_D^{20}$ −22°, m. p. 224−226°, undepressed on admixture with an authentic sample.

b) 1,4-Anhydro-D-glucitol (0.18 g). M. p. 116−117°, after recrystallisation from ethanol.

c) Glucitol, 0.40 g.

d) Lactitol, 1.49 g.

The lactitol contained small amounts of a substance with slightly higher R_F-value, which was isolated by chromatography on thick filter paper. It yielded galactose and glucitol on hydrolysis but was not further investigated.

REFERENCES

1. Abdel-Aker, M., Hamilton, J. K. and Smith, F. *J. Am. Chem. Soc.* **73** (1951) 4691.
2. Levene, P. A. and Kuna, M. *J. Biol. Chem.* **127** (1939) 49.
3. Ballou, C. E. *Advances in Carbohydrate Chem.* **9** (1954) 59.
4. Häggroth, S. and Lindberg, B. *Svensk Papperstidn.* **59** (1956) 870.
5. Soltzberg, S., Goepp, R. M. and Freudenberg, W. *J. Am. Chem. Soc.* **68** (1946) 919.

Received February 2, 1957.

ACTA CHEMICA SCANDINAVICA 11 (1957) 668—675

Separation of Mucopolysaccharides on a Cellulose Column

SVEN GARDELL

Chemistry Department II, Karolinska Institutet, Stockholm, Sweden

A column technique is described for the separation of mucopolysaccharides by fractional elution with alcohol.

The method has been applied on amounts from 10 mg up to 4 g of material.

The separation of mucopolysaccharides from nucleus pulposus and from cornea as well as the separation of chondroitinsulfuric acid and heparin monosulfuric acid is described.

Fractional precipitation from an aqueous solution with organic solvents is the most commonly used technique for the separation of the components of a mixture of polysaccharides. Sometimes clearcut separations can be obtained by varying the pH and the ionic strength and by adding metal ions such as calcium, barium or lead. In the majority of cases, however, and especially if the polysaccharides are closely related, the separation of the different types of polysaccharides is a tedious procedure. In spite of repeated precipitations and washings it is seldom possible to achieve complete separations. Moreover, the fractional precipitation methods can only be applied on a rather large scale, a drawback, which makes such methods of very limited value in metabolic studies in which frequently minute amounts of material have to be separated in pure form.

In such cases electrophoretic methods have been used (Boström and Gardell [1], Dorfman *et al.*[2]). However, these methods can be used only in such cases where a distinct difference in electrophoretic mobility exists, *e. g.* between hyaluronic acid and chondroitinsulfuric acid.

The use of partition methods is restricted mainly because of lack of suitable pairs of liquids. In a few cases this difficulty has been overcome by the use of "carriers" such as fatty amines [3–5]. The paperchromatographic separation of heparin and chondroitinsulfuric acid has also been reported [6].

Fractionation can also be obtained by a column technique, in which the column is used mainly as a carrier for the material to be separated. These are selectively brought into solution and eluted from the column by stepwise or

gradual changes in the composition of the eluting solvent. This principle has been used by Desreux and Ghauysen [7] for the separation of nucleic acids and by Zahn and Stahl [8] and recently by Zittle and Della Monica [9] for the separation of proteins.

In this work closely related acid mucopolysaccharides have been separated on a cellulose column by means of fractional or gradient elution. Ethanol of varying concentrations together with barium acetate has been used as the eluting solvent. The method has been applied on a micro scale as well as on preparative scale.

EXPERIMENTAL

Preparation of the column. Columns of different sizes are prepared from Whatman cellulose powder *. A suitable quantity of the powder for the preparation of a 20 cm long column is mixed with water to a rather thin slurry. This mixture is poured into a suction flask care being taken that the flask is not filled to more than one fifth of its total volume. The flask is connected to a water pump and gently rotated during evacuation. In this way most of the air present in the cellulose is removed, a procedure which greatly facilitates the even packing of the column.

The slurry is then poured into a chromatographic tube and allowed to settle to constant height. About one bed volume of water is then passed through the column with air pressure of 30—40 cm Hg. After washing with water under hydrostatic pressure of about 2 m until no carbohydrate can be detected in the effluent, the column is equilibrated with 80 % ethanol containing 0.3 % barium acetate.

Preparation of the sample. The polysaccharide mixture to be separated is dissolved in a 0.3 % aqueous solution of barium acetate. A solution containing about 10 % of the polysaccharide mixture is prepared.

Addition of the sample to the column. About 0.5 ml of the polysaccharide solution per cm^2 of cross section area of the column is added on top of the latter and allowed to drain in slowly. The walls of the tube are then washed with a small amount of 0.3 % barium acetate.

Elution of the material. The elution of the material from the column can be accomplished either by the use of ethanol in stepwise decreasing concentrations or by an arrangement where it is possible to decrease the ethanol concentration continuously. In the latter procedure the effluent is collected by means of a suitable fraction collector.

In both cases the column is first washed with at least three bed volumes of 80 % ethanol containing 0.3 % barium acetate in order to ascertain complete precipitation of the material on top of the column. With this washing little or no carbohydrates appears in the effluent.

In order to find the best conditions for a stepwise elution, *i. e.* the concentration of alcohol and the volume in each step, it is advisable to make a preliminary run. In such a run a suitable difference in ethanol concentration in the elution solvents between each step would be 5 %. A volume of three to four bed volumes is sufficient.

In the case of a continuous decrease of the ethanol concentration a suitable gradient is also chosen on the basis of a preliminary run either stepwise or made with an arbitrarily chosen gradient.

The concentrations and volumes as well as the concentration gradients used in actual experiments are given below.

The flow rate through the column must not exceed 5—10 ml per h per cm^2 cross section area of the column.

Analyses of the fractions. The fractions can be treated according to the purpose of the experiment. In general a qualitative or quantitative carbohydrate reaction is performed on the fractions.

* Whatman cellulose powder standard grade obtained from W. and R. Balston Ltd, England.

In the present investigation the carbazole [10] and the cysteine [11] reactions of Dische were carried out. Column chromatography of aminosugars [12] and neutral monosaccharides [13] were also used.

RESULTS AND DISCUSSION

The fractionation of the polysaccharides from nucleus pulposus by means of stepwise elution

The polysaccharides were prepared as described earlier [14,15]. Fifty mg of the polysaccharide preparation was dissolved in about 0.5 ml of 0.3 % barium acetate solution and applied on top of a column 1 × 20 cm prepared according to the principles given above. The polysaccharides were then eluted with solutions of decreasing alcohol concentrations. All solvents contained 0.3 % barium acetate. Fifty ml of each solution was used. The composition of the elution solvents as well as the aminosugar analysis of the fractions are given in Table 1.

Table 1. Fractionation of the nucleus pulposus polysaccharides by means of stepwise elution.

Per cent EtOH in elution solvent	Glucosamine-HCl			Galactosamine-HCl		
	mg	Per cent of total hexosamine	Per cent recovery	mg	Per cent of total hexosamine	Per cent recovery
80	0.0	0	0	0.0	0	0
50	6.02	99.2	10.2	0.05	0.8	0.6
45	17.30	95.4	29.3	0.84	4.6	1.0
40	12.9	92.6	21.9	1.03	7.4	1.3
35	4.82	89.1	8.2	0.59	10.9	0.7
30	4.70	81.0	8.0	1.10	19.0	1.3
25	1.60	50.0	2.7	1.60	50.0	2.0
20	0.82	16.1	1.4	4.26	83.9	5.2
15	0.60	3.3	1.0	17.80	96.7	21.8
10	0.60	2.2	1.0	27.08	97.8	33.2

In another experiment 4 g of the same material was fractionated on a column 6.5 × 23 cm. The elution was carried out with 80, 50, 35, 25 and 20 % of ethanol containing 0.3 % of barium acetate, and finally with 0.3 % barium acetate solution. Two litres of each of the solvents was used. The fraction eluted with 35 % ethanol and that eluted with barium acetate solution were concentrated *in vacuo* to about 50 ml each, made faintly acid with acetic acid and precipitated with alcohol. The precipitates were dissolved in 50 ml of water and reprecipitated with alcohol. The analysis of these fractions are given in Table 2.

From these experiments it is evident that the mucopolysaccharides from nucleus pulposus can be fractionated into at least two components, one appear-

Table 2. Analysis of the two main fractions from the nucleus pulposus polysaccharides (air dry substance).

	Fraction I eluted with 35 % ethanol	Fraction II eluted with barium acetate solution
Weight	1.33 g	2.14 g
Ash	24.3 %	31.9 %
Nitrogen	2.60 »	2.00 »
Micro Kjeldahl		
Sulfur in ester sulfates	5.45	4.83
Glucosamine-HCl	21.1 » (59.1 of the total glucosamine)	0.3 »
Galactosamine-HCl	0.3 »	22.8 » (82.4 % of the total galactosamine)
Galactose	16.8 »	—
Fucose	2.3 »	—

ing at an ethanol concentration of about 10—15 %. Most of the glucosamine was found in the first component and correspondingly most of the galactosamine was found in the second component.

Fractionation of the polysaccharides from nucleus pulposus by means of gradient elution

The arrangement used in order to obtain the concentration gradient was described by Lindberg and Wickberg [16].

A column 1 × 20 cm was used, prepared as described above. After the application of the polysaccharide mixture (145.5 mg dissolved in about 1.5 ml of the barium acetate solution) the column was first washed with 60 ml of 80 % ethanol containing barium acetate in the concentration described above. The column was then connected to the gradient arrangement. Vessel I, closest to the column, was filled with 350 ml of 80 % ethanol containing 0.3 % barium acetate, and vessel II was filled with 0.3 % barium acetate solution alone to hydrostatic equilibrium with the solvent in vessel I. The ratio between cross section area of the vessels was vessel I / vessel II = 2.7. The effluent was collected in 5—7 ml fractions. Each fraction was analysed with Dische's carbazole method as modified by Gurin and Hood [10] and by the cysteine method of Dische and Shettles [11]. 0.5 ml aliquots were used for each test.

In Fig. 1 the results of these analyses are plotted against the fraction numbers. The cysteine reaction showed a peak for hexoses and methyl pentoses with a maximum in fraction 25 and after this peak practically no colour was found. The carbazole reaction, on the other hand, showed several peaks one of which coincides with the peak given by the cysteine reaction. In the later part of the curve a large unsymmetrical peak, probably composed of several small peaks, is visible.

It is claimed [11] that the cysteine reaction is specific for hexoses and methyl pentoses, and that no colour is given by uronic acids. The carbazole reaction on the other hand is known to give much stronger colour for uronic acids than

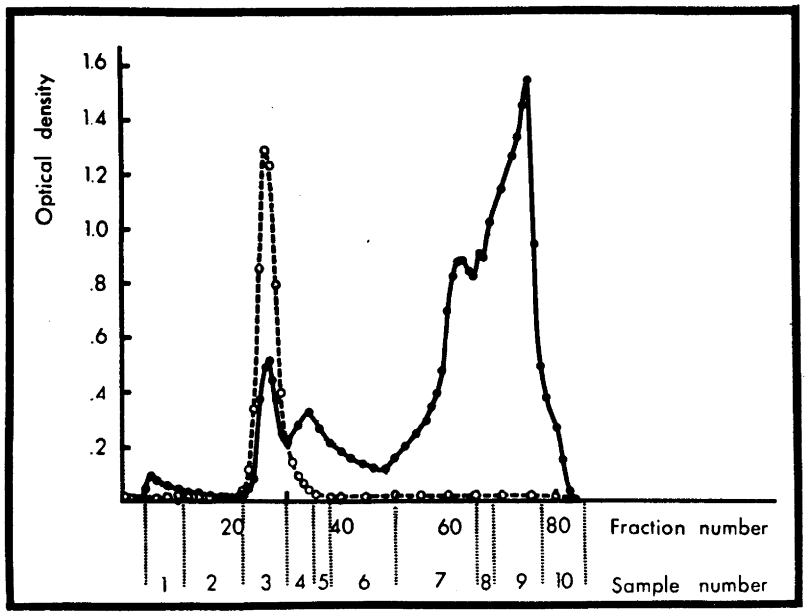


Fig. 1. Gradient elution from a cellulose column 1 × 20 cm of 145.5 mg of the polysaccharide mixture from nucleus pulposus. The fractions are analysed with the cysteine method of Dische and Shettels [11] and the carbazol method as modified by Gurin and Hood [10]. The fractions are pooled in ten samples as shown by the dotted lines.

for the hexoses. It is thus evident that in the peak given by the cysteine reaction a polysaccharide containing hexose — and methyl pentose — is present whilst the other peaks indicate uronic acid-containing substances.

The fractions were pooled as indicated in the figure and each of the ten samples thus obtained were evaporated to dryness and dissolved in 2 ml of water. 0.5 ml of this solution was hydrolyzed with an equal volume of concentrated hydrochloric acid for 8 h on a boiling water bath and the aminosugars determined as described by Gardell [12]. The result is given in Table 3.

Although two main components can be distinguished, the purity of the components obtained by gradient elution is not the same as that obtained by stepwise elution.

In the method of Zahn and Stahl [8] and in that of Zittle and Della Monica [9], the mixture to be separated was precipitated on the supporting medium suspended in the precipitating solvent. As this principle might give better conditions for the separation it was also tested in this case. Five g of Hyflo-Super Cel or cellulose powder was suspended in 50 ml of 80 % ethanol containing 0.3 % barium acetate, and 50 mg of the nucleus pulposus polysaccharides dissolved in about 5 ml of 0.3 % barium acetate solution was added. After thorough mixing the mixture was poured on a glass filter funnel and eluted with the aid of the same gradient as used above. In both cases the separation was very poor.

Table 3. Aminosugar analysis of the fractions obtained by gradient elution of the nucleus pulposus polysaccharides. The fractions are pooled as indicated in Fig. 1.

Sample	Glucosamine		Galactosamine	
	mg	Per cent of total hexosamine	mg	Per cent of total hexosamine
1	0		0	
2	trace		0	
3	9.05	91.1	0.88	8.9
4	1.18	89.4	0.14	10.6
5	0.31	88.6	0.04	11.4
6	0.37	36.6	0.64	63.4
7	0.36	5.8	5.86	94.2
8	0.06	1.8	3.25	98.2
9	0.19	2.6	7.21	97.4
10	trace	—	1.40	98—100

Table 4. Amino sugar analysis of the fractions obtained by fractional precipitation of the nucleus pulposus polysaccharides (analysis of air dry substances).

Fraction number	Per cent ethanol	Weight mg	Glucosamine-HCl			Galactosamine-HCl		
			Per cent of substance	Per cent of total hexosamine	Per cent recovery	Per cent of substance	Per cent of total hexosamine	Per cent recovery
1	11	21.5	1.5	6.0	0.5	23.6	94.0	6.1
2	14	144.1	0.7	2.8	1.7	24.5	97.2	42.4
3	20	19.6	2.9	9.5	1.0	27.7	90.5	6.5
4	28	26.4	20.8	86.3	9.1	3.6	14.7	1.2
5	33	62.8	18.9	86.3	19.7	3.0	14.7	2.3
6	37	21.2	22.1	89.5	7.8	2.6	10.5	0.7
7	45	28.0	20.4	89.5	9.5	2.4	10.5	0.8
8	10 volumes of ethanol	11.7	25.0	92.9	4.9	1.9	7.1	0.2

Fractional precipitation of the nucleus pulposus polysaccharides

In order to compare the efficiency of the column technique with that of the conventional fractional precipitation methods an alcohol fractionation of the nucleus pulposus polysaccharides was performed.

511 mg of the polysaccharide fraction was dissolved in 50 ml of a 3 % solution of barium acetate and fractionated at $\pm$ 0 °C with ethanol. The solution to be fractionated was constantly stirred and the alcohol was added very slowly until a turbidity appeared. The stirring was then continued for half an hour and the precipitate was then centrifuged in a Spinco centrifuge at 30 000 *g*, washed and dissolved in water and reprecipitated with several

volumes of alcohol from a faintly acid solution. The supernatant from the high speed centrifugation and the washings were combined and the fractionation continued on this solution. The result of the fractionation is given in Table 4.

Although it is possible to obtain the galactosamine containing portion in a rather pure state the glucosamine-containing one is not obtained with the same purity as with the column technique. The yield of the pure fractions is also much smaller.

Fractionation of a polysaccharide mixture from bovine cornea

As the cornea is known to contain different mucopolysaccharides [17–19] a fractionation experiment was also carried out on a polysaccharide fraction from this tissue.

The polysaccharides were prepared by proteolytic digestion of bovine corneas followed by extraction with 90 % phenol as described earlier [14,15]. A preparation was obtained which contained 2.99 % N and 18.3 and 13.2 % of glucosamine and galactosamine, respectively, calculated as the hydrochlorides. This polysaccharide was fractionated on a micro scale.

11.2 mg was dissolved in about 0.15 ml of the 0.3 % barium acetate solution and fractionated on a column 0.5 × 7 cm. The carbohydrate content of the fractions was determined by the cysteine reaction [11] and by the carbazole [10] reaction. 0.5 ml aliquots were taken for each determination. The rest of the fractions were evaporated to dryness and hydrolyzed with 0.5 ml of 6 N hydrochloric acid for the determination of their aminosugar composition. The result of the fractionation is given in Table 5.

Table 5. Analysis of the fractions obtained by stepwise elution of the polysaccharide mixture from bovine cornea. 6 ml of each solvent was used. D_{396} and D_{426} represent the optical densities given by the fractions in the cysteine reaction [11] at 396 mμ and 426 mμ, respectively. D_{530} represents the optical density given by the carbazole reaction [10] at 530 mμ.

Per cent EtOH in elution solvent	D_{396}	D_{426}	$D_{396} - D_{426}$	D_{530}	Glucosamine-HCl in per cent of total hexosamine	Galactosamine-HCl in per cent of total hexosamine
80	0.142	0.112	0.030	0.026	—	—
60	0.114	0.093	0.021	0.008	?	?
50	0.260	0.225	0.035	0.032	100	trace
45	0.235	0.206	0.029	0.052	96.4	3.6
40	0.290	0.255	0.035	0.071	87.1	12.9
35	0.105	0.082	0.023	0.342	71.9	28.1
30	0.033	0.019	0.014	0.242	6.8	93.2
25	0.013	0.005	0.008	0.118	trace	100
20	0.016	0.007	0.009	0.100	8.6	91.4
15	0.014	0.006	0.008	0.098	9.3	90.7
10	0.006	0.002	0.004	0.021	trace	trace
5	—	—	—	—	—	—
0	—	—	—	—	—	—

Fractionation of chondroitinsulfuric acid and heparin monosulfuric acid

These two polysaccharides are isomers with almost the same electrophoretic mobility and can be fractionated by means of fractional precipitation of their barium salts with alcohol [20]. They can also be completely separated using the column technique described above.

10 mg of heparin monosulfuric acid prepared from ox lung and 10 mg of chondroitinsulfuric acid from costal cartilage prepared according to Boström and Månsson [21] were mixed and the mixture was fractionated on a column 1 × 20 cm. In the fraction eluted with 20 % ethanol only galactosamine was found and correspondingly only glucosamine was found in the fraction eluted with 10 per cent ethanol.

This work has been aided by grants from the *Swedish State Medical Research Council.*

REFERENCES

1. Boström, H. and Gardell, S. *Acta Chem. Scand.* **7** (1953) 216.
2. Schiller, S., Matthews, M. B., Goldfaber, L., Ludowieg, J. and Dorfman, A. *J. Biol. Chem.* **212** (1955) 531.
3. O'Keffe, A. A., Dolliver, M. A. and Stiller, E. T. *J. Am. Chem. Soc.* **71** (1949) 2452.
4. Wolfrom, M. L., Montgomery, R., Karabinos, J. W. and Rothseb, P. *J. Am. Chem. Soc.* **72** (1950) 5796.
5. Berenson, G. S., Roseman, S. and Dorfman, A. *Biochim. et Biophys. Acta* **17** (1955) 75.
6. Kerby, G. *Proc. Soc. Exptl. Biol. Med.* **83** (1955) 263.
7. Desreux, V. and Ghauysen, E. M. *Bull. soc. chim. Belges* **60** (1954) 410.
8. Zahn, R. K. and Stahl, I. *Hoppe-Seyler's Z. physiol. Chem.* **293** (1953) 1.
9. Zittle, C. A. and Della Monica, S. E. *Arch. Biochem. and Biophys.* **58** (1955) 31.
10. Gurin, S. and Hood, D. B. *J. Biol. Chem.* **131** (1939) 211.
11. Dische, Z. and Shettles, L. B. *J. Biol. Chem.* **175** (1948) 595.
12. Gardell, S. *Acta Chem. Scand.* **7** (1953) 207.
13. Gardell, S. *Acta Chem. Scand.* **7** (1953) 201.
14. Gardell, S. *Arkiv Kemi* **4** (1952) 449.
15. Gardell, S. *Acta Chem. Scand.* **8** (1954) 362.
16. Lindberg, B. and Wickberg, B. *Acta Chem. Scand.* **8** (1954) 562.
17. Suzuki, M. *J. Biochem. Japan* **30** (1939) 185.
18. Woodin, A. M. *Biochem. J. London* **51** (1952) 319.
19. Meyer, K., Linker, A., Davidson, E. A. and Weissman, B. *J. Biol. Chem.* **205** (1953) 611.
20. Jorpes, J. E. and Gardell, S. *J. Biol. Chem.* **176** (1948) 267.
21. Boström, H. and Månsson, B. *Arkiv Kemi* **6** (1953) 17.

Received February 2, 1957.

ACTA CHEMICA SCANDINAVICA 11 (1957) 676—684

The Crystal Structure of $InOHF_2$

HANS-ERIK FORSBERG

Department of Inorganic and Physical Chemistry, University, and Department of Inorganic Chemistry, Royal Institute of Technology, Stockholm, Sweden

$InOHF_2$ has been investigated by X-ray methods. It has a monoclinic unit cell and the unit cell dimensions are

$a = (5.780 \pm 0.005)$ Å
$b = (5.157 \pm 0.005)$ Å
$c = (3.874 \pm 0.005)$ Å
$\beta = 98.74° \pm 0.02°$
$V = 114.1$ Å^3
$Z = 2$

A structure is proposed with atomic positions for the indium, oxygen and fluorine atoms in space group No. 5-*C*2. The parameters of the atoms (p. 681) were determined from Patterson projections and improved by back shift calculations.

The indium atoms are surrounded by two oxygen and four fluorine atoms so that a coordination In-6X is obtained.

The hydrogen atoms are situated either between the fluorine atoms forming F-H-F bonds or between the fluorine and oxygen atoms forming F-H-O bonds.

The structure may be described as a three dimensional framework (distorted ReO_3 structure).

The crystal structure of the isomorphous compounds InOCl and InOBr has recently been determined [1] and in connection with this investigation attempts were made to prepare indium oxide fluoride. With the method described by Enslin and Dreyer [2], no crystals large enough for single crystal X-ray investigations were obtained but, by hydrothermal hydrolysis of almost saturated indium(III) fluoride solutions of different acidities, a new compound could be prepared. Its formula proved to be $InOHF_2$ while Enslin and Dreyer gave the formula of their substance as InOF·aq. This paper presents the structure determination of $InOHF_2$.

PREPARATION OF THE CRYSTALS

Indium (III) fluoride [2,3] was obtained by dissolving indium hydroxide, prepared by treating a solution of indium(III) nitrate with aqueous ammonia, in 40 % hydrofluoric acid. The solution was then evaporated until crystals of $InF_3(H_2O)_3$ separated. After cooling, the crystals were filtered off, washed with water and dried in air.

Indium oxide fluoride was prepared as follows. A solution of 400 mg $InF_3(H_2O)_3$ dissolved in 6.5 ml HF (2 M) was poured into a Pt-crucible which was then kept at 300° C in an autoclave. After 18 h, the autoclave was cooled and the precipitate filtered off. It consisted of small transparent crystals of $InOHF_2$.

The crystals are insoluble in water but dissolve completely in hot dilute hydrochloric or nitric acid.

ANALYSIS

A sample, which had been dried in air, was decomposed by fusion with sodium and potassium carbonates. After cooling, the melt was leached with water and the residue filtered off. The amount of *fluoride* in the filtrate was determined gravimetrically as PbClF [4].

For the determination of *indium*, a sample was dissolved in nitric acid, evaporated, and then ignited and weighed as In_2O_3.

The *hydroxide* was determined as water by Hartwig-Bendig's modification of Penfield's method as described by Kolthoff and and Sandell [5].

The *density* of the crystals was determined from the loss of weight in benzene.

	Found		Calculated for $InOHF_2$
% In	67.8	67.6	67.60
% F	22.9	23.0	22.38
% OH	9.5	9.5	10.01
Density	4.8_9	4.9_1	4.94 (*cf.* below)

UNIT CELL AND SPACE GROUP

From rotation (around [100], [010] and [001]) and Weissenberg photographs (0*kl*, 1*kl*, *h*0*l*, *h*1*l*, *hk*0 and *hk*1), taken with Cu*K* radiation, it was concluded that the crystals are monoclinic with $a \approx 5.8$ Å, $b \approx 5.1$ Å, $c \approx 3.9$ Å and $\beta \approx 99°$. More accurate values of the unit cell dimensions were calculated from a powder photograph in a focusing camera of Guinier type (*cf.* Table 1). (Cu$K\alpha$ radiation, internal standard KCl with $a = 6.2930$ Å).[6]

$$\begin{aligned} a &= (5.780 \pm 0.005) \text{ Å} \\ b &= (5.157 \pm 0.005) \text{ Å} \\ c &= (3.874 \pm 0.005) \text{ Å} \\ \beta &= 98.74° \pm 0.02° \\ V &= 114.1 \text{ Å}^3 \end{aligned}$$

The mean value of the density is 4.90 so that there should be $1.98 \approx 2$ formula units $InOHF_2$ in the unit cell.

The only reflections systematically absent are

$$hkl \text{ with } h+k \text{ odd}$$

which is characteristic of the space groups No. 12-$C2/m$, No. 8-Cm and No. 5-$C2$.

Table 1. Powder photograph of $InOHF_2$. Cu$K\alpha$ radiation. Internal standard KCl. $a = 6.2930$ Å.

hkl	$10^4 \sin^2 \Theta$ calc	$10^4 \sin^2 \Theta$ obs	pF^2 calc	*I* obs
001	405	405	53	st
110	405		100	
200	727	728	35	st
11$\bar{1}$	727		73	
111	891	893	55	st
020	892		30	
20$\bar{1}$	967	968	10	vvw
201	1 297	1 297	26	m
021	1 297		51	
002	1 618	1 620	35	m—
220	1 619		78	
11$\bar{2}$	1 858	1 860	92	m+
310	1 859		94	
22$\bar{1}$	1 859		89	
20$\bar{2}$	2 016	2 016	24	w
31$\bar{1}$	2 023		55	
112	2 188	2 188	52	m-
221	2 189		49	
130	2 190		59	
311	2 505	2 512	52	m-
02$\bar{2}$	2 510		54	
13$\bar{1}$	2 512		48	
202	2 676	2 677	44	m-
131	2 676		86	
22$\bar{2}$	2 908	2 911	58	vw
400	2 909		24	
40$\bar{1}$	2 983	2 985	24	vw-
31$\bar{2}$	2 983		49	
222	3 568	3 569	33	vw
040	3 570		16	
003	3 641	3 644	9	vw
401	3 643		9	
132	3 643		19	
330	3 644		19	
11$\bar{3}$	3 799	3 798	30	w
420	3 801		56	
33$\bar{1}$	3 808		35	
40$\bar{2}$	3 867	3 876	34	vw
20$\bar{3}$	3 872		17	
42$\bar{1}$	3 875		33	
312	3 973	3 974	43	w
132	3 973		49	
041	3 975		44	
331	4 290	4 292	29	vw+
113	4 293		32	
240	4 297		29	
023	4 533	4 531	48	w-
421	4 535		29	
24$\bar{1}$	4 537		49	
31$\bar{3}$	4 759	4 762	27	w br
42$\bar{2}$	4 759		28	
51$\bar{1}$	4 761		40	
22$\bar{3}$	4 764		33	
510	4 768		34	
33$\bar{2}$	4 768		46	
203	4 862	4 856	23	vw-
241	4 867		40	

Reflections systematically absent according to space group No.5-$C2$ have been omitted.

The intensities were calculated from the expression $0.05 \cdot \frac{p}{\quad} F^2$ where p is the number

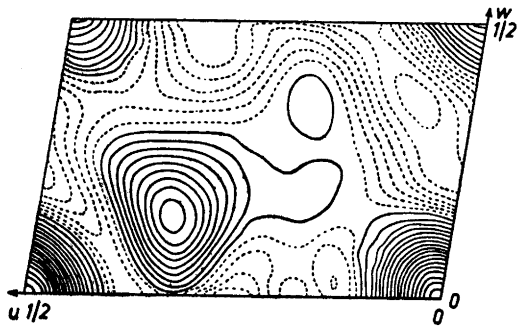


Fig. 1. The Patterson projection $P(upw)$ for $InOHF_2$. In the peaks at $P(0p0)$ and $P(\frac{1}{2}p0)$ only every second contour has been drawn. Dashed lines indicate negative values.

PATTERSON SYNTHESES

In the unit cell there are two indium, two oxygen and four fluorine atoms. To determine their positions, the Patterson projections, $P(upw)$, $P(pvw)$, and $P(uvp)$ were calculated. (Figs. 1 and 2.) Relative intensities of the reflections were estimated visually and the F^2-values were then calculated using the curves given by Lu[8]. No corrections have been applied for the absorption. In all syntheses, the value of $F^2(000)$ has been omitted. The maxima have been located by an interpolation table given by Booth [9]. In the space groups suggested by the extinctions, the possible point positions are as follows:

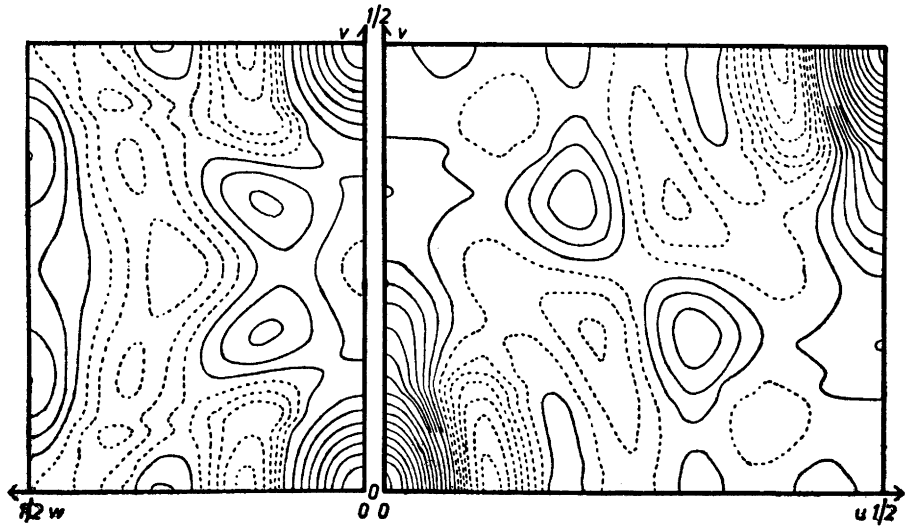


Fig. 2. The Patterson projections $P(pvw)$ and $P(uvp)$ for $InOHF_2$. In the peaks at $P(p00)$ and $P(00p)$ only every third and second contour has been drawn. Dashed lines indicate negative values.

$C2/m$	$(0,0,0;\ \frac{1}{2},\frac{1}{2},0)+$		
$2(a)$	$0,0,0;$	$4(e)$	$\frac{1}{4},\frac{1}{4},0;\ \frac{1}{4},\frac{3}{4},0$
$2(b)$	$0,\frac{1}{2},0;$	$4(f)$	$\frac{1}{4},\frac{1}{4},\frac{1}{2};\ \frac{1}{4},\frac{3}{4},\frac{1}{2}$
$2(c)$	$0,0,\frac{1}{2};$	$4(g)$	$0,y,0;\ 0,\bar{y},0$
$2(d)$	$0,\frac{1}{2},\frac{1}{2};$	$4(h)$	$0,y,\frac{1}{2};\ 0,\bar{y},\frac{1}{2}$
		$4(i)$	$x,0,z;\ \bar{x},0,\bar{z}$

Cm	$(0,0,0;\ \frac{1}{2},\frac{1}{2},0)$	$C2$	$(0,0,0;\ \frac{1}{2},\frac{1}{2},0)$
$2(a)$	$x,0,z$	$2(a)$	$0,y,0$
$4(b)$	$x,y,z;\ x,\bar{y},z;$	$2(b)$	$0,y,\frac{1}{2}$
		$4(c)$	$x,y,z;\ \bar{x},y,\bar{z}$

The indium atoms can be given arbitrarily the twofold point position $2(a)$ with $x = 0$, $y = 0$ and $z = 0$ for all three space groups. The In-In distances of $\pm(\frac{1}{2},\frac{1}{2},0)$ appear as pronounced maxima in the Patterson projections at $\frac{1}{2},p,0$, $p,\frac{1}{2},0$ and $\frac{1}{2},\frac{1}{2},p$.

In addition to the In-In peaks, the Patterson projections show other distinct maxima which should correspond to distances between indium and oxygen atoms and indium and fluorine atoms.

Since the unit cell contains two oxygen and four fluorine atoms the oxygen atoms should be situated in a twofold point position and the fluorine atoms either in two twofold or in one fourfold point position. In the Patterson projections $P(uvp)$ and $P(pvw)$ we observe a distinct maximum at $u \approx 0.325$, $v \approx 0.179$ and $w \approx 0.141$ which can only be explained as being due to atoms in the fourfold point position $4(b)$ in Cm or $4(c)$ in $C2$. Thus the fluorine atoms should be situated in one of these point positions.

The other distinct maximum in $P(pvw)$ at $v \approx 0.125$ and $w = \frac{1}{2}$ (the corresponding maximum in $P(uvp)$ is hidden by the In-In peak) must be explained as an In-O distance with the oxygen atoms in the point position $2(b)$ in $C2$. Thus we get the following parameters for the oxygen atoms (we need only consider the range $0 \leq x \leq \frac{1}{2}$, $0 \leq y \leq \frac{1}{2}$ and $0 \leq z \leq 1$).

$$2\ \mathrm{O}\ \text{in}\ C2\ 2(b)\ \text{with}\ y \approx 0.125$$

The remaining maxima in $P(uvp)$ and $P(pvw)$ on the u and w axes are small and probably caused by vectors between light atoms or by diffraction effects.

The parameters of the fluorine atoms are determined from the maximum at $u \approx 0.325$, $v \approx 0.179$, and $w \approx 0.141$ and we then notice that there are two possibilities for the sites of the atoms (we need only consider the range $0 \leq x \leq \frac{1}{2}$, $0 \leq y \leq \frac{1}{2}$ and $0 \leq z \leq 1$).

$$4\ F\ \text{in}\ C2\ 4(c)\ \text{with}\ x \approx 0.325,\ y \approx\ \ 0.179,\ z \approx 0.141\ \text{or}$$
$$x \approx 0.325,\ y \approx -0.179,\ z \approx 0.141$$

The latter alternative is excluded by the too short oxygen-fluorine distance of 1.9 Å.

FINAL PARAMETERS

The parameters given below are the mean values of those found in the Patterson projections. The only exception is the oxygen y parameter which is obtained only from the $P(pvw)$ projection (in the $P(uvp)$ projection, the In-O distance is hidden by the In-In peak). All values have been corrected by back shift calculations.

Thus the following structure is proposed for $InOHF_2$:

Space group No. 5-$C2$. Two formula units per unit cell.

	x	y	z
2 In in 2(a)	0	0	0
2 O in 2(b)	0	$0.14_9 \pm 0.01$	½
4 F in 4(c)	$0.32_8 \pm 0.01$	$0.18_0 \pm 0.01$	$0.15_4 \pm 0.01$

In Tables 2—4, the calculated structure factors are compared with the observed ones in the Weissenberg photographs $h0l$, $hk0$ and $0kl$. The reliability index

$$R = \frac{||F_{obs}| - |F_{calc}||}{|F_{obs}|}$$

is, for $h0l$, $hk0$ and $0kl$ 0.18, 0.20 and 0.15, respectively. However, for crystals like these containing both heavy and light atoms, the reliability index should not be taken as a definite proof that the structure as a whole is true but only that the arrangement proposed for the heavy atoms is essentially correct.

DESCRIPTION OF THE STRUCTURE

Figs. 3 and 4 show the structure of $InOHF_2$, projected along the b and c axes. In both projections, four adjacent unit cells are given so that the building principles of the structure will be more obvious.

If we describe our C-centered monoclinic lattice by a primitive triclinic lattice, the following unit cell dimensions are obtained: $a = b = c = (3.874 \pm$

Table 2. Comparison between calculated and observed structure factors $h0l$ from a Weissenberg photograph of $InOHF_2$. CuK radiation.

	$l\rightarrow$									
	h	4	3	2	1	0	$\bar{1}$	$\bar{2}$	$\bar{3}$	$\bar{4}$
calc	↓ 0					—	45	37	19	21
obs							52	33	14	21
calc	2	26	30	42	32	38	20	31	26	27
obs		23	20	48	39	30	15	46	28	30
calc	4	—	21	23	19	31	29	37	27	24
obs			17	19	20	32	21	51	30	25
calc	6	—	—	24	25	31	24	22	16	—
obs				17	23	31	28	25	23	

Table 3. Comparison between calculated and observed structure factors *hk*0 from a Weissenberg photograph of $InOHF_2$. Cu*K* radiation.

		h→							
	k ↓		0	1	2	3	4	5	6	7
calc		0	—	—	38	—	31	—	31	—
obs					43		43		41	
calc		1	—	44	—	43	—	25	—	23
obs				32		41		38		32
calc		2	31	—	37	—	31	—	20	—
obs			25		31		33		23	
calc		3	—	33	—	19	—	26	—	
obs				28		16		33		
calc		4	25	—	26	—	23	—		
obs			21		22		24			
calc		5	—	23	—	28	—			
obs				14		26				
calc		6	28	—	21					
obs			25		17					

Table 4. Comparison between calculated and observed structure factors 0*kl* from a Weissenberg photograph of $InOHF_2$. Cu*K* radiation.

		l→	0	1	2	3	4
	k ↓						
calc		0	—	46	37	19	21
obs				44	39	24	33
calc		2	33	33	32	30	26
obs			26	30	30	39	30
calc		4	26	29	24	27	—
obs			21	24	23	28	
calc		6	29	23			
obs			24	19			

0.005) Å and $\alpha = \beta = \gamma = 83.48° \pm 0.02°$ *. The triclinic cell can be regarded as a distorted cubic cell with approximately the same atomic arrangement as that found in ReO_3 [10]. It is thus obvious that the indium atoms have a six coordination in which the calculated distances In-O and In-F are approximately the same.

Alternatively, the structure might be formally described as being built up of layers of $(InF_2^+)_\infty$ separated by oxygen atoms (Fig. 3) or as containing chains of In-O-In separated by HF_2^- ions (*cf.* below).

The interatomic distances for the structure proposed will be (in Å):

In-In	= 3.87	F_1—F_2	= 2.9_3 and 3.87
In-O_1	= 2.08	F —F	= 3.0_8 and 3.9_2 (between layers)
In-F_1	= 2.06	O —O	= 3.87
In-F_2	= 2.11	O —F_1	= 2.8_7 and 3.7_4
F_1-F_1	= 2.4_6	O —F_2	= 2.4_9 and 2.9_3
F_2-F_2	= 3.8_0		

* The agreement of the unit cell dimensions with those of a rhombohedral unit cell must be accidental since reflexions which should be of equal intensity according to rhombohedral indices differ in intensity in the Weissenberg photographs.

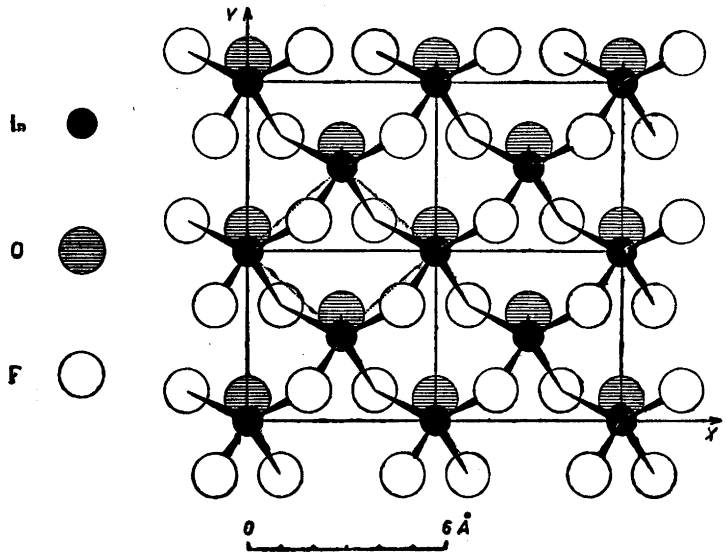


Fig. 3. The structure of $InOHF_2$, viewed along [001]. The dotted lines indicate the triclinic unit cell. (The range for the z parameter is $-0.859 \leq z \leq 0.141$.)

The error in the In-O and In-F distances is estimated to be $\pm$ 0.05 Å and in the F-F and O-F distances $\pm$ 0.1 Å. The In-O distances are about the same as those found in In_2O_3 [11] and InOCl and InOBr [1]. The shortest distance between oxygen and fluorine is somewhat shorter than that found in CeOF [12] and BiOF [13] (2.83 and 2.88 Å).

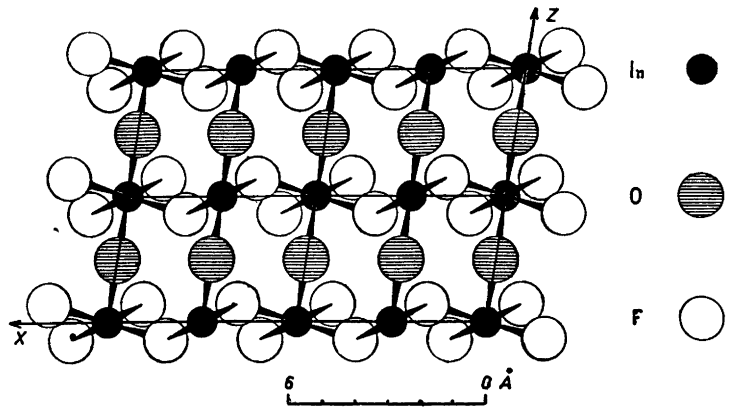


Fig. 4. The structure of $InOHF_2$, viewed along [010]. (The range for the y parameter $-0.375 \leq y \leq 0.625$.)

The long O-O distances of 3.87 Å exclude the possibility that hydrogen bonds are present between the oxygen atoms. The short distances O-F (2.49 Å) and F-F (2.46 Å) do not differ significantly. They both seem to be consistent with probable values of hydrogen bond lengths (*cf.* Pauling [14], Wells [15]). The fact that fluorine is more electronegative than oxygen might appear in favour of the existence of F-H-F bonds. On the other hand F-H-O bonds would give a more even distribution of the charge of the atoms.

Acknowledgements. The author is indebted to Professor Lars Gunnar Sillén for his helpful criticism and provision of laboratory facilities and to Professor Arne Ölander for his kind interest. The author wishes to thank Dr. Arne Magnéli and Dr. Georg Lundgren for many valuable discussions and Mr. D. G. Gillam for revising the English text.

Thanks are due to the *Consolidated Mining and Smelting Company of Canada, Ltd.* for generously supplying a large amount of indium metal of high purity.

REFERENCES

1. Forsberg, H.-E. *Acta Chem. Scand.* **10** (1956) 1287.
2. Enslin, F. and Dreyer, H. *Z. anorg. allgem. Chem.* **249** (1943) 119.
3. *Gmelins Handbuch der anorganischen Chemie* No. 37 Indium, Verlag Chemie, Berlin 1936.
4. Scott, W. W. *Standard Methods of Chemical Analysis*, D. van Nostrand Company Inc., New York 1948, Vol. 1, p. 404.
5. Kolthoff, I. M. and Sandell, E. B. *Textbook of Quantitative Inorganic Analysis*, Mac Millan Company, New York 1943, p. 753.
6. Hambling, P. G. *Acta Cryst.* **6** (1953) 98.
7. *International Tables for X-ray Crystallography*, Kynoch Press, Birmingham 1952, Vol. 1.
8. Lu, C.-S. *Rev. Sci. Instr.* **14** (1943) 331.
9. Booth, A. D. *Fourier Technique in X-ray Organic Structure Analysis*, University Press, Cambridge 1948, p. 64 and 101.
10. Meisel, K. *Z. anorg. allgem. Chem.* **207** (1932) 121.
11. Pauling, L. and Shappel, M. *Z. Krist.* **75** (1930) 128.
12. Finkelnburg, W. and Stein, A. *J. Chem. Phys.* **18** (1950) 1926.
13. Aurivillius, B. *Arkiv Kemi, Mineral. Geol.* **26B** (1948) 6.
14. Pauling, L. *The Nature of the Chemical Bond*, Cornell University Press, New York 1945, p. 284.
15. Wells, A. F. *Structural Inorganic Chemistry*, Clarendon Press, 1950, p. 237.

Received January 25, 1957.

ACTA CHEMICA SCANDINAVICA 11 (1957) 685—689

On the Production of Vitamins by Protein-rich and Protein-poor *Rhodotorula gracilis* Yeast

NIELS NIELSEN and GOTTFRIED SCHNEIDER

Research Department, AB Kabi, Stockholm, Sweden

When *Rhodotorula gracilis* was grown in nutrient solutions containing 0.1 or 1 % asparagine or ammonium sulphate as the nitrogen source, the crude protein content of the yeast varied between 8.4 and 60.7 %, calculated on a dry yeast basis. The fat content of the yeast also varied greatly, between 71.0 and 11.6 % of the yeasts dry weight. A marked correlation was noticeable, the fat content being high if the crude protein content was low and vice versa.

The sum of the contents of crude protein and fat was relatively constant, varying between 70 and 79 % of the dry yeast when asparagine was used as the nitrogen source. When ammonium sulphate was the nitrogen source this sum varied between 60 and 67 %. This difference between asparagine and ammonium sulphate media was probably caused by the increasing acidity of the latter.

The four vitamins investigated, *viz.* riboflavin, pantothenic acid, nicotinic acid and pyridoxine were present mainly in the nutrient solution (about 50 to 80 %). On calculating the vitamin contents as μg per g dry yeast, the amounts present at the end of the fermentations were much smaller for the yeast poor in crude protein. However, expressing the amounts as μg per g crude protein, no significant difference was found between the protein-poor and protein-rich types, with the exception of pantothenic acid and possibly nicotinic acid. Nicotinic acid had a tendency to be formed in higher amounts — calculated per g of protein — in the protein-poor yeast. Pantothenic acid was not formed to any appreciable extent in the protein-poor yeast, most probably due to the fact that β-alanine was not formed.

When *Rhodotorula gracilis* was cultivated in a nutrient solution low in nitrogen but containing an excess of sugar, considerable amounts of fat were produced [1]. The fat content of the yeast was found to be very high, amounting to 60 % or more calculated on a dry weight basis. Concomittantly the crude protein content decreased and a yeast with only 12 % crude protein might be obtained. If the yeast was cultivated with an excess of nitrogen a yeast with about 50 % crude protein and 10 % fat was obtained. Thus the protein content of this yeast can be varied between wide limits only by altering the nitrogen content of the nutrient solution.

Some comparative studies on the metabolism and the chemical composition of both the protein-rich and the protein-poor *Rh. gracilis* yeast have already been carried out. Nielsen, Sandegren and Ljungdahl [2] compared the amino acid content in these two yeast types and found certain differences. The protein-poor yeast had a relatively high content of glutamic acid and alanine compared with the protein-rich yeast. β-Alanine which is a component of pantothenic acid was present in the protein-rich but not in the protein-poor yeast. Later, Nielsen and Lundin [3] made quantitative determinations of some amino acids and found that whereas the amount of *iso*leucine, leucine, lysine, phenylalanine and tryptophane was practically the same in both the protein-rich and the protein-poor yeast (expressed per g of protein), the protein-poor yeast was very low in cystine and methionine. Accordingly the sulfur-content of the protein-poor yeast was also very low. Sandegren, Ekström and Nielsen [4] found that the protein-poor yeast contained fewer sulfhydryl-groups than the protein-rich yeast. The amount of phosphatides was small in the protein-poor yeast when the results were based on the weight of the yeast but no significant differences were found between the two yeast types when the phosphatide content was expressed per g of protein [5].

These investigations demonstrated important differences in the chemical composition of protein-rich and protein-poor *Rh. gracilis*. In this paper we have investigated the formation of some vitamins, *i. e.* riboflavin, pantothenic acid, nicotinic acid and pyridoxine, in these two yeast types.

METHODS

The variations in the protein content of the yeast were induced by altering the nitrogen content of the nutrient solution. The nutrient solution used for the protein-rich yeast had the following composition: 10 g asparagine or ammoniumsulphate, 4 g KH_2PO_4 – 3 g $MgSO_4$, $7H_2O$ – 1.5 g $CaCl_2$, $6H_2O$ – 0.015 g $FeCl_3$, $6H_2O$ and 40 g glucose, made up to 1 000 ml with distilled water. The nutrient solution for the protein-poor yeast had the same composition with the exception that only 1 g of asparagine or ammoniumsulphate was used.

The yeast was cultivated in 5 litre fermentors containing 3 litres of nutrient solution. The fermentors were kept at 25° and were aerated with 0.5 litre air per 1 litre solution per min. Each fermentor was seeded with 250 ml of a culture grown for 3 days in 250 ml Erlenmeyer flasks each containing 50 ml of the nutrient solution used for the production of protein-rich yeast. This amount of yeast corresponded to about 0.4 g of dry material.

During the experiments the pH of the nutrient solution and the amount of yeast present was determined daily. After the yeast had been removed by centrifuging, the amount of nitrogen was determined in the yeast-free solution, *i. e.* the amount of nitrogen not assimilated. From these analysis the crude protein content of the yeast could be calculated. At the end of the fermentations the yeasts was collected by centrifuging and washed twice with water. The yeast was then dried at 45° and a part was used for the determination of nitrogen and fat. Another part was dried at 105° in order to express the contents of nitrogen and fat on a dry weight basis. By the fat analysis [6] the total lipid content was determined. From the nitrogen analysis the crude protein was calculated as $N \times 6.25$.

The vitamins were determined microbiologically using the methods described by Barton-Wright [7]. The yeast was separated by centrifuging and the vitamin content determined on the nutrient solution directly and on the yeast after treatment according to Ref. [7].

RESULTS

Five experiments with a nitrogen-rich and five with a nitrogen-poor nutrient solution were carried out. Four of these experiments (2 with a nitrogen-rich and 2 with a nitrogen-poor nutrient solution) were made with ammonium sulphate as the nitrogen source and in the others asparagine was used.

At the beginning of the fermentations growth was as good in the nutrient solution low in nitrogen as in that containing excess nitrogen. After about 2 days, however, the nitrogen in the nitrogen-poor medium was practically consumed and the growth in these fermentors became slower. This reduction in growth rate becames apparent first when the crude protein content of the yeast is below 20 %. The growth rate of a yeast with 20 or 60 % crude protein is almost the same which was found to be the case in all experiments independent of the nitrogen source used.

A remarkable and important difference between the fermentations with ammonium sulphate as the nitrogen source and those with asparagine, is the resulting pH of the nutrient solution. Whereas the pH remains about 5 during the fermentations with asparagine the final pH is about 2 in the fermentations with ammonium sulphate as the nitrogen source. The acidity of the latter nutrient solution is due to the well known fact that the ammonium ions are taken up and the solution becomes more acid. This acidity is no doubt the reason why the growth is somewhat slower when ammonium sulphate is the nitrogen source. Most probably it is also the reason why the fat production is slightly less and the production of nicotinic acid is higher (see below).

The values obtained for the crude protein and fat content of the yeast at the end of the fermentations are summarized in Table 1. In this table the fermentations are arranged according to the crude protein content of the yeast.

The values given in Table 1 clearly show that both the crude protein content and the fat content of the yeast can be varied greatly by altering the nitrogen content of the nutrient solution. The crude protein content varied between 8.4 and 60.7 % and the fat content between 11.6 and 71.0 %. When the crude protein content is low the fat content is high and vice versa, which shows an inter-relationship between the two.

Table 1. Crude protein and fat content of the yeast at the end of the fermentation.

Expt. No.	Crude protein, % of dry weight	Fat, % of dry weight	Crude protein + fat, % of dry weight	Nitrogen source
10	8.4	71.0	79.4	asparagine
5	10.0	64.0	74.0	asparagine
6	10.2	63.2	73.4	asparagine
1	18.4	47.1	65.5	am. sulphate
2	25.4	41.2	66.6	am. sulphate
3	43.2	17.5	60.7	am. sulphate
4	43.8	15.7	59.5	am. sulphate
9	50.8	19.4	70.2	asparagine
7	53.5	16.7	70.2	asparagine
8	60.7	11.6	72.3	asparagine

The sum of the contents of crude protein and of fat is relatively constant, varying between 70 and 79 % of dry yeast, when the yeast is grown in the nutrient solutions containing asparagine as the nitrogen source. When the yeast is grown with ammonium sulphate as the nitrogen source this value is appreciably lower, ranging between 59 and 65 % of the dry yeast. Relatively little fat is formed when ammonium sulphate is the nitrogen source. The difference between the composition of the yeast grown with asparagine and with ammonium sulphate is probably caused by the different pH values during the fermentation, the nutrient solution being more acid when ammonium sulphate is employed. It must, however, be remembered that no determinations of protein *per se* were made but that only the nitrogen content multiplied by 6.25 was taken as a measure of the protein content of the yeast. If the yeast contains a large number of non protein compounds this would be included in the figures for crude protein.

The vitamins riboflavin, pantothenic acid, nicotinic acid and pyridoxine were determined both in the cell-free nutrient solution and in the yeast both during fermentation and at the end of the fermentation. It was found that the largest quantity of the vitamins was present in the nutrient solution, the yeast only contained some 20—50 % of the total amount.

Table 2 gives the amounts of the vitamins found at the end of the fermentations. The values are calculated both per g dry yeast and per g of protein. The 10 fermentations are arranged according to the crude protein content of the yeast.

Table 2. Vitamin content of protein-rich and protein-poor yeast at the end of the fermentation.

Expt. No. Experiment	10	5	6	1	2	3	4	9	7	8
Nitrogen source	asp.	asp.	asp.	ams.	ams.	ams.	ams.	asp.	asp.	asp.
Crude protein, %	8.4	10.0	10.2	18.4	25.4	43.2	43.8	50.8	53.5	60.7
Riboflavin										
μg/g yeast	28	61	65	100	124	161	187	250	140	150
μg/g protein	333	610	637	543	488	373	427	492	262	247
Pantothenic acid										
μg/g yeast	0	4	5	0	0	35	45	150	420	420
μg/g protein	0	40	49	0	0	81	103	295	785	692
Nicotinic acid										
μg/g yeast	30	97	86	190	210	465	421	105	77	124
μg/g protein	357	970	843	1 033	827	1 076	961	207	144	204
Pyridoxine										
μg/g yeast	4	3	4	12	14	16	17	10	13	16
μg/g protein	48	30	39	65	55	37	39	20	24	26

As can be seen from Table 2, the amounts of pantothenic acid present depended on the crude protein content of the yeast. If the crude protein content was low, no or very little pantothenic acid was present. The reason for the low pantothenic acid content in the protein-poor yeast may be that one of the components of this vitamin, β-alanine, is not formed when the nutrient solution is deficient in nitrogen. Nielsen, Sandegren and Ljungdahl [2] found β-alanine to be absent in protein-poor *Rh. gracilis* yeast whereas it was present in the protein-rich yeast.

With regard to the other vitamins the differences between the amounts present in the protein-rich and protein-poor yeast were not so striking. The amounts, calculated per g of yeast are somewhat smaller for the protein-poor yeast compared with the protein-rich one; for nicotinic acid this difference is rather insignificant. If calculated on g of protein, however, the amounts present are at least as high for the protein-poor yeast as for the protein-rich. There seems to be a tendency for the protein-poor yeast to be somewhat richer in the vitamins estimated than the protein-rich one, when calculated on a protein basis, which especially holds true for nicotinic acid. With regard to pantothenic acid the amounts present were, as mentioned above, very small in the protein-poor yeast.

The nicotinic acid appeared to be produced in higher amounts when the yeast was cultivated in the ammonium sulphate medium which was probably due to the low pH of the nutrient solution.

The vitamin contents of the protein-poor yeast, when calculated per litre nutrient solution, were of course much smaller than for the protein-rich one, due to the fact that the production of yeast was much less.

The amounts of vitamins calculated as μg per g did not vary much during the fermentation in the case of the protein-rich yeast. With regard to the protein-poor type a decrease could be noticed due to the fact that the yeast was growing poorer in protein, but if the vitamin content is expressed as μg per g protein the values were relatively constant during the fermentation. Calculated per litre nutrient solution a marked increase naturally occurs during the fermentation because of the increase in the amount of yeast.

In earlier investigations [8] it was found that the addition of thiamine and pantothenic acid stimulated the growth of *Rh. gracilis*, whereas the addition of nicotinic acid, riboflavin or pyridoxine had no effect. This is in good agreement with the fact that pantothenic acid under certain conditions is not formed at all or only in small amounts.

REFERENCES

1. Enebo, L., Anderson, L. G. and Lundin, H. *Arch. Biochem.* **11** (1946) 383.
2. Nielsen, N., Sandegren, E. and Ljungdahl, L. *Nature* **164** (1949) 1055.
3. Nielsen, N. and Lundin, H. *Ann. Acad. Sci. Fennicæ, Sér. A II. Chemica* **60** (1955) 455.
4. Sandegren, E., Ekström, D. and Nielsen, N. *Acta Chem. Scand.* **4** (1950) 1311.
5. Nilsson, N. G. and Nielsen, N. *Acta Chem. Scand.* **7** (1953) 1067.
6. *Methods of the milk products sub-committee of the Soc. Publ. Analyst* **61** (1936) 105.
7. Barton-Wright, E. C. *The microbiological assay of the vitamin B-complex and amino acids.* Pitman and Sons, London 1952.
8. Lundin, H. *J. Inst. Brewing* **56** (1950) 17.

Received January 29, 1957.

ACTA CHEMICA SCANDINAVICA 11 (1957) 690—692

Studies on the Hydrolysis of Metal Ions

20. The Hydrolysis of the Cd Ion, Cd^{2+}

Y. MARCUS

Department of Inorganic Chemistry, Royal Institute of Technology, Stockholm 70, Sweden *

Potentiometric (glass electrode) titrations of Cd^{2+} with NaOH in 3 M (Na^+) ClO_4^- ionic medium at 25° C were made. At first a slight hydrolysis was observed (not much more than 1 %), according to $Cd^{2+} + H_2O \rightleftharpoons CdOH^+ + H^+$, $\log K_{a1} = -9.0 \pm 0.2$, and subsequently precipitation of $Cd(OH)_2$ was found with $pL \geq 15.6$. There was no evidence for polynuclear species.

The method of study employed was the one in general use in this laboratory. Cadmium solutions were titrated with NaOH at 25.0 ± 0.1° C, at constant Cd concentrations (= B), and in an ionic medium of 3 000 mM (Na^+) ClO_4^-. The cell used was: Ag, AgCl / 10 mM Ag^+, 2 990 mM Na^+, 3 000 mM ClO_4^-/ 3 000 mM $NaClO_4$ / B mM Cd^{2+}, H mM H^+, 3 000—2B—H mM Na^+, 3 000 mM ClO_4^- / glass electrode. In the range of pH under consideration the liquid junction potential could be neglected, and the electromotive force E in mV followed the expression

$$E = E_0 - 59.16 \log h = E_0 + 59.16\ ph \qquad (1)$$

where h is the concentration of free hydrogen ions. The solutions were swept with purified nitrogen during titrations to guard against CO_2. The titrations proved to be completely reversible and reproducible. Above ph 6 considerable time was needed for attainment of equilibrium, and at a definite higher ph precipitation could be observed.

H_0, the excess acid present in the solutions, and E_0 were calculated by successive approximations from the portion of the titration data where no hydrolysis occurred (ph below 4). The average number of hydroxyl ions bound per metal ion, Z, was calculated from

$$Z = (h - H_0 - H)\ B^{-1} \qquad (2)$$

where H was the analytical excess acid (acid added — base added / total volume), and h was obtained from the measured electromotive force by (1).

---

* Permanent address: Israel Atomic Energy Commission, Hakiryah, Tel Aviv, Israel.

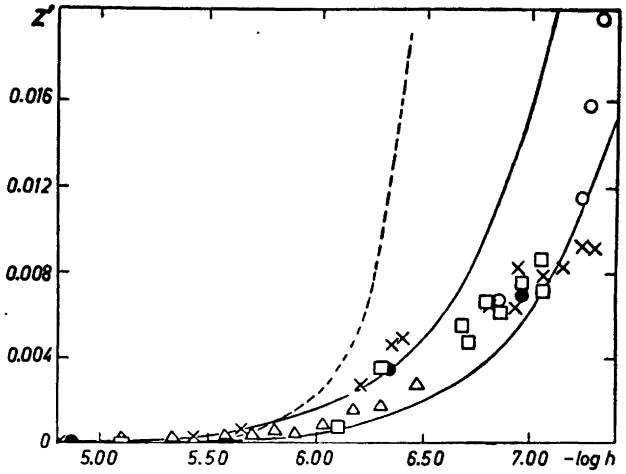


Fig. 1. The average number of hydroxyl ions bound per metal ion, Z', as function of the free hydrogen ion concentration $-\log h$. The symbols refer to the Cd concentrations B: × 10.7 mM, ○ 26.8 mM, □ 53.6 mM, ● 107.1 mM, △ 910 mM. The curves ——— were calculated with the limiting values of log K_{a1} −8.8 and −9.2, while - - - - - was calculated with the constant for reaction (4), log $K_{a2} = -14.6$. Selection of a different value for K_{a2} will only shift the curve horizontally to left or right, but it will not fit the data.

Titrations were made for five B values between 10 and 900 mM, and the data $Z(-\log h)_B$ calculated. The scattering was very considerable, because Z was usually much smaller than 0.01. Some acid impurity was found to be titrated together with the Cd, and its contribution, about 0.001 units, was subtracted from the Z values to give Z'. A plot of Z' against -log h is shown In Fig. 1.

Fig. 1 shows that B has no significant effect, as all points seem to fall on the same curve. A plot of log Z' against -log h gave a straight line log $Z' = (-8.09 \pm 0.17) - (0.86 \pm 0.03) \log h$ as was found by a least squares treatment.

The following mechanisms were considered:

$$p\ Cd^{2+} + q\ H_2O \rightleftharpoons Cd_p(OH)_q^{2p-q} + q\ H^+,\ p \neq 1 \quad (3)$$

$$Cd^{2+} + 2\ H_2O \rightleftharpoons Cd(OH)_2 + 2\ H^+ \quad (4)$$

$$Cd^{2+} + H_2O \rightleftharpoons Cd(OH)^+ + H^+ \quad (5)$$

Mechanism (3) requires the data to show an effect due to B, and is ruled out. Mechanism (4) requires a slope of +2 in a log Z against $-\log h$ plot, and does not agree with the data (see also Fig. 1). Mechanism (5) is therefore the most likely. The equilibrium constant K_{a1} is given by

$$K_{a1} = [CdOH^+]\ h\ [Cd^{2+}]^{-1} \approx Z\ h \quad (6)$$

Table 1. The ph of beginning precipitation and the solubility product of $Cd(OH)_2$.

pB	1.970	1.572	1.271	0.970	0.041
ph	7.43	7.29	6.91	6.85	6.50
pL	15.5	15.4	15.8	15.7	15.5

because $Z = [CdOH^+]\ B^{-1}$ and as Z was very small, $B \approx [Cd^{2+}]$. From (6) follows $\log Z = \log K_{a1} - \log h$, and a plot of $\log Z$ against $-\log h$ should have unit slope. The observed slope of 0.86 is fairly near to unity, and the best straight line with unit slope through the points has $\log K_{a1} = -(9.0 \pm 0.2)$.

Chaberck, Courtney and Martell [1] found with a glass electrode $pk = \log [CdOH^+]\ [H^+]\ [Cd^{2+}]^{-1} = -11.6$ at 30° and 0.1 M KCl ionic medium. These authors state, however, that "at best the value of k listed is reliable to only one significant figure". Earlier, the value $\log K_w - \log K_{a1} = -5.52$ was calculated by Jellinek [2] from distribution data of Löfman [3], while Kullgren [4] found by a kinetic method $\log K_{a1} = -9.49$ at 100°. The last two constants are of the same magnitude as the value found here. Hayek [5] found negligible solubility of CdO in $Cd(ClO_4)_2$ solutions, which shows negligible formation of polynuclear hydrolysis products.

The approximate ph of beginning precipitation enables one to calculate a lower limit of the solubility product L

$$pL \geq 2\ pK_w - 2\ ph + pB \qquad (7)$$

Assuming pK_w, the dissociation constant of water, to be 14.22, the data in Table 1 give the average $pL \geq 15.6$.

The following values of pL were previously reported in literature: Akselrud [6] 14.58, Kertman [7] 13.65, Bodländer [8] 13.65, Tananaev [9] 12.62, all at 18° C, Kovalenko [10] 15.81 at 22° C and Piater [11] 14.22 at 25° C, all for infinite dilution.

Note added in proof: Since the completion of this work Gayer and Woontner [12] have published results of their solubility measurements at 25°C: $\log K_{a1} = -9.3$ and $pL = 14.31$, besides values for species formed in alkaline solutinos.

The author wishes to thank the *Israel Atomic Energy Commission* for a research grant abroad, and Professor Lars Gunnar Sillén for his helpful discussion of the work.

REFERENCES

1. Chaberek, S. Jr., Courtney, R. L. and Martell, R. E. *J. Am. Chem. Soc.* **74** (1952) 5057.
2. Jellinek, E. *Lehrbuch der physikalischen Chemie*, 2nd Ed., Stuttgart 1933, **IV**: 62.
3. Löfman, N. *Z. anorg. u. allgem. Chem.* **107** (1919) 241.
4. Kullgren, C. *Z. physik. Chem.* **85** (1913) 466.
5. Hayek, E. and Schnell, E. *Monatsh.* **85** (1954) 472.
6. Akselrud, N. V. and Fialkov, Y. A. *Ukrain. Khim Zhur.* **16** (1950) 283.
7. Kertman, L. N. *Kurs Kachest Analisa O.N.T.I.* **1927** 568.
8. Bodländer, E. *Z. physik. Chem.* **27** (1898) 66.
9. Tananaev, N. A. *Analiticheskaya Khimiya O.N.T.I.* **1934** 304.
10. Kovalenko, P. N. *Zhur. Priklad. Khim.* **26** (1953) 814.
11. Piater, A. *Z. anorg. u. allgem. Chem.* **174** (1928) 339.
12. Gayer, K. H. and Woontner, L. *J. Phys. Chem.* **61** (1957) 364.

Received February 15, 1957.

ACTA CHEMICA SCANDINAVICA 11 (1957) 693—702

Surface Balance Studies of Bile Acid Monolayers

I. Cholanic and Glycocholanic Acid Monolayers

PER EKWALL, REINO EKHOLM and ARNE NORMAN*

Institute of Physical Chemistry, Åbo Akademi, Åbo, Finland

A continuously recording surface balance has been employed to study monomolecular layers of cholanic and glycocholanic acids spread on acid substrates of pH 2. Both acids form monolayers of the condensed type on compression. Already at the point 0, where the surface pressure begins to increase, the monolayer molecules are densely packed and oriented more or less vertical to the substrate surface with the alkyl chain and its terminal carboxyl group projecting into the surface. The differences between bile acid and cholesterol monolayers are discussed.

The cholanic acid monolayer is liquid at 20°C; the surface layer solidifies only after the collapse point has been passed. At temperatures below 14°C the glycocholanic acid monolayer is solid already at point 0 and remains so on further compression. Between 15° and 22°C a transition from a liquid to solid state occurs on compression; above 26°C the surface layer solidifies only after its collapse. The phase transformation in the monolayer is accompanied by a decrease in the internal energy amounting to 1 000 to 2 000 cal/mole. An increase in the sodium chloride content of the substrate has the same effect on the transformation as a moderate decrease in temperature.

There appears to be only one investigation that has dealt with the monolayer properties of bile acids. Adam, Askew and Danielli [1] studied the properties of apocholic and β-apocholic acid monolayers which they seem to have compressed to an area of about 100 Å^2 per molecule and to a surface pressure of 9 dynes / cm. They found that both acids form gaseous monolayers in which the longitudinal axes of the molecules apparently lie parallel to the surface owing to the fact that the molecules contain three hydrophilic groups that are situated fairly far apart.

In connection with investigations of micelle formation in bile acid salt solutions in progress at the Institute of Physical Chemistry of the Åbo Aka-

* Present address: Department of Physiological Chemistry, University of Lund, Lund, Sweden.

demi [2-7,15], we considered it of interest to study the monolayer properties of the bile acids [8]. We present the results of a surface balance study of the monolayer properties of cholanic and glycocholanic acids on acid substrates in this paper.

MATERIALS AND METHODS

The bile acids were synthesized by one of us (A. N.) at the Department of Physiological Chemistry of the Lund University. The methods of synthesis and the physical properties of the acids have been described in earlier publications [9].

The cholesterol which was included as a reference compound was from Hoffmann-La Roche AG, Basel; it melted at 148.5°C.

Owing to the low solubilities of the bile acids in benzene, chloroform was employed as solvent. The chloroform solutions of the bile acids contained 2×10^{18} molecules per ml. (It was found that cholanic acid and cholesterol monolayers yield slightly smaller area values (by 0.8 Å^2 per molecule) when chloroform than when benzene is the solvent. The surface pressures were not affected by the solvent. The observed difference may be due to the fact that the solubility of chloroform in water is ten times greater than that of benzene.)

The chloroform solutions of the bile acids were added to the surface of the aqueous substrate in a Langmuir trough from an Agla micrometer syringe. The surface pressure-area curves of the monolayers were recorded with an automatic, self-recording surface balance of the Wilhelmy-Dervichian type (as improved by Andersson-Groth, Ställberg-Stenhagen and Stenhagen [10]). Compression of the monolayer was begun 2 min after the substance had spread on the substrate surface. The rate of compression was 13 – 14 cm/min; the area values were found to be completely, and the pressure areas practically, independent of the rate of compression in this range. (When much lower rates of compression were employed, this was no longer the case; the area values tended to decrease and the pressure values to increase as the rate of compression was diminished. When the rate of compression was appreciable higher, from 25 – 50 cm/min, the pressure-area curves were no longer reproducible.)

The substrate was water or a 3 M sodium chloride solution; in both cases the pH was lowered to 1.9 – 2.0 with hydrochloric acid.

The viscosities of the monolayers were examined by a modified talcum powder method. If the powder did not move when a weak current of air was blown on the layer, the monolayer was judged to be solid.

EXPERIMENTAL RESULTS

Typical pressure-area curves recorded for the cholanic and glycocholanic acid monolayers are shown in Figs. 1 and 2. Curves for cholesterol monolayers recorded under identical conditions have also been drawn in the figures. The notations used to designate various characteristic points on the pressure-area curves in these figures will be employed for reference in the following.

Characteristic data for bile acid and cholesterol monolayers are given in Table 1. The thicknesses of the monolayers at the collapse point, K_{extr} or K_{max}, have been calculated by assuming that the densities of all the monolayer substances are 1.067 g/ml, *i. e.*, that of crystalline cholesterol. (In the literature we have found only the density value for norcholanic acid, $d = 1.13$).

On a salt-free substrate the bile acid monolayers must be compressed to an area of 44 Å^2 per molecule before the surface pressure begins to increase. With cholanic acid the pressure then increases steeply up to the collapse point. (The peak at the collapse point disappears when a lower rate of compression is employed.) In the pressure-area curve for glycocholanic acid a curvature

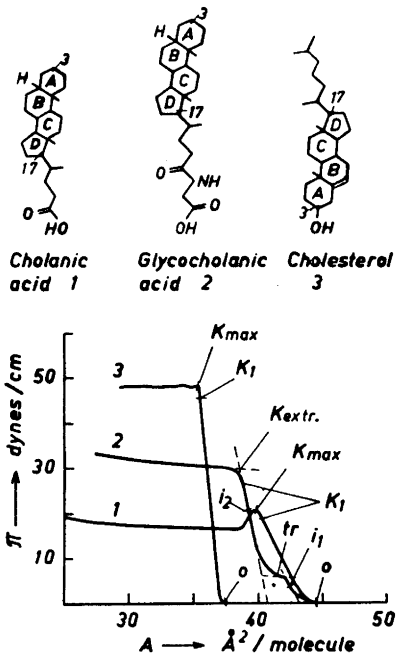


Fig. 1. Structural formulae of cholanic acid (1), glycocholanic acid (2) and cholesterol (3). Typical monolayer pressure-area curves. Substrate: water of pH 2. 20°C. 1. Cholanic acid; 2. Glycocholanic acid; 3. Cholesterol. Notation: 0, the point where the pressure begins to increase on compression.
K_1, K_{extr}, K_{max}, points where collapse occurs.
i_1, i_2, inflexion points.
tr, transition point.

showing that a transition takes place is seen at a pressure of 6.0 dynes / cm; on both sides of the transition region, the curves have a large slope. The pressure required to effect collapse of the glycocholanic acid monolayer is almost 50 % greater than that required for the cholanic acid monolayer. The area per molecule at the collapse point is 40 Å² for cholanic acid and 39 Å² for glycocholanic acid.

The area and pressure values recorded on a 3 M sodium chloride substrate are generally slightly higher than those recorded with pure water as substrate. An exception is the area value at point 0 for glycocholanic acid which is 1.4 Å² per molecule lower. This is due to the fact that the transition range and the

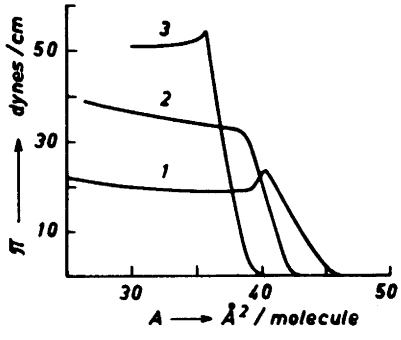


Fig. 2. Typical monolayer pressure-area curves of bile acids and cholesterol on 3M sodium chloride of pH 2. 20 °C. 1. Cholanic acid; 2. Glycocholanic acid; 3. Cholesterol.

Table 1. Characteristic monolayer data for cholanic acid, glycocholanic acid and cholesterol at 20 °C, pH 2.

Compound	Substrate	Areas in Å² per molecule					Surface pressures in dynes / cm				Thickness of monolayer at the collapse point Å
		A_0	A_{tr}	A_{K_1}	A_{Kextr}	A_{Kmax}	tr	K_1	Kextr	Kmax	
Cholanic acid	Water	44.2	—	40.2	40.1	39.7	—	19.2	21.0	21.0	14
	3M NaCl	45.8	—	40.6	40.5	40.2	—	21.8	23.0	23.0	
Glycocholanic acid	Water	44.5	41.6	38.8	38.8	—	6.0	27.3	29.5	—	17
	3M NaCl	43.1	—	39.3	38.8	—	—	27.3	32.2	—	
Cholesterol	Water	37.4	—	35.5	35.4	35.3	—	47.2	48.0	48.2	17
	3M NaCl	40.0	—	35.7	35.8	35.6	—	53.1	51.0	53.9	

lower section in the pressure-area curve of glycocholanic acid do not become evident when the sodium chloride content of the substrate is high enough; this is shown by the curves in Fig. 3 recorded with increasing salt concentration.

In order to determine the effect of temperature on the transition that occurs in the glycocholanic acid monolayer, pressure-area curves were recorded at different temperatures (Fig. 4). It was found that at temperatures below 14 °C the monolayer is solid already at point 0 and remains so on further

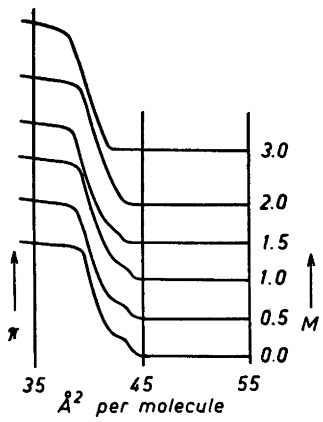


Fig. 3. Effect of substrate salt content on the glycocholanic acid monolayer. Range 0—3 M NaCl. pH 2. 20°C.

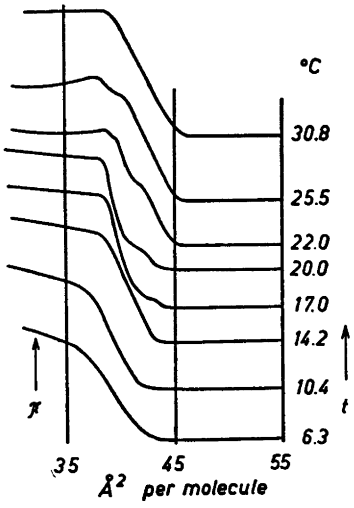


Fig. 4. Effect of temperature on the glycocholanic acid monolayer. Water of pH 2.

compression. At temperatures where the transition is observed, the monolayer is liquid up to the transition point (the point "tr"), but is solid above the latter, at least up to 22 °C. At temperatures above 26 °C, however, the surface layer becomes solid only after the monolayer has collapsed. A transition from a liquid to a solid phase thus occurs at the point tr, at least at temperatures between 15° and 22 °C.

DISCUSSION

In contrast to apocholic acid, cholanic and glycocholanic acids form monolayers of the condensed type (Figs. 1—4). This is obviously due to the presence of only one hydrophilic group in their molecules, *i. e.*, the carboxyl group at the end of the alkyl chain.

On the basis of information reported in the literature on the configurations of the bile acids and cholesterol [11] and with the aid of molecular models constructed from Stuart atomic calottes, we have attempted to compute the smallest areas that the molecules can take up in densely packed monomolecular layers (Table 2).

Table 2. Lengths and smallest cross-sectional areas of bile acids. Calculations based on molecular models.

Compound	Length of molecule Å	Molecular area perpendicular to major axis Å²	Smallest projection area with the molecule inclined 12° from the vertical Å²
Cholanic acid	18.5	45.5	44
Glycocholanic acid	22.0	45.5	44
Cholesterol	21.8	35	35

The experimentally found areas per molecule at point 0 (A_0) are of the same magnitude as the computed areas. This shows that the bile acid molecules are densely packed already at this point. A further compression can occur only if the molecules are fitted into each other. Between the points 0 and K, the molecules are oriented almost perpendicular to the substrate surface with the alkyl chain and its terminal carboxyl group projecting into the surface. Lacking exact values for the densities of the acids, only approximate values can be calculated for the thicknesses of the monomolecular layers. They are somewhat lower than the calculated maximum lengths of the molecules, apparently because the monolayer molecules at the collapse point are inclined about 12° from the vertical and because the molecules are somewhat curved. The experimental value for cholanic acid agrees fairly well with the value for desoxycholic acid (13.5 Å) calculated from data obtained in X-ray investigations of choleic acid crystals [12].

It is interesting to compare the monolayers of the bile acids with that of cholesterol. From molecular models, Harkins, Ries and Carman [13] have estimated the smallest cross-sectional area of a cholesterol molecule (assumed

to be a parallelepiped) to be 37 Å². Our calculations gave for the minimum projection area of cholesterol the value 35 Å². The former value is in fairly good agreement with our experimentally determined area requirement at point 0, $A_0 = 37.4$ Å², and the latter with the experimental value at the collapse point, $A_{Kextr} = 35.4$ Å². The molecules in the cholesterol monolayer are thus densely packed and nearly perpendicular to the surface at the point 0. The carbon atom 3 bearing the hydrophilic hydroxyl group and the carbon atom 17 which carries the alkyl chain with its terminal carboxyl group are at opposite ends of the molecule. As a consequence the arrangement of the cholesterol and the bile acid molecules is different in compressed monolayers. The former stand with the hydrophenanthrene skeleton pointing downwards, whereas the latter stand with their alkyl chains projecting into the substrate and the ring skeleton pointing upwards. It should further be noted that the alkyl chain of the bile acids is shorter than that of cholesterol and that the rings A and B are in the *cis* positions in the bile acid molecule but in the *trans* positions in the cholesterol molecule. There is further a double bond in the 5, 6 position in cholesterol. In a study of sterol monolayers, Adam, Askew and Danielli [1] found that the introduction of a double bound in the 5, 6 position increases the area requirement by approximately 1.8 Å² and that the change in the positions of the rings A and B from *trans* to *cis* configuration increases the molecular area by approximately 2.8 Å² at a surface pressure of 20 dynes / cm. From this it may be concluded that the area requirement of the bile acid ring skeleton is larger than that of cholesterol by about 1 Å². The observed difference of 3—5 Å² between the molecular areas in bile acid and cholesterol monolayers (Table 1) is thus for the most part due to the different orientations of the molecules in the monolayers. The appreciably lower collapse pressures found for the bile acid monolayers are apparently due to the same factor. The arrangement with the alkyl chain pointing downwards and the hydrophenanthrene ring system upwards apparently results in a less dense packing and a weaker cohesion than the opposite arrangement.

Since the only difference between cholanic and glycocholanic acids is that the latter contains a conjugated glycine molecule, this must be responsible for the curvature observed in the pressure-area curve of the latter acid at temperatures between 16° and 26 °C. At the lowest temperature studied (6—7°C), the solid glycocholanic acid monolayer gives a smooth pressure-area curve (Fig. 4) and the area can be reduced to about 37 Å² per molecule before a gradual collapse occurs. The A_0 values are 45—46 Å² per molecule, and the compressibilities calculated from the slopes of the curves at the inflexion points are rather high ($-\varkappa = 5—6 \times 10^{-3}$). When, however, the temperature rises above 10°C, the compressibility diminishes gradually, the curvature at the collapse point becomes sharper, and A_{Kextr} increases to a slightly higher value. The values of the surface pressures, areas per molecule and the compressibilities at different temperatures are given in Figs. 5, 6 and 7. In the temperature range 14°—26° where the transformation is observed, the properties of the liquid phase at low pressures (Phase 1), and those of the solid phase at high pressures (Phase 2) are well defined; the compressibilities of the two phases remain constant ($-\frac{\partial A}{A \partial \pi} = -\varkappa = 3—6 \times 10^{-3}$ and 1.8×10^{-3} cm / dyne)

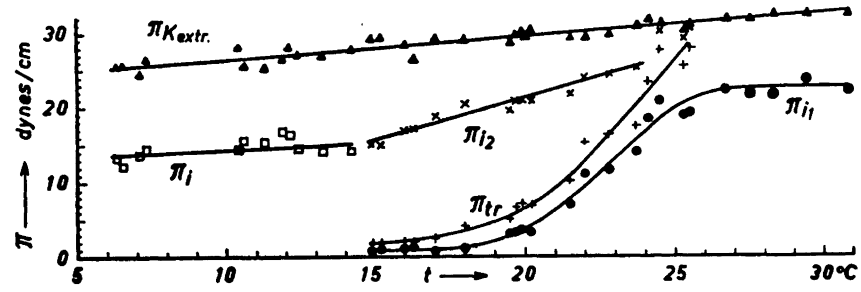


Fig. 5. Variation of the surface pressure of glycocholanic acid monolayer with the temperature. Water of pH 2.

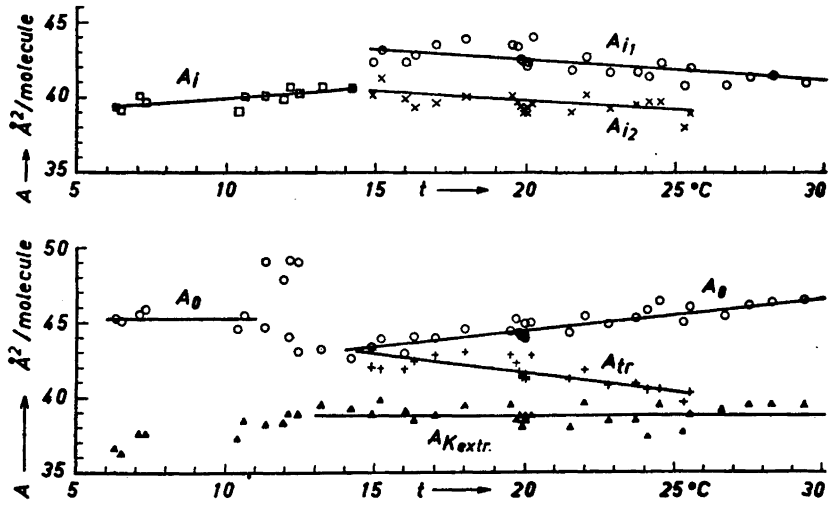


Fig. 6. Variation of molecular area with the temperature in the glycocholanic acid monolayer. Water of pH 2.

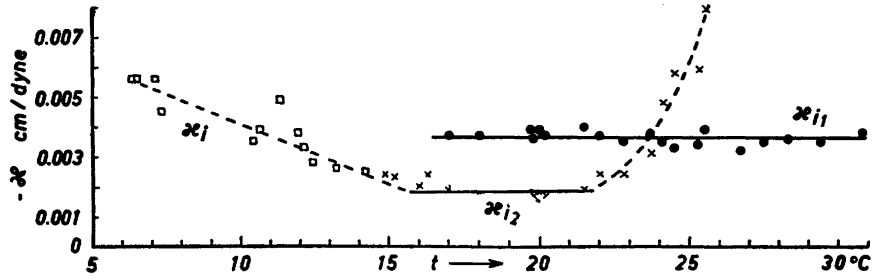


Fig. 7. Variation of compressibility at the inflexion point with the temperature in the glycocholanic acid monolayer. Water of pH 2.

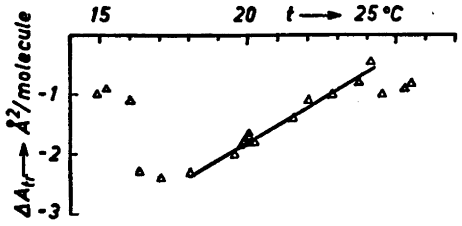


Fig. 8. The change in the molecular area at the transition point, ΔA_{tr}, of glycocholanic acid monolayer.

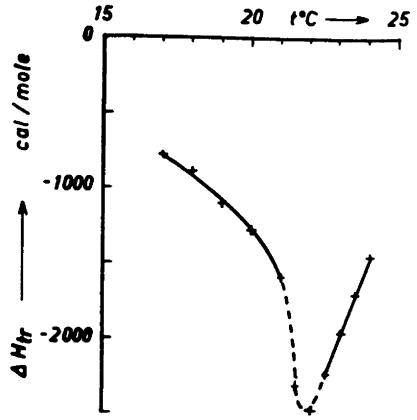


Fig. 9. The change in molal heat content when transition takes place in the glycocholanic acid monolayer.

(Fig. 7) and the areas at the inflexion points decrease linearly with rising temperature. Above 22°C, however, the high pressure phase (Phase 2) becomes less well defined, and is no longer observed above 26°C. At temperatures above the latter the surface layer solidifies only after the collapse point has been passed.

On the basis of the two dimensional analogue of the Clausius-Clapeyron equation [14]

$$\frac{d\pi_{tr}}{dT} = \frac{\Delta H_{tr}}{T \cdot \Delta A_{tr}} \qquad (1)$$

we have calculated the changes in molar heat content, ΔH_{tr}, accompanying the monolayer transformation in the range from 17° to 24 °C. In this equation π_{tr} is the equilibrium transition pressure of the monolayer at temperature T and ΔA_{tr} is the net change in molar area. We have taken ΔA_{tr} equal to the difference between the tangents drawn to the curves at the inflexion points. The value of ΔA_{tr} decreases linearly with rising temperature between 17° and 24°C (Fig. 8).

The calculated ΔH_{tr} values vary from about —1 000 to about —2 500 cal/mole (Fig. 9). The expression $\frac{\partial \Delta H_{tr}}{\partial T}$ is negative up to 22°C, but positive above the latter temperature. Since $\left(\frac{\partial \Delta H_{tr}}{\partial T}\right)_{\pi} = C_{\pi_2} - C_{\pi_1} = \Delta C_{\pi}$ (where C_{π} is the molar heat content of the phase), the values of this expression suggest that whereas the degrees of kinetic freedom of phase 2 are restricted compared to those of phase 1 below 22 °C, the opposite is true above this temperature. Our observations show that Phase 2 is solid and has a constant low compressibility up to the latter temperature, but that the properties of this phase are

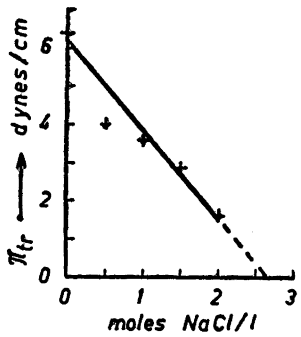


Fig. 10. Variation of the transition surface pressure with salt content of the substrate in the glycocholanic acid monolayer. 20°C.

less well defined (the compressibility increases continuously) between 22° and 24 °C. Further conclusions cannot be drawn owing to the limited experimental information available at present.

For a transformation at constant pressure, the net change in molar heat content is

$$\Delta H_{tr} = \Delta E_{tr} + \pi_{tr}\Delta A_{tr} \qquad (2)$$

where ΔE_{tr} is the net change in the molar internal energy of the monolayer system and $\pi_{tr}\Delta A_{tr}$ the work done by the system. At zero transition pressure, $\Delta H_{tr} = \Delta E_{tr}$. For the observed transition pressures, the values of ΔE_{tr} are only 10—25 cal/mole more positive than the ΔH_{tr} values; the temperature dependence of both is the same. The phase transformation is accompanied by a decrease in the internal energy, and the magnitude of ΔE_{tr} (—1 000 to —2 000 cal/mole) suggests that hydrogen bond formation takes place between the molecules in the monolayer. If this is true, it is probable that the hydrogen atom of the imino group is involved. In the range 14—22° a liquid monolayer is thus first formed which on compression is transformed into a solid layer, obviously with the formation of hydrogen bonds. This transition does not occur above 26°C, and above this temperature the glycocholanic acid monolayer is liquid up to the collapse point similarly as that of cholanic acid.

An increase in the sodium chloride content of the substrate has the same effect as a moderate decrease in temperature. The transition pressure decreases and the liquid phase 1 disappears (Fig. 10). When the salt content of the substrate becomes sufficiently high, the monolayer is directly transformed on compression into phase 2 with a low compressibility.

REFERENCES

1. Adam, N. K., Askew, F. A. and Danielli, J. F. *Biochem. J. London* **29** (1935) 1786.
2. Ekwall, P. *Acta Acad. Aboensis, Math. Phys.* **XVII** (1951) 8.
3. Ekwall, P. *Svensk Kem. Tidskr.* **63** (1951) 973.
4. Ekwall, P. *Koninkl. Vlaam. Acad. Wetenschap van Belgie. Intern. conference on Biochemical Problems of Lipids*, Brüssel **1953**, p. 103.
5. Ekwall, P. *J. Colloid Sci. Suppl.* **1** (1954) 66.
6. Ekwall, P. and Fontell, K. *Acta Chem. Scand.* **10** (1956) 327.

7. Ekwall, P., Sten, A. and Norman, A. *Acta Chem. Scand.* **10** (1956) 681.
8. Ekwall, P. and Ekholm, R. *9nde Nordiska Kemistmötet, Aarhus* 1956.
9. Norman, A. *Arkiv Kemi* **8** (1955) 331.
10. Andersson, K., Ställberg-Stenhagen, S. and Stenhagen, E. *The Svedberg* 1884–1944, Uppsala 1944, p. 11.
11. Fieser, L. F. and Fieser, M. *Natural products related to phenanthrene*, New York 1949.
12. Kratky, O. and Giacomello, G. *Monatsh.* **69** (1936) 427.
13. Harkins, W. D., Ries, H. E. and Carman, E. F. *J. Am. Chem. Soc.* **57** (1935) 2224.
14. Glaser, J. and Alexander, A. E. *Trans. Faraday Soc.* **47** (1951) 401.
15. Ekwall, P., Rosendahl, T. and Löfman, N. *Acta Chem. Scand.* **11** (1957) 590.

Received December 22, 1956.

ACTA CHEMICA SCANDINAVICA 11 (1957) 703—709

Surface Balance Studies of Bile Acid Monolayers

II. Monolayers of Litocholic and Glycolitocholic Acids

PER EKWALL, REINO EKHOLM and ARNE NORMAN*

Institute of Physical Chemistry, Åbo Akademi, Åbo, Finland

Litocholic and glycolitocholic acid monolayers have been studied with the same experimental technique as described in Part I [2]. The pressure-area curves for both the lithocholic acids differ appreciably from the curves for the cholanic acids, evidently due to the fact that there are two hydrophilic groups in the former and only one in the latter molecules. The molecules lie flat on the substrate surface and on compression the layer is first composed of densely packed lying molecules. When this monolayer collapses, pairs of lithocholic acid molecules, probably with their hydrophilic groups opposite each other, slide up on the monolayer and form a termolecular layer of lying molecules. This triple layer collapses in turn at a somewhat higher pressure. The transformation of the monolayer to a triple layer is accompanied by an increase in internal energy amounting to about 3 000 cal/mole.

Conclusions about the probable arrangement of the bile acid ions in the micelles present in bile salt solutions are drawn from the results of the monolayer studies.

The samples of litocholic and glycolitocholic acids were synthesized as previously described by one of us (A.N.) [1]. The methods used in the investigation of the monolayers have been described in Part I of this series [2]. Chloroform was employed as solvent for the acids. The solution of litocholic acid contained 2×10^{18} molecules per ml and that of glycolitocholic acid 0.67×10^{18} molecules per ml. Moderate variations in the rate with which the monolayers were compressed was not found to have any influence on the shape of the surface pressure-area curves.

EXPERIMENTAL RESULTS

Figs. 1 and 2 show typical pressure-area curves for litocholic and glycolitocholic acid monolayers recorded on salt-free and salt-containing substrates of pH 2. In some cases also a 3 M sodium chloride solution saturated with lito-

* Present address: Department of Physiological Chemistry, University of Lund, Lund, Sweden.

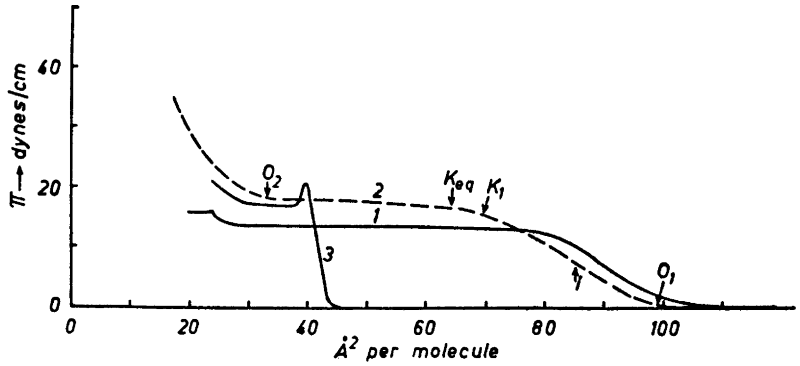


Fig. 1. Typical monolayer pressure-area curves of bile acids. Substrate: water of pH 2. 20 °C.
1. Litocholic acid.
2. Glycolitocholic acid.
3. Cholanic acid.

cholic acid was used as substrate; the solubility of the acid is so low that no transfer of the acid from the bulk of the solution to the surface was detected with the surface balance during 3 h; the pressure-area curves for litocholic acid recorded on this substrate were both qualitatively and quantitatively identical with the curves recorded on 3 M sodium chloride without prior saturation of the latter with the acid.

The pressure-area curves of litocholic acid monolayers on 3 M sodium chloride were recorded at various temperatures between 10° and 40 °C. Temperature had no effect on the shape of the curve; the area values were almost unchanged, but the surface pressure decreased linearly with increasing temperature (Fig. 3).

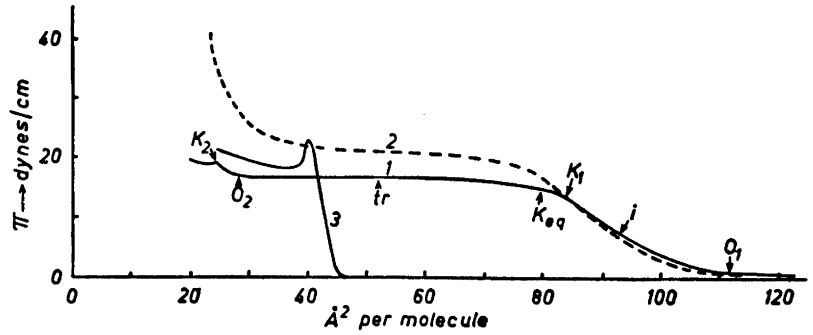


Fig. 2. Typical monolayer pressure-area curves of bile acids. Substrate: 3 M sodium chloride of pH 2. 20 °C.
1. Litocholic acid.
2. Glycolitocholic acid.
3. Cholanic acid.

Table 1. Characteristic data for litocholic acid and glycolitocholic acid monolayers.

Substance	Substrate moles NaCl per litre	Points on the π—A — curve							Physical property
		0	0_1	i	K_1	tr	O_2	K_2	
Litocholic acid	0	119	107.8	91.3	81.0	51.3	28.7	23.6	Area values, Å² per molecule
» »	3	121	112.0	93.4	84.0	52.0	29.8	24.5	
Glycolitocholic acid	0	105.2	98.7	86.9	69.6	—	33.8	—	
» »	3	113.7	106	88.4	76.4	—	43.6	—	
Litocholic acid	0	0.4	0.6	6.3	12.3	13.8	14.2	16.5	Surface pressure values, dynes per cm
» »	3	0.5	0.8	8.4	14.0	16.9	17.1	19.8	
Glycolitocholic acid	0	0.4	0.8	6.5	16.6	—	18.1	—	
» »	3	0.5	0.9	9.7	18.9	—	21.3	—	
Litocholic acid	0			—0.016					compressibility values $-\frac{\partial A}{A\partial\pi} = -\varkappa$ cm per dyne
» »	3			—0.013					
Glycolitocholic acid	0			—0.018					
» »	3			—0.014					

The notations used in Fig. 1 to designate various points on the pressure-area curves will be employed in the following discussion. For comparison, the pressure-area curve for cholanic acid has also been drawn in the figures.

Observations made with talcum powder indicated that the viscosities of the surface films of lito- and glycolitocholic acids undergo marked changes at two stages during the compression; at the first stage the film becomes much more viscous and in the second stage it becomes solid.

Characteristic monolayer data for the two bile acids at 20 °C are given in Table 1.

DISCUSSION

The pressure-area curves for the two litocholic acids differ appreciably from the curves for cholanic acids. The differences are evidently due to the fact that whereas the cholanic acid molecule contains only one hydrophilic group, *viz.* a carboxyl group at the end of the alkyl chain, the litocholic acids contain an additional hydroxyl group on carbon atom 3 at the opposite end of the molecule. Molecules with two hydrophilic groups separated a longer distance from each other, exhibit a tendency to lie more or less parallel to the substrate surface and generally form monolayers of the gaseous type. The pressure-area curves in Figs. 1 and 2, however, seem to suggest that the litocholic acids form monolayers of the condensed type on compression.

We have calculated with the aid of Stuart's molecule models the dimensions of the lithocholic acid molecules and the areas the molecules take up when they lie in different positions in densely packed monolayers (Table 2). The largest values in the table give the areas taken up by the molecules when they lie flat on the surface with their longitudinal axes parallel to the surface. The ring skeleton of the molecule is rigid but the alkyl chain can be folded; consequently

Table 2. Molecular dimensions and area requirements calculated from molecular models.

	Length of molecule Å	Area requirement in monolayer					Area requirement with molecules lying on edge in termolecular layer Å² per molecule
		molecules lying flat Å² per molecule		molecules on edge Å² per molecule		molecules vertical, minimum projection area Å² per molecule	
		max.	min.	max.	min.		
Litocholic acid	18.5	107	85	79	76	44.0	28—25
Glycolitocholic acid	22.0	122	85	93	76	44.0	28—25

it is possible for the area taken up by the molecule to decrease when the monolayer is compressed without the hydrophilic groups losing contact with the substrate surface. This minimum area requirement is also given in Table 2.

A comparison of the experimental data for the litocholic acids and the calculated area requirements shows that the observed value $A_0 = 100—110$ Å² per molecule closely corresponds to that of a molecule lying flat on the surface. Accordingly, already at the point 0 the monolayer is composed of densely packed molecules lying on the surface. The pressure-area curves exhibit no sharp break point in the range 120—70 Å²; the pressure increases slowly and at the inflexion points the monolayers have a compressibility, $-\varkappa$, equal to $0.013—0.018 \times 10^{-3}$ cm/dyne.

The monolayer can be compressed to an area of 85—65 Å² per molecule before the curve bends at the break point $K_1—K_{eq}$ and becomes almost horizontal. The latter area values approximately correspond to the smallest area requirements we have calculated for densely packed molecules which still have both hydrophilic groups in contact with the substrate surface. The high compressibility of the monolayer thus appears to be due to the fact that the molecules, while remaining in the horizontal position, rearrange themselves with increasing lateral pressure so that they first take up a smaller area and are then forced to fold to some extent.

In the relatively wide range of more or less constant surface pressure which follows after the break point at $K_1—K_{eq}$, the surface film is liquid but highly viscous. In the case of litocholic acid this state of the film prevails until it has been compressed to an area of about 29 Å² per molecule, after which the pressure begins to increase. When the area is decreased to 24 Å² per molecule, the curve shows a sharp break point at K_2 which resembles a normal collapse point, and after this point has been passed the film solidifies. When trying to interpret the pressure-area curve in this range the following facts may be considered. The fact that the area values for litocholic acid did not differ when the substrate was a pure 3 M sodium chloride solution and a similar solution saturated with the acid shows that the form of the pressure-area curve between the points K_1 and K_2 is not due to the transfer of litocholic acid from the monolayer into the substrate. If, after the break point $K_1—K_{eq}$,

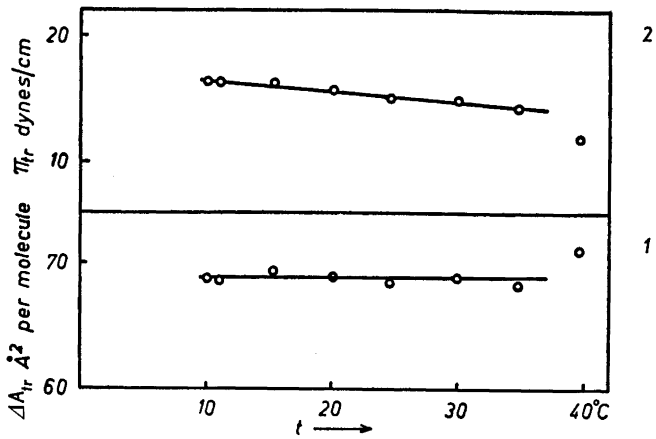


Fig. 3. 1. The change in the molecular area at the transition point, ΔA_{tr}, in the transformation of litocholic acid monolayer into a triple layer. 2. Variation of the surface pressure at the transition point.

larger and larger numbers of the monolayer molecules were forced to assume a vertical position in such a way that one of the hydrophilic groups (*e. g.* the hydroxyl group) is forced away from the substrate surface, this would finally lead to a monolayer composed of molecules in a more or less vertical position. Such a monolayer must, however, collapse after it has been compressed to an area of 44 Å² per molecule (*cf.* Part I[2]). The experimentally observed value of 24 Å² per molecule is, however, so low that it is impossible that such a monolayer of vertically oriented molecules can exist down to this point. The observed area value is on the other hand in fairly good agreement with the area requirement per molecule in a termolecular layer of molecules lying densely packed on their edges. From experiments performed using the built-up technique it is known that an arrangement of molecules such as that shown in Fig. 4 is very stable. In our case, conditions are furthermore suitable for the formation of hydrogen bonds between the hydrophilic groups when the molecules are arranged in this way. It therefore seems probable that the monomolecular layer "collapses" already at the break point K_1—K_{eq}, but when doing this pairs of litocholic acid molecules with their hydrophilic groups opposite each other slide up on the monolayer and form a termolecular layer of the type shown in Fig. 4. This transition of the monolayer into a triple layer seems to be reversible. The termolecular film collapses at K_2; here we have the real collapse point of the surface layer system. The termocular film is liquid, but

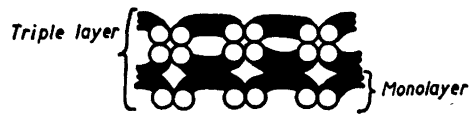


Fig. 4. Schematic arrangement of molecules in a triple layer of litocholic acid.

after the collapse at K_2, crystallization occurs, the earlier the lower the temperature.

As mentioned above, variation of the temperature between 10° and 40 °C does not effect any changes in the shape of the pressure-area curve of litocholic acid (Fig. 3). We are inclined to consider the transition from the liquid monolayer to the liquid triple layer as a transformation of the first order and have calculated the changes in molar heat content. ΔH_{tr}, in the transformation on the basis of the two-dimensional analogue of the Clausius-Clapeyron equation. The values of the equilibrium transition pressure, π_{tr}, and of the net change in monomolecular area, ΔA_{tr}, at the transformation point at different temperatures are given in Fig. 3. For the molar heat content, ΔH_{tr}, we have calculated in this way the value 1 800 cal/mole, and for the net change in the molar internal energy, ΔE_{tr}, we have found values of the order of 3 100—2 900 cal/mole.

The glycolitocholic acid monolayers behave in a similar manner as the litocholic acid monolayer. The phenomena are not, however, so distinct, primarily because the film becomes solid already before the triple layer collapses, *i. e.* when an area of 30 $Å^2$ per molecule is attained. The pressure rises but no collapse is observed to occur.

It may be mentioned that the "collapse" of the monolayers of both litocholic acids at appreciably lower surface pressures than that where the corresponding cholanic acid monolayer collapses (Figs. 1 and 2) can be ascribed to the prone arrangement of the litocholic acid molecules on the substrate surface. With this arrangement, the area of contact between the hydrocarbon parts of the molecules is only half that in a monolayer with the molecules in a vertical position. Accordingly the cohesion forces per unit area between the molecules in the monolayer must be weaker in the former case.

The results of our monolayer studies can be used to draw conclusions about the probable arrangement of bile acid ions in the micelles present in bile salt solutions. In cholanate solutions the conditions are probably such that micelles of essentially similar structure as those in the fatty acid salt solutions can be formed, *i. e.* micelles with the long anions arranged more or less parallel in double layers or in cylindrical or spheroidal aggregates in which all the hydrophilic groups face the surrounding water. In litocholate solutions a different micellar structure is more probable. In the smallest aggregates, it can be expected that the most advantageous arrangement from the energetic viewpoint is one in which 2 to 4 ions lie back to back with the hydrocarbon parts touching each other and the hydrophilic groups projecting outwards. Even larger aggregates may be assumed to be formed in a similar manner, for example, a double layer of ions with contiguous hydrocarbon parts. The size that such an aggregate can attain must however be very limited. When the aggregation proceeds further, a new arrangement must sooner or later result in which a part of the ions turn so that their hydrophilic groups approach each other, in the same way as in the termolecular films (Fig. 4). Ion-dipole interaction may play a role in keeping these anions together. A similar arrangement is possible in the micelles of the desoxycholates and cholates which have, respectively, two and three hydroxyl groups in their molecules. Our discussion thus leads to the conclusion that the association in these bile salt solutions

should result in the formation of different types of aggregates with different properties. This conclusion is to some extent confirmed by experimental findings. Our earlier investigations have revealed that the association in solutions of bile salts (desoxycholates and cholates) proceeds stepwise and that the properties of the micellar substance deviate from each other in different concentration ranges [3-4].

REFERENCES

1. Norman, A. *Arkiv Kemi* **8** (1955) 351.
2. Ekwall, P., Ekholm, R. and Norman, A. *Acta Chem. Scand.* **11** (1957) 693.
3. Ekwall, P. *Acta Acad. Aboensis, Math. Phys.* **XVII** (1951) 4.
4. Ekwall, P. *Koninkl. Vlaam. Acad. Wetenschap. van Belgie, Intern. Conference on Biochemical Problems of Lipids*, Brüssel 1953 p. 103.
5. Ekwall, P. *J. Colloid Sci. Suppl.* **1** (1954) 66.

Received December 27, 1956.

ACTA CHEMICA SCANDINAVICA 11 (1957) 710—716

The Complex between Hydroxamic Acids and Ferric Ions, and the Use of the Complex for Quantitative Determination of Hydroxamic Acids, Acylderivatives and Ferric Salts

GUNNAR AKSNES

Forsvarets forskningsinstitutt, Kjeller, Norway

The dissociation constants of the complex between ferric ions and acet- and benzhydroxamic acids have been determined in acid solution (pH = 1.4). The ratio between hydroxamic acid and ferric ions in the complex is 1:1.

When the complex is used for quantitative determination of acylderivatives the hydroxylamine, which must always be present in excess, will influence the stability of the complex.

In weakly alkaline solution the complex between iron and hydroxamic acids is probably $Fe(RCONHO)_3$. This complex can be used for quantitative determination of ferric salts.

Hydroxamic acids and ferric ions give complex compounds which absorb light in the visible region [1,2]. For the last 10 years there has been a growing interest in this reaction, because a variety of acylderivatives can be quantitatively converted into hydroxamic acids with the aid of hydroxylamine [3–6].

Hestrin [6] observed that, when using the hydroxamic acid-ferric complex method for determination of acetylcholin, the colour of the complex will fade when the pH of the solution is allowed to get below 1.2. The quantity of ferric chloride which is necessary to give complete transformation of hydroxamic acids to the complex, is very high. Hestrin therefore concluded that the dissociating tendency of the ferric-acethydroxamic acid complex must be fairly high at the pH used (1.4).

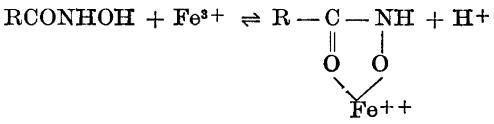
It will be shown in this work that the complex is very stable. It is further found that the dissociating tendency of the complex observed by Hestrin is partly caused by the reduction of ferric to ferrous iron by hydroxylamine.

DETERMINATION OF THE DISSOCIATION CONSTANTS OF ACET- AND BENZHYDROXAMIC ACIDS-FERRIC COMPLEXES

In order to determine the true dissociation constants for the two complexes it was necessary to work in the absence of hydroxylamine. The hydroxamic acids (acet- and benzhydroxamic acids) were therefore synthesized separately.

The absorption curves of the two complexes at pH 1.4 are shown in Fig. 1. In Fig. 2 log ε is given as a function of the ferric ion concentration with a fixed concentration of hydroxamic acid. In Fig. 3 log ε is given as a function of the acethydroxamic acid concentration with great excess of ferric chloride (lowest ratio approx. 20). The extinction of the complex follows Beer's law over a wide range of hydroxamic acid concentrations. This enables one to determine the dissociation constants from absorption measurements.

It is commonly believed that the complex between ferric ions and hydroxamic acids in acid solution is a 1:1 complex, though this has not yet been proved:



When the hydrogen ion concentration is fixed, we therefore have:

$$K_{\text{complex}} = \frac{C_{\text{hydroxamic acid}} \times C_{\text{Fe}}^{3+}}{C_{\text{complex}}}$$

If the concentration of complex is measured in a mixture of known amounts of hydroxamic acid and ferric ions, the dissociation constant, K_{complex}, can be evaluated from the equation:

$$K_{\text{complex}} = \frac{(a-c)(b-c)}{c}$$

a = initial concentration of hydroxamic acid
b = " " " ferric ions
c = the measured complex concentration

Because the extinction of the complex follows Beer's law we have:
$C = fI$
I = log extinction (log ε)
f = proportionality factor

From this one obtains:

$$K_{\text{complex}} = \frac{(a - fI)\,(b - fI)}{fI}$$

The proportionality factor f has been evaluated by two different methods:

a) Determination of the complex extinction when a given quantity of hydroxamic acid is quantitatively transformed to the ferric-hydroxamic acid complex. This can be done by using ferric ions in great excess. Then we have:

$$C = a = fI_{\max}, \text{ hence } f = \frac{a}{I_{\max}}$$

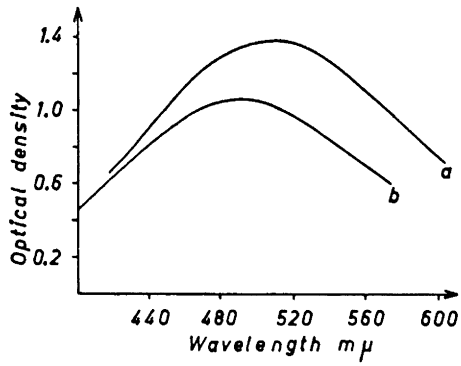


Fig. 1. (a) Absorption curves of complex between ferric ions and benzhydroxamic acid, and (b) complex between ferric ions and acethydroxamic acid. Concentration: 5 mg hydroxamic acid in 10 ml of 0.00925 M iron chloride adjusted to pH = 1.4 with hydrochloric acid.

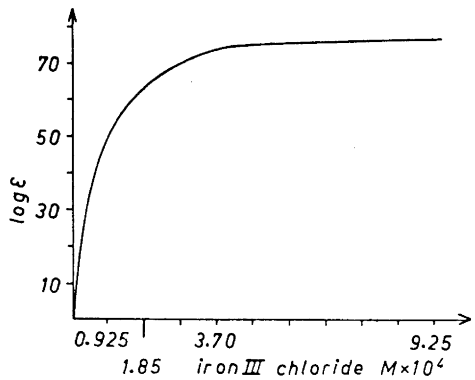


Fig. 2. Stability of ferric-acethydroxamic acid complex at constant pH (1.4). Concentration of acethydroxamic acid: 5×10^{-4} M. pH adjusted with hydrochloric acid.

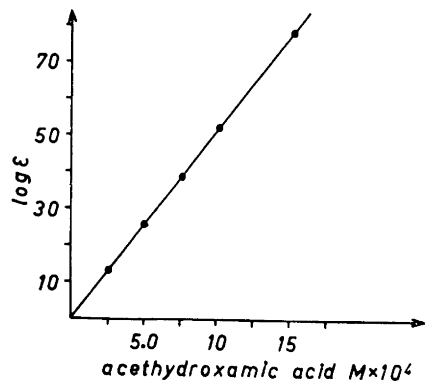


Fig. 3. log ε of ferric-acethydroxamic acid complex as function of acethydroxamic acid concentration (pH = 1.54). Concentration of ferric chloride: 0.0185 M. pH adjusted with hydrochloric acid.

b) If log ε of the complex is measured for two different sets of values for a and b, we get:

$$K_{\text{complex}} = \frac{(a_1 - fI_1)(b_1 - fI_1)}{fI_1} = \frac{(a_2 - fI_2)(b_2 - fI_2)}{fI_2}$$

f is found as the root in a second order equation.

The results are shown in Tables 1 and 2. The constancy of K_{complex} found for different values of a and b, indicates that the ratio between hydroxamic acid and ferric ions in the complex is 1:1.

Table 1. Determination of the complex constant of ferric-benzhydroxamic acid complex. Temperature: 20 °C, pH = 1.40.

$a \times 10^4$	$b \times 10^4$	I	I_{max}	$f = \frac{a}{I_{max}}$	$f_{calc.}$	$K_{complex}$
3.75	9.25	42.0	59.8	6.27×10^{-6}		2.76×10^{-4}
2.5	9.25	29.0	39.3	6.36×10^{-6}	6.20×10^{-6}	2.66×10^{-4}
1.25	9.25	15.0	19.8	6.31×10^{-6}		2.62×10^{-4}

Table 2. Determination of the complex constant of ferric-acethydroxamic acid complex. Temperature: 20 °C, pH = 1.40.

$a \times 10^4$	$b \times 10^4$	I	I_{max}	$f = \frac{a}{I_{max}}$	$f_{calc.}$	$K_{complex}$
3.75	18.5	31.4	39.5	9.49×10^{-6}		4.0×10^{-4}
1.875	18.5	16.1	20.1	9.33×10^{-6}	9.4×10^{-6}	4.2×10^{-4}
0.9375	18.5	7.9	9.9	9.45×10^{-6}		4.5×10^{-4}
3.75	9.25	23.9	39.5	9.49×10^{-6}		4.0×10^{-4}

THE INFLUENCE OF HYDROXYLAMINE ON THE STABILITY OF THE COMPLEX IN ACID SOLUTION

As mentioned in the introduction, hydroxylamine is always present in the solution when the complex is used for quantitative determination of acyl-derivatives.

The stability of the complex with and without a great excess of hydroxylamine, is shown in Fig. 4. The presence of hydroxylamine is seen to cause a rapid decrease in extinction during the first minutes; then the extinction drops more slowly. The reason for this rapid decrease in extinction is found in the ability of hydroxylamine to reduce ferric to ferrous ions according to the following equation:

$$2NH_2OH + 2Fe^{3+} \rightarrow 2Fe^{2+} + N_2O + 2H^+ + 2H_2O$$

The ferrous ions have been shown to give no complex formation with hydroxamic acids.

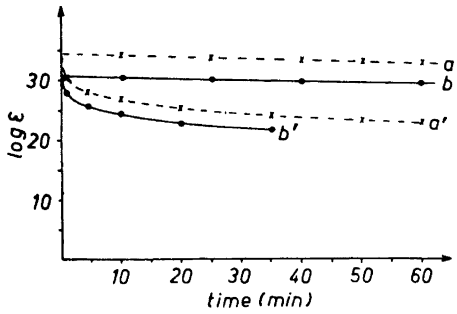


Fig. 4. Stability of ferric-hydroxamic acid complex as function of time.
a. 2.5 × 10^{-4} M benzhydroxamic acid + 1.85 × 10^{-3} M $FeCl_3$
b. 3.75 × 10^{-4} M acethydroxamic acid + 1.85 × 10^{-3} M $FeCl_3$
a'. 2.5 × 10^{-4} M benzhydroxamic acid + 1.85 × 10^{-3} M $FeCl_3$ + 0.05 M hydroxylamine
b'. 3.75 × 10^{-4} M acethydroxamic acid + 1.85 × 10^{-3} M $FeCl_3$ + 0.05 M hydroxylamine

The reaction is irreversible, but due to the formation of hydrogen ions the reaction will be greatly retarded with time in unbuffered solution (Fig. 4). The pH dependence of the reaction is shown in Fig. 5. The extinction and pH are measured 30 min after the start.

In an isolated experiment with benzhydroxamic acid and the same excess of Fe^{3+} the dissociation tendency of the complex was measured as function of pH. As seen from Fig. 5 the stability of the complex is greatly dependent on pH. The decrease in colour extinction in the presence of hydroxylamine is therefore dependent on both the reduction of the ferric concentration and the accompanying increase in hydrogen ion concentration.

Since the reduction of ferric ions by hydroxylamine will be greatly accelerated at higher pH, it is clear that when hydroxylamine is in excess, the extinction of the complex measured at fixed time intervals after mixing must show a maximum at a certain pH. On one side of the maximum (towards lower pH), the extinction of the complex will be reduced because the dissociation of the complex will increase; towards higher pH values the extinction will decrease because of rapid reduction of ferric to ferrous ions. This conclusion is clearly demonstrated in Fig. 5. The maximum is approximately pH 1.4 for both hydroxamic acids studied.

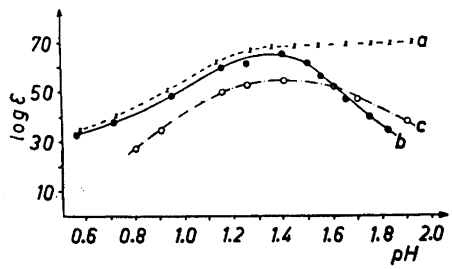


Fig. 5. pH dependence of the ferric-hydroxamic acid complex.
a. 8.41 × 10^{-3} M $FeCl_3$ + 4.57 × 10^{-4} M benzhydroxamic acid
b. 8.41 × 10^{-3} M $FeCl_3$ + 4.57 × 10^{-4} M benzhydroxamic acid + 0.182 M hydroxylamine.
c. 8.41 × 10^{-3} M $FeCl_3$ + 4.57 × 10^{-4} M acethydroxamic acid + 0.182 M hydroxylamine.
The extinction and pH were measured 30 min after start. pH was varied with hydrochloric acid.

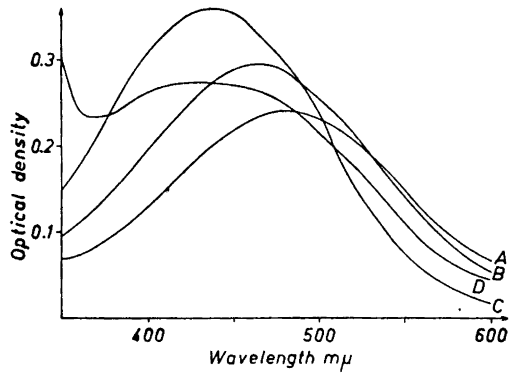


Fig. 6. Absorption curves of ferric-benzhydroxamic acid complex at different pH. A, pH = 2.59; B, pH = 3.5; C, pH = 6.8; D, pH = 10.0.

THE VARIATION OF THE STRUCTURE OF THE FERRIC-HYDROXAMIC ACID COMPLEX WITH pH, AND THE USE OF THE COMPLEX IN ALKALINE SOLUTION FOR QUANTITATIVE DETERMINATION OF FERRIC IRON

It was of interest to study the absorption spectrum of the complex as a function of pH. Because the experiments were performed in both acid and alkaline solution, the hydroxamic acid was here used in great excess to avoid formation of ferric hydroxide.

From the absorption curves at different pH (Fig. 6) it is seen that there is a successive shift of the absorption maximum towards shorter wave length with increasing pH. At the same time the extinction of the complex increases although the iron and hydroxamic acid concentrations are kept constant. A new maximum seems to be formed at 440 mμ in neutral or weakly alkaline solution. At very high pH values this maximum disappears.

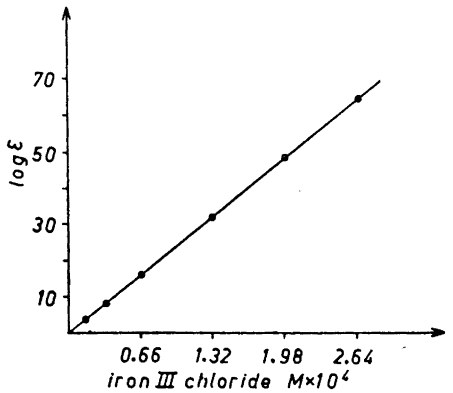


Fig. 7. Determination of ferric iron with acethydroxamic acid in alkaline solution. Concentration of acethydroxamic acid = 1.8×10^{-2} M. pH = 9.2 (*cf.* exptl. section).

The successive increase in extinction with pH suggests that the amount of hydroxamic acid in the complex increases successively with pH. This also explains the isolation of a neutral compound from alkaline alcoholic solution with an iron content corresponding to the formula $Fe(RCONHO)_3$. A possible variation of the structure of the complex with pH is the following:

$$\underset{\text{(acid)}}{Fe(RCONHO)^{++}} \rightleftharpoons \underset{\text{(weakly acid)}}{Fe(RCONHO)_2^{+}} \rightleftharpoons \underset{\text{(neutral or weakly alkaline)}}{Fe(RCONHO)_3} \rightleftharpoons \underset{\text{(strongly alkaline)}}{Fe(RCONO)_3^{---}}$$

It was of interest to examine whether the absorption maximum, which seems to be formed in weakly alkaline solution might be used for quantitative determination of ferric iron. The experiments were performed in a sodium carbonate-hydrogen carbonate buffer with great excess of hydroxamic acid. The results are shown in Fig. 7. It is seen that Beer's law is exactly valid over a wide range of ferric ion concentrations.

EXPERIMENTAL

Reagents. All reagents used were p.a. grade. The hydroxamic acids were synthesized according to descriptions in the literature [7].

Apparatus. The absorption curves were measured in a Beckman D.U. spectrophotometer. The colorimeter readings were taken with a Beckman electrophotometer. The hydrogen ion concentrations were measured with a Beckman pH meter, model H. 2.

Isolation of $Fe(C_6H_5CONHO)_3$. To a solution of 0.5 g ferric chloride and 3 g benzhydroxamic acid in 20 ml alcohol was added a 3 % solution of sodium alcoholate. A brownish precipitate was formed. It was filtered off and washed with alcohol and ether. (Found: Fe 12.20. Calc. for $Fe(C_6H_5CONHO)_3$ (464.22): Fe 12.46).

Determination of iron in alkaline solution. Reagents: Acethydroxamic acid 2 mg/ml. Buffer: 1.0 g sodium hydrogen carbonate + 0.5 g sodium carbonate in 100 ml water. Iron(III) chloride standard: 0.0001156–0.00185 M.

5 ml acethydroxamic acid solution was mixed with 1 ml iron chloride solution, and 1 ml buffer was thereafter added. The colorimeter readings were taken with a Beckman electrophotometer, filter 525 mμ.

REFERENCES

1. Feigl, F., Anger, V. and Frehden, O. *Mikrochemie* **15** (1934) 9.
2. Davidson, D. *J. Chem. Educ.* **17** (1940) 81.
3. Lipmann, F. and Tuttle, L. C. *J. Biol. Chem.* **159** (1945) 21.
4. Hill, U. *Anal. Chem.* **19** (1947) 932.
5. Hill, U. *Ind. Eng. Chem. Anal. Ed.* **18** (1947) 317.
6. Hestrin, S. *J. Biol. Chem.* **180** (1949) 249.
7. Vanino, L. Handbuch der preparativen Chemie, Verlag Ferdinand Enke, Stuttgart 1937, p. 686.

Received January 22, 1957.

ACTA CHEMICA SCANDINAVICA 11 (1957) 717—723

Paper Ionophoresis of Aldehydes and Ketones in the Presence of Hydrogen Sulphite

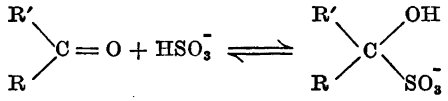
OLOF THEANDER

Organisk-kemiska Institutionen, Kungl. Tekniska Högskolan, Stockholm, and Träkemiska Avdelningen, Svenska Träforskningsinstitutet, Stockholm, Sweden

A number of aldehydes and ketones of different types have been studied by paper ionophoresis in hydrogen sulphite buffers of different concentrations and pH. The method is useful for the separation and characterisation of many carbonyl compounds.

Sugars have been studied by paper ionophoresis, generally in borate buffers [1], but electrophoretic methods for the separation of other aldehydes and ketones have not yet been developed. In a recent paper, Frahn and Mills [2] describe the ionophoretic behaviour of some sugars and glycols in aqueous solutions of borate, tungstate, vanadate, molybdate, arsenite, basic lead acetate and sodium hydroxide.

In the present publication a method is described for paper ionophoresis of aldehydes and ketones after conversion to the hydroxysulphonic acids. The ionophoresis is carried out in hydrogen sulphite buffers. The formation by aldehydes and many ketones of hydroxysulphonates, which can often be obtained in a crystalline state and are easily decomposed by alkali and acids, is well known.



(I)

The present method was worked out for fractionation and characterisation of a number of carbonyl compounds obtained from the oxidation of methyl glucosides [3]. Some other carbohydrates, and some aromatic aldehydes and other carbonyl compounds have also been investigated by this method.

Hydroxysulphonic acids are strong acids and can be considered as completely dissociated in the buffers used. The rate of migration of a carbonyl compound in a sulphite buffer should therefore depend largely upon the migration velocity of the ion and on the equilibrium I, assuming of course that the equilibrium is set up sufficiently fast that the carbonyl compound and its

sulphite adduct move as one substance. By using a low concentration of hydrogen sulphite, it is obviously possible to decrease the migration velocity of substances which give an adduct with a high dissociation constant, so that they separate better from substances with low dissociation constants. The equilibrium constants and the velocity coefficients are dependent on the temperature.

In a sugar solution there is an equilibrium between the different forms, the α and β pyranosides and furanosides. The interconversion of these forms, which is, of course, influenced by pH, temperature and other factors, probably takes place through the intermediate formation of the open aldehyde or keto forms of the sugar. The equilibrium constants for the hydrogen sulphite adducts of different sugars have been determined by Sundman [4]. He found that in each of the groups: glucose and the disaccharides with glucose at the reducing end, the remaining hexoses and pentoses, the methylpentoses and the uronic acids, the equilibrium constants were fairly closely related to the mutarotation constants. The higher the mutarotation constant the lower the equilibrium constant. The fractionation of sugars on ion exchange columns in the hydrogen sulphite form has been studied by Samuelsson [5].

Since the completion of this work a paper by Frahn and Mills [6] has been published describing the ionophoresis of some sugars and oligosaccharides in hydrogen sulphite solution. Under the conditions used (0.4 M unbuffered hydrogen sulphite at room temperature) the equilibrium between the sugar and the adduct was only slowly established. Each sugar gave two spots with streaking between, one representing the uncharged sugar with no migration and the other, which became quite faint after prolonged runs, the hydroxysulphonate ion. The distances between these spots were roughly equal for isomeric sugars but decreased with the molecular weight. This makes it possible to determine the chain length of lower oligosaccharides.

The addition of hydrogen sulphite to carbonyl compounds other than carbohydrates has been studied very little. Smith and Nichols [7] studied the addition to methylbenzaldehydes. The analogous cyanhydrin reaction has been more thoroughly investigated [8–11].

As an index of migration for the ions of hydrogen sulphite carbonyl compounds the term M_v is suggested, where for any substance

$$M_v = \frac{\text{true distance of migration of the substance}}{\text{true distance of migration of vanillin}}$$

Vanillin is chosen as reference substance since it migrates reasonably rapidly. The phenolic group is not ionized under the standard conditions used. The movement due to electro-endosmotic flow is corrected for by using methyl-β-glucoside as a reference compound.

Table 1 shows the influence of pH on the separation and shows for comparison the migration rates in some buffers not containing hydrogen sulphite. Sundman [4] worked with pH 4.7 as standard, and this pH has also been chosen here as standard. The concentration of hydrogen sulphite ion has a flat maximum at about pH 5 (the dissociation constants are $K_1 = 1.66 \times 10^{-2}$ and $K_2 = 1.02 \times 10^{-7}$). A better separation can be obtained in some cases at

higher pH values (*e. g.* between 6-aldehydo- and 3-keto-methyl-β-glucopyranoside) or by using pH 4.7 and a lower concentration of hydrogen sulphite. (Table 2). It is interesting to note that a good separation is obtained between glucuronic acid and galacturonic acid, but that the reversed order of migration is obtained in the absence of hydrogen sulphite. A disadvantage of using a higher pH is the increasing ionization of phenolic groups (*e. g.* in vanillin and formylvanillin). Unbuffered hydrogen sulphite was also tried but was found, to be less satisfactory. Freshly made it had a pH of 3.8 at 0.1 M concentration but after a few runs the pH was below 3.0.

Table 2 shows migration rates for some substances in hydrogen sulphite buffers at pH 4.7 and varying concentrations. It is evident that the migration velocity increases with increasing concentration. In agreement with the argument above, the separation is improved by decreasing the concentration of hydrogen sulphite. This is also shown in Table 4 for some aromatic aldehydes and oxidized glucosides. A disadvantage of using an electrolyte of too low a concentration is the tendency to tail and the lack of reproducibility after the solvent has been used for a few runs.

The M_v values at room temperature for some aldehydes and ketones in the buffer chosen as standard, 0.1 M hydrogen sulphite buffered to pH 4.7, are presented in Table 3. These values are reproducible to within ± 0.02 units or less. The spots obtained were round and sharp. As the unsubstituted sugars gave more or less long streaking spots under standard conditions, due to the relatively slow equilibrium between sugar and adduct they were also run at 60 °C (Table 5). At this temperature they gave single, concentrated spots, but the M_v values were approximately the same as those obtained at room temperature. The M_v values are in good qualitative agreement with the equilibrium constants of sugar hydrogen sulphite adducts estimated by Sundman [4]. It is obvious that for characterising and separating sugars the method is a good complement to the borate electrophoresis method and to paper chromatography.

It will be noticed that methyl β-3-ketoglucoside has a higher affinity for hydrogen sulphite than methyl α-3-ketoglucoside. The M_v values for the oxidized glucosides in the series are comparable with the M_v values of aldehydo-pentacetylglucose and *n*-heptanal and the aldehydo-glucoside is more reactive than the keto glucosides. On the other hand the difference in affinity between keto-glucosides and ketoses is remarkable. The separation of oxidized glucosides is improved by using a lower concentration of hydrogen sulphite (Table 3) or a higher temperature [3].

It is interesting to compare periodate oxidized methyl-β-glucopyranoside with periodate oxidized methyl-β-xylopyranoside. The first gave two spots of approximately the same intensity, with streaking between, and M_v values of about 1.0 and 1.5, respectively. The other gave only one spot with an M_v value of about 1.6. Those spots might indicate one (M_v 1.0) and two (M_v 1.5; 1.6) carbonyl groups available, respectively, for the formation of hydrogen sulphite adducts *.

* *Added in proof:* These results are confirmed by recent investigations of periodate oxidized methyl glycosides (Smith, F. *et al. J. Am. Chem. Soc.* **79** (1957) 691, and Mester, L. and Móczár, E. *Chemistry & Industry* **1957** 761).

The expected contribution to the M_v value when a new carbonyl group is introduced can be seen by comparison between the M_v values of *cyclo*hexanone and *cyclo*hexane-1:3-dione. In the group of substituted benzaldehydes investigated there is in some cases no separation at all and in others a good separation, particularly with low concentration of hydrogen sulphite. Lapworth and Manske [8] have investigated the effect of different substituents on the addition of hydrogen cyanide to substituted benzaldehyde. For *ortho*-, *meta*-, and *para*-hydroxy and *para*methoxy substituted benzaldehydes the M_v values and the equilibrium constants of the corresponding cyanhydrins were parallel. An exception was found in the *ortho*- and *para*-hydroxybenzaldehydes at 20 °C. At 60 °C, however, the order of their M_v values was reversed. There was no appreciable improvement in the separation of the aromatic aldehydes when higher temperatures were used during the runs. The distance of migration of the aromatic aldehydes over the same potential gradient and time was 10—20 % greater at 60 °C than at room temperature.

Barker, Bourne and Theander [12] used a borate containing eluant for the carbon column chromatography of some sugars which were difficult to separate by ordinary carbon column chromatography, but showed different electrophoretic mobilities in borate buffers. The analogous use of sulphite in the eluant is obvious and a mixture of methyl-β-glucoside and methyl β-2-ketoglucoside has recently been separated by that method [3].

Table 1. The migration of some aldehydes and ketones in electrolytes of different pH (Whatman No. 3, room temperature, 14.8 V/cm, 3—5 h; the migration of galacturonic acid is taken as 1.00).

	In the presence of hydrogen sulphite				In the absence of hydrogen sulphite		
pH	4.7	6.0	7.0	9.4	4.7	6.0	7.0
Xylose	0.24	0.21	0.17	0	0	0	0
Aldehydo-penta acetylglucose	0.60	0.63	0.64	0	0	0	0
Methyl β-D-3-keto-glucopyranoside	0.62	0.65	0.67	0	0	0	0
Methyl β-D-6-aldehydo-glucopyranoside	0.65	0.78	0.81	0.24	0	0	0
Glucuronic acid	0.67	0.82	0.83	1.11	0 1.13	0 1.06	0 1.06
Galacturonic acid	1.00	1.00	1.00	1.00	1.00	1.00	1.00
2-Ketogluconic acid	0.80	0.88	0.90	1.16	1.19	1.13	1.12
4-Hydroxy-3-methoxybenz-aldehyde (Vanillin)	0.71	0.77	0.90	0.75	0	0.08	0.29
3-Aldehydo-4-hydroxy-5-methoxybenzaldehyde (Formylvanillin)	1.07	1.21	1.33	0.89	0.23	0.84	0.88

Table 2. The migration (in cm) of some aldehydes and ketones in hydrogen sulphite buffers of various molarity and pH 4.7. (Whatman No. 3, room temperature, 12 V/cm for 5 h).

Molarity	0.01	0.05	0.10	0.20
Glucose	0	0.4	0.6	1.5
Xylose	2.5	4.6	6.1	12.4
Methyl β-D-3-keto-glucopyranoside	8.2	14.4	15.1	17.0
Methyl β-D-6-aldehydo-glucopyranoside	15.5	16.0	16.4	17.4
Galacturonic acid	21.1	23.8	25.0	27.7
2,4-Dihydroxy-benzaldehyde	6.2	12.0	14.2	16.9
Vanillin	16.3	17.0	17.5	19.3
Formylvanillin	26.2	26.8	27.1	28.7

Table 3. M_v values of some aldehydes and ketones. (0.1 M hydrogen sulphite, pH 4.7, Whatman No. 3, room temperature, 13—18.5 V/cm for 3—5 h.)

	M_v
Aldehydo-pentacetylglucose	0.86
Methyl α-D-3-ketoglucopyranoside	0.50
Methyl β-D-2-ketoglucopyranoside	0.88
Methyl β-D-3-ketoglucopyranoside	0.85
Methyl β-D-6-aldehydoglucopyranoside	0.92
Glucuronic acid	0.95
Galacturonic acid	1.43
2-Ketogluconic acid	1.13
5-Ketogluconic acid	1.02
Periodate oxidized methyl-β-glucopyranoside	1.02 1.48
Periodate oxidized methyl-β-xylopyranoside	1.62
n-Heptanal	0.98
Diacetyl	0.69
Citral	1.36
Cinnamic aldehyde	1.18
*Cyclo*hexanone	1.14
*Cyclo*hexane-1:3-dione	1.78
Furfural	1.29
ω-Hydroxymethyl furfural	1.07
Benzaldehyde	1.16
o-Hydroxybenzaldehyde (Salicylaldehyde)	0.95
m-Hydroxybenzaldehyde	1.16
3,4-Dimethoxybenzaldehyde (Veratraldehyde)	1.03
3,4,5-Trimethoxybenzaldehyde	1.01
4-Hydroxy-3-methoxybenzaldehyde (**Vanillin**)	**1.00**
2-Hydroxy-3-methoxybenzaldehyde (Orthovanillin)	1.10
4-Hydroxy-3,5-dimethoxybenzaldehyde (Syringaldehyde)	0.95
2,4-Dihydroxybenzaldehyde	0.82
3,4-Dihydroxybenzaldehyde (Protocatechualdehyde)	1.00
2,6-Dihydroxy-4-methylbenzaldehyde (Atranol)	0.74
3-Aldehydo-4-hydroxy-5-methoxybenzaldehyde (Formylvanillin)	1.53

Table 4. M_v values of some aromatic aldehydes and oxidized glucosides in 0.01 M hydrogen sulphite pH 4.7. (Whatman No. 3, room temperature, 12 V/cm for 5 h)

	M_v
Atranol	0.14
2,4-Dihydroxybenzaldehyde	0.38
o-Hydroxybenzaldehyde	0.91
Syringaldehyde	0.94
Vanillin	**1.00**
Protocatechualdehyde	1.02
3,4,5-Trimethoxybenzaldehyde	1.03
Veratraldehyde	1.04
Orthovanillin	1.10
p-Hydroxybenzaldehyde	1.12
Anisaldehyde	1.14
m-Hydroxybenzaldehyde	1.28
Benzaldehyde	1.31
Formylvanillin	1.61
Methyl α-D-3-ketoglucopyranoside	0.10
Methyl β-D-2-ketoglucopyranoside	0.55
Methyl β-D-3-ketoglucopyranoside	0.49
Methyl β-D-6-aldehydoglucopyranoside	0.95

EXPERIMENTAL

The apparatus and technique of the paper ionophoresis are essentially the same as described by Foster [13]. The ionophoresis was usually run at room temperature on Whatman No. 3 paper, but in some cases the temperature was held at 60 °C with a thermostat circulating warm water through the condensing block, which supports the glass plates and paper. The compounds were located by the use of UV light, dinitrophenylhydrazine, silver nitrate-sodium ethoxide or anisidine hydrochloride. Methyl-β-glucoside used to indicate the endosmotic effect, was placed on the margins together with vanillin, the standard reference substance. The latter, which was also put on the middle of the starting line, was located under UV, the margin strips were cut out, methyl-β-glucoside was located with the silver reagent, and the main paper was treated with a suitable reagent. The potential gradient used varied between 12 and 18.5 V/cm; the time between 3 and 5 h. The substances to be investigated were generally applied as 1 % solutions to the dry paper. The paper was dipped and the potential gradient was applied about 5 min after the electrolyte had risen from both sides up to the starting line.

Electrolytes. The 0.1 M hydrogen sulphite solution at pH 4.7 used as standard electrolyte contained per litre, 9.5 g of dry sodium *pyro*sulphite, 8.8 g of sodium acetate trihydrate and acetic acid to a pH of 4.7 (about 2.3 ml). The buffers of pH 6 and 7 contained the same concentrations of hydrogen sulphite and were buffered with potassium dihydrogen phosphate (0.05 M) and sodium hydroxide, the electrolyte of pH 9.4 was 0.1 M sodium sulphite. The electrolytes of varying hydrogen sulphite concentration, 0.01 – 0.2 M, all contained the same amount of sodium acetate as the standard hydrogen sulphite electrolyte (0.1 M) and were adjusted to pH 4.7 with acetic acid. The non-sulphite buffers of pH 6 and 7, respectively, contained 0.05 M potassium hydrogen phosphate adjusted to correct pH with sodium hydroxide and the electrolyte of pH 4.7 contained 0.1 M sodium acetate adjusted to correct pH with acetic acid.

The periodate oxidation of the glucosides was carried out with 0.03 M sodium periodate at 4 °C for 20 h in darkness. The aldehydo and ketoglucosides were obtained by chromate

Table 5. M_v values of some sugars at 60 °C and dissociation constants (K) of the hydrogen sulphite adducts at 19 °C (Sundman [4]). (0.1 M hydrogen sulphite, pH 4.7, Whatman No. 3, 13–18.5 V/cm for 3 h).

	M_v	K
Xylose	0.32	0.069
Arabinose	0.36	0.041
Ribose	0.40	0.028
Lyxose	0.55	0.019
Fucose	0.08	0.200
Rhamnose	0.13	0.127
Glucose	0.05	0.587
Allose	0.08	—
Galactose	0.19	0.104
Mannose	0.22	0.066
Altrose	0.32	—
Fructose, Sorbose, Tagatose, Allulose	0.00	—

oxidation of methyl-β-glucopyranoside [14] and of the 6-tritylethers of methyl-α-glucopyranoside and methyl-β-glucopyranoside [3].

The author is indebted to W. Roos's fund for financial support and to Dr. N.Richtmyer, National Institute of Health, Bethesda, Md., U.S.A. for a specimen of altrose.

REFERENCES

1. Lederer, M. *An Introduction to Paper Electrophoresis and Related Methods*, Elsevier, Amsterdam 1955, p. 70.
2. Frahn, J. N. and Mills, J. A. *Chemistry & Industry* **1956** 578.
3. Theander, O. *In preparation.*
4. Sundman, J. Diss. Helsingfors 1949.
5. Samuelson, O. *Ion Exchange in Analytical Chemistry*, Uppsala 1952, p. 198.
6. Frahn, J. L. and Mills, J. A. *Chemistry & Industry* **1956** 1177.
7. Smith, L. E. and Nichols, J. *J. Org. Chem.* **6** (1948) 498.
8. Lapworth, A. and Manske, R. H. F. *J. Chem. Soc.* **1928** 2533.
9. Lapworth, A. and Manske, R. H. F. *J. Chem. Soc.* **1930** 1976.
10. Baker, J. W. and Hemming, M. L. *J. Chem. Soc.* **1942** 191.
11. Baker, J. W. and Hopkins, H. B. *J. Chem. Soc.* **1949** 1089.
12. Barker, S. A., Bourne, E. J. and Theander, O. *J. Chem. Soc.* **1955** 4276.
13. Foster, A. B. *Chemistry & Industry* **1952** 1050.
14. Lindberg, B. and Theander, O. *Acta Chem. Scand.* **8** (1954) 1870.

Received February 6, 1957.

ACTA CHEMICA SCANDINAVICA 11 (1957) 724—730

The Synthesis of Some Organosilicon Alcohols. III

SUNE BRYNOLF

Department of Organic Chemistry, Chemical Institute of the University, Lund, Sweden

Some of the reactions of 4-trimethylsilylbutylene-1,2-oxide were studied from a synthetic point of view. Water and ammonia were added under formation of 4-trimethylsilylbutylene-1,2-glycol and 4-trimethylsilyl-1-aminobutanol-2, respectively. The oxide reacted with ethylmagnesium bromide under formation of 1-trimethylsilyl-3-methylpentanol-3 and 1-trimethylsilylhexanol-3.

In a previous paper [1] the synthesis of 4-trimethylsilylbutylene-1,2-oxide (I) from trimethylsilylmethylmagnesium bromide and epichlorohydrin *via* 4-trimethylsilyl-1-chlorobutanol-2 was reported. In this paper some of the reactions of (I) were studied from a synthetic point of view. The addition of water with perchloric acid as a catalyst yielded 4-trimethylsilylbutylene-1, 2-glycol.

$$(CH_3)_3SiCH_2CH_2CH\text{—}CH_2 + H_2O \rightarrow (CH_3)_3SiCH_2CH_2CHOHCH_2OH$$

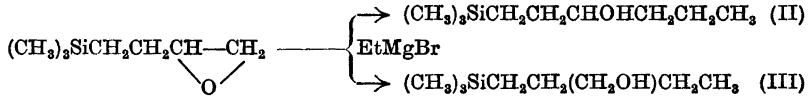
In analogy with the investigations carried out by Andersson [2] (I) reacted with ammonia under formation of only one product, 4-trimethylsilyl-1-amino-butanol-2 (A), resulting from interaction of one mole of (I) with one mole of ammonia.

$$(CH_3)_3SiCH_2CH_2CH\text{—}CH_2 + NH_3 \rightarrow (CH_3)_3SiCH_2CH_2CHOHCH_2NH_2 \text{ (A)}$$

The constitution of (A) followed from the fact that its phthalimidoderivative, 4-trimethylsilyl-1-phthalimidobutanol-2 (B), on oxidation with chromic acid in boiling acetic acid yielded a ketone whose analyses agreed with those calculated for 4-trimethylsilyl-1-phthalimidobutanone-2. (B) was partly synthesized from (A) and phthalic anhydride and partly from (I) and phthal-imide.

$$\left.\begin{array}{l}(CH_3)_3SiCH_2CH_2CHOHCH_2NH_2 \text{ (A)} + O(CO)_2C_6H_4 \\ (CH_3)_3SiCH_2CH_2CH\text{—}CH_2 \text{ (I)} + HN(CO)_2C_6H_4\end{array}\right\} \rightarrow (CH_3)_3SiCH_2CH_2CHOHCH_2N(CO)_2C_6H_4 \text{ (B)}$$

On interaction with ethylmagnesium bromide (I) reacted anomalously, inasmuch as it reacted both as a ketone and as an ethylene oxide. Theoretically four alcohols may be obtained; partly the oxide ring may be opened in two ways



and partly the oxide may react as if it had been rearranged to one or both of the isomeric oxo-compounds 4-trimethylsilylbutanone-2 and 4-trimethylsilylbutanal-1.

$$(CH_3)_3SiCH_2CH_2COCH_3 \xrightarrow{EtMgBr} (CH_3)_3SiCH_2CH_2COH(CH_3)CH_2CH_3 \quad (IV)$$

$$(CH_3)_3SiCH_2CH_2CH_2CHO \xrightarrow{EtMgBr} (CH_3)_3SiCH_2CH_2CH_2CHOHCH_2CH_3 \quad (V)$$

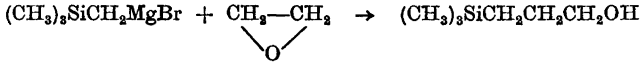
Out of the reaction mixture resulting from interaction of ethylmagnesium bromide with 4-trimethylsilylbutylene-1,2-oxide (I) two silicon-containing alcohols, (C) and (D), could be isolated. Those of their properties that were studied agreed with the corresponding properties of the alcohols (IV), 1-trimethylsilyl-3-methylpentanol-3 and (II), 1-trimethylsilylhexanol-3. (IV) was synthesized from 4-trimethylsilylbutanone-2, prepared according to Sommer and Marans [3], and ethylmagnesium bromide, and (II) from 1-trimethylsilylhexanone-3 by reduction with lithium aluminium hydride. The 1-trimethylsilylhexanone-3 was synthesized from β-trimethylsilylpropionyl chloride, prepared according to Sommer, Goldberg and Stone [4], and dipropylcadmium.

$$(CH_3)_3SiCH_2CH_2COCl + \tfrac{1}{2}(CH_3CH_2CH_2)_2Cd \rightarrow (CH_3)_3SiCH_2CH_2COCH_2CH_2CH_3$$

Besides it was shown that both (C) and (D) were non-identical with the alcohol (V), 1-trimethylsilylhexanol-4, which was obtained from 3-trimethylsilylpropylmagnesium bromide and propionaldehyde.

$$(CH_3)_3SiCH_2CH_2CH_2MgBr + OHCCH_2CH_3 \rightarrow (CH_3)_3SiCH_2CH_2CH_2CHOHCH_2CH_3 \quad (V)$$

The 3-trimethylsilylpropyl bromide was synthesized according to Sommer, Van Strien and Whitmore [5] from phosphorus tribromide and 3-trimethylsilylpropanol-1, which in its turn was prepared from trimethylsilylmethylmagnesium bromide and ethylene oxide.



It is often reported that ethylene oxides, especially the polysubstituted ones, rearrange into the isomeric ketones or aldehydes on reaction with Grignard reagents [6]. This isomerization is considered due to the presence of magnesium halide in the Grignard reagents according to the equation:

$$2RMgX \rightleftharpoons R_2Mg + MgX_2$$

In accordance with this theory no rearrangements have been observed when ethylene oxides are allowed to react with dialkylmagnesium [6]. In agreement with this the only silicon-containing alcohol (E) that could be obtained from (I) and diethylmagnesium was 1-trimethylsilylhexanol-3 (II).

In Table 1 the data of the alcohols (II), (IV), (V), (C), (D) and (E) and their 3,5-dinitrobenzoates are collected.

The diethylmagnesium was prepared from an ether solution of ethyl magnesiumbromide by precipitating magnesium bromide with dioxan and separating from the precipitate by centrifuging.

Table 1.

Alcohol	B. p. 13 mm Hg	n_D^{20}	d_4^{20}	3,5-dinitrobenzoate, M. p.
$(CH_3)_3SiCH_2CH_2CHOHCH_2CH_2CH_3$ (II)	91—92°	1.4370	0.830	82—83°
(D)	91—92°	1.4374	0.832	79—81°*
(E)	92—93°	1.4370	0.831	82—83°**
$(CH_3)_3SiCH_2CH_2COH(CH_3)CH_2CH_3$ (IV)	80—81°	1.4380	0.837	89—90°
(C)	81—82°	1.4377	0.837	88—90°***
$(CH_3)_3SiCH_2CH_2CH_2CHOHCH_2CH_3$ (V)	91—92°	1.4372	0.837	26—27°

* Mixed m.p. with (II) 81—82°.
** Mixed m.p. with (II) 82—83°.
*** Mixed m.p. with (IV) 88—90°.

EXPERIMENTAL

4-Trimethylsilylbutylene-1,2-glycol

14 g (0.10 mole) of 4-trimethylsilylbutylene-1,2-oxide (I) were shaken for one week with 1 liter of water mixed with 2 ml of 70 % perchloric acid. The resulting aqueous solution was extracted with 300 ml of ether in an extraction apparatus. The obtained ether solution was dried with anhydrous sodium sulphate and the ether removed by distillation. Fractionation at 15 mm Hg yielded 2.0 g (0.0014 mole) of unreacted 4-trimethylsilylbutylene-1,2-oxide at 53—55° and 6.6 g (0.041 mole) of 4-trimethylsilylbutylene-1,2-glycol at 130—131°; $n_D^{20} = 1.4519$; $d_4^{20} = 0.928$. (Found: C 51.1; H 11.1; Si 17.0; M_{RD} 47.1. Calc. for $C_7H_{18}O_2Si$: C 51.8; H 11.2; Si 17.3; M_{RD} 47.3.)

4-Trimethylsilyl-1-aminobutanol-2 (A)

10 g (0.069 mole) of 4-trimethylsilylbutylene-1,2-oxide (I) dissolved in 50 ml of ethanol were dropped into a stirred ice-cooled mixture of 150 ml of conc. ammonia and 200 ml of ethanol. The reaction mixture was allowed to come slowly to room temperature. After 3 days most of the ethanol was distilled off at ordinary pressure and the resulting water solution was extracted with ether. The ether solution was dried with anhydrous sodium sulphate and fractionated. 7.5 g (0.046 mole) of 4-trimethylsilyl-1-aminobutanol-2 (A) were collected at 113—114°, 13 mm Hg; $n_D^{20} = 1.4589$; $d_4^{20} = 0.898$. After some days the aminoalcohol (A) solidified to crystals melting at 31—33°. (Found: C 52.1; H 12.0; Si 17.4; M_{RD} 49.1. Calc. for $C_7H_{19}ONSi$: C 52.1; H 11.9; Si 17.4; M_{RD} 49.2.)

The distillation residue yielded after crystallization four times from petroleum ether (b. p. 40—60°) 1.9 g of crystals melting at 89.5—92.5°, probably consisting of di-(4-trimethylsilyl-2-hydroxibutyl-1)amine, $[(CH_3)_3SiCH_2CH_2CHOHCH_2]_2NH$. (Found: C 53.9; H 11.4; Si 18.3. Calc. for $C_{14}H_{35}O_2NSi$: C 55.0; H 11.5; Si 18.4.)

4-Trimethylsilyl-1-phthalimidobutanol-2 (B) from (A)

1.5 g (0.0093 mole) of (A) and 1.4 g (0.0093 mole) of phthalic anhydride were mixed with 5 ml of water. After removing of the water by warming on a water bath, the residue was distilled at 1.5 mm Hg. The main part distilled at about 205°. The distillate yielded after crystallization once from ligroin (b. p. 80—100°) 1.6 g (0.0059 mole) of 4-trimethylsilyl-1-phthalimidobutanol-2 (B). M. p. 85.5—87°. (Found: C 61.8; H 7.2; Si 9.6. Calc. for $C_{15}H_{21}O_3NSi$: C 61.8; H 7.2; Si 9.6.)

4-Trimethylsilyl-1-phthalimidobutanol-2 (B) from 4-trimethylsilylbutylene-1,2-oxide (I) and phthalimide

10 g (0.07 mole) of 4-trimethylsilylbutylene-1,2-oxide (I) and 10 g (0.07 mole) of phthalimide were warmed for 18 h in a sealed tube at 190°. The resulting reaction product was crystallized twice from ligroin (b. p. 80—100°) and yielded 10 g (0.035 mole) of (B). M. p. 86.5—87.5°. Mixed m. p. with the product prepared from 4-trimethylsilyl-1-aminobutanol-2 (A) 86—87.5°.

4-Trimethylsilyl-1-phthalimidobutanone-2 from (B)

4.0 g (0.014 mole) of 4-trimethylsilyl-1-phthalimidobutanol-2 (B) were dissolved in 20 ml of acetic acid and warmed on a boiling water bath. A solution of 1.2 g (0.012 mole) of chromium trioxide in 5 ml of water was slowly dropped into the acetic acid solution. When all the chromic acid had been added and the solution had become brightly green, the reaction mixture was diluted with 100 ml of water. After cooling in ice the crystals were filtered off and recrystallized from ethanol. 2.8 g (0.0097 mole) of 4-trimethylsilyl-1-phthalimidobutanone-2 were obtained. M. p. 92—92.5°. (Found: C 62.3; H 6.6; Si 9.7. Calc. for $C_{15}H_{19}O_3NSi$: C 62.2; H 6.6; Si 9.7.)

2,4-Dinitrophenylhydrazone. 1.0 g (0.0035 mole) of 4-trimethylsilyl-1-phthalimidobutanone-2 was boiled for one minute with a solution of 0.7 g (0.0035 mole) of 2,4-dinitrophenylhydrazine in 15 ml of ethanol and 2 ml of conc. hydrochloric acid. After cooling the formed crystals were filtered off and crystallized twice from ethanol. 1.1 g (0.0021 mole) of the 2,4-dinitrophenylhydrazone of 4-trimethylsilyl-1-phthalimidobutanone-2 were obtained. M. p. 208.5—210°. (Found: C 53.3; H 4.9; Si 6.0. Calc. for $C_{21}H_{23}O_6N_3Si$: C 53.6; H 4.9; Si 6.0.)

Reaction of 4-trimethylsilylbutylene-1,2-oxide (I) with ethylmagnesium bromide

10 g (0.07 mole) of 4-trimethylsilylbutylene-1,2-oxide in 50 ml of abs. ether were dropped into the stirred and ice-cooled Grignard reagent prepared from 21 g (0.2 mole) of ethyl bromide, 4.9 g (0.2 mole) of magnesium and 100 ml of abs. ether. When all had been added the ice-bath was removed, and when the solution had come to room temperature it was refluxed for 20 h. The reaction mixture was hydrolyzed with water and the basic salts were dissolved in dilute hydrochloric acid. The ether layer was separated and the water layer extracted with ether. The combined ether solutions were washed with some water and refluxed for 3 h with 8 g (0.2 mole) of pulverized sodium hydroxide in order to remove the formed chloro- and bromohydrines of 4-trimethylsilylbutylene-1,2-oxide. (In a previous experiment it proved difficult to separate these from the formed silicon-containing alcohols by distillation.) The excess of sodium hydroxide and the formed sodium halides were filtered off and washed with ether. After removal of the ether by distillation at ordinary pressure, fractionation at 13 mm Hg yielded 1.8 g (0.013 mole) of 4-trimethylsilylbutylene-1,2-oxide at 48—49°, 2.8 g (0.016 mole) of 1-trimethylsilyl-3-methylpentanol-3 (C) at 81—82° and 2.6 g (0.015 mole) of 1-trimethylsilylhexanol-3 (D) at 91—92°. Data for (C): $n_D^{20} = 1.4377$; $d_4^{20} = 0.837$. (Found: C 61.5; H 12.6; Si 16.1; M_{RD} 54.6.) Data for (D): $n_D^{20} = 1.4374$; $d_4^{20} = 0.832$. (Found: C 61.8; H 12.7; Si 15.9; M_{RD} 54.9.) (Calc. for $C_9H_{22}OSi$: C 62.0; H 12.7; Si 16.1; M_{RD} 54.9.)

3,5-Dinitrobenzoate. 3,5-Dinitrobenzoate was prepared according to a method described by Cameron and coworkers [7]. 1 g of the alcohol in question was mixed with 4 ml of pyridine (dried with potassium hydroxide), whereupon 2 g of 3,5-dinitrobenzoyl chloride were added. After heating for 3 h to 100° the cooled reaction mixture was diluted with 25 ml of ether. The ether solution was washed once with 15 ml of dilute hydrochloric acid and twice with 25 ml of a 5 % sodium hydroxide solution. The ether was evaporated from the obtained ethereal solution of the 3,5-dinitrobenzoate, and the resulting crystals were washed with some dilute hydrochloric acid followed by water and crystallized two times from ethanol.

1.0 g (0.0058 mole) of (C) yielded 1.5 g (0.0039 mole) of the 3,5-dinitrobenzoate. M. p. 88—90°. (Found: C 52.0; H 6.5; Si 7.5.)

1.0 g (0.0058 mole) of (D) yielded 1.2 g (0.0031 mole) of the 3,5-dinitrobenzoate. M. p. 79—81°. (Found: C 52.0; H 6.5; Si 7.5.) (Calc. for $C_{16}H_{24}O_8N_2Si$: C 52.2; H 6.6; Si 7.6.)

Reaction of 4-trimethylsilylbutylene-1,2-oxide (I) with diethylmagnesium

200 g of dioxan in 200 ml of abs. ether were dropped into the well stirred boiling Grignard reagent prepared from 109 g (1.0 mole) of ethyl bromide, 24.3 g (1.0 mole) of magnesium and 300 ml of abs. ether. The formed precipitate was removed by centrifuging. The resulting ether solution contained 0.2 mole of diethylmagnesium. 14.4 g (0.10 mole) of 4-trimethylsilylbutylene-1,2-oxide in 50 ml of abs. ether were dropped into the stirred and ice-cooled solution of diethylmagnesium mentioned above. After all had been added the mixture was allowed to come to room temperature and was then refluxed for 20 h. After decomposition with water and dilute hydrochloric acid the ether layer was separated and the water layer carefully extracted with ether. After drying of the resulting ether solution with anhydrous sodium sulphate, the ether and dioxan were removed by distillation at ordinary pressure. Fractionation at 13 mm Hg yielded 13.7 g (0.079 mole) of 1-trimethylsilylhexanol-3 (E) at 92—93°; n_D^{20} = 1.4370; d_4^{20} 0.831. (Found: C 61.4; H 12.4; Si 16.1; M_{RD} 54.9. Calc. for $C_9H_{22}OSi$: C 62.0; H 12.7; Si 16.1; M_{RD} 54.9.)

3,5-Dinitrobenzoate. 1.0 g (0.0058 mole) of (E) yielded 1.7 g (0.0044 mole) of 3,5-dinitrobenzoate. M. p. 82.5—83°. (Found: C 51.8; H 6.5; Si 7. 5. Calc. for $C_{16}H_{24}O_8N_2Si$: C 52.2; H 6.6; Si 7.6.)

1-Trimethylsilylhexanone-3

25.6 g (0.14 mole) of cadmium chloride (dried 10 h at 110°) were added to the stirred ice-cooled Grignard solution prepared from 34 g (0.28 mole) of *n*-propyl bromide, 6.5 g (0.27 mole) of magnesium and 300 ml of abs. ether. The main part of the ether was distilled off and 300 ml of anhydrous benzene added. The rest of the ether was now distilled off, whereupon 20 g (0.12 mole) of β-trimethylsilylpropionyl chloride were quickly dropped into the stirred boiling benzene solution. The mixture was refluxed for an hour and then hydrolyzed with water followed by dilute hydrochloric acid. The organic layer was separated and the water layer extracted twice with 25 ml of benzene. After drying with anhydrous sodium sulphate the benzene was distilled off at ordinary pressure. Fractionation of the rest at 20 mm Hg yielded 14 g (0.083 mole) of 1-trimethylsilylhexanone-3 at 99—100°; n_D^{20} = 1.4303. The semicarbazone melted at 73—74°. (Sommer, Bailey, Goldberg, Buck, Bye, Evans and Whitmore [8] report n_D^{20} = 1.4294 and m. p. of the semicarbazone 72—73°.) (Found: C 62.1; H 11.7; Si 16.3. Calc. for $C_9H_{20}OSi$: C 62.7; H 11.7; Si 16.3.)

2,4-Dinitrophenylhydrazone. 1.0 g (0.0058 mole) of 1-trimethylsilylhexanone-3 was boiled for one minute with a solution of 1.1 g (0.0056 mole) of 2,4-dinitrophenyl hydrazine in 20 ml of ethanol and 2 ml of conc. hydrochloric acid. After the mixture had come to room temperature, it was cooled in ice and the obtained crystals were filtered off. Two crystallizations from ligroin (b. p. 80—100°) yielded 1.6 g (0.0045 mole) of the 2,4-dinitrophenylhydrazone of 1-trimethylsilylhexanone-3. Orange-coloured crystals melting at 96—98°. (Found: C 51.0; H 6.8; Si 7.9. Calc. for $C_{15}H_{24}O_6N_4Si$: C 51.1; H 6.9; Si 8.0.)

1-Trimethylsilylhexanol-3 (II)

8.5 g (0.049 mole) of 1-trimethylsilylhexanone-3 in 25 ml of abs. ether were dropped into the stirred mixture of 3.5 g (0.10 mole) of lithium aluminium hydride and 50 ml of abs. ether. After refluxing for two hours the reaction mixture was decomposed with water and dilute hydrochloric acid. The organic layer was separated and the water layer extracted with ether. After drying with anhydrous sodium sulphate fractionation at 13 mm Hg yielded 5.8 g (0.034 mole) of 1-trimethylsilylhexanol-3 (II) at 91—92°; $n_D^{20} = 1.4370$; $d_4^{20} = 0.830$. The alcohol gave a negative result on testing for ketone with 2,4-dinitrophenyl hydrazine according to the description above. (Found: C 61.9; H 12.6; Si 15.9; M_{RD} 54.9. Calc. for $C_9H_{22}OSi$: C 62.0; H 12.7; Si 16.1; M_{RD} 54.9.)

3,5-Dinitrobenzoate. 1.0 g (0.0058 mole) of 1-trimethylsilylhexanol-3 yielded 1.6 g (0.0042 mole) of the 3,5-dinitrobenzoate; M. p. 82—83°. (Found: C 51.9; H 6.5; Si 7.6. Calc. for $C_{16}H_{24}O_8N_2Si$: C 52.2; H 6.6; Si 7.6.)

1-Trimethylsilyl-3-methylpentanol-3 (III)

2.9 g (0.002 mole) of 4-trimethylsilylbutanone-2 in 5 ml of abs. ether were dropped into the stirred Grignard reagent prepared from 3.3 g (0.03 mole) of ethyl bromide, 0.7 g (0.03 mole) of magnesium and 10 ml of abs. ether. After having been refluxed for two hours the reaction mixture was decomposed and worked up in the usual way. Fractionation yielded 2.0 g (0.012 mole) of 1-trimethylsilyl-3-methylpentanol-3 (III); B. p. 80—81° (13 mm Hg); $n_D^{20} = 1.4380$; $d_4^{20} = 0.837$. (Found: C 61.5; H 12.6; Si 16.0; M_{RD} 54.9. Calc. for $C_9H_{22}OSi$: C 62.0; H 12.6; Si 16.1; M_{RD} 54.9.)

3,5-Dinitrobenzoate. 0.8 g (0.0046 mole) of 1-trimethylsilyl-3-methylpentanol-3 (III) yielded 1.3 g (0.0034 mole) of the 3,5-dinitrobenzoate; M. p. 89—90°. (Found: C 51.8; H 6.5; Si 7.5. Calc. for $C_{16}H_{24}O_8N_2Si$: C 52.2; H 6.6; Si 7.6.)

3-Trimethylsilylpropanol-1

88 g (2.0 moles) of ethylene oxide in 175 ml of abs. ether were dropped into the stirred and ice-cooled Grignard reagent prepared from 167 g (1.0 mole) of bromomethyltrimethylsilane, 24 g (1.0 mole) of magnesium and 300 ml of abs. ether. When all had been added the ice-cooling was removed, whereupon the reaction mixture boiled spontaneously. After the boiling had stopped the stirred mixture was refluxed for four hours and was then allowed to stand over night. The next day the reaction mixture had solidified to a gel. After decomposition with water and dilute hydrochloric acid, the ether layer was separated and the water layer extracted with ether. The combined ether solutions were washed with some water and boiled for 3 h with 40 g (1.0 mole) of finely powdered sodium hydroxide in order to remove the formed ethylene chloro- and bromohydrines. (In a previous experiment it proved difficult to separate the ethylene bromohydrine from the formed siliconcontaining alcohol by distillation.) The excess of sodium hydroxide and the formed sodium halides were filtered off and washed with ether. After removal of the ether by distillation at ordinary pressure fractionation at 27 mm Hg yielded 82 g (0.62 mole) of 3-trimethylsilylpropanol-1; B. p. 83—85°; $n_D^{20} = 1.4294$ (Sommer, Van Strien and Whitmore [5] report b. p. 83° (27 mm Hg) and $n_D^{20} = 1.4290$). (Found: Si 21.0. Calculated for $C_6H_{16}OSi$: Si 21.2.)

1-Trimethylsilylhexanol-4 (IV)

1.2 g (0.002 mole) of propionaldehyde in 5 ml of abs. ether were dropped into the stirred Grignard reagent prepared from 3.8 g (0.002 mole) of 3-trimethylsilyl-1-bromopropane, 0.5 g (0.002 mole) of magnesium and 10 ml of abs. ether. After 2 h of refluxing the reaction mixture was worked up in the usual way and yielded 1.6 g (0.0092 mole) of 1-trimethylsilylhexanol-4 (IV); B. p. 91—92° (13 mm Hg); $n_D^{20} = 1.4372$; $d_4^{20} = 0.827$. (Found: C 61.8; H 12.6; Si 16.2; M_{RD} 55.1. Calc. for $C_9H_{22}OSi$: C 62.0; H 12.6; Si 16.1; M_{RD} 54.9.)

3,5-Dinitrobenzoate. 1.0 g (0.0058 mole) of 1-trimethylsilylhexanol-4 yielded 1.0 g (0.0026 mole) of the 3,5-dinitrobenzoate; M. p. 26–27°. (Found: C 51.5; H 6.5; Si 7.5. Calc. for $C_{16}H_{24}O_6N_2Si$: C 52.2; H 6.6; Si 7.6.)

The author wishes to express his appreciation to Professor Erik Larsson for his kind interest in this work.

REFERENCES

1. Brynolf, S. *Acta Chem. Scand.* **10** (1956) 883.
2. Andersson, S. *The Reaction Between Ethylene Oxides and Ammonia.* (Diss.) Lund 1955.
3. Sommer, L. H. and Marans, M. S. *J. Am. Chem. Soc.* **72** (1950) 1935.
4. Sommer, L. H., Goldberg, G. M. and Stone Jr, L. S. *J. Am. Chem. Soc.* **76** (1954) 1609.
5. Sommer, L. H., Van Strien, R. E. and Whitmore, F. C. *J. Am. Chem. Soc.* **71** (1949) 3056.
6. Gaylord, N. G. and Becker, E. I. *Chem. Revs.* **49** (1951) 413.
7. Cameron, M. D., McElrath, E. N., Heckle, W. A., White, E. R. and Williams, C. E. *J. Org. Chem.* **19** (1954) 1214.
8. Sommer, L. H., Bailey, D. L., Goldberg, G. M., Buck, C. E., Bye, T. S., Evans, F. J. and Whitmore, F. C. *J. Am. Chem. Soc.* **76** (1954) 1617.

Received February 21, 1957.

ACTA CHEMICA SCANDINAVICA 11 (1957) 731—740

On the Solubility Product of Precipitated Iron(III) Hydroxide

GEORGE BIEDERMANN and PAUL SCHINDLER

Department of Inorganic Chemistry, Royal Institute of Technology, Stockholm 70, Sweden; Department of Chemistry, University of Bern, Switzerland

The solubility equilibrium of precipitated iron(III) hydroxide was investigated at 25 °C by determining the $[Fe^{3+}]$ and $[H^+]$ of solutions in contact with the solid phase. $[Fe^{3+}]$ and $[H^+]$ were measured using the cells

$$- \text{ CE} \mid \text{solution S} \mid \text{Pt} + \qquad \text{(A)}$$

$$- \text{ Glass electrode} \mid \text{solution S} \mid \text{CE} + \qquad \text{(B)}$$

CE denotes the half-cell

$$\mid NaClO_4\text{: 3 M} \mid NaCl\text{: 0.010 M, } NaClO_4\text{: 2.990 M} \mid AgCl, Ag$$

and solution S had the general composition

$$[Fe(III)] = B_3 \text{ M}, [Fe(II)] = B_2 \text{ M}, [H^+] = H \text{ M}, [Na^+] = (3.000 - 3B_3 - 2B_2 - H) \text{ M}, [ClO_4^-] = 3.000 \text{ M},$$

where H is the hydrogen ion concentration assuming no hydrolysis or precipitation. B_3 was varied from 0.001 to 0.100 M and h, the actual hydrogen ion concentration of the solutions measured with cell (B), ranged from 2×10^{-2} to 2×10^{-3} M.

The precipitation reaction attains a steady state after about 200 h shown by the fact that after this period no further systematic change in $[Fe^{3+}]$ and $[H^+]$ could be detected; see Fig. 1.

The data for precipitates older than 200 h could be explained by assuming the reaction

$$Fe^{3+} + 2\ H_2O \rightleftharpoons FeOOH\ (s) + 3\ H^+$$

with $\log K = -3.96 \pm 0.10$. Since in 3 M $NaClO_4$ $\log K_{H_2O} = \log [H^+] + \log (OH^-) = -14.22$ [15],

$$\log K_s = \log ([Fe^{3+}]\ [OH^-]^3) = -38.7 \pm 0.2.$$

On the basis of Hedström's measurements [9] and the data obtained in this work, the experimental conditions for obtaining supersaturated solutions have been discussed.

A number of investigations have been devoted to the determination of the solubility product of precipitated iron(III) hydroxide. Previous work is summarized in Table 1.

Table 1.

Author	t °C	pK_s	anion present	method
Jellinek and Gordon [1] (1924)	14	37.9	Cl^-	E(H_2), Fe(III) analytically
Britton [2] (1925)	18	37.7	Cl^-	E(O_2)
Elder [3] (1930)	?	35.4–37.5	Cl^-	E(gl, H_2)
Kriukow and Awsejevitsch [4] (1933)	18	36.5	SO_4^{2-}	E(gl, $Fe^{2,3}$ redox)
Bézier [5] (1945)	18	36.9–38.2	ClO_4^-	E(gl)
Evans and Pryor [6] (1949)	20	35.5	SO_4^{2-}	E(gl)
Aksel'rud and Fialkov [7] (1950)	18	37.5	SO_4^{2-}	E(Sb, Sb_2O_3), Fe(III) analytically

E(H_2): hydrogen electrode, E(O_2): oxygen electrode, E(gl): glass electrode, E($Fe^{2,3}$) : Fe^{2+} — Fe^{3+} redox electrode, E(Sb, Sb_2O_3): Sb, Sb_2O_3 electrode.

All of these authors, with the exception of Aksel'rud and Fialkov, employed the same approach; a potentiometric titration was made by adding NaOH to a solution containing Fe(III) until a considerable part of the iron was precipitated. The majority of the investigators [2,3,5,6] determined the pH of the solutions in contact with the solid phase; the solubility product was calculated by making the assumptions that all iron(III) in the solution is present as Fe^{3+} and that the precipitate has the composition $Fe(OH)_3$. Jellinek and Gordon [1] supplemented the pH measurements with the colorimetric or gravimetric determination of the total iron(III) content of the solution. Kriukow and Awsejewitsch [4] utilized both pH and redox potential measurements. Aksel'rud and Fialkov's pK_s value [7] is based on the determination of the pH and of the total iron concentration of $Fe_2(SO_4)_3$ solutions in contact with iron(III) hydroxide.

Gayer and Woontner have studied recently [8] the total solubility of FeOOH in $HClO_4$ and NaOH solutions at 25 °C. For solutions of pH>5 the data could be explained by assuming the equilibrium

$$FeOOH(s) + H_2O \rightleftharpoons Fe(OH)_3 \text{ (dissolved)}$$

with pK = 6.5. For more acidic solutions the interpretation of the solubility data proved to be difficult because of the simultaneous presence of a series of hydrolysis products. In the pH range 1 to 3 the predominant part of the dissolved iron was found to exist as $Fe(OH)_2^+$.

The wide discrepancies among the reported results show that the experimental conditions were not chosen adequately to provide a reliable value of the solubility product.

Though it has been recognised very early [1] that the rate of precipitation is slow at room temperature and that freshly precipitated iron(III) hydroxide is far from being in equilibrium, no evidence has been given in any work that equilibrium was established under the described experimental conditions.

Precipitation with OH^- often yields a basic salt of a composition depending on the anion present in the solution and the temperature. Thus it cannot be assumed *a priori* that FeOOH is formed, but a method must be found to ascertain the composition of the solid phase.

Since Fe^{3+} is an acid of considerable strength [9], calculations made from pH measurements without taking into account the hydrolysis constants cannot give a correct value of the solubility product.

It is desirable to study the solubility equilibrium in a broad range of hydrogen and iron concentrations in order to test the validity of the assumptions made in computing the solubility product. Using solutions of varying ionic strengths the evaluation of the emf measurements is very difficult, since no method is available to estimate accurately the activity factors in mixed electrolytes containing a number of ions of various charges at appreciable concentrations.

The present work was undertaken to determine the solubility product of precipitated iron hydroxide by emf measurements in the constant ionic medium $[ClO_4^-] = 3$ M. The method of investigation was rather similar to that worked out in this laboratory to study the hydrolysis equilibria of metal ions. Though the results are applicable only in this ionic medium, the general approach might be of some value also under other experimental conditions.

Symbols used in the text

b = concentration of Fe^{3+}.
B_2 = total concentration of iron(II).
B_3 = total concentration of iron(III).
E_{0A} = a constant, defined by eqn. 1.
E_{0B} = a constant, defined by eqn. 2.
E_j = $-16.7\ h$ mV = liquid junction potential.
h = actual hydrogen ion concentration in the test solution.
H = hydrogen ion concentration, assuming no hydrolysis or precipitation.
K = equilibrium constant defined by eqn. 3.
K_s = equilibrium constant defined by eqn. 6.
M = moles/liter.

METHOD

To study this solubility equilibrium a series of test solutions were prepared. The iron(III) concentration of the test solutions was varied between 0.001 and 0.1 M, and in each of these the hydrogen ion concentration was adjusted so that a visible precipitate was slowly formed. The $[H^+]$ and $[Fe^{3+}]$ of the test solutions were periodically examined by emf measurements, and these were extended until no further systematic concentration change could be detected.

All test solutions (S) investigated had the general composition

$[Fe(III)] : B_3$ M, $[Fe(II)] : B_2$ M, $[H^+] : H$ M, $[Na^+] : (3.000 - 3B_3 - 2B_2 - H)$ M, $[ClO_4^-] : 3.000$ M

where B_3 denotes the total concentration of Fe(III), B_2 that of Fe(II), and H is the hydrogen ion concentration assuming no hydrolysis and precipitation. The test solutions were prepared by mixing an Fe(III)—Fe(II) stock solution and a $NaHCO_3$ solution (both containing 3 M ClO_4^-) in such a ratio that a visible precipitate was formed within a few days. $NaHCO_3$ has been used as the base, since preliminary experiments have shown, in accordance with Hedström [9], that NaOH causes an irreversible precipitation. The hydrolysis of CO_2 could be neglected since the pH of the test solutions never exceeded 3. Moreover a strong stream of N_2 was led through the solutions; thus the CO_2 concentration was always very low.

The $[H^+]$ and $[Fe^{3+}]$ of the test solutions were determined by measuring the emfs of the cells

$$- \text{ CE} \mid \text{solution S} \mid \text{Pt} + \qquad \text{(A)}$$

and

$$- \text{ Glass electrode} \mid \text{solution S} \mid \text{CE} + \qquad \text{(B)}$$

CE denotes the half-cell

Ag, AgCl | 0.010 M NaCl, 2.990 M $NaClO_4$ | 3.000 M $NaClO_4$ |

The emfs of the cells (A) and (B) can be written at 25 °C

$$E_A = E_{0A} + 59.16 \log (b / [Fe^{2+}]) + E_j \qquad (1)$$

and

$$E_B = E_{0B} - 59.16 \log h - E_j \qquad (2)$$

where E_{0A} and E_{0B} are constants, b and h are the actual $[Fe^{3+}]$ and $[H^+]$ of the test solutions, and E_j denotes the liquid junction potential at the junction 3 M $NaClO_4$ | solution S. E_j was calculated with the equation $E_j = -16.7\ h$ mV determined previously [10]. The acidity constant of Fe^{2+} is so low [11] that in the pH range studied the $[Fe^{2+}]$ could be set equal to B_2. The activity factors of the reacting species were assumed to be constants; this is certainly a good approximation since the solutions were rather dilute in Fe(III), Fe(II) and H^+.

E_{0A} and E_{0B} were determined by measuring E_A and E_B with solutions of so high an acidity that the hydrolysis of Fe^{3+} could be neglected. Each time before a test solution was measured, E_{0A} and E_{0B} were checked. The constancy of these quantities for a long period was an indication that the cell equipment functioned satisfactorily.

A few series of measurements were made as potentiometric titrations with the technique usually employed in this laboratory in order to study the degree of supersaturation attained under these experimental conditions. B_3 and B_2 were kept constant in each series while the $[H^+]$ was decreased stepwise by the addition of $NaHCO_3$ until a solid phase became visible.

MATERIALS AND ANALYSIS

Iron (III) perchlorate solutions were made from $Fe(NO_3)_3 \cdot 9\ H_2O$ "Baker's Analyzed" by adding 72 % $HClO_4$ in excess and expelling the HNO_3 and a large part of the excess $HClO_4$ by heating with an infra-red lamp. In the stock solution containing about 1 M Fe(III) no NO_3^-, Cl^- and SO_4^{2-} could be detected.

Iron (III) was determined potentiometrically according to the method described by Berecki-Biedermann [12], the accuracy was ± 0.1 %. The $Na_2S_2O_3$ solution was standardized against twice recrystallized KIO_3.

Iron (II) perchlorate solution was prepared from a portion of the iron(III) perchlorate stock solution by electrolytic reduction. The iron(II) concentration was determined by potentiometric titration using $K_2Cr_2O_7$. The $K_2Cr_2O_7$ preparation was purified by recrystallisation and made water-free by melting at 400 °C. The same result was found within 0.1 % when this $K_2Cr_2O_7$ or the KIO_3 was used to standardize the thiosulfate solution.

The total iron concentration of the iron(II) perchlorate stock solution was determined by oxidizing Fe^{2+} with H_2O_2 solution. The excess peroxide was expelled by boiling, and in the cooled solution Fe(III) was titrated by the same method [12] as above.

The excess hydrogen ion concentration, H, of the Fe(III) and Fe(II) stock solutions was determined using the ion exchange resin "Duolite C3" in the hydrogen form. The hydrogen ion concentration of the eluate which is equal to the $[ClO_4^-]$ was determined with standard NaOH. H was calculated according to the equation

$$[ClO_4^-] = H + 3\ B_3 + 2\ B_2$$

$HClO_4$, NaOH, $NaHCO_3$, $NaClO_4$, and NaCl solutions were prepared and analyzed as described previously [13].

Nitrogen taken from a cylinder was freed of oxygen by passing it through hot activated copper. Acid and basic impurities were absorbed in NaOH and H_2SO_4 solutions, and finally the gas was led through water and 3 M $NaClO_4$ to obtain the right vapor pressure.

Experimental details of the emf measurements

E_A was measured with a recently certified Leeds and Northrup potentiometer of type K2, which could be read to 0.01 mV. E_B was determined with a valve potentiometer "Radiometer PHM3" Copenhagen. The sensitivity of this instrument is ± 0.2 mV.

Ag, AgCl electrodes were prepared as usual in this laboratory [13]. Redox potentials were measured with bright Pt-foils. When two electrodes were simultaneously employed they always agreed within 0.05 mV.

The glass electrodes were prepared by Dr. E. Blomgren, Uppsala. They came to equilibrium within 10—15 min and have given constant and reproducible potentials within ± 0.2 mV.

All measurements were carried out in a paraffin oil thermostat at 25.0 ± 0.1 °C.

SURVEY OF MEASUREMENTS

Procedure. Test solutions with the following B_3 values were studied: 1.000×10^{-3}, 5.00×10^{-3}, 1.000×10^{-2}, 2.50×10^{-2} and 1.000×10^{-1} M. B_2 was always chosen to be approximately equal to B_3. With lower values of B_3 than 1 mM no satisfactory results could be obtained; this may be explained by the slow rate of precipitation and the low redox- and pH-buffer capacity of such dilute solutions. In order to avoid complications due to the variation of the activity factors, the higher limit of B_3 was set at 0.1 M.

O_2 and CO_2 were expelled from the test solutions by passing a strong stream of N_2 through them for about half an hour. The vessels were then closed with well fitting rubber stoppers, which were coated with paraffin and finally they were placed in the thermostat.

Though Fe^{2+} is rather slowly oxidized by air in $HClO_4$ solutions, it was important to check to what extent oxidation might have occurred during the long periods of measurement (10—20 days). For this purpose a number of solutions were transferred immediately after preparation to glass bottles, made

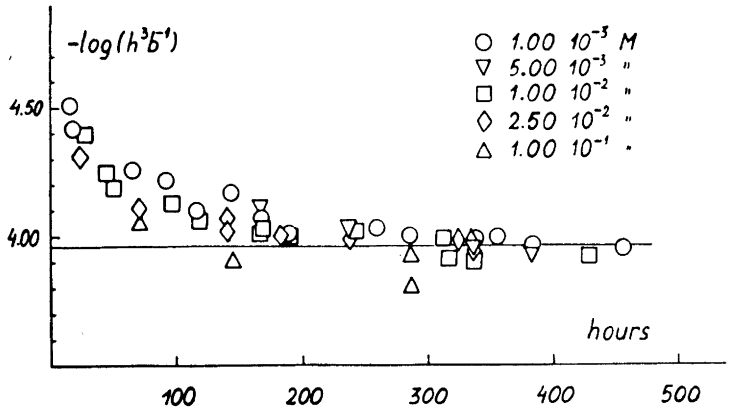


Fig. 1. Attainment of the steady state. $\log(h^3b^{-1})$ as a function of time. The horizontal line represents the solubility product $\log K = -3.96$ calculated by the plot given in Fig. 2.

free from O_2 and CO_2 by bubbling through N_2, and then the bottles were sealed and placed in the thermostat. After two weeks $\log h$ and $\log b$ were measured and found to agree within 0.01 units with the $\log h$ and $\log b$ values of solutions of the same composition, which were kept in the normal way and examined frequently. Thus no appreciable error could have been introduced by oxidation.

In the first week $\log h$ and $\log b$ varied rapidly and E_A and E_B were measured each day; later on measurements were generally made every second day.

Attainment of the steady state. The progress of the precipitation is illustrated in Fig. 1 which shows $\log(h^3b^{-1})$ as a function of the age of the test solution. The starting point of the reaction was taken when the solution was immersed in the thermostat. All test solutions were studied at least for 10 days; the majority of them were examined for a period of two weeks.

In the first 200 h the plot $\log(h^3b^{-1})^{-1}$ *versus* time is seen to give a gradually falling curve of monotonically decreasing slope; this type of time dependence indicates that the precipitation reaction is approaching to a steady state where the rate of reaction becomes negligible. This final state seems to be attained in about 200 h. As Fig. 1 shows, no further systematic variation of $\log(h^3b^{-1})$ can be detected within the limits of experimental error for test solutions older than 200 h, and all points, except one for $B_3 = 1 \times 10^{-1}$, are seen to lie in the interval —3.85 to —4.05. The uncertainty of the $\log(h^3b^{-1})$ values in the steady state may be estimated to be ± 0.05 on the basis of measurements made in solutions of the same B_3 value.

Composition of the precipitate. A chemical analysis of the precipitate could not be made, because no method was found to wash it free from the mother liquid. When the solid phase separated by centrifugation was washed with water, a colloidal solution was formed which could not be made to coagulate by centrifugation. Addition of SO_4^{2-} broke the sol very rapidly but the introduction of sulfate is of course not desirable.

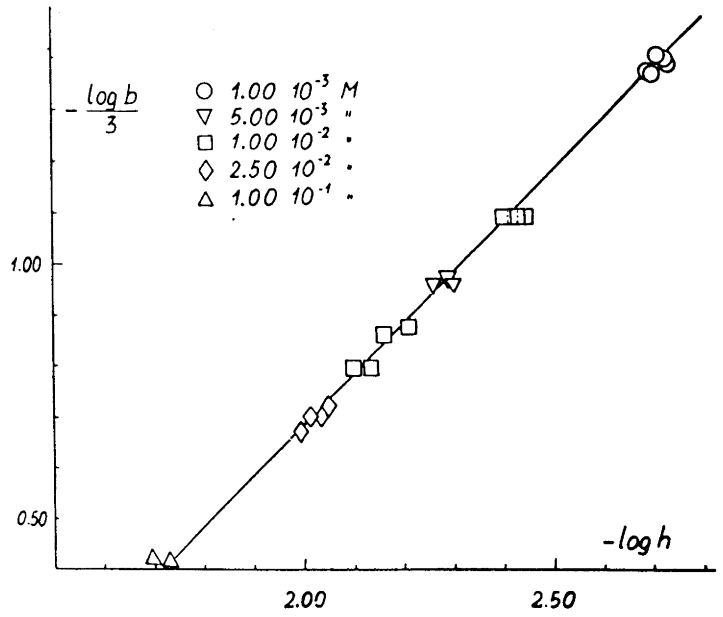


Fig. 2. Determination of log K. $\frac{\log b}{3}$ as a function of log h for test solutions older than 200 h. The line represents the equation $\frac{\log b}{3} = \log h + 1.32$.

There is, however, indirect evidence that no basic salt has been formed. Fig. 2 shows $\frac{\log b}{3}$ as a function of log h for all test solutions older than 200 h. The experimental points are seen to lie reasonably well on a straight line of unit slope. This indicates that these data may be explained by the reaction

$$Fe^{3+} + 2\ H_2O \rightleftharpoons FeOOH(s) + 3\ H^+ \quad K = h^3b^{-1} \qquad (3)$$

i. e. three hydrogen ions are set free when one Fe^{3+} is precipitated. By this type of argument it cannot be decided whether the precipitate contains OH groups ($Fe(OH)_3$), O atoms (Fe_2O_3), or both (FeOOH), because the water concentration was kept constant in all experiments. The precipitate may also contain H_2O and $NaClO_4$ but their presence cannot be ascertained because of similar reasons.

The compositions of aged precipitates formed from acidic iron(III) solutions were investigated with X-ray analyses by Weiser and Milligan [14]. They have found that, when no basic salt is formed, the solid phase always consists of FeOOH. Since there is strong evidence that no basic salt is formed from the solutions studied in this work, the precipitate has most likely the composition FeOOH. This was the reason for writing eqn. (3) in the form given.

An attempt was made to identify the fresh precipitate by X-ray diffraction using a Guinier camera with Cu$K\alpha$ radiation. All the lines in the X-ray photo-

graph could be ascribed to $NaClO_4$ except two very weak ones having 10^4 $\sin^2\Theta$ values 1 952 and 2 548. Thus by this method no definite conclusion could be made concerning the composition of the precipitate.

CALCULATION OF THE SOLUBILITY PRODUCT

Log K of eqn. (3) may be conveniently calculated by the plot $\log b^{\frac{1}{3}}$ (log h), Fig. 2. A line of unit slope was drawn through all experimental points, the intercept of which gives according to (3) $\frac{-\log K}{3}$. It was found

$$\log K = -3.96 \pm 0.10 \quad (4)$$

According to measurements made in this laboratory [15], the ionic product of water in 3 M $NaClO_4$ at 25 °C

$$\log K_{H_2O} = -14.22 \pm 0.10 \quad (5)$$

thus the solubility product expressed with OH^-, log K_s, will be

$$\log K_s = 3 \log K_{H_2O} - \log K = -38.7 \pm 0.2 \quad (6)$$

This log K_s value is considerably lower than any one reported previously; see Table 1. The discrepancy may be explained, besides other reasons, by the fact that previous work was done with quite fresh precipitates, far from being in equilibrium; see Fig. 1.

The data presented in this work give no evidence that the log K_s or the log K value calculated refers to a real equilibrium. In order to show that the steady state corresponds to a true equilibrium experiments are required which would show that the same state is attained from the reversed direction, *i. e.* by dissolving a part of the precipitate with the addition of hydrogen ions. A few experiments were made for this purpose but without success. It was found that the dissolution of the precipitate is a very slow process, and at about pH 2 no appreciable dissolution could be detected within two weeks.

Though it cannot be claimed that real equilibrium was attained in our experiments the data clearly indicate that when reaction (3) proceeds with the *formation* of the solid phase, a steady state is reached relatively rapidly which may be well described with the constant (4) or (6).

ON SUPERSATURATED SOLUTIONS

The solubility and hydrolysis equilibria of the Fe^{3+} ion are visualized in Fig. 3 where $\log(B_3/b)$ is plotted as a function of log h for the B_3 values 0.05, 0.010, 0.001 and 0.0001 M. The straight lines illustrate the solubility equilibrium (3), calculated with the constant (4) and the full-drawn curves represent the hydrolysis equilibria

$$Fe^{3+} + H_2O \rightleftharpoons FeOH^{2+} + H^+$$

$$Fe^{3+} + 2\ H_2O \rightleftharpoons Fe(OH)_2^+ + 2\ H^+$$

$$2\ Fe^{3+} + 2\ H_2O \rightleftharpoons Fe_2(OH)_2^{4+} + 2\ H^+$$

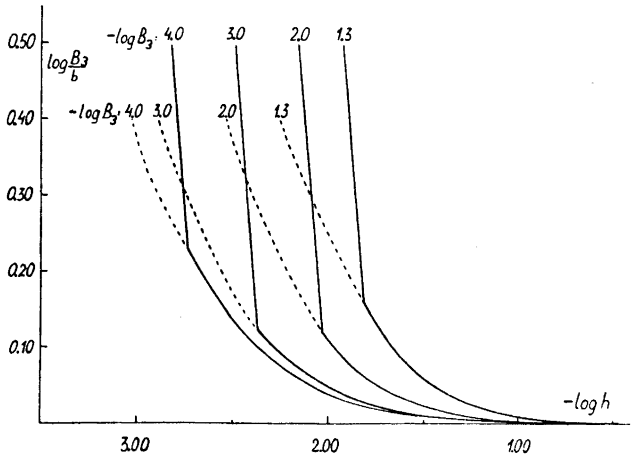


Fig. 3. The solubility and hydrolysis equilibria of the Fe^{3+} ion. $\log \frac{B_3}{b}$ as a function of $\log h$ for the $\log B_3$ values -4, -3, -2 and -1.3. The straight lines illustrate the solubility equilibrium calculated with $\log K = -3.96$; the full drawn curves represent the hydrolysis equilibria calculated with the constants given by Hedström [9]; the broken curves show Hedström's data obtained in supersaturated solutions.

calculated with the constants given by Hedström [9]. The broken curves show Hedström's experimental data obtained in supersaturated solutions with a potentiometric titration technique. He started from a practically unhydrolyzed solution and increased the pH stepwise by adding small amounts of a $NaHCO_3$ solution and a Fe^{3+} solution containing H^+ in excess. Hedström found that steady and reproducible redox and glass electrode potentials can be obtained until $\log (B_3/b)$ attains about 0.4; however above this value the potentials became unstable indicating a slow precipitation.

In order to study the conditions for obtaining supersaturated solutions a number of potentiometric titrations were made. Following carefully Hedström's technique his results could be wholly confirmed. A few series of measurements were made in a somewhat different manner. Starting from an unhydrolysed solution the pH was increased in big steps by adding each time a large amount of a $NaHCO_3$ solution and a Fe^{3+} solution containing H^+ in excess. In this case practically no supersaturation could be achieved. At the pH value where according to (4) a precipitate should be formed the potentials began to drift because of the formation of the solid phase, and no steady value was reached in one or two days.

For example when a single addition of $NaHCO_3$ solution was sufficient to cause a slight excess over the solubility product, precipitation started immediately, whereas if the same pH was attained in about ten steps no precipitation could be detected for 2—3 h.

The absence of supersaturation under these experimental conditions may be explained by the fact that, despite the vigorous agitation, a local excess of

HCO_3^- is very difficult to avoid when a relatively large amount of the base is added at once. In those regions of the solution where for a short period the pH is increased, crystal nuclei of FeOOH may be formed; when the acidity is so high that the solid phase is not stable these dissolve rapidly after the local concentration differences disappeared. In the stability region of the FeOOH (s), however, the presence of the nuclei assures that the solid phase will be formed with a high rate.

A considerable part of Hedström's measurements was made in supersaturated solutions, but this fact does not invalidate any of his conclusions concerning the hydrolysis equilibria, since under the experimental conditions chosen by him the rate of precipitation is negligible compared with that of the hydrolysis. By the study of supersaturated solutions the useful pH range could be much extended, and this has been of great help to provide a complete picture of the hydrolysis process.

This work which was carried out in the Stockholm laboratory was financially supported by *Statens Naturvetenskapliga Forskningsråd (Swedish Natural Science Research Council)* and by the *Theodor Kocher Institute*, Bern.

We are greatly indebted to Professor Walter Feitknecht and Professor Lars Gunnar Sillén for their great interest in this work and for their valuable criticism. We would like to thank to Dr. Clara Berecki-Biedermann for many valuable discussions and to Dr. Georg Johansson for his help especially in connection with the X-ray work. Mr. Frans Ericson has been of great help by making several parts of the equipment.

We are indebted to Dr. Stuart Tobias for helpful criticism of the manuscript.

REFERENCES

1. Jellinek, K. and Gordon, H. *Z. physik. Chem.* **112** (1924) 207.
2. Britton, H. T. S. *J. Chem. Soc.* **127** (1925) 2148.
3. Elder, L. W. Jr. *Trans. Electrochem. Soc.* **57** (1930) 383.
4. Kriukov, P. A. and Awsejewitsch, G. P. *Z. Elektrochem.* **39** (1933) 884.
5. Bézier, D. Thesis, University of Paris 1945.
6. Evans, U. R. and Pryor, M. J. *J. Chem. Soc.* **1949** 157.
7. Aksel'rud, N. V. and Fialkov, Ya. A. *Ukrain. Khim. Zhur.* **16** (1950) 283.
8. Gayer, K. H. and Woontner, L. *J. Phys. Chem.* **60** (1956) 1569.
9. Hedström, B. O. A. *Arkiv Kemi* **6** (1953) 1.
10. Biedermann, G. and Sillén, L. G. *Arkiv Kemi* **5** (1953) 425.
11. Hedström, B. O. A. *Arkiv Kemi* **5** (1953) 457.
12. Berecki-Biedermann, C. *To be published.*
13. Biedermann, G. *Arkiv Kemi* **9** (1956) 277.
14. Weiser, H. B. and Milligan, W. O. *J. Phys. Chem.* **39** (1935) 25.
15. Frydman, M., Ingri, N., Lagerström, G. and Sillén, L. G. *To be published.*

Received February 7, 1957.

ACTA CHEMICA SCANDINAVICA 11 (1957) 741—756

Short Communications

A New Cyclic α-Aminocarboxylic Acid in Berries of Cowberry

MAIJA-LEENA VÄHÄTALO and
ARTTURI I. VIRTANEN

Laboratory of the Foundation for Chemical Research, Biochemical Institute, Helsinki, Finland

In 1955, in a lecture on new amino acids isolated in this laboratory, one of us [1] presented a two-dimensional paper chromatogram on which also the presence of a new amino acid (No. 88 in this laboratory) was indicated: "α-Aminosäure isoliert aus Preisselbeeren; Struktur noch nicht sichergestellt". This amino acid is dealt with in the present paper.

Isolation of the amino acid 88. About 12 kg (fresh weight) of cowberries were crushed and amino acids were extracted from them with 70 % ethanol (the water content of the berries taken into account). The extract was concentrated and passed through an Amberlite IR-120 column. Amino acids were eluted from the resin with 1 N ammonium hydroxide. The eluate was evaporated to dryness *in vacuo* and the residue (very dark) dissolved in 20 ml distilled water. It was then passed through an Amberlite IR-4B column. Neutral amino acids were removed from the column by elution with water, while acidic amino acids remained in the resin. On a two-dimensional paper chromatogram (solvents: *n*-butanol--acetic acid-water (63:10:27) and phenol water-ammonia) an unknown spot appeared below alanine among neutral amino acids. On drying at 70° C the spot was yellow but soon turned orange-brown and then violet. The spot was unaffected by hydrolysis with 6 N HCl. It disappeared on deamination with nitrous oxides and was therefore apparently an α-amino acid.

The eluate was evaporated to dryness and the residue dissolved in a small volume of 1.5 N HCl. The new amino acid emerged in fractions 375—455 (of 10 ml each) together with valine and proline. The fractions were evaporated to dryness and suspended in butanol, to which cellulose powder was added. The dry powder obtained was sprinkled on the top of a cellulose powder column. The unknown amino acid was eluted by *n*-butanol from the cellulose powder column, by which treatment valine was separated. Finally the amino acid was separated from proline on a one-dimensional paper chromatogram, using phenol-NH_3 as solvent. The zone containing the amino acid 88 was cut out from the papers and the paper strips were extracted with distilled water. The residue, evaporated to dryness, was passed through an Amberlite IR-120 column. It was crystallized from hot ethanol. Almost white needle-shaped crystals were formed. The crystals were very soluble in water but not in absolute ethanol, acetone or ether.

Characteristics of the amino acid 88: R_F-values (Whatman No. 4):

	Phenol-water-NH_3	*n*-BuOH-AcOH-water
88	0.67	0.33
Alanine	0.62	0.25

Total hydrolysis (6 N HCl, 24 h, 108 °C): Spot stable, traces of homoserine (51) are formed. *Alkaline hydrolysis* (saturated $Ba(OH)_2$, 1 h, 100 °C; 10 % NaOH, 2 h, 108 °C, 5 % Na_2CO_3, 2 h, 108 °C): Stable. *Deamination* with nitrous oxide: Spot disappears (as controls: proline, γ-aminobutyric acid and 5-oxypiperidine-2-carboxylic acid which do not disappear); the acid is an α-amino acid. *Oxidation* with $KMnO_4$ in acid solution (4 % $KMnO_4$ solution, 20 %



Fig. 1. Two-dimensional paper chromatogram of amino acid 88 after reduction with HI and red P (butanol-acetic acid-water, and phenol-water-NH_3; same solvents in Fig. 2). Alanine (2) and valine (3) added. 51 = homoser, 81 = lactone of homoser, 27 = α-aminobut. acid.

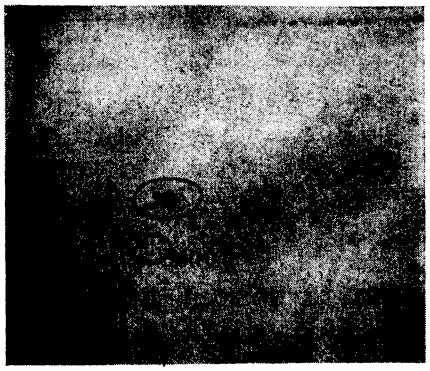


Fig. 2. Paper chromatogram of amino acid 88 after catalytic reduction. Alanine (2) and valine (3) added. 27 = α-aminobut. acid.

H_2SO_4) at +80 °C and with H_2O_2 at room temperature: No new amino acids were found on the paper chromatogram; part of the amino acids remained unoxidized. *Reduction* with HI and red P (140 °C, 1.5—4 h): Homoserine and its lactone as well as a small spot in the position for α-amino-*n*-butyric acid are formed (Fig. 1). Depending on circumstances either homoserine or the lactone of homoserine or both were formed. The reduction of pure homoserine gave a similar result as the reduction of 88. *Catalytic reduction* with PtO_2 and H_2 (Adams platinum oxide catalyst B 27, 6 h): α-NH_2-*n*-Butyric acid (27) is formed as well as faint spots in the position for alanine and in the vicinity of valine (Fig. 2). *UV spectrum:* Non-aromatic; resembling the uncharacteristic spectra of aliphatic amino acids. *Double bond:* Did not reduce alkaline $KMnO_4$ solution; no double bond. *Microtests:* The establishing of lactones as ferrihydroxamate; negative. The OH group in α-position to the amino group (Nessler); negative. The aldehyde or keto group (with 2,4-dinitrophenylhydrazine); negative. Isatin spraying (proline and its homologue); negative. Vanilline spraying; negative.

The above information on the new amino acid was obtained in the autumn of 1954 and in the winter of 1955. On the basis of the results we knew even then that the amino acid had a cyclic structure, and that homoserine or α-aminobutyric acid were formed from it on treatment with different reducing agents. The ring was very stable on hydrolysis, differing thus from the cyclic imino acid isolated from *Convallaria majalis* and *Polygonatum officinale*, respectively [2-4] (2-azetidinecarboxylic acid [3,4]). On paper chromatograms both substances also behaved differently. C, H, and N determinations of the new amino acid suggested a formula $(C_4H_{7-8}O_2N)_n$ but the molecular weight determination was lacking. At this stage the investigation was broken off because the younger author had to give up her research work for the time being and the amount (about 20 mg) of the pure amino acid isolated was used up.

In the autumn of 1956 the investigation was resumed. About 30 mg of the amino acid were isolated and the following additional information was obtained: *Microanalysis.* Found: C 47.62; H 6.89; N 13.91; O 32.59 (determ.). Calc. for $C_4H_7O_2N$: C 47.52; H 6.99; N 13.86; O 31.68. *Molecular weight* (Child's method): Values between 90 and 100 were found in different determinations; Calc. 101; n = 1. *Formation of CO_2 and NH_3* by ninhydrin (Linko's method): CO_2 is not formed, NH_3 to only about 30 % of the total N. Bromine is not taken up; no double bond. *Melting point:* Decomposes at about 234—236 °C. *Microtests:* Waser-Edlbacher (—N—CH_3); negative. Sodium nitroprusside + acet-

aldehyde . (secondary aliphatic amines); negative. α-Naphthoquinonesulphonate (secondary amino group):

	Solution A	Solution B
proline	blue	red
alanine	blue	blue
88	red	red

When at the end of February 1957 the molecular weight of the amino acid was established there were not many possibilities left for structure speculation. Then a paper was published by Burroughs [5] in which the isolation of 1-amino-*cyclo*propane-1-carboxylic acid from perry pears and cider apple was reported. The composition and characteristics of this amino acid are in complete agreement with the amino acid 88 isolated by us from cowberries. Any other structure than that presented by Burroughs cannot be given for the amino acid. Burroughs has also confirmed the structure of his amino acid by synthesis.

In August and September 1955 Mrs. Onerva Äyräpää performed isolation experiments of the amino acid 88 with ripe and unripe (on the one hand partly red and on the other hand quite green) cowberries. The amino acid was not found in unripe berries. The situation is thus the same in cowberries and in perry pears [5].

The content of the amino acid 88 in ripe cowberries is, according to paper chromatography determination, about 400 μg per 100 g fresh wt. and 3.2 mg per 100 g dry wt. or 0.4 % of ethanol soluble N.

Added in proof. Comparison of our preparation with a sample of Burrough's kindly sent by him has conclusively confirmed their identity.

1. Virtanen, A. I. *Angew. Chem.* **67** (1955) 381, Fig. 5.
2. Virtanen, A. I. and Linko, P. *Acta Chem. Scand.* **9** (1955) 551.
3. Fowden, L. *Nature* **176** (1955) 347.
4. Virtanen, A. I. *Nature* **176** (1955) 984.
5. Burroughs, L. F. *Nature* **179** (1957) 360.

Received March 23, 1957.

Paper Chromatography of Amino Acids, Sugars and Acids

GUNNAR HÖGSTRÖM

Dept. of Physiological Chemistry, Wenner Grens Institute, Stockholm, Sweden

The solvents commonly used for the paper chromatography of amino acids, namely phenol, collidine and butanol-acetic acid, popular for their good separatory powers, have several disadvantages: phenol and collidine are toxic, and the butanol-acetic acid mixture is subject to esterification with concomitant change of R_F-values. Their smell is also rather offensive. Many attempts have been made to replace them with less obnoxious solvents. In this article will be described an attempt to use methyl ethyl ketone in mixtures with acetone, water and formic acid for the separation of amino acids. These solvents have also been used successfully for sugars and acids belonging to the citric acid cycle.

Experimental: Methyl ethyl ketone of puriss and acetone of pure grade is used. No purification is necessary. The chromatography chambers are made of glass, $20 \times 30 \times 60$ cm, with glass-lids and glass-troughs supported on a glass-frame. Since the R_F-values of amino acids and sugars are very low in the solvents described here, a relatively fast paper, such as Whatman 4, has been used for these compounds, and its lower edge serrated so as to allow the solvent to drip off easily. Whatman 1 is used for the acids. The amino acids are developed by dipping the chromatogram in a 0.2 % solution of ninhydrin in acetone with 0.1 % acetic acid and a little collidine to bring out the right colours of the spots. The sugars are developed with silver nitrate or aniline hydrogen phthalate. The acids are developed by dipping in an indicator solution prepared from a 1 % solution of bromophenol blue in 95 % alcohol by neutralizing to the first tinge of red and then adding about five times its volume of petroleum ether.

In water-saturated methyl ethyl ketone alone the R_F-values of amino acids and sugars are too low to be practical. The addition of acetone makes it possible to introduce more water and increase the

aldehyde . (secondary aliphatic amines); negative. α-Naphthoquinonesulphonate (secondary amino group):

	Solution A	Solution B
proline	blue	red
alanine	blue	blue
88	red	red

When at the end of February 1957 the molecular weight of the amino acid was established there were not many possibilities left for structure speculation. Then a paper was published by Burroughs [5] in which the isolation of 1-amino-*cyclo*propane-1-carboxylic acid from perry pears and cider apple was reported. The composition and characteristics of this amino acid are in complete agreement with the amino acid 88 isolated by us from cowberries. Any other structure than that presented by Burroughs cannot be given for the amino acid. Burroughs has also confirmed the structure of his amino acid by synthesis.

In August and September 1955 Mrs. Onerva Äyräpää performed isolation experiments of the amino acid 88 with ripe and unripe (on the one hand partly red and on the other hand quite green) cowberries. The amino acid was not found in unripe berries. The situation is thus the same in cowberries and in perry pears [5].

The content of the amino acid 88 in ripe cowberries is, according to paper chromatography determination, about 400 μg per 100 g fresh wt. and 3.2 mg per 100 g dry wt. or 0.4 % of ethanol soluble N.

Added in proof. Comparison of our preparation with a sample of Burrough's kindly sent by him has conclusively confirmed their identity.

1. Virtanen, A. I. *Angew. Chem.* **67** (1955) 381, Fig. 5.
2. Virtanen, A. I. and Linko, P. *Acta Chem. Scand.* **9** (1955) 551.
3. Fowden, L. *Nature* **176** (1955) 347.
4. Virtanen, A. I. *Nature* **176** (1955) 984.
5. Burroughs, L. F. *Nature* **179** (1957) 360.

Received March 23, 1957.

Paper Chromatography of Amino Acids, Sugars and Acids

GUNNAR HÖGSTRÖM

Dept. of Physiological Chemistry, Wenner Grens Institute, Stockholm, Sweden

The solvents commonly used for the paper chromatography of amino acids, namely phenol, collidine and butanol-acetic acid, popular for their good separatory powers, have several disadvantages: phenol and collidine are toxic, and the butanol-acetic acid mixture is subject to esterification with concomitant change of R_F-values. Their smell is also rather offensive. Many attempts have been made to replace them with less obnoxious solvents. In this article will be described an attempt to use methyl ethyl ketone in mixtures with acetone, water and formic acid for the separation of amino acids. These solvents have also been used successfully for sugars and acids belonging to the citric acid cycle.

Experimental: Methyl ethyl ketone of puriss and acetone of pure grade is used. No purification is necessary. The chromatography chambers are made of glass, $20 \times 30 \times 60$ cm, with glass-lids and glass-troughs supported on a glass-frame. Since the R_F-values of amino acids and sugars are very low in the solvents described here, a relatively fast paper, such as Whatman 4, has been used for these compounds, and its lower edge serrated so as to allow the solvent to drip off easily. Whatman 1 is used for the acids. The amino acids are developed by dipping the chromatogram in a 0.2 % solution of ninhydrin in acetone with 0.1 % acetic acid and a little collidine to bring out the right colours of the spots. The sugars are developed with silver nitrate or aniline hydrogen phthalate. The acids are developed by dipping in an indicator solution prepared from a 1 % solution of bromophenol blue in 95 % alcohol by neutralizing to the first tinge of red and then adding about five times its volume of petroleum ether.

In water-saturated methyl ethyl ketone alone the R_F-values of amino acids and sugars are too low to be practical. The addition of acetone makes it possible to introduce more water and increase the

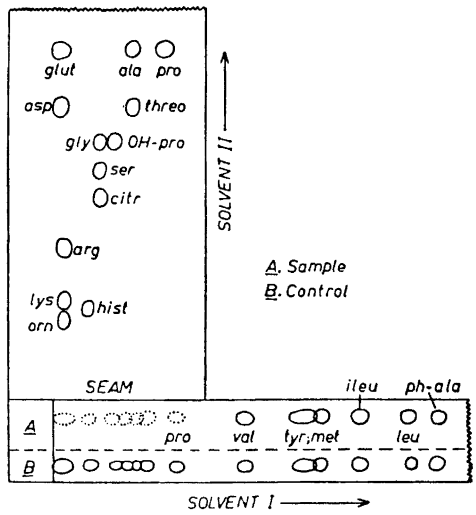


Fig. 1. Paper chromatogram of amino acids.

R_F-values. The following procedure has turned out to be useful for the amino acids:

On a 13 cm wide paper strip the unknown sample is applied on the starting-line 3 cm from one end and a mixture of the common amino acids 2 cm from the other end (Fig. 1). The chromatogram is run for about 30 h with a mixture of methyl ethyl ketone, acetone and water in the proportions 3:1:0.6 (solvent I) and dried at room temperature. A 4 cm wide strip containing the control mixture is separated from the main strip and developed with ninhydrin. The fastest amino acid, phenylalanine, will have travelled about 40 cm. The positions of proline and valine on the sample strip can be found with the aid of the control strip and the sample strip is cut between these two amino acids. The distal part is developed with ninhydrin. A new strip of paper is sewed on the undeveloped part at right angles to the direction of the first solvent and the remaining amino acids separated on this strip with solvent II — methyl ethyl ketone, acetone, water and formic acid in the proportions 3:1:1:0.1 — during 30 h. Here glutamic acid is the fastest amino acid. If the R_F-value of phenylalanine in solvent I and glutamic acid in solventII is arbitrarily designed as 1.00, the other amino acids will obtain the R_F-values collected in Table 1.

For sugars solvent I is used. Of the common sugars ribose is the fastest one and travels about 40 cm in 16 h. If its R_F-value is designed as 1.00, the other sugars will get the R_F-values collected in Table 2.

A mixture of methyl ethyl ketone, acetone, water and formic acid in the proportions 80:6:12:2 is convenient for the separation of some common acids, the R_F-values of which are found in Table 3. On Whatman 1 the front travels about 40 cm in 6 h.

Instead of solvent I a mixture with the proportions 15:3:? has sometimes been used with a little longer running time and somewhat improved separation. In this solvent tryptophan runs ahead of phenylalanine — in solvent I they coincide.

Salts in appreciable amounts have a pronounced effect on the separatory powers of these solvents, at least with respect to the amino acids. The only natural material, to which they have been applied so far, is acid-hydrolyzed *Neurospora*, and in this case this drawback has been obviated

Table 1. R_F-values of amino acids.

Solvent	I	II		I	II
Tryptophan	1.00		Hydroxyproline	0.19	0.73
Phenylalanine	1.00		Serine	0.16	0.64
Leucine	0.94		Glycine	0.14	0.73
*Iso*leucine	0.80		Histidine	0.09	0.28
Methionine	0.70		Citrulline	0.11	0.55
Tyrosine	0.67		Aspartic acid	0.04	0.74
Valine	0.48		Glutamic acid	0.04	1.00
Proline	0.28		Arginine	0.04	0.44
Alanine	0.21	1.00	Lysine	0.02	0.30
Threonine	0.21	0.82	Ornithine	0.02	0.25

Table 2. R_F-values of sugars.

Rhamnose	1.13
Ribose	1.00
Xylose	0.72
Arabinose	0.57
Fructose	0.52
Sedoheptulose	0.52
Mannose	0.50
Glucose	0.39
Mannoheptulose	0.39
Galactose	0.32
Lactose	0.09

Table 3. R_F-values of acids.

Fumaric acid	0.88
Aconitic acid	0.85
Succinic acid	0.83
Pyruvic acid	0.72
Lactic acid	0.72
α-Ketoglutaric acid	0.65
Malic acid	0.54
*Iso*citric acid	0.52
Citric acid	0.49
Glyceric acid	0.37
Tartaric acid	0.29
Oxalic acid	0.12

by using a simple desalting apparatus, illustrated in Fig. 2. The sample is applied along a line 5 cm from one end of a paper strip, 21 × 5 cm, pointed at the other end. The strip is placed between two glass sheets, 16 × 6 cm, in such a way that the pointed end is 1 cm outside the sheets. The other end is immersed in a mixture of acetone, water and ammonia in the proportions 7:3:0.4. After about 8 h all the amino acids have travelled to the pointed end of the strip, leaving most of the salts behind. The end is cut off and eluted with water. The eluate is concentrated and applied for chromatography. The application can, more conveniently, be made automatically by allowing the pointed end of the paper strip to touch the starting-line of the chromatography strip. A blast of air, directed from underneath this strip, accelerates the evaporation and prevents the spot from becoming too big.

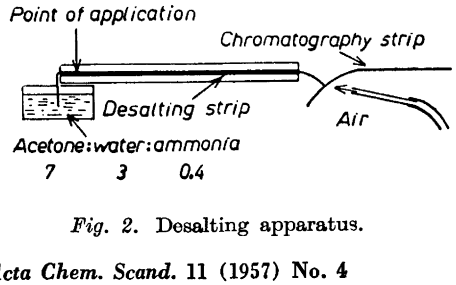


Fig. 2. Desalting apparatus.

About 20 cm has been found to be enough for the desalting strip in the case of *Neurospora*. Other materials may require greater length and time of desalting.

My thanks are due to Professor G. Ehrensvärd for much encouragement in this work.

Received April 10, 1957.

The Reflection Spectra of Anhydrous Nickel(II) Chlorides and Bromides and Their Double Salts with Monovalent Cations

R. W. ASMUSSEN and OLE BOSTRUP

Chemical Laboratory B, Technical University of Denmark, Copenhagen, Denmark

It is generally assumed that the nickel ions in anhydrous $NiCl_2$, $NiBr_2$ and their double salts $MeNiCl_3$ and $MeNiBr_3$ have the coordination number six. The magnetic properties of the double salts have previously been measured by Asmussen and Soling [1]. The reflection spectra of ten solid compounds are given in Fig. 1 and in Table 1. The excited levels corresponding to the absorption maxima agree with the ligand field theory for d^8-systems in fields of the cubic-octahedral symmetry O_h. Thus a ligand field parameter Δ (also denoted by $(E_1 - E_2)$ or 10Dq) can be found for each compound. Further the Slater-Condon-Shortley integrals F^k seem to be decreased [2] in the complexes relative to the Ni^{+2}.

Fig. 1 shows that the ten absorption spectra are remarkably similar. However, the values of Δ given in Table 1 vary within a range of 6 800 – 7 600 K. Δ decreases with increasing radius of the anion (Cl^-, Br^-) and with increasing radius of the cation (Rb^+, Cs^+, $C_5H_5NH^+$). It has previously been discussed [3] whether this behaviour can be explained by an electrostatic model. However, it is very probable that partly covalent bonding, *i. e.* intermixing of the partly filled 3d-shell with the orbitals of the ligands, occurs. The latter

Table 2. R_F-values of sugars.

Rhamnose	1.13
Ribose	1.00
Xylose	0.72
Arabinose	0.57
Fructose	0.52
Sedoheptulose	0.52
Mannose	0.50
Glucose	0.39
Mannoheptulose	0.39
Galactose	0.32
Lactose	0.09

Table 3. R_F-values of acids.

Fumaric acid	0.88
Aconitic acid	0.85
Succinic acid	0.83
Pyruvic acid	0.72
Lactic acid	0.72
α-Ketoglutaric acid	0.65
Malic acid	0.54
*Iso*citric acid	0.52
Citric acid	0.49
Glyceric acid	0.37
Tartaric acid	0.29
Oxalic acid	0.12

by using a simple desalting apparatus, illustrated in Fig. 2. The sample is applied along a line 5 cm from one end of a paper strip, 21 × 5 cm, pointed at the other end. The strip is placed between two glass sheets, 16 × 6 cm, in such a way that the pointed end is 1 cm outside the sheets. The other end is immersed in a mixture of acetone, water and ammonia in the proportions 7:3:0.4. After about 8 h all the amino acids have travelled to the pointed end of the strip, leaving most of the salts behind. The end is cut off and eluted with water. The eluate is concentrated and applied for chromatography. The application can, more conveniently, be made automatically by allowing the pointed end of the paper strip to touch the starting-line of the chromatography strip. A blast of air, directed from underneath this strip, accelerates the evaporation and prevents the spot from becoming too big.

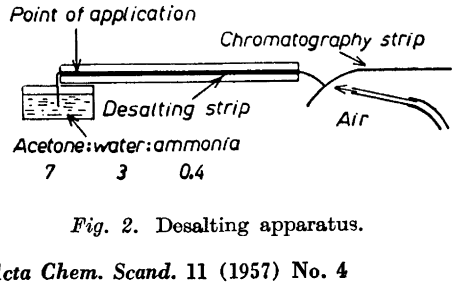


Fig. 2. Desalting apparatus.

About 20 cm has been found to be enough for the desalting strip in the case of *Neurospora*. Other materials may require greater length and time of desalting.

My thanks are due to Professor G. Ehrensvärd for much encouragement in this work.

Received April 10, 1957.

The Reflection Spectra of Anhydrous Nickel(II) Chlorides and Bromides and Their Double Salts with Monovalent Cations

R. W. ASMUSSEN and OLE BOSTRUP

Chemical Laboratory B, Technical University of Denmark, Copenhagen, Denmark

It is generally assumed that the nickel ions in anhydrous $NiCl_2$, $NiBr_2$ and their double salts $MeNiCl_3$ and $MeNiBr_3$ have the coordination number six. The magnetic properties of the double salts have previously been measured by Asmussen and Soling [1]. The reflection spectra of ten solid compounds are given in Fig. 1 and in Table 1. The excited levels corresponding to the absorption maxima agree with the ligand field theory for d^8-systems in fields of the cubic-octahedral symmetry O_h. Thus a ligand field parameter Δ (also denoted by $(E_1 - E_2)$ or 10Dq) can be found for each compound. Further the Slater-Condon-Shortley integrals F^k seem to be decreased [2] in the complexes relative to the Ni^{+2}.

Fig. 1 shows that the ten absorption spectra are remarkably similar. However, the values of Δ given in Table 1 vary within a range of 6 800 – 7 600 K. Δ decreases with increasing radius of the anion (Cl^-, Br^-) and with increasing radius of the cation (Rb^+, Cs^+, $C_5H_5NH^+$). It has previously been discussed [3] whether this behaviour can be explained by an electrostatic model. However, it is very probable that partly covalent bonding, *i. e.* intermixing of the partly filled 3d-shell with the orbitals of the ligands, occurs. The latter

Table 1. Spin-allowed bands of nickel(II) complexes and the parameters Δ and 15 B. Parentheses indicate the shoulders caused by intermixing with the singlet level $^1\Gamma_3$(D).

	$^3\Gamma_4$(F)		$^3\Gamma_4$(P)	Δ	15 B
Ni^{+2}	0		16 900	0	16 900
α-$NiCl_2$	(11 600),	12 900	22 100	7 600	11 300
β-$NiCl_2$	(11 600),	12 900	22 100	7 600	11 300
$RbNiCl_3$	(11 500),	(12 700)	21 600	7 200	11 700
$CsNiCl_3$	(11 300),	(12 500)	21 500	7 100	11 600
$C_5H_5NHNiCl_3$	11 200 ,	(12 500)	21 300	7 000	11 900
α-$NiBr_2$	(10 300),	12 100	20 700	7 300	10 900
β-$NiBr_2$	(10 300),	12 100	20 700	7 300	10 900
$RbNiBr_3$	(10 400),	11 500	20 200	7 000	11 500
$CsNiBr_3$	(10 300),	11 300	20 000	6 900	11 600
$C_5H_5NHNiBr_3$	(10 300),	11 200	19 900	6 800	11 700
$Ni(OH_2)_6^{+2}$	13 500),	(15 400)	25 300	8 500	14 100
$Nien_3^{+2}$	18 350		29 000	11 600	12 500

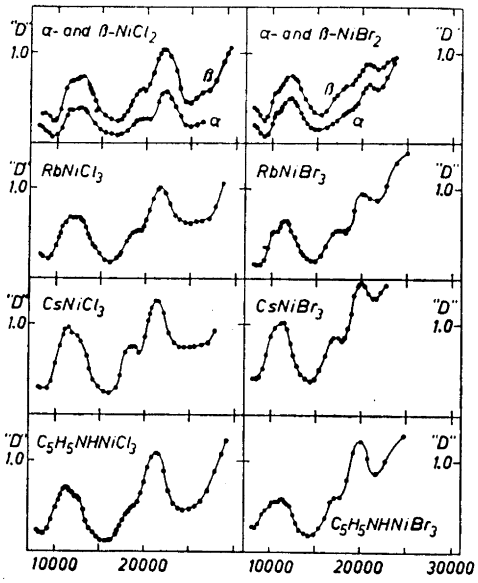


Fig. 1. Reflection spectra of nickel(II) halides measured by means of a Beckman DU spectrophotometer. (The optical density "D" is only a relative measure for the light absorbed).

possibility is supported by the fact that the values of a linear combination of F^k-integrals, *viz.* 15 B, is relatively more decreased among our examples, when Δ is large. For comparison with nickel(II) complexes with neutral ligands the values of Δ and 15 B for $Ni(OH_2)_6^{+2}$ and $Nien_3^{+2}$ are also given in Table 1. Even though the partly covalent bonding (as implied from decreased F^k-values) might seem rather important in nickel(II) halides compared with other nickel(II) complexes, it must be noted that similar or even stronger effects are observed in halide complexes of chromium(III) and rhodium(III) [2].

Further Fig. 1 shows that the wavenumbers of the absorption bands are identical for the α- and β-modifications of $NiCl_2$ and $NiBr_2$. Mr. P. Andersen [4] has demonstrated that α-$NiCl_2$ and α-$NiBr_2$ has more dis-ordered structure than the high-temperature β-forms. Generally the distribution of atoms, which are not directly coordinated to the transition group ion, has very small influence on the d^n-levels [5]. The nickel(II) halides, which do not contain monovalent cations, seem to be most tightly bound, *i. e.* Δ is large and 15 B much decreased.

Experimental. Preparation and analysis of the double halides are given elsewhere [1]. α- and β-$NiCl_2$ and α- and β-$NiBr_2$ were kindly supplied by Mr. P. Andersen [4].

1. Asmussen, R. W. and Soling, H. *Wilhelm Klemm-Festschrift Z. anorg. Chem.* **283** (1956) 3.
2. Jørgensen, C. Klixbull *Energy Levels of Complexes and Gaseous Ions.* (Thesis) Gjellerups Forlag, Copenhagen 1957.
3. Bostrup, O. and Jørgensen, C. Klixbüll *Acta Chem. Scand.* **10** (1956) 1501.
4. Andersen, P. *To be published.*
5. Bjerrum, J., Adamson, A. W. and Bostrup, O. *Acta Chem. Scand.* **10** (1956) 329.

Received April 15, 1957

Bound Homoserine in Fruits of Cowberry and Cranberry

MAIJA-LEENA VÄHÄTALO and ARTTURI I. VIRTANEN

Laboratory of the Foundation for Chemical Research, Biochemical Institute, Helsinki, Finland

The numerous new amino acids, found in recent years, generally occur as free amino acids. Only γ-hydroxyglutamic acid is found in bound form too in *Phlox* [1] and α-aminoadipic acid in proteins in maize [2]. Homoserine, which is a comparatively common free amino acid of plants and which is formed in germinating pea seeds in a surprisingly large quantity [3], has not been simultaneously found in free and bound form, whereas we have found it in bound form alone in berries and leaves of cowberry [1].

Fruits of cowberry were extracted with 70 % ethanol until no ninhydrin positive spots could be found on the paper chromatogram. The free amino acids in the ethanol extract can be seen in Fig. 1. No homoserine and hydroxyproline could be found on the chromatogram.

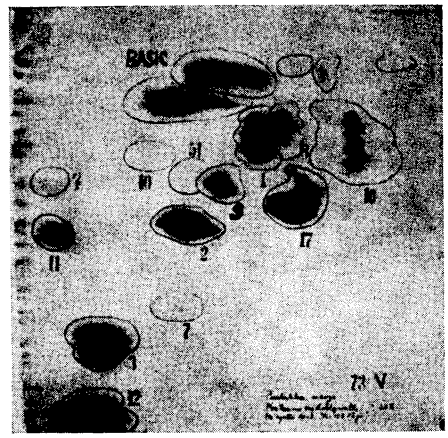


Fig. 2. Paper chromatogram of the hydrolyzed residue of 70 % ethanol extract of fruits of cowberry: 1 = gly, 10 = hydroxyproline, 51 = homoserine.

After ethanol extraction the residue of the berries was dried. 1 g of the residue was hydrolyzed with 15 ml of 6 N HCl for 24 h at 108 C°. Amino acids were separated in an Amberlite IR-120 column. Clear spots of homoserine and hydroxyproline were

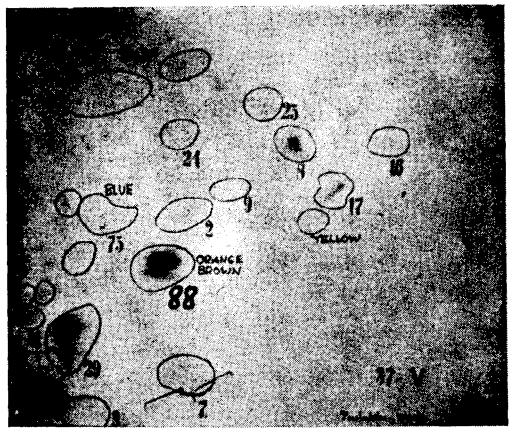


Fig. 1. Free amino acids of fruits of cowberry on a two-dimensional chromatogram (butanol-acetic acid-water, and phenol-water-NH_3; same solvents in Fig. 2). 2 = ala, 3 = val, 7 = tyr, 8 = ser, 9 = threo, 11 = pro,16 = asp, 17 = glu, 24 = glu-NH_2, 25 = asp-NH_2, 29 = γ-aminobut. acid, 60 = pipecolic acid, 75 = 5-hydroxypipecolic acid, 88 = new cyclic α-aminocarboxylic acid (1-*cyclo*propane-1-aminocarboxylic acid).

found on the paper chromatogram (Fig. 2). On the other hand *a*-aminobutyric acid (29), pipecolic acid (60), 5-hydroxypipecolic acid (75), and 1-*cyclo*propane-1-aminocarboxylic acid (88) which occur as free amino acids in the berries are not found on the paper chromatogram. Also in berries of cranberry *(Oxycoccus quadripetalus)* homoserine was found in bound form.

1. Virtanen, A. I. *Angew. Chem.* **67** (1955) 381.
2. Windsor, E. J. *J. Biol. Chem.* **192** (1951) 595.
3. Virtanen, A. I., Berg, A.-M. and Kari, S. *Acta Chem. Scand.* **7** (1953) 1423.

Received March 23, 1957.

Disubstitution of Ethyl Acetoacetate in one Step by Means of Sodium Hydride

RUNE SANDBERG

Chemical Institute, University of Uppsala, Uppsala, Sweden

Hitherto it has not been considered possible to prepare the disubstituted derivatives of acetoacetic ester in one step. For instance, Finar [1] points out that "the introduction of two alkyl groups must be carried out in two steps; it *cannot* be done in one step". However, Wallingford and Homeyer [2,3] have reported that dimetallation and disubstitution of β-ketoesters is possible with alcohol-free sodium alkoxide in alkyl carbonate solution, and Weizmann [4] was able to dialkylate acetoacetic ester by means of a complex formed between potassium hydroxide and an acetal or dialkyleter of ethylene glycol.

The present writer has found that ethyl β-acetotricarballylate can be prepared in good yields from ethyl acetoacetate and ethyl bromoacetate, using sodium hydride as metallating agent in benzene solution.

It is the author's intention to further investigate the extent to which this method is applicable.

Experimental: The apparatus used was a three-necked flask, fitted with a dropping funnel, a sealed Hersberg stirrer and a condenser, the top of which had connections to a source of nitrogen and a vacuum line. The apparatus was evacuated, flame-dried and filled with nitrogen. With nitrogen flowing, the dropping funnel was closed and removed, and sodium hydride (28.8 g, 1.2 mole) rapidly placed in the flask and covered with benzene (700 ml). The funnel was then replaced, the flow of nitrogen stopped and the funnel filled with a solution of freshly distilled ethyl acetoacetate (65 g, 0.5 mole) in dry benzene (150 ml) and then stoppered with a calcium chloride tube. With stirring, this solution was added during 30 min and the reaction mixture then stirred until the evolution of hydrogen had stopped. The apparatus was now swept with nitrogen, before a solution of freshly distilled ethyl bromoacetate (200 g, 1.2 mole) in dry benzene (75 ml) was placed in the dropping funnel. This solution was added with vigorous stirring during two hours, the flask being gently heated to maintain a slight reflux (the reaction is exothermic). When the addition was finished, the reaction mixture was stirred and refluxed for another 45 min.

After cooling, the reaction mixture was washed three times with water, the water washings extracted once with ether and the combined benzene and ether solutions dried over anhydrous magnesium sulphate. The solvents were removed and the residual oil fractionated, yielding 116.5 g (77 %) of β-acetotricarballylate, b. p. 142°—47°/1.0—1.2 mm. Phenylhydrazone m. p. 99°—100.5°. Emery [5] reports 190°/16 mm and 100°—101°, respectively.

The author wants to express his thanks to Professor Arne Fredga for his interest in this work.

1. Finar, I. L. *Organic Chemistry*, 2nd Ed., 1956, vol. I, p. 189.
2. Wallingford, V. H. and Homeyer, A. H. **U.S. 2, 391, 530;** *Chem. Abstr.* **40** (1946) 3770 [9].
3. Wallingford, V. H. and Homeyer, A. H. **U.S. 2, 438, 241;** *Chem. Abstr.* **42** (1948) 4606 d.
4. Weizmann, C. **Brit. 582, 191;** *Chem. Abstr.* **41** (1947) 2436a.
5. Emery, O. *Ber.* **23** (1890) 3755.

Received April 16, 1957.

found on the paper chromatogram (Fig. 2). On the other hand *a*-aminobutyric acid (29), pipecolic acid (60), 5-hydroxypipecolic acid (75), and 1-*cyclo*propane-1-aminocarboxylic acid (88) which occur as free amino acids in the berries are not found on the paper chromatogram. Also in berries of cranberry *(Oxycoccus quadripetalus)* homoserine was found in bound form.

1. Virtanen, A. I. *Angew. Chem.* **67** (1955) 381.
2. Windsor, E. J. *J. Biol. Chem.* **192** (1951) 595.
3. Virtanen, A. I., Berg, A.-M. and Kari, S. *Acta Chem. Scand.* **7** (1953) 1423.

Received March 23, 1957.

Disubstitution of Ethyl Acetoacetate in one Step by Means of Sodium Hydride

RUNE SANDBERG

Chemical Institute, University of Uppsala, Uppsala, Sweden

Hitherto it has not been considered possible to prepare the disubstituted derivatives of acetoacetic ester in one step. For instance, Finar [1] points out that "the introduction of two alkyl groups must be carried out in two steps; it *cannot* be done in one step". However, Wallingford and Homeyer [2,3] have reported that dimetallation and disubstitution of β-ketoesters is possible with alcohol-free sodium alkoxide in alkyl carbonate solution, and Weizmann [4] was able to dialkylate acetoacetic ester by means of a complex formed between potassium hydroxide and an acetal or dialkyleter of ethylene glycol.

The present writer has found that ethyl β-acetotricarballylate can be prepared in good yields from ethyl acetoacetate and ethyl bromoacetate, using sodium hydride as metallating agent in benzene solution.

It is the author's intention to further investigate the extent to which this method is applicable.

Experimental: The apparatus used was a three-necked flask, fitted with a dropping funnel, a sealed Hersberg stirrer and a condenser, the top of which had connections to a source of nitrogen and a vacuum line. The apparatus was evacuated, flame-dried and filled with nitrogen. With nitrogen flowing, the dropping funnel was closed and removed, and sodium hydride (28.8 g, 1.2 mole) rapidly placed in the flask and covered with benzene (700 ml). The funnel was then replaced, the flow of nitrogen stopped and the funnel filled with a solution of freshly distilled ethyl acetoacetate (65 g, 0.5 mole) in dry benzene (150 ml) and then stoppered with a calcium chloride tube. With stirring, this solution was added during 30 min and the reaction mixture then stirred until the evolution of hydrogen had stopped. The apparatus was now swept with nitrogen, before a solution of freshly distilled ethyl bromoacetate (200 g, 1.2 mole) in dry benzene (75 ml) was placed in the dropping funnel. This solution was added with vigorous stirring during two hours, the flask being gently heated to maintain a slight reflux (the reaction is exothermic). When the addition was finished, the reaction mixture was stirred and refluxed for another 45 min.

After cooling, the reaction mixture was washed three times with water, the water washings extracted once with ether and the combined benzene and ether solutions dried over anhydrous magnesium sulphate. The solvents were removed and the residual oil fractionated, yielding 116.5 g (77 %) of β-acetotricarballylate, b. p. 142°—47°/1.0—1.2 mm. Phenylhydrazone m. p. 99°—100.5°. Emery [5] reports 190°/16 mm and 100°—101°, respectively.

The author wants to express his thanks to Professor Arne Fredga for his interest in this work.

1. Finar, I. L. *Organic Chemistry*, 2nd Ed., 1956, vol. I, p. 189.
2. Wallingford, V. H. and Homeyer, A. H. **U.S. 2, 391, 530;** *Chem. Abstr.* **40** (1946) 3770 [9].
3. Wallingford, V. H. and Homeyer, A. H. **U.S. 2, 438, 241;** *Chem. Abstr.* **42** (1948) 4606 d.
4. Weizmann, C. **Brit. 582, 191;** *Chem. Abstr.* **41** (1947) 2436a.
5. Emery, O. *Ber.* **23** (1890) 3755.

Received April 16, 1957.

Studies of the Phospholipids of Human Bile and Small Intestinal Content

BENGT BORGSTRÖM

Department of Physiological Chemistry, University of Lund, Lund, Sweden

It has been demonstrated that lecithin is the only phospholipid present in human bile [1,2] and it is generally assumed that the bile lecithin is of importance for the digestion and absorption of fat from the small intestine.

Information as to the fate of the bile lecithin in the lumen of the small intestine during digestion is, however, incomplete, although different lecithin splitting enzymes have been demonstrated in pancreatic extracts and juice [3-5].

From preliminary studies with paper chromatography of small intestinal content collected from human beings by intubation, it appeared that most of the phospholipids present therein was in the form of lysolecithin. The studies were then extended and resulted in the isolation from human small intestinal content of β-palmitoyl-lysolecithin.

Ten ml of intestinal content collected from the upper jejunum of a normal adult human after a test meal free of phospholipids were mixed with 190 ml chloroform: methanol 2:1. After filtration the volumes were adjusted to 200 ml. Determination of total phosphorus [6] indicated a total of 2.40 mg P. The chloroform:methanol extract was mixed with 80 ml 0.9 % saline solution in a separatory funnel and the lower phase containing the lipid P (2.0 mg) passed through a 5 g column of silicic acid [7]. Three fractions were eluted: (I): chloroform, (II): chloroform with 30 volume % of 95 % ethanol, and (III): methanol.

(I) was free of phosphorus and contained neutral fat and free fatty acids [7]. (II) contained less than 5 μg phosphorus and (III) 1 960 μg phosphorus. In model experiment fraction II contains added lecithin and (III) added lysolecithin [8]. The phosphorus containing compound in fraction (III) from the intestinal content was identical with β-palmitoyl-lysolecithin prepared from egg lecithin by the action of *Crotalus adamanteus* venom [12] as indicated by paper chromatography [8,9], ester bond [10] to P ratio and hemolytic activity [11].

Similar results were obtained on several different samples of intestinal content, the percentage lysolecithin ranging from 62 to 100 of the total lipid phosphorus content.

After saponification the fatty acid of the isolated lysolecithin was identified as palmitic acid by chromatography on paper impregnated with liquid paraffin using 85 % acetic acid as the moving phase.

The fatty acid in the α-position of lecithin isolated from human bile was split off using lecithinase A from *Crotalus adamanteus* [12] and subsequently identified as oleic acid by chromatography directly and after hydrogenation.

The lecithin of human bile therefore is α-palmitoyl-β-oleyllecithin, thus conforming with other isolated lecithins in having an unsaturated fatty acid in the α-position and a saturated fatty acid in the β-position [13].

The occurrence of the highly surface-active lysolecithin in intestinal content has to be considered in connection with problems related to the digestion and absorption of fat.

1. Isaksson, B. *Acta Soc. Med. Upsaliensis* **56** (1951) 177.
2. Polonovski, M. and Bourrillon, R. *Bull. soc. chim. biol.* **34** (1952) 712.
3. Zeller, E. A., in Sumner, J. B. and Myrbäck, K. *The Enzymes* New York 1950, Vol. 1, Part 2.
4. Shapiro, B. *Nature* **169** (1952) 29.
5. Le Breton, E. and Pantaleon, J. *Arch. sci. physiol.* **1** (1947) 63.
6. Brante, G. *Acta Physiol. Scand. Suppl.* **63** (1949).
7. Borgström, B. *Acta Physiol. Scand.* **25** (1952) 101.
8. Lea, C. H., Rhodes, D. N. and Stoll, R. D. *Biochem. J.* **60** (1955) 353.
9. Rouser, G., Marinetti, G. V., Witter, R. F., Berry, J. F. and Stotz, E. *J. Biol. Chem.* **223** (1955) 193.
10. Rapport, M. M. and Alonzo, N. *J. Biol. Chem.* **217** (1955) 193.
11. Collier, H. B. *J. Gen. Physiol.* **35** (1952) 617.
12. Hanahan, D. J., Rodbell, M. and Turner, L. D. *J. Biol. Chem.* **206** (1954) 431.
13. Hanahan, D. J. *J. Biol. Chem.* **211** (1954) 313.

Received April 12, 1957.

The Enzymatic Hydrolysis of the β-Methyl Derivatives of Acetylcholine and Acetylthiocholine

KLAS-BERTIL AUGUSTINSSON and TORHILD ISACSHEN

Institute of Organic Chemistry and Biochemistry, University, Stockholm, Sweden

Since the observation made in 1938 by Glick [1] that horse serum splits only the D-isomer of acetyl-β-methylcholine, the only report on this subject has recently been published by Hoskin and Trick [2]. The latter authors, using rat brain homogenate, showed that the brain acetylcholinesterase also exhibits stereospecificity, the D-isomer only of the substrate used by Glick being split. Similar observations have been made in this laboratory with other enzyme preparations and other substrates. The results obtained will be briefly reported in the following.

The enzyme activity was measured with the Warburg technique and, in addition to acetyl-β-methylcholine, a series of thiocholine esters (as iodides) were used as substrates. Purified enzyme preparations of the electric organ of *Torpedo marmorata* and human blood plasma were employed; in addition, the esterase activity of cobra venom was similarly tested. The initial substrate concentration was 6.12 μmoles in a total reaction mixture of 2.40 ml. After complete hydrolysis of the substrate, the same amount of substrate was added to the reaction mixture from a second side bulb of the flask, and the hydrolysis reaction followed up to renewed completeness.

The results obtained with the electric tissue acetylcholinesterase (I) and human plasma cholinesterase (II) are recorded in Fig. 1. The experiments carried out with the cobra venom enzyme gave results which were identical with those obtained with the electric tissue enzyme. The enzymatic hydrolysis of a racemic mixture of acetyl-β-methylcholine (MeCh) came to completion when exactly 50 % of the amount of added substrate (6.12 μmoles) was hydrolysed. When a second portion of enzyme was added to this reaction mixture, no further hydrolysis was observed. If the same amount of substrate (MeCh) as the initial one was added to the reaction mixture after complete hydrolysis of the first added substrate (60 min for the electric tissue enzyme, 90 min for the plasma enzyme in the experiments shown in Fig. 1), hydrolysis started again, and was complete when 50 % of the second portion of substrate was hydrolysed. For comparison, the 100 % hydrolysis of acetylcholine is inserted in the figure. Human plasma cholinesterase splits acetyl-β-methylcholine at a very low rate, and therefore a 100 times higher concentration of this enzyme was used compared with the concentration used for the hydrolysis of acetylcholine. Furthermore, it was observed that after 50 % enzymatic hydrolysis of the β-methyl derivative by the plasma enzyme, the hydrolysis reaction continued with a very low rate, approximately 20 times lower than the initial rate. This infers that the plasma enzyme does split both the stereoisomers of acetyl-β-methylcholine, the hydrolysis rate for one of these (presumably the D-isomer) being about 20 times higher than that for the other isomer.

The experiments were repeated with some thiocholine esters. In all cases where thiocholine was the reaction product, the total amount of CO_2 produced was higher than expected from a theoretical point of view, when one mole of substrate hydrolysed is equivalent to one mole of CO_2 evolved from the bicarbonate system. For the thiocholine esters, CO_2 was not produced in equivalent amounts to the substrate hydrolysed, and this was probably due to the acidic property of thiocholine at the pH of the reaction mixture (7.4). Studies made by Hansen [3] with the tertiary amino analogue of thiocholine have shown that one of the two pK_a values observed for this derivative is approximately 8 which possibly may be due to the protolysis of the mercapto group. The mercapto group of thiocholine may be suggested to have similar acidic property. This, partly at least, explains the observation first made by Koelle [4], with a technique similar to that used in the present investigation, that acetylthiocholine is hydrolysed at a higher rate than acetylcholine by certain cholinesterase preparations. It may also explain the higher hydrolysis rates for the thiocholine esters at pH 8.0 than at pH 6.4, which difference is more marked than that for the corresponding reaction rates for choline esters.

Acetyl-β-methylthiocholine (MeThCh) gave similar results, 7.5 μmoles of CO_2 being produced instead of 6.12 μmoles ex-

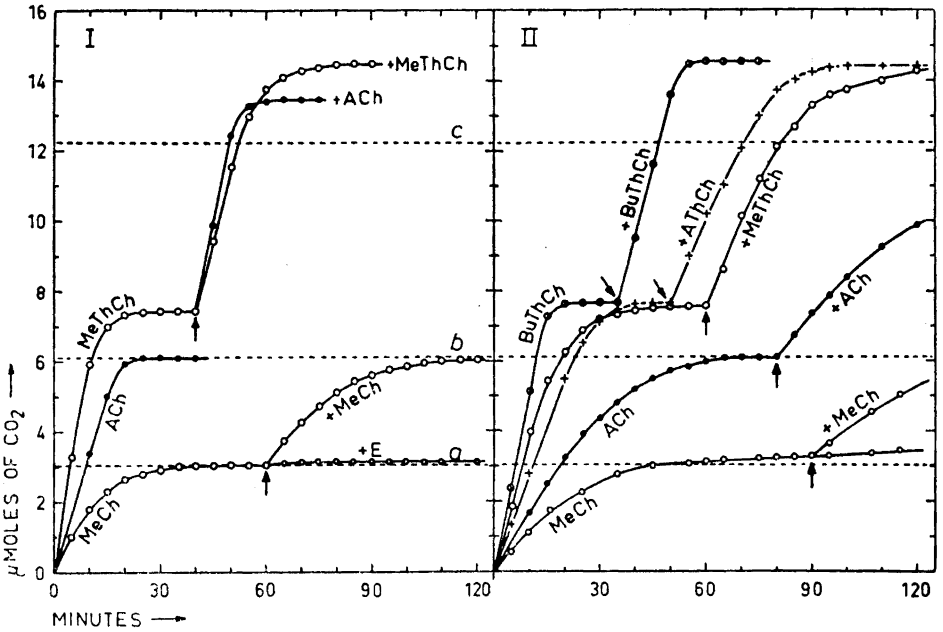


Fig. 1. The enzymatic hydrolysis of choline and thiocholine esters by purified cholinesterase preparations from *Torpedo* electric tissue (I) and human blood plasma (II). Initial amount of substrate 6.12 μmoles; total reaction mixture 2.40 ml. Arrows designate the addition of a second portion (6.12 μmoles) of substrate (or enzyme). The same enzyme concentration was used for various substrates, except in II where this concentration was 5 times higher for MeThCh and 100 times higher for MeCh. a = 3.06 μmoles; b = 6.12 μmoles; c = 12.24 μmoles. Symbols: ACh = acetylcholine chloride, MeCh = acetyl-β-methylcholine iodide, AThCh = acetylthiocholine iodide, BuThCh = butyrylthiocholine iodide, MeThCh = acetyl-β-methylthiocholine iodide. Symbols omitted for the initial hydrolysis curves in II for AThCh and MeThCh.

pected from a mole to mole basis. This optically active substrate used as racemic mixture thus behaved fundamentally different from its oxygen analogue. It has not been possible to find an explanation for this difference. It is very unlikely that the esterases show stereospecificity only for the choline esters and not for the thiocholine esters. It is more likely that the thioester is racemised during the enzymatic hydrolysis. A further difference between the S- and O-analogues of the β-methyl esters is that the former does not show the selective substrate specificity against acetylcholinesterases [5].

The thiocholine esters were kindly placed at our disposal by Messrs. Hoffmann-La Roche, Basel; for this generosity we wish to express our sincere thanks.

1. Glick, D. *J. Biol. Chem.* **125** (1938) 729.
2. Hoskin, F. C. G. and Trick, G. S. *Can. J. Biochem. and Physiol.* **33** (1955) 963.
3. Hansen, B. *Personal communication.*
4. Koelle, G. B. *J. Pharmacol. Exptl. Therap.* **100** (1950) 158.
5. Augustinsson, K.-B. *Scand. J. Clin. & Lab. Invest.* **7** (1955) 284.

Received April 17, 1957.

UV- und IR-Absorption von Kohlenstoffdiselenid

E. TREIBER, J. GIERER, J. REHNSTRÖM und K. E. ALMIN

Aus dem Centrallaboratorium der schwedischen Celluloseindustrie und dem schwedischen Holzforschungsinstitut, Stockholm, Schweden

Für Versuche, über die an anderer Stelle berichtet werden soll, war es notwendig, Kohlenstoffdiselenid (CSe_2) in grösserer Menge und grosser Reinheit darzustellen. Die Tatsache, dass wir so ein sehr reines Produkt zur Verfügung hatten, veranlasste uns, das bisher unbekannte Absorptionsverhalten im UV und IR zu untersuchen, worüber hier kurz referiert wird. Vorliegende Kurzmitteilung schliesst sich einer älteren Arbeit des einen von uns an [1,2], worin die UV-Absorption von Schwefelkohlenstoff und Kohlenoxysulfid studiert wurde.

Das ultraviolette Absorptionsspektrum. Kohlenstoffdiselenid, gelöst in Heptan, zeigt, wie erwartet, in Analogie zum Schwefelkohlenstoff 2 Absorptionsbanden im UV (2 660 mm^{-1} = 376 mμ und 4 115 mm^{-1} = 243 mμ). Beide Maxima sind gegenüber den analogen des Schwefelkohlenstoffs um ≈ 600 mm^{-1} gegen rot verschoben (Abb. 1). Die langwelligere Absorptionsbande dürfte vermutlich auch hier — wie beim CS_2 — als verbotener, angeregter Elektronenzustand interpretiert werden[1], der allerdings gegenüber CS_2 an Übergangswahrscheinlichkeit gewonnen hat. Die kurzwellige Bande darf dem CSe-Chromophor zugeordnet werden.

Die Infrarotabsorption. In Abb. 2 sind nun die analogen IR-Spektra von flüssigem CSe_2 und CS_2 wiedergegeben. Wie zu erwarten zeigen auch im IR beide Spektra sehr grosse Ähnlichkeit, wenn man von der Verschiebung zu niederer Wellenzahl im CSe_2-Spektrum absieht. Die bei 1 270 cm^{-1} beobachtbare Bande des CSe_2 besteht aus mindestens 3 getrennten Vibrationen und rührt offenbar von den Valenzschwingungen der C=Se-Bindung her. Diese Bande ist also analog der CS_2-Bande bei 1 523 cm^{-1}.

Experimentelles. Die Herstellung von Kohlenstoffdiselenid erfolgte in Anlehnung an die

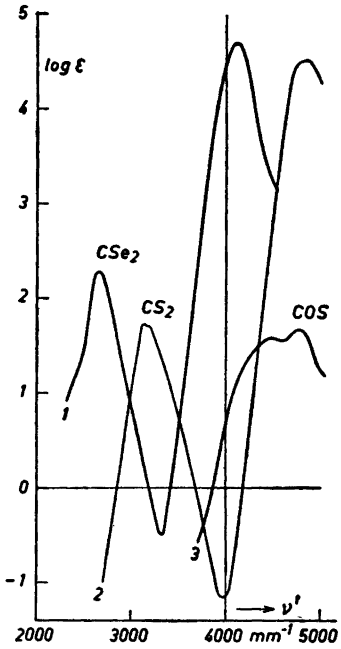


Abb. 1. UV-Absorptionsspektrum von: Kurve 1: CSe_2, Kurve 2: CS_2 [2], Kurve 3: COS [1].

von Ives u. Mitarb.[3] beschriebene Methode durch Einwirkung von Methylenchloriddämpfen auf schwach glühendes metallisches Selen. Die von uns verwendete Apparatur ist in Abb. 3 wiedergegeben. Zur Erhöhung der Ausbeute wurde das reichlich mit dem Gasstrom übergehende Selen wieder in den Reaktionsprozess zurückgeführt. Das im Kolben 3 kondensierte Substanzgemisch wurde nach Abfiltrierung des Selens einer Wasserdampfdestillation unterworfen. Die Methylenchlorid-Phase, die das Kohlenstoffdiselenid gelöst enthält, wurde abgetrennt, mit Natriumkarbonat sicc. getrocknet und im Vakuum bei ≈ 130 mm Hg fraktioniert. Kohlenstoffdiselenid — ein gelb gefärbtes Öl von äusserst widerlichem Geruch, die Schleimhäute reizend — wurde hierauf durch mehrfache Fraktionierung im Vakuum bei 110—115 mm Hg (Kp ≈ 66—67°C) über Hg-Metall und festem $Ca(OH)_2$ p.a. bis zur optischen Konstanz gereinigt.

In ähnlicher Weise erfolgte die Reinigung auf optische Konstanz von p.a. Schwefelkohlenstoff[2,4].

Die Reinigung von Heptan als optisch durchlässiges und inertes Lösungsmittel erfolgte in

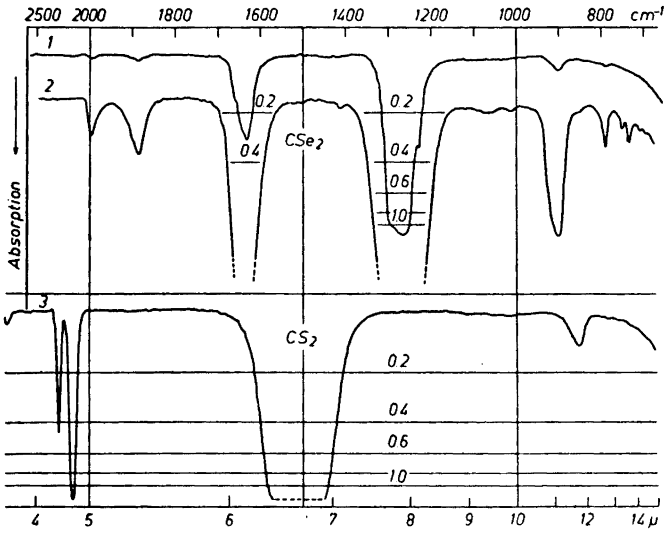


Abb. 2. Infrarotspektrum von CSe_2 (Kurve 1 und 2) und CS_2 (Kurve 3). (Kurve 1: CSe_2-Flüssigkeitsfilm zwischen zwei zusammengepressten Steinsalzplättchen; Kurve 2 und 3 flüssige Substanz in einer 0,1 mm Küvette.)

Anlehnung an übliche Reinigungsmethoden [4] durch Schütteln von Heptan mit konz. Schwefelsäure unter Zusatz von Silbersulfat, Waschen mit Wasser, alkal. Permanganatlösung und Wasser. Das abgetrennte Heptan wurde hierauf unter Zusatz von entsprechend gereinigtem Natriummetall fraktioniert; es erwies sich im gesamten, durch das Beckman-Spektrophotometer erfassbaren UV-Bereich als durchlässig.

Die IR-Aufnahme erfolgte in einem Perkin-Elmer-Spektrophotometer, Mod. 21 mit Steinsalzprisma. Für die Benutzung des Instruments danken wir Herrn Laborator A. Johansson von der analytisch-chemischen Abteilung der techn. Hochschule Stockholm.

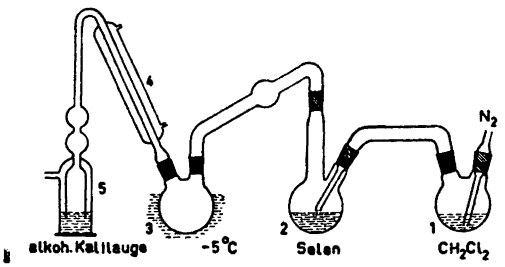


Abb. 3. Schema der Darstellungsapparatur.

1. Treiber, E. und Koren, H. *Monatsh.* **82** (1951) 1109.
2. Treiber, E., Lang, W. und Mader, E. *Holzforschg.* **8** (1954) 97. Vgl. auch Treiber, E., Porod, G. und Lang, W. *Österr. Chem. Ztg.* **53** (1952) 162.
3. Ives, D. J. G., Pittman, R. W. und Wardlaw, W. *J. Chem. Soc.* **1947** 1080.
4. Vgl. Pestemer, M. *Angew. Chem.* **63** (1951) 118.

Eingegangen am 23. April 1957.

N-Terminal Amino Acids Formed during Digestion of Bovine Fibrinogen by Plasmin

PER WALLÉN and KURT BERGSTRÖM

Kemiska Institutionen II, Karolinska Institutet, Stockholm, Sweden

The purpose of this work was to make a qualitative and quantitative estimation of the N-terminal amino acids, formed during the digestion of fibrinogen by plasmin, activated by urokinase. Besides the estimation of the N-terminal amino acids the decomposition of fibrinogen was followed by determination of coagulability. The determinations of N-terminal amino acids were carried out by Edman's phenyl-*iso*thiocyanate method [1]. The coagulability was determined after addition of lysine-ethylester in order to avoid further fibrinolysis [2]. The syneresis method of Morrison, as modified by Saifer and Newhouse [3], was applied.

The fibrinogen was prepared by the method recently published by Blombäck and Blombäck [4] and the coagulability of the preparations used by us varied from 95 to 99 %. Even these very pure preparations contain traces of plasminogen and after activation sufficient amounts of plasmin are formed to digest the fibrinogen.

The urokinase was prepared from human urine by adsorption on Hyflo Super Cel, and elution with ammonia. It was further purified by means of ammonium sulphate fractionation. By this method about 5 mg of dry substance was obtained from one liter of urine and the yield of activity was about 80 %.

500 mg of fibrinogen and 0.5 mg urokinase were dissolved in 50 ml of 0.02 M phosphate buffer pH 7.2 containing NaCl to a concentration of 0.3 M and incubated at 37 °C. At different times 10 ml of the reaction mixture was added to 10 ml pyridine containing 0.5 ml phenyl-*iso*-thiocyanate, thus interrupting the digestion. The coupling was continued for 2 h by keeping pH 8.5—9.0 with occasional addition of 1 N NaOH. The excess of phenyl-*iso*thiocyanate was removed by washing several times with benzene. The PTC-derivatives were transferred to the corresponding PTH-amino acids by heating with 1 N HCl at 100 °C for one hour. The PTH-amino acids were extracted and identified by paper chromatography. The solvents A, D, E and F of Edman and Sjöquist [5,6] and a solvent composed of D and E in equal parts [7] were used.

Blombäck and Yamashina [8] have recently reported that there are 2 tyrosyl and 2 glutamyl residues as N-terminal amino acids in the bovine fibrinogen molecule, when the molecular weight was estimated to be 340 000. During fibrinogenolysis the

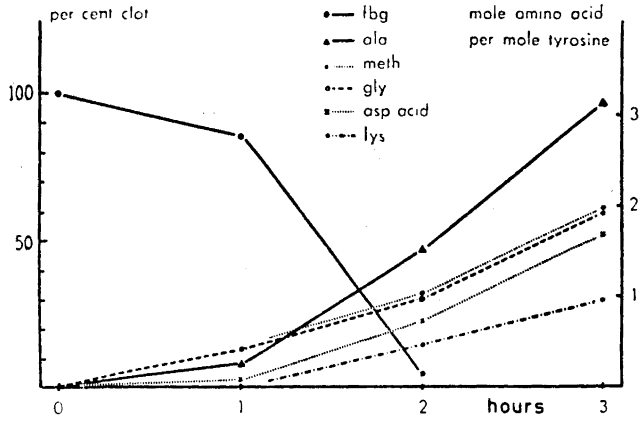


Fig. 1. N-Terminal amino acids released during fibrinogenolysis and correlated to coagulability.

following N-terminal amino acids appeared: aspartic acid, glycine, alanin, lysine and methionine. The glutamyl and tyrosyl residues did not show any significant change during the digestion time used. As the value of tyrosine was practically constant during the fibrinogenolysis, the released amounts of the N-terminal amino acids were expressed in relation to tyrosine (see Fig. 1). When the digestion of fibrinogen had proceeded so far that only traces could be coagulated with trombin, approximately one mole lysyl, two moles each of glycyl, aspartyl and methionyl, and three moles alanyl residues were formed from one mole of fibrinogen.

1. Edman, P. *Acta Chem. Scand.* **4** (1950) 283.
2. Blombäck, B., Blombäck, M., Senning, Å. and Wallén, P. *Nord. Med.* **53** (1955) 1019.
3. Saifer, A. and Newhouse, A. *J. Biol. Chem.* **208** (1954) 159.
4. Blombäck, B. and Blombäck, M. *Arkiv Kemi* **10** (1956) 415.
5. Edman, P. and Sjöquist, J. *Acta Chem. Scand.* **10** (1956) 1507.
6. Sjöquist, J. *Acta Chem. Scand.* **7** (1953) 447.
7. Blombäck, B. and Yamashina, I. *Arkiv Kemi* (In print).
8. Blombäck, B. and Yamashina, I. *Acta Chem. Scand.* **11** (1957) 194.

Received April 23, 1957.

An Antibiotic Related to the Streptothricin Group

J. A. CHRISTENSEN, O. ROSENLUND HANSEN, ALF LUND, and B. NOER

A/S Ferrosan, Copenhagen, Denmark

From an unidentified actinomycete No. 4279 isolated from a soil sample collected in North Zealand, Denmark, in 1953 we have succeeded in isolating a crude substance with antibiotic activity against a wide range of bacteria and fungi. This substance has properties very similar to those described by Schaffner, Rangaswami and Waksman [1,2] as regards the mycothricin complex though it differs from the latter in certain chemical respects. Optimum yield was obtained after 36 h at 25—28° in a medium containing the extractive material from 40 g of soy-meal per l in an aerated and stirred fermentator.

A crude preparation of the active substance was obtained from the broth by adsorption on activated carbon at pH 7—8 and elution with 80 % ethanol at pH 2.7. Purification was carried out (a) by treating a 20 % aqueous solution of the substance at pH 2.7 with activated carbon and subsequent precipitation by means of 10 volumes of acetone or ethanol and (b) by adsorption on Amberlite IRC-50 at pH 8 and elution with dilute hydrochloric acid; the active fractions were then neutralized with Amberlite IR-4B and evaporated *in vacuo* or, in some cases, lyofilized.

The substance is readily soluble in water and slightly soluble in ethanol. It is insoluble in chloroform, ether, benzene, toluene and *n*-butanol. Paper chromatograms developed with dilute ethanol at pH 3.0 showed the following R_F values: 0.38 (ethanol:water, 80:20), 0.70 (ethanol: water, 70:30), The total activity of the substance can be precipitated by ammonium reineckate, methyl orange, and picric acid, whereas only a fraction of the total activity can be precipitated by flavianic acid (pH between 5.0 and 5.5).

The following tests were negative: Ninhydrin, Pauly, Sakaguchi, Hopkins-Cole, Fehling, Tollens, Molisch, 9-hydrazinoacridin for hydrophilic aldehydes [3]. The biuret reaction was dubious. With sodium periodate the substance gave formaldehyde.

On hydrolysis in 2 N hydrochloric acid an amino acid and a sugar were formed.

Minimum inhibitory concentration

Test organism	μg/ml
Staph. aureus	0.25— 0.31
E. coli	12.5 — 25.0
Strept. hemolyticus	1.0 — 10.0
S. typhi	1.0 — 10.0
Corynebact. sp.	0.1 — 1.0
B. subtilis	0.1 — 1.0
B. dysenteriae Shiga	1.0 — 10.0
Pseud. aeruginosa	10 —100
Alternaria circinans	0.12— 0.25
P. notatum	0.25— 0.50
A. niger	1.0 — 10
P. pullulans	1.0 — 10
Candida albicans	12.5 — 25
Trichoderma viride	0.25— 0.50

following N-terminal amino acids appeared: aspartic acid, glycine, alanin, lysine and methionine. The glutamyl and tyrosyl residues did not show any significant change during the digestion time used. As the value of tyrosine was practically constant during the fibrinogenolysis, the released amounts of the N-terminal amino acids were expressed in relation to tyrosine (see Fig. 1). When the digestion of fibrinogen had proceeded so far that only traces could be coagulated with trombin, approximately one mole lysyl, two moles each of glycyl, aspartyl and methionyl, and three moles alanyl residues were formed from one mole of fibrinogen.

1. Edman, P. *Acta Chem. Scand.* **4** (1950) 283.
2. Blombäck, B., Blombäck, M., Senning, Å. and Wallén, P. *Nord. Med.* **53** (1955) 1019.
3. Saifer, A. and Newhouse, A. *J. Biol. Chem.* **208** (1954) 159.
4. Blombäck, B. and Blombäck, M. *Arkiv Kemi* **10** (1956) 415.
5. Edman, P. and Sjöquist, J. *Acta Chem. Scand.* **10** (1956) 1507.
6. Sjöquist, J. *Acta Chem. Scand.* **7** (1953) 447.
7. Blombäck, B. and Yamashina, I. *Arkiv Kemi* (In print).
8. Blombäck, B. and Yamashina, I. *Acta Chem. Scand.* **11** (1957) 194.

Received April 23, 1957.

An Antibiotic Related to the Streptothricin Group

J. A. CHRISTENSEN, O. ROSENLUND HANSEN, ALF LUND, and B. NOER

A/S Ferrosan, Copenhagen, Denmark

From an unidentified actinomycete No. 4279 isolated from a soil sample collected in North Zealand, Denmark, in 1953 we have succeeded in isolating a crude substance with antibiotic activity against a wide range of bacteria and fungi. This substance has properties very similar to those described by Schaffner, Rangaswami and Waksman [1,2] as regards the mycothricin complex though it differs from the latter in certain chemical respects. Optimum yield was obtained after 36 h at 25—28° in a medium containing the extractive material from 40 g of soy-meal per l in an aerated and stirred fermentator.

A crude preparation of the active substance was obtained from the broth by adsorption on activated carbon at pH 7—8 and elution with 80 % ethanol at pH 2.7. Purification was carried out (a) by treating a 20 % aqueous solution of the substance at pH 2.7 with activated carbon and subsequent precipitation by means of 10 volumes of acetone or ethanol and (b) by adsorption on Amberlite IRC-50 at pH 8 and elution with dilute hydrochloric acid; the active fractions were then neutralized with Amberlite IR-4B and evaporated *in vacuo* or, in some cases, lyofilized.

The substance is readily soluble in water and slightly soluble in ethanol. It is insoluble in chloroform, ether, benzene, toluene and *n*-butanol. Paper chromatograms developed with dilute ethanol at pH 3.0 showed the following R_F values: 0.38 (ethanol:water, 80:20), 0.70 (ethanol: water, 70:30), The total activity of the substance can be precipitated by ammonium reineckate, methyl orange, and picric acid, whereas only a fraction of the total activity can be precipitated by flavianic acid (pH between 5.0 and 5.5).

The following tests were negative: Ninhydrin, Pauly, Sakaguchi, Hopkins-Cole, Fehling, Tollens, Molisch, 9-hydrazinoacridin for hydrophilic aldehydes [3]. The biuret reaction was dubious. With sodium periodate the substance gave formaldehyde.

On hydrolysis in 2 N hydrochloric acid an amino acid and a sugar were formed.

Minimum inhibitory concentration

Test organism	μg/ml
Staph. aureus	0.25— 0.31
E. coli	12.5 — 25.0
Strept. hemolyticus	1.0 — 10.0
S. typhi	1.0 — 10.0
Corynebact. sp.	0.1 — 1.0
B. subtilis	0.1 — 1.0
B. dysenteriae Shiga	1.0 — 10.0
Pseud. aeruginosa	10 —100
Alternaria circinans	0.12— 0.25
P. notatum	0.25— 0.50
A. niger	1.0 — 10
P. pullulans	1.0 — 10
Candida albicans	12.5 — 25
Trichoderma viride	0.25— 0.50

The amino acid has R_F 0.15 (*n*-butanol: acetic acid:water, 4:1:5). A sugar test was made in the following way: The substance was heated in a solution of 2,4-dinitrophenylhydrazine in 2 N hydrochloric acid for a few hours. On cooling, a red precipitate of a tetranitrophenylosazone was formed. On adding a few drops of N sodium hydroxide to a solution of the precipitate in ethanol a blue colour was obtained (modified Bamberger reaction [4]).

The purest product obtained has been tested in broth-dilution assay against different microorganisms.

In mice LD 50 was about 1 200 mg/kg body weight when administered intravenously. In rats 50—500 mg/kg subcutaneously caused no acute toxic symptoms but anuria developed after 3 or 4 days. Examination of the kidneys showed severe tubular damage. Unlike streptothricin, a 1 % aqueous solution did not produce local irritation in rabbits' eyes.

1. Schaffner, C. P., Rangaswami, G. and Waksman, S. A. *Proc. 3rd Intern. Congr. Biochem.*, Brussels July 1955 (1956) 55.
2. Rangaswami, G., Schaffner, C. P. and Waksman, S. A. *Antibiotics and chemotheraphy* **6** (1956) 675.
3. Boxer, G. E. and Jelinek, V. C. *J. Biol. Chem.* **170** (1947) 491.
4. Bamberger, E. *Ber.* **32** (1899) 1806.

Received April 16, 1957.

Correction to "Determination of Small Amounts of Total Cholesterol by the Tschugaeff Reaction with a Note on the Determination of Lathosterol" *

HENRIK K. HANEL and HENRIK DAM

Department of Biochemistry and Nutrition, Polytechnic Institute, Copenhagen, Denmark

In Table 3, p. 681 the following corrections are made:

Compound		Absorbance mmoles/ml	
.....			
Cholesterol	*for*	9 593 *read*	9 067
Cholesterylacetate	*for*	8 349 *read*	6 348
.....			

* *Acta Chem. Scand.* **9** (1955) 677.

Received April 15, 1957.

ACTA CHEMICA SCANDINAVICA 11 (1957) 757—762

On the Glycogen in *Escherichia coli B*; Variations in Molecular Weight during Growth. I

T. HOLME, T. LAURENT and H. PALMSTIERNA

Bacteriological Department and Chemical Department I, Karolinska Institutet, Stockholm, Sweden

Molecular weight determinations have been performed on glycogen isolated from *Escherichia coli B* at different conditions of growth.

It was observed that the molecular weight increased when glycogen was accumulated by the cells. A decrease was noted when the glycogen was utilized.

In the experiments [1,2] published earlier it was shown that of the glucose residues incorporated into glycogen during an accumulation of this compound in *E. coli B*, those that were incorporated last were the first to be split off during a subsequent growth period, *i.e.* when the glycogen was utilized by the cells. A possible explanation of this could be that during accumulation the "excess synthesis" of glycogen proceeds by addition of glucose residues to the glycogen molecules that are already present at the beginning of the period. The glucose residues incorporated last would constitute a "peripheral tier" on the molecules, and would in turn be those most easily available during a subsequent utilization.

The purpose of the experiments described in this paper was to test this possibility. Molecular weight determinations by the light-scattering method revealed an increase in the molecular weight of the glycogen during the accumulation period, and a decrease during the utilization. These results seem to confirm the hypothesis, but the possibility that other types of glycogen rebuilding may proceed at the same time cannot be excluded.

METHODS

Molecular weight determination. The molecular weight of glycogen from different animal tissues has been measured by osmotic pressure [3], ultracentrifugation [4,5], and light scattering [6-9]. The values reported usually lie within a range of $1-10 \times 10^6$. The most recent report [9] gives values in the range of 50×10^6. Sedimentation studies on glycogen from *Mycobact. tuberculosis* [10] gave the value 12×10^6 and on glycogen from *Aerobacter aerogenes* [11] 9.2×10^6. The shape of the glycogen molecule has been reported to be spherical [12]. The present paper is the first report on glycogen from *E. coli B*. Light-scattering has been used to characterize the molecule.

Measurements were made in a Brice Phoenix Universal Light Scattering Photometer at a wavelength of 4 358 Å. The solutions to be measured were kept in a semioctagonal glass cell. The measurements were performed at 45°, 90° and 135° with respect to the direction of the direct beam. The molecular weight was calculated according to the formula [13]:

$$\frac{K \cdot c}{R_{90}^{\circ}} = \frac{1}{M \cdot P_{90}^{\circ}} + 2B \cdot c$$

where R_{90}° is the intensity scattered at 90° divided by the intensity of the direct beam, c the concentration of glycogen in g/ml, K a constant which includes the refractive increment of glycogen, M the molecular weight, P_{90}° a particle-scattering factor, and B a constant. The refractive increment used [7] was 0.136 ml/g, giving K a value of 2.94×10^{-7}. The particle-scattering factor can be obtained by using the relation $R_{45}^{\circ}/R_{135}^{\circ} = z = f(P_{90}^{\circ})$. This factor, z, is called the dissymmetry. P_{90}° has been tabulated for different values of z for spherical particles [13].

By measuring the scattering at several different concentrations, it was found that within the concentration range used, $2.5 \times 10^{-6} - 50 \times 10^{-6}$ g/ml, the scattering was independent of the concentration, and the constant B was thus zero. This agrees with light-scattering data on other glycogens [9]. The glycogen concentrations have been determined as described earlier [14].

The molecular weight obtained is a weight-average molecular weight, which is higher than the number-average obtained from, *e.g.*, osmotic pressure measurements. If a specimen is highly polydisperse, which is the case with glycogen, the results will be dominated by the highest molecular weight fraction.

It is possible to calculate the diameter of the molecules from dissymmetry data if the shape is spherical [13]. However, this value is a "z-average", which is even higher than a weight-average. The diameter of the molecules was found to be about 750 Å.

The glycogen specimens were quantitatively dissolved in an 0.1 M dust-free sodium chloride solution. The dust had been removed by filtration through a membrane filter with a pore diameter of 200—400 Å. When filtration or high speed centrifugation was used to take away dust from glycogen solutions, a large amount of glycogen was also removed. These solutions were therefore centrifuged in a small laboratory centrifuge in order to remove the largest extraneous particles. The amount of glycogen which sedimented during this centrifugation was within the limits of detection by the method of analysis. After this procedure, there conceivably may still remain some contamination of the glycogen specimens by dust; however this dust does not seem to disturb the measurements to any great extent. For one thing, the scattering from glycogen is very strong. Also, the dust would be expected to give high dissymmetries, but the measurements did not show excessively high values (1.60—2.50), or change if the solutions were kept overnight, when some of the dust ought to have settled. Finally, there was a high degree of reproducibility in the measurements, as shown in Table 1. Stetten *et al.*[9] also came to the conclusion that dust does not disturb the measurements.

Microbiological methods. Freeze-dried cultures of *Escherichia coli B* were cultivated in Friedlein's synthetic medium. Ammonium chloride was the sole nitrogen source and sodium lactate the carbon source. In the deficient media, ammonium chloride was used in 1.3×10^{-3} M (expt. B) or 1.0×10^{-3} M concentrations (expts .C and D). The cultivation methods and harvesting procedures have been reported earlier [14,15].

A typical nitrogen starvation experiment (expt. D) is presented graphically in Fig. 1. The amount of cells inoculated corresponded to about 20 mg of dry cells per litre of culture. The inoculum consisted of a suspension of cells grown for 16—18 h in Friedlein's medium, and washed once in nitrogen-free medium. Three h after the inoculation the dry weight of cells per litre of culture was about 90 mg. During the subsequent 90 min there was only a small increase; this period we call the starvation phase. This phase was interrupted by adding ammonium chloride to the culture. After this addition there was a second growth period. The glycogen per dry weight of cells in one litre of culture is recorded in the same figure. After collecting the cells of each sample by centrifugation, they were freeze-dried, and stored at −20°C until the material was weighed in for analysis.

Chemical methods. The glycogen was isolated by alkaline hydrolysis of the cells (30 % KOH, 100°C, 3 h), followed by precipitation with 66 % ethanol [14]. No shorter time

Table 1. Experiment A. Reproducibility of the methods used. For further details, see the text.

Sample	Molecular weight	Dissymmetry z
I	55.4×10^6	1.85
II	53.4	2.01
III	53.1	1.96
IV	50.0	1.93
V	51.6	1.92
VI	56.1	1.95
VII	54.9	1.99
Average	53.5×10^6	1.94

Table 2. Experiments B, C, and D.

Experiment	I Time after inoculation (min)	II Dry weight of cells per litre of culture (mg)	III Glycogen per litre of culture (mg)	IV II−III	V Molecular weight
B	120	39.8	2.6	37.2	27.8×10^6
	150	51.6	2.5	49.1	23.9
	300	174.0	26.0	148.0	78.2
	330	181.7	32.7	149.0	73.8
	330 addition of ammonium chloride				
	360	233.3	31.3	202.0	64.2
	405	313.8	23.8	290.0	82.2
	450	390.8	22.9	367.9	65.8
	480	454.3	20.0	434.3	66.6
C	270	122.6	27.0	95.6	79.1×10^6
	300	126.1	32.5	93.6	61.7
	330	134.5	36.2	98.3	72.6
	330 addition of ammonium chloride				
	420	217.1	41.8	175.3	53.7
	510	392.1	31.6	360.5	61.2
D	130	53.6	2.3	51.3	30.2×10^6
	150	70.1	3.1	67.0	25.7
	180	95.1	5.7	89.4	25.8
	270	119.1	20.8	98.3	52.3
	270 addition of ammonium chloride				
	360	257.8	18.5	239.3	76.6
	450	436.0	11.3	424.7	47.5
	540	562.8	9.6	553.2	37.4
	600	696.0	11.9	684.1	52.6

could be taken for the alkaline hydrolysis, nor could lower concentrations of the KOH be used if a low-nitrogen preparation was to be achieved. It was found necessary to perform the alkaline hydrolysis in new Pyrex tubes, since otherwise material was extracted from the glass, making it impossible to dissolve the glycogen completely. After the introduction of this modification, the molecular weight determinations were reproducible (see Table 1). The glycogen could be stored in neutral water solutions for several days at 0°C without undergoing any change in the molecular weight. The molecular weights of the bacterial

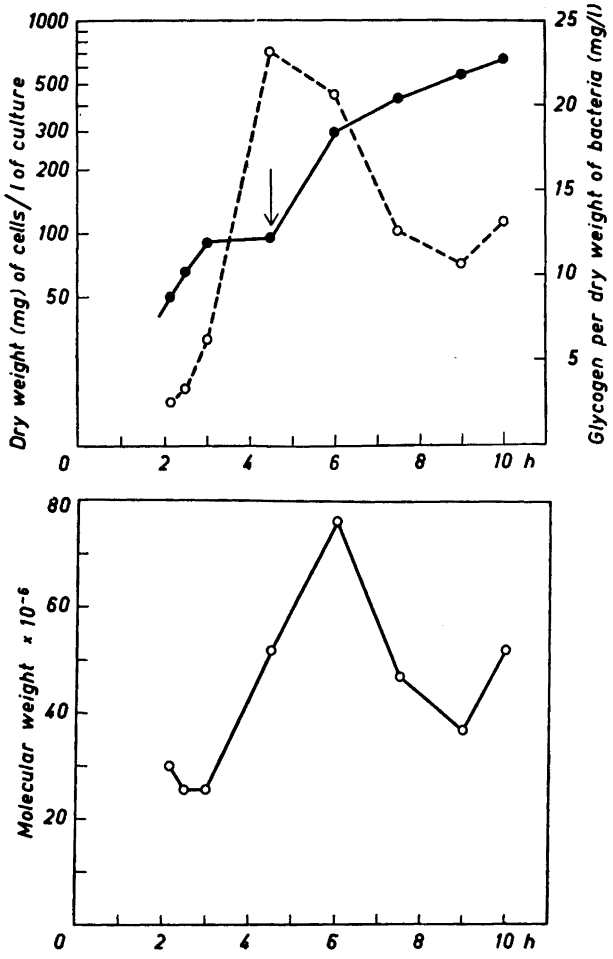


Fig. 1. Experiment D. Nitrogen-starved culture. The curve ● ——— ● represents the dry weight of cells per litre of culture (the glycogen content has been subtracted from the total weight). The arrow indicates the moment when ammonium chloride was added (see the text for further details regarding this experiment). The curve O — — — O represents the glycogen per litre of culture. In the lower part of the figure, the variation in molecular weight is shown.

glycogen isolated by the trichloro-acetic acid method used by Stetten *et al.*[9] were found to be considerably lower than those obtained by the alkaline isolation procedure.

In order to test the reproducibility of the methods used, the following experiment was carried out (expt. A). Cells from a 5-litre nitrogen-starved culture were harvested at 270 min after the inoculation, spun down and freeze-dried. The material was divided into eight equal parts. The glycogen was isolated separately from these samples by the methods described above. One part was taken for determination of the glycogen content of the cells; the molecular weights of the remaining seven samples of glycogen were then determined. The results are recorded in Table 1.

RESULTS

In determining the molecular weight, alkaline hydrolysis was found to be the most reliable method for the preparation of glycogen from *E. coli* cells (Table 1, expt. A).

During the accumulation of glycogen in the bacterial cells, the molecular weight of the glycogen increased considerably. When the glycogen content of the culture (calculated per dry weight of cells in one litre of culture) decreased during a subsequent utilization, the molecular weight decreased again (Table 2, Fig 1). This decrease was demonstrated most clearly in expt. D, in which the glycogen content of the culture reached lower values than in expts. B and C. The results are summarized in Table 2.

DISCUSSION

It is not possible to decide whether the glycogen isolated by one method is more "native" than that isolated by another. If a continuous change in the molecular weights is found during bacterial growth, however, extraction artefacts seem less likely.

On the basis of data obtained from isotope experiments (enzymatic degradation of ^{14}C-labelled rat liver glycogen), Stetten and Stetten [16,17] put forward the hypothesis that the glucose residues incorporated during glycogen synthesis may be added to pre-existing molecules, and preferentially attached to the end groups of these. This view was supported by the experiments reported earlier by Holme and Palmstierna [1,2], who investigated the glycogen metabolism of *E. coli B*. However, another explanation may be that the glycogen is inhomogeneous as regards its metabolic activity.

The possibility of obtaining accurate quantitative data on glycogen synthesis afforded by our system made it probable that molecular weight determinations on the glycogen would give valuable information. Our present results indicate that a correlation exists between the glycogen content of the bacteria and the molecular weight of this substance. However, the fact that the light-scattering method gives weight-average values, made a further analysis of the quantitative data impossible. It will probably be possible to obtain further information by fractionation of the glycogen.

In most cases there is no marked immediate decrease in glycogen per litre of culture after the addition of ammonium chloride to the nitrogen-starved cultures. A possible explanation may be that there has been a considerable overflow metabolism during the starvation period, *i.e.* low molecular intermediates have poured out into the medium [15,18]. These intermediates are possibly more easily utilized by the cells than the glycogen is. During this delay in glycogen utilization an increase in the molecular weight was observed. The explanation of this increase need not necessarily be that there has been a further synthesis of glycogen; it can just as well be due to the formation of larger molecules through the unification of smaller ones.

While this investigation was proceeding. Stetten *et al.*[9] published a work in which the light-scattering method was used for molecular weight determinations of liver and muscle glycogen from rat and rabbit. It was noted that the glycogens were metabolically inhomogeneous with regard to molecular weight.

The reproducibility of our results indicates that the nitrogen starvation technique offers definite advantages in the study of glycogen synthesis, and appears to be well suited for further investigation.

REFERENCES

1. Holme, T. and Palmstierna, H. *Acta Chem. Scand.* **10** (1956) 155.
2. Holme, T. and Palmstierna, H. *Acta Chem. Scand.* **10** (1956) 1557.
3. Oakley, B. H. and Young, F. G. *Biochem. J. London* **30** (1936) 868.
4. Bridgman, W. B. *J. Am. Chem. Soc.* **64** (1942) 2349.
5. Bell, D. J., Gutfreund, H., Cecil, R. and Ogston, A. G. *Biochem. J. London* **42** (1948) 405.
6. Staudinger, H. *Makromol. Chem.* **2** (1948) 88.
7. Putzeys, P. and Verhoeven, L. *Rec. trav. chim.* **68** (1949) 817.
8. Harrap, B. S. and Manners, D. J. *Nature* **170** (1952) 419.
9. Stetten, M. R., Katzen, H. M. and Stetten, D. Jr. *J. Biol. Chem.* **222** (1956) 587.
10. Chargaff, E. and Moore, D. H. *J. Biol. Chem.* **155** (1944) 493.
11. Levine, S., Stevenson, H.J.R., Tabor, E.C., Bordner, R.H. and Chambers, L.A. *J. Bacteriol.* **66** (1953) 664.
12. Meyer, K. H. *Advances in Enzymol.* **3** (1943) 109.
13. Stacey, K. A. *Light Scattering in Physical Chemistry.* Butterworth's Scientific Publications, London 1956.
14. Palmstierna, H. *Acta Chem. Scand.* **10** (1956) 567.
15. Holme, T. and Palmstierna, H. *Acta Chem. Scand.* **10** (1956) 578.
16. Stetten, M. R. and Stetten, D. Jr. *J. Biol. Chem.* **207** (1954) 331.
17. Stetten, M. R. and Stetten, D. Jr. *J. Biol. Chem.* **213** (1955) 723.
18. Dagley, S., Dawes, E. E. and Morrison, G. A. *J. Bacteriol.* **61** (1951). 433.

Received March 15, 1957.

ACTA CHEMICA SCANDINAVICA 11 (1957) 763—775

Continuous Culture Studies on Glycogen Synthesis in *Escherichia coli B*

T. HOLME

Bacteriological Department, Karolinska Institutet, Stockholm, Sweden

The correlation between the synthetic rates of nitrogen-containing compounds and of a nitrogen-free substance, glycogen, has been studied in *Escherichia coli B* by the continuous culture technique. The nitrogen source was used as the growth-rate-limiting factor. This kind of limitation did not reduce the synthetic rate of the glycogen in the cells. The net synthetic rate of glycogen was increased by a reduction in the synthetic rate of the nitrogen-containing compounds.

The possibility of maintaining steady-state growth in bacterial cultures was demonstrated in 1950 by Monod [1] and Novick and Szilard [2,3]. Since then a great number of continuous culturing devices have been described (for examples, see Refs. [1–7]), and some experimental work has been reported. Monod and Cohn [8] used the technique in studies on adaptive enzymes, and Novick and Szilard [2,9–11] demonstrated its usefulness in studies of bacterial genetics and physiology. Herbert and collaborators [5], using a 20-litre pilot-plant type apparatus, pointed out the advantages of the technique in industrial fermentation.

A continuous culture system consists in general of a growing bacterial culture, which is fed with a continuous flow of liquid, sterile nutrient medium at a constant rate. The culture volume is kept constant by removal of the bacterial suspension at the same rate as fresh medium enters the culture.

The increase of the bacterial mass in any exponentially growing culture may be expressed by

$$\frac{dx}{dt} = \mu x$$

where x is the dry weight of organisms per unit volume at time t and μ is the specific growth rate. If the flow-rate of fresh medium fed into a continuous culture is called f, the dilution rate, D, will be f/v, where v is the culture volume. In this case the expression for the increase in bacterial mass in the growth vessel is

$$\frac{dx}{dt} = \mu x - Dx$$

Equilibrium will be obtained, if $\mu = D$, *i.e.* if the flow-rate is equal to the specific growth rate. By utilizing the fact that the growth rate in a bacterial culture may be limited by reducing the concentration of one of the essential nutrients in the medium, it is possible to achieve equilibrium over a wide range of growth rates. While the concentration of one of the essential nutrients is low, all others are in excess. The low-concentration nutrient is called the limiting or controlling factor. The concentration of this factor is almost instantaneously reduced when the medium is mixed with the culture, and reaches a level which limits the growth rate. It can be shown that this system tends to attain a self-stabilizing equilibrium, where the growth rate is determined by the flow-rate of the incoming medium, and the bacterial mass is determined by the concentration of the limiting factor.

In equilibrium, the synthetic rate of every component of the cell is equal to the dilution rate, which in turn can be regulated by the experimenter at will to any values that do not exceed the maximum value of μ, *i.e.* the maximum synthetic capacity of the bacterium. Hence it should be clear that the continuous culture method provides definite advantages in the study of synthetic functions of bacteria, since the determinations of the rates of various processes are reduced to measurements of steady-state concentrations.

During continuous culture experiments with *Escherichia coli B* it was noted that the nature of the limiting factor had a profound influence on the chemical composition of the cells. Special attention was paid to the glycogen content of the bacteria. When the nitrogen source was used as the limiting factor, considerable variations in the glycogen content of the cells were noted at different growth rates.

In previous experiments in which conventional cultivation techniques were used Palmstierna [12] found that glycogen accumulated during the lag phase of growth in cultures of *E. coli B*. In collaboration with Palmstierna a number of experiments were carried out, the object of which was to throw light on different aspects of the glycogen synthesis in this bacterium [13–16].

In the experiments described in the present paper, the continuous culture technique has been used in a study of the correlation between the synthetic rates of glycogen and of nitrogen-containing compounds in *E. coli B*.* When the nitrogen source was used as the limiting factor, the synthetic rate of the nitrogen-containing compounds was selectively reduced. The rate of glycogen synthesis was not reduced by this limitation, and it attained its highest values at the lowest synthetic rates of the nitrogen-containing compounds. The main product of synthesis that accumulated inside the cells during nitrogen deficiency appeared to be glycogen.

METHODS

Continuous culture apparatus. In these studies it was possible to use a fairly simple device, which had the advantage of being easily operated. The culture vessel consisted of a 2-litre Erlenmeyer flask which was given a working volume of 1 litre by means of a

* In the present paper "synthesis" always refers to the net synthesis.

tubulature on the wall for removing the emergent bacterial culture. Good mixing and aeration was achieved by placing the flask on a rotary shaker working at 120 r.p.m., and by having the air stream forced through a sintered glass disc and entering the culture fluid as close to the wall of the flask as possible. The neck of the flask was sealed by a rubber stopper which was perforated by glass tubes for the supply of air and fresh medium, and for inoculation. Effluent air left the flask only through the tubulature mentioned, making the transfer of the emergent bacterial suspension to the cooling flask a matter of seconds. The air flow-rate was 1 litre per min, and was indicated by a rotameter. In some instances a small amount of carbon dioxide was added to the air, this also being indicated by a special rotameter. The rotary shaker with the culture vessel operated in a constant temperature-room at 37°C. Fresh medium was stored in 40-litre spherical pyrex flasks and supplied to the culture vessel by means of a hose pressure pump * through latex rubber tubes. The continuously expelled bacterial suspension was cooled on the walls of a cylindrical collecting vessel placed in ice water.

Operation. Deficient medium (40 litres in each storage flask) was sterilized separately. The culture vessel was sterilized containing 1 litre of the complete medium. It was inoculated with bacteria from an agar slant, and growth was allowed to proceed until the cell concentration reached a value of about 2×10^9 cells per ml, corresponding to about 500 mg of dry cells per litre. At this stage the continuous addition of deficient medium was started. In the steady-state, the dry weight of cells per litre of culture was usually kept about 120—200 mg. At the beginning of each experiment a dilution rate of about 0.3 h^{-1} was used. During the first 10 h of the continuous run, it was found necessary to add a certain amount of carbon dioxide to the air in order to prevent a complete wash-out of the cells (see Table 4 and Figs. 4 and 5).

When the steady-state was achieved at the selected flow-rate, two or three samples were taken daily. The duration of the test at each flow-rate was in most cases 2 days, but during a continuous run of 5—6 days at the same flow-rate, the variations in the polulation density and the glycogen content of the culture were found to be within the limits of the experimental errors. The flow-rate was changed to lower or higher values stepwise, big changes always being avoided. After a change of the flow-rate had been effected, the culture was run for about 18 h before sampling of the culture at the new steady-state was commenced. Control of the flow-rate was effected by measuring the volume of the bacterial suspension that had collected during a certain interval.

After a continuous run of about 12—14 days, wall-growth occurred in most cases, and the experiment was terminated. Wall-growth was never tolerated during the continuous run, because it affected both the yield of the bacteria and their glycogen content.

When the volume of the bacterial suspension in the collecting vessel was 800 ml, the cells of this sample were quantitatively spun down and dry weight determination was performed according to the method used by Palmstierna [12]. The freeze-dried material was kept at —20°C until it was weighed in for analysis.

The cell concentration was determined in 1 ml-samples taken directly from the outflowing culture. The bacteria were counted in a counting chamber under the phase contrast microscope.

Organism and culture media. Freeze-dried cultures of *Escherichia coli B* were used throughout. Two media were employed: one with sodium lactate ** and one with glucose *** as the carbon source. In both of the media, ammonium chloride was the sole nitrogen source. This nutrilite was used as the limiting factor in most of the experiments, but one experiment was also carried out with lactate as the limiting factor. In the nitrogen-deficient media, the concentration of ammonium chloride was usually about 1.5×10^{-3} M, but in one experiment a concentration of 3.9×10^{-3} M was used. After sterilization the ammonium-N concentration was determined, in every new batch of deficient medium. In the ex-

---

* Sigmamotor Inc., Middleport, N.Y., USA.

** Described by Friedlein [17] and having the following composition: sodium lactate 10 g, NH_4Cl 1 g, K_2HPO_4 0.7 g, KH_2PO_4 0.3 g, $Na_2SO_4 \cdot 10H_2O$ 0.25 g, $MgSO_4 \cdot 7H_2O$ 0.02 g, distilled water 1 000 ml.

*** Described by Hook and coworkers [18]: glucose 4 g, NH_4Cl 1 g, $Na_2HPO_4 \cdot 2H_2$ O7.5 g, KH_2PO_4 3.0 g, NaCl 0.5 g, $MgSO_4 \cdot 7H_2O$ 0.2 g, distilled water 1 000 ml.

periment with the carbon source as the limiting factor, the sodium lactate concentration was 1.0×10^{-2} M. The pH of the culture medium during the continuous run was 7.0 when the lactate medium was used, and 6.9 with the glucose medium.

Table 1.

Experiment	Dilution rate	Number of cells per ml $\times 10^{-6}$	Dry weight of cells per litre of culture (mg)	Glycogen-glucose, % of dry weight	Total nitrogen, % of dry weight	Total bacterial nitrogen per litre of culture (mg)	Synthetic rate of glycogen
A	0.18	6.5	153.1	21.9	11.2	17.2	35.1
	0.18	6.5	148.4	20.6	11.4	16.9	32.5
	0.18	6.6	153.1	19.3	11.2	17.2	30.9
	0.18	6.5	151.9	17.9	11.3	17.1	28.6
	0.33	6.0	132.0	8.2	13.1	17.3	20.7
	0.36	6.0	135.7	7.8	13.0	17.6	21.7
	0.36	6.0	131.7	7.7	13.1	17.2	21.2
	0.36	6.0	129.5	8.1	13.0	16.8	22 4
	0.59	5.2	130.9	4.1	13.5	17.7	17.9
	0.59	5.2	130.4	3.2	13.3	17.3	14.2
	0.75	5.0	123.7	2.2	14.3	17.7	11.5
	0.94	4.9	100.4	2.3	14.3	14.3	15.1
	0.94	4.9	104.0	2.3	14.1	14.7	15.3
B	0.21	7.7	153.9	16.1	11.8	18.1	28.7
	0.21	7.7	152.0	15.2	11.6	17.7	27.5
	0.47	7.7	133.0	5.7	13.3	17.7	20.2
	0.47	7.7	130.0	6.0	13.6	17.7	20.7
	0.48	6.2	144.0	5.8	13.3	19.2	20.9
	0.48	6.2	138.9	5.5	13.4	18.6	19.7
	0.49	5.4	141.5	5.4	13.4	18.9	19.8
	0.49	5.4	142.1	6.8	13.2	18.7	25.3
	0.49	5.4	138.5	4.8	13.5	18.7	17.4
	0.50	5.9	137.1	5.4	13.4	18.4	20.1
	0.50	5.9	139.4	5.9	13.2	18.4	22.3
	0.50	5.8	142.2	5.4	13.2	18.8	20.4
	0.61	5.4	129.6	2.2	14.0	18.2	9.6
	0.61	5.4	130.8	2.5	14.1	18.3	10.9
	0.66	5.4	141.6	2.3	13.9	19.7	10.9
	0.66	5.4	142.4	2.5	13.8	19.6	12.0
	0.66	5.4	137.3	2.7	13.7	18.8	13.0

Expts. A and B. Carbon source: sodium lactate. Input concentration of ammonium-N: expt. A 20 mg/l; expt. B 22 mg/l. The values given in the last column of the tables represent the amount of glycogen synthesized in one hour per 100 mg bacterial nitrogen. These values were plotted against the dilution rate. The data of the best straight line being fitted by the method of least squares are given below (the values at higher dilutions rates than 0.7 h^{-1} are not included in the calculations). As regards the statistical methods the reader is referred to Fisher [19].

Regression equation: $y = 37.6 - 38.1\,x$
Regression coefficient: -38.1 ± 3.25 ($t = 11.74$; $p < 0.001$)
Correlation coefficient: -0.920 ± 0.030 ($t = 30.7$; $p < 0.001$).

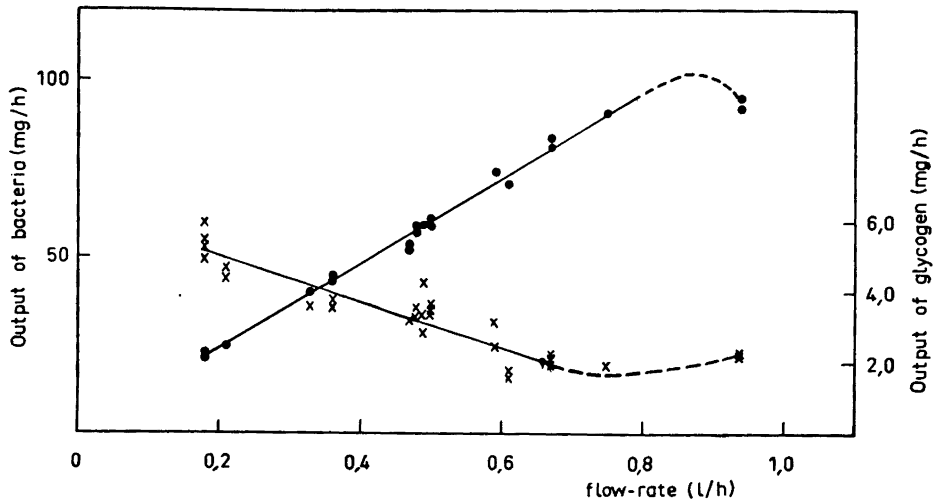


Fig. 1. Output of glycogen and bacteria at different flow-rates. Expts. A and B. Carbon source: sodium lactate. Culture volume: 1 litre. Input concentration of ammonium-N: 20 mg/l (the values of expt. B were corrected to correspond to this input concentration). The dry weight of cells per litre is indicated by dots (the glycogen content has been subtracted from the total dry weight values). The glycogen per litre is indicated by crosses, and the unbroken curve is fitted by the method of least squares.

Chemical methods. The isolation of glycogen and the estimation of the glycogen-glucose were performed as described by Palmstierna [12]. The micro-Kjeldahl method was used for the nitrogen determinations.

RESULTS

In continuous cultures of *Escherichia coli B* steady-state growth was obtained at different growth rates. Two media were employed: one with sodium lactate and the other with glucose as the carbon source. In other respects their composition was about the same. Using the nitrogen source as the limiting factor, specific growth rates * of 0.13—0.94 h^{-1} were established. The glycogen content and the total nitrogen content of the cells were determined. The results are presented in Tables 1 and 2. In experiments A and B (Table 1) sodium lactate was the carbon source; in experiments C and D (Table 2), it was glucose.

* The specific growth rate, μ, is defined by

$$\mu = \frac{1}{x}\frac{dx}{dt} = \frac{d\ (\log_e x)}{dt} = \frac{\log_e 2}{t_d}$$

where t_d is the doubling time, *i.e.* the time required for the concentration of organisms to double.

At equilibrium the specific growth rate (and the specific synthetic rate of every cell constituent) is equal to the dilution rate, D, defined as f/v, where f is the flow-rate in litres per hour and v is the culture volume.

The specific synthetic rate of glycogen increased considerably with decreasing dilution rates. The amount of glycogen synthesized in one hour at an input concentration of 20 mg ammonium-N per litre can be calculated by multiplying the per litre value of glycogen by the dilution rate value. In Figs. 1 and 2 the results are presented in that way. The output of bacterial cells (calculated as dry weight) is also recorded (the glycogen content has been subtracted from the total dry weight of the cells).

The values of the total nitrogen of the cells seemed to form a more accurate basis for the comparison of the synthetic rates of glycogen and nitrogen-

Table 2.

Experiment	Dilution rate	Input conc. of ammonium-N (mg/l)	Number of cells per ml $\times 10^{-6}$	Dry weight of cells per litre of culture (mg)	Glycogen-glucose, % of dry weight	Total nitrogen, % of dry weight	Total bacterial nirogen per litre of culture (mg)	Synthetic rate of glycogen
C	0.34	21	5.3	148.8	12.9	12.0	17.8	36.6
	0.34	21	5.3	146.5	12.5	12.2	17.9	34.8
	0.34	21	5.3	152.4	12.9	12.2	18.6	35.9
	0.35	21	6.0	147.8	11.8	12.2	18.1	33.8
	0.35	21	6.0	148.1	12.8	12.5	18.4	36.0
	0.35	21	6.1	148.4	12.1	12.4	18.4	34.2
	0.49	21	6.5	138.5	6.5	12.9	17.9	24.7
	0.49	21	6.0	139.3	7.2	13.1	18.3	26.9
	0.49	21	6.4	138.4	7.6	12.7	17.6	29.3
	0.66	21	4.1	130.1	5.5	13.6	17.7	26.6
	0.66	21	4.1	133.4	5.4	13.1	17.5	27.1
	0.66	21	4.0	133.5	5.6	14.1	18.8	26.2
	0.66	21	4.0	133.2	6.1	13.7	18.3	29.3
	0.72	21	3.6	135.6	5.4	13.4	18.2	28.9
	0.72	21	3.6	133.9	5.4	13.6	18.1	28.7
	0.72	21	3.7	133.6	4.5	13.8	18.5	23.4
	0.72	21	3.8	135.1	4.7	13.7	18.5	24.8
	0.84	22	6.0	148.4	3.6	13.1	19.4	23.1
	0.84	22	6.0	146.6	3.6	13.3	19.4	22.8
	0.86	22	6.0	146.3	3.4	13.2	19.3	22.2
	0.86	22	6.1	140.4	3.3	13.1	18.4	21.6
D	0.13	26	14	205.5	22.5	9.9	20.3	29.5
	0.17	26	14	205.5	20.0	10.8	22.2	31.5
	0.17	26	14	208.3	21.4	10.6	22.1	34.3
	0.24	26	14	199.2	15.4	11.5	22.9	32.1
	0.35	26	14	176.3	11.0	12.3	21.7	31.3
	0.35	26	14	176.8	11.2	12.3	21.7	31.9

Expts. C and D. Carbon source: glucose. The values of the synthetic rate of glycogen were plotted in the same way as for expts. A and B (the values at lower dilution rates than 0.2 h^{-1} were not included in the calculations).

Regression equation: $y = 40.2 - 20.4\,x$

Regression coefficient: -20.4 ± 2.43 ($t = 8.40$; $p < 0.001$)

Correlation coefficient: -0.872 ± 0.049 ($t = 17.8$; $p < 0.001$).

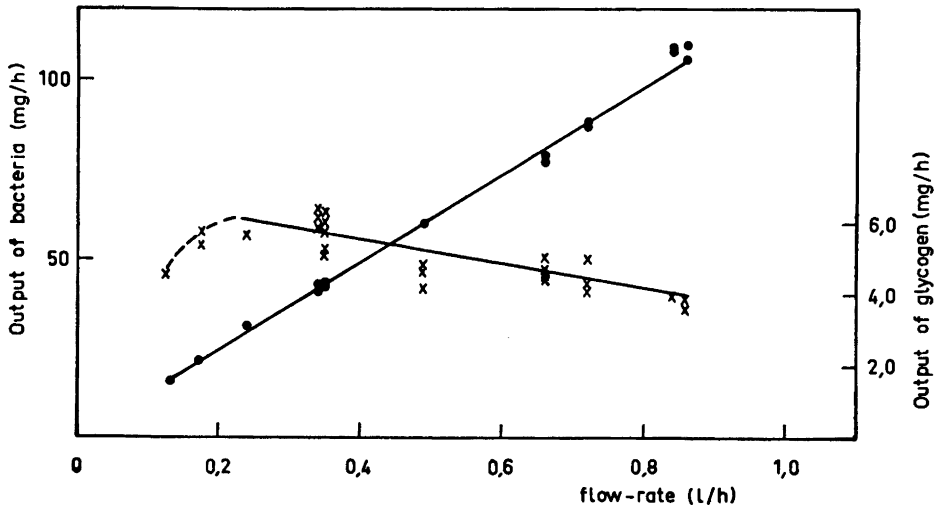


Fig. 2. Output of glycogen and bacteria at different flow-rates. Expts. C and D. Carbon source: glucose. Culture volume: 1 litre. The values are corrected to correspond to an input concentration of 20 mg ammonium-N per litre. For a description of the symbols see Fig. 1.

containing compounds. The amounts of glycogen synthesized in one hour per 100 mg bacterial nitrogen are recorded in the last column of the tables. It is seen that the synthetic rate of glycogen increases considerably when the dilution rate is diminished, *i.e.* when the synthetic rate of the nitrogen-containing compounds is reduced.

In the cultures grown in the lactate medium, the minimum content of glycogen in the continuously cultivated cells appeared to be reached at the highest dilution rates (>0.7 h^{-1}). A slight increase in the synthetic rate of glycogen might consequently have been expected with a further increase in the dilution rate. However, at the highest dilution rate, at which steady-state growth was obtained, the cell concentration was considerably lower than at the lower dilution rates. It is probable that the highest dilution rate, 0.94 h^{-1}, is very close to the maximum value of μ, and thus represents the highest dilution rate that can be attained. The quantitative relationships are best illustrated by the "output" curves in Fig. 1, representing the production of cells and glycogen by the continuous culture.

It appeared that the maximum content of glycogen in the continuously cultivated cells was reached in the cultures grown in glucose medium at the lowest dilution rates (<0.2 h^{-1}). The rate of glycogen synthesis, therefore, decreases at the lowest dilution rates in these cultures (Table 2, Fig. 2).

If the straight lines obtained from the values of the synthetic rate of glycogen in Tables 1 and 2 are drawn to the y axis, both will cut this axis at a value of about 40. This value is comparable with the initial synthetic rate of

glycogen * in batch cultures during nitrogen starvation, *i.e.* during a period when there is no synthesis of nitrogen-containing compounds [13]. This is also the case in the experiment recorded in Table 3, where continuously cultivated cells (dilution rate 0.46 h^{-1}) were used as inoculum in a batch culture. The medium contained no nitrogen source.

It was assumed in the calculations that the small differences in the input concentration of ammonium-N had no influence on the specific synthetic rate of glycogen. It was confirmed by one experiment in which the input concentration was increased to 54 mg ammonium-N per litre that this assumption was justified. The cell concentration was 385 mg dry weight per litre of culture. The synthetic rate of glycogen observed in this experiment was 26.5 ± 0.3 (mg per hour per 100 mg bacterial nitrogen; two determinations) at a dilution rate of 0.51 h^{-1} (carbon source: glucose).

In the continuous cultures where the carbon source was used as the limiting factor, no significant variations in the glycogen content of the cells were observed at different dilution rates. In one experiment in which sodium lactate was used as the limiting factor, glycogen determinations gave the following results: 1.5 % of the dry weight at a dilution rate of 0.33 h^{-1} and 1.1 % at a dilution rate of 0.14 h^{-1}.

Substances causing an absorption in the ultra-violet region poured out into the medium in the cultures with the nitrogen source as the limiting factor. The absorption increased considerably with decreasing dilution rates. The absorption curves for the cell-free culture medium from samples taken at different dilution rates are presented in Fig. 3.

During a certain period after the continuous addition of new medium had been started, it was found necessary to add carbon dioxide to the air

Table 3.

Time after inoculation (min)	Number of cells per ml $\times 10^{-8}$	Dry weight of cells per litre of culture (mg)	Glycogen-glucose, % of dry weight	Total nitrogen, % of dry weight	Total bacterial nitrogen per litre of culture (mg)
0	5.7	124.5	6.6	13.1	16.3
30	6.5	129.3	10.6	12.9	16.7
60	7.5	138.2	15.1	12.2	16.8
90	7.9	141.5	17.8	12.1	17.2

Cells from a continuous culture incubated in nitrogen-free medium. For further details, see the text.

* During the starvation phase in a nitrogen-starved culture the bacterial nitrogen per litre of culture is constant. The value of glycogen increase (calculated as mg glycogen per 100 mg bacterial nitrogen per h) was multiplied with $\log_e 2$ for the comparison with the values obtained in the continuous culture.

Calculated in this way the mean synthetic rate of glycogen during the first hour of the experiment recorded in Table 3 was 45.8.

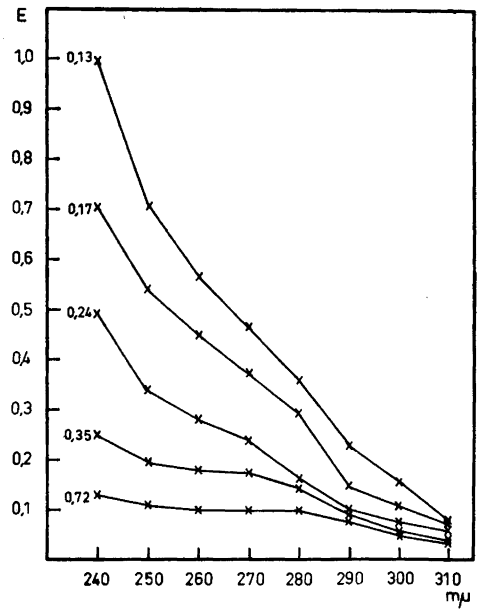


Fig. 3. Specific absorption (E) of the cell-free culture medium at different dilution rates, indicated by the figures at the end of each curve. Measurements were made on samples from expt. D, except those recorded at the dilution rate 0.72 h^{-1}, which were made on a sample from expt. C.

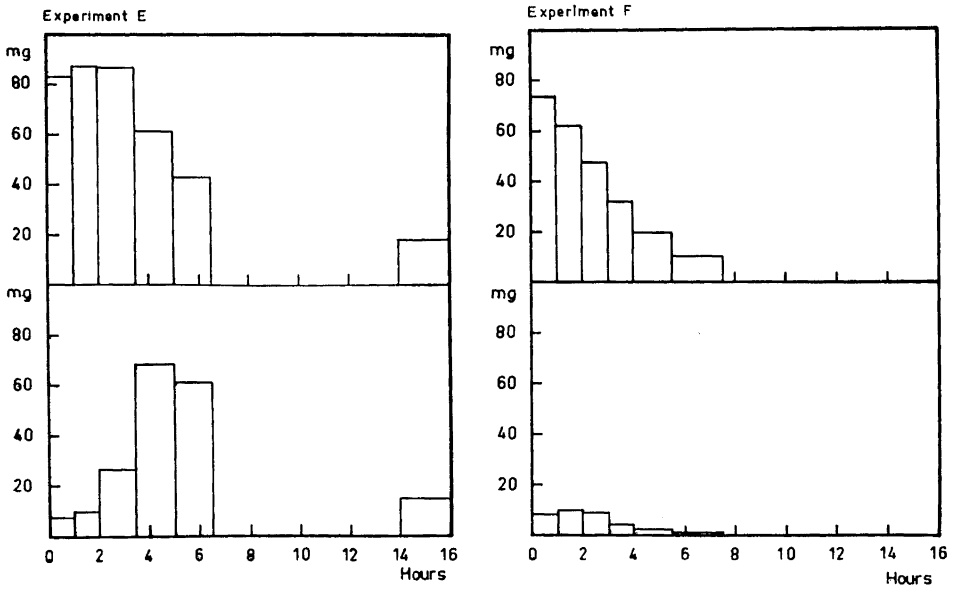


Fig. 4. Expts. E and F. The steeples in the upper parts of the figure indicate the total bacterial nitrogen per litre of culture. In the lower parts of the figure the glycogen per litre of culture is represented. At zero time the continuous addition of fresh medium was started. Dilution rate 0.29 h^{-1}.
Aeration: expt. E: Air+carbon dioxide (5 %); expt. F: Air only.

entering the culture, since otherwise the bacteria were completely washed-out. In order to investigate the role of the carbon dioxide during this period, the following experiment was carried out. Two cultures were allowed to grow in the lactate medium until they reached a cell concentration of about 2×10^9 whereupon the continuous addition of deficient medium (20 mg ammonium-N per litre) was begun. The dilution rate was 0.29 h^{-1} in both cultures. About 5 % carbon dioxide was added to the air entering one of the cultures (expt. E); the other was aerated with air alone (expt. F). The emergent bacterial suspensions were collected and the cells from each sample analyzed (Table 4, Fig. 4). The time required for collecting each sample was 1—2 h (see Table 4).

In expt. E, where carbon dioxide was added to the air, the glycogen content of the cells increased considerably during the first part of the contiunous run. The cell concentration decreased after an initial increase. Fourteen hours after the continuous addition of deficient medium had been started, steady-state concentrations of cells and glycogen were noted. Addition of carbon dioxide to the air in a culture in the steady-state had no measurable influence on the glycogen content of the cells. In expt. F, in which no carbon dioxide was added, the cell concentration decreased immediately. The glycogen content of the cells was low. Forteen hours after the start of the continuous run, no cells could be detected in the counting chamber.

Table 4.

Experiment	Sample (h)	Number of cells per ml $\times 10^{-8}$	Dry weight of cells per litre of culture (mg)	Dry weight per cell (mg $\times 10^{-10}$)	Glycogen-glucose, % of dry weight	Total nitrogen, % of dry weight	Glycogen-glucose per litre of culture (mg)	Total bacterial nitrogen per litre of culture (mg)
E	0—1	25	571.7	2.3	1.3	14.6	7.4	83.3
	1—2	39	609.7	1.6	1.6	14.3	9.8	87.0
	2—3.5	23	606.8	2.6	4.4	14.3	26.7	86.5
	3.5—5	21	511.8	2.4	13.4	11.9	68.6	60.8
	5—6.5	19	384.0	2.0	16.0	11.2	61.4	43.1
	14—16	5.4	149.6	2.8	9.9	12.1	14.8	18.1
F	0—1	27	509.3	1.9	1.6	14.4	8.1	73.5
	1—2	22	438.0	2.0	2.3	14.2	10.1	62.2
	2—3	18	335.4	1.9	2.6	14.1	8.7	47.4
	3—4	13	223.7	1.7	1.8	14.3	4.0	31.9
	4—5.5	9.0	136.7	1.5	1.4	14.3	1.9	19.5
	5.5—7.5	4.5	71.9	1.6	0.9	14.2	0.6	10.2
	14—16	<0.1	—					

Expts. E and F. Carbon source: sodium lactate. At zero time the continuous addition of fresh medium was started. Dilution rate 0.29 h^{-1}.
Aeration: expt. E: Air + carbon dioxide (5 %)
expt. F: Air only.

DISCUSSION

The application of the continuous culture technique to metabolic studies has given valuable information concerning the regulation of the rates of various synthetic processes [8,11]. A substance of general interest, namely glycogen, shown by Palmstierna [12] to be present in *E. coli* cells was the subject of continuous culture studies in the present investigation. Due to its function as a pool of energy and carbon in the cell, the regulation of its synthesis seemed to be of special interest.

Since the glycogen contains no nitrogen, its synthesis is not prevented by nitrogen deficiency in *E. coli* cells. On the other hand, energy-consuming processes like the syntheses of nucleic acids and protein are readily arrested by nitrogen starvation. When the nitrogen source was used as a growth-limiting substance in the continuous culture, the glycogen synthesis proceeded without being reduced by this limitation, and the synthetic rate could be shown to depend on the synthetic rate of the nitrogen-containing compounds.

This system also offers the possibility of studying the influence of various environmental factors on the synthetic rate of glycogen in the bacterial cells, *e.g.* temperature, pH, oxygen tension, concentration of different medium constituents and other substances. In the present investigation it was observed that the rate of glycogen synthesis depended on the nature of the carbon source in the culture medium. At a high synthetic rate of the nitrogen-containing compounds there was a lower synthetic rate of glycogen when lactate was the carbon source than when glucose was used. A possible explanation of this could be that the lactate must undergo a long series of transformations before it can be incorporated into the glycogen. The glucose on the other hand, is more easily incorporated in spite of the rapid breakdown. The difference in the synthetic rates appears to diminish when the synthetic rate of the nitrogen-containing compounds is reduced, *i.e.* when the carbon source is not utilized to any great extent for the synthesis of these compounds and consequently a greater part is available for glycogen synthesis.

It should be pointed out that glycogen appears to be the main substance that accumulates in the cells of *E. coli B* during nitrogen deficiency. This is made probable by the constant values obtained when the glycogen content of the cells is subtracted from the total dry weight. This has also been confirmed by using the nitrogen starvation technique in batch cultures.

As a rough method of estimating the "overflow metabolism" to the medium the ultra-violet absorption of the cell-free culture medium has been determined. The nature of these substances has not been investigated. It has been shown by Dagley *et al.* [20] that pyruvate is poured out at high rates during nitrogen starvation in batch cultures of *Aerobacter aerogenes*.

Different methods for starting the continuous run of the cultures have been applied. In experiment E the method used in the present investigation is demonstrated. Carbon dioxide was added to the air during the dilution period. In experiment F, where no carbon dioxide was added, there was a more rapid decrease than in experiment E during the first two hours, when the concentration of ammonium chloride could not be limiting. During the following period of rapid dilution, the decrease in bacterial nitrogen per litre of culture

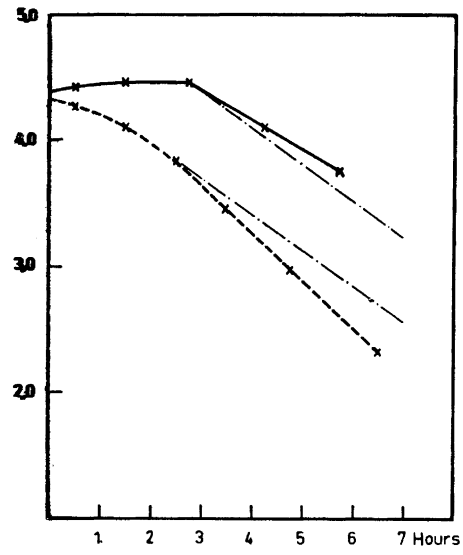


Fig. 5. The first part of the continuous run in expts. E (unbroken curve) and F (broken curve). The curves represent the $\log_e$ for the total bacterial nitrogen per litre of culture (the points are placed at the midpoints of the time intervals represented by the steeples in Fig. 4). The thin broken curves represent the "wash-out rate", *i.e.* the rate at which the organisms initially present in the vessel would be washed out if no growth occurred.

seemed to be more rapid than the wash-out rate (Fig. 5). This may be explained by a lysis of the cells. Fourteen hours after the start of the continuous addition, the number of cells in the culture vessel was less than 10^7 per ml and no increase was noted upon further incubation. In experiment E, where carbon dioxide was added to the air entering the culture the decrease in bacterial nitrogen per litre of culture seemed to be somewhat less rapid than the wash-out rate, but the difference is too small to be considered as significant (Fig. 5). It is however evident that during some part of the time required for stabilizing the culture, there must have been a stimulation of the synthesis of the nitrogen-containing compounds by the carbon dioxide since steady-state concentration of the cells was obtained at fourteen hours after the start of the continuous run.

Obviously the method of nitrogen limitation offers excellent possibilities for the control of glycogen yields. The relationships described might well serve as a model for the commercial production of nitrogen-free substances other than glycogen, cellular or extracellular.

REFERENCES

1. Monod, J. *Ann. Inst. Pasteur*, **79** (1950) 390.
2. Novick, A. and Szilard, L. *Proc. Natl. Acad. Sci. N.Y.* **36** (1950) 708.
3. Novick, A. and Szilard, L. *Science* **112** (1950) 715.
4. Hedén, C.-G., Holme, T. and Malmgren, B. *Acta Pathol. Microbiol. Scand.* **37** (1955) 42.
5. Herbert, D., Elsworth, R. and Telling, R. C. *J. Gen. Microbiol.* **14** (1956) 601.
6. Karush, F., Iacocca, V. F. and Harris, T. N. *J. Bacteriol.* **72** (1956) 283.
7. Perret, C. J. *J. Gen. Microbiol.* **16** (1957) 250.
8. Monod, J. and Cohn, M. *Advances in Enzymol.* **14** (1952) 67.
9. Novick, A. and Szilard, L. *Cold Spring Harbour Symposia Quant. Biol.* **16** (1951) 337.
10. Novick, A. and Szilard, L. *Nature* **170** (1952) 926.

11. Novick, A. and Szilard, L. *Dynamics of Growth Processes*, Princeton Univ. Press, Princeton, New Jersey 1954.
12. Palmstierna, H. *Acta Chem. Scand.* **10** (1956) 567.
13. Holme, T. and Palmstierna, H. *Acta Chem. Scand.* **10** (1956) 578.
14. Holme, T. and Palmstierna, H. *Acta Chem. Scand.* **10** (1956) 1553.
15. Holme, T. and Palmstierna, H. *Acta Chem. Scand.* **10** (1956) 1557.
16. Holme, T., Laurent, T. and Palmstierna, H. *Acta Chem. Scand.* **11** (1957) 757.
17. Friedlein, F. *Biochem. Z.* **164** (1928) 273.
18. Hook, A. E., Beard, D., Taylor, A. R., Sharp, D. G. and Beard, J. W. *J. Biol. Chem.* **165** (1946) 241.
19. Fisher, R.A. *Statistical Methods for Research Workers*, Oliver & Boyd, Edinburgh 1950.
20. Dagley, S., Dawes, E.E. and Morrison, G.A. *J. Bacteriol.* **61** (1951) 433.

Received March 15, 1957.

ACTA CHEMICA SCANDINAVICA 11 (1957) 776—779

On the Reaction between Urea and Formaldehyde in Neutral and Alkaline Solutions

VII. A Spectrophotometrical Method for Quantitative Determination of Urea and Methylol Ureas of the Reaction Mixture

NILS LANDQVIST

Rydboholms A.B., Rydboholm, Sweden

A spectrophotometrical method for quantitative determination of urea, mono- and dimethylol urea in reaction mixtures of urea and formaldehyde is described. The method is based on a colour reaction between the ureas and *p*-dimethylaminobenzaldehyde in the presence of hydrochloric acid. The influence of side reactions is sufficiently reduced when the reaction mixture sample is added to an excess of a methanolic solution of the reagent.

A comparatively selective colour reaction between urea and *p*-dimethylaminobenzaldehyde in acid solutions was described by Weltman and Barrenscheen [1], and was later on applied for spectrophotometrical determination of urea by Watt and Chrisp [2].

This kind of reaction has been found to be suitable for a quantitative determination of urea, mono- and dimethylol urea of urea-formaldehyde reaction mixtures, when combined with a determination of unreacted formaldehyde.

However, it is necessary to reduce the rates of reaction of the components of the reaction mixture in the presence of a strong acid, in order to obtain consistent results. This condition is realized when the reaction mixture sample is added to a large excess of a methanolic solution of the reagent.

In the following some experiments are described, on which the analytical method is based.

Reagent solution: 10 g/l *p*-dimethylaminobenzaldehyde, dissolved in methanol after addition of 10 ml/l concentrated hydrochloric acid. For one of the experiments a series of different concentrations was used. All chemicals of A. R. quality.

Other chemicals: Urea of A. R. quality; mono- and dimethylol urea prepared in accordance with Walter and Gewing [3]. Cryoscopic molecular weights: 90 ± 1 and 120 ± 1, respectively. Formaldehyde, containing only traces of methanol and formic acid.

Spectrophotometer: Hilger & Watt's "Uvispec". Cell length 20 mm.

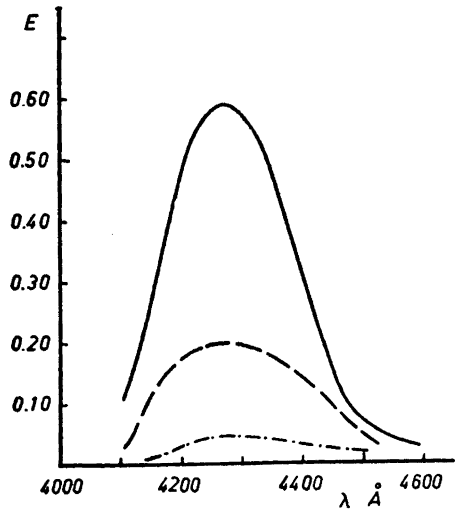


Fig. 1. Extinction curves of 0.0070 M urea (———), 0.0070 M monomethylol urea (— — —) and 0.0120 M dimethylol urea (—·—·). 2 ml sample + 10 ml reagent solution.

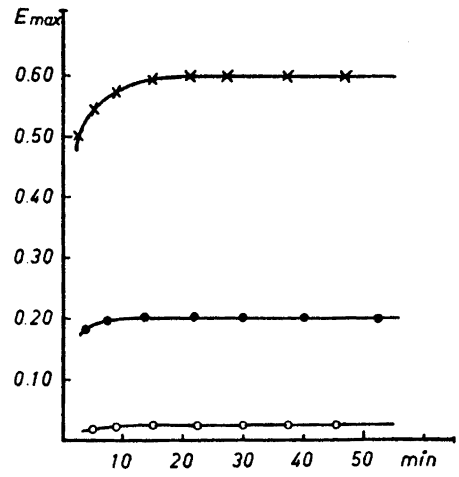


Fig. 2. Relationship between maximum extinction and time delay between preparation and spectrophotometry. 0.0070 M solutions of urea (×), mono- (●) and dimethylol urea (○). 2 ml sample + 10 ml reagent solution.

All experiments were carried out at 20 °C. The samples of the mono- and dimethylol urea solutions were added to the reagent solutions immediately after the dissolution of the ureas in distilled water. This was made in order to avoid disturbances from hydrolysis reactions.

A. To 2 ml of 0.0070 M urea, 0.0070 M mono- and 0.0120 M dimethylol urea, 10 ml of the reagent solution were added. When a constant extinction was attained (after ~20 min), the extinction curves were determined. The results are given i Fig. 1. From a preliminary study it was found that the wavelength at the extinction maximum is constant within the concentration range studied. $\lambda_{max} = 4\,270$ Å.

B. The dependence of the maximum extinction on the time elapsed between reagent addition and spectrophotometry is described by Fig. 2. The curves are related to 0.0070 M solutions, 2 ml sample and 10 ml reagent solution. At lower concentrations the asymptotic values were attained with less delay of time. As found from these measurements, 20—30 min interval between preparation and measurement is sufficient; the value attained is then constant during 1—2 h.

C. The relation between *p*-dimethylaminobenzaldehyde concentration of the reagent solution and maximum extinction is elucidated by Fig. 3, related to 0.0020 M urea, 2 ml sample + 10 ml reagent solution. The same behaviour was also observed for the methylol ureas. Below a reagent concentration of 20 g/l the curves are linear. From these results it might be concluded that the

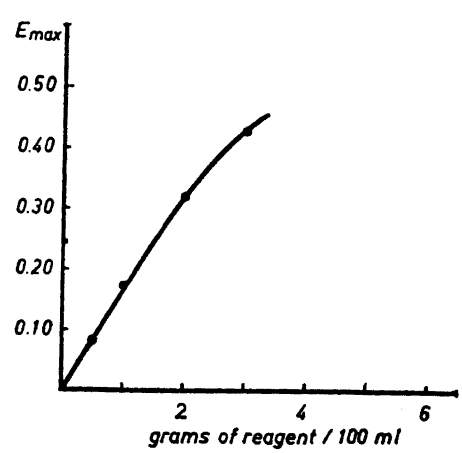


Fig. 3. Relationship between maximum extinction and reagent concentration. 0.0020 M urea. 2 ml sample + 10 ml reagent solution.

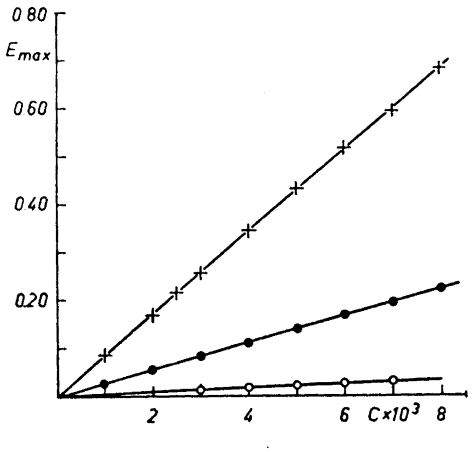


Fig. 4. Relationship between maximum extinction and sample concentration of urea (+), mono- (●) and dimethylol urea (○).

concentration of the coloured compound is determined by an equilibrium between the reagent and the ureas.

D. In Fig. 4 the relation between the concentration of urea, mono- and dimethylol urea of the reaction samples and the maximum extinction is shown. 2 ml sample added to 10 ml reagent solution; 30 min time delay between preparation and measurement.

A good linearity is present over the concentration range studied, $0 < C < 7 \times 10^{-3}$. The curves are described by the expressions:

$$C_U = 1.16 \times 10^{-2} \times E_{max} \quad (1)$$
$$C_M = 3.55 \times 10^{-2} \times E_{max} \quad (2)$$
$$C_D = 23 \times 10^{-2} \times E_{max} \quad (3)$$

where C_U = sample concentration of urea, C_M = sample concentration of monomethylol urea, C_D = sample concentration of dimethylol urea, E_{max} = maximum extinction.

E. To several of the solutions mentioned above formaldehyde was added in amounts corresponding to 0.1 M just before the addition of the reagent solution. No immediate or time dependent influence on the extinction was observed. The same behaviour was also found for mixtures of urea and methylol ureas.

F. In order to investigate whether the expressions (1)—(3) are valid also for solutions containing mixtures of urea and the methylol ureas, such mixtures were studied. The compositions and the results are given in Table 1. As can be seen, there is a good correlation between actual and calculated data. Thus, we can, for the concentration range investigated, accept the expression:

Table 1. Experimental and calculated maximum extinction data of urea, mono- and dimethylol urea solution mixtures.

$C_U \times 10^3$	$C_M \times 10^3$	$C_D \times 10^3$	E_{max}	
			measured	calculated
1.0	5.0	3.0	0.239	0.238
—	5.0	5.0	0.165	0.163
5.0	1.0	—	0.463	0.458
7.0	3.0	2.0	0.690	0.695
2.0	5.0	6.0	0.342	0.338
0.5	4.0	7.0	0.184	0.186
3.0	3.0	3.0	0.350	0.355
0.5	2.0	6.0	0.124	0.125
1.5	4.5	3.0	0.271	0.268
0.75	6.0	2.0	0.238	0.242

$$E_{max} = 86\ C_U + 28\ C_M + 4.3\ C_D \quad (4)$$

This expression is easily derived from (1)—(3).

For a reaction mixture of urea and formaldehyde, C_U° and C_F° are the initial urea and formaldehyde concentrations, and we have, provided mono- and dimethylol urea are the reaction products:

$$C_U^\circ = C_U + C_M + C_D$$
$$C_F^\circ = C_F + C_M + 2\ C_D$$

By means of this and eqn. (4) we obtain:

$$C_U = 0.0292\ E_{max} - 1.51\ C_U^\circ + 0.71\ C_F^\circ - 0.71\ C_F \quad (5)$$

Thus, from a determination of the concentration of unreacted formaldehyde, C_F, and the spectrophotometrical measurement, the actual composition of a reaction mixture might be determined with, from the technical point of view, good accuracy.

The author wishes to thank the board of Rydboholms A. B. for permission to publish this paper, and is also highly indebted to Mr. G. Johansson for his valuable assistance in the experimental work.

REFERENCES

1. Weltman, O. and Barrenscheen, H. K. *Klin. Wochschr.* **1922** 1100.
2. Watt, G. W. and Chrisp, J. H. *Anal. Chem.* **25** (1954) 452.
3. Walter, G. and Gewing, M. *Kolloid-Beih.* **34** (1934) 163.

Received February 26, 1957.

ACTA CHEMICA SCANDINAVICA 11 (1957) 780—785

On the Reaction between Urea and Formaldehyde in Neutral and Alkaline Solutions

VIII. Studies of the Reactions and Equilibria at Formaldehyde-Urea Molecular Ratios in the Range 1.4—2.0

NILS LANDQVIST

Rydboholms A.B., Rydboholm, Sweden

Reactions and equilibria at formaldehyde-urea ratios in the range 1.4—2.0 were investigated experimentally at 20 °C.

The general reaction rate equation was solved by means of an electronic differential analyser, using rate constants previously determined for the different reactions involved. The equilibrium concentrations were calculated, and both the course of reaction and equilibrium show a good agreement between experimental and theoretically determined data.

An empirical relationship between free formaldehyde and reaction time is also given.

For several practical purposes, *e. g.* the use of methylol ureas for textile finishing purposes, the reaction between formaldehyde and urea at molecular ratios within the range 1.4—2.0 is of a great interest. The purpose of the following paper is to describe studies of the kinetics of such reactions at 20 °C and to give the results of investigations on the equilibrium state of said reactions.

The experiments were carried out by means of the chemicals and the technique previously described [1,9].

We introduce the following symbols:

Concentrations: U = urea; U_0 = urea, initial; F = formaldehyde; F_0 = formaldehyde, initial; M = monomethylol urea; D = dimethylol urea.

Reaction rate constants: monomethylol urea: k = formation, k' = hydrolysis; dimethylol urea: k_1 = formation, k_2 = hydrolysis.

Reaction time: t.

If mono- and dimethylol urea are assumed to be the reaction products, see *e. g.* de Jong and de Jonge [2-4], the general reaction rate equations can be written:

$$\left.\begin{aligned}
&\frac{dM}{dt} = k \cdot U \cdot F - k' \cdot M - k_1 \cdot M \cdot F + k_2 \cdot D \\
&\frac{dD}{dt} = k_1 \cdot M \cdot F - k_2 \cdot D \\
&U = U_0 - M - D;\ F = F_0 - M - 2\ D \\
&t = 0:\ U = U_0;\ F = F_0;\ M = D = 0 \\
&t \to \infty\ \frac{dM}{dt} = \frac{dD}{dt} = 0
\end{aligned}\right\} \quad (1)$$

If we write: $\tau = k \cdot t$; $k'/k = \alpha$; $k_1/k = \beta$; $k_2/k = \gamma$; we have:

$$\left.\begin{aligned}
&\frac{dM}{d\tau} = U_0 \cdot F_0 - [U_0 + (1 + \beta) \cdot F_0 + \alpha] \cdot M + (1 + \beta) \cdot M^2 + \\
&\qquad (3 + 2\ \beta) \cdot M \cdot D - (2\ U_0 + F_0 - \gamma) \cdot D + 2\ D^2 \\
&\frac{dD}{d\tau} = \beta \cdot F_0 \cdot M - \beta \cdot M^2 - 2\ \beta \cdot M \cdot D - \gamma \cdot D \\
&\tau = 0:\ M = D = 0;\ \tau \to \infty\ :\ \frac{dM}{d\tau} = \frac{dD}{d\tau} = 0
\end{aligned}\right\} \quad (2)$$

Since a simple solution to the system of differential equations given above cannot easily be found, numerical solutions were obtained by means of an electronic differential analyser, the EIDA of Chalmers University of Technology, Gothenburg.

The accuracy of the solutions are, as calculated on the initial formaldehyde concentrations, of the order 3 %. Thus, the figures related to high τ values, $\tau > 4$, are moderately accurate. However, the equilibrium concentrations can be calculated exactly, as will be shown later on.

Numerical solutions given as $F = f(\tau)$ curves in Figs. 1—3 refer to 1 M urea and formaldehyde-urea ratios 1.4, 1.6 and 2.0. The buffer concentration was 0.050 M and the temperature 20 °C. The buffers were KH_2PO_4, pH = 6.70; borax, pH = 9.20; Na_2CO_3, pH = 10.00 at cationic strengths as in previous studies [1,5–7]. The reaction rate constants were taken from these studies. As can be seen, experimental data agree closely with the calculated curves. From this is might be concluded that the reaction rate constants, as previously determined under specialized conditions, are applicable to the more general case.

An example of the concentration-reaction time relationships of the reactants and the reaction products is given in Fig. 4, as calculated by means of the electronic differential analyser for 1.0 M urea + 1.7 M formaldehyde, 0.050 M Na_2CO_3, pH 10.00, 20 °C. The concentrations of urea, mono- and dimethylol urea were determined in accordance with Landqvist [9]. As seen from Fig. 4, experimental data and calculated curves are in a close agreement.

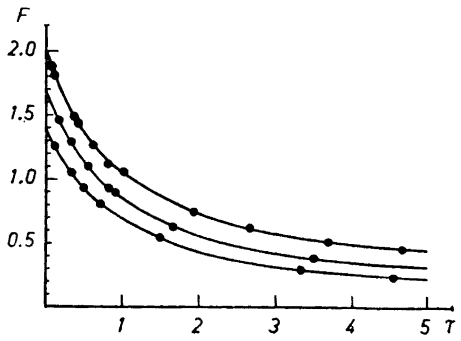


Fig. 1. Relationship between unreacted formaldehyde and the τ-value for the reactions between formaldehyde and 1 M urea at the molecular ratios 1.4, 1.7, 2.0; 0.050 M KH_2PO_4, pH 6.70. Temperature: 20 °C. The curve: theoretical solution, (●): experimental data.

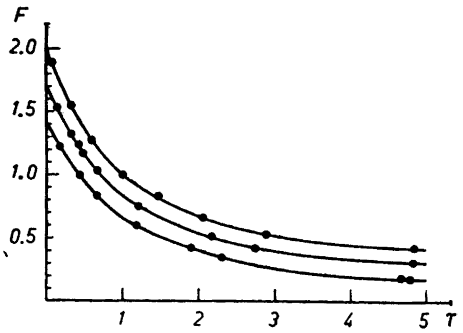


Fig. 2. Relationship between unreacted formaldehyde and the τ-value for the reactions between formaldehyde and 1 M urea at the molecular ratios 1.4, 1.7, 2.0; 0.050 M borax, pH 9.20. Temperature: 20 °C. The curve: theoretical solution, (●): experimental data.

In a previous paper [8], an empirical equation for the relationship between free formaldehyde and the reaction time was given:

$$\log \log \frac{F_0}{F} = A \cdot \log \log t + B \qquad (3)$$

This equation was found to be approximately valid in the case of equal con-

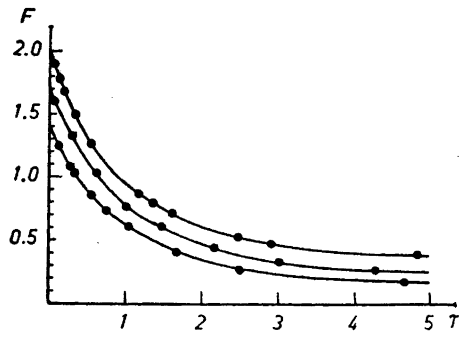


Fig. 3. Relationship between unreacted formaldehyde and the τ-value for the reactions between formaldehyde and 1 M urea at the molecular ratios 1.4, 1.7, 2.0; 0.050 M Na_2CO_3, pH 10.00. Temperature: 20 °C. The curve: theoretical solution, (●): experimental data.

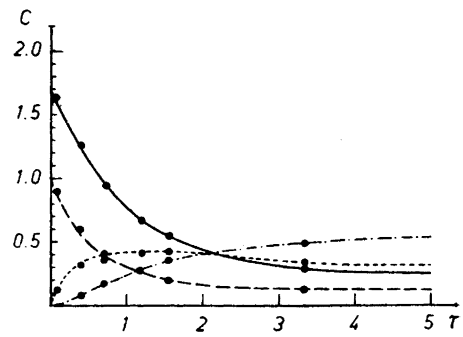


Fig. 4. Relationship between the reaction solution composition and the τ-value; 1.0 M urea and 1.7 M formaldehyde. 0.050 Na_2CO_3, pH 10.00, 20 °C. (———) formaldehyde, (— — —) urea, (. . . . .) monomethylol urea and (—.—.—) dimethylol urea. The curves: theoretical solutions, (●): experimental data.

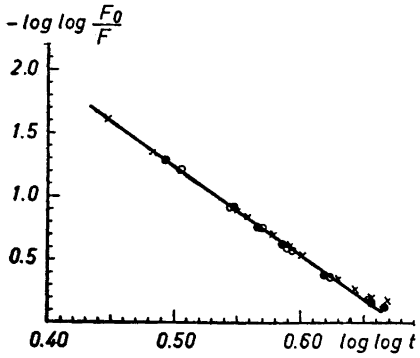


Fig. 5. The expression (3) applied to the reaction between formaldehyde and 1 M urea at the molecular ratios 1.4 (●), 1.7 (○) and 2.0 (×). 0.050 M KH_2PO_4, pH 6.70, 20 °C.

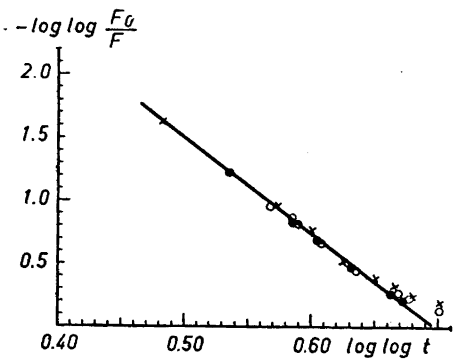


Fig. 6. The expression (3) applied to the reaction between formaldehyde and 1 M urea at the molecular ratios 1.4 (●), 1.7 (○) and 2.0 (×). 0.050 M borax, pH 9.20, 20 °C.

centrations of the reactants. The same equation applied to the solutions mentioned above is shown by the plots of Figs. 5—7. Curves of this kind may be of value when applied to practical work.

From the previous equations we find the equilibrium conditions:

$$t \rightarrow \infty : \frac{\mathrm{d}M}{\mathrm{d}t} = \frac{\mathrm{d}D}{\mathrm{d}t} = 0$$

$$M = \frac{k}{k'} \cdot U \cdot F = K_1 \cdot U \cdot F; \; D = \frac{k_1}{k_2} \cdot M \cdot F = \frac{k \cdot k_1}{k' \cdot k_2} \cdot U \cdot F^2 = K_2 \cdot U \cdot F^2$$

$$U_0 = U \; (1 + K_1 \cdot F + K_2 \cdot F^2); \; F_0 = F + U \; (K_1 \cdot F + 2 \cdot K_2 \cdot F^2)$$

and

$$\frac{F_0 - F}{U_0} = \frac{K_1 \cdot F + 2 \; K_2 \cdot F^2}{1 + K_1 \cdot F + K_2 \cdot F^2} \tag{4}$$

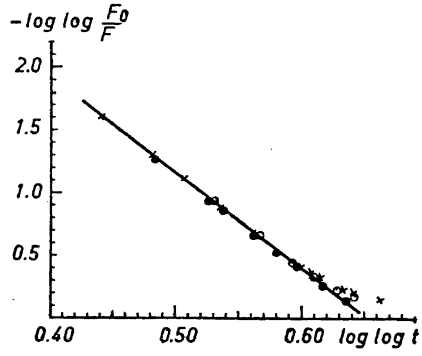


Fig. 7. The expression (3) applied to the reaction between formaldehyde and 1 M urea at the molecular ratios 1.4 (●), 1.7 (○) and 2.0 (×). 0.050 M Na_2CO_3, pH 10.00, 20 °C.

This equation can be solved straightforwardly, or by means of step by step approximation, starting from $F_0 - F \sim F_0$. Thus U, M and D can be calculated. The amounts of unreacted formaldehyde of the reaction solutions previously discussed in this paper were determined up to very long reaction times, ~100 h. From plots of the formaldehyde concentrations *versus* the inverse of the reaction time, the figures corresponding to infinite reaction time were found by extrapolation to zero. Further, these reaction solutions were diluted, and then subject to the same procedure. Finally, for some of the solutions the amounts of urea, mono- and dimethylol urea were determined in accordance with Landqvist [9]. The results can be found in Table 1, and we find that calculated equilibrium data agree with the observed values.

Table 1. Equilibrium data of reactions between formaldehyde and urea at the molecular ratios 1.4, 1.7 and 2.0. Temperature 20 °C. Buffer concentrations: 0.050 M.

Urea concentration U_0	Molecular ratio	Buffer	Calculated data				Observed data			
			U	M	D	F	U	M	D	F
1.0	1.4	KH_2PO_4	0.13	0.47	0.41	0.13	0.13	0.46	0.41	0.12
	1.7	pH 6.70	0.06	0.38	0.56	0.21	0.07	0.36	0.57	0.21
	2.0		0.03	0.28	0.69	0.34	0.03	0.27	0.70	0.33
	1.4	Borax	0.14	0.43	0.43	0.11	0.15	0.43	0.42	0.11
	1.7	pH 9.20	0.07	0.36	0.57	0.19	0.07	0.34	0.59	0.18
	2.0		0.03	0.26	0.71	0.32	0.02	0.28	0.70	0.32
	1.4	Na_2CO_3	0.15	0.40	0.45	0.10	0.16	0.43	0.41	0.10
	1.7	pH 10.00	0.07	0.33	0.60	0.17	0.08	0.32	0.60	0.18
	2.0		0.03	0.23	0.74	0.30	0.03	0.24	0.73	0.29
0.50	1.4	KH_2PO_4				0.10				0.10
	1.7	pH 6.70				0.16				0.16
	2.0					0.23				0.22
	1.4	Borax				0.09				0.09
	1.7	pH 9.20				0.15				0.15
	2.0					0.20				0.20
	1.4	Na_2CO_3				0.10				0.09
	1.7	pH 10.00				0.13				0.13
	2.0					0.20				0.20
0.33	1.4	KH_2PO_4				0.09				0.09
	1.7	pH 6.70				0.13				0.14
	2.0					0.18				0.18
	1.4	Borax				0.08				0.07
	1.7	pH 9.20				0.12				0.12
	2.0					0.16				0.16
	1.4	Na_2CO_3				0.09				0.08
	1.7	pH 10.00				0.11				0.11
	2.0					0.16				0.15

The author wishes to thank the board of Rydboholms A.B. for permission to publish this paper, and is also indebted to Dr. V. Wenzel and Mr. Ö. Karlsson for carrying out the work on the electronic differential analyser, and to Mr. G. Johansson for his valuable assistance in the experimental work.

REFERENCES

1. Landqvist, N. *Acta Chem. Scand.* **9** (1955) 1121.
2. de Jong, J. I. and de Jonge, J. *Rec. trav. chim.* **7** (1952) 643.
3. de Jong, J. I. and de Jonge, J. *Rec. trav. chim.* **7** (1952) 662.
4. de Jong, J. I. and de Jonge, J. *Rec. trav. chim.* **7** (1952) 840.
5. Landqvist, N. *Acta Chem. Scand.* **9** (1955) 1459.
6. Landqvist, N. *Acta Chem. Scand.* **9** (1955) 1466.
7. Landqvist, N. *Acta Chem. Scand.* **9** (1955) 1471.
8. Landqvist, N. *Acta Chem. Scand.* **9** (1955) 1477.
9. Landqvist, N. *Acta Chem. Scand.* **11** (1957) 776.

Received February 26, 1957.

ACTA CHEMICA SCANDINAVICA 11 (1957) 786—791

On the Reaction between Urea and Formaldehyde in Neutral and Alkaline Solutions

IX. The Influence of Methanol on the Rates of Reaction

NILS LANDQVIST

Rydboholms A.B., Rydboholm, Sweden

The effects of methanol on the rates of the urea-formaldehyde reactions were studied. Decreased rates were observed at increasing amounts of methanol in the case of urea or monomethylol urea and formaldehyde reactions. No influence on the hydrolysis reactions was found.

The formation of a hemiacetal between methanol and formaldehyde was studied cryoscopically as regards the rate constants and the equilibrium. On the basis of the theory that the hemiacetal does not take part in the reactions mentioned above some rate and equilibrium relationships were derived and found to be in agreement with experimental data.

It has been observed by, *e. g.*, Smythe [1] that the presence of methanol in urea-formaldehyde reaction mixtures decreases the rate of reaction. Since commercially available formaldehyde solutions very often contain methanol, added in order to prevent polymer precipitation, the effect mentioned is of some technical importance. The scope of the following paper is to describe some investigations carried out in order to study the influence of methanol on the rates of the different urea-formaldehyde reactions.

It is known that methanol and formaldehyde form a hemiacetal as follows:

$$HCHO + CH_3OH = CH_3 \cdot O \cdot CH_2OH \qquad (A)$$

The role of such a compound in water-methanol solutions containing different amounts of formaldehyde was investigated cryoscopically.

Chemicals: Formaldehyde stock solutions prepared by means of distillation of A. R. paraformaldehyde solutions.

Procedure: All experiments refer to 20 °C. Formaldehyde solutions were prepared by dilution of stock solutions at least 24 h before the addition of the methanol; this was made in order to allow any depolymerisation reactions to be completed. The alcohol was then stirred into these solutions and samples were taken and investigated cryoscopically until a constant value was obtained. This means that from time to time samples at 20 °C

were cooled quickly and the freezing temperature determined; the total change in this temperature was calculated as the difference between the temperatures at extrapolated zero and infinite reaction time. The figure corresponding to zero reaction time was always in good agreement with calculated data.

The equilibrium constants of reaction (A) were calculated from:

$$\frac{C_{CH_3OCH_2OH}}{C_{HCHO} \cdot C_{CH_3OH}} = K \tag{1}$$

The reaction solution composition and the results obtained can be found in Table 1.

Table 1. Equilibrium constants of the hemiacetal formation between methyl alcohol and formaldehyde. 20 °C.

C_{CH_3OH}	C_{HCHO}	K liter / moles
0.100	0.100	0.67
0.100	0.274	0.63
0.250	0.264	0.63
0.500	0.264	0.64
1.018	0.274	0.66
0.250	0.537	0.63
1.018	0.537	0.68
0.500	1.048	0.64
		Av. 0.65

As seen from this table, the K values are acceptably constant, thus reaction (A) may be the most important one under the conditions here studied.

The reaction rate equation can be written:

$$\frac{dy}{dt} = k_1 \, (C_M - y) \cdot (C_F - y) - k_2 \cdot y \tag{2}$$

where

y = concentration of the hemiacetal.
C_M = initial concentration of methanol.
C_F = initial concentration of formaldehyde.
k_1 = formation rate constant.
k_2 = dissociation rate constant.
t = time of reaction.

Initial conditions: $t = 0$, $y = 0$.

The solution to eqn. (2) can be written:

$$\varphi = k_1 \cdot t = \frac{1}{\sqrt{b^2 - 4\,a}} \cdot \ln \frac{(2\,y + b - \sqrt{b^2 - 4\,a}) \cdot (b + \sqrt{b^2 - 4\,a})}{(2\,y + b + \sqrt{b^2 - 4\,a}) \cdot (b - \sqrt{b^2 - 4\,a})} \tag{3}$$

where $a = C_M \cdot C_F$; $b = -\,(C_M + C_F + \frac{1}{K})$; $K = \frac{k_1}{k_2}$.

Applied to the reactions studied, eqn. (3) gives relationships as exemplified by Fig. 1, when the equilibrium constant mentioned previously is introduced into the equation. Since the rate of reaction is high as compared with the experimental technique — *i. e.* the cryoscopic measurements — figures corresponding to the initial part of the reaction could not be obtained. Despite of this lack of accuracy, we may accept

$$k_1 = 0.65 \times 10^{-3} \text{ liter/moles} \cdot \text{sec.}$$

$$k_2 = 1.0 \times 10^{-3} \text{ sec}^{-1}.$$

These figures are related to unbuffered solutions. Since addition of buffer substances considerably increases the reaction rates, no accurate measurements could be made on solutions containing such substances.

The reaction between urea or monomethylol urea and formaldehyde and the hydrolysis of mono- and dimethylol urea were investigated as previously described [2-5]. The solutions were the same as the 0.050 M KH_2PO_4, pH 6.70, series of the previous papers, but they also contained methanol.

The experimental results can be found in Table 2.

Table 2. Reaction rate constants of the reactions between urea or monomethylol urea and formaldehyde and of the hydrolysis of mono- and dimethylol urea in the presence of methanol; 0.050 M KH_2PO_4, pH 6.70, 20 °C.

$C_{methanol}$	C_{urea}	$C_{monomethylol\ urea}$	$C_{dimethylol\ urea}$	$C_{formaldehyde}$	$k \cdot 10^5$ *	$k_0 \cdot 10^5$ * calculated
0.000	4.0			0.40	10	10
0.094	4.0			0.40	10	11
0.72	4.0			0.40	8.3	10
1.34	4.0			0.40	6.4	10
0.000	2.0			0.20	10	10
0.063	2.0			0.20	10	11
0.69	2.0			0.20	8.2	11
1.31	2.0			0.20	6.2	10
0.72	2.0			0.80	8.0	11
0.00		1.0		1.0	3.8	3.8
0.22		1.0		1.0	3.5	3.8
0.85		1.0		1.0	2.6	3.6
1.47		1.0		1.0	2.1	3.6
0.00		1.0			0.35	
0.63		1.0			0.35	
1.25		1.0			0.34	
0.00			1.0		0.53	
0.63			1.0		0.52	
1.25			1.0		0.53	

* The rate constants of the formation reactions: liter / moles · sec.; the hydrolysis reactions: sec^{-1}.

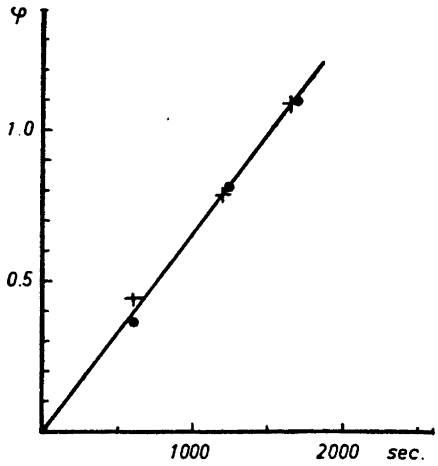


Fig. 1. Relationship in accordance with eqn. (3) of 0.500 M CH_3OH + 0.264 M HCHO (+) and 0.500 M CH_3OH + 1.048 M HCHO (●). 20 °C.

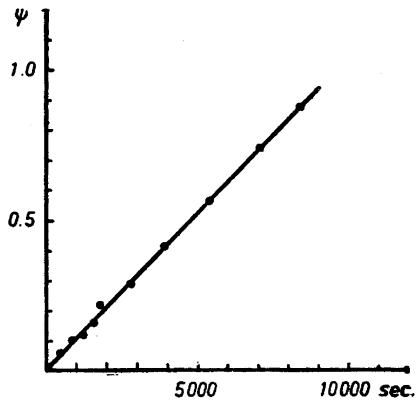


Fig. 2. Relationship in accordance with eqn. (6) for 4.0 M urea + 0.4 M formaldehyde; 0.050 M KH_2PO_4, pH 6.70, 20 °C; 1.34 M methanol.

If we compare the rate constant of hemiacetal hydrolysis and the rate constants of the urea — formaldehyde reaction systems, and remember that the hemiacetal hydrolysis appears to be catalysed by buffer substances, we may assume that the equilibrium in accordance with eqn. (1) is maintained throughout the urea or monomethylol urea and formaldehyde reactions. Assuming that the change in rates of the last mentioned reactions is dependent on the formation of a hemiacetal between methanol and formaldehyde [6], and further that this hemiacetal does not take part in the reactions with urea or monomethylol urea, we find that the rate constants *at zero reaction time* of the urea or monomethylol urea and formaldehyde reactions would be related as follows:

$$\frac{k_0}{k_{C_M}} = \frac{C_F}{C_F - y} \tag{4}$$

where

k_0 = reaction rate constant at zero methanol concentration.
k_{C_M} = reaction rate constant at C_M methanol concentration.
C_{C_F} = initial formaldehyde concentration.
y = initial hemiacetal concentration.

y as calculated from eqn. (2): $y^2 - (C_M + C_F + \frac{1}{K}) \cdot y + C_M \cdot C_F = 0$; symbols defined as previously.

The results, as found in Table 2, can be summarized: Within the range studied, 0—1.3 M methanol,

A. a considerable influence of methanol on the reaction rates of the urea or monomethylol urea and formaldehyde reactions is found;
B. the k_0-figures calculated by means of eqn. (4) are in agreement with the figures related to zero methanol concentration;
C. no effect of methanol on the rates of hydrolysis of mono- and dimethylol urea could be detected.

In the case of the urea-formaldehyde reactions, carried out with an excess of urea present (hydrolysis reactions negligible), we write:

$$\frac{dx}{dt} = k \cdot (C_U - x) \cdot (C_F - x - y)$$
$$\frac{y}{(C_M - y) \cdot (C_F - x - y)} = K = \frac{1}{\alpha} \qquad (5)$$

$t = 0$, $x = 0$;

Here is C_U = initial urea concentration; x = monomethylol urea concentration; k = rate constant and t = time of reaction. Other symbols as previously defined. If $y << C_M + C_F + \alpha - x$, we obtain the following solution to eqn. (5):

$$\psi = k \cdot t = \frac{\alpha + C_M + C_F - C_U}{(C_U - C_F) \cdot (C_U - C_F - \alpha)} \cdot \ln \frac{C_U}{C_U - x} + \frac{\alpha + C_M}{\alpha \cdot (C_U - C_F)} \cdot$$
$$\cdot \ln \frac{C_F}{C_F - x} - \frac{C_M}{\alpha \cdot (C_U - C_F - \alpha)} \cdot \ln \frac{C_F + \alpha}{C_F + \alpha - x} \qquad (6)$$

An example of the relationships according to this equation, plotted from experimental data, $C_M = 1.34$, $C_U = 4.0$, $C_F = 0.40$, in shown by Fig. 2. As seen a good linearity and agreement with the corresponding rate constant from Table 2 is present.

As a result of the fact that only the forward reaction rates are influenced by the presence of methanol, the equilibrium formaldehyde concentration, as determined analytically, may also be dependent on the amount of alcohol in the reaction mixtures.

Under the conditions used for the polarographic analysis of the amount of equilibrium formaldehyde of the reaction mixtures, all hemiacetal is completely hydrolysed. (The figures obtained on formaldehyde solutions with and without methanol present are the same, when samples of the solutions are added to the supporting electrolyte in accordance with the previous paper [2].) Thus, the analytically determined "equilibrium" formaldehyde concentration $C_{F\infty}$ is related to the concentration of "free" formaldehyde $C^{\circ}_{F\infty}$, *i. e.* the amount in actual equilibrium with urea, mono- and dimethylol urea, as follows: $C_{F\infty} = C^{\circ}_{F\infty} + y$; y is the concentration of the hemiacetal.

Eqn. (1) can be written

$$\frac{y}{(C_M - y) \cdot C^{\circ}_{F\infty}} = K \qquad (7)$$

Symbols defined as previously. If we combine this expression with $C_{F_\infty} = C^\circ_{F_\infty} + y$, we obtain:

$$C_{F_\infty} = C^\circ_{F_\infty} + \frac{C_M}{1 + \frac{1}{K \cdot C^\circ_{F_\infty}}} \quad (8)$$

From above we see that $C^\circ_{F_\infty}$ is independent of the presence of methanol and can be found from a determination of the analytical amount of formaldehyde in the urea-formaldehyde reaction mixtures at zero alcohol concentration. The validity of eqn. (8) is exemplified by the experimental data, extrapolated to infinite reaction time, obtained for the reactions between monomethylol urea and formaldehyde in accordance with the experiments of Table 2. The results are as follows:

$C_{methanol}$	C_{F_∞}	
	measured	calculated
0.00	0.22 *	—
0.22	0.25	0.25
0.85	0.33	0.33
1.47	0.40	0.39

* Thus, $C^\circ_{F_\infty} = 0.22$.

The principle introduced is, of course, generally applicable to these problems.

The influence of methanol on the reaction rates may also be attributed to influences on the ion activities of the catalysts. However, the behaviour of the mono- and dimethylol urea hydrolysis reactions, as seen from Table 2, shows that such effects may be negligible.

The conclusions to be drawn from the investigations described in this paper may be: The reduction in reaction rates of the urea or monomethylol urea and formaldehyde reactions caused by methanol depends mainly on the formation of a hemiacetal between methanol and formaldehyde. The hemiacetal does not take part in the reactions, and the equilibrium conditions of the hemiacetal are maintained throughout the reactions between the ureas and the formaldehyde.

The author wishes to thank the board of Rydboholms A. B. for permission to publish this paper, and is also indebted to Mr. A. Olofsson and Mr. L. Uppström for valuable assistance in the experimental work.

REFERENCES

1. Smythe, L. *J. Am. Chem. Soc.* **74** (1952) 2713.
2. Landqvist, N. *Acta Chem. Scand.* **9** (1955) 1127.
3. Landqvist, N. *Acta Chem. Scand.* **9** (1955) 1459.
4. Landqvist, N. *Acta Chem. Scand.* **9** (1955) 1466.
5. Landqvist, N. *Acta Chem. Scand.* **9** (1955) 1471.
6. Takahashi, A. *Chem. High Polymers (Japan)* **9** (1952) 48.

Received February 26, 1957.

ACTA CHEMICA SCANDINAVICA 11 (1957) 792—803

On the Reaction between Urea and Formaldehyde in Neutral and Alkaline Solutions

X. Notes on the Reaction Mechanism

NILS LANDQVIST

Rydboholms A.B., Rydboholm, Sweden

The rates of the reactions of the urea-formaldehyde system are compared with other experimental data connected with urea and formaldehyde. The conclusions drawn from such comparisons are partly in favour of previous assumptions, partly not.

Some of the conclusions are: It is probable that a tautomer of urea may be the activated state for reactions with formaldehyde, and the tautomer may be of a zwitter ion structure. If the reactive compound would be an anion, the anion is not present in any considerable quantities prior to the reaction collisions. Only dehydrated formaldehyde or a resonance structure of dehydrated formaldehyde may react with urea or monomethylol urea. The rates of the depolymerisation, dehydration or hydration reactions of formaldehyde are of such a magnitude that they do not influence the rates of the reactions of the urea-formaldehyde system. The buffer catalysis of the urea-formaldehyde reactions is probably not simply connected with a formation of a buffer-formaldehyde complex prior to the reactions with urea or monomethylol urea.

Some of the previous theories connected with the urea-formaldehyde reaction mechanism are:

A. An anion of urea is the reactive compound in reactions with formaldehyde [1–5].

B. Only dehydrated formaldehyde reacts with urea or monomethylol urea [1,2,4–6].

C. In concentrated solutions the slow depolymerisation of formaldehyde polymers influences the urea-formaldehyde reaction rates [7].

D. The main influence of the temperature on the urea-formaldehyde reactions is due to changes in the equilibrium between hydrated and dehydrated formaldehyde [4,5].

E. The hydrolysis of methylol ureas catalysed by hydroxyl ions is connected with a dissociation of the OH group of the compound: $—OH + OH^- = —O^- + H_2O$. The rate of hydrolysis is proportional to the concentration of the $—O^-$ compound [6].

THE STATE OF UREA SOLUTIONS

I. There are several reasons to assume that urea tautomers exist. In favour of this assumption is:

X-Ray analysis shows a decrease in the bond length between carbon and nitrogen atoms. This is a typical effect of resonance hybrids [8].

Raman- och infrared spectra of solid urea show that the force constants of the C — N and C = O bonds are 35 % above, respective 39 % below the expected figures. The occurrence of hydrogen bonds is not found to be probable [9]. The presense of such bonds was assumed by another author [10], and the occurrence of tautomers representing any considerable fraction of the total amount of urea was not found to be probable. However, in this latter investigation no force constant calculations were made. The differences in opinion are also connected with differences in the interpretation of the absorbtion bands.

II. A urea tautomer may be of a zwitter ion structure, and the reasons for this assumption are:

The dielectric constant decreases considerably when urea is added to water, and the same effect is produced by amino acids [8].

The melting point of urea is considerably above the figure to be expected. Amino acids show the same behaviour [8].

III. No alkaline dissociation of urea could be detected when titrations were made with a hydrogen electrode for the pH measurements [11].

As mentioned in a previous paper [12], pH measurements in highly alkaline solutions by means of hydrogen electrodes require a high degree of hydrogen purity. In order to examine the investigation referred to above, the titration curves of 1.0 M urea and of distilled water at 20 °C after addition of HCl have been determined by means of the glass electrode differential method [12]. Accuracy: $\pm$ 0.02 pH. The results are shown by Fig. 1. From this diagram it might be concluded that if any alkaline dissociation of urea occurs, $pK > 13$. Thus, the previous result is confirmed.

THE STATE OF FORMALDEHYDE SOLUTIONS

IV. In concentrated solutions is the formaldehyde partly present as linear polymers [13].

V. The rate of depolymerisation of the polymers is highly dependent on pH and temperature. A rate minimum exists in the pH range 3—4. From studies below and above this range the specific catalytic constants of hydrogen and hydroxyl ions were found to be 3.7 and 3.7×10^7 liter/moles $\times$ sec, respectively, at 20 °C. The activation energy is 17.4 kcal. The reaction is mainly monomolecular, and is assumed to include the formation of a polymer zwitter ion. Correspondingly, the polymerisation reaction would involve a monomer zwitter ion [14].

VI. From diamagnetic measurements it was found that the equilibrium between polymeric and monomeric aldehyde is dependent on pH; also at pH 10 the dependency is of a considerable magnitude [15].

In order to investigate this result further, cryoscopic measurements have

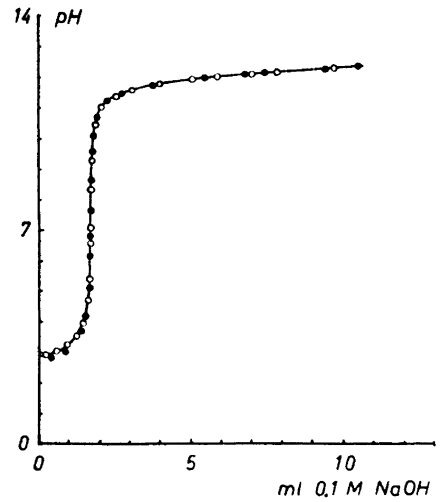


Fig. 1. Titration curve of 1.0 M urea (O) and of water (●) after addition of HCl to pH~3. 20 °C.

been made on pure formaldehyde solutions, pH 5.5, and after addition of NaOH to pH 10. A stock solution of formaldehyde, 12.6 M, was prepared by distillation of a paraformaldehyde-water mixture, and allowed to attain equilibrium before it was used for the experiments. The stock solution was then, with and without addition of NaOH, diluted to concentrations in the range 0—6 M. Temperature 20 °C. The cryoscopic measurements were made immediately after the dilution and after 24 h storage. The results obtained are shown by Table 1. As seen, there is a considerable deviation from unity in the $(t_C—t_0)_{pH\ 10}$ / $(t_C—t_0)_{pH\ 5.5}$ ratios * when the measurements were made immediately after the dilution. However, after the storage such a devia-

Table 1. The ratios between the differences in freezing temperatures at the formaldehyde concentrations C and zero at pH 10.0 and 5.5 when the measurements are made immediately after dilution from a 12.6 M stock solution and after 24 h storage. Temperature 20 °C.

$\sum_{n=1}^{\infty} nC_{(HCHO)_n}$	$(t_C-t_0)_{pH\ 10.0}$ / $(t_C-t_0)_{pH\ 5.5}$	
	Immediate measurements	After 24 h storage
1.0	1.67	1.00
2.0	1.43	1.00
3.0	1.35	1.00
4.0	1.31	1.00
6.0	1.28	1.00

* t_C and t_0 are the freezing temperatures at the formaldehyde concentrations C and zero, respectively.

tion does not exist. This effect may be a function of differences in rate of depolymerisation: after 24 h storage the equilibrium is probably attained at both pH values. Thus, it might be concluded that the pH influence referred to above is not found when the solutions are allowed to attain equilibrium conditions.

VII. The state of monomeric formaldehyde is described as an equilibrium between methylene glycol and dehydrated formaldehyde, and this equilibrium is highly in favour of the glycol [13]. The equilibrium constant [16,17] is $\sim 10^{-4}$. ($K = C_{HCHO} / C_{HOCH_2OH}$)

VIII. Both an acid and alkaline dissociation of formaldehyde is present [14,18,19]. At 20 °C the dissociation constants are: $pK = 5.8$ and 13.4, respectively.

IX. The methylene glycol dehydration is catalysed by buffer substances [17,20]. The activation energy of the dehydration reaction is 14 kcal [16]; the figure corresponding to the hydration reaction is close to zero [17]. The catalysis by buffer substances as studied in a previous paper [17], is further exemplified by Table 2.

X. The composition of formaldehyde solutions can be summarized as follows [21]; the data refer to 20 °C.

ΣC_{HCHO}	% polymers	% monomer
0.67	1	99
1.67	11	89
5.00	36	64
9.33	59	41

The temperature influence on the composition of the solutions was exemplified by the fact that the amount of polymers is below 1 % in 0.7 M solutions at 45 °C and in 7.3 M solutions at 100 °C.

Table 2. Polarographically determined dehydration rate constants of methylene glycol. Temperature 20 °C.

Analytical C_{HCHO}	Buffer *	pH	C_{buffer}	$k \times 10^2$ sec^{-1}
0.0157	KH_2PO_4	6.70	0.100	5.9
			0.050	3.4
			0.025	1.7
0.00392	borax	9.20	0.100	57
			0.050	40
			0.025	30
0.00785	Na_2CO_3	10.00	0.100	60
			0.050	49
			0.025	46

* To all solutions such amounts of the chloride of the buffer cation was added that a cationic strength corresponding to the most concentrated solution was obtained.

THE UREA OR MONOMETHYLOL UREA AND FORMALDEHYDE REACTIONS

When the collision theory of reaction will be used here for discussions, this does not mean that the theory is generally accepted. However, the frequency factors calculated can be used as a base for probability discussions: from a distribution curve, made from a great number of experimental data [22], it can be seen that 8 % of the frequency factors exceed 10^{13}, and only 4 % exceed 10^{14}.

In the following the calculations refer to data given in a series of previous papers [23–26]. The activation energy to be used is 15.4 kcal [27], equal for both the reactions.

The rate constants of the reactions between urea or monomethylol urea and formaldehyde are, within the range studied, 2×10^{-5} —2×10^{-3} liter/moles × sec. 20 °C, pH 6.70—11.50. Not only the formation reaction, but also the hydrolysis is catalysed by buffer substances [1,5,23–26]. The rate constants mentioned correspond to the frequency factors 5×10^{6} —5×10^{8}, *i.e.* the values are considerably below the figure to be expected from the collision theory, $\sim 3 \times 10^{11}$.

However, if we apply the assumption (B, see above) that only dehydrated formaldehyde reacts, and use the equilibrium constant 10^{-4} for the methylene glycol—fomaldehyde equilibrium (VII), the "corrected" rate constants corresponding to this would be 0.2—20 liter/moles. sec., and the frequency factors 5×10^{10} —5×10^{12}. When we compare these figures with the probability of different frequency factors as mentioned above, we find that if the dehydrated aldehyde is the formaldehyde reactant, the reactive structure of urea probably ought to be at least 1 % of the total amount. As previously mentioned (A,B), several reaction mechanism theories include the assumption that an anion of urea reacts with dehydrated formaldehyde. Since $pK > 13$ (III) for the formation of such an anion, it is not very probable that a reaction mechanism of this kind would be of any considerable importance in neutral and moderately alkaline solutions, if the anion is assumed to exist prior to the reaction stage. The complex relationships between pH and the logarithm of the reaction rate constants extrapolated to zero buffer concentration [23,24], show that the reaction mechanism is not solely including the presence of an anion of urea, as regards the effect of pH on the rates. Further, the catalytic effect of buffers cannot simply be explained by assumptions on the formation of the anion prior to the reaction stage.

The order of the dissociation constants of formaldehyde (VIII) shows that it is not very probable that formaldehyde ions would be of importance for the reactions in neutral and moderately alkaline solutions.

At this stage of the discussion some of the previous experimental results ought to be examined. From one of the papers [23] (Fig. 9 of Ref.[23]) it is seen that the rate relationship curves of the equimolecular urea—formaldehyde reactions are practically independent of the reactant concentrations in the interval studied, 0.5—4 M, 20 °C. As regards the monomethylol urea—formaldehyde reactions, the same behaviour was observed [24] in the studied range, 0.25—1 M, 20 °C. From above (X) it is known that at the upper concentrations of the ranges mentioned, the fraction of formaldehyde polymers is not

negligible. This would mean that the monomer fraction decreases when the concentration increases, and the fraction of the dehydrated formaldehyde too. A consequence of this would be a decrease in the rate constants.

This decrease in the concentration of the dehydrated aldehyde is exemplified by some data previously given [28]. When repeating the experiments on which these data are based, a fairly good agreement with the 60 °C figures was obtained. At 30 °C the very low absorption did not permit any accurate calculations.

An explanation to the non—influence of the presence of a considerable fraction of polymeric formaldehyde may be that collisions involving polymers also are active for producing a state of the aldehyde which is able to react with urea. The number of collisions is, from the theoretical point of view, more dependent on the number of HCHO groups than on their state: polymers or monomers.

This is seen from the well-known expression

$$Z = \sigma_{1;2}^2 n_1 n_2 \sqrt{8\pi RT\left(\frac{1}{M_1} + \frac{1}{M_2}\right)}$$

Z = number of collisions pr ml and sec between the molecules 1 and 2. $\sigma_{1;2}$ = sum of molecular radii, n_1 and n_2 = number of molecules pr ml. M_1 and M_2 = molecular weights. When the number, n, of one of the molecules decreases by polymer formation, σ increases since polymerisation means an increase in molecular dimensions.

Another explanation could be that a concentration effect connected with the formaldehyde is compensated by an opposite effect connected with the urea. When examining the results of the previous paper [23] (Table 1 and Figs. 15 and 16 of Ref.[23]), we find that such an assumption is improbable.

As mentioned previously, (V), the specific catalytic constant of hydroxyl ions for the formaldehyde polymer depolymerisation is 3.7×10^7 liter/moles $\times$ sec at 20 °C. If we compare this figure with the data of Table 2, we find that the rates of depolymerisation considerably exceed the rates of methylene glycol dehydration. Thus, when dehydrated formaldehyde is liberated in solutions containing polymers, the rate of methylene glycol dehydration might be the rate determining step.

It may also be of some interest to compare the catalytic effect of some buffer substances at a constant cationic strength on the dehydration rate constants of methylene glycol, as given in Table 2, with the catalytic effect of the same buffers on the reactions of the urea—formaldehyde system [23–26]. Such a comparison is given in Table 3, where the constants of the equation describing the rate constant — buffer concentration relationship

$$k = k_0 + a \cdot C_{\text{buffer}} \qquad (1)$$

can be found. k = rate constant at the buffer concentration C_{buffer}, k_0 = rate constant at the extrapolated zero buffer concentration.

If we examine the data of Table 3, we find that the rates of methylene glycol dehydration is considerably greater than the figures related to the urea—formaldehyde system. Thus, the dehydration rates have no influence on the rates of the urea—formaldehyde forward reactions. Since the hydration

Table 3. The constants of eqn. (1) of the methylene glycol dehydration and of the urea-formaldehyde reactions. Temperature 20 °C. Dehydration and hydrolysis reactions: k_0 sec^{-1}; a liter/moles · sec, Formation reactions: k_0 liter/moles · sec, a liter^2/moles^2 · sec.

Reactioo	Buffers						$a_{KH_2PO_4}$: a_{borax} : $a_{Na_2CO_3}$
	KH_2PO_4, pH 6.70		borax, pH 9.20		Na_2CO_3, pH 10.00		
	$k_0 \times 10^5$	$a \times 10^5$	$k_0 \times 10^5$	$a \times 10^5$	$k_0 \times 10^5$	$a \times 10^5$	
Methylene glycol dehydration	1 200	45 000	23 000	34 0000	41 000	18 0000	1 : 7.6 : 4.0
$H_2N \cdot CO \cdot NH_2$ + HCHO	3.4	126	4.3	37	6.7	133	1 : 0.29 : 1.1
$H_2N \cdot CO \cdot NH \cdot CH_2OH$ + HCHO	0.9	60	1.5	20	8.1	71	1 : 0.33 : 1.2
$H_2N \cdot CO \cdot NH \cdot CH_2OH$ hydrolysis	0.09	5.1	0.15	1.5	0.21	5.5	1 : 0.29 : 1.1
$HOCH_2 \cdot NH \cdot CO \cdot NH \cdot CHOH_2$ hydrolysis	0.11	8.7	0.18	2.4	0.72	7.3	1 : 0.28 : 0.8

reaction rates are 10^4 times greater than the dehydration rates, the same conclusion can be drawn regarding the hydrolysis reactions of the methylol ureas.

Another conclusion which might be drawn from Table 3 is that the mechanisms of methylene glycol dehydration and of the urea—formaldehyde reactions are probably not identical. This since the catalytic effect of the different buffers on the different reactions deviates considerably, as seen from the $a_{KH_2PO_4}$: a_{borax}: $a_{Na_2CO_3}$ ratios. The ratios connected with the urea—formaldehyde reactions are practically identical for all of these latter reactions. Thus, the catalysis of the rate determining step of the urea—formaldehyde reactions is probably not simply connected with the formation of an activated buffer—formaldehyde complex during the dehydration reaction, a complex which would represent an activated state for reactions with urea or monomethylol urea. However, the catalysts, *i.e.* buffers, H_2O and OH^-, increase the prior formaldehyde depolymerisation and dehydration reactions to such an extent that these reactions do not influence the rates of the urea—formaldehyde reactions.

Since polarographic investigation on formaldehyde in connection with the urea-formaldehyde reactions have previously [4] been used for discussions (A, B, D) regarding these reactions, some of the interpretations given will be examined.

The extent of formaldehyde dehydration was estimated from the ratios between actual "formaldehyde wave height" and the "total dehydrated wave height". The "total dehydrated wave height" was assumed to refer to a less steep slope appearing at increased temperatures when a log $i = f(1/T)$ curve is plotted from experimental data obtained on formaldehyde solutions containing buffer substances; (i = polarographic limiting current, T = temperature in °K). As easily seen from a previous paper [21], the change in slope mentioned does not mean that the formaldehyde is completely dehydrated; the less steep

slope appears when the rate of methylene glycol dehydration exceeds the rate of diffusion of this substance to such an extent that the latter rate controls the polarographic electrode process.

It was further found that the following expression, derived from the Arrhenius equation:

$$\log \frac{k_2}{k_1} = \frac{\Delta E_a}{\Delta E_{aa}} \cdot \log \frac{i_2}{i_1} \qquad (2)$$

is in a good agreement with experimental data. k_2 and k_1 = rate constants of the urea-formaldehyde reactions at two different temperatures but at the same buffer composition. i_2 and i_1 = the corresponding polarographic limiting currents of formaldehyde under the same conditions. ΔE_a and ΔE_{aa} = the "activation energies" of the urea-formaldehyde reaction, respectively the polarographic limiting current of formaldehyde. It is easily seen that eqn. (2) is self-consistent:

$$\log \frac{k_2}{k_1} = \log Z_k - \log Z_k - \frac{\Delta E_a}{M \cdot R} \cdot \left(\frac{1}{T_2} - \frac{1}{T_1}\right)$$

$$\log \frac{i_2}{i_1} = \log Z_i - \log Z_i - \frac{\Delta E_{aa}}{M \cdot R} \cdot \left(\frac{1}{T_2} - \frac{1}{T_1}\right)$$

(M = ln 10)

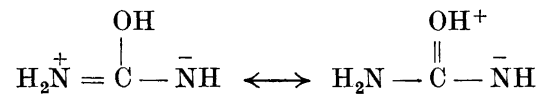
and thus eqn. (2) is obtained from these expressions. Any pair of reactions will give the coincidence observed, provided they obey the Arrhenius equation.

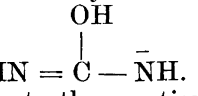
Finally, a relationship between urea-formaldehyde reaction rate constants and the polarographic limiting currents of formaldehyde at different pH values was given. However, this relationship is purely empirical [29].

It has previously been stated that the influence of the temperature on the urea—formaldehyde forward reaction rates is mainly due to changes in the equilibrium between hydrated and dehydrated formaldehyde (D); this assumption is also verified by comparisons between the activation energies referred to in this paper. Thus, the formation of an active state of urea would not be connected with any considerable change in energy.

Since our present knowledge of the state of urea in water solutions is highly limited, it is difficult to give any statement regarding the activated form of urea. However, it seems to be probable that urea tautomers exist, and that they may represent a considerable fraction of the total amount (I). Further, a zwitter ion structure of a tautomer is not improbable (II).

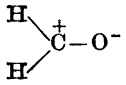
It has previously been assumed [3] that the urea structures



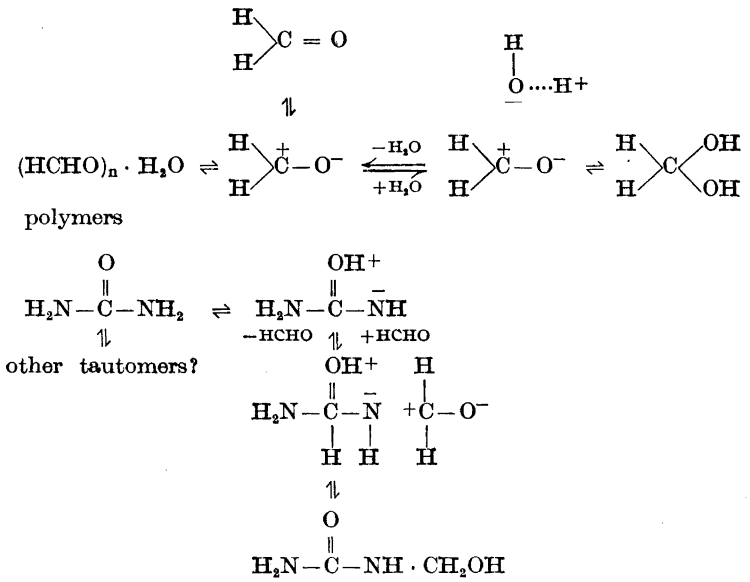
would be of importance for the urea—formaldehyde reactions. (The anion assumed to be necessary for the reactions would be obtained mainly through ionization to  The low probability of the formation of such an ion prior to the reaction with formaldehyde as a part of the reaction mechanism has been discussed above.)

The structures shown above may be in agreement with the requirements which follow from the experimental results regarding the state of urea previously mentioned in this paper. Further, a nitrogen atom is activated as a nucleophilic center.

In the polymerisation reactions of formaldehyde, a zwitter ion was assumed to be of importance (V), and the structure of the zwitter ion would be:



This structure may simply be regarded as a symbol for a resonance state of the dehydrated formaldehyde molecule, where the carbon atom is activated as an electrophilic center. With reference to the previous discussions regarding the formaldehyde polymers, and if we assume that the formaldehyde zwitter ion is in an activated state for both the hydration—dehydration reaction and for the reactions with urea or monomethylol urea, we get, *e.g.*, the following example of a possible reaction mechanism:



The proton exchange may be catalysed by proton donors and proton acceptors, *i.e.* buffer substances, and may represent the rate determining steps of the reactions.

A similar reaction scheme can also be applied to the monomethylol urea—formaldehyde system.

It will here be stressed that this scheme ought to be regarded as an example of a *possible* and not of a highly probable reaction mechanism description. Our present knowledge does not allow any conclusive statements.

THE HYDROLYSIS REACTIONS

A hydrolysis reaction mechanism previously assumed (E) may be within the scope of the scheme given above.

The shape of the rate constant—C_{OH^-} curve was shown to be in favour of the assumption that the anion of the methylol compound can be regarded as the activated complex for the hydrolysis reaction [6].

However, it is interesting to note that an assumption that the ionic form does *not* react, *i.e.* solely the -OH compound would be reactive and subject to a hydroxyl ion catalysis, is "verified" by the same experimental results.

This is found from the following:

$$R \cdot CH_2OH + OH^- = R \cdot CH_2O^- + H_2O$$

$$\frac{C_{R \cdot CH_2O^-}}{C_{R \cdot CH_2OH} \cdot C_{OH^-}} = K$$

$$C_{R \cdot CH_2OH} + C_{R \cdot CH_2O^-} = C_{total}$$

and

$$\frac{C_{total}}{C_{R \cdot CH_2OH}} - 1 = K \cdot C_{OH^-}$$

If only $R \cdot CH_2OH$ reacts and under the influence of hydroxyl ion catalysis, this means that the actual hydrolysis rate constant k is related to a rate constant k_0 at the same hydroxyl ion concentration and extrapolated from the slope of the $k = f(C_{OH^-})$ curve at $C_{OH^-} = 0$ as follows:

$$\frac{k_0}{k} = \frac{C_{total}}{C_{R \cdot CH_2OH}}$$

($C_{total} \ll C_{NaOH}$ in the experiments, thus $C_{OH^-} \sim C_{NaOH}$)
and thus:

$$K = \frac{1}{C_{OH^-}} \cdot \left(\frac{k_0}{k} - 1\right)$$

If we apply this expression to the figures taken from the experimental curves [6] related to monomethylol urea, MU, and also include the data for methylol benzamine, MB, methylol propioamide, MP and methylol chloroacetamide, MCh, we get the following K values:

C_{OH^-}	K_{MU}	K_{MB}	K_{MP}	K_{MCh}
0.2	1.7	6.9	5.6	16.0
0.3	2.0	6.7	5.7	15.3
0.4	2.1	6.8	6.0	15.1
0.6	2.1	7.0	6.0	14.6
1.0	2.1	7.1	6.2	14.7

When regarding the experimental accuracy to be expected, these results mean that no distinction between the two opposite reaction mechanism theories can be made.

However, the assumption (E) seems not to be unreasonable, even when there is a lack of significance in the experiments referred above. The initial stage of the hydrolysis reaction would, *e.g.*, be an ionization of the -OH group, followed by a proton transfer in accordance with the scheme above.

Table 4. The k_0 and a ratio between formation and hydrolysis reactions of the urea-formaldehyde system. k_0 and a formation, k_0' and a' hydrolysis. Temperature 20 °C.

Buffer	pH	Monomethylol urea		Dimethylol urea	
		k_0/k_0'	a/a'	k_0/k_0'	a/a'
KH_2PO_4	6.70	38	25	8.2	6 9
Borax	9.20	29	25	8.3	8.3
Na_2CO_3	10.00	32	24	11.3	9.7

It may be of some interest to compare the formation—hydrolysis k_0 and a ratios, respectively, at different buffer solution compositions calculated from the figures of Table 3. These ratios can be found in Table 4. As seen, the ratios of the urea or monomethylol urea and formaldehyde reaction systems are of the same order, and as regards the urea—formaldehyde reaction the a ratios are practically constant. This may be in favour of an assumption that the buffer catalysis mechanism of both the formation and the hydrolysis are identical. However, the variations in the other ratios do not exclude such an identity even in these cases; the ionization state of the reactants may influence the activites of the different buffer ions in different ways when these ions are approaching in order to promote a proton transfer.

The author whishes to thank the board of Rydboholms A.B. for permission to publish this paper.

REFERENCES

1. Smythe, L. *J. Phys. Colloid Chem.* **51** (1947) 369.
2. Smythe, L. *J. Am. Chem. Soc.* **73** (1951) 2735.
3. Smythe, L. *J. Am. Chem. Soc.* **75** (1953) 574.
4. Crowe, G. and Lynch, C. *J. Am. Chem. Soc.* **71** (1949) 3731.
5. de Jong, J. I. and de Jonge, J. *Rec. trav. chim.* **7** (1952) 643.
6. Ugelstad, J. *The Reaction of Formaldehyde with Amides and the Alkaline Hydrolysis of Alkoxymethyl Ureas* (Diss.) Leiden 1955, p. 54—61.
7. Smythe, L. *J. Am. Chem. Soc.* **74** (1952) 2713.
8. Sidgwick, N. V. *The Organic Chemistry of Nitrogen*, Clarendon Press, Oxford, 1937, p. 285.
9. Kellner, L. *Proc. Roy. Soc. London* **A 177** (1941) 456.
10. Sundara Rao, A. L. *J. Indian Chem. Soc.* **18** (1941) 337.
11. Bell, J., Gillespie, W. A. and Taylor, D. B. *Trans. Faraday Soc.* **39** (1943) 137.
12. Landqvist, N. *Acta Chem. Scand.* **9** (1955) 595.
13. Auerbach, F. and Barschall, H. *Arb. kaiserl. Gesundh.* **22** (1905) 594.
14. Wadano, M., Trogus, C. and Hess, K. *Ber.* **67** (1934) 174.
15. Sauterey, R. *Ann. chim. Paris (12)* **7** (1952) 1.
16. Bieber, R. *Über das polarografische Verhalten der niederen, gesättigten alifatische Aldehyde, besonders des Formaldehyds* (Diss.) Zürich 1948, p. 98—100.
17. Landqvist, N. *Acta Chem. Scand.* **9** (1955) 867.
18. Euler, H. and Lövgren, T. *Z. anorg. Chem.* **147** (1925) 123.
19. Lévy, M. *J. Biol. Chem.* **105** (1934) 157.
20. Veselý, K. and Brdička, R. *Collection Czechoslov. Chem. Communs.* **12** (1947) 313.

21. Walker, F. *Formaldehyde*, Reinhold Publishing Company, New York 1953, p. 53.
22. Meelwyn — Hughes, E. A. *The Kinetics of Reactions in Solution*, Clarendon Press, Oxford, 1933.
23. Landqvist, N. *Acta Chem. Scand.* **9** (1955) 1127.
24. Landqvist, N. *Acta Chem. Scand.* **9** (1955) 1459.
25. Landqvist, N. *Acta Chem. Scand.* **9** (1955) 1466.
26. Landqvist, N. *Acta Chem. Scand.* **9** (1955) 1471.
27. Landqvist, N. *Acta Chem. Scand.* **10** (1956) 244.
28. Walker, F. *Formaldehyde*, Reinhold Publishing Company, New York 1953, p. 51.
29. Crowe, G. *Private communication.*

Received April 1, 1957.

ACTA CHEMICA SCANDINAVICA 11 (1957) 804—810

Bestimmung kleiner Mengen von Ammoniak in Gasmischungen

YRJÖ KAUKO und SAADET DÖGER*

Aus dem Physikalisch-Chemischen Institut der Universität, Ankara, Türkei

Es wurde eine exakte potentiometrische Methode zur Ermittlung des Druckes von Ammoniak, p_{NH_3} ($< 10^{-3}$ Atm) in Gasmischungen ausgearbeitet. Die Bestimmung von p_{NH_3} wird als eine pH-Messung in einer NH_4Cl-Lösung, in Gleichgewicht mit dem unbekannten p_{NH_3}, ausgeführt. Zur Eichung wurde ein Gas mit bekanntem $p^b_{NH_3}$ benutzt. Die Messgenauigkeit is gut.

Ammoniak wird in Gasmischungen bekanntlich dadurch bestimmt, dass das Gas in Chlorwasserstoff absorbiert und die überschüssige Säure zurücktitriert wird [1]. Die Bestimmung des gelösten Ammoniaks kann man auch kolorimetrisch oder konduktometrisch nach verschiedenen Methoden ausführen [2,3]. Das Ammoniak kann durch verschiedene Oxydationsmittel zu Stickstoff oxydiert und dieser volumetrisch bestimmt werden [4].

Es lässt sich leicht feststellen, dass die Bestimmung von Ammoniak in Gasmischungen bis zu einem Druck von 10^{-3} Atm nach den obigen Methoden analytisch durchzuführen ist. Bei kleineren Gas-Konzentrationen aber müssen grosse Gasmengen und niedrige Durchströmungsgeschwindigkeiten angewandt werden. Deshalb wird die für die Analyse erforderliche Zeit lang und die Genauigkeit gering. Wenn man nämlich verdünnte Gase durch Flüssigkeiten leitet, ist eine ausserordentlich lange Zeit erforderlich zur vollständigen Diffusion der letzten Reste der Gase [5] aus der Gasphase in die flüssige Phase.

Airola [6] hat vorgeschlagen auf Grund des Gleichgewichtes zwischen gasförmiger und flüssiger NH_3-Phase aus dem pH-Wert der wässrigen Lösung den Ammoniakgehalt der Gasmischung zu ermitteln. Pekkarinen [7] hat festgestellt, dass zwar im Verlauf von etwa 5 Stunden ein Gleichgewicht zwischen den wässrigen und gasförmigen Phasen des Ammoniaks entsteht, dass aber die Methode in dieser Form praktisch kaum zu verwerten ist.

---

* Die Versuche dieser Arbeit wurden von Saadet Döger vorgenommen und als Doktorarbeit an der Universität Ankara in den *Communications de la Faculté des Sciences de l'Université d'Ankara* 1955 veröffentlicht.

THEORETISCHER TEIL

Ammoniak ist in Wasser leicht löslich (59 M/Atm bei 25°C) [8,9]. Der Übergang des Gases in die wässrige Phase nimmt eine verhältnismässig lange Zeit in Anspruch. Die Löslichkeit von Ammoniak kann durch Temperaturerhöhung und durch Anwendung von konzentrierten Ammoniumchloridlösungen herabgesetzt werden.

Das letztgenannte kann auf folgende Weise anschaulich gemacht werden. (Alle Molekelgattungen ausser $NH_3(g)$ sind in wässriger Lösung, [] Konzentration, {} Aktivität.) Nach den bekannten Gesetzen des Gleichgewichtes ist

$$NH_3\ (g) \rightleftharpoons NH_3 \qquad K_p = [NH_3] \cdot p_{NH_3}^{-1} \tag{1}$$

$$NH_3 + H_2O \rightleftharpoons NH_4^+ + OH^- \qquad K_b = \{NH_4^+\} \cdot \{OH^-\}\ [NH_3]^{-1} \tag{2}$$

Aus diesen Gleichungen kann abgeleitet werden:

$$NH_3(g) + H_2O \rightleftharpoons NH_4^+ + OH^- \qquad K_{pb} = \{NH_4^+\} \cdot \{OH^-\}\ p_{NH_3}^{-1} \tag{3}$$

$$K_{pb} = K_p \cdot K_b \tag{4}$$

Wenn wir nun annehmen, dass der Aktivitätskoeffizient für alle einwertige Ionen denselben Wert f_1 hat, erhalten wir unter Heranziehung der Gleichungen der Elektroneutralität für die Ammoniumchloridlösung:

$$[NH_4^+] + [H^+] = [OH^-] + [Cl^-] \tag{5}$$

$$[NH_3]_t = [NH_3] + [NH_4^+] = (\{OH^-\} + \{Cl^-\} - \{H^+\}) \cdot (\{OH^-\} \cdot K_b^{-1} + f_1^{-1}) \tag{6}$$

$$[NH_3]_t = K_{pb} \cdot \{OH^-\}^{-1} \cdot (\{OH^-\} \cdot K_b^{-1} + f_1^{-1}) \cdot p_{NH_3} \tag{7}$$

Die Konstanten K_p und K_b entnehmen wir der Literatur [8,9] und berechnen K_{pb}.

$K_p\ (25°) = 59\ M\ Atm^{-1}$ $\qquad K_p\ (40°) = 29{,}4\ \ M\ Atm^{-1}$

$K_b\ (25°) = 1{,}81 \times 10^{-5}\ M$ $\qquad K_b\ (40°) = 1{,}98 \times 10^{-5}\ M$

$K_{pb}(25°) = K_pK_b = 1{,}07 \times 10^{-3}\ M^2Atm^{-1}$ $\quad K_{pb}(40°) = K_pK_b = 0{,}582 \times 10^{-3}\ M^2Atm^{-1}$

Diese Werte sind auch mit Hilfe der thermodynamischen Daten der Reaktionskomponenten kontrolliert worden [10].

In der graphischen Darstellung der Fig. 1 haben wir als Freiheiten des Systems den totalen Ammoniakgehalt $[NH_3]_t$ und das pH der Lösung gewählt. Für Gleichung (6) wurde Konzentration bzw. Aktivität der Ammoniumchloridlösung als Parameter benutzt und für (7) der Druck von Ammoniak in der Lösung. Aus der Fig. 1 ergibt sich, dass für $p_{NH_3} < 10^{-3}$ Atm der $[NH_3]_t$-Gehalt der Lösung in den konzentrierten NH_4Cl-Lösungen eine schwache Abhängigkeit, pH dagegen eine starke Abhängigkeit von p_{NH_3} zeigt. In den konzentrierten NH_4Cl-Lösungen dürfte deswegen die Einstellung des Gleichgewichtes schnell vor sich gehen und infolgedessen die Empfindlichkeit der Methode gross sein.

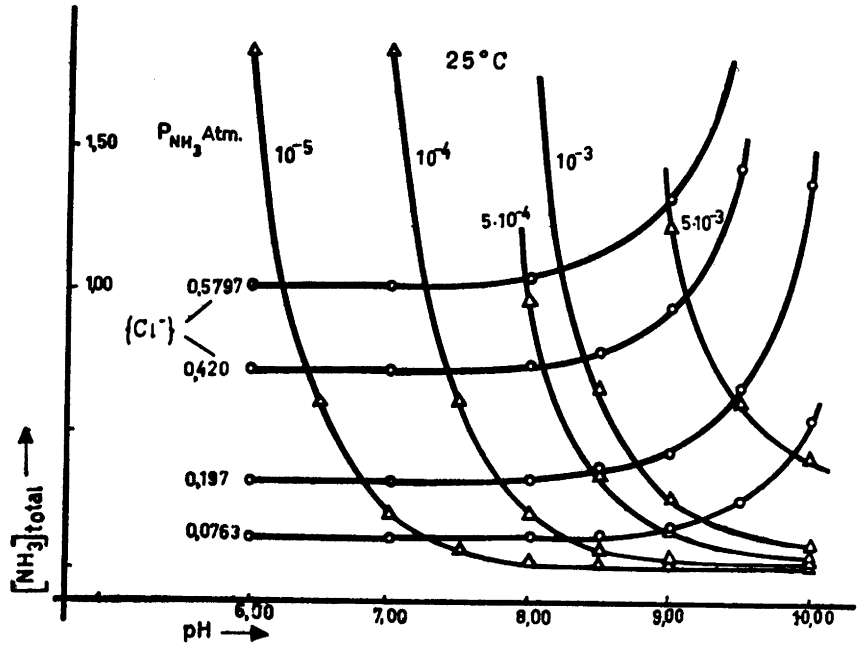


Fig. 1.

Für die praktische Anwendung lässt sich die Gleichung (3) auf folgende Weise schreiben, weil praktisch $[NH_4^+] = [Cl^-]$ ist:

$$\log p_{NH_3} = -\log [H^+] + \log C \qquad (8)$$
$$C = K_w \cdot K_{pb}^{-1} \cdot f_1 \cdot [Cl^-]$$

Wenn das gemessene "pH" mit einem (konstanten) Fehler Δ versehen ist

$$\text{"pH"} = -\log [H^+] + \Delta$$

so gilt

$$\log p_{NH_3} = \text{pH} + \log C' \qquad (9)$$
$$\log C' = \log C - \Delta$$

C und C' sind für eine bestimmte NH_4Cl-Lösung konstant. Durch Eichung mit einer Gasmischung mit bekanntem $p^b_{NH_3}$ kann man die Konstante C' bestimmen.

Wir erhalten schätzungsweise [11]

$$f_1 = 0{,}58 \qquad \text{für } [Cl^-] = 1 \text{ M}$$

Es berechnet sich folglich für $[Cl^-] = 1$ M

bei 25°C $\log C(25°) = -11{,}3 \pm 0{,}1$; $\log p_{NH_3} = \text{pH} - 11{,}3$

bei 40°C $\log C(40°) = -10{,}53 \pm 0{,}08$; $\log p_{NH_3} = \text{pH} - 10{,}53$ (10)

Die Bestimmung des NH_3-Druckes wird folglich auf die pH-Messungen in der folgenden Kette zurückgeführt:

Glaselektrode / 1 M NH_4Cl, $NH_3(g)$,H^+ / Bezugselektrode

EXPERIMENTELLER TEIL

Nach diesen Prinzipien haben wir Luft durch eine Ammoniaklösung, dessen $[NH_3]_t$ titrimetrisch genau bestimmt wurde, durch mehrere nacheinanderfolgende Waschflaschen im Ölthermostat geleitet. Das — mit NH_3-Druck der Lösung — gesättigte Gas ging zum Schluss durch eine NH_4Cl-Lösung, deren pH beobachtet wurde. Dass das pH konstant blieb, auch bei zunehmender Anzahl der Waschflaschen war ein Kennzeichen dafür, dass sich das Gleichgewicht sowohl zwischen den Gas- und Ammoniakphasen wie zwischen NH_3-Gas und NH_4Cl-Lösung eingestellt hatte.

Die pH-Messungen wurden mit Hilfe einer gesättigten Kalomelektrode als Bezugselektrode und mit einem Beckmann-Elektrometer (G-Model) von der Empfindlichkeit $\pm$ 0,01 pH ausgeführt. Der erhaltene pH-Wert wurde mit bekannten Pufferlösungen geeicht und noch mit einer Chinhydronelektrode in der *Veibel*schen Lösung (0,01 M HCl + 0,09 M KCl) mit angenommenem pH = 2,08 kontrolliert.

Aus der Konzentration der NH_3-Lösung wird $p^b_{NH_3}$ mit (1) errechnet und mit Hilfe des gemessenen "pH"-Wertes der obigen NH_4Cl-Lösung wird mit (9) ein Wert für C' erhalten.

Um das Gleichgewicht schnell herzustellen, haben wir kleine Mengen (0,2 bis 0,6 ml) NH_4Cl-Lösung in der Elektrode angewandt. Aus demselben Grunde werden die Flüssigkeit und das Gas durch dieselbe Kapillare von 1 m Länge und 0,3 mm Durchmesser (Fig. 2a) mit Geschwindigkeiten von 0,04 ml/St. und 25 ml/Min durchgeleitet. Es stellt sich schon in der Kapillare das Gleichgewicht ein, aber der Gasdruck ist jetzt nicht mehr derjenige der ursprünglichen Mischung. Aus diesem Grunde wurde nach einer Weile, etwa 20 Minuten, der Zustrom der Flüssigkeit abgestellt, und die vorhandene Elektrodenflüssigkeit mit dem Gas nachgesättigt, wonach das pH gemessen wurde.

Die Versuchsresultate sind in Tabelle 1 zusammengestellt. An Hand der Tabelle stellen wir fest, dass sich das Gleichgewicht schnell einstellt, falls beim Durchleiten des Gases der pH-Wert zunimmt (Kolonne 8 II). Dies wird erreicht, wenn die NH_4Cl-Lösung vermittels Durchleitens von Luft zuerst sauer gemacht wurde (Vgl. Fig. 1). Das Gleichgewicht wird in weniger als einer halben Stunde bei 25°C erreicht. Das endgültige Gleichgewicht stellt sich bei 40°C sehr schnell (in Minuten) sogar in der Kapillare ein. Die Anwendung von zwei Kapillaren hintereinander hatte keine nennenswerte Bedeutung.

In Kolonne 9 werden die log C'-Werte, die aus den $p^b_{NH_3}$ und pH-Werten errechnet wurden, wiedergegeben. Die Werte aus den verschiedenen Versuchen zeigen eine gute Übereinstimmung.

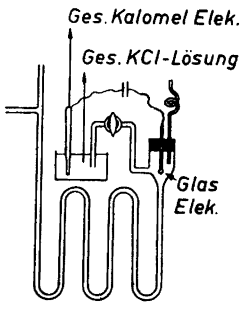


Fig. 2a.

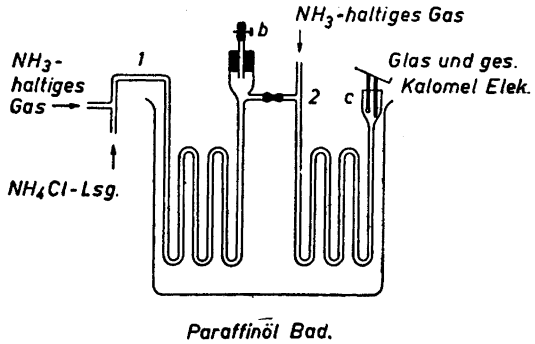


Fig. 2b.

Tabelle 1.

A. 25°C. p_{NH_3} der Ammoniaklösung aus der Gleichung $[NH_3] \times p_{NH_3}^{-1} = 59{,}1\ M\ Atm^{-1}$ berechnet. pH aus det Kette: Glaselektrode / $NH_4Cl, NH_3(g)$, H^+ / Kalomelelektrode erhalten.

a) mit einer Kapillare

1 Versuchsnummer	2 NH_3-Konzentr. Mol / l	Mittelwert	3 p_{NH_3} 10^{-3} Atm	4 Geschwindigkeit der Lösung ml/St	5 Geschwindigkeit der Gase ml/Min	6 Nachsättigungszeit Min	7 Anfangs pH	8 Gleichgewichts pH I	II	9 -log C'
5	0,0605	0,061	1,03	2,0	25	125	8,63	8,45	8,13	11,12
6	0,0595			0,4	23	25	8,63	8,17		
		0,060	1,02						8,11	11,10
7	0,0592			0,4	23	30	8,63	8,21		
9	0,0613			0,2	25	40	5,33	8,09		
		0,061	1,03						8,10	11,09
10	0,0610			0,2	25	6	5,33	8,09		

b) mit zwei Kapillaren

1	0,0605	0,061	1,03		30	10	6,20	8,04	8,09	11,08
2	0,0563			1,4	33	110	8,63	8,37		
		0,057	0,964						8,13	11,15
4	0,0577			0,5		50	8,63	8,21		

Mittelwert: $-\log C$ (25 °C) = 11,11 ± 0,04

B. 40°C. p_{NH_3} der Ammoniaklösung aus der Gleichung $[NH_3] \times p_{NH_3}^{-1} = 29{,}4\ M\ Atm^{-1}$

a) mit einer Kapillare

19	0,0611			0,7	25	0	8,50	7,97		
		0,061	2,07						7,96	10,64
20	0,0609			0,4	23	0	8,50	7,95		
21	0,0578			3,0	25	45	8,50	8,25		
		0,057	1,97						7,96	10,66
23	0,0570			0,5	25	10	8,50	8,04		
24	0,0602			0,3	25	0	5,55	7,95		
		0,060	2,04						7,95	10,64
25	0,0600			0,3	25	0	5,55	7,93		

b) mit zwei Kapillaren

11	0,0594			1,4	26	25	5,98	7,73	7,88	
12	0,0592			0,5	30	0	5,98	7,86	7,88	
13	0,0589			0,8	27	20	5,98	7,87		
		0,061	2,07						7,94	10,62
14	0,0615			1,8	30	0	5,98	7,94		
15	0,0604			0,6	30	0	5,98	7,86	7,86	
16	0,0588			0,4	30	70	8,50	8,04		
		0,059	2,01						7,95	
17	0,0579			0,3	34	0	8,50	7,97		10,65

Mittelwert: $-\log C$ (40 °C) = 10,64 ± 0,02

Die praktische Ausführung der Bestimmung von p_{NH_3}

Die zu untersuchende, Ammoniak enthaltende Gasmischung wird bei 25°C bzw 40°C durch eine 1 M NH_4Cl-Lösung bis zur Einstellung des Gleichgewichtes geleitet und das pH durch Messung der folgenden Kette bestimmt:

Glas-Elektrode / 1 M NH_4Cl, p_{NH_3}, H^+ / Besugselektrode

Der Ammoniakdruck p_{NH_3} (in Atm ausgedrückt) ergibt sich aus der Tabelle 1 wie folgt

$$\log p_{NH_3}\,(25°) = \mathrm{pH}\,(25°) - 11{,}11$$
$$\log p_{NH_3}\,(40°) = \mathrm{pH}\,(40°) - 10{,}64 \qquad (11)$$

Um das Gleichgewicht in der Elektrode schnell zu erreichen, werden etwa 0,2 ml 1 M NH_4Cl mit einer Geschwindigkeit von 0,6 ml/St. durch eine Kapillare (1 m lang, 0,3 mm Diameter) und das Gas mit einer Geschwindigkeit von 25 ml/Min in die Elektrode geleitet. Der Zustrom der Flüssigkeit wird eingestellt, die im Elektrodengefäss gesammelte Flüssigkeit mit dem Gasstrom nachgesättigt und pH bestimmt. Die Versuchsanordnung ist aus Fig. 2 ersichtlich. Wenn das pH der NH_4Cl-Lösung am Anfang vermittels Durchleitens von Luft auf pH 6 eingestellt wird, nimmt die Bestimmung bei 25°C etwa eine halbe stunde in Anspruch. Bei 40°C kann die Bestimmung in einer noch kürzeren Zeit ausgeführt werden.

DISKUSSION

Durch das beschriebene Verfahren wird in Wirklichkeit das Verhältnis $p^b_{NH_3}$ ermittelt. Die folgende Kette wurde gemessen, wobei das Diffusionspotential vernachlässigt werden kann [13]:

$$H_2 / NH_4Cl,\ p^b_{NH_3},\ \{H^+\}_b / \text{gesätt. } KCl / \{H^+\},\ p_{NH_3},\ NH_4Cl / H_2$$

Der erzielte p_{NH_3} ist insofern richtig wie $p^b_{NH_3}$ richtig ist. Der Vergleich zwischen den thermodynamisch berechneten C-Werten in Gleichung (10) mit den experimentell gefundenen C' in Gleichung (11) zeigt Differenzen von nur 0,2 bzw 0,1, obwohl der thermodynamische Wert unsicher ist, weil der Aktivitätskoeffizient approximativ ist, und weiter die gemessenen Werte etwaige prinzipielle Fehler von $p^b_{NH_3}$ und von pH enthalten.

Aus Gleichung (11) errechnet man z. B. für eine 1 M NH_4Cl-Lösung bei 25°C $\log p_{NH_3} = -5{,}11$ für pH=6 und $\log p_{NH_3} = -3$ für pH = 8,11.

Nur ein Druck von 10^{-3} Atm lässt sich nach den analytischen Methoden einigermassen bestimmen. Kleinere Werte sind ohne sehr umständliche Versuchsanordnungen nicht kontrollierbar [14].

LITERATUR

1. Treadwell, F. P. and Hall, W. T. *Analytical Chemistry*, IX Ed. New York 1943.
2. Snell, F. D. and Snell, C. T. *Colorimetric methods of analysis*, III Ed. 1949.
3. Kolthoff, I. M. and Stenger, V. A. *Ind. Eng. Chem. Anal. Ed.* **7** (1935) 79.
4. Hendricks, R. H. and Thomas, M. D. *Ind. Eng. Chem. Anal. Ed.* **14** (1942) 23.
5. Kauko, Y. and Carlberg, J. J. *Z. anorg. u. allgem. Chem.* **33** (1935) 223.
6. Airola, A. *Svensk Kem. Tidskr.* **53** (1941) 123.
7. Pekkarinen, A. *Teknillisen Korkeakoulun Tutkimuksia* No. 1. 1949 (Finland).
8. Gmelin's *Handbuch der Anorganischen Chemie*, VIII Aufl. **23** (1936) 74.
   Landolt-Börnstein, *Physikalisch-Chemische Tabellen* Hw. II 22, Eg. IIIc 2106, Eg. I. 649; *International Critical Tables* **7** (1930) 240.
9. Hougin, O. A. *Metallurgia* **32** (1925) 704.
   Galingaert, F. E. and Huggins, F. E. *J. Am. Chem. Soc.* **45** (1923) 916.
   Klarmann, E. *Z. anorg. u. allgem. Chem.* **139** (1923) 290.
   Scheffer, F. E. G., de Wijs, Hj. *Rec. Trav. Chim.* **44** (1925) 658.
   Scherwood, T. K. *Ind. Eng. Chem.* **17** (1925) 746.

10. Nikus, J. *Persönliche Mitteilung.*
11. Landolt-Börnstein: *Physikalisch Chemische Tabellen* Eg. IIIc 2151, IIb 1125.
12. MacInnes, D. A. and Belcher, D. *J. Am. Chem. Soc.* **55** (1933) 2630.
13. Airola, A. *Uber das Diffusionspotential der chemischen Ketten*, Akad. Abh. Helsinki, Finnland.
14. Kauko, Y. and Yli-Uotila, T. *Z. Anorg. u. allgem. Chem.* **229** (1936) 352.

Eingegangen am 24. Oktober 1956.

ACTA CHEMICA SCANDINAVICA 11 (1957) 811—825

Mercury(II) Halide Mixed Complexes in Solution

IV. Mixed Bromo-Iodo Complexes

Y. MARCUS*

Department of Inorganic Chemistry, Royal Institute of Technology, Stockholm 70, Sweden

Independent values for the mixed complex formation constants k_{ij} for $HgBr_{i-1}I_j + Br \rightleftharpoons HgBr_iI_j$ were obtained from mercury distribution data (D, a, r), where D is the Hg distribution ratio, a is free bromide concentration and r is ratio free iodide to free bromide, using cuts $D(a)_r$ and $D(r)_a$, and from iodine distribution data (D, a, B, M); D is the iodine distribution ratio, and B and M are total mercury and iodine. The constants are: $\log k_{21} = 1.85 \pm 0.03$, $\log k_{12} = 1.88 \pm 0.03$, $\log k_{31} = 1.49 \pm 0.06$, $\log k_{22} = 1.49 \pm 0.05$ and $\log k_{13} = 1.10 \pm 0.10$. Also, the constants for $HgBr_2 + 2I^- \rightleftharpoons HgI_2 + 2\ Br^-$, $\log p = 6.94 \pm 0.03$ and for $HgBr_2 + I^- \rightleftharpoons HgBrI + Br^-$, $\log q = 4.01 \pm 0.04$, and the distribution coefficient of HgBrI between benzene and the ionic medium $\log \lambda_{11} = 0.79 \pm 0.02$ were obtained. These constants are valid for 25° and 0.5 M (perchlorate + halide) ionic medium.

The mercury(II)-bromide-iodide system was subjected to a thorough study of possible mixed species. Use was made not only of mercury solvent distribution data but also of ligand—iodine—distribution. The rather difficult problem of having two independent variables was overcome in a number of ways, and complexity constants could be assigned to all mixed species.

Symbols. For a definition of the symbols used in this paper see part I, p. 330 [2]. The constants k'_{03} and k'_{04} will here be written k_{03} and k_{04}, since no mistake is possible. In addition, the terms $p = \beta_{02}\beta_{20}^{-1}$ and $q = \beta_{11}\beta_{20}^{-1}$ will be useful. The functions c_i and f_i are defined in eqns. (1), (1a), (2) and (8).

Experimental. For experimental details see part I, p. 331 [2]. Benzene was used as the organic solvent, the temperature was 25°, the ionic medium was 0.5 M (perchlorate + halide) and the phase volumes were equal.

General equations. In solutions of MA_2 and excess A^- and B^-, assuming maximum coordination number four [4], six mixed species might form. Introducing the ratio $r = ba^{-1}$, and selecting, for the sake of convenience, such formation reactions as either (I) are based on MA_2 for MB_j species, or (II) consist of the addition of one A^- to a precursor species for the mixed complexes, *e. g.*

* Permanent address: Israel Atomic Energy Commission, Hakiryah, Tel-Aviv, Israel.

(I) $MA_2+3\ B^- = MB_3^- + 2\ A^-$; pk_{03}, or (II) $MAB_2^- + A^- = MA_2B_2^=$; k_{22}, the concentration of the species present may be written as:

$[MA_2]$	$= u$	$[MB_2]$	$= upa^{-2}b^2 = upr^2$
$[MA_3]$	$= uk_{30}a$	$[MAB_2]$	$= upk_{12}a^{-1}b^2 = upk_{12}ar^2$
$[MA_4]$	$= uk_{30}k_{40}a^2$	$[MA_2B_2]$	$= upk_{12}k_{22}b^2 = upk_{12}k_{22}a^2r^2$
$[MAB]$	$= uqa^{-1}b = uqr$	$[MB_3]$	$= upk_{03}a^{-2}b^3 = upk_{03}ar^3$
$[MA_2B]$	$= uqk_{21}b = uqk_{21}ar$	$[MAB_3]$	$= upk_{03}k_{13}a^{-1}b^3 = upk_{03}k_{13}a^2r^3$
$[MA_3B]$	$= uqk_{21}k_{31}ab = uqk_{21}k_{31}a^2r$	$[MB_4]$	$= upk_{03}k_{04}a^{-2}b^4 = upk_{03}k_{04}a^2r^4$

At equilibrium with a benzene phase, the additional species

$$[MA_2]_{or} = u\lambda_{20} \quad [MAB]_{or} = uqa^{-1}b\lambda_{11} = uqr\lambda_{11} \quad [MB_2]_{or} = upa^{-2}b^2\lambda_{02} = upr^2\lambda_{02}$$

will be present.

The problem is to find the six mixed complex formation constants (q and the five k_{ij}) and also p.

EQUATIONS FOR MERCURY DISTRIBUTION

Cuts at constant r

In a recent paper [3] Sillén has described a way of treating data with three variables (here D, a and r), and the following derivation is based on this treatment.

Summing up the concentrations of the species listed above, the total concentration of mercury in the aqueous phase may be written as

$$M - M_{or} = u\ (c_0' + c_1'a + c_2'a^2)$$

$$c_0' = 1 + qr + pr^2 \qquad c_1' = k_{30} + qk_{21}r + pk_{12}r^2 + pk_{03}r^3$$

$$c_2' = k_{30}k_{40} + qk_{21}k_{31}r + pk_{12}k_{22}r^2 + pk_{03}k_{13}r^3 + pk_{03}k_{04}r^4 \qquad (1)$$

where the parameters c_i' are functions of r only, and constant for a series of experiments at constant r. Similarly, for the organic phase.

$$M_{or} = uc_0'' \qquad c_0'' = \lambda_{20} + q\lambda_{11}r + p\lambda_{02}r^2 \qquad (1a)$$

may be written, giving for the distribution ratio D the simple expression

$$D = M_{or}\ (M - M_{or})^{-1} = c_0\ (1 + c_1a + c_2a^2)^{-1} \qquad (2)$$
$$c_0 = c_0''c_0'^{-1} \quad c_1 = c_1'c_0'^{-1} \quad c_2 = c_2'c_0'^{-1}$$

The parameters c_i may then be obtained by curve fitting from plots log D (log a)$_r$. A set of $(c_i)_r$ values may then be obtained for a number of discrete values of r, and the resulting functions $c_i(r)$ solved for the equilibrium constants.

A provisional value of pq^{-1} may be obtained for high r by using the definition of c_0 (eqn. (2), (1a) and (1)) and neglecting the terms for MA_2: 1 in c_0' (1) and λ_{20} in c_0'' (1a):

$$pq^{-1} \approx (c_0 - \lambda_{11})\ (\lambda_{02} - c_0)^{-1}\ r^{-1} \tag{3}$$

(λ_{11} and λ_{02} being known [1,2]). With this, an estimate of q obtained at low r

$$q = c_0 r^{-1}\ [pq^{-1}\ (\lambda_{02} - c_0)r - (c_0 - \lambda_{11})]^{-1} \tag{4}$$

or, alternatively, $q = K(pq^{-1})$, with K from part III [1], may be used in the correction term to give a refined value for pq^{-1} by plotting the left hand side of

$$c_0\ (1 + q^{-1}r^{-1}) - \lambda_{11} = pq^{-1}\ (\lambda_{02} - c_0)r \tag{5}$$

against $(\lambda_{02} - c_0)\ r$.

From the definition of c_1 (eqn. (2) and (1)), the equation

$$c_1(q^{-1}r^{-1} + 1 + pq^{-1}\ r) - k_{30}q^{-1}r^{-1} - k_{03}pq^{-1}\ r^2 = k_{21} + k_{12}pq^{-1}\ r \tag{6}$$

is obtained. Since k_{30} and k_{03} are known [4], a plot of the left side of (6) against r gives the constants k_{21} and k_{12}.

Similarily, for c_2, knowing $k_{30}k_{40}$ and $k_{03}k_{04}$ [4], a plot of the left side of

$$c_2\ (q^{-1}r^{-1} + 1 + pq^{-1}\ r) - k_{30}k_{40}q^{-1}r^{-1} - pq^{-1}k_{03}k_{04}r^3 = k_{21}k_{31} + pq^{-1}k_{12}k_{22}r + pq^{-1}k_{03}k_{13}r^2 \tag{7}$$

against r yields the equilibrium constants $k_{21}k_{31}$, $k_{12}k_{22}$ and $k_{03}k_{13}$.

Cuts at constant a

A slightly different approach uses cuts at constant a instead of at constant r. Eqn. (1) may be written as

$$\begin{aligned} M - M_{or} &= uqr\ [f_0q^{-1}r^{-1} + f_1 + pq^{-1}f_2r + (f_3 + f(r))r^2] \\ f_0 &= 1 + k_{30}a + k_{30}k_{40}a^2 \\ f_1 &= 1 + k_{21}a + k_{21}k_{31}a^2 \\ f_2 &= 1 + k_{12}a + k_{12}k_{22}a^2 \\ f_3 &= pq^{-1}k_{03}k_{13}a^2 \qquad f(r) = pq^{-1}k_{03}a(1 + k_{04}ar) \end{aligned} \tag{8}$$

Eqns. (8) and (1a) — again neglecting λ_{20} — yield an expression for D, which, when rearranged, becomes

$$(\lambda_{11} + \lambda_{02}\ pq^{-1}r)D^{-1} - (f_0q^{-1}r^{-1} + f(r)r^2) = f_1 + pq^{-1}f_2r + f_3r^2 \tag{9}$$

Eqn. (9) may be solved graphically for f_i, and f_1 and f_2, in turn, for the required equilibrium constants, as will be shown below.

MERCURY DISTRIBUTION, EXPERIMENTAL RESULTS

Data (D, a, r) were obtained in the ranges $-2.1 < \log a < -1.0$ and $-3.4 < \log r < -1.5$. For experimental convenience, not r but $R = BA^{-1}$ was kept constant in a series of experiments with varying a. As A was about $10^3 - 10^4$ times M, $a \approx A$ is a very good approximation. B, however was not very large compared to M, since the specific

activity of the mercury did not permit the use of M values lower than about 10^{-5} M, and therefore the consumption of B by M made a correction necessary. Its magnitude was relatively large, but if $\bar{n}_B$ is obtained from any provisional constants (*e. g.* statistical values), $b = B - \bar{n}_B M$ is quite a good approximation. The values of $\bar{n}_B$ were mostly between 1.5 and 2.5. As a increased, b tended towards B and r towards R. A series of experiments log $D(a, B)_R$, where $\bar{n}_B M$ was particularily large is given in Table 1.

Table 1. Example of data log D(log a, log B)$_R$ converted into log D(log a)$_r$.

$-\log a$	$-\log B$	$\bar{n}_B$	$-\log b$	$-\log r$	log D	log $D_{r=0.010}$
1.945	3.945	1.95	4.66	2.71	1.22 ± 0.02	1.32 ± 0.03
1.842	3.842	1.96	4.28	2.44	1.28 ± 0.03	1.23 ± 0.03
1.742	3.742	1.96	4.046	2.305	1.208 ± 0.015	1.125 ± 0.020
1.644	3.644	1.96	3.870	2.226	1.072 ± 0.015	1.025 ± 0.020
1.541	3.541	1.97	3.710	2.169	0.963 ± 0.012	0.910 ± 0.015
1.439	3.439	1.98	3.567	2.128	0.858 ± 0.012	0.790 ± 0.015
1.340	3.340	1.99	3.440	2.100	0.711 ± 0.010	0.665 ± 0.015
1.237	3.237	2.01	3.313	2.076	0.610 ± 0.010	0.580 ± 0.015
1.137	3.137	2.03	3.198	2.062	0.380 ± 0.010	0.365 ± 0.015
1.059	3.059	2.05	3.110	2.051	0.273 ± 0.010	0.255 ± 0.015

In this series log $M = -4.330$, $\bar{n}_B$ about 2.0 and log $R = -2.000$.

Table 2. Mercury distribution : experimental data compared with calculated values.

$-\log a$	$-\log r$	log D_{obs}	log D_{calc}	$-\log a$	$-\log r$	log D_{obs}	log D_{calc}
1.28	1.52	0.34 ± 0.01	0.38	1.39	2.35	0.83 ± 0.02	0.78
1.38	1.53	0.47 ± 0.01	0.50	1.49	2.39	0.93 ± 0.01	0.88
1.48	1.54	0.66 ± 0.01	0.69	1.59	2.44	0.96 ± 0.01	0.98
1.58	1.56	0.78 ± 0.01	0.81	1.70	1.51	1.08 ± 0.01	1.06
1.68	1.58	0.91 ± 0.01	0.92	1.80	2.63	1.12 ± 0.01	1.13
1.78	1.61	1.04 ± 0.01	1.04	1.90	2.84	1.11 ± 0.01	1.12
1.88	1.64	1.13 ± 0.02	1.14	1.07	2.76	0.13 ± 0.01	0.14
1.98	1.68	1.32 ± 0.01	1.28	1.12	2.77	0.22 ± 0.01	0.23
1.28	2.08	0.57 ± 0.01	0.87	1.22	2.78	0.38 ± 0.01	0.36
1.46	2.07	0.89 ± 0.01	0.87	1.32	2.82	0.54 ± 0.01	0.51
1.76	2.17	1.22 ± 0.02	1.18	1.42	2.86	0.64 ± 0.01	0.62
1.86	2.23	1.31 ± 0.02	1.28	1.52	2.90	0.74 ± 0.02	0.72
2.06	2.44	1.40 ± 0.03	1.36	1.62	2.98	0.82 ± 0.02	0.80
1.06	2.05	0.27 ± 0.01	0.26	1.72	3.08	0.89 ± 0.03	0.85
1.14	2.05	0.38 ± 0.01	0.38	1.82	3.33	0.80 ± 0.02	0.78
1.24	2.08	0.61 ± 0.01	0.58	1.04	3.10	−0.12 ± 0.01	−0.11
1.34	2.10	0.71 ± 0.02	0.69	1.10	3.14	−0.09 ± 0.01	−0.05
1.44	2.13	0.86 ± 0.01	0.84	1.15	3.17	0.03 ± 0.01	0.02
1.54	2.17	0.96 ± 0.01	0.93	1.20	3.20	0.05 ± 0.01	0.06
1.64	2.23	1.07 ± 0.01	1.04	1.15	3.24	0.16 ± 0.01	0.13
1.74	2.31	1.21 ± 0.01	1.18	1.31	3.28	0.21 ± 0.01	0.18
1.84	2.44	1.28 ± 0.02	1.25	1.36	3.33	0.21 ± 0.01	0.22
1.95	2.71	1.22 ± 0.02	1.21	1.41	3.40	0.25 ± 0.01	0.24
1.21	2.31	0.54 ± 0.01	0.52	1.46	3.48	0.28 ± 0.01	0.24
1.29	2.32	0.65 ± 0.01	0.63	1.51	3.60	0.33 ± 0.01	0.23

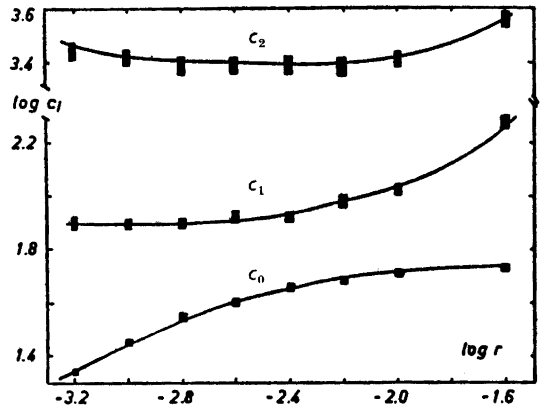


Fig. 1. The parameters c_i as function of r. ▮ values obtained by "curve fitting" log $D(\log a)_r$ plots, ———— calculated from the constants.

In Table 2 all the data are presented, with the observed D as function of the actual a and r values prevailing in the individual runs. The column D_{calc} is calculated for the individual a and r values with the constants found later, and summarized in Table 5.

Cuts at constant r

Values of log $D(\log a)_r$ were calculated by interpolation and were used to obtain the parameters $c_i(r)$ by curve fitting of eqn. (2). Plots of these parameters as log c_i(log r) are given in Fig. 1.

Considering c_0 first, a provisional value $pq^{-1} = 800$ was obtained from eqn. (3), using $\lambda_{11} = 6.1 \pm 0.6$ and $\lambda_{02} = 57.5 \pm 1.2$ from parts III and I[1,2]. From this and eqn. (4) the rough value of log $q = 4.2 \pm 0.2$, or using $q = Kpq^{-1}$ with log $K = 1.1 \pm 0.2$ from part III [1], log $q = 4.0 \pm 0.2$, was obtained. A refined value log $pq^{-1} = 2.90 \pm 0.05$ was then obtained by using eqn. (5) as shown in Fig. 2. A curve $c_0(r)$ calculated with the now known q and pq^{-1} is compared with the experimental values in Fig. 1.

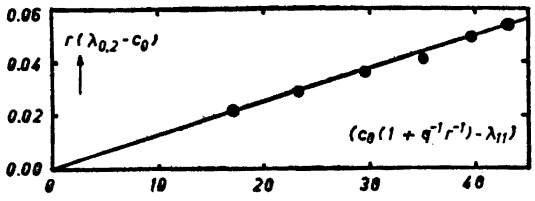


Fig. 2. Plots of eqn. (5) to find pq^{-1}, the slope of the best straight line through the origin and the points.

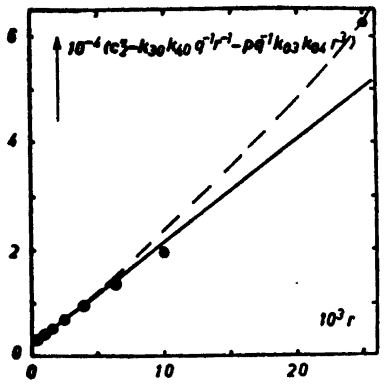


Fig. 3. Plots of eqn. (7). ● left side of (7) calculated from experimental points, ———— calculated with the constants $k_{12}k_{22}$ and $k_{22}k_{31}$. — — — — calculated with the additional constant k_{13}.

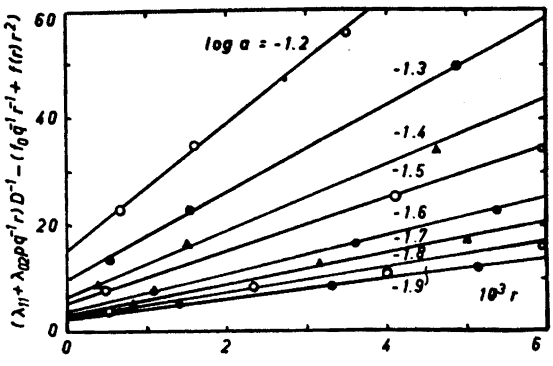


Fig. 4. Plot of eqn. (9) for low r values. ● ○ ▲ calculated from the experimental points, ———— best straight lines through the points.

The values of c_1 were inserted into eqn. (6) and the left side of it was plotted against r, and, divided by r, against r^{-1}, using $k_{30} = 185$ and $k_{03} = 4\,700$ [4]. From the slopes the values of the constants $\log k_{12} = 1.87 \pm 0.03$ and $\log k_{21} = 1.85 \pm 0.04$ were obtained. Inserted into a rearranged form of eqn. (6) they gave a $c_1(r)$ curve, which is compared with the experimental values in Fig. 1.

The values of c_2 were inserted into eqn. (7), and the resulting left hand term using $k_{30}k_{40} = 1.05 \times 10^4$ and $k_{03}k_{04} = 1.10 \times 10^6$ [4] was plotted against r in Fig. 3. Except for the last point, the plot is linear, and the constants $\log k_{12}k_{22} = 3.38 \pm 0.03$ and $\log k_{22}k_{31} = 3.35 \pm 0.04$ were obtained from it in the way outlined above for c_1. Using these two constants the straight line in Fig. 3 was obtained, which is seen to agree well with the data, except, again, for the last point. A value of $\log k_{13} \sim 1.0$ (eqn. (7)) may bring even the last point into line (the dashed curve in Fig. 3), although the fit for some of the remaining points is then somewhat poorer. The constants were inserted into a rearranged form of eqn. (7) to give a curve which is compared with the experimental c_2 in Fig. 1.

Cuts at constant a

Using data $\log D(\log r)_a$, again calculated by interpolation, and the constants $\log pq^{-1} = 2.90$ and $\log q \sim 4.2$ found above, the left hand term of eqn. (9) was calculated, and is plotted against r (up to $r = 0.005$) in Fig. 4. The best straight lines were drawn, one for each a value, with slopes f_2pq^{-1} and intercepts f_1. The functions $(f_1-1)a^{-1}$ and $(f_2-1)a^{-2}$ plotted against a gave straight lines of slopes $k_{21}k_{31} = 10^{3.34\pm0.05}$ and $k_{12}k_{22} = 10^{3.36\pm0.04}$,

while plots of $(f_1-1)a^{-2}$ and $(f_2-1)a^{-2}$ against a^{-1} yielded slopes $k_{21} = 10^{1.88\pm0.03}$ and $k_{12} = 10^{1.90\pm0.02}$. These constants agree very well with those obtained with cuts at constant r (see Table 5).

Using the functions f_1 and f_2pq^{-1} obtained above with eqn. (9) at $r > 0.005$, f_3 values were obtained for each a value, from which $\log k_{13} = 1.1 \pm 0.1$ was obtained. This value is a better approximation than that obtained with cuts at constant r.

The averages of the constants found for the two approaches were used to calculate the values of D_{calc} in Table 2.

EQUATIONS FOR IODINE DISTRIBUTION

The data for iodine distribution experiments will be discussed in terms of the species and complexity constants already employed above and listed on p. 812.

The experimental quantities studied are the independent variables a, B, and M, and the dependent variable D. Usually in solvent distribution studies, the concentration of free ligand is known, but in this case b = iodide is neither known nor negligible, and the situation is further complicated by the fact that the free ligand is a part of the material of which the distribution is studied.

The balances of mercury and iodine are:

$$M = \beta_{20}m[a^2(f_0+\lambda_{20})+qab(f_1+\lambda_{11})+pb^2(f_2+\lambda_{02})+pk_{03}b^3(1+k_{13}a+k_{04}b)] \quad (10)$$

$$B = b+\beta_{20}m\ [qab(f_1+\lambda_{11})+2pb^2(f_2+\lambda_{02})+3pk_{03}b^3(1+k_{13}+4/3k_{04}b)] \quad (11)$$

with the f_i defined in eqn. (8), and the distribution ratio of iodine:

$$D = \beta_{20}mb\ (qa\lambda_{11} + 2pb\lambda_{02})\ (B-\beta_{20}mb(aq\lambda_{11}+2pb\lambda_{02}))^{-1} \quad (12)$$

At sufficiently low B, and therefore b (for M values of the order of 10^{-5} M this means B lower than 2.10^{-4} M), the terms with b^3 are negligible. On the whole, it will be convenient to discuss the data in terms of three regions:
a) very low B, where terms with b^2 are negligible,
b) relatively high B, where terms with b (except for free B) are negligible, and
c) intermediate values of B, where terms with both b and b^2 are important.

Very low B

The very low range of B is practically defined by having

$$(\partial D/\partial B)_{a,M} \approx 0 \quad (13)$$

This means that b is eliminated from the expressions for D, which requires that the only B containing species be B and MA_iB.

Since B is very low, $\Sigma[MA_iB]$ will be negligible beside $\Sigma[MA_i]$, and therefore the mercury balance is

$$M = \beta_{20}ma^2\ (f_0 + \lambda_{20}) \quad (14)$$

where $a^2\ (f_0 + \lambda_{20})$ is known. The iodine balance is

$$B = b\ (1 + \beta_{20}qma\ (f_1 + \lambda_{11}) \tag{15}$$

Eliminating b and $\beta_{20}m$, the distribution of iodine will be

$$D = \lambda_{11}(f_0 + \lambda_{20})aq^{-1}M^{-1} + f_1) \tag{16}$$

Eqn. (16) may be transformed into a linear eqn. in M^{-1}

$$D^{-1} = (f_0 + \lambda_{20})a(q\lambda_{11})^{-1})\ M^{-1} + f_1\lambda_{11}^{-1} \tag{17}$$

whence the slope of a $D^{-1}\ (M^{-1})_a$ plot will give the value of $q\lambda_{11}$.

If plots $D^{-1}\ (M^{-1})_a$ are extrapolated to $M^{-1} = 0$ (*i. e.* $M = \infty$) and the values of log D (log $a)_{M=\infty}$ plotted, the constants λ_{11}, k_{21} and $k_{21}k_{31}$ may be obtained by curve-fitting methods. The constant q may then be obtained from λ_{11} and the value of $q\lambda_{11}$ obtained above from the slope of (17).

Relatively high B

The range of relatively high B will be defined by having as B containing species only B and MA_1B_2, whence

$$(\partial \log\ D\ /\ \partial \log\ (B/M))_a = -\ (1 - 2\lambda_{02}MB^{-1}\ (f_2+\lambda_{02})^{-1})^{-1} \approx -1 \tag{18}$$

The mercury and iodine balances are then

$$M = \beta_{02}mb^2\ (f_2 + \lambda_{02}) \tag{19}$$

$$B = b + 2\beta_{02}\ mb^2\ (f_2 + \lambda_{02}) = b + 2\ M \tag{20}$$

Introducing the distribution ratio D and eliminating b and $\beta_{02}\ m$,

$$f_2 = \lambda_{02}(2MB^{-1}\ (D + 1)\ D^{-1} - 1) \tag{21}$$

gives values for f_2, and plots log f_2 (log a) may be treated, *e. g.* by curve fitting methods, to yield values of k_{12} and $k_{12}k_{22}$.

Intermediate B

At intermediate values of B the species to be considered will be MA_i, MA_iB, MA_iB_2 and B. The mercury and iodine balances (10) and (11) combined, give then, neglecting terms with b^3

$$B/M = b\ /\ \mathrm{M} + \frac{qab\ (f_1+\lambda_{11})+2pb^2\ (f_2 + \lambda_{02})}{a^2\ (f_0 + \lambda_{20}) + qab\ (f_1 + \lambda_{11}) + pb^2\ (f_2 + \lambda_{02})} \tag{22}$$

Eliminating $\beta_{20}m$ from the iodine distribution ratio (12) and eqns. (10) and (11) gives

$$D = \frac{qa\lambda_{11} + 2\ pb\lambda_{02}}{(M^{-1}a^2(f_0+\lambda_{20})+qaf_1) + (M^{-1}qa(f_1+\lambda_{11}) + 2pf_2)b + (M^{-1}p(f_2+\lambda_{02}))\ b^2} \tag{23}$$

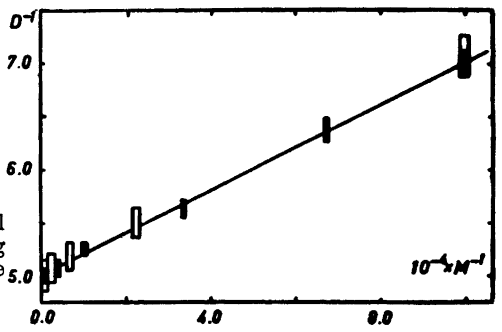


Fig. 5. Plot of eqn. (17). Experimental points: ■ for log $B = -5.9$, □ for log $B = -6.5$, ———— best straight line through the points.

Eqns. (22) and (23) are functions of b, known constants and the as yet unknown constant p (it is assumed that a and M are kept constant). The function log $D(\log p)_{a,b,M}$ is now plotted, calculated from (23) for discrete values of b. An approximate value for B/M may be obtained from

$$B/M \approx b/M + (1+a(f_0 + \lambda_{20})q^{-1}\ b^{-1}\ (f_1 + \lambda_{11})^{-1})^{-1} \qquad (22a)$$

Values of log $D(\log B/M)_{a,M}$ are now obtained experimentally, and the value of log D, corresponding to the B/M calculated for some value of b, gives then a provisional p value on the log $D(\log p)$ plot for this b value. The provisional values are used in conjunction with (22) to calculate a better value of B/M, the corresponding log D found from experiment is then used to give refined values of p, this process being repeated as much as necessary.

IODINE DISTRIBUTION, EXPERIMENTAL RESULTS

Very low B

One series of experiments was made at constant $a = 0.100$ M and at two log B values, -5.9 and -6.5, while log M changed from -4.0 to -2.0. At the highest M values, A was varied, so as to keep a constant, and was calculated from $A = a + n_A M$, n_A being calculated using the constants k_{i0} and a. The results, log $D(\log M)_{a,B}$, are given in Table 3 and were transformed to plots of eqn. (17), $D^{-1}(M^{-1})_{a,B}$, shown in Fig. 5.

As is seen the points for the two B values fall on the same straight line, so that eqn. (13) is fulfilled, and the slope is $(2.00 \pm 0.05) \times 10^{-4}$. Since $(f_0 + \lambda_{20})a = 12.6 \pm 1.1$ (part II[4]), the value found for log $q\lambda_{11}$ is 4.80 ± 0.04.

A second series of experiments, presented in Table 3, was made at constant log $B = -5.9$, and at two log M values: -4.00 and -3.00, for each a value, while log a varied from -3.5 to -1.0. The value of a was obtained by successive approximations from $a = A - n_A M$, when $A < 100\,M$. Two points were obtained for each a in plots $D^{-1}(M^{-1})$ and the best straight line with the known slope $a(f_0 + \lambda_{20})q^{-1}\lambda_{11}^{-1}$ was drawn through them, the points falling very neatly on the line. The intercept at $M^{-1} = 0$ gives log $D = \log \lambda_{11} - \log (1 + k_{21}a + k_{21}k_{31}a^2)$, which is plotted against log a in Fig. 6. The figure shows also the points log $D(M)_a$. At log $a < -2.3$, the points for the two M values coincide with that for $M^{-1} = 0$.

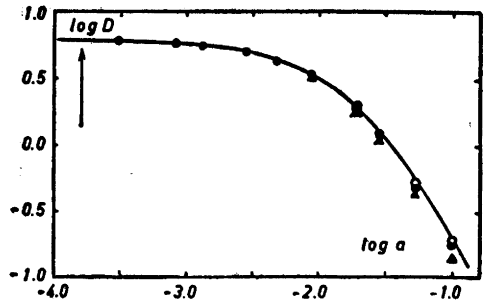


Fig. 6. Log D as function of log a for M^{-1} values extrapolated to zero: ○, and for experimental values $M^{-1} = 10^3$: ●, and $M^{-1} = 10^4$: ▲, ——— calculated with the constants λ_{11}, k_{21} and $k_{21}k_{31}$.

The plot of $\log D(\log a)_{M=\infty}$ was "curve fitted" and yielded the constants: $\log\lambda_{11} = 0.79 \pm 0.01$, $\log k_{21} = 1.84 \pm 0.02$ and $\log k_{21}k_{31} = 3.34 \pm 0.04$. The value of λ_{11} gave with the slope of eqn. (17) the value $\log q = 4.01 \pm 0.04$. A curve calculated with the constants is compared with the data in Fig. 6.

Relatively high B

Three series of experiments were made at constant $\log B = -3.70$, one having $\log M = -5.29$, the second having $\log M = -4.90$, and the third having $\log M$ varying between -4.70 and -5.28. In the first two series $\log a$ varied between -3.0 and -0.6, while in the third it was constant, $\log a = -1.00$ (see Table 4). The third series illustrates the validity of eqn. (18), since $(\triangle \log D/\triangle \log M)_a \approx 1$. The data were used to calculate f_2 by eqn. (21), and the values so found are plotted as $\log f_2(\log a)$ in Fig. 7.

As may be seen from the figure, points for different M values fall on the same curve, showing that the assumptions underlying eqn. (21) — in particular the species to be considered — are valid. The curve was "curve fitted" and

Table 3. Distribution of iodine at low B values.

Constant $a = 0.100$ M			Constant $\log B = -5.9$		
$-\log M$	$-\log D$		$-\log a$	$\log D$	
	$\log B = -5.9$	$\log B = -6.5$		$\log M = -4.0$	$\log M = -3.0$
2.00	0.700	0.700	1.00	−0.845	−0.720
2.34		0.705	1.27	−0.355	−0.310
2.52	0.705		1.55	0.045	0.075
2.82		0.715	1.73	0.250	0.270
3.00	0.720		2.06	0.525	0.535
3.34		0.740	2.32	0.630	0.630
3.52	0.750		2.55	0.710	0.705
3.82	0.805		2.88	0.750	0.750
4.00	0.845	0.850	3.09	0.765	0.770
			3.52	0.780	0.780

Values of $\log D$ for $\log B = -6.5$ are ± 0.012, all other $\log D$ values are ± 0.007.

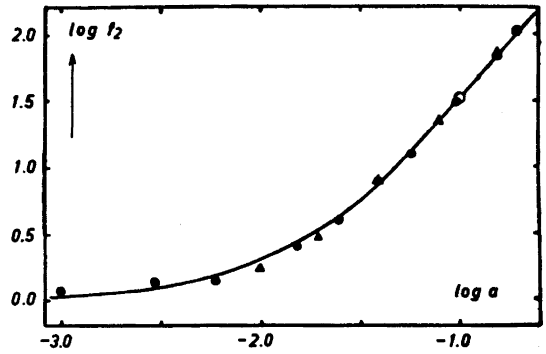


Fig. 7. Log f_2 obtained by eqn. (21) as function of log a. Experimental points ● log $M = -5.29$, ▲ log $M = -4.90$, O log M varying between -4.69 and -5.28, ——— calculated with the constants k_{12} and $k_{12}k_{22}$.

yielded the constants log $k_{12} = 1.87 \pm 0.03$ and log $k_{12}k_{22} = 3.37 \pm 0.05$. A curve calculated with these constants is compared with the data in Fig. 7.

Intermediate B

A series of experiments at constant log $M = -4.00$ and at constant $a = 0.100$ M was made, with log B/M varying between -1.5 and $+1.6$. The results are plotted as log $D(\log B/M)_{a,M}$ in Fig. 8. In the range of low B/M, D is independent of B/M as expected (eqn. (12)). At high B/M the slope of the curve is -1 as expected from eqn. (18). At intermediate values of B/M the curve rises slowly towards a maximum.

Curves log $D(\log p)_{a,b,M}$ were calculated, using the constants q, λ_{11} and k_{ij} previously found, and the constant values of a and M, for the nine values of b: log $b = -5.52 + 0.15\,i$, $i = 0, 1, 2 \ldots 8$. The curves are shown in Fig. 9. Values of B/M corresponding to the above b were obtained, first from (22a)

Table 4. Distribution of iodine at high B/M values.

log M = −5.29		log M = −4.90		log a = −1.00	
−log a	−log D	−log a	−log D	−log M	−log D
0.71	1.64	0.81	1.21	4.69	0.82
0.81	1.53	1.11	0.99	4.70	0.83
1.01	1.37	1.41	0.90	4.85	1.00
1.24	1.26	1.71	0.86	4.93	1.09
1.41	1.23	1.01	0.85	5.10	1.23
1.60	1.20			5.28	1.45
1.81	1.19				
2.23	1.18				
2.54	1.18				
3.00	1.18				

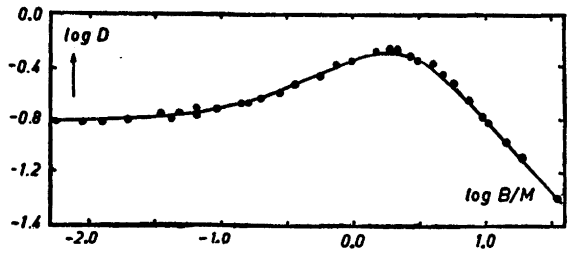


Fig. 8. Log D as function of log B/M for log $a = -1.00$ and log $M = -4.00$. ● experimental points, ———— calculated (eqns. (22), (23)) from the constants.

and then by successive approximations, using provisional values of p, from (22). Log D values for these B/M were obtained from the experimental plot in Fig. 8, and the corresponding log p values were read off from the log D(log p) plots, until log p proved constant $= 6.94 \pm 0.03$, and this value was accepted. The values so obtained are shown in Fig. 9.

A calculated curve, using all the constants, is compared with the data in Fig. 8.

REPRESENTATION OF RESULTS

The constants obtained from the various experimental and calculation methods are compared in Table 5.

The significance of the constants may be better understood when presented in graphical form.

One way of doing this is to show predominance areas, in a diagram with log a and log b as independent variables. Areas in it are marked with the indices ij of the complexes MA_iB_j, and correspond to a predominace of a single species (inside the shaded contour the concentration is >50 %). Lines mean equal concentrations of the complexes of the adjacent areas, and at triple points, three complexes are present at equal concentrations. This way gives at a

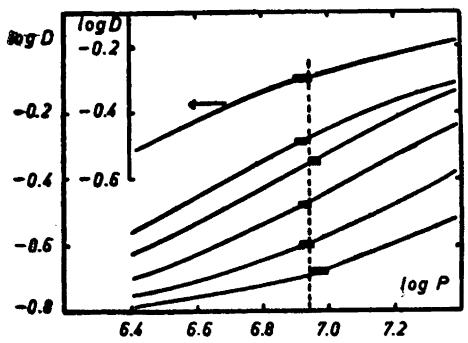


Fig. 9. Log D as function of log p, with b as parameter. ———— the calculated function (eqn. (23)), ■ experimental D corresponding to B/M calculated from b and p by eqn. (22).

Table 5. Complexity constants for ternary Hg—Br—I complexes.

Reaction	Constant	Hg distribution		Iodine distribution	Final values
		$D\ (a)_r$	$D\ (r)_a$		
$MA_2 + 2B^- \rightleftharpoons MB_2 + 2A^-$	log p	(7.1 ±0.2)		6.94±0.03	6.94±0.03
$MA_2 + B^- \rightleftharpoons MAB + A^-$	log q	4.2 ±0.2		4.01±0.04	4.01±0.04
$MAB + B^- \rightleftharpoons MB_2 + A$	log $q^{-1}p$	2.90±0.05		(2.91±0.05)	2.91±0.05
$MA_2 + MB_2 \rightleftharpoons 2\ MAB$	log K	(1.3 ±0.2)		(1.10±0.07)	1.10±0.07
$MAB \rightleftharpoons MAB_{or}$	log λ_{11}	(0.79±0.04)		0.79±0.02	0.79±0.02
$MAB + A^- \rightleftharpoons MA_2B^-$	log k_{21}	1.85±0.04	1.88±0.03	1.84±0.02	1.85±0.03
$MB_2 + A^- \rightleftharpoons MAB_2^-$	log k_{12}	1.87±0.03	1.90±0.02	1.87±0.03	1.88±0.03
$MA_2B^- + A^- \rightleftharpoons MA_3B=$	log k_{31}	1.50±0.06	1.46±0.06	1.50±0.05	1.49±0.06
$MAB_2^- + A^- \rightleftharpoons MA_2B_2=$	log k_{22}	1.51±0.04	1.46±0.04	1.50±0.06	1.49±0.05
$MB_3^- + A^- \rightleftharpoons MAB_3=$	log k_{13}	~1.0	1.10±0.10		1.10±0.10

The constants in parenthesis were calculated from others, directly obtained from the data, or were obtained from part III [1].

glance qualitative information as to the species important at given concentrations of both free A and free B. This diagram is shown in Fig. 10.

Another way to present two-dimensionally the three-dimensional diagram (% *formation*, *a*, *b*), is to present cuts at constant *a* (Fig. 11) or *b* (Fig. 12). This well known type of presentation shows the gradual addition of ligands, *e. g.* A in Fig. 12, while the ratios of the complexes with different numbers of the other ligand (*e. g.* B) remain constant (for cuts at constant *b*). Again, the complexes MA_iB_j are represented by their indices *ij* only.

DISCUSSION

A full discussion of the significance of the ternary complexity constants will be given in part V.

Previous work found on anionic mixed complexes of Hg(II) with halides is the Raman effect study of Delwaulle [5]. The mixed complexes HgA_nB_{4-n}

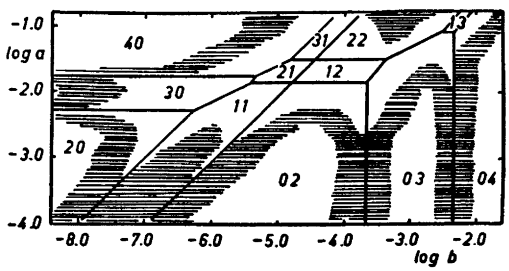


Fig. 10. Predominance area diagram. Areas correspond to predominance of the complexes MA_iB_j indicated by their indices *i j* (*e. g.* $HgBr_2I$ is (21)) (within shaded areas more than 50 %), as function of free bromide and free iodide concentrations.

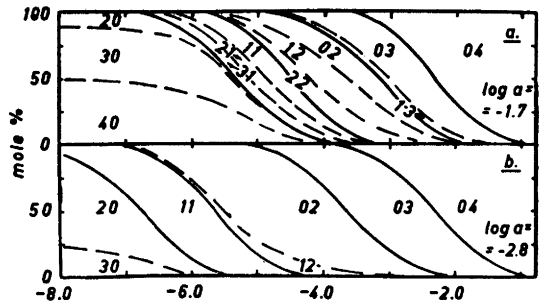


Fig. 11. Mole % of complexes as function of free iodide concentration, at constant bromide concentrations log $a = -1.7$ (a) and log $a = -2.8$ (b).

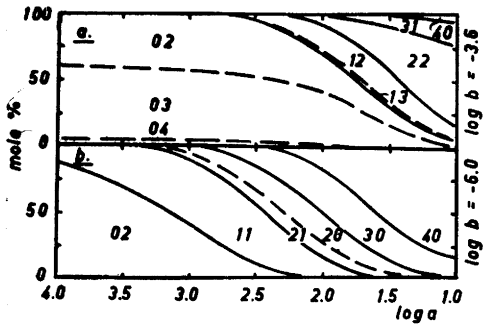


Fig. 12. Mole % of complexes as function of free bromide concentration, at constant iodide concentrations log $b = -3.6$ (a) and log $b = -6.0$ (b).

could all be identified for A and B being any two of Cl^-, Br^- and I^-, except that lines for $HgBrI_3^=$ could not be observed. This is in agreement with the rather weak formation of this complex found here, as is shown by its formation constant k_{13}. No complexity constants were, however, given by Delwaulle. A similar study, limited to the Br—I mixed complexes, is reported by Rolfe, Sheppard and Woodward [9].

The treatment of mercury distribution data is essentially similar to well known examples, like that mentioned in Ref.[3]. On the other hand, ligand distribution does not seem to have been used similarly to central-group distribution. In the present study, the system M—A—B has been studied by measuring the distribution of total B between two liquid phases, the relevant reactions being $M + iA + jB \rightleftharpoons MA_iB_j$ and $(MAB + MB_2)_{aq} \rightleftharpoons (MAB + MB_2)_{or}$. Of course, solvent distribution is but one example of employing a two-phase system where not all the components of the complex system are soluble in both phases. The following examples show in what ways the present method is similar to or different from other methods.

Consider, for instance, that the second phase is a gas, and J. Bjerrum's measurements of the ammonia vapour tension above metal-ammonia solutions [6] as an example of determining free A in a M—A system by two-phase distribution. The relevant reactions are then: $M + n\,A \rightleftharpoons MA_n$ and $A_{aq} \rightleftharpoons A_{vap}$ where M is the metal and A is ammonia.

If the second phase is a liquid, then the solvent distribution determination of free ligand may be illustrated by Dawson's study of the Hg—I system [7]. He determined the free iodide content of the solutions by measuring the iodine distribution between CS_2 or CCl_4 and the aqueous solutions, and, knowing the equilibrium constant for $I_2 + I^- \rightleftharpoons I_3^-$, he calculated $[I^-]$. In this case the relevant reactions are: $M + n\ A \rightleftharpoons MA_n$, $A + B \rightleftharpoons AB$ and $B_{aq} \rightleftharpoons B_{or}$, where M is again the metal, A is iodide, B is iodine and AB is triiodide.

For the second phase being a solid, Leden and Parck's work may be mentioned [8]. There the distribution of radioactive iodine between solid AgI and its solution in $AgClO_4$ was measured. The distributing species AgI is then a member of the series of complexes studied $Ag_nI^{(n-1)+}$. The relevant reactions are then: $MA + (n-1)\ M \rightleftharpoons M_nA$ and $MA_{aq} \rightleftharpoons MA_{solid}$.

The first two examples belong to a group where the concentration of free ligand is measured, and as such are analogous, for instance, to measuring the concentration of a free ligand that is the anion of a weak acid by measuring the pH (potentiometrically or otherwise), where the reaction $H^+ + Anion^- \rightleftharpoons H\ Anion$ is utilized.

The present work is similar to the third example in that the total distribution of an element is measured, the distributing species being members of the complex series to be studied. There is little real difference between measuring the distribution of the central group and of the ligand, and the polynuclear system of silver iodide complexes may be considered as "silvero" complexes of the central-group iodine.

Measurements of ligand distribution may be of wide applicability, particularly in cases where there is no convenient isotope of the metal, but there is of the ligand.

The author wishes to thank the *Israel Atomic Energy Commission* for a research grant abroad, Professor Lars Gunnar Sillén for the facilities provided, and particularly for his advice, comments and criticism, and Dr. Helen S. Dunsmore for improving the English presentation.

REFERENCES

1. Marcus, Y. *Acta Chem. Scand.* **11** (1957) 610, part III.
2. Marcus, Y. *Acta Chem. Scand.* **11** (1957) 329, part I.
3. Sillén, L. G. *Acta Chem. Scand.* **10** (1956) 803.
4. Marcus, Y. *Acta Chem. Scand.* **11** (1957) 599, part II.
5. Delwaulle, M. L. *Bull. soc. chim. France* **1955** 1294.
6. Bjerrum, J. *Metal Amine Formation in Aqueous Solutions*, Thesis, Copenhagen 1941.
7. Dawson, H. M. *J. Chem. Soc.* **95** (1909) 870.
8. Leden, I. and Parck, C. *Acta Chem. Scand.* **10** (1956) 535.
9. Rolfe, J. A., Sheppard, D. E. and Woodward, L. A. *Trans. Faraday Soc.* **50** (1954) 1275.

Received January 23, 1957.

ACTA CHEMICA SCANDINAVICA 11 (1957) 826—835

The Presence of Cinnamyl Alcohol Groups in Lignin

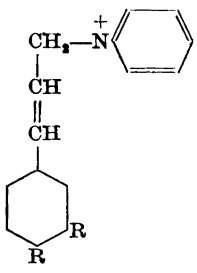
BENGT O. LINDGREN and HIROSHI MIKAWA

Department of Wood Chemistry, Swedish Forest Products Research Laboratory, Stockholm, Sweden

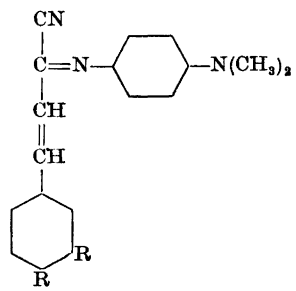
A colour reaction has been worked out for cinnamyl alcohol groups. It involves a transformation of these groups into *p*-dimethylamino-anilides of styryl-glyoxylonitriles (II). By this method the presence of a small amount of cinnamyl alcohol groups in spruce lignin has been indicated.

In 1896 Klason [1] found that coniferin is easily sulphonated when heated with an acid sulphite solution. This reaction was attributed to the presence of the cinnamyl alcohol group in coniferin. Partly because of this finding he suggested that the sulphonatable structures in lignin consist of cinnamyl alcohol groups. Later investigations [2] showed, however, that the main parts of these structures most probably are phenyl-carbinols and their ethers. On the other hand, the possibility of the presence of a small amount of cinnamyl alcohol groups in lignin has not been excluded.

This possibility may also be compatible with the modern view that gymnosperm lignin is formed by oxidative polymerization of coniferyl alcohol [3]. It may be possible that during such a process some of the coniferyl alcohol molecules are built into the lignin molecules without a change of their allyl alcohol side chains, thus forming cinnamyl alcohol groups in lignin.



Ia, R = H
b, R = OCH_3



IIa, R = H
b, R = OCH_3

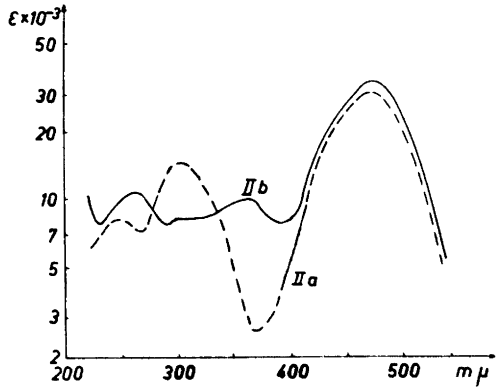


Fig. 1. The extinction curves for the *p*-dimethylamino anilides of styryl glyoxylonitrile (IIa) and for its 3,4-dimethoxy derivative (IIb). Alcoholic solution.

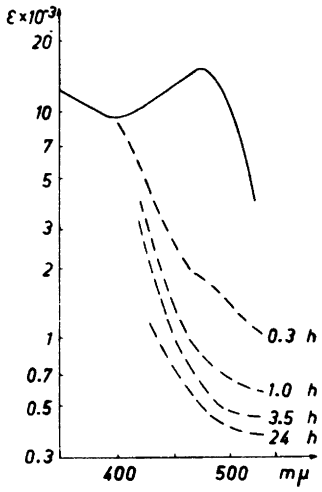


Fig. 2. Extinction curves. Alcoholic solution. The ε-values were calculated on the basis of the amount of (Ib) used.

Continuous line. The unfractionated reaction products from the reaction of (Ib) with *p*-nitrosodimethyl-aniline and potassium cyanide.

Dotted lines. The unfractionated products after being kept in 1/15 N alcoholic hydrochloric acid for varying times at room temperature.

We have therefore tried to find a colour reaction for these groups in lignin. It was found that cinnamyl alcohol and its 3,4-dimethoxy derivative could be transformed into the strongly red coloured *p*-dimethylamino-anilides of styryl-glyoxylonitriles (IIa and b, respectively) in a two-step process *via* the N-cinnamyl-pyridinium salts (Ia and b, respectively).

The first step was accomplished at room temperature by treating the alcohols with tosyl chloride dissolved in pyridine. The pyridinium salts (Ia and b) were obtained in good yields. The second step was carried out according to the method used by Kröhnke [4] to transform N-phenacyl-pyridinium bromide into the *p*-dimethylamino-anilide of benzoyl-glyoxylonitrile. The pyridinium salts (Ia and b) were treated at room temperature with a water-alcohol solution of *p*-nitrosodimethyl-aniline and potassium cyanide. The nitriles (IIa and b) were obtained, after chromatographic purification, in yields of 46 and 26 %, respectively.

On the other hand, when coniferyl alcohol was treated with tosyl chloride and pyridine no pyridinium salt was obtained. It is hardly probable, however, that lignin contains such reactive structures as *p*-hydroxy-cinnamyl alcohol groups because they would have been easily oxidized during the lignin biosynthesis. This failure is therefore of no great importance in the present case.

The extinction curves for the two nitriles (IIa and b) had strong maxima at 475 mμ, ε being 29 800 for (IIa) and 32 700 for (IIb) (Fig. 1).

The light absorption of the unfractionated reaction products obtained from the pyridinium salt (Ib) had $\varepsilon_{max} = 15\,500$ at 475 mμ (Fig. 2), calculated on the basis of the amount of pyridinium salt used. This absorption was considerably higher than that which corresponded to the yield of the nitrile (IIb). Therefore some coloured compounds other than this nitrile were formed by the Kröhnke synthesis. This inference must be considered if the colour reaction is used for the photometric estimation of the amount of cinnamyl alcohol groups.

The glyoxylonitrile derivatives are easily destroyed by acid [4] with the disappearance of the extinction maximum at 475 mμ. Fig. 2 shows that after treatment of the unfractionated mixture with 1/15 N hydrochloric acid at room temperature for 1 h the absorption at 475 mμ had decreased to 5 % of its original value.

The great reactivity of cinnamyl alcohol structures makes their presence in isolated lignin preparations unlikely even if the original lignin contained such structures. The colour reaction was therefore performed on extracted wood slices, the thickness of which was about 20 μ. If not otherwise stated, they were freshly prepared from a newly cut spruce tree. The slices were first treated with a solution of tosyl chloride in pyridine, and then, after careful washing, with one of *p*-nitrosodimethyl-aniline and potassium cyanide in water-alcohol. After another very careful washing, the light absorption of the slices was determined with a Beckman spectrophotometer. The light scattering was minimized by wetting the slices with benzene.

The suitability of this method was tested on slices containing an approximately known amount of cinnamyl alcohol groups derived from the cinnamyl *aldehyde* groups of lignin. The procedure was as follows.

First, the slices were heated with a neutral sulphite solution for 20 h at 135°C. In this way the cinnamyl alcohol groups which might have been present in lignin were destroyed by transforming them into alkali stable sulphonic acid structures.

The conditions for the sulphite treatment were chosen from a study of 3,4-dimethoxy-cinnamyl alcohol. Fig. 3 shows that this compound was almost completely sulphonated when heated at 135°C for about 20 h with a sulphite solution of pH 6.

During the sulphonation of the alcohol, its UV absorption curve changed considerably (Fig. 4). The 265 mμ maximum was shifted to 280 mμ and its ε value decreased. The absorption in the vicinity of 300 mμ disappeared. These changes indicated that the aliphatic double bond became saturated. Accordingly, the sulphonation probably involved an addition of sulphite to the aliphatic double bond of the alcohol.

The sulphite treatment of the slices would also transform the cinnamyl aldehyde structures of lignin more or less completely into the hydrosulphonic acid derivative (III) and its sulphite addition product (IV) [5]. The carbonyl group in structure (III) causes the sulphonic acid groups of (III) and (IV) to be split off easily by alkali with reforming of the double bond. To regenerate

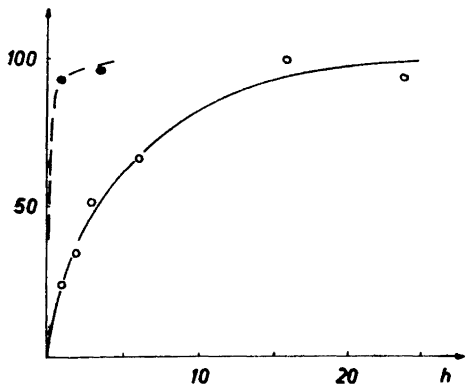


Fig. 3. The rate of sulphonation of 3,4-dimethoxy-cinnamyl alcohol (yield of sulphonic acid versus heating time). Temperature of the reaction 135°C. Total concentration of SO_2, 5 %.
— — — Sulphite solution at pH 3
———— Sulphite solution at pH 6
The yield was determined as described for similar experiments with vanillyl alcohol [6].

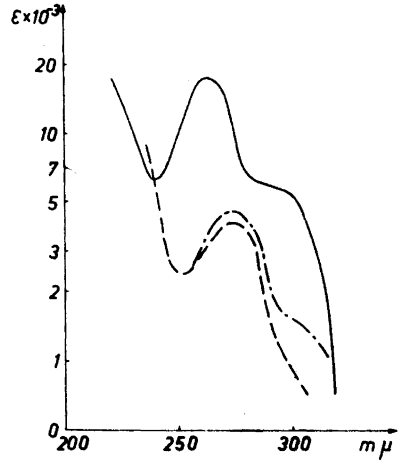
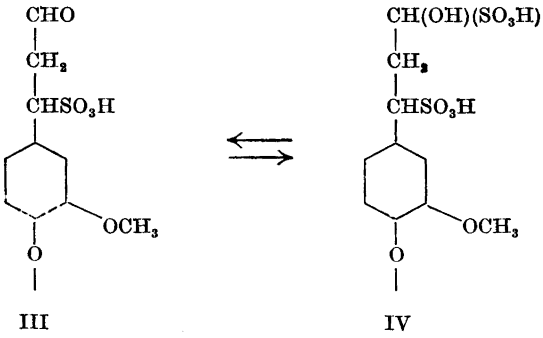


Fig. 4. The extinction curves for 3,4-dimethoxy-cinnamyl alcohol and its sulphonated products.
———— 3,4-Dimethoxy-cinnamyl alcohol
— — — Sulphonated at pH 6
— — — — Sulphonated at pH 1.5

the cinnamyl aldehyde structures the slices were therefore immersed in a sodium hydroxide solution.



Finally, the slices were treated with an aqueous sodium borohydride solution, to reduce the cinnamyl aldehyde groups of lignin to cinnamyl alcohol groups. As the yield of such a reduction is high, the amount of cinnamyl alcohol groups formed should be about the same as the amount of cinnamyl aldehyde structures originally present in lignin. Adler and Ellmer [5] have

estimated that spruce lignin contains one such aldehyde group per 40—60 phenylpropane monomers.

The presence of the cinnamyl alcohol groups in the treated slices was clearly demonstrated since the slices turned red when subjected to the colour reaction, and the absorption curve for the coloured slices had a distinct maximum at 475 mμ (Fig. 5). If the coloured slices were treated with acid the colour and the maximum disappeared (Fig. 5) in agreement with the acid labile nature of the glyoxylonitrile structures. (The wavelength of the maximum obtained on different slices varied between 475 ± 5 mμ. This uncertainty depended probably on the superposition of the absorption due to the aromatic structures of lignin, which caused the extinction to increase sharply at lower wavelengths as is shown in Fig. 5.)

As described above, slices which have been treated only with sulphite or with sulphite and alkali should contain no cinnamyl alcohol groups. In accordance with that no maximum was obtained when these slices were subjected to the colour reaction (Fig. 5).

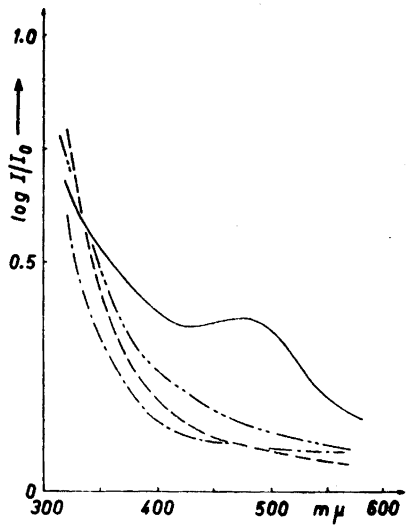


Fig. 5. Absorption curves on spruce wood slices first pretreated and then subjected to the colour reaction. Weight of the slices, 1.6 mg per cm². For the treatment conditions, see Table 1.
– – – – Pretreated with sulphite.
— — — — Pretreated with sulphite and sodium hydroxide.
——— Pretreated with sulphite, sodium hydroxide and sodium borohydride.
— – — – The last slice after treatment with hydrochloric acid.

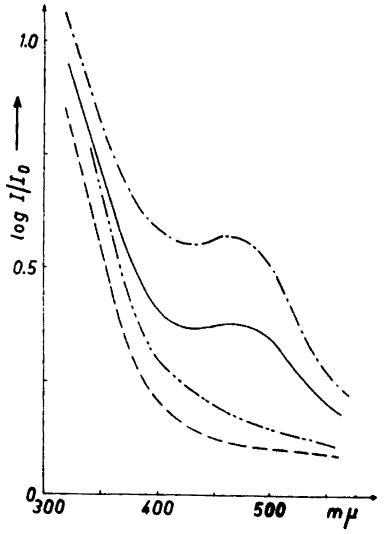


Fig. 6. Absorption curves on spruce wood slices subjected to the colour reaction. Weight of the slices, 1.6 mg per cm².
——— No pretreatment
— — — — The same slice after treatment with hydrochloric acid
— — — — Pretreated with sodium borohydride
— – — – The last slice after treatment with hydrochloric acid

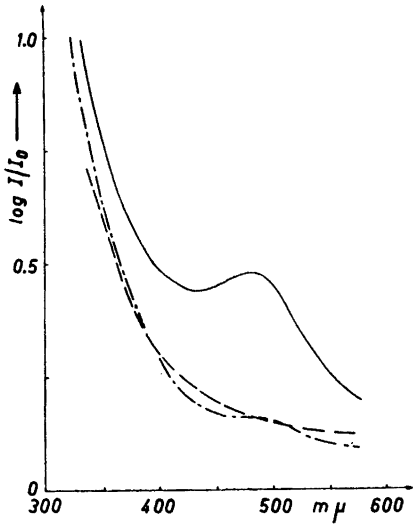


Fig. 7. Absorption curves on spruce wood slices stored for 6 months and then subjected to the colour reaction. Weight of the slices, 2.0 mg per cm².
- – – – – No pretreatment
——— Pretreated with sodium borohydride
— — — The last slice after treatment with hydrochloric acid

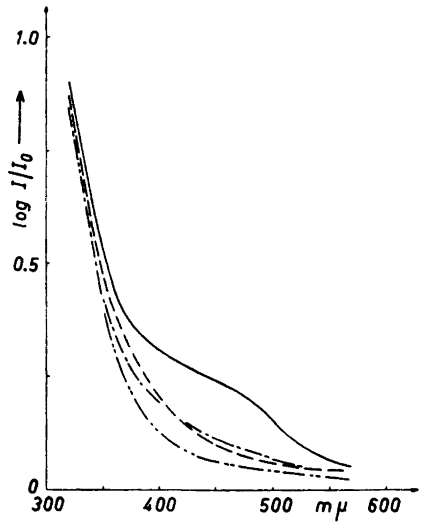


Fig. 8. Absorption curves for Brauns lignin subjected to the colour reaction. Concentration: 10 mg lignin in 50 ml of dioxan.
– – – – No pretreatment
– – – – The same material after treatment with hydrochloric acid
——— Pretreated with sodium borohydride
— — — The last material after treatment with hydrochloric acid

Thus, this experiment showed that even a small amount of cinnamyl alcohol groups in lignin can be demonstrated by this method.

The reaction was next performed on slices which had not been pretreated in any way but by extraction. A maximum was again obtained at about 475 mμ (Fig. 6). It disappeared when the coloured slices were treated with acid (Fig. 6). Accordingly, the presence of cinnamyl alcohol groups in lignin was indicated.

Slices which have been exposed to air during six months gave no maximum (Fig. 7). As cinnamyl alcohols are easily oxidized this could be expected. Stored Brauns lignin also gave no maximum (Fig. 8). After reduction with sodium borohydride, however, the presence of the cinnamyl alcohol groups formed was demonstrated in both materials (Figs. 7 and 8), even if the maximum obtained was not so distinct in the case of Brauns lignin.

The question now arises as to whether the 475 mμ maximum on coloured wood slices could be due to a type of group other than cinnamyl alcohol. Conceivable types might be phenyl and benzoyl-carbinols as the corresponding pyridinium salts (N-benzyl and N-phenacyl-pyridinium salts, respectively) are also transformed into anilides of glyoxylonitriles (phenyl and benzoyl-

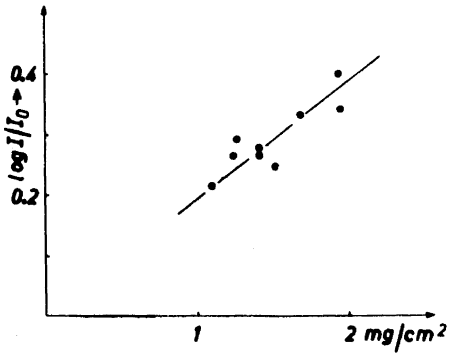


Fig. 9. The absorption at 475 mμ of coloured slices versus their weight per cm².

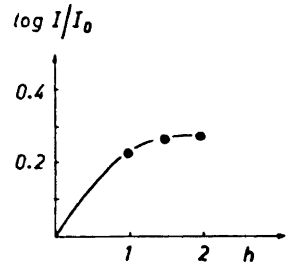


Fig. 10. The absorption at 475 mμ of coloured slices versus the time of treatment with the solution of *p*-nitrosodimethylaniline and potassium cyanide. The weight of the slices, 1.1 mg per cm².

glyoxylonitriles) by nitroso-dimethylaniline and potassium cyanide [4]. Furthermore, it was found that the anilide of benzoyl-glyoxylonitrile had a maximum in its extinction curve at 478 mμ (ε, 32 700) which was close to that of the nitriles obtained from cinnamyl alcohols. The maximum of the anilide of phenyl-glyoxylonitrile was determined to be at 458 mμ (ε, 21 200).

Only primary carbinols can be transformed into this type of nitrile as the central carbon atom in them is linked both with a double bond to a nitrogen atom and with a single bond to a nitrile group. If the 475 mμ maximum is caused by the presence in lignin of phenyl or benzoyl-carbinol structures lignin should then contain phenylmethane or phenylethane monomers, respectively. This does not seem probable according to the modern view of the lignin structure.

Another possibility is, however, not excluded. The maximum may be due to some type of structure which during the performance of the colour reaction is transformed into chromophoric groups structurally completely different from the anilides of glyoxylonitriles. However, the agreement between the maximum wavelength of the coloured slices and that of the model compounds, the destruction of the chromophoric groups by acid, and the inhibition of the colour reaction by pretreatment with sulphite and by air make it probable that the maximum is due to the presence of cinnamyl alcohol structures in lignin.

The data accounted for in Figs. 5—7 could be used to estimate approximately the concentration in lignin of the cinnamyl alcohol groups. In Table 1 the optical density at 475 mμ of the coloured slices (column 2) and of the same slices after decolourization with acid (column 3) have been put together. (The data in Figs. 5 and 6 have been determined on slices which had a weight of 1.6 mg per cm². On the other hand, the slices used for Fig. 7 had a weight of 2.0 mg. By using the fact that the absorption was roughly proportional to the weight per cm² of the slices (Fig. 9) the latter data were recalculated to correspond to a weight of 1.6 mg per cm².)

The optical density due to the glyoxylonitrile structures has been taken as the difference (Column 4) between the values in Columns 2 and 3 (Δ density). The table shows that the Δ density for the cinnamyl alcohol groups originally present in lignin was about 0.25. About the same value was obtained for the cinnamyl alcohol groups formed by reduction of the aldehyde structures with sodium borohydride. Consequently, the amount of cinnamyl alcohol structures in lignin is about the same as that of the cinnamyl aldehyde groups, *e. g.* one group per about 50 phenylpropane monomers.

If the slices were assumed to be optically homogeneous materials an approximate value of the concentration could be calculated in a simple way by using Beer's law. In this way it was estimated that lignin contained one cinnamyl alcohol group per 180 phenylpropane monomers. (The ε-value was assumed to be the same as that of the unfractionated reaction products from (Ib), which was $\varepsilon = 15\,500$ for $\lambda_{max} = 475$ mμ. The absorption due to the glyoxylonitrile structures was taken as the main value of Table 1, log $I_0/I = 0.22$.)

The difference between these two values may be caused by an incomplete reaction of the cinnamyl alcohol groups because of the failure of the reagents to penetrate the wood slices completely. As this obstacle ought to affect to a lesser degree the value obtained by a comparison with the cinnamyl aldehyde concentration, the latter value is assumed to be the more correct one.

Table 1. The optical density at 475 mμ of coloured and of acid decolourized slices.

Pretreated with [a]	Opt. density [b] for		Δdens. [d]	Structure [e]
	colour sl.	decol. sl. [c]		
no reagent	0.38	0.12	0.26	alc.
$NaBH_4$	0.57	0.17	0.40	alc. + ald.
sulphite	0.10	—	—	—
sulphite, alkali	0.10	—	—	—
sulphite, alkali and $NaBH_4$	0.38	0.15	0.23	ald.
air	0.13	—	—	—
air, $NaBH_4$	0.38	0.15	0.23	ald.

a) The conditions were:
$NaBH_4$; the slices were immersed in an aqueous sodium borohydride solution for 4 h.
Sulphite; the slices were heated with a sulphite solution (pH 6.1; total SO_2, 5 %) for 19 h at 135°C.
Alkali; the slices were immersed in N sodium hydroxide solution for 0.5 h.
Air; the slices were exposed for air during 6 months.
b) Determined as log I_0/I corrected to a slice weight of 1.6 mg per cm^2.
c) The coloured slices were immersed in N hydrochloric acid for about 15 h.
d) The difference of the values in columns 2 and 3.
e) The group in lignin which have been transformed into the glyoxylonitrile structure. Cinnamyl alcohol = alc; cinnamyl aldehyde = ald.

EXPERIMENTAL

The reaction of the model alcohols with tosyl chloride and pyridine

3,4-Dimethoxycinnamyl alcohol (2 g) and tosyl chloride (2 g) were dissolved in pyridine (3 ml). The solution was kept at room temperature for 2 days. Sodium hydroxide solution (2 N, 5 ml) was then added and the solution was concentrated *in vacuo* to a small volume. By repeated water additions and concentrations the solution was practically freed from pyridine. Dimethoxycinnamyl-pyridinium picrate was precipitated from the solution by addition of picric acid dissolved in alcohol. The product was recrystallized from aqueous alcohol. Obtained 2.9 g (yield 72 %), m. p. 139—141°. (Found: OCH_3 13.4. Calc. for $C_{22}H_{20}O_9N_4$: OCH_3 12.8.) The picrate was transformed into the perchlorate by using an anion exchanger. M. p. 106—107°. (Found: OCH_3 17.7; N 3.8. Calc. for $C_{16}H_{15}O_6NCl$: OCH_3 17.5; N 3.9.)

Cinnamyl alcohol (1.4 g) and tosyl chloride (1.9 g) were dissolved in pyridine (2 ml). The solution was kept at room temperature for 5 h. Perchloric acid solution (N, 20 ml) was added by which the cinnamyl-pyridinium perchlorate precipitated. It was collected and purified by precipitating from its methanol solution by ether addition. M. p. 70.5—71.5°, undepressed by authentic sample. Yield 60 %.

The synthesis of the *p*-dimethylamino-anilide of styryl-glyoxylonitrile (IIa) and its 3,4-dimethoxy derivative (IIb)

The pyridinium bromide (Ia or b) (1 g), *p*-nitrosodimethylaniline (0.6 g), and potassium cyanide (0.4 g) were dissolved in a mixture of water (2.5 ml) and alcohol (8 ml). The solution turned red. After being kept at room temperature for 1 h the solution was added to water (5 ml). The mixture obtained was extracted with benzene. The extract was passed through a column of alumina, and the column developed with benzene. The anilide was isolated from the coloured zone which moved most rapidly. It was recrystallized from alcohol.

The dimethylamino-anilide of styryl-glyoxylonitrile was obtained from N-cinnamyl-pyridinium bromide in a yield of 46 %. M. p. 116—117°. (Found: C 78.7; H 6.2; N 15.0. Calc. for $C_{18}H_{17}N_3$: C 78.5; H 6.2; N 15.3.)

The dimethylamino-anilide of 3,4-dimethoxy-styryl-glyoxylonitrile was obtained from N-(3,4-dimethoxycinnamyl)-pyridinium bromide in a yield of 26 %. M. p. 158—159°. (Found: C 71.7; H 6.4; N 12.5; OCH_3 18.9. Calc. for $C_{20}H_{21}O_3N_3$: C 71.7; H 6.3; N 12.5; OCH_3 18.5.)

The colour reaction performed on lignin samples

Wood slices. Radial slices about 20 μ thick of freshly cut spruce wood were extracted with hot water and benzene-alcohol (1:1). Some of the slices were then pretreated in accordance with the conditions given in Table 1. The slices were immersed in a solution of tosyl chloride (2 g) in pyridine (20 ml) for 24 h at room temperature. To facilitate penetration, the reaction mixture was placed in a desiccator which was repeatedly evacuated. After washing successively with benzene, alcohol, dilute hydrochloric acid and flowing water, the slices were immersed for 1.5 h (*cf.* Fig. 9) in a solution of *p*-nitrosodi methyl-aniline (1.1 g) and potassium cyanide (0.9 g) in aqueous alcohol (20 ml, 85 % v/v). The penetration was aided as before. The wood slices were then again carefully washed with alcohol and benzene. While wet with benzene they were pressed between two quartz plates, and their optical density was determined with a Beckman spectrophotometer.

Brauns lignin. Brauns lignin (10 mg) was dissolved in a solution of tosyl chloride (35 mg) in pyridine (300 mg), and left for 2 days at room temperature. Water was added and the precipitated lignin was washed well with water. The tosylated lignin was then

dissolved in dioxan-alcohol (0.5 ml, 1:1 v/v). To this solution *p*-nitrosodimethyl-aniline (65 mg) and potassium cyanide (52 mg) dissolved in water-dioxan (1.5 ml, 4:1 v/v) were added. The solution was kept at room temperature for 1 h. Water was added and the lignin suspension obtained was exhaustively extracted with benzene. The lignin was removed from the suspension by passage through a layer of fine sand. The sand was washed well with water, and then the lignin was extracted from it with dioxan. The optical density of the dioxan solution was determined with a Beckman spectrophotometer.

REFERENCES

1. Klason, P. *Svensk Kem. Tidskr.* **9** (1897) 133.
2. For a review, *cf.* Lindgren, B. O. *Svensk Papperstidn.* **55** (1952) 78; Adler, E. and Lindgren, B. O. *Svensk Papperstidn.* **55** (1952) 563.
3. Freudenberg, K. *Angew. Chem.* **68** (1956) 508.
4. Kröhnke, F. *Angew. Chem.* **65** (1953) 615.
5. Adler, E. and Ellmer, L. *Acta Chem. Scand.* **2** (1948) 839.
6. Lindgren, B. O. *Acta Chem. Scand.* **4** (1950) 1371.

Received February 9, 1957.

ACTA CHEMICA SCANDINAVICA 11 (1957) 836—838

On the Conversion of 3α,7α,12α-Trihydroxycoprostanic Acid to Cholic Acid in Rat Liver Homogenates

Bile Acids and Steroids 46

S. BERGSTRÖM, R. J. BRIDGWATER and U. GLOOR

Department of Physiological Chemistry, University of Lund, Lund, Sweden

With tritium labelled 3α,7α,12α-trihydroxycoprostanic acid it has been found that the main reactions in a rat liver homogenate are the degradation to cholic acid followed by the conjugation with taurine. A minor part of the C_{27} acid was directly conjugated with taurine.

Recently Haslewood [1] isolated 3α,7α,12α-trihydroxycoprostanic acid (»coprocholic acid») from various members of the *Crocodylidæ* and it has also been found in certain species of *Amphibia* (see Ref.[1]). The two coprocholic acids stereoisomeric at C—25 have been prepared by Bridgwater [11]. These C_{27}-bile acids with the intact cholesterol carbon skeleton might be intermediates in the conversion of cholesterol into C_{24} bile acids in higher animals.

This would be in agreement with the suggestion that hydroxylation of the steroid nucleus might precede the β-oxydation of the side chain [2,3]. In connection with work done at this institute on the *in vivo* metabolism of 3α,7α,12α-trihydroxycoprostanic acid [4] we have also studied the reactions of this substance in rat liver homogenates.

EXPERIMENTAL

Tritium labelled L-3α,7α,12α-trihydroxycoprostanic acid was material prepared by Bridgwater and Lindstedt [4]. The radioactivity was 2.2×10^6 counts per min per mg counted in infinite thin layer in a windowless gas flow counter. Directly before use, the substance was purified twice by reversed phase partition chromatography in a system with chloroform/heptane 9:1 as stationary phase and 50 % methanol as moving phase [5-7]. The peak of the titration curve was at 65—70 ml effluent on the standard 4.5 g column at 23°.

Rat liver homogenates were prepared in 4 parts of Bucher medium [8] per part liver fresh weight as described earlier [9]. Unbroken cells and cell debris were spun down at 800 × g for 15 min at 0° and the supernatant used as total homogenate. In a typical experiment we used the following conditions: 38 ml 20 % rat liver homogenate and 2 ml buffer containing 40 mg adenosine triphosphate (crystalline, disodium salt, 3 H_2O,

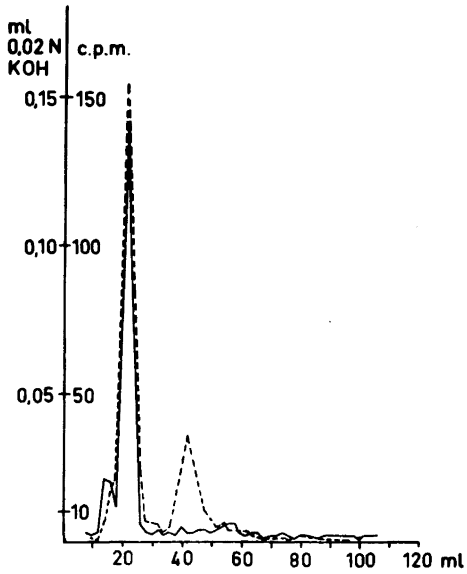


Fig. 1. Chromatography of the hydrolyzed taurine conjugates after incubating [T]-coprocholic acid with rat liver homogenates. Phase system F. Solid line: Titration values. Broken line: c.p.m. Absc. = ml effluent.

Sigma Chemical Corp., St. Louis, U.S.A.). 500 μg trihydroxycoprostanic acid sodium salt = 1.1×10^6 c.p.m. The incubation mixture was shaken in air for 2 h at 37°, pH 7.4 and at the end of this time 5 volumes ethanol were added to stop the reactions. The mixture was heated for 10 min in boiling water, cooled, the precipitate centrifuged off and the supernatant liquid evaporated under reduced pressure. The residue was partitioned between 1 N HCl and butanol and the combined butanol extracts again evaporated under reduced pressure. This gave the starting material for reversed phase column partition chromatography as worked out by Bergström, Sjövall and Norman [5-7]. The following solvent systems were used (Table 1).

Table 1. Solvent systems.

System	Stationary phase	Moving phase
C (Ref.[7])	chloroform / *iso*octanol 1:1	50 % methanol / water
D (Ref.[7])	butanol	water
F (Ref.[6])	chloroform / heptane 9:1	55 % methanol / water

Determinations of the radioactivity were done in "infinitely thin" layers on frosted aluminum or copper planchets in a windowless gas flow counter (Tracerlab).

After each experiment the extracts were first chromatographed with phase system D to separate the taurine conjugated acids from all distinctly less polar products, which stay in the stationary phase. The latter were then fractionated with phase system F. The taurine conjugated acids were saponified with 1 N NaOH for 8 h in sealed glass tubes at 120 °C, the acidified reaction mixture extracted with ether, washed, evaporated and chromatographed in phase system C together with unlabelled cholic acid.

RESULTS

In a typical experiment about 83 % of the activity was recovered in the taurine band (Phase system D). These fractions were combined and saponified and the isolated acids were rerun in phase system F together with unlabelled cholic acid. About 70 % were recovered in the cholic acid band near the front followed by a second band at 40—45 ml containing about 20 % *cf.* Fig. 1. When the material in the first band was rerun in system C the activity curve coincided with the titration curve of cholic acid. The identity of the labelled product with cholic acid was further strengthened by dilution with 100 mg unlabelled cholic acid and recrystallization four times from different solvents (aqueous ethanol, acetone, ethyl acetate) when the specific activity remained constant throughout the procedure.

The second band appeared at the same place as the coprocholic acid used. No unlabelled acid was available at that time for isotope dilution.

In vitro as *in vivo* the coprocholic acid was thus rapidly degraded to cholic acid that was conjugated with taurine. A minor part of the coprocholic acid was directly conjugated with taurine and thus protected from the degradation as has also been found *in vivo* [10].

The eluate of the butanol column, *i. e.* the acids that stayed on the column in this system, representing 17 % of the total activity, was rerun in phase system F when three distinct bands were obtained, with roughly equal isotope content, appearing at (a) 15, (b) 35, and (c) 75 ml. These minor peaks have not been identified with certainty but (b) follows coprocholic acid also in phase system C and might thus be unchanged coprocholic acid that has escaped conjugation, (a) is eluted before cholic acid in system C (glycocholic acid?). The structure of (c) is unknown. These compounds were not observed in the bile when labelled coprocholic acid had been injected intraperitoneally into bile fistula rats [4].

The investigation of the location of the various enzyme systems involved in the different fractions of the liver homogenate is being continued.

This work is part of investigations supported by *Statens medicinska forskningsråd* and *Knut och Alice Wallenbergs Stiftelse.*

REFERENCES

1. Haslewood, G. A. D. *Biochem. J. London* **62** (1956) 637.
2. Bergström, S. *Record Chem. Progr. Kresge-Hooker Sci. Lib.* **16** (1955) 63.
3. Bergström, S. and Lindstedt, S. *Biochim. et Biophys. Acta* **19** (1956) 556.
4. Bridgwater, R. J. and Lindstedt, S. *Acta Chem. Scand.* **11** (1957) 409.
5. Bergström, S. and Sjövall, J. *Acta Chem. Scand.* **5** (1951) 1267.
6. Sjövall, J. *Acta Physiol. Scand.* **29** (1953) 232.
7. Norman, A. *Acta Chem. Scand.* **7** (1953) 1413.
8. Bucher, N. L. R. *J. Am. Chem. Soc.* **75** (1953) 498.
9. Bergström, S. and Gloor, U. *Acta Chem. Scand.* **9** (1955) 34.
10. Lindstedt, S. and Norman, A. *Acta Chem. Scand.* **11** (1957) 414.
11. Bridgwater, R. J. *Biochem. J. London* **64** (1956) 593.

Received February 11, 1957.

ACTA CHEMICA SCANDINAVICA 11 (1957) 839—845

Determination of the Number of Free *ortho* and *para* Positions in Phenols

BENGT SMITH

Institutionen för Organisk Kemi, Chalmers Tekniska Högskola, Göteborg, Sweden

A method has been worked out for the determination of the number of free *ortho* and *para* positions in phenols, using bromide-bromate titration in glacial acetic acid and conductometric titration in ethyl alcohol-water. The majority of the phenols on which the method was tried gave the correct value for the number of free *ortho* and *para* positions. The significance of conductometric titration curves for the identification of various types of phenols has also been discussed.

On investigation of the structure of a phenol, a knowledge of the number of free *ortho* and *para* positions in the aromatic nucleus is of considerable value. The facile substitution by bromine of the hydrogen in the positions *ortho* and *para* to a phenolic hydroxyl should provide a suitable method for the determination of this number. However, there is no universal bromination procedure *, which can be used with confidence for the quantitative bromination of all types of phenols. This makes it more difficult to develop a successful application of the bromination method for the present structural problem. It is in general not possible to adapt the procedure to the type of phenol, since this is often unknown, and the same procedure must therefore be used in all cases. However, it must be remembered, that in this case a quantitative determination of the bromine consumption is not necessary since only an estimate of the number of bromine atoms entering the aromatic nucleus is required. Thus it is possible that a suitable compromise between the existing quantitative methods could be found which can give values accurate enough for this purpose. Recently [1] it was shown by the author that a large number of phenols could be quantitatively brominated in glacial acetic acid either by direct titration with bromide-bromate solution or by the use of an excess of this reagent. A hybrid between the two methods, applicable to the solution

* For a discussion of quantitative bromination methods for phenols, *cf.* Ref.[1].

of phenolic structural problems, has now been worked out and the results obtained are presented in this paper *.

The bromide-bromate titration gives only the number of equivalents of bromine consumed per gram of the phenol. To calculate the number of free *ortho* and *para* positions it is necessary to know the molecular weight of the phenol. Several methods are available for this purpose. Conductometric titration [8], titration in nonaqueous solvents [9,10] and, recently, high frequency titration [11] have been employed. Although the conductometric method might not be the most accurate one it has been chosen here because of its general applicability and its simplicity, which are important factors in identification work.

EXPERIMENTAL

Bromide-bromate titration. The phenol (50 mg) was weighed and dissolved in 20 ml of glacial acetic acid. Conc. hydrochloric acid (5 ml) was added and then 0.1 N potassium bromide-bromate dropwise until the solution of the sample had acquired a distinct yellow colour. Care should be taken not to add more than about 10 % excess of bromide-bromate solution. Five ml of a 10 % potassium iodide solution were then added and the iodine was titrated at once with 0.1 N thiosulphate using starch solution as indicator.

Conductometric titration. A Radiometer Conductometer model CDM2 was used. The phenol (300–500 mg) was weighed and dissolved in 25 ml of 96 % ethyl alcohol. The solution was then diluted with distilled water (usually 25 ml). For some phenols it was necessary to use a higher proportion of ethyl alcohol in order not to precipitate the phenol (see Table 1) but in all cases the total volume was 50 ml. From a microburette 0.5 N sodium hydroxide was added and the conductance read for each ml of the titrant. It is recommended that the addition should be carried on considerably beyond the first equivalence point in order to ascertain whether the molecule contains more than one acidic function. The observed conductance values were corrected for the dilution caused by the titrant by multiplying them by $(V+v) / V$ where V is the initial volume and v the volume of titrant added. The equivalence points were evaluated graphically by plotting the conductances against the volumes of titrant. The intersections of the straight lines drawn through these points define the equivalence points. The titration vessel was not thermostated but was shielded against rapid temperature changes.

RESULTS

Conductometric titrations. The accuracy of conductometric titrations of phenols is dependent on the concentration of the phenol in the solvent. Concentrations which are too low or too high should both be avoided. Here solutions which are 0.04 to 0.05 N have been titrated with good accuracy in most cases. It is of course difficult to weigh the correct amount of an unknown phenol. If, however, the first titration shows that the concentration of the solution has been considerably different from the values given above another titration should be made.

* Methods for the estimation of the number of free *ortho* and *para* positions in phenols by means of bromine have been described elsewhere. Veibel [2], for example, utilizes a modification of the well-known Koppeschaar procedure. In view of the reported inaccuracy of this method [3-7], which is partly connected with the replacement of various groups by bromine (Veibel mentions the risk of replacement of carboxyl groups) there is some doubt concerning the general usefulness of the Veibel procedure. There does not appear to be any published account of tests on different types of phenols of the procedure recommended.

Table 1. Bromide-bromate titration and conductometric titration of phenols.

No.	Compound	Equiv. wt bromide-bromate titration		Equiv. wt conductometric titration		Number of bromine atoms entering the molecule	
		Found	Calc.	Found	Calc.	Found	Calc.
1	Phenol	15.9	15.7	94.4	94.1	3.0	3
2	*o*-Cresol	27.0	27.0	108.6	108.1	2.0	2
3	*m*-Cresol	18.3	18.0	108.1	108.1	3.0	3
4	*p*-Cresol	26.9	27.0	108.0	108.1	2.0	2
5	*p-tert.*-Butylphenol	37.7	37.6	150.1	150.2	2.0	2
6	*p-tert.*-Amylphenol	41.3	41.1	164.5	164.2	2.0	2
7	*p*-Octylphenol	52.4	51.6	214.0*	206.3	2.0	2
8	2,3-Xylenol	30.7	30.5	123.0	122.2	2.0	2
9	2,4-Xylenol	62.1	61.1	122.5	122.2	1.0	1
10	2,5-Xylenol	31.0	30.5	123.0	122.2	2.0	2
11	2,6-Xylenol	51.0	61.1	123.6	122.2	1.2	1
12	3,4-Xylenol	30.1	30.5	121.6	122.2	2.0	2
13	3,5-Xylenol	20.8	20.4	122.7	122.2	2.9	3
14	Thymol	37.9	37.6	154.3	150.2	2.0	2
15	Carvacrol	45.0	37.6	156.8	150.2	1.7	2
16	2,3,5-Trimethylphenol	35.3	34.1	137.4	136.2	1.9	2
17	2,4,6-Trimethylphenol	53.8	—	142.8	136.2	1.3	0
18	2,6-Di*tert.*-butyl-*p*-cresol	96.6	—	244.0**	220.3	1.3	0
19	2,4-Di*tert.*-butyl-*m*(5)-cresol	101.3	110.2	235.6***	220.3	1.2	1
20	2,2-Bis-[*p*-hydroxyphenyl] propane	28.8	28.5	113.3	114.1	3.9	4
21	*o*-Hydroxymethylphenol	30.8	31.0	123.8	124.1	2.0	2
22	*m*-Hydroxymethylphenol	21.0	20.7	122.5	124.1	2.9	3
23	*p*-Hydroxymethylphenol	31.9	31.0	119.0	124.1	1.9	2
24	*o*-Hydroxybenzaldehyde	32.5	30.5	119.8	122.1	1.8	2
25	*m*-Hydroxybenzaldehyde	22.9	20.4	120.8	122.1	2.6	3
26	*p*-Hydroxybenzaldehyde	30.0	30.5	120.4	122.1	2.0	2
27	*o*-Hydroxyacetophenone	33.8	34.0	135.7	136.1	2.0	2
28	*p*-Hydroxyacetophenone	33.9	34.0	134.4	136.1	2.0	2
29	*p*-Hydroxypropiophenone	37.1	37.5	149.0	150.2	2.0	2
30	Salicylic acid	33.5	34.5	136.7	138.1	2.0	2
31	*m*-Hydroxybenzoic acid	23.8	23.0	69.4	69.1	2.9	3
32	*p*-Hydroxybenzoic acid	30.6	34.5	69.1	69.1	2.3	2
33	*o*-Chlorophenol	31.7	32.1	127.1	128.6	2.0	2
34	*m*-Chlorophenol	21.9	21.4	128.6	128.6	2.9	3
35	*p*-Chlorophenol	35.7	32.1	126.3	128.6	1.8	2
36	2,4-Dichlorophenol	82.4	81.5	160.9	163.0	1.0	1
37	2,4,5-Trichlorophenol	101.7	98.7	197.1	197.5	1.0	1
38	*p*-Chloro-*m*-cresol	36.2	35.7	142.7	142.6	2.0	2
39	2-Chloro-5-methylphenol	35.8	35.7	141.4	142.6	2.0	2
40	*o*-Nitrophenol	39.2	34.8	139.5	139.1	1.8	2
41	*m*-Nitrophenol	29.2	23.2	137.5	139.1	2.4	3
42	*p*-Nitrophenol	34.9	34.8	136.8	139.1	2.0	2
43	2,4-Dinitrophenol	122.5	92.1	182.1	184.1	0.7	1
44	Picric acid	no consumption of bromine	—	227.1	229.1	0	0

Table 1, continued.

45	*o*-Hydroxydiphenyl	42.7	42.6	170.7	170.2	2.0	2
46	*p*-Hydroxydiphenyl	41.6	42.6	169.6	170.2	2.0	2
47	2,2′-Dihydroxydiphenyl	24.6	23.3	183.6	186.2	3.7	4
48	α-Naphthol	33.6	36.1	143.4	144.2	2.1	2
49	β-Naphthol	68.1	72.1	143.2	144.2	1.1	1
50	*o*-Hydroxydiphenyl ether	42.2	46.6	184.8	186.2	2.2	2
51	Resorcinol	19.8	18.4	100.4 56.1	110.1 55.1	2.8	3
52	Phloroglucinol + $2H_2O$	27.2	27.0	78.3 52.5	81.1 54.0	2.9	3
53	2,4-Dihydroxybenzaldehyde	29.4	32.1	69.1	69.1	2.3	2
54	2,4-Dihydroxyacetophenone	38.1	38.0	150.5	152.1	2.0	2
55	*o*-Methoxyphenol	32.5	31.0	122.3	124.1	1.9	2
56	*m*-Methoxyphenol	22.7	20.7	126.0	124.1	2.8	3
57	*p*-Methoxyphenol	83.5	31.0	123.7	124.1	0.7	2

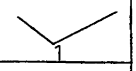
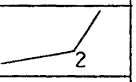
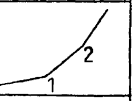
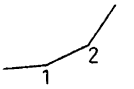
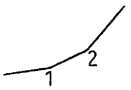
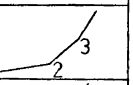
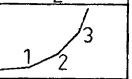
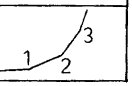
* Titrated in 75 % ethyl alcohol.
** Titrated in 96 % ethyl alcohol.
*** Titrated in 60 % ethyl alcohol.

The accuracy is sufficient for the purpose (*cf.* Table 1) except in a few cases such as some alkylphenols with several alkyl groups or large alkyl groups (*cf.* Nos. 7, 17, 18 and 19). One of the reasons for the decreased accuracy is that some of the compounds mentioned were not sufficiently soluble in 50 % ethyl alcohol and a solvent with less water had to be used which lowers the accuracy by increasing the angle at the equivalence point. In the case of phenols with several acidic functions one or more of the equivalence points were often of inferior accuracy. It was generally observed that the equiv. weight calculated from the last inflexion point was the most accurate one, provided that the inflexion was not too small (*cf.* No. 51 and below).

The shape of the titration curves will be discussed in some detail because of its significance in the identification of various types of phenols.

The phenols in Table 2 have been divided into nine groups according to the shape of their titration curves. The first group contains only picric acid, the titration curve being that of a strong acid titrated by a strong base. Group 2 contains the bulk of the phenols. Nearly all monobasic phenols yield the curve shown in the last column when titrated with sodium hydroxide under the present conditions. Pyrocatechol, salicylic acid and 2,2′-dihydroxydiphenyl also behave as monobasic compounds and give no indication of a second acidic function. 2,4-Dihydroxybenzaldehyde represents the third group. Both of the hydroxyls are titrated but only one break in the curve, at the second equivalence point, is obtained. *o*-Vanillic acid and 2,4-dihydroxyacetophenone (group 4) give two inflexion points on titration, the angle at the second one, however, is nearly 180°. Group 5 is composed of *m*-hydroxybenzoic acid, two *p*-hydroxybenzoic acids, ferulic acid (p-$HOC_6H_4CH_2$=$CHCOOH$), and *p,p′*-dihydroxydiphenyl-2,2-propan. As in group 4, one inflexion point is obtained for each equivalence point but this time the main inflexion is at point 2, the

Table 2. Conductometric titration curves for phenols.

Group No.	Compound	Number of acidic functions		Basicity	Shape of the titration curve
		Present	Found *		
1	Picric acid	1	1	1	
2	Monohydric phenols (except picric acid and phenols containing other acidic groups than hydroxyl groups)	1	1	1	
	Pyrocatechol	2	1	1	
	Salicylic acid	2	1	1	
	2,2′-Dihydroxydiphenyl	2	1	1	
3	2,4-Dihydroxy-benzaldehyde	2	1**	2	
4	*o*-Vanillic acid	2	2	2	
	2,4-Dihydroxy-acetophenone	2	2	2	
5	*m*-Hydroxybenzoic acid	2	2	2	
	p-Hydroxybenzoic acid	2	2	2	
	p-Vanillic acid	2	2	2	
	Ferulic acid	2	2	2	
	p,p′-Dihydroxydi-phenyl-2,2-propane	2	2	2	
6	Resorcinol	2	2	2	
	Hydroquinone	2	2	2	
7	Phloroglucinol + $2H_2O$	3	2**	3	
8	Pyrogallol	3	3	3	
9	Gentisic acid	3	3	3	

* Breaks in the titration curve.

** The values of the equiv. weights show, that these compounds cannot be monobasic and dibasic, respectively. It is also evident from the shape of the titration curve that the latter compound is tribasic.

angle at point 1 being nearly 180°. Resorcinol and hydroquinone which belong to group 6 are intermediate between the phenols in the two preceding groups, the angles at the two inflexion points being nearly alike.

Three phenols each with three acidic functions in the molecule were also titrated. The curves obtained for these compounds were all dissimilar and the

phenols accordingly placed into separate groups (Nos. 7, 8 and 9). According to Kolthoff * phloroglucinol behaves on conductometric titration as a dibasic acid and the curve has only one inflexion point. Under the present conditions phloroglucinol was found to behave as a tribasic acid. In addition to the inflexion point at the second equivalence point a slight change of the direction of the curve was obtained at the third equivalence point too. Pyrogallol also behaved as a tribasic acid, this time with an inflexion point at each equivalence point. Kolthoff [8] reported that pyrogallol behaved as a dibasic acid, giving two breaks in the curve. Gentisic acid (hydroquinonecarboxylic acid) also shows the three acidic functions, the main difference between this curve and that for pyrogallol being the large angle (small inflexion) at the third equivalence point.

It is evident from the foregoing that by using conductometric titration it is possible in most instances to determine the number of acidic functions present in a phenol molecule. For three phenols in group 2 the method failed, but in the case of 2,2′-dihydroxydiphenyl the bromide-bromate titration revealed the presence of two hydroxyl groups in the molecule (*cf.* below). Furthermore the shape of the titration curve often gives additional information about the structure.

Bromide-bromate titration. The results of the bromide-bromate titration of 57 phenols using the method previously described have been collected in Table 1, which gives the equiv. weights obtained and the number of bromine atoms entering each phenol molecule. The latter values were calculated from the molar weights determined by conductometric titration and the equiv. weights resulting from the bromide-bromate titration. As seen from the last column but one in Table 1 the results with few exceptions are satisfactory. For the 57 phenols collected in Table 1 the method gave the correct answer for the number of free *ortho* and *para* positions in 53 cases. It is, however, obvious that the method may give erroneous results in some cases.

The reaction, for example, between 2,4,6-trialkylsubstituted phenols (*cf.* Nos. 17 and 18) and bromine in acetic acid which proceeds easily with the formation of bromo*cyclo*hexadienones and other compounds [12–14] makes it difficult, using the present method, to ascertain the absence of free *ortho* and *para* positions in these compounds. The method also failed with *m*-nitrophenol, which has previously [1] been shown to be more resistant to attack by bromine than most other phenols. It has been pointed out that the quantitative bromination methods were less suited to the analysis of alkoxyphenols [1] and the same may be said about the method described in this paper. Although good values were obtained in many instances, rather divergent results were sometimes observed for phenols of similar structure (*cf.* Nos. 55 and 57). A contributory reason for this was that many of these compounds adopt a yellow colour as soon as the bromide-bromate solution is added, which makes it difficult to add the appropriate amount of this reagent.

Of the dihydric phenols tested, pyrocatechol consumed about 2 equivalents of bromine per mole and hydroquinone about 1. As seen from Table 1 the bromine consumption of phenols with the hydroxyl groups in *meta* position

* Kolthoff [8] used 1 N sodium hydroxide as titrant and water as solvent.

corresponds to the number of free *ortho* and *para* positions (*cf.* Nos. 51—54).

It is apparent from Table 1 that not more than 3 bromine atoms enter the molecule of a mononuclear phenol under the present conditions, provided that unsaturated or other bromine consuming side chains are absent. If the bromine consumption is found to exceed 6 equivalents per mole it is therefore an indication that a di- or polynuclear phenol may be present. Table 1 gives two examples of dinuclear phenols (Nos. 20 and 47). In the first case the presence of two hydroxyls was revealed by the conductometric titration, in the second, however, one break only was obtained in the titration curve. In both cases 4 bromine atoms entered, indicating that in the first the two hydroxyls were situated in separate rings and in the second not one but two hydroxyls were present, this time also in separate rings.

REFERENCES

1. Smith, B. *Acta Chem. Scand.* **10** (1956) 1589.
2. Veibel, S. *The Identification of Organic Compounds*, 4th Ed., G. E. C. Gad, Copenhagen 1954, p. 99.
3. Day, A. R. and Taggart, W. T. *Ind. Eng. Chem.* **20** (1928) 545.
4. Francis, A. W. and Hill, A. J. *J. Am. Chem. Soc.* **46** (1924) 2498.
5. Bielenberg, W., Goldhahn, H. and Zoff, A. *Oel u. Kohle* **37** (1941) 496.
6. Sprung, M. M. *Ind. Eng. Chem. Anal. Ed.* **13** (1941) 35.
7. Ruderman, J. W. *Ind. Eng. Chem. Anal. Ed.* **46** (1946) 753.
8. Kolthoff, I. M. *Z. anorg. u. allgem. Chem.* **112** (1920) 187.
9. Fritz, J. S. and Keen, R. T. *Anal. Chem.* **25** (1953) 179; see also *Anal. Chem.* **28** (1956) 784—797.
10. Fritz, J. S. *Acid-Base Titrations in Nonaqueous Solvents*, G. F. Smith Chemical Co., Columbus 1952.
11. Karrman, K. J. and Johansson, G. *Mikrochim. Acta* **11** (1956) 1573.
12. Fries, K. and Brandes, E. *Ann.* **542** (1939) 48.
13. Coppinger, I. M. and Campbell, T. W. *J. Am. Chem. Soc.* **75** (1953) 734.
14. Forman, L. E. and Sears, W. C. *J. Am. Chem. Soc.* **76** (1954) 4977.

Received February 22, 1957.

ACTA CHEMICA SCANDINAVICA 11 (1957) 846—853

Guanine Metabolism in Fishes

I. The Occurrence of a Guanine-Deaminating Enzyme in Fish Skin

PER ERIC LINDAHL and PER OLOV SVÄRD

Institute of Zoophysiology, University of Uppsala, Sweden

Some properties of the guanine-deaminating enzyme of fish skin have been studied. The deaminase activity was found to be stimulated by the metal-chelating agent ethylenediaminetetraacetate (EDTA), indicating a sensitiveness of the enzyme towards metal ions. Among a number of cations tested Cu++ and Zn++ were by far the most potent inhibitors and their effect was greatly influenced by the pH. In view of this it is likely that a salt-like complex is formed between the inhibiting ions and negatively charged groups of the enzyme molecule. Experiments with iodoacetate gave no evidence for the necessity of sulfhydryl groups for the deaminase activity. Dialysis experiments failed to demonstrate any metalic-ion requirement.

As is well known guanine, chiefly recognized as one of the purine bases of the nucleic acids, also occurs in large amounts in the skin and on the scales of fishes, causing the silvery appearance characteristic of many species. Hitchings and Falco [1] and more recently Neckel [2] have convincingly demonstrated the identity of this silvery matter with pure guanine.

Fishes — like spiders — are unique in their ability to produce large amounts of non-nucleic acid guanine. In fishes this production exhibits some peculiarities, *e. g.* the rather sudden appearance of this substance, which accompanies the metamorphosis of the Salmon parr to smolt, as well as the disappearance that can be induced merely by preventing the smolt from getting into seawater as it normally does on completion of the metamorphosis. Further it was shown by Sumner [3] that the production of guanine is subject to variations caused by visual stimuli. Thus it was found that prolonged stay of the fish upon a dark background led to a decrease in the amount of guanine, while a light background produced the reverse effect. — In view of these facts fishes appear to be interesting objects for a study of the enzymes involved in the metabolism of guanine. The present investigation was intended to determine, whether or not the fishes are provided with the same or similar enzymes for the breakdown of "skin guanine", as are known to affect nucleic acid guanine.

In the present paper the existence in fish skin of a guanine deaminating enzyme is demonstrated, and some of its properties are studied.

EXPERIMENTAL

Materials. The guanine and xanthine preparations used were commercial products obtained from Schuchardt and Hoffman-La Roche Chemical Co., respectively. They were not purified prior to use.

Because of the scanty solubility of guanine at neutrality colloidal solutions according to Schmidt [4] had to be prepared for ammonia determinations. For the spectrophotometric studies, which occupied the main part of this investigation, true solutions of guanine containing, unless otherwise indicated, 10 μg per ml could be used.

Preparation of the enzyme. The fish, roach *(Leuciscus rutilus* Lin.), was skinned immediately after being killed. The skin plus scales (wet weight 8—12 g) were ground as soon as possible, and extracted at room-temperature with 3 volumes of glass-distilled water or, when indicated, with a 0.01 M solution of ethylenediaminotetraacetic acid (EDTA). The extraction was performed for 30 min in a shaking device. The mixture was centrifuged at 1 200 *g* for 15 min in order to remove insoluble material; the supernatant was then subjected to 11 000 *g* for 20 min at 0 °C. The resulting fluid containing the enzyme was not further purified, since this was not found necessary for the present study.

Dialysis of the enzyme solution. Samples of the enzyme solution were dialysed through cellophane membranes against glass-distilled water or against a 0.005 M EDTA solution in an apparatus, providing frequent and thorough stirring of both the enzyme solution and the surrounding fluid.

In some cases samples were electrodialysed against 0.005 M EDTA solutions.

Analytical. The enzymatic activity was followed either by measuring the ammonia liberated or by a spectrophotometric procedure. The ammonia estimations were carried out essentially according to Schmidt [4], involving vacuum-distillation of pre-formed ammonia according to Parnas [5] with subsequent titration, employing the Tashiro indicator. Generally the spectrophotometric procedure was chosen. It is based upon the change in optical density in U.V. caused by the deamination of guanine to xanthine. The values reported by Roush and Norris [6] for the maximum density change at 245 mμ, (for pH values below 7.5) at 250 mμ (for pH values 8—8.5) and at 255 mμ (for pH values above 9.0) obtainable with 10 μg per ml solutions of guanine were checked, employing solutions of pure guanine and pure xanthine in buffer. These values were then used in computing the per cent deamination of guanine. A Beckman model DU spectrophotometer with U.V. attachment was used throughout.

Standard conditions. The incubation was carried out in 10 mm quartz cuvettes. 0.2 ml of the enzyme solution was incubated with 3.1 ml of the buffered solution of guanine containing 10 μg per ml. The pH was varied in the region 6.0—9.5, using 0.067 M phosphate or 0.05 M tris -(hydroxymethylaminomethane) buffers. The final pH was checked electrometrically at the end of the incubation. Readings were taken with one min intervals at 245, 250, or 255 mμ depending upon the actual pH against blanks without guanine. The time of incubation was generally 15 min, but was sometimes extended to 60 min. The temperature was kept at 21°C. The total volume of the samples was always kept at 3.3 ml.

RESULTS

Aqueous extracts of fish skin were found to contain a guanine deaminating enzyme. As seen from Fig. 1 there is good proportionality between the amount of enzyme added and the ammonia liberated. The spectrophotometric approach to the enzymic reaction elucidated that the ammonia formed is a result of an actual deamination and not of a breakdown of the ring structure, since xanthine, characterized by its U.V. absorption curve, appears as the other reaction product (Fig. 2).

The effect of EDTA. Preliminary experiments aiming at a determination of the enzymatic activity at different pH values showed that the time course curves for pH values above 8 were not linear. As is seen from Fig. 3 rather

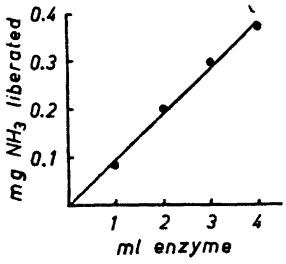


Fig. 1. The effect of varying enzyme concentration on the enzymatic activity as measured by the ammonia determination method. *Conditions:* 5.0 ml of a colloidal solution of guanine (0.88 mg per ml) and 10 ml of 0.067 M phosphate buffer pH 7.5 were incubated with the indicated amount of enzyme. The total volume of the samples was made up with distilled water to 20 ml. The incubation was carried out for 40 minutes at 40 °C, and was stopped by the addition of 4 per cent HCl. Aliquots were taken to ammonia estimations.

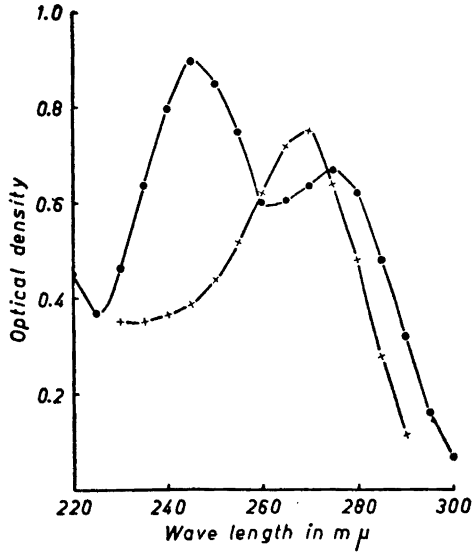


Fig. 2. The U.V. absorption changes caused by the deamination of guanine by the enzyme from fish skin. *Conditions:* 0.2 ml of the enzyme solution was incubated in a total volume of 3.3 ml with a buffered solution of guanine (15 μg per ml). Buffer: 0.067 M phosphate pH 7.5. Incubation time 30 minutes at 21 °C. ● — ●, the absorption curve at zero time, guanine. × — ×, the same after 30 minutes' incubation, xanthine.

abrupt drops in the activity occurred at these pH after about 10 min incubation. At pH 9.0 the enzyme seemed to be completely inactive. Pre-incubation of the enzyme for varying time periods with buffer at pH above 8 prior to the addition of substrate resulted in a considerably lowered deamination rate (Fig. 4). This effect of the pre-incubation increased with rising pH.

When EDTA was included in the reaction mixture this phenomenon disappeared (Fig. 3), the time course curves at all pH values being linear and the activity at pH 9.0 accounting for roughly 85 % of the optimum value. Although the activating effect of EDTA was more marked in the pH region above 8, it was also evident in the region below 8. Furthermore the stability of the enzyme solution was found to be greatly enhanced by the extraction of the enzyme with EDTA solution instead of glass-distilled water.

The effect of divalent cations. As a consequence of the above-mentioned findings the effect of divalent cations on the enzymatic activity was studied. For this purpose the enzyme was prepared by extraction with EDTA followed by

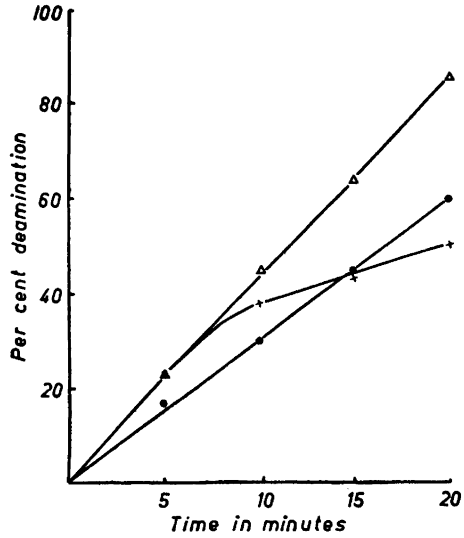


Fig. 3. The time course of the enzymatic activity. Standard conditions, 0.05 M TRIS buffer. ● — ●, obtained at pH 7.0. × — ×, obtained at pH 8.5. △ — △, obtained at pH 8.5 with the enzyme pre-treated with 0.01 M EDTA.

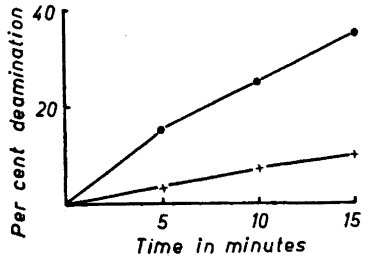


Fig. 4. The effect of pre-incubation on the enzymatic activity. Standard conditions, 0.05 M TRIS buffer pH 8.5, ● — ●, no pre-incubation. × — ×, pre-incubated for 10 minutes before the addition of substrate.

Table 1. The effect of cations on the enzymatic activity. Standard conditions: pH 8.5; 0.05 M TRIS buffer.

Inhibitor	Concentration	Relative activity
None	—	100
$CaCl_2$	1×10^{-2} M	96
$MgSO_4$	1×10^{-2} M	106
$MnCl_2$	1×10^{-2} M	104
$CoSO_4$	1×10^{-2} M	23
$ZnSO_4$	6×10^{-5} M	31
$Fe_2(SO_4)_3$	6×10^{-5} M	85
$FeSO_4$	6×10^{-5} M	85
$CoSO_4$	6×10^{-5} M	94
$CuSO_4$	6×10^{-5} M	29

Table 2. The effect of pH on the cationic inhibition. Standard conditions. The concentration of Cu^{2+} and Zn^{2+} = 6×10^{-5} M; 0.05 M TRIS buffer.

Inhibitor	Per cent inhibition at pH		
	7.3	8.5	9.0
$ZnSO_4$	0	69	100
$CuSO_4$	3	71	100

dialysis. By this treatment interferring ions together with EDTA were removed from the enzyme solution which was then suited for studies on ion promoted inhibition.

Among a number of ions tested (*cf.* Table 1) Cu^{2+} and Zn^{2+} were found to be by far the most potent inhibitors, effecting complete inhibition at concentrations of 6×10^{-5} M. The inhibition was found to be greatly influenced by the pH, being none or insignificant at pH 7, and complete at pH 9 (Table 2). When EDTA was included in the reaction mixture the mentioned ions were ineffective. However, once inhibited the enzymatic activity could not be restored by the addition of EDTA.

The effect of other inhibitors. The observation of Schmidt [4] that sodium fluoride inhibits the deamination of guanine could not be verified under the conditions of the present experiments. Neither when tested directly nor after pre-incubation with the enzyme before the addition of substrate did sodium fluoride exert any significant effect in concentrations as high as 0.01 M.

Iodoacetate was used for testing the possibility of an interaction between the inhibiting ions and sulfhydryl groups of the enzyme molecule. The enzyme was pre-incubated with iodoacetate at a concentration of 0.01 M for periods up to 60 min, yet without any effect (Table 4).

Table 3. The effect of sodium fluoride on the enzymatic activity. Standard conditions. 0.05 M Tris buffer pH 8.0.

Inhibitor	Per cent deamination	Per cent inhibition
None	37	0
NaF, 0.01 M not pre-incubated	36	2
NaF, 0.01 M pre-incubated for 20 min	35	5

Table 4. The effect of iodoacetate on the enzymatic activity. Standard conditions. 0.05 M Tris buffer pH 8.0.

Inhibitor	Per cent deamination	Per cent inhibition
None	35	0
Iodoacetate, 0.01 M not pre-incubated	35	0
Iodoacetate, 0.01 M pre-incubated for 20 min	33	5

Ammonia in a concentration of 0.01 M did not affect the enzymatic activity.

The effect of dialysis. When dialysis against 0.005 M EDTA was extended over 16 h no loss in activity occurred. On the contrary, when the enzyme had been prepared by extraction with glass-distilled water dialysis resulted in an activation (Fig. 5). No change in activity occurred when an enzyme solution prepared by extraction with EDTA was dialysed against glass-distilled water.

Electrodialysis during 5 h produced no inactivation.

The pH-activity curve and the effect of phosphate. The pH-activity curve is based on time course curves obtained for different pH values, while using enzyme solution freed from contaminating ions (Fig. 6). When studied in TRIS buffer the optimum pH was found to lie between pH 8.0 and 8.25. This is in agreement with Roush and Norris [6] using mammalian guanase. However, the

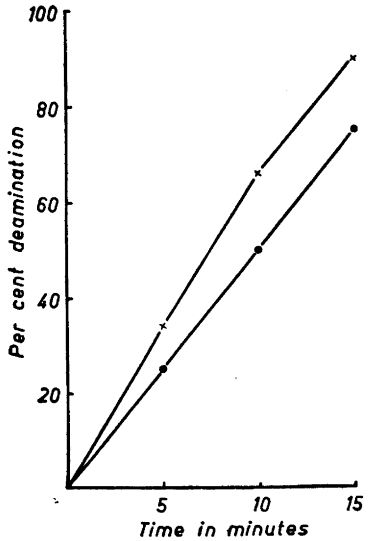


Fig. 5. The effect of dialysis on the enzymatic activity. The enzyme solution prepared by extraction with glass-distilled water was dialysed for 16 hours against 0.005 M EDTA. The activity was measured under standard conditions. ● — ●, non-dialysed enzyme. × — ×, dialysed enzyme.

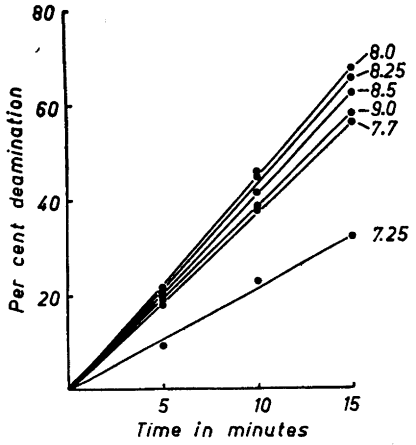


Fig. 6. Time course curve for the enzymatic activity at different pH values. Standard conditions, EDTA prepared enzyme, 0.05 M TRIS buffer, pH as indicated in the figure.

general appearance of the pH-activity curve for the enzyme in fish skin (Fig. 7) differs somewhat from that given by these authors, the discrepancies being essentially confined to the pH region below 8. This was found to be due to the kind of buffer substance used, and its concentration. When the reaction was studied in phosphate buffer of low concentration the curve more closely resembled that of mammalian guanase, the activity values at 7.3 accounting for 85 % of the optimum value as compared with 60 % in TRIS buffer (Fig. 8). With increasing concentration of the phosphate buffer the optimum pH was shifted towards the acid side. At a buffer concentration of 0.1 M the optimum was found to lie in the vicinity of 7.5.

DISCUSSION

In its pH dependency the guanine-deaminating enzyme of fish skin agrees with guanase of other origin studied previously [6]. The present authors could, however, not demonstrate any inhibition by sodium fluoride as reported by Schmidt [4]. Using bacterial guanase Rakosky, Zimmerman and Beck [7] were also unable to confirm this observation.

On account of the ineffectiveness of iodoacetate it is concluded that sulfhydryl groups are not essential for the enzymatic activity.

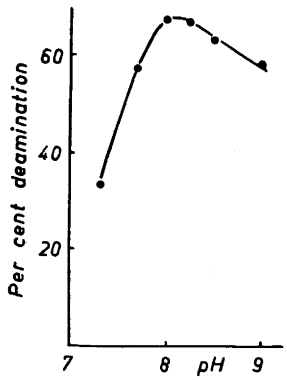


Fig. 7. The pH-activity curve of the fish skin enzyme. The curve is based on the time course curves in Fig. 6. The values corresponding to 10 minutes' incubation are plotted against the respective pH.

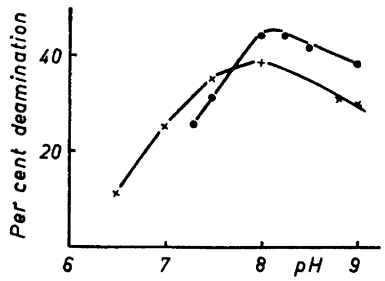


Fig. 8. The influence of the buffer system used on the pH-activity curve. Standard conditions, EDTA prepared enzyme solution. ● — ● Measured in 0.05 TRIS buffer. × — × Measured in 0.067 M phosphate buffer; the pH values 8.8 and 9.0 were obtained by the addition of phosphate up to 0.067 M concentration to TRIS buffer which latter determined the pH. The values correspond to 5 minutes' incubation time.

There is no evidence for a metal-ion requirement of the enzyme, as might be suspected from Schmidt's [4] observation. The dialysis experiments failed to demonstrate any need for a dialysable activator. On the contrary, some divalent cations were found to be potent inhibitors, and it was observed that their effect was counteracted by EDTA. On the basis of this fact the activating effect of EDTA was interpreted as being due to its metal-chelating property. It is likely that the enzyme solutions prepared by extraction with glass-distilled water are contaminated by ions which are thus removed by the action of EDTA.

As to the effect of dialysis illustrated in Fig. 5, the activation observed may most likely be ascribed to EDTA, since dialysis of an EDTA treated enzyme solution against glass-distilled water was unable to bring about any change in enzymatic activity.

In view of the dependency of the effect of the inhibiting ions on the pH it is likely that a salt-like complex is formed between the inhibiting cations and negatively charged groups of the enzyme molecule. This complex seems to be stable, since EDTA could not restore the activity when once inhibited. No macroscopic precipitate was, however, observed.

Ammonia, one of the reaction products, was found not to inhibit the activity at any concentration up to 0.1 M. Xanthine was not tested in this respect.

With respect to the pH-activity curve the enzyme from fish skin shows definite similarities with the mammalian guanase as studied by Roush and Norris [6], especially when measured in phosphate buffer of low concentration.

The mechanism behind the displacement of the optimum by increasing concentrations of the phosphate buffer as well as the somewhat different shape of the curve when measured in TRIS buffer remains, however, obscure.

REFERENCES

1. Hitchings, G. H. and Falco, E. A. *Proc. Natl. Acad. Sci. U. S.* **30** (1944) 294.
2. Neckel, I. *Mikroskopie* **9** (1954) 113.
3. Sumber, F. B. *Proc. Natl. Acad. Sci. U.S.* **30** (1944) 285.
4. Schmidt, G. *Hoppe-Seyler's Z. physiol. Chem.* **208** (1932) 185.
5. Parnas, I. K. *Biochem. Z.* **125** (1924) 1.
6. Roush, A. and Norris, E. A. *Arch. Biochem.* **29** (1950) 124.
7. Rakosky, J., Zimmerman, L. N. and Beck, J. V. *J. Bact.* **69** (1955) 566.

Received February 23, 1957.

ACTA CHEMICA SCANDINAVICA 11 (1957) 854—858

Guanine Metabolism in Fishes

II. A Guanosine Phosphorylase in Fish Skin

PER OLOV SVÄRD

Institute of Zoophysiology, University of Uppsala, Uppsala, Sweden

Aqueous extracts of fish skin, previously found to contain a guanine-deaminating enzyme, are also capable of splitting guanosine. The reaction has been studied spectrophotometrically and the enzyme has been found to be phosphorolytic.

Enzymatic splitting of guanosine may be either hydrolytic or phosphorolytic. Tarr [1] has shown recently the existence in fish muscles of two hydrolytic enzymes, one with specific action upon inosine at pH 8.6, and another, non-specific, acting upon guanosine at pH 5.6. Since Kalckar [2] elucidated the phosphorolytic action of the nucleosidases which had formerly been looked upon as hydrolytic enzymes, it has, on the other hand, become obvious that phosphorolytic splitting is a more wide-spread phenomenon than had been thought earlier. The purine nucleoside phosphorylase was proposed to catalyze the reaction:

$$\text{Purine-1-ribose} + H_3PO_4 \rightleftharpoons \text{Purine} + \text{Ribose-1-phosphate}$$

and it was found to be active only with guanine or hypoxanthine as the purine.

The present investigation was intended as a study of the mechanism of the fission of guanosine which was observed to be caused by an enzyme from fish skin. The use of a spectrophotometric method for the identification of guanine was made possible by the fact that the liberated purine base was not deaminated, although the enzyme extract contained guanase in addition to the nucleoside phosphorylase, as shown in an earlier investigation [3]. The apparent inhibition of guanase is probably competitive, but the problem will be followed up later. Because of this inhibition, the enzymatic method of Kalckar [4] could not be used for the quantitative determination of guanine.

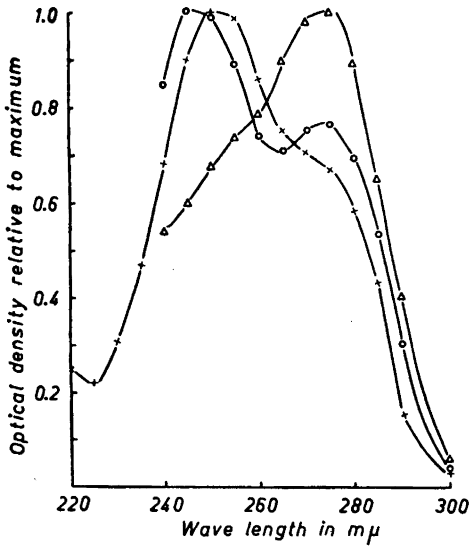


Fig. 1. Enzymatic splitting of guanosine by the fish skin enzyme. Conditions as described under Experimental. × — — — × absorption curve of the reaction mixture at zero time, pH 7.7. O — — — O absorption curve of the reaction mixture after 50 minutes incubation, pH 7.7. △ — — — △ the same as O — — — O made alkaline to pH > 11. The extinction at maximum (E_{max}) has been taken as 1.0.

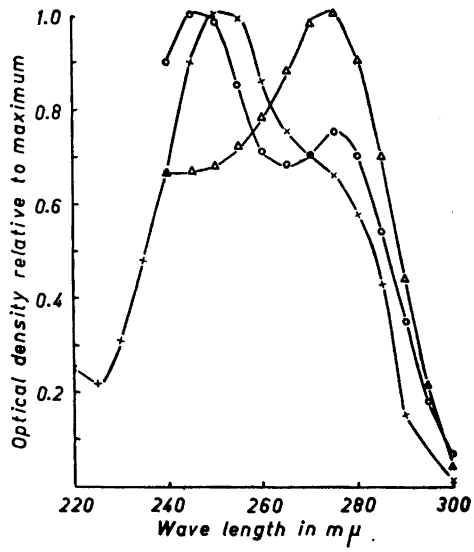


Fig. 2. Absorption curves of authentic guanosine and guanine. × — — — × guanosine at pH 7.7, O — — — O guanine at pH 7.7, △ — — — △ guanine at pH > 11, E_{max} = 1.0.

EXPERIMENTAL

Material. The guanosine and guanine preparations used were commercial products from Kebo Chemicals Ltd. and Schuchardt, respectively.

Preparation of enzyme. The fish (roach, *Leuciscus rutilus* Lin.) was skinned, the skins ground as soon as possible and extracted with 3 volumes of re-distilled water in a mechanical shaker at room-temperature for 30 min. The mixture was centrifuged at 1 200 *g* for 10 min, the supernatant was then subjected to 9 000 *g* for 15 min. The resulting fluid was used without further purification.

Analytical methods. The spectrophotometric method used for the identification of guanine, the reaction product, is based upon the characteristic absorption spectra of guanosine and guanine in U.V. The compounds are further differentiated and the identity of the reaction product is strengthened by raising the pH of the medium to pH > 11. A Beckman spectrophotometer model DU with U.V. attachment was used for the determinations.

3 ml of a solution of guanosine, containing 17 μg per ml in 0.067 M phosphate buffer of pH 7.7, was incubated in the Beckman cuvette with 0.3 ml of the enzyme solution. The absorption between 220 and 300 mμ was measured at zero time, and after the appropriate incubation time, usually 50 min, against a blank without guanosine. The reaction mixture was then made alkaline to pH > 11 with NaOH, and the absorption curve was re-read.

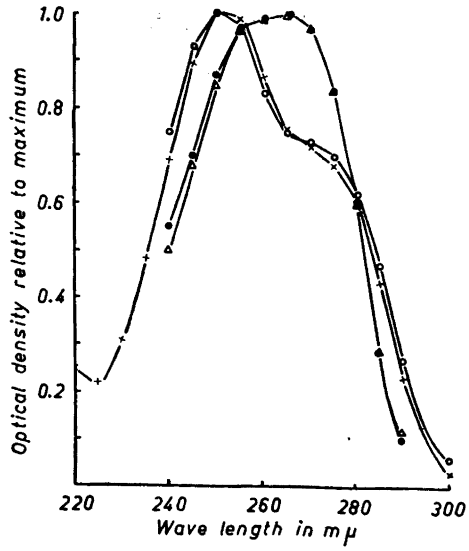


Fig. 3. The phosphate dependency of the fish skin enzyme. Conditions as described under Experimental except that phosphate buffer was exchanged for glycyl glycine buffer. × – – – × absorption curve of the reaction mixture at zero time, pH 7.8, O– – – O the same after 50 minutes incubation, pH 7.8, △– – – △ the same as O– – – O but pH > 11, ●– – – ● authentic guanosine at pH > 11.

The identification of the reaction product was further strengthened by subjecting to paper chromatography aliquots of a reaction mixture. This contained 5 μmoles of guanosine and 3 μmoles of phosphate in 0.02 M glycyl glycine buffer pH 7.8 which had been allowed to incubate with the enzyme at 37 °C for 60 min. A mixture of *iso*butyric acid-ammonia-ethylenediaminotetraacetic acid, according to Krebs and Hems [5], was used as solvent. The spots were detected with the aid of a U.V. lamp.

Guanine was determined quantitatively with Folin's phenol reagent as described by Hitchings [6] with minor modifications. Of reaction mixtures containing guanosine, phosphate, and enzyme solution in glycyl glycine buffer of pH 7.8, 1.0 ml was taken for guanine determination. The proteins were precipitated with 0.3 ml of 3 % perchloric acid, as recommended by Lowry and Lopez [7] for phosphate determination (see below). 1.0 ml of the protein-free centrifugate was mixed with 2.0 ml of the phenol reagent and 5.0 ml of a saturated solution of sodium carbonate. The mixture was brought up to 15 ml with distilled water, and readings were taken at 650 mμ in a Beckman spectrophotometer.

Compared with guanine, guanosine produces a very weak colour with the phenol reagent. This makes possible a quantitative determination of guanine in the presence of guanosine, as is also pointed out by Kalckar [4]. Before the addition of enzyme a 1.0 ml sample of the reaction mixture was taken and treated in the same way as the tests, and was used as a blank in these determinations.

Phosphate was determined according to Lowry and Lopez [7]. The colour reaction was made with 0.2 ml of the protein-free centrifugate mentioned in connection with the guanine determination.

RESULTS AND DISCUSSION

A comparison between Figs. 1 and 2 shows the similarity between the absorption curves of authentic guanine and the reaction product after 50 min incubation. The two figures in addition show the agreement between the respective absorption spectra at alkaline pH. The ratio values for authentic guanine at neutral pH: $E_{290} / E_{280} = 0.50$, $E_{250} / E_{260} = 1.37$, and $E_{280} / E_{250} =$

Table 1. Phosphorolysis of guanosine. 4.85 μmoles of guanosine and 3.35 μmoles of phosphate incubated with enzyme solution in glycyl glycine buffer at pH 7.8. Temp. 37 °C.

Incub. time, min	Inorg. phosph. μmoles	Inorg. + org. phosph. μmoles	Org. phosph. μmoles
0	3.33	3.35	0.02
200	2.55	3.31	0.76

Table 2. Phosphorolysis of guanosine and the formation of equivalent amounts of organic phosphate. 3.0 μmoles guanosine and 10.70 μmoles phosphate incubated with enzyme solution in glycyl glycine buffer. pH 7.8. Temp. 37 °C.

Incub. time, min	Inorg. phosph. μmoles	Org. phosph. μmoles	Guanine μmoles
0	10.68	0.02	—
10	9.99	0.71	0.76
20	9.24	1.46	1.53
30	8.91	1.79	1.81
40	8.76	1.94	2.04

0.71, given in the literature [8] should be compared with the corresponding values for the reaction product: 0.45, 1.35, and 0.70, respectively.

The paper chromatography confirmed the liberation of guanine during incubation of guanosine with the fish skin enzyme. The R_F values for authentic guanine and the fission product were identical and equal to 0.66, whereas guanosine had an R_F of 0.53.

Early experiments showed that the splitting of guanosine is effected only in the presence of inorganic phosphate. As is apparent from Fig. 3 no or only slight activity was noted when glycyl glycine was substituted for phosphate buffer.

The phosphate analysis indicated that inorganic phosphate disappears from the reaction mixture during the fission of guanosine. The phosphate obviously entered into a labile organic linkage, the substance formed being probably ribose-1-phosphate. The mild hydrolytic action of perchloric acid at 30 °C liberated all the organically bound phosphate (Table 1).

As is seen from the results of a typical experiment summarized in Table 2 there is good agreement between the liberated guanine and the phosphate bound in organic linkage. That the phosphate values throughout are somewhat too low might be explained by a slight, but unavoidable splitting of ribose-1-phosphate during the procedure of the determination as is pointed out by Lowry and Lopez [7], or by the existence in the enzyme solution of phosphatases as proposed by Kalckar [2].

The above-mentioned data show that the observed enzymatic splitting of guanosine by an enzyme extracted from fish skin is a phosphorolytic one.

The financial support of the Migratory Fish Committee is gratefully acknowledged.

REFERENCES

1. Tarr, H. L. A. *Biochem. J. London* **59** (1955) 386.
2. Kalckar, H. M. *J. Biol. Chem* **167** (1947) 477
3. Lindahl, P. E. and Svärd, P. O. *Acta Chem. Scand.* **11** (1957) 846.
4. Kalckar, H. M. *J. Biol. Chem.* **167** (1947) 429.
5. Krebs, H. A. and Hems, R. *Biochim et Biophys. Acta* **12** (1953) 172.
6. Hitchings, G. H. *J. Biol. Chem.* **139** (1941) 843.
7. Lowry, O. H. and Lopez, J. A. *J. Biol. Chem.* **162** (1946) 421.
8. Hotchkiss, R. *J. Biol. Chem.* **175** (1948) 315.

Received February 23, 1957.

ACTA CHEMICA SCANDINAVICA 11 (1957) 859—865

Methyl-fluoro-phosphorylcholines

Two Synthetic Cholinergic Drugs and Their Tertiary Homologues

L.-E. TAMMELIN

Research Institute of National Defence, Dept. 1, Sundbyberg 4, Sweden

The syntheses of ω-dimethylaminoethoxy-methyl-phosphoryl and ω-dimethylamino*iso*propoxy-methyl-phosphoryl fluorides and their methiodides, which are choline esters, are described. It is shown that the ω-dimethylaminoalkoxy-phosphoryl fluorides are liquid compounds which solidify by storage at room temperature. This is suggested to be caused by an intramolecular rearrangement that quaternizes the amino group and breaks the fluorine-phosphorus linkage giving the molecule a cyclic structure with a phosphorus-nitrogen bond. Hydrolysis of the fluorine-phosphorus bond has been shown in aqueous solutions of the synthesized methyl-fluoro-phosphoryl esters. At pH 8 and 25°C the tertiary amino esters are hydrolysed almost instantly and the choline esters considerably faster than the corresponding alkoxy esters. The choline esters are more toxic when injected intraperitoneally than alkoxy esters as *e. g.* methyl-*iso*propoxy-phosphoryl fluoride (Sarin) and are potent cholinesterase inhibitors.

Cholinesterase inhibitors can be classified as follows. *Compounds which in their chemical structure resemble the substrates* but are not or only slowly hydrolysed by the enzyme. They are bound to the enzyme by qualitatively the same kind of forces which primarily bind the substrates during the course of enzymic hydrolysis. An ionic bond between an ammonium group and the enzyme is essential in this case [1].

Compounds of the phosphorylating type which during the first step of the inhibition process are bound to the enzyme qualitatively in the same way as the carbonyl-ester group of the substrates. Neostigmine is one inhibitor of the first type and Sarin, Tabun, Parathion and DFP belong to the second type.

Sarin is *iso*-propoxy-methyl-phosphoryl fluoride [2]. Exchange of the *iso*-propanol residue in Sarin against a choline or β-methylcholine (ω-trimethylammonium*iso*propanol) halogenide residue leads to compounds which structurally have properties in common both with substrates of cholinesterase and phosphorylating inhibitors. The structural formulas of some compounds having affinity for cholinesterases are shown in the chart (Fig. 1) where the two last are the choline esters described in this paper.

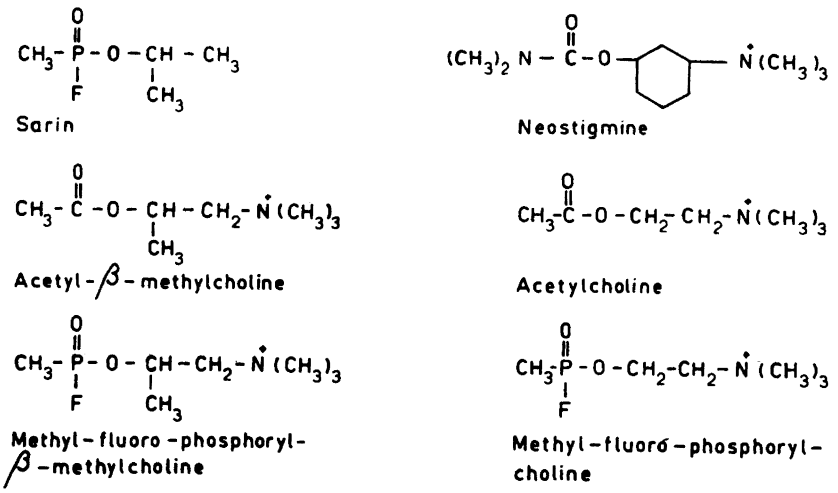
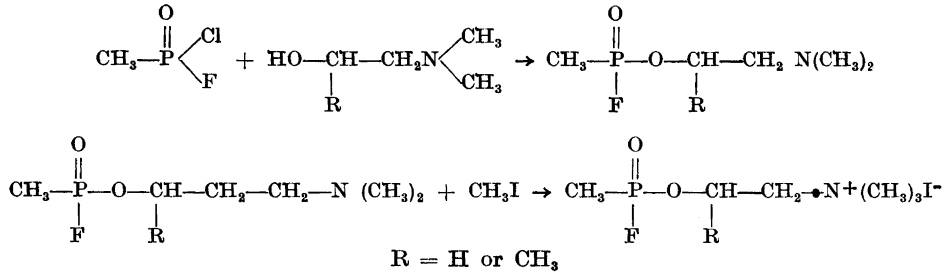


Fig. 1

SYNTHESES

The syntheses of the methyl-fluoro-phosphorylcholines were made according to the following scheme.



Both the dimethylaminoethoxy-methyl-phosphoryl fluoride and the dimethylamino*iso*propoxy-methyl-phosphoryl fluoride are colourless, water soluble oils with amine-like odours. They are unstable and are transformed into solid compounds by storage at room temperature.

Methyl-fluoro-phosphoryl choline iodide and methyl-fluorophosphoryl-β-methylcholine iodide are both colourless, water soluble crystalline compounds. *They are extremely toxic and care must be taken while handling them* to avoid direct contact with or the inhaling of the crystalline powder

Methyl-fluoro-phosphoryl chloride was synthesized from methyl-phosphoryl dichloride according to the schemes given by Collomp [4] as cited by Bocquet [5].

*ω-Dimethylaminoethoxy-methyl-phosphoryl fluoride and ω-dimethylamino*iso*propoxy-methyl-phosphoryl fluoride.* 2-dimethylaminoethanol (1 mole) is slowly added to 1 mole of methyl-fluoro-phosphoryl chloride which is dissolved in anhydrous ether (150 ml)

Table 1.

		M	% C		% H		% N		% F		B. p. °C/mm	M. p. °C	n_D^{25}	d_4^{25}	Yield %	R_D	
			calc.	found	calc.	found	calc.	found	calc.	found						calc.	found
2-Dimethylamino-ethoxy-methyl-phosphoryl fluoride	$C_5H_{13}FNO_2P$	169.1	35.5	34.9	7.8	7.7	—	—	11.3	10.7	40/0.2		1.4130	1.14	60	38.8	37.0
2-Dimethylamino-1-methylethoxy-methylphosphoryl fluoride	$C_6H_{15}FNO_2P$	183.2	39.3	39.2	8.3	8.2	—	—			40/0.1		1.4150	1.06	65	43.4	43.2
									% I								
Methyl-fluoro-phosphoryl-choline iodide	$C_6H_{16}FINO_2P$	311.1	23.2	23.2	5.2	5.1	4.5	4.6	40.8	40.5		152			75		
Methyl-fluoro-phosphoryl-β-methylcholine iodide	$C_7H_{18}FINO_2P$	325.1	25.9	25.9	5.7	5.6	4.3	4.1	39.1	38.5		84			85		

and 1.1 moles of triethylamine. The reaction mixture is refluxed for one hour. After cooling the precipitate formed is filtered off and the final product is isolated from the filtrate by means of distillation; for data see Table 1. The liquid compounds obtained are not very stable and form by storage at room temperature solid compounds which do not react with methyl iodide. It is thus recommended to do the next step immediately after the distillation.

Methyl-fluoro-phosphorylcholine iodide and methyl-fluorophosphoryl-β-methylcholine iodide The tertiary esters described earlier are quaternized by means of methyl iodide. One mole of the ester is treated with 1.1 moles of methyl iodide in ether solution at 25°C. A colourless precipitate is formed which is filtered off after six days and washed by ether and a small amount of alcohol; for data see Table 1.

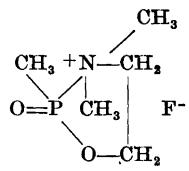
REARRANGEMENT OF THE DIMETHYLAMINOALKYL ESTERS

The dimethylaminoethoxy-methyl-phosphoryl and dimethyl-amino*iso*-propoxy-methyl-phosphoryl fluorides are liquid compounds which by storage at room temperature in sealed glass bottles are gradually transformed quantitatively into solid compounds. This occurs without noticeable pressure changes in the bottles and takes a few days for the ethyl derivative and a few months for the *iso*propyl derivative.

The solid ethyl derivative was used for an investigation in order to elucidate the kind of intramolecular rearrangement that causes the formation of the solid compounds.

The crystalline solid obtained has the same percent composition as the initial liquid. (Found: C 35.0; H 7.7; F 11.6. Calc. for $C_5H_{13}FNO_2P$ (169.1): C 35.5; H 7.8; F 11.3). The solubility in ether is low which is a difference from the liquid isomer. No melting point is found since the compound decomposes at 200°C. A reineckate precipitated from aqueous solution gives negative results when tested for fluorine according to Widmark [6]. Potentiometric titrations on aqueous solutions show that the compound has no protolytic properties in the pH range 3—10. The initial pH was slightly acid but the sodium hydroxide consumption is practically none between these pH limits. Investigations of hydrolytic properties using a "pH-stat" [7] shows no hydrolysis in a pH range from 10 to 6. In 0.1 M HCl, however, hydrolysis occurs and the hydrolysate has been shown to give equivalent amounts of three acids when investigated by means of potentiometric titration. One of the equivalents emanates from the hydrochloric acid yielding a salt with an amino group. Identical titration curves are obtained from hydrolysates of the liquid isomer. The amino pK_a is in both cases the same and about 7.6. Water solutions of the solid isomer give no Schoeneman [8] reaction whereas the liquid does. The Schoeneman reaction gives positive results on compounds containing $=\overset{\overset{\|}{O}}{P}-Hal$.

The high melting point, the low solubility in ether and the lack of protolytic properties indicate that a quaternary nitrogen compound has been formed. The lack of fluorine in the reineckate and the negative Schoeneman reaction indicate that an ammonium fluoride has been formed. The hydrolysis which occurs only at low pH values indicates a P—N bond [9]. A cyclic compound with the structure:



would have these properties and is thus suggested for this compound. By hydrolysis of the P—N bond in such a structure the same organophosphorus acid can be expected to be obtained as from hydrolysis of P—F in the liquid form. Identical amino pK_a values of the hydrolysis products have been found a fact which supports the suggested structure.

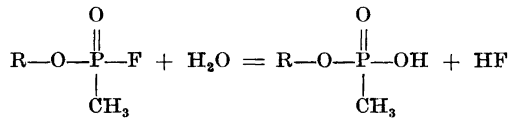
HYDROLYSIS

Sarin has been shown to be hydrolysed in aqueous solutions yielding the acid methyl-*iso*propoxy-hydroxy-phosphinoxide and hydrogen fluoride [10]. Choline and dimethylaminoethyl esters of the carboxylic acids have been shown to yield carboxylic acid and corresponding alcohol in aqueous solutions [1,11]. The P—O—C linkage is known to be hydrolyzable but the reaction rate at moderate pH values is known to be comparatively slow [12].

The qualitative course of the hydrolysis of the ω-dimethyl-aminoalkoxy-methyl-phosphoryl fluorides has been investigated as follows.

Aqueous solutions of the liquid compounds have been shown to yield fluorine ions which were precipitated as PbClF. The calculated amount of fluorine ions has been found after less than 2 h. Acidimetric potentiometric titrations have shown that equivalent amounts of two acids are obtained by the hydrolysis at room temperature.

The results show that the hydrolysis can be described with the following formula:



Using a "pH-stat" [7] the reaction rate of the hydrolysis has been determined at pH 8 with the following results. The half lives of the dimethylaminoethyl and dimethylamino*iso*propyl esters are very short and could not be determined. The choline and β-methyl-choline esters have half lives of 9 and 23 min, respectively. The corresponding value of Sarin [12] is 320 min. At pH = 6 the half life of the dimethylaminoethyl ester was 7 min. A more detailed investigation of the qualitative course and kinetics of the hydrolysis of the two choline esters has been done by Larsson [12]. The present results show, however, that the hydrolysis of these compounds is so fast, that special care must be taken in the determinations of toxicity and of enzyme inhibiting properties.

TOXICITY AND CHOLINESTERASE INHIBITION

Preliminary investigations of the toxicities have shown that aqueous solutions of dimethylaminoethoxy- and dimethylamino*iso*propoxy-methyl-phosphoryl fluorides show relatively low toxicity whereas the choline and β-methyl-choline esters are highly toxic. It was shown that when injected intraperitoneally into white mice both substances kill 50 % of the animals in doses close to 0.1 mg/kg body weight. The choline esters are thus more than three times

as toxic as Sarin, and they are among the most toxic synthetic compounds known. The low toxicity of the tertiary amino esters may be due to their rapid hydrolysis but also to other properties. A detailed description of the pharmacology of the compounds described in this paper is given by Fredriksson [13].

Preliminary investigations of the cholinesterase inhibiting properties have been done using an electrometric method [14]. The enzyme preparations were erythrocyte hemolysate and plasma from human blood. Before the addition of substrate the enzyme solution in Michel buffer solution was incubated for 30 min at 25°C with the inhibitors in varying concentrations. The substrate was acetylcholine, the concentration of which was 7.3×10^{-3} M. Starting pH was 8.

The negative logarithm of the inhibitor concentration in moles/l that causes 50 % inhibition of the enzyme activity in the system described above (pI_{50}) was determined. The rapid hydrolysis of the compounds made these determinations uncertain and the results obtained are to be considered as minimum values of pI_{50}. Methyl-fluoro-phosphorylcholine showed a pI_{50} of about 10 for erythrocytes and a pI_{50} of about 8.4 for plasma. Methyl-fluoro-phosphoryl-β-methyl-choline showed a $pI_{50} = 8.4$ for both erythrocytes and plasma. The corresponding pI_{50} values of Sarin are 8.8 for erythrocytes and 8.4 for plasma.

There are many factors influencing the pI_{50} values such as spontaneous or enzymic hydrolysis of the inhibitor. It is, however, evident from the experimental results that the inhibitors investigated are very potent, and it is highly probable that both of them are more potent than Sarin.

DISCUSSION

The present work originates from the idea that an ammonium group added to the structure of Sarin would yield a compound with more potent pharmacodynamic actions. On the whole this has been verified. It is, however, not quite evident that an added ionic bond between the inhibitor and vital proteins is the reason for the increased potency. Comparisons between Sarin and methyl-fluoro-phosphoryl-β-methylcholine on a simple structural basis are not very elucidating because of the great difference which has been found in the reactivity of the molecules by hydrolysis experiments. An increased reactivity of the P—F bond as an explanation for the increased inhibiting property of the ω-ammonium esters seems as valid as theories about the significanse of an ionic bond. Both effects are likely to contribute but it is impossible from the present experiments to judge which one is dominant.

The choline esters described in this paper are not very likely to become of direct practical value, as therapeutics or insecticides, and should not, contrary to Sarin, be considered as potential war gases, because of their physical properties and low chemical stability. However, Fredriksson [13] has shown that they are valuable tools in studies of cholinergic receptor effects.

My sincere thanks are due to the Director of the Research Institute of National Defence, Dept. 1, Professor G. Ljunggren, for his kind interest in this work.

REFERENCES

1. Wilson, I. B. *J. Biol. Chem.* **208** (1954) 123.
2. Bonnaud, X. *Protar* **14** (1948) 113.
3. Kinnear, A. M. and Perren, E. A. *J. Chem. Soc.* **1952** 3437.
4. Collomp, *Bull. Inf. Scient. Min. Guerre (Sect. techn. de l'Armée)*, 23/G., 28 (1949) Paris.
5. Bocquet, I. R. *Contribution á l'étude de la synthése des halogeno phosphates d'alkyle radioactifs et de l'inhibition de la cholinestérase par ces toxiques organophosphorés.* Diss. *Acta Med. Belgica* (1956).
6. Widmark, G. *Acta Chem. Scand.* **7** (1953) 1395.
7. Larsson, L. and Hansen, B. *Svensk Kem. Tidskr.* **68** (1956) 521.
8. Epstein, J. and Bauer, V. E. *Pittsburgh Conference on Analytical Chemistry and Applied Spectroscopy*, Feb 27 – March 2, (1956).
9. Larsson, L. *Acta Chem. Scand.* **7** (1953) 306.
10. Epstein, J., Bauer, V. E., Saxe, M. and Demek, M. M. *J. Am. Chem. Soc.* **78** (1956) 4068.
11. Larsson, L. *Acta Chem. Scand.* **8** (1954) 1017.
12. Larsson, L. *Acta Chem. Scand.* **11** (1957) *In press.*
13. Fredriksson, T. *Arch. int. pharmacodyn.* **XX** (1957) 394.
14. Tammelin, L.-E. *Scand. J. Clin. Lab. Invest.* **5** (1953) 267.

Received February 27, 1957.

ACTA CHEMICA SCANDINAVICA 11 (1957) 866—875

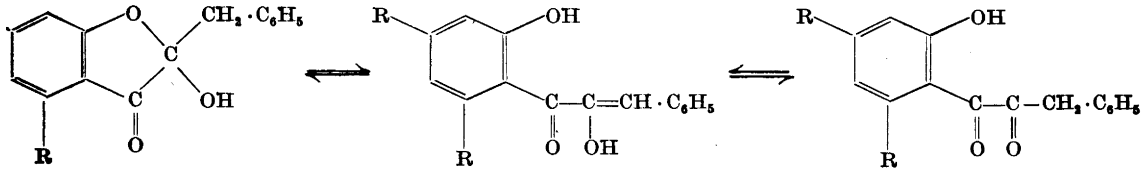
Confirmation of the Structure of 2-Benzyl-2-hydroxy-coumaran-3-ones

CARL ENEBÄCK and JARL GRIPENBERG

Department of Chemistry, Institute of Technology, Helsingfors, Finland

A number of hydroxy and methoxy derivatives of 2-benzylcoumaran-3-one, chalcone and 1,3-diphenylpropane-1,2-dione, corresponding to the tautomeric forms of 2-benzyl-2-hydroxycoumaran-3-ones [1], have been prepared. A comparison of the ultra-violet spectra and the carbonyl frequencies in the infra-red shows definitely the correctness of the 2-benzyl-2-hydroxycoumaran-3-one structure.

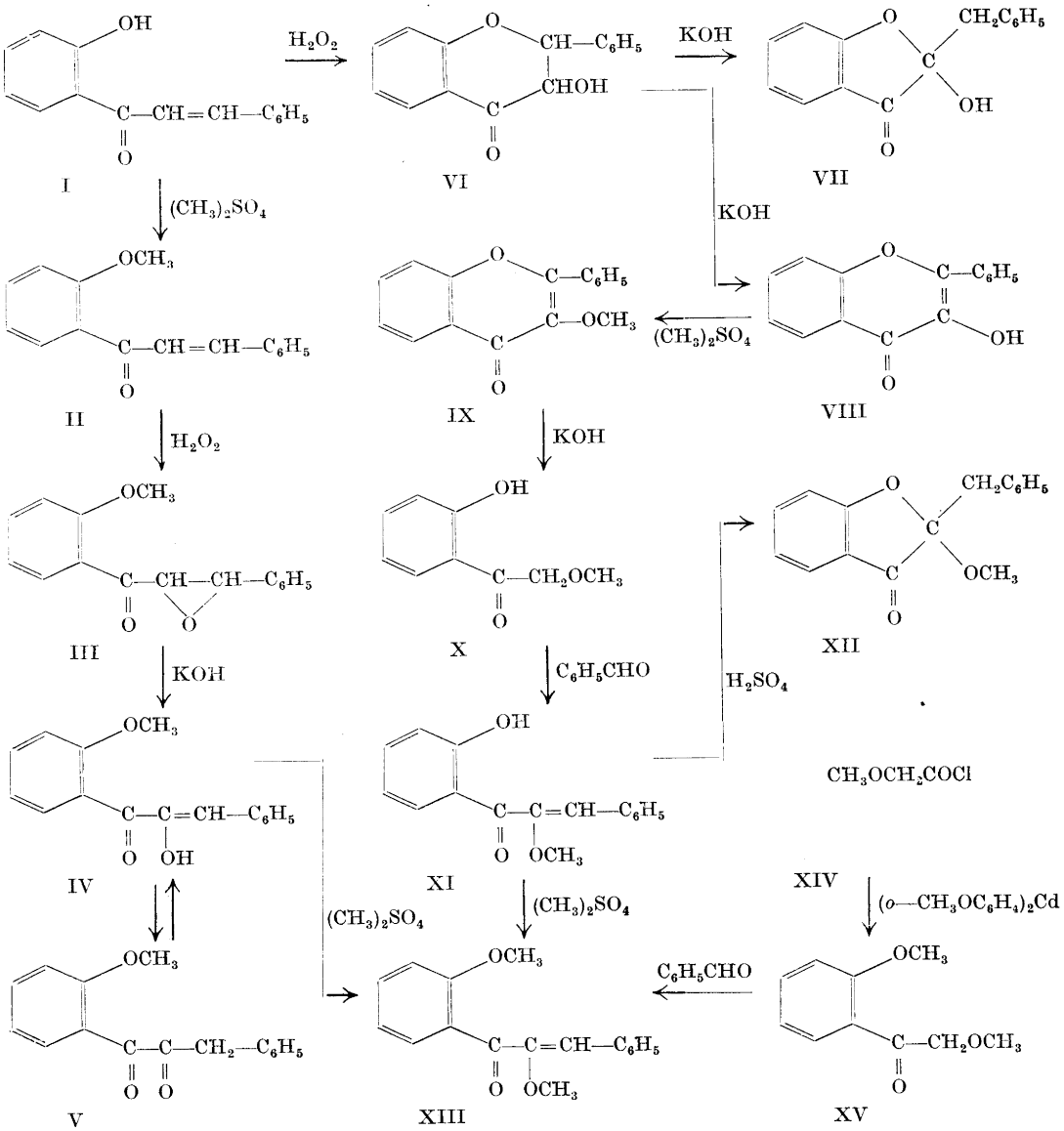
Some years ago, one of the present authors showed that a number of substances, earlier formulated as 3-hydroxyflavanones [1], were in all probability 2-benzyl-2-hydroxycoumaran-3-ones, a conclusion arrived at independently by Kubota [2] also. It was emphasised that the 2-benzyl-2-hydroxycoumaran-3-one(A) can be tautomeric with the hydroxychalcone (B) and the diketone (C)



The structure A could not be considered as definitely established, because of the possibility that this tautomeric shift takes place during the reactions used in the determination of structure.

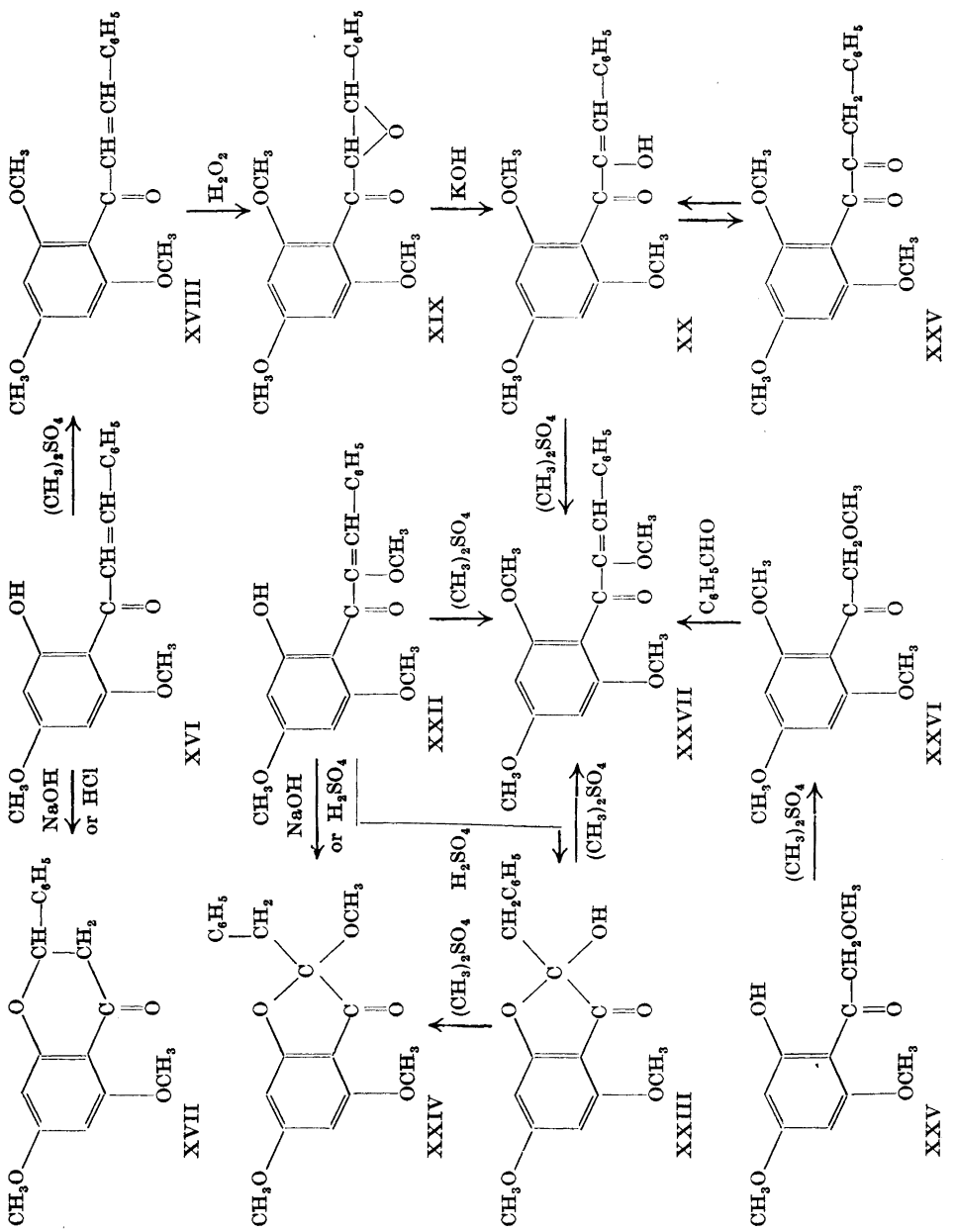
It was therefore decided to try to find further support for this formula from a comparison of the ultra-violet and infra-red spectra with those of compounds corresponding to the three tautomeric forms A, B and C, but where the tautomeric shift is made impossible. This can be achieved either by methylation of the hydroxyls or by removing them. The latter method is permissible only if the hydroxyl is in such a position that it does not have any influence on the spectral properties of the compound in question.

Chart I



Reference has already been made [1] to one case, where the ultra-violet spectrum could be taken as support for the 2-benzyl-2-hydroxycoumaran-3-one structure.

Chart II.



Of the three tautomeric structures, A and C can give rise to one methyl ether, whereas two monomethyl ethers and one dimethyl ether can be derived from B. All these methyl derivatives in the two series, where R = H and

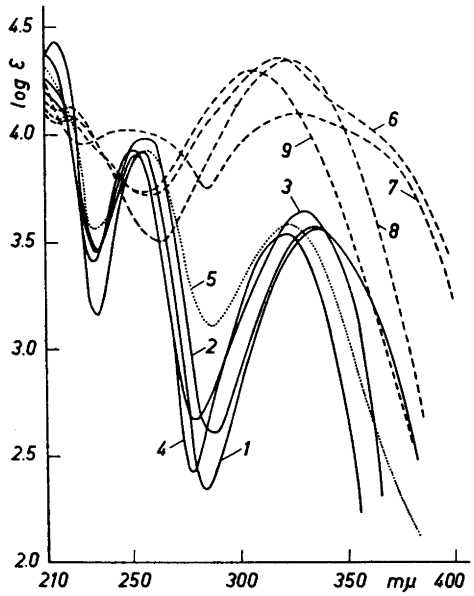


Fig. 1. Spectra of: 1. 2-Benzyl-2-hydroxycoumaran-3-one(VII), 2. 2-Benzyl-2-methoxycoumaran-3-one(XII), 3. 2-Benzylcoumaran-3-one, 4. Flavanone, 5. 1-(2-Methoxyphenyl)-3-phenylpropane-1,2-dione(V), 6. 2′-Hydroxychalcone(I), 7. 2′-Hydroxy-α-methoxychalcone(XI), 8. α-Hydroxy-2′-methoxychalcone(IV), 9. α,2′-Dimethoxychalcone(XIII) (all in ethanol).

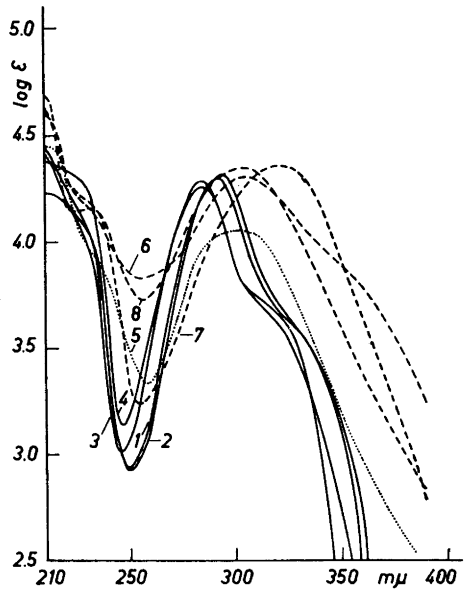


Fig. 2. Spectra of: 1. 2-Benzyl-2-hydroxy-4,6-dimethoxycoumaran-3-one(XXIII), 2. 2-Benzyl-2,4,6-trimethoxycoumaran-3-one(XXIV), 3. 2-Benzyl-4,6-dimethoxycoumaran-3-one, 4. 5,7-Dimethoxyflavanone(XVII), 5. 1-(2,4,6-Trimethoxyphenyl)-3-phenylpropane-1,2-dione(XXI), 6. 2′-Hydroxy-α,4′,6′-trimethoxychalcone (XXII), 7. α-Hydroxy-2′,4′,6′-trimethoxychalcone(XX), 8. α,2′,4′,6′-Tetramethoxychalcone(XXVII) (all in ethanol).

OCH_3, respectively, have been synthesised. The syntheses are outlined in Chart I and Chart II, which show the interrelationships between the different compounds, which serve to establish their structures.

The details of these reactions are given in the experimental part, but the following points require some further comments. Ring closure of 2′-hydroxychalcones to flavanones both by acids and by very dilute alkali is well established [3,4]. However, this does not hold when there is a methoxyl group in the α-position of the chalcone (*Cf.*, however Robertson *et al.*[5]). The formation of a 2-benzyl-2-hydroxycoumaran-3-one, when such a chalcone is treated with acids [1] was the starting point for this work, but it has now also been observed that the corresponding methoxy derivative is formed as well (*e. g.*, XXIV from XXII). A similar observation has been made also by Tsukamoto and Tominaga [6]. When 2′-hydroxy-α-methoxychalcone (XI) was treated in the same way only a neutral compound was obtained. This is thought to be 2-benzyl-2-methoxycoumaran-3-one (XII). Methylation of 2-benzyl-2-hydroxycoumaran-

3-one (VII) was expected to give the same compound, which should have confirmed its structure, but unfortunately all attempts to methylate VII failed. The structure of XII is therefore somewhat uncertain, although it is difficult to imagine any other structure, which could explain its properties.

It was further found that treatment of XXII with dilute alkali also gave XXIV, whereas XI was recovered unchanged from similar treatment.

The transformation of the enols IV and XX into the corresponding diketones V and XXI was achieved by distilling them in the presence of piperidine [7]. The enol was regenerated when an alkaline solution of the diketone was acidified.

The ultra-violet spectra of the different methyl derivatives and some other relevant compounds of the two series, where R = H and R = OCH_3 are reproduced in Figs. 1 and 2, respectively. (The spectra of compounds corresponding to the three structures A, B and C are drawn with different markings.)

From Fig. 1 it can be seen that the spectra of 2-benzyl-coumaran-3-one, 2-benzyl-2-hydroxycoumaran-3-one (VII), 2-benzyl-2-methoxycoumaran-3-one (XII) and flavanone are all very similar, but also that the spectrum of 1-(2-methoxyphenyl)-3-phenylpropane-1,2-dione (V) does not differ very much. The spectra of the chalcones IV and XIII are of a different type and close to that of I and chalcone (not shown in the figure).

The spectrum of 2′-hydroxy-α-methoxychalcone (XI) deserves further consideration, because it differs significantly from those of the other chalcones in having a maximum at 250 mμ, where the other have a minimum and having instead a minimum at 285 mμ. It thus shows some resemblance to the spectra of compounds with the *o*-hydroxyacetophenone chromophore. We would like to offer the following explanation for this difference (*Cf.* Black and Lutz [8]). Models show that when there is a methoxyl group in the α-position, the cinnamoyl group of the chalcone can be coplanar only if the other aromatic ring is out of this plane. In 2′-hydroxy-α-methoxychalcone the hydrogen bond between the hydroxyl and the carbonyl will, however, keep the carbonyl coplanar with this aromatic ring, whereby the coplanarity of the cinnamoyl group will be disturbed. The spectrum will therefore be more close to that of *o*-hydroxyacetophenone, than that of the other chalcones, where the cinnamoyl group will be the dominating factor.

From Fig. 2 it is obvious again that the spectra of the benzylcoumaranones are very close to that of the corresponding flavanone XVII, but in this case the diketone XXI differs clearly by the absence of the inflexion at 310—320 mμ. The spectra of the chalcones are very similar to those of the first series, but the difference between the chalcones on the one hand and the flavanones and benzylcoumaranones on the other hand is not so pronounced here. There is in this case no anomaly in the spectrum of 2′-hydroxy-α,4′,6′-trimethoxychalcone (XXII), although there is the same reason to expect a noncoplanarity of the cinnamoyl group as in XI. In this case, however, the absorption of the *o*-hydroxyacetophenone chromophore lies so close to that of the chalcones that it would not show up as a separate maximum.

As regards the tautomeric possibilities set forth in the beginning of this paper, it can be concluded that these spectra support strongly the benzyl-

hydroxycoumaranone structure (A), but that, particularly in the unsubstituted series, the diketone structure (C) cannot be definitely excluded. The spectra of the chalcones differ enough to make the structure B highly improbable.

In order to get more support for structure A the carbonyl frequencies in the infra-red were determined in chloroform solution (Table 1).

Table 1.

Compound	CO frequency cm^{-1}	Compound	CO frequency cm^{-1}
2-Benzyl-2-hydroxycoumaran-3-one (VII)	1 730	2-Benzyl-2-hydroxy-4,6-dimethoxycoumaran-3-one (XXIII)	1 706
2-Benzyl-2-methoxycoumaran-3-one (XII)	1 720	2-Benzyl-2,4,6-trimethoxycoumaran-3-one (XXIV)	1 696
2-Benzylcoumaran-3-one	1 713	2-Benzyl-4,6-dimethoxycoumaran-3-one [1]	1 690
Flavanone	1 695[9]	5,7-Dimethoxyflavanone (XVII)	1 665
3-Hydroxyflavanone (VI)	1 697	1-(2,4,6-Trimethoxyphenyl)-3-phenylpropane-1,2-dione (XXI)	1 710
1-(2-Methoxyphenyl)-3-phenylpropane-1,2-dione (V)	1 716 1 660	α,2′4′,6′-Tetramethoxychalcone (XXVII)	1 656 1 650
α,2′-Dimethoxychalcone (XIII)	1 650	α-Hydroxy-2′,4′,6′-trimethoxychalcone (XX)	1 666
α-Hydroxy-2′-methoxychalcone (IV)	1 655	2′-Hydroxy-α,4′,6′-trimethoxychalcone (XXII)	1 625
2′-Hydroxy-α-methoxychalcone (XI)	1 619		

All the coumaranone and flavanone derivatives in the series where $R = OCH_3$ have the carbonyl band at lower wave-numbers (24—30 cm^{-1}) than the corresponding compound in the unsubstituted series, in accord with expectation [10]. There is also a difference in the same direction between the diketones XXI and V but much smaller (4 and 6 cm^{-1} in the two bands). In the chalcone derivaties the differences are also small, but in the opposite direction. It should, however, be noted that the values for the chalcones are obtained from measurements in two different laboratories. The low values for XI and XXII are of course due to the hydrogen bond between the 2′-hydroxy group and the carbonyl [10].

The carbonyl frequency of a compound with structure B should be similar to XI and XXII, whereas a compound with structure C should show two carbonyl bands, one around 1 710 cm^{-1}, the other around 1 625 cm^{-1}. Instead the compounds VII and XXIII show only one carbonyl band close to that found in other coumaranone derivatives. The reason why the hydroxyl and, to a lesser extent, the methoxyl group in the 2-position of the benzylcoumaranones shifts the carbonyl frequency to higher wave-numbers is not clear, but it seems to be typical of these compounds.

The structure A must thus be correct, although the possibility that very small amounts of B and/or C exist in equilibrium in solution cannot be excluded on the present evidence. The infra-red data serve also to confirm the impossibility of a 3-hydroxyflavanone structure [1].

EXPERIMENTAL

(The analyses have been performed by Dr. A. Bernhardt, Mülheim, Germany.)

2'-Hydroxychalcone (I) was prepared according to Feuerstein and v. Kostanecki [11]. λ_{max} 222 mμ (log ε 4.09), 318 mμ (log ε 4.37), 355 mμ (infl.) (log ε 4.09), λ_{min} 216 mμ (log ε 4.07), 258 mμ (log ε 3.72).

2'-Methoxychalcone (II). 2'-Hydroxychalcone (I) (9 g) was methylated with dimethyl sulphate (3.9 ml) in acetone (100 ml) in the presence of potassium carbonate (10 g). Filtration and removal of the acetone was followed by washing the ether solution of the product with dilute sodium hydroxide and water. It was then twice distilled under vacuum, b. p. 214—215° / 8 mm. (Yield 6.1 g). v. Auwers and Brink [12] report b. p. 226° / 11.5 mm.

2'-Methoxychalcone oxide (III). 2'-Methoxychalcone (II) (6.1 g) was dissolved in methanol (50 ml) and the solution chilled in an ice-bath to +10°. Hydrogen peroxide (13 %; 9 ml) and 6 N potassium hydroxide (2.1 ml) were added, so that the temperature was kept below +35°. After a few minutes a volumious precipitate of 2'-methoxychalcone oxide was formed. This was recrystallised from methanol. Yield 5.8 g, colourless crystals, m. p. 125°. (Found: C 75.04; H 5.72. $C_{16}H_{14}O_3$ requires C 75.57; H 5.55).

α-Hydroxy-2'-methoxychalcone (IV). 2'-Methoxychalcone oxide (III) (2.5 g) was dissolved in ethanol (25 ml). To this was added 1 N potassium hydroxide (15 ml) and the mixture was refluxed for half an hour. About half of the ethanol was distilled off from the dark red solution. The cooled solution was then acidified with 2 N hydrochloric acid (15 ml), which precipitated a viscous mass. This was separated and crystallised when treated with methanol. Recrystallisation from methanol gave light yellow leaflets, m. p. 133.5°, λ_{max} 220 mμ (log ε 4.08), 234 mμ (infl.) (log ε 3.94), 325 mμ (log ε 4.36), λ_{min} 263 mμ (log ε 3.51). (Found: C 75.25; H 5.64. $C_{16}H_{14}O_3$ requires C 75.57; H 5.55). It gives a strong brown-violet colour with ferric chloride. Jörlander [13] has prepared the same compound in a different way, but he gives m. p. 118°.

1-(2-Methoxyphenyl)-3-phenylpropane-1,2-dione (V). α-Hydroxy-2'-methoxychalcone (IV) (100 mg) was placed together with 0.5 ml of a solution of piperidine in hexane (1 g/l) in a test tube with a side arm. The mixture was heated in an oil bath. When all the hexane had evaporated, a cold finger was inserted and the tube evacuated to 0.25 mm. The temperature of the oil bath was now regulated so that a slow distillation of the diketone to the cold finger was achieved. It formed an oil drop, which upon treatment with methanol gave yellow crystals, m. p. 72°, λ_{max} 259 mμ (log ε 3.93), 323 mμ (log ε 3.60), λ_{min} 233 mμ (log ε 3.57), 287 mμ (log ε 3.11). It gives no colour with ferric chloride. It dissolves in warm sodium hydroxide and acidification of this solution regenerates the enol form (IV), m. p. 133°.

2'-Hydroxy-α-methoxychalcone (XI). 3-Hydroxyflavanone [14] (VI), m. p. 188° was converted into a mixture of 2-benzyl-2-hydroxy-coumaran-3-one (VII) (λ_{max} 256 mμ (log ε 3.93), 336 mμ (log ε 3.58), λ_{min} 234 mμ (log ε 3.16), 284 mμ (log ε 2.34)) and 3-hydroxyflavone (VIII) upon treatment with alkali [1]. The last mentioned was also obtained according to v. Kostanecki and Szabrański [15]. Methylation of 3-hydroxyflavone with dimethyl sulphate and potassium carbonate in acetone gave 3-methoxyflavone (IX), m. p. 113°. Oyamada [16] reports m. p. 114°.

3-Methoxyflavone (4 g) was dissolved in 10 % potassium hydroxide in ethanol (100 ml) and the solution was refluxed for 4 h. Water (100 ml) was then added and the main part of the ethanol was distilled off. The remaining solution was extracted with ether and then acidified with acetic acid. The acid solution was extracted with ether, and the ether solution was washed with sodium hydrogen carbonate. Removal of the ether left 2-hydroxy-ω-methoxyacetophenone (X) (*Cf.* Ref.[17]) as an oil (1.5 g). This, without further purification, was dissolved in ethanol (15 ml) and benzaldehyde (2 ml), and 50 % sodium hydroxide (3 ml) were added. After standing for one day the solution was acidified with

2 N hydrochloric acid and extracted with ether. The ether solution was washed with sodium hydrogen carbonate and evaporated. The residue was crystallised from methanol and sublimed under vacuum, giving yellow needles of 2'-hydroxy-α-methoxychalcone, m.p. 52° (1.3 g), λ_{max} 250 mμ (log ε 4.03), 323 mμ (log ε 4.12), λ_{min} 227 mμ (log ε 3.96), 286 mμ (log ε 3.76). (Found: C 74.97; H 5.71. $C_{16}H_{14}O_3$ requires C 75.57; H 5.55).

2-Benzyl-2-methoxycoumaran-3-one (XII). 2'-Hydroxy-α-methoxychalcone (XI) (0.35 g) was boiled for 30 h with 2 N sulphuric acid (10 ml) in ethanol (50 ml). The ethanol was distilled off and the aqueous solution was extracted with ether. The ether solution was washed with sodium hydrogen carbonate and 2 N sodium hydroxide. Acidification of these washings gave only negligible amounts of material. The ether was removed, yielding an oil which soon crystallised. Recrystallisation from methanol gave 2-benzyl-2-methoxycoumaran-3-one (0.2 g) as colourless crystals, m. p. 50°, λ_{max} 257 mμ (log ε 3.99), 337 mμ (log ε 3.56), λ_{min} 233 mμ (log ε 3.45), 288 mμ (log ε 2.61). (Found: C 74.96; H 5.52; $C_{16}H_{14}O_3$ requires C 75.57; H 5.55). It gives no colour with magnesium and hydrochloric acid.

α,2'-Dimethoxychalcone (XIII). a). α-Hydroxy-2-methoxychalcone (IV) (0.5 g) was dissolved in acetone (10 ml) and dimethyl sulphate (0.3 ml) and potassium carbonate (4 g) were added and the mixture refluxed for 4 h. The α,2'-dimethoxychalcone (0.3 g), isolated in the usual way, was recrystallised from methanol, m. p. 55.5—56°, λ_{max} 221 mμ (log ε 4.13), 307 mμ (log ε 4.31), λ_{min} 215 mμ (log ε 4.11), 255 mμ (log ε 3.75). (Found C 76.06; H 6.42; $C_{17}H_{16}O_3$ requires C 76.10; H 6.01).

b) 2'-Hydroxy-α-methoxychalcone (XI) (0.3 g) was methylated in the same way as in a). Yield 0.2 g, m. p. 55—56°. It gives no depression of m. p. when mixed with material prepared according to a).

c) A benzene solution of bis-(*o*-methoxyphenyl)cadmium was prepared from *o*-bromoanisol (67 g) through the Grignard-compound. To this was added during 10 min methoxyacetyl chloride (XIV) (31 g), dissolved in benzene (53 ml). Heat was evolved and refluxing was continued for 15 min after the addition. The mixture was then poured into ice water (450 g) containing a little sulphuric acid. The benzene layer was separated, washed with sodium hydroxide and dried. Removal of the benzene left an oil from which 57 g of a fraction boiling at 88—182°/8 mm was obtained. 15 g of this fraction were treated with Girard-reagent-T (15 g) giving 2.3 g of ω,2-dimethoxyacetophenone (XV) as an oil. This (1.9 g), without further purification, was kept with benzaldehyde (5 g) and 10 % sodium hydroxide in 50 % ethanol (50 ml) for 1 day at room temperature and then for some days in the refrigerator. The crystals that had separated (1.3 g) were recrystallised from methanol. M. p. 55—56°, alone or mixed with material prepared according to a) or b).

5,7-Dimethoxyflavanone (XVII). A hot solution of 2'-hydroxy-4',6'-dimethoxychalcone [18] (XVI) (0.5 g) in ethanol (1.5 ml) was rapidly diluted with cold 1.5 % sodium hydroxide (15 ml). 5,7-Dimethoxyflavanone precipitated and was recrystallised from toluene, m. p. 145—146° (0.15 g). It gives no depression when mixed with material prepared from the same starting material by treatment with acid [19]. λ_{max} 284 mμ (log ε 4.26), 315 mμ (infl.) (log ε 3.65), λ_{min} 246 mμ (log ε 3.14).

2',4',6'-Trimethoxychalcone (XVIII). 2'-Hydroxy-4',6'-dimethoxychalcone [18] (XVI) (4.5 g) was methylated with dimethyl sulphate (2.4 ml) in acetone (40 ml) in the presence of potassium carbonate (6 g). 2',4',6'-Trimethoxychalcone (3.25 g) was obtained after recrystallisation from methanol as yellow crystals, m. p. 84°. (Found: C 73.01; H 6.11; $C_{18}H_{18}O_4$ requires C 72.46; H 6.08).

2',4',6'-Trimethoxychalcone oxide (XIX). 2',4',6'-Trimethoxychalcone (XVIII) (2 g) was dissolved in methanol (20 ml). This was cooled in an ice bath and hydrogen peroxide (13 %; 2.3 ml) and 6 N potassium hydroxide (0.52 ml) were added so that the temperature did not rise above + 20°. After a few minutes the 2',4',6'-trimethoxychalcone oxide precipitated. It was recrystallised from methanol, giving colourless crystals (1.8 g), m. p. 106.5°. (Found: C 68.21; H 6.01; $C_{18}H_{18}O_5$ requires C 68.78; H 5.77).

α-Hydroxy-2',4',6'-trimethoxychalcone (XX). 2',4',6'-Trimethoxychalcone oxide (XIX) (1.25 g) was dissolved in ethanol (10 ml) and 1 N potassium hydroxide was added. The mixture was refluxed for half an hour. Acidification produced a viscous mass, which rapidly solidified. After recrystallisation from methanol α-hydroxy-2',4',6'-trimethoxychalcone was obtained as light yellow needles (0.8 g), m. p. 138—139°. Recrystallisation from light petroleum (b.p. 60—80°) gave a mixture of bipyramidal crystals of m. p. 120° and the needles of the higher melting form. λ_{max} 230 mμ (log ε 4.17), 320 mμ (log ε 4.37),

λ_{min} 222 mμ (log ε 4.15), 255 mμ (log ε 3.24). (Found: C 68.67; H 5.91; $C_{18}H_{18}O_5$ requires C 68.78; H 5.77). It gives a dark brown-violet colour with ferric chloride.

1-(2,4,6-Trimethoxyphenyl)-3-phenylpropane-1,2-dione (XXI). This compound was obtained from α-hydroxy-2′,4′,6′-trimethoxychalcone in exactly the same way as described above for the preparation of 1-(2-methoxyphenyl)-3-phenylpropane-1,2-dione from the corresponding enol. Recrystallisation from methanol gave bright yellow leaflets, m. p. 98°. λ_{max} 303 mμ (log ε 4.06), λ_{min} 258 mμ (log ε 3.35). It gives no colour with ferric chloride, but dissolves upon warming in 1 N sodium hydroxide. Acidification regenerates the enol (XX), m. p. 138°.

2′-Hydroxy-α,4′,6′-trimethoxychalcone (XXII) was prepared according to Kimura and Hoshi [20]. M. p. 113°, λ_{max} 230 mμ (infl.) (log ε 4.18), 305 mμ (log ε 4.31), λ_{min} 255 mμ (log ε 3.84).

2-Benzyl-2-hydroxy-4,6-dimethoxycoumaran-3-one [1] (XXIII) was prepared according to Lindstedt [21] from 2′-hydroxy-α-,4′,6′-trimethoxychalcone (XXII). λ_{max} 290 mμ (log ε 4.30), 322 mμ (infl.) (log ε 3.66), λ_{min} 249 mμ (log ε 2.93).

2-Benzyl-2,4,6-trimethoxycoumaran-3-one (XXIV) a) 2-Benzyl-2-hydroxy-4,6-dimethoxycoumaranone (XXIII) (1.2 g) was methylated with dimethyl sulphate (0.57 ml) in acetone (18 ml) in the presence of potassium carbonate (2 g). The mixture was first allowed to stand 15 h at room temperature and then refluxed for 4 h. Treatment of the reaction mixture in the usual way gave a residue (1.2 g), which upon recrystallisation from methanol gave a mixture of colourless and yellow crystals. They were separated by hand picking, and further recrystallisation of the colourless crystals gave 2-benzyl-2,4,6-trimethoxycoumaran-3-one (0.57 g), m. p. 108—109°, λ_{max} 293 mμ (log ε 4.32), 325 mμ (infl.) (log ε 3.66), λ_{min} 251 mμ (log ε 2.92). (Found: C 68.66; H 6.03; $C_{18}H_{18}O_5$ requires C 68.78; H 5.77). It gives no colour with magnesium and hydrochloric acid. The yellow crystals, m. p. 134—135°, were identified as α,2′,4′,6′-tetramethoxychalcone (see below).

b) 2′-Hydroxy-α,4′,6′-trimethoxychalcone (XXII) (0.35 g) was dissolved in hot ethanol (0.75 ml). A cold 1.5 % sodium hydroxide solution (3.75 ml) was then added. The mixture was allowed to stand for 40 h, but no precipitation took place. After refluxing the mixture for one hour 2-benzyl-2,4,6-trimethoxycoumaran-3-one precipitated. Recrystallisation gave 0.13 g of m. p. 108—109°, not depressed by material prepared according to a).

c). In the preparation of 2-benzyl-2-hydroxy-4,6-dimethoxycoumaran-3-one (XXIII) according to Lindstedt [21] the ether solution remaining after washing with alkali was evaporated leaving a residue, which after recrystallisation from hexane and then from methanol gave a small amount of 2-benzyl-2,4,6-trimethoxycoumaran-3-one, m. p. 107—108°, undepressed by material prepared according to a) or b).

α,2′,4′,6′-Tetramethoxychalcone (XXVII). a). ω,2,4,6-Tetramethoxyacetophenone (XXV) was prepared by methylation of ω-methoxyphloracetophenone [22] (2 g) with dimethyl sulphate and potassium carbonate. It had m. p. 56.5—57°. (Slater and Stephen [22] report 50°). 0.1 g of this was dissolved in ethanol (2.5 ml) and benzaldehyde (0.4 ml), 10 % sodium hydroxide (2.5 ml) was added and the mixture allowed to stand at room temperature. Next day the yellow crystals of α,2′,4′,6′-tetramethoxychalcone were filtered off and recrystallised from methanol. Yield 0.1 g, m. p. 134—135°, λ_{max} 227 mμ (infl.) (log ε 4.23), 303 mμ (log ε 4.35), λ_{min} 255 mμ (log ε 3.73). (Found: C 69.41; H 6.10; $C_{19}H_{20}O_5$ requires C 69.50; H 6.13).

b). α-Hydroxy-2′,4′,6′-trimethoxychalcone (XX) (0.5 g) was methylated with dimethyl sulphate and potassium carbonate, giving 0.4 g of α,2′,4′,6′-tetramethoxychalcone, m. p. 135°.

c). 2′-Hydroxy-α,4′,6′-trimethoxychalcone (XXII) (1 g) was methylated with dimethyl sulphate and potassium carbonate, giving 0.7 g of α,2′,4′,6′-tetramethoxychalcone, m. p. 134—135°.

d). The yellow crystals obtained by methylation of 2-benzyl-2-hydroxy-4,6-dimethoxycoumaran-3-one (XXIII), m. p. 134—135° gave no depression when mixed with material prepared according to a), b) or c), which also gave no depression of m. p. when mixed.

2-Benzylcoumaran-3-one, was prepared according to v. Auwers [23] from ethyl 3-hydroxycoumarone-2-carboxylate. v. Auwers describes 2-benzylcoumaran-3-one as an oil, but in our hands the oil first obtained solidified after standing for some time. It had m. p. 50° but appeared to be still somewhat impure, because its infra-red spectrum shows a weak

peak at 1 750 cm^{-1}, attributable to an ester group. λ_{max} 252 mμ (log ε 3.94), 330 mμ (log ε 3.64), λ_{min} 231 mμ (log ε 3.41), 278 mμ (log ε 2.65).

2-Benzyl-4,6-dimethoxycoumaran-3-one [1] has λ_{max} 283 mμ (log ε 4.29), 315 mμ (infl.) (log ε 3.70), λ_{min} 246 mμ (log ε 3.01).

Some of the infra-red spectra were determined by Dr. L. A. Duncanson, ICI Research Department, Welwyn, and some by Mr. B. C. Fogelberg, Centrallaboratorium A. B., Helsingfors. We wish to thank also Mr. J. F. Grove and Professor W. Jensen, respectively, for these arrangements. This work has been financially supported by a grant from *Statens Naturvetenskapliga Kommission*, which is gratefully acknowledged.

REFERENCES

1. Gripenberg, J. *Acta Chem. Scand.* **7** (1953) 1323.
2. Kubota, T. *J. Chem. Soc. Japan* **73** (1952) 571, *J. Inst. Polytech. Osaka City Univ. Ser. C* **4** (1953) 253.
3. v. Kostanecki, S., Lampe, V. and Tambor, J. *Ber.* **37** (1904) 784.
4. Löwenbein, A. *Ber.* **57** (1924) 1515.
5. Cavill, G. W. K., Dean, F. M., McGookin, A., Marshall, B. M. and Robertson, A. *J. Chem. Soc.* **1954** 4573.
6. Tsukamoto, T. and Tominaga, T. *J. Pharm. Soc. Japan* **73** (1953) 1172; *Chem. Abstracts* **48** (1954) 12740.
7. Moureu, H. *Ann. chim.* [10] **14** (1930) 283.
8. Black, W. B. and Lutz, R. E. *J. Am. Chem. Soc.* **77** (1955) 5134.
9. Shaw, B. L. and Simpson, T. H. *J. Chem. Soc.* **1955** 655.
10. Bellamy, L. J. *Ultrarot Spektrum und chemische Konstitution* Übersetzt von Brügel, W. Verlag D. Steinkopff, Darmstadt 1955, p. 104 ff.
11. Feuerstein, W. and v. Kostanecki, S. *Ber.* **31** (1898) 710.
12. v. Auwers, K. and Brink, H. *Ann.* **493** (1932) 218.
13. Jörlander, H. *Ber.* **50** (1917) 406.
14. Murakami, M. and Irie, T. *Proc. Imp. Acad. Tokyo* **11** (1935) 229; *Chem. Abstracts* **29** (1935) 6598.
15. v. Kostanecki, S. and Szabrański, W. *Ber.* **37** (1904) 2819.
16. Oyamada, T. *J. Chem. Soc. Japan* **55** (1934) 1256; *Chem. Abstracts* **29** (1935) 4358.
17. Herzig, J. and Hofmann, B. *Ber.* **42** (1909) 155.
18. v. Kostanecki, S. and Tambor, J. *Ber.* **32** (1899) 2260.
19. v. Kostanecki, S., Lampe, V. and Tambor, J. *Ber.* **37** (1904) 2803.
20. Kimura, Y. and Hoshi, M. *Proc. Imp. Acad. Tokyo* **12** (1936) 285; *Chem. Abstracts* **31** (1937) 1807.
21. Lindstedt, G. *Acta Chem. Scand.* **4** (1950) 772.
22. Slater, W. K. and Stephen, H. *J. Chem. Soc.* **117** (1920) 309.
23. v. Auwers, K. *Ber.* **61** (1928) 408.

Received February 7, 1957.

ACTA CHEMICA SCANDINAVICA 11 (1957) 876—880

On the Oxidation of Benzidine and *o*-Dianisidine with Hydrogen Peroxide and Acetylcholine in Alkaline Solution

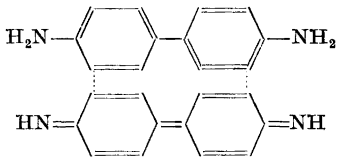
GUNNAR AKSNES and KJELL SANDBERG

Forsvarets forskningsinstitutt, Kjeller, Norway

The oxidation of benzidine and *o*-dianisidine with hydrogen peroxide and acetylcholine in alkaline solution at 20°C has been investigated. From benzidine one single oxidation product has been isolated and shown to be identical with synthesized 4-amino-4′-nitrobiphenyl. From the oxidation of *o*-dianisidine three compounds have been isolated. One of these is identical with the previously known *bis* (3,3′-dimethoxy-4-amino)azobiphenyl, whereas the other two have been identified as the previously undescribed compounds, 3,3′-dimethoxy-4-amino-4′-nitrobiphenyl and 3,3′-dimethoxy-4-amino-4′-nitrosobiphenyl.

Benzidine and many of its derivatives have been extensively used as sensitive reagents for several types of oxidizing agents. As examples may serve the detection of lead peroxide [1], phosphomolybdic acid [2], silicomolybdic acid [3], peroxy disulphuric acid [4], peroxide [5] and aldehydes [6].

The methods described for the detection of these oxidants have a common characteristic feature, inasmuch as the oxidation is invariably carried out in a neutral or faintly acidic solution. One of the coloured compounds formed when benzidine is oxidized under these conditions, is the meriquinoid oxidation product "benzidine blue" (I).



(I)

The oxidation of benzidine and its derivatives in alkaline solution, seems to have attracted less interest. In this work we intended to isolate and identify the oxidation products arising from the oxidation with hydrogen peroxide of benzidine and *o*-dianisidine in alkaline solution.

When highly purified reagents are used, it is known that at a moderate temperature (20°C), benzidine and *o*-dianisidine are very sparingly oxidized by hydrogen peroxide in alkaline solution. However, impurities of various kinds are able to promote the reaction. At least when heavy metal ions are involved, the effect is in all probability a catalytic one.

Among organic compounds, acid halogenides, acid anhydrides and esters all greatly accelerate oxidation with alkaline hydrogen peroxide. These agents, however, are consumed in certain stoichiometric proportions, so that their action is not strictly catalytic.

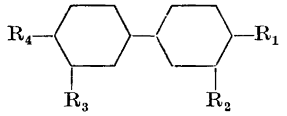
This paper is exclusively devoted to the isolation and identification of the coloured products formed in the oxidation reaction of benzidine and *o*-dianisidine with hydrogen peroxide in alkaline solution, and with acetylcholine as "activator".

REACTION CONDITIONS

An alkaline solution of benzidine or *o*-dianisidine is obtained by using acetone as mixing solvent. The oxidation was carried out at a pH approximately equal to 11. As alkaline buffer solution, dipotassium hydrogen phosphate-potassium hydroxide was used, the reaction being carried out at room temperature.

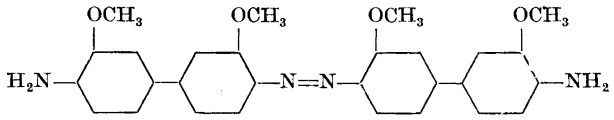
Under these conditions the solution containing benzidine or *o*-dianisidine, alkaline buffer solution, acetone and hydrogen peroxide, stayed colourless for at least one hour, provided that the most carefully purified reagents were used. When acetylcholine was added to this solution in the form of the bromide or the chloride, a rapidly developing colour could be detected after a few seconds. The colour which at first appeared yellow, quickly changed through orange and red, and finally attained a deep red tone when *o*-dianisidine was used, whereas in the case of benzidine the solution remained intensely orange-yellow even after half an hour.

The oxidation products were isolated by chromatographic methods. 4-Amino-4′-nitrobiphenyl was isolated from benzidine as the only oxidation product: II, $R_1 = NO_2$, $R_2 = R_3 = H$, $R_4 = NH_2$)



(II)

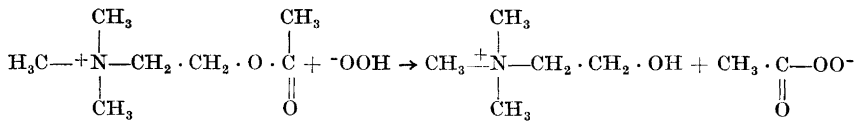
From the oxidation of dianisidine 3 substances were isolated, 3,3′-dimethoxy-4-amino-4′-nitrobiphenyl (II, $R_1 = NO_2$, $R_2 = R_3 = OCH_3$, $R_4 = NH_2$), 3,3′-dimethoxy-4-amino-4′-nitrosobiphenyl (II, $R_1 = NO$, $R_2 = R_3 = OCH_3$, $R_4 = NH_2$), and *bis*(3,3′-dimethoxy-4-amino)azobiphenyl(III).



(III)

DISCUSSION

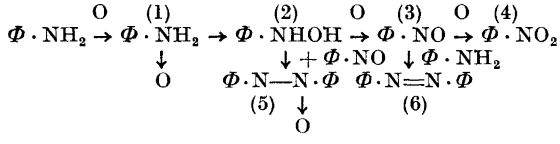
The ability of acetylcholine to enhance the oxidizing action of hydrogen peroxide in alkaline solution, is due to the formation of peracetic acid [7] in a nucleophilic reaction:



In alkaline solution peracetic acid is rapidly decomposed, yielding acetic acid and active oxygen. By volumetric measurement of the oxygen liberation from an alkaline solution of hydrogen peroxide after adding acetylcholine, it was clearly demonstrated that 1 mole oxygen is evolved from every 2 moles of acetylcholine. Peracetic acid has furthermore been qualitatively detected under these conditions [7].

The chemical compositions of the isolated oxidation products of benzidine and *o*-dianisidine supply further evidence in favour of the assumption that oxidation is brought about by oxygen uptake of one of the amino groups.

The series of oxidation products of *o*-dianisidine described in this paper, bears a striking resemblance to another series found earlier by Bamberger [8], who examined the oxidation products of aniline with per sulphuric acid. Bamberger showed that the following mechanism applies in the case of aniline oxidation:



Of these products (1) and (2) are very unstable, and Bamberger has not succeeded in isolating them. The nitroso compound (3) on the other hand, can be isolated provided sufficient care is taken, and products (4), (5) and (6) are relatively easily isolated.

In our case the isolated oxidation products of *o*-dianisidine correspond to the products (3), (4) and (6) in Bambergers aniline series. We have not succeeded in isolating the azoxy compound corresponding to product (5) in Bambergers series, but this might be due to deficiencies in the experimental methods used. However in our opinion the absence of this compound may be due to an even stronger tendency of the hydroxylamine derivative of our series to further oxidation, than is shown by phenylhydroxylamine. In our experiments we have not isolated any product in which both of the two amino groups have been oxidized.

Comparing the product obtained from benzidine with those from *o*-dianisidine, it is to be noted that in the former case only one oxidation product is isolated, *viz.* the nitro compound corresponding to (4) in Bambergers series. We have no reason to believe that the nitroso compound and the azo compound should be present here in detectable quantities and yet have escaped our attention as long as they did not do so in the *o*-dianisidine series. In our opinion, therefore, the two methoxy groups in the *ortho* positions to the amino

groups of *o*-dianisidine may play an important role by stabilizing the nitroso compound of this series, thus retarding further oxidation to the nitro compound.

EXPERIMENTAL

Our experiments were all carried out in the following way, with only slight modifications specified in each particular case.

500 mg *o*-dianisidine hydrochloride (or benzidine respectively) was dissolved in 50 ml water. To this solution 100 ml buffer solution (1.65 g K_2HPO_4 and 1.0 g KOH per 100 ml H_2O) was added, followed by 200 ml acetone, 20 ml 2 % H_2O_2 solution and finally 500 mg acetylcholine bromide in 10 ml H_2O.

The reaction was allowed to proceed for half an hour, and the mixture was filtered, water was added to the filtrate, and extraction effected using approx. 100 ml of chloroform. The extract was washed twice with 0.1 N HCl, then twice with water, dried with Na_2SO_4 and evaporated to dryness *in vacuo* at room temperature. The residue was dissolved in 5 ml benzene and transferred to a chromatographic coloumn packed with activated alumina.

In the case of benzidine, the chromatogram was developed and the product eluted with 50 % benzene and 50 % ether. The eluate was again evaporated *in vacuo*, and the residue dissolved in benzene and rechromatographed twice using 90 % benzene and 10 % ether.

The oxidation products of *o*-dianisidine were first chromatographed using 50 % benzene and 50 % ether as developer, and three coloured zones became visible. The first and the second zone from the bottom (a yellow (I) and a brown (II) zone) were not clearly separated. Above them a red zone (III), relatively well separated from the others, could be collected. The red zone was purified by twice repeated chromatography from benzene, and the two lower zones were separated and purified by chromatographing two or three times from benzene.

Care was taken not to leave the compound from the brown zone (II) on the alumina for any length of time, since purification has to be carried out as fast as possible because this nitroso compound is relatively unstable. Even when purified, passage of the compound through the column leaves behind a brown colouring because of polymerization, so that no sharply defined zone is obtained.

In our experiments we have observed that we can increase the amount of nitroso compound by using acetylcholine chloride instead of the bromide, and at the same time the reaction is shortened to 10—15 min. The best yields of the azo compound are obtained when the unwashed chloroform extract is allowed to stand overnight before proceeding.

Oxidation product from benzidine, *4-amino-4'-nitrobiphenyl:* M. p. 195°C (uncorr.)
Molecular weight 225 (Rast), theory 212.2
Ultraviolet spectrum: abs. max. at 370 mμ (in ethanol).
Infrared spectrum: abs. max. in mμ (NaBr-disk):
NH_2-frequency: 2.98 (s), 2.90 (d)
NO_2- » 6.28 (s), 7.45 (d)

4-amino-4'-nitrobiphenyl was synthesized according to Fittig [9]; m.p. 195°C (uncorr.). Mixed melting point with our substance showed no depression. Ultraviolet and infrared spectrum were identical.

Oxidation products from *o*-dianisidine, *3,3'-dimethoxy-4-amino-4'-nitrobiphenyl (zone 1):*

M. p. 101°C (uncorr.). (Found: C 61.53; H 5.19; N 9.97. Calc. for $C_{14}H_{14}O_4N_2$ (274.27): C 61.30; H 5.15; N 10.20).
Ultraviolet spectrum: abs.max. at 370 mμ (in ethanol).
Infrared spectrum: abs.max. in mμ (NaBr-disk)
NH_2-frequency: 2.98 (s) 2.90 (d)
NO_2- » 6.25 (s) 7.40 (d)

3.3'-dimethoxy-4-amino-4'-nitrosobiphenyl (zone II):
M. p. 148° (uncorr.)
Test for nitroso group according to Feigel [10] is positive.

The substance condenses easily with compounds containing active metylene groups. The substance is easily hydrolyzed by cold alkali [11].

Ultraviolet spectrum: abs. max. at 445 mμ (in ethanol).
Infrared spectrum: abs. max. in mμ (NaBr-disk):
NH_2-frequency: 3.0 (s) 2.92 (d)
NO^- » 7.18 6.28 (?)
The nitroso compound was oxidized with H_2O_2 and acetylcholine to give 3,3'-dimethoxy-4-amino-4'-nitrobiphenyl (see above).

bis (3 3'-dimethoxy-4-amino) azobiphenyl (zone III).
M. p. 240° C (uncorr.).
Ultraviolet spectrum: abs. max. at 435 mμ (in ethanol).
Infrared spectrum: abs. max. in mμ (NaBr-disk):
NH_2-frequency: 2.98 (s), 2.91 (d)
-N=N- — » 6.23

Bis (3 3'-dimethoxy-4-amino) azobiphenyl was synthesized according to Moir [12]. The two substances showed identical melting points identical ultraviolet and infrared absorption spectra. Mixed melting point showed no depression.

REFERENCES

1. Deniges, G. *Precis de Chemie analytique* 4th Ed., Paris 1913; Schlenk, W. *Ann.* **363** (1908) 313; Feigl, F., Spot Tests, 3th Ed. Elsevier Publishing Co., New York 1947.
2. Feigl, F. *Z. anal. Chem.* **61** (1922) 454; **74** (1928) 386; **77** (1929) 299.
3. Feigl, F. and Krumholz, P. *Microchemie, Pregl-Festschrift* **1929** 82.
4. Monnier, A. *Ann. chim. anal.* **21** (1916) 237; Smidt, J. and Hinderer, W. *Ber.* **65** (1932) 87.
5. Nosaka, K. *Mikrochim. Acta* **1** (1937) 78.
6. Woker, G. *Ber.* **47** (1914) 1024.
7. Aksnes, G. *Unpublished studies.*
8. Bamberger, E. *Ber.* **31** (1898) 1522; **32** (1899) 1675; **36** (1903) 685; Goldschmidt, H. *Ber.* **53** (1920) 28; **55** (1922) 3216.
9. Fittig, K. *Ann.* **124** (1862) 276.
10. Feigl, F. *Spot Tests* (Ref.[1]) p. 321.
11. Ehrlich, P. and Sachs, F. *Ber. 32* (1899) 2341.
12. Moir, J. *S. African J. Sci.* March 1914, p. 560.

Received January 24, 1957.

ACTA CHEMICA SCANDINAVICA 11 (1957) 881—892

The Lipids of a Lysozyme Sensitive *Bacillus* Species (*Bacillus* "M")

CLAES WEIBULL

Central Bacteriological Laboratory of Stockholm City, Stockholm, Sweden

The lipids extracted from cells of a lysozyme sensitive bacterium, closely related to *Bacillus megaterium*, have been studied with respect to chemical constitution and to their distribution between various cell fractions. The total lipid content of the organism (*Bacillus* "M") is about 4 %. Part of the lipids can be extracted only after acid hydrolysis of the cell material. About 65 % of the total lipids are located in the cytoskeletons ("ghosts") remaining after the cells have been lysed with lysozyme. The lipids seem to consist of a mixture of neutral fat or fatty acids and phosphatidic acids. Cholesterol and lipids of the sphingolipid type seem to be absent altogether or are present only in small amounts.

A great number of investigations have been carried out on bacterial lipids. Earlier investigations (reviewed in Refs. [1–3]) were as a rule carried out using whole bacterial cells as experimental material. In some of the more recent studies, on the other hand, a fractionation of the cell constituents has preceded the extraction and characterization of the lipids. The first step in the fractionation procedure has been either a mechanical disintegration of the cells [4,5], or, in the case of lysozyme sensitive bacteria, a treatment of the cells with this enzyme [6]. A fractionation of the released cell constituents has then followed, carried out by means of differential centrifugations.

The procedure including enzymatic disintegration has been used in the present work. As has been shown earlier, lysozyme treatment of sensitive bacteria results in the dissolution of the cell wall and in the formation of bacterial "ghosts" [7–9]. The peripheral part of the "ghosts" represent the cytoplasmic membrane but probably these structures contain additional elements [6,10]. The "ghosts" could to some extent be compared to the stroma or post-hemolytic residue of red blood cells.

When lysozyme is allowed to act on bacteria suspended in a strong sucrose solution, the cell wall can be dissolved without ensuing lysis of the protoplasm [9]. The resulting free protoplasts retain most of the biochemical and biological capabilities of the whole cells [11]. The protoplasts are rather resistant towards

single centrifugations and can be separated from the bulk of the degraded cell wall material remaining in the supernatant. When protoplasts are suspended in dilute salt solutions or distilled water, lysis occurs instantaneously causing release of soluble protoplasm and the formation of "ghosts". The "ghosts" are precipitable by centrifugation at 15 000 × *g*, whereas the constituents of the soluble protoplasm may be sedimented only by ultracentrifugation.

It is thus possible to obtain a division of the cell material into three portions: "ghosts", soluble protoplasm and cell wall material. Since the protoplasts are somewhat fragile it is not always easy to effect a complete separation of the two last-mentioned fractions by means of resuspension and washing procedures.

The present investigation has been carried out on a lysozyme sensitive *Bacillus* species, designed as *Bacillus* M by Tomcsik [12]. It is closely related to *Bacillus megaterium* and has even been classified as a strain of this bacterium [13]. The distribution of the lipids of *Bacillus* M has been studied by means of the disintegration and fractionation procedure outlined above. A chemical characterization of the extracted and purified lipids has also been carried out.

MATERIALS AND METHODS

Organism, growth conditions and harvesting. Bacillus M [13] was used in all experiments. Cultures for experimental work were grown at 30°C in a medium containing 2 % Difco peptone and 0.05 % Difco yeast extract. 8 l Fernbach flasks, each containing 1 l substrate, were incubated for 16 h on a rotary shaker. The bacteria, then being in the stationary growth phase, were harvested by centrifugation, repeatedly washed with distilled water and resuspended in the same medium. The suspension was either immediately freeze-dried or subjected to the fractionation procedures outlined below. As a rule batches of about 5 g bacterial dry weight were prepared.

Preparation of bacterial cell fractions. The fractionation aimed at a division of the cell material into three parts: cell wall material, "ghosts" and soluble protoplasm. Often, however, wall material and soluble protoplasm were not separated from each other. In such a case, lysozyme and sodium chloride (final concentrations 0.01 – 0.02 % and 0.01 M, respectively) were added to 100 – 200 ml of a suspension of *Bacillus* M in distilled water (dry weight content 10 – 20 mg/ml). After completion of the lytic process the "ghosts" were spun down by centrifugation at 15 000 × *g*, and after resuspension washed three times with distilled water. The supernatants from the centrifugations thus contained both cell wall material, solubilized by lysozyme, and soluble protoplasm. Both this material and the "ghost" fractions were freeze-dried.

When a division of the cell material into the three fractions of wall substances, soluble protoplasm and "ghosts" was tried, sucrose, sodium chloride and magnesium chloride were added to the bacterial suspension at final concentrations of 0.5, 0.01 and 0.005 M, respectively. Lysozyme was then added as described above. When the cells had been converted into protoplasts, these bodies were spun down by centrifugation. The supernatant, containing the bulk of the wall material, was removed and the protoplasts were resuspended in 0.02 M phosphate buffer of pH 7. Lysis occurred immediately, resulting in the formation of "ghosts" and in the release of soluble protoplasm. The "ghosts" were separated from soluble protoplasm as described in the preceding paragraph. – A quite satisfactory separation of the cell wall material from the cytoplasm was, however, not achieved. First, it was found that a few per cent of the ultraviolet absorbing substances of the protoplasts leaked out into the medium. (Thus, the protoplasts of *Bacillus* M seemed to be somewhat less stable than the same bodies obtained from *Bacillus megaterium*, strain KM [9].) Second, noticeable lysis occurred when after centrifugation washing of the protoplasts with sucrose was tried. A few per cent of the cell wall material, remaining between the precipitated protoplasts, could consequently not be removed.

Extraction and purification of the bacterial lipids: a. Lipids extractable without acid hydrolysis of the cell material ("free" lipids). Two methods were tried, that one introduced by Bloor, using an ethanol-ether mixture (3:1) as extraction fluid [14], and that recommended by Folch *et al.*[15], employing for the same purpose chloroform-methanol in the proportion 2:1. When the former procedure was applied, the material to be extracted was suspended in about 20 times the amount of extraction fluid. The mixture was brought to boil, then allowed to cool and filtered. The filtrate was evaporated to dryness at 35—40°C. The solid residue was reextracted with petroleum ether. The resulting solution was filtered, evaporated as already described, dried *in vacuo* and weighed.

The extraction with chloroform was, if not otherwise mentioned, preceded by refluxing with methanol for one hour in order to break lipid-protein complexes [16]. Twice the amount of chloroform was then added. The solution was brought to boil, allowed to cool and filtered. Evaporation was carried out as described in the preceding paragraph. Purification of the extracted lipids followed the method given by Folch *et al.*[17]. The crude lipids were dissolved in chloroform-methanol. An amount of water equal to 1/5 of the volume of the lipid solvents was added. The system was thoroughly shaken and left overnight. Two liquid phases had then formed. The upper phase was removed, the lower one containing the lipids, was washed with a dilute calcium chloride solution [18]. After evaporation the solid lipids were dried *in vacuo* and redissolved in pure chloroform. The resulting solution was filtered and evaporated. Finally the purified lipids were weighed after drying.

b. Lipids extractable only after acid hydrolysis of the cell material ("bound" lipids). The material remaining after the extraction with chloroform-methanol was refluxed for 2 h with 6 M hydrochloric acid. (The wash water obtained when purifying the crude "free" lipids was also acidified and refluxed.) The acid solutions were shaken repeatedly with ether one hour each time. The combined etheral extracts were evaporated at about 30°C in a stream of carbon dioxide, the solid residue dried and redissolved in a small amount of ether. The solution was filtered, the solvent evaporated as just described and the lipids weighed after drying.

Chemical characterization of the lipids: a. Phosphorus content. Total phosphorus was determined according to Allen [19]. The amount of phosphorus liberated by mild alkaline hydrolysis was determined according to Schmidt *et al.*[20] and Brante [21]. The lipids were treated with 1 M sodium hydroxide at 37°C for 24 h. After neutralization trichloroacetic acid was added to a final concentration of 6 %. The suspension was filtered and the phosphorus in the filtrate was determined according to Allen.

b. Estimation of choline, serine and ethanolamine. The lipids were hydrolyzed with 6 M hydrochloric acid at 100°C for 3 h. The acid was evaporated and the residue was redissolved in a small amount of distilled water.

Suitable amounts of the hydrolysate were chromatographed on Whatman No. 1 filter paper. Butanol-acetic acid-water (6:1:2) was used as the solvent. Serine and ethanolamine were detected on the chromatograms by means of the ninhydrin reaction. Choline was detected with phosphotungstic acid according to Levene and Chargaff [22] or with dipicrylamine according to Augustinsson and Grahn [23]. By comparison with known amounts of choline, *etc.*, chromatographed in parallel with the lipid hydrolysate, an approximate estimation of the content of these compounds in the lipids could be made.

c. Estimation of hexoses and inositol. The lipids were hydrolyzed with 6 M hydrochloric acid for 45 min (hexoses) or 6 h (inositol) [21]. After evaporation of the acid *in vacuo* at room temperature and redissolving the residue in distilled water chromatography was carried out. Ethyl acetate-pyridine-water (2:1:2) was used as the solvent. The carbohydrates were detected on the papers by means of silver nitrate and alcoholic sodium hydroxide according to Trevelyan *et al.*[24]

d. Determination of cholesterol. The Liebermann-Burchard reaction was used, carried out according to Schoenheimer and Sperry [25].

e. Circular paper chromatography of intact lipids. The procedure outlined by Hack [26] was adopted. Whatman No. 1 filter paper disks were extracted with chloroform-methanol (4:1). About 25 μl of a chloroform-methanol solution containing 10—40 μg of lipids was placed in the center of the disk. The solvent was evaporated and 25—50 μl of chloroform-methanol was added until the lipids had spread to a ring 10 mm in diameter. Finally the desired solvent was added at such a rate that the diameter of the wet spot increased about 2 mm per second, not allowing the diameter to exceed 30—40 mm. As solvents

Table 1. Mg of bacterial lipids extracted from 1 g of dried cell fractions of *Bacillus* M.

Cell fraction	Extraction fluid used:	
	Chloroform-methanol	Ethanol-ether
"Ghosts"	150	153
Cell walls + soluble protoplasm	10.9	4.0

were used chloroform-methanol (4:1), chloroform, methanol, acetone, benzene, ethyl acetate and pyridine. Sometimes two different solvents were used one after another on the same chromatogram, letting the paper dry in between. The first solvent was allowed to spread to a diameter of 40 mm, the second to 30 mm.

Lipids in general were detected on the chromatograms by staining with a 0.1 % solution of Sudan black in 50 % aqueous ethanol and by washing with the same solvent. Phospholipids were detected by exposing the chromatograms to acid ammonium molybdate followed by hydrogen sulphide [27]. Unsaturated fatty acids were detected by exposing the chromatograms to osmic tetroxide vapors.

Dry weight determinations. The dry weight of bacterial cells and proteinaceous cell fractions were determined after drying samples at 100°C. The dry weight of purified lipids was determined after evaporating the lipid solvents at 30—40°C in a stream of carbon dioxide. The residue was dried *in vacuo* at room temperature using anhydrous calcium sulphate as desiccant, and weighed.

RESULTS

Comparison between lipid extraction using chloroform-methanol and alcohol-ether, respectively

The freeze-dried material to be extracted was divided into two halves. One half was extracted with chloroform-methanol, the other one with ethanol-ether. The purification of the extracted crude lipids was carried out as described in the methodological section. Table 1 gives the results.

According to the figures in Table 1 cell material that contains only small amounts of lipids seems to be extracted most completely by means of the procedure involving treatment with chloroform-methanol. This procedure was used as a standard method in the present investigation.

Completeness of the extractions

Freeze-dried cells and cell fractions were subjected to four successive extractions before and after acid hydrolysis. As is shown by Fig. 1 the extraction process can then be regarded as completed.

Lipid content of the bacterial cells

Extraction of whole cells. Four different batches of *Bacillus* M were investigated. Table 2, column a, gives the amounts of lipid extractable with chloroform-methanol ("free lipids"). Column b gives the amounts of "bound" lipids,

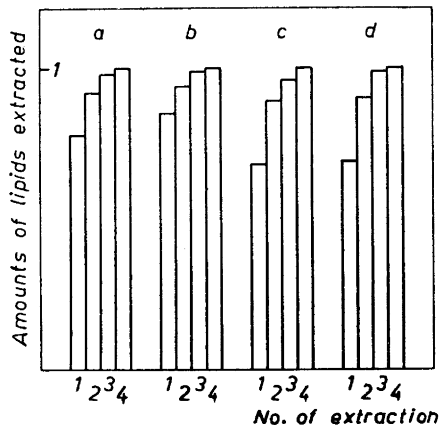


Fig. 1. Amounts of lipids extracted from cell material by repeated treatments with chloroform-methanol (experiments a, b and c) or with ether after acid hydrolysis (d). The total amount of lipids obtained in each of the experiments has been put equal to unity. "Ghosts" (a), cell wall + soluble protoplasm (b) and whole cells (c, d) were extracted.

i. e. the material obtained by acid hydrolysis of the residues from the chloroform-methanol extraction and by subsequent treatment of the hydrolysate with ether.

The figures in Table 2 (columns a—c) demonstrate rather wide variations in the lipid content of different batches of *Bacillus* M. On the other hand, the ratio "free" lipids/total lipids is remarkably constant (column d).

Table 2. Lipid content of whole cells of *Bacillus* M.

Batch	% lipids in dried cells			d. Free lip., % of total.
	a. Free lip.	b. Bound lip.	c. Total lip.	
IV	1.89	1.79	3.68	51
VII	1.96	2.14	4.10	48
VIII	1.54	1.40	2.94	52
IX	1.65	1.73	3.39	49

Extraction of cell fractions: a. "Ghosts". The results are summarized in Tables 3 and 4. Table 3 shows the amounts of extracted lipids, expressed as percentage of the dry weight of the "ghosts". In Table 4 the dry weight and the lipid content of the "ghosts" is given as percentage of the dry weight of the intact cells.

It could be mentioned that in the case of batches V and VI the "ghosts" were obtained from the cells *via* protoplasts stabilized with magnesium chloride. The somewhat high dry weight of this material, and hence a lower lipid content, may be due to some protoplasmic material precipitable by magnesium ions [28].

Two batches (VIII and IX) were first extracted with chloroform-methanol, then refluxed with methanol and again extracted (in all other cases refluxing preceded the extraction). Batch VIII was extracted in the wet state, all other ones after being freeze-dried.

Table 3. Lipid content of "ghosts" of *Bacillus* M.

Batch	% lipids in dried "ghosts"			d. Free lip., % of total
	a. Free lip.	b. Bound lip.	c. Total lip.	
V	10.9	2.4	13.3	82
VI	15.0	1.5	16.5	91
VII	15.8	2.8	18.6	85
VIII	14.8[x] + 1.3[z]	0.8	17.1	95
IX	19.1[y] + 0.4[z]	1.5	21.0	93

[x] Wet extraction without refluxing with methanol.
[y] Dry » » » » »
[z] Additional » after » » »

Table 4. Dry weight and total lipid content of "ghosts" of *Bacillus* M, expressed as % of dry weight of whole cells.

Batch	a. Dry weight	b. Lipid content
V	18.8	2.50
VI	19.8	3.27
VII	14.9	2.78
VIII	15.3	2.61
IX	15.1	3.19

b. Cell wall and soluble protoplasm. Most determinations were carried out on material obtained by treating *Bacillus* M with lysozyme in dilute phosphate buffer and removing the ensuing "ghosts" by centrifugation. This material thus represents a mixture of cell wall material and soluble protoplasm. Tables 5 and 6 show the amounts of extracted lipids, expressed as percentage of the dry weight of the cell fraction and the whole cells, respectively.

Experiments were also carried out on cell wall material and soluble protoplasm separated from each other. As has been pointed out in the methodological section, however, a complete separation could not be achieved. The great amount of sucrose present especially in the wall fraction also made a quantitative determination of the lipids difficult. It could be concluded, however, that lipids must be present both in the cell wall and in the soluble protoplasm.

Table 5. Lipid content of cell wall + soluble protoplasm of *Bacillus* M.

Batch	% lipids in dried cell fraction			d. Free lip. % of total
	a. Free lip.	b. Bound lip	c. Total lip.	
II	1.18	0.37	1.55	76
VII	2.09	0.66	2.75	76
VIII	0.84	0.28	1.12	75
IX	1.29	0.52	1.81	71

Table 6. Dry weight and total lipid content of cell wall + soluble protoplasm of *Bacillus* M, expressed as % of dry weight of whole cells.

Batch	a. Dry weight	b. Lipid content
II	86.1	1.34
VII	85.1	2.34
VIII	84.7	0.95
IX	84.9	1.54

Comparison between the amounts of lipids extracted from whole bacteria and from the sum of the cell fractions. Three batches of *Bacillus* M were divided into halves. One half was extracted in the form of whole cells. The other one was fractionated into "ghosts" and cell wall material + soluble protoplasm. Table 7 shows the total amounts of lipids extracted from the whole cells and from the sum of the fractions, respectively.

Table 7. Amounts of lipids (free + bound) extracted from whole cells of *Bacillus* M and from fractionated material expressed as % of dry weight of whole cells.

Batch	Intact cells	Sum of fractions
VII	4.10	5.12
VIII	2.94	3.56
IX	3.39	4.73

It can easily be calculated from the figures of Table 7 that about 25 % more lipid material is extracted from the fractionated material than from whole cells. This fact will be discussed later in this paper.

Chemical nature of the bacterial lipids

As mentioned earlier the total amounts of phospholipids in the "free" lipids was estimated by total phosphorus determinations. For the estimation of monoaminophospholipids and phosphatidic acids the lipids were hydrolyzed with 1 M alkali and the liberated phosphorus determined. Table 8 gives the results.

Since pure phospholipids contain about 4 % of phosphorus it can be concluded that the lipids isolated from the "ghosts" (phosphorus content 3.3—4.0 %) to the greater part consist of such compounds. The phosphorus content of the lipids extracted from other cell fractions and from whole cells is considerably lower.

The results of the estimations of choline, serine, ethanolamine, inositol, hexoses and cholesterol in the "free" bacterial lipids are summarized in Table 9.

Table 8. Phosphorus content of "free" bacterial lipids of *Bacillus* M, expressed as % of lipid dry weight.

Lipids extracted from		Batch					
		IV	V	VI	VII	VIII	IX
Whole cells	NH[x]	2.44			2.40	2.16	1.82
	H[y]	2.32			2.32		1.76
"Ghosts"	NH		3.46	3.49	4.02	3.28	3.71
	H		3.36	3.36	3.55	3.22	3.71
Cell wall	NH			1.06			
	H		1.92	1.06			
Soluble protopl.	NH		2.26	1.73			
	H		2.08	1.79			
Cell wall + sol. protopl.	NH				1.84	1.50	1.19
	H				1.65	1.50	1.19

x Phosphorus determined without previous alkaline hydrolysis.
y » » after » » »

It is seen that only small amounts, if any, of the various compounds are present. This fact suggest that the phospholipids isolated from *Bacillus* M mainly consist of phosphatidic acids. Cholesterol could well be absent altogether, since the Liebermann-Burchard test was completely negative. (The "bound" lipids were also tested for cholesterol but with equally negative result.) No traces of choline, inositol and hexoses could be detected on the chromatograms. On the other hand, small amounts of serine and ethanolamine were present. The presence of several other ninhydrin positive compounds was revealed on such chromatograms that were run on hydrolyzed lipids isolated from whole cells or from cell fractions other than the "ghosts".

The circular chromatography experiments, carried out according to Hack [26], revealed the following facts. Well defined coloured rings were obtained by treating the dried chromatograms with suitable reagents. The position of the

Table 9. Amounts of various constituents in "free" bacterial lipids of *Bacillus* M, expressed as % of lipid dry weight.

Constituent	Lipids extracted from		
	"Ghosts"	Soluble protopl. + cell wall.	Whole cells
Choline	< 0.3	< 0.5	< 0.3
Serine	< 0.2	< 0.5	< 0.5
Ethanolamine	< 0.3	< 0.5	< 0.5
Inositol	< 0.2	< 0.2	< 0.2
Hexoses	< 0.2	< 0.2	< 0.2
Cholesterol	< 0.2	< 0.2	< 0.2

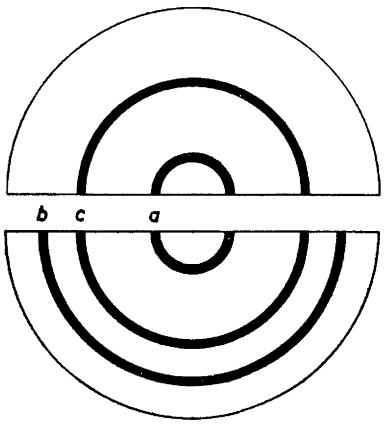


Fig. 2. Chromatograms of bacterial lipids, extracted with $CHCl_3$:CH_3OH. The chromatogram was developed to *a* with $CHCl_3$:CH_3OH (4:1), to *b* with acetone, to *c* with CH_3OH (this order) and dried in between. The lower half was treated with Sudan black (general test for lipids), the upper one with NH_4-molybdate and H_2S (test for phospholipids).

rings, compared to that of the solvent front, indicated that the lipids as a rule had a R_F value either close to unity or close to zero. The best differentiation was obtained by developing the chromatograms first with chloroform-methanol (radius of wet spot 10 mm), then with acetone (40 mm) and finally with methanol (30 mm). Three rings were obtained, all of which stained with Sudan black and osmic acid vapors. Only in the two central ones, however, could phospholipids be detected by means of the ammonium molybdate-hydrogen sulphide spot test. The results are illustrated by Fig. 2. A similar system of components was observed when commercial egg lecithin was chromatographed.

No certain differences could be detected in the chromatographic behavior of lipids extracted from "ghosts", cell wall, soluble protoplasm and whole cells, respectively. In all chromatograms the presence of both phospholipids and lipids free of phosphorus was indicated.

DISCUSSION

A great number of methods for the extraction and purification of lipids have been developed during the course of time. Of the two procedures for the isolation of "free" lipids that have been tried in the present study the one using chloroform-methanol seems to effect the most complete extraction of the investigated material. It is by no means excluded, however, that still more efficient methods could be developed by using other solvent mixtures or purification techniques.

As far as the "ghosts" are concerned, the refluxing technique recommended by Reichert [16] seems to increase the yield of chloroform-methanol extractable lipids by less than 10 %. The yield of such lipids remains approximately the same whether wet or freeze-dried material serves as starting material for the extractions (Table 3, column a, batches VIII and IX).

As is evident from Tables 2, 3 and 5 a considerable part of the bacterial lipids, the "bound" lipids, cannot be extracted without a chemical degradation (acid hydrolysis) of the cell material. This has earlier been pointed out by

Bloor and others [1]. From the tables it can be seen that the proportion of the "bound" lipids to totally extractable lipids diminishes from 50 to about 20 % as a consequence of the lysozyme treatment and the fractionation procedures. It remains to be investigated whether this change is due to breakage of chemical bonds or to the mere disintegration of the cell structure.

The decrease in the content of "bound" lipids that accompanies the preparation of the cell fractions may to some extent at least explain why more lipid material is obtained from these fractions, taken together, than from whole cells (Table 7). The acid hydrolysis of the cell material causes a degradation of the lipid molecules. Of the split products only the fatty acids are extracted when the hydrolysate is shaken with ether.

The total amount of lipid material extractable from *Bacillus* M ranges between 3 and 5 % (Table 7). Previous investigators have reported that cells of *Bacillus megaterium* contain 10—25 % of lipids [29]. The bulk of these lipids consists of polymerized β-hydroxy-butyric acid and is located in granules stainable with Sudan black [30,31]. The present author has only occasionally found similar granules in cells of *Bacillus* M. It could be mentioned in this connection that the presence or absence of lipid granules has been used as a means for the differentiation between various *Bacillus* species [29].

From the figures in Tables 4, 6 and 7 it can be calculated that 55—75 % of the bacterial lipids are located in the "ghosts". These structures represent about 15 % of the total cell dry weight(Table 4). Thus the greater part of the lipids are concentrated in a rather small fraction of the cell material. Lipid rich fractions of bacterial cells have earlier been described by Mitchell and Moyle [4], by Few [5] and by Georgi *et al* [6]. The "red fraction" obtained by the last-mentioned workers, containing about 50 % of the bacterial lipids, is probably equivalent to the "ghosts" described in the present paper. After the extraction with lipid solvents this "red fraction" was transformed into discrete granules. Some preliminary electron microscopical observations on the residue obtained after extraction of the "ghosts" of *Bacillus* M have not revealed characteristic granules but rather masses built up by not very well-defined subunits. On the other hand, granules are present in the intact "ghosts" of this bacterium [10].

The chemical analyses reported in this paper suggest a rather simple composition of the lipids of *Bacillus* M. Cholesterol is very probably absent altogether. The small differences between the phosphorus determinations carried out with and without alkaline hydrolysis indicate that the extracted phospholipids consist almost entirely of phosphatidic acids or of monoamino compounds. In addition since no hexoses could be detected in lipid hydrolysates (Table 9) sphingolipids are probably not present. This is in accordance with the findings of Čmelik [32]. He notes the absence of hexoses in lipids isolated from cells of *Salmonella paratyphi C*. Georgi *et al.*, on the other hand, report that the phospholipids of *Bacillus stearothermophilus* are mainly of the sphingomyelin type. The apparent dissimilarity between the lipids of the two *Bacillus* species could perhaps be explained by the fact that Georgi *et al.* used a weaker alkali (0.1 M) for the hydrolysis of the monoaminophospholipids [6].

The very low content of choline, serine, ethanolamine and inositol in the "free" bacterial lipids (Table 9) strongly suggests that the phospholipids pre-

sent in this material mainly consist of phosphatidic acids. This is in accordance with the findings of Few [5] and by Čmelik [32]. Few [5] reports that choline is absent in lipids isolated form a "small particle fraction" of disintegrated *Pseudomonas denitrificans* and *Staphylococcus aureus* cells. This fraction very probably represents disintegrated cytoplasmic membranes. Mostly phospholipids were isolated from *Pseudomonas denitrificans*, and these lipids had a high content of phosphatidic acids. Čmelik finds no choline in lipids extracted from whole cells of *Salmonella paratyphi C*.

It could be questioned, however, whether the phosphatidic acids exist as such in the living bacteria. Hanahan and Chaikoff have demonstrated the presence in plant tissues of an enzyme that rapidly splits nitrogen compounds from phosphatides [33]. Similar enzymes may be active in bacterial lysates as well. On the other hand, the "free" lipids isolated from whole cells also have a low content of choline, etc. In this case it seems less probable that a significant degradation of the lipids can have occurred as a consequence of lytic processes.

In the lipids isolated from cell wall and soluble protoplasm the presence of several ninhydrin-positive substances besides serine and ethanolamine was noted. Such substances, often identified as amino acids, have been found earlier in purified lipids [34,35]. Whether they represent contaminations or from complexes with the lipids does not seem quite clear [35].

The circular chromatography experiments indicate that the bacterial lipids contain phoshorus-free lipids in addition to the phospholipids or phosphatidic acids. The former substances probably represent neutral fat or fatty acids such compounds have been isolated from several bacteria [1–3].

The chromatographic characterisation of the phospholipids show in addition that these compounds can be divided into two fractions, one soluble in methanol, the other one methanol insoluble. A similar behavior of phospholipids isolated from typhoid bacteria has been demonstrated by Čmelik [32,35,36]. In the methanol-soluble fraction of Čmelik's lipids amino acids were present, whereas the fraction insoluble in the same solvent consisted of a mixture of cephalin and phosphatidic acids.

The greater part of the experimental work of this investigation was carried out by Mr. Ulf Nyström. His skilful assistance is gratefully acknowledged.

I also wish to thank Dr. Gunnar Brante for reading the manuscript and for valuable suggestions in this connection.

The investigation is part of a program on the submicroscopic structure of the bacterial cell, which is financially supported by the *Swedish Natural Science Research Council.*

REFERENCES

1. Bloor, W. R. *Biochemistry of the fatty acids and their compounds, the lipids*, Reinhold Publishing Co., New York 1943, p. 264.
2. Porter, J. R. *Bacterial Chemistry and Physiology*, John Wiley & Sons, New York, Chapman and Hall, London 1946, p. 406.
3. Werkman, C. H. and Wilson, P. W. (Ed.) *Bacterial Physiology*. Academic Press, New York 1952, p. 10.
4. Mitchell, P. and Moyle, J. *J. Gen. Microbiol.* **5** (1951) 981.
5. Few, A. W. *Biochim. et Biophys. Acta* **16** (1955) 137.

6. Georgi, C. E., Militzer, W. E. and Decker, T. S. *J. Bacteriol.* **70** (1955) 716.
7. Herbert, D. and Pinsent, J. *Biochem. J. London* **43** (1948) 193.
8. Tomcsik, J. and Guex-Holzer, S. *Schweiz. Z. Pathol. u. Bakteriol.* **15** (1952) 517.
9. Weibull, C. *J. Bacteriol.* **66** (1953) 688.
10. Weibull, C. and Thorsson, K. G. *Proc. I:st European Conf. on Electron Microscopy*, Stockholm, Almqvist & Wiksell 1956.
11. Spooner, E. T. C. and Stocker, B. A. D. (Ed) *Bacterial Anatomy*, The University Press, Cambridge 1956, p. 127.
12. Tomcsik, J. *Experimentia* **7** (1951) 459.
13. Spooner, E. T. C. and Stocker, B. A. D. (Ed.) *Bacterial Anatomy*, The University Press, Cambridge 1956, p. 41.
14. Bloor, W. R. *J. Biol. Chem.* **22** (1915) 133.
15. Folch, J., Ascoli, I., Lees, M., Meath, J. A. and Le Baron, F. N. *J. Biol. Chem.* **191** (1951) 833.
16. Reichert, R. *Helv. Chim. Acta* **27** (1944) 961.
17. Folch, J., Lees, M. and Sloan-Stanley, G. H. *Federation Proc.* **13** (1954) 209.
18. Glick, D. (Ed.) *Methods of Biochemical Analysis*, Interscience, New York 1955, Vol. II, p. 107.
19. Allen, R. J. A. *Biochem. J. London* **34** (1940) 858.
20. Schmidt, G., Benotti, J., Hershman, B. and Thannhauser, S. J. *J. Biol. Chem.* **166** (1946) 505.
21. Brante, G. *Studies on Lipids in the Nervous System* (Diss.) University, Uppsala 1949.
22. Levine, C. and Chargaff, E. *J. Biol. Chem.* **192** (1951) 465.
23. Augustinsson, K.-B. and Grahn, M. *Acta Chem. Scand.* **7** (1953) 906.
24. Trevelyan, W. E., Procter, D. P. and Harrison, J. S. *Nature* **166** (1950) 444.
25. Schoenheimer, R. and Sperry, W. M. *J. Biol. Chem.* **106** (1934), 745.
26. Hack, M. H. *Biochem. J. London* **54** (1953) 602.
27. Hanes, C. S. and Isherwood, F. A. *Nature* **164** (1949) 1107.
28. Weibull, C. *Exptl. Cell Research* **10** (1956) 214.
29. Lemoigne, M., Delaporte, B. and Croson, M. *Ann. inst. Pasteur* **70** (1944) 224.
30. Weibull, C. *J. Bacteriol.* **66** (1953) 696.
31. Widra, A. *J. Bacteriol.* **71** (1956) 689.
32. Čmelik, S. *Hoppe-Seyler's Z. physiol. Chem.* **296** (1954) 67.
33. Hanahan, D. J. and Chaikoff, I. L. *J. Biol. Chem.* **172** (1948) 191.
34. Lovern, J. A. *The Chemistry of Lipids of Biochemical Significance.* Methuen & Co., London 1955, p. 62.
35. Čmelik, S. *Hoppe-Seyler's Z. physiol. Chem.* **302** (1955) 20.
36. Čmelik, S. *Naturwiss.* **42** (1955) 489.

Received March 2, 1957.

ACTA CHEMICA SCANDINAVICA 11 (1957) 893—916

Short Communications

Refractometric Determination of Diffusion Constants in the Critical Region of Partly Miscible Liquids

HANS LUDVIG LORENTZEN and BJØRN BERGSNOV HANSEN

Universitetets Kjemiske Institutt, Blindern-Oslo, Norway

Owing to the convenient critical temperature of about 30° the system chosen for starting off diffusion measurements was ethyl alcohol-succinonitrile. The diffusion constant approaches zero at the critical point.

The sample of about 50 mm³ liquid mixture was contained in a hollow, vertical 60° prism of about 10 mm in height. An astigmatic optical system was employed which showed directly on a photographic diagram the refractive indices of the liquids at different levels inside the prism, and thereby the composition of the liquid. The system has been described earlier [1,2].

Before being sealed off the prism was filled with a liquid mixture of roughly critical composition. By agitating the prism at a temperature above the critical point (where the components are entirely miscible) a certain gradient of composition was obtained, the liquid at the bottom being richer in the denser component than at the top.

The prism was then lowered into the thermostat [3], which was set just above the critical temperature. When the thermostat was then regulated to temperatures just below the critical, two phases developed. Both these phases will have constant composition as indicated by vertical lines on the diagram. When now the thermostat was again raised to a temperature above the critical, a diffusion commenced at the former surface between the two phases. The vertical composition lines on the diagram will thereby be connected by a sigmoid curve. Fig. 1 shows in principle the photographically obtained diagram, while Fig. 2 shows an actual photograph. The inclination of the tangent at the sigmoid curve's inflexion point was determined from the photographs, as were also the compositions of the two phases of constant compositions (C_1 and C_2).

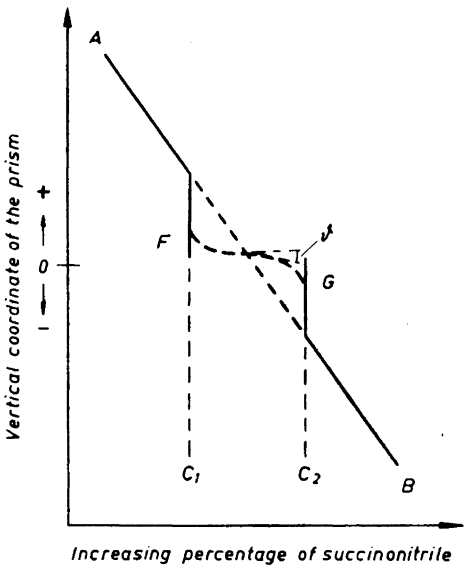


Fig. 1. Schematic drawing of photographically obtained diagram. Line AB shows the composition of the liquid at different levels inside the prism at the beginning of the experiment. The sigmoid curve FG is formed due to the diffusion when the temperature is raised to a selected temperature above the critical.

The composition was calculated to be the following function of the time and of the vertical coordinate z in the prism. z equals zero at the transition between the

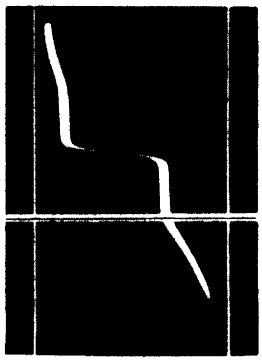


Fig. 2. Photographically obtained diagram. This belongs to a second system now under investigation, *i. e.*, triethylamine water. The straight lines are for orientation of the curve on the photographic plate, and are horizontal and vertical. The distance between the two vertical lines corresponds to a difference in refractive index of the sample of about 0.015. The total length of the curve corresponds to 17 mm vertically in the prism.

two phases, and the time t equals zero at the beginning of the diffusion. D is the diffusion constant to be determined.

$$C = \frac{C_2-C_1}{\sqrt{\pi}} \int_0^{z/2\sqrt{Dt}} e^{-x^2}\,dx + \tfrac{1}{2}(C_2-C_1)$$

This gives for $z = 0$ $\frac{\partial C(0)}{\partial z} = \frac{C_2-C_1}{2\sqrt{\pi Dt}}$ (1)

On the photographs we regard Z as ordinate, k_v as vertical magnification, X as abscissa, and k_h as horizontal proportional factor. Linearity was previously found to exist between the refractive index and X. Assuming linearity between the composition and the refractive index, we then get:

$$\frac{\partial c}{\partial z} = \frac{k_v}{k_h} \qquad \lim \frac{\delta X}{\delta Z} = \frac{k_v}{k_h}\,\frac{1}{\mathrm{tg}\vartheta}$$

On the other hand, when we assume that

$$C_2-C_1 = \frac{\Delta X}{k_h}, \text{ eqn. 1. gives } \frac{k_v}{\mathrm{tg}\vartheta} = \frac{\Delta X}{2\sqrt{\pi Dt}}$$

from which it will be seen that $\mathrm{tg}\vartheta$ is a function of time of the type: $\mathrm{tg}\vartheta = bt$

$$\text{This gives } D = \frac{k_v^2 \cdot b^2}{4\pi}\,\Delta X^2$$

From a series of photographs $\mathrm{tg}\vartheta$ was measured as a function of time and the factor b determined by the method of least squares.

The method employed presupposes equal diffusion constants for all compositions in the range between C_1 and C_2. The results seem to indicate that the presupposition is reasonably correct. In fact, when carrying out the measurements the difference between C_1 and C_2 has been kept rather on the low side (less than 5 %) and the compositions between C_1 and C_2 correspond to the very flat top of the coexistence curve.

The method requires the concentrations C_1 and C_2 to be constant during the individual series at the selected temperatures. The series had therefore to be terminated when the vertical lines C_1 and C_2 were disturbed due to diffusion. Actually the individual series has to be broken long before the vertical lines C_1 and C_2 on the photograph seem visually to be destroyed.

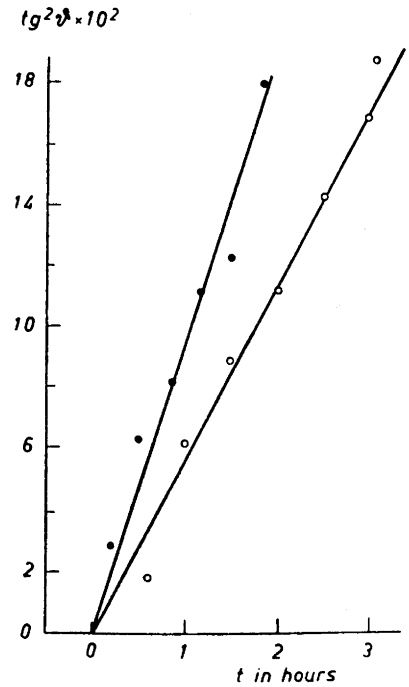


Fig. 3. $\mathrm{tg}^2\vartheta$ as function of time, for the two representative series 0.070° above Tc, C_1-C_2 = 4.6 % (solid dots) and 0.036° above Tc, C_1-C_2 = 4.9 % (open circles).

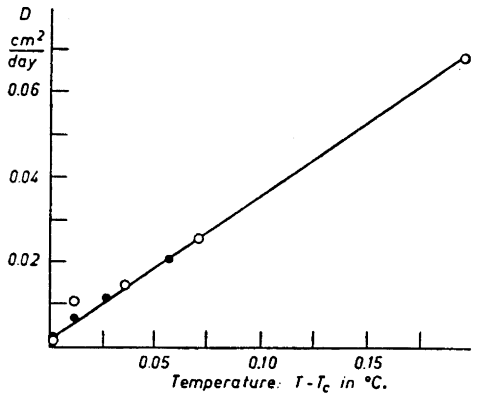


Fig. 4. Diffusion constant as function of temperature. The solid dots and the open circles belong to two different series. The deviation of the one open circle may be due to the thermostat working imperfectly.

In Fig. 4 the diffusion constants are plotted against the temperature distance from the critical point. The points belong to two different series with different prisms and samples used for filling up the prisms. Minor impurities in the samples are certainly different in the two series. Moreover, certain reactions seem to take place inside the prism. This is shown by the fact that the critical temperature has not been constant the whole time, but has decreased from day to day so that it had to be checked at all individual diffusion measurements at the selected temperatures.

In Fig. 4 the diffusion constant does not extrapolate exactly to zero at the critical temperature. However, no conclusions can be drawn from this, especially as the exact determination of the critical temperature has been a difficult undertaking, and the temperature regarded as critical may have been one or two millidegrees below the actual temperature.

The diffusion constant seems to approach zero by lowering the temperature down to the critical by 0.37 cm^2 per day and °C.

Thanks are extended to Professor Joseph E. Mayer of the University of Chicago and Dr. Bruno H. Zimm of General Electric Company, Schenectady, for valuable personal conferences, and to Cand. real O. Øgrim for his assistance with the calculations of the optical system.

Throughout the whole period of the investigations the encouragement and interest shown by Professor O. Hassel of the University of Oslo has been of inestimable value.

1. Svensson, H. and Forsberg, R. *J. Opt. Soc. Amer.* **44** (1954) 414.
2. Lorentzen, H. L. *Acta Chem. Scand.* **9** (1955) 1724.
3. Lorentzen, H. L. *Acta Chem. Scand.* **7** (1953) 1335.

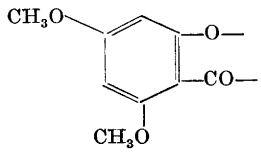
Received March 7, 1957.

The Ultraviolet Absorption Spectra of Some Aroyl Compounds Derived from Phloroglucinol

CARL ENEBÄCK

Department of Chemistry, Institute of Technology, Helsingfors, Finland

The electronic absorption spectra of 2-hydroxy-4,6-dimethoxybenzaldehyde (Fig, 1; max. 294 mμ, log ε = 4.31; infl. 330 mμ, log ε = 3.58), 2-hydroxy-4,6-dimethoxyacetophenone (Fig. 2; max. 288 mμ. log ε = 4.24; infl. 320 mμ, log ε = 3.60) and 2-hydroxy-ω,4,6-trimethoxyacetophenone (Fig. 3; max. 288 mμ, log ε = 4.31; infl. 323 mμ, log ε = 3.62) in 95 % ethanolic solution show a close resemblance to each other and to the spectra of flavanones [1,2] and 2-benzylcoumaran-3-ones [1] that have the group



in common and are unsubstituted in the isolated phenyl group. It is, therefore, to be concluded that this type of spectrum represents the absorptional properties of the aroyl group in question when coplanar or nearly coplanar.

Methylation of the two acetophenones mentioned leads to a quite different type

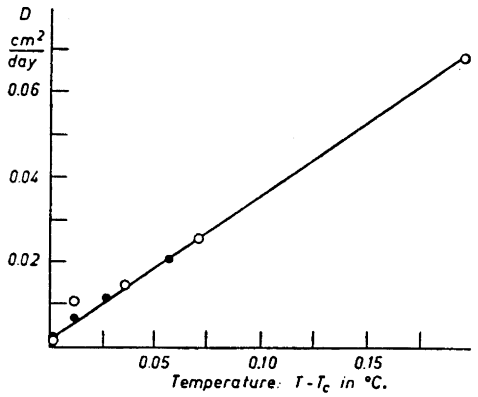


Fig. 4. Diffusion constant as function of temperature. The solid dots and the open circles belong to two different series. The deviation of the one open circle may be due to the thermostat working imperfectly.

In Fig. 4 the diffusion constants are plotted against the temperature distance from the critical point. The points belong to two different series with different prisms and samples used for filling up the prisms. Minor impurities in the samples are certainly different in the two series. Moreover, certain reactions seem to take place inside the prism. This is shown by the fact that the critical temperature has not been constant the whole time, but has decreased from day to day so that it had to be checked at all individual diffusion measurements at the selected temperatures.

In Fig. 4 the diffusion constant does not extrapolate exactly to zero at the critical temperature. However, no conclusions can be drawn from this, especially as the exact determination of the critical temperature has been a difficult undertaking, and the temperature regarded as critical may have been one or two millidegrees below the actual temperature.

The diffusion constant seems to approach zero by lowering the temperature down to the critical by 0.37 cm^2 per day and °C.

Thanks are extended to Professor Joseph E. Mayer of the University of Chicago and Dr. Bruno H. Zimm of General Electric Company, Schenectady, for valuable personal conferences, and to Cand. real O. Øgrim for his assistance with the calculations of the optical system.

Throughout the whole period of the investigations the encouragement and interest shown by Professor O. Hassel of the University of Oslo has been of inestimable value.

1. Svensson, H. and Forsberg, R. *J. Opt. Soc. Amer.* **44** (1954) 414.
2. Lorentzen, H. L. *Acta Chem. Scand.* **9** (1955) 1724.
3. Lorentzen, H. L. *Acta Chem. Scand.* **7** (1953) 1335.

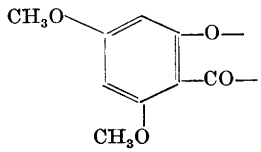
Received March 7, 1957.

The Ultraviolet Absorption Spectra of Some Aroyl Compounds Derived from Phloroglucinol

CARL ENEBÄCK

Department of Chemistry, Institute of Technology, Helsingfors, Finland

The electronic absorption spectra of 2-hydroxy-4,6-dimethoxybenzaldehyde (Fig, 1; max. 294 mμ, log ε = 4.31; infl. 330 mμ, log ε = 3.58), 2-hydroxy-4,6-dimethoxyacetophenone (Fig. 2; max. 288 mμ. log ε = 4.24; infl. 320 mμ, log ε = 3.60) and 2-hydroxy-ω,4,6-trimethoxyacetophenone (Fig. 3; max. 288 mμ, log ε = 4.31; infl. 323 mμ, log ε = 3.62) in 95 % ethanolic solution show a close resemblance to each other and to the spectra of flavanones [1,2] and 2-benzylcoumaran-3-ones [1] that have the group



in common and are unsubstituted in the isolated phenyl group. It is, therefore, to be concluded that this type of spectrum represents the absorptional properties of the aroyl group in question when coplanar or nearly coplanar.

Methylation of the two acetophenones mentioned leads to a quite different type

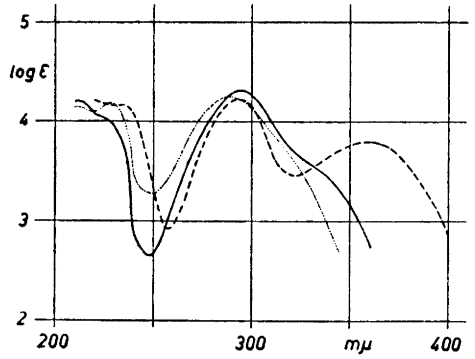


Fig. 1. ———— 2-hydroxy-4,6-dimethoxybenzaldehyde in 95 % ethanol. — — — — 2-hydroxy-4,6-dimethoxybenzaldehyde in 0.05 N NaOH in 48 % aqueous ethanol. ····· 2,4,6-trimethoxybenzaldehyde in 95 % ethanol.

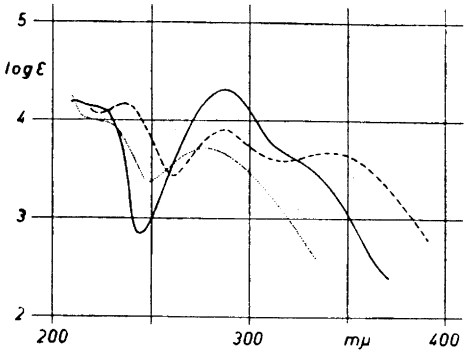


Fig. 3. ———— 2-hydroxy-ω,4,6-trimethoxyacetophenone in 95 % ethanol. — — — — 2-hydroxy-ω,4,6-trimethoxyacetophenone in 0.05 N NaOH in 48 % aqueous ethanol. ····· ω,2,4,6-tetramethoxyacetophenone in 95 % ethanol.

of spectra, characterised by much lower overall molar extinction, especially at longer wave-lengths. Cram and Cranz [3] already have observed this effect of two *o*-methoxyl groups in the case of the dimethyl ethers of 2,6-dihydroxyacetophenone and 2,6-dihydroxy-3-methylacetophenone. 2,4,6-Trimethoxyacetophenone (Fig. 2) has a maximum at 274 mμ, log $\varepsilon = 3.76$ and ω,2,4,6-tetramethoxyacetophenone (Fig. 3) a maximum at 278 mμ, log $\varepsilon = 3.72$. It cannot be seen from the spectra whether such a maximum results from two bands which presumably would correspond to the most intense band and the inflexion in the parent 2-hydroxy compound.

2,4,6-Trimethoxybenzaldehyde (Fig. 1), in contrast to the corresponding acetophenones, exhibits but a slightly lower molar extinction in the main band (max. 289 mμ, log $\varepsilon = 4.25$) compared with the parent 2-hydroxy compound. Again, the inflexion in the latter becomes less pronounced by methylation.

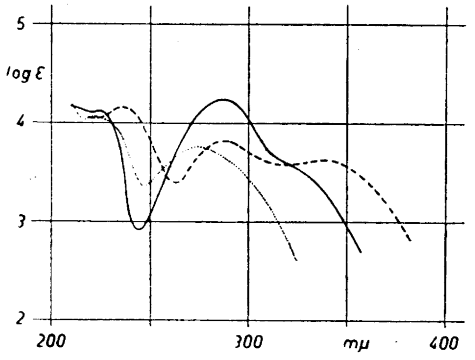


Fig. 2. ———— 2-hydroxy-4,6-dimethoxyacetophenone in 95 % ethanol. — — — — 2-hydroxy-4,6-dimethoxyacetophenone in 0.05 N NaOH in 48 % aqueous ethanol. ····· 2,4,6-trimethoxyacetophenone in 95 % ethanol.

The reduction of the *K*-band intensity due to steric hindrance of coplanarity in aroyl compounds with one or two ortho-methyl groups has been studied by Braude and Sondheimer [4]. They deduced a quantitative relation between the band intensity and the mean angle between the planes of the benzene nucleus and the acyl group in the ground electronic state of the molecule. The mean angles are smaller in the substituted benzaldehydes than in the acetophenones, as, beside the mere steric interaction between the carbonyl oxygen and an *o*-methyl group in the former, an overlap of an *o*-methyl group and the acetyl-methyl group is possible in the latter. This overlap, in addition, provides a much stronger hindrance to coplanarity than does the overlap of the carbonyl and *o*-methyl groups.

The low absorption intensities of the acetophenones with two *o*-methoxyl groups can be conveniently explained by the hindrance to coplanarity of the aroyl group mainly produced by the steric interaction of either of the *o*-

groups and the group forming the second link of the side carbon chain. In this respect, the effect of *o*-methoxyl resembles that of *o*-methyl groups. A hindrance to coplanarity by a steric interaction between the carbonyl oxygen and one *o*-methoxyl group is not evident from the intensity data, since the spectra of 2-methoxyacetophenone, 2-methoxybenzaldehyde, their parent hydroxy compounds, flavanone and 2-benzylcoumaran-3-one, are all very like each other [5,1]. In fact, slightly *higher* molar extinctions of the most intense bands are reported for the two mentioned methoxy compounds, of which 2-methoxyacetophenone shows rather marked hypsochromic shifts when compared with 2-hydroxyacetophenone: 5.5 mμ for the most intense band and 22 mμ for the band at the longer wave-length [5]. On the other hand, the slight reduction in the absorption intensity, which follows the methylation of 2-hydroxy-4,6-dimethoxybenzaldehyde, might be noted.

A steric interaction of the carbonyl group forming the second link of the carbon chain in 1-(2,4,6-trimethoxyphenyl)-3-phenylpropane-1,2-dione with either of the *o*-methoxyl groups possibly contributes to its somewhat individualistic spectral behaviour [1].

From the spectra in 0.05 N sodium hydroxide/48 % aqueous ethanol solution of 2-hydroxy-4,6-dimethoxybenzaldehyde (Fig. 1; max. 294 mμ, log ε = 4.21; max. 359 mμ, log ε = 3.79), 2-hydroxy-4,6-dimethoxyacetophenone (Fig. 2; max. 288 mμ, log ε = 3.82; max. 338 mμ, log ε = 3.62) and 2-hydroxy-ω,4,6-trimethoxyacetophenone (Fig. 3; max. 288 mμ, log ε = 3.90; max. 342 mμ, log ε = 3.67) it is seen that the phenolate ions of both acetophenone derivatives absorb much less intensely than the anion of 2-hydroxy-4,6-dimethoxybenzaldehyde. The overlap of the second chain link and either of two *o*-oxygen atoms thus seems to hinder coplanarity when the possibility of chelate ring formation is eliminated.

Experimental: 2-Hydroxy-4,6-dimethoxybenzaldehyde, m.p. 70.5° (71° reported [6]), was prepared by demethylation of 2 g of *2,4,6-trimethoxybenzaldehyde*, m.p. 120° (see acknowledgement) with aluminium bromide (1.05 moles) in benzene solution. It was purified by repeated recrystallisations from aqueous methanol and, finally, by sublimation under vacuum.

2-Hydroxy-4,6-dimethoxyacetophenone, m. p; 82° (various values from 80° to 88° reported. 83°, Ref.[7]) and *2-hydroxy-ω,4,6-trimethoxyacetophenone*, m. p. 104° (103—104° reported) were prepared by the procedure described for the latter compound [8]. They were purified by repeated recrystallisations from methanol and ethanol, respectively, and, finally, by sublimation under vacuum.

2,4,6-Trimethoxyacetophenone, m. p. 101.5° (102—103° reported [9]) was obtained by methylation of phloroacetophenone (2 g) in 30 ml of acetone with dimethyl sulphate (3.5 moles) and potassium carbonate. It was purified by washing the ether solution with alkali, recrystallisations from methanol-ethanol, and final sublimation under vacuum.

ω,2,4,6-Tetramethoxyacetophenone, m. p. 56.5°—57° [1], was purified by washing with alkali, repeated recrystallisation from ether and sublimation under vacuum.

The spectra were determined with a Beckman DU spectrophotometer from solutions of the sublimed compounds in concentrations of 10 to 20 mg/l. All determinations were carried out immediately after the dissolution. The measurement of 2-hydroxy-4,6-dimethoxybenzaldehyde in 0.05 N NaOH/48 % ethanol was repeated after 2 h and those of both aldehydes in neutral ethanol after 7 days, but the spectra were unchanged.

The author wishes to thank Mr. Kaj Silander, M. Sc., for the specimen of 2,4,6-trimethoxybenzaldehyde.

1. Enebäck, C. and Gripenberg, J. *Acta Chem Scand.* **11** (1957) 866.
2. Lindstedt, G. *Acta Chem. Scand.* **4** (1950) 772.
3. Cram, D. J. and Cranz, F. W. *J. Am. Chem. Soc.* **72** (1950) 595.
4. Braude, E. A. and Sondheimer, F. *J. Chem. Soc.* **1955** 3754.
5. Morton, R. A. and Stubbs, A. L. *J. Chem. Soc.* **1940** 1347.
6. Karrer, P., Lichtenstein, N. and Helfenstein, A. *Helv. Chim. Acta* **12** (1929) 991.
7. Sonn, A. and Buelow, W. *Ber.* **58** (1925) 1694.
8. Row, L. R. and Seshadri, T. R. *Proc. Indian Acad. Sci.* **23A**, 23; *Chem. Abstr.* **40** (1946) 5050.
9. Rennie, E. H., Cooke, W. T. and Finlayson, H. H. *J. Chem. Soc.* **117** (1920) 345.

Received March 26, 1957.

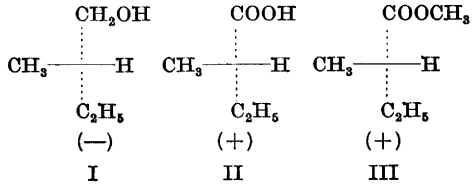
*iso*Thiocyanates XXVII *. The Absolute Configuration of Optically Active 2-Butylamine and 2-Butyl *iso*Thiocyanate

ANDERS KJÆR and SVEND ERIK HANSEN

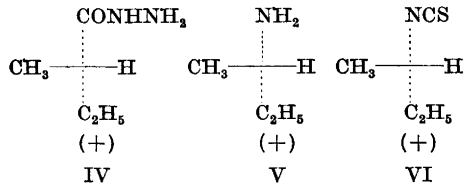
Chemical Laboratory of the University of Copenhagen, Denmark

The isolation from natural sources of 2-butyl *iso*thiocyanate was effected by Hofmann [1] in 1874. Gadamer [2] later established the glycosidic origin and dextrorotatory character of the mustard oil and accomplished its synthesis from (+)-2-butylamine. The configuration of the latter, relative to glyceraldehyde, can be inferred from the kinetically controlled interconversions of 2-butylamine, 2-butyl halides and 2-butanol established by the Ingold school [3]. Various authors have correlated 2-butanol with glyceraldehyde through lactic acid as a key intermediate (*cf.* Ref.[4]).

In the course of current investigations in this laboratory, it became of interest to correlate optically active 2-butylamine, and hence 2-butyl *iso*thiocyanate, with glyceraldehyde through transformations not involving inversions at the asymmetric centre. This has been achieved in the following way:



I II III



IV V VI

(—)-2-Methylbutanol ('active amyl alcohol') (I) was oxidized to (+)-2-methylbutyric acid (II), and the latter further converted into (+)-methyl 2-methylbutyrate (III) and (+)-2-methylbutyric acid hydrazide (IV). Curtius rearrangement of the corresponding azide, followed by acid hydrolysis of the intermediate urethan, ultimately furnished *dextrorotatory* 2-butylamine (V), characterized as its hydrochloride and benzoyl derivative. Since Jones and Wallis [5] first demonstrated the Curtius rearrangement to take place without racemization, evidence has become abundant that this intramolecular displacement reaction proceeds with full retention of configuration (*cf. e. g.* Ref.[6]).

The above symbols (I)—(VI), represent the absolute configurations on following grounds: (I) has been configuratively related with (—)-glyceraldehyde through a rather circumstantial series of transformations, recently summarized by Crombie and Harper [7]. The assignment has been verified by Freudenberg's ingenious application [8] of dihydroshikimic acid for determining the configuration of (+)-3-methylhexane, which has been correlated with (I) many years ago [9]. The X-ray evidence of Bijvoet *et al.*[10] finally renders established relationship with glyceraldehyde equal to knowledge of the absolute configuration.

Correlation of (I) with C-3 in natural *iso*leucine has been achieved in various ways (*cf. e. g.* Ref.[11]). Hence, natural *iso*leucine and (+)-2-butyl *iso*thiocyanate (VI) belong to the same configurational series. The direct determination of the absolute configuration of the former by means of X-ray crystallography [12] provides an independent confirmation of the above assignments, which may prove useful also for the purpose of establishing the correlation of (+)-2-butyl *iso*thiocyanate with its glucosidic progenitor (glucocochlearin) as suggested by Ettlinger and Lundeen [13].

Experimental. Melting points are uncorrected. Rotations are measured in a 1 dm tube.

(+)-2-Methylbutyric acid (II). An optically active acid, produced by oxidation of essentially pure (—)-2-methylbutanol, served as a starting material for the following syntheses. The acid had the rotation value: $[\alpha]_D^{21}$ +19.6° (neat), D_4^{21} 0.937, somewhat higher than most literature values.

(+)-Methyl 2-methylbutyrate (III). Esterification of the above acid (65 g) with methanol

* Part XXVI of this series: *Acta Chem. Scand.* **11** (1957) *In press.*

(600 ml), and a few drops of sulphuric acid, afforded the methyl ester (44 g) as a colourless liquid, b. p. 115°, n_D^{25} 1.3916, D_4^{22} 0.888, $[\alpha]_D^{22}$ +23.6° (neat), $[\alpha]_D^{21}$ +26.0° (*c* 1.8, MeOH).

Guye [14] reported the value $[\alpha]_D^{22}$ +22.03° for the ester, corrected to supposedly optically pure condition, while von Doering and Aschner [15] listed the value $[\alpha]_D^{27}$ +21.1° (*c* 1.7, MeOH) for a specimen prepared from 2-methylbutyric acid, having $[\alpha]_D^{27}$ +17.75° (neat) and claimed to be 98 % optically pure. The enantiomeric ester, deriving from an acid with $[\alpha]_D^{17}$ —17.35°, was reported by Prelog and Zalán [16] with the rotation value $[\alpha]_D^{15}$ —19.42° (neat).

(+)-2-Methylbutyric acid hydrazide (IV). The methyl ester (30 g) was slowly added to a large excess of boiling 90 % hydrazine hydrate, and the mixture was refluxed for 2 h. On removal of hydrazine *in vacuo*, the crude hydrazide separated (29 g). Three sublimations afforded an analytical specimen as thin, colourless needles, m. p. 96°. $[\alpha]_D^{22}$ +41.3° (*c* 2.6, H_2O). (Found: C 51.80; H 10.54; N 24.24. Calc. for $C_5H_{12}N_2O$: C 51.68; H 10.43; N 24.21).

(+)-2-Butylamine (V). To a stirred solution of the hydrazide (28 g) in 1 N HCl (400 ml), covered with ether and cooled to 0°, was added a concentrated aqueous solution of $NaNO_2$ (22 g). The ether phase was separated, combined with two additional ether extracts, and briefly dried over Na_2SO_4. Anhydrous ethanol (*ca.* 300 ml) was added and the solution was refluxed for 2 h, when the N_2-evolution had completely ceased. A small fraction of the oily urethan, remaining upon removal of the solvents, was refluxed with 20 % HCl for 10 h, when removal of water and acid resulted in separation of the crystalline amine hydrochloride. This was covered with ether and strong alkali was slowly added to liberate the amine. Ether was removed from the carefully dried extract by distillation through a 3-feet helix-packed column, and (+)-2-butylamine distilled as a colourless liquid, b. p. 62.5°, n_D^{25} 1.3853. The rotation value, $[\alpha]_D^{22}$ +6.1° (neat), was measured on a fore-run probably still containing traces of water. Literature values are: $[\alpha]_D^{15.5}$ +6.42° (neat)[2b], $[\alpha]_D^{20}$ +7.44° (neat)[17], and $[\alpha]_D$ +7.4° (*c ca.* 25, H_2O) [18].

The hydrochloride separated from acetone in colourless, hygroscopic needles, m. p. 152—153° (closed tube), $[\alpha]_D^{19}$ —1.05° (*c* 13.3, H_2O) (Found: N 12.47; Cl 32.50. Calc. for $C_4H_{12}ClN$: N 12.78; Cl 32.34). Literature values: $[\alpha]_D^{20}$ —2.05° (*c* 7.3, H_2O)[2b], $[\alpha]_D^{20}$ —1.13° (*c* 14.0, H_2O) [17] and, for the enantiomorphous salt, $[\alpha]_D^{20}$ +0.90° (*c.* 3.7, H_2O) [19].

(+)-N-(2-Methylbutyl)-benzamide. Benzoylation of the above amine, performed under customary Schotten-Baumann conditions, furnished the benzamide, separating from 50 % ethanol in colourless needles, m. p. 97°, $[\alpha]_D^{21}$ +34.9° (*c* 1.1, EtOH) (Found: C 74.60; H 8.40; N 7.82. Calc. for $C_{11}H_{15}NO$: C 74.56; H; 8.54 N 7.91.) Previously reported data: m. p. 92°, $[\alpha]_D^{21}$ +30.7 (*c* 1, EtOH)[19], m. p. 92.0—92.5°, $[\alpha]_D^{25}$ +30.74° (*c* 4, EtOH) [20].

Microanalyses were performed in this laboratory by Mr. P. Hansen. The optically active 2-methylbutyric acid was generously supplied by Dr. A. Klit. The work is part of investigations supported by *The Danish State Research Foundation* and *The Carlsberg Foundation*. A special grant from *Kai Hansen's Fond* is gratefully acknowledged.

1. Hofmann, A. W. *Ber.* **7** (1874) 508.
2. Gadamer, J. *Arch. Pharm.* (a) **237** (1899) 92, (b) **239** (1901) 283.
3. Brewster, P., Hiron, F., Hughes, E. D., Ingold, C. K. and Rao, P. A. D. S. *Nature* **166** (1950) 179.
4. Wiberg, K. B. *J. Am. Chem. Soc.* **74** (1952) 3891.
5. Jones, L. W. and Wallis, E. S. *J. Am. Chem. Soc.* **48** (1926) 169.
6. Newman, M. S. (Ed.) *Steric Effects in Organic Chemistry*, J. Wiley & Sons, Inc., New York 1956, p. 251.
7. Crombie, L. and Harper, S. H. *J. Chem. Soc.* **1950** 2685.
8. Freudenberg, K. and Hohmann, W. *Ann.* **584** (1953) 54.
9. Marckwald, W. *Ber.* **37** (1904) 1038.
10. Bijvoet, J. M., Peerdeman, A. F. and van Bommel, A. J. *Nature* **168** (1951) 271.
11. Winitz, M., Birnbaum, S. M. and Greenstein, J. P. *J. Am. Chem. Soc.* **77** (1955) 3106.
12. Trommel, J. and Bijvoet, J. M. *Acta Cryst.* **7** (1954) 703.
13. Ettlinger, M. G. and Lundeen, A. J. *J. Am. Chem. Soc.* **78** (1956) 4172.
14. Guye, P. A. *Bull. soc. chim. France* [3] **25** (1901) 544.
15. von E. Doering, W. and Aschner, T. C. *J. Am. Chem. Soc.* **75** (1953) 393.
16. Prelog, V. and Zalan, E. *Helv. Chim. Acta* **27** (1944) 545.
17. Thomé, L. G. *Ber.* **36** (1903) 582.

18. Fleury-Larsonneau, A. *Bull. soc. chim. France* [5] **6** (1939) 1576.
19. Pope, W. J. and Gibson, C. S. *J. Chem. Soc.* **101** (1912) 1702.
20. Leonard, N. J. and Nommensen, E. W. *J. Am. Chem. Soc.* **71** (1949) 2808.

Received May 13, 1957.

The Incorporation of $^{14}CO_2$-carbon into the Glycogen of *Escherichia coli* B

HANS PALMSTIERNA and RUNE STJERNHOLM*

Bacteriological Dept., Karolinska Institutet, Stockholm, Sweden, and Department of Biochemistry, School of Medicine, Western Reserve University, Cleveland 6, Ohio, U.S.A.

Under resting cell conditions *Escherichia coli* B ferments Na-lactate and accumulates a polysaccharide of glycogen-like nature. If aerated with a mixture of air and $^{14}CO_2$ in a 9:1 ratio (v/v) respectively, isotope is incorporated into the glucose units. A detailed description of the experimental conditions has been published previously [1]. A preliminary analysis by means of a bacterial degradation with *Lactobacillus casei* indicated that 95 % of the isotope was located in the 3 and 4 positions of the glucose molecule. However, the method of degradation did not permit differentiation of the individual carbon atoms in the glucose molecule. It is the purpose of this report to show the exact isotopic distribution pattern, since the value of this method for the preparation of glucose-3,4—^{14}C, rests upon an equal labeling of the 3 and 4 carbon atoms. In the standardized method the cells were allowed to ferment Na-lactate in the presence of $^{14}CO_2$ for 60 min. The glycogen was isolated by the usual alkaline hydrolysis method. Depolymerisation was accomplished by hydrolysis in 0.6 N HCl and the glucose thus obtained was purified by passing through Dowex 50 in the H^+-form and Dowex 2 in the acetate form. The ion exchangers must be used in the order mentioned. The glucose was further purified by chromatography according to Gardell [2]. The sugar was finally subjected to a bacterial degradation by means of *Leuconostoc mesenteroides*, which allows a complete separation of all C-atoms in the glucose molecule [3]. Carbon 1 is split off as carbon dioxide, carbon atoms 2 and 3 appear as ethanol, and carbons 4, 5 and 6 as lactic acid. Ethanol and lactic acid were chemically degraded by conventional methods. All samples were counted as CO_2 in a proportional gas counter [4].

The following specific activities for the different carbon atoms were found:

C-atom	c/min/mmole C
1	600
2	200
3	15 600
4	15 000
5	140
6	80

Total oxidation of glucose by the van Slyke combustion method gave 33 700 c/min/mole glucose. The counting accuracy was ± 2 % for the carbons 3 and 4, and ± 15 % for the other carbons. The activities were thus fairly evenly distributed in the 3 and 4 positions. Furthermore very little of the activity was found in the other carbon atoms.

The method described previously [1], thus provides a simple method of preparation of glucose-3,4-^{14}C.

1. Palmstierna, H. and Ehrensvärd, G. *Acta Chem. Scand.* **10** (1956) 691.
2. Gardell, S. *Acta Chem. Scand.* **7** (1953) 201.
3. Bernstein, I. A., Lentz, L., Malm, M., Schambye, P. and Wood, H. G. *J. Biol. Chem.* **215** (1955) 137.
4. Bernstein, W. and Ballentine, R. *Rev. Sci. Instr.* **21** (1950) 158.

Received May 13, 1957.

* Du Pont Predoctoral Fellow 1956—1957.

The Base Strength of Hydrazoic Acid

THOR A. BAK and EIGIL L. PRÆSTGAARD

Universitetets Fysisk-Kemiske Institut, Copenhagen, Denmark

In his early work on the base strength of nitrogen compounds Hantzsch [1] investigated the cryoscopic behaviour of hydrazoic acid in concentrated sulfuric acid. From his measurements he concluded that in 100 % H_2SO_4 hydrazoic acid takes up three protons to form $H_4N_3^{+++}$. (Strictly speaking he stated that the salt $N_3H_4(HSO_4)_3$ is formed.)

Recalculation of Hantzsch's data shows that at most two protons are taken up. Using the value [2] −10.6 for Hammett's acidity function H_0 for 100 % H_2SO_4 we can from Hantzsch's data estimate the dissociation-constant for the acid $H_3N_3^{++}$. We get $pK = -10.1$, but this value should undoubtedly be taken with some reservation.

Since it is of importance to know the base strength of hydrazoic acid in order to study the mechanism of, *e. g.*, the Schmidt reaction [3,4] we have determined the dissociation constant for the acid $H_2N_3^+$ at 25.0°C by the following simple technique. HN_3 was equilibrated between a sulfuric acid phase and a chloroform phase, and the concentrations of HN_3 and $H_2N_3^+$ in the two phases were determined cerimetrically [5].

We use the symbols

$[HN_3]s$	concentration of HN_3 in the sulfuric acid phase
$[H_2N_3^+]s$	concentration of $H_2N_3^+$ in the sulfuric acid phase
$[HN_3]c$	concentration of HN_3 in the chloroform phase

The concentration of $H_2N_3^+$ in the chloroform phase is neglected. We also neglect the concentration of the ion $H_3N_3^{++}$ in both phases. The justification for this lies in the experimental data given below.

Defining two distribution constants:

$$f = \frac{[HN_3]s + [H_2N_3^+]s}{[HN_3]c}$$

$$n = \frac{[HN_3]s}{[HN_3]c}$$

we have, as a simple consequence of the definition [6] of H_0:

$$pK = H_0 + \log\left(\frac{f}{n} - 1\right). \qquad (1)$$

pK is the negative logarithm of the dissociation constant of the acid $H_2N_3^+$.

Since we neglect the concentration of $H_3N_3^{++}$ the distribution-constant f can be determined directly and proves to be constant over the range 25−40 % H_2SO_4. We conclude therefore that in this range $f = n$. The value of n is (accidentally) equal to one, $n = 1.00 \pm 0.04$.

Assuming that n will be constant equal to one also for higher sulfuric acid concentrations we can determine an approximate value of pK from the measurement of f, using eqn. (1). Under this assumption we obtained as an average of six measurements $pK = -6.21$ (see Table 1).

Table 1.

% H_2SO_4	H_0	f	pK
77.96	—6.55	3.22	—6.20
78.12	—6.57	4.22	—6.07
78.54	—6.64	3.84	—6.19
81.20	—7.04	6.66	—6.29
83.76	—7.44	15.80	—6.27
84.56	—7.54	19.95	—6.26

f is the distribution constant for hydrazoic acid between sulfuric acid and chloroform.

This approach is of course somewhat unsatisfactory, since we only know that n is constant over the range 25−40 % H_2SO_4. We therefore proceded to treat n, for higher sulfuric acid concentration, as an unknown, constant only over a small range in H_0.

Using the first four measurements for which H_0 is practically constant we determined the value of n by requiring that the mean square deviation of pK, regarded as a function of n, be minimum. This gives a value for n slightly below one ($n \sim 0.98$), but the correction in pK introduced in this way is immaterial. The above value for pK is therefore the best estimate of the dissociation constant we can give on basis of this method.

For higher concentrations of sulfuric acid we find unexpectedly small values of f (*e. g.*, $f \sim 85$ for 95 % H_2SO_4), indicating that n decreases rapidly with increasing concentration of sulfuric acid. This effect, which has nothing to do with the basicity

of HN_3, makes the present method unsuitable for studying the dissociation constant of, *e. g.*, $H_3N_3^{++}$. Similar effects have recently been reported by Deno and Perizzolo [7].

We thank Professor J. A. Christiansen for his interest in this investigation, and E. L. P. gratefully acknowledges financial support from *Carlsbergfondet.*

1. Hantzsch, A. *Ber.* **63 B** (1930) 1782.
2. Deno, N. C. and Taft Jr., R. W. *J. Am. Chem. Soc.* **76** (1954) 244.
3. Schmidt, K. F. *Ber.* **57 B** (1924) 704.
4. Bak, T. A. *Acta Chem. Scand.* **8** (1954) 1733.
5. Martin, J. *J. Am. Chem. Soc.* **49** (1927) 2133.
6. See for instance Hammett, L. P. *Physical Organic Chemistry.* New York 1940.
7. Deno, N. C. and Perizzolo, C. *J. Am. Chem. Soc.* **79** (1957) 1345.

Received May 13, 1957.

The Chemistry of the Natural Order Cupressales

XIX *. The Occurrence of Manool in *Cupressus sempervirens* L.

C. ENZELL and H. ERDTMAN

Organisk-kemiska Institutionen, Kungl. Tekniska Högskolan, Stockholm, Sweden

During routine examinations of the heartwood extractives of the conifers belonging to the genera *Cupressus* and *Chamaecyparis*, the heartwood of the Mediterranean cypress *Cupressus sempervirens* has been subjected to a brief study. Like Di Modica and Rossi [1] we have found that the main neutral constituents are carvacrol methyl ether and cedrol. The high boiling material, rather surprisingly gave manool [2](I). This diterpene alcohol is characteristic of a section of the genus *Dacrydium*, N. O. Podocarpales, and this is the first time it has been found in another genus of the conifers. Minor neutral constituents of the wood extractives are *d*-borneol, *d*-bornyl acetate and sesquiterpenes. From the acid material carvacrol, β-thujaplicin and nootkatin were isolated.

Experimental. Melting points were taken on the Koflerblock. Only upper limits of b.p. range of the fractions are given.

Finely divided heartwood (4.8 kg, from Le Lavandou, Provence, S. France) was extracted with acetone for 48 h. The acetone was removed and the residue poured, with vigorous stirring, into a tenfold volume of ether, which was filtered, concentrated and similarly poured into light petroleum. The filtered solution was successively shaken with 5 % aqueous potassium hydroxide, 10 % ethanolic potassium hydroxide and water. The alkaline fractions were combined, washed with light petroleum, acidified and extracted with light petroleum. The combined neutral solutions and the acid solution were dried (Na_2SO_4) and the solvent evaporated. The neutral fraction yielded 276 g (5.8 %) of a slightly coloured oil (N) and the acid fraction 20.4 g (0.4 %) of a yellow brown oil (A).

The neutral oil, N, (166 g) was fractionally distilled through a vacuum jacketed, packed column. Pressure 26 mm. Back pressure 10 mm. Fraction N_1, b. p. up to 104°, 1.9 g; N_2, 109°, 11.4 g; N_3, 110°, 70.0 g; N_4, 140°, 16.6 g; N_5, 162°, 9.6 g; N_6, 172°, 15.2 g; N_7, 178°, 2.1 g; N_8 (at lower pressure), 5.0 g. The remainder, after a simple distillation at lower pressure, yielded a distillate N_9 (31.9 g) and a residue (2.3 g, discarded).

Fractions N_{1-2} deposited a solid (2.5 g) which was recrystallized from ligroin and from nitromethane and sublimed. M. p. and mixed m. p. with *d*-borneol 204—207° (sealed tube, uncorr.), $[\alpha]_D^{22}$ +36.5° ($CHCl_3$; *c* 1.7).

Judging from the distillation curve the non-crystalline part of N_2 and fraction N_3 (total 79 g) contained the same compound, namely carvacrol methylether. Demethylation with HBr followed by etherification with chloroacetic acid yielded carvacroxy acetic acid, m. p. and mixed m. p. 150—152°. Fraction N_4 and the non-crystalline part of N_5 (see below) were combined (23.7 g) and distilled through a spinning band column. Pressure 26 mm.

Fraction N_{41}, b. p. up to 118°, 3.24 g, $[\alpha]_D^{22}$ +6.6°, n_D^{21} 1.4973; N_{42}, 120°, 3.59 g, +18.0°, 1.4882; N_{43}, 120°, 3.03 g, +29.5°, 1.4716; N_{44}, 128°, 2.31 g, +18.3°, 1.4800; N_{45}, 142°, 2.16 g, —7.7°, 1.4968; N_{46}, 144°, 2.96 g, —17.8°, 1.5003; N_{47}, 156°, 1.17 g, —22.8°, 1.5029; N_{48}, 173°, 2.76 g, —17.8°, 1.5071; N_{49}, tailings/10 mm 1.31 g, +8.5°; Residue 1.25 g.

* Part XVIII *Acta Chem. Scand.* **11** (1957) *In press.*

of HN_3, makes the present method unsuitable for studying the dissociation constant of, *e. g.*, $H_3N_3^{++}$. Similar effects have recently been reported by Deno and Perizzolo [7].

We thank Professor J. A. Christiansen for his interest in this investigation, and E. L. P. gratefully acknowledges financial support from *Carlsbergfondet.*

1. Hantzsch, A. *Ber.* **63 B** (1930) 1782.
2. Deno, N. C. and Taft Jr., R. W. *J. Am. Chem. Soc.* **76** (1954) 244.
3. Schmidt, K. F. *Ber.* **57 B** (1924) 704.
4. Bak, T. A. *Acta Chem. Scand.* **8** (1954) 1733.
5. Martin, J. *J. Am. Chem. Soc.* **49** (1927) 2133.
6. See for instance Hammett, L. P. *Physical Organic Chemistry.* New York 1940.
7. Deno, N. C. and Perizzolo, C. *J. Am. Chem. Soc.* **79** (1957) 1345.

Received May 13, 1957.

The Chemistry of the Natural Order Cupressales

XIX *. The Occurrence of Manool in *Cupressus sempervirens* L.

C. ENZELL and H. ERDTMAN

Organisk-kemiska Institutionen, Kungl. Tekniska Högskolan, Stockholm, Sweden

During routine examinations of the heartwood extractives of the conifers belonging to the genera *Cupressus* and *Chamaecyparis*, the heartwood of the Mediterranean cypress *Cupressus sempervirens* has been subjected to a brief study. Like Di Modica and Rossi [1] we have found that the main neutral constituents are carvacrol methyl ether and cedrol. The high boiling material, rather surprisingly gave manool [2](I). This diterpene alcohol is characteristic of a section of the genus *Dacrydium*, N. O. Podocarpales, and this is the first time it has been found in another genus of the conifers. Minor neutral constituents of the wood extractives are *d*-borneol, *d*-bornyl acetate and sesquiterpenes. From the acid material carvacrol, β-thujaplicin and nootkatin were isolated.

Experimental. Melting points were taken on the Koflerblock. Only upper limits of b.p. range of the fractions are given.

Finely divided heartwood (4.8 kg, from Le Lavandou, Provence, S. France) was extracted with acetone for 48 h. The acetone was removed and the residue poured, with vigorous stirring, into a tenfold volume of ether, which was filtered, concentrated and similarly poured into light petroleum. The filtered solution was successively shaken with 5 % aqueous potassium hydroxide, 10 % ethanolic potassium hydroxide and water. The alkaline fractions were combined, washed with light petroleum, acidified and extracted with light petroleum. The combined neutral solutions and the acid solution were dried (Na_2SO_4) and the solvent evaporated. The neutral fraction yielded 276 g (5.8 %) of a slightly coloured oil (N) and the acid fraction 20.4 g (0.4 %) of a yellow brown oil (A).

The neutral oil, N, (166 g) was fractionally distilled through a vacuum jacketed, packed column. Pressure 26 mm. Back pressure 10 mm. Fraction N_1, b. p. up to 104°, 1.9 g; N_2, 109°, 11.4 g; N_3, 110°, 70.0 g; N_4, 140°, 16.6 g; N_5, 162°, 9.6 g; N_6, 172°, 15.2 g; N_7, 178°, 2.1 g; N_8 (at lower pressure), 5.0 g. The remainder, after a simple distillation at lower pressure, yielded a distillate N_9 (31.9 g) and a residue (2.3 g, discarded).

Fractions N_{1-2} deposited a solid (2.5 g) which was recrystallized from ligroin and from nitromethane and sublimed. M. p. and mixed m. p. with *d*-borneol 204—207° (sealed tube, uncorr.), $[\alpha]_D^{22}$ +36.5° ($CHCl_3$; *c* 1.7).

Judging from the distillation curve the non-crystalline part of N_2 and fraction N_3 (total 79 g) contained the same compound, namely carvacrol methylether. Demethylation with HBr followed by etherification with chloroacetic acid yielded carvacroxy acetic acid, m. p. and mixed m. p. 150—152°. Fraction N_4 and the non-crystalline part of N_5 (see below) were combined (23.7 g) and distilled through a spinning band column. Pressure 26 mm.

Fraction N_{41}, b. p. up to 118°, 3.24 g, $[\alpha]_D^{22}$ +6.6°, n_D^{21} 1.4973; N_{42}, 120°, 3.59 g, +18.0°, 1.4882; N_{43}, 120°, 3.03 g, +29.5°, 1.4716; N_{44}, 128°, 2.31 g, +18.3°, 1.4800; N_{45}, 142°, 2.16 g, —7.7°, 1.4968; N_{46}, 144°, 2.96 g, —17.8°, 1.5003; N_{47}, 156°, 1.17 g, —22.8°, 1.5029; N_{48}, 173°, 2.76 g, —17.8°, 1.5071; N_{49}, tailings/10 mm 1.31 g, +8.5°; Residue 1.25 g.

* Part XVIII *Acta Chem. Scand.* **11** (1957) *In press.*

For the fractions N_{41-44} the above data, the carbonyl absorption in the I.R. and the odour indicated *d*-bornylacetate. Saponification and back titration showed the presence of 45 % of the ester. *d*-Borneol was easily isolated by chromatography from the hydrolysate. M. p. and mixed m. p. 204—207° (sealed tube, uncorr.) $[\alpha]_D^{22}$ +36.3° ($CHCl_3$, *c* 3.2). Fractions N_{45-48} showed carbon-carbon double bond absorptions in I.R. and the main part behaved chromatographically as a hydrocarbon while N_{49} was fairly pure cedrol. The hydrocarbon, boiling between bornylacetate and cedrol, may therefore possibly be a mixture of cedrenes.

Fractions N_{6-7} and the crystalline material from N_5 were combined (19.9 g), recrystallized from aqueous methanol and sublimed *in vacuo*. M. p. and mixed m. p. with cedrol 87.5—88° $[\alpha]_D^{22}$ +10.0° ($CHCl_3$, *c* 1.1).

Fraction N_9 (31.9 g) was distilled through the spinning band column. Pressure 14 mm.

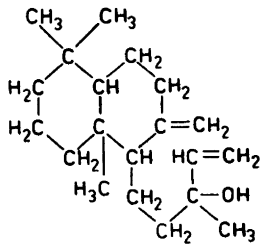
Fraction N_{91}, b. p. up to 110°, 0.45 g, $[\alpha]_D^{22}$ —8.5°, n_D^{21} 1.5029; N_{92}, 184°, 3.61 g, —6.5°, 1.5136; N_{93}, 189°, 2.4 g, +20°, 1.5178; N_{94}, 190°, 3.61 g, +29°, 1.5160; N_{95}, 192°, 3.40 g, +30°, 1.5148; N_{96}, 192°, 2.13 g, +28°, 1.5147; N_{97}, 198°, 2.83 g, +30°, 1.5139; N_{98}, 210°, 1.86 g, +30°, 1.5167; N_{99}, 217°, 1.42 g, +32°, 1.5273; N_{910}, 224°, 0.71 g, +23°, 1.5344; N_{911}, 229°, 2.34 g, +16°, 1.5348; N_{912}, 233°, 0.83 g, +25°, 1.5412; Residue 6.3 g.

Fractions N_{94-97} (12 g or 0.3 %) distilled at fairly constant temperature. Molecular weight determinations (Rast, 289, 292), optical rotation, refractive index and I.R. absorption properties indicated manool. When the thick oily material was seeded with authentic manool it immediately started to crystallise. The solid was recrystallized from light petroleum, m. p. and mixed m. p. 53—53.5°. The infra red absorption spectra were identical.

The acid fraction A on standing deposited nootkatin (0.2 g). The remaining oil was distilled at low pressure yielding 13.9 g volatile material, which was subjected to a fractional distillation in the spinning band column. Pressure 27 mm.

Fraction A_1, b. p. up to 129°, 1.44 g; A_2, 129°, 1.33 g; A_3, 156°, 0.86 g; A_4, 175°, 0.94 g; A_5, 175°, 0.43 g; A_6, 216°, 2.46 g; tailings/13 mm, 1.03 g. Residue 5.7 g. The rotation of all fractions was close to zero.

Fractions A_1 and A_2 according to I. R. data and paper chromatography (in light petroleum, on dimethyl sulphoxide impregnated paper)[3] contained carvacrol and etherification with chloracetic acid gave carvacroxy acetic acid, m. p. and mixed m. p. 150—2°. Fractions A_3 and A_4, according to paper chromatographic results [4] contained β-thujaplicin (0.5 g), which crystallized when seeded with this compound. M. p. and mixed m. p. 51.5—52.0°. The solid fractions A_6 and A_7 were largely nootkatin, identified by paper chromatography [4], m. p. and mixed m. p. 95—96°.



I.

The authors wish to express their gratitude to Prof. O. Jeger, Zürich, and to I. R. Mc Donald, Wellington, for samples of manool, and to *Statens Naturvetenskapliga Forskningsråd* for a grant.

1. Di Modica, G. and Rossi, P. F. *Ann. chim. (Rome)* **45** (1955) 354; **46** (1956) 842.
2. Hosking, J. R. and Brandt, C. W. *Ber.* **68** (1935) 1311.
3. Wickberg, B. *Unpublished method.*
4. Zavarin, E. and Anderson, A. B. *J. Org. Chem.* **21** (1956) 332.

Received May 29, 1957.

Syntheses of Nonan-1,2-diol and Nonan-1,3-diol

GERD BENDZ and MARGARETA KARTH

Chemical Institute, University of Uppsala, Uppsala, Sweden

During the investigation of the structure of some natural products two diols hitherto not prepared *viz.* nonan-1,2-diol and nonan-1,3-diol have been synthesised. The two diols are, when solid, white, odorless and waxy products, soluble in all the common organic solvents. They react with 3,5-dinitrobenzoyl chloride and yield, under mild conditions, mono-dinitroben-

For the fractions N_{41-44} the above data, the carbonyl absorption in the I.R. and the odour indicated *d*-bornylacetate. Saponification and back titration showed the presence of 45 % of the ester. *d*-Borneol was easily isolated by chromatography from the hydrolysate. M. p. and mixed m. p. 204—207° (sealed tube, uncorr.) $[\alpha]_D^{22}$ +36.3° ($CHCl_3$, *c* 3.2). Fractions N_{45-48} showed carbon-carbon double bond absorptions in I.R. and the main part behaved chromatographically as a hydrocarbon while N_{49} was fairly pure cedrol. The hydrocarbon, boiling between bornylacetate and cedrol, may therefore possibly be a mixture of cedrenes.

Fractions N_{6-7} and the crystalline material from N_5 were combined (19.9 g), recrystallized from aqueous methanol and sublimed *in vacuo*. M. p. and mixed m. p. with cedrol 87.5—88° $[\alpha]_D^{22}$ +10.0° ($CHCl_3$, *c* 1.1).

Fraction N_9 (31.9 g) was distilled through the spinning band column. Pressure 14 mm.

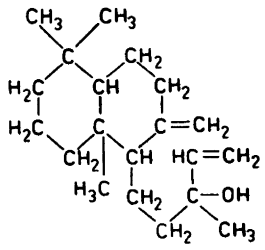
Fraction N_{91}, b. p. up to 110°, 0.45 g, $[\alpha]_D^{22}$ —8.5°, n_D^{21} 1.5029; N_{92}, 184°, 3.61 g, —6.5°, 1.5136; N_{93}, 189°, 2.4 g, +20°, 1.5178; N_{94}, 190°, 3.61 g, +29°, 1.5160; N_{95}, 192°, 3.40 g, +30°, 1.5148; N_{96}, 192°, 2.13 g, +28°, 1.5147; N_{97}, 198°, 2.83 g, +30°, 1.5139; N_{98}, 210°, 1.86 g, +30°, 1.5167; N_{99}, 217°, 1.42 g, +32°, 1.5273; N_{910}, 224°, 0.71 g, +23°, 1.5344; N_{911}, 229°, 2.34 g, +16°, 1.5348; N_{912}, 233°, 0.83 g, +25°, 1.5412; Residue 6.3 g.

Fractions N_{94-97} (12 g or 0.3 %) distilled at fairly constant temperature. Molecular weight determinations (Rast, 289, 292), optical rotation, refractive index and I.R. absorption properties indicated manool. When the thick oily material was seeded with authentic manool it immediately started to crystallise. The solid was recrystallized from light petroleum, m. p. and mixed m. p. 53—53.5°. The infra red absorption spectra were identical.

The acid fraction A on standing deposited nootkatin (0.2 g). The remaining oil was distilled at low pressure yielding 13.9 g volatile material, which was subjected to a fractional distillation in the spinning band column. Pressure 27 mm.

Fraction A_1, b. p. up to 129°, 1.44 g; A_2, 129°, 1.33 g; A_3, 156°, 0.86 g; A_4, 175°, 0.94 g; A_5, 175°, 0.43 g; A_6, 216°, 2.46 g; tailings/13 mm, 1.03 g. Residue 5.7 g. The rotation of all fractions was close to zero.

Fractions A_1 and A_2 according to I. R. data and paper chromatography (in light petroleum, on dimethyl sulphoxide impregnated paper)[3] contained carvacrol and etherification with chloracetic acid gave carvacroxy acetic acid, m. p. and mixed m. p. 150—2°. Fractions A_3 and A_4, according to paper chromatographic results [4] contained β-thujaplicin (0.5 g), which crystallized when seeded with this compound. M. p. and mixed m. p. 51.5—52.0°. The solid fractions A_6 and A_7 were largely nootkatin, identified by paper chromatography [4], m. p. and mixed m. p. 95—96°.



I.

The authors wish to express their gratitude to Prof. O. Jeger, Zürich, and to I. R. Mc Donald, Wellington, for samples of manool, and to *Statens Naturvetenskapliga Forskningsråd* for a grant.

1. Di Modica, G. and Rossi, P. F. *Ann. chim. (Rome)* **45** (1955) 354; **46** (1956) 842.
2. Hosking, J. R. and Brandt, C. W. *Ber.* **68** (1935) 1311.
3. Wickberg, B. *Unpublished method.*
4. Zavarin, E. and Anderson, A. B. *J. Org. Chem.* **21** (1956) 332.

Received May 29, 1957.

Syntheses of Nonan-1,2-diol and Nonan-1,3-diol

GERD BENDZ and MARGARETA KARTH

Chemical Institute, University of Uppsala, Uppsala, Sweden

During the investigation of the structure of some natural products two diols hitherto not prepared *viz.* nonan-1,2-diol and nonan-1,3-diol have been synthesised. The two diols are, when solid, white, odorless and waxy products, soluble in all the common organic solvents. They react with 3,5-dinitrobenzoyl chloride and yield, under mild conditions, mono-dinitroben-

zoates and, under somewhat more rigorous conditions, di-dinitrobenzoates.

A diol with the molecular formula $C_9H_{20}O_2$ was obtained by Anchel [1] on catalytic reduction of the polyacetylene biformin. Later Bohlmann [2] and Bu'Lock [3] mention that biformin is probably nona-4,6,8-triyne-1,2-diol, as its hydrogenation product on oxidation with chromic acid gave octanic acid. Consequently the glycol obtained from biformin ought to be nonan-1,2-diol. According to the figures published there is, however, a small discrepancy as to its melting point compared to that of the glycol now synthesised. Anchel [1] reports that the glycol from biformin, after purification in a sublimation vessel, melted at 40—43°, whereas the synthetic glycol, purified by several sublimations at reduced pressure, melted at 33.5—34°. The derivatives of the glycol from biformin, *viz.* mono-3,5-dinitrobenzoate and the α-naphthylamine addition compound of the di-3,5-dinitrobenzoate melt 6—9° lower than the corresponding derivatives of the nonan-1,2-diol, but these low melting points may depend on the difficulties to purify small amounts of natural products. If the hydrogenation product of biformin really is nonan-1,2-diol the different melting points of the two glycols can either be due to the fact that nonan-1,2-diol can exist in two different modifications as for instance nonan-4,5-diol [4], or that the glycol from biformin is an optical antipode whereas the synthetic one is a racemic compound.

Experimental. Nonan-1,2-diol was prepared by hydroxylation of 1-nonen with performic acid according to the method used by Swern *et al.*[5] for the preparation of octan-1,2-diol.

To a well stirred mixture of 1-nonen [6] in formic acid 25.6 % hydrogen peroxide (in 2.5 % excess) was added in one portion. The mixture was heated and stirred at 40° for about 15 h at which time the solution was homogeneous. The formic acid was removed by distillation at reduced pressure and the residue was refluxed for about one hour with excess of 3 N alcoholic potassium hydroxide. After the alcohol had been evaporated, the residue was treated with ether and water. The ether was removed and the residue distilled. The glycol boiled at 155°/17 mm and solidified at once to a crystalline product which after several sublimations in vacuum melted at 33.5—34° (Found: C 67.90; H 12.43. Calc. for $C_9H_{20}O_2$: C 67.45; H 12.58).

Nonan-1,3-diol was prepared by a Grignard reaction. To an ether solution of *n*-hexylmagnesium bromide β-hydroxypropionaldehyde [7] was added dropwise. The solution was refluxed for half an hour and then worked up in the usual way. The diol boiled at 144—146°/12 mm and after cooling in an ice mixture solidified to a waxy product melting at 14—16°. Purification in a sublimation vessel did not raise the melting point (Found: C 67.13; H 12.42).

The mono-3,5-dinitrobenzoates of the diols were prepared by treating their benzene solutions with an equimolecular amount of 3,5-dinitrobenzoyl chloride and a few drops of pyridine. The solutions were heated to boiling, cooled and worked up as usual. The benzoates were recrystallised from benzene-petroleum ether and that of the 1,2-diol melted at 60—61° (Found: C 54.30; H 6.21. Calc. for $C_{16}H_{22}O_7N_2$: C 54.23; H 6.26). The corresponding derivative from biformin is reported [1] to melt at 50—55°. The benzoate of the 1,3-diol melted at 66.5—67° (Found: C 54.03; H 6.03).

In order to obtain the di-3,5-dinitrobenzoates the benzene solutions of the diols were treated as before but with the reagent in excess and by refluxing the solutions for half an hour before they were worked up. As the di-ester of the 1,2-diol was obtained as an oil its ethereal solution was treated with α-naphthylamine in excess. After recrystallisation from absolute ethanol, the addition compound with two moles of α-naphthylamine was obtained as rosettes of orange needles melting at 120—121°. (Found: C 61.90; H 4.88. Calc. for $C_{43}H_{42}O_{12}N_6$: C 61.86; H 5.07). The corresponding addition compound obtained by Anchel [1] melted at 111—112°.

The di-ester of the 1,3-diol, after recrystallisation from aqueous acetone, melted at 113.5—114° (Found: C 50.21; H 4.34. Calc. for $C_{23}H_{24}O_{12}N_4$: C 50.37; H 4.41).

Our thanks are due to *A. B. Astra*, Södertälje, for financial support and to Mr. R. Öhberg for the analyses.

1. Anchel, M. and Cohen, M. P. *J. Biol. Chem.* **208** (1954) 319.
2. Bohlmann, F. *Angew. Chem.* **67** (1955) 389.
3. Bu'Lock, J. D. *Quart. Rev. London* **10** (1956) 371.
4. Pierce, J. S. and Adams, R. *J. Am. Chem. Soc.* **47** (1925) 1098.
5. Swern, D., Billen, G. N. and Scanlan, J. T. *J. Am. Chem. Soc.* **68** (1946) 1504.
6. Wilkinson, R. *J. Chem. Soc.* **1931** 3057.
7. Glattfeld, J. W. E. and Sander, F. V. *J. Am. Chem. Soc.* **43** (1921) 2675.

Received May 27, 1957.

Crystalline Cytochrome c from Beef Heart Muscle

SVEN PALÉUS and HUGO THEORELL

Medicinska Nobelinstitutet, Biokemiska avdelningen, Stockholm, Sweden

For the past two years we have been concerned with the crystallization of beef cytochrome c. The yield of crystals by the alcohol precipitation method [1] is, however, very poor. In order to get a starting material for crystallization with reproducible properties we worked out the following preparation method *. 6 kg fresh cow hearts were minced, 15 liters of distilled water added and the pH adjusted to 4.1 with 1 N H_2SO_4. After passing cheese cloth the mince was extracted further with 6 liters of water, all at 4° C. The extract was neutralized with 4 N ammonia and centrifuged. 140 g of Amberlite XE-64 (in the ammonia form) were added to the supernatant. The resin with the adsorbed cytochrome was collected on a Büchner funnel, washed with 30 liters of distilled water and eluted with 2 500 ml 0.15 M phosphate of pH 7.0. The eluate was dialyzed against 0.002 M ammonia and centrifuged. The cytochrome was adsorbed again on 10 g of the same resin and eluted with a volume of 250–300 ml 0.09 M phosphate of pH 7.5. The eluate was saturated to 85 % with ammonium sulphate, centrifuged and filtered. The filtrate was dialyzed against 0.01 M glycine buffer pH 8.5. The cytochrome, about 500 mg, now had an iron content of 0.41 % and $E^{1\,\%}_{1\,cm}$ 550 mμ = 20.9. It was now placed on a column of CM–W cellulose (1.5 × 15 cm) prepared according to Peterson and Sober [2], buffered with 0.01 M glycine of pH 8.5. On chromatographing cytochrome c with this buffer and 0.01 M glycine buffer of pH 10.5 some small, colored fractions separated. The main part was finally eluted with 0.05 M glycine buffer of pH 10.5, dialyzed and concentrated by lyophilization.

During the course of this work Hagihara *et al.*[3] published the crystallization of cytochrome c from yeast, beef and pig. Since they gave no analytical data, except the ratio E_{550}/E_{280}, or any convincing proofs of homogeneity of their material we repeated their procedure to produce beef cytochrome c. Crystals were obtained entirely in agreement with their description. Electrophoresis at pH 7.2 in the large Spinco apparatus * revealed three different peaks of the completely reduced cytochrome, all moving towards the cathode. The main component, comprising about 80 %, was the fastest one.

The cytochrome c prepared according to our method, described above, was now submitted to electrophoresis under the same conditions. It was found to show a similar electrophoretic pattern. The main fraction was isolated electrophoretically. This material crystallized in a few hours from ammonium sulphate and ammonia, whereas the crystallization before electrophoresis took a couple of days, just as described by the Japanese workers. Crystals and supernatant showed practically the same spectrophotometrical data. However, for some reason, the ratio E_{550}/E_{280} does not seem to be a very reliable criterion. The crystals contained 0.435 % Fe. Somewhat higher values for the iron content have been reported [4,5] but traces of non-heme iron cannot be excluded in these cases. The light absorption per dry weight (E_{550}, 1 %, 1 cm) was found to be 22.7.

Our conclusion is that crystallization of cytochrome c does not give homogeneous preparations unless followed by further purification, for example by electrophoresis. This is a common experience in protein chemistry.

1. Kuby, S. A., Paléus, S., Paul, K. G. and Theorell, H. *Acta Chem. Scand.* **10** (1956) 148.
2. Peterson, E. A. and Sober, H. A. *J. Am. Chem. Soc.* **78** (1956) 751.
3. Hagihara, B., Morikawa, I., Sekuzu, I., Horio, T. and Okuniki, K. *Nature* **178** (1956) 629.
4. Paléus, S. and Neilands, J. B. *Acta Chem. Scand.* **4** (1950) 1024.
5. Margoliash, E. *Biochem. J.* **56** (1954) 529.

* This part of the work was done in collaboration with Dr. S. A. Kuby, Enzyme Research Institute, University of Wisconsin, Madison, Wisconsin.

* We are indebted to Professor T. Storgårds, AB. Mjölkcentralen, Stockholm, for the permission to use this apparatus.

Received June 1, 1957.

*iso*Thiocyanates XXVIII *. A New *iso*Thiocyanate Glucoside (Glucobarbarin) Furnishing (-)-5-Phenyl-2-oxazolidinethione upon Enzymic Hydrolysis

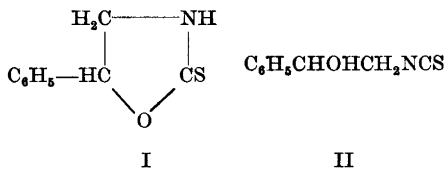
ANDERS KJÆR and ROLF GMELIN

Chemical Laboratory of the University of Copenhagen, Denmark

Paperchromatographic analysis in this laboratory of the *iso*thiocyanate glucoside contents in seed extracts of several species of the genus *Barbarea (Cruciferae)* revealed the presence of two glucosides, one of which was gluconasturtiin, enzymically hydrolyzed to the steam-volatile 2-phenylethyl *iso*thiocyanate and recognized many years ago by Gadamer [1] as a constituent of, *inter alia*, *Barbarea praecox* R. Br.

The second, and preponderant, glucoside, for which we propose the name *glucobarbarin*, does not seem to have been recognized previously. Its identity has now been established by investigation of a purified seed extract of *Barbarea vulgaris* R. Br.** On paper chromatography in *n*-butanol: ethanol:water (4:1:4), glucobarbarin travels at the same rate as glucotropaeolin, the glucoside producing benzyl mustard oil, while gluconasturtiin possesses a definitely higher R_F-value. The new glucoside does not afford steam-volatile material on enzymatic hydrolysis but possesses the notable property of yielding a compound with ultra-violet absorption data suggestive of a cyclic thiocarbamate structure (*cf. e. g.* Ref.[2]), in keeping also with the blue-green colour produced with Grote's reagent. In addition, the enzymic hydrolysis results in the formation of the traditional fragments, sulphate and glucose, the latter identified by paper chromatography in two solvent systems.

On a preparative scale, a seed extract of *B. vulgaris*, purified by passing through a column of anionotropic alumina, was buffered to pH 6.7 and subjected to enzymic hydrolysis with a cell-free myrosinase preparation. The semi-crystalline, Grote-positive reaction product, isolated by chloroform extraction, was transformed into thin, colourless needles on repeated recrystallizations from aqueous ethanol and ethyl acetate-hexane mixtures, m. p. 125° (uncorr.), $[\alpha]_D^{23} = -70.8° \pm 1.5°$ (*c* 2.0, MeOH). Analytical data suggested the composition C_9H_9NOS for the new compound (Found: C 60.30; H 4.96; N 7.76; S 17.78. Calc. C 60.31; H 5.06; N 7.82; S 17.89). Its UV-spectrum in 96 % ethanol exhibited a minimum at 224 mμ (ε 4 300), and a maximum at 245 mμ (ε 19 000), the latter displace hypsochromically on addition of alkali, a pattern characteristic for 2-oxazolidinethiones [2,3]. Subtraction of the elements of the heterocyclic ring from the empirical formula above, leaves a phenyl grouping to be accommodated. Previous evidence that 5-substituted 2-oxazolidinethiones are secondarily formed from enzymically liberated 2-hydroxysubstituted *iso*thiocyanates [2,5,6], renders it very likely that the new compound is (−)-5-phenyl-2-oxazolidinethione (I), a cyclic artifact deriving from one of the stereoisomeric 2-hydroxy-2-phenylethyl *iso*thiocyanates (II), enzymically liberated from glucobarbarin.



I II

For the purpose of comparison, (±)-5-phenyl-2-oxazolidinethione (I) has been synthesized. Racemic 2-amino-1-phenylethanol, prepared by lithium aluminium hydride reduction of (±)-mandelonitrile, was transformed into optically inactive (I), following the procedure designed by Hodgkins and Ettlinger [4] for the synthesis of *iso*thiocyanates from amines. An analytical specimen separated from benzene in colourless needles, m. p. 140° (uncorr.) (Found: C 60.25; H 5.16; N 7.88. Calc. for C_9H_9NOS: C 60.31; H 5.06; N 7.82). On paper chromatography in three solvent systems, the racemic compound was indistinguishable from the

* Part XXVII of this series: *Acta Chem. Scand.* **11** (1957) 898.

** The seed material was commercially obtained from H. Bornträger, Offstein/Kr. Worms, Germany.

levorotatory, natural isomeride. Their identity, save for the steric arrangement around 5-C, is further supported by their nearly coinciding infra-red spectra.

More recently, the synthesis of both isomerides of (I) from the enantiomeric 2-amino-1-phenylethanols [7] has been accomplished in this laboratory. Upon critical comparison, the synthetic, levorotatory enantiomorph proved identical with the specimen of natural origin.

The synthesis of levorotatory (I) from (−)-2-amino-1-phenylethanol further establishes its absolute configuration, and hence that of the mustard oil derivable from glucobarbarin, because the (−)-amine results from a series of reactions not involving inversions and starting with (−)-mandelic acid [7] whose relationship with (+)-glyceraldehyde has been established by several investigators (*cf.* Ref.[8]). Consequently, the heterocyclic enantiomorph of natural provenance should be depicted as (I), yet with the bonds to the hydrogen atom and phenyl grouping in 5-position projecting above and below the plane of the paper, respectively.

The work is part of investigations supported by *The Danish State Research Foundation* and *The Carlsberg Foundation*. A special grant from *Kai Hansen's Fond* is gratefully acknowledged.

1. Gadamer, J. *Ann.* **237** (1899) 507, p. 518.
2. Kjær, A., Gmelin, R. and Boe Jensen, R. *Acta Chem. Scand.* **10** (1956) 432.
3. Astwood, E. B., Greer, M. A. and Ettlinger, M. G. *J. Biol. Chem.* **181** (1949) 121.
4. Hodgkins, J. E. and Ettlinger, M. G. *J. Org. Chem.* **21** (1956) 404.
5. Greer, M. A. *J. Am. Chem. Soc.* **78** (1956) 1260.
6. Schultz, O.-E. and Wagner, W. *Arch. Pharm.* **289/61** (1956) 597.
7. Pratesi, P. and Grassi, M. *Farm. sci. e tec. (Pavia)* **8** (1953) 86.
8. Mislow, K. *J. Am. Chem. Soc.* **73** (1951) 3954.

Received May 16, 1957.

Infrared Investigation of the Location of the Ethylenic Bonds in the Newly Discovered Palustric Acid

HENRIK H. BRUUN

Department of Medical Biochemistry, Institute of Medical Chemistry, University of Uppsala, Uppsala, Sweden and The Institute of Wood Chemistry, Åbo Akademi, Åbo, Finland

Recently Loeblich, Baldwin and Lawrence [1,2] isolated a new acid, which they named palustric acid, from the oleoresin of *Pinus palustris* and *Pinus caribaea* by means of partition chromatography. Palustric acid is a primary acid of the abietic type which these authors also isolated as an intermediate product in the acid and heat isomerization of levopimaric acid to abietic acid. This new member of the abietic series is interesting from the standpoint of rosin acid chemistry and may be of value for the elucidation of the conversion of rosin acids into one another.

Palustric acid is reported to contain two conjugated double bonds which according to the location of the maximum in the ultraviolet spectrum appear to be situated between carbon atoms 5—6 and 7—8 (Fig. 1). On the other hand, the close relationship between palustric and *l*-abietic acid shown by the heat isomerization of levoabietic suggests a structure for palustric acid in which the double bonds are located between carbon atoms 7—8 and 13—14 [1,2].

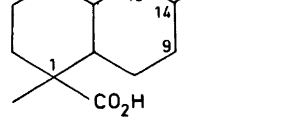


Fig. 1.

levorotatory, natural isomeride. Their identity, save for the steric arrangement around 5-C, is further supported by their nearly coinciding infra-red spectra.

More recently, the synthesis of both isomerides of (I) from the enantiomeric 2-amino-1-phenylethanols [7] has been accomplished in this laboratory. Upon critical comparison, the synthetic, levorotatory enantiomorph proved identical with the specimen of natural origin.

The synthesis of levorotatory (I) from (−)-2-amino-1-phenylethanol further establishes its absolute configuration, and hence that of the mustard oil derivable from glucobarbarin, because the (−)-amine results from a series of reactions not involving inversions and starting with (−)-mandelic acid [7] whose relationship with (+)-glyceraldehyde has been established by several investigators (*cf.* Ref.[8]). Consequently, the heterocyclic enantiomorph of natural provenance should be depicted as (I), yet with the bonds to the hydrogen atom and phenyl grouping in 5-position projecting above and below the plane of the paper, respectively.

The work is part of investigations supported by *The Danish State Research Foundation* and *The Carlsberg Foundation*. A special grant from *Kai Hansen's Fond* is gratefully acknowledged.

1. Gadamer, J. *Ann.* **237** (1899) 507, p. 518.
2. Kjær, A., Gmelin, R. and Boe Jensen, R. *Acta Chem. Scand.* **10** (1956) 432.
3. Astwood, E. B., Greer, M. A. and Ettlinger, M. G. *J. Biol. Chem.* **181** (1949) 121.
4. Hodgkins, J. E. and Ettlinger, M. G. *J. Org. Chem.* **21** (1956) 404.
5. Greer, M. A. *J. Am. Chem. Soc.* **78** (1956) 1260.
6. Schultz, O.-E. and Wagner, W. *Arch. Pharm.* **289/61** (1956) 597.
7. Pratesi, P. and Grassi, M. *Farm. sci. e tec. (Pavia)* **8** (1953) 86.
8. Mislow, K. *J. Am. Chem. Soc.* **73** (1951) 3954.

Received May 16, 1957.

Infrared Investigation of the Location of the Ethylenic Bonds in the Newly Discovered Palustric Acid

HENRIK H. BRUUN

Department of Medical Biochemistry, Institute of Medical Chemistry, University of Uppsala, Uppsala, Sweden and The Institute of Wood Chemistry, Åbo Akademi, Åbo, Finland

Recently Loeblich, Baldwin and Lawrence [1,2] isolated a new acid, which they named palustric acid, from the oleoresin of *Pinus palustris* and *Pinus caribaea* by means of partition chromatography. Palustric acid is a primary acid of the abietic type which these authors also isolated as an intermediate product in the acid and heat isomerization of levopimaric acid to abietic acid. This new member of the abietic series is interesting from the standpoint of rosin acid chemistry and may be of value for the elucidation of the conversion of rosin acids into one another.

Palustric acid is reported to contain two conjugated double bonds which according to the location of the maximum in the ultraviolet spectrum appear to be situated between carbon atoms 5—6 and 7—8 (Fig. 1). On the other hand, the close relationship between palustric and *l*-abietic acid shown by the heat isomerization of levoabietic suggests a structure for palustric acid in which the double bonds are located between carbon atoms 7—8 and 13—14 [1,2].

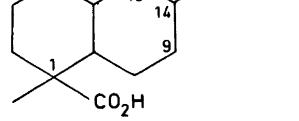


Fig. 1.

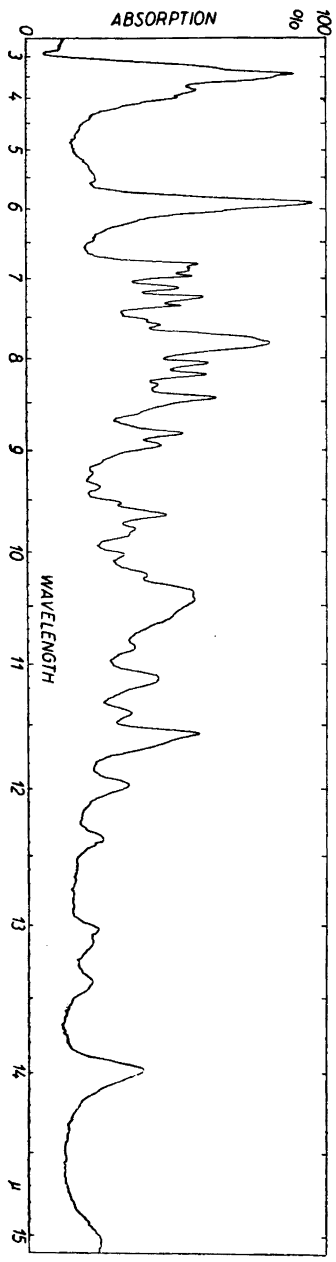


Fig. 2. Infrared absorption spectrum of palustric acid.

The infrared absorption spectrum of the acid could be expected to permit a decision as to the actual locations of the double bonds. Their locations between carbon atoms 5—6 and 7—8 would imply that both would absorb in the infrared range since the bonds would be di- and trisubstituted ethylenic bonds with properties similar to those of the double bonds in *l*-abietic, levopimaric and neoabietic acids, while with the alternative locations between carbon atoms 7—8 and 13—14, only the former double bond would be expected to give rise to infrared absorption bands resembling those of the trisubstituted ethylenic bond in a dihydroabietic acid.

The infrared absorption spectrum of palustric acid is reproduced in Fig. 2. A comparison of this spectrum with the spectra for the other resin acids mentioned above (*l*-abietic acid [3], levopimaric acid [4], dihydroabietic acid [5,3]) * shows that the former spectrum most closely resembles the spectrum of dihydroabietic acid. The following interpretation of bands is presented which confirms that the second alternative, *i. e.* double bonds between carbon atoms 7—8 and 13—14, is the most probable one.

The C=C stretching vibration gives rise to a sharp peak at 6.15—6.17 μ in the spectra of abietic, levopimaric and neoabietic acid, while in the spectra for dihydroabietic and palustric acids there is no peak or possibly only very indistinct shoulder at 6.04 μ. The =C—H out-of-plane vibration gives rise to a sharp absorption band at 12.65 μ in the abietic acid spectrum and at 12.62 μ in the levopimaric acid spectrum. In the spectra of dihydroabietic, neoabietic and palustric acid which, in contrast to the preceding acids, have only one bond of this type (assuming palustric acid to have its double bonds at 7—8 and 13—14), weak bands are seen at 12.48, 12.50 and 12.38 μ, respectively.

Levopimaric and neoabietic acids have in their spectra a band at 14.35 and 14.42 μ, respectively, that is possibly due to the vibration of the ethylenic bond. No bands of this kind are seen in the spectra for dihydroabietic and palustric acids. If the first alternative for the location of the

* The spectrum of neoabietic acid in the solid state differs in several respects from the spectra of the other resin acids, evidently owing to intramolecular transformation and shows a double peak due to the carbonyl group (at 5.93 and 5.80 μ) and a band due to polymer associated OH (at 3.12 μ[4]).

double bonds were correct for palustric acid, one would expect to find bands due to the *cis*-disubstituted double bond between atoms 5 and 6 in its spectrum.

Experimental. The palustric acid employed in the study was kindly sent to the author by E. L. Patton, Head of the Naval Stores Research Section, Naval Stores Section, The United States Department of Agriculture.

The absorption spectrum was recorded with an automatic double-beam spectrophotometer of the type described by Hornig, Hyde and Adcock [6]. The sample was examined using the potassium bromide technique. For further informations, see Ref.[3].

Acknowledgements. I wish to express my sincere gratitude to Dr. Ingrid Fischmeister of the Department of Medical Biochemistry for the spectrophotometric measurements and to Professor Einar Stenhagen for placing the facilities of the Department at my disposal.

1. Loeblich, D., Baldwin, D. E. and Lawrence, R. V. *J. Am. Chem. Soc.* **77** (1955) 2823.
2. Loeblich, D. Baldwin, D. E. and Lawrence, R. V. *J. Am. Chem. Soc.* **77** (1955) 6311.
3. Bruun, H. H. *Paper and Timber, Finland* **38** (1956) 577.
4. Bruun, H. H. *Paper and Timber, Finland* **39** (1957).
5. Bruun, H. H. *Acta Chem. Scand.* **10** (1956) 481.
6. Hornig, D. F., Hyde, G. E. and Adcock, W. A. *J. Opt. Soc. Amer.* **40** (1950) 498.

Received May 31, 1957.

The Formation of Anhydro Vitamin A_1 in the Study of Vitamin A_1 Isomers

B. BARNHOLDT

Statens vitamin-laboratorium, Copenhagen, Denmark

As described by Edisbury *et al.*[1] and later by Meunier *et al.*[2] and Schantz *et al.*[3] the action of an anhydrous (N/30) ethanolic solution of hydrogen chloride on vitamin A_1 results in the conversion of the vitamin into the hydrocarbon anhydro vitamin A_1. Robeson and Baxter [4] have shown that the two isomers 13-*cis* and all-*trans* vitamin A_1 form the same substance when treated with hydrogen chloride in ethanol, but the rate of reaction (in 0.02 N ethanolic hydrogen chloride) is not the same in the two cases.

During recent years a number of new vitamin A_1 isomers [5-7] have been added to those already known, and when faced with the problem of identifying the individual components — isolated for instance by chromatography — of a mixture of vitamin A_1 isomers, it will be natural, side by side with other identification tests, to utilize the process of anhydro vitamin A_1 formation. The aim of the present work has been to develop a convenient procedure for the formation of anhydro vitamin with a view to the utilisation of this reaction for purposes of identification.

It is possible to follow the course of the reaction by spectrophotometry of the reaction mixture, since the formation of anhydro vitamin A_1 causes an increase in the extinction at wavelengths above approx. 340 mμ. Maximum increase is observed at wavelengths of approx. 350, 368.5 and 390 mμ, *i. e.* very near the three maxima of anhydro vitamin A_1 — 351, 371, 392 mμ[3]. Under the action of the hydrogen chloride solution the process continues, and anhydro vitamin A_1 is converted into *iso*anhydro vitamin A_1 (maxima at approx. 330, 350 and 370 mμ [3,8,9]), causing the maximum at 390 mμ to disappear again. The value of E_{390} measured for the reaction mixture thus does not only comprise the extinction due to the anhydro vitamin A_1, but also the extinction of unconverted vitamin A_1 and *iso*-anhydro vitamin A_1. However, the maximum value of E_{390} will almost exclusively be due to anhydro vitamin A_1.

For the purpose of following the process of anhydro vitamin formation the following two magnitudes may be used: (1) the maximum value of the ratio $E_{390} / E°_{max.}$ and (2) the corresponding time $t_{max.\ anh.}$ In the ratio $E_{390} / E°_{max.}$ is E_{390} the extinction (cell length 1 cm) of the reaction mixture at 390 mμ. $E°_{max.}$ is the extinction (cell length 1 cm) of the reaction mixture being due to vitamin A_1 at zero time, *i. e.* at the moment when the vitamin A_1 solution and the hydrogen chloride solution are mixed. $E°_{max.}$ is not measured directly, but is calculated from the value of $E_{max.}$ already measured for the vitamin A_1 solution. The value of these two magnitudes, $E_{390} / E°_{max.}$ and $t_{max.\ anh.}$ have been determined for all-

double bonds were correct for palustric acid, one would expect to find bands due to the *cis*-disubstituted double bond between atoms 5 and 6 in its spectrum.

Experimental. The palustric acid employed in the study was kindly sent to the author by E. L. Patton, Head of the Naval Stores Research Section, Naval Stores Section, The United States Department of Agriculture.

The absorption spectrum was recorded with an automatic double-beam spectrophotometer of the type described by Hornig, Hyde and Adcock [6]. The sample was examined using the potassium bromide technique. For further informations, see Ref.[3].

Acknowledgements. I wish to express my sincere gratitude to Dr. Ingrid Fischmeister of the Department of Medical Biochemistry for the spectrophotometric measurements and to Professor Einar Stenhagen for placing the facilities of the Department at my disposal.

1. Loeblich, D., Baldwin, D. E. and Lawrence, R. V. *J. Am. Chem. Soc.* **77** (1955) 2823.
2. Loeblich, D. Baldwin, D. E. and Lawrence, R. V. *J. Am. Chem. Soc.* **77** (1955) 6311.
3. Bruun, H. H. *Paper and Timber, Finland* **38** (1956) 577.
4. Bruun, H. H. *Paper and Timber, Finland* **39** (1957).
5. Bruun, H. H. *Acta Chem. Scand.* **10** (1956) 481.
6. Hornig, D. F., Hyde, G. E. and Adcock, W. A. *J. Opt. Soc. Amer.* **40** (1950) 498.

Received May 31, 1957.

The Formation of Anhydro Vitamin A_1 in the Study of Vitamin A_1 Isomers

B. BARNHOLDT

Statens vitamin-laboratorium, Copenhagen, Denmark

As described by Edisbury *et al.*[1] and later by Meunier *et al.*[2] and Schantz *et al.*[3] the action of an anhydrous (N/30) ethanolic solution of hydrogen chloride on vitamin A_1 results in the conversion of the vitamin into the hydrocarbon anhydro vitamin A_1. Robeson and Baxter [4] have shown that the two isomers 13-*cis* and all-*trans* vitamin A_1 form the same substance when treated with hydrogen chloride in ethanol, but the rate of reaction (in 0.02 N ethanolic hydrogen chloride) is not the same in the two cases.

During recent years a number of new vitamin A_1 isomers [5-7] have been added to those already known, and when faced with the problem of identifying the individual components — isolated for instance by chromatography — of a mixture of vitamin A_1 isomers, it will be natural, side by side with other identification tests, to utilize the process of anhydro vitamin A_1 formation. The aim of the present work has been to develop a convenient procedure for the formation of anhydro vitamin with a view to the utilisation of this reaction for purposes of identification.

It is possible to follow the course of the reaction by spectrophotometry of the reaction mixture, since the formation of anhydro vitamin A_1 causes an increase in the extinction at wavelengths above approx. 340 mμ. Maximum increase is observed at wavelengths of approx. 350, 368.5 and 390 mμ, *i. e.* very near the three maxima of anhydro vitamin A_1 — 351, 371, 392 mμ[3]. Under the action of the hydrogen chloride solution the process continues, and anhydro vitamin A_1 is converted into *iso*anhydro vitamin A_1 (maxima at approx. 330, 350 and 370 mμ [3,8,9]), causing the maximum at 390 mμ to disappear again. The value of E_{390} measured for the reaction mixture thus does not only comprise the extinction due to the anhydro vitamin A_1, but also the extinction of unconverted vitamin A_1 and *iso*-anhydro vitamin A_1. However, the maximum value of E_{390} will almost exclusively be due to anhydro vitamin A_1.

For the purpose of following the process of anhydro vitamin formation the following two magnitudes may be used: (1) the maximum value of the ratio $E_{390} / E°_{max.}$ and (2) the corresponding time $t_{max.\ anh.}$ In the ratio $E_{390} / E°_{max.}$ is E_{390} the extinction (cell length 1 cm) of the reaction mixture at 390 mμ. $E°_{max.}$ is the extinction (cell length 1 cm) of the reaction mixture being due to vitamin A_1 at zero time, *i. e.* at the moment when the vitamin A_1 solution and the hydrogen chloride solution are mixed. $E°_{max.}$ is not measured directly, but is calculated from the value of $E_{max.}$ already measured for the vitamin A_1 solution. The value of these two magnitudes, $E_{390} / E°_{max.}$ and $t_{max.\ anh.}$ have been determined for all-

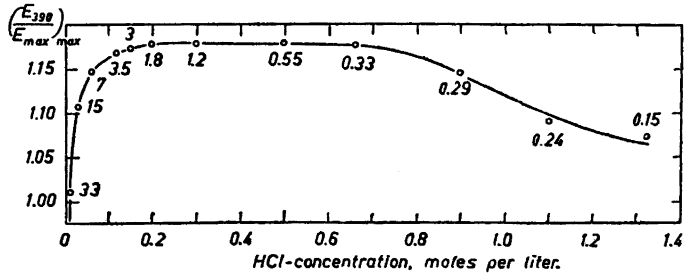


Fig. 1. Maximum values of E_{390}/E°_{325} obtained in the conversion of all-*trans* vitamin A_1 into anhydro vitamin A_1 at different concentrations of hydrogen chloride in ethanol. For each of the experimentally determined points,, the value of $t_{max.\ anh.}$ (in minutes) are stated $t_{max.\ anh.}$ being the time which has elapsed from the moment when the vitamin A solution and the hydrogen chloride solution are mixed and until the reaction mixture exhibits maximum extinction at 390 mμ.

trans vitamin A_1 at different hydrogen chloride concentrations. After mixture of for instance 2.5 ml ethanolic hydrogen chloride solution and 2.5 ml vitamin A_1 solution (containing about 10 μg vitamin A_1 per ml) the reaction mixture was poured into a quartz cuvette, and the course of the reaction was followed by measurements by means of a Beckman DU spectrophotometer. The temperature of the reaction mixture was 25—26°C.

In Fig. 1 the maximum value of the ratio E_{390} / E°_{325} and the corresponding reaction time have been represented as a function of the hydrogen chloride concentration in the reaction mixture. It will be seen that $(E_{390}$ / $E^{\circ}_{325})$ max. does not assume values above 1.18. If a further conversion of anhydro vitamin A_1 did not take place, complete conversion of all-*trans* vitamin A_1 into anhydro vitamin A_1 should be expected to result in a value of $\frac{3\,180 \times 268}{1\,850 \times 286} = 1.61$ of E_{390} / E°_{325} [E (1 %, 1 cm, 390 mμ) = 3 180[3] of anhydro vitamin A_1, molecular weight 268, E (1 %, 1 cm, 325 mμ) = 1 850 [5] of all-*trans* vitamin A_1, molecular weight 268].

When ethanolic hydrogen bromide (0.15 —0.50 N) is used, the same values of $(E_{390}$ / $E^{\circ}_{325})$ max. are obtained as when using 0.15—0.50 N hydrogen chloride. The use of ethanolic sulphuric acid or acetic acid results in lower values of E_{390} / E°_{325} and higher $t_{max.\ anh.}$ values than those obtained with hydrogen chloride in the same molar concentration. Even 50 % (v/v) acetic acid in ethanol results in a considerably slower rate of reaction with a lower value of E_{390} / E°_{325} than that obtained with, for instance, 0.01 N ethanolic hydrogen chloride. If anhydro vitamin A_1 is formed in a mixture of 1 volume of sulphuric acid (95—97 %) and 9 volumes of absolute ethanol, $t_{max.\ anh.}$ is found to be about 1.0 min, while E_{390} / E°_{325} reaches a value of 1.04 only. Lower concentrations of sulphuric acid result in higher values of $t_{max.\ anh.}$ and lower values of E_{390} / E°_{325}.

The course of the dehydration reaction for all-*trans* vitamin A_1 dissolved in ethanolic *p*-toluenesulphonic acid has also been examined. Schantz [10] used *p*-toluenesulphonic acid as catalyst in the preparation of anhydro vitamin A_1. A 10 % (w/v) solution of *p*-toluenesulphonic acid hydrate (anhydrous *p*-toluenesulphonic acid was not available commercially) in absolute ethanol gives $t_{max.\ anh.}$ = about 1 min, while E_{390} / E°_{325} reaches a value of about 0.5 only. Reduction of the *p*-toluenesulphonic acid concentration changes the course of the reaction in the same way as decribed with respect to the other acids.

To prepare anhydro vitamin in ethanolic solution at room temperature hydrogen chloride thus seems to be the most suitable of the dehydration agents examined in the present investigation. It may be added that the presence of merely a few per cent of water in the hydrogen chloride mixture will cause a considerable increase in $t_{max.\ anh.}$ and reduce the maximum value of E_{390} / $E^{\circ}_{max.}$.

The influence of variations in the vitamin A_1 concentration on $t_{max.\ anh.}$ and E_{390} / $E^{\circ}_{max.}$ at constant hydrogen chloride concentration has been examined for all-

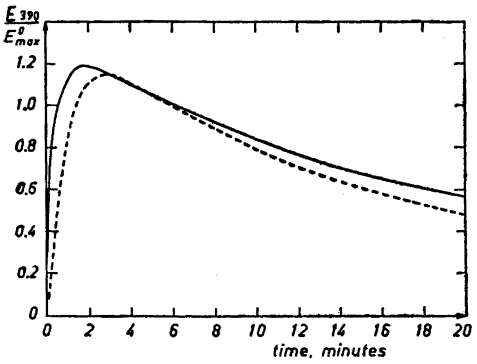


Fig. 2. Conversion of all-*trans* (————) and 13-*cis* (— — — —) vitamin A_1 into anhydro vitamin A_1 in anhydrous 0.20 N ethanolic hydrogen chloride. The graph represents $E_{390}/E°_{max.}$ plotted against time.

trans and 13-*cis* vitamin A_1 in 0.20 N ethanolic hydrochloric acid, and both magnitudes were found to be independent of $E°_{max.}$ in a concentration range corresponding to $E°_{max.} = 0.1-1$.

Fig. 2 illustrates the difference in the dehydration reactions in the case of all-*trans* vitamin A_1 and 13-*cis* vitamin A_1, respectively, in 0.20 N ethanolic hydrochloric acid. It must be considered probable that the magnitudes $t_{max.\ anh.}$ and the maximum values of $E_{390} / E°_{max.}$ for the different vitamin A_1 isomers will depend on the number of *cis* configurations and their positions in the molecule and on the molar extinction-coefficient of the vitamin A_1 isomer concerned.

An example of the application of the identification test described in the above will be published elsewhere [11].

The author wishes to thank Dr. phil. Willy Hjarde for his very kind interest in this study and for many valuable discussions.

1. Edisbury, J. R., Gillam, A. E., Heilbron, J. M. and Morton, R. A. *Biochem. J.* **26** (1932) 1164.
2. Meunier, P., Dolou, R. and Vinet, A. *Compt. rend.* **216** (1943) 907.
3. Schantz, E. M., Cawley, J. D. and Embree, N. D. *J. Am. Chem. Soc.* **65** (1943) 901.
4. Robeson, C. D. and Baxter, J. G. *J. Am. Chem. Soc.* **69** (1947) 136.
5. Robeson, C. D., Cawley, J. D., Weisler, L., Stern, M. H., Eddinger, C. C. and Chechak, A. J. *J. Am. Chem. Soc.* **77** (1955) 4111.
6. Dieterle, J. M. and Robeson, C. D. *Science* **120** (1954) 219.
7. Wald, G., Brown, P. K. and Hubbard, R. *Proc. Natl. Acad. Sci. U.S.* **41** (1955) 438.
8. Isler, O., Huber, W., Ronco, A. and Kofler, M. *Helv. chim. Acta* **30** (1947) 1911.
9. Oroshnik, W. *Science* **119** (1954) 660.
10. Schantz, E. M. *J. Biol. Chem.* **182** (1950) 515.
11. Barnholdt, B. and Hjarde, W. *Acta Physiol. Scand.* (1957) *In press.*

Received June 7, 1957.

Depolymerization of 1,2-Dithiolane and 1,2-Diselenolane Polymers

GÖRAN BERGSON and GÖRAN CLAESON*

Chemical Institute, University of Uppsala, Uppsala, Sweden

On hydrolysing trimethylendiselenocyanate, according to Hagelberg [1], Morgan and Burstall [2] a yellow powder is formed which was regarded as the monomer of 1,2-diselenolane (1,2-diselena-*cyclo*pentane) by Morgan and Burstall. Since this molecule is of great interest in connection with the spectrochemical investigations of diselenides, which are in progress at this institute by one of us [3], we tried to dissolve it in the common spectroscopic solvents. It was, however, found to be quite insoluble at ordinary temperatures, but when heated to about 60° the yellow powder darkened and went into solution. This solution was yellow and showed an absorption maximum at about 4 500 Å (Fig. 1). The colour persisted for several days at room temperature and then the yellow powder slowly precipitated. These facts indicate that the solution contains the monomer and that the yellow powder is a polymer, which depolymerizes when heated.

The corresponding sulphur compound (m. p. *ca.* 73°) prepared from trimethylendibromide and sodium disulphide [4] was also investigated. It dissolved without

* Both authors contribute equally.

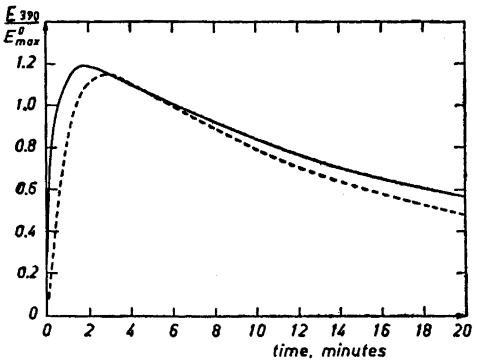


Fig. 2. Conversion of all-*trans* (————) and 13-*cis* (— — — —) vitamin A_1 into anhydro vitamin A_1 in anhydrous 0.20 N ethanolic hydrogen chloride. The graph represents $E_{390}/E°_{max.}$ plotted against time.

trans and 13-*cis* vitamin A_1 in 0.20 N ethanolic hydrochloric acid, and both magnitudes were found to be independent of $E°_{max.}$ in a concentration range corresponding to $E°_{max.} = 0.1-1$.

Fig. 2 illustrates the difference in the dehydration reactions in the case of all-*trans* vitamin A_1 and 13-*cis* vitamin A_1, respectively, in 0.20 N ethanolic hydrochloric acid. It must be considered probable that the magnitudes $t_{max.\ anh.}$ and the maximum values of $E_{390} / E°_{max.}$ for the different vitamin A_1 isomers will depend on the number of *cis* configurations and their positions in the molecule and on the molar extinction-coefficient of the vitamin A_1 isomer concerned.

An example of the application of the identification test described in the above will be published elsewhere [11].

The author wishes to thank Dr. phil. Willy Hjarde for his very kind interest in this study and for many valuable discussions.

1. Edisbury, J. R., Gillam, A. E., Heilbron, J. M. and Morton, R. A. *Biochem. J.* **26** (1932) 1164.
2. Meunier, P., Dolou, R. and Vinet, A. *Compt. rend.* **216** (1943) 907.
3. Schantz, E. M., Cawley, J. D. and Embree, N. D. *J. Am. Chem. Soc.* **65** (1943) 901.
4. Robeson, C. D. and Baxter, J. G. *J. Am. Chem. Soc.* **69** (1947) 136.
5. Robeson, C. D., Cawley, J. D., Weisler, L., Stern, M. H., Eddinger, C. C. and Chechak, A. J. *J. Am. Chem. Soc.* **77** (1955) 4111.
6. Dieterle, J. M. and Robeson, C. D. *Science* **120** (1954) 219.
7. Wald, G., Brown, P. K. and Hubbard, R. *Proc. Natl. Acad. Sci. U.S.* **41** (1955) 438.
8. Isler, O., Huber, W., Ronco, A. and Kofler, M. *Helv. chim. Acta* **30** (1947) 1911.
9. Oroshnik, W. *Science* **119** (1954) 660.
10. Schantz, E. M. *J. Biol. Chem.* **182** (1950) 515.
11. Barnholdt, B. and Hjarde, W. *Acta Physiol. Scand.* (1957) *In press.*

Received June 7, 1957.

Depolymerization of 1,2-Dithiolane and 1,2-Diselenolane Polymers

GÖRAN BERGSON and GÖRAN CLAESON*

Chemical Institute, University of Uppsala, Uppsala, Sweden

On hydrolysing trimethylendiselenocyanate, according to Hagelberg [1], Morgan and Burstall [2] a yellow powder is formed which was regarded as the monomer of 1,2-diselenolane (1,2-diselena-*cyclo*pentane) by Morgan and Burstall. Since this molecule is of great interest in connection with the spectrochemical investigations of diselenides, which are in progress at this institute by one of us [3], we tried to dissolve it in the common spectroscopic solvents. It was, however, found to be quite insoluble at ordinary temperatures, but when heated to about 60° the yellow powder darkened and went into solution. This solution was yellow and showed an absorption maximum at about 4 500 Å (Fig. 1). The colour persisted for several days at room temperature and then the yellow powder slowly precipitated. These facts indicate that the solution contains the monomer and that the yellow powder is a polymer, which depolymerizes when heated.

The corresponding sulphur compound (m. p. *ca.* 73°) prepared from trimethylendibromide and sodium disulphide [4] was also investigated. It dissolved without

* Both authors contribute equally.

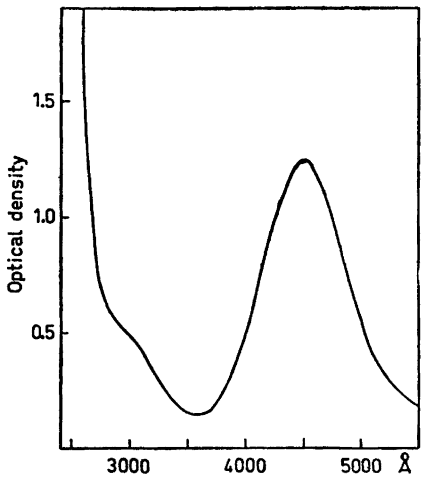


Fig. 1. UV-absorption of 1,2-diselenolane in nujol.

colour change in hot lowboiling solvents and precipitated on cooling. On treating the above mentioned sulphur compound with paraffin oil or nujol a yellow solution was obtained at about 160°. The U.V.-absorption of the cooled, still yellow solution was recorded. It showed a peak at 2 630 Å and a weak shoulder at about 3 300 Å (Fig. 2). The peak comes from the normal absorption of linear disulphide and the shoulder indicates the presence of the 1,2-dithiolane. To confirm the presence of the characteristic 1,2-dithiolane peak (3 300 Å), we heated the solution and collected the vapors in ethanol. The U.V.-spectrum of the ethanol solution showed two distinct peaks; one from the polymer (2 620 Å) and one from the monomer (3 270 Å). The small shifts from the normal values of λ_{max} are in the expected directions for an absorption curve composed of two functions D_1 (λ) and D_2 (λ).

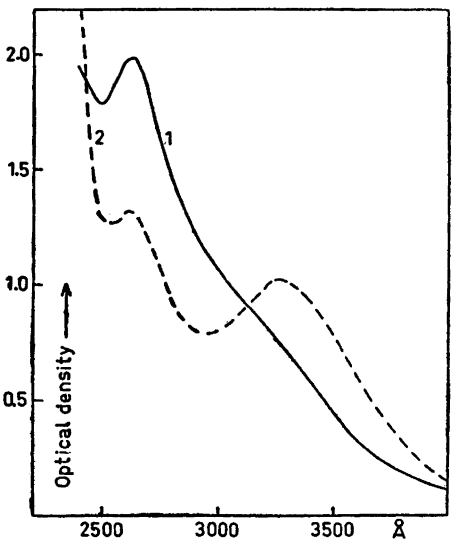


Fig. 2. Curve 1: UV-absorption of 1,2-dithiolane and polymer in nujol. Curve 2: UV-absorption of vapors collected in ethanol.

To complete our investigation of the depolymerization we determined the molecular weights by the Rast camphor-method. The molecular weight of the selenium compound was found to be 240 (calc. 200). This high value is in agreement with the shoulder in the spectrum (Fig. 1), indicating the presence of small amounts of polymer. Morgan and Burstall [2] found the molecular weight 225 in benzene. This misled them to believe that the substance was a monomer also in solid state.

No boiling point elevation could be detected, when an attempt was made to determine the molecular weight of the sulphur compound in benzene. This is in agreement with our assumption that the substance is dissolved as a polymer in lowerboiling solvents. The compound has earlier been considered as a dimer [5]. In molten camphor, however, it should be expected to be partly depolymerized. This was also found. The molecular weight depended on the time which the sample was in molten state. A rapid determination gave the molecular weight 740. After 3 h at 180° the mol.wt. was 205.

A similar depolymerization method for thioctic acid has recently been reported by Thomas and Reed [6].

The very easy depolymerization of the selenium compound as compared with the sulphur compound is remarkable.

The investigations on cyclic disulphides and diselenides are being continued.

Experimental. The spectra were determined with a Beckman model DU (2 450—4 000 Å) and a Beckman model B (4 000—5 500 Å) photoelectric spectrophotometer.

The molecular weights were determined in a Kofler hot-stage microscope.

We are indebted to Dr. Lennart Schotte for valuable discussions. We also wish to thank

Professor Arne Fredga for all the facilities placed at our disposal. A grant from the *Swedish Natural Science Research Council* to one of us (G.B.) is gratefully acknowledged.

1. Hagelberg, L. *Ber.* **23** (1890) 1090.
2. Morgan, G. T. and Burstall, F. H. *J. Chem. Soc.* **1930** 1497.
3. Bergson, G. *Arkiv Kemi* **9** (1956) 121; 9. Nordiske Kemikermøde i Aarhus 1956, p. 47.
4. Barltrop, J. A., Hayes, P. M. and Calvin, M. *J. Am. Chem. Soc.* **67** (1954) 4348.
5. Autenrieth, W. and Wolff, K. *Ber.* **32** (1899) 1368.
6. Thomas, R. C. and Reed, L. J. *J. Am. Chem. Soc.* **78** (1956) 6148.

Received June 17, 1957.

Eine verbesserte Methode zur Synthese neuer Nitrophenylester

SELMA KREISKY

Institut für klinische Chemie der Universität Gotenburg, Gotenburg, Schweden

Ester des *p*-Nitrophenols wurden mit folgenden Säuren hergestellt: Essigsäure, Propionsäure, *Iso*buttersäure, Buttersäure, *Iso*valeriansäure, *n*-Valeriansäure, Capronsäure, Laurinsäure, Myristinsäure, Stearinsäure und Ölsäure.

Ein Teil dieser Ester war bereits von Huggins und Lapides [1] hergestellt worden, doch waren die flüssigen Produkte nicht durch ihre Siedepunkte charakterisiert worden. Für diese Ester und die vom Verfasser erstmalig hergestellten Ester sind Schmelz- und Siedepunkte in der Tabelle 1 angegeben.

Für die Synthese der Ester wurde die Methode von Spasov [2] abgeändert, da es sich erwies, dass die Wirkung des Magnesiums bei der Veresterung katalytisch und nicht stöchiometrisch ist. Daher wurde statt eines Äquivalents Magnesium (1/2 Mol) bloss 10 % der theoretischen Menge (1/20 Mol) verwendet. Um die Reaktion in Gang zu setzen wurde die Lösung mit einigen Körnchen Jod versetzt.

Durchführung der Synthesen. Zur Herstellung der niederen Fettsäureester bis inkl. der *Iso*buttersäure werden 13,9 g *p*-Nitrophenol, 0,12 Mol Säurechlorid, 0,12 g Magnesiumspäne, 30 g Benzol und einige Körnchen Jod eine Stunde, zur Herstellung der höheren Fettsäureestern vier Stunden unter Rückflusskühlung gekocht. Nach dem Abkühlen setzt man 150 ml Äthyläther, bei Myristinsäure- und Stearinsäureestern jedoch 150 ml Chloroform zu. Die Lösung wird darauf einmal mit 100 ml Wasser, zweimal mit 100 ml gesättigter Natriumbikarbonatlösung und schliesslich zweimal mit dest. Wasser gewaschen. Die nichtwässrige Schicht wird dann mit wasserfreiem Natriumsulfat getrocknet und mit Tierkohle behandelt. Nach dem Filtrieren wird die Lösung unter vermindertem Druck eingedampft. Die höheren

Tabelle 1.

p-Nitrophenyl ester der	Schmp. °C	Siedepunkt		Ausbeute %	*p*-Nitrophenolgehalt nach erfolgter Hydrolyse %	
		°C	Torr		Ber.	Gef.
*Iso*buttersäure	36,5—37					
n-Buttersäure	12—14	162—164	7	92		
*Iso*valeriansäure		158—160	6	86		
n-Valeriansäure		155—156	3	88	62,35	62,3
n-Capronsäure		174—175	6	84	58,8	61,8—63
Laurinsäure	44,5—45			79	43,36	43,5
Myristinsäure	54,5—55			85	39,85	39,9
Stearinsäure	66,5—67			86	34,34	34,4
Ölsäure		194—198	3	50		

Professor Arne Fredga for all the facilities placed at our disposal. A grant from the *Swedish Natural Science Research Council* to one of us (G.B.) is gratefully acknowledged.

1. Hagelberg, L. *Ber.* **23** (1890) 1090.
2. Morgan, G. T. and Burstall, F. H. *J. Chem. Soc.* **1930** 1497.
3. Bergson, G. *Arkiv Kemi* **9** (1956) 121; 9. Nordiske Kemikermøde i Aarhus 1956, p. 47.
4. Barltrop, J. A., Hayes, P. M. and Calvin, M. *J. Am. Chem. Soc.* **67** (1954) 4348.
5. Autenrieth, W. and Wolff, K. *Ber.* **32** (1899) 1368.
6. Thomas, R. C. and Reed, L. J. *J. Am. Chem. Soc.* **78** (1956) 6148.

Received June 17, 1957.

Eine verbesserte Methode zur Synthese neuer Nitrophenylester

SELMA KREISKY

Institut für klinische Chemie der Universität Gotenburg, Gotenburg, Schweden

Ester des *p*-Nitrophenols wurden mit folgenden Säuren hergestellt: Essigsäure, Propionsäure, *Iso*buttersäure, Buttersäure, *Iso*valeriansäure, *n*-Valeriansäure, Capronsäure, Laurinsäure, Myristinsäure, Stearinsäure und Ölsäure.

Ein Teil dieser Ester war bereits von Huggins und Lapides [1] hergestellt worden, doch waren die flüssigen Produkte nicht durch ihre Siedepunkte charakterisiert worden. Für diese Ester und die vom Verfasser erstmalig hergestellten Ester sind Schmelz- und Siedepunkte in der Tabelle 1 angegeben.

Für die Synthese der Ester wurde die Methode von Spasov [2] abgeändert, da es sich erwies, dass die Wirkung des Magnesiums bei der Veresterung katalytisch und nicht stöchiometrisch ist. Daher wurde statt eines Äquivalents Magnesium (1/2 Mol) bloss 10 % der theoretischen Menge (1/20 Mol) verwendet. Um die Reaktion in Gang zu setzen wurde die Lösung mit einigen Körnchen Jod versetzt.

Durchführung der Synthesen. Zur Herstellung der niederen Fettsäureester bis inkl. der *Iso*buttersäure werden 13,9 g *p*-Nitrophenol, 0,12 Mol Säurechlorid, 0,12 g Magnesiumspäne, 30 g Benzol und einige Körnchen Jod eine Stunde, zur Herstellung der höheren Fettsäureestern vier Stunden unter Rückflusskühlung gekocht. Nach dem Abkühlen setzt man 150 ml Äthyläther, bei Myristinsäure- und Stearinsäureestern jedoch 150 ml Chloroform zu. Die Lösung wird darauf einmal mit 100 ml Wasser, zweimal mit 100 ml gesättigter Natriumbikarbonatlösung und schliesslich zweimal mit dest. Wasser gewaschen. Die nichtwässrige Schicht wird dann mit wasserfreiem Natriumsulfat getrocknet und mit Tierkohle behandelt. Nach dem Filtrieren wird die Lösung unter vermindertem Druck eingedampft. Die höheren

Tabelle 1.

p-Nitrophenyl ester der	Schmp. °C	Siedepunkt		Ausbeute %	*p*-Nitrophenolgehalt nach erfolgter Hydrolyse %	
		°C	Torr		Ber.	Gef.
*Iso*buttersäure	36,5—37					
n-Buttersäure	12—14	162—164	7	92		
*Iso*valeriansäure		158—160	6	86		
n-Valeriansäure		155—156	3	88	62,35	62,3
n-Capronsäure		174—175	6	84	58,8	61,8—63
Laurinsäure	44,5—45			79	43,36	43,5
Myristinsäure	54,5—55			85	39,85	39,9
Stearinsäure	66,5—67			86	34,34	34,4
Ölsäure		194—198	3	50		

Ester werden durch Umkristallisieren aus *n*-Butanol, die flüssigen Ester durch fraktionierte Destillation gereinigt (Tabelle 1).

Analyse. Die von Huggins und Lapides [1] beschriebene Methode wurde für die Bestimmung der Ester bis zur *n*-Valeriansäure verwendet, bei Estern höherer Säuren musste jedoch die Methode abgeändert werden. 0,33 Millimol des Esters werden in 100 ml 0,1 N methylalkoholischer Natronlauge gelöst und 6 Stunden unter Rückfluss gekocht. Von dem Hydrolysat werden 1 ml auf 100 ml mit wässriger 0,1 N Natronlauge verdünnt. An dieser Lösung werden die kolorimetrischen Bestimmungen ausgeführt. Als Standardlösungen werden Lösungen von *p*-Nitrophenol verwendet, welche 100 bis 700 Mikromol per Liter enthalten. Die Messungen wurden bei einer Wellenlänge von 400 mμ durchgeführt. Zur Verwendung gelangte ein Beckmann B Spektrophotometer.

Herrn Laborator Dr. Gunnar Jungner danke ich für die Förderung dieser Arbeit.

1. Huggins, C. und Lapides, J. *J. Biol. Chem.* **170** (1947) 477.
2. Spasov, A. *Ann. Univ. Sofia, II. Faculté phys.-math.* **35** (1938—39) 289.

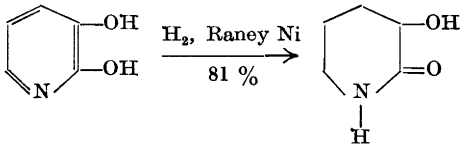
Eingegangen am 11. Juni 1957.

New Synthesis of 3-Hydroxy-2-piperidone

NIELS ELMING*

Centrallaboratoriet, Sadolin & Holmblad A/S, Copenhagen, Denmark

Catalytic hydrogenation of 2,3-pyridinediol has been shown to give the expected 3-hydroxy-2-piperidone *cf.* [1, 2]. This compound has previously been obtained by cyclization of *α*-hydroxy-*δ*-amino-*n*-valeric acid, but no detailed directions were reported [3].



* Present address: A/S Pharmacia, Copenhagen, Denmark.

Experimental. 2,3-Pyridinediol [4-6] (0.56 g) and anhydrous methanol (40 ml) were shaken (6 h) with Raney nickel (0.2 g) under hydrogen (140 atm) at 160—180°. The Raney nickel was removed by filtration and the filtrate evaporated in a vacuum. The crystalline residue was crystallized from methanol-ether. The yield was 0.47 g (81 %) of 3-hydroxy-2-piperidone [white crystals, m. p. 133—135° (Hershberg apparatus, corr.), previously found [3] 134.3°]. (Found: C 52.3; H 7.8; N 12.2. Calc. for $C_5H_9NO_2$ (115.1): C 52.2; H 7.9; N 12.2).

Sublimation (100—110°/0.05 mm) also gave white crystals, m. p. 133—135°.

In a first experiment carried out at 95—100° under 110 atmospheres of hydrogen for one hour only starting material was isolated.

1. Nielsen, J. T., Elming, N. and Clauson-Kaas, N. *Acta Chem. Scand.* **9** (1955) 30.
2. Nielsen, J. T., Elming, N. and Clauson-Kaas, N. *Acta Chem. Scand.* **9** (1955) 9.
3. Hunter, A. and Woodward, H. E. *Biochem. J.* **35** (1941) 1298.
4. Kudernatsch, R. *Monatsh.* **18** (1897) 613.
5. v. Schickh, O., Binz, A. and Schulz, A. *Ber.* **69 B** (1936) 2593.
6. Clauson-Kaas, N. and Nedenskov, P. *Acta Chem. Scand.* **9** (1955) 14.

Received April 27, 1957.

On the Mechanism of Alkylation of β-Keto Esters

I. Methylation of β-Hydroxycoumarilic Acid Ethyl Ester

ARNE BRÄNDSTRÖM and INGEMAR FORSBLAD

Chemical Institute, University of Uppsala, Uppsala, Sweden

The mechanism of the alkylation of metallic derivatives of tautomeric substances has been the subject of many investigations and theories [1]. As late as 1953 Brändström [2,3] published a new theory and in 1955 Kornblum *et al.* [4] proposed a theory seen from a different aspect.

In an attempt to elucidate the mechanism we have begun to study the alkylation of *β*-keto esters. The methylation of *β*-hydroxycoumarilic acid ethyl ester was

Ester werden durch Umkristallisieren aus *n*-Butanol, die flüssigen Ester durch fraktionierte Destillation gereinigt (Tabelle 1).

Analyse. Die von Huggins und Lapides [1] beschriebene Methode wurde für die Bestimmung der Ester bis zur *n*-Valeriansäure verwendet, bei Estern höherer Säuren musste jedoch die Methode abgeändert werden. 0,33 Millimol des Esters werden in 100 ml 0,1 N methylalkoholischer Natronlauge gelöst und 6 Stunden unter Rückfluss gekocht. Von dem Hydrolysat werden 1 ml auf 100 ml mit wässriger 0,1 N Natronlauge verdünnt. An dieser Lösung werden die kolorimetrischen Bestimmungen ausgeführt. Als Standardlösungen werden Lösungen von *p*-Nitrophenol verwendet, welche 100 bis 700 Mikromol per Liter enthalten. Die Messungen wurden bei einer Wellenlänge von 400 mμ durchgeführt. Zur Verwendung gelangte ein Beckmann B Spektrophotometer.

Herrn Laborator Dr. Gunnar Jungner danke ich für die Förderung dieser Arbeit.

1. Huggins, C. und Lapides, J. *J. Biol. Chem.* **170** (1947) 477.
2. Spasov, A. *Ann. Univ. Sofia, II. Faculté phys.-math.* **35** (1938—39) 289.

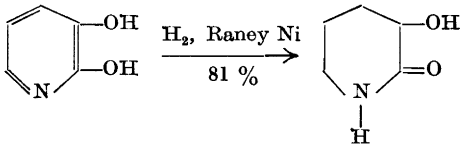
Eingegangen am 11. Juni 1957.

New Synthesis of 3-Hydroxy-2-piperidone

NIELS ELMING*

Centrallaboratoriet, Sadolin & Holmblad A/S, Copenhagen, Denmark

Catalytic hydrogenation of 2,3-pyridinediol has been shown to give the expected 3-hydroxy-2-piperidone *cf.* [1, 2]. This compound has previously been obtained by cyclization of *α*-hydroxy-*δ*-amino-*n*-valeric acid, but no detailed directions were reported [3].



* Present address: A/S Pharmacia, Copenhagen, Denmark.

Experimental. 2,3-Pyridinediol [4-6] (0.56 g) and anhydrous methanol (40 ml) were shaken (6 h) with Raney nickel (0.2 g) under hydrogen (140 atm) at 160—180°. The Raney nickel was removed by filtration and the filtrate evaporated in a vacuum. The crystalline residue was crystallized from methanol-ether. The yield was 0.47 g (81 %) of 3-hydroxy-2-piperidone [white crystals, m. p. 133—135° (Hershberg apparatus, corr.), previously found [3] 134.3°]. (Found: C 52.3; H 7.8; N 12.2. Calc. for $C_5H_9NO_2$ (115.1): C 52.2; H 7.9; N 12.2).

Sublimation (100—110°/0.05 mm) also gave white crystals, m. p. 133—135°.

In a first experiment carried out at 95—100° under 110 atmospheres of hydrogen for one hour only starting material was isolated.

1. Nielsen, J. T., Elming, N. and Clauson-Kaas, N. *Acta Chem. Scand.* **9** (1955) 30.
2. Nielsen, J. T., Elming, N. and Clauson-Kaas, N. *Acta Chem. Scand.* **9** (1955) 9.
3. Hunter, A. and Woodward, H. E. *Biochem. J.* **35** (1941) 1298.
4. Kudernatsch, R. *Monatsh.* **18** (1897) 613.
5. v. Schickh, O., Binz, A. and Schulz, A. *Ber.* **69 B** (1936) 2593.
6. Clauson-Kaas, N. and Nedenskov, P. *Acta Chem. Scand.* **9** (1955) 14.

Received April 27, 1957.

On the Mechanism of Alkylation of β-Keto Esters

I. Methylation of β-Hydroxycoumarilic Acid Ethyl Ester

ARNE BRÄNDSTRÖM and INGEMAR FORSBLAD

Chemical Institute, University of Uppsala, Uppsala, Sweden

The mechanism of the alkylation of metallic derivatives of tautomeric substances has been the subject of many investigations and theories [1]. As late as 1953 Brändström [2,3] published a new theory and in 1955 Kornblum *et al.* [4] proposed a theory seen from a different aspect.

In an attempt to elucidate the mechanism we have begun to study the alkylation of *β*-keto esters. The methylation of *β*-hydroxycoumarilic acid ethyl ester was

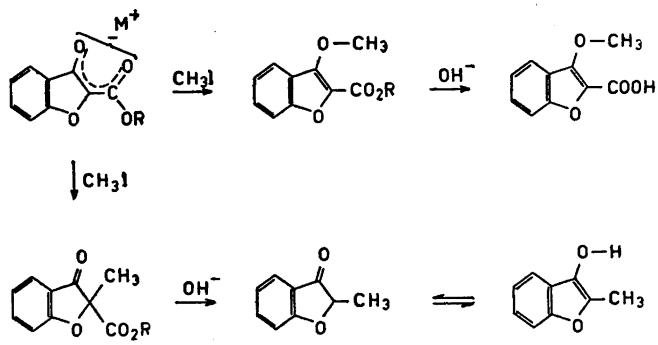


Fig. 1.

selected for study. The reaction has earlier been the subject of a somewhat superficial investigation [5,6] and is well suited to the present purpose as it gives both the C- and O-alkyl product. In order to find out the extent to which the free anion and the metal chelate give C- and O-alkylation, the rate and order of the different reactions must be studied under conditions which lead to different degrees of dissociation.

The β-hydroxycoumarilic acid ethyl ester was prepared in a pure enol-form by an improved method according to Friedländer [7]. Through IR-spectra we have shown that it changes only very slowly into the keto-form at 0°C.

A method to determine the proportion of C- and O-alkyl product formed in alkylation has been worked out. The alkylation reaction is stopped by adding acid; the mixture is diluted with water and the ester extracted with carbon tetrachloride. The residue is titrated with NaOH to determine the velocity of the total reaction. From the carbon tetrachloride solution the unalkylated ester is extracted with 1 N KOH and the residue saponificated, decarboxylated, acidified and extracted with ether.

The acid from the O-alkyl product, which does not decarboxylate, is titrated to pH 6.5—7.0. At that pH the enol-form of 2-methyl coumarone does not interfere. The difference between the rate of the total reaction and that of the O-alkylation is taken as the rate of C-alkylation.

Table 1. Methylation in CH_3OH.

Metal	k_{C+O}	k_C	k_O	C/O
Li	1.20	1.03	0.17	6.0
Na	2.96	2.26	0.70	3.2
K	3.45	2.78	0.67	4.2

Table 2. Methylation with Li.

Solution	k_{C+O}	k_C	k_O	C/O
CH_3OH	1.20	1.03	0.17	6.0
C_2H_5OH	0.89	0.76	0.13	5.7
n-C_3H_7OH	0.54	0.44	0.10	4.5
n-C_4H_9OH	0.36	0.27	—0.09	—3

k_{C+O}, k_C and k_O are, respectively, the velocity constants for the total, C- and O-alkylation. They are given in units of $10^{-2} \cdot$ l/mole $\cdot$ min. C/O is the quotient of the rates of the C- and O-alkylation.

Hitherto the methylation reaction has been studied at 50°C with methyl iodide in methanol solution using Li, Na and K as catalysts, and in ethanol, *n*-propanol and *n*-butanol with Li as catalyst. The concentration of alkali was 0.1 M; the ester was used in 5 % and the methyl iodide in 100 % excess. Both the C- and O-alkylation reactions are of the second order. The preliminary results are shown in Tables 1 and 2.

It has been found that the rate of the C-alkylation decreases more rapidly than that of the O-alkylation through the solvent series $CH_3OH > C_2H_5OH > n\text{-}C_3H_7OH > n\text{-}C_4H_9OH$. Thus the yield of C-alkyl product falls in the same series. In methanol the rate of C-alkylation increases through the series Li<Na<K and the O-alkylation through the series Li < Na ~ K. Thus the ratio C/O decreases in the series Li > K > Na.

This suggests that the mechanism is rather complicated and depends on more factors than the dissociation degree.

In order to find out the extent to which the results depend on the occurence of the alkali salts as ions or a chelate in the reaction medium, the degree of dissociation must be known. We have begun to determine this quantity, by a method due to Brändström [8], from electrical conductance measurements. The complete elucidation of the mechanism requires that other aspects of the reaction should be investigated. Further studies along these lines are in progress at this institute.

Experimental: Salicyl-O-acetic acid [O-(carboxymethoxy)-benzoic acid] was prepared from salicylic acid and chloroacetic acid [9]. Unchanged salicylic acid was separated from the product by continued extraction with benzene.

Salicyl-O-acetic acid diethyl ester was prepared by esterification in the usual way with benzene as water-removing agent [10]. Yield 84 %; m. p. 43.0—44.5°C (not earlier published).

β-Hydroxycoumarilic acid ethyl ester was prepared according to Friedländer [7] with the following modification: After condensation and acidification with 50 % H_2SO_4 at 0°C the product was dried in air at room temperature for a few hours, and than in a desiccator over night. Yield 93 %; m. p. 70.5—71.5°C. The ester contained a little Na_2SO_4 and after recrystallization from dry ether it was obtained as white needles with the same m. p. The low m. p. (65°) earlier reported is probably due to the change of ester into its keto-form during recrystallization from water-alcohol mixture (The velocity of tautomerisation increases with the temperature and polarity of the solvent [11]). It is important that the ester after acidification be kept at as low a temperature as possible.

The authors are indebted to Professor Arne Fredga and to Dr. Lennart Schotte for valuable discussions. A grant from the *Swedish Natural Science Research Council* is gratefully acknowledged.

1. Henecka, H. *Chemie der Beta-Dicarbonyl-verbindungen*, Springer-Verlag, Berlin 1950.
2. Brändström, A. *Arkiv Kemi* **6** (1953) 155.
3. Brändström, A. *Arkiv Kemi* **7** (1954) 81.
4. Kornblum, N., Smiley, R. A., Blookwood, R. K. and Iffland, D. C. *J. Am. Chem Soc.* **77** (1955) 6269.
5. von Auwers, K. *Ann.* **393** (1912) 338.
6. von Auwers, K. *Ber.* **61** (1928) 408.
7. Friedländer, P. *Ber.* **32** (1899) 1868.
8. Brändström, A. *Arkiv Kemi* **11** (1957) *In press.*
9. Meyer, R. and Duczmal, C. *Ber.* **46** (1913) 3370.
10. Brändström, A. *Arkiv Kemi* **1** (1950) 481.
11. Ref. 1, p. 10.

Received June 20, 1957.

Den kgl. Veterinær- og

Ester werden durch Umkristallisieren aus *n*-Butanol, die flüssigen Ester durch fraktionierte Destillation gereinigt (Tabelle 1).

Analyse. Die von Huggins und Lapides [1] beschriebene Methode wurde für die Bestimmung der Ester bis zur *n*-Valeriansäure verwendet, bei Estern höherer Säuren musste jedoch die Methode abgeändert werden. 0,33 Millimol des Esters werden in 100 ml 0,1 N methylalkoholischer Natronlauge gelöst und 6 Stunden unter Rückfluss gekocht. Von dem Hydrolysat werden 1 ml auf 100 ml mit wässriger 0,1 N Natronlauge verdünnt. An dieser Lösung werden die kolorimetrischen Bestimmungen ausgeführt. Als Standardlösungen werden Lösungen von *p*-Nitrophenol verwendet, welche 100 bis 700 Mikromol per Liter enthalten. Die Messungen wurden bei einer Wellenlänge von 400 mμ durchgeführt. Zur Verwendung gelangte ein Beckmann B Spektrophotometer.

Herrn Laborator Dr. Gunnar Jungner danke ich für die Förderung dieser Arbeit.

1. Huggins, C. und Lapides, J. *J. Biol. Chem.* **170** (1947) 477.
2. Spasov, A. *Ann. Univ. Sofia, II. Faculté phys.-math.* **35** (1938—39) 289.

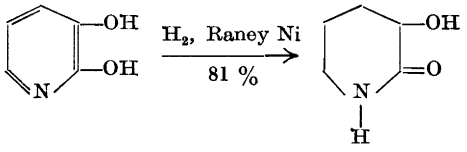
Eingegangen am 11. Juni 1957.

New Synthesis of 3-Hydroxy-2-piperidone

NIELS ELMING*

Centrallaboratoriet, Sadolin & Holmblad A/S, Copenhagen, Denmark

Catalytic hydrogenation of 2,3-pyridinediol has been shown to give the expected 3-hydroxy-2-piperidone *cf.* [1, 2]. This compound has previously been obtained by cyclization of *α*-hydroxy-*δ*-amino-*n*-valeric acid, but no detailed directions were reported [3].



* Present address: A/S Pharmacia, Copenhagen, Denmark.

Experimental. 2,3-Pyridinediol [4-6] (0.56 g) and anhydrous methanol (40 ml) were shaken (6 h) with Raney nickel (0.2 g) under hydrogen (140 atm) at 160—180°. The Raney nickel was removed by filtration and the filtrate evaporated in a vacuum. The crystalline residue was crystallized from methanol-ether. The yield was 0.47 g (81 %) of 3-hydroxy-2-piperidone [white crystals, m. p. 133—135° (Hershberg apparatus, corr.), previously found [3] 134.3°]. (Found: C 52.3; H 7.8; N 12.2. Calc. for $C_5H_9NO_2$ (115.1): C 52.2; H 7.9; N 12.2).

Sublimation (100—110°/0.05 mm) also gave white crystals, m. p. 133—135°.

In a first experiment carried out at 95—100° under 110 atmospheres of hydrogen for one hour only starting material was isolated.

1. Nielsen, J. T., Elming, N. and Clauson-Kaas, N. *Acta Chem. Scand.* **9** (1955) 30.
2. Nielsen, J. T., Elming, N. and Clauson-Kaas, N. *Acta Chem. Scand.* **9** (1955) 9.
3. Hunter, A. and Woodward, H. E. *Biochem. J.* **35** (1941) 1298.
4. Kudernatsch, R. *Monatsh.* **18** (1897) 613.
5. v. Schickh, O., Binz, A. and Schulz, A. *Ber.* **69 B** (1936) 2593.
6. Clauson-Kaas, N. and Nedenskov, P. *Acta Chem. Scand.* **9** (1955) 14.

Received April 27, 1957.

On the Mechanism of Alkylation of β-Keto Esters

I. Methylation of β-Hydroxycoumarilic Acid Ethyl Ester

ARNE BRÄNDSTRÖM and INGEMAR FORSBLAD

Chemical Institute, University of Uppsala, Uppsala, Sweden

The mechanism of the alkylation of metallic derivatives of tautomeric substances has been the subject of many investigations and theories [1]. As late as 1953 Brändström [2,3] published a new theory and in 1955 Kornblum *et al.* [4] proposed a theory seen from a different aspect.

In an attempt to elucidate the mechanism we have begun to study the alkylation of *β*-keto esters. The methylation of *β*-hydroxycoumarilic acid ethyl ester was

ACTA CHEMICA SCANDINAVICA 11 (1957) 917—926

Thiamine Phosphates and Phosphate Transport in Liver Mitochondria

KARL-HEINZ KIESSLING

Institute of Zoophysiology, Uppsala, Sweden

Incubation of mitochondria with radioactive inorganic phosphate results in an incorporation of ^{32}P into the intramitochondrial thiamine diphosphate. The incorporation is localized mainly to the terminal phosphate group (βP), and is higher with, than without pyruvate as a substrate.

Synthetic thiamine compounds (thiamine, thiamine mono-, di-, tri-, and tetraphosphate) added to mitochondria do not, however, take part in the phosphate turnover in the same degree as the endogenous compound. No further synthesis from the added compounds could be found, nor did the thiamine phosphates transfer their phosphate directly to the adenylic system at any appreciable rate. Only a very slight incorporation of ^{32}P into the added thiamine phosphates could be obtained.

In animal tissues thiamine occurs mainly as thiamine diphosphate and only to a smaller extent as thiamine. The occurrence of thiamine triphosphate * in rat liver has been reported by Rossi-Fanelli, Siliprandi, and Fasella [1].

Only few investigations dealing with the role of thiamine phosphates in the phosphate transport have been published. Kiessling and Lindahl [2] found a turnover of the phosphorus of TDP in a cyclophorase system isolated from guinea pig liver when incubated with inorganic ^{32}P, and the turnover rate was higher when pyruvate is metabolized than without added "sparker". No synthetic TDP was added, *i. e.* the only TDP present during the incubation was that initially existing in the liver (endogenous TDP) **.

* The following abbreviations have been used: T thiamine, TMP thiamine monophosphate, TDP thiamine diphosphate, TTP thiamine triphosphate, TTeP thiamine tetraphosphate, ADP adenosine diphosphate, ATP adenosine triphosphate, G-6-P glucose-6-phosphate, P_i inorganic phosphate, ^{32}P radioactive phosphate, TCA trichloroacetic acid, P/O ratio of number of micromoles of esterified phosphate to the number of microatoms of oxygen consumed.

** Endogenous thiamine phosphate: thiamine phosphate originating from the tissue. In this paper two types of endogenous thiamine phosphate have been distinguished between, *viz.* intra- and extramitochondrial thiamine phosphate.

Synthetic thiamine phosphate: thiamine phosphate added to the samples and hence not originating from the tissue.

Bartley [3] on the other hand was able to demonstrate only a rather low turnover of phosphate in TDP, when adding this substance to a kidney cyclophorase system with pyruvate or α-ketoglutarate as a substrate.

However, using ^{32}P-labelled synthetic TDP, Ogata, Nohara, Morita, and Kawai [4] found a direct transport of phosphate from TD^{32}P to ADP with a liver cyclophorase system.

The first part of this paper deals with the incorporation of radioactive phosphorus into endogenous TDP in mitochondria. In the second part the participation in the phosphate transport of synthetic thiamine phosphates added to mitochondria has been studied (Fig. 1).

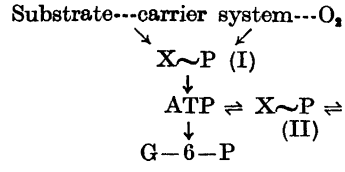


Fig. 1.

Two possibilities for the participation of thiamine compounds in the phosphate metabolism are proposed in Fig. 1. X~P indicates a thiamine phosphate. This thiamine phosphate can either be involved in the phosphate transport from the substrate-carrier level to glucose (I), or be in equilibrium with ATP in a side reaction (II). The second part of the investigation has been carried out along these alternative possibilities.

MATERIALS AND METHODS

Mitochondria were prepared from rat and guinea pig liver mainly according to the method of Schneider and Hogeboom [5]. The medium for isolation was 0.25 M sucrose, and after two washings the mitochondria were suspended in 0.25 M sucrose. The pH of the suspension was adjusted to 7.4 with TRIS-buffer or potassium phosphate buffer to a final concentration of 0.03 M.

In the experiments with rat liver, mitochondria from 10 g of liver were suspended in the buffers mentioned, and made up with sucrose to a final volume of 20 ml. To each Warburg vessel 1 ml of the mitochondrial suspension was added together with 1.2 ml of other solutions (*cf.* below); 0.2 ml KOH 2 M was added to the center well.

When isolated from guinea pig liver, large quantities of mitochondria were used in each sample (mitochondria from 5—10 g of liver). For this reason these incubations were performed in Fernbach flasks. The size of the flasks was about 200 ml. 3 ml from each sample were transferred to Warburg vessels for respiration measurements. At the end of the experiment 0.2 ml H_2SO_4 5 M was added to the Warburg vessels, and TCA to a concentration of 9 % to the Fernbach flasks in order to stop the reaction. The precipitate formed was centrifuged down and pH adjusted to 3.

From the Warburg incubations with rat mitochondria the thiamine phosphates were separated by paper chromatography [13] directly after pH had been adjusted to 3. From the Fernbach incubations with guinea pig mitochondria TDP was isolated, except in one case, by adsorption on Fuller's earth, eluated with pyridine, and purified by paper chromatography as described by Kiessling [6]. Finally a second paper chromatographic solvent (Siliprandi and Siliprandi [7]) was used in both cases as an additional purification of the thiamine phosphates. With the two solvents used the R_F values of the thiamine phosphates and of P_i differ greatly, and after the application of the two methods no inorganic phosphate could be found to contaminate the thiamine phosphates.

In the experiments with guinea pig mitochondria only endogenous TDP was present during the incubations. To facilitate the isolation synthetic TDP (2–5 mg) was added after the proteins were detached, and pH adjusted to 3. The TDP isolated in this way was a mixture of endogenous and synthetic TDP. According to Goethart [8] mitochondria from 1 g of liver contain about 4 μg TDP. Hence a rough estimate of the radioactivity of the intramitochondrial TDP can be obtained by multiplication with a dilution factor.

ATP+ADP was precipitated with Lohmann's reagent [9], and isolated by means of paper chromatography [10]. In the experiments with hexokinase present the amount of ATP was low. The specific radioactivity therefore was determined on hydrolyzable phosphate from ATP+ADP isolated from the samples.

The radioactivity was measured in an M 6 standard liquid counter tube from 20th Century Electronics Ltd. The radioactivity figures always refer to counts per 5 min.

Phosphorus was determined according to Berenblum and Chain [11]. TDP supplied by Roche Products Ltd. contained only traces of TMP. ATP and ADP in the form of the sodium salt were purchased from Sigma Chemical Company.

In my experiments I needed TDP, TTP, and TTeP labelled only in their hydrolyzable phosphate groups. By heating thiamine and unhydrous phosphoric acid Viscontini *et al.*[12] had obtained a mixture of thiamine phosphates from which they could separate TMP, TDP, and TTP by means of paper chromatography. Using another solvent I had been able to isolate from this mixture, besides the compounds mentioned, also TTeP and four additional thiamine phosphates with more than four phosphate groups [13]. By heating TDP (or TMP) with a mixture of anhydrous phosphoric acid and radioactive inorganic phosphate I obtained a mixture of thiamine phosphates labelled in the desired way. They could be separated by paper chromatography as described for the non-labelled compounds above [13]. The radioactivity of the hydrolyzable and non-hydrolyzable phosphate (the latter value in brackets) was for TDP 70 700 (600), TTP 31 600 (208), and TTeP 10 600 (160). These figures are intended only to give an idea of the relative distribution of ^{32}P within the molecules *.

The yeast hexokinase was prepared at the Wenner Gren Institute in Stockholm according to Berger *et al.*[14], except for the cytolysis in toluene, which was performed as described by Bailey and Webb [15]. The purification was followed up to step five.

RESULTS

Incorporation of ^{32}P into endogenous TDP in liver mitochondria

The mitochondria from a guinea pig liver (20 g liver) were isolated, and distributed on two Fernbach flasks, one with and one without substrate. The supernatant obtained at the preparation of the mitochondria from 10 g of liver was added to a third flask together with substrate. The substrate was pyruvate together with small amounts of α-ketoglutarate (*cf.* Table 1). To all flasks ATP, glucose, hexokinase, cytochrome c and cozymase were added. Besides these additions each flask contained radioactive inorganic phosphate. The final volume was 45 ml. From each sample 3.0 ml were transferred to Warburg vessels for respiration measurements. The oxygen consumption is shown in Fig. 2. 5 mg synthetic TDP was added to each sample to facilitate the isolation of endogenous TDP.

From the figures in Table 1 it appears that the highest specific radioactivity of TDP has been obtained in the sample with mitochondria and substrate (1.6×10^3 counts/100 μg hydrolyzable P). In accordance with the calculations

* Ogata *et al.*[4] have prepared radioactive TDP in which, however, the αP and βP were equally labelled.

Table 1.

Incubation	Radioactivity of endogenous + synt. TDP	Radioactivity of endogenous TDP	Radioactivity of ATP—ADP	Radioactivity of inorg. P
Mitoch. + substrate	1.6×10^3	2.00×10^5	4.20×10^5	1.34×10^6
Supernatant + substrate	0.30×10^3	0.30×10^5	1.20×10^5	1.05×10^6
Mitoch. without substrate	0.46×10^3	0.57×10^5	0.53×10^5	1.09×10^6

Radioactivity of TDP, inorganic and organic phosphate after incubation of mitochondria and supernatant from guinea pig liver with radioactive inorganic phosphate.

No synthetic TDP was added to the samples until the incubation was terminated, and then only to make possible the isolation of endogenous TDP. The figures given in the table for TDP refer to 100 μg synthetic + endogenous TDP, or to 100 μg endogenous TDP only.

The vessels contain 10 mg ATP, 0.5 ml cytochrome c 0.1 %, 0.5 ml DPN (0.3 mg/ml), 0.3 ml α-ketoglutarate 0.3 M, 1.0 ml pyruvate 0.3 M, 1.0 ml $MgCl_2$ 0.1 M, 75 mg glucose, hexokinase in excess, non-radioactive and radioactive inorganic phosphate. Mitochondria or supernatant was added as is seen in the table, and the volume made up to 45 ml with sucrose 0.25 M. In the third flask α-ketoglutarate and pyruvate were omitted. The figures refer to 100 μg phosphorus (for TDP and ATP this means hydrolyzable phosphorus). Time of incubation 20 min.

mentioned above 100 μg hydrolyzable intramitochondrial TDP phosphorus gives 2.0×10^5 counts, *i. e.* nearly half that of ATP—ADP (4.2×10^5 counts/100 μg hydrolyzable P).

In the sample with supernatant and substrate the TDP exhibited radioactivity, possibly depending on synthesis of TDP from thiamine as the synthesis of TDP is mainly localized to the supernatant according to Leuthardt and Nielsen [16]. The radioactivity was about 1/5 of that of intramitochondrial

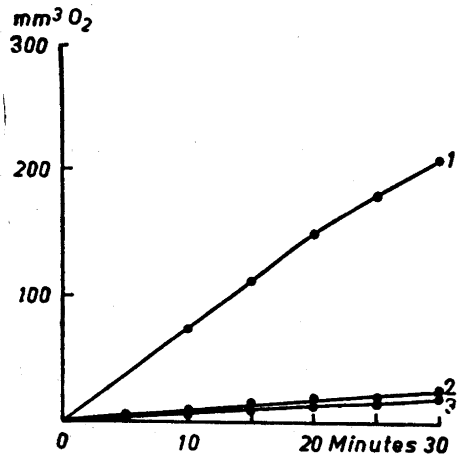


Fig. 2. Oxygen consumption in mitochondria and supernatant from guinea pig liver. 3 ml from each Fernbach flask (Table 1) were added to Warburg vessels. The center wells contained 0.2 ml KOH 2 M, and the gas phase was air.
1. mitochondria + substrate.
2. supernatant + substrate.
3. mitochondria without substrate.

TDP. Thus the radioactivity of the intramitochondrial TDP cannot, to any great extent, come from TDP synthesized in the mitochondria during the incubation.

A modification of the previous type of experiment was carried out as a control. The mitochondria were incubated with substrate as described above. The vessel contained mitochondria from 5 g of liver, the final volume being 20 ml. The radioactivity of the added phosphate was six times stronger than in the experiment above. After 20 min at 30°C the sample was rapidly cooled down to 0°C, the mitochondria centrifuged down, and washed once with sucrose. By this procedure most of the radioactive inorganic phosphate and other additions were removed, and in this way a small extract could be obtained for isolation of TDP. TCA was added to the washed mitochondria to a final volume of 5 ml giving a concentration of 9 %. After removal of the precipitated proteins and adjustment of pH to 3, 2 mg synthetic TDP were added. One ml of the sample was put as a line on a Whatman No. 1 paper, and TDP isolated by chromatography [13].

The radioactivity of the hydrolyzable phosphate, referred to 100 μg of endogenous TDP-phosphate was 2.87×10^6 counts and 4.3×10^6 for ATP—ADP. The inorganic phosphate gave 7.6×10^6 counts per 100 μg P.

In a third type of experiment the ratio between the amount of mitochondria present and the radioactive labelling of the intramitochondrial TDP was examined. Mitochondria from 10 g of liver were added to vessel 1, and from 5 g to vessel 2. Otherwise the additions were the same to both vessels. The same amount of radioactive inorganic phosphate was added to the two vessels, and the final volume of both made up to 33 ml with 0.25 M sucrose. After incubation the proteins were removed with TCA, 2 mg synthetic TDP added, and the synthetic + intramitochondrial TDP isolated by adsorption on Fuller's earth and by paper chromatography as described above. The results are given in Table 2.

Table 2.

Sample	Oxygen consumption	Radioactivity of endogenous + synt. TDP	Radioactivity of endogenous TDP	Radioactivity of ATP—ADP	Radioactivity of inorg. P
1. (10 g liver)	121	3.30×10^4	1.66×10^6	2.26×10^6	4.23×10^6
2. (5 g liver)	54	1.77×10^4	1.77×10^6	3.11×10^6	5.68×10^6

Results from an experiment with various amounts of mitochondria.
The oxygen consumption is given as mm^3/20 min/3 ml sample. The radioactivity of TDP and ATP—ADP is expressed as counts/100 μg hydrolyzable P, and of inorganic phosphate as counts/100 μg P. Apart from mitochondria the Fernbach flasks contained 10 mg ADP, 1 mg cytochrome c, 0.3 mg cozymase, 0.3 ml α-ketoglutarate 0.3 M, 1.5 ml pyruvate 0.3 M, 1.0 ml Mg^{2+} 0.1 M, 75 mg glucose, hexokinase and radioactive inorganic phosphate. Mitochondria from 10 g of liver suspended in 20 ml sucrose-phosphate medium pH 7.4 were added to sample 1 and from 5 g to sample 2, and the volume made up to 33 ml with 0.25 M sucrose. The samples were incubated at 30°C for 20 min.

The figures show that the specific radioactivity of the total TDP (synthetic + intramitochondrial) from sample 1 (10 g of liver) is about twice that of sample 2 (5 g of liver). The specific radioactivity is the same in both samples as far as only the intramitochondrial TDP is concerned.

Comparing the radioactivity in TDP of the βP with that of the αP it appears that mainly the βP becomes labelled. The ratio between the radioactivity of βP and αP varies from 8—14 in the three types of experiments reported above.

The figures from the experiments show that the intramitochondrial TDP incorporates ^{32}P, and mainly in the hydrolyzable phosphate (βP). This incorporation is more rapid when a substrate as pyruvate is metabolized than when no substrate is added.

In the following experiments the role of added synthetic thiamine phosphates in a mitochondrial system is studied.

Synthetic thiamine derivatives as phosphate acceptors in mitochondria

Rat liver mitochondria in a 0.01 M phosphate buffer in 0.25 M sucrose were incubated with T, TMP, TDP, or TTP. One mg of the thiamine compound in 0.5 ml water was added to each vessel. Besides, the vessels contained 0.8 mg ATP, 0.1 ml 0.3 M glutamate, hexokinase, 4 mg glucose, 0.05 ml Mg^{2+} 0.1 M, and 0.05 mC radioactive inorganic phosphate. The samples were made isotonic by addition of 1 M sucrose. Finally 1 ml mitochondria suspension was added. After 20 min incubation at 30°C 0.2 ml of 5 M H_2SO_4 was added, samples were taken for determination of organic and inorganic ^{32}P and, after neutralization, the thiamine phosphates were isolated on paper chromatograms. The presence of synthetic thiamine compounds did not affect the P/O value which was about 2. No spots could be found on the chromatograms suggesting any further phosphorylation of the thiamine compounds during the incubation. On the contrary a slight hydrolysis of the thiamine phosphates had taken place. TTeP had partly been hydrolyzed to TTP, and TTP to about 20 % to TDP.

TTeP did not contain any radioactivity at all. The hydrolyzable phosphate of TTP gave 600 counts/100 μg hydrolyzable P and of TDP 520 counts/100 μg hydrolyzable P.

The results show that added thiamine or thiamine phosphates do not at all or only at a very low rate act as phosphate acceptors in a respirating mitochondria system. The incorporation of ^{32}P into TDP is slow compared with that of the mitochondrial TDP, described above.

Possibly thiamine phosphates are in equilibrium with ATP in a side reaction (Fig. 1, alternative II). In the presence of glucose and hexokinase, however, no AT^{32}P would accumulate and, as a consequence, no formation of thiamine phosphates would occur to give rise to radioactive thiamine phosphates. An accumulation of AT^{32}P could experimentally be effected by excluding hexokinase. Incubation of TMP and TDP with ADP in the same way as described above but without hexokinase did, however, not give rise to TTP from TDP or TDP from TMP, nor was a higher incorporation of ^{32}P obtained compared with that found in the experiments with hexokinase present. Neither

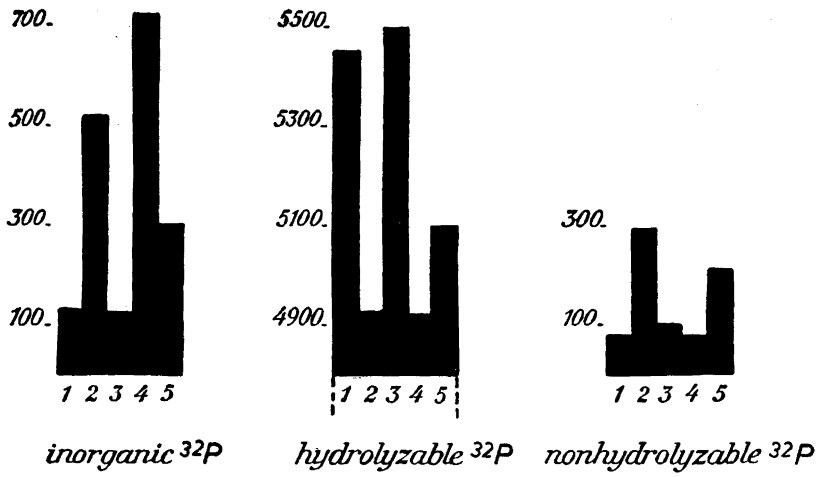


Fig. 3. The radioactivity in the inorganic, hydrolyzable, and non-hydrolyzable phosphate fraction from a mitochondria experiment with labelled TDP.

1. mitochondria + ADP + $TD^{32}P$ + hexokinase + glucose (0 min)
2. mitochondria + ADP + $TD^{32}P$ + hexokinase + glucose (20 min)
3. mitochondria + ADP + $TD^{32}P$ (20 min)
4. ADP + $TD^{32}P$ + hexokinase + glucose (20 min)
5. mitochondria + ADP + $TD^{32}P$ + hexokinase + glucose + inorganic non-radioactive phosphate (50 μM) + 0.1 ml glutamate 0.3 M (20 min)

The rat mitochondria were suspended in a TRIS-sucrose medium pH 7.4. 0.4 ml $TD^{32}P$ (1 000 μg/ml) was added to each flask together with 1 mg ADP, hexokinase, and 4 mg glucose (except in flask 3). To vessels 1—3 and 5 was added 1 ml mitochondria, and the volumes of all samples were made up to 2.2 ml with sucrose. Incubation time 20 min at 30°C. The oxygen consumption in sample 5 was 108 mm^3 in 20 min. The radioactivity was measured on 0.1 ml of the samples.

did exclusion of substrate influence upon the radioactivity in the added thiamine phosphates.

In the experiments without hexokinase no hydrolysis of the thiamine phosphates was observed. It therefore seems that the hexokinase preparation, purified to this special stage, still contains a phosphatase which attacks thiamine phosphates.

Synthetic thiamine phosphates as phosphate donors in mitochondria

From the above results it is obvious that added thiamine phosphates do not take part in the phosphate transport from the substrate-carrier level *via* ATP to glucose in the system used (Fig. 1, alternative I). Neither was the supposition confirmed that thiamine phosphates are in equilibrium with ATP in a side reaction (Fig. 1, alternative II), as it was impossible to transfer ^{32}P to the thiamine phosphates when $AT^{32}P$ was accumulated by excluding hexokinase.

This indicates that no equilibrium exists between added thiamine phosphates and ATP in a side reaction, or that the equilibrium is displaced far towards ATP.

In order to examine the second alternative thiamine phosphates were prepared containing radioactive phosphorus only in their hydrolyzable phosphate groups. If a direct phosphate transfer exsists from thiamine phosphates to ADP, the ATP formed would be radioactive. The γP should be trapped off by the hexokinase and the glucose, and rediscovered as non-hydrolyzable glucose-6-phosphate. Thus a decrease in the hydrolyzable phosphate and an increase in the non-hydrolyzable phosphate would be easy to follow without previously isolating the thiamine phosphates or the phosphate acceptor.

The results of an experiment are seen in Fig. 3.

As was pointed out earlier the hexokinase preparation used is contaminated with a phosphatase which slowly hydrolysis thiamine phosphates. When hexokinase is present the phosphatase splits off phosphate from TDP, and this gives rise to the radioactivity in the inorganic fraction in samples 2 and 4 (Fig. 3). With hexokinase present but no mitochondria (sample 4) the radioactivity in the inorganic fraction is higher than when mitochondria have been added. Very likely this is effected by ADP being phosphorylated to ATP in the presence of mitochondria, as these may contain traces of substrate. In the sample without mitochondria (sample 4) no inorganic phosphate is eliminated in this way. Therefore the radioactivity of the inorganic fraction in this sample is somewhat higher than in sample 2.

The radioactivity in the non-hydrolyzable fraction rises in the sample where both mitochondria and hexokinase are present (sample 2). This rise is, however, not larger than what corresponds to the decrease in the inorganic fraction in sample 2, which fraction can be assumed initially to have been as high as in sample 4.

In the fifth sample the components present were the same as in samples 1 and 2. In addition glutamate and inorganic non-radioactive phosphate were added. With a substrate and inorganic phosphate present TDP was not hydrolyzed to the same degree as without these additions as is seen in Fig. 3. The radioactivity peak of the hydrolyzable phosphate in sample 5 is somewhat higher than in 2 and 4, and the radioactivity of the inorganic fraction is lower than in 2. The radioactivity of the non-hydrolyzable fraction is even lower than the inorganic fraction. This indicates that the phosphate of the glucose-6-phosphate can not originate directly from the highly labelled TDP-phosphate. It must have been diluted primarily with inorganic non-labelled phosphate before being transferred *via* ATP to glucose. From this it may be concluded that intact mitochondria do not contain an enzyme system which transfers phosphate from added TDP to ADP without previous hydrolysis to inorganic phosphate, or if such an enzyme system exists, the rate of transfer must be very low.

The same results were obtained by using TTeP or TTP instead of TDP. With TMP no liberation of inorganic phosphate took place, nor could any rise in the radioactivity of the non-hydrolyzable fraction be observed.

DISCUSSION

In this paper the incorporation of radioactive phosphorus into intramitochondrial TDP has been studied as well as the extent to which synthetic thiamine phosphates added to mitochondria take part in the phosphate metabolism.

The results show that intramitochondrial TDP and added synthetic thiamine phosphates do not take part in the phosphate metabolism to the same extent.

The specific radioactivity of the intramitochondrial TDP was high after incubation (1/2—2/3 of that of ATP—ADP), whereas the added synthetic thiamine phosphates neither incorporated ^{32}P in any appreciable degree, nor supplied phosphate to ADP.

In a previous note [2] an incorporation of ^{32}P into TDP was found to take place in a cyclophorase system from guinea pig liver. Only the endogenous TDP was present during the incubation. The incorporation into TDP depended on the metabolization of a substrate, in this case pyruvate, and was proportional to the oxygen consumption.

Bartley could not verify these results [3]. He used a kidney cyclophorase system to which synthetic thiamine phosphates were added. The specific radioactivity of the added thiamine phosphates was fairly low. These investigations on incorporation of ^{32}P into thiamine phosphates by a cyclophorase system are in keeping with the results obtained with mitochondria in the present paper which show that intramitochondrial TDP incorporates ^{32}P in a much higher degree than added synthetic thiamine phosphates.

From Bartley's experiments it is not possible to decide to what extent the thiamine phosphates furnish ADP with phosphate, and then appear as phosphate compounds with a reduced number of phosphate groups, as he only determines the incorporation of ^{32}P into the added thiamine compounds. The transfer of phosphate from added synthetic TDP to ADP in a cyclophorase system has been examined by Ogata *et al.*[4]. They found a direct transfer of phosphate from TD^{32}P to ADP. My experiments, however, supply no evidence for the existence of an active enzyme system in intact mitochondria which catalyses phosphate transport from added thiamine phosphates to ADP.

These discrepancies may depend on the fact that no intact mitochondria exist in a cyclophorase system. TDP added to the system might easily come in contact with the actual enzyme. In so doing it forms a short-lived and unstable combination and, after delivering one phosphate, leaves room for another TDP. In the intact mitochondria the intramitochondrial TDP would be much stronger bound in the enzyme. Hence it would not be split off after delivering phosphate, but the generated TMP would be rephosphorylated to TDP.

To explain the differences as depending exclusively on difficulties of TDP to penetrate the membrane of the intact mitochondria is not convincing, as TDP in the tissues is mainly synthesized outside the mitochondria [16], and thus must penetrate the membrane to reach its apoenzyme.

Acknowledgements. I am indebted to Prof. P. E. Lindahl for valuable discussion and to Prof. O. Lindberg for the privilege of carrying out part of this work in his laboratory, and for the interest he has shown in it. I also wish to express my thanks to Dr. L. Ernster and Dr. H. Löw for stimulating discussions and helpful criticism. Thanks are also due to Mrs. Margot Aunver for technical assistance, to the technical staff at the Wenner-Gren Institute for help with preparation of rat mitochondria, and to Dr. A. L. Morrison, Messrs. Roche Products Ltd., for the gift of TDP.

This work was made possible by grants from the *Swedish Natural Science Research Council*, and from *Magn. Bergvalls Stiftelse*.

REFERENCES

1. Rossi-Fanelli, A., Siliprandi, N and Fasella, P. *Science* **116** (1952) 711.
2. Kiessling, K.-H. and Lindahl, P. E. *Arkiv Kemi* **4** (1952) 285.
3. Bartley, W. *Biochem. J. London* **56** (1954) 379.
4. Ogata, K., Nohara, H., Morita, T. and Kawai, K. *J. Biochem. Japan* **42** (1955) **13.**
5. Schneider, W. and Hogeboom, G. *J. Biol. Chem.* **183** (1950) 123.
6. Kiessling, K.-H. *Biochim. et Biophys. Acta* **20** (1956) 293.
7. Siliprandi, D. and Siliprandi, N. *Biochim. et Biophys. Acta* **14** (1954) 52.
8. Goethart, G. *Biochim. et Biophys. Acta* **8** (1952) 479.
9. Carter, H. *Biochem. Preparations* **1** (1949) 5.
10. Krebs, H. A. and Hems, R. *Biochim. et Biophys. Acta* **12** (1953) 172.
11. Berenblum, I. and Chain, F. *Biochem. J. London* **32** (1938) 295.
12. Viscontini, M., Bonetti, G. and Karrer, P. *Helv. Chim. Acta* **32** (1949) 1478.
13. Kiessling, K.-H. *Acta Chem. Scand.* **10** (1956) 1356.
14. Berger, L., Slein, M., Colowick, S. and Cori, C. *J. Gen. Physiol.* **29** (1946) 379.
15. Bailly, K. and Webb, E. *Biochem. J. London* **42** (1948) 60.
16. Leuthardt, F. and Nielsen, H. *Helv. Chim. Acta* **35** (1952) 1196.

Received March 7, 1957.

ACTA CHEMICA SCANDINAVICA 11 (1957) 927—931

The Structure of Xanthoperol

JOHAN B-SON BREDENBERG

Department of Chemistry, Institute of Technology, Helsingfors, Finland

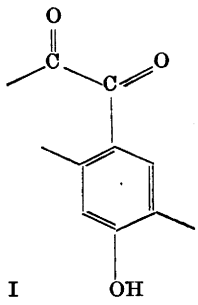
The structure V is proposed for xanthoperol, an artefact from the wood of *Juniperus communis* L. Xanthoperol is formed, without intervention of atmospheric oxygen, during the alkaline hydrolysis of wood extract from a substance having a *p*-ketophenol chromophore.

In a previous paper, the isolation of the diterpene phenol xanthoperol has been described [1], *. In the same paper, a partial structure (I) was proposed and the possibility that xanthoperol might have the structure 9,10-diketoferruginol (II) was discussed and regarded with doubt.

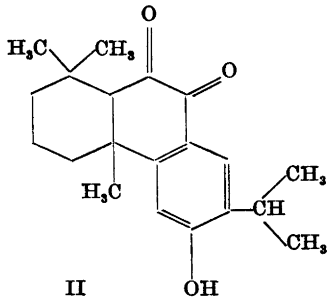
In continuation of the work, xanthoperol was subjected to Clemmensen reduction. As it is an α-diketone, it was considered possible that it might yield a mixture of various stages of reduction. This was also borne out by the experiment. The bulk of the reduction product was a mixture corresponding in its properties to a mixture of ferruginol (III), Δ^9-dehydroferruginol and hydroxyferruginols. As a side product a substance was isolated which showed properties corresponding to 9-ketoferruginol. On chromic oxide oxidation of the acetylated main part this same substance was obtained, besides xanthoperol. The substance, melting between 240 and 250° with decomposition, had an ultraviolet spectrum with the same shape as that of 9-ketoferruginol, *i. e.* a sharp maximum at 236 mμ (log ε 4.17) and a broad maximum at 286 mμ (log ε 4.09). The infrared spectrum likewise confirmed the conclusion that it was analogous to 9-ketoferruginol.

The reduced xanthoperol was dehydrogenated with selenium, but owing to the small amount of starting material, no pure product could be isolated. The ultraviolet spectra of some fractions of the chromatographed reaction product, however, showed full correlation with the spectrum of retenol-6 (IV) with maxima where retenol-6 has its major bands and plateaus or inflexions where retenol-6 has its side bands. These must be regarded as a strong indication that the dehydrogenation yielded retenol-6. Further evidence for the

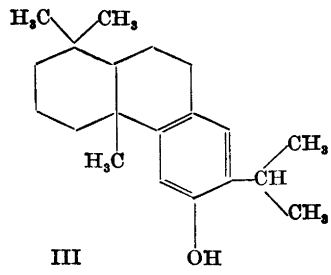
* In the theoretical part of this paper the wave-number of the hydroxyl band is erroneously given as 3 436 cm^{-1}; it should be 3 380 cm^{-1}.



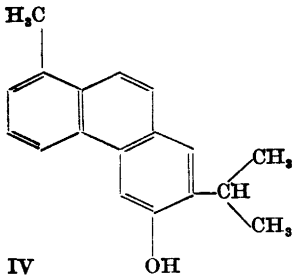
I



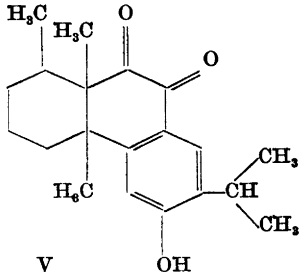
II



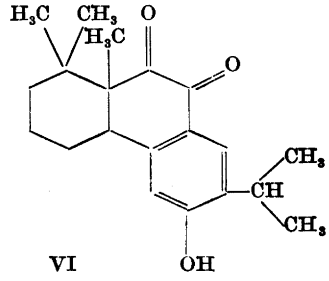
III



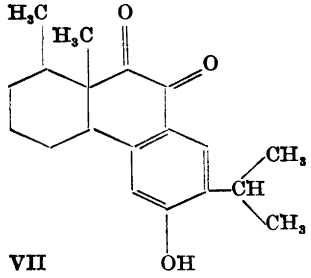
IV



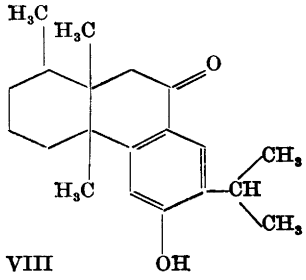
V



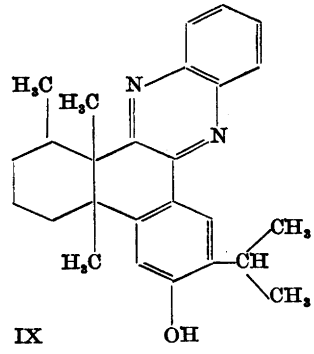
VI



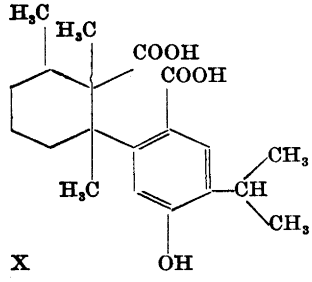
VII



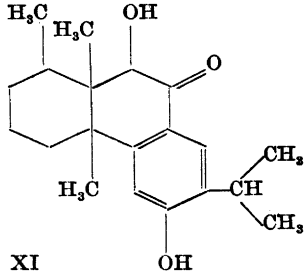
VIII



IX



X



XI

presence of an *iso*propyl group in xanthoperol is afforded by the occurrence of bands at 1 163 cm^{-1} in xanthoperol and 1 172 cm^{-1} in the reduction product.

The retenol accounts for 18 carbon atoms. The remaining two carbon atoms, in the form of two methyl groups or, less probably, an ethyl group, must be placed in such positions that they are lost during the dehydrogenation, *i. e.* in the positions 1, 11 or 12, on the assumption that the aromatic ring in the partial structure (I) corresponds to the C-ring. This last assumption is strongly supported by the nature of the other compounds isolated from the wood of the juniper: ferruginol, Δ^9-dehydroferruginol and 9-ketoferruginol [2,3]. In the previous paper [1], it was shown that all structures proposed for xanthoperol where the 10-ketogroup could be enolised must be regarded with doubt. One methyl group must consequently be placed in the 11-position to hinder the enolisation. This leaves two structures: V, where a methyl group from the 1-position has migrated to the 11-position in comparison with the common diterpene phenols, and VI, where the methyl group from the 12-position has migrated to the 11-position. A third structure, the C_{19}-structure VII, which must also be taken into consideration at this stage, would apparently imply that the migration C-1—C-11 and C-12—C-13 of the methyl groups has occurred, as postulated in the case of columbin [4], with subsequent loss of the methyl group at the 13-position by aromatisation of the C-ring.

Decision can be made from among these structures by a C-methyl determination. The model 9-ketoferruginol gives the value 1.12, while xanthoperol gives 1.98. This at once excludes the structure VI as well as 9,10-diketoferruginol (II), which have the same side chains as 9-ketoferruginol. A short calculation shows that structure VII can also be ruled out. It is known that a *gem.*-dimethyl group contributes to the C-methyl determination with a value of 0.4 [5]. Hence the *iso*propyl group and the angular methyl group contribute with a joint value of 0.72. This would give the value 1.98—0.72 = 1.26 for the methyl group in the 1-position in structure VII, an obviously impossible value. If we assume that the *iso*propyl group also contributes with a value of 0.4 (the angular methyl group = 0.32), we would obtain the value 0.94 for the methyl group in the 1-position in structure V, which tallies well with the expected value. Even if one must be cautious in drawing inferences from detailed calculations of the C-methyl values, the results, nevertheless, strongly support the correctness of structure V. The reduction product, m. p. 240—250°, consequently has the structure VIII.

In most of the experiments performed, the diketo group proved to be sterically hindered. An attempt to prepare a disemicarbazone thus failed and oximation yielded only a nonresolvable mixture. Condensation with *o*-phenylene diamine gave in low yield a substance, m. p. 250—252°, which can be regarded as the corresponding quinoxaline (IX). Oxidation with periodic acid gave a quantitative recovery of xanthoperol. Treatment of xanthoperol with a large excess of alkaline hydrogen peroxide at room temperature for a long period (two days) yielded a small amount of an impure substance, m. p. 200—202°, to which the corresponding dicarboxylic acid structure X must be assigned.

Xanthoperol has a structure with no known counterpart in diterpene chemistry. It was therefore of special interest to study its formation. As

previously remarked [1], xanthoperol does not occur as such in wood. Closer examination, especially by spectrophotometry in ultraviolet, revealed that the precursor is a substance which is eluted directly after 9-ketoferruginol and that it has a chromophore which is the same or very nearly the same as the chromophore of 9-ketoferruginol. Atmospheric oxygen does not take part in the formation of xanthoperol during hydrolysis. The yield is actually higher in an atmosphere of hydrogen. The results appear to point to the structure XI or its equivalent, which would be oxidised during the hydrolysis by substances occurring simultaneously in the fractions. In spite of several attempts, the precursor could not be obtained in pure form.

EXPERIMENTAL

(All m. p. s are determined on a Kofler microscope. The microanalyses have been performed by Dr. A. Bernhardt, Mülheim, and the infrared spectra by Mr. B. C. Fogelberg, B. Sc.).

Clemmensen reduction of xanthoperol. Xanthoperol (60 mg) in ethanol-benzene (10 ml, 1:1) was reduced with amalgamated zinc (5 g) and concentrated hydrochloric acid (4 ml) at reflux temperature. After 1 1/2 h, when both layers were colourless, the heating was stopped, conc. hydrochloric acid (10 ml) was added and the mixture was allowed to stand overnight. Water was added and the solution was extracted with ether. The solvent was evaporated and the residue extracted with light petroleum, which left undissolved 0.5 mg of crystals, m. p. 240—250° (decomp.). The ultraviolet spectrum of these crystals in ethanol showed a sharp maximum at 236 mμ and a broad maximum at 286 mμ. The part soluble in light petroleum, having a maximum at 285 mμ, was acetylated with acetic anhydride and pyridine. The acetylation yielded a slowly crystallising sticky mass (44 mg), m. p. 75—95°, λ_{max} (in ethanol) 271 mμ (log k 0.92). Purification by chromatography or crystallisation did not sharpen the melting point.

Oxidation of the reduction product with chromic oxide. Xanthoperol (85 mg) was reduced as before. The reduced product was oxidised with chromic oxide (40 mg) in acetic acid (8 ml) on the water bath for 1 h. After dilution with water, the product was extracted with ether and the ether was evaporated. The residue was chromatographed on an Al_2O_3 column with light petroleum-ether-methanol. Ether-methanol eluted xanthoperol. In the ether eluates, before xanthoperol came out, about 20 mg of impure 10-deketoxanthoperol (VIII) could be demonstrated spectrophotometrically. These fractions were purified by crystallisation and sublimation, yielding 3 mg of needles, m. p. 240—250° (decomp.), λ_{max} (in ethanol) 236 mμ (log ε 4.17) 286 mμ (log ε 4.09). Principal IR-maxima (KBr): 3 280 (s), 2 920 (s), 2 835 (m), 1 642 (s), 1 590 (s), 1 568 (s), 1 502 (m), 1 464 (m), 1 385 (w), 1 366 (m), 1 340 (s), 1 309 (w), 1 288 (m), 1 257 (s), 1 192 (m), 1 172 (m), 1 055 (w), 970 (w) and 876 cm^{-1} (w). The properties of the compound resembled those of 9-ketoferruginol.

Selenium dehydrogenation of reduced xanthoperol. Reduced xanthoperol (80 mg) was mixed with selenium (300 mg) and heated at 290° for 24 h. The product was extracted with ether and the ether evaporated. The residue was chromatographed on an Al_2O_3 column with benzene-ether-methanol. The fractions eluted by ether-methanol, showing the expected ultraviolet spectra of phenanthrene derivatives, were rechromatographed. The elution was followed by spectrophotometry, but no fraction having a pure spectrum could be obtained. The purest fractions had UV-spectra of the following form: (in ethanol) maxima at 223, 258, 342 and 360 mμ, plateaus or inflexions at 270 and 308 mμ; (in *cyclo*hexane) maxima at 222, 260 and 360 mμ and plateaus or inflexions at 277, 306, 327 and 340 mμ.

Retenol-6 (IV) from 6-aminoretene. Retenol-6 was obtained from an authentic sample of 6-aminoretene by diazotisation. The product formed needles, m. p. 178—179°. (Found C 86.3; H 7.7. Calc. for $C_{18}H_{18}O$ C 86.4; H 7.3.) UV-spectrum of retenol-6: (in ethanol) mμ (log ε): 220 (4.44), 257 (4.68), 279 (4.19), 310 (4.03), 342 (3.39) and 359 (3.40); (in *cyclo*hexane) mμ (log ε): 221 (4.40), 258 (4.69), 278 (4.25), 295 (3.98), 308 (4.11), 325 (3.11), 340.5 (3.32), 357.5 (3.38).

Derivatives of xanthoperol. In attempts to prepare the disemicarbazone from xanthoperol and semicarbazide hydrochloride by heating on a water bath with sodium acetate in ethanol for one day or in pyridine-water for three days, a quantitative recovery of xanthoperol was obtained. Oximation with hydroxylamine hydrochloride in pyridine-ethanol for two days on a water bath gave crystals, m. p. 111—114°, but a sharp melting point could not be obtained by further purification.

Condensation with o-phenylene diamine. Xanthoperol (26 mg) and *o*-phenylene diamine (20 mg) were heated in acetic acid (1 ml) for 19 h on a water bath and thereafter for 2 h with reflux. Water was added and the precipitate was filtered. The precipitate was dissolved in ether and unreacted xanthoperol was extracted with 2 N sodium carbonate. After evaporation of the ether, the residue was crystallised from benzene-light petroleum, m. p. 250—252° (4 mg). The compound (IX), which was shown by paper chromatography to be free from xanthoperol, gave a deep red to violet colour with conc. sulphuric acid. λ_{max} (in ethanol) 241 mμ (log ε 4.19), 383 mμ (log ε 4.25), plateau at 260—290 mμ (log ε 4.1).

Oxidation with periodic acid. No reaction occurred between xanthoperol and periodic acid in acidic aqueous ethanol, even at water-bath temperature. The recovery of xanthoperol was quantitative in all experiments.

Oxidation with alkaline hydrogen peroxide. After preliminary experiments had shown that no reaction occurred in milder conditions, the oxidation was carried out by keeping xanthoperol (17 mg) and 30 % hydrogen peroxide (0.5 ml) in N sodium hydroxide (5 ml) for two days at room temperature. The now colourless solution was acidified and the flocky precipitate (4 mg) filtered. The precipitate (X), m. p. 200—202°, sublimed as needles from 150°. λ_{max} (in ethanol) 247 mμ (log ε 3.72), 290 mμ (log ε 3.62), Principal IR-maxima (KBr): 3 300 (broad) 2 900 (broad), 1 720 (broad), 1 680, 1 595, 1 558, 1 513, 1 460, 1 415, 1 343, 1 235, 1 165, 1 115, 940 and 872 cm^{-1}.

The formation of xanthoperol. The neutral non-hydrolysed part of the wood extract was chromatographed on an Al_2O_3 column with light petroleum-ether. Samples were taken from the fractions, which had been eluted by light petroleum-ether and ether, and UV-spectra were run in ethanol and in alkaline solution. After hydrolysis, spectra were again taken in ethanol and in alkaline solution. These spectra showed that the precursor was eluted after 9-ketoferruginol, and that it had an ultraviolet spectrum resembling that of 9-ketoferruginol: maxima at about 230 and 280 mμ in neutral and at 350 mμ in alkaline solution. The yield of xanthoperol was higher when the hydrolysis was performed in an atmosphere of hydrogen than in an atmosphere of oxygen. The precursor could not be obtained pure.

The author is indebted to Dr. J. Gripenberg for valuable suggestions. He also wishes to express his thanks to Dr. K. J. Karrman for a sample of 6-aminoretene.

REFERENCES

1. Bredenberg, J. B. and Gripenberg, J. *Acta Chem. Scand.* **10** (1956) 1511.
2. Bredenberg, J. B. and Gripenberg, J. *Acta Chem. Scand.* **8** (1954) 1728.
3. Bredenberg, J. B. *Acta Chem. Scand.* **11** (1957) 932.
4. Barton, D. H. R. and Elad, D. *J. Chem. Soc.* **1956** 2090.
5. Müller, E. (Ed) *Methoden der Organischen Chemie*, Georg Thieme, Stuttgart 1953, Vol. II, p. 274.

Received February 26, 1957.

ACTA CHEMICA SCANDINAVICA 11 (1957) 932—935

Ferruginol and Δ^9-Dehydroferruginol

JOHAN B-SON BREDENBERG

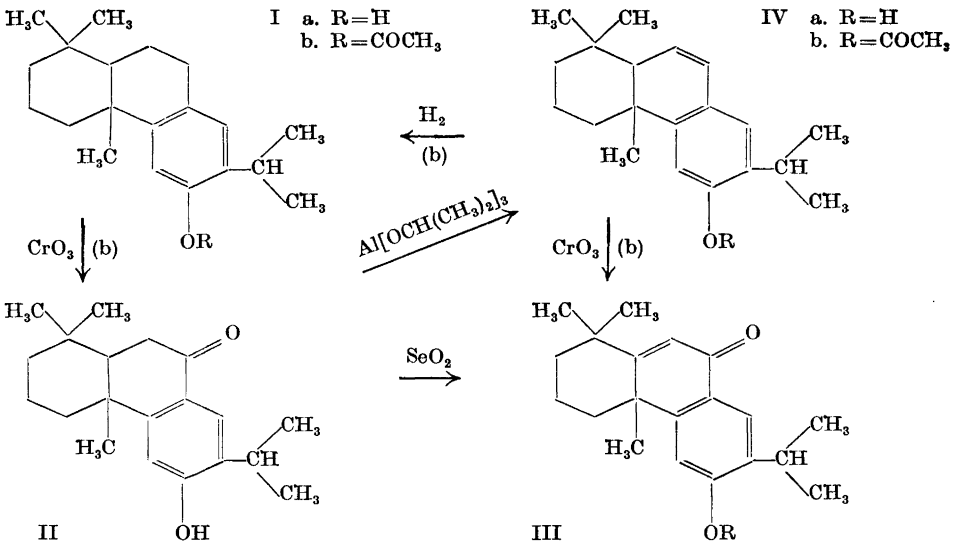
Department of Chemistry, Institute of Technology, Helsingfors, Finland

The phenolic substance, acetate m. p. 92—93°, from the wood of *Juniperus communis* L. has been shown to be a mixture of ferruginol and Δ^9-dehydroferruginol. The previously isolated ferruginol from *Podocarpus ferrugineus* D. Don and *Dacrydium cupressinum* Solander also contains small amounts of Δ^9-dehydroferruginol. This compound has been synthesised.

The isolation of a phenolic substance in the form of a crystalline acetate, m. p. 92—93°, has previously been described [1]. This substance was at first thought to represent a pure compound "katajol" [2], but later this was doubted. In particular, the fact that only partial crystallisation of the phenol could be effected, was taken as an indication of non-homogeneity. It was suggested that the substance was a mixture of ferruginol (Ia) and a dehydro derivative [1]. Definite evidence of its nature came from an oxidation of the acetate with chromic oxide. After hydrolysis, this yielded a substance which was identified as a mixture of 9-ketoferruginol (II) and 9-keto- Δ^{10}-dehydroferruginol (III) by comparison of its ultraviolet and infrared spectra with those of the authentic compounds. On selenium dioxide dehydrogenation of the mixture, pure 9-keto- Δ^{10}-dehydroferruginol was obtained.

The acetate was subjected to catalytic hydrogenation, and it consumed 0.42 moles of hydrogen per mole of substance. The hydrogenated acetate formed rods, m. p. 81—82°, $[\alpha]_D^{20}$ +62° (ethanol). On hydrogenation, the ultraviolet spectrum (in ethanol) was altered from one absorption maximum at 268 mμ (log ε 3.71) to two maxima at 269 mμ (log ε 3.08) and 278 mμ (log ε 3.12). There is only one position, the conjugated 9-position, where the double bond could be placed in order to explain the large hypochromic shift in the ultraviolet spectrum and the formation of 9-keto- Δ^{10}-dehydroferruginol. During the chromic oxide oxidation the double bond in the 9-position obviously migrates to the 10-position. The acetate, m. p. 92—93°, thus consist of ferruginyl acetate (Ib) and Δ^9-dehydroferruginyl acetate (IVb). In order to verify this, Δ^9-dehydroferruginyl acetate was prepared in a 70 % yield by aluminium *iso*propoxide reduction of 9-ketoferruginol and acetylation of the reduced product. The reduction yielded in one stage the desired dehydro

derivative as a result of the easy dehydration that occurred in the intermediate 9-hydroxyferruginol. The Δ^9-dehydroferruginyl acetate had the constants m. p. 108—109°, $[\alpha]_D^{20}$ —92° (ethanol), λ_{max} (in ethanol) 220 mμ (log ε 4.39), 266 mμ (log ε 4.01), all of which are in good correlation with the constants



calculated from the pure ferruginyl acetate, the acetate mixture and the hydrogen consumed by it. Ferruginyl acetate and Δ^9-dehydroferruginyl acetate were investigated by the contact method of Kofler [3] and found to form mixed crystals of Roozebom's type I.

Ferruginol, $[\alpha]_D^{18}$ +65° (ethanol), λ_{max} (in ethanol) 284 mμ (log ε 3.50) prepared from ferruginyl acetate resisted crystallisation. By prolonged chromatography a few crystals, m. p. 56—57°, could be obtained, but the greater part could not be crystallised. Even a trace of impurity seems to be able to inhibit crystallisation. Δ^9-Dehydroferruginol, $[\alpha]_D^{20}$ —60° (ethanol), λ_{max} (in ethanol) 218 mμ (log ε 4.29), 280 mμ (log ε 3.97) also resists crystallisation.

The formation of mixed crystals between ferruginyl acetate and its dehydro derivative explains some discrepancies in the literature and our observations. From *Podocarpus ferrugineus* D. Don, Brandt and Neubauer [4] isolated ferruginol, $[\alpha]_D^{16}$ +40.6° (ethanol). A sample of the acetate from this ferruginol was kindly supplied by Prof. H. Erdtman. After catalytic hydrogenation, this acetate, m. p. 82—83°, $[\alpha]_D^{20}$ +57° (ethanol), λ_{max} (in ethanol) 269 mμ (log ε 3.19), 278 mμ (log ε 3.19) gave the values m. p. 81—2°, $[\alpha]_D^{20}$ +62° (ethanol), λ_{max} (in ethanol) 269 mμ (log ε 3.09), 278 mμ (log ε 3.12). Hence it contained about 3 % Δ^9-dehydroferruginyl acetate. For the acetate of ferruginol obtained from *Dacrydium cupressinum* Solander, Brandt and Thomas [5] reported

log ε 3.3 at λ_{max} 269 mμ (in ethanol). This would be equivalent to a content of about 9 % of the dehydro form.

In the partial synthesis of ferruginol from dehydroabietic acid and podocarpic acid, Campbell and Todd [6] reported rotations of the ferruginyl acetates and of the crude ferruginols, which are in good correlation with the present values, but in the purification of ferruginol from podocarpic acid the rotation was lowered from $[\alpha]_{Hg}^{25}$ +59° to $[\alpha]_{Hg}^{27}$ +37.8° (ethanol). No explanation for this behaviour has been found.

The isolation of ferruginol from the wood of *Juniperus communis* L. in a yield of 0.1 % would at least partially explain the durability of the wood, for this phenol is a fungicide [7].

EXPERIMENTAL

(All m. p.'s are determined on a Kofler microscope. The microanalyses have been performed by Dr. A. Bernhardt, Mülheim.)

Oxidation of the acetate, m. p. 92—93°, with chromic oxide. The acetate (200 mg) and chromic oxide (80 mg) in acetic acid (10 ml) were heated on the water bath for 45 min. After dilution with water, the product was extracted with ether. The crystals obtained from the ether melted after recrystallisation between 115 and 130°. This mixture was chromatographed, yielding 48 mg of colourless prisms, m. p. 287—289°. Both the UV- and the IR-spectrum proved that the crystals consisted of a mixture of 9-ketoferruginol and 9-keto-Δ^{10}-dehydroferruginol.

9-Keto-Δ^{10}-dehydroferruginol (III). 9-Ketoferruginol (30 mg) and selenium dioxide (11 mg) in nitrobenzene (2 ml) were heated at 190° for 2 h. The dark-coloured solution was filtered and the precipitate washed with ether and ethanol. The combined filtrates were washed with sodium carbonate, and the ether and ethanol evaporated. After chilling, 13 mg of pink-coloured rods, m. p. 281—283°, crystallised out. Recrystallisation from benzene-light petroleum yielded colourless crystals, m. p. 288—290°. (Found C 80.2; H 8.9. Calc. for $C_{20}H_{26}O_2$ C 80.5; H 8.8.) UV-spectrum: λ_{max} (in ethanol) 246 mμ (log ε 4.21), 316 mμ (log ε 4.02); (in 0.05 N Na_2CO_3) 245 mμ (log ε 4.30), 381 mμ (log ε 4.18). IR-spectrum, principal bands (KBr): 3 060 (s), 2 905 (s), 2 840 (m), 1 630 (s), 1 610 (s), 1 575 (s), 1 555 (s), 1 500 (s), 1 460 (s), 1 383 (s), 1 340 (s), 1 310 (s), 1 282 (s), 1 258 (s), 1 178 (s), 1 150 (m), 1 090 (m), 887 (s), 875 (m) and 866 cm^{-1} (s).

A sample of the previously obtained mixture of 9-ketoferruginol and 9-keto-Δ^{10}-dehydroferruginol (25 mg) was oxidised with selenium dioxide (9 mg) as described above. After purification, 9 mg of rods, m. p. 287—289°, were isolated. The IR- and UV-spectra of this product were identical with those of authentic 9-keto-Δ^{10}-dehydroferruginol.

Hydrogenation of the acetate, m. p. 92—93°. The acetate (300 mg) in ethanol (10 ml) was subjected to catalytic hydrogenation with a Pt-catalyst (16 mg PtO_2). The reduction stopped after 1 h, 0.38 mmoles of hydrogen having been consumed. The product (290 mg) crystallised from ethanol as rods, m. p. 81—82°, $[\alpha]_D^{20}$ +62° ± 2° (ethanol, *c* 2.2). (Found C 80.1; H 9.8. Calc. for $C_{32}H_{32}O_2$ C 80.4; H 9.8), λ_{max} (in ethanol) 269 mμ (log ε 3.08), 278 mμ (log ε 3.12).

Hydrogenation of the "Brandt-Neubauer" ferruginyl acetate. The ferruginyl acetate, m. p. 82—83°, $[\alpha]_D^{20}$ +57° ± 2° (ethanol, *c* 2.3), λ_{max} (in ethanol) 269 mμ (log ε 3.19), 278 mμ (log ε 3.19), was hydrogenated as above, yielding crystals, m. p. 81—82°, $[\alpha]_D^{20}$ + 62° ± 2° (ethanol, *c* 2.1), λ_{max} (in ethanol) 269 mμ (log ε 3.09), 278 mμ (log ε 3.12). The mixed m. p. of the hydrogenated acetates was 81—82°.

Ferruginol (Ia). Ferruginyl acetate (hydrogenated) (100 mg) was refluxed in N potassium hydroxide (20 ml) for 40 min. The product, 85 mg of a nearly colourless resin, $[\alpha]_D^{18}$ + 65° ± 2° (ethanol, *c* 2.4), λ_{max} (in ethanol) 284 mμ (log ε 3.50), resisted crystallisation. By chromatography a few crystals, m. p. 56—57°, could be obtained in one fraction, but crystallisation could not be effected by seeding in the bulk.

Δ^9-Dehydroferruginyl acetate (IVb). 9-Ketoferruginol (145 mg) and aluminium *iso*-propoxide (350 mg) (Riedel-de Haën) in abs. *iso*propanol (5 ml) were heated on a water bath in a flask equipped with a 40 cm Vigreux column. After 5 h, no acetone could be detected in the distillate. Abs. *iso*propanol (5 ml) was added and the solution was kept at total reflux for 1 h. The acetone reaction was negative in the distillate taken after this time. The cooled solution was hydrolysed with 2 N hydrochloric acid (30 ml) and extracted with ether. The ether was evaporated on the water bath and the residue was acetylated with acetic anhydride and pyridine at room temperature (two days). The mixture was poured into water and the precipitate crystallised from aqueous ethanol, giving 110 mg (70 %) of prisms, m. p. 108–109°, $[\alpha]_D^{20}$ −92° ± 2° (ethanol, *c* 2.3), λ_{max} (in ethanol) 220 mμ (log ε 4.39), 266 mμ (log ε 4.01), inflexion at 298 mμ (log ε 3.2). (Found C 80.3; H 9.3. Calc. for $C_{22}H_{30}O_2$ C 80.9; H 9.3). The acetate was partially hydrolysed by chromatography on alumina.

Δ^9-Dehydroferruginol (IVa). *Δ^9*-Dehydroferruginyl acetate (90 mg) was refluxed in N potassium hydroxide (10 ml) for 30 min. The product (75 mg) was a light yellow resin, $[\alpha]_D^{20}$ −60° ± 2° (ethanol, *c* 3.2), λ_{max} (in ethanol) 218 mμ (log ε 4.29), 280 mμ (log ε 3.97). All attempts to effect crystallisation failed.

Isomorphy of ferruginyl acetate and Δ^9-dehydroferruginyl acetate. The acetates were brought into contact by the method of Kofler [3]. On cooling and heating the acetates formed mixed crystals of Roozebom's type I.

The author is indebted to Dr. J. Gripenberg for valuable advice. He also wishes to thank Mr. B. C. Fogelberg, B. Sc., Centrallaboratorium Ab., Helsingfors, who has taken the infrared spectra.

REFERENCES

1. Bredenberg, J. B. and Gripenberg, J. *Acta Chem. Scand.* **10** (1956) 1511.
2. Bredenberg, J. B. *Meddelande 9:de nordiska kemistmötet*, Aarhus 1956.
3. Kofler, L. and Kofler, A. *Thermo-Mikro-Methoden*, Verlag Chemie, Weinheim 1954, p. 151.
4. Brandt, C. W. and Neubauer, L. G. *J. Chem. Soc.* **1939** 1031.
5. Brandt, C. W. and Thomas, B. R. *New Zealand J. Sci. Technol.* **33B** (1951) N:o 1, 30.
6. Campbell, W. P. and Todd, D. *J. Am. Chem. Soc.* **64** (1942) 928.
7. Erdtman, H. *Progr. Org. Chem.* **1** (1952) 22.

Received February 26, 1957.

ACTA CHEMICA SCANDINAVICA 11 (1957) 936—939

A New Approach to the Determination of Distribution Functions, Especially for Polymers

KARL ERIK ALMIN and BÖRJE STEENBERG

Swedish Forest Products Research Laboratory, Paper Technology Department, Stockholm, Sweden

Inherent weaknesses in current methods for the determination of molecular weight distribution functions are pointed out and a new method based on liquid-liquid distribution at equilibrium conditions is outlined.

The object in characterisation of a sample by fractionation methods is to determine the distribution function of the sample under study in respect to a chosen parameter. The experimental method involves a series of physical or chemical processes, resulting in a number of fractions, the weights of which are determined. From the experimental data the distribution function can then be calculated. The mathematical treatment is a simple one provided that any fraction does not contain such parts of the original sample, which appear in other fractions. This is the case for instance at the fractionation of spheres of different sizes by a series of screens.

If, and this is the important case, each fraction contains all types of units represented in the unfractionated sample, the problems become more complicated.

Let us assume that the original sample has a weight frequency function which, in respect to the separation parameter, γ, is

$$y = f(\gamma)$$

then the quantity of substance in the fraction numbered p can be written

$$W_p = \int_0^\infty F(\gamma, p) \cdot f(\gamma) \mathrm{d}\gamma \qquad (1)$$

where $F(\gamma,p)$ is a function determined by the program used in the fractionation and by the nature of the physical or chemical process used.

The first condition required to solve the integral equation given in (1) with respect to $f(\gamma)$ using the experimentally determined W_p values is that the functions $F(\gamma,p)$ are known. These functions may be derived from theoretical considerations or from independent experiments. It is true that even with this function unknown, it is possible to characterize the sample by a relation between W_p and p, provided that the fractionating process is completely standardized. The basic information which was sought for is, however, not reached.

In the determination of molecular weight distribution functions of high polymers (see *e. g.* Ref.[1]) it is customary to utilize methods with maximum selectivity. Even so the fractions are far from homogeneous in molecular weight. It may very well be so that the width of the frequency function of single fractions are comparable to that of the original sample. The reaction mechanism in such fractionation methods is incompletely understood which, in other terms, implies that the function $F(\gamma, p)$, where now γ stands for the molecular weight, is unknown.

It is customary in the mathematical treatment of the experimental results of the type discussed to make some assumptions concerning the shape of the distribution functions of the fractions. In the method described by Mark and Raff [2] it is supposed that the fractional frequency curves are symmetrical and narrow. Beall [3], working on the basis that the fractional frequency curves "must tend to be unimodal", worked out a time-consuming but probably more reliable method. Such methods may imply a gross oversimplification especially at low and high molecular weights. The chief weakness of these methods is that basic assumptions are introduced at early stages of the calculations.

What possibilities exist to surmount these difficulties? The possibilities to derive the function $F(\gamma, p)$ theoretically or from experimental data seem small. In precipitation or dissolution fractionation methods knowledge regarding the relation between the activities of the polymer in the solution and the precipitate have to be known. Although such relations have been worked out by Huggins [4] and Flory [5], they are still incomplete and their usefulness in this case at least debatable. Experimental determination of the function $F(\gamma, p)$ requires access to preparations with unique molecular weight or known distribution functions. Preparations of polymers of medium or high DP undisputably of this type are unknown.

The solution must consequently rest in a new method of fractionation, where the mechanism of reaction is known. As far as the authors know nobody has explicitely stated that the problem is composed of two parts. The first part is to determine the distribution function with respect to some suitable parameter. The second part is to determine a relation between this parameter and the molecular weight. Only then the molecular weight distribution function can be derived. The method should preferably be chosen in such a way that the function $F(\gamma, p)$ is theoretically known.

The reason why it is desirable to treat the problem in this way is that the relation between the parameter and the molecular weight is not necessarily a monotonous function. Thus Morey and Tamblyn [6] investigating the precipitation method report that low molecular weight material under certain conditions can precipitate before high molecular weight material.

Let us discuss the possibilities to solve the problem. It seems obvious that only a chemical equilibrium method can be useful. This implies that diffusion methods or chromatographic methods have to be ruled out.

The liquid distribution methods, closely related to the precipitation and dissolution methods, can, however, be expected to fulfill the requirements. Such a method has been used by Schulz and Nordt [7]. They concluded that the method is relatively ineffective in fractionation. These writers have, however, used different composition of the liquid system at different stages of the fractionation procedure. Such a procedure is certainly efficient if the object is to obtain fractions of as widely different molecular weights as possible, but if the object is to determine the molecular weight distribution function of the original sample it will result in the same difficulties as classical precipitation procedures.

It must be a pre-requisite that the fractionation parameter γ is kept constant for every type of molecules present at all steps of the fractionation.

If the partition coefficient is chosen as the parameter this implies that it is necessary to have constant composition of the liquid system at all steps in the procedure.

It is obvious that this will lead to a decreased fractionation effect, but this can be compensated by a method of multiplication. The Craig countercurrent system seems to lend itself admirably to investigations of this type. Countercurrent fractionation according to related principles for high polymers have been used successfully by Swenson and coworker [8,9] in this laboratory. His method did, however, not involve equilibrium conditions.

In a series of papers of one of the authors the possibilities to apply countercurrent methods to this problem will be analyzed theoretically and experimentally. It will be shown that if the polymer is distributed between two immiscible liquids in a counter current apparatus the quantity of polymer in each fraction can be written

$$W_p = \binom{n}{p} \int_0^\infty \frac{k^p}{(1+k)^n} f(k)\, \mathrm{d}k$$

where k is the partitition coefficient for a specific size of molecules and $f(k)$ denotes the weight frequency function for the polymer with respect to the parameter k. The number of the fractions is p ($p = 0,1,2.....n$), the total number of fractions being $n + 1$. From this integral equation $f(k)$ can be derived by a properly chosen approximation method.

If the average molecular weight $\overline{M}_p$ in each fraction is determined experimentally one can write

$$\overline{M}_p^a = \frac{1}{W_p} \cdot \binom{n}{p} \int_0^\infty \frac{k^p}{(1+k)^n} \cdot f(k) \cdot M^a\, \mathrm{d}k$$

where a is a parameter fixed by the conditions of the method [10]. Because $f(k)$ is known it is possible to calculate M as a function of k. The molecular weight frequency function can be derived from the formula

$$g(M) = f(k) \cdot \frac{dk}{dM}$$

DISCUSSION

The principle for the determination of molecular weight distribution functions outlined has its merits in the possibilities of a more precise mathematical treatment than is theoretically possible with earlier used methods.

From a practical point of view it is first of all necessary to find a pair of immiscible liquids, both being solvents for the polymer to be studied. It seems probable that such systems are not easily found except in a few cases, but already the existence of one such system may allow studies leading to deeper insight into the laws of high polymers.

It is also necessary that a thermodynamic equilibrium is reached when the polymer is distributed between the liquids. Interaction between molecules of different size should be negligible, or in other words the partition coefficient shall be independent of the presence of reasonable quantities of other size molecules. From a mathematical point of view this means that the function $F(\gamma, p)$ shall be independent of the molecular frequency function of the sample.

Only experimental studies can ascertain whether the mentioned conditions can be realized. Preliminary experiments with polyglycols and two phase liquid systems composed of trichloroethylene, chloroform, ethanol and water are promising, and detailed results will be published.

REFERENCES

1. Cragg, L. H. and Hammerschlag, H. *Chem. Rev.* **39** (1946) 79.
2. Mark, H. and Raff, R. *High Polymeric Reactions (High Polymers*, Vol. III), Interscience, N. Y. 1941.
3. Beall, G. *J. Polymer Sci.* **4** (1949) 483.
4. Huggins, M. L. *J. Phys. Chem.* **46** (1942) 151.
5. Flory, P. J. *J. Chem. Phys.* **10** (1942) 51.
6. Morey, D. R. and Tamblyn, J. W. *J. Phys. & Colloid Chem.* **51** (1947) 721.
7. Schulz, G. V. and Nordt, E. *J. prakt. Chem.* **155** (1940) 115.
8. Swenson, H. *Acta Chem. Scand.* **9** (1955) 572.
9. Swenson, H. and Rosenberg, A. *Acta Chem. Scand.* **10** (1956) 1393.
10. Ott, E. and Spurlin, H. M. *Cellulose and Cellulose Derivatives (High Polymers*, Vol. V), Part III, Interscience, N. Y. 1955.

Received March 4, 1957.

ACTA CHEMICA SCANDINAVICA 11 (1957) 940—944

The Crystal Structure of $N_4S_4H_4$

E. WANG LUND and SVEN R. SVENDSEN*

Kjemisk Institutt, Universitetet i Oslo, Blindern, Norway

An X-ray crystallographic study of $N_4S_4H_4$ has been carried out. The analysis shows that that the molecule has the form of a puckered eight-membered ring with alternating sulphur and nitrogen atoms. The positions of the hydrogen atoms have not been determined.

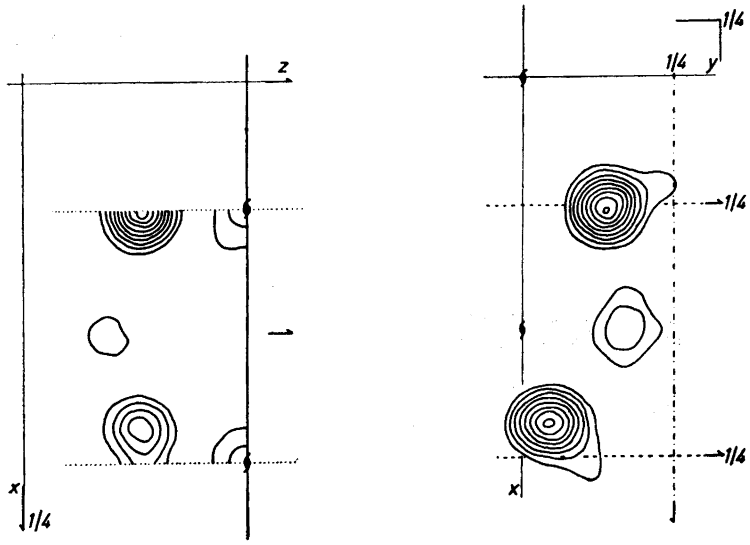
Several authors have regarded as a plausible structure of $N_4S_4H_4$ one which is based on an 8-membered ring with alternating sulphur and nitrogen atoms [1,2]. For the attachment of the hydrogen atoms two different opinions have been held. Some chemical evidence [1,5] is said to point in favour of a structure with hydrogen atoms linked to sulphur atoms. A study of the infrared spectrum [6] indicates, however, the presence of NH rather than SH bonds in the molecule.

The aim of the present investigation is to establish the arrangement of sulphur and nitrogen atoms in the molecule by means of X-ray crystallographic methods. It has not been possible or even tried to locate hydrogen atoms. A crystal structure determination of the same substance has been performed previously by Jaeger and Zanstra [3], using rotation and powder X-ray diagrams. We have, however, not been able to find correspondence between some of their data and results and ours.

The substance was prepared by the method described by Meuwsen. N_4S_4 in benzene was reduced by stannous chloride in alcoholic solution. From acetone needle-shaped crystals of $N_4S_4H_4$ were obtained, but also small bipyramidal plates were observed.

Oscillation and rotation X-ray diagrams showed that $N_4S_4H_4$ crystallizes in the orthorhombic system. The unit cell dimensions were found to be $a = 6.75$ Å, $b = 7.97$ Å, $c = 12.19$ Å. These values are assumed to be accurate to within one half per cent. With four molecules in the unit cell the dimensions lead to a calculated density of 1.907 gcm^{-3} which compares favourably with the observed value [3] of 1.88 gcm^{-3}.

* Present address: Statens råstofflaboratorium, Trondheim, Norway.



Figs. 1 and 2. Projections of the asymmetric unit of $N_4S_4H_4$ on (001) and (010), respectively. Electron density maps with interval between contour lines corresponding to 10 electrons per Å^2, the lowest lying at 10 electrons per Å^2.

Weissenberg diagrams, taken with Cu-*K* radiation show extinctions of reflexions characteristic of the space groups *Pbnm* or *Pbn*. The Wilson ratio $\langle|F|\rangle^2 / \langle|F|^2\rangle$ was computed for seven different sets of reflexions lying within concentric areas in reciprocal *h0l* plane. The mean value of the ratio was found to be 0.63, which indicates the most symmetric space group *Pbnm*. With four molecules in the unit cell this space group requires two halves of a molecule to be crystallographically equivalent.

Intensities of *h0l* and *hk*0 reflexions were estimated visually by means of a standard scale, using the multiple film technique. Patterson projections were computed and found to be compatible with a structure based on an 8-membered ring with alternating S and N atoms and having the point symmetry 4 *mm*. If this is the main feature of the structure one of the symmetry planes of the molecule has to coincide with the symmetry plane of the space group.

A model was tentatively assumed with N—S distance equal to 1.77 Å and with the angles N—S—N and S—N—S equal to 105° and 109°, respectively. Patterson projections served to locate such a model in the unit cell with a satisfactory degree of correspondence between observed and calculated structure factors. Fourier projections on (001) and (010) planes were computed. The contour maps are shown in Figs. 1 and 2. The interval between contour lines corresponds to 10 electrons per Å^2.

From these electron density maps rather reliable coordinates of sulphur atoms can be derived. Only one nitrogen atom gives rise to a well separated peak. The other two nitrogen atoms of the molecule cannot be located accu-

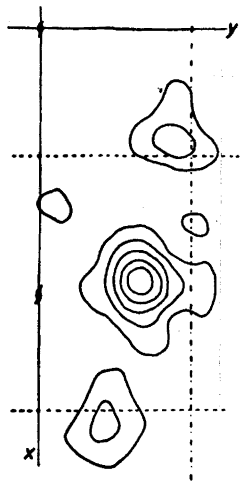


Fig. 3. Difference electron density projection on (001), amplitudes being $F_0 - F_s$. Interval between contour lines corresponding to 3 electrons per Å², the lowest lying at 3 electrons per Å².

rately due to overlap from other atoms in the projections. In order to determine the coordinates of these nitrogen atoms a difference synthesis $F_0 - F_s$ was performed in the projections on (001), F_s being the calculated contribution of the sulphur atoms to the structure factor. In Fig. 3 the resulting difference electron density map is reproduced. From this map the x and y coordinates of the nitrogen atoms were derived. Figs. 4 and 5 show the arrangement of the molecules in the unit cell.

In Table 1 the final coordinates are listed. These coordinates lead to four independent determinations of the N—S distance of the magnitude 1.65 ± 0.02 Å and further to three independent values of the angle S—N—S lying in the range 122° ± 3° and two values of the angle N—S—N within 109° ± 1°.

In Table 2 observed and calculated structure factors are given. The calculated values include temperature factors B equal to 3.00 and 3.65 Å² for the projections on (010) and (001), respectively. No correction for absorption has

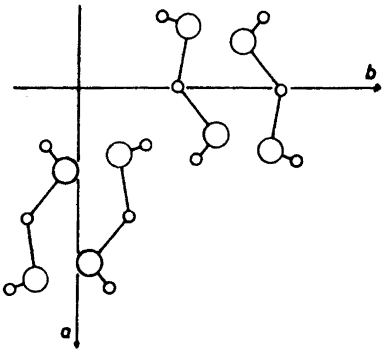


Fig. 4. Projection of the structure of $N_4S_4H_4$ along the c-axis.

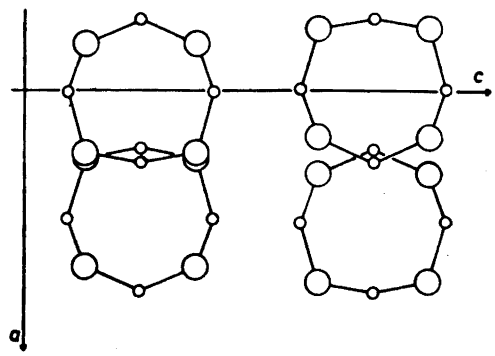


Fig. 5. Projection of the structure of $N_4S_4H_4$ along the b-axis.

Table 1. Coordinates of sulphur and nitrogen atoms.

	x	*y*	*z*
S_1	0.259	0.137	0.131
S_4	0.680	0.043	0.131
N_1	0.221	0.225	0.250
N_3	0.774	0.108	0.250
N_4	0.494	0.171	0.094

been made. Nor has the contribution of hydrogen atoms to the structure factors been considered. The 'reliability index' $R = \Sigma||F_0| - |F_c|| / \Sigma |F_0|$ is found to be 0.13 for the projections on (010) and 0.17 for the projection on (001).

Table 2. Observed and calculated structure factors. (One eighth of absolute values.)

hkl	$\|F_0\|$	$\|F_c\|$	*hkl*	$\|F_0\|$	$\|F_c\|$	*hkl*	$\|F_0\|$	$\|F_c\|$
020	3.1	4.0	470	1.7	2.4	1 011	0	0.2
040	5.4	5.2	480	1.6	1.5	1 013	0	0.2
060	2.5	2.1	490	0.2	0.5	202	7.3	6.9
080	1.4	0.8	510	4.8	5.0	204	8.5	8.8
0 100	1.6	2.0	520	5.1	5.6	206	2.1	2.6
110	7.2	8.5	530	0.6	0.4	208	10.5	10.7
120	4.3	4.4	540	0	0.4	2 010	4.5	5.0
130	1.4	1.1	550	0	0.6	2 012	4.8	4.5
140	8.4	9.5	560	0.9	0.3	2 014	1.6	1.6
150	1.3	1.5	570	0.4	0.4	301	4.1	4.5
160	6.9	7.3	580	1.3	1.4	303	3.2	3.4
170	0.6	0.1	600	0.9	0.3	305	3.7	4.3
180	0	0.6	610	0	0.5	307	2.1	1.9
190	2.6	1.2	620	2.8	2.6	309	2.8	3.1
1 100	0.7	0.8	630	0	0.2	3 011	1.3	0.9
200	15.1	18.2	640	3.7	3.2	3 013	2.0	1.7
210	1.4	1.3	650	1.9	2.1	402	1.2	1.3
220	4.8	4.6	660	0.5	0.2	404	4.2	4.6
230	2.6	3.2	670	0.3	0.8	406	1.0	1.8
240	3.7	3.6	710	0	0.3	408	3.4	4.2
250	4.3	5.0	720	3.2	3.1	4 010	0.9	0.9
260	0	0.4	730	0	0.1	4 012	0.6	0.8
270	1.7	2.4	740	1.1	1.2	501	5.5	6.4
280	1.9	1.9	750	0.6	0.5	503	5.1	5.4
290	0	0.6	800	0.6	0.5	505	4.8	5.0
310	6.2	6.7	810	0.4	0.6	507	2.7	3.1
320	5.0	5.3	820	2.2	1.7	509	3.1	4.2
330	6.2	6.1	830	1.1	1.1	5 011	1.8	1.4
340	3.8	3.4	840	0.8	1.8	602	1.0	1.1
350	0	0.3	002	5.7	5.7	604	0.5	1.1
360	3.7	3.5	004	17.5	20.1	606	0.6	0.4
370	0	0.6	006	3.9	2.0	608	1.1	0.5
380	0.7	0.6	008	15.0	14.3	6 010	1.1	0.9
390	0.3	0.9	0 010	3.3	3.7	701	3.7	4.3
400	9.5	9.1	0 012	5.8	4.8	703	3.2	3.5
410	1.5	1.1	0 014	1.2	1.6	705	4.2	4.5
420	3.4	3.3	101	1.0	1.0	707	1.9	2.0
430	2.2	2.2	103	0.8	0.9	709	2.6	3.4
440	5.7	5.3	105	0.8	0.7	802	0	0.1
450	4.2	4.7	107	0.6	0.4	804	0	0.2
460	1.4	1.7	109	0.5	0.4	806	0	0.6

In order to establish the position of the hydrogen atoms in the molecule it would be of interest to study derivatives in which hydrogen is replaced by a heavier atom or group. The formaldehyde derivative $N_4S_4(CH_2OH)_4$ has been prepared according to Meuwsen. X-Ray diagrams show that this compound belongs to the space group *Pbca* with axial lengths 12.0 Å, 13.1 Å and 15.8 Å. The observed density is 1.55 gcm^{-3} whereas the calculated density assuming eight molecules in the unit cell is 1.74 gcm^{-3}. A more detailed crystallographic study of this compound has not been carried out. The preparation of a compound $N_4S_4F_4$ has been reported [4] and the compound is said to belong to the space group $P\ \bar{4}\ 2_1c$ with two molecules in the unit cell. The point symmetry of the molecule must then necessarily be $\bar{4}$. Assuming that the structure of this molecules also is based on an 8-membered ring, this point symmetry leads to a structure different from that found for $N_4S_4H_4$. It will be of interest to see a more detailed analysis of the structure of the fluorine derivative.

One of the authors (E. W. L.) wants to thank *Norsk Hydros Fond* for financial aid.

REFERENCES

1. Meuwsen, A. *Ber.* **62** (1929) 1959.
2. Arnold, M. H. M. *J. Chem. Soc.* **1938** 1596.
3. Jaeger, F. M. and Zanstra, J. E. *Proc. Koninkl. Akad. Wetenschap Amsterdam* **34** (1931) 782.
4. Glemser, O., Schröder, H. and Haeseler, H. *Z. anorg. allgem. Chem.* **279** (1955) 28.
5. Sidgwick, N.V. *The Chemical Elements and Their Compounds*, Oxford University Press, London, 1950, p. 893.
6. Lippincott, E.R. and Tobin, M.C. *J. Am. Chem. Soc.* **73** (1951) 4990.

Received March 1, 1957.

ACTA CHEMICA SCANDINAVICA 11 (1957) 945—949

Syntheses of some Thiolacetic Acid Derivatives

I. Trichlorothiolacetic Acid

BERTIL SJÖBERG

Research Laboratories, Skoghallsverken, Uddeholms AB, Skoghall, Sweden

The trichlorothiolacetic acid has been synthesised by addition of hydrogen sulfide to trichloroacetic acid anhydride. The infra-red spectrum of the trichlorothiolacetic acid has been recorded and compared with the corresponding spectra of trichloroacetic acid and trichloroacetyl chloride.

Thiolacetic acid reacts easily with many olefins giving thiolacetates, from which by hydrolysis thiols in good yield can be obtained [1–3]. Cunneen [4] has shown that the chloro-substituted thiolacetic acids have still more additive activity depending on their higher acidity. From rubber and chlorinated thiolacetic acids Cunneen easily obtained adducts, but the reaction was difficult to bring about with thiolacetic acid.

Cunneen prepared the chlorinated thiolacetic acids by reacting the corresponding acetyl chlorides with hydrogen sulfide in the presence of aluminium chloride.

Trichlorothiolacetic acid, the most reactive of these acids, was conveniently prepared in this laboratory through addition of hydrogen sulfide to trichloroacetic acid anhydride:

$$(CCl_3CO)_2O + H_2S = CCl_3COSH + CCl_3COOH.$$

In a similar way we had earlier prepared thiolacetic acid from hydrogen sulfide and acetic anhydride [5].

The necessary trichloroacetic acid anhydride was obtained by dehydration of trichloroacetic acid with phosphoric anhydride and was purified by distillation in vacuum.

The addition of hydrogen sulfide to the trichloroacetic acid anhydride was carried out at room temperature. As a catalyst a small amount of pyridine was added. From the reaction mixture trichlorothiolacetic acid was isolated and purified. Physical data for trichloroacetic anhydride and trichlorothiolacetic acid do not seem to be reported in literature. Some data obtained are therefore given in Table 1.

Table 1. Physical data.

Compound	Boiling point °C/mm Hg	d_4^{20}	n_D^{20}	MR_D	AR_D of S
Trichloroacetic anhydride	105/12	1.6900	1.4857	52.43	—
Trichlorothiol-acetic acid	40/4	1.6136	1.5300	34.36	8.31

In Table 1 the molar refraction MR_D is calculated from the physical data, using the Lorentz-Lorenz formula. According to the values given by Eisenlohr [6] for the atomic refractions the molar refraction of the trichloroacetic acid anhydride ought to be only 51.54. The higher value we have found indicates a considerable exaltation.

Using the values of Eisenlohr for the atomic refractions of carbon, hydrogen, chlorine and oxygen we have calculated the atomic refraction for the sulfur atom in the trichlorothiolacetic acid from the found molecular refrac-

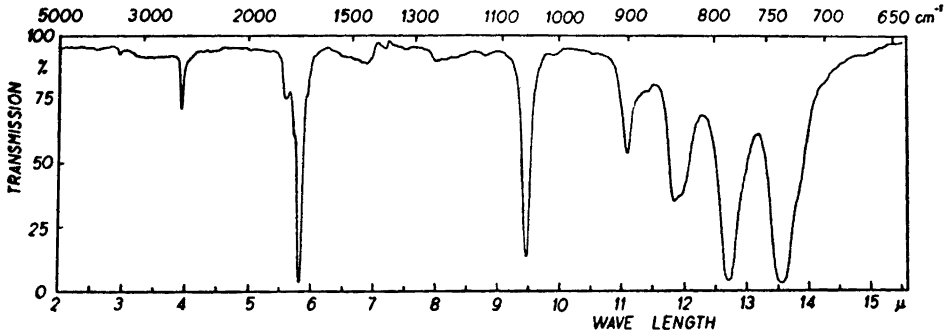


Fig. 1. The infra-red spectrum of trichlorothiolacetic acid in CS_2-solution.

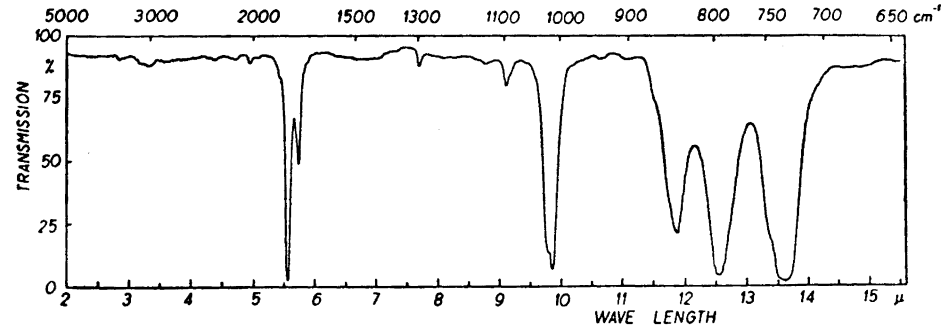


Fig. 2. The infra-red spectrum of trichloroacetyl chloride in CS_2-solution.

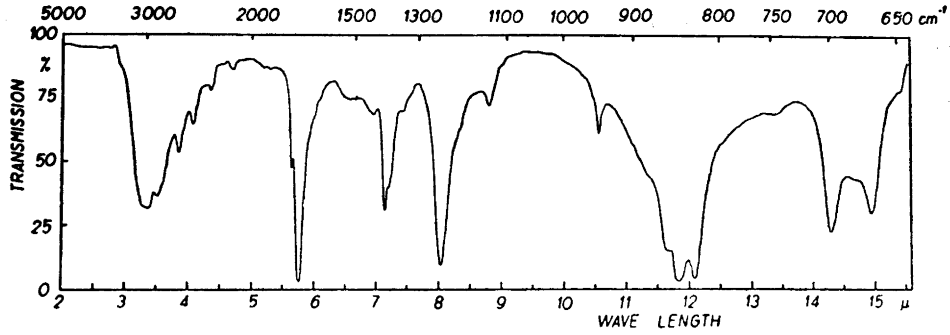


Fig. 3. The infra-red spectrum of trichloroacetic acid in CS_2-solution.

tion. The calculated value 8.31 is in good agreement with the values we have found for other thiolacetic acids.

The infra-red spectrum of the trichlorothiolacetic acid has been recorded in a solution of carbon disulfide (Fig. 1). As a comparison the infra-red spectrum of the trichloroacetyl chloride (Fig. 2) and trichloroacetic acid (Fig. 3) are also given.

It is apparent from the spectra that the trichlorothiolacetic acid is free from trichloroacetic acid. The similarity of the spectra of trichlorothiolacetic acid and trichloroacetyl chloride is striking. The same relation between thiolacetic acid and acetyl chloride has been pointed out by Sheppard [7]. The absence of carbon-hydrogen bonds makes the spectrum of the trichlorothiolacetic acid comparatively simple, and the absorption bands in the region of the group-frequencies are very few. At 2 554 cm^{-1} we find the weak S—H stretching band. At 1 726 cm^{-1} the C = O stretching gives a strong absorption. The band at 1 058 cm^{-1} seems to correspond to the trichloroacetyl chloride band at 1 017 cm^{-1}, which has been assigned by Seewann-Albert [8] to C—C stretching. The weak band of the trichlorothiolacetic acid at 903 cm^{-1} has no counterpart in the trichloroacetyl chloride spectrum and therefore seems to belong to the S—H deformation. The three absorption bands at the end of the spectrum

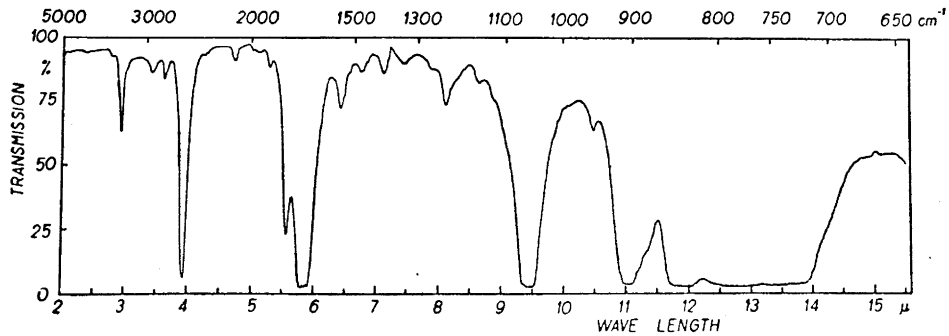


Fig. 4. The infra-red spectrum of liquid trichlorothiolacetic acid.

belong to chlorine stretching and skeletal vibrations and cannot safely be assigned without corresponding Raman-spectra.

From the spectrum of the trichlorothiolacetic acid and the similarity of this spectrum with that of the trichloroacetyl chloride, it can be concluded that trichlorothiolacetic acid predominantly must exist in form of CCl_3COSH. Earlier Sheppard [7] and later Mecke and Spiesecke [9] have stated the same relation for the thiolacetic acid. In the thiolacetic acid, however, a small percentage of the isomeric thionform CH_3CSOH was found. This isomer could be identified by a weak band at 1 225 cm^{-1} belonging to the C=S stretching. The two isomeric forms are in equilibrium and the amount of the thionform increases at higher temperature.

In order to further investigate the spectrum of the trichlorothiolacetic acid we made a recording of the liquid acid in a thin layer (Fig. 4).

The absorption at the higher wave lengths is too strong but in the shorter wave length region there are interesting absorption bands. The absorption band at 3 431 cm^{-1} most probably can be assigned to the O—H group. Since there is also a distinct band at 1 232 cm^{-1}, which can be attributed to the C=S stretching, the existence of a small quantity of the thionform CCl_3CSOH must be assumed.

EXPERIMENTAL

Preparation of trichloroacetic acid anhydride: 300 g pure trichloroacetic acid was heated in an oil bath with 130 g phosphoric anhydride (the theoretical amount) at 210 °C for 10 h. After cooling to room temperature the liquid layer was decanted from the viscous phosphoric acid and distilled in vacuum. At 93—97 °C and 8 mm Hg 207 g trichloroacetic acid anhydride was obtained (yield 73 %). This product was redistilled in vacuum in a fractionation column according to Todd [10] with about 40 theoretical plates. The main fraction boiled at 105 °C and 12 mm Hg. (Found: Cl 68.5. Calc. for $C_4O_3Cl_6$: Cl 68.9).

Preparation of trichlorothiolacetic acid: Hydrogen sulfide was disperged through a fritted glass disc into 183 g trichloroacetic anhydride and 1 ml pyridine at room temperature. To get a sufficient absorption height a narrow glass tube was used for the mixture. The rate of absorption was followed by weighing the reaction tube and titrating the reaction product with iodine (*cf.* the preparation of thiolacetic acid [5]). The reaction velocity was comparatively low and came to a stop after 40 h. Vacuum distillation gave 60 g trichlorothiolacetic acid (yield 56 %). The acid was purified by vacuum distillation with a Widmer-column, b. p. 40 °C at 4 mm Hg. (Found: Cl 59.4; S 17.73; equiv. wt. 180.5. Calc. for C_2HOSCl_3: Cl 59.3; S 17.87; equiv. wt. 179.45).

The infra-red spectra

The infra-red spectra were recorded with a *Perkin-Elmer* double-beam spectrometer Model 21 a with rock-salt prism. Slit schedule 927, corresponding to program 4. Speed: 3 min/μ. The frequencies of the absorption bands are given below.

Trichlorothiolacetic acid (Fig. 1). 100 g/l CS_2-solution. Cell: 0.1 mm 2 554 (w), 1 787(w), 1 726(s), 1 058(s), 903(m), 846(s), 788(s), and 738(s).

Trichloracetyl chloride (Fig. 2). 26.4 g/l CS_2-solution. Cell: 0.459 mm 1 803(s), 1 750(w), 1 023(m), 1 017(s), 844(s), 797(s), and 736(s).

Trichloroacetic acid (Fig. 3). 99.9 g/l CS_2-solution. Cell: 0.1 mm. At 3 008 broad band with small peaks at 2 878, 2 628, 2 478, and 2 323. 1 787(w), 1 747(s), 1 407(s), 1 252(s), 1 141(w), 951(w), 847(s), 830(s), 701(s), and 671(s).

Trichlorothiolacetic acid, liquid. Cell: 0.052 mm. 3 431(m), 2 937(w), 2 782(w), 2 554(s), 2 112(w), 1 803(m), 1 690—1 730(vs), 1 559(w), 1 483(w), 1 404(w), 1 340(w), 1 232(w), 1 050—1 070(vs), 956(w), 900—915(vs), and 720—860(vs).

The author gratefully acknowledges the assistance of ing. Bengt Axelsson (synthetic work), ing. Bengt Berglund (infra-red spectrometry) and ing. Esse Zetterqvist (chemical analyses).

REFERENCES

1. Holmberg, B. *Arkiv Kemi, Mineral. Geol.* **12B** (1938) No. 47.
2. Holmberg, B. and Schjånberg, E. *Arkiv Kemi, Mineral. Geol.* **14A** (1940) No. 7.
3. Sjöberg, B. *Ber.* **74** (1941) 64.
4. Cunneen, J. I. *J. Chem. Soc.* **1947** 134.
5. Sjöberg, B. *Sv. Kem. Tidskr.* **63** (1951) 90.
6. Landolt-Börnstein: *Physikalisch-Chemische Tabellen*, Vol. II, 986, 1923.
7. Sheppard, N. *Trans. Faraday Soc.* **45** (1949) 693.
8. Seewann-Albert, H. *Acta Phys. Austriaca* **1** (1947/48) 346.
9. Mecke, R. and Spiesecke, H. *Chem. Ber.* **89** (1956) 1110.
10. Todd, F. *Ind. Eng. Chem. Anal. Ed.* **17** (1945) 175.

Received March 16, 1957.

ACTA CHEMICA SCANDINAVICA 11 (1957) 950—956

The Influence of Water Content on the Action of Ionizing Radiation on Starch

L. EHRENBERG, M. JAARMA, and E. C. ZIMMER

Institute for Organic Chemistry and Biochemistry, University, Stockholm, Sweden

In order to elucidate the "protective effect" of water in various biologic materials irradiations of polysaccharides of various water contents have been carried out and some chemical changes measured. It was found that the number of breaks produced in the polysaccharide chains of the molecules per energy absorbed decreases with increasing water content, in quantitative parallelism to the effects in biologic materials. This effect can be explained by assuming that in materials of low water content excitations lead to chemical changes with higher efficiency than in materials containing more water. There were also found chemical effects showing an entirely different dependence on water content.

When studying the induction of mutations by irradiating plant seeds, it was found at an early stage of the investigations that the material showed a radiation sensitivity varying irregularly between the individuals in a sample as well as between different samples. The variation was observed to be greater with sparsely ionizing radiations (such as γ- and X-rays) than with densely ionizing radiations (secondaries produced by neutrons). An analysis of possible causes led to the conclusion that the seemingly irregular variation obtained in experiments with sparsely ionizing radiation could be explained by the influence of the water content of the seeds on the radiation sensitivity.[1]

Desiccated seed material with a water content of 6—8 % was found to be most sensitive to X- and γ-rays, and a maximum "protective effect" was observed at a water content of about 20 % (the water content corresponding to minimum sensitivity somewhat depending on the material and on the test reaction studied). The dose reduction factors brought about by increased water content range from 2.5 for mutation rate in barley [2] to 3—4.5 for inhibition of growth in the same material [1]. In contradistinction no dependence of sensitivity on water content has been found using fast neutron irradiation [1-4]. At water contents above 20 % the sensitivity increases for all kinds of radiation, due, partly at least, to an increase in metabolic activities, involving, *e.g.*, chromosome multiplication and initiation of germinative processes [6].

Qualitatively, the influence of the water content is the same for all radiation effects studied: gene mutation, chromosome aberrations, sterility, growth inhibition and lethality, all these effects possibly resulting from disturbances in the nuclear material. The phenomenon is, decidedly, a very general one, since it has been observed in seeds of many different species (barley [1–5], tomato [7], pea [8], and others) and also in pollen [9] and in bacteria [10].

A more detailed analysis of the ways by which water brings about this very pronounced effect might well furnish important clues as to the mechanisms of action of radiations in general. No physiological or biochemical factors have thus far been found that depend on water content in such a way as to explain the modifying action of water on radiosensitivity [6]. On the other hand the water content exerts a qualitatively and quantitatively very similar influence on the radiation induced chemical changes in non-living hydrophilic colloids [6,11]. Consequently, it seems quite reasonable to look for an explanation on the physicochemical level.

The present paper describes investigations into the radiation induced changes in systems of polysaccharides of the starch type (α-polyglucosides), irradiated at different water contents. In a way these experiments are exploratory, as they strive to find which chemical changes depend on water content in the same manner as the biological effects, and which do not.

EXPERIMENTAL

Samples of potato starch, amylose from potato starch, or maize amylopectin ("Amioca" from National Starch Products) were treated, in desiccators, with streaming air of different relative humidities in the range of 0 to 95 %. When, after 4—6 days at 20°C, equilibrium was reached, the samples were irradiated in glass stoppered test tubes.

γ-Irradiation was carried out at distances 3—18 cm from a 70 Curie ^{60}Co source. The (average) dose rates at these distances and in the tubes used were determined actinometrically [12] by measuring the oxidation of $FeSO_4$ in 0.8 N H_2SO_4, a G-value of 15.5 Fe^{3+} per 100 eV absorbed being used. At a distance of 3 cm the dose rate amounted to 10^5 r/h.

Roentgen irradiation was given by means of a therapy apparatus run at 175 kV; filtering 2 mm Al; dose rate 800 r/min. The dose was measured during the irradiation by means of a wave-length independent thimble chamber connected to a valve electrometer and integrating counter calibrated in Roentgens (r).

The analytical methods are mentioned in connection with the experimental results.

RESULTS

Common potato starch becomes soluble in water after irradiation by about 10^5 r of γ- or X-rays, and aqueous solutions can therefore be investigated above this dose.

Solutions of irradiated starch are acidic. In order to get amounts of acid groups, easy to titrate, starch was irradiated with 10 and 24 Mr and the groups were titrated electrometrically with 10^{-3} M NaOH. Within this dose range, the amount of acid groups is proportional to the dose. Probably a mixture of different groups is obtained, with an average pK_s amounting to 4 or a somewhat lower value. The titrations are disturbed by the presence of starch, and therefore the values obtained somewhat approximate. Up to 16 % water the

Table 1. Effects of γ-radiation in starch.

Water content %	Acid groups	Reducing groups	Dose giving $\eta_{sp} = 2.5$ Mr
	per ion pair (32.5 eV of energy absorbed)		
6.4	0.78	2.0	0.35
13.2	0.54	1.9	0.48
16.0	0.50	2.0	0.60
20.8	1.4	1.8	0.78
Dose range:	10—24 Mr		0.3—1 Mr

yield of acid groups per ion pair * is fairly constant or slowly decreasing (Table 1), whereas a much higher value is obtained at 20 % water. Considering the fact that the decomposition of starch decreases monotonically with increasing water content, as measured by the viscosity (Table 1, last column), there is no simple correlation of acidity to decomposition. The number of reducing groups determined according to Somogyi [13] (column 3), is totally independent of the water content, and cannot be related at all to the net degradation. The reducing groups are also formed in proportion to the dose. — When intact seeds were irradiated by 5×10^5 r of X-rays the number of glucosidic bonds split was somewhat greater at 17 % H_2O than at 8 % H_2O [14]. Obviously biochemical and physiological factors have to be considered in the irradiation of tissue.

It seems logical to assume that the formation of one reducing group, *i.e.*, the hydrolysis of a glucoside bond, leads to a break of the polysaccharide chain (although the formation of a new bond not affecting the reducing group is, of course, not excluded). Since the net degradation of starch, in contradistinction to the formation of reducing groups, depends on the water content at irradiation, it was of interest to estimate the total number of breaks in the polysaccharide chains obtained per unit dose. Obviously chemical reactions other than the hydrolysis of glucoside bonds are responsible for part, at least, of the net degradation.

A prerequisite for a direct determination of the number of breaks in the polysaccharide chains would be, of course, the use of a material permitting the study of aqueous solutions of the unirradiated material. Starch derivatives made soluble by chemical treatments, *e.g.*, the carboxymethyl ether used in preliminary experiments, were regarded unsuitable for the purpose due to a possible disturbing influence of the introduced groups or changes. Moreover, since the average molecular weights of α-polyglucosides obtained, for instance, from determinations of viscosity, are rather uncertain, we preferred the following indirect method of estimating the number of chain breaks at a given degree of degradation.

* The term "ion pair produced" is used for convenience and in a strictly formal way, implying no other meaning than the absorption of 32.5. eV of radiation energy in the medium.

In amylose, irradiated at different water contents by 30 Mr of γ-radiation, the degradation was estimated from the displacement towards shorter wavelengths of the absorption maximum of the complex with iodine, and from the decrease of the optical density at 650 mμ. The number of breaks in the polysaccharide chains was calculated from the reduction values measured at the same optical changes caused by very dilute solutions of α-amylase. Since amylose consists mainly of long unbranched chains, both agents can be supposed to attack the molecules at randomly situated points. The optical properties can be supposed to depend exclusively on the chain length, irrespective of the chemical nature of the end groups. This assumption is supported by the fact that the displacement of the absorption maximum agrees fairly well with that expected from the degree of decomposition calculated (see Table 2), *i.e.*, the absorption curve changes equally after irradiation and enzymatic hydrolysis. The yield of chain breaks per ion pair produced is found to decrease from 4—5 at 6 % H_2O to about 2 at 20 % H_2O.

A similar result was obtained with the branched polysaccharide, amylopectin, from which stable 1 % solutions could be prepared. A 50 % decrease of the viscosity of 1 % solutions was obtained by irradiating desiccated samples

Table 2. Amylose, irradiated with 30 Mr (5.0×10^{19} ion pairs) γ-radiation, at different water contents. Number of chain breaks calculated from the extinction decrease at 650 mμ. The colorimetric determinations were done with 0.0002—0.0006 % amylose solutions containing excess iodine (0.004 %)

Water content %	Decrease of extinction at 650 mμ, %	Maximum extinction at mμ	No. of chain breaks		Maximum extinction expected from degree of hydrolysis, mμ
			per g amylose	per ion pair (32.5 eV of energy absorbed)	
6.6	70	570	$23.5 \cdot 10^{19}$	4.4 ($\pm$2)	555
10.1	49	590	$16.7 \cdot 10^{19}$	3.2 ($\pm$2)	580
13.6	37.5	600	$12.5 \cdot 10^{19}$	2.4 ($\pm$1)	595
19.8	29.0	595	$9.8 \cdot 10^{19}$	1.8 ($\pm$1)	605

Table 3. Doses of γ- and X-rays causing 50 % reduction of the viscosity of 1 % amylopectin solutions, and ionic yields for chain breaks.

Water content at irradiation %	50 % dose of γ-rays, Mr	50 % dose of X-rays, Mr	No. of chain breaks per ion pair (32.5 eV of energy absorbed)
4—6	0.2	0.200	4.7$\pm$0.6
14	0.6		1.6 *
20	1.0		0.9 *

* Calculated from dose reduction according to column 2.

(4—6 % H_2O) at 200 kr of X-rays or γ-rays (Table 3). The dose reduction factor for obtaining the same viscosity at higher water contents (about 20 % H_2O) was somewhat greater for this compound than for starch and amylose, amounting to about 5 times. From simultaneous determinations of viscosity and reduction value, the number of breaks at different viscosities could be estimated. Since the reduction value is too low to be measured at 50 % viscosity, an extrapolation backwards had to be done on the reduction/time curve; this extrapolation is justified, the curve being linear at the beginning. The yield of chain breaks per ion pair was found, in agreement with the amylose value, to be about 5 in the desiccated material, and about 1 at 20 % H_2O.

DISCUSSION

Genetic as well as many other biologic radiation effects can possibly be ascribed to changes in desoxyribonucleic acids (DNA) or their complexes with proteins. The polysaccharides might therefore seem to constitute systems, which are chemically too unrelated to the biological materials mentioned to permit drawing any conclusions. The influence of the moisture content on radiation sensitivity seems to be a general phenomenon, however, also being at work for certain changes in proteins (unpublished) and DNA (after UV irradiation [15]). The possible significance of the present results for biological effects might therefore be discussed on general terms.

Different chemical effects induced in the polysaccharides depend differently on the water content: Some effects, as the degradation measured spectrometrically or viscosimetrically, are greatest at low water contents and are inhibited by the presence of water quantitatively to the same degree as the biological effects. The degradation of amylopectin irradiated at different water contents was followed also in pure nitrogen atmosphere, and quantitatively identical results were obtained; in the biologic material water exerts the same protective influence in nitrogen (which, in addition, causes some protection).[1] From the similar displacement of spectra after irradiation and enzymatic hydrolysis it does not seem plausible that the degradation measured can be ascribed to a breaking of great numbers of hydrogen bonds [16]. Chemical changes involving rupture of the polysaccharide chains are certainly at work. That chemical changes involving covalent bonds do follow the degree of degradation is further indicated by the ability of irradiated starch to reduce iodine in solution, the ionic yield for this ability decreasing from about 0.5 at 6 % H_2O to 0.2 at 20 % H_2O. (The chemical nature of the iodine consuming groups is being studied further.) Other reactions show the inverse dependence on the water content, especially the oxidation of adsorbed iodide [11] and possibly also the induction of acid groups at high water contents. Still other reactions are independent of the water content, such as the rupture of glycosidic bonds, probably also the induction of acid groups below 16 % H_2O. The occurrence of these different modes of reaction gives, in principle, means to elucidate the chemical changes, leading to moisture-dependent biologic radiation effects.

The validity of the estimations of the number of chain breaks per ion pair is strengthened by the quantitative agreement between the two very different

systems: amylose, *i.e.*, an unbranched polysaccharide, irradiated with 10—24 Mr, and the branched amylopectin irradiated with a 100 times lower dose. It is therefore reasonable to assume that per ion pair, *i.e.*, 32.5 eV absorbed, about 5 breaks occur when the material is irradiated at about 6 % H_2O. Taking into consideration the many experimental difficulties and possible sources of error, the latter value can be said to be certainly higher than 3 breaks per ion pair and accordingly greater than the yields of acid groups or glucosidic bonds hydrolyzed. An increase of the water content to about 20 % at irradiation decreases the yield of chain breaks by 2—5 times, in similarity with the biological experience, bringing it to a value close to one break per ion pair. The high ionic yield obtained when irradiating the desiccated material may be taken as an indication that excitations are chemically effective here. — The possible biologic importance of excitations has but infrequently been discussed. As a rule they have been regarded unimportant (*cf.* Lea [17]).

Due to difficulties in measuring the number of excitations in materials such as those we are considering here, the frequency at which they occur is still a matter of dispute. For various materials values amounting to 1—3 excitations per ion pair have been given [16–18]. If all of them were leading to chemical reactions, ionic yields amounting to 2—4 would be obtained. We have therefore some justification to suppose, at present as a working hypothesis, that in biologic materials as well as in non-living model systems, water exerts its maximum "protection" at high water contents (about 20 % H_2O) by eliminating the chemical rearrangements following excitation, whereas the chemical consequences of ionization are not affected to the same degree. Regarding the number of excitations per ion pair this would mean a dose reduction factor of 2—4, in agreement with the experiments. The idea is further supported by the fact that Kaplan [15], irradiating by UV bacteria as well as DNA at different water contents, finds a dose reduction factor, in both systems amounting to about 22. The low energy of the UV-photons makes the frequency of ionizations relatively much more rare, and, consequently, a protection against excitation leads to a much more pronounced "protective effect" than in the case of ionizing radiations.

Thanks are due to Professor Karl Myrbäck and Dr. K. G. Zimmer for valuable discussions. The investigation was supported financially by grants from the *Agricultural Research Council* and from the *Hierta-Retzius Research Foundation.*

REFERENCES

1. Ehrenberg, L. *Botan. Notiser* **108** (1955) 184.
2. Ehrenberg, L. *Hereditas* **41** (1955) 123.
3. Ehrenberg, L. *Acta Radiol. Suppl.* **116** (1954) 680.
4. Ehrenberg, L. and Nybom, N. *Acta Agr. Scand.* **4** (1954) 396.
5. Caldecott, R. S. *Science* **120** (1954) 809.
6. Ehrenberg, L. *Svensk Kem. Tidskr.* **67** (1955) 207.
7. Lefort, M. and Ehrenberg, L. *Arkiv Botan.* [2] **3** (1955) 121.
8. Lambert, J. *Arch. biol. Liége* **44** (1933) 621; Unpubl. investigations by L. Ehrenberg, O. Gelin and H. Lamprecht.
9. Kaplan, R. W. *Biol. Zentr.* **60** (1940) 298.
10. Houtermans, T. *Z. Naturforsch.* **11 b** (1956) 636.

11. Ehrenberg, L. *Radiobiology Symposium Cambridge* 1955, p. 114.
12. Ehrenberg, L. and Saeland, E. *JENER Publ. No. 8* (1954).
13. Somogyi, M. *J. Biol. Chem.* **160** (1945) 61.
14. Ehrenberg, L. and Jaarma, M. *Acta Chem. Scand.* **9** (1955) 539.
15. Kaplan, R. W. *Naturwiss.* **42** (1955) 466.
16. Bacq, Z. M. and Alexander, P. *Fundamentals of Radiobiology.* London 1955.
17. Lea, D. E. *Actions of Radiations on Living Cells.* Cambridge 1946.
18. Fano, U. in Hollaender, A. *Radiation Biology I:1.* New York 1954, p. 1.

Received March 27, 1957.

ACTA CHEMICA SCANDINAVICA 11 (1957) 957—958

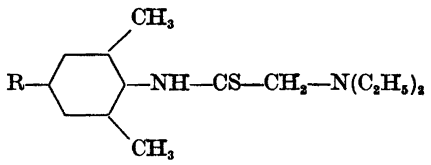
Studies on Local Anesthetics XIII *

BJÖRN LÜNING

Institute of Organic Chemistry and Biochemistry, University of Stockholm, Stockholm, Sweden

Two compounds related to xylocaine *i.e. α-diethylamino-2,6-dimethylthioacetanilide* and *α-diethylamino-2,4,6-trimethylthioacetanilide* have been synthesized, and tested for their local anesthetic potency by subcutaneous anesthesia on man. Furthermore, the lethal dose in white mice was determined.

The compounds synthesized in this work have the following structure:



I: R = H
II: R = CH_3

They were both prepared from the corresponding oxygen compounds (xylocaine and LL 31) [2] by replacing the carbonyl oxygen with sulphur, P_2S_5 in pyridine solution being used for the exchange reactions. The compounds were tested for their anesthetic potency by subcutaneous injection on man, and for compound I the duration was found to be approximately 40 % shorter than that of xylocaine whereas compound II gave practically no effect. The LD_{50} values measured by subcutaneous injection in white mice and calculated as g of I, II and xylocaine per kg of body weight are 0.9, 1.2 and 0.4, respectively **.

EXPERIMENTAL

α-Diethylamino-2,6-dimethylthioacetanilide

α-Diethylamino-2,6-dimethylthioacetanilide (xylocaine[2]), 23.4 g (0.100 mole), was mixed with 33 g (0.15 mole) of phosphorus pentasulphide, dissolved in 300 ml of dry pyridine (dried by CaH_2) and the mixture was gently refluxed for two hours. The product was

* For paper XII of this series see Löfgren, Lundquist, Lindström [1].
** Experiments performed by S. Wiedling.

allowed to cool, and was poured under vigorous stirring, into 2 000 ml of 6 N hydrochloric acid containing 500 g of ice. A thick grey precipitate (sulphur) formed. After standing overnight, the precipitate was filtered off. The solution was extracted three times with 300 ml of carbon disulphide and twice with 300 ml of ether. The aqueous solution was made weakly alkaline (pH 8—9) with 25 % ammonia and was then extracted twice with 150 ml of ether. The ether was distilled off at atmospheric pressure until a quantity of about 40 ml of pyridine remained, which was evaporated at 18 mm Hg (bath temperature 40°). The last traces of pyridine were removed in a desiccator over silica gel. The resulting brownish crystals were dissolved in ether which was extracted with 60 ml of 1 N hydrochloric acid. The aqueous solution was made alkaline (pH 9) with 2 N ammonia and extracted with ether (60 ml). This purification step was repeated once. The ethereal solution thus obtained was dried over Na_2SO_4 and then chromatographed through an aluminium oxide (Brockmann's Standardized) column (diam. 14 mm; height, 50 mm), coloured impurities being retained at the top of the column. The resulting ethereal solution — after evaporation — gave 9.2 g (0.037 mole; 37 %) of almost colourless crystals. Recrystallization from a mixture of 20 ml of ligroin (b.p. 110°—125°) and 10 ml of *n*-butyl ether yielded 7.4 g (0.029 mole, 29 %) of colourless prisms; m.p. 106.5°—107° (corr.). (Found: C 67.0; H 8.92; equiv. wt.* 250. Calc. for $C_{14}H_{22}N_2S$ (250.4): C 67.1; H 8.86; equiv. wt. 250.)

Nitrate. Long colourless prisms from absolute ethanol; m.p. 150° (decomp.). (Found: C 53.7; H 7.35. Calc. for $C_{14}H_{23}N_3O_3S$ (313.4): C 53.7 ;H 7.40.)

Picrate. Yellow needles from 96 % ethanol; m.p. 193°—194° (corr.). (Found: C 50.2; H 5.12. Calc for. $C_{20}H_{25}N_5O_7S$ (479.5): C 50.1; H 5.25.)

Perchlorate. Colourless rhomboidal prisms from absolute ethanol; m.p. 188° (decomp.). (Found: C 47.9; H6.59. Calc. for $C_{14}H_{23}ClN_2O_4S$ (350.9): C 47.9; H 6.60.)

α-Diethylamino-2,4,6-trimethylthioacetanilide

α-Diethylamino-2,4,6-trimethylacetanilide,[2] 51 g (0.21 mole), was treated with phosphorus pentasulphide as described above. The yield was 4.75 g (0.0180 mole; 8.7 %) of an almost colourless crystalline mass. After two subsequent recrystallizations from *iso*propyl ether, 3.3 g (0.0125 mole; 6 %) of colourless needles were obtained; m.p. 121° (corr.). (Found: C 68.1; H 9.15; equiv. wt. 264. Calc. for $C_{15}H_{24}N_2S$ (264.4): C 68.2; H 9.15; equiv. wt. 264.)

Nitrate. Short prisms from ethanol, melting at 119°—120°. (Found: C 55.0; H 7.82. Calc. for $C_{15}H_{25}N_3O_3S$ (327.4): C 55.0; H 7.70.)

Picrate. Small yellow prisms from 70 % ethanol; m.p. 207°—208° (decomp., corr.). (Found: C 51.2; H 5.60. Calc. for $C_{21}H_{27}N_5O_7S$ (493.5): C 51.1; H 5.52.)

Perchlorate. Small colourless laths from absolute ethanol-*iso*propyl ether; m.p. 164°—165° (corr.). (Found: C 49.2; H 6.90. Calc. for $C_{15}H_{25}N_2O_4SCl$ (364.9): C 49.4; H 6.91.)

REFERENCES

1. Löfgren, N. Lundquist, B. † and Lindström, S. *Acta Chem. Scand.* **9** (1955) 1079.
2. Löfgren, N. *Studies on Local Anesthetics. Xylocaine, a new Synthetic Drug.* (Diss.) Stockholm 1948.

* The determination of equivalent weights of the synthesized bases was made by titrating them in 30 % ethanol with 0.1 N HCl; mixed indicator, methylene blue-methyl red.

Received March 27, 1957.

ACTA CHEMICA SCANDINAVICA 11 (1957) 959—961

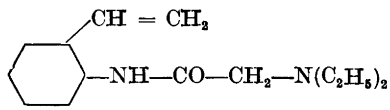
Studies on Local Anesthetics XIV *

BJÖRN LÜNING

Institute of Organic Chemistry and Biochemistry, University of Stockholm, Stockholm, Sweden

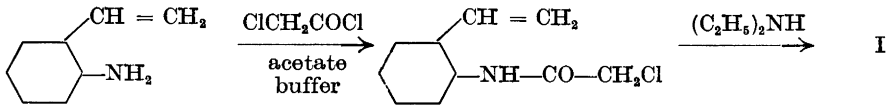
A new compound related to xylocaine [2] *i. e. α-diethylamino-2-vinylacetanilide* has been synthesized, and tested for its local anesthetic potency by subcutaneous anesthesia on man. Furthermore, the lethal dose in white mice was determined.

The compound synthesized in this work has the following structure:



I

Synthesis of the compound was carried out according to the following scheme:



2-Nitrostyrene was prepared as described by Einhorn [3] with some minor alterations. By reduction of this nitro compound according to Komppa [4], 2-vinylaniline was obtained. Due to the instability of the pure amine, it was not isolated. The amine was obtained as an ethereal solution which directly was used in the reaction with chloroacetyl chloride.

The ultraviolet absorption curves of I and α-diethylamino-2-ethylacetanilide are given in Fig. 1. Compound I was tested for its anesthetic activity by subcutaneous injection on man. The duration was found to be approximately 30 % shorter than that of xylocaine. The LD_{50} value measured by intravenous injection on mice was found to be the same as for xylocaine, *i.e.* 0.041 g of base per kg of white mouse **.

* For paper XIII of this series see Lüning [1].
** Experiments performed by S. Wiedling.

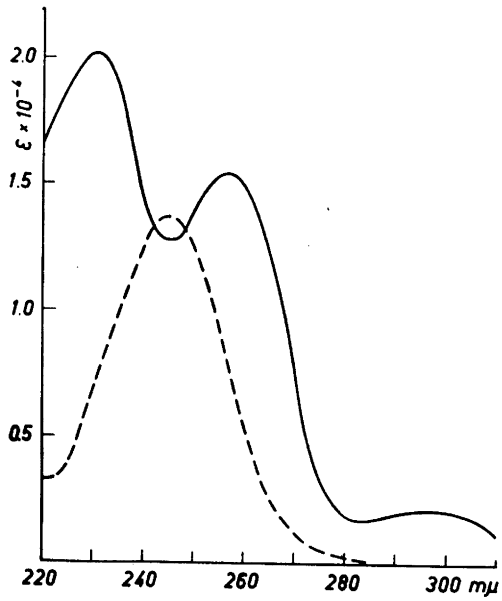


Fig. 1. Ultraviolet absorbtion curves of I (————) and α-dimethylamino-2-ethylacetanilide (— — — — —).

EXPERIMENTAL

β-Bromo-β-(2-nitrophenyl)propionic acid. This acid was prepared according to Einhorn [3]. Since Einhorn's description is rather incomplete, the experimental conditions had to be determined. Acetic acid saturated with hydrogen bromide at 0° was prepared in the following manner. Acetyl bromide, 50 g ,was mixed with 34 g of glacial acetic acid in a thick walled tube of resistant glass. The tube was cooled to 0°, and 10 ml of aqueous hydrobromic acid (d = 1.49) were added in 0.5 ml portions. If in this procedure addition be too fast, hydrogen bromide will escape resulting in an unsaturated solution. In this operation the temperature should be kept at 0°.

To the solution thus prepared, 2-nitrocinnamic acid, 10 g (0.052 mole), was added and the tube sealed. Under shaking, the tube was heated in a water bath at 75°—80° for one hour. During this time all 2-nitrocinnamic acid went into solution and a brown syrup formed. The tube was cooled to about —25° and then opened. Excess of HBr was removed at a bath temperature of 60° and the contents poured into 500 ml of ice-water. The brown precipitate thus formed was sucked off and washed with 100 ml of benzene. The yield was 9.9 g (0.036 mole; 72 %) of a brown crystalline powder; m.p. 138° (decomp.).

2-Nitrostyrene. 2-Nitrostyrene was prepared from β-bromo-β-(2-nitrophenyl)propionic acid according to the method given by Einhorn [3]. However, since Einhorn's yield of 2-nitrostyrene is very low (10 %) some improvements were made. A solution of 30 g of dry sodium carbonate in 150 ml of boiling water was introduced into the distilling flask of a steam distillation apparatus. β-Bromo-β-(2-nitrophenyl)propionic acid, 4 g, was added and the 2-nitrostyrene formed was steam distilled until no more came over. Another portion of 4 g of acid was added and the procedure repeated until a total amount of 23 g (0.084 mole) of the acid had been added. The distillate was made acid with a few drops of concentrated hydrochloric acid and the 2-nitrostyrene was taken up in 50 ml of ether. The ether was washed with 25 ml of dilute sodium carbonate solution and twice with 50 ml of water. The ethereal solution was dried over Na_2SO_4 and the ether evaporated.

The residue consisted of 2.2 g (0.015 mole; 17 %) of a brownish oil which solidified in the refrigerator. The crude 2-nitrostyrene was dissolved in ether and chromatographed through an Al_2O_3 (Brockmann's Standardized) column (diam. 14 mm; height 40 mm), coloured impurities being retained at the top of the column. After evaporation of the solvent the remaining oily material was crystallized from a solvent mixture ether-light petroleum 1 : 1 (v/v) at a temperature of −27°. Long pale yellow needles melting at 13°−14° (corr.) were obtained. (Found: C 64.4; H 4.73. Calc. for $C_8H_7NO_2$ (149.2): C 64.7; H 4.69.)

2-Vinylaniline. This compound was prepared according to Komppa's [4] method by reduction of 2-nitrostyrene with $SnCl_2$; however, the following alterations were made: (1) the reduction was carried out in a vessel that was cooled in a bath of running cold tap water, (2) the base obtained as an ethereal solution in the procedure was used directly for the synthesis of α-chloro-2-vinylacetanilide (*cf.* above).

α-Chloro-2-vinylacetanilide. To a mixture of a solution of 2-vinylaniline, prepared from 5.0 g (0.034 mole) of 2-nitrostyrene in 100 ml of ether (*cf.* above), and 12 g (0.15 mole) of dry sodium acetate, a solution of 3.0 g (0.038 mole) of chloroacetyl chloride in 50 ml of dry ether was added under vigorous stirring. After a period of 5 min, 25 ml of water were added and stirring was continued for another 15 min. Without separation of the two phases the ethereal layer was driven off under reduced pressure. α-Chloro-2-vinylacetanilide which precipitated during the evaporation was sucked off and dried. The dry product was dissolved in benzene and purified with charcoal. After evaporation, the residue was recrystallized once from absolute ethanol and once from benzene. Yield (based on 2-nitrostyrene): 1.9 g (0.0095 mole; 30 %) of colourless needles m.p. 92°−92.5° (corr.). Found: C 60.9; H 5.15. Calc. for $C_{10}H_{10}NOCl$ (195.65): C 61.4; H 5.15.)

α-Diethylamino-2-vinylacetanilide. α-Chloro-2-vinylacetanilide 1.8 g (0.0092 mole), was mixed with 2 g (0.0273 mole) of diethylamine in 16 ml of benzene (dried over $CaCl_2$) and the mixture refluxed for 5 h. After cooling, 20 ml of ether were added. The precipitated diethylamine hydrochloride was filtered off and the solution evaporated to dryness. The residue consisted of 2.0 g (0.0086 mole; 94 %) of a pale brownish oil. The oil was dissolved in ether and chromatographed through an Al_2O_3 (Brockmann's Standardized) column (diam. 14 mm; height, 40 mm), coloured impurities being retained at the top of the column. The effluent was washed with 100 ml of water. The base was extracted from the ether with 250 ml of 0.5 N hydrochloric acid. This solution was washed three times with 100 ml of ether. The base was liberated by means of saturated sodium carbonate solution and taken up in 50 ml of ether.

From this ethereal solution the *perchlorate* was prepared. The salt was recrystallized twice from absolute ethanol m.p. 166° (corr.). (Found: C 50.6; H 6.50. Calc. for $C_{14}H_{21}ClN_2O_5$ (332.8): C 50.5; H 6.36.)

The pure perchlorate was dissolved in 20 ml of water and 3 g of dry sodium carbonate were added. The separated oily base was taken up into ether. This ethereal solution was dried over potassium carbonate and then filtered. The ether was evaporated, leaving 1.45 g (0.0063 mole; 68 %) of a colourless oil; $n_D^{20} = 1.5480$. (Found: C 72.0; H 8.67. Calc. for $C_{14}H_{20}N_2O$ (232.3): C 72.4; H 8.68.)

REFERENCES

1. Lüning, B. *Acta Chem. Scand.* **11** (1957) 957.
2. Löfgren, N. *Studies on Local Anesthetics, Xylocaine, a new Synthetic Drug.* (Diss.) Stockholm 1948.
3. Einhorn, A. *Ber.* **16** (1883) 2208.
4. Komppa, G. *Über kernsubstituierte Styrole.* (Diss.) Helsinki 1893.

Received March 27, 1957.

ACTA CHEMICA SCANDINAVICA 11 (1957) 962—970

Studies on Local Anesthetics XV *

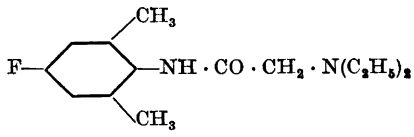
SVEN LINDSTRÖM

Institute of Organic Chemistry and Biochemistry, University of Stockholm, Stockholm, Sweden

The thermodynamic ionization constants, the apparent molar refractions and the ultraviolet absorption spectra of α-diethylamino-4-fluoro-2,6-dimethylacetanilide and of xylocaine have been determined. The electronic effect induced by the fluorine atom is discussed, and finally, a possible explanation is offered for the fact that α-diethylamino-4-fluoro-2,6-dimethylacetanilide as compared with xylocaine has such a low local anesthetic potency.

In a previous work [2] some xylocaine analogues, each with a fluorine atom in the benzene nucleus, were synthesized and studied for their local anesthetic activity. In comparison with xylocaine, the fluoro derivatives were found to have a lower potency, and contrary to xylocaine they exercised an irritant action.

One of these compounds, α-diethylamino-4-fluoro-2,6-dimethylacetanilide, with the formula



had a duration on rabbit cornea which was about one tenth of that of xylocaine. As this compound is so closely related to xylocaine, (the non-fluorinated derivative), the low potency is rather astonishing.

Löfgren [3], Fischer and Löfgren [4] investigated some physico-chemical properties of xylocaine and closely related compounds. In making a comparison between xylocaine and its nuclear isomers and homologues, xylocaine was found to have: (a) a very low exaltation in its molar refraction, (b) a low pK_a value, (c) the ultraviolet absorption bands displaced towards shorter wave lengths, and (d) the intensities of the bands appreciably lowered. Now, it seemed to be of interest to us to study how the fluorine atom in the

* For paper XIV of this series see Lüning [1].

4-position affects these properties of xylocaine. The fluorinated compound and also xylocaine have therefore been subjected to measurements of thermodynamic ionization constants in water at 25°, apparent molar refractions in benzene solutions at 20° and ultraviolet absorption spectra in hexane solution.

Determination of the thermodynamic ionization constant. For the thermodynamic ionization constant, K_a, we have

$$pK_a = pH - \log \frac{C_B}{C_{BH^+}} - pf_{BH^+} \quad (1)$$

C_B is the concentration of the uncharged base B, C_{BH^+} is the concentration of the acid BH^+, $pf_{BH^+} = -\log f_{BH^+}$, and f_{BH^+} is the activity coefficient of BH^+. The pH values were measured with the aid of a cell of the type:

(—) "Glass electrode" / H^+ (aq) / / KCl (satd.) / Hg_2Cl_2, Hg (+)

For this cell we have

$$pH = \frac{E - E'}{k} \quad (2)$$

where E is the e.m.f. of the cell in mV and E' is the standard potential of the cell including the liquid junction potential (assumed to be constant). At 25°, k is 59.16 mV. Kielland [5] has calculated activity coefficients for a large number of ions at different concentrations in water at 25° by use of the Debye-Hückel formula:

$$-\log f_i = pf_i = \frac{0.358 \cdot z_i^2 \cdot \Gamma^{1/2}}{1 + 10^8 \cdot d_i \cdot 0.2325 \cdot \Gamma^{1/2}} \quad (3)$$

where f_i is the activity coefficient of the ith ion with valence z_i and effective diameter d_i. Γ is the ionic concentration, given by $\Gamma = \Sigma C_i z_i^2$ with C_i in moles per litre.

According to measurements by Löfgren [3] the effective diameter for the BH^+ ions were assumed to be 8×10^{-8} cm. The values of f_i for ions with this effective diameter were logarithmed, and pf_{BH^+} was plotted against $\frac{1}{2}\Gamma = C_{salt}$ in a diagram from which pf_{BH^+} could be read off directly at any concentration.

Since it is difficult to obtain a clear survey of the systematic errors, (above all, errors caused by liquid junction potentials) we have confined ourselves to an accuracy of two decimals for pK_a. For mutual comparison, however, the values can be given with greater accuracy; the error here seldom exceeds $\pm$ 0.005.

The experimental data from the measurements of the ionization constants are compiled in Table 1. The double e.m.f. values arise from the two glass electrodes used. From Table 1 it is seen that the fluorinated compound ($pK_a = 7.78_1$) is a weaker base than xylocaine ($pK_a = 7.84_8$; previously found (Löfgren [3]) 7.85_5).

Determination of the apparent molar refraction. For a mixture, the following equation is valid

$$\frac{n^2 - 1}{n^2 + 2} \cdot \frac{m_0 + m_1}{d} = \frac{n_0^2 - 1}{n_0^2 + 2} \cdot \frac{m_0}{d_0} + (r_1)_{app.} \cdot m_1 \quad (4)$$

Table 1. Determination of the ionization constants. NaOH-solution = 0.0265_0 M; test solution = 100 ml. $AHNO_3$ = xylocaine hydronitrate; $BHNO_3$ = α-diethylamino-4-fluoro-2,6-dimethylacetanilide hydronitrate.

Compound	salt weighed (g)	NaOH added (ml)	$\log \frac{C_B}{C_{BH^+}}$	pf_{BH^+}	$-E'$ (mV)	$+E$ (mV)	pH	pK_a	pK_a average
	0.1315	9.05	+0.073	0.029	135.1 120.0	335.1 350.0	7.948	7.846	
	0.1439	9.15	+0.002	0.031	135.1 120.0	331.2 346.1	7.882	7.849	
$AHNO_3$	0.1622	9.33	−0.082	0.032	135.1 120.0	326.6 341.3	7.802	7.852	7.84_8
	0.2142	9.14	−0.296	0.037	135.1 120.0	313.6 328.8	7.586	7.845	
	0.1426	9.20	+0.068	0.030	135.1 119.9	331.0 346.2	7.880	7.782	
	0.1552	9.10	−0.018	0.031	135.1 119.9	326.4 341.2	7.795	7.782	
$BHNO_3$	0.1710	9.26	−0.083	0.032	135.1 119.9	321.9 337.3	7.727	7.778	7.78_1
	0.2203	9.14	−0.275	0.035	135.1 119.9	311.2 326.2	7.542	7.782	

where n is the refractive index, d is the absolute density, m is the amount weighed and $(r_1)_{app.}$ is the apparent specific refraction of the solute; quantities referring to the solution are designated by no index, those referring to the solvent by the index 0 and those referring to the solute by the index 1. The apparent molar refraction is obtained from $(r_1)_{app.}$

$$(R_1)_{app.} = (r_1)_{app.} \cdot M_1 \tag{5}$$

The figures from the measurements of the molar refractions are compiled in Table 2. For the computation of the molar refraction from atomic refractions, the usual published values have been employed; see Table 3. Whereas xylocaine has a small exaltation = 0.16 (previously [3] found to be 0.24), the fluorinated compound has a small depression = 0.17.

Calculation of the errors in the molar refractions. According to Kohner and Johnson (see Weissberger [6]) an expression for the maximum error is

$$(\nabla R_1)_{app.} = \frac{1\,000}{C}\left[\frac{6n_0}{(n_0^2+2)^2}\cdot\nabla(\Delta n) + \frac{\Phi_0}{d_0}\cdot\nabla(\Delta d)\right] \tag{6}$$

where C is the concentration in moles per litre,

$$\Delta n = n - n_0,\ \Delta d = d - d_0 \text{ and } \Phi_0 = \frac{n_0^2 - 1}{n_0^2 + 2}$$

The "Pulfrich" used gave a maximum error in reading = ± 30″. This means that $(\nabla n)_a = \pm 4 \times 10^{-5}$. For a temperature change = 0.02° we obtain for

Table 2. Determination of apparent molar refractions [a]). A = xylocaine; B = α-diethylamino-4-fluoro-2,6-dimethylacetanilide.

Compound	Weighed amount (g) of		d_{20}	$(n_D^{20})^2$	$(R_1)_{app.}$	$(R_1)_{app.}$ average	Exalt.
	compound	benzene					
A	2.17328	7.29727	0.90513	2.26646	71.13		
	2.22808	7.56269	0.90498	2.26646	71.13	71.14	+0.16
	2.17145	7.40230	0.90483	2.26646	71.16		
B	2.24338	7.08697	0.91698	2.25695	70.72		
	2.27927	7.59943	0.91529	2.25639	70.67	70.71	−0.17
	2.26824	7.44430	0.91587	2.25695	70.73		

[a] The calculations are based on the refractive index $n_D^{20} = 1.50110$ for benzene. If, however, one should use another recorded value [20] ($n_D^{20} = 1.50144$) for benzene, the mean values of the apparent molar refractions will be 71.18 and 70.75 for A and B, respectively.

Table 3. Atomic refraction (D-line) of element or structural feature.

C	H	F	O in carbonyl group	Double bond	N in tert. amine	N in sec. amide
2.418	1.100	0.997 [a]	2.211	1.733	2.840	2.676

[a] Value according to Schiemann [21] (*cf.* also v. Auwers [22]).

benzene [7] $(\nabla n)_t = \pm 1.3 \times 10^{-5}$ and for aniline [7] the change is about the same. For these reasons we take ∇n for our substances to be $\pm 5 \times 10^{-5}$. For the same inaccuracy of temperature $(\nabla d)_t$ is estimated [8] to 2×10^{-5} and $(\nabla d)_{weight}$ to 5×10^{-5}. The total error ∇d is therefore estimated to be 1×10^{-4}.

For the following values

$$\nabla(\Delta d) = \pm (|\nabla d| + |\nabla d_0|) = \pm 2 \times 10^{-4}$$

$$\nabla(\Delta n) = \pm (|\nabla n| + |\nabla n_0|) = \pm 1 \times 10^{-4}$$

$$n_0 \sim 1.50,\ C \sim 1.0,\ d_0 \sim 0.88$$

is obtained $(\nabla R_1)_{app.} = \pm 0.1$.

The apparent molar refraction has therefore been given to two decimals.

In a previous paper [2], the nitration of 3,5-dimethylfluorobenzene yielding two mononitro derivatives was described. One of them was proved to be 4-nitro-3,5-dimethylfluorobenzene. The other nitro derivative was consequently considered to consist of 2-nitro-3,5-dimethylfluorobenzene. This assumption has now been proved experimentally. By heating 2-nitro-3,5-dimethylfluoro-

benzene with KOH in methanolic solution, the fluorine atom was replaced by the methoxy group and the resulting methoxy compound was identified as 2-nitro-3,5-dimethylanisole.

DISCUSSION

The strengths of aromatic bases are influenced by methyl groups in the *ortho*-position in a way which could not be predicted on the basis of the inductive and mesomeric effects. Thus *o*-toluidine and 2,6-xylidine are weaker bases than aniline (Thomson [9]). This means that the methyl groups decrease the electron-availability of the nitrogen atom. "In o-$CH_3C_6H_4NH_2$ the proton from the methyl group may go to the unshared pair of electrons of the amino group" (Branch and Calvin [10]), *i. e.* in this compound it is supposed that there is a hydrogen bond between the amine nitrogen and the methyl group. This type of hydrogen bond should, of course, be more pronounced in the di-*ortho*-methylated compound.

From measurements of ionization constants, Löfgren [3] suggests that the same type of hydrogen bond occurs in α-diethylamino-2,6-dimethylacetanilide ("xylocaine"). This compound, when compared with α-diethylaminoacetanilide, has a pK_a value about 0.2 units lower. It is particularly interesting to note that the *ortho*-effect is so strongly emphasized throughout the relatively long chain. From investigations on molar refractions and spectra, Löfgren concludes that the mobility in the resonance system is suppressed. Further, the steric conditions in this molecule indicate strongly that the interaction between the unshared electron pair of the amide nitrogen and the π-electronic system of the nucleus is suppressed. In other words, the electron-attracting capacity of the benzene nucleus is smaller in the 2,6-xylidide than in the anilide. One would then think that the pK_a value of the xylidide should be greater than that of the anilide. Supposing, however, that the unshared electron pair of the amide nitrogen is not only prevented from interfering with the nucleus but is also so influenced (by the *o*-methyl groups) that it becomes "bound", this would influence the electronic state at the carbonyl group. In the anilide, for instance, the key-oxygen-atom may have its electronic density increased by a mesomeric effect from the unshared electron pair of the amide nitrogen, but also by an inductive attraction which also affects the unshared electron pair of the diethylamino group at the end of the molecule. Through the *ortho*-effect described above, the mesomeric effect of the amide group on the carbonyl group in the 2,6-xylidide may be considered reduced, and therefore the inductive electron-attraction of the key-atom is more strongly pronounced. This means a weaker proton-binding capacity and appears in a low pK_a value.

Concerning *p*-substituted fluorine, it is known to induce a weak electron-attractive effect; in some cases *p*-F is even weakly electron-repulsive. *m*-F, however, exerts throughout clearly an electron-attractive effect (Watson [11], Hammet [12]). For our investigations it is of special value to recognize the influence of *p*-substituted fluorine on the amino group. From measurements of ionization constants (Bennet *et al.*[13], *cf.* also Watson [11]) of aniline and of *p*-fluoroaniline it is evident that there is an approximate equality between the

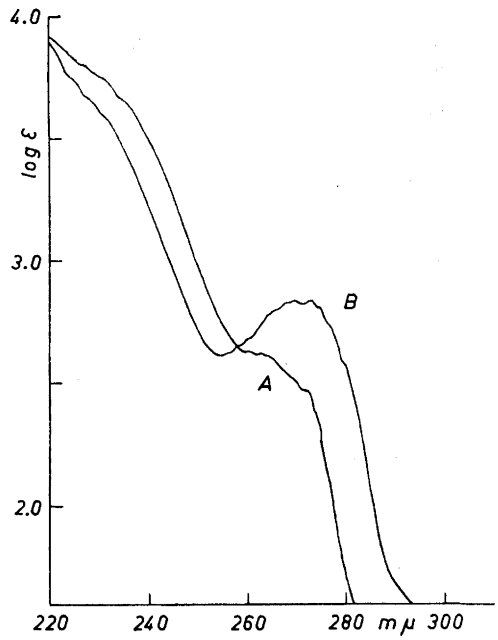


Fig. 1. Ultraviolet absorption spectra of hexane solutions of xylocaine (A) and α-diethylamino-4-fluoro-2,6-dimethylacetanilide (B)

constants of the two bases. Hence, we consider that *p*-F has very little influence on the electron pair of the amine nitrogen. On account of the steric conditions, the influence of the fluorine atom *para* to the nitrogen in 4-fluoro-2,6-dimethylaniline must be still less than in *p*-fluoroaniline.

We therefore conclude that the fluorine atom in α-diethylamino-4-fluoro-2,6-dimethylacetanilide has a negligible effect on the unshared electron pair of the amide nitrogen, but that the fluorine atom must exert a certain electron-attractive effect on the methyl groups (*cf.* above concerning *m*-substituted fluorine), *i. e.* the methyl groups must to a certain degree be "protonized". This should favour chelation of hydrogen bond type methyl group — amide nitrogen. The electron pair of the amide nitrogen in the fluorinated compound is therefore supposed to exert less interference with the carbonyl group than in the non-fluorinated compound, and for that reason (*cf.* above) the fluorinated compound has a lower pK_a value than the non-fluorinated compound, *i. e.* xylocaine. — To sum up, we put forward as a theory that the lower basicity of the fluorinated compound as compared with xylocaine is due to a stronger hydrogen bonding methyl group — amide nitrogen.

The differences in the molar refractions and absorption spectra are too small to permit any assumptions as regards the difference in the electronic states of the actual molecules. However, the findings from those measurements

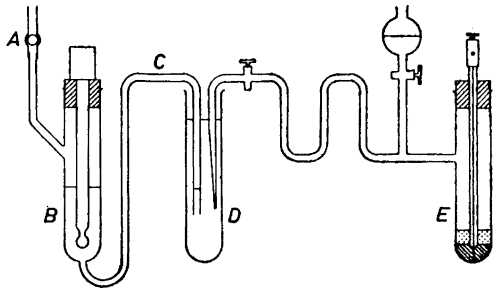


Fig. 2. Diagram of the cell. A = rubber tube with glass pellet (valve). B = glass electrode vessel. C = junction tube. D = junction vessel. E = satd. KCl calomel electrode.

do not in any way contradict what has been said above concerning the electronic effect of fluorine.

Finally, we want to make a possible explanation of the fact that the fluorinated compound, in comparison with xylocaine, has such a low local anesthetic potency. Generally it may be stated that the introduction of a fluorine atom in a physiologically active molecule changes to a marked degree its physiological activity, and this change in activity is probably due to the introduction of a strongly polarized C—F bond (*cf.* Burger *). According to Löfgren [3,15], there is a general rule for anilides of this type, *viz.* that the introduction of a strongly polar group in *p*-position to the amide nitrogen results in a low local anesthetic potency.

EXPERIMENTAL

Benzene, "Merck pro anal." was subjected to the usual purifying procedure, stored over sodium wire and distilled immediately before use; $d^{20} = 0.87902$; $n_D^{20} = 1.50110$ (recorded value [16]).

α-Diethylamino-2,6-dimethylacetanilide (xylocaine), prepared according to Löfgren [3], was recrystallized six times from petroleum ether; m. p. 67°. — The hydronitrate was prepared according to Löfgren [3], and then recrystallized three times from absolute ethanol; m. p. 133° (decomp.).

α-Diethylamino-4-fluoro-2,6-dimethylacetanilide, prepared according to Löfgren *et al.*[2], was recrystallized six times from petroleum ether; m. p. 56°. — The hydronitrate was obtained as colourless, thin needles from methyl ethyl ketone; m. p. 98°. (Found: C 53.2; H 6.99. Calc. for $C_{14}H_{22}FN_3O_4$ (315.3): C 53.3; H 7.03).

Solutions for pK_a determinations were made by dissolving the hydronitrates in water, neutralizing to 30—60 % with sodium hydroxide and diluting to definite volume.

The sodium hydroxide solution, practically carbonate free, was standardized against potassium hydrogen phthalate using phenolphthalein as an indicator. The distilled water had a specific conductivity of about 6×10^{-6} ohm^{-1} cm^{-1}.

The complete cell (see Fig. 2) was placed in a thermostat at 25° ± 0.05 °C. The vessel containing the glass electrode was filled by sucking up the solution through the junction

* According to Burger [14] fluorinated compounds appear to be much less physiologically active than derivatives containing other halogens, and even less than the corresponding non-fluorinated substances.

tube. To be able to measure the test solution with two different glass electrodes, the junction vessel was connected with two glass electrode vessels. Before use, each glass electrode vessel, with its electrode in place, was rinsed several times with distilled water and three times with the test solution. The boundary surface, originally at the end of the junction tube, was automatically raised 1.5 cm into the tube when the tube was lowered into the saturated potassium chloride solution. After ten minutes, readings were taken every other minute on each electrode until they became constant to within 0.1 mV (15—20 min.). With this apparatus the constancy and reproducibility of the measurements were very good.

The electromotive force was measured with an accuracy of 0.1 mV by a valve potentiometer (type PHM 3a made by Radiometer, Copenhagen). The standard cell of the potentiometer was checked against a Weston cell from the Cambridge Instrumental Company.

As a standard for the pH measurements, the buffer solutions recommended by Hitchcock and Taylor [17] were used.

The E' values of the glass electrodes (type G102A, Radiometer) were based on measurements with two freshly prepared different buffers, both before and after each day's work. The glass electrodes were also tested with the borate buffer (pH = 9.180) and no alkaline errors could be found.

The indices of refraction for the sodium D line, n_D, were determined with a Zeiss-Pulfrich refractometer at a temperature of 20° ± 0.02 °C. Repeated readings were taken in order to get a mean value. The refractive index of the prism was determined by means of carefully purified benzene. In this determination two different benzene preparations, "Merck pro anal." and "Stockholms Gasverk pro anal.", were used. Both benzene preparations showed the same angle of emergence.

The *absolute* density, d^{20}, of benzene and the benzene solutions were determined in Sprengel-Ostwald pyknometers, the weight being reduced to vacuum. The same thermostat and the same calibrated thermometer (graduated in 0.1°) were used in the measurements of the indices of refraction and the density. The density of benzene was determined by six separate measurements and the mean value agreed with a recorded value [16].

The ultraviolet absorption spectra were measured on a Beckman quartz spectrophotometer with a hydrogen lamp as a light source. The solvent was spectroscopically pure hexane and the concentrations were about 3×10^{-4} M. The interval between two readings was 1 mμ, except in the more interesting regions where the interval was 1/4 mμ

Proof of the position of the nitro group in 2-nitro-3,5-dimethylfluorobenzene. The nitro compound was treated with KOH in methanol in the same manner as described previously [2] for the determination of the position of the nitro group in the 4-nitro derivative. The melting point of the crude product was found to be 43—44°; yield 93 % (assuming the product to be a nitro-3,5-dimethylanisole). The substance was recrystallized from methanol. Pale yellow crystals melting at 44—45° were obtained; yield 75 % (*cf.* above). This melting point agrees with that of 2-nitro-3,5-dimethylanisole [18,19]. 2-Nitro-3,5-dimethylanisole was prepared according to the method of Rowe *et al.*[18] (nitration of 3,5-dimethylphenol and subsequent methylation of the 2-nitro derivative). The mixed m. p. showed no depression, and therefore the nitro compound must be 2-nitro-3,5-dimethylfluorobenzene.

The author wishes to thank Dr. N. Löfgren for valuable discussions.

REFERENCES

1. Lüning, B. *Acta Chem. Scand.* **11** (1957) 959.
2. Löfgren, N., Lundqvist, B. and Lindström, S. *Acta Chem. Scand.* **9** (1955) 1079.
3. Löfgren, N. *Studies on Local Anesthetics. Xylocaine a New Synthetic Drug* (Diss.) University, Stockholm 1948.
4. Fischer, I. and Löfgren, N. *Acta Chem. Scand.* **4** (1950) 1408.
5. Kielland, J. *J. Am. Chem. Soc.* **59** (1937) 1675.
6. Weissberger, A. *Technique of Organic Chemistry*, 2nd Ed., Interscience, New York 1949, Vol. I, p. 1161.

7. Landolt-Börnstein *Physikalisch-Chemische Tabellen*, Hw II, p. 971, 972.
8. Landolt-Börnstein *Physikalisch-Chemische Tabellen*, Erg. IIIa, p. 340.
9. Thomson, G. *J. Chem. Soc.* **1946** 1113.
10. Branch, G. and Calvin, M. *The Theory of Organic Chemistry*, Prentice-Hall, New York 1945, p. 262.
11. Watson, H. *Modern Theories of Organic Chemistry*, 2nd Ed., Oxford University Press, London 1941, p. 103.
12. Hammet, L. *Physical Organic Chemistry*, McGraw-Hill, New York and London 1940, p. 188.
13. Bennet, G., Brooks, G. and Glasstone, S. *J. Chem. Soc.* **1935** 1821.
14. Burger, A. *Medicinal Chemistry*, Interscience, New York 1951, Vol. I, p. 34.
15. Löfgren, N. *Private communication.*
16. Forziati, A., Glasgow, A., Willingham, C. and Rossini, F. *J. Research Natl. Bur. Standards* **36** (1946) 129.
17. Hitchcock, D. and Taylor, A. *J. Am. Chem. Soc.* **59** (1937) 1812.
18. Rowe, F., Bannister, S., Seth, R. and Storey, R. *J. Soc. Chem. Ind. London* **T49** (1930) 469.
19. Wilds, A. and Djerassi, C. *J. Am. Chem. Soc.* **68** (1946) 1862.
20. Landolt-Börnstein *Physikalisch-Chemische Tabellen*, Hw II, p. 977.
21. Schiemann, G. *Z. physik. Chem.* **(A) 156** (1931) 397.
22. v. Auwers, K. *Z. physik. Chem.* **(A) 158** (1932) 411.

Received February 19, 1957.

ACTA CHEMICA SCANDINAVICA 11 (1957) 971—980

Ultraviolet Absorption Spectra of Chain Molecules Consisting of Alternating Benzene Rings and Ethylenic Bonds

JOHANNES DALE

Forsvarets Forskningsinstitutt, Kjeller, Norway

The electronic absorption spectra of styrene, stilbene, 1,4-diphenylbutadiene, *p*-distyrylbenzene, *p*-(phenylbutadienyl)stilbene, *p,p'*-distyrylstilbene and diphenylacetylene have been measured, most of them down to 195 mμ. Mono-*cis*-isomers of *p*-distyrylbenzene and *p*-(phenylbutadienyl)stilbene have been prepared and their spectra also recorded. The observed bands are of three types: 1) a stationary band at 200—210 mμ; 2) a semi-stationary band at 210—250 mμ; and 3) polyene-like bands which can be interpreted as fundamental- and overtone-transitions of the full chromophore.

The spectra of the cross-conjugated compounds *m*-terphenyl and *m*-distyrylbenzene have been measured and compared with the spectra of biphenyl and stilbene.

The syntheses of *p,p'*-distyrylstilbene, *p*-chloro-*p'*-styryl-stilbene and *o*-chloro-*p'*-styrylstilbene are described.

Compounds of structure intermediate between the polyphenyls and the pure polyenes are of considerable interest for the interpretation of electronic absorption spectra of conjugated chain molecules in general. The chemical structure of alternating benzene nuclei and ethylenic bonds is such that a multiplicity of "partial chromophores" would be expected to be active in addition to the "full chromophore", if it is at all justified to divide a conjugated system arbitrarily into independent partial chromophores in order to explain the more complex spectra. It has already been shown that the concept of partial chromophores had to be rejected in discussions of polyene and polyenyne spectra [1,2] in favour of the simple, and more successful, overtone interpretation, which requires that the wave length position of the minor bands must be independent of the detailed structure and correspond to integral fractions of the total chromophore length. The transitions are, however, subject to selection rules which depend on the over-all shape of the molecule.

Among compounds of this type, styrene [3,4], as well as *cis*- and *trans*-stilbene [5,6], have already been investigated in the ultraviolet; for the stilbene isomers an interpretation based on rather implausible assumptions of several partial chromophores has been given by Braude [7]. For the first stilbene

homolog, *p*-distyrylbenzene, only an incomplete spectrum has been reported [8]. The solution spectra of these compounds have now been remeasured to down below 200 mμ (Figs. 1—3).

The next stilbene homolog, *p,p'*-distyrylstilbene, has been synthesized for the first time (see Experimental Part), but its extremely low solubility made it difficult to obtain a spectrum in the lowest wave length region (Fig. 4).

In addition, the closely related compounds, 1,4-diphenylbutadiene and *p*-(phenylbutadienyl)stilbene have also been investigated, the latter for the first time (Figs. 5—6).

The spectra of mono-*cis*-isomers of stilbene [6] and 1,4-diphenylbutadiene [9] have been redrawn from the literature (Figs. 2 and 5). Mono-*cis*-isomers of *p*-distyrylbenzene and *p*-(phenylbutadienyl)stilbene were not known and have been prepared by illumination of the all-*trans*-isomers; the spectra are given in Figs. 3 and 6.

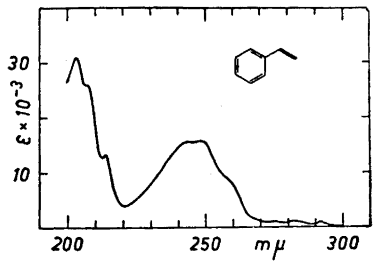


Fig. 1. Molecular extinction curve of styrene in hexane.

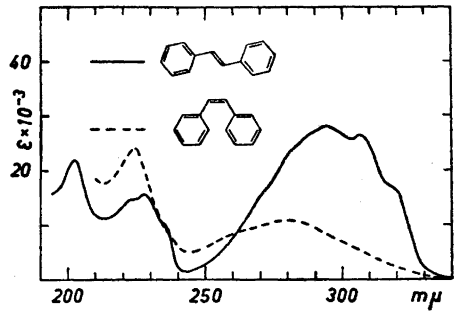


Fig. 2. Molecular extinction curves of *trans*-stilbene in hexane, and of *cis*-stilbene in ethanol (the latter curve from Beale and Roe [6]).

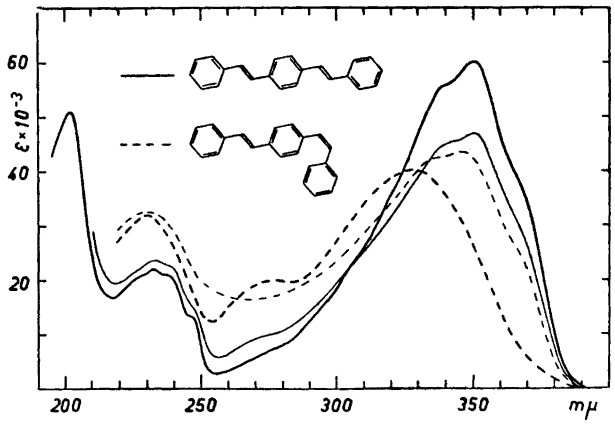


Fig. 3. Molecular extinction curves of all-*trans*- and of mono-*cis*-*p*-distyrylbenzene in hexane. Heavy lines represent fresh solutions; thin lines the same solutions after iodine catalysis.

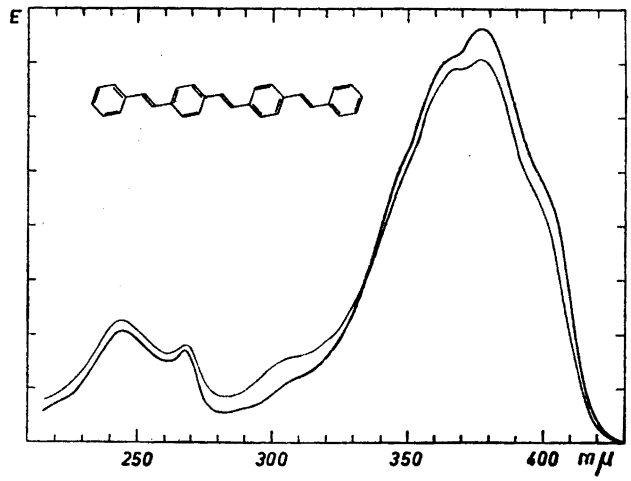


Fig. 4. Extinction curve of all-*trans*-*p,p'*-distyrylstilbene in *cyclo*hexane. Heavy line represents a fresh solution; thin line the same solution after iodine catalysis. Cell length 5 cm.

None of the compounds mentioned above contain benzene nuclei linked in other than the *para* position. It was the plan of this work to prepare similar chains containing also *ortho*-disubstituted benzene links, but none of the numerous attempts were successful (see Experimental Part), either because the methods that were used may not be suitable, or because the compounds may not be obtainable in crystalline form. It is noteworthy that only one such compound has been reported in the literature, namely, *o*-distyrylbenzene, claimed to be obtained in a Meerwein reaction between *o*-aminostilbene and cinnamic acid[10], and that a sample of this product proved, on closer examination, to be impure stilbene (see Experimental Part). The experience of the present writer indicates that the Meerwein reaction proceeds readily in the *para* position, but is replaced mainly by a Sandmeyer reaction in the *ortho* position (see Experimental Part). It should be mentioned, however, that chromatographically separated oily fractions showing the spectra expected for the desired *ortho* compounds could be obtained in some cases, but the quantities were far too small for identification.

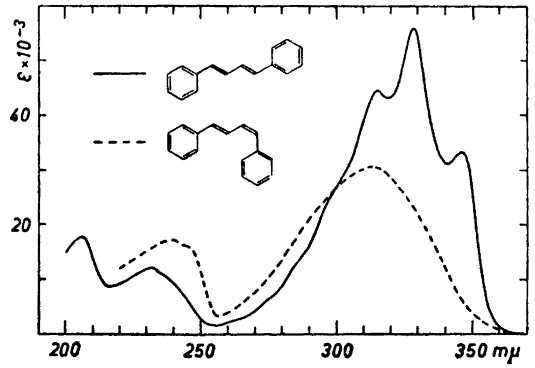


Fig. 5. Molecular extinction curves of all-*trans*- and of mono-*cis*-1,4-diphenylbutadiene in hexane (the latter curve from Pinckard, Wille and Zechmeister[9]).

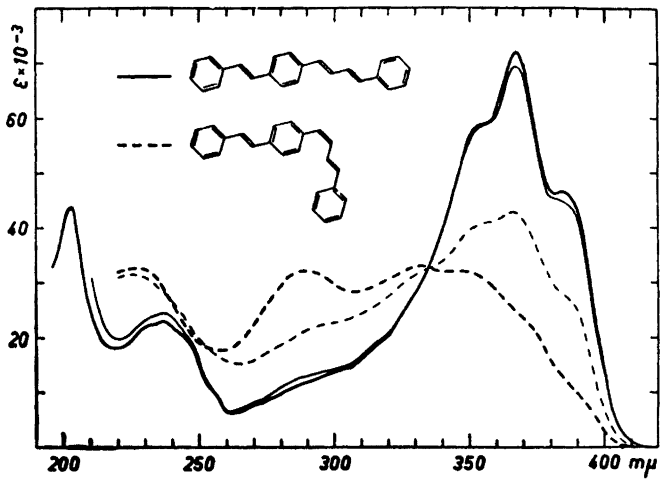


Fig. 6. Molecular extinction curves of all-*trans*- and of mono-*cis*-*p*-(phenylbutadienyl)-stilbene in hexane. Heavy lines represent fresh solutions; thin lines the same solutions after iodine catalysis.

In order to predict the wave length position of overtone bands [1] the wave lengths of the main bands have been plotted against the number of chromophoric units in Fig. 7. It was found that the smoothest curve could be obtained if each benzene ring is set equal to two ethylenic bonds. This choice is also in agreement with the molecular orbital picture of such systems [4].

The predicted and observed wave lengths have been compared in Table 1.

The polyene-like bands

From Figs. 3, 4 and 6 it is at once seen that there are no bands in the spectra of these compounds that could be assigned to any of the partial chromophores that would seem most reasonable. For instance, in the spectrum

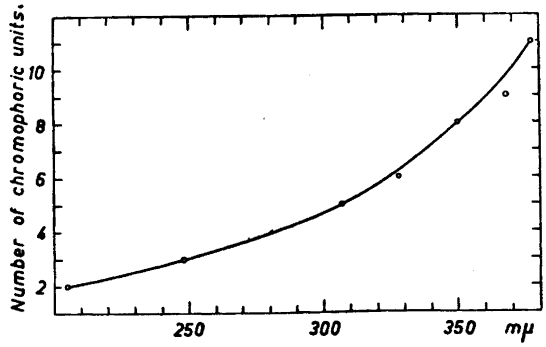


Fig. 7. Wave length position of the main band of the compounds from the preceding figures, plotted against number of chromophoric units (benzene ring = 2; ethylenic bond = 1).

Table 1. Predicted and observed wave lengths of overtone bands (in mμ).

	Number of chromophoric units	λ_2		λ_3		λ_4	
		calc.	obs.	calc.	obs.	calc.	obs.
Stilbene	5	228	224				
1,4-Diphenylbutadiene	6	248	~246	205	(~207)		
p-Distyrylbenzene	8	280	~275	235	~230	205	
p-(Phenylbutadienyl)-stilbene	9	295	~288	248	(~246)	217	~225
p,p'-Distyrylstilbene	11	315	~305	270	268	240	(~244)

of *p*-distyrylbenzene (Fig. 3) there is no band in the 300 mμ region where the stilbene chromophore should absorb; and in the *p*-(phenylbutadienyl)stilbene spectrum (Fig. 6) no bands appear that can be due to either the stilbene- or the diphenyl-butadiene-chromophore. Furthermore, in the *p,p'*-distyryl-stilbene spectrum (Fig. 4) bands corresponding to the stilbene- and the *p*-distyrylbenzene-chromophore are both lacking.

On the other hand, the spectra can be satisfactorily explained in terms of overtone transitions of the total chromophore (Table 1). Thus, in the region predicted for the first overtone (λ_2-band) no bands are observed as long as the ethylenic bonds remain in the stable *trans*-configuration obtained by synthesis (no dipole moment for this transition in a straight chain), but bands appear upon *cis*-isomerization. This behaviour is just what should be expected [1], and the bands correspond with the "*cis*-peak" in polyene spectra. It can also be inferred from this spectral behaviour that the *p*-divinylbenzene system must assume the "*trans*-like" configuration already implied in the drawings of the skeleton models shown in the figures.

In the lower wave length region the situation is complicated by the presence of typical bands which are relatively stationary at 210—250 mμ and at 200—210 mμ through the whole series, and which apparently must have another origin than the polyene-like bands (for further discussion see below). Thus, in *cis*-stilbene (Fig. 2) a λ_2-band at 224 mμ must be superimposed on the stationary band which is at 228 mμ in *trans*-stilbene, while in mono-*cis*-diphenylbutadiene (Fig. 5) the λ_2-band is on the long wave side of the stationary band.

The λ_3-band, which should be allowed in all isomers, seems to be superimposed on the short wave side of the stationary band in *p*-distyrylbenzene; it coincides with it in *p*-(phenyl-butadienyl)stilbene; and in *p,p'*-distyrylstilbene it appears well separated on the long wave side. A λ_4-band must be held responsible for the increased absorption at 225 mμ in mono-*cis*-*p*-(phenylbutadienyl)stilbene (Fig. 6); it is forbidden in the all-*trans*-isomer [1].

The stationary bands

A discussion of the origin of the "stationary" bands is strictly beyond the scope of this paper, but it is tempting to correlate the strong band at 200—210 mμ with allowed transitions between orbitals with no longitudinal node

localized in each benzene ring, $e \rightarrow e$ in Platt's notation [4], although the intensity does not seem to be a clear function of the number of rings. The strongest band in the polyphenyl spectra is always found very constantly at the same wave length, and has been given this interpretation as a real "partial" [11].

A further confirmation of these assignments could be obtained by checking experimentally a few predictions based on the following reasoning: In each benzene ring there are two sets of doubly degenerate π-orbitals, one filled and one empty, between which the electron jumps observable as absorption bands in the accessible ultraviolet region occur. When the rings are either mono-substituted or *para*-disubstituted links in a conjugated chain, one orbital of each set has a longitudinal node and remains isolated, whereas the other orbital of each set interacts with neighbouring π-orbitals to give polyene-like whole-molecular orbitals [4]. If, however, a *para*-disubstituted link is replaced by a *meta*-disubstituted ring, one orbital of each set will interact mainly with one conjugated system, while the other two orbitals interact mainly with another conjugated system, so that, instead of through-conjugation, we get cross-conjugation in Dewar's sense [12]. The whole situation is very analogous to what happens if an allenic link is introduced into an aliphatic unsaturated system [13,14]. The effect is to break the conjugation; one double bond in the allenic grouping being conjugated with an unsaturated system in one plane, while the other allenic bond is conjugated with another planar system rotated by 90° from the former plane.

It is thus understandable that *m*-terphenyl should show a conjugation band corresponding to twice that of biphenyl *, which was already noted by Gillam and Hey in 1939 [16]. In contrast, the band at 205 mμ should be expected to have the same intensity in both compounds since isolated orbitals will now be present only in the phenyl groups at both ends. This prediction could be

* The spectra of a series of polyphenyls containing *m*-disubstituted benzene rings [15], acting like insulating groups, can be similarly explained as superpositions of bands due to cross-conjugated partial chromophores corresponding to biphenyl, *p*-terphenyl or *o*-terphenyl.

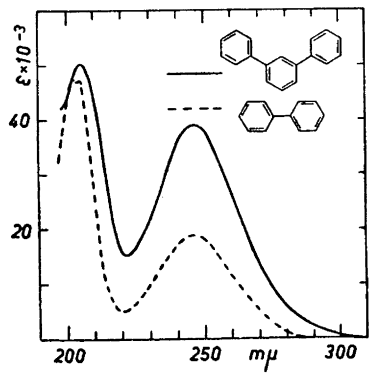


Fig. 8. Molecular extinction curves of *m*-terphenyl and biphenyl in hexane.

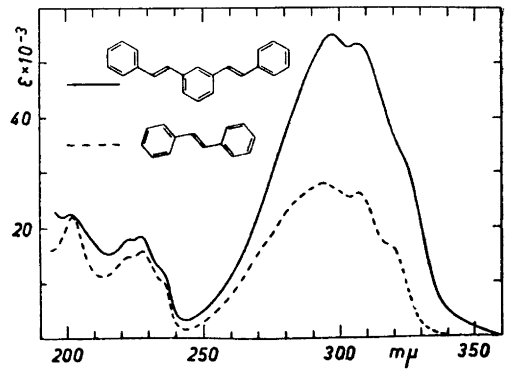


Fig. 9. Molecular extinction curves of *m*-distyrylbenzene and stilbene in hexane.

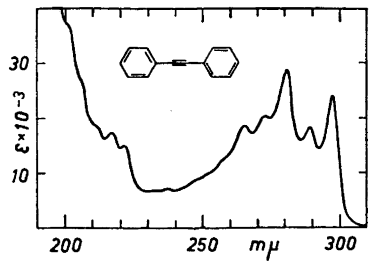


Fig. 10. Molecular extinction curve of diphenylacetylene (tolan) in hexane.

verified as shown in Fig. 8. Exactly the same relationships were found between the spectrum of *m*-distyrylbenzene and that of stilbene (Fig. 9).

The other "stationary" band at 228 mμ shows an intensity change intermediate between that of the conjugation band at 300 mμ and that of the true "partial" at 200 mμ. With increasing length of the conjugated system it undergoes a slight red-shift, from about 228 mμ in stilbene to about 244 mμ in *p,p'*-distyrylstilbene, so that the band is really only semi-stationary. We may therefore have to do with the transitions between an isolated π-orbital (*e*) and a polyenelike π-orbital (*p*) discussed by Platt [4]. The difficulty is that there is no counterpart in the polyphenyl spectra; furthermore, there should be two different transitions, $e \rightarrow p$ and $p \rightarrow e$ in Platt's notation, and they should be weak. There does not seem to be more than one band, and it is rather strong. The alternative assignment of both stationary bands to $e \rightarrow p$ and $p \rightarrow e$ transitions has been proposed [17], but the arguments do not seem decisive.

It may be significant that the pattern of vibrational structure in the semi-stationary band is very similar to that of the conjugation band [6]. Even for styrene this feature is apparent; it now seems to overlap on the long wave side of the stationary band at 204 mμ (Fig. 1). When the vibrational spacings of the conjugation band change and the peaks sharpen, as upon replacement of the ethylenic bond in stilbene with an acetylenic bond (Fig. 10), the structure of the semi-stationary band, now at 205—25 mμ, changes correspondingly.

Band width and steric hindrance

The absorption spectrum of mono-*cis*-*p*-(phenyl-butadienyl)stilbene requires a few comments. As is well known, the introduction of sterically hindered *cis*-bonds in a polyene- or diphenylpolyene-chain *etc.* shifts the absorption maximum of the main band considerably towards the ultraviolet. This is usually explained as an increase in the pure electronic transition energy due to a greater reduction of the resonance energy in the excited state than in the ground state. The present spectrum, however, shows rudimentary vibrational structure with the peaks not far from the positions in the all-*trans*-isomer (Fig. 6). The observed shift of the maximum, also in the completely structureless bands of *cis*-isomers of stilbene, diphenylbutadiene, *etc.*, must therefore be due mainly to a larger change in bond order upon excitation, so that according to the Franck-Condon principle more vibrational quanta are co-excited, and the maximum in the intensity distribution shifted towards the ultraviolet.

Similar spectral evidence is also available from Karrer's hindered *cis*-isomers of lycopene [18] and diphenyl-tetramethyl-octadecanonaene [19]. It is here quite clear that the pure electronic transition energy is only increased from that of the all-*trans*-compound by the same small amount as for the unhindered *cis*-isomers [20], but the transition probability maximum is shifted to much higher vibrational levels, and a greater band width results.

EXPERIMENTAL

The *spectra* were recorded in a Beckman DK-1 instrument using hexane as a solvent except when otherwise noted. In the lowest wave length region 2 mm silica cells were used. The sparingly soluble compounds were also measured in 5 cm cells.

Biphenyl, *m*-terphenyl, styrene, stilbene, 1,4-diphenylbutadiene, and diphenylacetylene (tolan) were purified commercial samples. Professor L'Ecuyer, Québec, most kindly provided samples of *m*-distyrylbenzene, *p*-distyrylbenzene and *p*-(phenylbutadienyl)-stilbene prepared by the Meerwein reaction [10].

p-Distyrylbenzene could also be prepared in good yield from *p*-dibromobenzene and phenylacetaldehyde in a Grignard reaction. The intermediate diol was dehydrated by boiling with toluenesulfonic acid. M. p. 265 °C.

p,p'-Distyrylstilbene. *p,p'*-Dinitrostilbene, prepared according to Walden and Kernbaum [21], was reduced with stannous chloride [22] to *p,p'*-diaminostilbene, m. p. 228 °C. 1.05 g of this compound (0.005 moles) was dissolved in 2.2 ml of 25 % HCl, and, after cooling and addition of 2.2 g of ice, diazotized with 0.37 g of $NaNO_2$ in 0.75 ml of water. The solution of the diazonium salt was poured into a cooled mixture (0 °C) of cinnamic acid (0.74 g), acetone (7.5 ml), anhydrous sodium acetate (0.8 g), and cupric chloride (0.23 g). The mixture was stirred vigorously and allowed to warm up slowly until the gas evolution started. The reaction mixture was steam-distilled, the water decanted off while hot, and the dry residue successively extracted in a Soxhlet apparatus with ethanol, acetone, hexane and chloroform. The earlier fractions contained *p,p'-dichlorostilbene*, m. p. 170 °C (Sandmeyer reaction), and a yellow substance which proved to be *p-chloro-p'-styryl-stilbene*, m. p. 238—40°, λ_{max} in hexane 353 mμ; this product is to be expected in a combination of the Meerwein and Sandmeyer reactions. The boiling chloroform deposited orange-yellow crystals of *p,p'-distyrylstilbene* already during the extraction. These were redissolved in chlorobenzene and precipitated with hexane. The very fine crystals were centrifuged, washed several times with hexane and finally sublimed *in vacuo*. The substance decomposes without melting at 310 °C, and is so extremely insoluble in the solvents commonly used for ultraviolet spectroscopy that even with chloroform quantitative extinction values could not be obtained.

Attempts to prepare o-*distyrylbenzene.* In a Grignard reaction between α,α'-dibromo-*o*-xylene and benzaldehyde no crystalline material was obtained. In a Grignard reaction between benzyl bromide and *o*-phthalaldehyde the only crystalline product was bibenzyl. In a Meerwein reaction between the diazonium salt of *o*-aminostilbene and cinnamic acid, following the prescription of L'Ecuyer and Turcotte [10], only stilbene and *o*-chlorostilbene could be isolated as crystalline materials. Furthermore, a sample of the compound described by these authors as *o*-distyrylbenzene, m. p. 120—22 °C, and kindly put at my disposal by professor L'Ecuyer, was examined spectroscopically both in the U.V. and the I.R. and proved to be stilbene, which melts at 124 °C when pure, admixed with some yellow impurity.

Attempt to prepare o,o'-distyrylstilbene. *o,o'*-Dinitrostilbene was prepared according to Bischoff [23] and reduced with stannous chloride [22] to *o,o'*-diaminostilbene, m. p. 174—75 °C. An attempted Meerwein reaction gave as the only crystalline material a good yield of the Sandmeyer product *o,o'-dichlorostilbene*, m. p. 98 °C.

Attempt to prepare o,p'-distyrylstilbene. *o,p'*-Dinitrostilbene was made in a cross-reaction between *o*- and *p*-nitrobenzylchloride. In order to keep the less reactive *o*-compound in excess during the reaction, the procedure was as follows: A solution of 17 g of *o*-nitrobenzylchloride and 2 g of *p*-nitrobenzylchloride in 72 ml of ethanol was placed in a three-necked flask equipped with a stirrer and two dropping funnels. A solution of 15 g of

p-nitrobenzylchloride in 56 ml of warm ethanol in one of the funnels and a solution of 11.5 g of KOH in 140 ml of ethanol in the other funnel were allowed to run slowly into the flask over the same period of time. After cooling, the crystal mass was filtered off and boiled with benzene. The insoluble residue was recrystallized from acetone; it consisted of *p,p'*-dinitrostilbene. Upon cooling the benzene solution, white-yellowish needles of *o,o'*-dinitrostilbene deposited. On further cooling, yellow needles of *o,p'*-dinitrostilbene started growing from the bottom of the vessel. The reaction products could also be resolved by chromatography of the benzene solution on alumina; the *o,o'*-compound is adsorbed less strongly than the *o,p'*-compound. After recrystallization, *o,p'*-dinitrostilbene melts at 143 °C, as compared with 138—140 °C reported for a sample made by a different method [24]. *o,p'-Diaminostilbene* was obtained by reduction with stannous chloride, and melted at 125 °C. A Meerwein reaction of its diazonium salt with cinnamic acid gave as the only crystalline products, *o,p'-dichlorostilbene*, m. p. 71 °C, and a good yield of a yellow substance which proved to be *o-chloro-p'-styrylstilbene*, m. p. 200 °C, λ_{max} in hexane 350 mμ.

Isomerization of p-distyrylbenzene. A solution of *p*-distyrylbenzene in benzene was exposed to daylight for several weeks. Extensive destruction took place. The benzene was distilled off and the residue dissolved in hexane and chromatographed on alumina with benzene/hexane as developer. The first few fractions that were collected were empty. Then came the only fraction containing more than traces of substance; it yielded a compound melting at about 95° C, which must be the mono-*cis*-isomer. Upon illumination in the presence of catalytic amounts of iodine the spectrum changed towards the characteristic spectrum of the all-*trans*-isomer, but the rearrangement was apparently accompanied by much destruction.

Isomerization of p-(phenylbutadienyl)stilbene. The illumination and the separation of the mixture was performed as for *p*-distyrylbenzene (see above). The only fraction containing any quantity of substance was collected quite early. The substance did not crystallize and may be one or more of the three possible mono-*cis*-isomers. In view of the intense *cis*-peak in the U.V. spectrum the *cis*-bond is most probably centrally located. Upon illumination in the presence of iodine the spectrum reverted very quickly to the characteristic spectrum of the all-*trans*-isomer.

Acknowledgements. The author is indebted to Professor P. L'Ecuyer, Québec, for generous gifts of some of the compounds, and to siv.ing. Eirik Raknes for valuable help in preparing the diaminostilbenes and *p,p'*-distyrylstilbene.

REFERENCES

1. Dale, J. *Acta Chem. Scand.* **8** (1954) 1235.
2. Dale, J. *Acta Chem. Scand.* **11** (1957) 265.
3. Price, W. C. and Walsh, A. D. *Proc. Roy. Soc. London* **A191** (1947) 22.
4. Platt, J. R. *J. Chem. Phys.* **19** (1951) 101.
5. Smakula, A. and Wassermann, A. *Z. physik. Chem.* **A155** (1931) 353.
6. Beale, R. N. and Roe, E. M. F. *J. Chem. Soc.* **1953** 2755.
7. Braude, E. A. *J. Chem. Soc.* **1949** 1902.
8. Hertel, E. and Siegel, U. *Z. physik. Chem.* **B52** (1942) 174.
9. Pinckard, J. H., Wille, B. and Zechmeister, L. *J. Am. Chem. Soc.* **70** (1948) 1938.
10. L'Ecuyer, P. and Turcotte, F. *Can. J. Research* **25B** (1947) 575.
11. Dale, J. *Acta Chem. Scand.* **11** (1957) 650.
12. Dewar, M. J. S. *J. Chem. Soc.* **1952** 3544.
13. Celmer, W. D. and Solomons, I. A. *J. Am. Chem. Soc.* **74** (1952) 1870, 2245.
14. Oroshnik, W., Mebane, A. D. and Karmas, G. *J. Am. Chem. Soc.* **75** (1953) 1050.
15. Woods, G. F., Artsdale, A. L. V. and Reed, F. T. *J. Am. Chem. Soc.* **72** (1950) 3221.
16. Gillam, A. E. and Hey, D. H. *J. Chem. Soc.* **1939**, 1170.
17. Birnbaum, P. P., Linford, J. A. and Style, D. W. G. *Trans. Faraday Soc.* **49** (1953) 735.
18. Garbers, C. F. and Karrer, P. *Helv. Chim. Acta* **36** (1953) 828.

19. Garbers, C. F., Eugster, C. H. and Karrer, P. *Helv. Chim. Acta* **35** (1952) 1850; **36** (1953) 562.
20. Eugster, C. H., Garbers, C. F. and Karrer, P. *Helv. Chim. Acta* **35** (1952) 1179.
21. Walden, P. and Kernbaum, A. *Ber.* **23** (1890) 1958.
22. Bergmann, F. and Schapiro, D. *J. Org. Chem.* **12** (1947) 57.
23. Bischoff, C. A. *Ber.* **21** (1888) 2071.
24. Ruggli, P. and Dinger, A. *Helv. Chim. Acta* **24** (1941) 173.

Received February 16, 1957.

ACTA CHEMICA SCANDINAVICA 11 (1957) 981—989

Absorption Spectra of Dysprosium(III), Holmium(III), and Erbium(III) Aquo Ions

CHR. KLIXBÜLL JØRGENSEN

Chemistry Department A, Technical University of Denmark, Copenhagen, Denmark

The narrow f^n-bands of aqueous Dy(III), Ho(III), and Er(III) perchlorates are measured in the range 800—210 mμ. The application of the theory of Slater, Condon, Shortley, and Racah to the distribution of multiplet terms is discussed. The lowest term with the total spin S one unit lower than of the groundstate often decays with fluorescence in the lanthanides and actinides, *e.g.* Sm(III), Eu(III), Sm(II), Dy(III), Pu(III), and Am(III).

Stewart [1] investigated trivalent lanthanides lighter than terbium. The present author has studied thulium [2]. The remaining three lanthanides, Dy, Ho, Er, have not been completely measured in aqueous solutions by modern spectrophotometry. Thus, Gorter *et al.*[3] do not report the spectra below 360—370 mμ, and Holleck and Hartinger [4] and Banks and Klingman [5] indicate only the wavelengths of the high peaks of analytical interest. The former authors [4] assume the absorption limit at a wavelength so high that they do not recognize the erbium(III) band at 255.2 mμ, discovered by Moeller and Brantley [6]. Therefore, the present author has procured the pure Dy_2O_3, Ho_2O_3, and Er_2O_3, prepared by Professor F. H. Spedding, and has measured the spectra with high dispersion on a Cary spectrophotometer. It was not felt useful to duplicate the measurements [3-6] above 800 mμ on a Beckman DU. Tables 1—3 give the band groups.

A conspicuous result is the absence of strong bands, such as those caused by $4f^n \rightarrow 4f^{n-1}5d$ transitions in Ce(III), Sm(II), and Eu(II). The molar extinction coefficient ε of Dy(III), Ho(III), and Er(III) is well below 2 at 220 and 3 at 210 mμ. Likewise, Yb (III) does not exhibit such bands [7].

SEXTET AND QUARTET LEVELS OF DYSPROSIUM(III)

Dieke and Singh [8] have recently expressed doubt whether the present author [9] is correct in assuming the multiplet ^6F in the infra-red and ^6P in the near ultra-violet part of the Dy(III) spectrum. This illustrates two different opinions on the most practical method of identifying f^n-energy levels. Dieke and

Table 1. Absorption bands of dysprosium(III) aquo ions. The bands are arranged in groups thought to correspond with the levels of the gaseous ion. Shoulders are given in parenthesis. λ denotes the wavelength in mμ and σ the wavenumber in K = cm^{-1} (not corrected for the refraction of air) of the maxima. δ is the half-width in K, *i.e.* the distance from the maximum to the wavenumber with half the value of ε, the molar extinction coefficient. (−) and (+) indicate the values of δ of unsymmetrical bands, towards lower and higher σ, respectively. The oscillator strength P is given in units of 10^{-6} from the equation $P = 9.2 \times 10^{-9}\ \varepsilon\delta$.

Group	λ	σ	ε	δ	P
1	760	13 160	0.32	100	0.3
2	475	21 050	0.09	—	0.11
3	453	22 080	0.23	—	0.4
	(451)	22 170	0.21	—	
4	427	23 420	0.08	—	0.1
5	394.5	25 350	0.22	250	0.5
6	(389.3)	25 620	0.40	—	1.0
	385.8	25 920	0.81	125	
	(378.6)	26 410	0.34	—	0.4
7	(366.1)	27 310	0.94	—	2.2
	364.5	27 430	2.00	(−)115	
8	(352.8)	28 340	1.39	—	3.1
	350.6	28 520	2.40	(−)130	
9	338.6	29 530	0.27	100	0.25
10	(326.6)	30 630	1.35	75	2.0
	325.5	30 720	1.68	85	
	(321.3)	31 120	0.15	—	
11	302.6	33 050	0.09	—	0.07
12	299.6	33 380	0.19	—	0.2
	298.7	33 480	0.19	—	
13	295.5	33 840	0.63	90	0.5
14	292.3	34 210	0.18	—	0.15
15	278.7	35 880	0.03	—	0.02
16	275.3	36 320	0.12	—	0.2
	274.5	36 430	0.15	—	
17	264.5	37 810	0.09	—	0.1
18	258.0	38 760	0.28	75	0.2
19	256.2	39 030	0.64	70	0.4
20	239.6	41 740	0.05	—	—
21	235 ?	42 550	0.04	—	—

Singh prefer the (physically very sound) way to identify J of each level by different methods: selection rules for polarized light, Zeeman effect and, most important, the maximum number of possible sub-levels ($2J+1$ for an even and $J+\frac{1}{2}$ for an odd number of electrons). When J is known for all levels, they can be assembled in multiplets with defined L and S if the deviations from Russell—Saunders' coupling are not too large.

Although the success of this method is evident in some cases, it must be realized that it has developed rather slowly. The present author attempted to stimulate the search for correct assignments of energy levels by drawing attention [9,10] to the fact that the theory of Slater, Condon, and Shortley [11] as refined for f^n-configurations by Racah [12] seems remarkably close to the large-scale distribution of multiplets in the absorption spectra of lanthanides and actinides. Thus, the large gap between 10 000 K (= cm^{-1}) and a fairly

Table 2. Absorption bands of holmium(III) aquo ions. Notation as in Table 1.

Group	λ	σ	ε	δ	P
1	655.7	15 250	1.05	(+)60	0.6
	652.3	15 330	1.03	—	0.6
	640.3	15 620	3.17	80	2.4
2	(548.4)	18 230	0.42	—	5.0
	542.9	18 420	1.78	—	
	536.5	18 640	4.42	(−)70	
3	(490.5)	20 390	0.37	—	1.3
	484.9	20 620	1.85	75	
	(483.2)	20 690	0.95	—	
4	479.5	20 850	0.48	—	0.1
5	473.4	21 120	0.86	100	0.8
6	467.6	21 390	0.84	45	0.3
7	(456.8)	21 890	0.73	—	5.5
	(454.0)	22 030	1.96	—	
	451.4	22 150	3.94	150	
	450.5	22 200	3.92		
	(447.5)	22 350	1.67	—	
8	421.2	23 740	0.86	20	3.0
	(418.4)	23 890	1.41	130	
	(416.4)	24 010	2.33		
	415.7	24 060	2.55		
9	393.0	25 450	0.13	—	0.1
	389.0	25 710	0.31	—	0.1
	384.7	26 000	0.50	35	0.2
	381.3	26 220	0.13	—	0.05
10	(363.6)	27 500	0.66	—	2.7
	361.1	27 690	2.20	—	
	(359.6)	27 810	1.50	—	
11	(347.8)	28 750	0.24	—	0.6
	345.6	28 940	0.57	120	
12	333.9	29 420	0.82	90	0.7
13	(295.0)	33 900	0.44	230	1.1
	293.8	34 030	0.55		
14	289.4	34 550	1.36	(−)25	1.5
	287.6	34 770	3.37	(+)50	
	(284.3)	35 170	0.04	—	
15	278.6	35 870	2.07	100	1.9
16	274.5	36 430	0.09	—	0.06
17	272.0	36 760	0.07	60	0.04
18	261.9	38 180	0.04	—	0.05
	260.2	38 430	0.06	—	
	258.8	38 640	0.03	—	
19	(251.2)	39 810	0.09	—	0.2
	250.0	40 000	0.20	105	
20	(242.4)	41 250	0.55	—	2.0
	241.8	41 360	1.54	—	
	241.1	41 470	3.52	(+)85,(−)35	
21	238.6	41 910	0.11	80	0.1
22	(233.7)?	42 790	0.06	—	—

high wavenumber in the middle of the lanthanide series is explained by the expected terms with the same S as the groundstate [10].

When the theory [11] has been previously applied to f^n-systems, unprobable ratios have been assumed between the parameters F^2, F^4 and F^6. Since the

Table 3. Absorption bands of erbium(III) aquo ions. Notation as in Table 1.

Group	λ	σ	ε	δ	P
1	666.8	15 000	0.51	(+)60	0.3
	652.9	15 320	1.92	(+)80	1.4
	(649.2)	15 400	1.04	(−)45	0.4
2	549.1	18 210	0.21	75	0.15
	542.0	18 450	0.72	50	0.3
3	(527.8)	18 950	0.40	—	
	523.3	19 110	3.10	(+) 45, (−) 105	
	(521.1)	19 190	1.98	—	2.1
	(518.3)	19 290	1.07	—	
4	491.4	20 350	0.94	(+)125	
	487.2	20 530	1.89	60	1.5
	(485.0)	20 620	0.81	—	
5	(455.6)	21 950	0.21	—	0.3
	453.5	22 050	0.38	—	
	449.8	22 230	0.89	50	0.4
	442.2	22 610	0.45	60	0.3
6	(410.5)	24 360	0.13	—	0.1
	407.0	24 570	0.53	110	0.6
	404.9	24 700	0.66		0.6
7	378.4	26 420	5 25	(+)55, (−) 90	
	(377.6)	26 480	3.81	—	3.8
	(376.0)	26 600	1.58	—	
8	(366.8)	27 260	0.45	(+)65	
	364.4	27 440	2.09	(+)38	0.8
	363.7	27 490	1.68	(−)34	
9	359.3	27 830	0.28	—	0.1
	356.2	28 070	0.81	43	0.3
10	317.0	31 550	0.11	50	0.05
11	(295.9)	33 800	0.08	—	0.02
	(294.4)	33 970	0.13	—	0.02
	293.5	34 070	0.17	23	0.04
12	287.2	34 820	0.17	48	0.1
13	275.1	36 350	0.32	33	0.2
	274.0	36 500	0.30	34	
14	261.0	38 310	0.06	—	
	260.3	38 420	0.11	—	0.1
	259.1	38 600	0.23	—	
15	255.2	39 180	6.45	(+)130, (−)145	8.2
16	243.3	41 100	0.64	70	0.4
	240.1	41 650	0.19	170	0.3
	236.1	42 350	0.08	35	0.03
17	230.1	43 460	0.49	80	0.4

energy differences between the terms with maximum S are multipla of one linear combination, E^3, of these parameters, Bethe and Spedding [13] and Satten [14] succeeded in identifying the spin-allowed bands of Tm(III) and Nd(III), respectively, while the spinforbidden bands of Nd(III) agree better [9] with ratios $F^2 \cong 1.5\, F^4 \cong 2\, F^6$. Independently, Judd [15] applied similar ratios to Eu(III) and Gd(III). Hence, it would be a surprising irregularity, if the order of ^{6}F and ^{6}P was reversed in Dy(III), especially since the hole-equivalent systems Sm(III) and Pu(III) exhibit analogous behaviour [9].

The present author does not believe that this reversal is finally proven. Dieke and Singh [8] have not observed the levels with $J = 11/2$, $9/2$, and $1/2$ of ^6F and hence concluded that the remaining levels actually are ^6P. It would not be surprising if the observed and calculated levels in Table 7, Ref. [9], were shifted one unit in J, since the interest was concentrated more on the multiplets than on the individual levels. However, the behaviour reported by Dieke and Singh [8] is more remarkable: the level called $^6P_{5/2}$ has five sub-levels, two more than the highest possible number. The collision between ^6H and ^6F may produce rather strong overlapping between levels, even with identical J, since the non-diagonal elements in intermediate coupling are zero [10] between levels with the maximum value of S. If $^6F_{1/2}$ is not the excited level at 13 200 K, the transition may be too weak to be observed with the large decrease of J from $^6H_{15/2}$. The two levels $^6F_{11/2}$ and $^6F_{9/2}$ may be hidden by the other levels, or simply be too improbable as final states for the fluorescence (in absorption they should occur below 9 000 K).

The fluorescent level at 20 958.8 K has seven sub-levels [8]. Dieke and Singh do not assume $J = 13/2$, but identify the level * as $^6F_{11/2}$ with subsequent ^6F-levels in the blue. Dieke and Singh [8] maintain that the intensity is too high for spin-forbidden transitions to quartet levels. However, in Table 1 there are three bands at 325.5, 350.6, and 364.5 mμ, which are 20 times stronger than the bands in the blue (*cf.* Fig. 1). The sextet character is evidently concentrated in the former bands. If they are identified as transitions to ^6P (they do not necessarily all have different values of J, but may be intermixed), E^3 is slightly greater than assumed previously [9], since the bands below 360 mμ were not known [3]. The new value $E^3 = 575$ K is more likely, compared to 480 K in Sm (III) and 630 K in Tm(III), than the old value 520 K.

Since $\zeta_{4f} = 1\,920$ K in Dy(III)[16], the quartet levels $\sim$21 000 K are expected to have $\sim$6 % sextet character, as actually observed.

FLUORESCENCE OF TRIVALENT LANTHANIDES AND ACTINIDES

Dieke and Singh [8] remark, "Moreover, the whole intensity of the fluorescence spectrum is due to the transitions from the resonance level to sextet levels. It would be hard to explain this as quartet-sextet transitions. This could only be so if there were no quartet levels below the resonance level." In the author's opinion, the latter hypothesis corresponds to a rather necessary condition for a f^n-level to decay with fluorescence: it shall be the lowest level with S one unit lower than the groundstate. This condition is satisfied by $^5D_0$ in Eu(III)[17] (however, $^5D_1$ can also be observed) and by $^5D_4$ in Tb(III)[18]. Butement [19] observed a fluorescent level at 14 514 K of Sm(II) in $BaCl_2$. This result implies [28] that the F_k-integrals in Sm(II) are $\sim$16 % smaller than in the iso-electronic Eu(III).

The fluorescent level of Sm(III) at 17 800 K agrees well with the spin-forbidden band of lowest wavenumber; there is a gap without absorption bands

* It can hardly have one of the very high J-values of ^4M, but is rather $^4I_{15/2}$ or $^4I_{13/2}$.

10 500—17 800 K in Sm(III), as there is between * 13 200—20 900 K in Dy(III). In Pu(III), the analogous gap [9] between 17 900 and 19 800 K is much smaller. Actually, a fluorescent level has been observed [20] of Pu(III) in $LaCl_3$ at 19 200 K, while Am(III)[21] in $LaCl_3$ has a group of fluorescent levels in the blue. The fluorescent levels of actinides can be utilized to find the excited levels of the ground multiplet (as initiated by Gobrecht [22] in the case of lanthanides) and hence to determine the large values of ζ_{5f}. Thus, a level seems to occur at 3 100 K in Pu(III), implying $\zeta_{5f} = 4\,400$ K, if the effects of intermediate coupling are neglected. (However, ζ_{5f} is probably 20 % smaller, since Judd [16] has proven that the distances between the lowest levels of a ground multiplet generally are increased, and the distances between the highest levels decreased, compared to the Landé interval rule). It is interesting to compare the ^7F levels of Sm(II)[19], Eu(III), and Am(III) implied by fluorescence (f) and absorption (a):

$J =$	0	1	2	3	4	5	6
Sm(II)	0	269f	834f	1 493f	2 296f	?	?
Eu(III)	0	370f	1 058f	1 906f	2 872f	3 936f	4 964f
Am(III)	0	~800f	2 600f	5 300f	?	9 500a	12 300a

The wavenumbers have roughly the ratios 0.8 : 1 : 2.5. Although the determinants of intermediate coupling are not known, $^7F_4$ seems to be somewhat decreased in all cases.

ENERGY LEVELS OF HOLMIUM(III) AND ERBIUM(III)

It is common to f^2-, f^5-, f^9-, and f^{12}-systems that the P-term with maximum spin is 42 E^3 above ** the ground term H, and the F-term only 9 E^3 above H. Thus, Pr(III), Sm(III), Dy(III), and Tm(III) all have a P-term at a high wavenumber, preceded by a large gap with no bands towards the red and spin-forbidden bands towards the blue limit. f^3-, f^4-, f^{10}-, and f^{11}-systems have another characteristic distribution of terms with the maximum value of S: I, F, S, G, and D at 0, 21, 21, 33, and 54 E^3, respectively. Hence, two gaps exist, one in the near infra-red between I and F, and one in the near ultra-violet between G and D. The behaviour of Nd(III) and Pm(III) has previously been discussed [9]. Tables 2 and 3 and Fig. 1 present similar evidence from Ho(III) and Er(III).

The lowest triplet level of Ho(III) appears to occur at 20 600 K, probably $^3K_8$. It has a small chance to be fluorescent. It would be interesting to know, whether the excited states (before the fluorescent level is reached) decay with internal conversion into vibrational energy, or infra-red light is irradiated by sharp transitions.

* The extremely weak bands reported [8] of $DyCl_3$, $6H_2O$ at 17 151, 18 462, and 18 486 K may be caused by impurities of Nd(III), Ho(III), etc.

** These energies refer to the baricenters, *i.e.* the average of the energy levels, when weighted by their degeneracy numbers.

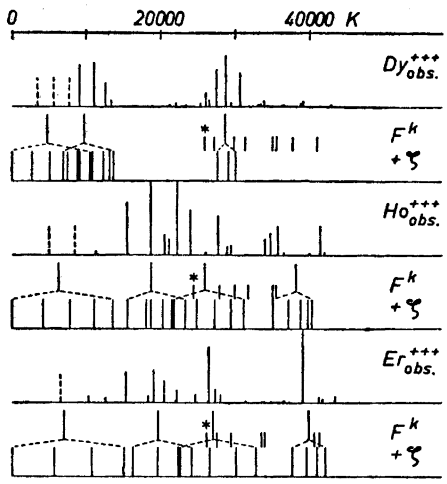


Fig. 1. The energy levels of dysprosium(III), holmium(III), and erbium(III). Three rows are given for each element: First, the wavenumbers of the observed band groups are indicated by lines, whose heights are proportional to the oscillator strength P (except the dotted lines in the infra-red, where P is not known). Second, the predicted baricenters of multiplets are given as high and low lines, representing terms with the maximum value of S and lower values, respectively. Third, the splitting of the terms with maximum value of S, assuming Russell-Saunders' coupling, is given. E^3, a linear combination of F_k-integrals [9], is estimated to 575 K, 590 K, and 610 K in the three ions (it is 460 K in Pr(III) and 630 K in Tm(III)) while the three values [16, 9] of ζ_{4f} are 1 920, 2 080, and 2 350 K (the values in Ce(III) is 644 K and in Yb(III) 2 950 K). The lowest multiplet with S one unit lower than of the groundstate is marked by an asterisk.

Especially in Fig. 1, a large gap is evident between the last level of Ho(III) with largely ^{5}G-character at 27 800 K and the likely ^{5}D-levels at 34 800—41 500 K. In the red, no bands are reported between the last ^{5}I-level * at 11 200 K and the first ^{5}F-level at 15 300 K.

The effects of intermediate coupling are very large in Er(III)[9], and the property "lowest spin-forbidden transition" to $^2H_{11/2}$ and to $^2H_{9/2}$ must be rather dispersed among the ^{4}I levels with the same J. The very high band at 39 200 K has probably some ^{4}D-character, but the exact nature is perhaps rather complicated. It has not been possible to observe an extremely narrow band of the type $^2P_{1/2}$ at 23 400 K of Nd(III). It may be connected with the low transition probablity of a transition in Er(III) from $^4I_{15/2}$ to a level with $J = 1/2$ (the $^2P_{1/2}$ of Nd(III) has ~30 % quartet character, and nevertheless, the oscillator strength is only ~2 % of ordinary $^4I_{9/2} \rightarrow$ quartet transitions in Nd(III)). Generally, transitions where J decreases strongly have rather low

* The author has not been able to observe $^5I_4$ reported [22] at 13 300 K. This may be due either to vanishing intensity (the transition to $^5I_5$ is also very weak, *cf.* Fig. 1) or to a partial reversal of the upper-most levels of ^{5}I, as is perhaps the case in ^{4}I of Er(III) and certainly in ^{3}H of Tm(III). The latter effect corresponds to strong effects of 'averaged' intermediate coupling, as studied by Judd [16].

probabilities [9]. However, the absolute oscillator strengths, which probably are caused by forced electric dipole radiation induced by vibrations or ligand fields without a centre of inversion [23], are not easily calculated. Thus, some, but not all, bands of the acetylacetonates [24] are much higher than of the aquo ions. In particular, some bands of Ho aca_3 and Er aca_3 have ~50 times larger oscillator strengths than the corresponding bands of the aquo ions.

SUMMARIZING REMARKS

It is seen from Fig. 1 that the general distribution of spin-allowed and spin-forbidden transitions in Dy(III), Ho(III), and Er(III) agrees with the theory [9,10], as is also the case for the other trivalent lanthanides. This agreement is caused mainly by the fact that radial functions of highly different shape produce a smooth decrease of F_k with increasing k. Since interactions probably occur with other electron configurations (but not much more in the aquo ions than in the gaseous ions), the theory has always an uncertainty between 500 and 2 000 K of the baricenter of a given multiplet. On the other hand, it does not usually predict a multiplet 5 000 K in error.

It is hoped that this treatment may aid the future identification work, as J of a few levels of Ho(III) and Er(III) recently have been reported [25]. Especially the ultraviolet regions have been very little studied by more refined methods. It must be admitted that the determination of J of the individual levels is not yet completed, even in the much studied Nd(III) (the present author is inclined to believe that the groups at 680 and 630 mμ are caused by $^2H_{9/2}$ and $^2H_{11/2}$, respectively, and that the low J-values of ^4G must be dispersed in an irregular way between the stronger quartet bands of this ion). The intentions of ligand field studies of lanthanide salts at low temperature [26, 27] are very admirable, but they seem to be more fruitful when connected with the general theory of multiplet distribution in the f^n-systems.

EXPERIMENTAL

0.5 g Dy_2O_3 was dissolved by boiling with a slight excess of 2 M $HClO_4$ and measured in 2 cm silica cells. In the same way, 0.3 g Ho_2O_3 and 0.3 g Er_2O_3 were measured in1 cm silica cells. The purity of the rare earths is better than 99.9 %. The spectra were measured twice (in opposite directions) at the lowest possible rate of dispersion change, *viz.* 1.25 mμ per division (0.83 cm of paper) in the visible and 0.5 mμ in the ultraviolet. No attempt was made to compare with $HClO_4$ in the double-beam Cary spectrophotometer 11 MS-50; rather, water was placed in the reference cell, and 2 M $HClO_4$ later measured against this water in order to evade spurious behaviour of the multipots.

Acknowledgement. I am grateful to Professor F. H. Spedding, Iowa State College, Ames, for the supply of the pure rare earths.

REFERENCES

1. Stewart, D. C. *Light Absorption . . .* I, AECD-2389.
2. Jørgensen, C. Klixbüll, *Acta Chem. Scand.* **9** (1955) 540.
3. Hoogschagen, J. and Gorter, C. J. *Physica* **14** (1948) 197.
4. Holleck, L. and Hartinger, L. *Angew. Chem.* **67** (1955) 648.

5. Banks, C. V. and Klingman, D. W. *Anal. Chim. Acta* **15** (1956) 356.
6. Moeller, Th. and Brantley, J. C. *Anal. Chem.* **22** (1950) 433.
7. Jørgensen, C. Klixbüll, *Kgl. Danske Videnskab. Selskab, Mat.fys.Medd.* **30** (1956) No. 22.
8. Dieke, G. H. and Singh, S. *J. Opt. Soc. Amer.* **46** (1956) 495.
9. Jørgensen, C. Klixbüll, *Kgl. Danske Videnskab.Selskab, Mat.fys.Medd.* **29** (1955) No. 11.
10. Jørgensen, C. Klixbüll, *Energy Levels of Complexes and Gaseous Ions.* Gjellerups Forlag. Copenhagen 1957.
11. Condon, E. U. and Shortley, G. H. *Theory of Atomic Spectra.* Cambridge 1953.
12. Racah, G., *Phys. Rev.* **76** (1949) 1352.
13. Spedding, F. H. *Phys. Rev.* **58** (1940) 255.
14. Satten, R. A. *J. Chem. Phys.* **21** (1953) 637.
15. Judd, B. R. *Proc. Roy. Soc. London* **A228** (1955) 120.
16. Judd, B. R. *Proc. Phys. Soc. London* **A69** (1956) 157.
17. Sayre, E. V. and Freed, S. *J. Chem. Phys.* **24** (1956) 1213.
18. Geisler, H. F. and Hellwege, K. H. *Z. Physik* **136** (1953) 293.
19. Butement, F. D. S. *Trans. Faraday Soc.* **44** (1948) 617.
20. Cunningham, B. B., Gruen, D. M., Conway, J. G. and McLaughlin, R. D. *J. Chem. Phys.* **24** (1956) 1275.
21. Gruen, D. M., Conway, J. G., McLaughlin, R. D. and Cunningham, B. B. *J. Chem. Phys.* **24** (1956) 1115.
22. Gobrecht, H. *Ann. Physik* [5] **28** (1937) 673; **31** (1938) 755.
23. Broer, L. J. F., Gorter, C. J. and Hoogschagen, J. *Physica* **11** (1945) 231.
24. Moeller, Th. and Ulrich, W. F. *J. Inorg. Nucl. Chem.* **2** (1956) 164.
25. Kahle, H. G. *Z. Physik* **145** (1956) 347, 361.
26. Paskin, A. and Keller, J. M. *Absorption Spectrum of* $Tm_2(SO_4)_3 8H_2O$. ISC-310. Ames, 1953.
27. Dieke, G. H. and Heroux, L. NYO-3977, 1955; *Phys. Rev.* **103** (1956) 1227.
28. Jørgensen, C. Klixbüll, *J. Inorg. Nucl. Chem.* **4** (1957) 369.

Received March 20, 1957.

ACTA CHEMICA SCANDINAVICA 11 (1957) 990—996

Electroorganic Preparations III. Polarography and Reduction of N-Nitrosamines

HENNING LUND

Leo Pharmaceutical Products, Copenhagen, Denmark

N-Nitrosamines of secondary aliphatic, heterocyclic, and aromatic amines are investigated polarographically. The formation of N-nitrosamines is used for the polarographical determination of secondary amines. The polarographic reductions of the N-nitrosamines are shown by controlled potential electrolysis to be, in acid solution a four electron reduction to the hydrazine, whereas the reduction in alkaline solution is a two electron reduction to the secondary amine with the formation of nitrous oxide.

Dimethylamine has been determined by polarography of its N-nitroso derivative [1,2], but no polarographic investigation of other N-nitrosamines has been reported. N-Nitroso phenylhydroxylamine has been investigated by Kolthoff and Liberty [3]. As there might be a possibility to determine secondary amines in the presence of primary and tertiary amines by polarography of their N-nitrosamines a polarographic investigation of N-nitrosamines was undertaken. The course of the reduction of the N-nitrosamines at a macro mercury electrode was proved by means of controlled potential electrolysis.

POLAROGRAPHIC INVESTIGATION

Effect of pH on half-wave potentials. In Table 1 are compiled the half-wave potentials and diffusion currents of N-nitroso dimethylamine (I), N,N'-dinitroso piperazine (II), N-nitroso morpholine (III), N-nitroso N-methylaniline (IV), and N-nitroso diphenylamine (V) at different pH-values.

The half-wave potentials of (I), (II) and (III) vary linearly with pH from pH about 0 to pH about 6. The slopes of the $E_{\frac{1}{2}}$ *vs* pH plots in this pH interval were 0.100, 0.097 and 0.098 V per pH-unit for (I), (II) and (III), respectively. At pH-values higher than about 7 the half-wave potentials were independent of pH. The half-wave potentials of (IV) vary from pH 1 to pH 7 linearly with pH with a slope of 0.082 and are independent of pH at higher pH-values. At pH-values lower than 1 the half-wave potentials are less negative than required

Table 1. Half-wave potentials (*vs* S.C.E.) and diffusion currents at different pH-values of N-nitroso dimethylamine (I), N,N'-dinitroso piperazine (II), N-nitroso morpholine (III), N-nitroso N-methylaniline (IV), and N-nitroso diphenylamine (V). Concentration 1.00×10^{-3} M, 0.01 % gelatin added as maximum suppressor.

pH		0.20	0.60	0.95	2.75	3.60	5.05	7.15	10.35	12.5
(I)	$-E_{\frac{1}{2}}$ V	0.87	0.91	0.94	1.12	1.21	×	1.53§	1.54	1.55
	i_d μA	13.5	13.5	13.5	13.4	13.3		8	6.5	6.4
(II)	$-E_{\frac{1}{2}}$ V	0.74	0.78_5	0.85	1.00	1.07	1.24	1.29	1.34	1.35
	i_d μA	26.3	26.3	26.3	26.3	26.2	25.9	25.5	14.1	13.3
(III)	$-E_{\frac{1}{2}}$ V	0.75	0.79	0.83	0.99_5	1.09	1.26_5	1.38	1.40	1.40
	i_d μA	12.8	12.8	12.8	12.7	12.3	11.9	11.7	6.9	6.4
(IV)	$-E_{\frac{1}{2}}$ V	0.58_5	0.64_5	0.68	0.86	0.92	1.02	1.23	1.30	1.31
	i_d μA	12.0	12.0	11.9	11.9	11.8	11.7	11.6	6.0	5.95
(V)	$-E_{\frac{1}{2}}$ V	0.47	0.51	0.56_5	0.71_5	0.76_5	0.85_5	0.98	1.03	1.03
	i_d μA	10.5	10.5	10.5	10.4	10.4	10.4	10.1	5.43	5.20

× No wave § Poorly defined wave

by the straight line in the $E_{\frac{1}{2}}$ *vs* pH plot. The half-wave potentials of (V) vary linearly with pH at pH values lower than 1 with a slope of 0.130 V per pH-unit. From pH about 2 to pH about 7 the slope of the $E_{\frac{1}{2}}$ *vs* pH plot is 0.063 and at pH-values higher than 8 the half-wave potentials are independent of pH.

In Table 2 are given the half-wave potentials and diffusion currents at different pH-values for *p*-nitroso N,N-dimethylaniline. The half-wave potentials vary linearly with pH in the examined pH interval with a slope of 0.068 V per pH-unit.

Effect of pH on diffusion current. The diffusion currents are for the N-nitrosamines fairly constant from pH 0 to pH about 5. In an interval around pH 7 the diffusion currents drop to a value which is half the value in acid solution. At pH-values higher than about 9 the diffusion currents again are fairly independent of pH. As shown in Fig. 1 the plot of the diffusion current *vs* pH has its highest slope at the same pH as that, at which the half-wave potentials start to be independent of pH. The diffusion currents of *p*-nitroso N,N-dimethylaniline are fairly constant in the examined pH-interval and have

Table 2. Half-wave potentials (*vs* S.C.E.) and diffusion currents at different pH-values of *p*-nitroso N,N-dimethylaniline. Concentration 1.0×10^{-3} M, 0.01 % gelatin added as maximum suppressor.

pH	4.0	5.0	6.5	8.0	10.0	12.5
$-E_{\frac{1}{2}}$ V	-0.01_5	0.05	0.16	0.26	0.38	0.55
i_d μA	12.1	12.1	11.9_5	11.8	11.7	11.6

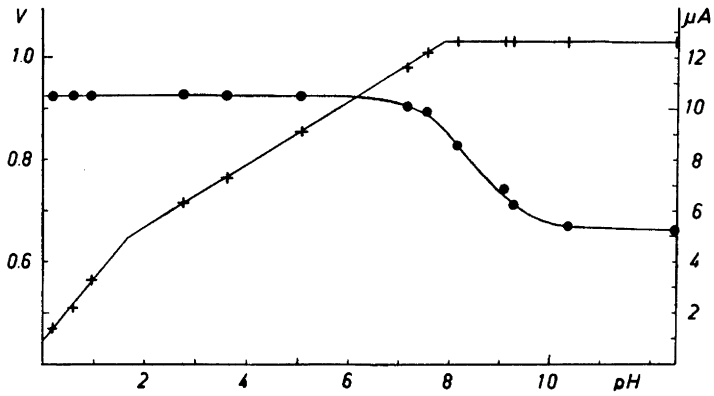


Fig. 1. Half-wave potentials +(V *vs* S.C.E.) and diffusion currents ● (μA) of N-nitroso diphenylamine plotted against pH. Concentration 10^{-3} M, 0.01 % gelatin added as maximum suppressor.

a value nearly equal to the value of the diffusion current of N-nitroso N-methylaniline in acid solution.

Effect of mercury height on limiting current. The data presented in Table 3 for limiting currents of N-nitroso dimethylamine and N-nitroso diphenylamine at different mercury column heights indicate that the limiting currents both in acid and alkaline solution are diffusion controlled. A diffusion controlled limiting current is nearly proportional to the square root of the corrected mercury column height and it is seen in Table 3 that $i_d/h^{1/2}$ is fairly constant.

Variation of diffusion currents with concentration. The variation of diffusion currents with concentration is substantially linear for the compounds between 1.5×10^{-4} and 2×10^{-3} M. At higher concentrations there is a slight negative deviation.

Wave form. The waves of N-nitroso dimethylamine, N,N'-dinitroso piperazine, and N-nitroso morpholine are somewhat drawn out whereas those of

Table 3. Dependence of limiting currents on mercury column heights for N-nitroso dimethylamine and N-nitroso diphenylamine in acid and alkaline solution. Concentration 10^{-3} M, 0.01 % gelatin added as maximum suppressor.

pH	N-nitroso dimethylamine				N-nitroso diphenylamine			
	1.0		12.5		1.0		12.5	
h cm	i_dμA	$i_d/h^{\frac{1}{2}}$	i_dμA	$i_d/h^{\frac{1}{2}}$	i_dμA	$i_d/h^{\frac{1}{2}}$	i_dμA	$i_d/h^{\frac{1}{2}}$
28.5	10.4	1.95	4.87	0.914	7.80	1.46	3.90	0.732
38.5	12.1	1.95	5.55	0.895	9.30	1.50	4.59	0.740
48.5	13.5	1.94	6.40	0.919	10.50	1.51	5.20	0.747
58.5	15.2	1.99	6.92	0.907	11.55	1.51	5.64	0.738

N-nitroso N-methylaniline and N-nitroso diphenylamine more approach the form of a reversible wave. None of them are, however, reversible. The plots of log $(i/i_d—i)$ *vs* the electrode potential at pH about 1 yield straight lines for N-nitroso N-methylaniline and N-nitroso diphenylamine with the slopes of 0.068 and 0.047, respectively. For N-nitroso dimethylamine, N,N'-dinitroso piperazine, and N-nitroso morpholine the first part of the waves yield a straight line with the slopes of 0.080, 0.125 and 0.115, respectively, whereas the second part of the waves yield a curve which deviates from the straight line corresponding to a drawn out wave. As a reversible one-electron reduction would yield a straight line with the slope of 0.059 the slope of N-nitroso diphenylamine 0.047 suggests that more than one electron is involved in the potential determining step.

Discussion. The half-wave potentials depend upon the structure in a manner which was to be expected. The introduction of a phenyl group lowers the half-wave potential, but at the same time both the form of the wave and the dependence of the half-wave potential upon pH approach the behaviour of a reversible reduction. This is probably due to the increased resonance possibilities of the primarily formed radical present when a phenyl group participates in the resonance system.

The polarographic analysis shows that the electrode reaction in acid solution involves twice as many electrons as the electrode reaction in alkaline solution as the limiting currents are twice as high in acid as in alkaline solution and both of them are diffusion controlled. This would be in accordance with the assumption that the reduction in acid solution yielded the hydrazine and in alkaline solution either the tetrazene or the amine and nitrous oxide. It seems reasonable to assume that in acid solution it is the protonated nitrosamine $RR'N—NOH^+$ which is reduced whereas the free nitrosamine is reduced in alkaline solution. This is consistent with the fact that the half-wave potentials in alkaline solution are independent of pH, whereas they in acid solution have a linear dependence upon pH. It seems necessary to assume the reduction of a doubly protonated molecule $(C_6H_5)_2NH^+—N=OH^+$ in order to explain the behaviour of N-nitroso diphenylamine in strongly acid solution, where the half-wave potentials are dependent upon the square of the hydrogen ion concentration. A similar pH dependence was found [3] for N-nitroso phenylhydroxylamine. The electrode reaction of N-nitroso diphenylamine in strong acid solution is a four electron reduction.

The reduction of *p*-nitroso N,N-dimethylaniline requires the same number of electrons in acid and alkaline solution, whereas the reduction of N-nitroso phenylhydroxylamine in acid solution involves six electrons and in alkaline solution four electrons [3]. The polarographic behaviour of N-nitrosamines, N-nitroso phenylhydroxylamine, and *p*-nitroso N,N-dimethylaniline is thus different.

ANALYTICAL INVESTIGATION

English [2] found that methylamine on reaction with nitrous acid in strong acetic acid yielded some nitromethane which interfered with the determination of dimethylamine. Trimethylamine in high concentration yielded some N-nitroso dimethylamine under the same conditions.

Using the procedure described below only negligible side reactions took place for the following primary amines: methylamine, ethylamine, and *cyclo*-hexylamine. Trimethylamine was nitrosated to some extent, whereas triethylamine was only slightly attacked and N-ethylpiperidine reacted only to a slight degree with nitrous acid when the concentration of the tertiary amine was less than 5×10^{-3} M in the final solution.

Primary aromatic amines form diazonium compounds on reaction with nitrous acid and these [4] or their coupling products are reducible at potentials in the neighbourhood of those of secondary nitrosamines. Tertiary aromatic amines form *p*-nitroso compounds on reaction with nitrous acid and these are reducible at potentials lower than those of N-nitrosamines. High concentrations of primary and tertiary aromatic amines will thus make a determination of secondary amines difficult.

In a mixture containing secondary aromatic and aliphatic amines it is possible to determine both kinds of amines as there is a difference of more than 0.2 volt between the half-wave potentials of the nitrosamines of secondary aromatic and aliphatic amines.

Nitrosation of amines. Attempts to nitrosate amines in dilute hydrochloric acid with excess of sodium nitrite were successful for amines as diphenylamine and N-methylaniline, whereas diethylamine and piperidine did not yield the nitrosamines under these conditions. Morpholine and diethanolamine yielded some nitrosamine but the yield was not quantitative. As it apparently was the weak bases which reacted with nitrous acid under acid conditions it was tried to nitrosate the strong amines at higher pH-values. It was found that in an acetate buffer, pH about 4, all the amines tried gave quantitative yields of the nitrosamines.

Procedure. For the quantitative determination of secondary amines the following procedure was found suitable. To 1.00 ml of an amine solution containing about 1 mg of the amine is added 1 ml of acetate buffer (10 ml glacial acetic acid + 10 ml 2 N NaOH + 80 ml water) and 1 ml 20 % aqueous sodium nitrite (prepared daily). The mixture is warmed for about 15 min in a water bath at 80°. After cooling there is added 1 ml 4 N HCl, 5 ml saturated potassium chloride solution, 5 ml ethanol and 1 ml of an aqueous 5 % ammonium sulfamate solution and the volume is adjusted to 25.0 ml. This is quantitatively transferred to the polarographic cell and purified nitrogen is bubbled through for 10 min. At the end of that time the last traces of nitrite are destroyed by adding 1.00 ml 5 % ammonium sulfamate solution and the solution is polarographed.

By using this procedure a linear connection between wave height and concentration (from about 2×10^{-4} to about 4×10^{-3} M) was found for the following amines: diphenylamine, N-methylaniline, diethylamine, piperidine, piperazine, morpholine and diethanol amine.

As mentioned above high concentrations of aromatic amines will invalidate the results. The same is the case with ethylene diamine. The reason is probably that ethylene diamine forms ethylene oxide on treatment with nitrous acid [5]. The ethylene oxide reacts with excess of nitrous acid [6] or nitrogen dioxide [7] with the formation of nitroethanol [6] or nitroethanol nitrate [7] which is reduced at about the same potential as aliphatic nitrosamines.

PREPARATIVE REDUCTIONS

Preparative reductions at controlled potential at a macro mercury electrode have been used to prove the course of the polarographic reduction. It was found that the N-nitrosamines at pH 1 and 5 yielded the corresponding unsymmetric hydrazine by a four electron reduction in isolated yields of about 80 %. No other reduction products were isolated.

$$RR'N-N=OH^+ + 4\,e^- + 4\,H^+ \rightarrow RR'N-NH_3^+ + 2\,H_2O$$

In alkaline solution the reduction consumed two electrons per molecule and the secondary amine was isolated in high yield. Besides nitrous acid could be isolated.

$$2\,RR'N-N=O + 4\,e^- + 3\,H_2O \rightarrow 2\,RR'NH + N_2O + 4\,OH^-$$

The course of the reductions is not surprising in view of the facts that the nitrosamines in acid solution by chemical reduction mostly yield the hydrazines and that as found by Schueler and Hanna [8] N-nitroso diphenylamine by reduction with $LiAlH_4$ yielded diphenylamine as the main product.

EXPERIMENTAL

The polarograph was a recording polarograph Radiometer Type PO 3a. The capillary delivered 2.346 mg of mercury per second at a corrected mercury column height of 48.5 cm; the drop time t = 3.12 sec (20 % alcohol, 1 N KCl, open circuit); the capillary constant $m^{2/3}t^{1/6}$ = 2.14 $mg^{2/3}\,sec^{-\frac{1}{2}}$.

The reference electrode was a silver/silver chloride electrode in aqueous saturated KCl solution separated from the test solution with an agar plug and a fritted glass diaphragm. The reference electrode was measured against the saturated calomel electrode (S.C.E.).

The cell and circuit used for the controlled potential reductions was the same as used in part I[9]. The coulometer was an oxygen-hydrogen coulometer adapted from Lingane [10].

To the polarographic investigation was used a medium consisting of 1 M KCl in 20 % aqueous ethanol. The buffer solutions were the same as used in part I. The nitrosamines were prepared according to wellknown procedures. The compounds were distilled or recrystallized before use. The solvents and reagents were analytical grade.

Reduction of N-nitroso diphenylamine in acetate buffer. 1.0 g of N-nitroso diphenylamine was dissolved in 120 ml methanolic 2 N LiCl + 10 ml glacial acetic acid + 15 ml aqueous 2 N LiOH. The nitrosamine was reduced at a cathode potential of −1.05 V (*vs.* S.C.E.) with an initial current of 0.4 A. The reduction was followed polarographically. In the coulometer were evolved 385 ml (22°, 760 mm) corresponding to a consumption of 4 electrons per molecule. After completion of the reduction the reaction mixture was diluted with water, made alkaline and extracted several times with ether which was dried over potassium carbonate. To the ether was added alcoholic hydrogen chloride and the precipitate (980 mg) was recrystallized from alcohol-ether (870 mg 78 %). (Found: C 65.25; H 6.00; N 12.55; Cl 15.99. Calc. for $C_{12}H_{13}N_2Cl$: C 65.31; H 5.93; N 12.70; Cl 16.06). The compound was identified as unsymmetric diphenylhydrazine hydrochloride by its analysis.

Reduction of N-nitroso diphenylamine in alkaline solution. 4.0 g of N-nitroso diphenylamine was dissolved in 140 ml methanolic 2 N LiCl + 15 ml methanolic 1 N LiOH and reduced at −1.15 V *vs* S.C.E. The initial current was 0.3 A, 540 ml $O_2 + H_2$ were evolved (23°, 756 mm) corresponding to a consumption of 2 electrons per molecule. When the reduction was completed the reaction medium was diluted with water and the precipitate filtered off. The mother liquor was extracted with ether, which was dried and evaporated.

The precipitate and the residue (3.15 g) were recrystallized from dilute ethanol yielding 2.80 g (82 %) of a compound which was identified as diphenylamine by its m.p. 50–51° (53°), its analysis (Found: C 85.08; H 6.78; N 8.09. Calc. for $C_{12}H_{11}N$: C 85.17; H 6.55; N 8.28) and the analysis of the hydrochloride (Found: C 70.13; H 5.86; N 6.80; Cl 17.26. Calc. for $C_{12}H_{12}NCl$: C 70.14; H 5.89; N 6.82; Cl 17.25).

Reduction of N-nitroso morpholine. 7.0 g of N-nitroso morpholine was dissolved in 150 ml aqueous 2 N potassium chloride and 10 ml 2 N sodium hydroxide. The cathode chamber was deaerated with purified nitrogen and a slow current of nitrogen was passed through the solution during the reduction. After bubbling through the catholyte the nitrogen passed through a wash bottle immersed in an acetone-carbon dioxide cooling bath, then through a cold finger immersed in boiling nitrogen and finally through a solution of ferrous sulfate. The reduction was conducted at a cathode potential of −1.30 V with an initial current of 1.2 A. After completion of the reduction the cooling of the cold finger with boiling nitrogen was stopped. The cold finger contained a white solid which disappeared rapidly when not cooled in boiling nitrogen. No colour was detected in the ferrous sulfate solution. The white solid was identified as nitrous oxide by the following facts: Its m.p. and b.p. were between −80° and −200° (N_2O has b.p. −88° and m.p. −102°), it was colourless and did not react with ferrous sulfate.

The reaction mixture was saturated with potassium hydroxide and repeatedly extracted with ether. The ether was dried with potassium carbonate. On addition of alcoholic hydrogen chloride a precipitate, 3.9 g, was obtained. It was identified as morpholine hydrochloride by its analysis. (Found: C 39.09; H 8.30; N 11.24; Cl 28.69. Calc. for $C_4H_{10}NOCl$: C 38.87; H 8.16; N 11.33; Cl 28.68).

REFERENCES

1. Smales, A. A. and Wilson, H. N. *J. Soc. Chem. Ind.* **67** (1948) 210.
2. English, F. L. *Anal. Chem.* **23** (1951) 344.
3. Kolthoff, I. M. and Liberti, A. *J. Am. Chem. Soc.* **70** (1948) 1885.
4. Elofson, R. M., Edsberg, R. L. and Mecherly, P. A. *J. Electrochem. Soc.* **97** (1950) 166.
5. Hofmann, A. W. *Jahresber. Fortschr. Chem.* **1859** 386.
6. Japan 156256 (1943); *Chem. Abstr.* **44** (1950) 2008.
7. Darzens, G. *Compt. rend.* **229** (1949) 1148.
8. Schueler, F. W. and Hanna, C. *J. Am. Chem. Soc.* **73** (1951) 4996.
9. Lund, H. *Acta Chem. Scand.* **11** (1957) 283.
10. Lingane, J. J. *Electroanalytical Chemistry.* Interscience Publishers, New York, London 1953, p. 349.

Received March 20, 1957.

ACTA CHEMICA SCANDINAVICA 11 (1957) 997—1002

The Sterols of Coconut Oil

BENT ANDERSEN and BØRGE KRAWACK

Aarhus Oliefabrik A/S, Århus, Denmark

The investigations were first and foremost carried out on sterols from the pitch, which is produced at the distilling of coconut fatty acids ("pitchsterols"), but in addition a preliminary investigation has been made on sterols extracted from crude coconut oil ("crude oil sterols").

For the separation of the sterol mixtures was used fractional crystallization from ethyl ether, ethanol-hexane mixture or propanol, and as a measure for the separation was used the consumption of bromine according to Rosenmund-Kuhnhenn.

In the pitch sterols, the presence of α-spinasterol, stigmasterol, β-sitosterol, and fucosterol was proved. No pure compound was isolated from the crude oil sterols, but it contained in addition to the four sterols found in the pitch one sterol with conjugated double bonds in the 5,7-position and one sterol with a 7-double bond.

In search for raw materials for the production of steroide hormons it was found that coconut oil sterols had a comparatively high content of sterols with more than one double bond. As the literature only contained one statement about coconut sterols, namely that they contain stigmasterol [1], an investigation was made, which may not have solved all problems, but which does give a fairly comprehensive account of the composition of this complicated mixture.

The coconut sterols were obtained from the fatty pitch which results from the distillation of the soap-stock fatty acids from the refining of coconut oil. These sterols will be referred to as "pitch sterols". Besides, a preliminary investigation has been made on sterols from crude coconut oil ("crude oil sterols").

For an initial characterization of the two kinds of sterols, the following determinations were made:

1. By saponification of the acetate, the average molecular weight of the pitch sterols was determined as 414 (29 carbon atoms).

2. On quantitative hydrogenation of the pitch sterols, 1.31 moles H_2 per mole sterol were consumed, which means that there is 31 % sterol with two hydrogenatable double bonds. In the same way the crude oil sterols were found to contain 36 % sterols with two hydrogenatable double bonds.

3. On bromination according to Rosenmund-Kuhnhenn [2], 1.53 moles bromine per mole pitch sterol and 1.84 moles bromine per mole crude oil sterol were consumed. This means that substitution takes place at the brominations, and that sterols with non-hydrogenatable double bonds may occur.

4. Idler and Baumann's modified Lieberman-Burchard reaction [3] shows that the pitch sterols contain 3 %, and the crude oil sterols 10 % sterol with a double bond at carbon atom No. 7.

5. The pitch sterols have only a negligible absorption in the ultraviolet region down to 2 500 Å, so that sterols with conjugated double bonds cannot occur. The crude oil sterols, on the other hand, have their absorption maxima at 2 930, 2 820, and 2 715 Å, which is characteristic of sterols with conjugated double bonds in the 5,7 position [4]. The intensities of the maxima indicate 4.5 % sterol of this kind.

6. Addition of bromine to the acetate of the pitch sterols according to Windaus and Haut [5] produced a precipitate corresponding to 18—20 % stigmasterol in the pitch sterols. This precipitate, however, was a mixture, and only after a fractional crystallization from ethanol, pure tetrabromostigmasteryl acetate was obtained in a quantity corresponding to 4—8 % stigmasterol in the pitch sterol. Some derivates of stigmasterol have been prepared, and their melting points and specific rotations are compared with values from the literature (Table 1).

THE PITCH STEROLS

The pitch sterols were further investigated by fractional crystallization. A number of solvents was examined for their fractionating power, the change in the consumption of bromine after one re-crystallization being used as the criterion. Ethyl ether proved to be the best, but considerable fractionation was also obtained from a mixture consisting of equal portions of 96 % ethanol and hexane, and from *n*-propanol.

The fractional crystallization was performed in the usual way [6]. So much solvent was used that about half the quantity of substance was crystallized off each time. First ethyl ether was applied, and after 10 series of crystallizations, the least soluble component, fraction A, was found to consume 3.10 moles bromine per mole sterol, whereas the most soluble component, fraction B, consumed 1.25 moles bromine. Further crystallization from ether brought no alteration in these values.

Fraction A could not be separated into its constituents by crystallization as sterol or acetate. From the benzoate pure stigmasteryl benzoate was isolated by crystallization from a mixture of chloroform and ethanol, while other components could not be isolated.

Eventually the separation was successful by fractional crystallization of the ketone (Oppenauer-oxidation [7]) from ethanol, and pure α-spinastadienone was isolated as the less soluble and stigmastadienone as the more soluble component.

Fraction A, then, is a mixture of α-spinasterol and stigmasterol, and a quantitative hydrogenation shows that it consists of 70 % stigmasterol and 30 % α-spinasterol, the 7-double bond not being hydrogenated. The optical rotation of sterol, acetate, and benzoate, is in accordance with this (Table 1).

Table 1. Melting points and optical rotations of sterols and their derivatives.

	Stigmasterol				α-Spinasterol				Fraction A			β-Sitosterol				γ-Sitosterol	
	m.p.		$[\alpha]_D$		m.p.		$[\alpha]_D$		m.p.	$[\alpha]_D$		m.p.		$[\alpha]_D$		m.p.	$[\alpha]_D$
Ref. No.	Exp	7,15	Exp	7,15	Exp	16,17	Exp	16,17	Exp	Exp	*	Exp	7,18	Exp	7,18	19,20	
Sterol	169	168	—51	—51	—	169	—	—2.7	163	—35	—36	138	136 —37	—36	—37	147	—43
Acetate	147	143	—55	—55	—	180 —82	—	—6.4	143	—38	—40	126	125 —26	—40	—41	143	—48
Benzoate	162	164	—25	—26	—	196 —99	—	+2.1	156	—18	—18	149	146 —47	—15	—14	152	—19
Ketone	124	126	+60	+62	176	176	22	20	—	—	—	—	—	—	—	—	—
Stanyl-acetate	131	131	+14	+15	—	—	—	—	—	—	—	133	131	+12	+15	143 —44	+9— 10

* Calculated for 30 % α-spinasterol and 70 % stigmasterol.

Fraction B consumed 1.25 moles bromine per mole sterol ,and as mentioned above, fractional crystallization from ethyl ether gave no further separation. But by a great number of fractional crystallizations from a mixture of ethanol and hexane (1:1), the following four main fractions were obtained: B 1 consuming 1.50, B 2 1.17, B 3 1.65, and B 4 1.50 moles bromine per mole sterol.

In fraction B 1 stigmasterol and α-spinasterol have again been concentrated.

Fraction B 2 was exposed to fractional crystallization from *n*-propanol, and it was possible to reduce the consumption of bromine to 1.08 moles per mole, which figure was also found on quantitative hydrogenation. Although, then, the substance is not entirely pure, melting points and optical rotations of sterol, acetate, and benzoate show that it is β-sitosterol (Table 1).

Fraction B 3 could not be further separated. Attempts were made with several other solvents and with fractional crystallization of ketone and benzoate; but in no case could a pure substance be isolated.

As mentioned above, the fraction B 3 consumes 1.65 moles bromine per mole sterol, and the same value is found on a quantitative hydrogenation, so that the mixture must consist of 35 % of a sterol with one double bond and 65 % of a sterol with two double bonds.

On ozonizing according to Mac Phillamy [8] acetaldehyde was isolated as carboxyphenylhydrazone and as 2,4-dinitrophenylhydrazone, the latter in a yield corresponding to 32 % of the available quantity of sterol with two double bonds.

On ozonizing the acetate according to Idler and Fagerlund [9] acetaldehyde was again obtained as 2,4-dinitrophenylhydrazone, while the non-volatile portion was chromatographed on a mixture of celite and silicagel, as described by Idler and Fagerlund. Unreacted sterol was eluted with benzene, after which a ketone was eluted with a mixture of benzene and chloroform (4:1 by volume).

Melting point and optical rotation of this ketone, as well as the melting point of the 2,4-dinitrophenylhydrazone showed that the ketone was 24-ketocholesterylacetate, whereby the easily soluble component with 2 double bonds has been identified as fucosterol.

Fraction B 4 is slightly yellow, indicating that it contains decomposition products of the sterols. In the ultraviolet absorption curve of the fraction there is an obvious maximum at 2 400 Å, whereas all the other fractions here have only a faint shoulder on the absorption curve rising steeply towards the absorption maximum of the isolated double bonds at 2 050 Å.

The maximum at 2 400 Å is no doubt caused by a conjugated system of C = C and C = O-double bonds, a ketone group at the allylic 7-carbon atom constituting such a system with the C-5-double bond This theory is in accordance with Bergström and Wintersteiner [10] who have shown that by oxidation of a colloid solution of cholesterol with oxygene, the 7-keto compound is actually produced, this compound having its absorption maximum at 2 400 Å.

Fraction B 4 consumes less bromine than fraction B 3, and this is due to the fact that the conjugated system is more stable than the isolated double bond. Thus cholestenone, which has a conjugated system analogous with the 7-ketosterols, consumes only approximately 25 % of the theoretical quantity of bromine at the Rosenmund-Kuhnhenn-bromination.

As will be mentioned later the more soluble fractions of the crude oil sterols contain sterols with a double bond at C-7, but no evidence of such sterols was found in fraction B 4 from the pitch sterols.

Consequently, fraction B 4 is supposed to consist of the same sterols as fraction B 3, but contaminated by 7-ketosterols formed during the many crystallizations.

Hence, the structure of the pitch sterols must be as shown in Table 2, the percentages being rather uncertain.

THE CRUDE OIL STEROLS

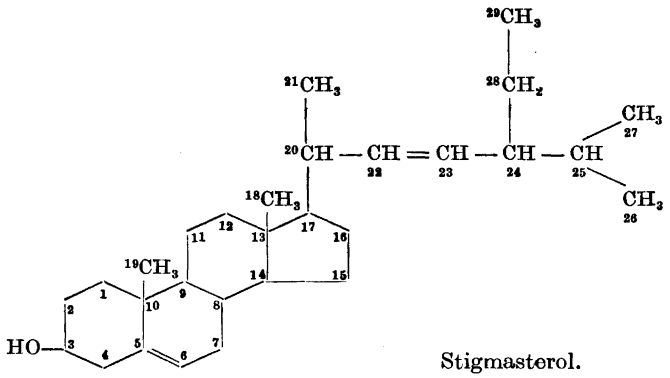
The attempt at isolating pure substances from the crude oil sterols was unsuccessful, but it is, however, possible to indicate their composition with some accuracy.

On fractional crystallization from ethanol-hexane mixture (1:1) the sterol with conjugated double bonds was concentrated in the least soluble fractions, together with stigmasterol and possibly α-spinasterol. A quantitative hydrogenation showed that the conjugated sterol has 2 hydrogenatable double bonds. Hence, there is some reason to presume that it is $\Delta^{5,7,22}$-stigmastatrienol.

At the fractional crystallization an additional series of fractions of medium solubility was obtained, probably consisting of fucosterol and β-sitosterol, and, finally, an easily soluble fraction, which shows strong substitution at bromination. Presumably it contains a Δ^{7}-stenol, analogous with Fieser's lathosterol [11], which is also concentrated in the more soluble fractions.

Hence, the composition of the crude oil sterols can be as indicated in Table 2.

When the composition of the two kinds of sterols is compared, it is seen that the sterol with the conjugated double bonds has been totally destroyed



Stigmasterol.

All the sterols from coconut oil are derivatives of stigmasterol.

Table 2. The composition of the sterols from coconut oil.

	Double bonds	Pitch Sterols, %		Crude Oil Sterols, %	
Stigmastatrienol	5, 7, 22	0		4.5	
Stigmasterol	5, 22	6—10	31		31.5
Fucosterol	5, 24 (28)	20—25			
α-Spinasterol	7, 22	3			6.0
Stenol	7	0			
β-Sitosterol	5	66		58.0	

at the high temperature during the distillation of the fatty acids, whereas the quantity of sterols with an isolated double bond at C-7 has been considerably reduced. On the other hand, the ratio of the quantity of β-sitosterol to the total quantities of stigmasterol and fucosterol has not been substantially changed.

EXPERIMENTAL

The melting points were determined on Kofler Heizbank and optical rotations in 1 dm macro tubes (about 0.2 g in 10.0 ml chloroform). U.V.spectra were measured on a Beckman model DU instrument.

To obtain the pitch sterols, the pitch, which contained 15—30 % unsaponifiable matter, was saponified with alcoholic KOH and extracted with hexane. After the distilling of the hexane a viscous, dark brown substance containing 50—70 % sterol was obtained. By re-crystallization from a mixture consisting of equal portions of hexane and ethanol, the pitch sterols were obtained as a yellowish product, and it was difficult to obtain perfectly white crystals. Accordingly, the yield was only 50—60 % of the sterols in the pitch.

From crude coconut oil 0.17 % unsaponifiable matter was obtained, and from this again 30 % sterol.

Bromination according to Rosenmund-Kuhnhenn was carried out according to *Handbuch der Lebensmittelchemie* [2]. Surplus of bromide (15—25 %) was titrated iodometrically. The transformation into acetate, recommended by B.I.O.S.[12] was found unnecessary.

Benzoates and acetates were prepared by the usual methods. The yields were 90—95 % of theory. Derivatives of fraction A were only re-crystallized once in order to avoid

fractionation, while pure substances were re-crystallized until the melting points remained constant.

Quantitative hydrogenations were carried out in an apparatus which was a modification of the apparatus of Prater and Haagen-Smit [13], and of Savacol and Ullyot [14].

Derivatives of fucosterol: 2,4-dinitrophenylhydrazone of acetaldehyde m.p. 162—64° (lit. value [21] 163.5—64.5°); *p*-carboxyphenylhydrazone of acetaldehyde m.p. 209—10° (210—11°). Molecular weight found [22] 178 and 186 (theoretical 178). 24-Ketocholesteryl-acetate m.p. 126.5°, $[\alpha]_D$ −42° (lit. value [9] 126—27° and −43°). 2,4-Dinitrophenylhydrazone of 24-ketocholesterylacetate m.p. 169° (lit. value [9] 170°).

Acknowledgements. The authors wish to thank Aarhus Oliefabrik A/S for permission to publish this paper and Mr. O. T. Meyer for many valuable suggestions during the work.

REFERENCES

1. Juckenack, A., Bames, E., Bleyer, B. and Crossfeld, J. *Handbuch der Lebensmittelchemie*, Julius Springer, Berlin 1939, p. 363.
2. *Handbuch der Lebensmittelchemie*, Berlin 1939, Vol. IV, p. 104.
3. Idler, D. R. and Baumann, C. A. *J. Biol. Chem.* **203** (1953) 389.
4. Ewing, G. W. and Krieger, J. *J. Am. Chem. Soc.* **67** (1945) 609.
5. Windaus, A. and Haut, A. *Ber.* **39** (1906) 4378.
6. Riesenfeld, E. H. *Lehrbuch der anorganischen Chemie*, 3rd Ed., Rascher, Zürich 1943, p. 481.
7. Fernholz, E. and Stavely, H. E. *J. Am. Chem. Soc.* **61** (1939) 142, 2956.
8. MacPhillamy, H. B. *J. Am. Chem. Soc.* **64** (1942) 1732.
9. Idler, D. R. and Fagerlund, U. H. M. *J. Am. Chem. Soc.* **77** (1955) 4142.
10. Bergström, S. and Wintersteiner, O. *J. Biol. Chem.* **141** (1941) 597.
11. Fieser, L. F. *J. Am. Chem. Soc.* **73** (1951) 5007.
12. *German Medical Target B.I.O.S.*, Final Rep., 449, 24.
13. Prater, A. N. and Haagen-Smit, A. J. *Ind. Eng. Chem. Anal. Ed.* **12** (1940) 705.
14. Savacool, R. V. and Ullyot, G. E. *Anal. Chem.* **24** (1952) 714.
15. Barton, D. H. R. and Cox, J. D. *J. Chem. Soc.* **1948** 783.
16. Simpson, J. C. E. *J. Chem. Soc.* **1937** 730.
17. King, L. C. and Ball, C. D. *J. Am. Chem. Soc.* **64** (1942) 2488.
18. Wallis, E. S. and Chakravorty, P. N. *J. Org. Chem.* **2** (1937) 335.
19. Ichiba, A. *Sci. Papers. Inst. Phys. Chem. Research Tokyo* **28** (1935) 112.
20. Anderson, R. J. and Shriner, R. L. *J. Biol. Chem.* **71** (1927) 401.
21. Strain, H. H. *J. Am. Chem. Soc.* **57** (1935) 758.
22. Veibel, S. *Acta Chem. Scand.* **1** (1947) 54.

Received January 25, 1957.

ACTA CHEMICA SCANDINAVICA 11 (1957) 1003—1012

Acid-soluble Nucleotides of the Earthworm (*Lumbricus terrestris*)

ROY NILSSON

Department of Zoophysiology, University of Lund, Sweden

The acid-soluble nucleotides of the body wall musculature of the earthworm have been analysed by chromatographic methods. The following nucleotides were identified:* AMP, ADP, ATP, ADPR, DPN, IMP, GMP, GDP, GTP, UMP, UTP and CTP. The identifications are based on elution positions in ion-exchange, paper chromatography before and after hydrolysis, ultraviolet absorption spectra and estimation of the phosphorus, pentose and base contents. Two fractions, a CMP derivative and an UDP derivative containing ninhydrin-positive components have not been fully identified.

In recent years the isolation of ATP from muscle [1,2] has been supplemented by the isolation of further nucleoside polyphosphates. It was shown [3,4] that the muscle of vertebrates contains beside AMP, ADP and ATP, the corresponding derivatives of guanosine, uridine and cytidine. In the muscle of invertebrates, however, only adenosine nucleotides have hitherto been demonstrated [5–8]. An investigation of the acid-soluble nucleotides in invertebrate material was therefore undertaken. The earthworm is a suitable object for such work as it has a well defined body wall musculature which is easy to handle, and furthermore it is easy to obtain large numbers of the animal. In the present work, therefore, earthworm was chosen for the analysis of the acid-soluble nucleotides of invertebrate muscle.

* AMP = adenosinemonophosphate
ADP = adenosinediphosphate
ATP = adenosinetriphosphate
ADPR = adenosinediphosphoribose
DPN = diphosphopyridine nucleotide
IMP = inosinemonophosphate
GMP = guanosinemonophosphate
GDP = guanosinediphosphate
GTP = guanosinetriphosphate
UMP = uridinemonophosphate
UTP = uridinetriphosphate
CTP = cytidinetriphosphate

MATERIAL AND METHODS

Preparation of trichloroacetic acid extract. The earthworm species *Lumbricus terrestris* was used and the animals were handled immediately after collection. Before extraction the animals were dipped into cold alcohol (−60°C) for a few seconds. They could then easily be gutted, and the muscle was immersed into cold alcohol. After enough tissue had been collected (usually 100−125 g) it was homogenized with one volume of ice-cold 10 % trichloroacetic acid in a Turmix blendor and pressed through madapolam. The extraction was repeated three times with 5 % trichloroacetic acid and the combined extracts filtered through Hyflo Supercel. The filtrate was shaken six times with ether to remove the bulk of the trichloroacetic acid, neutralized with a drop of ammonia and freed from ether by aeration. The protein free extract thus obtained was used for phosphorus analysis and paper chromatography.

The crude extract could also be used directly for ion-exchange chromatography. The presence of non-nucleotide constituents (amino acids etc.) results, however, in high background absorption and impairs on the separation and quantitative analysis of the smaller nucleotide fractions. These disadvantages could be avoided by treatment of the extract with norite prior to chromatography.

Purification of the nucleotide fraction by the norite method. The extract containing the nucleotides was acidified with hydrochloric acid to pH 1 and shaken for 30 min with an appropriate amount of norite. After filtration the norite was washed free from acid and sucked dry. The nucleotides were eluted with 50 % ethanol containing 1 % ammonia. In order to obtain a quantitative yield several elutions were necessary. Table 1 shows the nucleotide content of consecutive eluates as measured by ultraviolet absorption at 260 mμ. No differences in the type of ultraviolet absorption were seen between the first and the seventh eluate (Fig. 1).

Ion-exchange chromatography. Dowex-1 (200−400 mesh) in the formate form was used and elution was carried out with a modification of the formate system used by Bergkvist and Deutsch [9]. Fractions were collected by a time-operated fraction collector and every fraction was read at 250, 260 and 270 mμ in a Beckman DU spectrophotometer. Appropriate fractions were pooled and the nucleotides concentrated by the norite method.

Paper chromatography. Two dimensional chromatography [10] was used to resolve the nucleotides in the crude trichloroacetic acid extract, with *n*-propanol-ammonia (*d* 0.880)-water (60:30:10) in the first direction and saturated ammonium sulphate solution-water-*iso*propanol (79:19:2) in the second.

One dimensional chromatography in *iso*propanol-hydrochloric acid-water (97:25:28) was used for the separation of the products obtained on hydrolysis of the different nucleotide fractions from ion-exchange chromatography. Hydrolysis was carried out in N hydrochloric acid for one hour at 100 °C.

For determination of the individual nucleotides before hydrolysis the fractions were run in the *n*-propanol-ammonia-water system, together with the authentic substances.

Descending chromatography on Whatman No. 1 paper was used throughout and the spots on the finished chromatogram were located by ultraviolet photography.

For quantitative estimations, the spots were cut out together with blank areas and eluted with 0.1 N hydrochloric acid over night; the eluates were used for ultraviolet spectrophotometry and phosphorus analysis.

Analytical procedures. Phosphorus was determined by the method of Allen [11] using a Klett Summerson photoelectric colorimeter with a red filter and was differentiated in

Table 1. Elution of nucleotides from norite. Elution with 50 % ethanol containing 1 % ammonia. Every eluate *ca* 6 ml.

Elution-number	1	2	3	4	5	6	7
ΣE_{260}	1 485	909	455	241	153	109	56

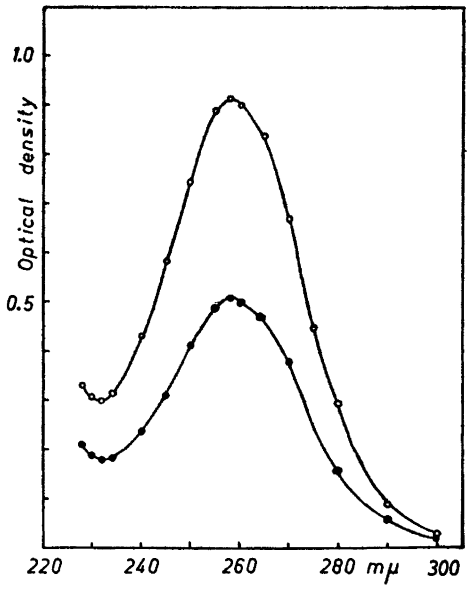


Fig. 1. Ultraviolet absorption curves for norite-eluates. O—O—O Eluate No. 1. 10 μl eluate + 3.0 ml 0.1 M hydrochloric acid. ●—●—● Eluate No. 7. 150 μl eluate + 3.0 ml 0.1 M hydrochloric acid.

separate analyses into total phosphorus (P_T) inorganic phosphorus (P_i) and acid-labile phosphorus (P_{10}) determined after 10 min hydrolysis in N hydrochloric acid at 100°C.

Pentose was determined by the method of Mejbaum as modified by Albaum and Umbreit [12]. A Klett Summerson photoelectric colorimeter was used with a red filter.

Optical densities were measured in a Beckman Universal Spectrophotometer Model DU in 0.1 N hydrochloric acid, the molecular extinction coefficients of 14 200 at 260 mμ for adenosine phosphates, 13 200 at 250 mμ for inosine phosphates, 10 850 at 256 mμ for guanosine phosphates, 10 050 at 262 mμ for uridine phosphates and 13 000 at 280 mμ for cytidine phosphates, being used.

Cyanide complex formation for the identification of DPN was carried out in M NaCN according to Colowick, Kaplan and Ciotti [13], using the increase in absorption at 325 mμ as a measure for N-substituted nicotinamide derivatives.

Oxidation with periodate for the estimation of 5′-substitution was carried out by the method of Dixon and Lipkin [14].

Table 2. Phosphorus analysis of crude and norite-purified trichloroacetic acid extracts of *Lumbricus* muscle expressed as μg P per gram muscle wet weight.

	P_i μg / g	P_{10} μg / g	P_T μg / g	$P_{10}-P_i$ μg / g	P_T-P_{10} μg / g
Crude extract	215	583	858	368	275
Crude extract	188	398	787	210	389
Norite eluate	0	172	283	172	109

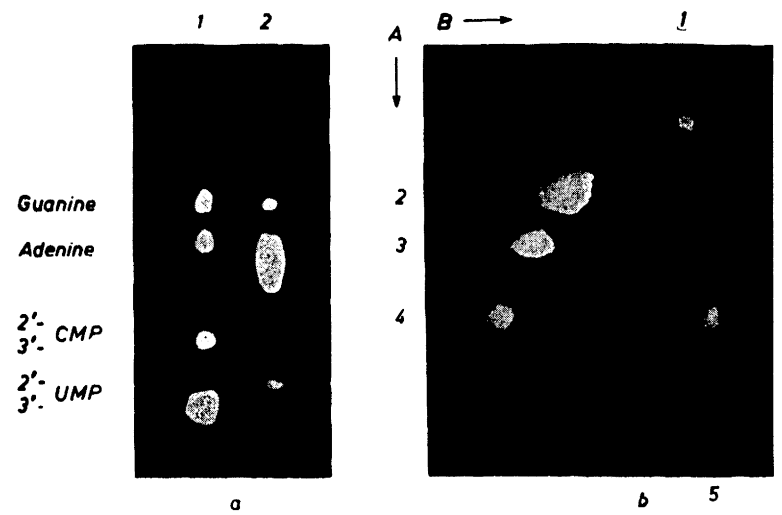


Fig. 2. (a) paper chromatography of the extract from *Lumbricus* muscle after hydrolysis for 1 h in N hydrochloric acid at 100 °C. Solvent: *iso*propanol-hydrochloric acid-water (97:25:28). Time 24 h. Whatman No. 1 paper. (1) RNA-hydrolysate, (2) hydrolysed extract. (b) twodimensional chromatography of the unhydrolysed extract. Solvent: (A) propanol-ammonia-water (60:30:10) 72 h, (B) saturated ammoniumsulphate-*iso*-propanol-water (79:2:19) 8 h, Whatman No. 1 paper. (1) GTP, (2) ATP, (3) ADP, (4) AMP, (5) uridinederivative.

RESULTS

Phosphorus analysis of the trichloroacetic acid extract showed that *Lumbricus* muscle contains considerable quantities of acid-soluble phosphorus both as inorganic phosphate and as acid-labile and acid-stable phosphates (Table 2). Nearly all acid-labile phosphate was adsorbed on norite and recovered in the norite eluate indicating that most of this phosphorus fraction consists of nucleotides. Only about one-third of the acid-stable phosphorus, however, was adsorbed on norite; the phosphate fraction not adsorbed was probably composed of lombricine [15] and of sugar phosphates. Lombricine was isolated from the norite filtrate by precipitation of the barium-salt with three volumes of alcohol and was identified as guanidoethylserylphosphoric acid by paper chromatography of the compound and its products of hydrolysis, as previously described by Thoai and Robin [15].

Paper chromatography of the hydrolysed extract (Fig. 2a) gave a large spot for adenine besides smaller spots for guanine and uridylic acid, indicating that the main ultraviolet-absorbing components of the extract before hydrolysis were adenine derivatives besides guanine- and uridine nucleotides. The slightly lower R_F-value of the uridylic acid spot as compared with that from RNA may possibly indicate the presence of 5′-derivative in the extract (Fig. 2a). Two dimensional chromatography of the unhydrolyzed extract comfirmed these results. The major components as shown by Fig. 2b were

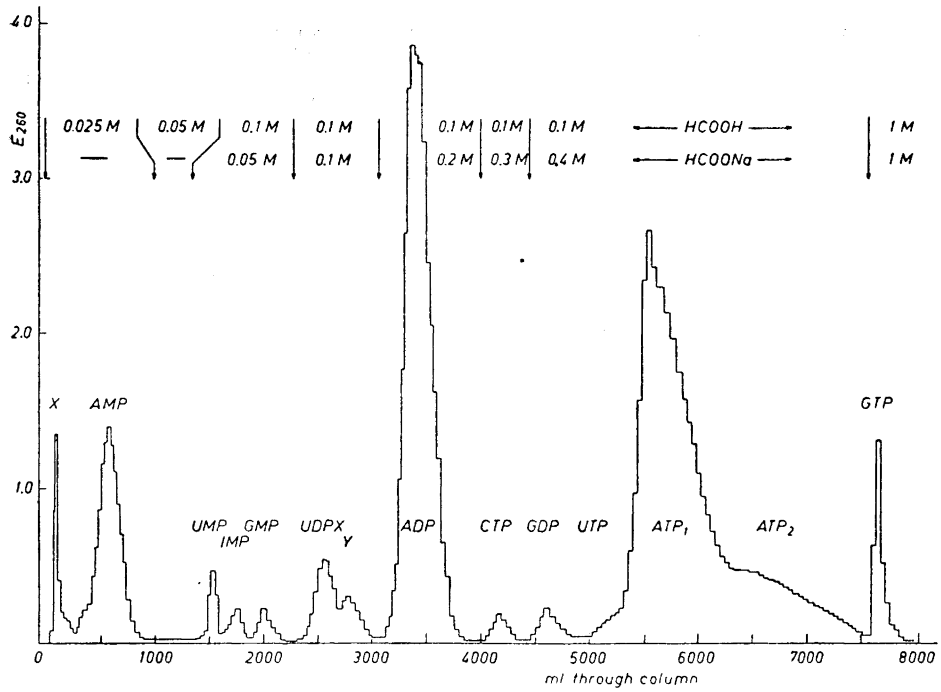


Fig. 3. Ion-exchange chromatography of a purified trichloroacetic acid extract from earthworm muscle. Dowex-1 (200–400 mesh) column, 1 cm^2 × 13 cm in the formate system. Adsorbed material: extract with optical density E_{260} = 3 900. Recovery 101 %.

ATP, ADP and AMP besides weak spots indicating the presence of other nucleotide compounds.

Paper chromatography of a complex mixture like that in the trichloroacetic acid extract, however, gave only a rough picture of the main components. For the detailed analysis of all the different nucleotides ion-exchange chromatography is the method of choice. Therefore, both the crude trichloroacetic acid extract and the purified norite-eluates were analysed by chromatography on Dowex-1 in a formate system, giving in the main the same results. However, the purified extract gave — for the reason mentioned above — the clearer separation. Fig. 3 shows the results of ion-exchange analysis of the acid-soluble nucleotides from the body wall musculature of the earthworm.

The first tentative identification of the components was made according to elution positions in ion-exchange and the ultraviolet absorption curves. For further identification, the appropriate fractions were pooled and concentrated *via* norite adsorption-elution as described above. In the next step the base components were determined by chromatography of the fractions after hydrolysis in N hydrochloric acid at 100°C for one hour. The R_F-values of the products of hydrolysis are shown in Table 3 together with those for the authentic compounds.

Table 3. R_F-values of ion-exchange fractions from earth-worm muscle after hydrolysis in N hydrochloric acid at 100 °C for one hour, compared with the R_F-values of known substances. Solvent: *iso*propanol-hydrochloric acid-water (97 : 25 : 28). Descending chromatography on Whatman No. 1 paper for 24 h.

Fraction	R_F	Marker	R_F
AMP	0.30		
Y	0.29	Adenine	0.28
ADP	0.28		
ATP_1	0.28		
ATP_2	0.29		
IMP	0.28	Hypo-xanthine	0.29
GMP	0.21		
GDP	0.21	Guanine	0.21
GTP	0.21		
		2′-UMP	
UMP	0.69	3′-	0.76
UDPX	0.69	5′-UMP	0.70
UTP	0.68		
		2′-CMP	
X	0.55	3′-	0.57
CTP	0.48	5′-CMP	0.50

As seen from the table, the nucleotides from *Lumbricus* muscle comprise derivatives of the five bases adenine, hypoxanthine, guanine, uracil and cytosine. Adenine and hypoxanthine have the same R_F-values but are easily distinguished by their different ultraviolet absorption curves. The fractions containing pyrimidine derivatives showed R_F-values corresponding to the 5′-monophosphates with the exception of fraction X. This fraction had the elution position of CMP and yields on paper chromatography after hydrolysis a spot with nearly the same R_F-value as 2′- and 3′-CMP. The ultraviolet spectrum, however, was different from that of the cytidylic acids, the absorption maximum in 0.1 N hydrochloric acid being at 270 mμ instead of around 280 mμ.

After the purine and pyrimidine components of the different nucleotides had been established, the degree of phosphorylation was determined by phosphorus analysis. The purity of the fractions was checked by paper chromatography before analysis. The propanol-ammonia-water system was used which separates the different phosphates of the same nucleoside well, and gave a further qualitative identification of the compounds. Table 4 gives the R_F-values of the different fractions in comparison with those of the authentic compounds.

With a few exceptions (fractions UDPX, X and Y) the R_F-values found are in good agreement with those expected from the elution positions in ion-exchange and the results of paper chromatography after hydrolysis.

The pure fractions were analysed for pentose, acid-labile and total phosphates. In those cases where paper chromatography indicated an impure fraction

Table 4. R_F-values of ion-exchange fractions from earthworm muscle, compared with the R_F-values of authentic substances. Solvent: propanol-ammonia-water (60 : 30 : 10). Descending chromatography on Whatman No. 1 paper (a 120 cm long strip) for 70 h.

Fraction	R_F	Marker	R_F	Fraction	R_F	Marker	R_F
AMP	0.30	AMP	0.30	GDP	0.13	—	—
ADP	0.21	ADP	0.21	GTP	0.11	GTP	0.12
ATP_1	0.17	ATP	0.17	UMP	0.23	5′-UMP	0.23
ATP_2	0.18			UDPX	0.30	—	—
Y	0.30			UTP	0.13	UTP	0.13
IMP	0.21	IMP	0.21	X	0.25	5′-CMP	0.23
GMP	0.15	GMP	0.14				

the analysis was made on the eluted spots after further purification by paper chromatography. Only purinebound pentose was determined quantitatively. The presence of pyrimidinebound pentose was detected by qualitative orcinol tests before and after treatment with bromine [16]. No quantitative data were, however, obtained. The results of the analyses are shown in Table 5.

The analytical data together with evidence both from ion-exchange and paper chromatography confirm the identifications made in Fig. 3. After hydrolysis the purine derivatives AMP, ADP, ATP, IMP, GMP, GDP and GTP gave the corresponding bases: adenine, hypoxanthine and guanine, respectively (Table 3). The state of phosphorylation was determined by paper chromatography and direct analysis (Tables 4 and 5). Furthermore, all the nucleotides were established as 5′-phosphates by periodate oxidation, which showed that the 2′- and 3′-positions of pentose were unsubstituted. On a molar base, every nucleotide consumed 0.95—0.99 moles of periodate.

The ATP-fraction appears in the ion-exchange chromatogram as a very asymmetric peak, which could indicate a heterogeneous fraction. For this reason the fraction was divided into two parts, ATP_1 and ATP_2, each of which were analysed separately. They gave, however, identical ultraviolet absorption curves, the same R_F-values on paper chromatography both before and after hydrolysis. In addition they gave the same values for acid-labile and acid-stable phosphorus, for pentose and on periodate oxidation. For these reasons both fractions were considered to be ATP.

The pyrimidine derivatives were identified as UMP, UTP and CTP as shown in Fig. 3 and Tables 3, 4 and 5. They are 5′-phosphates: on hydrolysis 5′-uridylic and 5′-cytidylic acid are formed and not the 2′- or 3′-derivatives as shown by paper chromatography.

Three fractions are not yet fully identified, namely those designed X, Y and UDPX. Fraction Y is in all probability 5'-adenosinediphosphoribose derived from DPN by degradation with alkali during elution. It contains two moles of phosphate and two moles of pentose per mole adenine and has a higher R_F-value than ADP on paper chromatography (Table 4).

The UDPX fraction was shown to be a derivative of 5′-UMP by the ultraviolet absorption curve and the R_F-value after hydrolysis which was identical

Table 5. Analysis of the fractions obtained by ion-exchange-chromatography of the norite-purified trichloroacetic acid extract from *Lumbricus* body wall musculature.

Fraction	labile P μg	total P μg	base μg	pentose μg	base : pentose: labile P: total P
AMP	0	3.7	13.1	15.3	1:1.02:0:1.20
UMP	0	3.6	11.6	—	1:—: 0:1.10
IMP	0	9.5	40.3	48.0	1:1.07:0:1.02
GMP	0.2	2.7	12.1	11.4	1:0.95:0.11:1.07
UDPX	7.2	14.6	23.3	—	1:—:0.99:2.01
Y	2.7	11.1	23.2	50.2	1:1.93:0.50:2.08
ADP	4.0	8.1	16.9	18.7	1:0.99:1.03:2.02
CTP	3.8	6.0	6.9	—	1:—:1.94:3.08
GDP	1.8	3.7	9.3	9.2	1:0.99:0.91:1.93
UTP	5.6	8.4	10.2	—	1:—:1.99:2.98
ATP_1	3.9	5.6	8.1	9.8	1:1.00:2.04:2.99
ATP_2	4.1	6.1	8.7	9.7	1:1.00:2.04:2.99
GTP	3.0	4.5	8.1	8.2	1:1.03:1.81:2.74

with that of 5′-UMP. Phosphorus analysis gave the uracil: acid-labile phosphate: total phosphate ratio (1:1:2) of UDP. The R_F-value of the unhydrolysed fraction in propanol-ammonia-water, however, was much higher than that of UDP indicating a derivative of UDP. On chromatography after hydrolysis in N hydrochloric acid at 100 °C for 10 min the fraction gave only one ultraviolet absorbing spot, corresponding to 5′-UMP and phosphorus spots corresponding to UMP and orthophosphate. Spraying with ninhydrin revealed a strongly positive spot which did not coincide with the ultraviolet absorbing one. The unhydrolysed fraction gave, however, only a very weak ninhydrin reaction. Spraying with carbohydrate reagents gave no definite results. Oxidation with periodate gave a consumption of 0.95 mole periodate per mole base indicating that the 2′- and 3′-positions of the ribose moiety of UDP were unsubstituted. Our results so far characterize the UDPX fraction as a 5′-UDP derivative which on hydrolysis liberates a strongly ninhydrinpositive component.

Fraction X gave one ultraviolet absorbing spot both before and after hydrolysis in N hydrochloric acid at 100 °C. The ultraviolet absorption curve

Table 6. The nucleotide content of earthworm muscle obtained by ion-exchange chromatography of crude and norite-purified trichloroacetic acid extracts.

Fraction	μmoles per 100 g		Fraction	μmoles per 100 g	
	purified extract	crude extract		purified extract	crude extract
AMP	20.6	20.6	IMP	2.5	3.9
ADP	53.2	67.5	UMP	2.5	2.4
ATP	108.0	102.0	UDPX	8.0	9.4
ADPR (Y)	4.4	1.0	UTP	3.6	3.5
GMP	2.8	4.2	CTP	2.5	1.5
GDP	3.4	2.8	DPN	—	4.0
GTP	8.0	8.5			

and the elution position in ion-exchange chromatography indicate the presence of a cytidine derivative. The R_F-value after hydrolysis was that of 2′- or 3′-CMP. Beside the ultraviolet absorbing spot several ninhydrinpositive components were revealed by paper chromatography of this fraction, the complexity of which hindered further identification with the small amounts hitherto available.

The same results were obtained on ion-exchange chromatography of the crude trichloroacetic acid extract as with the norite eluates. The amounts of the different nucleotides from the earthworm muscle obtained by ion-exchange chromatography of the two types of extracts are shown in Table 6. There are a few qualitative differences in the nucleotide fractions between these two types of extracts. DPN was not eluted from norite by our procedure unless degraded to adenosinediphosphoribose and was consequently not found in the norite-purified extract. From the crude extract, however, DPN was obtained in the first chromatographic fractions together with other phosphorus compounds. DPN was estimated as the cyanidecomplex according to Colowick, Kaplan and Ciotti [13]. The earthworm muscle contains 4 μmoles DPN per 100 g, calculated from the molar extinction coefficient (6×10^{-6}) for the DPN—CN complex at 325 mμ.

Fraction Y is almost lacking in the DPN containing crude extract but is present in the DPN free extract obtained after norite adsorption, in further support of the identification of fraction Y as ADP-ribose originating from DPN. 4 μmoles of fraction Y were obtained from 100 g muscle, in good agreement with the figures for the DPN content of the crude extract. Otherwise the same nucleotides are obtained in both types of extracts, as seen from Table 6.

The acid-soluble nucleotide content of the earthworm muscle shows the following general pattern: predominance of adenine nucleotides (nearly 90 %), equal amounts of guanine and uridine derivatives (about 5 % of each) and a small amount of cytidine compounds. The same pattern is shown by rabbit skeletal muscle although the absolute amount of nucleotides was about 3 times greater in the latter case.

The resemblance in nucleotide composition between these two muscles of widely different origin is not surprising since their functions are similar.

The earthworm muscle, however, can hardly be considered as true striated muscle and is — compared with vertebrate skeletal muscle — a slow working muscle, a fact which may explain the quantitative difference in the nucleotide contents.

The author wishes to thank Laborator A. Deutsch, Statens Mejeriförsök, Alnarp, for his kind advice and stimulating criticism. This work was carried out with grants from *Kungl. Fysiografiska Sällskapet i Lund* and the *Lilly Foundation.*

REFERENCES

1. Lohmann, K. *Naturwiss.* **17** (1929) 624.
2. Fiske, C. H. and Subbarow, Y. *Science* **70** (1929) 281.
3. Bergkvist, R. and Deutsch, A. *Acta Chem. Scand.* **7** (1953) 1307.
4. Schmitz, H., Potter, V. R., Hurlbert, R. B. and White, D. M. *Cancer Research* **14** (1954) 66.
5. Lohmann, K. *Biochem. Z.* **233** (1931) 467.
6. Lohmann, K. and Schuster, Ph. *Biochem. Z.* **272** (1935) 24.
7. Biró, N. A. and Nagy, B. *Acta Physiol. Acad. Sci. Hung.* **8** (1955) 311.
8. Rey, C. *Biochim. et Biophys. Acta* **19** (1956) 300.
9. Bergkvist, R. and Deutsch, A. *Acta Chem. Scand.* **8** (1954) 1877.
10. Deutsch, A. and Nilsson, R. *Acta Chem. Scand.* **7** (1953) 858.
11. Allen, R. J. L. *Biochem. J. London* **34** (1940) 858.
12. Albaum, H. G. and Umbreit, W. W. *J. Biol. Chem.* **167** (1947) 369.
13. Colowick, S. P., Kaplan, N. O. and Ciotti, M. M. *J. Biol. Chem.* **191** (1951) 447.
14. Dixon, J. S. and Lipkin, D. *Anal. Chem.* **26** (1954) 1092.
15. Thoai, N. V. and Robin, Y. *Biochim. et Biophys. Acta* **14** (1954) 76.
16. Massart, L. and Hoste, J. *Biochim. et Biophys. Acta* **1** (1947) 83.

Received March 12, 1957.

ACTA CHEMICA SCANDINAVICA 11 (1957) 1013—1016

Conversion of Yohimbine into β-Yohimbine and 3-*epi*-β-Yohimbine

W. O. GODTFREDSEN and S. VANGEDAL

Leo Pharmaceutical Products, Copenhagen, Denmark

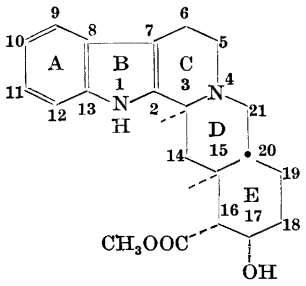
A four step conversion of yohimbine into β-yohimbine is described. Epimerization of β-yohimbine at C_3 affords a new yohimbine stereoisomer, 3-*epi*-β-yohimbine. Finally, the correlation between R_F-values and conformations of some yohimbine stereoisomers is discussed.

Three of the four possible 16-carbomethoxy-17-hydroxy-(—)-yohimbanes are known, *viz.* yohimbine, corynanthine, and β-yohimbine *.

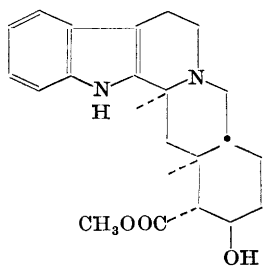
In yohimbine (I) the 16-carbomethoxy group is equatorially and the 17-hydroxyl group axially oriented [2,3]. Corynanthine is the 16-epimer of yohimbine [4] and, consequently, β-yohimbine must contain an equatorial 17-hydroxyl group. The 16-carbomethoxy group is considered to be of equatorial conformation since β-yohimbic acid is not epimerized by prolonged treatment with alkali [5].

In the following, a four step conversion of yohimbine (I) into β-yohimbine (II) will be described.

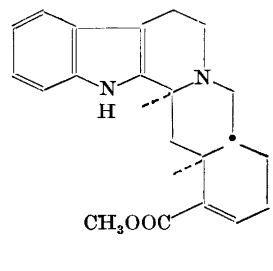
The first step, which consists in dehydration of yohimbine (I) to apoyohimbine (III), is well known [6].



I



II

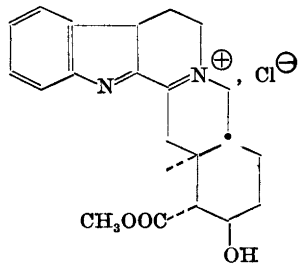


III

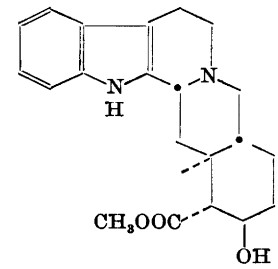
* The fourth stereoisomer is possibly represented by the alkaloid Serpine [1].

Treatment of apoyohimbine (III) with sodium methoxide in boiling methanol causes addition of methanol to the 16,17-double bond with the formation of a 16-carbomethoxy-17-methoxy-(—)-yohimbane, which upon heating with 48 % hydrobromic acid and subsequent esterification of the resulting 16-carboxy-17-hydroxy-(—)-yohimbane with diazomethane yields β-yohimbine, identical in every respect with an authentic sample.

In a previous paper [7] the dehydrogenation of alkaloids of the yohimbine type with *tert*-butyl hypochlorite was described. When β-yohimbine (II) is dehydrogenated in this way 3-dehydro-β-yohimbine chloride (IV) is obtained in good yield.



IV



V

Reduction of this compound with zinc and 50 % acetic acid according to Weisenborn and Diassi [8] yields a mixture of β-yohimbine (II) and a new yohimbine stereoisomer, 3-*epi*-β-yohimbine (V). For the separation of these two epimers their different solubilities in acetone were utilized. While β-yohimbine is readily soluble in this solvent, 3-*epi*-β-yohimbine forms a practically insoluble solvate.

The new yohimbine stereoisomer crystallizes nicely from alcohol, ethyl acetate, and benzene, but in solvated forms from which the solvent, in spite of intensive drying, could not be completely removed. For analysis the recrystallized material was therefore sublimed.

The melting point (203—204°C) and the optical rotation ($[\alpha]_D^{25}$ —83° in pyridine (c = 1)) seem to exclude that 3-*epi*-β-yohimbine is identical with any of the unidentified yohimbine isomers isolated from *Rauwolfia* species.

Table 1. R_F-values in Bush's B5-system.

Substance	R_F-value	D/E ring juncture	Orientation of the		
			C_3-hydrogen	16-carbomethoxy group	17-hydroxyl group
Corynanthine [4]	0.37	*trans*	axial	axial	axial
β-Yohimbine [5]	0.43	—	—	equatorial	equatorial
Yohimbine [2,3]	0.55	—	—	equatorial	axial
Allo-yohimbine [11]	0.67	*cis*	—	axial	equatorial
α-Yohimbine [12]	0.79	—	—	equatorial	equatorial
3-*epi*-β-Yohimbine	0.28	*trans*	equatorial	equatorial	equatorial
Pseudo-yohimbine [2]	0.40	—	—	equatorial	axial

In accordance with the equatorial orientation of the hydrogen atom at C_3, 3-*epi*-β-yohimbine is not dehydrogenated by mercuric acetate [8].

It has previously been pointed out [7] that Bush's B5 system [9] is well suited for paper chromatographic separation of alkaloids of the yohimbine type; in Table 1, the R_F-values of seven yohimbine stereoisomers are given. It will be seen that a substance containing an equatorial hydroxyl group is absorbed more strongly than its axial epimer (β-yohimbine — yohimbine; 3-*epi*-β-yohimbine — *pseudo*yohimbine), a phenomenon which is well known from the steroid series [10]. In addition, it appears from the table that compounds with an equatorial hydrogen atom at C_3 have lower R_F-values than their C_3-epimers (3-*epi*-β-yohimbine—β-yohimbine; *pseudo*yohimbine—yohimbine), and that compounds with an axial 16-carbomethoxy group are absorbed more strongly than their equatorial epimers (corynanthine — yohimbine; *allo*yohimbine — α-yohimbine).

EXPERIMENTAL

All melting points are corrected.

16-Carbomethoxy-17-methoxy-(—)-yohimbane (β-yohimbine methyl ether)

Apoyohimbine (22.4 g) and methyl acetate (25 ml) were added to a sodium methoxide solution containing 12.0 g of sodium in 350 ml of absolute methanol, and the mixture was refluxed for three days. The resulting clear solution was cooled and the crystals were collected on a filter and washed with methanol and water. Addition of water to the filtrate gave a further crop of crystals.

The combined precipitates were dissolved in 10 % acetic acid, reprecipitated with aqueous ammonia, and dried over P_2O_5 to give 21.7 g of white crystals with m.p. 196—200 °C. Recrystallization from *iso*propanol yielded 21.6 g of a product containing one mole of *iso*propanol. M.p. 204—206 °C (sealed tube). $[\alpha]_D^{20}$ −49° in pyridine (c = 1). (Found: C 70.05; H 8.57; N 6.40. Calc. for $C_{22}H_{28}N_2O_3$, C_3H_7OH: C 70.06; H 8.47; N 6.54).

Three recrystallizations from benzene gave solvent free crystals with m.p. 214.5—215.5 °C (sealed tube). $[\alpha]_D^{20}$ −54.5°±1 in pyridine (c = 1). (Found: C 71.53; H 7.76; N 7.68. Calc. for $C_{22}H_{28}N_2O_3$: C 71.71; H 7.66; N 7.60).

β-Yohimbine (II).

β-Yohimbine methyl ether, C_3H_7OH (2.0 g), was triturated in a mortar with a few ml of 48 % hydrobromic acid. The resulting paste was transferred to a 100 ml round-bottomed flask fitted with a reflux condenser; freshly distilled 48 % hydrobromic acid (20 ml) was added, and the mixture was heated cautiously with occasional shaking. When the excessive foaming which occurred during the first period of heating had ceased (about 30 min), the mixture was refluxed until a clear solution was obtained (another 30 min).

The solution was evaporated *in vacuo* and the last traces of hydrobromic acid were removed by drying over potassium hydroxide The residue was dissolved in methanol (30 ml) and excess of an ethereal solution of diazomethane was added. The solution was warmed on the steam bath to expel excess reagent and then evaporated *in vacuo* to a volume of 20 ml. After standing, 1.3 g of white plates, m.p. 234.5—235.5°C, were collected by filtration. Recrystallization from methanol raised the melting point to 236—237°C, and this was not depressed by admixture with an authentic sample of β-yohimbine, 2 CH_3OH. The I.R.-spectra of the two products and their R_F-values were identical too.

The optical rotation was found to be: $[\alpha]_D^{23}$ −42° in pyridine (c = 1). Le Hir and Goutarel [5] report $[\alpha]_D^{18}$ −46.6° in pyridine (c = 0.5).

3-Dehydro-β-yohimbine chloride (IV).

To a stirred solution of 1 360 mg (3.25 mmoles) of β-yohimbine, 2 CH_3OH and 0.50 ml of triethylamine in 25 ml of dry methylene chloride, a solution of 0.50 ml of *tert*-butyl hypochlorite in 5 ml of carbon tetrachloride was added at −25 °C during a period of 10 min. The cooling bath was removed and, after standing for about 15 min, the solution was washed with two 10 ml portions of water, and dried. The solvent was removed *in vacuo*, the residue dissolved in 5 ml of methanol, and the solution acidified with methanolic hydrogen chloride. Upon standing, 1 025 mg of yellow needles m.p. 267—269 °C (decomp.) were obtained. Recrystallization from methanol raised the melting point to 268—269.5 °C (decomp.). Ultraviolet absorption spectrum: λ_{max}^{MeOH} 246 mμ, log ε 4.03; 354 mμ, log ε 4.38. (Found: C 63.97; H 6.74; Cl 9.06. Calc. for $C_{21}H_{25}ClN_2O_3$, ½ CH_3OH: C 63.78; H 6.72; Cl 8.76).

3-*epi*-β-Yohimbine (V)

Zinc dust (800 mg) was added to a solution of 3-dehydro-β-yohimbine chloride, ½ CH_3OH (1 600 mg) in 50 % acetic acid (40 ml) and the mixture was shaken at room temperature until all zinc had dissolved (about 4 h). After addition of crushed ice, the solution was made alkaline with conc. aqueous ammonia (pH 9) and extracted three times with 30, 15 and 10 ml, respectively, of methylene chloride.

The combined extracts were dried over $MgSO_4$ and the solvent was removed *in vacuo* The residue was treated with 20 ml of boiling acetone to bring the β-yohimbine into solution. Cooling, filtration and washing with acetone gave 680 mg of crude 3-*epi*-β-yohimbine. Recrystallization from absolute ethanol afforded 505 mg of pure material which sintered at 141—142 °C (loss of solvent) and melted at 203—204 °C (dec.).

Recrystallizations from ethyl acetate and benzene gave also solvated forms and, for analysis the material was therefore sublimed. The sublimed material had m.p. 203—204 °C (decomp.) and $[\alpha]_D^{25}$ −83° in pyridine (c = 1).

Ultraviolet absorption spectrum: λ_{max}^{EtOH} 225 mμ, log ε 4.54; 282 mμ, log ε 3.88; 290 mμ, log ε 3.81. λ_{min}^{EtOH} 248 mμ, log ε 3.29; 288 mμ, log ε 3.80. (Found: C 70.99; H 7.25; N 7.71. Calc. for $C_{21}H_{26}N_2O_3$: C 71.16; H 7.39; N 7.90).

The acetone filtrate, containing mainly β-yohimbine, was evaporated to dryness *in vacuo* and the residue dissolved in 10 ml of boiling methanol. After cooling, 660 mg of β-yohimbine, 2 CH_3OH, m.p. 233—235 °C, were recovered.

Acknowledgement. The authors wish to thank professor M.-M. Janot, Paris, for an authentic sample of β-yohimbine. We are also indebted to Dr. P. Mørch for the ultraviolet and infrared spectra, and to Mr. G. Cornali for the microanalyses.

REFERENCES

1. Chatterjee, A., Pakrashi, S. C. and Werner, G. *Fortschr. Chem. org. Naturstoffe* **13** (1956) 356.
2. Janot, M-M., Gouratel, R., Le Hir, A., Amin, M. and Prelog, V. *Bull. soc. chim. France* **1952** 1085.
3. Cookson, R. C. *Chemistry & Industry* **1953** 337.
4. Janot, M-M. and Goutarel, R. *Bull. soc, chim. France* **1949** 509.
5. Le Hir, A. and Goutarel, R. *Bull, soc. chim. France* **1953** 1023.
6. Barger, G. and Field, E. *J. Chem. Soc.* **123** (1923) 1038.
7. Godtfredsen, W. O. and Vangedal, S. *Acta Chem. Scand.* **10** (1956) 1414.
8. Weisenborn, F. L. and Diassi, P. A. *J. Am. Chem. Soc.* **78** (1956) 2022.
9. Bush, I. E. *Biochem. J. London* **50** (1952) 370.
10. Savard, K. *J. Biol. Chem.* **202** (1953) 457.
11. Le Hir, A., Janot, M-M. and Goutarel, R. *Bull. soc. chim. France* **1953** 1027.
12. Wenkert, E. and Liu, L. H. *Experientia* **11** (1955) 302.

Received February 17, 1957.

ACTA CHEMICA SCANDINAVICA 11 (1957) 1017—1033

A New Interferometric Method for the Determination of Diffusion Coefficients of Very Dilute Solutions

OLOF BRYNGDAHL

Institute of Optical Research, The Royal Institute of Technology, Stockholm 70, Sweden

A new simple and rapid interferometric method is described for studying diffusion and other phenomena giving rise to a refractive index gradient in a solution. The method utilizes birefringence interferences and is found to possess a high degree of precision which probably cannot be attained by methods where the optical power of resolution sets a serious limit to the amount of accuracy attainable. In addition the method is particularly valuable in the study of cases where the refractive index gradient has a low value. By virtue of this fact, measurements can be extended to very low concentration differences. The possibility of arranging differential diffusion experiments with very low concentration gradients also provides a convenient means of studying the concentration dependance of the diffusion coefficient. The new method should further offer a possibility of verifying the Fuoss and Onsager theory for the diffusion coefficients of very dilute electrolytic solutions.

The observation of diffusion processes includes delicate and troublesome measuring problems because of the difficulty in arranging the experiments and the great demands made upon the optical methods. The methods used most for the determination of diffusion coefficients are: the "scale"- and schlieren methods of Lamm with a series of modifications and the Gouy interference method. To enhance the precision of the diffusion measurements the resolution of the optical method must be increased and the influence of the concentration dependance decreased. In order to diminish the influence of the concentration dependance of the diffusion coefficient, it is necessary to work with a small concentration difference, implying that the relative accuracy of the concentration measurement must be correspondingly increased. Under these conditions all the methods mentioned are subject to the fundamental difficulty of the limitation of the optical resolution. This is primarily based on a wave uncertainty principle, analogous to that of Heisenberg to which Wolter, among others, has called attention.[1] A method using birefringence interferences, which contains no resolution-limiting stops, has been introduced in this field by Ingelstam [2a,2b]. As will be described below, there were indi-

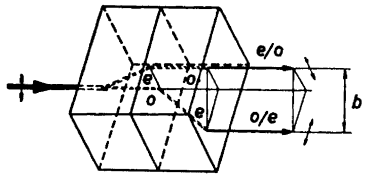


Fig. 1. The Savart plate. The splitting up of an entering ray into an extraordinary-ordinary and an ordinary-extraordinary ray is shown. The arrows at the rays indicate polarization directions.

cations *a priori* that this method would be capable of giving a greater accuracy than earlier ones, and would be especially convenient for very low concentrations. The experiments described in the following sections seem to confirm these expectations.

I. THE OPTICAL METHOD

A plane wave front is distorted in passing through a diffusion cell (of rectangular cross section with plane parallel glass windows) in accordance with the variation of the concentration within the solution. A wave front, defined as the locus of the same optical paths traversed by an originally plane wave front, gives a representation of the optical paths Z. In the diffusion process examined here, Z varies with one space coordinate x (the diffusion direction), and with time t. The relation between Z and the refractive index n and the cell thickness a is as follows:

$$Z(x,t) = n(x,t)a = [k_0 + k_1c(x,t) + k_2c^2(x,t) + \ldots]a \approx [k_0 + k_1c(x,t)]\ a, \quad (1)$$

the last form presupposing that the linear relation between the concentration and the refractive index holds (with is a good approximation in most cases).

By means of a shearing interferometer [3] the derivative of such a concentration curve can be conveniently measured. The wave front is to be split up, in the x-direction, into two parts separated from each other a small distance Δx. This shearing is easily realizable using a birefringent double crystal plate in parallel light. The Savart plate, (Fig. 1), with the incident light plane polarized in such a direction that the oscillation plane bisects the two principle planes of the crystal plate, divides the wave front into two equally strong, perpendicularly polarized, and coherent wave fronts which are at the same time sheared. In Fig. 1 it is also seen how the shear, $\Delta x = b$, results from the fact that the extraordinary rays are oblique in both parts of the Savart plate. The double plate makes the oscillations of the two wave fronts perpendicular, and by means of an analyzer introduced at 45° in relation to the principal planes of the crystal plates, the two wave fronts are enabled to interfere. As will be described below, the interference pattern consists of a set of horizontal fringe pairs. The number of fringe pairs corresponds to the total Z-increment Z_0, in the notation of eqn. (1) $Z_0 = Z(+\infty, t) - Z(-\infty, t)$, *i.e.*, the cell thickness times the total refractive increment of the solution. There is a difference of the optical thickness Z of one wave length between two fringes.

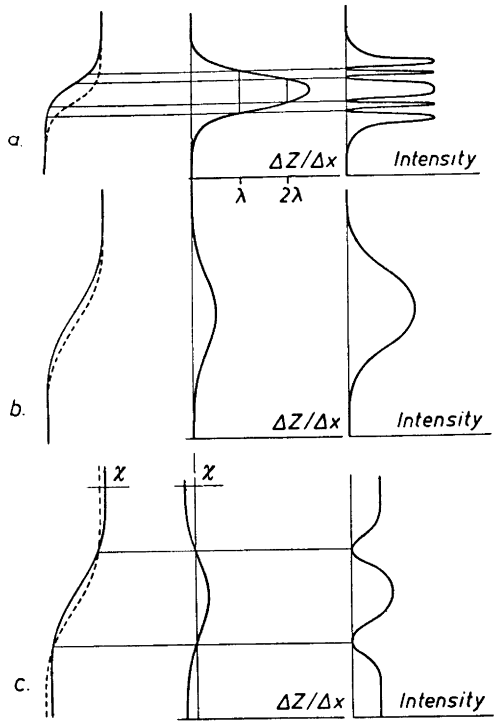


Fig. 2. The optical path as a function of x governed by the concentration gradient is shown (left). The optical path difference between the two separated wave fronts is seen in the middle and the light intensity of the interference pattern at the right. *a* represents an earlier time than *b* when the derivative curve has diminished so that no fringe pair remains. By tilting the Savart plate a constant path difference, χ, between the two wave fronts is introduced and a fringe pair has arisen as shown in *c*.

To the left in Fig. 2, the two laterally displaced wave fronts are shown. The path difference, ΔZ, between two rays emerging from the double crystal plate at the same spot, but originating from different parts, at the distance b, of the entering wave front (Fig. 2) is measured interferometrically. The resulting wave fronts interfere destructively or constructively when the path difference $\Delta Z = m\,\lambda/2$ (m = whole number). If the axes of the two polarizers, P_1 and P_2 in Fig. 3, are perpendicular to each other, the light is extinguished when $m = 0, 2, 4$, etc., and dark fringes are obtained at the corresponding x-coordinates. Similarly for polarizers whose axes are parallel dark fringes arise when $m = 1, 3, 5$, etc. The situation with crossed polarizers is represented in Fig. 2. As shown in Fig. 2a, the fringe pairs correspond to path differences of 0, λ, 2λ, etc., and the possibility of constructing $\Delta Z/\Delta X$ as function of x from the positions of the fringe pairs is clear. When the derivative curve is so low that $\Delta Z < \lambda/2$, which means that no fringes are obtained (Fig. 2b), the Savart plate can be tilted a slight amount and, on account of this, the wave fronts

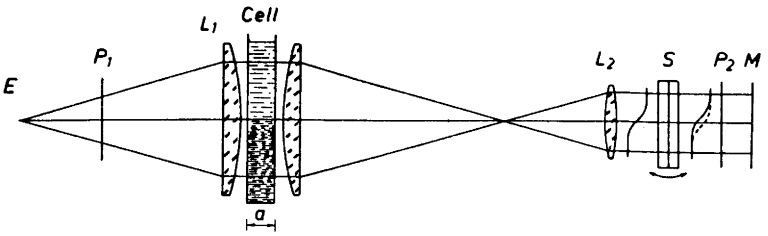


Fig. 3. Optical arrangement. For notation see text.

are displaced a desired path difference χ and a fringe pair has arisen according to Fig. 2c. Thus this method makes it possible to work with concentration differences corresponding to an optical path difference as small as about one wave length.

The interference pattern produced is related to the Gaussian curve, which represents the ideal concentration gradient. An evaluation method used by Lamm in the schlieren method is modified here and the diffusion coefficient is deduced from the rate at which the fringe pattern changes.

II. APPARATUS

1. *The lens system.* The lens system is shown schematically in Fig. 3. E is a horizontal slit illuminated by monochromatic light. It is located in the focal plane of the first lens in the system L_1. The system L_1 is composed of two equal lenses, each having a focal length of 1 m, and corrected for both chromatic and spherical aberrations. By means of the lens L_2, $f = 12$ cm, an image of the cell plane is obtained in the object plane M. The strict collimation necessary in the wavefronts traversing the crystal plate is accomplished by the displacement of L_2. During the experiments the cell is placed between the lenses L_1 where the light is parallel. The numerical value of the optical magnification, G, is 0.120.

2. *The Savart plate.* The crystal plate, which is traversed by strictly parallel light, introduces a displacement between of the wavefronts in the x-direction equal to b. If the Savart plate is adjusted so as to be perpendicular to the optical axis, so that no phase shift is introduced between the two wavefronts, b is determined by the equation,

$$b = e\sqrt{2}\ \frac{n_e^2 - n_0^2}{n_e^2 + n_0^2} \tag{2}$$

where e is the thickness of each part of the double plate and n_e and n_o are the principal refractive indices. The quartz plate, which is used in the experiments with very dilute solutions, has $e = 10$ mm and $b = 84.2\ \mu$. If the magnification is G, the real distance at the object is not b but b_1 which is equal to b/G.

3. *The cell.* The diffusion cell used was a flowing-junction cell, having a stainless steel body, kindly lent to us by Dr. H. Svensson, who designed and

used it in his earlier developmental work.[4] In this type of cell the initially sharp boundary is formed by allowing solution and solvent to flow together into a narrow horizontal exit slit in the side wall of the diffusion channel, the horizontal cross section of which is 3×50 mm^2 and the height of which is 70 mm. The cell windows are 10 mm thick and the flatness before clamping is about one wave length.

4. *The monochromator.* The horizontal entrance slit is illuminated by a 100 W mercury lamp with a filter that transmits only the green Hg-line (5 461 Å).

5. *The camera.* In the experiments with liquid gradients, where a quick registration of the beginning of the run is desired (an exposure every tenth second), a Robot camera which automatically feeds the film is used. Together with this a Leitz bellow adjustment apparatus and an Elmar objective ($f = 5$ cm) is used.

6. *Photography.* For all photographic recordings Ilford HPS film is used with Ilford Microphen fine grain developer. HPS film is used to attain a minimum time of exposure (about 2 sec).

7. *Control of temperature.* Unfortunately, no thermostat is available during the experiments, but they are carried out in a room with a remarkably constant temperature, held within $\pm$ 1 degree with an electric radiator for 10 h before the experiment. The cell part of the arrangement is shielded with an aluminium box to give radiation equilibrium. A thermometer placed close to the cell shows, in general, a variation in temperature of less than $\pm$ 0.05° during an experiment. Care was taken not to warm up the thermostat by touching or by radiation from the body.

8. *Support.* All the optical components are mounted on a 3 m steel beam resting on sheets of sponge rubber on concrete tubes which stand on the floor. In this way vibrations communicated to the optical system through the floor are effectively damped out.

III. CALCULATION

At small concentration differences, the skewness of the gradient arising from the concentration dependance of the coefficient disappears and Fick's second law is presumed to be valid. The derivative of the optical path gradient can be written

$$\frac{\partial Z(x,t)}{\partial x} = \frac{Z_0}{2} \cdot \frac{1}{\sqrt{\pi Dt}} \cdot e^{-(x/\sqrt{4Dt})^2} \qquad (3)$$

The correction between the path difference $\Delta Z/b_1 = \Delta Z/\Delta x$ that is measured, and the path derivative desired, eqn. (3), can easily be calculated [2a, 2b]. In the neighbourhood of the inflexion points the magnitude of the corrections is extremely small, and for a birefringence displacement, b_1, less than 3 σ, where $\sigma = \sqrt{2Dt}$ is half the distance between the inflexion points of the Gaussian curve, the correction is practically negligible over the whole curve.

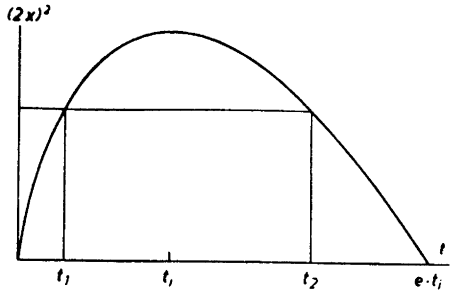


Fig. 4. The square of the distance between the fringes as function of time. The diffusion coefficient is obtained from pairs at certain distances and their corresponding times, as

$$D = \frac{(2x)^2(1/t_1 - 1/t_2)}{8 \ln t_2/t_1}$$

The difference ratio measured can be expanded in a series and the derivatives substituted by polynomists in x/σ as follows:

$$\frac{\Delta Z(x)}{b_1} = \frac{Z(x + \frac{1}{2}b_1) - Z(x - \frac{1}{2}b_1)}{b_1}$$

$$= Z'(x)\left\{1 + \frac{1}{3!}\left(\frac{b_1}{2}\right)^2 \frac{Z^{III}(x)}{Z'(x)} + \frac{1}{5!}\left(\frac{b_1}{2}\right)^4 \frac{Z^{V}(x)}{Z'(x)} + \cdots\right\} \quad (4)$$

$$= Z'(x)\left\{1 + \frac{1}{2^2 \cdot 3!}\left(\frac{b_1}{\sigma}\right)^2 (x^2 - \sigma^2) + \frac{1}{2^4 \cdot 5!}\left(\frac{b_1}{\sigma}\right)^4 (x^4 - 6x^2\sigma^2 + 3\sigma^4) + \cdots\right\}$$

From this it appears that when b_1/σ is small the corrections for obtaining the gradient are conveniently small.

The curve constructed from the interference pattern (the fringe pairs represent symmetrical points with a fixed value of $\Delta Z/\Delta x$) can easily be corrected and the derivative determined.

An accurate evaluation method, due to Lamm [5], having the advantages of using only the region not far from the inflexion points of the Gaussian curve, is modified for this method. From the set of fringes, a distance $2x$ between corresponding fringes in the interference pattern is measured. Following a definite fringe pair with time, we may plot $(2x)^2$ *vs.* t (Fig. 4). The diffusion coefficient is then obtained from a value of $(2x)^2$ and its co-ordinate times t_1 and t_2 by the equation

$$D = \frac{(2x)^2 (1/t_1 - 1/t_2)}{8 \ln t_2/t_1} \quad (5)$$

The equation of the curve in Fig. 4 is

$$(2x)^2 = 8Dt \left(1 + \ln \frac{t_i}{t}\right) \quad (6)$$

where t_i represents the time corresponding to maximum distance between the fringes. When $t = t_i$

$$(2x_i)^2 = 8Dt_i \quad (7)$$

and $2x_i = 2\sigma$, which is the distance between the inflexion points of the Gaussian curve.

At higher concentration differences a group of such curves is obtained and the information about the diffusion process is very copious.

IV. ZERO-TIME CORRECTION

Since the infinitely sharp initial boundary, required for rigorous application of the equations, cannot be obtained experimentally, the observed time, t, after a certain time zero point in the formation of a boundary must be corrected by a small constant increment Δt, in order to arrive at the zero point where the boundary would have been infinitely sharp.

Method 1. In experiments with concentration differences giving many fringes, a *rough* estimate of the diffusion coefficient and the zero-time correction can be made. By combining the maximum points in Fig. 9 a straight line, $(2x)^2 = 8Dt$, is obtained. The slope of the line is $8D$ and from the intersection with the abscissa axis the zero-time correction is determined.

Method 2. A more accurate method exploiting only the variation of one fringe pair is obtained by the following.

A diffusion coefficient D' is computed by using the measured time in eqn. (5). The true diffusion coefficient D is related to D' by the expression

$$D = \frac{(2x)^2 \left(\frac{1}{t_1 + \Delta t} - \frac{1}{t_2 + \Delta t}\right)}{8 \ln \frac{t_2 + \Delta t}{t_1 + \Delta t}}$$

$$\approx \frac{(2x)^2 \left(\frac{1}{t_1} - \frac{1}{t_2}\right)}{8 \ln \frac{t_2}{t_1}} \cdot \frac{1}{\left(1 + \Delta t \frac{t_1 + t_2}{t_1 t_2}\right)\left(1 - \Delta t \frac{\frac{1}{t_1} - \frac{1}{t_2}}{\ln \frac{t_2}{t_1}}\right)}$$

$$\approx \frac{D'}{1 + \Delta t \cdot \vartheta} \qquad (8)$$

$$\text{where} \quad \vartheta = \frac{t_1 + t_2}{t_1 t_2} - \frac{\frac{1}{t_1} - \frac{1}{t_2}}{\ln \frac{t_2}{t_1}}$$

and D and Δt are readily obtained from a plot of D' *vs.* ϑ (Fig 10). This method is not applicable at very short experimental times, *i.e.*, when $(\Delta t)^2$ no longer can be neglected in comparison with $t_1 \cdot \Delta t$.

Method 3. An iteration method has been adopted for obtaining higher accuracy and an estimation of the precision of the calculation. Fig. 11 shows how D varies with $(2x)^2$ for different values of the parameter Δt. In this way a Δt giving the most constant D can be determined.

V. EXPERIMENTAL TEST

Work with the present apparatus has been confined to solutions of glycine and sucrose. In the experiments with glycine a small downward drift of the diffusion coefficients was observed. Reaction products between glycine and iron were found which is equivalent to an absorption process. In the experiments, discussed here, sucrose of analytical purity has been used. Accurate measurements of the diffusion of this material have recently been performed elsewhere [6-8].

The solvent and solution are put in the thermostat, and after about 10 h when thermal equilibrium is obtained, the stopcocks of the reservoirs, which are provided with handles for operation from outside the aluminium box, are opened. After another half an hour, when the gradient is very sharp and temperature equilibrium is obtained, the stopcocks are closed and the outflow stopped so that diffusion may take place. About 50 exposures are taken during the diffusion process, more frequently at the beginning.

For obtaining the highest precision measurement of the films, a photometer is used. The distance, $2x$, between corresponding centres of the density minima are measured with an accuracy of 1 μ. In one of the experiments, (II), a comparator reading to 1 μ has been used.

From the data taken in these experiments it is evident that, in general, no advantage is gained from photometric measurements. Photometry is advisable in working with concentration differences corresponding to an optical path difference of about one wave length. At the very end of the diffusion process, when the derivative curve is low (Fig. 2 b and c), the asymmetry and blurring of the fringes are troublesome when the distance between coordinate fringes is small (representing points at the very top of the derivative curve). As a rule, in these cases, one has no interest in following the fringes so long that the asymmetry and broadness of the fringes will be troublesome. The higher the concentration difference, the sharper the fringes, since this depends on the slope of the gradient curve (*cf.* Fig. 2). For determination of the fringe pair positions at smaller concentration differences (with a small broadening of the density minima in the film) an increase of the exposure time will give sharper fringes ("Minimumstrahlkennzeichnung", Wolter [1]).

A procedure, "Äquidensitenverfahren", designed by Krug and Lau [9] has been tried for obtaining greater measuring accuracy at wide interference strips. It must be stressed that this procedure has only an advantage for wide fringes, which appear here when working with concentration differences corresponding to an optical thickness of about one wave length.

For density curves, running more or less steep, points with the same density (these curves are called Äquidensiten) can be connected by a photographic procedure [9]. Practically this can be done by making a positive on hard film from the original negative. When it is nearly developed, the film is illuminated by uniform light, which has most influence on the positions not illuminated before. So by the Sabattiereffect a plate is obtained in which a positive and a negative are in precise covering and the Äquidensiten arise where the negative and positive have about the same density.

Here, however, one is looking for the minima in the negatives, but then the method fails because of the impossibility of computing the density values corresponding to the Äquidensiten, neither does it give a comprehension of the amount of asymmetry. Thus it is impossible to find the minimum point by producing Äquidensiten at different density values and extrapolating to the minimum.

The difference between the refractive index of water and a solution of 1 g sucrose in 100 cm^3 water gives a retardation of 132 (air) wave lengths for the cell used (around 50 mm thick). From this it is evident, that as low a concentration as about 0.01 %, corresponding to an optical path difference of 1.32 wave lengths, can be used.

A series of exposures taken during a diffusion run is shown in Fig. 5. The position of the fringes is very accurately determined by constructing the medians in the photograms (Fig. 6).

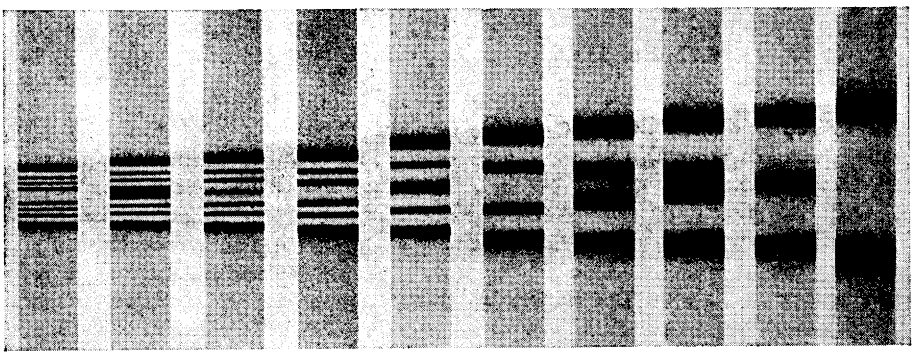


Fig. 5. Exposures taken during a diffusion experiment (Expt. IV).

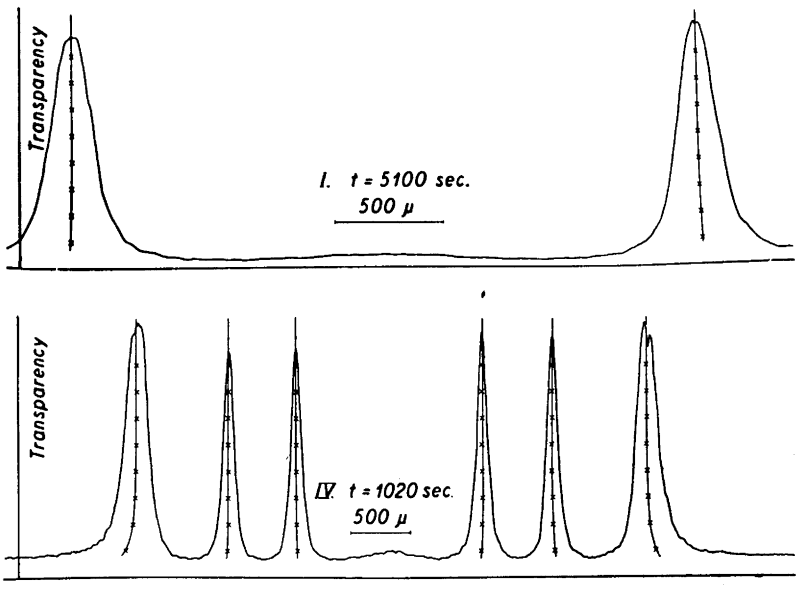


Fig. 6. Photograms showing how the exact positions of the fringes are found by constructing the medians of the curves. Observe how precisely the position can be measured with such low a concentration difference as in expt. I.

Four experiments with different concentrations were performed (Table 1). Every run has been calculated in detail.

Table 1.

Run	Sucrose conc. above/under the boundary %	Thermostat temp. °C	Fringe pairs at the beginning (in air wavelengths)	χ Å
I 31.1.57	0/0.0112	21.33±0.07	1.48	470
II 30.1.57	0/0.0500	20.76±0.20	6.60	1 890
III 4.2.57	0/0.1018	23.62±0.05	13.48	3 680
IV 5.2.57	0.7249/0.8253	23.84±0.06	13.25	2 430

Eqn. (6) has been adapted to the experimental points of run I in Fig. 7. Good agreement over the whole curve, except for very low time values, is clear from the diagram. Despite the fact that the method gives high values at the very beginning of the process, all distances were found to be smaller than the theoretical ones. This indicates that a high zero-time correction is obtained, owing to the difficulties of producing sharp boundaries at such a low concentration. The results obtained using the iteration method on run I (concentration corresponding to an optical path difference of 1.48 wave lengths) are shown in Fig. 8. The dotted part of the curves, represents disturbances at the beginning, which are found to die out very quickly. With the parameter $\Delta t = 205$ sec, the curve runs well horizontally and the corresponding value of the diffusion coefficient is determined very accurately.

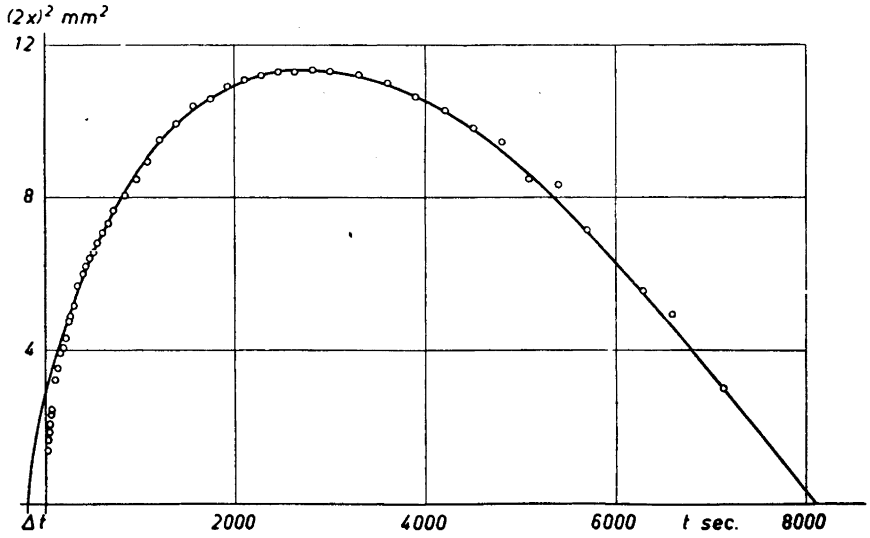


Fig. 7. $(2x)^2$ as function of time for expt. I. Eqn. (6) has been adapted to the experimental points.

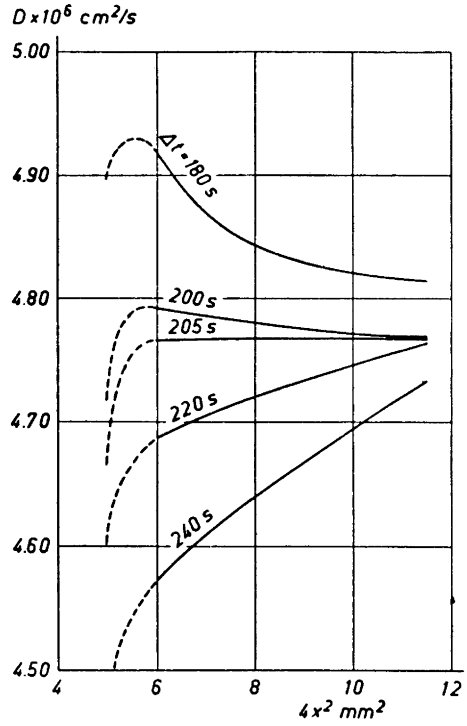


Fig. 8. D as a function of $(2x)^2$. The dotted part represents disturbances. *Cf.* Fig. 7.

In order to illustrate the simplicity, rapidity, accuracy and amount of information given by this method, the above mentioned ways of finding the zero-time correction are applied to run III (Figs. 9, 10 and 11). In Figs. 10 and 11 the curves refer to the next outermost fringe pair. From a comparison with the values calculated from the curves corresponding to the other fringe pairs a good agreement, within 0.02 %, is obtained. In Fig. 11 the influence of the correction between the difference and the derivative appears. The dotted parts represent the uncorrected values. It must be observed that this curve at the beginning corresponds to points far from the inflexion points of the Gaussian curve. Nevertheless, the influence of the correction is dying out very fast and can be ignored in all practical measurements. In order to compare the diffusion coefficients obtained with the values given in Refs.[6–8], corrections were applied to 25.0 °C using Stoke-Einstein's relation. These data are given in Table 2, where values extrapolated from the measurements in Ref.[7] are also found.

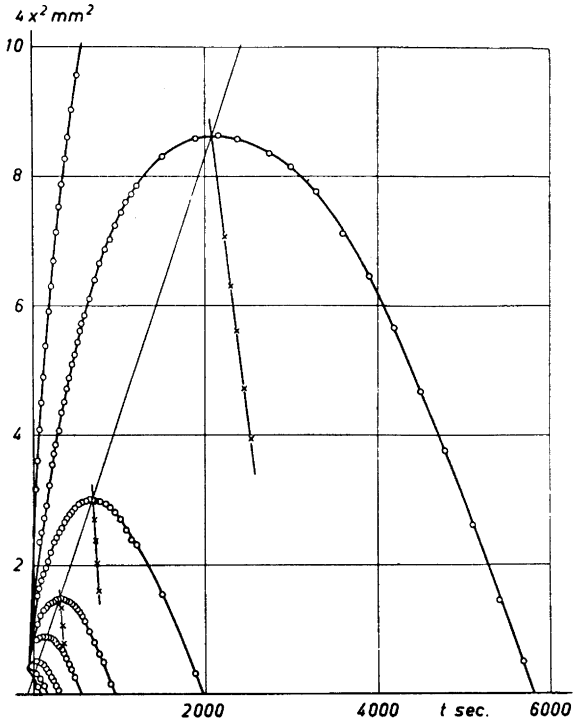


Fig. 9. $(2x)^2$ as a function of time for expt. III. The maximum points of the curves are easily found by constructing the medians, and the line combining the maximum points gives a rough estimate of the diffusion coefficient and the zero-time correction.

Table 2.

Run	c %	Δc %	Δt sec.	$D_{25} \times 10^6$ cm²/s	$D_{25} \times 10^6$ cm²/s extracted from Ref.[7]
I	0.0056	0.0112	205	5.229±0.011	5.228
II	0.0250	0.0500	54	5.193±0.042	5.224
III	0.0509	0.1018	47	5.235±0.008	5.222
IV	0.7751	0.1004	55	5.193±0.011	5.170

In Fig. 12 it is clearly seen how the results obtained by this method agree with the values extracted from the equation of the concentration dependance of the diffusion coefficient stated in Ref.[7]. From this diagram it is evident that a *very* small concentration difference can be used. The exactness of the measurements is also indicated. Experiment II with poor temperature control has given too low a value.

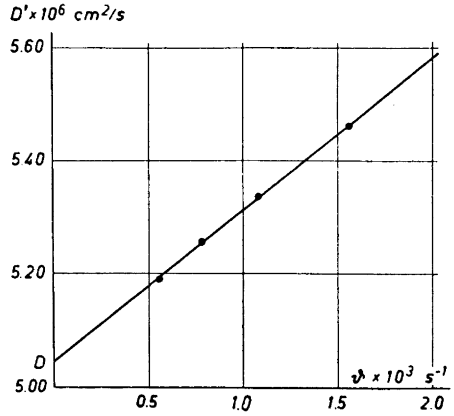


Fig. 10. The calculated diffusion coefficient D' as a function of the factor ϑ (see IV, 2). D is obtained from the intersection with the ordinate axis. The slope of the line is $\Delta t D$.

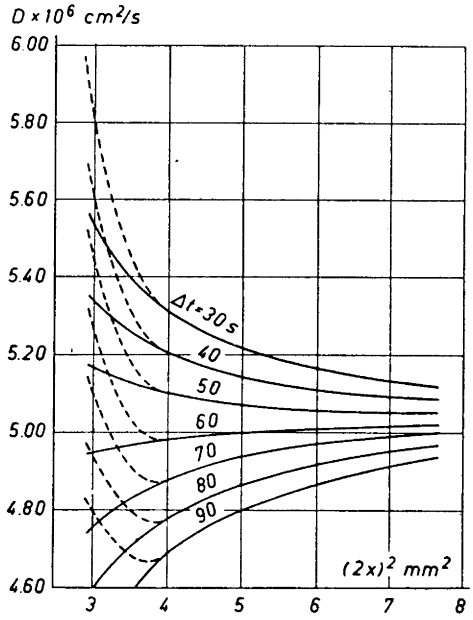


Fig. 11. D as a function of $(2x)^2$ obtained from the next outermost fringe pair. The dotted parts represent values obtained without regard to the correction between difference and derivative. Observe in this curve, that in the part representing points far from the inflexion points (for $(2x)^2 < 5$ mm^2), the corrections are obtainable and die out fast.

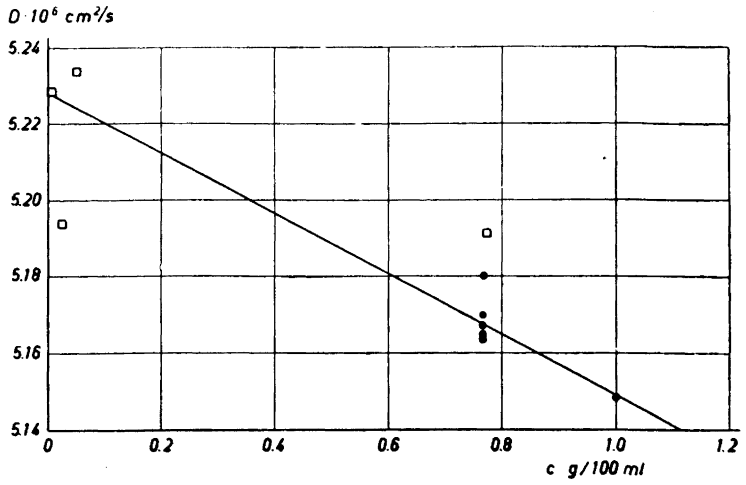


Fig. 12. Determination of diffusion coefficients for sucrose. Filled circles, Refs. [6-8], having been determined with the Gouy interference method. The line drawn is obtained from Akeley and Gosting [7]. Empty squares, results from the investigations presented in this paper.

VI. DISCUSSION

The determined diffusion coefficients deviate from the values in Refs.[6-8] by less than 0.5 %, which is very small compared with the accuracy in the referenced values quoted above. It should be stressed that the results do not really give the method full justice, since these experiments were carried out without careful thermostating and that large temperature corrections (the uncertainty in the absolute value of temperature is about 0.1 °) have been applied.

It is difficult to give a quantitative estimate of the effect of the sources of error on the accuracy and precision of the measurements. In the method described the following factors have an influence on the calculated diffusion coefficient:

a. insufficient control of temperature (about 0.2 %),

b. overlapped thermal gradient (a temp. gradient of 0.1 ° corresponds to an optical path difference of about 5 000 Å, this effect dies out in a few minutes),

c. the concentration dependance of the diffusion coefficient (about 0.05 % in these experiments),

d. correction between difference and derivative (has an exceedingly small influence in these calculations, where only points not far from the inflexion points of the Gaussian curve have been used),

e. determination of the distance between the fringes; the measurements are performed with an accuracy of 1 μ at the beginning and about 3 μ

at the end (consistent with the sharpness of the fringes), see Fig. 4. Here also a possible error in the magnification factor has an influence,

f. calculation (the last two sources introduce an error of about 0.05 %),
g. error of focusing,
h. non-parallel light through the cell,
i. lens effect of the cell (can be compensated by displacement of L_2),
j. a wedge shaped diffusion column (has an extremely small influence in this method).

The maximum error in the estimates (except II with bad temperature constancy) is about 0.2 % (with regard to the uncertainty in the absolute temperature about 0.5 %) which in its greater part arises from the variation of temperature. With accurate temperature control, it would easily be possible with the present method to determine the diffusion coefficient within 0.1 %.

The cell used gives an extremely great zero-time correction compared with other measurements with flowing-juction diffusion cells. Longsworth [10], for example, stated 4—6 sec. Thus, in general, the determination of the zero-time correction will not give rise to such a marked problem. It should be emphasized that the zero-time correction does not appreciably increase with the dilution and so the values found here show good agreement with those obtained by Svensson [11] with the same cell at higher concentration difference.

Contrary to expectation the method is not extremely sensitive to minor imperfections in the optical system, nor to contaminations in the cell. However, good quality optical equipment is essential in order that the advantages of the method be fully utilized. The importance of proper focusing is naturally also more prominent in working with a method giving such a precision in the measurements as the above mentioned, than in less sensitive methods. We owe a good deal to Svensson for his prethought of developing the theory of second and third order aberrations in the interferometric measurement of concentration gradients. The adjustment of our optical system was carried out in conformity with his prescriptions.

Svensson has shown [12, 13] that the aberration corresponding to the Wiener skewness of the gradient curve disappears if the camera is focused on a plane 1/3 of the cell thickness from the front wall. The photographic enlargement factor is determined experimentally by placing an object in the plane of the middle of the cell, although this is not optically conjugate to the plate. If the light through the cell is converging, it gives rise to an aberration, which may be corrected for by determining the optical magnification factor of the cell from the slightly defocused plane through the middle of the cell [12].

A result of Svensson's calculations [14] is that the third order aberrations depend on the entrance angle, and that there is a certain entrance angle (the light source should be situated below the optical axis) that is more favourable than any other angle. The third order aberrations are found to decrease very rapidly with time. The critical time of diffusion (when all aberrations have decreased to 1/50 of a light wave) in these measurements with low concentration differences is surprisingly small, about a few seconds.

There seems to be little justification in stating a diffusion coefficient within a few tenths of a per cent, using a total concentration difference corresponding to an optical path difference of about 100 wave-lengths, bearing in mind that the coefficient varies to the extent of several per cent in the concentration region examined. The present method on the contrary works with very low concentration differences and thus the concentration dependance of the diffusion coefficient is correspondingly smaller. This is one of the great advantages of this method. Other advantages are that only part of the Gaussian curve near the inflexion points is used and that an image of the whole diffusion column is obtained.

Another striking feature of the new method is that it enables diffusion experiments to be carried out in a very short time — 20 min or even less (observing inner fringe pairs or very dilute solutions). No doubt, this is to be ascribed to the greatly enhanced power of resolution, which makes the method equally well suited to measurements on medium and very low refractive index gradients.

The present method has by no means an unlimited power of resolution — this would rule out the wave uncertainty relation completely. But a great enhancement results from choosing the conditions of the experiment and the method of registration in a suitable way. The described method possesses the same degree of high precision which is achieved by Wolter [1] who modified the schlieren method by changing the slit to a 180° phase plate. "Minimumstrahlkennzeichnung" and all advantages attaching thereto (as *e.g.*, unlimited high beam sharpness and enhancement of the measuring precision making photometry superfluous) are exploited by birefringence interferometry in polarized light. *The Savart plate has some advantages compared to the phase plate:* it is simpler to realize in practical measurements and gives more information (many fringe pairs) about the process.

The fact that the extrapolated values obtained by Akeley and Gosting [7] show a fair agreement with the results of the exceedingly accurate experiments reported in this paper is probably a mere coincidence.

The conductance method of Harned and French [15], which implied a considerable improvement in accuracy at concentrations ten times lower than optical methods existing at that time, was applicable to cases where the original concentration differences was of an order of magnitude not less than 0.0025 molal in KCl. Our method enables measurements to be carried out with a concentration difference of 0.0015 molal in KCl. The precision of our measurements would be of the order of $\pm$ 0.1 % while the accuracy reported by Harned and French is approximately $\pm$ 0.9 % which was later reduced to about $\pm$ 0.1 % with concentrations down to 0.00125 molal [16].

As pointed out by Svensson [12], it is desirable to carry out experiments with very low concentration gradient when studying polydisperisity, in order that the influence of the concentration dependance of the diffusion coefficient can be disregarded and the effect of polydispersity studied separately.

REFERENCES

1. *Handbuch der Physik*, Bd XXIV, p. 577–88, Springer Verlag, Berlin 1956.
2a. Ingelstam, E. *Arkiv Fysik*, **9** (1955) 197.
2b. Ingelstam, E. *J. Opt. Soc. Amer.* **47** (1957) 536.
3. *Handbuch der Physik*, Bd XXIV, p. 452–5, Springer Verlag, Berlin 1956.
4. Svensson, H. *Acta Chem. Scand.* **3** (1949) 1170.
5. Lamm, O. *Private communication.*
6. Gosting, L. J. and Morris, M. S. *J. Am. Chem. Soc.* **71** (1949) 1998.
7. Akeley, D. F. and Gosting, L. J. *J. Am. Chem. Soc.* **75** (1953) 5685.
8. Riley, J. F. and Lyons, P. A. *J. Am. Chem. Soc.* **77** (1955) 261.
9. Krug, W. and Lau, E. *Feingerätetechnik*, **1** (1952) 391.
10. Longsworth, L. G. *Rev. Sci. Instr.* **21** (1950) 72.
11. Svensson, H. *Acta Chem. Scand.* **5** (1951) 72.
12. Svensson, H. *Optica Acta* **1** (1954) 25.
13. Forsberg, R. and Svensson, H. *Optica Acta* **2** (1954) 90.
14. Svensson, H. *Optica Acta* **3** (1956) 164.
15. Harned, H. S. and French, D. M. *Ann. N. Y. Acad. Sci.* **46** (1945) 267.
16. Harned, H. S. and Nuttall, R. L. *Ann. N.Y. Acad. Sci.* **51** (1949) 781.

Received April 4, 1957.

ACTA CHEMICA SCANDINAVICA 11 (1957) 1034—1058

Equilibrium Studies of Polyanions

II Polyborates in $NaClO_4$ Medium

NILS INGRI, GÖSTA LAGERSTRÖM, MINA FRYDMAN, and LARS GUNNAR SILLÉN

Department of Inorganic Chemistry, The Royal Institute of Technology, Stockholm 70, Sweden

The pH equilibria of boric acid and borate ion have been studied in 3 M sodium (perchlorate) medium at 25°C by electrometric titration using a hydrogen electrode. The total boron concentration B had values between 0.010 and 0.600 M. With the total boron concentration $B \leqq 0.025$ M, essentially only the mononuclear species boric acid $B(OH)_3$ and the ion $B(OH)_4^-$ seem to be present; the data for $B > 0.025$ M give evidence also for two polynuclear species, $B_3O_3(OH)_4^-$ and $B_3O_3(OH)^{2-}$. (The data may also be explained, though not so well, by assuming $^5B_3O_3(OH)_4^-$ and $B_4O_4(OH)_6^{2-}$).

Reactions and constants:

$B(OH)_3 + H_2O \rightleftharpoons B(OH)_4^- + H^+$ $\quad \log K_{11} = -9.00 \pm 0.05$

$3B(OH)_3 \rightleftharpoons B_3O_3(OH)_4^- + H^+ + 2H_2O$ $\quad \log K_{13} = -6.84 \pm 0.10$

$3B(OH)_3 \rightleftharpoons B_3O_3(OH)_5^{2-} + 2H^+ + H_2O$ $\quad \log K_{23} = -15.44 \pm 0.20$

In aqueous solution boric acid shows a number of irregularities which indicate the existence of polyborate ions. The aim of this work has been to investigate the pH equilibria of boric acid at various total boron concentrations (B), and from this to deduce the formulas of the predominating species, and the equilibrium constants for their formation.

In the following survey we shall for brevity, and to conform with the notations in the general papers [1], use the symbols

$$A^- \text{ or } A = -H^+ \qquad\qquad B = H_3BO_3$$

The charge of the species A_pB_q will then be $p-$; we shall sometimes write it out, sometimes not. When we apply the law of mass action to the equilibria, we shall write

$$[A] = a = [H^+]^{-1} = h^{-1}; \quad [B] = b$$

and denote by K_{pq} the equilibrium constant for the reaction

$$p\,A + q\,B \rightleftharpoons A_pB_q; \quad [A_pB_q] = K_{pq}a^pb^q = K_{pq}h^{-p}b^q \qquad (1\,a)$$

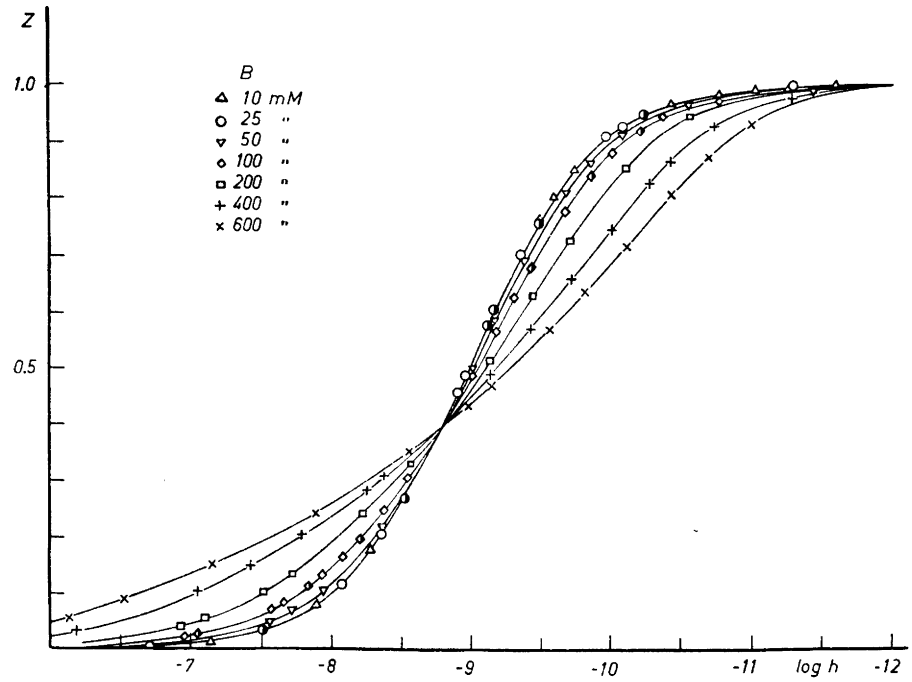


Fig. 1. Average number of OH bound per boron, Z, as a function of $-\log h$. The curve through the points for the two lowest concentrations is that calculated for a normal weak acid with $\log K_a = -9.00$. For the other concentrations smooth curves have been drawn through the experimental points. Half-filled symbols represent points from backtitrations.

or

$$n\,H_2O\text{—}p\,H^+ + q\,H_3BO_3 \rightleftharpoons B_q(OH)_{3q+p}(H_2O)_{n-p}^{p-}; \qquad (1\,b)$$

$$[B_q(OH)_{3q+p}^{-p}] = K_{pq}h^{-p}[H_3BO_3]^q = K_{pq}h^{-p}b^q$$

The important factors are the number of protons and H_3BO_3 groups. The number of water molecules n cannot be determined from the equilibria.

Then K_{11} for the simplest mononuclear reaction is the acidity constant of boric acid

$$A^- + B \rightleftharpoons AB^-; \quad K_{11} = [AB]a^{-1}b^{-1} = [AB]hb^{-1} \qquad [(2\,a)$$

$$H_3BO_3\text{—}H^+ + H_2O \rightleftharpoons B(OH)_4^-; \; K_{11} = h[B(OH)_4^-][H_3BO_3]^{-1} = K_a' \quad (2\,b)$$

The behavior of boric acid is well illustrated by Fig. 1, which gives our data for the titration of B (H_3BO_3) with A (Na^+OH^-). Each set of points represents a titration (or rather two duplicate titrations) where the total boron concentration B was maintained constant, at 0.010, 0.025, 0.050, 0.100, 0.200, 0.400 or 0.600 M. The activity factor effects were largely eliminated by keeping $[Na^+] = 3$ M in all experiments by addition of $NaClO_4$. The abscissas represent $\log h$ and the ordinates Z, the average charge per boron atom.

With decreasing B, all of the curves approach the steepest curve, which is the one calculated for a normal weak acid with log $K_a = -9.00$. At these low concentrations, the only species that need be considered would be B and AB^-. According to Konopik and Leberl [2], H_3BO_3 should split off two more protons, with log K_a values of —12.3 and —13.3; in our notation A_2B^{2-} and A_3B^{3-} would be formed. With the present data, Z does not seem to exceed 1.0, so there was no definite indication of a dissociation beyond the step AB^-. However, our measurements were not pursued to very high values of the pH.

At higher total concentrations of B, the curves deviate from the mononuclear one; for low values of Z, the solutions are more acidic and at high values of Z more alkaline, than would be expected, if the mononuclear reaction were the only one.

The curves intersect at $Z \approx 0.40$. Such an intersection point was referred to as an isohydric point by Carpéni [3]. Byé [4] and Souchay [5] have pointed out that at such a point the condensation to polyions must be at a maximum.

Before trying to analyse these curves, we shall survey some previous work on borates in solutions.

PREVIOUS SOLUTION DATA

Reversibility of equilibria. Kahlenberg and Schreiner [6] were the first to check that whatever reactions there may be between monoborate ions, boric acid, and polyborate ions, they must come very rapidly to equilibrium. For instance, no difference was found between a solution prepared from water and $Na_2B_4O_7(H_2O)_{10}$, and one prepared by mixing the corresponding amounts of NaOH and H_3BO_3. All subsequent work, including our own, seems to lead to the same conclusion.

Freezing point data. According to Menzel [7] the freezing point depression of aqueous solutions of H_3BO_3 is quite normal up to the highest concentrations studied by him, 0.358 M; thus the formation of uncharged polyboric acids, B_q, seems to be negligible Also freezing point data for Na^+AB^- ("$NaBO_2(H_2O)_2$", $Na^+B(OH)_4^-$) up to 2 m solution do not deviate significantly from those of other 1—1 salts like $K^+HCO_3^-$ (Menzel [7], Menzel and Schulz [8]). Doucet and Rollin [9] measured the depression of the freezing point of $Na_2SO_4(H_2O)_{10}$, which largely eliminates the uncertainty caused by ionic strength effects, and still found no association for B (up to 0.25 M) or Na^+AB^- (up to 0.11 M).

Freezing point data for salts like borax, $Na_2B_4O_7(H_2O)_{10}$, and $NaB_5O_8(H_2O)_5$ in dilute solution indicate that they give chiefly mononuclear species B and AB^-. At higher concentrations there are, however, signs of association (Menzel [7]). Souchay [10] gives curves for the freezing point depression for a series of solutions corresponding to a titration at constant total concentration B (0.10 or 0.25 M) and constant ionic medium. He found that the number of molecules per boron atom is 1.0 at the B and AB^- sides, whereas at the isohydric point it has a minimum value, approximately 0.7 at the higher value for B.

We may thus conclude that the polynuclear species formed are neither polymers B_q nor polymers $(AB)_q^{q-}$ but rather of the mixed type $A_pB_q^{p-}$.

Conductance and pH of pure B solutions. Owen [11] has found log $K_a^\circ = -9.236$ for H_3BO_3 (B) at 25°C, using cells without liquid junctions, and extrapolating to zero concentration.

Concentrated solutions of B are more acidic than would correspond to the dissociation of B to H^+ and AB^-. Kolthoff [12] and Thygesen [13] measured the conductivity of B solutions as a function of concentration. Both assumed that the high acidity is due to the single reaction

$$qB \rightleftharpoons H^+ + AB_q^-; \text{ equilibrium constant } = K_{1q}, \tag{3}$$

and neglected all other species. Kolthoff moreover assumed $q = 4$ and found values for log $K_{14} \approx -9$ at 18°C. Thygesen tested various values for q; the equilibrium constant

calculated showed the smallest variation with $q = 3$ ($\log K_{13} \approx -7.5$ at 18°C). However, Thygesen preferred to assume $q = 4$ ($\log K_{14} \approx -7.1$), with a small amount of $q = 2$; probably he was (like Kolthoff) influenced by the net formula of borax. The complexes would then be AB_4^- and AB_2^-; no attempt was made to estimate the formation constant of the latter.

Stetten [14] measured the pH of various B solutions. Assuming the main reaction (3), he found an average $q = 3.2$ and $\log K_{1,3.2} = -6.86$. From similar pH measurements, Edwards [15] concluded that the main species is AB_3^- with $\log K_{13} \approx -7.5$; deviations at the highest concentrations were ascribed to AB_6^- with $\log K_{16} \approx -6.8$.

Antikainen [16] titrated boric acid of various concentrations B in a number of salt media. From the slope of the titration curve at the isoelectric point (which gives the buffer value of a pure B solution), he calculated the apparent ionization constant of B and concluded the average value for q to be 3.87 ± 0.04. This would indicate that the main species is AB_4^-, and $\log K_{14} = -7.06$ (extrapolated to zero ionic strength).

Solubilities. From the solubility of B in Na^+AB^- solutions of increasing concentration, Auerbach [17] concluded that the complex formed contained 4 to 5, probably 5, B per Na (B per A^-, in our notation).

pH titrations. A number of pH titrations of B were carried out by Kolthoff and Bosch [18]. The data were discussed qualitatively, and the formula AB_5 was favored, in all probability because of the existence of a salt $KB_5O_8(H_2O)_4$. Carpéni and Souchay [19] carried out a series of titrations in 1 M NaCl medium. They obtained curves very much like those given in Fig. 1. These curves gave rise to a rather long discussion in French journals between Carpéni, Souchay and Byé. Whereas Carpéni and Souchay [19] originally concluded that $HB_2O_4^-(AB_2^-)$ and $B_5O_8^-(AB_5^-)$ are formed, Carpéni [3] in 1948 coined the name "isohydric point" for such a point of intersection and claimed [20,21] (1949, 1952) that it proved the existence of a single complex with $Z = 0.40$, which should be $HB_5O_9^{2-}(A_2B_5^{2-})$. To some extent, Carpéni [22] corroborated this conclusion by the preparation of a new solid borate, $K_2HB_5O_9(H_2O)_3$. On the other hand, Byé [4] has criticized Carpéni's mathematical arguments. Souchay [5] prefers to think that the solutions contain the ions $B_5O_8^-(AB_5^-)$ and $B_4O_7^{2-}(A_2B_4^{2-})$, corresponding to "well known types" of salts.

LIST OF SYMBOLS

A	total concentration of A $= -H^+$, proton deficiency $= -H$
a	"concentration of free A" $= h^{-1}$
B	total concentration of B $= B(OH)_3$
B_1	total concentration of mononuclear species, $[B]+[AB^-] = [B(OH_3)] + [B(OH)_4^-]$.
B	a normalized quantity corresponding to B (21)
E	the measured emf in mV.
E_{oa}	$= E+59.15 \log h - 59.15 \log K_w - E_j$ (eqn. 5 c)
E_{oh}	$= E+59.15 \log h - E_j$ (eqn. 5 a)
E_j	$= 17\,h - 8[OH^-]$ (eqn. 7), liquid junction emf
H	total analytical excess concentration of hydrogen ions assuming no hydrolysis; in most experiments H was negative
h	concentration of free hydrogen ions

K_a	acidity constant
K_{1q}	equilibrium constant for the formation of AB_q^- (3)
K_w	ionic product of water
K_{pq}	equilibrium constant for formation of A_pB_q from B and A (1 a)
p	number of A in complex A_pB_q
$\bar{p}_{poly}$	average number of A per polynuclear complex
q	number of B in complex A_pB_q
$\bar{q}_{poly}$	average number of B per polynuclear complex
R^{-1}	average degree of condensation of B
R_{poly}	$= (\bar{q}_{poly})^{-1}$
u	a normalized quantity corresponding to a (22)
v	a normalized quantity corresponding to b (22)
α	constant defined by (21)
Z	average number of A per B (4)
Z_1	average number of A per B in the mononuclear species

Chemical symbols are in Roman, concentrations in italic type. Concentrations and equilibrium constants will be expressed in M (mole/l) throughout (except that in Fig. 1 mM is used for B).

METHOD OF MEASUREMENT

This study of the hydrolysis of boric acid has been carried out as a number of potentiometric titrations at 25°C. In order to use concentrations instead of activities in the formulas for emf and equilibrium constants, all solutions were made 3 M in Na^+ by the addition of sodium perchlorate. For the mathematical analysis we decided to give the experimental data in the form $Z(\log h)_B$ or $\log B(\log h)_Z$.

In each titration the total boron concentration, B, was kept constant while the analytical proton deficiency $A = -H$ was varied. A hydrogen electrode was used to determine h. The quantity Z which is the average negative charge per B and may be described as the average number of hydroxyl ions bound per boric acid unit, was calculated from each point of the titration using the relationship

$$BZ = h - H - K_w h^{-1} \qquad (4)$$

where K_w is the ionic product of water in 3 M $NaClO_4$.

The hydrogen electrode was used in combination with the half-cell

SE = Ag,AgCl/0.010 M $AgClO_4$, 2.990 M $NaClO_4$/3 M $NaClO_4$.

For the cell

— Pt, H_2 (1 atm)/H^+ // SE +

the measured emf, assuming the activity factors to be constant, may be represented by the equations

$$E = E_{oh} - 59.15 \log h + E_j \qquad (5\ a)$$
$$E = E_{oa} + 59.15 \log[OH^-] + E_j \qquad (5\ b)$$
$$E = E_{oa} + 59.15 \log K_w - 59.15 \log h + E_j \qquad (5\ c)$$

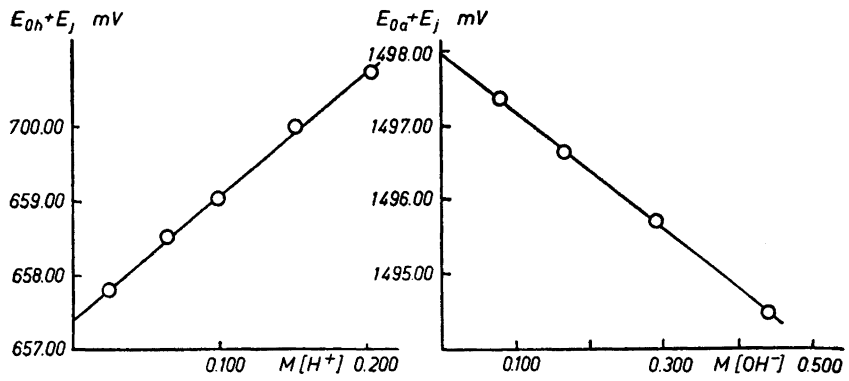


Fig. 2. $E+59.15 \log h = E_{oh}+E_j$ as a function of $[H^+] = h$, and $E-59.15 \log [OH^-] = E_{oa}+E_j$ as a function of $[OH^-]$.

where E_{oh} and E_{oa} are constants, E_j the liquid junction potential and K_w the ionic product of water in 3 M $NaClO_4$.

The ionic product of water was determined in separate titrations by adding a $NaOH+NaClO_4$ solution to a $HClO_4+NaClO_4$ solution. The sum $E+59.15 \log h$ was plotted as a function of h and $E-59.15 \log [OH^-]$ as a function of $[OH^-]$. These functions were approximately straight lines, as shown in Fig. 2, and the slope of the lines was a measure of E_j/h and $E_j/[OH^-]$. By extrapolation to $h = 0$ and $[OH^-] = 0$ the constants E_{oh} and E_{oa} were obtained and the ionic product of water in 3 M $NaClO_4$ was determined as

$$-\log K_w = \frac{E_{oa}-E_{oh}}{59.15} = 14.22 \pm 0.02 \qquad (6)$$

Ågren [23] has obtained $\log K_w = -14.15 \pm 0.10$ in 3 M sodium perchlorate.

From the slopes E_j/h and $E_j/[OH^-]$ in the determination of K_w, we found for *the liquid junction potential* the relation

$$E_j = 17\ h - 8[OH^-] \qquad (7)$$

where h and $[OH^-]$ are in M, and E_j in mV. For acid solutions this agrees well with the relation $E_j = +18\ h$ found by Biedermann and Sillén [24].

The *constants* E_{oh} *and* E_{oa} were, moreover, determined in most borate titrations; E_{oh} was obtained from points in the acid range where boron is practically not hydrolysed ($Z \approx 0$), and E_{oa} from the points with the highest values of $-\log h$ ($Z \approx 1$).

We could then calculate $-\log h$ for each point of the titration in two different ways from E, using either E_{oh} or E_{oa}.

$$-\log h = \frac{E-E_{oh}-17h+8[OH^-]}{59.15} \qquad (8\ a)$$

$$-\log h = \frac{E-(E_{oa}+59.15 \log K_w)-17h+8[OH^-]}{59.15} \qquad (8\ b)$$

These two values of —log h were not identical. The difference was very small at low total concentrations B but appreciable at higher B.

Since both h and $[OH^-]$ in (4) are usually negligible in comparison with $-H$ (except for the highest values of —log h), the variation of the E_0 does not significantly affect the values of Z but only —log h.

The variation of E_{oh} and E_{oa} with the boron concentration

In different titrations with the same B, E_{oh} was always the same within ± 1 mV, but in titrations with different B, E_{oh} decreased with increasing boric acid concentration.

In order to investigate this variation we made a separate titration where B was varied and H was constant and positive. The relationship between E_{oh} and B (Table 1) proved to be approximately linear

$$E_{oh} = \text{const} - 8\,B \qquad (9\text{ a})$$

if E_{oh} is expressed in mV and B in M.

This deviation is probably due to a variation of the activity coefficients with the ionic medium. If some more acidic species like $H_4BO_3^+$ were formed, this would cause a trend in the opposite direction.

In titrations with the same B, E_{oa} was the same within ± 1 mV but varied in titrations with different B. In a separate titration, where $[OH^-]$ was constant ($Z \approx 1.00$) and B was varied, we found the relationship between E_{oa} and B to be approximately linear (Table 1)

$$E_{oa} = \text{const} + 5\,B \qquad (9\text{ b})$$

if E_{oa} is expressed in mV and B in M. This deviation must also be due to a variation of the activity factors. The formation of species like $H_3BO_4^{2-}$ would cause a deviation in the other direction.

Table 1. The variation of E_{oa} and E_{oh} with B.

The variation of E_{oh} at $[H^+] = 0.0260$ M		The variation of E_{oa} at $[OH^-] = 0.0500$ M	
B M	E_{oh} mV	B M	E_{oa} mV
0.0000	657.81	0.0000	1498.44
0.0545	657.36	0.0545	1498.63
0.1000	657.03	0.1000	1498.88
0.1384	656.72	0.1384	1499.10
0.2000	656.22	0.2000	1499.45
0.1471	655.84	0.2470	1499.70
0.2842	655.52		
0.4000	654.69	0.4000	1500.03
0.5000	653.83		
0.6000	653.20	0.6000	1501.34

EXPERIMENTAL DETAILS

Reagents and analysis

Sodium perchlorate was prepared by carefully neutralizing recrystallized Na_2CO_3 (p.a.) with perchloric acid (p.a.). The sodium perchlorate solution was concentrated until a thin layer of the salt formed on the surface, filtered while hot, and the filtrate stirred vigorously while cooling. The salt crystallized well with one molecule of water. The salt was recrystallized twice, after which no Cl^-, ClO_3^- or silica could be detected, and was then found to be free from acid impurities. The $NaClO_4$ solutions were analysed by evaporating a known weight of solution at 120°C and drying at the same temperature until a constant weight was attained.

Perchloric acid. The ordinary p.a. product was used, and was standardized against $KHCO_3$ and standard NaOH. The determinations with different standard substances agreed within ± 0.1 %.

Sodium hydroxide. A 50 % solution was prepared from the commercial p.a. material, filtered through a G4 Jena glass filter, and stored in a polyethylene bottle. Dilute solutions were prepared from de-aerated water and 50 % stock solution. The alkali solutions were standardized against $HClO_4$ which had been standardized in turn against $KHCO_3$. Hydrazine sulfate and acid potassium iodate have also been used for the standardizations giving values in good agreement (± 0.1 %) with the $HClO_4$ value.

The carbonate ion concentration in the NaOH solutions used was about 0.1 % of the NaOH concentration, as estimated from the difference between the methyl red and the phenolphthalein points in a titration.

Boric acid. The ordinary crystallized p.a. product was used. A stock solution was prepared by weighing a known amount of boric acid and diluting with water to a certain volume. The concentration was checked by adding mannitol and titrating with standard alkali using α-naphtholphthalein as indicator.

Silver perchlorate solutions were prepared by adding a slight excess of Ag_2O to a boiling $HClO_4$ solution. The excess of Ag_2O was filtered off, and the Ag^+ content in the solution was determined by Volhard's method using a silver wire as a standard.

Titration vessel solution (S_0). Measured quantities of boric acid, perchloric acid, and sodium perchlorate were added to a volumetric flask to give the concentrations wanted. After waiting until the temperature had become equalized, the flask was carefully filled to the mark with de-aerated water.

Buret solution (T). The procedure was the same as described for the titration vessel solution, S_0, except that the solutions were mixed in a CO_2-free N_2 atmosphere.

Apparatus

Since the work was carried out with alkaline solutions, all glassware may be appreciably attacked by alkali. To avoid this, polythene or alkali resistant glass vessels may be used. Lagerström [25] pointed out in his study of silicate solutions that polythene has so many disadvantages that the use of Jena-Geräte glass was to be preferred. He estimated that an amount of silica corresponding to 0.03 mM is dissolved from the glass vessel during a titration similar to ours (to pH $\approx$ 12). Since this is negligible, Jena-Geräte glass has been used all through this work.

The electrode vessel and the salt bridge were of the "Wilhelm" type described in previous papers [26] from this institute.

Commercially available hydrogen was purified by passing it through a) a column of activated copper at around 180°C to remove traces of oxygen, b) a wash bottle containing 10 % H_2SO_4 to remove alkaline impurities, and c) a wash bottle with 10 % NaOH to remove acidic impurities. Before entering the titration vessel, the gas was saturated with water by passage through two wash bottles containing the ionic medium, 3.0 M $NaClO_4$.

The *hydrogen electrode* was prepared according to Bates [27] (p. 166). Immediately after the preparation, the electrode was electrolysed as the cathode in 0.1 M H_2SO_4 for 20 min. An even distribution of H_2 bubbles on the electrode surface was good evidence of a completely active surface. Electrodes with an uneven distribution of bubbles were immediately taken out of service. A new hydrogen electrode was prepared for each titration,

and the electrode gave a steady potential after 10 to 20 min, regardless of the velocity of the hydrogen stream.

The *silver-silver chloride electrode* was prepared by electro-depositing Ag on a Pt foil and afterwards electrolysing the silver electrode in dilute HCl.

The emf measurements were made with a Jensen compensator (type 10A) and a Multiflex galvanometer. The compensator could be read to a hundredth of a mV.

Titration procedure

The titrations were carried out at 25.0±0.1°C with the cell and the titration vessel immersed in an oil thermostat and the whole equipment in a thermostated room at 25.0±0.5°C.

For each titration two solutions were prepared: S_o (in the titration vessel) and T (in the buret) ,with the following analytical composition.

Solutions	[Na+] M	B M	H M	[ClO_4^-] M
Titration vessel (S_o)	3	B	C_1(C_1M H^+)	$3+C_1$
Buret (T)	3	B	$-C_2$(C_2M OH^-)	$3-C_2$

The manner of titration is best described by an example, and Table 2 gives a representative part of a titration with B = 0.100 M.

In the titration shown in Table 2, the analytical hydrogen ion concentration was checked with aid of the points obtained in the unhydrolysed acid range and in the alkaline part with Z = 1. The end-point was found by Gran's method[28] of extrapolation. The two straight lines, corresponding to free H^+ and free OH^-, intersect in two points on the volume axis. The total hydrogen ion concentration obtained from the intersection of the H^+ line agreed very well with that calculated from the analytical concentrations of solutions S_o and T. The distance between the intersections of the H^+ and OH^- lines on the volume axis corresponds to the amount of A, necessary to give the species AB^-.

In some cases the hydrolysed solution was back-titrated with acid; the points $Z(\log h)$ always fell on the same curve as the points obtained by adding alkali, indicating that the equilibria are completely reversible. (Half-filled symbols in Fig. 1.)

TREATMENT OF THE DATA AND RESULTS

Using the eqns. (4), (8 a) and (8 b), the $Z(\log h)_B$ curves have been obtained from the emf measurements. The data are shown in Table 3 and plotted in Fig. 1.

For values of $B \leqq 0.025$ essentially the same $Z(\log h)$ curve was obtained, which indicates that for these low boron concentrations only the mononuclear species B = $B(OH)_3$ and AB^- = $B(OH)_4^-$ need be considered. Moreover, the curve has the shape characteristic of equilibria with only two mononuclear species.

Table 2. A titration with $B = 0.100$ M

S_0 : $H_3BO_3 = 0.100$ M, $HClO_4 = 0.0434$ M, $NaClO_4 = 3.000$ M, 50.0 ml
T_1 : $H_3BO_3 = 0.100$ M, NaOH = 0.1083 M, $NaClO_4 = 2.892$ M, v_1 ml
T_2 : $H_3BO_3 = 0.100$ M, NaOH = 0.3777 M, $NaClO_4 = 2.622$ M, v_2 ml

Atmospheric pressure = 772.0 mm Hg. The vapor pressure of pure water at 25.0°C = 23.7 torr. This value has been used instead of that valid for 3 M $NaClO_4$. The correction 29.58 log p_{H_2} is +0.20 mV. E_{oh} from the first acid points (8 a) = 658.20 mV. E_{oa} = 1500.00 mV at $Z \approx 1.0$; E_{oh} from E_{oa} and K_w (8 b) = 658.89 mV.

v_1 ml	v_2 ml	Total volume	E mV	E_{corr} mV	−log h calc with E_{oh}	−log h calc with $E_{oa} + 59.15 \log K_w$	$K_w h^{-1} \cdot 10^{-3}$ M	$H \cdot 10^{-3}$ M	$\frac{h - H - K_w h^{-1}}{B} = Z$
0.00		50.00	739.00	739.20				43.40	
3.52		53.52	745.54	745.74				33.42	
7.13		57.13	753.66	753.66				24.47	
10.56		60.56	762.85	763.05				16.95	
16.08		66.08	788.10	788.30				6 48	
20.04		70.04	1011.07	1011.27					
	1.28	71.32	1107.00	1107.20	7.590	7.580		− 6.78	0.068
	2.28	72.32	1125.29	1125.49	7.899	7.890		−11.90	0.119
	3.27	73.31	1139.00	1139.20	8.131	8.121		−16.84	0.168
	5.19	75.24	1154.04	1154.24	8.440	8.430		−26.05	0.261
	7.52	77.56	1174.10	1174.30	8.724	8.715		−36.62	0.366
	9.32	79.36	1185.09	1185.29	8.910	8.900		−44.35	0.444
	12.28	82.32	1201.05	1201.25	9.179	9.170		−56.34	0.563
	13.92	83.96	1209.20	1209.40	9.317	9.308	0.01	−62.62	0.626
	15.33	85.37	1216.21	1216.41	9.436	9.426	0.02	−67.82	0.678
	16.84	86.88	1223.75	1223.95	9.563	9.554	0.02	−73.20	0.732
	18.10	88.14	1230.38	1230.58	9.675	9.666	0.03	−77.56	0.775
	20.04	90.08	1241.66	1241.86	9.866	9.857	0.04	−84.02	0.838
	21.32	91.36	1250.71	1250.91	10.019	10.009	0.06	−88.14	0.881
	23.39	93.43	1271.74	1271.94	10.374	10.365	0.14	−94.55	0.944
	24.54	94.58	1295.88	1296.08	10.782	10.773	0.37	−98.00	0.973
	26.22	96.26	1352.68	1352.88				−102.88	
	29.38	99.42	1385.48	1385.68				−111.61	
	34.75	104.79	1405.00	1405.20				−125.25	
	40.08	110.12	1414.98	1415.18				−137.47	
	45.21	115.25	1421.35	1421.55				−148.16	
	49.77	119.81	1425.54	1425.74				−156.90	
	60.12	130.16	1432.25	1432.45				−174.46	

For concentrations >0.025 M, different $Z(\log h)$ curves were obtained for different values of B. This shows that besides the mononuclear complexes there must also be polynuclear complexes.

The first step in our calculation has been an approximate determination of the average number of boron atoms and the average charge of the polynuclear complexes, $\bar{q}_{poly}$ and $\bar{p}_{poly}$.

With aid of the values $\bar{q}_{poly}$ and $\bar{p}_{poly}$, we have then tested various hypotheses and determined the equilibrium constant for the most probable complexes.

Table 3. Experimental data. The $-\log h$ values calculated with ($E_{oa} + 59.15 \log K_w$) are omitted in the table for $B = 0.010$, 0.020, 0.025 and 0.050 M since these values are approximately the same as calculated with E_{oh}.

$B = 0.010$ M		$B = 0.020$ M		$B = 0.025$ M		$B = 0.050$ M		$B = 0.100$ M		
Z	$-\log h$ calc. with E_{oh}	Z	$-\log h$ calc. with E_{oh}	Z	$-\log h$ calc. with E_{oh}	Z	$-\log h$ calc. with E_{oh}	Z	$-\log h$ calc. with E_{oh}	$-\log h$ calc. with $E_{oa} + 59.15 \log K_w$
0.010	7.137	0.052	7.757	0.033	7.510	0.006	6.538	0.024	7.090	
0.062	7.794	0.107	8.065	0.116	8.073	0.047	7.573	0.068	7.590	7.580
0.174	8.293	0.200	8.367	0.202	8.361	0.068	7.717	0.108	7.833	
0.265	8.541	0.302	8.608	0.287	8.572	0.105	7.938	0.119	7.899	7.890
0.530	9.052	0.398	8.792	0.459	8.843	0.105	7.960	0.131	7.939	
0.609	9.194	0.513	9.996	0.488	8.874	0.182	8.293	0.168	8.131	8.121
0.705	9.385	0.803	9.587	0.583	9.141	0.191	8.269	0.202	8.232	
0.752	9.488	0.986	10.657	0.604	9.160	0.217	8.372	0.261	8.440	8.430
0.847	9.751			0.700	9.354	0.298	8.558	0.300	8.530	
0.896	9.946			0.749	9.490	0.345	8.680	0.366	8.724	8.715
0.944	10.238			0.911	9.973	0.371	8.719	0.444	8.910	8.900
0.985	10.769			0.925	10.091	0.461	8.902	0.563	9.179	9.170
0.993	10.911			0.965	10.441	0.459	8.920	0.607	9.254	
0.999	11.241			0.984	10.801	0.586	9.161	0.626	9.317	9.308
1.002	11.416			1.001	11.317	0.611	9.203	0.678	9.436	9.426
						0.690	9.387	0.732	9.563	9.554
						0.709	9.445	0.775	9.675	9.666
						0.812	9.683	0.838	9.866	9.857
						0.869	9.864	0.881	10.019	10.009
						0.917	10.081	0.897	10.073	
						0.972	10.583	0.944	10.374	10.365
						0.990	11.433	0.973	10.782	10.773
						0.991	11.835			
						0.999	12.031			

Table 3. Continued.

B = 0.200 M			B = 0.400 M			B = 0.600 M		
Z	$-\log h$ calc. with E_{oh}	$-\log h$ calc. with $E_{oa} + 59.15 \log K_w$	Z	$-\log h$ calc. with E_{oh}	$-\log h$ calc. with $E_{oa} + 59.15 \log K_w$	Z	$-\log h$ calc. with E_{oh}	$-\log h$ calc. with $E_{oa} + 59.15 \log K_w$
0.040	6.927	6.894	0.030	6.192		0.032	5.820	5.700
0.050	7.085	7.050	0.035	6.298	6.222	0.053	6.139	6.020
0.052	7.104		0.064	6.691		0 090	6.540	6.420
0.099	7.484	7.451	0.066	6.680	6.605	0.102	6.712	6.592
0.100	7.506		0.102	7.051	6.975	0.148	7.162	7.042
0.130	7.723	7.688	0.119	7.173	7.097	0.177	7.396	7.276
0.148	7.812		0.136	7.337		0.240	7.891	7.771
0.173	7.913	7.880	0.149	7.429	7.353	0.266	8.071	7.952
0.186	8.020	7.984	0.178	7.619	7.542	0.283	8.185	8.065
0.237	8.231		0.201	7.788	7.712	0.348	8.573	8.453
0.241	8.223	8.190	0.219	7.921		0.369	8.684	8.564
0.263	8.356	8.320	0.222	7.904	7.828	0.405	8.870	8.751
0.304	8.457	8.425	0.281	8.259	8.183	0.431	8.992	8.872
0.327	8.572		0.304	8.384		0.466	9.159	9.040
0.357	8.695	8.661	0.333	8.505	8.429	0.536	9.452	9.332
0.374	8.700	8.667	0.374	8.700	8.624	0.565	9.572	9.453
0.411	8.837		0.388	8.774		0.631	9.817	9.697
0.427	8.861	8.828	0.415	8.879	8.803	0.653	9.906	9.786
0.482	9.022	8.989	0.471	9.093	9.017	0.715	10.119	9.999
0.511	9.134		0.485	9.152		0.733	10.187	10.067
0.550	9.209	9.177	0.545	9.365	9.288	0.793	10.389	10.269
0.557	9.288	9.253	0.567	9.443		0.803	10.444	10.324
0.603	9.351	9.319	0.597	9.543	9.467	0.862	10.648	10.528
0.626	9.438		0.642	9.691		0.872	10.698	10.578
0.661	9.563	9.528	0.655	9.720	9.644	0.933	10.993	10.874
0.661	9.501	9.468	0.711	9.866	9.790			
0.728	9.726		0.717	9.931				
0.730	9.686	9.653	0.745	10.010	9.933			
0.753	9.811	9.776	0.787	10.158	10.082			
0.849	10.053	10.020	0.799	10.192				
0.852	10.117	10.082	0.826	10.280	10.204			
0.860	10.123		0.865	10.434				
0.941	10.532		0.868	10.448	10.372			
0.947	10.576	10.541	0.901	10.573	10.497			
0.989	11.301		0.929	10.740				
			0.983	10.804	10.728			
			0.990	11.583				

The average charge and the average number of boron atoms in the polynuclear complexes.

It has been possible to obtain the average composition of the polynuclear complexes from the experimental $Z(\log h)_B$ curves without any special assumptions about the complexes formed using the formulas given by Sillén [29], which give the quantities B_1 and R.

$$\log B_1 = \log B - \int_{-11.60}^{\log h} \left[(Z_1 - Z) - \left(\frac{\partial Z}{\partial \log B} \right)_h \right] \mathrm{d} \log h \text{ at constant } B \quad (10)$$

$$R = 1 - \int_{-11.60}^{\log h} \left(\frac{\partial Z}{\partial \log B} \right)_h \mathrm{d} \log h \text{ at constant } B \quad (11)$$

where B is the total concentration of boron, B_1 the boron concentration in the mononuclear species, R the reciprocal of the average degree of condensation of B and Z_1 = the average number of A per B in the mononuclear species.

The average charge of the polynuclear complexes $\bar{p}_{\mathrm{poly}}$, has been calculated from the equation

$$\bar{p}_{\mathrm{poly}} = \frac{Z_{\mathrm{poly}}}{R_{\mathrm{poly}}} = \frac{BZ - B_1 Z_1}{BR - B_1} \quad (12)$$

and the average number of boron, $\bar{q}_{\mathrm{poly}}$, from

$$\bar{q}_{\mathrm{poly}} = \frac{1}{R_{\mathrm{poly}}} = \frac{B - B_1}{BR - B_1} \quad (13)$$

where BZ = the number of moles A that are bound to B per liter, $B_1 Z_1$ = the number of moles A that are bound to B in the mononuclear species, and BR = the sum of the molar concentration of B and of all complexes containing boron.

Previous solution data, especially the freezing-point data [9], make it appear very likely that the species at the highest and lowest pH are mononuclear, *i.e.* H_3BO_3 (B) at the acid, and $B(OH)_4^-$ (AB) at the alkaline end. In the above formulas borate is assumed to be mononuclear with $Z = 1.00$ for $-\log h \geqq 11.60$.

The integration has been carried out numerically from the experimental $Z(\log h)$ curves at given value of B. As is clear from the above formulas, the determination of R is a step in calculating B_1. Keeping h constant, the slope $(\partial Z/\partial \log B)_h$ from any experimental value for B was assumed to be the average of the difference quotients $(\Delta Z/\Delta \log B)$ for the two neighboring intervals.

An example of the various steps in the calculation is given in Table 4. As follows from (10) and (11), the values of B_1 and R have a minimum at the intersection point. B_1 approaches the value B, and R approaches 1 at the highest values of h when $Z \approx 0$; this fact corroborates our assumption that boric acid and borate ion are chiefly mononuclear at $Z = 0$ and $Z = 1.00$. In Table 4, natural logarithms were used when (10) and (11) were applied.

Table 5 gives $\bar{p}_{\mathrm{poly}}$ and $\bar{q}_{\mathrm{poly}}$ for $B = 0.100$, 0.200, and 0.400 M at various $-\log h$. The data in this table indicate that the most probable complexes in the solution contain three boron and have the charge one or two; however, the

Table 4. Analysis of the Z (log h) curve for $B = 0.100$ M

$-\log h$	Z_1-Z	$-\left(\frac{\partial Z}{\partial \ln B}\right)_a$	$\Delta \ln a$	$\Delta \ln B/B_1$	$\ln B/B_1$	$\ln B_1$	$\log B_1$	B_1	Δ (1—R)	R	BR	q_{poly}	p_{poly}
11.80	0.000								0.001	1.000			
			0.461	0.001									
11.60	0.002	0.002			0.001	—2.304	—1.000	99.9	0.001	0.999	99.9		
			0.461	0.003									
11.40	0.003	0.004			0.004	—2.307	—1.002	99.6	0.002	0.998	99.8	2.0	0.5
			0.461	0.004									
11.20	0.006	0.006			0.008	—2.311	—1.004	99.2	0.002	0.996	99.6	2.0	0.5
			0.461	0.005									
11.00	0.007	0.004			0.013	—2.316	—1.006	98.7	0.003	0.994	99.4	1.9	0.6
			0.461	0.007									
10.80	0.010	0.009			0.020	—2.323	—1.009	98.0	0.006	0.991	99.1	1.8	0.9
			0.461	0.011									
10.60	0.013	0.016			0.031	—2.334	—1.014	97.0	0.010	0.985	98.5	2.0	1.1
			0.461	0.017									
10.40	0.017	0.027			0.048	—2.351	—1.021	95.3	0.016	0.975	97.5	2.1	1.3
			0.461	0.025									
10.20	0.022	0.041			0.073	—2.376	—1.032	93.0	0.023	0.959	95.9	2.4	1.5
			0.461	0.035									
10.00	0.032	0.057			0.108	—2.411	—1.047	89.8	0.026	0.936	93.6	2.7	1.6
			0.461	0.042									
9.80	0.045	0.055			0.150	—2.453	—1.065	86.1	0.027	0.910	91.0	2.8	1.5
			0.461	0.049									
9.60	0.052	0.062			0.199	—2.502	—1.086	82.0	0.028	0.883	88.3	2.9	1.5
			0.461	0.053									
9.40	0.055	0.061			0.252	—2.555	—1.109	77.7	0.024	0.855	85.5	2.9	1.4
			0.461	0.048									
9.20	0.048	0.042			0.300	—2.603	—1.130	74.1	0.014	0.831	83.1	2.9	1.2
			0.461	0.032									
9.00	0.027	0.020			0.332	—2.635	—1.144	71.8	0.005	0.817	81.7	2.9	1.2
			0.461	0.011									
8.80	±0.000	±0.000			0.343	—2.646	—1.149	71.0	—0.006	0.812	81.2	2.8	1.1
			0.461	—0.011									
8.60	—0.024	—0.024			0.332	—2.635	—1.144	71.8	—0.015	0.818	81.8	2.8	1.1
			0.461	—0.030									
8.40	—0.040	—0.041			0.302	—2.605	—1.131	74.0	0.021	0.833	83.8	2.8	1.0
			0.461	—0.042									
8.20	—0.047	—0.052			0.260	—2.563	—1.113	77.1	—0.024	0.854	85.4	2.8	1.0
			0.461	—0.046									
8.00	—0.048	—0.054			0.214	—2.517	—1.093	80.7	—0.024	8.878	87.8	2.5	0.9
			0.461	—0.045									
7.80	—0.044	—0.049			0.169	—2.472	—1.073	84.5	—0.021	0.902	90.2	2.7	0.8
			0.461	—0.039									
7.60	—0.035	—0.043			0.130	—2.433	—1.057	87.8	—0.019	0.923	92.3	2.7	1.1
			0.461	—0.033									
7.40	—0.026	—0.038			0.097	—2.400	—1.042	90.8	—0.016	0.942	94.2	2.7	0.9
			0.461	—0.029									
7.20	—0.018	—0.031			0.068	—2.371	—1.030	93.4	—0.013	0.958	95.8	2.8	0.8
			0.461	—0.020									
7.00	—0.013	—0.024			0.040	—2.343	—1.017	96.1		0.971	97.1	3.9	1.3

Table 5. The values of $\bar{q}_{poly}$ and $\bar{p}_{poly}$

$-\log h$	0.100 M $-\log h$ calc. with E_{oh}		0.100 M $-\log h$ calc. with $E_{oa}+59.15 \log K_w$		0.200 M $-\log h$ calc. with E_{oh}		0.200 M $-\log h$ calc. with $E_{oa}+59.15 \log K_w$		0.400 M $-\log h$ calc. with E_{oh}		0.400 M $-\log h$ calc. with $E_{oa}+59.15 \log K_w$	
	$\bar{q}_{poly}$	$\bar{p}_{poly}$	$\bar{q}_{poly}$	$\bar{p}_{poly}$	$\bar{q}_{poly}$	$\bar{p}_{poly}$	$\bar{q}_{poly}$	$\bar{p}_{poly}$	$\bar{q}_{poly}$	$\bar{p}_{poly}$	$\bar{q}_{poly}$	$\bar{p}_{poly}$
11.60	1.0				1.7				2.0			
11.40	2.0	0.5		0.5	1.9	0.1	2.3		3.0		2.0	
11.20	2.0	0.5	2.0	0.8	2.1	0.9	2.5	0.5	2.2	0.7	1.8	
11.00	1.9	0.6	2.3	0.8	2.1	1.1	2.3	0.8	2.3	1.0	1.9	0.4
10.80	1.8	0.9	2.1	0.8	2.2	1.4	2.2	1.1	2.5	1.4	2.0	0.9
10.60	2.0	1.1	2.1	0.9	3.1	1.6	2.2	1.1	2.8	2.5	2.1	1.0
10.40	2.1	1.3	2.9	1.2	3.0	1.5	2.4	1.3	2.8	1.5	2.8	1.0
10.20	2.4	1.5	2.3	1.5	2.7	1.4	2.5	1.3	3.0	1.5	2.7	1.1
10.00	2.7	1.6	2.6	1.5	2.8	1.4	2.5	1.2	3.1	1.5	2.3	1.0
9.80	2.8	1.5	2.8	1.5	2.9	1.3	2.4	1.2	3.1	1.5	2.7	1.4
9.60	2.9	1.5	2.9	1.5	2.9	1.4	2.4	1.1	3.2	1.5	2.7	1.2
9.40	2.9	1.4	3.0	1.5	1.9	1.4	2.5	1.1	3.3	1.5	2.7	1.2
9.20	2.9	1.2	3.0	1.4	3.0	1.3	2.5	1.0	3.6	1.4	2.6	1.2
9.00	2.9	1.2	3.1	1.3	3.1	1.3	2.5	1.0	3.7	1.6	2.6	1.1
8.80	2.8	1.1	3.0	1.2	3.1	1.2	2.4	1.0	3.8	1.5	2.6	1.1
8.60	2.8	1.1	3.0	1.1	3.1	1.2	2.4	0.9	3.8	1.4	2.5	1.1
8.40	2.8	1.0	2.9	1.0	3.1	1.1	2.3	0.9	3.8	1.3	2.6	1.1
8.20	2.8	1.0	2.9	1.0	3.1	1.1	2.2	0.8	3.8	1.3	2.6	1.1
8.00	2.5	0.9	2.9	1.0	3.1	1.1	2.1	0.8	3.8	1.2	2.6	1.2
7.80	2.7	0.8	2.8	1.0	3.0	1.0	2.1	0.8	3.8	1.4	2.6	1.2
7.60	2.7	1.1	3.0	1.0	3.1	0.9	2.3	0.8	3.8	1.2	2.8	1.4
7.40	2.7	0.9	2.9	1.0	3.1	0.9	2.5	1.2	4.0	1.4	3.1	1.9
7.20	2.8	0.8	2.8	0.9	3.0	0.8	1.4	1.0	4.2	1.3		
7.00	3.9	1.3	2.6	1.0	3.0	0.8	1.1	1.1	4.3	1.1		

solution may also contain species with two or four boron atoms. In order to see which complexes occur, we have in the following tested various hypotheses with the aid of normalized graphs [30] $\boldsymbol{B}(\log u)_Z$.

The method of normalized $\boldsymbol{B}(\log u)_Z$ graphs [30].

It may be instructive to illustrate by an example the use of normalized graphs in the analysis of the experimental data. If we assume the four species B, AB, AB_3 and A_2B_3 — the combination that we finally have found the most likely one — the law of mass action gives the following equations:

$$[AB] = K_{11} b h^{-1} \quad (14)$$
$$[AB_3] = K_{13} b^3 h^{-1} \quad (15)$$
$$[A_2B_3] = K_{23} b^3 h^{-2} \quad (16)$$

where b is the concentration of free B

$$B = [B] + [AB] + 3[AB_3] + 3[A_2B_3] = b + K_{11} b h^{-1} + 3K_{13} b^3 h^{-1} + + 3K_{23} b^3 h^{-2} \quad (17)$$

$$BZ = [AB] + [AB_3] + 2[A_2B_3] = K_{11} b h^{-1} + K_{13} b^3 h^{-1} + 2\ K_{23} b^3 h^{-2} \quad (18)$$

We wish to transform these expressions to the normalized form:

$$\boldsymbol{B} = v(1 + u) + 3v^3 u(1 + \alpha\ u) \quad (19)$$
$$\boldsymbol{BZ} = uv + v^3 u(1 + 2\alpha\ u) \quad (20)$$

where $$\alpha = \frac{K_{23}}{K_{11} K_{13}} \quad (21)$$

This is achieved by the substitutions:

$$u = K_{11} h^{-1};\ \ v = b(K_{13} K_{11}^{-1})^{\frac{1}{2}};\ \ \boldsymbol{B} = B(K_{13} K_{11}^{-1})^{\frac{1}{2}} \quad (22)$$

From the normalized eqns. (19) and (20) we can get

$$2 \log \boldsymbol{B} = 2 \log [1 - 2u(1 - \alpha) - \alpha u^2] + \log (2 + Zu - u) - 3 \log [(1 + 2\alpha u) - -3Z\ (1 + \alpha u)] - \log u \quad (23)$$

If the constant α is known one may calculate $\boldsymbol{B}$ as a function of Z and $\log u$.

Graphs $\log \boldsymbol{B}\ (\log u)_Z$ were calculated for some values of α and compared with the experimental graph. From the graph which fitted best with the experimental data we obtained the constants K_{11} and K_{13} as differences along the coordinate axes.

$$\log \boldsymbol{B} - \log B = \tfrac{1}{2} (\log K_{13} - \log K_{11}) \quad (24)$$
$$\log u - \log h = \log K_{11} \quad (25)$$

and the constant K_{23} from the value of α giving the best fit.

Survey of the projection map

The normalized $\log \boldsymbol{B}\ (\log u)_Z$ graph calculated from (22) with $\alpha = 0.25$ is given in Fig. 3c, and the various complexes have been put down in the range where they dominate.

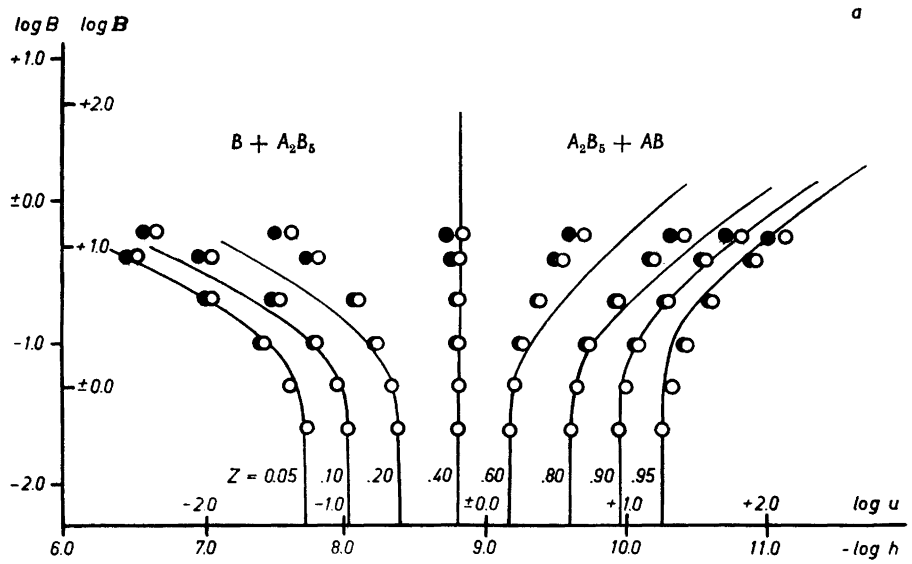


Fig. 3. "Surface-fitting" of the experimental data for the hydrolysis of boric acid and borate ion plotted as log B(log h)$_Z$ (open circles, experimental $-\log h$ calculated from E_{oh} and filled circles $-\log h$ calculated from $E_{ca} + 59.15 \log K_w$). The curves give the projection map log B (log u)$_Z$ in the best fit, calculated for the following species:

a) B, AB and A_2B_5 (the hypothesis of Carpéni [22])

$AB + B$. In the lower part of the graph the value of (log u)$_Z$ does not change with B, and the vertical lines correspond to a system with two mononuclear species AB and B. The u values for different Z are given by

$$u \approx \frac{Z}{1-Z} \tag{26}$$

as may be derived from (19) and (20), with $v \ll 1$.

$B + AB_3$ From the eqns. (19) and (20) for $u \ll 1$ and $\alpha u \ll 1$ we get

$$B = v + 3v^3u; \quad B\bar{Z} = v^3u \tag{27}$$

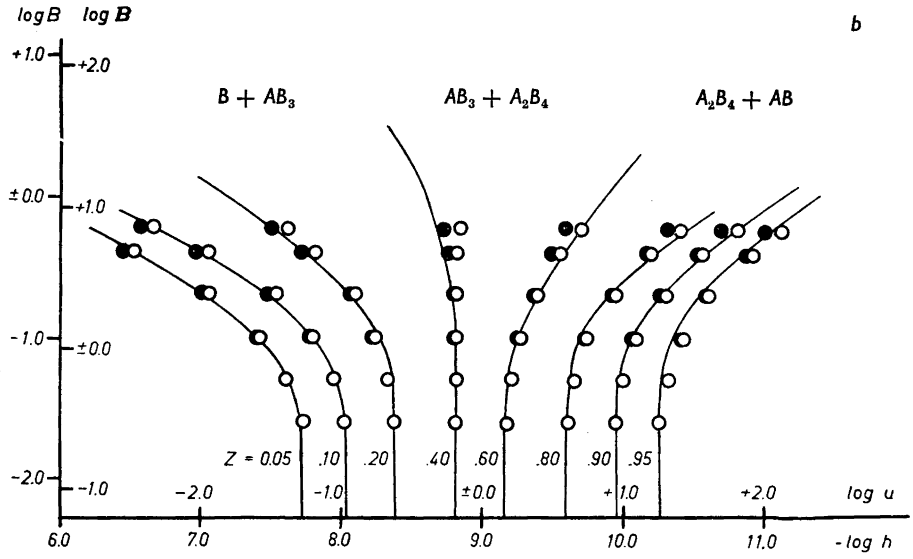
which means that practically only the complexes B and AB_3 are formed and

$$\log B = \tfrac{1}{2} \log \frac{Z}{(1-3Z)} - \tfrac{1}{2} \log u \tag{28}$$

Thus log B (log u)$_Z$ is the family of straight lines with the slope $-\frac{1}{2}$ in the left upper part of the graph.

$A_2B_3 + AB$. In a similar way the rectilinear curves to the right in the graph correspond to a range with practically only the complexes AB and A_2B_3, and log B(log$u$)$_Z$ is given by

$$\log B = \tfrac{1}{2} \log \frac{Z-1}{(3Z-2)^3} - \tfrac{1}{2} \log \alpha + \tfrac{1}{2} \log u \tag{29}$$



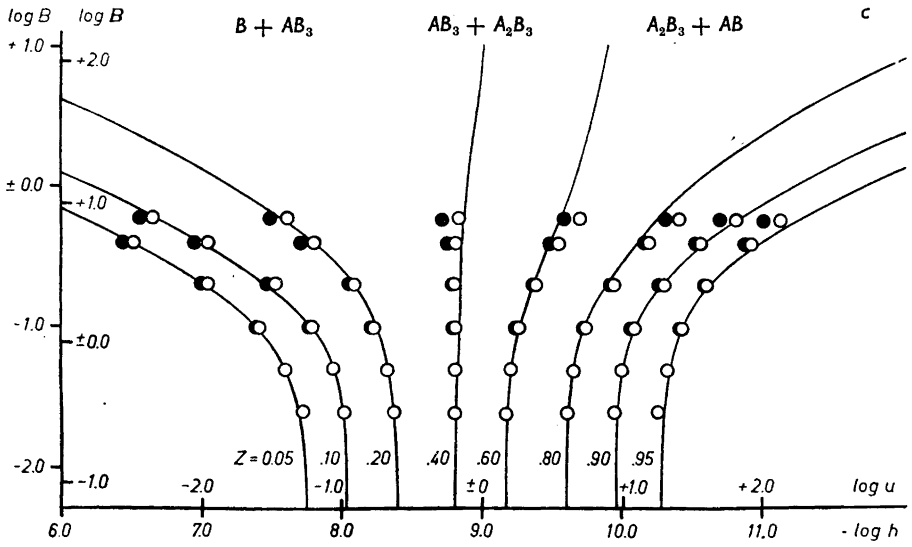


Fig. 3. (Continued) -

b) B, AB, AB_3 and A_2B_4 assuming $\frac{K_{24}}{K_{11} \cdot K_{13}} = 1.25$

c) B, AB, AB_3 and A_2B_3 assuming $\frac{K_{23}}{K_{11} \cdot K_{13}} = 0.25$

$AB_3+A_2B_3$. The upper almost vertical lines in the graph correspond to the predominance of the two polynuclear complexes AB_3 and A_2B_3, and the log u value for different Z is given by

$$\log u = \log (1-3Z) - \log \alpha - \log (3Z-2) \qquad (30)$$

Hypotheses tested

We have tried to explain the experimental data with as few polynuclear complexes as possible. The value of $\bar{p}_{poly}$ and $\bar{q}_{poly}$ indicates that the number of boron atoms does not rise above four and the charge not above minus two in any complex.

If only *one polynuclear complex* exists, the Z value ≈ 0.40 of the intersection point of the curves would correspond to the formula of that complex. The only possible formula is then A_2B_5 which has been suggested by Carpéni [20,21]. Although the value of $\bar{q}_{poly}$ indicated that the complex A_2B_5 was not to be expected, normalized graphs were constructed with the function B, assuming B, AB and A_2B_5 to be the species present. For all values of Z the agreement was so poor (Fig 3a) that an explanation with only the complex A_2B_5 can be ruled out.

Next it was assumed that *B, AB and only two polynuclear* complexes exist and that these contain two, three or four boron and the charge minus one or two. All such combinations that can give an intersection at $Z \approx 0.40$ are as follows:

$B + AB_3 + A B_2 + AB$	$(1_3 1_2)$
$B + AB_3 + A_2B_4 + AB$	$(1_3 2_4)$
$B + AB_3 + A_2B_3 + AB$	$(1_3 2_3)$
$B + AB_3 + A_2B_2 + AB$	$(1_3 2_2)$
$B + AB_4 + A B_2 + AB$	$(1_4 1_2)$
$B + AB_4 + A_2B_4 + AB$	$(1_4 2_4)$
$B + AB_4 + A_2B_3 + AB$	$(1_4 2_3)$
$B + AB_4 + A_2B_2 + AB$	$(1_4 2_2)$

Normalized graphs log B (log $u)_Z$ were constructed for the combinations $(1_3 1_2)$, $(1_3 2_4)$, $(1_3 2_3)$ and $(1_4 2_4)$.

The calculated graph with *the combination* $(1_4 2_4)$ gave a fair fit in the range of A_2B_4 and AB, but did not fit at all at the low values of Z where B and AB_4 would predominate. We thus concluded that there is no range where B and AB_4 predominate *which rules out all the combinations containing* 1_4 ($1_4 1_2$, $1_4 2_4$, $1_4 2_3$ *and* $1_4 2_2$).

In *the combination* $1_3 2_2$ the intersection Z must vary between 0.33 and 1.00. Higher B increases the ratio $AB_3(A_2B_3)^{-1}$ and consequently decreases the intersection point. However, from the experimental Z (log $h)_B$ we found a tendency of the intersection point to increase or to be constant; therefore *the combination* $1_3 2_2$ *has been ruled out* as being unlikely.

The calculated graph *for the combination* $1_3 1_2$ *agreed too poorly* with the experimental curves to explain them.

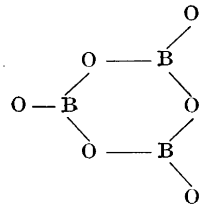
The normalized graph for the *combination* $1_3 2_4$ fitted fairly well with the experimental data (Fig. 3b) but not as well as the remaining *combination* $1_3 2_3$ (Fig. 3c).

Before a discussion of possible structures for the complexes found, it is necessary to survey some previous works on borate in crystals.

STRUCTURAL DATA

Structures of anhydrous borates. In such hydrogen-free compounds as may be obtained at high temperatures, isolated BO_3 triangles are very often encountered. For instance BO_3^{3-} triangles are found in $LaBO_3$ with the aragonite structure, in $InBO_3$ and $ScBO_3$ with the calcite structure (Wells [31], p. 598), and in $Co_3(BO_3)_2$ and $Mg_3(BO_3)_2$ (Berger [32]).

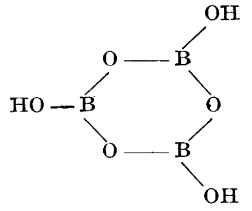
An almost planar group $B_2O_5^{4-}$, consisting of two BO_3 triangles sharing a corner, was found in $Co_2B_2O_5$ (Berger [33]) and $Mg_2B_2O_5$ (Takéuchi [34]). In CaB_2O_4 the BO_3 triangles form infinite chains, each BO_3 group sharing two of its O atoms with neighbors (Zachariasen and Ziegler [35]). Finally, the BO_3 groups can also join to form planar rings $B_3O_6^{3-}$ in the salts $K_3B_3O_6$ and $Na_3B_3O_6$ previously written as KBO_2 and $NaBO_2$ (Zachariasen [36] and Fang [37]).



Four-coordinated B (BO_4 tetrahedra) is found in B_2O_3 (Berger [38,39]), in BPO_4 and $BAsO_4$ (Schulze [40]), and in $CaB_2Si_2O_8$ (Machatschki and Stradner [41]). According to Ito, Morimoto and Sadanaga [42], $Mg_3B_7O_{13}Cl$ (boracite) contains both BO_4 tetrahedra and flat BO_3 pyramids.

Structures of borates containing hydrogen. The crystal structure of boric acid is built up of layers with flat $B(OH)_3$, triangles, joined by hydrogen bonds (Zachariasen [43,44]). The metaboric acid, $HBO_2(\beta)$, contains chains with boron both in three- and four-coordination, according to a preliminary report by Zachariasen [45].

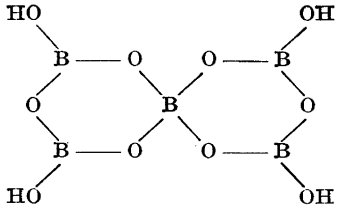
The α-form of metaboric acid has been investigated by Tazaki [64]. According to him the structure is built up of ringshaped trimeric units:



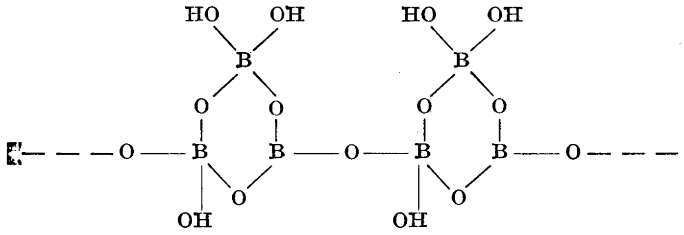
These units are bound together by hydrogen bridges to give a layer structure.

Tetrahedral ions $B(OH)_4^-$ have been found in the structures of the minerals teepleite, $Na_2B(OH)_4Cl$ (Formaseri [46]) and bandylite, $CuB(OH)_4Cl$ (Collin [47]). From the close similarity of the Raman spectra of teepleite and of concentrated potassium borate solutions, Edwards *et al.*[48] concluded that the mononuclear borate ion in solution has the formula $B(OH)_4^-$.

Only two polyborates, to our knowledge, have been thoroughly studied. One is the salt "$KB_5O_8(H_2O)_4$", which is more properly written as $KH_4B_5O_{10}(H_2O)_2$. According to Zachariasen [49], this salt contains the group B_5O_{10}, where two B_3O_3 rings have one B atom in common; this B has a tetrahedral configuration, whereas the others are triangular. From measurements of nuclear magnetic resonance, Smith and Richards [50] concluded that there are four protons attached to this group, the remaining protons being bound in H_2O (Zachariasen originally proposed two H in the B_5O_{10} group, and two H_3O^+ ions). The formula of the group would thus be (the planes of the two rings form right angles)



The crystal structure of colemanite, $CaB_3O_4(OH)_3H_2O$ has been described as containing chains of three-boron rings:



where one B has triangular, two tetrahedral surroundings (Christ, Clark, and Evans [51]).

A Spanish research group has proposed structures for some other polyborates, but according to the *Structure Reports* (1947—45, p. 428—432, 1949, p. 264) these cannot be considered as certain. If they are correct, the structures contain BO_3 and B_3O_6 rings, combined to form sheets.

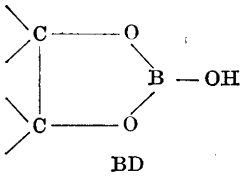
The fact that the mineral kernite, $Na_2B_4O_7(H_2O)_4$, has a fibrous structure indicates that it contains polyborate chains (Menzel and Schulz [52]). This is also indicated by a preliminary X-ray structure analysis (Berger [53]).

It seems very likely that the "sodium metaborate" $NaBO_2(H_2O)_2$ is really $Na^+B(OH)_4^-$. However, from the mere existence of salts like $Na_2B_4O_7(H_2O)_{10}$ and $NaB_5O_8(H_2O)_5$, it is not safe to conclude that ions $B_4O_7^{2-}$ and $B_5O_8^-$ would exist as separate units, even in the crystal structures. The structures of silicate

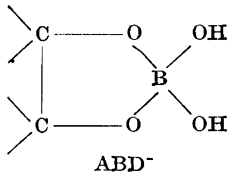
minerals would give a warning against such conclusions; the structures may well contain infinite units (chains, sheets) or several different ionic species.

Complexes with polyols. Boric acid forms complexes with a number of polyols, *i.e.* organic compounds containing several OH groups. Such complexes are put to practical use, as for instance, when mannitol is added before titration of boric acid; the latter then behaves like a strong acid. Since these complexes may show analogies with the polyborate ions, we shall here try to summarize the main facts about them.

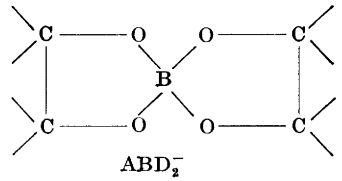
Most of the borate complexes prepared or proved to exist from equilibrium data may be written in one of the following three forms (see *e.g.* Böeseken [54]):



BD



ABD^-

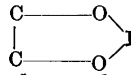


ABD_2^-

(D = diol). Compounds of type BD, when they have been prepared, have proved to be very weak acids, still weaker than boric acid (Hermans [55]). It has not been definitely proved whether the ions ABD^- formed with polyols have the four-coordinated configuration written above, or a three-coordinated configuration with a single O bound to B instead of 2 OH. However, considering the general weakness of the B—O—H acidity, it seems likely that negative ions which can exist where $B(OH)_3$ would not be ionized are generally four-coordinated. For ions of the form ABD_2^- the tetrahedral configuration has been proved by the resolution of optical isomers.

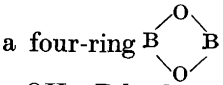
The existence of complexes ABD^- and ABD_2^- has been proved in many instances by analysis of pH and conductance data (later work, *e.g.* Deutsch and Osoling [56], mannitol; Ross and Catotti [57], mannitol; Schäfer [58], pyrocatechol, salicylic acid, and mannitol; Torsell [59], mannitol and fructose). In all of the cases quoted only ABD^- and ABD_2^- were found. Occasionally there is evidence for uncharged BD (which has then probably the form above, Böeseken and Niks [60]) but never for uncharged BD_2.

Boric acid is rather particular in the choice of diol (Schäfer [61], Isbell *et al.* [62], and especially Böeseken [54]). With glycol or glycerol it reacts only at high concentrations, whereas a strong reaction is observed with polyols like mannitol and erythritol. Considering aromatic diols, it reacts only with the ortho-compounds, but with *cyclo*pentane-1,2-diol it reacts only with the *cis*form. It does not seem to react at all with any form of *cyclo*hexane-diol. Steric explanations have been proposed (Böeseken [54]).

It seems essential that a five-membered-ring  is formed (a six-membered-ring with one more C has occasionally been obtained). Complexes where a carbonyl C—O may react like a $C(OH)_2$ group are known; however, such OH groups do not seem to react with the same B atom forming a four-ring.

General rules for borate structures. From the equilibrium data, we may deduce the number of boron atoms and the charge for a certain polyborate ion

in solution. This still leaves us a number of possible formulas that differ by one or several H_2O, like $B_3O_3(OH)_4^-$, $B_3O_4(OH)_2^-$, $B_3O_5^-$ etc; one cannot decide between them from equilibrium data alone. However, the structures of borate crystals and organic borate complexes may give some aid in proposing a formula and a reasonable structure.

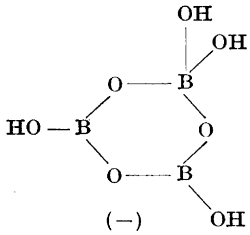
BO_3 or BO_4 groups, as a rule, are joined by sharing an O atom, thus forming a B—O—B bridge. In B_2O_3, some oxygen atoms are said to be shared between three B atoms (Berger [39]); however, no case with a four-ring  seems to be known. There is also no structure known with B—OH—B bridges.

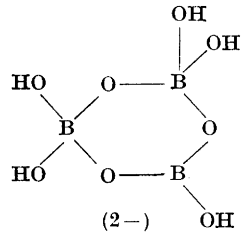
The sharing of an oxygen between more than two B has not been proved in any other compound than B_2O_3 where there is a great shortage of oxygen. We shall assume that it does not occur in aqueous solutions, where a large number of oxygen atoms are available.

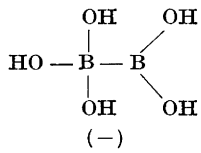
It seems very unlikely that polyborate ions in aqueous solution would be held together by hydrogen bonds between OH groups attached to different B, considering that solutions of pure boric acid show no association (Menzel [7]).

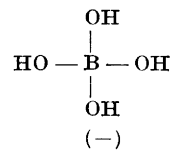
As for the *unshared oxygen* atoms bound to boron, it seems reasonable to assume as a working hypothesis that they are *always OH groups*. Thus Edwards *et al.*[48] suggest that $B(OH)_3$ forms an ion not by splitting off H^+ to form $BO(OH)_2^-$, but by addition of OH^- to boron $B(OH)_4^-$. This also agrees with the crystal structures of $KH_4B_5O_{10}(H_2O)_2$ and $CaB_3O_4(OH)_3H_2O$ given above.

If these rules are general, we can easily see that in any borate ion there will be one negative charge for each four-coordinated boron atom, *e.g.*









The ion $H_4B_5O_{10}^-$ agrees well with these principles.

The ease with which boron can switch over between three- and four-coordination is probably one of the reasons why the polyborate equilibria are so rapidly achieved.

CONCLUSIONS

From the measurements made in this work, we have obtained the following equilibria:

$$B(OH)_3 + H_2O \rightleftharpoons B(OH)_4^- + H^+; \quad \log K_{11} = -9.00 \pm 0.05$$
$$3\,B(OH)_3 \rightleftharpoons B_3O_3(OH)_4^- + H^+ + 2H_2O; \quad \log K_{13} = -6.84 \pm 0.10$$
$$3\,B(OH)_3 \rightleftharpoons B_3O_3(OH)_5^{2-} + 2H^+ + H_2O; \quad \log K_{23} = -15.44 \pm 0.20$$

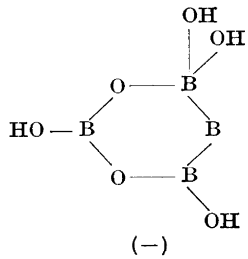
The experimental data may also be explained if the last equilibrium is replaced with

$$4\,B(OH)_3 \rightleftharpoons B_4O_4(OH)_6^{2-} + 2H^+ + 2H_2O; \quad \log K_{24} = -15.71 \pm 0.20$$

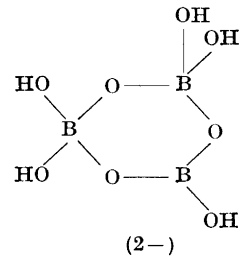
In both cases the agreement between the experimental and calculated data is satisfactory except for small deviations at high values of Z and B. These deviations may be explained as a variation in the activity factors. The agreement between the constant obtained in this investigation and in other investigations seems to be satisfactory — Owen [11] (log $K_a^\circ = -9.236$), Thygesen [13] (log $K_{13} = -7.5$ at 18°C), Stetten [14] (log $K_{1,3.2} = -6.86$) and Edwards [15] (log $K_{13} = -7.5$).

From general chemical considerations, the polynuclear combination AB_3 and A_2B_4 seems to be very unlikely.

The possibility that AB_3 and A_2B_3 could be chains must be ruled out since it would be very hard to explain why a certain number should be preferred. It seems to be more likely that the complexes contain a six membered B—O—B ring



(−)



(2−)

Note. When our work was completed a structure determination by Christ and Clark [63] appeared which corroborated our conception that the most likely two-charged polynuclear complex was to be $B_3O_3(OH)_5^{2-}$. Christ and Clark [63] showed in a X-ray investigation of the mineral mayerhofferite, $2CaO \cdot 3B_2O_3 \cdot 7H_2O$ that the crystal contains polyions consisting of two $BO_2(OH)_2$ tetrahedra and a $BO_2(OH)$ triangle linked to form a ring of the composition $B_3O_3(OH)_5^{2-}$, which is the same complex that we have proposed above.

This work is part of a program financially supported by *Statens Naturvetenskapliga Forskningsråd (Swedish Natural Science Research Council)*. It has also received much stimulation from research work supported by Columbia-Southern Chemical Corporation, in this laboratory.

REFERENCES

1. Hietanen, S. and Sillén, L. G. *Acta Chem. Scand.* **8** (1954) 1607; Sillén, L. G. *Acta Chem. Scand.* **8** (1954) 299; Biedermann, G. and Sillén, L. G. *Acta Chem. Scand.* **10** (1956) 1011.
2. Konopik, N. and Leberl, O. *Monatsh.* **80** (1949) 655.
3. Carpéni, G. *Compt. rend.* **226** (1948) 807.
4. Byé, J. *Bull. soc. chim. France* **1953** 390.
5. Souchay, P. *Bull. soc. chim. France* **1953** 395.
6. Kahlenberg, L. and Schreiner, O. *Z. physik. Chem.* **20** (1896) 547.
7. Menzel, H. *Z. anorg. allgem. Chem.* **164** (1927) 1, 22.
8. Menzel, H. and Schulz, H. *Z. anorg. allgem. Chem.* **251** (1943) 167.

9. Doucet, Y. and Rollin, M. *Compt. rend.* **226** (1948) 1967.
10. Souchay, P. *Bull. soc. chim. France* **1951** 932.
11. Owen, B. D. *J. Am. Chem. Soc.* **56** (1934) 1695.
12. Kolthoff, I. M. *Rec. trav. chim.* **45** (1926) 501.
13. Thygesen, J. E. *Z. anorg. allgem. Chem.* **237** (1938) 101.
14. Stetten, D. Jr. *Anal. Chem.* **23** (1951) 1177.
15. Edwards, J. O. *J. Am. Chem. Soc.* **75** (1953) 6151.
16. Antikainen, P. *Ann. Acad. Sci.Fennicae, Ser A II*, No. 56.
17. Auerbach, F. *Z. anorg. Chem.* **37** (1903) 353.
18. Kolthoff, I. M. and Bosch, W. *Rec. trav. chim.* **46** (1927) 180.
19. Carpéni, G. and Souchay, P. *J. Chem. Phys.* **42** (1945) 149.
20. Carpéni, G. *Compt. rend.* **228** (1949) 89.
21. Carpéni, G. *Bull. soc. chim. France* **1952** 1010.
22. Carpéni, G. *Compt. rend.* **239** (1954) 1500.
23. Ågren, A. *Acta Chem. Scand.* **9** (1955) 49.
24. Biedermann, G. and Sillén, L. G. *Arkiv Kemi* **5** (1953) 425.
25. Lagerström, G. *To be published.*
26. Forsling, W., Hietanen, S. and Sillén, L. G. *Acta Chem. Scand.* **6** (1952) 901.
27. Bates, R. G. *Electrometric pH determinations*, John Wiley and Sons Inc. 1954.
28. Gran, G. *Analyst* **77** (1952) 661.
29. Sillén, L. G. *To be published.*
30. Sillén, L. G. *Acta Chem. Scand.* **10** (1956) 803.
31. Wells, A. F. *Structural inorganic chemistry*, Oxford 1950.
32. Berger, S. V. *Acta Chem. Scand.* **3** (1949) 660.
33. Berger, S. V. *Acta Chem. Scand.* **4** (1950) 1054.
34. Takéuchi, Y. *Acta Cryst.* **5** (1952) 574.
35. Zachariasen, W. H. and Ziegler, G. E. *Z. Krist.* **83** (1932) 354.
36. Zachariasen, W. H. *J. Chem. Phys.* **5** (1937 a) 919.
37. Fang, S. M. *Z. Krist*, **99** (1938) 1.
38. Berger, S. V. *Acta Cryst.* **5** (1952) 389.
39. Berger, S. V. *Acta Chem. Scand.* **7** (1953) 611.
40. Schulze, G. E. R. *Z. physik. Chem.* **B24** (1934) 215.
41. Machatschki, F. and Stradner, E. *Österr. Akad. Wiss. Math-naturw. Kl. Anz* **2** (1953) 26.
42. Ito, T., Morimoto, N. and Sadanaga, R. *Acta Cryst*, **4** (1951) 310.
43. Zachariasen, W. H. *Z. Krist.* **88** (1943) 150.
44. Zachariasen, W. H. *Acta Cryst.* **7** (1954) 305.
45. Zachariasen, W. H. *Acta Cryst.* **5** (1952) 68.
46. Fornaseri, M. *Periodico mineral. Rome* **18** (1949) 103. (*Structure Reports* **12**, 263).
47. Collin, R. L. *Acta Cryst.* **4** (1951) 204.
48. Edwards, J. O., Morrison, G. C., Ross, V. F. and Schultz, J. W. *J. Am. Chem. Soc* **.77** (1955) 266.
49. Zachariasen, W. H. *Z. Krist.* **98** (1937 b) 266.
50. Smith, J. B. S. and Richards, R. E. *Trans. Faraday Soc.* **48** (1952) 307.
51. Christ, C. L., Clark, J. R. and Evans, H. T. Jr. *Acta Cryst.* **7** (1954) 149.
52. Menzel, H. and Schulz, H. *Z. anorg. allgem. Chem.* **245** (1940) 157.
53. Berger, S. V. *Private communication* (1955).
54. Böeseken, J. *Advances in Carbohydrate Chem.* **4** (1949) 189.
55. Hermans, P. H. *Z. anorg. allgem. Chem.* **142** (1925) 83.
56. Deutsch, A. and Osoling, S. *J. Am. Chem. Soc.* **71** (1949) 1637.
57. Ross, S. D. and Catotti, A. J. *J. Am. Chem. Soc.* **71** (1949) 3563.
58. Schäfer, H. *FIAT Rev. Ger. Sci.* 1939—1946 (1948), Inorg. Chem. III, 225.
59. Torssell, K. *Arkiv Kemi* **3** (1952) 571.
60. Böeseken, J. and Niks, A. *Rec trav. chim.* **59** (1940) 1062.
61. Schäfer, H. *Z. anorg. allgem. Chem.* **247** (1941) 96.
62. Isbell, H. S., Brewster, J. F., Holt, N. B. and Frush, H. L. *J. Research Natl. Bur. Standards* **40** (1948) 129.
63. Christ, C. L. and Clark, J. R. *Acta Cryst.* **9** (1956) 830.
64. Tazaki, H. *J. Sci. Hiroshima Univ. Ser A*, **10** (1940) 55—61.

Received March 25, 1957.

ACTA CHEMICA SCANDINAVICA 11 (1957) 1059—1076

Short Communications

Some Electron Diffraction Studies of 1,4-Dibromo-butyne-2

A. ALMENNINGEN, O. BASTIANSEN and F. HARSHBARGER

Universitetets Kjemiske Institutt, Blindern, and Institutt for teoretisk kjemi, N.T.H., Trondheim, Norway

Heat capacity measurements [1,2] of $CH_3-C\equiv C-CH_3$ have indicated an almost free rotation between the methyl groups. In the case of $CH_3-C\equiv C-CF_3$ there have been contraversial views [3-5] over the possibility of internal free rotation. It seemed of interest to study the internal rotation in a similar molecule by electron diffraction. The diffraction power of bromine made $CBrH_2-C\equiv C-CBrH_2$ suitable for our studies.

The diagrams were taken by the Oslo electron diffraction apparatus [6] using distances between the diffraction point and photographic plate of 48 cm and 19 cm. The intensity data went out to $s = 27$. The data were treated in our usual manner [7], but with a very strong damping factor of 0.006, as we were primarily interested in the longer distances. The information about these distances is found in the inner part of the intensity curve.

The radial distribution curve is presented in Fig. 1 and is compared with the theoretically determined distances. The positions of the distances are indicated by perpendicular lines. These values were calculated using the following parameters: $C_1-H_1 = 1.09$ Å, $C_2-C_3 = 1.21$ Å, $C_1-C_2 = 1.45$ Å and $Br_1C_1C_2 = 111.5°$. The height of each line is proportional to $n\,Z_1Z_2/r$, where Z_1 is the atomic number of one atom, Z_2 is the atomic number of the second atom, n is the number of times the distance occurs in the molecule, and r is the distance.

If we subtract from the radial distribution curve the contribution of distances which would be invariable under rotation, we obtain the contribution of the distances which are dependent upon the rotation. This curve is presented in Fig. 2 as the solid line and should give information about the Br_1-Br_4 and the Br_1-H_4 distances.

If the molecule were rigid, there would be only one Br—Br peak. For a *cis* molecule the peak would occur at 5.55 Å and for a *trans* molecule at 6.63 Å. The difference curve shows no single simple peak. On the contrary, the double peak in Fig. 2 suggests free rotation.

The theoretical radial distribution curves for the Br_1-Br_4 distance were calculated assuming free rotation. These curves were made by assuming normal curves whose areas were proportional to the probability of the corresponding r-value. Gaussian normal curves were used. The three different theoretical curves (Fig. 2)

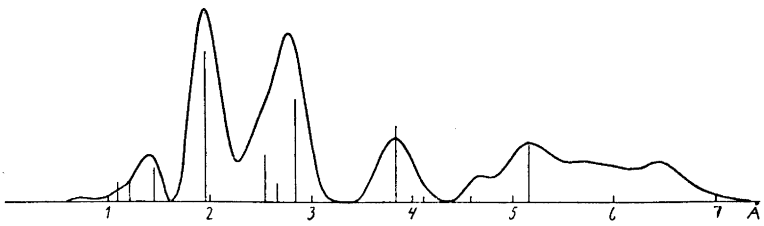


Fig. 1. Radial distribution curve for $BrH_2C-C\equiv C-CH_2Br$ ($k = 0.006$).

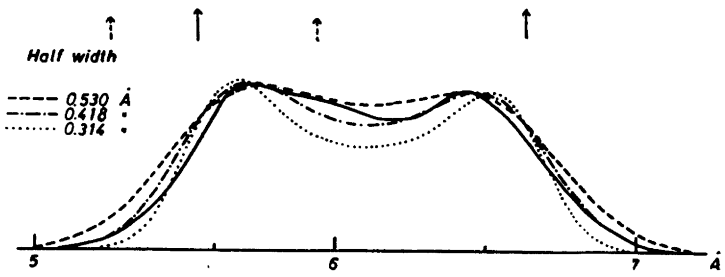


Fig. 2. Experimental difference curve and theoretical curves calculated on the assumption of free rotation.

represent three different choices for the half-width, *i. e.*, 0.314 Å, 0.418 Å, and 0.530 Å. The theoretical curves were normalized to the experimental curve.

The agreement between the theoretical and experimental curves is good. The discrepancies are easily understood: 1) The choice of the subtracted envelope [7] is somewhat arbitrary, 2) the subtraction of the invariable distances leaves some uncertainty, and 3) the Br_1-H_4 distances are expected to give rise to a detectable effect. The Br_1-H_4 distances should have a probability curve similar to that for Br_1-Br_4, but with peaks at about 5.37 Å and 5.87 Å and a total area about 15 % of the Br_1-Br_4 area. The maximum and minimum Br_1-H_4 distances are marked by dashed arrows in Fig. 2. The maximum and minimum Br_1-Br_4 distances are marked by solid arrows.

There remains one unexplained point in the radial distribution curve, namely the comparatively large area located at 4.67 Å. The C_1-H_4 distance at 4.58 Å should not give rise to such a large area. Even though we are not able to interpret this point, we feel it has no essential effect on our conclusion that there is internal rotation in the gaseous $CBrH_2-C\equiv C-CBrH_2$ molecule.

One of the authors (F. H.) wishes to express his gratitude to the *United States Educational Foundation in Norway* for a stipend during the 1956—57 academic year.

We also wish to thank siv.ing. Marit Trætteberg for the preparative work.

1. Kistiakowsky, G. B. and Rice, W. W. *J. Chem. Phys.* **8** (1940) 618.
2. Yost, D. M., Osborne, D. W. and Garner, C. S. *J. Am. Chem. Soc.* **63** (1941) 3492.
3. Bak, B., Hansen, L. and Rastrup-Andersen, J. *J. Chem. Phys.* **21** (1953) 1612.
4. Lide, Jr., D. and Kivelson, D. *J. Chem. Phys.* **23** (1955) 2191.
5. Bak, B., Christensen, D., Hansen-Nygaard, L. and Tannenbaum, E. *J. Chem. Phys.* **26** (1957) 241.
6. Bastiansen, O., Hassel, O. and Risberg, E. *Acta Chem. Scand.* **9** (1955) 232.
7. Almenningen, A. and Bastiansen, O. *Acta Chem. Scand.* **9** (1955) 815.

Received June 20, 1957.

Phenol Dehydrogenations

VII. *. Dehydrogenation of Chavicol to Magnolol

H. ERDTMAN and J. RUNEBERG

Institutionen för organisk kemi, Kungl. Tekniska Högskolan, Stockholm, Sweden

The biosynthetic importance of dehydrogenative coupling of phenols with the formation of diphenyl or diphenyl-oxide derivatives has recently been discussed by Erdtman and Wachtmeister [1]. Magnolol (II) is a particularly simple example with a structure indicating that it has been formed by the coupling of two molecules of chavicol (I) or an aromatic precursor.

* Part VI: *Svensk Kem. Tidskr.* **47** (1935) 223.

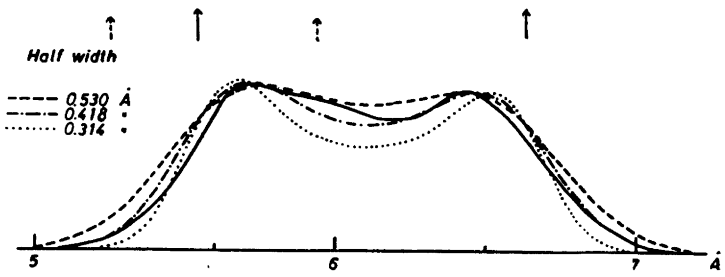


Fig. 2. Experimental difference curve and theoretical curves calculated on the assumption of free rotation.

represent three different choices for the half-width, *i. e.*, 0.314 Å, 0.418 Å, and 0.530 Å. The theoretical curves were normalized to the experimental curve.

The agreement between the theoretical and experimental curves is good. The discrepancies are easily understood: 1) The choice of the subtracted envelope [7] is somewhat arbitrary, 2) the subtraction of the invariable distances leaves some uncertainty, and 3) the Br_1-H_4 distances are expected to give rise to a detectable effect. The Br_1-H_4 distances should have a probability curve similar to that for Br_1-Br_4, but with peaks at about 5.37 Å and 5.87 Å and a total area about 15 % of the Br_1-Br_4 area. The maximum and minimum Br_1-H_4 distances are marked by dashed arrows in Fig. 2. The maximum and minimum Br_1-Br_4 distances are marked by solid arrows.

There remains one unexplained point in the radial distribution curve, namely the comparatively large area located at 4.67 Å. The C_1-H_4 distance at 4.58 Å should not give rise to such a large area. Even though we are not able to interpret this point, we feel it has no essential effect on our conclusion that there is internal rotation in the gaseous $CBrH_2-C\equiv C-CBrH_2$ molecule.

One of the authors (F. H.) wishes to express his gratitude to the *United States Educational Foundation in Norway* for a stipend during the 1956—57 academic year.

We also wish to thank siv.ing. Marit Trætteberg for the preparative work.

1. Kistiakowsky, G. B. and Rice, W. W. *J. Chem. Phys.* **8** (1940) 618.
2. Yost, D. M., Osborne, D. W. and Garner, C. S. *J. Am. Chem. Soc.* **63** (1941) 3492.
3. Bak, B., Hansen, L. and Rastrup-Andersen, J. *J. Chem. Phys.* **21** (1953) 1612.
4. Lide, Jr., D. and Kivelson, D. *J. Chem. Phys.* **23** (1955) 2191.
5. Bak, B., Christensen, D., Hansen-Nygaard, L. and Tannenbaum, E. *J. Chem. Phys.* **26** (1957) 241.
6. Bastiansen, O., Hassel, O. and Risberg, E. *Acta Chem. Scand.* **9** (1955) 232.
7. Almenningen, A. and Bastiansen, O. *Acta Chem. Scand.* **9** (1955) 815.

Received June 20, 1957.

Phenol Dehydrogenations

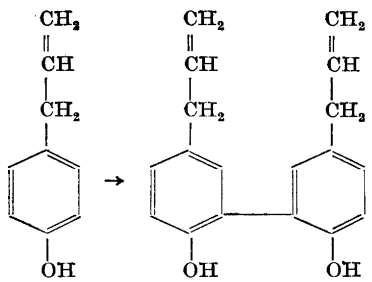
VII. *. Dehydrogenation of Chavicol to Magnolol

H. ERDTMAN and J. RUNEBERG

Institutionen för organisk kemi, Kungl. Tekniska Högskolan, Stockholm, Sweden

The biosynthetic importance of dehydrogenative coupling of phenols with the formation of diphenyl or diphenyl-oxide derivatives has recently been discussed by Erdtman and Wachtmeister [1]. Magnolol (II) is a particularly simple example with a structure indicating that it has been formed by the coupling of two molecules of chavicol (I) or an aromatic precursor.

* Part VI: *Svensk Kem. Tidskr.* **47** (1935) 223.



I II

Magnolol occurs in the bark of a number of *Magnolia* species. The compound was isolated and its structure elucidated by Sugi [2] who also synthesised tetrahydro-magnolol.

We have now obtained magnolol in a yield of about 25 % by dehydrogenation of chavicol with ferric chloride. During this work Ohta and Mori [3] reported the formation of tetrahydromagnolol from *p*-(*n*-propyl)-phenol by dehydrogenation with a mixture of hydrogen peroxide and aqueous ferrous sulphate. Tetrahydro-magnolol was also obtained recently by Haynes, Turner and Waters [4] during their studies on the dehydrogenation of various phenols with potassium ferricyanide.

Experimental *. *Dehydrogenation of 1-allyl-4-hydroxy-benzene (chavicol):* Ferric chloride (28 g) was dissolved in distilled water (2 500 ml) in a three-neck flask. 1-Allyl-4-hydroxy-benzene (10 g) in 95 % ethanol (40 ml) was added dropwise during 4 h with stirring while a stream of air was bubbled through. The solution turned first green and then black. Stirring and aeration was continued for 48 h more. When the stirring was stopped at the end of this period, a viscous red oil collected at the bottom of the flask. The reaction mixture was acidified and extracted with ether, the ether solution extracted with 2 N sodium hydroxide and the alkaline solution acidified and extracted with ether. After washing and drying the ether extract was evaporated and the remaining oil distilled yielding first, unchanged starting material (5.9 g), then a liquid fraction (0.79 g) boiling at 120—130°/0.8 mm which was not further investigated and finally a crystalline fraction (1.02 g) consisting of magnolol boiling at 175—177°/0.8 mm. Allowing for recovered starting material the yield of crude magnolol was 25 %.

Magnolol phenylurethan: The above crude magnolol (1.0 g) was heated with phenyl *iso*-cyanate (1.2 g) at 110° for one hour in a sealed tube. Excess reagent was evaporated under vacuum on a waterbath. A benzene solution of the crystalline residue was filtered through a 20 cm column of aluminum oxide soaked with ligroin. The first product leaving the column was the phenylurethan. The impurities moved at a slower rate. Evaporation of the solvent gave the phenylurethan (1.3 g) which after recrystallisation from 95 % ethanol melted at 143.5—144.5° undepressed by magnolol phenylurethan obtained synthetically from 2,2-dihydroxydiphenyl [5].

Magnolol from magnolol phenylurethan: Magnolol phenylurethan (2.0 g) was heated overnight in a high vacuum at 200° in a tube sealed at one end and surrounded by a coil providing a decreasing thermogradient towards the open end of the tube where the magnolol formed was deposited. Yield 0.87 g. The product was resublimed twice; m. p. 101.0—101.5° (lit. 103°), undepressed by magnolol obtained synthetically from 2,2′-dihydroxydiphenyl [5].

Isomagnolol: In a nickel crucible, powdered potassium hydroxide (0.25 g) was dissolved in hot amyl alcohol (0.36 g). Magnolol (0.1 g) was added and the melt heated at 140° for 20 h. After cooling, water (10 ml) was added and the amyl alcohol removed by steam distillation. The remaining solution was filtered and acidified. The crystalline precipitate formed was collected, washed with water, dried and recrystallised from ligroin, m. p. 142—143° (lit. 143.5°).

1. Erdtman, H. and Wachtmeister, C. A. *Festschrift Arthur Stoll*, Sandoz AG, Basel 1957, p. 144.
2. Sugi, Y. *J. Pharm. Soc. Japan* **50** (1930) 23.
3. Ohta, T. and Mori, Y. *Ann. Rept. Tokyo Coll. Pharm.* **3** (1953) 206; *Chem. Abstr.* **49** (1955) 7513 i.
4. Haynes, C. G., Turner, A. H. and Waters, William A. *J. Chem. Soc.* **1956** 2829.
5. Runeberg, J. *Forthcoming publication.*

* Melting points are uncorrected.

Received June 26, 1957.

The Incorporation of ^{32}P into Mitochondrial Thiamine Diphosphate* in the Presence of Different Substrates and Inhibitors

KARL-HEINZ KIESSLING

Institute of Zoophysiology, Uppsala, Sweden

The incorporation of radioactive phosphate into intramitochondrial TDP has been studied in a series of investigations [1-4]. The incorporation was found to depend on the simultaneous metabolization of pyruvate or succinate, whereas α-ketoglutarate was less effective [4]. These results are partly in agreement with those of Bartley [5], who, when incubating a kidney cyclophorase enzyme complex with synthetic TDP and $^{32}P_i$ found a somewhat higher incorporation in the presence of pyruvate and succinate than when using α-ketoglutarate. However, in Bartley's experiments the incorporation was slow compared with that observed by me, since added thiamine phosphates do not take part in mitochondrial phosphate metabolism to the same degree [2] as intramitochondrial TDP. That the incorporation of ^{32}P into TDP was higher with succinate than with α-ketoglutarate was surprising, for since the investigations of Auhagen [6] and Lohmann and Schuster [7], TDP has been known especially to function as a coenzyme in the decarboxylation of α-ketoacids. However the incorporation with succinate as a substrate might depend on succinate being transformed into pyruvate in the mitochondria and, when the pyruvate thus formed was oxidatively decarboxylated, an exchange of the phosphate in TDP might take place. If this were the case fumarate, which is primarily formed when succinate gives rise to pyruvate, should have the same effect as succinate on the incorporation into TDP. Results from an experiment aiming to answer this question are seen in Table 1. The experimental conditions were the same as in the previous paper [3] except that the concentration of phosphate buffer present in the mitochondrial suspension was twice that of the earlier amount (3 ml 0.5 M, pH 7.4, instead of 1.5 ml) and pyruvate and α-ketoglutarate were replaced by succinate or fumarate. From the table it is seen that when fumarate is metabolized the incorporation of ^{32}P into intramitochondrial TDP is slower than when succinate is present, the incorporation being of the same extent as that during incubation without added substrate. Thus the incorporation into TDP with succinate as a substrate does not depend on succinate being transformed into pyruvate.

Amytal (5-ethyl-5-*iso*amylbarbiturate), in a concentration of 1.8 mM has been shown by Ernster *et al.*[8] to inhibit completely hydrogen transfer from mitochondrial dehydrogenases to oxygen in DPN-linked oxidation systems, while at the same time having no effect on the aerobic oxidation of succinate, or on the phosphorylations coupled to it. This is explained as depending on the action of amytal on the electron transport pathway between FAD and Slater's factor at a site not present in the succinate oxidation pathway.

Incubating mitochondria in the same way as in the experiments described in Table 1 with succinate and amytal gave the same or only slightly lower incorporation of ^{32}P into TDP than when amytal was omitted (Table 2). The oxidation of fumarate was completely inhibited with the same concentration of amytal. This provides further evidence that the incorporation into TDP is not caused only by oxidative decarboxylation of the pyruvate eventually formed from succinate.

Succinic dehydrogenase has been shown not to contain TDP. Up to now the only known reaction including succinate which requires the presence of TDP is the decarboxylation of succinate to propionate found by Whitely [9] to occur in certain bacteria, and the carboxylation of propionate recently shown by Lardy and Adler [10] to occur in liver mitochondria. However, the reverse reaction of the propionate carboxylation they found to proceed slowly, at least in extracts of mitochondria, making this reaction less probable as a possible explanation of the results above.

Sodium fluoride (final concentration 0.02 M), when used in my experiments, inhibited the incorporation into TDP completely and reduced the oxygen consumption to

* Abbreviations: TDP, thiamine diphosphate; ADP, adenosine diphosphate; DPN, diphosphopyridine nucleotide; DNP, 2,4-dinitrophenol; FAD, flavin adenine dinucleotide; $^{32}P_i$, radioactive inorganic phosphate; P/O = the ratio of μmoles esterified phosphate to μatoms consumed oxygen.

Table 1. Incorporation of radioactive phosphate into intramitochondrial TDP in the presence of succinate or fumarate. Experimental conditions see text. Volume of sample 14.22 ml. Two ml of this volume were transferred to Warburg vessels for determination of the O_2-consumption. Incubation temp. 30°C. Incubation time 25 min. No synthetic TDP was present during incubation. In order to facilitate the isolation of the intramitochondrial TDP three mg were, however, added after the reaction had been stopped with TCA. The radioactivity of intramitochondrial TDP was estimated according to values given in an earlier paper [3].

Substrate	TDP counts/μg hydrolyzable P	Oxygen consumption mm^3/25 min/2 ml sample	P/O
Succinate	1.45×10^4	151	2.45
Fumarate	0.66×10^4	145	2.28
None	0.72×10^4	40	1.86

Table 2. The effect of amytal on the incorporation of radioactive phosphate into intramitochondrial TDP with succinate as a substrate. Experimental conditions see Table 1. Incubation time 20 min. When amytal is present its final concentration is 1.8 mM.

Substrate	Inhibitor	TDP counts/μg hydrolyzable P	Oxygen consumption mm^3/20 min/2 ml sample	P/O
Succinate	None	4.6×10^4	133	2.3
Succinate	Amytal	4.4×10^4	135	2.1
None	None	2.1×10^4	48	1.9

20 %. DNP (final concentration 10^{-4} M) had no effect on the incorporation. The substrate was in both cases pyruvate.

Ochoa [11] when investigating the enzymic synthesis of TDP in animal tissues found that NaF in a concentration of 0.04 M only slightly affected the synthesis. This may be taken as additional evidence, aside from that given earlier [2], that the incorporation of ^{32}P into TDP, reported above, is not only the result of a mere synthesis of TDP from thiamine present in the mitochondria.

The results with DNP are in agreement with those of Ogata *et al.*[12] who found no inhibition with DNP of the transfer of ^{32}P from labelled TDP to ADP in a liver cyclophorase system.

Acknowledgements. I am indebted to Prof. P. E. Lindahl for valuable discussions, to Dr. Hans Löw for the supply of hexokinase and to Mrs. Margot Persson for technical assistance. Thanks are also due to Dr. A. L. Morrison, Messrs. Roche Products Ltd., for the gift of TDP. This work is part of investigations made possible by support from the *Swedish Natural Science Research Council.*

1. Kiessling, K.-H. and Lindahl, P. E. *Arkiv Kemi* **4** (1952) 285.
2. Kiessling, K.-H. *Acta Chem. Scand.* **11** (1957) 917.
3. Kiessling, K.-H. *Arkiv Kemi* **11** (1957) 451.
4. Kiessling, K.-H. *Arkiv Kemi* **11** (1957) 469.
5. Bartley, W. *Biochem. J.* **56** (1954) 379.
6. Auhagen, E. *Biochem. Z.* **258** (1933) 330.
7. Lohmann, K. and Schuster, Ph. *Biochem. Z.* **294** (1937) 188.
8. Ernster, L., Jalling, O., Löw, H. and Lindberg, O. *Exptl. Cell Research*, Suppl. **3** (1955) 124.
9. Whiteley, H. R. *J. Am. Chem. Soc.* **75** (1953) 1518.
10. Lardy, H. and Adler, J. *J. Biol. Chem.* **219** (1956) 933.
11. Ochoa, S. *Biochem. J.* **33** (1939) 1262.
12. Ogata, K., Nohara, H., Morita, T. and Kawai, K. *J. Biochem. Japan* **42** (1955) 13.

Received August 29, 1957.

Quantitative Mass Spectrometric Analysis of Mixtures of Unsaturated and Saturated Fatty Acids

BO HALLGREN, EINAR STENHAGEN and RAGNAR RYHAGE

Department of Medical Biochemistry, Institute of Medical Chemistry, University of Uppsala, and Laboratory for Mass Spectrometry, Biochemical Institute, Karolinska Institutet, Stockholm

It has been shown [1] that with the aid of a high-resolution mass spectrometer it is possible to obtain excellent mass spectra of methyl esters of saturated long chain carboxylic acids. Two series of peaks are prominent, *viz.* ionized hydrocarbon fragments and methoxycarbonyl-containing fragments, respectively. The latter type of fragments dominates quantitatively over the former. The spectra show comparatively large parent peaks due to the ionized unfragmented molecules. These allow a direct determination of the molecular weights of the compounds studied. In mixtures, the peak heights of the parent peaks can be used for the quantitative analysis of mixtures of normal chain fatty acids of high molecular weight (*cf.* Ref.[1]). The general principles of the analysis of mixtures in the mass spectrometer are outlined in standard texts (*cf.*, *e.g.*, Refs. [2-4]).

If we have a mixture of a saturated methyl ester and methyl esters of mono- or poly-ethenoid acids having the same number of carbon atoms the mass spectrum will show a series of parent peaks corresponding to the different molecular weights. The high-mass range of the mass spectrum for a mixture of C_{18} acids is reproduced in Fig. 1. The saturated ester (methyl stearate) has a parent peak at m/e = 298, the mono-ethenoid ester (methyl oleate) at 296, the di-ethenoid ester (methyl linoleate) at 294 and the tri-ethenoid ester (methyl linolenate) at 292 (*cf.* Figs. 1 and 2). The strong isotope peaks (m/e = M+1) are at odd mass numbers and do not overlap the parent peaks. The sensitivity coefficients of the parent peaks in the mass spectrum of the different esters studied are not the same, and in order to derive the quantitative composition of the mixture it

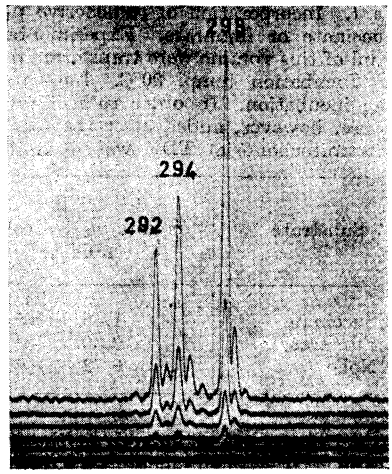


Fig. 1. High-mass end of the mass spectrum of a mixture containing 25 % methyl stearate, 38 % methyl linoleate, 36 % methyl linolenate and approximately 1 % methyl oleate.

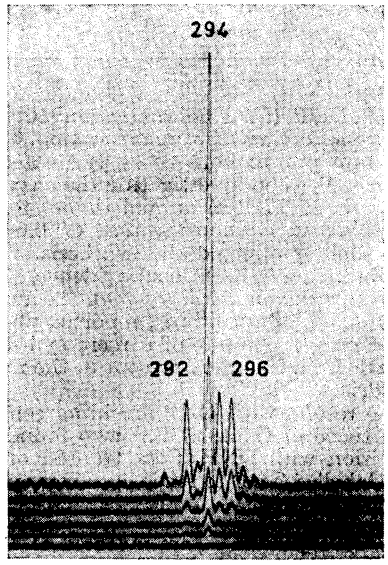


Fig. 2. High-mass end of the mass spectrum of a mixture containing 31 % methyl oleate, 55 % methyl linoleate and 14 % methyl linolenate.

is necessary to apply empirical corrections. If this is properly carried out it is possible to determine the percentage of the various components of the mixture directly. If pure components are available it is easy to check the results by running artificial mixtures and thus to get a very high accuracy in the quantitative analysis.

The mass spectra of the samples of methyl linoleate and methyl linolenate studied show a peak at $m/e = 290$. In the case of methyl linoleate the height of this peak is 1.7 % of the parent peak ($m/e = 294$). For methyl linolenate the height of the $m/e = 290$ peak is 18 % of the parent peak at $m/e = 292$. This peak appears to be the parent peak of the methyl ester of a C_{18} acid containing four double bonds. Whether this acid is present as an impurity in the original samples or whether it is formed by a dehydration reaction in the heated intake system of the mass spectrometer cannot be said at present. The present evidence, however, is in favour of the first mentioned possibility. It has been proposed that acids of this type may be formed from linoleic and linolenic acids by dehydrogenation between the existing double bonds and the carboxyl group in such a way that all unsaturation is methylene-interrupted and all *cis*. (*cf.* Ref.[5]). C_{18} tetra-ethenoid acids have been found in the fats of marine animals [5,6].

In a complex mixture it is not possible to distinguish between geometrical and positional isomers within each group of unsaturated esters. The peak at $m/e = 296$ in the figure might thus be due to, *e.g.*, methyl oleate (methyl *cis*-$\Delta^{9,10}$-octadecenoate), methyl elaidate (methyl *trans*-$\Delta^{9,10}$-octadecenoate), or methyl petroselinate (methyl *cis*-$\Delta^{6,7}$-octadecenoate) or due to a mixture of mono-ethenoid esters. It may be possible to overcome this difficulty by examining suitable derivatives.

The high-mass, high-resolution mass spectrometer thus offers a convenient method for determining the fatty acid distribution ("fatty acid spectrum") of natural or synthetic fats. The analysis can be performed on a few milligrams of material.

The financial support of *Statens Tekniska Forskningsråd* and *Statens Medicinska Forskningsråd* is gratefully acknowledged. We are indebted to Dr. W. O. Lundberg, The Hormel Institute, Austin, Minnesota, for the gift of methyl esters of unsaturated fatty acids.

1. Asselineau, J., Ryhage, R. and Stenhagen, E. *Acta Chem. Scand.* **11** (1957) 196.
2. Brewer, A. K. and Dibeler, V. H. *J. Research Natl. Bur. Standards* **35** (1945) 125.
3. Robertson, A. J. B. *Mass Spectrometry*, London 1954, p. 84.
4. Barnard, G. P. *Modern Mass Spectrometry*, The Institute of Physics, London 1953, p. 192.
5. Holman, R. T. in Glick, D. *Methods of Biochemical Analysis*, N.Y. 1957, p. 99.
6. *Cf.* Hilditch, T. P. *The chemical constitution of natural fats*, 3 rd. Ed., London 1956.

Received June 26, 1957.

Note on the Crystal Structure of Niobium Monoxide

GEORG ANDERSSON and ARNE MAGNÉLI

Institute of Chemistry, University of Uppsala, Uppsala, and Institute of Inorganic and Physical Chemistry, University of Stockholm, Stockholm, Sweden

In connection with studies on transition metal compounds of defective sodium chloride structure, *e.g.* vanadium monoxide [1] and titanium monoxide [2], the powder pattern of niobium monoxide was registered by means of an X-ray G.M. diffractometer (CuK radiation). The structure derived by Brauer [3] for this substance (a defective sodium chloride structure with the positions 000 and $\frac{1}{2}\frac{1}{2}\frac{1}{2}$ vacant) is supported by our measurements, but as our investigation is based on quantitative data it may be worth mentioning.

The lattice parameter of the niobium monoxide sample as obtained from a Guinier powder photograph (internal standard potassium chloride $a = 6.2919$ Å at 20°C) was found to be 4.210_8 Å in excellent agreement with the value given by Brauer 4.2103 ± 0.0004 Å (21°C). The density was found to be 7.3 likewise in perfect agreement with Brauer's value of 7.30 and the value 7.27 calculated for a cell content of three formula units of NbO.

Table 1 gives the F values for the first fourteen reflexions as obtained from the diffractogram. The alternative structures (2)—(4) are among those discussed by Brauer *viz.* 3 Nb in $\frac{1}{2}\frac{1}{2}0$, $\frac{1}{2}0\frac{1}{2}$, $0\frac{1}{2}\frac{1}{2}$ for (2)

is necessary to apply empirical corrections. If this is properly carried out it is possible to determine the percentage of the various components of the mixture directly. If pure components are available it is easy to check the results by running artificial mixtures and thus to get a very high accuracy in the quantitative analysis.

The mass spectra of the samples of methyl linoleate and methyl linolenate studied show a peak at $m/e = 290$. In the case of methyl linoleate the height of this peak is 1.7 % of the parent peak ($m/e = 294$). For methyl linolenate the height of the $m/e = 290$ peak is 18 % of the parent peak at $m/e = 292$. This peak appears to be the parent peak of the methyl ester of a C_{18} acid containing four double bonds. Whether this acid is present as an impurity in the original samples or whether it is formed by a dehydration reaction in the heated intake system of the mass spectrometer cannot be said at present. The present evidence, however, is in favour of the first mentioned possibility. It has been proposed that acids of this type may be formed from linoleic and linolenic acids by dehydrogenation between the existing double bonds and the carboxyl group in such a way that all unsaturation is methylene-interrupted and all *cis*. (*cf.* Ref.[5]). C_{18} tetra-ethenoid acids have been found in the fats of marine animals [5,6].

In a complex mixture it is not possible to distinguish between geometrical and positional isomers within each group of unsaturated esters. The peak at $m/e = 296$ in the figure might thus be due to, *e.g.*, methyl oleate (methyl *cis*-$\Delta^{9,10}$-octadecenoate), methyl elaidate (methyl *trans*-$\Delta^{9,10}$-octadecenoate), or methyl petroselinate (methyl *cis*-$\Delta^{6,7}$-octadecenoate) or due to a mixture of mono-ethenoid esters. It may be possible to overcome this difficulty by examining suitable derivatives.

The high-mass, high-resolution mass spectrometer thus offers a convenient method for determining the fatty acid distribution ("fatty acid spectrum") of natural or synthetic fats. The analysis can be performed on a few milligrams of material.

The financial support of *Statens Tekniska Forskningsråd* and *Statens Medicinska Forskningsråd* is gratefully acknowledged. We are indebted to Dr. W. O. Lundberg, The Hormel Institute, Austin, Minnesota, for the gift of methyl esters of unsaturated fatty acids.

1. Asselineau, J., Ryhage, R. and Stenhagen, E. *Acta Chem. Scand.* **11** (1957) 196.
2. Brewer, A. K. and Dibeler, V. H. *J. Research Natl. Bur. Standards* **35** (1945) 125.
3. Robertson, A. J. B. *Mass Spectrometry*, London 1954, p. 84.
4. Barnard, G. P. *Modern Mass Spectrometry*, The Institute of Physics, London 1953, p. 192.
5. Holman, R. T. in Glick, D. *Methods of Biochemical Analysis*, N.Y. 1957, p. 99.
6. *Cf.* Hilditch, T. P. *The chemical constitution of natural fats*, 3 rd. Ed., London 1956.

Received June 26, 1957.

Note on the Crystal Structure of Niobium Monoxide

GEORG ANDERSSON and ARNE MAGNÉLI

Institute of Chemistry, University of Uppsala, Uppsala, and Institute of Inorganic and Physical Chemistry, University of Stockholm, Stockholm, Sweden

In connection with studies on transition metal compounds of defective sodium chloride structure, *e.g.* vanadium monoxide [1] and titanium monoxide [2], the powder pattern of niobium monoxide was registered by means of an X-ray G.M. diffractometer (CuK radiation). The structure derived by Brauer [3] for this substance (a defective sodium chloride structure with the positions 000 and $\frac{1}{2}\frac{1}{2}\frac{1}{2}$ vacant) is supported by our measurements, but as our investigation is based on quantitative data it may be worth mentioning.

The lattice parameter of the niobium monoxide sample as obtained from a Guinier powder photograph (internal standard potassium chloride $a = 6.2919$ Å at 20°C) was found to be 4.210_8 Å in excellent agreement with the value given by Brauer 4.2103 ± 0.0004 Å (21°C). The density was found to be 7.3 likewise in perfect agreement with Brauer's value of 7.30 and the value 7.27 calculated for a cell content of three formula units of NbO.

Table 1 gives the F values for the first fourteen reflexions as obtained from the diffractogram. The alternative structures (2)—(4) are among those discussed by Brauer *viz.* 3 Nb in $\frac{1}{2}\frac{1}{2}0$, $\frac{1}{2}0\frac{1}{2}$, $0\frac{1}{2}\frac{1}{2}$ for (2)

Table 1. X-Ray diffractometer data for niobium monoxide.

hkl	F_{obs}	F_{obs}—F(Nb)	Structure (2)		Structure (3)		Structure (4)	
			F_{calc}	F(O)	F_{calc}	F(O)	F_{calc}	F(O)
100	$\overline{32}$	4	$\overline{29}$	8	$\overline{36}$	0	$\overline{25}$	11
110	$\overline{38}$	$\overline{4}$	$\overline{40}$	$\overline{6}$	$\overline{34}$	0	$\overline{34}$	0
111	73	$\overline{21}$	78	$\overline{16}$	78	$\overline{16}$	86	$\overline{8}$
200	100	11	104	14	104	14	104	14
210	$\overline{25}$	3	$\overline{24}$	4	$\overline{28}$	0	$\overline{22}$	6
211	$\overline{34}$	$\overline{7}$	$\overline{31}$	$\overline{4}$	$\overline{27}$	0	$\overline{27}$	0
220	79	4	85	10	85	10	85	10
221	$\overline{22}$	2	$\overline{21}$	3	$\overline{24}$	0	$\overline{20}$	5
300	$\overline{22}$	2	$\overline{21}$	3	$\overline{24}$	0	$\overline{20}$	5
310	$\overline{26}$	$\overline{2}$	$\overline{27}$	$\overline{3}$	$\overline{24}$	0	$\overline{24}$	0
311	58	$\overline{11}$	61	$\overline{8}$	61	$\overline{8}$	65	$\overline{4}$
222	80	13	75	8	75	8	75	8
320	$\overline{22}$	0	$\overline{20}$	2	$\overline{22}$	0	$\overline{18}$	4
321	$\overline{24}$	$\overline{3}$	$\overline{24}$	$\overline{2}$	$\overline{21}$	0	$\overline{21}$	0

—(4) and 3 O in $\frac{1}{2}00$, $0\frac{1}{2}0$, $00\frac{1}{2}$ (structure (2)), 3 O randomly distributed in $\frac{1}{2}\frac{1}{2}\frac{1}{2}$, $\frac{1}{2}00$, $0\frac{1}{2}0$, $00\frac{1}{2}$ (structure (3)) and 3 O randomly arranged in 000, $\frac{1}{2}00$, $0\frac{1}{2}0$, $00\frac{1}{2}$ (structure (4)). For each of the structure alternatives, the values of F_{calc} for the two components of the unresolved reflexion (221 + 300) are identical and the corresponding values of F_{obs} are thus calculated considering the multiplicity of the reflexions. The signs alloted to F_{obs} are those determined by the arrangement of the Nb atoms.

The consistency is definitely better for structures (2) and (3) than for (4) (and for still another structure (5) discussed by Brauer). The difference between F_{calc} and F_{obs} for (2) and (3) is relatively small, as may be anticipated from the similarity of these two alternatives, but the data speak in favour of structure (2) in accordance with Brauer's opinion. The quotients $\Sigma||F_{obs}| - |F_{calc}||/\Sigma|F_{obs}|$ are 0.058, 0.079 and 0.109 for (2), (3) and (4), respectively. The table also gives the differences between F_{obs} and F(Nb) (the contribution of the niobium atoms to F_{calc}) which may represent the share in F_{obs} of the oxygen atoms. The quotients $\Sigma||F_{obs}-F(\mathrm{Nb})| - |F(\mathrm{O})||/\Sigma|F_{obs} - F(\mathrm{Nb})|$ are 0.44 for (2), 0.56 for (3) and 0.78 for (4).

Melting of niobium monoxide (small tablets) in an electric arc furnace with subsequent rapid quenching from the melting temperature did not change the structure of this compound. Evidently there is no indication of a phase transition similar to that found in titanium monoxide [2]. Thus high-temperature studies would be necessary to decide definitely whether there occurs a rapid transition to a random niobium monoxide at a certain temperature.

This investigation forms part of a research program on metal oxides and related compounds, financially supported by the *Swedish Natural Science Research Council.*

1. Andersson, G. *Acta Chem. Scand.* **8** (1954) 1599.
2. Kuylenstierna, U. and Magnéli, A. *Acta Chem. Scand.* **10** (1956) 1195.
3. Brauer, G. *Z. anorg. Chemie* **248** (1941)1.

Received July 8, 1957.

Preparation of Some Hydroxycoprostanes; 3α, 7α- and 3α, 12α-dihydroxycoprostane

Bile Acids and Steroids 49

SUNE BERGSTRÖM and
LENNART KRABISCH

Department of Physiological Chemistry, University of Lund, Lund, Sweden

In connection with studies on the transformation of cholesterol into bile acids it was of interest to study the metabolism of the coprostanes corresponding to the common bile acids. These compounds have now all been prepared through electrolysis of the appropriate bile acid with *iso*valeric acid. The data for 3α, 7α, 12α-trihydroxycoprostane, that was described recently,[1,2] has also been included for comparison. Some results of the metabolic studies with these compounds have already been published [1,3,4].

Experimental. 3α,12α-dihydroxycoprostane. Deoxycholic acid (2.0 g) was dissolved in methanol (450 ml) and *iso*valeric acid (13.5 ml, isomer-free) and a solution of sodium (290 mg) in methanol (50 ml) was added. The solution was placed in a beaker surrounded by ice. The electrolysis was run for 80 min with 4.2 A between platinum electrodes (5.2 cm^2) placed 0.2 cm from each other.

The mixture was then evaporated to dryness *in vacuo*, the residue was dissolved in a mixture of water and ether, the phases were separated and the aqueous phase reextracted twice with ether. The combined ether phases were washed with dilute sodium hydroxide and water and taken to dryness. The residue (1.84 g) was brought onto a column of silicic acid (30 g, dried at 120° for 24 h) prepared with methylene dichloride. The column was eluted with methylene dichloride containing 1.5 % of methanol, each fraction being 30 ml. Fractions 4 and 5 that contained the bulk of the material (1.35 g) were combined and recrystallized from aqueous acetone three times, when a constant melting point had been reached. Yield 550 mg, m.p. 108—110°C.

In the same way 3α, 7α-dihydroxy and 3α-hydroxycoprostane were prepared from chenodeoxycholic and lithocholic acid, respectively. The 3α-hydroxycoprostane was chromatographed in the system described by Danielson [5] for the reversed phase partition chromatography of monosubstitued C_{27}-steroids.

The data for these compounds together with those obtained earlier for the 3α-7α,12α-trihydroxycoprostane are listed in Table 1. Analysis by Microanalytical Laboratory, Department of Chemistry, University of Copenhagen. All rotations were made in chloroform, m.p.'s are corrected.

This work is part of investigations supported by *Statens medicinska forskningsråd* and *Knut och Alice Wallenbergs Stiftelse.*

1. Bergström, S. *Acta Chem. Scand.* **8** (1954) 1109.
2. Kazuno, T. and Mori, A. *Proc. Japan. Acad.* **30** (1954) 486.
3. Bergström, S. *Record Chem. Progr. Kresge Hooker Sci.* **16** (1955) 63.
4. Bergström, S. and Lindstedt, S. *Biochem. et Biophys. Acta* **19** (1956) 556.
5. Danielson, H. *Biochem. et Biophys. Acta. In press.*
6. Dorée, C. and Gardner, J. *J. Chem. Soc.* **93** (1908) 1630.
7. Dutcher, J. and Wintersteiner, O. *F. Am. Chem. Soc.* **61** (1939) 1992.

Received July 8, 1957.

Table 1.

	m.p. °C	$[\alpha]_D^{20°}$	M_D	conc g/100 ml CHLFORM	% C		% H	
					calc.	found	calc.	found
1. 3α-hydroxycoprostane (*cf* [6,7]) $C_{27}H_{48}O$	116—118	30.7	120	1.62	83.4	83.2	12.4	12.5
2. 3α,7α-dihydroxycoprostane $C_{27}H_{48}O_2 \cdot H_2O$	84—86	14.1	59	2.21	76.9	76.7	11.9	11.9
3. 3α,12α-dihydroxycoprostane $C_{27}H_{48}O_2$	108—110	45.0	182	1.06	80.1	80.1	12.0	11.7
4. 3α,7α,12α-trihydroxycoprostane $C_{27}H_{48}O_3$	185—186	30.4	128	1.24	77.1	76.7	11.5	11.4

Theoretical Determination of the Electronic Polarizability of Lithium and Scandium

INGA FISCHER-HJALMARS and MARIANNE SUNDBOM

Institute of Theoretical Physics, University of Stockholm, Stockholm, Sweden

Different experimental investigations, *e.g.* of the crystal structure of certain Al-Si-Me compounds [1], make it plausible to assume that the electronic polarizability of atoms and ions with partly filled *d*-shells (transition elements) should be considerably larger than the polarizability of closed shell atoms. This assumption can be supported by simple, theoretical considerations. However, no detailed theoretical investigation of this problem seems to have been published before. As the problem is of great interest in several connections, we have made an attempt to find the order of magnitude of this polarizability from a simple perturbation calculation.

The electronic polarizability of atoms with rare-gas-like configurations, *i.e.* s^2p^6 and $s^2p^6d^{10}$, has recently been treated as a perturbation problem by Sternheimer [2]. We have carried out a similar perturbation calculation for the case of atoms with one electron outside the closed shells and applied the result to Li $1s^22s$ and Sc $3d\,4s^2$. Using an one-electron model the unperturbed wave function can be written as a single Slater determinant of unperturbed one-electron functions φ_i. The first-order perturbation of these functions, φ_i', is determined by the equation

$$(H_0 - E_0)\ \varphi_i' = -V\ \varphi_i, \qquad (1)$$

where V is the perturbing potential. The electronic polarizability α is

$$\alpha = -\frac{2}{E^2}\sum_i \int \varphi_i^*\, V\, \varphi_i'\, d\tau \qquad (2)$$

where the sum is to be taken over all filled orbitals.

In the case of Sc the $3d$ orbital of the unperturbed atom cannot be given a definite m-value. We have shown, however, that the correct zeroth-order wave function for the $3d$ electron corresponds to $m = 0$. The differential equations (1) have been solved by numerical methods, using the Swedish electronic digital computor BESK. Hitherto, we have programmed the problem for one-electron orbitals of the simple analytic form $r^n e^{-\mu r}$. However, the programme can easily be modified so that also numerically given orbitals can be used. As the computed value of α is strongly depending on the choice of unperturbed functions, we can only expect to get a rough estimate by the use of simple analytical orbitals. As a check on our programme we have computed the polarizability of Ca^{2+}, previously calculated by Sternheimer [2].

Preliminary results for the polarizabilities of Li and Sc are given in Table 1. In the case of Li the contribution to α from the inner shell is negligible. In the case

Table 1. Calculated and experimental values of the electronic polarizability α.

Atom	α in units 10^{-24} cm^3	Method	Author
Li	16 ± 3	exptl.	Drechsler and Müller [4]
	20	theor., μ chosen to fit the best SCF orb.	present inv.
Ca^{2+}	0.47—1.1	exptl.	Tessmann, see [2]
	0.73	theor., SCF orb.	Sternheimer [2]
	0.83	theor., μ chosen to fit the best SCF orb.	present inv.
Ca	92	theor., μ from Slater's rules	present inv.
	52	theor., μ chosen to fit SCF orb.	present inv.
Sc	90	theor., μ from Slater's rules	present inv.

of Sc the same is true and the main contribution orginates from $3d\ 4s^2$. In order to discriminate between $3d$ and $4s^2$ we have also computed a of Ca $4s^2$. Table 1 shows that a of Ca and Sc both are much larger than a of Ca^{2+}.

An extension of the present investigation to include atoms with several d-electrons outside the closed shell is going on. It would be of special interest to look at Ni, for which an experimental value of a is available [3].

We are indebted to Dr. P. Spiegelberg, Stockholm, who has drawn our attention to this problem. The present investigation has been supported by *Statens Naturvetenskapliga Forskningsråd (The Swedish Natural Science Research Council)*. Full details of the work will be published by one of us (M.S.).

1. Spiegelberg, P. *Private communication.*
2. Sternheimer, R. M. *Phys. Rev.* **96** (1954) 951.
3. Liepack, H. and Drechsler, M. *Naturwiss.* **43** (1956) 52.
4. Drechsler, M. and Müller, E. W. *Z. Physik* **132** (1952) 195.

Received July 31, 1957.

Note on the Crystal Structures of Hexagonal HgO and Hg_2O_2NaI

KARIN AURIVILLIUS and
INGA-BRITT CARLSSON

Institute of Inorganic and Physical Chemistry, University of Stockholm, Stockholm, Sweden

The hexagonal modification of mercury (II)oxide and the compound Hg_2O_2NaI have been prepared according to Laruelle [1] and studied by X-ray diffraction methods.

HgO. Hexagonal form. Space group $P3_121$ No. 152. Unit cell dimensions $a = 3.577$ Å, $c = 8.681$ Å in agreement with the values given by Laruelle. The cell content is 3 formula units of HgO. The positions of the mercury atoms have been derived by means of trial methods from powder data registered with a Geiger-Mueller diffractometer using Cu$K\alpha$ radiation. A probable arrangement of the oxygen atoms has been obtained from space considerations. The point positions are:

3Hg in $3(a)$:$x0\frac{1}{3}$, $0x\frac{2}{3}$, $\bar{x}\bar{x}0$ with $x = 0.745$
3O in $3(b)$:$x0\frac{5}{6}$, $0x\frac{1}{6}$, $\bar{x}\bar{x}\frac{1}{2}$ with $x = 0.46$

This structure is built up of infinite spiral chains -O-Hg-O- running parallel to the c axis of the hexagonal unit cell. The distances and angles within the chains are:

Hg-O 2.03 Å The angle Hg-O-Hg 109°
Hg-Hg 3.30 Å The angle O-Hg-O 180°

This atomic arrangement is isostructural with the hexagonal modification of mercury(II)sulphide (cinnabar)[2]. The Hg-O distance and the bond angles are identical with those found in the planar zigzag chains -O-Hg-O- in orthorhombic mercury(II)oxide [3].

This investigation is to be continued by means of neutron diffraction methods in order to investigate the proposed oxygen arrangement. Studies on the stability relations between the modifications of mercury(II)oxide are in progress.

Hg_2O_2NaI. Space group $P6_222$ No. 180. Unit cell dimensions $a = 6.667$ Å, $c = 10.054$ Å. Cell content 3 formula units of Hg_2O_2NaI.

The positions of the mercury and iodine atoms have been derived on the basis of single crystal data.

6 Hg in $6(f)$:$\frac{1}{2}0z\frac{2}{3}, 0\frac{1}{2}\frac{2}{3}+z, \frac{1}{2}\frac{1}{2}\frac{1}{3}+z$
$\frac{1}{2}0\bar{z}, 0\frac{1}{2}\frac{2}{3}-z, \frac{1}{2}\frac{1}{2}\frac{1}{3}-z$ with $z=\frac{1}{3}$
3 I in $3(c)$:$\frac{1}{2}00, 0\frac{1}{2}\frac{2}{3}, \quad \frac{1}{2}\frac{1}{2}\frac{1}{3}$

This investigation is being continued in order to find the positions of the sodium and oxygen atoms.

These studies form part of a research program financially supported by the *Swedish Natural Science Research Council.*

1. Laruelle, M. P. *Compt. rend.* **241** (1955) 802.
2. Aurivillius, K. *Acta Chem. Scand.* **4** (1950) 1413.
3. Aurivillius, K. *Acta Chem. Scand.* **10** (1956) 852.

Received July 11, 1957.

of Sc the same is true and the main contribution orginates from $3d\ 4s^2$. In order to discriminate between $3d$ and $4s^2$ we have also computed a of Ca $4s^2$. Table 1 shows that a of Ca and Sc both are much larger than a of Ca^{2+}.

An extension of the present investigation to include atoms with several d-electrons outside the closed shell is going on. It would be of special interest to look at Ni, for which an experimental value of a is available [3].

We are indebted to Dr. P. Spiegelberg, Stockholm, who has drawn our attention to this problem. The present investigation has been supported by *Statens Naturvetenskapliga Forskningsråd (The Swedish Natural Science Research Council)*. Full details of the work will be published by one of us (M.S.).

1. Spiegelberg, P. *Private communication.*
2. Sternheimer, R. M. *Phys. Rev.* **96** (1954) 951.
3. Liepack, H. and Drechsler, M. *Naturwiss.* **43** (1956) 52.
4. Drechsler, M. and Müller, E. W. *Z. Physik* **132** (1952) 195.

Received July 31, 1957.

Note on the Crystal Structures of Hexagonal HgO and Hg_2O_2NaI

KARIN AURIVILLIUS and
INGA-BRITT CARLSSON

Institute of Inorganic and Physical Chemistry, University of Stockholm, Stockholm, Sweden

The hexagonal modification of mercury (II)oxide and the compound Hg_2O_2NaI have been prepared according to Laruelle [1] and studied by X-ray diffraction methods.

HgO. Hexagonal form. Space group $P3_121$ No. 152. Unit cell dimensions $a = 3.577$ Å, $c = 8.681$ Å in agreement with the values given by Laruelle. The cell content is 3 formula units of HgO. The positions of the mercury atoms have been derived by means of trial methods from powder data registered with a Geiger-Mueller diffractometer using Cu$K\alpha$ radiation. A probable arrangement of the oxygen atoms has been obtained from space considerations. The point positions are:

3Hg in $3(a)$:$x0\frac{1}{3}$, $0x\frac{2}{3}$, $\bar{x}\bar{x}0$ with $x = 0.745$
3O in $3(b)$:$x0\frac{5}{6}$, $0x\frac{1}{6}$, $\bar{x}\bar{x}\frac{1}{2}$ with $x = 0.46$

This structure is built up of infinite spiral chains -O-Hg-O- running parallel to the c axis of the hexagonal unit cell. The distances and angles within the chains are:

Hg-O 2.03 Å The angle Hg-O-Hg 109°
Hg-Hg 3.30 Å The angle O-Hg-O 180°

This atomic arrangement is isostructural with the hexagonal modification of mercury(II)sulphide (cinnabar)[2]. The Hg-O distance and the bond angles are identical with those found in the planar zigzag chains -O-Hg-O- in orthorhombic mercury(II)oxide [3].

This investigation is to be continued by means of neutron diffraction methods in order to investigate the proposed oxygen arrangement. Studies on the stability relations between the modifications of mercury(II)oxide are in progress.

Hg_2O_2NaI. Space group $P6_222$ No. 180. Unit cell dimensions $a = 6.667$ Å, $c = 10.054$ Å. Cell content 3 formula units of Hg_2O_2NaI.

The positions of the mercury and iodine atoms have been derived on the basis of single crystal data.

6 Hg in $6(f)$:$\frac{1}{2}0z\frac{2}{3}, 0\frac{1}{2}\frac{2}{3}+z, \frac{1}{2}\frac{1}{2}\frac{1}{3}+z$
$\frac{1}{2}0\bar{z}, 0\frac{1}{2}\frac{2}{3}-z, \frac{1}{2}\frac{1}{2}\frac{1}{3}-z$ with $z=\frac{1}{3}$
3 I in $3(c)$:$\frac{1}{2}00, 0\frac{1}{2}\frac{2}{3}, \quad \frac{1}{2}\frac{1}{2}\frac{1}{3}$

This investigation is being continued in order to find the positions of the sodium and oxygen atoms.

These studies form part of a research program financially supported by the *Swedish Natural Science Research Council.*

1. Laruelle, M. P. *Compt. rend.* **241** (1955) 802.
2. Aurivillius, K. *Acta Chem. Scand.* **4** (1950) 1413.
3. Aurivillius, K. *Acta Chem. Scand.* **10** (1956) 852.

Received July 11, 1957.

A Simple Procedure for the Preparation of Single Crystals of Orthorhombic Mercury(II)oxide

KARIN AURIVILLIUS and
INGA-BRITT CARLSSON

Institute of Inorganic and Physical Chemistry, University of Stockholm, Stockholm, Sweden

The procedures described in the literature for the preparation of single crystals of orthorhombic mercury(II)oxide [1] have been found to be rather uncertain and give poor results. In connection with studies on the hexagonal modification of this substance a simple method was found for the synthesis of beautiful crystals of the orthorhombic form. One part of 0.1 M K_2HgI_4 was mixed with two parts of 10–13 M NaOH and poured into a gold tube which was covered with a gold lid. The tube was slid into a pyrex glass tube which was sealed and placed in an oven at 100–175°C for about 70 h.

The crystals appeared in the form of light red rods with lustrous faces of up to 2 mm extension. Amply exposed powder patterns obtained in a Guinier focusing camera did not show any reflexions not belonging to the pattern for orthorhombic mercury(II)oxide.

This convenient method has been discovered in connection with work on mercury compounds which has been financially supported by the *Swedish Natural Science Research Council.*

Gmelin-Kraut, *Handbuch der anorganischen Chemie* V: II 507—508, 1695, 1914.

Received July 11, 1957.

Separation of Acid Mucopolysaccharides by Paper Electrophoresis

STIG D. SCHULTZ-HAUDT*

Johan Throne Holst's Institute for Nutrition Research, University of Oslo, Blindern, Norway

The separation of acid mucopolysaccharides from various sources by means of paper electrophoresis has been reported by several investigators [1-4]. The conditions for the electrophoresis as well as the methods of locating the separated mucopolysaccharide fractions have differed in each particular case. For the purpose of investigating the mucopolysaccharide contents of mucous membranes a number of methods were tested, but no particular procedure was found to be entirely satisfactory. However, a system was developed which allowed a distinct separation of hyaluronic acid and chondroitin sulphate. This system represents a combination of some of the methods referred to above.

Methods. A box, similar to that described by Grassmann [5], was constructed from parts cut out of 0.5 cm thick Perspex acrylic sheet to serve as support for the paper.

The buffer solution employed was made by combining 100 ml of 0.9 M sodium chloride with 50 ml of 0.2 M phosphate buffer (pH 7.0) and diluting to a total volume of one liter with distilled water.

The paper used was Whatman No. 3 MM ilter paper for chromatography.

The electrophoresis was carried out at 160 V for 18 h at room temperature.

Prior to electrophoresis, a paper strip, 57 cm in length and 4 cm wide, was moistened with buffer from both ends to within 1 cm from the midline and blotted dry with filter paper. The paper was next placed in the box, and the vertical ends of the paper were dipped into the buffer. The horizontal stretch of the paper strip in position in the box was 40 cm. Buffer equilibration was allowed to proceed for 30 min. From 50 to 100 μl of a crude mucopolysaccharide mixture dissolved in the buffer were then applied along the midline to the wet paper. Another 30 min were allowed to pass before the current was connected.

Following electrophoresis, the paper strip was dried at 110°C for 30 min. Acid mucopolysaccharide fractions were next located in the manner described by Bera *et al.*[2] In order to obtain satisfactory results, however, it was necessary subsequent to the immersion of the paper in Cetavlon to wash it in hot running tap water for 45 min. The paper was then dried at 110°C for one hour, sprayed with the bromocresol purple reagent, and again dried at 110°C for 15 min.

* The present investigations are supported financially by the *Norwegian Dental School*, by the *Norwegian Institute of Dental Research* and by *New York Community Trust.*



Fig. 1.

In order to identify the separated fractions, two paper strips were run at the same time. Following electrophoresis, one paper was developed with Cetavlon/bromocresol purple [2]. The areas of the second paper corresponding to the spots on the first paper were cut out and eluted in the manner described by Rienits [1]. Concentrated hydrochloric acid was added to the eluates in amounts sufficient to make the solution 7 N in terms of the acid. Hydrolysis was carried out in sealed test tubes at 100°C for 4 h. The solutions were treated with Norit A for a few minutes, centrifuged, and the supernates were taken to dryness by lyophilization. The residues were dissolved in appropriate amounts of distilled water and paper chromatography of these solutions were carried out by the method of Stoffyn and Jeanloz [6] for the identification of the aminosugars present.

In cases where larger amounts of mucopolysaccharide mixtures were applied to paper strips for electrophoretic separation, milligram amounts of each fraction could be obtained after elution by precipitating with ethanol in the presence of sodium acetate. Following hydrolysis, the mucopolysaccharides obtained in this fashion were shown by paper chromatography and paper electrophoresis to be of a satisfactory purity.

Results and discussion. Fig. 1 represents a typical result of paper electrophoresis of a crude mucopolysaccharide mixture obtained from human gingiva, followed by staining with Cetavlon/bromocresol purple.

By means of the method described, it was shown that the slowest moving component contained glucosamine as the only aminosugar, whereas the fastest moving component contained galactosamine, but no glucosamine.

Paper electrophoresis of a number of crude mucopolysaccharide mixtures extracted in different manners from various tissues and of widely different purities were carried out. The results obtained showed that acid mucopolysaccharides could readily be separated and identified in the manner described, and the results were entirely reproduceable. Amounts of 5—6 mg of crude mixtures could be applied on the paper for electrophoresis. When amounts of a particular acid mucopolysaccharide were below 100 μg the spot produced by the staining reaction was very weak.

None of the other staining reagents tested gave as distinct results as those obtained with the Cetavlon/bromocresol purple method.

The separation of hyaluronic acid and chondroitin sulphate in the manner described compared favorably to all of the other systems tested.

The above described system provides a simple tool for a comparatively rapid demonstration of the presence of acid mucopolysaccharides in biological materials and for a ready separation of hyaluronic acid and chondroitin sulphate from a mixture.

1. Rienits, K. G. *Biochem. J.* **53** (1953) 79.
2. Bera, B. C., Foster, A. B. and Stacey, M. *J. Chem. Soc.* **1955** 3788.
3. Odell, T. T., Jr. and Anderson, B. *Proc. Soc. Exptl. Biol. Med.* **94** (1957) 151.
4. Hall, D. A., Lloyd, P. F., Happey, F., Horton, W. G. and Naylor, A. *Nature* **179** (1957) 1078.
5. Grassmann, W. in *A Manual of Paper Chromatography and Paper Electrophoresis.* Academic Press, Inc., New York 1955.
6. Stoffyn, P. J. and Jeanloz, R. W. *Arch. Biochem. Biophys.* **52** (1954) 373.

Received June 26, 1957.

A Simple Procedure for the Preparation of Single Crystals of Orthorhombic Mercury(II)oxide

KARIN AURIVILLIUS and
INGA-BRITT CARLSSON

Institute of Inorganic and Physical Chemistry, University of Stockholm, Stockholm, Sweden

The procedures described in the literature for the preparation of single crystals of orthorhombic mercury(II)oxide [1] have been found to be rather uncertain and give poor results. In connection with studies on the hexagonal modification of this substance a simple method was found for the synthesis of beautiful crystals of the orthorhombic form. One part of 0.1 M K_2HgI_4 was mixed with two parts of 10–13 M NaOH and poured into a gold tube which was covered with a gold lid. The tube was slid into a pyrex glass tube which was sealed and placed in an oven at 100–175°C for about 70 h.

The crystals appeared in the form of light red rods with lustrous faces of up to 2 mm extension. Amply exposed powder patterns obtained in a Guinier focusing camera did not show any reflexions not belonging to the pattern for orthorhombic mercury(II)oxide.

This convenient method has been discovered in connection with work on mercury compounds which has been financially supported by the *Swedish Natural Science Research Council.*

Gmelin-Kraut, *Handbuch der anorganischen Chemie* V: II 507—508, 1695, 1914.

Received July 11, 1957.

Separation of Acid Mucopolysaccharides by Paper Electrophoresis

STIG D. SCHULTZ-HAUDT*

Johan Throne Holst's Institute for Nutrition Research, University of Oslo, Blindern, Norway

The separation of acid mucopolysaccharides from various sources by means of paper electrophoresis has been reported by several investigators [1-4]. The conditions for the electrophoresis as well as the methods of locating the separated mucopolysaccharide fractions have differed in each particular case. For the purpose of investigating the mucopolysaccharide contents of mucous membranes a number of methods were tested, but no particular procedure was found to be entirely satisfactory. However, a system was developed which allowed a distinct separation of hyaluronic acid and chondroitin sulphate. This system represents a combination of some of the methods referred to above.

Methods. A box, similar to that described by Grassmann [5], was constructed from parts cut out of 0.5 cm thick Perspex acrylic sheet to serve as support for the paper.

The buffer solution employed was made by combining 100 ml of 0.9 M sodium chloride with 50 ml of 0.2 M phosphate buffer (pH 7.0) and diluting to a total volume of one liter with distilled water.

The paper used was Whatman No. 3 MM ilter paper for chromatography.

The electrophoresis was carried out at 160 V for 18 h at room temperature.

Prior to electrophoresis, a paper strip, 57 cm in length and 4 cm wide, was moistened with buffer from both ends to within 1 cm from the midline and blotted dry with filter paper. The paper was next placed in the box, and the vertical ends of the paper were dipped into the buffer. The horizontal stretch of the paper strip in position in the box was 40 cm. Buffer equilibration was allowed to proceed for 30 min. From 50 to 100 μl of a crude mucopolysaccharide mixture dissolved in the buffer were then applied along the midline to the wet paper. Another 30 min were allowed to pass before the current was connected.

Following electrophoresis, the paper strip was dried at 110°C for 30 min. Acid mucopolysaccharide fractions were next located in the manner described by Bera *et al.*[2] In order to obtain satisfactory results, however, it was necessary subsequent to the immersion of the paper in Cetavlon to wash it in hot running tap water for 45 min. The paper was then dried at 110°C for one hour, sprayed with the bromocresol purple reagent, and again dried at 110°C for 15 min.

* The present investigations are supported financially by the *Norwegian Dental School*, by the *Norwegian Institute of Dental Research* and by *New York Community Trust.*

On the Action of Peroxidase on 3,5-Diiodotyrosine

JAN-GUSTAF LJUNGGREN

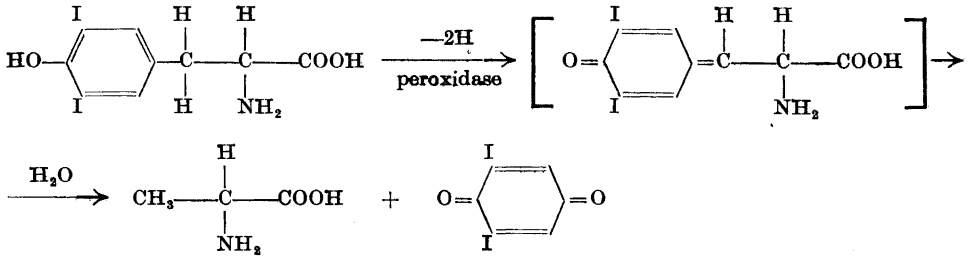
Medicinska Nobelinstitutet, Biokemiska avdelningen, Stockholm, Sweden

It has been suggested [1] that thyroxine is formed from 3,5-diiodotyrosine through the action of peroxidase but no attempts to verify this theory experimentally seem to have been made.

When 3,5-diiodotyrosine, hydrogen peroxide and peroxidase were incubated no formation of thyroxine could in fact be detected. However, another reaction product was observed which might be a possible intermediate in the conversion of 3,5-diiodotyrosine into thyroxine.

3,5-diiodotyrosine was incubated as described below with crystallized verdoperoxidase and hydrogen peroxide and a sample of the solution was studied by paper chromatography. The chromatograms were developed with butanol:acetic acid:water (4:1:1) and the spots visualised with ninhydrin. Alanine was thus identified as one of the reaction products.

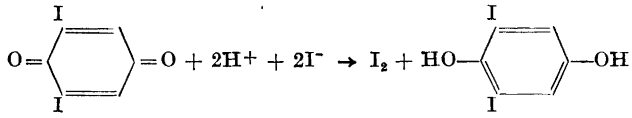
A possible reaction giving alanine as a reaction product would be the following:



The other hypothetical reaction product, 2,6-diiodobenzoquinone, was identified in the reaction mixture by extraction with petroleum ether and crystallization from the same solvent. The melting point of the product was 177°C, as reported for 2,6-diiodobenzoquinone [2], and the mixed melting point with an authentic sample of the quinone prepared according to Ref.[2] was unchanged.

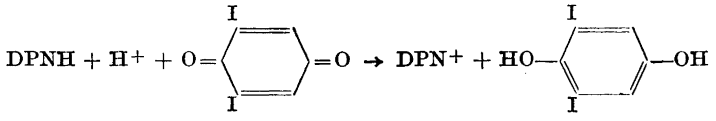
The identity of this reaction product was also confirmed by incubating the latter with potassium iodide in acid solution. Free iodine and a compound identified by paper chromatography as 2,6-diiodohydroquinone were found.

Thus the reaction was the following:



The 2,6-diiodobenzoquinone might be a precursor to thyroxine. It is, however, evident that it must first be reduced to 2,6-diiodohydroquinone.

Wosilait and Nason [3] have previously found that some benzoquinones, *e.g.* 2,6-dichlorobenzoquinone, were easily reduced by DPNH to hydroquinones non enzymatically. We have found that 2,6-diiodobenzoquinone also reacts rapidly with DPNH. The oxidation of DPNH to DPN+ by 2,6-diiodobenzoquinone was followed in a Beckman DU spectrophotometer at 340 mμ



When 2,6-diiodobenzoquinone was incubated with DPNH, 2,6-diiodohydroquinone could be isolated by extraction with ethyl ether, the ether evaporated and the product crystallized from water. The melting point was as reported for 2,6-diiodohydroquinone [4] (144°C) and the mixed melting point between the isolated substance and an authentic sample of 2,6 diiodohydroquinone was the same. They also had the same R_F value on paper chromatogram.

The 2,6-diiodohydroquinone was quantitatively determined both by paper chromatography and a colorimetric method [5]. The latter is based upon the reduction of ferric ions to ferrous ions by a hydroquinone followed by a colorimetric determination of the ferrous ions with *o*-phenantroline. Here DPN^+ does not interfere but the solution must be free from DPNH in order to prevent a new formation of hydroquinone from the benzoquinone formed when ferric ions are reduced to ferrous ions.

The yield of 2,6-diiodohydroquinone was found to be 20 % of theory when 20 ml 3,5-diiodotyrosine (10^{-3} M) in 0.05 M phosphate buffer, pH = 7.2, temperature = 20°C, was incubated with 0.5 ml crystallized verdoperoxidase (3.2 mg VPO/ml) and 0.5 ml H_2O_2 (10^{-2} M). The hydrogen peroxide was added slowly by means of a motor driven micrometer syringe; the 0.5 ml volume requiring 10 h. The hydrogen peroxide had to be added slowly in order to prevent a destruction of the verdoperoxidase, as observed by Agner. When all the hydrogen peroxide had been consumed 1.85 ml DPNH (1 mg DPNH/ml) was added and its oxidation followed spectrophotometrically at 340 mμ.

We have verified that peroxidase is present in the thyroid gland and probably in higher amounts than previously reported [6].

Thus, 2,6-diiodobenzoquinone and 2,6-diiodohydroquinone might be intermediates in the conversion of 3,5-diiodotyrosine into thyroxine. The formation of thyroxine by the condensation of one molecule 3,5-diiodotyrosine and one molecule 2,6-diiodohydroquinone, is now being investigated. Attempts are also being made to purify peroxidase from the thyroid gland. The results of these studies will be reported in this journal.

Acknouledgements. The author wishes to thank Professor Hugo Theorell for valuable help and encouragement during this work. Thanks are also due to Dr. K. Agner for kindly supplying the crystalline verdoperoxidase, to Drs. B. Sörbo, K. G. Paul and S. Åkerfeldt for valuable discussions and to Dr. George D. Ludwig for correction of the language.

1. Westerfeld, W. W. and Lowe, C. *J. Biol. Chem.* **145** (1942) 463.
2. Kehrmann, F. and Messinger, J. *Ber.* **26** (1893) 2377.
3. Wosilait, W. D. and Nason, A. *J. Biol. Chem.* **206** (1954) 255.
4. Seifert, B. *J. prakt. Chem.* **28** (1883) 437.
5. Stephen, W. J. *Metallurgia* **37** (1948) 333.
6. Glock, G. E. *Nature* **154** (1944) 460.

Received July 25, 1957.

Hexadecenoic Acid as a Feature of Beef and Horse Subcutaneous Fat

OLLE DAHL

Scans Centrallaboratorium, Malmö, Sweden

Recently the fatty acid composition of some typical fats from domestic animals was examined by the author [1]. Among these fats a beef subcutaneous fat from hide trimmings showed a remarkably high content of hexadecenoic acid, *viz.* 13.0 mole-%. Subsequently, when studying the relationship between iodine value and content of various fatty acids as well as between the content of the fatty acids themselves in natural fats [2], the said subcutaneous fat behaved differently from the others, evidently dependent on the high content of hexadecenoic acid. Furthermore, in an extensive investigation of the characteristics of more than 700 animal fats [3], the beef subcutaneous fats showed a lower saponification equivalent throughout and, besides, the relations between the characteristics were divergent from those of other fats. (In various investigations (for references, *cf.* Ref.[2]) pig subcutaneous fat (back fat) was proved to contain but moderate amounts of hexadecenoic acid, about 3 mole-%.)

These findings gave rise to a further confirmation of hexadecenoic acid as a feature of beef subcutaneous fat. The most abundant depot of subcutaneous fat is the brisket. The brisket fat from 10 cows was collected, mixed and extracted by means of ethyl ether, saponified and esterified by

When 2,6-diiodobenzoquinone was incubated with DPNH, 2,6-diiodohydroquinone could be isolated by extraction with ethyl ether, the ether evaporated and the product crystallized from water. The melting point was as reported for 2,6-diiodohydroquinone [4] (144°C) and the mixed melting point between the isolated substance and an authentic sample of 2,6 diiodohydroquinone was the same. They also had the same R_F value on paper chromatogram.

The 2,6-diiodohydroquinone was quantitatively determined both by paper chromatography and a colorimetric method [5]. The latter is based upon the reduction of ferric ions to ferrous ions by a hydroquinone followed by a colorimetric determination of the ferrous ions with *o*-phenantroline. Here DPN^+ does not interfere but the solution must be free from DPNH in order to prevent a new formation of hydroquinone from the benzoquinone formed when ferric ions are reduced to ferrous ions.

The yield of 2,6-diiodohydroquinone was found to be 20 % of theory when 20 ml 3,5-diiodotyrosine (10^{-3} M) in 0.05 M phosphate buffer, pH = 7.2, temperature = 20°C, was incubated with 0.5 ml crystallized verdoperoxidase (3.2 mg VPO/ml) and 0.5 ml H_2O_2 (10^{-2} M). The hydrogen peroxide was added slowly by means of a motor driven micrometer syringe; the 0.5 ml volume requiring 10 h. The hydrogen peroxide had to be added slowly in order to prevent a destruction of the verdoperoxidase, as observed by Agner. When all the hydrogen peroxide had been consumed 1.85 ml DPNH (1 mg DPNH/ml) was added and its oxidation followed spectrophotometrically at 340 mμ.

We have verified that peroxidase is present in the thyroid gland and probably in higher amounts than previously reported [6].

Thus, 2,6-diiodobenzoquinone and 2,6-diiodohydroquinone might be intermediates in the conversion of 3,5-diiodotyrosine into thyroxine. The formation of thyroxine by the condensation of one molecule 3,5-diiodotyrosine and one molecule 2,6-diiodohydroquinone, is now being investigated. Attempts are also being made to purify peroxidase from the thyroid gland. The results of these studies will be reported in this journal.

Acknouledgements. The author wishes to thank Professor Hugo Theorell for valuable help and encouragement during this work. Thanks are also due to Dr. K. Agner for kindly supplying the crystalline verdoperoxidase, to Drs. B. Sörbo, K. G. Paul and S. Åkerfeldt for valuable discussions and to Dr. George D. Ludwig for correction of the language.

1. Westerfeld, W. W. and Lowe, C. *J. Biol. Chem.* **145** (1942) 463.
2. Kehrmann, F. and Messinger, J. *Ber.* **26** (1893) 2377.
3. Wosilait, W. D. and Nason, A. *J. Biol. Chem.* **206** (1954) 255.
4. Seifert, B. *J. prakt. Chem.* **28** (1883) 437.
5. Stephen, W. J. *Metallurgia* **37** (1948) 333.
6. Glock, G. E. *Nature* **154** (1944) 460.

Received July 25, 1957.

Hexadecenoic Acid as a Feature of Beef and Horse Subcutaneous Fat

OLLE DAHL

Scans Centrallaboratorium, Malmö, Sweden

Recently the fatty acid composition of some typical fats from domestic animals was examined by the author [1]. Among these fats a beef subcutaneous fat from hide trimmings showed a remarkably high content of hexadecenoic acid, *viz.* 13.0 mole-%. Subsequently, when studying the relationship between iodine value and content of various fatty acids as well as between the content of the fatty acids themselves in natural fats [2], the said subcutaneous fat behaved differently from the others, evidently dependent on the high content of hexadecenoic acid. Furthermore, in an extensive investigation of the characteristics of more than 700 animal fats [3], the beef subcutaneous fats showed a lower saponification equivalent throughout and, besides, the relations between the characteristics were divergent from those of other fats. (In various investigations (for references, *cf.* Ref.[2]) pig subcutaneous fat (back fat) was proved to contain but moderate amounts of hexadecenoic acid, about 3 mole-%.)

These findings gave rise to a further confirmation of hexadecenoic acid as a feature of beef subcutaneous fat. The most abundant depot of subcutaneous fat is the brisket. The brisket fat from 10 cows was collected, mixed and extracted by means of ethyl ether, saponified and esterified by

Table 1. Component fatty acids of beef brisket fat and horse wither fat.

Brisket fat: iodine value 56.4; sapon. equiv. 278.1; unsap. matter 0.33 %
Wither » » » 84.2; » » 279.8; » » 0.42 %

Component fatty acids	Beef brisket fat		Horse wither fat	
	% (weight)	% (mole)	% (weight)	% (mole)
Saturated:				
Myristic	3.2	3.7	4.4	5.1
Palmitic	31.3	32.5	26.0	27.1
Stearic	5.4	5.0	2.1	2.0
Unsaturated:				
Tetradecenoic	1.9	2.2	1.7	2.0
Hexadecenoic	16.9	17.7	14.2	14.9
Oleic	38.9	36.6	35.2	33.3
Octadecadienoic	2.4	2.3	6.4	6.1
Octadecatrienoic	—	—	9.6	9.2
C_{20}-acids	—	—	0.4	0.3

methyl alcohol. The component fatty acids were determined by fractional distillation of the methyl esters as previously described [1]. The cows were killed at the end of March, *i. e.* prior to the pasture-feeding.

With regard to pure horse subcutaneous fat, no data of its composition are available whatsoever. It was decided, therefore, to examine the wither fat, which generally is the most abundant horse subcutaneous fat, in the same way as the brisket fat from cows. For this purpose the wither fat from 4 horses — 3 geldings and 1 mare — was collected. The animals were slaughtered at the same time as the cows. The results are summarized in Table 1.

As is seen from Table 1 the content of hexadecenoic acid is considerable both in brisket and in wither fat, the content of the former being still higher than that previously found in beef hide fat [1].

Dugan *et al.*[4] investigated the composition of beef brisket fat but disregarded the hexadecenoic acid, the content of which was simply included in that of oleic acid. In a review of the formation of animal fats Shorland [5] refers to unpublished data on the composition of beef subcutaneous fat, indicating a content of 4.6 mole-% hexadecenoic acid only.

The fairly high content of hexadecenoic acid previously found by the author in horse fats [1] may partly be due to the presence of 17 % wither fat in the fatty tissue mixture.

Finally it may be mentioned that, among fats of land animals, bone fat occasionally holds significant amounts of hexadecenoic acid. Thus, beef bone fat contains up to 10 or even 11 mole-% of this acid (for references, see Ref.[2]). In hoof oil and "offal oil" from horse, the latter deriving from bones and trimmings mixed in indefinite proportions, Brooker and Shorland [6] found no less than 20.5 and 11.5 mole-% hexadecenoic acid, respectively.

1. Dahl, O. *Z. Lebensm.-Untersuch. u. Forsch.* **106** (1957) 81.
2. Dahl, O. *Z. Lebensm.-Untersuch. u. Forsch.* **106** (1957) 349.
3. Dahl, O. *Acta Agr. Scand. To be published.*
4. Dugan, L. R., Maroney, J. E. and Petheram, M. *J. Am. Oil Chemists' Soc.* **29** (1952) 298.
5. *Progress in the Chemistry of Fats and Other Lipids*, Vol. 3; Pergamon Press, London & New York, 1955, p. 276: Shorland, F. B. *Formation of Animal Fats.*
6. Brooker, E. G. and Shorland, F. B. *Biochem. J.* **46** (1950) 80.

Received August 13, 1957.

Plant Growth Regulators II

Methyl- and Methoxysubstituted Naphthylboronic Acids

SVEN-OLOV LAWESSON*

Department of Organic Chemistry, Chemical Institute, University of Uppsala, Sweden

1- and 2-Naphthylmethylboronic acids have earlier been shown to be conspicuous anti-auxins [1]. As the aralkylboronic acids are very sensitive to atmospheric oxygen and difficult to handle, arylboronic acids have also been included in the investigation. Thus the writer has recently prepared a number of thiopheneboronic acids[2]. As he is not in a position to pursue these investigations for the time being, the data for some lately prepared naphthylboronic acid are given here.

Substituted phenylboronic acids have been investigated biologically by several authors [3-7] and Professor B. Åberg is now testing the thiophene- and naphthylboronic acids. According to preliminary reports, they have about the same effect [8] as those investigated by Torssell [7]. The results will be published elsewhere.

The naphthyl boronic acids were prepared *via* the lithium reagents at a low temperature following usual procedures. The lithium reagents were obtained by lithium-halogen exchange reactions from the corresponding bromine compounds, except for 3-methoxy-2-naphthylboronic acid; in this case the lithium reagent was prepared by metalating 2-methoxynaphthalene by the method of Sunthankar and Gilman [9].

Experimental. Reactions with lithium were performed under dry oxygen-free nitrogen in a standard assembly.

As a typical example we will describe the preparation of 2-methyl-1-naphthylboronic acid: 11 g of 1-bromo-2-methylnaphthalene in 75 ml of absolute ether was cooled to 0°C and then treated with 50 ml of 1 M butyllithium in ether. After stirring for 15 min the lithium reagent was slowly added with stirring to 20 g of tributyl borate in dry ether, cooled to —70°C. The stirring was continued for 4 h and then the reaction mixture was treated with 1 M hydrochloric acid, the ether layer separated and the aqueous phase extracted with ether. The combined ether layers were extracted with sodium hydroxide. The alkaline solution was acidified with hydrochloric acid, precipitating the acid as a white powder. After recrystallisation from water-ethanol and drying in air the acid was obtained as small, white needles. M. p. 125—127 °C. Weight 3.8 g. Yield 41 %.

The data for this and the other boronic acids are tabulated in Table 1.

The author is indebted to Professor B. Åberg for private communications. A grant from the *Swedish Natural Science Research Council* is gratefully acknowledged.

* Present address: Department of Organic Chemistry, University of Chicago, Chicago 37, Ill.

Table 1. Preparation of substituted naphthylboronic acids *via* the lithium reagent.

Boronic acid	M. p. °C	Yield °C	Boron	
			Calc. %	Found %
2-Methyl-1-naphthyl-	125—127	41	5.83	5.85
4-Methyl-1-naphthyl-	205—207	54	5.83	5.87
2-Methoxy-1-naphthyl-	143—145	50	5.36	5.35
3-Methoxy-2-naphthyl-	153—155	39	5.36	5.39

1. Lawesson, S.-O. *Arkiv Kemi* **10** (1956) 171.
2. Lawesson, S.-O. *Arkiv Kemi* **11** (1957) 387.
3. Caujolle, F. and Bergal, G. *Compt. rend.* **228** (1949) 1516.
4. Caujolle, F. and Bergal, G. *Ibid* **230** (1950) 1101.
5. Caujolle, F. and Bergal, G. *Ibid.* **231** (1950) 1550.
6. Caujolle, F. and Bergal, G. *Ibid* **232** (1951) 109.
7. Torssell, K. *Physiol. Plantarum* **9** (1956) 652.
8. Åberg, B. *Private communication.*
9. Sunthankar, S. V. and Gilman, H. *J. Org. Chem.* **16** (1950) 8.

Received August 16, 1957.

ACTA CHEMICA SCANDINAVICA 11 (1957) 1077—1096

Proceedings of the Danish Biochemical Society

Papers read at the joint meeting of the Scandinavian Biochemical Societies in Copenhagen, June 3—4, 1957

The Enzymic Amination of Xanthosine-5-phosphate to Guanosine-5-phosphate

Ulf Lagerkvist

Biochemical Department, Karolinska institutet, Stockholm, Sweden

In a previous communication [1] the occurrence of two enzyme-catalyzed reactions in extracts of pigeon liver acetone powder was reported, leading from inosine-5-phosphate to guanosine-5-phosphate *via* xanthosine-5-phosphate. The first reaction took place only in the presence of DPN * while the second reaction required ATP, Mg^{++}-ions and L-glutamine as an aminogroup donor. NH_4^+-ions or L-aspartate could not substitute for L-glutamine while L-glutamate was active at higher concentrations owing to the presence of glutamine synthease in the crude extract.

Inosine-5-phosphate $\xrightarrow{\text{DPN}}$ Xanthosine-5-phosphate (1)

Xanthosine-5-phosphate $\xrightarrow[\text{L-glutamine}]{\text{ATP}}$ Guanosine-5-phosphate (2)

At the same time Abrams and Bentley [2,3] demonstrated the occurrence of similar reactions in extracts of rabbit bone marrow while Gehring and Magasanik [4] reported on the partial purification of an enzyme catalyzing reaction (1) from *Aerobacter aerogenes*. Magasanik *et al.*[5] have later reported briefly on the purification of an enzyme from *E. coli* that aminated XMP by a different mechanism using NH_4^+-ions as aminogroup donors.

The enzyme (or enzymes) catalyzing reaction (2) has been purified 80—90 fold over the crude extract. Acetone powder of pigeon liver was extracted with dilute phosphate buffer pH 7.4 and after acidification to pH 6 fractionated with ammonium sulfate between 30 and 50 % saturation. The precipitate was dissolved in phosphate buffer pH 7.4 and inactive protein removed by adding $MnCl_2$. The centrifugate was again fractionated with ammonium sulfate between 39 and 55 % saturation. The precipitate was dissolved in dilute phosphate buffer pH 7.4, dialyzed shortly and chromatographed on DEAE-cellulose in PO_4-form by gradient elution with phosphate buffer pH 6.0. A typical preparation is shown in Table 1.

Table 1. Purification of the enzyme.

Purification step	mg protein	Spec. act.	Total units
Crude extract	8 600	0.21	1 810
1st ammonium sulfate precipitate	3 660	0.54	1 970
Adsorption on manganous phosphate	1 830	0.93	1 700
2nd ammonium sulfate precipitate	500	1.70	850
Chromatography on DEAE-cellulose	14	19	266

Using the purified enzyme no amination of XMP was obtained in the presence of L-glutamate instead of L-glutamine. Balance experiments indicate the following stoichiometry for reaction (2):

XMP + L-glutamine + ATP → GMP + L-glutamate + AMP + pyrophosphate

* The following abbreviations are employed: AMP = adenosine-5-phosphate, ATP = adenosine-5-triphosphate, DEAE = diethylaminoethyl, DPN = diphosphopyridine nucleotide, XMP = xanthosine-5-phosphate.

1. Lagerkvist, U. *Acta Chem. Scand.* **9** (1955) 1028.
2. Abrams, R. and Bentley, M. *J. Am. Chem. Soc.* **77** (1955) 4179.
3. Bentley, M. and Abrams, R. *Federation Proc.* **15** (1956) 218.
4. Gehring, L. B. and Magasanik, B. *J. Am. Chem. Soc.* **77** (1955) 4685.
5. Magasanik, B., Moyed, H. S. and Karibian, D. *J. Am. Chem. Soc.* **78** (1956) 1510.

Enzymic Formation of Uridine-5′-phosphate from Uracil

Ola Sköld and Peter Reichard

Biochemical Department, Karolinska Institutet, Stockholm, Sweden

Most mammalian tissues studied show a relatively poor utilization of uracil for pyrimidine nucleotide synthesis. In the Ehrlich ascites tumor, however, uracil was incorporated into polynucleotide pyrimidines as rapidly as orotic acid. In a study of the enzymic mechanism of this process it was found that uridine-5′-phosphate(UMP) formation from uracil in acetone powder extracts of the tumor proceeded according to:

$$\text{Uracil} + \text{ribose-1-phosphate} \xrightarrow[\text{phosphorylase}]{\text{nucleoside}} \text{uridine} + \text{phosphate}$$

$$\text{Uridine} + \text{ATP} \xrightarrow[\text{kinase}]{\text{uridine}} \text{UMP} + \text{ADP}$$

Both enzymes involved are known to occur in mammalian organs, *e. g.* liver, which form very little UMP from uracil.

We have now investigated the amount of these two enzymes in the ascites tumor and in rat liver. Furthermore, the breakdown of uracil to CO_2 was also studied, since it had been proposed that this process might determine uracil utilization in different tissues [2].

A significant difference was found in the amount of nucleoside phosphorylase as measured by a spectrophotometric assay. Uridine kinase was consistently *ca.* 10 times more active in extracts of the tumor than in liver extracts. A high concentration of uridine was necessary for optimum UMP synthesis. In accordance with earlier findings of other investigators we observed a quite rapid breakdown of uracil to CO_2 in rat liver preparations. No such degradation was observed in tumor extracts, however. In both cases a high TPNH level was maintained during the reaction.

It seems likely that uracil utilization by different tissues will depend on a competition between catabolic reactions which degrade uracil to CO_2 and the anabolic formation of UMP.

1. Reichard, P. and Sköld, O. *Acta Chem. Scand.* **11** (1957) 17.
2. Canellakis, E. S. *J. Biol. Chem.* **221** (1956) 315.

Dephosphorylation of Nucleoside Triphosphates by Rat Diaphragm *in vitro* *

Aa. Rye Alertsen, O. Walaas and E. Walaas

Institute of Medical Biochemistry and Physiology, Department of Biochemistry, University of Oslo, Norway

When the isolated rat diaphragm is incubated in saline phosphate medium at pH 7.4 at 37 °C a marked ATPase and adenylic acid deaminase activity is present. These properties have been studied by determination of the degradation products of ATP in the diaphragm during incubation. The products formed have been separated by an ion exchange resin method on Dowex-1. By the same technique the conversion products of nucleoside triphosphates added to the medium during incubation of rat diaphragm have been studied

The breakdown of ATP in the diaphragm has been studied in experiments where diaphragms from 20 rats, weighing 6—7 g, were incubated in 15 ml saline phosphate medium. During incubation for 30 min in oxygen, 25 % of ATP initially present in the diaphragm (2.2 μmole per g initial level) was broken down and almost quantitatively recovered as IMP and inosine. In anaerobiosis the breakdown of ATP was greatly accelerated, amounting to 90 % in 30 min. The same high rate of breakdown was observed in oxygen if 5×10^{-5} M 2,4-dinitrophenol or 0.01 M NaCN was present in the medium. In these experiments nucleotides were not detected in the medium which, however, contained a considerable amount of inosine.

The breakdown of nucleotides added to the medium was studied by incubating 2 hemidiaphragms weighing 250 mg in 2 ml saline phosphate medium. 10 μmole ATP added at the start of the experiment was rapidly broken down in oxygen atmosphere. Thus after 30 min 95 % of ATP was broken down and accumulation of ADP, AMP, IMP and inosine was demonstrated. The dephosphorylation and deamination probably did occur on the surface of the diaphragm muscle as no enzyme activity was liberated into the medium when 2 hemidiaphragms were incubated for 30 min. The experiments indicate that the following sequence of reactions takes place:

ATP → ADP → AMP → IMP → Inosine

* Supported by grants from *Eli Lilly and Co.* and from *Norwegian Research Council for Science and the Humanities.*

Experiments on studies of the breakdown of other nucleoside triphosphates CTP, UTP, GTP and ITP will be reported.

Some Properties of the Uridine Diphosphate Glucose Pyrophosphorylase

Agnete Munch-Petersen

The Fibiger-Laboratory, University of Copenhagen, Denmark

In a previous communication [1] the purification and isolation of uridine diphosphate glucose (UDPG) pyrophosphorylase from yeast is described. This enzyme catalyses the following reversible reaction:

$$UDPG + P—P \rightleftharpoons UTP + G—1—P$$

Experiments were described, which showed that incubation of uridine triphosphate (UTP) and ^{32}P-labelled pyrophosphate (P—P) with the enzyme rendered ^{32}P-labelled UTP. Likewise incubation of UDPG with ^{32}P-labelled glucose-1-phosphate (G-1-P) rendered ^{32}P-labelled UDPG. These exchange experiments have been interpreted as an indication of the formation of a free uridyl-enzyme complex as an intermediate in the pyrophosphorolytic transfer of uridyl groups.

In view of the findings of Neufeld *et al.*[2] that UDPG pyrophosphorylase, isolated from seedlings of mungbeans, does not bring about an incorporation of $^{32}P—^{32}P$ into UTP as described above, the exchange experiments with the yeast enzyme have been repeated under more quantitative conditions. The incorporation rate of $^{32}P—^{32}P$ into UTP has been measured by an assay, similar to that described by Berg [3], *i. e.* after incubation of the enzyme with UTP and ^{32}P-labelled P—P, the incubation mixture is treated with charcoal; the charcoal is suspended in 50 % ethanol, and the radioactivity of an aliquot of this suspension is measured. During the purification procedure for the enzyme the different fractions have been tested for exchange activity, measured by the above described charcoal assay, as well as for UDPG pyrophosphorylase activity measured spectrophotometrically [2], and the ratio between these two activities per mg protein remains constant during the different stages (35 fold purification).

If, however, the purified UDPG pyrophosphorylase is treated with crystalline phosphoglucomutase, the exchange activity may be completely abolished; at the same time the enzyme activity as measured spectrophotometrically remains unchanged. This finding together with the fact that addition of G-1-P or UDPG greatly enhances the exchange indicates that the exchange ability of the purified UDPG pyrophosphorylase is not an intrinsic quality of the enzyme, but rather caused by some tightly bound UDPG or G-1-P which cannot be removed by the ordinary purification methods.

The charcoal assay offers an extremely sensitive assay for the pyrophosphorylase reaction. Less than 0.005 μmoles of UDPG or G-1-P may be easily detected and, since this assay, contrary to the spectrophotometric assay, requires no other enzyme system present, it is well suited for kinetic investigations. Measured with this technique the purified UDPG pyrophosphorylase shows specificity for G-1-P as uridyl acceptor among a number of hexose and pentose phosphate esters tested, while crude yeast extract and extracts of fresh spinach leaves contain several uridyl-linked pyrophosphorylases.

1. Munch-Petersen, A. *Acta Chem. Scand.* **9** (1955) 1523.
2. Neufeld, E. F., Ginsburg, V., Putman, E. W., Fanshier, D. and Hassid, W. Z. *Arch. Biochem. and Biophys. In press.*
3. Berg, P. *J. Biol. Chem.* **222** (1956) 991.

Some Studies on Amino Acid Decarboxylases

Gunnar Steensholt and P. E. Joner

Biochemical Institute, University of Oslo, Norway

Glutamic acid decarboxylase is known to have pyridoxal-5-phosphate as cofactor. We found it to require in addition a metal cofactor, namely Zn^{++}, Fe^{+++} or Co^{++} for the enzyme from carrots, and Mn^{++} for the rat brain enzyme. SH-groups appear to be essential. Cysteic acid decarboxylase also requires pyridoxal-5-phosphate as cofactor, and also Fe^{++}, Zn^{++} or Mn^{++}. The presence of SH-groups in this enzyme is doubtful. Cysteine sulphinic acid decarboxylase is also a pyridoxal-5-phosphate enzyme, with essential SH-groups and requiring Fe^{++}, Fe^{+++} or Zn^{++}. The authors consider cysteic acid decarboxylase and cysteine sulphinic acid decarboxylase to be two different enzymes. All three enzymes have been purified to some extent.

Enzymic Formation of Uridine-5′-phosphate from Uracil

Ola Sköld and Peter Reichard

Biochemical Department, Karolinska Institutet, Stockholm, Sweden

Most mammalian tissues studied show a relatively poor utilization of uracil for pyrimidine nucleotide synthesis. In the Ehrlich ascites tumor, however, uracil was incorporated into polynucleotide pyrimidines as rapidly as orotic acid. In a study of the enzymic mechanism of this process it was found that uridine-5′-phosphate(UMP) formation from uracil in acetone powder extracts of the tumor proceeded according to:

$$\text{Uracil} + \text{ribose-1-phosphate} \xrightarrow[\text{phosphorylase}]{\text{nucleoside}} \text{uridine} + \text{phosphate}$$

$$\text{Uridine} + \text{ATP} \xrightarrow[\text{kinase}]{\text{uridine}} \text{UMP} + \text{ADP}$$

Both enzymes involved are known to occur in mammalian organs, *e. g.* liver, which form very little UMP from uracil.

We have now investigated the amount of these two enzymes in the ascites tumor and in rat liver. Furthermore, the breakdown of uracil to CO_2 was also studied, since it had been proposed that this process might determine uracil utilization in different tissues [2].

A significant difference was found in the amount of nucleoside phosphorylase as measured by a spectrophotometric assay. Uridine kinase was consistently *ca.* 10 times more active in extracts of the tumor than in liver extracts. A high concentration of uridine was necessary for optimum UMP synthesis. In accordance with earlier findings of other investigators we observed a quite rapid breakdown of uracil to CO_2 in rat liver preparations. No such degradation was observed in tumor extracts, however. In both cases a high TPNH level was maintained during the reaction.

It seems likely that uracil utilization by different tissues will depend on a competition between catabolic reactions which degrade uracil to CO_2 and the anabolic formation of UMP.

1. Reichard, P. and Sköld, O. *Acta Chem. Scand.* **11** (1957) 17.
2. Canellakis, E. S. *J. Biol. Chem.* **221** (1956) 315.

Dephosphorylation of Nucleoside Triphosphates by Rat Diaphragm *in vitro* *

Aa. Rye Alertsen, O. Walaas and E. Walaas

Institute of Medical Biochemistry and Physiology, Department of Biochemistry, University of Oslo, Norway

When the isolated rat diaphragm is incubated in saline phosphate medium at pH 7.4 at 37 °C a marked ATPase and adenylic acid deaminase activity is present. These properties have been studied by determination of the degradation products of ATP in the diaphragm during incubation. The products formed have been separated by an ion exchange resin method on Dowex-1. By the same technique the conversion products of nucleoside triphosphates added to the medium during incubation of rat diaphragm have been studied

The breakdown of ATP in the diaphragm has been studied in experiments where diaphragms from 20 rats, weighing 6—7 g, were incubated in 15 ml saline phosphate medium. During incubation for 30 min in oxygen, 25 % of ATP initially present in the diaphragm (2.2 μmole per g initial level) was broken down and almost quantitatively recovered as IMP and inosine. In anaerobiosis the breakdown of ATP was greatly accelerated, amounting to 90 % in 30 min. The same high rate of breakdown was observed in oxygen if 5×10^{-5} M 2,4-dinitrophenol or 0.01 M NaCN was present in the medium. In these experiments nucleotides were not detected in the medium which, however, contained a considerable amount of inosine.

The breakdown of nucleotides added to the medium was studied by incubating 2 hemidiaphragms weighing 250 mg in 2 ml saline phosphate medium. 10 μmole ATP added at the start of the experiment was rapidly broken down in oxygen atmosphere. Thus after 30 min 95 % of ATP was broken down and accumulation of ADP, AMP, IMP and inosine was demonstrated. The dephosphorylation and deamination probably did occur on the surface of the diaphragm muscle as no enzyme activity was liberated into the medium when 2 hemidiaphragms were incubated for 30 min. The experiments indicate that the following sequence of reactions takes place:

ATP → ADP → AMP → IMP → Inosine

* Supported by grants from *Eli Lilly and Co.* and from *Norwegian Research Council for Science and the Humanities.*

Experiments on studies of the breakdown of other nucleoside triphosphates CTP, UTP, GTP and ITP will be reported.

Some Properties of the Uridine Diphosphate Glucose Pyrophosphorylase

Agnete Munch-Petersen

The Fibiger-Laboratory, University of Copenhagen, Denmark

In a previous communication [1] the purification and isolation of uridine diphosphate glucose (UDPG) pyrophosphorylase from yeast is described. This enzyme catalyses the following reversible reaction:

$$UDPG + P—P \rightleftharpoons UTP + G—1—P$$

Experiments were described, which showed that incubation of uridine triphosphate (UTP) and ^{32}P-labelled pyrophosphate (P—P) with the enzyme rendered ^{32}P-labelled UTP. Likewise incubation of UDPG with ^{32}P-labelled glucose-1-phosphate (G-1-P) rendered ^{32}P-labelled UDPG. These exchange experiments have been interpreted as an indication of the formation of a free uridyl-enzyme complex as an intermediate in the pyrophosphorolytic transfer of uridyl groups.

In view of the findings of Neufeld *et al.*[2] that UDPG pyrophosphorylase, isolated from seedlings of mungbeans, does not bring about an incorporation of $^{32}P—^{32}P$ into UTP as described above, the exchange experiments with the yeast enzyme have been repeated under more quantitative conditions. The incorporation rate of $^{32}P—^{32}P$ into UTP has been measured by an assay, similar to that described by Berg [3], *i. e.* after incubation of the enzyme with UTP and ^{32}P-labelled P—P, the incubation mixture is treated with charcoal; the charcoal is suspended in 50 % ethanol, and the radioactivity of an aliquot of this suspension is measured. During the purification procedure for the enzyme the different fractions have been tested for exchange activity, measured by the above described charcoal assay, as well as for UDPG pyrophosphorylase activity measured spectrophotometrically [2], and the ratio between these two activities per mg protein remains constant during the different stages (35 fold purification).

If, however, the purified UDPG pyrophosphorylase is treated with crystalline phosphoglucomutase, the exchange activity may be completely abolished; at the same time the enzyme activity as measured spectrophotometrically remains unchanged. This finding together with the fact that addition of G-1-P or UDPG greatly enhances the exchange indicates that the exchange ability of the purified UDPG pyrophosphorylase is not an intrinsic quality of the enzyme, but rather caused by some tightly bound UDPG or G-1-P which cannot be removed by the ordinary purification methods.

The charcoal assay offers an extremely sensitive assay for the pyrophosphorylase reaction. Less than 0.005 μmoles of UDPG or G-1-P may be easily detected and, since this assay, contrary to the spectrophotometric assay, requires no other enzyme system present, it is well suited for kinetic investigations. Measured with this technique the purified UDPG pyrophosphorylase shows specificity for G-1-P as uridyl acceptor among a number of hexose and pentose phosphate esters tested, while crude yeast extract and extracts of fresh spinach leaves contain several uridyl-linked pyrophosphorylases.

1. Munch-Petersen, A. *Acta Chem. Scand.* **9** (1955) 1523.
2. Neufeld, E. F., Ginsburg, V., Putman, E. W., Fanshier, D. and Hassid, W. Z. *Arch. Biochem. and Biophys. In press.*
3. Berg, P. *J. Biol. Chem.* **222** (1956) 991.

Some Studies on Amino Acid Decarboxylases

Gunnar Steensholt and P. E. Joner

Biochemical Institute, University of Oslo, Norway

Glutamic acid decarboxylase is known to have pyridoxal-5-phosphate as cofactor. We found it to require in addition a metal cofactor, namely Zn^{++}, Fe^{+++} or Co^{++} for the enzyme from carrots, and Mn^{++} for the rat brain enzyme. SH-groups appear to be essential. Cysteic acid decarboxylase also requires pyridoxal-5-phosphate as cofactor, and also Fe^{++}, Zn^{++} or Mn^{++}. The presence of SH-groups in this enzyme is doubtful. Cysteine sulphinic acid decarboxylase is also a pyridoxal-5-phosphate enzyme, with essential SH-groups and requiring Fe^{++}, Fe^{+++} or Zn^{++}. The authors consider cysteic acid decarboxylase and cysteine sulphinic acid decarboxylase to be two different enzymes. All three enzymes have been purified to some extent.

Incorporation *in vitro* of Purine Ribosides into Deoxyribonucleic Acids of Ehrlich's Ascites Tumor Cells

Hans Klenow and
Eleanor Lichtler
The Fibiger-Laboratory, University of Copenhagen, Denmark

In *in vivo* experiments with rats Roll *et al.*[1] have found that the adenosine part of adenylic acid b may serve as a precursor of the deoxyribose of all four deoxyribonucleosides of deoxyribonucleic acid (DNA), and that some of the adenosine may have been converted to an adenine deoxyriboside derivative with the glycosidic linkage intact. There was no suggestion that the guanosine part of guanylic acid b was directly converted to a guanosine deoxyriboside derivative.

We have studied the incorporation *in vitro* of purine ribosides into deoxyribonucleic acids of ascites tumor cells. Suspensions of Ehrlich's ascites tumor cells in Tyrode's solution were incubated with glucose (10 mg/ml cell suspension), sodium succinate (10 mg/ml cell suspension), deoxycytidine (3 μmole/ml cell suspension), and uniformly ^{14}C-labelled adenosine or uniformly ^{14}C-labelled guanosine. After incubation at 37 °C with shaking for 3—4 h the suspensions were treated with ice-cold perchloric acid. The precipitate was washed with alcohol and with an alcohol-ether mixture (3:1), and digested with KOH overnight. After neutralization and dialysis of the digest the DNA present was degraded by incubation with DNA'ase and snake venom phosphodiesterase. The individual deoxyribonucleotides formed were separated and isolated by paper chromatography, and their specific radioactivity was determined.

It was found that when the cells had been incubated with uniformly ^{14}C-labelled adenosine most of the radioactivity (70—90 %) of the DNA was present in the deoxyadenylic acid, whereas the pyrimidine deoxyribotides contained insignificant amounts of radioactivity. The deoxyribose-5-phosphate of DNA-deoxyadenylic acid from such experiments was obtained by paper chromatography after acid hydrolysis. It was found that the average radioactivity per μmole carbon of this compound ranged from 70—100 % of to the average radioactivity per μmole carbon of the deoxyadenylic acid from which it had been derived. The experiments suggest, therefore, that under the conditions used adenosine serves as a precursor of DNA-deoxyadenylic acid, and that 50 % or more of labelled DNA-deoxyadenylic acid could have been formed from adenosine without cleavage of the glycosidic linkage.

In a similar way it was found that guanosine could serve as a precursor of DNA-deoxyguanylic acid. Furthermore, the average specific activity of the carbon atoms in DNA-deoxyguanylic acid obtained from such experiments ranged from 70—100 % of the average specific activity of the carbon atoms of its deoxyribose-5-phosphate part. This suggests that 50 % or more of the labelled DNA-deoxyguanylic acid could have been formed from guanosine without cleavage of the glycosidic linkage.

These results are only in partial agreement with the *in vivo* experiments of Roll *et al.* carried out with uniformly labelled purine ribotides.

1. Roll, P. M., Weinfeld, H., Carroll, E. and Brown, G. B. *J. Biol. Chem.* **220** (1956) 439.

Reversible Inactivation of Ribonuclease

Lars Josefsson
Department of Physiological Chemistry, University of Lund, Lund, Sweden

It has previously been shown that anhydrous formic acid induces an N,O-acyl migration in lysozyme followed with a loss of the enzymatic activity. However, titration of the inactivated enzyme with alkali at pH 7.5 reversed the peptidyl shift and restored the activity completely [1-3].

In the same way ribonuclease now has been studied to elucidate the mechanism of the enzymatic activity. In contrast to lysozyme the inactivation and reactivation of ribonuclease proceed slower. Furthermore the activity of ribonuclease is not completely restored at pH 7.5 but requires a further reaction at pH 8.5. However, the reactivation and alkali consumption strictly follow each other.

1. Josefsson, L. and Edman, P. *Acta Chem. Scand.* **10** (1956) 148.
2. Edman, P. and Josefsson, L. *Nature. In press.*
3. Josefsson, L. and Edman, P. *Biochim. et Biophys. Acta. In press.*

A General Method for Reduction of Pyrimidine Nucleosides and Nucleotides

S. Laland, J. McKinley McKee and E. Roth

Biochemistry Department, The University, Blindern, Oslo, Norway

The reduction of the pyrimidine ring in nucleosides and nucleotides has recently attracted considerable attention. Burke [1] reported the reduction of pyrimidine nucleosides with sodium in liquid ammonia and ethanol. Cohn and Doherty [2] reduced catalytically pyrimidine nucleosides and nucleotides using a rhodium catalyst and simultaneously with this latter work the reduction of thymidine with sodium amalgam and the subsequent isolation of the sugar component was reported [3].

This simple reduction method has now been extended to the following substances: deoxycytidine, deoxycytidylic acid, thymidylic acid, thymidine diphosphate, deoxycytidine diphosphate, cytidylic acid, uridylic acid, cytidine and uridine. In all cases the reduction is carried out by shaking for a few hours at room temperature an aqueous solution of the substance with 3 % sodium amalgam. The complete reduction of the 4,5-ethylenic linkage in the pyrimidine ring was demonstrated by the disappearance of the UV absorption at 260 mμ[4]. With thymidylic acid and thymidine diphosphate the rate of reduction was slower. The present report concerns in particular the reduction of the deoxyribose nucleosides and nucleotides. The completeness of the reduction was also shown by the fact that the modified Dische diphenylamine test [5] after the reduction revealed the presence of between 90 and 100 % of the theoretical amount of 2-deoxy-D-ribose. Examination of the reduction products by paper chromatography, paper electrophoresis and ion exchange chromatography revealed the presence of several deoxyribosyl substances as was the case with thymidine [3]. This is due to the fission of the dihydropyrimidine ring under the prevailing alkaline condition. The reduction products are interesting. First some of them may be intermediates in the biosynthesis of nucleosides and nucleotides. Work to establish this is in progress. Secondly, for tracer work where the isolation of sugar and sugar phosphates is necessary, these reduction products are convenient because of the lability of the glycosidic linkage towards acid, which enables isolation of the free sugar or the sugar phosphate. After short heating of reduction mixtures of thymidine, deoxycytidine, deoxycytidylic and thymidylic acid, respectively, with Amberlite IR-120 (H), 2-deoxy-D-ribose and 2-deoxy-D-ribose 5-phosphate were isolated in good yield by paper chromatography in propanol-ammonia (conc.), 6:4. Finally, subsequent to reduction, colour tests for the sugar component may be used for detecting and estimating pyrimidine nucleosides and nucleotides. Using the modified Dische diphenylamine method [5] for 2-deoxy-D-ribose, standard curves for the determination of thymidine, deoxycytidine, deoxycytidylic acid and thymidylic acid after reduction with 3 % sodium amalgam were made. Linear curves were obtained. It was shown that quantities of 50 μg of nucleosides or nucleotides could be estimated. This method for deoxyribose pyrimidine nucleosides and nucleotides is particularly useful when the presence of other UV absorbing material, prevents the use of UV absorption spectroscopy.

1. Burke, D. C. *J. Org. Chem* **20** (1955) 643.
2. Cohn, W. E. and Doherty, D. G. *J. Am. Chem. Soc.* **78** (1956) 2863.
3. Laland, S. and Roth, E. *Acta Chem. Scand.* **10** (1956) 1058.
4. Cavalieri, L. F., Bendich, A., Tinker, J. F. and Brown, G. B. *J. Am. Chem. Soc.* **70** (1948) 3875.
5. Burton, K. *Biochem. J.* **62** (1956) 315.

The Synthesis and Characterization of Some AMP-Sulphates

N. R. Ringertz and Peter Reichard

Department of Cell Research and Biochemical Department, Karolinska Institutet, Stockholm, Sweden

Adenosine-5′-phosphosulphate has been implicated as an intermediate in the enzymic activation of sulphate [1]. It has been synthesized by the condensation of a sulphur trioxide-pyridine complex with adenosine-5′-monophosphate [2] (AMP), and by the carbodiimide method [3].

The carbodiimide method was used for the synthesis of some structurally related AMP-sulphates, containing sulphate linked to the hydroxyl groups of the ribose moiety. The following compounds were synthesized and characterized:

AMP-monosulphates: Adenosine-5′-phosphosulphate (APS). Inorganic sulphate was rapidly liberated from this compound by acid hydrolysis. It was somewhat more resistant to alkaline and CaO hydrolysis. It was degraded to adenosine, phosphate and sulphate by snake venom and prostatic phosphatases. It was an intermediate in the enzyme system for sulphate activation [4]. Adenosine-2′-sulphate-5′-phosphate and adenosine-3′-sulphate-5′-phosphate decomposed at a slower rate than APS during acid hydrolysis and were very slowly degraded by alkaline and CaO hydrolysis. Digestion with snake venom phosphatase produced adenosine, phosphate and sulphate. Prostatic phosphatase produced adenosine-sulphates + phosphate.

AMP-disulphates: The disulphates were probably a mixture of three different compounds, which were not further separated. Two of the compounds conceivably contained one phosphosulphate and one ribose-sulphate linkage. The third compound contained both sulphates attached to ribose.

AMP-trisulphate: Adenosine-2′,3′-disulphate-5′-phosphosulphate was degraded to adenosine-2′,3′ - disulphate - 5′-phosphate and sulphate during acid, alkaline and CaO hydrolysis. Further decomposition occurred at a slower rate. Snake venom phosphatase produced adenosine-2′,3′-disulphate-5′-phosphate + sulphate. Prostatic phosphatase produced adenosine-2,3′-disulphate, phosphate and sulphate.

The factors influencing the yield of the different AMP-sulphates were studied. APS appeared as the primary product. By increasing the amount of sulphuric acid in the reaction mixture and prolonging the reaction time a total yield of AMP-sulphates amounting to 90—100 % (calc. on AMP) could be obtained. It was possible to obtain a 40—50 % conversion of AMP to APS without more than small amounts of other AMP-sulphates.

The different AMP-sulphates could be separated from each other by column electrophoresis on a gram scale.

1. Robbins, P. W. and Lipmann, F. *J. Am. Chem. Soc.* **78** (1956) 6409; Bandurski, R. S. Wilson, L. G. and Squires, C. C. *J. Am. Chem. Soc.* **78** (1956) 6408.
2. Baddiley, J., Buchanan, J. G. and Letters, R. *J. Chem. Soc.* **1957** 1067.
3. Reichard, P. and Ringertz, N. R. *J. Am. Chem. Soc.* **79** (1957) 2026.
4. We wish to thank Dr. P. W. Robbins for testing the enzymic activity of our APS.

Complex Formation of Nucleoside Triphosphates with Metal Ions *

E. Walaas

Institute of Medical Biochemistry and Physiology, Department of Biochemistry, University of Oslo, Norway

Transphosphorylation reactions with nucleoside triphosphates as the phosphate donor require metals as cofactors, especially Mg^{2+}, Mn^{2+} or Ca^{2+}. It has therefore been suggested that metal nucleotide complexes are the actual coenzymes. In the present work the dissociation constants of several nucleoside triphosphates of Ca^{2+}, Mg^{2+}, Co^{2+} and Mn^{2+} have been determined. An ion exchange method according to the principle reported by Schubert has been adopted. An anion exchange resin (Dowex-1) in the chloride form has been used. The dissociation constants of mononucleotides with different metals have been determined under the following conditions. A total volume of 20 ml contained (concentrations): 0.5×10^{-4} M nucleotide, 0.1 M NaCl, 0.005 M tris(hydroxymethyl)aminomethane buffer, pH 8.2, and usually 50 mg resin. Equilibration was obtained without and with addition of metal salts to the mixture by shaking for 3 h at 23 °C. The concentration of nucleotide not bound to the resin was determined by reading the extinction at appropriate wavelenghts in ultraviolet region on a Beckman spectrophotometer. From these data the dissociation constants k_c for ATP with metals have been calculated.

$$k_c\ \mathrm{Ca} > k_c\ \mathrm{Mg} > k_c\ \mathrm{Co} > k_c\ \mathrm{Mn}$$
$$1.7 \times 10^{-4}\quad 0.9 \times 10^{-4}\quad 0.23 \times 10^{-4}\quad 0.17 \times 10^{-4}$$

Dissociation constants for different metal complexes with ADP and AMP show the same sequence as reported for ATP. However, as an approximation complexes with ADP are 10 times more dissociated and complexes with AMP are 100 times more dissociated than the corresponding ATP metal complexes. This can be illustrated in the case of complexes with Mg

$$\mathrm{ATP} < \mathrm{ADP} < \mathrm{AMP}$$
$$0.9 \times 10^{-4}\quad 6.4 \times 10^{-4}\quad 1.1 \times 10^{-3}$$

The dissociation constants for CTP, GTP, UTP and ITP with the different metals show, with a few exceptions, the same sequence as reported for ATP. The values approximately correspond to those given for ATP metal complexes.

* Supported by grants from *Eli Lilly and Co.* and from *Norwegian Research Council for Science and the Humanities.*

A General Method for Reduction of Pyrimidine Nucleosides and Nucleotides

S. Laland, J. McKinley McKee and E. Roth

Biochemistry Department, The University, Blindern, Oslo, Norway

The reduction of the pyrimidine ring in nucleosides and nucleotides has recently attracted considerable attention. Burke [1] reported the reduction of pyrimidine nucleosides with sodium in liquid ammonia and ethanol. Cohn and Doherty [2] reduced catalytically pyrimidine nucleosides and nucleotides using a rhodium catalyst and simultaneously with this latter work the reduction of thymidine with sodium amalgam and the subsequent isolation of the sugar component was reported [3].

This simple reduction method has now been extended to the following substances: deoxycytidine, deoxycytidylic acid, thymidylic acid, thymidine diphosphate, deoxycytidine diphosphate, cytidylic acid, uridylic acid, cytidine and uridine. In all cases the reduction is carried out by shaking for a few hours at room temperature an aqueous solution of the substance with 3 % sodium amalgam. The complete reduction of the 4,5-ethylenic linkage in the pyrimidine ring was demonstrated by the disappearance of the UV absorption at 260 mμ[4]. With thymidylic acid and thymidine diphosphate the rate of reduction was slower. The present report concerns in particular the reduction of the deoxyribose nucleosides and nucleotides. The completeness of the reduction was also shown by the fact that the modified Dische diphenylamine test [5] after the reduction revealed the presence of between 90 and 100 % of the theoretical amount of 2-deoxy-D-ribose. Examination of the reduction products by paper chromatography, paper electrophoresis and ion exchange chromatography revealed the presence of several deoxyribosyl substances as was the case with thymidine [3]. This is due to the fission of the dihydropyrimidine ring under the prevailing alkaline condition. The reduction products are interesting. First some of them may be intermediates in the biosynthesis of nucleosides and nucleotides. Work to establish this is in progress. Secondly, for tracer work where the isolation of sugar and sugar phosphates is necessary, these reduction products are convenient because of the lability of the glycosidic linkage towards acid, which enables isolation of the free sugar or the sugar phosphate. After short heating of reduction mixtures of thymidine, deoxycytidine, deoxycytidylic and thymidylic acid, respectively, with Amberlite IR-120 (H), 2-deoxy-D-ribose and 2-deoxy-D-ribose 5-phosphate were isolated in good yield by paper chromatography in propanol-ammonia (conc.), 6:4. Finally, subsequent to reduction, colour tests for the sugar component may be used for detecting and estimating pyrimidine nucleosides and nucleotides. Using the modified Dische diphenylamine method [5] for 2-deoxy-D-ribose, standard curves for the determination of thymidine, deoxycytidine, deoxycytidylic acid and thymidylic acid after reduction with 3 % sodium amalgam were made. Linear curves were obtained. It was shown that quantities of 50 μg of nucleosides or nucleotides could be estimated. This method for deoxyribose pyrimidine nucleosides and nucleotides is particularly useful when the presence of other UV absorbing material, prevents the use of UV absorption spectroscopy.

1. Burke, D. C. *J. Org. Chem* **20** (1955) 643.
2. Cohn, W. E. and Doherty, D. G. *J. Am. Chem. Soc.* **78** (1956) 2863.
3. Laland, S. and Roth, E. *Acta Chem. Scand.* **10** (1956) 1058.
4. Cavalieri, L. F., Bendich, A., Tinker, J. F. and Brown, G. B. *J. Am. Chem. Soc.* **70** (1948) 3875.
5. Burton, K. *Biochem. J.* **62** (1956) 315.

The Synthesis and Characterization of Some AMP-Sulphates

N. R. Ringertz and Peter Reichard

Department of Cell Research and Biochemical Department, Karolinska Institutet, Stockholm, Sweden

Adenosine-5′-phosphosulphate has been implicated as an intermediate in the enzymic activation of sulphate [1]. It has been synthesized by the condensation of a sulphur trioxide-pyridine complex with adenosine-5′-monophosphate [2] (AMP), and by the carbodiimide method [3].

The carbodiimide method was used for the synthesis of some structurally related AMP-sulphates, containing sulphate linked to the hydroxyl groups of the ribose moiety. The following compounds were synthesized and characterized:

AMP-monosulphates: Adenosine-5′-phosphosulphate (APS). Inorganic sulphate was rapidly liberated from this compound by acid hydrolysis. It was somewhat more resistant to alkaline and CaO hydrolysis. It was degraded to adenosine, phosphate and sulphate by snake venom and prostatic phosphatases. It was an intermediate in the enzyme system for sulphate activation [4]. Adenosine-2′-sulphate-5′-phosphate and adenosine-3′-sulphate-5′-phosphate decomposed at a slower rate than APS during acid hydrolysis and were very slowly degraded by alkaline and CaO hydrolysis. Digestion with snake venom phosphatase produced adenosine, phosphate and sulphate. Prostatic phosphatase produced adenosine-sulphates + phosphate.

AMP-disulphates: The disulphates were probably a mixture of three different compounds, which were not further separated. Two of the compounds conceivably contained one phosphosulphate and one ribose-sulphate linkage. The third compound contained both sulphates attached to ribose.

AMP-trisulphate: Adenosine-2′,3′-disulphate-5′-phosphosulphate was degraded to adenosine-2′,3′ - disulphate - 5′-phosphate and sulphate during acid, alkaline and CaO hydrolysis. Further decomposition occurred at a slower rate. Snake venom phosphatase produced adenosine-2′,3′-disulphate-5′-phosphate + sulphate. Prostatic phosphatase produced adenosine-2,3′-disulphate, phosphate and sulphate.

The factors influencing the yield of the different AMP-sulphates were studied. APS appeared as the primary product. By increasing the amount of sulphuric acid in the reaction mixture and prolonging the reaction time a total yield of AMP-sulphates amounting to 90—100 % (calc. on AMP) could be obtained. It was possible to obtain a 40—50 % conversion of AMP to APS without more than small amounts of other AMP-sulphates.

The different AMP-sulphates could be separated from each other by column electrophoresis on a gram scale.

1. Robbins, P. W. and Lipmann, F. *J. Am. Chem. Soc.* **78** (1956) 6409; Bandurski, R. S. Wilson, L. G. and Squires, C. C. *J. Am. Chem. Soc.* **78** (1956) 6408.
2. Baddiley, J., Buchanan, J. G. and Letters, R. *J. Chem. Soc.* **1957** 1067.
3. Reichard, P. and Ringertz, N. R. *J. Am. Chem. Soc.* **79** (1957) 2026.
4. We wish to thank Dr. P. W. Robbins for testing the enzymic activity of our APS.

Complex Formation of Nucleoside Triphosphates with Metal Ions *

E. Walaas

Institute of Medical Biochemistry and Physiology, Department of Biochemistry, University of Oslo, Norway

Transphosphorylation reactions with nucleoside triphosphates as the phosphate donor require metals as cofactors, especially Mg^{2+}, Mn^{2+} or Ca^{2+}. It has therefore been suggested that metal nucleotide complexes are the actual coenzymes. In the present work the dissociation constants of several nucleoside triphosphates of Ca^{2+}, Mg^{2+}, Co^{2+} and Mn^{2+} have been determined. An ion exchange method according to the principle reported by Schubert has been adopted. An anion exchange resin (Dowex-1) in the chloride form has been used. The dissociation constants of mononucleotides with different metals have been determined under the following conditions. A total volume of 20 ml contained (concentrations): 0.5×10^{-4} M nucleotide, 0.1 M NaCl, 0.005 M tris(hydroxymethyl)aminomethane buffer, pH 8.2, and usually 50 mg resin. Equilibration was obtained without and with addition of metal salts to the mixture by shaking for 3 h at 23 °C. The concentration of nucleotide not bound to the resin was determined by reading the extinction at appropriate wavelenghts in ultraviolet region on a Beckman spectrophotometer. From these data the dissociation constants k_c for ATP with metals have been calculated.

$$k_c\ \mathrm{Ca} > k_c\ \mathrm{Mg} > k_c\ \mathrm{Co} > k_c\ \mathrm{Mn}$$
$$1.7 \times 10^{-4}\quad 0.9 \times 10^{-4}\quad 0.23 \times 10^{-4}\quad 0.17 \times 10^{-4}$$

Dissociation constants for different metal complexes with ADP and AMP show the same sequence as reported for ATP. However, as an approximation complexes with ADP are 10 times more dissociated and complexes with AMP are 100 times more dissociated than the corresponding ATP metal complexes. This can be illustrated in the case of complexes with Mg

$$\mathrm{ATP} < \mathrm{ADP} < \mathrm{AMP}$$
$$0.9 \times 10^{-4}\quad 6.4 \times 10^{-4}\quad 1.1 \times 10^{-3}$$

The dissociation constants for CTP, GTP, UTP and ITP with the different metals show, with a few exceptions, the same sequence as reported for ATP. The values approximately correspond to those given for ATP metal complexes.

* Supported by grants from *Eli Lilly and Co.* and from *Norwegian Research Council for Science and the Humanities.*

Equilibrium Constants of Thiol-Disulphide Systems. The Relative Oxidation-Reduction Potential of Cysteine-Glutathione *

Alexander Pihl and Lorentz Eldjarn

Norsk Hydro's Institute for Cancer Research, The Norwegian Radium Hospital, Oslo, Norway

Previously we have presented evidence that the accessible thiols and disulphides of the body exist in a state of dynamic equilibrium, governed by the appropriate equilibrium constants and by the total SH/SS-ratio [1,2]. Clearly, information on the relevant equilibrium constants and reaction rates is necessary for the understanding of the role and mode of action of thiols and disulphides in biochemical processes.

* Supported by grants from the *Norwegian Cancer Society*.

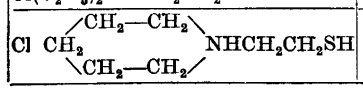
A method for the analysis of thiol-disulphide equilibria has previously been presented [1,2]. Recently, by a modification of this procedure, we have succeeded in measuring directly the concentrations of three of the five constituents of thiol-disulfide equilibria, permitting the straight-forward calculation of the appropriate equilibrium constants. In the improved method, which is described in detail elsewhere [3], the ^{35}S-labeled constituents of the systems tested are separated by electrophoresis at pH 2 in mercuric acetate treated paper.

The procedure has been used for the determination of the equilibrium constants, at pH 7.4 and 37 °C, of systems containing cystine or oxidized glutathione and various sulphur containing X-ray protective thiols. The data are summarized in Table 1. Here is also given the approximate time needed to obtain equilibrium under these conditions.

The K-values found, imply that in these systems high amounts of mixed disulphides are present at equilibrium. The data confirm our previous findings [4,5] that sulphur-containing agents possessing high ability to protect animals against ionizing radiation, exhibit a pronounced tendency to form mixed disulphides with biological thiols and disulphides.

Table 1. The equilibrium constants K_2 and K_3 of various thiol-disulphide systems *.

$$\mathrm{ASH} + \mathrm{BSSB} \overset{K_2}{\rightleftharpoons} \begin{matrix}\mathrm{ASSB} + \mathrm{BSH} \\ \mathrm{ASSB} + \mathrm{ASH}\end{matrix} \overset{K_3}{\rightleftharpoons} \mathrm{ASSA} + \mathrm{BSH}$$

ASH	BSSB						**
	Cystine			Oxidized glutathione			
	Time needed to reach equilibrium min	K_2	K_3	Time needed to reach equilibrium min	K_2	K_3	E_0' CSSC/CSH
$CH_3CONHCH_2CH_2SH$	10	5.00	0.62	12	2.86	0.28	0.0180
$ClNH_3CH_2CH_2SH$	1	4.76	0.75	1.5	5.09	0.34	0.0099
$Cl\ (CH_3)_2NHCH_2CH_2SH$	2	2.30	0.36	2	1.56	0.32	0.0068
$Cl(C_2H_5)_2NHCH_2CH_2SH$	2.5	2.79	0.36	3	1.92	0.29	0.0079
	3	2.81	0.31	2	1.89	0.25	0.0081
						Mean	0.0101

* The measurements were carried out at pH 7.4 and 37 °C.

** E_0' = standard oxidation-reduction potential, at pH 7.4 and 37 °C, relative to that of glutathione ($E_{0\,GSSG/GSH}' = 0$ volts), with sign opposite to that used by Latimer [6].

From the equilibrium constants the relative oxidation-reduction potential of the 15 thiol-disulphide couples involved in the 10 systems studied, can be calculated. Of particular interest is the fact that the above equilibrium constants can be used for the calculation of the oxidation-reduction potential of cysteine, relative to that of glutathione. It is clear from Table 1 that the calculations, based on 5 independent sets of data, show good agreement. The results seem to present a solution to this controversial question.

1. Eldjarn, L. and Pihl, A. *Acta Chem. Scand.* **10** (1956) 1054.
2. Eldjarn, L. and Pihl, A. *J. Biol. Chem.* **225** (1957) 499.
3. Eldjarn, L. and Pihl, A. *J. Am. Chem. Soc. In press.*
4. Eldjarn, L. and Pihl, A. *Proc. of the 4th Internat. Conf. on Radiobiology*, Oliver and Boyd, London 1956, p. 249.
5. Pihl, A. and Eldjarn, L. *Proc. of the 5th Internat. Conf. on Radiobiology*, Oliver and Boyd, London. *In press.*
6. Latimer, W.M. In *Oxidation Potentials.* Prentice Hall, New York 1952.

Enzyme Kinetics in Univalent Buffers

J. S. McKinley McKee

Biochemical Institute, University of Oslo, Blindern, Oslo

Many ions have different effects on the kinetics of the fumarase-catalyzed reaction [1]:

$$\text{fumarate} + H_2O \rightleftharpoons \text{L-malate}$$

With buffer ions specific effects arise due to the binding of the different buffer ions. Kinetic studies in phosphate buffers [2] proved unsatisfactory due to the presence of HPO_4^{--} and $H_2PO_4^-$ ions, each with its own effect on the enzyme and the relative concentration of which varied with pH. As the kinetic constants are unaffected by the buffer cation, while being very sensitive to the anion concentration and type, univalent buffers of the uncharged base type (*e. g.* imidazole, tris, ammidol-chloride, fluoride or perchlorate) have been used. Thus specific buffer effects can be studied as there is a single anion, the concentration of which can be held constant over a wide pH range.

The experiments have consisted of determining the pH variation of the maximum velocities (V_M, V_F) and Michaelis constants (K_M, K_F) for the forward and reverse reactions. These were obtained from Liveweaver-Burk plots. It was important to use substrate concentrations (range 4K—K/4) which gave neither substrate activation or inhibition [2], as otherwise erroneous kinetic constants resulted. The enzyme solutions were prepared from crystalline fumarase, and the kinetics were followed on the 80—100 % transmission expanded scale of a Beckman DUR spectrophotometer [2]. The Michaelis constants for malate and fumarate in 5 mM chloride, perchlorate or acetate buffers rise markedly above pH 8.0. With malate, the K_M values are approximately constant below pH 7.0, while with fumarate this represents a minimum. Plots of V_M, V_F, V_M/K_M, and $V_F/4.4K_F$ *vs.* pH are symmetrical and bell shaped. For each buffer the data were consistent with the ionisation of two groups in the enzymatic site, having different ionisation constants in the free enzyme and the fumarase and L-malate complexes. In the various buffers the pK values vary markedly. Good agreement was found between the experimental points and theoretical curves calculated from pH independent kinetic constants and the pK values [3]. In interpreting the data the secondary ionisations of the substrates have to be taken into account at the lowes pH values. A comparison of the kinetic constants in phosphate (approximate values) with those in the univalent buffers shows that while neither buffer type or concentration markedly affect the pH independent maximum velocity or turnover number, yet the corresponding Michaelis constants are much greater in phosphate, presumably due to the divalent ions present. As both substrates give the same ionisation constants for two essential groups in the free enzyme (V_M/K_M and $V_F/K_{eq}K_F$ superimposable) it seems that it is the same enzymatic site that is involved in the proton transfer reactions resulting in hydration or dehydration.

The author wishes to thank professor R. A. Alberty for many helpful discussions.

1. Massey, V. *Biochem. J.* **53** (1953) 67.
2. Alberty, R. A., Massey, V., Frieden, C. and Fuhlbrigge, A. R. *J. Am. Chem. Soc.* **76** (1954) 2485.
3. Alberty, R. A. *J. Cellular Comp. Physiol.* **47** (1956) 245.

From the equilibrium constants the relative oxidation-reduction potential of the 15 thiol-disulphide couples involved in the 10 systems studied, can be calculated. Of particular interest is the fact that the above equilibrium constants can be used for the calculation of the oxidation-reduction potential of cysteine, relative to that of glutathione. It is clear from Table 1 that the calculations, based on 5 independent sets of data, show good agreement. The results seem to present a solution to this controversial question.

1. Eldjarn, L. and Pihl, A. *Acta Chem. Scand.* **10** (1956) 1054.
2. Eldjarn, L. and Pihl, A. *J. Biol. Chem.* **225** (1957) 499.
3. Eldjarn, L. and Pihl, A. *J. Am. Chem. Soc. In press.*
4. Eldjarn, L. and Pihl, A. *Proc. of the 4th Internat. Conf. on Radiobiology*, Oliver and Boyd, London 1956, p. 249.
5. Pihl, A. and Eldjarn, L. *Proc. of the 5th Internat. Conf. on Radiobiology*, Oliver and Boyd, London. *In press.*
6. Latimer, W.M. In *Oxidation Potentials.* Prentice Hall, New York 1952.

Enzyme Kinetics in Univalent Buffers

J. S. McKinley McKee

Biochemical Institute, University of Oslo, Blindern, Oslo

Many ions have different effects on the kinetics of the fumarase-catalyzed reaction [1]:

$$\text{fumarate} + H_2O \rightleftharpoons \text{L-malate}$$

With buffer ions specific effects arise due to the binding of the different buffer ions. Kinetic studies in phosphate buffers [2] proved unsatisfactory due to the presence of HPO_4^{--} and $H_2PO_4^-$ ions, each with its own effect on the enzyme and the relative concentration of which varied with pH. As the kinetic constants are unaffected by the buffer cation, while being very sensitive to the anion concentration and type, univalent buffers of the uncharged base type (*e. g.* imidazole, tris, ammidol-chloride, fluoride or perchlorate) have been used. Thus specific buffer effects can be studied as there is a single anion, the concentration of which can be held constant over a wide pH range.

The experiments have consisted of determining the pH variation of the maximum velocities (V_M, V_F) and Michaelis constants (K_M, K_F) for the forward and reverse reactions. These were obtained from Liveweaver-Burk plots. It was important to use substrate concentrations (range 4K—K/4) which gave neither substrate activation or inhibition [2], as otherwise erroneous kinetic constants resulted. The enzyme solutions were prepared from crystalline fumarase, and the kinetics were followed on the 80—100 % transmission expanded scale of a Beckman DUR spectrophotometer [2]. The Michaelis constants for malate and fumarate in 5 mM chloride, perchlorate or acetate buffers rise markedly above pH 8.0. With malate, the K_M values are approximately constant below pH 7.0, while with fumarate this represents a minimum. Plots of V_M, V_F, V_M/K_M, and $V_F/4.4K_F$ *vs.* pH are symmetrical and bell shaped. For each buffer the data were consistent with the ionisation of two groups in the enzymatic site, having different ionisation constants in the free enzyme and the fumarase and L-malate complexes. In the various buffers the pK values vary markedly. Good agreement was found between the experimental points and theoretical curves calculated from pH independent kinetic constants and the pK values [3]. In interpreting the data the secondary ionisations of the substrates have to be taken into account at the lowes pH values. A comparison of the kinetic constants in phosphate (approximate values) with those in the univalent buffers shows that while neither buffer type or concentration markedly affect the pH independent maximum velocity or turnover number, yet the corresponding Michaelis constants are much greater in phosphate, presumably due to the divalent ions present. As both substrates give the same ionisation constants for two essential groups in the free enzyme (V_M/K_M and $V_F/K_{eq}K_F$ superimposable) it seems that it is the same enzymatic site that is involved in the proton transfer reactions resulting in hydration or dehydration.

The author wishes to thank professor R. A. Alberty for many helpful discussions.

1. Massey, V. *Biochem. J.* **53** (1953) 67.
2. Alberty, R. A., Massey, V., Frieden, C. and Fuhlbrigge, A. R. *J. Am. Chem. Soc.* **76** (1954) 2485.
3. Alberty, R. A. *J. Cellular Comp. Physiol.* **47** (1956) 245.

Insulin-like Activity of a Dialyzable Factor in Human Blood Plasma *

R. Haavaldsen and O. Walaas

Institute of Medical Biochemistry and Physiology, Department of Biochemistry, University of Oslo, and Lier Mental Hospital, Norway

Human blood serum or plasma exerts an insulin-like activity shown by the stimulating effect on glucose uptake of the rat diaphragm *in vitro*. Based on this observation a method for determination of the insulin content in plasma or serum has been worked out by Groen *et al.*[1] and later by others. However, a definite proof that the effect of serum is due solely to the content of insulin is lacking. This can be questioned from the fact that wide variations in values obtained by different investigators have been reported, as well as from a theoretical point of view.

The present investigation has been undertaken to show if the insulin-like activity of plasma specifically can be related to the content of insulin or if other compounds contribute to this effect. The following experimental technique has been adopted. Blood is drawn into a syringe previously heparinized and plasma immediately separated by centrifugation. A sample of plasma was dialysed against Krebs Ringer solution for 12 h at +2 °C. The solution was buffered either with bicarbonate or with phosphate to pH 7.4 and glucose added to a final concentration of 140 mg per 100 ml. The effect of plasma and dialysate on glucose uptake of the rat diaphragm has been investigated by a procedure used for some years in our laboratory.

The dialysate from serum as well as from plasma stimulated glucose uptake in the isolated rat diaphragm. This was a significant and reproducible effect. As an average of 10 experiments 30 % stimulation was obtained. The stimulating effect was stable against heat. Thus, if the dialysate was kept at 80 °C for 20 min or boiled for 5 min the stimulating effect was increased by another 30 %. This indicated thermal inactivation of an inhibitory factor in the dialysate. The stimulating effect in the dialysate was not due to insulin. 0.1 unit crystalline insulin added to plasma did not influence the effect of the dialysate on glucose uptake of the rat diaphragm and insulin could be recovered in the plasma inside the bag after dialysis. — The insulin like effect of plasma was reduced after dialysis. After prolonged dialysis for 48 h even inhibition of the glucose uptake in rat diaphragm by the dialysed plasma has been observed.

So far, we have not been able to confirm that the insulin-like activity of plasma solely is due to the content of insulin. Of particular interest is that a dialysable factor from plasma or serum exerts insulin-like activity in the rat diaphragm method. Further studies on the nature of this factor is in progress.

* Supported by grants from *Eli Lilly and Co.*

1. Groen, J., Kamminga, C. E., Willebrands, A. F. and Blickman, J. R. *J. Clin. Invest.* **31** (1952) 97.

The Interaction of Cysteamine and Cysteine with various Carbonyl Compounds *

Lorentz Eldjarn, Karl F. Nakken** and Alexander Pihl

Norsk Hydro's Institute for Cancer Research, The Norwegian Radium Hospital, Oslo, Norway

Numerous important metabolites and several therapeutic agents possess reactive carbonyl groups. A study of the interaction of thiols with carbonyl compounds has therefore been undertaken.

In the present paper data on the interaction of the 1-mercapto-2-amines cysteamine and cysteine with several carbonyl compounds, will be reported. The procedure previously described for the analysis of thiol-disulphide interactions [1,2], was found suitable for this purpose. The sulphur labeled thiols were incubated with the carbonyl compound at 37 °C and the desired pH. After acidification the labeled products were separated from the reactants by paper electrophoresis in phthalate buffer at pH 2.

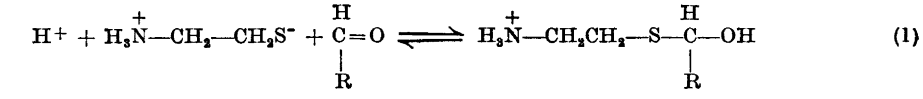
The reaction mechanism has been studied in some detail in the system cysteamine and glyceraldehyde. It was observed that at pH 6.8—7.4 the rate of formation of the labeled product followed the kinetics of a bimolecular one-way reaction of the type $A+B \rightarrow C$. No evidence for the formation of dithials was

* Supported by grants from the *Norwegian Cancer Society.*

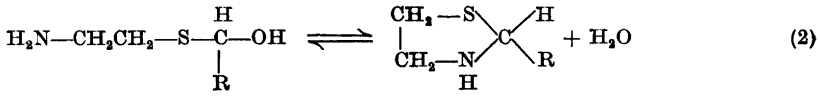
** Fellow of the Norwegian Cancer Society.

obtained, even when a large excess of cysteamine was used. Over a wide pH range (1.4—8.3) the observed reaction rate paralleled the concentration of the ionized thiol ($pK_{SH}=8.6$), which constitutes evidence that in this reaction thiol is indeed the reactive molecular species. It also demonstrates that, in the pH range studied, no marked proton activation of the carbonyl group takes place. At pH 7.4 and 37 °C the radioactivity of the labeled product did not decrease when an excess of non-labeled cysteamine was added.

On the basis of the above data the following reaction mechanism is suggested:



(1)



(2)

Since the formation of cyanohydrins, acetals and bisulphite addition products are known to be reversible [3], reaction 1 would similarly be expected to be reversible. The fact that the formation of the product appears as a one-way reaction, can be explained by assuming that reaction 2 is faster than reaction 1 and is displaced to the right.

The rate of interaction of cysteamine with cortisone was found to be negligible at pH 7.4 and 37 °C. However, significant reaction rates were found with glyceraldehyde, methylglyoxal [4], dihydroxyacetone and α-ketoglutaric acid. The rate constants

$$k = \frac{[\text{Product}]}{[RS^-]\,[R'\text{—}CO\text{—}R'']}\ \text{min}^{-1} \times \text{M}^{-1} \times (10^3)\text{l}$$

were 2.5, 1.2, 0.2 and 0.01 respectively.

Since streptomycin is known to be inactivated by cysteamine and cysteine [5], it is of interest that cysteine was found to react stoichiometrically with streptomycin at a fairly rapid rate, whereas no interaction was observed with dihydrostreptomycin. This latter finding indicates that the reaction takes place at the carbonyl group of streptomycin.

1. Eldjarn, L. and Pihl, A. *Acta Chem. Scand.* **10** (1956) 1054.
2. Eldjarn, L. and Pihl, A. *J. Biol. Chem.* **225** (1957) 499.
3. Bartlett, P. D. in *Organic Chemistry* **3**, John Wiley & Sons, Inc. New York 1953, p. 1.
4. Franzen, V. *Angew. Chem.* **11** (1956) 381.
5. Denkelwater, R., Cook, M. A. and Tishler, M. *Science* **102** (1945) 12.

The Isolation of Prostaglandin

S. Bergström and J. Sjövall

Department of Physiological Chemistry, University of Lund, Lund, Sweden

The presence of a smooth muscle stimulating factor in sperm and in extracts of the accessory genital glands of man and certain animals was demonstrated by Goldblatt [1] and von Euler [2]. A concentrate of the factor from sheep prostate gland was prepared by von Euler [3] who studied some of its chemical properties.

Some preliminary data on the further purification of this concentrate have been published [4].

We have succeeded in isolating one "prostaglandin" factor (PGF) in crystalline form The. compound (102°—103°) is an unsaturated hydroxyacid, that does not contain nitrogen. A good response is obtained on a rabbit's duodenum at a concentration of $\sim 5 \times 10^{-9}$ g per ml.

At least one other active acidic factor is present in sheep prostate glands.

The isolation procedure and some of the properties of the pure compound will be discussed.

1. Goldblatt, M. W. *Chemistry & Industry* **52** (1933) 1056.
2. von Euler, U. S. *Arch. exptl. Pathol. Pharmakol* **175** (1934) 78.
3. von Euler, U. S. *Scand. Arch. Physiol.* **81** (1939) 65.
4. Bergström, S. *Nord. Med.* **42** (1949) 1465.

Insulin-like Activity of a Dialyzable Factor in Human Blood Plasma *

R. Haavaldsen and O. Walaas

Institute of Medical Biochemistry and Physiology, Department of Biochemistry, University of Oslo, and Lier Mental Hospital, Norway

Human blood serum or plasma exerts an insulin-like activity shown by the stimulating effect on glucose uptake of the rat diaphragm *in vitro*. Based on this observation a method for determination of the insulin content in plasma or serum has been worked out by Groen *et al.*[1] and later by others. However, a definite proof that the effect of serum is due solely to the content of insulin is lacking. This can be questioned from the fact that wide variations in values obtained by different investigators have been reported, as well as from a theoretical point of view.

The present investigation has been undertaken to show if the insulin-like activity of plasma specifically can be related to the content of insulin or if other compounds contribute to this effect. The following experimental technique has been adopted. Blood is drawn into a syringe previously heparinized and plasma immediately separated by centrifugation. A sample of plasma was dialysed against Krebs Ringer solution for 12 h at +2 °C. The solution was buffered either with bicarbonate or with phosphate to pH 7.4 and glucose added to a final concentration of 140 mg per 100 ml. The effect of plasma and dialysate on glucose uptake of the rat diaphragm has been investigated by a procedure used for some years in our laboratory.

The dialysate from serum as well as from plasma stimulated glucose uptake in the isolated rat diaphragm. This was a significant and reproducible effect. As an average of 10 experiments 30 % stimulation was obtained. The stimulating effect was stable against heat. Thus, if the dialysate was kept at 80 °C for 20 min or boiled for 5 min the stimulating effect was increased by another 30 %. This indicated thermal inactivation of an inhibitory factor in the dialysate. The stimulating effect in the dialysate was not due to insulin. 0.1 unit crystalline insulin added to plasma did not influence the effect of the dialysate on glucose uptake of the rat diaphragm and insulin could be recovered in the plasma inside the bag after dialysis. — The insulin like effect of plasma was reduced after dialysis. After prolonged dialysis for 48 h even inhibition of the glucose uptake in rat diaphragm by the dialysed plasma has been observed.

So far, we have not been able to confirm that the insulin-like activity of plasma solely is due to the content of insulin. Of particular interest is that a dialysable factor from plasma or serum exerts insulin-like activity in the rat diaphragm method. Further studies on the nature of this factor is in progress.

* Supported by grants from *Eli Lilly and Co.*

1. Groen, J., Kamminga, C. E., Willebrands, A. F. and Blickman, J. R. *J. Clin. Invest.* **31** (1952) 97.

The Interaction of Cysteamine and Cysteine with various Carbonyl Compounds *

Lorentz Eldjarn, Karl F. Nakken** and Alexander Pihl

Norsk Hydro's Institute for Cancer Research, The Norwegian Radium Hospital, Oslo, Norway

Numerous important metabolites and several therapeutic agents possess reactive carbonyl groups. A study of the interaction of thiols with carbonyl compounds has therefore been undertaken.

In the present paper data on the interaction of the 1-mercapto-2-amines cysteamine and cysteine with several carbonyl compounds, will be reported. The procedure previously described for the analysis of thiol-disulphide interactions [1,2], was found suitable for this purpose. The sulphur labeled thiols were incubated with the carbonyl compound at 37 °C and the desired pH. After acidification the labeled products were separated from the reactants by paper electrophoresis in phthalate buffer at pH 2.

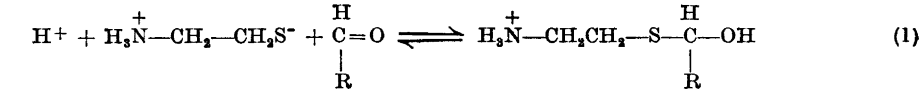
The reaction mechanism has been studied in some detail in the system cysteamine and glyceraldehyde. It was observed that at pH 6.8—7.4 the rate of formation of the labeled product followed the kinetics of a bimolecular one-way reaction of the type $A+B \rightarrow C$. No evidence for the formation of dithials was

* Supported by grants from the *Norwegian Cancer Society.*

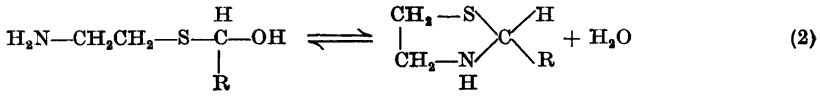
** Fellow of the Norwegian Cancer Society.

obtained, even when a large excess of cysteamine was used. Over a wide pH range (1.4—8.3) the observed reaction rate paralleled the concentration of the ionized thiol ($pK_{SH}=8.6$), which constitutes evidence that in this reaction thiol is indeed the reactive molecular species. It also demonstrates that, in the pH range studied, no marked proton activation of the carbonyl group takes place. At pH 7.4 and 37 °C the radioactivity of the labeled product did not decrease when an excess of non-labeled cysteamine was added.

On the basis of the above data the following reaction mechanism is suggested:



(1)



(2)

Since the formation of cyanohydrins, acetals and bisulphite addition products are known to be reversible [3], reaction 1 would similarly be expected to be reversible. The fact that the formation of the product appears as a one-way reaction, can be explained by assuming that reaction 2 is faster than reaction 1 and is displaced to the right.

The rate of interaction of cysteamine with cortisone was found to be negligible at pH 7.4 and 37 °C. However, significant reaction rates were found with glyceraldehyde, methylglyoxal [4], dihydroxyacetone and α-ketoglutaric acid. The rate constants

$$k = \frac{[\text{Product}]}{[RS^-]\,[R'\text{—}CO\text{—}R'']}\ \text{min}^{-1} \times \text{M}^{-1} \times (10^3)\text{l}$$

were 2.5, 1.2, 0.2 and 0.01 respectively.

Since streptomycin is known to be inactivated by cysteamine and cysteine [5], it is of interest that cysteine was found to react stoichiometrically with streptomycin at a fairly rapid rate, whereas no interaction was observed with dihydrostreptomycin. This latter finding indicates that the reaction takes place at the carbonyl group of streptomycin.

1. Eldjarn, L. and Pihl, A. *Acta Chem. Scand.* **10** (1956) 1054.
2. Eldjarn, L. and Pihl, A. *J. Biol. Chem.* **225** (1957) 499.
3. Bartlett, P. D. in *Organic Chemistry* **3**, John Wiley & Sons, Inc. New York 1953, p. 1.
4. Franzen, V. *Angew. Chem.* **11** (1956) 381.
5. Denkelwater, R., Cook, M. A. and Tishler, M. *Science* **102** (1945) 12.

The Isolation of Prostaglandin

S. Bergström and J. Sjövall

Department of Physiological Chemistry, University of Lund, Lund, Sweden

The presence of a smooth muscle stimulating factor in sperm and in extracts of the accessory genital glands of man and certain animals was demonstrated by Goldblatt [1] and von Euler [2]. A concentrate of the factor from sheep prostate gland was prepared by von Euler [3] who studied some of its chemical properties.

Some preliminary data on the further purification of this concentrate have been published [4].

We have succeeded in isolating one "prostaglandin" factor (PGF) in crystalline form The. compound (102°—103°) is an unsaturated hydroxyacid, that does not contain nitrogen. A good response is obtained on a rabbit's duodenum at a concentration of $\sim 5 \times 10^{-9}$ g per ml.

At least one other active acidic factor is present in sheep prostate glands.

The isolation procedure and some of the properties of the pure compound will be discussed.

1. Goldblatt, M. W. *Chemistry & Industry* **52** (1933) 1056.
2. von Euler, U. S. *Arch. exptl. Pathol. Pharmakol* **175** (1934) 78.
3. von Euler, U. S. *Scand. Arch. Physiol.* **81** (1939) 65.
4. Bergström, S. *Nord. Med.* **42** (1949) 1465.

Studies of Transphosphorylating Enzymes. The Incorporation Rate of ^{32}P into Trichloroacetic Acid Soluble Nucleotides, Protein-Phosphoserine and Phosphothreonine of Baker's Yeast

Gunnar Ågren and Lorentz Engström

Institute of Medical Chemistry, University of Uppsala, Sweden

In a recent paper [1] it was demonstrated that radioactive phosphoserine could be isolated from a yeast hexokinase preparation incubated with AT^{32}P or glucose-6-^{32}P. The results were interpreted in the way that the transfer of phosphorus in the hexokinase system is at least a two-step reaction with the formation of an enzyme-phosphate as an intermediate. It seemed to be of considerable interest if similar types of transphosphorylations could be demonstrated in later steps of the carbohydrate metabolism.

As in animal cells [2] the only phosphorylated amino acids present in partial hydrolysates of the Schneider protein residue from yeast cells were phosphoserine and phosphothreonine [3]. Recently Schmitz [4] also found that the perchloric acid soluble mononucleotides from yeast were the same as present in the corresponding extracts from animal cells [5]. Yeast cells were accordingly cultivated in a glucose medium and the rate of phosphorus incorporation into the phosphorylated amino acids and some of the metabolically active nucleotides were determined and compared.

In preliminary experiments the cells were preincubated in a 1 % glucose medium for 30 min followed by the addition of ^{32}P-phosphate at the beginning of each series. The specific activity values of the trichloroacetic acid soluble mononucleotides were determined at 0.5, 2, 5, 10, and 20 min of cultivation, mainly in the same way as Brumm *et al.*[6]. The values were compared with the specific activity values of the phosphoserine and phosphothreonine fractions isolated from the Schneider protein residues of each batch of cells [1,2]. With the increase in time there was a parallel increase of the phosphorus incorporation into the different mononucleotides and phosphoamino acids.

In several experiments the yeast cells were grown in the presence of enzyme inhibitors acting on enzymes in metabolic steps after the initial hexokinase system. In each series one of the inhibitors was added after 20 min of preincubation in a 1 % glucose medium. 10 min later the radioactive phosphate was added. The specific activities of the different compounds were determined after 2 and 20 min of cultivation. A control without inhibitor was always run parallel. The inhibitors, iodoacetic acid, potassium fluorid, sodium azide [7] or phlorhizin [8] were added to a final concentration of 2×10^{-3} M in the different series.

As compared with the controls there was always a decrease of the specific activity values of the trichloroacetic acid soluble nucleotides in the different inhibitor series. A parallel decrease in the specific activity values of the phosphorylated amino acids from the Schneider protein residues was also observed. This is taken as further evidence that several phosphoproteins in the later steps of the carbohydrate metabolism may also function as transphorylating enzymes in the same way as has previously been demonstrated for the hexokinase system.

1. Ågren, G. and Engström, L. *Acta Chem. Scand.* **10** (1956) 489.
2. Ågren, G., de Verdier, C.-H. and Glomset, J. *Acta Chem. Scand.* **8** (1954) 1570.
3. Ågren, G. and Engström, L. *Acta Chem. Scand.* **10** (1956) 877.
4. Schmitz, H. *Biochem. Z.* **325** (1954) 555.
5. Schmitz, H., Hurlbert, R. B., Brumm, A. F. and Potter, V. R. *J. Biol. Chem.* **209** (1954) 41.
6. Brumm, A. F., Potter, V. R. and Siekevitz, P. *J. Biol. Chem.* **220** (1956) 713.
7. Spiegelman, S., Kamen, M. D. and Sussman, M. *Arch. Biochem.* **18** (1948) 409.
8. Meyerhof, O. and Wilson, J. R. *Arch. Biochem.* **17** (1948) 153.

Yeast Lactic Dehydrogenase

Agnar P. Nygaard

Johan Throne Holst's Institutt for Ernæringsforsking, Blindern, Oslo, Norway

The enzyme has been isolated from bakers yeast after mechanical disruption of the cells. Preparations of the enzyme are able to reduce cytochrome c to a remarkable extent without substrate added. Enzymatic properties will be discussed.

The Use of Mixed Solvents in the Study of Enzyme Kinetics

E. W. Westhead and
Bo G. Malmström

Biokemiska Institutionen, Uppsala Universitet, Uppsala, Sweden

Possible advantages to be obtained through the use of aqueous-organic solvent mixtures in the study of enzyme kinetics are twofold: the influence of the nature of the solvent on the reaction might give information on the mechanism of the reaction, as it has in the case of many non-enzymic reactions, and the resultant depression of the freezing point of the solution might be useful in extending the temperature range over which the reaction can be studied.

To determine the extent to which these possibilities may be realized, the effects of dioxan, ethanol, methanol, and glycerol on the enolase reaction have been studied in detail. To avoid the danger of artefacts, the solvent study was accompanied by careful investigation of all factors influencing the kinetic behavior. This led, for example, to the discovery that buffer ions played an unexpected role in the reaction, resulting in changes of apparent activation energy and in low-temperature inhibition.

The results of this investigation have shown that serious misinterpretations of data may be made by assuming that the same factors are involved in solvent effects on enzymic reactions as on nonenzymic reactions. Specifically, dielectric constant changes in the medium were found to have no appreciable effect on the reaction.

The use of organic solvents to lower the freezing point of the medium was found to be justified for the enolase reaction since it did not cause any change in the temperature dependance of the reaction; hence the reaction mechanism is apparently unaffected despite the lowering of the activity. Through this technique it has been found possible to lower the reaction rate sufficiently to investigate kinetic behavior at higher enzyme concentration than would otherwise be possible without the use of advanced electronic equipment, such as that used by Chance and others [1]. The use of high enzyme concentrations is desirable both to avoid certain types of artefacts (*e. g.* inactivation by surface denaturation or traces of metal ions) and to increase the information obtainable by kinetic means. Results of these investigations, including studies of "low temperature inhibition", will be presented.

1. Roughton, F. J. W. and Chance, B. in Friess, S. L. and Weissberger, A. *Investigations of Rates and Mechanisms*, Interscience, New York 1953, p. 669.

Ornithine Carbamyl Transferase

Peter Reichard

Biochemical Department, Karolinska Institutet, Stockholm, Sweden

The enzyme which catalyzes the formation of citrulline [1,2] was purified from rat liver mitochondria. The final preparation moved as a single compound during paper electrophoresis between pH 5 and 8.5. During ultra centrifugation an impurity amounting to *ca.* 5—8 % was detected.

The enzyme catalyzed the following stoichiometric reaction:

L-ornithine + carbamyl phosphate ⇌ L-citrulline + phosphate

Out of 26 tested amino acids only L-ornithine could accept the carbamyl group of carbamyl phosphate. The name ornithine carbamyl transferase is proposed for the enzyme. The reversibility of the reaction was demonstrated with the aid of isotopic substrates and the equilibrium constant was found to be about 10^5. The liver enzyme described by Krebs *et al.*[3] which catalyzed the phosphorolysis or arsenolysis of citrulline was found to be identical with ornithine carbamyl transferase.

The reaction is strongly inhibited by *p*-chloromercuribenzoate. Ornithine and carbamyl phosphate can to some extent protect the enzyme from inhibition. Isotope exchange experiments gave no indication for the formation of a carbamylated enzyme. The reaction mechanism will be discussed.

Carbamyl aspartate was formed from citrulline + aspartate in the presence of phosphate by the combined action of ornithine carbamyl transferase and aspartate carbamyl transferase [4].

1. Grisolia, S. and Cohen, P. P. *J. Biol. Chem.* **198** (1952) 561.
2. Jones, M. E., Spector, L. and Lipmann, F. *J. Am. Chem. Soc.* **77** (1955) 819.
3. Krebs, H. A., Eggleston, L. V. and Knivett, V. A. *Biochem. J. London* **59** (1955) 185.
4. Reichard, P. and Hanshoff, G. *Acta Chem. Scand.* **10** (1956) 548.

On the Migration of the Phosphoryl Group in Phosphoproteins

Gunnar Ågren and
Carl-Henric de Verdier

Institute of Medical Chemistry, University of Uppsala, Sweden

In a previous paper [1] on the phosphorus-containing proteins of cells we discussed the possible migration of phosphorus from a phospho-amide linkage in serine to the hydroxyl groups. Plapinger and Wagner-Jauregg [2] have shown this to occur, when N-di*iso*propylphosphorylserine is hydrolysed with aqueous hydrochloric acid. Elliott [3] also found a transfer of approximately 60 % of the peptide chains linked to the nitrogen atoms of serine residues to the hydroxyl groups of these residues. Possible migration within the serine molecule when the corresponding phenylthiohydantoin is formed has been discussed by Edman and Lauber [4].

Müller *et al.*[5] recently published an interesting report where they demonstrated that aminophosphate (AP) at 25° and pH 7.2 phosphorylated the imidazole group of histidine. They also isolated a phosphorylated insulin containing 1 % of phosphorus when the protein was incubated with AP. They suggested that the phosphoryl group was linked to histidine in the protein molecule. This compound offered an unique opportunity to investigate a possible phosphorus migration within a phosphoprotein with known amino acid sequences, probably only containing nitrogen-bound phosphorus.

AP was synthesized according to Stokes [6] as modified by Müller *et al.*[5] 7 g of bovine crystalline insulin * was incubated at pH 8.0 and 25° with 4.37 g AP, divided in five equal parts and added with intervals of 2 h. Samples of the incubation mixture containing 120 mg of insulin were purified from AP by electrodialysis for 1 h at pH 8. pH was kept constant by adding ammonia. The yield was 6 g of lyophilised material containing 0.48 % P. After partial acid hydrolysis and repeated purification on Dowex-50 colums it was possible to isolate a ninhydrin-positive substance which on paper chromatograms with different solvents and on paper-electrophoresis strips at different pH moved as O-phosphoserine. It contained about 0.4 % of the phosphorus present in phosphoinsulin. The partial hydrolysis used always gives a mixture of phosphopeptides [1,7]. In a similar manner the partial hydrolysis of phosphoinsulin resulted in several phosphopeptides containing serine and threonine.

Model experiments with several basic and neutral amino acids including serine, threonine and cysteine are in agreement with the hypothesis that the phosphoryl group is primarily attached to the imidazole- and ε-amino groups of histidine and lysine, respectively. The isolation of O-phosphoserine seems to demonstrate a nitrogen to oxygen migration of the phosphoryl-group from one amino acid to another within the molecule. Perlmann [8] recently showed that the phosphate in some phosphoproteins can be N-, O-, and pyrophosphate bound. The amide-bound phosphorus, as representing high-energy linked phosphorus, is of special interest in metabolic reactions. Recent results from this laboratory [1,9-11] seem to demonstrate that several of the intracellular phosphoproteins must function as transphosphorylating enzymes. It is likely that many of these phosphoproteins contain the nitrogen-linked type of phosphate. The O-phosphoserine and O-phosphothreonine isolated from such proteins by our standard procedure originally may have been nitrogen-linked as in phosphoinsulin and then by the partial acid hydrolys migrated to the O-position in serine and threonine.

* The gift of crystalline insulin from professor E. Jorpes is gratefully acknowledged.

1. Ågren, G., de Verdier, C.-H. and Glomset, J. *Acta Chem. Scand.* **8** (1954) 1570.
2. Plapinger, R. E. and Wagner-Jauregg, T. *J. Am. Chem. Soc.* **75** (1953) 5757.
3. Elliott, D. F. *Biochem. J.* **50** (1952) 548.
4. Edman, P. and Lauber, K. *Acta Chem. Scand.* **10** (1956) 466.
5. Müller, Th., Rathlev, T. and Rosenberg, Th. *Biochim. et Biophys. Acta* **19** (1956) 563.
6. Stokes, H. N. *Am. Chem. J.* **15** (1893) 198.
7. de Verdier, C.-H. *Acta Soc. Med. Upsaliensis* **60** (1955) 48.
8. Perlmann, G. *Advances in Protein Chem.* **10** (1955) 1.
9. Engström, L. and Ågren, G. *Acta Chem. Scand.* **10** (1956) 877.
10. de Verdier, C.-H. *Acta Physiol. Scand.* **39** (1957) 1.
11. Ågren, G. and Engström, L. *Acta Chem. Scand.* **11** (1957) 1087.

Yeast Carboxylase and Cell Permeability

Heikki Suomalainen and Erkki Oura

Research Laboratories of the State Alcohol Monopoly, Helsinki, Finland

The effect of cell permeability on the metabolic functions of micro-organisms has been repeatedly discussed in the literature, but very little direct evidence has been presented [1-3]. In this work the question has been studied by comparing the decarboxylating activity of yeast carboxylase preparations and of intact yeast cells.

Yeast carboxylase decarboxylates not only pyruvic acid but also other straight-chain α-keto acids, at least up to acids with 8 carbon atoms. Our results with dried brewer's yeast as a crude carboxylase preparation show that, in accordance with earlier observations [4,5], the decarboxylating power of the enzyme decreases with increase of the carbon chain length (Table 1).

It has been generally supposed that the enzyme carboxylase is located in the interior of the yeast cell. Thus the cell wall may form a barrier tending to prevent the substrate from coming in contact with the enzyme. The longer the carbon chain the faster the normal fatty acids penetrate into a yeast cell [6,7].

Table 1. Decarboxylation of different α-keto acids by dried brewer's yeast at pH 5.8. α-Keto acids were used at a concentration (0.04 M) at which the enzyme was saturated with the substrate.

Substrate	CO_2, μl/3 min/10 mg dry yeast
Pyruvic acid	192
α-Ketobutyric acid	143
α-Ketovaleric acid	122
α-Ketocaproic acid	58
α-Ketooenanthic acid	33
α-Ketocaprylic acid	28

The same tendency in decarboxylating power was found both in dried baker's yeast and in brewer's or baker's yeast disintegrated by freeze-thawing.

Table 2. Decarboxylation of different α-keto acids by intact brewer's yeast, in two substrate concentrations.

Substrate	CO_2, μl/3 min/80 mg fresh yeast Concentration of the keto acid	
	0.0015 M	0.0075M
Pyruvic acid	2	11
α-Ketobutyric acid	7	31
α-Ketovaleric acid	8	38
α-Ketocaproic acid	11	51
α-Ketooenanthic acid	22	—
α-Ketocaprylic acid	27	—

Analogous results were obtained with intact baker's yeast.

Consequently it is possible that in intact yeast the permeability of the cell wall determines the velocity of the decarboxylation of α-keto acids. Because only undissociated acid molecules can penetrate, the experiments with intact yeast were performed at a lower pH, at which, however, the longer-chain keto acids can be used in low concentrations only. Examples of the results are given in Table 2.

From these results it would appear that the velocity of decarboxylation of α-keto acids by intact yeast bears an inverse relation to the velocity of decarboxylation of dried yeast preparations or of disintegrated yeast cells. The explanation that this difference is due to the limiting effect of the cell permeability has been confirmed by potentiometric measurements of the penetration velocities of the α-keto acids.

1. Malm, M. *Physiol. Plantarum* **3** (1950) 376.
2. Suomalainen, H. and Oura, E. *Exptl. Cell Research* **9** (1955) 355.
3. Collander, R. *Protoplasma* **46** (1956) 123.
4. Green, D. E., Herbert, D. and Subrahmanyan, V. *J. Biol. Chem.* **138** (1941) 327.
5. Kobayasi, S. *J. Biochem. Japan* **33** (1941) 301.
6. Conway, E. J. and Downey, M. *Biochem. J.* **47** (1950) 347.
7. Collander, R., Oura, E. and Suomalainen, H. *To be published.*

Pasteur Effect, Malonate Pasteur Effect and Crabtree Effect in Ehrlich Ascites Tumor Cells

Elling Kvamme

Ullevål sykehus, Centrallaboratoriet, Oslo, Norway

In confirmation of earlier reports by others, it was found that ascites tumor cells exhibit a clear cut Pasteur effect, *i. e.*, they have a lower aerobic than anaerobic glucose utilization. A similar type effect was also demonstrated in malonate blocked cells, incubated aerobically. Under these conditions, fumarate stimulated the oxygen uptake markedly and reduced the glucose uptake as well as the lactic acid formation (malonate Pasteur effect). In the absence of malonate, fumarate had no such action upon glycolysis and respiration.

It has been shown that the concentration of inorganic phosphate in the incubation medium is limiting for the rate of aerobic glycolysis in the Ehrlich ascites cells. The same was found when the cell suspensions were incubated in partial vacuum, as well as in the presence of malonate. It has further been demonstrated that the concentration of inorganic phosphate within the cells decreased to immeasurable values during aerobic glycolysis. An almost complete depletion of intracellular inorganic phosphate was also found to accompany the malonate Pasteur effect.

The Pasteur effect as well as the malonate Pasteur effect decreased by increasing the phosphate concentration of the medium. More ^{32}P was taken up by the cells during aerobic glycolysis than during anaerobic glycolysis. In the latter case, phosphate was given off from the cells to the medium.

An accumulation of acid soluble phosphate esters, including fructose-diphosphate, glucose-6-phosphate and adenosine-triphosphate (ATP), did only accompany aerobic glycolysis. The ATP concentration increased at the expence of ADP and AMP. The amount of acid labile phosphate esters which accumulated, declined by reducing the phosphate concentration of the medium, in contrast to the acid stable phosphate esters. In the presence of iodoacetic acid (10^{-4} M) glucose further reduced the ADP and AMP, a reduction which was not counteracted by the corresponding increase in ATP.

The data indicate that the accumulation of phosphate esters during aerobic glycolysis further restrict the intracellular availability of inorganic phosphate, resulting in a reduced rate of aerobic glycolysis, *i. e.* a Pasteur effect.

The aerobic accumulation, especially of acid labile phosphate esters in the presence of glucose and phosphate, may also have some bearing upon the Crabtree effect. As this effect was more or less counteracted by removal of phosphate from dilute suspensions of glycolyzing cells, it is probably not directly caused by intracellular phosphate limitation. The Crabtree effect may possibly be explained by a depletion of mitochondrial phosphate acceptors, due to the ATP accumulation during aerobic glycolysis.

Chromatographic Separation of Urinary Corticoids

R. Emberland and K. F. Stöa

The Endocrinological Research Laboratory, University Clinic, Bergen

Dirscherl *et al.* [1] have found that individual steroid hormones can be separated by means of partition-chromatography on cellulose columns.

This principle has been applied to the fractionation of urinary corticosteroids, and several individual hormone metabolites have been separated and identified.

The procedure involves hydrolysis of the urinary steroid conjugates, either with acid or by means of β-glucuronidase. The steroids are then extracted with ether, the ether extract washed with 0.1 M NaOH and with water. After evaporation of the ether, the residue is dissolved in 2 ml toluene saturated with 1,2-propylene glycol. This solution is chromatographed on a cellulose column impregnated with 1,2-propyleneglycol. Elution fluid: toluene saturated with 1,2-propyleneglycol. The corticoids are determined as reducing steroids.

By means of this method we have determined the loss of several individual corticosteroids when the urine is hydrolyzed with acid and with β-glucuronidase, respectively.

Likewise we have determined the percentage of free and glucuronic acid bound urinary corticoids.

1. Dirscherl, W., Korus, W. and Schriefers H. Hoppe-Seyler's *Ztschr. f. physiolog. Chemie* **305** (1956) 116.

Fragmentation of Mast Cells Caused by Some Phenothiazine Derivatives

Bertil Högberg

Research Department, AB Leo, Hälsingborg

and Börje Uvnäs

Department of Pharmacology, Karolinska Institutet, Stockholm, Sweden

Chlorpromazine has been reported to give rather frequent side effects such as pruritus, dermatitis and other cutaneous reactions, rhinitis and icterus. The side effects have been proposed to be of an allergic nature. If so, the manifestations should be due to or accompanied with release of histamine. As phenothiazine derivatives have a pronounced antihistamine effect, it is, however, difficult to use current methods for biological testing of histamine liberated by these derivatives. Since "histamine releasers" have been observed to disrupt mast cells we have tested some phenothiazine derivatives on their ability to cause disruption of mast cells. A slight modification of the technique described by Norton was used [1].

The disrupting actions of chlorpromazine, chlorpromazine sulfoxide, oxypromazine, promethazine and promazine are compared with that of compound 48/80, a very potent "histamine liberator". All the phenothiazine derivatives except chlorpromazine sulfoxide, the major metabolite of chlorpromazine, have a disrupting action on mast cells, although to a lesser degree than 48/80. The ED_{50} value (50 % disruption of mast cells) is for 48/80 0.32 μg/ml (0.18—0.56), and for chlorpromazine, the most active of the phenothiazine derivatives studied, ED_{50} is 45 μg/ml (42.1—48.2). The log-dose response curve obtained for chlorpromazine is of the same character as that obtained for 48/80, a fact indicating that the mechanism of action on the mast cell membrane is identical for the two substances.

It is of interest to note that chlorpromazine produces an action in cases of essential hyperlipemia similar to that produced by intravenous heparin [2]. The "clearing effect" of chlorpromazine might be explained as the result of its disruptive action on mast cells. These cells contain, at least in some species and in some tissues, not only histamine but also heparin, which substances occur in the blood on fragmentation of the mast cells.

On treatment of mental illnesses it has been proved that chlorpromazine is the most active of the phenothiazine derivatives studied. It can therefore be discussed if not only the side effects but also the clinical effect may be explained partly by the disruption of the mast cells.

1. Högberg, B., Südow, G., Thon, I.-L. and Uvnäs, B. *Acta Physiol. Scand.* **38** (1957) 265.
2. Hollister, L. E. and Kanter, S. L. *Gastroenterology* **29** (1955) 1069.

Formic Acid Oxidation in *Aspergillus niger*

J. G. Hauge

Institute for Nutrition Research, University of Oslo, Norway

Preformed mycelial pads of *Aspergillus niger* discharge large amounts of oxalate when incubated with sodium formate. Based on this finding Bernhauer postulated a C_1—C_1 condensation to take place in the organism [1]. As noticed by Butkewitsch, oxalate is, however, also produced when the mycelium is incubated on a buffer in the absence of organic carbon [2].

These findings were confirmed in the present investigation. When ^{14}C-labelled formate was employed, a small but significant incorporation into oxalate was observed. This incorporation may well have passed through carbonate as an intermediate, since labelled carbonate was converted to oxalate to the same extent as formate.

Carbonate is readily formed from formate by the organism or extracts thereof, provided the organism has been exposed to formate during growth. The inducible and soluble enzyme catalyzing this reaction has been partly purified and some of its properties studied. It carries out the oxidative decarboxylation of formate with oxygen as the only effective electron acceptor and H_2O_2 as the reaction product together with CO_2. No dialyzable cofactors participate in the reaction. The enzyme has a pH optimum of 6.2 and a Michaelis constant of 0.013 M.

1. Bernhauer, K. and Slalina, F. *Biochem. Z.* **274** (1934) 97.
2. Butkewitsch, W. S. *Biochem. Z.* **276** (1935) 451.

Bile Acids in Newborn and Adult Humans

Jan-Carl Encrantz and Jan Sjövall

Department of Physiological Chemistry, University of Lund, Lund, Sweden

Using quantitative paper chromatography [1] taurocholic (TC), taurochenodeoxycholic + taurodeoxycholic (TCD+TD), glycocholic (GC), glycochenodeoxycholic (GCD) and glycodeoxycholic (GD) acids have been determined in human bile and intestinal contents. In 34 analyses of the bile acids in the duodenal contents of 21 newborn babies (1—7 days old) the total bile acid concentration expressed as free bile acids varied between 84 and 1 182 mg/100 ml. Only conjugated bile acids could be found. With the method used free bile acids should have been detected when present as 2—3 % of the total amount of bile acids. The ratio of glycine conjugated acids to taurine conjugated acids (G/T) rose with age. Thus in children between one and four days old a mean value of 0.45 was found whereas the ratio 0.93 was obtained in children 5—7 days of age. No TD or GD could be found but an unidentified spot moving slightly faster than GD was in some cases observed on the paper chromatograms. There was approximately 2.5 times more cholic acid than chenodeoxycholic acid. When the children had reached an age of about eight months the bile acids were again analyzed in some subjects. The G/T ratio had risen to about 2 and deoxycholic acid could still not be found.

The proportions between the various bile acids in the duodenal contents of 19 medical students has been determined. No free bile acids could be detected. The mean G/T ratio was 3.1 and the proportions between cholic, chenodeoxycholic and deoxycholic acids were 1.2:1:0.6. When several analyses were made on the same subject at different times variations were noted in the G/T ratio as well as in the proportions between the different bile acids. Some factors influencing the G/T ratio will be discussed.

Cholic acid was by far dominating in human fistula bile. It was noteworthy that deoxycholic acid was usually absent. This resembles the bile acid composition of the newborn babies. In the normal adult, however, the relative amount of cholic acid is diminished and deoxycholic acid is now present. This suggested that deoxycholic acid is formed by bacterial action on cholic acid during the entero-hepatic circulation. At the same time Lindstedt in his work on the turnover of cholic acid in man observed that radioactive cholic acid gave rise to a labelled dihydroxycholanic acid which was identified as deoxycholic acid [2].

1. Sjövall, J. *Acta Chem. Scand.* **10** (1956) 1051.
2. Lindstedt, S. *Arkiv Kemi* **11** (1957) 145.

The Influence of Whole Body X-Irradiation of the Biosynthesis of Cholesterol in Liver

H. K. Hanel, G. Hjort, G. Johansen and P. R. Purser

Radium Centre Copenhagen, Radiobiological Laboratory, Copenhagen, Denmark

Earlier work [1] has shown disturbances in hepatic synthesis of cholesterol in rats after 2 400 r whole body X-irradiation. We have preferred to study the effects of 400 r whole-body irradiation, considering that this would throw more light on the biochemical changes in "radiation sickness" and induce negligible histological changes. Three series of experiments are reported here.

In the first series we studied the *in vivo* incorporation of 2-^{14}C acetate injected intraperitoneally, in liver cholesterol in mice, and the disturbances caused by whole body X-irradiation. We found a decrease in synthesis immediately after X-irradiation, probably a response to the X-irradiation, and a subsequent rise, probably a response to the liver cholesterol concentration.

In the next series we studied in vitro synthesis by incubation of rat liver slices with 2-^{14}C acetate after whole body X-irradiation. Here we found an immediate rise in the rate of synthesis as a response to the X-irradiation. Subsequent changes in the rate of synthesis could be attributed to the effect of the liver cholesterol concentration. The changes in carbon dioxide metabolism were studied simultaneously.

The third series was carried out *in vivo* with mice. We studied the effects of synkavit (naphthohydroquinone) injected intraperitoneally alone and followed by irradiation. The amount of synkavit we used, 2 mg, gave an effect, similar to but greater than that produ-

ced by radiation alone. The conbined treatment gave an immediate depression in synthesis rate though smaller than that produced by radiation or synkavit alone; this was followed by an increase above normal, which was not produced by either treatment alone.

1. *Progress in Radiobiology, Proc. of Fourth International Conference of Radiobiology*, Cambridge (1955), p. 71.

The Formation of Bile Acids from Cholesterol in the Rabbit

Sven Lindstedt

Department of Physiological Chemistry, University of Lund, Lund, Sweden

Cholesterol-4-^{14}C has been administered intravenously into rabbits with a bile fistula. More than 90 % of the activity in the bile acids was present as cholic acid, which normally constitutes only about 10 % of the total bile acids in the rabbit. The origin of deoxycholic acid — the main bile acid in intact animals — will be discussed.

Thiamine in Baker's Yeast

Olof Forsander and Heikki Suomalainen

Research Laboratories of the State Alcohol Monopoly, Helsinki, Finland

During the anaerobic growth of the common industrial yeasts, thiamine added to the medium is taken up by the cells and mainly esterified to cocarboxylase. During the aerobic cultivation of brewer's yeast and of *Torulopsis utilis*, however, the whole amount of thiamine lost from the medium has not been traced in the yeast cells by the thiochrome method [1].

A balance experiment on the uptake of thiamine by baker's yeast was performed on an industrial scale. The cultivation was performed in the usual way for the production of commercial baker's yeast under strongly aerobic conditions. Thiamine was added to two out of three batches. After cultivation, the thiamine content of the yeast cells was determined by the thiochrome method. Table 1 shows the result of the experiment.

The loss may depend on a transformation of thiamine into some compound which cannot be determined by the thiochrome method. It is known that as pyrophosphate ester thiamine has different functions under aerobic and under anaerobic conditions but it is assumed that it acts aerobic in some other form too. Myrbäck [2] suggested that thiamine or cocarboxylase may be transformed into a disulfide form.

In order to study the question baker's yeast was cultivated under aerobic conditions on a laboratory scale with the addition of ^{35}S-labelled thiamine. After the cultivation, thiamine compounds were extracted from the yeast with TCA at pH 1—2. The extract was examined by paper chromatography [3]. No thiamine disulfide compounds could be found in this extract. The only labelled compounds found in this extract were cocarboxylase and free thiamine.

1. Fink, H. and Just, F. *Biochem. Z.* **311** (1942) 61.
2. Myrbäck, K. and Vallin, I. *Svensk Kem. Tidskr.* **57** (1945) 72.
3. Paladini, A. C. and Leloir, L. F. *Biochem. J.* **51** (1952) 426.

Table 1. Balance experiment on the uptake of thiamine by baker's yeast during cultivation under strongly aerobic conditions.

	Thiamine in yeast, μg/g	Total amount of thiamine in yeast, g	Loss of thiamine, %
No thiamine added	2.8	23.8	
15 g thiamine added	3.5	30.3	43.3
30 g thiamine added	3.7	29.2	54.3

Bile Acids in Newborn and Adult Humans

Jan-Carl Encrantz and Jan Sjövall

Department of Physiological Chemistry, University of Lund, Lund, Sweden

Using quantitative paper chromatography [1] taurocholic (TC), taurochenodeoxycholic + taurodeoxycholic (TCD+TD), glycocholic (GC), glycochenodeoxycholic (GCD) and glycodeoxycholic (GD) acids have been determined in human bile and intestinal contents. In 34 analyses of the bile acids in the duodenal contents of 21 newborn babies (1—7 days old) the total bile acid concentration expressed as free bile acids varied between 84 and 1 182 mg/100 ml. Only conjugated bile acids could be found. With the method used free bile acids should have been detected when present as 2—3 % of the total amount of bile acids. The ratio of glycine conjugated acids to taurine conjugated acids (G/T) rose with age. Thus in children between one and four days old a mean value of 0.45 was found whereas the ratio 0.93 was obtained in children 5—7 days of age. No TD or GD could be found but an unidentified spot moving slightly faster than GD was in some cases observed on the paper chromatograms. There was approximately 2.5 times more cholic acid than chenodeoxycholic acid. When the children had reached an age of about eight months the bile acids were again analyzed in some subjects. The G/T ratio had risen to about 2 and deoxycholic acid could still not be found.

The proportions between the various bile acids in the duodenal contents of 19 medical students has been determined. No free bile acids could be detected. The mean G/T ratio was 3.1 and the proportions between cholic, chenodeoxycholic and deoxycholic acids were 1.2:1:0.6. When several analyses were made on the same subject at different times variations were noted in the G/T ratio as well as in the proportions between the different bile acids. Some factors influencing the G/T ratio will be discussed.

Cholic acid was by far dominating in human fistula bile. It was noteworthy that deoxycholic acid was usually absent. This resembles the bile acid composition of the newborn babies. In the normal adult, however, the relative amount of cholic acid is diminished and deoxycholic acid is now present. This suggested that deoxycholic acid is formed by bacterial action on cholic acid during the entero-hepatic circulation. At the same time Lindstedt in his work on the turnover of cholic acid in man observed that radioactive cholic acid gave rise to a labelled dihydroxycholanic acid which was identified as deoxycholic acid [2].

1. Sjövall, J. *Acta Chem. Scand.* **10** (1956) 1051.
2. Lindstedt, S. *Arkiv Kemi* **11** (1957) 145.

The Influence of Whole Body X-Irradiation of the Biosynthesis of Cholesterol in Liver

H. K. Hanel, G. Hjort, G. Johansen and P. R. Purser

Radium Centre Copenhagen, Radiobiological Laboratory, Copenhagen, Denmark

Earlier work [1] has shown disturbances in hepatic synthesis of cholesterol in rats after 2 400 r whole body X-irradiation. We have preferred to study the effects of 400 r whole-body irradiation, considering that this would throw more light on the biochemical changes in "radiation sickness" and induce negligible histological changes. Three series of experiments are reported here.

In the first series we studied the *in vivo* incorporation of 2-^{14}C acetate injected intraperitoneally, in liver cholesterol in mice, and the disturbances caused by whole body X-irradiation. We found a decrease in synthesis immediately after X-irradiation, probably a response to the X-irradiation, and a subsequent rise, probably a response to the liver cholesterol concentration.

In the next series we studied in vitro synthesis by incubation of rat liver slices with 2-^{14}C acetate after whole body X-irradiation. Here we found an immediate rise in the rate of synthesis as a response to the X-irradiation. Subsequent changes in the rate of synthesis could be attributed to the effect of the liver cholesterol concentration. The changes in carbon dioxide metabolism were studied simultaneously.

The third series was carried out *in vivo* with mice. We studied the effects of synkavit (naphthohydroquinone) injected intraperitoneally alone and followed by irradiation. The amount of synkavit we used, 2 mg, gave an effect, similar to but greater than that produ-

ced by radiation alone. The conbined treatment gave an immediate depression in synthesis rate though smaller than that produced by radiation or synkavit alone; this was followed by an increase above normal, which was not produced by either treatment alone.

1. *Progress in Radiobiology, Proc. of Fourth International Conference of Radiobiology*, Cambridge (1955), p. 71.

The Formation of Bile Acids from Cholesterol in the Rabbit

Sven Lindstedt

Department of Physiological Chemistry, University of Lund, Lund, Sweden

Cholesterol-4-^{14}C has been administered intravenously into rabbits with a bile fistula. More than 90 % of the activity in the bile acids was present as cholic acid, which normally constitutes only about 10 % of the total bile acids in the rabbit. The origin of deoxycholic acid — the main bile acid in intact animals — will be discussed.

Thiamine in Baker's Yeast

Olof Forsander and Heikki Suomalainen

Research Laboratories of the State Alcohol Monopoly, Helsinki, Finland

During the anaerobic growth of the common industrial yeasts, thiamine added to the medium is taken up by the cells and mainly esterified to cocarboxylase. During the aerobic cultivation of brewer's yeast and of *Torulopsis utilis*, however, the whole amount of thiamine lost from the medium has not been traced in the yeast cells by the thiochrome method [1].

A balance experiment on the uptake of thiamine by baker's yeast was performed on an industrial scale. The cultivation was performed in the usual way for the production of commercial baker's yeast under strongly aerobic conditions. Thiamine was added to two out of three batches. After cultivation, the thiamine content of the yeast cells was determined by the thiochrome method. Table 1 shows the result of the experiment.

The loss may depend on a transformation of thiamine into some compound which cannot be determined by the thiochrome method. It is known that as pyrophosphate ester thiamine has different functions under aerobic and under anaerobic conditions but it is assumed that it acts aerobic in some other form too. Myrbäck [2] suggested that thiamine or cocarboxylase may be transformed into a disulfide form.

In order to study the question baker's yeast was cultivated under aerobic conditions on a laboratory scale with the addition of ^{35}S-labelled thiamine. After the cultivation, thiamine compounds were extracted from the yeast with TCA at pH 1—2. The extract was examined by paper chromatography [3]. No thiamine disulfide compounds could be found in this extract. The only labelled compounds found in this extract were cocarboxylase and free thiamine.

1. Fink, H. and Just, F. *Biochem. Z.* **311** (1942) 61.
2. Myrbäck, K. and Vallin, I. *Svensk Kem. Tidskr.* **57** (1945) 72.
3. Paladini, A. C. and Leloir, L. F. *Biochem. J.* **51** (1952) 426.

Table 1. Balance experiment on the uptake of thiamine by baker's yeast during cultivation under strongly aerobic conditions.

	Thiamine in yeast, μg/g	Total amount of thiamine in yeast, g	Loss of thiamine, %
No thiamine added	2.8	23.8	
15 g thiamine added	3.5	30.3	43.3
30 g thiamine added	3.7	29.2	54.3

Adaptation of *E. coli* to 2-Deoxy-D-ribose

J. Jonsen and S. Laland

Biochemistry Department, The University, Blindern, Oslo, Norway

The degradation of the sugar component of deoxyribonucleosides has been demonstrated with whole cells and extracts of *E. coli* [1,2] but little is known concerning the bacterial utilization of the free pentose.

The present paper describes preliminary studies on the adaptation of *E. coli* to utilize 2-deoxy-D-ribose.

Standard techniques, *i. e.* incubation of the microorganisms on solid media in the presence of 0.25 % of specific substrate, was not practical because of a limited supply of 2-deoxy-D-ribose. A technique was therefore worked out in which a fairly large yield of adapted cells (1 g dry weight) was obtained in a fluid medium containing 20 mg of 2-deoxy-D-ribose. To obtain a similar yield of adapted cells on solid medium, 2.5 g of 2-deoxy-D-ribose was needed. The adaptation was made as follows: A loop inoculum from a slope was seeded into 5 ml of broth containing 1 % glucose. After 4 h growth at 37 °C, 0.2 ml of the culture was evenly distributed on each of 50 agar plates containing 1 % glucose. After 12 h at 37 °C the bacterial growth was scraped off the agar. The bacteria were suspended in ice-cold 0.05 M tris-HCl buffer (pH 7.4), filtered through gauze, centrifuged down at 0° and washed five times with cold buffer. The washed sediment was then suspended in 200 ml of fluid medium containing 2-deoxy-D-ribose (0.01 %), tryptic digested peptone (1 %), and sodium chloride (0.5 %). The mixture was stirred slowly in a 500 ml beaker at 37 °C. The degradation of 2-deoxy-D-ribose was followed by the disappearance of the Dische diphenylamine colour on aliquots withdrawn after different times of incubation. When about 90 % of the sugar was degraded, the bacteria were rapidly centrifuged down at 0° and washed repeatedly with cold 0.9 % saline. The degradation of 2-deoxy-D-ribose by cells adapted in this manner is shown in Table 1. A comparison is made with cells adapted on solid medium and non adapted cells.

Adapted cells could be lyophilized or stored at 4 °C without appreciable loss of activity. In the presence of glucose no adaptation occurred. By subcultivation of adapted cells in media containing no 2-deoxy-D-ribose, the adaptive ability was lost in one generation.

With cell free extracts, no significant degradation has been obtained in the presence of ATP and Mg++, neither could the formation of deoxyribose-5-phosphate be demonstrated. Under similar conditions the same strain of *E. coli* readily gave cell free extracts which metabolized D-ribose when adapted to this pentose. Under certain conditions [3] 44 % of the available D-ribose was isolated as D-ribose-5-phosphate. The formation of ribose-5-phosphate is the first step in the degradation of this sugar [3] by *E. coli*, and a similar pathway was anticipated for 2-deoxy-D-ribose. The

Table 1. Degradation of 2-deoxyribose by *E. coli.*

Incubation period (37°) min	2-Deoxy-D-ribose (DR) in mixture with					
	cells adapted on solid medium		cells adapted in fluid medium		not adapted cells	
	DR µg/ml	DR consumed µg/ml	DR µg/ml	DR consumed µg/ml	DR µg/ml	DR consumed µg/ml
0	370	0	370	0	330	0
10	345	25	355	15	325	5
35	270	100	265	105		
70	145	225	150	220	320	10
110	0	370	10	360	315	15
450					60	270

Experiments were made in tris-HCl-buffer (0.05 M pH 7.4). Each mixture contained the same quantity of cells.

failure to prepare a deoxyribokinase extract, compared to the ease with which a ribokinase could be prepared from *E. coli* make us believe that the degradation of 2-deoxy-D-ribose does not start with the formation of 2-deoxy-D-ribose-5-phosphate. It is also possible that the difference is due to extreme lability of the enzymes attaching 2-deoxy-D-ribose.

1. Manson, L. A. and Lampen, J. O. *J. Biol. Chem.* **193** (1951) 539.
2. Hoffmann, C. E. and Lampen, J. O. *J. Biol. Chem.* **198** (1952) 885.
3. Long, C. *Biochem. J.* **59** (1955) 322.

The Effect of Estradiol Pretreatment on Hexokinase Activity of Rat Uterine Muscle *

O. Walaas and R. Lange

Institute of Medical Biochemistry and Physiology, Department of Biochemistry, University of Oslo, Norway

Previous investigations in this laboratory have shown that administration of estradiol monobenzoate to rats increases glycogen content of uterine muscle and stimulates glucose uptake of the surviving uterine muscle. These findings indicated a study of whether hexokinase activity is increased after pretreatment with estradiol.

Hexokinase activity of extracts from uterine muscle of rats has been determined 48 h after subcutaneous injection of 50 μg estradiol monobenzoate in previously ovariectomized animals. 10 % homogenate of uterine muscle was prepared in 0.03 M tris(hydroxymethyl)-aminomethane buffer, pH 8.2, which contained 0.0012 M EDTA (versene). After centrifugation at 4 000 × *g* for 20 min the supernatant was used for determination of hexokinase activity. Aliquots of the extract (usually 20 mg tissue equivalent) were incubated with 1.5 μM glucose, 4 μM ATP, 5 μM $MgCl_2$, 20 μM KF at 37 °C for 30 min. Incubation was made in 0.033 M tris buffer in a total volume of 1.0 ml. Hexokinase activity was determined by the glucose disappearence method.

Hexokinase activity increased in linear correlation with time during incubation up to 30 min and was proportional with the amounts of extract added. After pretreatment with estradiol monobenzoate hexokinase activity was increased by 100 % above the control values in ovariectomized rats. This was a relatively specific effect as the "specific activity" (μmole glucose phosphorylated per mg protein in 30 min) was increased by 75 %.

Experiments were performed to decide if the increased hexokinase activity was due to activation of pre-existing enzyme or to stimulation of enzyme synthesis by pretreatment with estradiol. Therefore several properties of hexokinase activity of uterine muscle in controls and after administration of estradiol were studied. These experiments included the effect of pH, the affinity to ATP, protection by EDTA, inhibition by glucose-6-phosphate, inhibition by *p*-chloromercuribenzoate. No indication was obtained that these properties were changed after pretreatment with estradiol. The results indicate that administration of estradiol monobenzoate increases hexokinase activity of uterine muscle by stimulation of enzyme synthesis.

* Supported by grants from *Eli Lilly and Co.* and from *Norwegian Research Council for Science and the Humanities.*

Studies in the Mechanism of Bile Acid Formation

S. Bergström, S. Lindstedt and B. Samuelsson

Department of Physiological Chemistry, University of Lund, Lund, Sweden

and E. J. Corey

Department of Chemistry, University of Illinois, Urbana, Ill., U.S.A.

In order to study the mechanism of the reactions involved in the transformation of cholesterol into bile acids we have prepared cholesterol stereospecifically labelled with tritium in the 7α- or 7β-position.

Some data on the metabolism of these compounds will be presented and discussed.

failure to prepare a deoxyribokinase extract, compared to the ease with which a ribokinase could be prepared from *E. coli* make us believe that the degradation of 2-deoxy-D-ribose does not start with the formation of 2-deoxy-D-ribose-5-phosphate. It is also possible that the difference is due to extreme lability of the enzymes attaching 2-deoxy-D-ribose.

1. Manson, L. A. and Lampen, J. O. *J. Biol. Chem.* **193** (1951) 539.
2. Hoffmann, C. E. and Lampen, J. O. *J. Biol. Chem.* **198** (1952) 885.
3. Long, C. *Biochem. J.* **59** (1955) 322.

The Effect of Estradiol Pretreatment on Hexokinase Activity of Rat Uterine Muscle *

O. Walaas and R. Lange

Institute of Medical Biochemistry and Physiology, Department of Biochemistry, University of Oslo, Norway

Previous investigations in this laboratory have shown that administration of estradiol monobenzoate to rats increases glycogen content of uterine muscle and stimulates glucose uptake of the surviving uterine muscle. These findings indicated a study of whether hexokinase activity is increased after pretreatment with estradiol.

Hexokinase activity of extracts from uterine muscle of rats has been determined 48 h after subcutaneous injection of 50 μg estradiol monobenzoate in previously ovariectomized animals. 10 % homogenate of uterine muscle was prepared in 0.03 M tris(hydroxymethyl)-aminomethane buffer, pH 8.2, which contained 0.0012 M EDTA (versene). After centrifugation at 4 000 × *g* for 20 min the supernatant was used for determination of hexokinase activity. Aliquots of the extract (usually 20 mg tissue equivalent) were incubated with 1.5 μM glucose, 4 μM ATP, 5 μM $MgCl_2$, 20 μM KF at 37 °C for 30 min. Incubation was made in 0.033 M tris buffer in a total volume of 1.0 ml. Hexokinase activity was determined by the glucose disappearence method.

Hexokinase activity increased in linear correlation with time during incubation up to 30 min and was proportional with the amounts of extract added. After pretreatment with estradiol monobenzoate hexokinase activity was increased by 100 % above the control values in ovariectomized rats. This was a relatively specific effect as the "specific activity" (μmole glucose phosphorylated per mg protein in 30 min) was increased by 75 %.

Experiments were performed to decide if the increased hexokinase activity was due to activation of pre-existing enzyme or to stimulation of enzyme synthesis by pretreatment with estradiol. Therefore several properties of hexokinase activity of uterine muscle in controls and after administration of estradiol were studied. These experiments included the effect of pH, the affinity to ATP, protection by EDTA, inhibition by glucose-6-phosphate, inhibition by *p*-chloromercuribenzoate. No indication was obtained that these properties were changed after pretreatment with estradiol. The results indicate that administration of estradiol monobenzoate increases hexokinase activity of uterine muscle by stimulation of enzyme synthesis.

* Supported by grants from *Eli Lilly and Co.* and from *Norwegian Research Council for Science and the Humanities.*

Studies in the Mechanism of Bile Acid Formation

S. Bergström, S. Lindstedt and B. Samuelsson

Department of Physiological Chemistry, University of Lund, Lund, Sweden

and E. J. Corey

Department of Chemistry, University of Illinois, Urbana, Ill., U.S.A.

In order to study the mechanism of the reactions involved in the transformation of cholesterol into bile acids we have prepared cholesterol stereospecifically labelled with tritium in the 7α- or 7β-position.

Some data on the metabolism of these compounds will be presented and discussed.

ACTA CHEMICA SCANDINAVICA 11 (1957) 1097--1102

On the Possible Existence of Tetrahedral Nickel(II) Complexes

R. W. ASMUSSEN and OLE BOSTRUP

The Chemical Laboratory B, Technical University of Denmark, Copenhagen, Denmark

The magnetic moments and the reflection spectra of a series of apparently tetrahedral Ni(II) complexes have been measured. Comparison with corresponding data for definitively octahedral complexes seems to show that most of the complexes investigated in reality are octahedral.

The magnetic susceptibilities of several Ni(II) complexes have been measured by one of us [1]. The calculated magnetic moments are in agreement with the Pauling theory for bond type and spatial arrangement of the ligands in the complexes. Representative compounds and experimental data are given in Table 1.

It should, however, be pointed out that the distinction between tetrahedral and octahedral configurations cannot be founded upon magnetic measurements and moments alone but should principally be based upon a knowledge of the chemical properties of the ligands, in particular their usual coordination capa-

Table 1. Magnetic properties of Ni(II)complexes. Analysis.

Substance	χ_g	χ_M	$\chi_M^{corr.}$	$\mu_{eff.}$	Analysis Calc.	Found
$Ni(NH_3)_6Br_2$	12.7	4 099	4 251	3.16	18.28	18.50 Ni
$Ni(NH_3)_4(SCN)_2$	17.6	4 286	4 418	3.23	24.15	24.01 Ni
$Nien_3(SO_4)$	12.1	4 053	4 240	3.16	17.52	17.67 Ni
$Nien_2(SCN)_2$, H_2O	12.1	3 787	3 972	3.06	18.75	18.88 Ni
$Nipy_4(SCN)_2$	9.04	4 436	4 704	3.32	11.96	11.95 Ni
$Nitren(SCN)_2$	12.88	4 135	4 325	3.19	18.28	18.38 Ni
$Nitren(SO_4)$, $7H_2O$	9.78	4 176	4 422	3.23	22.49	22.68 SO_4
$Nitren(SO_4)$	14.11	4 245	4 400	3.22	31.92	32.20 SO_4
$Ni(DH_2)_2Cl_2$	11.70	4 233	4 415	3.23	16.22	16.42 Ni

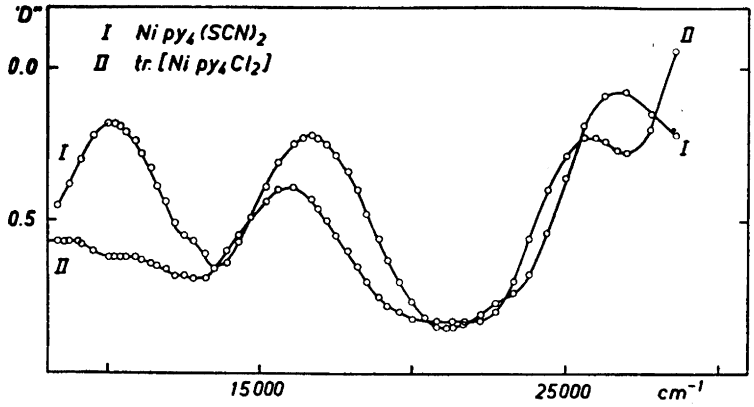


Fig. 1. Reflection spectra of $Ni(NC_5H_5)_4(SCN)_2$ and *trans* $Ni(NC_5H_5)_4Cl_2$.

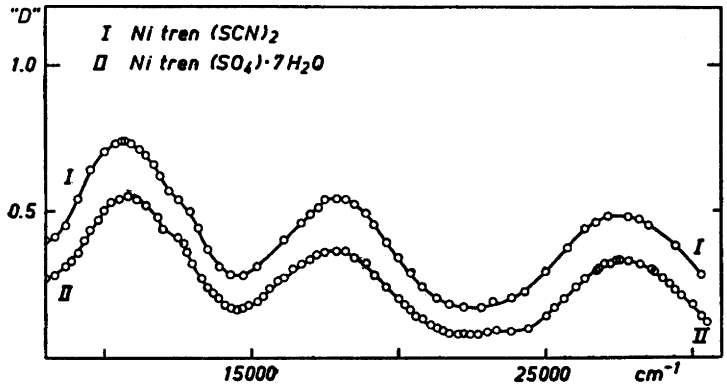


Fig. 2. Reflection spectra of Nitren$(SCN)_2$ and Nitren (SO_4) $7H_2O$.

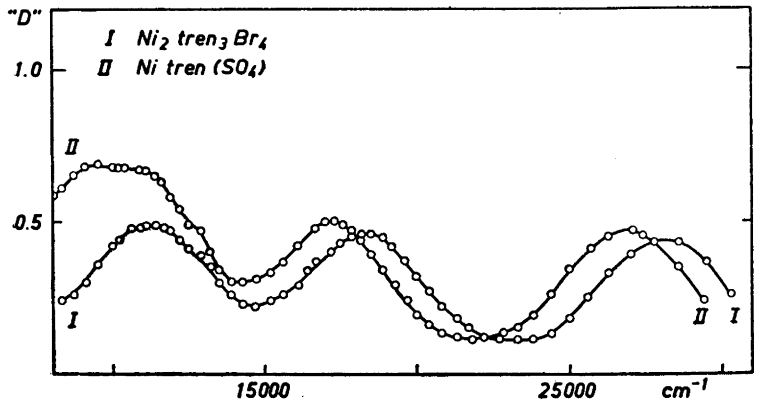


Fig. 3. Reflection spectra of $Ni_2tren_3Br_4$ and Nitren(SO_4).

Table 2. Reflection spectra of some Ni(II) complexes. σ_1, σ_2 and σ_3 are the wavenumbers in cm^{-1} of the three main bands. The wavenumbers for some small bands are also given. The ratio σ_2/σ_1 has been discussed by Ballhausen [10].

Substance	σ_1	σ_2	σ_3	Small bands	Δ	15 B	σ_2/σ_1
$NiSO_4 . 7H_2O$	8 500	14 700	25 700	15 500 19 000 22 000	8 500	14 900	1.73
$Nipy_4Cl_2$	9 500	15 900	25 700	11 000	9 500	13 100	1.67
$Nitren(SO_4)$	10 000	17 200	26 800	12 500	10 000	14 000	1.72
$Nien_2(SCN)_2 . H_2O$	10 000	17 900	28 000	12 000	10 000	15 900	1.79
$Nipy_4(SCN)_2$	10 200	16 600	26 700	14 000	10 200	12 700	1.63
$Ni(NH_3)_6Br_2$	10 800	17 500	28 200		10 800	13 500	1.62
$Nitren(SO_4) . 7H_2O$	10 800	17 800	27 600	13 000	10 800	13 000	1.65
$Nitren(SCN)_2$	10 800	17 800	27 800	12 500	10 800	13 200	1.65
$Nien_3(SO_4)$	11 300	18 500	29 000	12 800	11 300	13 600	1.64
$Ni_2tren_3Br_4$	11 400	18 400	28 200		11 400	12 400	1.61
$Ni\ ptn_2\ SO_4$	12 100	19 300	29 500		12 100	12 500	1.59
$Ni(DH_2)_2Cl_2$	10 900	17 100		12 900	10 900		1.57

city. This means, *e.g.*, that a complex as $Nitren(SCN)_2$ can either be considered as $[Nitren(SCN)_2]$ or as $[Nitren]\ (SCN)_2$, both structures are in agreement with the magnetic moment found.

Magnetic measurements on paramagnetic Ni(II) complexes show that the orbital magnetic moment contributes in higher or lesser degree to the total moment. The Penney-Schlapp approximation makes it probable that the orbital contribution will be smaller in octahedral complexes than in tetrahedral [2]. According to Table 1 we may consider some of these complexes, which hitherto have been formulated as tetrahedral, as octahedral.

Our study of the reflection spectra of some of the tabulated apparently tetrahedral complexes has shown that in all cases three bands approximately situated as the three bands in undoubtedly octahedral Ni(II) complexes and reasonable values for the parameters Δ and 15 B can be found. Table 2 gives a summary of our results. Some examples of the measured reflection spectra are given in Figs. 1—3.

An X-ray investigation carried out by Cox and Webster [3] showed that $Nitren(SCN)_2$ either has the tetrahedral structure $[Nitren]\ (SCN)_2$ or the *cis*-octahedral $[Nitren(SCN)_2]$. Our measurements of magnetism and reflection spectrum seem to indicate the latter possibility. If the compound $Nitren(SO_4)$, $7\ H_2O$ has octahedral structure (*cis*) then it is either an aquo or a sulphato complex. Since two of the seven water molecules in $Nitren(SO_4)$, $7\ H_2O$ are

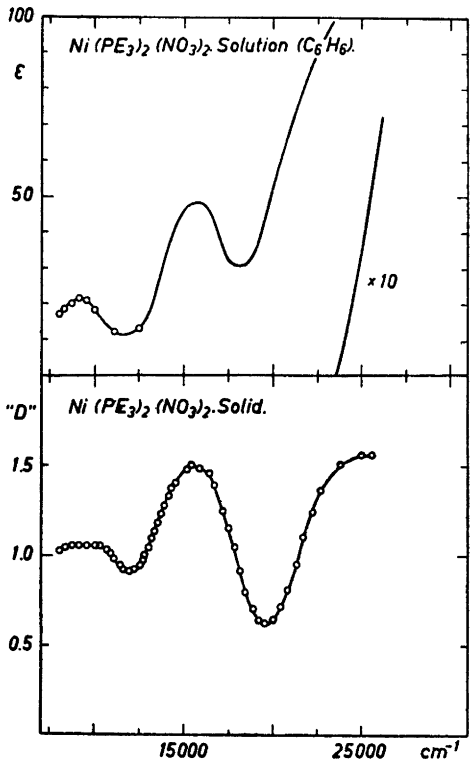


Fig. 4. Absorption spectrum and reflection spectrum of $[Ni(P(C_2H_5)_3)_2(NO_3)_2]$

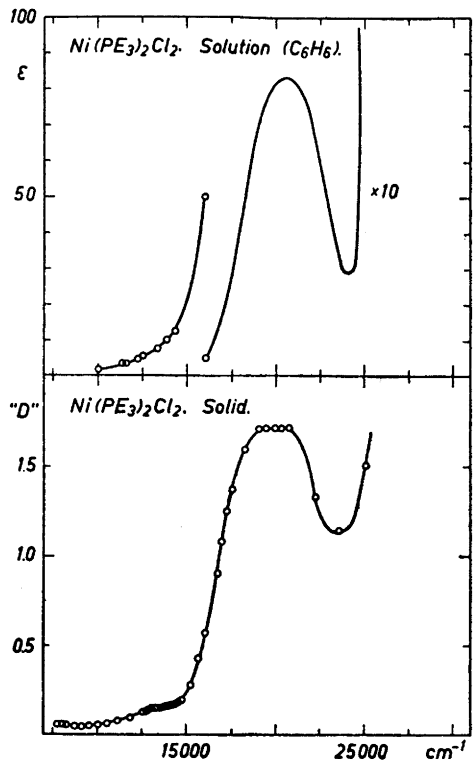


Fig. 5. Absorption spectrum and reflection spectrum of $[Ni(P(C_2H_5)_3)_2Cl_2]$

stronger bound than the others [4], and since the absorption bands are situated at the same places as in the aqueous solution of equivalent amounts of tren and $Ni(NO_3)_2$ investigated by Ballhausen and Klixbüll Jørgensen [5] it is reasonable to consider the heptahydrat as a *cis* diaquo complex. It is, however, difficult for the authors to imagine the anhydrous complex Nitren(SO_4) with octahedral configuration since as far as we know it has never been verified that SO_4^{-2} can act as a ligand with the coordination capacity 2. However, the experimental data indicate nothing unique with the properties of this compound.

Particular interest is connected with the paramagnetic green compound $Ni(P(C_2H_5)_3)_2(NO_3)_2$. The absorption spectrum in solution (benzene) and the reflection spectra are shown in Fig. 4. In Fig. 5 we give the spectra for the diamagnetic red chloro-compound [6]. The similarity between the spectra in Fig. 4 indicates that a monomer is also present in the crystal. The magnetic moment [6] is 3.10 μ_B which may be interpreted as corresponding with an octahedral structure. This assumption requires the ligand NO_3^- to be bidendate;

this seems to be rather unprobable although the isoster ion CO_3^{-2} can have the coordination capacity two, *e.g.* in $[Co(NH_3)_4(CO_3)]^{+1}$. Furthermore we do not observe 3 bands in the spectra and are forced to postulate that the band corresponding to $^3F(\Gamma_4)$ is masked of the high electron-transfer band in ultraviolet. The octahedral structure thus involves 2 unproven assumptions. However, it must be admitted that the 2 bands observed occur nearly at the wavenumbers required for an octahedral Ni(II)-complex. The possibility of the tetrahedral configuration cannot be ruled out, but we want in this connection to point out that the absorption curves for $Ni(P(C_2H_5)_3)_2(NO_3)_2$ and for $[Ni(OH_2)_6]^{+2}$ differ less than the corresponding curves for $[Co(OH_2)_6]^{+2}$ and $[CoCl_4]^{-2}$. The last ion has after all experimental evidences tetrahedral structure. The last possibility for the structure of $Ni(P(C_2H_5)_3)_2(NO_3)_2$ is the *cis*-planar configuration. As for the present we have no knowledge of how far it is possible that the action of this asymmetric field may result in such splittings that the configuration will allow for the observed magnetic moment, we are of the opinion that the lack of theoretical and experimental evidence makes it impossible to solve this problem with security. We consider an X-ray structure analysis to be more conclusive than the conclusions drawn from the spectra and magnetic moments alone.

EXPERIMENTAL

The solid samples were prepared according to the methods previously described [1,6]. The following abbreviations are used:

tren = β,β',β''-triaminotriethylamin
ptn = 1,2,3-triaminopropane
DH_2 = dimethylglyoxime

The magnetic measurements were carried out by means of the Guoy method described in earlier papers [9].

The reflection spectra were measured by means of a Beckman DU spectrophotometer equipped with a photomultiplier. In order to estimate the accuracy of the apparatus we measured the reflection spectrum of $NiSO_4$, $7H_2O$ and compared it with the known absorption curves for $[Ni(OH_2)_6]^{+2}$-solutions. These results will be published elsewhere [7] but it is worth while to note that all the bands known from solutions [8] were found in the reflection spectrum.

Acknowledgement. Our thanks are due to Professor, Dr. F. G. Mann, Cambridge, who kindly supplied us with a collection of trencomplexes, and to Mr. S. E. Rasmussen, who kindly supplied us with a sample of Nitren(SCN)$_2$. One of the authors (R.W.A.) thanks "*Statens teknisk-videnskabelige Forskningsraad*" for a grant which made it possible to procure the Beckman DU spectrophotometer and photomultiplier.

REFERENCES

1. Asmussen, R. W. *Studies in the Magnetochemistry of Inorg. Complex Compounds* (in Danish), Copenhagen 1944.
2. Nyholm, R. S. *Quart. Rews.* **53** (1953) 263.
3. Cox, E. G. and Webster, K. C. *Z. Krist.* **92** (1935) 478.
4. Mann, F. G. and Pope, W. J. *J. Chem. Soc.* **1926** 482.
5. Jørgensen, C. Klixbüll *Acta Chem. Scand.* **10** (1956) 887.
6. Asmussen, R. W., Jensen, A. and Soling, H. *Acta Chem. Scand.* **9** (1955) 1391.

7. Bostrup, O. and Jørgensen, C. Klixbüll, *Acta Chem. Scand.* **11** (1957) 1223.
8. Orgel, L. E. *J. Chem. Phys.* **23** (1955) 1004.
9. Christiansen, J. A. and Asmussen, R. W. *Kgl. Danske Videnskab. Selskab, Mat. fys. Medd.* **12** (1934) No. 10.
Asmussen, R. W. and Soling, H. *Acta Chem. Scand.* **8** (1954) 558; *Wilhelm Klemm-Festschrift, Z. anorg. Chem.* **283** (1956) 3.
10. Ballhausen, C. J. *Rec. trav. chim.* **75** (1956) 665.

Received April 15, 1957.

ACTA CHEMICA SCANDINAVICA 11 (1957) 1103—1110

Electrophoresis of Proteins in the Presence of Interacting Ions *

KURT SCHILLING

Biological Institute of the Carlsberg Foundation, Copenhagen, Denmark

The interaction of human, bovine and equine serum proteins with various protein precipitating ions was investigated by means of moving boundary electrophoresis. As these reactions are reversible, the total buffer used for the electrophoresis contained the interacting ion in the equilibrium concentration.

A detailed study of the interaction of cadmium ions with bovine serum albumin showed that at low concentrations the mass action law was obeyed with a binding constant in agreement with that found by earlier authors to apply for attachment to the histidine residues. At higher concentrations further binding, presumably to carboxyl groups, could be demonstrated.

Certain correlations were found between degree of interaction and precipitating power of the various ions.

Human, bovine, and equine serum albumin could be resolved in two separate peaks in the positive branch, when electrophoresis was performed in acetate buffer pH 6, $\Gamma/2 = 0.1$.

A change in the pattern of whole serum was observed by electrophoresis in the presence of various interacting ions.

Addition of interacting ions resulted in electrophoretic separations, which are not obtained in ordinary buffers.

It has previously been reported, that a number of anions and cations, such as tungstate, sulfosalicylate, cadmium, and lead can be used for the fractional precipitation of the serum proteins from various species [1, 2]. The interaction is reversible, and it was possible to remove the ions by dialysis, the regenerated proteins showing no signs of denaturation in subsequent electrophoresis. Marked differences were encountered between the behaviour of the various ions used, as well as between the proteins of different species.

Whether a protein is precipitated by addition of these ions under certain conditions will depend partly on the degree of interaction and partly on the solubility of the compounds formed. In order to investigate these factors, the

* A preliminary account of this work was presented at the Third International Congress of Biochemistry, Brussels 1955.

interaction was studied at pH-values, where a precipitation did not occur. As the combination with the ions is accompanied by a change in the net charge of the protein molecule, electrophoresis was considered an adequate approach to the problem. One important feature of this method is the possibility to investigate the interaction with the various components of a complex protein mixture. As the examined reactions are fully reversible, all electrophoreses were performed with the total buffer containing the interacting ion in the equilibrium concentration. The observed boundary velocities would then directly yield the constituent mobilities of the complexes.

MATERIALS AND METHODS

Human, bovine and equine serum were obtained from spontaneously coagulated blood. The samples were either used immediately or stored at −20°C.

Crude albumin fractions were prepared by precipitation with 55 % saturated ammonium sulfate and dialysis of the supernatant against distilled water followed by lyophilization. A bovine albumin of high purity prepared by lead and cresol precipitation [2] was used in some of the experiments.

Crude γ-globulin fractions were prepared by repeated precipitation with 38 % saturated ammonium sulfate. The precipitate was separated by centrifugation and used immediately or stored at −20°C.

The composition of the various buffers is recorded in Table 1. The samples were dissolved in the buffer and dialyzed against an excess until equilibrium had been established. Electrophoresis was then performed using the same buffer. A moving boundary Tiselius apparatus with Philpott-Svensson optical system was employed. The temperature of the bath was 1.5°C, and the duration of the experiments 2−3 h with a potential gradient of 5−8 V/cm.

RESULTS AND DISCUSSION

Effect of ion concentration. As a typical example Fig. 1 shows the influence of increasing cadmium concentration on the mobility of bovine serum albumin at pH 6.0. There is evidence of a strong interaction. The addition of cadmium

Table 1. Composition of the buffers.

No.		pH	$\Gamma/2$
1	0.1 M NaAc + HAc to	4.1	0.1
2	0.1 M Ag lactate + lactic acid to	4.2	0.1
3	0.0333 M $PbAc_2$ + HAc to	4.2	0.1
4	0.0333 M $PbAc_2$ + HAc to	4.5	0.1
5	0.0333 M $CdAc_2$ + HAc to	4.5	0.1
6	0.1 M NaAc + HAc to	5.3	0.1
7	0.1 M $ZnAc_2$ + HAc to	5.3	0.3
8	0.05 M Sulfosalicylic acid + 0.05 M NaAc + NaOH to	5.3	0.2
9	0.048 M KH_2PO_4 + 0.009 M Na_2HPO_4 + 0.025 M NaCl	6.0	0.1
10	0.05 M NaAc + 0.05 M NaCl + HAc to	6.0	0.1
11	0.1 M NaAc + HAc to	6.0	0.1
12	0.0917 M NaAc + 0.00278 M $CdAc_2$ + HAc to	6.0	0.1
13	0.075 M NaAc + 0.00833 M $CdAc_2$ + HAc to	6.0	0.1
14	0.05 M NaAc + 0.0167 M $CdAc_2$ + HAc to	6.0	0.1
15	0.0333 M $CdAc_2$ + HAc to	6.0	0.1
16	0.0667 M $CdAc_2$ + HAc to	6.0	0.2
17	0.014 M KH_2PO_4 + 0.029 M Na_2HPO_4	7.1	0.1
18	0.02 M Sulfosalicylic acid + 0.0174 M Na_2HPO_4 + NaOH to	7.2	0.1
19	0.04 M Na_2WO_4 + 0.02 N HCl	7.1	0.1

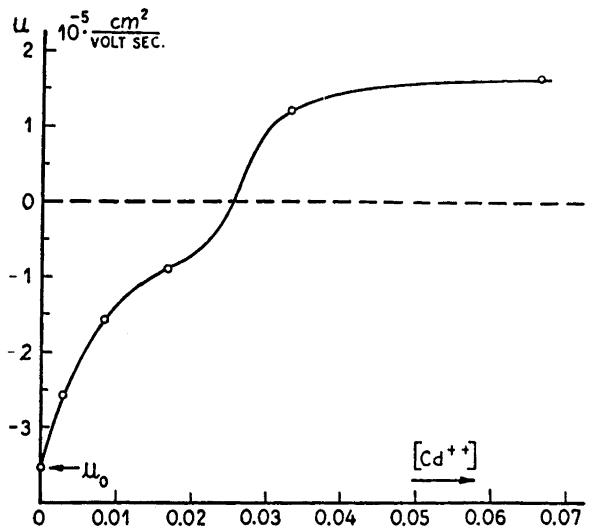


Fig. 1. Electrophoretic mobility of bovine serum albumin in acetate buffer pH 6.0 containing increasing amounts of cadmium ions. The composition of the buffers is recorded in Table 1. Nos. 11—16.

in low concentrations reduces the mobility markedly and higher concentrations even cause a reversal of the direction of migration. This shows that cadmium is still being bound after the protein compound has acquired a positive net charge.

It is possible to arrive at a quantitative interpretation of these results and to compare them with earlier investigations on the combination of cadmium ions with bovine serum albumin. From polarographic studies Tanford [3] concluded that cadmium as well as zink are bound chiefly to the histidine residues of the albumin. In the case of zink Gurd and Goodman [4] arrived at the same result by means of equilibrium dialysis.

If we thus assume that the cadmium-ions are bound by n equal sites, where they are competing with hydrogen ions, we get the following mass law equations

$$\frac{\nu}{(n-\nu-\nu_H)} = K \cdot [Cd^{++}]$$

$$\frac{\nu_H}{(n-\nu-\nu_H)} = K_H \cdot [H^+]$$

where ν denotes the number of sites occupied by cadmium, ν_H those occupied by hydrogen, and K and K_H the equilibrium constants including a possible electrostatic correction. The observed mobility change (Δu) in the electrophoresis experiment would be determined by

$$\Delta u = \frac{2\nu + \nu_H - \nu_{Ho}}{f}$$

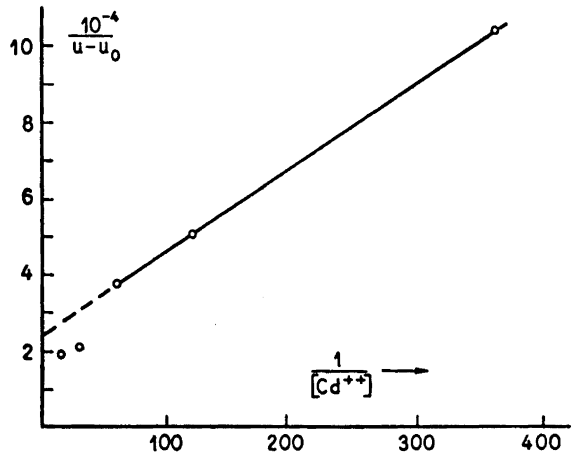


Fig. 2. Reciprocal mobility change by addition of cadmium ions to bovine serum albumin in acetate buffer plotted against reciprocal cadmium concentration.

where f denotes the number of charges corresponding to a mobility change of 1 unit, and ν_{Ho} the number of the n sites occupied by hydrogen at zero cadmium concentration. Combining these equations we get

$$\frac{1}{f \cdot \Delta u} = a \cdot \frac{1}{[Cd^{++}]} + b$$

with

$$a = \frac{(1+K_H \cdot [H^+])^2}{nK(2+K_H \cdot [H^+])}; \quad b = \frac{1+K_H \cdot [H^+]}{n(2+K_H \cdot [H^+])}$$

Plotting $1/\Delta u$ against $1/Cd^{++}$ we should expect a straight line, provided the electrostatic corrections contained in K and K_H do not change appreciably. Considering the great variation in the net charge of the protein over the experimental range this assumption appears rather questionable. However, as shown in Fig. 2, at low cadmium concentrations a straight line is obtained. Adopting the value $5.0 \cdot 10^5$ for f according to Longsworth and Jacobsen [5] and making n equal to 17 (the probable number of histidine residues in bovine albumin), the constants obtained for the working temperature of 1.5°C are log $K = 2.8$ and log $K_H = 6.7$, which is in satisfactory agreement with the intrinsic constants determined by Tanford [3].

Taking the electrostatic effect of the protein charge into account we should expect the experimental points at higher cadmium concentrations to lie above the straight line. The fact that they are situated below the line indicates, that at these concentrations further sites with lower affinity, presumably carboxyl groups, participate, resulting in binding of more cadmium ions. It should be pointed out that these concentrations greatly exceed those used by Tanford [3].

Table 2. Relative amounts of the two components obtained with various albumin samples in the positive (ascending) branch after electrophoresis in acetate buffer, pH 6.

Buffer (*cf.* Table 1)	Sample	Fast comp. %	Slow comp. %
11	Bovine serum albumin, crude	40	60
11	Bovine serum albumin, purified	43	57
10	Bovine serum albumin, crude	39	61
11	Human serum albumin, crude	50	50
10	Human serum albumin, crude	31	69
11	Equine serum albumin, crude	39	61

Heterogeneity of the serum albumin. Interestingly, all albumin preparations, which appeared quite homogeneous in phosphate buffer, showed a sharp separation into two peaks in the positive branch during electrophoresis in acetate buffer of pH 6.0 (Fig. 3). When the pH was decreased to 5.3, no separation was observed.

The total area of the two peaks was equal to that found in the negative branch and to that found in phosphate buffer. The relative amounts of the two components as determined by planimetry of the electrophoresis curves are recorded in Table 2.

When half of the acetate was substituted by chloride in the buffer the separation became less sharp. In the case of the human albumin a different

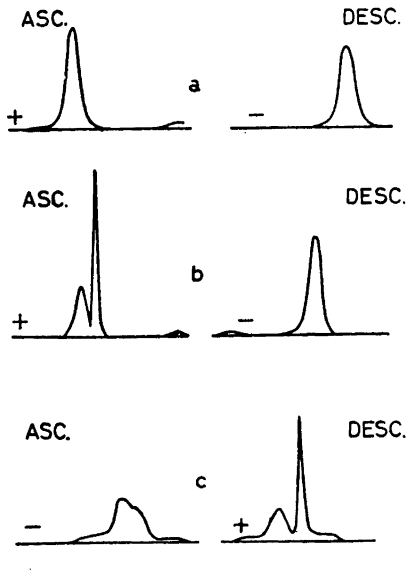


Fig. 3. Electrophoretic pattern of bovine serum albumin in (a) phosphate, (b) sodium acetate and (c) cadmium acetate buffer at pH 6.0, $\Gamma/2$ 0.1. Buffers Nos. 9, 11 and 15 (Table 1).

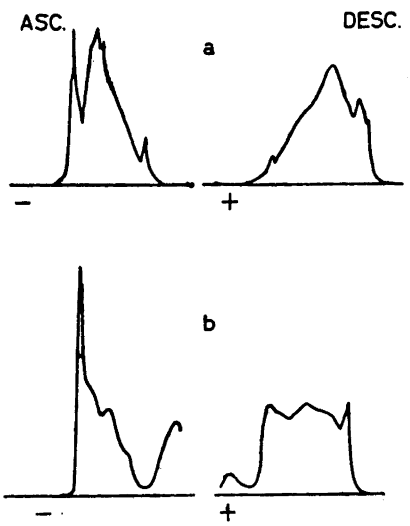


Fig. 4. Electrophoretic pattern of equine serum in (a) lead and (b) cadmium acetate at pH. 4.5, $\Gamma/2$ 0.1.

Table 3. Mobility of bovine serum albumin in various buffers. In the column denoted Δu the change in mobility is recorded relative to that found in buffers consisting of the sodium salt (cation interaction) or of phosphate or acetate (anion interaction). The values used for subtraction at pH 4.2, pH 4.5 and pH 7.2 have been interpolated.

Buffer (*cf.* Table 1)	Interacting ion	pH	u cm^2V^{-1} sec^{-1}	Δu
1	Ac	4.1	2.37	
2	Ag	4.2	5.60	3.63
3	Pb	4.2	6.76	4.79
4	Pb	4.5	5.41	4.63
5	Cd	4.5	2.33	1.55
6	Ac	5.3	−2.42	
7	Zn	5.3	0.51	2.93
8	Sulf.	5.3	−4.47	−2.05
17	Phosph.	7.1	−5.50	
18	Sulf.	7.2	−6.50	−0.85

value for the percentage of the two components was found, but on account of the poor separation of the peaks this change may not be real. On the other hand it might be explained by accepting a specific reversible ion interaction with a fraction of the albumin resulting in different mobility.

With bovine albumin exactly the same result was obtained, whether the albumin had been prepared solely by ammonium sulfate fractionation or by purification through precipitation with lead ions and cresol.

The shape of the electrophoresis curves indicates that the separation is due to a pronounced boundary sharpening effect with one albumin component. It was not obtained with whole serum and could be abolished by adding the globulin fraction. Addition of cadmium ions had no effect on the relative mobilities of the two components. Fig. 3 shows the electrophoretic diagrams of bovine serum albumin in sodium and in cadmium acetate buffer. In cadmium acetate the direction of migration is reversed, but the shape of the two peaks in the positive, now descending branch remains on the whole unaltered. They can, however, be distinguished in the negative branch and, in addition, minor components seem to separate.

It is well known that albumin is split up electrophoretically at pH 4, well below its isoelectric point. At other pH-values separations have been attained using long lasting experiments or buffers of extremely low ionic strength. A specific effect of acetate ions on the electrophoretic pattern at pH 4.7 was reported by Phelps and Cann [6]. In the present experiments other conditions are described, which lead to similar separation effects. The heterogeneity of bovine serum albumin is thus emphasized. Experiments by Christiansen *et al.*[7] indicate that molecules of different size may exist in solutions of bovine serum albumin. Investigations are in progress to show whether this could explain the present observations.

Correlation between ion interaction and precipitation behaviour. One purpose of the present work was to see if electrophoresis experiments of this kind may yield information, which can be used for fractionation by means of specific precipitations.

The interaction of bovine serum albumin with cadmium ions was described above. When compared with earlier fractionation experiments [2] it seems probable that precipitation produced by cadmium addition is mainly due to the ions bound to carboxyl groups, as at this pH an extensive binding as well as precipitation occurs only at high cadmium concentrations.

This assumption is confirmed by experiments with lead. At pH 4.5 where the metal ions will be attached chiefly to carboxyl groups, the change in mobility with 0.033 M lead acetate is thrice that noted with cadmium at the same concentration (Table 3). Correspondingly, lead ions added to bovine serum precipitate the albumin selectively at a pH about 5 in contrast to cadmium [2] which, in the same concentration range, precipitates the albumin only at pH-values above 7. Gurd and Murray [8] using purified human mercaptalbumin found intensive binding of lead ions to carboxyl groups and insolubility of the compounds formed, in close analogy to the present findings.

Various anions which previously [1] had proved suitable for serum protein fractionation were included in the investigation.

Sulfosalicylate showed a marked interaction with bovine serum albumin at pH 5.3, well above the isoelectric point (Table 3). At pH 7.0 the mobility still changed considerably when sulfosalicylate was partly substituted for phosphate in the buffer.

With bovine γ-globulin a notable interaction was observed with various ions. The isoelectric point of the preparation was found to be about pH 5.9, indicating that it contained mainly γ_1-globulin. The mobilities measured in phosphate and sulfosalicylate buffer at pH 7.2 were —1.69 and —2.66 $cm^2 V^{-1} sec^{-1}$, respectively. The change in mobility is thus of the same magnitude as that of albumin at the same pH (Table 3).

In tungstate buffer at pH 7.1 the mobility increased even to —3.37 $cm^2 V^{-1} sec^{-1}$ which is in accordance with the fact that γ-globulin is precipitated from bovine serum by tungstate [1] at relatively high pH.

The electrophoresis experiments reported have thus proved valuable for estimating the interaction with the various anions used for precipitation, and distinct correlations have been found. It is on the other hand evident that the mobility change due to addition of a certain ion is no strict criterion of the efficiency of this ion as a precipitating agent, as the solubility of the compound will also greatly depend on the binding sites and on other factors.

In this connection electrophoresis experiments performed in phosphate buffer pH 7.7 in the presence of phenol may be mentioned. Addition of phenols is known to influence profoundly the precipitation properties of the serum proteins [9, 10]. The experiments demonstrated that the mobilities of the proteins were unchanged by phenol addition. The change in their solubility is thus in the present case not associated with variation in the net charge.

Experiments with whole serum. In a number of experiments electrophoresis of whole sera was performed in the presence of interacting ions at different pH-values. The purpose was to see if better separations could be obtained, and if any qualitative differences from the usual electrophoretic diagrams could be observed. Addition of lead or cadmium at pH 4.5 caused striking changes in the electrophoretic pattern, corresponding to the different interaction with

the various components (Fig. 4). However, the exact interpretation of the electrophoresis diagrams awaits further experimental study.

Mehl and Golden [11] recommended electrophoresis of pathological sera at pH 4.5 as a valuable supplement to those generally performed at pH 8—9. The present results render it probable, that further informations may be gained by addition of suitable ions such as lead or cadmium.

Electrophoresis of bovine serum in the presence of tungstate at pH 7 gave a pattern rather similar to that achieved with phosphate buffer. Since tungstate interaction is strongest with the slower moving globulins, a more compressed picture was obtained, which made it desirable to prolong the analysis. On the other hand a considerable boundary sharpening was observed, which made the various fractions better discernible than in phosphate buffer.

Specific separation effects. It might have been expected, that mixtures of protein components of very similar mobilities would show greater variations when combined with added ions, resulting in better electrophoretic separation. The result with bovine albumin in cadmium buffer (Fig. 3) indicates, that this is indeed the case, and that the procedure can be used analytically. With human albumin in cadmium acetate buffer at the same pH a similar effect was obtained. Electrophoresis of bovine γ-globulin in the presence of sulfosalicylate made it possible to distinguish several subfractions, but the separation was poor. In this case the effect of the added sulfosalicylate may possibly be due to a suppression of the protein-protein interactions between the various γ-globulin components. A number of further experiments indicate that the best conditions for such separations will probably be found with low ionic strengths of strongly interacting ions.

Acknowledgement. This investigation was supported by a grant from »*Teknisk kemisk Fond*».

REFERENCES

1. Astrup, T., Birch-Andersen, A. and Schilling, K. *Acta Chem. Scand.* **8** (1954) 901.
2. Astrup, T., Schilling, K., Birch-Andersen, A. and Olsen, E. *Acta Chem. Scand.* **8** (1954) 1361.
3. Tanford, C. *J. Am. Chem. Soc.* **74** (1952) 211.
4. Gurd, F. R. N. and Goodman, D. S. *J. Am. Chem. Soc.* **74** (1952) 671.
5. Longsworth, L. G. and Jacobsen, C. F. *J. Phys. Colloid Chem.* **53** (1949) 126.
6. Phelps, R. A. and Cann, J. R. *J. Am. Chem. Soc.* **78** (1956) 3539.
7. Christiansen, J. A., Jensen, C. E. and Marcker, K. *Acta Chem. Scand.* **11** (1957) 402.
8. Gurd, F. R. N. and Murray, G. R., Jr. *J. Am. Chem. Soc.* **76** (1954) 187.
9. Harms, A. J. *Nature* **157** (1946) 514.
10. Schilling, K. *Acta Chem. Scand.* **7** (1953) 1007.
11. Mehl, J. W. and Golden, F. *J. Clin. Invest.* **29** (1950) 1214.

Received April 24, 1957.

ACTA CHEMICA SCANDINAVICA 11 (1957) 1111—1130

The Stability of Metal Halide Complexes in Aqueous Solution

III. The Chloride, Bromide and Iodide Complexes of Bismuth

STEN AHRLAND and INGMAR GRENTHE

Department of Inorganic and Physical Chemistry, Chemical Institute, University of Lund, Lund, Sweden

The chloride, bromide and iodide complexes of Bi^{3+} have been studied in an acid perchlorate medium by means of emf and solubility measurements. The overall stability of these complex systems increases in the order mentioned; Bi^{3+} thus belongs to the central ions of the second group (*cf.* Ref.[1]). The first bromide complex is however a little weaker than the first chloride one. Thus Bi^{3+} also possesses certain properties of the first group central ions, as could perhaps be expected from its position in the outskirts of the second group area. The sixth complex is the one finally formed in all the systems measured; in the case of chloride and bromide the fifth complex has a remarkably wide range of existence.

With respect to the strength of their halide complexes, central ions may be divided into two groups. The first one shows decreasing stability of the complexes in the order $F^- \gg Cl^- > Br^- > I^-$, the second one in the opposite order $F^- < Cl^- < Br^- < I^-$. In part I of this series [1] it was pointed out that the ions of the second group were all situated within a roughly triangular area of the periodic system, centered around the noble metals. The primary aim of the present investigation has been to decide whether Bi^{3+} is also within this area, a question which was left open in the previous paper.

As Bi^{3+} is readily hydrolysed [2], the measurements have to be performed in acid solutions so that the halide complex formation is not mixed up with intricate hydrolytic reactions. In this work all solutions had $[H^+] = 1$ M, an acidity ensuring that no perceptible amounts of soluble hydroxo complexes exist at the bismuth concentrations used. Due to their very low solubility, the oxyhalides BiOCl and BiOBr are nevertheless precipitated even from solution of quite low $[Bi^{3+}]$. When further halide is added the precipitates however dissolve again owing to the strong decrease of $[Bi^{3+}]$ caused by the increasing complex formation. In the case of the iodide, the neutral third complex

BiI_3 is precipitated, as being the least soluble solid phase in the medium used. This precipitate also dissolves with the formation of higher complexes when further amounts of ligand are added.

As to methods available for the investigation, emf measurements of the concentration of free central ion, $[Bi^{3+}]$, by means of a bismuth amalgam electrode seemed most convenient (*cf.* Ref.[2]). According to the experience gained here this method worked well if the total bismuth concentration, C_M, was $\gtrsim 0.5$ mM. Where the halide concentration, C_A, of the solutions allowed such values of C_M, the complex formation could therefore be followed by emf measurements. This turned out to be the case for the greatest part of the complex formation of the chloride and bromide systems, where only the first constant could not be determined. In the case of the iodide, on the other hand, only the constant of the final (*i. e.* the sixth) complex could be obtained in this way.

The investigation could, however, be extended to lower ligand concentrations by means of solubility determinations (*cf.*, *e. g.*, Leden [3,4]). With the method employed here, solutions of a C_M (= the solubility l) as low as ≈ 0.02 mM could be analysed. For the calculation of the stability constants, the solubility products of the solid phases BiOCl, BiOBr and BiI_3 were also needed. The determination of these quantities sometimes required the measurement of $[Bi^{3+}]$ in solutions of $C_M \approx 0.2$ or even 0.1 mM. This was often successfully accomplished especially if C_A was not too low, but great care had to be exercised in these measurements and evidently this range of C_M is not very suitable for emf measurements.

Good values of the first constant of the chloride and bromide system could be determined by these solubility measurements, which also confirmed some of the constants previously determined potentiometrically. For the iodide system values of the last three constants could be obtained. The two methods employed thus complement each other rather satisfactorily.

All values of constants found refer to the acid perchlorate medium used which had a total ionic strength $I = 2$ M. As usual, sodium perchlorate was used as supplementary neutral salt. The temperature has been kept at 20°C.

CALCULATION OF COMPLEXITY CONSTANTS FROM MEASUREMENTS OF $[Bi^{3+}]$ (=[M]) WITH THE BISMUTH AMALGAM ELECTRODE

Experimentally, the emf E of cells of the following type were measured

$$+ \text{RE} \;\Big|\; \begin{matrix} C_M \text{ mM Bi(III)} \\ C_A \text{ mM ligand} \\ [H^+] = 1 \text{ M};\ I = 2 \text{ M} \end{matrix} \;\Big|\; \text{Bi-Hg} \; -$$

where RE is a quinhydrone reference electrode. This emf can be written as

$$E = E_{RE} + E_d - E^\circ - \frac{RT}{3F} \ln f_M \cdot [M] \qquad (1)$$

In this expression E_{RE} and E° are of course independent of variations of C_M and C_A and the same will be very nearly true for the liquid junction potential

E_d and the activity factor f_M in the approximately constant medium used. Hence (1) can be written

$$E = E_k - \frac{RT}{3F} \ln [M] \tag{2}$$

where E_k is a constant. If the emf of the special case of $C_A = 0$, $[M] = C_M$ is denoted E' we obtain:

$$E - E' = E_M = \frac{RT}{3F} \ln \frac{C_M}{[M]} \tag{3}$$

From the quantity $C_M/[M]$ thus found, the stability constants β were calculated by Leden's [5,6] method as developed by Fronæus [7] (*cf.* also Ref.[8]):

If only mononuclear complexes MA_n are formed then

$$C_M / [M] = 1 + \sum_{n=1}^{N} \beta_n [A]^n = X([A]) \tag{4}$$

The value of [A] for a certain value of X thus found is obtained by a method of extrapolation. E_M is determined as a function of C_A in solutions containing different C_M. From the resulting family of curves values of C_A are read off for a number of values of E_M. Every value of E_M then corresponds to a certain constant value of [A], as seen from (3) and (4), andt herefore also to a constant ligand number $\bar{n}$ (*cf.* Ref. [5-8]). Thus if corresponding values of C_A and C_M are plotted for a certain E_M a straight line $C_A = \bar{n} \cdot C_M + [A]$ will result, with the intercept on the C_A-axis = [A] and the slope = $\bar{n}$. When corresponding values of X and [A] have thus been found, the constants β are calculated from (4). Different methods of calculation have however to be used for the chloride and bromide on the one hand and the iodide system on the other.

For the chloride and bromide systems where, at the pH used in this investigation, most of the complex formation can be covered by the emf measurements, the constants are calculated in the usual way [9], by extrapolation of functions X_n. Thereby β_1 is obtained first and then successively the following constants up to β_N.

In the case of the iodide system on the other hand emf measurements can be performed only for the very last part of the complex formation due to the low solubility of the neutral complex MA_3. In the whole measurable range, MA_N is the dominating species. Its constant is conveniently calculated by forming a new function

$$X'_N = \frac{X}{[A]^N} = \beta_N + \beta_{N-1} \cdot [A]^{-1} + \sum_{n=2}^{N-1} \beta_{N-n} [A]^{-n} + [A]^{-N} \tag{5}$$

When X'_N is plotted against $1 / [A]$, β_N will be found as the intercept of the X'_N -axis, and β_{N-1} as the slope of the curve at the point of intersection * (*cf.*[6] p. 16).

* In the present case only β_N can be calculated, owing to the predominance of the highest complex in the range measured. In principle however further constants may be calculated by successively forming new functions X', in the first instance

$$X'_{N-1} = (X'_N - \beta_N) \cdot [A] = \beta_{N-1} + \beta_{N-2}[A]^{-1} + \sum_{n=3}^{N-1} \beta_{N-n} \cdot [A]^{1-n} + [A]^{1-N}$$

If the complex formation is not entirely mononuclear, (4) no longer holds, C_M / [M] being a function of both [A] and [M]. By extrapolating the C_M, C_A-lines of constant E_M to $C_M = 0$ (implying [M] = 0), corresponding values of [A] and X will nevertheless be found and hence correct values of β calculated, as shown by Fronæus (Ref.[7], p. 20). The slope of these lines will however not be $= \bar{n}$ in this case but a quantity $< \bar{n}$. By comparing the genuine complex formation function $\bar{n} = f([A])$, calculated from the found values of β with the values obtained from the C_A, C_M slopes, the existence of polynuclear complexes can thus be revealed.

CALCULATION OF COMPLEXITY CONSTANTS FROM MEASUREMENTS OF THE SOLUBILITY OF Bi(III) IN HALIDE SOLUTIONS

If only mononuclear complexes are assumed to exist in solutions of Bi(III), the solubility l can written as

$$l = [M]\left(1 + \sum_{n=1}^{N} \beta_n [A]^n\right) = [M] \cdot X \tag{6}$$

bearing in mind that soluble hydroxo complexes certainly do not exist in the medium used [2]. Now in the cases of chloride and bromide the formula of the solid phase is MOA which we may consider as formed according to the reaction $M + 2\ OH^- + A \rightleftharpoons MOA + H_2O$. Thus

$$[M][OH^-]^2[A] = L = [M][A] \cdot \frac{K_w^2}{[H^+]^2} \tag{7}$$

As $[H^+]$ is kept constant throughout the measurements a new constant L' may be introduced:

$$[M][A] = \frac{L}{K_w^2} \cdot [H^+]^2 = L' \tag{8}$$

Combining (6) and (8) we arrive at

$$l - \frac{L'}{[A]} = L'\left(\beta_1 + \sum_{n=2}^{N} \beta_n [A]^{n-1}\right) = L' \cdot X_1 \tag{9}$$

The value of [A] corresponding to a certain value of l is given by

$$[A] = C_A - (C'_M - l) - \bar{n} \cdot l \tag{10}$$

where C'_M is the stoicheiometric concentration of Bi(III) added, most of it $(= C'_M - l)$ being precipitated. In all the solubility measurements, l is fairly low and $\bar{n} \cdot l$ only a correction term. Therefore a sufficiently good value of $\bar{n}$ is obtained by taking from the complex formation curve of the emf measurements the value corresponding to $[A] = C_A - (C'_M - l)$. Using this value of $\bar{n}$, a value of [A] is calculated from (10). This value of [A] gives in turn a better value of $\bar{n}$ which however when inserted in (10) does not appreciably change the value of [A] already obtained.

Provided only that L' can be found, $L' \cdot X_1$ is therefore known as a function of [A]. From this function the constants β can be calculated in the same way

as from the simple X-functions, *cf.* p. 000. The function $L'\cdot X_1$ has an intercept on the ordinate axis $= L'\cdot\beta_1$. The next constant β_2 is conveniently found by forming the function

$$\frac{L'X_1 - L'\beta_1}{[\mathrm{A}]} = L'\Big(\beta_2 + \sum_{n=3}^{N} \beta_n[\mathrm{A}]^{n-2}\Big) = L'\cdot X_2 \qquad (11)$$

whose extrapolation to $[\mathrm{A}] = 0$ gives $L'\cdot\beta_2$. Analogously further constants may be found.

For the determination of $L' = [\mathrm{M}]\,[\mathrm{A}]$, [M] of saturated solutions of known [A] has to be measured. This is done by measuring emf of cells of the type written on p. 1112. From the values of L' thus determined it is further possible to calculate the solubility product L of the oxyhalides if K_w of the solvent medium is measured.

In the case of the iodide system where MA_3 is present as solid phase,

$$L = [\mathrm{M}][\mathrm{A}]^3 \qquad (12)$$

which combined with (6) gives

$$l\,[\mathrm{A}]^3 = L\Big(1 + \sum_{n=1}^{N} \beta_n[\mathrm{A}]^n\Big) = L\cdot X \qquad (13)$$

When calculating the value of [A] belonging to a certain value of l, correction must be applied for that part of the iodide which has been oxidized during the time of equilibration. Even at the lowest values of [A] used here, the iodine formed will appear mainly [10] as I_3^-. If it is assumed that this species does not form complexes with Bi^{3+}, [A] is then given by the formula

$$[\mathrm{A}] = C_A - 3(C_M' - l) - \bar{n}\cdot l - 3[\mathrm{I}_3^-] \qquad (14)$$

Here $[I_3^-]$ is determined by analysis of a sample of the saturated solution. As to $\bar{n}$, a sufficiently correct value (*viz.* $\bar{n} = 6$) is known only in the range of [A] covered by the emf measurements where the highest complex MA_N ($= MA_6$) is practically the only one existing. At lower [A], $\bar{n} = 3$ has been used as a first approximation. This value certainly represents a lower limit of $\bar{n}$ in the range of [A] used, as shown by the following evidence. At the value of [A] where $\bar{n} = 3$ is correct, the concentration of the complex MA_3 relative to the other complexes will be at a maximum [7, p. 30]. The concentration of MA_3 in the solution is however constant, because of its presence as a solid phase. The total solubility, l, will therefore show a minimum when $\bar{n} = 3$. As seen from Fig. 1, the iodide solubility curve is in fact flattening out very much at the lowest [A] measured, but it does not reach its minimum. So $\bar{n}$ must be >3 along the whole curve.

As it can be foreseen that the upper complexes are also the dominating ones in the range covered by the solubility measurements, the constants are calculated downwards in much the same manner as that used for the potentiometric measurements. From (13) the following function is formed

$$l\,/\,[\mathrm{A}]^{N-3} = L\left(\beta_N + \sum_{n=1}^{N-1} \beta_{N-n}[\mathrm{A}]^{-n} + [\mathrm{A}]^{-N}\right) = L\cdot X_N' \qquad (15)$$

When $1 / [A] \rightarrow 0$, $l / [A]^{N-3} \rightarrow L \cdot \beta_N$. Then the following function is formed:

$$(l/[A]^{N-3} - L \cdot \beta_N) \cdot [A] = L\left(\beta_{N-1} + \sum_{n=2}^{N-1} \beta_{N-n}[A]^{1-n} + [A]^{1-N}\right) = L \cdot X'_{N-1} \quad (16)$$

which gives $L \cdot \beta_{N-1}$ when $1 / [A] \rightarrow 0$. Further constants $L \cdot \beta_n$ are calculated analogously, and as L can be determined in the same way as L' of the chloride and bromide systems, all the constants β can be found. From these constants a complex formation curve is calculated allowing us to insert approximately correct values of $\bar{n}$ in (14). Better values of [A] are thus obtained giving a better set of constants β. In fact this second approximation gives the final values of β of the present system as the correction term $\bar{n} \cdot l$ of (14) is fairly small.

EXPERIMENTAL

Chemicals: All chemicals were, if not otherwise stated, of analytical grade and used without further purification.

Liquid *bismuth amalgam*, containing ≈1 % bismuth, was prepared [2] by dissolving Bi in Hg under water at about 90 °C. To prevent formation of oxide films it was stored under dilute perchloric acid. Before use it was washed with boiled water. During the measurements, no changes of emf due to changes of the bismuth activity in the amalgam could be detected, therefore no perceptible oxidation of the amalgam seems to occur.

Bismuth perchlorate solution was prepared by dissolving Bi_2O_3 in an approximately 50 % excess of ≈ 6 M $HClO_4$. By diluting this solution, a stock solution for the measurements was prepared and analysed for C_M and free acid.

The determination of C_M was carried out by precipitating and weighing BiOI, in the main according to the procedure described by Vogel [11]. Due to the slight solubility of $KClO_4$, NaI had to be used instead of KI as a precipitant. It was necessary to adjust pH to about 4.5 with sodium acetate to ensure that all the originally precipitated brown-black BiI_3 and all the yellow iodide complexes of the solution were converted into purple BiOI. The final value of the pH was checked by spots tests, as the addition of an indicator would have masked the decolourization which accompanies complete hydrolysis of the bismuth solution. The stock solution had C_M = 0.496 M.

The concentration of free acid in this solution was determined by alkalimetric titration after the removal of the bismuth by means of cation exchange, *cf.* Ref.[12]. A value of $[H^+]$ = 0.92 M was found, in good agreement with the value of $[H^+]$ = 0.93 M which was calculated from the amount of acid used in the preparation.

Two preparations of *sodium perchlorate* was used. The first one (from G. Frederick Smith) was recrystallized twice. The second one was made by neutralization of perchloric acid. The main part of the acid was neutralized by sodium carbonate, the carbon dioxide boiled off, and the last trace of acid finally neutralized with sodium hydroxide. Both the preparations contained <0.01 % of Cl^- and ClO_3^-. A 2 M stock solutions was prepared by weighing the dried salt.

Stock solutions, close to 2 M, were also prepared of *perchloric, hydrochloric* and *hydrobromic acids*, as well as of *sodium chloride, bromide and iodide*, and their exact concentrations determined by analysis.

The potentiometric measurements: Two different reference electrodes were used, *viz.*:

Au	0.01 M $HClO_4$ 1.99 M $NaClO_4$ quinhydrone(s).	2 M $NaClO_4$	and	Au	1 M $HClO_4$ 1 M $NaClO_4$ quinhydrone(s).	1 M $HClO_4$ 1 M $NaClO_4$

denoted RE (0.01) and RE(1), respectively. RE (0.01) was used in the earlier measurements, RE(1) in the later ones. The change of RE(0.01) for RE(1) ought to improve the constancy of E_d of (1). Moreover the risk of diffusion or flow between the cell compartments should be much less.

Table 1. The validity of Nernst's law for the bismuth amalgam electrode in 2 M perchlorate medium. — Series I: $[H^+]_0$ = 9.99 mM; 2 M $NaClO_4$ in the junction between the half-cells. Series II: $[H^+]$ = 1 M throughout the whole cell.

	I		II	
C_M mM	E' mV	E_k mV	E' mV	E_k mV
0.496	368.6	304.6	461.6	397.6
0.985	363.3	305.0	455.4	397.1
1.91	357.5	304.7	449.5	396.7
4.52	350.6	305.1	442.0	396.5
11.5	343.0	305.4	434.0	396.4
24.9	337.0	305.9	427.7	396.6
33.2			425.5	396.8
39.7	333.4	306.2		

First, the behaviour of the bismuth amalgam electrode in the medium used was investigated. In the amalgam half-cell, a known volume was placed of a solution containing 1 M $HClO_4$, and 1 M $NaClO_4$. Portions of bismuth perchlorate solution of the same $[H^+]$ and I were then added and the emfs of the resulting cells measured. As no complexing agent is present, these cells have $[M] = C_M$, and E_k can therefore be calculated according to (2). From Table 1 it is evident that E_k really is a constant. Thus a variation of C_M within the given limits does not cause appreciable changes of E_d or f_M. Nernst's law is obeyed in the form (2).

The main measurements were also carried out as titrations mostly in the following way. A solution, S, of known C_M but containing no ligand was prepared in the amalgam half-cell and the cell connected. Dissolved air was then expelled by bubbling nitrogen gas, free from oxygen, through the bismuth solution, the bubbling being continued through the whole titration in order to keep the solution free from air and thoroughly mixed. After E' had been read, a ligand solution T, of the same C_M, $[H^+]$ and I as the solution S, was added in portions. In the beginning a precipitate (BiOCl, BiOBr or BiI_3) was formed which however was dissolved by further addition of ligand solution. When a clear solution had thus been obtained, measurements of E could begin. Titrations were performed at four or five different values of C_M and they were continued to as high C_A as could conveniently be reached within the ionic strength used.

In order to extend the measurements to as low values of C_A as possible titrations were also performed in the opposite direction, with decreasing C_A. Portions of S were then added to a solution S′ in the electrode vessel, S′ containing a ligand concentration high enough to secure a clear solution. In this way values of E could be determined even in solutions somewhat supersaturated with respect to the slightly soluble halide. When at last precipitation really occurred, this was at once indicated by a rapid drift in the emf measured, even in cases where the precipitate was hardly visible. A value of E' could however not be directly determined in these titrations. As the value of E' varied a little between parallel titrations, being dependent on small differences in E_k between different cells, it was desirable to find the value of E' corresponding to the values of E measured in a particular titration. This was done by comparing the values of E found when titrating over a common range with increasing and decreasing C_A. The difference between E of such series leads to a fairly safe estimate of the difference between E'. The value of E' for the series with decreasing C_A can then be found as E' for its companion series was measured directly.

In the case of the iodide, a ligand solution of $[H^+]=1$ M would have been rather unstable. In these titrations, neutral iodide solution was therefore added from one burette and perchloric acid from another. In this way iodide was kept in acid solution only in the electrode vessel, where its oxidation was minimized by the presence of an inert atmosphere.

The values of E_M given in the following tables are as a rule the mean of three titrations. In the chloride and bromide systems the values of emf measured were very stable. They were reached, moreover, almost immediately after the solutions had been mixed, with the exception of E' whose adjustment to the final value sometimes took about half an hour. The emfs could be reproduced within about ± 0.5 mV, as a rule somewhat better at lower values of C_A and somewhat worse at higher ones. In the iodide system it often took 5—10 min for the emfs to reach their final value; they were also markedly less reproducible, especially at high values of C_A. At the very highest values of C_A tried, they were even unstable and drifted erratically, especially if C_M was also high. Often a tarnishing of the amalgam surface was observed in such solutions and their colour gradually faded to light yellow on standing.

The solubility measurements: Solutions of 50 ml total volume, with known initial concentrations of bismuth and ligand were prepared in glass-stoppered bottles of 100 ml volume. The concentrations were chosen so that a precipitate formed. The bottles were shaken in a thermostat for about a week. After that time equilibrium had been established, as was proved by shaking a few bottles for another week. The same results were obtained in both cases.

Samples of the saturated solutions thus obtained were filtered by suction through a sintered glass disc (filter stick) direct into a pipette. The total bismuth concentration of these solutions, *i.e.* the solubility l, was then determined spectrophotometrically by the iodide method [13].

This method utilized the very intense colours of the bismuth iodide complexes, especially that of the highest. In order to bring about maximum absorption, the iodide concentration should be at least ≈ 100 mM. At this value of [A] the formation of the highest complex is practically completed, therefore further addition of iodide does not alter the absorption appreciably. The extinction curve has a maximum at 4 600 Å, where the iodide complex has a molar extinction coefficient $\varepsilon \approx 11\,000$ $M^{-1} \cdot cm^{-1}$. This very high value of ε permits a convenient determination of bismuth concentrations down to $\approx 10^{-5}$ M. The extinction values are however not very reproducible if steps are not taken to prevent the formation of I_3^- which also absorbs strongly at 4 600 Å. Following Wiegand *et al.*[13] we have successfully used hypophosphorous acid (≈ 0.3 M) to prevent the formation of I_3^-. In the absence of Bi(III) the medium used is completely colourless, and distilled water can therefore be used in the solvent absorption cell of the spectrophotometer (Beckman DU). A calibration curve giving the connexion between C_M and the specific extinction* e was constructed by measuring solutions of known C_M. Only slight deviation from Beer's law was found.

The statement above that practically all the bismuth is present as the highest iodide complex when the iodide concentration = 100 mM may of course be invalidated if other ligands are present in the solution, competing with the iodide. This is the case when analysing chloride or bromide solutions. It was found experimentally however that if the iodide concentration was increased to 250 mM, chloride or bromide could be present in a concentration of at least 50 mM, without changing the extinction perceptibly. This could also have been expected from the values of the stability constants of the different systems, previously found by the potentiometric measurements.

The solubility l for a certain C_A could as a rule be reproduced within ≈ 10 % except at the lowest values of C_A in the chloride and iodide system where the reproducibility was very poor. This is evident from Tables 4, 7 and 10 where the solubility experiments have been tabulated.

In most cases a second sample of the saturated solutions was filtered off and used for a potentiometric determination of $[Bi^{3+}]$ in order to find L' and L. For the bromide system useful values of E_M could then be obtained in the whole range of C_A used, whereas C_A must be at least 20 or 30 mM in chloride or iodide solutions before even acceptable values of E_M could be read. At lower values of C_A, unsteady and drifting potentials were obtained. This is of course mainly due to the very low value of C_M ($= l$) in such solutions, but to judge from the figures of the chloride system, the value of C_A (or [A]) itself must also be of importance. Thus E_M can be measured for $C_A = 20$ mM, but not at lower C_A in spite of the fact that l has already reached its minimum value at $C_A = 20$ mM (Table 4).

* $e = E/d$, where E = extinction measured and d = thickness of absorbing layer.

Table 2. The chloride system. E_M as a function of C_A for different values of C_M.

$C_M \rightarrow$ mM	2	1	0.5		20	10	2	1	0.5
C_A mM	E_M mV			C_A mM	E_M mV				
25.0*			20.0	136.4			59.3	59.9	59.7
28.6*		21.9	22.4	160.7			64.6	65.5	64.9
33.3*		25.2	25.5	184.2		63.0	69.0	69.5	69.4
40.0*		28.8	29.0	217.9		69.3	74.3	75.2	75.1
50.0*		33.7	33.6	250		74.7	80.0	80.1	80.1
57.6		36.8		300		81.9	86.6	86.8	86.7
58.8*	36.1	37.5	37.2	346	81.9	87.7	92.1	92.3	92.0
66.7*	39.1	40.4	40.3	429	91.6	96.6	100.4	100.6	100.2
71.4		41.9	42.2	500	98.7	103.2	106.7	106.8	106.3
76.9*	42.6	43.5	44.1	618	108.4	112.2	115.2	115.3	114.7
83.3*	44.7	45.7	46.1	711	114.8	118.3	121.0	120.9	120.6
84.9		46.2	46.7	818	121.3	124.5	126.9	126.9	126.4
90.9*	47.0	48.1	48.4	900	125.7	128.7	130.7	130.8	130.2
98.1		50.1	50.4	1000	130.2	133.2	135.2	135.2	134.5
100.0*	49.7	51.0	51.0	1071	133.4	136.2	138.0	137.9	137.3
111.1	53.0	53.7	53.9	1200	138.4	140.8	142.1	142.6	142.1

* These values belong to the series titrated from higher to lower values of C_A, while all other values belong to the series titrated in the opposite direction.

Evidently the bismuth species dominating at [A] = 20 mM have a more favourable electrode kinetics than those dominating at lower [A], as has also been directly proved by the impedance measurements of Randles and Somerton [14].

In the case of the iodide system a third sample of the saturated solution was filtered off and analysed by thiosulphate titration for the amount of I_3^- formed during the shaking, in order to find the true value of [A] according to (14).

In order to find L from L', K_w of the medium used was finally determined by measuring $[H^+]$ of solutions of known $[OH^-]$ by means of a hydrogen electrode. As mean of three determinations a value of $K_w = (0.75 \pm 0.05) \cdot 10^{14}$ M^{-2} was found.

RESULTS

The chloride and bromide systems: In Tables 2 and 5, E_M is given as a function of C_A with C_M as a parameter. These functions are cut at a number of E_M, thus giving corresponding values of [A] and X, Tables 3 and 6. An accurate value for the constant β_1 cannot, however, be found from the function X_1 thus formed, as the latter is not known at sufficiently low values of [A]. Reliable values of β_1 can, however, be found from the solubility measurements, where the lowest values of [A] measured are 3.94 mM for the chloride and 2.12 mM for the bromide, as compared with 23.4 mM and 8.5 mM, respectively, in the potentiometric measurements. In order to find the value of [A] corresponding to a certain value of l measured, it is, however, necessary to know beforehand $\bar{n}$ approximately as a function of [A] (*cf.* eqn. (10)). By calculating a set of provisional stability constants from the X-functions found potentiometri-

Table 3. The chloride system. Computation of the complexity constants.

Table 3 A. The functions X at low values of [A].

$C_M \rightarrow$ mM	2	1	0.5	0					
E_M mV	C_A mM			C_A = [A]	X	$X_1 \times 10^{-2}$ M^{-1}	$X_2 \times 10^{-4}$ M^{-2}	$X_3 \times 10^{-5}$ M^{-3}	$X_4 \times 10^{-6}$ M^{-4}
20		26.0	24.8	23.6	10.8	4.13	0.77	2.1	
25		33.2	32.3	31.4	19.5	5.88	1.14	2.76	1.58
30		42.7	42.0	41.3	35.2	8.29	1.45	2.86	1.45
35		53.8	53.2	52.6	63.9	11.9	1.83	2.96	1.33
40	69.3	66.3	65.5	64.1	116	17.9	2.43	3.37	1.73
45	84.3	80.8	79.8	78.1	209	26.7	3.12	3.64	1.77
50	101.0	97.3	96.5	94.6	379	40.0	3.97	3.91	1.74
55	119.5	116.0	115.9	113.4	687	60.3	5.11	4.26	1.76

cally, using a value of $\beta_1 = 0$, complex formation functions good enough for this purpose are obtained.

For both the systems, the values of L' found are constant within the experimental error in the whole range of [A] covered. Thus the solid phases really do have a ratio M:A = 1, as postulated in (7) and (8). Furthermore, samples of the precipitates have been filtered off, and, after drying, analysed for bismuth, and in the case of the bromide, halide also. For bismuth the complexometric method of Malat *et al.*[15] has been used, and it was then found that direct titrations with EDTA could be performed for the chloride also. Bromide was determined according to Volhard. (Found for the chloride: Bi 80.4 %, calc. for BiOCl: 80.2 %. Found for the bromide: Bi 68.0 %, Br 26.23 %, calc. for BiOBr: Bi 68.4 %, Br 26.21 %.)

Table 3 B. The functions X at high values of [A].

$C_M \rightarrow$ mM	20	10	2	1	0						
E_M mV	C_A mM				C_A = [A]	$X \times 10^{-4}$	$X_1 \times 10^{-4}$ M^{-1}	$X_2 \times 10^{-4}$ M^{-2}	$X_3 \times 10^{-5}$ M^{-3}	$X_4 \times 10^{-6}$ M^{-4}	$X_5 \times 10^{-7}$ M^{-5}
60		166.5	140.0	137.3	134.5	0.124	0.92	6.70	4.79	1.88	4.61
65		192.0	162.5	160.5	157.4	0.225	1.43	8.92	5.50	2.06	5.08
70		221	190.0	185.2	182.3	0.407	2.23	12.12	6.50	2.32	5.81
80	330	283	253	250	246	1.34	5.45	22.1	8.85	2.68	5.77
90	414	365	328.5	326	320	4.39	137	42.8	13.3	3.45	6.84
100	515	464	425.5	423	417.5	14.4	344	82.4	19.7	4.16	6.95
110	640	589	544.5	541.5	538	47.1	875	163	30.3	5.20	7.32
120	794	739	695	695	686	155	2 260	329	47.9	6.65	7.85
130	996	929	882	882	872	506	5 800	665	76.1	8.46	8.25

Table 4. The chloride system. The solubility l as a function of [A]. Determination of the constant L', with subsequent calculation of the complexity constants β_1 and β_2.

$C_{M'}$ mM	C_A mM	E_M mV	[M] $\times 10^3$ mM	l mM	[A] mM	$L' \times 10^9$ M^2	$L' \cdot X_1 \times 10^6$ M	$L' \cdot X_2 \times 10^5$
1	5			0.108	3.94		55.2	
1	5			0.0792	4.02		(27.5)	
1	7.5			0.0857	6.47		53.5	
1	7.5			0.0949	6.52		63.0	
1	10			0.0857	8.98		62.5	
1	10			0.0871	8.99		64.0	
1	12.5			0.0880	11.48		69.9	
1	15			0.1036	13.89		88.6	
1	20			0.0949	18.91		83.9	
1	20	38.1	10.81	0.0958	18.91	204	84.8	
1	25	38.2	10.69	0.1045	23.88	255	95.8	201
1	25	38.4	10.45	0.123	23.89	250	114	276
2	30	41.8	6.97	0.116	27.85	194	108.5	215
2	35	42.3	6.56	0.149	32.9	215	143	288
2	40			0.168	37.7		162.5	304
2	40	45.2	4.66	0.165	37.8	176	159.5	296
2	50	47.1	3.72	0.1985	47.6	177	194	306
2	60	47.8	3.42	0.328	57.2	196	342	484

Table 5. The bromide system. — E_M as a function of C_A for different values of C_M.

$C_M \rightarrow$ mM	5	2	1	0.5		10	5	2	1
C_A mM	E_M mV				C_A mM	E_M mV			
8.3 *				13.7	111.1	71.2	80.8	87.1	88.9
10.0 *			15.5	16.3	136.4	82.2	90.4	95.8	97.4
12.5 *			18.6	20.2	160.7	91.0	98.2	103.0	104.5
14.9			22.6	23.5	184.2	98.4	104.7	109.0	110.3
16.7 *			24.4	26.1	217.9	107.2	112.7	116.5	117.6
20.8 *				31.5	250.0	114.5	119.1	122.7	123.5
25.0 *			35.0	36.5	300	123.9	127.8	130.8	131.6
29.4		37.0	40.0	41.4	346	131.4	134.6	137.3	137.9
35.7 *				47.6	429	142.2	144.7	146.9	147.6
41.6 *			51.7	52.6	500	150.1	152.5	154.0	154.5
43.7 *		50.5	53.1	54.4	618	160.3	162.1	163.6	164.1
45.5 *			54.6	55.8	711	167.4	168.9	170.2	170.6
50.0 *			58.2	59.2	818	174.4	175.7	176.6	177.1
57.6	51.2	60.7	63.2	64.1	900	179.2	180.8	180.8	181.3
71.4	60.5	68.9	71.4	72.2	1000	184.3	186.0	185.6	186.1
84.9	68.4	76.1	78.1		1071	187.8	189.3	188.6	189.1
98.1	75.0	82.0	83.8		1200	193.3	194.6	193.4	194.1

* See note of Table 2.

Table 6. The bromide system. Computation of the complexity constants.

Table 6 A. The functions X at low [A].

C_M mM	5	2	1	0.5	0	X	$X_1 \times 10^{-2}$ M^{-1}	$X_2 \times 10^{-4}$ M^{-2}	$X_3 \times 10^{-6}$ M^{-3}	$X_4 \times 10^{-8}$ M^{-4}	$X_5 \times 10^{-9}$ M^{-5}
E_A mV	C_A mM				C_A = [A]						
15			9.9	9.2	8.5	5.94	5.81	4.71	2.25		
20			13.2	12.3	11.4	10.75	8.55	5.92	2.74		
25			16.7	15.8	14.9	19.5	12.4	7.11	2.90		
30			20.7	19.6	18.5	35.2	18.5	9.03	3.35		
35			24.9	23.7	22.5	63.8	27.9	11.60	3.92		
40		32.5	29.5	28.2	26.7	116	42.9	15.4	4.72	1.02	
45		37.7	34.7	33.2	31.7	209	65.7	20.2	5.49	1.10	
50		43.3	40.0	38.6	37.0	379	102	27.0	6.55	1.23	
55	63.0	49.4	46.1	44.5	42.3	686	162	37.8	8.26	1.48	2.32
60	70.6	56.7	52.8	51.3	48.9	1242	254	51.5	9.95	1.63	2.31
65	78.9	64.6	60.6	59.0	56.1	2250	401	71.0	12.1	1.80	2.32

Table 6 B. The functions X at high values of [A].

C_M mM	10	5	2	1	0	$X_1 \times 10^{-5}$ M^{-1}	$X_2 \times 10^{-6}$ M^{-2}	$X_3 \times 10^{-7}$ M^{-3}	$X_4 \times 10^{-8}$ M^{-4}	$X_5 \times 10^{-9}$ M^{-5}
E_M mV	C_A mM				C_A = [A]					
70	109	88	73	69	64.5	0.63	0.976	1.47	1.92	2.20
80	131	109	94	89.5	84.5	1.58	1.87	2.18	2.33	2.16
90	157	135	119	114.5	109.5	4.01	3.66	3.32	2.85	2.14
100	190	167	150	145	140	10.2	7.29	5.19	3.56	2.18
110	230	206	188	183	178	25.6	14.4	8.09	4.45	2.23
120	278	255	235	230	224	69.0	30.8	13.7	6.03	2.47
130	337	314	294	289	283	179	63.3	22.4	7.85	2.60
140	411	388	368	363	358	464	130	36.3	10.1	2.68
150	499	476	459	452	447	1 220	273	61.0	13.6	2.94
160	615	588	570	564	558	3 200	574	103	18.4	3.21
170	749	725	709	701	696	8 410	1 210	174	25.0	3.52
180	914	886	884	873	873	22 000	2 520	288	33.0	3.72
190	1 123	1 091	1 109	1 094	1 101	57 100	5 180	470	42.6	3.82

The mean value of L' is found to be $(208 \pm 20) \times 10^{-9}$ M^2 for the chloride and $(303 \pm 10) \times 10^{-9}$ M^2 for the bromide. Using these values of L', β_1 is calculated from the corresponding values of l and [A], according to (9). The values of β_1 thus found are then used for calculating X_2 from the potentiometrically found X_1. From X_2 (Tables 3 and 6), β_2 is found by extrapolation to [A] = 0. Further X-functions are then formed and the corresponding constants determined. For both the chloride and the bromide the function X_5 is found to be a straight line, the sixth complex thus being the highest one existing in the range of [A] investigated. The complex formation curves, as

Table 7. The bromide system. The solubility l as a function of [A]. Determination of the constant L', with subsequent calculation of the complexity constants β_1 to β_4.

C_M' mM	C_A mM	E_M mV	[M] $\times 10^3$ mM	l mM	[A] mM	$L' \times 10^9$ M^2	$L' \cdot X_1 \times 10^6$ M	$L' \cdot X_2 \times 10^3$	$L' \cdot X_3$ M^{-1}	$L' \cdot X_4$ M^{-2}
1	3	15.2	164	0.202	2.12	345	59			
1	3	17.4	126.5	0.200	2.12	266	57			
1	4	19.0	104.7	0.169	3.07	314	70			
1	4	20.4	88.5	0.183	3.08	269	85	9.7		
1	5	22.8	66.7	0.164	4.02	265	89	8.5		
2	7.5	26.0	45.5	0.147	5.46	247	82	6.8		
4	10	24.3	55.7	0.150	5.95	329	99	7.4		
2	10	27.7	37.2	0.182	7.87	292	144	11.3	0.74	
2	10	27.4	38.6	0.166	7.88	302	128	9.3	0.48	
2	10	29.2	31.1	0.171	7.88	244	133	9.9	0.56	
2	12.5	28.5	33.8	0.207	10.28	346	177	11.9	0.62	
2	12.5	28.5	33.8	0.216	10.27	347	186	12.8	0.71	
2	15			0.267	12.63		243	14.9	0.75	
5	20			0.309	14.51		288	16.0	0.72	
2	20	33.0	19.8	0.461	17.15	340	443	22.6	1.00	33
2	20	33.6	18.5	0.418	17.23	318	400	20.0	0.84	23
5	25	33.8	18.0	0.534	18.94	342	518	24.4	1.00	30
5	25	35.2	15.3	0.525	18.95	290	509	24.0	0.98	29
5	25			0.502	19.00		486	22.7	0.91	25
5	27.5			0.659	21.14		645	27.9	1.06	29
5	27.5			0.667	21.12		653	28.4	1.09	31
5	30			0.797	23.25		784	31.4	1.12	29
10	45			1.63	30.8		1616	50.7	1.47	34
10	50			2.17	34.1		2165	61.9	1.65	36

calculated from the constants found, show very distinct tendencies of asymptotically approaching $\bar{n} = 6$, Fig. 2. The coordination number of bismuth in these two halide systems thus seems to be $N = 6$. In fact even the sixth complex is a little reluctant to form from the fifth one. In addition to the values of β_1 used in connexion with the potentiometric data, values of some of the higher constants can also be determined from the solubility measurements (*cf.* eqn. (11)). In this way β_2 of the chloride system and β_2 to β_4 of the bromide system are calculated and found to be in reasonable agreement with the values found potentiometrically, as seen from Table 11, where all the constants are tabulated.

As C_M must be kept rather low in the potentiometric measurements in order to avoid precipitation as much as possible, the determination of the slopes of the C_A, C_M lines of constant E_M becomes rather uncertain, all the more as the error in E_M is not very small (*cf.* p. 1118). In such cases the slopes found cannot be expected to coincide completely with the complex formation curve even if the complex formation is in fact entirely mononuclear. As seen from Fig. 2, discrepancies are found for the chloride system especially, but they can most certainly be explained by the poor accuracy of the slope values. The general trends of these nevertheless coincide with the curve found from the

Table 8. The iodide system. E_M as a function of C_A for different values of C_M.

$C_M \rightarrow$ mM	10	5	2	1	$C_M \rightarrow$ mM	10	5	2	1
C_A mM	E_M mV				C_A mM	E_M mV			
60.2				232.7	346	304.7	312.7	320.4	324.4
73.9				243.5	375	310.0	317.1	324.5	328.6
87.2			245.5	252.5	424	317.4	324.0	331.0	335.1
100.2			253.2	259.9	465	322.8	329.0	335.6	339.9
124.8		253.4	265.4	271.6	499	327.1	333.2	339.4	343.6
147.9		263.3	274.5	280.1	553	333.1	338.8	344.6	349.0
180.2	264.9	274.4	285.5	290.4	595	337.1	342.9	348.3	352.7
209.7	274.9	283.2	293.8	298.5	627	340.0	345.7	350.8	355.5
245.5	284.6	292.7	302.5	306.7	675	344.0	349.5	354.8	359.0
278	291.9	300.2	308.8	313.0	715	352.0	352.3	357.6	362.3
314	299.0	307.2	315.2	319.4					

stability constants and no doubt the complex formation is mononuclear for both systems.

The iodide system: In Table 8, E_M is given as a function of C_A at different C_M. A fairly high value of C_A is necessary in order to prevent precipitation of BiI_3 even at C_M as low as 1 mM. As the values of E_M obtained for a certain C_A are remarkably high the system must be strongly complex. Only the highest complexes can therefore be expected to exist in the range of [A] covered by the emf measurements. The calculation should in such a case start with β_N (*cf.* p. 1113). From the results of the chloride and bromide systems, it may be

Table 9. The iodide system. Calculation of β_6 from potentiometric measurements

$C_A \rightarrow$ mM	10	5	2	1	0	$X \times 10^{-12}$	$X'_6 \times 10^{-19}$ M^{-6}
E_M mV	C_A mM				C_A = [A]		
245			86	74	62	4.32	7.8
250			94	82	70	7.82	6.7
255		128	103	91	83	14.2	4.3
260		139	113	100	92	25.6	4.2
265	180	152	123	110	107	46.4	2.9
270	193	166	135	121	119	84.1	3.0
275	209	182	148	134	131	152.3	3.0
280	227	199	162	148	145	276	3.0
285	247	216	177	163	158	499	3.2
290	268	235	194	179	176	904	3.1
300	318	278	234	216	212	2960	3.3
310	375	331	282	262	255	9720	3.5
320	443	394	342	319	315	$3.19 \cdot 10^4$	3.3
330	525	472	415	386	386	$10.45 \cdot 10^4$	3.2
340	626	564	502	466	468	$34.3 \cdot 10^4$	3.3
350		683	614	565	541	$112.2 \cdot 10^4$	4.5

Table 10. The iodide system. The solubility l as a function of [A]. Determination of the solubility product L, with subsequent calculation of the complexity constants β_6 to β_4.

C'_M mM	C_A mM	E_M mV	[M] × 10^{17} M	l mM	$[I_3^-]$ mM	[A] mM	$L \times 10^{18}$ M^4	$L \cdot X'_6$ M^{-2}	$L \cdot X'_5$ M^{-1}
1	7.5			0.0255	0.14	4.08		375	1.51
1	10			0.0239	0.19	6.41		90.8	0.547
1	10			0.0130	0.09	6.72		42.8	0.252
1	12.5			0.0277	0.14	9.05		37.4	0.289
1	15			0.0450	0.25	11.20		32.0	0.297
1	15			0.0437	0.10	11.65		27.6	0.258
1	17.5			0.0506	0.35	13.38		21.2	0.210
1	20			0.0580	0.60	15.11		16.8	0.171
1	20			0.0663	0.44	15.57		17.6	0.188
1	20			0.0731	0.33	15.86		18.3	0.203
1	22.5			0.0867	0.27	18.52		13.6	0.150
1	25			0.0892	1.10	18.53		14.0	0.158
1	25			0.1077	0.42	20.5		12.5	0.144
1	25			0.0980	0.36	20.8		11.0	0.114
1	30			0.151	1.07	23.5		11.7	0.145
1	30	197.9	6220	0.163	0.59	24.9	0.96	10.6	0.127
1	30			0.185	0.50	25.1		11.8	0.158
1	35			0.236	0.59	29.7		9.1	0.106
1	40	207.4	2010	0.337	0.85	33.6	0.76	8.9	0.114
1	40			0.349	0.67	34.1		8.8	0.113
1	40	208.3	1810	0.340	0.15	35.7	0.82	7.5	0.070
1	50	209.5	1570	0.596	1.19	41.8	1.15	8.2	0.111
2	65	218.8	520	1.077	1.24	52.3	0.75	7.6	0.107
3	80	225.0	249	1.82	0.84	63.3	0.63	7.2	
5	100	226.7	203	2.44	1.80	72.6	0.78	6.4	
5	100	227.7	181	2.65	1.08	74.1	0.74	6.5	
10	150	233.9	87	5.82	1.08	99.8	0.86	5.9	

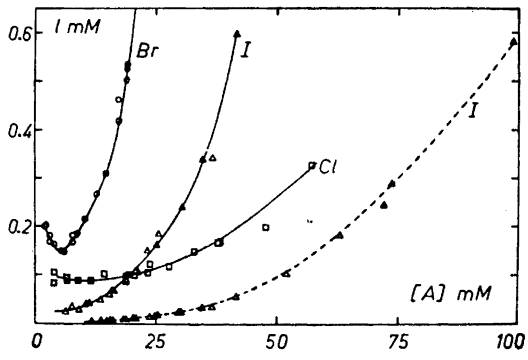


Fig. 1. The solubility l of Bi(III) as a function of [A] in halide solutions. Squares, circles and triangles refer to the chloride, bromide and iodide systems respectively. The dashed curve of iodide refers to values of l ten times greater than those given on the ordinate axis.

assumed that $N = 6$ also for the iodide. In Table 9, where corresponding values of X and [A] are found, the function X_6' is also given, calculated according to (5). It is found to be a constant, $= \beta_6$, from the highest value of [A] down to [A] $\approx$ 80 mM, thereby confirming that $N = 6$. For [A] $<$ 80 mM, X_6' increases as lower complexes become perceptible, but further constants cannot be safely calculated from the present figures.

A substantial extension of the measured range of [A] is obtained by the solubility measurements, Table 10. A value of [A] $\approx$ 4 mM can be reached, as compared with [A] $\approx$ 60 mM in the emf measurements. In that range of [A] (>25 mM) where [M] can be measured and thus values of L determined (from eqn. (12)), L is found to be constant within the experimental errors (Table 10). Thus the solid phase really is MA_3, as postulated in (12). Using the established value of $N = 6$, $L \cdot X_6' = l / [A]^3$ is then calculated, *cf.* eqn. (15), and from the extrapolation to $1 / [A] = 0$, $L \cdot \beta_6$ and hence β_6 is found. Then $L \cdot X_5'$ is formed according to (16), and from this function β_5 and β_4 are found from the intercept on the axis and the slope at the point of intersection. The function is not linear, so the third complex must be present in appreciable amounts, at least in the solutions of lowest [A]. The accuracy of l is not good enough however to permit the calculation of a further constant from a function $L \cdot X_4'$, formed analogously to $L \cdot X_5'$.

The constants found are given in Table 11. As can be seen, the two values of β_6 found agree tolerably well. We believe, however, that the figure found by the solubility measurements is the more reliable one, on the following grounds. As pointed out above (p. 1118) a reaction involving the amalgam electrode is evidently taking place in iodide solutions of high [A]. From the bleaching of the solutions it is obvious that Bi(III) is being reduced by the metallic Hg. Such a reduction is rendered possible by the formation of very strong iodide complexes of Hg(II) which greatly stabilize this oxidation state relative to Hg(0). A calculation based on the data of Sillén [16] for Hg(II) and those of the present paper for Bi(III) also confirms that the reduction is possible. On the other hand Sillén's data seem to indicate that the existence of Hg(I) in appreciable amounts (as solid Hg_2I_2) is not to be expected at those values of [A] where a perceptible reduction of Bi(III) can take place. Similar calculations for the chloride and bromide system prove that no reduction of Bi(III) is to be feared in these cases, as is also experimentally confirmed.

Even at lower values of C_A where the function of the amalgam electrode is not obviously erratic, minor irregularities occur which may indicate the beginning of its break-down. Thus the corresponding values of C_M and C_A at constant values of E_M do not fall as well as they should along straight lines. Moreover the best straight lines which can be drawn have slopes much greater than $\bar{n}$. Obviously the values of E_M measured cannot be considered as quite realiable, and more weight should therefore be placed on the measurements of solubility.

The observed slopes of course do not suggest any polynuclear complex formation, being greater than $\bar{n}$. As their value seems doubtful however, no conclusions ought to be drawn. But from the behaviour of the other halide systems it may perhaps be concluded that the iodide system also is probably mononuclear.

CONCLUSIONS. COMPARISON WITH PREVIOUS WORK

The halide complexes of Bi^{3+} increase in strength in the order $Cl^- < Br^- < I^-$, and Bi^{3+} thus belongs to the second group of central ions, *i. e.* those centered about the noble metals. This is evident from Table 11 and also from Fig. 2, where the complex formation curves are drawn as calculated according to Ref.[9], p. 785.

Fig. 2 also shows that the curves of the chloride and bromide systems are similar, implying that the complex formation proceeds in much the same way

Table 11. The logarithms of the stability constants β and the solubility products L, with maximum random errors indicated. Comparison with the results of other investigations.

		log β_n (M^{-n})						log L (M^4)
$n \rightarrow$		1	2	3	4	5	6	
Present authors								
Cl^-	emf		3.5 ±0.2	5.35 ±0.06	6.10 ±0.15	7.72 ±0.06	7.56 ±0.12	BiOCl −34.93 ±0.09
	sol	2.36 ±0.10	3.8 ±0.3					
Br^-	emf		4.45 ±0.06	6.30 ±0.06	7.70 ±0.08	9.28 ±0.04	9.38 ±0.08	BiOBr −34.77 ±0.06
	sol	2.26 ±0.06	4.26 ±0.10	6.18 ±0.12	7.8 ±0.2			
I^-	emf						19.4 ±0.4	BiI_3 −18.09 ±0.10
	sol				14.95 ±0.2	16.8 ±0.2	18.8 ±0.2	
Babko and Golub *								
Cl^-, Br^-, I^-	emf				5.42 7.82	7.5 7.3	6.42 7.9 11.51	
Newman **								
Cl^-	sp	2.43 ±0.01	4.4	5.8	6.2	6.7		

* β_4 and β_5 measured in 1.5 M HNO_3 for the chloride, in 1.2 M HNO_3 for the bromide. β_6 of all systems measured in 0.6 M HNO_3. The solutions also contain KNO_3 to a total $I = 2.3$ or 3 M. Temperature 20°C.

** The first two consecutive constants (β_n/β_{n-1}) were measured in 1 M $HClO_4$, the three following ones in a medium of the same $[H^+]$, but with $I = 5$ M.

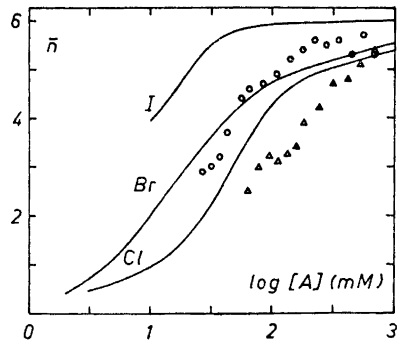


Fig. 2. The complex formation functions of the bismuth chloride, bromide and iodide systems. The curves are calculated from the values of β found. The points obtained from the slopes of the C_A, C_M-lines of constant E_M are indicated by circles for the bromide and by triangles for the chloride system.

in these two systems. A characteristic feature is the slow formation of the sixth complex, which means that the fifth one has a broad range of existence. This stands out well in Fig. 3, where the distribution of Bi(III) on the different complexes is given as a function of log [A] (*cf.* Ref.[9], p. 787). The graphical representation is the one first used by Bjerrum [17], *cf.* also J. Bjerrum [18] (p. 287). A still more interesting thing is that the value of β_1 for bromide is about the same as that for chloride (or even a little less). In this respect Bi^{3+} thus behaves as an intermediate between the two groups of central ions, in accord with its position in the outskirts of the second group. As the formation curve of the bromide is much steeper than that of the chloride, the overall complexity of the former system is nevertheless considerably stronger. As to the solubility products of the oxyhalides, that of the bromide seems to be just greater than that of the chloride, which is also contrary to the general rule for halide systems of the second group ions, as exemplified by the halides of Cu^+, Ag^+, Hg_2^{+2} and Hg^{2+}.

In the iodide system, on the other hand, the fifth complex does not have a wide range of existence, instead the formation curve goes steeply up $\bar{n} = N = 6$. Moreover the difference in stability between the iodide and bromide complexes is much greater than between the bromide and chloride ones.

Quantitative investigations of the complex formation in solutions of the bismuth halides have also been performed by Babko and Golub [19] and by Newman [20]. Babko and Golub measured $[Bi^{3+}]$ by means of bismuth metal electrodes, as well as measuring the corresponding $[Cl^-]$ or $[Br^-]$ by silver halide electrodes. The pure metal electrodes did not give emfs as reproducible as those of the present amalgam electrodes, in accordance with the general observation that electrodes of hard metals are not easy to get working satisfactorily. The measurements were performed in nitrate media of such high acidity that a definite risk of oxidation of the metal electrode certainly must have existed, especially in solutions of high halide concentration where bismuth is much less noble than in non-complexing media. In the case of iodide, moreover, it was necessary to add sulphite in order to prevent oxidation of the ligand. This addition, however, is objectionable, as sulphate and sulphite are

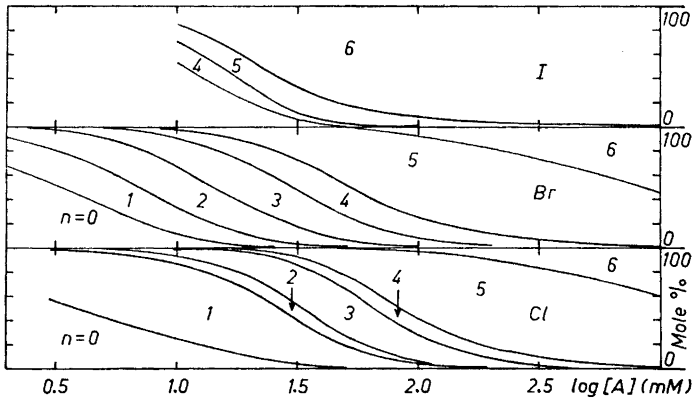


Fig. 3. The distribution of bismuth between the various complexes as a function of [A].

thereby introduced as new ligands in the solution whose concentration of acid is simultaneously reduced.

Dissociation constants, K_n, have been calculated for the three highest complexes of the chloride and bromide systems and for the highest (= sixth) iodide complex. The corresponding stability constants, $\beta_n = 1/K_n$, are as a rule perceptibly lower than those found by the present authors, Table 11. As to the chloride and bromide systems, they are nevertheless of the same order of magnitude. The value of β_6 of the iodide system is however quite different.

Newman has measured spectrophotometrically the consecutive constants of the first five complexes of the chloride system, as well as constants for mixed chloride bromide complexes containing one bromide ion. The constants β calculated from his data, Table 11, agree on the whole tolerably well with ours, especially if the differences of method and medium are taken into account. The most remarkable discrepancy is found for β_5. The sixth complex has escaped discovery because the measurements were not extended into that range of [A] where it exists in perceptible amounts, according to the present investigation.

This investigation has been supported by a generous grant from *Statens naturvetenskapliga forskningsråd (Swedish Natural Science Research Council)*. Our thanks are due to Dr George Gamlen, I.C.I. Dyestuffs Division, Blackley, Manchester, for his kind and thorough revision of the English in our manuscript.

Note added in proof: Slightly revised, Newman's [20] work has recently been definitively published (Newman, L. and Hume, D. N. *J. Am. Chem. Soc.* **79** (1957) 4571, 4576, 4581.

REFERENCES

1. Ahrland, S. *Acta Chem. Scand.* **10** (1956) 723.
2. Granér, F. and Sillén, L. G. *Acta Chem. Scand.* **1** (1947) 631; *cf.* also Granér, F Olin, Å. and Sillén, L. G. *Acta Chem. Scand.* **10** (1956) 476.
3. Leden, I. *Svensk Kem. Tidskr.* **64** (1952) 249.
4. Leden, I. *Symposium on Co-ordination Chemistry, Copenhagen, August 9—13, 1953.* Copenhagen 1954, p. 77.

5. Leden, I. *Z. physik. Chem.* **A 188** (1941) 160.
6. Leden, I. *Potentiometrisk undersökning av några kadmiumsalters komplexitet*, (Diss.) University, Lund 1943.
7. Fronaeus, S. *Komplexsystem hos koppar*, (Diss.) University, Lund 1948.
8. Ahrland, S., Chatt, J., Davies, N. R. and Williams, A. A. *J. Chem. Soc. In press.*
9. Ahrland, S. *Acta Chem. Scand.* **3** (1949) 783.
10. *Gmelins Handbuch*, 8th ed., **8 I** (1933) 426.
11. Vogel, A. I. *Quantitative Inorganic Analysis*, 2. ed., London 1951, p. 426.
12. Ahrland, S. and Larsson, R. *Acta Chem. Scand.* **8** (1954) 137.
13. Wiegand, C. J. W., Lann, G. H. and Kalich, F. W. *Ind. Eng. Chem. Anal. Ed.* **13** (1941) 912.
14. Randles, J. E. B. and Somerton, K. W. *Trans. Faraday Soc.* **48** (1952) 951.
15. Malát, M., Suk, V. and Rybá, O. *Collection Czechoslov. Chem. Communs* **19** (1954) 258 (from Schwarzenbach, G. *Die komplexometrische Titration*, 2. ed., Stugttart 1956, p. 88).
16. Sillén, L. G. *Acta Chem. Scand.* **3** (1949) 539.
17. Bjerrum, N. *Kgl. Danske Videnskab. Selskabs Skrifter, Naturvidenskab. math. Afdel.* [7] **12** (1915) No. 4.
18. Bjerrum, J. *Metal Ammine Formation in Aqueous Solution*, (Diss.) University, Copenhagen 1941.
19. Babko, A. K. and Golub, A. M. *Sbornik Statej Obsh. khim. SSSR* **I** (1953) 64.
20. Newman, (Diss.) M. I. T., Cambridge, Mass. 1956.

Received May 5, 1957.

ACTA CHEMICA SCANDINAVICA 11 (1957) 1131—1142

The Alkaline Hydrolysis of *iso*Propoxy-methyl-phosphoryl Fluoride (Sarin) and some Analogues

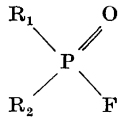
LENNART LARSSON

Research Institute of National Defence, Dept. 1, Sundbyberg 4, Sweden

The alkaline hydrolysis of Sarin and ten analogues have been studied at different temperatures with an electrometric method. The bimolecular rate constants and the energies and entropies of activation of the reactions have been calculated. The hydrolysis products have been examined with paper chromatographic technique. The results indicate that the hydrolysis proceeds as an one-stage reaction (S_N2) and involves a nucleophilic attack of the hydroxyl ion on the phosphorus atom. The attraction between them is controlled by the inductive and mesomeric effects of the substituents which also influence the strength of the P—F bond. On the basis of the theories of Kirkwood and Westheimer a semi-quantitative treatment of the electrostatic effects of the substituents on the rates has been performed, and a fairly good agreement between calculated and found rate constants has been obtained.

Since the fundamental investigation of the hydrolysis of di-*iso*propoxyphosphoryl fluoride, DFP, performed by Kilpatrick [1], several papers concerning different reactions of fluorine derivatives of organic phosphorus compounds have been published. Especially the reactions of Sarin and of DFP with catechols [2,3], hydroxamic acids [4,5] and oximes [6] have attracted attention. The hydrolysis of Sarin catalyzed by hydroxyl ions has also been touched in some papers [4,7].

Sarin has caught interest because of its potent effects on the cholinergic transmission. It has also been considered as a potential war gas. The hydrolysis of Sarin is thus of practical importance for chemical and pharmacological studies as well as for its decontamination. The purpose of this investigation was to determine the pH-dependence of the hydrolysis of Sarin and to elucidate the reaction mechanism of its alkaline hydrolysis. It was also of interest to study the effect of substituents on the rates of hydrolysis of compounds with the general formula



Because the hydrolysis of Sarin as well as the hydrolysis of its analogues is catalyzed by several ions, it is rather complicated to study the pH-dependence of the reaction in various buffer solutions. The hydrolysis has instead been studied by an electrometric method developed by Larsson and Hansen [8]. The nomenclature used in this paper conforms to the Swedish proposition [9].

EXPERIMENTAL

Materials. The methyl-fluoro-phosphorylcholine derivatives were synthesized in this institute by Tammelin [10]. The other organic phosphorus compounds except the bromoethoxy- and dimethylbutoxy-derivatives were synthesized by Tammelin and Fagerlind [11]. 2-Bromoethoxy-methyl-phosphoryl fluoride and 3,3-dimethylbutoxy-methyl-phosphoryl fluoride were synthesized by reacting methyl-fluoro-phosphoryl chloride with 2-bromoethanol and 3,3-dimethylbutanol [12], respectively, according to the scheme given by Tammelin [10]. Analytical data of these two compounds are shown in Table 1. The densities, determined with a self-filling pycnometer [13], and refractive indices of the liquid compounds as well as the formulae of all the compounds are given in Table 2. Methylphosphoryl-dichloride used in the chromatographic study was prepared according to Kinnear and Perren [14]. The salts were recrystallized and the liquids freshly distilled before use.

Paper chromatographic technique. The phosphorus compounds to be chromatographed were hydrolyzed in 0.1 M ammonium hydroxide. The choline chloride used was dissolved in distilled water. Five μl of 0.5 % solutions of the compounds were placed with micropipettes on a filter paper, Whatman No. 1, Ascending technique was used, and the chromatograms were run at 25°C. Both acid and alkaline solvents were tested. The composition of the acid solvent was: *n*-butanol : ethanol : acetic acid : water (8 : 2 : 1 : 3)[15], and that of the alkaline solvent was: *tert.*-butanol : *iso*propanol : 2 M ammonium hydroxide (2 : 2 : 1).

The development of the spots from the phosphorus compounds was carried out by spraying the paper with an acid solution of ammonium molybdate and treating the dried paper with hydrogen sulfide [16].

An attempt to develop the chromatographed hydrolyzate of one of the phosphorylcholine derivatives in respect of the choline group was made in three different ways: by spraying with a solution of dipicrylamine [15], by immersing in a solution of Reinecke salt [17], and by immersing in a solution of phosphomolybdic acid with subsequent reduction with stannous chloride [18]. Choline chloride was developed with dipicrylamine.

Kinetic measurements. The rates of the hydrolysis of the compounds were studied by means of an automatic recording titrator [8]. The principle of this instrument is that acid products formed in the hydrolysis are neutralized by addition of alkali in such a rate

Table 1. Analytical data.

Compound	Formula	Molecular weight	% C		% H		% Br		B.p. °C/mm Hg
			calc.	found	calc.	found	calc.	found	
2-Bromoethoxy-methyl-phosphoryl fluoride	$C_3H_7BrFO_2P$	205.0	17.6	17.9	3.4	3.4	39.0	38.9	58/0.7
3,3-Dimethylbutoxy-methyl-phosphoryl fluoride	$C_7H_{16}FO_2P$	182.2	46.1	45.7	8.9	8.9	—	—	50/0.5

Table 2. The formulae, densities and refractive indices of the organic phosphorus compounds studied.

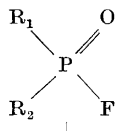
Compound			d_4^{25}	n_D^{25}
	R_1	R_2		
Methoxy-methyl-phosphoryl fluoride	CH_3	CH_3O	1.2355	1.3740
Ethoxy-methyl-phosphoryl fluoride	CH_3	CH_3CH_2O	1.1524	1.3785
2-Bromoethoxy-methyl-phosphoryl fluoride	CH_3	$BrCH_2CH_2O$	1.6708	1.4480
Methyl-fluoro-phosphorylcholine iodide	CH_3	$(CH_3)_3N^+CH_2CH_2O$	—	—
n-Propoxy-methyl phosphoryl fluoride	CH_3	$CH_3CH_2CH_2O$	1.1008	1.3885
Methyl-fluoro-phoshorylhomocholine iodide	CH_3	$(CH_3)_3N^+CH_2CH_2CH_2O$	—	—
*iso*Propoxy-methyl-phosphoryl fluoride (Sarin)	CH_3	$(CH_3)_2CHO$	1.0941	1.3815
Methyl-fluoro-phosphoryl-β-methylcholine iodide	CH_3	$(CH_3)_3N^+CH_2CHO$ $\quad\quad\quad

Table 3. The pH values of the standard buffer solutions, the ion products of water, pK_w, and activity coefficients of hydroxyl ions, f_{OH^-}, at different temperatures.

t °C	pH		pK_w	f_{OH^-} $\mu = 0.100$
	0.05 M potassium hydrogen phthalate	0.01 M sodium tetraborate		
20	4.00	9.22	14.17	0.767
25	4.01	9.18	14.00	0.766
30	4.01	9.14	13.83	0.764
35	4.02	9.10	13.68	0.762

of potassium chloride; in dilute alkali solutions this value seems to be more reasonable to use than that given for potassium hydroxide [21].

The choline derivatives were dissolved in abs. ethanol; the solutions were freshly prepared every day. The other compounds studied were dissolved in dioxan, *E. Merck c.p.*, purified from peroxides and redistilled over sodium. The concentration of the compounds in the stock solutions were 10 mM. In the reaction vessel 1 to 2 ml of the stock solution was diluted to 40.0 ml with 0.100 M solution of potassium chloride which before the addition of the stock solution had been adjusted to the desired pH-value. The concentration of the sodium hydroxide added was 0.050 M. The slight dilution during the reaction due to the volume of the alkali was neglected. The potassium chloride solution was used to maintain the ionic strength constant. In one series of experiments the concentration of potassium chloride was varied and in one case sodium fluoride was used. The final concentrations of the compounds varied between 0.25 and 0.50 mM.

RESULTS

Hydrolysis products

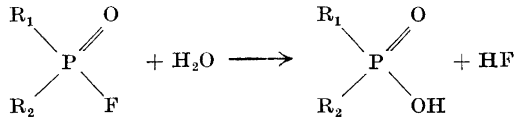
When Sarin or its analogues studied in this paper are hydrolysed in alkaline solution exactly two equivalences of acid are formed. In the hydrolyzates fluoride ion was indicated with zirkon alizarin paper.

The hydrolyzates of Sarin and of methyl-fluoro-phosphorylcholine were analysed with paper chromatographic technique to investigate the products which were formed. Only one spot indicating a phosphorus compound was obtained on the two chromatograms. As comparison solutions of methyl-dihydroxy-phosphine oxide, obtained from methylphosphoryl dichloride, and of choline chloride were analysed in the same manner. The R_F value of the hydrolyzate of Sarin does not agree with that of methyl-dihydroxy-phosphine oxide. It is thus proved that this compound is not formed in the hydrolysis and that the hydrolysis product containing phosphorus must be methyl-*iso*propoxy-hydroxy-phosphine oxide. Neither the R_F value of choline nor that of methyl-dihydroxy phosphine oxide agree with the R_F value of the hydrolyzate of methyl-fluoro-phosphorylcholine. This indicates that these compounds are not formed in the hydrolysis, and that the hydrolysis product must be methyl-hydroxy-phosphorylcholine. The R_F values of the four compounds in acid and alkaline solvents are given in Table 4. It is, however, remarkable that the choline group in methyl-hydroxy-phosphorylcholine was impossible to indicate with any of the three developers used for choline.

Table 4. The R_F values in acid and alkaline solvents.

Compound	R_F	
	Acid solvent	Alkaline solvent
Methyl-dihydroxy-phosphine oxide	0.26	0.02
*iso*Propoxy-methyl-hydroxy-phosphine oxide	0.64	0.48
Methyl-hydroxy-phosphorylcholine	0.22	0.18
Choline chloride	0.43	0.31

These results indicate that the hydrolysis proceeds according to the following scheme:



and that any further hydrolysis of the reaction products does not seem to occur under the present conditions.

pH-Dependence of the hydrolysis of Sarin

The pH-dependence of the hydrolysis of Sarin was studied at 25°C at the pH-values 8.00, 8.40, 8.70, 9.00, 9.40 and 9.80 and at 35°C at the pH-values 8.30, 8.68 and 9.13. The hydrolysis curves obtained from the recorder were treated according to the method given by Guggenheim [22]. Straight lines were obtained indicating that the hydrolysis proceeds as a first-order reaction when the pH is maintained constant. If the rate of the hydrolysis only depends upon the hydroxyl ion activity and the reaction with water molecules can be neglected, the pH-dependence of the hydrolysis at constant ionic strength may be equated as

$$k_1 = k_2' \cdot a_{OH^-} = k_2' \cdot \frac{K_w}{a_{H^+}} \tag{2a}$$

or in logarithmic form

$$\log k_1 = \log k_2' - \text{pOH} \tag{2b}$$

where k_1 is the pseudo first-order rate constant, k_2' the second-order rate constant at constant ionic stregth and K_w the ionic product of water.

When the logarithms of the pseudo first-order constants in sec.$^{-1}$ obtained from three runs at each pH are plotted against pOH, using the values of pK_w given in Table 3, straight lines are obtained as shown in Fig. 1. The equations of the two lines were calculated by the method of least squares, and were found to be:

$$\log k_1 = 1.519 - 0.995 \times \text{pOH at } 25°C, \text{ and}$$
$$\log k_1 = 1.731 - 0.995 \times \text{pOH at } 35°C.$$

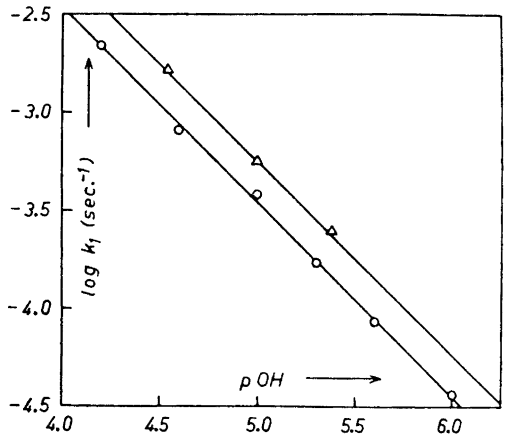


Fig. 1. The pOH dependence of the hydrolysis of Sarin ○ at 25°C and △ at 35°C. The sizes of the points indicate the standard deviations in log k_1.

The error in the found coefficients of pOH is ± 0.013 and ± 0.021, respectively. The coefficients are within the limits of error equal to 1.00 which thus confirms the correctness of the proposed eqn. (2).

Effect of ions on the hydrolysis of Sarin

It appears from Table 5 that the rate of the hydrolysis of Sarin is increased when increasing the ionic strength at constant pH. If, however, the second-order rate constant, k_2, is calculated from the hydroxyl ion concentrations in question, this constant is found to be independent of the ionic strength within the limits of error. This will probably depend upon the activity coefficient of the hydroxyl ion canceling the activity coefficient of the charged activated complex and the activity coefficient of the uncharged Sarin molecule being unaffected in the ionic strength range in question. For that reason eqn. (2 a) has been transformed to the following equation:

$$k_1 = k_2 \cdot c_{OH^-} = k_2 \cdot \frac{a_{OH^-}}{f_{OH^-}} \qquad (3)$$

where the bimolecular rate constant k_2 is independent of the ionic strength to at least 0.5.

From Table 5 it is also shown that the fluoride ions have no effect on the the rate of the hydrolysis.

Temperature dependence of the hydrolysis of Sarin and its analogues

The temperature dependence of the hydrolysis of Sarin was determined at 20°C, 25°C, 30°C and 35°C. The pseudo first-order rate constants obtained

Table 5. The effect of ionic strength and fluoride ions on the hydrolysis of Sarin at pH 9.00 and 25°C.

M_{KCl}	M_{NaF}	f_{OH^-}	$c_{OH^-} \times 10^5$	$k_1 \times 10^4$ sec.$^{-1}$	k_2 l mole^{-1} sec.$^{-1}$
0.050	—	0.813	1.23	3.73	30.3
0.100	—	0.766	1.31	3.81	29.1
0.200	—	0.715	1.40	4.32	30.9
0.500	—	0.649	1.54	4.42	28.7
—	0.100	0.766	1.31	3.83	29.2

were converted into second-order rate constants by means of eqn. (3). The first-order rate constants at 20°C and 30°C were calculated from three runs at each temperature at pH 9.17 and 8.83, respectively, *i.e.* at pOH 5.00. The second-order rate constants at 25°C and 35°C were calculated from the results of the study of the pH-dependence.

The Arrhenius activation energy, E_a, was calculated in usual manner by plotting log k_2 against $1/T$ as shown in Fig. 2. The line was drawn according to the method of least squares and the equation obtained was found to be

$$\log k_2 = 8.049 - 1.979 \times 10^3 \; 1/T$$

The value of the activation energy of Sarin obtained from this equation is given in Table 6.

In the same table there is also given the entropy of activation of the reaction, $\Delta S^{\ddagger}$; which is calculated according to Eyring [23a] for reactions in solution:

$$k_2 = e \cdot \frac{kT}{h} \cdot e^{-Ea/RT} \cdot e^{\Delta S^{\ddagger}/R} \qquad (4)$$

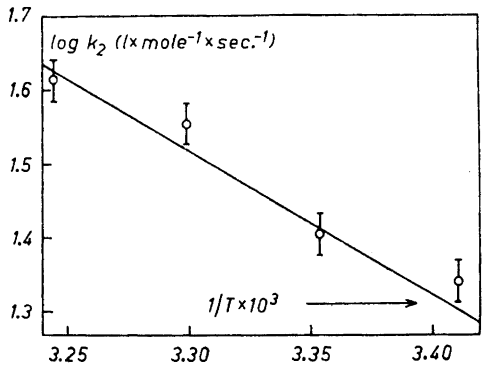


Fig. 2. The temperature dependence of the hydrolysis of Sarin. The values at 20°C, 25°C, 30°C and 35°C are mean values of 3, 18, 9 and 3 determinations, respectively. The lines through the points indicate the standard deviations in log k_2.

Table 6. Rate constants and energies and entropies of activation of Sarin and its analogues.

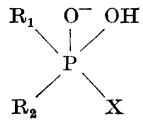
Compound	t = 25°C		t = 35°C			
	$k_1 \times 10^4$ sec.$^{-1}$ pOH = 5.50	k_2 l mole^{-1} sec.$^{-1}$	$k \times 10^4$ sec.$^{-1}$ pOH = 5.50	k_2 l mole^{-1} sec.$^{-1}$	E_a kcal. mole^{-1}	$\Delta S^{\neq}$ E.U.
hoxy-methyl- sphoryl fluoride	4.29 4.53	106	7.87 7.77	188	10.5 ±0.7	−16 ±2
oxy-methyl- sphoryl fluoride	2.45 2.56	60.7	4.77 4.53	112	11.2 ±0.8	−15 ±3
romoethoxy-methyl- sphoryl fluoride	6.74 6.64	162	12.6 12.4	301	11.3 ±0.3	−13 ±1
hyl-fluoro-phosphoryl ine iodide	38.8 38.6	935	20.2* 20.0*	1530	9.0 ±0.2	−17 ±1
ropoxy-methyl- sphoryl fluoride	2.24 2.22	54.0	4.06 3.82	95.3	10.4 ±0.7	−18 ±2
hyl-fluoro-phospho- homocholine iodide	12.5 12.7	305	24.1 23.6	575	11.6 ±0.4	−10 ±1
ropoxy-methyl-phos- ryl fluoride (Sarin)	—	25.8	—	42.4	9.1 ±0.3	−24 ±1
hyl-fluoro-phosphoryl- ethylcholine iodide	15.8 15.6	381	27.5 27.5	663	10.1 ±0.2	−15 ±1
Dimethylbutoxy- hyl-phosphoryl fluo-	2.05 2.02	49.3	3.88 4.03	95.3	12.0 ±0.6	−13 ±2
ropoxy-ethyl- phoryl fluoride	1.20† 1.23†	9.35	2.16† 2.24†	16.8	10.7 ±0.6	−20 ±2
ropoxy-*iso*propyl- phoryl fluoride	0.258† 0.272†	2.03	0.443† 0.435†	3.35	9.2 ±0.7	−28 ±2

* pOH = 6.00 ; † pOH = 5.00

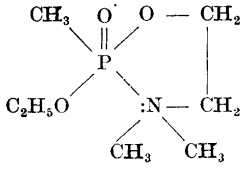
The pseudo first-order rate constants of the hydrolysis of the ten analogues to Sarin were determined at 25°C and 35°C and most of the experiments at pOH 5.50; the most rapid hydrolyses were measured at pOH 6.00 and the slowest ones at pOH 5.00. The values are shown in Table 6. The second-order rate constants were calculated on the presumption that the rate of the hydrolysis in conformity to the hydrolysis of Sarin is direct proportional to the hydroxyl ion concentration. This proved to be valid for the hydrolysis of methylfluoro-phosphorylcholine within the limits of error, when the rates of hydrolysis were determined at pOH 5.50 and pOH 6.00 at 25°C. From the rate constants obtained, the energy and entropy of activation of the ten Sarin analogues are calculated by means of Arrhenius' and Eyring's equations. The values of the second-order rate constants calculated from the mean values of the first order constants, and the energies and entropies of activation are given in Table 6. The errors reported are maximum errors with the exception of those of Sarin which are the standard deviations.

DISCUSSION

The direct proportionality of the reaction rate to the hydroxyl ion concentration in the hydrolysis of Sarin and its analogues indicates a bimolecular reaction mechanism. In the study of the hydrolysis of Tabun [24] the author suggested the hypothesis that the hydrolysis proceeded as a two-stage reaction involving an intermediate like

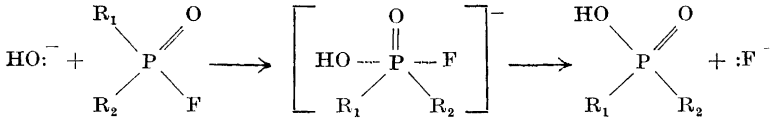


formed by utilization of one of the vacant 3d orbitals of phosphorus. If phosphorus shows such a tendency to expand its valence shell, it would be expected to coordinate the unshared electron pair on the nitrogen of ethoxy-dimethylaminoethoxy-methyl-phosphine oxide the formula of which can be designed:



If a bond of marked strength is established between the phosphorus and nitrogen atoms, this compound would be a considerably weaker base than the corresponding acetyl ester. Tammelin [25] has, however, shown that the difference between their dissociation constants is relatively small ($\Delta pK_a = 0.21$) which indicates that no expansion of the valence shell of phosphorus occurs, and that only a weak bond of dipole-dipole character thus may be formed. This contradicts the hypothesis of the formation of an intermediate in the hydrolysis of Sarin and its analogues and favours a simple one-stage displacement mechanism (S_N2). Dostrovsky [26] has also come to the same conclusion from his study of the hydrolysis of ^{18}O-labelled diethoxy-phosphoryl chloride.

The low effect of the ionic strength as well as the negligible effect of the fluoride ion concentration exclude a S_N1 mechanism and support the S_N2 mechanism. The alkaline hydrolysis can thus be described with the usual bimolecular scheme:



A polarimetric examination of the hydrolysis of one of the optical isomers of for example methyl-fluoro-phosphorylcholine is likely to give further evidence of the mechanism. The proposed mechanism would thus lead to inversion of the configuration without racemization.

The influence of the substituents on the rate of hydrolysis has been discussed on the basis of the theory of the inductive and mesomeric effects of the substituents (Ingold's terminology) and on the presumption that the reaction involves a nucleophilic attack of the hydroxyl ion on the phosphorus atom which will carry a small positive charge. A change from methyl to *iso*propyl in the alkyl or akoxy group involves a decrease in the rate of the hydrolysis as appears from Table 6. This can be explained by the increasing positive inductive effect, *i.e.* electron-releasing effect, when passing from methyl to *iso*propyl. This effect tends to increase the electronic density of the phosphorus atom and in this way to diminish the attraction of the hydroxyl ion. The decrease in rate is especially pronounced in the variation of the alkyl group. The low values of entropy of activation in these cases indicate a decreased probability of the transition state caused by steric hindrance. A substitution of hydrogen in the alkoxy group with an electron-attracting group such as bromine or a trimethylammonium group, which lower the electronic density of the phosphorus atom, causes a strong increase in the rate of hydrolysis.

If the methyl group in Sarin is exchanged against a *iso*propoxy group, the rate is decreased ($k_2 = 0.83$ l mole^{-1} sec.$^{-1}$ at 25°C)[1] which depends upon the increased mesomeric effect of the unshared electrons in the added oxygen atom. This effect is expected to be still greater in a dimethylamino group which is illustrated by the strong decrease in rate in the hydrolysis of bis-dimethylamido-phosphoryl fluoride ($k_2 = 5.7 \times 10^{-5}$ l mole^{-1} sec.$^{-1}$ at 25°C)[27]. The very strong decrease of the rate may also be attributed to the steric effect of the two dimethylamino groups.

As appears from Table 6 the activation energies of the reactions studied are approximately independent of the different substituents, even though some variations were expected. Similar results have been obtained in the alkaline hydrolysis of alkyl halides [28]. It is, however, essentially the free energy of activation which determines the rate of a reaction because the entropy of activation is not constant in the various reactions. The activation energy or really the heat of activation is rather to consider as an expression for the temperature dependence of the reaction.

From the results of the influence of the substituents on the rate of hydrolysis one can conclude that the rate of hydrolysis of Sarin and its analogues is mainly controlled by the strength of the P-F bond and by the ease with which the hydroxyl ion can attack the phosphorus atom. The approach of the hydroxyl ion depends upon the electronic density of the phosphorus atom, which is controlled by inductive and mesomeric effects of the substituents, and upon the steric hindrance by these substituents. The strength of the P-F bond is also influenced by the electron distribution of the substituents.

An attempt to a semi-quantitative treatment of the electrostatic effects of the substituents on the rates of hydrolysis has been performed on the basis of the theories improved by Kirkwood and Westheimer [29], and their equations for charged substituents (5) and dipolar substituents (6) have been used in the computation of the rate constants:

$$\ln k_2''/k_2 = \frac{e^2}{kTD_E d} \qquad (5) \qquad\qquad \ln k_2''/k_2 = \frac{e\mu \cos v}{kTD_E d^2} \qquad (6)$$

where k_2'' is the rate constant of the substituted compound to be calculated and k_2 is the found rate constant of the unsubstituted compound.

The computations were made on the assumptions that the molecule was a sphere with the radius R, and that the oxygen atom of the hydroxyl ion in the transition state and the charged atom or the center of the dipole were placed equidistant from the center on a diameter of the sphere. The diameter, $2R$, of the molecule was estimated from molecular models (Catalin Products Ltd.) as the geometric mean value of the lengths of three axes at right angles. The mean square distance, d, between the oxygen atom and the charged atom or the center of the dipole was calculated on the basis of free rotation about all the bonds [29]. The effective dielectric constant, D_E, is defined by the expression [29]: $1/D_E = f_1/D + f_2/D_i$, where D is the dielectric constant of the medium, D_i is the internal dielectric constant estimated as 2.0, and f_1 and f_2 are functions of the ratio $\frac{d}{2R}$. The value 1.48×10^{-18} e.s.u. was used for the dipole moment of the C-Br bond [30], and the angle, v, between the dipole and the line joining it to the oxygen atom was estimated to 31° from the fully extended molecule. Values of the angle found in this manner differ in general only little from those obtained from successive approximations [31].

The calculated rate constants, k_2'', and the found rate constants, k_2°, are given in Table 7. The found rate constants of the choline derivatives have been corrected to infinite dilution according to the theory of the influence of ionic strength on reactions between ions[23b]. The computations from eqns. (6) and (5) of the rate constants, k_2'', of bromoethoxy-methyl-phosphoryl fluoride and of methyl-fluoro-phosphorylcholine are based on the rate constant, k_2, of ethoxy-methyl-phosphoryl fluoride. Those of the homocholine- and β-methylcholine-derivatives are analogously based on the rate constants of propoxy-methyl-phosphoryl fluoride and Sarin, respectively.

Table 7. The rate constants of the hydrolysis of 2-bromoethoxy-methyl-phosphoryl fluoride and the choline derivatives at 25°C calculated according to Kirkwood and Westheimer.

Compound	$2R$ Å	d Å	D_E	$\log k_2''/k_2$	$\log k_2''$	$\log k_2^\circ$
2-Bromoethoxy-methyl-phosphoryl fluoride	6.45	4.65	5.38	0.55	2.33	2.21
Methyl-fluoro-phosphoryl-choline iodide	7.02	4.87	24.2	2.06	3.84	3.29
Methyl-fluoro-phosphoryl-homocholine iodide	7.25	5.34	31.5	1.45	3.18	2.80
Methyl-fluoro-phosphoryl-β-methylcholine iodide	7.27	4.87	21.2	2.36	3.77	2.90

The calculated rate constants agree fairly well with the found ones. The discrepancies are mainly due to the low accuracy in the estimation of the distances R and d and the disregard of the influence of the substituents on the strength of the P-F bond. The relatively great discrepancy between the calculated and found rate constants of methyl-fluoro-phosphoryl-β-methylcholine is probably caused by no consideration being taken of the steric effect of the β-methyl group in the estimation of the distance d. To compensate for

the steric effect of the trimethylammonium group the rate constant of methyl-fluoro-phosphorylcholine has also been calculated from the rate constant of 3,3-dimethylbutoxy-methyl-phosphoryl fluoride, at which calculation the logarithm of the rate constant was reduced from 3.84 to 3.75. These results demonstrate that the employment of the theories of Kirkwood and Westheimer leads to reasonable values in the calculation of the rate constants of the hydrolysis of organo-phosphorus compounds.

My sincere thanks are due to Professor G. Ljunggren, Director of this Institute, for the kind interest he has shown in this work.

The author wishes also to express his sincere thanks to Docent L. Melander, Nobel Institute of Chemistry, for stimulating criticism and discussions.

REFERENCES

1. Kilpatrick, M. and Kilpatrick, M. L. *J. Phys. & Colloid Chem.* **53** (1949) 1371, 1385.
2. Augustinsson, K.-B. *Acta Chem. Scand.* **6** (1952) 959.
3. Epstein, J., Rosenblatt, D. H. and Demek, M. M. *J. Am. Chem. Soc.* **78** (1956) 341.
4. Hackley, B. E., Plapinger, R., Stolberg, M. and Wagner-Jauregg, T. *J. Am. Chem. Soc.* **77** (1955) 3651.
5. Swidler, R. and Steinberg, G. M. *J. Am. Chem. Soc.* **78** (1956) 3594.
6. Green, A. L. and Saville, B. *J. Chem. Soc.* **1956** 3887.
7. Epstein, J., Bauer, V. E., Saxe, M. and Demek, M. M. *J. Am. Chem. Soc.* **78** (1956) 4068.
8. Larsson, L. and Hansen, B. *Svensk Kem. Tidskr.* **68** (1956) 521.
9. Larsson, L., Holmstedt, B. and Tjus, E. *Acta Chem. Scand.* **8** (1954) 1563.
10. Tammelin, L.-E. *Acta Chem. Scand.* **11** (1957) 859.
11. Tammelin, L.-E. and Fagerlind, L. *Unpublished results.*
12. Ipatieff, V. N., Thompson, W. W. and Pines, H. *J. Am. Chem. Soc.* **73** (1951) 553.
13. Hennion, G. F. *Ind. Eng. Chem., Anal. Ed.* **9** (1937) 479.
14. Kinnear, A. M. and Perren, E. A. *J. Chem. Soc.* **1952** 3437.
15. Augustinsson, K.-B. and Grahn, M. *Acta Chem. Scand.* **7** (1953) 906.
16. Hanes, C. S. and Isherwood, F. A. *Nature* **164** (1949) 1107.
17. Hack, M. H. *Biochem. J.* **54** (1953) 602.
18. Levine, C. and Chargaff, E. *J. Biol. Chem.* **192** (1951) 465.
19. Bates, R. G. *Electrometric pH determinations.* John Wiley & Sons, Inc., New York 1954, pp. 74, 314.
20. Manov, G. G., Bates, R. G., Hamer, W. J. and Acree, S. F. *J. Am. Chem. Soc.* **65** (1943) 1765.
21. Harned, H. S. and Owen, B. B. *The Physical Chemistry of Electrolytic Solutions.* Reinhold Publishing Corp., New York 1950, p. 381.
22. Guggenheim, E. A. *Phil. Mag.* **2** (1926) 538.
23. Glasstone, S., Laidler, K. J. and Eyring, H. *The Theory of Rate Processes.* McGraw-Hill Book Company, Inc., New York 1941, a) p. 199, b) p. 428.
24. Larsson, L. *Acta Chem. Scand.* **7** (1953) 306.
25. Tammelin, L.-E. *Acta Chem. Scand.* **11** (1957). *In press.*
26. Dostrovsky, I. and Halmann, M. *J. Chem. Soc.* **1956** 1004.
27. Heath, D. F. and Casapieri, P. *Trans. Faraday Soc.* **47** (1951) 1093.
28. Hinshelwood, C. N., Laidler, K. J. and Timm, E. W. *J. Chem. Soc.* **1938** 848.
29. Kirkwood, J. G. and Westheimer, F. H. *J. Chem. Phys.* **6** (1938) 506.
30. Ferguson, L. N. *Electron Structures of Organic Molecules.* Prentice-Hall, Inc., New York 1952, p. 133.
31. Westheimer, F. H. and Shockhoff, M. W. *J. Am. Chem. Soc.* **61** (1939) 555.

Received May 9, 1957.

ACTA CHEMICA SCANDINAVICA 11 (1957) 1143—1152

Die Geschwindigkeit der Äthanolyse und der Hydrolyse des Äthylbromids in Wasser-Äthanolgemischen

S. KILPI

Chemisches Institut der Universität Helsinki, Finnland

Auf Grund der Geschwindigkeitskoeffizienten der Solvolyse des Äthylbromids in Wasser-Äthanolgemischen wurden die Geschwindigkeitskoeffizienten der Hydrolyse und der Äthanolyse berechnet. In den wasserärmsten Gemischen ist die Geschwindigkeit der Äthanolyse und der Hydrolyse nach den Messungen annähernd proportional der stöchiometrischen Konzentration des Äthanols bzw. des Wassers. Die auf Grund der Geschwindigkeitskoeffizienten bei verschiedenen Temperaturen berechneten Temperaturkoeffizienten ändern sich mit der Zusammensetzung des Gemisches. In den wasserärmsten Gemischen wurde diese Abhängigkeit der Temperaturkoeffizienten von der Zusammensetzung des Lösungsmittels als von der Veränderung der Solvatationsverhältnisse verursacht erklärt.

Aus den Geschwindigkeitskoeffizienten der Solvolyse des Äthylbromids in wasserfreiem Äthanol und in einem Gemische, welches Wasser und Äthanol im Molverhältnis von 1:10 enthielt, berechnete der Verfasser [1] die Geschwindigkeitskoeffizienten der Äthanolyse und der Hydrolyse. Die Reaktionsgeschwindigkeit hat sich bei vielen Reaktionen, insbesondere in wasserarmen Äthanollösungen, als von der Zusammensetzung des Gemisches stark abhängig erwiesen. Es war deshalb von Interesse, zu untersuchen, inwieweit die Koeffizienten der obigen Solvolyse von der Zusammensetzung der Lösung abhängig sind. Zu diesem Zweck wurden in der vorliegenden Arbeit die Geschwindigkeitskoeffizienten der Solvolyse bei verschiedenen Temperaturen in wasserfreiem Äthanol und in Gemischen mit den stöchiometrischen Molverhältnissen 1:10, 1:6, 1:3 und 1:1 für $[H_2O]/[C_2H_5OH]$ bestimmt.

Die Materialien. Wasserfreies Äthanol wurde aus 96 %igem Äthanol durch Behandeln mit CaO und darauf mit Magnesium, welches mit Jod aktiviert worden war [2], und zuletzt mit wasserfreiem $CuSO_4$ hergestellt. Das in den folgenden Messungen verwendete Äthanol war 99,95—99,99 %ig.

Äthylbromid wurde aus Äthanol und Kaliumbromid durch Behandeln mit konz. Schwefelsäure bereitet.[3] Sp. 38,5°C bei 765 mm.

DIE MESSUNGEN

Die Messungen wurden bei 45°, 55°, 65° und 75°C ausgeführt und in einigen Fällen auch bei 25°, 35° und 40°C. Die Temperatur des Thermostaten verblieb innerhalb 0,02°C konstant. Der durch die Solvolyse gebildete Bromwasserstoff wurde titrimetrisch mit ca. 0,01 N $Ba(OH)_2$ oder mit kohlensäurefreiem NaOH gemessen. Als Indikator wurde Phenolphthalein verwendet. Da das Lösungsmittel zur Farbenveränderung selbst Alkali verbrauchte, wurden alle Titrationen in der Weise ausgeführt, dass die Lösung am Ende der Titration ca. 10 ml Äthanol und 40 ml Wasser enthielt. Dann verbrauchte das Lösungsmittel 0,40 ml 0,01 N Base, welche von der verbrauchten Basenmenge abgezogen wurde.

Bei den Titrationen wurden geeichte Mikrobüretten von 2 oder 5 ml Inhalt mit Einteilung von 0,01 bzw. 0,02 ml verwendet.

Alle Konzentrationen sind im folgenden in Mol pro 1 000 g Lösungsmittel angegeben. Das Äthylbromid wurde in dünnwandige Ampullen eingewogen und diese in abgewogenen Mengen Äthanol zerbrochen. Wenn die Reaktionsgeschwindigkeit in einem Wasser-Äthanolgemisch bestimmt werden sollte, wurde zu der alkoholischen Lösung eine berechnete Menge Wasser hinzugefügt. Etwa 10 ml Lösung wurden in eine gewogene, mit einem kapillaren Hals versehene Ampulle abgefüllt, die Ampulle zugeschmolzen und gewogen. In der Ampulle befand sich nur so viel Luft, dass ein Zerspringen der Ampulle wegen der Ausdehnung der Flüssigheit nicht zu befürchten war.

Die Konzentration des Äthylbromids war ca. 0,1 M. Der Geschwindigkeitskoeffizient verblieb in dem Konzentrationsbereich 0,05 — 0,15 M des Äthylbromids innerhalb der Versuchsfehler konstant. Nach einer gewissen Zeit wurde der gebildete Bromwasserstoff titriert. Die Titrationen wurden möglichst am Anfang der Reaktion ausgeführt, denn die von dem gebildeten Bromwasserstoff verursachte Gegenreaktion erschwert die Berechnung des Geschwindigkeitskoeffizienten der Solvolyse wegen der starken Elektrolytwirkung auf die Reaktion von HBr mit Äthanol.[5,6]

Entsprechend den Geschwindigkeitsgleichungen bei der Einwirkung von Chlorwasserstoff auf Äthanol[4] gilt bei der Solvolyse von Äthylbromid[5]:

$$dx/dt = k_2 (a - x) - k_1 x^2 \qquad (1)$$

wo k_2 und k_1 die Geschwindigkeitskoeffizienten der Solvolyse bzw. der Einwirkung von Bromwasserstoff auf Äthanol sind. Die Anfangskonzentration des Äthylbromids wird mit a bezeichnet und x ist die Konzentration des gebildeten Bromwasserstoffs. Wenn die Wirkung der Gegenreaktion zu vernachlässigen ist, erhält man k_2 nach der Gleichung:

$$k_2 = \frac{2{,}303}{t} \log \frac{a}{a-x} \qquad (2)$$

Im allgemeinen konnte die Gleichung (2) verwendet werden. Nur in absolutem Äthanol musste bei höheren Temperaturen die Berechnung nach der Gleichung (1) ausgeführt werden wegen der Gegenreaktion des Bromwasserstoffs mit Äthanol. Weil der Wert des Geschwindigkeitskoeffizienten k_1,

insbesondere bei kleinen Konzentrationen des Bromwasserstoffs, sich mit der Zunahme der Konzentration von Bromwasserstoffsäure sehr stark verändert, war die Integration der Gleichung (1) graphisch auszuführen [2] nach den Gleichungen:

$$k_2 t = \int_0^x dx/\{(a-x)-(k_1/k_2)_0 x^2/\varphi(x)\}$$
$$\log\varphi(x) = 2A'\sqrt{x}/(1 + a\sqrt{x}) \qquad (3)$$

Durch die Funktion (x) wird die Elektrolytwirkung nach der Debye-Hückelschen Theorie bei kleinen Elektrolytkonzentrationen ausgedrückt. Der Koeffizient A' wurde unter Anwendung der von Åkerlöf [7] bestimmten Werte der Dielektrizitätskonstante in den Wasser-Äthanolgemischen berechnet. Auf Grund der Werte von Grunwald und Winstein [5] wurde für a bei 55°C der Wert 1,20 berechnet. In der Tabelle 1 sind die Werte von $2A'$ und a bei 55°C und die gemäss der Debye-Hückelschen Gleichung auf 65°C und 75°C reduzierten Werte bezeichnet. Diese Werte gelten für die Darstellung der bezüglichen Elektrolytwirkung, wenn die Konzentration des Bromwasserstoffs nicht über 0,01 N steigt.

Tabelle 1.

t °C	$2A'$	a	pk_1 bei 0,00373 N	$pk_{1,0}$
75	7,54	1,24		2,02
65	7,02	1,22	3,05	2,65
55	6,70	1,20	3,70	3,32

Die Werte von $pk_{1,0}$ sind aus den von uns bei 55° und 65°C in 0,00373 N Bromwasserstofflösung gemessenen Werten mit Anwendung von $2A'$ und a der Tabelle berechnet worden. Der Wert 2.02 für $pk_{1,0}$ bei 75°C wurde mit der Arrheniusschen Gleichung aus den Werten bei 55° und 65°C berechnet. Wenn die Konzentration in Mol pro Liter Lösung ausgedrückt wird, erhält man mit $d_{55} = 0{,}7585$ aus 3,32 für $pk_{1,0}$ bei 55°C den Wert 3,20, der gut mit dem von Grunwald und Winstein [5] erhaltenen 3,185 übereinstimmt.

Aus den Tabellen 2—4, in denen die Messresultate in Äthanol bei 55°, 65° und 75°C angeführt sind, ist der Einfluss der Gegenreaktion des Bromwasserstoffs auf k_2 zu ersehen. Diese Messungen sind zugleich Beispiele für die Bestimmung der Geschwindigkeitskoeffizienten in dieser Arbeit. In den Tabellen bezeichnet g das Gewicht der Lösung in Gramm, v die von HBr verbrauchte Menge 0,01056 N $Ba(OH)_2$ in ml. x_∞ ist die Konzentration von HBr im Gleichgewicht, ermittelt mit Hilfe der entsprechenden nach der Debye-Hückelschen Gleichung aus $(k_1/k_2)_0$ berechneten Werten k_1/k_2. Beim graphischen Integrieren kann zuerst der nach der Gleichung (2) sich ergebende Wert für k_2 verwendet werden. Wenn nötig, muss man mit dem durch die graphische Integration erhaltenen Wert von k_2 die Berechnung von neuem ausführen.

Tabelle 2. Äthanollösung; 75°C; $a = 0{,}1347$; $(k_1/k_2)_0 = 5\,200$.

g	t (sec.)	v	$x \times 10^3$	pk_2 (nach 2)	pk_2 (nach 3)	k_1/k_2	$x_\infty \times 10^3$
10,014	$1{,}80 \times 10^4$	3,66	3,87	5,78	5,74	1 980	7,9
10,121	$1{,}80 \times 10^4$	3,74	3,91	5,78	5,74	1 980	7,9
9,522	$2{,}16 \times 10^4$	3,97	4,42	5,80	5,76	1 882	8,1
10,504	$2{,}52 \times 10^4$	5,00	5,04	5,81	5,76	1 775	8,4

Tabelle 3. Äthanollösung; 65 °C; $a = 0{,}1430$; $(k_1/k_2)_0 = 3\,700$.

g	t (sec.)	v	$x \times 10^3$	pk_2 (nach 2)	pk_2 (nach 3)	k_1/k_2	$x_\infty \times 10^3$
9425	$7{,}47 \times 10^4$	5,05	5,75	6,25	6,23	1205	
8891	$8{,}17 \times 10^4$	5,19	6,25	6,25	6,22	1150	10,7

Tabelle 4. Äthanollösung; 55°C; $a = 0{,}1430$; $(k_1/k_2)_0 = 2\,340$.

g	t (sec.)	v	$x \times 10^3$	pk_2 (nach 2)	pk_2 (nach 3)	k_1/k_2	$x_\infty \times 10^3$
9,904	$7{,}35 \times 10^4$	1,97	2,13	6,69	6,69	1198	
8,978	$1{,}292 \times 10^5$	3,00	3,58	6,71	6,69	987	
10,220	$1{,}292 \times 10^5$	3,48	3,65	6,70	6,68	975	
9,938	$1{,}358 \times 10^5$	3,72	4,02	6,68	6,66	942	
8,400	$1{,}418 \times 10^5$	3,17	4,05	6,69	6,67	935	
10,727	$1{,}637 \times 10^5$	4,70	4,70	6,69	6,67	880	12,19

Der Einfluss der Gegenreaktion auf die Berechnung des Geschwindigkeitskoeffizienten der Solvolyse ist bei 75°C am grössten, weil die Geschwindigkeit der Einwirkung von Bromwasserstoff auf Äthanol viel stärker mit der Temperatur steigt als die der Solvolyse. Dennoch hält sich der mit Hilfe der Gleichung (2) berechnete Geschwindigkeitskoeffizient beim Fortlaufen der Reaktion innerhalb der Versuchsfehler konstant. Dies wird dadurch verursacht, dass sich der Geschwindigkeitskoeffizient der Gegenreaktion bei der Zunahme von HBr wegen der Elektrolytwirkung stark vermindert. Zugleich wächst die Konzentration x_∞ des Bromwasserstoffs bei dem Gleichgewicht, das dem bezüglichen Wert von k_1/k_2 entspricht. Bei 65° und 55°C sind die nach den Gleichungen (2) und (3) berechneten Werte innerhalb der Versuchsfehler gleich gross. In den wasserhaltigen Gemischen braucht die Gegenreaktion nicht berücksichtigt zu werden.

Die von Grunwald und Winstein [5] für den Geschwindigkeitskoeffizienten der Solvolyse bei 55°C erhaltenen Werte, welche mit dem Fortschreiten der Reaktion kleiner werden, nähern sich bei zunehmender HBr-Konzentration dem von uns erhaltenen Wert. Der grössere Unterschied im Anfang der Reaktion bei niedrigerer HBr-Konzentration ist wahrscheinlich dadurch verursacht, dass in unseren Messungen die von dem Lösungsmittel verbrauchte Basenmenge von der in der Titration verbrauchten Menge abgezogen wurde (s. 1144).

In Tabelle 5 sind die gemessenen Geschwindigkeitskoeffizienten k_2 zusammengefasst. Mit Hilfe der bei 45°, 55°, 65° und 75°C gemessenen Werte wurden die in den Tabellen 6 und 7 angeführten Geschwindigkeitskoeffizienten $k_2'/[C_2H_5OH]$ und $k_2''/[H_2O]$ der Äthanolyse und der Hydrolyse berechnet, wobei die folgende Bezeichnung angewendet wurde:

$$k_2 = k_2' + k_2''$$

Tabelle 5. Die bei verschiedenen Temperaturen gemessenen pk_2-Werte in Äthanol (I) und in den Äthanol-Wassergemischen II, III, IV und V.

Lösungsmittel / Temperatur in °C.	I $[C_2H_5OH]$ = 21,73		II $[C_2H_5OH]$ = 20,9 $[H_2O]$ = 2,09		III $[C_2H_5OH]$ = 20,4 $[H_2O]$ = 3,40		IV $[C_2H_5OH]$ = 19,23 $[H_2O]$ = 6,41		V $[C_2H_5OH]$ = 16,51 $[H_2O]$ = 16,51	
	beob.	ber.	beob.	ber.	beob.	ber.	beob.	ber.	beob.	ber.
75	5,75	5,77	5,54	5,53	5,46	5,47	5,28	5,31	4,93	4,93
65	6,22	6,21	5,97	5,98	5,92	5,91	5,76	5,73	5,36	5,35
55	6,68	6,68	6,43	6,46	6,37	6,37	6,20	6,18	5,77	5,79
45	7,18	7,18	6,98	6,96	6,84	6,85	6,62	6,65	6,26	6,25
40			7,23	7,23						
35					7,35	7,36	7,16	7,15		
25			8,05	8,07						

Tabelle 6. $k_2'/[C_2H_5OH]$, erhalten aus den Werten von k_2 in I bzw. in I, II, III und IV; $k_2''/[H_2O]$ erhalten aus den Werten von k_2 in I und II bzw. in I, II, III und IV.

°C	$p(k_2'/[C_2H_5OH])$				$p(k_2''/[H_2O])$	
	I		I, II, III, IV		I, II	I, II, III, IV
	erhalten aus k_2	ber. nach *a*)	aus k_2	ber. nach *b*)	aus k_2	aus k_2
75	7,09	7,11	7,10	7,07	6,24	6,25
65	7,56	7,55	7,52	7,54	6,65	6,76
55	8,02	8,02	8,00	8,03	7,09	7,16
45	8,52	8,52	8,58	8,55	7,69	7,54

Tabelle 7. $p(k_2''/[H_2O])$ in verschiedenen Äthanol-Wassergemischen.

Lösungsmittel / °C	II		III		IV		V	
	aus k_2 erhalten	ber.	aus k_2 erhalten	ber.	aus k_2 erhalten	ber.	aus k_2 erhalten	ber.
75	6,27	6,24	6,29	6,31	6,25	6,29	6,18	6,18
65	6,65	6,67	6,75	6,72	6,74	6,69	6,60	6,59
55	7,08	7,13	7,16	7,15	7,15	7,12	7,00	7,02
45	7,65	7,61	7,59	7,61	7,54	7,57	7,49	7,48
40	7,87	7,87						

Die auf Grund der Werte von k_2 in absolutem Äthanol (Lösung I) berechneten Werte von $k_2'/[C_2H_5OH]$ befinden sich in der zweiten Kolumne der Tabelle 6. Aus diesen Werten ergeben sich für die Koeffizienten E und A der Arrheniusschen Gleichung:

$$k = Ae^{-E/RT}$$

folgende Werte:

a) $E = 24{,}05$ kcal; $\log A = 7{,}90$

Diese, sowie alle anderen hier angegebenen Werte von E und A sind nach der Methode der kleinsten Quadrate berechnet worden. Die berechneten Werte der Kolumne 3 in Tabelle 6 sind mit Anwendung der Werte *a*) berechnet worden. Die 6. Kolumne enthält die Werte $k_2''/[H_2O]$, aus den Werten von k_2 in den Lösungen I und II berechnet. Ausserdem wurden $k_2'/[C_2H_5OH]$ und $k_2''/[H_2O]$ auf Grund der Werte von k_2 in den Lösungen I, II, III und IV nach der Methode der kleinsten Quadrate berechnet. Die in dieser Weise erhaltenen Werte befinden sich in den Kolumnen 4 und 7 der Tabelle 6. Ein Vergleich der letztgenannten, unter Berücksichtigung aller mit Lösungen I, II, III und IV erhaltenen Werte, mit den Werten der Kolumnen 2 bzw. 6 zeigt, dass die Übereinstimmung in Bezug auf $k_2'/[C_2H_5OH]$ besser ist als in Bezug auf $k_2''/[H_2O]$. Die Unterschiede bei $k_2'/[C_2H_5OH]$ übersteigen kaum die Versuchsfehler. Doch ist auch in Bezug auf $k_2'/[C_2H_5OH]$ mit Änderung der Temperatur ein merkbarer Gang zu erkennen. Dies ist ersichtlich, wenn man die sich aus den Angaben der Kolumne 4 ergebenden Werte

b) $E = 25{,}11$ kcal ; log $A = 8{,}59$

mit den Werten *a*) vergleicht. Die Kurven 1 der Abbildung 1 zeigen die nach den Werten *a*) und *b*) berechnete Abhängigkeit des Geschwindigkeitskoeffizienten von der Temperatur.

Wegen der verhältnismässig nahen Übereinstimmung der Werte $k_2'/[C_2H_5OH]$ der Kolumnen 2 und 4 der Tabelle 6 sind die Werte der Kolumne 4 wahrscheinlich annähernd gleich den Werten von $k_2'/[C_2H_5OH]$ in je einem der Gemische II, III und IV. Deshalb wurde $k_2''/[H_2O]$ mit Hilfe der nach den Werten *b*) sich ergebenden Werte von $k_2'/[C_2H_5OH]$ in jeder der Lösungen II, III und IV einzeln berechnet. Auch in dem von den übrigen Gemischen betreffend Zusammensetzung am meisten abweichenden Gemische V wurde $k_2''/[H_2O]$ in derselben Weise berechnet, obgleich es in die obigen Berechnungen nicht aufgenommen war, da in diesem Fall die Äthanolyse neben der Hydrolyse von untergeordneter Bedeutung ist und die Berechnung von $k_2''/[H_2O]$ deshalb weniger von der Genauigkeit des Wertes von $k_2'/[C_2H_5OH]$ abhängt. Die nach dem obigem erhaltenen Werte von $k_2''/[H_2O]$ sind in Tabelle 7 angegeben.

Ausser den Messungen bei 45°, 55°, 65° und 75°C sind in den Tabellen 5 und 7 auch die Ergebnisse der Messungen bei einigen niedrigeren Temperaturen angegeben. Die berechneten Werte der Tabellen 5, 6 und 7 sind mit den in der Tabelle 9 angeführten Werten von $\log A$ und E erhalten worden. Die Übereinstimmung der berechneten Werte mit den gemessenen ist auch bei den Temperaturen 25°, 35°, und 40°C gut; die bei diesen Temperaturen

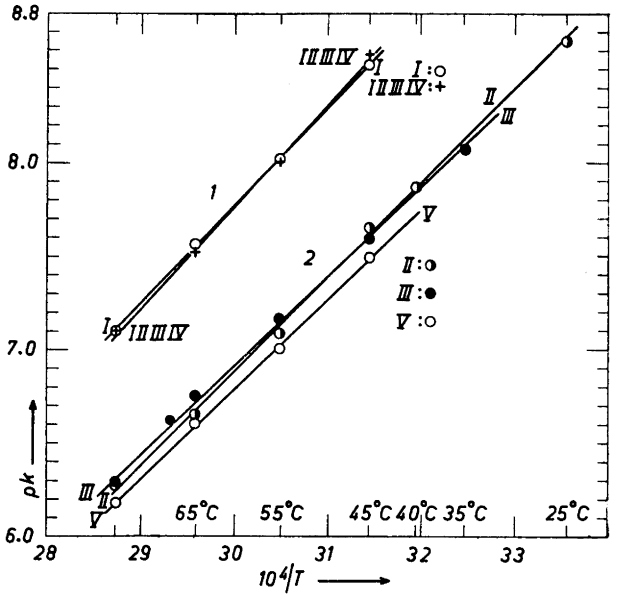


Abbildung 1. Die Abhängigkeit der Geschwindigkeitskoeffizienten von der Temperatur. 1 : p(k_2'/[C_2H_5OH]) nach den Messungen in Äthanol (I) und in den Gemischen I, II, III und IV. 2 : p (k_2''/[H_2O]) in den Gemischen II, III und V.

ausgeführten Messungen wurden zur Berechnung der Temperaturkoeffizienten nicht verwendet.

Die Abhängigkeit der Geschwindigkeitskoeffizienten k_2'/ [C_2H_5OH] und k_2''/ [H_2O] von der Temperatur in verschiedenen Gemischen ist aus der Abbildung 1 ersichtlich.

DISKUSSION

Wie aus Tabellen 6 und 7 und aus der Abbildung 1 zu ersehen ist, übersteigt die Änderung von k_2'/ [C_2H_5OH] mit der Zusammensetzung des Wasser-Äthanolgemisches kaum die Versuchsfehler der bei 45° bis 75° ausgeführten Messungen der Gemische I, II, III und IV. Auch betreffend k_2''/ [H_2O] ist ist die Änderung der Gemische II, III und IV verhältnismässig klein. Danach ist die Geschwindigkeit der Äthanolyse und der Hydrolyse in den genannten Gemischen annähernd proportional der stöchiometrischen Konzentration des Äthanols bzw. des Wassers. In dem Gemisch V weicht der erhaltene Wert von k_2''/ [H_2O] etwas mehr von den in den anderen Gemischen berechneten Werten ab, als sich die in diesen erhaltenen Werte voneinander unterscheiden.

In Tabelle 8 ist der Wert des Verhältnisses k_2''/ [H_2O] : k_2'/[C_2H_5OH] in verschiedenen Wasser-Äthanolgemischen und bei verschiedenen Temperaturen dargestellt. Der Wert nimmt beim Abnehmen der Temperatur zu. Das Gemisch V unterscheidet sich von den übrigen Gemischen II, III und IV

dadurch, dass der Geschwindigkeitskoeffizient der Hydrolyse im Gemisch V im Vergleich mit dem Geschwindigeitskoeffizienten der Äthanolyse grösser ist in den anderen Gemischen.

Tabelle 8. Das Verhältnis $k_2''/[H_2O]:k_2'/[C_2H_5OH]$.

Lösungsmittel / °C	II	III	IV	V
75	6,7	5,7	6,0	7,8
65	7,3	6,6	7,0	9,0
55	8,0	7,6	8,1	10,2
45	8,6	8,8	9,5	10,7

Tommila, Tiilikainen und Voipio [8] haben die Geschwindigkeitskoeffizienten der Hydrolyse verschiedener Alkylhalogenide in Aceton-Wassergemischen gemessen und auf Grund der Abhängigkeit der Aktivierungsenergie und der Aktivierungsentropie von der Zusammensetzung des Gemisches den Einfluss der Solvatation auf die Hydrolysegeschwindigkeit diskutiert.

Auch in den Wasser-Äthanolgemischen ist wegen der Bildung der Wasser-Äthanolsolvate die Solvatation bei der Diskussion der Abhängigkeit der Hydrolyse- und Äthanolysegeschwindigkeit von der Zusammensetzung des Gemisches zu berücksichtigen. Der Einfluss der Zusammensetzung des Wasser-Äthanolgemisches auf die Geschwindigkeit der Solvolyse von Äthylbromid erscheint am deutlichsten in der Abhängigkeit der Geschwindigkeitskoeffizienten von der Temperatur und dementsprechend auch in den in der Tabelle 9 dargestellten Werten der Aktivierungsenergie E, der Aktionskonstante A und der Aktivierungsentropie ΔS^*.

Tabelle 9. Aktivierungsenergie, Aktionskonstante und Aktivierungsentropie der Solvolyse von Äthylbromid in Wasser-Äthanolgemischen.

Reaktion	Lösungsmittel	E (kcal)	log A	ΔS^* (cal)
Äthanolyse	I	24,05	7,90	−22,8
»	I II III IV	25,11	8,59	−19,6
Hydrolyse	II	23,28	8,28	−21,5
»	III	21,95	7,38	−25,2
»	IV	21,79	7,30	−25,6
»	V	22,17	7,65	−24,0

Der verhältnismässig geringe Einfluss der Änderung der Zusammensetzung des Lösungsmittels auf die Geschwindigkoeffizienten der Äthanolyse und der Hydrolyse wird von den miteinander parallelen Veränderungen von E und ΔS^* verursacht. Entgegen der durch das Steigen von E verursachten Verkleinerung des Geschwindigkeitskoeffizienten wirkt das gleichzeitige Steigen

der Aktivierungsentropie, welches auf den Geschwindigkeitskoeffizienten nach der Gleichung [9].

$$A = 2{,}1 \times 10^{10}\ T\ e^{\Delta S^*/T}$$

erhöhend einwirkt.

Beim Hinzufügen von Wasser zu Äthanol steigt sowohl E als ΔS^* der Äthanolyse. Dieses kann als von der Solvatation der Äthanolmoleküle durch die Wassermoleküle verursacht erklärt werden. Denn hierdurch sinken die Äthanolemoleküle auf ein niedrigeres Energieniveau, was eine Vergrösserung der Aktivierungsenergie veranlasst. Zugleich wirkt die Solvatation auf die Ordnung der Atome der reagierenden Komponente vergrössernd, weshalb die Verkleinerung der Entropie bei der Bildung des einen grösseren Ordnungsgrad und eine niedrigere Entropie besitzenden Übergangskomplexes geringer ist als in dem wasserfreien Äthanol. Dementsprechend ist die Aktivierungsentropie der Äthanolyse in wasserhaltigem Äthanol weniger negativ als in wasserfreiem Äthanol.

Weil die Berechnung von $k_2''/[H_2O]$ nur indirekt aus k_2 durch Anwendung der mit gewissen Annahmen berechneten Werte von $k_2'/[C_2H_5OH]$ auszuführen ist, kann die Abhängigkeit der Aktivierungsenergie und der Aktivierungsentropie von der Zusammensetzung des Gemisches in Bezug auf $k_2''/[H_2O]$ nur in grossen Zügen betrachtet werden. In entsprechender Weise wie bei der Äthanolyse kann das Steigen von E und ΔS^* der Hydrolyse bei Zunahme der Äthanolkonzentration in den Gemischen II, III und IV als von der Solvatation verursacht erklärt werden. Denn in diesem Fall ist die Solvatation der Wassermoleküle durch die Äthanolmoleküle verhältnismässig um so vollständiger, je geringer die Konzentration des Wassers ist. Beim Übergang von IV zu V ist die Veränderung von E und ΔS^* von den erwähnten Verhältnissen abweichend, indem sowohl E als ΔS^* bei der Abnahme der Äthanolkonzentration steigen. Das Ansteigen des ΔS^* beim Übergang von IV zu V könnte erklärt werden durch Abnahme der Entropie der Wassermoleküle, z.B. durch Assoziation, welche bei kleineren Äthanolkonzentrationen eine grössere Wirkung auf die Aktivierungsentropie hat als die Solvatation durch die Äthanolmoleküle.

Nach der obigen Betrachtung kann bezüglich der Werte von E und ΔS^* der behandelten Solvolysereaktionen die Abhängigkeit von der Zusammensetzung des Lösungsmittels in den wasserärmsten Gemischen als von den veränderten Solvatationshältnissen verursacht erklärt werden. Die trotz der Änderung von E und ΔS^* relativ gute Konstanz der Geschwindigkeitskoeffizienten bei der Veränderung der Zusammensetzung des Gemisches beruht darauf, dass die Veränderung von E und die von ΔS^* in ihrer Wirkung auf die Geschwindigkeitskoeffizienten sich zum grössten Teil gegenseitig kompensieren.

Bei der Ausführung der Messungen sind mir K. Arnala, Eva Lindell, P. Ollari, Hilkka Siltanen, und L. Uino behilflich gewesen.

Die Ausführung dieser Arbeit ist von *Valtion Luonnontieteellinen Toimikunta* mit einem Stipendium unterstützt worden, wofür ich meinen Dank ausspreche.

LITERATUR

1. Kilpi, S. *Suomen Kemistilehti* **26 B** (1953) 9.
2. Lund, H. und Bjerrum, J. *Ber.* **64** (1931) 210.
3. Gattermann-Wieland, *Die Praxis des organischen Chemikers*, 36. Aufl., Walter de Gruyter & Co., Berlin 1954, S. 86.
4. Kilpi, S. *Z. physik. Chem.* **86** (1914) 427.
5. Grunwald, E. und Winstein, S. *J. Am. Chem. Soc.* **69** (1947) 2051.
6. Kilpi, S., *Z. physik. Chem.* **A 166** (1933) 289.
7. Åkerlöf, G. *J. Am. Chem. Soc.* **54** (1932) 4125.
8. Tommila, E., Tiilikainen, M. und Voipio, A. *Ann. Acad. Sci. Fennicae, Ser* **A II** *65* (1955).
9. Glasstone, S., Laidler, K. J. und Eyring, H. *The Theory of Rate Processes.* New York 1941, S. 416, 452.

Eingegangen am 3. Mai 1957.

ACTA CHEMICA SCANDINAVICA 11 (1957) 1153—1156

Amines Related to Adrenaline Containing Nuclear Chlorine

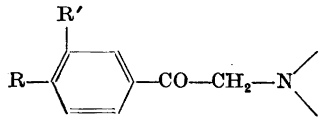
RICHARD DAHLBOM and ALFONS MISIORNY

Research Laboratories, AB Astra, Södertälje, Sweden

A number of amines related to adrenaline and noradrenaline containing nuclear chlorine have been prepared and tested for antiadrenaline and antinoradrenaline activity.

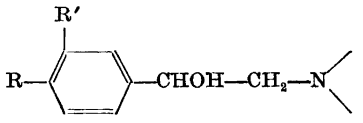
Several investigators have been interested in amines related to adrenaline and noradrenaline containing chlorine in the 3- and/or 4-position of the benzene nucleus. Thus Glynn and Linnell [1] prepared α-3,4-dichlorophenyl-β-aminoethanol from 3,4-dichloro-ω-aminoacetophenone. Edkins and Linnell [2] synthesised a number of ω-aminoacetophenones containing halogen substituents in 3- or 4-position but were unable to reduce them to the corresponding alcohols. Similar difficulties met Hansen [3] who prepared 3-chloro-4-hydroxy-ω-methylaminoacetophenone. However, the synthesis of α-(3-chloro-4-hydroxyphenyl)-β-methylaminoethanol and its ethyl analogue was performed by Fosdick, Fancher and Urbach [4] by catalytic hydrogenation of the corresponding N-benzylated acetophenones. Finally Lutz *et al.*[5] during their search for new antimalarials prepared a number of halogen substituted dialkylaminoacetophenones which were reduced to the corresponding alcohols by means of aluminium *iso*propoxide.

In the course of an investigation on drugs with potential antiadrenaline effect, a number of compounds of type I and II were synthesised. As amino components, piperidine and substituted piperazines were mainly used because of the presence of these amines in well-known adrenergic blocking drugs [6,7].



R = Cl, OH; R′ = H, Cl

I

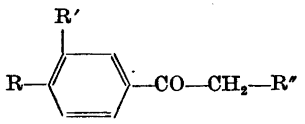


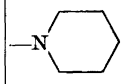
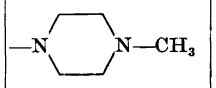
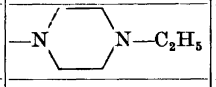
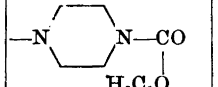
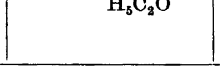
R = Cl; R′ = H, Cl

II

The compounds of type I were easily obtained from the appropriate ω-chloroacetophenone and the desired amine. The compounds of type II were prepared by the reduction of the corresponding amino ketone with lithium

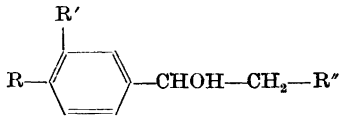
Table 1.

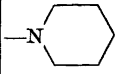
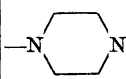


No.	R	R′	R″	Yield [a] %	Derivative analysed	M. p. °C	Recryst. solvent [b]	Formula	Analyses, %					
									Calc.			Found		
									C	H	N	C	H	N
1	Cl	H		85	Base	52— 53	P	$C_{13}H_{16}ClNO$	65.7	6.78	5.89	65.3	6.46	5.55
					HCl	222—223	A	$C_{13}H_{16}ClNO \cdot HCl$	56.9	6.25	5.11	56.5	6.33	5.39
2	OH	Cl		87	HCl	268—270 (decomp.)	A—E	$C_{13}H_{16}ClNO_2 \cdot HCl$	53.8	5.91	4.83	53.6	6.14	4.50
3	Cl	Cl		70	HCl	249—251	A—P	$C_{13}H_{15}Cl_2NO \cdot HCl$	50.6	5.23	4.54	50.6	5.53	4.57
4	Cl	H	—NH—C_2H_5	41	HCl	246—248 (decomp.)	A	$C_{10}H_{12}ClNO \cdot HCl$	51.3	5.59	5.98	51.5	5.65	5.91
5	Cl	H		55	HCl	248—249 (decomp.)	A—Aq	$C_{13}H_{17}ClN_2O$ 2 HCl · 2 H_2O	43.2	6.41	7.75	43.7	6.62	7.81
6	Cl	Cl		69	HCl	252—254 (decomp.)	A	$C_{13}H_{16}Cl_2N_2O \cdot 2$ HCl	43.4	5.04	7.78	43.4	5.09	7.66
7	Cl	H		56	HCl	266—268 (decomp.)	A—Aq	$C_{14}H_{19}ClN_2O \cdot 2$ HCl	49.5	6.23	8.25	49.3	6.26	8.24
8	Cl	H		87	HCl	196—197 (decomp.)	A—E	$C_{15}H_{19}ClN_2O_3 \cdot HCl$	51.9	5.80	8.07	52.1	5.86	8.02
9	Cl	Cl		67	Base	108—109	M	$C_{15}H_{18}Cl_2N_2O_3$	52.2	5.25	8.12	52.2	5.06	7.85
					HCl	212—214 (decomp.)	A—E	$C_{15}H_{18}Cl_2N_2O_3 \cdot HCl$				c		

a Calc. on the crude products.
b A, ethanol; Aq, water; E, ether; M, methanol; P, petroleum ether.
c Calc. Cl 27.9; found 27.9.

Table 2.



No.	R	R′	R″	Yield [a] %	Derivative analysed	M. p. (B. p.) °C	Recryst. solvent [b]	Formula	Analyses, %					
									Calc.			Found		
									C	H	N	C	H	N
10	Cl	H		71	Base	68.5—70	A—Aq	$C_{13}H_{18}ClNO$	65.1	7.56	5.84	65.1	7.46	5.61
11	Cl	Cl		72	Base	89—90	M	$C_{13}H_{17}Cl_2NO$	56.9	6.25	5.11	57.4	6.37	5.05
12	Cl	H	—NH—C_2H_5	37	Base	190/0.8 mm Hg 87—88 [c]		$C_{10}H_{14}ClNO$	60.1	7.07	7.02	59.9	6.84	7.06
13	Cl	H		55	Base	85—85.5	M—Aq	$C_{13}H_{19}ClN_2O$	61.3	7.52	11.0	61.2	7.45	10.7
					HCl	236—237 (decomp.)	A	$C_{13}H_{19}ClN_2O \cdot 2\,HCl$			8.55	*d*		8.42
14	Cl	Cl		49	Base	121—122	A—Aq	$C_{13}H_{18}Cl_2N_2O$	54.0	6.27	9.69	53.8	6.20	9.49

a, *b* See Table 1.
c M. p. of solidified distillate.
d Calc. Cl 32.5; found 32.3.

aluminium hydride. The new compounds are listed in Tables 1 and 2. They have been tested for antiadrenaline and antinoradrenaline activity by Professor U.S. von Euler, Department of Physiology, Karolinska Institutet, Stockholm. In experiments on the blood pressure of cats, a weak antagonism towards adrenaline and noradrenaline was shown by the piperidino compounds 1, 10, and 11.

EXPERIMENTAL

Preparation of the amino ketones. The halogen substituted ω-chloroacetophenones required as starting material were prepared according to procedures described in literature [1,3,8].

The amino ketones were all prepared in essentially the same way. The appropriate ω-chloroacetophenone (0.025 mole) and the amine (0.065 mole) were dissolved in toluene (usually 25 ml) and the reaction mixture was kept at room temperature overnight. The amine hydrochloride was removed by filtration and the toluene solution was washed with water and then extracted with 2 N hydrochloric acid. The extract was made alkaline with sodium carbonate solution and the precipitated base was extracted with ether. The ether was dried over sodium sulphate and the amino ketone was then isolated as the hydrochloride by the addition of ethereal hydrogen chloride and recrystallised. The physical properties of these compounds are listed in Table 1.

Preparation of the amino alcohols. A solution of the free amino ketone (0.02 mole) in ether (100 ml) was prepared from the pure hydrochloride and was added, with mechanical stirring, to a suspension of lithium aluminium hydride (0.015 mole) in ether (100 ml). The mixture was stirred under reflux for 15 min. Excess hydride was destroyed with water and the mixture was made alkaline with 2 ml of 5 N sodium hydroxide. The ethereal layer was then decanted and dried over sodium sulphate. Evaporation of the solvent yielded the almost pure crystalline amino alcohol. In one case (compound 12), an oily product was obtained which was purified by distillation. The physical properties of the amino alcohols are listed in Table 2.

REFERENCES

1. Glynn, H. E. and Linnell, W. H. *Quart. J. Pharmacol.* **5** (1932) 480.
2. Edkins, R. P. and Linnell, W. H. *Quart. J. Pharmacol.* **9** (1936) 75.
3. Hansen, H. L. *J. Am. Chem. Soc.* **59** (1937) 280.
4. Fosdick, L. S., Fancher, O. and Urbach, K. F. *J. Am. Chem. Soc.* **68** (1946) 840.
5. Lutz, R. E., Allison, R. K., Ashburn, G., Bailey, P. S., Clark, M. T., Codington, J. F., Deinet, A. J., Freek, J. A., Jordan, R. H., Leake, N. H., Martin, T. A., Nicodemus, K. C., Rowlett, R. J. Jr., Shearer, N. H. Jr., Smith, J. D. and Wilson, J. W. III, *J. Org. Chem.* **12** (1947) 617.
6. Bovet, D. and Simon, A. *Arch. intern. pharmacodynamie* **55** (1937) 15.
7. Swain, A. P. and Naegele, S. K. *J. Am. Chem. Soc.* **76** (1954) 5091.
8. Collet, A. *Compt. rend.* **125** (1897) 717.

Received March 19, 1957.

ACTA CHEMICA SCANDINAVICA 11 (1957) 1157—1161

The Chemistry of the Natural Order Cupressales

XVIII *. Nootkatene, a New Sesquiterpene Type Hydrocarbon from the Heartwood of *Chamaecyparis nootkatensis* (Lamb.) Spach.

H. ERDTMAN and J. G. TOPLISS

Organisk-kemiska institutionen, Kungl. Tekniska Högskolan, Stockholm, Sweden

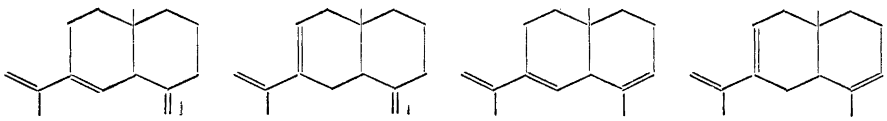
A preliminary study of the neutral constituents of the heartwood extractives of "Alaska yellow cedar" (*Chamaecyparis nootkatensis*) has been carried out. Terpenoid hydrocarbons, alcohols and carbonyl containing compounds were obtained in addition to carvacrol methyl-ether previously reported. A sesquiterpene hydrocarbon "nootkatene" was isolated in an apparently pure state. It contains three double bonds, two of which are conjugated and since it yields eudalene on dehydrogenation appears to be a dehydroselinene. The alcohol fraction similarly yielded 1-methyl-7-ethyl-naphthalene. Like the carbonyl fraction it appears to contain C_{14}-components, presumably related to nootkatene

Earlier investigations [1] have shown that the heartwood of *Chamaecyparis nootkatensis* contains a large quantity of extractable neutral material in addition to nootkatin [2], carvacrol [1] and chamic and chaminic acids [3]. A previous examination of the low boiling neutral oils revealed the presence of carvacrol methyl ether [4].

The sesquiterpene fraction of the neutral oil has now been examined and we wish to give a preliminary account of the findings. Fractional distillation has shown the main hydrocarbon component to be a liquid b.p. 134°/11 mm, n_D^{25} 1.5222, $[\alpha]_D$ —177° ($CHCl_3$), d_{24}^{24} 0.933, $[R_L]_D$ 66.86, for which the name *nootkatene* is proposed. The carbon-hydrogen analysis corresponds to a molecular formula of $C_{15}H_{22}$ and catalytic hydrogenation revealed the presence of 3 double bonds in the molecule. Dehydrogenation with selenium gave eudalene in moderate yeld, identified as the picrate. Moreover, the ultraviolet absorption spectrum of the compound shows a maximum at 235 mμ, ε 13 500, indicative of a conjugated diene system with three or four substituents, and the infra-red absorption spectrum (very strong band at 890 cm^{1-} and strong

* Part XVII *Acta Chem.Scand.* **10** (1956) 1563.

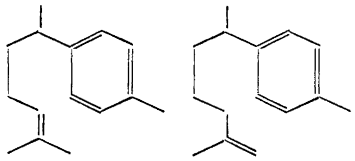
band at 827 cm^{-1}) points to the presence of a terminal methylene group and a trisubstituted double bond. Ozonolysis afforded formaldehyde but no acetone. Hence these preliminary studies reveal that nootkatene can be regarded as a dehydroselinene, the most probable structral possibilities being I to IV although certain other structures are not rigidly excluded on the basis of the present evidence.



I II III IV

The conjugated double bond system as given in formulae I to IV would give on 1,4-addition a tetrasubstituted double bond which might be expected to be rather unreactive. Since catalytic hydrogenation of nootkatene using 10 % palladium charcoal in ethanol and the action of bromine in chloroform resulted in incomplete addition to the third double bond the results may be cited as evidence in favour of the position of the diene system as shown.

The only previously reported naturally occurring $C_{15}H_{22}$ sesquiterpene type hydrocarbon appears to be *ar*- curcumene [5] (V and VI). Further studies on the structure of nootkatene are in progress.



V VI

The sesquiterpene "alcohol" fraction of *Chamaecyparis nootkatensis* has also been briefly examined. Selenium dehydrogenation yielded 1-methyl-7-ethylnaphthalene in fair yield, identified as the picrate. Chromatography of the fraction revealed the presence of a small proportion of a component or components having an α/β-unsaturated carbonyl function. Both the latter and the alcohol portion appear to be mixtures containing mainly C_{14} compounds. Efforts are now being made to find a suitable procedure for separating these compounds.

EXPERIMENTAL

Isolation of sesquiterpene components from the heartwood. Finely divided heartwood (12 kg) was extracted with acetone and the extract separated into crude acidic, phenolic and neutral fractions as described previously [1]. The crude "neutral" material (294 g) thus obtained, was distilled *in vacuo* yielding 215 g of distillate b.p. 100–190°/5 mm. This oil was then subjected to careful fractional distillation *in vacuo* using a silvered, vacuum jacketed double glass spiral column. A section of the distillation data obtained is given in Table 1.

Table 1. Pressure 11 mm. Back pressure 15 mm. Reflux ratio 25:1. Take off rate *ca.* 10 ml/hour

Fraction	Vol. of fraction (ml)	Temp.* °C	$n_D^{16.5}$	$[\alpha]_D$ ($CHCl_3$)
a	3	132.0	1.5171	−41.5
b	3	132.5	1.5175	−53
c	4	133.25	1.5298	−82
d	3	133.75	1.5211	−107
e	3	133.75	1.5220	−126
f	3	134.0	1.5233	−146
g	3	134.0	1.5240	−160
h	3	134.0	1.5247	−169
i	3	134.0	1.5250	−175
j	3	134.0	1.5256	−177
k	3	134.0	1.5256	−166
l	3	141.5	1.5247	−149

* Temperatures were taken at the end of each fraction.

Fraction (j) was analysed by the sorption method of Blohm [6] with the following results. Sample n_D^{25} 1.5221. Fractions, as removed from silica gel column (1) n_D^{25} 1.5212 (2) n_D^{25} 1.5221 (3) n_D^{25} 1.5222 (4) n_D^{25} 1.5222 (5) n_D^{25} 1.5222 (6) n_D^{25} 1.5220. Thus this result coupled with the distillation data provides good evidence for the fact that fraction (j) is an essentially pure sample of a new sesquiterpene hydrocarbon, *nootkatene*. The physical data relating to nootkatene (all determined on fraction j) may then be stated as follows: b.p. 134°/11 mm; n_D^{25} 1.5222; $[\alpha]_D$ −177° (*c* 2.02 in $CHCl_3$); d_{24}^{24} 0.933; $[R_L]_D$ 66.86; ultra-violet spectrum, max 235 mμ (ε 13 500); infra-red spectrum, very strong band at 890 cm^{-1} and strong band at 827 cm^{-1}. (Found: C 88.60; H 10.77. $C_{15}H_{22}$ requires: C 89.02; H 10.96)

Nootkatene did not give a crystalline adduct on refluxing with maleic anhydride in dry xylene for 5 h nor a crystalline hydrochloride on treatment with dry hydrogen chloride in dry ether at −10° for 1 h.

Hydrogenation experiments. (a) Nootkatene (0.268 g) was hydrogenated in glacial acetic acid solution (25 ml) in the presence of Adams' catalyst (0.051 g) at room temperature and atmospheric pressure. Hydrogenation ceased after 108 ml (3.1 mole) of hydrogen had been absorbed in 40 min. The rate of uptake of the third mole was somewhat slower than that of the first two.

(b) A further sample of the hydrocarbon (0.202 g) in ethanol (20 ml) was reduced at atmospheric pressure and room temperature in the presence of a 10 % palladium charcoal catalyst (0.071 g). 51 ml (2 mole) of hydrogen were absorbed in 18 min. The rate of uptake then dropped noticeably and 70 % of a third mole of hydrogen was absorbed over 65 min at which point the hydrogenation ceased.

Bromine titration. To nootkatene (0.5111 g) in chloroform (10 ml) was added a solution of bromine in chloroform of known concentration from a burette. 39.4 ml of the bromine solution (≡ 2 mole of bromine) was rapidly decolourised. A further 8.7 ml was then decolourised at an appreciably slower rate after which the uptake became too slow for effective measurement.

Dehydrogenation. Nootkatene (0.53 g) was heated with selenium powder (1 g) for 13 h at 300°±10°. The product was extracted with ether and after filtration the ether was evaporated and the residue distilled *in vacuo*, giving a faintly coloured oil (0.423 g), b.p. *ca.* 130°/7 mm, showing an ultra-violet absorption spectrum typical of a naphthalene hydrocarbon *viz.* max 227, 280, and 320 mμ, ε 36 000, 2 000 and 240, respectively. The picrate which crystallised out on mixing concentrated warm ethanolic solutions of the hydrocarbon (0.40 g) and picric acid (0.40 g) had m.p. 93−94° (corr) and amounted to 0.110 g. The mother liquors on concentration yielded a further 0.125 g of picrate m.p. 89−91° (corr). Recrystallisation of the first picrate batch from ethanol gave pure eudalene picrate as fine needles m.p. 93.5−94.5 (corr.), undepressed on admixture with authentic eudalene picrate.

Ozonolysis. Nootkatene (0.483 g) dissolved in a mixture of dry chloroform (8 ml) and dry carbon tetrachloride (2 ml) was ozonised until no more ozone was being taken up as indicated by iodine titration (*ca.* 30 min). The exit gases were bubbled through a trap containing a small quantity of water and after the ozonolysis was complete the water in the trap was mixed with an equal volume of concentrated aqueous dimedone solution and on scratching a small quantity of formaldehyde-dimethone separated m.p. 190—191° (corr), undepressed on admixture with authentic formaldehyde-dimethone. The ozonide was obtained as a glass by evaporation of the solvent under water pump vacuum at 0°. The exient vapours during this evaporation were passed through an aqueous solution of 2,4-dinitrophenylhydrazine hydrochloride but no significant precipitate was obtained. Water was added to the ozonide and the mixture was refluxed for 30—60 min with precautions for trapping any outgoing vapours with 2,4-dinitrophenylhydrazine hydrochloride solution. However no volatile aldehydes or ketones were detected during this period. The mixture was then distilled into aqueous 2,4-dinitrophenylhydrazine hydrochloride solution whereupon an insoluble 2,4-dinitrophenylhydrazone was precipitated. After a short time this was collected by filtration and dried, m.p. 162—165° (corr), undepressed on admixture with authentic formaldehyde 2,4-dinitrophenylhydrazone, m.p. 167—168° (corr). The non-steam volatile product was extracted with ether and the acidic material was separated by alkali extraction and isolated as a gum by acidification and ether extraction in the usual way (0.193 g). The neutral portion, obtained as an oil, amounted to 0.083 g. Both the acidic and neutral products failed to crystallise.

Sesquiterpene "alcohol" fraction. From the continuation of the fractional distillation of the oil described in the isolation of nootkatene a considerable number of fractions, amounting in all to 50—60 ml of viscous oil, b.p. 140—150°/3 mm, $n_D^{16.5}$ 1.5179—1.5254, $[\alpha]_D$ +31 — +107°, were obtained. The physical constants of the various fractions showed a definite drift between the limits given but it was clear that no clear cut separation of the components had occurred. The middle fractions, which showed an appreciable absorption in the ultra-violet with a maximum at 235 mμ and ε values of 2 000—3 000 were further investigated as described.

Dehydrogenation. "Alcohol fraction" (1.2 g) was heated with selenium powder (2.0 g) at 290—300°. After 4 h a further 1.0 g of selenium was added and the dehydrogenation was continued for a further 18 h at the same temperature. The product was isolated by ether extraction and distilled *in vacuo* affording 0.482 g of distillate b.p. 120—160°/7 mm (bath temp) which was then passed through a short alumina column in petroleum ether (40—60°) yielding 0.334 g of purified product. The ultra-violet absorption spectrum of the product showed maxima at 228, 280 and 321 mμ typical of a naphthalene hydrocarbon. The hydrocarbon picrate prepared in the usual manner melted at 95.5—96.5° (corr) after recrystallisation from ethanol (Found: C 57.03; H 4.78; N 10.54. Calc. for $C_{19}H_{17}O_7N_3$: C 56.99; H 4.28; N 10.50). Thus the analysis of the picrate suggests that the molecular formula of the hydrocarbon is $C_{13}H_{14}$. The hydrocarbon trinitrobenzene adduct prepared from the hydrocarbon and somewhat less than the theoretical quantity of 1,3,5-trinitrobenzene in methanol crystallised from methanol as yellow needles, m.p. 106.5—107.5° (corr.) (Found: N 11.12. $C_{19}H_{17}O_6N_3$ requires N, 10.96). The melting point of the picrate was not depressed on admixture with a synthetic specimen of 1-methyl-7-ethylnaphthalene picrate, kindly supplied by Prof. D. H. R. Barton, or with a specimen of the same compound prepared from santonin and kindly supplied by Prof. W. Cocker.

Chromatography of "Alcohol fraction". "Alcohol fraction" (1.89 g) was dissolved in a small volume of petroleum ether (40—60°) and chromatographed on a column of alumina (175 g). Elution with 15 % ether in benzene removed a component (0.317 g) having the following constants: n_D^{22} 1.5269, $[\alpha]_D$ +189 (*c* 1.7 in $CHCl_3$), ultra-violet absorption spectrum: max 235 mμ (ε 10 900); 306 mμ (ε 74). (Found: C 81.50; H 10.13. $C_{14}H_{20}O$ requires C 82.30; H 9.87. $C_{14}H_{22}O$ requires C 81.30; H 10.75). The ultra-violet absorption data is compatible with the component containing an α/β-unsaturated carbonyl function which was confirmed by the preparation of a semicarbazone using semicarbazide hydrochloride and sodium acetate in aqueous ethanol. The semicarbazone crystallised in ill defined prisms from ethanol or ethyl acetate, m.p. 190—192° (corr), unchanged on further recrystallisation, $[\alpha]_D$ +210° (*c* 0.2 in $CHCl_3$). Ultra-violet absorption, max 268 mμ (ε 28 500). (Found: C 68.47; H 9.05; N 14.61; 14.77. $C_{15}H_{24}ON_3$ requires C 68.68; H 9.21; N 16.02).

The indications are that the semicarbazone is not a single compound. The chromatography did not appear to give a very good separation of the other components of the mixture.

We are indebted to *Statens Naturvetenskapliga Forskningsråd* for financial support and to Dr. G. Widmark, Stockholms Högskola, for the sorption analysis.

REFERENCES

1. Carlsson, B., Erdtman, H., Frank, A. and Harvey, W. E. *Acta Chem. Scand.* **6** (1952) 690.
2. Duff S. R., Erdtman, H. and Harvey, W. E. *Acta Chem. Scand.* **8** (1954) 1073.
3. Erdtman, H., Harvey, W. E. and Topliss, J. G. *Acta Chem. Scand.* **10** (1956) 1381.
4. Duff, S. R. and Erdtman, H. *Chemistry & Industry* **1953** 747.
5. Carter, F. D., Copp, F. C., Sanjiva Rao, B., Simonsen, J. L. and Subramaniam, K. S. *J. Chem. Soc.* **1939** 1504.
6. Blohm, S. G. *Arkiv Kemi* **6** (1953) 317.

Received April 13, 1957.

ACTA CHEMICA SCANDINAVICA 11 (1957) 1162—1168

Characterization of Polyelectrolyte Solutions

I. Molecular Fractionating on Ion Exchange Resins

NILS HARTLER

Uddeholms Aktiebolag, Cellulose Research Laboratory, Skoghall, Sweden *

The screening effect of anion exchange resins upon a polyelectrolyte solution containing anions of varying size is discussed. In experiments with polystyrene sulphonic acid no change in this screening effect has been found when under equilibrium conditions resins of varying degree of cross-linking are used. However, a variation in the porosity of the resin gives a change in the screening properties; a resin of high porosity being able to retain larger ions as compared with a resin of low porosity.

Resins of varying porosity are used in an ion exchange battery for the fractionation, based on differing ion size, of polyelectrolyte solutions. The limitations of the method are pointed out.

Several years ago Samuelson [1] demonstrated that anion exchange resins have a screening effect on the ions in a solution of a polyelectrolyte. When such a solution is passed through a column containing an anion exchange resin, the ions whose size is large enough to prevent penetration into the resin structure will pass through together with any non-ionic components whereas low-molecular-weight anions are retained by the resin. This arbitrary separation into low and high-molecular-weight anions is governed by a number of experimental conditions. There are indications [2] that this method classifies a low-molecular-weight anion as one with the ionic size equal to or less than 30 Å. The use of this separation has been reported by many authors in later years.

As is pointed out in many papers [3,4,5], it would be reasonable to expect a change in the screening effect by varying the degree of cross-linking of the resin, *i. e.* a resin with low degree of cross-linking (highly swollen) should be able to retain larger ions than a resin with a normal degree of cross-linking. In the present paper it is shown that under the conditions obtained in a laboratory ion exchange column with a flow-rate of about 1 ml $cm^{-2}min^{-1}$ there exists no difference in screening properties between anion exchange resins of varying

* The main part of the experimental work was done during 1953 at the College of Forestry in Syracuse, N.Y., U.S.A.

degree of cross-linking as far as a solution of polystyrene sulphonic acid is concerned. This means that under the conditions and in the system in question, a variation in the degree of cross-linking of the resin does not affect the screening properties. On the other hand, under non-equilibrium conditions a difference in screening properties between resins of different degree of cross-linking is obtained as a result of the differences in penetration rate between ions of varying size which are obtained when the degree of cross-linking is altered [6].

The above statements seem to be true for all resins of the translucent type. As demonstrated in the present paper, resins of the porous type (obtained from the Chemical Process Company, Redwood City, California, U.S.A., under the special trade name Porous Duolite) show, however, varying screening properties.

The promising results with the porous resins justified investigating them as possible fractionating agents for polyelectrolytes. Provided that a porous resin gives a sharp fractionation based on the degree of polymerisation or preferably the ionic size, the prime requisite for satisfactory fractionation exists.

EXPERIMENTAL

Materials

The resins. All the resins were ground and screened to a particle size 0.25—0.42 mm. The cation exchange resins were regenerated with 3 N hydrochloric acid and the anion exchange resins with a 2 N ammonium hydroxide solution.

The polyelectrolyte solution. The ammonium salt of sulphonated polystyrene, stated by the manufacturer to have an average molecular weight of about 10 000 was obtained from the Monsanto Chemical Company. The salt was dissolved in water and the free acid liberated by passing the solution through a column containing a cation exchange resin of the sulphonic acid type in the hydrogen form.

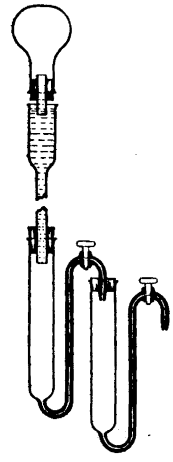


Fig. 1. Apparatus with two columns coupled in series and with arrangement for constant flow-rate through the system.

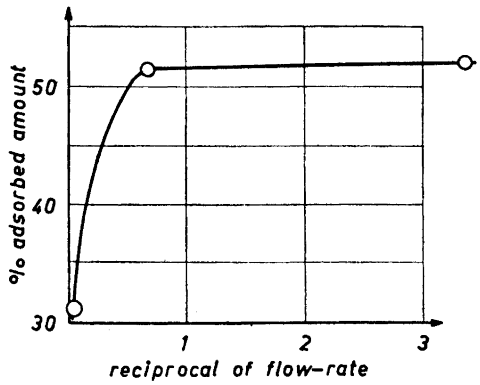


Fig. 2. The adsorbed amount of acid at different flow-rates. Column: Dowex 3.

Experiments

Fractionations with anion exchange resins of the translucent type. The separation of the polyelectrolyte into two fractions by the passage through an anion exchange column was studied under varying experimental conditions. For this study the weakly basic anion exchange resin Dowex 3 was used. The arrangements to get a constant flow-rate and to couple two columns in series are shown in Fig. 1. The polystyrene sulphonic acid liberated in the first column entered the second column, containing the anion exchange resin under study (Dowex 3). Part of the anions was adsorbed and the larger ions that were not adsorbed were found in the effluent. After washing the column with distilled water, the effluent plus the washings were titrated with 0.1 N sodium hydroxide solution using phenolphthalein as indicator. Knowing the amount of acid in the original solution, the adsorbed amount of acid was calculated by

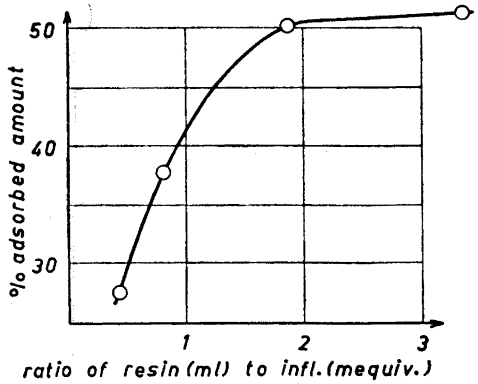


Fig. 3. Variation of the amount of adsorbed acid with varying ratios of resin to influent. Column: Dowex 3.

Table 1. Effect of resin cross linkage on ion adsorbtion. Influent: 2.8 % solution containing 1.38 mequiv acid; flow-rate: 1 ml min^{-1}; ratio resin (ml) to influent (mequiv): 7.

Type of resin	Degree of cross-linking	Amount of acid in the effluent, mequiv	Adsorbed acid as per cent of acid in influent
Dowex 1	about 8	0.645	53.2
» 1	1	0.652	52.8
» 1	10	0.654	52.6
Amberlite IRA-400	—	0.643	53.4
Amberlite IR-4B	—	0.647	53.1

difference. In some experiments this procedure was checked by elution with 1 N sodium hydroxide solution and estimation of the retained acids, and good agreement was obtained.

As is seen from Fig. 2, a flow-rate of 1 ml per min or lower represents equilibrium conditions. Furthermore, a resin to influent ratio of 2 or higher is needed to give a sharp fractionation, Fig. 3. The exchange capacity of the resin is about 0.5 mequiv/ml for this particular range of ionic size as compared with 2.7 mequiv/ml for really low-molecular-weight ions.

The same experimental technique was used in order to study the influence of the degree of cross-linking of the resin. In Table 1 the fractionation results are given for the strongly basic anion exchange resin (Dowex 1) against varying degrees of cross-linking which is given as per cent and is equal to the amount of divinylbenzene used in the polymerisation step in the preparation of the resin. In Table 1 two Amberlite resins are also included, one strongly basic (Amberlite IRA-400) the other weakly basic (Amberlite IR-4B).

As seen in Table 1 a variation from 1 to 10 in the degree of cross-linking does not give any difference, within experimental error, in the screening properties of the resin.

Fractionation with a combination of anion exchange resins of the translucent and of the porous type. With the same experimental conditions, porous resins adsorb a greater amount of acids from a given polyelectrolyte solution in comparison with translucent ones, and furthermore, there are resins with different acid retaining capacity, representing a variation in porosity. For one and the same resin, however, the capacity changes with the ratio resin (ml) to influent (mequiv) with the range that has been studied (Fig. 4). For fractionating on an absolute basis this is a very great draw-back that cannot be overcome but for comparative purposes, on a qualitative basis, this type of resin can be used to obtain a rapid answer as to the distribution of the degree of polymerisation for a polyelectrolyte.

As an illustration the following experiment was made. An exchange battery of the type illustrated in Fig. 1 was used with four columns coupled in series according to Fig. 5. In the first column the conversion to polystyrene

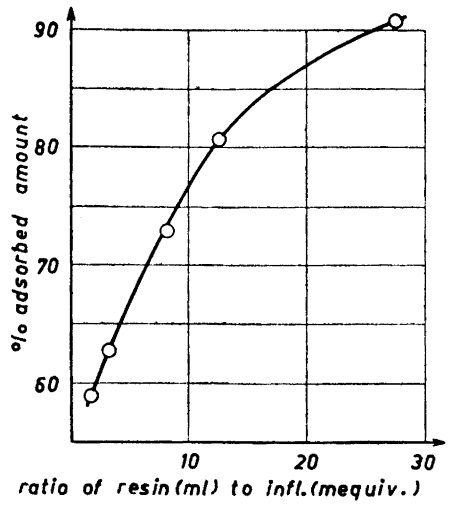


Fig. 4. Variation of the amount of adsorbed acid with varying ratios of resin to influent. Column: Duolite A2.

sulphonic acid occurred and in the last three columns the anions were selectively adsorbed. 50 ml of the polyelectrolyte solution containing 14.11 mequiv were passed through the battery followed by washing with distilled water. The effluent was collected, reference fraction 4, and the columns were separated. Each column was separately eluted with 100 ml 1 N sodium hydroxide solution with subsequent washing with distilled water. In order to remove excess of sodium hydroxide and to convert the salts into the corresponding acids, the collected eluates were passed through columns containing a sulphonic acid cation exchange resin in the hydrogen form. The processed eluate from column 2 was termed fraction 1, that from column 3 fraction 2, and that from column 4 fraction 3. The amount of acid in each fraction was then determined by titration with 0.1 N sodium hydroxide solution against phenolphthalein.

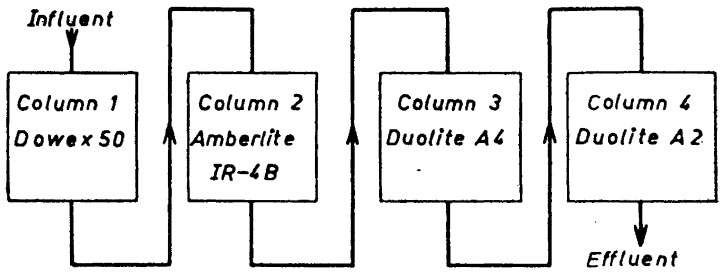


Fig. 5. Ion exchange battery for fractionation.

Table 2. Fractionation of a sample with an average molecular weight of 10 000. Influent: 50 ml containing 14.11 mequiv; flow-rate: 1 ml min^{-1}.

Fraction No.	Amount of acid		Specific viscosity at 25°C of a solution containing 8 mequiv per litre
	mequiv	%	
1	7.26	52.4	0
2	1.278	9.2	0.08
3	1.502	10.8	0.30
4	3.805	27.5	0.71
total	13.85	99.9	

An aliquot of each fraction was diluted to a concentration of 8 mequiv acid per litre and the specific viscosity was measured at 25°C in Ostwald viscometers. The results are given in Table 2.

There is no doubt that the procedure used separated the polystyrene sulphonic acid into fractions with gradually increasing molecular weight. However, as already pointed out, the great disadvantage is that the amount of acid in each fraction depends not only on the properties of the sample and of the resins used but also to a great extent on the experimental conditions.

The fractionating battery according to Fig. 5 gave results as reported in Table 2 for a sulphonated polystyrene with an average molecular weight of 10 000. Another sample of sulphonated polystyrene with a higher average molecular weight (70 000) has been fractionated on the same battery and with the same experimental conditions. The results are given in Table 3. As might be expected the polyelectrolyte with the higher average molecular weight gives smaller amounts of acid in fractions 2 and 3 and higher in fraction 4.

CONCLUSIONS

A variation in the degree of cross-linking from 1 to 10 % for the strongly basic anion exchange resin Dowex 1 did not cause any change in the screening properties of the resin (Table 1). This means that the various resins when used

Table 3. Fractionation of a sample with an average molecular weight of 70 000. Influent: 60 ml containing 15.60 mequiv acid; flow-rate: 1 ml min^{-1}.

Fraction No.	Amount of acid	
	mequiv	%
1	8.21	53.1
2	0.95	6.15
3	0.50	3.23
4	5.80	37.7
total	15.46	100.2

in excess in column operation, retained the same amount of acid from a given polystyrene sulphonic acid solution. It is further interesting to note that the same amount of acid is taken up also by the strongly basic resin (Amberlite IRA-400) and the weakly basic resin (Amberlite IR-4B).

It should be pointed out that the above observations have been made under equilibrium conditions, *i. e* at a low flow-rate. Under non-equilibrium conditions, however, the uptake may very well be different for different resins of the translucent type.

As shown in Tables 2 and 3 porous resins with the general trade name Duolite can retain larger ions in comparison with translucent resins. If three columns containing resins of varying porosity are coupled in series, Fig. 5, this ion exchange battery can, as shown in Tables 2 and 3, be used for fractionating the polystyrene sulphonic acid. The solution to be analysed is passed through resins of successively increasing porosity. Each resin retains ions within a specific size range. Hence, a fractionation based on ionic size takes place.

The results from fractionations according to the proposed method can, however, only be used for comparative purposes, because the range of size of retained ions for a particular resin is not constant but varies with the ratio of the amount of resin to the amount of added ions.

REFERENCES

1. Samuelson, O. *Svensk Papperstidning* **46** (1943) 583.
2. Kunin, R. *Anal. Chem.* **21** (1949) 87.
3. Kressman, T. R. E. and Kitchener, J. A. *Discussions Faraday Soc.* **1949** No. 7, 90.
4. Partridge, S. M. *Nature* **169** (1952) 496.
5. Samuelson, O. *Ion exchange resins in analytical chemistry* John Wiley New York 1953.
6. Richardson, R. W. *J. Chem. Soc.* **1951** 910.

Received April 10, 1957.

ACTA CHEMICA SCANDINAVICA 11 (1957) 1169—1172

Characterization of Polyelectrolyte Solutions

II. Separation of Strong and Weak Acids by means of Ion Exclusion

NILS HARTLER

Uddeholms Aktiebolag, Cellulose Research Laboratory, Skoghall, Sweden *

Ion exclusion as applied to quantitative separation on a laboratory scale is described in detail. A separation based on ionic size of the acid components in sulphite waste liquor by means of ion exchange and on the basis of acid strength by means of ion exclusion reveals interesting facts as regards the composition of such a liquor.

The method as applied to a mixture of weak and strong acids gives information as to whether the weak acid groups are attached to the same or to separate molecules as the strong acid groups.

When an electrolyte solution is brought into contact with an ion exchange resin and the counter ions in the resin and in the solution are the same, no ion exchange takes place but a redistribution of the ions between the outer solution and the inner resin phase results. A strong electrolyte is excluded from the resin phase (usually by as much as a factor of 10), whereas a weak electrolyte will be almost evenly distributed. These phenomena have formed a basis for the development of a new technique termed ion exclusion [1]. The method is used for the separation of strong electrolytes from weak or non-electrolytes. As is evident, the main feature with ion exclusion as compared with ion exchange chromatography is that no regeneration of the resin is needed.

EXPERIMENTAL

A. Experiment to establish suitable experimental conditions

A mixture of hydrochloric and acetic acid was passed at constant flow-rate through an ion exchange column containing a cation exchange resin of the sulphonic acid type in the hydrogen form. The mixture was followed immediately by distilled water. The effluent was collected in small fractions and each fraction analysed for the total acid content by titration with sodium hydroxide solution. Furthermore, each fraction was tested for the presence of chloride ions.

* The main part of the work was done during 1953—54 at the College of Forestry in Syracuse, N.Y., U.S.A.

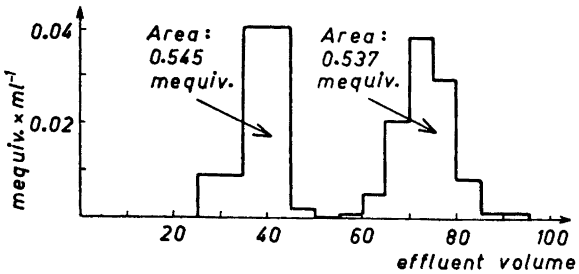


Fig. 1. Separation of hydrochloric and acetic acids by means of ion exclusion.

A number of resins with varying degree of cross-linking and of varying particle size were tested, the effect of varying the ratio of influent volume to resin volume was examined and the flow-rate varied. Only with one type of resin and with one set of variables was the separation found to operate satisfactorily. These were: Dowex 50 with 4 % cross-linking and a particle size 50—100 mesh, a ratio of influent volume to resin volume of 1 : 7, and a flow-rate of 1 ml min^{-1} cm^{-2}. A column was charged with 70 ml of such a resin in the hydrogen form and 10 ml of a solution containing 0.542 mequiv of hydrochloric acid and 0.526 mequiv of acetic acid was passed through, followed by distilled water. Fractions of 5 ml were collected and the acid concentration was plotted against the effluent volume, Fig. 1. After 50 ml had passed through the column, *i.e.* after the first peak in the curve, Fig. 1, no chloride was detected in the subsequent fractions. The total amount of acid between 25 and 50 ml effluent volume corresponded within experimental error, to the amount of hydrochloric acid in the influent, and a similar correspondance was found between the total amount of acid between 50 and 100 ml effluent volume and the amount of acetic acid in the influent.

Other mixtures of a strong and a weak acid have been tested and in all instances the strong acids have been found in the effluent fraction between 25—50 ml and the weak acids between 50—100 ml with the intermediate 50—10 ml containing no acid at all.

B. Ion exclusion and ion exchange as applied to the analysis of sulphite waste liquor

A mixture of strong and weak acid polyelectrolytes can be analysed both by means of ion exchange based on ionic size [2] and by means of ion exclusion as described above. These methods were applied to a waste liquor from a laboratory sulphite paper pulp cook

Table 1. Analytical data for the various fractions. All measurements of optical density were made at a dilution of 1 : 5 000.

Fraction	Description	Acidity		Optical density at 280 mμ
		Strong acids mequiv/ml	Weak acids mequiv/ml	
a	Original liquor	—	—	0.138
b	Hydrogen ion exchanged liquor	0.315	0.113	0.135
c	Strong acids in fraction b	0.317	0.042	0.133
d	Weak acids in fraction b	—	0.063	0.002
e	High polymer acids in fraction b after "screening" by ion exchange	0.169	0.093	0.132
f	Strong acids in fraction e	0.170	0.032	0.133
g	Weak acids in fraction e	—	0.055	0.004

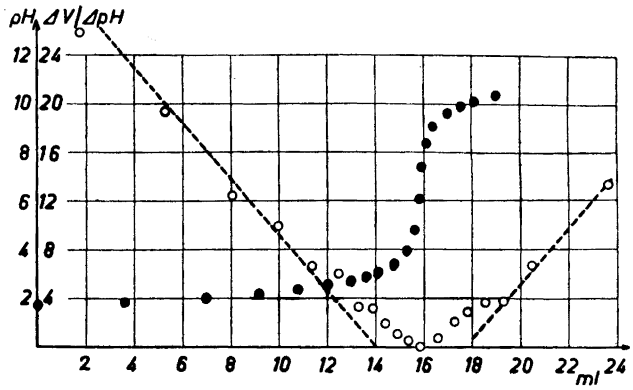


Fig. 2. Potentiometric titration plot according to Gran [3] for fraction c (Table 1).

on spruce. The metal cations in the liquor were first replaced by hydrogen ions by using a cation exchange resin of the sulphonic acid type (resulting in fraction b, Table 1). Part of this acid fraction was passed through a column containing the weakly basic anion exchange resin, Amberlite IR-4B. The high polymer acids were found in the effluent (fraction e, Table 1), whereas the low-molecular-weight acids were adsorbed by the resin. By means of the ion exclusion technique described above the original hydrogen ion exchanged liquor (fraction b) and the high polymer acid fraction (fraction e) were each separated into two fractions, *viz.* the strong acid fraction and weak acid fraction. The various fractions were analysed for the total content of acid by potentiometric titration with 0.1 N sodium hydroxide solution and for lignin content by measuring the optical density in a Beckman spectrophotometer, model DU, at 280 mμ after suitable dilution. The results from the potentiometric titrations were evaluated according to the Gran method [3] in order to determine separately the weak and strong acids. The results are given in Table 1.

In fraction c and f only strong acids should be present but when a molecule contains strong as well as weak acid groups, the latter will necessarily be found in the strong acid fraction. The potentiometric titration diagrams are given in Fig. 2 for fraction c and in Fig. 3 for fraction d. The abnormal shape of the curve in Fig. 2 between pH 7 and 10 is caused by the alkali consumption of the originally present phenolic groups as well as those formed during the titration. The weak acid fraction, Fig. 3, does not contain any appreciable amount of strong acids and in addition the curve shows normal behaviour in the alkaline pH-range.

DISCUSSION

Although the necessary conditions to obtain a satisfactory separation by means of ion exclusion require the maintenance of rather critical experimental variables within narrow limits, the method operates very well according to the procedure described above. This method is most useful when a separation of weak and strong electrolytes is desired for purification purposes. The method also gives information as to whether the weak acid groups are attached to the same molecule as the strong acids or whether they belong to separate molecules. In the former case the weak acid groups appear in the strong acid fraction but in the latter case they are found in the weak acid fraction.

The results reported in Table 1 show that the lignin sulphonic acids are found quantitatively in the high polymer fraction and in the strong acid frac-

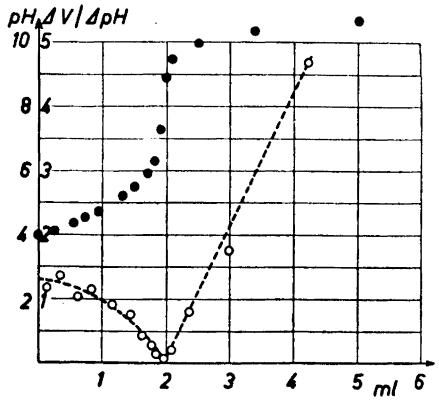


Fig. 3. Potentiometric titration plot according to Gran [3] for fraction d (Table 1).

tions. From this it can be concluded that all the lignin sulphonic acids are of high polymer nature. Similar experiments with a waste liquor from a sulphite rayon pulp cook show that the lignin sulphonic acids in this instance are partly of a low-molecular-weight nature, *i. e.* they are partly retained by an Amberlite IR4B resin. Further, it can be concluded from the results in Table 1 that only about 50 % of the strong acids in the liquor are of a high polymer nature and that the high polymer molecules containing strong acid groups also contain about 15 % weak acid groups. The liquor contains about 15 % of molecules containing only weak acid groups (calculated on an acidity basis).

REFERENCES

1. Wheaton, R. M. and Bauman, W. C. *Ind. Eng. Chem.* **45** (1953) 228.
2. Hartler, N. *Acta Chem. Scand.* **11** (1957) 1162.
3. Gran, G. *Acta Chem. Scand.* **4** (1950) 559.

Received April 10, 1957.

ACTA CHEMICA SCANDINAVICA 11 (1957) 1173—1182

Studies on the Extraction of Metal Complexes

XXVIII. The Distribution of some Actinides and Fission Products between Tributyl Phosphate (TBP) and Aqueous Solutions of HNO_3 and $Ca(NO_3)_2$

BRITA BERNSTRÖM and JAN RYDBERG

Research Institute of National Defence, Dept. 1, Sundbyberg 4, Sweden

The distribution ratios of U(VI), Pu(VI), Pu(IV), Th(IV), Ru, Zr(IV), Nb(V), La(III), Sr(II) and Ca(II) between tributyl phosphate (TBP) and aqueous solutions of varying concentrations of HNO_3 have been determined at room temperature for different (constant) concentrations of $Ca(NO_3)_2$ in the aqueous phase. The extraction curves are discussed with respect to the different complexes formed and to the possibility of using the investigated systems for separating plutonium and uranium from the fission products.

In the previous paper of this series of investigations (Part XXVII [1]) the extraction of plutonium, uranium and some fission products from aqueous solutions into the organic solvent methyl *iso*butyl ketone (hexone) was studied as a function of the HNO_3 and $Ca(NO_3)_2$ concentrations in the aqueous phase. These investigations have here been extended to the organic solvent tributyl phosphate (TBP); in this paper, only the case of pure TBP is reported (*i.e.* no organic diluent added). No extensive investigations of metal extractions with 100 % TBP seem to have been reported previously [2,3].

The following metals (valency states in aqueous solutions — if known — are given within parenthesis) have been studied: U(VI), Pu(VI), Pu(IV), Th(IV), Ru, Zr(IV), Nb(V), La(III), Sr(II) and Ca(II). The concentration of the metal nitrates never exceeded 0.1 M (except for Ca), while the HNO_3 concentration was varied from $\sim$ 0.1 to 10 M, and the $Ca(NO_3)_2$ concentration from 0 to $\sim$ 4 M. The results are given in the form of curves (Figs. 1—7) showing the distribution ratio of a metal as a function of the equilibrium HNO_3 concentration in the aqueous phase at constant $Ca(NO_3)_2$ concentration.

EXPERIMENTAL

Chemicals. Tributyl phosphate, $(C_4H_9)_3PO_4$, of technical grade was obtained from AB Kebo. The solvent was treated with 5 % sodium carbonate and then washed with several portions of water.

UO_3 obtained from AB Atomenergi was dissolved in concentrated HNO_3, filtered and diluted. The uranium content was determined by weighing the oxide U_3O_8 after evaporation and ignition.

^{234}Th (UX_1) was used as tracer for thorium. The solutions were made $\sim 10^{-5}$ M by the addition of ^{232}Th.

A tracer solution of Pu(IV) in 10 M HNO_3 was available. Pu(VI) was obtained by oxidizing the Pu(IV) solution with 0.1 M $K_2S_2O_8$ in 1 M HNO_3 using Ag^+ as catalyst immediately before use. In one case the oxidizing agent was 0.2 M $KBrO_3$.

A carrier free solution of $^{95}Zr + ^{95}Nb$ in 0.3 M HCl and with 2 % oxalic acid was obtained from AERE, Harwell. In the distribution experiments this solution was diluted 1:50.

^{106}Ru in 0.4 M HCl was purchased from AERE, Harwell. The solution was carrier free and diluted 1:1000 before use.

^{140}La was obtained as the neutron irradiated oxide. The oxide was dissolved in 1 M HNO_3 to make the metal concentration $\sim 10^{-5}$ M.

^{89}Sr-carbonate was dissolved in concentrated HNO_3 and diluted.

The $Ca(CO_3)_2$ used was of reagent grade as were all other reagents.

Distribution experiments. All distribution experiments were carried out at room temperature (20 ± 2°C) and were run with each metal separately. The metal nitrate was mixed with varying amounts of HNO_3 and $Ca(NO_3)_2$ and shaken vigorously for 5 min with an equal volume of TBP; equilibrium is usually attained within a few minutes. The two phases were separated by centrifuging. Samples of each phase were withdrawn to determine the HNO_3 concentration of the aqueous phase as well as the metal concentration in each phase. The distribution ratio q, *i.e.* the ratio of the metal concentration in the organic phase to that in the aqueous phase, could then be calculated.

Analyses. Ca was determined by a substitution titration with EDTA (ethylenediamine tetraacetic acid) at pH 10 using Eriochrome Black T as indicator [4]. Before the titration, Ca in the TBP phase was transferred to an aqueous phase by mixing 20 ml of water with 0.5 ml of the TBP phase diluted with 20 ml of benzene.

Uranium was determined spectrophotometrically by the thiocyanate method [5,6]. Only the water phase which contained the smallest fraction of U was analysed, whereas the uranium content of the TBP phase was obtained as the difference between the initially added uranium concentration (0.1 M) and that found in the aqueous phase.

HNO_3 was determined by titration with NaOH.

The α activity of Pu was measured by an argon-methane proportional counter. By means of the TEG-method [7] dry, thin samples were obtained.

The β, γ counting of ^{140}La, ^{106}Ru (^{106}Rh) and ^{234}Th (UX_1) was made on dry samples, whereas ^{89}Sr was measured with a liquid counter. In order to increase the sensitivity of the determinations at very low and at very high distribution ratios, the volume ratio V_{TBP}/V_{aq} was varied, *i.e.* for $q_{Sr} \leq 10^{-2}$ $V_{TBP}/V_{aq} = 5$, for $q_{Th} \geq 10^2$ $V_{TBP}/V_{aq} = 0.1$. In the latter case, the small amount Th in the water phase was concentrated by a hydroxide precipitation with La as carrier thus increasing the counted activity.

For the determination of Zr and Nb separately in a mixture of both of them, the following procedure was used. By means of a lead absorber (200 mg/cm²) the β-activity was filtered away and the total γ-activity of the solution of ^{95}Zr (0.40 MeV β,; 0.71 MeV γ) $+ ^{95}Nb$ (0.15 MeV β, 0.76 MeV γ) was determined from measurements on dry samples. The fraction of γ-activity contributed by ^{95}Zr on this solution was determined by precipitating [8] the zirconium as $BaZrF_6$ and counting the precipitate through the same absorber; inactive zirconium was added as a carrier. From an average of four determinations 37.5 % of the total γ-activity was ascribed to ^{95}Zr. For the ratio $R = I_{Zr}/I_{Nb}$ we then calculate the value 0.60.

In the distribution experiments, the total γ-activity of each phase was determined (I_{TBP} respectively I_{aq}) as well as the Zr content of the water phase ($I_{Zr\ aq}$), by measuring precipitated $BaZrF_6$. q_{Zr} was calculated from the relation

$$q_{Zr} = \frac{R}{(R+1)} \cdot \frac{(I_{TBP} + I_{aq})}{I_{Zr,aq}} - 1$$

The ratio I_{TBP}/I_{aq} was found to depend on the time of mixing and increased with time, probably because equilibrium was slowly attained for Nb. For a shaking time of 5 min the distribution ratio q_{Nb} was calculated according to

$$q_{Nb} = \frac{1}{(R+1)} \cdot \frac{(I_{TBP} + I_{aq})}{(I_{aq} - I_{Zr,aq})} - 1$$

Good material balance was obtained.

RESULTS AND DISCUSSION

The distribution curves

The distribution ratio q_M (subscript refers to the metal investigated) has been plotted against the molarity of HNO_3 in the aqueous phase at equilibrium. The curves are shown in Figs. 1—7 for initial $Ca(NO_3)_2$ concentrations of 0, 1, 2, 3 and 4 M. In all cases the distribution ratios increase with increasing $Ca(NO_3)_2$ concentration. The distribution ratios also increase with increasing HNO_3 concentration except at high $Ca(NO_3)_2$ concentrations.

The distribution of HNO_3 is presented in two different ways. Fig. 1a shows the HNO_3 concentration of the TBP phase as a function of the aqueous HNO_3 concentration. Fig. 1b shows q_H as a function of the HNO_3 concentration.

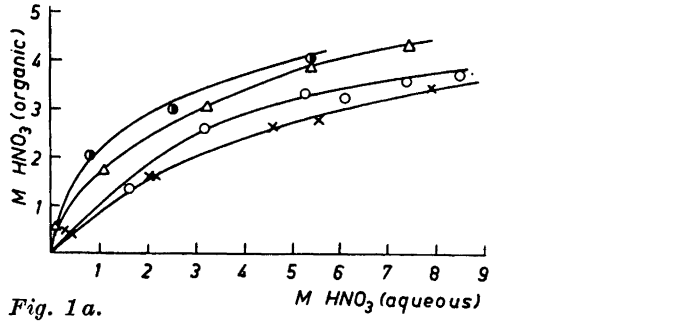


Fig. 1 a.

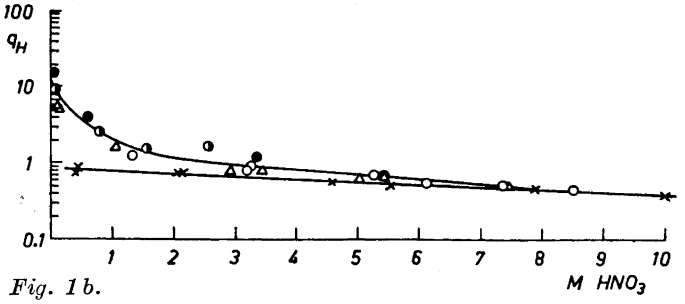


Fig. 1 b.

The distribution of HNO_3 as a function of the equilibrium concentration of HNO_3 in the aqueous phase in two different graphical representations. Concentrations of initial $Ca(NO_3)_2$: ● 4M, ◑ 3 M, △ 2 M, ○ 1 M, × no $Ca(NO_3)_2$ present.

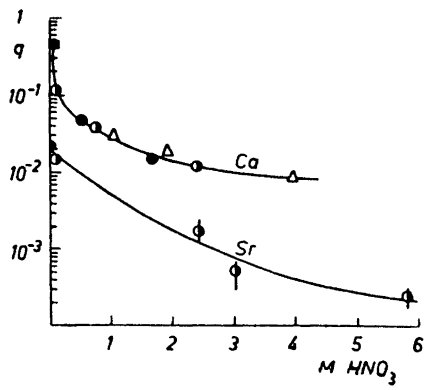


Fig. 2. The distribution ratio q of calcium and strontium as a function of the equilibrium concentration of HNO_3 in the aqueous phase. Concentrations of initial $Ca(NO_3)_2$: ● 4 M, ◑ 3 M, △ 2 M.

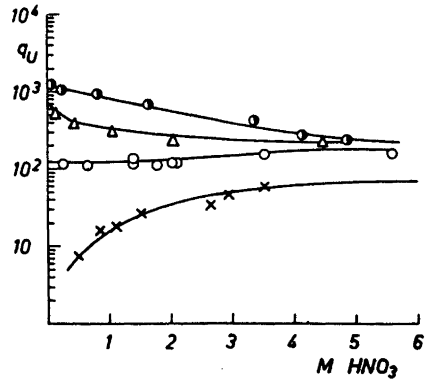


Fig. 3. The distribution ratio q_U of hexavalent uranium as a function of the equilibrium concentration of HNO_3 in the aqueous phase. Concentration of initial $Ca(NO_3)_2$: ◑ 3 M, △ 2 M, ○ 1 M, × no $Ca(NO_3)_2$ present.

These results can be compared with some data available in the literature. The distribution curve of HNO_3 with no $Ca(NO_3)_2$ present (Fig. 1a) agrees closely with that determined by Alcock *et al.*[10] It is noteworthy that at low HNO_3 concentration our results agree better with their calculated curve for a 1:1 complex of $HNO_3 \cdot TBP$ than their experimental data do[Ref. 10, Fig. 4]. Peppard *et al.*[11] report the extraction of Th and Zr into 100 % TBP from HNO_3 solutions containing no $Ca(NO_3)_2$. Their results for Th agree

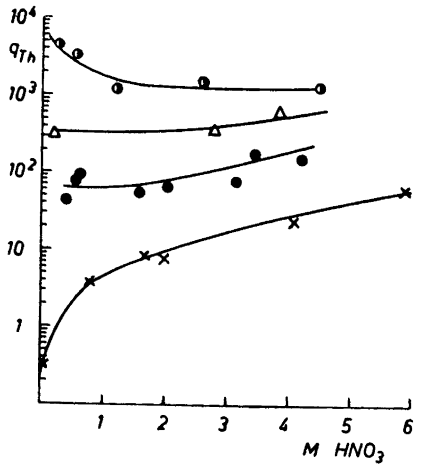


Fig. 4. The distribution ratio q_{Th} of thorium as a function of the equilibrium concentration of HNO_3 in the aqueous phase. Concentration of initial $Ca(NO_3)_2$: ◑ 3 M, △ 2 M, ● 1 M, × no $Ca(NO_3)_2$ present.

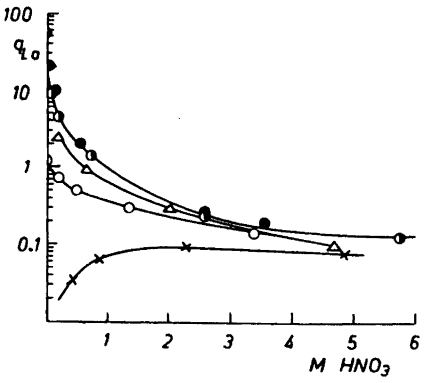


Fig. 5. The distribution ratio q_{La} of lanthanum as a function of the equilibrium concentration of HNO_3 in the aqueous phase. Concentration of initial $Ca(NO_3)_2$: ● 4 M, ◑ 3 M, △ 2 M, ○ 1 M, × no $Ca(NO_3)_2$ preser t.

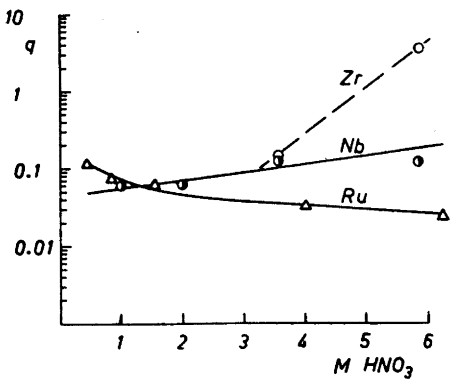


Fig. 6. The distribution ratios of ruthenium △, zirconium ○ and niobium ◑ as a function of the equilibrium concentration of HNO_3 in the aqueous phase. No $Ca(NO_3)_2$ present.

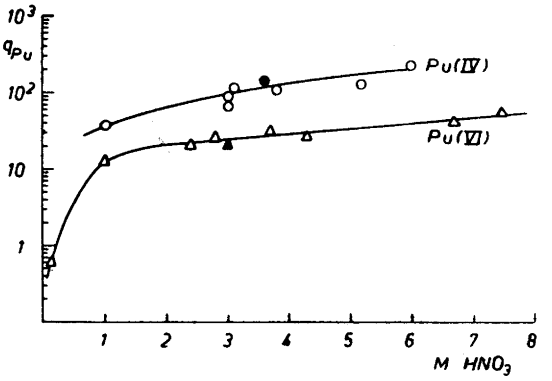


Fig. 7. The distribution ratio q_{Pu} of tetravalent and hexavalent plutonium as a function of the equilibrium concentration of HNO_3 in the aqueous phase. No $Ca(NO_3)_2$ present. Plutonium pretreated with 10 M HNO_3 ○, $NaNO_2$ ● (*cf.* Ref. 9), BrO_3^- ▲, and $S_2O_8^{2-}$ △.

with the present work except for high acidities where we obtain a lower value of q_{Th}. The presence of $H_2C_2O_4$ in our stock solution of Zr probably explains our lower value of q_{Zr} compared with Peppard's (*cf.* Bruce [12] who shows the effect of $H_2C_2O_4$ on q_{Zr}). Scadden and Ballou [13] report the extraction of Zr and Nb from HNO_3 solutions into 100 % TBP. Their data are, however, for TBP as received, which yields quite different results because of small impurities of hydrolysis products as, *e.g.*, dibutylphosphate (DBP). Peppard *et al.*[14] report $q_{La} = 0.33$ for 100 % TBP and an aqueous phase 15.6 M in HNO_3, a value which is of the same order as that determined here *.

The extraction mechanism

It can be shown [15] that if a metal M (charge N+) is extracted as a nitrate complex into TBP, the distribution Q_M of the metal between the two phases should follow eqn. (1), if only mononuclear complexes of the type $M(NO_3)_n(TBP)_s^{N-n}$ are formed (neglecting waters of hydration).

$$Q_M = \frac{\sum_0^S \lambda_{Ns}\varkappa_{Ns} \{NO_3^-\}^N \{TBP\}^s}{1 + \sum_{1,1}^{ns} \varkappa_{ns} \{NO_3^-\}^n \{TBP\}^s} \qquad (1)$$

Here { } are used to indicate activities, which all refer to the aqueous phase; $\varkappa_{ns}$ is defined as the complexity constant and λ_{Ns} as the distribution constants of the uncharged complexes $M(NO_3)_N(TBP)_s$. If the concentration of all

* *Note added in proof.* D. Scargill *et al.*[21] report q_{La} for 100 % TBP and varying HNO_3 solutions in close agreement with our data.

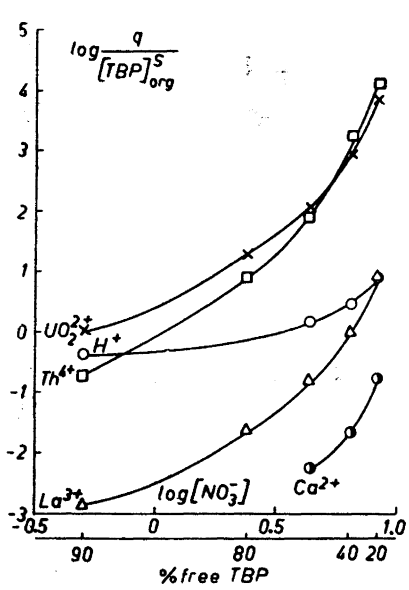


Fig. 8. The variation of $\log \frac{q}{[TBP]^S_{org}}$ with the nitrate concentration for constant $[HNO_3]_{(aq)} = 0.5$ M.

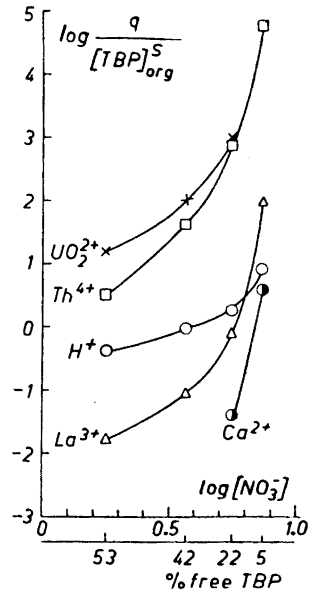


Fig. 9. The variation of $\log \frac{q}{[TBP]^S_{org}}$ with the nitrate concentration for constant $[HNO_3]_{(aq)} = 2$ M.

complexes of M in the aqueous phase is small compared to the concentration of M^{N+}, the second term in the denominator of eqn. (1) can be neglected. If it is further assumed that only one complex of M is extracted, *e.g.* $M(NO_3)_N(TBP)_S$, eqn. (1) can then be rewritten (using [ ] for concentration):

$$\log \frac{q_M}{[TBP]^S_{org}} - (N+1) \log f_{\pm} + \log \frac{f_{MC}}{f^S_{TBP}} = N \log [NO_3^-]_{aq} + \log K \quad (2)$$

Here all constants are included in K. The activity factor $f_{\pm}$ refers to the metal nitrate in the aqueous phase, f_{MC} to the metal complex and f_{TBP} to the free TBP in the organic phase; for 100 % TBP we define $f_{TBP} = 1$; f_{MC} is also = 1 in this case since the organic phase is infinitely dilute with respect to the metal complex. Q_M in eqn. (1) has been substituted by q_M to indicate that the distribution ratio in eqn. (2) refers to the concentration of the metal.

If the concentrations of the species present in large (molar) amounts are unaltered throughout the experiments, the activity factors can usually be regarded as constant. It is seen from eqn. (2) that a plot of $\log q_M/[TBP]^S_{org}$ against $\log [NO_3^-]_{aq}$ should then give a straight line of slope N. Such plots have been made in Figs. 8 and 9.

The q-values corresponding to different $Ca(NO_3)_2$ concentrations were taken from Figs. 1—5 at a constant acidity of 0.5 M and 2 M. $Ca(NO_3)_2$ was assumed to be completely

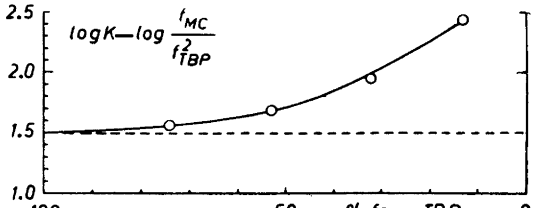


Fig. 10. Plot for $UO_2(NO_3)_2$ of $\log (q \cdot [TBP]_{org}^{-2}[NO_3^-]^{-2} \cdot f_{\pm}^{-3}) = \log K - \log \frac{f_{MC}}{f^2_{TBP}}$ at varying concentration of free TBP in the organic phase. *Cf.* equation 2, p. 1178.

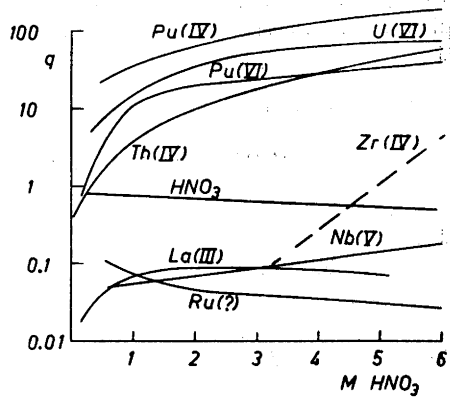


Fig. 11 The distribution ratios of the investigated metal ions and HNO_3 as a function of HNO_3 in the aqueous phase, when no $Ca(NO_3)_2$ is present.

dissociated in HNO_3 solutions <2 M, whereas a small correction for undissociated HNO_3 at high NO_3^- concentrations has been made [16].

The concentration of free, uncomplexed TBP in the organic phase, $[TBP]_{org}$, was calculated by subtracting the TBP bound to HNO_3[10] and to metal complexes [17,18] (see below) from the original TBP concentration ($[TBP]_{org,init}$) according to the equation

$$[TBP]_{org} = [TBP]_{org,init} - [HNO_3]_{org} - \Sigma S[M(NO_3)_N]_{org} \quad (3)$$

which is valid if HNO_3 and $M(NO_3)_N$ are bound to a constant number (1 or S, respectively) of TBP molecules in the organic phase. $[TBP]_{org,init} = 3.4$ M when 100 % TBP is equilibrated with water and 3.2 M when at equilibrium with 2 M HNO_3[22] due to a small volume change.

S has been taken from investigations by McKay *et al.* for the complexes $UO_2(NO_3)_2 \cdot 2TBP$ [17,18], $Th(NO_3)_4 \cdot 2TBP$ [17,18], $La(NO_3)_3 \cdot 3TBP$ [18], $Ca(NO_3)_2 \cdot 3TBP$ [18] and $HNO_3 \cdot TBP$ [10].

It is seen from Figs. 8 and 9 that a straight line is not obtained in any case; all curves (except for HNO_3) start at low NO_3^- concentrations with a slope $<$ N and end up with a slope $>$ N. Apparently it is impossible to adequately describe the systems without considering activity factors (the ionic strength of the aqueous phase varies from 3 to 12 molar, or 0.5 to 8 molal, and the concentration of free TBP from 90 to only 10 %).

The activity factors are only known for one of the metal complexes in these systems. They have been determined by McKay [19] for $UO_2(NO_3)_2$ in solutions of $Ca(NO_3)_2$; these activity factors include possible complex formation between UO_2^{2+} and NO_3^- ions in the aqueous phase. Introducing these values for $f_{\pm}$ in eqn. (2), one can calculate $\log K - \log f_{MC}/f^2_{TBP}$ as a function of $[TBP]_{org}$; this has been graphed in Fig. 10 where, on the abscissae, % free TBP is given instead of molarity. With increasing percentage of

TBP, the concentration of HNO_3 as well as of the metal complex in the organic phase decreases. By extrapolating the curve in Fig. 10 to 100 % TBP, we thus obtain log $K = 1.5$, since by definition $f_{TBP} = 1$ and also $f_{MC} = 1$.

It can easily be shown that this K is the equilibrium constant for the reaction

$$UO_2^{++}{}_{(aq)} + 2NO_3^-{}_{(aq)} + 2\ TBP_{(org)} = UO_2(NO_3)_2(TBP)_{2(org)}$$

It follows from Fig. 10 that the vertical distance between the curve and the horizontal line represented by log K must be equal to log f_{MC}/f_{TBP}^2. For 13 % free TBP one obtains $f_{MC}/f_{TBP}^2 = 0.1$. It can be deduced from this ratio that one or both of the activity factors f_{MC} and f_{TBP} must deviate from 1 by a factor of at least 2. Much greater variations have in fact been shown by McKay to exist for solutions of TBP, though in his case the solutions consisted of mixtures of highly polar TBP and HNO_3 in a solvent (kerosene) of low dipole moment *; in our case, when all components most probably are very polar, the change in the activity factors is expected to be smaller, which is in agreement with the findings.

The deviation of the curves in Figs. 8 and 9 from straight lines may not solely be due to variations in activity factors. Since at high NO_3^- concentrations a considerable part of the TBP is tied up in complexes with HNO_3 and $M(NO_3)_N$, it seems probable that the HNO_3 and metal complexes here are deficient in TBP. This is definitely indicated by the result in Fig. 9, where the TBP concentration according to eqn. (3) is < 0 at the highest NO_3^- concentration. It can also be seen from Fig. 1a that the ratio $[HNO_3]_{org}/[TBP]_{org}$ exceeds 1 (*i.e.* $[HNO_3]_{org} > 3.4$ M) at high values of HNO_3, indicating that HNO_3 is extracted in other forms than the complex $HNO_3 \cdot TBP$. This means that eqn. (3) is no longer correct; the concentration of free TBP is probably somewhat higher. The consequence of this is that the ordinate values log $q/[TBP]_{org}^N$ in Figs. 8 and 9 should be lowered, and the higher the NO_3^- concentration is the greater the decrease, which would give the curves a less steep slope at high values of log $[NO_3^-]$. It should further be noted that the formation of complexes of M in the aqueous phase (*i.e.* $[M^{N+}] \gg \sum_{1,1}^{n,s} [M(NO_3)_n(TBP)_s]_{aq}$) will lead to the same consequence, *i.e.* to a less steep slope of the curves at high NO_3^- concentrations. Thus, *e.g.*, Ahrland [20] has shown that in 2 M NO_3^- about 50 % of U(VI) is in the form of $UO_2NO_3^+$. It therefore seems incorrect to explain the deviation from straight lines in Figs. 8 and 9 solely as due to variations in activity factors. Certainly part of the deviations are due to the formation of more than one type of complex for HNO_3 and for the metals in the organic as well as in the aqueous phase.

* It should be observed that in Ref.[10] another reference state for the activity factor of TBP is used, *i.e.* $f_{TBP} = 1$ for 0 % TBP in 100 % kerosene.

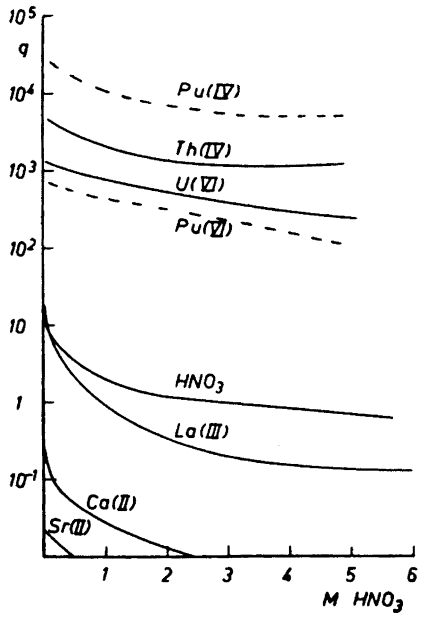


Fig. 12. The distribution ratios of the investigated metal ions and HNO_3 as a function of HNO_3 in the aqueous phase. Concentration of $Ca(NO_3)_2$: 3 M. (The curves for Pu(VI) and Pu(IV) have been extrapolated assuming Pu(VI) parallels U(VI) and Pu(IV) parallels Th(IV)).

Separation of uranium and plutonium from other metals.

The distribution curves for the different metals and HNO_3 are given in Fig. 11 for no $Ca(NO_3)_2$ present, and in Fig. 12 for 3 M $Ca(NO_3)_2$. The dashed curves for Pu(IV) and Pu(VI) in Fig. 12 are calculated on the assumption that $q_{Pu(IV)}$ changes approximately like q_{Th}, and $q_{Pu(VI)}$ like $q_{U(VI)}$, when going from 0 M to 3 M $Ca(NO_3)_2$ solutions. Similar curves for 1, 2 and 4 M $Ca(NO_3)_2$ can be obtained from Figs. 2—7.

By comparing Figs. 11 and 12 it is seen that the distribution factors increase with increasing $Ca(NO_3)_2$ concentration, and that this increase is greatest for the tetravalent and hexavalent actinides. As a consequence of this, highly salted aqueous solutions and pure TBP would seem to be a suitable system for separating Th, U and Pu from the other metals. Now it is a well-known fact that the best separation between two metals *e.g.* M_1 and M_2, is obtained if $q_{M_1} = q_{M_2}^{-1}$ at equal phase volumes. If M_1 represents Th, U or Pu, and M_2 represents the other metals, it can be seen from Fig. 12 that this optimum relation between q_{M_1} and q_{M_2} cannot be obtained with 3 M $Ca(NO_3)_2$ solutions. In fact, it is difficult to obtain an organic phase containing Th, U and Pu, which is free of the other metals. It can therefore be concluded that 3 M $Ca(NO_3)_2$ solutions are not suitable for separating U and Pu from the fission products.

In certain instances it may be of importance to determine small amounts of plutonium or uranium in aqueous solutions very dilute with respect to these elements. If the aqueous phase then is strongly salted, as with $Ca(NO_3)_2$, and mixed with a small volume of pure TBP, practically all Pu(IV), Pu(VI)

and U will move over into the organic phase. This concentration of Pu and U which may amount to a factor of 50, will make it easier to analyse for these metals.

It is seen from Fig. 11 where no $Ca(NO_3)_2$ is present that between 1 and 3 M HNO_3 the difference in distribution ratios between the tetravalent or hexavalent actinides and the other metals is about a factor 100. The conditions for separating U and Pu from the fission products (F.P.) at equal phase volumes are here optimum ($q_U \approx q_{Pu} \approx q_{F.P.}^{-1}$). It can be calculated[1] that in a counter-current extraction with 3 extraction stages and 3 stripping stages, about 99.9 % of Pu(IV), Pu(VI) and U are extracted, with a decontamination factor from the fission products investigated in Fig. 11 of the order of 10^6.

Acknowledgement. The authors wish to thank the head of FOA 1, Prof. G. Ljunggren, for his continuous support of this work and for the permission to publish the results. Sincere thanks are also due to Miss V. Dahlberg for elaborate experimental aid, and to Dr. S. Tobias for correcting the English text.

REFERENCES

1. Rydberg, J. and Bernström, B. *Acta Chem. Scand.* **11** (1957) 86.
2. *Proceedings of the International Conference on the Peaceful Uses of Atomic Energy*, Sessions 21.B and 10B.2, United Nations, New York 1956.
3. *Progress in Nuclear Chemistry*, Series III, "*Process Chemistry*, Vol. 1", Pergamon Press Ltd, London 1956.
4. Schwarzenbach, G. *Die Komplexometrische Titration*, Ferdinand Enke Verlag, Stuttgart 1956.
5. Rodden, C. J. and Warf, J. C. *Analytical Chemistry of the Manhattan Project*, Ch. 1, *N.N.E.S.** *VIII, 1* (1950).
6. Hök, B. *Svensk Kem. Tidskr.* **65** (1953) 105.
7. Hurst, R. and Glover, K. M. *A.E.R.E. Report* C/M 100, 1951.
8. Hume, D. N., Paper 245 of *Radiochemical Studies. The Fission Products* (Ed. C.D. Coryell and N. N. Sugerman), N.N.E.S.* *IV—9* (1951).
9. Flanary, J. R., Paper P/539 in Vol. 9 of Ref.[2]
10. Alcock, K., Grimley, S. S., Healy, T. V., Kennedy, J. and McKay, H. A. C. *Trans. Faraday Soc.* **52** (1956) 39.
11. Peppard, D. F., Mason, G. W. and Maier, J. L. *J. Inorg. Nucl. Chem.* **3** (1956) 215.
12. Bruce, F. R., Paper P/719 in Vol. 7 of Ref.[2].
13. Scadden, E. M. and Ballou, N. E. *Anal. Chem.* **25** (1953) 1602.
14. Peppard, D. F., Faris, J. P., Gray, P. R. and Mason, G. W. *J. Phys. Chem.* **57** (1953) 294.
15. Rydberg, J. *Arkiv Kemi* **8** (1955) 101; *Rec. trav. chim.* **75** (1956) 737.
16. Redlich, O. *Monatsh.* **86** (1955) 329.
17. McKay, H. A. C., Paper P/441 in Vol. 7 of Ref.[2]
18. Healy, T. V. and McKay, H. A. C., *Rec. trav. chim.* **75** (1956) 730; *Trans. Faraday Soc.* **52** (1956) 633.
19. McKay, H. A. C. *Chemistry & Industry* **1954** 1549.
20. Ahrland, S. *Acta Chem. Scand.* **5** (1951) 1271.
21. Scargill, D., Alcock, K., Fletcher, J. M., Hesford, E. and McKay, H. A. C. *J. Inorg. Nucl. Chem.* **4** (1957) 304.
22. Peppard, D. F., Driscoll, W. J., Sironen, R. J. and McCarty, S. *Ibid.* **4** (1957) 326.

* N.N.E.S. = National Nuclear Energy Series, McGraw-Hill Book Co., New York.

Received May 4, 1957.

ACTA CHEMICA SCANDINAVICA 11 (1957) 1183—1190

Local Anaesthetics I.
N-Alkyl Pyrrolidine and N-Alkyl Piperidine Carboxylic Acid Amides

BO af EKENSTAM, BÖRJE EGNÉR and GÖSTA PETTERSSON

The research Laboratory, AB Bofors Nobelkrut, Bofors, Sweden

General methods and detailed examples are given for the preparation of 35 new aromatic amides of N-alkyl pyrrolidine and N-alkyl piperidine carboxylic acids. The compounds were prepared in order to test them as local anaesthetics. Pharmacological and clinical work has proved these compounds to be good local anaesthetics. The effect of compounds orginating from α-, β- and γ-carboxylic acids, respectively, compare as 7 : 2 : 1, while corresponding values for the toxicity compare as 2.7 : 1 : 1.

An extension of the N-alkyl group attached to the heterocyclic ring and an increase of the number of alkyl groups in the aromatic ring causes an increase in the effect as well as in the toxicity. The introduction of alkoxygroups in the aromatic ring lowers the toxicity but causes an increase in the irritation of living tissue. Alkylation of the amidic nitrogen as well as the introduction of an alkyl group between the amide and the aryl group decreases the effect. There appears to be no difference in pharmacological respect between the optical isomers.

dl-N-Methyl pipecolic acid 2,6-xylidide (Carbocaine) has proved suitable for clinical use.

In a number of papers [1-9], covering a period of some fifty years, local anaesthetics of amide type have been described. Though, as far as we know, no compounds were prepared where the carbonyl group of the amide was directly linked to one of the carbon atoms in a saturated or partly saturated heterocyclic ring.

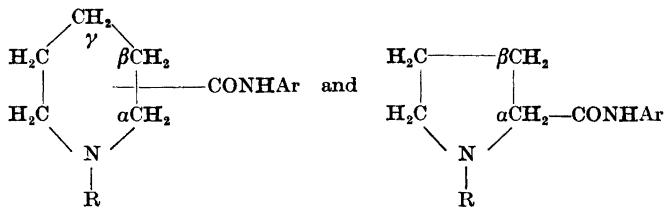
As it could be of interest to test compounds of this type, a number of aryl amides were synthesized starting from pyrrolidine and piperidine carboxylic acids.

A juxtaposition of the compounds prepared is given in Table 1. Their structure is apparent from the formulae.

Table 1

No.	Ar	R	Mol.weight	Melting point °C Base	Hydrochloride
		dl-N-Alkyl pipecolic acid amides			
1	C_6H_5	C_2H_5	232.15	108–110	186–188
2	C_6H_5	n-C_4H_9	260.17	83–84	158–160
3	C_6H_4, 2-CH_3	C_2H_5	246.16	97–98	224–225
4	C_6H_4, 2-CH_3	n-C_4H_9	274.18	oil	213–215
5	C_6H_4, 3-CH_3	C_2H_5	246.16	50–52	140–143
6	C_6H_4, 4-CH_3	C_2H_5	246.16	88–90	224–226
7	C_6H_3, 2,4-$(CH_3)_2$	C_2H_5	260.17	59–60.5	241–243
8	C_6H_3, 2,6-$(CH_3)_2$	CH_3	246.16	150–151	262–264
9	C_6H_3, 2,6-$(CH_3)_2$	C_2H_5	260.17	132–133	252–254
10	C_6H_3, 2,6-$(CH_3)_2$	n-C_3H_7	274.18	121	262
11	C_6H_3, 2,6-$(CH_3)_2$	n-C_4H_9	288.19	107.5–108	258.5
12	C_6H_3, 2,6-$(CH_3)_2$	*cyclo*-C_5H_9	300.20	158	268–269
13	C_6H_3, 2-Cl-6-CH_3	C_2H_5	280.61	101	261–261.5
14	C_6H_4, 2-C_2H_5	C_2H_5	260.17	94–95	234–235
15	C_6H_4, 4-OC_2H_5	C_2H_5	276.17	120	174–176
16	C_6H_3, 2-CH_3-4-OC_4H_9	CH_3	304.19	96–97	177
17	C_6H_2, 2,6-$(CH_3)_2$-4-OC_4H_9	CH_3	328.21	85–87	221–223
18	C_6H_2, 4,6-$(CH_3)_2$-2-OC_4H_9	C_2H_5	342.22	85–86	234–236
19	C_6H_2, 2,4,6-$(CH_3)_3$	C_2H_5	274.18	117	271–272.5
20	$C_6H_5CH_2$	CH_3	231.15	80–81	200–203
21	C_6H_5*	CH_3	246.16	oil	184–186
		dl-N-Alkyl nipecotic acid amides			
22	C_6H_3, 2,6-$(CH_3)_2$	CH_3	246.16	154–155	193–195
23	C_6H_3, 2,6-$(CH_3)_2$	C_2H_5	260.17	145	233–235
24	C_6H_3, 2,6-$(CH_3)_2$	n-C_3H_7	274.18	136–137	196–197
25	C_6H_3, 2,6-$(CH_3)_2$	*iso*-C_3H_7	274.18	157–158	219–220
26	C_6H_3, 2,6-$(CH_3)_2$	n-C_4H_9	288.19	114–115	207–208
27	C_6H_3, 2-Cl-6-CH_3	C_2H_5	280.61	122–123	223–224
28	C_6H_2, 2,6-$(CH_3)_2$-4-OC_2H_5	CH_3	290.18	110–112	oil
29	C_6H_2, 4,6-$(CH_3)_2$-2-OC_2H_5	CH_3	290.18	127–128	192–193
		N-Alkyl isonipecotic acid amides			
30	C_6H_5	CH_3	218.14	140–142	254–255
31	C_6H_3, 2,6-$(CH_3)_2$	C_2H_5	260.17	181–182	247–248
		dl-N-Alkyl proline amides			
32	C_6H_3, 2,6-$(CH_3)_2$	CH_3	232.15	68–70	215–217
33	C_6H_3, 2,6-$(CH_3)_2$	C_2H_5	246.16	91–93	235–237
34	C_6H_3, 2,6-$(CH_3)_2$	n-C_3H_7	260.17	110–112	257–258
35	C_6H_3, 2-Cl-6-CH_3	n-C_4H_9	294.62	77–78	233–235

* Amide nitrogen also ethylated



Yet in No. 20 a methylene group has been introduced between NH and Ar, and in No. 21 an alkyl group has been coupled to the amidic nitrogen.

For the preparation of these compounds there are several possible ways; only the most suitable will be described here. In the following survey of the methods there is for every reaction a roman numeral which refers to the corresponding description in the experimental part.

Method A. A pyridine carboxylic acid is transferred into an aryl amide (I), which is then catalytically (II) hydrogenated and alkylated at the ring nitrogen (III). (I) is most conveniently carried out over the acid chloride, which is prepared by treating a suspension of the sodium salt in toluene with phosphorus pentachloride. The hydrogenation was carried out according to a method by Barnes [10] for the preparation of piperidine carboxylic acid esters. The pressure was however kept at 4—5 atm and the temperature at *ca.* 80°. The alkylation is easily carried out according to common methods.

The pyrrole carboxylic acid amide cannot be hydrogenated in this way.

Method B. The amides of the saturated carboxylic acids (IV) are prepared before (V) or after (VI, VII) the alkylation of the ring nitrogen. (V) was carried out over the acid chloride, which was prepared according to Fischer [11] in acetyl chloride with phosphorus pentachloride. It should be observed that for a complete reaction piperidine carboxylic acid requires a temperature of 35°, while the formation of prolyl chloride according to Fischer occurs at 0°. This causes a racemization during the preparation of the amide from optically active pipecolic acid, while the amide of *l*-proline can be prepared with unchanged optical activity. N-Alkylated piperidine carboxylic acids were preferably prepared by alkylation and hydrolysis of the corresponding ester. β- and γ-Amides are easily prepared *via* the acid chlorides, which are obtained by treating the acids with thionyl chloride (VI). The acid chlorides of the α-carboxylic acids cannot be prepared in this way. The amides of these can also be prepared by treatment with *iso*cyanate (VII).

Method C. By modifying methods given by Albertson *et al.*[12] and Putochin [13] for the synthesis of proline, the heterocyclic nitrogen ring was obtained by ring closure as the last step before the N-alkylation. Thus an acid with the formula $H_2N \cdot (CH_2)_n \cdot CHClCOOH$ was prepared according to Albertson and thereafter transferred into an arylamide. Ring closure was then achieved in alkaline environment (VIII). The method of Putochin was modified so that as the first step one of the carbonyl groups in diethyl malonate was reacted with the desired arylamine to give a monoamide according to Chattaway and Olmsted [14] (IX). The synthesis was continued essentially according to Putochin. From the monoaryl amide the *iso*nitroso compound (X) was prepared,

nitrosylchloride being used as nitrosating agent as suggested by Whiteley [15]. After reduction to amine (XI), this was reacted with alkylene dibromide, whereafter ring closure was achieved in strongly acid environment (XII).

Only α-compounds were prepared according to method C. Tetrahydro quinaldinic acid amides and tetrahydro *iso*quinaldinic acid amides were also prepared according to the methods A—B. In a forthcoming communication an account will be given of these compounds.

In order to investigate if there was any difference in pharmacological respect between the optical isomeres of the α- and β-compounds *l*- and *dl*-N-ethyl proline 2,6-xylidide was synthesized. In addition *dl*-N-methyl pipecolic acid 2,6-xylidide was separated into its optical isomeres with the aid of tartaric acid.

PHARMACOLOGY

A full account of the pharmacological characteristics of the substances will be published elsewhere. However, some results of general interest will be reported here. Thus it has been established that the α-amides possess the best local anaesthetic effect. Derivatives where R was C_2H_5 and Ar was C_6H_3-2,6-$(CH_3)_2$ (Nos. 9, 23 and 31 in Table 1) and where the only difference was in the amide position were compared at blockage of *N. ulnaris*. With respect to duration α-, β- and γ-derivatives compared roughly as 7 : 2 : 1. The corresponding proline amide gave approximately the figure 3. These results agree well with the observation of Erdtman and Löfgren [5] of a decreasing effect in the amide series of aliphatic amino acids with an increasing distance between the amide and amino groups. β- and γ-Amides turned out to have about the same toxicity while the α-amide was 2.7 times as toxic. As, however, the effect is manifolded the α-amides appear to possess a better therapeutic index.

At weal tests and determination of LD_{50} on mice no statistical difference could be established between the two optical isomers.

An extension of the heterocyclic hydrocarbon chain R results in an increase in effect at the same time as the toxicity is aggravated. N-Alkyl-proline amides have a lower effect than the corresponding pipecolic acid amides even if the shortening of the hydrocarbon chain in the heterocyclic ring is considered. Alkylation of the arylamide nitrogen (No. 21) and the introduction of an alkyl group between the amide and aryl groups (No. 20) appear to decrease the local anaesthetic power.

The introduction of side chains into the aryl group cause an increase both in effect and toxicity. The replacement of an alkyl chain in the aryl group by an alkoxy group causes a decrease in the toxicity but makes the substance irritating on living tissues. Replacement of the group by chlorine increases the toxicity while the effect decreases.

The one for clinical use most suitable compound appeared to be No. 8, *dl*-N-methyl pipecolic acid 2,6-xylidide. The compound was given the name Carbocain and has been subjected to pharmacological examination by Ulfendahl [16] and to clinical by Dhunér *et al.* [16, 17]

The toxicity values for some comparable derivatives are summarised in Table 2.

Table 2.

No. in Table 1				R	Ar	LD_{50} on mice, mg/kg			
α	*β*	*γ*	prolyl			*α*	*β*	*γ*	prolyl
8	22			CH_3	C_6H_3, 2,6-$(CH_3)_2$	43.3	84.3		
9	23	31	33	C_2H_5	C_6H_3, 2,6-$(CH_3)_2$	24.5	68.0	67.8	37.9
10	24		34	*n*-C_3H_7	C_6H_3, 2,6-$(CH_3)_2$	13.5	37.9	—	22.3
	25			*iso*-C_3H_7	C_6H_3, 2,6-$(CH_3)_2$	—	30.5		
11	26			*n*-C_4H_9	C_6H_3, 2,6-$(CH_3)_2$	12.7	20.2		
13	27			C_2H_5	C_6H_3, 2-Cl-6-CH_3	16.9	38.3		
1				C_2H_5	C_6H_5	60.4			
3				C_2H_5	C_6H_4, 2-HC_3	36.7			
15				C_2H_5	C_6H_4, 4-OC_2H_5	51.7			
12				*cyclo*-C_5H_9	C_6H_3, 2,6-$(CH_3)_2$	4.6			
19				C_2H_5	C_6H_2, 2,4,6-$(CH_3)_3$	26.8			
17				CH_3	C_6H_2, 2,6-$(CH_3)_2$-4-*n*-OC_4H_9	38.0			
		30		CH_3	C_6H_5				

EXPERIMENTAL

A description of the synthesis of every compound in Table 1 is not given. However, an account is rendered below of all the methods mentioned in the introduction.

Iso*nicotinic acid 2,6-xylidide (I)*. *Iso*nicotinic acid sodium salt (145 g) was suspended in toluene (550 ml) and phosphorus pentachloride (80 g) added. After 1 h at 90° the solution was filtered, and 2,6-xylidine (120 g) added drop by drop to the filtrate under vigorous stirring. The precipitate was drawn off on a funnel, and washed with toluene and ether to give the hydrochloride as white crystals. Yield 210 g (93 %); m.p. 250—251°C. The hydrochloride (150 g) was dissolved in water (500 ml), carbon treated and precipitated with NaOH. Yield 123 g (95 %); m.p. after recrystallization from alcohol and ether 154—155°C. (Found: N 12.27. Calc. for $C_{14}H_{14}ON_2$: N 12.39).

Iso*nipecotic acid 2,6-xylidide (II)*. *Iso*nicotinic acid 2,6-xylidide (36 g) was dissolved in abs. alcohol (100 g) and acetic acid (20 g) and hydrogenated in the presence of platinum oxide (0.5 g) at 80° and *ca.* 4 atm. The catalyst was filtered off and to the filtered solution was added 50 % caustic soda lye (27 g) and ether (150 ml). After filtering off, precipitated sodium acetate the solution was evaporated to dryness under vacuum. The residue was dissolved in diluted hydrochloric acid, carbon treated and the base was precipitated with NaOH. Yield 33 g (89 %); m.p. after recrystallization from alcohol and ether 181—182°C. (Found: N 11.99. Calc. for $C_{14}H_{20}ON_2$: N 12.07).

N-Ethyl iso*nipecotic acid 2,6-xylidide (III)*. *Iso*nipecotic acid 2,6-xylidide (50 g) was heated on a steambath together with diethyl sulphate (100 g) for 30 min. Complete dissolution was obtained. After cooling down, the solution was washed with water (400 ml). The layer consisting of unreacted diethyl sulphate was separated and washed with a further lot of water (100 ml). The combined water phases were washed with ether (3 × 200 ml), the remaining ether removed from the water solution and this was then treated with carbon. The reaction product was precipitated with NaOH. Yield 53 g (92 %); m.p. after recrystallization from alcohol 181—182°C (gives a depression with unalkylated product). (Found: N 10.71. Calc. for $C_{16}H_{24}ON_2$: N 10.77).

dl-Pipecolic acid hydrochloride (IV). Picolinic acid (70 g) was dissolved in abs. alcohol (300 g) and acetic acid (70 g) and hydrogenated in the presence of platinum oxide (1 g) at *ca.* 80°C and 4—5 atm. When no more hydrogen was absorbed (after 1,5—2 h), the mixture was cooled and filtered. Conc. hydrochloric acid (60 g) was added to the filtrate and cooled to —20°C. Yield 75 g (80 %); m.p. 262—264 °C. (Found: Cl 21.40. Calc. for

$C_6H_{12}O_2NCl$: Cl 21.42). By evaporating the mother liquor to dryness more product was obtained. The total yield amounted to 92—95 %.

dl-Pipecolic acid 2,6-xylidide (V). *dl*-Pipecolic acid hydrochloride (100 g) was suspended in acetylchloride (1 000 ml). Phosphorus pentachloride (100 g) was added under vigorous agitation. After a reaction time of 8 h at 35° with a second addition of phosphorus pentachloride (50 g) after 6 h the mixture was cooled to 10—15° and filtered. The precipitate was washed with toluene and acetone and suspended in acetone (600 ml). All in one 2,6-xylidine (180 g) was added under stirring. The mixture was heated to boiling for 30 min. After cooling the precipitate formed was drawn off and washed with acetone and dryed. In order to remove remaining xylidine the product was steam distilled at pH 5.5, carbon treated and precipitated with NaOH. Yield 112 g (80)); m.p. 116—117°. After recrystallization from alcohol the m.p. rose to 121°. (Found: N 12.03. Calc. for $C_{14}H_{20}ON_2$: N 12.07).

dl-N-Methyl pipecolic acid 2,6-xylidide (III). *dl*-Pipecolic acid 2,6-xylidide (100 g) was dissolved in methyl alcohol (200 ml) and potassium carbonate (45 g) added. Dimethyl sulphate (55 g) was added under stirring, and the mixture refluxed for 6 h. After cooling the mixture was filtered, and the filtrate evaporated to dryness. The residue was dissolved in conc. hydrochloric acid (37 ml) and water (750 ml), carbon treated and precipitated with NaOH. Yield 80.5 g (76 %); m.p. 148°C. After recrystallization from ether the m.p. rose to 150—151°C. (Found: N 11.37. Calc. for $C_{15}H_{22}ON_2$: N 11.38).

dl-Proline-2-chloro-6-methyl anilide (V). To a suspension of the hydrochloride of *dl*-prolinechloride (prepared according to Fischer [11]) (5 g) in acetone (30 ml) 2-chloro-6-methyl aniline (10 g) was added. The mixture was heated on a water bath for 30 min. Water was added until complete solution of any precipitate formed, and the acetone driven off under vacuum. The pH of the solution was adjusted to 5 and the excess of amine removed by extraction with ether. The water solution was made strongly alkaline with NaOH, and the base then extracted with ether. After drying the ether solution with sodium sulphate the ether was evaporated, and *dl*-proline 2-chloro-6-methyl anilide was obtained as an oil. Yield 6 g (85,5 %). (Found: N 11.63. Calc. for $C_{12}H_{15}ON_2Cl$: N 11.74).

dl-N-n-Butyl proline 2-chloro-6-methyl anilide (III). *dl*-Proline 2-chloro-6-methyl anilide (6 g) was dissolved in *n*-butyl alcohol (30 ml) and then under stirring refluxed with potassium carbonate (3 g) and *n*-butyl bromide (3.6 g) for 20 h. The reaction mixture was filtered and the filtrate evaporated under vacuum. The residue was dissolved in diluted hydrochloric acid and carbon treated. A crystalline precipitate was obtained with NaOH. Yield 6 g (81 %); m.p. after recrystallization from ether 77—78°C. (Found: N 9.41. Calc. for $C_{16}H_{23}ON_2Cl$: N 9.52).

dl-N-Ethyl nipecotic acid 2-chloro-6-methyl anilide (VI). *dl*-N-Ethyl nipecotic acid (50 g) was treated with thionyl chloride (150 g). When the reaction subsided, the mixture was heated on a water bath for 30 min, when a clear solution was obtained. The excess of thionyl chloride was driven off under vacuum, until crystallization occurred. In order to make the crystallization complete, ether (100 ml) was added and the mixture shaken, after which the crystal slurry was drawn off and washed with ether. Without drying the crystals were suspended in acetone (300 ml). To the suspension 2-chloro-6-methyl aniline (65 g) was added drop by drop. The mixture was refluxed for 15 min after which the acetone was driven off under vacuum. The residue was dissolved in water (500 ml). The pH was adjusted to 5.5 and unreacted 2-chloro-6-methyl aniline removed by ether extraction. The water solution was cleared from ether and the base precipitated with NaOH. Yield 75 g (84 %); m.p. after recrystallization from alcohol and ether 122—123°C. (Found: N 9.99. Calc. for $C_{15}H_{21}ON_2Cl$: N 9.98).

dl-N-Ethyl pipecolic acid o-toluidide (VII). *dl*-N-Ethyl pipecolic acid (50 g) was heated on a steam bath under stirring with 2-methyl phenyl *iso*cyanate (100 g). When the evolution of carbon dioxide had ceased the excess of *iso*cyanate was driven off under vacuum. The residue was boiled for 15 min with 27 ml of conc. hydrochloric acid and 250 ml of water. The mixture was cooled down and filtered. After carbon treatment and precipitation with NaOH the base was obtained in the form of crystals. Yield 52 g (65 %); m.p. after recrystallization 97—98°C. (Found: N 11.40. Calc. for $C_{15}H_{22}ON_2$: N 11.38).

dl-Proline 2,6-xylidide (VIII). 2-Chloro-5-aminovaleric acid hydrochloride (94 g) prepared according to Albertson *et al.*[12] was chlorinated in acetyl chloride (450 ml) with phosphorus pentachloride (188 g) under cooling with ice water. After 7 h the crystals

formed were washed with toluene and suspended in acetone. 2,6-Xylidine (120 g) was added to the suspension, and the mixture heated on a water bath for 30 min. Water was added and the acetone driven off under vacuum. The pH was adjusted to 5 and the excess of xylidine removed by ether extraction. The water solution was carbon treated and NaOH added to pH 12, when an oil began to precipitate. After stirring for 2 days at room temperature a crystalline product was formed. This was extracted with ether, and after evaporation of the ether an oil was obtained which crystallized after some time. Yield 53.5 g (49 %). (Found: N 12.71. Calc. for $C_{13}H_{18}ON_2$: N 12.84).

After ethylation with diethyl sulphate according to III, a product was obtained, identical with *dl*-N-ethyl proline 2,6-xylidide prepared from *dl*-proline.

Malonic acid ethylester 2,6-xylidide (IX). 2,6-Xylidine (121 g) was heated with diethyl malonate (400 g) at 155—160° for 1 h and the ethanol distilled off as it was formed. Then the excess of diethyl malonate was distilled off under vacuum. To the crystalline residue ethanol (500 ml) was added. After cooling down the crystals of malonic acid dixylidide formed were filtered off. The alcohol solution was diluted with water (2 l) under agitation, when malonic acid ethylester xylidide crystallized out. The monoxylidide was filtered, washed with water and recrystallized from 50 % ethyl alcohol. Yield 138 g (58.8 %); m.p. 100—101°C. (Found: N 6.08. Calc for $C_{13}H_{17}O_3N$: N 5.96.)

Isonitrosomalonic acid ethylester 2,6-xylidide (X). To a solution of malonic acid ethylester 2,6-xylidide (60 g) in chloroform (400 ml) nitrosyl chloride was added during 6 h at 0°C. The crystals of the *iso*nitroso compound formed were filtered off washed with chloroform and dryed in vacuum. Yield 56 g. From the mother liquor a further 5 g were obtained by vacuum evaporation. Total yield 61 g (90.5 %); m.p. 193—194°C. (Found: N 10.51. Calc. for $C_{13}H_{16}O_4N_2$: N 10.60).

Aminomalonic acid ethylester 2,6-xylidide (XI). *Iso*nitrosomalonic acid ethylester 2,6-xylidide (60 g) was dissolved in formic acid (200 ml). Zinc powder (36 g) was added in portions during 1 h at 90—95°. After a further hour at 90° the hot solution was filtered and evaporated under vacuum. The evaporation residue was dissolved in hot amyl alcohol, washed neutral with 5 % bicarbonate solution and filtered. The amyl alcohol was driven off under vacuum and the residue recrystallized from 50 % ethyl alcohol. Yield: 47.2 g (83 %); m.p. 195°C. (Found: N 11.18. Calc. for $C_{13}H_{18}O_3N_2$: N 11.20).

dl-Pipecolic acid 2,6-xylidide (XII). In a sodium ethylate solution, prepared by dissolving sodium (4.6 g) in abs. alcohol (125 ml), aminomalonic acid ethylester 2,6-xylidide (50 g) was dissolved. Tetramethylene dibromide (87 g) was added at 70° during 20 min. The reaction mixture was then refluxed for 6 h, cooled down and filtered. The ethanol and excess of tetramethylene dibromide were distilled off with steam. The remaining oil was separated from the water and refluxed with conc. hydrochloric acid (150 ml) for 3 h, after which the solution was evaporated to dryness under vacuum. The residue was dissolved in water and the pH adjusted to 5 with caustic soda. The water solution was extracted with ether, carbon treated and precipitated with NaOH at pH 13. Yield: 16 g (34.5 %). M.p. 115—116°C. After recrystallization from ethyl alcohol the m.p. rose to 120—121°C. (Found: N 11.98. Calc. for $C_{14}H_{20}ON_2$: N 12.07).

REFERENCES

1. Einhorn, A. and Oppenheimer, M. *Ann.* **311** (1900) 154.
2. Einhorn, A. and Uhlfelder, E. *Ann.* **371** (1910) 162.
3. Miescher, K. *Helv. Chim. Acta* **15** (1932) 163.
4. Erdtman, H. and Löfgren, N. *Svensk Kem. Tidskr.* **49** (1937) 163.
5. Löfgren, N. *Arkiv Kemi Mineral. Geol.* **22A** (1946) No. 18.
6. Garmid, K. N., Ray, J. N. and Yajnik, J. N. *J. Indian Chem. Soc.* **17** (1940) 400.
7. Garmid, K. N., Ray, J. N. and Sarni, B. *J. Indian Chem. Soc.* **17** (1940) 619.
8. Hofstetter, E. *Nature* **170** (1952) 980.
9. Ehrhardt, G., Ruschiz, H., Stein, L. Anmüller, W. and Ther, L. Ger. 942993.
10. Barnes, A. *J. Am. Chem. Soc.* **49** (1927) 1308.
11. Fischer, E. och Reif, G. *Ann.* **363** (1908) 123.
12. Albertson, N. F. and Fillman, J. L. *J. Am. Chem. Soc.* **71** (1949) 2819.

13. Putochin, N. J. *Ber.* **56** (1923) 2213.
14. Chattaway, F. D. and Olmsted, J. M. D. *J. Chem. Soc.* **97** (1910) 939.
15. Whiteley, M. A. *J. Chem. Soc.* **83** (1903) 29.
16. af Ekenstam, B., Egnér, B., Ulfendahl, H., Dhunér, K. G. and Oljelund, O. *Brit. J. Anaesthesia* **11** (1956) 503.
17. Dhunér, K. G., Oljelund, O. and Aageson, G. *Acta Chir. Scand.* **1957**. *In Press.*

Received April 8, 1957.

ACTA CHEMICA SCANDINAVICA 11 (1957) 1191–1200

On Vitamins in Sewage Sludge

V. The Effect of Antibiotics on Vitamin B_{12} Contents of Microbially Decomposing Sewage Sludge

HALINA Y. NEUJAHR

Division of Food Chemistry, Royal Institute of Technology, Stockholm, Sweden

The effect of the addition of antibiotics to microbially decomposing sewage sludge was studied with respect to the amount of vitamin B_{12} activity formed and its distribution between the different factors. *Aureomycin* was found to stimulate the formation of vitamin B_{12} activity if added at a sludge decomposition stage characterized by pH 6.5–7.0. Under anaerobic conditions the addition of aureomycin caused an enhanced synthesis of factors with R_F-values related to that of factor III, whereas under aerobic conditions the synthesis of cyanocobalamin was stimulated. — Under aerobic conditions *terramycin* was found to have a similar, but less pronounced, effect. — Both active and inactivated *penicillin* stimulated the synthesis of cyanocobalamin and of other vitamin B_{12} factors when incubated with sludge. The effect was more pronounced with the inactivated agent, thus suggesting the possibility that the latter may be the factor stimulating the vitamin B_{12} synthesis. — *Neomycin* stimulated the synthesis of cyanocobalamin and of other vitamin B_{12} factors. Heat and alkali treated (but not inactivated) neomycin had a detrimental effect on the synthesis of cyanocobalamin.

Antibiotics are known to exert a vitamin B_{12} "sparing action" on several animals and are extensively used as "feed supplement" for pigs and chickens. The mechanism of this action has not yet been elucidated and the experimental evidence is contradictory on some points.

Many investigators support the view that antibiotics enhance the growth of young poultry and swine merely through alterations of the normal intestinal microflora, whereas others postulate that the antibiotic molecule or a fragment thereof is involved as a metabolite in the host. The latter hypothesis is based on experiments with inactivated antibiotics, administered perorally and parenterally to chickens [1] and pigs [2].

Peterson and Johanson [3] in their experiments with rats have shown that both the active and inactivated agents, regardless of the route of administration, induced marked changes in the intestinal microflora which, however,

were not always accompanied by a growth effect in the host. It has been shown by several workers that feeding with a diet containing antibiotics — but limited in vitamin B_{12} — results in increased synthesis (or contents) of vitamin B_{12} in the intestines of chickens [4] and rats [5].

According to Pawe kiewicz [6] the addition of aureomycin to a culture of propionic acid bacteria increases the formation of cyanocobalamin and cobalamin X at the expense of vitamin B_{12p} (which has been identified as factor B). Mannino and Pipitone [7], however, have reported that in *Bacterium coli* the amount of vitamin B_{12} produced in the presence of antibiotics was less than in their absence.

The process of formation of vitamin B_{12} factors during aerobic and anaerobic fermentation of municipal sewage sludge has previously been studied in this laboratory [8].

The attempt has now been made to investigate in what way this process may be influenced by addition of antibiotics.

Fresh sewage sludge with graded levels of aureomycin, terramycin, penicillin and neomycin was fermented aerobically and anaerobically. Samples were taken at definite time intervals and analyzed for vitamin B_{12} activity by means of microbiological tests; the different vitamin B_{12} factors were identified by bioautographic methods.

EXPERIMENTAL

Fresh sludge from a settling tank of the Stockholm municipal sewage plant was disintegrated in a "Turmix" blendor, mixed with *ca.* 20 % of digested sludge and diluted with water. The substrate thus obtained had a dry solid content of *ca.* 4 % and pH 5.0—5.5. It was fermented aerobically and anaerobically at 33°C with addition of some antibiotics. The experimental conditions of the different investigations are summarized in Table 1. Experiments Nos. 2 and 3 were performed in glass fermenters each of 10 litres capacity, provided with stirrers, heating coils, arrangements for inlet of gas and for removal of samples. The appropriate temperature (33°C) was obtained by circulating warm water from constant temperature baths through the coils of the fermenters with simultaneous stirring. In the anaerobic fermentation (expt. No. 2) a gas mixture of CH_4 and CO_2 (6:4) was blown through the sludge until all air was removed, this procedure being used every time the sludge came in contact with air, *e. g.* after removal of a sample. In expt. No. 3 air was blown through the sludge, 2 × 30 min every day.

Experiments Nos. 1, 4, 5, 6, and 7 were performed in conical flasks placed in rooms with thermostatically controlled air temperature. Shaking table was used for the aerobic fermentations, whereas for the anaerobic fermentations no special arrangements were made — the flasks were filled with sludge with only a very small space left above and incubated in the thermostat. Samples were treated as described elsewhere [8]. Vitamin B_{12} activity was estimated with the aid of the cup plate, the tube and the bioautographic methods using *Escherichia coli* 113—3. In some few cases ionophoretic estimations in combination with bioautography were carried out.

Bioautography. For chromatography it proved to be more convenient to modify the technique used in the earlier experiments [9]. In the present investigation the following procedure was adapted:

Paper: Whatman 1. Each spot corresponded to 1 μl of the solution to be tested. The paper strips were prepared in duplicate and developed for 48 h in two different solvent systems at 18°C.
Solvent system I: *sec.* butanol: H_2O:HAc (75:24:1) + 0.01 % KCN.
Solvent system II: *sec.* butanol: H_2O:NH_3 (75:24:1) + 0.01 % KCN.
Two standard solutions were used:
Standard solution 1 (S1): cyanocobalamin + factor III + factors (Z2 + Z3) [10].
Standard solution 2 (S2): factor A + factor B.

The resolution of factors Z2 and Z3 could not be achieved by this technique but instead factor III could be separated from factor A in solvent system II.

However, after the chromatographic resolution of the initial spots of the samples, the spots with R_F-values corresponding to that of factor A may not represent this factor or perhaps not only this factor. In an earlier investigation [10] it has been shown that sewage sludge contains at least 6 different factors with R_f-values closely related to that of factor A and of ψ -B_{12}. As only the two latter factors had been obtained in crystalline state [11,12], the author found it appropriate to use factor A as standard instead of a mixture of factors isolated from sewage sludge. In the following the spots corresponding to factor A will be designated as "A". Obviously, "A" may signify a mixture of the following factors: A + ψ-B_{12} + XI + X2 + X3 + X4 + III + W in solvent system I, whereas in solvent system II factors III + W can be resolved from the other factors. The spots corresponding to factor III may also contain factor W.

Paper electrophoresis of the samples in combination with bioautography revealed in several instances that "A" corresponded to more than one factor but it was not possible to obtain sufficient information about the nature of these factors.

Following preparations of antibiotics were used in the different experiments:

Aureomycin: Aureomycin HCl crystalline, Lederle.
Terramycin: Terramycin HCl crystalline, Pfizer.
Penicillin: Benzylpenicillin, AB Kabi.
Neomycin: Mycifradin sulphate, The Upjohn Company.

Heat and alkali treatment of penicillin and neomycin. The solutions were autoclaved at 121°C for 15 min at pH 12.

Table 1.

Expt. No.	Antibiotic added	Type of fermentation	Apparatus	Amount of sludge fermented ml	Time of addition: Days after the start of the ferment.	Time of addition: pH of the sludge
1	Aureomycin	Anaerobic	conical flasks (2 l); no stirring	1 800	0	5.5
2	Aureomycin	Anaerobic	glass fermenter (10 l) filled with a mixture of CH_4 and CO_2 gas (6:4); stirring	5 000	40	6.8
3	Aureomycin	Aerobic	glass fermenter (10 l); intermittent aeration; stirring	5 000	40	6.5
4	Auremycin	Aerobic	conical flasks (300 ml); shaking	100	20	7.5
5	Terramycin	Aerobic	conical flasks (300 ml); shaking	100	20	7.5
6	Penicillin	Anaerobic	conical flasks (300 ml);			
	a) active			280	0	5.5
	b) inactivated *			280	0	5.5
7	Neomycin	Anaerobic	conical flasks (300 ml); no stirring			
	a) active			280	0	5.5
	b) heat and alkali treated, but not inactivated			280	0	5.5

* by heat and alkali.

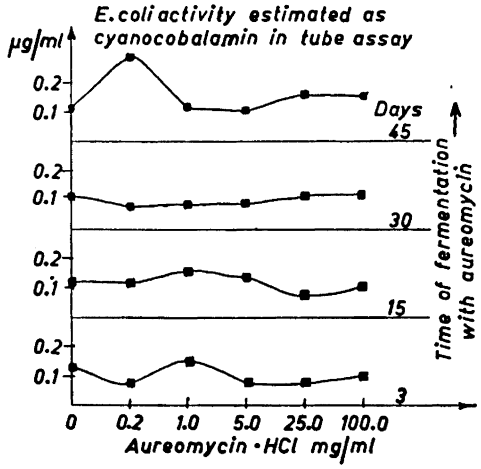


Fig. 1. (Expt. No. 1). Effect of the addition of aureomycin to fresh sewage sludge, subsequently anaerobically fermented.

RESULTS

The pH changes of the fermenting sludges to which antibiotics had been added were essentially the same as the corresponding changes in sludges containing no added antibiotics.

The results of the different experiments are shown in Figs. 1—7 *.

Experiment No. 1. The bioautographic estimation of vitamin B_{12} activity in samples taken 3, 15, 30, and 45 days after the start of the fermentation did not reveal any significant variations in the distribution of *E. coli* activity between the different vitamin B_{12} factors. The estimation in tube assay gave somewhat varying values of the total *E. coli* activity. These values are represented in Fig. 1. A slight maximum in *E. coli* activity can be noticed after 3 days of anaerobic fermentation of the sludge to which 1 mg aureomycin/l sludge had been added. This maximum is still maintained after 15 days of fermentation and it disappears after 30 days while, after 45 days, an unexpected maximum appears in the sludge with 0.2 mg aureomycin/l added. In view of the instability of aureomycin at the actual pH ($\sim$ 6) the results can hardly be explained by the antibiotic effect of aureomycin.

Experiments Nos. 2 and 3. The addition of aureomycin (10 mg/l) to sewage sludge which had already undergone certain microbial decomposition (pH $\sim$6.5) resulted in enhanced formation of cyanocobalamin under aerobic condi-

* Abbreviations used in Figs. 1—7.

I — solvent system I
II — solvent system II
t — time of fermentation
S1 — standard solution 1
S2 — standard solution 2
Z — factors Z2 + Z3
III — factor III
Cy — cyanocabalamin
A — factor A
B — factor B

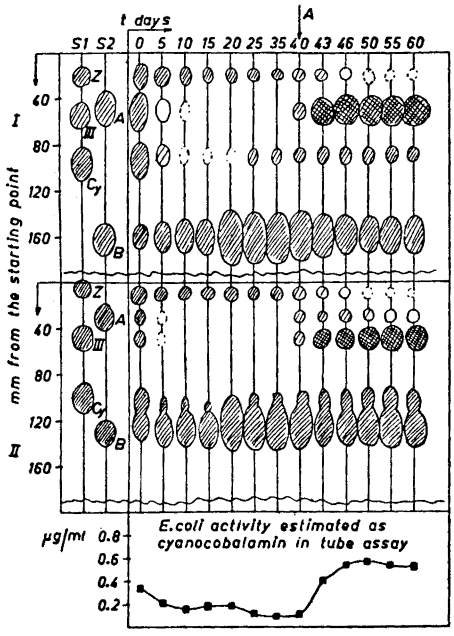


Fig. 2. (Expt. No. 2). Effect of the addition of aureomycin to anaerobically fermenting sewage sludge. Bioautogram *. A — addition of aureomycin . HCl (10 mg/l sludge).

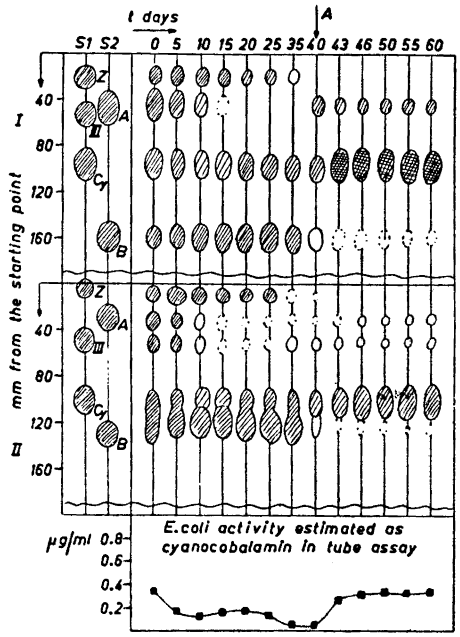


Fig. 3. (Expt. No. 3). Effect of the addition of aureomycin to aerobically fermenting sewage sludge. Bioautogram *. A — addition of aureomycin · HCl (10 mg/l sludge).

tions (*cf.* Fig. 3) and of factor III under anaerobic conditions (*cf.* Fig. 2). This is also clearly reflected in the significant increase of the total *E. coli* activity as estimated in tube assay (*cf.* Figs. 2 and 3).

Experiment No. 4. The results of this experiment further confirm the finding (expt. No. 3) that aureomycin stimulates the formation of cyanocobalamin in aerobically fermented sludge if added at the stage when the pH of the sludge has risen to about 7. The effect was most pronounced with 5—25 mg aureomycin per litre sludge after 40—90 h of fermentation, but was partly abolished by further fermentation as seen in the samples taken after 160 h **. During the first 40 h aureomycin also seemed to stimulate the formation of factors Z, whereas after 90 and 160 h its effect was the opposite. The same phenomenon could be observed with factors "A". The formation of factor III was only slightly stimulated by the addition.

* For abbreviations see footnote on p. 1194.

** This is apparently not fully in agreement with the results of expt. No. 3, where the increased contents of cyanocobalamin persisted for several days (*cf.* Fig. 3). It is possible that the relatively quicker destruction of cyanocobalamin in expt. No. 4 as compared with expt. No. 3 was due to the more vigorous aeration employed in this experiment (*cf.* Table 1).

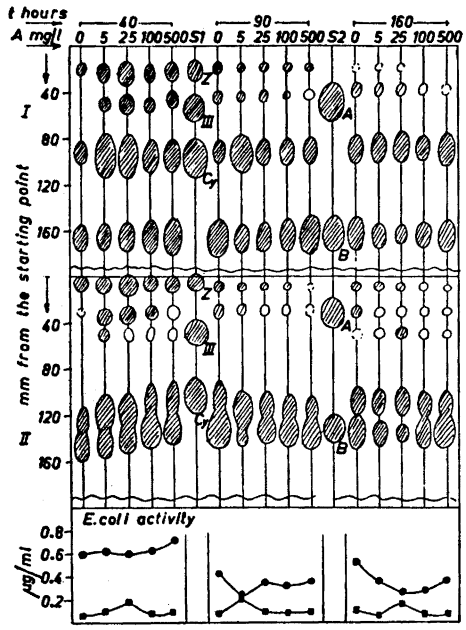


Fig. 4. (Expt. No. 4). Effect of the addition of aureomycin to aerobically fermenting sludge. Bioautogram *. A — aureomycin · HCl, graded amounts. ●—● cup assay; ■—■ tube assay.

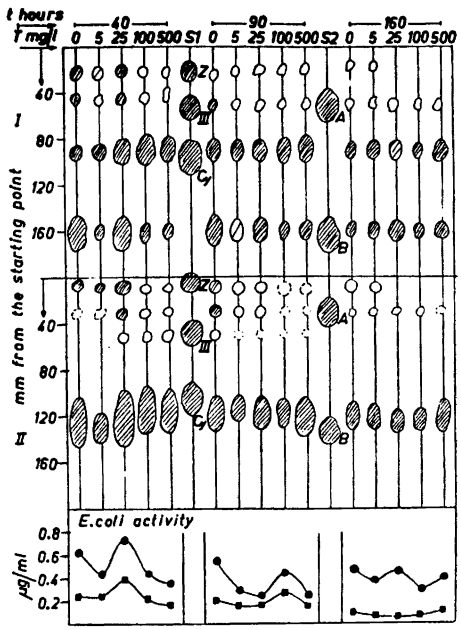


Fig. 5. (Expt. No. 5). Effect of the addition of terramycin to aerobically fermenting sewage sludge. Bioautogram *. T — terramycin · HCl, graded amounts. ●—● cup assay; ■—■ tube assay.

Experiment No. 5. 25—100 mg terramycin per litre aerobically fermented sludge stimulated formation of cyanocobalamin after 40 h of fermentation. This effect was partly abolished during continued fermentation. The effect upon other factors was more obscure. 5 mg terramycin/l sludge seemed to cause a minimum in the amount of factors B and Z, while 25 mg/l caused a maximum in the amounts of these factors as well as in those of factors "A".

Experiment No. 6. a) Addition of active penicillin stimulated the formation of cyanocobalamin; the effect was strongest with 20 mg penicillin/l sludge and could be noted after 10 days as well as after 30 days of anaerobic fermentation. With increasing amounts of penicillin increasing amounts of factors Z could be observed after 10 days of fermentation; the amount of factors "A" and factor III simultaneously decreased. The amount of factor B was almost unaffected. The effect was quite different after 30 days of fermentation. A pronounced maximum in the amounts of factor B, cyanocobalamin and factor III could then be observed with 20 mg/l. Factors Z disappeared.

b) The addition of increasing amounts of inactivated penicillin caused an increased formation of cyanocobalamin. The effect was strongest with 50

* For abbreviations see footnote on p. 1194.

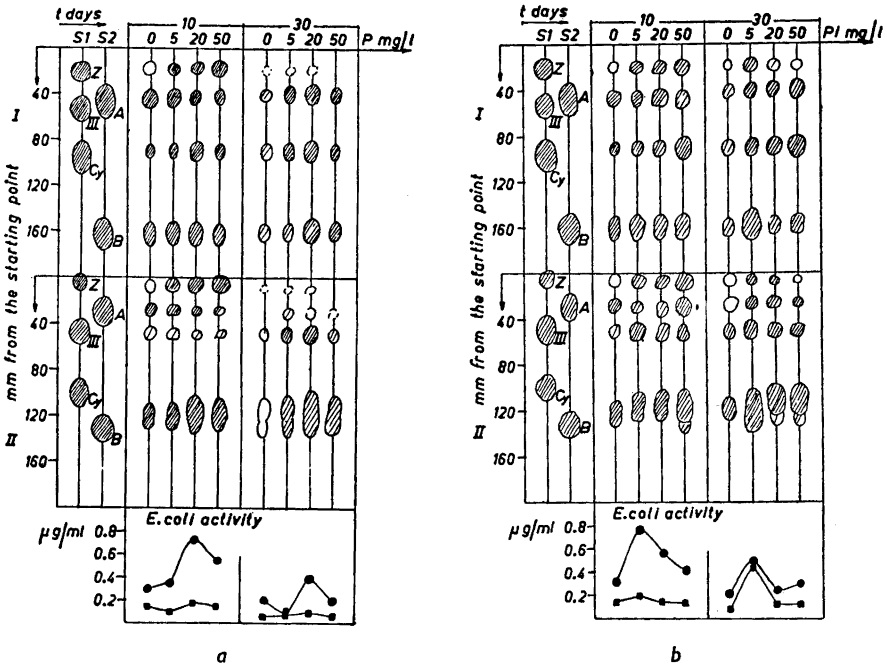


Fig. 6. (Expt. No. 6). Effect of the addition of penicillin to fresh sewage sludge, subsequently anaerobically fermented. Bioautograms *. a) P — active benzyl penicillin; b) Pi — heat and alkali inactivated benzyl penicillin. ●—● cup assay; ■—■ tube assay.

mg/l and could be noted after 10 days of fermentation as well as after 30 days. With increasing amounts of penicillin added, increased amounts of factors Z were observed after 10 days; after 30 days a maximum in the amount of these factors corresponded to the addition of 5 mg/l. The effect on the formation of factors "A" and III was less pronounced although a slight stimulation of their synthesis could be observed also here. The amount of factor B was unaffected after 10 days, but showed a clear maximum after 30 days in the sludge to which 5 mg/l had been added.

Experiment No. 7. a) 5—25 mg neomycin/l sludge caused an increased synthesis of cyanocobalamin and of factors Z, "A" and III after 10 days, but after 30 days the effect of neomycin upon the two latter factors was abolished. The synthesis of factor B was slightly stimulated by the addition of neomycin.

b) Increasing amounts of heat and alkali treated (but not inactivated) neomycin caused a decrease in the vitamin B_{12} activity as estimated in tube assay. The detrimental influence was exerted mainly upon cyanocobalamin, whereas the amount of factor Z showed a slight maximum after 10 days of fermentation in the sludge to which 5 mg neomycin per litre had been added. The amount of factor B was essentially unaffected by the addition.

* For abbreviations see footnote on p. 1194.

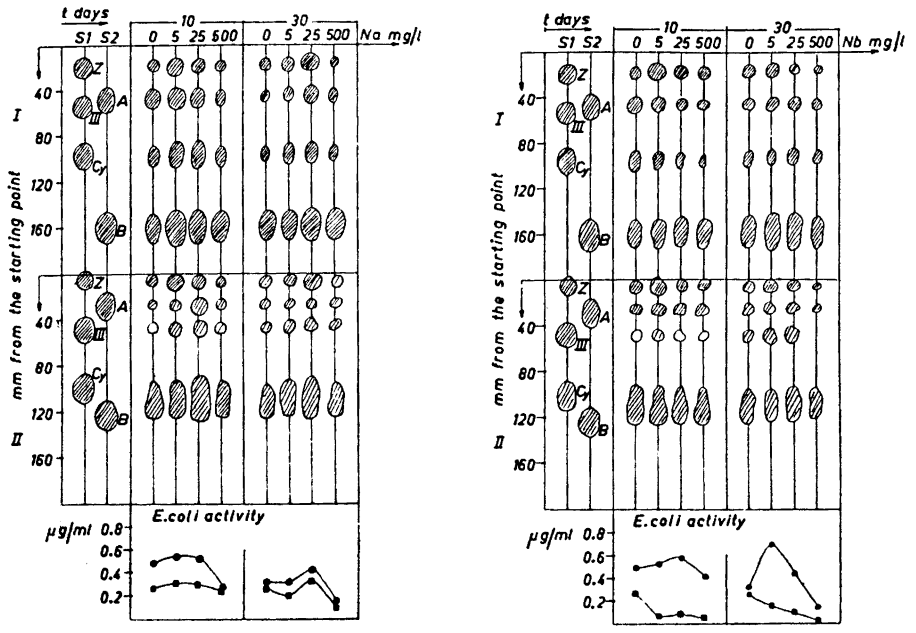


Fig. 7. (Expt. No. 7). Effect of the addition of neomycin to fresh sewage sludge, subsequently anaerobically fermented. Bioautograms *. a) Na — mycifradin sulphate; b) Nb — heat and alkali treated but not inactivated mycifradin sulphate. ●—● cup assay; ■—■ tube assay.

As can be seen in Table 2, antibiotics (except for the heat and alkali treated neomycin) generally increased the total vitamin B_{12} activity of microbially decomposing sewage sludge and most of them caused an increase of that part of the activity which is due to cyanocobalamin. The following circumstances seemed to exert a particular influence on this phenomenon.

1) the type of fermentation: aerobic or anaerobic.

2) the degree of decomposition of the sludge at the moment of addition, as characterized by the pH of the sludge.

Thus, under anaerobic conditions aureomycin had only a very slight effect on the vitamin B_{12} activity of decomposing sludge if added to "fresh" sludge (pH 5.5). Under similar conditions its addition to partly decomposed sludge (pH 6.5—6.8) caused a significant increase in the vitamin B_{12} content mainly due to the synthesis of *factor III*. Corresponding addition to intermittently aerated sludge resulted in an increased synthesis of *cyanocobalamin* accompanied by the disappearance of factor B, whereas with continuous aeration (shaking) a simultaneous formation of cyanocobalamin and of factor B was obtained. It is difficult to decide whether the effect of aureomycin depended on its antibiotic action or whether it was used as a "metabolite" enhancing the synthesis of vitamin B_{12} (*cf.* Pawelkiewicz, 1955[6]). The "immediate"

Table 2. Effect of the addition of antibiotics upon the vitamin B_{12} activity of sewage sludge.

+ = increase
— = decrease
0 = no change
+,— = slight effect
++,—— = medium effect
+++,——— = strong effect
+;— = initial increase followed by a decrease.

Antibiotic added mg/l sludge	Type of sludge	Type of fermentation after the addition	Effect on					
			Total vit. B activity, tube assay	Cyanocobalamin	Factor III	Factors "A"	Factors Z	Factor B
Aureomycin 0.2—5.0	fresh, pH 5.5	anaerobic	+ (?)	0	0	0	0	0
Aureomycin 10	fermenting, pH 6.8	anaerobic	+++	0	+++	0	0	—
Aureomycin 10	fermenting, pH 6.5	aerobic (intermittent aeration)	+++	+++	0	0	0	———
Aureomycin 5—25	fermeuting, pH 7.5	aerobic (continuous aeration)	++	+++	+;—	+;—	+;—	++
Terramycin 25—100	fermenting, pH 7.5	aerobic (continuous aeration)	++	++;—	(+;—)	(+;—)	(+;—)	(—;+;—)
Penicillin								
a) active 5—50	fresh, pH 5.5	anaerobic	+	+++	——	——	+++	0;++
b) inactivated 5—50	fresh, pH 5.5	anaerobic	+++	+++	+	+	+++	+
Neomycin								
a) untreated 5—25	fresh, pH 5.5	anaerobic	++	+++	++	++	++	+
b) heat and alkali treated 5—25	fresh, pH 5.5	anaerobic	———	——	(?)	0	+;—	0

(40 h) effect of the addition of aureomycin to partially decomposed sludge (expts. Nos. 2 and 3) may suggest the latter possibility, or it may indicate that the growth of some strains consuming different vitamin B_{12} factors has been inhibited, thus causing the accumulation of the corresponding factors in the sludge. Probably both mechanisms were involved *.

The results obtained with penicillin differ from those obtained with aureomycin (expt. No. 1) in that the addition to *fresh sludge* of active as well as of inactivated penicillin followed by anaerobic fermentation caused an increase of the vitamin B_{12} activity. Both agents seemed to enhance the synthesis of

* The reservation must here be made that due to some variations in experimental conditions as stirring, shaking, amount of sludge fermented (*cf.* Table 1) not all the experiments are fully comparable.

cyanocobalamin, strikingly accompanied by the synthesis of factors Z which may suggest the possibility of a metabolic relationship between cyanocobalamin and these factors. Active penicillin caused a decrease in the amounts of factors III and "A" and did not affect the amount of factor B in the beginning but increased it during continued fermentation. On the other hand inactivated penicillin increased the amount of all these factors. It seems likely, therefore,, that inactivated penicillin is the agent responsible for an enhanced synthesis of vitamin B_{12} factors in digesting sewage sludge, as the benzylpenicillin used in the experiments must have been inactivated very soon after the beginning of the fermentation.

Acknowledgements. The author is grateful to Professor H. Lundin, Head of the Division, for his encouraging interest in and valuable advice on the execution of this work; she also wishes to thank AB Kabi, Stockholm, for their kind gift of antibiotics. Thanks are also due to Miss R. Wolf for technical assistance. The financial support from *Statens Tekniska Forskningsråd* is gratefully acknowledged.

REFERENCES

1. Elam, J. F., Gee, L. L. and Couch, J. R. *Proc. Soc. Exptl. Biol. Med.* **78** (1951) 832.
2. Taylor, J. H. and Gordon, W. S. *Nature* **176** (1955) 312.
3. Peterson, G. E. and Johansson, K. R. *Antibiotics Annual* **1953—54**, p. 386.
4. Jenkins, K. J., Bell, J. M., O'Neil, J. B. and Spinks, J. W. T. *Can. J. Biochem. Physiol.* **32** (154) 628.
5. Peterson, G. E., Dick, E. C. and Johansson, K. R. *J. Nutrition* **51** (1953) 171.
6. Pawelkiewicz, J. *Acta Biochim. Polon.* **2** (1955) 321.
7. Mannino, N. and Pipitone, V. *Boll. soc. ital. biol. sper.* **30** (1954) 308.
8. Neujahr, H. Y. *Acta Chem. Scand.* **9** (1955) 622.
9. Sjöström, A. G. M., Neujahr, H. Y. and Lundin, H. *Acta Chem. Scand.* **7** (1953) 1036.
10. Neujahr, H. Y. *Acta Chem. Scand.* **10** (1956) 917.
11. Ford, J. E., Kon. S. K. and Porter, J. W. G. *Chemistry & Industry* **44** (1952) 132.
12. Pfiffner, J. J., Dion, H. W. and Calkins, D. G. *Federation Proc.* **11** (1952) 269.

Received April 9, 1957.

ACTA CHEMICA SCANDINAVICA 11 (1957) 1201—1208

An Ultra Micromethod for the Determination of Total Cholesterol in Bile Based on the Tschugaeff Color Reaction

KLAVS H. JØRGENSEN and HENRIK DAM

Department of Biochemistry and Nutrition, Polytechnic Institute, Copenhagen, Denmark

In the present method all operations, including the development of the color, take place in one and the same vessel (a centrifuge tube). The final volume of the reaction mixture is small (0.5 ml). Hence the method permits the determination of as little as 2 μg cholesterol. When used on a hamster bladder bile extract the Tschugaeff reaction gives rise to a yellow color besides the red color due to cholesterol. A correction for this yellow color is described.

The method was developed for the purpose of determining cholesterol in bladder bile of syrian hamsters where the volume obtainable from one animal usually is between 5 and 50 microliter. The amount of cholesterol present in such a sample may be as low as 2 μg. In principle it may be possible to use the method on other biological fluids than bile, such as blood plasma.

EXPERIMENTAL

Reagents

Standard cholesterol, prepared from crude cholesterol by purification through the dibromide,

Aqueous KOH solution, 1 M.

Chloroform, Ph.Dan.

Acetyl chloride, analytical grade (E. Merck, A.G.). This reagent should not be used for a longer period than 1 month after the first opening of the ampoule, and should be stored at a temperature below 5°C.

Glacial acetic acid, analytical grade (E. Merck, A.G.).

$ZnCl_2$, anhydrous, in sticks, analytical grade (M & B, Ltd.).

A 20 % solution (w/w) of $ZnCl_2$ in glacial acetic acid was prepared by heating on a water bath at 65°C under occasional shaking. The solution which is turbid is clarified by standing or centrifugation. It can be used for at least one month.

Procedure

A. Extraction. 0.003 to 0.010 ml hamster bladder bile * is introduced by means of a Carlsberg pipette [1] into a centrifuge tube having a standard taper female joint 10/15 (shown in Fig. 1). The shape and size of the tube is so chosen that with a content up to

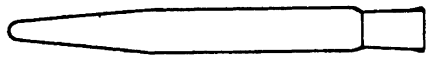


Fig. 1. The vessel in which all operations take place. It is furnished with a standard taper female joint 10/15. Total length: 116 mm, max. diameter: 12 mm, volume up to the joint: about 7 ml.

1 ml nothing will escape from the vessel during violent shaking on a "Microid Flask Shaker" (Griffin & George Ltd.). 0.5 ml of a 1 M KOH solution is added and mixed with the bile by shaking on the just mentioned shaker. The bile alkalized in this way is quite clear. 0.3 ml of chloroform is added and the tube is shaken violently on the shaker for 1/2 min, whereby an emulsion is formed. The tube is then centrifuged (3 000 r.p.m.). In order to ensure extraction of that part of the layer which at the beginning of the shaking may have been thrown up on the upper interior surface of the tube, the latter is again shaken 1/2 min and centrifuged until a yellow, clear aqueous layer is completely separated from a bottom layer which consists of an upper white emulsion and a lower colorless chloroform part. As much as possible of the clear aqueous layer is carefully removed by suction by means of a Carlsberg pipette equipped with a rubber cap. 1/2 ml of water is poured down along the inner wall of the tube. The tube is shaken on the shaker for about 10 sec, centrifuged, and the clear supernatant sucked off. This washing procedure is carried out 4 times in all. The last aqueous layer which is sucked off shall be of neutral reaction, and the emulsion layer shall have disappeared or be reduced to a thin white film between the chloroform and water layers. After the last sucking off, 0.3 ml chloroform is poured down along the inner wall of the tube.

Simultaneously with two samples of bile, a blank and a known amount of cholesterol, 4 μg for instance, serving as a standard, are treated similarly. The cholesterol standard is introduced into the tube by pipetting, say 0.5 ml of a chloroform solution, which is thereafter evaporated.**

B. Evaporation. The evaporation of the 0.3 + 0.3 ml chloroform and about 0.050 ml water (the rest of the washing liquid) is carried out in the following way: The tube is placed in one of the clamps of the shaker and furnished with a standard taper male joint which through a rubber tube fixed in an other clamp of the shaker can be connected with a water suction pump or an oil pump. First the water suction pump is connected with the tube and the chloroform evaporated under shaking while the tube is immerged in a water bath of room temperature. When the pressure has fallen to 15 – 20 mm Hg the temperature of the water bath is raised to 40 – 50°C. Hereby the water in the tube is evaporated. The last trace of water is removed by means of the oil pump. The evaportion procedure requires only a few minutes for each tube.

C. The color reaction. To the residue in each of the tubes (2 with cholesterol from bile, one with standard cholesterol and one with the blank) is added 0.100 ml freshly prepared reagent mixture *** consisting of chloroform, acetyl chloride and 20 % $ZnCl_2$ acetic solution in the proportion 3 : 1 : 1 (by vol.). The tubes are sealed with polyethylene stoppers coated on the upper part of the conical surface with a thin layer of starch-glycerol

* After puncture of the gallbladder of the killed animal the bile is taken out in a capillary tube by suction (not directly with the Carlsberg pipette).

** Concerning the technique of evaporation, see under B.

*** For the pipetting of $CHCl_3$ and reagent mixture Carlsberg pipettes equipped with rubber caps were used.

grease [2]. The stoppers are turned down into the grounds until they fit quite tightly *. The whole inner surface, but not the stopper, is brought in contact with the reagent mixture by suitable gentle turning of the tube. The tubes are then placed in a water bath of 65°C and remain there for exactly 6 min, whereafter they are cooled in ice water for some minutes and are then warmed to room temperature. The stoppers are removed, and the contents of the tubes are diluted with 0.400 ml of the reagent mixture. The stoppers are again inserted and the tubes shaken on the shaker, whereafter the contents are transferred by pipettes to semimicro cuvettes (internal measures: height 40 mm, width 4 mm, and length (ligth path) 10 mm). These cuvettes may be used for contents of about 0.5 ml in a Beckman Spectrophotometer DU when the slit of the instrument is covered with a metal plate furnished with a small opening and the cuvettes are raised about 5 mm from the bottom of the holder. Finally, the extinctions ($E = -\log (I/I_0)$) are measured within 15 min against the blank at 522 mμ and at 440 mμ.

CALCULATION OF THE CHOLESTEROL CONTENT

As mentioned later, the red color developed in the Tschugaeff reaction will be accompanied by a yellow color when the reaction is applied to a hamster bladder bile extract. This yellow color will absorb to a certain extent at the maximum of the red color (522 mμ). It is possible, however, to compute the extinction E'^{bile}_{522} caused by cholesterol alone, by making use of the observed extinctions E^{bile}_{522} and E^{bile}_{440} for the bile sample examined, and the corresponding values E^{st}_{522} and E^{st}_{440} for the standard:

$$E'^{\text{bile}}_{522} = E^{\text{bile}}_{522} \frac{1-0.43\ E^{\text{bile}}_{440}/E^{\text{bile}}_{522}}{1-0.43\ E^{\text{st}}_{440}/E^{\text{st}}_{522}}$$

Thereby the cholesterol content m_{bile} of the sample may be calculated from the amount of standard cholesterol m_{st}:

$$m_{\text{bile}} = m_{\text{st}}\ E'^{\text{bile}}_{522}/E^{\text{st}}_{522}$$

or

$$m_{\text{bile}} = \frac{E^{\text{bile}}_{522} - 0.43\ E^{\text{bile}}_{440}}{E^{\text{st}}_{522} - 0.43\ E^{\text{st}}_{440}}\ m_{\text{st}}$$

DISCUSSION OF THE METHOD

Experiments with standard cholesterol

The colorimetric determination of as little as 2 μg of cholesterol with a reasonable accuracy in cuvettes with a light path of 1 cm and a final volume of the reaction mixture of 0.5 ml requires the use of either the Tschugaeff or the Zlatkis reaction [3]. The Tschugaeff reaction is preferred because of the relative unspecificity of the Zlatkis reaction as pointed out by Lovern [4].

Several methods based on the Tschugaeff reaction are described in the literature, but they all use a final volume of 5 ml or more.

* Polyethylene stoppers fitting to standard taper joints are now commercially available.

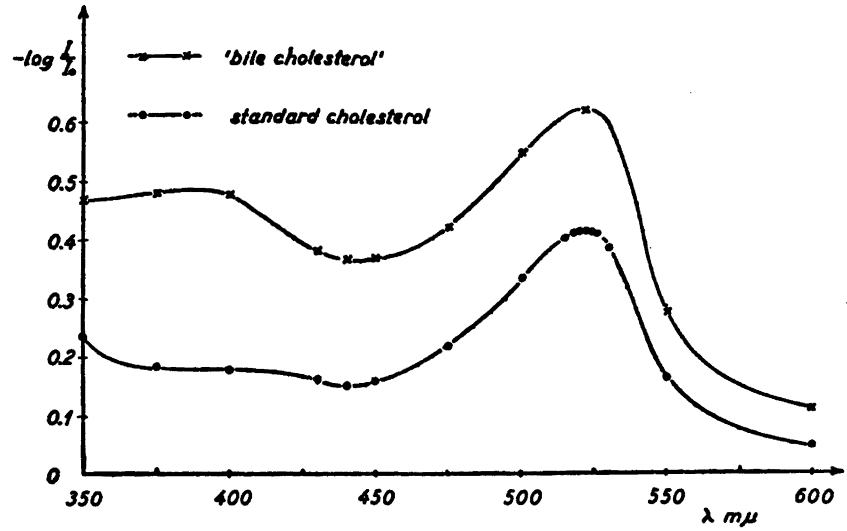


Fig. 2. Absorption curves for the Tschugaeff reaction on 8 μg standard cholesterol and "bile cholesterol" from 0.025 ml hamster bladder bile. Total volume of reaction mixture: 1/2 ml.

Recently, Schön and Gey [5] have described a method in which the color is developed by standing 3 h at room temperature. We could, however, not obtain the agreement with Beer's law reported by these authors.

The same applies to methods using a reaction temperature of 65°C, *e.g.* that of Hanel and Dam [6], when only a few μg of cholesterol shall be determined. The reason for these discrepancies is not clear.

If the reaction mixture is diluted 5 fold after the color has been developed (at 65°C and at a ratio by vol. between chloroform, acetyl chloride and $ZnCl_2$ reagent of 3 : 1 : 1) we have found that Beer's law will be followed in the extinction interval 0.1 to 1.7.

With a final volume of 0.5 ml it was necessary to use primarily 0.100 ml reagent mixture which is later diluted with 0.400 ml of the reagent mixture.

Table 1. Extinctions for various amounts of standard cholesterol per 0.5 ml total volume.

cholesterol μg	E_{522}	E_{522} per 2 μg	E_{440}	E_{440} per 2 μg
0.8	0.036	0.090	0.014	0.035
2	0.105	0.105	0.035	0.035
4	0.215	0.108	0.070	0.035
8	0.420	0.105	0.145	0.036
16	0.860	0.108	0.295	0.037
32	1.750	0.109	0.552	0.035

In order to prevent the escape of part of the volatile reaction mixture the afore-mentioned small tubes with polyethylene stoppers are required. When such stoppers are greased with starch-glycerol grease and turned firmly into the standard taper joints, they can withstand the vapor pressure during the heating of the reaction mixture.

Fig. 2 shows the results of measurements at different wavelengths for a cholesterol standard. A maximum occurs at 522 mμ and a minimum at 440 mμ.

The results obtained for various concentrations of cholesterol at the maximum and the minimum are shown in Table 1.

Beer's law is followed with sufficient accuracy in the concentration interval 2 to 32 μg per 0.5 ml total volume.

If the solution of $ZnCl_2$ had been stored for several weeks deviation from Beer's law occurred. However, the solution could be used at least 1 month after its preparation. Deviation from Beer's law was also found if the acetyl chloride had been stored for a longer time after the first opening of the bottle. If stored cool the acetyl chloride could be used for at least 1 month.

The red color developed in the reaction was not absolutely stable. However, the decrease in intensity during 15 min was low (3—4 %) and nearly proportional to the concentration of cholesterol. Thus, the instability of the color is not an important source of error if only the photometer reading is carried out within 15 min after the development of the color and as simultaneously as possible for the bile sample and the reference standard.

Experiments with hamster bladder bile

As postulated by Zuckerman and Natelson [7], diluted alkali will split cholesterol from protein without heating in the presence of chloroform. This is confirmed by the results presented in Table 2.

Hydrolysis by heating with KOH is, therefore, superfluous. It is possible that esters of cholesterol will not be hydrolysed by the treatment chosen in our method, but cholesterol esters are not known to occur in bile, and, further, in the Tschugaeff reaction esters give the same extinction on a molar basis as free cholesterol [4].

In order to examine the purity of the "Tschugaeff color" when the reaction is applied to bile, the formerly described procedure was carried out on a bile sample and the extinction was measured at different wavelengths (Fig. 2.).

Table 2. Analytical results for bile heated for various lengths of time on steam bath with 0.5 ml 1 M KOH before the extraction with $CHCl_3$.

Sample No. 1 0.005 ml bladder bile		Sample No. 2 0.005 ml bladder bile	
Heating time, h	E_{522}	Heating time, h	E_{522}
0	0.138	0	0.238
0.25	0.143	0.5	0.242
0.5	0.139	1	0.239

Table 3. Extinctions at 522 mμ and 440 mμ for the colors obtained with the 1st, 2nd and 3rd extracts of alkalized bile.

Sample No.	Extraction No.	E_{522}	E_{440}	E_{522}/E_{440} Extract No. 1	2	3
I	1	0.137	0.093	1.47		
0.010 ml	2	0.012	0.028		0.429	
bile	3	0.003	0.003			—
II	1	0.622	0.366	1.70		
0.025 ml	2	0.058	0.137		0.424	
bile	3	0.029	0.067			0.433
III	1	1.08	0.541	2.00		
0.025 ml	2	0.076	0.168		0.452	
bile	3	0.035	0.086			0.407
IV	1	>3	1.60	—		
0.025 ml	2	0.114	0.235		(0.485)	
bile	3	0.090	0.205			0.439
				Average:	0.435	0.426

The absorption curve for "bile cholesterol" has another shape than the curve for standard cholesterol. In both cases the maximum is found at 522 mμ and the minimum at 440 mμ, but the absorption at the lower wavelengths is relatively higher for "bile cholesterol" than for standard cholesterol. Thus, $E^{st}_{522}/E^{st}_{440}$ is about 2.7, whereas $E^{bile}_{522}/E^{bile}_{440}$ is about 1.7. Therefore, the color obtained with "bile cholesterol" has a yellow tinge.

Several attempts to eliminate the yellow color were carried out such as heating of the alkalized bile before the extraction, further washing of the chloroform extract with water, alkali or acid, or the use of other solvents than chloroform, but without success.

In order to isolate the chromogenic impurities, and to ensure that the proposed procedure gives a complete extraction of cholesterol the following experiment was carried out: bile+0.5 ml 1 M KOH were shaken on the shaker with 0.3 ml chloroform and centrifuged in the usual way. The first supernatant was pipetted into another tube with 0.3 ml chloroform. After shaking for 1 min and subsequent centrifugation the supernatant was pipetted into a third tube with 0.3 ml chloroform. After renewed shaking for 1 min and subsequent centrifugation the supernatant was discarded. The 3 portions of chloroform were washed as usual and the analytical procedure was carried out as formerly described on all three samples and a blank. The colors given by the second and third extracts were not visibly red, but in most cases distinctly yellow. The results are presented in Table 3.

The experiments show that the yellow color given by the second and third extracts gives a certain extinction at 522 mμ. Therefore, the same must be the

Table 4. Experiment showing that the yellow color and the red "Tschugaeff color" do not interfere with each other.

Sample	No.	E_{522}	E_{440}
"Bile cholesterol" from 0.0125 ml bile	1	0.189	0.114
The same amount of "bile cholesterol" + 8 μg standard	2	0.595	0.261
8 μg standard	3	0.404	0.146

case for the yellow color included in the color from the first extract. Thus, a correction for the yellow color is necessary.

The table shows that the values E_{522}/E_{440} are increasing with increasing cholesterol concentration: this means that the relative contamination by the yellow color decreases.

Excluding the high value E_{522}/E_{440} for the second extract from sample IV, which apparently is extremely rich in cholesterol, the average values of E_{522}/E_{440} for the second and third extracts are nearly identical: about 0.43. This suggests that the cholesterol is completely extracted by the first extraction as a small amount of cholesterol in the second extract would have caused a significant increase of E_{522}/E_{440} compared with the corresponding value for the third extract.

To see whether the red color produced by cholesterol and the yellow color from the impurities interfered with each other, the following experiment was made: The extraction and evaporation procedures were carried out on 0.050 ml bile. The residue was dissolved in 1 ml chloroform. From this solution 0.250 ml was pipetted into a tube. 0.250 ml of the same solution was pipetted into another tube containing 8 μg of the standard cholesterol. A third tube contained only 8 μg of standard cholesterol. Thereafter, the rest of the procedure was carried out on the three samples and the blank, *cf.* Table 4.

Table 5. Double analyses of some samples of bile.

Sample No.	Bile for analysis ml	Cholesterol per ml bile μg	Mean	Deviation between single determinations in % of mean
I	0.005	765	779	3.6
	0.010	793		
II	0.003	1360	1290	10.9
	0.006	1220		
III	0.005	645	633	3.8
	0.010	621		
IV	0.005	571	597	8.9
	0.010	624		
V	0.005	540	537	1.1
	0.010	534		
			Average:	5.7

It is seen that the sum of the extinctions for samples 1 and 3 is equal to the extinction for sample 2 at 522 mμ as well as at 440 mμ. Thus, the yellow color which is included in the color for sample 1 does not interfere with the "Tschugaeff color" but is directly superposed on the latter.

Since, further, Beer's law is followed for the "Tschugaeff color" both at 522 and 440 mμ it is possible to correct for the yellow color in the following way:

With the designations

E^{bile}_{522} and E^{bile}_{440} = the observed extinctions for bile cholesterol,

E'^{bile}_{522} and E'^{bile}_{440} = the corrected extinctions, *viz.* the extinctions obtained if the yellow color were not present in the bile,

E^{st}_{522} and E^{st}_{440} = the observed extinctions for the standard,

and supposing that E_{522}/E_{440} for the yellow color is 0.43 (*cf.* Table 3), the following equation is obtained:

$$E'^{bile}_{522} = E^{bile}_{522} - (E^{bile}_{440} - E'^{bile}_{440})\ 0.43.$$

Introducing $E'^{bile}_{440} = E'^{bile}_{522} \frac{E^{st}_{440}}{E^{st}_{522}}$, the equation is transformed to:

$$E'^{bile}_{522} = E^{bile}_{522} \frac{1-0.43\ E^{bile}_{440}/E^{bile}_{522}}{1-0.43\ E^{st}_{440}/E^{st}_{522}}$$

The ratio $E'^{bile}_{522}/E^{bile}_{522}$ is usually between 0.8 and 0.9.

The content of cholesterol in the bile sample is thereafter calculated as formerly described (p. 1203).

In addition to the afore-mentioned recovery experiment (*cf.* Table 4), three recovery experiments were carried out in which the added cholesterol was introduced already at the beginning of the procedure. The results showed full recovery of the added cholesterol, *viz.* 102, 102, and 99 %, respectively.

In order to evaluate the accuracy with which cholesterol can be determined in hamster bile, a series of double estimations were carried out (Table 5).

To introduce as great a variation in the experimental conditions as possible, different amounts of the two samples corresponding to one double analysis were used. Further, the two samples were treated at different times, and the colors developed were measured together with different amounts of standard.

The average deviation between the individual determinations corresponding to a double analysis is 5.7 %.

REFERENCES

1. Linderstrøm-Lang, K. and Holter, H. In Bamann, E. and Myrbäck, K. *Die Methoden der Fermentforschung*, Thieme, Leipzig. 1941, pp. 1138–39.
2. Herrington, B. L. and Starr, M. P. *Ind. Eng. Chem. Anal. Ed.* **14** (1942) 62.
3. Zlatkis, A., Zak, B. and Boyle, A. J. *J. Lab. Clin. Med.* **41** (1953) 486.
4. Lovern, J. A. *Proc. Nutrition Soc. (Engl. and Scot.)* **15** (1956) 46.
5. Schön, H. and Gey, F. *Hoppe-Seyler's Z. physiol. Chem.* **303** (1956) 81.
6. Hanel, H. K. and Dam, H. *Acta Chem. Scand.* **9** (1955) 677.
7. Zuckermann, J. L. and Natelson, S. *J. Lab. Clin. Med.* **33** (1948) 1322.

Received April 15, 1957.

ACTA CHEMICA SCANDINAVICA 11 (1957) 1209—1215

Ion Exchange Equilibria

I. Sodium-Zinc, Sodium-Copper, Sodium-Manganese in Nitrate Solutions

RALPH DJURFELDT and OLOF SAMUELSON

Department of Engineering Chemistry, Chalmers Tekniska Högskola, Göteborg, Sweden

Results from measurements of ion exchange equilibria and swelling with a sulfonated resin in solutions of Na-Zn, Na-Cu, and Na-Mn nitrate are presented. The selectivity coefficient is independent of a dilution of the outer solution, but depends on the ionic composition of the resin. As the variations in swelling are very small this dependency must be ascribed to variations in the activity coefficients in the resin phase.

Exhange equilibria in ion exchange resins have been the object of numerous investigations, but most published work deals with the exchange between ions of the same valence. In the present paper data on the exchange in nitrate solutions between sodium ions and the following bivalent ions will be given: zinc, copper and manganese. The ion exchanger was a sulfonated resin of phenolic type (Wofatit KS). The aim of the investigation was to calibrate the resin so that it could be used for determinations of the complexity of metaphosphate solutions [1,2], but as the experimental results may be of general interest it seemed appropriate to present the experiments with nitrate solutions as a separate paper. Ion exchange equilibria with metaphosphate solutions will be given in Part II of the present series.

EXPERIMENTS

Ion exchange resin. The ion exchanger used was Wofatit KS of 0.4—0.5 mm particle size, which, after purification [2], was completely converted into the sodium form by treatment with a sodium chloride solution. This treatment was followed by washing with distilled water and drying in the air. The air dried resin was stored in flasks with close-fitting stoppers. The exchange capacity was determined by displacing the sodium ions with hydrochloric acid, evaporation to dryness and chloride titration according to Mohr. The exchange capacity per gram of air dry resin is given in the tables. The same resin was used in several experimental series and the differences in exchange capacity depend upon the somewhat varying moisture content after air drying.

For resins of the same type as used in the present investigation it has been shown that under similar conditions the counter ions have a negligible effect upon the exchange

Table 1. Exchange capacity and swelling

Counter ion	Exchange capacity mequiv./g Na+ resin (air dried)		n_r equiv./1000 g water		Average
Na	2.24;	2.24	3.76;	3.78	3.77
Cu	2.24;	2.24	3.63;	3.64	3.64
Zn	2.26;	2.26	3.67;	3.65	3.66
Mn	2.25;	2.25	3.71;	3.74	3.73

capacity [3]. This was checked by percolating 0.05 M nitrate solutions of the bivalent cations through columns containing a known weight of the sodium form of the resin until the effluent concentration was unchanged. After washing with water the bivalent cations were eluted with hydrochloric acid and transformed to sulfates by addition of sulfuric acid and evaporation to dryness. The sulfates were determined using the alkalimetric ion exchange method [4]. The results presented in Table 1 confirm that the differences in exchange capacity are small.

In the same table are given results from swelling determinations performed in pure water. For this type of resin the deswelling in the dilute solutions used in the ion exchange experiments can be neglected [4]. The experiments were performed according to the centrifuge technique [5]. In all experiments the sodium form of the resin (air dried) was weighed in and transformed into other forms as described above. The moisture content of the air dried Na-resin (26.1 % H_2O) was determined by drying over magnesium perchlorate in vacuum at 55°C.

A correction was applied for the increase in weight because of the ion exchange and instead of tabulating the amount of water per unit weight of resin the results are given as equivalents of metal ions per 1 000 g of water (n_r). In a separate series of experiments the swelling was studied for resins containing varying amounts of sodium and manganese ions. The results are given in Table 2.

Table 2. Swelling of Na—Mn-resin

Equivalent fraction, X_{Mn}	0.00	0.09	0.27	0.48	0.68	0.87	1.00
Equivalent concentration, n_r	3.77	3.74	3.74	3.74	3.73	3.73	3.73

Solutions. Solutions of 0.1 M sodium nitrate (for some experiments 0.2 M) and of 0.05 M copper-, zinc- and manganese-nitrate were prepared by dissolving calculated amounts of c.p. reagents in distilled water. The concentration of the solutions was determined according to the ion exchange method by passing known volumes through a cation exchange resin in the hydrogen form and titrating the liberated acid [3].

Procedure. In each experiment 40.00 ml 0.1 M sodium nitrate solution, a certain volume (a ml) of the nitrate solution containing the bivalent metal and (10—a) ml water were mixed in an Erlenmeyerflask. After addition of 1.000 g dry resin the flasks were closed and shaken for 17—18 h in a shaking apparatus. Preliminary experiments showed that equilibrium was attained within 4 h. After shaking, the solution was analyzed. In some experiments the order of the additions was altered in order to make sure that the equilibrium was reversible. — With manganese, experiments were performed also at higher dilution (at a total volume of 150 and 500 ml).

The determination of copper was made iodometrically in a biphthalate buffer [6]. For zinc a polarographic method was applied [7], using the Radiometer polarograph, PO3. Manganese was determined colorimetrically with a Coleman spectrophotometer after oxidation to permanganate with potassium periodate in phosphoric and nitric acid solution [6]. A number of duplicate experiments were performed and at least two analytical determinations were made in each experiment. The agreement was very good and only the average values are presented in the tables and diagrams. Some duplicate experiments were made about three months after the first experiments with manganese. In the meantime the resin had been run through three or four exchange cycles with metaphosphate solutions. In spite of this only small deviations could be detected.

CALCULATIONS

From the concentration of the bivalent cation in the equilibrium solution the amount of bivalent ions in the resin is calculated by difference. In this calculation the change in volume of the outer solution caused by the swelling of the resin is not taken into consideration. For the ion exchanger used the swelling was very small compared to the volume of the outer solution. Therefore, the errors in the calculations are insignificant. Furthermore, the nitrate concentration in the resin has been neglected. For this type of resin this is permitted when working at a low concentration in the outer solution [4].

The equivalent fraction of the bivalent ion in the resin (X) is obtained as the ratio between milliequivalents of M found in the resin and the total exchange capacity of the resin. Under the conditions used in these experiments the exchange capacity can be considered as a constant independent of X.

It has proved useful to calculate the selectivity coefficient K_X which for the exchange between sodium ions and a bivalent ion (M) can be defined by the following expression:

$$K_X = \frac{X}{(1-X)^2} \frac{n^2_{Na}}{n_M} \quad (1)$$

In this equation the equivalent concentrations (n) in the outer solution and equivalent fraction (X) of the bivalent ion in the resin phase are used to express the equilibrium.

DISCUSSION

According to the thermodynamic treatment by Donnan and Guggenheim [8] the exchange between sodium ions and a bivalent ion (M) may be represented by the following equation

$$\pi(2v_{Na} - v_M) = RT \ln \left[\frac{x_{MR} \cdot f_{MR}}{x_M \cdot f_M} \times \left(\frac{x_{Na} \cdot f_{Na}}{x_{NaR} \cdot f_{NaR}} \right)^2 \right] \quad (2)$$

where π is the swelling pressure [9], v the partial molar volume, and RT the product of the gas constant and the absolute temperature. Mole fractions and rational activity coefficients are represented by x and f. The subscript R is used for ions belonging to the resin phase.

Combining eqns (1) and (2) and substituting practical (molal) activity coefficients (γ) for rational activity coefficients gives

$$\pi(2v_{Na} - v_M) / RT = \ln(K_X / n_r) + \ln \gamma_{MR} / \gamma^2_{NaR} + \ln \gamma^2_{Na} / \gamma_M$$

where n_r is the total ion concentration in the resin phase in equivalents per 1 000 g water.

The left hand side in this equation contains the pressure-volume term. Data, which permit a calculation of this term, are not available for the resin used in the present investigation, but as the swelling has been shown to be independent of X (Tables 1 and 2) this term may be considered as constant [9,10]. In addition, for the systems investigated n_r is independent of X and, as the

Table 3. Ion exchange equilibria Na—Mn in nitrate solution.

	Reagents added:	
I.	1.000 g Na+ resin (= 2.17 mequiv.) 40 ml 0.100 M $NaNO_3$ a ml 0.0500 M $Mn(NO_3)_2$ 10—a ml dist. water	II. 1.000 g Na+ resin (=2.17 mequiv.) 20 ml 0.200 M $NaNO_3$ a ml 0.0490 M $Mn(NO_3)_2$ 30—a ml dist. water

	a ml	X	n_{Mn} equiv./l	n_{Na} equiv/l.	K_X
I.	1	0.0429	0.135×10^{-3}	81.8×10^{-3}	2.32
	2	0.0848	0.320	83.8	2.22
	3	0.126	0.547	85.4	2.20
	4	0.165	0.823	87.2	2.19
	5	0.204	1.15	88.8	2.21
	6	0 241	1.55	90.4	2.21
	7	0.277	1.98	92.0	2.27
	8	0.311	2.49	93.5	2.30
	9	0.344	3.07	95.0	2.35
	10	0.376	3.68	96.4	2.44
II.	12	0.429	4.92	98.7	2.61
	14	0.478	6.68	100.8	2.67
	16	0.521	8.75	102.6	2.73
	18	0.558	11.05	104.2	2.81
	20	0.590	13.6	105.6	2.88
	22	0.615	16.4	106.5	2.87
	24	0.641	19.2	107.8	3.01

Table 4. Ion exchange equilibria Na—Mn in nitrate solution.

	Reagents added:	
I.	1.000 g Na+ resin (= 2.17 mequiv.) 40 ml 0.100 M $NaNO_3$ a ml 0.0500 M $Mn(NO_3)_2$ 110—a ml dist. water	II. 1.000 g Na+ resin (= 2.17 mequiv.) 40 ml 0.100 M $NaNO_3$ a ml 0.0490 M $Mn(NO_3)_2$ 110—a ml dist. water

	a ml	X	n_{Mn} equiv./l	n_{Na} equiv./l	K_X
I.	1	0.0452	0.0143×10^{-3}	27.3×10^{-3}	2.58
	2	0.0899	0.0344	28.0	2.47
	3	0.134	0.062	28.6	2.36
	4	0.177	0.098	29.3	2.29
	5	0.221	0.141	29.9	2.31
	6	0.263	0.193	30.5	2.33
	7	0.305	0.250	31.1	2 44
	8	0.347	0.321	31.7	2.55
II.	9	0.377	0.420	32.1	2.38
	10	0.415	0.530	32.7	2.45
	12	0.484	0.840	33.7	2.46
	14	0.549	1.21	34.6	2.67
	16	0.604	1.72	35.4	2.81
	18	0.647	2.40	36.0	2.80
	20	0.682	3.20	36.6	2.82
	22	0.712	4.07	37.0	2.89
	24	0.741	4.96	37.4	3.12

Table 5. Ion exchange equilibria Na—Mn in nitrate solution.

Reagents added: 1.000 g Na+ resin (2.17 mequiv.)
40 ml 0.100 M $NaNO_3$
a ml 0.0500 M $Mn(NO_3)_2$
460—a ml dist. water

a ml	X	n_{Mn} equiv./l	n_{Na} equiv./l	K_X
5	0.228	0.0128×10^{-3}	8.98×10^{-3}	2.41
8	0.361	0.0314	9.56	2.57
9	0.405	0.0420	9.76	2.59
10	0.448	0.0550	9.96	2.65
12	0.531	0.093	10.30	2.75
16	0.675	0.269	10.94	2.84
20	0.772	0.675	11.34	2.83
24	0.823	1.23	11.58	2.86

experiments have been performed at a low concentration, the last term on the right hand side can be neglected.

Therefore, it must be concluded that any variations in K_X with varying X must be ascribed to variations in the ratio $\gamma_{MR}/\gamma^2_{NaR}$. A reservation must be made for the intervals in which one of the components is present in very small amounts, since here certain complications may occur [11].

The experiments presented in Tables 3—5 show that for the system Na-Mn the volume of the outer solution, which has been varied between 50 and 500 ml, has no or in any case only a very small influence upon the selectivity coefficient K_X. On the other hand, there is in all experimental series with manganese a significant variation in the selectivity coefficient when the composition changes in the resin phase, K_X being higher for increasing equivalent fraction

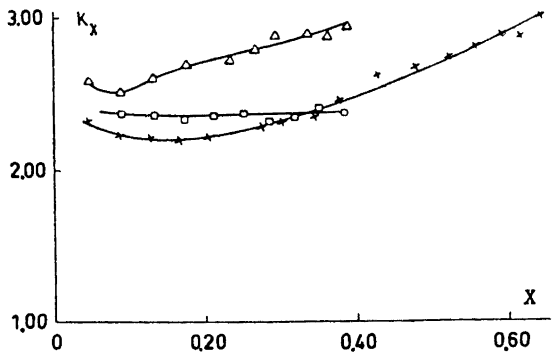


Fig. 1. The selectivity coefficient (K_X) as a function of the equivalent fraction (X) of the bivalent ion in the resin. △ System Na—Cu, □ System Na—Zn, × System Na—Mn.

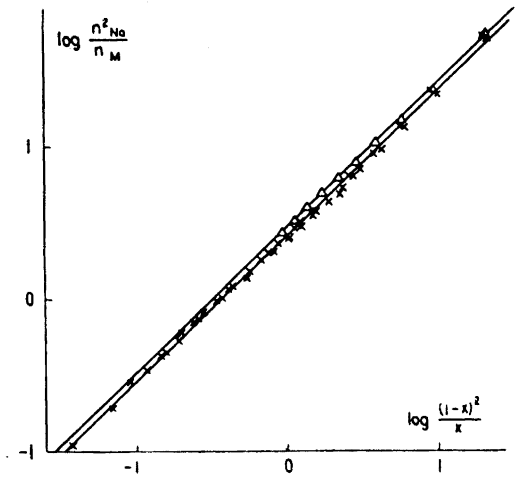


Fig. 2. Log n^2/n_M *versus* log $(1-X)^2/X$. △ System Na—Cu, × System Na—Mn.

(X) of the bivalent ion in the resin phase. As may be seen from Fig. 1 similar variations are obtained also for copper. For zinc the variations in K_X are very small within the interval in X covered in the present investigation. Diagrams of the type given in this figure are useful for calculations of ion exchange equilibria and this type of diagram has been used in the investigations on metaphosphate solutions presented in Part II.

For all three systems the variations in K_X when the equivalent fraction in the resin phase is altered are comparatively small compared with the variations established in other ion exchange reactions. Furthermore the ions studied in the present investigation give remarkably small differences in swelling (Tables 1 and 2). As already mentioned it must be concluded that the variations in K_X arise from variations in the ratio $\gamma_{MR}/\gamma^2_{NaR}$. It may also be pointed out that the differences in K_X for the three systems are comparatively small.

From a practical point of view it may be of interest to find out if the results can be represented by a simple empirical equation. The two-parameter equation proposed by Rothmund and Kornfeld [12] for equilibria in inorganic zeolites has also proved useful to describe the distribution between organic ion exchangers, sulfonated coal[13] as well as resinous exchangers [4,14] and an electrolyte

Table 6. Parameters in Rothmund and Kornfeld's equation

System	k	p
Na—Cu	0.33	1.06
Na—Mn	0.37	1.05

solution. For the exchange between monovalent and bivalent cations the equation can be written:

$$\frac{(1-X)^2}{X} = k\left(\frac{n^2_{Na}}{n_M}\right)^p \quad (3)$$

where k and p are empirical parameters. A plot of log n^2_{Na}/n_M against log $(1-X)^2/X$ is presented in Fig. 2 and as may be seen from the figure a straight line is obtained. From this graph the parameters have been determined. The results are given in Table 6.

REFERENCES

1. Samuelson, O. *Iva* **17** (1946) 9.
2. Samuelson, O. *Ion Exchangers in Analytical Chemistry*, Wiley & Sons, New York 1953 and Almqvist & Wiksell, Stockholm 1952.
3. Samuelson, O. *Iva* **17** (1946) 17.
4. Samuelson, O. *Diss.* Tekn. Högskolan, Stockholm 1944.
5. Gregor, H. P., Held, K. M. and Bellin, J. *Anal. Chem.* **23** (1951) 620.
6. Kolthoff, I. M. and Sandell, E. B. *Textbook of Quantitative Inorganic Analysis*, MacMillan, New York 1943.
7. Hohn, H. *Chemische Analysen mit dem Polarographen*, Springer, Berlin 1937.
8. Donnan, F. G. and Guggenheim, E. A. *Z. physik. Chem.* **162A** (1932) 346; Donnan, F. G. *Z. physik. Chem.* **168A** (1934) 369.
9. Boyd, G. E. and Soldano, B. A. *Z. Elektrochem.* **57** (1953) 162.
10. Glückauf, E. *Proc. Roy. Soc. London* **214A** (1952) 207.
11. Fronaeus, S. *Acta Chem. Scand.* **7** (1953) 469.
12. Rothmund, V. and Kornfeld, G. *Z. anorg. Chem.* **103** (1918) 129.
13. Walton, H. F. *Trans. Illinois State Acad. Sci.* **34** (1941) No. 2.
14. Högfeldt, E. *Acta Chem. Scand.* **9** (1955) 151.

Received April 3, 1957.

ACTA CHEMICA SCANDINAVICA 11 (1957) 1216—1222

Ion Exchange Equilibria

II. A Study of the Association in Sodium Polymetaphosphate Solutions Containing Zinc, Copper, and Manganese

RALPH DJURFELDT and OLOF SAMUELSON

Department of Engineering Chemistry, Chalmers Tekniska Högskola, Göteborg, Sweden

Using a cation exchange resin, the exchange of sodium ions for bivalent ions (Zn, Cu, Mn) has been studied in polymetaphosphate solutions. The experiments indicate that not only the bivalent ions but also sodium ions are associated with the polyanion and that there is a competition between the bivalent cations and the sodium ions for places in the polymer coil. The results suggest that the association equilibrium in metaphosphate solutions can as a first approximation be calculated using the Rothmund and Kornfeld formula originally suggested to describe ion exchange equilibria between a solid exchanger and electrolyte solutions.

Sodium polymetaphosphate (Graham's salt) is known as an efficient complex forming agent, which gives complexes with various metal cations. Several methods have been used to study the properties of these complexes but the results are contradictory.

In the present paper solutions containing zinc, copper, and manganese polymetaphosphate have been studied by means of an ion exchange method. The method is in principle the same as described in an earlier paper on iron(III)polymetaphosphate [1] (*cf.* also Ref. [2]).

EXPERIMENTS

Materials. The ion exchange resin and the nitrate solutions were the same as described in Part I [3]. Polymetaphosphate was prepared by heating $NaH_2PO_4 \cdot 2\ H_2O$ at 725°C for 2 h in a platinum dish and subsequently quenching with ice water. The metaphosphate glass was dissolved in a calculated volume of water to obtain a 0.1 N solution. The molecular weight of the metaphosphate was about 12 000 determined according to the end group method [4]. The solution was kept in a refrigerator to depress depolymerization, which occurs more rapidly at higher temperature. The solutions used in the experiments have never been more than a week old. The concentrations were checked according to the ion exchange method by passing the solution through a cation exchanger in the hydrogen form and subsequent titration against standard alkali using methyl red as

Table 1. Ion exchange equilibria Na—Mn in metaphosphate solution.

Reagents added:

I. 1.000 g Na+ resin (= 2.17 mequiv.)
5 ml 0.0490 M $Mn(NO_3)_2$
a ml 0.098 N $NaPO_3$
40—a ml 0.100 M $NaNO_3$
5 ml dist. water

II. 1.000 g Na+ resin (= 2.17 mequiv.)
15 ml 0.0500 M $Mn(NO_3)_2$
a ml 0.098 N $NaPO_3$
$20-\frac{a}{2}$ ml 0.200 M $NaNO_3$
$15-\frac{a}{2}$ ml dist. water

	a ml	$n_{PO_3^-}$ equiv./l ×10³	X	$\frac{n_{Mn^{2+}}}{n^2_{Na^+}}$ ×10⁴	Calculations acc. to Method I: n_{Na^+} equiv./l ×10³	$n_{Mn^{2+}}$ equiv./l ×10⁶	n_{Mn_P} equiv./l ×10³	Calculations acc. to Method II: n_{Na^+} equiv./l ×10³	$n_{Mn^{2+}}$ equiv./l ×10⁶	n_{Mn_P} equiv./l ×10³
I.	10	19.6	0.0419	211	81.4	140	7.84	69.6	102	7.88
	15	29.4	0.0127	58.7	80.0	37.6	9.21	59.8	21.0	9.23
	20	39.2	0.00392	17.8	79.4	11.2	9.62	49.8	4.41	9.63
	25	49.0	0.00179	8.05	79.0	5.03	9.72	39.7	1.27	9.72
	30	58.8	0.00099	4.45	78.8	2.76	9.75	29.8	0.395	9.76
	35	68.6	0.00063	2.84	78.6	1.75	9.77	19.8	0.111	9.77
	40	78.4	0.00054	2.43	78.4	1.49	9.78	9.8	0.0233	9.78
II.	20	39.2	0.177	1140	86.9	861	21.44	69.1	544	21.76
	25	49.0	0.117	655	84.0	462	24.46	59.5	232	24.69
	30	58.8	0.0728	378	82.0	254	26.59	49.8	93.7	26.75
	35	68.6	0.0452	222	80.6	144	27.90	39.9	35.3	28.01

Table 2. Ion exchange equilibria Na—Mn in metaphosphate solution.

Reagents added:
1.000 g Na+ resin (= 2.17 mequiv.)
10 ml 0.0490 M $Mn(NO_3)_2$
a ml 0.098 N $NaPO_3$
40—a ml 0.100 M $NaNO_3$
100 ml dist. water

a ml	$n_{PO_3^-}$ equiv./l ×10³	X	$\frac{n_{Mn^{2+}}}{n^2_{Na^+}}$ ×10⁴	Calculations acc. to Method I: n_{Na^+} equiv./l ×10³	$n_{Mn^{2+}}$ equiv./l ×10⁶	n_{Mn_P} equiv./l ×10³	Calculations acc. to Method II: n_{Na^+} equiv./l ×10³	$n_{Mn^{2+}}$ equiv./l ×10⁶	n_{Mn_P} equiv./l ×10³
6	3.92	0.275	2200	30.6	206	2.35	29.0	185	2.37
8	5.23	0.234	1680	30.0	151	3.00	27.8	130	3.02
10	6.53	0.193	1250	29.3	107	3.64	26.4	87.1	3.66
12	7.84	0.158	950	28.8	78.8	4.17	25.1	59.9	4.19
15	9.80	0.113	620	28.1	49.0	4.84	23.2	33.4	4.86
20	13.1	0.0594	290	27.3	21.6	5.65	19.9	11.5	5.66
25	16.3	0.0265	122	26.7	8.70	6.14	16.5	3.32	6.15
30	19.6	0.0128	57	26.5	4.00	6.34	13.2	0.993	6.35
35	22.9	0.00627	27.4	26.3	1.90	6.44	9.8	0.263	6.44
40	26.1	0.00371	16.2	26.2	1.11	6.48	6.6	0.0706	6.48

Table 3. Ion exchange equilibria Na—Mn in metaphosphate solution.

Reagents added:

I. 1.000 g Na^+ resin (= 2.17 mequiv.)
5 ml 0.0500 M $Mn(NO_3)_2$
a ml 0.098 N $NaPO_3$
40—a ml 0.100 M $NaNO_3$
105 ml dist. water

II. 1.000 g Na^+ resin (= 2.17 mequiv.)
15 ml 0.0500 M $Mn(NO_3)_2$
a ml 0.098 N $NaPO_3$
40—a ml 0.100 M $NaNO_3$
95 ml dist. water

III. 1.000 g Na^+ resin
20 ml 0.100 M $NaNO_3$
20 ml 0.098 N $NaPO_3$
a ml 0.0500 M $Mn(NO_3)_2$
110—a ml dist. water

	a ml	$n_{PO_3^-}$ equiv./l $\times 10^3$	X	$\frac{n_{Mn^{2+}}}{n^2_{Na^+}}$ $\times 10^4$	Calculations acc. to Method I: n_{Na^+} equiv./l $\times 10^3$	$n_{Mn^{2+}}$ equiv./l $\times 10^6$	n_{Mn_P} equiv./l $\times 10^3$	Calculations acc. to Method II: n_{Na^+} equiv./l $\times 10^3$	$n_{Mn^{2+}}$ equiv./l $\times 10^6$	n_{Mn_P} equiv./l $\times 10^3$
I	10	6.53	0.0456	218	27.2	16.1	2.66	23.3	11.8	2.66
	15	9.80	0.0136	60.6	26.7	4.32	3.13	20.0	2.42	3.13
	20	13.1	0.00406	17.7	26.5	1.24	3.27	16.7	0.494	3.27
	25	16.3	0.00189	8.20	26.3	0.567	3.31	13.3	0.145	3.31
	30	19.6	0 00111	4.90	26.3	0.339	3.32	10.0	0.0490	3.32
	35	22.9	0.00076	3.30	26.2	0.227	3.32	6.62	0.0145	3.32
	40	26.1	0.00058	2.50	26.1	0.170	3.33	3.33	0.00277	3.33
II	15	9.80	0.283	2270	30.6	213	5.69	26.5	159	5.74
	20	13.1	0.198	1300	29.3	112	7.02	23.2	70.0	7.06
	25	16.3	0.132	750	28.3	60.1	8.03	20.0	30.0	8.06
	30	19.6	0.0829	423	27.5	32.0	8.77	16.7	11.8	8.79
	35	22.9	0.0507	243	26.9	17.6	9.25	13.3	4.30	9.26
	40	26.1	0.0288	132	26.5	9.27	9.57	10.0	1.32	9.58
III	2	13.1	0.00028	1.24	26.4	0.0864	1.33	14.6	0.0264	1.33
	4	13.1	0.00171	7.4	26.4	0.516	2.64	15.9	0.187	2.64
	6	13.1	0.00876	38.6	26.5	2.71	3.87	17.3	1.16	3.87
	8	13.1	0.0302	140	26.9	10.1	4.89	18.7	4.90	4.89
	10	13.1	0.0677	337	27.4	25.3	5.66	20.0	13.5	5.67
	12	13.1	0.114	620	28.1	49.0	6.30	21.3	28.1	6.33

indicator [2]. As a check the sodium ions taken up by the resin were eluted with hydrochloric acid and determined as chlorides. Good agreement was obtained for the two methods.

Procedure. The ion exchange equilibria were studied in a way similar to that used in Part I. Instead of sodium nitrate, varying proportions of sodium nitrate solution and polymetaphosphate solution were added. The flasks were shaken for 17—18 h in a shaking apparatus. Preliminary experiments had shown that equilibrium was attained within 4 h and that the equilibrium was independent of the sequence in which the reagents were added. Afterwards the resin was separated from the solution and collected quantitatively on a small glass filter. The equilibrium solution was drained off as completely as possible and subsequently the resin was washed with water. The ions taken up by the ion exchanger were displaced with 3 N hydrochloric acid, the hydrochloric acid driven off by evaporation and the bivalent ion determined in the residue.

Table 4. Ion exchange equilibria Na—Mn in metaphosphate solution.

Reagents added: 1.000 g Na^+ resin (= 2.17 mequiv.)
10 ml 0.0490 M $Mn(NO_3)_2$
a ml 0.098 N $NaPO_3$
40—a ml 0.100 M $NaNO_3$
450 ml dist. water

a	$n_{PO_3^-}$	X	$\frac{n_{Mn^{2+}}}{n^2_{Na^+}}$	Calculations acc. to Method I			Calculations acc. to Method II		
				n_{Na^+}	$n_{Mn^{2+}}$	n_{Mn_P}	n_{Na^+}	$n_{Mn^{2+}}$	n_{Mn_P}
ml	equiv./l $\times 10^3$		$\times 10^4$	equiv./l $\times 10^3$	equiv./l $\times 10^6$	equiv./l $\times 10^3$	equiv./l $\times 10^3$	equiv./l $\times 10^6$	equiv./l $\times 10^3$
6	1.18	0.288	2320	9.24	19.8	0.690	8.75	17.8	0.692
8	1.57	0.251	1860	9.06	15.3	0.855	8.35	13.0	0.857
10	1.96	0.208	1410	8.86	11.1	1.05	7.95	8.91	1.05
12	2.35	0.168	1060	8.68	7.99	1.22	7.55	6.04	1.22
15	2.94	0.122	679	8.46	4.86	1.43	6.95	3.28	1.43
20	3.92	0.0613	299	8.18	2.00	1.69	5.95	1.06	1.69
25	4.90	0.0281	128	8.02	0.823	1.84	4.96	0.315	1.84
30	5.88	0.0133	58.6	7.94	0.369	1.90	3.96	0.0919	1.90
35	6.86	0.00682	29.7	7.88	0.184	1.93	2.95	0.0258	1.93
40	7.84	0.00401	17.3	7.86	0.107	1.94	1.96	0.00665	1.94

The analycital methods were those described in Part I. In the case of manganese the equilibrium solution was also analysed in some experiments. It was observed that the colorimetric determination of manganese was not affected by the presence of metaphosphate. Good agreement was obtained between the two methods. The calculations presented in Tables 1—4 are based upon the analysis of the resin when the main part of the manganese was present in the solution and vice versa.

Calculations. From the determination of the bivalent ion (M) in the resin or in the solution the equivalent fraction X in the resin is calculated and inserted in eqn. (1) in Part I. The selectivity coefficient K_X at a given value for X is taken from the experimental data obtained for nitrate solutions (*cf.* Part I) and the ratio n_M/n^2_{Na} calculated from eqn. (1) in Part I. The results obtained with solutions containing manganese are given in the Tables 1—4.

If it is valid to assume that sodium metaphosphate is completely dissociated (and that there is no associate formation of any kind between sodium ions and metaphosphate ions) the equivalent concentration of free M-ions (n_M) can be calculated by putting n_{Na} equal to the total concentration of sodium ions in the solution. The activity coefficients can, at least at present, not be accounted for in these polyelectrolyte systems and in the present work all deviations from ideality are included in the degree of dissociation. The calculations presented under Method I were made with the assumption that sodium metaphosphate is completely dissociated.

However, as discussed below, this approach cannot explain the behaviour of the metaphosphate solutions and therefore the assumption had to be made that not only bivalent ions but also sodium ions are strongly bound to metaphosphate. This is in agreement with results recently published by Schindewolf and Bonhoeffer [5] as well as by Wall *et al.*[6] Sufficient data are lacking for a quantitative interpretation of the systems studied in the present work. Therefore as a first approximation we have chosen the alternative of considering every PO_3-unit, which is not bound to a bivalent cation as being bound to sodium. The results are given in the tables under Method II.

As may be seen from the tables the two methods of calculation give values for n_M which differ considerably, the differences being largest for systems which contain a considerable excess of metaphosphate in comparison with the bivalent ion. Independent

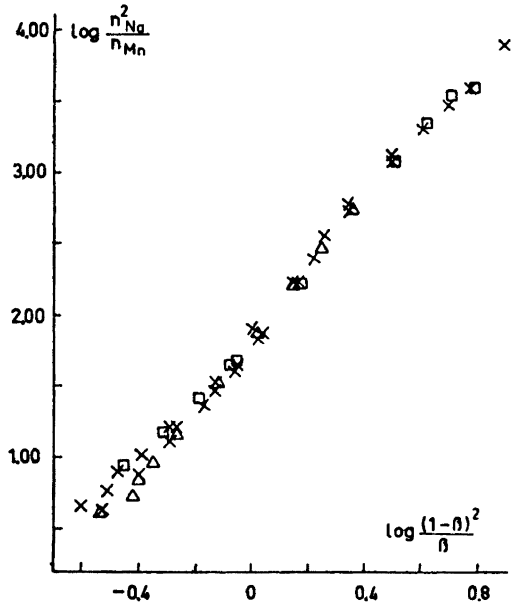


Fig. 1. log n^2_{Na}/n_{Mn} *versus* log $(1-\beta)^2/\beta$. Volume of solution: □ 50 ml; × 150 ml; △ 500 ml.

of the method of calculation the equivalent concentration of M-ions bound to the metaphosphate (n_{MP}) is calculated as the difference between the total concentration of M-ions in the solution and n_M. The data presented in the tables show that the differences in n_{MP} when calculations are made according to the two methods are rather small and in certain cases negligible. Consequently it may be of interest to find a correlation between n_{MP} and the ratio n_M/n^2_{Na}. The discussion in the subsequent part of this paper is restricted to calculations based upon Method II, but from the above it is obvious that even if Method I had been chosen the influence upon the empirical constants in the equation representing this correlation would be small. The symbol β is used for the ratio n_{MP}/n_{PO_4} where n_{PO_4} is the total equivalent concentration of metaphosphate. In accordance with the assumption made in the calculations according to Method II, the concentration of sodium ions bound to the metaphosphate is $(1-\beta)n_{PO_4}$.

DISCUSSION

When a solution containing a complex salt is diluted, the complex equilibrium is changed in the direction towards a decomposition of the complex. For the metaphosphate solutions studied in the present investigation this rule does not hold true. A probable explanation is that not only the bivalent ions but also the sodium ions are associated in some way with the metaphosphate. An attempt has been made to find an empirical equation which can represent the experimental results.

Figs. 1 and 2 show a plot of log n^2_{Na}/n_M against log $(1-\beta)^2/\beta$. It is observed that over a considerable range of concentration all experimental points fall upon one curve. Fig. 1 contains all experimental data with manganese from

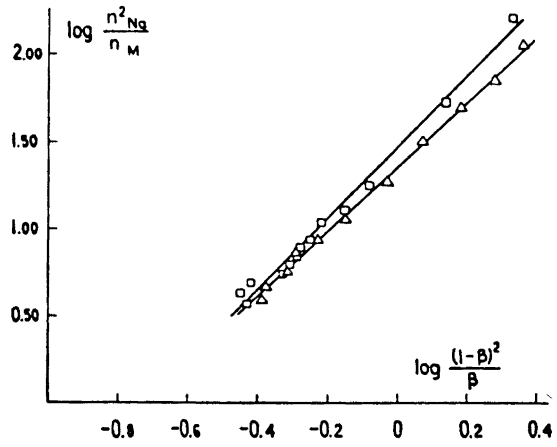


Fig. 2. log n^2_{Na}/n_M *versus* log $(1-\beta)^2/\beta$. □ System Na—Zn; △ System Na—Cu.

Tables 1—4. At low values for n^2_{Na}/n_{Mn}, *i.e.* at high values for β, there seems to be some deviations, but as the experimental errors may have a considerable influence no attempt will be made to account for these deviations. As a first approximation the curve can be considered as a straight line represented by the following equation:

$$(1-\beta)^2/\beta = k\ (n^2_{Na}/n_M)^p \qquad (1)$$

The numerical values for the parameters are reproduced in Table 5.

Experiments have been performed over a large concentration interval (volume 50—500 ml) and it is obvious that β, *i.e.* the association of manganese to metaphosphate, increases when diluting the solution. This peculiar behaviour might be explained by the polyelectrolyte character of the metaphosphate. For ion exchange resins, which are cross-linked polyelectrolytes, it is known that the uptake of bivalent ions by the resin increases when a solution containing bivalent and monovalent ions is diluted. Furthermore eqn. 1 shows that there is a competition between bivalent ions and sodium ions for metaphosphate in a similar manner as in a solid cation exchanger. Formally eqn. (1) is equivalent to the Rothmund and Kornfeld equation [7]

Table 5. Parameters in equation (1).

System	k	p
Na—Zn	0.19	0.49
Na—Cu	0.18	0.54
Na—Mn	0.17	0.42

which is an empirical formula used to represent ion exchange equilibria. This equation has been used successfully to describe ion exchange equilibria in inorganic as well as in organic ion exchangers. In general this equation has proved to be the best among the numerous formulas proposed for this purpose. From the present investigations it is evident that this equation can be useful also for calculations of the association equilibrium in solutions, which besides metaphosphate contain an ordinary salt, *e.g.* nitrate, the polymer metaphosphate being formally considered as an ion exchanger, *i.e.* as a separate phase. The coincidence might be explained by the ability of linear polyelectrolytes to coil, the cations being held in the coil in a similar manner as the counter ions in an ion exchanger.

The results from experiments with metaphosphate solutions, containing zinc and copper, are reproduced in an analogous manner in Fig. 2. As may be seen from the figure, the curves can as a good approximation be considered as straight lines. The parameters are given in Table 5. From these data it is obvious that the differences in behaviour between manganese, zinc and copper are rather small. Manganese is associated more strongly with the metaphosphate than zinc and copper.

The present approach can only be considered as a first approximation, the use of which is restricted to polymetaphosphate solutions containing besides another electrolyte. It has been observed that besides associated sodium ions, a considerable amount of free sodium ions are present in a pure solution of sodium polymetaphosphate [5], but sufficient data are not available to permit the application of a correction.

The experimental work reported in the present series of papers was performed during the years 1947—1949 at the Department of Inorganic Chemistry, The Royal Institute of Technology, Stockholm. Thanks are due to Professor Oscar Collenberg for putting the resources of his institute at our disposal and for his great interest in the investigations. The financial support of the *State Technical Research Council* (*Statens Tekniska Forskningsråd*) is gratefully acknowledged.

REFERENCES

1. Samuelson, O. *Iva* **17** (1946) 9.
2. Samuelson, O. *Ion Exchangers in Analytical Chemistry*, Wiley & Sons, New York, 1953 and Almqvist & Wiksell, Stockholm 1952.
3. Djurfeldt, R. and Samuelson, O. *Acta Chem. Scand.* **11** (1957) 1209.
4. Samuelson, O. *Svensk Kem. Tidskr.* **56** (1944) 343.
5. Schindewolf, U. and Bonhoeffer, K.-F. *Z. Elektrochem.* **57** (1953) 216.
6. Wall, F. T. and Doremus, R. H. *J. Am. Chem. Soc.* **76** (1954) 868.
7. Rothmund, V. and Kornfeld, G. *Z. anorg. Chem.* **103** (1918) 129.

Received April 3, 1957.

ACTA CHEMICA SCANDINAVICA 11 (1957) 1223—1231

The Decrease of F^k-Integrals, Tetragonal Perturbations and Effects of Average Environment in the Reflection Spectra of Nickel(II) Complexes

OLE BOSTRUP and CHR. KLIXBÜLL JØRGENSEN

Chemical Laboratories B and A, Technical University of Denmark, Copenhagen, Denmark

The reflection spectra of 25 paramagnetic nickel(II) complexes are compared with the predictions of the ligand field theory for d^8 in O_h. The results are: the ligand field strength Δ can be implied in mixed complexes from the "rule of average environment" and is within 2 % independent of atoms outside the first co-ordination sphere. The effects of tetragonal contributions to the ligand field are surprisingly small and can be empirically described by a certain deviation of the band differences. The integrals F^k, inversely proportional to the extension of the partly filled shell, are decreased 15—40 % relative to the gaseous ion. As also found in molybdenum(III), the decrease has the same order of magnitude for γ_6- and γ_3-electrons.

It is possible to apply [1,2] the ligand field theory [3,4] for d^8 in the symmetry O_h to the absorption spectra of nickel(II) complexes in solution with some effects of intermediate coupling, intermixing levels with total spin $S = 1$ and 0. Hence, a nickel(II) complex can be characterized by two parameters, Δ (also called $(E_1—E_2)$ or 10 Dq) and the percentage decrease of the Slater-Condon-Shortley integrals F^k. The deviation of the ligand field from spherical to octahedral-cubic symmetry determines Δ, while the decrease of F^k is an effect of partly covalent bonding, decreasing the central field of spherical symmetry [5], compared to the central field in the gaseous ion.

The present paper is a comparison of the absorption spectra of solutions with the reflection spectra of solid nickel(II) complexes. The study of absorption spectra of solutions and solids have differing advantages: In the former case, physico-chemical methods [6] can prove the existence of complexes, of which no solid compounds are known. With modern spectrophotometers, the measurements of solutions can be made more easily, and a reliable molar extinction coefficient ε can be found, while the reflection spectra present a monotonic, but not a linear, function of ε. The latter function cannot be predicted and depends on the pulverization etc.; although the effective light

Table 1. Wavenumbers of band maxima of nickel(II) complexes. The excited levels are indicated. The unit is 1 kK = 1 000 K = 1 000 cm^{-1}.

	$^3\Gamma_5$(F)	$^1\Gamma_3$(D)	$^3\Gamma_4$(F)	$^1\Gamma_b$	$^1\Gamma_c$	$^3\Gamma_4$(P)
pyHNiBr$_3$	—	(10.3)	11.2	17.4	—	19.9
CsNiBr$_3$	—	(10.3)	11.3	17.2	—	20.0
RbNiBr$_3$	—	(10.4)	11.5	17.3	—	20.2
NiBr$_2$	—	(10.3)	12.1	(16.8)	—	20.7
pyHNiCl$_3$	—	(12.5)	11.2	(18.4)	—	21.3
CsNiCl$_3$	—	(12.5)	(11.3)	18.7	—	21.5
RbNiCl$_3$	—	(11.5)	(12.7)	18.6	(25.6)	21.6
NiCl$_2$	—	(11.6)	12.9	19.4	(26.3)	22.1
NiSO$_4$, 7H$_2$O	8.5	(15.4)	(14.1)	(18.8)	(21.8)	25.7
NiSO$_4$, 6H$_2$O	8.6	(14.2)	(15.4)	(19.0)	(21.9)	25.7
(NH$_4$)$_2$Ni(SO$_4$)$_2$, 6H$_2$O	8.9	(14.4)	(15.5)	(18.0)	(22.0)	25.8
Ni(H$_2$O)$_6$++	8.5	(15.4)	(13.5)	(18.3)	(22.0)	25.3
Nipy$_4$Cl$_2$	8.5; 10.9	—	15.9	—	—	25.7
Nipy$_4$(SCN)$_2$	10.1	(12.8)	16.7	—	(22.7)	26.7
Ni(NO$_3$)$_2$ in py	10.15	13.5	16.5	—	—	27.0
Ni(dgmH)$_2$Cl$_2$	10.9	(12.9)	17.1	—	—	—
Nien$_2$(SCN)$_2$, H$_2$O	9.7	(12.3)	17.7	(15.6)	—	28.0
NitrenSO$_4$	10.0	(12.9)	17.2	—	—	26.9
NitrenSO$_4$, 7H$_2$O	10.6	(12.9)	17.9	—	(23.3)	27.5
Nitren(SCN)$_2$	10.9	(12.8)	17.9	—	(23.3)	27.8
Nitren(H$_2$O)$_2$++	10.5	(12.8)	17.8	—	—	27.8
Nitren$_3$Br$_4$	11.2	(12.9)	18.4	—	—	28.1
Ni$_3$tren$_3$++++	10.7	(12.5)	18.3	—	—	28.7
Ni(NH$_3$)$_6$Br$_2$	10.8	—	17.7	—	—	28.2
Ni(NH$_3$)$_6$++	10.75	13.15	17.5	—	—	28.2
Nien$_3$SO$_4$	11.3	(12.8)	18.5	—	—	29.0
Nien$_3$++	11.2	(12.4)	18.35	—	(24.0)	29.0
Nidtn$_2$(NO$_3$)$_2$	11.0	(12.6)	18.1	—	—	28.2
Niden$_2$(NO$_3$)$_2$	11.2	(12.4)	18.9	(16.3)	—	28.6
Niden$_2$++	11.5	—	18.7	—	—	29.1
Niptn$_2$SO$_4$	(11.6)	(12.6)	19.3	(17.5)	—	29.5
Niptn$_2$++	11.2	(12.5)	19.0	—	—	29.7

path is larger for coarse-grained than for fine-powdered material, it decreases with increasing ε, and for very high values of ε, a flat "roof" is observed of the band (corresponding to light scattering from the surface). Thus, only the position of the band can be measured exactly in the reflection spectrum; the relative heights of the bands and their half-widths cannot easily be deduced from the data. On the other hand, the crystallographic structure of solids may be known, and several complexes cannot be dissolved in any solvent without decomposition or isomerization.

Table 1 gives the observed maxima, while the Figures illustrate selected examples. The material of Table 1 is taken partly from other papers [1,2,7,17]. One of the most conspicuous results is the similarity between the spectra of a given complex in solution and in solid state. This is a special case of N. Bjerrum's rule [8] that atoms outside the first co-ordination sphere have a very small influence on the absorption spectrum. This rule is valid mainly for the Laporte-forbidden transitions within the partly filled shell of the complex (as explained by ligand field theory) while the electron transfer spectra can be more depend-

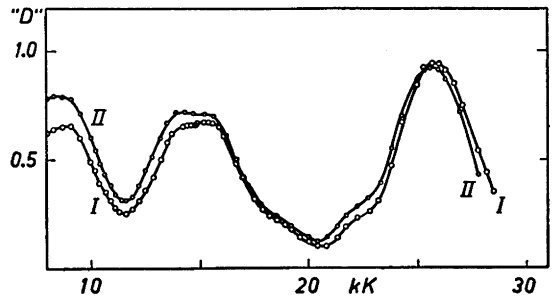


Fig. 1. Reflection spectra of I. $(NH_4)_2Ni(SO_4)_2$, $6H_2O$ and II. $NiSO_4$, $7H_2O$.

ent on the solvent [9,23]. The high bands of Fe *o*-phen$_2$(CN)$_2$ are, *e.g.*, shifted 10 %, while most other solvent effects do not exceed 2 %.

It is seen from Fig. 1 that the Tutton salt $(NH_4)_2Ni(SO_4)_2$, $6H_2O$ exhibits a slightly larger deviation from $Ni(H_2O)_6^{++}$ in solution or in other salts. It is interesting that the double band in the red [6], having $^3\Gamma_4$(F) and $^1\Gamma_3$(D) as excited levels [1], evolves in the manner predicted [1] for a larger Δ in the Tutton salt, *viz.* that the triplet percentage (and hence the intensity) wanders from the part with low to that with high wavenumber. Analogous to this greenish blue salt at room temperature, other samples, containing nickel(II) hexaaquo ions, turn sky-blue at the temperature of liquid air. Both the effects of crystal environment and temperature seem to be larger for aquo ions than for other complexes, perhaps caused by the changed polarization of the loosely bound water molecules.

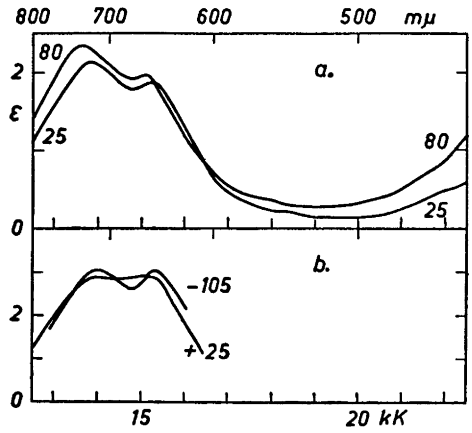


Fig. 2 a. Absorption spectra of 0.1 M $Ni(ClO_4)_2$ in 0.01 M $HClO_4$ measured in 5 cm cells on a recording Cary spectrophotometer. at 25° and 80°C. *b.* Absorption spectra of 0.5 M $Ni(NO_3)_2$ in 10 % water, 40 % glycerol 50 % ethanol, measured by Mr. Arne Jensen by photographic methods at −105° and 25°C as described in the experimental section.

Mr. A. Jensen of the Pharmaceutical College has kindly informed us about photographic measurements * of the spectrum of 0.05 M $Ni(NO_3)_2$ in 10 % H_2O, 40 % glycerol, and 50 % ethanol at —105°C, demonstrating similar effects (Fig. 2 b). Schäffer and Klixbüll Jørgensen have later measured the spectra of aqueous $Ni\,ClO_4)_2$ at 25°C and 80°C on a Cary spectrophotometer (Fig. 2 a). In all cases, the effect of cooling resembles that of Tutton salt, compared to other nickel(II) salts.

Fig. 1 of Ref. [7] demonstrates similar effects in the anhydrous chlorides and bromides. The position of $^1\Gamma_3$(D) might seem anomalously low. This effect is caused by the low values of F^k-integrals in anion complexes [4,5,10]. Δ is slightly larger in $NiCl_2$ than in the double chlorides $MNiCl_3$ and larger in $NiBr_2$ than in $MNiBr_3$, decreasing for increasing radii of the occurring anions and cations. All these compounds have an octahedral environment of six halide atoms around each nickel atom.

Table 2 gives the values of Δ and [2,4] the two quantities $B = \frac{1}{49} F^2 - \frac{5}{441} F^4$ and $C = \frac{5}{63} F^4$, derived from

$$^3\mathrm{P}-{}^3\mathrm{F} = 15\,B = \sigma_2 + \sigma_3 - 3\,\Delta \text{ with } \Delta = \sigma_1$$

$$\frac{4}{7}(^1\mathrm{D}) + \frac{3}{7}(^1\mathrm{G})-{}^3\mathrm{F} = 8\,B + 2\,C = \sigma(^1\Gamma_3)_{\mathrm{corr}}$$

σ_1, σ_2, σ_3 are the wavenumbers of the baricenters of the bands, representing transitions from $^3\Gamma_2$(F) to $^3\Gamma_5$(F), $^3\Gamma_4$(F), and $^3\Gamma_4$(P), respectively. σ_1 is corrected for the effects of intermediate coupling [1] and in some complexes inferred from the Orgel diagram, when σ_1 cannot be directly observed in the infra-red. σ_2 and $\sigma(^1\Gamma_3)$ are also corrected for the influence of intermediate coupling, when needed.

Table 2 gives the ratios β_1 and β_2 between the values of 15 B and 8 B+2 C in the complex and the gaseous ion, assuming the latter values to be 16 900 K (= cm^{-1}) and 17 900 K, respectively. However, this is equivalent to assuming an effect of (L, S)-coupling = $-\frac{3}{2}\zeta_{3d}$ = —950 K on the groundstate $^3I'_2$(F). If the effect of (L, S)-coupling is completely quenched, all the ratios β_1 and β_2 mentioned above are increased by 0.06 from the values, given in Table 2. If the interaction with $^1\Gamma_3$(G) is considered, β_2 is increased by ~0.03.

The decrease of β from 1 seems to be a rather monotonic function of the extent of the partly covalent bonding. However, it cannot be assumed that $\sqrt{\beta}$ is exactly equal to the intermixing in the squares of the wavefunctions, [5,12,15] forming linear combinations of atomic orbitals from the ligands and the nickel ion. It could not be assumed *a priori* that the molecular orbital theory might be applied to the complexes, assuming sharply defined configurations. However, the agreement of the Orgel diagram (the energy levels as function of Δ or rather [3] of Δ/β) with the gerade levels of d^n-complexes suggest that configuration interaction is relatively unimportant in the case of the γ_3- and γ_5-subshells.

* These measurements were carried out at Chemistry Department A, where Mr. Arne Jensen worked as a guest with Professor J. Bjerrum.

Table 2. The values of the parameters $\triangle$, 15 B, and 8 $B+2\,C$ in kK for nickel(II)-complexes in solid state and in aqueous solution. The ratios β_1 and β_2 of the two latter parameters, compared to those for the gaseous Ni^{++}, are given. The observed energy difference X_{obs} between $^3\Gamma_4(F)$ and $^3\Gamma_4(P)$ is compared to X_{calc} calculated from the ligand field symmetry O_h and the parameters $\triangle$ and β_1.

	$\triangle$	15 B	β_1	8 $B+2\,C$	β_2	X_{obs}	X_{calc}	$X_{calc}-X_{obs}$
$pyHNiBr_3$	6.8	11.7	0.71	10.6	0.59	—	—	—
$NiBr_2$	7.3	10.9	0.65	10.4	0.58	—	—	—
$pyHNiCl_3$	7.0	11.9	0.71	12.1	0.68	—	—	—
$NiCl_2$	7.6	11.3	0.67	12.0	0.67	—	—	—
$Ni(H_2O)_6^{++}$	8.5	14.1	0.84	14.7	0.82	11.0	11.3	0.3
$NiSO_4$, $7H_2O$	8.5	14.9	0.88	14.8	0.83	11.0	11.9	0.9
$NiSO_4$, $6H_2O$	8.6	14.7	0.87	14.8	0.83	10.9	11.7	0.8
$(NH_4)_2Ni(SO_4)_2$, $6H_2O$	8.9	14.1	0.84	14.9	0.83	10.8	11.6	0.8
$Niata^-$	9.5	13.1	0.78	13.3	0.74	9.6	10.6	1.0
Niata gly^{--}	9.9	13.6	0.80	13.0	0.73	9.1	11.1	2.0
β-$Nienta^{--}$	9.9	13.6	0.80	12.8	0.71	9.5	11.1	1.6
α-$Nienta^{--}$	10.1	12.9	0.76	12.7	0.71	9.2	10.6	1.4
$Nigly_2^-$	10.1	13.9	0.82	13.1	0.73	11.0	11.3	0.3
Nienta en^{--}	10.1	14.1	0.84	12.5	0.70	9.8	11.4	1.6
$Nienta(NH_3)^{--}$	10.2	13.5	0.80	12.7	0.71	9.7	11.0	1.3
Ni^{++}in py	10.2	12.9	0.76	13.5	0.75	10.5	10.6	0.1
$Nipy_4(SCN)_2$	10.2	12.8	0.76	12.8	0.71	10.0	10.5	0.5
$NitrenSO_4$	10.3	13.2	0.78	12.7	0.71	9.7	10.8	1.1
Nien gly_2, aq	10.7	13.3	0.79	13.0	0.73	10.8	11.0	0.2
$Ni(NH_3)_6^{++}$	10.8	13.4	0.79	13.1	0.73	10.7	11.0	0.3
$Ni(NH_3)_2Br_2$	10.8	13.5	0.80	—	—	11.0	11.3	0.6
$Nitren(H_2O)_2^{++}$	10.9	12.9	0.76	12.6	0.70	10.0	10.8	0.8
$NitrenSO_4$, $7H_2O$	11.0	12.4	0.73	12.7	0.71	9.6	10.5	0.9
$Niata\ den^-$	11.1	13.0	0.77	12.5	0.70	11.1	10.9	−0.2
$Nien_2gly^+$	11.1	13.2	0.78	12.5	0.70	10.7	11.0	0.3
$Nitren(SCN)_2$	11.3	11.8	0.70	12.6	0.70	9.9	10.3	0.4
$Nitetren^{++}$	11.3	13.0	0.77	12.4	0.69	10.1	11.0	0.9
$Nitn_3^{++}$	11.3	12.1	0.72	12.3	0.69	10.4	10.5	0.1
$Nidtn_2(NO_3)_2$	11.4	12.1	0.72	12.4	0.69	10.1	10.5	0.4
$Nibdn_3^{++}$	11.4	12.4	0.73	12.5	0.70	10.6	10.7	0.1
$Nitren(NH_3)_2^{++}$	11.4	12.4	0.73	12.2	0.68	10.0	10.7	0.7
Nitren en^{++}	11.4	13.5	0.80	12.2	0.68	10.3	11.3	1.0
$NitetrenNH_3^{++}$	11.5	12.8	0.76	12.2	0.68	9.9	10.9	1.0
$Niden_2^{++}$	11.5	13.3	0.78	—	—	10.4	11.1	0.7
Nitren gly^+	11.6	12.2	0.72	12.4	0.69	9.4	10.6	1.2
$Niden_2(NO_3)_2$	11.6	12.7	0.75	12.2	0.68	9.7	11.0	1.3
$Ni_2tren_3Br_4$	11.6	11.7	0.69	12.6	0.70	9.7	10.5	0.8
$Nien_3^{++}$	11.6	12.5	0.74	12.2	0.68	10.7	10.8	0.1
$Nien_3SO_4$	11.7	12.4	0.73	12.6	0.70	10.5	10.8	0.3
$Niptn_2^{++}$	11.8	13.3	0.79	12.3	0.69	10.7	11.3	0.6
$Niptn_2SO_4$	12.1	12.5	0.74	12.4	0.69	10.2	11.0	0.8

There is no doubt that γ_3-electrons are more anti-bonding than γ_5-electrons in all octahedral d^n-complexes, *i.e*, $\triangle$ is positive, agreeing with σ-bonding in the direction from the ligands to the central ion, or π-bonding in the opposite direction. If π-bonding from the ligands occurs, it decreases $\triangle$. It might thus be presumed that sub-shell configurations with many γ_3-electrons would exhibit larger effects of partly covalent bonding than the less anti-bonding configurations. It is seen from Table 2 that β is not essentially different for 15 B,

derived from $\gamma_5^5\gamma_3^3$ and $\gamma_5^4\gamma_3^4$ and for 8 B+2 C, derived from $\gamma_5^6\gamma_3^2$. Similar evidence is obtained [14] from molybdenum(III) in $MoCl_5(H_2O)^{--}$, where both the positions of $^2\Gamma_3$ and $^2\Gamma_5$ of γ_5^3 and $^4\Gamma_5$ and $^4\Gamma_4$ of $\gamma_5^2\gamma_3$ and $\gamma_5\gamma_3^2$, relative to the γ_5^3-groundlevel $^4\Gamma_2$, can be explained by the set B = 450 K and C = = 1 800 K. Hence, the decrease of β is equally effective for γ_5 and γ_3 electrons.

It is surprising that Jahn-Teller distorted systems such as vanadium(IV) [14] and copper(II) [1,2,15] have a ligand field of distinctly tetragonal symmetry, D_{4h}, even when the ligands are nearly or completely identical, while on the other hand, the regular d^3-, d^5-, d^6- and d^8-systems (with $S = \frac{3}{2}, \frac{5}{2}$, 0 and 1, respectively) agree very nicely with the theory for the cubic-octahedral symmetry O_h with only one ligand field parameter Δ.

In chromium(III) and cobalt(III) complexes [10], the deviations from O_h are not conspicuous, even in the case of highly different ligands. This is even more pronounced in the case of nickel(II) complexes [1,2] in solution. The latter effect can be explained by the insufficient difference between N and O in Tsuchida's spectrochemical series, which can be written [16]

$$Br < Cl < F < O < N < C$$

according to the bonding atom of the ligand. Table 1 gives one probable case of tetragonal splitting *, *trans*-Ni py_4Cl_2, where the level $^3\Gamma_5$(F) is markedly split, analogous [10] to $^4\Gamma_5$(F) of *trans*-Cr $en_2Cl_2^+$, corresponding to the larger difference between Cl and N.

Since no tetragonal splitting generally can be perceived, the rule of "average environment" can be directly applied to the absorption bands, *viz.* that they correspond to an average value of Δ, found by interpolation between Δ for the complexes with six equal ligand atoms. Tables 1 and 2 extend the investigated class of "average environments" considerably, as discussed by Asmussen and Bostrup in the case of polyamine nickel(II) complexes [17]. Especially, the tetradentate amine tren is shown to form no tetrahedral complexes in solid state [17], but to have two residual places for other ligands [2] (*cf.* also Ref.[18]).

Even though a genuine tetragonal splitting has been found only in Ni py_4Cl_2, it is possible to dinstinguish between purely cubic and tetragonally distorted complexes by a closer study of the observed wavenumbers: The two levels $^3\Gamma_4$(F) and $^3\Gamma_4$(P) have energies, which are the roots E in the weak field determinant

$$\begin{vmatrix} 0.6\,\Delta - E & 0.4\,\Delta \\ 0.4 & 15\,B - E \end{vmatrix} = 0$$

* The *trans*-configuration is demonstrated by Porai-Koshits [11] from crystallographic X-ray studies. The compound has the same spectrum in anhydrous pyridine and in ethanol with maxima at the same wavenumbers as the solid. By addition of 10 % water to the ethanolic solution, or more water to the pyridine, the greenish blue colour is changed to sky-blue with the same maxima as produced by $Ni(NO_3)_2$ in pyridine. Hence, the Katzin effect [12] seems to occur in the exchange of chloride and water on the two residual places of Ni py_4^{++}, when dissolved in an organic solvent.

or the equivalent strong field determinant

$$\begin{vmatrix} 3B + 0.8\,\Delta - E & 6B \\ 6B & 12B - 0.2\,\Delta - E \end{vmatrix} = 0$$

if the energy of the groundlevel $^3\Gamma_2$(F) is written -1.2Δ. Thus, with two parameters Δ and B, the three spin-allowed bands σ_1, σ_2, and σ_3 can be described. It is possible to compare the distance X_{obs} between the two bands σ_2 and σ_3 with the distance between the two roots E

$$X_{calc} = \sqrt{225\,B^2 - 18\,B\,\Delta + \Delta^2}$$

Table 2 demonstrates that within the uncertainty of the parameters Δ and B (amounting to 0.2 or 0.3 kK in X_{calc}) the complexes with six identical ligands have $X_{obs} = X_{calc}$, while for the tetragonal complexes, X_{calc} is 600—2 000 K *larger* than X_{obs}. When $X_{calc} - X_{obs}$ is very large, the treatment in Table 2 loses some of its validity; in this case, Δ is undoubtedly larger than indicated by σ_1, and 15 B thus calculated too large.

The deviation from the conservation of baricenters is probably caused by the interaction of the three $^3\Gamma_{t_5}$ levels. Schäffer and one of the authors [19] have discussed this problem. On the analogy of chromium(III) complexes, the tetragonal splitting is expected to occur in a complex with weaker ligand field along the tetragonal axis than along the two axes in the plane:

$^3\Gamma_2$(F)	$^3\Gamma_5$(F)	$^3\Gamma_4$(F)	$^3\Gamma_4$(P)
↓	↙ ↘	↙ ↘	↙ ↘
$^3\Gamma_{t_3}$	$^3\Gamma_{t_5}$ $^3\Gamma_{t_4}$	$^3\Gamma_{t_2}$ $^3\Gamma_{t_5}$	$^3\Gamma_{t_5}$ $^3\Gamma_{t_2}$

However, the splitting is smaller than expected from any electrostatic model. The effect in Table 2 is probably connected with the fact that the maximum absorption occurs in the doubly degenerate part $^3\Gamma_{t_5}$ of the bands $^3\Gamma_4$.

It is seen from Table 2 that SCN^- introduces a slightly larger value of Δ than the corresponding aquo complexes. By comparison of the data for $Ni\,py_4(SCN)_2$ and nickel(II) nitrate in 90 % pyridine [2], the latter complex probably contains only four molecules py, as previously foreseen. It is seen from Table 1 that the blue hydrochloride of nickel(II) dimethylglyoximate [20] has a large ligand field strength Δ.

The last problem to be discussed in this paper is the identification of the two next singlet levels $^1\Gamma_b$ and $^1\Gamma_c$ of Table 1. The three most probable levels are $^1\Gamma_1$(G) of $\gamma_5^6\gamma_3^2$ and $^1\Gamma_5$(D) and $^1\Gamma_4$(G) of $\gamma_5^5\gamma_3^3$. The slope of $^1\Gamma_c$ as function of Δ indicates that it is $^1\Gamma_5$(D) with the wavenumber $\sigma \simeq \Delta + 8\,B + 2\,C$, except in $RbNiCl_3$ and $NiCl_2$. It has previously been discussed [2] whether $^1\Gamma_b$ $\sim$15 kK is caused by a tetragonal splitting or is $^1\Gamma_1$(G) with a highly decreased value of $\sigma \simeq 16\,B + 4\,C$. Hence, $^1\Gamma_4$(G) with $\sigma \simeq \Delta + 12\,B + 2\,C$, is probably in most cases situated at a slightly higher wavenumber than $^3\Gamma_4$(P).

The main result of this paper is that the ligand field theory can be applied to paramagnetic nickel(II) complexes, both in solid state and in solution, with assumption of octahedral symmetry and one ligand field parameter Δ, if one

further variation is admitted: the parameters F^k (*i.e.* B and C) are multiplied by a factor $0.5 < \beta < 1$ in complexes, compared to gaseous Ni^{++}. Even though the levels may show individual behaviour, caused by interaction with other levels having the same S and Γ_n, it seems demonstrated that the partly filled shell is expanded, relative to the 3d-shell in Ni^{++}. This expansion has the same order of magnitude in the γ_3- and γ_5-sub-shells. The final explanation of this by molecular orbital theory will probably be rather complicated. However, the present authors believe that the ligand field theory is remarkably close, ~2 %, in predicting the d^n-energy levels, if the wavefunctions of the partly filled shell are written as antisymmetrized products of orbitals, each being the product of a hydrogen-like angular part (influenced by the group-theoretical conditions of the complex) and a radial part. The latter varies from one complex to another as indicated by the variation of the parameters F^k of electrostatic interaction between the electrons in a mainly spherical symmetrical field [5].

EXPERIMENTAL

The preparation and the analyses of the solid nickel(II) compounds are described elsewhere [7,11,17,20]. The ligands are abbreviated:

py	=	pyridine (1 N)
en	=	ethylenediamine (2 N)
den	=	diethylenetriamine = bis(2-aminoethyl)imine (3 N)
tetren	=	tetraethylenepentamine (5 N)
tn	=	trimethylenediamine = 1,3 diaminopropane (2 N)
bdn	=	1.3 diaminobutane (2 N)
dtn	=	bis (3-aminopropyl)imine (3 N)
ptn	=	1,2,3-triaminopropane (3 N)
tren	=	tris (2-aminoethyl(nitrogen (4 N)
$enta^{-4}$	=	ethylenediaminetetraacetate (2 N, 4 COO)
ata^{-3}	=	nitrogentriacetate (1 N, 3 COO)
gly^-	=	aminoacetate (1 N, 1 COO)
dmg H	=	dimethylglyoxime

The numbers in parentheses denote the number of nitrogen atoms and carboxyl groups available for co-ordination.

The reflection spectra were measured on the Beckman DU spectrophotometer. The absorption spectra of solutions were measured in the infra-red on this instrument and in the visible on the Cary MS-11 recording spectrophotometer.

Mr. Arne Jensen determined the absorption spectra of 0.05 M $Ni(NO_3)_2$ in a mixture of 10 volume % H_2O, 40 % glycerol and 50 % ethanol with a Zeiss spectrograph. The solutions were contained in a test tube, suspended in a double-wall plastic box, 20 × 20 × 20 cm. In the bottom of this box, liquid air was placed in order to evade condensation of ice inside the box, and the test tube was cooled by immersion in the liquid air. The temperature was measured with a thermoelement. The Schwarzschild exponent p was determined for the photographic plate, according to Kortüm [21]. The extinction coefficients were determined by comparison with the spectrum of the mixture, which was both photographed and measured on the Cary spectrophotometer. Since ε is definitely larger than for the aquo ion (*cf.* Ref. [22]), solvates with glycerol or nitrate must occur. It cannot be excluded that the composition of the solution changes with temperature, caused by the heat of formation of these complexes. However, a definite narrowing and shift towards higher wavenumbers by cooling can be inferred from Mr. Arne Jensen's measurements, and Mr. Claus E. Schäffer and Klixbüll Jørgensen have later determined on the Cary the effect on 0.1 M $Ni(ClO_4)_2$ in 5 cm layer of aqueous solution of warming from 25°C to 80°C, and obtained the predicted change: broadening and bathochromic shift of the bands, and the change of singlet-triplet intermixing corresponding to a decreased value of Δ.

Acknowledgments: We thank Mr. C. J. Ballhausen and Professor Jannik Bjerrum for having drawn our attention to the effect of temperature on the absorption spectrum of nickel(II) salts. Further, we are indebted to Dr. F. G. Mann, Cambridge, who provided samples of tren- and ptn-complexes. Finally, we want to thank Professor R. W. Asmussen for many valuable discussions.

REFERENCES

1. Jørgensen, C. Klixbüll, *Acta Chem. Scand.* **9** (1955) 1362.
2. Jørgensen, C. Klixbüll, *Acta Chem. Scand.* **10** (1956) 887.
3. Tanabe, Y. and Sugano, S. *J. Phys. Soc. Japan* **9** (1954) 753, 766.
4. Jørgensen, C. Klixbüll, *Quelques Problèmes de Chimie Minérale. Dixieme Conseil de Chimie. Institut International de Chimie Solvay.* R. Stoops, Bruxelles 1956, p. 355.
5. Jørgensen, C. Klixbüll, *Energy Levels of Complexes and Gaseous Ions.* Gjellerups Forlag, Copenhagen 1957.
6. Bjerrum, J. *Metal Ammine Formation in Aqueous Solution.* Thesis. Copenhagen 1941.
7. Asmussen, R. W. and Bostrup, O. *Acta Chem. Scand.* **11** (1957) 745.
8. Bjerrum, N. *Z. anorg. Chem.* **63** (1909) 140.
9. Bjerrum, J., Adamson, A. W., and Bostrup, O. *Acta Chem. Scand.* **10** (1956) 329.
10. Schäffer, C. E. *To be published.*
11. Porai-Koshits, M. A. *Trudy Inst. Krist. Akad. Nauk SSSR* **10** (1954) 117 and *Doklady Akad. Nauk SSSR* **92** (1953) 333.
12. Jørgensen, C. Klixbüll, *Kgl. Danske Videnskab. Selskab, Mat. fys. Medd.* **30** (1956) No. 22.
13. Jørgensen, C. Klixbüll, *Acta Chem. Scand.* **11** (1957) 53.
14. Jørgensen, C. Klixbüll, *Acta Chem. Scand.* **11** (1957) 73.
15. Bjerrum, J., Ballhausen, C. J. and Jørgensen, C. Klixbüll, *Acta Chem. Scand.* **8** (1954) 1275.
16. Bostrup, O. and Jørgensen, C. Klixbüll, *Acta Chem. Scand.* **10** (1956) 1501.
17. Asmussen, R. W. and Bostrup, O. *Acta Chem. Scand.* **11** (1957) 1097.
18. Jørgensen, C. Klixbüll, *Acta Chem. Scand.* **11** (1957) 399.
19. Schäffer, C. E. and Jørgensen, C. Klixbüll, *Acta Chem. Scand. To be published.*
20. Asmussen, R. W. *Studies in the Magnetochemistry of Inorg. Complex Compounds* (in Danish) Copenhagen. 1944.
21. Kortüm, G. *Kolorimetrie, Photometrie und Spectrophotometrie,* 3. ed. 1955, p. 388.
22. Jørgensen, C. Klixbüll, *Acta Chem. Scand.* **8** (1954) 175.
23. Nakamoto, K., Kobayashi, M., and Tsuchida, R. *J. Chem. Phys.* **22** (1954) 957.

Received April 15, 1957.

ACTA CHEMICA SCANDINAVICA 11 (1957) 1232—1239

O-Phosphorylserine

GEORG FÖLSCH and OLOF MELLANDER

Department of Medical Biochemistry, University of Gothenburg, Sweden

A synthesis of the L-, D- and DL-forms of O-phosphorylserine (phosphoserine, serinephosphoric acid or 2-amino-2-carboxy-ethyl-phosphoric acid) is described. The L-isomer was shown to be identical with the phosphorylated serine isolated from phosphoproteins.

A large part of the phosphoprotein phosphorus is considered to be ester bound to serine hydroxyl groups. This view was first expressed by Lipmann after the isolation of O-phosphorylserine from casein and vitellin hydrolysates [1–4]. Later, phosphorylated serine was obtained from several phosphoproteins [5–12], and was also found in free form [13–14]. The occurrence of phosphoric acid diester bound serine in phospholipids such as phosphatidyl serine is well known, and, in addition, serine-guanidoethanol- [15] and serine-aminoethanol [16] diesters have been found. Furthermore, O-phosphorylserine has been isolated from enzymes deactivated by *diiso*propylphosphoryl fluoride and related compounds [17].

Phosphoproteins and phosphopeptides have been studied for a long time [18] in our laboratory. We have observed that, when cow's casein is hydrolysed by proteolytic enzymes under conditions similar to the physiological ones [19] a considerable part of the casein molecule is left as an enzyme-resistant residue. This residue consists of a complex mixture of phosphorylated peptides. The amino acid composition and the phosphorus content of this peptide fraction [20] allow all of the serine hydroxyl groups to be bound as monophosphate esters, although other structures are possible, *e. g.* diester bridges, polyphosphate bridges, N-phosphoryl groups *etc.*[21] The enzyme resistance of these peptides seems to be due to their phosphorylation. Another property of these phosphorylated peptides, the tendency for metal complex formation, is of great biological interest. The calcium salts are, for example well utilised in bone calcification [22,23]. One of us (F.) has made a study of the synthesis of phosphorylated serine peptides as a link in this chain of investigation [24,25]. Here a new synthesis of the keycompound in such peptides, O-phosphorylserine, will be described.

An esterification of serine was mentioned by Langheld in 1911 [26], but the first synthesis of O-phosphorylserine was reported by Levene and Schormüller [27]. These obtained the racemic form in a yield of about 15 % by esteri-

fication of DL-serine with a mixture of phosphoric acid and phosphorus pentoxide. The barium salt of the naturally occurring L-isomer was later isolated after fractional crystallisation of the brucine salts of the racemic mixture [28].

Modifications of this phosphoric acid esterification were reported by Plimmer, who obtained somewhat higher yields [29]. More recently, appreciably higher yields, 40 %, were reported by Canali *et al*[30]. who replaced the aforegoing phosphorylation mixture with polyphosphoric acid. Unlike Canali *et al.*, Cherbuliez and Rabinowitz [31], however, found no phosphorylation of serine with polyphosphoric acid of low degree of polymerisation. Cherbuliez and Rabinowitz obtained a yield of 15 % when serine methyl ester was used instead of the free amino acid [31].

It has been stated several times that the direct esterifications of serine as reported by Levene and Schormüller or by Plimmer give low yields and impure compounds [32]. The same drawbacks seem to accompany the method of Canali *et al.* by which method we have obtained at most a 10 % yield.

These difficulties have forced us to work out a new way to synthesise O-phosphorylserine. The route we used is very similar to the one we used for synthesising phosphorylated peptides [24] and to that used by Baer and Stancer in their synthesis of phosphorylethanolamine [33]. N-Carbobenzoxyserine benzyl esters are phosphorylated by diphenylphosphoryl chloride [34], and the resulting triesters are cleaved by catalytic hydrogenolysis. By this procedure, L-, D- and DL-forms of O-phosphorylserine are obtained in pure, crystalline state and in good yields.

The pure compounds were characterised by their melting points, optica rotations, elementary compositions, R_F-values in different solvents, X-ray powder diffraction patterns and by their infrared absorption spectra *.

In preliminary experiments, dibenzylphosphoryl chloride [36] and di-(*p*-nitrobenzyl) phosphoryl chloride [37] were used as phosphorylating agents. These acid chlorides reacted readily with serine hydroxyl groups ** but the yields were not satisfactory in some cases. Better results were obtained with the easily available and stable diphenyl derivative [34]. The phosphorylation step takes place practically quantitatively (*cf.* Riley *et al.*[39]). The triesters obtained are hydrogenolyzed more slowly than the corresponding benzyl esters, but the yields are good. Two intermediates, O-diphenylphosphorylserine and O-monophenylphosphorylserine can easily be isolated during the hydrogenolysis. This indicates the stepwise elimination of blocking benzyl- and phenyl groups shown in the reaction scheme.

EXPERIMENTAL

When not otherwise stated, the compounds were before analysis dried at room temperature *in vacuo* over phosphorus pentoxide. The melting or decomposition points were determined by using sealed capillary tubes and a well stirred oil bath. They are uncorrected.

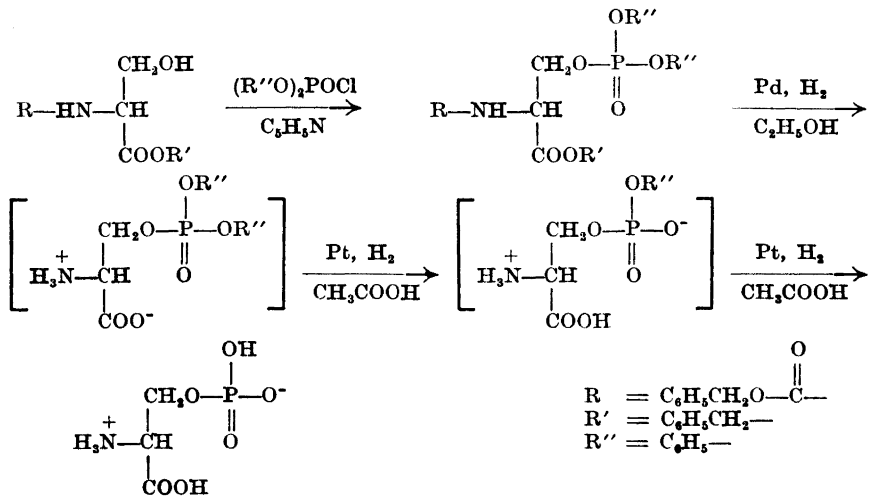
Elementary analyses were made in the Microanalytical Laboratory of the Institute of Medical Chemistry, Uppsala University.

Infrared absorption spectra were recorded with a double beam in time spectrophotometer of the Hornig type built by Dr. M. Skogh at the Institute of Medical Chemistry,

* A study of some metal complexes of the DL-compound has been reported by Österberg [35].

** Li and Eakin [38] observed no reaction between dibenzylphosphoryl chloride and DL-serine methyl ester.

Reaction scheme



Uppsala University. Sodium chloride prism was used. The compounds (1.4 mg) were pressed into freeze dried potassium bromide (300 mg) pellets.

X-Ray powder diffraction patterns were taken with a Guinier camera using quartz monochromated Cu$K\alpha$-radiation (λ = 1.5418 Å). The solvent mixtures used in the paper chromatography were: (I) Phenol-water (80/20 v/v), ascending, about 6 h. (II) *n*-Butanol-acetic acid-water (40/10/50 v/v), descending; 18 h.

N-Carbobenzoxyserine benzyl esters

These compounds were obtained by an azeotrope distilling procedure similar to that of Cipera and Nicholls [40]. Ten g of N-carbobenzoxyserine [41] and 20 ml of benzyl alcohol were distilled with 100 ml of carbon tetrachloride in the precence of 0.5 g of *p*-toluenesulphonic acid. Carbon tetrachloride was added periodically to keep the volume constant. After a reaction time of 5 h the carbon tetrachloride solution was allowed to cool and was then washed with 50 ml of 20 % sodium bicarbonate solution and three 50 ml portions of water. It was dried over anhydrous sodium sulphate. Light petroleum (b. p. 20—40°) was added to the warmed solution. After some hours at room temperature most of the ester had crystallised and was filtered off. More material was obtained by cooling of the concentrated mother liquor to —16°. The yields varied between 70 and 78 %. The physical constants of the three isomers agreed well with the values reported by Baer and Maurukas [41]. Jones and Lipkin [42] recently prepared the DL- and L-compounds, and Skinner *et al.*[43] the D-compound by other procedures.

N-Carbobenzoxy-L-serine benzyl ester, m. p. 83—84°, $[\alpha]_D^{21}$ + 5.5° (chloroform, *c* 4.1, *l* 1); N-Carbobenzoxy-D-serine benzyl ester, m. p. 84—85°, $[\alpha]_D^{21}$ —5.6° (chloroform, *c* 4.0, *l* 1); N-Carbobenzoxy-DL-serine benzyl ester, m. p. 72—73°.

O-Diphenylphosphoryl-N-carbobenzoxy-L-serine benzyl ester

To a solution of 6.6 g (20 mmole) of N-carbobenzoxy-L-serine benzyl ester in 10 ml of anhydrous pyridine 6.4 g (24 mmole) of diphenylphosphoryl chloride [34] was added within 10 min. The reaction mixture was shaken and was held below 40° by occasional cooling in

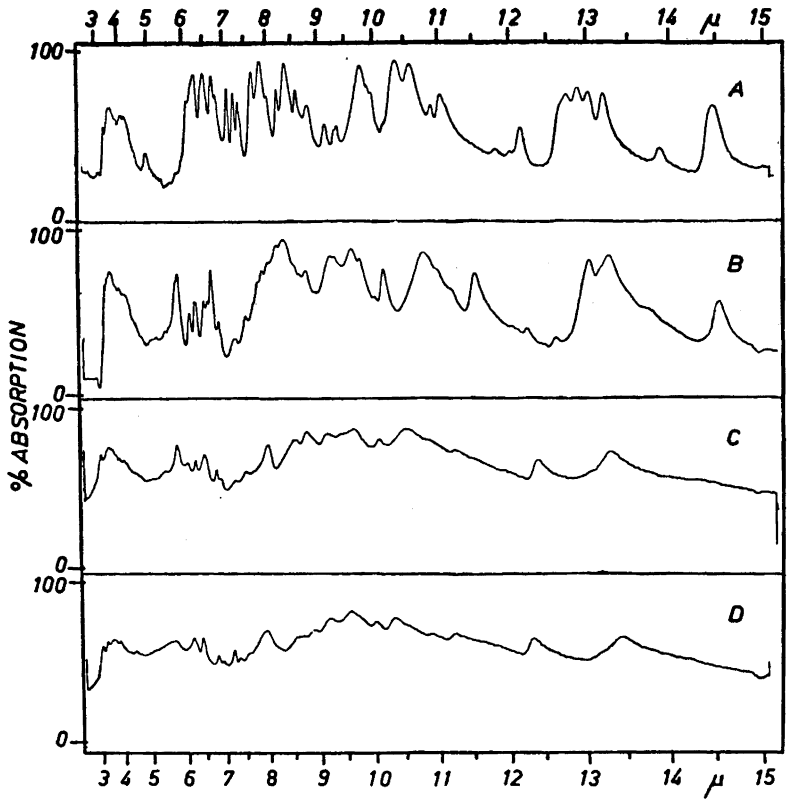


Fig. 1. Infrared absorption spectra of O-diphenylphosphoryl-DL-serine (A), O-monophenylphosphoryl-DL-serine (B), O-phosphoryl-DL-serine (C) and O-phosphoryl-L-serine (D). Compounds in potassium bromide pellets.

cold water. A crystalline precipitate of pyridinium chloride was formed. After 4 h at room temperature, the excess of diphenylphosphoryl chloride was decomposed with 1 ml of water. After an additional hour the mixture was poured into 150 ml of ice water and 150 ml of ether. The ether extract was washed successively with 2 × 50 ml of cold 4 N sulphuric acid, 50 ml of water, 50 ml of 20 % sodium bicarbonate and 50 ml of water.

After drying over anhydrous sodium sulphate the ether was distilled off at reduced pressure, finally at 0.1 mm Hg. The triester remained as a colourless oil, weighing 10.8 g (96 % of theory), $n_D^{22°}$ 1.5640. It was dissolved in 30 ml of 99 % ethanol, and light petroleum (b. p. 20—40°) was added to slight turbidity whereupon O-diphenyl phosphoryl-N-carbobenzoxy-L-serine benzyl ester slowly crystallised out. After a night at room temperature and a few hours at 4° the chrystallisation was complete: 10.5 g (95 % of theory); m. p. 53—53.5°; $[\alpha]_D^{18}$ −3.8° (abs. ethanol, *c* 10.1, *l* 1); $[\alpha]_D^{18}$ +18.0° (chloroform, *c* 5.3, l 1). (Found: C 64.29; H 5.15; N 2.58; P 5.12. Calc. for $C_{30}H_{28}O_8NP$ (561.5): C 64.17; H 5.03; N 2.49; P 5.52).

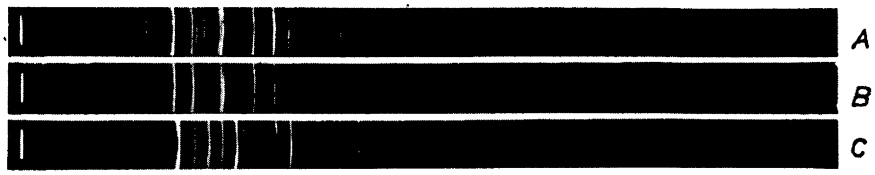


Fig. 2. X-Ray powder diffraction patterns of synthetic (A) and natural (B) O-phosphoryl-L-serine and of O-phosphoryl-DL-serine (C). The strongest reflections are listed in the following table.

Synthetic O-phosphoryl-L-serine		Reported [45] for natural O-phosphoryl-L-serine		Synthetic O-phosphoryl-DL-serine	
intensity	Å	intensity	Å	intensity	Å
—	—	v.w.	6.82	v.s.	4.94
—	—	v.w.	6.21	m.	4.50
—	—	v.w.	5.88	m.	4.16
s.	5.10	s.	5.10	m.	3.88
s.	4.53	s.	4.53	s.	3.63
—	—	m.	4.40	m.	3.60
—	—	w.	4.26	m.	3.07
s.	3.92	s.	3.93	m.	2.91
s.	3.88	s.	3.85		
—	—	v.w.	3.56		
s.	3.36	s.	3.36		
s.	3.10	w.	3.10		

v.s. = very strong s. = strong m. = medium w. = weak v.w. = very weak

O-Diphenylphosphoryl-N-carbobenzoxy-D-serine benzyl ester

The D-isomer was prepared in the same way as the aforegoing compound from 3.3 g of N-carbobenzoxy-D-serine benzyl ester. The yield was 5.3 g (95 % of theory); m. p. 52—53°; $[\alpha]_D^{18}$ +3.7° (abs. ethanol, *c* 10.2, *l* 1); $[\alpha]_D^{18}$ −18.3° (chloroform, *c* 5.0, *l* 1). (Found: C 64.37; H 5.10; N 2.67; P 5.06. Calc. for $C_{30}H_{28}O_8NP$ (561.5): C 64.17; H 5.03; N 2.49; P 5.52).

O-Diphenylphosphoryl-N-carbobenzoxy-DL-serine benzyl ester

The DL-compound was prepared in the same way as the enantiomers. From 16.5 g of N-carbobenzoxy-DL-serine benzyl ester was obtained 25.8 g (92 % of theory); m. p. 47—48°; Found: C 64.21; H 5.20; N 2.62; P 5.26. Calc. for $C_{30}H_{28}O_8NP$ (561.5): C 64.17; H 5.03; N 2.49; P 5.52).

O-Phosphoryl-L-serine

To a solution of 5.6 g (10 mmole) of O-diphenylphosphoryl-N-carbobenzoxy-L-serine benzyl ester in 50 ml of 99 % ethanol was added 1.5 g of palladium oxide catalyst [44], and the mixture was shaken in an atmosphere of pure hydrogen. Eight hours later,

practically no more hydrogen was being consumed and a precipitate, largely consisting of O-diphenylphosphoryl-L-serine, had been formed. This material was dissolved by adding 50 ml of a warm water and acetic acid (1:1) mixture. The catalyst was filtered off and washed with more hot water. The combined solutions were then evaporated to dryness at reduced pressure (bath temperature 40°). The solid residue was redissolved in 50 ml of glacial acetic acid and again shaken in a hydrogen atmosphere, now together with 1 g of platinum oxide catalyst [44]. After about 20 h no more hydrogen was absorbed *. Twenty-five ml of hot water was added to dissolve some precipitated material and the catalyst filtered off. The filtrate and water washings were evaporated to dryness at reduced pressure and the residue dissolved in 100 ml of water. Ten g of cation exchange resin Amberlite IR-120 (H^+-form) was added and the mixture was shaken for 1.5 h. The resin was filtered off and washed with water. The combined solutions were again evaporated to dryness *in vacuo*. The solid residue was finally dissolved in 8 ml of boiling water, and 99 % ethanol was added to faint turbidity. The solution was left to slowly attain room temperature **, when crystals of O-phosphoryl-L-serine were formed. These were washed with ethanol-water (2:1) and dried *in vacuo* at room temperature over phosphorus pentoxide. The yield was 1.55 g (84% of theory); m. p.*** 168—172° (decomp.); reported 167° (decomp.)[9]; $[\alpha]_D^{19}$ +7.4° (water, *c* 3.4, *l* 1); $[\alpha]_D^{21}$ +16.2° (2 N HCl, *c* 3.0, *l* 1); reported $[\alpha]_D^{23}$ +7.2° (water, *c* 4.2)[9]; $[\alpha]_D^{25}$ +16.3° (10 % HCl, *c* 6). (Solution prepared from the *barium* salt) [28]. (Found: C 19.81; H 4.45; N 7.57; P 16.73. Calc. for $C_3H_8O_6NP$ (185.1): C 19.47; H 4.36; N 7.57; P 16.74). R_F-values ****: In solvent I 0.08, in II 0.05.

The infrared absorption spectrum (Fig. 1) and the X-ray powder diffraction pattern (Fig. 2) of this compound were both identical with those obtained from O-phosphoryl-L-serine isolated from casein by Ågren and de Verdier [9] (a sample was kindly given us by Dr. Carl-Henric de Verdier).

O-Phosphoryl-D-serine

This isomer, which has not been reported before, was prepared from 2.80 g of the corresponding triester by hydrogenolysis in exactly the same way as the preceding isomer. The yield was 0.76 g (80 % of theory); m. p. 170—173° (decomp.); $[\alpha]_D^{21}$ −7.0° (water, *c* 3.0, *l* 1); $[\alpha]_D^{21}$ −15.6° (2 N HCl, *c* 3.2, *l* 1). (Found: C 19.62; H 4.40; N 7.55; P 16.81. Calc. for $C_3H_8O_6NP$ (185.1): C 19.47; H 4.36; N 7.57; P 16.74).

The infrared absorption spectrum and X-ray powder diffraction pattern were identical with those of the L-derivative.

O-Phosphoryl-DL-serine

The racemic compound was prepared from the corresponding racemic triester. 22.4 g of this gave a yield of 5.8 g (72 % of theory) of the well crystallising and hitherto unreported *monohydrate;* m. p. 153—156° (decomp.) after sintering at 135°. (Found: C 17.62; H 5.00; N 6.79; P 15.16. Calc. for $C_3H_8O_6NP$, H_2O (203.1): C 17.73; H 4.96; N 6.90; P 15.25).

---

* The progress of the hydrogenolysis after different times can easily be determined by paper chromatography in solvent II. At the end of the reaction only traces of O-diphenylphosphoryl-serine (R_F 0.59) and O-monophenylphosphorylserine (R_F 0.18) should be present beside O-phosphorylserine (R_F 0.05).

** To obtain complete crystallisation, it was often necessary to gradually add several volumes of absolute ethanol and to store the solution in the icebox for some days.

*** The melting points of O-phosphorylserines and O-phosphorylated serine peptides vary appreciably with the conditions during the determination. When heated very slowly, they decompose at temperatures below those reported here. Much more characteristic are the infrared spectra and the X-ray diffraction patterns.

**** Practically the same R_F values were obtained for the L-, D, and DL-forms.

The water of hydration was not removed by drying *in vacuo* at 100°. When the compound was dried at 120°, considerable decomposition occurred.

The anhydrous compound could be prepared by precipitation with ethanol and ether from the 5 % solution of the *monohydrate* in water; m. p. 167—170° (decomp.); reported 165—166° (decomp.) [29], 166—167° [32]. (Found: C 19.45; H 4.52; N 7.52; P 16.50. Calc. for $C_3H_8O_6NP$ (185.1): C 19.47; H 4.36; N 7.57; P 16.74).

The infrared absorption spectrum of the racemic product could be distinguished from the spectra of the optically active isomers, although they were very similar (Fig. 1). The X-ray powder diffraction pattern of the racemic compound was quite different from the pattern of the L- and D-isomers (Fig. 2). However, its infrared spectrum and X-ray diffraction pattern were identical with those obtained from O-phosphoryl-DL-serine prepared according to Plimmer [29] and Canali *et al* [30].

O-Diphenylphosphoryl-DL-serine

O-Diphenylphosphoryl-N-carbobenzoxy-DL-serine benzyl ester in ethanol solution was shaken as usual in a hydrogen atmosphere together with palladium oxide catalyst. The precipitate formed during the hydrogenolysis was filtered off and dissolved in a minimum amount of a hot mixture of acetic acid and water (2:1). The solution was filtered to remove the palladium catalyst and was then allowed to cool. After some hours at +4° the crystals of O-diphenylphosphoryl-DL-serine were collected and dried *in vacuo* over potassium hydroxide; m. p. 129—130° (decomp.). (Found: C 53.39; H 4.76; N 4.14; P 9.16. Calc. for $C_{15}H_{16}O_6NP$ (337.3): C 53.41; H 4.78; N 4.15; P 9.19).

Further hydrogenolysis of this compound in glacial acetic acid solution using platinum oxide catalyst, gave O-phosphorylserine, identified by paper chromatography.

Free amino group was indicated by the colour reaction of the compound with ninhydrin. R_F value in solvent I 0.9, in II 0.59. The infrared absorption spectrum is shown in Fig. 1. In contradistinction to the O-phosphorylserines and to O-monophenylphosphorylserine, there was no carbonyl absorption band near 5.75 μ. Instead, the strong band at 6.04 μ indicated the presence of an ionised carboxyl group.

O-Monophenylphosphoryl-DL-serine

This phosphoric diester was isolated in another hydrogenolytic experiment. O-Diphenylphosphoryl-N-carbobenzoxy-DL-serine benzyl ester was hydrogenated as usual using palladium as a catalyst and, after evaporation of the ethanol, the residue was dissolved in glacial acetic acid. The hydrogenolysis was started again, now with platinum oxide catalyst. After an hour, during which the hydrogen was rapidly consumed, the reaction slowed down and was interrupted. The catalyst was removed and the solvent distilled off *in vacuo*. The solid residue was then dissolved in a minimum amount of boiling water, and the filtered solution was left at room temperature for four hours. Crystals of O-monophenylphosphoryl-DL-serine were formed. After one more recrystallization from hot water, the crystals were collected, washed with ice-cold distilled water and dried (the mother liquor and washings contained O-phosphorylserine); m. p. 163—165° (decomp.). (Found: C 41.62; H 4.69; N 5.38; P 12.01. Calc. for $C_9H_{12}O_6NP$ (261.2): C 41.39; H 4.33; N 5.36; P 11.86).

The compound was ninhydrin positive. The R_F value in solvent I was 0.36, in II 0.18. Hydrogenolysis in glacial acetic acid solution and with platinum oxide catalyst gave O-phosphorylserine, identified by paper chromatography. The infrared absorption spectrum is shown in Fig. 1.

Acknowledgements. The authors are much indebted to Professor Einar Stenhagen for valuable discussions, to Mrs. Karin Nilsson, Uppsala, for the infrared absorption spectra, to Miss Ulla-Britt Dahlberg, Uppsala, for the elementary analyses, to Mr. Gösta Vannerberg, Department of Inorganic Chemistry, Chalmers University of Technology, for the X-ray diffraction patterns and measurements and to Mrs. Birgit Boman for technical assistance.

The work was supported by grants from the *Swedish Medical Research Council* and from the *Medical Faculty, University of Gothenburg.*

REFERENCES

1. Lipmann, F. and Levene, P. A. *J. Biol. Chem.* **98** (1932) 109.
2. Lipmann, F. *Naturwiss.* **21** (1933) 236.
3. Lipmann, F. *Biochem. Z.* **262** (1933) 3.
4. Lipmann, F. *Biochem. Z.* **262** (1933) 9.
5. Posternak, S. and Posternak, T. *Compt. rend.* **197** (1933) 429.
6. Rapoport, S. *Biochem. Z.* **289** (1937) 420.
7. Sorimati, T. *J. Biochem. Japan* **29** (1939) 289.
8. Mechan, D. K. and Olcott, H. S. *J. Am. Chem. Soc.* **71** (1949) 3670.
9. Ågren, G. deVerdier, C.-H. and Glomset, J. *Acta Chem. Scand.* **5** (1951) 324.
10. deVerdier, C.-H. *Acta Chem. Scand.* **8** (1954) 1302; *cf.* also deVerdier, C.-H. *Thesis*, University of Uppsala 1955.
11. Kennedy, E. P. and Smith, S. W. *J. Biol. Chem.* **207** (1954) 153.
12. Flavin, M. *J. Biol. Chem.* **210** (1954) 771.
13. Malatesta, C. *Boll. oculist.* **31** (1952) 685.
14. Hiller, E. and Bischof, H. *Die Medizinische* **1953** 1541.
15. Thoai, N. and Robin, Y. *Biochim. et Biophys. Acta* **14** (1954) 76.
16. Roberts, E. and Lowe, I. *J. Biol. Chem.* **211** (1954) 1.
17. Schaeffer, N. K., May, S. C. and Summerson, W. H. *J. Biol. Chem.* **202** (1953) 67.
18. Mellander, O. *Biochem. Z.* **300** (1939) 240.
19. Mellander, O. *Upsala Läkareförен. Förh.* **52** (1947) 107.
20. Løvtrup, S., Mellander, O. and Roos, K. *Arch. Mikrobiol.* **26** (1957) 83.
21. Pearlman, G. E. *Advances in Protein Chem.* **10** (1955) 1.
22. Mellander, O. and Isaksson, B. *Acta S c. Med. Upsaliensis* **55** (1950) 239.
23. Mellander, O. *Acta Soc. Med. Upsaliensis* **55** (1950) 247.
24. Fölsch, G. *Acta Chem. Scand.* **9** (1955) 1039.
25. Fölsch, G. *Acta Chem. Scand.* **10** (1956) 686.
26. Langheld, K. *Ber.* **44** (1911) 2087.
27. Levene, P. A. and Schormüller, A. *J. Biol. Chem.* **105** (1934) 547.
28. Levene, P. A. and Schormüller, A. *J. Biol. Chem.* **106** (1934) 595.
29. Plimmer, R. H. A. *Biochem. J.* **35** (1941) 461.
30. Canali, V., Casciotti, G., De Luca, R. and Baldantoni, A. *Boll. soc. ital. sper.* **27** (1951) 1479.
31. Cherbuliez, E. and Rabinowitz, J. *Helv. Chim. Acta* **39** (1956) 1461.
32. Plapinger, R. E. and Wagner-Jauregg, T. *J. Am. Chem. Soc.* **75** (1953) 5755.
33. Baer, E. and Stancer, H. C. *Can. J. Chem.* **34** (1956) 436.
34. Baer, E. *Biochemical Preparations* **1** (1949) 51; **2** (1952) 96.
35. Österberg, R. *Nature* **179** (1957) 476.
36. Atherton, F. A., Openshaw, H. T. and Todd, A. R. *J. Chem. Soc.* **1945** 382.
37. Zervas, L. and Dilaris, I. *J. Am. Chem. Soc.* **77** (1955) 5354.
38. Li, S. O. and Eakin, R. E. *J. Am. Chem. Soc.* **77** (1955) 1866.
39. Riley, G., Turnbull, J. H. and Wilson, W. *Chemistry & Industry* **1953** 1181.
40. Cipera, J. D. and Nicholls, R. V. V. *Chemistry & Industry* **1955** 16.
41. Baer, E. and Maurukas, J. *J. Biol. Chem.* **212** (1955) 25.
42. Jones, E. E. and Lipkin, D. *J. Am. Chem. Soc.* **78** (1956) 2408.
43. Skinner, C. G., Mc Cord, T. J., Ravel, J. M. and Shive, W. *J. Am. Chem. Soc.* **78** (1956) 2412.
44. Adams, R., Voorhees, V. and Shriner, R. L. *Organic Synthesis* Coll. Vol. I (1944) 463.
45. de Verdier, C.-H. *Upsala Läkareförен. Förh.* **60** (1955) 48.

Received April 18, 1957.

ACTA CHEMICA SCANDINAVICA 11 (1957) 1240—1247

On the Chemical Composition of some Mucous Substances of Fish

ERLAND WESSLER and IVAR WERNER

Institute of Medical Chemistry, University of Upsala, Sweden

The mucous substances of some fishes have been studied. The predominant component of the external surface mucus seems to be a simple protein, in the case of myxinoids a protein which precipitates in fibres. Together with the simple protein there are also small, varying amounts of nucleic acid and glycoproteins. The glycoproteins contain hexosamine, galactose, fucose, and sialic acid, and thus seem to be of the same types as are present in mucous secretions of other vertebrates.

In addition to ribose (nucleic acid) and in some cases small amounts of fucose, and/or glucose, the fish-roe preparations contained hexosamine, galactose, mannose, and sialic acid as monosaccharide constituents. The carbohydrate moiety probably forms the substantial part of the jelly coat of the roe.

The epithelial mucus of mammals has a fairly uniform composition, its main components being two glycoproteins[1]. One of these has a prosthetic group containing acetylated hexosamine, galactose, and fucose; the other contains acetylated hexosamine and sialic acid. As a rule they occur together, and are usually inseparable by ordinary physico-chemical procedures. The chemical differences found in mucus specimens from different organs, species, or individuals may be differences in proportion between the two types of prosthetic groupings, differences in the relative content of some monosaccharide constituent such as fucose or galactosamine, or slight variations in the acyl groups substituted to the sialic acid molecule. Up to now no exception from this pattern has been reported.

Investigations on frog spawn have shown the mucous, gelatinous coating of the spawn to contain the same main carbohydrate constituents, *viz.* hexosamine, galactose, fucose, and probably, sialic acid [2,3].

Preliminary analyses of mucosal scrapings from birds (pheasants and geese) have shown the same main carbohydrate components (Werner, unpublished data).

Thus the same types of glycoproteins seem to be prevalent in the epithelial mucus of mammals, birds, and amphibians. We therefore decided to investigate some mucous substances of the lower vertebrates, fishes, and cyclostomes.

MATERIAL

The external mucous coatings of plaice (*Pleuronectes platessa*), cod (*Gadus callarias*), whiting (*Gadus merlangus*), eel (*Anguilla vulgaris*), pike (*Esox lucius*), ray (*Raja sp.*), and hagfish (*Myxine glutinosa*) were collected, care being taken to avoid contamination from both external and internal sources (roe, milt, *etc*,). The preparations were dehydrated in ethanol, acetone, and ether, and subsequently analysed.

Samples of roe from perch (*Perca fluviatilis*), pike-perch (*Lucioperca sandra*), cod (*Gadus callarias*), burbot (*Lota vulgaris*), whitefish (*Coregonus lavaretus*), and Baltic herring (*Clupea harengus*), and of milt from burbot (*Lota vulgaris*) were freed from membranes, washed with aqueous (50 %) ethanol, dehydrated by treatment with ethanol, acetone, and ether, and analysed.

Some other samples of roe from pike-perch, burbot, and whitefish, and of milt from burbot were instead lyophilized, and subsequently analysed. These preparations, however, gave slightly turbid solutions in the orcinol-sulphuric-acid reaction, probably owing to the presence of some lipid constituents, and they were therefore not used for quantitative analysis.

ANALYTICAL METHODS

Nitrogen was determined by the Kjeldahl method [4].

Hexosamine was assayed according to Blix's modification of the Morgan-Elson method [5]. Before analysis the samples were hydrolysed for 14 and 18 h with 2 N hydrochloric acid at 100°C. The two hydrolysis-times gave nearly identical hexosamine values. The readings were made at 530 mμ in a Beckman B spectrophotometer.

Hexose, *pentose*, and *methylpentose* were determined by the orcinol-sulphuric-acid method in Vasseur's modification [6]. After a heating time of 20 min the absorbancies were measured at 495 mμ, where the sugars present have roughly the same extinction coefficients. As chromatography revealed galactose to be the predominant sugar in most preparations this sugar was chosen as standard.

The *methylpentose* content was determined separately by Dische's method [7]. A heating time of 10 min was used. A standard with 10 μg of fucose was run simultaneously with the unknown samples. The readings were made 4 to 6 h after the addition of cysteine, because at this time the absorbancy depending on the fucose content has reached a maximum and nearly constant value [8,9].

Most of the preparations were found to contain material interfering with the determination. When cysteine was added, a colour with maximum absorption at about 395 mμ developed instantly, and then gradually disappeared in 2 to 3 h. The absorption due to fucose seemed to develop, independently of the interfering reaction, in the course of 4 to 6 h. Thus when very little or no fucose was present there was only a fading of the initial colour after addition of cysteine; but when the fucose content was higher, the absorption first decreased and later increased. When the fucose content exceeded about 1 % there was no fading, the colour intensity rising from the beginning. Thus the influence of the interfering material was probably eliminated by not making the readings until at least 4 h after the addition of cysteine.

The absorptions developing during the heating with sulphuric acid were read off before the addition of cysteine, and subtracted from the values obtained 4 to 6 h after cysteine had been added.

The methylpentose values found are reported as fucose, because this sugar was the only methylpentose revealed by chromatography.

Sialic acid was assayed by the quantitative Ehrlich and Bial reactions described previously [10]. The results obtained with the two methods tallied very well, and it is thus probable that the preparations contain a sialic acid. This is further supported by the fact that the absorption spectra in all but two cases (ray and hagfish) showed absorption maxima at the same wavelengths as crystalline sialic acid.

For qualitative demonstration of *hexuronic acid* most of the preparations were examined by the naphthoresorcinol method of Fishman *et al.*[11] No hexuronic acid could be traced by this method.

Table 1. Percentage composition of the dried external mucus of some fishes. The figures are corrected for ash and moisture content.

Species	N	Carbohydrate (total)	Hexosamine	Hexose + Pentose + Methylpentose	Fucose	Sialic acid	P
Teleostei							
Pleuronectes platessa	13.5	8.5	3.0	5.0	2.1	0.5	
Gadus callarias	15.2	4.0	0.6	2.6	0.1	0.8	1.0
Gadus merlangus	13.8	4.8	0.9	3.1	0.1	0.8	
Anguilla vulgaris	14.1	3.7	1.0	1.3	[0.1][1]	1.4	
Esox lucius	13.8	8.3	3.5	3.2	0.4	1.6	
Elasmobranchii							
Raja sp.	12.7	14.4	4.2	10.2	1.4	<0.2	
Cyclostomi							
Myxine glutinosa	13.6	3.3	1.8	1.5	[0.1][2]	<0.2	0.2

[1] No fucose spot could be detected on the chromatogram.
[2] A fucose spot could not with certainty be detected on the chromatogram.

All analytical figures given are means of at least two separate determinations, and are corrected for ash and moisture content.

Chromatography. The carbohydrate composition was studied by one-dimensional chromatography on Munktell OB filter-paper. Lutidine-*n*-amyl alcohol [12] proved to be the most suitable solvent. The papers were sprayed with the aniline hydrogen phthalate reagent of Partridge [13]. The preparations were hydrolysed with 2 N sulphuric acid at 100°C for one hour. $Ba(OH)_2$ was added to pH 6, and, after centrifuging, the clear supernatant was taken for analysis. A hydrolysis time of one hour was found suitable. Mannose was the sugar most slowly split from the protein. After about one hour it had reached a concentration high enough to be demonstrable by chromatography. A ribose spot was visible on all chromatograms after hydrolysis for one hour, but after a hydrolysis time of 2 h no ribose could be traced by paper chromatography.

The amino acids were assayed by two-dimensional paper chromatography, using ascending phenol-ammonia-cupron in one direction and descending pyridine—amyl-

Table 2. Percentage composition of dried roe and milt from some fishes. The figures are corrected for ash and moisture content.

Material	Carbohydrate (total)	Hexosamine	Hexose + Pentose + Methylpentose	Fucose	Sialic acid	P
Roe from						
Perca fluviatilis	12.5	1.8	8.6	[0.3] [1]	2.1	
Lucioperca sandra	8.5	2.0	3.9	0.0	2.6	
Gadus callarias	3.3	0.9	1.9	0.0	0.5	1.1
Lota vulgaris	4.8	1.3	2.2	0.0	1.3	1.0
Coregonus lavaretus	7.9	1.6	3.9	0.3	2.4	
Clupea harengus	5.1	1.3	3.0	0.2	0.8	
Milt from						
Lota vulgaris	4.0	0.4	3.2	0.0	0.4	3.3

[1] No fucose spot could be detected on the chromatogram.

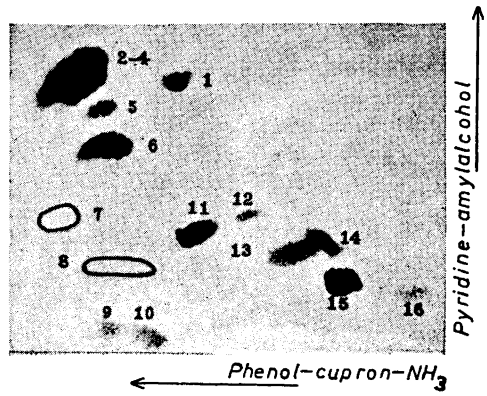


Fig. 1. Two-dimensional chromatogram showing the amino acid pattern of the external mucus of eel. Solvents, phenol-cupron-ammonia/pyridine-amyl alcohol.

1. Tyrosine
2. Phenylalanine
3. *Iso*-leucine
4. Leucine
5. Methionine
6. Valine
7. Proline
8. Histidine
9. Arginine
10. Lysine
11. Alanine
12. Threonine
13. Glycine
14. Serine
15. Glutamic acid
16. Aspartic acid

alcohol in the other. The technique described by de Verdier and Ågren was employed [14]. This procedure allows good separation of all ordinary amino acids except phenylalanine, leucine, and isoleucine.

RESULTS

In the dried state the preparations of external mucus were light white-greyish powder, except the one from the hagfish. The hagfish mucus maintained throughout the drying and grinding procedure (several different methods were used) a distinct fibrous structure and was, in the dry state, similar to

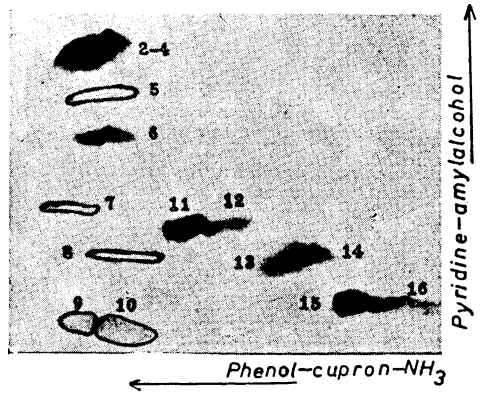


Fig. 2. Two-dimensional chromatogram showing the amino acid pattern of the external mucus of ray. Solvents and designation as in Fig. 1.

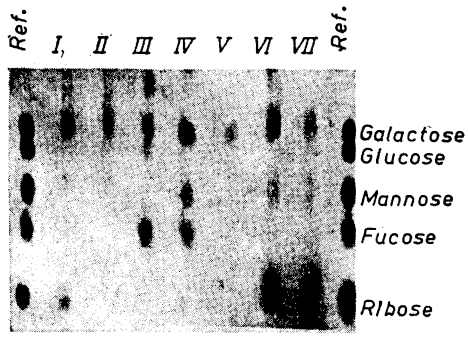


Fig. 3. Chromatogram showing sugar components of the external mucous coatings of some fishes. I, cod; II, eel; III, plaice; IV, ray; V, hagfish; VI, pike; VII, whiting. Solvent, lutidine-*n*-amyl alcohol.

short-clipped cotton wool. The dried roe and milt preparations were yellowish powders.

The analytical figures are given in Tables 1 and 2.

Amino acid chromatography of the mucous coatings revealed in most preparations the presence of all the common amino acids. A characteristic chromatogram is shown in Fig. 1. In the mucus of the ray no tyrosine could be demonstrated (Fig. 2).

The sugar chromatograms are shown in Fig. 3 and 4. A rough quantitative evaluation based on the size and intensity of the spots is given (Tables 3 and 4). This evaluation holds only for the individual chromatograms, and should not be used for mutual comparison of different chromatograms.

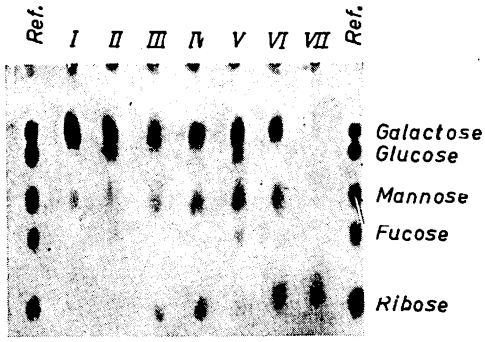


Fig. 4. Chromatogram showing sugar components of roe from I, perch; II, Baltic herring; III, cod; IV, pike-perch; V, whitefish; VI, burbot; and VII, milt from burbot. Solvent, lutidine-*n*-amyl alcohol.

DISCUSSION

The presence of carbohydrate in some piscine mucins has been observed earlier. In a study of the surface slime of the Pacific hagfish (*Polistotrema stouti*), Ferry [15] found carbohydrate contents of 1.4 and 2.9 % (expressed as glucose) in two different preparations. From loach (*Misgurnus anguilli caudatus*) Turumi and Saito [16] obtained a mucous product said to contain 17.9 % glucosamine, 9.8 % galactose, and sialic acid.

Hammarsten [17] examined roe from perch and found that the yolk protein was not a glycoprotein, whereas the egg-jelly gave, after acid hydrolysis, large quantities of a reducing substance, the nature of which he did not further investigate. Young and Inman [18] found 1.0 % glucosamine in the protein of the egg-casings of the salmon. A few per cent of reducing substance has also been reported in roe from *Barbus fluviatus* [19], pike [19], king salmon [20], trout [21], herring [22-24], and salmon [25].

All our preparations of external fish mucus contained carbohydrate. The carbohydrate content is comparatively low, and the quantitative variation between different species is small, except that the ray mucus contains about twice as much as that of other fishes.

The main constituent of the mucus seems to be a simple protein component containing very little or no carbohydrate. In all species investigated the amino-acid pattern of the protein seemed to be mainly the same except in the ray, the mucus protein of which does not contain tyrosine and thus also differs in this respect.

Besides this simple protein component, the mucus also contains variable amounts of one or more glycoproteins. The presence of hexosamine, galactose, fucose, and sialic acid indicates the same types of glycoproteins as are present in mucous secretions of higher vertebrates, *viz.* fucomucin and sialomucin [1]. It is interesting to note that sialic acid is present in the mucus of all ordinary fishes, but not in the mucus of the ray and the hagfish.

In addition to the sugars mentioned, all the preparations except perhaps that of the hagfish, contained ribose and mannose, and one of them also glucose. The ribose probably derives from nucleic acid. The presence of nucleic acids in the mucus is not unexpected, as it is known that many of the epidermal cells discharge their entire contents directly onto the surface. Mannose is

Table 3. Relative sugar composition (hexoses + pentoses + methylpentoses) of the external mucous coatings of some fishes, as shown by chromatography after acid hydrolysis.

Material	Galactose	Glucose	Mannose	Fucose	Ribose
External mucus from					
Pleuronectes platessa	++	+	(+)	+++	+
Gadus callarias	+		(+)	(+)	++
Gadus merlangus	+		(+)	(+)	++
Anguilla vulgaris	+		(+)		+
Esox lucius	++		+	(+)	+
Raja sp.	+++		++	++	+
Myxine glutinosa	+		?	?	(+)

Table 4. Relative sugar composition (hexoses + pentoses + methylpentoses) of the roe and the milt of some fishes, as shown by chromatography after acid hydrolysis.

Material	Galactose	Glucose	Mannose	Fucose	Ribose
Roe from					
Perca fluviatilis	++++		+		+
Lucioperca sandra	+++	+	++		++
Gadus callarias	+++		+		+++
Lota vulgaris	+++		++	(+)	++
Coregonus lavaretus	+++	++	++	+	+
Clupea harengus	+++	++	+	+	++
Milt from					
Lota vulgaris	+				++

a well-known component in many serum and tissue glycoproteins, and is often found in small amounts in mucous secretions of mammals. The mannose might thus be explained as belonging to some tissue protein present. The possibility of mannose belonging to some of the mucous glycoproteins mentioned above cannot of course be excluded. The glucose probably derives from glycogen, which has been shown to be present in the epidermal cells [26].

The view that the mucus is a mixture of one major, simple protein component and smaller amounts of one or more glycoproteins is supported by histological observations. Firstly, there are in most fishes several different types of "glands", specific glandular structures such as the large mucous glands of the myxinoids, the simple pouch-like epidermal organs, and the monocellular "glands" of the goblet-type, indicating a complex nature of the secretion [27]. Secondly, the mucus and some of the epidermal cells, especially the goblet cells, take various degrees of staining with fuchsin after pretreatment with per-iodic acid. They also show metachromasia with toluidine blue in the same way as do many glycoproteins [26, 28].

The finding of fucose- and sialic acid containing glycoproteins in secretion from external mucous epithelium is notable. Glycoproteins of this type so far known have all been of entodermal or closely related origin. Here we find tissues of obviously ectodermal origin producing the same types of substance.

The same monosaccharides as in the external mucus are also found in hydrolysates of fish roe. It is reasonable to assume here, too, that the ribose derives from nucleic acid. Galactose, mannose, hexosamine, and sialic acid are invariable constituents, and are probably due to the presence of glycoproteins. Some of the preparations also contained glucose and/or fucose. The origin of the glucose is obscure. The method of preparation employed (treatment of the pulverized roe with aqueous ethanol) is certain to remove free glucose, which is known to occur in fish eggs [29]. Glycogen has not been found in undeveloped fish eggs [21, 25]. Fucose may indicate the presence of small quantities of mucus of the usual epithelial mucus type.

The largest carbohydrate content is found in those roe specimens that have the thickest mucous layers, *viz.* whitefish and perch, and the smallest content in those with very thin layers, *e.g.* cod and burbot. Considering that

the mucous layer only contributes a minor part of the total dry weight of the roe, and assuming that the carbohydrates are mainly derived from this, it is clear that the relative carbohydrate content of this mucous layer must be high and similar to that of frog-spawn mucin [2].

Ribose was the predominant sugar in the milt sample examined.

REFERENCES

1. Werner, I. *Acta Soc. Med. Upsaliensis* **58** (1953) 1.
2. Folkes, B. F., Grant, R. A. and Jones, J. K. N. *J. Chem. Soc.* **1950** 2136.
3. Hiyama, N. *Tohoku J. Exptl. Med.* **50** (1949) 373.
4. Friedrich, A. *Mikroanalyse*, F. Deuticke, Leipzig 1933.
5. Blix, G. *Acta Chem. Scand.* **2** (1948) 467.
6. Vasseur, E. *Acta Chem. Scand.* **2** (1948) 693.
7. Dische, Z. and Shettles, L. B. *J. Biol. Chem.* **175** (1948) 595.
8. Aminoff, D. and Morgan, W. T. J. *Biochem. J.* **48** (1951) 74.
9. Gibbons, M. N. *Analyst* **80** (1955) 268.
10. Werner, I. and Odin, L. *Acta Soc. Med. Upsaliensis* **57** (1952) 230.
11. Fishman, W. H., Smith, M., Thompson, D. B., Bonner, C. D., Kasdon, S. C. and Homburger, F. *J. Clin. Invest.* **30** (1951) 685.
12. Werner, I. and Odin, L. *Acta Soc. Med. Upsaliensis* **54** (1949) 69.
13. Partridge, S. M. *Nature* **164** (1949) 443.
14. De Verdier, C.-H. and Ågren, G. *Acta Chem. Scand.* **2** (1948) 783.
15. Ferry, J. D. *J. Biol. Chem.* **138** (1941) 263.
16. Turumi, K. and Saito, Y. *T hoku J. Exptl. Med.* **58** (1953) 247.
17. Hammarsten, O. *Skand. Arch. Physiol.* **17** (1905) 113.
18. Young, E. G. and Inman, W. R. *J. Biol. Chem.* **124** (1938) 189.
19. McCrudden, F. H. *J. Biol. Chem.* **9** (1911) VIII.
20. Greene, Ch. W. *J. Biol. Chem.* **48** (1921) 429.
21. Fauré-Fremiet, M. E. and Garrault, H. *Compt. rend.* **174** (1922) 1375.
22. Steudel, H. and Osato, S. *Z. physiol. Chem., Hoppe-Seyler* **127** (1923) 220.
23. Steudel, H. and Osato, S. *Z. physiol. Chem., Hoppe-Seyler* **131** (1923) 60.
24. Inoue, Y. and Kudô, Y. *J. Agr. Chem. Soc. Japan* **22** (1948) 53; *Chem. Abstr.* **45** 9481 c.
25. Hayes, F. R. and Hollett, A. *Can. J. Research, Section D*, **18** (1940) 53.
26. Björkman, N. *Acta Anat.* **16** (1952) 191.
27. Bolk, L., Göppert, E., Kallius, E., Lubosch, W. *Handbuch der vergleichenden Anatomie der Wirbeltiere*, Urban & Schwarzenberg, Berlin-Wien 1931.
28. Wallin, O. *Personal communication.*
29. Needham, J. *Biochemistry and Morphogenesis*, Cambridge Univ. Press 1942, p. 618.

Received May 7, 1957.

ACTA CHEMICA SCANDINAVICA 11 (1957) 1248—1256

Insulin Crystals

VII. The Growth of Insulin Crystals

JØRGEN SCHLICHTKRULL

Novo Terapeutisk Laboratorium, Copenhagen, Denmark

Pig insulin is crystallized from a clear solution containing sodium citrate and acetone. The decreasing concentration of insulin is determined during the process. The final distribution of crystal sizes is similar to that found earlier in the crystallization of beef insulin from a saline suspension of amorphous insulin [2].

The rate of pig insulin crystallization is

$$\frac{dC}{dt} = 2.8 \times 10^{-7} \times C(95.8-C)^3$$

where C is the crystalline fraction in per cent of total insulin (1.43 mg insulin nitrogen/ml), and t stands for time in min.

The linear rate, R_d, of deposition of insulin on the crystal faces is calculated from the previous [2] and the present data:

saline, beef: $R_d = 1.63\ (c_i-0.080)^2\ \mu$/min
citrate, pig: $R_d = 0.38\ (c_i-0.066)^3\ \mu$/min

where c_i is the concentration of dissolved insulin in millimoles per l, each molecule containing 65 atoms of nitrogen (M = ca. 5 700).

Rhombohedral insulin crystals of perfect shape may be obtained either from pig insulin or by crystallizing beef insulin from a saline solution containing precipitated amorphous insulin [1]. The latter process of crystallization has been analyzed by an experiment using mathematics devised for the purpose [2]. The ratio, r, between the total surface, S, and volume, V, of crystals was found to be constant during crystallization, except for the initial stage. It was assumed that crystals grow with identical rates of linear growth and it was then concluded by mathematical argument that the logarithm of the cumulative size distribution, $P(l)$, is linear, having the slope

$$\frac{d\ln P}{dl} = -3r = -3S/V \qquad (1)$$

This relation was confirmed by the $P(l)$ estimates obtained by counting the crystals according to size. From the constancy of r it was further concluded that the rate of nucleation is proportional to the product of the linear growth

rate and the total number of crystals present. It was demonstrated that this number is proportional to the total length, L, surface, S, and volume, V, of the crystals during crystallization. A chemical interpretation was suggested to the effect that the crystals are self-reproducing at a rate proportional to their linear growth rate. This rate could be expressed by

$$\dot{l} = \text{const.} \ (c_s - c)^2$$

where c_s was the actual and c the final concentration of dissolved insulin, the dot symbol indicating differentiation with respect to time.

The crystallization of pig insulin from a clear solution without addition of sodium chloride has been examined by counting the crystals according to size when crystallization was finished [2]. The cumulative size distribution was found to be very similar to that found for beef insulin, indicating crystal self-reproduction and proportionality during crystallization between the total surface and volume.

It is the purpose of the present investigation to determine the rate of linear growth as a function of the insulin concentration also in this crystallization.

The relation between the rate of growth, $\dot{l}$, and the rate, R_d, of insulin deposition on the crystal faces has been established in experiments with stained crystals [3]. Thus, the rates of deposition will be calculated from the rates of growth.

SYMBOLS

l = size of crystals, *i.e.* the largest diagonal in the crystal projection on a plane through one of the faces. As the crystals lie on their faces, the plane is parallel to the slide on the microscope stage. l is measured in μ.

$\dot{l}$ = $\mathrm{d}l/\mathrm{d}t$ = rate of linear growth of crystals. The time is counted in minutes.

$P(l,t)$ = cumulative distribution of crystal sizes at the moment t, *i.e.* the number per ml of suspension of crystals which are greater than l at the moment t.

$p(l,t) = -\frac{\delta P(l,t)}{\delta l}$, *i.e.* distribution of crystal sizes at the moment t.

$N(t) = \int_0^{l_{max}} p(l,t)\mathrm{d}l$ is the number of crystals per ml of suspension.

$L(t) = \int_0^{l_{max}} lp(l,t)\mathrm{d}l$ is the total length of crystals per ml of suspension

$S(t) = \int_0^{l_{max}} l^2 p(l,t)\mathrm{d}l$ is the total surface of crystals per ml of suspension, the unit area being the area of a rhombohedron with size $l = 1\mu$.

$V(t)$ = $\int_0^{l_{max}} l^3 p(l,t) dl$ is the total volume of crystals per ml of suspension, the unit volume being that of the rhombohedron with size $l = 1\mu$.

r = S/V.

λ = distance in μ between parallel crystal faces.

α = obtuse angle of the rhombohedron ($\alpha = 114°22'$) [1].

R_d = $\dot{\lambda}$ = the linear rate of deposition of insulin on the faces of the growing crystal.

c_s = the concentration of dissolved insulin in per cent of the initial concentration which is 1 % or 1.43 mg insulin nitrogen per ml.

C = the crystallized fraction in per cent of the initial insulin concentration ($C = 100 - c_s$).

c_i = insulin concentration in millimoles per l. An amount of insulin containing 65 atoms of nitrogen is considered equivalent to one molecule (M = 5 778).

METHOD

Crystallization. The method of crystallization has been described recently [1,4]. The crystallization mixture contains: 1 % insulin, 0.04 % Zn^{++}, 0.05 M sodium citrate, 15 % (v/v) acetone, pH = 6.4. Two solutions are made, one of them contains insulin, the other one is a buffer solution.

(A) 10 g recrystallized insulin from pig pancreas is dissolved in 500 ml water containing 9 ml 1 N HCl. The solution is sterilized by filtering through an asbestos filter previously rinsed with diluted HCl. 125 ml acetone and water are added to the filtrated solution to make a total of 875 ml.

(B) 0.05 mole sodium citrate, 0.80 g $ZnCl_2$, 25 ml acetone+water to make 125 ml. When (A) and (B) are mixed in the proportion 7 : 1, pH = 6.4. It may be necessary to add NaOH or HCl to solution (B) in order to produce this pH

The solutions (A) and (B) are mixed at the time $t = 0$ in a glass beaker The surface of the liquid is covered with a layer of paraffin oil to prevent evaporation and the beaker is covered with a glass lid. The mixture is stirred slowly for 24 h at 21°—22°C.

Determination of the insulin concentration, c_s. At intervals, 20—50 ml samples are filtered on sintered glass. The moments, t_1, at the beginning of filtration and those at the end, t_2, are noted. The averages of t_1 and t_2 are used as the t-estimates in the calculations. The concentrations of nitrogen in the filtrates are determined by semi-micro Kjeldahl analyses. Determinations of total nitrogen are also made to check that evaporation is insignificant.

Determination of the cumulative distribution of crystal sizes, $P_*(l)$. $P_*(l)$, the number per ml of suspension of crystals greater than l, is determined when crystallization is finished, using the technique described earlier [5].

THEORY

The linear growth rate, $\dot{l}$. It follows from the definition of S and V (see list of symbols) that

$$dV = 3Sdl \tag{3}$$

and

$$\dot{V} = 3S\dot{l}. \tag{4}$$

Assuming a constant ratio, r, between surface and volume, it follows that

$$(\dot{\ln} V) = 3r\dot{l} \tag{5}$$

and, as V and C are proportional,

$$\dot{l} = \frac{(\dot{\ln} C)}{3r} \tag{6}$$

from which $\dot{l}$ can be calculated by the t, C data when r is known. The ratio r is calculated from *eqn.* (1)

$$r = -\frac{d\ln P_*(l)}{3dl} \tag{7}$$

Hence

$$\dot{l} = -\frac{(\dot{\log}\ C)}{d\log P_*(l)/dl} \tag{8}$$

The linear rate, R_d, of insulin deposition on the crystal faces. During crystallization insulin is deposited on the plane crystal faces which thereby move outwards in directions perpendicular to the faces. The relation between the linear rate of deposition, R_d, and the linear growth rate, $\dot{l}$, is found by geometrical calculus. The distance between the parallel faces of the obtuse rhombohedron is called λ. It can be demonstrated that

$$\lambda = \sin\left(\frac{\alpha}{2}\right) \cdot \sqrt{1 + 2\cos\alpha} \cdot l \tag{9}$$

where α is the obtuse angle of the rhomb and l is the crystal size, *i.e.* the greatest diagonal in the crystal projection on a plane through a face. The angle, α, has been estimated by goniometric measurement [1] as 114°22′. Thus,

$$\dot{\lambda} = 0.351\ \dot{l} \tag{10}$$

It has been shown by experiment that the insulin is not deposited on the three crystal faces meeting in one of the obtuse vertices, but that it is deposited on the three remaining faces, with identical rates of deposition [3]. Hence,

$$R_d = 0.351\ \dot{l} \tag{11}$$

ANALYSIS OF THE DATA

The ratio between surface and volume ($r = S/V$). In the crystallization of beef insulin from a saline suspension of amorphous insulin, perfectly shaped rhombohedral single crystals were developed. However, in the pig insulin crystallization from clear solution, crystal agglomeration occurs to such an extent as to weaken the significance of the notions. The crystals are counted, irrespective of whether they are single or attached to other crystals, and as the shape of attached crystals varies, it follows that the relations between size, surface and volume of a crystal also vary. Thus, the equations set up on the assumption of geometrical similarity do not strictly hold true in this crystallization. It is nevertheless assumed that the deviations from similarity do not significantly alter the significance of the relations leading to eqn. (1). It is assumed that

$$S/V = r = -\frac{\mathrm{d}\ln P_*(l)}{3\mathrm{d}l} \tag{12}$$

in the main part of crystallization, *i.e.* from the moment when a few per cent of insulin have crystallized onwards. This assumption is based upon the similarity between the observed distributions of sizes in this experiment and in the former experiment on cattle insulin crystallization, but it may be incorrect.

The $P_*(l)$ estimates from three countings are shown in Fig. 1.

The slope, $-3r\mathrm{M} = -0.029$ was calculated by using the method of least squares on the section $l < 75\ \mu$. Thus, $r = 0.022$ which is identical with the ratio found earlier in beef-insulin crystallizations [2].

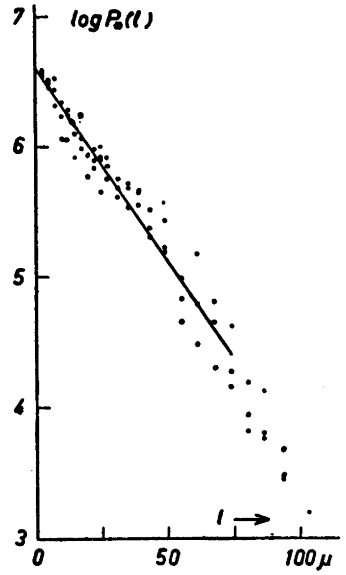


Fig. 1. The cumulative distribution of crystal sizes.

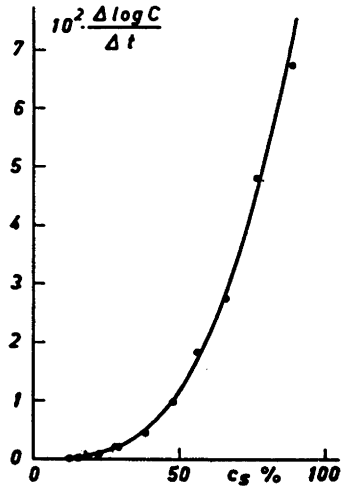


Fig. 2. ($\dot{\log}\ C$) as a function of c_s.

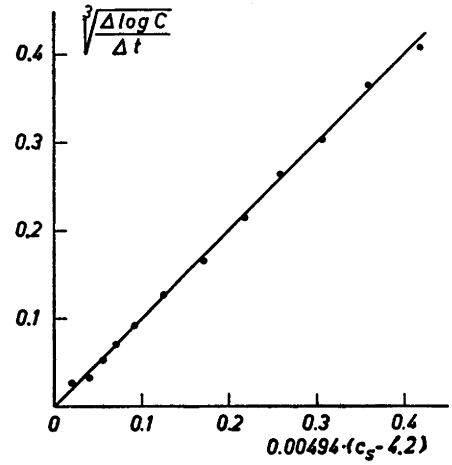


Fig. 3. The third root of ($\dot{\log}$ C) as a function of c_s.

The growth rate, $\dot{l} = (\dot{lnC})/3r$. The t and C estimates are listed in Table 1. Estimates of ($\dot{\log}$ C) are obtained by the approximation

$$(\dot{\log} C_i) \approx \frac{\log C_{i+1} - \log C_{i-1}}{t_{i+1} - t_{i-1}} \tag{13}$$

where i is the sample number. The estimates are plotted in Fig. 2 against the concentration of insulin, c_s.

It appears that $\dot{l}$ is a power function of c_s. The curve drawn into the figure is

$$\frac{\Delta \log C}{\Delta t} = 1.206 \times 10^{-7} \, (c_s - 4.2)^3 \tag{14}$$

The constants in this equation were determined by trial and error using the chronometric integral below and aiming at the best agreement between observed and calculated C-values.

The third root of $\Delta \log C/\Delta t$ is plotted in Fig. 3 against the third root of $1.206 \times 10^{-7} \, (c_s - 4.2)^3$.

Thus, using eqns. (8) and (14)

$$\dot{l} = \frac{1.206}{0.029} \times 10^{-7} \, (c_s - 4.2)^3 = 4.2 \times 10^{-6} \, (c_s - 4.2)^3 \tag{15}$$

The chronometric integral, $t(C)$. is calculated from eqn. (14) which (since $C + c_s = 100$) is written as follows:

$$\mathrm{d}t = \frac{10^7 \cdot \mathrm{M} \cdot \mathrm{d}C}{1.206 \cdot C(95.8 - C)^3} \qquad (\mathrm{M} = 0.4343) \tag{16}$$

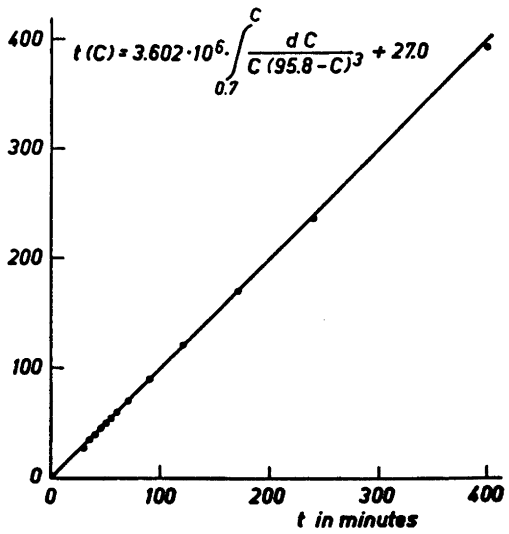


Fig. 4. The chronometric integral as calculated for each of the observed C-values.

It follows by integration that

$$t(C)—t(C_1) = 3.60 \times 10^6 \int_{C_1}^{C} \frac{dC}{C \cdot (95.8—C)^3} \tag{17}$$

Estimates of $t(C)—t(C_1)$ have been calculated for $C_1 = 0.7$ using the formula

$$\int \frac{dx}{x(a—x)^3} = (3a—2x)/2a^2(a—x)^2 + a^{-3} \cdot \ln[x/(a—x)] \tag{18}$$

By subtracting these estimates from the experimental $t(C)$ values, t (C_1) was found to be 27.0 min (in the average). Thus,

$$t(C) = 3.60 \times 10^6 \int_{0.7}^{C} \frac{dC}{C \cdot (95.8—C)^3} + 27.0 \tag{19}$$

The t-values calculated from eqn. (19) are tabulated (Table 1) and plotted (Fig. 4) against the experimental t-values. The discrepancies are within the range of the experimental error.

The analytical estimates, $C(t)$, of insulin which has crystallized at the time t are plotted against t in Fig. 5. The curve in the figure represents eqn. (19), the chronometric integral. The difference between the observations and the curve is insignificant. Hence, it is possible to account for the course of crystallization by a simple mathematical expression.

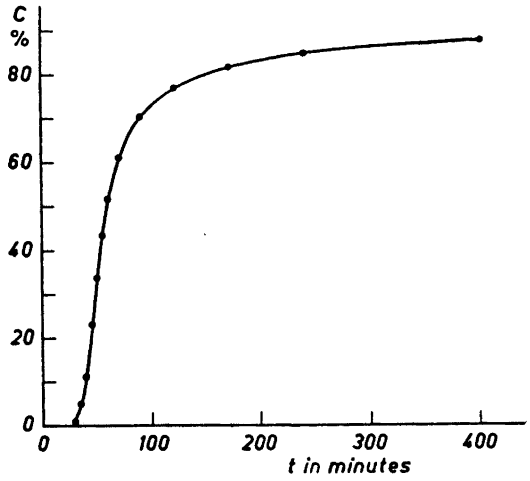


Fig. 5. The percentage of crystalline insulin, C, as observed — the dots — and as calculated from eqn. (19) — the curve.

THE RATE OF DEPOSITION ON THE CRYSTAL FACES

Saline. When beef insulin was recrystallized from a saline medium it was found [2] that

$$\dot{l} = 4.64\ (c_i - 0.080)^2\ \mu/\text{min} \qquad (20)$$

where c_i is the concentration of insulin in millimoles per l. An amount of insulin containing 65 atoms of nitrogen is considered equivalent to one molecule, M = 5 734. It follows from eqns. (11) and (20) that

$$R_d = 1.63\ (c_i - 0.080)^2\ \mu/\text{min} \qquad (21)$$

Table 1. The experimental data.

i	t_1	t_2	t	C	$10^2 \Delta \log C/\Delta t$	$t(C)$
1	1'30″	2'30″	1.8	0.0		
2	29'45″	30'00″	29.9	0.7		27.0
3	34'45″	35'15″	35.0	4.9		35.6
4	39'35″	40'10″	39.9	11.2	6.73	39.9
5	44'45″	45'15″	45.0	23.1	4.81	45.2
6	49'50″	49'55″	49.9	33.9	2.75	49.7
7	54'55″	55'00″	55.0	43.5	1.83	54.6
8	59'45″	60'05″	59.9	51.7	0.98	60.2
9	70'00″	70'15″	70.1	61.1	0.45	70.2
10	89'30″	90'05″	89.8	70.6	0.20	90.3
11	119'45″	120'20″	120.1	77.1	0.078	121.5
12	170'35″	171'00″	170.8	81.7	0.034	170.6
13	239'45″	240'15″	240.0	84.7	0.014	237
14	399'50″	400'20″	400.1	87.8	0.003	394
15	1400'	1400'	1400	91.7		1268

The maximum $R_d = 0.7$ μ/min occurred at $c_i = 0.73$.

Citrate buffer. Provided that eqn. (12) is valid in this crystallization just as in the former, it follows from eqn. (15) that

$$\dot{l} = 1.1\ (c_i - 0.066)^3\ \mu/\text{min} \tag{22}$$

from which

$$R_d = 0.38\ (c_i - 0.066)^3\ \mu/\text{min} \tag{23}$$

The maximum $R_d = 1.3$ μ/min occurred at $c_s = 100$ %, *i.e.* at $c_i = 1.57$ mmole/l.

Acknowledgements. My thanks are due to Dr. Hallas-Møller for his critical advice which has been of considerable benefit to the work. In the mathematical part of the study I have received encouragement, advice and technical assistance from Dr. A. Hald, Professor of Statistics at the University of Copenhagen. It is with pleasure I express my sincere gratitude for this kind help.

I also want to thank K. Petersen, with whom I have had many discussions, my colleagues I. Nøring and F. Sundby who contributed to the experimental work.

REFERENCES

1. Schlichtkrull, J. *Acta Chem. Scand.* **10** (1956) 1459.
2. Schlichtkrull, J. *Acta Chem. Scand.* **11** (1957) 439.
3. Schlichtkrull, J. *Acta Chem. Scand.* **11** (1957) 484.
4. Schlichtkrull, J. *Acta Chem. Scand.* **10** (1956) 1455.
5. Schlichtkrull, J. *Acta Chem. Scand.* **11** (1957) 291.

Received April 15, 1957.

ACTA CHEMICA SCANDINAVICA 11 (1957) 1257—1270

Determination of Molecular Weights and Diffusion Coefficients in the Ultracentrifuge

ANDERS EHRENBERG

Nobel Medical Institute, Biochemical Department, Stockholm, Sweden

A simple method of using the boundary condition at the meniscus in the sector shaped centrifuge cell for the determination of the ratio S/D or M is described. Some pure proteins are studied and the results compared to other data, especially analytical ones. The diffusion coefficients are also computed separately. The homogeneity of the sample is investigated by following the time dependence of M at the meniscus. Information about inhomogeneous samples is thus gained, and reversible dimerizations or polymerizations can be studied.

The possibility of obtaining a value of the ratio of the sedimentation coefficient and the diffusion coefficient from the boundary condition at the meniscus in the centrifuge cell was demonstrated by Archibald [1]. Its value as a purity test has been emphasized by Pedersen [2] and the importance of simplifying and standardizing the method has been discussed [2]. The method seems to have been experimentally applied only in a few cases, first by Li *et al.*[3] and by Porath [4] using an oil turbin centrifuge, and more recently by Brown *et al.*[5] and by Klainer and Kegeles [6,7] using an electrically driven Spinco centrifuge. In these cases the methods of evaluation appears to be rather involved and time consuming. In the present work Archibald's method has been applied in a fashion rather similar to that used by Klainer and Kegeles, but the mode of evaluation has been simplified considerbly.

TECHNICAL

A Spinco analytical ultracentrifuge, model E, was used. The diaphragm of the schlieren optics had been replaced by a phaseplate [6,8,9], and a Wratten light filter, 77A, was used in all the experiments, where it was possible to work with the green monochromatic light of 546 mμ wavelength. A 12 mm synthetic boundary cell with a rubber valve was employed throughout the work. An automatic temperature control, also supplied by the centrifuge manufacturer, was an important additional facility, since the sedimentation and diffusion coefficients depend differently on the temperature and since any convection in the cell would have decreased the accuracy of the method. All the experiments were conducted at temperatures between 18 and 23°C. The surface measurements were made by means of a mechanical planimeter.

DETERMINATION OF THE RATIO S/D AND THE MOLECULAR WEIGHT

Let us consider a sector shaped cell in a rotor revolving at the angular velocity ω. The amount of sedimenting and diffusing solute transported per second through a concentric cylindrical surface in the cell at a distance r from the axes of rotation is Φ (r).

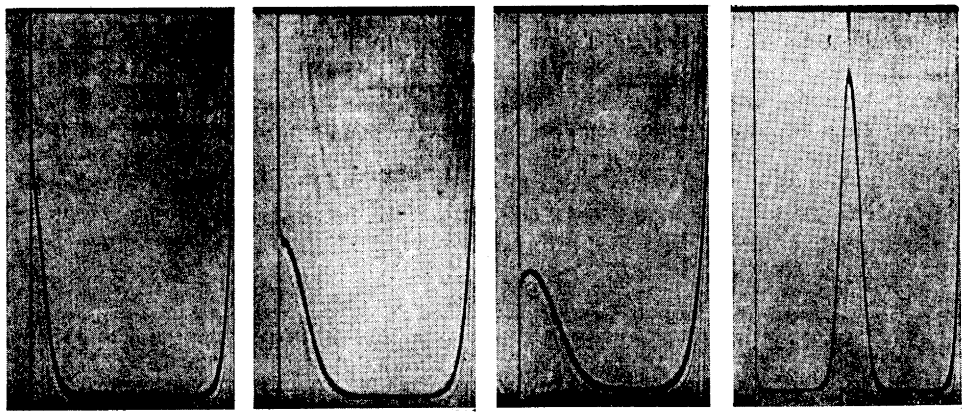
$$\Phi(r) = \Theta r h \left(\omega^2 rcS - D\frac{\partial c}{\partial r}\right) = D\,\omega^2 rc\Theta h \left(\frac{S}{D} - \frac{1}{\omega^2 rc}\cdot\frac{\partial c}{\partial r}\right) \qquad (1)$$

Here Θ denotes the sector angle and h the cell height; c is the concentration, S the sedimentation coefficient and D the diffusion coefficient of the solute. At equilibrium $\Phi(r) = 0$ and

$$\frac{S}{D} = \frac{1}{\omega^2 rc}\cdot\frac{\partial c}{\partial r} \qquad (2)$$

at every distance r in the cell. The same condition (2) is valid during the whole experiment at the meniscus and at the bottom of the cell as both are impervious to the substance. The ratio $\frac{\partial c}{\partial r}/c$, between the concentration grandient and the concentration, at these boundaries the whole time adjusts itself to fulfill eqn. (2). How this boundary condition is utilized for the determination of the quantity S/D will be made clear from the description of an actual experiment.

A solution of the substance under investigation is prepared in a suitable buffer and dialyzed against the same buffer for at least 12 h. After the dialysis some of the buffer is saved. In experiment I a centrifuge run is made at



a b c d

Fig. 1. Some of the photographs taken in the experiments on the old yellow enzyme. Experiment I a) 3 700 s, b) 11 400 s, and c) 19 050 s. Experiment II d) 3 700 s after that 12 590 rpm was attained.

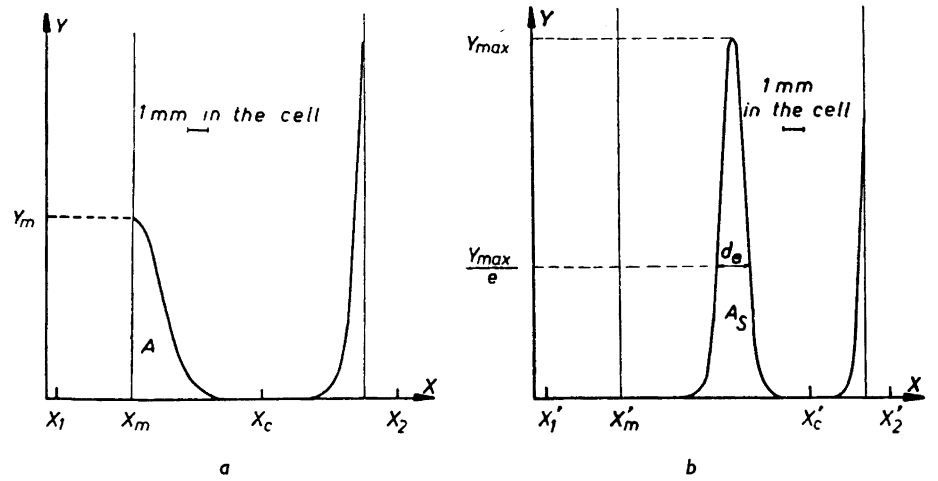


Fig. 2. Reproductions of drawings, with inlayed coordinate axes, made from photographs corresponding to a) Fig. 1 b and b) Fig. 1 d. 1 cm on the original drawings corresponds to 1 mm in the cell. For further explanation see text.

a low speed in the 12 mm synthetic boundary cell but without using the layering technique. Fig. 1 a — c shows three of the exposures taken, one in the beginning, one in the middle and one at the end of the experiment. The pictures are placed in a magnifying apparatus and drawings made of the refractive index gradient curves in a convenient scale (1 cm on the paper corresponded to 1 mm in the cell). Fig. 2 a shows such a drawing with inlaid coordinate axes. The y-coordinate of the refractive index gradient is proportional to the concentration gradient of the substance. At the meniscus we thus have

$$\left(\frac{\partial c}{\partial r}\right)_m = k_1 y_m \tag{3}$$

where the subscript m refers to the meniscus and k_1 is the constant of proportion. Because of optical distortion near the meniscus the curve has to be extrapolated the last few millimeters on the paper. The most accurate values of y_m are hence obtained from the exposures in the middle period of the experiment for which the refractive index gradient curves are horizontal or nearly so at the meniscus *. A relation similar to (3) is also valid at the bottom of the cell, but because of the piling up of material the curves are usually steep there and the y-coordinate of the intercept at the bottom is difficult to determine with the precision needed. Because of these reasons we have so far only treated the data obtained at the meniscus.

* *Note added in proof:* This eliminates to a large extent the influence of the error in the meniscus image, recently discussed by P. J. Cheng, *J. Phys. Chem.* **61** (1957) 695.

It is essential that a region in the middle of the cell remains with a flat baseline and with the concentration varing according to the formula given by Pedersen [10]

$$c = c_0 e^{-2\omega^2 St} \tag{4}$$

Here c is the concentration of solute at time t and c_0 the initial concentration. The concentration at the meniscus at time t is thus obtained by the equation

$$c_m = c - \int_{r_m}^{r_c} \frac{\partial c}{\partial r}\, \omega r \tag{5}$$

or

$$c_m = c_0 e^{-2\omega^2 St} - k_1 k_2 \int_{x_m}^{x_c} y \mathrm{d}x \tag{6}$$

x_m is the x-coordinate of the meniscus, x_c that of a point in the part of the cell where eqn. (4) is valid. k_2 is the inverse of the enlargement in the x-direction. y corresponds to an exposure taken at time t. The integral of eqn. (6) is the surface A between the curve, the meniscus and the x-axes of Fig. 2a:

$$A = \int_{x_m}^{x_c} y \mathrm{d}x \tag{7}$$

Insertion of expressions (3), (6) and (7) in eqn. (2) gives

$$\frac{S}{D} = \frac{k_1 y_m}{\omega^2 r_m \left(c_0 e^{-2\omega^2 St} - k_1 k_2 A\right)} \tag{8}$$

The first term in the denominator is determined in a separate experiment, II, a principle that was also used by Klainer and Kegeles [6]. The same synthetic boundary cell is used as in the previous experiment, and the equilibrated buffer is layered over the sample at a speed of 5 000—7 000 rpm. In all other details, such as acceleration time, rotational speed, temperature, phaseplate angle, exposure times and, if possible, exposure intervals, this experiment is an exact duplicate of the previous one. Fig. 1 d shows a typical exposure and Fig. 2 b the corresponding enlarged diagram. This time it is essential that there are two flat regions of the curve, one between the meniscus and the peak where the concentration is zero and one between the peak and the bottom with the concentration varying according to eqn. (4). In analogy with the previous discussion we now get the relation

$$c = c_0 e^{-2\omega^2 St} = k_1 k_2 \int_{x'_m}^{x'_c} y \mathrm{d}x = k_1 k_2 A_s \tag{9}$$

where A_s is the surface under the curve in Fig. 2 b. If expression (9) is inserted in (8) we obtain the simple relation

$$\frac{S}{D} = \frac{y_m}{\omega^2 r_m k_2 (A_s - A)} \tag{10}$$

y_m is the distance from the baseline to the intersection of the curve and the meniscus of the enlarged drawing of an exposure of experiment I and can be determined to better than $\pm$ 1 %. A is the surface between curve, baseline and meniscus of the same exposure, A_s the surface between the curve and the baseline in the corresponding exposure of experiment II. These surfaces are easily determined with a planimeter and the error in their difference is usually smaller than $\pm$ 1 %. The factor k_2 is suitably adjusted to 0.1000 $\pm$ 0.0002. The radius of the meniscus, r_m, is determined from the position of x_m relative to the two indices x_1 and x_2 on the drawing, the factor k_2, and the radius of the center of the cell. The latter is known to be better than $\pm$ 0.1 % at the moderate speeds used; at higher speeds, say exceeding 40 000 rpm, the accuracy is somewhat less due to elastic distortion of the rotor. This figure might be taken as an estimate of the error in r_m. ω is determined from the selected rotor speed which is kept constant to better than $\pm$ 0.5 % over any period of time. In ω^2, which enters in the expression (10), this means an error of $\pm$ 1 %. The temperature is kept constant within $\pm$ 0.1°C. As the viscosity effects S and D identically, the temperature error enters in S/D only because D is proportional to the absolute temperature. The error due to the temperature is thus about $\pm$ 0.04 %. All these contributions added together give a maximum error in a single determination of S/D of 3.4 %.

By means of a blank experiment with the buffer it is possible to evaluate a correction for gradients due to sedimenting salt and for curvature of the baseline. This correction was found to be negligible for rotor speeds below 20 000 rpm. Whenever such a correction is needed the maximum error is greater than 3.4 %. Other possible optical distortions or imperfections have not been considered.

Klainer and Kegeles [6] did not use the same cell in their experiments corresponding to I and II. This technique has been tried but found to be inferior since the two cells usually have slightly different depths and since the properties of the quartz windows might be slightly different.

The simple eqn. (10) can be used as long as the time schedules of experiments I and II are identical. If A_s can be determined only in an early period of experiment II, because of the diffusion which after some time violates the flat regions at both sides of the peak (Fig. 2 b), A_s in (10) has to be replaced by $A_{so} \cdot e^{-2\omega^2 S t_I} \approx A_{so}(1 - 2\ \omega^2\ S t_I)$, where the time t_I refers to experimet I. A_{so} is determined from experiment II as a mean of the values $A_s \cdot e^{2\omega^2 S t_{II}} \approx A_s (1 + 2\ \omega^2\ S t_{II})$. This means that a knowledge of S under the actual experimental conditions is necessary. If it is not known beforehand, it may be determined accurately enough at the end of experiment II. The rotor is then accelerated to a higher speed, and a few exposures are taken from which S can be calculated in the usual way. Because of the adiabatic cooling of the rotor this S-value corresponds to a slightly lower temperature than the orginal

and a proper correction has to be made before it is used in the calculation of S/D. If necessary a separate experiment has to be made in the synthetic boundary cell for the determination of S.

If the sedimentation constant is not known from the beginning and the wrong speed of rotation is chosen initially in experiment I, the rotor might be stopped, the cell taken out and shaken a little to make the solution homogeneous again. The experiment may then be started again and a more suitable speed of rotation selected. The two experiments I and II are usually performed within 6—8 h. All the calculations are made in 3 or 4 h by one person. If the plates instead were evaluated in a microcomparator and numerical integrations were made, the calculations were much more timeconsuming without much gain in accuracy.

The value of S/D thus obtained is used for the calculation of the molecular weight by insertion in the well known equation

$$M = \frac{S}{D} \cdot \frac{RT}{1 - V\varrho} \tag{11}$$

Here R is the gas constant and equal to 8.313×10^7 erg.mole^{-1}. degree^{-1}, T is the absolute temperature at which the experiment was performed, ϱ is the density of the buffer at that temperature and V is the partial specific volume of the solute at the same temperature.

The behaviour of a sample with several components of different S/D is easy to predict if it is permitted to superpose the systems. Each component, n, alone would give

$$\frac{S_n}{D_n} = K \frac{y_{mn}}{A_{sn} - A_n}$$

The observed ratio is

$$\frac{S}{D} = K \frac{y_m}{A_s - A}$$

where $y_m = \Sigma\, y_{mn}$ and $A_s - A = \Sigma\, (A_{sn} - A_n)$

Hence we obtain

$$\frac{S}{D} = \frac{\sum \frac{S_n}{D_n} (A_{sn} - A_n)}{\Sigma\, (A_{sn} - A_n)} \tag{12}$$

At time zero all the A_n are zero. If the specific refractive index increments are equal for all the components the value of S/D extrapolated to zero time is the mean of the different S_n/D_n weighted with their corresponding relative concentrations (the weight-average value). As the experiment goes on all the A_n values increase. Those corresponding to the higher S_n/D_n increase faster than the others and hence the contribution of these S_n/D_n in S/D will be relatively smaller and the observed S/D will decrease towards the lowest value S_n/D_n. The speed of this decrease depends on the ratio between the different values of S_n/D_n and on the rotor velocity. Only a solute that is

homogeneous with respect to the ratio S/D and for which this ratio is independent of the concentration will exhibit a value of S/D that does not change with time during the experiment.

A sample where the solute molecules are in a monomer-dimer equilibrium will also show a decrease with time in the ratio S/D or the proportional M. This decrease is due to the dilution of the solute close to the meniscus which favours the monomer.

DETERMINATION OF DIFFUSION COEFFICIENTS

The diffusion coefficients were determined from the exposures of the type II experiments in which a boundary between solution and solvent was formed in the centre of the cell. The data were evaluated in two different ways which both are easily derived from the solution of the differential equation of diffusion.

In the "maximum ordinate — area" method the following relationship is used:

$$\frac{A_s^2}{y_{max}^2} = 4\ k_2^2\ \pi\ D\ (t - t_0) \tag{13}$$

where A_s is the area between the gradient curve and the baseline at time t, measured from the instance when the synthetic boundary was formed. y_{max} is the maximum height of that curve (Fig. 2 b), k_2 is the magnification along the baseline and D is the diffusion coefficient.

According to the "maximum ordinate" method the relation

$$d_e^2 = 16\ k_2^2\ D\ (t - t_0) \tag{14}$$

is used. Here d_e is the distance along the baseline between the points on the gradient curve having $y = y_{max}/e$.

D is obtained from the slope of the line obtained by plotting either A_s^2/y_{max}^2 or d_e^2 *versus* t. Agreement between the two methods in combination with slightly negative values of t_0 has been taken as evidence of a successful experiment. Positive values of t_0 indicate that the boundary formation had been disturbed and made the results less reliable.

The right hand sides of eqns. (13) and (14) also should contain the factor $[1 + \frac{1}{2}\ \omega^2\ S(t - t_0)]$ corresponding to the correction factor given by Lamm [11]. The correction term, however, never caused a deviation of more than 0.5 % from the straight line.

MATERIALS

The old yellow enzyme, myoglobin I and apymyoglobin I were prepared by Theorell and Åkeson as they have recently described [12,13]. The rhodanese was prepared by Sörbo [14], the myeloperoxidase by Agner [15], and the liver alcohol dehydrogenase by Dalziel [16]. The growth hormone samples have been described elsewhere [17]. The bovine serum albumin was obtained from Armour Laboratories, lot No. J 10603.

The cytochrome c was prepared in the crystalline form from beef heart by Paléus and Theorell, and two different samples were used. One sample was prepared according to Hagihara *et al.*[18], had an iron content of 0.42 %, and was used for the centrifuge experi-

ments. The other sample was prepared according to Paléus and Theorell [19] and had an iron content of 0.46 %. It was used for the determination of the partial specific volume.

The pituitary growth hormones were dissolved in a 0.05 M borate buffer of pH 9.9. In all other cases a 0.05 M phosphate buffer of pH 7.0 was used. All the solutions contained 1 % NaCl.

In all cases the partial specific volume was assumed to depend on temperature in the same way as that of haemoglobin [10].

RESULTS AND DISCUSSION

A few proteins considered to be essentially pure and homogeneous have been investigated. The substances were chosen because of availability and because of possibility to compare with other data, especially analytical values. The main results have been collected in Table 1 and Fig. 3 a.

In spite of the fact that *bovine serum albumin* is known not to be completely homogeneous [20], it was subjected to several experiments because it has been so thoroughly investigated by many investigators and by means of many methods. The sedimentation coefficient of the sample was determined at a few concentrations and it was found to depend on the concentration according to the formula

$$S_{20}^{\circ} = 4.44\ (1 - 0.0060 \cdot a)\ S \qquad (15)$$

where a is the mean concentration in mg/ml. This concentration dependence agrees well with the data reported by Schulman [21]. A small fraction amounting to less than 5 % could be seen to move somewhat faster in the centrifuge.

In three experiments at a protein-concentration of 20 mg/ml the calculated M was found to increase with about 0.18 % in every period of 1 000 sec. No such increase could be identified in one experiment at half that protein

Table 1.

Protein	V_{sp}	S_{20}° (S-units)	D_{20}° (F-units)		M			
			in a diffusion cell	in the centrifuge	from S and D (diffusion cell)	from S and D (centrifuge)	from S/D at the meniscus	from analysis
Cytochrome c[18,19] (beef heart)	0.728	1.71 *	—	11.4	—	13 300	13 300	13 300
Apomyoglobin I[13]	0.743[26]	1.89	—	10.4	—	17 200	18 800	18 200[13]
CO-myoglobin I[13]	0.743[24]	2.01	—	10.3	—	18 500	18 300	18 800[13]
Rhodanese [14]	0.742[14]	3.03 *[14]	7.5 *[14]	8.2	38 000	35 600	36 300	—
Serum albumin (bovine)	0.7434[35]	4.44	5.805[20]	5.7	72 200	73 500	73 200	—
Alcohol dehydrogenase[16] (liver)	0.750[27]	5.11[27]	5.95 *[27]	5.9	83 300[27]	84 000	84 400	88 000[27]
Old yellow enzyme [12]	0.753[12]	5.82	—	5.54	—	102 000	106 000	104 000[12]
Myeloperoxidase [15]	0.731[29]	7.93[29]	4.81 *[29]	4.9	149 000[29]	145 000	157 000	151 000[29]

1 S (Svedberg unit) = 10^{-13} s
1 F (Fick unit) = 10^{-7} cm^2 s^{-1}
* indicates that the value has not been extrapolated to infinite dilution. None of the diffusion coefficients determined in the centrifuge has been extrapolated in this way.

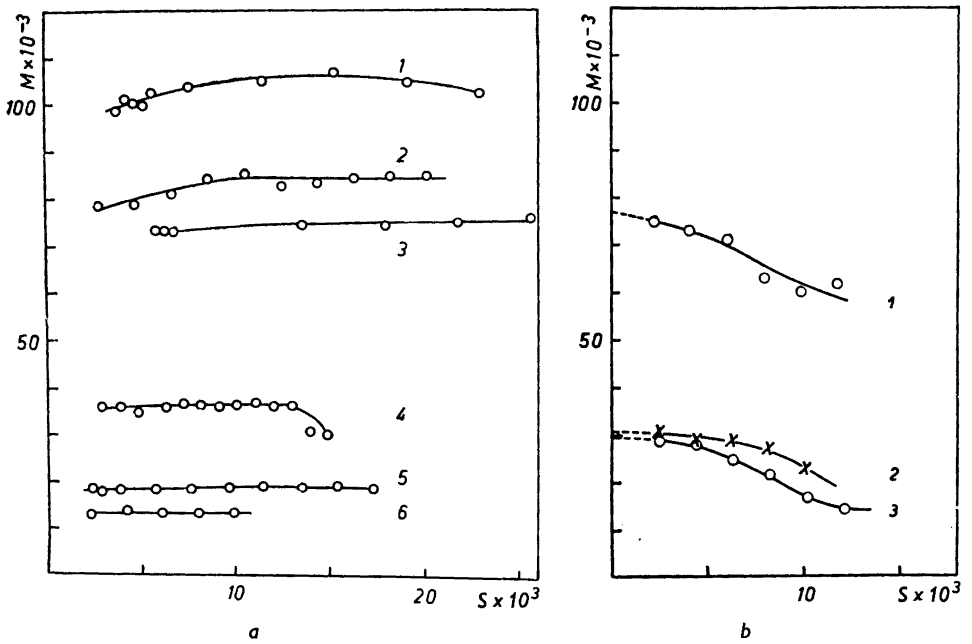


Fig. 3. Time dependence of the molecular weights of different proteins as evaluated from the boundary condition at the meniscus. The time is measured from the instance when the rotor attained equilibrium at the selected speed. a) Curve 1) old yellow enzyme (12 590 rpm); 2) liver alcohol dehydrogenase (12 590 rpm); 3) bovine serum albumin (12 590 rpm); 4) rhodanese (17 980 rpm); 5) apomyoglobin (23 150 rpm) and 6) cytochrome c (23 150 rpm). b) Curve 1) ox pituitary growth hormone (14 290 rpm); 2) human pituitary growth hormone (17 250 rpm) and 3) human pituitary growth hormone (23 150 rpm).

concentration. In the parts of these experiments later than 10 000 sec after the rotor had attained equilibrium speed the following mean molecular weights were ontained: 75 200, 69 900 and 72 700. One experiment at 10 mg/ml gave a value of 75 000. At concentrations of 5 mg/ml or lower the experiments were more difficult to evaluate and the results were no longer consistent.

The *Old yellow enzyme* was investigated because it was uncertain whether the molecule contained one or two prosthetic groups. The new analytical data [12] required a molecular weight of $n \times 52\,000$, while earlier studies [22] on a less pure preparation had given a value of 82 000, or 76 000 when corrected for the slightly elevated rotor temperature in the centrifuge used [2]. The partial specific volume of the crystallized enzyme was redetermined [12] and was found to be 0.753 at 25°C as compared with the previous value of 0.731 at 20°C. The difference accounts for an increase in M of 9 % which would bring it up to 83 000 again. Also the sedimentation coefficient has been redetermined. The concentration dependence was investigated and the following formula was found to be valid:

$$S_{20}^{\circ} = 5.82\ (1—0.0046 \cdot a)\ S \qquad (16)$$

where a is the concentration in mg/ml. The previously reported value [22] was 5.76 S, or 5.33 S, when corrected for the rotor temperature. The protein concentration in these experiments was not reported but must have been of the order of 10—20 mg/ml. Correction for this according to the formula (16) yields 5.5—5.7 S, which is only slightly lower than the present value. $S_{20}^{\circ} =$ 5.82 S instead of 5.33 S, however, adds another 8.5 % to M and brings it to 90 500.

The molecular weight has now been determined in one experiment at a protein concentration of 18.4 mg/ml. The calculated M appeared to increase in the first part of the experiment with about 0.45 %/1 000 s and to decrease in the later part having a maximum about 15 000 s after that the full speed had been reached. The maximum of 106 000 is taken as the best value of M.

The diffusion coefficient has been determined from two experiments with undisturbed synthetic boundary formation, one at 18.4 mg/ml and the other at 7.8 mg/ml. It was found to be 5.54 ($\pm$0.05) F, which is appreciably lower than the old value [13] of 6.3 F. Together with S_{20}° and V reported here it gives $M = 102\,000$.

These data definitely prove that there are two flavin mononucleotide molecules bound per molecule of the old yellow enzyme, for which case the M-value derived from analysis becomes 104 000. The great difference between the value of M determined now and the old value appears to be an unfortunate combination of errors in all the three quantities S, D and V.

The purified *myoglobin I* [13] has been investigated both in the form of apomyoglobin and in the form of CO-myoglobin. In both cases a partial specific volume of 0.743 has been used. This value has been determined [24] for ferri Mb and the same can be calculated for apo Mb on the basis of the amino acid analysis [25,26]. The sedimentation coefficient determined earlier [13] in the same centrifuge have been used. At that time the automatic temperature control had not yet been installed and no correction was made for the adiabatic cooling of the rotor. In a set of experiments this cooling has been found to be 0.87°C when the rotor is accelerated up to 59 780 rpm. A correction of 2.15 % had thus to be added to the previous data. Another small correction of 0.5 % has also been added according to Lamm's formula [11]. The data thus become:

$$S_{20}^{\circ} = 1.89\ (1-0.00682 \cdot a)\ S \text{ for apoMb I} \qquad (17)$$

and

$$S_{20}^{\circ} = 2.01\ (1-0.00642 \cdot a)\ S \text{ for Mb I} \qquad (18)$$

The colourless apo Mb I has been investigated in one experiment at a protein concentration of 12.5 mg/ml. Because of the high rotor speed of 23 150 rpm a minor correction had to be explored in a separate run on the buffer. Again M was found to increase slightly in the first part of the experiment (0.70 %/1 000 s). An asymptotic level of $M = 18\,800$ was reached.

A much less reliable experiment was conducted on a less concentrated sample of the carbon monoxide compound of Mb I. This derivative was used because of its low absorption above 600 mμ, and a red filter was used cutting off below this wavelength. The phaseplate, however, is manufactured for the green mercury line of 546 mμ, and long exposure times had to be used because

of the low efficiency of the lamp in the red region. Hence the pictures were not very sharp and the calculated molecular weight of 18 300 cannot be considered to be accurate to better than ± 4 %.

The diffusion coefficients of 10.4 and 10.3 F, respectively, are, as would be expected, rather smaller than the value of 11.25 F, that was earlier determined by Polsen [23] on an old preparation of Mb, which had an iron content 0.34 % as compared to 0.297 % for Mb I [13].

The M-values, as calculated from S/D or S and D, do not agree completely with the data obtained from iron-analysis of Mb I (Table 1). It is obvious that there might be an error in the determination of either $S_{20}°$ or $D_{20}°$ of apo Mb I. It is probable that $S_{20}°$ should be greater than 1.89 S, since the drop from 2.01 S for Mb I appears to be rather big, if not the removal of the haem is accompanied by a rather drastic change of molecular shape.

One experiment on *liver alcohol dehydrogenase* was performed at a protein concentration of 10 mg/ml. The M-value increased in the early part of the experiment but a level of 84 400 was reached before 10 000 s. This value is in good agreement with the other data discussed elsewhere [27] and referred to in Table 1, but it is considerably higher than the value of 67 500 (corrected for the rotor temperature [2]) that was determined on an earlier and less pure preparation of the enzyme [28].

Rhodanese was investigated at a protein concentration of 10 mg/ml. The M-value appeared to be practically constant until the decrease at the end due to back diffusion. The sedimentation constant of 2.97 S given by Sörbo [14] has in the table been corrected for the adiabatic cooling of the rotor. The present values of M are lower than the old one, which is also reflected in the greater diffusion constant obtained now. The absence of an initial increase in the calculated M-values might indicate the presence of some smaller molecular fragments, which would have caused an increase in D. The previous diffusion experiments [14] were made, however, under rather different conditions; the protein concentrations were low, the temperature was low and the observations were made over time periods of more than 30 h. The most likely explanation of the low diffusion coefficients obtained seems to be that some denaturation and aggregation occurred in the samples.

The partial specific volume of the *crystallized cytochrome c* was determined in a 10 ml pycnometer at 21.7°C as described elsewhere [29]. The protein concentration of the electrolyte free solution was 18.73 mg/ml. Two experiments gave $V = 0.728$ (mean of 0.7273 and 0.7282), which is appreciably higher than the old value 0.702—0.707 [30,31]. The new value implies that the sterical configuration of the helices in cytochrome c does not need to be as closely packed as was recently suggested [26].

The molecular weight was determined on cytochrome c in its reduced form at a concentration of 10 mg/ml, and the red filter cutting off below 600 mμ had to be used. The reduction was achieved by adding a small amount of ascorbic acid to the sample in the cellophane bag before starting the dialysis. This was made against a previously degassed buffer in a closed vessel filled with nitrogen. The calculated M did not change with time and it is in perfect agreement with the value obtained from the iron content.

The diffusion coefficient comes out rather close to the value 11,1 F determined by Theorell [31] on an old preparation of cytochrome c.

A few experiments have been performed with the crystallized *myeloperoxidase*. In spite of its green colour, the light absorption at 546 mμ made it impossible to work with concentrations higher than 5 mg/ml. In combination with the high sedimentation velocity this circumstance made the results rather unreliable. The mean M-value of three experiments, however, came out as 157 000, in rough agreement with the other data listed for this enzyme in Table 1 [29].

The slow increase of M with time in the early parts of the experiments, that has been observed for several of the proteins now discussed, might to a large extent have been caused by the concentration dependence of S. From eqns. (15)—(18) and the speed of dilution at the meniscus this effect can be calculated for serum albumin, old yellow enzyme and myoglobin. It amounts to about 0.3 %/1 000 s in the early part of the experiments and decreases to less than 0.1 %/1 000 s after 15 000 s. Part of the increase might, however, be an artefact due to difficulties in making the extrapolation to the meniscus from the first few photographs.

Some experiments have been made at pH 9.9 on *growth hormones* obtained from human and ox pituitaries, and the main results have already been reported [17]. The time dependence of the calculated M-values is seen from Fig. 3 b. The M-values decrease from the very beginning of the experiment instead of increasing slightly or remaining practically constant as observed for substances that are homogeneous. It has been shown in eqn. (13) that such a decrease of M is due to inhomogeneity with respect to S/D or the proportional M. In sedimentation studies at pH 9.9 the hormones seem to be quite homogeneous, but the sedimentation coefficients increase with increasing concentration [17,32]. These facts show that the hormone is in a state of equilibrium between molecules of different sizes, presumably a monomer-dimer equilibrium [17]. The M-values extrapolated to the time when the rotor obtained its equilibrium speed can thus be taken as a weight-average M of the sample, valid for the concentration used: M_{mean} = 30 000 for human hormone at 5—10 mg/ml and M_{mean} = = 75 000—80 000 for ox hormone at 10 mg/ml. The molecular weights extrapolated in the later part of the experiment would correspond to the monomeric molecules (or a mean of the smallest molecules): $M_{monomer}$ is hence approximately 15 000 and 50 000, respectively.

Similar more or less drastic decreases of M have been observed for impure protein preparations or for preparations known to be very inhomogeneous, *e.g.* cheese extracts [33] and stomach juice [34]. Also in these cases a mean value of M for the whole sample may be estimated as well as a mean M for the smaller molecules. If the components can be resolved by sedimentation analysis it is also possible to estimate M of the larger molecules.

CONCLUSIONS

The determination of molecular weights of homogeneous substances from the boundary condition at the meniscus appears to be quite accurate. The data generally agree within 2—3 % with those obtained from separate determina-

tions of sedimentation and diffusion coefficients or from analysis. As in case of sedimentation equilibrium the method is based on the balance between sedimentation and diffusion of the molecules, but the time requirement is much smaller. The diffusion coefficients are determined separately and appear to be reliable within a few percent. Only a small amount of material is needed, 15 mg is usually sufficient, and the method described here is simple and rapid to evaluate.

It is possible to investigate a rather wide range of molecular sizes. With a low speed attachment that makes it possible to run the centrifuge at a few thousands rpm molecular weights up to several hundred thousands might be determined. At the highest speed, 59 780 rpm, molecular weights as low as a few hundreds can be determined, as has been shown by Klainer and Kegeles [6].

By studying the time dependence of the ratio S/D or the proportional M the homogeneity of the sample might be explored. A constant or slightly increasing value indicates that the substance is homogeneous. A value that immediately starts to decrease shows that the sample is not monodisperse. Comparison with sedimentation analysis reveals the eventual presence of a reversible dimerization or polymerization.

Acknowledgements. The author wishes to thank all those who kindly put the various samples at his disposal. He also wishes to express his special gratitude to Professor H. Theorell for his interest and support in the work. Able technical assistance has been given by Mr. N. Ekman and Mr. K. Ingebrigtsen. Thanks are further due to the *Knut and Alice Wallenberg Foundation* for financial support.

REFERENCES

1. Archibald, W. J. *J. Phys. Chem.* **51** (1947) 1204.
2. Pedersen, K. O. on *Les Protéines, Rapport et Discussion, 9eme Conceil de Chimie*, Bruxelles 1953, p. 19—62.
3. Li, C. H., Tiselius, A., Pedersen, K. O., Hagdahl, L. and Carstensen, H. *J. Biol. Chem.* **190** (1951) 317.
4. Porath, J. *Acta Chem. Scand.* **6** (1952) 1237.
5. Brown, R. A., Kritchevsky, D. and Davies, M. *J. Am. Chem. Soc.* **76** (1954) 3342.
6. Klainer, S. M. and Kegeles, G. *J. Phys. Chem.* **59** (1955) 952.
7. Klainer, S. M. and Kegeles, G. *Arch. Biochem. and Biophys.* **63** (1956) 247.
8. Wolter, H. *Ann. Physik* **7** (1950) 182.
9. Trautman, R. and Burns, V. W. *Biochim. et Biophys, Acta* **14** (1954) 26.
10. Svedberg, T. and Pedersen, K. O. *The Ultracentrifuge*, Clarendon Press, Oxford, 1940.
11. Lamm, O. *Z. physik. Chem.* **143 A** (1929) 177.
12. Theorell, H. and Åkeson, Å. *Arch. Biochem. and Biophys.* **65** (1956) 439.
13. Theorell, H. and Åkeson, Å. in *Biochemistry of Nitrogen*, Helsinki, 1955, p. 303.
14. Sörbo, B. H. *Acta Chem. Scand.* **7** (1953) 1129.
15. Agner, K. *Acta Chem. Scand.* **12** (1958). *In press.*
16. Dalziel, K. *To be published.*
17. Ehrenberg, A. and Heijkenskjöld, F. *Acta Chem. Scand.* **10** (1956) 1675.
18. Hagihara, B., Morikawa, I., Sekuzu, I., Hono, T. and Okumuki, K. *Nature* **178** (1956) 630.
19. Paléus, S. and Theorell, H. *Acta Chem. Scand.* **11** (1957) 905.
20. Wagner, M. L. and Scheraga, H. A. *J. Phys. Chem.* **60** (1956) 1066.
21. Shulman, S. *Arch. Biochem. and Biophys.* **44** (1953) 230.
22. Kekwick, R. A. and Pedersen, K. O. *Biochem. J. London* **30** (1936) 2201.
23. Polson, A. G. *Kolloid, Z.* **87** (1939) 149.

24. Theorell, H. and Ehrenberg, A. *Acta Chem. Scand.* **5** (1951) 823.
25. Tristram, G. R. *Advances in Protein Chem.* **5** (1949) 83.
26. Ehrenberg, A. and Theorell, H. *Acta Chem. Scand.* **9** (1955) 1193.
27. Dalziel, K. and Ehrenberg, A. *In press.*
28. Theorell, H. and Bonnichsen, R. K. *Acta Chem. Scand.* **5** (1951) 1105.
29. Ehrenberg, A. and Agner, K. *Acta Chem. Scand.* **12** (1958). *In press.*
30. Pedersen, K. O. quoted by Paul, K. G. in Sumner, J. B. and Myrbäck, K. *The Enzymes*, Vol. II, Part I, Academic Press Inc., New York 1951, p. 375.
31. Theorell, H. *Biochem. Z.* **285** (1936) 207.
32. Li, G. H. and Pedersen, K. O. *J. Biol. Chem.* **201** (1953) 595.
33. Lindqvist, B. and Ehrenberg, A. *Unpublished data.*
34. Gräsbeck, R. and Ehrenberg, A. *Unpublished data.*
35. Dayhoff, M. O., Perlmann, G. E. and MacInnes, D. A. *J. Am. Chem. Soc.* **74** (1952) 2515.

Received April 5, 1957.

ACTA CHEMICA SCANDINAVICA 11 (1957) 1271—1284

Short Communications

The Magnetic Properties of the Elements Molybdenum and Tungsten

Studies in Magnetochemistry 17 *

R. W. ASMUSSEN and J. POTTS JENSEN

The Chemical Laboratory B, Technical University of Denmark, Copenhagen, Denmark

The first magnetic measurements concerning molybdenum and tungsten were published by Koenigsberger [1] in 1898. The author reports the χ_g-value 1.80×10^{-6} for molybdenum and 0.70×10^{-6} for tungsten. The susceptibility was dependent on the field strength. In 1899 Meyer [2] gave the χ_g-values 0.25×10^{-6} and 0.55×10^{-6}, respectively. The metal samples cannot be considered chemically and magnetically pure.

Magnetic measurements at different temperatures (room-temperature to 1 200°C) were published in 1910 by Honda [3]. For *molybdenum* a slight increase of χ_g with increasing temperature was observed; χ_g for *tungsten* was temperature independent. Mo: Metal lump (regulus) from Kahlbaum (nach Moissan), specific gravity 8.6 g/cm³. $\chi_g = 0.039 \times 10^{-6}$ is given as an average value. W: A metal lump and a powder sample both with a specific gravity 19.1 g/cm³ (from prof. Tammann); $\chi_g = 0.334 \times 10^{-6}$ and 0.336×10^{-6}, respectively.

In 1912 Owen [4] published the following results. *Molybdenum:* Powder specimen from Merck, the specific gravity 8.6 g/cm³ and $\chi_g = 0.603 \times 10^{-6}$ (0.558×10^{-6} for $H \rightarrow \infty$) at room-temperature and decreasing slightly with increasing temperature in the temperature range — 180°C to 20°C. *Tungsten:* Several samples with different (temperature independent but field strength dependent) χ_g-values. The author assumed the best value $\chi_g = 0.22 \times 10^{-6}$.

In 1933 de Haas and Alphen [5] published measurements on *molybdenum*, in which no impurities could be detected by chemical methods; spectroscopically, however, the presence of traces of certain metals were proved. Iron did not occur. The authors report $\chi_g = 0.949 \times 10^{-6}$ at 289°K. The susceptibility increases strongly with decreasing temperature. At 14.2°K, χ_g is 1.819×10^{-6}. For *tungsten* the following χ_g-values were found: 0.284×10^{-6}, 0.287×10^{-6} and 0.292×10^{-6} at the temperatures 289°K, 20.4°K and 14.2°K, respectively.

Finally Kriessman [6] in 1953 has published results of susceptibility measurements on molybdenum and tungsten. For *molybdenum:* $\chi_g = 0.93 \times 10^{-6}$ at 25°C increasing with increasing temperature being 1.11×10^{-6} at 1 825°C, (estimated from the χ_g, T-curve, no tables are published). The measurements on *tungsten* gave $\chi_g = 0.32 \times 10^{-6}$ at room-temperature; a slight increase in χ_g with increasing temperature was observed. The χ_g-value is 0.37×10^{-6} at 1 850°C. The samples used were spectroscopically pure metal-rods prepared by Johnson, Matthew and Co., London.

In this laboratory we have measured the magnetic susceptibility of molybdenum and tungsten at varying temperatures (80°K to 530°K) and at different values of the magnetic field strength.

The metal samples used for the measurements were spectroscopic standards prepared by Johnson, Matthew and Co., London. For *molybdenum* the specific gravity was determined to 10.3 g/cm³ (Landolt-Börnstein's tables give 10.2 g/cm³). The cylindrical rod had the dimensions: Diameter 4.98 mm and length 10.10 cm. In the spectra the sensitive

* No. 16 of this series: *Acta Chem. Scand.* 11 (1957) *in press.*

Table 1. Magnetic susceptibilities $\chi_g \times 10^6$ at different temperatures and field strengths.

	W			Mo		
Temp. °K / H Ørsteds	80	195	294	80	198	372
2 138	0.278	0.292	0.294	0.838	0.868	
2 657	0.278	0.292	0.294	0.839	0.875	0.875
3 040	0.278	0.293	0.296	0.839	0.874	0.874
3 346	0.281	0.293	0.296	0.839	0.837	0.872

lines of the elements Fe and Cu were barely visible and those of Ag, Al, As, Ca, Cd, Co, Cr, K, Li, Mn, Na, Nb, Ni, Pb, Rb, Sb, Sn, Si, Ta, Ti, V, W, Zn and Zr were not observed. The specific gravity of *tungsten* was determined to 19.1 g/cm³ (Landolt-Börnstein's tables give 19.1 g/cm³). The shape of the specimen was cylindrical (diameter 4.01 mm and length 10.10 cm). In the spectra the sensitive lines of the elements Fe and Si were very faint. No lines of the elements Ag, Al, Ca, Co, Cr, K, Li, Mg, Mn, Na, Ni, Pb, Sn, Ti, V, Zn, and Zr were observed.

The magnetic measurements were carried out as previously described [7].

The susceptibilities for both metals were measured at 2 138, 2 657, 3 040 and 3 346 Ørsteds at the temperatures 291, 198 and 80°K for molybdenum and at 294, 195 and 80°K for tungsten. The high-temperature measurements were carried out at 2 657, 3 040 and 3 346 Ørsteds, while in the temperature intervals: CO_2-temperature to liquid air temperature and CO_2-temperature to room-temperature, the susceptibilities were measured at 3 346 Ørsteds.

Our measurements of the gram susceptibilities are plotted against the temperature (°K) in Fig. 1. The straight lines have been determined by means of the method of least squares and have the equations:

$$\text{Mo: } \chi_g \times 10^6 = 0.8544 + 0.000053\ T$$
$$\text{W: } \chi_g \times 10^6 = 0.2798 + 0.000037\ T$$

For both metals there seems to be, at the lowest temperatures, a more rapid

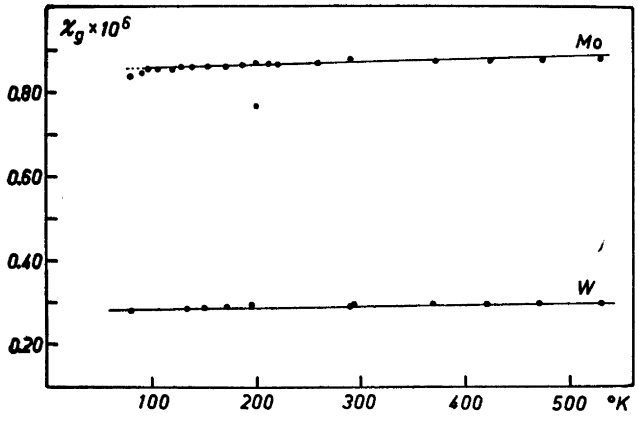


Fig. 1. Temperature dependence of the magnetic gram susceptibilities of molybdenum and tungsten.

decrease in χ_g with decreasing temperature, mostly pronounced in the case of molybdenum. Since we have no possibilities of carrying out magnetic measurements at lower temperatures than that of liquid air, we cannot decide, if this decrease in χ_g is a physical reality. Consequently the susceptibility of molybdenum at 80°K and 91°K have not been incorporated in the calculations mentioned above.

As average values for the specific magnetic susceptibilities in the temperature interval 97°K to 530°K for *molybdenum* and 80°K to 530°K for *tungsten* may be accepted the values 0.868×10^{-6} and 0.289×10^{-6}, respectively. The corresponding susceptibilities per gram-atom are 83.3×10^{-6} and 53.2×10^{-6}, respectively.

The susceptibilities were found to be independent of the field strength. The measurements arbitrarily selected for Table 1 exemplify this constancy.

1. Koenigsberger, J. *Ann. Phys. u. Chem.* **66** (1898) 698.
2. Meyer, S. *Ann. Phys. u. Chem.* **68** (1899) 325.
3. Honda, K. *Ann. Phys. u. Chem.* **4** 32 (1910) 1027.
4. Owen, M. *Ann. Phys. u. Chem.* **4** 37 (1912) 657.
5. de Haas, W. J. and Alphen, P. M. *Koninkl. Akad. v. Wetenschap. Amsterdam.* **36** (1933) 263.
6. Kriessman, C. J. *Rev. modern Physics* **25** (1953) 122.
7. Asmussen, R. W. and Soling, H. *Acta Chem. Scand.* **8** (1954) 558, 563.

Received July 2, 1957.

The Structure of Ammines of Ammonium Halides

IVAR OLOVSSON

Institute of Chemistry, University of Uppsala, Uppsala, Sweden

In a project covering structure investigations of ammines, formed with salts of alkali metal, alkaline earth metal and ammonium, the compounds $NH_4Cl \cdot 3NH_3$, $NH_4Br \cdot 3NH_3$, $NH_4I \cdot 3NH_3$ and $NH_4I \cdot 4NH_3$ have been studied. The structures of these are essentially solved but they will be further refined by least square methods. A full account of the structure determinations will be given after these refinements are finished. Some preliminary data are given below.

The crystal structure determinations are based on three-dimensional X-ray data taken in a low temperature Weissenberg camera. Exposures made at −35°, −80° and −140°C give identical photographs for each compound, apart from effects due to different temperature factors and cell dimensions.

$NH_4Cl \cdot 3NH_3$: The crystals (m.p. +10°C) are orthorhombic, space group $P\ 2_12_12_1$ with four formula units in a cell of dimensions $a = 8.795$, $b = 8.68$, $c = 8.989$ Å (at −35°C). The atomic coordinates for chlorine were obtained from Patterson-Harker sections $P(\frac{1}{2}; y; z)$, $P(x; \frac{1}{2}; z)$ and $P(x; y; \frac{1}{2})$ and the coordinates for the nitrogens thereafter from electron density projections and sections. The preliminary atomic coordinates are: Cl: (0.042; 0.000; 0.443); N_0: (0.477; 0.120; 0.284); N_1: (0.049; 0.106; 0.025); N_2: (0.232; 0.761; 0.191); N_3: (0.232; 0.342; 0.319). The ammonium ion (to which N_0 belongs) is tetrahedrally surrounded by three ammonia molecules (nitrogens N_1, N_2 and N_3) and one chloride ion; distances N−Cl: 3.26 Å; N−N: 2.83, 2.88 and 2.93 Å. The hydrogen atoms of the ammonium ions are evidently involved in these bonds.

The bromide and iodide compounds are isostructural with the chloride and possess the following cell dimensions:

$NH_4Br \cdot 3NH_3$: $a = 8.96$, $b = 8.996$, $c = 9.263$ Å (−35°C). (This work was done in collaboration with R. Liminga.)

$NH_4I \cdot 3NH_3$: $a = 8.32$, $b = 9.91$, $c = 9.96$ Å (−35°C). (The work was done together with G. Larsson.)

$NH_4I \cdot 4NH_3$: The work on this compound has been quite recently started and the structure is not yet completely elucidated. The crystals are probably tetragonal, space group $P\ 4/n$ with two formula units in a cell of dimensions $a = 8.94$, $c = 6.55$ Å (−140°C). (The work was done together with E. Hadler Vihovde, Oslo.)

Received August 31, 1957.

The Preparation of 3α,12α-Dihydroxy-25-methylcoprostane Bile Acids and Steroids 56

DEBABRATA SEN*

Department of Physiological Chemistry, University of Lund, Lund, Sweden

The compound 3α,12α-dihydroxy-25-methyl-coprostan, which does not seem to have been described in literature before, was needed for metabolic studies. We have prepared it through anodic (Kolbe) synthesis from desoxycholic acid and *t*-butylacetic acid [1]. In order to promote mixed coupling, a 20 to 22 fold excess of *t*-butylacetic acid has been used resulting in a 17 % yield of the compound calculated on the basis of the bile acid used.

The pure substance was isolated from the neutral product of the electrolysis through chromatography on silicic acid. Reversed phase partition chromatography on hydrophobic Supercel according to the method of Danielsson [2] has also been used.

The molecular rotation of our compound has been found to be the same as that of coprostan-3α,12α-diol [3].

Experimental. All melting points were taken on electrically heated aluminium block and are corrected. Desoxycholic acid, crystallised from ethanol-water, was used without further drying.

A mixture of 504 mg of desoxycholic acid, 3 ml (23 mmole) of *t*-butylacetic acid [1] and 56 mg (2.42 mmole) of sodium was dissolved in 50 ml of methanol. This solution was electrolysed using the procedure reported before. Temperature of the electrolyte 25°–40°.

The solution was then taken to dryness in vacuum, water (40 ml) was added and it was extracted with ether (5 × 40 ml). The ethereal solution was washed with 10 % sodium hydroxide solution, water, 1 N hydrochloric acid and then water and then evaporated to dryness.

Adsorption chromatography on silicic acid. The residue (500 mg) was chromatographed on a column (i.d. of tube 24 mm) made with a mixture of silicic acid (16 g) (Silicic Acid powder, Baker-analysed-reagent; dried at 120° for 30 h) and Hyflo Supercel (8 g). Effluent-fractions 50 ml.

Fraction	*Eluent*	*Eluate*
1	methylenechloride	2 mg oil
2—5	Methylenechloride/ methanol (99:1 v/v)	0.5—2 mg oil in each;
6	—»—	74.0 mg, crystallised on addition of methanol
7	—»—	165.7 mg, crystallised on addition of methanol
8, 9, 10	—»—	20.2, 9.7 and 6 mg, respectively, oil, did not crystallise as above.

Several crystallisations from methanol and from acetone yielded 68 mg of white needles, m.p. 131.3°—132.3° from fractions 6 and 7.

Reversed phase partition chromatography. The combined mother liquors were taken to dryness and then crystallised once from methanol. The crystals (76 mg) were subjected to reversed phase partition chromatography [3] on hydrophobic Supercel (13.5 g) with 55 % *iso*propanol in water as moving phase and chloroform/heptane (1:4) (12 ml) as stationary phase. Fractions of about 3 ml were collected and the solvent was removed from them in a vacuum oven at about 55°.

The main band of crystalline material appeared in the fractions corresponding to 120—142 ml effluent. After two crystallisations of the material from these fractions from methanol 14 mg of white needles, m.p. 131.3°—132.3°, were obtained from them.

Total yield 82 mg (17 % calculated on the amount of bile acid used). Further crystallisations did not raise the melting point. (Found: C 80.2; H 12.1. Calc. for $C_{28}H_{50}O_2$: C 80.4; H 12.0).

$[\alpha]_D^{20} = +43.7° \pm 0.4°$ (in chloroform, $c = 0.0230$ g/ml solution). $M_D = +182$.

This work is part of investigations supported by *"Statens Medicinska Forskningsråd"*.

1. Widequist, S. *Arkiv Kemi* **23B** (1947) No. 4.
2. Danielsson, H. *Biochim. et Biophys. Acta. In press.*
3. Bergström, S. and Krabisch, L. *Acta Chem. Scand.* **11** (1957) 1067.

Received August 6, 1957.

* Present address: Department of Applied Chemistry, University College of Science and Technology, Calcutta 9, India.

A Note on the Tritiation of Organic Compounds in Tritium Gas

SUNE BERGSTRÖM and SVEN LINDSTEDT

Department of Physiological Chemistry, University of Lund, Lund, Sweden

It was recently found by Wilzbach [1] that an exchange reaction occurs when organic compounds are exposed to tritium gas, resulting in the incorporation of tritium into stable positions. This important observation thus makes tritium labelled compounds easily available for purposes when a specific labelling is not required.

This communication describes a simple glass apparatus shown in Fig. 1 that we have used to carry out the tritiation on a milligram-scale. It was constructed from 8 mm Pyrex tubing except for the parts drawn with heavy lines in the figure which were made from 1 mm capillary tubing. At A the line was connected to a mercury diffusion pump through a ball joint. The tritium ampoule was connected at B. The substance to be exposed was put into a small glasstube which holds about 10 mg of material covered with a small plug of glass wool. Six of these tubes were placed in the reaction vessel (shown in scale), which was then connected at C. By this arrangement several substances can conveniently be exposed simultaneously.

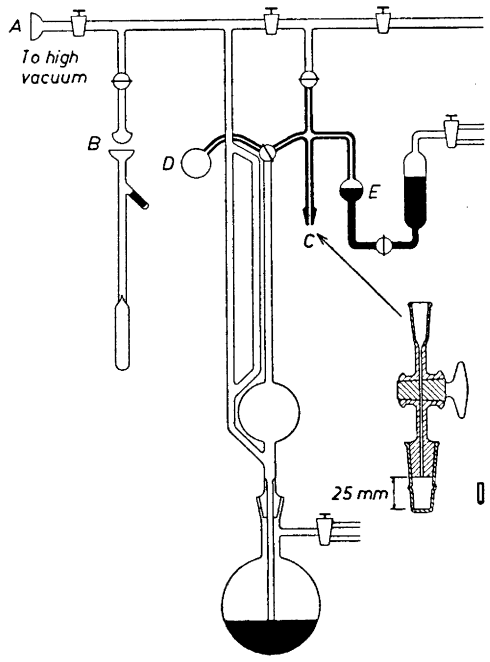


Fig. 1.

When the apparatus has been evacuated, the tritium is pumped into the reaction vessel with the Toepler pump. The pump is calibrated for volume measurements (10 μl—2 ml). After the desired time of exposure the Toepler pump is used to transfer the tritium gas to the glass bulb D (10 ml) where it is kept for further use.

As the apparatus is also used to carry out catalytic hydrogenations with tritium, it includes a device to alter the capacity of the reaction space, by varying the volume of the bulb E.

This apparatus has been used to label a large number of different compounds. As an example the labelling of cholic acid will be described. Six tubes loaded with 5 mg of crystalline cholic acid in each were kept for different times in 1 Curie of tritium gas (~80 % pure) at a pressure of approximately 100 mm Hg. The cholic acid was then purified by chromatography [2]. After 36 h the cholic acid had a specific activity of ~7 μC per mg that increased to ~3.2 mC per mg after 28 days. Less than 5 % of decomposition products had been formed.

The possibility of utilizing these high activities for analytical purposes is being investigated.

Time of exposure Days	Total activity in cholic acid sample (5 mg) c.p.m. × 10^{-6} plated in infinit thinness and measured in gas flow chamber
1.5	28
3	73
5	223
9	512
16	2 200
28	12 000

1. Wilzbach, K. E. *Chem. Eng. News* **34** (1956) 4616; *J. Am. Chem. Soc.* **79** (1957) 1013.
2. Norman, A. *Acta Chem. Scand.* **7** (1953) 1413.

Received August 6, 1957.

On the Isomerism of Hydroxyurea

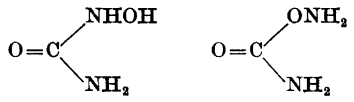
IX. Absorption Spectra in the Infra-Red

HELMER KOFOD

Royal Danish School of Pharmacy, Dept. of Organic Chemistry, Copenhagen, Denmark

Absorption spectra in the frequency-region 3 600—600 cm^{-1} have been recorded of the two isomeric "oxyureas" melting at approximately 72°C (OU_{72}) and at approximately 140°C (OU_{140}), respectively [1].

The absorption spectrum of OU_{140} confirmed brief information previously published by other investigators [2]. It showed an intense, incompletely resolved pair of bands at about 1 650 cm^{-1}, similar to that produced by urea. It should undoubtedly, as also suggested by Runti and Deghenghi [2], be assigned to the carbonyl group.



(I) (II)

Urea as well as the two "oxyureas" showed an identical set of bands at 3 300 —3 400 cm^{-1}. These are tentatively assigned to N—H stretching vibrations. In the spectrum of OU_{140} there was observed an additional intense band at approximately 2 800 cm^{-1}, absent in the other two compounds. A possible assignment of this band to the (hydrogen-bonded) N—OH group would, together with the established carbonyl frequency, be in favour of formula (I) for OU_{140}. This structure can also account for most other physical and chemical properties (*vide, e. g.* previous publications in the present series) and may now be regarded as reasonably well established.

The IR-spectrum of OU_{72} has not previously been on record. In the region 1 500 —600 cm^{-1} it is much more complex than those of urea and OU_{140}. At higher frequencies it is similar to that of urea; it has, like urea, an intense absorption band in the carbonyl region (1 700 cm^{-1}). The strong absorption at 2 800 cm^{-1}, which was observed in OU_{140} is absent in OU_{72}. If the assignment of this frequency to the N—OH group is correct it follows that OU_{72} does not contain a hydroxy-group. Since, furthermore, there seems to be evidence for a carbonyl group, the absorption spectrum appears to support the formula (II) for OU_{72}; this was recently proposed on the basis of classical chemical arguments by Exner [3].

The structure (II) is one of more than twenty formally possible combinations of hydroxylamine and cyanic acid, considered by the present author [5]. It can account for a number of the observed properties, such as the solubility in ether, which is greater than that of the isomeride (I), the existence of only one methoxyurea [6, p. 491] corresponding to structure (I), the absence of a colour reaction with ferric chloride, and finally also for the basic properties [7] of OU_{72} (weak, though stronger than those of urea) contrary to the weak acidic properties of OU_{140}. Other observations are, however, difficult to explain on the basis of structure (II), *e. g.* the polarographic properties [8] and the relative amounts of the isomerides formed in different solvents [9] by the reaction of hydroxylamine with cyanic acid. In these experiments it was found possible to correlate the isomerism with well-established knowledge on the tautomerism of cyanic acid. Structure I/II on the other hand implies that the structural ambiguity of cyanic acid is unimportant, and that the isomerism arises from the hydroxylamine molecule being added in two different manners to cyanic acid. These are, however, formalistic arguments, which may be weakened by future knowledge of the true reaction mechanism of the formation (*cf.* Ref.[10]).

Although plausible the formula (II) cannot be regarded as definitely proved. The classical chemical arguments [3,4] have the usual weaknesses characteristic for structure determination on the basis of chemical reactivity, and the absorption spectra need expert interpretation. Since the pressed-plate technique was employed, the spectral data refer to the crystalline state only.

A more detailed account of the spectroscopic investigations and the results of a kinetic examination of the rearrangement $OU_{72} \rightarrow OU_{140}$ will be presented in forthcoming publications.

The assistance of Mr. Henry E. Andersen in recording the spectra is gratefully acknowledged. The instrument was a Perkin Elmer spectrophotometer, model 21.

1. Kofod, H. *Acta Chem. Scand.* **7** (1953) 938.
2. Runti, C. and Deghenghi, R. *Ann. Triestini* **22—23** (1952—53) sez. 2a, p. 9.
3. Exner, O. *Collection Czechoslov. Chem. Communs.* **22** (1957) 335.
4. Exner, O. *Chem. listy* **51** (1957) 497.
5. Kofod, H. *Final discussion. (In print).*
6. Kofod, H. *Acta Chem. Scand.* **8** (1954) 485, p. 486.
7. Kofod, H. *Acta Chem. Scand.* **8** (1954) 494.
8. Kofod, H. *Acta Chem. Scand.* **9** (1955) 455.
9. Kofod, H. *Acta Chem. Scand.* **10** (1956) 256.
10. Kofod, H. *Acta Chem. Scand.* **11** (1957) 5, p. 9.

Received July 15, 1957.

Table 1. Distribution of ^{90}Y between $CHCl_3$—DBP and 0.1 M HNO_3.

Conç. of DBP in $CHCl_3$ M	I_{aq} cpm	I_{org} cpm	log q	log K
0.003	1 471	13.1	—2.05	3.42
0.007	1 463	96.6	—1.18	3.19
0.01	1 162	276	—0.63	3.27
0.015	741	634	—0.07	3.31
0.02	457	900	+0.29	3.29
0.03	209	1 194	+0.76	3.23
0.05	47.3	1 493	+1.50	3.31
0.1	48.3	7 154	+2.17	3.07
			Mean value:	3.26±0.12

Separation of Strontium-90 and Yttrium-90 and the Preparation of Carrier-free Yttrium-90

DAVID DYRSSEN

The Research Institute of National Defence, Dept. 1 (FOA 1), Sundbyberg 4, Sweden

In investigations with the radioactive isotope ^{90}Sr it is often valuable to have a simple and rapid method of separating ^{90}Sr and its daughter ^{90}Y. Methods that have been used for this separation include ion exchange [1-3], precipitation [4-6], electrolysis [7], and solvent extraction [8-10]. As solvent extraction procedures usually are very efficient and rapid, it seemed worth while to develop such a method. Previously the TTA-benzene [8,9] and the DBP-dibutyl ether [10] systems have been used. As DBP (dibutyl phosphoric acid) extracts metal ions at lower pH values than TTA (thenoyl trifluoroacetone), we preferred to work out a procedure using DBP as a complexing agent.

The extraction with DBP and chloroform can also be used for the preparation of carrier-free ^{90}Y which is a suitable isotope for tracer experiments. A 0.1 M nitric acid solution of the long-lived parent ^{90}Sr will constitute a continuous supply of ^{90}Y.

Reagents. The fission product ^{90}Sr was obtained in 1 M HNO_3 from AERE, Harwell, England. ^{89}Sr was also purchased from Harwell as neutron-irradiated $SrCO_3$. The chloroform (analytical grade) was washed with water to remove the alcohol present. The di-*n*-butyl phosphate (DBP) was kindly supplied by Albright & Wilson Ltd, London. Titration with alkali and analysis of C and H. (Found: C 45.0; H 8.7. Calc. for $C_8H_{19}PO_4$: C 45.7; H 9.1) showed the compound to be at least 99 % pure.

General procedure. The experiments were carried out at 25°C. The aqueous phase (5 ml) with 0.1 to 10 M HNO_3 and ^{90}Sr was shaken 3 to 5 minutes with an equal volume of 0.003 to 1 M DBP in chloroform. After centrifugation 0.1—0.5 ml of each phase was withdrawn. The dried samples were then counted with a total absorber thickness of 200 mg/cm². Corrections were made for counting efficiency, background, and the *bremsstrahlung* from ^{90}Sr.

Table 2. Distribution of ^{90}Y between 0.1 M DBP in $CHCl_3$ and HNO_3.

Conc. of HNO_3 in the aqueous phase M	I_{aq} cpm	I_{org} cpm	log q	log K
0.1	48.3	7 154	+2.17	3.07
0.15	119	7 890	+1.82	3.25
0.2	180	7 634	+1.63	3.44
0.3	762	6 818	+0.95	3.28
0.5	2 310	5 120	+0.35	3.35
0.7	4 667	2 505	—0.27	3.17
1	6 544	1 134	—0.76	3.14
1.5	7 183	298	—1.38	3.05
2	6 952	180	—1.59	3.22
3	7 144	110	—1.81	(3.52)
5	7 292	53.4	—2.14	(3.86)
5	7 857	72.2	—2.04	(3.96)
7	7 630	20.4	—2.57	(3.87)
7	7 776	18.5	—2.62	(3.82)
10	7 132	89.2	—1.90	(5.00)
			Mean value:	3.22±0.13

1. Kofod, H. *Acta Chem. Scand.* **7** (1953) 938.
2. Runti, C. and Deghenghi, R. *Ann. Triestini* **22—23** (1952—53) sez. 2a, p. 9.
3. Exner, O. *Collection Czechoslov. Chem. Communs.* **22** (1957) 335.
4. Exner, O. *Chem. listy* **51** (1957) 497.
5. Kofod, H. *Final discussion. (In print).*
6. Kofod, H. *Acta Chem. Scand.* **8** (1954) 485, p. 486.
7. Kofod, H. *Acta Chem. Scand.* **8** (1954) 494.
8. Kofod, H. *Acta Chem. Scand.* **9** (1955) 455.
9. Kofod, H. *Acta Chem. Scand.* **10** (1956) 256.
10. Kofod, H. *Acta Chem. Scand.* **11** (1957) 5, p. 9.

Received July 15, 1957.

Table 1. Distribution of ^{90}Y between $CHCl_3$—DBP and 0.1 M HNO_3.

Conç. of DBP in $CHCl_3$ M	I_{aq} cpm	I_{org} cpm	log q	log K
0.003	1 471	13.1	—2.05	3.42
0.007	1 463	96.6	—1.18	3.19
0.01	1 162	276	—0.63	3.27
0.015	741	634	—0.07	3.31
0.02	457	900	+0.29	3.29
0.03	209	1 194	+0.76	3.23
0.05	47.3	1 493	+1.50	3.31
0.1	48.3	7 154	+2.17	3.07
			Mean value:	3.26±0.12

Separation of Strontium-90 and Yttrium-90 and the Preparation of Carrier-free Yttrium-90

DAVID DYRSSEN

The Research Institute of National Defence, Dept. 1 (FOA 1), Sundbyberg 4, Sweden

In investigations with the radioactive isotope ^{90}Sr it is often valuable to have a simple and rapid method of separating ^{90}Sr and its daughter ^{90}Y. Methods that have been used for this separation include ion exchange [1-3], precipitation [4-6], electrolysis [7], and solvent extraction [8-10]. As solvent extraction procedures usually are very efficient and rapid, it seemed worth while to develop such a method. Previously the TTA-benzene [8,9] and the DBP-dibutyl ether [10] systems have been used. As DBP (dibutyl phosphoric acid) extracts metal ions at lower pH values than TTA (thenoyl trifluoroacetone), we preferred to work out a procedure using DBP as a complexing agent.

The extraction with DBP and chloroform can also be used for the preparation of carrier-free ^{90}Y which is a suitable isotope for tracer experiments. A 0.1 M nitric acid solution of the long-lived parent ^{90}Sr will constitute a continuous supply of ^{90}Y.

Reagents. The fission product ^{90}Sr was obtained in 1 M HNO_3 from AERE, Harwell, England. ^{89}Sr was also purchased from Harwell as neutron-irradiated $SrCO_3$. The chloroform (analytical grade) was washed with water to remove the alcohol present. The di-*n*-butyl phosphate (DBP) was kindly supplied by Albright & Wilson Ltd, London. Titration with alkali and analysis of C and H. (Found: C 45.0; H 8.7. Calc. for $C_8H_{19}PO_4$: C 45.7; H 9.1) showed the compound to be at least 99 % pure.

General procedure. The experiments were carried out at 25°C. The aqueous phase (5 ml) with 0.1 to 10 M HNO_3 and ^{90}Sr was shaken 3 to 5 minutes with an equal volume of 0.003 to 1 M DBP in chloroform. After centrifugation 0.1—0.5 ml of each phase was withdrawn. The dried samples were then counted with a total absorber thickness of 200 mg/cm². Corrections were made for counting efficiency, background, and the *bremsstrahlung* from ^{90}Sr.

Table 2. Distribution of ^{90}Y between 0.1 M DBP in $CHCl_3$ and HNO_3.

Conc. of HNO_3 in the aqueous phase M	I_{aq} cpm	I_{org} cpm	log q	log K
0.1	48.3	7 154	+2.17	3.07
0.15	119	7 890	+1.82	3.25
0.2	180	7 634	+1.63	3.44
0.3	762	6 818	+0.95	3.28
0.5	2 310	5 120	+0.35	3.35
0.7	4 667	2 505	—0.27	3.17
1	6 544	1 134	—0.76	3.14
1.5	7 183	298	—1.38	3.05
2	6 952	180	—1.59	3.22
3	7 144	110	—1.81	(3.52)
5	7 292	53.4	—2.14	(3.86)
5	7 857	72.2	—2.04	(3.96)
7	7 630	20.4	—2.57	(3.87)
7	7 776	18.5	—2.62	(3.82)
10	7 132	89.2	—1.90	(5.00)
			Mean value:	3.22±0.13

Results. The results of the distribution experiments are given in Tables 1 and 2. It can be seen that ^{90}Y is more than 99 % extracted from 0.1 M HNO_3 with 0.1 M DBP in chloroform. Experiments with ^{89}Sr showed no activity in the organic phase under these conditions. However, with 1 M DBP small amounts of ^{89}Sr are extracted ($\log q = -2.216$). From this value we may calculate the extraction of ^{90}Sr to be less than 10^{-2} % ($\log q = -4.22$) with 0.1 M DBP.

Other measurements [11] have shown that DBP (HA) is highly dimerizised in chloroform. Within the concentration ranges of HNO_3 and DBP investigated here, the following equilibria may then explain the extraction of yttrium.

$$Y^{3+}\ (aq) + 3\ H_2A_2\ (org) \rightleftharpoons Y(HA_2)_3\ (org) + 3\ H^+\ (aq)$$

If the distribution of Y is given by

$$q = [Y(HA_2)_3]_{org}/[Y^{3+}]_{aq}$$

the equilibrium constant K will follow

$$\log K = \log q + 3 \log [H^+] - 3 \log C_A + 3 \log 2$$

where the DBP concentration in chloroform, $C_A = 2\ [H_2A_2]_{org}$.

The equilibrium constant K is calculated in the tables. The complex $Y(HA_2)_3$ is of a new type and will be further investigated. Other metal ions seem to form similar complexes [12].

Recommended procedure. a) Separation of ^{90}Sr and ^{90}Y. The sample is dissolved in 2—5 ml 0.1 M HNO_3 (HCl, $HClO_4$) and shaken with an equal volume of 0.1 M DBP in alcohol-free chloroform. The two phases are centrifuged and samples are withdrawn and evaporated to dryness. 80 % of the DBP in the chloroform sample may be removed at 190°C.

b) Preparation of carrier-free ^{90}Y. 5 ml of a 0.1 M HNO_3 solution with ^{90}Sr is shaken with 5 ml 0.1 M DBP in alcohol-free chloroform. The chloroform phase is then extracted with 5 ml of 5 M HNO_3. This nitric acid solution then contains 98 % of the ^{90}Y and 0.001 M of DBP. The DBP concentration can be lowered to 10^{-6} M, which is negligible for most purposes, by extraction first with 5 ml of chloroform and then twice with 5 ml of hexone (methyl *iso*butyl ketone). If carrier-free ^{90}Y is not wanted, inert yttrium may be added to the nitric acid solution and then precipitated with aqueous ammonia. This may be a convenient method of preparing an yttrium tracer, since neutron irradiated Y_2O_3 often contains some radioactive impurities.

The author wishes to thank the head of FOA 1, Professor Gustaf Ljunggren, for his kind interest and Mr. Bengt Carlsson and Mr. Ebbe Johansson for their technical assistance.

1. Herrmann, G. and Strassmann, F. *Z. Naturforsch.* **11a** (1956) 946.
2. Marathe, E. V. *J. Sci. Ind. Research India* **14B** (1955) 354.
3. Tompkins, E. R., Khym, J. X. and Cohn, W. E. *J. Am. Chem. Soc.* **69** (1947) 2769.
4. Salutsky, M. L. and Kirby, H. W. *Anal. Chem.* **27** (1955) 567.
5. Volchok, H. L. and Kulp, J. L. *Phys. Rev.* **97** (1955) 102.
6. Herrmann, G. and Strassmann, F. *Z. Naturforsch.* **10a** (1955) 146.
7. Lange, G., Herrmann, G. and Strassmann, F. *J. Inorg. & Nuclear Chem.* **4** (1957) 146.
8. Chetham-Strode, Jr., A. and Kindermann, E. M. *Phys. Rev.* **93** (1954) 1029.
9. Goldin, A. S. *U.S. AEC TID-7517* (1956) 323.
10. Scadden, E. M. and Ballou, N. E. *Anal. Chem.* **25** (1953) 1602.
11. Dyrssen, D. *Acta Chem. Scand. In press.*
12. Dyrssen, D. *To be published.*

Received August 13, 1957.

The Influence of Some Amino Acids on the Growth of and Vitamin B_{12} Production by *Streptomyces griseus* NzC5

W. KURZ and NIELS NIELSEN

Division of Food Chemistry, Royal Institute of Technology, Stockholm, and Research Department, AB Kabi, Stockholm, Sweden

The purpose of this investigation was to study the influence of different amino acids on both the growth and the vitamin B_{12} formation of *Streptomyces griseus*.

Methods. The organism used for this investigation was a strain of *Streptomyces*

Results. The results of the distribution experiments are given in Tables 1 and 2. It can be seen that ^{90}Y is more than 99 % extracted from 0.1 M HNO_3 with 0.1 M DBP in chloroform. Experiments with ^{89}Sr showed no activity in the organic phase under these conditions. However, with 1 M DBP small amounts of ^{89}Sr are extracted ($\log q = -2.216$). From this value we may calculate the extraction of ^{90}Sr to be less than 10^{-2} % ($\log q = -4.22$) with 0.1 M DBP.

Other measurements [11] have shown that DBP (HA) is highly dimerizised in chloroform. Within the concentration ranges of HNO_3 and DBP investigated here, the following equilibria may then explain the extraction of yttrium.

$$Y^{3+}\ (aq) + 3\ H_2A_2\ (org) \rightleftharpoons Y(HA_2)_3\ (org) + 3\ H^+\ (aq)$$

If the distribution of Y is given by

$$q = [Y(HA_2)_3]_{org}/[Y^{3+}]_{aq}$$

the equilibrium constant K will follow

$$\log K = \log q + 3 \log [H^+] - 3 \log C_A + 3 \log 2$$

where the DBP concentration in chloroform, $C_A = 2\ [H_2A_2]_{org}$.

The equilibrium constant K is calculated in the tables. The complex $Y(HA_2)_3$ is of a new type and will be further investigated. Other metal ions seem to form similar complexes [12].

Recommended procedure. a) Separation of ^{90}Sr and ^{90}Y. The sample is dissolved in 2—5 ml 0.1 M HNO_3 (HCl, $HClO_4$) and shaken with an equal volume of 0.1 M DBP in alcohol-free chloroform. The two phases are centrifuged and samples are withdrawn and evaporated to dryness. 80 % of the DBP in the chloroform sample may be removed at 190°C.

b) Preparation of carrier-free ^{90}Y. 5 ml of a 0.1 M HNO_3 solution with ^{90}Sr is shaken with 5 ml 0.1 M DBP in alcohol-free chloroform. The chloroform phase is then extracted with 5 ml of 5 M HNO_3. This nitric acid solution then contains 98 % of the ^{90}Y and 0.001 M of DBP. The DBP concentration can be lowered to 10^{-6} M, which is negligible for most purposes, by extraction first with 5 ml of chloroform and then twice with 5 ml of hexone (methyl *iso*butyl ketone). If carrier-free ^{90}Y is not wanted, inert yttrium may be added to the nitric acid solution and then precipitated with aqueous ammonia. This may be a convenient method of preparing an yttrium tracer, since neutron irradiated Y_2O_3 often contains some radioactive impurities.

The author wishes to thank the head of FOA 1, Professor Gustaf Ljunggren, for his kind interest and Mr. Bengt Carlsson and Mr. Ebbe Johansson for their technical assistance.

1. Herrmann, G. and Strassmann, F. *Z. Naturforsch.* **11a** (1956) 946.
2. Marathe, E. V. *J. Sci. Ind. Research India* **14B** (1955) 354.
3. Tompkins, E. R., Khym, J. X. and Cohn, W. E. *J. Am. Chem. Soc.* **69** (1947) 2769.
4. Salutsky, M. L. and Kirby, H. W. *Anal. Chem.* **27** (1955) 567.
5. Volchok, H. L. and Kulp, J. L. *Phys. Rev.* **97** (1955) 102.
6. Herrmann, G. and Strassmann, F. *Z. Naturforsch.* **10a** (1955) 146.
7. Lange, G., Herrmann, G. and Strassmann, F. *J. Inorg. & Nuclear Chem.* **4** (1957) 146.
8. Chetham-Strode, Jr., A. and Kindermann, E. M. *Phys. Rev.* **93** (1954) 1029.
9. Goldin, A. S. *U.S. AEC TID-7517* (1956) 323.
10. Scadden, E. M. and Ballou, N. E. *Anal. Chem.* **25** (1953) 1602.
11. Dyrssen, D. *Acta Chem. Scand. In press.*
12. Dyrssen, D. *To be published.*

Received August 13, 1957.

The Influence of Some Amino Acids on the Growth of and Vitamin B_{12} Production by *Streptomyces griseus* NzC5

W. KURZ and NIELS NIELSEN

Division of Food Chemistry, Royal Institute of Technology, Stockholm, and Research Department, AB Kabi, Stockholm, Sweden

The purpose of this investigation was to study the influence of different amino acids on both the growth and the vitamin B_{12} formation of *Streptomyces griseus*.

Methods. The organism used for this investigation was a strain of *Streptomyces*

griseus, NzC5, which gives low yields of vitamin B_{12} and streptomycin.

The nutrient solution had the following composition: 0.5 g K_2HPO_4, $3H_2O$ – 0.5 g $MgSO_4$, $7H_2O$ – 0.015 g $CuSO_4$, $5H_2O$ – 0.015 g $MnSO_4$, $4H_2O$ – 0.03 g $ZnSO_4$, $7H_2O$ – 0.025 g $FeSO_4$, $7H_2O$ – 0.05 g $CaCl_2$, $2H_2O$ – 0.005 g $Co(NO_3)_2$, $6H_2O$ and 20 g glucose made up to 1 000 ml with distilled water. Different amino acids were added to the solution as the nitrogen source so that the nitrogen content of the medium was 0.60 to 0.66 g per litre.

The experiments were made either with 50 ml of nutrient solution in 250 ml Ehrlenmeyer flasks, shaken continuosly at 25°, or with 3 litres of nutrient solution in 5 litre fermentors at the same temperature. The results of these two experiments were in good agreement. The amount of mycelium and vitamin B_{12} was determined daily; the former by weighing the washed and dried mycelium and the latter microbiologically using *Escherichia coli*. Vitamin B_{12} was determined both in the mycelium and in the nutrient solution; most of the vitamin B_{12} was found to be present in the nutrient solution. The amount of nitrogen was determined periodically to ensure that an excess of assimilable nitrogen was present. All experiments were performed in duplicate.

Results. A number of experiments were made in which the nutrient solution contained only one amino acid as the nitrogen source. The amino acids used in these experiments were: arginine, aspartic acid, cystine, glutamic acid, glycine, *iso*leucine, leucine, serine and valine. The amounts of the amino acids used corresponded to 0.60 g nitrogen per litre nutrient solution. The maximum values for mycelium and vitamin B_{12} content are given in Table 1 where the amino acids are tabulated according to the growth obtained. Maximum growth was obtained after 4 to 6 days and the maximum vitamin content somewhat later, after the commencement of autolysis.

Only three of the nine amino acids tried maintained good growth, *viz.* glutamic acid, glycine and aspartic acid. The vitamin B_{12} formation, however, was not proportional to the growth obtained. Whereas the growth obtained with aspartic acid was almost as vigorous as that obtained with glycine, the amount of vitamin B_{12} formed with aspartic acid was much smaller (See column 4 which gives the ratio μg B_{12} : g mycelium).

Table 1. Growth and vitamin B_{12} formation with different amino acids.

Nitrogen source	Mycelium max. amount, g dry weight per litre	Vitamin B max. amount, μg per litre	Ratio $\frac{\mu g \text{ vitamin } B_{12}}{g \text{ mycelium}}$
Glutamic acid	4.5	400	88
Glycine	3.1	360	116
Aspartic acid	2.6	60	23
Arginine	0.4	10	25
Leucine	0.4	7	18
Valine	0.4	20	50
Cystine	0.3	15	50
*Iso*leucine	0.3	6	20
Serine	0.3	5	17

With regard to the other six amino acids only slight growth occurred. The vitamin formation was accordingly low as the presence of a certain amount of mycelium is a necessary condition for good formation of the vitamin. Two of these six amino acids, *viz.* valine and cystine, produced higher amounts of vitamin B_{12} than the other four. From these experiments it appears that no strict proportionality exists between growth and vitamin B_{12} formation.

The experiments summarized in Table 1 show that aspartic acid promotes good growth whereas the vitamin B_{12} production is small, calculated on g mycelium formed. Other amino acids maintain only weak growth, but the vitamin B_{12} formation is relatively high. In a series of experiments it was investigated whether aspartic acid together with the last mentioned amino acids would result in an increased vitamin B_{12} formation. In each experiment to one litre of nutrient solution 0.60 g nitrogen as aspartic acid and 0.06 g as one of the other amino acids was added. The total amount of nitrogen thus amounted to 0.66 g per litre. The fact that this increased amount of nitrogen is of no importance *per se* was demonstrated in an experiment in which the amount of aspartic acid was increased by 10 %.

While the addition of the amino acids had no marked effect on growth there was in most cases an increase in the vitamin B_{12} formation. In all cases except when β-alanine, arginine and leucine were used, the vitamin formation was increased by about

Table 2. Growth and vitamin B_{12} formation with aspartic acid + one of the following amino acids.

Amino acids added	Mycelium max. amount, g dry weight per litre	Vitamin B_{12} max. amount, μg per litre	Ratio $\frac{\mu g \text{ vitamin } B_{12}}{g \text{ mycelium}}$
β-alanine	3.3	60	18
Arginine	2.2	70	32
Glutamic acid	2.9	95	33
Glycine	3.0	100	33
Histidine	2.7	100	37
Leucine	2.9	80	28
Lysine	2.6	100	38
Proline	3.3	100	30
Serine	2.8	130	46
Tryptophane	2.7	95	35
Valine	2.4	100	42
No addition	2.6	60	23

50 %. Column 4, Table 2, shows that the greatest stimulation of the vitamin production was obtained with serine and valine (in the presence of aspartic acid). In the case of valine this is in good agreement with the experiments given in Table 1. Serine, however, when being the sole nitrogen source, was found to give a very low vitamin formation. The reason for this must be, that if serine is the only nitrogen source such a small amount of mycelium is formed that a high vitamin formation is impossible.

Glutamic acid and glycine have, when added in small amounts, a less marked effect on the vitamin B_{12} production than would be expected from Table 1 (if these amino acids constitute the sole nitrogen source they give rise to vigorous growth and vitamin production). The reason for this peculiar behaviour (Table 2) is probably that these amino acids, when added in small amounts, are used for the nitrogen assimilation and accordingly hardly anything remains for the formation of vitamin B_{12} which, as mentioned above, mainly takes place after the cessation of the growth. Serine and valine, on the other hand, are very bad nitrogen sources for growth and are thus not used during the growth phase but are left over to the vitamin forming phase.

Received September 3, 1957.

An Efficient Method for the Separation and Identification of Alkaloids in Biological Material

R. BONNICHSEN, A. C. MAEHLY and S. NORDLANDER

Statens Rättskemiska Laboratorium, Stockholm, Sweden*

The detection of alkaloids in biological material has long been based largely on colorreactions and crystal precipitation methods under the microscope. In recent years, paper chromatography has been employed to an increasing degree, pioneered by Munier *et al.*[1] and used by Jatzkewitz [2,3], Vidic [4] and others.

Buffered paper was employed by Carless and Woodhead [5], Goldbaum and Kazyak [6] and others. Schmall *et al.*[7] refined this technique by buffering zones to different pH values on the same paper. We have modified their technique for toxicological work and extended it to the identification of more than 30 compounds mainly of the alkaloid group. Quantitative estimation by spectrophotometry has also been worked out for many alkaloids. The basic principle of the method is as follows:

The tissue (whenever possible urine is employed, otherwise kidney, liver or blood) is heated with hydrochloric acid for 1 h for hydrolytic cleavage of adducts with glucuronic acid etc., and extracted in the usual way *via* amylacetate, 0.1 N HCl and chloroform.

The chloroform extract is dried, and evaporated to dryness. The residue is dissolved in hot 75 % ethanol and the ethanolic solution applied to a filter paper.

The migration and efficient separation of alkaloids and some other toxicologically important compounds on filter paper is achieved only if the free base is allowed to migrate in the direction of descending pH values and depends on the pH of the buffered zones as well as on the partition coefficients between the buffers and the mobile organic phase. The most efficient way to prepare the filter paper was the subject of extensive experimentation.

* The Government Laboratory for Forensic Chemistry.

Table 2. Growth and vitamin B_{12} formation with aspartic acid + one of the following amino acids.

Amino acids added	Mycelium max. amount, g dry weight per litre	Vitamin B_{12} max. amount, μg per litre	Ratio $\frac{\mu g \text{ vitamin } B_{12}}{g \text{ mycelium}}$
β-alanine	3.3	60	18
Arginine	2.2	70	32
Glutamic acid	2.9	95	33
Glycine	3.0	100	33
Histidine	2.7	100	37
Leucine	2.9	80	28
Lysine	2.6	100	38
Proline	3.3	100	30
Serine	2.8	130	46
Tryptophane	2.7	95	35
Valine	2.4	100	42
No addition	2.6	60	23

50 %. Column 4, Table 2, shows that the greatest stimulation of the vitamin production was obtained with serine and valine (in the presence of aspartic acid). In the case of valine this is in good agreement with the experiments given in Table 1. Serine, however, when being the sole nitrogen source, was found to give a very low vitamin formation. The reason for this must be, that if serine is the only nitrogen source such a small amount of mycelium is formed that a high vitamin formation is impossible.

Glutamic acid and glycine have, when added in small amounts, a less marked effect on the vitamin B_{12} production than would be expected from Table 1 (if these amino acids constitute the sole nitrogen source they give rise to vigorous growth and vitamin production). The reason for this peculiar behaviour (Table 2) is probably that these amino acids, when added in small amounts, are used for the nitrogen assimilation and accordingly hardly anything remains for the formation of vitamin B_{12} which, as mentioned above, mainly takes place after the cessation of the growth. Serine and valine, on the other hand, are very bad nitrogen sources for growth and are thus not used during the growth phase but are left over to the vitamin forming phase.

Received September 3, 1957.

An Efficient Method for the Separation and Identification of Alkaloids in Biological Material

R. BONNICHSEN, A. C. MAEHLY and S. NORDLANDER

Statens Rättskemiska Laboratorium, Stockholm, Sweden*

The detection of alkaloids in biological material has long been based largely on colorreactions and crystal precipitation methods under the microscope. In recent years, paper chromatography has been employed to an increasing degree, pioneered by Munier *et al.*[1] and used by Jatzkewitz [2,3], Vidic [4] and others.

Buffered paper was employed by Carless and Woodhead [5], Goldbaum and Kazyak [6] and others. Schmall *et al.*[7] refined this technique by buffering zones to different pH values on the same paper. We have modified their technique for toxicological work and extended it to the identification of more than 30 compounds mainly of the alkaloid group. Quantitative estimation by spectrophotometry has also been worked out for many alkaloids. The basic principle of the method is as follows:

The tissue (whenever possible urine is employed, otherwise kidney, liver or blood) is heated with hydrochloric acid for 1 h for hydrolytic cleavage of adducts with glucuronic acid etc., and extracted in the usual way *via* amylacetate, 0.1 N HCl and chloroform.

The chloroform extract is dried, and evaporated to dryness. The residue is dissolved in hot 75 % ethanol and the ethanolic solution applied to a filter paper.

The migration and efficient separation of alkaloids and some other toxicologically important compounds on filter paper is achieved only if the free base is allowed to migrate in the direction of descending pH values and depends on the pH of the buffered zones as well as on the partition coefficients between the buffers and the mobile organic phase. The most efficient way to prepare the filter paper was the subject of extensive experimentation.

* The Government Laboratory for Forensic Chemistry.

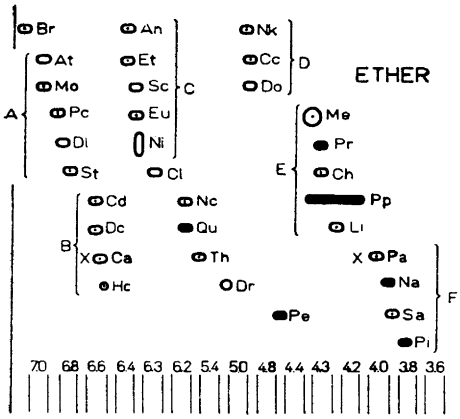


Fig. 1. The R_F or pH values of common alkaloids and other compounds of toxicological importance. The descending technique was used, the solvent (here ether) appears to migrate from left to right. The buffered zones of the paper are labelled with the corresponding pH value. The abbreviations shown stand for the following 33 compounds (if the name does not correspond to that given in the "Merck Index", the "Merck" name is added in brackets).

An Antipyrin (phenazone)
At Atropine
Br Brucine
Ca Coffeine
Cc Cocaine
Cd Codeine
Ch Chloropromethazine
Cl Cliradon (ketobemidone)
Dc Dicodid (dihydrocodeinone)
Dl Dilaudid (dihydromorphinone)
Do Dolantine (meperidine)
Dr Dromorane (3-hydroxy-N-methyl-morphinan)
Et Ethylmorphine
Eu Eucodal (dihydrooxycodeinon)
Hc Hydrocodeinon (synkonin)
Le Lergitin (N-benzyl-N′, N′-dimethyl-N-phenylethylene-diamine)
Me Methadone
Mo Morphine
Na Narcotine
Nc Novocaine
Ni Nicotine
Nk Nikethamide (nicamide)
Pa Phenacetin
Pc Paracodin (dihydrocodeine)
Pe Percaine (dibucaine)
Pi Piperine
Pp Papaverin
Pr Promethazine
Qu Quinine
Sa Santonin
Sc Scopolamine
St Strychnine
Th Thebaine

Compounds that are not clearly resolved from all others are indicated in groups (A—F).

The following symbols are used for the individual spots:

⊙ colored by Dragendorff's reagent and absorbing ultraviolet light.
○ colored by Dragendorff's reagent but not absorbing ultraviolet light.
● colored by Dragendorff's reagent and fluorescing in ultraviolet light.
× ⊙ not colored by Dragendorff's reagent but absorbing ultraviolet light.

The pH values finally adopted for ether and chloroform respectively as the mobile phases are shown in Figs. 1 and 2.

Fig. 1 shows the distribution on the chromatography sheat of 33 standard substances. The positions of spots are averaged from a number of runs on different days and with somewhat varying amounts of material (10—50 μg of each compound). The solvent was *ether* and the descending method was used at room temperature and in the dark. The buffer

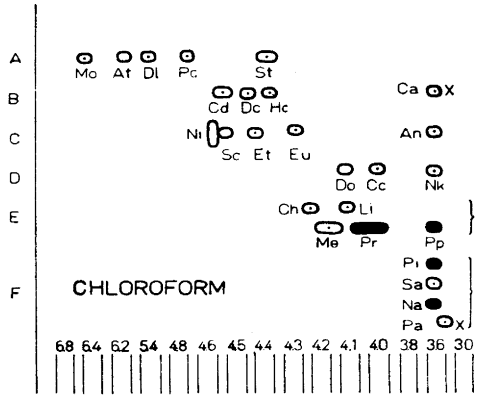


Fig. 2. Those compounds that are not cleary resolved when using ether as the mobile phase are here shown on a chromatogram where chloroform is the moving solvent. Groups A to F of Fig. 1 are each shown on 1 or 2 horizontal lines. The symbols used are the same as in Fig. 1.

Table 1. Buffer solutions employed. The amounts of 0.10 M citric acid and 0.20 M disodium phosphate listed were diluted to a final volume of 100 ml with distilled water.

pH	X ml 0.1 M citric acid	Y ml 0.2 M Na_2HPO_4	pH	X ml 0.1 M citric acid	Y ml 0.2 M Na_2HPO_4
3.0	39.3	10.2	4.8	25.2	24.8
3.6	33.9	16.1	5.0	24.3	25.7
3.8	32.3	17.7	5.4	22.2	27.8
4.0	30.7	19.3	6.2	16.9	33.1
4.1	30.0	20.0	6.3	16.2	33.8
4.2	29.4	20.6	6.4	15.4	34.6
4.3	28.6	21.4	6.6	13.6	36.4
4.4	27.8	22.2	6.8	9.1	40.9
4.5	27.2	22.8	7.0	6.5	43.6
4.6	26.7	23.3	—	—	—

composition as it is presently employed is listed in Table 1. Only disodium phosphate and citric acid are needed. The compounds are quite evenly distributed over the whole paper and some of them show distinct R_F values or "pH values", a term better suited for this technique. However, most of them appear in groups marked A to F in Fig. 1. Fortunately these groups are almost all clearly separated with *chloroform* as the mobile phase (Fig. 2).

Exceptions are chloro-promazin, methadone and phenbenzamine in group E and also all of group F. In the latter case, optical properties help in identification: piperine and narcotine show a blue fluorescence and the former also gives a distinct yellow color with Dragendorff's spraying reagent. Santonine and phenacetine both absorb ultraviolet light (UV-lamp in conjunction with fluorescein treated paper) but only the former reacts with Dragendorff's reagent.

The position of a spot (R_F or pH value) is never regarded as an absolute invariable and standards of known purity and concentration are always run on the same sheet of paper. Qualitative identification was sometimes aided by cutting the spot into a narrow rectangle, wetting it with liquid paraffin oil and measuring its spectrum *vs.* a blank treated in the identical way. If the paper had been sprayed with Dragendorff's reagent, a short treatment with ammonia vapour to restore the free base preceded the oiling.

Semi-quantitative evaluation was usually possible by extracting the spot with dilute ammonia and chloroform, evaporating and dissolving the residue in 75 % ethanol for spectrophotometric analysis. In cases where the spectrum did not show any characteristic bands or where the amount of material was insufficient, known amounts of standard solutions were run simultaneously on the same paper as the unknown, and the amount of the unknown estimated by matching spot sizes.

Transfers of individual "spots" to another paper for re-chromatography proved to be a useful and often indispensible means for separation and purification. If sufficient amounts of material were present, elution and evaporation were used. In other cases, a simple transfer could be achieved by sandwiching the cut-out spot between a new filter paper and a small glassplate with the help of paper clips and running the paper in the usual manner.

Some of the main advantages of the method for the toxicologist are: The need of only very small amounts of material (10 μg for qualitative identification is usually the lower limit), the relative speed of the process and the possibilities for purifying individual compounds from an often complex array of "spots" from tissue extracts.

A detailed report together with application of the method to actual toxicological cases will be published later.

1. Munier, R., Macheboeuf, M. and Cherrier, N. *Bull. soc. chim. biol.* **34** (1952) 204.
2. Jatzkewitz, H. *Z. physiol. Chem. Hoppe-Seyler* **292** (1953) 94.
3. Jatzkewitz, H. *Deut. med. Wochschr.* **79** (1954) 541.
4. Vidic, E. *Arzneimittel-Forsch.* **5** (1955) 291.
5. Carless, J. E. and Woodhead, H. B. *Nature* **168** (1951) 203.
6. Goldbaum, L. R. and Kazyak, L. *Anal. Chem.* **28** (1956) 1289.
7. Schmall, M., Wollish, E. G. and Schafer, E. G. E. *Anal. Chem.* **28** (1956) 1373.

Received August 13, 1957.

Isotope Effect in the Methanolysis of Grignard Compounds

LARS OLOF ASSARSSON

Nobel Institute of Chemistry, Stockholm 50, Sweden

Measurements of the hydrogen isotope effect in the hydrolysis of methylmagnesium iodide, phenylmagnesium iodide and phenylmagnesium bromide in different solvents, *i. e.* anisole-pyridine and anisole-tetrahydrofuran, have been reported in previous preliminary papers [1,2].

Decomposition of Grignard compounds by tritiated methanol has now been carried out under the same or similar conditions. The reactions investigated are the methanolysis of methylmagnesium iodide in anisole-tetrahydrofuran and in *n*-butyl ether and that of dimethylmagnesium, *n*-butylmagnesium bromide, and phenylmagnesium bromide in *n*-butyl ether. Determination of the deuterium isotope effect in the methanolysis of a number of organometallic compounds has earlier been carried out by Wiberg [3], who found a small inversed isotope effect.

The methanolysis of dimethylmagnesium was done in an attempt to throw some light upon the reaction mechanism. It has been found [4], for instance, that acetone reacts about 50 times faster with dimethylmagnesium than with methylmagnesium iodide, and it has been concluded that dimethylmagnesium is probably the reactive component of the Grignard solution, the reaction rate of the ordinary reagent being determined by that of the generation of dimethylmagnesium by the well-known Schlenk-disproportionation.

If in the present experiments with methylmagnesium iodide and dimethylmagnesium, the methanolysis takes place with the dimethylmagnesium in both cases, then it could be expected that the mechanism of the decomposition, and hence the isotope effect, should be independent of the origin of the dimethylmagnesium. The results do not confirm such an expectation, as they do not confirm any hypothesis of a reactive species common to both reagents, *e. g.* the methyl carbanion. The mechanisms might be analogous but not identical, the difference being at least some kind of interaction with the mother reagent.

It has further been found [5] that diethylmagnesium reacts about 3 times faster with 1-alkynes than does ethylmagnesium bromide and that the isotope effect deuterium-protium is of considerable magnitude but not equal in the two cases. The isotope effect has its largest value with ethylmagnesium bromide. Since the isotope effect is large, the C—H bond concerned is believed to be cleaved in the rate-determining step. The reaction with ethylmagnesium bromide was shown to be a simple reaction of the second-order, and the kinetics of that with diethylmagnesium could be explained by the assumption of a competitive, consecutive, second-order reaction.

An analogous reaction scheme might be assumed for the methanolysis of dimethylmagnesium and methylmagnesium iodide, but the cleavage of the O—H bond has to take place in a step which is kinetically nearly insignificant, since the isotope effect is small, although not equal for the two compounds. Another, less likely alternative would be that the cleavage from oxygen is part of the rate-determining step but involves almost no loss of zero-point energy.

The methylmagnesium iodide reagent used was a solution of the compound in anisole-tetrahydrofuran and in *n*-butyl ether. The *n*-butyl ether solutions are known to contain practically no dimethylmagnesium [4,6]. This was confirmed in the present investigation by precipitating a solution of methylmagnesium iodide in *n*-butyl ether with a large excess of dioxan, *i. e.* 4 moles per g-ion of halogen [6]. The supernatant when tested both directly, as well as after vigorous shaking for 175 h (in order to reach equilibrium), evolved no appreciable amount of gas on hydrolysis.

The dimethylmagnesium reagent was prepared by precipitating a boiling ethyl ether solution of methylmagnesium iodide with dioxan in the excess mentioned above and boiling the mixture. The hot mixture was centrifuged to separate the precipitate from the clear supernatant, which was transferred into *n*-butyl ether. The ethyl ether and dioxan were distilled off in an argon atmosphere at reduced pressure from the *n*-butyl ether solution of dimethylmagnesium. Possible traces of dioxan in the solution are probably without significance, because it has been shown [7], that the presence of dioxan in dialkylmagnesium solutions is generally without influence on the reaction kinetics.

After the preparation of *n*-butylmagnesium bromide and phenylmagnesium bro-

Table 1. Results in the decomposition of Grignard compounds with methanol at 20°C

Grignard compound	Reaction medium	k_T/k_H	Number of parallel determinations of tritium in combustion water	Mean value (including error in determination of tritium in combustion water from the methanol)
CH_3MgI	Anisole-tetrahydrofuran	0.823 0.827 0.843 0.810	1 1 1 1	0.83 ± 0.02
CH_3MgI	*n*-butyl ether	0.953 0.938 0.950	2 1 2	0.95 ± 0.02
$(CH_3)_2Mg$	—»—	0.802 0.864 0.868	1 1 1	0.84 ± 0.04
n-C_4H_9MgBr	—»—	0.979 0.916 0.848	2 1 1	
C_6H_5MgBr	—»—	0.857 0.843	2 four different 2 combustions	0.85 ± 0.02

mide, a fraction of the solvent was distilled off at reduced pressure in order to eliminate hydrocarbons formed by moisture or other side reactions.

The technique of the decompositions was the same as the one used earlier, *i. e.* the Grignard reagent was added by means of an injection syringe or a dropping funnel into a solution of tritiated methanol. The methanol was present in at least 8-fold excess over the Grignard compound.

The anisole and the *n*-butyl ether were dried by refluxing over and distilling from metallic sodium, while the dioxan was dried in the same manner after standing for some weeks over anhydrous calcium chloride. The tetrahydrofuran was dried by shaking it with anhydrous calcium chloride, thereafter with metallic sodium and finally distilling it from methylmagnesium iodide. The ethyl ether was made absolute according to current methods.

The tritiated methanol (CH_3OT + CH_3OH) was made by addition of tritiated water to dry methanol, drying the mixture with gypsum, decanting and distilling.

The hydrocarbons formed in the methanolysis as well as the methanol were burnt over cupric oxide, and the radioactivity of the water of combustion was determined by means of a Geiger-Müller counter after reduction to hydrogen.

The results, all obtained at 20°C, are given in Table 1. The reported values have not been corrected for the small change in the specific activity of the methanol occurring during the reaction. The decreasing values of the ratio k_T/k_H in the *n*-butylmagnesium bromide methanolysis are probably due to small amounts of moisture gradually entering the flask containing the Grignard reagent.

1. Assarsson, L. O. *Acta Chem. Scand.* **9** (1955) 1399.
2. Assarsson, L. O. *Acta Chem. Scand.* **10** (1956) 1509.
3. Wiberg, K. B. *J. Am. Chem. Soc.* **77** (1955) 5987.
4. Aston, J. G. and Bernhard, S. A. *Nature* **165** (1950) 485.
5. Dessy, R. E., Wotiz, J. H. and Hollingsworth, C. A. *J. Am. Chem. Soc.* **79** (1957) 358.
6. Cope, A. C. *J. Am. Chem. Soc.* **57** (1935) 2238.
7. Wotiz, J. H., Hollingsworth, C. A. and Dessy, R. E. *J. Am. Chem. Soc.* **78** (1956) 1221.

Received August 27, 1957.

ACTA CHEMICA SCANDINAVICA 11 (1957) 1285—1289

Studies on Pyrazolones

XI. Reactions between 1-Phenyl-3-methyl-2-pyrazolin-5-one and Some Aliphatic Carbonyl Compounds

GUNNEL WESTÖÖ

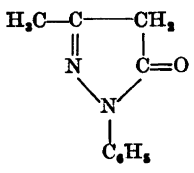
Institute of Organic Chemistry, University of Lund, Lund, Sweden

Aliphatic aldehydes and 1-phenyl-3-methyl-2-pyrazolin-5-one (I) react with the formation of 4,4′-alkylidenebis[1-phenyl-3-methyl-2-pyrazolin-5-ones] (II a—e). No 1-phenyl-3-methyl-4-alkylidene-2-pyrazolin-5-ones (III a) could be isolated.

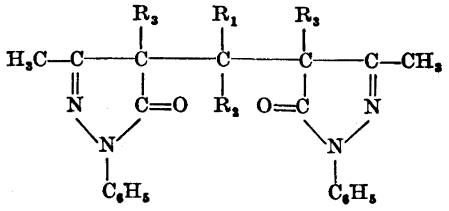
Methylalkyl ketones and I yield 1-phenyl-3-methyl-4-(1-methylalkylidene)-2-pyrazolin-5-ones (III b, c) and 4,4′-(1-methylalkylidene)-bis[1-phenyl-3-methyl-2-pyrazolin-5-ones] (II f, g). In solution II f and g — contrary to II a—e — are strongly dissociated into I and III (b, c).

1-Phenyl-3-methyl-2-pyrazolin-5-one (I) reacts rapidly at room temperature with aliphatic aldehydes, colourless, crystalline, stable acids, 4,4′-alkylidenebis[1-phenyl-3-methyl-2-pyrazolin-5-ones] (II a—e) being formed. In anhydrous 1,2-diaminoethane they can be titrated as dibasic acids with sodium methoxide in benzene-methanol solution using *o*-nitroaniline as indicator [1,2], but under ordinary conditions — in ethanol - water using phenolphthalein as indicator — they are titrated as monobasic acids. They form 4,4′-dibromo compounds, *e.g.*, II h. Only one alkylidene compound, preparable from an aliphatic aldehyde and I, has been described in the literature before, *viz.* the methylene compound [3-5].

A comparison between the acidic properties of II a—e and 1,1′,1″-triphenyl-3,3′,3″-trimethyl-4,4′,4″-ter-[2-pyrazoline-5,5′,5″-trione] [IV][6] shows a great difference in the dissociability of the second 4-H atom, caused by the different electron affinity of the alkylidene and pyrazolonylidene groups, the electron donating alkylidene groups weakening the acidic strength, the electron attracting pyrazolonylidene group increasing the acidity remarkably. Thus IV is titrated as a dibasic acid in aqueous ethanol with barium hydroxide using phenolphthalein as indicator, whereas even on titration in dimethylformamide solution with sodium methoxide in benzene-methanol using azo violet as indicator [7], II a—e turn out as monobasic acids.

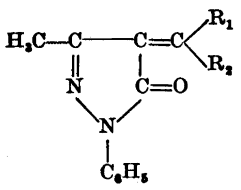


I



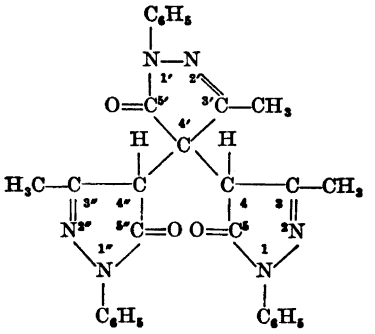
II

a. $R_1 = R_3 = H$; $R_2 = CH_3$.
b. $R_1 = R_3 = H$; $R_2 = C_2H_5$.
c. $R_1 = R_3 = H$; $R_2 = n\text{-}C_3H_7$.
d. $R_1 = R_3 = H$; $R_2 = i\text{-}C_3H_7$.
e. $R_1 = R_3 = H$; $R_2 = n\text{-}C_6H_{13}$.
f. $R_1 = R_2 = CH_3$; $R_3 = H$.
g. $R_1 = CH_3$; $R_2 = C_2H_5$; $R_3 = H$.
h. $R_1 = H$; $R_2 = CH_3$; $R_3 = Br$.



III

(a. $R_1 = H$; R_2 = alkyl.)
b. $R_1 = R_2 = CH_3$.
c. $R_1 = CH_3$; $R_2 = C_2H_5$.
(d. $R_1 = R_2 = C_2H_5$.)

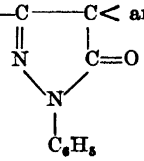


IV

From reactions between acetone and I Knorr [8], with excess of acetone, isolated 1-phenyl-3-methyl-4-*iso*propylidene-2-pyrazolin-5-one (III b) and, with equivalent amounts of reactants, an acid for which he proposed the structure 4,4′-*iso*propylidenebis [1-phenyl-3-methyl-2-pyrazolin-5-one] (II f), though without proof.

A closer investigation of the reaction showed that I rapidly adds to III b with formation of a bispyrazolone. Accordingly, even with great excess of acetone, bispyrazolone is formed in the beginning of the reaction when the concentration of I is large. However, there exists an equilibrium *

$$PyH_2 + Py{=}C(CH_3)_2 \rightleftharpoons PyHC(CH_3)_2PyH$$

* Py represents the group  and tautomeric forms.

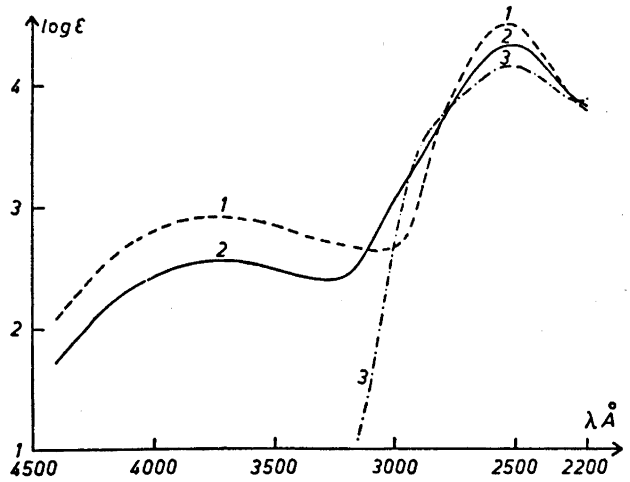


Fig. 1. UV absorption curves of 1) 1-phenyl-3-methyl-4-*iso*propylidene-2-pyrazolin-5-one (III b), 2) 4,4′-*iso*propylidenebis[1-phenyl-3-methyl-2-pyrazolin-5-one] (II f) and 3) 4,4′-propylidenebis[1-phenyl-3-methyl-2-pyrazolin-5-one] (II b), showing the stability of II b and the dissociation of II f.

and on prolonged boiling with acetone all pyrazolone is therefore transformed into III b.

The structure of the bispyrazolone is difficult to settle by direct study on account of its strong dissociation into I and III b in solution. But the analogy to the corresponding compounds (II a—e) obtained from aldehydes and the plausibility that a Michael addition takes place between I and III b are in favour of the structure II f. The equivalent weight of II f cannot be determined, for both I and III b consume alkali, III b probably mainly by addition of the ethanol used as solvent to form a salt of the unstable acid 1-phenyl-3-methyl-4-(1-ethoxy-1-methylethyl)-2-pyrazolin-5-one (*cf.* Westöö [9]).

Methylethylketone reacts with I analogously to acetone, 1-phenyl-3-methyl-4-*sec*-butylidene-2-pyrazolin-5-one (III c) and 4,4′-*sec*-butylidenebis-[1-phenyl-3-methyl-2-pyrazolin-5-one] (II g) being formed. III c is rather unstable at room temperature. The corresponding diethyl compound, III d, is still more unstable and could not be isolated from the reaction between diethylketone and I. Similar to II f, but contrary to II a—e, II g is strongly dissociated into I and III c in solution. The difference in stability between the alkylidene and 1-methylalkylidene compounds (see Fig. 1), may be caused by III a being less stabilized by hyperconjugation and presenting less hindrance towards addition than III b or c (steric and inductive effects).

EXPERIMENTAL

4,4'-Ethylidenebis[1-phenyl-3-methyl-2-pyrazolin-5-one] (II a). Finely divided 1-phenyl-3-methyl-2-pyrazolin-5-one (I), recrystallized from ethyl acetate, (10 g) was dissolved in acetaldehyde (30 ml). On scratching colourless crystals separated. They were collected by filtration and washed with light petroleum. The product was purified by solution in benzene and precipitation with light petroleum, yield 9.3 g. After recrystallization from ethanol (solution in 15 ml at room temperature, crystallization on scratching, yield 8.4 g) it melted at 173° (decomp.). (Found: C 70.3; H 5.9; N 14.9; equiv. wt. 372 on titration in aqueous ethanol with barium hydroxide using phenolphthalein as indicator, 185 on titration in 1,2-diaminoethane with sodium methoxide in benzene-methanol using *o*-nitroaniline as indicator. Calc. for $C_{22}H_{22}N_4O_2$: C 70.6; H 5.9; N 15.0; equiv. wt. 374.4 or 187.)

4,4'-Ethylidenebis[1-phenyl-3-methyl-4-bromo-2-pyrazolin-5-one] (II h). II a (0.97 g) was dissolved in acetic acid, a few pieces of ice were added, and bromine (0.83 g) in acetic acid was poured into the solution. More ice and water precipitated the bromo compound, which was filtered, washed with water and air-dried. Yield: 1.47 g. After one crystallization from ethanol it melted at 119—120° (decomp.). The bromine was split off quantitatively at room temperature by dilute sodium hydroxide solution. (Found: C 49.4; H 3.8; N 10.6; Br 29.9; mol.wt. 520. Calc. for $C_{22}H_{20}N_4O_2Br_2$: C 49.6; H 3.8; N 10.5; Br 30.0; mol.wt. 532.)

4,4'-Propylidenebis[1-phenyl-3-methyl-2-pyrazolin-5-one] (II b). A mixture of 1-phenyl-3-methyl-2-pyrazolin-5-one (6 g) and propionaldehyde (15 ml) was stirred until an almost clear solution was obtained. After filtration the aldehyde was evaporated under reduced pressure and the residue was recrystallized from ether. Yield of colourless crystals: 5.3 g. After recrystallization from ethanol the product melted at 152° (decomp.). (Found: C 71.1; H 6.3; N 14.4; equiv. wt. 386 on titration in ethanol — water with barium hydroxide using phenolphthalein as indicator, 197 on titration in 1,2-diaminoethane with sodium methoxide in benzene-methanol solution using *o*-nitroaniline as indicator. Calc. for $C_{23}H_{24}N_4O_2$: C 71.1; H 6.2; N 14.4; equiv. wt. 388.5 or 194.)

4,4'-Butylidenebis [1-phenyl-3-methyl-2-pyrazolin-5-one] (II c). A mixture of I (6 g) and *n*-butyraldehyde (15 ml) was shaken until an almost clear solution was obtained and was then filtered after addition of ether. In the filtrate colourless crystals separated. More ether was added and the crystals were collected by filtration and washed with ether, yield 5.5 g. After recrystallization from ethanol, the product melted at 145° (decomp.). (Found: C 71.4; H 6.5; N 13.9; equiv. wt. 398 on titration with barium hydroxide using phenolphthalein as indicator. $C_{24}H_{26}N_4O_2$ requires: C 71.6; H 6.5; N 13.9; equiv. wt. 402.5.)

*4,4'-*Iso*butylidenebis[1-phenyl-3-methyl-2-pyrazolin-5-one] (II d)* was prepared from I (6 g) and *iso*butyraldehyde (15 ml) analogously to II c, yield 5.4 g, m.p. 210° (decomp.). (Found: C 71.4; H 6.7 ;N 14.0; equiv. wt. 398 on titration with barium hydroxide solution using phenolphthalein as indicator. $C_{24}H_{26}N_4O_2$ requires: C 71.6; H 6.5; N 13.9; equiv. wt. 402.5.)

4,4'-Heptylidenebis[1-phenyl-3-methyl-2-pyrazolin-5-one] (II e). Heptanal (10.3 g) and I (15.1 g) were stirred overnight. The following day the excess of aldehyde and impurities were extracted with light petroleum. Colourless crystals (19 g) remained. They were recrystallized from ethanol, m.p. 134—135° (decomp.). (Found: C 72.8; H 7.2; N 12.5; equiv. wt. 439 on titration in aqueous ethanol with barium hydroxide (phenolphthalein) and 219 on titration in 1,2-diaminoethane with sodium methoxide in benzene-methanol solution (*o*-nitroaniline). Calc. for $C_{27}H_{32}N_4O_2$: C 72.9; H 7.3; N 12.6; equiv. wt. 445 or 222.)

*1-Phenyl-3-methyl-4-*iso*propylidene-2-pyrazolin-5-one (III b).* This compound has been prepared by a modification of the method of Knorr [8]. Acetone (30 ml) and I (5.0 g) were refluxed overnight. The acetone was then evaporated under reduced pressure, and the 1-phenyl-3-methyl-4-*iso*propylidene-2-pyrazolin-5-one left was recrystallized once from ethanol. Yield: 4.2 g; m.p. 116°. If the product obtained contains traces of II f, it can be purified by extraction with ether at room temperature, filtration of the extract and evaporation of the solvent at reduced pressure.

*1-Phenyl-3-methyl-4-*sec*-butylidene-2-pyrazolin-5-one (III c).* III c was prepared from methylethylketone (35 ml) and I (5.0 g) analogously to III b. Yield: 3.9 g; m.p.

88—89°. (Found: C 73.5; H 7.0; N 12.3. Calc. for $C_{14}H_{16}N_2O$: C 73.7; H 7.1; N 12.3.) The product should be stored in an ice-box.

4,4'-sec-Butylidenebis[1-phenyl-3-methyl-2-pyrazolin-5-one] (II g). I (10 g) was refluxed in methylethylketone (40 ml) for 3 h. The ketone was evaporated under reduced pressure, and the III c formed was extracted with small amounts of ether. The colourless residue (II g) was crystallized once from ethanol, m.p. 106°. Michaelis and Zilg [10] give quite a different m.p., 248°, which is, however, surprisingly high compared to the m.p. of the corresponding *iso*propylidene compound, 138° (Knorr [8]). (Found: C 71.4; H 6.5; N 13.9; O 8.0. Calc. for $C_{24}H_{26}N_4O_2$: C 71.6; H 6.5; N 13.9; O 8.0.)

The analyses were performed by the Department of Analytical Chemistry, University of Lund, or by Mikroanalytisches Laboratorium im Max-Planck-Institut für Kohlenforschung, Mülheim, Germany.

The financial support of *Statens naturvetenskapliga forskningsråd* is gratefully acknowledged.

REFERENCES

1. Moss, M. L., Elliot, J. H. and Hall, R. T. *Anal. Chem.* **20** (1948) 784.
2. Fritz, J. S. *Anal. Chem.* **24** (1952) 674.
3. Pellizzari, G. *Ann.* **255** (1889) 230.
4. Schiedt, B. *J. prakt. Chem.* **157** (1941) 203.
5. Amâl, H. and Özger, A. *Rev. fac. sci. univ. Istanbul* **16A** (1951) 71; *Chem. Abstr.* **46** (1952) 4534b.
6. Westöö, G. *Acta Chem. Scand.* **7** (1953) 355.
7. Fritz, J. S. *Anal. Chem.* **24** (1952) 306.
8. Knorr, L. *Ann.* **238** (1887) 137.
9. Westöö, G. *Acta Chem. Scand.* **7** (1953) 449.
10. Michaelis, A. and Zilg, A. *Ber.* **39** (1906) 370.

Received April 15, 1957.

ACTA CHEMICA SCANDINAVICA 11 (1957) 1290—1297

Studies on *Cyclo*propanes

I. Preparation and Properties of Some Hexasubstituted *Cyclo*propanes

GUNNEL WESTÖÖ

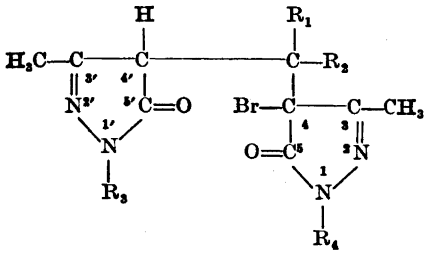
Institute of Organic Chemistry, University of Lund, Lund, Sweden

Alkali salts of 4-bromo-4,4′-*iso*propylidenebis[1-phenyl-3-methyl-2-pyrazolin-5-one] (I a) and related compounds, *e.g.*, I b—f, in solution are rapidly converted to hexasubstituted *cyclo*propanes, II a—f. These *cyclo*propane derivatives under proper conditions isomerize quantitatively to bispyrazolones of the structure III a, b or substituted III a, b, cleavage of the *cyclo*propane ring with migration of a hydrogen atom from a methyl group taking place.

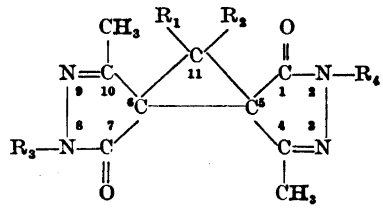
In a preceding paper [1] it was shown that 1,1′,1″-triphenyl-3,3′,3″-trimethyl-4-bromo-[4,4′,4″-ter-2-pyrazoline]-5,5′,5″-trione (IV) splits off hydrogen bromide with formation of furlone yellow (V) in good yield. The isomeric *cyclo*propane derivative was not detected among the reaction products and could only have been formed in a small amount, in spite of the fact that the analogous reaction between *e.g.*, 1-phenyl-3,4-dimethyl-4-bromo-2-pyrazolin-5-one and 1-phenyl-3,4-dimethyl-2-pyrazolin-5-one takes place with formation of a C—C bond, 1,1′-diphenyl-3,3′-dimethyl-[4,4′-bi-2-pyrazoline]-5,5′-dione being formed [2]. Besides for steric reasons, the non-appearance of a carbon-carbon coupling in the case of IV may be caused by a lack of electrons in the 4 and 4″ positions.

Experiments have now been performed to investigate whether an exchange of the second pyrazolonylidene group in IV for small, electron-releasing groups will cause formation of substituted *cyclo*-alkanes. Preparations of *cyclo*propane derivatives by ring closure of halogen compounds having an active hydrogen atom in the γ-position of the halogen atom have been described by several authors [3-5].

The sodium salt of 4-bromo-4,4′-*iso*propylidenebis[1-phenyl-3-methyl-2-pyrazolin-5-one] (I a) could be prepared by a Michael addition of the sodium salt of 1-phenyl-3-methyl-4-bromo-2-pyrazolin-5-one to 1-phenyl-3-methyl-4-*iso*propylidene-2-pyrazolin-5-one (VI a) in ethanol solution (equilibrium reaction, *cf.* Westöö [1, 6, 7]). The addition compound rapidly splits off sodium bromide with formation of a neutral product of the empirical formula $C_{23}H_{22}N_4O_2$.

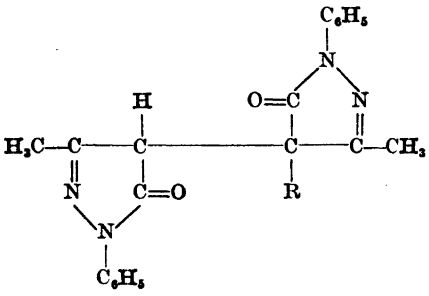


I

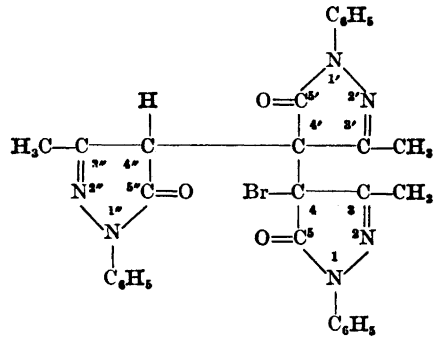


II

a. $R_1 = R_2 = CH_3$; $R_3 = R_4 = C_6H_5$.
b. $R_1 = R_2 = CH_3$; $R_3 = C_6H_5$; $R_4 = p\text{-}CH_3C_6H_4$.
c. $R_1 = R_2 = CH_3$; $R_3 = C_6H_5$; $R_4 = p\text{-}BrC_6H_4$.
d. $R_1 = CH_3$; $R_2 = C_2H_5$; $R_3 = R_4 = C_6H_5$.
e. $R_1 = CH_3$; $R_2 = C_2H_5$; $R_3 = C_6H_5$; $R_4 = p\text{-}CH_3C_6H_4$.
f. $R_1 = CH_3$; $R_2 = C_2H_5$; $R_3 = C_6H_5$; $R_4 = p\text{-}BrC_6H_4$.

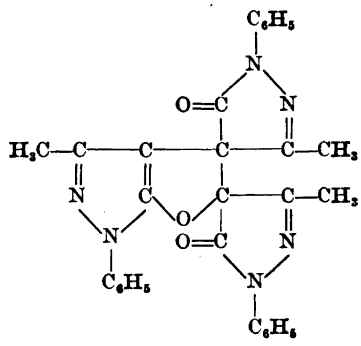


III

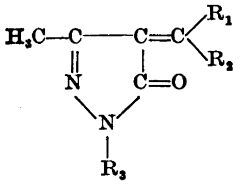


IV

a. R = $-C(=CH_2)-CH_3$
b. R = $-C(=CH_2)-C_2H_5$
c. R = $-C(Cl)(CH_3)-CH_3$
(d. R = $-C(=CHCH_3)-CH_3$)

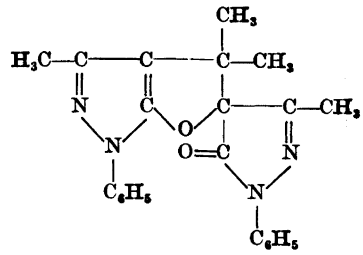


V



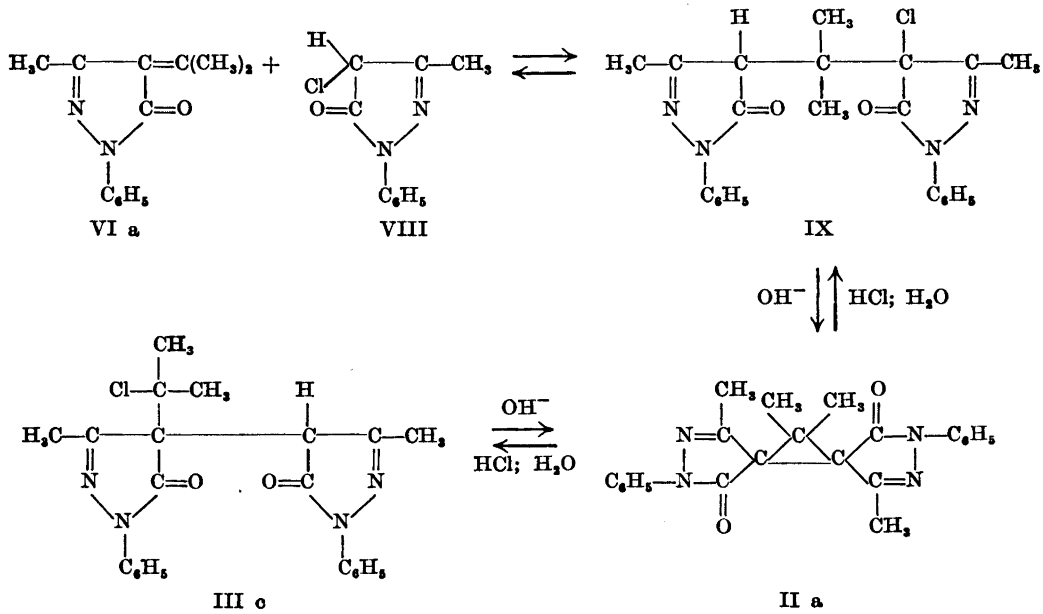
VI

a. $R_1 = R_2 = CH_3$; $R_3 = C_6H_5$.
b. $R_1 = R_2 = CH_3$; $R_3 = p\text{-}BrC_6H_4$.
c. $R_1 = CH_3$; $R_2 = C_2H_5$; $R_3 = C_6H_5$.



(VII)

From the two possible structures of $C_{23}H_{22}N_4O_2$, II a and VII, VII may be excluded, for after addition of hydrogen chloride to a benzene solution of the product, 1,1′-diphenyl-3,3′-dimethyl-4-(1-chloro-1-methylethyl)-[4,4′-bi-2-pyrazoline]-5,5′-dione (III c) could be isolated in good yield. The dissociation products of 4-chloro-4,4′-*iso*propylidenebis[1-phenyl-3-methyl-2-pyrazolin-5-one] (IX), *viz.* VI a and VIII, were also formed. Dilute alkali splits off hydrogen chloride from III c, the main reaction being ring closure with reformation of II a (Scheme 1). Thus the structure of $C_{23}H_{22}N_4O_2$ is 2,8-diphenyl-4,10,11,11-tetramethyl-2,3,8,9-tetrazadispiro[4.0.4.1]undeca-3,9-diene-1,7-dione (II a). The formation of the *trans* isomer is most probable, but the existence of the *cis* isomer cannot be excluded.



Scheme 1.

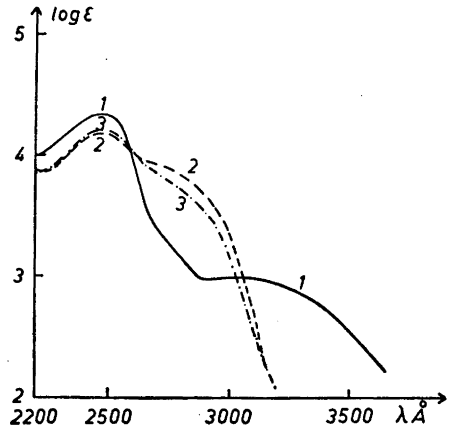


Fig. 1. UV absorption in ethanol of 1) II a, 2) III a, 3) III c.

A bromo derivative of II a, II c, has been prepared in two different ways a) by addition of the sodium salt of 1-*p*-bromophenyl-3-methyl-4-bromo-2-pyrazolin-5-one to 1-phenyl-3-methyl-4-*iso*propylidene-2-pyrazolin-5-one (VI a) and b) by addition of the sodium salt of 1-phenyl-3-methyl-4-bromo-2-pyrazolin-5-one to 1-*p*-bromophenyl-3-methyl-4-*iso*propylidene-2-pyrazolin-5-one (VI b). The identity of the compounds obtained was demonstrated by UV and IR absorption measurements and affords another indication of the *cyclo*propane structure of II.

When boiled with ethanol for a few minutes or when left in acetone or alcohol solution at room temperature for some days, II a is quantitatively isomerized to a monobasic acid, for which the structure 1,1′-diphenyl-3,3′-dimethyl-4-*iso*propenyl-[4,4′-bi-2-pyrazoline]-5,5′-dione (III a) is proposed. The acid is stable towards hydrogen chloride and presents an UV absorption curve similar to the corresponding curve of 1,1′-diphenyl-3,3′-dimethyl-[4,4′-bi-2-pyrazoline]-5,5′-dione [2]. The existence of a $CH_2{=}C$ group in the acidic isomer was demonstrated by the method of Bricker and Roberts [8].

A total of five derivatives of II a have been synthesized, *viz.* II b—f. Their UV absorption curves are almost identical with the curve of II a. According to various authors [9–13] the IR spectra of *cyclo*propane derivatives contain a ring deformation band at 1 000—1 050 cm^{-1}. The spectra of II a—f show absorption at the long wave limit of this region. The steric arrangement of the groups in II b-f has not been investigated.

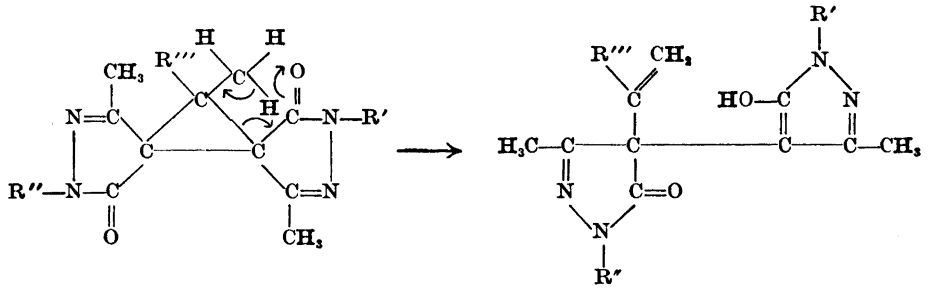
II b and c, like II a, when heated in dry state or in solution for a short time or when kept in solution at room temperature for some days, undergo ring cleavage with a hydrogen shift from one of the methyl groups attached to the *cyclo*propane ring to the 4 position of one of the pyrazolone rings. The para substituents do not appreciably affect the rate of isomerization. In acetone-ethanol solution (1:1, v/v) at 25° the monomolecular rate constants were found to be for II a 9.8×10^{-4}, for II b 9.6×10^{-4} and for II c 9.95×10^{-4}. In the case of II b and c two isomeric acids, e.g., 1-phenyl-1′-*p*-tolyl-3,3′-dimethyl-4-*iso*propenyl-[4,4′-bi-2-pyrazoline]-5,5′-dione and 1-phenyl-1′-*p*-tolyl-3,3′-di-

methyl-4′-*iso*propenyl-[4,4′-bi-2-pyrazoline]-5,5′-dione, can be formed. The rate constants indicate that about equal amounts of the two isomers are obtained. The mixtures have not been resolved.

2,8-Diphenyl-11-ethyl-4,10,11-trimethyl-2,3,8,9-tetrazadispiro[4.0.4.1]undeca-3,9-diene-1,7-dione, II d, and its *p*-methyl and *p*-bromo derivatives, II e and f, isomerize with formation of acids under the same conditions as II a—c, though with greater ease. The monomolecular rate constants of the isomerization in acetone-ethanol solution (1:1, v/v) at 25° are for II d 1.36×10^{-3}, for II e 1.25×10^{-3} and for II f 1.35×10^{-3}.

For the isomerization product of II d there are two possible structures, III b and d. A test of end unsaturation [8] was positive. A determination of the amount of C-methyl gave the same value as for III a. Accordingly 1,1′-diphenyl-3,3′-dimethyl-4-(1-ethylvinyl)-[4,4′-bi-2-pyrazoline]-5,5′-dione, III b, is the correct structure of the acid.

The isomerizations take place also in solvents like benzene which cannot supply protons for addition to the carbonyl groups. The acids formed during the reactions have no influence on the rates. An intramolecular rearrangement seems plausible (Scheme 2).



Scheme 2.

EXPERIMENTAL

1-p-Bromophenyl-3-methyl-4-isopropylidene-2-pyrazolin-5-one (VI b). This product was prepared in the same way as 1-phenyl-3-methyl-4-*iso*propylidene-2-pyrazolin-5-one (VI a) (Westöö [7]). M.p. 155° (decomp.). (Found: C 53.3; H 4.5; Br 27.21; N 9.6; O 5.6. Calc. for $C_{13}H_{13}BrN_2O$: C 53.3; H 4.5; Br 27.26; N 9.6; O 5.5.)

2,8-Diphenyl-4,10,11,11-tetramethyl-2,3,8,9-tetrazadispiro[4.0.4.1]undeca-3,9-diene-1,7-dione (II a). 1-Phenyl-3-methyl-4-bromo-2-pyrazolin-5-one (2.16 g) was dissolved in an equivalent amount of N sodium hydroxide solution (7.2 ml) and ethanol (25 ml) at room temperature and immediately poured into a solution of 1.83 g of 1-phenyl-3-methyl-4-*iso*propylidene-2-pyrazolin-5-one (VI a) in ethanol (100 ml). Almost colourless crystals of II a separated. After 3—4 h the precipitate (2.32 g) was filtered, washed with ethanol and water and air-dried. The combined filtrate and washings were left overnight when another 0.51 g of II a separated. Both products were pure, yield 2.83 g. (Found: C 71.4; H 5.8; N 14.5; mol.wt. 379 (freezing point depression of benzene solutions). Calc. for $C_{23}H_{22}N_4O_2$: C 71.5; H 5.7; N 14.5; mol.wt. 386.) No sharp melting point was obtained because the compound isomerized into III a on heating. The solid product is stable at room temperature. For UV absorption curve, see Fig. 1.

2-p-Bromophenyl-8-phenyl-4,10,11,11-tetramethyl-2,3,8,9-tetrazadispiro[4.0.4.1]undeca-3,9-diene-1,7-dione (II c). a) 1-*p*-Bromophenyl-3-methyl-4-bromo-2-pyrazolin-5-one (crude product) was dissolved in ethanol (25 ml) and the equivalent amount of 2.5 N sodium hydroxide solution, and was then immediately poured into a solution of 1.81 g

of 1-phenyl-3-methyl-4-*iso*propylidene-2-pyrazolin-5-one (VI a) in ethanol (125 ml). After a few minutes II c started separating. When the separation was complete, the crystals were filtered and washed with ethanol and water, yield 4.42 g. (Found: C 59.2; H 4.55; Br 17.26; N 12.0; O 7.0. Calc. for $C_{23}H_{21}BrN_4O_2$: C 59.4; H 4.55; Br 17.17; N 12.0; O 6.9.)

b) II c was also prepared from 1-phenyl-3-methyl-4-bromo-2-pyrazolin-5-one and 1-*p*-bromophenyl-3-methyl-4-*iso*propylidene-2-pyrazolin-5-one (VI b) in the same way as described above. Analyses, UV and IR absorption curves were identical for the product obtained here and the one obtained according to a).

2-Phenyl-8-p-tolyl-4,10,11,11-tetramethyl-2,3,8,9-tetrazadispiro[4.0.4.1]undeca-3,9-diene-1,7-dione (II b). 1-Phenyl-3-methyl-4-*iso*propylidene-2-pyrazolin-5-one (8.32 g) was dissolved in ethanol (600 ml). Hydrobromide of 1-*p*-tolyl-3-methyl-4-bromo-2-pyrazolin-5-one (13.55 g of crude product) in ethanol (30 ml) was neutralized with 2.5 N sodium hydroxide solution using thymolphthalein as indicator and immediately poured into the above solution. The II b formed was filtered and washed with ethanol and water, yield 13.4 g, m.p. about 125° (decomp.). (Found: C 72.0; H 6.0; N 13.9. Calc. for $C_{24}H_{24}N_4O_2$: C 72.0; H 6.0; N 14.0.)

2,8-Diphenyl-11-ethyl-4,10,11-trimethyl-2,3,8,9-tetrazadispiro[4.0.4.1]undeca-3,9-diene-1,7-dione (II d). 1-Phenyl-3-methyl-4-bromo-2-pyrazolin-5-one (9.7 g) was dissolved in the equivalent amount of 1.63 N ethanolic piperidine (23.6 ml). The solution was immediately poured into a solution of 1-phenyl-3-methyl-4-*sec*-butylidene-2-pyrazolin-5-one [7] (VI c) (10 g) in ethanol (125 ml). On scratching II d started separating. After 4 h the precipitate was filtered and washed with ethanol and water, yield 7.5 g. (Found: C 71.9; H 6.1; N 14.1. Calc. for $C_{24}H_{24}N_4O_2$: C 72.0; H 6.0; N 14.0.)

2-Phenyl-8-p-tolyl-11-ethyl-4,10,11-trimethyl-2,3,8,9-tetrazadispiro[4.0.4.1]undeca-3,9-diene-1,7-dione (II e) and 2-p-bromophenyl-8-phenyl-11-ethyl-4,10,11-trimethyl-2,3,8,9-tetrazadispiro[4.0.4.1]undeca-3,9-diene-1,7-dione (II f). II e and f were prepared analogously to II d from 1-phenyl-3-methyl-4-*sec*-butylidene-2-pyrazolin-5-one and 1-*p*-tolyl-3-methyl-4-bromo-2-pyrazolin-5-one or 1-*p*-bromophenyl-3-methyl-4-bromo-2-pyrazolin-5-one. (Found for II e: C 72.2; H 6.3; N 13.6. Calc. for $C_{25}H_{26}N_4O_2$: C 72.4; H 6.3; N 13.5. Found for II f: C 60.0; H 5.0; Br 16.65; N 11.7. Calc. for $C_{24}H_{23}BrN_4O_2$: C 60.1; H 4.8; Br 16.67; N 11.7.)

Addition of hydrogen chloride to $C_{23}H_{22}N_4O_2$ (neutral isomer). A solution of $C_{23}H_{22}N_4O_2$ in benzene was cooled in ice, and dry hydrogen chloride was passed into the solution for 15 min. After removal of the benzene under reduced pressure, the residue was dissolved in ethanol and precipitated with water, filtered, washed with water and air-dried. A yellow product was obtained.

When sodium acetate solution and a small amount of cupric sulphate were added to the filtrate, pyrazole blue precipitated, indicating the presence of 1-phenyl-3-methyl-4-chloro-2-pyrazolin-5-one.

With light petroleum at room temperature 1-phenyl-3-methyl-4-*iso*propylidene-2-pyrazolin-5-one could be extracted from the yellow, solid mixture. After recrystallization from ethanol, it melted at 116° alone and mixed with authentic 1-phenyl-3-methyl-4-*iso*propylidene-2-pyrazolin-5-one.

It is evident that a hydrochloride of 4-chloro-4,4'-*iso*propylidenebis[1-phenyl-3-methyl-2-pyrazolin-5-one] is primarily formed from part of the $C_{23}H_{22}N_4O_2$, and that it is decomposed into hydrogen chloride, 1-phenyl-3-methyl-4-chloro-2-pyrazolin-5-one and 1-phenyl-3-methyl-4-*iso*propylidene-2-pyrazolin-5-one on addition of ethanol and water. As this chlorobispyrazolone is a minor part of the addition product, VII can not be the structure of $C_{23}H_{22}N_4O_2$. (According to light absorption measurements the mixture obtained contained about 20 % of 1-phenyl-3-methyl-4-*iso*propylidene-2-pyrazolin-5-one, corresponding to about 35 % cleavage of the C_5-C_6 bond of II a).

The main addition compound, which was not extracted by the light petroleum, was an almost colourless, acidic product. For UV curve see Fig. 1. (Found: C 65.3; H 5.6; Cl 8.29; N 13.15. Calc. for $C_{23}H_{23}ClN_4O_2$: C 65.3; H 5.5; Cl 8.38; N 13.25.) On addition of dilute alkali, the product split off hydrogen chloride with formation of the original 3-ring in about 75 % yield. The acidity of the addition product, its slight solubility in light petroleum and easy ring closure together with the lack of oxidative power (*cf.* Westöö [14]) show that the product is 1,1'-diphenyl-3,3'-dimethyl-4-(1-chloro-1-methylethyl)-[4,4'-bi-2-pyrazoline]-5,5'-dione (III c).

Isomerization of II a into 1,1'-diphenyl-3,3'-dimethyl-4-isopropenyl-[4,4'-bi-2-pyrazoline]-5,5'-dione (III a). II a (1.35 g) was boiled in ethanol (30 ml) until about 15 ml remained (30 min). On cooling colourless crystals separated (1.20 g). They were filtered, washed with cold ethanol and air-dried, m.p. 201° (decomp.). (Found: C 71.5; H 5.7; N 14.6; O 8.3; equiv.wt. 384. Calc. for $C_{23}H_{22}N_4O_2$: C 71.5; H 5.7; N 14.5; O 8.3; equiv.wt. 386). The existence of $CH_2=$ in the molecule was demonstrated by the method of Bricker and Roberts [8], though only qualitatively. A quantitative determination did not succeed. For UV absorption curve, see Fig. 1.

When a weighed amount of II a was boiled in excess of ethanol for 5 min, cooled and titrated with barium hydroxide solution using thymolphthalein as indicator, the consumption of base corresponded to a quantitative isomerization into 1,1'-diphenyl-3,3'-dimethyl-4-*iso*propenyl-[4,4'-bi-2-pyrazoline]-5,5'-dione (III a). The same isomerization took place in a couple of days at room temperature in acetone or acetone-ethanol solution. Heating of solid II a at 140° for one hour also gave III a together with degradation products.

1,1'-Diphenyl-3,3'-dimethyl-4-isopropenyl-4'-bromo-[4,4'-bi-2-pyrazoline]-5,5'-dione. Because the mol.wt. of III a could not be determined on account of the slight solubility in benzene and glacial acetic acid of the product, the 4-bromo derivative was prepared for mol.wt. determination.

III a (0.80 g) was dissolved in acetic acid. A few pieces of ice were added, and bromine (0.34 g) in acetic acid was dropped into the solution. More ice and water precipitated the reaction product, which was filtered, washed with water and air-dried. The 4-bromobispyrazolone was isolated by solution of the mixture obtained in acetic acid and dropwise addition of water until yellow crystals started separating. The solution was then cooled in ice and the crystals formed were filtered and washed with dilute acetic acid and water. The product could be recrystallized from acetic acid. (Found: C 59.1; H 4.6; Br 17.3; N 11.9; mol.wt. 455. Calc. for $C_{23}H_{21}BrN_4O_2$: C 59.35; H 4.6; Br 17.2; N 12.0; mol.wt. 465.)

Isomerization of II d to form 1,1'-diphenyl-3,3'-dimethyl-4-(1-ethylvinyl)-[4,4'-bi-2-pyrazoline]-5,5'-dione (III b). II d (1.18 g) was refluxed in ethanol (10 ml) for 15 min. On cooling and scratching colourless crystals separated (0.92 g), m.p. 188° (decomp.). (Found: C 72.0; H 6.0; N 14.0; equiv.wt. 400. Calc. for $C_{24}H_{24}N_4O_2$: C 72.0; H 6.0; N 14.0; equiv.wt. 400.)

For the acid formed there are two possible structures, III b and d. A qualitative test of end unsaturation according to Bricker and Roberts [8] was positive, thus supporting the formula III b. Furthermore, a determination of C-methyl on this product and on III a gave in both cases 10.1 %. III a requires 11.7 %, III b 11.3 % and III d 15.0 %. Accordingly III b must be the structure of the acid.

Isomerization of II b, c, e and f. The mono-*p*-methyl and mono-*p*-bromo derivatives, II b, c, e and f, could be isomerized by boiling them in ethanol or by keeping their solutions in acetone or acetone-ethanol at room temperature for some days. Two isomeric acids can be formed in each case, *e.g.*, from II c 1-phenyl-1'-*p*-bromophenyl-3,3'-dimethyl-4-*iso*propenyl-[4,4'-bi-2-pyrazoline]-5,5'-dione and 1-phenyl-1'-*p*-bromophenyl-3,3'-dimethyl-4'-*iso*propenyl-[4,4'-bi-2-pyrazoline]-5,5'-dione. They have not been separated.

Reaction rates of the isomerizations. About 2 g of the *cyclo*propane derivatives were dissolved in 250 ml of acetone (25 ml) and so much commercial, anhydrous ethanol (warmed to 39° to compensate the decrease of temperature when the solvents are mixed) was added that the total volumes were 500 ml at 25.0°. The solutions were placed in a thermostat at 25.00°±0.05°. At intervals samples of 50.0 ml were titrated with barium hydroxide solution using thymophthalein as indicator. The constants were calculated from the moment when the first sample was titrated.

The analyses were performed by the Department of Analytical Chemistry, University of Lund, or by Mikroanalytisches Laboratorium im Max-Planck-Institut für Kohlenforschung, Mülheim, Germany.

The financial support of *Statens naturvetenskapliga forskningsråd* is gratefully acknowledged.

REFERENCES

1. Westöö, G. *Acta Chem. Scand.* **7** (1953) 360.
2. Westöö, G. *Acta Chem. Scand.* **7** (1953) 352.
3. Cloke, J. B., Stehr, E., Steadman, T. R. and Westcott, L. C. *J. Am. Chem. Soc.* **67** (1945) 1587.

4. Radulescu, D. and Georgescu, V. *Bull. soc. chim. France* [4] **37** (1925) 187.
5. Prelog, V., Bauer, W., Cookson, G. H. and Westöö, G. *Helv. Chim. Acta* **34** (1951) 736.
6. Westöö, G. *Acta Chem. Scand.* **7** (1953) 355.
7. Westöö, G. *Acta Chem. Scand.* **11** (1957) 1285.
8. Bricker, C. E. and Roberts, K. H. *Anal. Chem.* **21** (1949) 1331.
9. Derfer, J. M., Pickett, E. E. and Boord, C. E. *J. Am. Chem. Soc.* **71** (1949) 2482.
10. Slabey, V. A. *J. Am. Chem. Soc.* **76** (1954) 3604.
11. Wiberley, S. E. and Bunce, S. C. *Anal. Chem.* **24** (1952) 623.
12. Bridson-Jones, F. S., Buckley, G. D., Cross, L. H. and Driver, A. P. *J. Chem. Soc.* **1951** 2999.
13. Bridson-Jones, F. S. and Buckley, G. D. *J. Chem. Soc.* **1951** 3009.
14. Westöö, G. *Acta Chem. Skand.* **6** (1952) 1499.

Received April 15, 1957.

ACTA CHEMICA SCANDINAVICA 11 (1957) 1298—1307

*iso*Thiocyanates XXVI*. Straight-Chain ω-Methylthioalkyl *iso*Thiocyanates and some Derivatives

ANDERS KJÆR and BO CHRISTENSEN

Chemical Laboratory of the University of Copenhagen, Denmark

The occurrence in plants of straight-chain compounds, containing a methylthio-grouping in terminal position, is briefly surveyed. Special attention is given to a number of *iso*thiocyanates of this general type encountered in Nature.

The preparation as well as properties of the homologous series, $CH_3S(CH_2)_nNCS$, with values of n ranging from two to nine, are reported, together with the corresponding thiourea-derivatives resulting from interaction of the *iso*thiocyanates with ammonia and benzylamine (Tables 1, 2 and 3).

The ω-methylthioalkylamines, (XXI), serving as intermediates in the syntheses of the mustard oils, are produced by varying methods and characterized as crystalline thiourea-derivatives formed upon reaction with phenyl *iso*thiocyanate (Table 4).

Comparison of a synthetic specimen of 1-benzyl-3-(9-methylthiononyl)-urea, (XXIII), with a product directly derivable from the *Arabis* mustard oil, on which we recently reported [16], establishes beyond doubt the proposed structure of the latter as (−)-9-methylsulphinylnonyl *iso*thiocyanate (XI).

The biosynthetic origin of the methylthio-grouping in natural products is briefly discussed.

About fifty years ago, Schneider isolated the *iso*thiocyanates cheirolin [1] (I) and erysolin [2] (II) from seeds of the crucifers *Cheiranthus cheiri* L. and *Erysimum Perofskianum* Fisch. *et* M.**, respectively. The structural analogy of cheirolin and methionine was commented upon by Barger and Coyne [3] in 1928 when these authors first announced the structure and synthesis of the new amino acid. Since then, an additional number of straight-chain compounds, having a terminally located methylthio-grouping in common, has been recognized in Nature. Thus, 3-methylthiopropanol (III), a constituent of soya-sauce [4], methyl 3-methylthiopropionate (IV), present in the essential oil of pineapple [5], and the adenylthiomethylpentose recognized in yeast many years ago (*cf.* Ref.[6]), all belong to this structural type.

* Part XXV of this series: *Acta Chem.Scand.* 11 (1957) 577.

** Thus far, it has not been possible in this laboratory to confirm the occurrence of an erysoline glucoside in this or other botanical species.

$CH_3S(O)(CH_2)_nNCS$

I: n = 3
II: n = 4

$CH_3SCH_2CH_2CH_2OH$ III

$CH_3SCH_2CH_2COOCH_3$ IV

$CH_3S(O)CH_2CH(NH_2)COOH$ V

$CH_3SCH_2CH(NH_2)COOH$ VI

$CH_3SCH=CHCOOH$ VII

Other examples can be adduced from more recent work. Independently, Synge and Wood [7] and Morris and Thompson [8] announced the discovery of (+)-S-methyl-L-cysteine sulphoxide (V) in various crucifers, a finding recently supplemented by the discovery also of the corresponding S-methyl-L-cysteine (VI) as a constituent of higher plants [9]. The stereoisomeric 3-methylthioacrylic acids (VII), demonstrated by Stoll *et al.* [9a] to occur as the acid moieties of two esters present in rhizomes of *Petasites officinalis* Moench, also deserve attention in this connexion.

Besides (I) and (II), a number of straight-chain *iso*thiocyanates, carrying a terminal methylthio grouping as such or oxidized to the sulphoxide stage, has been encountered in various members of the family *Cruciferae*. Thus, Schmid and Karrer [10] established the structure (VIII) for sulphoraphene, derivable from a glucoside in radish seeds, whereas Schultz and Gmelin [11] assigned the formula (IX) to a mustard oil enzymically liberated from an analogous glucoside in seeds of *Iberis amara* L. In this laboratory, 3-methylthiopropyl [12] (XIII), 4-methylthiobutyl [13] (XIV) and 5-methylthiopentyl [14] (XV) *iso*thiocyanates have been established as products of enzymic hydrolysis of glucosides present, *inter alia*, in seeds of *Iberis sempervirens* L., *Eruca sativa* Mill. and *Berteroa incana* (L.) DC., respectively. More recently, we have proved also the existence in Nature of glucosides corresponding to the *levo*rotatory sulphoxide *iso*thiocyanates, (X)—(XII), *viz.* in seeds of *Alyssum argenteum* Vitm.[15], *Arabis alpina* L.[16] and *Camelina sativa* (L.) Crantz [17], respectively. It appears likely that these sulphoxides should be regarded as secondary products, biogenetically deriving from the corresponding 5-methylthiopentyl (XV), 9-methylthiononyl (XIX) and 10-methylthiodecyl (XX) *iso*thiocyanates.

$CH_3S(O)CH=CHCH_2CH_2NCS$ VIII

$CH_3S(O)(CH_2)_nNCS$

IX : n = 3
X : n = 5
XI : n = 9
XII: n = 10

$CH_3S(CH_2)_nNCS$

XIII: n = 3
XIV: n = 4
XV : n = 5
XVI: n = 6
XVII : n = 7
XVIII: n = 8
XIX : n = 9
XX : n = 10

On this background, and for various other reasons, it became desirable to have at disposal the individual mustard oils of the general series $CH_3S(CH_2)_n$-NCS, with values of *n* ranging from two to nine. The present paper records the

Table 1. ω-Methylthioalkyl *iso*thiocyanates, $CH_3S(CH_2)_nNCS$.

n	Formula	B.p.	mm Hg	n_D^{25}	Analyses					
					Carbon		Hydrogen		Nitrogen	
					Found	Calc.	Found	Calc.	Found	Calc.
2[a]	$C_4H_7NS_2$	85	2	1.5767	36.00	36.07	5.18	5.30	10.66	10.52
3[b]	$C_5H_9NS_2$	121	12	1.5610	40.35	40.77	5.98	6.16	9.64	9.51
4[c]	$C_6H_{11}NS_2$	136[d]	12	1.5518	44.59	44.68	6.75	6.87	8.54	8.69
5[e]	$C_7H_{13}NS_2$	155	10	1.5422	48.25	47.97	7.51	7.48	8.09	7.99
6	$C_8H_{15}NS_2$	119	0.5	1.5336	50.75	50.77	7.76	7.94	7.43	7.40
7	$C_9H_{17}NS_2$	117	0.3	1.5274	53.50	53.16	8.41	8.43	6.82	6.89
8	$C_{10}H_{19}NS_2$	122	0.3	1.5242	55.25	55.25	8.46	8.81	6.50	6.45
9	$C_{11}H_{21}NS_2$	130	0.2	1.5189	56.95	57.10	9.09	9.15	6.05	6.05

[a] Apparently, Weller *et al.*[17] synthesized this compound, yet without presenting any physical or analytical data for the mustard oil. [b] *cf.* Ref.[13]. [c] *cf.* Ref.[13]. [d] Reported b.p. 130–140°/9 mm[26]. [e] *cf.* Ref.[14].

preparation and properties of these *iso*thiocyanates, together with data for the thiourea-derivatives formed upon their reactions with ammonia and benzylamine. For particular reasons, the symmetric *bis*-(ω-methylthioalkyl)-thioureas, wherein the alkyl represents hexyl, heptyl, octyl, and nonyl, have also been synthesized. In general, the *iso*thiocyanates, (XIII)–(XIX), were produced from the corresponding amines by reaction with thiocarbonyl chloride in a slightly modified version of the traditional reaction. They all distilled as colourless, pungent oils possessing a characteristic taste and odour, reminiscent

Table 2. N-(ω-Methylthioalkyl)-thioureas, $CH_3S(CH_2)_nNHCSNH_2$.

n	Formula	M.p.°	Analyses					
			Carbon		Hydrogen		Nitrogen	
			Found	Calc.	Found	Calc.	Found	Calc.
2	$C_4H_{10}N_2S_2$	68	32.15	31.96	6.72	6.71	18.70	18.64
3[a]	$C_5H_{12}N_2S_2$	66–67[b]	36.60	36.55	7.30	7.36	16.98	17.06
4[c]	$C_6H_{14}N_2S_2$	53[d,e]	40.38	40.41	7.90	7.91	15.80	15.72
5[f]	$C_7H_{16}N_2S_2$	67.5[e]	43.70	43.71	8.22	8.39	14.35	14.57
6	$C_8H_{18}N_2S_2$	73	46.55	46.56	8.93	8.79	13.35	13.58
7	$C_9H_{20}N_2S_2$	79	49.20	49.05	9.09	9.15	12.55	12.71
8	$C_{10}H_{22}N_2S_2$	76	51.30	51.24	9.34	9.46	11.86	11.95
9	$C_{11}H_{24}N_2S_2$	88	53.07	53.10	9.74	9.81	11.28	11.08

[a] *cf.* Ref.[12]. [b] Recrystallized from a mixture of ethyl acetate and pentane. [c] *cf.* Ref.[13]. [d] Reported[26] m.p. 55–56°. [e] Recrystallized from a mixture of chloroform and pentane. [f] *cf.* Ref.[14].

Table 3. 1-Benzyl-3-(ω-methylthioalkyl)-2-thioureas, $C_6H_5CH_2NHCSNH(CH_2)_nSCH_3$.

n	Formula	M.p.°	Analyses					
			Carbon		Hydrogen		Nitrogen	
			Found	Calc.	Found	Calc.	Found	Calc.
2	$C_{11}H_{16}N_2S_2$	59[a]	55.05	54.96	6.56	6.71	11.53	11.65
3	$C_{12}H_{18}N_2S_2$	57	56.77	56.65	6.93	7.13	11.07	11.02
4[b]	$C_{13}H_{20}N_2S_2$	77–78[c]	58.25	58.15	7.55	7.51	10.45	10.44
5[d]	$C_{14}H_{22}N_2S_2$	56–57	59.45	59.54	8.06	7.85	9.97	9.92
6	$C_{15}H_{24}N_2S_2$	45	60.80	60.79	7.96	8.16	9.40	9.45
7	$C_{16}H_{26}N_2S_2$	64	61.85	61.90	8.34	8.44	8.95	9.02
8	$C_{17}H_{28}N_2S_2$	59	63.00	62.92	8.50	8.70	8.49	8.63
9	$C_{18}H_{30}N_2S_2$	73	63.86	63.87	9.01	8.93	8.18	8.28
10[e]	$C_{19}H_{32}N_2S_2$	73	65.10	64.73	9.06	9.15	8.00	7.95

[a] Crystallization of this previously described derivative[27] could be induced only after seeding with crystalline material (m.p. 58°), kindly placed at our disposal by Dr. H. M. Sell. [b] *cf.* Ref.[13]. [c] Recrystallized from a mixture of ethyl acetate and pentane. [d] *cf.* Ref.[15]. [e] *cf.* Ref.[17].

of those of fresh radish root. Physical and analytical data for the mustard oils are presented in Table 1, whereas the two series of thioureas are summarized in Tables 2 and 3. For the sake of completeness a few compounds, recorded in previous papers in this series, are included.

The requisite ω-methylthioalkylamines (XXI), whence the mustard oils derive, were synthesized by a number of different routes as briefly outlined in the sequel. 2-Methylthioethylamine (XXI, n = 2), the lowest member of the series, was obtained from ethyleneimine and methanethiol according to Wie-

Table 4. 1-Phenyl-3-(ω-methylthioalkyl)-2-thioureas, $C_6H_5NHCSNH(CH_2)_nSCH_3$.

n	Formula	M.p.°	Analyses					
			Carbon		Hydrogen		Nitrogen	
			Found	Calc.	Found	Calc.	Found	Calc.
2	$C_{10}H_{14}N_2S_2$	94	53.15	53.05	6.46	6.23	12.30	12.38
3	$C_{11}H_{16}N_2S_2$	87–88	54.90	54.96	6.60	6.71	11.87	11.65
4	$C_{12}H_{18}N_2S_2$	48–49[a]	56.84	56.65	7.03	7.13	11.04	11.02
5	$C_{13}H_{20}N_2S_2$	67	58.31	58.15	7.45	7.51	10.68	10.44
6	$C_{14}H_{22}N_2S_2$	55	59.46	59.54	7.82	7.85	9.83	9.92
7	$C_{15}H_{24}N_2S_2$	55.5	60.76	60.79	8.25	8.16	9.50	9.45
8	$C_{16}H_{26}N_2S_2$	57–58	61.73	61.90	8.37	8.44	9.26	9.02
9	$C_{17}H_{28}N_2S_2$	44	62.90	62.92	8.59	8.70	8.78	8.63

[a] Reported as an oil by Schmid and Karrer [26].

land *et al.*[18] The synthesis of the following two homologues, (XXI, n = 3 and 4) was accomplished by lithium aluminium hydride reduction of the corresponding nitriles, as described in earlier papers from this laboratory [19, 20]. Again, details on the preparation of 5-methylthiopentylamine (XXI, n = 5) were presented in a previous memoir [14] of this series *. 6-Chlorohexanol was readily transformed into 6-methylthiohexanol, and the latter, in turn, into 6-chlorohexyl methyl sulphide which served as a common intermediate for the syntheses of 6-methylthiohexylamine (XXI, n = 6), *via* N-(6-methylthiohexyl)-phthalimide, and 7-methylthioheptylamine (XXI, n = 7), the latter resulting from lithium aluminium hydride reduction of 7-methylthioheptanenitrile. This, in turn, was accessible from the above chlorosulphide by employing the general conditions developed by Brändström [22] for the synthesis of organic cyanides. 1,8-Octanediol was converted into its chlorohydrin as described elsewhere [23, 24]. Again, the further transformations into 8-methylthiooctanol and 8-chloro-octyl methyl sulphide were accomplished according to established methods [25]. The latter intermediate was processed to N-(8-methylthiooctyl)-phthalimide and 8-methylthiooctylamine (XXI, n = 8) in straight-forward reactions. Essentially the same procedure was employed in the preparation of 9-methylthiononylamine (XXI, n = 9), characterized as its N-benzoyl derivative, from N-(9-methylthiononyl)-phthalimide and the previously known 9-chlorononyl methyl sulphide [25]. For the purpose of characterization, the whole series of amines was converted into crystalline phenylthioureas upon reaction with phenyl *iso*thiocyanate. The properties of these derivatives are recorded in Table 4.

$CH_3S(CH_2)_nNH_2$ XXI

$CH_3S(CH_2)_9NHCXNHCH_2C_6H_5$ XXII : X = S; XXIII: X = O

The preparation of the thioureas, summarized in Tables 2 and 3, calls for no comments. It is of interest, however, that the synthetic preparation of 1-benzyl-3-(9-methylthiononyl)-thiourea, (XXII), permitted the unequivocal structure determination of the *levo*rotatory mustard oil which we recently demonstrated to be liberated on enzymic hydrolysis of a glucoside in seeds of *Arabis alpina* L., and to which we assigned the structure (XI) on strong, though admittedly inconclusive, evidence [16]. On treatment of (XXII) with a solution of silver nitrate in dilute ethanol 1-benzyl-3-(9-methylthiononyl)-urea (XXIII) resulted. Its identity with the product of m.p. 99.5°, formerly attained by stepwise degradation of the natural mustard oil [16], was established by mixed melting point determination and coinciding infra-red spectra. Hence, there remains no uncertainty as to the mustard oil, derivable from glucoarabin, being (−)-9-methylsulphinylnonyl *iso*thiocyanate (XI).

The numerous and diverse plant constituents, containing a terminal methylthio-grouping, raise the question as to a possible common biogenetic origin of

* Professor P. Karrer kindly informed us that analyses and physical constants for this amine have been recorded in 1950 from his laboratory in a thesis [21] the existence of which we regret not to have known at the time our manuscript was submitted for publication.

the latter. Positive evidence in favour of any general pathway is lacking. It rather appears that more than one route is needed in order to account for the biosynthesis of these compounds. Thus, very little is known about methionine formation in higher plants, but in *E. coli* and *Neurospora* strains it proceeds, according to general belief, from cysteine and *homo*serine, *via* cystathionine, to *homo*cysteine, followed by S-methylation of the latter (*cf.* Ref.[28]). The recent observation by Wolff *et al.*[29], that an extract of yeast can accomplish an enzymic synthesis of S-methyl-L-cysteine from L-serine and methanethiol, indicates an alternative mode of introduction of the CH_3S-moiety, involving again, however, the exchange of a terminal hydroxy-grouping with a sulphur-containing fragment. In principle, the newly reported cysteine synthesis in yeast from serine and hydrogen sulphide [30] also fits this general scheme. Hence, the function of ω-hydroxyalkyl chains as intermediate stages in the biosynthesis of the various natural ω-methylthioalkyl *iso*thiocyanates, or rather their glucosides, is an attractive possibility. The hypothesis further accomodates the appearance in Nature of several terminally unsaturated *iso*thiocyanates, as well as of masked hydroxyalkyl species such as the 3-benzoyloxypropyl mustard oil lately recognized in this laboratory as a constituent arising from a glucoside in seeds of *Malcolmia maritima* (L.) R. Br [31]. The investigations on the occurrence and biogenesis of *iso*thiocyanates in higher plants are being continued in this laboratory.

EXPERIMENTAL

All melting points are uncorrected and determined in capillary tubes (soft glass) in a slowly heated bath.

Hexamethylene series

6-Methylthiohexanol. Methanethiol (27 g) was introduced into a solution of sodium (13 g) in methanol (350 ml). 6-Chlorohexanol [32] (75 g) was slowly added to this solution, and the stirred reaction mixture was refluxed for 3 h. The salt was then filtered off, the methanol removed by distillation, and water was added to the residue to cause the alcohol to separate. After extraction with ether, it distilled as a colourless, hygroscopic oil, b.p. 125°/9 mm, n_D^{25} 1.4821 (Found: C 56.15; H 10.98; S 21.70. Calc. for $C_7H_{16}OS$: C 56.71; H 10.88; S 21.63). Yield: 71 g.

6-Chlorohexyl methyl sulphide. In a three-necked flask, provided with a sealed stirrer, reflux condenser and dropping funnel, was placed a solution of 6-methylthiohexanol (69 g) in dry chloroform (40 ml). Purified thionyl chloride (58 g) was added at such a rate as to maintain a steady reflux (about 2 h). Towards the end of the reaction occasional heating was needed to keep the desired refluxing rate. After removal of the solvent, the chlorosulphide was distilled *in vacuo*, b.p. 72–74°/0.3 mm (63 g, 81 %). Redistillation furnished a colourless specimen for analysis, b.p. 103–104°/9 mm, n_D^{25} 1.4818 (Found: C 50.60; H 9.08; S 19.39. Calc. for $C_7H_{15}SCl$: C 50.42; H 9.07; S 19.23).

N-(6-Methylthiohexyl)-phthalimide. A solution of 6-chlorohexyl methyl sulphide (30 g) and potassium phthalimide (36.5 g) in dimethylformamide (310 ml) was heated and stirred at 100° for 5 h. After cooling, ice water (300 ml) was added and the solution extracted thrice with 250 ml portions of ether. The combined ether extracts were washed with 0.5 N NaOH (300 ml), 0.5 N HCl (300 ml) and water (300 ml). On removal of the solvent from the dried extract a crystalline mass remained. Recrystallization from aqueous ethanol furnished essentially pure material (42 g, 84 %). An analytical specimen separated from pentane as colourless plates, m.p. 51° (Found: C 64.85; H 6.83; N 5.06. Calc. for $C_{15}H_{19}NO_2S$: C 64.95; H 6.90; N 5.05).

6-Methylthiohexylamine (XXI, n = 6). A solution of the phthalimide (39 g) in 96 % ethanol (250 ml) was refluxed for 1 h with 90 % hydrazine hydrate (7.8 g). After being digested with 7 N HCl (400 ml) for another hour the separated phthalhydrazide was removed by filtration. The filtrate was made alkaline with strong NaOH and the amine was extracted with ether (3 × 200 ml). The combined extracts were dried over solid KOH, the ether removed over a small column, and the 6-methylthiohexylamine distilled *in vacuo* care being taken to minimize its exposure to the atmosphere. The colourless amine was obtained in analytically pure form after one redistillation, b.p. 104—105°/10 mm, n_D^{25} 1.4814 (Found: C 56.85; H 11.58; N 9.40. Calc. for $C_7H_{17}NS$: C 57.08; H 11.64; N 9.51).

1,3-bis-(6-Methylthiohexyl)-thiourea. A solution of 6-methylthiohexyl *iso*thiocyanate, prepared according to the general directions given below, and 6-methylthiohexylamine (1.5 mole) in ether, deposited on standing the symmetric thiourea as crystalline material, which was recrystallized thrice from aqueous ethanol before analysis, m.p. 41° (Found: C 53.60; H 9.51; N 8.31. Calc. for $C_{15}H_{32}N_2S_3$: C 53.55; H 9.59; N 8.33).

Heptamethylene series

7-Methylthioheptanenitrile. The reaction between 6-chlorohexyl methyl sulphide (16 g) and NaCN (7 g) was performed in polyethylene glycol (35 ml), essentially following the directions given by Brändström for analogous reactions [22]. The reflux temperature gradually rose from 180° to about 210° within half an hour, when it remained constant, indicating that the reaction had gone to an end. The organic cyanide was removed in a vacuum and redistilled to furnish 9.5 g (68 %) of a product, b.p. 135—137°/10 mm, n_D^{25} 1.4755, which, according to analyses, may have contained traces of the solvent (Found: C 60.30; H 9.68; N 8.00. Calc for $C_8H_{15}NS$: C 61.09; H 9.61; N 8.91).

7-Methylthioheptylamine (XXI, n = 7). In a three-necked flask, equipped with a Hershberg-stirrer, reflux condenser, dropping funnel and nitrogen inlet, was placed a solution of $LiAlH_4$ (5.0 g) in anhydrous ether (100 ml). In nitrogen atmosphere, a solution of 7-methylthioheptanenitrile (9.8 g) in an equal volume of ether, was added at such a rate as to maintain a steady reflux. The reaction was completed by heating for an hour on the water bath. After cooling, water (6 ml) and 15 % NaOH (6 ml) were carefully added, the precipitate filtered off and thoroughly washed with liberal amounts of ether. The combined filtrates were dried over KOH pellets, the solvent removed over a small column, and the amine distilled. The colourless oil had b.p. 118°/10 mm, n_D^{25} 1.4799, (7.5 g, 75 %) (Found: C 59.30; H 12.12; N 8.68. Calc. for $C_8H_{19}NS$: C 59.59; H 11.88; N 8.69).

1,3-bis-(7-Methylthioheptyl)-thiourea. A pure specimen of this derivative, prepared exactly as described above for the lower homologue, was secured by repeated crystallizations from aqueous ethanol, m.p. 45° (Found: C 56.25; H 9.89; N 7.70. Calc. for $C_{17}H_{36}N_2S_3$: C 56.00; H 9.95; N 7.69).

Octamethylene series

8-Methylthiooctanol. This was prepared, essentially as described above for 6-methylthiohexanol, in 80 % yield from 8-chlorooctanol [23, 24] and sodium methyl mercaptide. The alcohol distilled as a colourless oil, b.p. 143—145°/10 mm, n_D^{25} 1.4788 (Found: C 61.30; H 11.26; S 17.85. Calc. for $C_9H_{20}OS$: C 61.33; H 11.44; S 18.19). Previously recorded [25]: b.p. 135—138°/10 mm.

8-Chlorooctyl methyl sulphide. 8-Methylthiooctanol was converted in 73 % yield into the chlorosulphide following the directions given above for the production of 6-chlorohexyl methyl sulphide. The colourless chloride distilled at 86°/0.2 mm, n_D^{25} 1.4783 (Found: C 55.50; H 9.83. Calc. for $C_9H_{19}ClS$: C 55.50; H 9.83). Ref.[25] reports: b.p. 113—116°/3 mm, n_D^{20} 1.4821.

N-(8-Methylthiooctyl)-phthalimide. This intermediate was prepared in 90 % yield from the chlorosulphide as described above for the analogous 6-methylthiohexyl-derivative. It separated from hexane in nacreous plates, m.p. 46° (Found: C 66.95; H 7.44; N 4.62. Calc. for $C_{17}H_{23}NO_2S$: C 66.86; H 7.59; N 4.59).

8-Methylthiooctylamine (XXI, n = 8). The amine resulted from hydrazinolysis of the phthalimide-derivative performed exactly as reported above for the hexamethylene compound. It distilled as a colourless oil, b.p. 133°/10 mm, n_D^{25} 1.4780 (Found: C 61.30; H 12.06; N 8.24. Calc. for $C_9H_{21}NS$: C 61.66; H 12.07; N 7.99).

1,3-bis-*(8-Methylthiooctyl)-thiourea.* This was prepared in the usual way and separated from aqueous ethanol in colourless needles, m.p. 52° (Found: C 58.30; H 10.21; N 7.06. Calc. for $C_{19}H_{40}N_2S_3$: C 58.10; H 10.27; N 7.14).

Nonamethylene series

9-Methylthiononanol. The preparation of a correctly analyzing specimen of this compound was performed from 9-chlorononanol [24] and methanethiol according to the established procedure [25], b.p. 161°/12 mm, m.p. 17°, n_D^{25} 1.4783. Yield: 82 %. Ref.[25] reports: b.p. 138—142°/9 mm, m.p. 22°.

9-Chlorononyl methyl sulphide. Upon reaction with thionyl chloride in the usual way, the foregoing alcohol furnished the chlorosulphide in satisfactory yield as a colourless liquid, b.p. 96°/0.1 mm, n_D^{25} 1.4775. Previously reported [25]: b.p. 118—124°/2 mm, n_D^{25} 1.4811.

N-(9-Methylthiononyl)-phthalimide. This resulted in almost quantitative yield from the usual reaction of the chlorosulphide with potassium phthalimide. An analytical specimen separated from dilute ethanol in colourless plates, m.p. 69° (Found: C 67.60; H 7.61; N 4.29. Calc. for $C_{18}H_{25}NO_2S$: C 67.69; H 7.89; N 4.39).

9-Methylthiononylamine (XXI, n = 9). Hydrazinolysis in the usual way afforded an 80 % yield of 9-methylthiononylamine from the phthalimide-derivative, b.p. 145°/11 mm. Because of the extreme readiness of the amine to take up carbon dioxide from the atmosphere, it was preferred to perform the analyses on the crystalline *N-(9-methylthiononyl)-benzamide,* produced under ordinary Schotten-Baumann conditions. It separated from dilute ethanol as colourless needles, m.p. 50° (Found: C. 69.20; H 9.12; N 4.70. Calc. for $C_{17}H_{27}NOS$: C 69.59; H 9.28; N 4.77).

1,3-bis-*(9-Methylthiononyl)-thiourea.* This derivative crystallized in colourless needles from dilute ethanol, m.p. 60° (Found: C 60.20; H 10.60; N 6.42. Calc. for $C_{21}H_{44}N_2S_3$: C 59.94; H 10.54; N 6.66).

1-Benzyl-3-(9-methylthiononyl)-urea (XXIII). An ethanolic solution of 1-benzyl-3-(9-methylthiononyl)-thiourea (*cf.* Table 3) (581 mg) was treated on the steam bath with another solution, containing silver nitrate (585 mg) in 50 % ethanol. Gradually, enough 1 N NaOH was added to keep the mixture at pH 7. After filtering off precipitated silver sulphide, water was added to the filtrate resulting in precipitation of the urea, which was collected and recrystallized twice from ethyl acetate (Found: C 66.95; H 9.47; N 8.53. Calc. for $C_{18}H_{30}N_2OS$: C 67.02; H 9.38; N 8.68). The colourless product had the m.p. 99.5°, alone or in admixture with a specimen obtained by step-wise degradation of the *Arabis* mustard oil derivative [16]. Coinciding infra-red spectra further served to establish the identity of the two specimens.

General synthetic methods

*iso*Thiocyanates $CH_3S(CH_2)_nNCS$ (n = 2—9). The following procedure was adopted as a standard method of converting the ω-methylthioalkyl amines into the corresponding mustard oils.

To a solution of thiocarbonyl chloride (0.02 mole) in chloroform (20 ml) was added the appropriate amine (0.02 mole) and 12 ml of a 5 % solution of sodium bicarbonate. An exothermic reaction set in upon mixing the components and the flask was thoroughly shaken until all thiophosgene had disappeared (about 10 min). The yellow chloroform layer was separated and the aqueous phase extracted with two additional portions of chloroform. After removal of the solvent, distillation *in vacuo* furnished the mustard oil as a colourless or slightly yellow liquid. In all preparations, considerable quantities of dark-brown by-products were formed, accounting for the fact that yields never exceeded 50 %. Most likely, however, runs on a larger scale would proceed in more satisfactory yields. The physical and analytical data of the individual *iso*thiocyanates are summarized in Table 1.

Thioureas. All mono-substituted thioureas (Table 2) were obtained in practically quantitative yields by keeping the *iso*thiocyanates overnight at room temperature in methanol, saturated with ammonia. The mostly oily products, remaining upon removal of the solvent, crystallized on chilling and scratching. The thioureas were recrystallized to constant melting points from aqueous ethanol, when not otherwise indicated. Their properties are presented in Table 2.

Similarly, reaction of the *iso*thiocyanates in anhydrous ether with 1.5 molecular proportion of benzylamine at room temperature furnished the benzylthioureas in high yields. Analytical specimens, produced by repeated recrystallizations from aqueous ethanol, possessed the properties recorded in Table 3.

The phenylthioureas, summarized in Table 4, were obtained by reaction of the ω-methylthioalkylamines (XXI) with slightly less than one equivalent of phenyl *iso*thiocyanate in ether solution at reflux temperature for 2 h. The mostly oily, crude products crystallized usually in contact with a few drops of dilute HCl. Some of the products, however, needed cooling to $-80°$ for crystallization to commence. Again, aqueous ethanol was the preferred solvent for recrystallization of the derivatives to constant melting points.

Paper chromatography. The mono-substituted thioureas (Table 2) could be chromatographed on paper according to our previously published method [33], yet modified to the descending technique. Using Whatman paper No. 1, and water-saturated chloroform as the mobile phase, the thioureas, containing 2, 3, 4, 5 and 6 methylene-groupings, could be clearly distinguished, possessing the R_{Ph}-values [33]: 0.58, 0.83, 0.99, 1.12 and 1.15, respectively. The higher members of the series travelled too near the solvent front to make a clean separation possible in this solvent system. It was found, however, that on paper chromatography with formamide as the stationary and chloroform as the mobile phase, a complete and satisfactory separation of even the long-chain thioureas was easily achieved.

Microanalyses were performed in this laboratory by Mr. P. Hansen. The work is part of investigations supported by *Statens Almindelige Videnskabsfond (The Danish State Research Foundation)* and *Carlsbergfondet (The Carlsberg Foundation)*. A special grant from *Kai Hansen's Fond* is gratefully acknowledged.

REFERENCES

1. Schneider, W. *Ann.* **375** (1910) 207.
2. Schneider, W. and Kaufmann, H. *Ann.* **392** (1912) 1.
3. Barger, G. and Coyne, F. P. *Biochem. J. London* **22** (1928) 1417.
4. Akabori, S. and Kaneko, T. *Proc. Imp. Acad. Tokyo* **12** (1936) 131; *cf. Chem. Zentr.* **1936 II** 2391.
5. Haagen-Smit, A. J., Kirchner, J. G., Deasy, C. L. and Prater, A. N. *J. Am. Chem. Soc.* **67** (1945) 1651.
6. Weygand, F., Junk, R. and Leber, D. *Hoppe-Seyler's Z. physiol. Chem.* **291** (1952) 191.
7. Synge, R. L. M. and Wood, J. C. *Biochem. J. London* **64** (1956) 252.
8. Morris, C. J. and Thompson, J. F. *J. Am. Chem. Soc.* **78** (1956) 1605.
9. Thompson, J. F., Morris, C. J. and Zacharius, R. M. *Nature* **178** (1956) 593.
9a. Stoll, A., Morf, R., Rheiner, A. and Renz, J. *Experientia* **12** (1956) 360.
10. Schmid, H. and Karrer, P. *Helv. Chim. Acta* **31** (1948) 1017.
11. Schultz, O.-E. and Gmelin, R. *Arch. Pharm.* **287/59** (1954) 404.
12. Kjær, A., Gmelin, R. and Larsen, I. *Acta Chem. Scand.* **9** (1955) 1143.
13. Kjær, A. and Gmelin, R. *Acta Chem. Scand.* **9** (1955) 542.
14. Kjær, A., Larsen, I. and Gmelin, R. *Acta Chem. Scand.* **9** (1955) 1311.
15. Kjær, A. and Gmelin, R. *Acta Chem. Scand.* **10** (1956) 1100.
16. Kjær, A. and Gmelin, R. *Acta Chem. Scand.* **10** (1956) 1358.
17. Kjær, A., Gmelin, R. and Boe Jensen, R. *Acta Chem. Scand.* **10** (1956) 1614.
18. Wieland, T., Möller, E. F. and Dieckelmann, G. *Chem. Ber.* **85** (1952) 1035.
19. Kjær, A., Marcus, F. and Conti, J. *Acta Chem. Scand.* **7** (1953) 1370.
20. Kjær, A. and Conti, J. *Acta Chem. Scand.* **8** (1954) 295.
21. Scheitlin, E. *Zur Kenntnis der Senföle* (Diss.) University, Zürich 1950.

22. Brändström, A. *Acta Chem. Scand.* **10** (1956) 1197.
23. Coleman, W. R. and Bywater, W. G. *J. Am. Chem. Soc.* **66** (1944) 1821.
24. Perrine, T. D. *J. Org. Chem.* **18** (1953) 1356.
25. Bennett, G. M. and Gudgeon, H. *J. Chem. Soc.* **1938** 1891.
26. Schmid, H. and Karrer, P. *Helv. Chim. Acta* **31** (1948) 1497.
27. Weller, L. E., Ball, C. D. and Sell, H. M. *J. Am. Chem. Soc.* **74** (1952) 1104.
28. Davis, B. D. *Advances in Enzymol.* **16** (1955) 247, p. 271.
29. Wolff, E. C., Black, S. and Downey, P. F. *J. Am. Chem. Soc.* **78** (1956) 5958.
30. Schlossmann, K. and Lynen, F. *Angew. Chem.* **69** (1957) 179.
31. Kjær, A. and Gmelin, R. *Acta Chem. Scand.* **10** (1956) 1193.
32. Campbell, K. N. and Sommers, A. H. *Org. Syntheses* **28** (1948) 65.
33. Kjær, A. and Rubinstein, K. *Acta Chem. Scand.* **7** (1953) 528.

Received April 26, 1957.

ACTA CHEMICA SCANDINAVICA 11 (1957) 1308—1312

Studies on the Stability of Aluminium Chelates of Catecholdisulphonic Acid in Aqueous Solutions

REINO NÄSÄNEN

Institute of Chemistry, University of Helsinki, Finland

The complex formation between the aluminium ion and catecholdisulphonic acid (H_4A) has been investigated. The stability constant of AlA^- was determined. The effect of some added electrolytes on the stabilities of AlA^- and AlA_2^{5-} has been studied. The effects of potassium chloride and nitrate on the stability of AlA_2^{5-} were nearly equal. The effects of sodium perchlorate, chloride and nitrate were mutually nearly equal but differed considerably from the effect of potassium salts. The effect of one pentavalent ion (AlA_2^{5-}) appeared to be nearly equal to that of five monovalent ions.

In a recent paper from this laboratory [1], it was concluded that the types of the complexes formed between the aluminium ion and catecholdisulphonic acid (H_4A) are AlA^-, AlA_2^{5-} and AlA_3^{9-}. At that time the equilibrium

$$Al^{3+} + H_2A^{2-} = AlA^- + 2H^+ \quad (1)$$

was not investigated in detail. Data concerning equilibrium (1) are now presented.

The previous potentiometric method was used and the equilibrium constant

$$K_I = [AlA^-][H^+]^2 / [Al^{3+}][H_2A^{2-}] \quad (2)$$

was calculated from the equations

$$[H_2A^{2-}] = (c - 0.5c_B - 0.5[H^+]) / (1 + 0.5K_3 / [H^+])] \quad (3)$$

$$c' = c - [H_2A^{2-}](1 + K_3 / [H^+]) \quad (4)$$

$$x = [H_2A^{2-}] / [H^+]^2 \quad (5)$$

$$K_I = c' / x(c_{Al} - c') \quad (6)$$

where c, c_B and c_{Al} are the total molar concentrations of tiron, sodium hydroxide and aluminium perchlorate, respectively.

Table 1. Determination of constant K_I at 25°C.

Titration I:			Titration II:				Titration III:			
$c \cdot 10^3$ / $c_{Al} \cdot 10^3$	$\sqrt{I}$	pK_I	$c \cdot 10^3$	$c_{Al} \cdot 10^3$	$\sqrt{I}$	pK_I	$c \cdot 10^3$	$c_{Al} \cdot 10^3$	$\sqrt{I}$	pK_I
1.364	0.092	2.69	4.092	1.364	0.179	2.84	14.21	4.737	0.34	3.01
1.357	0.089	2.68	4.071	1.357	0.178	2.84	13.93	4.639	0.34	3.06
1.351	0.087	2.66	4.053	1.351	0.176	2.82	13.64	4.545	0.33	3.05
1.341	0.084	2.64	4.023	1.341	0.174	2.82	13.37	4.455	0.32	3.06
1.339	0.081	2.64	4.017	1.339	0.173	2.83	13.11	4.369	0.31	3.05
1.333	0.077	2.63	3.999	1.333	0.172	2.84				

In Table 1 the results of some titrations for the determination of the constant K_I are presented. The ionic strength is calculated from $I = \frac{1}{2}\Sigma z_i^2 c_i$. The constant K_I is seen to vary in a way to be expected from the Debye-Hückel equation, which in this case has the form

$$pK_I = pK_I^\circ + \frac{5.09\sqrt{I}}{1 + a\sqrt{I}} - BI. \qquad (7)$$

The results do not suggest the formation of the complex AlHA, a type which is found among the Fe(III) complexes of tiron [2]. The effect of addition of potassium chloride on the constant K_I was also investigated and the results are presented in Table 2. These results can be represented satisfactorily by the equation

$$pK_I = 2.32 + \frac{5.09\sqrt{I}}{1 + 2.35\sqrt{I}} + 0.06I \qquad (8)$$

On comparing the values in Tables 1 and 2, one sees they differ at higher ionic strengths, as would be expected from the differences in ionic medium.

The equilibrium constant of the reaction

$$AlA^- + H_2A^{2-} = AlA_2^{5-} + 2H^+ \qquad (9)$$

defined by

$$K_{II} = [AlA_2^{5-}][H^+]^2 / [AlA^-][H_2A^{2-}] \qquad (10)$$

has been determined previously by Näsänen and Veivo [1]. They became aware that the points of both the second and the third buffer ranges of the titration curve give almost constant values for K_{II} and K_{III}, respectively,

Table 2. Constant K_I in potassium chloride solutions at 25°C.

$\sqrt{I}$	pK_I exptl.	pK_I eqn. (8)	$\sqrt{I}$	pK_I exptl.	pK_I eqn (8)
0.084	2.67	2.67	1.02	3.90	3.91
0.32	3.26	3.25	1.39	4.10	4.09

Table 3. The effect of pentavalent ions AlA_2^{5-} on the equilibrium constant K_{II}.

Titration I. $c/c_{Al} = 3$

$c \cdot 10^3$	c_B/c_{Al}	c'/c_{Al}	pH	$\sqrt{\frac{1}{2}\Sigma z_i^2 c_i}$	$\sqrt{\frac{1}{2}\Sigma z_i c_i}$	pK_{II}
3.974	2.12	1.07	4.801	0.110	0.104	8.06
3.965	2.29	1.15	5.017	0.118	0.105	8.09
3.947	2.62	1.31	5.246	0.127	0.107	8.08
3.930	2.91	1.48	5.438	0.134	0.108	8.11
3.913	3.08	1.64	5.607	0.145	0.110	8.10
3.896	3.62	1.81	5.820	0.152	0.112	8.09
3.888	3.79	1.89	5.972	0.155	0.113	8.04

Titration II. $c/c_{Al} = 3$

$c \cdot 10^3$	c_B/c_{Al}	c'/c_{Al}	pH	$\sqrt{\frac{1}{2}\Sigma z_i^2 c_i}$	$\sqrt{\frac{1}{2}\Sigma z_i c_i}$	pK_{II}
12.86	2.18	1.09	4.373	0.203	0.188	7.51
12.62	2.71	1.31	4.732	0.225	0.190	7.52
12.24	3.07	1.53	4.973	0.244	0.192	7.51
12.16	3.51	1.75	5.235	0.262	0.196	7.53
12.05	3.73	1.87	5.421	0.270	0.198	7.54

Titration III. $c/c_{Al} = 3$

$c \cdot 10^3$	c_B/c_{Al}	c'/c_{Al}	pH	$\sqrt{\frac{1}{2}\Sigma z_i^2 c_i}$	$\sqrt{\frac{1}{2}\Sigma z_i c_i}$	pK_{II}
58.8	2.35	1.18	3.802	0.435	0.404	6.63
57.7	2.75	1.33	4.064	0.515	0.410	6.62
56.6	3.17	1.58	4.240	0.550	0.416	6.59
55.6	3.55	1.78	4.522	0.580	0.421	6.68

although the increase in the concentrations of the ions AlA_2^{5-} and AlA_3^{9-} during the titrations causes a considerable change in ionic strength as calculated from $I = \frac{1}{2}\Sigma z_i^2 \cdot c_i$. More complete measurements have since been carried out by the present author in the case of AlA_2^{5-}. In Table 3 some titrations with the ratio $c / c_{Al} = 3$ but with different total concentrations are recorded. The results are in agreement with Brönsted's theory of specific ionic interaction [3] in the sense that one pentavalent negative ion has nearly the same effect on K_{II} as five univalent negative ions. The quantity $\frac{1}{2}\Sigma z_i c_i$ also varies during the titration but much less than $\frac{1}{2}\Sigma z_i^2 \cdot c_i$ and obviously the variation of K_{II} with $\frac{1}{2}\Sigma z_i c_i$ is of the same order of magnitude as the accuracy reached in the case in question.

The specific ionic interaction in the case of equilibrium (9) was further investigated by means of some neutral salts. These results are presented in Table 4. From this table and from Fig. 1 one can see that sodium chloride, nitrate and perchlorate have a nearly equal effect. The effects of potassium chloride and nitrate are also mutually nearly equal but differ considerably from the effect of sodium salts. Thus these results are also in accordance with the theory of specific ionic interaction.

Table 4. The dependence of K_{II} on ionic strength in solutions of some neutral salts.

	pK_{II}				pK_{II}	
$\sqrt{\frac{1}{2}\Sigma z_i c_i}$	($NaClO_4$)	(NaCl)	($NaNO_3$)	$\sqrt{\frac{1}{2}\Sigma z_i c_i}$	(KCl)	(KNO_3)
0.108	8.13	8.13	8.14	0.108	8.13	8.13
0.316	6.98	6.95	6.96	0.294	6.57	—
0.612	6.28	—	—	0.313	—	6.43
0.971	—	—	5.84	0.598	5.68	—
0.998	—	5.79	—	0.962	—	5.34
1.300	—	—	5.66	1.070	5.26	—
1.375	—	5.71	—	1.305	—	5.24
				1.700	5.14	

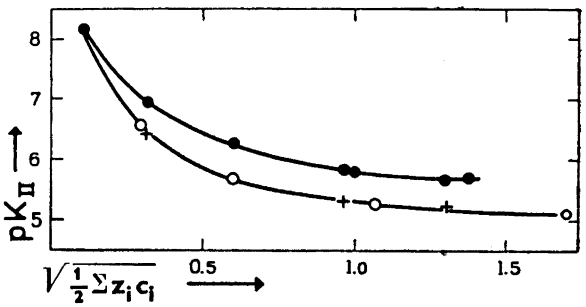


Fig. 1. The effect of some salts on the constant K_{II}. ● NaCl, $NaNO_3$, $NaClO_4$. ○ KCl, +KNO_3.

Besides concentrations of negative ions, eqn. (10) also contains the concentration of hydrogen ion. The change in the activity coefficient of hydrogen ion with ionic medium is small compared with the respective changes of the activity coefficients of the high valent ions and obviously does not much influence the results.

For the calculation of the stability constants

$$k_\nu = [AlA_\nu^{(4\nu-3)-}] / [Al^{3+}][A^{4-}]^\nu, \qquad (11)$$

the ionisation constants

$$K_3 = [H^+]\,[HA^{3-}] / [H_2A^{2-}] \text{ and } K_4 = [H^+]\,[A^{4-}] / [HA^{3-}] \qquad (12)$$

Table 5. Some values of the stability constants of aluminium chelates of catecholdisulphonic acid in potassium chloride solutions at 25°C.

$\sqrt{\frac{1}{2}\Sigma z_i c_i}$	$\log k_1$	$\log k_2$
0.1	16.6	30.0
1.0	14.9	28.4
2.0	14.6	28.1

are needed. One obtains

$$k_1 = K_I/K_3K_4\,; \quad k_2 = K_IK_{II}/K_3^2K_4^2 \text{ and } k_3 = K_IK_{II}K_{III}/K_3^3K_4^3 \quad (13)$$

The third and fourth ionisation constants have been determined recently by the present author [4]. The values of k_1 and k_2 at various ionic strength in potassium chloride solutions are given in Table 5.

REFERENCES

1. Näsänen, R. and Veivo, J. *Suomen Kemistilehti* B 29 (1956) 213.
2. Schwarzenbach, G. and Willi, A. *Helv. Chim. Acta* 34 (1951) 528.
3. Brönsted, J. N. *J. Am. Chem. Soc.* 44 (1922) 877, 938; 45 (1923) 2898. *Cf.* Olson, A. R. and Simonson, T. R. *J. Chem. Phys.* 17 (1949) 348, 1167, 1322; Kilpi, S., Mikkola, K. S. and Valanki, M. K. *Ann. Acad. Sci. Fennicae II. Chem.* 52 (1953).
4. Näsänen, R. *Suomen Kemistilehti* B 30 (1957) 61.

Received May 9, 1957.

ACTA CHEMICA SCANDINAVICA 11 (1957) 1313—1316

1 : 1 Complexes of Acid Chromate Ion with Alcohols or Acetaldehyde

ULRIK KLÄNING

Laboratoriet for Fotokemi, Fotografi og Reproduktionsteknik, Polyteknisk Læreanstalt, Copenhagen, Denmark

Evidence for 1:1 complexes of acid chromate ion with some aliphatic alcohols or acetaldehyde is presented. The stability constants and spectra have been measured, and the heat of formation of one of the complexes (the 2-propanol complex) has been determined. In view of these complexes, the light sensitiveness of the acid chromate-alcohol solutions will be discussed.

Westheimer *et al.* [1-3] have investigated the kinetics of the oxidation of 2-propanol to acetone by acid chromate ions in aqueous solution, and have shown that the primary step in the reaction is the formation of a complex (an ester)

$$CH_3CHOHCH_3 + HCrO_4^- + H^+ = H_2CrO_4 \cdot CH_3CHOHCH_3$$

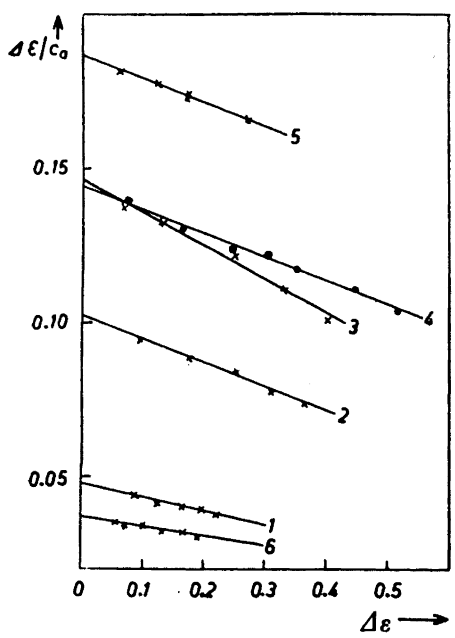
Edwards has postulated the existence of a similar complex [4].

At low acidities, 10^{-2} M to 10^{-3} M, and temperatures below 40°C, the above mentioned oxidation is extremely slow. Under these conditions the present author has found evidence for an equilibrium of the type:

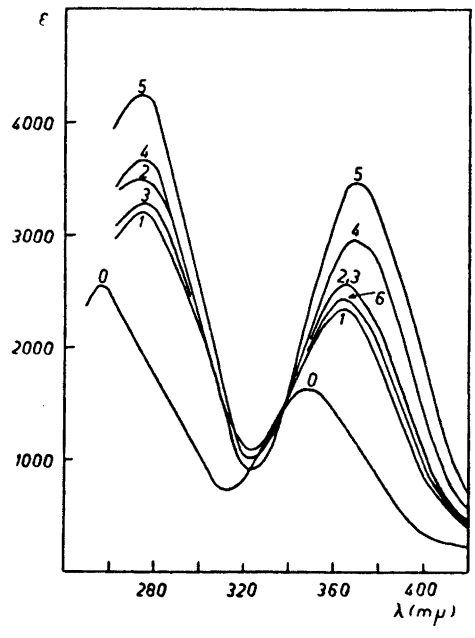
$$X + HCrO_4^- = X \cdot HCrO_4^-$$

where X stands for an alcohol or acetaldehyde. In more acid solutions these complexes (probably esters) may react with a proton to form unstable complexes (esters) similar to those proposed by Westheimer.

Measurements were made of the difference in extinction $\Delta\varepsilon$ of two solutions, both containing 10^{-4} M acid chromate and 10^{-3} M perchloric acid, one of them, furthermore, an alcohol or acetaldehyde. Under these conditions less than 1 % of the acid chromate is present as dichromate. For constant alcohol concentration $\Delta\varepsilon$ was measured at wavelengths between 260 mμ and 420 mμ; at 375 mμ $\Delta\varepsilon$ was measured at various concentrations of alcohol or acetaldehyde.



Figur 1. $\Delta\varepsilon/c_a$ *versus* $\Delta\varepsilon$ for acid chromate solutions containing 1) methanol, 2) ethanol, 3) *n*-propanol, 4) 2-propanol, 5) 2-butanol and 6) acetaldehyde.



Figur 2. The absorption spectrum of the acid chromate ion 0), and the absorption spectra of the complexes of acid chromate with 1) methanol, 2) ethanol, 3) *n*-propanol, 4) 2-propanol, 5) 2-butanol and 6) acetaldehyde.

The following relation was established, indicating the existence of a 1:1 complex:

$$\frac{\Delta\varepsilon}{c_a} = K \cdot \Delta\varepsilon_{K1} \cdot l \cdot c_0 - K \cdot \Delta\varepsilon$$

where K is the stability constant, l the length of the optical path in cm, c_a the concentration of alcohol or acetaldehyde, c_0 the concentration of acid chromate, and $\Delta\varepsilon_{K1}$ the difference between the extinction coefficient of the complex and that of the acid chromate ion at 375 mμ.

From the straight line representing $\Delta\varepsilon/c_a$ as a function of $\Delta\varepsilon$, K and $\Delta\varepsilon_{K1}$ were calculated for methanol, ethanol, *n*-propanol, 2-propanol, 2-butanol and acetaldehyde (Fig. 1). The stability constants in litre · mole^{-1} at 25°C were, for methanol 0.043, ethanol 0.077, *n*-propanol 0.109, 2-propanol 0.078, 2-butanol 0.082 and for acetaldehyde 0.034. The spectra were obtained from measurements of $\Delta\varepsilon$ at varying wavelengths, knowing the absorption spectrum of the acid chromate ion [5]. The spectra of the complexes are shown in Fig. 2.

The equilibrium constant for 2-propanol was measured also at 11°C, 0.0884, and at 35°C, 0.0746, giving a value for the heat of formation of $-\Delta H$ = 1.31 kcal/mole.

Furthermore it was found that $\Delta\varepsilon$ is independent of the concentration of perchloric acid in the interval 2×10^{-4} — 0.2 M, indicating that the complexes, like the acid chromate ion, are weak both as acids and as bases. At the highest acidities the oxidation is rather fast, $\Delta\varepsilon$ therefore was found by extrapolating log ε to zero time, assuming a first order reaction rate.

Westheimer [1] has found that the dichromate ion is inactive in the above mentioned oxidation. In agreement with this, measurements of the extinction per cm, ε, at 366 mμ of solutions containing dichromate and 2-propanol indicated that the interaction between 2-propanol and dichromate ions is weak. In these experiments the concentration of 2-propanol was 3 M, the ionic strength was 10^{-2} and the total chromium concentration c_0 was varied between 5×10^{-4} M and 1.5×10^{-3} M. Assuming that the dichromate ion does not form a complex with 2-propanol, we may write for the extinction ε:

$$\varepsilon = \varepsilon_1 \cdot c_0 + 2c_2\Delta\varepsilon_{21} + c_K\Delta\varepsilon_{K1}$$

where ε_1 is the extinction coefficient of acid chromate and $\Delta\varepsilon_{21}$ the difference between the extinction coefficient of dichromate and that of acid chromate. c_2 and c_K are concentrations of dichromate and of the complex, respectively. c_K is given by:

$$2c_K^2K_2 + c_K(K \cdot c_a + K^2c_a^2) - K^2c_a^2c_0 = 0$$

c_2 is given by

$$4K_2c_2^2 - (1 + 4K_2(c_0 - c_K))c_2 + (c_0 - c_K)^2K_2 = 0$$

where K_2 is the constant for the equilibrium between acid chromate and dichromate. From these equations ε has been calculated. For $\Delta\varepsilon_{K1}$ and K the values at $c_0 = 10^{-4}$ M have been used. $\Delta\varepsilon_{21}$ is known [6], 873 litre·mole^{-2} cm^{-2}. K_2 has been determined by Tong and King [7], $K_2 = 45$ litre·mole^{-1}. Table 1 shows the calculated and the measured values of ε at various concentration c_0.

Table 1. 25.0°C

c_0 mole/litre	ε measured	ε calculated
1.5×10^{-3}	2.445	2.462
1.0×10^{-3}	1.632	1.623
7.5×10^{-4}	1.210	1.215
5.0×10^{-4}	0.805	0.807

We introduce the coefficient $\gamma_0 = \dfrac{c_a \cdot K \cdot \varepsilon_K}{c_a \cdot K \cdot \varepsilon_K + \varepsilon_1}$, where ε_K is the extinction coefficient of a complex. γ_0 is that fraction of the absorbed photons, which are absorbed by the complexes. At small values for c_a, γ_0 becomes $\dfrac{c_a \cdot K \cdot \varepsilon_K}{\varepsilon_1}$

In Table 2 the γ_0/c_a values at 366 mμ are given for the 5 alcohols and acetaldehyde. The quantum yields for the photochemically induced oxidation of some of the above mentioned alcohols and acetaldehyde by acid chromate at 366 mμ have been determined by Bowen and Chatwin [8]. Their values for the quantum yields

Table 2. 25.0°C

Complex	γ_0/c_a	γ/c_a
Acetaldehyde-	0.065	0.0396
Methanol-	0.079	0.0130
Ethanol-	0.155	0.0416
n-Propanol-	0.217	0.0470
2-Propanol-	0.179	0.0470
n-Butanol-	—	0.081
2-Butanol-	0.220	—
*Iso*butanol-	—	0.0775

in dilute solutions divided by the alcohol or acetaldehyde concentrations, γ/c_a, are also given in Table 2. We note that γ_0/c_a varies parallel to γ/c_a (except for acetaldehyde), suggesting that it is the complexes, which are photochemically active.

EXPERIMENTAL

Acetaldehyde was distilled just before use. The alcohols were purified by distillation. The normal alcohols were distilled over NaOH and $Pb(CH_3COO)_2$ to remove aldehydes. The solutions were made with redistilled water.

The extinction measurements were made with a Beckman DU spectrophotometer. The temperature was held within 0.2°C by circulating thermostated water through the Beckman Thermospacer.

REFERENCES

1. Westheimer, F. H. *Chem. Revs.* **45** (1949) 419. Errata June 1950.
2. Holloway, F., Cohen, M. and Westheimer, F. H. *J. Am. Chem. Soc.* **75** (1951) 65.
3. Westheimer, F. H. and Novick, A. *J. Chem. Phys.* **11** (1943) 506.
4. Edwards, J. *Chem. Revs.* **50** (1952) 455.
5. Danies, W. G. and Prue, J. E. *Trans. Faraday Soc.* **51** (1953) 1045.
6. Kobsa, H. *Monatsh.* **86** (1955) 662.
7. Tong, J. Y. and King, E. L. *J. Am. Chem. Soc.* **75** (1953) 6180.
8. Bowen, E. J. and Chatwin, J. E. *J. Chem. Soc.* **1932** 2081.

Received May 17, 1957.

ACTA CHEMICA SCANDINAVICA 11 (1957) 1317—1322

Fractionation of Casein by Distribution in a Liquid Two-Phase System

NILS ELLFOLK

Laboratory of Valio, Biochemical Institute, Helsinki, Finland

The distribution of casein between a two-phase system of collidine, ethanol, and water has been studied. α-Casein was found to distribute in favour of the water-rich phase and β- and γ-casein in favour of the collidine-rich. Electrophoretically pure α-casein was prepared by extracting a neutralized casein solution with the collidine-rich phase of the collidine-ethanol-water system.

Until recently it has generally been assumed that casein is a pure protein, although there was some evidence to the contrary. Linderstrøm-Lang [1] first demonstrated that casein was a mixture of several distinct proteins. Later on Mellander [2] showed that casein is composed of at least three components which he denoted α-, β-, and γ-casein in order of decreasing mobility.

It was apparent from previous attempts to fractionate casein that the separation of the different electrophoretic components would be difficult. Warner [3] devised the first chemical method for the separation of α- and β-casein, a repeated isoelectric precipitation at low temperature. This technique was further developed by Cherbuliez and Baudet [4]. Hipp *et al.*[5] separated the different electrophoretic fractions of casein by precipitation from 50 % alcohol by means of variations in temperature, pH, and ionic strength. Another method, developed by the same authors, was based on the solubility of the different casein components in aqueous urea. Walter [6] succeeded in fractionating α- and β-casein between a liquid two-phase system containing phenol. This system was found to be highly specific to casein.

Fractionation of casein by means of distribution in a two-phase system containing collidine is studied in the present paper.

METHODS

Description of the three-component system of collidine-ethanol-water (C-E-W). A three-component system is usually described in a triangular diagram. The composition of any ternary system can be represented by a point in the diagram, when the side of the equi-

lateral triangle is taken as unity and the amounts of the three components are expressed as fractions of the whole. The corners of the triangle represent the pure component. The distance from one point to any side, measured parallel to either of the others, gives the proportion of the component occupying the opposite corner. Any point within the triangle represents three components, but a point situated on one of the sides indicates two components only.

To determine the diagram, 10 g of collidine were titrated in an Erlenmayer flask with distilled water under thorough mixing to a permanent turbidity showing the presence of two phases. 1 ml of ethanol (96 %) was then added, and the titration was again carried out with water to slight turbidity. By repeating this procedure the ascending part of the curve could be constructed to its vertex. The descending part of the curve was determined in a similar way by titrating 10 g of distilled water with collidine and adding ethanol after the endpoint of the titration was shown by a slight turbidity. Any point outside the constructed curve represents one liquid layer only. Inside the curve two liquid layers are in equilibrium, the components being given by the appropriate points on the curve. One known concentration term allows the position of one layer to be fixed on the constructed curve and defines the system completely. In order to determine the composition of the layers an analysis of collidine was made.

Determination of collidine. Collidine was determined on the basis of the absorption at 280 mμ, using a Beckman spectrophotometer. For the analysis the samples were diluted with distilled water. The amount of collidine was read from a curve constructed by diluting a known amount of collidine with distilled water.

Electrophoresis. Moving boundary electrophoresis was carried out with a Klett electrophoresis apparatus. The optical system was that of Philpot-Svensson. In the runs a 15 ml analytical cell was used. All samples were diluted with veronal buffer of pH 8.6 and of ionic strength 0.12 and dialyzed against 2 l of the same buffer for a week. In all experiments so much buffer was added to the samples as to make the total protein concentration 1.0 %. The runs were carried out with a potential gradient of 9 volt/cm at 4°C.

Since the area enclosed by the electrophoresis curve of the gradient and the basis line is proportional to the concentration of the gradient, the relative amounts of the different protein components can be determined by calculating their corresponding areas. This was done by enlarging the films on millimeter paper and drawing the diagrams on the paper. From the drawings the areas were easily determined by means of a planimeter.

Determination of the pH. The pH of the solutions was measured with a glass electrode (Beckman).

RESULTS AND DISCUSSION

Preliminary experiments were carried out with the phase-pair collidine-water. When casein solutions of different concentrations, neutralized to a pH of about 7, were mixed with an equal volume of collidine, stable milk-white emulsions were formed. It is well known that proteins act as emulsifying agents. In order to prevent the formation of these emulsions, some lower alcohols were tested as de-emulsifying agents. Methanol as well as ethanol were found to have strong de-emulsifying effects. A diagram of the three-component system C-E-W can be seen in Fig. 1. The phases obtained at both temperatures are extremely temperature-labile. A mere warming with the hand caused turbidity. In the following experiments the two-phase system was obtained by mixing the three components at 20°C in the following proportion: 30 ml of collidine, 16.5 ml of ethanol, and 60 ml of distilled water. The pH of the mixture was 9.5. The pH value as measured with a glass electrode is not exact beacuse of the high content of organic solvents.

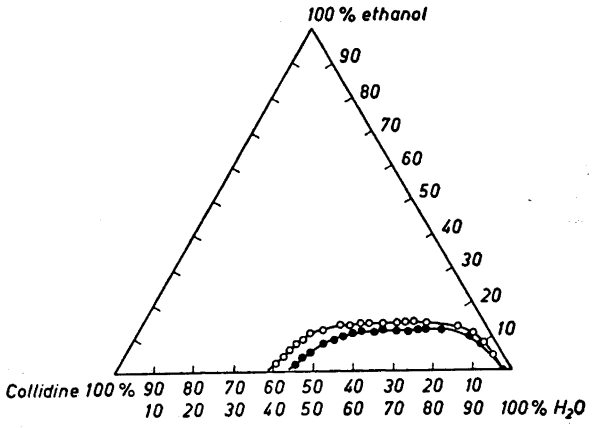


Fig. 1. Phase diagrams of the C-E-W system at 15°C (●) and at 20°C (○).

When the bottom and the top phase had separated completely, their composition was determined and found to be as follows:

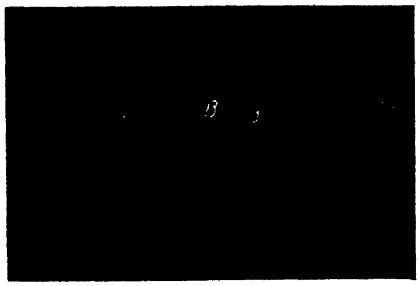
Collidine phase (top phase)	Water phase (bottom phase)
41.9 % collidine	13.7 % collidine
46.1 % water	72.3 % water
12.0 % ethanol	14.0 % ethanol

It can be seen from Fig. 1 that these points are situated in the homogenous part of the diagram when the temperature is 15°C.

Acid Hammarsten's casein (Merck) was found to be easily soluble in the top phase without any neutralizing. When in a two-phase system in equilibrium different columes of the top phase were replaced by the corresponding volume of the top phase containing casein, and the two phases were mixed, no separation in two phases occurred, but the solution was completely clear and homogeneous. When, however, the casein in the top phase was neutralized with NaOH, dissolved in the top phase, a separation again occurred. It is evident that casein neutralized by collidine functioned as a homogenizing agent in the liquid two-phase system. In order to avoid this, the casein solutions in the following experiments were neutralized to a slight alkalinity.

Fractionation of casein in the C-E-W system. 1 g of Hammarsten's casein (Merck) was dissolved in water by neutralizing it to pH 8.7 and made up to 60 ml. 30 ml of collidine and 16.5 ml of ethanol were added to this solution, well mixed and kept at room temperature (20°C) until both phases had separated completely. Samples of the two phases were taken and evaporated to dryness *in vacuo*, the temperature of the bath not rising over 45°C. Both these dried fractions were dissolved in veronal buffer, dialyzed against the same buffer and analyzed by electrophoresis. The diagrams of the ascending limbs of the different preparations can be seen in Figs. 2—4.

2



3



4



Fig. 2. Electrophoresis diagram of Hammarsten's casein.

Fig. 3. Electrophoresis diagram of casein isolated from the collidine-rich phase after distribution in the C-E-W system.

Fig. 4. Electrophoresis diagram of casein isolated from the water-rich phase after distribution in the C-E-W system. (Ascending boundaries, pH 8.6, $\mu = 0.12$, $F = 9$ Volt/cm, $t = 90-120$ min, α, β, and γ denote the different casein fractions and B the buffer peak.)

It is apparent from these diagrams that α-, β-, and γ-casein vary considerably, and that a distinct enrichment of the β-component occurs in the collidine phase after only one distribution. By quantitative evaluation of the electrophoretic diagrams the following values were obtained for α-, β-, and γ-casein (Table 1). The diagrams of the ascending limbs were used in the calculations, because it was found that the ascending limbs showed values for β-casein more closely to the real value of 25 % than those of the descending limbs. Nitschmann and Zürcher [7] have shown that the concentration of β-casein, shown in electrophoresis diagrams of descending limbs, decreases, continuously with increasing casein concentration, a fact which is due to a formation of a reversible complex or association between α- and β-casein. At infinite dilution the complex was found to be completely dissociated, the amount of

Table 1. Distribution of α-, β-, and γ-casein in the C-E-W system at 20°C.

Fraction	Relative amount present in %		
	α-	β-	γ-casein
Hammarsten's casein	76	22	2
Collidine phase	46	37	17
Water phase	91.5	8.5	—

Table 2. Concentrations and distribution constants of α- and β-casein in the C-E-W system at 20°C.

Fraction	Collidine phase c_{coll} %	Water phase c_w. %	Distribution factor $K = c_w/c_{coll}$
α-Casein	0.294	1.35	$K_\alpha = 4.6$
β-Casein	0.236	0.117	$K_\beta = 0.5$

β-casein being 25 %, whereas in a 1 % casein solution the amount of β-casein was 18 % and in a 2 % solution only 14 %.

In order to evaluate the distribution constants of α- and β-casein, the protein concentrations of the two phases were determined on a dry weight basis. It was found that the protein concentration of the collidine-rich phase was 0.64 % and that of the water-rich phase 1.48 %. Compared with the amount of casein added, the sum of the protein concentrations in the two phases was a little too high, but, owing to the semiquantitative nature of the calculation, it was assumed to be satisfactory. The α- and β-casein concentrations of the two phases, calculated from the electrophoretic diagrams, and the distribution constants of the two casein fractions in the C-E-W system can be seen in Table 2. The distribution coefficient of α-casein is high compared with that of β-casein. The separation factor, β, defined as the ratio of the partition coefficients, was found to be:

$$\beta = K\beta/K_\alpha = 9.2$$

Preparation of electrophoretically pure α-casein. On the basis of the above findings electrophoretically pure α-casein was prepared in the following way: 1 g of casein was dissolved in 60 ml as earlier, and the same amounts of collidine and ethanol were added, mixed and kept at room temperature until both phases separated completely, after which the top phase was carefully removed. The remaining bottom phase was now treated three times with fresh top phase (50 ml each time), the top phase being removed after each treatment. At the end of the experiment the bottom phase was evaporated to dryness

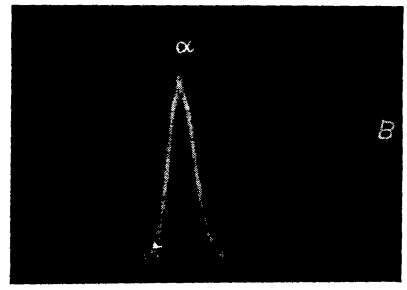


Fig. 5. Electrophoresis diagram of the bottom fraction from a four step distribution of casein in the C-E-W system at 20°C. (Conditions as in Figs. 2—4).

in vacuo, dissolved in veronal buffer as earlier and analyzed by electrophoresis in the usual way. The diagrams of the ascending and descending limbs can be seen in Fig. 5. Since both boundaries are completely symmetric it is assumed that the concentration of β-casein is very low. It is, however, to be assumed that the tendency for complex formation between α- and β-casein is greater at a low β-casein concentration when the concentration of α-casein is high.

I am deeply indebted to Professor Eero Uroma, head of the State Serum Institute, for his kindness in letting me use the electrophoresis equipment of his institute, and to Mr. Antti Louhivuori, M.A., for valuable advice.

REFERENCES

1. Linderstrøm-Lang, K. *Compt. rend. trav. lab. Carlsberg* **17** (1929) No. 9.
2. Mellander, O. *Biochem. Z.* **300** (1939) 240.
3. Warner, R. C. *J. Am. Chem. Soc.* **66** (1944) 1725.
4. Cherbuliez, E. and Baudet, P. *Helv. Chim. Acta* **33** (1950) 398.
5. Hipp, N. J., Groves, M. L., Custer, J. H. and McMeekin, T. L. *J. Dairy Sci.* **35** (1952) 272.
6. Walter, J. O. *Untersuchungen über die Fraktionierung von Casein mit zwei Fluessigen nicht-mischbaren Phasen, Diss.*, Bern 1952.
7. Nitschmann, Hs. and Zürcher, H. *Helv. Chim. Acta* **33** (1950) 1698.

Received June 1, 1957.

ACTA CHEMICA SCANDINAVICA 11 (1957) 1323—1330

Electroorganic Preparations

IV. Oxidation of Aromatic Hydrocarbons

HENNING LUND

Leo Pharmaceutical Products, Copenhagen, Denmark

It is shown that aromatic hydrocarbons can be oxidized at a platinum electrode in acetonitrile containing sodium perchlorate. The half-wave potentials of the voltammetric curves are found to be directly related to the wave numbers of the *p*-bands in the ultraviolet absorption spectra of the hydrocarbons. The reaction product of the controlled potential oxidation of anthracene in acetonitrile containing pyridine and sodium perchlorate is shown to be 9,10-dihydroanthraquinyldipyridinium diperchlorate.

Electrolytic oxidation of aromatic hydrocarbons [1] yields mostly a mixture of hydroquinones, quinones, and acids, when the current density is used as the controlling factor. No controlled potential oxidations of aromatic hydrocarbons have been reported.

In the second part of this series [2] it was shown that some aromatic alcohols by controlled potential oxidation in acetonitrile containing sodium perchlorate and pyridine could be oxidized to the aldehydes and it was postulated that the first step of the oxidation in this inert medium was a loss of electrons from the aromatic sytem.

This investigation is concerned with the controlled potential oxidation of some aromatic hydrocarbons and their derivatives. The technique used to determine the optimal potential for the oxidation is the same as that used in Part II [2]. The current-potential curve of the compound in acetonitrile is determined with a platinum microelectrode and the oxidation is performed at a potential about 0.15 V more positive than the half-wave potential of the compound in the medium used.

VOLTAMMETRIC INVESTIGATION

In Table 1 are compiled the results of the voltammetric investigation. In column 1 are given the compounds, in column 2 the wave numbers of the first *p*-band in their ultraviolet spectrum as defined by Clar [3]. The wave numbers were obtained from Clar [3]. Most of the spectra have been

Table 1. Half-wave potentials of the investigated compounds in unbuffered acetonitrile containing 0.5 M sodium perchlorate measured against the 0.1 N silver ion/silver electrode in acetonitrile.

Compound	wave number cm^{-1}	$E_{\frac{1}{2}}$ V	shape
Benzene	48 100	2.00	deformed
Naphthalene	35 090	1.31	nearly normal
Anthracene	26 700	0.84	normal
Tetracene, 1. wave	21 230	0.54	normal
2. wave		1.20	normal
5,12-Dihydrotetracene		1.16	normal
Phenanthrene	34 190	1.23	nearly normal
1,2-Benzanthracene	27 860 *	0.92	normal
1,2,5,6-Dibenzanthracene, 1. wave	28 490 *	1.00	normal
2. wave		1.26	normal
Chrysene	31 350	1.13	normal
Pyrene, 1. wave	29 990	0.86	normal
2. wave		1.12	deformed
Benzo-*a*-pyrene	26 010	0.76	deformed
Biphenyl	40 000	1.48	deformed
Bianthryl, 1. wave		0.87	normal
2. wave		1.2	drawn out
Indene		1.23	normal
Fluorene	38 310	1.25	deformed
Fluoranthene	27 890	1.18	deformed
Toluene		1.93	deformed
Acenaphthene		1.11	deformed
Retene		1.18	normal
9,10-Dimethylanthracene		0.65	normal
Methylcholanthrene		0.69	normal
a-Nitronaphthalene		1.62	deformed
9-Nitroanthracene		1.25	normal
9-Anthrylpyridinium perchlorate		1.20	normal
9-Bromoanthracene, 1. wave		0.99	normal
2. wave		1.48	normal
9,10-Dibromoanthracene, 1. wave		1.15	normal
2. wave		1.47	normal
(9-Bromo-10-anthryl)pyridinium perchlorate		1.47	normal
Aniline		0.65	normal
Anisol		1.35	normal

* The spectrum measured in benzene solution.

measured in alcohol, but those marked with an asterisk were measured in benzene. The wave numbers used in Fig. 1 were, for comparative purposes, corrected to ethanol by the relationship: ν (ethanol)= ν (benzene) + 300 cm^{-1}, which is characteristic of *p*-bands. In column 3 are compiled the anodic half-wave potentials corrected for iR-drop in the solution measured against the 0.1 N silver ion/silver electrode, and in column 4 the shape of the voltammetric curve.

As the half-wave potentials of the compounds depend upon the surface of the microelectrode and the reaction products often alter the surface slightly

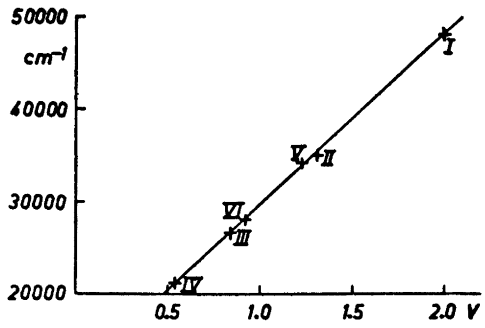


Fig. 1. The anodic half-wave potentials of some acenes and phenes plotted against the wave number of the first *p*-band in their ultraviolet absorption spectrum in alcohol. Benzene (I), naphthalene (II), anthracene (III), tetracene (IV), phenanthrene (V), 1,2-benzanthracene (VI).

the half-wave potentials are only reproducible within about 0.03 V although a standard procedure of wiping off the electrode before the measurement was used.

DISCUSSION

The cathodic half-wave potentials at the dropping mercury electrode of aromatic hydrocarbons [4-8] have been related to wave-mechanical calculations [5,8] and to absorption spectra [4,6,7]. It has been shown [6] that in a series of related hydrocarbons the half-wave potentials are proportional to the wave number of the first *p*-band as defined by Clar [3] in the ultraviolet absorption spectrum of the hydrocarbon following the equation $E_{\frac{1}{2}} = a + b\,\nu$, where a and b are constants and ν the wave number of the first *p*-band. When the wave numbers are replaced by the corresponding energies in electron volts, the slope ($\Delta E_\nu / \Delta E_{\frac{1}{2}}$) has been predicted [4] to be two.

As shown in Fig. 1 a similar relation is found between the wave number of the first *p*-band and the anodic half-wave potential at a platinum microelectrode, $E_{\frac{1}{2}} = 0.543 \times 10^{-4}\nu - 0.61$, and it seems reasonable to expect that there in a series of related hydrocarbons would be a relation between the energy required to exite an electron corresponding to a defined band in the spectrum and the energy necessary to remove an electron completely from the aromatic system.

It was attempted to correlate the anodic half-wave potentials of a series of acenes with their *para*-localization energy as computed by Brown [9], but only a semi-quantitative accordance was found.

When the resonance system of a benzene ring in a polynuclear aromatic hydrocarbon loses two electrons the system acts as if the loss is restricted to a single benzene ring and the remaining separated resonance systems are apparently only affected to a minor degree. Thus tetracene yields a second wave at about the same potential as does 5,12-dihydrotetracene and both potentials are of the value which would be expected for a 2,3-dialkyl naphthalene.

The qualitative influence of a substituent on the half-wave potential can be predicted from its electron-attracting or electron-releasing properties as long as the steric circumstances permit the expected interaction between the substituent and the nucleus. An electron-releasing group as the methoxy

group or the amino group lowers the half-wave potential whereas an electron-attracting group as the nitro group or the quaternary ammonium group raises the half-wave potential in comparison with the unsubstituted hydrocarbon. A qualitative connection between the influence of a substituent on the half-wave potential and its σ-value as defined by Hammett was found, but no quantitative connection was detected.

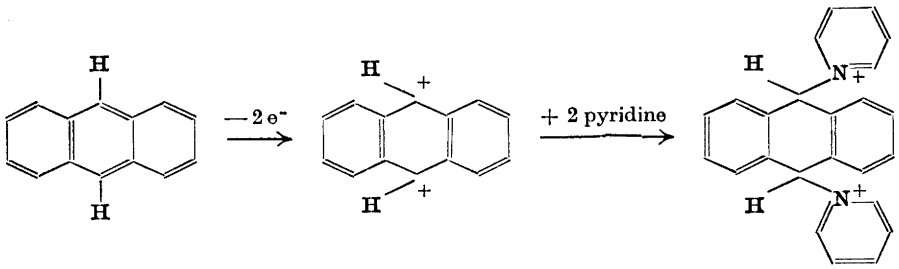
In an attempt to find the reason why some compounds yield deformed waves whereas other produce normal waves it is interesting to note the difference between indene and fluorene as indene yields a normal wave whereas fluorene produces a pronounced deformed wave. As will be shown in the preparative oxidation, anthracene yields in the presence of pyridine a product which is a derivative of dihydroanthracene. Assuming a similar reaction path in the oxidation of indene and fluorene the analogous oxidation product of indene would be a derivative of indane and would very likely be a stable compound, whereas a derivative of dihydrofluorene would be expected to be very unstable and to polymerize to a more or less defined product, in agreement with the fact that the reaction product covers the electrode with a black, insoluble layer which insulates the electrode from the solution.

The same considerations can be applied to other compounds giving deformed waves as benzene, diphenyl, fluoranthene and benzpyrene. In all cases the dihydro derivatives are unstable compounds. Naphthalene gives a slightly deformed wave and correspondingly dihydronaphthalene is only moderately stable.

The hydrocarbons which give a Diels-Alder adduct produce normal waves and there is a qualitative connection between the rate of formation of such adducts and the anodic half-wave potentials in such a way that the hydrocarbons having the lowest half-wave potential react most readily with maleic anhydride [9]. The presence of methyl substituents in the meso positions of anthracene lowers the half-wave potential and increases the rate of the addition of maleic anhydride whereas it decreases the percentage adduct in the equilibrium mixture of anthracene derivative and maleic anhydride [10].

As may be expected, there is a qualitative connection between the anodic half-wave potentials of the acenes and the tendency to form photo oxides. The influence of substituents is mostly the same in both cases, meso methyl groups greatly facilitate the photochemical addition of oxygen and lowers the half-wave potential. 9,9'-Bianthryl, however, forms no photo oxide, whereas it is oxidized at the anode. The half-wave potential is not, however, as low as might be expected from the analogy between benzene-diphenyl and anthracene-9, 9'-bianthryl substantiating the assumption that the plane of one of the anthracene molecules forms an angle of nearly 90° with the plane of the other anthracene molecule in 9,9'-bianthryl [11].

The first step in the oxidation is probably a localization of two π-electrons either at the same carbon atom or at two carbon atoms due to the attraction of the positive electrode. In either case they are extracted from the aromatic resonance system leaving a divalent carbonium ion. In the case of anthracene the electron deficiency is localized most of the time in the 9 and 10 positions. In presence of an electron donor as pyridine the pyridine donates its unpaired electrons to the carbonium ion thus forming a pyridinium ion:



The compound thus formed contains only isolated benzene rings which further are somewhat deactivated by the presence of the pyridinium groups and the compound is therefore not further attacked anodically at the potential used for the oxidation of anthracene. If the oxidation had consisted of a dimerization to 9,9'-bianthryl a further oxidation of the reaction product would be expected.

The addition of anhydrous perchloric acid in acetonitrile does not change the anodic half-wave potentials of the hydrocarbons, whereas the presence of pyridine lowers the half-wave potentials from 0.05—0.1 V. This can be explained by assuming the electron transfer to be a reversible reaction. In the presence of pyridine the concentration of the carbonium ion would be very much lower than in the absence of an electron donor, and the measured half-wave potential is, therefore, lowered. As hydrogen ions are not involved in the oxidation the addition of hydrogen ions is of no effect.

In view of the fact that the anodic half-wave potentials of the aromatic carbinols mostly differ only about 0.1 V from the half-wave potentials of their parent compounds (α-naphthyl carbinol 1.25 V, naphthalene 1.31 V; anisyl alcohol 1.22 V. anisol 1.35 V; cinnamyl alcohol 1.36 V, methyl styrene 1.47 V) it seems likely to assume that the first step in this case also is a loss of two electrons from the resonance system as postulated in Part II [2].

PREPARATIVE OXIDATION

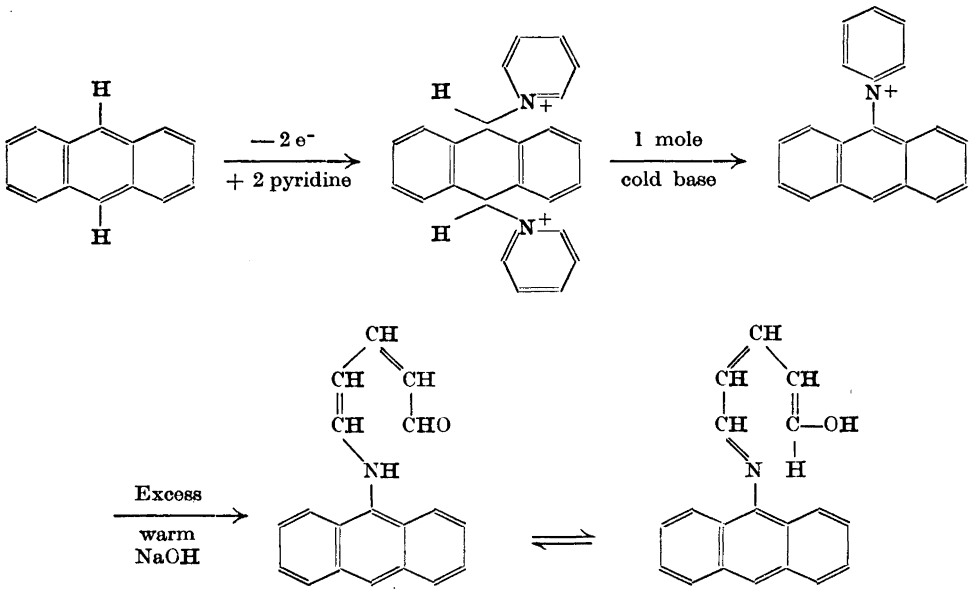
The controlled potential oxidations were performed in anhydrous acetonitrile or acetone containing sodium perchlorate and pyridine. It was found that the oxidation of anthracene at an anode potential of + 0.95 V *vs* the 0.1 N silver ion/ silver electrode yielded a watersoluble ionic compound which was identified as 9,10-dihydroanthranyldipyridinium diperchlorate by analysis of the diperchlorate, the diiodide and the dipicrate, m.p. 169.5°—171° (168.5°—170°, Barnett and Cook [12]) and by its infrared and ultraviolet spectrum. The ultraviolet spectrum showed only a very slight absorption at wave lengths above 280 mμ indicating that the compound did not contain the anthracene resonance system.

The 9,10-dihydroanthranyldipyridinium diperchlorate was also formed by addition of sodium perchlorate to an aqueous solution of the dibromide prepared according to Barnett and Cook [12], and the compounds were found to be identical.

As 9,10-dihydroanthracene is not planar three isomers (two *cis* and one *trans* isomer) of the 9,10-dihydroanthranyldipyridinium diperchlorate are theoretically possible, but only one has been isolated. The configuration of the isolated isomer is not known.

As described for the dibromide [12] the diperchlorate yielded on addition of a little less than 1 equiv. cold base or contact with an ion exchange resin IRC-50 9-anthrylpyridinum perchlorate. This conversion could be detected simply on heating the diperchlorate with water and it also proceeded to a certain degree during the electrolytic oxidation in the presence of the excess of pyridine giving the reaction mixture a yellow colour.

Barnett and Cook [12] treated 9,10-dihydroanthranyldipyridinium dibromide with excess of warm sodium hydroxide and isolated in a yield of 3.5 % a chocolate-brown compound to which they suggested the formula $C_{14}H_9$-NH-CH=CH-CH=CH-CH=O. The 9,10-dihydroanthranyldipyridinium diperchlorate was treated with excess of warm sodium hydroxide and there was isolated in a yield of 55 % a chocolate-brown compound with an analysis close to that found by Barnett and Cook. The infrared spectrum of the compound (in chloroform solution) showed a band at 1 648 cm^{-1}. As 2,4-hexadienal [13] shows a band (in chloroform solution) at 1 642 cm^{-1} the infrared spectrum of the compound supports the proposed formula containing a dienal. The band did not, however, possess the intensity to be expected of a dienal, but this can be explained by a strong enolisation. By enolisation the unsaturation of the side chain comes into conjugation with the anthracene resonance system. A high degree of enolisation is also suggested by the strong dark-red colour of the solution in chloroform, as a solution of the pure dienal would be expected to give a faint, yellow solution.



The oxidation of 9,10-dibromoanthracene in the presence of pyridine followed the same reaction path as the oxidation of anthracene, but only (9-bromo-10-anthranyl)pyridinium perchlorate was isolated probably due to instability of the analogous product 9,10-dibromo-9,10-dihydroanthranyldipyridinium diperchlorate. In this connection it is interesting to note that the half-wave potential of the second wave of 9-bromoanthracene (1.48 V) and that of 9,10-dibromoanthracene (1.47 V) is close to the half-wave potential of (9-bromo-10-anthryl)pyridinium perchlorate (1.47 V).

EXPERIMENTAL

The apparatus used for the voltammetric investigation and the preparative oxidations was the same as described in Part I[14], II[2], and III[15].

The acetonitrile, sodium perchlorate and silver perchlorate were purified in the same manner as described in Part II[2]. The acetone was Riedel-de-Haën analytical grade.

The following compounds were prepared according to the given references: anthracene [16], 9,9'-bianthryl [17], 9-nitroanthracene [18], 9-bromoanthracene [19], 9,10-dibromoanthracene [20], and 9,10-dimethylanthracene [21].

The other compounds investigated were commercially available or were obtained from Dr. L. F. Fieser, Dr. Hakon Lund or Mr. F. Lund. The author wishes to acknowledge with thanks the receipt of these hydrocarbon samples.

Oxidation of anthracene. In 150 ml of a deaerated solution of 15 g anhydrous sodium perchlorate and 4 ml pyridine in acetonitrile was suspended 1.00 g of anthracene, and the anthracene was oxidized at an anode potential of +0.90 – +0.95 V *vs* the 0.1 N silver ion/silver electrode. The anolyte was stirred with a magnetic stirrer and purified nitrogen was bubbled through the solution during the oxidation. As the oxidation proceeded the anthracene gradually dissolved. The amount of electricity required for the oxidation corresponded to a two-electron oxidation. After completion of the reaction the acetonitrile was evaporated *in vacuo* at temperatures not exceeding 30°. To the dry residue were added 40 ml of water, the precipitate was filtered off and washed with small portions of cold water. After drying the precipitate was dissolved in acetonitrile and precipitated with dry ether. One further recrystallization from acetonitrile/ether yielded a white compound (1.35 g). The compound turns yellow at about 170° and decomposes at about 215°. (Found: C 53.71; H 3.70; N 5.17; Cl 13.30. Calc. for $C_{24}H_{20}O_8N_2Cl_2$: C 53.72; H 3.76; N 5.24; Cl 13.41.) The compound had an absorption maximum at 251 mμ and showed only a very faint absorption at wave lengths above 280 mμ. Its infrared spectrum contained no carbonyl absorption. The compound was readily soluble in acetonitrile and acetone, soluble in 50 % aqueous alcohol, but less soluble in absolute alcohol and water and insoluble in benzene and ether. The compound formed a picrate, m. p. 169.5–171°. (Found: C 54.47; H 2.94; N 14.03. Calc. for $C_{36}H_{24}O_{14}N_8$: C 54.55; H 3.05; N 14.14). By adding an excess of sodium iodide in acetone to a solution of the compound in acetone an iodide was obtained, m. p. 143° (decomp.). (Found: C 49.17; H 3.27; N 4.80; I 43.19. Calc. for $C_{24}H_{20}N_2I_2$: C 48.86; H 3.41; N 4.75; I 42.98). The compound was identified as 9,10-dihydroanthranyldipyridinium diperchlorate.

Analogous to the preparation of 9-anthrylpyridinium bromide [12] the 9-anthrylpyridinium perchlorate was obtained by adding a little less than one equivalent of sodium hydroxide to a 50 % aqueous alcoholic solution of the diperchlorate and evaporating part of the solvent after the reaction was completed. M. p. 269–272°. (Found: C 64.28; H 4.14; N 3.90; Cl 10.03. Calc. for $C_{19}H_{14}O_4NCl$: C 64.13; H 3.97; N 3.94; N 9.97). On addition of excess of sodium iodide in acetone to a solution of the compound in acetone the iodide was obtained, m. p. 260–64°. (Found: C 59.67; H 3.83; N 3.44; I 33.25. Calc. for $C_{19}H_{14}NI$: C 59.55; H 3.68; N 3.65; I 33.12). The 9-anthrylpyridinium perchlorate had maxima (in alcohol) at 389, 369, and 352 mμ.

Treatment of 9,10-dihydroanthranyldipyridinium diperchlorate with excess of sodium hydroxide. To 1.0 g of the diperchlorate were added 50 ml 1 N sodium hydroxide and 50 ml chloroform. The mixture was refluxed for 1 h and cooled. The dark-purple chloroform layer was separated from the aqueous layer, to which were added 25 ml 1 N sodium

hydroxide and 50 ml chloroform. The mixture was again refluxed for 1 h, cooled and the layers were separated. The pooled chloroform layers were washed with water and most of the chloroform evaporated *in vacuo*. On addition of ether a chocolate-brown compound was obtained, 290 mg (55 %). (Found: C 80.85; H 5.30; N 4.88. Calc. for $C_{19}H_{15}ON$, $\frac{1}{2}H_2O$: C 80.83; H 5.71; N 4.96). The infrared spectrum of the compound showed a relatively weak carbonyl band at 1 648 cm^{-1} (in chloroform solution).

Oxidation of 9,10-dibromoanthracene. A suspension of 2.0 g 9,10-dibromoanthracene in 150 ml of a solution of 15 g sodium perchlorate and 4 ml pyridine in acetone was oxidized at an anode potential of +1.2 V *vs* the 0.1 N silver ion/silver electrode in acetone. The oxidation was not run to completion, but was stopped after a consumption of electricity of 910 coulomb (80 % of the theoretical amount). The current was rather low as it was governed by the rate of dissolving the 9,10-dibromoanthracene. The undissolved, unreacted dibromoanthracene was filtered off, part of the solvent was evaporated *in vacuo* and the residue diluted with water. The precipitate was filtered off, dried and extracted in a Soxhlet extractor with carbon tetrachloride, which dissolved unreacted dibromoanthracene. The residue, 1.3 g, was dissolved in hot acetone. On addition of carbon tetrachloride a precipitate, 0.95 g, was obtained. M. p. 270–272°. (Found: C 52.18; H 3.05; N 3.24; Br 18.75; Cl 8.51. Calc. for $C_{19}H_{13}O_4NBrCl$: C 52.50; H 3.02; N 3.22; Br 18.38; Cl 8.16). The compound formed a picrate, m. p. 237–240°. (Found: C 52.90; H 2.53; N 9.93; Br 14.18. Calc. for $C_{25}H_{15}O_7N_4Br$: C 53.35; H 2.68; N 9.94; Br 14.17). The compound showed maxima (in 50 % aqueous ethanol) at 399, 378 and 359 mμ. The compound was identified as (9-bromo-10-anthryl)pyridinium perchlorate.

Oxidation of naphthalene. 1.0 g of naphthalene was dissolved in 150 ml of a solution of 15 g sodium perchlorate and 4 ml pyridine in acetonitrile. The naphthalene was oxidized at an anode potential of +1.4 V *vs* the 0.1 N silver ion/silver electrode. The current decreased rapidly from 0.2 A to about 5 mA. No visible layer covered the electrode, but after the electrode had been wiped off the current again started at about 0.2 A. The current decreased, however, rapidly to a negligible value. The amount of electricity consumed was less than 5 % of the theoretical amount and no oxidation products could be isolated from the reaction mixture.

REFERENCES

1. Fichter, F. *Organische Elektrochemie*, Theodor Steinkopff, Dresden und Leipzig 1942.
2. Lund, H. *Acta Chem. Scand.* **11** (1957) 491.
3. Clar, E. *Aromatische Kohlenwasserstoffe*, 2nd Ed., Springer-Verlag, Berlin-Göttingen-Heidelberg 1952.
4. Watson, A. T. and Matsen, F. A. *J. Chem. Phys.* **18** (1950) 1305.
5. Pullman, A., Pullman, B. and Berthier, G. *Bull. soc. chim. France* **1950** 591.
6. Bergman, I. *Trans. Faraday Soc.* **50** (1954) 829.
7. Bergman, I. *Trans. Faraday Soc.* **52** (1956) 690.
8. Hoijtink, G. J. and Van Schooten, J. *Rec. trav. chim.* **71** (1952) 1089.
9. Brown, R. D. *J. Chem. Soc.* **1950** 691.
10. Bachmann, W. E. and Kloetzel, M. C. *J. Am. Chem. Soc.* **60** (1938) 481.
11. Magnus, A. and Becker, F. *Erdöl u. Kohle* **4** (1951) 115.
12. De Barry Barnett, E. and Cook, J. W. *J. Chem. Soc.* **1921** 901.
13. Blout, E. R., Fields, M. and Karplus, R. *J. Am. Chem. Soc.* **70** (1948) 194.
14. Lund, H. *Acta Chem. Scand.* **11** (1957) 283.
15. Lund, H. *Acta Chem. Scand.* **11** (1957) 990.
16. Fieser, L. F. *Experiments in Organic Chemistry*, 3rd Ed., D. C. Heath and Co., Boston 1955, p. 163.
17. Bell, F. and Waring, D. H. *J. Chem. Soc.* **1949** 1579.
18. Braun, C. E., Cook, C. D., Merritt, C. and Rousseau, J. E. *Org. Syntheses* **31** (1951) 77.
19. De Barry Barnett, E. and Cook, J. W. *J. Chem. Soc.* **1924** 1084.
20. Heilbron, I. M. and Heaton, J. S. *Org. Syntheses, Coll. Vol.* **1** (1941) 207.
21. Phillips, D. D. and Cason, J. *J. Am. Chem. Soc.* **74** (1952) 2934.

Received May 22, 1957.

ACTA CHEMICA SCANDINAVICA 11 (1957) 1331—1339

The Magnetic Properties of Manganous Complexes

Studies in Magnetochemistry 18 *

R. W. ASMUSSEN and H. SOLING

The Chemical Laboratory B, Technical University of Denmark, Copenhagen, Denmark

The effective magnetic moments at room temperature of representative manganous complexes are reported. The temperature dependence of the susceptibility in the interval 85—295°K is studied for Mn(II)-bis-salicylaldehyde, Mn(II)-bis-salicylaldehyde-ethylenediimine and Mn(II)-bis-salicylaldehyde-*o*-phenylenediimine. Preparative details are given for these chelates. The magnetic moments found are compared with the predictions of the valence bond theory and the ligand field theory. A qualitative explanation of the apparent non-existence of planar manganous complexes with magnetic moment 3.87 μ_B is suggested. A slight discontinuity in the χ^{-1}, T-diagram of Mn(II)-bis-salicylaldehyde-ethylenediimine is reported. The reflection spectrum of the pink $Mnpy_2Cl_2$ is interpreted as originating in a halogenbridged polymeric structure. Evidences for the non-existence of Reitzenstein's brown "isomer" $Mnpy_2Cl_2$ are given.

The ground level of the $3d^5$ electron system of the free Mn^{+2} ion is ^6S. Assuming ideal Russell-Saunders coupling the magnetic moment of the free manganous ion is 5.92 μ_B. When the manganous ion is the central-ion in complexes more or less pronounced deviations from the ideal free ion value of the magnetic moment may be expected according to the type of bond and the spatial arrangement of the ligands. The valence bond theory thus predicts three different magnetic moments, *viz.* 5.92 μ_B, 3.87 μ_B, and 1.73 μ_B. In the two last mentioned cases, with reduced spin multiplicity, the bonding electrons are supposed to utilize the planar dsp^2-hybrid and the octahedral d^2sp^3-hybrid, respectively.

The magnetic moments actually found in manganous complexes are almost invariably about 5.9 μ_B corresponding to the sextet ground level. A slightly higher value, 6.2 μ_B is reported by Wiley, Tyson, and Stellar [1] in the case of the manganous-kojate. However, only the manganous hexacyanides exemplify the case of the lowest spin multiplicity, while no certain instances of compounds with a quartet ground level are reported. As an illustration of the

* No. 17 of this series is published in *Acta Chem. Scand.* 11 (1957) 1271.

Table 1. Effective magnetic moments in Bohr magnetons of complex manganous compounds.

	Temp. °C	μ_{eff}/μ_B
$MnSO_4$	19	5.85
$[Mn(OH_2)_4]SO_4$	19	5.96
$[Mn(C_2O_4)_2](NH_4)_2$, $2H_2O$	17	5.84
$Mnpy_2Cl_2$ I brown	17	5.67
$Mnpy_2Cl_2$ II pink	18	5.89
$Mnpy_2Cl_2$ III pink	18	5.96
$Mnpy_2Br_2$	18	5.96
$Mnpy_6Br_2$	18	6.00
$[Mn(SCN)_6]K_4$, $3H_2O$	18	6.06
$[Mn(CN)_6]K_4$, $3H_2O$	17	2.13

experimental results some manganous complexes earlier prepared and measured magnetically by one of us [2] are stated in Table 1.

The magnetic results mentioned in Table 1 are equally well described by the theory of crystalline field potential (v. Vleck and his school [3]). According to this theory the electric field from the ligands causes a sort of intramolecular Stark splitting of the energy levels of the central ion. In case of the manganous ion the Stark splitting leaves a sextet level lowest in octahedral and tetrahedral ligand fields of weak and intermediate strength, while at strong ligand fields a doublet becomes the ground level, and a reduction of the magnetic moment occurs as observed for $K_4Mn(CN)_6$.

The value of the magnetic moment of $K_4Mn(CN)_6$ stated in Table 1 is somewhat higher than the "spin only" value 1.73 μ_B of one unpaired electron. It is rather difficult to prepare this substance of a sufficient purity as the presence of even minute amounts of other manganese compounds may increase the susceptibility considerably. The rather large range of moments quoted in the literature reflects this. However, it is interesting that the deviation from the value 1.73 μ_B may also be explained theoretically. A quantum mechanical calculation by Kotani [4], taking into account the spin-orbit interaction, leads to an effective magnetic moment of about 2.5 μ_B at room temperature. According to Kotani's calculations the effective magnetic moment decreases slowly when the temperature is lowered and converges against the "spin only" value when the temperature approaches the absolute zero. A study of the temperature dependence of the susceptibility of this and a few other manganous-cyano-complexes is being carried out in this laboratory at present.

Particular interest is connected to the measurements of the three preparates $Mnpy_2Cl_2$ I, II and III. Reitzenstein [5] prepared a pink compound of this composition and furthermore a brown substance of apparently the same composition, which have been considered as *cis-trans* isomers. The magnetic moment of the brown preparation I is lesser than the moment of the pink preparation III, which may be due to the presence of higher oxidation states of manganese. This assumption is supported by the fact that preparation I becomes darker brown when exposed to the air for some time. After recrystalli-

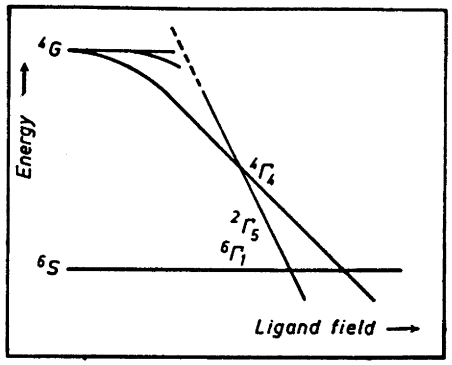


Fig. 1. Theoretical Orgel diagram for octahedral manganous complexes. (For explanation of terms see Ref. 7).

zation of I from ethanol the pink preparation II was obtained having nearly the theoretical value 5.92 μ_B for the magnetic moment (compare also the results of the Cl-determinations in the three cases). The brown "isomer" is probably not a chemically pure substance. Neither the directions given by Reitzenstein nor systematic variations of the experimental conditions yielded well defined products. In one of the more or less brownish powders now obtained, the presence of higher oxidation states of manganese could be demonstrated. X-Ray powder photograms (19 cm Bradley camera) supplied by P. F. Andersen M.sc. of this laboratory prove that all the lines in the powder-photogram of the pink compound appear in the powder photos of the brownish products with identical Bragg-angles and intensities. The powder photos of the brown products contain besides these lines a few foreign lines. In our opinion the only existing compound of the composition $Mnpy_2Cl_2$ is the pink crystalline com-

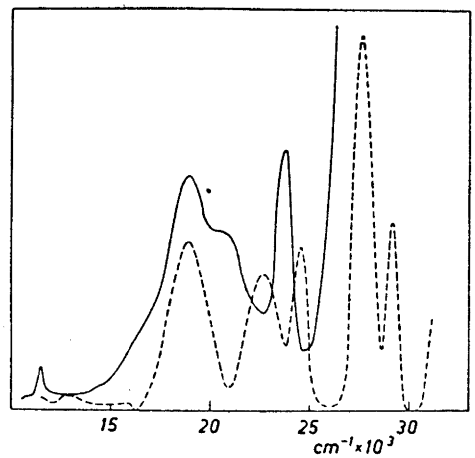


Fig. 2. Reflectionspectra of $MnCl_2 \cdot 4\,H_2O$ (punctuated) and $Mnpy_2Cl_2$ (full drawn) measured with a Beckman spectrophotometer model DU. Ordinate in arbitrary units. Abscissae frequencies in Kayser-units = cm^{-1}.

pound with the magnetic moment 5.96 μ_B which moment, according to the valence bond theory, excludes a planar configuration.

Concerning the non-existence of planar manganous complexes with magnetic moment 3.87 μ_B Dr. Klixbüll Jørgensen has kindly pointed out to us that referring to the energy level diagram in Fig. 1 the following arguments might be given, (for further details and explanation of the terms used compare for instance Ref.[7]).

In octahedral complexes the $^2\Gamma_5$-level crosses the $^6\Gamma_1$-level at a smaller ligand field strength than is the case with $^4\Gamma_4$. When the octahedron of 6 ligands are tetragonally deformed the quartet and the doublet levels are further split, but in view of the relative slopes of the $^2\Gamma_5$ and $^4\Gamma_4$-lines it seems rather improbable that this splitting should cause an interchange of the sequence of the crossing points with the $^6\Gamma_1$-level. Thus one may conclude that provided the intramolecular Stark-pattern caused by four co-planar ligands is comparable with that caused by a tetragonally deformed octahedral arrangement of 6 ligands, the existence of planar manganous-complexes with the magnetic moment 3.87 μ_B seems energetically less probable.

In the particular case of $Mnpy_2Cl_2$ the results of the magnetic measurements are in conformity with the formula

$$[Mnpy_4][MnCl_4]$$

and with a halogenbridged chain-like structure as well. In view of the reflection spectrum discussed below we prefer the latter possibility.

The reflection spectra of $Mnpy_2Cl_2$ and of $MnCl_2,4H_2O$ are shown in Fig. 2. Following the arguments of Orgel [6] the bands of the latter are identified as follows (frequencies in Kayser units = cm^{-1}).

18 800 $^4\Gamma_4$ (G)	22 700 $^4\Gamma_5$ (G)	24 600 $^4\Gamma_1$ (G) and $^4\Gamma_3$ (G)
27 600 $^4\Gamma_5$ (D)	29 200 $^4\Gamma_3$ (D)	

By analogy the spectrum of $Mnpy_2Cl_2$ is interpreted in the following way: The narrow band at 23 800 K is due to the transition $^6\Gamma_1$ (S)$\rightarrow$$^4\Gamma_1$ (G) and $^4\Gamma_3$ (G). The red shift of this band gives evidence for an increased anionic character of the complex [7]. The broad band in the region 15 000 K to 23 000 K shows two maxima and a shoulder towards the red. The maximum with the highest wavenumber, being due to the transition $^6\Gamma_1$ (S)$\rightarrow$$^4\Gamma_5$ (G), is also shifted towards the red. This red shift is at least partly a consequence of the former, but an increased ligand field strength probably also contributes. The last maximum together with the shoulder is believed to originate in a tetragonal splitting of the $^4\Gamma_4$ (G) level. This interpretation suggests that $Mnpy_2Cl_2$ has a halogen-bridged polymeric structure *i.e.* octahedra sharing 2 Cl^- and with 2 pyridine molecules in *trans* position analogous to that found by X-ray analysis of the violet $Copy_2Cl_2$[8].

From the magnetochemistry of nickel(II)-complexes several planar, diamagnetic chelates with tetradentate Shiff-base ligands of the type salicylaldehyde-ethylenediimine are well known. In the light of the above discussion it was therefore considered worth while to study the magnetic behaviour of similar manganous compounds. We have prepared and studied the magnetic properties of manganous-bis-salicylaldehyde-ethylenediimine and manganous-

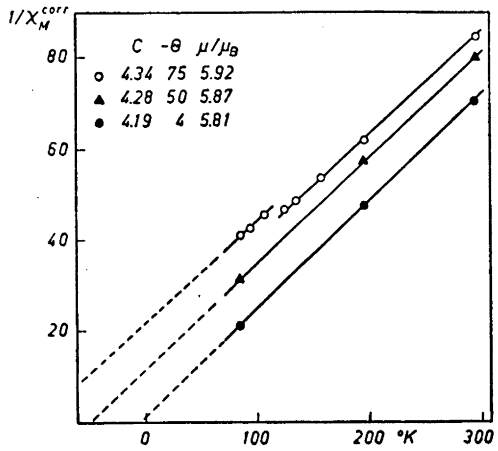


Fig. 3. Reciprocal corr. molar susceptibility of manganous-bis-salicylaldehyde ▲, manganous-bis-salicylaldehyde-ethylenediimine O, and manganous-bis-salicylaldehyde-o-phenylenediimine ● plotted against the abs. temperature.

bis-salicylaldehyde-*o*-phenylene-diimine and for comparison also manganous-bis-salicylaldehyde, although this latter compound could not be obtained in a quite satisfactory purity.

Fig. 3 illustrates the results of the magnetic measurements over a range of temperatures. The reciprocal molar susceptibility corrected for the diamagnetism of the ligands and the diamagnetism of the electron system of the manganous ion is plotted against the absolute temperature. The straight lines, representing the Curie-Weiss relation, are fixed by means of a least square analysis of the data. In the figure is also stated the values of the Curie constant C, the Weiss-correction Θ and the mean magnetic moment calculated from the formula $\mu = 2.84 \sqrt{\chi_M^{cor}(T-\Theta)}\mu_B$. The magnetic moments are only a little smaller than the "spin only" value of five unpaired electrons, thus indicating a sextet ground level clearly.

It is noteworthy that while the Weiss correction for the salicylaldehyde-*o*-phenylenediimine-compound is only $-4°$, this constant has a considerably higher value for the salicylaldehyde- and the salicylaldehyde-ethylenediimine-compounds *viz.* $-50°$ and $-75°$, respectively. Since a residual orbital contribution and anisotropy effects are not expected for manganous compounds the Θ-values may be ascribed to exchange interactions. It is in accordance with this point of view that the presumably most diluted *o*-phenylene-diimine-compound has the smallest Θ-value.

In the temperature range 85—107°K the susceptibilities of the salicylaldehyde-ethylenediimine-complex are from 8 to 10 % lower than calculated from the Curie-Weiss line based upon the susceptibilities measured between 125 and 295°K. A rough estimate of the values gives the relation $\chi_M^{cor} = \frac{4.48}{T+99}$

for $85 < T < 107$°K. In this temperature interval obviously a change in the crystals occurs, which increases the exchange forces (Θ). A decrease in the atomic distances explains this effect; however, since no X-ray information is available this question cannot be settled for the present.

EXPERIMENTAL

Preparation and analysis of the compounds

The materials used for the preparation of the compounds were the tetrahydrates of manganous chloride and manganous sulphate, anhydrous manganous bromide prepared from the oxide and hydrogen bromide, potassium cyanide, potassium thiocyanate and furthermore pyridine, salicylaldehyde, ethylenediamine and *o*-phenylenediamine. The potassium cyanide was the purest product available. The other substances were c.p. chemicals. The Schiff-bases prepared from salicylaldehyde and the amines were recrystallized from 96 % ethanol.

Manganese was determined as manganous sulphate or potentiometrically according to *Lingane* and *Karplus* [9] after destruction of the complexes and chelates with concentrated sulphuric acid to which was added a small amount of concentrated nitric acid. Chloride was determined argentometrically after Volhard.

Anhydrous manganous sulphate was obtained by dehydration of the tetrahydrate (constant weight).

Manganous sulphate tetrahydrate. Some of the most well developed and apparently not dehydrated crystals were selected for the magnetic measurement. The evidence for the composition of this salt is of course not entirely satisfactory. A slight deviation in the water content has, however, no significant influence upon the value of $\mu_{eff.}$

Ammonium manganous dioxalate dihydrate. This compound was prepared after the method of Sonchay and Lenssen [10]. No higher hydrates were isolated. (Found: Mn 18.30, Calc.: Mn 18.13).

Potassium manganous thiocyanate trihydrate. The method used to prepare the complex is essentially that of Walden [11]. Only red crystals were used for the analysis and the magnetic measurement. Brownish crystals were discarded. (Found: Mn 9.04. Calc. Mn 8.95).

Potassium manganous hexa-cyanide trihydrate. The procedure given by Christensen [12] was followed. (Found: Mn 13.14. Calc.: Mn 13.04).

Dipyridinomanganous chloride. Preparation No. I, brown powder, was obtained as described in the paper of Reitzenstein [5]. (No. I. Found: Cl. 24.65. Calc. Cl 24.98). The preparation of this brown substance was carried out with success only once.

A portion of No. I was recrystallized from ethanol. The pink crystals were washed with ether and dried in vacuum; thus we obtained preparate No. II, the composition of which also is $Mnpy_2Cl_2$. (No. II. Found: Cl 24.61. Calc. Cl 24.98).

The third specimen, preparation No. III, was produced by addition of pyridine to a solution of manganous chloride in ethanol. Further treatment as in the case of No. II. (No. III. Found: Cl 24.88. Calc. Cl 24.98).

It seems to be a mere accident if Reitzenstein's "kaffeebraune" compound is precipitated. If the aqueous solution of manganous chloride is saturated with oxygen, one obtains a substance of a light brown colour. In other experiments oxygen was continuously passed through the solution during the preparation. In these cases deeper brown solids were precipitated. Specimens selected for analysis gave 24.26 % Cl and 24.87 % Cl. However, the substance was not homogeneous. The total yield was ground in a mortar and the content of Cl was now 26.85 % and 26.95 %. In another series of experiments the ratio of the concentration of manganous chloride to pyridine was varied from 1 : 4 to 1:20. The colour of the precipitates became deeper brown when decreasing this ratio. One of the deepest brown products gave evolution of chlorine when boiled with hydrochloric acid (potassium iodide paper).

These evidences, the X-ray results above mentioned, and the magnetic measurements on preparations I, II, and III discussed above indicate that the existence of a well defined brown or darkbrown compound of the composition $Mnpy_2Cl_2$ is doubtful. The reason for

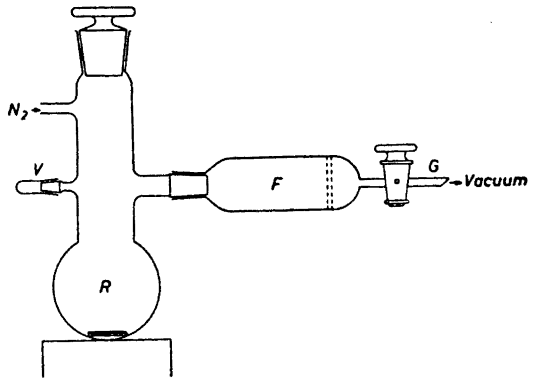


Fig. 4. Apparatus for preparation of manganous-bis-salicylaldehyde.

the brown colour may be that the pink compound is contaminated with a manganese compound in which the oxidation state of manganese is higher than 2. In our opinion the pink, crystalline substance above described as II or III is the only existing defined compound of the composition $Mnpy_2Cl_2$.

Dipyridinomanganous bromide. This complex was prepared following the method of Grossmann [13]. (Found: Mn 14.89. Calc. Mn 14.73).

Hexapyridinomanganous bromide. Crystals of this compound were obtained by cooling a boiling solution of anhydrous manganous bromide in pyridine (Grossmann [13]). The substance gives off pyridine easily at room temperature. (Found: Mn 7.87. Calc. Mn 7.97).

Manganous-bis-salicylaldehyde. Emmert, Gsottschneider and Stanger [14] prepared a hydrate containing $1\frac{1}{2}$ H_2O from manganous chloride and salicylaldehyde in aqueous ammonia (Found for C and H respectively, 51.84 % and 4.01 % calc 51.83 % and 3.81 %, respectively). Ray and Mukherjee [15] in a similar way prepared a dihydrate (Found: Mn 16.68. Calc. Mn 16.51). Our preparation was carried out as follows: The apparatus shown in Fig. 4 was evacuated and a current of nitrogen passed through. This operation was repeated several times. The following reagents were introduced into the reaction bulb *R* while a continuous stream of nitrogen was passed through: 1.0 g $MnCl_2 \cdot 4H_2O$ was dissolved in 40 ml 50 % aqueous acetone (oxygen-free), 1.5 ml salicylaldehyde was added and furthermore drop by drop 10 ml water-acetone mixture +5 ml conc. ammonia while stirring the mixture.

The apparatus was closed and the reaction mixture vigorously stirred for half an hour (magnetic stirrer). The liquid and the strawcoloured crystals were transferred to the filterbulb *F*. The crystals were filtered off by suction through *G* and washed with aqueous acetone and next with acetone, which was introduced through *V* by means of a long funnel. The washing operation was carried out in an atmosphere of nitrogen.

The apparatus was again closed and the precipitate was dried by pumping through *G* for some hours. The substance was finally dried in a high vacuum over P_2O_5 at 110 – 120°C until the weight was constant. The dry compound does not become darker when exposed to the atmosphere. Seven different preparates were produced. (No. 1: Mn 19.42. No. 2: Mn 19.47; No. 3: Mn 19.15. Calc. Mn 18.49).

These particular 3 compounds were applied for the magnetic measurement in spite of their manganese content being too high. The magnetic moments of these substances are practically identical and equal to 5.87 μ_B and the Curie-Weiss line is nearly *parallel* to that of manganous-bis-salicylaldehyde-*o*-phenylenediimine. The surplus of manganese does not increase the magnetic moment more than 1 % of the theoretical value for ionic- or sp^3-bonds (5.92 μ_B). The main point is that the presence of the impurity does not make our statement concerning the non-planar configuration doubtful.

Manganous-bis-salicylaldehyde-ethylenediimine. 750 ml redistilled ethanol was placed in a 1 000 ml round-bottomed flask fitted with a mechanical stirrer and a fractionating column with condenser. A current of nitrogen was passed through the system and 100 ml ethanol was distilled over. Together with 3.0 g $MnCl_2 \cdot 4H_2O$ this distillate was returned to the remanens. 100 ml ethanol were again distilled off and returned to the flask together with 4.0 g salicylaldehyde-ethylenediimine. 100 ml ethanol was distilled over and 0.9 g solid NaOH was added to the reaction mixture. The column was adjusted so that the destillation was now very slow. Red crystals separated after 45 min, and after 4—5 h 2—3 g of red crystals were formed, which were filtered off (glassfilter-crucible) and washed with ethanol, acetone, and ether. These operations were all carried out in an atmosphere of nitrogen. Sometimes the red crystals were contaminated with a yellow precipitate, which was easily eliminated by washing with 0.04 M acetic acid.

Three independent specimens were prepared for the magnetic measurement. (No. 1: Mn 17.14; No. 2: Mn 17.19; No. 3: Mn 17.03. Calc. Mn 17.10).

Manganous-bis-salicylaldehyde-o-phenylenediimine. This substance was obtained by a method similar to the preceding. The reaction-mixture turned strongly red after half an hour. After one hour the precipitate was so dense that the preparation had to be interrupted. A dark yellow spongy mass of 1 cm long crystals was obtained.

Two independent preparates were produced for the magnetic measurement. (No. 1: Mn 14.80; No. 2: Mn 15.02. Calc. Mn 14.88).

In a previous publication by Asmussen [2] it was pointed out that it is very difficult to prepare manganous chelates by means of Schiff-bases as chelating agents in so well defined composition that a magnetic measurement has any sense. The preparation methods here described seem to give compounds for which the magnetic susceptibilities are sufficiently reproducible. However, it must be admitted that we have not succeeded in preparing the analoguous chelates with bis-salicylaldehyde-putrescine and bis-salicylaldehyde-cadaverine. Manganous-bis-salicylaldehyde could not be prepared following the method described above for manganous-bis-salicylaldehyde-ethylenediimine.

Magnetic measurements

The determination of the magnetic susceptibilities were carried out by the Gouy-method as described by Asmussen and Soling [16]. The susceptibilities were measured at room temperature, then at 195°K and at 85°K and finally for control again at room temperature. Manganous-bis-salicylaldehyde-ethylenediimine No. 3 was measured at 5 temperatures between 85°K and 195°K. These temperatures were realized by means of a brass block which fitted in the Dewar vessel. The amounts of liquid air were so adjusted that the different temperatures were fixed within 5° intervals. At all temperatures except room temperature the measurements were performed 20—30 min after the specimen tube had been suspended in the cooling system. The measurement was repeated after 20—30 min. In some cases a third measurement was performed after another 20—30 min interval. The agreement between the results was in general excellent. The temperature dependence of the susceptibility for the preparate mentioned is illustrated by the data given in Table 2.

Table 2. Temperature dependence of χ_M (corr) and μ_{eff} for manganous-bis-salicylaldehyde-ethylenediimine No. 3.

°K	$\chi_M^{cor} \times 10^6$	μ_{eff}/μ_B	°K	$\chi_M^{cor} \times 10^6$	μ_{eff}/μ_B
290	11 965	5.29	125	21 374	4.64
195	16 157	5.04	107	21 949	4.35
157	18 634	4.88	94	23 488	4.22
135	20 529	4.73	85	24 416	4.09

Table 3. Susceptibilities and μ_{eff} values for the 3 different manganous-bis-salicylaldehyde-ethylenediimine preparates.

Preparation number	°K	$\chi_g \times 10^6$	$\chi_M \times 10^6$	$\chi_M^{cor} \times 10^6$	$1{:}\chi_M^{cor}$	μ_{eff}/μ_B
1	291	36.11	11 600	11 760	85.03	5.25
2	294	36.10	11 596	11 756	85.06	5.28
3	294	36.20	11 629	11 789	84.82	5.29
1	195	49.58	15 927	16 087	62.15	5.03
2	195	49.63	15 943	16 103	62.11	5.03
3	195	49.96	16 047	16 207	61.69	5.05

The values for χ_M^{corr} are calculated from χ_M by means of the corrections for the diamagnetism of the ligands and the diamagnetism of the electron system of the Mn^{+2} ion. The values used for these corrections are -122×10^{-6} and -160×10^{-6} and -175×10^{-6} for the bis-salicylaldehyde, the bis-salicylaldehyde-ethylenediimine and the bis-salicylaldehyde-*o*-phenylenediimine chelates, respectively. These corrections were calculated from Pascal's constants and the experimental value $\chi_M = -64.4 \times 10^{-6}$ for salicylaldehyde measured by Rumpf and Leguin [17]. The diamagnetism of the Mn^{+2} ion was calculated [2] to $-21 \cdot 10^{-6}$.

The results of the measurements are shown in Fig. 3. We point out that the "points" in the diagram at each temperature are mean values of all measurements on different preparations of the compound in question. The data in Table 3 give an impression of the reproducibility of the measurements of the 3 different preparates of manganous-bis-salicylaldehyde-ethylenediimine.

The field strength dependence was investigated at room temperature. The susceptibilities of all compounds were field strength independent in the interval 700 to 8 000 Ørsted.

REFERENCES

1. Wiley, J. W., Tyson, G. N. and Stellar, J. S. *J. Am. Chem. Soc.* **64** (1942) 963.
2. Asmussen, R. W. *Studies in the Magnetochemistry of Inorganic Complex Compounds* (in Danish), Copenhagen 1944.
3. v. Vleck, J. H. *J. Chem. Phys.* **3** (1955) 807.
4. Kotani, M. *J. Phys. Soc. Japan* **4** (1949) 293.
5. Reitzenstein, F. *Z. anorg. allgem. Chem.* **18** (1898) 292.
6. Orgel, L. E. *J. Chem. Phys.* **23** (1955) 1824.
7. Klixbüll Jørgensen, Chr. *Acta Chem. Scand.* **11** (1957) 66.
8. Dunitz, J. D. *Acta Cryst.* **10** (1957) 307.
9. Lingane, J. J. and Karplus, R. *Ind. Eng. Chem. Anal. Ed.* **18** (1946) 191.
10. Sonchay, A. and Lenssen, E. *Ann.* **102** (1857) 50.
11. Walden, F. *Z. anorg. allgem. Chem.* **23** (1900) 373.
12. Christensen, O. T. *J. prakt. Chem.* **31** (1885) 171.
13. Grossmann, H. *Ber.* **37** (1904) 564.
14. Emmert, B. Gsottschneider, H. and Stanger, H. *Ber.* **69** *B* (1936) 1319.
15. Ray, P. and Mukherjee, A. *J. Ind. Chem. Soc.* **27** (1950) 716.
16. Asmussen, R. W. and Soling, H. *Acta Chem. Scand.* **8** (1954) 558, 563.
17. Rumpf, F. and Leguin, M. *Bull soc. chim. France* **1949** 366.

Received June 6, 1957.

ACTA CHEMICA SCANDINAVICA 11 (1957) 1340—1349

Dialkoxy-phosphorylthiocholines, Alkoxy-methyl-phosphorylthiocholines and Analogous Choline Esters.

Syntheses, pK_a of Tertiary Homologues and Cholinesterase Inhibition

L-E. TAMMELIN

Research Institute of National Defence Dept. 1, Sundbyberg 4, Sweden

The syntheses of S,ω-dimethylaminoethyl-dialkylthiophosphate, ω-dimethylaminoeththio-alkoxy-methyl-phosphine oxide and their corresponding oxygen phosphates are described. These tertiary amino esters have been quaternized with methyl iodide, yielding esters of thiocholine and choline. The alkoxy groups were ethoxy and *iso*-propoxy groups. The protolytic dissociation constants in water $(pK)_a$ at 25°C of the dimethylaminoethyl esters have been determined and results obtained have been used in a discussion of the properties of the substituted phosphoryl groups. Compounds with sulfur-phosphoryl groups have significantly lower pK_a values than other analogous compounds investigated. The cholinesterase inhibiting properties of the compounds have been determined as pI_{50}. The esterase preparations were human plasma and hemolysate of human red cells. Thio derivatives are potent inhibitors and about 10^4 times as potent as their oxygen analogues. The chemical structures of the inhibitors in relation to their cholinesterase-inhibiting properties are discussed.

Choline esters of the aliphatic carboxylic acids, as *e.g.* acetylcholine, are considered to form addition compounds with cholinesterases as a first step in the sequence of reactions which lead to enzymic hydrolysis. The anchor points of the substrate are considered to be the carbonyl-ester and the ammonium parts of the molecule [1]. It has been shown that methyl-fluoro-phosphorylcholines are potent inhibitors of cholinesterases and it has been pointed out that phosphorylcholines are likely to react with the enzyme, as the first step in inhibition, in qualitatively the same way as substrates [2,3] do. The phosphoryl group in the inhibitors resembles the carbonyl group in substrates.

A new group of compounds related to choline esters has been introduced by Gosh and Newman [4]. It has been shown that S, ω-dialkyl-aminoethyl-dialkyl-thiophosphates are insecticides and methods for their syntheses are

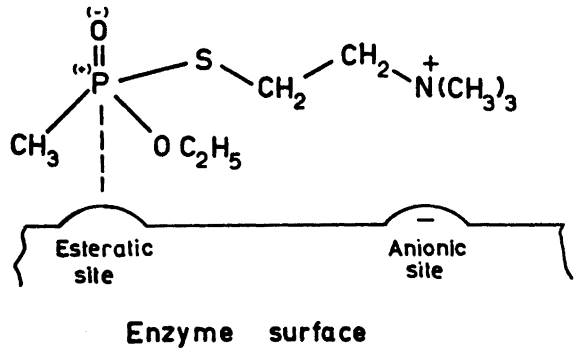


Fig. 1. Hypothetical model of the enzyme inhibitor complex formed during the inhibition of acetylcholinesterase by organophosphorylcholines.

given [5]. Diethoxy-phosphorylthiocholine and S, ω-dimethylaminoethyl-diethylthiophosphate have been shown to be potent cholinesterase inhibitors [6].

The present work deals with the syntheses and description of thio compounds of the types mentioned above, their oxygen analogues and alkoxymethyl-phosphorylthiocholines (See Fig. 1.), their tertiary homologues and corresponding oxygen compounds.

The earlier described dialkoxy-phosphorylthiocholines, and the alkoxymethyl-phosphorylthiocholines described in this paper, do presumably react with the cholinesterases as described above. (See Fig. 1.)

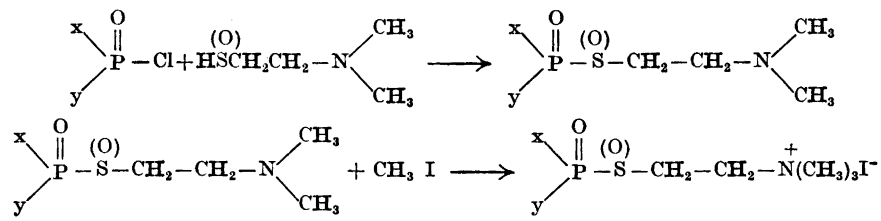
The bond energy between the esteratic site of the enzyme and the phosphoryl group is part of the total affinity to the enzyme. The degree of polarity in insecticides has been correlated to the toxicity by Perkow [7] and his general view can be applicated to the organo-phosphorylcholines. In the following an attempt will be made to use K_a values of the acid base equilibrium

$$RCH_2—CH_2—NH(CH_3)_2^+ = RCH_2—CH_2—N(CH_3)_2 + H^+$$

where R is the organophosphorus residue, for a discussion of the electronic distribution in the phosphoryl part of the inhibitor molecules. Through determinations of K_a values and inhibiting properties it is thus possible to discuss the affinity to cholinesterases in relation to the polarity.

EXPERIMENTAL

The phosphorylcholine and phosphoryl-thio-choline esters were synthesized according to the scheme [5]



Two series were synthesized 1) x = y = C_2H_5O or *iso*-C_3H_7O and 2) x = CH_3 and y = C_2H_5O or *iso*-C_3H_7O.

The thio compounds (tertiary or quaternary) are extremely toxic and care must be taken while handling them to avoid direct contact with, or inhaling of, the compounds.

The free amino bases. One mole of dialkoxyphosphoryl chloride or alkoxy-methylphosphoryl chloride and one mole of dimethylaminoethanol or dimethylaminoethanthiol were mixed in 400 ml of ether with 1.05 moles of triethylamine. The reaction mixture was refluxed for one hour. Triethylammonium chloride was filtered off and the filtrate fractionated by distillation at reduced pressure. Yield ~60 %.

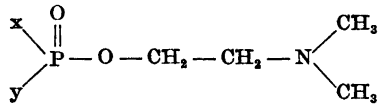
Hydrogen oxalates. One mole of the amino base (25 % solution in methanol) and 1.05 moles of oxalic acid (10 % solution in methanol) were mixed. The hydrogen oxalate which was precipitated by evaporation of the methanol is recrystallized from acetone to constant melting point (as a rule only once). Yield ~70 %.

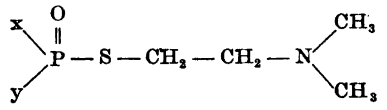
Choline and thiocholine esters. One mole of the tertiary amino base and 1.5 moles of methyl iodide were refluxed in 2.5 l of ether. The methiodides precipitate in 5 h and were filtered off. Yield ~85 %.

Verification of the composition. The boiling points were rather approximately determined by the distillation by means of an ordinary thermometer and a McLeod manometer and shall not be considered as characteristic physical constants though reproducible in our distillation set up. Densities were determined by a pycnometer and the refractive index in an Abbe refractometer. Molar refractions were calculated from group and atomic refractions given by Vogel [8] and Holmstedt [9]. Melting points were determined on a Kofler Heizbank. Carbon and hydrogen contents were determined in an ordinary combustion oven which is possible if the sample is mixed with the double amount of vanadium pentoxide. Nitrogen content was determined according to Kjeldahl and sulfur content was determined by combustion with sodium peroxide in a Parr bomb and precipitation as barium sulfate. The content of oxalic acid was determined by permanganate titration at 60°C. The end point is rather vague but after some exercise reproducible results were obtained. (For data see Table 2). Finally the number of acid protons per molecule were determined by means of sodium hydroxide titration. (See determination of pK_a and Fig. 2).

The choline and thiocholine esters were prepared as iodides. The iodine content was determined by directly applied potentiometric argentometric titration. For data see Table 3.

Table 1. Physical data of the amino ester distillation fractions.





x y	M	B.p. °C/mm	d_4^{25}	n_D^{25}	R_D calc.	 found	M	B.p. °C/mm	d_4^{25}	n_D^{25}	R_D calc.	 found
CH_3 C_2H_5O	195.2	56/0.05	1.0294	1.4320	49.3	49.2	211.3	80/0.06	1.0725	1.4780	55.8	55.8
CH_3 *i*-C_3H_7O	209.2	70/0.3	0.9992	1.4285	53.9	53.9	225.3	77/0.1	1.0501	1.4675	60.4	59.6
C_2H_5O C_2H_5O	225.2	60/0.05	1.0486	1.4220	54.9	54.6	241.3	85/0.1	1.0772	1.4655	61.4	61.8
i-C_3H_7O *i*-C_3H_7O	253.3	75/0.05	1.0042	1.4215	64.2	64.0	269.3	85/0.1	1.0296	1.4570	70.7	71.4

Determination of the acid equilibrium constants, pK_a, of the ω-dimethylaminoesters

When hydrogen oxalates of the amino esters, *i.e.* BHOxH (see also heads of Tables 2 and 3) are dissolved in water, BH^+ and HOx^- are formed. Both ions show protolysis. The values of pK_a for the equilibrium, $BH^+ = B + H^+$, were determined at 25°C with an automatic recording titrator as described by Larsson and Hansen [10]. Hydrogen oxalates (BHOxH) of the compounds (B) were dissolved in 0.100 M potassium chloride (yielding $10^{-2.4}$ M solutions) and titrated with 0.1000 M sodium hydroxide. All solutions were kept carbon dioxide free. The titration curves were recorded and showed pH as a function of the amount of sodium hydroxide added. The pH scale of the equipment was standardized against two buffer solutions, 0.05 M potassium hydrogen phtalate, pH = 4.01, and 0.01 M borax, pH = 9.18.

For evaluation of pK_a the curves were converted to curves where the number of protons split off per BHOxH, Z, was shown as a function of pH [11] (Fig. 2). At every point of the recorded curve Z can be calculated from the equation:

$$Z = \frac{[H^+] + [Na^+] - [OH^-]}{[B] + [BH^+]}$$

where $[H^+]$ and $[OH^-]$ were computed from pH and $[Na^+]$ from the added amount of sodium hydroxide, and $[B]+[BH^+]$ is the total concentration of B or oxalate, that is $[B]+[BH^+] = [H_2Ox]+[HOx^-]+[Ox^{2-}]$. Using the law of electro-neutrality and the following relationships:

$$K_1' = \frac{a_{H^+}[HOx^-]}{[H_2Ox]} \; ; \; K_2' = \frac{a_{H^+}[Ox^{2-}]}{[HOx^-]} \; ; \; K_a' = \frac{a_{H^+}[B]}{[BH^+]}$$

Z may be expressed as

$$Z = \frac{\dfrac{a_{H^+}}{K_2'} + 2}{\dfrac{a_{H^+}^2}{K_1'K_2'} + \dfrac{a_{H^+}}{K_2'} + 1} - \frac{\dfrac{a_{H^+}}{K_a'}}{\dfrac{a_{H^+}}{K_a'} + 1}$$

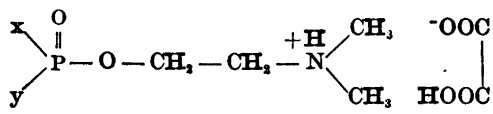
Evaluation of the mixed diss. const. K_2' and K_a'. The curves in Fig 2 show that pK_2' and pK_a' are rather well apart and it was decided to use the preceding expression of Z to test if A—B and B—C in Fig 2 could be treated as separate titration curves. In this case pH at $Z = 0.5$ gives pK_2' and pH at $Z = 1.5$ gives pK_a'. Using the approximate values $K_2' = 10^{-4}$; $K_a' = 10^{-8}$ and $K_1' = 6.5 \times 10^{-2}$, Z was calculated at $a_{H^+} = K_2'$ giving $Z = 0.4995$ and at $a_{H^+} = K_a'$ giving $Z = 1.5001$. This shows that $pK_2' =$ pH at $Z = 0.5$ and $pK_a' =$ pH at $Z = 1.5$ with satisfactory accuracy. Moreover the experimental pH/Z curves have been shown to follow the theoretical curve, yielding equivalence points at $Z = 1$ and $Z = 2$. Errors in analysis, impurities in the substanses or simultaneous hydrolysis of the esters are easily recognized as deviations from the theoretical curves [11].

Evaluation of the second thermodynamic diss. const. K_2 of oxalic acid. The eight pH/Z curves at $Z = 0.5$ (part A—B, Fig. 2) showed pH = 3.93 ± 0.01. Thus $pK_2 = 3.93 \pm 0.01$

$pK_2 = pK_2' + \log \frac{f_{HOx^-}}{f_{Ox^{2-}}}$ where f is the activity factor of the ion indicated. The ionic strength was 0.10. Values of f are from Bates [12]. $pK_2 = pK_2' + 0.324 = 4.25$.

Evaluation of the thermodynamic diss. const. K_a of the ammonium ions. The titration curves of the eight different substances showed at $Z = 1.5$ different pH values between the

Table 2. Analytical data of the ammonium ester hydrogen oxalates.



x y	Formula	M	% C		% H		% N		% oxalic acid		M.p. °C
			cacl.	found	calc.	found	calc.	found	calc.	found	
CH_3 C_2H_5O	$C_9H_{20}NO_7P$	285.2	37.9	37.3	7.1	6.8	4.9	4.8	31.6	32.4	85
CH_3 *i*-C_3H_7O	$C_{10}H_{22}NO_7P$	299.3	40.2	40.2	7.4	7.5	4.7	4.6	30.1	29.8	100
C_2H_5O C_2H_5O	$C_{10}H_{22}NO_8P$	315.3	38.1	37.6	7.0	7.0	4.5	4.4	28.6	28.6	112
i-C_3H_7O *i*-C_3H_7O	$C_{12}H_{26}NO_8P$	343.3	42.1	42.1	7.7	7.8	4.1	4.1	26.3	26.3	122

limits indicated in Fig. 2 part B—C. The pK'_a values found were converted to pK_a as follows:

$$pK_a = pK'_a + \log f_{BH^+} = pK'_a - 0.08$$

f_{BH^+} is the activity factor of the ammonium ions. The ionic strength was 0.10. The value of f_{BH^+} was estimated from values given by Kielland[13]. The pK_a values of the organophosphorus ammonium esters are shown in Table 5.

Determination of the cholinesterase inhibiting effect, pI_{50}.

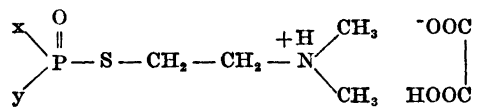
The ability to inhibit cholinesterase was determined by means of an electrometric method[14]. The enzyme preparations were erythrocyte hemolysate and plasma from human blood. Hemolysate diluted 1/30 and plasma diluted 1/20 in a Michel buffer solution (pH = 8) were incubated at 25°C with the inhibitor and thereafter acetylcholine was added to a final concentration of $10^{-2.3}$ M. Two compounds, methyl-etoxy-phosphoryl thiocholine and the corresponding dimethylaminoethanthiol ester were tested on enzyme preparations free from phosphorylphosphatases, the plasma fraction IV. 6 and a homogenate of the electric organ from *Torpedo*. In both cases I_{50}-values were obtained which were in good agreement with those obtained from human blood.

The results from preliminary tests with varying incubation time indicated that two hours are sufficient to obtain maximum inhibition at 25° with the actual concentrations of enzymes and inhibitors. The enzyme activity (v) was measured at various inhibitor concentrations (I) and pI_{50} determined by plotting v/v' against pI (v' = uninhibited enzymic activity) and taking the pI value at $v/v' = 0.5$ as pI_{50}[15]. The results are given in Table 6. Inhibitor solutions stored overnight gave the same results as those freshly prepared. Reproducibility of the pI_{50} values is shown by the maximum deviations in series of three determinations being ± 0.2.

RESULTS

S,ω-Dimethylaminoethyl-O,O′-dialkylthiophosphates, ω-dimethylaminoeththio-alkoxy-methyl-phosphine oxides and the corresponding compounds with oxygen instead of sulfur have been prepared as free amines, hydrogen oxalates

Table 3. Analytical data of the ammonium thioester hydrogen oxalates.

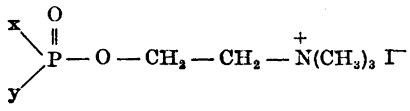


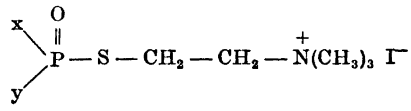
x y	Formula	M	% C		% H		% N		% S		% oxalic acid		M.p. °C
			calc.	found	calc.	found	calc.	found	calc.	found	calc.	found	
CH_3 C_2H_5O	$C_9H_{20}NO_6PS$	301.3	35.9	36.3	6.7	6.8	4.7	4.6	10.6	10.8	30.0	30.1	102
CH_3 i-C_3H_7O	$C_{10}H_{22}NO_6PS$	315.3	38.1	38.5	7.0	7.2	4.5	4.4	10.1	10.2	28.6	29.0	143
C_2H_5O C_2H_5O	$C_{10}H_{22}NO_7PS$	331.3	36.3	37.7	6.7	7.1	4.2	4.1	9.6	9.7	27.2	26.8	116
i-C_3H_7O i-C_3H_7O	$C_{12}H_{26}NO_7PS$	359.4	40.2	40.0	7.3	7.7	3.9	3.8	8.9	9.0	25.8	25.8	120

and methiodides (see Tables 1, 2, 3 and 4). The methiodides are choline or thiocholine ester iodides.

The dimethylaminoethyl-phosphoryl esters are water soluble colorless liquid compounds which are faintly discolored by storage in closed bottles at room temperature. The S,ω-dimethyl aminoethyl-diethylthiophosphate is not quite stable and preparations solidify after some months of storage. The hydrogen oxalates and methiodides are water soluble colorless crystalline compounds. It is apparent that the compounds hydrolyse very slowly because there is no effect on pK_a determinations nor on the cholinesterase inhibition studies if the experiments are performed within a few hours after preparation of solutions.

Table 4. Analytical data of the quaternary ammonium ester iodides.





x y	Formula	M	% I		M.p. °C	Formula	M	% I		M.p. °C
			calc.	found				calc.	found	
CH_3 C_2H_5O	$C_8H_{21}INO_3P$	337.2	37.7	37.0	100	$C_8H_{21}INO_2PS$	353.2	35.9	35.9	110
CH_3 i-C_3H_7O	$C_9H_{23}INO_3P$	351.2	36.2	36.2	114	$C_9H_{23}INO_2PS$	367.2	34.6	34.9	164
C_2H_5O C_2H_5O	$C_9H_{23}INO_4P$	367.2	34.6	35.3	100	$C_9H_{23}INO_3PS$	383.2	33.1	33.2	138
i-C_3H_7O i-C_3H_7O	$C_{11}H_{27}INO_4P$	395.2	32.2	32.1	172	$C_{11}H_{27}INO_3PS$	411.3	30.9	30.7	154

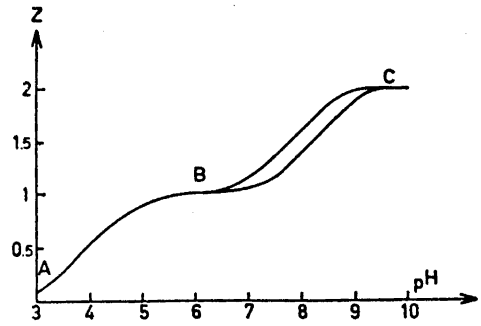


Fig. 2. Titration curves obtained with hydrogen oxalates of ω-dimethylaminoethyl-organo-phosphoryl esters (BHOxH) as titrand and sodium hydroxide as titrator. Z is the number of protons split off per mole BHOxH. A—B shows titration of OxH^- and B—C of BH^+. The two B—C curves limits the family of curves obtained from different B shown together with pK_a in Table 5.

Hydrogen oxalates of dimethylaminoethyl esters can be prepared in a pure state, as has been shown in the preparative part of this paper and confirmed by the titration curves (Fig. 2). The pH-scale was fixed by means of two buffer solutions. In determinations of the thermodynamic equilibrium constants pK_a, pH at $Z = 0.5$ offers a third possibility in controlling the pH-scale. The obtained value of the second dissociation constant (pK_2) of oxalic acid is well in accordance with earlier determinations. (Found 4.25, earlier values 4.22 and 4.29)[16]. The pH-scale is thus satisfactorily fixed and the reproducability of the ammonium pK_a determinations can be controlled by the A-B part of the (Z/pH) diagram (Fig 2). This part of the titration curve, which admittedly could be considered to be a complication, has thus been shown to be of value in checking the reliability of the experiments. Hydrogen oxalates of amines are therefore suitable for determinations of ammonium pK_a. The pK_a values of the compounds investigated in this paper are shown in Table 5.

It has been confirmed that the *dialkoxy-phosphorylthiocholines* and tertiary homologues are potent inhibitors of acetylcholinesterase. Koelle [6] used rabbit

Table 5. The thermodynamic acid constants (pK_a) at 25°C of some ω-dimethylaminoethyl organo-phosphoryl esters. Carboxylic acid esters are from an earlier paper [19]. Reproducability ±0.01.

Amino ethyl residue \ Organo phosphorus residue	CH_3, O, P—, C_2H_5O	CH_3, O, P—, C_3H_7O	$(C_2H_5O)_2P(O)-$	$(isoC_3H_7O)_2P(O)-$	$CH_3C(O)-$	$C_2H_5C(O)-$	$C_3H_7C(O)-$
$-OC_2H_4N(CH_3)_2$	8.14	8.24	8.03	8.06	8.35	8.29	8.31
$-SC_2H_4N(CH_3)_2$	7.80	7.77	7.73	7.70	8.27	8.28	8.32

Table 6. The negative logarithm of the molar concentrations of some organophosphorylcholines and corresponding dimethylaminoethyl esters which reduce cholinesterase activity to 50 % in enzyme preparations of human plasma (P) and erythrocytes (E). Reproducability ±0.2

Organo phosphorus residue / Amino ethyl residue	CH_3, C_2H_5O		CH_3, C_3H_7O		C_2H_5O, C_2H_5O		C_3H_7O, C_3H_7O	
	P	E	P	E	P	E	P	E
$-SC_2H_4N(CH_3)_2$	7.3	8.8	6.4	8.1	8.0	7.9	7.0	5.8
$-SC_2H_4N^+(CH_3)_3$	7.9	9.1	7.1	8.4	8.9	8.4	7.6	6.4
$-OC_2H_4N(CH_3)_2$	<4	<4	<4	4.6	<4	4.6	<4	<4
$-OC_2H_4N^+(CH_3)_3$	<4	<4	4.4	4	4.5	<4	<4	4.7

brain and rabbit erythrocytes as enzyme sources. In the present experiments human erythrocytes were used. Moreover, it has been shown that these organophosphorus compounds are equally or more potent inhibitors of the cholinesterase from human plasma than of the cholinesterase from human erythrocytes.

It has been shown that *alkoxy-methyl-phosphorylthiocholines* and tertiary homologues are more potent inhibitors than the dialkoxy derivatives of the acetylcholinesterase from human erythrocytes. The alkoxy-methyl-phosphoryl compounds are however less potent as inhibitors of human blood plasma cholinesterase.

It has been found that the dialkoxy-phosphorylcholines, alkoxy-methyl-phosphorylcholines and tertiary homologues are weak inhibitors of cholinesterases.

It was found that complete reaction between cholinesterases and the inhibitors is obtained in two hours. The pI_{50} values obtained after two hours incubation time are summarized in Table 6.

DISCUSSION

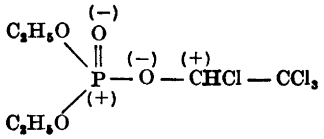
A question of importance in syntheses of the thio compounds is the position of the sulfur atom. The method of synthesis results in compounds where the sulfur is genetically situated between the dimethylaminoethyl and phosphoryl groups. A subsequent isomerisation is not probable since it has been made probable that

$$=\overset{\overset{S}{\|}}{P}-O-CH_2-CH_2-N(CH_3)_2 \text{ yields } =\overset{\overset{O}{\|}}{P}-S-CH_2-CH_2-N(CH_3)_2$$

when heated [5,20]. Moreover the Z/pH diagrams show that the products obtained are homogeneous, which would be improbable if rearrangements occurred. The distillates described in Table 1 are rather crude due to difficulties in the dis-

tillation of the compounds which combine high boiling points with thermolability. However, the molar refractions show that the distillates on the whole have the predicted composition.

According to Perkow [7] the electronic distribution in organophosphorus insecticides can be described by the following formula:



which seems rather probable. The same author has shown that a fewer number of chlorine atoms in the chloroethyl group gives less potent insecticides. This is interpreted as being due to a decreased polarity in the organophosphorus residue. It is also pointed out that the reaction with proteins is favored by a high polarity in cases where the reaction is an addition of the insecticide or if it is a phosphorylation as in cholinesterase. In the last case the increased polarity is said to cause a weakening of the $\overset{(+)}{P}-\overset{(-)}{O}-\overset{(+)}{C}$ bridge with consequently enhanced phosphorylation.

The thio compounds show as a group considerably higher cholinesterase inhibiting properties than corresponding oxygen compounds. The present data are not sufficient to make it possible to judge definitely whether the present organophosphorus compounds phosphorylate cholinesterases, or are added as such or as metabolites although the first alternative seems probable for the thio inhibitors. However, a difference might be that the oxygen compounds are added as such and the thio compounds phosphorylate through breakage of the P—S bond. The relatively high hydrolysability of compounds containing the P-S-C group [17] supports the hypothesis of phosphorylation.

The thio compounds show also as a group lower pK_a values than the oxygen compounds. If the viewpoints of Eucken [18] on chloroacetic acid are applied qualitatively on these admittedly more complicated compounds the low pK_a values in the organophosphorus compounds can be understood as follows. The dipole resulting from the formal charges of atoms in the sphere around the phosphoryl group has, because of the found low pK_a values, a repellent effect on the proton added to the amino group and is, due to asymmetry, more efficient in the thio compounds. The difference in polarity indicated by the pK_a values in oxygen and thio compounds seems, however, too small to explain the relatively high cholinesterase inhibiting potency of the thio compounds as being due only to an increased dipole-dipole attraction between inhibitor and enzyme. A comparison between the pK_a values in phosphoryl esters [19] (*e.g.*, ω-dimethylaminoethhyl acetate)

$$-\overset{\overset{O}{\|}}{C}-S-C$$

indicates that the polarity of the system is lower than of the

$$=\overset{\overset{O}{\|}}{P}-S-C$$

system.

Steric effects of the alkoxy groups in the thio compounds on the affinity for cholinesterases has been demonstrated in two ways. Di*iso*propoxy-phosphorylthiocholine is less active an inhibitor than the diethoxy compound and the same difference is shown by the tertiary homologues although the pK_a values and thus the reactivities should be similar. Moreover, dialkoxy and alkoxy-methyl compounds showed different patterns in affinity for acetylcholinesterase and serum esterase, effects which should be contributed to steric phenomena. The relatively high affinity for acetylcholinesterase compared to that for serum esterases of the alkoxy-methyl-phosphoryl compounds is unique among organophosphorus esters.

It seems probable that the compounds studied in this paper will become valuable tools in pharmacological studies of cholinergic effects due to their stability and interesting relations to cholinesterases. The comparison between thiocholine and dimethylaminoethanthiol diethoxy-phosphoryl esters made by Koelle and Steiner [6] is already one excellent example.

My thanks are due to the Director of this Institute, Professor G. Ljunggren, for his kind interest in this work.

REFERENCES

1. Wilson, I. B. and Bergmann, F. *J. Biol. Chem.* **186** (1950) 693.
2. Tammelin, L.-E. *Acta Chem. Scand.* **11** (1957) 859.
3. Fredriksson, T. *Arch. int. pharmacodyn. To be published.*
4. Ghosh, R. and Newman, J. F. *Chemistry & Industry* **1955** 118.
5. Ghosh, R. *Brit. Pat.* 738839.
6. Koelle, G. B. and Steiner, E. C. *J. Pharmacol. Exptl. Therap.* **118** (1956) 420.
7. Perkow, W. *Z. Naturforsch.* **126** (1957) 33.
8. Vogel, A. I. *J. Chem. Soc.* **1948** 1833.
9. Holmstedt, B. *Acta Physiol. Scand.* **25** (1951) Suppl. 90.
10. Larsson, L. and Hansen, B. *Svensk Kem. Tidskr.* **68** (1956) 521.
11. Sillén, L. G. *Acta Chem. Scand.* **10** (1956) 186.
12. Bates, R. G. *Electrometic pH Determinations*, New York 1954.
13. Kielland, J. *J. Am. Chem. Soc.* **59** (1957) 1675.
14. Tammelin, L.-E. *Scand. J. Clin. Lab. Invest.* **5** (1953) 267.
15. Augustinsson, K.-B. *Acta Physiol. Scand.* **15** (1948) Suppl. 52.
16. Harned, H. S. and Fallon, L. D. *J. Am. Chem. Soc.* **61** (1939) 3111.
17. Heath, D. F. *J. Chem. Soc.* **1956** 247.
18. Eucken, A. *Angew. Chem.* **45** (1932) 203.
19. Tammelin, L.-E. *Acta Chem. Scand.* **11** (1957) 487.
20. Tammelin, L.-E. *Acta Chem. Scand.* **11** (1957). *In press.*

Received May 20, 1957.

ACTA CHEMICA SCANDINAVICA 11 (1957) 1350—1354

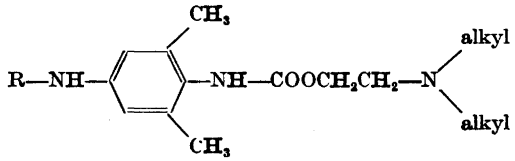
Further Studies on Amino Esters of Substituted Phenylcarbamic Acids

RICHARD DAHLBOM and ALFONS MISIORNY

Research Laboratories, AB Astra, Södertälje, Sweden

The synthesis of some amino esters of 2,6-dimethylphenylcarbamic acid substituted in the *para* position with an amino group or substituted amino group is described. Two amino esters of 2-chloro-6-methylphenylcarbamic acid were also prepared. The new compounds have been tested for local anesthetic activity.

In a previous paper the synthesis of some esters and amides of 2,6-dimethyl and 2,4,6-trimethylphenylcarbamic acids with basic substituents was described [1]. As an extension of these investigations a number of related compounds of the following type were prepared, R being H, n-C_4H_9 or an acyl group.



The starting material for these syntheses was ethyl 2,6-dimethyl-4-nitrophenylcarbamate (I) which could be prepared from 2,6-dimethyl-4-nitroaniline and ethyl chloroformate. It could also be obtained in good yield by nitration of ethyl 2,6-dimethylphenylcarbamate. The smooth formation of the 4-nitro compound in this case is rather interesting since the nitration of 2,6-dimethylacetanilide and 2,6-dimethylformanilide mainly gives the 3-nitro derivatives [2]. As ethyl 2,6-dimethyl-4-nitrophenylcarbamate is easily hydrolysed to 2,6-dimethyl-4-nitroaniline in almost quantitative yield, this method opens a new satisfactory route to this amine in addition to the method devised by Wepster [2]. The different steps involved in the synthesis of the amino esters (V, VI) and their alkyl and acyl derivatives (VIII-XI) are shown in Fig. 1.

In addition, the β-diethylaminoethyl and β-piperidinoethyl esters of 2-chloro-6-methylphenylcarbamic acid were prepared (XIII, XIV).

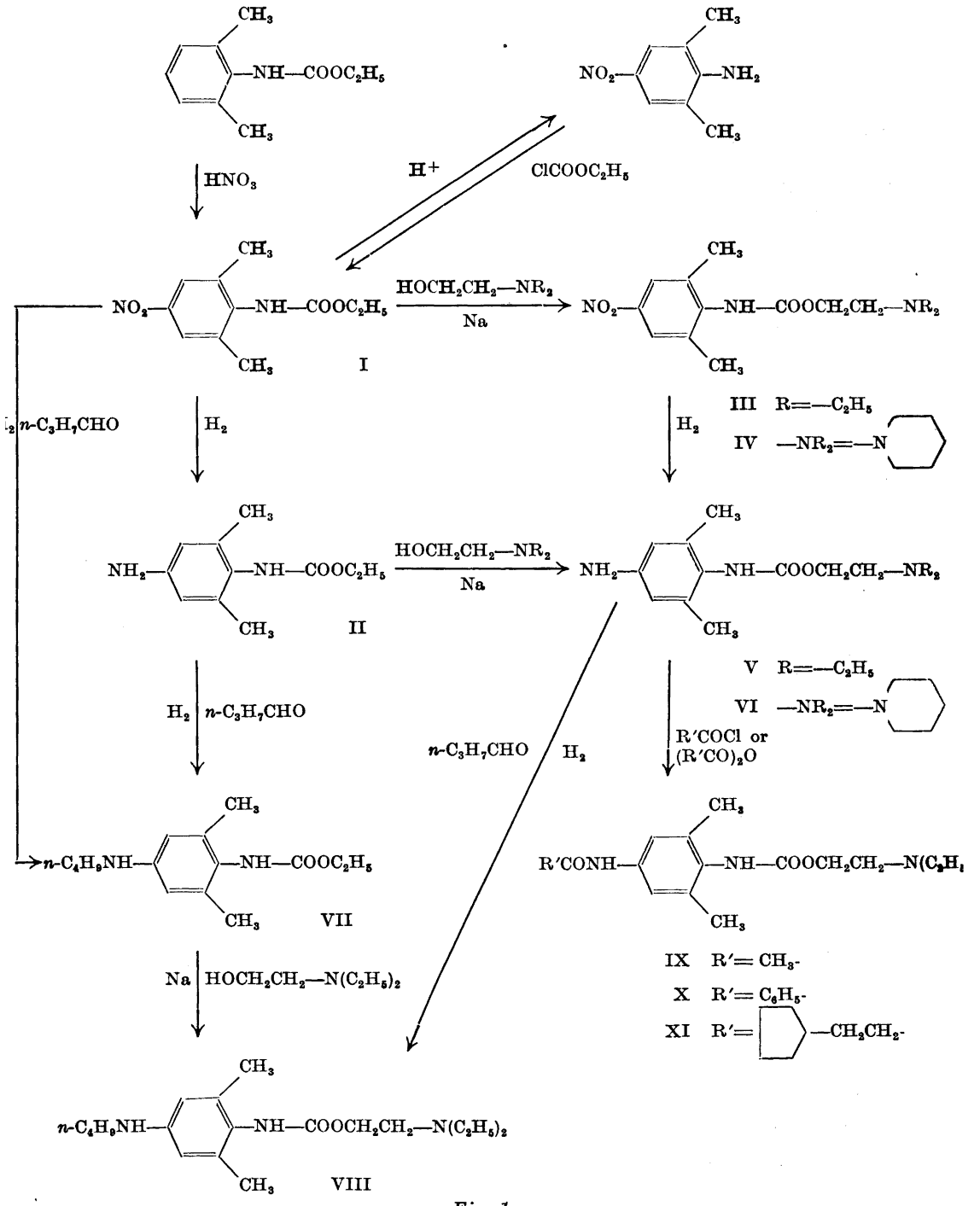

HNO3
H+
ClCOOC2H5
HOCH2CH2—NR2
Na
I
III R=—C2H5
IV —NR2=—N
H2
n-C3H7CHO
II
V R=—C2H5
VI —NR2=—N
R'COCl or
(R'CO)2O
n-C4H9NH—
VII
IX R'=CH3-
X R'=C6H5-
XI R'=
—CH2CH2-
Na
HOCH2CH2—N(C2H5)2
VIII

Fig. 1.

The new compounds were tested for local anesthetic action on the rabbit cornea and compared with Xylocaine *. The *p*-amino derivatives V and VI were devoid of anesthetic activity. The *n*-butylamino derivate VIII had an effect comparable with that of Xylocaine but had a longer latency time, low frequency of anesthesia and more than twice the toxicity. The acyl derivate IX was inactive, and X was only slightly active but XI had a strong anesthetic effect. It was, however, irritating to the rabbit eye and had a long latency time and a low frequency of anesthesia. Strong activity was also displayed by the amino esters of 2-chloro-6-methylphenylcarbamic acid (XIII, XIV), but they were too toxic to be of any clinical value.

EXPERIMENTAL

Ethyl 2,6-dimethyl-4-nitrophenylcarbamate (I). (*a*) 2,6-Dimethyl-4-nitroaniline (8.3 g, 0.05 mole), prepared by hydrolysis of 2,6-dimethyl-4-nitro-1-(*p*-toluenesulfonyl)-aniline according to the method of Wepster [3], and pyridine (5.15 g, 0.065 mole) were dissolved in benzene (600 ml) and ethyl chloroformate (7.0 g, 0.065 mole) was added dropwise with mechanical stirring. The mixture was refluxed for 2.5 h and then filtered hot. The benzene was evaporated and the residue dissolved in ether (800 ml) and extracted with conc. hydrochloric acid (150 + 100 ml) in order to remove unreacted starting material. The ether solution was washed with water, dried over sodium sulphate and the solvent was then evaporated. The crystalline residue (6.9 g, 58 %) melted at 165—168°; recrystallisation from ethanol yielded pale yellow crystals of m.p. 172—173°. (Found: C 55.3; H 5.95; N 11.8. Calc. for $C_{11}H_{14}N_2O_4$: C 55.45; H 5.92; N 11.8).

(*b*) To a solution of nitric acid (76 ml, 2 moles; *d* 1.50) in water (600 ml) were added successively ethyl 2,6-dimethylphenylcarbamate [1] (58 g, 0.3 mole), glacial acetic acid (600 ml) and sodium nitrite (2.1 g, 0.03 mole). The mixture was refluxed for 1.5 h and after cooling to room temperature it was poured into water (1.2 l). The crude nitro compound (56 g, 78 %) of m.p. 169—171° was recrystallised from ethanol giving yellow crystals melting at 172—173°. A mixed m.p. with the product prepared by procedure (*a*) showed no depression.

Hydrolysis of ethyl 2,6-dimethyl-4-nitrophenylcarbamate (I) to 2,6-dimethyl-4-nitroaniline. A mixture of compound I (2.4 g, 0.01 mole) and 85 % sulphuric acid (25 ml) was heated in an oil bath at 140—150°. Evolution of carbon dioxide began at once and had subsided after 45 min. The reaction mixture was then poured into ice water (200 ml) and made alkaline with 5 N sodium hydroxide. The light yellow product (1.55 g, 94 %) melted at 163—164° alone or in admixture with a sample of 2,6-dimethyl-4-nitroaniline prepared according to the method of Wepster [3]. Recrystallisation from aqueous ethanol did not raise the m.p.

Ethyl 4-amino-2,6-dimethylphenylcarbamate (II). Ethyl 2,6-dimethyl-4-nitrophenylcarbamate (14.3 g), dissolved in ethanol (125 ml), was hydrogenated at about 50° and normal pressure with Raney nickel as catalyst. The calculated amount of hydrogen was consumed after 4 h. The solution was filtered and the solvent evaporated. The crystalline residue (12.5 g, 100 %) was recrystallised from benzene giving a product (10.0 g) of m.p. 107—108°. (Found: C 63.9; H 8.01; N 13.1. Calc. for $C_{11}H_{16}N_2O_2$: C 63.4; H 7.74; N 13.4).

β-Diethylaminoethyl 2,6-dimethyl-4-nitrophenylcarbamate (III). A mixture of ethyl 2,6-dimethyl-4-nitrophenylcarbamate (71.4 g, 0.3 mole) and β-diethylaminoethanol (195 g, 1.65 mole) in which a piece of sodium (1.5 g) had been dissolved was heated at 75—80° for 3 h at a pressure of 80—100 mm/Hg. The excess of the amino alcohol was evaporated off and the residue washed with water and extracted with 2 N hydrochloric acid. The acid solution was extracted with ether and made alkaline with dilute sodium hydroxide. The precipitated, semisolid base was extracted with ether. Evaporation of the ether yielded a crystalline residue (75.0 g, 81 %) of m.p. 46—48°. Since further purification of the base proved to be difficult, it was converted to the *hydrochloride* which was recrystallised

* Acknowledgement is made to Dr. S. Wiedling for performing these tests.

from ethanol-ether; m.p. 164—165°. (Found: C 51.9; H 6.94; Cl 10.4. Calc. for $C_{15}H_{21}ClN_2O_4$: C 52.1; H 6.99; Cl 10.25).

β-Piperidinoethyl 2,6-dimethyl-4-nitrophenylcarbamate (IV). This compound was prepared in 90 % yield from ethyl 2,6-dimethyl-4-nitrophenylcarbamate and β-piperidinoethanol by the same method as that described for III. The amino ester base was recrystallised from methanol-water; m.p. 139—140°. (Found: C 60.0; H 7.52; N 12.7. Calc. for $C_{16}H_{23}N_3O_4$: C 59.8; H 7.21; N 13.1).

β-Diethylaminoethyl 4-amino-2,6-dimethylphenylcarbamate (V). (*a*) The nitro compound III (4.2 g) was dissolved in ethanol (50 ml) and hydrogenated at about 50° and normal pressure with Raney nickel as catalyst. The calculated amount of hydrogen was consumed in 2 h. The catalyst was removed by filtration and the solvent evaporated. The colourless oily residue (3.6 g, 95 %) was converted to the *dihydrochloride;* m.p. 299—301° after recrystallisation from ethanol-ether. (Found: C 51.3; H 7.85; Cl 20.4. Calc. for $C_{15}H_{27}Cl_2N_3O_2$: C 51.1; H 7.72; Cl 20.1).

(*b*) Transesterification of ethyl 4-amino-2,6-dimethylphenylcarbamate with diethylaminoethanol as described for III yielded the *dihydrochloride* of V in 50 % yield. M.p. after recrystallisation from ethanol-ether 300—302°.

β-Piperidinoethyl 4-amino-2,6-dimethylphenylcarbamate (VI). The nitro compound IV was hydrogenated as described above for V (*a*) and the piperidino ester was isolated as the *dihydrochloride* in 80 % yield. M.p. 291—293° (decomp.) after recrystallisation from ethanol-ether. (Found: C 52.55; H 7.54; N 11.3. Calc. for $C_{16}H_{27}Cl_2N_3O_2$: C 52.7; H 7.47; N 11.5).

Ethyl 4-n-butylamino-2,6,dimethylphenylcarbamate (VII). (*a*) A solution of ethyl 4-amino-2,6-dimethylphenylcarbamate (4.15 g, 0.02 mole), *n*-butyraldehyde (0.04 mole) and fused sodium acetate (1 g) in ethanol (50 ml) was hydrogenated with Raney nickel as catalyst at normal pressure and room temperature for one hour. The catalyst was removed by filtration and the solvent evaporated. The residue was dissolved in 2 N hydrochloric acid, the acid solution was extracted with ether and then made alkaline with dil. sodium hydroxide. The precipitate was extracted with ether and the solvent was evaporated yielding a crystalline residue (4.7 g, 90 %) of m.p. 73—74°. Recrystallisation from aqueous methanol raised the m.p. to 76—77°. (Found: C 68.15; H 9.01; N 10.5. Calc. for $C_{15}H_{24}N_2O_2$: C 68.15; H 9.15; N 10.6).

(*b*) This compound could also be prepared in 82 % yield by using ethyl 2,6-dimethyl-4-nitrophenylcarbamate (I) as starting material in the reductive alkylation described above (*a*). The reaction was, however, rather sluggish; the calculated amount of hydrogen was consumed after 6 h.

β-Diethylaminoethyl 4-n-butylamino-2,6-dimethylphenylcarbamate (VIII). (*a*) A solution of β-diethylaminoethyl 4-amino-2,6-dimethylphenylcarbamate (3.9 g, 0.014 mole), *n*-butyraldehyde (1.3 g, 0.018 mole) and sodium acetate (1.0 g) in ethanol (50 ml) was hydrogenated at normal pressure and room temperature over Raney nickel for one hour. The reaction mixture was worked up as described above for compound VII (*a*). The product was isolated as the *dihydrochloride* (3.6 g, 62 %); m.p. 236—237° (decomp.) after recrystallisation from ethanol-ether. (Found: C 55.6; H 8.72; N 9.93. Calc. for $C_{19}H_{35}Cl_2N_3O_2$: C 55.9; H 8.64; N 10.3).

(*b*) This compound was also obtained by transesterification of ethyl 4-*n*-butylamino-2,6-dimethylphenylcarbamate with β-diethylaminoethanol according to the procedure described for compound III. The yield of the *dihydrochloride* was 63 %.

β-Diethylaminoethyl 4-acetamido-2,6-dimethylphenylcarbamate (IX). A suspension of compound V (2.8 g free base, 0.01 mole) in acetic anhydride (10 ml) was heated to 60° for 30 min and was then poured into water (100 ml). The mixture was made alkaline and extracted with ether. The ether solution was filtered through a short column of aluminium oxide and evaporated. The solid residue (1.7 g, 53 %) was recrystallised from benzene; m.p. 122—123°. (Found: C 63.0; H 8.45; N 13.1. Calc. for $C_{17}H_{27}N_3O_3$: C 63.5; H 8.47; N 13.1).

β-Diethylaminoethyl 4-benzamido-2,6-dimethylphenylcarbamate (X). Compound V was treated with benzoyl chloride in pyridine-benzene. A heavy precipitate consisting of the hydrochloride of X was formed. The salt was suspended in water, the suspension made alkaline and the base extracted with ether. Evaporation of the ether yielded a crystalline residue which was recrystallised from benzene; m.p. 144—145°. (Found: 69.4; H 7.65; N 10.8. Calc. for $C_{22}H_{29}N_3O_3$: C 68.9; H 7.62; N 11.0).

β-Diethylaminoethyl 4-(β-cyclopentylpropionamido)-2,6-dimethylphenylcarbamate (XI) was prepared similarly in 71 % yield from V and *β-cyclo*pentylpropionyl chloride; m.p. 115—116° after recrystallisation from benzene-light petroleum. (Found: C 68.4; H 9.19; N 10.45. Calc. for $C_{23}H_{37}N_3O_3$: C 68.45; H 9.24; N 10.4).

Ethyl 2-chloro-6-methylphenylcarbamate (XII). To a stirred solution of 2-chloro-6-methylaniline (28.3 g, 0.2 mole) and pyridine (20 g, 0.25 mole) in benzene (200 ml), ethyl chloroformate (27.1 g, 0.25 mole) was added dropwise over a period of one hour. The temperature gradually rose to 45°. The stirring was then continued for one hour and the pyridine hydrochloride formed was removed by filtration. The benzene solution was washed successively with water, 2 N hydrochloric acid and water and was then evaporated to dryness. The residue (38.5 g, 90 %) melted at 75—77° and was recrystallised from aqueous methanol; m.p. 76—77°. (Found: C 56.3; H 5.69; N 6.62. Calc. for $C_{10}H_{12}ClNO_2$: C 56.2; H 5.66; N 6.56).

β-Diethylaminoethyl 2-chloro-6-methylphenylcarbamate (XIII). This compound was prepared by transesterification of the ethyl ester XII with β-diethylaminoethanol by the method described for compound III. The oily base was converted to the *oxalate*. Yield 51 %; m.p. 127—128° after recrystallisation from 80 % ethanol. (Found: C 51.7; H 6.51; N 7.35. Calc. for $C_{16}H_{23}ClN_2O_2$: C 51.3; H 6.18; N 7.48).

β-Piperidinoethyl 2-chloro-6-methylphenylcarbamate (XIV) was prepared similarly from β-piperidinoethanol and XII. The oily base was isolated as the *hydrochloride*. Yield 87 %; m.p. 172—173° after recrystallisation from ethanol-ether. (Found: C 54.1; H 6.47; N 8.39: Calc. for $C_{15}H_{22}Cl_2N_2O_2$: C 54.05; H 6.66; N 8.41).

REFERENCES

1. Dahlbom, R. and Österberg, L.-E. *Acta Chem. Scand.* 9 (1955) 1553.
2. Wepster, B. M. *Rec. trav. chim.* 73 (1954) 809.

Received May 20, 1957.

ACTA CHEMICA SCANDINAVICA 11 (1957) 1355—1358

The Occurrence of 3-Oxoglucose Units in Oxidised Cellulose

BENGT LINDBERG and OLOF THEANDER

Institutionen för träkemi, Kungl. Tekniska Högskolan, and Träkemiska avdelningen, Svenska Träforskningsinstitutet, Stockholm, Sweden

D-Allose has been isolated from the hydrolysate of a cellulose which was first oxidised with chromate and subsequently reduced with borohydride. The mannose content was roughly the same as found in the hydrolysate of an unmodified cellulose. These results strongly indicate that most of the keto-groups in the oxidised cellulose are present as 3-oxoglucose units and that the contribution from 2-oxoglucose units is rather insignificant.

The oxidation of cellulose is technically an important although usually most undesirable reaction, which takes place during the bleaching of pulp, aging of paper etc. The alcoholic hydroxyl groups of the cellulose are converted to oxo or carboxyl groups, and more drastic oxidation also cleaves carbon-carbon linkages. Fairly satisfactory methods are available for the analytical determinations of these groups, but these are complicated by the heterogeneous nature of the reactions upon which they are based. Meesook and Purves [1] have also developed methods which distinguish between aldo and keto groups. The assignment of definite structures to different oxidised units in the modified celluloses is, with few exceptions, based upon assumptions only. The structure of periodate oxidised cellulose, however, has been proved both by further oxidation and by reduction of the material and subsequent identification of the products of hydrolysis [2]. The isolation of 3,5-dioxo-tetrahydro-4-pyrone [3] after acid hydrolysis of a cellulose oxidised with nitrogen dioxide, indicated the presence of 2,3-dioxoglucose units.

Whistler *et al.*[4] have recently studied a hypochlorite oxidised starch; after hydrolysis they isolated glyoxylic acid and D-erythronic acid, which demonstrates that the link between $C_{(2)}$ and $C_{(3)}$ in the glucose units has been broken. Purves *et al.*[5,6] have investigated chromate and hypochlorite oxidised starch. The modified polysaccharides were first subjected to a cyanohydrin synthesis and then to hydrolysis and reduction with hydrogen iodide. 4-Hydroxy-2-methylhexanoic acid was isolated from the reaction product and is obviously formed from 2-oxoglucose units. As no products derived from

potential 3-oxoglucose units were obtained, they draw the conclusion that the main part of the keto-groups in these modified starches were due to 2-oxoglucose units.

When methyl β-D-glucopyranoside was oxidised with chromate, the 6-oxoglucoside was the dominating oxo-derivative, follwed by the 3-oxoglucoside [7]. We have since found that the 2-oxoglucoside is also formed, but in a much lower yield [8]. From these results one would, by analogy, expect to find more 3- than 2-oxoglucose units in chromate oxidised cellulose.

The present paper describes an investigation of cellulose, cotton linters, oxidised with chromate; the modified product contained 6.9 oxo groups per 100 glucose units, as determined by the borohydride method [9]. The oxidised cellulose was reduced with borohydride. By reduction under similar conditions [8] methyl β-D-2-oxoglucoside yielded glucoside and mannoside in the proportions 41:59 and methyl β-D-3-oxoglucoside yielded glucoside and alloside in the proportions 48:52. In neither case were other sugars formed in detectable amounts, which indicates that no isomerisations took place. It is reasonable to assume that the reduction of potential 2- and 3-oxoglucose units in the cellulose should follow a similar course. The reduced polysaccharide was then hydrolysed to a mixture of glucose and other sugars, and the glucose was selectively removed by enzymatic oxidation to gluconic acid with the aid of notatin and subsequent treatment with ion exchange resins. In the residue, the presence of mannose, xylose, allose and traces of glucose could be demonstrated by paper chromatography and by paper electrophoresis in borate buffer. Glucose and xylose, however, were not separated by the last method. A weak spot, probable due to arabinose, was also obtained both in the modified and unmodified sample. Mannose and xylose were also found in the hydrolysate of the unmodified cellulose. The quantitative determination of the sugars was complicated by the presence of unknown material, possibly proteins or peptides from the enzyme preparation which interfered with various reactions tried. These difficulties were finally overcome by estimating the sugars from the sizes of the spots in comparison with those of reference spots, using anisidine hydrogen chloride as spraying reagent. Fairly reproducible results were obtained and the agreement between the values determined by paper chromatography and by paper electrophoresis was satisfactory (Table 1). The analytical figures were corrected for sugar decomposition during the acid hydrolysis and also for the formation of 1,6-anhydro-D-allose [10]. Losses during the manipulations were also corrected for by adding a known amount of rhamnose to the hydrolysate and determining rhamnose in the final sugar mixture. The oxidation of sugars other than glucose by notatin was considered insignificant and was not corrected for (*cf.* Ref.[11]) In a separate experiment, the losses of mannose during this treatment were found to be less than 1 % of the total amount.

The figures in Table 1 show that the cellulose contained small but detectable amounts of mannose and xylose. The modified cellulose contained comparable amounts of these sugars, and no increase in the mannose content was observed. Allose, which of course was not present in the linters, was found in the modified cellulose. In a separate and essentially analogous experiment, crystalline D-allose was isolated from an oxidised and reduced cellulose and

Table 1. Sugars other than glucose, before and after oxidation reduction of the cellulose. E and C, determined by paper electrophoresis and paper chromatography, respectively.

Sample	Mannose %		Xylose %		Allose %	
	E	C	E	C	E	C
Cotton linters,	0.18	0.13	—	0.26	0	0
» » modified	0.16	0.14	—	0.24	0.17	0.17

proved to be identical with an authentic sample. These results, which are in agreement with our earlier model experiments, demonstrate the presence of 3-oxoglucose units in chromate oxidised cellulose. There may be 2-oxogroups also present, but to a much lesser extent. If practically no mannose is formed by the reduction of the 2-oxoglucose units, the percentage of the latter could of course be quite high, but the results of model experiments [8] make this assumption improbable. It is also possible that the original mannose in the sample, as present in the form of a highly accessible hemicellulose, was destroyed during the oxidation and that the mannose found in the modified cellulose should come from 2-oxoglucose units. This assumption, however, seems highly improbable as the xylose content is the same in both samples, and xylose units, by the same argument, should also be preferentially oxidised. Thus, of the oxogroups present, 6.9 in 100 glucose units, only 0.34 or 5 % should be in 3-oxoglucose units. This, of course, is a very crude estimation, which is valid only for the actual sample investigated, since the proportions between different groups may vary considerably with the conditions of preparation.

EXPERIMENTAL

Preparation of the modified cellulose. Cotton linters (20 g) was treated with a solution of potassium dichromate (7.86 g) in 0.4 N sulphuric acid (1 600 ml) at 25° for 120 h and was then carefully washed with water and dried in air. The oxogroups were determined by the borohydride method as 6.9 groups in 100 glucose units. The copper number, determined according to Hägglund [12], was 18.9. The modified cellulose (10 g), reduced by treatment for 6 hours at 25° with an aqueous solution (400 ml) containing potassium borohydride (0.56 g), buffered to pH 9.6 by boric acid (3.70 g) and sodium hydroxide (1.60 g) was filtered off, washed and air-dried.

Hydrolysis and enzymatic oxidation of the hydrolysate. Unmodified or modified cellulose (3 g) was treated with 72 % sulphuric acid (7.5 ml), a vacuum being applied and released a number of times to obtain a better contact with the solvent. After 17 h at room temperature the solution was diluted with water (105 ml) and refluxed 3 h. The cooled solution was then neutralised with barium carbonate using vigorous agitation and keeping the temperature below 15°. After filtering and washing, the solution was deionised, using the ion exchange resins Amberlite IR 120 and IR 4B and concentrated under reduced pressure to an almost colourless syrup (3.5 g). The syrup was dissolved in 0.5 M acetate buffer (90 ml) at pH 5.5 and the enzyme preparation (Dee 0 Takamine Laboratory) (30 mg) was added. Oxygen was bubbled through the solution, which was kept at 35° and vigorously agitated. At intervals the pH was adjusted to 5.5 by addition of solid sodium hydrogen carbonate. After one day further enzyme preparation (30 mg) was added and after 2 ½ days the oxidation was stopped. Rhamnose monohydrate (30 mg) was added and the solution was deionised as above and concentrated to a syrup under reduced pressure.

Analysis of the hydrolysate. The syrup above was dissolved in water and the volume adjusted to 5 ml. A qualitative chromatographic analysis revealed the presence of significant amounts of rhamnose, xylose, mannose and allose, the latter, however, only in the hydrolysate from the modified cellulose. Smaller amounts of glucose and arabinose were also found together with some substances that were obviously oligosaccharides, since they gave spots with low R_F-values and positive reactions with anisidine hydrogen chloride. A fast spot, which gave a weak reaction with the silver nitrate-sodium ethoxide reagent, and which had the R_F-value of 1,6-anhydroallose, was also obtained from the hydrolysate of the modified cellulose.

For the quantitative estimations, aliquot amounts of the hydrolysate were spotted on sheets of Whatman No. 1 filter papers, together with varying amounts of reference substances (5—75 μg). The chromatograms were run, first with solvent A, ethyl acetate-acetic acid-water, 3:1:3 (upper phase), for 16 h, dried and then run with solvent B, butanol-pyridine-water, 3:1:1.5, for 24 h. The spots were developed with the anisidine hydrogen chloride reagent, the areas of the reference spots were plotted against the amounts of sugars and the amounts of sugars in the hydrolysates determined by interpolation. The electrophoretic separations were carried out on Whatman No. 3 filter paper in a 0.1 M borate buffer at pH 10 for 2 h at 1 500 V. The quantitative estimations were made as described above. The results of analyses are given in Table 1.

Isolation of D-*allose.* A sample of the modified cellulose (10 g) was hydrolysed, enzymatically oxidised and worked up as described above. A rather large amount of enzyme preparation, 0.50 g, was used. The syrup (525 mg) was fractionated as above on ten sheets of Whatman No. 3 filter paper (width 23 cm), which had previously been carefully washed with water. The bands containing the allose, mixed with mannose, were cut out, the sugars were eluted and the solution concentrated to a syrup (70 mg) under reduced pressure. This syrup was now fractionated on three sheets of the same paper, run for 24 h with solvent B. A fraction (42 mg) containing allose as the only sugar was obtained. The syrup was extracted with boiling 75 % aqueous ethanol, and the extract was concentrated to dryness, dissolved in water, decolourised with carbon, deionised and concentrated again. When anhydrous ethanol was added to the syrup, it crystallised. The crystals (8 mg) were recrystallised from ethanol, yielding pure D-allose (4.2 mg) m. p. 127—128°, undepressed on admixture with authentic material. In its behaviour on paper chromatography in various solvents and in paper electrophoresis, the substance was undistinguishable from authentic D-allose.

The authors wish to thank Mrs. S. Lidman-Safwat for her skilful assistance.

REFERENCES

1. Meesook, B. and Purves, C. B. *Paper Trade J.* **123** (1946) 35.
2. Purves, C.B., in Wise, L. E. and Jahn, E. C. *Wood Chemistry*, Vol. I, Reinhold, New York 1952, p. 168.
3. Battenberg, E. and Berg, A. *Ber.* **86** (1953) 640.
4. Whistler, R. L., Linke, E. G. and Kazeniac, S. *J. Am. Chem. Soc.* **78** (1956) 4704.
5. Ellington, A. C. and Purves, C. B. *Can. J. Chem.* **31** (1953) 801.
6. McKillican, Marg. E. and Purves, C. B. *Can. J. Chem.* **32** (1954) 312.
7. Lindberg, B. and Theander, O. *Acta Chem. Scand.* **8** (1954) 1870.
8. Theander, O. *Unpublished results.*
9. Lindberg, B. and Theander, O. *Svensk Papperstidning* **57** (1954) 83.
10. Pratt, J. W. and Richtmyer, N. K. *J. Am. Chem. Soc.* **77** (1955) 1906.
11. Whittaker, V. P., in Klyne, W. *Progress in Stereochemistry*, Vol. I, Butterworth, London 1954, p. 297.
12. *Central Laboratory of the Swedish Cellulose Industry Standards, CCA* **3** (1940).

Received May 22, 1957.

ACTA CHEMICA SCANDINAVICA 11 (1957) 1359—1364

Studies on *Cyclo*propanes

II. Preparation and Properties of Some Penta- and Tetrasubstituted *Cyclo*propanes

GUNNEL WESTÖÖ

Institute of Organic Chemistry, University of Lund, Lund, Sweden

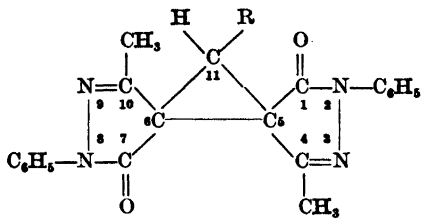
The pentasubstituted *cyclo*propanes, I b—e, and the tetrasubstituted one, I a, have been prepared. They are more stable towards isomerization than the hexasubstituted *cyclo*propane derivatives described in a previous paper [1]. On heating I a and I e are transformed into III a and III b.

2,8,11-Triphenyl-4,10-dimethyl-2,3,8,9-tetrazadispiro[4.0.4.1]undeca-3,9-diene-1,7-dione, I e, could be prepared from 1-phenyl-3-methyl-4-benzylidene-2-pyrazolin-5-one and 1-phenyl-3-methyl-4-bromo-2-pyrazolin-5-one analogously to the hexasubstituted products [1]. For the preparation of I a—d the corresponding 4,4′-alkylidenebis[1-phenyl-3-methyl-2-pyrazolin-5-ones] [2] (II a—d) were used as starting materials. When their sodium salts were brominated or iodinated to form II h or II i, ring closure took place immediately at room temperature, I a—d precipitating in good yields (>90 %). The bromination was performed with a bromopyrazolone, *e.g.*, 1-phenyl-3-methyl-4-bromo-2-pyrazolin-5-one or preferably 1-phenyl-3-methyl-4,4-dibromo-2-pyrazolin-5-one [3].

Analogous ring closures have been made with alkylidenebis[indanedione] and 2,2′-methylenebis[5,5-dimethyl-1,3-*cyclo*hexanedione] by Radulescu and Georgescu [4] and with methyl β-phenyl-γ-bromo-γ-benzoyl-ethylmalonate by Kohler and Conant [5].

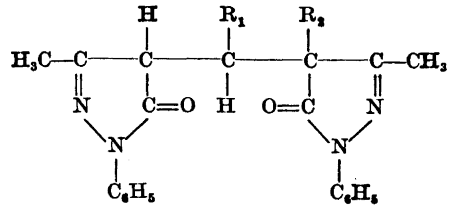
Good support for the *cyclo*propane structure of the reaction products is afforded by the UV curves (Fig. 1), which are almost identical with the corresponding curves of the hexasubstituted *cyclo*propanes described earlier [1]. The IR spectra [1,6,7] show absorption at 1 000—1 010 cm^{-1}. — The steric arrangement of the groups in I a—e has not been studied.

Hydrogen chloride adds to the compounds I a, b or c with formation of 4-chloro-4,4′-alkylidenebis[1-phenyl-3-methyl-2-pyrazolin-5-ones], II e, f or g, as proved by the following facts. The products obtained are acids which in



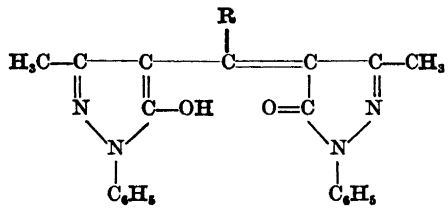
I

a. R = H.
b. R = CH_3.
c. R = C_2H_5.
d. R = *i*-C_3H_7.
e. R = C_6H_5.



II

a. R_1 = R_2 = H.
b. R_1 = CH_3; R_2 = H.
c. R_1 = C_2H_5; R_2 = H.
d. R_1 = *i*-C_3H_7; R_2 = H.
e. R_1 = H; R_2 = Cl.
f. R_1 = CH_3; R_2 = Cl.
g. R_1 = C_2H_5; R_2 = Cl.
h. R_1 = H or alkyl; R_2 = Br.
i. R_1 = H or alkyl; R_2 = I.



III

a. R = H.
b. R = C_6H_5.
(c. R = alkyl.)

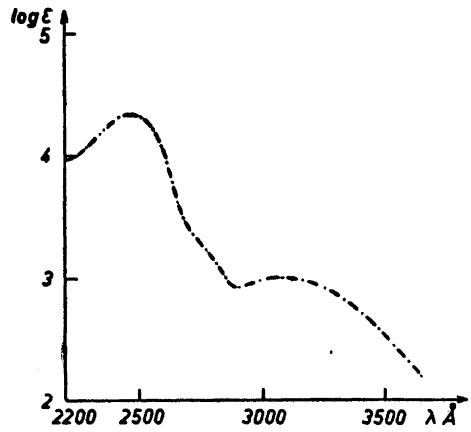


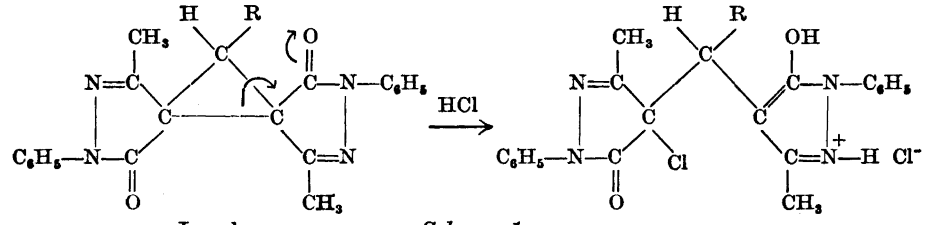
Fig. 1. UV curve of I b in ethanol.

acetate-buffered solution split off hydrogen chloride with reformation of I a, b or c. They oxidize iodides almost quantitatively to iodine at room temperature according to the equation (*cf.* Westöö [8]):

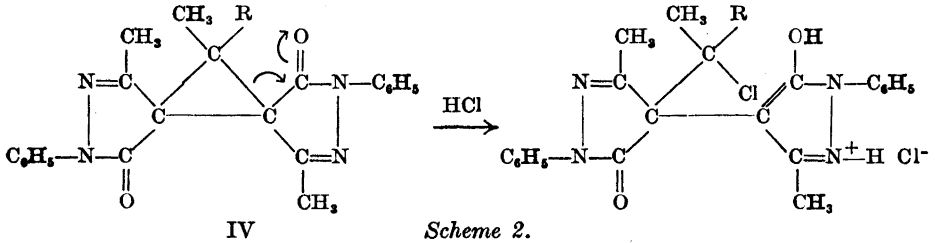
$$PyClCHRPyH\,{}^{*}+2KI \rightarrow PyHCHRPyK+I_2+KCl.$$

Contrary to 4-chloro-4,4′-*iso*propylidenebis[1-phenyl-3-methyl-2-pyrazolin-5-one] [1] and 1,1′,1″-triphenyl-3,3′,3″-trimethyl-4-bromo-[4,4′,4″-ter-2-pyrazoline]-5,5′,5″-trione [9], II e, f and g do not dissociate into 1-phenyl-3-methyl-4-halogeno-2-pyrazolin-5-one and an α,β-unsaturated carbonyl compound.

The opening of the *cyclo*propane ring by hydrogen chloride is probably started by the addition of a proton to a carbonyl group, followed by an electron transfer from a *cyclo*propane bond to the pyrazolone ring and the uptake of a chloride ion by the most positive carbon atom. When C_{11} carries one methyl or ethyl group only, it is too electron-deficient to allow a displacement of the $C_5—C_{11}$ bonding electrons to the pyrazolone, and the $C_5—C_6$ bond breaks exclusively (Scheme 1). However, when C_{11} has two electron-releasing groups, a cleavage of the $C_5—C_{11}$ bond is instead the main reaction [1] (Scheme 2). Under the conditions described in the experimental part only about 20 % of the $C_5—C_6$ bonds were cleaved in the 11,11-dimethyl compound (IV a), 5 % in the 11-ethyl-11-methyl compound (IV b) in accordance with the increased inductive effect on C_{11}.



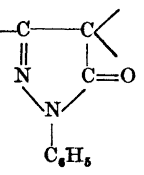
I a, b, c *Scheme 1*



IV *Scheme 2.*

a. R = CH_3.
b. R = C_2H_5.

* Py represents the group



The quantitative rearrangement, which was found in solution even at room temperature with the hexasubstituted *cyclo*propanes (cleavage of the *cyclo*propane ring with migration of a hydrogen atom from an 11-methyl group), has no analogue with the pentasubstituted products I b—d. These are quite stable at room temperature and are markedly more resistant towards heat than are the hexasubstituted ones. On prolonged heating of I b or c in dioxan-water at 95°, amorphous products were obtained. Besides degradation products the isomer Py = C(CH_2R)PyH has probably been formed, but it has not been isolated. I d is even more stable than I b and c and could be recovered to 90 % after heating at 95° for 24 h in dioxan-water solution.

Heating in solid form or in solution of the phenyl compound, I e, yielded 4,4'-benzylidynebis[1-phenyl-3-methyl-2-pyrazolin-5-one] (III b)[10]. The same form of isomerization was found with the tetrasubstituted product I a, methylidynebis[1-phenyl-3-methyl-2-pyrazolin-5-one][11] (III a) being formed.

EXPERIMENTAL

2,8-Diphenyl-4,10-dimethyl-2,3,8,9-tetrazadispiro[4.0.4.1]undeca-3,9-diene-1,7-dione (I a). 4,4'-Methylenebis[1-phenyl-3-methyl-2-pyrazolin-5-one] (II a) (2.5 g of crude product, obtained from the reaction of 1-phenyl-3-methyl-2-pyrazolin-5-one in benzene solution with formaldehyde at room temperature) was dissolved in ethanol (50 ml) and poured into a neutralized solution of 1-phenyl-3-methyl-4-bromo-2-pyrazolin-5-one (1.5 g) in ethanol (15 ml). I a (2.0 g) separated immediately. It was collected by filtration and washed with ethanol and water. M.p. after crystallization from ethanol 162° (decomp.). (Found: C 70.5; H 5.0; N 15.7; mol.wt. 350 *. Calc. for $C_{21}H_{18}N_4O_2$: C 70.4; H 5.1; N 15.6; mol.wt. 358.)

2,8-Diphenyl-4,10,11-trimethyl-2,3,8,9-tetrazadispiro[4.0.4.1]undeca-3,9-diene-1,7-dione (I b). a) 4,4'-Ethylidenebis[1-phenyl-3-methyl-2-pyrazolin-5-one][3] (II b) (1.53 g) in ethanol (5 ml) was neutralized with 2.5 N sodium hydroxide solution using phenolphthalein as indicator. Excess of 1-phenyl-3-methyl-4,4-dibromo-2-pyrazolin-5-one (1.36 g) dissolved in ethanol (20 ml) was added. I b separated at once as a soft mass which on scratching was transformed into crystals. The product was filtered, washed with ethanol, dilute sodium hydroxide solution and water. Yield: 1.40 g of crude product, m.p. 130—131° (decomp.). After one crystallization from ethanol it melted at 131—132° (decomp.). (Found: C 71.0; H 5.4; N 15.1; mol.wt. 370 *. Calc. for $C_{22}H_{20}N_4O_2$: C 70.95; H 5.4; N 15.05; mol.wt. 372.) b) 4,4'-Ethylidenebis[1-phenyl-3-methyl-2-pyrazolin-5-one] (II b) (2.60 g) was dissolved in ethanolic sodium hydroxide solution (10 ml of ethanol + 5.65 ml of 2.46 N aqueous NaOH solution). Iodine (1.76 g) dissolved in ethanol (25 ml) was added with stirring. Crystals of I b separated. They were filtered and washed with 50 % ethanol. Yield: 2.35 g, m.p. of crude product 131° (decomp.).

2,8-Diphenyl-4,10-dimethyl-11-ethyl-2,3,8,9-tetrazadispiro[4.0.4.1]undeca-3,9-diene-1,7-dione (I c) and 2,8-diphenyl-4,10-dimethyl-11-isopropyl-2,3,8,9-tetrazadispiro[4.0.4.1]-undeca-3,9-diene-1,7-dione (I d). These compounds were prepared from equimolar amounts of the sodium salts of the corresponding alkylidenebis[1-phenyl-3-methyl-2-pyrazolin-5-one][3] (II c and d) and 1-phenyl-3-methyl-4,4-dibromo-2-pyrazolin-5-one or iodine in the way described for I b. The yields were 90—95 % of the theoretical amounts. The m.p. of I c was 110° and of I d 163—164° (decomp.). (Found for I c: C 71.4; H 5.7; N 14.6. Calc. for $C_{23}H_{22}N_4O_2$: C 71.5; H 5.7; N 14.5. Found for I d: C 71.6; H 6.0; N 13.9. Calc. for $C_{24}H_{24}N_4O_2$: C 72.0; H 6.0; N 14.0.)

2,8,11-Triphenyl-4,10-dimethyl-2,3,8,9-tetrazadispiro[4.0.4.1] undeca-3,9-diene-1,7-dione (I e). 1-Phenyl-3-methyl-4-benzylidene-2-pyrazolin-5-one[12] (1.93 g) was dissolved in ether (80 ml) and ethanol (40 ml) and mixed with a neutralized solution (phenolphthalein) of 1-phenyl-3-methyl-4-bromo-2-pyrazolin-5-one (1.87 g) in ethanol (40 ml). When the

* determined by measurements of the freezing-point depressions of benzene solutions.

mixture had been decolorized, the ether was evaporated under reduced pressure. The precipitate was filtered and washed with ethanol and water. Yield: 3.10 g, m.p. 132°. (Found: C 74.5; H 5.1; N 12.8. Calc. for $C_{27}H_{22}N_4O_2$: C 74.6; H 5.1; N 12.9.)

Cleavage of the cyclopropane ring of I c with hydrogen chloride. I c (0.55 g) was dissolved in benzene, and dry hydrogen chloride was introduced with ice-cooling until the solution was saturated. After one hour the solvent was removed under reduced pressure; the solid residue was dissolved in ethanol, precipitated with water, filtered and washed with water. Yield: 0.48 g. (Found: C 65.0; H 5.5; Cl 8.5; N 13.0. Calc. for $C_{23}H_{23}ClN_4O_2$: C 65.3; H 5.5; Cl 8.4; N 13.25.)

When a buffered ethanol solution (50 ml of 1.8 N aqueous sodium acetate solution + ethanol to 500 ml) of the acid obtained was left for a few hours, hydrogen chloride was split off, and the three-ring was reformed quantitatively, as could be shown by UV measurement.

The chloro compound oxidized hydrogen iodide to iodine rapidly at room temperature.

0.0984 g of the addition product was dissolved in ethanol (10 ml) and mixed with an excess of potassium iodide dissolved in water (3 ml). After 3 min 5 N hydrochloric acid (3 ml) was added and the solution was titrated with 0.0998 N sodium thiosulphate solution. 4.65 ml was consumed. This corresponds to pure $PyClCH(C_2H_5)PyH$, II g. Another sample gave 97 % of $PyClCH(C_2H_5)PyH$.

Cleavage of the cyclopropane ring of I b with hydrogen chloride. I b (1.00 g) was dissolved in benzene (10 ml). Dry hydrogen chloride was introduced for 15 min into the ice-cooled solution, which was then kept in the ice bath for 2 h. The benzene was evaporated under reduced pressure, the solid residue was dissolved in ethanol (25 ml) and the solution was poured into water (200 ml) with stirring. The precipitate formed (II f) was filtered and washed with water. Yield: 1.02 g of almost colourless acid. It was purified by solution in ether and precipitation with light petroleum. (Found: C 64.5; H 5.3; Cl 8.6; N 13.6; O 7.7. Calc. for $C_{22}H_{21}ClN_4O_2$: C 64.6; H 5.2; Cl 8.7; N 13.7; O 7.8.)

Ring closure and oxidation of iodide were performed as for II g and with the same results.

Cleavage of I a by hydrogen chloride. I a was cleaved with hydrogen chloride in the same way as described for I b and c, II e being the main product formed. (Found: C 63.7; H 5.0; Cl 9.0; N 14.1; O 8.2. Calc. for $C_{21}H_{19}ClN_4O_2$: C 63.9; H 4.85; Cl 9.0; N 14.2; O 8.1.)

The addition product oxidized hydrogen iodide to iodine in about 90 % yield according to the procedure described for II g (time of reaction 1 min instead of 3). The low iodine yield may be caused by some hydrogen iodide splitting off from $PyICH_2PyH$.

When an ethanol solution of the product was titrated with barium hydroxide solution, I a (identified by its m.p. 162° (decomp.), UV curve and neutrality) separated during the titration. In acetate-buffered solution ring closure also took place as could be shown by UV measurements. When a concentrated ethanol solution of the addition product was left for some weeks, methylidynebis[1-phenyl-3-methyl-2-pyrazolin 5-one][11] (III a) separated, m.p. alone and mixed with an authentic sample 182.5°.

Cleavage of 2,8-diphenyl-11-ethyl-4,10,11-trimethyl-2,3,8,9-tetrazadispiro[4.0.4.1]undeca-3,9-diene-1,7-dione (IV b) by hydrogen chloride [1]. IV b (0.25 g) was dissolved in ice-cooled benzene [20 ml) saturated with hydrogen chloride. After 15 min the solvent was removed under reduced pressure, the residue was dissolved in ethanol (5 ml) and poured into water (50 ml) with stirring. The precipitate formed was filtered and washed with water. Yield: 0.25 g of faintly yellow product. According to light absorption measurements less than 3 % of 1-phenyl-3-methyl-4-*sec*-butylidene-2-pyrazolin-5-one was present in the mixture, indicating that the C_5-C_6 bond had been cleaved to about 5 %.

When 2,8-diphenyl-4,10,11,11-tetramethyl-2,3,8,9-tetrazadispiro[4.0.4.1]undeca-3,9-diene-1,7-dione (IV a) was treated in the way described above, about 12 % of the reaction product was 1-phenyl-3-methyl-4-*iso*propylidene-2-pyrazolin-5-one.

Bromination of $C_{23}H_{23}ClN_4O$. The chloro compound II g (0.19 g) was dissolved in acetic acid, and the equimolar amount of bromine (0.07 g) in acetic acid and a few pieces of ice were added. The product formed was precipitated with more ice and water, filtered, washed with water and air-dried. Yield: 0.22 g of yellow crystals, m.p. 123° (decomp.). Recrystallization from ethanol did not change the m.p. (Found: C 55.2; H 4.5; Br 16.1; Cl 7.2. Calc. for $C_{23}H_{22}BrClN_4O_2$: C 55.0; H 4.4; Br 15.9; Cl 7.1.)

Isomerization of I e to form 4,4'-benzylidynebis[1-phenyl-3-methyl-2-pyrazolin-5-one] (III b). I e was heated in an oil bath at 135° for two hours or in dioxan-water (10:1)

solution at 95° for 20 h. Recrystallization from ethanol gave orange crystals, which melted at 240–241.5° (decomp.). Michaelis and Zilg [10] give m.p. 242° for III b. (Found: C 74.8; H 5.1; N 12.9. Calc. for $C_{27}H_{22}N_4O_2$: C 74.6; H 5.1; N 12.9.)

Isomerization of I a to form 4,4'-methylidynebis[1-phenyl-3-methyl-2-pyrazolin-5-one] (III a). I a (0.50 g) in ethanol (30 ml) was refluxed for 24 h. On cooling orange crystals (0.43 g) separated. After crystallization from ethanol they melted at 183°. According to Ionescu and Georgescu [11] III a melts at 180°. (Found: C 70.1; H 5.2; N 15.6; equiv.wt. 354. Calc. for $C_{21}H_{18}N_4O_2$: C 70.4; H 5.1; N 15.6; equiv.wt. 358.)

Attempts to isomerize I b, I c, and I d. Boiling of I b or I c in ethanol solution overnight was not sufficient to decompose the *cyclo*propane rings completely. More than 25 % of unaltered I b or c could be isolated from the orange-red products.

Heating at 95° in dioxan-water (10:1, v:v) for 24 h destroyed the three-rings of I b and c. However, when I d was heated in the same way, about 90 % of the starting material could be recovered unchanged.

The analyses were performed by the Department of Analytical Chemistry, University of Lund, or by Mikroanalytisches Laboratorium im Max-Planck-Institut für Kohlenforschung, Mülheim.

The financial support of *Statens naturvetenskapliga forskningsråd* is gratefully acknowledged.

REFERENCES

1. Westöö, G. *Acta Chem. Scand.* **11** (1957) 1290.
2. Westöö, G. *Acta Chem. Scand.* **11** (1957) 1285.
3. Westöö, G. *Acta Chem. Scand.* **7** (1953) 456.
4. Radulescu, D. and Georgescu, V. *Bull. soc. chim. France* [4] **37** (1925) 187.
5. Kohler, E. P. and Conant, J. B. *J. Am. Chem. Soc.* **39** (1917) 1404.
6. Derfer, J. M., Pickett, E. E., and Boord, C. E. *J. Am. Chem. Soc.* **71** (1949) 2482.
7. Slabey, V. A. *J. Am. Chem. Soc.* **76** (1954) 3604.
8. Westöö, G. *Acta Chem. Scand.* **6** (1952) 1499.
9. Westöö, G. *Acta Chem. Scand.* **7** (1953) 355.
10. Michaelis, A. and Zilg, A. *Ber.* **39** (1906) 370.
11. Ionescu, M. V. and Georgescu, V. N. *Bull. soc. chim. France* [4] **41** (1927) 881.
12. Knorr, L. *Ann.* **238** (1887) 137.

Received May 23, 1957.

ACTA CHEMICA SCANDINAVICA 11 (1957) 1365—1370

Isolation of Disaccharides from Golden Apple Gum

BENGT O. LINDGREN*

Queen's University, Kingston, Ontario, Canada

The structure of Golden Apple gum has been studied by the method of partial hydrolysis. After a mild acid treatment 3-*O*-α-[4(?)-*O*-methyl-D-glucuronopyranosyl]-L-arabinose was obtained. This acid thus is an integral part of the easily split side-chains of the gum molecule. The partially hydrolysed material yielded after further hydrolysis the following three disaccharides: 3-*O*-β-D-galactopyranosyl-D-galactose, 6-*O*-β-D-galactopyranosyl-D-galactose, and 6-*O*-β-[4(?)-*O*-methyl-D-glucuronopyranosyl]-D-galactose. Consequently, these acids are parts of the more resistant, pyranoside framework of the gum.

A previous investigation [1] of the gum exuded from Golden Apple tree (*Spondias cytheria* Sonner; family *Anacardiaceae*) showed that it was composed of residues of arabinose, galactose, a uronic acid (probably 4-*O*-methyl-D-glucuronic acid), xylose, and traces of rhamnose and fucose. The isolation of 3-*O*-β L-arabopyranosyl-L-arabinose from a hydrolysate of the gum showed that some of the arabinose units were present in the pyranose form. At least some of the xylose units must be linked to arabinose since 3-*O*-α-D-xylopyranosyl-L-arabinose was also obtained from the hydrolysate.

This paper reports a further study of the gum. The sample examined contained 51 % of pentose anhydride units and 15 % of uronic anhydride units. Its equivalent weight was 1 070. $[\alpha]_D$ — 5° (*c* 1.1; water).

Many gums are considered to be built up of a framework of galactopyranose units to which are attached side chains, composed largely of arabofuranose residues. The gum was therefore first hydrolysed under conditions such that practically all of the furanoside bonds, but only a small part of the pyranoside ones should be split. This was done in the usual way by heating a solution of the gum in its acidic form (autohydrolysis) until the reducing power did not further increase (80 h at 98°C).

The hydrolysate obtained was divided by conventional methods into i) the acidic mono- and oligosaccharides, ii) the neutral mono- and oligosaccharides, and iii) the degraded gum which constituted the pyranoside framework of the gum.

* Present address: Swedish Forest Products Research Laboratory, Stockholm, Sweden.

i) The weight of the acidic sugars was 13 % of that of the gum. The main component was an aldobiuronic acid, which is called acid A in the following. If formed about a third of the fraction. The rest was composed mainly of higher oligosaccharides, as revealed by paper chromatography of the fraction.

The hydrolysate of acid A showed on a paper chromatogram spots of arabinose and of a monomethyl-uronic acid, which probably was 4-*O*-methyl-D-glucuronic acid. The high positive rotation of A, $[\alpha]_D$ + 123°, suggested that its components were linked by an *alpha*-glycosidic bond.

The structure of A was determined by degradation in the following steps: complete methylation, reduction of the ester group to a carbinol group, methylation of the carbinol group, and hydrolysis of the glucosidic bond. A paper chromatogram of the hydrolysate obtained showed three spots. Two of the components were isolated in pure form by paper sheet chromatography. One of them was identified as 2,4-di-*O*-methyl-L-arabinose by conversion into the corresponding *N*-phenyl-glycosyl amine. The other was shown to be 2, 3, 4, 6-tetra-*O*-methyl-D-glucose by comparing its infra-red spectrum with that of an authentic sample.

The third component did not move when subjected to paper electrophoresis using a borate buffer. This implied that the hydroxyl group on C_2 was methylated since the α-glycol group on C_1 and C_2 should otherwise form a borate complex. (For instance, the rate of movement of 3, 4-di-*O*-methyl-L-arabinose was found to be 40 % of that of glucose.)

On paper chromatograms, the component gave a brown spot with *p*-anisidine hydrochloride, and had an R_F greater than that of 2, 4-dimethyl-arabinose. Two of the dimethyl-arabinoses, 2, 3- and 2, 5-dimethyl-arabinose, move faster than the 2, 4-derivative [1]. Only the 2, 5-derivative, however, gives a brown spot with anisidine; that of the other is coloured red [1]. The third component was therefore probably 2,5-di-*O*-methyl-L-arabinose.

From this followed that acid A should be 3-*O*-α-(4-*O*-methyl-D-glucurono-pyranosyl)-L-arabinose, which has not earlier been reported as having been isolated from a polysaccharide. The fact that *two* arabinose methyl ethers were obtained obviously indicated that the completely methylated disaccharide contained both arabopyranose and arabofuranose residues.

The identification of 4-*O*-methyl-glucuronic acid as the acidic component of A was, however, made only by paper chromatography. As the rates of the movement of the other monomethyl-glucuronic acids are not known, the position of the methoxyl group in acid A is not definitely established. 4-*O*-Methyl-D-glucuronic acid is, however, a common component in polysaccharides while the other monomethyl-glucuronic acids are comperatively rare in nature.

ii) The weight of the neutral sugars was 59 % of that of the gum. The fraction was composed mainly of arabinose (about 58 %). The other constituents were xylose (7 %), oligosaccharides (32 %) and small amounts of galactose and rhamnose (1—2 % each). This fraction had already been examined in the earlier investigation [1], which led to the isolation of 3-*O*-β-L-arabopyranosyl-L-arabinose and 3-*O*-α-D-xylopyranosyl-L-arabinose, and was therefore not examined further.

iii) The degraded gum constituted 28 % of the total gum. It contained 30.5 % of pentose anhydride units and 20 % of uronic anhydride units. $[\alpha]_D$—41° (*c* 1.0; water).

Its hydrolysate contained mainly galactose, arabinose, and an aldobiuronic acid, which is called acid B in the following. Acid A was not present.

From the hydrolysate of another sample of degraded gum, acid A was isolated (see experiment B in the experimental part). This sample of degraded gum had not been prepared by such a prolonged hydrolysis as the above mentioned sample and was obtained in a higher yield. It was therefore probable that it still contained considerable amounts of arabofuranose residues.

The difficulty of removing all of the arabinose units from the gum by autohydrolysis has already been pointed out[1]. It follows from the above that practically all of the remaining arabinose units in the degraded gum most probably are in the pyranose form.

The aldobiuronic acid isolated from the degraded gum, acid B, was built up of galactose and monomethyl-uronic acid, probably 4-*O*-methyl-D-glucuronic acid. It yielded, on methylation, the crystalline methyl ester of hepta-*O*-methyl-6-*O*-*β*-D-glucuronopyranosyl-D-galactose. Consequently, B should be 6-*O*-*β*-(4-*O*-methyl-D-glucuronopyranosyl)-D-galactose, which has previously been isolated from gum myrrh [2]. As in the case of acid A, the position of the methyl group in acid B is not definitely established. The rate of movement of B on a paper chromatogram and its $[\alpha]_D$ value agreed, however, with the corresponding figures for the acid from gum myrrh.

From the hydrolysate of the degraded gum small amounts of two disaccharides were isolated. They crystallised readily from methanol. One of them, disaccharide C, had m.p. 156—159 °C. The crystals of the other, disaccharide D, rapidly liquefied when kept in air. They probably contained methanol of crystallisation, which easily evaporated causing the destruction of the crystal lattice. Both disaccharides on hydrolysis gave only galactose, which was identified by paper chromatography.

Disaccharide C was found to be identical with 3-*O*-*β*-D-galactopyranosyl-D-galactose, which has been isolated from *Acacia pycnantha* gum[3].

Disaccharide D yielded no formaldehyde on periodate oxidation in slightly alkaline solution, which is characteristic for hexose containing disaccharides with 1,5 or 1,6-linkages [4]. The low positive optical rotation, $[\alpha]_D$ + 30°, indicated a *beta*-glucosidic link between the sugar units. D should accordingly be 6-*O*-*β*-D-galactopyranosyl-D-galactose, and this was confirmed by a comparison of the infra-red spectrum of D with that of a synthetic sample. This disaccharide has recently been obtained from the water-soluble arabogalactan which is present in the wood of *Larix occidentalis* [5].

EXPERIMENTAL

Analyses etc.

Paper chromatography. Solvents:

a. Ethyl acetate:acetic acid-formic acid:water (18:3:1:4 v/v).
b. Ethyl acetate:acetic acid:water (7:2:1: v/v) .
c. *n*-Butanol:ethanol:water:conc. ammonia (200:50:244:5 v/v, the top layer).

d. *n*-Butanol:pyridine:water (10:3:3 v/v).
Paper: Whatman No. 1.
Spray: *p*-Anisidine hydrochloride dissolved in butanol.
R_{gal}: the rate of movement relative to galactose.
R_G: the rate relative to 2,3,4,6-tetra-*O*-methyl-D-glucose.

Paper electrophoresis. The experiment was performed according to Foster [6]. The pH of the borate buffer was 10. Voltage 900 V. Time 2 h. The correction for electroendosmosis was determined by running parallel tests with 2,3,4,6-tetra-*O*-methyl-D-glucose.

M_G: the rate of movement relative to glucose.

Infra-red spectra. If not otherwise stated, they were determined on potassium bromide pellets with a Perkin-Elmer double beam spectrophotometer. The maxima in the most characteristic part of the spectra, the region 700 – 1 000 cm^{-1}, are recorded in this paper.

Pentose anhydride. This analysis was carried out according to a Tappi standard method [7], by which the amount of furfural formed is determined by oxidation with bromate-bromide solution. As the predominant pentose sugar in the gum was arabinose, the yield of furfural was assumed to be 74 %, which is the yield obtained from arabinose [7]. The correction for the amount of furfural formed from the uronic acid units was applied by assuming that the yield was one half of that from arabinose [8]. No correction was made for the small amount of hydroxymethylfurfural formed from the galactose units.

Uronic anhydride. The determinations were carried out according to Browning [9].

Reducing power. This was determined iodometrically according to Ingles and Israel [10]. The oxidation was carried out at pH 11.5.

Hydrolysis

Autohydrolysis. An aqueous solution of the gum (5.00 g) was passed through a column of a cation exchanger (Amberlite IR-120) saturated with hydrogen ions. The eluate (150 ml) was heated in a water bath at 98°C, The consumption of 0.1 N iodine solution per ml of the solution was after 0 h, 0.04 ml; after 3 h, 0.74 ml; after 9 h, 1.25 ml; after 21 h, 1.57 ml; after 45 h, 1.77 ml; after 68 h, 1.79 ml, and after 75 h, 1.75 ml.

After 80 hours' heating a part of the solution (78 ml) was passed through a column (diameter 4.5, height 7.5 cm) of a "weak" anion exchanger (Amberlite IR-4B) saturated with acetate ions. The column was then washed with water until the water gave a negative Molisch test.

The column was eluted with N formic acid. The residue after evaporation of the eluate (334 mg, corresponding to 13 % of the weight of the gum) showed on a paper chromatogram (solvent a) a faint, red spot at R_{gal} = 2.70 (probably 4-methyl-glucuronic acid), a strong, red spot at R_{gal} = 1.3 (acid A), and a series of spots having lower R_{gal} values (different oligosaccharides).

The residue (38 mg) was separated on a paper sheet using solvent a. The strip containing acid A was extracted with water. Evaporation of the extract yielded 12 mg of acid A.

The solution which passed directly through the anion exchanger column was neutralised with barium carbonate and concentrated to 20 ml. Ethanol (100 ml) was added and the precipitate of degraded gum (728 mg, corresponding to 28 % of the weight of the gum) was removed by centrifugation.

The residue on evaporation of the alcohol-water solution weighed 1 525 mg (corresponding to 59 % of the weight of the gum). A part of the residue (124 mg) was separated on paper sheets using solvent a. The strips containing the different components were extracted with water and the extracts were evaporated to dryness. The weight of the residue from the arabinose strips was 71 mg; from the xylose strips, 8 mg; from the rhamnose and galactose strips, 2 mg each; from the strips with 3-xylopyranosyl-arabinose, 9 mg; from the strips with 3-arabopyranosyl-arabinose, 15 mg; and from the strips containing the remaining oligosaccharides, 15 mg. Total 122 mg.

Hydrolysis of degraded gum. Experiment A. The degraded gum (681 mg obtained from the experiment described above) dissolved in N sulphuric acid (10 ml) was heated on a water bath for 5 h. The solution was neutralised with barium carbonate, passed through a column of a cation exhanger (Amberlite IR-120) saturated with hydrogen ions, and

evaporated to dryness. The weight of the residue was 480 mg. A paper chromatogram (solvent a) showed at R_{gal} = 2.70 a red, faint spot (probably 4-methyl-glucuronic acid), at R_{gal} = 1.63 a strong, red spot (arabinose), at R_{gal} = 1.00 a strong, brown spot (galactose), and at R_{gal} = 0.58 a strong, brown spot (acid B). No spot was observed at R_{gal} = 1.3 (which would be due to acid A). With solvent d spots were obtained at R_{gal} = 1.53 (arabinose), at R_{gal} = 1.00 (galactose), and at low R_{gal} values (acidic components).

Experiment B. The degraded gum for this experiment was obtained by heating an aqueous solution (2 000 ml) of the acidic gum (38.4 g) at 83°C for 24 h. The product (15.3 g, 40 % of the weight of the gum) was precipitated from the neutral part of the hydrolysate by addition of alcohol as described above.

The degraded gum (15.0 g) dissolved in 2 N sulphuric acid (200 ml) was heated at 53°C for 8 days. The solution was neutralised with barium hydroxide, and passed through a column of a cation excanger (Amberlite IR-120) saturated with hydrogen ions. The components of the solution were fractionated into *a*) neutral and *β*) acidic compounds by passing the solution through a column (diameter 4.5, height 11 cm) of a "weak" anion exchanger (Amberlite IR-4B) in its acetate form.

a) Evaporation of the solution which passed through the column yielded a syrup of the neutral components (4.9 g). The syrup was passed through a carbon-Celite column 1:1 w/w, diameter 3, height 27 cm). The column was eluted with water containing stepwise increasing amounts of ethanol in the usual way. The fractions obtained were examined by paper chromatography.

0 % ethanol. Weight 3.65 g. Contained: galactose, arabinose, and traces of rhamnose.

2 % ethanol. Weight 0.02 g. Contained: galactose, arabinose, 3-xylopyranosyl-arabinose (?), and traces of rhamnose.

5 % ethanol. Weight 0.18 g. Contained: 3-xylopyranosyl-arabinose (?), 3-arabopyranosyl-arabinose (?), disaccharides C and D.

The last fraction was chromatographed on paper sheets using solvent a. C (39 mg) and D (16 mg) were obtained.

b) The acidic fraction absorbed on the column was eluted with N formic acid. The eluate was continuously extracted with ether for 24 h (to remove formic acid), then evaporated to dryness, residue 6.1 g.

The residue (3.0 g) was fractionated on a cellulose column using solvent b. The following fractions were collected and examined by paper chromatography.

Fraction a) contained 4-methyl-glucuronic acid (?); weight, 67 mg. b) contained acid A; weight, 165 mg. c) contained acid B; weight 402 mg.

Structures of the disaccharides

Acid A. R_{gal} = 1.3 (solvent a). $[\alpha]_D$ +123° (*c* 1.0; water). Paper chromatograms of the hydrolysate of A showed three spots: i) unchanged A, ii) arabinose, and iii) a sugar, which moved at the same rate as 4-methyl-glucuronic acid in solvents a and d.

A (300 mg) was methylated with dimethyl sulphate and sodium hydroxide, and then with Purdie reagent. The infra-red absorption curve of the product (in carbon tetrachloride solution) showed no maximum in the vicinity of 3 400 cm^{-1} indicating the absence of hydroxyl groups.

The completely methylated A was then dissolved in ether (about 5 ml, distilled from lithium aluminium hydride). Lithium aluminium hydride (0.5 g) was added to the solution and the mixture was left at room temperature for 24 h. After addition of ice and water, the solution was continuously extracted with chloroform.

The extract was dried (Drierite) and evaporated to dryness. After methylation with Purdie reagent the product was hydrolysed (N hydrochloric acid, steam bath, 20 h). The hydrolysate was neutralised with silver carbonate, filtered, and evaporated to dryness. Residue 140 mg.

Paper chromatograms of the residue showed three spots with the R_G values (solvent c): 0.63 (red), 0.86 (brown), and 1.00 (red). Paper electrophoresis showed only one spot: M_g = 0.0.

The components of the hydrolysate were separated on paper sheets. By a mishap most of the components were lost during the separation. Only about 5 mg each of the fastest moving and the slowest moving components were obtained. The fast moving component

crystallised, m.p. 60—70°C. Its infra-red spectrum and that of 2,3,4-6-tetra-*O*-methyl-D-glucose were identical. They showed maxima at 700, 768 (broad), 853 (strong), 887 (weak), 905 (weak), 917 (weak), 964, and 990 (strong) cm^{-1}.

The slow moving component (5 mg), aniline (5 mg), and methanol (0.5 ml) were heated together on a water bath for 2 h. Evaporation of the solvent yielded crystals, m.p. 128—130°C. The infra-red spectrum of the crystals and that of *N*-phenyl-2,4-di-*O*-methyl-L-arabinosyl amine were identical. In the region 600—1 100 cm^{-1} they showed maxima at: 660, 695 (strong), 746 (strong), 760 (strong), 820, 825 (masked), 860, 880, 900, 928 (strong), 973, 990, 1 037 (strong), 1 055, 1 080 (strong, broad) cm^{-1}.

Acid B. R_{gal} = 0.58 (solvent a). $[\alpha]_D$ −1° (*c* 0.4; water). Paper chromatograms of the hydrolysate of B gave three spots; i) unchanged B, ii) galactose, and iii) a sugar which moved with the same rate as 4-methyl-glucuronic acid in solvents a and d.

Methylation of B (380 mg) with dimethyl sulphate and sodium hydroxide, and after that with Purdie reagent yielded the crystalline methyl ester of hepta-*O*-methyl-6-β-D-glucuronopyranosyl-D-galactose (195 mg). After recrystallisation from light petroleum, the compound had m.p. 92—93°C, undepressed on admixture with an authentic sample. (Found: C 51.2; H 7.8; OCH_3 52.8. Calc. for $C_{20}H_{36}O_{12}$: C 51.2; H 7.7; OCH_3 52.8.)

Disaccharide C. R_{gal} = 0.27 (solvent a), and 0.25 (solvent d). Paper chromatograms of the hydrolysate showed only one spot, that of galactose. C crystallised readily from methanol, m.p. 156—159°C, undepressed by addition of 3-β-D-galactopyranosyl-D-galactose. The behaviour of C with lead-tetracetate [11] and its X-ray powder diagram were identical with those of this disaccharide. (The oxidation and the determination of the X-ray diagram were kindly carried out by Dr. A. S. Perlin.)

Disaccharide D. R_{gal} = 0.16 (solvent a), and 0.11 (solvent d). $[\alpha]_D$ +30° (*c* 1.2; water). Paper chromatograms of the hydrolysate showed only one spot, that of galactose. D crystallised in needles from methanol. If kept in a dessiccator or in air, the crystals decomposed.

The periodate oxidation in slightly alkaline solution was carried out as described by Hough and Perry [4]. The pH of the periodate solution was 8. Oxidation time, 24 h. Formaldehyde was determined colorimetrically using the chromotropic acid method. In the test D gave the same reading as a blank. (This experiment was kindly performed by Mr. M. B. Perry.)

6-β-D-galactopyranosyl-D-galactose was synthesised according to Freudenberg and co-workers [12]. Its infra-red spectrum had maxima at 703, 775, 790 807, 876, 894, 916, 950, 973, 998 cm^{-1} in the region 700—1 000 cm^{-1}. Outside this region the spectrum had distinct maxima at 1 150, 1 213, and 1 248—1 252 (broad) cm^{-1}.

Since there was insufficient amount of D available the distinct maxima only showed up in the comparison diagram for D. They were at 703, 775, about 890, 916, 950, 1150, 1 213, and about 1 250 cm^{-1}.

Acknowledgement. I would like to express my thanks to Dr. J. K. N. Jones for suggesting this subject and for his kind interest. I am also indebted to the *Swedish America Foundation* for a fellowship.

REFERENCES

1. Andrews, P. and Jones, J. K. N. *J. Chem. Soc.* **1954** 4134.
2. Jones, J. K. N. and Nunn, A. S. *J. Chem. Soc.* **1955** 3001.
3. Hirst, E. L. and Perlin, A. S. *J. Chem. Soc.* **1954** 2622.
4. Hough, L. and Perry, M. B. *Chemistry & Industry* **1956** 768.
5. Bouveng, H. and Lindberg, B. *Acta Chem. Scand.* **10** (1956) 1515.
6. Foster, A. B. *J. Chem. Soc.* **1953** 982.
7. *Tappi standard method* T 223 m-43.
8. Pigman, W. W. and Goepp, R. M. *Chemistry of the Carbohydrates*, New York 1948, p. 308.
9. Browning, B. C. *Tappi* **32** (1949) 119.
10. Ingles, O. G. and Israel, G. C. *J. Chem. Soc.* **1948** 810.
11. Charlson, A. J. and Perlin, A. S. *Can. J. Chem.* **34** (1956) 1200.
12. Freudenberg, K., Wolf, A., Knopf, E. and Zaheer, S. H. *Ber.* **61** (1928) 1743.

Received June 17, 1957.

ACTA CHEMICA SCANDINAVICA 11 (1957) 1371—1377

Enzymatic Hydrolysis of Organophosphorus Compounds

VII. The Stereospecificity of Phosphorylphosphatases

KLAS-BERTIL AUGUSTINSSON

Institute of Organic Chemistry and Biochemistry, University, Stockholm, Sweden

The enzymatic hydrolysis of dimethylamido-ethoxyphosphoryl cyanide (tabun) by purified phosphorylphosphatase preparations from human blood plasma, swine kidney and liver, and by the plasma of rabbit and rat was studied from a kinetic point of view. The hydrolysis was a first-order reaction for the human plasma enzyme. When the kidney and liver enzymes were used, the reactions were composed of two simultaneous first-order reactions; the numerical values of the rate constants for the kidney enzyme were 5.70 h^{-1} and 0.39 h^{-1}. The results were interpreted as being due to stereospecificity for the kidney and liver enzymes, the stereoisomers of tabun being hydrolysed at two different rates by these enzymes. In studies with mixed enzymes it was demonstrated that the isomer of tabun, being slowly hydrolysed by the kidney enzyme, was readily hydrolysed by both the human plasma phosphorylphosphatase and the rabbit plasma enzyme. Both the rat and rabbit plasma phosphorylphosphatases also showed stereospecificity, but to a lower degree compared with the kidney enzyme.

The existence and properties of phosphorylphosphatases have recently been reported by this [1] and other laboratories [2-4]. In most of our studies, tabun (dimethylamido-ethoxyphosphoryl cyanide) was used as substrate. From the reaction curves (see paper I of the present series of reports [1]) for the system tabun-phosphorylphosphatase using various animal tissues as enzyme sources, it can be concluded that the reaction, in certain cases at least, might be composed of two different hydrolysis rates. Hoskin and Trick [5] recently obtained experimental evidence for this proposal and suggested that tabun, containing an asymmetric phosphorus atom, exists in two optically active forms which are enzymatically hydrolysed at different rates. Rat serum was employed in their experiments, and polarimetric determinations indicated that the dextrorotatory form of tabun is more rapidly hydrolysed. Similar experiments have been performed in this laboratory, and extended to a variety of enzyme preparations. The present report deals with the results obtained.

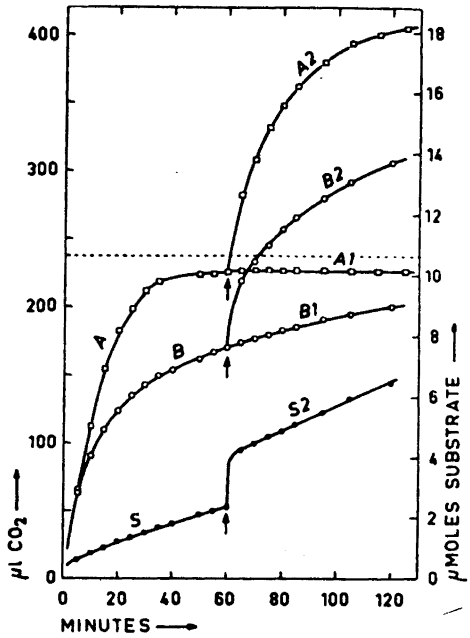


Fig. 1. Enzymatic hydrolysis of tabun by purified phosphorylphosphatase preparations from human serum (A) and swine kidney, and the effects of the addition (indicated by an arrow) of a second portion of enzyme (1) and substrate (2) respectively. S, spontaneous substrate hydrolysis. Dotted line refers to total substrate hydrolysis (273.5 µl CO_2 or 10.6 µmoles).

METHODS AND MATERIAL

Enzyme activity was measured by the Warburg manometric technique at 25°C using flasks with two side bulbs [1]. All determinations were carried out in 0.040 M sodium bicarbonate solution of pH 7.6 (equilibrated with a mixture of 95 % N_2 and 5 % CO_2) and tabun, dissolved in water immediately before use, was used as substrate throughout. The total volume of the reaction mixture was 2.00 ml after adding the first portion of substrate from one of the side bulbs. In most experiments, 1.60 ml of the enzyme solution was placed in the main compartment, and 0.40 ml of the substrate or enzyme solution in each of the two side bulbs. The amount of substrate added to the enzyme from the beginning was 10.6 µmoles of tabun, and this amount was also used when a second portion of substrate was added to the reaction mixture.

Human plasma enzyme was prepared from postpartum serum according to a partly modified method No. 6 of Cohn *et al.*[6]. It was identical with Fraction IV−1 used in previous investigations of this series.

Rabbit plasma enzyme and *rat plasma enzyme.* Fresh plasma was used as such without any treatment.

Kidney and *liver enzymes* were prepared from fresh swine organs, the first part of the method being similar to that described by Mounter *et al.*[2] for DFPase, and continued with ammonium sulphate fractionation according to a procedure to be described in a following report.

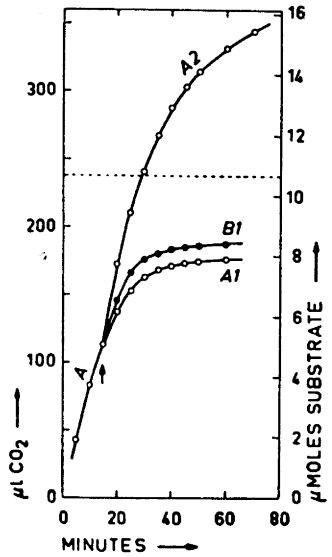


Fig. 2. Enzymatic hydrolysis of tabun by rat plasma (A), and the effects of the addition of a second portion of enzyme (rat plasma, A1; purified kidney enzyme, B1) and substrate (2). *Cf.* Fig. 1.

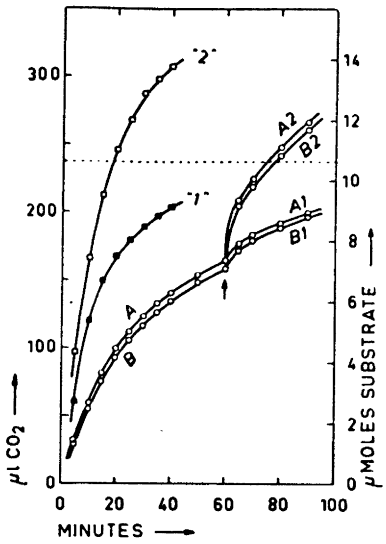


Fig. 3. Enzymatic hydrolysis of tabun by two purified preparations (A and B) of swine liver phosphorylphosphatase, and the effects of the addition of a second portion of enzyme (1) and substrate (2); prepn. A purer than prepn. B. Curves "1" and "2" refer to systems where the concentrations of enzyme and substrate respectively were doubled from the beginning of the reaction. *Cf.* Fig. 1.

RESULTS

Human plasma phosphorylphosphatase. The hydrolysis curve (Fig. 1) showed that tabun was hydrolysed to almost 100 %, suggesting that both the optical isomers of the substrate were split by this preparation. Two identical reaction mixtures were used, and after 60 min when the reaction had come to completion, the same amounts of substrate and enzyme, respectively, as present from the beginning of the experiment were added in order to double the concentration of the two constituents. The addition of more enzyme had no effect, confirming that all the substrate had been used up. After adding the second portion of substrate, on the other hand, the hydrolysis reaction started again with a rate somewhat lower than was observed with untreated enzyme. The lower reaction rate was probably due to enzyme inhibition by the degradation product(s) of tabun.

It will be noted in Fig. 1 and also in the following figures that the theoretical 100 % hydrolysis of the substrate was never reached. This was due to the spontaneous hydrolysis of tabun, *i.e.*, the substrate concentration at the moment of mixing enzyme and substrate is lower than the actual amount of substrate dissolved; it is impossible to avoid such spontaneous hydrolysis

of the substrate solution before use, for practical reasons. The spontaneous hydrolysis curve is inserted in Fig. 1, and was obtained by replacing the enzyme solution with the bicarbonate solution. The acid degradation product of tabun formed (dimethylamido-ethoxy-hydroxy-phosphine oxide) gives rise to an instantaneous production of CO_2, when the substrate solution is mixed with the bicarbonate containing enzyme solution.

Rat plasma phosphorylphosphatase. Rat plasma splits tabun at about the same rate as human plasma. In the experiment shown in Fig. 2 the second portion of substrate and enzyme, respectively, were added before the reaction had come to completion. The rat plasma enzyme seems to split one of the stereoisomers at higher rate than the other isomer. This result confirms the observation reported previously by Hoskin and Trick [3].

With the *rabbit plasma phosphorylphosphatase* similar results were obtained, but the stereospecificity of this enzyme is less pronounced than that of the rat plasma enzyme. This was obvious from an experiment where the rabbit plasma was added to a mixture in which one of the isomers of tabun had been split completely by the kidney phosphorylphosphatase (Fig. 4).

Swine kidney phosphorylphosphatase. The hydrolysis of tabun by purified enzyme of swine kidney (Figs. 1 and 4) is readily interpreted on the basis of enzyme stereospecificity with respect to the substrate. After the gas evolution during the first minutes due to the decomposition of tabun before the addition of the substrate solution to the bicarbonate system, a rapid hydrolysis was observed which came to completion when about one-half (120 μl) of the theoretical yield of gas was evolved. Then the reaction rate became relatively low; this slow reaction was partly due to the spontaneous (non-enzymatic) hydrolysis of the other stereoisomer of tabun and partly to the enzymatic hydrolysis of that isomer. The addition of a second portion of enzyme did not change the reaction rate; after adding a second portion of substrate, on the other hand, the reaction started again with a rate which was lower than following the addition of the first portion of substrate. It is suggested that the phosphorus containing reaction product inhibits the enzymatic hydrolysis, thus explaining the lower reaction rate.

The composition of the reaction curve by two hydrolysis rates are further illustrated in Fig. 5.

Swine liver phosphorylphosphatase. A purified preparation of this enzyme behaved similarly to the kidney enzyme, but the difference between the hydrolysis rates of the two stereoisomers was less pronounced for the former enzyme (Fig. 3).

Studies with mixed enzymes. In order to find confirmation for the suggestion put forward above that human plasma phosphorylphosphatase splits both the stereoisomers of tabun, the following experiment was performed (Fig. 4). The substrate was hydrolysed by the kidney enzyme, and when the enzymatic hydrolysis had come to completion a purified preparation of human plasma enzyme was added to the reaction mixture. It was found that the plasma enzyme split that isomer of the substrate which had not been attacked by the kidney enzyme. A similar result was obtained when the rabbit phosphorylphosphatase was added to the reaction mixture. The same amount

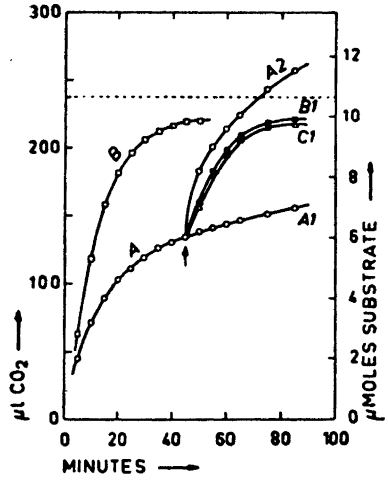


Fig. 4. Enzymatic hydrolysis of tabun by a purified phosphorylphosphatase preparation from swine kidney (A) and the effect of purified phosphorylphosphatase from human serum (B1) and of rabbit plasma (C1) on the reaction mixture. The hydrolysis curve for the purified enzyme from human serum (B) is inserted for comparison. *Cf.* Fig. 1.

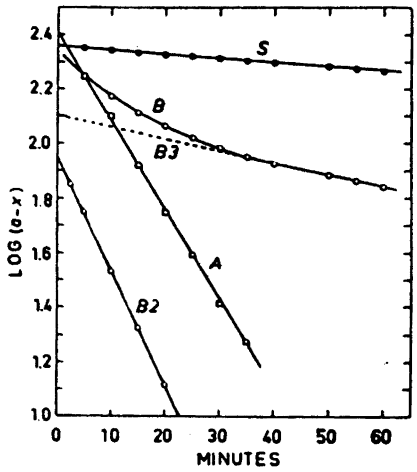


Fig. 5. Graphical evaluation of first-order reaction constants for the enzymatic hydrolysis of tabun by purified phosphorylphosphatase preparations from human serum (A) and swine kidney (B) and the spontaneous (non-enzymatic) hydrolysis of the substrate (S). B3, extrapolated line to estimate k_3 (actually $k_1 + k_3$), and to obtain B2, the line necessary for the estimation of k_2. Experimental values taken from Fig. 1. *Cf.* text.

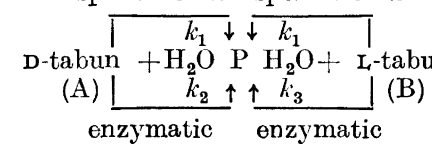
of gas was finally evolved as when the human plasma enzyme hydrolysed the substrate alone from the beginning.

Rat plasma behaved differently in these experiments compared with human and rabbit plasma: it was not found possible to hydrolyse the "non-attacked" isomer. In a similar experiment performed, the result of which is shown in Fig. 2, it was likewise demonstrated that the rat plasma enzyme split the same isomer of tabun as did the kidney enzyme.

DISCUSSION

The results reported above show that the enzymatic hydrolysis of tabun by certain enzyme preparations (especially those from the kidney and liver) is composed of at least two simultaneous reactions. The explanation, is, most probably, that tabun contains an asymmetric phosphorus atom and thus exists in two optically active isomers which are hydrolysed enzymatically at different rates. This idea, first pointed out by Hoskin and Trick [5], is clearly demostrated by a purified enzyme preparation from swine kidney (Fig. 1). The data obtained in this experiment were used to calculate the reaction constants according to a classical graphical technique, and the results are recorded in Fig. 5.

When a racemic mixture of tabun is used as substrate for this particular enzyme (kidney phosphorylphosphatase), the following four first-order reactions are suggested to take place simultaneously (rate constants in brackets): the spontaneous hydrolysis (k_1 which is the same for the two isomers), the enzymatic hydrolysis of the D-isomer (k_2) and the enzymatic hydrolysis of the L-isomer (k_3). Whether the reaction products (P) contain dimethylamido-ethoxy-hydroxy-phosphine oxide in an optically active form or as a racemic mixture has not been investigated:



The four reactions are represented by the following differential equations:

Spontaneous:	Enzymatic + spontaneous:
$-\frac{d(A)}{dt} = k_1(A)$	$-\frac{d(A)}{dt} = k_1(A) + k_2(A)$
$-\frac{d(B)}{dt} = k_1(B)$	$-\frac{d(B)}{dt} = k_1(B) + k_3(B)$

If $\log (a - x)$ (a = original amount of substrate, x = amount of substrate hydrolysed spontaneously and/or enzymatically after t min) is plotted against t, a straight line is obtained for the spontaneous hydrolysis, and from the slope of the line the rate constant, k_1, was found to be 0.21 h^{-1}. The curved line (B) representing the enzymatic hydrolysis by the kidney enzyme (*cf.* Fig. 1, B) indicates that this reaction can be resolved into two first-order reactions, represented by the line B3 (extrapolation of line B to the ordinate) and the line B2 (obtained by subtracting line B3 from B) (Fig. 5). The line B3 in its turn is composed of the spontaneous (k_1) substrate hydrolysis and the enzymatic (k_3) hydrolysis of the slow reacting stereoisomer. The numerical values of k_3 and k_2 obtained were 0.39 h^{-1} (= 0.60 — 0.21) and 5.71 h^{-1}.

The enzymatic hydrolysis of tabun by the purified human plasma phosphorylphosphatase is a first-order reaction, indicated by the straight line obtained when the experimental values from Fig. 1 are analysed according to the same graphical method. The numerical value of the reaction constant in this case was 4.45 h^{-1}. This enzyme, therefore, split both the stereoisomers of tabun at the same rate.

It will be noted that the hydrolysis reaction proceeded in a medium of pH 7.6 at which pH the P-CN is the only linkage broken, both spontaneously [7] and enzymatically [1].

In the experiments reported by Hoskin and Trick [5], using rat serum as the enzyme source, the reaction constant for the spontaneous hydrolysis of tabun was found to be approximately five times greater than that for the slow reaction observed during the enzymatic hydrolysis. It is difficult to

find a plausible explanation for this observation. Such an unexpected difference between the two rate constants has not been found in any of our experiments.

It has not been possible to supplement this investigation by observing changes in optical rotation during the reactions. This is mainly due to technical reasons: a comparatively high tabun concentration is necessary for polarimetric determination, and there are difficulties in getting the enzyme solutions clear enough to make observations of optical rotation possible. Using rat serum, Hoskin and Trick [5] reported some data from polarimetric determinations which indicated that the dextrorotatory isomer of tabun is more rapidly hydrolysed enzymatically. It is likely that this isomer also is the form of tabun which is more readily attacked, for example, by the kidney phosphorylphosphatase.

The results obtained in the present investigation with various enzyme preparations support the idea that there exists a variety of phosphorylphosphatases. The enzyme present in human plasma differs from those present in the kidney and liver by not showing stereospecificity. Furthermore, the enzymes of rat and rabbit plasmas behave differently in this respect both from the human plasma enzyme and the enzymes present in the organs studied. In a report to be published in due course, further support for the complexity of phosphorylphosphatases will be discussed.

The author wishes to express his sincere thanks to Professor Gustaf Ljunggren, Chief of the Research Institute of National Defence, Department 1, for his continual interest in these investigations. He is greatly indebted to Miss Toril Isachsen for skilful technical accistance.

REFERENCES

1. Augustinsson, K.-B. and Heimbürger, G. *Acta Chem. Scand.* **8** (1954) 753 [I], 762 [II], 915 [III], 1533 [IV]; **9** (1955) 310 [V], 383 [VI]. See also *Biochim. et Biophys. Acta* **13** (1954) 303 [preliminary].
2. Mounter, L. A. *J. Biol. Chem.* **209** (1954) 813; **215** (1955) 705; **219** (1956) 677. See also *ibid.* **204** (1953) 221, 837; **210** (1954) 219; **215** (1955) 691, 699; **219** (1956) 695; **221** (1956) 537.
3. Hoskin, F. C. G. *Can. J. Biochem. and Physiol.* **34** (1956) 75, 743.
4. Adie, P. A. *Can. J. Biochem. and Physiol.* **34** (1956) 1091; See also *ibid.* **34** (1956) 80.
5. Hoskin, F. C. G. and Trick, G. S. *Can. J. Biochem. and Physiol.* **33** (1955) 963.
6. Cohn, E. J. *et al. J. Am. Chem. Soc.* **72** (1950) 465.
7. Larsson, L. *Acta Chem. Scand.* **7** (1953) 306.

Received June 13, 1957.

ACTA CHEMICA SCANDINAVICA 11 (1957) 1378—1380

On the Synthesis of Protein and Polynucleotides in Spores of *Penicillium brevicompactum*

E. HAMMARSTEN and H. PALMSTIERNA

Department of Bacteriology, Karolinska Institutet, Stockholm, Sweden

Spores of *Penicillium brevicompactum* have been cultivated in submerged cultures, until, after 10 hours, the very first morphological signs showed a beginning development of mycelia.

In this system the net synthesis of ribonucleic acid (RNA) started during the first 30 minutes of cultivation and preceded the net synthesis of protein.

No measurable net synthesis of desoxyribonucleic acid (DNA) was found before 8 to 10 hours of cultivation. The amounts of DNA present in the spores is very low compared to animal and bacterial cells.

The net syntheses were determined by direct measurements of amounts and were investigated by tracer methods.

EXPERIMENTAL

Microbiological methods. Spores of *P. brevicompactum* were spread on Czapek-Dox maltose agar plates and grown two weeks at 25°C. After this period the plates were placed at room temperature for another three weeks. The spores were then removed by a soft sterilized brush. The pooled material was freed from contaminating mycelia by filtering a suspension in glass-distilled water at 0°C through Pyrex glass wool. No mycelia were found in the filtrate, as checked by means of phase contrast microscopy. In order to reduce the culture volume and to ascertain a rapid growth of the spores, the cells were kept submerged by continuous shaking and aeration. The medium used was the salt-glucose medium devised by Czapek-Dox. The glucose concentration, however, was only one tenth (0.4 %) of the one commonly used in their medium. The glucose was labeled in all carbon atoms with ^{14}C. The specific activity was 190 c.p.m. per μg of glucose carbon.

The culture volume was 10 litres. Inoculation was made with approximately 5 g of spores calculated as dry weight. The culture was aerated at a rate of 1.5 litres per min and litre of medium. The air was dispersed by a sintered glass filter.

In order to check if the spores would develop into mycelia in this medium, a 1 litre culture had previously been inoculated with about 5 mg of spores. After 3 days 700 mg of dry mycelium were harvested. The first sign of morphological changes were found between 10 and 12 h after inoculation in the form of a small bud on some cells. The spores in the main experiment were controlled in this way too, and the buds after 10 h were found to be extremely rare.

Chemical methods. The cells were disintegrated in a Griffith shaker with glass beads (0.28 mm in diameter) in 30 % ethanol (v/v) at 0°C. After 24 h no spores remained, and the disintegration seemed to be complete as checked by phase contrast microscopy. The poly-

nucleotides were isolated from samples of about 500 to 800 mg of dry spores according to Hammarsten [1]. RNA was degraded to mononucleotides by alkaline hydrolysis. The hydrolysates of RNA were chromatographed on Dowex 2 resin according to Cohn [2] and Hurlbert *et al.*[3] with 4 N formic acid-0.2 M ammoniumformate for elution. DNA was degraded enzymatically according to the method of Hurst *et al.*[4] as modified by Cohn [5]. Elution from Dowex 2 resin was accomplished according to Hurlbert and Potter [3] with 1 M ammonium formate-formic acid (pH = 4.8). Guanine was isolated after acid hydrolysis of guanylic acid (Dowex 50). Adenine from RNA and the pyrimidine nucleotides from RNA and DNA were only so far purified that it could be shown that their labeling did not significantly deviate from that of guanine. Adenine from DNA could not be isolated on account of the minute amounts of DNA in our material. The labeling of purines and polynucleotides followed the pattern found for *Escherichia coli B* in the lag-phase [6].

The activity of guanine was determined by measuring the activity at "infinite" thinness on lead planchets in a windowless gas flow counter. The amount of guanine was estimated from spectrophotometric data.

The protein fraction was isolated by the trichloracetic acid method of Schneider after mechanical disintegration of the cells in the way mentioned. The precipitate was boiled in 6 N hydrochloric acid for 18 h. The hydrolysate was filtered through Pyrex glass wool and the hydrochloric acid removed *in vacuo*. The nitrogen to carbon ratio was determined in four samples and found to be 0.26 ± 0.03.

All samples with a low labeling were counted to an accuracy of 10 % and the others to 5 %.

RESULTS AND DISCUSSION

It is shown in Table 1 that the RNA-phosphorus increased rapidly during the first half hour after inoculation. Since there was no corresponding high activity in the RNA-guanine, it is possible that the net synthesis to a large part derived from unlabeled procursors within the cells and only to a smaller part from the medium. Another possibility is the formation of phosphopentose backbone before incorporation of guanine. In recent work on *E. coli* in the lagphase [6] the cells had been labeled with ^{13}C before the actual culti-

Table 1.

Cultivation time, h	mg dry spores per litre of culture	mg phosphorus in RNA per litre of culture	mg phosphorus in DNA per litre of culture	mg nitrogen in protein per litre of culture	Counts per min per μg carbon in:		
					RNA guanine	DNA guanine	Protein
0	598	1.78	0.010	28.1	—	—	—
1/2	596	2.47	0.010	33.4	0.7	0.4	0
1	592	2.56	0.013	33.5	1.6	0.4	0
2	622	2.74	0.008	37.2	5.7	0.4	0.9
4	636	2.96	0.006	37.7	8.2	1.2	3.6
6	693	3.44	0.007	33.3	18.0	1.0	13.1
8	801	4.43	0.016	46.2	43.2	0.5	21.5
10	944	5.41	0.015	61.0	68.5	6.8	38.1

vation experiment. It was found in that work that the syntheses of polynucleotides and also of proteins used material from cell precursors in the earliest stages of growth in the lagphase.

During the period that followed, the increase per hour in RNA-phosphorus in the spores was between 7 and 12 %. Owing to the very small amounts of DNA present in the spores no very exact estimates could be made of the DNA-phosphorus. In contrast to the rapid incorporation of ^{14}C into RNA, the DNA did not show any appreciable incorporation.

The proteins did not incorporate ^{14}C during the first hour of growth. Compared to the RNA the specific activity of the protein carbon remains at low values during the first 4 to 5 h. Thereafter the incorporation of ^{14}C had still a lower gradient than the incorporation into RNA. In view of the incorporation and protein synthesis from labeled precursors within the cells found in *E. coli* [6] it is quite probable that some protein in the spores has been synthesized from precursors within the cells during the period when proteins remain unlabeled. If the protein had derived all its carbon from medium carbon exclusively, the specific activity of the protein carbon at 10 h after inoculation would have been approximately half that of the carbon in the medium glucose. It is, however, only 20 % of the specific activity of the medium glucose. This probably means that a large part of the protein carbon was derived from cellular carbon sources present at the moment of inoculation (or partly from CO_2). The figures for protein net synthesis are irregular owing to technical difficulties arising from the capsular substances.

REFERENCES

1. Hammarsten, E. *Acta Med. Scand.* **Suppl. 196** (1947) 634.
2. Cohn, W. E. *J. Am. Chem. Soc.* **72** (1950) 1471.
   Cohn, W. E. and Volkin, *Nature* **167** (1951) 483; *Arch Biochem. and Biophys.* **35** (1952) 465; *J. Biol. Chem.* **203** (1953) 319.
3. Hurlbert, R. B., Schmitz, H., Brumm, A. F. and Potter, V. R. *J. Biol. Chem.* **209** (1954) 1.
4. Hurst, R. O., Little, J. A. and Butler, G. L. *J. Biol. Chem.* **188** (1951) 705.
   Hurst, R. O. and Butler, G. L. *J. Biol. Chem.* **193** (1951) 91.
5. Cohn, W. *Personal communication.*
6. Eliasson, N. A., Hammarsten, E., Palmstierna, H., Åqvist, S. and Reio, L. *Acta Chem. Scand.* **11** (1957) 1381.

Received June 3, 1957.

ACTA CHEMICA SCANDINAVICA 11 (1957) 1381—1389

Studies on *Escherichia coli* B in the Lag Phase of Growth

N. A. ELIASSON, E. HAMMARSTEN, H. PALMSTIERNA and S. ÅQVIST

Karolinska Institutet, Departments of Chemistry and Bacteriology, Stockholm, Sweden
and

L. REIO

Wenner-Gren Institute, Department of Physiological Chemistry, Stockholm, Sweden

The growth of *E. coli* B in the lag-phase of growth was investigated by analysis of the amounts of proteins, RNA, DNA and glycogen. The cells had been labeled with ^{13}C in a preculture running into the stationery phase, and were then cultivated in a medium labeled with ^{14}C and ^{15}N.

The relative increase in amount per litre culture followed the sequence: Glycogen>RNA>DNA>protein.

The role of cell precursors relative to that of the medium is discussed.

Previous work [1,2] led us to investigate some processes during the lag phase that starts when *E. coli* B cells, harvested from a culture in the stationary phase, are incubated in a fresh medium and prepare themselves for fission. Preliminary experiments with cells labeled with ^{15}N had shown that a redistribution of the nitrogen in the cells occurred simultaneously with an incorporation of nitrogen from the medium. This implies a very complex metabolic pattern in the lag-phase which may correspond to similar stages of growth in other cells. In spite of this anticipated complexity we have tried the method of prelabeling the cells and then cultivating them in a fresh medium labeled in another way. The cells were prelabeled with ^{13}C. The new medium contained lactate ($^{14}CH_3CH(OH)COO^-$) as the only carbon source and ^{15}N-labeled ammonium chloride as the only nitrogen source. Samples were taken at zero time and after 5, 25, 50 and 80 min of cultivation.

The rates of relative increase in amounts were found to be: Glycogen > RNA > DNA > Proteins (Fig. 1.). This is in accordance with earlier findings [1,2]. No carbon, once incorporated, disappeared from the cells. The proteins incorporated carbon from cell sources during the first 50 min. The same was the case

with glycogen during the first 50 min. The proteins incorporated practically all their nitrogen from the medium but RNA and DNA used rather much nitrogen, that was present in the cells at the moment of inoculation.

EXPERIMENTAL

E. coli B was grown in Friedleins salt-sodium lactate medium. The lactate was labeled with ^{13}C in the methyl group. The atom per cent excess ^{13}C in the medium was 5.45 at zero time and 2.35 after 18 h cultivations. The cells were harvested and washed in tracer-free medium and then inoculated into fresh medium with ^{14}C label in carbon 3 of the lactate and ^{15}N label in the ammonium chloride. The cultivation was carried out in four 30 litres pyrex flasks in a waterbath at 37°C. The culture volume was 20 litres. The cultures were aerated at a rate of 1 litre per min and litre of medium. The flasks were arranged around a vertical axis and were driven back and forth by a compressed-air motor. The flasks were emptied at appropriate times and the cultures cooled with a cooling coil. The taking of a sample and its cooling to +3° to +4°C took 3,5—4 min. A small sample was taken for counting the number of cells under the phase contrast microscope in a Bürker chamber and the rest of the culture was centrifuged at 0°C at 2 500 × *g* for 2 h in stainless steel tubes fitted with baffles and a netting of stainless steel at the bottoms of the tubes to prevent the cells from whirling up during the retardation of the centrifuge. The number of cells remaining in the supernatant was determined by counting the number of colonies produced on endo agar plates. Less than 1.5×10^4 cells/ml were left in the supernatant. Tests on blood and endo agar plates did not show any contamination with foreign cells. The sediment was washed 3 times at 0°C with tracer-free medium in a centrifuge at 25 000 × *g*. The harvesting of the cells and the centrifuging were carried out on a quantitative basis in order to ensure the calculation of the number of cells per unit final dry weight.

Previously we had tried to calculate the number of cells in a freeze-dried sample by resuspending part of the sample and counting the cells. No accurate estimate could be made in this way, since part of the cells disappeared, possibly due to a fragility induced by the freeze-drying process. For this reason the cell concentration in the culture was estimated and the cells harvested and lyophilized in a quantitative way. The dry weight was estimated by weighing a small part of the lyophilized material and drying it to constant weight (90°C, P_2O_5 vacuum). The figures listed in Table 1 are calculated on dry weight and this weight is corrected for the amount of medium solids enclosed in the sample (about 5 % of the dry weight). It was assumed that the loss in weight during the drying procedure corresponded to water from a solution with the same content of solute as the medium. This approximation may be justified, especially as the corrections were too small to affect the main conclusions.

The extractions of DNA and RNA were carried out on 400 to 500 mg dry cells. The cells were mixed with 10 ml of pyrex beads (0.28 mm diam.) and 30 ml of 30 % (v/v) cold ethanol and disintegrated by shaking them at high rates in a Griffith shaker at — 15°C. The contents remained in the same tube through all manipulations. After freeze-drying and extraction with boiling ethanol-ethylether (3:1) the lipidfree cells were extracted for DNA and RNA according to Hammarsten [8]. The hot TCA-extractable phosphorus in the undissolved residue was determined after combustion. The following values were obtained and are expressed as per cent of the total phosphorus in the extracted polynucleotides:

Cultivation times in min	0	5	25	50	80
Phosphorus in per cent of phosphorus in polynucleotides	7.1	9.0	8.3	6.6	7.6

Over 90 % of the polynucleotides were thus extracted.

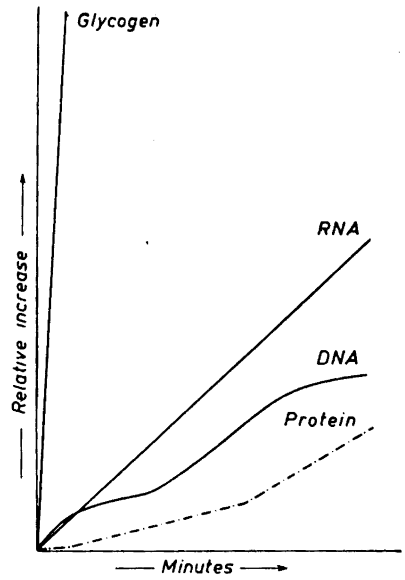


Fig. 1. (From Table 2.)

After hydrolysis with alkali the mononucleotides of RNA were separated [4] on Dowex 2 (elution with formic acid). Cytidylic and adenylic acids were further purified on Dowex 2 (elution with 0.01 N HCl). These two fractions and uridylic and guanylic acids from the formic acid elution were separated together on Dowex 50 in the H^+ form, previously washed with water until the eluate was neutral. Uridylic acid was eluted with water, cytidylic acid with 0.01 N HCl, guanylic and adenylic acids (well separated from each other) with 0.02 N HCl.

Uridylic and cytidylic acids were analysed for tracer content without any further purification. Parts of the guanylic and adenylic acids were analysed in the same way and the rest hydrolysed (1 h, 100°C, N HCl). The products of each nucleotide were separated on Dowex 50 as above. By elution with water the first few tubes showed a very weak light absorption at 260 mμ. This fraction was considered as ribose. Guanine and adenine

Table 1.

Cultivation time in min	Number of cells per ml $\times 10^{-8}$	Dry weight per cell, mg $\times 10^{10}$	Mg $\times 10^{12}$ per cell of:					
			Protein nitrogen	Glycogen	RNA phosphorus	DNA phosphorus	Total nitrogen	Lipid phosphorus
0	2.3	1.8	18.8	2.2	1.23	0.43	26.0	0.43
5	2.2	2.1	19.9	12.2	1.53	0.57	27.9	0.43
25	2.2	2.6	23.8	29.1	2.47	0.68	33.9	0.37
50	2.1	3.2	29.0	41.6	3.72	1.05	43.2	0.53
80	2.9	3.5	32.1	32.8	3.93	0.93	47.8	0.38

Table 2. Relative increase of cellular constituents during the lag phase.

Cultivation time in min	Dry weight	Total nitrogen	Glycogen	Protein nitrogen	RNA phosphorus	DNA phosphorus	Lipid phosphorus
0	1.00	1.00	1.00	1.00	1.00	1.00	1.00
5	1.11	1.03	5.55	1.01	1.19	1.26	0.96
25	1.40	1.26	12.9	1.22	1.94	1.52	0.83
50	1.67	1.56	17.9	1.45	2.84	2.29	1.15
80	2.44	2.33	19.1	2.16	4.05	2.72	1.13

were then eluted with 2 N HCl. The bases were mixed and run on a Dowex 50 column (6 × 0.6 cm) and eluted again with 2 N HCl. They were obtained in very small volumes. The different fractions were evaporated and dissolved in water. The amounts of nucleotide carbon were calculated from the determinations of phosphorus. The amounts of purine carbon were calculated from determinations of nitrogen. In both cases (nucleotides and purines) samples were combusted (dry) and total carbon determined as barium carbonate. The amounts of "ribose" were calculated from combustion. The measurements of the radioactivity were performed in a windowless gas flow counter with less than 20 μg of material per cm^2. The corrections for foreign carbon (total carbon by combustion divided by the carbon calculated from determinations of P and N) ranged from 1.2 – 3.0 but was in most cases 1.2 – 2.0. No correction could be made in the case of ribose.

The degradation of DNA was carried out according to Hurst *et al.*[5]. The chromatographic separations were in all essentials the same as for the nucleotides from RNA. The correction terms for foreign carbon were within the same limits as those for the RNA-products.

The protein fractions were determined in separately weighed samples of lyophilized cells. These were disintegrated in the way described above, lyophilized and treated accord-

Table 3.

Atom per cent excess of ^{15}N					Specific activity of ^{14}C: c.p.m. per μg C			Atom per cent excess ^{13}C				
Cultivation time in min	Protein	RNA	Hot trichloro-acetic acid extract of total cells	Total cells	Protein	Hot trichloro-acetic acid extract of total cells	Glycogen	Protein	Glycogen	Total cells	Specific activity ^{14}C; c.p.m. per μg C of lactate in medium	Atom per cent excess of ^{15}N in medium
0	—	—	—	—	—	—	—	2.32	1.55	3.15	—	4.27
5	0.10	0.30	0.34	0.16	0.82	4.28	5.94	2.65	0.87	2.70	35	4.25
25	0.64	1.11	1.12	0.73	4.52	6.47	8.22	2.13	0.59	2.31	30	4.22
50	1.40	1.92	2.01	1.64	7.33	6.32	8.69	1.77	0.59	1.76	31	4.17
80	2.22	2.75	2.63	2.40	9.46	—	10.28	1.24	0.44	1.24	30	—

Table 4. Isotopic data on the components in the protein and nucleic acid fractions. Atom per cent excess ^{15}N.

Cultivation time in minutes		5	25	50	80
RNA	Uridylic acid	0.12	0.66	1.77	2.51
	Cytidylic acid	0.25	0.90	1.94	2.69
	Adenine	0.34	1.32	2.15	2.74
	Guanine	0.37	1.41	2.44	2.76
DNA	Thymidylic acid	0.06	0.30	0.72	1.58
	Cytidylic acid	0.11	0.49	1.22	1.78
	Adenine	0.06	0.62	1.27	1.59
	Guanine	0.12	0.64	1.32	1.89
Protein	Glutamic acid	0.14	0.71	1.48	2.28
	Glycine	0.09	0.60	1.38	2.22
	Methionine	0.08	0.56	1.25	1.81
	Serine	0.10	0.62	1.36	2.17
	Leucine+*iso*leucine	0.12	0.67	1.43	2.24
	Valine	0.11	0.64	1.41	2.21
	Alanine	0.07	0.36	1.10	2.02
	Threonine	0.08	0.61	1.37	2.20
	Aspartic acid	0.12	0.64	1.37	2.18
	Proline	0.04	0.42	1.16	1.91
	Tyrosine	0.13	0.60	1.31	2.14

ing to Schneider. The protein precipitate was hydrolysed for 18 h in 6 N HCl. The hydrolysate was carefully washed out from the glass beads, evaporated and dissolved to a suitable volume. Protein carbon was directly determined by combustion. No correction was made for foreign carbon. The part that was not used for analyses (Tables 1 and 3) was separated on Dowex 50 and starch [6] and 11 of the amino acids were isolated (the two leucines as one fraction). The individual amino acids were run again on very small columns. Total carbon was determined as for the RNA derivatives and amino carbon was calculated from determinations of nitrogen. The quotients for correction varied between 1.1 and 2.0. Most of the amino acids, however, did not contain over 30 % foreign carbon.

The lactates labeled with ^{13}C and ^{14}C in β-position were synthesized according to Reio [7]. Isotopic barium carbonate (^{13}C and ^{14}C labeled) was reduced in two different batches with lithium aluminium hydride into methanol, which in turn was converted to methyl iodide and condensed with acetamino-malonic ester. After hydrolysis alanine was isolated and treated with sodium nitrite yielding sodium DL-lactate. The synthesis of ^{14}C-labeled compounds from barium carbonate to alanine was carried out in a closed apparatus-system, whereby all reaction steps were performed in a short time with a minimum loss of activity. The lactic acids were purified from remaining alanine and salts by passing them through Dowex 50 columns. The determinations of specific activity in the medium at different times were based on direct determinations of lactic acid [8] and countings of 8—4 μg lactic acid before and after a second separation on Dowex 2 and stepwise elution with water to 0.4 N HCl.

DISCUSSION AND RESULTS

The values for the atom per cent excess ^{13}C depend on the rather high corrections for foreign carbon. The determination of carbon as barium carbonate after dry combustion is admittedly not a very exact method. This has certainly

Table 4a. Isotopic data on the components in the protein and nucleic acid and glycogen fractions.

		Spec.activity ^{14}C: c.p.m. per μg				Atom per cent excess ^{13}C				
Cultivation time in minutes		5	25	50	80	0	5	25	50	80
RNA	Uridylic acid	3.03	9.25	6.74	5.96		3.32	1.59	0.97	0.74
	Cytidylic acid	1.80	4.52	6.50	5.87		2.10	1.49	1.13	0.61
	Adenylic acid	2.67	6.04	8.17	7.83		1.63	—	1.42	0.58
	Guanylic acid	2.08	9.39	8.10	7.00		1.16	0.89	0.98	0.95
	Adenine	2.08	8.53	8.54	7.65		1.96	1.38	0.90	0.54
	Guanine	1.51	5.73	7.78	6.16		1.75	0.58	0.36	0.43
DNA	Thymidylic acid	0	2.75	4.10	2.63		3.33	2.51	1.70	0.88
	Cytidylic acid	0	2.04	3.04	4.76		2.72	2.48	2.28	1.17
	Adenine	0	2.28	—	3.79		3.21	2.03	—	0.88
	Guanine	0	1.95	1.88	3.28		2.45	2.23	1.27	1.16
RNA	Adenine-ribose	1.76	7.15	4.00	2.79		1.31	0.83	0.54	0.36
	Guanine-ribose	1.74	5.44	3.96	4.06		1.29	1.22	0.62	0.63
DNA	Desoxyribose from purine nucleosides	0.23	1.42	—	0.59		0.23	0.17	0.16	0.11
Protein	Glutamic acid	1.55	4.88	7.79	11.04	2.05	3.03	3.17	2.26	1.75
	Glycine	0.05	0.35	0.64	0.26	0.60	0.64	0.45	0.54	0.43
	Methionine	0.27	1.01	2.05	2.69	—	3.01	2.90	1.89	0.99
	Serine	1.78	4.75	4.85	5.91	2.38	1.64	2.03	1.01	0.93
	Leucine + *iso*leucine	0.93	3.55	7.99	12.50	2.56	2.66	2.45	2.12	1.51
	Valine	1.26	5.29	10.57	13.45	1.87	2.75	1.94	1.75	1.32
	Alanine	3.90	11.17	12.93	14.19	2.62	2.07	2.46	1.81	2.19
	Threonine	1.17	3.82	2.15	6.74	3.35	3.96	3.25	2.45	2.78
	Aspartic acid	0.05	0.95	2.65	5.58	3.43	3.65	3.24	3.02	1.57
	Proline	0.02	3.32	5.23	9.80	—	3.01	2.82	2.23	1.45
	Tyrosine	1.31	3.17	5.23	5.88	—	2.48	2.35	1.73	1.94
	Glucose from glycogen	5.9	8.2	8.7	10.3	1.55	0.87	0.59	0.59	0.44

Table 5. Amount of ^{13}C in the cells per litre of culture.

Cultivation time in min	I Dry weight of cells per litre, mg	II ^{13}C Atom per cent excess in total cell	I × II
0	41.2	3.15	130
5	45.7	2.75	123
25	57.2	2.31	134
50	58.6	1.76	121
80	100.5	1.24	136
			M = 126±5

to be considered when using the labeling of carbon for calculations. ^{14}C was determined on plates at "infinite" thinness. The lactates used as substrates were racemic. It was still racemic after the harvesting of the cells. In experiments in which the amount of new synthesized glycogen could be determined accurately and in which probably no "old glycogen" was degraded, this new synthesized glycogen had the same specific activity as the medium glucose, when totally labeled glucose was used. This was certainly not the case when β-labeled lactate was used, as in the present experiments. The specific activity in glycogen was only 30 % of the specific activity of the medium lactate. In recent work[10] on spores from *Penicillium brevicompactum* with ^{14}C-labeled glucose as carbon source it was shown that RNA in the lag phase incorporated considerable amounts of cellular carbon. It seems also that the methyl carbon in lactate has not been used to the same extent as carbon atoms 1 and 2.

Table 5, col. 4, demonstrates that the product of ^{13}C in total cells and their dry weight per litre was constant. The variations are irregularly distributed. This indicates that little if any carbon had left the cells during the cultivation time. The assumption is made that all carbon-containing substances in the cells from the stationary phase of preculture were labeled with ^{13}C. The same calculation for RNA, protein and glycogen show greater irregularities which could be expected on account of the difficulties of the tracer analyses in the purified substances. Still, the figures show that there cannot be any considerable exchange of the carbon present in RNA at zero time with other cellular components during the 80 min incubation (Table 6).

The protein fraction incorporated carbon from other cellular sources during the first 5 min of incubation which is indicated by the rise in ^{13}C content (Table 7, col. 4) and by the rise in ^{13}C-labeling in several amino acids during the same period (Table 4). During the following period from 5 to 80 min after incubation the product of protein carbon per litre and atom per cent excess ^{13}C remains fairly constant, demonstrating that the original carbon in proteins was not, or only to a small extent exchanged during this period. Glycogen had incorporated carbon from other cellular sources during the first 50 min (Table 7, col. 7). Protein carbon was higher labeled than glycogen and the amount of this was not more than 1 to 15 % of the protein carbon. The incorporation of carbon from the medium into glycogen starts during the first 5 min (Table 3, col. 8). It may well be that cell carbon, incorporated into glycogen, is derived from remaining ^{13}C-lactate or other low molecular precursors. A small part may have been derived from broken-down protein.

In Table 8 the quotients are given between the increases from zero time at each investigated cultivation time in amounts per litre found by direct analysis (numerator) and the same amounts (denominator) calculated from the labeling. In this calculation the total amount per litre at each investigated cultivation time was multiplied with the labeling at the corresponding time in relation to the labeling in the medium.

The net synthesis of protein in 80 min, determined by nitrogen analysis (54 %) agrees well with the synthesis as calculated from the labeling with ^{15}N (53 %). This shows that the incorporation of ^{15}N into protein may be

Table 6. Amount of ^{13}C in RNA per litre of culture.

Cultivation time in min	I RNA-phosphorus per litre of culture	II Atom per cent excess ^{13}C in RNA	I × II
0	0.28	—	—
5	0.33	2.28	0.76
25	0.59	1.25	0.68
50	0.79	0.84	0.67
80	1.31	0.58	0.76

Table 7. Amount of ^{13}C in protein and glycogen in the cells per litre of culture.

	Protein			Glycogen		
Cultivation time in min	I Protein carbon per litre, mg [1]	II Atom per cent excess ^{13}C	I × II	I Glycogen carbon per litre, mg	II Atom per cent excess ^{13}C	I × II
0	17.4	2.32	40	0.22	1.55	0.34
5	17.6	2.65	47	1.21	0.87	1.05
25	21.3	2.13	45	2.80	0.59	1.65
50	25.2	1.77	45	3.90	0.59	2.30
80	37.7	1.24	47	4.16	0.44	1.83

[1] 4.08 × Nitrogen = Carbon.

Table 8. Ratio between the increase in amount, as measured by direct analysis to the increase, as measured by isotopic labeling.

	Total cell	Protein		RNA		DNA		Glycogen
Cultivation time in min	calc. from ^{15}N	calc. from ^{15}N	calc. from ^{14}C	calc. from ^{15}N	calc. from ^{14}C	calc. from ^{15}N	calc. from ^{14}C	calc. from ^{14}C
5	0.83	(0.50)	(0.43)	2.25	2.70	(8.6)	—	1.30
25	1.20	1.19	1.22	1.86	2.12	2.8	4.6	1.40
50	0.92	0.92	1.35	1.42	2.70	2.1	2.7	1.42
80	1.00	1.02	1.27	1.21	3.56	1.6	3.5	1.53

taken as a measure of the net synthesis of protein during active growth in bacterial cells at least when the sole source of nitrogen is NH_4Cl.

The quotients (Table 8) calculated for protein at 5 min are probably not significant, since the figure for net synthesis is too near the limits of the analytical error. Otherwise the quotients both for total cells and for proteins show no systematical variation. Thus the protein incorporated its nitrogen

exclusively or nearly so from the medium. The quotients from the calculation from ^{14}C increase with the cultivation time. As protein incorporates very little if any carbon from the cell carbon between 5 and 80 min, the possibility is not excluded that during this period of carbon incorporation some change in selectivity occurs in the use of the three lactate carbons. The same relative decrease of the incorporation of labeled carbon from the lactates in the medium turns up in the quotients for glycogen, though less marked. The quotients for RNA as calculated from the content of ^{15}N go in opposite way from 2.30 to 1.21, showing that RNA in earlier stages incorporates comparatively much nitrogen from the cells, whilst the medium as time passes on is furnishing more and more of the nitrogen. The quotients calculated from ^{14}C are probably too inaccurate for being safely interpreted. It was shown (Table 6) that RNA does not change its total ^{13}C-content much. The fact that the quotients (Table 8) are high may signify that carbon atoms 1 and 2 in the medium-lactate are more extensively used than carbon 3. The quotients for DNA are even more erratic than those for RNA but show the same general tendency. The most rapidly formed of the four components investigated, glycogen, was using cell carbon proportionally more than any of the others, and RNA (and DNA) acted in a similar way in respect to nitrogen in early stages of synthesis. Except for a small uptake of cellular carbon during the first 5 min protein was mainly synthesized from the medium.

The very first part of the lag-phase seems thus to be characterized by a redistribution of the cellular carbon. This redistribution still operates later on in the lag-phase, but to a smaller extent. In the later part of the lag-phase the synthesis from medium constituents dominates.

REFERENCES

1. Cavanna, R., Chain, E. B., Hedén, C. G., Malmgren, B., Eliasson, N. A., Hammarsten, E. and Åqvist, S. *Rendiconti Dell Instituto Superiore Di Sanità:* **17** (1954) 1284.
2. Palmstierna, H. *Studies on a glycogenlike polysaccharide in Escherichia coli B, Diss.*, Stockholm 1956.
3. Hammarsten, E. *Acta Med. Scand. Suppl.* **196** (1947) 634.
4. Cohn, W. E. *J. Am. Chem. Soc.* **72** (1950) 1471.
   Cohn, W. E. and Volkin, *Nature*, **167** (1951) 483; *Arch. Biochem. and Biophys.* **35** (1952) 465; *J. Biol. Chem.* **203** (1953) 319.
5. Hurst, R. O., Little, J. A. and Butler, G. L. *J. Biol. Chem.* **188** (1951) 705.
6. Åqvist, S. *Acta Chem. Scand.* **5** (1951) 1031.
7. Reio, L. *To be published.*
8. Koenemann, R. H. *J. Biol. Chem.* **135** (1940) 105.
9. Hammarsten, E. and Palmstierna, H. *Acta Chem. Scand.* **11** (1957) 1378.

Received June 3, 1957.

ACTA CHEMICA SCANDINAVICA 11 (1957) 1390—1404

The Infra-Red Absorption Spectra of Some Amide- and Dipeptide-Metal Chelates

ANDREAS ROSENBERG

Institute of Biochemistry, University of Uppsala, Uppsala, Sweden

Changes in the infra-red absorption spectra of amino acid amides and dipeptides after chelate formation with Cu(II) are interpreted as a result of the shift in the resonance equilibrium of the peptide group. The magnitude of these changes for chelates of Cu(II), Ni(II) and Zn(II) has been used as a measure for the interaction of metal ions with the peptide group.

The behaviour of the infra-red (IR) absorption frequencies of $-NH_2$ and -COOH groups in amino acid-metal chelates was examined in a previous publication.[1] In the present investigation the behaviour of the amide group, as represented by its IR absorption spectra, is studied in some amide- and dipeptide-metal chelates. The chelation of peptides and amides by metal ions has mainly been studied in solutions, by methods aimed at the determination of complex constants.[2-4] A number of crystalline chelates has been prepared and analyzed and the ratio of metal to ligand thus determined.[5,6] The need for a better elucidation of metal-peptide bond interaction has arisen from studies of metal-activated enzymes. Smith and Spackman [7], for example, explain the role of metal ions in proteolytic enzyme systems by assuming a metal chelate bridge between the enzyme and the substrate molecule. The interaction of the peptide group with the metal ion is viewed as resulting in an electron displacement rendering the bond susceptible to nucleophilic attack by hydroxyl ions. If this were the case, the IR frequencies of the amide linkage should be considerably influenced by the metal ion. An IR study of chelate formation between metals and peptides has been published by Chouteau [8]. Since Chouteau's main interest was the investigation of the biuret reaction, the solid chelate compounds were precipitated or evaporated at extremely high pH values. Working at the pH values of 12—13, Chouteau found that the frequencies ascribed to the amide group did change considerably. The behaviour of the amide group at such extreme pH values has probably no direct bearing on the biological role of the metal ions. The solid chelates of peptides used in the present examination are all of neutral character, isolated from aqueous solutions where the pH value never exceeded 9.

PREPARATIONS

Bis-glycinamido-Cu(II)monohydrate, $(GA)_2Cu,H_2O$, Bis-L-leucinamido-Cu(II), $(La)_2Cu$, and Bis-L-leucinmethylamido-Cu(II) trihydrate, $(LMA)_2Cu,3H_2O$, were prepared from the corresponding amides with Cu(II) acetate as described by Rising and Yang [9] with the modification that the volume of the reaction mixture was increased to prevent an instantaneous precipitation. The solution was then slowly evaporated until the reddish-blue crystals appeared. The crystals were dried over P_2O_5 and analyzed . The $(LMA)_2$-Cu(II) showed a tendency to crystallize with varying numbers of water molecules. These differences were not essential for the IR investigation, as the different species showed only changes in the diffuse background absorption.

Glycylglycino-Cu(II) trihydrate, GG-Cu,$3H_2O$, DL-alanylglycino-Cu(II) dihydrate, AG-Cu,$2H_2O$, DL-leucylglycino-Cu(II) hydrate, LG-Cu,H_2O and Glycyl-L-leucino-Cu(II) hydrate GL-Cu, H_2O were prepared from commercial dipeptides and $CuCO_3$ according to Tomita *et al.*[5]. The crystalline chelates were recrystallized from water and washed with alcohol. When dried over P_2O_5, the dark blue trihydrate of glycylglycine is converted to a blue monohydrate. The monohydrate of GG-Cu(II) can be obtained directly when the chelate is precipitated from aqueous solution by ethanol.

The Bis-glycylglycino-Ni(II) didhydrate, $(GG)_2Ni,2H_2O$, was obtained as pale blue crystals. An aqueous solution of GG was vigorously shaken with an excess of freshly precipitated Ni(II) hydroxide. The pH of the suspension was adjusted to approx. 8. The residual Ni(II) hydroxide was removed by filtration. The volume of the blue solution was reduced and ethanol added. The chelate crystallized even from a solution of GG and $NiCl_2$ in proportions 2 to 1 when the pH of the solution was adjusted to 8 and ethanol added.

Bis-glycylglycino-Zn(II) dihydrate, $(GG)_2Zn,2H_2O$, was prepared from $Zn(OH)_2$ and GG. An excess of freshly precipitated and washed $Zn(OH)_2$ was added to an aqueous solution of GG. The pH of the suspension was adjusted approx. to 8 and the suspension shaken vigorously before filtration. The chelate crystallized as white needles upon addition of ethanol. Bis DL-alanylglycino-Zn(II) dihydrate was obtained by the same method.

Table 1. Analyses.*

Chelate	% N		% Metal	
	Calc.	Found	Calc.	Found
$(GA)_2Cu,H_2O$	24.61	24.41	27.91	27.79
$(LA)_2Cu$	17.40	17.26	19.74	19.53
$(LMA)_2Cu,3H_2O$	13.87	14.20	15.73	15.58
GG-Cu,$3H_2O$	11.31	11.53	25.65	25.71
GG-Cu,H_2O	13.23	12.98	29.90	30.02
AG-Cu,$2H_2O$	11.49	11.56	26.07	26.01
LG-Cu,H_2O	10.46	10.47	23.72	23.68
GL-Cu,H_2O	10.46	10.54	23.72	23.83
$(GG)_2Ni,2H_2O$	15.69	15.52	16.44	16.36
$(GG)_2Zr,2_2HO$	15.40	15.38	17.97	18.01
$(AG)_2Zn,2H_2O$	14.31	14.26	16.69	16.74

* N was determined according to Dumas and the metals titrated with EDTA.

Glycinamide-hydrochloride, GA, HCl, was prepared according to Bergell and Wülfing [10]. Mp. for hydrochloride: 185—187° and for free glycinamide 64—65°.

L-Leucinamide, LA, was prepared from L-leucine ethyl ester according to Yang and Rising [11]. The L-leucine ester used was obtained according to Fischer [12] M.p. found for L-leucinamide hydrochloride 235°. L-Leucine methylamide, LMA, was prepared from

L-leucine ethyl ester. The ester was cooled with dry CO_2 in ethanol and an equal volume of liquid methyl amine was added. The glass tube containing the mixture was sealed and kept at 50° for 3 days. The amide was then distilled *in vacuo*; bp/9 mm Hg 139°C. (Found: N 19.17. Calc. 19.46).

Glycylglycine ethyl ester, GGet, was obtained by the same method as L-leucine ester. (Found: N 14.30. Calc. 14.25).

A Perkin-Elmer model 21 spectrophotometer equipped with CaF_2 and NaCl prisms was used for the IR-absorption measurements. The chelates were pressed into transparent KBr discs as described by Schiedt and Reinwein [13]. Ir order to achieve the best resolution possible, the IR absorption of the chelates was generally measured at low temperature. The low-temperature cell and the effects of low temperature have been described previously [1]. The values obtained at normal temperatures are directly compared with those obtained at low temperatures only when the temperature change has no effect on the position of the absorption bands.

The deuterium exchange was obtained by recrystallizing the substance under investigation from 99.7 % D_2O.

RESULTS OF THE ABSORPTION MEASUREMENTS

The first chelates investigated were the Cu(II)-amide chelates. Fig. 1—3 show the IR-absorption in the 3 μ region for 3 pairs of substances. GA and $(GA)_2$ Cu, H_2O, LA and $(LA)_2$ Cu, LMA and $(LMA)_2$ Cu, $3H_2O$. All the absorption curves except that for the pure LMA were obtained at low temperatures. The spectra of LMA can still be compared with the spectra of its Cu(II) chelate as the positions of the chelate frequencies were not influenced by a change of temperature.

The positions of the absorption bands due to N-H or O-H stretching frequencies are compiled in Table 2.

Table 2.

	Stretching frequencies in the 3 μ region		
GA	3 347	3 279	3 137, 3 084
$(GA)_2,Cu,H_2O$	3 329	3 218	3 106
LA	3 349	3 279	3 096
$(LA)_2Cu$	3 323	3 202	3 112
LMA	3 312		3 086
$(LMA)_2Cu,3H_2O$	3 232		3 117

Figs. 4—6 show the 6 μ region of the same chelates.

The amides themselves show, in this region, two well-known bands produced by the amide group frequencies. In the following these bands are referred to as the amide I and amide II bands.

The dashed curves in Figs. 4—6 represent the absorption of the deuterated compounds.

Deuterization removes from this region the possible amide II band and all the bands due to N-H bending movements. The frequencies of the free amides and amide hydrochlorides are presented in Table 3 together with the corresponding values for Cu-amide chelates.

Table 3.

	Solid		Solution	
	Amide I	Amide II	Amide I	Amide II
GA	1 695	1 608	1 686	1 553
GA, HCl	1 709	1 597		
$(GA)_2Cu,H_2O$	1 570			
LA	1 664 1 681	1 600	1 678	1 548
LA, HCl	1 678 1 686	1 618		
$(LA)_2Cu$	1 588 1 554			
LMA	1 658	1 541	1 678	1 520
LMA, HCl	1 675	1 572		
$(LMA)_2 Cu,3H_2O$	1 567			

The next group of substances examined, were the metal chelates of simple dipeptides. Fig. 7 shows the 3 μ region of GG and GG-Cu(II) trihydrate.

Fig. 8 shows the same spectral region of three further dipeptide-Cu(II) chelates. The AG-Cu(II) has two molecules of water attached to the chelate molecule, the other two LG-Cu(II) and GL-Cu(II) posess only one molecule of water each. The next two figures (9 and 10) show the IR absorption of the chelates in the 6 μ region. Fig. 9 represents the absorption of GG-Cu, H_2O.

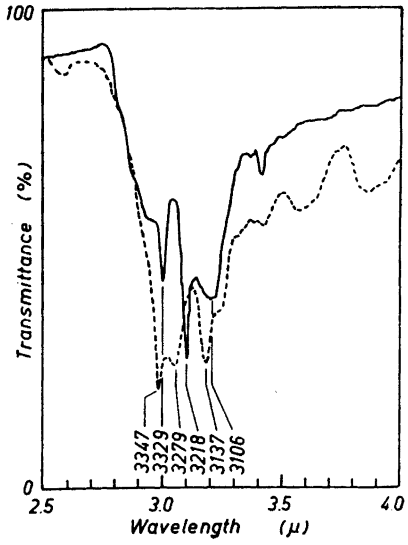


Fig. 1. IR absorption of glycinamide, GA, ---------- and of $(GA)_2Cu,H_2O$ ————

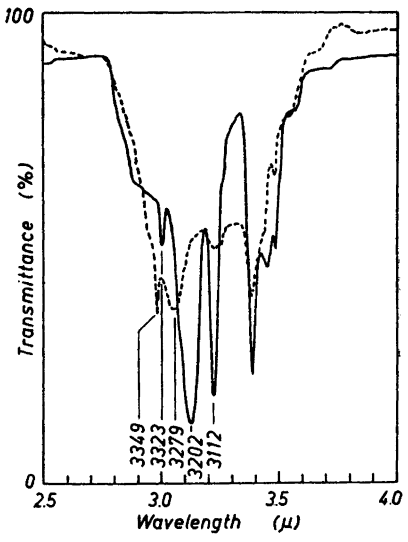


Fig. 2. IR absorption of L-leucinamide, ---------- LA, and of $(La)_2Cu$ ————

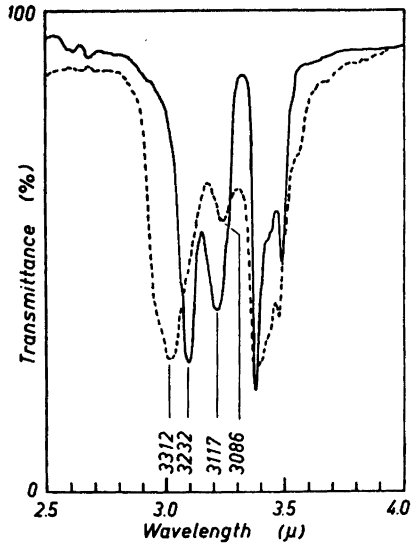


Fig. 3. IR absorption of L-leucinmethylamide, LMA, ---------- and of $(LMA)_2Cu,3H_2O$ ————

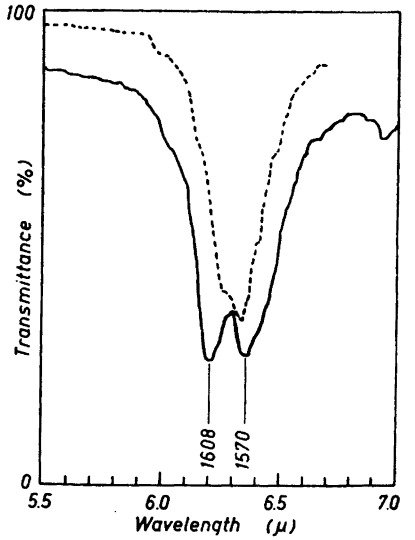


Fig. 4. IR absorption of $(GA)_2Cu,H_2O$ ———— and of the deuterated compound ----------

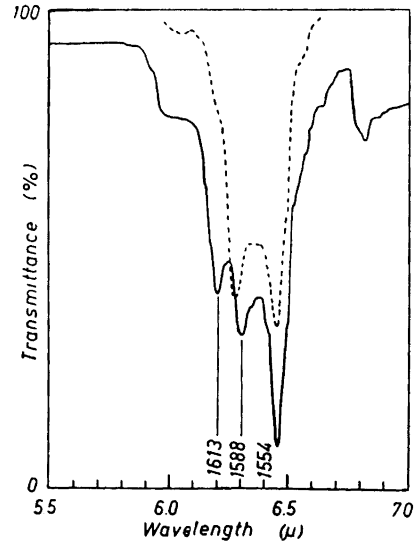


Fig. 5. IR absorption of $(LA)_2Cu$ ———— and of the deuterated compound ----------

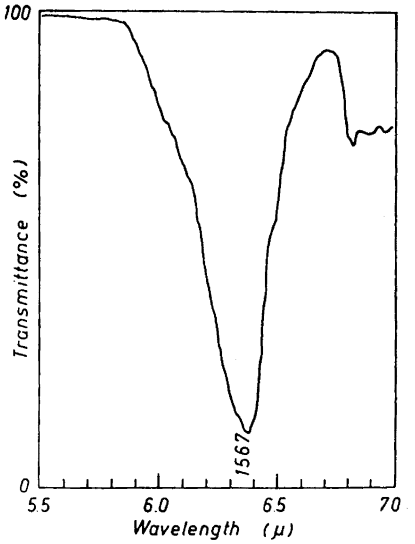


Fig. 6. IR absorption of $(LMA)_2Cu,3H_2O$

The spectrum of the trihydrate shown in Fig. 11 is complicated due to the three water molecules. In order to simplify the picture the chelate was recrystallized from D_2O. The IR absorption of the deuterated compound is represented by the broken curve in Fig. 9. The absorption spectra of the deuterated products of GG-Cu, H_2O and GG-Cu, $3H_2O$ were identical in this wavelength region.

Fig. 10 shows the 6 μ region for three further dipeptide chelates. The values of the two main bands, ν (COO^-) and ν ($-C\overset{O}{\underset{N-}{\ll}}$), are collected in Table 4. The extra bands visible in the figure are due to N-H or O-H bendings as they all vanish after deuterization.

Table 4.

	ν (COO^-)	ν ($-C\overset{O}{\underset{N-}{\ll}}$)
GG-Cu,H_2O	1 592	1 541
AG-Cu,$2H_2O$	1 587	1 548
LG-Cu, H_2O	1 597	1 534
GL-Cu,H_2O	1 595	1 524

Fig. 11 represents the IR absorption of Cu(II), Ni (II) and Zn(II) chelates of glycylglycine (GG). The absorption in wavelength regions between 2.5-4 μ and 5.5-7.0 μ was measured with a CaF_2 prism, for the region from 7 to 14 μ a NaCl prism was utilized. Low temperature has been used for all of the measurements. As the absorption from water molecules conceals most of the absorption bands of GG-Cu, $3H_2O$ in the 6 μ region, the absorption of the monohydrate, represented by the broken curve, was added to the original spectrum.

The frequencies of the peptide and carboxyl groups for the different forms of GG are collected in Table 5.

Table 5.

	Amide I	Amide II	COO^-		Amide I	Amide II	COO^-
GG	1 678 1 657	d	1 608	GG-Cu,$3H_2O$	1 541		1 613[c]
GG, HCl	1 686	1 562	1 748[a]	$(GG)_2Ni,2H_2O$	1 653 1 631	1 583	1 600
GG-et	1 664	1 536	1 745[b]				
GG-et $CHCl_3$ sol.	1 672	1 536	1 748[b]	$(GG)_2Zn,2H_2O$	1 661 1 642	1 577	1 600

a Frequency of the COOH group.
b Frequency of the COOet group; et = ethylgroup.
c Deuterated compound.
d assignment uncertain.

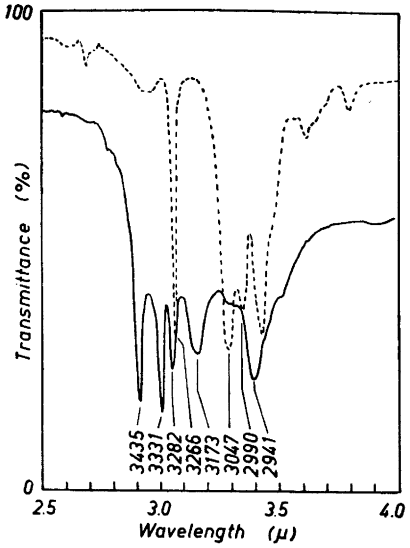


Fig. 7. IR absorption of glycylglycine, GG, ---------- and of GG-Cu,$3H_2O$ ————

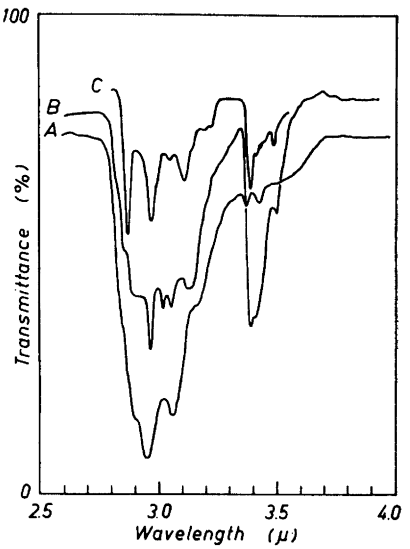


Fig. 8. IR absorption of AG-Cu,$2H_2O$ curve A, of GL-Cu,H_2O curve B, and of LG-Cu,H_2O curve C.

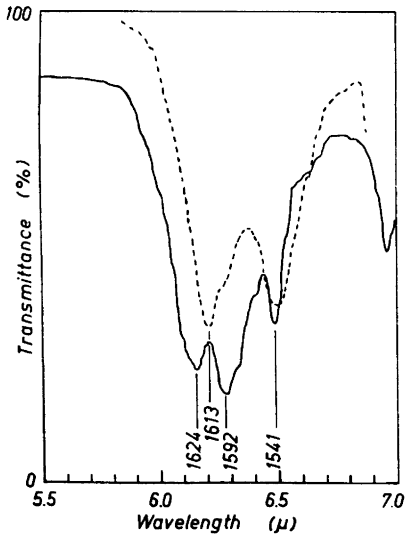


Fig. 9. IR absorption of GG-CuH_2O ———— and of the deuterated compound ----------

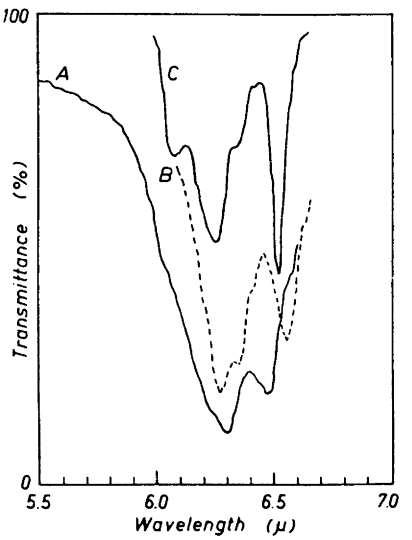


Fig. 10. IR absorption of AG-Cu,$2H_2O$ curve A, of GL-Cu,H_2O curve B and of LG-Cu,H_2O curve C.

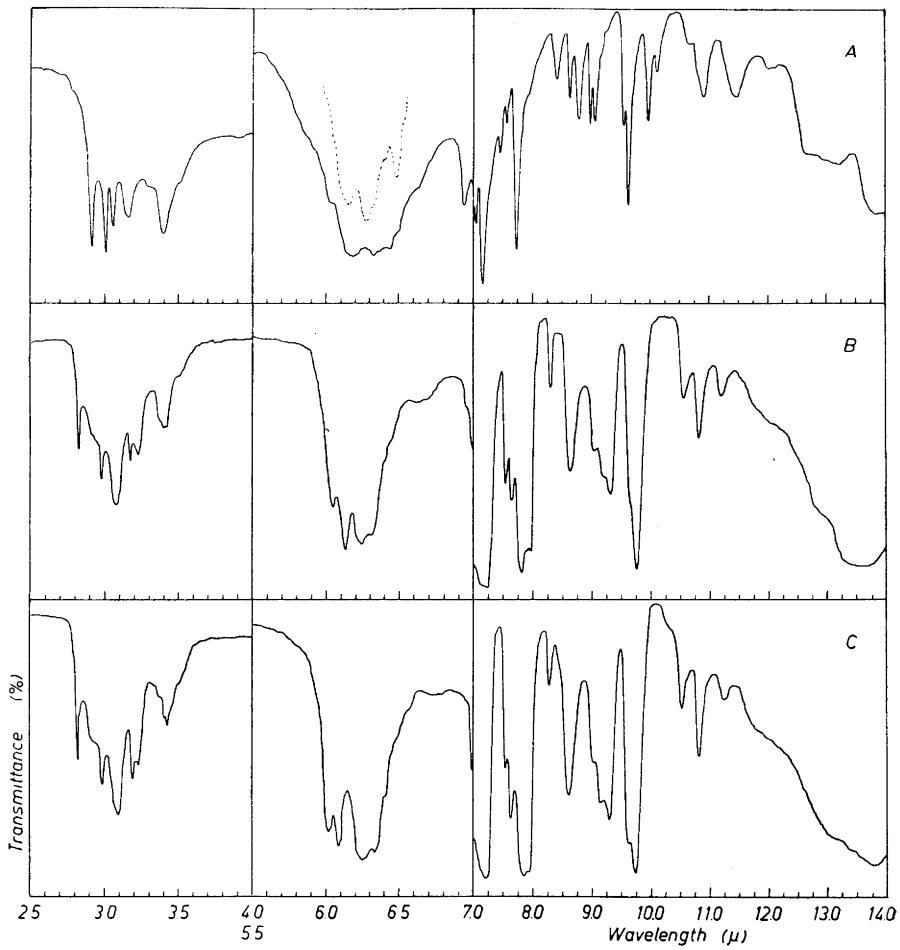
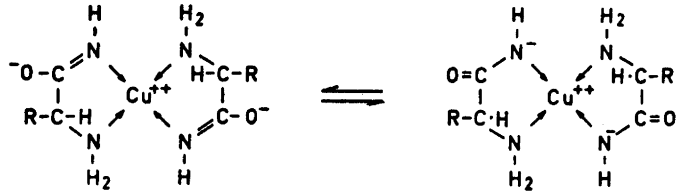


Fig. 11. IR absorption of GG-Cu,$3H_2O$ curve A, of $(GG)_2Ni,2H_2O$ curve B and of $(GG)_2Zn,2H_2O$ curve C.

In order to check the assignments of absorption frequencies in the Zn(II) chelates, the Zn(II) chelates of DL-alanylglycine and glycyl-L-leucine were prepared. $(AG)_2Zn,2H_2O$ crystallized beautifully and showed an IR spectrum in the 6 μ region that was almost identical with the spectrum of $(GG)_2Zn,2H_2O$. The amide I doublet was found at 1 658 and 1 639 cm^{-1}, the absorption of the carboxyl group appearing at 1 600 cm^{-1}. The Zn(II) chelate with glycyl-L-leucine is not included in the experimental part because a chelate with a definite number of water molecules could not be isolated. The product with an undefined number of water molecules exhibited broad absorption bands in the same region as $(GG)_2Zn,2H_2O$ and $(AG)_2Zn,2H_2O$, no absorption being visible below 1 580 cm^{-1}.

DISCUSSION

Amide-Cu(II) chelates. The interpretation of the observed changes in the IR absorption spectra of amide molecules after chelate formation is comparatively simple. The red Cu(II) chelates of DL-leucinamide and glycinamide have previously been isolated and analyzed by Rising and Yang [9]. They found that two amide molecules combine with one Cu(II) ion to form a neutral chelate. $(GA)_2Cu(II)$ crystallizes with one molecule of water whereas $(LA)_2$ Cu(II) lacks water of crystallization. This eliminates the possibility that the neutral molecule is formed by dissociation of hydrogen ions from coordinatively bound water molecules. The results of analyses of the amide chelates prepared for this investigation are in accordance with the values given by Rising and Yang. Potentiometric measurements, recently described by Datta and Rabin [16], confirm the assumption that, in each of the two amide molecules, one hydrogen is ionized from the amide nitrogen so that the chelate formed carries no net charge. The structure of the Cu(II) chelates with amino acid amides can be represented by Fig. 12.



I II

Fig. 12.

These changes in the amide molecule ought to be accompanied by changes in the IR absorption due to hydrogen stretching movements in amino and amide groups and in the intense vibration bands of the amide group in the neighbourhood of 6 μ.

The chelate formation results in a shift of the N-H bond stretching frequencies of amides towards lower wavenumbers. The shift is generally exhibited by amino groups when the free electron pair of the nitrogen is used for bond formation [1,17]. The behaviour of the N-H frequencies observed follows this rule. The spectrum of amides in the 3 μ region is rather complicated as the unsubstituted amides exhibit at least four N-H absorption bands in this region, some of these being certainly influenced by hydrogen bonds with the oxygen of the peptide group. The band structure of the Cu(II) chelates seems to be somewhat simpler. The amino group contributes with two frequencies and the remaining amide N-H with one frequency. It can be inferred from studies of the metal chelates of amino acids [1] that amino frequencies appear at slightly lower wavenumbers than the N-H frequencies in free amides. The Cu(II) chelate of leucine, for example, has its main amino frequencies at 3 308 and 3 240 cm^{-1}. The Cu(II) chelates of GA and LA show 3 frequencies in this region. The band, at 3 106 cm^{-1} for $(GA)_2Cu$ and at 3 112 cm^{-1} for $(LA)_2Cu$,

can thus tentatively be ascribed to the N-H stretching of the amide group. The Cu(II) chelate of LMA shows as expected only two absorption bands in this region. The interpretation of the absorption data of N-H stretchings is not entirely unambiguous as some of the bands are broad enough so that the possibility of two overlapping frequencies is not excluded. At the same time some of these frequencies might be split into two bands due to crystal effects. It must be stressed that, owing to above mentioned difficulties, the position or absence of the amide N-H frequency can scarcely be used as a general indication of the influence of the metal ion on the peptide linkage.

The region of 6 μ is far more suitable for this purpose as the intense amide I frequency can easily be identified. The amide I, at approx. 6 μ, is usually considered to be a stretching frequency of the amide carbonyl in resonance with the C-N bond. Amide I is only slightly influenced by deuterization. The amide II, at approx. 6.2—6.4 μ, is a combination band where the N-H bending movement participates. It is strongly influenced by deuterization. These assignments have recently been reviewed and discussed by Miyazawa *et al.*[14] in connection with the calculation of frequencies for monosubstituted amides. The frequencies of the chelates show a vastly changed picture. The region for amide I is devoid of any absorption, the band structure being markedly shifted towards lower wavenumbers. The picture is further completed by the deuterized compounds, where the absorption due to hydrogen bending movements is removed from this wavelength region. The band remaining must be the stretching frequency of the resonating structure corresponding to the amide I band ($-C\begin{matrix}O\\ \diagdown N-\end{matrix}$). The only deviation from the simple picture expected is the split of this band for $(LA)_2$ Cu. When interpreting these changes, the influence of the hydrogen bonds on the amide I frequency ought to be considered. The positions of the frequencies of free amides in the solid state and in dilute $CHCl_3$ solutions can be compared in Table 3. The frequency changes do not exceed the value of approx. 20 cm^{-1}.

Further, the effect of metal ion-amino group interaction on the amide frequency ought to be considered.

A comparison between the free amide and its hydrochloride can be considered as relevant, the hydrogen ion taking the place of the metal ion. The observed shift of the amide I frequency is at its height approximately 20 cm^{-1} towards higher wavenumbers. The difference between the normal amide I frequency and the frequency observed in Cu(II) chelates is of the order 90—100 cm^{-1}. This can hardly be due to other effects than to the definite shift of the resonance equilibrium of the amide group towards the canonical form (I) in Fig. 12. From his IR studies of the biuret reaction of amides at high pH values, Chouteau [8] puts forth the same explanation.

Dipeptide-Cu(II) chelates. The next step is to compare these results with the IR-absorption of dipeptide-metal chelates. GG-Cu, $3H_2O$ and LG-Cu, H_2O have been crystallized and analyzed by Tomita *et al.*[5] and GG-Cu,H_2O by Manyak *et al.*[6] In all these chelates one dipeptide molecule combines with one Cu(II) ion, Manyak *et al.* proposed the structure III in Fig. 13 for the glycylglycine chelate.



III IV

Fig. 13.

The neutral chelate is formed either by the dissociation of the amide hydrogen or by dissociation from the coordinatively bound water molecule. From titrimetric and spectrometric data Dobbie and Kermack [2], and later Datta and Rabin [4,16], arrive at the conclusion that the dissociation takes place from the peptide group.

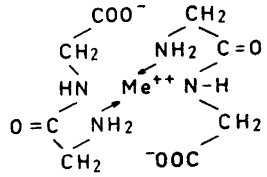
The IR absorption of Cu dipeptides in the 3 μ region is exemplified by Figs. 7 and 8. The absorption of amide chelates, and especially that of the secondary amide $(LMA)_2Cu$, indicates that GG-Cu is liable to exhibit two N-H frequencies in the neighbourhood of 3 200—3 300 cm^{-1}. Of the 4 possible absorption bands in Fig. 7, those at 3 331 and 3 282 cm^{-1} are most likely to belong to the N-H stretching frequencies. When the two other peaks present are considered it must be borne in mind that OH frequencies can appear in this wavelength region originating from the three molecules of water attached to the chelate. It is evident from a comparision with the N-H bands of the amide-Cu(II) chelates that the band at 3 435 cm^{-1} in GG-Cu(II),$3H_2O$ appears at a wavenumber too high for the N-H stretching frequency; it must be assigned to an OH stretching frequency. The band at 3 173 cm^{-1} is possibly the other OH frequency of the coordinated water molecule. It is obvious from Fig. 8 that the 4 main bands found in GG-Cu(II),$3H_2O$ dominate also the spectra of Cu dipeptide chelates with only one water of crystallization as LG-Cu (II),H_2O. This indicates that the OH bands originate from the water molecule bound to the metal ion as a fourth ligand (Fig. 13). The other two water molecules in GG-Cu(II),$3H_2O$ contribute presumably only with broad and undefined absorption. The special position of one water molecule is even emphasized by the fact that whereas it is easy to remove two molecules of water from GG-Cu (II),$3H_2O$ the third molecule is retained even at high temperatures.

The OH absorption and the fact that some of the absorption bands are not sharp enough to exclude an overlapping of frequencies, are the reasons why the IR-absorption in the 3 μ region does not give a conclusive answer to the question of metal ion influence on the peptide linkage. We have, as in the case of amide-Cu(II) chelates, to rely mainly on the results obtained in the double bond region. The IR absorption of dipeptide-Cu (II) chelates in the 6 μ region is characterized by two strong bands unaffected by deuterization. The frequency due to the stretching of the carboxyl group is generally found [15] in the neighbourhood of 1 590 cm^{-1}. When the carboxyl group participates in some kind of covalent bound formation with the metal ion, the stretching frequency shifts to higher wavenumbers as observed for Pt(II) chelates of glycine and, to a certain extent, for the water-free Cu(II) chelates

of some amino acids [1]. Table 4 summarizes the behaviour of the carboxyl frequency for Cu-dipeptide chelates. The COO^- frequencies show no appreciable trend towards higher wavenumbers so that the interaction between the carboxyl group and the metal ion ought to be of the same kind as in alkali salts of carboxylic acids. The only change in the position of the carboxyl frequency is displayed by the deuterization product of GG-Cu(II) as shown by Fig. 9. The position of similar bands in other dipeptide-Cu chelates, uninfluenced by deuterization, indicates that of the two bands remaining after deuterization, the carboxyl frequency at 1 613 cm^{-1} is represented in the monohydrate by the band at 1 592 cm^{-1} and not by the band at 1 624 cm^{-1}.

The band at 1 541 cm^{-1} in GG-Cu(II),H_2O must be ascribed to the amide I frequency, representing the same mode of vibration of the peptide group as observed in the Cu(II) chelates of amino acid amides. The position of this band in different Cu(II) dipeptides is fairly constant. The wavenumbers of these bands are gathered in Table 4. The observed shift of the amide I band, due to chelate formation, is for the peptides examined, approx. 100 cm^{-1}, which is in close agreement with the values observed for amide-Cu(II) chelates. The frequency is thus found at a considerably lower wavenumber than the normal peptide group vibration or a conjugated C = N bond frequency, indicating that the resonance structure of the peptide group is preserved but the equilibrium shifted towards the canonical structure III in Fig. 13.

Dipeptide chelates with Ni(II) and Zn(II). Manyak *et al.*[6] presume that the chelates formed by dipeptides with Ni(II) and Zn(II) are of the same type as the corresponding Cu(II) chelates. The Ni(II) and Zn(II) chelates isolated for this investigation are, as the analysis results show, neutral compounds consisting of two dipeptide molecules and one metal ion. These proportions and the absence of alkali ions rule out the possibility of further hydrogen ionisation in addition to the carboxyl group dissociation. The structure can be represented by *V* in Fig. 14.



V

Fig. 14.

A comparison of the IR curves in Fig. 11 reveals that the IR spectra of Ni(II) and Zn(II) chelates are almost identical and of another type than that of the Cu(II) chelate. The difference between Ni(II) and Zn(II) chelates lies in the position of the amide I band. This suggests a difference in the influence of metal ions on the peptide link. A second more prominent feature, common for both Ni(II) and Zn(II) chelates, is the splitting of the amide I frequency. Such splitting is frequently observed in crystalline peptides. Glycylglycine

itself, for example, shows a similar double peak. It is presumably due to hydrogen bond effects between the peptide groups in the crystal lattice.

Table 5 summarizes the behaviour of the important frequencies of GG under different conditions. We choose the value of the amide I band of GG-ester at 1 672 cm^{-1} measured in dilute $CHCl_3$ solution, as a standard for the uninfluenced peptide group. When the solution of the GG-ester is evaporated to dryness, the remaining film of liquid ester shows a shift of the amide I band by 8 cm^{-1} towards lower wavenumbers. The effect is undoubtedly due to hydrogen bond formation. The same kind of shift is observed when the GG-ester is compared with free GG. The shift of the mean of two amide I frequencies is in this case 5 cm^{-1}. That the shift is so small is probably due to the fact that the GG molecule exists in the solid state as a "zwitterion" where the extra hydrogen at the amino group shifts the amide frequency in the opposite direction. This kind of influence was observed in the hydrochlorides of amides and is also exhibited by the hydrochloride of GG, where the shift of the amide I frequency is 14 cm^{-1} towards higher wavenumbers. The hydrochloride of the GG-ester, when compared to the free ester, shows a similar shift of 14 cm^{-1} in the same direction.

Thus the shifts of the amide I band due to changes in hydrogen bond structure and bond formation at the amino group do not exceed the value of 20 cm^{-1}.

The amide I band of the Cu(II) chelate of GG shows, as previously demonstrated, a shift of 131 cm^{-1} towards lower wavenumbers. The Ni(II) chelate displays a similar shift of 32 cm^{-1} and the Zn(II) chelate a shift of 20 cm^{-1} in the same direction. The mean value of the two amide I frequencies has been used for the Ni(II) and Zn(II) chelates. The shift in Ni(II) chelates is big enough to permit the conclusion that the metal ion has an influence on the resonance of the peptide bond. The influence of the Zn(II) ion is smaller and the shift of the amide I band exceeds only with 12 cm^{-1} the value shown by the free GG. The position of the amide I band in $(GG)_2Zn(II)$, $2H_2O$ at 1 653 cm^{-1} lies in a region where the normal amid I frequencies of secondary amides are due to appear [18]. For example the methylamide of L-leucine (Table 1) has its amide I band as near as at 1 658 cm^{-1}. The influence of the Ni(II) ion is not unexpected as Maynak *et al*[6]. have isolated, from a more alkaline solution, a chelate of the same proportions as the neutral compound investigated here, but with two Na ions attached. The presence of the Na ions indicates that the chelate formed has lost two protons in analogy to the GG-Cu(II) chelate. The observation that Ni(II) forms, at high pH values, a chelate of the same character as the Cu(II) ion can also be inferred from the titration curves [6,16]. The existence of such a chelate with Zn(II) ions has not been demostrated.

These differences observed for the chelates of different metal ions lead to the conclusion that, although Cu(II), Ni(II) and Zn(II) all form chelate structures with the amino group of the GG molecule, differences between the various ions are large enough, so that, for example, the neutral chelate of GG with Cu(II) isolated at pH 8, shows a major change in the peptide group resonance, whereas the neutral chelate with Zn(II) scarcely shows any change in the peptide group.

The question whether the neutral chelate with Cu(II) is formed by proton dissociation from the amide nitrogen or from the coordinatively bound water molecule cannot be solved directly from changes in hydrogen stretching frequencies due to the complexity of the absorption band structure in the 3 μ region. However, as the changes in the 6 μ region for GG-Cu(II)H_2O are of the same type as for $(LA)_2$Cu(II), where the existence of two OH groups is excluded by the analysis results, the IR-investigation strongly supports the view that the proton dissociation takes place from the peptide group. The proton dissociation is also essential for the interpretation of the resonance shift in the peptide group, as in a chelate where the nitrogen binds both a proton and a metal ion, the peptide group resonance is blocked and the carbonyl frequency (amide 1) shifted towards higher wavenumbers. This kind of behaviour has been observed by Penland *et al.*[19] for different metal chelates of urea. The evidence that the metal ion-peptide group interaction in Cu(II) chelates is characterized by the substitution of the amide hydrogen with a metal ion does not imply that the observed interaction of Ni(II) with the peptide group does involve the nitrogen atom. On the contrary, the conclusions from urea chelates when applied to dipeptide chelates indicate that in case the amide hydrogen is retained after chelate formation and the amide I frequency still shows a shift towards lower wavenumbers, as in $(GG)_2$-Ni (II), the interaction between the metal ion and the peptide group probably takes place through the oxygen of the peptide link.

Although it is not quite correct to apply results obtained with solid chelates to aqueous solutions, it is interesting to note that the Zn(II) ion, which activates several proteolytic enzymes, shows practically no tendency to interact with the peptide group. This means that if chelate formation with the peptide group of the substrate molecule with a resulting electron displacement is a necessary step in the mechanism of metal activated enzymes, the role of the metal ion must be considerably influenced by the protein molecule [20].

Acknowledgements. The author wants to express his gratitude to Professor Arne Tiselius for encouraging interest and to make grateful acknowledgement to Mr. Stig Bergwall for able technical assistance. This investigation is a part of a program of infrared research financially supported by grants from the *Royal Swedish Academy of Sciences*, the *State Technical Research Council* and the *Rockefeller Foundation.*

REFERENCES

1. Rosenberg, A. *Acta Chem. Scand.* **10** (1956) 840.
2. Dobbie, H. and Kermack, W. O. *Biochem. J. London* **59** (1955) 246.
3. Perkins, D. J. *Biochem. J. London* **57** (1954) 702.
4. Datta, S. P. and Rabin, B. R. *Biochim. et Biophys. Acta* **19** (1956) 572.
5. Tomita, M., Hamamura, N., Tamiya, H., Takehara, M. and Tomita, K. *Hoppe-Seyler's Z. physiol. Chem.* **295** (1953) 128.
6. Manyak, A. R., Murphy, C. B. and Martell, A. E. *Arch. Biochem. and Biophys.* **59** (1955) 373.
7. Smith, E. L. and Spackman, D. H. *J. Biol. Chem.* **212** (1955) 271.
8. Chouteau, J. *Thesis*, Paris 1954.
9. Rising, M. M. and Yang, P. S. *J. Biol. Chem.* **99** (1932) 755.
10. Bergell, P. and Wülfing, Z. *Hoppe-Seyler's Z. physiol. Chem.* **64** (1910) 353.
11. Yang, P. S. and Rising, M. M. *J. Am. Chem. Soc.* **53** (1931) 3183.

12. Fischer, E. *Ber.* **34** (1901) 444.
13. Schiedt, U. and Reinwein, H. Z. *Z. Naturforsch.* **7b** (1952) 270.
14. Miyazawa, T., Shimanouchi, T. and Mizushima, S. *J. Chem. Phys.* **24** (1956) 408.
15. Bellamy, L. J. *The Infra Red Spectra of Complex Molecules*, Methuen, London 1954, p. 150.
16. Datta, S. P. and Rabin, B. R. *Trans. Faraday Soc.* **52** (1956) 1117.
17. Svatos, G. F., Curran, C. and Quagliano, J. V. *J. Am. Chem. Soc.* **77** (1955) 6159.
18. Ref.[15], p. 176.
19. Penland, R. B., Mizushima, S., Curran, C. and Quagliano, J. V. *J. Am. Chem. Soc.* **79** (1957) 1575.
20. Malmström, B. G. *Arch. Biochem. and Biophys.* **58** (1955) 381.

Received June 5, 1957.

ACTA CHEMICA SCANDINAVICA 11 (1957) 1405—1417

Studies on Cobaltammines

I. Equilibrium Measurements of Inner-Sphere Thiocyanato- and Nitro-Complexes

RAGNAR LARSSON

Department of Inorganic and Physical Chemistry, Chemical Institute, University of Lund, Lund, Sweden

The exchange of ammonia in the hexammine cobalt(III) ion for one and two thiocyanate ions or one nitrite ion has been achieved by the use of active carbon as a catalyst. By measurement of the total cobalt concentration in solutions saturated with hexammine cobalt (III) perchlorate, the equilibrium constants at ionic strength 1 M have been calculated. The influence of outer-sphere complexes has been considered.

Ever since the beginning of coordination chemistry in the days of Jørgensen and Werner the ammino compounds of tervalent cobalt have been intensely studied. Little has been known, however, about the equilibrium constants of reactions between these compounds. This situation is obviously related to those properties that made Co(III) complexes so suitable for preparative work; the low solubility of many of them and — above all — their sluggish reaction.

Until the work of J. Bjerrum [1], no reactions had been quantitatively studied, involving an ammonia displacement from the hexammine cobalt(III) ion. In the present paper, equilibrium measurements of the reaction of the hexammine cobalt(III) ion with thiocyanate and nitrite ions, respectively, will be presented.

METHOD OF INVESTIGATION

To overcome the slow attainment of equilibrium J. Bjerrum [1,2] has used active carbon as a catalyst. Other workers have also studied this catalytic effect.[3,4] They agree that the efficiency of the carbon is gradually decreased as time progresses. The probable explanation is that the carbon is poisoned by a layer of cobalt(III) hydroxide; a proposal strengthened by the observation of Bjerrum [1, p. 255], that there is a decrease in the total concentration of cobalt when equilibrium has been attained. Though experiments of the

present author have shown platinum black and finely dispersed silver to be catalysts as well, active carbon has been used in this investigation because of its cheapness and (compared to silver) greater inertness.

The measurements should be performed in a medium of high and constant ionic strength in order to justify the assumption that the coefficients of activity are constant, so that the law of mass action may be expressed in concentration units instead of activities.

Furthermore, the concentration of ammonium ions should be as great as possible in order to suppress the hydrolysis:

$$Co(NH_3)_6^{3+} + H_2O \rightleftharpoons Co(NH_3)_5OH^{2+} + NH_4^+$$

As the neutral salt, therefore, 1 M NH_4ClO_4 has been used. At the temperature of measurement, 20°C, the solubility of $Co(NH_3)_6(ClO_4)_3$ in 1 M NH_4ClO_4 is 0.21 mM.

It therefore seemed natural to measure the degree of complex formation from the increase in solubility of this rather sparingly soluble salt.

For easy concentration determinations the hexammine cobalt(III) salt was labelled with radioactive ^{60}Co.

NOTATIONS AND GENERAL FORMULAE

The notations used and methods of calculation will conform as closely as possible to those used by Fronæus [5].

In formulae M will stand for Co, A for ammonia and B for thiocyanate or nitrite.

C_A will mean the total and [A] the free concentration of A. Equivalent notations apply to other molecular species.

The equilibrium constant for the reaction

$$MA_6 + nB \rightleftharpoons MA_{6-n}B_n + nA$$

will be denoted by γ_n

$$\gamma_n = \frac{[MA_{6-n}B_n][A]^n}{[MA_6][B]^n} \tag{1}$$

In recent years the conception of "outer-sphere complexes" has been used in connection with the explanation of kinetical data on cobalt(III) complexes [6–8]. The eventual formation of such outer-sphere complexes will be duly accounted for in this investigation.

An outer-sphere coordination of the ligand B to the unsubstituted ion MA_6 may be written:

$$MA_6 + B \rightleftharpoons (MA_6)B$$

The equilibrium constant is denoted

$$\beta^o_{B,1} = \frac{[(MA_6)B]}{[MA_6][B]} \tag{2a}$$

In the general case, with n ligands B in the inner (hexacoordination-) sphere and m ligands B in the outer sphere we write:

$$MA_{6-n}B_n + mB \rightleftharpoons (MA_{6-n}B_n)B_m$$

$$\beta^{(n)}_{B,m} = \frac{[(MA_{6-n}B_n)B_m]}{[MA_{6-n}B_n][B]^m} \tag{2b}$$

Analogously, with ammonia in the outer coordination sphere we write in the general case

$$MA_{6-n}B_n + mA \rightleftharpoons (MA_{6-n}B_n)A_m$$

$$\beta^{(n)}_{A,m} = \frac{[(MA_{6-n}B_n)A_m]}{[MA_{6-n}B_n][A]^m} \tag{2c}$$

It is further defined:

$$X^{(n)}_A = \sum_{m=1}^{M} \beta^{(n)}_{A,m}[A]^m \tag{3a}$$

$$X^{(n)}_B = \sum_{m=1}^{M} \beta^{(n)}_{B,m}[B]^m \tag{3b}$$

Combining the expressions (1), (2 b), (2 c), (3 a) and (3 b) we may write the total metal concentration C_M

$$C_M = [MA_6]\Big[1 + X^{\circ}_A + X^{\circ}_B + \gamma_1 \frac{[B]}{[A]}(1 + X^{(1)}_A + X^{(1)}_B) + \cdots + \gamma_n \frac{[B]}{[A]}(1 + X^{(n)}_A + X^{(n)}_B)\Big] \tag{4}$$

For the sake of simplicity in writing, we denote the expression inside the large brackets as Y.

Thus $$C_M = [MA_6]Y \tag{5}$$

Though the concentration of ammonium ions is kept high, the hydrolytic reactions may still be of significance.

For the first step of hydrolysis

$$MA_6 + H_2O \rightleftharpoons MA_5OH + HA$$

we put $$k_{\overline{OH}} = \frac{[MA_5OH][HA]}{[MA_6]}$$

Now $$[HA] = C_{NH_4} = 1 \text{ M}$$

Thus $$[MA_5OH] = [MA_6]k_{\overline{OH}} \tag{6}$$

From the value of the second constant of hydrolysis reported by Bjerrum [1, p. 272] (for another temperature and another ionic medium) it may be inferred that the second hydrolytic step

$$MA_5OH + H_2O \rightleftharpoons MA_4(OH)_2 + HA$$

will not contribute to an appreciable amount.

Adding eqn. (6) to the expression (5) for the total metal concentration we finally get

$$C_M = [MA_6](Y + k_{OH}) \tag{7}$$

As the solution is saturated with $MA_6(ClO_4)_3$ we have

$$[MA_6][ClO_4]^3 = l \tag{8}$$

where l is the solubility product of $MA_6(ClO_4)_3$ in the actual solution. When $C_B = C_A = 0$ we write

$$[MA_6]_0[ClO_4]_0^3 = l_0 \tag{9}$$

By dividing eqn. (8) with eqn. (9) we get

$$[MA_6] = [MA_6]_0 \cdot \frac{[ClO_4]_0^3}{[ClO_4]^3} \cdot \frac{l}{l_0} \tag{10}$$

Inserting eqn. (10) in eqn. (7) we get

$$C_M = (Y+k_{OH}) \cdot [MA_6]_0 \cdot \frac{[ClO_4]_0^3}{[ClO_4]_3} \cdot \frac{l}{l_0} \tag{11}$$

As previously mentioned the cobalt determination was a radiometric one. The counting intensity for a given volume of the suturated solution (I cpm) is proportional to C_M.

Thus

$$I = \text{const.}C_M \tag{12 a}$$

$$I_0 = \text{const.}[MA_6]_0 \tag{12 b}$$

Combining eqns. (11), (12 a) and (12 b) we get

$$Y + k_{OH} = \frac{I}{I_0} \cdot \frac{[ClO_4]^3}{[ClO_4]_0^3} \cdot \frac{l_0}{l} \tag{13}$$

The above deduction is made under the assumption that no polynuclear complexes are formed. This may be regarded as reasonable, because of the small value of C_M. Furthermore, as it is known that most polynuclear Co(III) complexes involve the formation of OH or NH_2 bridges [9], and only a small contribution to C_M is due to hydrolytic products, the assumption made is so much more plausible.

EXPERIMENTAL

Chemicals used. Unlabelled $Co(NH_3)_6Cl_3$ was prepared from analytical grade $CoCl_2$ aq, following the prescriptions of Bjerrum [1, p. 241].

$Co(NH_3)_6(ClO_4)_3$, *labelled with* ^{60}Co, was prepared from neutron irradiated metallic cobalt (from AERE, Harwell) which was dissolved in dilute hydrochloric acid, some platinum black acting as a catalyst. Thereafter $Co(NH_3)_6Cl_3$ was prepared as above, and the perchlorate was precipitated with concentrated perchloric acid, filtered and washed with alcohol and ether.

From these two preparations a stock solution was made containing 5 mM $Co^*(NH_3)_6(ClO_4)_3$ and 55 mM $Co(NH_3)_6Cl_3$.

Ammonium thiocyanate and *sodium nitrite.* Analytical grade reagents were used and the stock solutions were checked by titration according to Volhard and by cerimetric titration, respectively.

Ammonium perchlorate was of analytical grade. The concentration of the stock solution was checked by evaporation of a sample on the steam bath. No loss of weight could be detected on prolonged heating at this temperature.

Sodium perchlorate. A *purum* quality preparation was recrystallized once from hot water and dried at 110°.

Carbon dioxide-free *ammonia* was used together with ammonium perchlorate to make buffer solutions (C_{NH_4}:C_{NH_3} = 1 : 5, 1 : 0.5 and 1 : 0.05), the ammonia content of which was determined by acidimetric titration using bromocresol green as indicator.

Active carbon. A gas adsorption carbon was used. Once every month it was heated in an oven to 150 °C to increase the acurate attainment of equilibrium. (*Cf.* Fig. 1 and the foot-note on p. 217 of Ref.[10])

Procedure. In 100 ml flasks with ground glass stoppers 30 ml aliquots of solutions of the following general composition were mixed from stock solutions:

C_B M ammonium thiocyanate (or sodium nitrite)
C_A M ammonia
1.000 − C_B M ammonium perchlorate
2.0 mM $Co^*(NH_3)_6^{3+}$

The amount of $Co(NH_3)_6(ClO_4)_3$ will then be about ten times that of a saturated solution. After a while a precipitation takes place. In the experiments aiming at an inner-sphere equilibration, weighed amounts of active carbon were added. Three (or sometimes four) flasks were charged with solution of the same composition, each flask being charged with different amounts of active carbon, approximately 25, 40 and 70 mg. The flasks, with the stoppers shielded and kept in place by a rubber nipple, were placed in a shaker and vigorously shaken for some days.

Thereafter a 10 ml sample was withdrawn from each flask, using a pipette with two small disks of filter paper kept in place at the tip of the pipette by means of a set of small cut rubber tubings. The samples were poured into small Petri dishes and the activity was measured with a Tracerlab P-20 QG Scintillation Counter, combined with a Tracerlab SC-18 Superscaler. The Petri dishes used were internally calibrated with an equal amount of a solution of known activity.

At no time less then 10 000 counts, more often 20 000 counts, were registered. Thus the error of counting was always less than 1 %.

Using the value of 5.3 years for the half-life of ^{60}Co, the measured intensities (I cpm) have been corrected to a common time.

Sodium nitrite was chosen instead of ammonium nitrite because of its easy availability. This choice does not invalidate the assumptions made on the constancy of the ammonium ion concentration, as the concentration of sodium nitrite will in no case be more than 3 % of the total salt concentration. Furthermore, an extrapolation to $C_{NO_2^-} = 0$ is undertaken in the course of calculation, thus completely eliminating any errors introduced.

Temperature control. The shaking of the flasks and the separation of aliquots to be measured, were made in a thermostatically controlled room, the temperature of which was 20.0°±0.2°. The pipettes used had been stored in the same room and had thus attained the same temperature.

The temperature dependency of the solubility of $Co(NH_3)_6(ClO_4)_3$ was determined by raising the temperature of the room to 22.9°. The increase in the solubility was then 25 %, corresponding to 0.9 % for every tenth of a degree.

Calculation of the concentration of perchlorate ions. As seen from the composition of the solutions examined and the stock solution of hexammine cobalt(III) salts, the perchlorate concentration will depend on C_B and on the amount of cobalt complexes formed. The following formula may be derived:

$$[ClO_4] = 1000 - 5.5 - C_B + 3 \times 0.21 \times I/I_0 = 994.5 - C_B + 0.63 \times I/I_0 \text{ mM}$$

The second term on the right side of the formula corresponds to the chloride ions brought into the solution from the cobalt stock solution. The fourth term represents the increase in $[ClO_4]$ as the solubility rises.

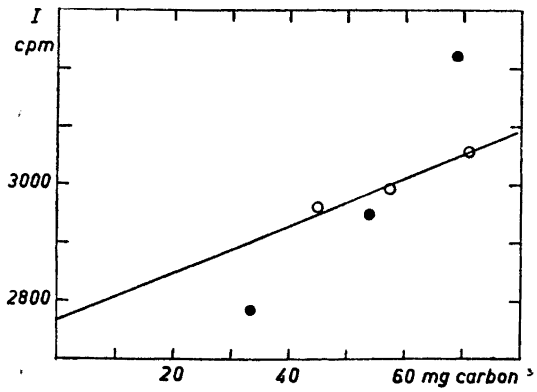


Fig. 1. The dependency of the equilibration on the amount of carbon in the thiocyanate measurements. Filled circles denote experiments with carbon that had long been exposed to air, unfilled circles denote experiments with carbon heated to 150° for several hours.

The solubility of $Co(NH_3)_6(ClO_4)_3$ in pure 1 M NH_4ClO_4 was determined by radiometric isotope dilution analysis to be 0.21 mM.

On the action of carbon. The criterion that equilibrium has been reached should be that the intensities of the solutions equilibrated by different amounts of carbon are the same. As long as the solution is saturated with respect to $Co(NH_3)_6(ClO_4)_3$, any adsorption of cobalt on the carbon would not affect this result. As a matter of fact this criterion has been found to be fulfilled in the measurements on the nitrite-substitution and the hydrolysis. In these cases the value of I, recorded in the following, is the mean value of the measurements with different amounts of carbon.

In the case of the thiocyanate-substitution, however, it was found that I increased as the carbon amount was increased. This effect was most prominent in experiments with low ammonia concentration. Those values of I reported in this system and denoted by an asterisk are attained by a linear extrapolation to zero amount of carbon. For series, notably those at high ammonia concentration, where the spreading is $< \pm 2$ %, the mean values have been reported. In Fig. 1 this effect is illustrated together with the effect of heating the carbon.

The nature of this effect is rather dubious. A probable explanation is perhaps that there occurs a catalytic decomposition of the thiocyanate ions on carbon, yielding cyanide ions, which react with the cobaltammine ions. This reaction may well be favoured by a decrease in the pH, as it is known that the thiocyanic acid is not stable in acid solution. It is strengthened by the fact that the slope of the line I *versus* the amount of carbon is increased on prolonged shaking, indicating the occurrence of a time reaction.

RESULTS

In order to obtain information on the hypothetic existence of outer-sphere complexes of the hexammine cobalt(III) ion, measurements were made of the solubility of the perchlorate at varying concentrations of thiocyanate or nitrite ions and of ammonia, *without any addition of carbon.* For the two first-mentioned ligands the value of $\frac{I}{I_0} \cdot \frac{[ClO_4]^3}{[ClO_4]_0^3}$ are reported in Figs. 2 and 3. Within the limits of experimental error the quotient is found to have a constant

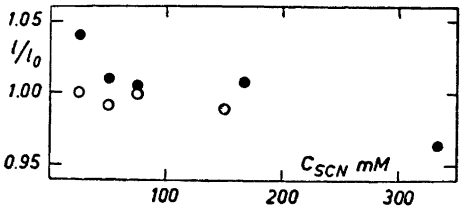


Fig. 2. The function l/l_0 plotted against C_{SCN^-}. Filled circles correspond to C_{NH_3} = 194 mM, unfilled circles to $C_{NH_3} = 0$.

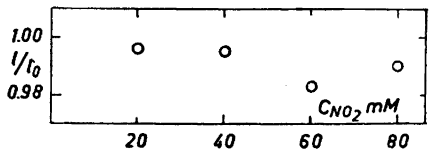


Fig. 3. The function l/l_0 plotted against $C_{NO_2^-} \cdot C_{NH_3} = 69$ mM.

value of 1. Thus it might be concluded that no outer-sphere complexes with charged ligands are formed and secondly that there is no medium effect affecting the solubility product l. However, the possibility of these two factors just compensating each other over the rather small concentration range used, must still be kept in mind. Two facts favour such an explanation.

Firstly, there has been observed quite distinct changes of the absorption spectrum of the hexammine cobalt(III) perchlorate, when part of the perchlorate ions is exchanged for halide or azide ions (Ref. [12,13]) and also for thiocyanate ions (Sonesson [14]).

Secondly, it is seen from Table 1, that an exchange of one fifth of the ammonium perchlorate for sodium perchlorate effects a distinct change of the solubility of $Co(NH_3)_6(ClO_4)_3$. As thiocyanate and nitrite ions are more unequally shaped compared to perchlorate ions than sodium ions are compared to ammonium ions, the change in solubility in the cases considered might be expected to be at least as large as that indicated in Table 1.

In the case of ammonia, conditions are quite different. The measurements are recorded in Table 1, showing a steady increase of solubility as C_{NH_3}

Table 1. The influence of the ammonia concentration on the solubility of $Co(NH_3)_6(ClO_4)_3$.

$C_{NH_4ClO_4} = 1$ M						$C_{NH_4ClO_4} = 0.8$ M $C_{NaClO_4} = 0.2$ M		
C_{NH_3} M	I cpm	x_A^o	C_{NH_3} M	I cpm	x_A^o	C_{NH_3} M	I cpm	x_A^o
0.0	1 387					0.0	1 267	
0.1976	1 409	0.016	2.122	1 882	0.36	0.499	1 336	0.055
0.355	1 430	0.031	2.217	1 936	0.40	1.239	1 493	0.136
0.503	1 461	0.053	2.992	2 266	0.63	2.124	1 717	0.36
0.739	1 509	0.088	3.24	2 465	0.78	3.01	2 037	0.61
1.047	1 596	0.151	3.70	2 712	0.96			
1.770	1 815	0.31	3.94	2 903	1.09			

increases. This effect may be due to any of two causes; an increase in the solubility product of $Co(NH_3)_6(ClO_4)_3$ as the solvent dielectric constant is changed with increasing ammonia, or an outersphere complex formation with one or more molecules of ammonia. As no value of the dielectric constant of ammonia water solutions has been found in literature, we are not able to tell the direction of such a change of solubility. However, some data of J. Bjerrum [11] on the solubility of $Ba(IO_3)_2$ in 2 M NH_4NO_3 and varying C_{NH_3} suggests that this medium effect should be one to decrease the solubility, not to increase it. The possibility of outer-sphere ammine complexes has then been accepted as a working-hypothesis.* In the third column of Table 1 the function x_A° is recorded.

$$x_A^\circ = \frac{I}{I_0} - 1$$

This notation is chosen to distinguish the thus defined quantity from the quantity X_A° defined by eqn. (3 a). X_A° might be calculated from x_A°, if the dependency of the solubility product on C_{NH_3} was known. Then, however, this correction would have to be used also when calculating Y in the inner-sphere equilibration measurements.

In the following the quantity $Y - x_A^\circ$ is used in calculation, Y being formed under the assumption that $l/l_0 = 1$, *i.e.* is independent of C_{NH_3}. The measurements recorded in Table 1 with the ionic medium 0.2 M $NaClO_4$, 0.8 M NH_4ClO_4 show that the increase in solubility is independent of the pH, thus there is (at this pH) no reaction like $Co(NH_3)_6^{3+} \rightleftharpoons Co(NH_3)_5NH_2^{2+} + H^+$.

THE HYDROLYTIC EQUILIBRIUM

By adding active carbon to an ammonium perchlorate solution with $C_B = 0$ we can get an estimation of the constant of hydrolysis, defined by eqn. (6). As this constant will be obtained at a difference of two almost equal quantities, the random error will be consequently large. The values reported in Fig. 4 are mean values of five or more independent determinations. It is seen that there is a slight increase in the values as C_{NH_3} increases. However, it is uncertain if this is a real effect or follows from experimental error. If the change is significant, it is of interest to note that the trend is the inverse to that found by Bjerrum [1, p. 257]. This might be seen as a support of the hypothesis of outersphere ammonia complexes.

THE THIOCYANATE SYSTEM

Measurements were made at the thiocyanate concentrations 25.0, 75.0 and 166.7 mM. The results are tabulated in Table 2. The values of x_A° are obtained by a graphical interpolation of the data given in Table 1, and those of k_{OH} from the line drawn in Fig. 4.

* Light absorption measurements of the present author, the results of which are soon to be published, strengthen this view.

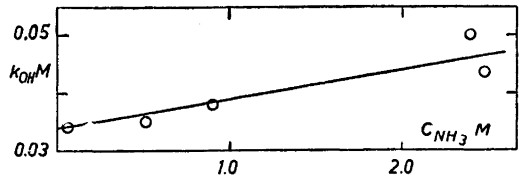


Fig. 4. The experimentally determined values of k_{OH} plotted against C_{NH_3}. The line is drawn to fit the points as closely as possible.

In Fig. 5 the quantity $Y-x_A^0$ is plotted against C_B/C_A. Actually the quotient [B]/[A] should be used in the subsequent calculations, but for small values of C_B/C_A the number of B bound per metal atom, $\bar{n}$, is small and thus $[B] = C_B - \bar{n}\ C_M$ is almost equal to C_B. (Analogous reasoning, of course, is to be applied to C_A and [A].) For greater values of C_B/C_A where $\bar{n}$ is rather large and a distinct difference exists between [B] and C_B, the degree of reproducibility of measurements is rather low, so there is no point in making extra corrections of the quotient C_B/C_A. Thus C_B/C_A will be used as the ligand quotient throughout the calculations.

Table 2. The thiocyanate system. Calculation of $Y-x_A^0$ as a function of C_B/C_A.

$I_0 = 1\ 387$ cpm; $[ClO_4]_0 = 995$ mM							
Time of shaking (h)	C_B mM	C_A mM	$\frac{C_B}{C_A}$	I cpm	$[ClO_4]$ mM	$Y+k_{OH}$	$Y-x_A^0$
27	25.0	274.6	0.0910	1 680	970	1.122	1.065
17		113.1	0.2210	1 737	970	1.160	1.119
60		56.5	0.442	1 856*	970	1.240	1.202
55		35.5	0.704	2 060*	970	1.376	1.340
60		25.0	1.00	2 440*	971	1.64	1.60
55		19.36	1.29	2 875*	971	1.93	1.89
60		15.33	1.63	3 900*	971	2.74	2.7
60		12.91	1.94	4 000*	971	2.81	2.8
71	75.0	1 532	0.0490	2 260	921	1.292	1.018
71		1 140	0.0658	2 178	921	1.245	1.046
71		796	0.0942	2 116	921	1.210	1.075
118		274.6	0.2731	2 170	920	1.237	1.180
118		193.8	0.387	2 265	921	1.295	1.240
133		112.7	0.665	2 500	921	1.430	1.389
66		79.9	0.94	3 004	921	1.72	1.68
100		56.5	1.33	3 250	921	1.86	1.82
>150	166.7	1 409	0.1183	3 493	829	1.457	1.206
>150		488	0.342	3 358	829	1.400	1.316
115		274.6	0.607	3 580	829	1.493	1.436
41		113.1	1.47	5 370*	830	2.25	2.21
>150		100.5	1.66	4 912*	829	2.05	2.0
88		79.7	2.09	7 290	831	3.1	3.0

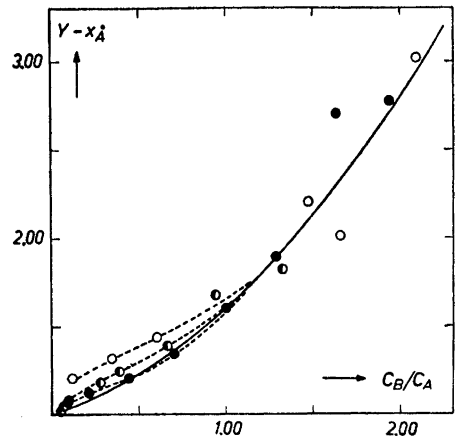


Fig. 5. The thiocyanate system. $Y-x_A^\circ$ as a function of C_B/C_A. Filled, half-filled and unfilled circles correspond to C_B = 25.0, 75.0 and 167 mM, respectively. The dotted lines are those used for the extrapolation of Table 3. The full-drawn curve is obtained from the reported constants.

However, there is no difficulty in calculating $\bar{n}$, and for systems where greater accuracy might be obtained, this correction may be worth while.

Applying the method of calculation used by Fronaeus [5], we get

$$\bar{n} \approx \frac{[B]}{[A]} \cdot \frac{1}{Y} \cdot \frac{dY}{d([B]/[A])}$$

From graphical estimation on the curve $Y-C_B/C_A$ we can get an approximate value of $\frac{dY}{d([B]/[A])}$ and of [B]/[A] and thus the more correct expression:

$$\frac{[B]}{[A]} = \frac{C_B - \bar{n}C_M}{C_A + \bar{n}C_M}$$

It is seen in Fig. 5 that we obtain different curves for the different values of C_B. At about $C_B/C_A = 1.3$ they seem to coalesce. This means that in the expression Y of eqn. (4) *either* we have still some terms dependent on [A] or [B] only and not on [B]/[A], *i.e.* the correction with x_A° corresponding to outer-sphere ammonia attachment to the MA_6^{3+} ion has not made account for all possible outer-sphere complexes, so that there may also exist, *e.g.*, $(MA_6)B$- and $(MA_5B)A$-complexes, *or*, and this is as plausible an explanation as the preceding one, the equilibrium constants γ_n will be effected by the change in the dielectric constant of the solvent as C_{NH_4} increases. Such an effect is well known for dissociation constants of weak acids [15], and has also been observed in studies on complex formation [16,17].

Both these effects may be thought to combine to give the effect of Fig. 5. Whatever the cause, however, an extrapolation to $C_A = C_B = 0$ for constant values of C_B/C_A will make all these effects vanish, *i.e.* the function Y will transform to

$$Y_0 = 1 + \gamma_1 \frac{C_B}{C_A} + \gamma_2 \left(\frac{C_B}{C_A}\right)^2 + \text{----}$$

where the constants γ are valid in 1 M NH_4ClO_4.

Table 3. The thiocyanate system. Extrapolation to $C_B = 0$ and calculation of equilibrium constants.

$\gamma_1 = 0.3 \pm 0.1$ $\gamma_2 = 0.3 \pm 0.1$

$\frac{C_B}{C_A}$	$Y - x_A^0$			Y_0	$\frac{C_A}{C_B}(Y_0 - 1)$
	$C_B = 167$ mM	$C_B = 75.0$ mM	$C_B = 25.0$ mM		
0.100	1.182	1.091	1.063	1.037	0.37
0.250	1.265	1.179	1.131	1.106	0.42
0.400	1.337	1.245	1.186	1.160	0.40
0.600	1.432	1.348	1.277	1.254	0.42
0.900	1.592	1.538	1.490	1.477	0.53
1.300	1.89	1.88	1.88	1.88	0.67
1.47	2.21			2.21	0.82
1.63			2.7	2.7	1.04
1.66	2.0			2.0	0.61
1.94			2.8	2.8	0.93
2.09	3.0			3.0	0.96

In Table 3 such an extrapolation is performed for $C_B/C_A \leq 1.3$, above this region of coalescence the experimental Y-x_A^0 values have been used. The function $\frac{C_A}{C_B}(Y_0 - 1)$ are, within the limits of the rather large experimental errors, linear, showing the existence of the first and second substituted complex to be formed for these values of the ligand quotient.

THE NITRITE SYSTEM

As the nitro-ligand was found to be more strongly attached to the Co(III) nucleus, much smaller values of the ligand quotient had to be used than was the case in the preceding investigation on the thiocyanate system. The nitrite concentrations used were 9.00, 18.00 and 27.00 mM. In Table 4 the experimental results are recorded. As before, C_B/C_A is used instead of [B]/[A]. In Fig. 6 a line with the slope 43 has been drawn through the upper points.

The points corresponding to $(Y$-$x_A^0)$-values less than about 2.5 are found to lie above that line and the ones corresponding to $C_B = 27$ mM and $C_B = 18$ mM are lying progressively higher than those corresponding to $C_B = 9$ mM. An extrapolation to $C_B = 0$ would, within the limits of experimental error, bring about a complete coincidence with the above-mentioned line. Thus it may be concluded that at these values of the ligand quotient only the first substitution complex exists, γ_1 being 43 ± 2. The colour of the solutions when the carbon had been filtered off was clear yellow. Thus the nitropentammine complex is formed and not the nitritopentammine one.

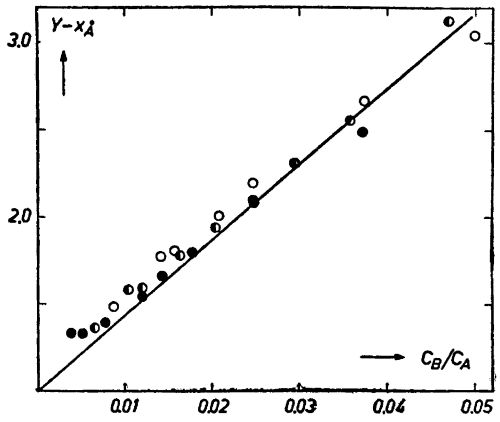


Fig. 6. The nitrite system. $Y-x_A^\circ$ as a function of C_B/C_A. Filled, half-filled and unfilled circles correspond to C_B = 9.00, 18.00 and 27.0 mM, respectively.

Table 4. The nitrite system. Calculation of $Y-x_A^\circ$ as a function of C_B/C_A.

I_0 = 1 387 cpm; $[ClO_4]_0$ = 995 mM

Time of shaking (h)	C_B mM	C_A M	$\frac{C_B}{C_A} \cdot 10^3$	I cpm	$[ClO_4]$ mM	$Y+k_{OH}$	$Y-x_A^\circ$
87	9.00	0.2419	37.2	3 710	986	2.54	2.49
87		0.363	24.8	3 061	986	2.15	2.08
61		0.509	17.7	2 688	986	1.89	1.80
61		0.629	14.3	2 524	986	1.77	1.66
61		0.750	12.0	2 385	986	1.67	1.55
64		1.155	7.8	2 284	985	1.60	1.40
64		1.774	5.1	2 364	986	1.66	1.33
64		2.393	3.8	2 594	986	1.82	1.33
63	18.00	0.383	47.0	4 669	978	3.20	3.13
63		0.503	35.8	3 862	977	2.64	2.55
63		0.608	29.6	3 533	977	2.41	2.31
63		0.729	24.7	3 243	977	2.21	2.09
63		0.882	20.4	3 064	977	2.09	1.94
63		1.107	16.3	2 887	977	1.97	1.78
63		1.501	12.0	2 726	977	1.86	1.59
63		1.727	10.4	2 787	977	1.90	1.59
72		2.767	6.5	2 888	977	1.97	1.36
64	27.00	0.601	49.9	4 721	969	3.14	3.04
64		0.721	37.4	4 195	968	2.79	2.66
52		0.920	29.4	3 719	968	2.47	2.31
64		1.099	24.6	3 595	968	2.39	2.20
52		1.299	20.8	3 360	968	2.23	2.01
64		1.719	15.7	3 195	968	2.12	1.81
52		1.918	14.1	3 217	968	2.14	1.78
72		3.10	8.7	3 353	968	2.23	1.48

My sincere appreciation is due to Professor S. Bodforss for his having awakened my interest in the chemistry of cobaltammines and having kindly placed at my disposal the facilities of this laboratory.

The helpful interest of Dr. S. Ahrland and Dr. S. Fronaeus is also acknowledged.

REFERENCES

1. Bjerrum, J. *Metal Ammine Formation in Aqueous Solution*, (Diss.) University, Copenhagen 1941.
2. Bjerrum, J. and Rasmussen, S. E. *Acta Chem. Scand.* **6** (1952) 1265.
3. Bailar, J. C. and Work, J. B. J. *J. Am. Chem. Soc.* **67** (1945) 176.
4. Douglas, B. E. *J. Am. Chem. Soc.* **76** (1954) 1020.
5. Fronaeus, S. *Komplexsystem hos koppar*, (Diss.) University, Lund 1948.
6. Taube, H. and Posey, F. A. *J. Am. Chem. Soc.* **75** (1953) 1463; **78** (1956) 15.
7. Adamson, A. W. and Basolo, F. *Acta Chem. Scand.* **9** (1955) 1261.
8. Ašperger, S. and Ingold, C. K. *J. Chem. Soc.* **1956** 2862.
9. Abegg, *Handbuch der Anorg. Chemie*, IV, 3 Abt. Vol. 3, Leipzig 1935.
10. Fernelius, W. C. (Ed.) *Inorganic Synthesis*, Vol. II, McGraw-Hill Book Company, Inc, New York 1946.
11. Bjerrum, J. *Kgl. Danske Videnskab. Selskab, Mat.-fys. Medd.* **11** (1931–32) No. 10.
12. Linhard, M. *Z. Elektrochem.* **50** (1944) 224.
13. Evans, M. G. and Nancollas, G. H. *Trans. Faraday Soc.* **49** (1953) 363.
14. Sonesson, A. *Private communication.*
15. Robinson, R. A. and Stokes, R. H. *Electrolyte Solutions*, Butterworth's Scientific Publications, London 1955, p. 340.
16. Kratohvil, J. and Težak, B. *Rec. trav. chim.* **75** (1956) 775.
17. Jonassen, H. B., Fagley, T. F., Rolland, C. C. and Yates, P. C. *J. Phys. Chem.* **58** (1954) 286.

Received June 19, 1957.

ACTA CHEMICA SCANDINAVICA 11 (1957) 1418—1444

Short Communications

Tocopherol Levels in Normal Pigs and in Pigs with Waxy Muscle Degeneration and *Hepatosis diaetetica*

HANS WANNTORP and ANNA-LISA OBEL

Departments of Chemistry and Pathology, State Veterinary Medical Institute, Stockholm, Sweden

Vitamin E or tocopherol was first considered to be a fertility or antisterility vitamin on the basis of early experiments with rats. Numerous investigations have since demonstrated, however, that this vitamin has a much wider range of activity. In animals other than rats including domestic animals, the major activity seems to be as an antioxidant in metabolic processes.

The most commonly used pig feeds are relatively deficient in vitamin E. It is, therefore, to be expected that lesions often occur in pigs which may be the expression of a deficiency of this vitamin. Many of the changes which can be observed in experimental vitamin E deficiency in the rat such as waxy degeneration of the muscles, ulceration in the cutaneous partition of the mucous membrane of the stomach, and so-called yellow fat can also be seen in many pig autopsies. Vitamin E deficiency is also an aetiological factor contributing towards the production of the hepatosis diaetetica syndrome. Obel [1] was able to produce this disease experimentally through a deficiency of vitamin E and sulphur-containing amino acids.

In order to establish whether or not the tocopherol level in the tissues of pigs with waxy degeneration of the muscles and *hepatosis diaetetica* is lower than is the case for healthy animals, determinations were carried out for various groups of animals. The tocopherol content of the heart, liver, and spleen was determined by the method of Wanntorp and Nordlund [2].

The average values for tocopherol in the heart, liver, and spleen of normal slaughter pigs (group 1) was 1.42, 0.96, and 0.59 mg/100 g, respectively. Group 2 consisted of pigs submitted for autopsy and which were affected by diseases other than those which could be associated with vitamin E deficiency. Average values for the hearts, livers, and spleens from this group were 1.07, 0.67, and 0.45 mg/100 g, respectively. Both these groups can be taken as comparison material for the other groups which consisted of animals probably deficient in vitamin E, *i. e.*, pigs with waxy degeneration of the skeletal musculature, group 3, pigs with *hepatosis diaetetica*, group 4, and pigs with experimental vitamin E deficienty, group 5. The average values obtained for tocopherol in group 3 were 0.76, 0.52, and 0.34 mg/100 g, respectively, in group 4, 0.59, 0.38, and 0.24 mg/100 g, respectively, and in group 5, 0.65, 0.44, and 0.26 mg/100 g, respectively.

Statistical treatment of the results showed that pigs with *hepatosis diaetetica* and the animals in group 5 which had received a diet deficient in vitamin E had significantly lower tocopherol levels in the heart, liver, and spleen than the pigs in group 2 which represent the normal levels for autopsy material.

The tocopherol levels in the heart and spleen of pigs with waxy muscle degeneration may possibly be significantly lower than the normal levels in group 2.

In order to study more closely the relationships between the tocopherol levels in different organs, an analysis of covariance was made using the tocopherol values for heart and liver as one variant pair and the values for heart and spleen as another. If, in a coordinate system, the x-axis repre-

sents the tocopherol level for heart and the y-axis the tocopherol level for liver and spleen, respectively, the regression lines for the averages of the groups will pass through zero and they are significantly straight lines. This indicates that the relationship between the tocopherol levels in heart, liver, and spleen are linear. From the angle of the regression lines for the average values of the groups, it is possible to state the general relationship between the tocopherol content of heart, liver, and spleen to be about 8: 5: 3. This relationship applies to all groups, fresh normal material, autopsy material in which the tocopherol level may sink after death, and material from animals with vitamin E deficiency.

1. Obel, A.-L. *Acta Pathol. Microbiol. Scand. Suppl.* **94** (1953).
2. Wanntorp, H. and Nordlund, G. *Arkiv Kemi Mineral. Geol.* **25 A** (1947) No. 6.

Received April 27, 1957.

Metal Ammine Formation in Solution

XI. Stability of Ethylenediamine Complexes and the Coordination Number of Chromium(II)

R. L. PECSOK* and JANNIK BJERRUM

Chemistry Department A, Technical University of Denmark, Copenhagen, Denmark

The coordination compounds of chromium(II) have been studied for many years; however, no stability constants have been reported for any of its complexes, nor has any experimental evidence been given of its coordination number. The difficulty of preparing chromium(II) solutions free from other metals (or acetate), the instability of chromium(II) toward oxidation, and the strong tendency of chromium(II) to form insoluble basic salts are serious obstacles to such an investigation. From the ligand field theory it is postulated [1] that chromium(II) complexes should show similarity with copper(II) complexes, *i. e.* have a tetragonal bipyramidal configuration and the metal ion a characteristic coordination number of four. This has been verified by establishing the formation curve for the chromium(II) ethylenediamine complexes. Studies with other amines are in progress and will be reported elsewhere.

Solutions containing *ca.* 0.04 M chromous chloride, 0.35 M hydrochloric acid, and 1 M potassium chloride were titrated with concentrated solutions of ethylenediamine (*ca.* 5 M, and 1 M KCl), the hydrogen ion concentration being determined with the glass electrode. It was shown spectrophotometrically that below 6 M chloride ion, chloro complexes are insignificant. The formation curves giving the average ligand number as function of the exponent of the free ethylenediamine concentration were calculated according to Bjerrum [2]. Three independent titrations are represented in Fig. 1. The fulldrawn curve is the theoretical formation curve calculated from the stability constants obtained. With a concentration of free amine higher than *ca.* 0.1 M, there is a considerable scatter in the experimental points because of the high initial acid concentration required to prevent precipitation of hydroxy compounds during the course of the titration. However, it is evident that the formation function of Cr(II)-en levels off at $\bar{n} = 2$. Preliminary spectrophotometric measurements show qualitatively that the bis(ethylenediamine) chromous ion has only a very slight tendency to take up more ethylenediamine. Further it is interesting to see that there is a distinct "pentammine" effect in the spectra just as in the corresponding cupric systems [3,4] (see Table 1).

Table 1. Data for the absorption maximum of the aquo chromous ion and two chromium (II) ethylenediamine solutions.

$C_{Cr(II)}$	C_{en}	λ_{max}	$1/\lambda_{max}$	ε_{max}
mole/l	mole/l	mμ	cm^{-1}	
0.212	0	714	14 000	4.7
0.0375	0.57	547	18 300	25.1
0.0351	10.8	571	17 500	17.1

The consecutive formation constants were calculated in the usual way [2,5], and found to be $\log K_1 = 5.145$, $\log K_2 = 4.035$ at 25°. In Table 2 these values are compared with the earlier determined constants for the other divalent transition group

* Guggenheim Fellow 1956—57, on leave from the University of California, Los Angeles.

sents the tocopherol level for heart and the y-axis the tocopherol level for liver and spleen, respectively, the regression lines for the averages of the groups will pass through zero and they are significantly straight lines. This indicates that the relationship between the tocopherol levels in heart, liver, and spleen are linear. From the angle of the regression lines for the average values of the groups, it is possible to state the general relationship between the tocopherol content of heart, liver, and spleen to be about 8: 5: 3. This relationship applies to all groups, fresh normal material, autopsy material in which the tocopherol level may sink after death, and material from animals with vitamin E deficiency.

1. Obel, A.-L. *Acta Pathol. Microbiol. Scand. Suppl.* **94** (1953).
2. Wanntorp, H. and Nordlund, G. *Arkiv Kemi Mineral. Geol.* **25 A** (1947) No. 6.

Received April 27, 1957.

Metal Ammine Formation in Solution

XI. Stability of Ethylenediamine Complexes and the Coordination Number of Chromium(II)

R. L. PECSOK* and JANNIK BJERRUM

Chemistry Department A, Technical University of Denmark, Copenhagen, Denmark

The coordination compounds of chromium(II) have been studied for many years; however, no stability constants have been reported for any of its complexes, nor has any experimental evidence been given of its coordination number. The difficulty of preparing chromium(II) solutions free from other metals (or acetate), the instability of chromium(II) toward oxidation, and the strong tendency of chromium(II) to form insoluble basic salts are serious obstacles to such an investigation. From the ligand field theory it is postulated [1] that chromium(II) complexes should show similarity with copper(II) complexes, *i. e.* have a tetragonal bipyramidal configuration and the metal ion a characteristic coordination number of four. This has been verified by establishing the formation curve for the chromium(II) ethylenediamine complexes. Studies with other amines are in progress and will be reported elsewhere.

Solutions containing *ca.* 0.04 M chromous chloride, 0.35 M hydrochloric acid, and 1 M potassium chloride were titrated with concentrated solutions of ethylenediamine (*ca.* 5 M, and 1 M KCl), the hydrogen ion concentration being determined with the glass electrode. It was shown spectrophotometrically that below 6 M chloride ion, chloro complexes are insignificant. The formation curves giving the average ligand number as function of the exponent of the free ethylenediamine concentration were calculated according to Bjerrum [2]. Three independent titrations are represented in Fig. 1. The fulldrawn curve is the theoretical formation curve calculated from the stability constants obtained. With a concentration of free amine higher than *ca.* 0.1 M, there is a considerable scatter in the experimental points because of the high initial acid concentration required to prevent precipitation of hydroxy compounds during the course of the titration. However, it is evident that the formation function of Cr(II)-en levels off at $\bar{n} = 2$. Preliminary spectrophotometric measurements show qualitatively that the bis(ethylenediamine) chromous ion has only a very slight tendency to take up more ethylenediamine. Further it is interesting to see that there is a distinct "pentammine" effect in the spectra just as in the corresponding cupric systems [3,4] (see Table 1).

Table 1. Data for the absorption maximum of the aquo chromous ion and two chromium (II) ethylenediamine solutions.

$C_{Cr(II)}$	C_{en}	λ_{max}	$1/\lambda_{max}$	ε_{max}
mole/l	mole/l	mμ	cm^{-1}	
0.212	0	714	14 000	4.7
0.0375	0.57	547	18 300	25.1
0.0351	10.8	571	17 500	17.1

The consecutive formation constants were calculated in the usual way [2,5], and found to be $\log K_1 = 5.145$, $\log K_2 = 4.035$ at 25°. In Table 2 these values are compared with the earlier determined constants for the other divalent transition group

* Guggenheim Fellow 1956—57, on leave from the University of California, Los Angeles.

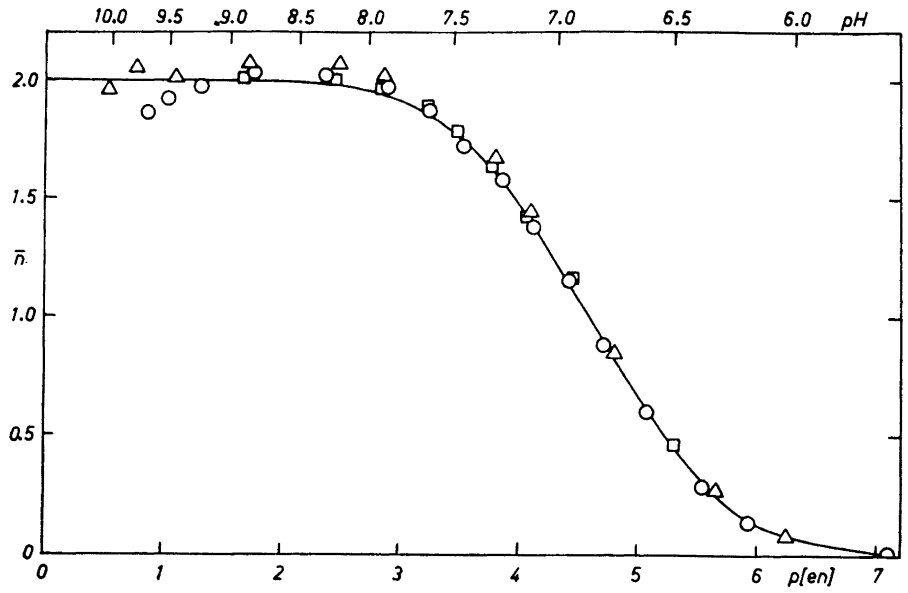


Fig. 1. Formation curve for Cr(II)-ethylenediamine system at 25°.
Titration with initial concentrations:
○, 0.344 M HCl, 0.0459 M $CrCl_2$, 0.96 M KCl
△, 0.355 M HCl, 0.0366 M $CrCl_2$, 1.02 M KCl
□, 0.355 M HCl, 0.0366 M $CrCl_2$, 1.02 M KCl

metals under similar conditions (25°, $\mu \sim 1.4$) *.

The crystal field stabilization is calculated as previously described [1,7], and the data show that chromium(II) has a rather high stabilization compared to the other transition group metals. From Table 1 it is seen that the bis(ethylenediamine)-chromium(II) ion is displaced 18 300—14 000 = 4 300 cm^{-1} relative to the aquo ion. The corresponding displacement of the planar bis(ethylenediamine)copper(II) ion is not much higher, 18 200—12 600 = 5 600 cm^{-1}. This shows that the tetragonal distortion is of the same order of magnitude in the two cases, and considering that the

* See Refs. [2,4-6]. The manganous constants are converted from 30° to 25° by addition of 0.04 to log K_n, the ferrous constants by addition of 0.06, and the cobaltous constants by addition of 0.08.

Table 2. Consecutive formation constants K_n and estimated ligand field stabilizations for the ethylenediamine complexes of the divalent transition group metals.

	d^4 Cr++	d^5 Mn++	d^6 Fe++	d^7 Co++	d^8 Ni++	d^9 Cu++	d^{10} Zn++
log K_1	5.15	2.77	4.34	5.97	7.51	10.72	5.92
Stabilization	3.00	0	0.94	1.94	2.85	5.43	0
log K_2	4.04	2.10	3.31	4.91	6.35	9.31	5.15
Stabilization	2.55	0	0.60	1.59	2.42	4.77	0
log K_3	—	0.92	2.05	3.18	4.42	—1.0	1.86
Stabilization	< -1	0	0.94	1.88	2.93	—2.7	0

complexity constants are much higher in the copper than in the chromium system, it can be concluded that the 3rd formation constant must be exceedingly small in the last mentioned case. Also the relatively small "pentammine" effect in the chromous system gives evidence for this.

Experimental. Chromous solutions were prepared by dissolving electrolytically purified chromium metal (kindly furnished by E. I. du Pont de Nemours and Co.) in hot oxygenfree hydrochloric acid to give solutions containing *ca.* 0.2 M chromous chloride and 0.2 M hydrochloric acid. Chromium(II) was determined by titration with potassium iodate [8], hydrochloric acid by potentiometric titration with sodium hydroxide, and chromium(III) spectrophotometrically. The solution used contained less than 2 % of the chromium as chromic ion which was ignored. The chromium(II) solution was always under a positive pressure of nitrogen, and all other solutions were made oxygenfree by bubbling with nitrogen. The ethylenediamine hydrate was specially purified by Carbide and Carbon Chemicals Company and distilled through a column. It was diluted with an equal volume of 2 M potassium chloride and swept with nitrogen before use.

The titrations were performed under nitrogen in a thermostated cell at 25°C. The cell E.M.F. was measured with a Radiometer pH meter, model PHM 3, using a glass electrode which had been tested for linear response to pH. The acidity constants of the ethylenediamine ($pK_{enH_2} = 7.44$, $pK_{enH} = 10.06$) were determined by titrating solutions of the same composition as for the complexity titrations, replacing the chromous chloride with an equivalent amount of barium chloride [2].

1. Bjerrum, J. and Jørgensen, C. K. *Rec. trav. chim.* **75** (1956) 658.
2. Bjerrum, J. *Metal Ammine Formation in Aqueous Solution.* Thesis 1941, p. 198 ff. Reprinted 1957, P. Haase and Son, Copenhagen.
3. Bjerrum, J., Ballhausen, C. J. and Jørgensen, C. K. *Acta Chem. Scand.* **8** (1954) 1275.
4. Bjerrum, J. and Nielsen, E. J. *Acta Chem. Scand.* **2** (1948) 297.
5. Bjerrum, J. and Andersen, P. *Kgl. Danske Videnskab. Selskab, Mat. fys. Medd.* **22** (1945) No. 7.
6. Poulsen, I. and Bjerrum, J. *Acta Chem. Scand.* **9** (1955) 1412.
7. *Dixième Conseil de Chimie Solvay, Bruxelles 1956. Rapport et Discussions*, p. 340.
8. Stone, H. W. *Anal. Chem.* **20** (1948) 747.

Received August 14, 1957.

The Preparation of Benzene-1,2,4-trisulphonic Acid

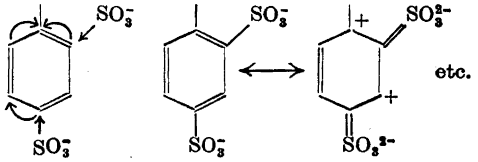
ROLF LUNDQVIST

Chemical Institute, University of Uppsala, Uppsala, Sweden

As a part of the preliminaries for an investigation on the adsorption of benzene sulphonic acids and naphtalene sulphonic acids on aluminium oxide, asymmetrical benzene trisulphonic acid has been prepared.

After unsuccessful experiments with the method of Gattermann [1,2], involving the use of aniline-2,4-disulphonic acid, and after attempts to develop sulphonation products of thiophenyl derivatives, refluxing [3] a solution of the sodium salt of bromobenzene-2,4-disulphonic acid [4-7] and sodium sulphite for 6 h in the presence of some cupric sulphate turned out to be a simple and successful method. [8] Benzene-1,4-disulphonic acid [8] was prepared from bromobenzene-4-sulphonic acid [9] as a preparatory study of this method.

Compared with the preparation of benzene sulphonic acid from bromobenzene, which is achieved by heating bromobenzene with a solution of sodium sulphite and cupric sulphate at 180—200°C for 7 h, the displacement of bromine from bromobenzene-2,4-disulphonic acid is clearly facilitated. As the reaction is carried out in a neutral solution, it gives some valuable information on the relative strengths of the inductive and mesomeric effects operating from the two sulphonate groups. The inductive effect (I) is opposite to the mesomeric effect (II).



I. + I effect II. — M effect

The displacement of bromine is a nucleophilic reaction:

complexity constants are much higher in the copper than in the chromium system, it can be concluded that the 3rd formation constant must be exceedingly small in the last mentioned case. Also the relatively small "pentammine" effect in the chromous system gives evidence for this.

Experimental. Chromous solutions were prepared by dissolving electrolytically purified chromium metal (kindly furnished by E. I. du Pont de Nemours and Co.) in hot oxygenfree hydrochloric acid to give solutions containing *ca.* 0.2 M chromous chloride and 0.2 M hydrochloric acid. Chromium(II) was determined by titration with potassium iodate [8], hydrochloric acid by potentiometric titration with sodium hydroxide, and chromium(III) spectrophotometrically. The solution used contained less than 2 % of the chromium as chromic ion which was ignored. The chromium(II) solution was always under a positive pressure of nitrogen, and all other solutions were made oxygenfree by bubbling with nitrogen. The ethylenediamine hydrate was specially purified by Carbide and Carbon Chemicals Company and distilled through a column. It was diluted with an equal volume of 2 M potassium chloride and swept with nitrogen before use.

The titrations were performed under nitrogen in a thermostated cell at 25°C. The cell E.M.F. was measured with a Radiometer pH meter, model PHM 3, using a glass electrode which had been tested for linear response to pH. The acidity constants of the ethylenediamine ($pK_{enH_2} = 7.44$, $pK_{enH} = 10.06$) were determined by titrating solutions of the same composition as for the complexity titrations, replacing the chromous chloride with an equivalent amount of barium chloride [2].

1. Bjerrum, J. and Jørgensen, C. K. *Rec. trav. chim.* **75** (1956) 658.
2. Bjerrum, J. *Metal Ammine Formation in Aqueous Solution.* Thesis 1941, p. 198 ff. Reprinted 1957, P. Haase and Son, Copenhagen.
3. Bjerrum, J., Ballhausen, C. J. and Jørgensen, C. K. *Acta Chem. Scand.* **8** (1954) 1275.
4. Bjerrum, J. and Nielsen, E. J. *Acta Chem. Scand.* **2** (1948) 297.
5. Bjerrum, J. and Andersen, P. *Kgl. Danske Videnskab. Selskab, Mat. fys. Medd.* **22** (1945) No. 7.
6. Poulsen, I. and Bjerrum, J. *Acta Chem. Scand.* **9** (1955) 1412.
7. *Dixième Conseil de Chimie Solvay, Bruxelles 1956. Rapport et Discussions*, p. 340.
8. Stone, H. W. *Anal. Chem.* **20** (1948) 747.

Received August 14, 1957.

The Preparation of Benzene-1,2,4-trisulphonic Acid

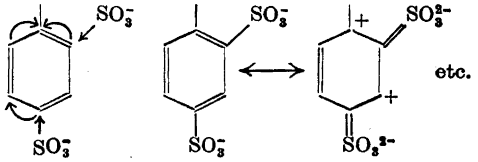
ROLF LUNDQVIST

Chemical Institute, University of Uppsala, Uppsala, Sweden

As a part of the preliminaries for an investigation on the adsorption of benzene sulphonic acids and naphtalene sulphonic acids on aluminium oxide, asymmetrical benzene trisulphonic acid has been prepared.

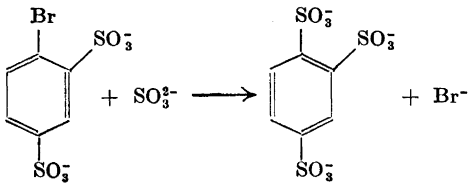
After unsuccessful experiments with the method of Gattermann [1,2], involving the use of aniline-2,4-disulphonic acid, and after attempts to develop sulphonation products of thiophenyl derivatives, refluxing [3] a solution of the sodium salt of bromobenzene-2,4-disulphonic acid [4-7] and sodium sulphite for 6 h in the presence of some cupric sulphate turned out to be a simple and successful method. [8] Benzene-1,4-disulphonic acid [8] was prepared from bromobenzene-4-sulphonic acid [9] as a preparatory study of this method.

Compared with the preparation of benzene sulphonic acid from bromobenzene, which is achieved by heating bromobenzene with a solution of sodium sulphite and cupric sulphate at 180—200°C for 7 h, the displacement of bromine from bromobenzene-2,4-disulphonic acid is clearly facilitated. As the reaction is carried out in a neutral solution, it gives some valuable information on the relative strengths of the inductive and mesomeric effects operating from the two sulphonate groups. The inductive effect (I) is opposite to the mesomeric effect (II).



I. + I effect II. — M effect

The displacement of bromine is a nucleophilic reaction:



and thus the statement is justified that the mesomeric effect of the two sulphonate groups in the bromobenzene-2,4-disulphonate ion is stronger than the corresponding inductive effect.

The common method of isolating and characterizing the sulphonic acid as the sulphonyl chloride was found not to be the proper way in this case due to the formation of chlorobenzene-2,4-disulphonyl chloride[10] (m. p. 88—89°C, diamide m. p. 205—208°C) in most experiments, and so the S-benzyl*iso*thiouronium salt was chosen for this purpose. — The benzene-1,2,4-trisulphonyl chloride was prepared afterwards using mild conditions during the treatment with phosphorus pentachloride.

A convenient method of preparing bromobenzene-2,4-disulphonic acid has also been developed.

Experimental. Bromobenzene - 2,4 - disulphonic acid: A mixture of 76 g of bromobenzene and 260 ml of chlorosulphonic acid was heated at 145°C on an oil bath for 4 h with stirring. After cooling the excess of chlorosulphonic acid was carefully hydrolysed on ice. A substance insoluble in water was obtained and was thoroughly washed with 1 500 ml of ether in small portions. The volume of the ether solution was reduced to 100 ml by evaporating and after adding 200 ml of light petrol 41 g of bromobenzene-2,4-disulphonyl chloride crystallized out on cooling at 0°C (m.p. 102—104°C, diamide m.p. 241—242°C). The yield corresponds to 24 % of the theoretical amount. — The sodium salt was prepared by hydrolysing the dimethyl ester with boiling water and neutralizing with NaOH.

Benzene-1,2,4-trisulphonic acid: 25.6 g of the sodium salt of bromobenzene-2,4-disulphonic acid was refluxed for 6 h with a solution of 13.4 g (= 3 equiv.) of sodium sulphite and 1.3 g of cupric sulphate in 190 ml of water. During the reaction a red coating of Cu_2O was formed on the walls of the vessel. After cooling the solution was acidified with hydrochloric acid and air was passed through to displace the SO_2 until the odor of the gas abated. The solution was freed from precipitated CuCl by filtering, cooled in an ice bath and poured with stirring into an ice cooled solution of 44.5 g of S-benzyl*iso*thiouronium chloride in 200 ml of water. A pale yellow precipitate was at once obtained and after a few hours' cooling on ice a white substance crystallized out. Both substances were recrystallized from 50 % alcohol and yielded 30.7 g of rectangular prisms, m. p. 240—241°C (decomp.). Another 7.5 g of the same substance was obtained from the mother liquors by evaporating and cooling.

Analysis: Found H 4.57; C 44.03; N 10.15; S 23.87. Calculated for $C_6H_3[SO_3 \cdot (NH_2)_2 C \cdot S \cdot CH_2 \cdot C_6H_5]_3$: H 4.44; C 44.11; N 10.29; S 23.55. The equivalent weight of the substance was obtained by passing it through a cation exchanger (Amberlite IR-100) and titrating with NaOH. Found 272.3, calc. 272.3. Infrared spectra showed the presence of a 1,2,4-trisubstituted benzene nucleus.

The yield of S-benzyl*iso*thiouronium benzene-1,2,4-trisulphonate, 38.2 g, was 66 % of the theoretical amount, calculated on sodium bromobenzene-2,4-disulphonate.

The sodium salt was prepared by passing a 50 % alcoholic solution of the S-benzyl*iso*-thiouronium salt through a cation exchanger and neutralizing the eluate with NaOH. After evaporating the solvent the sodium salt was crystallized from 70 % alcohol and was obtained as a white powder.

Benzene-1,2,4-trisulphonyl chloride was prepared by heating the sodium salt with excess of phosphorus pentachloride at 110°C for 5 min with stirring. The reaction mixture was hydrolysed with ice water and the sulphonyl chloride was dissolved in ether and crystallized twice from light petrol; irregularly shaped crystals, m. p. 114—116°C. (Found: C 19.39. Calc. for $C_6H_3(SO_2Cl)_3$: C 19.29).

The writer is indebted to Professor A. Fredga and Fil. lic. G. Bendz for advice and interest.

1. Gattermann, L. *Ber.* **32** (1899) 1136.
2. Bellavita, V. *Gazz. chim. ital.* **62** (1932) 658.
3. Rosenmund, K. W. *Ber.* **54** (1921) 439.
4. Meyer, V. *Ber.* **7** (1874) 1311.
5. Fischer, P. *Ber.* **24** (1891) 3805.
6. Heinzelmann, G. *Ann.* **190** (1878) 227.
7. Zander, O. *Ann.* **198** (1879) 10.
8. Zincke, Th. and Frohneberg, W. *Ber.* **42** (1909) 2728.
9. Baxter, R. R. and Chattaway, F. D. *J. Chem. Soc.* **107** (1915) 1815.
10. Davies, W. and Wood, E. S. *J. Chem. Soc.* **1928** 1125.

Received September 17, 1957.

*iso*Thiocyanates XXIX* Separation of Volatile *iso*Thiocyanates by Gas Chromatography

ANDERS KJÆR and AAGE JART

Chemical Laboratory of the University of Copenhagen, Denmark

The frequent occurrence in crucifers and certain other higher plants of mixtures of mustard oil glucosides (*cf. e. g.* Ref.[1]), enzymically hydrolyzed to corresponding mixtures of *iso*thiocyanates, renders the analytical separation of the latter a matter of considerable interest. Although liquid partition chromatography, on paper as well as columns, has served this purpose extensively, alternative methods of separation have occasionally been felt desirable. The present communication records preliminary results of an investigation, undertaken in order to study the applicability of gas chromatography for the separation of volatile *iso*thiocyanates.

All separations were performed in a 2 m column at various, but closely controlled and constant temperatures. Dixon helices served as support for the stationary phase, consisting of silicon grease, and nitrogen was used throughout as a carrier gas at a rate of 10 mg per min. The output pressure was 20 mm, and the total pressure drop through the entire column about 4 mm.

A typical separation of a five-component system, with a total weight of 6.7 mg, is reproduced in Fig. 1, A. The mixture had the composition:

Methyl *iso*thiocyanate	14	%
Ethyl *iso*thiocyanate	18	»
*iso*Propyl *iso*thiocyanate	17	»
n-Butyl *iso*thiocyanate	18.5	»
*iso*Pentyl *iso*thiocyanate	32.5	»

and a temperature of 68.5° was selected. Under these conditions the components emerged from the column in the above order, yet with the ethyl and *iso*propyl bands unresolved. However, some separation of these was achieved at 50°, and in an experiment conducted at 30.5° the two *iso*thiocyanates were recognizable as distinct bands (Fig. 1, B). Separate runs on the individual compounds indicated that the small peaks appearing briefly after the start, and the slight inflexion just ahead of the butyl derivative (Fig. 1, A), could be attributed to unknown impurities in the specimens of *iso*pentyl and *iso*propyl *iso*thiocyanates employed, respectively. Preliminary runs at fixed temperatures in the range 40° – 50° have further provided satisfactory separations of 3-butenyl and allyl *iso*thiocyanate, as well as of the latter and *iso*propyl *iso*thiocyanate.

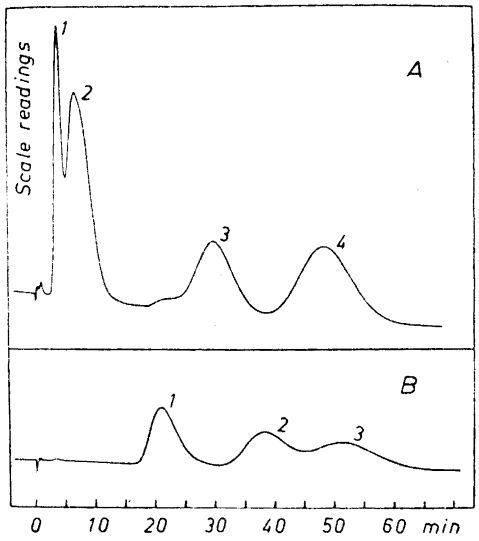


Fig. 1. A: Separation by gas chromatography of: 1. methyl, 2. ethyl and *iso*propyl, 3. *n*-butyl, and 4. *iso*pentyl *iso*thiocyanates. Total weight: 6.7 mg. Column temperature: 68.5°. *B:* Separation of: 1. methyl, 2. ethyl, and 3. *iso*propyl *iso*thiocyanate. Total weight: 4.4 mg. Column temperature: 30.5°.

Gas chromatography thus appears to be a method of great promise for the separation, analysis and identification of volatile *iso*thiocyanates, including those of natural provenance. Further work along this line is in progress and a more detailed account will appear at a later date.

The work is part of investigations supported by *Statens Almindelige Videnskabsfond (The Danish State Research Foundation)* and *Carlsbergfondet (The Carlsberg Foundation)*. A special grant to one of us (A.K.) from *Kai Hansen's Fond* is gratefully acknowledged.

* Part XXVIII of this series: *Acta Chem. Scand.* **11** (1957) 906.

1. Kjær, A. *Dansk Tidsskr. Farm.* **30** (1956) 117.

Received August 23, 1957.

Unit Cells and Space Groups of Some Carboxylic Acid Derivatives of 1,2-Dithiolane, 1,2-Dithiane, 1,2-Diselenane and 1,2-Dithiepane

OLAV FOSS and LENNART SCHOTTE

Chemical Institute, University of Bergen, Bergen, Norway, and Chemical Institute, University of Uppsala, Uppsala, Sweden

The X-ray crystallographic survey of saturated cyclic disulphides reported below serves as a preliminary to attempts at complete crystal structure determinations of suitable representatives. Of special interest is the stereochemistry of the disulphide group, particularly in five-membered rings where the CSS/SSC dihedral angle is expected to be considerably smaller than the normal value of about 90°.

The data were obtained from oscillation and Weissenberg photographs of single-crystal specimens, using Cu$K\alpha$ radiation, $\lambda = 1.542$ Å. Axial lengths are believed to be accurate to within 0.5 %. Densities were determined by flotation in suitable solvent mixtures.

1,2-Dithiolane-4-carboxylic acid [1-3] (I). Triclinic, irregularly shaped crystals, with $a = 5.34$ Å, $b = 5.85$ Å, $c = 10.75$ Å, $\alpha = 93\frac{1}{2}°$, $\beta = 89\frac{1}{2}°$, $\gamma = 109\frac{1}{2}°$. There are two molecules per unit cell; density, calc. 1.58, found 1.54 g/cm³. The space group is $C_i^1-P\bar{1}$.

The projection of the structure along the a axis has been solved [4], and the complete structure will be worked out. The a-axis projection indicates that the dithiolane ring is not planar, the CSS/SSC dihedral angle being different from 0°.

Racem - *1,2 - dithiolane - 3,5 - dicarboxylic acid* [2,5-7] (II). Monoclinic prismatic, $a = 8.47$ Å, $b = 18.20$ Å, $c = 10.14$ Å, $\beta = 98°$. Eight molecules per unit cell; density, calc. 1.67, found 1.67 g/cm³. The space group, from systematic absences, is $C_{2h}^5-P2_1/c$, from which follows that the asymmetric unit consists of two molecules.

The crystals were plates {010} sometimes elongated along the c axis.

Racem - *1,2-dithiane - 3,6-dicarboxylic acid* [2,6,8,9] (III). Monoclinic prismatic, $a = 9.62$ Å, $b = 9.26$ Å, $c = 9.70$ Å, $\beta = 102\frac{1}{2}°$. There are four molecules per unit cell; density, calc. 1.64, found 1.65 g/cm³. The space group, from systematic absences and from Patterson and Fourier projections along the b axis, is C_{2h}^6-I2/c. In the conventional $C2/c$ setting, $a = 12.09$ Å, $\beta = 129°$, otherwise as above.

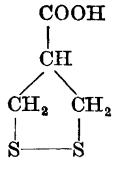
The crystals occurred as thick prisms {110}.

With four molecules per unit cell, each molecule must possess twofold symmetry in the crystals, and were found to lie on twofold axes. The dithiane ring has the chair form, with the substituents in equatorial positions. A detailed structure determination is being made [10].

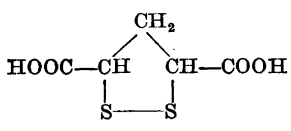
Meso - *1,2 - dithiane - 3,6 - dicarboxylic acid* [2,6,8,9]. Monoclinic prismatic, $a = 6.36$ Å, $b = 13.63$ Å, $c = 10.31$ Å, $\beta = 110°$. Four molecules per unit cell; density, calc. 1.65, found 1.64 g/cm³. The space group, from systematic absences, is $C_{2h}^5-P2_1/c$.

The crystal studied was a thick prism extended along the a axis, bounded by {010}, {001} and {011}, and terminated by {100}.

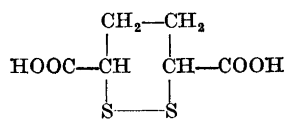
The *meso* acid, granted that its disulphide group is non-planar. will in the crystals occur in two equivalent mirror image forms, since the space group is not enantiomorphous. In solution, conversion of the dithiane ring, *i. e.*, of one enantiomorph of the *meso* acid into the other, takes place. In view of the relatively high barrier, 10—14 kcal/mole [11], towards rotation through the planar *cis* form of a disulphide group, it may be expected that conversion of the 1,2-dithiane ring takes place less rapidly than the conversion of *cyclo*hexane itself and its derivatives.



(I)



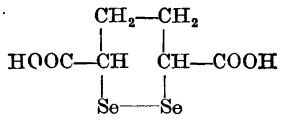
(II)



(III)

Racem - *1,2 - diselenane - 3,6 - dicarboxylic acid* [12,13] (IV). Monoclinic, probably prismatic, $a = 9.97$ Å, $b = 9.43$ Å, $c = 9.78$ Å, $\beta = 105°$. There are four molecules per unit cell; density, calc. 2.26, found 2.27 g/cm³. Systematic absences, *hkl* when $h + k$ is odd, *h0l* when *l* is odd. Similarities with the dithiane analogue, particularly of the *h0l* zones of reflections, indicate that the space group is the centrosymmetric one, C_{2h}^6-C2/c. In the *I2/c* setting, $a = 12.01$ Å, $\beta = 127°$. As in the case of the dithiane analogue, the crystals occur as prisms {110}.

The *racem* 1,2-dithiane- and 1,2-diselenane-3,6-dicarboxylic acids thus crystallize in the same space group, with very similar unit cell dimensions, but, once the *a* axes and β angles are chosen so as to conform dimensionally, the *C*- and *I*-centered settings are interchanged in the two crystals. Thus, the photographs of the 0*kl* zones of reflections have different symmetries, corresponding to the plane groups *cmm* and *pmg*, respectively. The difference corresponds to interchange of locations of twofold screw axes and symmetry centres at $x = \frac{1}{4}$ and $\frac{3}{4}$, and to different arrangements of the molecules relatively to each other as seen along the *a* axes. Otherwise, the two structures should be very similar.



(IV)

(+) - *1,2 - diselenane - 3,6 - dicarboxylic acid* [12,13]. Orthorhombic sphenoidal, $a = 9.57$ Å, $b = 9.91$ Å, $c = 9.50$ Å. Four molecules per unit cell; density, calc. 2.23, found 2.21 g/cm³. The systematic absences are those of the space group $D_2^4-P2_12_12_1$.

The crystals occurred as flat prisms extended along the *c* axis, with {100} dominant. {110} and {101} were also observed. There is a pronounced tendency of cleavage along the *c* plane.

Racem - *1,2-dithiepane - 3,7 - dicarboxylic acid* [2,14,15] (V). Monoclinic prismatic, $a = 12.97$ Å, $b = 8.20$ Å, $c = 8.90$ Å, $\beta = 96°$. There are four molecules per unit cell; density, calc. 1.57, found 1.57 g/cm³. The space group is $C_{2h}^5-P2_1/c$, from systematic absences.

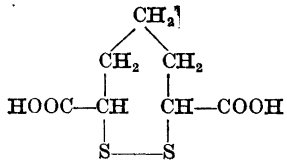
The crystals were mostly poorly developed; the one studied was a prism extended along the *b* axis.

Meso - *1,2 - dithiepane - 3,7 - dicarboxylic acid* [2,14,15]. Monoclinic, $a = 25.91$ Å, $b = 5.82$ Å, $c = 13.21$ Å, $\beta = 91\frac{1}{2}°$. Eight molecules per unit cell; density, calc. 1.48, found 1.49 g/cm³. Systematic absences, *hkl* when $h + k$ is odd, *h0l* when *l* is odd. The morphology of the crystals indicates that a twofold axis is present, and thus that the space group is the centrosymmetric one, C_{2h}^6-C2/c.

The sample consisted of prisms elongated along the *b* axis and bounded by {100} and {201}.

The disulphide group of the 1,2-dithiepane ring almost certainly being non-planar, two enantiomorphous forms of the *meso* acid occur in the crystals. Analogous considerations as to interconversion of the enantiomorphs in solution should apply as indicated above for *meso*-1,2-dithiane-3,6-dicarboxylic acid.

In the course of the work, data were obtained also for meso-*α,α'-dibromo-adipic acid* (m. p. 193 °C). The crystals were monoclinic prismatic, and occurred as prisms {011} terminated by {101}, with $a = 5.00$ Å, $b = 10.42$ Å, $c = 9.78$ Å, $\beta = 111°$. There are two molecules per unit cell; density, calc. 2.12, found 2.12 g/cm³. The space group from systematic absences, is $C_{2h}^5-P2_1/c$, from which follows that the molecules are centrosymmetric in the crystals.



(V)

The authors wish to express their thanks to Professor Arne Fredga for his kindness in placing samples of the selenium compounds at their disposal.

1. Schotte, L. and Ström, H. *Acta Chem. Scand.* **10** (1956) 687.
2. Schotte, L. *Arkiv Kemi* **9** (1956) No. 37.
3. Jansen, E. F. *J. Biol. Chem.* **176** (1948) 657.
4. Foss, O. and Tjomsland, O. *Acta Chem. Scand.* **11** (1957) 1426.

5. Schotte, L. *Acta Chem. Scand.* **8** (1954) 130.
6. Schotte, L. *Arkiv Kemi* **8** (1955) No. 56.
7. Schotte, L. *Arkiv Kemi* **9** (1956) No. 36.
8. Fredga, A. *Ber.* **71** (1938) 289.
9. Fredga, A. *Arkiv Kemi, Mineral. Geol.* **12 A** (1938) No. 27.
10. Foss, O. and Reistad, T. *Acta Chem. Scand.* **11** (1957) 1427.
11. Scott, D. W. *et al. J. Am. Chem. Soc.* **72** (1950) 2424; **74** (1952) 2478; **76** (1954) 1488.
12. Fredga, A. *Arkiv Kemi, Mineral. Geol.* **11 B** (1933) No. 15.
13. Fredga, A. *Studien über Selen-di-Karbonsäuren und Diselen-di-Karbonsäuren* (Diss.) Uppsala 1935.
14. Schotte, L. *Acta Chem. Scand.* **8** (1954) 131.
15. Schotte, L. *Arkiv Kemi* **9** (1956) No. 34.

Received August 24, 1957.

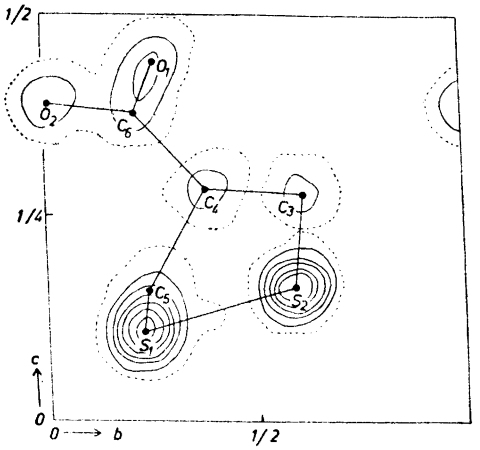


Fig. 1. Electron density projection of 1,2-dithiolane-4-carboxylic acid along the a axis, showing one asymmetric unit (one molecule). Contours at intervals of 3 e · Å^{-2}, beginning with 3 e · Å^{-2} (dashed).

Structure of Crystalline 1,2-Dithiolane-4-carboxylic Acid

OLAV FOSS and OLAV TJOMSLAND

Chemical Institute, University of Bergen, Bergen, Norway

As part of a program for the study of crystal structures of five-, six- and seven-membered cyclic disulphides, with the view of obtaining information about the stereochemistry of the disulphide group in the rings, unit cell and space group determinations have recently been made of some 1,2,4-dithiazolidine derivatives [1] and of some 1,2-dithiolane-, 1,2-dithiane-, 1,2-diselenane- and 1,2-dithiepane-carboxylic acids [2]. Also, the detailed structure of thiuret (3,5-diimino-1,2,4-dithiazolidine) hydroiodide has been worked out [3,4]. The present note gives the preliminary results of a crystal structure determination of 1,2-dithiolane-4-carboxylic acid [5,6].

The crystals are triclinic, with the unit cell dimensions [2], $a = 5.34$ Å, $b = 5.85$ Å, $c = 10.75$ Å, $\alpha = 93\frac{1}{2}°$, $\beta = 89\frac{1}{2}°$, $\gamma = 109\frac{1}{2}°$. The space group is $C_i^1 - P\bar{1}$, and there are two molecules per unit cell. The intensities of the $0kl$ reflections were estimated visually from Weissenberg photographs taken with CuK radiation, and were converted to relative structure factors in the usual way. The positions of the two sulphur atoms were found from a F_0^2 synthesis of the $0kl$ data, and a subsequent F_0 synthesis with signs based on the sulphur contributions showed the outline of the molecule and gave approximate coordinates for the carbon and oxygen atoms. After a few F_0 and $(F_0 - F_c)$ refinements the $0kl$ electron density map is as shown in Fig. 1, and the y and z coordinates as listed in Table 1. The reliability index R is at this stage 15.7 %.

Provided that the chemically equivalent S_1-C_5 and S_2-C_3 bonds and $S_1-S_2-C_3$ and $S_2-S_1-C_5$ bond angles do not have too different dimensions, the a-axis projection shows that the disulphide group of the 1,2-dithiolane ring is not planar. If, pending the determination of the x coordinates through a projection along another axis, the assumption is made that the S—C bond lengths are equal and approximately 1.81 Å, and that the S—S—C bond angles are equal, the y and z coordinates of the sulphur atoms and the C_3 and C_5 atoms lead to a disulphide group with dimensions approximately as follows: S—S bond length = 2.09 Å, S—S—C bond angles = 95°, and CSS/SSC dihedral angle = 20°.

The carboxyl groups of different molecules appear to be arranged around symmetry centres at $z = \frac{1}{2}$, and non-bonded S—S contacts only to occur across the c plane at $z = 0$.

5. Schotte, L. *Acta Chem. Scand.* **8** (1954) 130.
6. Schotte, L. *Arkiv Kemi* **8** (1955) No. 56.
7. Schotte, L. *Arkiv Kemi* **9** (1956) No. 36.
8. Fredga, A. *Ber.* **71** (1938) 289.
9. Fredga, A. *Arkiv Kemi, Mineral. Geol.* **12 A** (1938) No. 27.
10. Foss, O. and Reistad, T. *Acta Chem. Scand.* **11** (1957) 1427.
11. Scott, D. W. *et al. J. Am. Chem. Soc.* **72** (1950) 2424; **74** (1952) 2478; **76** (1954) 1488.
12. Fredga, A. *Arkiv Kemi, Mineral. Geol.* **11 B** (1933) No. 15.
13. Fredga, A. *Studien über Selen-di-Karbonsäuren und Diselen-di-Karbonsäuren* (Diss.) Uppsala 1935.
14. Schotte, L. *Acta Chem. Scand.* **8** (1954) 131.
15. Schotte, L. *Arkiv Kemi* **9** (1956) No. 34.

Received August 24, 1957.

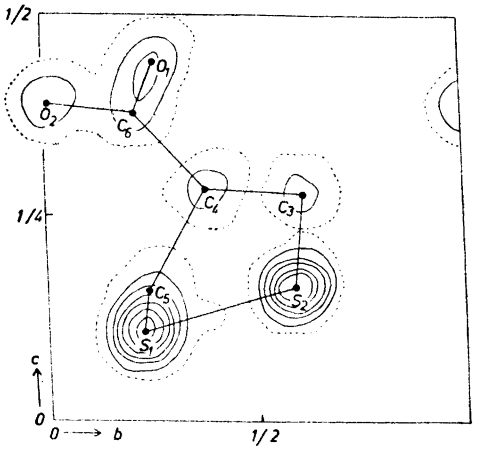


Fig. 1. Electron density projection of 1,2-dithiolane-4-carboxylic acid along the a axis, showing one asymmetric unit (one molecule). Contours at intervals of 3 e · Å^{-2}, beginning with 3 e · Å^{-2} (dashed).

Structure of Crystalline 1,2-Dithiolane-4-carboxylic Acid

OLAV FOSS and OLAV TJOMSLAND

Chemical Institute, University of Bergen, Bergen, Norway

As part of a program for the study of crystal structures of five-, six- and seven-membered cyclic disulphides, with the view of obtaining information about the stereochemistry of the disulphide group in the rings, unit cell and space group determinations have recently been made of some 1,2,4-dithiazolidine derivatives [1] and of some 1,2-dithiolane-, 1,2-dithiane-, 1,2-diselenane- and 1,2-dithiepane-carboxylic acids [2]. Also, the detailed structure of thiuret (3,5-diimino-1,2,4-dithiazolidine) hydroiodide has been worked out [3,4]. The present note gives the preliminary results of a crystal structure determination of 1,2-dithiolane-4-carboxylic acid [5,6].

The crystals are triclinic, with the unit cell dimensions [2], $a = 5.34$ Å, $b = 5.85$ Å, $c = 10.75$ Å, $\alpha = 93\frac{1}{2}°$, $\beta = 89\frac{1}{2}°$, $\gamma = 109\frac{1}{2}°$. The space group is $C_i^1 - P\bar{1}$, and there are two molecules per unit cell. The intensities of the $0kl$ reflections were estimated visually from Weissenberg photographs taken with CuK radiation, and were converted to relative structure factors in the usual way. The positions of the two sulphur atoms were found from a F_0^2 synthesis of the $0kl$ data, and a subsequent F_0 synthesis with signs based on the sulphur contributions showed the outline of the molecule and gave approximate coordinates for the carbon and oxygen atoms. After a few F_0 and $(F_0 - F_c)$ refinements the $0kl$ electron density map is as shown in Fig. 1, and the y and z coordinates as listed in Table 1. The reliability index R is at this stage 15.7 %.

Provided that the chemically equivalent S_1-C_5 and S_2-C_3 bonds and $S_1-S_2-C_3$ and $S_2-S_1-C_5$ bond angles do not have too different dimensions, the a-axis projection shows that the disulphide group of the 1,2-dithiolane ring is not planar. If, pending the determination of the x coordinates through a projection along another axis, the assumption is made that the S—C bond lengths are equal and approximately 1.81 Å, and that the S—S—C bond angles are equal, the y and z coordinates of the sulphur atoms and the C_3 and C_5 atoms lead to a disulphide group with dimensions approximately as follows: S—S bond length = 2.09 Å, S—S—C bond angles = 95°, and CSS/SSC dihedral angle = 20°.

The carboxyl groups of different molecules appear to be arranged around symmetry centres at $z = \frac{1}{2}$, and non-bonded S—S contacts only to occur across the c plane at $z = 0$.

Table 1. Atomic coordinates, in fractions of triclinic cell edges. Origin at a centre of symmetry.

	y	*z*
S_1	0.230	0.108
S_2	0.593	0.164
C_3	0.620	0.280
C_4	0.385	0.286
C_5	0.243	0.161
C_6	0.218	0.379
O_1	0.265	0.443
O_2	0.012	0.390

It is intended to refine the *a*-axis projection further, and to carry out a detailed structure analysis.

The work has been aided by a grant from *L. Meltzers Høyskolefond.*

1. Foss, O. *Acta Chem. Scand.* **10** (1956) 868.
2. Foss, O. and Schotte, L. *Acta Chem. Scand.* **11** (1957) 1424.
3. Foss, O. and Tjomsland, O. *Acta Chem. Scand.* **10** (1956) 869.
4. Foss, O. and Tjomsland, O. *To be published.*
5. Schotte, L. and Ström, H. *Acta Chem. Scand.* **10** (1956) 687.
6. Schotte, L. *Arkiv Kemi* **9** (1956) No. 37.

Received August 24, 1957.

Structure of Crystalline *Racem*-1,2-dithiane-3,6-dicarboxylic Acid

OLAV FOSS and TORBJØRN REISTAD

Chemical Institute, University of Bergen, Bergen, Norway

In two preceding notes [1,2], crystal data on some carboxylic acid derivatives of five-, six- and seven-membered cyclic disulphides, and preliminary results of a crystal structure determination of the five-membered one, 1,2-dithiolane-4-carboxylic acid, have been reported. A corresponding study of a six-membered representative, *racem*-1,2-dithiane-3,6-dicarboxylic acid[3-6], has so far given the following results.

The crystals are monoclinic prismatic, with a four-molecule unit cell based on the space group C_{2h}^6-I2/c, and with the unit cell dimensions [1], $a = 9.62$ Å, $b = 9.26$ Å, $c = 9.70$ Å, $\beta = 102\frac{1}{2}°$. The correctness of the centrosymmetric space group was first assumed, and confirmed through the subsequent work. The intensities of the *h0l* reflections were estimated visually from Weissenberg photographs taken with Cu*K* radiation; 51 reflections out of 57 attainable were recorded with measurable intensities. The position of the one sulphur atom of the asymmetric unit was derived

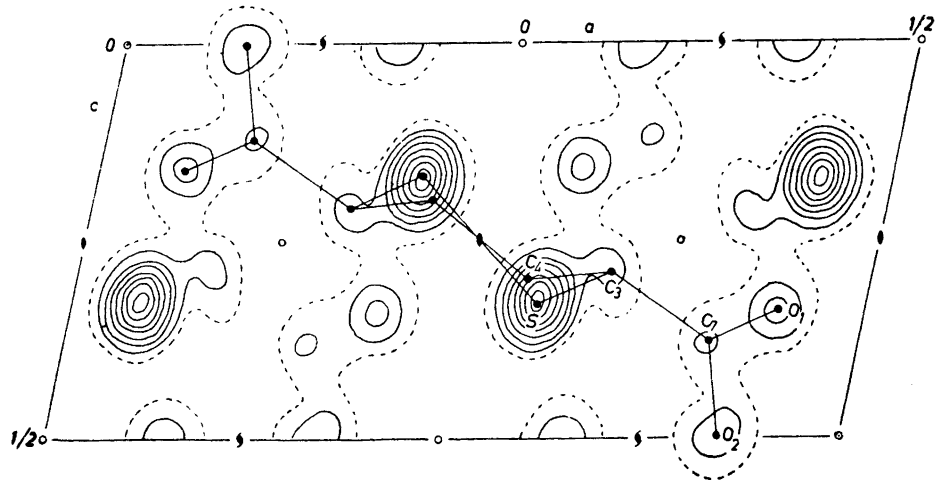


Fig. 1. Electron density projection of *racem*-1,2-dithiane-3,6-dicarboxylic acid along the *b* axis. Four asymmetric units (half a unit cell) are shown, and lines are drawn to indicate the outline of one molecule. Contours at intervals of 3 e · Å^{-2}, beginning with 4 e · Å^{-2} (dashed).

Table 1. Atomic coordinates, in fractions of triclinic cell edges. Origin at a centre of symmetry.

	y	*z*
S_1	0.230	0.108
S_2	0.593	0.164
C_3	0.620	0.280
C_4	0.385	0.286
C_5	0.243	0.161
C_6	0.218	0.379
O_1	0.265	0.443
O_2	0.012	0.390

It is intended to refine the *a*-axis projection further, and to carry out a detailed structure analysis.

The work has been aided by a grant from *L. Meltzers Høyskolefond.*

1. Foss, O. *Acta Chem. Scand.* **10** (1956) 868.
2. Foss, O. and Schotte, L. *Acta Chem. Scand.* **11** (1957) 1424.
3. Foss, O. and Tjomsland, O. *Acta Chem. Scand.* **10** (1956) 869.
4. Foss, O. and Tjomsland, O. *To be published.*
5. Schotte, L. and Ström, H. *Acta Chem. Scand.* **10** (1956) 687.
6. Schotte, L. *Arkiv Kemi* **9** (1956) No. 37.

Received August 24, 1957.

Structure of Crystalline *Racem*-1,2-dithiane-3,6-dicarboxylic Acid

OLAV FOSS and TORBJØRN REISTAD

Chemical Institute, University of Bergen, Bergen, Norway

In two preceding notes [1,2], crystal data on some carboxylic acid derivatives of five-, six- and seven-membered cyclic disulphides, and preliminary results of a crystal structure determination of the five-membered one, 1,2-dithiolane-4-carboxylic acid, have been reported. A corresponding study of a six-membered representative, *racem*-1,2-dithiane-3,6-dicarboxylic acid[3-6], has so far given the following results.

The crystals are monoclinic prismatic, with a four-molecule unit cell based on the space group C_{2h}^6-I2/c, and with the unit cell dimensions [1], $a = 9.62$ Å, $b = 9.26$ Å, $c = 9.70$ Å, $\beta = 102\frac{1}{2}°$. The correctness of the centrosymmetric space group was first assumed, and confirmed through the subsequent work. The intensities of the *h0l* reflections were estimated visually from Weissenberg photographs taken with Cu*K* radiation; 51 reflections out of 57 attainable were recorded with measurable intensities. The position of the one sulphur atom of the asymmetric unit was derived

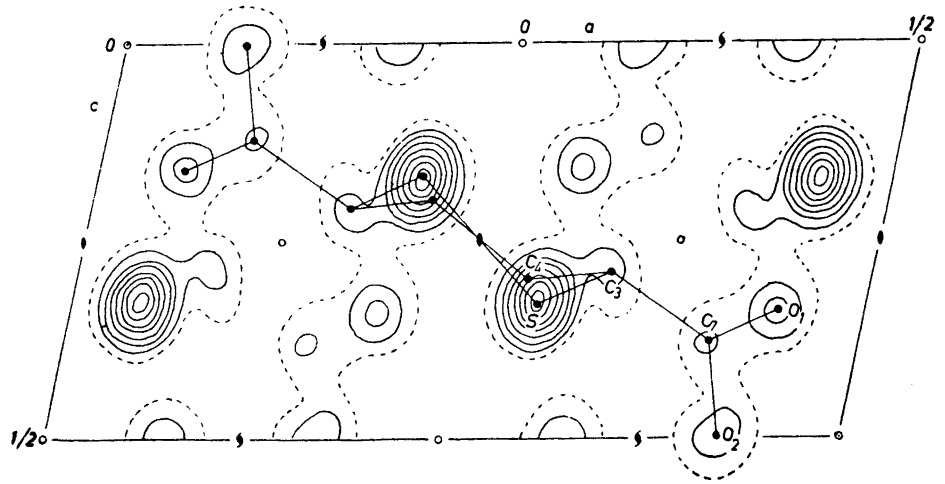


Fig. 1. Electron density projection of *racem*-1,2-dithiane-3,6-dicarboxylic acid along the *b* axis. Four asymmetric units (half a unit cell) are shown, and lines are drawn to indicate the outline of one molecule. Contours at intervals of 3 e · Å^{-2}, beginning with 4 e · Å^{-2} (dashed).

from a F_0^2 synthesis of the *h0l* data, and the sulphur atom then served as a heavy atom for the determination of the carbon and oxygen positions through F_0 syntheses. Refinement was carried out by means of successive (F_0-F_c) syntheses, and led to a standard deviation in electron density of about 0.45 e · Å^{-2} for the *h0l* zone, and a corresponding reliability index R of 10.4 %.

The *h0l* electron density map is shown in Fig. 1, and the x and z coordinates are listed in Table 1. They give a S—S bond length of 2.069 Å across the twofold axis, with an estimated standard deviation of about 0.014 Å.

Table 1. Atomic coordinates, in fractions of monoclinic cell edges. Origin at a centre of symmetry.

	x	z
S	0.0885	0.3325
C_3	0.173	0.292
C_4	0.070	0.302
C_7	0.313	0.379
O_1	0.393	0.342
O_2	0.348	0.499

The molecule possesses, by space group requirements, a twofold axis of symmetry. The 1,2-dithiane ring occurs in the chair form, and has the substituents in equatorial positions. The difference maps indicated a pronounced anisotropic thermal vibration for the sulphur atom. In the temperature factor $\exp[-B(\sin^2\Theta/\lambda^2)]$ finally chosen B was 4.0 Å^2 for the carbon and oxygen atoms and $(6.5-4.0\sin^2\varphi)$ Å^2 for the sulphur atom, where φ is the angle between the normal of the reflecting plane and the direction of maximum vibration of the atom. This direction lies about 16° from c in the acute angle, and is very close to the axial direction of the 1,2-dithiane ring, *i. e.*, to the direction of movement of the atom for conversion of the ring.

The work will be continued, and details published later.

1. Foss, O. and Schotte, L. *Acta Chem. Scand.* **11** (1957) 1424.
2. Foss, O. and Tjomsland, O. *Acta Chem. Scand.* **11** (1957) 1426.
3. Fredga, A. *Ber.* **71** (1938) 289.
4. Fredga, A. *Arkiv Kemi, Mineral. Geol.* **12 A** (1938) No. 27.
5. Schotte, L. *Arkiv Kemi* **8** (1955) No. 56.
6. Schotte, L. *Arkiv Kemi* **9** (1956) No. 37.

Received August 24, 1957.

Aberrations Chromosomiques Produites dans des Graines par de Hautes Pressions d'Oxygène

L. EHRENBERG, J. MOUTSCHEN-DAHMEN * et M. MOUTSCHEN-DAHMEN **

Institut de chimie organique et de biochimie, Université de Stockholm; Institut de recherche forestière, Département de génétique, Stockholm 51, Suède

En 1951, Conger et Fairchild ont trouvé que l'oxygène pur produit des aberrations chromosomiques dans les microspores de *Tradescantia* [1].

Dans d'autres expériences, des résultats contradictoires ont été obtenus [2]. Ceci peut indiquer que, alors que l'oxygène, sous certaines conditions, est capable de casser les chromosomes, le matériel biologique change dans son aptitude à résister à cet effet.

Dans une étude biochimique des mutations spontanées et de leurs mécanismes, nous nous sommes posé la question de savoir si l'oxygène peut produire des aberrations chromosomiques dans les graines de plantes supérieures.

Méthodes. Des graines sèches d'orge var. *Bonus*, dont la teneur en eau est de 11 %, ont été traitées pendant une ou deux semaines, respectivement, dans une bombe de fer sous 60 atmosphères de pression d'oxygène. Dans le but d'étudier l'effet d'une haute pression, *per se*, une expérience parallèle fût réalisée avec 60 atmosphères d'azote. Lors de ces traitements, on a pris soin de changer la pression très lentement afin d'éviter les effets thermiques.

Après une semaine de traitement, les graines sons mises à germer. Les pointes de racines sont fixées 30 à 90 h après la fin du traitement afin de pouvoir observer les successions des trois premières mitoses consécutives au traitement.

Après le traitement de deux semaines, nous avons attendu un délai de trois semaines avant de les mettre à germer.

---

* Chargé de recherche au *Fonds National belge de la Recherche Scientifique* (F.N.R.S.).

** Chargée de recherche à *l'Institut pour l'encouragement de la Recherche Scientifique dans l'Industrie et l'Agriculture* (I.R.S.I.A.).

from a F_0^2 synthesis of the *h0l* data, and the sulphur atom then served as a heavy atom for the determination of the carbon and oxygen positions through F_0 syntheses. Refinement was carried out by means of successive (F_0-F_c) syntheses, and led to a standard deviation in electron density of about 0.45 e · Å^{-2} for the *h0l* zone, and a corresponding reliability index R of 10.4 %.

The *h0l* electron density map is shown in Fig. 1, and the x and z coordinates are listed in Table 1. They give a S—S bond length of 2.069 Å across the twofold axis, with an estimated standard deviation of about 0.014 Å.

Table 1. Atomic coordinates, in fractions of monoclinic cell edges. Origin at a centre of symmetry.

	x	z
S	0.0885	0.3325
C_3	0.173	0.292
C_4	0.070	0.302
C_7	0.313	0.379
O_1	0.393	0.342
O_2	0.348	0.499

The molecule possesses, by space group requirements, a twofold axis of symmetry. The 1,2-dithiane ring occurs in the chair form, and has the substituents in equatorial positions. The difference maps indicated a pronounced anisotropic thermal vibration for the sulphur atom. In the temperature factor $\exp[-B(\sin^2\Theta/\lambda^2)]$ finally chosen B was 4.0 Å^2 for the carbon and oxygen atoms and $(6.5-4.0\sin^2\varphi)$ Å^2 for the sulphur atom, where φ is the angle between the normal of the reflecting plane and the direction of maximum vibration of the atom. This direction lies about 16° from c in the acute angle, and is very close to the axial direction of the 1,2-dithiane ring, *i. e.*, to the direction of movement of the atom for conversion of the ring.

The work will be continued, and details published later.

1. Foss, O. and Schotte, L. *Acta Chem. Scand.* **11** (1957) 1424.
2. Foss, O. and Tjomsland, O. *Acta Chem. Scand.* **11** (1957) 1426.
3. Fredga, A. *Ber.* **71** (1938) 289.
4. Fredga, A. *Arkiv Kemi, Mineral. Geol.* **12 A** (1938) No. 27.
5. Schotte, L. *Arkiv Kemi* **8** (1955) No. 56.
6. Schotte, L. *Arkiv Kemi* **9** (1956) No. 37.

Received August 24, 1957.

Aberrations Chromosomiques Produites dans des Graines par de Hautes Pressions d'Oxygène

L. EHRENBERG, J. MOUTSCHEN-DAHMEN * et M. MOUTSCHEN-DAHMEN **

Institut de chimie organique et de biochimie, Université de Stockholm; Institut de recherche forestière, Département de génétique, Stockholm 51, Suède

En 1951, Conger et Fairchild ont trouvé que l'oxygène pur produit des aberrations chromosomiques dans les microspores de *Tradescantia* [1].

Dans d'autres expériences, des résultats contradictoires ont été obtenus [2]. Ceci peut indiquer que, alors que l'oxygène, sous certaines conditions, est capable de casser les chromosomes, le matériel biologique change dans son aptitude à résister à cet effet.

Dans une étude biochimique des mutations spontanées et de leurs mécanismes, nous nous sommes posé la question de savoir si l'oxygène peut produire des aberrations chromosomiques dans les graines de plantes supérieures.

Méthodes. Des graines sèches d'orge var. *Bonus*, dont la teneur en eau est de 11 %, ont été traitées pendant une ou deux semaines, respectivement, dans une bombe de fer sous 60 atmosphères de pression d'oxygène. Dans le but d'étudier l'effet d'une haute pression, *per se*, une expérience parallèle fût réalisée avec 60 atmosphères d'azote. Lors de ces traitements, on a pris soin de changer la pression très lentement afin d'éviter les effets thermiques.

Après une semaine de traitement, les graines sons mises à germer. Les pointes de racines sont fixées 30 à 90 h après la fin du traitement afin de pouvoir observer les successions des trois premières mitoses consécutives au traitement.

Après le traitement de deux semaines, nous avons attendu un délai de trois semaines avant de les mettre à germer.

---

* Chargé de recherche au *Fonds National belge de la Recherche Scientifique* (F.N.R.S.).

** Chargée de recherche à *l'Institut pour l'encouragement de la Recherche Scientifique dans l'Industrie et l'Agriculture* (I.R.S.I.A.).

Tableau 1.

Traitement		Cassures par métaphase	Cassures par anaphase	Ponts par anaphase	Nombre de cellules en méta- ou anaphase
O_2	1 semaine	0.102	0.021	0	600
	2 semaines	0.213	0.041	0.03	600
N_2	2 semaines	0	0	0	600

Le fixateur utilisé est le mélange de Çarnoy et les observations sont effectuées en "Feulgen-squashes".

Résultats. Nous avons observé les effets suivants:

Après une semaine de traitement par O_2, la première mitose consécutive au traitement montre une profusion d'effets primaires fortement marqués. De l'érosion chromosomique parfois discrète mais plus fréquemment généralisée se présente dans environ 45 % des anaphases et des métaphases. Du collage "stickiness" des chromosomes est observé en métaphases et en anaphases et les "pseudo-ponts" sont très peu abondants (0.12 % des anaphases sticky).

Dans les figures mitotiques perturbées, les chromosomes sont souvent effilochés et fréquemment hyper-colorés et montrent dès lors, une structure en "lamp-brush"[3]. Cet effet fréquemment considéré comme étant nécrotique s'est néanmoins montré réversible et labile. Lors de la première mitose, les effets primaires sont donc présents dans environ 90 % des mitoses. Lors de la seconde mitose après le traitement, on ne note plus de l'érosion que dans environ 30 % des métaphases et anaphases.

Pour le traitement pendant 2 semaines, aucun phénomène précédemment décrit n'a pu être observé lors de la première mitose à l'exception de l'érosion chromosomique présente dans 45 % des cas. Nous avons attribué cette absence au temps de latence entre la fin du traitement et la mise en germination. Pour les deux temps de traitement, lors de la seconde mitose consécutive à ces traitements, nous avons observé des effets radio-mimétiques résumés dans le Tableau 1.

Ce tableau montre que les effets radiomimétiques (cassures métaphasiques et anaphasiques avec quelques ponts vrais) ont augmenté avec le temps de traitement. Aucun effet analogue n'a été observé chez le témoin sous N_2. Chez celui-ci, la première mitose montre seulement une certaine fréquence (40—50 %) d'érosion chromosomique parfois assez marquée. Il est donc probable qu'une partie au moins des perturbations cellulaires conduisant à des modifications matricielles soient imputables à un effet de pression mais il n'en est pas de même en ce qui concerne les effets radio-mimétiques.

Il est donc démontré qu'un traitement par l'oxygène à de très hautes pressions (60 atmosphères étant 300 fois la pression du milieu normal) produit un nombre d'aberrations appréciable: 0.1 des secondes métaphases perturbées correspond à l'effet d'une dose de rayons X d'environ 1 000 r appliquée à des graines ayant la même teneur en eau. L'effet semble d'autant plus remarquable que la fréquence d'aberrations spontanées chez l'orge est extrêmement basse. L'effet semble plutôt général étant donné que, après des traitements similaires sur des graines de légumineuses (*Pisum sativum* et *Vicia faba*), les feuilles de ces plantes montrent des fréquences accrues des types de panachures qui pourraient être imputées à des aberrations chromosomiques [4,5].

Cette recherche a été subsidiée par le *Conseil national suédois de la recherche agronomique.*

1. Conger, A. D. et Fairchild, L. M. *Genetics* **36** (1951) 547: *Proc. Nat. Acad. Sci.* **38** (1952) 289.

2. *cfr.* Giles, N. H. Jr. in Hollaender, A. *Radiation Biology* I, New York 1954, p. 745.
3. Ris, H. in Mc Elroy, N.D. and Glass B. *Chemical Basis of Heredity*, Johns Hopkins Press, Baltimore 1957 p. 48.
4. Kaplan, R. W. *Strahlentherapie* **94** (1954) 106.
5. Zacharias, M. *à publier in Hereditas* (1958).

Manuscrit reçu le 12 Septembre 1957.

Preparation of the Laevorotatory Enantiomer of Methylallylacetic Acid

GUNNEL STÄLLBERG

Department of Medical Biochemistry, Institute of Medical Chemistry, University of Uppsala, Uppsala, Sweden

The dextrorotatory form of methylallylacetic acid ((+)-2L-methyl-$\Delta^{4:5}$-pentenoic acid) was first obtained by Ställberg-Stenhagen [1] by resolution of the racemic acid *via* the quinine salt. The configuration was determined by Ställberg-Stenhagen and Stenhagen [2], who oxidized the (+)-acid to (−)-methylsuccinic acid. The laevorotatory enantiomer has so far not been reported in the literature. In connection with work on the synthesis of phthiocerol in this laboratory, both enantiomers were needed for the synthesis of the different stereoisomeric forms of the 3-methoxy-4-methyl-grouping of the phthiocerol molecule [3]. It has now been found that the laevorotatory enantiomer of methylallylacetic acid ((−)-2D-methyl-$\Delta^{4:5}$-pentenoic acid) can be obtained *via* the (+)-1-phenylethylamine salt. The optical rotation found was numerically equal to that reported for the dextrorotatory enantiomer [4,5].

Experimental. (−)-2D-*Methyl-*$\Delta^{4:5}$*-pentenoic acid.* Partially resolved laevorotatory acid (43 g, a_D^{25} −5.3° (undiluted, *l* 1)), obtained from the mother liquor of the first crystallization of the quinine salt of the dextrorotatory enantiomer, was dissolved in ether (700 ml) and a solution of (+)-phenylethylamine (44.5 g) in ether (800 ml) was added cautiously (heat is evolved during the formation of the salt). Crystallization was allowed to take place overnight at a temperature of −15°. The salt crystallized in the form of long thin needles. Acid isolated from the mother liquor of this crystallization had an optical rotation of a_D^{25} −2.2° (undiluted, *l* 1). The salt was recrystallized from successively smaller volumes of ether and the course of the resolution followed by measuring the rotation of acid isolated from the mother liquors. Nine crystallizations were needed before the rotation attained the constant value a_D^{25} −7.80° (undiluted, *l* 1). Decomposition of the salt gave 6.6 g of (−)-methylallylacetic acid of b.p. 87−88° at 12 mm; n_D^{25} 1.4275, n_D^{18} 1.4305; d_4^{25} 0.946; R_D calcd. 31.02, found 31.01.

Optical rotation: a_D^{25} −7.80° (undiluted, *l* 1); $[\alpha]_D^{25}$ −8.25°; $[M]_D^{25}$ −9.41°.

The specimen of the dextrorotatory enantiomer, prepared in the course of the present work had $[\alpha]_D^{25}$ +8.25°. Ställberg-Stenhagen [4] gives a_D^{20} +7.88° (undiluted, *l* 1), which corresponds to $[\alpha]_D^{20}$ +8.28°. Fray and Polgar [5] give $[\alpha]_D^{19}$ +8.24°.

I am indebted to Prof. A. Fredga for placing the (+)-phenylethylamine used at my disposal. The expenses involved in this work were defrayed by a grant from *Statens Medicinska Forskningsråd* to Prof. E. Stenhagen.

1. Ställberg-Stenhagen, S. *Arkiv Kemi, Mineral. Geol.* **23 A** (1946) No. 15.
2. Ställberg-Stenhagen, S. and Stenhagen, E. *Arkiv Kemi, Mineral. Geol.* **24 B** (1947) No. 9.
3. Ryhage, R., Stenhagen, E. and von Sydow, E. *Acta Chem. Scand.* **11** (1957) 180.
4. Ställberg-Stenhagen, S. *Arkiv Kemi* **1** (1949) 153.
5. Fray, G. I. and Polgar, N. *J. Chem. Soc.* **1956** 2036.

Received September 10, 1957.

2. *cfr.* Giles, N. H. Jr. in Hollaender, A. *Radiation Biology* I, New York 1954, p. 745.
3. Ris, H. in Mc Elroy, N.D. and Glass B. *Chemical Basis of Heredity*, Johns Hopkins Press, Baltimore 1957 p. 48.
4. Kaplan, R. W. *Strahlentherapie* **94** (1954) 106.
5. Zacharias, M. *à publier in Hereditas* (1958).

Manuscrit reçu le 12 Septembre 1957.

Preparation of the Laevorotatory Enantiomer of Methylallylacetic Acid

GUNNEL STÄLLBERG

Department of Medical Biochemistry, Institute of Medical Chemistry, University of Uppsala, Uppsala, Sweden

The dextrorotatory form of methylallylacetic acid ((+)-2L-methyl-$\Delta^{4:5}$-pentenoic acid) was first obtained by Ställberg-Stenhagen [1] by resolution of the racemic acid *via* the quinine salt. The configuration was determined by Ställberg-Stenhagen and Stenhagen [2], who oxidized the (+)-acid to (−)-methylsuccinic acid. The laevorotatory enantiomer has so far not been reported in the literature. In connection with work on the synthesis of phthiocerol in this laboratory, both enantiomers were needed for the synthesis of the different stereoisomeric forms of the 3-methoxy-4-methyl-grouping of the phthiocerol molecule [3]. It has now been found that the laevorotatory enantiomer of methylallylacetic acid ((−)-2D-methyl-$\Delta^{4:5}$-pentenoic acid) can be obtained *via* the (+)-1-phenylethylamine salt. The optical rotation found was numerically equal to that reported for the dextrorotatory enantiomer [4,5].

Experimental. (−)-2D-*Methyl-*$\Delta^{4:5}$*-pentenoic acid.* Partially resolved laevorotatory acid (43 g, a_D^{25} −5.3° (undiluted, *l* 1)), obtained from the mother liquor of the first crystallization of the quinine salt of the dextrorotatory enantiomer, was dissolved in ether (700 ml) and a solution of (+)-phenylethylamine (44.5 g) in ether (800 ml) was added cautiously (heat is evolved during the formation of the salt). Crystallization was allowed to take place overnight at a temperature of −15°. The salt crystallized in the form of long thin needles. Acid isolated from the mother liquor of this crystallization had an optical rotation of a_D^{25} −2.2° (undiluted, *l* 1). The salt was recrystallized from successively smaller volumes of ether and the course of the resolution followed by measuring the rotation of acid isolated from the mother liquors. Nine crystallizations were needed before the rotation attained the constant value a_D^{25} −7.80° (undiluted, *l* 1). Decomposition of the salt gave 6.6 g of (−)-methylallylacetic acid of b.p. 87−88° at 12 mm; n_D^{25} 1.4275, n_D^{18} 1.4305; d_4^{25} 0.946; R_D calcd. 31.02, found 31.01.

Optical rotation: a_D^{25} −7.80° (undiluted, *l* 1); $[\alpha]_D^{25}$ −8.25°; $[M]_D^{25}$ −9.41°.

The specimen of the dextrorotatory enantiomer, prepared in the course of the present work had $[\alpha]_D^{25}$ +8.25°. Ställberg-Stenhagen [4] gives a_D^{20} +7.88° (undiluted, *l* 1), which corresponds to $[\alpha]_D^{20}$ +8.28°. Fray and Polgar [5] give $[\alpha]_D^{19}$ +8.24°.

I am indebted to Prof. A. Fredga for placing the (+)-phenylethylamine used at my disposal. The expenses involved in this work were defrayed by a grant from *Statens Medicinska Forskningsråd* to Prof. E. Stenhagen.

1. Ställberg-Stenhagen, S. *Arkiv Kemi, Mineral. Geol.* **23 A** (1946) No. 15.
2. Ställberg-Stenhagen, S. and Stenhagen, E. *Arkiv Kemi, Mineral. Geol.* **24 B** (1947) No. 9.
3. Ryhage, R., Stenhagen, E. and von Sydow, E. *Acta Chem. Scand.* **11** (1957) 180.
4. Ställberg-Stenhagen, S. *Arkiv Kemi* **1** (1949) 153.
5. Fray, G. I. and Polgar, N. *J. Chem. Soc.* **1956** 2036.

Received September 10, 1957.

α-Keto Acids in Cultures of Lactic and Propionic Acid Bacteria and in some Cheese Varieties

MATTI KREULA and ARTTURI I. VIRTANEN

Laboratory of Valio, Biochemical Institute, Helsinki, Finland

Using the same method (hydrogenolysis of 2,4-dinitrophenylhydrazones with tin in hydrochloric acid solution to the corresponding amino acids and establishing these by paper chromatography) as Alfthan and Virtanen used for the estimation of many new keto acids in plants, the present authors established the α-keto acids shown in Table 1 in cultures of lactic and propionic acid bacteria as well as in some cheese varieties. When determining keto acids in the nutrient and culture solutions, proteins were first removed by adding 10 % solution of sodium tungstate and 2/3 N sulphuric acid in the proportion test solution: tungstate solution:sulphuric acid 2:1:2 (v/v). 200 ml of test solution was generally used. The filtrate was further treated according to Alfthan and Virtanen [1] (*cf.* also Kreula and Virtanen [2]). When investigating cheese, "tear fluid", and yeast, 100 ml of 10 % sodium tungstate and 14 ml of 5 N sulphuric acid were added to 50 g of the substance to be investigated. The mixture was diluted with water to 500 ml, homogenized, and filtered. The filtrate was treated as mentioned in connection with bacterial cultures.

Table 1. The corresponding amino acids of α-keto acids found in bacterial cultures, yeast, and some cheese varieties.

Material	Corresponding amino acids of α-keto acids *
Lactic acid bacteria	
Milk	1, 2, 8, 17
Milk + *Streptococcus thermophilus* (45°C, 1 day)	1, 2, 8, 17
Milk + *Lactobacillus helveticus* (42°C, 1 day)	1, 2, (3), (5), 8, (9), 16, 17
Propionic acid bacteria	
Nutrient solution (whey fermented with *L. helveticus*, addition of chalk, + yeast extract + peptone; pH 6.5)	1, 2, 16, 17
Nutrient solution + *Propionibacterium* V (30°C, 3 days)	2, 3, 7, 16, *17*
Nutrient solution + *Propionibacterium* V (30°C, 3 days)	1, *2*, 7, 16, 17
Nutrient solution + *Propionibacterium* V (30°C, 16 days)	1, 2, 8, 16, 17
Nutrient solution + *Propionibacterium* 101 (30°C, 16 days)	1, 2, 8, 16, 17
Nutrient solution + *Propionibacterium* V (30°C, 29 days)	2, 17
Baker's yeast	1, 2, 8, 17
Cheeses	
Emmental cheese, 3 months old	1, *2*, 8, 16, 17
Emmental cheese, 6 months old	1, 2, 8, 16, 17
Emmental cheese, over 12 months old	1, 2, 3, 5, 8, 16, 17
"Tear fluid" of Emmental cheese	2, 3, 17
Mouldy cheese (Roquefort)	1, 2, 3, 4, 5, 16, 17

* The keto acids are: 1 = glyoxylic acid, 2 = pyruvic acid, 3 = α-keto*iso*valeric acid, 4 = α-keto*iso*capronic acid, 5 = α-ketocapronic acid, 7 = *para*-OH-phenylpyruvic acid, 8 = OH-pyruvic acid, 9 = β-OH-butyric acid, 16 = oxalacetic acid, 17 = α-ketoglutaric acid; italics = +++, parenthesis = +.

As can be seen from Table 1 new keto acids, in addition to 1, 2, 8, and 17, originally found in milk, were not found in the milk culture of *Str. thermophilus*, whereas in the culture of *L. helveticus* small amounts of 3, 5, and 9, and a larger amount of 16 were found. In the culture solution of propionic acid bacteria keto acid 7 was found after 3 days in addition to 1, 2, 16, and 17 which were present in the nutrient solution from the beginning, after 16 days keto acid 8, whereas after 19 days only keto acids 2 and 17 remained.

3- to 6-month-old Emmental cheese contains keto acids 1, 2, 8, 16, and 17; 12-month-old Emmental cheese keto acids 3 and 5 in addition. In the fluid secreted in the eyes of older cheese only keto acids 2, 3, and 17 were found.

In mouldy cheese (Roquefort) keto acids 1, 2, 3, 4, 5, 16, and 17 were found.

1. Alfthan, M. and Virtanen, A. I. *Acta Chem. Scand.* **9** (1955) 86.
2. Kreula, M. and Virtanen, A. I. *Proceedings of the XIVth International Dairy Congress*, Roma **1** (1956) 802.

Received July 25, 1957.

Über einen antifungalen Faktor aus den grünen Teilen der Heidelbeerpflanze *(Vaccinium myrtillus)*

K. RAIBLE* und ARTTURI I. VIRTANEN

Laboratorium der Stiftung für chemische Forschung, Biochemisches Institut, Helsinki, Finnland

In früheren Arbeiten aus diesem Laboratorium konnte gezeigt werden, dass alle bisher untersuchten Kulturpflanzen Stoffe enthalten, die das Wachstum des pflanzenpathogenen Pilzes *Fusarium nivale* und vieler anderer Pilze zu hemmen vermögen, und dass mit der Anwesenheit solcher Stoffe die Resistenz bezw. die Anfälligkeit der betreffenden Pflanze gegenüber dem genannten Mikroorganismus erklärt werden kann [1]. Aktive Substanzen sind bisher in reinem Zustand aus jungen Roggen[2]-, Weizen- und Maispflanzen [3] sowie auch aus Rotklee [4] isoliert und chemisch charakterisiert worden. Wir haben in lezter Zeit auch einige wilde Pflanzen auf das Vorkommen antifungaler Substanzen untersucht. In den grünen Teilen der Heidelbeerpflanze *(Vaccinium myrtillus)* haben wir eine ungewöhnlich hohe Aktivität gegen *Fusarium nivale* gefunden. Die Aktivität ist im frischen Laub während der Frühjahrsmonate ebenso nachzuweisen wie in altem Laub und auch in den Stengeln während des Winters, wobei auch stets die Menge an dem aktiven Stoff etwa die gleiche ist. Die antifungale Wirksamkeit 70 % alkoholischer Extrakte (Pressäfte können wegen des geringen Wassergehaltes der Pflanzen meist nur in unzureichendem Mass gewonnen werden) beträgt etwa 15 Einheiten, d.h. aus 1 g Pflanzenmaterial gewonnener Extrakt reicht aus um das Wachstum von *Fusarium nivale* auf 15 ml Hafermehlagarmedium völlig zu hemmen. Zusammensetzung des Mediums: 50 g Hafermehl, 5 ml Glycerin, 1,5 ml Milchsäure, 7 g $KHPO_4$, 35 ml 0,2 M Na_2HPO_4-Lösung, 1 000 ml Wasser. pH des Mediums 4,7—4,8.

Untersuchungen über die Art des antifungalen Faktors ergaben, dass es sich hierbei offenbar um eine gerbstoffartige Substanz oder um ein Gemisch von solchen Stoffen handelt. Der antifungale Faktor ist gut löslich in Wasser, Äthanol, Methanol und Aceton, unlöslich hingegen in wasserfreiem Äther, Petroläther und Benzol. Die Substanz reagiert neutral und passiert daher sowohl den saueren Amberlite-Jonenaustauscher IR 120 als auch die stark basischen Harze IRA 410 und IRA 400.

Aktive Extrakte mit 10—15 Einheiten pro 1 g Pflanzenmaterial konnten erhalten werden beim Variieren der Extraktionsmethoden und -temperaturen wie folgt:

1) 100 g Pflanzenmaterial + 500 ml 60 % Äthanol, 3 Std digeriert, abgepresst, Presskuchen nochmals ebenso behandelt.
2) Wie 1, jedoch 12—14 Std digeriert bei Zimmertemperatur oder bei —5°C.
3) 100 g Pflanzenmaterial + 1 l Methanol 12 und 48 Std digeriert, dann weiter wie bei 1.
4) Wie 3, jedoch Zusatz von 5 und auch 10 g K-metabisulfit (Extrakt vor dem Test selbstverständlich durch sauren und basischen Jonenaustauscher geleitet).

* Die jetzige Adresse: Deutsche Forschungsanstalt für Lebensmittelchemie, München 23, Leopoldstrasse 175, Deutschland.

As can be seen from Table 1 new keto acids, in addition to 1, 2, 8, and 17, originally found in milk, were not found in the milk culture of *Str. thermophilus*, whereas in the culture of *L. helveticus* small amounts of 3, 5, and 9, and a larger amount of 16 were found. In the culture solution of propionic acid bacteria keto acid 7 was found after 3 days in addition to 1, 2, 16, and 17 which were present in the nutrient solution from the beginning, after 16 days keto acid 8, whereas after 19 days only keto acids 2 and 17 remained.

3- to 6-month-old Emmental cheese contains keto acids 1, 2, 8, 16, and 17; 12-month-old Emmental cheese keto acids 3 and 5 in addition. In the fluid secreted in the eyes of older cheese only keto acids 2, 3, and 17 were found.

In mouldy cheese (Roquefort) keto acids 1, 2, 3, 4, 5, 16, and 17 were found.

1. Alfthan, M. and Virtanen, A. I. *Acta Chem. Scand.* **9** (1955) 86.
2. Kreula, M. and Virtanen, A. I. *Proceedings of the XIVth International Dairy Congress*, Roma **1** (1956) 802.

Received July 25, 1957.

Über einen antifungalen Faktor aus den grünen Teilen der Heidelbeerpflanze *(Vaccinium myrtillus)*

K. RAIBLE* und ARTTURI I. VIRTANEN

Laboratorium der Stiftung für chemische Forschung, Biochemisches Institut, Helsinki, Finnland

In früheren Arbeiten aus diesem Laboratorium konnte gezeigt werden, dass alle bisher untersuchten Kulturpflanzen Stoffe enthalten, die das Wachstum des pflanzenpathogenen Pilzes *Fusarium nivale* und vieler anderer Pilze zu hemmen vermögen, und dass mit der Anwesenheit solcher Stoffe die Resistenz bezw. die Anfälligkeit der betreffenden Pflanze gegenüber dem genannten Mikroorganismus erklärt werden kann [1]. Aktive Substanzen sind bisher in reinem Zustand aus jungen Roggen[2]-, Weizen- und Maispflanzen [3] sowie auch aus Rotklee [4] isoliert und chemisch charakterisiert worden. Wir haben in lezter Zeit auch einige wilde Pflanzen auf das Vorkommen antifungaler Substanzen untersucht. In den grünen Teilen der Heidelbeerpflanze *(Vaccinium myrtillus)* haben wir eine ungewöhnlich hohe Aktivität gegen *Fusarium nivale* gefunden. Die Aktivität ist im frischen Laub während der Frühjahrsmonate ebenso nachzuweisen wie in altem Laub und auch in den Stengeln während des Winters, wobei auch stets die Menge an dem aktiven Stoff etwa die gleiche ist. Die antifungale Wirksamkeit 70 % alkoholischer Extrakte (Pressäfte können wegen des geringen Wassergehaltes der Pflanzen meist nur in unzureichendem Mass gewonnen werden) beträgt etwa 15 Einheiten, d.h. aus 1 g Pflanzenmaterial gewonnener Extrakt reicht aus um das Wachstum von *Fusarium nivale* auf 15 ml Hafermehlagarmedium völlig zu hemmen. Zusammensetzung des Mediums: 50 g Hafermehl, 5 ml Glycerin, 1,5 ml Milchsäure, 7 g $KHPO_4$, 35 ml 0,2 M Na_2HPO_4-Lösung, 1 000 ml Wasser. pH des Mediums 4,7—4,8.

Untersuchungen über die Art des antifungalen Faktors ergaben, dass es sich hierbei offenbar um eine gerbstoffartige Substanz oder um ein Gemisch von solchen Stoffen handelt. Der antifungale Faktor ist gut löslich in Wasser, Äthanol, Methanol und Aceton, unlöslich hingegen in wasserfreiem Äther, Petroläther und Benzol. Die Substanz reagiert neutral und passiert daher sowohl den saueren Amberlite-Jonenaustauscher IR 120 als auch die stark basischen Harze IRA 410 und IRA 400.

Aktive Extrakte mit 10—15 Einheiten pro 1 g Pflanzenmaterial konnten erhalten werden beim Variieren der Extraktionsmethoden und -temperaturen wie folgt:

1) 100 g Pflanzenmaterial + 500 ml 60 % Äthanol, 3 Std digeriert, abgepresst, Presskuchen nochmals ebenso behandelt.
2) Wie 1, jedoch 12—14 Std digeriert bei Zimmertemperatur oder bei —5°C.
3) 100 g Pflanzenmaterial + 1 l Methanol 12 und 48 Std digeriert, dann weiter wie bei 1.
4) Wie 3, jedoch Zusatz von 5 und auch 10 g K-metabisulfit (Extrakt vor dem Test selbstverständlich durch sauren und basischen Jonenaustauscher geleitet).

* Die jetzige Adresse: Deutsche Forschungsanstalt für Lebensmittelchemie, München 23, Leopoldstrasse 175, Deutschland.

5) Wie 3, jedoch Zusatz von 5 g Ascorbinsäure.

6) Wie weiter unten angeführt wird.

Als der einfachste Weg zur Gewinnung weitgehend vorgereinigter Rohkonzentrate erwies sich folgende Arbeitsweise: 1 kg grüne Pflanzenteile werden in 4 l *n*-Butanol mit Hilfe eines Mix-Gerätes zerkleinert und über Nacht bei Zimmertemperatur digeriert. Dann wird abgepresst. Der Presssaft wird verworfen, der Presskuchen einige Stunden in 5 l 70 % Äthanol digeriert. Man presst wiederum ab und erhält eine gelb gefärbte Lösung, die den aktiven Faktor enthält. Sie wird sodann im Vakuum auf etwa 1 l wässerige Lösung konzentriert. Man schickt sie dann durch die Jonenaustauscher IR 120 und IRA 410 oder IRA 400. Sodann wird wiederum im Vakuum konzentriert und schliesslich durch Lyophilisation völlig getrocknet. Man erhält etwa 20 g gelb-braunes, stark hygroskopisches Pulver, das die gesamte Aktivität enthält.

Mit diesem Lyophilisat angestellte Versuche zeigten, dass aus wässerigen Lösungen durch Zugabe von NaCl bis zur Sättigung der grösste Teil der gelösten Stoffe als voluminöser brauner Niederschlag gefällt wird, wobei der aktive Faktor in der Fällung enthalten ist. Pb-Acetat fällt aus 60 % äthanolischer Lösung ebenfalls den grössten Teil der Trockensubstanz und auch den aktiven Faktor. Bei Zusatz von Essigsäure geht die gesamte Fällung wieder in Lösung. Ebenso ist aus alkoholischer Lösung der Hauptteil der Trockensubstanz und des antifungalen Faktors mit K-Acetat fällbar. Aluminium-Oxyd wirkt in wässerigen, alkoholischen und auch essigsäurehaltigen Lösungen stark absorbierend sowohl auf die gesamten gelösten Stoffe als auch auf den antifungalen Faktor.

Bei längerer Aufbewahrung nimmt die antimikrobielle Wirksamkeit des Lyophilisates allmählich ab, wobei auch seine Farbe dunkler wird. Dies ist auch in wässerigen und alkoholischen Lösungen zu beobachten. Alkalische Reaktion fördert diesen Prozess stark. Es ist noch nicht eindeutig geklärt, ob diese Veränderungen allein durch Polymerisations- oder Kondensationsvorgänge bedingt sind, oder ob dabei auch Oxydationsprozesse mitspielen.

Bei chromatographischer Analyse des Lyophilisates auf Whatman-1-Papier ergab lediglich die Anwendung des folgenden Fliessmittels eine Auftrennung: Äthyl-acetat (2 Teile), Eisessig (1 Teil), Wasser (2 Teile), Äthanol (0,35 Teile). Hierbei liess sich bei R_F 0,9 eine abgegrenzte, im UV-Licht hellblau fluorescierende Zone erkennen, gefolgt von einem schwach absorbierenden Schwanz bis R_F etwa 0,2. Beräuchern mit Ammoniak verstärkt die Fluorescenz. Die fluorescierende Zone gibt auf dem Papier folgende Reaktionen: Mit $FeCl_3$ dunkelgrüne Färbung, mit Benzidin-Reagenz erst hell-orange-rote Färbung, die aber rasch etwas dunkler wird, mit ammoniakalischer Silbernitrat-Lösung schwarzbraune Färbung. Im Gegensatz dazu ergibt der Schwanz auf dem Papier mit Eisenchlorid eine blaue Färbung und mit Benzidin eine orange Farbe, wie sie sich bei der fluorescierenden Zone im nachgedunkelten Zustand erst einstellt.

Bei präparativer Chromatographie an der Zellulosesäule mit dem oben angegebenen Fliessmittel konnten wir auch bei sehr schön gleichmässig laufenden Säulen nur eine gewisse Anreicherung der fluorescierenden Substanz erzielen, nicht jedoch deren Isolierung. Es zeigte sich nämlich bei papierchromatographischer Untersuchung, dass alle Fraktionen um R_F 0,9, die allein aus der fluorescierenden Substanz hätten bestehen müssen, auch die nicht fluorescierende, schwanzbildende Substanz mitenthielten. Diese Substanz entsteht wahrscheinlich aus dem fluorescierenden Stoff. Die Ergebnisse des mikrobiologischen Tests lassen darauf schliessen, dass der antifungale Faktor wahrscheinlich nicht die fluorescierende Substanz selbst ist, sondern eines oder mehrere ihrer Umwandlungsprodukte, welche aber auch schon in der Pflanze vorhanden sind.

Alle diese Beobachtungen, sowie eine Reihe weiterer Feststellungen führten zu der bereits ausgesprochenen Annahme, dass der antimikrobiell wirkende Faktor von *Vaccinium myrtillus* ein gerbstoffartiger Stoff ist und vermutlich der Gruppe der nicht hydrolysierbaren oder kondensierten Gerbstoffe angehört (vgl. hierzu Schmidt [5]). Hierfür spricht des weiteren die Feststellung, dass sich bei Hydrolyse des Lyophilisates durch 1 stündiges Kochen in 1 N HCl-Lösung — offenbar durch Polymerisation — lediglich schwarzbraune, wasserunlösliche, amorphe Produkte ohne antimikrobielle Wirksamkeit bilden, in denen sich auch in einer grossen Anzahl verschiedener Fliessmittel auf papierchromatographischem Weg keine irgendwie definierbaren phenolischen oder zuckerartigen Stoffe nachweisen lassen.

1. Virtanen, A. I. *Giorn. Microbiol.* **2** (1956) 15.

2. Virtanen, A. I. und Hietala, P. K. *Acta Chem. Scand.* **9** (1955) 1543.
3. Virtanen, A. I., Hietala, P. K. und Wahlroos, Ö. *Suomen Kemistilehti B* **29** (1956) 143.
4. Virtanen, A. I. und Hietala, P. K. *Suomen Kemistilehti B* **30** (1957) 99.
5. Schmidt, O. Th. *Natürliche Gerbstoffe* in Paech, K. und Tracey, M. V. *Moderne Methoden der Pflanzenanalyse*, Springer-Verlag, Berlin, Göttingen, Heidelberg 1955, Bd. 3, S. 517.

Eingegangen am 5. August 1957.

Structure of Elastin

1. Analysis of Some Acid Peptides

A. KÄRKELÄ and E. KULONEN

Department of Medical Chemistry, University of Turku, Finland

This preliminary communication is meant to contribute to the discussion on the relations between collagen and elastin. Burton and co-workers [1] claimed, mainly on electronmicroscopic evidence, that collagen is transformed to elastin without being degraded to amino acids. If this theory were correct, the peptides from elastin should present similarities with those known from collagen [2-3].

Elastin was prepared from bovine nuchal ligament. Other non-collagenous proteins were extracted from the finely ground tissue exhaustively with 0.2 M disodium phosphate solution, and collagen subsequently with boiling water for five days.

Partial hydrolysates were made with hydrochloric acid [2] (5 % protein in 4 N acid was kept for a week at +37° C). The acid was removed by repeated evaporations and a sirupy dark-brown mass obtained. It dissolved completely in 10 % trichloroacetic acid. This material was fractionated using the method by Moore and Stein [4] with slight modifications. The resulting curve is presented as Fig. 1.

It is quite obvious that this procedure does not provide a very suitable method for structural analysis of elastin. The separations are not clear and the number of peptides produced seems small.

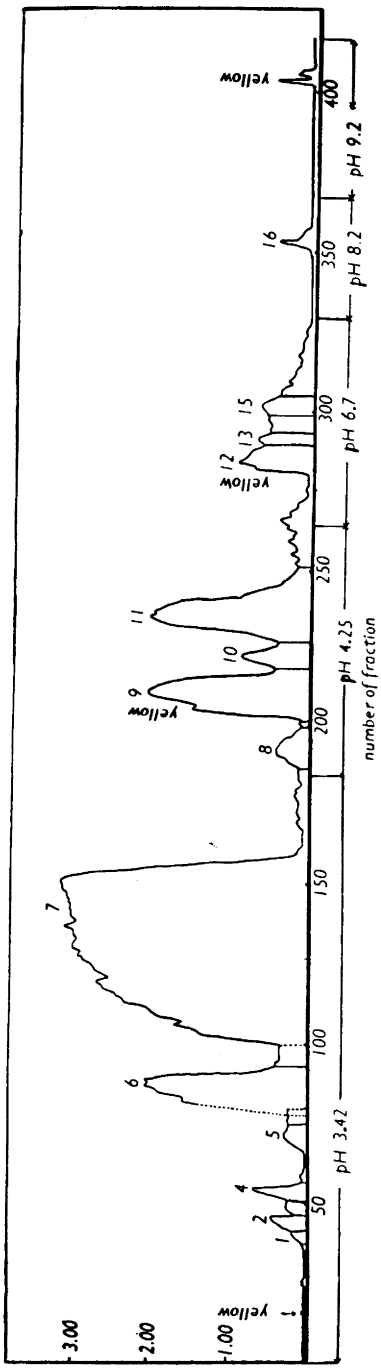


Fig. 1. Fractionation of partial hydrolysate of elastin (360 mg, for preparation see the text) in Dowex-50 column [4]. The last peak was obtained with 0.2 N NaOH. Two-ml fractions were collected (from pH 9.2 onwards 4 ml). The colour was developed from 0.2 ml samples taken from the fractions and the ordinate indicates the extinction in 1 cm cell. The numbers outside the curve refer to the text.

2. Virtanen, A. I. und Hietala, P. K. *Acta Chem. Scand.* **9** (1955) 1543.
3. Virtanen, A. I., Hietala, P. K. und Wahlroos, Ö. *Suomen Kemistilehti B* **29** (1956) 143.
4. Virtanen, A. I. und Hietala, P. K. *Suomen Kemistilehti B* **30** (1957) 99.
5. Schmidt, O. Th. *Natürliche Gerbstoffe* in Paech, K. und Tracey, M. V. *Moderne Methoden der Pflanzenanalyse*, Springer-Verlag, Berlin, Göttingen, Heidelberg 1955, Bd. 3, S. 517.

Eingegangen am 5. August 1957.

Structure of Elastin

1. Analysis of Some Acid Peptides

A. KÄRKELÄ and E. KULONEN

Department of Medical Chemistry, University of Turku, Finland

This preliminary communication is meant to contribute to the discussion on the relations between collagen and elastin. Burton and co-workers [1] claimed, mainly on electronmicroscopic evidence, that collagen is transformed to elastin without being degraded to amino acids. If this theory were correct, the peptides from elastin should present similarities with those known from collagen [2-3].

Elastin was prepared from bovine nuchal ligament. Other non-collagenous proteins were extracted from the finely ground tissue exhaustively with 0.2 M disodium phosphate solution, and collagen subsequently with boiling water for five days.

Partial hydrolysates were made with hydrochloric acid [2] (5 % protein in 4 N acid was kept for a week at +37° C). The acid was removed by repeated evaporations and a sirupy dark-brown mass obtained. It dissolved completely in 10 % trichloroacetic acid. This material was fractionated using the method by Moore and Stein [4] with slight modifications. The resulting curve is presented as Fig. 1.

It is quite obvious that this procedure does not provide a very suitable method for structural analysis of elastin. The separations are not clear and the number of peptides produced seems small.

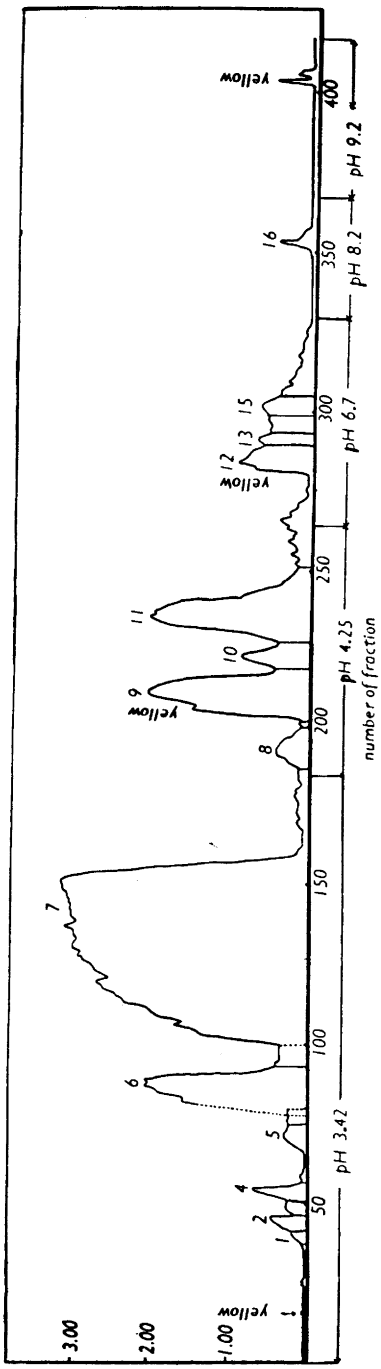


Fig. 1. Fractionation of partial hydrolysate of elastin (360 mg, for preparation see the text) in Dowex-50 column [4]. The last peak was obtained with 0.2 N NaOH. Two-ml fractions were collected (from pH 9.2 onwards 4 ml). The colour was developed from 0.2 ml samples taken from the fractions and the ordinate indicates the extinction in 1 cm cell. The numbers outside the curve refer to the text.

Fractions 6 and 7 were analysed by the dinitrofluorobenzene method following mainly Schroeder's instructions. The chromatography of DNP-compounds was, however, made according to Blackburn and Lowther [5]. The non-terminal amino acids were also converted to DNP-compounds and chromatographed. DNP-proline was identified additionally by the spectrum. All the DNP-amino acids were chromatographed with mixed crystallised references.

The following results could be obtained for peptides eluted at pH 3.42. (The asterisk indicates comparatively small amount.)

Fraction 6, peptide 1*: Glu-(Asp, Gly, Val*, Leu *)
peptide 2: Pro-(Asp, Glu, Gly, Val *, Leu*);

this peptide may be contaminated with another with valine as N-terminal amino acid.

Fraction 7, peptide 1: Gly-(Asp, Glu, Val*, Leu*, Gly?)
peptide 2: Ala-(Asp, Glu, Gly, Val*, Ala?)
peptide 3*: Val-(Asp, Glu, Gly, Ala, Pro)

The remarkable point is the abundance of aspartic and glutamic acids, which are present in small amounts in elastin, and the peptide breaks easily at aspartic acid. Common constituents are in these peptides Asp, Glu, Gly and in traces Val. Further investigation will show whether they form a characteristic sequence. In gelatin this region (pH 3.42) contains only two peptides Ala-Asp and Gly-Asp in quite small amounts, while proline and glycine peptides form the main part of the hydrolysate[2].

The form of the fractionation curve or the composition of the peptides which emerge at pH 3.42 do not support the concept of conversion of collagen to elastin at peptide level.

This work forms a part of a program which is generously supported by the *Finnish Medical Society Duodecim.*

1. Burton, D., Hall, D. A., Keech, M. K., Reed, R., Saxl, H., Tunbridge, R. E. and Wood, M. J. *Nature* **176** (1955) 966.
2. Schroeder, W. A., Kay, L. M., Legette, J., Honnen, L. and Green, F. C. *J. Am. Chem. Soc.* **76** (1954) 3556.
3. Grassmann, W., Hannig, K., Endres, H. and Riedel, A. *Hoppe-Seyler's Z. physiol. Chem.* **306** (1956) 123.
4. Moore, S. and Stein, W. H. *J. Biol. Chem.* **192** (1951) 663; for the colour development *J. Biol. Chem.* **176** (1948) 367.
5. Blackburn, S. and Lowther, A. G. *Biochem. J.* **48** (1951) 126.

Received August 23, 1957.

Diamagnetism of LiNO, NaNO and KNO

Studies in Magnetochemistry 19 *

R. W. ASMUSSEN

Chemical Laboratory B, Technical University of Denmark, Copenhagen, Denmark

The direct reaction between sodium metal and nitric oxide results in a reduction of nitric oxide. If, however, the process is carried out in liquid ammonia the result of the reaction is the formation of sodium nitrosyl (NaNO). Joannis [1], who first studied this reaction, prepared the sodium and potassium compounds and considered these substances as hyponitrites. Zintl and Harder [2] reprepared the sodium nitrosyl. Frazer and Long [3] measured the magnetic susceptibility of sodium nitrosyl and state that the compound is diamagnetic but give no numerical value.

The alkali metal nitrosyls are colourless or nearly colourless crystalpowders. The X-ray powder photo of the sodium compound is different from that of anhydrous sodium hyponitrite. The lines are very diffuse, an indexing could not be carried out (cf. also Zintl and Harder [2]). The aqueous solution is not stable; also at 0°C the solution is decomposed under evolution of nitrous oxide. Under corresponding conditions a sodium hyponitrite solution is stable or decomposes very slowly. These facts indicate that the compounds are not $hypo_n$ nitrites but may be considered as $(NaNO)_n$ and $(KNO)_n$. We may propose the ionic structures

$$\overset{+}{Na}(N\overline{O}) \text{ and } \overset{+}{K}(N\overline{O}).$$

* No. 18 of this series: *Acta Chem. Scand.* **11** (1957) 1331.

Fractions 6 and 7 were analysed by the dinitrofluorobenzene method following mainly Schroeder's instructions. The chromatography of DNP-compounds was, however, made according to Blackburn and Lowther [5]. The non-terminal amino acids were also converted to DNP-compounds and chromatographed. DNP-proline was identified additionally by the spectrum. All the DNP-amino acids were chromatographed with mixed crystallised references.

The following results could be obtained for peptides eluted at pH 3.42. (The asterisk indicates comparatively small amount.)

Fraction 6, peptide 1*: Glu-(Asp, Gly, Val*, Leu *)
peptide 2: Pro-(Asp, Glu, Gly, Val *, Leu*);

this peptide may be contaminated with another with valine as N-terminal amino acid.

Fraction 7, peptide 1: Gly-(Asp, Glu, Val*, Leu*, Gly?)
peptide 2: Ala-(Asp, Glu, Gly, Val*, Ala?)
peptide 3*: Val-(Asp, Glu, Gly, Ala, Pro)

The remarkable point is the abundance of aspartic and glutamic acids, which are present in small amounts in elastin, and the peptide breaks easily at aspartic acid. Common constituents are in these peptides Asp, Glu, Gly and in traces Val. Further investigation will show whether they form a characteristic sequence. In gelatin this region (pH 3.42) contains only two peptides Ala-Asp and Gly-Asp in quite small amounts, while proline and glycine peptides form the main part of the hydrolysate[2].

The form of the fractionation curve or the composition of the peptides which emerge at pH 3.42 do not support the concept of conversion of collagen to elastin at peptide level.

This work forms a part of a program which is generously supported by the *Finnish Medical Society Duodecim.*

1. Burton, D., Hall, D. A., Keech, M. K., Reed, R., Saxl, H., Tunbridge, R. E. and Wood, M. J. *Nature* **176** (1955) 966.
2. Schroeder, W. A., Kay, L. M., Legette, J., Honnen, L. and Green, F. C. *J. Am. Chem. Soc.* **76** (1954) 3556.
3. Grassmann, W., Hannig, K., Endres, H. and Riedel, A. *Hoppe-Seyler's Z. physiol. Chem.* **306** (1956) 123.
4. Moore, S. and Stein, W. H. *J. Biol. Chem.* **192** (1951) 663; for the colour development *J. Biol. Chem.* **176** (1948) 367.
5. Blackburn, S. and Lowther, A. G. *Biochem. J.* **48** (1951) 126.

Received August 23, 1957.

Diamagnetism of LiNO, NaNO and KNO

Studies in Magnetochemistry 19 *

R. W. ASMUSSEN

Chemical Laboratory B, Technical University of Denmark, Copenhagen, Denmark

The direct reaction between sodium metal and nitric oxide results in a reduction of nitric oxide. If, however, the process is carried out in liquid ammonia the result of the reaction is the formation of sodium nitrosyl (NaNO). Joannis [1], who first studied this reaction, prepared the sodium and potassium compounds and considered these substances as hyponitrites. Zintl and Harder [2] reprepared the sodium nitrosyl. Frazer and Long [3] measured the magnetic susceptibility of sodium nitrosyl and state that the compound is diamagnetic but give no numerical value.

The alkali metal nitrosyls are colourless or nearly colourless crystalpowders. The X-ray powder photo of the sodium compound is different from that of anhydrous sodium hyponitrite. The lines are very diffuse, an indexing could not be carried out (cf. also Zintl and Harder [2]). The aqueous solution is not stable; also at 0°C the solution is decomposed under evolution of nitrous oxide. Under corresponding conditions a sodium hyponitrite solution is stable or decomposes very slowly. These facts indicate that the compounds are not $hypo_n$ nitrites but may be considered as $(NaNO)_n$ and $(KNO)_n$. We may propose the ionic structures

$$\overset{+}{Na}(N\overline{O}) \text{ and } \overset{+}{K}(N\overline{O}).$$

* No. 18 of this series: *Acta Chem. Scand.* **11** (1957) 1331.

Since $N\bar{O}$ and O_2 are isosteres it is possible that the ground state of the $N\bar{O}$-ion is a triplet state. This state gives a magnetic moment $\mu = 2.83\ \mu_B$. In order to settle this question the metal nitrosyls LiNO, NaNO and KNO were prepared and measured magnetically; LiNO was prepared for the first time. The results of the chemical analyses and the magnetic measurements are given in Table 1. The results prove that $N\bar{O}$ is in a singlet state — if present in these compounds.

Table 1. Analyses and diamagnetic susceptibilities of alkali metal nitrosyls.

Substance	% Metal calc.	% Metal found	$\chi_g \times 10^6$	$\chi_M \times 10^6$	$\chi_{N\bar{O}} \times 10^6$
LiNO	18.78	18.50	-0.56_2	−20.8	−20.1
NaNO	43.37	42.98	-0.40_0	−21.2	−17.2
KNO	56.57	56.42	-0.46_4	−32.1	−18.1

The metals were determined as sulphates. The metal nitrosyls were measured magnetically in evacuated glass tubes (Gouy method) at 20—22°C.

The gram ionic susceptibilities for NO^- were calculated from the χ_M values by means of the gram ionic susceptibilities -0.7×10^{-6}, -4×10^{-6} and -14×10^{-6} for the ions Li^+, Na^+ and K^+, respectively. *A reasonable mean value for the gram ionic susceptibility of* NO^- *is* -18×10^{-6}. This number is calculated from the 3 values in Table 1 giving the values for NaNO and KNO double weight because the analytical data for these substances are in better accordance with the theoretical values than is the case for LiNO.

1. Joannis, A. *Ann. Chim. Phys.* (8) **7** (1906) 96.
2. Zintl, E. and Harder, A. *Ber.* **66** (1933) 760.
3. Frazer, J. H. and Long, N. O. *J. Chem. Phys.* **6** (1938) 462.

Received September 12, 1957.

On the Existence of Oscillating Enzymatic Reactions and on a Possible Interpretation of Spontaneous Spike Potentials in Nerves

J. A. CHRISTIANSEN

Københavns Universitets Fysisk-Kemiske Institut, Copenhagen, Denmark

An overall reaction

$$A_1 + A_2 + A_3 \rightleftharpoons B_2 + B_3 + B_1 \qquad (B)$$

is supposed to be catalyzed by an enzyme according to the mechanism (A)

$$\begin{aligned} A_1 + X_1 &\rightleftharpoons X_2 + B_2 \quad (\pm 1) \\ A_2 + X_2 &\rightleftharpoons X_3 + B_3 \quad (\pm 2) \\ A_3 + X_3 &\rightleftharpoons X_1 + B_1 \quad (\pm 3) \end{aligned} \qquad (A)$$

where X_1, X_2, X_3 are three different forms of the enzyme or complexes thereof with the substrates (A_i, B_i). The sum of the concentrations of the three forms is the total constant enzyme concentration E, which is supposed to be stoichiometrically small as compared to the concentrations of the substrates. Let x_1, x_2 and x_3 be the fractions of the enzyme present in the three states, and let s_1, s_2 and s_3 be the resulting rates of the three partial reactions, divided by E.

We then have the four equations

$$\begin{aligned} x_1 w_1 - x_2 w_{-2} &= s_1 \\ x_2 w_2 - x_3 w_{-3} &= s_1 \\ x_3 w_3 - x_1 w_{-1} &= s_2 \end{aligned} \qquad (1)$$

$$x_1 + x_2 + x_3 = 1 \qquad (2)$$

where w_1 is the probability in unit time for X_1 to react according to $(+1)$ in (A), w_{-1} the probability for X_2 to react with B_2 according to (-1) in (A), *etc.*

The steady state solution of the system (1) in connection with the condition (2) is well known [12]. It is characteristic for this, that if the probabilities w are exactly known the result of the calculation is of unlimited accuracy.

There exists, however, another solution of (1) and (2) for which this is not true in so far as in this case the (weighted) sums of the squared deviations from mean values have well defined constant values, different from zero.

This solution seems therefore to be inherently more probable than the usual one.

Since $N\bar{O}$ and O_2 are isosteres it is possible that the ground state of the $N\bar{O}$-ion is a triplet state. This state gives a magnetic moment $\mu = 2.83\ \mu_B$. In order to settle this question the metal nitrosyls LiNO, NaNO and KNO were prepared and measured magnetically; LiNO was prepared for the first time. The results of the chemical analyses and the magnetic measurements are given in Table 1. The results prove that $N\bar{O}$ is in a singlet state — if present in these compounds.

Table 1. Analyses and diamagnetic susceptibilities of alkali metal nitrosyls.

Substance	% Metal calc.	% Metal found	$\chi_g \times 10^6$	$\chi_M \times 10^6$	$\chi_{N\bar{O}} \times 10^6$
LiNO	18.78	18.50	-0.56_2	−20.8	−20.1
NaNO	43.37	42.98	-0.40_0	−21.2	−17.2
KNO	56.57	56.42	-0.46_4	−32.1	−18.1

The metals were determined as sulphates. The metal nitrosyls were measured magnetically in evacuated glass tubes (Gouy method) at 20—22°C.

The gram ionic susceptibilities for NO^- were calculated from the χ_M values by means of the gram ionic susceptibilities -0.7×10^{-6}, -4×10^{-6} and -14×10^{-6} for the ions Li^+, Na^+ and K^+, respectively. *A reasonable mean value for the gram ionic susceptibility of* NO^- *is* -18×10^{-6}. This number is calculated from the 3 values in Table 1 giving the values for NaNO and KNO double weight because the analytical data for these substances are in better accordance with the theoretical values than is the case for LiNO.

1. Joannis, A. *Ann. Chim. Phys.* (8) **7** (1906) 96.
2. Zintl, E. and Harder, A. *Ber.* **66** (1933) 760.
3. Frazer, J. H. and Long, N. O. *J. Chem. Phys.* **6** (1938) 462.

Received September 12, 1957.

On the Existence of Oscillating Enzymatic Reactions and on a Possible Interpretation of Spontaneous Spike Potentials in Nerves

J. A. CHRISTIANSEN

Københavns Universitets Fysisk-Kemiske Institut, Copenhagen, Denmark

An overall reaction

$$A_1 + A_2 + A_3 \rightleftharpoons B_2 + B_3 + B_1 \qquad (B)$$

is supposed to be catalyzed by an enzyme according to the mechanism (A)

$$\begin{aligned} A_1 + X_1 &\rightleftharpoons X_2 + B_2 \quad (\pm 1) \\ A_2 + X_2 &\rightleftharpoons X_3 + B_3 \quad (\pm 2) \\ A_3 + X_3 &\rightleftharpoons X_1 + B_1 \quad (\pm 3) \end{aligned} \qquad (A)$$

where X_1, X_2, X_3 are three different forms of the enzyme or complexes thereof with the substrates (A_i, B_i). The sum of the concentrations of the three forms is the total constant enzyme concentration E, which is supposed to be stoichiometrically small as compared to the concentrations of the substrates. Let x_1, x_2 and x_3 be the fractions of the enzyme present in the three states, and let s_1, s_2 and s_3 be the resulting rates of the three partial reactions, divided by E.

We then have the four equations

$$\begin{aligned} x_1 w_1 - x_2 w_{-2} &= s_1 \\ x_2 w_2 - x_3 w_{-3} &= s_1 \\ x_3 w_3 - x_1 w_{-1} &= s_2 \end{aligned} \qquad (1)$$

$$x_1 + x_2 + x_3 = 1 \qquad (2)$$

where w_1 is the probability in unit time for X_1 to react according to $(+1)$ in (A), w_{-1} the probability for X_2 to react with B_2 according to (-1) in (A), *etc.*

The steady state solution of the system (1) in connection with the condition (2) is well known [12]. It is characteristic for this, that if the probabilities w are exactly known the result of the calculation is of unlimited accuracy.

There exists, however, another solution of (1) and (2) for which this is not true in so far as in this case the (weighted) sums of the squared deviations from mean values have well defined constant values, different from zero.

This solution seems therefore to be inherently more probable than the usual one.

The essential points in the derivation are: 1) the introduction of a system of "weights" m_1, m_2 and m_3; 2) the description of the deviations as vectors.

The weights are defined in terms of the w's by the "auxiliary equations" (3).

$$\begin{aligned} m_1w_1 - m_3w_{-3} &= 1 \\ m_2w_2 - m_1w_{-1} &= 1 \\ m_3w_3 - m_2w_{-2} &= 1 \end{aligned} \tag{3}$$

whose solutions may be written in the form (4)

$$\begin{aligned} (1-\beta)m_1w_1 &= 1 + \beta_2\beta_3 + \beta_3 \\ (1-\beta)m_2w_2 &= \beta_1 + 1 + \beta_3\beta_1 \\ (1-\beta)m_3w_3 &= \beta_1\beta_2 + \beta_2 + 1 \end{aligned} \tag{4}$$

where $\beta_i = w_{-i}/w_i$ and $\beta = \beta_1\beta_2\beta_3$

If β is small as compared to 1 the overall reaction (B) is irreversible, which we shall assume.

We define further a set g_1, g_2 and g_3 of pure numbers by

$$g_1 = m_iw_i - 1/2 \tag{5}$$

The calculations which will be published later, then lead to the following description of the deviations of x_1, x_2 and x_3 from their mean values λ_1, λ_2 and λ_3.

1) Draw a triangle with the sides λ_1, λ_2 and λ_3 where

$$\begin{aligned} \lambda_1 &= A\sqrt{g_2 + g_3} \\ \lambda_2 &= A\sqrt{g_3 + g_1} \\ \lambda_3 &= A\sqrt{g_1 + g_2} \end{aligned} \tag{6}$$

A is determined by the condition that the perimeter of the triangle $\lambda_1 + \lambda_2 + \lambda_3$ shall equal 1.

2) Project the sides of the triangle on a pointer which rotates in the direction 123 with the constant angular velocity $2\pi\nu$.

These projections then represent the (real) deviations from the fixed values λ_1, λ_2 and λ_3, respectively. The (real) sum of the deviations is evidently zero, but separately at most one of them can be zero at a certain time.

To calculate ν we use the relations

$$\begin{aligned} dq_1/dt &= \sigma_3 - \sigma_1 \\ dq_2/dt &= \sigma_1 - \sigma_2 \\ dq_3/dt &= \sigma_2 - \sigma_3 \end{aligned} \tag{7}$$

and their complex conjugates. q_1 is the (complex) deviation of x_i from λ_i and σ_i the (complex) deviation of s_i from s. Eqns. (7) follow directly from the law of conservation of matter.

(By use of (3) and the condition (2) it can be shown that

$$m_1s_1 + m_2s_2 + m_3s_3 = s(m_1 + m_2 + m_3) = 1 \tag{8}$$

The first equation (8) shows that s is the weighted mean of the different possible values of s_i and the second that this mean is exactly the steady state value. It should be noted that our mean values λ are different from the usual steady state values, the reason being that the system is never in its steady state.

The real frequency ν can then be calculated from

$$8\pi g\nu = (g_1+g_2)/m_1 + (g_2+g_3)/m_3 + (g_3+g_1)/m_3 \tag{9}$$

where

$$g^2 = g_1g_2 + g_2g_3 + g_3g_1 \tag{10}$$

By use of (5) eqn. (9) may be simplified into

$$8\pi g\nu = (w_1+w_{-1}+w_2+w_{-2}+w_3+w_{-3}) \tag{11}$$

Finally to arrive at the actual values of x_1, x_2 and x_3 we simply add to the sides of the fixed triangle λ_1, λ_2, λ_3 the respective varying deviations from our geometrical construction. The sum of the resulting lengths will then be constant, but they will vary periodically with time. The lengths separately will represent the distribution on the different forms of the enzymes at different times. Considering x_1 it will be seen that it performs harmonic oscillations between zero and $2\lambda_1$, and similarly for the others, but the oscillations are never in the same phase.

Now these oscillations may be registered by an oscillograph as spike potentials [3-5] if the enzymatic system is electrochemically active.

The source of the periodically occurring potentials is usually believed to be located in some "end-organ" from which they are transmitted through the nerve.

Such spike-potentials may perhaps not be expected to be generally observable in vessels of macroscopic dimension as the whole spectrum then may be diffuse. This is because of the vague definition of time "zero" in such cases. But in nerves whose diameters are of the order of magnitude 1 μ no such difficulty arises. It may therefore be, that we should assume the presence of an enzyme which catalyses some irreversible process, perhaps in the membrane of the end-organ or / and of the nerve.

1. Christiansen, J. A. *Acta Chem. Scand.* **3** (1949) 493.
2. Christiansen, J. A. *Advances in Catalysis* **5** (1953) 311.
3. Loewenstein, O. and Sand, A. *J. Exptl. Biol.* **13** (1936) 416.
4. Sand, A. *Proc. Roy. Soc. London* **B 125** (1938) 524.
5. Loewenstein, O. and Roberts, T. D. M. *J. Physiol. London* **110** (1949) 392.

Received September 17, 1957.

On Hydroxylamine Compounds in *Azotobacter* Cultures. I. Formation of Hydroxylamine Compounds

NILS-ERIK SARIS and ARTTURI I. VIRTANEN

Laboratory of the Foundation for Chemical Research, Biochemical Institute, Helsinki, Finland

Blom [1] was the first to demonstrate small amounts of hydroxylamine in nitrogen-fixing *Azotobacter* cultures, and later on bound hydroxylamine was found by Endres [2]. Hydroxylamine was formed only from nitrate or molecular nitrogen but not from ammonium nitrogen. On the other hand Virtanen and Hakala [3] observed that about the same amount of bound hydroxylamine was found in the nutrient solutions of *Azotobacter vinelandii* both when nitrate nitrogen, ammonium nitrogen, and molecular nitrogen were the sources of nitrogen. Virtanen and Järvinen [4] investigated the formation of bound hydroxylamine in the cell suspension of *Azotobacter vinelandii* and found that it was formed both from N_2-, NO_3-, and NH_4-N, although more rapidly from molecular nitrogen and nitrate nitrogen than from ammonium nitrogen. These authors determined bound hydroxylamine in the cell mass separated by centrifugation.

The present authors have now further studied the formation of hydroxylamine compounds found in the nutrient solution of *Azotobacter*. Under the experimental conditions used the enrichment of hydroxylamine compounds in cells was too scant to make a closer investigation of these compounds possible. On the other hand bound hydroxylamine was enriched in the nutrient solution in such amounts that a closer investigation of them could be attempted.

Nutrient solution. 1.5 g Burk's salt, 10 mg $Fe_2(SO_4)_3$, 15 mg $FeSO_4$, $7H_2O$, 0.25 mg Na_2MoO_4 per litre, pH 7.2. In the experiments proper glycerol was the source of carbon (*cf.* below); the source of nitrogen is mentioned in connection with the experimental results.

Determination of bound hydroxylamine. Csáky's method was used, with the modification that the hydrolysis time was shortened to one hour. To destroy nitrite a pinch of urea was added. Determinations were made both from 2 and 10 ml.

Azotobacter strain. In preliminary experiments the largest amount of bound hydroxylamine was found in cultures of *Azotobacter chroococcum* K 1. In cultures of other investigated strains (*A. vinelandii* Kluyver, *vinogradsky* Kluyver, *beijerinckii*, and a not closer characterized strain isolated from soil) a much smaller amount of bound hydroxylamine, if any, was enriched.

Effect of the carbon source. Because Endres obtained the largest amount of bound hydroxylamine when lactate was the source of carbon, growth experiments were performed with different carbon compounds (glycerol, Ca-lactate, saccharose, ethanol, acetone, sorbitol). In the concentrations investigated glycerol was as good a carbon source as lactate, and it was used in the experiments proper. The large amounts of hydroxylamine found by Endres in lactate nutrient solutions were not, however, even approximately obtained. He found maximum 2×10^{-4} mole NH_2OH per 10 ml, the present authors about 10^{-5} only. This circumstance made the isolation of hydroxylamine compounds and their characterization difficult.

Cultivation methods. Method 1. Azotobacter was allowed to grow without shaking in 1 litre flat flasks containing 200 ml of nutrient solution each. 200 ml of nutrient solution without combined nitrogen was inoculated with 2.5 ml of a 4-day-old *Azotobacter* culture. The experiment was terminated after 3 days, the maximum amount of bound hydroxylamine being then found in the solution. The influence of the age of the cultures on the content of bound hydroxylamine in the nutrient solution can be seen from the following results with *Azotobacter chroococcum* K 1:

1. Christiansen, J. A. *Acta Chem. Scand.* **3** (1949) 493.
2. Christiansen, J. A. *Advances in Catalysis* **5** (1953) 311.
3. Loewenstein, O. and Sand, A. *J. Exptl. Biol.* **13** (1936) 416.
4. Sand, A. *Proc. Roy. Soc. London* **B 125** (1938) 524.
5. Loewenstein, O. and Roberts, T. D. M. *J. Physiol. London* **110** (1949) 392.

Received September 17, 1957.

On Hydroxylamine Compounds in *Azotobacter* Cultures. I. Formation of Hydroxylamine Compounds

NILS-ERIK SARIS and ARTTURI I. VIRTANEN

Laboratory of the Foundation for Chemical Research, Biochemical Institute, Helsinki, Finland

Blom [1] was the first to demonstrate small amounts of hydroxylamine in nitrogen-fixing *Azotobacter* cultures, and later on bound hydroxylamine was found by Endres [2]. Hydroxylamine was formed only from nitrate or molecular nitrogen but not from ammonium nitrogen. On the other hand Virtanen and Hakala [3] observed that about the same amount of bound hydroxylamine was found in the nutrient solutions of *Azotobacter vinelandii* both when nitrate nitrogen, ammonium nitrogen, and molecular nitrogen were the sources of nitrogen. Virtanen and Järvinen [4] investigated the formation of bound hydroxylamine in the cell suspension of *Azotobacter vinelandii* and found that it was formed both from N_2-, NO_3-, and NH_4-N, although more rapidly from molecular nitrogen and nitrate nitrogen than from ammonium nitrogen. These authors determined bound hydroxylamine in the cell mass separated by centrifugation.

The present authors have now further studied the formation of hydroxylamine compounds found in the nutrient solution of *Azotobacter*. Under the experimental conditions used the enrichment of hydroxylamine compounds in cells was too scant to make a closer investigation of these compounds possible. On the other hand bound hydroxylamine was enriched in the nutrient solution in such amounts that a closer investigation of them could be attempted.

Nutrient solution. 1.5 g Burk's salt, 10 mg $Fe_2(SO_4)_3$, 15 mg $FeSO_4$, $7H_2O$, 0.25 mg Na_2MoO_4 per litre, pH 7.2. In the experiments proper glycerol was the source of carbon (*cf.* below); the source of nitrogen is mentioned in connection with the experimental results.

Determination of bound hydroxylamine. Csáky's method was used, with the modification that the hydrolysis time was shortened to one hour. To destroy nitrite a pinch of urea was added. Determinations were made both from 2 and 10 ml.

Azotobacter strain. In preliminary experiments the largest amount of bound hydroxylamine was found in cultures of *Azotobacter chroococcum* K 1. In cultures of other investigated strains (*A. vinelandii* Kluyver, *vinogradsky* Kluyver, *beijerinckii*, and a not closer characterized strain isolated from soil) a much smaller amount of bound hydroxylamine, if any, was enriched.

Effect of the carbon source. Because Endres obtained the largest amount of bound hydroxylamine when lactate was the source of carbon, growth experiments were performed with different carbon compounds (glycerol, Ca-lactate, saccharose, ethanol, acetone, sorbitol). In the concentrations investigated glycerol was as good a carbon source as lactate, and it was used in the experiments proper. The large amounts of hydroxylamine found by Endres in lactate nutrient solutions were not, however, even approximately obtained. He found maximum 2×10^{-4} mole NH_2OH per 10 ml, the present authors about 10^{-5} only. This circumstance made the isolation of hydroxylamine compounds and their characterization difficult.

Cultivation methods. Method 1. Azotobacter was allowed to grow without shaking in 1 litre flat flasks containing 200 ml of nutrient solution each. 200 ml of nutrient solution without combined nitrogen was inoculated with 2.5 ml of a 4-day-old *Azotobacter* culture. The experiment was terminated after 3 days, the maximum amount of bound hydroxylamine being then found in the solution. The influence of the age of the cultures on the content of bound hydroxylamine in the nutrient solution can be seen from the following results with *Azotobacter chroococcum* K 1:

Time after inoculation, days	1	2	3	4	5	6
Cells formed, mg/10 ml	0	30	120	165	190	205
NH_2OH after hydrolysis, μg N/10 ml	0	0.54	1.40	0.95	0.30	0

The effect of the nitrogen source on the enrichment of hydroxylamine compounds in the nutrient solution was determined after 3 days of growth in glycerol nutrient solutions in which KNO_3, $(NH_4)_2CO_3$, urea, or N_2 (without combined nitrogen) were the sources of nitrogen. The amount of each nitrogen compound used was 60 mg N per 200 ml nutrient solution. The results can be seen in Table 1.

Table 1. Effect of the nitrogen source on the enrichment of bound hydroxylamine in the nutrient solution of *A. chroococcum.*

Nitrogen nutrition	NH_2OH-N μg/10 ml	Cells mg/10 ml	Assimilated N mg/10 ml	Excret. total N mg/10 ml
N_2	1.46	160	2.15	0.08
KNO_3	1.04	85	1.23	—
$(NH_4)_2CO_3$	1.80	40	0.52	—
$CO(NH_2)_2$	1.62	140	2.05	—

Method 2. 1 Litre Kluyver flasks contained 200 ml of the above-mentioned nutrient solution. A vigorous current of air was passed through the solution after addition of bacterial mass. Under these conditions hydroxylamine was accumulated in the solution only when a large amount of bacteria was suspended in the nutrient solution.

The bacterial mass used was separated by centrifugation from two-days-old liquid cultures and suspended into the nutrient solution using a Waring-Blendor homogenisator. 250 mg of *Azotobacter* mass were added to each nutrient solution. KNO_3 (60 mg N/200 ml), urea (60 mg N/200 ml), and N_2 (no combined nitrogen in the nutrient solution) were the sources of nitrogen. The results can be seen in Fig. 1.

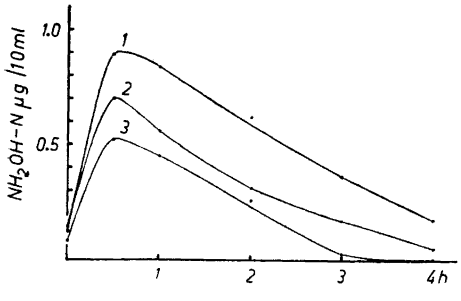


Fig. 1. Bound hydroxylamine in a vigorously aerated suspension of *A. chroococcum* in nutrient solutions with potassium nitrate (1), molecular nitrogen (2), and urea (3) as nitrogen source.

The results recorded above show that bound hydroxylamine, accumulated in the nutrient solution, disappears from flask cultures after the 4th day and from aerated suspensions of bacteria within a few hours. This disappearance may depend on assimilation or decomposition of the substance in the nutrient solution. It was also found that the yield of hydroxylamine decreases when the pH falls below 7.3. Hydroxylamine compounds were not demonstrable in cultures with a pH below 6.8.

In order to find out to what extent bound hydroxylamine, accumulated in the nutrient solution, disappears in a vigorously aerated suspension at different pH values, a fraction containing bound hydroxylamine, separated with Amberlite IR-120, was added to two suspensions of *A. chroococcum* K 1 in the nutrient solution. The pH of the one solution was regulated to 7.3 and that of the other to 6.5. An equally strong current of air was

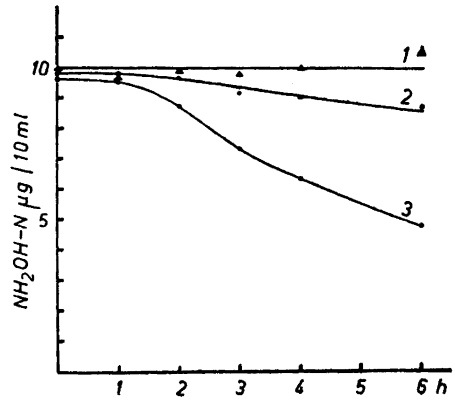


Fig. 2. Disappearance of added hydroxylamine fraction without *Azotobacter* (1), with *Azotobacter* suspension, pH 6.5 (2), and with *Azotobacter* suspension, pH 7.3 (3).

passed through both suspensions in a Kluyver flask. In the control the nutrient solution containing the hydroxylamine fraction but no bacteria was aerated. The results can be seen in Fig. 2.

These results indicate that the hydroxylamine fraction is stable without *Azotobacter* during the experimental period, *i. e.* for 6 h, and that in experiments with *Azotobacter* bound hydroxylamine disappears much faster at pH 7.3 than at pH 6.5. The results suggest accordingly that the absence of bound hydroxylamine in *Azotobacter* cultures at pH 6.5 is due to a reduced formation of hydroxylamine compounds.

Since hydroxylamine compounds are formed in our *Azotobacter* cultures from NH_4—N as rapidly as from N_2, and identical compounds seem to be in question (*cf.* paper II), there is no evidence any longer of an oxidative step in aerobic N_2 fixation. On the basis of their results with *Clostridium* Virtanen and Hakala [5] years ago suggested that N_2 fixation by anaerobic organisms is a pure reduction, di-imide being the first intermediate, and the same mechanism can now be suggested also for aerobic N_2 fixation.

1. Blom, J. *Zentr. Bakteriol. Parasitenk. II* **84** (1931) 60.
2. Endres, G. *Ann.* **518** (1935) 109.
3. Virtanen, A. I. and Hakala, M. *Unpublished.*
4. Virtanen, A. I. and Järvinen, H. *Acta Chem. Scand.* **5** (1951) 220.
5. Virtanen, A. I. and Hakala, M. *Suomen Kemistilehti B* **22** (1949) 23; *Acta Chem. Scand.* **3** (1949) 1044.

Received September 22, 1957.

On Hydroxylamine Compounds in *Azotobacter* Cultures. II. On the Chemical Nature of the Bound Hydroxylamine Fraction in *Azotobacter* Cultures

NILS-ERIK SARIS and ARTTURI I. VIRTANEN

Laboratory of the Foundation for Chemical Research, Biochemical Institute, Helsinki, Finland

In the previous communication [1] it was reported that bound hydroxylamine was accumulated in the nutrient solution of *Azotobacter*. Attempts to isolate and characterize these hydroxylamine compounds are reported in this paper.

Behaviour on ion exchange columns. Bound hydroxylamine from the nutrient solution passed through a slightly basic resin (Amberlite IR-4B), but was absorbed by a strongly basic one (IR-400). It was eluted quantitatively with diluted acetic or formic acid from the latter. On the other hand it was also absorbed almost quantitatively by acid resins from more concentrated solutions. Only some per cent of the total bound hydroxylamine passed through the Amberlite IR-120 column. From this column the amino acids and part of the hydroxylamine compounds could be eluted by 1 N ammonia, the latter compounds quantitatively only with 10 % ammonia. Paper chromatographic characteristics showed that the bound hydroxylamine eluted together with amino acids by dilute ammonia was similar to that eluted by more concentrated ammonia.

Separation of the bound hydroxylamine absorbed by the Amberlite IR-120 column. The fraction obtained from the glycerol cultures (N_2 as source of nitrogen) of *Azotobacter* was investigated by paper chromatography. The fraction was obtained by evaporating the culture solution to a small volume *in vacuo*, precipitating mucous substances with ethanol, evaporating ethanol *in vacuo* from the clear solution, passing the solution through the Amberlite IR-120 column, eluting the column

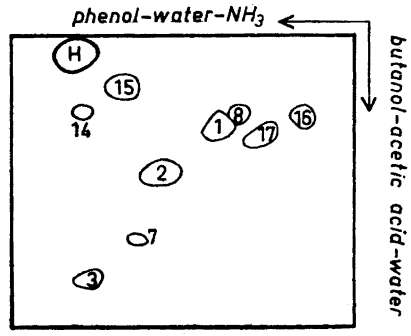


Fig. 1. Two-dimensional run of amino acids and bound hydroxylamine (formed in the culture solution of *A. chroococcum* K 1 grown in glycerol-flask-cultures for 3 days) after absorption in Amberlite IR-120 resin and elution with 1 N ammonia. H = bound hydroxylamine (a weak greyish spot with ninhydrin), 1 = gly, 2 = ala, 3 = val, 7 = tyr, 8 = ser, 14 = arg, 15 = lys, 16 = asp, 17 = glu.

passed through both suspensions in a Kluyver flask. In the control the nutrient solution containing the hydroxylamine fraction but no bacteria was aerated. The results can be seen in Fig. 2.

These results indicate that the hydroxylamine fraction is stable without *Azotobacter* during the experimental period, *i. e.* for 6 h, and that in experiments with *Azotobacter* bound hydroxylamine disappears much faster at pH 7.3 than at pH 6.5. The results suggest accordingly that the absence of bound hydroxylamine in *Azotobacter* cultures at pH 6.5 is due to a reduced formation of hydroxylamine compounds.

Since hydroxylamine compounds are formed in our *Azotobacter* cultures from NH_4—N as rapidly as from N_2, and identical compounds seem to be in question (*cf.* paper II), there is no evidence any longer of an oxidative step in aerobic N_2 fixation. On the basis of their results with *Clostridium* Virtanen and Hakala [5] years ago suggested that N_2 fixation by anaerobic organisms is a pure reduction, di-imide being the first intermediate, and the same mechanism can now be suggested also for aerobic N_2 fixation.

1. Blom, J. *Zentr. Bakteriol. Parasitenk. II* **84** (1931) 60.
2. Endres, G. *Ann.* **518** (1935) 109.
3. Virtanen, A. I. and Hakala, M. *Unpublished.*
4. Virtanen, A. I. and Järvinen, H. *Acta Chem. Scand.* **5** (1951) 220.
5. Virtanen, A. I. and Hakala, M. *Suomen Kemistilehti B* **22** (1949) 23; *Acta Chem. Scand.* **3** (1949) 1044.

Received September 22, 1957.

On Hydroxylamine Compounds in *Azotobacter* Cultures. II. On the Chemical Nature of the Bound Hydroxylamine Fraction in *Azotobacter* Cultures

NILS-ERIK SARIS and ARTTURI I. VIRTANEN

Laboratory of the Foundation for Chemical Research, Biochemical Institute, Helsinki, Finland

In the previous communication [1] it was reported that bound hydroxylamine was accumulated in the nutrient solution of *Azotobacter*. Attempts to isolate and characterize these hydroxylamine compounds are reported in this paper.

Behaviour on ion exchange columns. Bound hydroxylamine from the nutrient solution passed through a slightly basic resin (Amberlite IR-4B), but was absorbed by a strongly basic one (IR-400). It was eluted quantitatively with diluted acetic or formic acid from the latter. On the other hand it was also absorbed almost quantitatively by acid resins from more concentrated solutions. Only some per cent of the total bound hydroxylamine passed through the Amberlite IR-120 column. From this column the amino acids and part of the hydroxylamine compounds could be eluted by 1 N ammonia, the latter compounds quantitatively only with 10 % ammonia. Paper chromatographic characteristics showed that the bound hydroxylamine eluted together with amino acids by dilute ammonia was similar to that eluted by more concentrated ammonia.

Separation of the bound hydroxylamine absorbed by the Amberlite IR-120 column. The fraction obtained from the glycerol cultures (N_2 as source of nitrogen) of *Azotobacter* was investigated by paper chromatography. The fraction was obtained by evaporating the culture solution to a small volume *in vacuo*, precipitating mucous substances with ethanol, evaporating ethanol *in vacuo* from the clear solution, passing the solution through the Amberlite IR-120 column, eluting the column

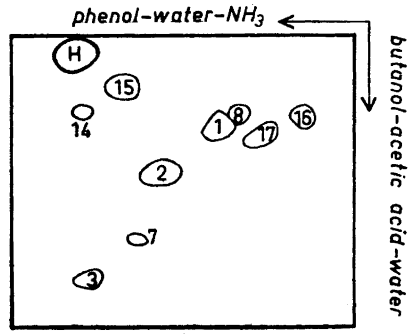


Fig. 1. Two-dimensional run of amino acids and bound hydroxylamine (formed in the culture solution of *A. chroococcum* K 1 grown in glycerol-flask-cultures for 3 days) after absorption in Amberlite IR-120 resin and elution with 1 N ammonia. H = bound hydroxylamine (a weak greyish spot with ninhydrin), 1 = gly, 2 = ala, 3 = val, 7 = tyr, 8 = ser, 14 = arg, 15 = lys, 16 = asp, 17 = glu.

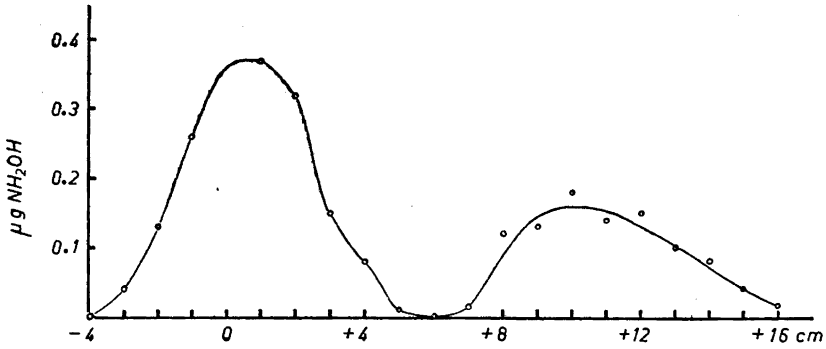


Fig. 2. Paper electrophoresis of bound hydroxylamine, pH 6.5, pyridine-acetic acid buffer, 1 000 V, 10 mA, 4 h.

with 10 % ammonia, upon which both amino acids and bound hydroxylamine went into solution quantitatively, and evaporating ammonia *in vacuo*. Phenol-water-ammonia and butanol-acetic acid-water were used as solvents. In a one-dimensional run the paper sheets were cut crosswise into narrow strips and hydroxylamine was determined from the water extracts after hydrolysis. The following R_F-values for bound hydroxylamine were found: 0.8 with phenol-water-ammonia, ~0.02 with butanol-acetic acid-water as solvents. (In parallel runs made for comparison the R_F-values for β-aspartylhydroxamic and γ-glutamylhydroxamic acids with butanol-acetic acid as solvents were 0.09 and 0.15.) Fig. 1 shows the position of bound hydroxylamine on a two-dimensional paper chromatogram. Independently of the nitrogen source (N_2-, NH_4-, NO_3—N) the same bound hydroxylamine spot was found on paper chromatograms. The spot was slightly ninhydrin positive and could thus be seen on the same chromatogram as the amino acids. No red colour was formed with ferric chloride, which indicates that simple aminohydroxamic acids were not in question. It was generally found that in the position for bound hydroxylamine a faint yellow colour was to be seen before ninhydrin spraying.

The bound hydroxylamine found in the culture solutions of *Azotobacter* cells grown with different nitrogen nutrition (N_2, NO_3^-, NH_4^+) behaved in much the same way on ion exchangers. On reduction with sodium amalgam amino acids were not formed from the bound hydroxylamine which had passed through the Amberlite IR-120 column, and hence the oximes of keto acids were not found in this fraction. This fraction, the quantity of which varied in different experiments generally constituting only a few per cent of the total bound hydroxylamine, was not closer investigated.

It is remarkable that from a one-dimensional paper chromatogram a thorough extraction brought only about 20 % of the bound hydroxylamine originally placed on the paper into water solution and about 30 % into water containing ammonia.

Bound hydroxylamine was freed from amino acids in the cellulose powder column using butanol-acetic acid as solvent. Bound hydroxylamine travelled slowest (*cf.* above), and the yellow colour made it easy to follow its run. It cannot be said for certain if the colour belongs to the hydroxylamine fraction or if it is only an impurity in this fraction. Generally it was found, however, that there was some parallelism between the yellow colour and the content of bound hydroxylamine in *Azotobacter* cultures.

On hydrolysis with 6 N HCl two unknown amino acids were formed from the bound hydroxylamine fraction and in addition glutamic acid and smaller amounts of glycine, serine, alanine, valine, and *iso*leucine. On a two-dimensional paper chromatogram the unknown amino acids travelled slowly both in phenol and butanol-acetic acid and formed one spot, provided that the run with butanol-acetic acid was not continued for 4 to 5 days. In the latter case the spot divided into two. The faster travelling spot was chromatographically identical with synthetic hydroxyaspartic acid (R_F 0.05 in both solvents). When this spot was cut off from the paper and the water extract reduced with HI and red phosphorus, mainly aspartic acid, but also small amounts of glycine, serine and alanine were formed, *i. e.* the same products as from syn-

thetic hydroxyaspartic acid. On the basis both of chromatographic behaviour and reduction products it can be regarded as proved that the amino acid studied is hydroxyaspartic acid.

The spot which travelled slower in butanol-acetic acid (R_F ~0.04) gave on reduction with HI and phosphorus glutamic acid and in addition glycine, serine, and alanine. It may be dihydroxyglutamic acid, but this cannot be regarded as proved.

Because there was no proof of the homogeneity of the isolated bound hydroxylamine fraction, it was subjected to paper electrophoresis (pyridine-acetic acid buffer, 1 000 V, 10 mA, pH 6.5, 4 h). Upon this bound hydroxylamine divided into two fractions, one of which behaved neutral and the other slightly basic (Fig. 2). On hydrolysis the neutral fraction gave hydroxyaspartic acid, glutamic acid, and alanine (in addition traces of valine and leucine), the basic fraction again the other unknown amino acids and besides the same amino acids as the neutral one. From the results it can be concluded that there are two hydroxylamine compounds, one giving hydroxyaspartic acid on hydrolysis, the other a still slower in butanol-acetic acid moving acidic amino acid (*cf.* above). If the components separated by electrophoresis are homogeneous they may be polypeptides, in which hydroxylamine is perhaps bound to one amino acid. The small amount of hydroxylamine formed on hydrolysis of these compounds — only about 1.5 % of the total N — arouses, however, the suspicion that the electrophoretically separated fractions may contain peptides as foreign substances. If this is the case nothing can be said about the chemical nature of the hydroxylamine compounds. Attention should, however, be called to the fact that hydroxyaspartic acid and another not fully characterized acid amino acid apparently belong to bound hydroxylamine in some way, since in *Azotobacter* cultures in which bound hydroxylamine was not formed, these amino acids were not found either.

A further elucidation of the problem demands more material and, accordingly, cultivation of *Azotobacter* on a larger scale. In any case it was proved that structurally complicated hydroxylamine compounds are accumulated in the culture solution of *Azotobacter;* that these compounds can be separated from amino acids by chromatography, and from each other by electrophoresis; that hydroxyaspartic acid is formed from one of these compounds on total hydrolysis and another not fully characterized amino acid from the other. In addition to these glutamic acid and alanine were formed from both.

1. Saris, N.-E. and Virtanen, A. I. *Acta Chem. Scand.* **11** (1957) 1438.

Received September 22, 1957.

X-Ray Crystallographic Data on Miscellaneous Sulphur Compounds

OLAV FOSS

Chemical Institute, University of Bergen, Bergen, Norway

The unit cells and space groups of the following derivatives of divalent sulphur, selenium and tellurium were determined some years ago in the course of crystal structure work on analogous compounds, and have not been published before. The data were derived from oscillation and Weissenberg photographs on single-crystal specimens, using iron radiation, $\lambda(\mathrm{Fe}K\alpha) = 1.934$ Å, and in one case (tellurium dibenzenethiosulphonate) copper radiation, $\lambda(\mathrm{Cu}K\alpha) = 1.542$ Å.

Tellurium dimethylxanthate [1], $\mathrm{Te(S_2C\text{-}OCH_3)_2}$. Monoclinic prismatic, $a = 4.24$ Å, $b = 14.18$ Å, $c = 17.28$ Å, $\beta = 93°$. There are four molecules per unit cell; density, calc. 2.19, found 2.18 g/cm³. The space group, from systematic absences, is $C_{2h}^5 - P2_1/c$.

The crystals occur as brownish red prisms, extended along [100] and with {001} dominant. The repeat distance along the a axis, 4.24 Å, is shorter than twice the value, 2.2 Å, listed by Pauling [2] for the van der Waals radius of tellurium, but is not in discord with Briegleb's value [3], 1.9 Å, or with the non-bonded Te-Te approaches of 4.18 Å and 4.28 Å, respectively, found in *p,p'*-dichlorodiphenyl ditelluride [4] and monoclinic barium telluropentathionate dihydrate [5].

The crystals liberate tellurium more rapidly than do those of the ethyl compound described below, perhaps because of the close Te-Te contact.

Tellurium diethylxanthate [1], $\mathrm{Te(S_2C\text{-}OC_2H_5)_2}$. Monoclinic prismatic, $a = 9.35$ Å, $b = 6.17$ Å, $c = 21.21$ Å, $\beta = 91°$. Four

thetic hydroxyaspartic acid. On the basis both of chromatographic behaviour and reduction products it can be regarded as proved that the amino acid studied is hydroxyaspartic acid.

The spot which travelled slower in butanol-acetic acid (R_F ~0.04) gave on reduction with HI and phosphorus glutamic acid and in addition glycine, serine, and alanine. It may be dihydroxyglutamic acid, but this cannot be regarded as proved.

Because there was no proof of the homogeneity of the isolated bound hydroxylamine fraction, it was subjected to paper electrophoresis (pyridine-acetic acid buffer, 1 000 V, 10 mA, pH 6.5, 4 h). Upon this bound hydroxylamine divided into two fractions, one of which behaved neutral and the other slightly basic (Fig. 2). On hydrolysis the neutral fraction gave hydroxyaspartic acid, glutamic acid, and alanine (in addition traces of valine and leucine), the basic fraction again the other unknown amino acids and besides the same amino acids as the neutral one. From the results it can be concluded that there are two hydroxylamine compounds, one giving hydroxyaspartic acid on hydrolysis, the other a still slower in butanol-acetic acid moving acidic amino acid (*cf.* above). If the components separated by electrophoresis are homogeneous they may be polypeptides, in which hydroxylamine is perhaps bound to one amino acid. The small amount of hydroxylamine formed on hydrolysis of these compounds — only about 1.5 % of the total N — arouses, however, the suspicion that the electrophoretically separated fractions may contain peptides as foreign substances. If this is the case nothing can be said about the chemical nature of the hydroxylamine compounds. Attention should, however, be called to the fact that hydroxyaspartic acid and another not fully characterized acid amino acid apparently belong to bound hydroxylamine in some way, since in *Azotobacter* cultures in which bound hydroxylamine was not formed, these amino acids were not found either.

A further elucidation of the problem demands more material and, accordingly, cultivation of *Azotobacter* on a larger scale. In any case it was proved that structurally complicated hydroxylamine compounds are accumulated in the culture solution of *Azotobacter;* that these compounds can be separated from amino acids by chromatography, and from each other by electrophoresis; that hydroxyaspartic acid is formed from one of these compounds on total hydrolysis and another not fully characterized amino acid from the other. In addition to these glutamic acid and alanine were formed from both.

1. Saris, N.-E. and Virtanen, A. I. *Acta Chem. Scand.* **11** (1957) 1438.

Received September 22, 1957.

X-Ray Crystallographic Data on Miscellaneous Sulphur Compounds

OLAV FOSS

Chemical Institute, University of Bergen, Bergen, Norway

The unit cells and space groups of the following derivatives of divalent sulphur, selenium and tellurium were determined some years ago in the course of crystal structure work on analogous compounds, and have not been published before. The data were derived from oscillation and Weissenberg photographs on single-crystal specimens, using iron radiation, $\lambda(\mathrm{Fe}K\alpha) = 1.934$ Å, and in one case (tellurium dibenzenethiosulphonate) copper radiation, $\lambda(\mathrm{Cu}K\alpha) = 1.542$ Å.

Tellurium dimethylxanthate [1], $\mathrm{Te(S_2C\text{-}OCH_3)_2}$. Monoclinic prismatic, $a = 4.24$ Å, $b = 14.18$ Å, $c = 17.28$ Å, $\beta = 93°$. There are four molecules per unit cell; density, calc. 2.19, found 2.18 g/cm³. The space group, from systematic absences, is $C_{2h}^5 - P2_1/c$.

The crystals occur as brownish red prisms, extended along [100] and with {001} dominant. The repeat distance along the a axis, 4.24 Å, is shorter than twice the value, 2.2 Å, listed by Pauling [2] for the van der Waals radius of tellurium, but is not in discord with Briegleb's value [3], 1.9 Å, or with the non-bonded Te-Te approaches of 4.18 Å and 4.28 Å, respectively, found in *p,p'*-dichlorodiphenyl ditelluride [4] and monoclinic barium telluropentathionate dihydrate [5].

The crystals liberate tellurium more rapidly than do those of the ethyl compound described below, perhaps because of the close Te-Te contact.

Tellurium diethylxanthate [1], $\mathrm{Te(S_2C\text{-}OC_2H_5)_2}$. Monoclinic prismatic, $a = 9.35$ Å, $b = 6.17$ Å, $c = 21.21$ Å, $\beta = 91°$. Four

molecules per unit cell; density, calc. 2.01, found 2.03 g/cm³. Space group, from systematic absences, $C_{2h}^5-P2_1/c$.

The crystals were obtained as long, red prisms, bounded by {001} and {100}, with the latter occasionally dominant.

Tellurium dibenzenethiosulphonate, $Te(S_2O_2C_6H_5)_2$, *monoclinic dimorph.* $a = 13.93$ Å, $b = 7.71$ Å, $c = 15.72$ Å, $\beta = 96°$. Density, calculated for four molecules per unit cell, 1.88 g/cm³, as compared with 1.86 g/cm³ for the orthorhombic dimorph [6]. The space group, from systematic absences, is $C_{2h}^5-P2_1/c$.

The orthorhombic dimorph (I) of this compound, the crystal structure of which was described recently [7], was obtained on crystallization from chloroform [6]. The monoclinic dimorph (II) usually occurred when benzene was used as a crystallization medium instead of chloroform, and also when the compound was crystallized from dilute chloroform solutions on addition of ether. Occasionally, mixtures were obtained, small amounts of I separating along with II from benzene, and II together with I from chloroform. Chemical analysis of the X-ray sample of II gave 26.6 % Te, calc. 26.9 %. The dimorphs appear to be about equally stable, no transition between them being observed at room temperature or on heating to about 150°C.

Tetragonal crystals, containing 75 mole % of tellurium dibenzenethiosulphonate and 25 mole % of sulphur dibenzenethiosulphonate, have been observed. The latter compound, and also the selenium analogue, crystallize in a tetragonal space group [6,8].

Disulphur dibenzenethiosulphonate [9], $S_2(S_2O_2C_6H_5)_2$. Orthorhombic bipyramidal, $a = 11.36$ Å, $b = 12.90$ Å, $c = 22.47$ Å. Density, calculated for eight molecules per unit cell, 1.66 g/cm³. This figure may be compared with the X-ray densities, 1.58, 1.57 and 1.62 g/cm³, respectively, of the analogues containing one, two and three sulphur atoms less [8,10]. The space group, from systematic absences, is $D_{2h}^{15}-Pbca$.

This hexathionic compound crystallized as plates {001} with plate edges parallel to the *ab* diagonals.

Strontium selenopentathionate dihydrate, $SrSe(S_2O_3)_2 \cdot 2H_2O$. Orthorhombic bipyramidal, $a = 4.94$ Å, $b = 10.19$ Å, $c = 21.83$ Å. Density, calculated for four formula units per unit cell, 2.58 g/cm³. Systematic absences, $0kl$ when $k + l$ is odd, $hk0$ when h is odd. These data indicate that the salt is isomorphous with orthorhombic barium pentathionate [11] and selenopentathionate [12] dihydrates, the space group of which is $D_{2h}^{16}-Pnma$. The crystals have the same morphology as the barium salts, and show the same perfect cleavage along the *c* plane.

The crystals were obtained by recrystallization from aqueous methanol of a crude sample prepared from the sodium salt [13] by metathesis with strontium perchlorate. No chemical analysis was made, but the X-ray data in connection with the known composition of the barium salts appear sufficient to establish the formula given above.

No further crystallographic work on the compounds is contemplated.

1. Foss, O. *Acta Chem. Scand.* **3** (1949) 1385.
2. Pauling, L. *The Nature of the Chemical Bond.* Cornell University Press, Ithaca, New York 1945, p. 189.
3. Briegleb, G. *Fortschr. chem. Forsch.* **1** (1950) 642.
4. Kruse, F. H., Marsh, R. E. and McCullough, J. D. *Acta Cryst.* **10** (1957) 201.
5. Foss, O. and Tjomsland, O. *Acta Chem. Scand.* **12** (1958). *In press.*
6. Foss, O. *Acta Chem. Scand.* **6** (1952) 521.
7. Øyum, P. and Foss, O. *Acta Chem. Scand.* **10** (1956) 279.
8. Dawson, I. M., Mathieson, A. McL. and Robertson, J. M. *J. Chem. Soc.* **1948** 322.
9. Troeger, J. and Hornung, V. *J. prakt. Chem.* [2] **60** (1899) 113.
10. Foss, O. *Acta Chem. Scand.* **8** (1954) 469.
11. Foss, O. and Zachariasen, H. *Acta Chem. Scand.* **8** (1954) 473.
12. Foss, O. and Tjomsland, O. *Acta Chem. Scand.* **8** (1954) 1701.
13. Foss, O. *Acta Chem. Scand.* **3** (1949) 435.

Received September 15, 1957.

The Nature of the Sulphur-Sulphur Bond in Thiosulphate and Thiosulphonate Ions

OLAV FOSS and ASBJØRN HORDVIK

Chemical Institute, University of Bergen, Bergen, Norway

Thiosulphate and thiosulphonate ions, $[S-SO_3]^{--}$ and $[S-SO_2R]^-$, are apparently (beside the polysulphide ions) the only relatively stable species with sulphur-sulphur bonds where one of the sulphur

molecules per unit cell; density, calc. 2.01, found 2.03 g/cm³. Space group, from systematic absences, $C_{2h}^5-P2_1/c$.

The crystals were obtained as long, red prisms, bounded by {001} and {100}, with the latter occasionally dominant.

Tellurium dibenzenethiosulphonate, $Te(S_2O_2C_6H_5)_2$, *monoclinic dimorph.* $a = 13.93$ Å, $b = 7.71$ Å, $c = 15.72$ Å, $\beta = 96°$. Density, calculated for four molecules per unit cell, 1.88 g/cm³, as compared with 1.86 g/cm³ for the orthorhombic dimorph [6]. The space group, from systematic absences, is $C_{2h}^5-P2_1/c$.

The orthorhombic dimorph (I) of this compound, the crystal structure of which was described recently [7], was obtained on crystallization from chloroform [6]. The monoclinic dimorph (II) usually occurred when benzene was used as a crystallization medium instead of chloroform, and also when the compound was crystallized from dilute chloroform solutions on addition of ether. Occasionally, mixtures were obtained, small amounts of I separating along with II from benzene, and II together with I from chloroform. Chemical analysis of the X-ray sample of II gave 26.6 % Te, calc. 26.9 %. The dimorphs appear to be about equally stable, no transition between them being observed at room temperature or on heating to about 150°C.

Tetragonal crystals, containing 75 mole % of tellurium dibenzenethiosulphonate and 25 mole % of sulphur dibenzenethiosulphonate, have been observed. The latter compound, and also the selenium analogue, crystallize in a tetragonal space group [6,8].

Disulphur dibenzenethiosulphonate [9], $S_2(S_2O_2C_6H_5)_2$. Orthorhombic bipyramidal, $a = 11.36$ Å, $b = 12.90$ Å, $c = 22.47$ Å. Density, calculated for eight molecules per unit cell, 1.66 g/cm³. This figure may be compared with the X-ray densities, 1.58, 1.57 and 1.62 g/cm³, respectively, of the analogues containing one, two and three sulphur atoms less [8,10]. The space group, from systematic absences, is $D_{2h}^{15}-Pbca$.

This hexathionic compound crystallized as plates {001} with plate edges parallel to the *ab* diagonals.

Strontium selenopentathionate dihydrate, $SrSe(S_2O_3)_2 \cdot 2H_2O$. Orthorhombic bipyramidal, $a = 4.94$ Å, $b = 10.19$ Å, $c = 21.83$ Å. Density, calculated for four formula units per unit cell, 2.58 g/cm³. Systematic absences, $0kl$ when $k + l$ is odd, $hk0$ when h is odd. These data indicate that the salt is isomorphous with orthorhombic barium pentathionate [11] and selenopentathionate [12] dihydrates, the space group of which is $D_{2h}^{16}-Pnma$. The crystals have the same morphology as the barium salts, and show the same perfect cleavage along the *c* plane.

The crystals were obtained by recrystallization from aqueous methanol of a crude sample prepared from the sodium salt [13] by metathesis with strontium perchlorate. No chemical analysis was made, but the X-ray data in connection with the known composition of the barium salts appear sufficient to establish the formula given above.

No further crystallographic work on the compounds is contemplated.

1. Foss, O. *Acta Chem. Scand.* **3** (1949) 1385.
2. Pauling, L. *The Nature of the Chemical Bond.* Cornell University Press, Ithaca, New York 1945, p. 189.
3. Briegleb, G. *Fortschr. chem. Forsch.* **1** (1950) 642.
4. Kruse, F. H., Marsh, R. E. and McCullough, J. D. *Acta Cryst.* **10** (1957) 201.
5. Foss, O. and Tjomsland, O. *Acta Chem. Scand.* **12** (1958). *In press.*
6. Foss, O. *Acta Chem. Scand.* **6** (1952) 521.
7. Øyum, P. and Foss, O. *Acta Chem. Scand.* **10** (1956) 279.
8. Dawson, I. M., Mathieson, A. McL. and Robertson, J. M. *J. Chem. Soc.* **1948** 322.
9. Troeger, J. and Hornung, V. *J. prakt. Chem.* [2] **60** (1899) 113.
10. Foss, O. *Acta Chem. Scand.* **8** (1954) 469.
11. Foss, O. and Zachariasen, H. *Acta Chem. Scand.* **8** (1954) 473.
12. Foss, O. and Tjomsland, O. *Acta Chem. Scand.* **8** (1954) 1701.
13. Foss, O. *Acta Chem. Scand.* **3** (1949) 435.

Received September 15, 1957.

The Nature of the Sulphur-Sulphur Bond in Thiosulphate and Thiosulphonate Ions

OLAV FOSS and ASBJØRN HORDVIK

Chemical Institute, University of Bergen, Bergen, Norway

Thiosulphate and thiosulphonate ions, $[S-SO_3]^{--}$ and $[S-SO_2R]^-$, are apparently (beside the polysulphide ions) the only relatively stable species with sulphur-sulphur bonds where one of the sulphur

atoms forms one bond only. Bonds of this type may be coordinate bonds, or double bonds. It was predicted by one of us [1] in 1950, on the basis of a discussion of the non-existence of branched sulphur chains, that the sulphur-sulphur bonds of thiosulphate and thiosulphonate ions possess a considerable degree of double-bond character. The argument was [1] that, since a sulphur atom, as acceptor, can be expected to add to another sulphur atom, as donor, only if the donor is *less* electronegative than the acceptor, and since the sulphur atom of sulphite and sulphinate ions is, presumably, *more* electronegative than electroneutral sulphur, the bonds cannot be pure coordinate bonds.

In the same year, Gerding and Eriks [2], on the basis of force constants from Raman spectra of aqueous sodium thiosulphate solutions, concluded that in the thiosulphate ion "the sulphur-sulphur bond undoubtedly possesses a strong double bond character".

Taylor and Beevers [3], in 1952, determined the crystal structure of sodium thiosulphate pentahydrate and found the sulphur-sulphur bond to be 1.97 Å, with a maximum error given as 0.06 Å. The present authors have now [4] made a crystal structure determination of sodium methanethiosulphonate monohydrate, $CH_3SO_2SNa \cdot H_2O$. The crystals [5] are orthorhombic bipyramidal, space group D_{2h}^{16}—*Pnma* with four formula units per unit cell, and the methanethiosulphonate ion possesses mirror plane symmetry in the crystals. The sulphur-sulphur bond was found to be 1.98 Å and the sulphur-oxygen bonds 1.45 Å, with standard deviations of probably less than 0.01 Å and 0.02 Å, respectively.

There is some uncertainty as to the length of a S—S single bond. Abrahams [6] has recently proposed 2.08 Å, and the true value may be a little larger. The double-bond length is probably [6] as in the S_2 molecule in the ground state, 1.89 Å. The S—S bonds in the thiosulphate and thiosulphonate ions, of lengths 1.97—1.98 Å, are next to that in the S_2 molecule the shortest S—S bonds measured, and correspond, according to Abrahams' tentative bond order-bond length curves [6-8], to between 50 % and 60 % double-bond character.

There may, of course, be various causes for the shortening of the sulphur-sulphur bonds of the thiosulphate and thiosulphonate ions. One picture is that, as predicted, double bonds (π bonds) exist to a considerable degree, arising from overlap of the $p\pi$ electron pairs of the outer sulphur atom with available 3*d* orbitals of the central sulphur atom. In view of the smaller tendency of the $p\pi$ electron pairs of a larger atom to participate in π-bond formation (*cf.* Ref.[9]), the amount of π-bond character of the sulphur-sulphur bonds should be smaller than in the sulphur-oxygen bonds of the same ions. The S—O distance in the methanethiosulphonate ion, 1.45 Å, corresponds [6,10] to about 90 % π-bond character. The estimate arrived at above for the S—S bond does thus not appear unreasonable.

It is interesting to note that when the thiosulphate and methanethiosulphonate ions undergo oxidation to the corresponding tetrathionic compounds, the double-bond character of the outer S—S bonds is lost, the length changing from 1.97—1.98 Å to 2.10—2.12 Å. The latter figures are from crystal structure determinations of barium tetrathionate dihydrate [11] and dimethanesulphonyl disulphide [12]. On the other hand, the new S—S bond formed on oxidation, *i. e.*, the middle S—S bond of the tetrathionic compounds, is about 2.04 Å and thus shorter than the outer bonds, probably due to *pd* π-bond formation now occurring between the divalent sulphur atoms.

1. Foss, O. *Acta Chem. Scand.* **4** (1950) 404.
2. Gerding, H. and Eriks, K. *Rec. trav. chim.* **69** (1950) 659.
3. Taylor, P. G. and Beevers, C. A. *Acta Cryst.* **5** (1952) 341.
4. Foss, O. and Hordvik, A. *To be published.*
5. Foss, O. *Acta Chem. Scand.* **10** (1956) 871.
6. Abrahams, S. C. *Quart. Rev. London* **10** (1956) 407.
7. Abrahams, S. C. and Grison, E. *Acta Cryst.* **6** (1953) 206.
8. Abrahams, S. C. *Acta Cryst.* **7** (1954) 423.
9. Baddeley, G. *J. Chem. Soc.* **1950** 663.
10. Moffitt, W. *Proc. Roy. Soc. London* **200 A** (1950) 409.
11. Foss, O., Furberg, S. and Zachariasen, H. *Acta Chem. Scand.* **8** (1954) 459.
12. Sörum, H. *Acta Chem. Scand.* **7** (1953) 1.

Received September 15, 1957.

ACTA CHEMICA SCANDINAVICA 11 (1957) 1445—1456

Studies on the Hydrolysis of Metal Ions

19. The Hydrolysis of Bismuth(III) in Perchlorate Medium

ÅKE OLIN

Department of Inorganic Chemistry, The Royal Institute of Technology, Stockholm 70, Sweden

The hydrolysis of the Bi(III) ion has been studied at 25 °C in 3 M sodium perchlorate medium by means of the cells:

$$-\text{Bi}-\text{Hg} \mid \text{S} \mid \text{ref}+$$
$$-\quad \text{glass} \mid \text{S} \mid \text{ref}+$$

where S had the general composition,

$$B \text{ mM Bi(III)}, H \text{ mM } H^+, 3\,000 - 3B - H \text{ mM } Na^+, 3\,000 \text{ mM } ClO_4^-.$$

It has been possible to vary B between 50 and 0.1 mM.

The data can be explained assuming the equilibria:

$$Bi^{3+} + H_2O \rightleftharpoons BiOH^{2+} + H^+ \qquad \log \beta_1 = -1.58 \pm 0.02$$

$$6\,Bi^{3+} + 12\,H_2O \rightleftharpoons Bi_6(OH)_{12}^{6+} + 12\,H^+ \qquad \log \beta_{12,6} = 0.330 \pm 0.005$$

For a summary of the work on the hydrolysis of bismuth up to 1947, the reader is referred to a paper by Granér and Sillén [1]. Since the appearance of their paper, in which a continuous polymerization was proposed, a photometric study has been published by Souchay and Peschanski [2], who found evidence for the formation of a complex that might be written as $Bi_4O_4^{4+}$. They state, however, that the complexes $Bi_5O_5^{5+}$ and $Bi_6O_6^{6+}$ are just as likely. In more basic solutions than correspond to $BiOClO_4$, Faucherre [3] has proposed the complex $Bi_8O_{10}^{4+}$. In none of these three investigations has any evidence been found for the simple complexes $BiOH^{2+}$ and $Bi(OH)_2^+$. Holmberg, Kraus, and Johnson [4] have ultracentrifuged bismuth(III) solutions and found only one complex, but it was not possible to state if the complex contained 5 or 6 bismuth atoms. The present work is an electrometric investigation of bismuth(III) perchlorate solutions similar to that of Granér and Sillén but carried out over a much broader range of concentrations.

THE METHOD OF INVESTIGATION

The experimental approach to this problem is essentially the same as similar investigations carried out in this laboratory [1,5]. In short a titrating solution rich in H^+ was added to a solution low in H^+, the total Bi(III) being kept constant. This is the only possible way in this case, since starting from the acid side would require too strong a base to be convenient. The solutions had the general composition:

$[Bi(III)] : B\text{mM}, [H^+]_{tot} : H\text{mM}, [Na^+] : 3\,000—3B—H\text{mM}, [ClO_4^-] : 3\,000\text{mM},$

where B denotes the total Bi(III) concentration and $[H^+]_{tot}$ is the "analytical" hydrogen ion concentration assuming no hydrolysis. The following cells were used to measure $[H^+] = h$ and Bi^{3+}

$$-\text{glass} \mid h \mid \text{ref} + \qquad E = E^\circ_g - 59.16 \log h - E_j \qquad (1)$$

$$-\text{Bi}-\text{Hg} \mid Bi^{3+} \mid \text{ref} + \qquad E = E^\circ_{am} - 19.72 \log [Bi^{3+}] - E_j \qquad (2)$$

The reference half-cell was in both cases

Ag, AgCl | 10 mM Ag^+, 2 990 mM Na^+, 3 000 mM ClO_4^- | 3 000 mM $NaClO_4$

The salt bridge was of the "Wilhelm" type designed by Forsling, Hietanen, and Sillén [6].

MATERIALS AND ANALYSIS

Sodium perchlorate was prepared by neutralizing Na_2CO_3 (Merck p.a.) with $HClO_4$ (Kebo p.a.) following the directions given by Biedermann [7]. The filtered solution gave no reaction for heavy metals, NO_3^- or SO_4^{2-}. It contained, however, minute quantities of chloride. The solution was therefore evaporated and allowed to crystallize. By working with not-too-concentrated solutions and stirring vigorously during the crystallization, it is possible to obtain readily-filterable crystals. A yield of *ca.* 70 % is obtained under proper conditions. The crystals were redissolved in water and the stock solution analysed by evaporating a known weight of solution and weighing the residue as $NaClO_4$.

Perchloric acid solutions were prepared from $HClO_4$ p.a. (70—72 %) and standardized against $KHCO_3$ and standard NaOH. The sodium hydroxide was standardized both against $N_2H_4 \cdot H_2SO_4$ and $KH(IO_3)_2$.

Bismuth (III) perchlorate was prepared by dissolving known amounts of Bi_2O_3 in standardized $HClO_4$. The Bi_2O_3 was prepared as follows: $Bi(NO_3)_3$ aq (p.a.) was recrystallized from nitric acid and ignited in an electric resistance furnace at *ca.* 700 °C to constant weight. In this way a lemon-yellow powder was obtained which dissolved completely in *ca.* 3 M $HClO_4$ to give a colorless solution. No foreign anions could be detected in it. The bismuth perchlorate stock solution was analysed for bismuth by precipitating it as the phosphate according to Blasdale and Parle [8] or as the oxide chloride as described by Winkler [9]. Both methods gave the same result within 0.2 %. The ClO_4^- concentration was determined by passing the solution through an ion exchanger and titrating the liberated acid with NaOH. The analytical hydrogen ion concentration was obtained as the difference $[ClO_4^-] - 3[Bi^{3+}]$. The agreement between the calculated and found concentrations of ClO_4^- and Bi^{3+} was within 0.2 %.

Bismuth amalgam was prepared electrolytically using mercury (redist.) as the cathode and a platinum spiral as the anode. An attempt was made to prepare the amalgam by dissolving metallic bismuth in mercury in a CO_2 atmosphere. This failed, however, since the metal contained traces of oxide which could not be completely removed. The amalgam was kept under the acid electrolyte in an inert atmosphere. A small portion of the stock amalgam was taken out for each titration by an arrangement similar to a wash bottle. Preliminary tests showed that no electrolyte came along with the amalgam. The concentration of bismuth in the amalgam was about 0.25 % (weight).

EXPERIMENTAL DETAILS OF THE EMF MEASUREMENTS

Almost all concentrations were measured in two series with stock solutions completely independent of each other, and in each series duplicate titrations were made. The glass electrode (Blomgren) was calibrated up to 750 mM of acid, giving the sum of the liquid junction potential and the deviation of the glass electrode from ideality as a function of h. The calibration curve was the same from one time to another for acid concentrations below *ca.* 450 mM. In more acid solutions fluctuations were observed amounting to 0.5 mV.

The liquid junction potential was determined by means of the cell,

$$\text{Ag, AgCl} \;\Big|\; \text{10 mM } Ag^+,\ \text{2 990 mM } \begin{Bmatrix} H^+ \\ Na^+ \end{Bmatrix},\ \text{3 000 mM } ClO_4^- \;\Big|\; \text{ref}$$

and found to agree with the values given by Biedermann and Sillén [10] to within 0.1 mV. For higher acidities (600 mM) the potentials were uncertain to 0.3 mV.

The amalgam electrode, which consisted of a pool on the bottom of the titration vessel, gave very constant and reproducible potentials. For identical points in each series, the difference between the emf values very seldom exceeded 0.05 mV. Under the same conditions the glass electrode showed a reproducibility of 0.2 mV. The overall reproducibility between the two series can be estimated by interpolation to be, for the amalgam electrode 0.1—0.2 mV, and for the glass electrode 0.3—0.4 mV. These limits, of course, contain analytical and other errors as well. Exceptions to the behavior stated above were given by the 0.1 mM titrations. Here the amalgam potential took at least half an hour to attain a constant value, and the reproducibility was only ± 0.2 mV.

Equilibrium seems to be attained immediately, and the potential remained constant within 0.05 mV for at least 3 h. It was observed that if a large amount of acid was added at one time, exactly the same potential was obtained (as fast as it could be measured), as if the same amount of acid was added during the course of about 5 h.

RESULTS AND CALCULATIONS

Since the amount of data obtained in this investigation is very large (600 equilibrium compositions were measured), it is not possible to give them all in detail. One representative titration is given in full in Table 1 and the others from the second series in compact form in Table 2. Fig. 2 shows the data from the second series. Those from the first series agree so closely that no difference would be seen in the figure. η denotes $\log \frac{[\text{Bi(III)}]_{\text{total}}}{[\text{Bi}^{3+}]_{\text{free}}}$ and h the hydrogen ion concentration at equilibrium. All concentrations in tables and figures, and E°_{am}, are on the mM scale, whereas E°_{g} and the final equilibrium constants are on the M scale.

Determination of E°_{am} *and* E°_{g}. In order to evaluate h and $[\text{Bi}^{3+}]$ from eqns (1) and (2), it is necessary to know the E°. By assuming that at sufficiently high acidities the hydrolysis is completely repressed, one can calculate the E° values by inserting the analytical concentrations. In this way it was possible to get the E° for the glass electrode, since the effect of the hydrolysis on the hydrogen ion concentration is small in the most acid solutions. The E°_{g} so obtained agreed with the E° from separate acid-base titrations substantiating the assumption made. For the amalgam electrode, a slight but definite trend in E°_{am} was always observed. Thus only a rough value was obtained, which was used for the preliminary calculations.

Table 1. Measurements with amalgam and glass electrodes. S_1 : Bi(III) : 10 mM, H^+ : 0.00 mM, Na^+ : 2970 mM, ClO_4^- : 3000 mM, S_2 : Bi(III) : 10 mM, H^+ : 1198 mM, Na^+ : 1772 mM, ClO_4^- : 3000 mM, $E°_{am}$ = 418.1 mV.

S_2 ml	E_g mV	E_{Bi-Hg} mV	H mM	$E°_g$ mV	log h mM	$-E_j$ mV	η
0	398.4	436.74	0		1.297	0.32	1.929
0.2	393.1	433.24	4.77		1.386	0.39	1.748
0.5	387.0	429.18	11.87		1.490	0.49	1.537
0.7	383.6	426.95	16.55		1.549	0.57	1.420
1.0	379.2	424.18	23.50		1.625	0.68	1.274
1.5	373.6	420.52	34.90		1.723	0.84	1.080
2.0	369.2	417.71	46.09		1.801	1.01	0.929
2.5	365.6	415.40	57.07		1.863	1.17	0.804
3.0	362.3	413.50	67.83		1.923	1.34	0.699
3.5	359.9	411.90	78.40		1.966	1.48	0.611
4.0	357.6	410.53	88.77		2.006	1.62	0.534
4.5	355.4	409.35	98.95		2.046	1.78	0.466
5.0	353.6	408.32	108.9		2.080	1.92	0.407
5.5	351.9	407.42	118.8		2.111	2.06	0.354
6.0	350.3	406.63	128.4		2.142	2.22	0.306
6.5	349.1	405.95	137.9		2.163	2.33	0.266
7.0	347.8	405.36	147.2		2.188	2.46	0.229
7.5	346.6	404.86	156.3		2.210	2.59	0.197
8.0	345.5	404.44	165.3		2.230	2.72	0.169
8.5	344.4	404.08	174.1		2.250	2.85	0.145
9.0	343.3	403.80	182.8	296.7	2.272	2.98	0.124
9.5	342.3	403.58	191.3	296.8	2.290	3.10	0.107
10	341.5	403.42	199.7	296.9	2.305	3.20	0.093
11	340.0	403.26	216.1	297.2	2.335	3.41	0.075
12	338.5	403.24	231.9	297.2	2.365	3.64	0.062
13	337.2	403.31	247.3	297.3	2.393	3.87	0.054
14	335.9	403.43	262.2	297.3	2.418	4.10	0.048
15	334.7	403.56	276.6	297.2	2.442	4.32	0.044
17	332.7	403.85	304.1	297.2	2.483	4.70	0.039
19	331.0	404.16	330.0	297.2	2.519	5.04	0.038
21	329.5	404.44	354.4	297.1	2.550	5.35	0.036
23	328.3	404.72	377.6	297.3	2.577	5.65	0.035
25	327.3	404.97	399.4	297.4	2.601	5.93	0.034
				$E°_g$ = 297.2 mV			

In the following the same notations as those of Hietanen and Sillén [11] will be used. The calculations will chiefly be based on the η function, since this is much more accurate than the Z function.

A plot of η against log h revealed two characteristic features. For higher values of η, a different curve for each Bi_{tot} was found, thus indicating polynuclearity. For low η values the curves coincided showing that only mononuclear complexes appear besides Bi^{3+}. To evaluate a more accurate $E°_{am}$ the following method was adopted:

Table 2. Corresponding values of η and log h at equilibrium calculated with $E°_{am}$ = 418.10 mV.

50 mM		25 mM		5 mM		2.5 mM	
η	log h	η	log h	η	log h	η	log h
1.756	1.664	2.071	1.393	1.918	1.173	2.057	0.987
1.635	1.725	1.887	1.484	1.714	1.277	1.757	1.134
1.504	1.797	1.674	1.592	1.485	1.391	1.447	1.292
1.423	1.834	1.559	1.649	1.361	1.455	1.291	1.371
1.317	1.890	1.414	1.721	1.209	1.530	1.105	1.461
1.170	1.963	1.330	1.767	1.121	1.576	0.868	1.589
1.051	2.024	1.221	1.820	1.007	1.631	0.695	1.673
0.947	2.080	1.069	1.897	0.849	1.714	0.555	1.754
0.859	2.124	0.944	1.961	0.721	1.783	0.445	1.814
0.783	2.165	0.840	2.014	0.615	1.836	0.354	1.867
0.714	2.200	0.750	2.060	0.525	1.887	0.281	1.914
0.653	2.234	0.672	2.102	0.448	1.928	0.223	1.952
0.600	2.260	0.604	2.137	0.381	1.965	0.165	1.991
0.551	2.288	0.543	2.170	0.323	2.002	0.142	2.025
0.504	2.312	0.488	2.201	0.273	2.033	0.118	2.054
0.466	2.332	0.439	2.228	0.230	2.062	0.100	2.085
0.430	2.354	0.394	2.253	0.193	2.090	0.090	2.108
0.394	2.377	0.354	2.274	0.161	2.114	0.082	2.135
0.363	2.393	0.316	2.297	0.135	2.137	0.076	2.160
0.329	2.417	0.283	2.316	0.115	2.160	0.068	2.199
0.306	2.430	0.254	2.337	0.099	2.179	0.062	2.236
0.253	2.464	0.226	2.356	0.086	2.201	0.054	2.296
0.176	2.513	0.199	2.375	0.077	2.218	0.049	2.348
0.119	2.561	0.176	2.391	0.069	2.236	0.044	2.391
0.084	2.600	0.138	2.420	0.060	2.266	0.040	2.429
0.062	2.643	0.104	2.452	0.054	2.296	0.036	2.461
0.045	2.678	0.081	2.476	0.051	2.323	0.036	2.490
0.043	2.705	0.063	2.500	0.048	2.347	0.034	2.515
0.039	2.732	0.052	2.522	0.045	2.370	0.033	2.538
0.038	2.757	0.041	2.564	0.041	2.410		
0.036	2.780	0.037	2.598	0.037	2.445		
0.035	2.800	0.034	2.628	0.034	2.476		
				0.032	2.503		

Consider the following mononuclear equilibria

$$Bi^{3+} + H_2O \rightleftharpoons BiOH^{2+} + H^+ \qquad \beta_1 = \frac{[BiOH^{2+}][H^+]}{[Bi^{3+}]}$$

$$Bi^{3+} + 2H_2O \rightleftharpoons Bi(OH)_2^+ + 2H^+ \qquad \beta_2 = \frac{[Bi(OH)_2^+][H^+]^2}{[Bi^{3+}]}$$

Together with

$$[Bi(III)]_{tot} = [Bi^{3+}] + [BiOH^{2+}] + [Bi(OH)_2^+] + \ldots\ldots$$

$$[Bi(III)]_{tot} = B\,;\ [Bi^{3+}] = b\,;\ [H^+] = h$$

Table 2 (continued)

1 mM		0.5 mM		0.1 mM	
η	log h	η	log h	η	log h
2.001	0.839	2.502	0.481	2.215	0.301
1.608	1.041	2.293	0.588	1.981	0.455
1.240	1.223	2.058	0.699	1.535	0.653
1.065	1.318	1.771	0.833	1.327	0.763
0.861	1.418	1.561	0.940	1.164	0.845
0.753	1.474	1.396	1.025	1.042	0.943
0.617	1.547	1.259	1.097	0.929	0.997
0.442	1.646	1.135	1.155	0.716	1.112
0.315	1.731	0.963	1.250	0.622	1.173
0.225	1.794	0.821	1.320	0.516	1.232
0.168	1.850	0.705	1.387	0.411	1.320
0.136	1.900	0.610	1.436	0.356	1.362
0.116	1.944	0.530	1.476	0.306	1.427
0.105	1.982	0.463	1.521	0.269	1.504
0.096	2.017	0.406	1.559	0.237	1.575
0.089	2.041	0.340	1.598	0.214	1.629
0.083	2.078	0.287	1.642	0.195	1.676
0.079	2.106	0.229	1.684	0.168	1.749
0.074	2.132	0.183	1.742	0.134	1.831
0.071	2.152	0.159	1.788	0.126	1.905
0.068	2.174	0.141	1.829	0.103	1.967
0.065	2.195	0.120	1.869	0.099	2.020
0.061	2.214	0.113	1.903	0.079	2.110
0.059	2.232	0.100	1.937	0.071	2.180
0.054	2.265	0.092	1.993	0.057	2.240
0.051	2.295	0.082	2.039	0.057	2.291
0.049	2.322	0.076	2.083	0.053	2.335
0.047	2.347	0.071	2.130	0.048	2.374
0.044	2.370	0.066	2.158	0.044	2.409
0.040	2.410	0.062	2.191	0.040	2.440
0.036	2.445	0.058	2.221	0.037	2.468
0.034	2.475	0.051	2.248	0.036	2.495
0.033	2.502	0.047	2.297	0.032	2.518
0.032	2.526	0.043	2.340		
		0.040	2.378		
		0.036	2.412		
		0.034	2.443		

these equations give

$$\left(\frac{B}{b} - 1\right)h = \beta_1 + \beta_2 \cdot h^{-1} + \beta_3 \cdot h^{-2} + \ldots\ldots$$

The problem is then to find an E° value which gives a curve of the right shape when $\left(\frac{B}{b} - 1\right) h$ is plotted against h^{-1}. In Fig 1 three such curves are shown for different E° values, namely 418.30, 418.10 and 417.90 mV . The figure shows that the curves deviate appreciably for too high or too low E° values, leaving a range in which the correct value may be found. The "best

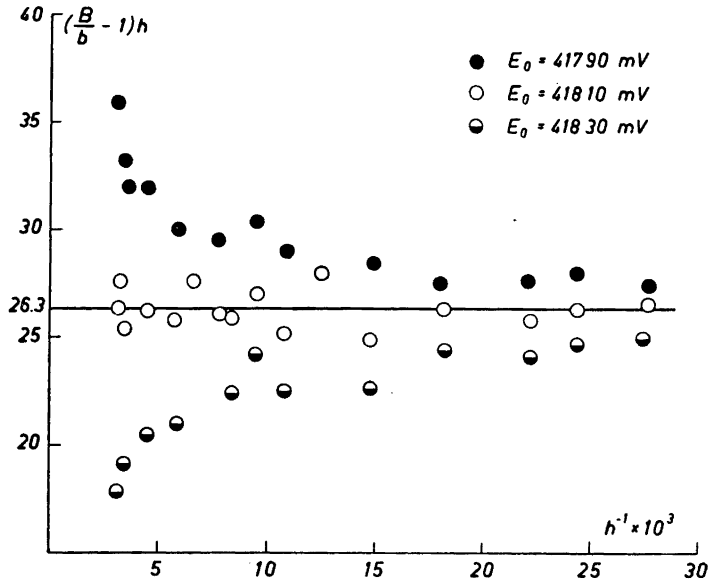


Fig 1. Determination of $E°_{am}$, β_1 and β_2. The middle curve represents $E°_{am}$ = 418.10 mV and $\left(\frac{B}{b} - 1\right)h$ = 26.3 mM.

$E°''$ = 418.10 mV was found to give an almost horizontal line with an intercept (equal to β_1) on the $\left(\frac{B}{b} - 1\right)h$ axis = 26.3 mM. Since the scatter is necessarily great a constant correct to more than 5 % cannot be expected; furthermore, it is hard to decide if the line is horizontal or has a small slope. The second mononuclear constant seems to be very small, and has not been considered in the further calculations. An analysis of the mononuclearity thus gives for the first hydrolysis stage an equilibrium constant 26.3 ± 2 mM with the second stage almost absent.

Determination of the main hydrolysis products. The recalculated η *vs.* log h curves (Fig 2) with $E°_{am}$ = 418.10 mV revealed the following features for larger η values. The curves were almost parallel with a spacing $\left(\frac{\Delta \log B}{\Delta \log h}\right)_\eta = 2.4$ and had a slope of -2. It may be pointed out that these properties are independent of any chosen $E°_{am}$, since changing this parameter only means that the curves are shifted along the ordinate axis.

Let it be assumed that the general composition of the complexes may be written Me_qH_{-p};

$$B = b + \Sigma q\beta_{pq}b^q h^{-p} \simeq \Sigma q\beta_{pq}b^q h^{-p} \quad (3)$$

$$10\eta = \frac{B}{b} = 1 + \Sigma q\beta_{pq}b^{q-1}h^{-p} \simeq \Sigma q\beta_{pq}b^{q-1}h^{-p} \quad (4)$$

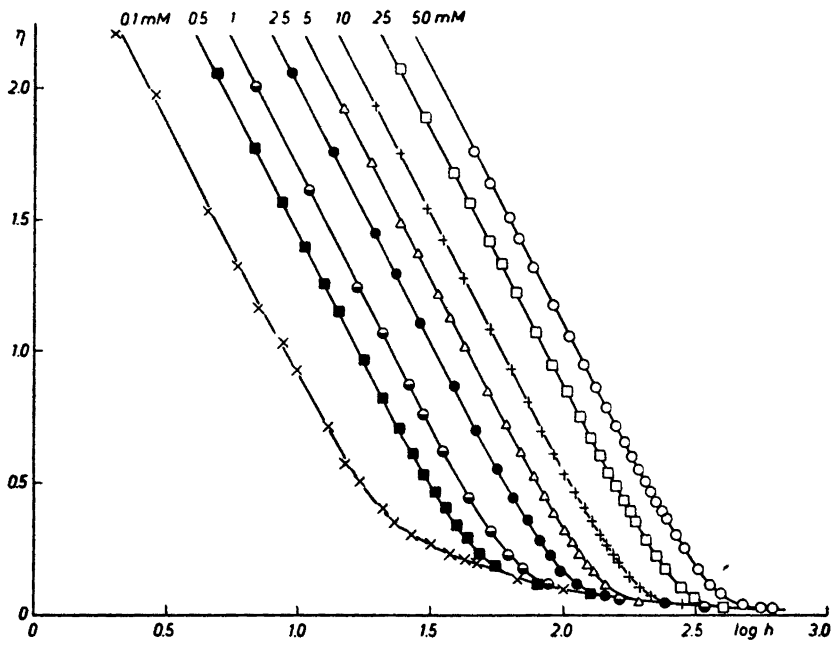


Fig 2. $\eta = \log \frac{[\mathrm{Bi(III)}]_{tot}}{[\mathrm{Bi^{3+}}]}$ as a function of log h. Curves are calculated with $\beta_1 = 26.3$ mM and $\beta_{12.6} = 2.14$ M^7. For clarity not all of the experimental points are shown for low η values.

The curves give

$$B \text{ constant} ; \eta = \mathrm{f}(B) - 2 \log h \tag{5}$$

$$\frac{B}{b} \text{ constant} ; \log B - 2.4 \log h = \text{const. or } 10\eta = \mathrm{f}(b^{-1}h^{2.4}) \tag{6}$$

Eqns (6) and (4) give

$$\Sigma q\beta_{pq} b^{q-1} h^{-p} = \mathrm{f}(b^{-1}h^{2.4})$$

which can be fulfilled only if

$$p = 2.4(q - 1) \tag{7}$$

If (5) is rewritten as $\log B - \log b = \mathrm{f}(B) - 2 \log h$, it is seen that $bh^{-2} = \mathrm{f}'(B)$. This gives with (3)

$$bh^{-2} = \mathrm{f}'(\Sigma q\beta_{pq} b^q h^{-p}) \text{ or } q = \frac{p}{2} \tag{8}$$

Eqns (7) and (8) give $q = 6$ and $p = 12$. The main complex may therefore be written $Bi_6(OH)_{12}^{6+}$ or more generally $Bi_6O_n(OH)_{12-2n}^{6+}$. The lines of argument in this discussion follow closely those of Sillén in AB I and II [12,13], and indeed the same result appears with his methods.

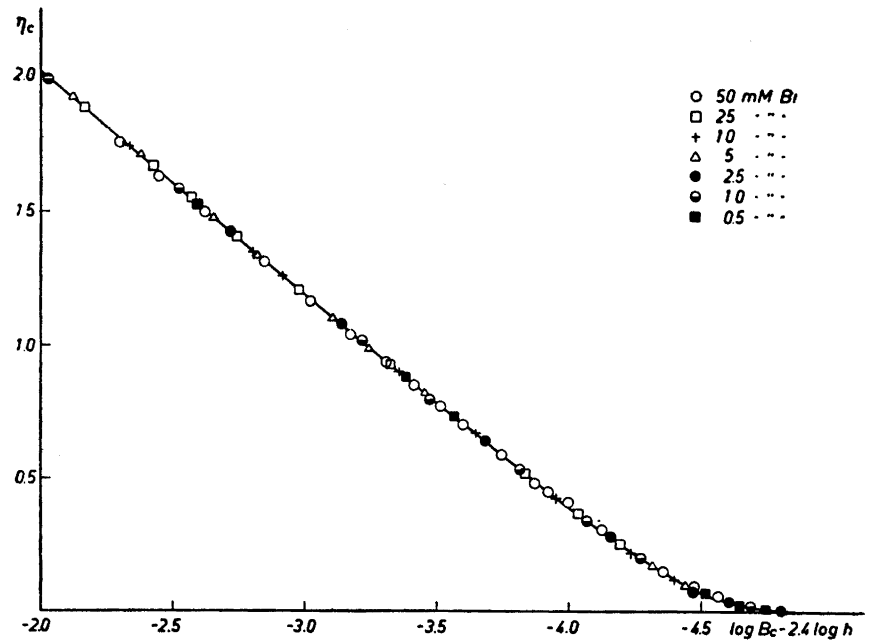


Fig 3. η_c as a function of log B_c — 2.4 log h (see text). The curve is calculated with log $\beta_{12,6} = 0.330$.

To evaluate the equilibrium constants for the hexamer the following method may be adopted. We define the functions B_c and η_c so that they have their usual meaning, except that the mononuclear part has been subtracted. From the relations,

$$B = b + \beta_1 b h^{-1} + 6\beta_{12,6} b^6 h^{-12}$$

$$B_c = B - \beta_1 b h^{-1} = b + 6\beta_{12,6} b^6 h^{-12}$$

$$\frac{B_c}{b} = 10^{\eta_c} = 1 + 6\beta_{12,6} b^5 h^{-12} = 1 + \frac{6\beta_{12,6}}{10^{5\eta_c}} [B_c h^{-2.4}]^5$$

it follows that η_c is a function of the single variable log B_c — 2.4 log h. In Fig 3, η_c is shown as a function of log B_c — 2.4 log h. Since all the experimental points fall on a single curve, we might conclude that the concentrations of complexes other than $BiOH^{2+}$ and $Bi_6(OH)_{12}^{6+}$ must be small. By comparing this curve with a "normalized" one the equilibrium constant of the hexamer is obtained as log $\beta_{12,6} = 0.330 \pm 0.005$, M scale. The uncertainty in this value lies in the E°_{am} determination.

It might at this point be asked with what certainty one can say that there are 6 Bi in the complex and not for instance 5 or 7. These complexes correspond to the spacings 2.50 and 2.33, thus lying very near to 2.4. It

was therefore decided to make calculations using these assumptions too. These calculations showed, however, that a good fit could not be obtained over the whole B range but when only a narrow concentration range in B is considered, it is not easy to draw any definite conclusions. This shows the desirability of covering as wide a concentration range as possible.

The graphic methods developed by Biedermann and Sillén [14] using "normalized" curves should be applicable to this case. On account of the preceding discussion the assumption is made that the only species present, apart from Bi^{3+}, are $BiOH^{2+}$ and $Bi_6(OH)_{12}^{6+}$. This leads to a three-parameter problem since $E°_{am}$ is unknown in addition to the equilibrium constants. The method is based on cuts for constant η. The family of experimental curves for constant η values

$$x = \log B - 2.4 \log h$$
$$y = \log h$$

are plotted and compared with a graph of the theoretical, normalized curves

$$X = \log B - 2.4 \log h + \log k = \eta + \log v$$
$$Y = -\log \alpha = \log h - \log \beta_1 = -\log(10^{\eta} - 1 - v^5)$$

where $k^5 = 6\ \beta_{12.6}$; $v = kbh^{-2.4}$.

By eliminating the parameter v, we obtain

$$Y = -\log(10^{\eta} - 1 - 10^{5(X-\eta)})$$

From this equation we can calculate the family of curves $Y(X)_\eta$. The two graphs are laid on top of each other to coincide as closely as possible and the differences on the x and y axes in this position give the equilibrium constants.

The correct $E°_{am}$ is obtained by considering the smallest η values; since in this range η is dependent on log h only, Y must be independent of v which happens only when v equals zero. Corresponding values between η and log α are obtained by putting $v = 0$. A curve $\eta(\log \alpha)$ may thus be found. From experimental data based on different $E°_{am}$, a family of curves $\eta(\log h)_{E°_{am}}$ is obtained. It is now possible to plot log $\alpha(\log h)_{E°_{am}}$ for each of the chosen $E°_{am}$. The curve for the right $E°_{am}$ should give a straight line of slope -1. In this way the same $E°_{am} = 418.1$ mV was obtained as by the earlier method. In Fig 4 the normalized curves are shown together with the experimental points in the position of "best fit". The equilibrium constants found are log $\beta_1 = -1.585$ ($\beta_1 = 0.026$ M) and log $\beta_{12.6} = 0.325$ (M scale), comparing favorably with the earlier results. It may be pointed out that in this method the constants may be varied simultaneously and independently of each other.

Since the Z values $\left(\frac{h-H}{B}\right)$ must necessarily be quite uncertain in such acid solutions as have been used in this investigation, they were thought not to be worth a separate treatment. This gap, it is hoped, will be filled by conductimetric measurements; however, there was no doubt that the limiting value of Z is 2. In addition, the quantity $\frac{h-H}{B-b}$ (the number of hydrogen

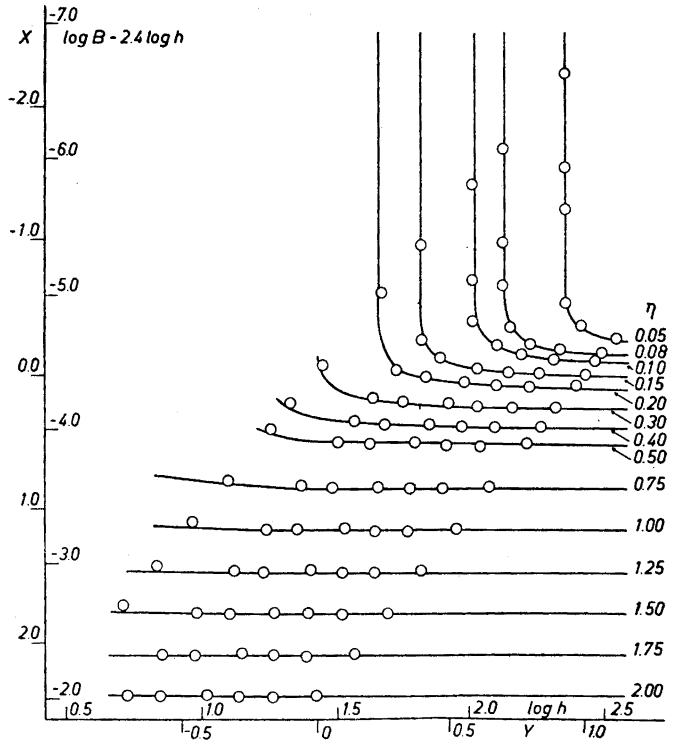


Fig 4. X, Y curves and experimental points *x, y* (see text) in position of »best fit». O experimental points.

ions set free by the complexed bismuth) was found to vary between 1.95 and 2.05 in the region where polynuclear species predominate. This strongly indicates that in the most hydrolysed solutions the ratio Bi:OH in the complex (es) formed is 1:2.

DISCUSSION

The present investigation of the hydrolysis of Bi^{3+} leads to a different mechanism from that proposed by Granér and Sillén [1], who used the same type of investigation. As has already been pointed out, it is difficult to decide what mechanism is the most likely, when only a rather small concentration range has been measured: a small error may completely change the picture. In the case of Granér and Sillén, who only studied the concentration range 10—50 mM of Bi(III), one probable error can be pointed out. They calculated with liquid junction potentials obtained from quinhydrone measurements. As was found later by Biedermann and Sillén [10] the quinone acts as a base [15] and the liquid junction potentials are not applicable to a quinhydrone-free system. This leads to an error of 0.1 units in η in the most unfavorable cases.

The most recent works on bismuth perchlorate all seem to indicate the presence of only one complex. Its composition was, however, not definitely established. There seems to be no doubt that the ratio Bi:O is 1:1, but the number of bismuth atoms in the complex has not hitherto been ascertained. The work of Faucherre [3] is not comparable since it was carried out in solutions of so low acidity, that they cannot be obtained when working in a strong ionic medium because of precipitation. In the present investigation the most hydrolysed solutions gave η values around 3. These points lie on the extensions of the curves in Fig. 3 and give no indication of a new reaction. The solutions were not quite stable but gave a small precipitate after standing for about a week. We hope, however, to be able to carry out titrations at lower ionic strength to find out what happens at higher pH values.

If only one complex is formed, it is hard to imagine it as a chain or a layer, since a complex with a certain, relatively high number of atoms in it would not be expected to dominate; however, for a complex containing six metal atoms one can visualise models of high symmetry. This symmetry could then account for the extreme stability and presence of only one predominating complex. These models must, however, be accepted with scepticism and need confirmation from structural data both in solution and in the solid state. Work in this direction is planned. The absence of $Bi(OH)_2^+$ is remarkable. The reason for this may be that the "hexamer" is so stable compared to $Bi(OH)_2^+$ that the equilibrium concentration of this complex is too low to be detected.

Acknowledgements. The author wishes to express his gratitude to Professor Lars Gunnar Sillén for suggesting this work and for his guidance in carrying it out. He also wishes to thank Dr. George Biedermann and Dr. Gösta Lagerström for the many discussions held with them on various aspects of this problem. Dr. Helen S. Dunsmore and Dr. R. Stuart Tobias are thanked for having corrected the English. Mr. Frans Ericson has been a valuable aid in constructing the apparatus.

This work has been made possible by a fellowship from *Statens Tekniska Forskningsråd (Swedish Technical Research Council)*.

REFERENCES

1. Granér, F. and Sillén, L. G. *Acta Chem. Scand.* **1** (1947) 631.
2. Souchay, P. and Peschanski, D. *Bull. soc. chim. France* **1948** 439.
3. Faucherre, J. *Bull. soc. chim. France* **1954** 253.
4. Holmberg, R. W., Kraus, K. A. and Johnson, J. S. *J. Am. Chem. Soc.* **78** (1956) 5506.
5. Hietanen, S. *Acta Chem. Scand.* **8** (1954) 1626.
6. Forsling, W., Hietanen, S. and Sillén, L. G. *Acta Chem. Scand.* **6** (1952) 903.
7. Biedermann, G. *Arkiv Kemi* **9** (1956) 277.
8. Blasdale, W. C. and Parle, W. C. *Ind. Eng. Chem. Anal. Ed.* **8** (1936) 352.
9. Winkler, L. W. *Die chemische Analyse* Bd. 29, Ferdinand Enke Verlag, Stuttgart 1931.
10. Biedermann, G. and Sillén, L. G. *Arkiv Kemi* **5** (1953) 425.
11. Hietanen, S. and Sillén, L. G. *Acta Chem. Scand.* **8** (1954) 1607.
12. Sillén, L. G. *Acta Chem. Scand.* **8** (1954) 299.
13. Sillén, L. G. *Acta Chem. Scand.* **8** (1954) 318.
14. Biedermann, G. and Sillén, L. G. *Acta Chem. Scand.* **10** (1956) 1011.
15. Biedermann, G. *Acta Chem. Scand.* **10** (1956) 1340.

Received May 15, 1957.

ACTA CHEMICA SCANDINAVICA 11 (1957) 1457—1464

The Acid-soluble Nucleotides of Barley and Oat Plants

ROLF BERGKVIST

Institute of Biochemistry, University of Lund, Sweden

The acid-soluble nucleotides of barley and oat plants are isolated and fractionated by ion exchange chromatography; they are shown to include the 5′-triphosphates of adenosine, guanosine, cytidine and uridine besides mono- and diphosphates. The identifications are based on ultraviolet absorption measurements and chromatographic and ionophoretic evidence before and after hydrolysis together with chemical and enzymic analysis.

Besides as a constituent of nucleic acids, adenosine-5′-phosphate has been known for a long time to occur in combined forms in smaller molecules which act as coenzymes in many metabolic processes. None of the other three nucleotides from ribonucleic acid had been found to occur in biological material either free or forming part of small molecules. Seven years ago Leloir and coworkers [1] studying the galactose metabolism in yeast, and Park and Johnson [2] studying the effects of penicillin on bacteria, observed independently the occurrence of acid-soluble uridine-containing compounds in living tissues. Following these important contributions to the progress of nucleotide biochemistry, derivatives of uridine-5′-phosphate, guanosine-5′-phosphate and cytidine-5′-phosphate have been isolated from different sources with the result that the number of derivatives of these nucleotides known to occur in living tissues is about the same as that in the adenosine-5′-phosphate series, so that the latter compounds have now lost the unique position, as building blocks of coenzymes, which they were believed to have.

The main difficulties encountered in the demonstration of these compounds in plants have centered around the problem of their isolation free from interfering substances and their separation. Methods developed primarily for the isolation of the nucleotides from animal tissues have proven unsatisfactory for the isolation of these compounds from plants. From mung beans, which have a low content of disturbing substances, an ATP *-like compound [3] and

* Abbreviations used: A, adenosine; G, guanosine; U, uridine; C, cytidine; MP, monophosphate; DP, diphosphate; TP, triphosphate; UDPG, uridine diphosphate glucose; UDPAG, uridine diphosphate acetylglucosamine; DPN, diphosphopyridine nucleotide; TPN, triphosphopyridine nucleotide.

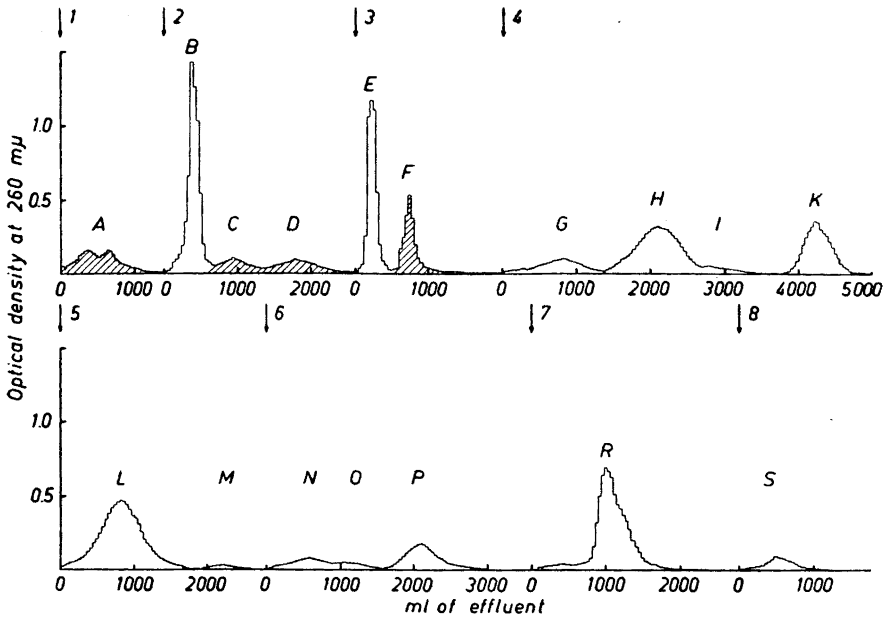


Fig. 1. Ion exchange chromatogram of acid-soluble nucleotides from 500 g of barley plants. The crossed fractions varied in amounts in different preparations.

Exchanger: Dowex 1, X-10, 200 to 400 mesh, 1.6 × 40 cm., formate form; flow rate 1.5 ml/min.

Eluting agents:

1)	0.02	M	formic	acid				
2)	0.1	M	»	»				
3)	0.1	M	»	»	+	0.05	M	sodium formate
4)	0.1	M	»	»	+	0.3	M	» »
5)	0.1	M	»	»	+	0.4	M	» »
6)	0.1	M	»	»	+	0.6	M	» »
7)	0.2	M	»	»	+	0.8	M	» »
8)	0.5	M	»	»	+	1.0	M	» »

Identity of peaks:

A) 2′- and 3′-CMP
B) 5′-AMP
C) 2′-AMP
D) 3′-AMP
E) 5′-UMP
F) 2′- and 3′-UMP; 2′- and 3′-GMP; CDP and TPN.
G) UDPAG
H) UDPG
I) ADP derivative
K) UDP
L) ADP
M) CTP
N) GDP
O) ATP derivative
P) UTP
R) ATP
S) GTP

quite recently a mixture of uridine diphosphate sugar compounds [4] have been isolated. Paper chromatographic evidence for the presence of adenosine and uridine containing compounds in plants has been presented by several authors [5–7].

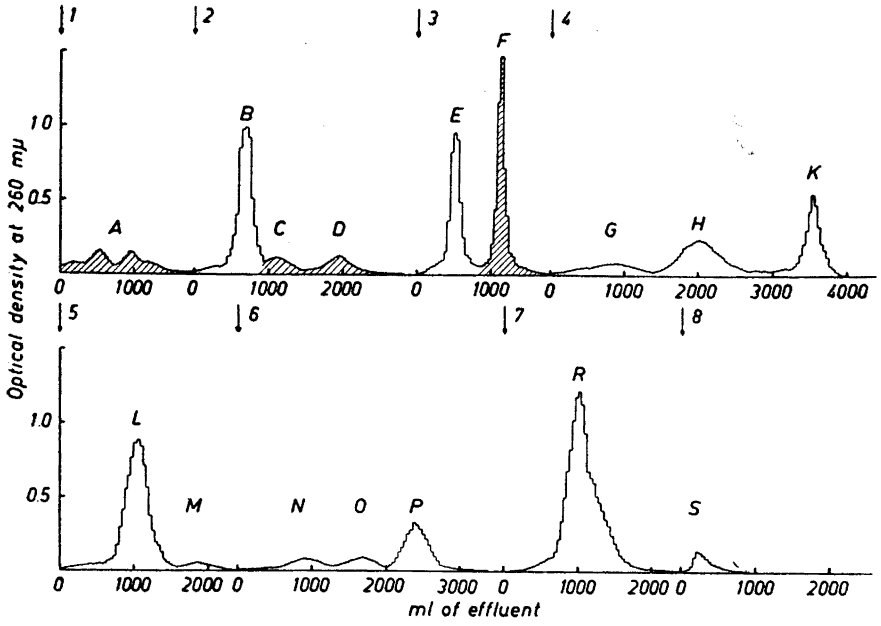


Fig. 2. Ion exchange chromatogram of acid-soluble nucleotides from 500 g of oat plants. The crossed fractions varied in amounts in different preparations.

Exchanger: Dowex 1,X-10, 200 to 400 mesh, 1.6 × 40 cm., formate form; flow rate 1.5 ml/min.
The eluting agents and identity of peaks are the same as in Fig. 1.

An improved method for the isolation and quantitative estimation of the acid-soluble nucleotides from plant tissues has been described in a previous paper [8]. The application of this method to wheat plants established the occurrence of all the four ribonucleosides in the form of acid-soluble 5′-mononucleotides at different levels of phosphorylation [8]. Of interest is the predominance of uridine, besides adenosine derivatives in wheat plants, in contrast to the dominating role of the latter compounds in animal tissue.

The present paper deals with the isolation and identification of the acid-soluble nucleotides of two other kinds of grain, namely oats and barley. Because of very marked similarities in nucleotide content the two plants are described together. From oats, the isolation in low yield of a nucleotide of low purity which appeared to be related to, but not identical with 5′-ADP, had been reported by Albaum and Umbreit [9].

The acid-soluble nucleotides were isolated by homogenizing the plant material in cold perchloric acid and freed from other phosphorus-containing or ultraviolet-absorbing substances according to the method previously elaborated. After adsorption on a column of 200 to 400 mesh strong base anion exchanger in the formate form, the individual nucleotides were eluted with

formic acid solutions containing increasing concentrations of sodium formate. Elution of the nucleotides was followed by the changes in optical densities of the eluate at 250, 260 and 270 mμ. The optical densities at 260 mμ of the effluent fractions were plotted against effluent volume to obtain the chromatographs shown in Figs. 1 and 2.

The elution position and the absorbance ratios gave a preliminary identification of the individual fractions. Since the nucleotides from the column were distributed in large volumes of formate buffer, it was desirable to concentrate them and remove the excess salt by readsorption on norite and elution with ammoniacal ethanol.

The solutions thus obtained were used to identify the nucleotides and establish the purity of the peaks by comparison of their chromatographic and ionophoretic behaviour with that of the corresponding authentic nucleotides. Further characterization of the nucleotide fractions was obtained by the following criteria: (a) ultraviolet absorption spectra at different pH values; (b) determination of total phosphorus content and of phosphorus content and phosphorus liberated after hydrolysis for 10 min with 1 N hydrochloric acid; (c) determination of the sugar content; (d) paper chromatographic identification of the sugars; (e) paper chromatographic behaviour of the bases after hydrolysis with acids; and (f) ultraviolet absorption curves of the products of hydrolysis.

The position of the phosphate groups was confirmed by oxidation with periodate and by the action of rattle snake venom. All these analyses have already been described in detail [8]. In addition, special analyses of certain nucleotides were undertaken, which are described later.

The quantities of the nucleotides were calculated by using molecular extinction coefficients at 260 mμ of 14 500 for the adenine nucleotides, 10 800 for the guanine nucleotides, 6 300 for the cytosine nucleotides, and 10 000 for the uracil nucleotides. The amounts of the different components are summarized in Table 1.

An amount of ultraviolet-absorbing material, representing about 2—4 % of the total absorbancy of the sample was not adsorbed on the column but was recovered in the wash water. This fraction contained nucleosides and free bases and as main components non-nucleotide material.

Peaks A, C and D appeared to contain the 2′- and 3′-phosphates of cytidine and adenosine, respectively, together with larger amounts of ultraviolet absorbing non-nucleotide material. These nucleotides could, however, easily be separated from interfering substances and estimated by paper chromatography or ionophoresis.

The main component of the sixth peak (F) comprising 60—80 % of the total nucleotide material of that peak was found to be TPN. The minor components behaved ionophoretically and chromatographically like CDP, 2′- and 3′-UMP and 2′- and 3′- GMP.

Analysis of the nucleotides of peaks G and H gave spectra similar to that of uridine; they contained 1 μmole of acid-stable and 1 μmole of acid-labile phosphorus per μmole of base. Treatment with acid at pH 2 during 5 min at 100°C led to the formation of UDP and acetylglucosamine and glucose, respectively. With stronger acid one phosphate group was split off leaving

Table 1. Amounts and identity of effluent fractions obtained on ion exchange chromatography of the acid-soluble nucleotides from barley and oat plants. The 2′- and 3′-phosphates were obtained in varying amounts and the maximum values are given.

Compound	Identity	μmoles/1 000 g of barley plants	μmoles/1 000 g of oat plants
A	2′- and 3′-CMP	11	13
B	5′-AMP	33	35
C	2′-AMP	4	7
D	3′-AMP	5	8
E	5′-UMP	37	38
F	2′- and 3′-UMP	4	9
F	2′- and 3′-GMP	6	4
F	TPN	9	12
F	CDP	3	4
G	UDPAG	14	12
H	UDPG	44	38
I	ADP derivative	3	
K	UDP	29	30
L	ADP	43	47
M	CTP	5	8
N	GDP	8	7
O	ATP derivative	4	6
P	UTP	18	26
R	ATP	40	76
S	GTP	7	8
Adenosine 5′-phosphates		123	164
Uridine 5′-phosphates		142	144
Guanosine 5′-phosphates		15	15
Cytidine 5′-phosphates		8	12

5′-UMP. The sugars were identified by chromatography in three solvent systems and by ionophoresis in borate buffer at pH 9.2. The sugar moiety of the substance in peak G gave the same spectrum as that from authentic UDPAG after treatment with dilute alkali and *p*-dimethylaminobenzaldehyde.

The unhydrolyzed samples from the two peaks behaved also ionophoretically and chromatographically like UDPAG and UDPG, respectively.

The acid-soluble nucleotides of barley included a small amout of an adenosine diphosphate derivative obtained as peak I, which followed closely UDPG. Both plant extracts contained another adenosine derivative, which could either be eluted between GDP and UTP or overlapped partly these fractions. The three substances could, however, be separated by ionophoresis at pH 4.15. The adenosine derivative contained 3 μmoles of phosphorus per μmole of base. A typical adenosine spectrum was obtained from both adenosine derivatives and no spectral change was observed after addition of cyanide. Paper chromatography of the base gave in both cases R_F values identical with that of adenine. Amounts sufficient for detailed structural studies have not been available yet of either substance.

The results of the present investigation establish further the occurrence in plant tissues of 5′-ribonucleotide derivatives of all the four bases present in ribonucleic acids. A preponderance of uracil derivatives besides those of adenine confirms previous findings on wheat plants. These nucleotides — without which metabolic processes would come to a standstill — are apparently involved in metabolism as coenzymes, as precursors of coenzymes and as building blocks for nucleic acids, and as such they may participate in the energy-requiring process of protein synthesis. Ever since Caputto *et al.* have shown that UDPG participates in the interconversion of D-glucose and D-galactose in yeast, it has become more and more apparent that the sugar nucleotides and specially 5′-UDP derivatives play a fundamental role in carbohydrate metabolism, and it is therefore according to expectations that these nucleotides are present or even dominate in plant tissues.

Only very small and varying amounts of the 2′- and 3′-monophosphates were detected in some experiments; they originate presumably from the degradation of ribonucleic acids. No quantitative estimation of DPN and TPN was attained with the present method; for the determination of these nucleotides other methods are available.

EXPERIMENTAL

Isolation and separation of acid-soluble nucleotides

Only the aerial portion of mature plants grown out of doors under normal field conditions, which had begun to fruit when harvested, were investigated. 1 000 g of fresh plants were homogenized in 3 000 ml of ice cold 10 % perchloric acid in a Waring Blendor and after re-extraction with 1 000 ml of 5 % perchloric acid the nucleotides were isolated and freed from disturbing substances according to the method[8] previously elaborated.

Fractionation of the isolated nucleotide mixture was carried out by ion exchange chromatography using Dowex 1, X-10, 200 to 400 mesh in the formate form. The individual nucleotides were eluted with increasing concentrations of formic acid or a mixture of formic acid and sodium formate. The eluting agents and the column size are seen from Figs. 1 and 2. The nucleotides were recovered from the pooled fractions by norite adsorption and elution with small volumes of 50 % aqueous ethanol containing 0.5 % ammonia.

Analytical methods

Ultraviolet absorption. The chromatographic fractions were analyzed by measurement of their light absorption at 250, 260 and 270 mμ in a Beckman spectrophotometer, Model DU, with photomultiplier. Each peak was also identified by determining its optical density over the range 220 to 320 mμ in acid and alkaline solution. The molar absorbancy and the absorbance ratios E_{250}/E_{260} and E_{270}/E_{260} were given in an earlier report [8].

Phosphate. Phosphorus was determined by the method of Allen [10] adapted to a total volume of 5.0 ml, and acid-labile phosphorus was determined after 10 min hydrolysis in 1 N hydrochloric acid at 100°C.

Pentose. Pentose estimations were carried out with the orcinol reagent according to Albaum and Umbreit [11]. The results were calculated by use of authentic samples as standards.

Acetylglucosamine. Mild acid hydrolysis of UDPAG liberated the hexosamine, which gave a positive Morgan-Elson reaction according to the modified test by Reissig *et al.*[12]

Periodate oxidation. Oxidation with periodate was performed according to Dixon and Lipkin [13].

Action of snake venom. The action of rattle snake venom was studied as previously described [8].

Paper chromatography

Whatman No. 1 filter paper was used, and the papers were in equilibrium with the solvent mixture before the runs were started. Standard substances were run in every chromatogram. The temperature was 20 to 22°C.

The nucleotides were located in ultraviolet light of 254 mμ photographically, eluted, and estimated spectrophotometrically. For paper chromatography of the nucleotides the following solvent systems were used: (I) *n*-propanol-ammonia-water (60:30:10); (II) ethanol-1 M ammonium acetate, pH 7.5 (75:30); (III) ethanol- 1 M ammonium acetate buffer, pH 3.8 (75:30); (IV) *iso*propanol-saturated ammonium sulphate solution-water (2:79:19); and (V) *iso*butyric acid-ammonia-water (66:1:33).

The bases obtained after hydrolysis by heating at 100°C for one hour in 1 N hydrochloric acid for the purines, and in 70 % perchloric acid for the pyrimidines, were identified with the following systems: (VI) *iso*propanol-hydrochloric acid (*d* 1.180) — water (65:17:18); (VII) *n*-butanol-acetic acid-water (4:1:5); and No. IV.

The sugar released on mild acid hydrolysis was identified by chromatography in the following solvents: (VIII) ethyl acetate-pyridine-water (2:2:1); (IX) phenol-water saturated at room temperature; and system No. VII. The positions of the sugar spots were demonstrated by spraying with aniline hydrogen phthalate or benzidine.

Paper ionophoresis

Ionophoresis on paper was performed with the technique described in the following paper [14]. Separation of the nucleotides was obtained using the acetate buffer of ionic strength 0.1 and pH 4.15. The sugars were studied in 0.1 M sodium tetraborate buffer at pH 9.2.

Materials

The nucleotides used as standard substances were obtained from Sigma Chemical Company.

This work has been supported by a grant from the *Swedish Natural Research Council*, and financial support for purchase of the reference substances has been obtained from *Sigma Chemical Company*.

REFERENCES

1. Caputto, R., Leloir, L. F., Cardini, C. E. and Paladini, A. C. *J. Biol. Chem.* **184** (1950) 333.
2. Park, J. T. and Johnson, M. *J. Biol. Chem.* **179** (1949) 585.
3. Albaum, H. G., Ogur, M. and Hirshfeld, A. *Arch. Biochem.* **27** (1950) 130.
4. Ginsburg, V., Stumpf, P. K. and Hassid, W. Z. *J. Biol. Chem.* **223** (1956) 977.
5. Buchanan, J. G., Lynch, V. H., Benson, A. A., Bradley, D. F. and Calvin, M. *J. Biol. Chem.* **203** (1953) 935.
6. Simonis, W. and Schwinck, L. *Naturwiss.* **40** (1953) 245.
7. Sebesta, K. and Sorm, F. *Chem. Listy*, **48** (1954) 1585.
8. Bergkvist, R. *Acta Chem. Scand.* **10** (1956) 1303.
9. Albaum, H. G. and Ogur, M. *Arch. Biochem.* **15** (1947) 158.
10. Allen, R. J. L. *Biochem. J. London* **34** (1940) 858.
11. Albaum, H. G. and Umbreit, W. W. *J. Biol. Chem.* **167** (1947) 369.
12. Reissig, J. L., Strominger, J. L. and Leloir, L. F. *J. Biol. Chem.* **217** (1955) 959.
13. Dixon, J. S. and Lipkin, D. *Anal. Chem.* **26** (1954) 1092.
14. Bergkvist, R. *Acta Chem. Scand.* **11** (1957) 1465.

Received June 5, 1957.

ACTA CHEMICA SCANDINAVICA 11 (1957) 1465—1472

The Separation and Estimation of Nucleotides

ROLF BERGKVIST

Institute of Biochemistry, University of Lund, Sweden

A method is presented for the separation and estimation of the 5′-mono-, di- and triphosphates of adenosine, guanosine, cytidine and uridine together with uridine diphosphate glucose, uridine diphosphate acetylglucosamine, diphospho- and triphosphopyridine nucleotides. The nucleotides are separated by a combination of paper chromatography and ionophoresis, and an apparatus is described which allows the ionophoretic separation of substances with very small differences in mobility.

In the course of studies of the nucleotide content of different plant materials a method has been developed for the isolation of the acid-soluble nucleotides without interfering substances [1]. A quantitative separation of the mono-, di- and triphosphates of adenosine, guanosine, cytidine and uridine has been effected by means of a column of the strong base anion exchange resin Dowex-1. The resin was used in the formate form, and separation of the nucleotides was achieved by stepwise elution with formic acid solutions containing progressively increasing amounts of formate.

The use of ion exchange resins for chromatography is particularly well suited to the study of nucleoside derivatives because of the number and variety of charged groups which these compounds possess. Ion exchange chromatography has several great advantages. It is capable of handling both large and small quantities of material. The method is suitable for preparative work, great resolving power is attained and contaminants are of smaller importance than in paper chromatography and ionophoresis. As an analytical method this procedure suffers of slowness and of the disadvantage that considerable volumes of liquid may have to be handled. In order to get a more rapid and sufficiently accurate method for preliminary analysis, a procedure has been developed in this laboratory for the fractionation of nucleotides based upon chromatography together with ionophoresis on filter paper.

In spite of numerous trials with different solvent systems including those already reported in the literature together with a great number of other solvents, no method has so far been found to be entirely satisfactory for the separation of all the purine and pyrimidine nucleotides to be found in plant

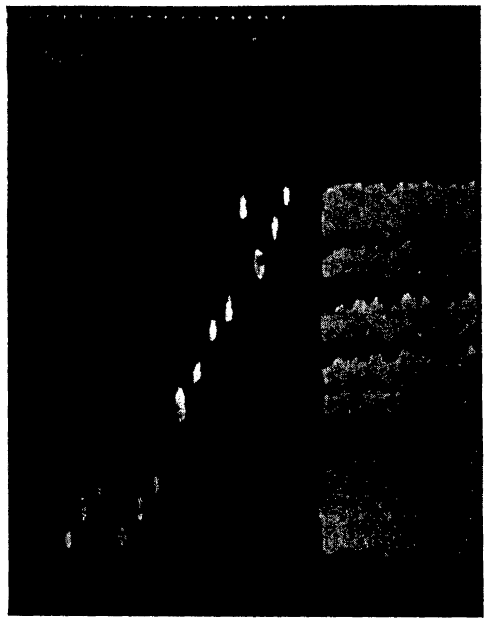


Fig. 1. One-dimensional chromatogram showing the group separation of a nucleotide mixture in comparison with the individual constituents. Solvent system: saturated ammonium sulphate solution-water-*iso*propanol (79:19:2); duration of the run: 35 h.

1) AMP;	4) DPN;	6) GMP;	9) CMP;	12) UMP;
2) ADP;	5) TPN;	7) GDP;	10) CDP;	13) UDP;
3) ATP;		8) GTP;	11) CTP;	14) UTP;
				15) UDPG;
				16) UDPAG;

materials. Two-dimensional paper chromatography has been used for the resolution of mixtures containing the 5′- mono-, di- and triphosphates of adenosine, guanosine, inosine and uridine giving adequate resolution of all the twelve components [2]. In the first direction, the chromatogram was developed with *n*-propanol-ammonia-water (60:30:10) and in the second direction with a solvent system consisting of saturated ammonium sulphate solution-water-*iso*propanol (79:19:2). The cytosine and uracil nucleotides are not separated from each other by means of these or any other solvent mixtures described in the literature. For the present purpose the use of the strongly alkaline first solvent system had the disadvantage of hydrolysing labile nucleotides like UDPG, UDPAG, DPN and TPN *. The ammonium sulphate mixture, originally introduced for the separation of the nucleotides obtained

* Abbreviations used: A, adenosine; G, guanosine; U, uridine; C, cytidine; MP, monophosphate; DP, diphosphate; TP, triphosphate; UDPG, uridine diphosphate glucose; UDPAG, uridine diphosphate acetylglucosamine; DPN, diphosphopyridine nucleotide; TPN, triphosphopyridine nucleotide.

by hydrolysis of nucleic acids [3] and for the separation of adenosine and inosine polyphosphates [4] has, however, been retained from the previous method for obtaining a separation of the very complex nucleotide mixture into smaller groups.

The grade of filter paper most frequently used was Whatman No. 1, and when larger quantities were to be separated the thick Whatman No. 3 paper was used. For successful separation of the different groups it was necessary to use large sheets of paper (50 × 110 cm). Descending chromatography was used and the development was continued until the distance travelled by the solvent front was about 100 cm. The mixture to be analysed was applied to the paper in a series of small spots along a line across the paper, and in this way milligram amounts could be separated, which were even sufficient for the analysis of the weaker components. Emphasis must be laid on the necessity of always providing appropriate controls in chromatography with large papers thereby greatly decreasing the chances of erroneous deductions arising from unforseen variables, such as temperature changes etc.

Fig. 1 shows the fractionation of the actual nucleotides possible with this solvent system which, it will be noted, has a tendency to separate the compounds into four clear-cut bands. The components in the different bands are seen from the figure and are summarized in Table 1.

For quantitative estimations, each ultraviolet-absorbing band with the appropriate blank was cut out and eluted with 0.1 N hydrochloric acid. The optical densities of the extracts were read at the appropriate wavelengths and the total amount of nucleotides in the different bands could then be calculated. In order to concentrate the extracts sufficiently for further analysis, the substances were adsorbed on norite and eluted with small volumes of ethanol-ammonia.

The application of the method of paper ionophoresis to the separation of nucleotides has been extensively studied by various workers [5-8] but only a few papers are concerned with the separation of more than a few nucleotides. None of the techniques hitherto described has been found to give a satisfactory separation of all the nucleotides. With the following method a complete separation of all the nucleotides in the different groups was obtained, except for the uridine diphosphate sugar compounds.

Ionophoresis was carried out in sodium acetate buffer of pH 4.15 and of ionic strength 0.1. Higher and lower pH values resulted in overlapping of

Table 1. The nucleotides in the different groups obtained by paper chromatography as shown in Fig. 1.

Group	A	B	C	D
Compound	AMP ADP ATP DPN	TPN GMP	GDP GTP	CMP CDP CTP UMP UDP UTP UDPG UDPAG

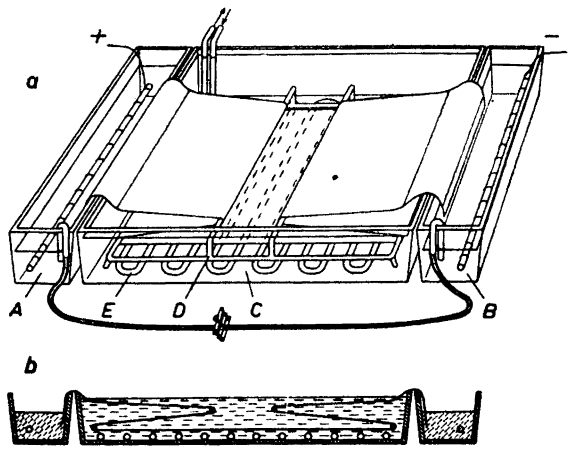


Fig. 2. Apparatus for paper ionophoresis, a) total view and b) cross section. A large sheet of filter paper, kept cool by immersion in the carbon tetrachloride vessel C (50 × 40 × 8 cm), is held in position by a glass frame D as shown in the cross section. The two ends of the paper dip into the electrode vessels A and B (50 × 10 × 8 cm). The liquid in the vessel C is cooled by running tap water in the coil E.

two or more of the cytosine and uracil nucleotides. Because of only small differences in mobility of several of the compounds it was necessary to use long travelling distances for getting sharp separations and therefore the apparatus shown in Fig. 2 has been used.

The equipment is a modification of the apparatus described by Markham and Smith [6], where the paper is kept cold by immersion in carbon tetrachloride. The apparatus consists of two vessels containing the buffer solutions and a third one containing carbon tetrachloride. Either carbon or platinum electrodes were used. Ionophoresis was carried out on large sheets of Whatman No.1 paper (40 × 110 cm) washed three times with N hydrochloric acid and finally with water for removing trace impurities. The samples to be analysed were applied to the paper at a line 15 cm from one end at right angles to the long axis of the paper. For getting compact spots the samples were applied as narrow bands instead of spots about 15 mm in length and about 3 cm from each other. The buffer was carefully brought up on either side of the samples through dipping in the desired electrolyte solution and the surplus moisture was removed by pressure between sheets of thick blotting paper. Then the paper, held in position by a frame made of glass, was immersed in the carbon tetrachloride vessel so that the two ends dipped into the electrode vessels, as shown in Fig. 2 b. The electrodes were connected to a d. c. power supply adjusted to 1 000 V giving a voltage gradient of about 10 V/cm. Under these conditions a run for 12 h gave a resolution of fractions A, B, C and D as shown in Fig. 3 in comparison with authentic nucleotides.

During the passage of the current through the long paper for several hours the carbon tetrachloride warmed up and to prevent this and to hold the

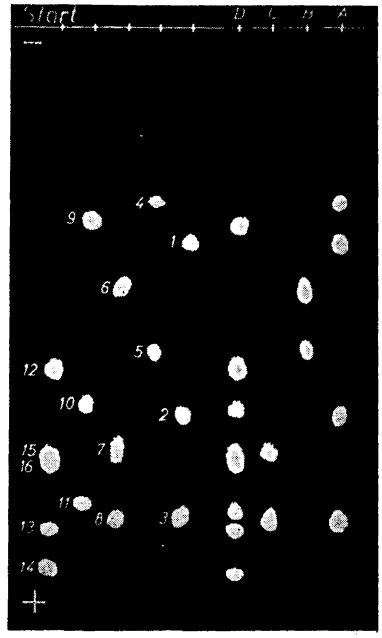


Fig. 3. Fractionation of the groups obtained in Fig. 1 by paper ionophoresis. Sodium acetate buffer of pH 4.15 and of ionic strength 0.1; 10 V/cm; 12 h. The mobility of the substances is compared with that of the authentic nucleotides and the numbers refer to the same substances as in Fig. 1.

temperature constant the liquid was cooled with tap water. The whole apparatus was placed under a cover which prevented the evaporation of the carbon tetrachloride.

When it is desirable to make a separation of a certain fraction on a large scale, it is advisable to apply the mixture as a line and if the substances to be separated have greatly differing mobilities a shorter paper can be used

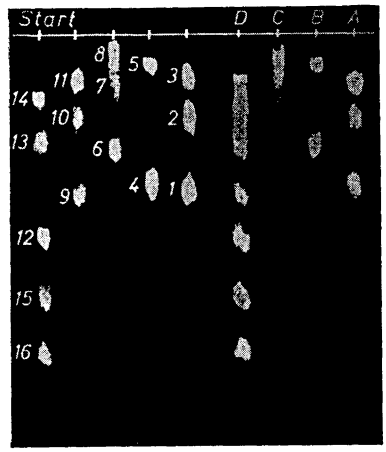


Fig. 4. One-dimensional chromatogram of the groups from Fig. 1 in 95 % ethanol-1 M ammonium acetate, pH 7.5 (75:30), 75 h. The reference substances have the same numbers as in Fig. 1.

to effect the fractionation. The length of the paper can be shortened by the use of other frames. The apparatus is suitable for two-dimensional ionophoresis and for a combination of ionophoresis and chromatography too, but these methods were not used in the present work.

When ionophoresis was completed, the paper was hung up to dry and then printed in ultraviolet light in the usual way. Then the spots containing the substances were located, cut out and eluted with 1 ml of 0.1 N hydrochloric acid. To allow for ultraviolet absorbing substances in the paper, densities were measured against the appropriate blanks. In this way the amounts of all the nucleotides could be calculated with the exception of UDPG and UDPAG, which were not separated from each other. The latter substances could be separated by chromatography in a solvent composed of 7.5 volumes of 95 % ethanol and 3 volumes of 1 M ammonium acetate solution of pH 7.5 [9]. Since the R_F values are rather low, it is advantageous to use the descending method and to cut notches in the papers at the bottom, from which the solvent is allowed to drip. Development for 75 h gave the separation shown in Fig. 4 in relation to authentic substances. Besides UDPG and UDPAG some other nucleotides were separated and another value of their concentration could be calculated. Several nucleotides, such as UDP, UTP, CDP and CTP or DPN and AMP, overlap in this solvent system. The guanosine polyphosphates form tails and are also badly separated.

Several mixtures of authentic nucleotides were analysed by the present procedure; the results of one of these analyses are summarized in Table 2.

Recoveries of 90—100 % were obtained regularly, the losses being mainly manipulational and no decomposition of any nucleotide could be detected. The method has been applied with success to the analysis of the acid-soluble nucleotide fraction from different plant materials.

EXPERIMENTAL

Paper chromatography

The group separation of the nucleotide mixture was performed in a large rectangular chromatographic chamber, 60 cm long, 30 cm wide and 115 cm high, which is large enough to handle up to 4 paper sheets, 50 × 110 cm. The atmosphere of the chamber must be saturated with the solvent mixture and therefore the walls of the chamber were lined with filter paper extending to the whole height of the chamber. Approximately 150 ml of the solvent mixture were poured into the tank, care being taken to wet the lining paper thoroughly. Before a run was started the papers were equilibrated with the solvent mixture for 8 h. When the solvent has run a convenient distance (in about 35 h) the paper was removed and dried at room temperature.

The nucleotides were located by making a contact print in monochromatic ultraviolet light of 254 mμ and then the bands were eluted and the quantitative evaluation of the amounts of material in each group performed as previously described. The nucleotides from each group were adsorbed on norite and eluted by repeated shaking with small volumes of an aqueous solution containing 50 % ethanol and 1 % ammonia. The elution was repeated in the cold until no more ultraviolet absorbing material was eluted, and the eluates were immediately adjusted to pH 7 with hydrochloric acid. In this way the concentrated solutions were also freed from salts which interfere with the ionophoretic separation.

Table 2. Analysis of a mixture of authentic nucleotides. The concentrations expressed in μmoles were calculated using the molecular extinction coefficients previously reported [1].

Compound	μmoles of nucleotide		Recovery %
	Calculated	Found	
AMP	2.39	2.28	95
ADP	3.02	3.05	101
ATP	3.24	3.08	95
DPN	2.89	2.72	94
TPN	2.16	2.10	97
GMP	2.77	2.74	99
GDP	2.74	2.74	100
GTP	2.95	2.77	94,
CMP	3.26	3.13	96
CDP	2.94	2.82	96
CTP	3.04	2.95	97
UMP	2.60	2.65	102
UDP	3.02	2.96	98
UTP	3.11	2.99	96
UDPG	2.68	2.55	95
UDPAG	2.40	2.33	97

The paper chromatographic separation in ethanol — 1 M ammonium acetate of pH 7.5 (75:30) was carried out with the standard size of paper (46 × 57 cm) and a conventional type of box was used. For quantitative estimations, the spots were cut out and eluted with 1.0 ml of 0.1 N hydrochloric acid. The optical densities of the extracts were measured in a 1.00 cm quartz cuvette in a Beckman Universal Spectrophotometer, Model DU, adapted for measuring small volumes.

Paper ionophoresis

Ionophoresis was carried out on Whatman No. 1 papers (40 × 110 cm) purified by washing three times with N hydrochloric acid and finally with water until the pH of the paper was about 7. The removal of interfering substances is particularly important in paper ionophoresis where the movement of nucleoside polyphosphates is otherwise severely retarded.

The material was applied to the dry paper at a cross line 15 cm from one edge; placing the substances in lines rather than circular spots gave much sharper separations. Sodium acetate buffer of pH 4.15 and of ionic strength 0.1 was used. Phosphate buffers were avoided because of the desirability of making phosphorus analyses on material eluted from the spots.

The paper was impregnated with buffer by dipping one edge of the paper into the buffer solution; when the buffer front has almost reached the samples, further movement

was arrested by dipping the other edge of the paper into the buffer and allowing this second front to meet the first. The excess moisture was removed and then the paper was placed on a glass frame and immersed into the vessel containing the carbon tetrachloride. After a run for 10 to 12 hours the paper was dried and then the nucleotides were revealed by taking an ultraviolet contact print. The quantitative estimations were performed as described above.

Materials

The nucleotides used were obtained from the Sigma Chemical Company. Stock solutions were first prepared of all the compounds and the composition of these solutions was carefully analysed by paper chromatography and ionophoresis. The mixture to be analysed was obtained by mixing carefully measured volumes of these stock solutions.

The author wishes to express his gratitude to *Sigma Chemical Company* for gifts of many of the nucleotides.

This work has been supported by grants from the *Swedish Natural Science Research Council.*

REFERENCES

1. Bergkvist, R. *Acta Chem. Scand.* **10** (1956) 1303.
2. Bergkvist, R. and Deutsch, A. *Acta Chem. Scand.* **9** (1955) 1398.
3. Markham, R. and Smith, J. D. *Biochem. J. London* **49** (1951) 401.
4. Deutsch, A. and Nilsson, R. *Acta Chem. Scand.* **7** (1953) 858.
5. Turba, F. and Enenkel, H. J. *Naturwiss.* **38** (1951) 189.
6. Markham, R. and Smith, J. D. *Biochem. J. London* **52** (1952) 552.
7. Wollenberger, A. *Nature* **173** (1954) 205.
8. Wade, H. E. and Morgan, D. M. *Biochem. J. London* **56** (1954) 41.
9. Paladini, A. C. and Leloir, L. F. *Biochem. J.* **51** (1952) 426.

Received June 5, 1957.

ACTA CHEMICA SCANDINAVICA 11 (1957) 1473—1476

L'Action du Tétra-acétate de Plomb sur l'α-D-Galactopyranosyl-2-D-glucose, Préparé à Partir de l'Umbelliférose

ALF WICKSTRØM

Universitetets farmasøytiske institutt, Blindern-Oslo, Norvège

The reaction between lead tetra-acetate and 2-α-D-galactopyranosyl-D-glucose has been studied. The disaccharide was prepared from umbelliferose and the presence of a (1→2)-linkage in this trisaccharide was confirmed. The cyclic hemiacetal form of the reducing disaccharide examined is not so easily opened during the oxidation with lead tetra-acetate as in the case of 2-O-methyl-D-glucose, reported in the literature.

Par hydrolyse partielle de l'umbelliférose (α-D-galactopyranosyl-2′-α-D-glucopyranosyl-β-D-fructofuranoside) nous obtenons un disaccharide réducteur, l'α-D-galactopyranosyl-2-D-glucose. Ce disaccharide, possédant la liaison (1 → 2) assez rare, a été soumis à l'oxydation au moyen du tétra-acétate de plomb (T.A.Pb.).

Selon Perlin et coll.[2,3] le T.A.Pb. est un réactif généralement utile dans l'étude de la structure des disaccharides réducteurs. Dans des conditions bien définies le résultat de l'action du T.A.Pb. sur les disaccharides réducteurs dépend de la position du pont osidique.

Le comportement des disaccharides (1 → 2) vis-à-vis de cet oxydant a été établi par analogie avec l'oxydation des O-méthyl-2-aldoses [2,3] et ensuite confirmé par l'étude de l'α-D-mannopyranosyl-2-D-mannose [4]. En présence de catalyseur (acétate de potassium) le T.A.Pb. paraît oxyder les sucres, O-substitués sur C_2, sous leur forme linéaire en libérant une molécule de formaldéhyde. En absence de catalyseur et à la température du laboratoire ces sucres sont pratiquement résistants vis-à-vis du T.A.Pb. pendant les premiéres 30 minutes de contact. Cette rèsistance, ainsi que la libération d'une molécule de formaldéhyde pendant la réaction catalysée, distingueraient les disaccharides (1 → 2) de tous les autres disaccharides réducteurs [2,3].

Les résultats de l'oxydation non catalysée de l'α-D-galactopyranosyl-2-D-glucose se trouvent dans le Tableau 1. Ils sont conformes à ceux de Perlin et coll.

Tableau 1. Oxydations au moyen du tétra-acétate de plomb (T.A.Pb.) en absence de catalyseur.

Durée de contact à 18° (minutes)		15	30	45
Molécules [a] de T.A.Pb. réduites	I [b]	0.20	0,24	0,49
	II [c]	0,80	1,23	1,55

a) par molécule de substance mise en oeuvre.
b) α-D-galactopyranosyl-2-D-glucose
c) β-D-galactopyranosyl-4-D-glucose (lactose)

Dans le Tableau 2 sont exposé les résultats de l'oxydation catalysée de la même substance. Ils ne sont pas tout à fait conformes aux faits rapportés par Perlin et coll., notre substance ne libérant que 0,55 molécules de formaldéhyde et après 5 heures seulement. Les quantités de T.A.Pb. réduite et d'anhydride carbonique dégagée correspondent bien à la quantité de formaldéhyde retrouvée après l'oxydation. Tout se passe donc comme si la partie réductrice du disaccharide étudié est stabilisée sous forme cyclique et comme si la réaction-se passe par deux étapes (v. schéma I), la première étant la plus rapide.

La comparaison du Tableau 2 avec le schéma I fait ressortir l'influence des réactions secondaires, déjà signalées par Perlin et coll. Ces réactions sont probablement dues à l'hydrogène du carbone 2 activé par la formation d'une fonction carbonyle sur le carbone 3. Ils impliquent une consommation supplémentaire de l'oxydant. A une température légèrement plus haute (32° au lieu de 27°) les réactions secondaires sont plus importantes, la quantité de formaldéhyde libérée ne changeant guère.

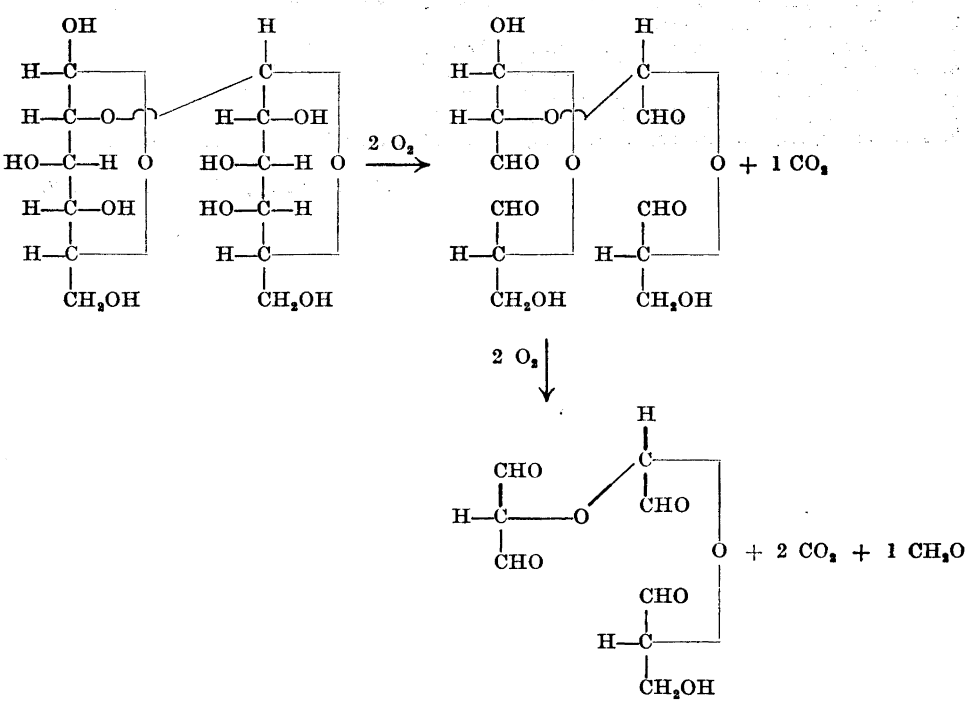
Le mémoire présent donne un exemple d'un disaccharide (1 → 2) qui, soumis à l'oxydation au moyen du T.A.Pb., se comporte d'une façon légèrement différente du seul disaccharide (1 → 2) étudié jusqu'ici. La libération

Tableau 2. Oxydation de l'α-D-galactopyranosyl-2-D-glucose au moyen du tétra-acétate de plomb (T.A.Pb) dans l'acide acétique en présence d'acétate de potassium.

Durée de contact à 27° (heures)	0,5	1	2	3	4	5
Molécules [a] de T.A.Pb. réduites	3,70	4,28	5,17	5,85	6,70	7,23
Molécules [a] de CO_2 dégagées dans l'appareil de Warburg	0,70	1,12	1,46	1,84	2,05	2,30
Molécules [a] de formaldéhyde libérées	0,22					0,55
Molécules [a] de formaldéhyde libérées des substances témoins suivantes:						
Erythritol	1,90					
Mannitol	1,93					
Lactose	0					0,05

a) pour une molécule de substance mise en oeuvre.

Schéma I. Oxydation de l'α-D-galactopyranosyl-2-D-glucose au moyen du tétra-acétate de plomb (T.A.Pb.)



partiellement empechée du formaldéhyde ne semble pas nuir à l'utilité du T.A.Pb. dans l'étude de la structure des disaccharides réducteurs. L'ensemble de nos résultats confirme donc la présence d'une liaison (1 → 2) dans l'umbelliférose.

PARTIE EXPERIMENTALE

1. *Préparation de l'α-D-galactopyranosyl-2-D-glucose.* L'umbelliférose (0,8 g) dissous dans l'acide sulfurique 0,01 N (70 ml) fut chauffé à reflux (100°) jusqu'à libération complète du fructose terminal (2 à 3 h, controlée par chromatographie sur papier). L'hydrolysat fut neutralisé ($BaCO_3$) et le disaccharide réducteur fut isolé et purifié à l'aide des colonnes de charbon-celite [5]. Rendement: 0,30 g d'un poudre blanc, chromatographiquement homogène, qui cristallise après quelque temps sous vide. Analyses: (substance séchée au poids constant dans le vide sur le P_2O_5 à 60°) F: 118°—120°, $[\alpha]_D^{20}$ + 145° (c = 2, eau, équilibre), pouvoir réducteur vis-à-vis de l'hypoiodite de sodium [6]: calc. pour $C_{12}H_{22}O_{11}$: 52,64 % de celui du D-glucose, tr: 52,75 %. Traité par la phénylhydrazine il ne donne pas d'osazone.

2. *Oxydations au moyen du T.A.Pb.* Nous avons suivi les modes opératoires décrits par Perlin et coll. [3-4]. Le formaldéhyde fut dosé par photométrie selon Alexander et coll.[7]. Dans quelques expériences où la prise d'essai fut rélativement importante (12—14 mg) le formaldéhyde libéré après 5 h d'oxydation à 30° a été isolé à l'aide de dimédon. Rendement: 55—60 % de la théorie. Point de fusion de la combinaison dimédon-formaldéhyde: 190°.

BIBLIOGRAPHIE

1. Wickström, A. et Bærheim Svendsen, A. *Acta Chem. Scand.* **10** (1956) 1199.
2. Perlin, A. S. *Anal. Chem.* **27** (1955) 396.
3. Charlson, A. J. et Perlin, A. S. *Can. J. Chem.* **34** (1956) 1200.
4. Gorin, P. A. J. et Perlin, A. S. *Can. J. Chem.* **34** (1956) 1796.
5. Whistler, R. L. et Durso, D. F. *J. Am. Chem. Soc.* **72** (1950) 677.
6. Willstätter, R. et Schudel, G. *Ber.* **51** (1918) 780.
7. Alexander, B., Landwehr, G. et Selignan, A. M. *J. Biol. Chem.* **160** (1945) 51

Manuscrit reçu le 30 Avril 1957.

ACTA CHEMICA SCANDINAVICA 11 (1957) 1477—1484

Studies on the Chemistry of Lichens

II *. Chemical Components of *Haematomma ventosum* (L.) Mass. var. *lapponicum* (Räs.)

YNGVE JOHANNES SOLBERG

Universitetets Kjemiske Institutt, Blindern-Oslo, Norway

Thamnolic acid and a new lichen substance, called *ventosic* acid, $C_{22}H_{44}O_6$, have been isolated from *Haematomma ventosum* (L.) Mass. var. *lapponicum* (Räs.). The new substance is an aliphatic compound. It contains four hydroxyl and one carboxyl group. Reaction with hydriodic acid and reduction with zinc and glacial acetic acid affords n-*docosanoic* acid (behenic acid). This result is in harmony with the new substance being tetrahydroxy behenic acid.

Haemotomma ventosum is a crustose lichen and is rather common on boulders and rocks on mountain-wilds. Sometimes it covers large areas. Our material was collected in Trabelia, the middle part of Gudbrandsdal, Norway, and the greatest possible care was taken to avoid contamination by other species.

The lichen *Haematomma ventosum* (L.) Mass. is known in two varieties. The one is *lapponicum* giving a bright red colour with *p*-phenylenediamine, the other does not give any colour with this reagent.

Knop, Hesse and Zopf [1–5] were the first to examine samples of this lichen, but they did not indicate which of the varieties they dealt with. The obsolete methods employed could not yield complete information regarding the composition of the lichen.

A thorough examination of *Haematomma ventosum* (L.) Mass. var. *lapponicum* (Räs.) has now been made using a series of solvents in succession for extraction. During the years 1955 and 1956 in all about four kilogrammes were extracted. As a result of this investigation it has been found that the important components of this lichen are usnic, divaricatic and thamnolic acid and a new lichen substance, for which the name *ventosic* acid was adopted. Previous investigators did not obtain thamnolic acid from this lichen. The structure of thamnolic acid has been established by Asahina and coworkers, both by degradation and by synthesis [6–10].

* Part I. *Acta Chem. Scand.* 9 (1955) 1234.

The crude thamnolic acid obtained from ether and acetone extracts was collected and thoroughly washed with chloroform and ethanol. Recrystallisation was effected several times conveniently from dioxan giving thamnolic acid with one molecule dioxan as light yellow prisms [11], m.p. 210—211° (decomp.). After drying *in vacuo* thamnolic acid gave analytical values agreeing with the formula $C_{19}H_{16}O_{11} \cdot C_4H_8O_2$. The crystalline product gave the same colour reactions and has the same properties as mentioned for thamnolic acid in the literature [12,13]. Thamnolic acid is very sparingly soluble in most organic solvents but may be crystallised from acetone or dioxan.

With barium hydroxide the substance gave the same characteristic yellow crystals as reported by Zopf for hirtellic acid [12] (identical with thamnolic acid).

A proof of the identity was possible by mixed melting point determination and X-ray diffraction patterns. The comparison of X-ray diffraction patterns of authentic thamnolic acid and the substance isolated here, both crystallised from dioxan, gave the spacing values in Å, recorded in Table 1.

Table 1. Spacing values in Å. (w = weak, m = medium, s = strong, vs = very strong).

Substance from *Haematomma ventosum* var. *lapponicum*	Authentic thamnolic acid.
15.77 m	15.77 m
9.02 »	9.02 »
7.64 »	7.65 »
7.16 s	7.17 »
6.56 m	6.58 »
5.34 »	5.25 s
4.57 »	4.59 w
4.35 »	4.33 »
3.60 vs	3.60 vs
3.17 m	3.17 w
2.92 w	2.91 »
2.76 »	2.77 »»

By working up the mother liquors from the acetone extractions another aldehydic substance was obtained which was found to be identical with decarboxythamnolic acid. This substance has so far not been detected in lichens and it is most likely produced during the extraction with acetone. Asahina [8] made the same observation.

Zopf [3] and Hesse [5] isolated small quantities of an aldehydic substance from *Haematomma ventosum*, for which the name *ventosaric* acid was adopted by Zopf. Zopf gave the melting point at 205—207°, Hesse at 190° which is not far from that of thamnolic acid. Ventosaric acid further resembles thamnolic acid in having a low solubility in ethanol and acetone and in its colour reactions with ferric chloride, sodium hydroxide and concentrated sulphuric acid. These facts would suggest that ventosaric acid is identical with thamnolic acid.

When the extraction was carried out with acetone and ethanol a white amorphous, sparingly soluble precipitate was formed in the extraction flask. This precipitate gave after purification, as described in the experimental part, ventosic acid as a white amorphous powder, m.p. 183—185°. The substance was soluble in hot ethanol, glacial acetic acid, dioxan, aniline and pyridine. In other organic solvents it had a very low solubility. After drying the acid gave analytical values agreeing with the formula $C_{22}H_{44}O_6$. Several attempts were made by means of the method of Pirsch to obtain a molecular weight, but without result. Ventosic acid did not contain methoxyl groups and exhibited no carbonyl function. It was recovered unchanged after boiling with sodium hydroxide solution as well as on diluting its solution in cold concentrated sulphuric acid.

Ventosic acid on treatment with acetic anhydride and a trace of concentrated sulphuric acid gave a colourless glassy compound, m.p. about 54°, the composition of which corresponded to a tetra-acetate. The acetate has so far not crystallised. On boiling with ethanolic potassium hydroxide it was deacetylated to the orginal substance.

With *p*-phenylazobenzoyl chloride [14] the substance yielded an orange-red tetrabenzoate, $C_{37}H_{38}O_5N_4$, m.p. 153—157°.

Treated with hydriodic acid ($d = 1.7$) ventosic acid yielded a dark brown oil which could not be purified or crystallised. As the crude oily product contained iodine it was reduced with zinc dust in glacial acetic acid. The resulting product crystallised in colourless needles, m.p. 75°. Repeated recrystallisations from different solvents did not raise the melting point discernibly and no evidence was obtained for the presence of more than one component. It contained no hydroxyl groups and was identified as behenic acid, $C_{22}H_{44}O_2$, by preparation of the methyl ester, m.p. 52—53°, and by X-ray analysis. All these values correspond well with those given in the literature. (Similar reduction has been made with 13,14-dihydroxy-behenic acid by Urwanzopp [15]. The behenic acid obtained in this manner had the m.p. 74—76°)

The higher fatty acids exhibit at least three polymorphic forms and X-ray measurements show that these crystal modification possess different spacings. The most important of these modifications are designated as α- and β-, the former showing a C crystal spacing and the latter a somewhat longer B spacing, (Ref.[16]). The X-ray investigations of Müller and Shearer [17–19] showed that the fatty acids exhibit three characteristic lines d_1, d_2 and d_3. The last two

Table 2.

	Behenic acid obtained by reduction of ventosic acid	Authentic sample of behenic acid	Behenic acid, Refs.[16–18]
Melting point	75°	78—79°	80.0°
d_1 B spacing	54.2 Å	53.2 Å	53.6 Å
d_1 C spacing	49.6 »	49.0 »	48.5 »
d_2	4.14 »	—	4.1 »
d_3	3.73 »	—	3.7 »

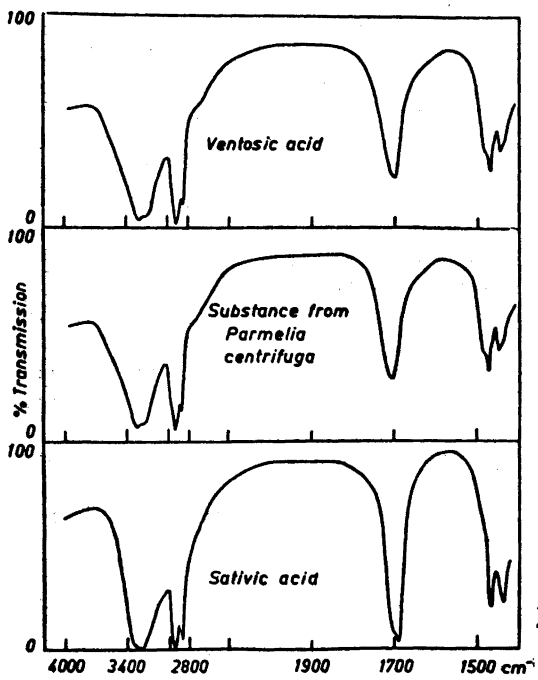


Fig. 1. Infrared absorption spectra from 4 000 — 1 450 cm^{-1}. All substances as pressed KBr — disks.

lines are essentially constant for a specific series and are the diffractions from planes parallel to the long axes of the molecules. The long spacing d_1 is a function of the number of carbon atoms in the chain.

The results of X-ray examinations of the behenic acid obtained by reduction of ventosic acid and of authentic sample of behenic acid are shown in Table 2. The acids gave extremely good reflections.

Infrared analysis of ventosic acid ascertained the presence of an aliphatic carbonyl-hydroxy-compound. The infrared absorption spectrum in the region 4 000 cm^{-1} — 700 cm^{-1} showed strong bands at 3 280 cm^{-1} and at 1 710 cm^{-1}. The observed values indicate the presence of hydroxyl and carbonyl groups, respectively. The frequency at 1 710 cm^{-1} would suggest the presence of a dimer aliphatic acid [20,21]. Further bands at 2 920 cm^{-1} and at 1 470 cm^{-1} — 1 445 cm^{-1} corresponded to C-H and C-H_2 stretching frequencies in saturated aliphatic compounds. The 1 382 cm^{-1} band shows that a C-CH_3 group is present. There were only few bands below 1 450 cm^{-1}.

An infrared spectrum of sativic acid (tetrahydroxystearic acid), m.p. 168—171°, was very similar to that of ventosic acid in the region 4 000 cm^{-1} — 1 450 cm^{-1}. The same characteristic bands were observed (Fig. 1). This adds strength to the conclusion that ventosic acid must be an aliphatic hydroxy acid.

X-Ray diffraction patterns of sativic acid showed a certain similarity with that of ventosic acid. Characteristic are the two strong peaks in the region 4.0—4.9 Å, (Fig. 2).

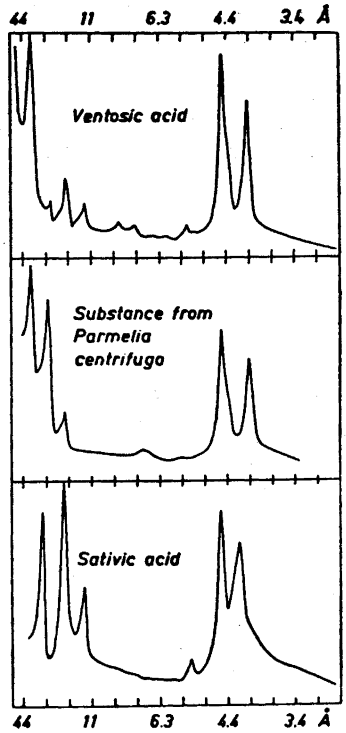


Fig. 2. X-Ray powder diagrams taken with Cu-$K\alpha_1$ radiation.

It was quite impossible to obtain an ester of ventosic acid. This is remarkable because the isolated substance most probably is an aliphatic tetrahydroxy carboxylic acid. On the other hand sativic acid was easily converted into the methyl ester by reaction with methanol and concentrated sulphuric acid.

Both ventosic and sativic acid were practically insoluble in sodium hydroxide solution.

Metabolic products of *Parmelia physodes* (L.) Ach. and *Parmelia furfuraceae* (L.) Ach. have been studied in detail by Zellner [22,23]. He obtained two white, amorphous substances which he called *hypogymnole*. The physical and chemical properties of these substances are in agreement with those of ventosic acid from *Heamatomma ventosum*. An allied substance has been isolated by Klima [24] from *Alectoria ochroleuca* (Ehrh.) Nyl. Zellner and Klima did not, however, establish the chemical composition of these substances.

A preliminary examination of these three lichens showed that the substances detected by Zellner and Klima most likely are identical with ventosic acid from *Haematomma ventosum*. Also the lichens *Parmelia centrifuga* (L.) Ach., *Cetraria nivalis* (L.) Ach. and *Cladonia alpestris* (L.) Rabh. were investigated. Hereby substances either identical or closely related to ventosic acid have been isolated. X-Ray and infrared analysis have been used.

As an example X-ray diffraction pattern and infrared absorption spectrum of the substance isolated from *Parmelia centrifuga* are shown in Figs. 1 and 2.

Lack of material has so far not permitted degradative experiments on ventosic acid on a larger scale. However, it is of interest to note that ventosic rapidly acid is oxidised by periodic acid. It is hoped to establish the structure of ventosic acid by investigation of the oxidation products.

EXPERIMENTAL

(Melting points are uncorrected.)

Extraction and isolation of the lichen substances

Usnic acid. The fresh lichen obtained was air-dried and ground into coarse powder (1 000 g), and exhaustively extracted with ether in a Soxhlet apparatus. During the extraction usnic acid separated as large yellow crystals in the flask. After 20 h when the extraction was found to be completed the crystals were removed by filtration and washed with ethanol. Usnic acid was recrystallised from chloroform-ethanol (1:3). Yield 24.5 g; m.p. 199–200°; $[\alpha]^{21}_D$ +500° (chloroform, c = 2.355).

Divaricatic acid. The ether extract was evaporated. The residue which consisted of crystals and an oily substance was treated with small quantities of ether. The ether-soluble portion was evaporated and the residue recrystallised from 60 % ethanol. The substance was identified as divaricatic acid. Repeated recrystallisations from ethanol and glacial acetic acid yielded 3.7 g; m.p. 135–137°. The acid dissolved readily in ether and ethanol at room temperature, and also in hot chloroform, benzene and glacial acetic acid. An alcoholic solution of the substance turned violet on the addition of a drop of ferric chloride solution.

The ether insoluble portion was washed with alcohol. Pale yellow crystalline product (Fraction A).

The residual lichen was subsequently extracted with acetone for 20 h. During the extraction the new compound (ventosic acid) separated as a colourless amorphous powder. It was removed by filtration and washed with acetone, ethanol and ether. Finally dried at 70° for 30 min (Fraction B). The dark red extract was concentrated by distilling off the solvent. More yellow crystalline product separated (Fraction D). The solid was filtered off and the mother liquid evaporated. The residue, a reddish brown resinous mass was shaken with 800 ml ethanol for one hour. The alcohol-soluble part was not further investigated. The insoluble part could be divided into two portions by treatment with hot chloroform. The chloroform-insoluble portion was collected by filtration and washed with alcohol (Fraction D).

Decarboxythamnolic acid. The chloroform extract yielded a pale yellow crystalline product on standing in a refrigerator. This was filtered off and washed with small quantities of ether, (1.6 g). Repeated recrystallisations from ethyl acetate yielded decarboxythamnolic acid in a pure state. Yield 23 mg; m.p. 213–215° (decomp). (Found: C 57.18; H 4.12; Calc. for $C_{18}H_{16}O_9$: C 57.46; H 4.29). As described by Asahina the decarboxythamnolic acid was soluble in hot acetone, ethanol, ethyl acetate and chloroform. On heating with potassium hydroxide and chloroform the substance gave a deep red solution. With barium hydroxide no characteristic crystals were obtained.

Thamnolic acid. Fraction A from the ether extraction and the fractions C and D from the acetone extraction of the lichen were found to be the same substance. The fractions were collected (17.7 g), and recrystallised repeatedly from dioxan. Pale yellow needles, m.p. 210–212° (decomp.). Mixed melting point with authentic sample of thamnolic acid showed no depression. (Found: C 54.43; H 4.70; Calc. for $C_{19}H_{16}O_{11} \cdot C_4H_8O_2$: C 54.33; H 4.76).

Ventosic acid. The residual lichen powder was finally extracted with 96 % ethanol for 48 h. On standing the extract gave some ventosic acid. Together with the fraction B from the acetone extract, the yield of crude ventosic acid was about 0.8 %. The sub-

stance was purified by recrystallisation from dioxan, ethanol and glacial acetic acid. White, amorphous powder, m.p. 183°. (Found: C 65.29; H 10.88; Calc. for $C_{22}H_{44}O_6$: C 65.30; H 10.96). It gave none of the colour reactions characteristic for lichen substances. The compound was without taste.

Derivatives of ventosic acid

Acetylation. Ventosic acid (1.0 g) was heated on a steam bath for 45 min with 30 ml of the following mixture: 30 g acetic anhydride +220 ml pyridine. During the reaction the solution became brown. The reaction mixture was then poured into ice-water with good stirring. The brown oily product which separated was extracted with ether and the ether solution evaporated. The dark oily residue was dissolved in ethanol and treated with active carbon, filtered and the colourless solution evaporated to dryness. The acetyl compound was thus obtained as a colourless glassy product, m.p. 54°. It could not be crystallised. (Found: for material dried *in vacuo* over KOH: C 62.67; H 9.21; Calc. for $C_{30}H_{52}O_{10}$: C 62.92; H 9.15).

Deacetylation. The acetyl compound (0.31 g) was boiled with alcoholic potassium hydroxide (25 ml 0.5 N) for 30 min. After a short time a white amorphous powder precipitated. After cooling the powder was removed by filtration and washed with water and alcohol. To remove ash-components the product was recrystallised from glacial acetic acid and washed with alcohol and ether; m.p. 182°. It was found to be identical with the original substance, ventosic acid, the mixed melting point being undepressed. X-Ray diffraction patterns were also identical. (Found: C 65.19; H 10.68; Calc. for $C_{22}H_{44}O_6$: C 65.30; H 10.96).

p-*Phenylazobenzoate.* A mixture of ventosic acid (1.0 g), *p*-phenylazobenzoylchloride (2.4 g) and dried pyridine (6 ml) was refluxed for one hour. The reaction mixture was filtered, cooled and poured into a solution of 10 % sodium hydrogen carbonate and ice. The orange-red precipitate obtained was filtered off and thoroughly washed with water. Recrystallisation from a benzene-ethanol mixture gave orange-red powder. Yield 0.68 g; m.p. 153—157°. (Found: C 71.59; H 6.63; N 8.15; Calc. for $C_{74}H_{76}O_{10}N_8$: C 71.89; H 6.19; N 9.06). The benzoate was easily soluble in benzene and ether with a dark red colour.

Reduction to behenic acid. Ventosic acid (4.35 g) was refluxed with 100 ml hydriodic acid (b.p. 126°) for 10 min. The solid rapidly turned to a dark brown oily product. The reaction mixture was diluted with water and extracted with ether. The ether extract was shaken with an aqueous solution of sodium thiosulphate and at last washed with water. The ether solution, dried and concentrated, yielded a light yellow viscous liquid, (3.1 g). As the liquid contained halogen it was boiled with zinc powder in glacial acetic acid (25 ml) for one hour. The reduction product was obtained in a crystalline state when the filtered solution was evaporated *in vacuo*. The residue was washed with much water and recrystallised several times from diluted acetic acid and petroleum ether (30—50°); m.p. 74—75°, undepressed on admixture with authentic behenic acid (m.p. 78—79°). Yield about 1 g. The substance was readily soluble in ether, acetone, ethanol and benzene. (Found: C 77.54; H 12.82; mol.wt. (Landsberger) 313, 314; Calc. for $C_{22}H_{44}O_2$: C 77.55; H 13.02; mol.wt. 341).

Behenic acid methyl ester. The methyl ester was prepared from behenic acid (110 mg) with diazomethane. The ester recrystallised from methanol (10 ml) gave a quite colourless and crystalline product; m.p. 52—53°. No depression of the melting point when mixed with an authentic sample of behenic acid methyl ester. (Found: C 78.10; H 13.01; CH_3O 9.89; $C_{23}H_{46}O_2$ requires C77.89; H 13.07; CH_3O 8.75).

Tetrahydroxystearic acid (Sativic acid). The hydroxy acid was prepared from linolic acid tetrabromide (m.p. 115—116°) in the same manner as described by Rollett [25] and Hazura [26]. The crude product of sativic acid was recrystallised from dilute hydrochloric acid, washed with water and dried. Then shaken with hot benzene and at last recrystallised from alcohol. Colourless, crystalline product; m.p. 168—171°. (Found: C 62.18; H 10.51; $C_{18}H_{36}O_6$ requires C 62.10; H 10.41).

Sativic acid methyl ester. Sativic acid (300 mg) was suspended in a solution of methanol (30 ml) and concentrated sulphuric acid (3.3 ml) and refluxed for 2 h. After cooling the solution was diluted with water. A white precipitate was formed. This was filtered off and recrystallised from methanol-water (1:1). The colourless, crystalline product was

removed by filtration and washed with methanol and ether. Yield 170 mg; m.p. 146–156°. Once more purified by recrystallisation from white spirit (160–180°) (50 ml). M.p. 147–151°. (Found: C 63.14; H 10.33. $C_{19}H_{38}O_6$ requires C 62.95; H 10.57).

By the X-ray diffraction analysis, a small amount of the substance was melted on a glass plate and spread out so as to form a very thin film. The instrument used was a Philips X-ray Geiger Counter Spectrometer with Cu-$K\alpha_1$ radiation.

The author wishes to express his indebtness to Dr. Carl Axel Wachtmeister, Stockholm, for a sample of thamnolic acid, and to Professor Dr. Endre Berner and Cand. real. Eilif Dahl for their advice and interest in this work.

Behenic acid was kindly provided by Jahres Kjemiske Fabrikker, Sandefjord, Norway.

REFERENCES

1. Knop, W. *Ann.* **49** (1844) 122.
2. Zopf, W. *Ann.* **288** (1895) 31.
3. Zopf, W. *Ann.* **295** (1897) 252.
4. Zopf, W. *Ann.* **300** (1898) 354.
5. Hesse, O. *J. prakt. Chem.* **62** (1900) 467.
6. Asahina, Y. and Ihara, S. *Ber.* **62** (1929) 1196.
7. Asahina, Y. and Fuzikawa, F. *Ber.* **65** (1932) 58.
8. Asahina, Y. and Hiraiwa, M. *Ber.* **69** (1936) 330.
9. Asahina, Y. and Hiraiwa, M. *Ber.* **72** (1939) 1402.
10. Asahina, Y. and Ihara, S. *Ber.* **65** (1932) 55.
11. Wachtmeister, C. A. *Acta Chem. Scand.* **9** (1955) 1395.
12. Zopf, W. *Die Flechtenstoffe in Chemischer, botanischer, pharmakologischer und technischer Beziehung*, Jena 1907, p. 259.
13. Asahina, Y. and Shibata, S. *Chemistry of Lichen Substances*, Japan Soc. for the Promotion of Science, Tokyo 1954.
14. Woolfolk, E. O., Beach, F. E. and McPherson, S. P. *J. org. Chem.* **20** (1955) 391.
15. Urwanzoff, L. *J. prakt. Chem.* **39** (1889) 334, p. 337.
16. Ralstone, A. W. *Fatty Acids and their Derivatives*, John Wiley & Sons, Inc., New York 1948.
17. Müller, A. *J. Chem. Soc.* **123** (1923) 2043.
18. Shearer, G. *J. Chem. Soc.* **123** (1923) 3152.
19. Müller, A. and Shearer, G. *J. Chem. Soc.* **123** (1923) 3156.
20. Grove, J. F. and Willis, H. A. *J. Chem. Soc.* **1951** 877.
21. Bowling Barnes, R., Gore, R. C., Stafford, R. W. and Williams, V. Z. *Anal. Chem.* **20** (1948) 402.
22. Zellner, J. *Monatsh.* **64** (1934) 6.
23. Zellner, J. *Monatsch.* **66** (1935) 81.
24. Klima, J. *Monatsch.* **62** (1932) 209.
25. Rollett, A. *Z. physiol. Chem.* **62** (1909) 410.
26. Hazura, K. *Monatsch.* **8** (1887) 147, p. 153.

Received June 18, 1957.

ACTA CHEMICA SCANDINAVICA 11 (1957) 1485—1492

Fungus Pigments

V*. Degradations of Cinnabarin

JARL GRIPENBERG, ERKKI HONKANEN and ORA PATOHARJU

Department of Chemistry, Finland Institute of Technology, Helsinki, Finland

Fungus material from Central-Africa, labelled as *Polystictus sanguineus*, gave, in addition to the desired cinnabarin, a second pigment, $C_{14}H_8O_4N_2$, termed cinnabarinic acid. Oxidation of cinnabarin with potassium permanganate gives benzoxazolone-4-carboxylic acid and with hydrogen peroxide oxalic or oxamic acid. No pure substances were isolated after zinc dust distillation but the spectra of some fractions indicated the occurrence of carbazole and phenoxazin-3-one derivatives. A partial formula based on the phenoxazin-3-one ring system is proposed for cinnabarin.

Shortly after publication of our first paper on cinnabarin [1], the pigment of *Trametes cinnabarina* Jacq., there appeared two papers by Australian authors [2,3] describing a pigment, polystictin, isolated from *Coriolus sanguineus* (Fr.) (*Polystictus cinnabarinus* Jacq.). However, these names are regarded as synonymous with *T. cinnabarina* [3]. Although there are some minor differences between the properties reported for cinnabarin and polystictin, both Lemberg [2] and Cavill and coworkers [3] regarded polystictin as identical with cinnabarin. This has now been confirmed by a comparison of the IR-spectrum of cinnabarin with that of polystictin published by Cavill *et al.*[3].

Although Lemberg, who had priority in the isolation of the pigment, used the name polystictin, he has proposed that the name cinnabarin should be adopted [2]. We have therefore continued to use this name.

Further work on the structure of cinnabarin was for a long time hampered by lack of material, but through kind help of Professor H. Erdtman, Stockholm, it was finally possible to secure a substantial amount of fungus material, labelled as *Polystictus sanguineus*, from tropical Africa. This material came from three different sources, namely from the Belgian Congo, Nigeria and the Gold Coast sent by Mr. J. Frasell, Dr. T. S. Robertson and Dr. M. F. Madelin, respectively.

* Part IV *Acta Chem. Scand.* **10** (1956) 1111. A preliminary account of the present work has been published in *Chemistry & Industry* **1956** 1505.

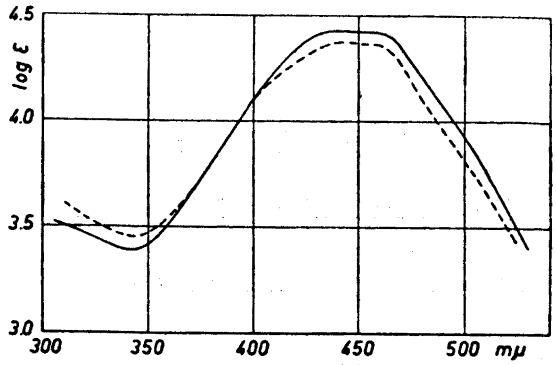


Fig. 1. Absorption curves of cinnabarin (————) and cinnabarinic acid (— — —) in pyridine.

The crude pigment obtained by extraction of this fungus material as previously described [1] was found to be a mixture of cinnabarin and another pigment, for which we propose the name cinnabarinic acid. Cinnabarinic acid differs clearly from cinnabarin in its greater acidity, being readily soluble in sodium hydrogen carbonate. The separation of the two pigments can be achieved either by using this property or by fractional extraction with hot pyridine, in which cinnabarinic acid is much more soluble.

Lemberg [2] has described a pigment, polystictinin, accompanying his polystictin. A comparison of the properties of polystictinin with those of cinnabarinic acid shows, however, that these two cannot be identical.

The analytical figures for cinnabarinic acid agree well with those required for $C_{14}H_8O_6N_2$, but it should be kept in mind that this result is from analysis of a single preparation, the purity of which is difficult to assess, owing to lack of a melting point. As cinnabarin has the composition $C_{14}H_{10}O_5N_2$ cinnabarinic acid thus differs in having one oxygen atom more and two hydrogen atoms less. A close relationship between cinnabarin and cinnabarinic acid is also indicated by the almost identical absorption curves (Fig. 1). Work is in progress aimed at relating cinnabarinic acid with cinnabarin.

Earlier work had given very little information about the structure of cinnabarin. Each group had observed that cinnabarin on alkaline hydrolysis gives one molecule of ammonia [1-3]. Cavill *et al.*[3] inferred from the IR-spectrum that cinnabarin contains a carboxamide group and also concluded that cinnabarin contains an acidic hydroxyl group and an ether oxygen, as well as a quinonoid system. Nothing was known about the basic ring system.

In the hope of obtaining some products containing a smaller or larger part of the basic skeleton, we have treated cinnabarin with different oxidants under varying conditions and submitted it to zinc dust distillation.

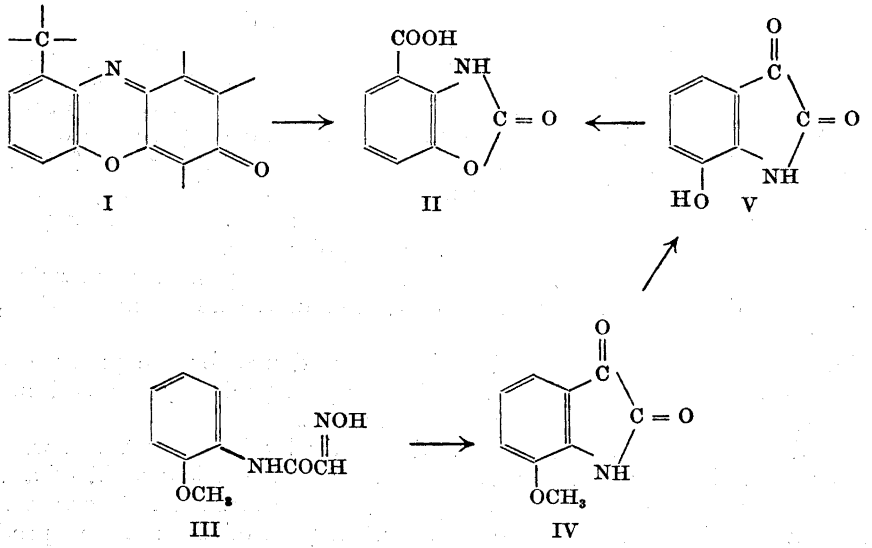
Oxidation with potassium permanganate proved to be most informative. It gave a substance, m.p. 279—281°, of the composition $C_8H_5O_4N$. With diazomethane this gave a dimethyl derivative, $C_{10}H_9O_4N$, with however, only one methoxyl. At this stage of the investigation the electronic spectrum of

cinnabarin which shows a close similarity to that of actinomycin, suggested that cinnabarin might be structurally related to the group responsible for the spectrum of the actinomycin molecule. According to Brockmann and Muxfeldt [4] this is derived from phenoxazin-3-one, and Johnson and coworkers [5,6] showed that oxidation with alkaline hydrogen peroxide followed by acid hydrolysis to remove the amino acids, gives 7-methylbenzoxazolone-4-carboxylic acid. Our oxidation product could therefore be benzoxazolone-4-carboxylic acid (II) a view further supported by the similarity of the UV-spectrum of our product with that found by Bullock and Johnson [6] for 7-methylbenzoxazolone-4-carboxylic acid.

Benzoxazolone-4-carboxylic acid was synthesised and was found to be identical with our oxidation product. The identity was established by mixed melting points of both the free acid and its dimethyl derivative with the corresponding synthetic substances. The dimethyl derivative must be methyl N-methyl-benzoxazolone-4-carboxylate; Zinner and Herbig [7] have shown that methylation of the benzoxazolone system with diazomethane leads to the N-methyl derivative.

It was therefore concluded that cinnabarin is a derivative of phenoxazin-3-one. Cavill and Tetaz [8] have also arrived at this conclusion. The recently reported observations that on oxidation phenoxazin-3-one gives benzoxazolone [6] and 2-amino-1,9-diacetylphenoxazin-3-one gives 4-acetylbenzoxazolone [9] gives further support to this view.

The benzoxazolone-4-carboxylic acid was synthesised by an analogous method to the synthesis of 7-methylbenzoxazolone-4-carboxylic acid [6]. The starting material was 7-methoxyisatin (IV). This was prepared by a modification of the Sandmeyer reaction from *o*-anisidine. Although Sandmeyer [10] explicitly states that the ring closure to an isatin derivative cannot be affected with *iso*nitroso-acet-*o*-anisidide (III) we found that use of polyphosphoric



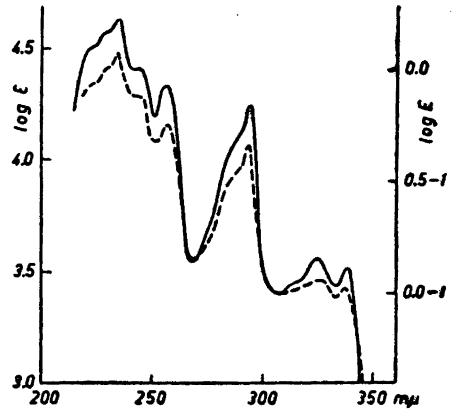


Fig. 2. Absorption curves of carbazole (————) and fraction e from zinc dust distillation (— — —) in hexane. The extinction values for the former are on the left hand side and for the latter on the right hand side.

acid instead of sulphuric acid brings about the desired ring closure, giving 7-methoxyisatin (IV). This was identified by mixed m.p. determination with an authentic sample kindly supplied by Professor A. W. Johnson, Nottingham, and originally sent to him by Professor A. Mangini, Bologna. Demethylation of 7-methoxyisatin was accomplished with pyridine hydrochloride [6] and the 7-hydroxyisatin (V) was oxidised with hydrogen peroxide in the presence of sodium hydrogen carbonate giving benzoxazolone-4-carboxylic acid (II).

The formation of benzoxazolone-4-carboxylic acid (II) places a carbon atom in position 9 in the phenoxazin-3-one nucleus leading to the partial structure I. If this carbon atom were a carboxyl group or a derivative, which would give a carboxyl group on alkaline hydrolysis, it would have been expected that benzoxazolone-4-carboxylic acid would also have been formed on oxidation with hydrogen peroxide in alkaline solution, as in the oxidation of actinomycin [5,6]. The only identifiable product from hydrogen peroxide oxidation was either oxalic acid or oxamic acid according to the alkalinity of the solution. In addition a product was formed which is very difficultly soluble in organic solvents, and is non-volatile under vacuum. It has not been possible to purify this product, which appears to be polymeric.

It is therefore concluded that the carboxyl group in benzoxazolone-4-carboxylic acid has been formed by oxidation of a side chain by the permanganate.

The formation of oxamic acid is further evidence for the presence of a carboxamide group in cinnabarin. This group is probably situated in the quinonoid ring of the phenoxazin-3-one nucleus.

Zinc dust distillation had been tried already by Lemberg [2], but without much success. Even in our hands the reaction gave a low yield of a very complex mixture. No crystalline compounds were obtained but certain fractions from the chromatography of the neutral part of the reaction product

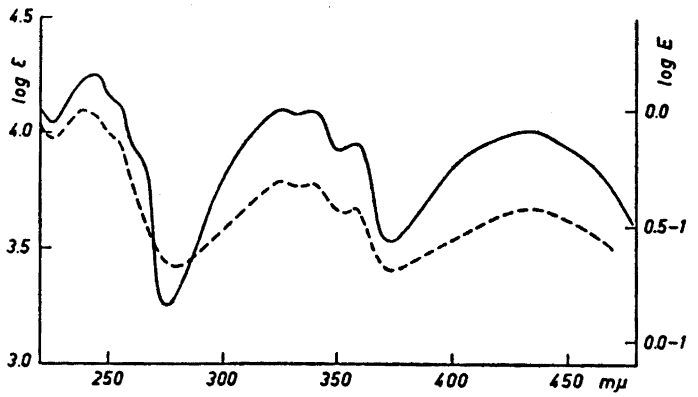


Fig. 3. Absorption curves of phenoxazin-3-one (————) and fraction 8 from zinc dust distillation (— — —) in hexane. The extinction values for the former are on the left hand side and for the latter on the right hand side.

had UV-spectra from which it has been possible to draw some conclusions about the substances present. The spectrum of one fraction was practically identical with that of carbazole (Fig. 2). This means that carbazole or a homologue (or a mixture of homologues) had been formed. Because the UV-spectra of carbazole and C-alkylated carbazoles are almost identical [11,12] it is not possible to distinguish between these alternatives.

This result was somewhat surprising. Firstly because Lemberg [2] had found no reactions typical of carbazole in his reaction product. Secondly, if cinnabarin is a derivative of phenoxazin-3-one, this means that the ring is opened at the oxygen atom which is lost, followed by ring closure again. Such an opening of the oxygen bridge during zinc dust distillation is not usually met with in simple systems such as dibenzofuran [13] and dibenzopyran [14] but there seems to be no information available about the behaviour of phenoxazines upon zinc dust distillation.

In view of the very low yield obtained, the possibility cannot be completely ruled out, that this substance was formed from some impurity in the starting material. The fact that fractions with identical UV-spectra have been obtained from two samples of cinnabarin of completely different origin can, however, be taken as evidence against such a possibility.

A further fraction had a spectrum closely similar to that of phenoxazin-3-one (Fig. 3) and this fraction evidently corresponds to the product (H) reported by Cavill and Tetaz [8].

EXPERIMENTAL

(The analyses have been performed by Dr. A. Bernhardt, Mülheim)

Separation of cinnabarin from cinnabarinic acid. a) The mixture of pigments obtained by acetone extraction of the fungus material was treated on a filter with sodium hydrogen carbonate and washed with water. This was repeated until the filtrate was no longer red.

The filtrate was run directly into dilute acid to give cinnabarinic acid as a red amorphous precipitate. This was recrystallised from pyridine giving dark brown glistening crystals, which decompose above 300° without melting. (Found: C 55.98; H 2.80; N 9.18; O 31.74. $C_{14}H_8O_6N_2$ requires C 56.01; H 2.69; N 9.33; O 31.98).

The cinnabarin remaining on the filter was purified by recrystallisation from pyridine.

b) The mixture was boiled with a small amount of pyridine, filtered hot, and allowed to crystallise. The crystals which were a mixture enriched in cinnabarinic acid, were filtered off. The mother liquor was used again for re-extraction of the undissolved material. This was repeated until the crystallisate contained pure cinnabarin, as judged by the absence of colouration upon treating a sample with sodium hydrogen carbonate. The cinnabarin was then recrystallised from fresh pyridine. Although this method readily gives cinnabarin, free from cinnabarinic acid, it is more difficult to obtain pure cinnabarinic acid and for this purpose it is better to combine it with method a).

Oxidation of cinnabarin with potassium permanganate. Cinnabarin (3.0 g) was suspended in 5 % sodium carbonate solution (120 ml) and finely powdered potassium permanganate was added with stirring until the permanganate colour persisted. The mixture was acidified with sulphuric acid and the precipitate of manganese dioxide was dissolved by adding sodium hydrogen sulphite. The solution was extracted with ten portions of ether (50 ml each). The residue from the ether extract was washed with a little water and then with benzene and sublimed (200—210°/2 mm). The sublimate was recrystallised from methanol giving benzoxazolone-4-carboxylic acid (240 mg) as slightly yellow crystals; m.p. 279—281°. (Found: C 53.17; H 2.84; N 7.74; O 34.28. $C_8H_5O_4N$ requires C 53.64; H 2.81; N 7.82; O 35.73) λ_{max} (ethanol) 239 mμ (log ε 4.05), 302 mμ (log ε 3.20); λ_{min} 224 mμ (log ε 3.80), 262 mμ (log ε 2.60); λ_{max} (0.05 N NaOH) 226 mμ (log ε 4.17), 250 mμ (log ε 4.08), 310 mμ (log ε 3.92); λ_{min} 238 mμ (log ε 3.90), 270 mμ (log ε 2.97).

Benzoxazolone-4-carboxylic acid (45 mg) was dissolved in methanol and an ether solution of diazomethane was added until the yellow colour persisted. The solution was evaporated and the residue sublimed (140—150°/2 mm) giving methyl N-methylbenzoxazolone-4-carboxylate (43 mg), m.p. 141—142° (Found: C 58.00; H 4.62; N 6.98; O 30.88; OCH_3 14.84. $C_9H_6O_3N(OCH_3)$ requires C 57.97: H 4.38; N 6.76; O 30.89; OCH_3 14.98) λ_{max}(ethanol) 240 mμ (log ε 3.90), 304 mμ (log ε 3.76); λ_{min} 226 mμ (log ε 3.74), 264 mμ (log ε 2.76).

Oxidation of cinnabarin with hydrogen peroxide. a) Cinnabarin (200 mg) was suspended in sodium hydrogen carbonate (4 %, 5 ml) and hydrogen peroxide (30 %; 5 ml) was added. More hydrogen peroxide was added from time to time until a clear almost colourless solution resulted. This took about 2 days. The solution was acidified with conc. hydrochloric acid and evaporated at room temperature in a vacuum desiccator over sodium hydroxide. The residue was extracted with several portions of hot dioxan. The dioxan solution was evaporated almost to dryness in vacuum and the crystals which formed were filtered off (*ca.* 35 mg) and recrystallised from dioxan, m.p. 210—211°. (Found N 15.40. $C_2H_3O_3N$ requires N 15.73). It gave no depression of m.p. when mixed with oxamic acid [15].

b) Cinnabarin (200 mg) was dissolved in 2 N sodium hydroxide (2 ml) and allowed to stand overnight. Hydrogen peroxide (30 %) was then added dropwise and the solution allowed to stand until it was light yellow. It was then acidified with conc. hydrochloric acid and evaporated in a vacuum desiccator over sodium hydroxide. The residue was extracted with ether and the ether evaporated giving oxalic acid.

c) Hydrogen peroxide (30 %; 2 ml) was added to cinnabarin (200 mg) followed by dropwise addition of 2 N sodium hydroxide. When the solution tended to acquire a darker colour more hydrogen peroxide was added. This was continued until a clear light yellow solution was obtained. Oxamic acid and oxalic acid were isolated from this as described in a) and b).

Zinc dust distillation of cinnabarin. A mixture of cinnabarin (252 mg) and Zn-dust (2.54 g), divided into 5 portions, was distilled in a stream of hydrogen. The volatile products were collected in a trap cooled to −70°. The distillation residue was extracted with ether which was combined with an ether solution of the volatile part. Altogether 30 mg of ether soluble material was obtained. This was divided into basic, acidic and neutral parts by extraction of the ether solution with hydrogen chloride and sodium hydroxide. Each fraction was then chromatographed on alumina using hexane, ether and methanol in that order for elution. The chromatograms on inspection by U. V., showed

several fluorescent zones. The different zones were collected in different fractions and the ultra violet spectrum of each fraction was recorded. Only the neutral part gave fractions that showed any selective absorption in the ultra-violet. Fractions Nos. 5—7 (eluted by hexane) showed two distinct maxima at 232 and 291 mμ. Further chromatography of these fractions gave finally a noncrystalline fraction with maxima at 234, 257, 293, 327 and 337 mμ, and minima at 251, 269, 307 and 332 mμ (Fig. 2).

Fraction 8 had maxima at 240, 326, 340, 358, and 528—533 mμ and minima at 225, 279, 334, 352 and 370 mμ (Fig. 3).

Fractions 9—10 had maxima at 240 and 302 mμ and minima at 227 and 280—285 mμ.

7-Methoxyisatin. (IV). *Iso*nitroso-acet-*o*-anisidide [10] (III) (0.5 g) was added to polyphosphoric acid [16] (5 ml) kept on a boiling water bath. Heating was continued until all the material had dissolved giving a dark violet-brown solution. This was cooled and a large volume of water was added. The precipitate was filtered off and treated with chloroform. The chloroform solution was chromatographed on alumina. The dark red eluate was evaporated to a small volume. 7-Methoxyisatin (0.1 g) crystallised, m.p. 242—243°, undepressed on admixture with an authentic sample.

7-Hydroxyisatin. (V). 7-Methoxyisatin (150 mg) was added to pyridine hydrochloride (1.5 g) and the mixture was heated for 20 minutes to 200° in an oil bath. Water was added to the mixture after cooling and the product was taken up in ethyl acetate. A considerable amount of dark coloured material was removed by filtering the ethyl acetate solution through a short column of silicic acid. Evaporation of the solvent gave 7-hydroxyisatin (80 mg) as brown-red crystals, which decompose around 270° without melting. (Found: C 59.01; H 3.75. $C_8H_5O_3N$ requires C 58.90, H 3.09).

Benzoxazolone-4-carboxylic acid. (II). 7-Hydroxyisatin (80 mg) was suspended in sodium hydrogen carbonate (5 %; 15 ml) and hydrogen peroxide (30 %; 2 ml) was added. After about one hour the originally dark red solution had become almost colourless. Acidification produced a crystalline precipitate of benzoxazolone-4-carboxylic acid, m.p. 279—281°. By treatment with diazomethane this was converted into methyl N-methylbenzoxazolone-4-carboxylate m.p. 140—141°. In neither case was there any depression of melting point when mixed with the corresponding substances obtained by oxidation of cinnabarin.

The authors wish to thank Mr. J. Fraselle, Yangambi, Belgian Congo, Dr. T. S. Robertson, West African Institute for Oil Research, Benin City, Nigeria, and Dr. M. F. Madelin, Botany Department, University College of the Gold Coast, Achimoto, Gold Coast, for their great kindness in collecting the fungus material used in this investigation. Our thanks are also due to Professor H. Erdtman, Stockholm, for arranging these contacts.

We wish also to thank Professor A. W. Johnson, Nottingham, for a sample of 7-methoxyisatin and for much information on the oxidation of actinomycin prior to publication.

This investigation has been financially supported by a grant from the *State Commission for Natural Sciences* (*Valtion Luonnontieteellinen Toimikunta*), which is gratefully acknowledged.

REFERENCES

1. Gripenberg, J. *Acta Chem. Scand.* **5** (1951) 590.
2. Lemberg, R. *Australian J. Exptl. Biol. Med. Sci.* **30** (1952) 271.
3. Cavill, G. W. K., Ralph, B. J., Tetaz, J. R. and Werner, R. L. *J. Chem. Soc.* **1953** 525.
4. Brockmann, H. and Muxfeldt, H. *Angew. Chem.* **68** (1956) 69.
5. Angyal, S. J., Bullock, E., Hanger, W. G. and Johnson, A. W. *Chemistry & Industry* **1955** 1295.
6. Bullock, E. and Johnson, A. W. *J. Chem. Soc.* **1957** 1602.
7. Zinner, H. and Herbig, H. *Chem. Ber.* **88** (1955) 693.
8. Cavill, G. W. K. and Tetaz, J. R. *Chemistry & Industry* **1956** 986.
9. Butenandt, A. *Angew. Chem.* **69** (1957) 16.

10. Sandmeyer, T. *Helv.* **2** (1919) 234.
11. Schmid, H., Ebnöther, A. and Karrer, P. *Helv.* **33** (1950) 1486.
12. Robinson, R. and Saxton, J. E. *J. Chem. Soc.* **1952** 976.
13. Hoffmeister, W. *Ann.* **159** (1871) 191.
14. Richter, R. *J. prakt. Chem.* [2] **28** (1883) 273.
15. Oelkers, L. *Ber.* **22** (1889) 1569.
16. Bachmann, W. E. and Horton, W. J. *J. Am. Chem. Soc.* **69** (1947) 58.

Received June 18, 1957.

ACTA CHEMICA SCANDINAVICA 11 (1957) 1493—1495

Side-chain Reactions with Furans

NIELS ELMING*

Centrallaboratoriet, Sadolin & Holmblad A/S, Copenhagen, Denmark

As part of attempts to transform furans into other aromatic systems 9 new α-substituted furans have been prepared.

In the course of attempts to transform furans into other aromatic systems [1-8] a number of new α-substituted furans (II—IV, VI, VIII, X—XIII) have been prepared by the reactions shown below. Further syntheses employing these compounds failed, but it was found worth while to publish directions for their preparation since all the compounds at any time may become of use for synthetic work in this field.

The acid chloride of 2,5-dimethoxy-2,5-dihydrofuroic acid (XI) was not isolated pure but identified by transformation to the corresponding methyl ester (IX).

EXPERIMENTAL

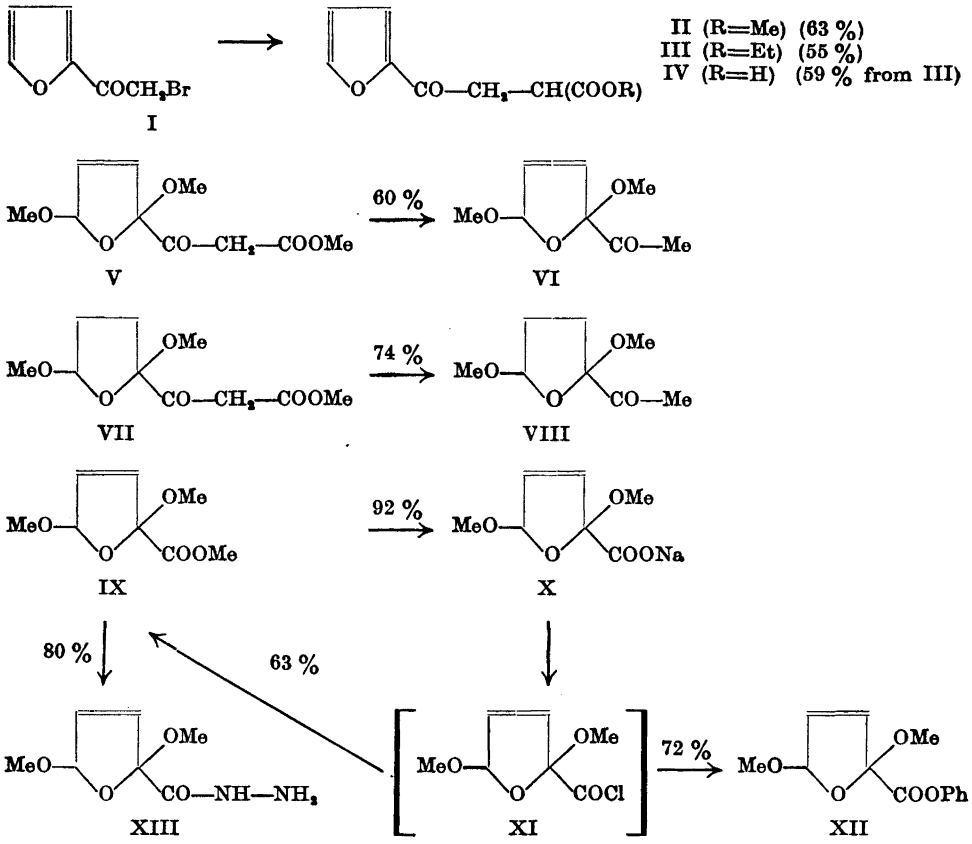
Microanalyses by E. Boss and K. Glens

2-(α-Oxo-β-bromoethyl)-furan (I) was prepared after Brown [9]. The yield was 51 % [b.p.$_{0.1}$ 66—67°; n_D^{25} 1.5718; m.p. 32—34° (Hershberg apparatus, corr.)]. Brown obtained 85 % of a product with b.p.$_{20}$ 121—123°; n_D^{25} 1.5783 and m.p. 36—37° (after two crystallizations from petroleum ether). (Found: C 38.4; H 2.9; Br 41.8. Calc. for $C_6H_5BrO_2$ (189.0): C 38.1; H 2.7; Br 42.3).

2-(α-Oxo-γ,γ-(dicarbomethoxy)-propyl)-furan (II). I (25.0 g, 0.13 mole) was dissolved in anhydrous ether (20 ml) and the solution added during 15 min with stirring to a suspension of sodium dimethyl malonate [from powdered sodium (3.22 g, 0.14 mole) and dimethyl malonate (19.4 g, 0.15 mole)] in anhydrous ether (140 ml) (gentle reflux). The reaction mixture was heated under reflux with stirring for 2 h and cooled. Cold water was added, the etheral layer separated, washed twice with cold water and dried. The ether was evaporated in a vacuum and the crystalline residue removed by filtration, washed with ether and dried. The yield was 16.7 g of II (white crystals, m.p. 67—69°). (Found: C 54.8; H 5.2; OCH_3 25.0. Calc. for $C_9H_6O_4(OCH_3)_2$ (240.2): C 55.0; H 5.0; OCH_3 25.8). After crystallization from ether the m.p. was 69—71°.

The filtrate from the above 16.7 g of II was distilled and the distillate (4.0 g, b.p.$_{0.1}$ 132—135°) crystallized from ether. Hereby another 3.2 g of II was obtained (white crystals, m.p. 68—70°). (Found: C 54.9; H 5.4; OCH_3 26.8). The total yield of II thus was 19.9 g (63 %).

* Present address: Aktieselskabet Pharmacia, Copenhagen, Denmark.



2-(α-Oxo-γ,γ-(dicarbethoxy)-propyl)-furan (III) was prepared from I (19.0 g), dissolved in 20 ml of anhydrous ether, and sodium diethyl malonate [from powdered sodium (2.30 g) and diethyl malonate (16.0 g) suspended in anhydrous ether (95 ml)] as described above for the preparation of II. The reaction product was isolated by distillation. The yield was 14.7 g (55 %) of III (colorless liquid; b.p.$_{0.1}$ 141—143°; n_D^{25} 1.4853). (Found: C 58.5; H 6.2; OC_2H_5 33.5. Calc. for $C_9H_8O_4(OC_2H_5)_2$ (268.3): C 58.2; H 6.0; OC_2H_5 33.6).

2-(α-Oxo-γ,γ-(dicarboxy)-propyl)-furan (IV). III (2.20 g) and a solution of potassium hydroxide (1.02 g) in methanol (20 ml) were heated under reflux (1 h). Water (5 ml) was added, the methanol distilled in a vacuum and the mixture adjusted to pH 3 with conc. hydrochloric acid. The precipitate formed was removed by filtration, washed twice with water and dried. The yield of crude IV was 1.49 g (86 %) [light-brown crystals; m.p. 158—161° (decomp.)]. Treatment with active carbon in methanol followed by crystallization from methanol-ether gave 1.02 g (59 %) of pure IV [white crystals, m.. 159—162° (decomp.)]. (Found: C 50.7; H 3.8; neut.equiv. (phenolphthalein indicator) 105.6. Calc. for $C_9H_8O_6$ (212.2): C 51.0; H 3.8).

2,5-Dimethoxy-2-(α-oxoethyl)-2,5-dihydrofuran (VI). V[5] (17.3 g) and a solution of potassium hydroxide (5 %, 200 ml) were mixed and heated under reflux (6 h). After cooling, the mixture was extracted continuously with ether and the etheral extract dried and distilled. The yield was 7.74 g (60 %) of VI (colorless liquid; b.p.$_{11}$ 91—94°;

n_D^{25} 1.4431). (Found: C 55.6; H 7.2; OCH_3 35.3. Calc. for $C_6H_6O_3(OCH_3)_2$ (172.2): C 55.8; H 7.0; OCH_3 36.0).

2,5-Dimethoxy-2-(α-oxoethyl)-tetrahydrofuran (VIII). VIII was prepared from VII[8] (4.64 g) as described for the preparation of VI. The yield was 2.57 g (74 %) of VIII (colorless liquid; b.p.$_{12}$ 92—93°; n_D^{25} 1.4347). (Found: C 55.3; H 8.1; OCH_3 34.8. Calc. for $C_6H_8O_2(OCH_3)_2$ (174.2): C 55.2; H 8.1; OCH_3 35.6).

Sodium 2,5-dimethoxy-2,5-dihydrofuroate (X). Methyl 2,5-dimethoxy-2,5-dihydrofuroate[10] (7.52 g, 0.040 mole) and sodium hydroxide (1.05 N, 40.0 ml, 0.042 mole) were mixed and heated under reflux (19 h). After cooling, the mixture was washed with ether, filtered and evaporated in a vacuum, at last for 4 h under 0.1 mm at 60—70°. The residue was pulverized in a mortar and dried further for 2 h. The yield was 7.24 g (92 %) of X (white powder with a yellow tinge). (Found: OCH_3 30.7. Calc. for $C_6H_7O_5Na(OCH_3)_2$ (196.1): OCH_3 31.6).

2,5-Dimethoxy-2,5-dihydrofuroyl chloride (XI). X (1.96 g, 0.010 mole), anhydrous benzene (10 ml) and a drop of pyridine were mixed and the mixture cooled to 0°. Oxalyl chloride (1.55 g, 0.012 mole) was added at 0° and the mixture shaken (20 min) at 0—10° and evaporated three times under 35 mm from a water bath of 20° with anhydrous benzene. A precipitate of sodium chloride was removed by filtration and washed with a little anhydrous ether. The slightly yellow filtrate consists of about equal parts of XI and solvent (benzene and ether) and is used directly for further syntheses without isolation of the acid chloride.

In order to identify XI the solution was added to a solution of sodium acetate (1.20 g) in anhydrous methanol (20 ml) during 10 min at 0°. After standing for 15 min without cooling anhydrous ether was added, the mixture filtered and the filtrate distilled. Hereby 1.18 g (63 %) of methyl 2,5-dimethoxy-2,5-dihydrofuroate (b.p.$_{14}$ 120—122°; n_D^{25} 1.4472; previously found[10] b.p.$_{13-14}$ 119—121°; n_D^{25} 1.4476) was obtained. (Found: C 51.5; H 6.7; OCH_3 48.1. Calc. for $C_6H_7O_3(OCH_3)_3$ (188.2): C 51.1; H 6.4; OCH_3 49.4).

Phenyl 2,5-dimethoxy-2,5-dihydrofuroate (XII). A solution of XI prepared as above was added to a solution of phenol (1.04 g, 0.011 mole) in pyridine (10 ml) during 10 min at −5°. After shaking for 2 h without cooling the mixture was evaporated partly in a vacuum and ether was added. A precipitate of pyridinium hydrochloride was removed by filtration and the filtrate washed with water, dried and distilled. The yield was 1.80 g (72 %) of XII (colorless liquid; b.p.$_{0.1}$ 129—132°; n_D^{25} 1.5076). (Found: C 62.3; H 5.8; OCH_3 24.3. Calc. for $C_{11}H_8O_3(OCH_3)_2$ (250.2): C 62.4; H 5.6; OCH_3 24.8).

2,5-Dimethoxy-2,5-dihydrofuroic acid hydrazide (XIII). Methyl 2,5-dimethoxy-2,5-dihydrofuroate[10] (3.76 g) and hydrazine hydrate (90 %, 7 ml) were mixed, the mixture left standing overnight and distilled. The yield was 3.01 g (80 %) of XIII (colorless liquid; b.p.$_{0.5}$ 140—145°; n_D^{25} 1.5008). (Found: C 44.7; H 6.5; N 15.0; OCH_3 32.4. Calc. for $C_6H_6N_2O_2(OCH_3)_2$ (188.2): C 44.7; H 6.4; N 14.9; OCH_3 33.0).

After standing for some days the sample crystallized completely (m.p. 60—75°). Crystallization from methanol-ether gave a product melting at 86—91°. (Found: C 44.6; H 6.7; N 14.8; OCH_3 32.4).

Three further crystallizations from methanol-ether gave products with the following m.p.'s: 86—90°, 100—102° and 105—106°. Probably all the products are mixtures of the *cis* and the *trans* isomer (*cf.*[10]).

REFERENCES

1. Clauson-Kaas, N., Elming, N. and Tyle, Z. *Acta Chem. Scand.* **9** (1955) 1.
2. Nielsen, J. T., Elming, N. and Clauson-Kaas, N. *Acta Chem. Scand.* **9** (1955) 9.
3. Clauson-Kaas, N. and Nedenskov, P. *Acta Chem. Scand.* **9** (1955) 14.
4. Elming, N. and Clauson-Kaas, N. *Acta Chem. Scand.* **9** (1955) 23.
5. Clauson-Kaas, N. and Nedenskov, P. *Acta Chem. Scand.* **9** (1955) 27.
6. Nielsen, J. T., Elming, N. and Clauson-Kaas, N. *Acta Chem. Scand.* **9** (1955) 30.
7. Elming, N. and Clauson-Kaas, N. *Acta Chem. Scand.* **10** (1956) 1603.
8. Elming, N. *Acta Chem. Scand.* **10** (1956) 1664.
9. Brown, E. V. *Iowa State Coll. J. Sci.* **11** (1937) 221.
10. Clauson-Kaas, N. and Limborg, F. *Acta Chem. Scand.* **6** (1952) 551.

Received April 27, 1957.

ACTA CHEMICA SCANDINAVICA 11 (1957) 1496—1498

3-Hydroxypicolinaldehyde

NIELS ELMING*

Centrallaboratoriet, Sadolin & Holmblad A/S, Copenhagen, Denmark

3-Hydroxypicolinaldehyde triacetate was obtained by rearrangement of 2-hydroxymethyl-3-pyridinol-1-oxide. Hydrolysis of this compound gave pure 3-hydroxypicolinaldehyde.

The following derivatives of 3-hydroxypicolinaldehyde were prepared: the diethyl acetal, the dimethyl acetal, the aldoxime, the 2,4-dinitrophenylhydrazone hydrochloride and the hydrochloride.

As part of an investigation of oximes of the pyridine series Ginsburg and Wilson [1] prepared 3-hydroxypicolinaldehyde and certain of its derivatives. Starting from 2-acetoxymethyl-3-acetoxypyridine (obtained from 3-pyridinol after Stempel and Buzzi [2]) they prepared the 1-oxide which was transformed into 3-hydroxypicolinaldehyde triacetate (method of Boekelheide and Linn [3]). The triacetate was then hydrolyzed to 3-hydroxypicolinaldehyde. The intermediate products were not isolated. The aldehyde was obtained in a 12 % yield as an oil which was not analyzed.

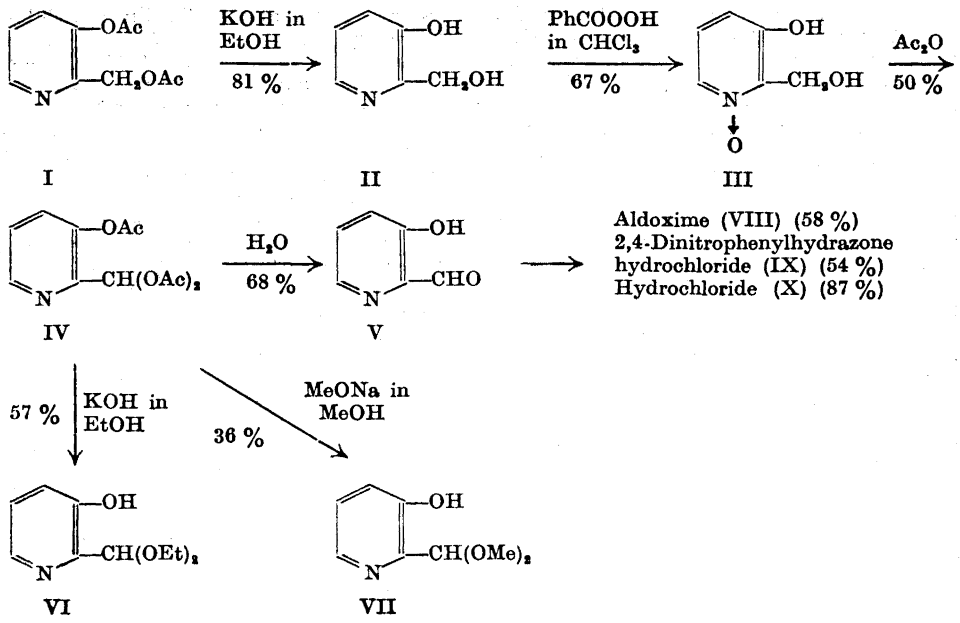
In connection with other experiments in the 3-pyridinol field 3-hydroxypicolinaldehyde has been prepared by a modification of the route used by Ginsburg and Wilson. Better yields were obtained and all intermediate products and derivatives were isolated pure. The reactions carried out are summarized below.

EXPERIMENTAL

Microanalyses by K. Glens and P. Hansen

2-Hydroxymethyl-3-pyridinol (II). 2-Acetoxymethyl-3-acetoxypyridine (I) (prepared from 3-pyridinol after Stempel and Buzzi [2]) (2.09 g, 0.010 mole) and 1 N potassium hydroxide in ethanol (40 ml, 0.040 mole) were mixed and heated under reflux for 2 h. Water (15 ml) was added and the ethanol evaporated in a vacuum. The solution was neutralized by adding conc. hydrochloric acid, solid potassium carbonate was added and the mixture then continuously extracted with ether overnight. The ether was evaporated and the residue washed twice with ether and dried. The yield was 1.02 g (81 %) of II [yellowish-white crystals; m.p. 136—139° (Hershberg apparatus, corr.), previously found [4] 132°]. (Found: N 11.0. Calc. for $C_6H_7NO_2$ (125.1): N 11.2).

* Present address: Aktieselskabet Pharmacia, Copenhagen, Denmark.



Sublimation (110—125°/0.05 mm) gave white crystals, m.p. 137—139°.

In another experiment I (2.09 g, 0.010 mole) and conc. hydrochloric acid (20 ml) were mixed and refluxed for 12 h. The solution was evaporated to dryness in a vacuum, dissolved in water and solid potassium carbonate added. Continuous extraction with ether overnight gave 0.91 g (73 %) of II (yellowish-white crystals, m.p. 136—139°).

2-Hydroxymethyl-3-pyridinol hydrochloride. II (125 mg, 0.0010 mole) was dissolved in N hydrochloric acid (5 ml) and the solution evaporated to dryness in a vacuum. Dissolution of the residue in 99 % ethanol and precipitation with ether gave 148 mg (92 %) of 2-hydroxymethyl-3-pyridinol hydrochloride (white crystals; the m.p. was not sharp, but the compound darkened at 209—211°; previously found [4] m.p. 206°). (Found: N 8.8; Cl 22.9. Calc. for $C_6H_8ClNO_2$ (161.6): N 8.7; Cl 21.8).

2-Hydroxymethyl-3-pyridinol-1-oxide (III). II (8.00 g, 0.064 mole) was dissolved in methanol (32 ml) and chloroform (60 ml) was added. A solution of perbenzoic acid (13.8 g, 0.10 mole) in chloroform (180 ml) was added and the mixture left standing at room temperature overnight. The solution was concentrated to about 100 ml in a vacuum, the precipitate removed by filtration, washed with chloroform and dried. Crystallization from methanol gave 6.00 g (67 %) of III [white crystals; m.p. 175—177°). (Found: C 50.9; H 5.2; N 9.8. Calc. for $C_6H_7NO_3$ (141.1): C 51.1; H 5.0; N 9.9).

III gave a red color with aqueous ferric chloride.

3-Hydroxypicolinaldehyde triacetate (IV). III (6.30 g) was dissolved in acetic anhydride (63 ml) and the solution heated under reflux for 30 min. Distillation gave 8.0 g of a pale yellow liquid ($b.p._{0.1}$ 140—145°), which crystallized completely on standing. Crystallization from ether gave 5.9 g (50 %) of III [white crystals; m.p. 79—81° (Hershberg apparatus, corr.)]. (Found: C 53.7; H 5.0; N 5.2; $COCH_3$ 49.1. Calc. for $C_6H_4NO_3(COCH_3)_3$ (267.2): C 53.9 ;H 4.9; N 5.2; $COCH_3$ 48.3). IV gave no color reaction with aqueous ferric chloride.

3-Hydroxypicolinaldehyde (V). IV (1.34 g) and water (25 ml) were heated under reflux overnight. The crystalline reaction product sitting in the reflux condenser was dissolved in ether (the remaining solution in the flask was made alkaline with potassium carbonate and continuously extracted with ether for 5 h, whereby only 40 mg of an oil was obtained), washed with a little 2 M potassium hydrogen carbonate and dried with magne-

sium sulfate. Evaporation gave 0.53 g of a yellow crystalline residue. Sublimation (40—50°/0.05 mm) gave 0.42 g (68 %) of V (yellowish-white crystals, m.p. 81—82°). Crystallization from ether followed by sublimation did not change the m.p. (Found: C 58.1; H 4.4; N 11.1. Calc. for $C_6H_5NO_2$ ((123.1): C 58.5; H 4.1; N 11.4). V gave a red color with aqueous ferric chloride. When V is placed on the skin a persistent green color develops.*

3-Hydroxypicolinaldehyde diethyl acetal (VI). IV (0.67 g, 0.0025 mole) and 0.5 N potassium hydroxide in 96 % ethanol (30 ml, 0.015 mole) were mixed, heated under reflux for 1.5 h and then evaporated in a vacuum to about 10 ml. A little water was added, the solution neutralized under cooling with acetic acid and then made alkaline by adding potassium carbonate. The solution was extracted twice with ether, the ether extract washed with a little water and dried with magnesium sulfate. Evaporation gave 0.34 g of a white crystalline residue. Sublimation (75°/0.05 mm) gave 0.28 g (57 %) of VI (white crystals; m.p. 82—83°). Crystallization from ether followed by sublimation did not change the m.p. (Found: C 61.0; H 7.7; N 7.1; OC_2H_5 44.4. Calc. for $C_6H_5NO(OC_2H_5)_2$ (197.2): C 60.9; H 7.7; N 7.1; OC_2H_5 45.7). VI gave a red color with aqueous ferric chloride.

3-Hydroxypicolinaldehyde dimethyl acetal (VII). IV (1.34 g, 0.0050 mole) was dissolved in methanol (10 ml) and sodium methoxide in methanol [prepared from 0.24 g of sodium (0.011 mole) and methanol (5 ml)] was added. After 30 min at room temperature the reaction mixture was worked up essentially as described above for the preparation of VI. The yield after sublimation (90°/0.1 mm) was 0.30 g (36 %) of VII (white crystals; m.p. 104—105°). Crystallization from ether followed by sublimation did not change the m.p. (Found: C 56.4; H 6.3; N 8.5; OCH_3 36.4. Calc. for $C_6H_5NO(OCH_3)_2$ (169.2): C 56.8; H 6.6; N. 8.3; OCH_3 36.7). VII gave a red color with aqueous ferric chloride.

3-Hydroxypicolinaldehyde aldoxime (VIII). V (0.37 g, 0.0030 mole) was dissolved in a mixture of pyridine (6 ml) and 99 % ethanol (6 ml). Hydroxylamine hydrochloride (0.33 g, 0.0048 mole) was added, the mixture heated under reflux for 1 h and then evaporated. Ether (50 ml) was added to the residue and the mixture heated under reflux for 10 min. The ether extract was washed with water, dried with magnesium sulfate and evaporated. The crystalline residue was sublimed (120°/0.05 mm). The yield was 0.24 g (58 %) of VIII (white crystals; m.p. 173—174°; previously found [5] 170°). Crystallization from ether followed by sublimation did not change the m.p. (Found: C 52.2; H 4.4; N 20.0. Calc. for $C_6H_6N_2O_2$ (138.1): C 52.2; H 4.4; N 20.3).

3-Hydroxypicolinaldehyde 2,4-dinitrophenylhydrazone hydrochloride (IX). V (10 mg) was dissolved in water (2 ml) and 15 ml of a 0.2 % solution of 2,4-dinitrophenylhydrazine in 2 N hydrochloric acid was added. A yellow precipitate was formed at once. After 1 h the precipitate was removed by filtration, washed with water and dried. The yield was 15 mg (54 %) of IX [orange-red crystals; m.p. 305—310° (decomp.); previously found [6] 219—221° (decomp.)] (Found: C 42.5; H 3.1; N 19.7. Calc. for $C_{12}H_{10}ClN_5O_5$ (339.7): C 42.4; H 3.0; N 20.6).

IX was also obtained from IV after hydrolysis (1 h) as described above for the preparation of V. Crystallization from 96 % ethanol gave 50 % of IX, m.p. 305—310° (decomp.).

3-Hydroxypicolinaldehyde hydrochloride (X). V (40 mg) was dissolved in anhydrous ether (10 ml), gaseous hydrogen chloride was passed into the solution, the white precipitate was removed by filtration, washed with ether and dried. The yield was 45 mg (87 %) of X (white crystals, m.p. 218—221°). (Found: N 8.6; Cl 21.9. Calc. for $C_6H_6ClNO_2$ (159.6): N 8.8; Cl 22.2).

REFERENCES

1. Ginsburg, S. and Wilson, I. B. *J. Am. Chem. Soc.* **79** (1957) 481.
2. Stempel, A. and Buzzi, E. C. *J. Am. Chem. Soc.* **71** (1949) 2969.
3. Boekelheide, V. and Linn, W. J. *J. Am. Chem. Soc.* **76** (1954) 1286.
4. Urbanski, T. *J. Chem. Soc.* **1946** 1104.
5. Kuhn, R. and Hensel, H. R. *Chem. Ber.* **86** (1953) 1333.
6. Metzler, D. E., Ikawa, M. and Snell, E. E. *J. Am. Chem. Soc.* **76** [1954) 648.

* *Note added in proof:* Mathes, W. and Sauermilch, W. (*Chem. Ber.* **90** (1957) 758), have prepared V(m.p. 83°) by gas phase oxidation of 2-methyl-3-pyridinol. The yield of crude product was 26.5 %.

Received April 27, 1957.

ACTA CHEMICA SCANDINAVICA 11 (1957) 1499—1504

Calculation of Standard Deviations for Interatomic Distances in Benzene Based upon Spectroscopic Data

S. J. CYVIN

Institutt for teoretisk kjemi, N.T.H., Trondheim, Norway

A set of force constants in a harmonic potential function for in-plane vibrations of benzene has been computed and used for a normal coordinate determination. The ten types of interatomic distances are studied by group theory methods and the normal coordinate analysis is performed. Finally the standard deviation for all interatomic distances in benzene is given at the temperatures 0, 273, 298 and 323°K.

The subject of this paper is the calculation of standard deviations for interatomic distances in the benzene molecule by making use of a normal coordinate analysis for in-plane vibrations. The vibrations are treated as harmonic oscillations. As for the theory, the treatment given by Wilson, Decius and Cross [1] is followed. The treatment is extended to deal with all types of interatomic distances. Crawford and Miller [2] have previously evaluated a set of force constants for benzene. In this paper another set is used, as obtained by recalculation with a newer set of experimental frequencies [3].

SYMMETRY COORDINATES

The applied symmetry coordinates are of the VFSC type (linear combinations of valence force coordinates) and are specified in Table 1. The notation for valence force coordinates is: σ for C—H stretching (s in Wilson's notation [1]), τ for C—C stretching (t in Wilson's notation), α for C—C—C bending and β for C—H bending (identical with the notations by Wilson). According to Table 1, for instance, $s_{12} = 6^{-\frac{1}{2}} (\alpha_1 - \alpha_2 + \alpha_3 - \alpha_4 + \alpha_5 - \alpha_6)$. The symmetry coordinates, as well as the normal coordinates, are numbered in the same way as Wilson's [1] and Langseth's [3] numbering of fundamental frequencies.

Table 1. Symmetry coordinates for in-plane vibrations of benzene.

Species	VFSC	N	1	2	3	4	5	6	
A_{1g}	S_2	$6^{-1/2}$	1	1	1	1	1	1	σ
	S_1	$6^{-1/2}$	1	1	1	1	1	1	τ
	S_r	$6^{-1/2}$	1	1	1	1	1	1	a
A_{2g}	S_3	$6^{-1/2}$	1	1	1	1	1	1	β
B_{1u}	S_{13}	$6^{-1/2}$	1	−1	1	−1	1	−1	σ
	S_{12}	$6^{-1/2}$	1	−1	1	−1	1	−1	a
B_{2u}	S_{14}	$6^{-1/2}$	−1	1	−1	1	−1	1	τ
	S_{15}	$6^{-1/2}$	1	−1	1	−1	1	−1	β
E_{2g}	S_{7a}	$12^{-1/2}$	2	−1	−1	2	−1	−1	σ
	S_{8a}	$12^{-1/2}$	1	−2	1	1	−2	1	τ
	S_{6a}	$12^{-1/2}$	2	−1	−1	2	−1	−1	a
	S_{9a}	$1/2$	0	1	−1	0	1	−1	β
	S_{7b}	$1/2$	0	1	−1	0	1	−1	σ
	S_{8b}	$1/2$	1	0	−1	1	0	−1	τ
	S_{6b}	$1/2$	0	1	−1	0	1	−1	a
	S_{9b}	$12^{-1/2}$	−2	1	1	−2	1	1	β
E_{1u}	S_{20a}	$12^{-1/2}$	2	1	−1	−2	−1	1	σ
	S_{19a}	$1/2$	1	0	−1	−1	0	1	τ
	$S_{r;a}$	$12^{-1/2}$	2	1	−1	−2	−1	1	a
	S_{18a}	$1/2$	0	1	1	0	−1	−1	β
	S_{20b}	$1/2$	0	−1	−1	0	1	1	σ
	S_{19b}	$12^{-1/2}$	−1	−2	−1	1	2	1	τ
	$S_{r,b}$	$1/2$	0	−1	−1	0	1	1	a
	S_{18b}	$12^{-1/2}$	2	1	−1	−2	−1	1	β

Three redundants (see Table 1) are occurring among the symmetry coordinates. These have been removed by the conditions:

$$S_r = 0 \tag{1}$$

$$S_{r;a} = -S_{19a}/l_2 \tag{2}$$

$$S_{r;b} = -S_{19b}/l_2 \tag{3}$$

l_2 is the C—C equilibrium distance.

FORCE CONSTANTS

The adopted force constants of the potential function in terms of symmetry coordinates are given in Table 2. The calculation has been based on fundamental frequencies for benzene and benzene-d_6 from spectroscopic data by Brodersen and Langseth [3].

l_1 and l_2 denote the C—H and C—C equilibrium distances, respectively.

Table 2. Force constants of the potential function in symmetry coordinates (10^5 dyn cm^{-1})

	s_2	s_1	s_3	s_{13}	s_{12}	s_{14}	s_{15}
s_2	5.029	−0.468					
s_1		7.883					
s_3			$0.863\ l_1^2$				
s_{13}				4.994	$0.095\ l_2$		
s_{12}					$0.680\ l_2^2$		
s_{14}						4.363	$0.718\ l_1$
s_{15}							$0.837\ l_1^2$

	s_7	s_8	s_6	s_9	s_{20}	s_{19}	s_{18}
s_7	5.184	0	0	0			
s_8		5.508	0	0			
s_6			$0.799\ l_2^2$	$-0.160\ l_1^2$			
s_9				$0.869\ l_1^2$			
s_{20}					5.098	0	0
s_{19}						11.645	$1.586\ l_1$
s_{18}							$0.825\ l_1^2$

NORMAL COORDINATE ANALYSIS FOR SYMMETRY COORDINATES

A symmetry coordinate is approximated to a linear combination of normal coordinates from the respective symmetry species,

$$s_i = \sum_j B_{ij} Q_j \qquad (4)$$

The transformation coefficients have been determined by Wilson's method [1], and their squares are given in Table 3. M denotes the mass of the carbon atom.

GROUP THEORY TREATMENT OF THE INTERATOMIC DISTANCES

In benzene there are ten types of interatomic distances, each type forming a symmetric equivalent set. The notation used for deviations from the equilibrium distances is as follows.

σ for the distances of type C_1—H_1, σ^* for C_2—H_1, σ^{**} for C_3—H_1 and σ^{***} for C_4—H_1;

τ for the type C_1—C_2 (*ortho*), τ^* for C_1—C_3 (*meta*) and τ^{**} for C_1—C_4 (*para*);

ϱ for the type H_1—H_2, ϱ^* for H_1—H_3 and ϱ^{**} for H_1—H_4.

Each of the equivalent sets is taken as basis for a reducible representation of the group D_{6h}. The characters of these representations are given in Table 4. Then it is a simple matter to determine the symmetric structure of the represen-

Table 3. Numerical values of the terms $B_{ij}^2 M$.

	Q_2	Q_1	Q_3	Q_{13}	Q_{12}	Q_{14}	Q_{15}
s_2	12.8664	0.05041					
s_1	0.1141	0.8860					
s_3			$15.0709/l_1^2$				
s_{13}				12.8754	0.04145		
s_{12}				$1.3244/l_2^2$	$10.6756/l_2^2$		
s_{14}						2.1944	0.8056
s_{15}						$0.8717/l_1^2$	$12.0452/l_1^2$

	Q_7	Q_8	Q_6	Q_9	Q_{20}	Q_{19}	Q_{18}
s_7	12.8867	0.02608	0.001646	0.002454			
s_8	0.04313	2.0696	0.1074	0.2798			
s_6	$0.6952/l_2^2$	$2.9623/l_2^2$	$2.9158/l_2^2$	$0.9267/l_2^2$			
s_9	$0.09629/l_2^2$	$10.3134/l_2^2$	$0.2417/l_2^2$	$12.0711/l_2^2$			
s_{20}					12.8798	0.03574	0.001341
s_{19}					0.09085	1.0503	0.3588
s_{18}					$0.03141/l_1^2$	$0.2034/l_1^2$	$14.5233/l_1^2$

tations by usual methods from group theory. The results can be expressed in the following way:

$$\Gamma(\tau\,\varrho) = A_{1g} + B_{2u} + E_{2g} + E_{1u} \tag{5}$$

$$\Gamma(\sigma,\sigma^{***},\tau^*,\varrho^*) = A_{1g} + B_{1u} + E_{2g} + E_{1u} \tag{6}$$

$$\Gamma(\sigma^*,\sigma^{**}) = A_{1g} + A_{2g} + B_{1u} + B_{2u} + 2E_{2g} + 2E_{1u} \tag{7}$$

$$\Gamma(\tau^{**},\varrho^{**}) = A_{1g} + E_{2g} \tag{8}$$

The above results show which of the normal coordinates build up a given interatomic distance coordinate. Thus for instance only normal coordinates from species A_{1g} and E_{2g} will enter into the expression of τ^{**} and ϱ^{**} as linear combinations of normal coordinates.

Table 4. Characters for reducible representations of the group D_{6h}

χ	E	$2C_6$	$2C_3$	C_2	$3C_2'$	$3C_2''$	I	$2S_3$	$2S_6$	σ_h	$3\sigma_d$	$3\sigma_v$
τ,ϱ	6	0	0	0	0	2	0	0	0	6	2	0
$\sigma,\sigma^{***},\tau^*,\varrho^*$	6	0	0	0	2	0	0	0	0	6	0	2
σ^*,σ^{**}	12	0	0	0	0	0	0	0	0	12	0	0
τ^{**},ϱ^{**}	3	0	0	3	1	1	3	0	0	3	1	1

NORMAL COORDINATE ANALYSIS FOR INTERATOMIC DISTANCE COORDINATES

A representative set of ten interatomic distance deviations has been expressed by the set of symmetry coordinates,

$$r = Vs \tag{9}$$

V being the transformation matrix. The connection between symmetry coordinates and normal coordinates, eqn. (4), is given in matrix notation by

$$s = BQ \tag{10}$$

Then the transformation matrix in

$$r = CQ \tag{11}$$

can easily be found, since

$$C = VB \tag{12}$$

The squares of the matrix elements rather than the elements themselves have been calculated. The values $l_1 = 1.084$ Å and $l_2 = 1.397$ Å for C—H and C—C equilibrium distances have been adopted. The results are listed in Table 5.

Table 5. Numerical values of the terms $C_{ki}^2 M$.

	σ	σ^*	σ^{**}	σ^{***}	τ	τ^*	τ^{**}	ϱ	ϱ^*	ϱ^{**}
Q_2	2.1444	1.1828	1.2835	1.4129	0.01901	0.05703	0.07603	1.7596	5.2789	7.0385
Q_1	0.008402	0.1778	0.5517	0.7399	0.1477	0.4430	0.5906	0.2265	0.6795	0.9060
Q_3		0.7922	0.3177							
Q_{13}	2.1459	1.2314	1.2933	2.1459		0.05518			5.3008	
Q_{12}	0.006908	0.1292	0.5419	0.006908		0.4448			0.6576	
Q_{14}		0.5751	0.001537		0.3657			1.6000		
Q_{15}		0.2171	0.3161		0.1343			4.3583		
Q_7	4.2956	2.4215	3.4386	2.9434	0.01438	0.01873	0.1274	0.9277	2.6603	14.3505
Q_8	0.008694	0.4713	0.07046	0.2900	0.6899	0.04949	0.1983	0.8968	0.8308	0.3991
Q_6	0.000549	0.09576	0.4498	0.9444	0.03581	0.4314	0.8995	0.03121	0.4578	0.9905
Q_9	0.000818	1.3166	0.3463	0.1276	0.09328	0.000179	0.1080	8.0724	2.0096	0.1489
Q_{20}	4.2933	2.3747	3.3563	4.2933	0.03028	0.03028		2.5849	2.5849	
Q_{19}	0.01191	0.6332	0.7062	0.01191	0.3501	0.3501		1.5777	1.5777	
Q_{18}	0.000447	1.2978	0.2431	0.000447	0.1196	0.1196		1.7957	1.7957	

STANDARD DEVIATIONS OF INTERATOMIC DISTANCES

At this point the standard deviations of interatomic distances,

$$u = \overline{(r^2)}^{1/2} \tag{13}$$

can be calculated by means of the formula

$$u^2 = \overline{r_k^2} = \sum_i C_{ki}^2 \frac{h}{8\pi^2 \nu_i} \coth \frac{h\nu_i}{2kT} \tag{14}$$

Table 6. Standard deviations for interaromic distances in benzene

Distance	Calculated standard deviations in Å units $T = 0$	273.16	298.16	323.16
C_1-H_1	0.0771	0.0771	0.0771	0.0771
C_2-H_1	0.1000	0.1003	0.1004	0.1006
C_3-H_1	0.0952	0.0958	0.0960	0.0963
C_4-H_1	0.0928	0.0939	0.0942	0.0946
C_1-C_2	0.0457	0.0459	0.0459	0.0460
C_1-C_3	0.0534	0.0544	0.0547	0.0551
C_1-C_4	0.0576	0.0592	0.0597	0.0603
H_1-H_2	0.1556	0.1559	0.1561	0.1563
H_1-H_3	0.1313	0.1318	0.1321	0.1323
H_1-H_4	0.1179	0.1188	0.1191	0.1195

(see, *e.g.*, Morino *et al.*[4]) C_{ki} denotes the coefficients of eqn. (11), the squares of which have been enumerated in the previous section. ν_i is a fundamental frequency, h Planck's constant, k Boltzmann's constant and T is the absolute temperature.

Table 6 shows the calculated values for u at the temperatures $T = 0$, 273.16, 298.16 and 323.16°K. The values have been compared with results from electron diffraction data as obtained by Karle [5] and later by Bastiansen *et al.*[6] A report about this has been submitted for publication elsewhere [7].

It is planned to work out the same calculations also for benzene-d_6.

REFERENCES

1. Wilson, E. B. Jr., Decius, J. C. and Cross, P. C. *Molecular Vibrations*, N.Y., Toronto, London 1955.
2. Crawford, B. L. Jr. and Miller, F. A. *J. Chem. Phys.* **17** (1949) 249.
3. Brodersen, S. and Langseth, A. *Mat. Fys. Skr. Dan. Vid. Selsk.* **1** (1956) 1.
4. Morino, Y., Kuchitsu, K. and Shimanouchi, T. *J. Chem. Phys.* **20** (1952) 726.
5. Karle, I. *J. Chem. Phys.* **20** (1952) 65.
6. Almenningen, A., Bastiansen, O. and Fernholt, L. *Kgl. Norske Videnskabs Selskabs Skrifter* (1957). *In press.*
7. Bastiansen, O. and Cyvin, S. J. *Nature* (1957). *In press.*

Received June 20, 1957.

ACTA CHEMICA SCANDINAVICA 11 (1957) 1505—1511

The Crystal Structure of Phosphorous Acid

SVEN FURBERG and PER LANDMARK

Chemical Institute, University of Bergen, Bergen, Norway

The crystal structure of phosphorous acid, H_3PO_3, has been determined by X-ray methods. The space group is $Pna2_1$ and there are eight molecules per unit cell. Two of the P—O bonds in the molecule, presumably the P—OH bonds, are found to be about 1.54 Å, whereas the bond to the third oxygen atom is significantly shorter, 1.47 Å. There are two hydrogen bonds for each molecule. These observations are in agreement with the accepted structural formula $H_2(HPO_3)$.

As phosphorous acid, H_3PO_3, is dibasic, it is generally assumed that one of the hydrogen atoms is linked directly to the phosphorus atom. In connection with our work on phosphoric acid [2] we thought it of value to study the structure of this interesting molecule by X-ray crystallographic methods, especially as no such investigation of phosphites was reported in the literature. Only very recently the first crystal structure determination of a phosphite, $MgHPO_3.6H_2O$, was published [1], showing HPO_3^{--} ions with trigonal symmetry.

EXPERIMENTAL

Phosphorous acid was prepared by hydrolysis of phosphorus trichloride and recrystallized from water and alcohol. The best crystals were obtained from the latter solvent. Mp. 73°C (uncorr.). The crystals are hygroscopic and were kept in thinwalled glass capillaries during the exposures. Weissenberg and oscillation diagrams were taken about the *a*- and *c*-axes using Cu$K\alpha$ radiation (λ = 1.542 Å). The intensities were estimated visually, and corrected for Lorentz and polarization effects. Very small crystals with even cross-sections were used and no correction for absorption was made.

CRYSTAL DATA

The crystals are orthorhombic, generally elongated along *a*, with unit cell dimensions a = 7.27 Å, b = 12.06 Å and c = 6.85 Å. These values are probably accurate to within 0.5 %. By flotation in mixtures of carbon tetrachloride and ethylene dibromide a density of 1.806 g/cm^3 was found, corresponding to eight (calc. 7.96) molecules H_3PO_3 in the unit cell.

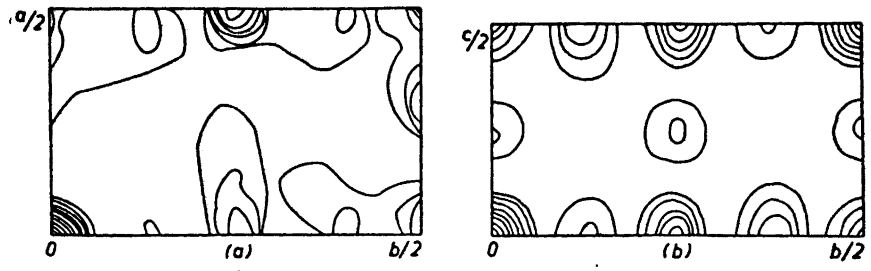


Fig. 1. Patterson projections on the (001) plane (a) and the (100) plane (b).

Systematic absences occur in the $0kl$-reflections for $k+l$ odd and in the $h0l$-reflections for h odd. The space groups $Pna2_1$ and $Pnam$ are both compatible with these observations. The crystals were tested for piezoelectric effects with a sensitive apparatus built by one of us (P.L.), but no effect was found. The space group $Pna2_1$ was nevertheless tentatively assumed on the basis of space considerations, and the subsequent structure analysis showed the choice to be correct. As this space group has four general positions, the asymmetric unit consists of two molecules H_3PO_3. Reflections $0k0$ are extremely weak when k is not 4n, and the crystals have in fact pseudotetragonal symmetry.

THE STRUCTURE DETERMINATION

Projections of the structure along the c and a axes were determined by Patterson, F and $(F_o—F_c)$ syntheses. The c projection was tackled first as it is the only one with apparent centres of symmetry.

The c-projection. The Patterson synthesis reproduced in Fig. 1a indicates that one phosphorus atom lies at $y = 1/8$ and the other at $y = 3/8$, and that approximately $x = 0$ for one or both of them. Coordinates (0, 1/8) and (0, 3/8) were chosen for the first Fourier synthesis, from which some information on the positions of the oxygen atoms was obtained. Because of the pseudotetragonal symmetry a difference of $b/4$ in the y coordinates of corresponding atoms in the two crystallographically independent molecules was assumed. Some agreement between F_o and F_c was obtained by Fourier refinement. However, the value of F_c remained very small for some strong reflections. The likely signs of these were then derived by the "multiplication rule" (Sayre [3]). The corresponding Fourier map indicated clearly radical shifts in the x coordinates of some of the oxygen atoms, and by further refinement the final electron density map given in Fig. 2a was obtained. Four further refinements of the atomic coordinates were carried out by $(F_o—F_c)$ synthesis. The same temperature factor $\exp(-2.2 \sin^2\Theta/\lambda^2)$ was used for all the atoms, although the final difference map shows this to be only approximately correct. The atomic scattering factors employed are those given by Viervoll and Øgrim [4]. No attempt was made to derive the positions of the hydrogen atoms from the difference maps, and their contribution to the structure factors was calculated from assumed positions. The final value of the reliability index $R = (\Sigma|F_o—F_c|)/\Sigma|F_o|$ is

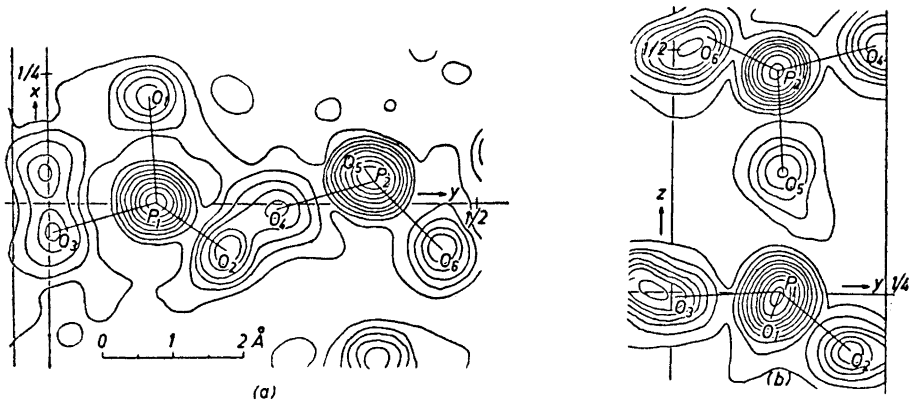


Fig. 2. Electron density projections on the (001) plane (a) and the (100) plane (b). Contours at 2, 4, 6, . . . e . Å^{-2}, every second contour being omitted above 12 e . Å^{-2}. Calculated at 1/60 of b and 1/30 of a and c.

0.10. The strongest reflection, 200, which evidently suffers from extinction (as well as 002 in the a projection), is not included in the calculation of R. Reflections not observed are only taken into account when F_c exceeds the observable limit.

The a-projection. The Patterson synthesis (Fig. 1b) shows that the difference in z-coordinates of the two phosphorus atoms probably is near $c/2$. Approximate z-coordinates for the oxygen atoms were derived from the known coordinates and the P—O distances found in phosphoric acid [2]. Two different mutual orientations of the molecules were possible, which both gave $R = 0.33$. The one chosen changed in the course of the refinement to the other possibility. Three Fourier refinements brought R down to 0.20, followed by five difference syntheses which made R drop to 0.10. As this projection is non-centrosymmetric, the atoms were in each refinement moved approximately twice the amount indicated by the Fourier- and difference-maps. The process would have been speedier if the atoms had been moved even more than this in each refinement. The final electron density map is shown in Fig. 2b, and the atomic coordinates are given in Table 1. The temperature factor is the same as in the c-projection. In Table 3 observed and calculated structure factors are given.

Table 1. Atomic coordinates as fractions of the corresponding cell edge.

Atom	x	y	z
P_1	0.002	0.1265	0.003
P_2	0.046	0.378	0.461
O_1	0.208	0.116	0.951
O_2	0.910	0.209	0.874
O_3	0.940	0.004	0.985
O_4	0.994	0.259	0.518
O_5	0.075	0.369	0.241
O_6	0.909	0.459	0.518

DESCRIPTION AND DISCUSSION OF THE STRUCTURE

From the atomic coordinates in Table 1 the bond lengths and bond angles given in Table 2 were calculated.

Table 2. Bond lengths (in Å units) and bond angles.

Molecule I		Molecule II	
P_1-O_1	1.544	P_2-O_5	1.526
P_1-O_2	1.485	P_2-O_6	1.451
P_1-O_3	1.552	P_2-O_4	1.535
$O_1-P_1-O_2$	111°	$O_5-P_2-O_6$	114°
$O_1-P_1-O_3$	101°	$O_5-P_2-O_4$	103°
$O_2-P_1-O_3$	117°	$O_6-P_2-O_4$	114°

The standard deviation of the atomic coordinates were estimated by applying the formula given by Cruickshank [5]. The following values were found: $\sigma(x) = 0.004$ Å, $\sigma(y) = 0.003$ Å, $\sigma(z) = 0.005$ Å for the phosphorus atoms; $\sigma(x) = 0.016$ Å, $\sigma(y) = 0.012$ Å, $\sigma(z) = 0.024$ Å for the oxygen atoms. In the case of $\sigma(z)$ the lack of a centre of symmetry is taken into account by multiplication by 2. The standard deviation in the bond lengths vary between 0.013 Å for the bond $P_1—O_3$ and 0.024 Å for $P_2—O_5$. Unfortunately, an oxygen atom is very close to a phosphorus atom in each projection (O_5 and O_1, respectively), and the error in the position of these atoms may be considerably greater than should be expected from the calculated standard deviations. This does not influence the bond lengths appreciably, but makes the values derived for the bond angles rather uncertain. The maximum error is estimated to about 5° for the angles $O_1—P_1—O_2$ and $O_5—P_2—O_6$ and to about 3° for the other angles.

It will be seen that the two crystallographically independent molecules are found to be identical within the limits of error. The differences observed in the bond angles may also partly be due to deformation by van der Waals forces [6]. In each of the molecules there is one shorter and two longer P—O bonds, and one of the bond angles is considerably smaller than the others. The mean dimensions of the two molecules are given in Fig. 3. The short P—O bond, which presumably corresponds to the "lone" oxygen, has the length of 1.47 Å, and is significantly shorter than the two bonds to the "hydroxyl" oxygens, for which values close to 1.54 Å are found. The angle between the two P—OH bonds is as small as 102°, whereas all the angles involving the short P—O bond are greater than the tetrahedral angle, their mean value being 114°. The O—O distance across the small angle is only 2.39 Å in both molecules. Approximate positions for the hydrogen atoms of the hydroxyl groups may be derived from the directions of the hydrogen bonds. All O—H bonds lie roughly in the plane of the two P—OH bonds, and the whole molecule has thus approximately a plane of symmetry. These molecular dimensions are, as might be expected, somewhat different from those reported for the phosphite ion, which is found to have threefold symmetry about the P—H bond direction with P—O bonds of length 1.51 Å and O—P—O bond angles of 110°.

Table 3. Observed and calculated structure factors. The values given are one quarter of the absolute values.

hkl	F_o	F_c	*hkl*	F_o	F_c
011	1.8	1.5	0 14 0	<0.8	+ 0.1
031	8.8	6.5	110	0.9	− 0.9
051	12.2	12.4	120	0.7	+ 0.5
071	2.7	3.1	130	1.2	+ 1.1
091	3.9	3.9	140	6.0	+ 5.5
0 11 1	2.2	2.3	150	7.1	+ 7.3
0 13 1	2.3	2.1	160	<1.0	− 0.2
0 15 1	1.2	1.5	170	1.3	+ 1.5
002	18.0	38.4	180	1.4	− 1.2
022	5.8	6.4	190	2.8	+ 2.1
042	4.8	5.8	1 10 0	<1.2	− 0.6
062	2.2	1.2	1 11 0	2.6	+ 3.0
082	13.5	14.7	1 12 0	<1.2	− 0.6
0 10 2	3.6	3.4	1 13 0	1.5	+ 1.6
0 12 2	5.7	5.9	1 14 0	<1.0	− 0.4
0 14 2	1.5	1.3	1 15 0	2.3	+ 2.3
013	8.1	8.3	200	16.8	+34.6
033	5.8	5.4	210	2.3	− 2.2
053	8.3	8.4	220	2.7	− 2.7
073	2.2	1.8	230	9.4	− 9.4
093	<1.2	0.3	240	4.6	− 4.8
0 11 3	<1.2	0.3	250	10.6	+11.0
0 13 3	1.3	0.7	260	<1.2	+ 0.7
004	17.4	21.1	270	8.9	+ 8.4
024	4.9	5.1	280	12.8	+12.9
044	11.3	11.3	290	3.5	− 2.9
064	1.8	0.9	2 10 0	<1.2	− 1.1
084	11.8	12.5	2 11 0	<2.1	− 1.1
0 10 4	2.6	3.2	2 12 0	5.4	+ 5.3
0 12 4	4.6	4.2	2 13 0	<1.0	+ 0.9
015	4.2	4.5	310	3.7	+ 1.8
035	5.0	5.1	320	12.4	+13.9
055	7.4	8.1	330	3.7	+ 2.7
075	3.1	3.3	340	5.5	− 5.4
095	1.4	1.9	350	<1.2	+ 1.3
0 11 5	2.4	2.5	360	8.7	− 8.5
006	7.8	6.8	370	4.4	+ 3.2
026	2.9	2.8	380	4.3	− 3.5
046	5.8	5.5	390	<1.2	− 0.9
066	1.1	0.7	3 10 0	5.6	+ 5.2
086	5.3	4.9	3 11 0	<1.2	− 0.8
0 10 6	1.6	1.7	3 12 0	<1.2	+ 0.9
017	2.2	2.2	3 13 0	<1.0	+ 0.4
037	2.1	1.9	3 14 0	2.6	− 2.5
057	3.4	3.8	400	10.0	+10.4
077	1.8	1.8	400	10.0	+10.4
008	4.9	4.3	410	1.2	− 0.9
028	1.1	1.0	420	3.3	− 3.0
048	3.4	2.7	430	5.1	− 4.5
020	0.6	− 0.5	440	9.4	− 8.5
040	12.2	−13.9	450	7.5	+ 7.5
060	<0.8	+ 0.4	460	2.5	− 2.1
080	18.4	+19.6	470	5.5	+ 5.0
0 10 0	1.2	− 1.6	480	9.8	+ 9.6
0 12 0	8.9	− 9.3	490	2.2	− 2.7

Table 3. Continued.

hkl	F_o	F_c	*hkl*	F_o	F_c
4 10 0	<1.2	− 0.6	660	1.6	− 1.9
4 11 0	<1.2	− 0.7	670	3.7	+ 3.8
4 12 0	2.9	− 2.0	680	3.4	+ 3.3
4 13 0	1.6	+ 1.5	690	1.9	− 2.0
510	7.3	+ 7.6	6 10 0	1.1	− 1.3
520	6.0	+ 6.8	6 11 0	2.8	− 3.1
530	3.7	− 3.0	710	3.2	+ 3.2
540	<1.2	− 0.7	720	3.3	+ 2.7
550	7.4	− 7.3	730	3.7	− 3.7
560	5.1	− 5.1	740	1.9	+ 1.9
570	6.3	+ 5.7	750	3.8	− 4.7
580	<1.2	− 0.5	760	2.4	− 2.1
590	1.8	+ 0.8	770	2.9	+ 3.5
5 10 0	3.6	+ 3.6	780	0.9	+ 1.0
5 11 0	3.2	− 3.1	790	0.9	+ 0.1
5 12 0	<1.0	+ 0.5	800	<1.0	− 0.7
600	<1.2	− 0.1	810	1.9	− 1.7
610	5.5	− 5.3	820	1.3	− 2.0
620	2.0	− 2.7	830	<1.0	− 1.1
630	5.9	− 5.7	910	2.3	+ 2.5
640	5.4	− 3.4	920	1.2	+ 0.9
650	4.0	+ 3.9	930	3.3	− 4.4

It would seem to be of interest to compare the molecule of phosphorous acid with that of phosphoric acid [2]. In phosphoric acid the short P—O bond is found to be 1.52 Å and the P—OH bonds to be 1.57 Å. Values of 106° and 112° were found for the two types of bond angles. Phosphorous acid may be derived from phosphoric acid by substituting a hydroxyl group by a hydrogen atom. It is seen that this change appears to make all the bond angles deviate more from the tetrahedral angle and all the P—O bonds shorter, especially the short P—O bond. Correspondingly, the angles involving this bond are greater in H_3PO_3 than in H_3PO_4, and the angles between P—OH bonds smaller. Although these differences are small, they are probably significant in view of the agreement in the dimensions of the two independent molecules of H_3PO_3.

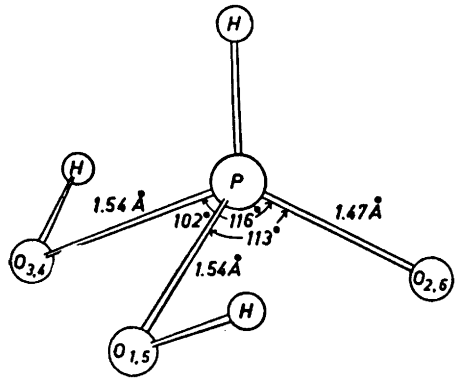


Fig. 3. Bond lengths and bond angles in H_3PO_3.

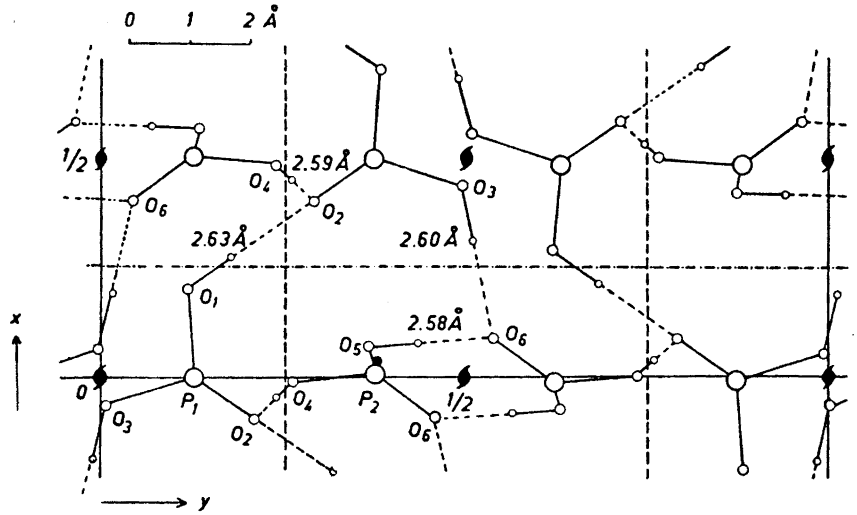


Fig. 4. The c projection of the structure. Broken lines indicate hydrogen bonds.

The molecules are linked together by hydrogen bonds, as shown in Fig. 4. There are two such bonds for each molecule, as to be expected from the formula $HPO(OH)_2$, but not from $P(OH)_3$. The four bonds are of nearly equal length, the values 2.59 Å, 2.63 Å, 2.58 Å and 2.60 Å being found. All other intermolecular O—O distances are greater than 3.0 Å. The two "lone" oxygen atoms O_2 and O_6 each take part in two hydrogen bonds, whereas each of the other oxygen atoms is involved in only one such bond. As generally found in crystal structures, the angles between the hydrogen bonds and the P—O bonds are least distorted at the oxygen atoms to which the hydrogen atoms are bonded. The two hydrogen bonds to the "lone" oxygen atom in H_3PO_4 are 2.53 Å of length, somewhat shorter than in the present case.

The structure has pseudo-tetragonal symmetry, with an approximate 4_1 axis roughly at (0, y, 1/4). This holds not only for the atomic coordinates and the molecular dimensions, but also for the hydrogen bonding scheme.

One of us (S.F.) wishes to thank *Nansenfondet og de dermed forbundne fond* for a grant.

REFERENCES

1. Corbridge, D. E. C. *Acta Cryst.* **9** (1956) 991.
2. Furberg, S. *Acta Chem. Scand.* **9** (1955) 1557.
3. Sayre, D. M. *Acta Cryst.* **5** (1952) 60.
4. Viervoll, H. and Øgrim, O. *Acta Cryst.* **2** (1949) 277.
5. Cruickshank, D. W. J. *Acta Cryst.* **2** (1949) 65.
6. Dunitz, J. D. and Rollett, J. S. *Acta Cryst.* **9** (1956) 327.

Received June 22, 1957.

ACTA CHEMICA SCANDINAVICA 11 (1957) 1512—1515

Nucleation in Barium Sulfate Precipitation *

ARNE E. NIELSEN

Universitetets fysisk-kemiske institut, Copenhagen, Denmark

In precipitation experiments with barium sulfate the number of crystals per unit volume was reduced to one-tenth or less by first cleaning the glass mixing vessel with condensing steam. During the precipitation higher order Tyndall spectra were observed.

It is concluded that under normal conditions the greater part of the nuclei does not originate from a homogeneous process but from the walls of the glass.

In theories of the precipitation of sparingly soluble salts such as barium sulfate different authors assume that the nuclei (i) exist before the mixing of the stable solutions, or (ii) are formed spontaneously at the moment of mixing, or (iii) originate from a homogeneous chemical process during a certain period of time in the beginning of the experiment.

As shown in a previous paper [1], the kinetics of the precipitation process measured for instance as the electric conductance in dependence of time can be made to agree with all three assumptions. It is therefore of interest to obtain a different kind of quantitative information such as the number of crystals formed per unit volume or, what is equivalent, their final size. Fischer and Rhinehammer [2] showed that the particle size and O'Rourke and Johnson [3] that the number of crystals depend on the age of the solutions used. It seems impossible to account for this phenomenon by means of any sort of theory with a nucleation process starting at the moment of mixing, that is (ii) or (iii) above.

In the experiments reported below it was found that the number of crystals formed also depends on the method of cleaning the glass vessel. The introduction of a new cleaning technique (proposed by J. A. Christiansen) reduced this number to one tenth or even less.

* This is a part of the paper that was read before the 9. Nordiske Kemikermøde in Århus, August 1956.

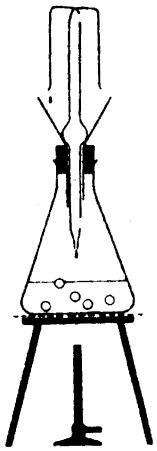


Fig. 1. The steam condenses at the inside of the beaker and through the funnel the water returns to the flask.

EXPERIMENTAL

50 ml 0.002 M $BaCl_2$ and 50 ml 0.002 M K_2SO_4 were taken up in pipettes, which were then emptied in less than 3 s in such a way that the two liquids met before reaching the bottom of the 250 ml Pyrex beaker. The solution was allowed to rest for 5 min, the precipitate became visible in 10 to 15 s and settled in a few minutes. 5 min after the moment of mixing the mixture was stirred with a glass rod and a drop of the slurry transferred to a blood cell counting chamber. It was found important to place the cover glass in less than 2 s since the precipitate sediments very quickly. At least either some 100 crystals — or all crystals inside the 9 mm^2 (0.9 mm^3) counting field were counted.

The results were controlled through sedimentation experiments. The level of the uppermost crystals was easily measured during the first two or three minutes. From a plot the sedimentation velocity was found. If v = velocity in cm/s, r = radius of a sphere with the same volume as the crystal, g = acceleration of gravity, d = density of crystal, d_0 = density of medium, f = a form factor determined from the experiments ($f = 1$ for spheres of radius r), η = viscosity, n = number of crystals per liter, $c = 0.001$ = molarity of $BaSO_4$ just after mixing, M = molecular weight, m = weight of a crystal, — then

$$v = (4/3)\pi r^3 g(d-d_0)f/6\pi\eta r$$
$$n = cM/m;\ m = (4/3)\pi r^3 d$$
$$\therefore \log f = \log v + (2/3)\log n - 3.60$$

The f-values found lie between 0.38 and 0.65 which is very reasonable.

The 250 ml Pyrex beaker used as a mixing chamber was cleaned before every experiment except the first one in a series by first rubbing it with a brush and rinsing in hot water. Then it was placed, bottom up, over boiling water, see Fig. 1, so that the steam condensed on the inside of the glass. After 10 min it was placed on a few layers of filter paper and allowed to cool.

RESULTS

In the beginning of a series of experiments usually about 2 000 or more crystals were found per mm^3. After one or two cleanings of the beaker the number decreased to about a hundred of crystals per mm^3, or 10^8 per liter, and the counts might seem to obey a Poisson distribution. But occasionally, without change in technique, the counts were as low as 25 mm^{-3} several times. See Figs. 2 and 3.

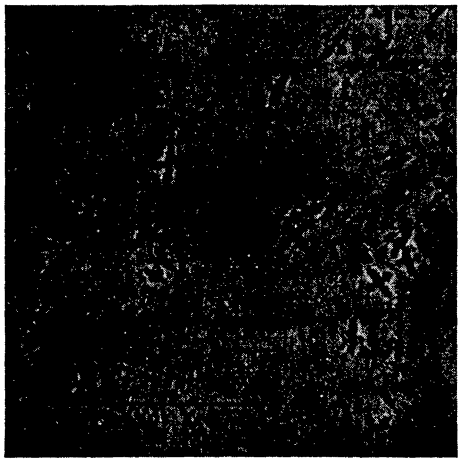


Fig. 2. The barium sulfate precipitate from an experiment where the glass had only been ordinarily cleaned. 2 050 crystals were found per mm^2. In order to get more than one crystal on the photo (at a reasonable magnification) the precipitate was concentrated by sedimentation.

These results may be compared with those of O'Rourke and Johnson [3] who in the same sort of experiments (except for the cleaning technique) found 1.1×10^9 particles per liter. That is about ten to fifty times as many as found in the present work.

Very often it was observed that *after* the sample had been withdrawn for counting, the solution became milky, and during the second sedimentation two distinct bands separated. Under the microscope another sample now displayed that new, much smaller crystals had appeared. These must be attributed to the stirring: either are new nuclei brought into the system with the stirring rod, or, what is more likely, the crystals already formed are crushed yielding nuclei. The easy breaking of the crystals upon handling was also observed by Fischer and Rhinehammer [2].

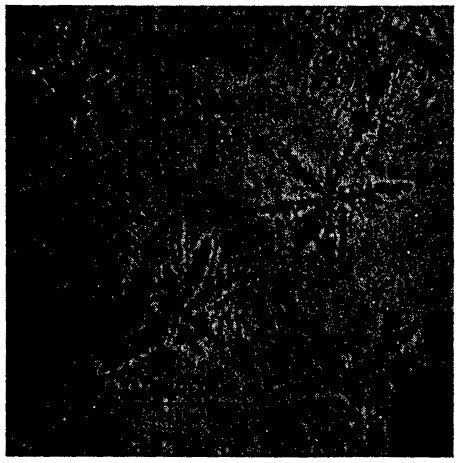


Fig. 3. The precipitate from an experiment where the glass had been cleaned as shown in Fig. 1; everything else was performed as in the experiment of Fig. 2. Only 30 crystals appeared per mm^2. The magnification is the same in Figs. 2 and 3.

When the precipitation was observed in parallel light higher order Tyndall spectra [3-5] were observed. In these experiments the glass was not treated with steam.

When looking in a direction 135° to that of the original light beam, a red and a green light were observed during 5 to 15 s after the moment of mixing. When the concentrations were 0.0025 M before mixing both first and second order red and green were observed, together with violet in between.

After about 25 s all colours had disappeared, and only white light was observed.

These colours were obtained with Merck's K_2SO_4 but not with Analar's Na_2SO_4. The cause of this difference was not sought.

The appearance of the colours imply that the crystals are equally large since otherwise the lights would mix to yield white in all directions.

CONCLUSION

It seems impossible to explain that improving of the cleaning technique of the glass can reduce the number of crystals without assuming that those extra crystals formed when the glass is not cleaned so well originate from the walls of the glass. Since this number amounts to between 90 and 98 % of all the crystals formed under ordinary conditions we may conclude that by far the greater part of these, and perhaps all of them, do not originate from spontaneous nucleation but from impurities on the glass.

The appearance of higher order Tyndall spectra indicates that the precipitate at this time is very monodisperse and from this fact, too, we may conclude that the nuclei are not formed in a homogeneous process, since they must have all started growing at very nearly the same time.

The author is much indebted to professor J. A. Christiansen who suggested the experiments reported.

REFERENCES

1. Nielsen, A. E. *J. Colloid Sci.* **10** (1955) 576.
2. Fischer, R. B. and Rhinehammer, T. B. *Anal. Chem.* **25** (1953) 1544.
3. O'Rourke, J. D. and Johnson, R. A. *Anal. Chem.* **27** (1955) 1699.
4. Sinclair, D. and LaMer, V. K. *Chem. Rev.* **44** (1949) 245.
5. LaMer, V. K. and Dinegar, R. H. *J. Am. Chem. Soc.* **72** (1950) 4847.

Received June 29, 1957.

ACTA CHEMICA SCANDINAVICA 11 (1957) 1516—1529

Über die Reaktionen des Lignins bei der Sulfatkochung

Der Einbau des Schwefels in das Lignin

JOSEF GIERER und BO ALFREDSSON

Schwedisches Holzforschungsinstitut, Holzchemische Abteilung, Stockholm, Schweden

The sulphidizing reaction of lignin has been studied using model compounds of the *p*-hydroxybenzyl alcohol, -benzylalkyl ether and -dibenzy lether type as well as isolated lignin preparations and finely ground wood powders.

It was shown that model substances of the above-named types react readily with sodium sulfhydrate solutions at 100°C to yield the corresponding sulfides, unless this reaction is sterically hindered by the presence of a substituent in the β-position of the side-chain.

p-Hydroxybenzyl alcohols and *p*-hydroxybenzylalkyl ethers were found to react with ethylmercaptan to yield *p*-hydroxybenzylethyl-sulfides. This is in harmony with previous views regarding the course of lignin sulfidation.

After using an "acid mixture" (hydroiodic acid, hydrochloric acid and hypophosphorous acid) the major part of the sulphur from the various thiolignins was determined to be present in an "acid-labile" fraction. On the basis of model experiments described in a previous communication [1] this fraction is considered to have benzyl-sulphidic structures as principal building units.

Im Jahre 1911 wiesen Klason und Segerfelt [2] nach, dass das nach einer Sulfatkochung aus der Schwarzlauge isolierbare Thiolignin organisch gebundenen Schwefel enthält. In der Folgezeit wurde aufgrund von Vergleichen zwischen Alkali- und Sulfatkochungen dem Schwefel die wichtige Rolle zugeschrieben, durch Umsetzung mit reaktionsfähigen Gruppen des Lignins Kondensationsreaktionen zu verhindern und dadurch den Delignifizierungsprozess zu erleichtern [3]. Damit erhob sich die Frage nach der chemischen Natur der reaktionsfähigen Gruppen im Lignin, welche für den Einbau des Schwefels verantwortlich sind.

Holmberg fand, dass sich die Sulfitierung des Lignins [4], die Reaktion mit Thioglykolsäure [5] sowie die Alkylierung mit alkoholischer Salzsäure [6] durch die Annahme von Benzylalkohol- und Benzylätherstrukturen im Lignin erklären lassen. Diese Vorstellung wurde in den letzten 20 Jahren durch zahlreiche Modellversuche und vor kurzem durch den direkten Nachweis von *p*-Hydroxybenzylalkoholgruppen in Nativlignin [7] stark gestützt.

Es lag nahe, auch die Ursache der Sulfidierungsreaktion in erster Linie bei derartigen Gruppen zu suchen. Enkvist und Moilanen [8] konnten in Modellversuchen zeigen, dass Vanillylalkohol durch Behandlung mit gepufferten Schwefelwasserstofflösungen (pH 7) bei 100°C zum Teil in Divanillyldisulfid übergeführt wird. Mikawa [9] fand, dass bei dieser Umsetzung Divanillylmonosulfid als Hauptprodukt entsteht und wies darauf hin, dass die Bildung des Disulfids durch Dehydrierung des intermediär auftretenden Vanillylthiols nur als Nebenreaktion aufzufassen ist. Er beschrieb kürzlich [10] eine analoge Sulfidierungsreaktion für die homologe Modellsubstanz II (Äthyl-(3-methoxy-4-hydroxy-phenyl)-carbinol). Unter Einhaltung ähnlicher Reaktionsbedingungen hatte Zentner [11] früher aus letztgenannter Substanz nur *Iso*eugenol erhalten.

MODELLVERSUCHE

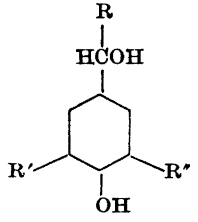
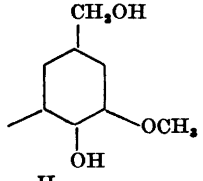
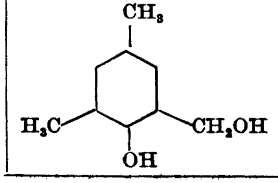
Bei der Untersuchung des Verhaltens einer Reihe einfacher Modellsubstanzen des *p*-Hydroxybenzylalkohol- und des *p*-Hydroxybenzylalkyläthertypus unter den Bedingungen einer milden Sulfidierung (8-stündiges Erhitzen auf 100°C in einer Natriumsulfhydratlösung vom pH 9) fanden wir, dass sämtliche in Tabelle 1 angeführten Verbindungen zu einem grossen Teil in die entsprechenden Sulfide übergeführt werden. Diese wurden entweder als solche isoliert oder als entsprechende Acetate bzw. acetylierte Sulfoxyde charakterisiert. Wie aus den Versuchen mit Vanillylalkoholmethyläther (VIII) und mit den beiden Dibenzyläthern IX und X hervorgeht, wird die Sulfidierungsreaktion der *p*-Hydroxybenzylalkohole unter den oben angegebenen Bedingungen durch Verätherung der benzylalkoholischen Hydroxylgruppe nicht gehemmt. Bei Verätherung der phenolischen Hydroxylgruppe hingegen tritt — wie ein Versuch mit Veratrylalkohol zeigte (vgl. Ref. 8 und 9) — vollkommene Blockierung der Sulfidierungsreaktion ein.

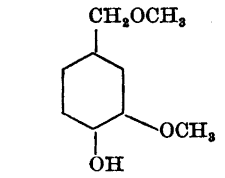
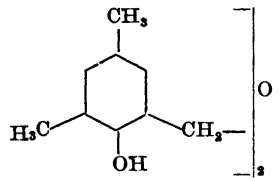
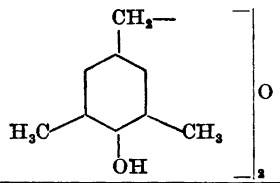
In Übereinstimmung mit früheren Versuchen [8] erwiesen sich auch Vanillin und Acetovanillon sowie *Iso*eugenol als nicht sulfidierbar.

Damit ist gezeigt, dass unter den gewählten Bedingungen die Sulfidierungsreaktion allen *p*-Hydroxybenzylalkoholen und -benzylalkyläthern mit einfacher Seitenkette (R = H, Alkyl oder $HOCH_2$-CHOH—) gemeinsam ist. Um die Abhängigkeit dieser Reaktion von der Struktur des Substituenten R weiter zu untersuchen wurden die vier dimeren Substanzen XI—XIV den gleichen Sulfidierungsbedingungen unterworfen. Ihr Verhalten war von besonderem Interesse, da das Vorkommen ähnlicher Strukturelemente im Lignin sowohl aufgrund von Modellstudien über die Alkoholyse mit alkoholischer Salzsäure [12] bzw. Acidolyse mit Chlorwasserstoff in Dioxan-Wasser [13] und über die Sulfitierung [12,14] als auch aufgrund von Untersuchungen über die Biosynthese des Lignins [15] in Erwägung gezogen wurde.

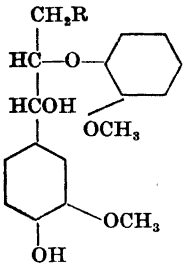
Es zeigte sich, dass die 3 Substanzen XII, XIII und XIV unter den oben angegebenen Sulfidierungsbedingungen nahezu vollkommen stabil sind und zum grössten Teil (91—96 %) unverändert zurückgewonnen werden können. Im Fall der Substanz XI konnte papierchromatographisch lediglich eine teilweise Wasserabspaltung unter Ausbildung einer zum aromatischen Kern kon-

Tabelle 1. Sulfidierungsprodukte aus *p*-(bzw. *o*-)Hydroxybenzylalkoholen, -benzylalkyl- und -dibenzyläthern.

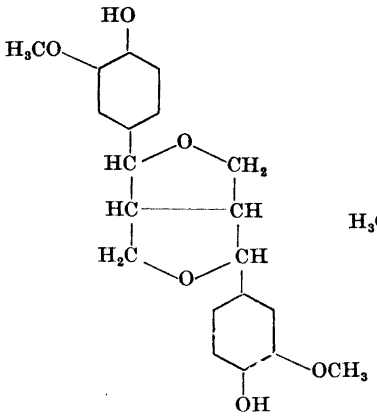
p-Hydroxybenzylalkohole	Nr.	R	R′	R″	Sulfid				
					isoliert als	S (%) ber.	S (%) gef.	Schmp.	Ausbeute (%)
	I	H	H	OCH_3	solches	10.50	10.35	84.5—85.5	45
	II	C_2H_5	H	OCH_3	solches	8.84	8.70	Öl	64
	III	H		OCH_3	solches	10.53	10.63	amorph	75
	IV	CH_2OH | CHOH |	H	OCH_3	solches	7.53	6.02*	Öl	47
	V	H	OCH_3	OCH_3	Diacetat	7.12	6.94	137—138	90
	VI	H	CH_3	CH_3	Sulfoxyddiacetat	7.97	7.92	235—237	51
o-Hydroxybenzylalkohol 	VII	—	—	—	Sulfoxyddiacetat	7.97	8.28	204—207	67

p- bzw. *o*-Hydroxybenzyl alkyläther 	VIII	—	—	—	solches			83—84 (keine Schmp. Depression mit Sulfid aus I)	46
	IX	—	—	—	Sulfoxyd-diacetat			206—207.5 (keine Schmp. Depression mit Sulfoxyd-diacetat aus VII)	84
	X	—	—	—	solches diacetat			95.5—97 127.5—128.5 (keine Schmp. Depression mit Sulfid aus VI)	70

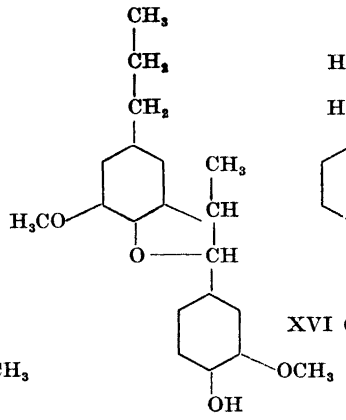
* Das Sulfidierungsprodukt erwies sich bei papierchromatographischer Kontrolle (Lösungsmittelgemisch: Benzol-gesättigtes Wasser; Entwicklungsmittel: diazotiertes Benzidin) als uneinheitlich und dürfte sowohl mit unverändertem Ausgangsmaterial als auch mit verschiedenen Kondensationsprodukten verunreinigt sein. Auf eine weitere Reinigung musste wegen Substanzmangels verzichtet werden.



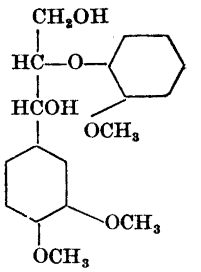
XI R=OH
XII R=H



XIII



XIV



XV

XVI CO statt HCOH

jugierten Doppelbindung nachgewiesen werden (siehe exp. Teil). Da die Substanzen XI und XII je eine *p*-Hydroxybenzylalkoholgruppe und die Substanz XIII (Pinoresinol) zwei *p*-Hydroxybenzylalkyläthergruppen enthalten, muss der negative Ausfall der Sulfidierungsreaktion bei diesen Verbindungen wohl auf eine sterische Hinderung durch den β-ständigen Substituenten (in XI bis XIII) bzw. auf eine besondere Stabilität der beiden Hydrofuranringe (in XIII) zurückzuführen sein. Eine ähnliche Erklärung dürfte auch im Falle der Substanz XIV (Dihydro-dehydro-di*iso*eugenol) gelten. Ein Vergleich des Verhaltens der letztgenannten Substanz mit dem einfacher (nicht cyklischer) *p*-Hydroxybenzylaryläther ist jedoch nicht möglich, da derartige Verbindungen bisher noch nicht synthetisiert worden sind. Das Vorkommen nicht cyklischer Benzylarylätherstrukturen im Lignin konnte jedoch durch Modellversuche über die Alkylierung mit methanolischer Salzsäure [16] ausgeschlossen werden.

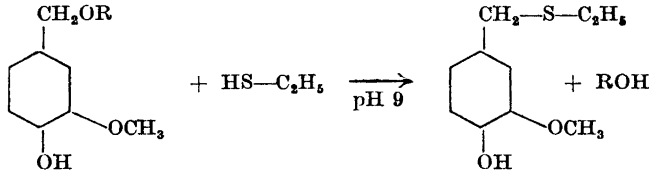
Die Sulfidierungsreaktion in α- (= Benzyl) Stellung wird demnach unter den angegebenen Bedingungen durch geeignete β-ständige Substituenten (z.B. Aroxyl) fast vollkommen gehemmt. Die Alkylierung der Carbinolgruppe mit methanolischer Salzsäure bei 20°C verläuft bei XI und XII in normaler Weise — wenngleich erheblich langsamer als bei Carbinolen ohne Aroxylsubstituent in β-Stellung [13] — während XIII nur schlecht und XIV überhaupt nicht alkyliert werden [16]. Die Sulfitierung gelingt mit XI [17], XII [17], XIII [14] und XIV [18] in neutraler Lösung.

Die Einwirkung von Natriumsulfhydratlösungen auf einfache, sterisch nicht gehinderte *p*-Hydroxybenzylalkohole, -benzylalkyläther und -dibenzyläther führt demnach überwiegend zur Bildung der entsprechenden Dibenzylsulfide. Hägglund und Enkvist [3] schlugen für diese Sulfidbildung einen Verlauf vor, der sich durch folgendes Schema formulieren lässt:

$$1)\ ROH + SH^- \rightarrow SR^- + H_2O$$

$$2)\ R'OH + SR^- \rightarrow RSR' + OH^-$$

Die erste Stufe dieser Reaktionsfolge ist wegen der grossen Reaktionsfähigkeit der *p*-Hydroxy- (und *p*-Alkoxy-) benzylthiole mit Hilfe von Modellsubstanzen bisher nicht gezeigt worden *. Hingegen konnte die zweite Stufe durch Umsetzung von Äthylmerkaptan mit Vanillylalkohol (I) sowie mit dessen Methyläther (VIII) in alkalischem Medium und Isolierung des gebildeten Sulfids anschaulich gemacht werden [1]:



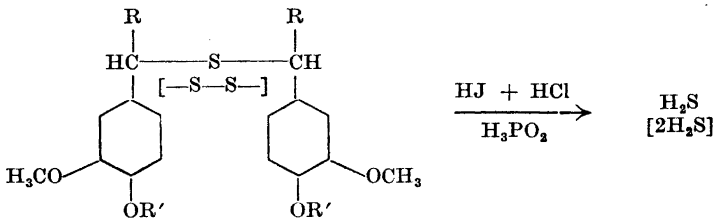
R = H oder CH_3

VERSUCHE MIT THIOLIGNINEN

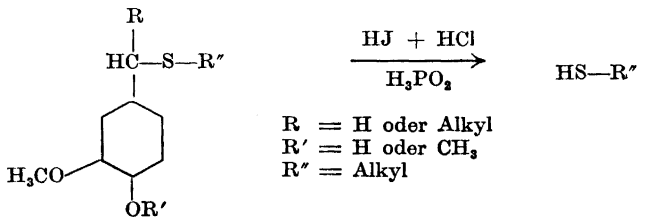
Die eben erwähnten Modellversuche stützen die Annahme, dass zumindest ein Teil des Schwefels in α-Stellung zu den aromatischen Kernen (= Benzylstellung) des Lignins eingebaut wird. Um dies direkt an Thioligninen zeigen zu können, wurde versucht, eine Methode zur Bestimmung des in Benzylstellung gebundenen Schwefels auszuarbeiten, worüber wir bereits an anderer Stelle [1] ausführlich berichteten.

Die Methode beruht auf der besonders leichten Spaltbarkeit der Benzylkohlenstoff-Schwefelbindung in *p*-Hydroxy- und *p*-Alkoxybenzylsulfiden und -disulfiden bei Behandlung mit einer Säuremischung,bestehend aus Jodwasserstoffsäure, Salzsäure und unterphosphoriger Säure. Hierbei bildet sich aus Bis-(*p*-hydroxybenzyl)- oder Bis-(*p*-alkoxybenzyl)-sulfiden oder -disulfiden die stöchiometrisch erforderliche Menge Schwefel-

A.)



B.)



R = H oder Alkyl
R′ = H oder CH_3
R″ = Alkyl

* Versuche zur Darstellung von Veratrylthiol aus Veratrylchlorid und Natriumsulfhydrat führten zur intermediären Bildung des gewünschten Produktes, das jedoch an der Luft sofort zum Diveratryldisulfid oxydiert wurde (17).

wasserstoff (Vorgang A) und aus *p*-Hydroxy- oder *p*-Alkoxybenzylalkylsulfiden das entsprechende Alkylmerkaptan (Vorgang B). Der Schwefelmwasserstoff bzw. das Alkylmerkaptan wird mit Stickstoff übergetrieben und in der Vorlage jodometrisch bestimmt.

Ein getrennter Nachweis von Schwefelwasserstoff und Alkylmerkaptan ist nach der Methode von Bergström und Trobeck [19] möglich, wobei das Gas zunächst eine 10 %ige Lösung von Cadmiumchlorid in 1 %iger Salzsäure und hierauf eine 5 %ige Quecksilber(II)-cyanidlösung passiert. Eventuell vorhandener Schwefelwasserstoff wird in der ersten Lösung als Cadmiumsulfid aufgefangen, während Alkylmerkaptane infolge der Säureunbeständigkeit der Cadmiummerkaptide die erste Lösung passieren und sich in der zweiten Lösung zu den entsprechenden schwer löslichen Quecksilbermerkaptiden umsetzen.

Dieses Verfahren erlaubt eine Differenzierung des im Sulfatlignin enthaltenen organisch gebundenen Schwefels in eine "säurelabile" und eine "säurestabile" Fraktion, von denen die erstgenannte zum Grossteil aus benzylsulfidischen und — eventuell — -disulfidischen Einheiten bestehen dürfte. Eine Unterscheidung zwischen sulfidischen und disulfidischen Bindungen ist auf diesem Weg nicht möglich.

Ausser *p*-Hydroxy- und *p*-Alkoxybenzylsulfiden und -disulfiden werden auch entsprechend substituierte Phenacyl- und Cinnamylsulfide von der Säuremischung glatt gespalten. Die Spaltbarkeit der *p*-Hydroxy- und *p*-Alkoxyphenacylsulfide kann jedoch durch $NaBH_4$-Reduktion der Carbonylgruppe bedeutend herabgesetzt werden [1].

Die Methode wurde zunächst auf zwei Thiolignine angewandt, die durch Sulfidierung (8-stündiges Erhitzen in einer Natriumsulfhydratlösung von pH 9 bei 100°C) von Björkman-Lignin und von Brauns "native lignin" gewonnen wurden.

Das nach Björkman [20] dargestellte Nativlignin aus Fichte * nahm hierbei rund 3 % Schwefel auf, wovon ca. 70 % durch die Säuremischung als Schwefelwasserstoff abgespalten werden konnten (siehe Tabelle 2). Brauns' "native lignin" aus Fichtenholzmehl [21] ,das einen höheren Gehalt an freien phenolischen Hydroxylgruppen als Björkman-Lignin aufweist [22], enthält erwartungsgemäss auch eine grössere Anzahl sulfidierbarer Gruppen. Insgesamt wurden 6.28 % Schwefel eingebaut, wovon ebenfalls ca. 70 % bei Behandlung mit der Säuremischung als Schwefelwasserstoff abgespalten wurden (siehe Tabelle 2). Der Gehalt an Totalschwefel und v.a. an "säurelabilem" Schwefel ändert sich nur wenig, wenn die Reaktionszeit von acht auf vierundzwanzig Stunden verlängert wird (siehe Tabelle 2).

Die Abspaltung des Hauptteiles des Schwefels bei der Säurebehandlung der beiden Thioligninpräparate stützt demnach die Auffassung, dass dieser zum Grossteil in Benzylstellung eingebaut war und die oben beschriebenen Modellversuche lassen in Übereinstimmung mit früheren Untersuchungen [8-10] als wahrscheinlich erscheinen, dass *p*-Hydroxybenzylalkohol- und *p*-Hydroxybenzylalkyläthergruppen im nativen Lignin für diesen Einbau verantwortlich sind.

Die Menge des durch Behandlung mit der Säuremischung abspaltbaren Schwefels ist bei beiden Thioligninpräparaten auffallend hoch. Bei Überführung aller Phenylpropaneinheiten (mittleres Molekülgewicht ca. 210) in Dibenzylsulfideinheiten würde der Gehalt an "Benzylschwefel" rund 7.6 % betragen. Der tatsächliche Gehalt macht also beim Thiolignin aus Björkman-Lignin rund 28 % und beim Thiolignin aus Brauns' "native lignin" rund 59 % dieses Maximalwertes aus, d.h. fast 30 % (bei Björkman-Lignin) bzw. etwas

* Hrn. Dr. A. Björkman danken wir für die freundliche Überlassung eines Präparates.

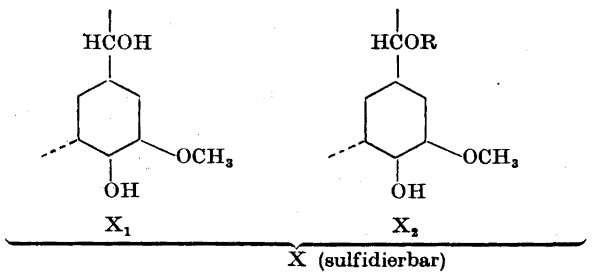
Tabelle 2. Gehalte der Thiolignine an Total- und an "säurelabilem" Schwefel.

Thiolignin aus	Total S	säurelabiler S	säurelabiler S in % des Total S	säurelabiler S in % der max. mögl. Menge *
Björkman-Lignin (Kochung mit NaSH)	3.08	2.12	68.8	27.9
Brauns' "native lignin" (Kochung mit NaSH, 8h)	6.28	4.51	71.9	59.4
(Kochung mit NaSH, 24h)	7.47	4.73	63.2	62.0
Björkman-Lignin (Kochung mit C_2H_5SH)	3.67	3.08	84.0	25.2
technischer Schwarzlauge	1.09	0.53	48.6	7.0
technischem Sulfatlignin (Kochung mit NaSH)	2.13	1.36	63.9	17.9
technischem Sulfatlignin (Kochung mit NaSH, Behandlung mit 1N NaOH)	1.33	0.50	37.6	6.59
Holzmehl, feinstgemahlen (Kochung mit NaSH)	3.79	2.05	54.1	27.0
Holzmehl, feinstgemahlen (Kochung nit NaSH, Behandlung mit 0,1 N NaOH, bei Zimmertemp.)	3.70	1.49	40.3	19.6
Holzmehl, feinstgemahlen (Kochung mit NaSH, Behandlung mit $NaBH_4$ bei Zimmertemp.)	3.31	1.42	42.9	18.7
Holzmehl, feinstgemahlen (Kochung mit C_2H_5SH)	3.72	3.10	83.4	25.4

* 1 S/C_{10}-Einheit bei Kochung mit C_2H_5SH bzw. 1 S/2C_{10}-Einheiten bei Kochung mit NaSH

mehr als die Hälfte (bei Brauns' "native lignin") aller Phenylpropaneinheiten nehmen an der Sulfidierungsreaktion teil. Diese Anteile entsprechen ungefähr dem Gehalt der beiden Ligninpräparate an Einheiten mit freier phenolischer Hydroxylgruppe, die — wie die Modellversuche ergaben — eine Voraussetzung für das Eintreten der Sulfidierungsreaktion in α-Stellung darstellen.

Die Sulfidierungsreaktion — zusammen mit der Säurespaltungsmethode — scheint somit eine neue Möglichkeit zu eröffnen, die Frage der Menge der Gruppen X_1 und X_2 in Ligninpräparaten zu beleuchten.



Die Gruppen X_1 sind durch die Indophenolreaktion [7] bestimmbar. Der Rest der phenolischen Einheiten ($X—X_1 = X_2$), der offenbar auch sulfidierbar ist, dürfte — nach den obigen Modellversuchen zu urteilen — aus reaktionsfähigen Benzylalkyläthergruppen (X_2) bestehen. Eine einwandfreie Bestimmung der letztgenannten Gruppen auf diesem Weg wird jedoch erst möglich, wenn es gelingt, die strenge Reproduzierbarkeit der Sulfidierungsreaktion zu zeigen und die unten erwähnten denkbaren Komplikationen (teilweise Disulfidbildung, Sulfidierung in anderen Stellungen als in der Benzylstellung) experimentell auszuschliessen.

Da Sulfidierbarkeit in α-Stellung ausser freien p-ständigen phenolischen Hydroxylgruppen auch noch die Abwesenheit von sterisch hindernden Substituenten in β-Stellung erfordert und somit die Strukturtypen XI bzw. XII, XIII und XIV ausschliesst (vgl. Modellversuche S. 1517) ist der gefundene, relativ hohe Gehalt der beiden Thioligninpräparate an "säurelabilem" Schwefel nicht ohne weiteres mit den gegenwärtigen Vorstellungen über die Struktur der Ligninbausteine und deren gegenseitige Verknüpfung vereinbar. Diese Vorstellungen rechnen ja z.B. mit β-aroxylsubstituierten Einheiten als wesentlichem Bauprinzip des Lignins [23, 13, 24], wobei wenigstens ein Teil dieser Einheiten freies phenolisches Hydroxyl enthalten sollte.

Eine Möglichkeit zur teilweisen Beseitigung dieser Diskrepanz liegt in der Annahme, dass ausser sulfidischen auch disulfidische Bindungen vorliegen könnten, zwischen welchen — wie bereits erwähnt — die Säurespaltungsmethode nicht zu unterscheiden vermag. Die Umsetzung von Björkman-Lignin mit Äthylmerkaptan (siehe unten), bei welcher eine Ausbildung von Disulfidstrukturen nicht möglich ist, lieferte jedoch ein Präparat, dessen "säurelabile" Schwefelfraktion der des entsprechenden Thiolignins (hergestellt durch Umsetzung mit Natriumsulfhydrat) nahezu äquivalent ist (siehe Tabelle 2.). Aus diesem Grund scheidet die Annahme von Disulfidgruppen in den beiden oben erwähnten Thioligninpräparaten als Erklärung für deren hohen Gehalt an "säurelabilem" Schwefel aus. Eine weitere Möglichkeit zur Deutung des erwähnten Sachverhaltes könnte sich dadurch ergeben, dass eventuell auch andere als Benzylsulfidbindungen von der Säuremischung gespalten werden könnten. Ein solches Verhalten wäre nach vorläufigen Modellversuchen [17] vor allem von γ-sulfidischen Einheiten mit bereits vorliegender oder während der Säurebehandlung entstehender, zum Kern konjugierter Doppelbindung (Coniferylsulfidtypus) zu erwarten, da sie zu den benzylsulfidischen Einheiten vinylog sind. Genauere Untersuchungen über die eventuelle Ausbildung γ-sulfidischer Strukturen während der Sulfidierung stehen noch aus. Doch zeigt z.B. das Verhalten des Ketols XVI, das unter den obigen Sulfidierungsbedingungen z.T. in das entsprechende γ-Sulfid übergeführt wird (siehe exp. Teil), dass mit einer solchen Möglichkeit gerechnet werden muss.

Das Vorkommen von Strukturelementen des p-Hydroxy- bzw. p-Alkoxyphenacylcarbinoltypus, deren Thioderivate ebenfalls die Spaltungsreaktion geben [1], konnte ausgeschlossen werden. Die Menge des aus dem Thiolignin abgespaltenen Schwefelwasserstoffs ist nämlich nach Behandlung mit $NaBH_4$ genau so gross wie nach einfacher Alkalibehandlung (siehe Tabelle 2) während Modellsubstanzen dieses Typus — wie oben erwähnt — durch Reduktion der Carbonyl- zu den entsprechenden Carbinolgruppen einen Grossteil ihrer Spaltbarkeit einbüssen.

Der zweite Schritt der Benzylsulfidbildung, welcher — wie oben erwähnt — modellmässig durch Umsetzung von Vanillylalkohol (I) und von dessen Methyläther (VIII) mit Äthylmerkaptan illustriert werden konnte, liess sich auch direkt am Lignin zeigen. Bei Behandlung von Björkman-Lignin mit Äthylmerkaptan nimmt das Präparat 3.67 % Schwefel auf, der zum grössten Teil (84 %) bei Einwirkung der Säuremischung wieder als Äthylmerkaptan abgespalten wird. Die Menge des mit der Säuremischung abspaltbaren Schwefels (3.08 %) entsprach hier — wie beim Produkt der Umsetzung von Björkman-Lignin mit Natriumsulfhydrat (vgl. entsprechende Werte in Tabelle 2) — ca. einem Viertel des theoretisch möglichen Maximalwertes (1 S/Phenylpropaneinheit, mittleres Molekülgewicht 263, entsprechend 12.16 %). Aufgrund der obigen Modellversuche (siehe S. 1521) lassen sich diese Befunde wohl am besten durch die Annahme erklären, dass auch bei der Reaktion des Lignins mit Äthylmerkaptan *p*-Hydroxybenzylalkohol- bzw. -benzylalkyläthergruppen eine massgebende Rolle spielen und in die entsprechenden "säurelabilen" Benzyläthylsulfidgruppen übergeführt werden.

Sulfatlignin aus technischer Schwarzlauge enthält bedeutend weniger Schwefel als die aus den isolierten Ligninen dargestellten Thiolignine (siehe Tabelle 2). Dies kann mit der Annahme erklärt werden, dass während des unter radikaleren Bedingungen verlaufenden technischen Prozesses entweder ein Teil der sulfidierbaren Einheiten durch Kondensationsreaktionen blockiert oder dass aus zunächst sulfidierten Einheiten durch Alkali wieder Schwefel abgespalten wird. Die letztgenannte Alternative konnte durch Modellversuche mit Divanillyldisulfid [8] und mit Divanillylmonosulfid [9,10] gestützt werden.

Um zu untersuchen, ob bei einer derartigen Schwefelabspaltung sulfidierbare Einheiten regeneriert werden, wurde das technische Präparat einer Sulfidierung unter gleichen Bedingungen wie die beiden Nativlignine unterworfen. Hierbei stieg zwar der Gehalt an Totalschwefel auf das Doppelte und der an "säurelabilem" Schwefel auf das fast Dreifache an (siehe Tabelle 2), jedoch erreichten beide Werte nur ca. 2/3 der beim Thiolignin aus Björkman-Lignin beobachteten Schwefelgehalte. Ein grosser Teil (64 %) des bei dieser milden Sulfidierung in das technische Sulfatlignin eingebauten Schwefels kann durch Einwirkung der Säuremischung wieder als Schwefelwasserstoff abgespaltet werden. Bei 8-stündiger Behandlung dieses mild sulfidierten technischen Thiolignins mit 1 N Natronlauge (170°C) sinken der Gehalt an Total- und an "säurelabilem" Schwefel wieder fast auf die Ausgangswerte (= Werte für das technische Thiolignin) ab und es zeigt sich, dass die Gesamtmenge des mit Alkali wieder abspaltbaren Schwefels (0.8 %) der "säurelabilen" Fraktion (0.86 %) angehört. Vielleicht kommt man daher den tatsächlichen Verhältnissen mit der Annahme am nächsten, dass unter technischen Bedingungen sowohl eine irreversible Zerstörung sulfidierbarer Strukturen als auch eine sekundäre Schwefelabspaltung aus primär sulfidierten Strukturelementen eintritt.

VERSUCHE MIT HOLZMEHLPRÄPARATEN

Um einen eventuellen Einfluss der Kohlenhydratbestandteile des Holzes auf die Sulfidierungsreaktion des Lignins festzustellen, wurde abschliessend auch ein nach Björkman [20] durch Ultrafeinmahlung (Schwingkugelmühle) ge-

wonnenes Fichtenholzmehlpräparat direkt Kochungen mit Natriumsulfhydrat und mit Äthylmerkaptan unterworfen und die entstandenen Thiolignine isoliert und analysiert. Durch die weitgetriebene Feinmahlung ist es möglich, begrenzende Faktoren der Sulfidierung und Delignifizierung, welche auf Penetrierungsschwierigkeiten beruhen, weitgehend auszuschalten. Die so gewonnenen Ergebnisse sind ausserdem direkt mit den beim Björkman-Lignin erzielten vergleichbar.

Sowohl bei Kochung mit Natriumsulfhydrat als auch bei Kochung mit Äthylmerkaptan werden Thiolignine erhalten, die im Gehalt an Totalschwefel und an "säurelabilem" Schwefel mit den entsprechenden Präparaten aus isoliertem Björkman-Lignin weitgehend übereinstimmen (siehe Tabelle 2).

Somit scheinen die Kohlenhydratbestandteile des Holzes unter den angegebenen Bedingungen den Einbau des Schwefels in das Lignin chemisch nicht nennenswert zu beeinflussen.

EXPERIMENTELLER TEIL

Darstellung der Modellsubstanzen

Die für die Untersuchung der Sulfidierungsreaktion verwendeten Modellsubstanzen wurden wie in der Literatur beschrieben dargestellt.

Kochung der Modellsubstanzen mit Natriumsulfhydratlösung

Die Kochung der in Tabelle 1 angeführten Modellsubstanzen wurde unter einheitlichen Bedingungen durchgeführt und soll daher nur an einem Beispiel (Syringaalkohol, V) näher beschrieben werden:

285 mg Syringaalkohol (V) wurden in einer Druckflasche mit 10 ml "Sulfidierungslösung" (3 g $Na_2S \cdot 9\ H_2O$ in 100 ml Schwefelwasserstoffwasser) versetzt und auf 100°C erwärmt. Hierbei ging die gesamte Substanz in Lösung, aus der sich im Laufe der 8-stündigen Reaktionszeit allmählich ein Öl abschied. Nach Abkühlen wurde durch Einleiten von Kohlendioxyd neutralisiert, wobei eine weitere Menge Öl ausfiel. Durch 5-malige Ätherextraktion des Reaktionsansatzes konnten 254 mg (entsprechend 90 % d.Th.) farbloses Öl isoliert werden, das beim Anreiben mit etwas Toluol zum grössten Teil kristallisierte. Dieses Rohprodukt wurde mit Essigsäureanhydrid-Pyridin (1 : 1) in üblicher Weise acetyliert und 2 mal aus Äthanol umkristallisiert. Nadeln vom Schmp. 137—138°. (Die analytischen Daten, Schmelzpunkte und Ausbeuten der einzelnen Sulfidierungsprodukte bzw. ihrer Derivate sind in Tabelle 1 zusammengestellt.)

Die Stabilität der fünf dimeren Substanzen XI—XV unter den angegebenen Sulfidierungsbedingungen und ihre Wiedergewinnung soll am Beispiel des *p*-Hydroxybenzylalkohols XII genauer beschrieben werden:

295 mg XII (Schmp. 94—96°) wurden in einer Druckflasche in 30 ml Äthanol gelöst, mit 30 ml "Sulfidierungslösung" versetzt und 8 Stunden auf 100°C erwärmt. Die gesamte Substanz war nach der Kochung in Lösung. Nach Neutralisieren durch Einleiten von Kohlendioxyd und Abdestillieren des Alkohols wurde die Lösung einigemale mit Äther ausgeschüttelt. Die vereinigten Ätherextrakte enthielten ein Öl (279 mg, entsprechend 95 % der Einwage), das sich papierchromatographisch (Lösungsmittelgemisch : Benzol-gesättigtes Wasser; Entwicklungsflüssigkeit : diazotiertes Benzidin) als einheitlich erwies und den gleichen R_F-Wert (0.64) wie das Ausgangsmaterial (XII) besass. Nach Reinigung durch Adsorption an Al_2O_3 und Umkristallisieren aus sehr wenig Methyläthylketon wurden Kristalle vom Schmp. 94—96° erhalten, die mit dem Ausgangsmaterial (XII) keine Schmp.-Depression ergaben.

Pinoresinol (XIII) und Dihydro-dehydro-di*iso*eugenol (XIV) konnten nach der gleichen Behandlung in 91 %iger bzw. 96 %iger Ausbeute zurückgewonnen werden.

Das Diol XI gab bei gleicher Behandlung und Aufarbeitung ein viskoses schwefelfreies Öl, das papierchromatographisch (Lösungsmittelgemisch: Benzol-gesättigtes Wasser) näher untersucht wurde. Es zeigte sich, dass es ausser unverändertem Ausgangsmaterial (R_F = 0.67) eine weitere phenolische Komponente (R_F = 0.52) enthielt. Diese gab beim Entwickeln mit einer alkoholischen Lösung von Chinonmonochlorimid und mit verdünnter Natronlauge eine vorübergehende Violettfärbung und beim Besprühen mit Phloroglucin-Salzsäure eine stabile Rotfärbung. Die Bildung eines instabilen Indophenolfarbstoffes beim Entwickeln mit Chinonmonochlorimid deutet auf das Vorliegen eines durch Wasserabspaltung aus dem Ausgangsmaterial entstandenen Coniferylalkoholderivates hin [7]. Die positive Phloroglucin-Reaktion zeigt, dass dieses teilweise zum entsprechend substituierten Coniferylaldehyd oxydiert worden sein dürfte [25].

Die der Guajacylverbindung XI entsprechende Veratrylverbindung XV konnte bei Einhaltung der oben erwähnten Bedingungen ebenfalls nicht sulfidiert werden. Das resultierende farblose Öl enthielt keinen Schwefel, erwies sich papierchromatographisch (Lösungsmittelgemisch: Benzol-gesättigtes Wasser; Entwicklung durch Joddämpfe) als einheitlich und besass sowohl den gleichen R_F-Wert (0.82) als auch den gleichen Methoxylgehalt (28.2 %) wie das Ausgangsmaterial.

Dagegen gab das dem Diol XV entsprechende Ketol XVI unter den gleichen Bedingungen ein kristallisiertes Sulfidierungsprodukt. Ausbeute: 21 % d. Th. Schmp. 134—136°. (Gef.: S 5.29. Ber. für $C_{36}H_{38}O_{10}S$: S 4.85.) Das Sulfid wurde von der "Säuremischung" langsam gespalten.

Kochung der Modellsubstanzen mit Äthylmerkaptan

Die Kochung erfolgte wie bereits für den Vanillylalkohol (I) beschrieben [1]. Vanillylalkoholmethyläther (VIII, Schmp. 35—36°) lieferte hierbei in 86 %iger Ausbeute Vanillyläthylsulfid.

Darstellung der Thiolignine

1) *aus Björkman-Lignin* [20]

a) *Kochung mit Natriumsulfhydratlösung.* 224 mg Björkman-Lignin wurden in einer Druckflasche mit 20 ml Äthanol und 20 ml "Sulfidierungslösung" versetzt und 8 Stunden auf 100°C erwärmt. Nach Abdestillieren des Äthanols im Vakuum wurde etwas Wasser hinzugefügt und mit 2N Salzsäure schwach angesäuert. Das hierbei ausfallende Thiolignin konnte durch kurzes Erwärmen auf 60° in eine leicht filtrierbare Form übergeführt werden. Nach Trocknung über P_2O_5, Extraktion mit Toluol und Petroläther sowie erneuter Trocknung über Paraffin gab das Produkt die in Tabelle 2 angeführten analytischen Werte. Das Ultraviolett-Spektrum war dem des Ausgangsmaterials überaus ähnlich, das Absorptionsmaximum bei 280 mμ war gleich ausgeprägt. Die Reaktion mit Phloroglucin-Salzsäure war — wie bei den anderen hier beschriebenen Thioligninpräparaten aus Nativligninen — positiv. Da jedoch — wie der Modellversuch mit der Substanz XI zeigte — während der Sulfidierungsreaktion eventuell mit der Neubildung Coniferylaldehyd-artiger Gruppierungen zu rechnen ist, darf dies nicht als Beweis für das Überleben der ursprünglich vorhandenen Coniferylaldehydgruppen betrachtet werden. Ausbeute 121 mg.

b) *Kochung mit Äthylmerkaptan.* 404 mg Björkman-Lignin wurden mit 40 ml 1/15 M Phosphatpufferlösung vom pH 6.9, 55 ml Äthanol und 5 ml Äthylmerkaptan versetzt und nach Sättigung mit Stickstoff in einem rotierenden Stahlautoklaven 24 Stunden auf 100° erwärmt. Nach Abdestillieren des Alkohols im Vakuum wurden 150 ml dest. Wasser zugesetzt und nochmals im Vakuum eingeengt. Hierbei fiel das "Äthylmerkaptan-Lignin" teilweise aus. Durch schwaches Ansäuern mit verdünnter Salzsäure wurde ein weiterer Teil ausgefällt, die gesamte Fällung sofort abzentrifugiert und einigemale mit dest. Wasser gewaschen. Nach Trocknung an der Luft wurden 364 mg hellgelbes Pulver erhalten. Zur Reinigung wurde dieses dreimal mit Hexan ausgezogen und hierauf im Vakuum über Paraffin und P_2O_5 getrocknet. (Analysenwerte siehe Tabelle 2.)

2) *aus Brauns "native lignin"* [21]

Kochung mit Natriumsulfhydratlösung. Die Darstellung erfolgte wie oben für das Thiolignin aus Björkman-Lignin beschrieben. Aus 220 mg wurden 164 mg säurefällbares Thiolignin erhalten. (Analysenwerte siehe Tabelle 2.)

Isolierung und Natriumsulfhydrat-Kochung des technischen Thiolignins

Die Schwarzlauge einer technischen Sulfatkochung von Fichtenholz wurde durch Einleiten von Kohlendioxyd neutralisiert. Das hierbei ausgefällte Thiolignin flockte bei kurzem Erwärmen auf 60° aus. Es wurde abzentrifugiert, mit Kohlendioxyd-gesättigtem Wasser gewaschen und im Vakuum über P_2O_5 getrocknet. Schliesslich wurde das Präparat mit Schwefelkohlenstoff und mit Petroläther gründlich extrahiert.

880 mg dieses Thiolignins wurden mit 180 ml "Sulfidierungslösung" versetzt und in einer Druckflasche 8 Stunden auf 100° erwärmt. Nach Einengen auf kleines Volumen wurde mit Essigsäure angesäuert und das Reaktionsprodukt auf gleiche Weise wie das Ausgangsmaterial isoliert und gereinigt. Bei Behandlung dieses Präparates mit der Säuremischung konnte nur Schwefelwasserstoff als flüchtiges Spaltprodukt nachgewiesen werden.

378 mg dieses sulfidierten technischen Thiolignins wurden in 10 ml 1 N NaOH gelöst und in einem rotierenden Stahlautoklaven 8 Stunden auf 170° erhitzt. Die Wiederisolierung und Reinigung erfolgte wie oben beschrieben. (Analysenwerte siehe Tabelle 2.)

Kochung von feinstgemahlenem Holzmehl

a) *mit Natriumsulfhydratlösung.* 3.80 g feinstgemahlenes Fichtenholzmehl [20] wurden in einer Lösung von 1.0 g Natriumsulfhydrat in 60 ml Äthanol und 40 ml dest. Wasser suspendiert und 24 Stunden in einem rotierenden Stahlautoklaven auf 100° erwärmt. Der nach dieser Kochung ungelöste Rest betrug 2.46 g (= 65 % der Einwage) und enthielt 2.59 % OCH_3. Aus dem Filtrat dieses Rückstandes wurde — auf gleiche Weise wie bei der Kochung von Björkman-Lignin beschrieben — ein Thiolignin in Form eines gelbbraunen Pulvers isoliert. Ausbeute 0.45 g (= 12 % der Einwage), Das Präparat ergab bei Totalhydrolyse 7 % reduzierende Monosaccharide, deren prozentuelle Zusammensetzung ebenso wie die der im Kochungsrückstand enthaltenen Zucker durch quantitative Papierchromatographie ermittelt und in Tabelle 3 zusammengestellt wurde.

Eine kleine Probe (60 mg) des Präparates wurde in 10 ml 0.1 N NaOH gelöst und 12 Stunden bei Zimmertemperatur aufbewahrt. Hierauf wurde das Thiolignin wie üblich isoliert und gereinigt. Ausbeute 51 mg. Eine weitere Probe (60 mg) wurde in 10 ml 80 %igem Äthanol suspendiert und mit 50 mg $NaBH_4$ versetzt. Nach 12 Stunden Schütteln bei Zimmertemperatur wurde der Versuchsansatz wie üblich aufgearbeitet. Ausbeute an reduziertem Thiolignin 53 mg. (Analysenwerte siehe Tabelle 2.)

b) *mit Äthylmerkaptan.* 3.80 g feinstgemahlenes Holzmehl wurden in einer Mischung bestehend aus 100 ml Äthänol, 80 ml 1/15 M. Phosphatpufferlösung vom pH 6.9 und 10 ml Äthylmerkaptan suspendiert, die Suspension wurde mit Stickstoff gesättigt und in einem rotierenden Stahlautoklaven 24 Stunden auf 100° erwärmt. Der nach dieser Kochung erhaltene Rückstand (1.60 g = 42 % der Einwage) enthielt 2.73 % OCH_3. Aus dem Filtrat dieses Kochungsrückstandes wurde auf übliche Weise ein "Äthylmerkaptan-Lignin" in Form eines hellbraunen Pulvers isoliert. Ausbeute 0.39 g . (Analysenwerte siehe Tabelle 2.) Bei Behandlung dieses Präparates mit der Säuremischung in der auf Seite 1521 angegebenen Weise konnte als flüchtiges Spaltprodukt nur Äthylmerkaptan nachgewiesen und nach Überführung in das Quecksilbersalz durch Schmp. identifiziert werden [72—73.5°).

Herrn Prof. E. Hägglund, Schwedisches Holzforschungsinstitut, Stockholm, danken wir für die Anregung zu dieser Arbeit, Herrn Prof. E. Adler, Chalmers Technische Hochschule, Göteborg, für sein reges Interesse, sowie für die Überlassung der Modellsubstanzen IV, XI und XII. Für wertvolle experimentelle Hilfe sei Herrn S. Söderberg bestens gedankt.

Tabelle 3. Prozentuelle Zusammensetzung der Kohlenhydrate im Rückstand und im säurefällbaren Thiolignin nach Natriumsulfhydrat-Kochung von feinstgemahlenem Holzmehl.

	Glucose und Galaktose	Mannose	Xylose	Arabinose
Rückstand	77	18	4	1
mit Säure fällbares Thiolignin	31	42	20	7

LITERATUR

1. Gierer, J. und Alfredsson, B. *Chem. Ber.* **90** (1957) 1240.
2. Klason, P. und Segerfelt, B. *Arkiv Kemi, Mineral. Geol.* **4** (1911) Nr. 6.
3. Enkvist, T. und Hägglund, E. Festschrift, J. A. Hedvall, Göteborg **1948**, S. 149; Enkvist, T. *Svensk Papperstidn.* **51** (1948) 225; Hägglund, E. *Chemistry of Wood*, Academic Press Inc. N.Y. 1951, S. 487.
4. Hedén, S. und Holmberg, B. *Svensk Kem. Tidskr.* **48** (1936) 207.
5. Holmberg, B. *J. prakt. Chemie* (2) **141** (1934) 93.
6. Berg, G. A. und Holmberg, B. *Svensk Kem. Tidskr.* **47** (1935) 257.
7. Gierer, J. *Acta Chem. Scand.* **8** (1954) 1319; *Chem. Ber.* **89** (1956) 257.
8. Enkvist, T. und Moilanen, M. *Svensk Papperstidn.* **52** (1949) 183; **55** (1952) 668.
9. Mikawa, H. *Bull. Chem. Soc. Japan* **27** (1954) 50.
10. Mikawa, H., Sato, K., Takasaki, C. und Ebisawa, K. *Bull. Chem. Soc. Japan* **29** (1956) 265.
11. Zentner, T. G. *TAPPI* **36** (1953) 517.
12. Adler, E., Lindgren, B. O. und Saedén, U. *Svensk Papperstidn.* **55** (1952) 245.
13. Adler, E., Pepper, J. M. und Eriksoo, E. *Am. Chem. Soc. Meeting, Atlantic City 16—21. Sept. 1956 Abstract of Papers*, S. 18 E.
14. Lindgren, B. O. *Acta Chem. Scand.* **6** (1952) 91.
15. Freudenberg, K. und Schlüter, H. *Chem. Ber.* **88** (1955) 617; Freudenberg, K. und Rasenack, D. *Chem. Ber.* **86** (1953) 755; Freudenberg, K. und Hübner, H. H. *Chem. Ber.* **85** (1952) 1181.
16. Adler, E. und Delin, S. *Privatmitteilung.*
17. Gierer, J. und Alfredsson, B. *Unveröffentlicht.*
18. Häggroth, S. *Privatmitteilung;* vgl. Mikawa, H., Sato, K., Takasaki, C. und Ebisawa, K. *Bull. Chem. Soc. Japan* **29** (1956) 209.
19. Bergström, H. und Trobeck, K. G. *Svensk Papperstidn.* **22** (1939) 554.
20. Björkman, A. *Svensk Papperstidn.* **59** (1956) 477; Björkman, A. und Person, B. *Ibid.* **60** (1957) 158.
21. Brauns, F. E. *J. Am. Chem. Soc.* **61** (1939) 2120.
22. Adler, E. und Gierer, J. in E. Treiber, *Chemie der Pflanzenzellwand*, Springer Verlag, Heidelberg 1957, S. 455; Hernestam, S. *Svensk Kem. Tidskr.* **67** (1955) 37.
23. Adler, E. und Lindgren, B. O. *Svensk Papperstidn.* **55** (1952) 563; Adler, E. und Yllner, S. *Svensk Papperstidn.* **57** (1954) 78.
24. Freudenberg, K. *Angew. Chem.* **68** (1956) 84, 508.
25. Adler, E., Björkvist, K. J. und Häggroth, S. *Acta Chem. Scand.* **2** (1948) 93.

Eingegangen am 28. Juni 1957.

ACTA CHEMICA SCANDINAVICA 11 (1957) 1530—1533

Polarographic Reduction of Hydroxamic Acids

MILDA PRYTZ and TH. ØSTERUD

Universitetets Kjemiske Institutt, Blindern-Oslo, Norway

Acethydroxamic acid and propionhydroxamic acid were polarographically reduced in aqueous alcoholic solutions of tetraethyl ammonium iodide.

Over a pH range from 4.7 to 9.5 two distinct waves occur. For the acethydroxamic acid the more positive one levels off in the prescribed manner, giving a very well defined wave. The half wave potential of the more negative one has so great negative value that erratic dripping or streaming of the mercury occurs and deranges the polarographic curve, which shows a maximum. The first wave was therefore found most suitable for practical analytical purposes and accordingly studied thoroughly. For the propionhydroxamic acid the first waves also show some tendency to form rounded maxima but are still sufficiently well defined for analytical purposes.

The values of the half wave potentials seem to be practically independent of the pH of the solutions until the pH has increased to about 10. For acethydroxamic acid the values with respect to the saturated calomel electrode lie about 1.7 V, for propionhydroxamic acid about 1.85 V.

The form of the curves seems to indicate that the reaction at the cathode is irreversible and we have therefore not found it expedient to calculate $I/(I_{dc}-I)$.

Our reason for studying hydroxamic acids is their general utility in organic analysis. They owe their analytical application to the fact that they may be identified by their formation of soluble, red to violet coloured ferric salts [1]. Since esters are readily hydroxylaminolyzed in the presence of alkali, this reaction can also be employed as a test for esters. Being interested in instrumental analysis and especially in polarographic methods we wanted to use hydroxamic acids for polarographic determination of esters. The saturated aliphatic esters are not capable of producing polarographic reduction waves [2–4], and can therefore not be polarographically determined as such. The hydroxamic acids, however, which may be looked upon as oximes of the original acids, ought to be polarographically reducible, inasmuch as the corresponding oximes lend themselves to polarographic methods [4]. The authors made many negative attempts at obtaining reduction waves for hydroxamic acids, in different buffer solutions, but were nevertheless convinced that the problem could be solved

if only a suitable supporting electrolyte could be found. It must give no hydrogen wave, and only contain components with greatly negative reduction potentials. We have found that hydroxamic acids are not electro-reducible within the potential range given by buffers containing alkali salts in aqueous solution, the only resulting waves obviously being hydrogen waves. Consequently we had to make use of tetraalkylammonium salts. We noticed that Bobrowa and Matwejewa [5] by polarographic reduction of unsaturated esters had used tetramethylammonium iodide in alcoholic solution, and their curves show that the usable potential range reaches to about —2.5 V. For our experiments we used a supporting electrolyte consisting of 0.1 M $N(C_2H_5)_4I$ in 50 % C_2H_5OH with 0.005 % tylose. The pH was raised by addition of $N(C_2H_5)_4OH$. Trying to lower pH was inexpedient inasmuch as it only resulted in the reduction of hydrogen ions. Most measurements were carried out with a mercury pool anode. In order to get significant values of the half-wave potentials, however, some polarograms were recorded with a saturated calomel electrode as external anode. The hydroxamic acids studied were acethydroxamic acid and propionhydroxamic acid.

EXPERIMENTAL PROCEDURE

In these experiments a recording polarograph from Radiometer, Copenhagen, was used. Instead of the usual lead batteries an arrangement with Nife batteries in series with a rectifyer was employed. It gave high stability to the potential across the bridge. The usual precautions against oxygen interference were taken, a mixture of pure nitrogen and hydrogen being bubbled through the supporting electrolyte in the electrolysis vessel until it showed no trace of any oxygen wave. The solutions to be measured were kept under the inert gas, the flow of which was only stopped during the recording of the polarograms.

The acethydroxamic acid was prepared by Farmaceutisk Industri A/S and the propionhydroxamic acid by Dr. Else Kloster Jensen at *Sentralinstitutt for industriell forskning*. Both acids were recrystallized several times to make sure that they were chemically pure. Their molar concentration in the electrolysis vessel during the analysis was of the order 10^{-3}. The pH of the solutions was measured at the start and at the completion of the experiments.

EXPERIMENTAL RESULTS

The polarographic waves were very distinct even without the use of counter current, which was found to be superfluous in this case.

For the acethydroxamic acid as well as for the propionhydroxamic acid the polarograms consist of two waves. Of these the first wave is the best defined reduction wave, while the second wave is apt to show a somewhat irregular behaviour that need not be ascribed to the hydroxamic acids, because the occurrence of variable and erratic drops is always apt to be troublesome in aqueous alcoholic solutions near the decomposition potential of tetraalkyl ammonium halides. The irregular form of the more negative wave therefore made us limit our efforts to the more positive one, as this wave lends itself readily to analytical purposes. Both waves were registered, but we find it adequate to render only the first one. For acethydroxamic acid the curves are given in Fig. 1. The curves all start at V = 1.05, and for each of them the curve for the corresponding supporting electrolyte was always taken.

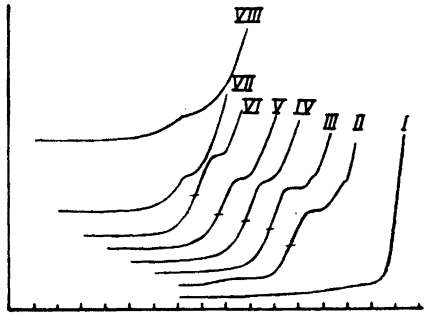


Fig. 1. Electro-reduction of the acethydroxamic acid at the pH values 4.7, 5.5, 6.5, 7.5, 8.5, 9.5 and 10.5, the pH increasing from curve II to curve VIII. Curve I represents the supporting electrolyte. Mercury pool anode.

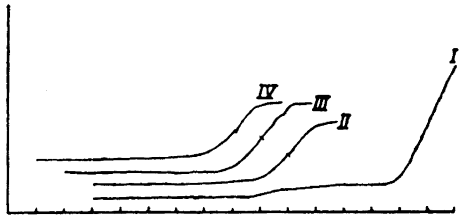


Fig. 2. Electro-reduction of acethydroxamic acid at the pH values 4.7, 7.0 and 9.0, the pH increasing from curve II to curve IV. Curve I represents the supporting electrolyte. Saturated calomel electrode as anode.

In order to express the half wave potentials with reference to the S.C.E., according to general practice, some records were made with a saturated calomel electrode as the second electrode. For the acethydroxamic acid the results are given in Fig. 2.

The value of the half wave potentials seemed to be independent of the pH except for the highest value, and referred to the mercury pool anode it was 1.7 V. Referred to the saturated calomel electrode it was 2.1 V in slightly acid solution and rose to 2.14 V only in distinctly basic solution.

The propionhydroxamic acid is also reduced in two steps. The first wave is apt to show a small rounded maximum. The second wave, on the other hand, is somewhat more regular than we were able to obtain it with the acethydroxamic acid. The value of the half wave potential as referred to the mercury pool was 1.8 V, *versus* the saturated calomel electrode 2.13 V.

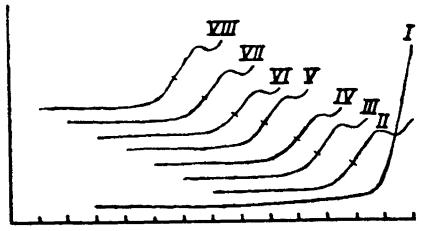


Fig. 3. Electro-reduction of propionhydroxamic acid at the pH values 4.7, 5.5 ,6.0, 6.5, 7.0, 9.0 and 10.0, the pH increasing from curve II to curve VIII. Curve I represents the supporting electrolyte. Mercury pool anode.

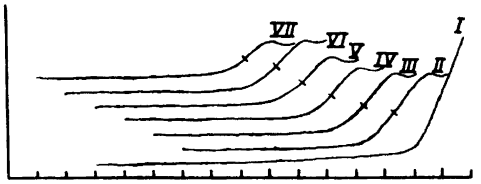


Fig. 4. Electro-reduction of propionhydroxamic acid at the pH values 4.7, 6.0, 7.0, 8.0, 9.5 and 10.5, the pH increasing from curve II to curve VII. Curve I represents the supporting electrolyte. Saturated calomel electrode as anode.

The results are given in Figs. 3 and 4. As a potential of 3 V had been laid across the bridge each interval on the abscissa represents 1.5 V. These curves were also started at 1.05 V.

DISCUSSION

If we compare the structure of the oxime tautomeric forms of the hydroxamic acids with the corresponding oximes, to wit: acethydroxamic acid $CH_3—C\begin{smallmatrix}OH\\NOH\end{smallmatrix}$ with ethanal oxime $CH_3—C\begin{smallmatrix}H\\NOH\end{smallmatrix}$, or propionhydroxamic acid $CH_3CH_2—C\begin{smallmatrix}OH\\NOH\end{smallmatrix}$ with propanal oxime $CH_3CH_2—C\begin{smallmatrix}H\\NOH\end{smallmatrix}$, we must be justified in assuming that a polarographic reduction will affect the double bond of the group $>C = NOH$ between the carbon and the nitrogen atom. Whereas the oximes have both weakly acid and weakly basic properties, the hydroxamic acids, on the other hand, are classed as acids in aqueous solution. This tends to make their reduction somewhat more sluggish and require a higher reduction potential. Even though they may be forced to accept electrons, this takes place polarographically only at relatively high negative potentials. As was to be expected, both the forms of the curves and the independence of the half wave potentials of the pH suggest irreversibility in the process.

The object of this investigation was to find an instrumental method for indication of the analytically very serviceable hydroxamic acids. This problem found its solution in a polarographic reduction of the acids in a supporting electrolyte consisting of a solution of tetraethyl ammonium iodide in an ethanol-water mixture. The curves were very well defined and always gave the same half-wave potential. This was practically independent of the pH of the solution, so that an addition of tetraethyl ammonium hydroxide seems superfluous.

The authors are indebted to Cand.mag. Per Kolsaker for the recording of the polarograms.

REFERENCES

1. Feigl, F. *Spot Tests*, Nordemann Publishing Co., New York 1937, p. 267.
2. Brdička, R. *Chem. Listy* **39** (1945) 35.
3. Stackelberg, M. V. and Stracke, W. Z. *Z. Elektrochem.* **53** (1949) 118.
4. Østerud, Th. and Prytz, M. *Acta Chem. Scand.* **10** (1956) 451.
5. Bobrowa, M. J. and Matwejewa, A. N. *Zhur. Obshchei Khim.* **24** (1954) 1741.

Received June 24, 1957.

ACTA CHEMICA SCANDINAVICA 11 (1957) 1534—1540

Evidence for the Diamagnetism of $Co(NO)_2Hal.$ and $Fe(NO)_2Hal.$

Studies in Magnetochemistry 20 *

H. SOLING and R. W. ASMUSSEN

The Chemical Laboratory B, Technical University of Denmark, Copenhagen, Denmark

The magnetic susceptibilities of $Co(NO)_2X$, X = I, Br, Cl, and $Fe(NO)_2Y$, Y = I, Br, have been measured at temperatures ranging from 85 to 295°K. The compounds are found to be diamagnetic or nearly so. This result is compatible with the generally accepted binuclear structures, if in the particular case of the iron compounds an intermetallic bond be supposed. The preparation and the purification of the compounds are described in detail.

In the years 1939 and 40 Hieber and coworkers [1, 2] prepared a series of metal-NO-halides of the composition $Co(NO)_2X$ and $Fe(NO)_2Y$, where X = I, Br, Cl and Y = I, Br. All the compounds are very instable, black solids with low melting points. They can be prepared by the action of NO-gas on the appropriate anhydrous metal-di-halide eventually under addition of metal powder, *e.g.*

$$FeI_2 + Fe + 4NO \rightarrow 2Fe(NO)_2I$$

In the present paper a magnetochemical investigation of the above mentioned compounds is reported.

The results of the measurements of the magnetic susceptibility of several samples of $Co(NO)_2I$, $Co(NO)_2Br$, $Co(NO)_2Cl$ and $Fe(NO)_2I$ are given in Table 1 together with the results of the chemical analyses of the compounds. The independent samples Nos. I to V of $Co(NO)_2I$ have been prepared by consecutive sublimations of the crude product. Considering the measurements at room temperature it is seen that the gram susceptibility decreases from No. I to No. IV; the difference between Nos. IV and V is considered of no significance. (*Cf.* the remarks below concerning the accuracy of the measurements). The low-temperature measurements of the samples No. I to No. IV display the

* No. 19 of this series: *Acta Chem. Scand.* 11 (1957) 1435.

Table 1. Analyses and magnetic gram susceptibilities of the compounds $Me(NO)_2Hal$

Compound	Analyses	% Metal	% Halg	$\chi_g \cdot 10^6$ at 295°K	$\chi_g \cdot 10^6$ at 195°K	$\chi_g \cdot 10^6$ at 85°K
$Co(NO)_2I$	calc.	23.97	51.61			
No. I	found	24.05	51.24	0.173	0.309	0.85
No. II	»	23.89	51.55	−0.017	0.018	0.39
No. III	»	24.09	51.65	−0.034	−0.017	0.19
No. IV	»	24.04	51.47	−0.105	−0.109	−0.01
No. V	»		51.40	−0.108		
$Co(NO)_2Br$	calc.	29.64	40.18			
No. I	found	29.77	40.09	0.023		
No. II	»	29.63	40.20	−0.027		
$Co(NO)_2Cl$	calc.	38.17	22.96			
No. I	found	38.36	22.96	0.076		
No. II	»	38.12	22.88	0.025		
$Fe(NO)_2I$	calc.	23.00	52.28			
No. I	found	23.08	52.21	−0.142	−0.143	−0.18
No. II	»	22.96	52.05	−0.139	−0.149	−0.16

same features. On the other hand, when considering each preparation separately χ_g increases when the temperature is decreased. The absolute increase is the largest for preparate No. I, which has a positive susceptibility. Remembering that $Co(NO)_2$ I is undergoing some decomposition when exposed to the air even for a short time and that the products of decomposition must be strongly paramagnetic or even ferromagnetic, it seems safe to conclude that chemically pure $Co(NO)_2$ I is diamagnetic. The good accordance between the analysed and the calculated composition of the substances rather strengthens than weakens this conclusion since the amount of an ordinary paramagnetic cobaltous-compound necessary to mask completely even a strong diamagnetism is beyond the limits of what can be found by a chemical analysis.

In the cases of $Co(NO)_2Br$ and $Co(NO)_2Cl$ magnetic measurements have been performed at room temperature only. A faint diamagnetism was ultimately found for the bromide while an equally small paramagnetism was the best result we could reach with the chloride. These two compounds are even more liable to undergo decomposition than the iodide. It is furthermore highly improbable that the magnetic properties of the bromide and the chloride should be essentially different from that of the iodide. We consequently conclude that also $Co(NO)_2Br$ and $Co(NO)_2Cl$ are diamagnetic when chemically pure.

$Fe(NO)_2I$ is the only substance for which we found a reproducible, although very small, diamagnetism independent of the temperature. The apparently increased diamagnetism at lower temperatures is not considered significant. Usually we claim a much higher accuracy, but remembering that the magnetic susceptibility is found from the difference between the force exerted by the magnetic field upon the Gouy-tube + substance and that exerted upon the

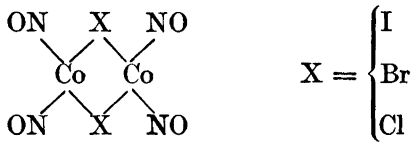
Table 2. Magnetic gram susceptibilities of $Fe(NO)_2I$ at different temperatures and different field strengths.

Temperature, °K	295		195		85	
Field Strength, Ørsted	6 226	7 636	3 346	4 194	3 346	4 194
Force (in mg) exerted on:						
a: Container + Sample	1.238	1.890	0.364	0.567	0.622	0.732
b: Container	0.894	1.363	0.261	0.409	0.452	0.549
c: Sample	0.344	0.527	0.103	0.158	0.170	0.183
$-\chi_g \times 10^6$	0.139	0.144	0.145	0.141	0.183	0.170

empty tube, it is obvious that the experimental error must be rather large when so small susceptibilities are measured as the case is here. Furthermore, during the measurements at low temperatures a continuous condensation of ice upon the tube occurs, which considerably augments the experimental errors. As an illustration of these effects a series of measurements on $Fe(NO)_2I$ is shown in Table 2.

Besides the compounds listed in Table 1 we also prepared $Fe(NO)_2Br$ and attempted to measure it magnetically. In spite of several efforts shortly reported in the experimental section we did not succeed in obtaining even a qualitative impression of its susceptibility. We suppose, by extrapolation from the above results, that this compound is so instable that an experimental demonstration of its — presumed — diamagnetism is impossible.

Hieber and coworkers [1,2] have proposed a binuclear formula for the cobalt-compounds:



The NO-metal bond contributes, according to the detailed discussion given by Seel [3], three electrons to the electron system of the acceptor metal. The four-coordinated Co-atom thus obtains an EAN = 36 which accounts for the diamagnetism. However, it must be pointed out, that since the monomer also contains an even number of electrons the above formula is no necessary consequence of the observed diamagnetism.

The four ligands around each Co-atom may utilize either the tetrahedral sp^3-hybrid or the planar dsp^2-hybrid. The latter necessitates the promotion of two electrons from the 3d orbitals to the 4p orbital not participating in the hybridization, and is therefore considered energetically less favourable.

$Fe(NO)_2Y$ contains an uneven number of electrons in the monomer form. A binuclear structure analogous to that shown above for the cobalt-compounds leaves one unpaired electron on each iron atom. The assumption of a high-

polymer structure is not in accordance with the low melting points and the fact that the compounds are easily sublimed. We consider a binuclear structure with an intermetallic bond the most acceptable explanation of the diamagnetism.

EXPERIMENTAL

Preparation and analysis of the compounds

The preparation of the compounds was carried out according to the method given by Hieber *et al.*[1,2] We have modified the technique in order to prepare the compounds in the highest possible degree of magnetic purity, and for the reason of easy handling the samples used for the magnetic measurements.

$Co(NO)_2I$. 4 g of powdered anhydrous CoI_2 were introduced in the apparatus shown in Fig. 1 and dried at 110—120°C in a current of dry nitrogen. After cooling to room temperature the nitrogen was displaced by pure, dry NO and the temperature slowly raised. At 60—80°C the powder began to react with the NO-gas under liberation of iodine which was collected on the "cold finger". When the reaction began to slow down, the temperature was cautiously raised to 105°C. The reaction vessel was maintained at this temperature until the evolution of iodine ceased. The apparatus was then cooled to room temperature. While a current of dry nitrogen was passed through, the "cold finger" was withdrawn, cleaned, dried and inserted again. The pressure was then reduced to about 1 mm Hg and the sublimation of $Co(NO)_2I$ was started by heating the apparatus to 80°C as quickly as possible. In the course of 5 to 6 h a brush of black crystals was collected on the "cold finger". This crude sublimate must be stored in an evacuated vessel. The purification of the product was accomplished by several resublimations.

$Co(NO)_2Br$ was prepared analogously from an intimate mixture of powdered, anhydrous $CoBr_2$ and freshly reduced cobalt powder (from cobaltous-oxalate). The reaction started at 100°C. $Co(NO)_2Br$ forms black crystals.

$Co(NO)_2Cl$ was obtained from anhydrous $CoCl_2$ and cobalt powder just as the corresponding bromide. Black crystals.

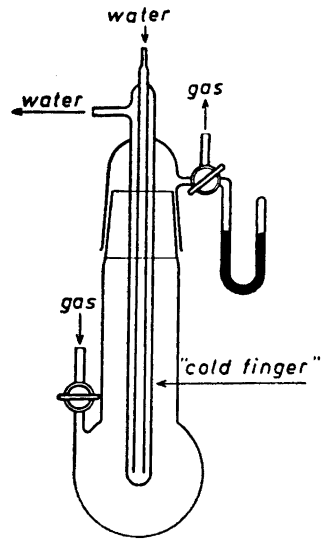


Fig. 1. Reaction- and sublimation-apparatus.

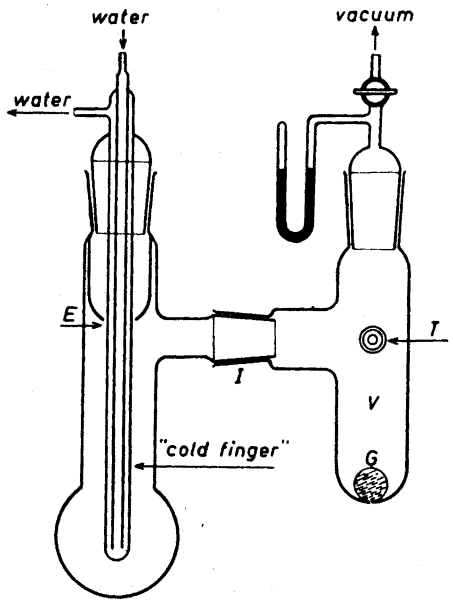


Fig. 2. Sublimation apparatus with vessel (*V*), where the sublimate is powdered by means of the glass-sphere (*G*), and filled into the Gouy-tube (*T*). The edge (*E*) scratches the sublimate off the "cold finger".

While $Co(NO)_2I$ could be sublimed nearly without decomposition, the bromide and the chloride underwent a slight decomposition during the sublimation. All three substances are very sensitive to oxygen.

The *anhydrous cobaltous-halides* used were prepared from Ni-free $CoCO_3$ which was dissolved in the appropriate halogen acid. The solution was then evaporated to dryness under dropwise addition of acid to prevent hydrolysis. $CoCl_2$ was finally dried in a current of dry HCl at 120°C, while $CoBr_2$ and CoI_2 were dried at 130—140°C *in vacuo*. The substances were all completely soluble in water.

$Fe(NO)_2I$. 4 g of powdered anhydrous FeI_2 thoroughly mixed with 1 g of freshly reduced iron powder were treated with NO-gas as described above. The reaction started at room temperature under evolution of a considerable amount of heat, and was allowed to continue without further heating. From time to time slight cooling was necessary in order to keep the reaction under control. When the temperature exceeded 80°C the reaction mixture began to melt. No free iodine was observed during the reaction. The crude nitrosate was sublimed at 80—90°C under reduced pressure. In order to obtain a sublimate of a crystal size suitable for the further manipulations, the sublimation had to be carried out in three stages: *i*, 80°C, 10 mm Hg; the substance melted and gave off NO rather vigorously. *ii*, When the evolution of NO ceased, the temperature was raised to 85°C and the pressure was reduced to 5 mm Hg. The majority of the substance was volatilized at this stage. *iii*, Finally the temperature was raised to 90°C and the pressure was lowered to about 1 mm Hg. The sublimation was now continued until only a small remanence of iron powder and decomposed substance was left. The resublimations were carried out in the same way. No liberation of NO was then observed and the yield was nearly quantitative. $Fe(NO)_2I$ forms black crystals, sensitive to oxygen.

$Fe(NO)_2Br$ was prepared in the same way as the iodide. This substance, which also forms black crystals, is the most delicate of the compounds described here. Like the

iodide' it sublimes easily, but far from quantitatively. $Fe(NO)_2I$, on the other hand, is the most stable of the five substances in question. A specimen of this substance stored in an evacuated glass-tube for three years did not show any sign of decomposition, while the other substances were more or less decomposed.

The *anhydrous ferrous-halides* used were prepared from iron powder and elementary halogens, according to standard procedures, and finally sublimed in high vacuum.

Analysis. Cobalt-compounds: Cobalt was determined as $CoSO_4$ by weighing. The compounds were converted into the sulphate, which was heated at 500°C until constant weight. Owing to the small amounts of substance available at that stage of development of the preparation technique the usual method of determination of iodine as AgI by weighing could not be used. The iodine was therefore oxidized to IO_3^- and determined iodometrically. Bromine and chlorine were weighed as the silver-halides.

$Fe(NO)_2I$: Iron was determined as Fe_2O_3 and the iodine as AgI. The results of the analyses are given in Table 1 together with the results of the magnetic measurements.

Magnetic measurements

The magnetic susceptibilities were measured by means of the Gouy method as described in earlier papers [4]. The susceptibility quoted for each sample and temperature in Table 1 is the mean value of several measurements at at least two field strengths ranging from 3 346 to 7 636 Ørsted (*cf.* Table 2). No sign of field strength dependence of the susceptibilities was found within the limits of experimental errors. In view of the obvious risk of ferromagnetic impurities in the preparates, measurements of the susceptibilities over a broader range of field strengths would have been desirable, but owing to the very feeble magnetism observed, the measurements could only be carried out with a reasonable accuracy (a few per cent) in the above mentioned interval of field strengths, 7 636 Ørsted being the maximum field strength obtainable with our magnet. On the other hand, a slight ferromagnetism would not invalidate our conclusion that the pure compounds are diamagnetic.

The delicacy of the compounds to oxygen complicated the packing of the substance into the tubes used for the magnetic measurements. The following procedure, which is the final result of several attempts, fulfils the demands for simplicity and efficiency to a reasonable degree. The resublimations were carried out in the apparatus shown in Fig. 2 as described above. After cooling to room temperature, the apparatus was tilted and while a current of dry nitrogen was passed through, the "cold finger" was slowly drawn out with a screwing movement. When reaching the edge E the crystals were scratched off and fell down into the vessel V, which then was disconnected at J and closed with a ground stopper. The vessel was evacuated, the crystals were powdered by aid of the glass-sphere G and could now be packed into the tube T by aid of a little glass rod (not shown in Fig. 2) containing an iron core, so that it could be manipulated from outside by means of a magnet. However, great difficulties were experienced at this point due to adhesion of the fine powder to the glass walls. We were therefore forced to abandon the fine-powdering and instead adapted the following way of packing. The crystals were only crushed coarsely with the glass-sphere and next filled into the tube in small portions. Each time the tube was tapped gently at the bottom until the packing appeared uniform by inspection with a magnifying glass. From our general experience concerning the packing of Gouy-tubes this procedure is judged to be sufficiently reproducible for the purpose, provided the size of the particles is nearly uniform and not too large. The apparatus was again connected to the vacuum-pump and the tube T was sealed off, while the pump was working. During the sealing-off process the upper surface of the packing melts slightly and locks the packing when it again solidifies, thus securing a defined length of the substance column. Since the upper surface of the packing is situated well outside the magnetic field during the measurements an eventual slight decomposition due to the melting cannot commit the measurements.

Several samples of $Fe(NO)_2Br$ were prepared as described above and measured magnetically. Rather large positive and completely irreproducible susceptibilities were found. Assuming that the crushing of the crystals might cause some decomposition, we finally filled the sublimate into the Gouy-tube without any crushing at all. Of course the packing became highly imperfect in this way, but still we might obtain some qualitative inform-

ation about the susceptibility. The glass-tube with the crystals was, however, still attracted by the magnetic field, and the attraction slightly increased with time. This clearly shows, that the substance is steadily decomposed even in the sealed-off tube. We therefore gave up further investigations of the magnetic properties of $Fe(NO)_2Br$.

REFERENCES

1. Hieber, W. and Marin, R. *Z. anorg. allgem. Chem.* **240** (1939) 241.
2. Hieber, W. and Nast, R. *Z. anorg. allgem. Chem.* **244** (1940) 23.
3. Seel, F. *Z. anorg. allgem. Chem.* **249** (1942) 308.
4. Asmussen, R. W. and Soling, H. *Acta Chem. Scand.* **8** (1954) 558, 563.

Received July 1, 1957.

ACTA CHEMICA SCANDINAVICA 11 (1957) 1541—1549

Fractionation of Polymers by Liquid-Liquid Distribution

I. Theory

KARL ERIK ALMIN

Swedish Forest Products Research Laboratory, Paper Technology Department, Stockholm, Sweden

Equations for the calculation of molecular frequency functions of polymers from counter current experiments are deduced provided that ideal conditions prevail.

The method of fractionating polymers by distribution between two immiscible solvents was first applied by Schulz and Nordt [1]. By shaking a water solution of polyglycol with mixtures of chloroform and benzene of different composition they obtained a number of fractions of different molecular weights. The volume ratio of the two phases was kept very high.

The theory of the process was first treated by Brønsted [2]. On the basis of the assumption that in chemically similar materials the potential energy of the molecule is proportional to its magnitude he deduces the formula

$$k = \exp \frac{P \cdot \varepsilon}{RT} \tag{1}$$

where k = partition coefficient, P = degree of polymerisation and ε is a constant dependent of the composition of the solvent system. By experiments Schulz [3] found that a simple relation exists between the constant ε and the composition of the solvent system. By applying these laws Schulz and Nordt [1] could conclude that the efficiency of separation is improved by increasing the volume ratio of the two phases. The conclusion which was drawn from these investigations is that fractional precipitation can be considered more efficient, as in the latter case the volume ratio of the two phases is much higher than can be attained in practice at distribution between two solvents.

By the use of statistical thermodynamics several equations have been derived to account for the activity of polymer solutions. (For a review see *e.g.*, Ref.[4]). These equations confirm at least qualitatively the results of Schulz and Nordt [1].

As was pointed out by Almin and Steenberg [5] the liquid-liquid distribution method as carried out by Schulz and Nordt suffers from the same weakness as the solution and precipitation methods, as to the calculation of the molecular frequency function from the experimental data. By keeping the composition of the solvent system constant at all steps of the fractionation and compensating for the decreased fractionation effect by a method of multiplication, data can be obtained, making it possible to carry out the calculations in a theoretically correct way.

The scope of this work is to make use of this by distributing polymers between two immiscible solvents according to the Craig counter current method.

FREQUENCY CURVES WITH RESPECT TO PARTTION COEFFICIENT

When a pure substance is distributed between two solvents in a Craig distribution apparatus according to the fundamental procedure [6], the amount of substance present in the pth tube is

$$w(p) = m_0 \cdot \binom{n}{p} \cdot \frac{k^p}{(k+1)^n} \quad (= 0,1,2, \ldots\ldots n) \tag{2}$$

where m_0 is the total amount of substance added to the apparatus and k is the partition coefficient for the substance between the phase to be transferred and the stationary phase, n being the number of transfers. Equal volumes of the two phases are presupposed. If the substance contains molecules of different partition coefficients and the weight frequency function with respect to partition coefficients is $f(k)$, the amount of those molecules which have a partition coefficient in the range between k and $k + \mathrm{d}k$ in the pth tube is

$$\delta w(p) = m_0 \cdot \binom{n}{p} \cdot \frac{k^p}{(k+1)^n} \cdot f(k) \cdot \mathrm{d}k$$

or

$$W_n(p) = \frac{m_0}{w(p)} = \int_0^\infty \binom{n}{p} \cdot \frac{k^p}{(k+1)^n} \cdot f(k) \cdot \mathrm{d}k \tag{3}$$

$W_n(p)$ is the weight fraction of the original substance present in the pth tube.*

The condition precedent for the validity of this formula is that no interaction of molecules of different size occurs and that the partition coefficient is independent of concentration. Of course it is a prerequisite that the presence of the polymer does not cause a change in the composition of the solvents, and that real equilibrium conditions are fulfilled.

As $W(p)$ is known from experiments the integral eqn. (3) can be solved with respect to $f(k)$ according to some approximation method. The author has adopted the following method for the solution of the equation.**

* When confusion is out of question the index n of $W_n(p)$ will be omitted.

** By access of an electronic computor somewhat different treatment of the problem is conceivable.

It is considered that the frequency function $f(k)$ can be expressed as a sum of several functions $\psi_i(k)$:

$$f(k) = \sum_i \psi_i\ (k)$$

The functions ψ_i are chosen so that 1) they are bell shaped and $= 0$ for $k = 0$ and ∞, 2) the integral

$$\int_0^\infty \binom{n}{p} \cdot \frac{k^p}{(k+1)^n} \cdot \psi_i\ (k) \cdot \mathrm{d}k$$

can be expressed by elementary functions. These conditions are fulfilled if, *e.g.*,

$$\psi_i\ (k) = A_i \cdot k^{r_i} \cdot (k+1)^n \cdot \exp(-a_i \cdot k^{s_i}) \tag{4}$$

where r_i, s_i, A_i and a_i are properly chosen numbers. For the sake of simplicity r_i, s_i and a_i ought to be integers and if possible s_i shall be put equal to 1. For the special case $s_i = 1$ one obtains

$$W(p) = \binom{n}{p} \cdot \sum_i A_i \cdot \frac{(p+r_i)!}{a_i^{p+r_i+1}} \tag{5}$$

By trial and error it is posssible to find values of A_i, a_i and r_i to have the calculated and the experimentally determined $W(p)$ values agree. This can be done in a systematic way.

The method will be explained by a fictive experiment. A polymer is assumed to be defined by the frequency function

$$f(k) = 5.784 \times 10^5 \cdot k^4\ (k+1)^{19} \cdot \exp\ (-27 \cdot k^{\frac{1}{2}}) \tag{6}$$

The corresponding curve is drawn in Fig. 1. If this preparation is distributed in a 20-tube countercurrent distribution apparatus ($n = 19$) one obtains in accordance with eqn. (3)

$$W(p) = 1.157 \times 10^6 \cdot \frac{(2p+9)!}{27^{2p+10}} \tag{7}$$

The $W(p)$ values calculated from this formula are listed in Table 1.

Starting from these values $f(k)$ shall be calculated considering that it can be expressed by a sum of functions of the type

$$A \cdot k(k+1)^{19} \cdot \exp(-ak)$$

From the table can be seen that $W(p)$ has its highest value for $p = 11$. A preparation with a frequency function of the type mentioned has its highest $W(p)$ value for $p = 11$ when $a = 9$. The difference

$$\Delta W(p)' = W(p) - A'_1 \cdot \binom{19}{p} \cdot \frac{(p+1)!}{9^{p+2}} \tag{8}$$

Table 1.

p	$W(p)$ (Eqn. 7)	$\Delta W(p)$ (Eqn. 8)	$\Delta W(p)$ (Eqn. 9)
0	0.0020	19×10^{-4}	-1×10^{-4}
1	0.0058	54	3
2	0.0113	100	5
3	0.0184	153	4
4	0.0274	205	0
5	0.0386	247	−3
6	0.0519	267	−4
7	0.0669	253	−1
8	0.0826	202	2
9	0.0972	124	3
10	0.1083	47	2
11	0.1130	0	0
12	0.1091	3	−1
13	0.0959	48	0
14	0.0751	100	0
15	0.0509	123	−2
16	0.0286	104	−4
17	0.0125	61	−4
18	0.0038	23	−1
19	0.0006	4	0
	$\Sigma = 0.9999$		$\Sigma = -2 \times 10^{-4}$

is calculated assuming such a value of A_1 that the difference = 0 for $p = 11$ (*i.e.* where $W(p)$ is maximum). As can be seen from the table this difference has its highest values for p = 6 and $p = 15$. The new difference

$$\Delta W(p)'' = W(p) - \binom{19}{p} \cdot (p+1)! \cdot \left[\frac{A_1''}{9^{p+2}} + \frac{A_2''}{16^{p+2}} + \frac{A_3''}{5^{p+2}} \right]$$

is calculated assuming such values of the A''-s that $\Delta W(p)'' = 0$ for $p = 6$, 11 and 15. (It shall be borne in mind that the two last terms within the parenthesis have their highest values for $p = 6$ and 15, resp.) When the difference

$$\Delta W(p)''' = W(p) - A_1'' \cdot \binom{19}{p} \cdot \frac{(p+1)!}{9^{p+2}}$$

is now calculated, it is found that its highest values occur when $p = 7$ and 14. This means that the choice of the two last functions was not appropriate. Thus a new attempt is made with functions which give their highest $W(p)$ values for $p = 7$, 11 and 14. This procedure is now repeated until agreement is attained at least in the tubes containing the chief part of the preparation. In this case it is found that this new approach gives good agreement exept for $p = 1$, 2 and 3, but by further subtraction with an expression of the type

$$A_4 \cdot \binom{19}{p} \cdot \frac{(p+1)!}{25^{p+2}}$$

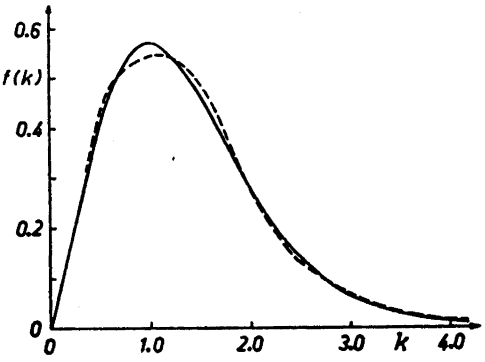


Fig. 1. Comparison between theoretical and calculated frequency curves.
———— Frequency curve according to eqn. 6.
— — — — — Frequency curve according to eqn. 10.

(this expression has its highest value for $p = 2$) good agreement is obtained. In column No. 4 of Table 1 the difference

$$\Delta W(p)'''' = W(p) - \binom{19}{p} \cdot (p+1)! \cdot \left[\frac{4.441 \times 10^{-6}}{6^{p+2}} + \frac{5.934 \times 10^{-3}}{9^{p+2}} + \frac{3.550 \times 10^{-1}}{14^{p+2}} + \frac{1.4 \times 10^{-2}}{25^{p+2}} \right] \quad (9)$$

is calculated. As can be seen, the differences can be regarded as small in comparison to experimental errors in a real experiment. If the amount of original substance had been 1 g, no error exceeds 0.5 mg. These calculations thus lead to the conclusion that the frequency curve can be expressed by

$$f_1(k) = k \cdot (k+1)^{19} \cdot [4.441 \times 10^{-6} \cdot \exp(-6k) + 5.934 + 10^{-3} \cdot \exp(-9k) + 3.550 \times 10^{-1} \cdot \exp(-14k) + 1.4 \times 10^{-2} \cdot \exp(-25k)] \quad (10)$$

The corresponding curve is drawn in Fig. 1. The agreement with the theoretical curve must be regarded as good.

In this connection it seems justified to mention that the moments of the frequency functions can easily be obtained from the data of experiments of this type. According to definition the νth moment about the origin is

$$\mu_\nu = \int_0^\infty k^\nu \cdot f(k) \cdot \mathrm{d}k = \int_0^\infty \frac{k^\nu \cdot (k+1)^n}{(k+1)^n} \cdot f(k) \cdot \mathrm{d}k = \sum_{p=0}^{n} \binom{n}{p} \cdot \int_0^\infty \frac{k^{p+\nu}}{(k+1)^n} \cdot f(k) \cdot \mathrm{d}k =$$

$$= \sum_{p=0}^{n} \frac{\binom{n}{p}}{\binom{n}{p+\nu}} \cdot W(p+\nu) = \mu_\nu' + \Delta\mu_\nu \quad (11)$$

where $$\mu_\nu' = \sum_{p=0}^{n-\nu} \frac{\binom{n}{p}}{\binom{n}{p+\nu}} \cdot W(p+\nu) \quad (12\,a)$$

$$\text{and} \quad \Delta\mu_\nu = \sum_{p=n-\nu+1}^{n} \frac{\binom{n}{p}}{\binom{n}{p+\nu}} \cdot W(p+\nu) \qquad (12\,b)$$

Although μ'_ν can be calculated from the experimental $W(p)$ values, $\Delta\mu_\nu$ cannot because all terms in this expression are of the indefinite form 0/0. Thus the calculation of the moments cannot be done completely and it can only be regarded as justified if $\Delta\mu_\nu$ is a small number in comparison to μ'_ν. In any case calculation of moments of high order cannot be done with any accuracy. In Table 2 the first three moments are calculated for the curve given in eqn. (6) and compared to those calculated from the $W(p)$ values given in Table 1. As can be seen from the table the accuracy diminishes as the order of the moment increases.

Table 2.

Order of moment	Theoretical moment	Moment calc. from eqn. 12 a
1	1.366	1.364
2	2.450	2.40_9
3	5.369	4.90_5

The fitting of the frequency curve by the method of moments as for instance developed by Pearsom (see, *e.g.*, Ref.[7]) can of course be done, but this method presupposes a frequency function of only one mode. If the frequency curve contains more than one peak this method will fail. With the first one given, however, more details can be detected.

As far as the author knows no mathematical analytical method exists to determine (calculate) the accuracy of the frequency curve. It is quite evident that a very sharp peak in the curve cannot be detected only by mathematical means. This can only be done by changing the experimental conditions so that the resolving power of the distribution apparatus is increased, *e.g.* by increasing the number of fractions or choosing another solvent system.

The result is no doubt dependent on the mathematical method chosen for the calculations. In the method adopted by the author it is considered that the frequency function can be represented by a sum of a limited number of functions of a special type. It is of course not certain that this approach is correct, but as long as it is not unreasonable it must be considered justified. The only possibility to check the results is to vary the experimental conditions and to test whether the same result is obtained when the resulting frequency curve in respect to distribution coefficient is converted into a molecular frequency curve. Negative $\Delta W(p)$ values should of course be avoided at early stages of the calculations.

RELATION BETWEEN MOLECULAR WEIGHT AND PARTITION COEFFICIENT

When the frequency function with respect to the partition coefficient in a certain solvent system is known, it remains to determine the relation between the partition coefficient and the molecular weight before the molecular frequency function can be determined. The fractionation method suggested in this paper is not selective and thus the procedure will depend upon the way and method of measuring molecular weights. As was pointed out by Almin and Steenberg [5] the average molecular weight $\overline{M(p)}$ in fraction No. p can be written

$$\overline{M(p)}^{\alpha} = \frac{1}{W(p)} \cdot \binom{n}{p} \cdot \int_0^{\infty} \frac{k^p}{(k+1)^n} \cdot f(k) \cdot M^{\alpha} \cdot \mathrm{d}k \tag{13}$$

where M is the molecular weight of molecules with the partition coefficient k, and α is a parameter fixed by the conditions of the method of molecular weight determination. This formula is valid in cases when number averages ($\alpha = -1$), weight averages ($\alpha = 1$) or viscosity averages ($0.5 < \alpha < 1$) of the molecular weight are measured.

Eqn. (13) can be solved with respect to $f(k) \cdot M^{\alpha}$ according to a method quite analogous to the one suggested for eqn. (3). By dividing the solution of eqn. (13) with the solution of eqn. (3) one obtains M^{α} as a function of k. By applying such a method serious errors can be expected because errors from the two approximate solutions are introduced. For this reason other methods to calculate M^{α} as a function of k ought to be tried. By introducing a model for the relation between M^{α} and k as below a solution is obtained which is independent of the solution of eqn. (3):

$$M^{\alpha} = B \cdot \ln\, k + \sum_i C_i \cdot k^i \tag{14}$$

where it is considered that i can only adopt small negative or positive values (including 0).

From eqns. (13) and (14) one obtains

$$S(p) \cdot \overline{M(p)}^{\alpha} = B \cdot \int_0^{\infty} \frac{k^p}{(k+1)^n} \cdot f(k) \cdot \ln k \cdot \mathrm{d}k + \sum_i C_i \int_0^{\infty} \frac{k^{p+i}}{(k+1)^n} \cdot f(k) \cdot \mathrm{d}k$$

$$= B \cdot \frac{\mathrm{d}S(p)}{\mathrm{d}p} + \sum_i C_i \cdot S(p+i) \tag{15}$$

where

$$S(p) = \frac{W_p}{\binom{n}{p}} \tag{16}$$

By dividing with $S(p)$ one obtains

$$\overline{M(p)}^{\alpha} = B \cdot \frac{\mathrm{d}\ln S(p)}{\mathrm{d}p} + \sum_i C_i \cdot \frac{S(p+\mathrm{i})}{S(p)} \tag{17}$$

As $\overline{M(p)}$ and $S(p)$ are known from the experiments and $\frac{\mathrm{d}\ln S(p)}{\mathrm{d}p}$ can be obtain-

ed graphically it is possible to calculate B and C_i for instance by the method of least squares. If a good correlation between observed and calculated values is not obtained when only a few terms of the sigma of eqn. (17) are made use of, this method is not to be recommended. Then another model must be tried or the first mentioned method must be used. The expression in eqn. (14) is, however, not chosen only because it gives a rather simple solution (eqn. 17), but also for theoretical reasons. According to the Brønsted formula (eqn. 1) ln k is proportional to the degree of polymerisation. The real relation between these quantities is certainly more complex and therefore the author has chosen a modified approach. The formula can be considered especially convenient in cases when $\alpha = 1$ or close to one, as for instance in viscometric measurements.

The range of validity of the relation obtained between the molecular weight and the partition coefficient is difficult to estimate from one experiment only. Especially at high and low molecular weights appreciable errors can be expected. By investigating several samples of different mean molecular weights of the same polymer at the same experimental conditions it would be possible to obtain a curve which covers an appreciable molecular weight range.

MOLECULAR FREQUENCY CURVES

The final problem is to convert the frequency functions of partition coefficient to molecular weight frequency functions. This can be achieved by applying the formula

$$g(M) = f(k) \cdot \frac{\mathrm{d}k}{\mathrm{d}M} \tag{18}$$

where $g(M)$ is the molecular weight frequency function. The derivative $\frac{\mathrm{d}k}{\mathrm{d}M}$ is obtained from the relation between partition coefficient and the molecular weight by graphical or other means.

DISCUSSION

The mathematical methods for treating the experimental data from counter current fractionations are based on the assumptions that the quantities involved can be represented by models. These models are chosen so that a rather simple numerical treatment is possible.

The basic assumptions which are made are discussed by Almin and Steenberg [5]. It is, however, very probable that the laws which are used to deduce eqns. (3) and (13) do not hold in practice. The relation between the molecular weight and the partition coefficient affords a special problem. The experimental conditions ought to be chosen so that this relation is a monotonous one. These problems will be discussed in the experimental parts of this series.

REFERENCES

1. Schulz, G. V. and Nordt, E. *J. prakt. Chem.* **155** (1940) 115.
2. Brønsted, J. N. *Z. physik. Chem., Bodenstein-Festband* **1931** 257.
3. Schulz, G. V. *Z. physik. Chem.* **A 179** (1937) 321.
4. Stuart, H. A. *Die Physik der Hochpolymeren*, Springer-Verlag, Berlin 1953.
5. Almin, K. E. and Steenberg, B. *Acta Chem. Scand.* **11** (1957) 936.
6. Craig, L. C. and Craig, D. in Weissberger, A. *Technique of Organic Chemistry*, Vol. III, Interscience Publ. New York 1956.
7. Kendall, M. G. *The Advanced Theory of Statistics*, Griffin & Comp. London 1943.

Received June 29, 1957.

ACTA CHEMICA SCANDINAVICA 11 (1957) 1550—1556

Some $\Delta\varepsilon$-Curves for Dissociations of Tropolones and Salts of Organic Bases

GUNHILD AULIN-ERDTMAN and LAILA HEGBOM

Cellulosaindustriens Centrallaboratorium and Organisk-Kemiska Institutionen, Kungl. Tekniska Högskolan, Stockholm, Sweden

In order to explore the applicability of the $\Delta\varepsilon$-method to ionisable compounds other than phenols, the $\Delta\varepsilon$-curves have been determined for a series of simple tropolones, arylamines and heterocyclic bases. It is shown that the $\Delta\varepsilon$-method should be useful for the characterisation and estimation of these types of compounds.

The analytical value of the changes in light absorption which take place when chromophores undergo certain reactions, such as substitutions, hydrogenation, ionisation and complex formation, has been pointed out earlier[1]. The changes on ionisation have been used in the so-called "$\Delta\varepsilon$-method" worked out in these laboratories primarily for the study of the nature and frequency of the phenolic groups in lignin. With phenols this reaction causes a characteristic, not too small absorption change in the easily accessible ultra-violet region. To our knowledge, ionisation $\Delta\varepsilon$-studies have so far been carried out mainly with phenolic materials (lignin, tanning agents *etc.*), and a reasonable number of model $\Delta\varepsilon$-curves relating to the ionisation of phenols is now available in the literature (*cf.* Refs.[2,3] and references given therein). However, some further types of ionisation have also been studied. The work by Goldschmid referred to in Ref.[3] includes $\Delta\varepsilon$-studies of the addition of a proton to CO-groups[4]. Investigations of a similar type have also been reported for some heterocyclic bases[5].

An examination of other types of ionisable compounds was of interest as part of an investigation into the applicability of the $\Delta\varepsilon$-method to other classes of natural and technical products. The present study includes some tropolones and a series of simple aromatic and heterocyclic bases.

MATERIALS, SOLVENTS AND MEASUREMENTS

The compounds investigated are listed in Table 1 together with brief data on their purification and properties.

Table 1.

Compound	Solvent	UV absorption maxima mμ	logε	mμ	logε	*Cf.* Ref.
I. Tropolone, prepd. from Ba salt *, distd. *in vacuo*, recryst. from heptane, m.p. 49—49.5°	95 % EtOH, 0.01 N in HCl	228	4.37	319	3.86	
		351	3.77	366	3.70	6
	95 % EtOH, N in KOH	240	4.37	263	3.85	
		334	4.10	398	4.07	
II. α-Thujaplicin (α-*iso*propyltropolone), distd. *in vacuo*, recryst. from heptane, m.p. 33—34°	95 % EtOH, 0.01 N in HCl	239—40	4.46	318	3.82	
		354—5	3.78	367	3.76	7
	95 % EtOH, N in KOH	247	4.39	336—7	4.10	
		402—3	4.10			
III. β-Thujaplicin (β-*iso*propyltropolone, hinokitiol), distd. *in vacuo*, recryst. from heptane, m.p. 50.5—51°	95 % EtOH, 0.01 N in HCl	239—40	4.49	320—1	3.82	
		349	3.81			7
	95 % EtOH, N in KOH	244—5	4.44	266	3.96	
		334—5	4.09	393	4.09	
IV. γ-Thujaplicin (γ-*iso*propyltropolone), recryst. from heptane, m.p. 79—79.5°	95 % EtOH, 0.01 N in HCl	233	4.40	321—2	3.97	7
	95 % EtOH, N in KOH	242—3	4.40	336	4.20	
		403	4.05			
V. Pyridine, anal. grade (contg. 0.07 % water)	0.1 N H_2SO_4	255	3.72			8
	pH 10 carbonate buffer soln.	251	3.39	256	3.44	
		262	3.27			9
VI. Quinoline, purif. *via* sulphate (m.p. 161.5—162.5°), distd., n_D = 1.6251	0.1 N H_2SO_4	233	4.58	313	3.83	10
	pH 10 carbon. buffer soln.	224—5	4.48	276—7	3.53	
		299	3.50	312	3.50	10
VII. Isoquinoline, purif. *via* sulphate (m.p. 207—209°), distd., n_D = 1.6147, m.p. 25.5—26°	0.1 N H_2SO_4	227	4.65	265—6	3.28	
		273	3.29	331	3.60	11
	pH 10 carbon. buffer soln.	259	3.51	268	3.53	
		277	3.40	306	3.38	
		319	3.48			11
VIII. Aniline, anal. grade (contg. 0.31 % water), n_D = 1.5841.	0.1 N H_2SO_4	248	2.11	254	2.19	
		259—60	2.05			12
	pH 10 carbon. buffer soln.	230	3.90	280	3.13	13
IX. *o*-Toluidine, purif. *via* oxalate (m.p. 160—160.5°), distd. *in vacuo*, n_D = 1.5716	0.1 N H_2SO_4	259	2.40	266	2.29	14
	pH 10 carbon. buffer soln.	230	3.89	280	3.25	
X. *m*-Toluidine, anal. grade (contg. 0.16 % water) n_D = 1.5669	0.1 N H_2SO_4	260—1	2.47	268	2.39	14
	pH 10 carbon. buffer soln.	232—3	3.88	281—2	3.16	
XI. *p*-Toluidine, purif. *via* oxalate (m.p. 168—169°), recryst. from water and dil. EtOH, m.p. 43—44°	0.1 N H_2SO_4	260	2.35	268	2.24	14, 15
	pH 10 carbon. buffer soln.	233	3.88	286	3.12	
XII. 1-Naphthylamine, recryst. from dil. EtOH, m.p. 48—49°	0.1 N HCl	268	3.74	277	3.80	
		285	3.62			16
	pH 10 carbon. buffer soln.	236—7	4.36	304	3.70	16
XIII. 2-Napththylamine, recryst. from water and dil. EtOH, m.p. 110—110.5°	0.1 N HCl	220	4.93	266—7	3.65	
		273—4	3.68			16
	pH 10 carbon. buffer soln.	234	4.73	269	3.68	
		278	3.75	289	3.61	
		334—5	3.23			16

* Compound supplied by Dr. H. Fernholz.

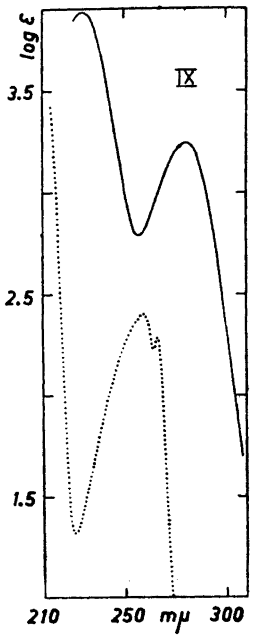


Fig. 1. Absorption curves for *o*-toluidine in 0.1 N H_2SO_4 (·····) and in pH 10 carbonate buffer solution (————).

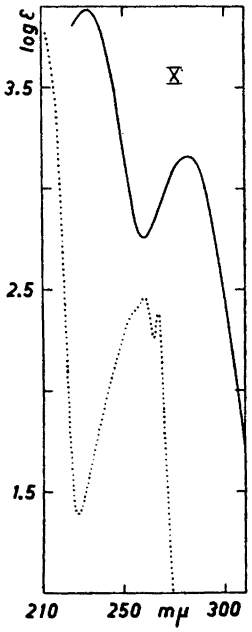


Fig. 2. Absorption curves for *m*-toluidine in 0.1 N H_2SO_4 (·····) and in pH 10 carbonate buffer solution (————).

The ultra-violet absorption curves were determined for solutions of these substances in the acidic and alkaline solvents listed in the same table. The solvents were chosen so as to give a complete set of curves for the tropolones and the tropolonate ions in ethanol and for the bases and their ions in water.

A Beckman Model DU spectrophotometer with 1 cm calibrated silica cells was used for the measurements. The concentrations of the solutes were varied so as to keep $\log(I_0/I)$ within the limits of 0.1 and 1.5. In critical regions readings were made at 1—2 mμ intervals, otherwise at every 5 mμ.

The difference curves were calculated by subtracting the ε-values for the acidic solutions from the corresponding ε-values for the alkaline solutions.

RESULTS AND DISCUSSION

The absorption maxima found are listed in Table 1. The ultra-violet absorption curves for these compounds have already been studied in various solvents and reported in the literature. It is true that earlier data in many cases show great discrepancies, but for all compounds it was possible to find curves or figures in the literature (references in Table 1) which agree well with the results reported here.

The absorption curves are not reproduced except for the toluidines (Figs. 1—3) for which the literature does not give complete information.

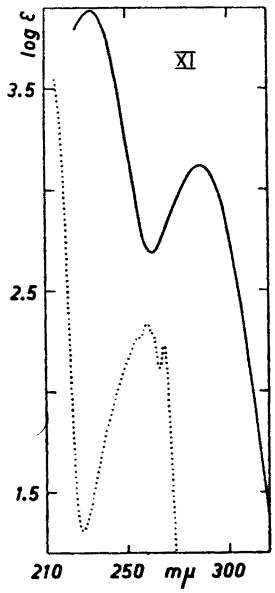


Fig. 3. Absorption curves for *p*-toluidine in 0.1 N H_2SO_4 (·····) and in pH 10 carbonate buffer solution (————).

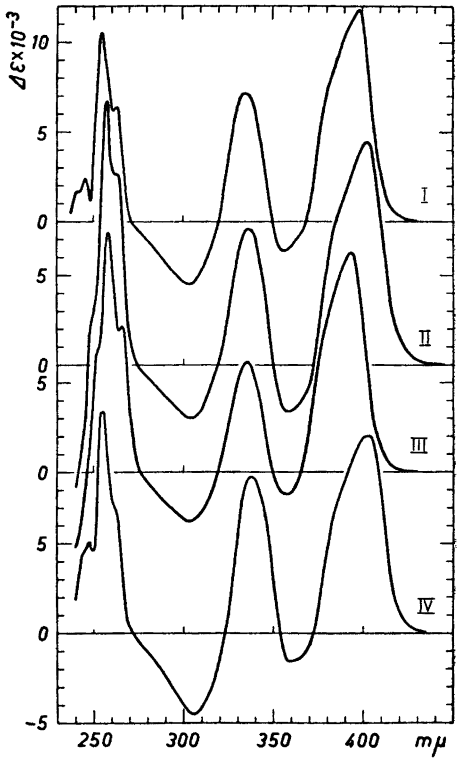


Fig. 4. $\Delta\varepsilon$-curves for ionisation of tropolone (I), *α*-thujaplicine (II), *β*-thujaplicine (III) and *γ*-thujaplicine (IV) in ethanol.

The ionisation difference curves for tropolone and its C-*iso*propyl derivatives are given in Fig. 4. Because of their similar electronic structures these compounds give closely related $\Delta\varepsilon$-curves. The curves are quite characteristic and distinct from those of any phenols so far investigated. This type of $\Delta\varepsilon$-curve is, of course, by no means characteristic of all tropolones. Changes such as the introduction of additional hydroxyl groups in the ring or ring-conjugated double bonds give rise to marked changes in the electronic structure and, hence, in the $\Delta\varepsilon$-curve.

Fig. 5 gives the $\Delta\varepsilon$-curves for the conversion of the pyridinium, quinolinium and *iso*quinolinium ions into the corresponding bases. Like most carboxylic acids these heterocyclic ammonium ions show a hypsochromic shift, hence a long-wave $\Delta\varepsilon$-minimum on loss of a proton (*cf.* Ref.[3]).

Due to the spectrochemically similar electronic structures of the arylamines and the phenolate ions and of the arylammonium ions and the phenols, the conversion of anilinium ion and the toluidinium ions into the bases gives $\Delta\varepsilon$-curves (Fig. 6) which are similar to the ionisation $\Delta\varepsilon$-curves for the corre-

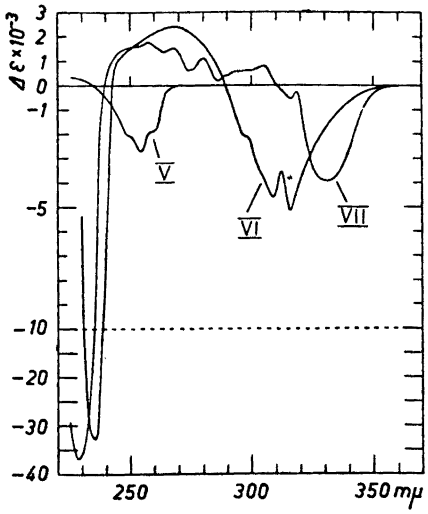


Fig. 5. $\Delta\varepsilon$-curves for loss of a proton from the pyridinium (V), quinolinium (VI) and *iso*quinolinium (VII) ions in aqueous solutions.

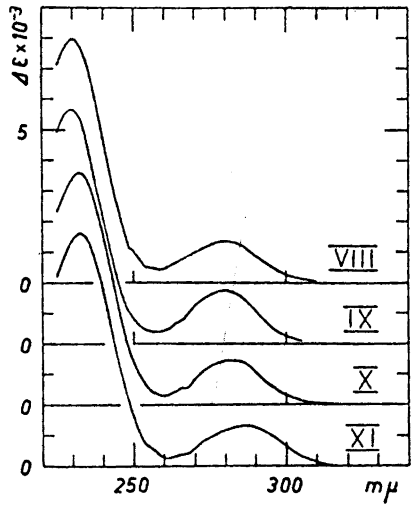


Fig. 6. $\Delta\varepsilon$-curves for loss of a proton from the anilinium (VIII), *o*-toluidinium (IX), *m*-toluidinium (X) and *p*-toluidinium (XI) ions in aqueous solutions.

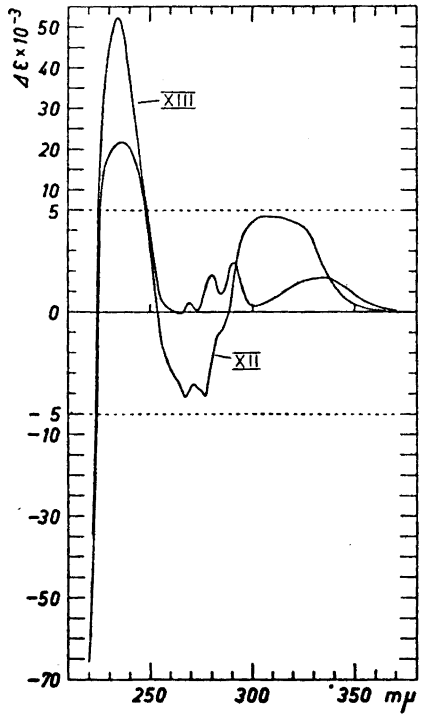


Fig. 7. $\Delta\varepsilon$-curves for loss of a proton from the α-naphthylammonium (XII) and β-naphthylammonium (XIII) ions in aqueous solutions.

Table 2. Ionisation of tropolones (95 % EtOH, 0.01 N in HCl → 95 % EtOH, N in KOH)

Compound	$\Delta\varepsilon$-maxima				$\Delta\varepsilon$-minima			
	mμ	$\Delta\varepsilon$	mμ	$\Delta\varepsilon$	mμ	$\Delta\varepsilon$	mμ	$\Delta\varepsilon$
I	241	1 700	245	2 400	242	1 700	248	1 200
	254	10 600	263	6 400	261	6 200	303–4	−3 500
	334–5	7 200	398	11 800	356	−1 600		
II	257	14 800	263	10 700	262	10 700	304–5	−2 900
	336	7 600	402	12 500	358	−2 600		
III	258	13 400	266	8 200	264	7 900	304	−2 700
	335	6 200	393	12 300	357	−1 300		
IV	247–8	5 100	255	12 400	250	4 600	306	−4 500
	337–8	8 700	403	11 200	359	−1 600		

sponding phenols [3]. The similarity in $\Delta\varepsilon$-curves between the naphthylammonium ions (Fig. 7) and the corresponding naphthols [3] is, however, less pronounced.

The maxima and minima of the difference curves just discussed are given in Tables 2 and 3. The accuracies of these $\Delta\varepsilon$-values were estimated approximately, assuming [2] $e_\varepsilon/\varepsilon = 0.02$. The $\Delta\varepsilon$-values were rounded off accordingly, so that errors will generally occur only in the last figure.

It follows from the results presented that all the simple tropolones and bases investigated give characteristic $\Delta\varepsilon$-curves. There is considerable similarity within groups of closely related compounds. The differences between different types of compounds are also marked. All of the substances, except perhaps pyridine, give reasonably high, sometimes very high, $\Delta\varepsilon$-values above 230 mμ. It should, therefore, be possible to characterise and estimate the above compounds by means of the $\Delta\varepsilon$-method.

Table 3. Conversion of amine salts into amines (0.1 N H_2SO_4→pH 10 carbonate buffer solution)

Compound	$\Delta\varepsilon$-maxima				$\Delta\varepsilon$-minima			
	mμ	$\Delta\varepsilon$	mμ	$\Delta\varepsilon$	mμ	$\Delta\varepsilon$	mμ	$\Delta\varepsilon$
V	250	−2 100			249	−2 100	254	−2 700
VI	268–9	2 410	312	−3 600	236	−32 900	309	−4 600
					316	−5 200		
VII	257	1 770	269	1 500	228–9	−37 000	264	1 300
	280	1 110	305	800	274	590	286	200
	318	−300			316	−600	331–2	−3 940
VIII	230	8 000	280	1 350	259	440		
IX	230	7 700	280	1 770	257	370		
X	232–3	7 600	266	530	260–1	280	267	530
	281–2	1 440						
XI	233	7 600	286–7	1 320	261	280		
XII	237	21 700	271	−3 500	267	−4 100	277	−4 100
	305–6	4 700						
XIII	234	52 000	269	400	264	−100	273	100
	279–80	1 800	291	2 400	285	900	301	310
	334–5	1 680						

The $\Delta\varepsilon$-method is particularly useful for the analysis of difficultly separable mixtures and for the structural elucidation of complex molecules containing two or more separate chromophores. It might for example be used to locate hydroxyl groups in the heterocyclic or in the phenyl moiety in alkaloids of the benzyl-*iso*quinoline and angostura types. There are also obvious applications in the fields of purines, pterines, nucleic acids[5] and proteins. In addition to the $\Delta\varepsilon$-curve the pH region at which the absorption change occurs is also indicative of the ionisable chromophore. One of the chief advantages of the method is that only small amounts of material are needed.

The authors would like to acknowledge the financial assistance of *Fonden för skoglig forskning* and *Statens Tekniska Forskningsråd.*

REFERENCES

1. Aulin-Erdtman, G. *Chemistry & Industry* **1955** 581.
2. Aulin-Erdtman, G. *Svensk Papperstidn.* **56** (1953) 287.
3. Aulin-Erdtman, G. and Hegbom, L. *Svensk Papperstidn.* **60** (1957) 671.
4. Goldschmid, O. *J. Am. Chem. Soc.* **75** (1953) 3780.
5. Hakala, M. T. and Schwert, G. W. *Biochem. et Biophys. Acta* **16** (1955) 489.
6. Cook, J. W., Gibb, A. R., Raphael, R. A. and Somerville, A. R. *J. Chem. Soc.* **1951** 503.
7. Erdtman, H. and Gripenberg, J. *Acta Chem. Scand.* **2** (1948) 625.
8. Lyons, L. E. *J. Proc. Roy. Soc. N. S. Wales* **83** (1949) 75.
9. Brown, H. C. and Mihm, X. R. *J. Am. Chem. Soc.* **77** (1955) 1723.
10. Ewing, G. W. and Steck, E. A. *J. Am. Chem. Soc.* **68** (1946) 2181.
11. Osborn, A. R. and Schofield, K. *J. Chem. Soc.* **1956** 4191.
12. Flexser, L. A., Hammett, L. P. and Dingwall, A. *J. Am. Chem. Soc.* **57** (1935) 2103.
13. Kumler, W. D. and Strait, L. A. *J. Am. Chem. Soc.* **65** (1943) 2349.
14. Marchlewski, L. and Pizlo, J. *Bull. intern. acad. polon., Classe sci. math. nat.* **1934** A 22.
15. Ramart-Lucas, P. *Bull. soc. chim. France* [5] **3** (1936) 723.
16. Boaz, H. and Rollefson, G. K. *J. Am. Chem. Soc.* **72** (1950) 3435.

Received July 3, 1957.

ACTA CHEMICA SCANDINAVICA 11 (1957) 1557—1564

The Oxidation of Glycosides

V. Oxidation of Methyl 6-*O*-Trityl-α-D-glucopyranoside and Methyl 6-*O*-Trityl-β-D-glucopyranoside with Chromium Trioxide *

OLOF THEANDER

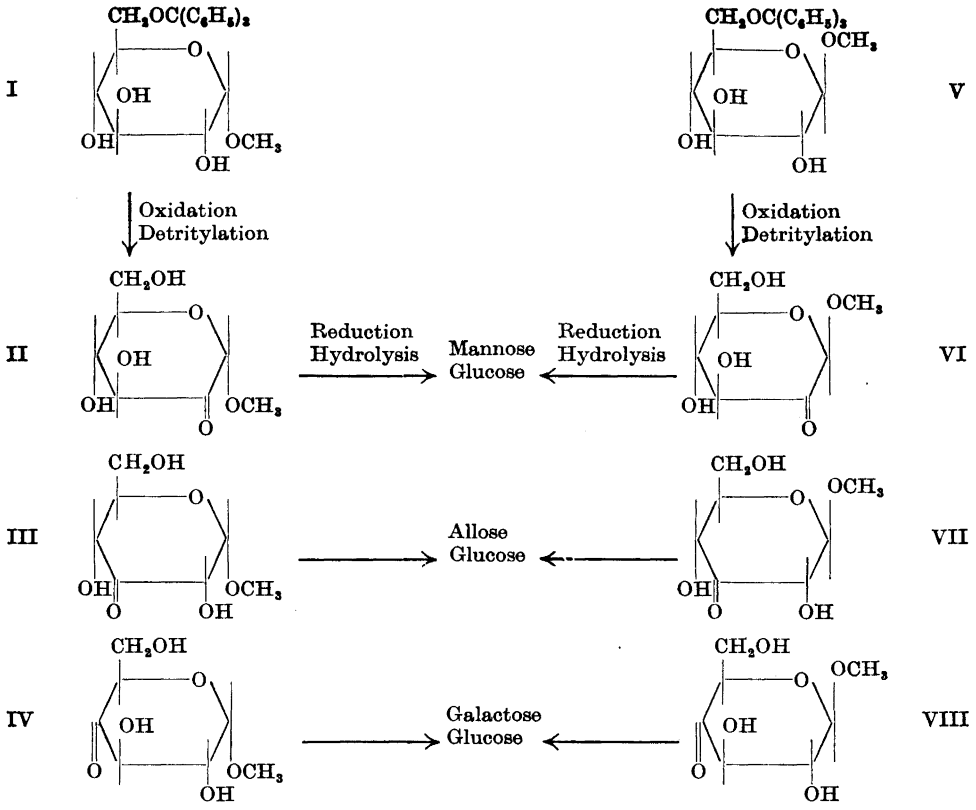
Organisk-kemiska Institutionen, Kungl. Tekniska Högskolan, Stockholm and Träkemiska avdelningen, Svenska Träforskningsinstitutet, Stockholm, Sweden

Methyl 6-*O*-trityl-α-D-glucopyranoside and methyl 6-*O*-trityl-β-D-glucopyranoside have been oxidised with chromium trioxide in acetone. After detritylation of the resulting mixture, the 2-oxo-, 3-oxo and 4-oxo-methylglucosides in both the α- and the β-series were isolated. The position of the oxo-groups were shown by characterising the sugars formed after hydrolysis of the reduced oxoglucosides.

In part IV [1] the isolation of methyl β-D-3-oxoglucopyranoside and methyl β-D-6-oxoglucopyranoside from the reaction mixture after oxidation of methyl β-D-glucopyranoside with dichromate in the presence of oxalic acid was described. These two oxocompounds were isolated only in low yield with the aldehyde predominating. In order to improve the yields of the 3-oxo-glucoside and the other potential oxidation products, the primary hydroxyl at $C_{(6)}$ was now protected by tritylation prior to oxidation (V). The oxidation of methyl 6-*O*-trityl-α-D-glucopyranoside (I) was also investigated.

Chromium trioxide-pyridine [2] was tried as oxidant, but chromium trioxide in acetone was found to give better yields of oxoglucosides. After oxidation (see Experimental) the brown precipitate of chromium oxides was filtered off and the trityl groups were removed by mild hydrolysis. The chromium in the solution was reduced by ethanol at the same time. The water soluble, neutral part of the oxidation mixture, obtained after separation of triphenylcarbinol and other water insoluble products followed by deionizing, was investigated by paper chromatography and was found to contain at least a dozen different components. The mixture was separated by chromatography on a carbon column and by chromatography and electrophoresis on thick filter paper. The yields are given in Table 1 of the methyl β-3-oxoglucoside (VII) and the

* Part. IV. *Acta Chem. Scand.* 8 (1954) 1870.



unoxidised methyl β-glucoside, obtained after carbon column chromatography of the reaction product from the oxidation of V with varying amounts of chromium trioxide.

The yield of VII has a flat maximum of about 4.5 % at 1—2 moles oxidant per mole of sugar; at the same time there is still much unchanged methyl glucoside left. The amount of oxoglucosides is obviously limited by further oxidation of these compounds and perhaps also by side reactions, *e.g.* oxidation of glucose at $C_{(1)}$. In addition to VII which was crystalline and identical to the substance m.p. 129.5-131°, $[\alpha]_D$-62° in water, previously isolated, there were also isolated two other ketoglucosides in the β-series (VI and VIII), and the corresponding compounds in the α-series (II, III and IV). VI was crystalline, m.p. 120-121°, and $[\alpha]_D$-47° in water. VIII and the last three were amorphous, but chromatographically and electrophoretically pure. The specific rotation of III was $[\alpha]_D$ +84° in water. The structure of the oxoglucosides was proved by characterising the sugars obtained after reduction with Raney nickel[3] and hydrolysis of the glucoside formed (compare the scheme above). Each sugar gave glucose and one of the sugars mannose, allose or galactose. Constants and details of the separation are given in Table 2.

Table 1. Oxidation of methyl 6-*O*-trityl-β-D-glucopyranoside with chromium trioxide in acetone (The yields are given as a percentage of amount of starting material calculated as methyl β-glucoside

Moles chromium trioxide per mole of trityl sugar	Water soluble, neutral products	Methyl glucoside	Methyl 3-oxo-glucoside
1.0	64	46	4.0
1.5	53	31	4.4
1.5	57	33	4.9
4.0	18	9	3.2

The amounts of 3-oxoglucosides formed were much higher than those of the 2- and 4-oxoglucosides. This is obvious also from the direct paper chromatogram of the hydrolysed oxidation mixture, before the separation procedure. On the other hand it was found in preliminary experiments that the 2-oxo and 4-oxoglucosides are more labile than the corresponding 3-oxo-compound at a pH near the neutral point and give epimerisation and decomposition products. As they emerge from the carbon column together with unchanged methyl glucoside their separation is more complicated than that of 3-oxoglucoside, which is obtained directly from the carbon column almost pure, crystallises readily (in the β-series) and is less labile.

The differences in the R_F values and the relative rates of the electrophoretic migration in hydrogen sulphite buffer between the various oxoglucosides is remarkable and much more marked than for, *e.g.*, hexoses. All oxoglucosides gave strong reducing reactions with the silver nitrate-sodium ethoxide reagent and a particularly sensitive and characteristic colour reaction was given by the resorcinol-hydrochloric acid reagent. In addition to unchanged methyl glucoside and mono-ketoglucosides there were many other compounds present in small amounts, amongst which were: (in the order of emergence from the carbon column) salts, traces of arabinose, glucose (about 0.1 %), methyl 6-oxoglucoside (isolated in the β-series only), a group of substances probably condensation products, with low R_F values and finally products with high R_F values, which might be dioxo compounds, emerging from the column at about 10 % ethanol. One or more of the latter group gave a strong red-violet colour reaction with the resorcinol-hydrochloric acid reagent and one gave a strong yellow colour with anisidine hydrogen chloride. A small amount (0.3 %) of the last mentioned compound was isolated both in the α-series and β-series and after reduction and subsequent hydrolysis gave spots corresponding to glucose, galactose and also arabinose in smaller amount on paper chromatograms. They gave positive Schiff reactions, consumed hypoiodite [5] (corresponding to a purity of about 70 %), and the electrophoretic migration in hydrogen sulphite had the magnitude expected for a dioxo compound. On the paper chromatograms they gave one dominating spot with a high R_F value and a minor one with low R_F value with trailing between, probably explained by a slow equilibrium between different forms (behaving similarly to methyl-β-6-

Table 2. Oxo-glucosides; preparation and characteristics.
Oxidant per mole = 1.5. The yields are calculated as percentage of the amount of glucoside before oxidation. Data of the carbon column chromatography and the solvents and buffers used by the paper chromatography and electrophoresis are given in Experimental. f. = fluorescence; a. = absorption.

	Methyl α-D-oxoglucopyranosides			Methyl α-D-glucopyranoside
	2-oxo	3-oxo	4-oxo	
Yield (%)	0.3	2.0	0.4	31
Percentage of ethanol in the eluant, when the substance emerged from the carbon column	3.8	6.9	4.9	4.0
Paper chromatography $R_{Glucose}$ values				
Solvent A	1.78	3.38	2.47	2.63
Solvent B	1.42	2.05	1.61	1.64
Paper electrophoresis M_V values, buffer D (50°)	0.93	0.07	0.75	0
Colour reactions on paper chromatograms (the data in brackets refer to the colour in UV-light):				
Anisidine hydrogen chloride	yellow (brownish yellow a.)	yellow (brownish yellow a.)	yellow (brownish yellow a.)	
Resorcinol-hydrochloric acid	brick red (red-brown a.)	orange (orange f.)	brick red (red-brown a.)	

oxoglucoside [1]). These facts might indicate the presence of methyl-4.6-dioxoglucosides in the α- and β-series, respectively.

Only 0.5 % of the material was soluble in water directly after the oxidation and this gave approximately the same chromatographic picture as the main mixture obtained after hydrolysis, (*i.e.* methyl glucoside and methyl 3-oxoglucoside predominated) showing that the protecting trityl group is hydrolysed to a very small extent during the oxidation. In spite of that the 6-oxoglucoside and a possible dioxo compound containing an aldehyde-group were formed (about 0.7 % isolated altogether), which might indicate tritylation on secondary hydroxyls to some extent leaving the primary hydroxyl group free.

An interesting observation was made on the rate of detritylation in a case where the strength of the acid for the hydrolysis following the oxidation of V was unintentionally lower than usual. Methyl β-glucoside and VII were isolated by carbon column chromatography from this "weak" hydrolysate and from the hydrolysate obtained after further hydrolysis of the water insoluble material with the usual strength of acid. The total amount of methyl

Table 2. (continued)

	Methyl β-D-oxoglucopyranosides				Methyl β-D-glucopyranoside
	2-oxo	3-oxo	4-oxo	6-oxo	
Yield (%)	0.5	4.7	0.4	0.4	32
Percentage of ethanol in the eluant, when the substance emerged from the carbon column	3.0	6.6	4.6	5.3	3.4
Paper chromatography $R_{Glucose}$ values					
Solvent A	1.54	3.69	2.21	1.10	2.44
Solvent B	1.19	1.87	1.41	0.87 2.20	1.55
Paper electrophoresis M_V values, buffer D (50°)	0.79	0.56	0.81	1.25	0
Colour reactions on paper chromatograms (the data in brackets refer to the colour in UV-light):					
Anisidine hydrogen chloride	yellow (brownish yellow a.)	yellow (brownish) yellow a.)	yellow (brownish yellow a.)	reddish brown (grey yellow a.)	
Resorcinol-hydrochloric acid	brick red (red brown a.)	orange (orange f.)	brick red (red. brown a.)	weak pink (reddish a.)	

β-glucoside was distributed 65 to 35 % between the "weak" and "normal" hydrolysates, respectively, but the corresponding values for the oxoglucoside were 10 to 90 %, indicating that removal of the trityl group from the latter is more difficult.

EXPERIMENTAL

Melting points corrected. All evaporations were made under reduced pressure and at a bath temperature under 40°, unless freeze-drying was used. Whatman 1 filter papers were used for paper chromatography and electrophoresis except for the preparative separations, which were made on Whatman 3 MM filter papers, previously washed thoroughly with water.

Solvents and buffers used:

A. Ethyl acetate-acetic acid-water, 3 : 1 : 3 (the upper phase).
B. Butanol-ethanol-water, 10 : 3 : 5.
C. Butanol-pyridine-water, 3 : 1 : 1.5.
D. Hydrogen sulphite buffer [4] pH 4.7, 0.1 M. (The electrophoresis was run at 50° if not otherwise stated.)
E. Borate buffer [6] pH 10.0, 0.1 M.

Oxidation of methyl 6-*O*-trityl-β-D-glucopyranoside and fractionation of the product

Methyl 6-*O*-trityl-β-D-glucopyranoside (V)[7], dried in a vacuum over P_2O_5 at 70° (65.0 g) was dissolved in acetone (800 ml), which had been purified by refluxing in the presence of potassium permanganate, drying over potassium carbonate and distilling. A solution of chromium trioxide (22.5 g), corresponding to 1.5 moles of oxidant per mole of sugar, in purified acetone (800 ml), at about 5°, was poured in a slow stream with agitation into the sugar solution which was kept in an ice water bath. This procedure took about 20 min and the temperature was kept below 15°. As has been previously observed[8], it is important to add the chromium trioxide to the solvent in small portions with agitation; it then dissolves readily to give a reddish brown solution. If the two chemicals are mixed in the reverse order, *i.e.* acetone to chromium trioxide it usually inflames!

The oxidation was carried out by refluxing the mixture for 30 min (leaving the mixture at room temperature for a day gave almost the same result). During the oxidation a dark brown precipitate formed. The solution was cooled and filtered and the precipitate was washed with acetone, refluxed with fresh acetone (400 ml) for 10 min and again filtered and washed. This procedure was repeated three times. After the last treatment the amount of extractable material was negligible. The brown chromium oxides, probably hydrated, were heated to about 300—400°, giving green Cr_2O_3 (77 % of the theoretical amount). The combined filtrates and washings were evaporated to a dark brown clear solution (adjusted to 540 ml with acetone), which was mixed with 6 N ethanolic hydrogen chloride (60 ml). The acid treatment was performed at 25° for 30 min. The colour turned to green and there was a typical odour of acetaldehyde, indicating a reduction of chromium in the solution. Silver carbonate was added with agitation and cooling (the temperature kept below +10°) until a drop of the solution showed pH 5 when put on a moist pH paper. The silver precipitate was filtered off and washed first with acetone and then with water. The aqueous acetone solution was evaporated to a small volume and the crops of triphenyl carbinol separating during this process were removed (82 % of the theoretical amount, m.p. 159—161°). The concentrated aqueous solution was extracted with chloroform several times and then passed through columns of the ion exchange resins Amberlite IR-120 (H^+) and IR-4B (free base). The solution, which had a pH about 4.5 was evaporated to a thick, light green-yellow syrup (15.9 g). To make sure that the detritylation was complete, the concentrated chloroform extract (3.3 g), was given a further treatment with hydrogen chloride as described above using hydrogen chloride at twice the concentration but yielded negligible amounts of water soluble material (0.1 g), which gave the same paper chromatographic picture as the main water extract. The possibility of detritylation during the oxidation procedure was checked by taking an aliquot of the acetone solution directly after oxidation, shaking it with water and chloroform several times and evaporating the water phase, which had a pH of about 5. The water soluble material (0.15 g) gave approximately the same paper chromatographic picture as the main water extract.

The water soluble, deionised material (15.9 g) was fractionated on a charcoal-Celite column (48 × 6 cm) using linear gradient elution (16 l 0—20 % aqueous ethanol) in the usual way. The substances present emerged in the following order: salts, arabinose (traces only), glucose, unknown substances (small amounts), methyl-β-glucoside together with 2-, 4- and 6-oxoglucoside, 3-oxoglucoside and unknown substances, probably condensation or decomposition products of oxocompounds, and also dioxo compounds. Methyl β-glucoside crystallised directly on evaporation of the fractions containing this substance (m.p. 110—111° after recrystallisation from ethanol). Further amounts of methyl β-glucoside and the 2-, 4- and 6-oxoglucosides were isolated from the mother liquors by repeated separations on Whatman 3 MM papers run in solvent A. The final separation of the 4-oxoglucoside was carried out by electrophoresis in buffer D at room temperature and subsequent ion exchange of eluants from the paper strips. The 3-oxoglucoside was obtained quite pure from the column, in a fraction with only small amounts of methyl β-glucoside and other substances. It crystallised directly on evaporation, and was recrystallised from *n*-propanol. The yield was increased by working up the mother liquors and higher fractions from the column by separations on thick papers. The amounts isolated and the characteristics of the oxoglucosides and methyl β-glucoside are given in Table 2.

The figures are averages of two similar batches. Glucose (0.03 g) and the 6-oxoglucoside (0.12 g) were isolated only in one case. By fractionation on thick papers a compound which might be a dioxoglucoside was isolated (0.09 g) from the late fractions from the carbon column.

As the oxo compounds were quite labile, particularly the 2- and 4-oxoglucosides, which were epimerised to 3-oxoglucoside and further transformed to other products even at pH 4—7, the eluants from the final thick paper separations were evaporated by freeze-drying in silicone treated flasks.

Oxidations were also carried out with 1.0 and 4.0 moles of oxidant, respectively, per mole of sugar and the product formed worked up as described above. but only methyl β-glucoside and the 3-oxoglucoside were isolated (Table 1).

In one case, with 1.5 moles oxidant per mole of sugar, the strength of the acid used for the hydrolysis was unintentionally lower than usual. The water soluble material obtained from this "weak" hydrolysis and from a further hydrolysis of the chloroform extract using the normal conditions were both worked up separately on a carbon column in the usual way. The total amount of methyl β-glucoside was distributed as 64 and35% in the "weak" and "normal" hydrolysate, respectively, and the corresponding figures for methyl β-3-oxoglucoside were 10 and 90 %.

Characterisation of methyl β-oxoglucosides

Methyl-β-D-3-oxoglucopyranoside (VII) was identical with that previously isolated [1], but the physical data, m.p. 129.5—131°, $[\alpha]_D^{22}$ −62° (c = 2, water), recorded now are more accurate since more substance was available. After reduction of VII (1.00 g) with Raney nickel [3], hydrolysis with 0.5 N sulphuric acid for 16 h at 100° and neutralisation with the ion exchange resin Amberlite IR-4B, the sugars formed were separated on thick papers using solvent A (2 × 16 hours). After elution, evaporation and recrystallisation from ethanol, D-allose (0.32 g, m.p. and mixed m.p. 127°) was isolated.

A small amount of *methyl β-D-2-oxoglucopyranoside* (VI) was obtained in crystalline form from ethanol but the values given here, m.p. 120—121° and $[\alpha]_D^{22}$ −47° (c = 2, water) (Found: C 44.1; 6.43; OCH_3 16.9. Calc. for $C_7H_{12}O_6$ (192.2): C 43.7; H 6.26; OCH_3 16.1) were obtained when more substance became available from a procedure which will be described in a later publication.

Small amounts (about 40 mg) of VI and *methyl β-D-4-oxoglucopyranoside* (VIII), respectively, were reduced, hydrolysed and deionised as above and the sugars formed fractionated on thick filter paper in solvent C for two days. It was shown by paper chromatography and electrophoresis in solvents A—C and buffers D and E, that the only sugars formed were glucose and mannose (from VI) and glucose and galactose (from VIII). Glucose was characterised as the phenylosazone, m.p. 206—208° from VI and VIII, undepressed on admixture with authentic material, mannose as the phenylhydrazone, m.p. and mixed 195—196°, and galactose as the methylphenylhydrazone, m.p. and mixed m.p. 188—189°, in the usual way.

The Methyl β-D-6-oxoglucopyranoside was shown to be identical with that previously isolated [1] by paper chromatography and electrophoresis; it gave a positive reaction with Schiff's reagent and gave only glucose on reduction and subsequent hydrolysis as above.

The possible *methyl β-D-4,6-dioxoglucopyranoside* had the $R_{Glucose}$ values 2.92, 0.65 (B) and M_V value 2.25 (D, at 50°), gave a strong lemon yellow reaction with anisidine hydrogen chloride, a positive Schiff's reaction and consumed hypoiodite [5] (corresponding to a purity of 70 %). After reduction and subsequent hydrolysis, glucose, galactose and smaller amounts of arabinose were shown by paper chromatography.

Oxidation of methyl 6-*O*-trityl-α-D-glucopyranoside

Methyl 6-*O*-trityl-α-D-glucopyranoside (I) [7] was oxidised and the product worked up using the same amounts and conditions as described above for the corresponding β-compound. Data for the isolation and characteristics of the mono-oxoglucosides isolated are given in Table 2. The methyl α-glucoside recovered had m.p. 165—165.5° after recrystallisation from ethanol. A possible 4,6-dioxoglucoside corresponding to that in the β-series was also isolated (0.07 g).

Characterisation of methyl α-oxoglucosides

The same technique of reduction, hydrolysis, neutralisation and preparative isolation and characterisation of the sugars formed was used as in the β-series.

Methyl α-D-*2-oxoglucopyranoside* (II) gave glucose phenylosazone, m.p. and mixed m.p. 207—208°, and mannose phenylhydrazone, m.p. and mixed m.p. 196—198°.

Methyl α-D-*3-oxoglucopyranoside* (III) gave very little glucose, sufficient only for characterisation by paper chromatography and electrophoresis. The predominant D-allose was isolated, m.p. and mixed m.p. 126—127°. Amorphous III showed $[\alpha]_D^{22}$ +84° (c = 2, water).

Methyl α-D-*4-oxoglucopyranoside* (IV) gave glucose phenylosazone, m.p. and mixed m.p. 206—208°, and galactose methylphenylhydrazone, m.p. and mixed m.p. 186—187°.

The possible *methyl* α-D-*4,6-dioxoglucopyranoside* had the $R_{Glucose}$ values 2.64, 0.62 (B) and M_V values 2.06 (D, at 50°), gave a strong lemon yellow reaction with anisidine hydrogen chloride, a positive Schiff's reaction, consumed hypoiodite [5] (corresponding to a purity of 69%) and gave glucose, galactose and small amounts of arabinose on reduction and subsequent hydrolysis.

Acknowledgement. The author is indebted to *Statens Tekniska Forskningsråd* for financial support and to Mr. A. Assarsson for his skilful assistance.

REFERENCES

1. Lindberg,B . and Theander, O. *Acta Chem. Scand.* **8** (1954) 1870.
2. Poos, G. I., Arth, G. E., Beyler, R. E. and Sarett, L. H. *J. Am. Chem. Soc.* **75** (1953) 422.
3. Karabinos, J. V. and Ballun, A. T. *J. Am. Chem. Soc.* **75** (1953) 4501.
4. Theander, O. *Acta Chem. Scand.* **11** (1957) 717.
5. Jeanloz, R. *Helv. Chem. Acta* **29** (1945) 57.
6. Foster, A. B. *J. Chem. Soc.* **1953** 982.
7. Helferich, B. and Becker, J. *Ann.* **440** (1924) 1.

Received July 3, 1957.

ACTA CHEMICA SCANDINAVICA 11 (1957) 1565—1575

On the Presence of Nucleoproteins and Lipoproteins in the Salt-soluble Protein Fraction of Barley

TEUVO ÄYRÄPÄÄ

Forskningslaboratoriet LKB, Åppelviken, Sweden

Considerable amounts of nucleic acids and protein-bound lipids are found in extracts obtained from ground barley grain with 1 M sodium chloride. About 5 % of the nitrogenous material precipitated from such extracts with cold trichloroacetic acid (TCA) consists of nucleic acids (both RNA and DNA), representing about a third of the total nucleic acids of barley. The lipids bound to salt-soluble proteins, represent only 2.5—5 % of the total barley lipids. Distilled water dissolves no nucleoprotein below pH 7 and only moderate amounts (only RNA) above this value. The solubility of the lipoproteins is also lower when extracted with distilled water. Calcium ion at a concentration of 0.01 moles/l completely inhibits the extraction of TCA-stable phosphorus-containing protein complexes at low ionic strengths.

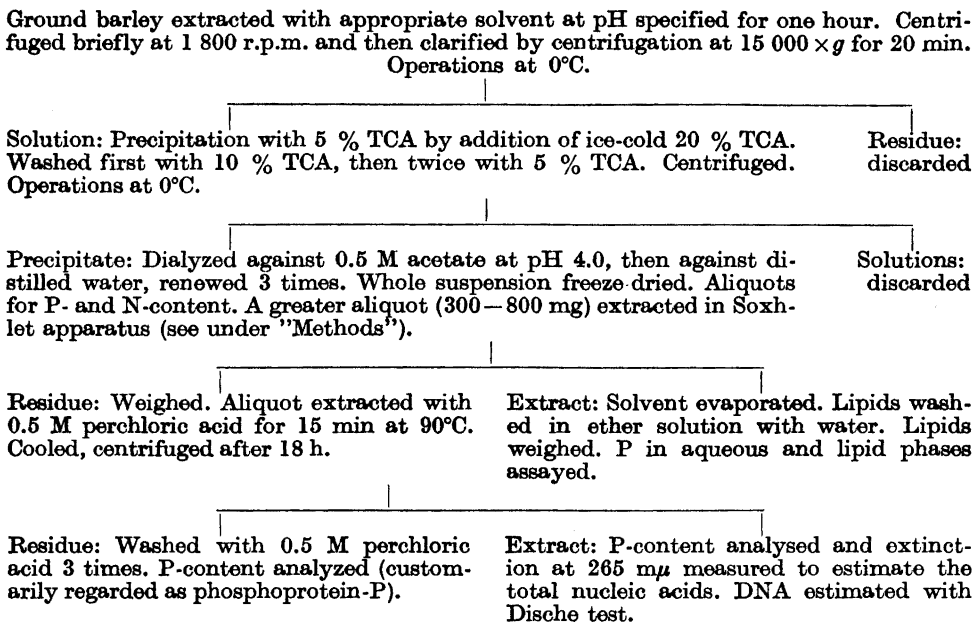
The methods used for nucleic acid and lipid assays, and for the determination of phosphorus distribution, and the origin and character of the nucleoproteins and lipoproteins are discussed.

Our knowledge of the nucleoproteins and lipoproteins of barley is very limited. Pool and Shooter [1] showed that small amounts of nucleic acid were present in a protein fraction. Similar observations have been made by Äyräpää [2], who also found lipids in the same fraction. A phosphorus-containing protein fraction supposed to be nucleoprotein has been found in brewery wort by Hopkins, Amphlett and Berridge [3]. The presence in brewery products of purine and pyrimidine derivatives, supposed to be degradation products of nucleic acids, has been demonstrated by several workers [4–6].

The corresponding protein complexes of wheat, which could be supposed to have their analogues in barley, are somewhat better worked out, but the investigations are almost exclusively limited to the nucleic acid complexes of wheat germ [7,8] (first recognized by Osborne [9]) and gluten-lipid complexes (*cf. e. g.* Olcott and Mecham [10]). A peculiar wheat lipoprotein has been isolated and described by Balls, Hale and Harris [11].

This paper gives no complete picture of the nucleoproteins and lipoproteins of barley grain. The aim of this investigation is to elucidate the extent to which such complexes occur in the much investigated so-called salt-soluble

Fig. 1. Outlines of the analytical procedure.



protein fraction of barley. Hence the extraction has been limited to the "natural" pH range (pH 5—8) mostly used in such investigations.

Trichloroacetic acid (TCA) at 0—+2°C has been chosen as the protein-precipitating agent, because cold TCA separates loosely bound phosphates [12–14], especially inositol phosphates [15], from the more stable posphorus-containing complexes (nucleoproteins, lipoproteins and phosphoproteins). It was also used to wash the tissues before lipid extraction [16]. TCA is generally regarded as the most selective protein-precipitating agent [17].

The TCA-precipitates from different extracts were freeze-dried and then subjected to an analytical procedure which may be regarded as a combination and modification of the methods of Schneider [12] and of Ogur and Rosen [18]. The outlines of the procedure are given in Fig. 1; the details are described under "Materials and Methods".

RESULTS

I. *Orientation experiments; comparison between barley and malt.* The amounts of phosphorus and nitrogen precipitated with 5 % TCA from different barley and malt extracts are shown in Figs. 2 and 3. (The experimental procedure was similar to the first two steps described in Fig. 1, with the exception that the extraction was performed at +25°C for 2 h.) The solubility properties of the phosphorus-containing protein complexes in barley and malt

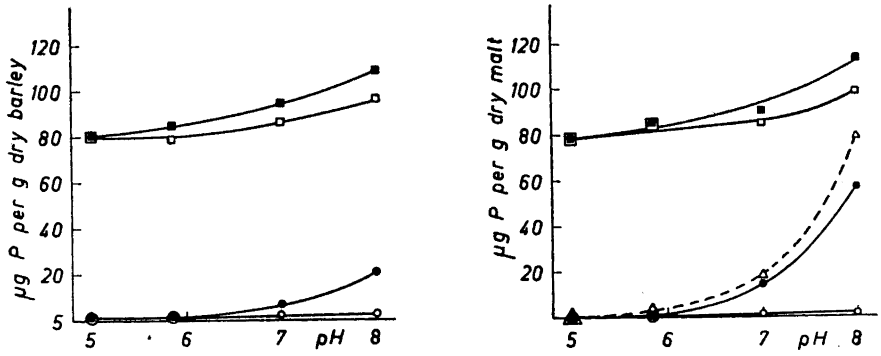


Fig. 2. The amounts of TCA-precipitated phosphorus in barley and malt extracts. Ordinate: μg precipitated P corresponding to 1 gram of dry barley or malt. Asbcissa: pH at extraction. Extraction solutions: -●—●- distilled water, -○—○- 0.01 M $CaCl_2$, -■—■- 1 M NaCl, -□—□- 1 M NaCl+0.01 M $CaCl_2$ and -△--△- 0.01 M EDTA.

are evidently very similar. Distilled water, however, in the alkaline range dissolves more protein-bound phosphorus, probably nucleic acid, from malt.

The nitrogen curves presented in Fig. 3, indicating the amounts of TCA-precipitable nitrogen extracted, suggest that a relatively phosphorus-rich fraction would be extracted with 1 M sodium chloride at pH 8 if the bulk of protein were first removed at pH 7 with distilled water. The activity of nucleases necessitates a rapid extraction and centrifugation procedure. A nucleic-acid rich protein fraction has been prepared in this way, but has not yet been further investigated.

The other conclusions drawn from these figures will be presented together with the results of phosphorus distribution analyses.

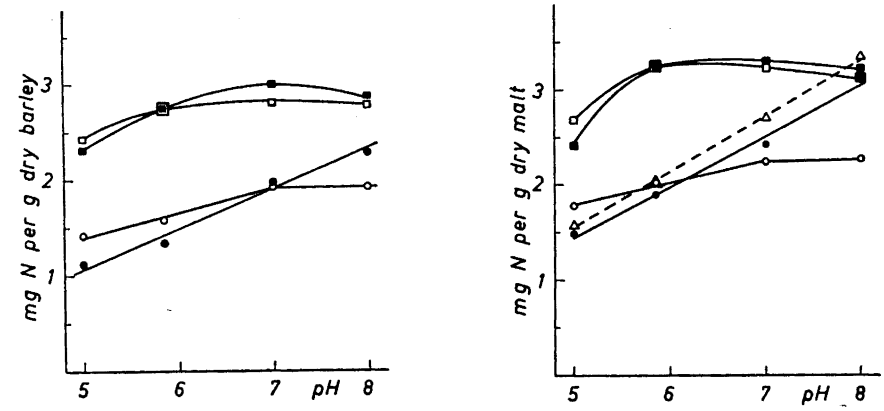


Fig. 3. The amounts of TCA-precipitated nitrogen in barley and malt extracts. Ordinate: mg precipitated N corresponding to 1 gram of dry barley or malt. Otherwise as in Fig. 2.

Table 1. The amounts of TCA-precipitates obtained from barley extracts and their nitrogen and phosphorus content.

Solvent and pH at extraction	Yield mg dry matter per g dry barley	% N in dry matter	% P in dry matter
Distilled water, pH 5.85	8.04	14.4	0.025
» » pH 7.0	9.48	14.5	0.040
» » pH 8.0	13.1	14.0	0.175
1 M NaCl, pH 5.85	22.1	13.7	0.440
» » pH 7.0	21.0	14.4	0.445
» » pH 8.0	20.4	14.3	0.545

II. *The distribution of phosphorus.* The amounts of freeze-dried TCA-precipitates obtained from barley extracts and their nitrogen and phosphorus contents are shown in Table 1. The distribution of phosphorus in these precipitates is shown in Table 2. The results presented in Table 2 and in Figs. 2 and 3 may be condensed to the following conclusions:

1) The nucleic acids are extracted by 1 M sodium chloride in considerable amounts at all the pH values investigated. The amounts extracted at pH 8 are only slightly higher than those obtained at pH 5.85. Distilled water dissolves moderate amounts of nucleic acids at pH values above 7 but not at lower values.

2) The lipoprotein phosphorus is found in considerable amounts only in sodium chloride extracts at pH 8, but small amounts are present in all the extracts, somewhat more in sodium chloride extracts than in distilled water extracts.

3) The other phosphorus-containing fractions are small. The phosphorus left in the residue after extraction with perchloric acid, customarily designated as phosphoprotein phosphorus, and another unknown phosphorus fraction, extracted with neutral alcohol-ether mixture but found in the aqueous phase after the washing of the lipids, are both present in greater amounts in sodium

Table 2. The distribution of phosphorus in TCA-precipitates from barley extracts.

Solvent at extraction	Lipid-P µg/g barley	Nucleic acid-P µg/g barley	Unknown P		Control	
			P in rest substance "Phosphoprotein-P"	P extracted with alcohol-ether but water-soluble	P by direct assay	P by addition
Dist. water pH 5.85	0.7	0.6	0.3	0.2	2.0	1.8
» » pH 7.0	1.1	1.9	0.3	0.8	3.8	4.1
» » pH 8.0	2.6	16.1	0.5	1.0	22.9	20.2
1 M NaCl pH 5.85	3.7	86.4	2.8	2.9	97.0	95.8
» pH 7.0	3.3	83.6	1.5	2.2	93.0	90.6
» pH 8.0	19.3	97.0	1.8	2.4	111.5	120.5

chloride extracts. Their amounts are not much influenced by the pH value at extraction.

4) The influence of calcium ion is marked in distilled water extracts: at a concentration of 0.01 M it inhibits the extraction of practically all the protein-bound phosphorus. In 1 M sodium chloride extracts, the presence of similar amounts of calcium has only a slight inhibiting effect above pH 7 (as seen in Figs. 1 and 2).

III. *Nucleic acids.* The amounts of nucleic acids calculated on the basis of phosphorus analyses compared with the amounts calculated from the ultraviolet absorption data are shown in Table 3. The agreement (except when only traces of phosphorus are present) is generally good. Only in the sodium chloride extract obtained at pH 5.85 is there appreciably more phosphorus. This excess of phosphorus seemed to be acid-stable (it was not hydrolysed to inorganic phosphate by 1 M hydrochloric acid at 100°C in 10 min). Since, in the course of attempts to prepare nucleic acid from whole barley, phytic acid was found in some combination with nucleic acid, the presence of phytic acid was especially tested for, but with negative results.

Table 3. The amounts of nucleic acids in TCA-precipitates from barley extracts. (Phosphorus and U.V. extinction values compared).

Solvent at extraction	Nucleic acid by P-det. µg/g barley	Nucleic acid by extinction µg/g barley	DNA by Dische reaction µg/g barley	% nucleic acid N of the total N of TCA-ppt. (by extinction)
Dist. water pH 5.85	6(?)	0	0	—
» » pH 7.0	20(?)	11	0	0.15
» » pH 8.0	169	165	0	1.9
1 M NaCl, pH 5.85	890	748	274	4.0
» » pH 7.0	870	835	300	4.4
» » pH 8.0	1000	978	344	5.4

The nucleic acids are calculated to constitute 4.0—5.5 % of the TCA-precipitable nitrogen in the sodium chloride extracts.

In order to estimate how much of the total nucleic acid of barley is extracted by 1 M sodium chloride solution, an attempt to estimate the nucleic acid content of barley is made by the cupric precipitation method, as described by Vendrely [19] (but on a larger scale, see under "Methods"). By assuming that the nucleic acids contain 10.7 % purine nitrogen and by neglecting the presence of free nucleotides, the nucleic acid content is calculated to be 0.27 % of the barley dry matter. Thus 1 M sodium chloride dissolves about 35—40 % of barley nucleic acid under the conditions described above.

The differentiation of RNA and DNA by hydrolytic methods [13,18] has not been found successful (*cf.* the experiences of Martin and Morton [20]). Thus the presence of DNA in the perchloric acid extracts containing total nucleic acid

was tested by the method of Dische [21], which is often considered to give too high values (*cf.* Markham [22]). The color given by perchloric acid-extracted nucleic acids, derived from sodium chloride extracts was the same as that of standard DNA (maximum at 595 mμ), whereas the nucleic acids derived from distilled water extracts gave no color. Moreover, in preliminary experiments starting from sodium chloride extracts we have obtained appreciable amounts of fibrous DNA, which is not digested by ribonuclease and shows an intense Feulgen reaction. Although the amounts given in Table 3 may be approximate, the presence of considerable amounts of DNA in sodium chloride extracts thus seems well established.

IV. *Lipids.* The amounts of lipids obtained from the TCA-precipitates and the phosphorus contents of these lipids are shown in Table 4.

Table 4. The lipids in TCA-precipitates from barley extracts and their phosphorus content.

Solvent at barley extraction	Lipid extracted with alcohol-ether		Lipid extracted with acidified alcohol-ether		Lipid as % of total barley lipid	Lipid as % of TCA-precipitated dry matter
	μg per g barley	% P in lipid	μg per g barley	% P in lipid *		
Dist. water pH 5.85	110	0.09	30	1.9	0.4	1.8
» » pH 7.0	330	0.16	30	1.9	1.1	3.6
» » pH 8.0	820	0.21	30	3.0	2.6	6.5
1 M NaCl pH 5.85	920	0.15	110	1.2	3.1	4.7
» » pH 7.0	820	0.12	100	2.4	2.8	4.4
» » pH 8.0	1460	1.25	50	2.8	4.6	7.4

* See under »Methods» how these values are estimated.

The amounts of lipids extracted with the HCl-containing alcohol-ether mixture is in most cases of the same order of magnitude as the error in the lipid analysis. But since the phosphorus content of this fraction is relatively important and since the removal of this fraction is necessary for the subsequent estimation of nucleic acids (*cf.* Ogur and Rosen [18]), this step cannot be omitted.

The nature of these lipids has not yet been investigated. Since their phosphorus content is generally low, the majority probably consist of various neutral components. (Abundance of neutral fat seems to be characteristic of plant lipoproteins [20,23]).

It has hitherto been possible to demonstrate the presence of steroids only in the lipids from the sodium chloride extract at pH 8 (by the method of Pijoan and Walter [24]; they amount to about 5 % of the protein-bound lipids).

DISCUSSION

1) *Accuracy of results.* The values presented above must be regarded as tentative only. In the first place, the extraction cannot be made exhaustively, as the enzymic degradation of nucleic acids, which is found to be appreciable

even in ice-cold solutions, necessitates a rapid extraction and clarification procedure. The long washing in TCA-solutions may also remove some of the nucleic acids.

As the clarification of the extract is another critical point, the barley cannot be ground too finely. Pool and Shooter [1] have shown that extracts from fine meal are difficult to clarify by centrifugation. Vendrely, Palmade and Vendrely [25], have found that the grinding of microorganisms in a ball mill renders the extraction of DNA more difficult. Filtration through filter pads (*e. g.* Seitz K 10) removes an appreciable fraction of the soluble high molecular nitrogen components, as was also pointed out by Pool and Shooter [1]. Hence we have chosen a grinding giving 70 % fine meal (as recommended by E.B.C.-Analytica [26]), extraction at 0°C for one hour and the clarification of extracts by centrifugation at 15 000 × *g*, as described under "Methods". Under other conditions, different values may be found.

As seen in Table 2, the accuracy of the values obtained in the phosphorus distribution analyses is scarcely greater than ±10 %. The lipid extraction and washing procedures may be somewhat incomplete. Further, the evaluation of nucleic acids is approximate owing to the use of standards obtained from different organisms. It must be emphasized that the method described in this paper is limited to TCA-precipitates from barley extracts. It is not applicable to whole barley, which contains both UV-absorbing and phosphorus-containing disturbing components.

2) *The origin of complexes.* The solubility properties of the nucleoproteins and lipoproteins of barley are similar to those of such complexes in general. For instance, from animal mitochondria the nucleoproteins may be extracted with 1 M sodium chloride at neutrality and the lipoproteins then with a more alkaline solution (for complete extraction a pH value of about 11 is needed) [27]. To what extent the nucleoprotein and lipoprotein complexes of saline barley extracts are derived from cytoplasmic particles remains to be shown. Some observations suggest that a part of the RNA may be derived from particles centrifuged down at 15 000 × *g* (probably plastids and mitochondria present in all the parts of the grain [28]). As the extraction of the nucleoproteins and lipoproteins is enhanced by the same factors, the lipoproteins may partially originate from similar particles. The submicroscopic particles (microsomes), if present, are probably left in solution after centrifugation at 15 000 × *g*, and may thus contribute to the nucleic acid and lipid content of the TCA-precipitates. (A centrifugation experiment at 150 000 × *g* has yielded slightly opaque pellets from sodium chloride extracts, previously clarified at 15 000 × *g*).

The DNA found in sodium chloride extracts may also partly originate from cytoplasmic particles, for Martin and Morton [23] have found appreciable quantities of DNA in cytoplasmic particles from wheat rootlets. On the other hand, when we tried to prepare nucleic acid from saline extracts of wheat flour (= endosperm fraction), a preparation consisting mainly of DNA was obtained. As RNA always preponderates in cytoplasmic particles, the presence of nuclear constituents in the saline extracts cannot be excluded.

3) *On the general character of nucleoproteins and lipoproteins.* The fractionation methods hitherto used in the study of barley proteins cannot be expected to give much information about native nucleoprotein and lipoprotein com-

plexes. During the slow fractionation procedures, an appreciable degradation by different enzymes is probable, since plant ribonucleases [29] and some lipases [30] are stable and active in a wide variety of conditions. Such procedures as salt fractionation may result in a dissociation of nucleoproteins, and in the subsequent dialysis the nucleic acid may then combine with new protein components [7,31,32].

In some preliminary fractionation experiments, we have certainly found lipids and nucleic acids in the globulin fraction and in the insoluble dialysis precipitate but never in the albumins. But just as phytic acid, on combining with proteins, may change their solubility properties [33,34], so nucleic acids and lipids may behave in a similar manner. For the reasons mentioned above, these experiments warrant no definite conclusions.

The presence of artificial lipoprotein complexes in barley extracts is possible, as evidenced with respect to wheat gluten by Olcott and Mecham [10]. But as all organisms contain lipoproteins, at least a part of those found in barley extracts may be expected to be natural.

The observations made in the course of this work suggest that greater attention paid to the structure of the grain, along the lines introduced by Säverborn, Danielsson and Svedberg [35], Danielsson [36] and Hess [37], might be fruitful in continued investigations on cereal proteins in general. In examination of lipoproteins and nucleoproteins, the separation of different cell fractions by differential centrifugation would be especially useful.

MATERIALS AND METHODS

Barley, Variety Herta, grown in 1955 in South Sweden, was used. It was milled immediately before the experiments with an Electrolux mill, adjusted to give about 70—75 % "fine meal" (passing through a Pfungstadt No. 3 sieve). N 1.69 %, P 0.37 % and total lipid 3.27 % (dry basis). Moisture 10.1 %.

Malt, Herta, grown in 1953 in South Sweden, was used. Milled as barley, about 90 % fine meal was obtained. N 1.57 % and P 0.42 % (dry basis). Moisture 6.8 %.

Nucleic acid standards. As RNA-standard, yeast nucleic acid from the Nutritional Biochemical Co. was used. It was deproteinized according to the method of Sevag, Lackmann and Smolens [38], dialyzed for one day and reprecipitated with 2 vols. ethanol. P 8.0 %, N 14.0 %, after heating with 0.5 M perchloric acid for 15 min at 90°C the extinction measured in 0.1 M HCl at 260 mμ was 10 800 per mole phosphorus.

The DNA standard was prepared from calf thymus according to the procedure of Mirsky and Pollister [39]. It was digested with crystalline pancreatic ribonuclease (Sigma Chemical Co.) and then deproteinized (as RNA above); dialyzed and reprecipitated with 1 vol. ethanol. P 8.53 %, N 14.1 %; the extinction measured as above was at 268 mμ (maximum) 10 100 per mole phosphorus.

The calculations of nucleic acid amounts are based on the assumption that the purine: pyrimidine ratio is unity, that RNA contains 9.6 % P and DNA 9.9 % P. Thus the DNA-RNA mixture present in sodium chloride extracts is considered to have a molar extinction of 10 600 at 265 mμ and a phosphorus content of 9.7 %.

Extraction of barley. The extraction was made on an ice bath or at room temperature. The flour was added as a fine stream to the stirred solution, in order to avoid the formation of artificial lipid complexes on moistening the flour by doughing (*cf.* Olcott and Mecham[10]). The pH value was repeatedly checked and adjusted by addition of 2 M sodium hydroxide or hydrochloric acid through a capillary to the vortex of the stirred solution.

Centrifugation. The extracts were first centrifuged at 1 800 r.p.m. and the turbid solution then clarified by centrifugation at high speed for 20 min at 15 000 × *g*. The clear or slightly opalescent middle layer was collected by pipette, contamination with the lipid-

containing top layer being avoided. Extraction and clarification of a sufficient quantity of extract generally required 3 h.

Precipitation with TCA and dialysis. This was performed as described in Fig. 1. The precipitate was washed ready for dialysis 10—12 h after the beginning of the extraction. Practically no nitrogen and little phosphorus (less than 10 %) was lost during the dialysis, which required 42 h.

Extraction of lipids. Generally 300—800 mg of the freeze-dried TCA-precipitate was extracted in a semimicro Soxhlet apparatus, first with 80 ml of ethanol-ether (3:1) for 48 h, then with 60 ml of absolute ethanol to which had been added 0.8 ml of concentrated hydrochloric acid per 100 ml (about 0.1 M). After 24 h 20 ml of ether was added to the solvent and extraction continued for a further 24 h. The two extracts were dealt with separately. They were evaporated on a water bath, the last 10 ml *in vacuo* without heating. The residues were moistened with 0.6 ml of absolute ethanol, after which 20 ml of ether and 20 ml of distilled water were added and the mixtures shaken in separatory funnels. The separated ether phases were washed twice with water and the original aqueous phases (probably containing proteinaceous material, carbohydrates and polyphenols) shaken again twice with 15 ml of ether, which was likewise washed with water. The ether phases were transferred to 50 ml volumetric flasks with 2 g of anhydrous sodium sulphate. The flasks were filled to the volume. After drying overnight aliquots of 40—45 ml were removed and evaporated and the residues transferred with ether to small weighed capsules through a little funnel with a minute filter paper disk in the stem. The ether was finally evaporated in a desiccator by cautious suction, with ether in the vacuum trap. The capsules with their contained lipid droplets were finally weighed after 24 h drying *in vacuo*.

It may be mentioned that we have tried many different lipid extraction methods, including enzymatic proteolysis and acid pressure hydrolysis, extraction with chloroform and *n*-butanol (Morton [40]). The hydrolytic methods seem not to offer any advantage: they are tedious and much evidently non-lipid material which is soluble in alcohol-ether is obtained. The chloroform extracts gave a dark and solid residue. Extraction with *n*-butanol seemed in some cases suitable, but in other cases gave definitely less lipids; it is evidently useful but has not yet been systematically investigated.

The method described above is not ideal. Phospholipids are hydrolyzed during the acid extraction, which is proved by treating known amounts of soybean lecithin in the same manner. The lipids obtained contain some other material (they often give a positive Molisch reaction). Actually, it cannot be said if this material is an integral part of the lipid or not (*cf.* Lovern [41], p. 42).

From experiments with soybean lecithin it appears that the lipid phosphorus extracted with acid alcohol and ether is to be found in the aqueous phase after the washing of lipids. The phosphorus content of the "firmly bound" lipids listed in Table 4 is only a rough approximation. Owing to the various possible sources of error, the phosphorus percentage is calculated without regard to the lost unknown lipid fragments.

Extraction of nucleic acids. As already mentioned, we did not obtain any reproducible results with the differential hydrolytic extraction method of Ogur and Rosen [18]. The amounts of RNA extracted with cold perchloric acid were generally low. Thus the total nucleic acids were extracted with hot perchloric acid. Heating at +70°C for 20 min produced extracts which were difficult to clarify and which showed an appreciable extinction at 300—330 mμ. When the heating temperature was raised to +90°C and the extracts cooled overnight at 4°C, the turbidity was easy to centrifuge off and the absorption curve between 220 and 330 mμ was close to those of the nucleic acids, as shown in Fig. 4. The heating time seemed not to be critical; 10 and 30 min gave practically identical results.

Purine nitrogen determination. The method of Vendrely [19] was adopted, but on a larger scale. Barley samples of 2 g were hydrolyzed in 20 ml of 1 M hydrochloric acid by gently boiling for 6 h with reflux. After centrifugation, the brown solutions were neutralized (with bromocresol purple as indicator), acidified with acetic acid to about pH 5, heated to 100°C and centrifuged again. A sample of the solution corresponding to a known amount of original extract was then taken for the copper precipitation, performed according to the original method but with sixfold amounts of reagents (3 drops was taken to be 0.1 ml). The nitrogen was determined in the second precipitate by the usual Kjeldahl method (modification of Blom and Schwartz [42], see below).

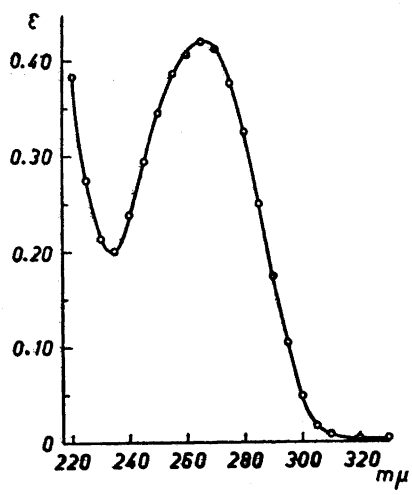


Fig. 4. The ultraviolet absorption spectrum of hot perchloric acid extract containing nucleic acids. (Delipidated TCA-precipitate from sodium chloride extract, obtained at pH 8).

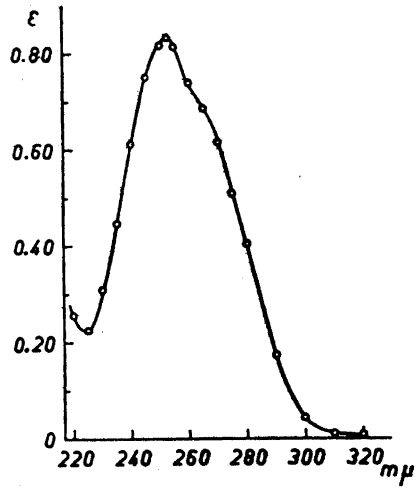


Fig. 5. The ultraviolet absorption spectrum of the decomposed copper-purine complex from barley hydrolysate, measured in 0.1 M hydrochloric acid.

Since the values given by the cupric precipitation method may be too high, they were checked for some samples by measuring the ultraviolet absorption of the decomposed cupric precipitate as follows: The second cupric precipitate was decomposed by 1 % sodium sulphide (exactly as the first precipitate according to the original method). The cleared supernatant was diluted with 0.1 M hydrochloric acid and the ultraviolet absorption measured. Fig. 5 shows the absorption curve of such a solution, corresponding well to the curve of an adenine-guanine mixture. If the molar extinction coefficient of an equimolar adenine-guanine mixture is considered to be 12 000 (at 253 mμ) [22], virtually equal values were found by nitrogen determination and by extinction measurement.

Assay of nitrogen. The semimicro modification of the Kjeldahl method suggested by Blom and Schwartz [42] was used. Distillation was performed in Markham's apparatus.

Assay of phosphorus. The Fiske-SubbaRow method as modified by King [43] was used. Especially when the presence of phytic acid was suspected, a droplet of 0.4 % ammonium molybdate was added to the digestion tube to ensure rapid hydrolysis of phytic acid [44].

Phytic acid analysis. The method of Leva and Rappoport [45] was adopted, since preliminary experiments showed that relatively large amounts of mucleic acid do not interfere.

The author is indebted to the head of the laboratory, Dr. S. Brohult, to Dr. E. Sandegren and to Mr. H. Nihlén for valuable advices and discussions. For the revision of the English text I wish express my cordial thanks to Mrs. Jean-Margaret Perttunen, B. Sc.

REFERENCES

1. Pool, A. A. and Shooter, E. M. *J. Sci. Food Agric.* **6** (1955) 524, 534.
2. Äyräpää, T. *Acta Chem. Scand.* **9** (1955) 1403.
3. Hopkins, R. H., Amphlett, P. H. and Berridge, N. J. *J. Inst. Brewing* **47** (1941) 106.
4. Laufer, L., Gutcho, M., Stewart, E. D. and McCully, R. *Am. Soc. Brewing Chemists*, Proceedings, Annual Meeting 1951, p. 68.

5. Harris, G. and Parsons, R. *J. Inst. Brewing* **61** (1955) 29.
6. Bolinder, A., Kurz, W. and Lundin, N. *J. Inst. Brewing* **61** (1955) 497.
7. Belozerskij, A. N. and Bazhilina, G. D. *Biokhimiya* **9** (1944) 134.
8. Lusena, C. V. *Cereal Chem.* **28** (1951) 400; Kay, E. R. M. and Dounce, A. L. *J. Am. Chem. Soc.* **75** (1953) 4041.
9. Osborne, T. B. and Campbell, G. F. *J. Am. Chem. Soc.* **22** (1900) 379.
10. Olcott, H. S. and Mecham, D. K. *Cereal Chem.* **24** (1947) 407.
11. Balls, A. K., Hale, W. S. and Harris, T. H. *Cereal Chem.* **19** (1942) 279.
12. Schneider, W. C. *J. Biol. Chem.* **161** (1945) 293.
13. Schmidt, G. and Thannhauser, S. J. *J. Biol. Chem.* **161** (1945) 83.
14. Eggman, L., Singer, S. J. and Wildman, S. G. *J. Biol. Chem.* **205** (1953) 969.
15. Barré, R. and Courtois, J.-E. *Ann. pharm. franç.* **11** (1953) 653.
16. Johnson, R. M. and Dutch, P. R. *Proc. Soc. Exptl. Biol. Med.* **78** (1951) 662.
17. Kirk, P. L. *Advances in Protein Chem.* **3** (1947) 139.
18. Ogur, M. and Rosen, G. *Arch. Biochem.* **25** (1950) 262.
19. Vendrely, R. *Biochim. et Biophys. Acta* **1** (1947) 95.
20. Martin, E. M. and Morton, R. K. *Biochem. J. London* **64** (1956) 221.
21. Dische, Z. *Mikrochemie* **8** (1930) 4.
22. Markham, R. *Moderne Methoden der Pflanzenanalyse.* Springer-Verlag, Berlin 1955, Vol. IV, p. 246.
23. Martin, E. M. and Morton, R. K. *Biochem. J. London* **64** (1956) 687.
24. Pijoan, M. and Walter, C. W. *J. Lab. Clin. Med.* **22** (1937) 968.
25. Vendrely, R., Palmade, C. and Vendrely, C. *Nature* **178** (1956) 1044.
26. *European Brewery Convention.* Analytica. Elsevier, Amsterdam 1953.
27. Dallam, R. D. *Arch. Biochem. and Biophys.* **54** (1955) 24.
28. Engel, Chr. and Bretschneider, L. H. *Biochim. et Biophys. Acta* **1** (1947) 357.
29. Holden, M. and Pirie, N. W. *Biochem. J. London* **60** (1955) 39.
30. Lea, C. H. *J. Sci. Food Agric.* **8** (1957) 1.
31. Magasanik, B. *The Nucleic Acids.* Academic Press Inc. New York 1955, Vol. I, p. 373.
32. Belozerskij, A. N. *Trav. Inst. Bot. Univ. Moscou* **36** (1940) 5.
33. Barré, R. and Courtois, J.-E. *Bull. soc. chim. biol.* **35** (1953) 913.
34. Rondelet, J. and Lontie, R. *European Brewery Convention,* Proc. Congr. Baden-Baden 1955, p. 90.
35. Säverborn, S., Danielsson, C.-E. and Svedberg, T. *Svensk Kem. Tidskr.* **56** (1944) 75.
36. Danielsson, C.-E. *Biochem. J. London* **44** (1949) 387.
37. Hess, K. *Kolloid Z.* **136** (1954) 84.
38. Sevag, M. G., Lackman, D. B. and Smolens, J. *J. Biol. Chem.* **124** (1938) 425.
39. Mirsky, A. E. and Pollister, A. W. *J. Gen. Physiol.* **30** (1946) 117.
40. Morton, R. K. *Nature* **166** (1950) 1092.
41. Lovern, J. A. *The Chemistry of Lipids of Biochemical Significance.* Methuens Monographs. London 1955.
42. Blom, J. and Schwarz, B. *Acta Chem. Scand.* **3** (1949) 1439.
43. King, E. J. *Biochem. J. London* **26** (1932) 292.
44. Seligson, N. *Arch. Pharm.* **268** (1930) 147.
45. Leva, E. and Rapoport, S. *J. Biol. Chem.* **141** (1941) 343.

Received July 5, 1957.

ACTA CHEMICA SCANDINAVICA 11 (1957) 1576—1586

The Effect of Ions on the Catalytic Activity of Enzymes: Yeast Glucose-6-phosphate Dehydrogenase

WILLIAM J. RUTTER*

Medicinska Nobelinstitutet, Biokemiska avdelningen, Stockholm 60, Sweden

1. The catalytic activity of yeast glucose-6-phosphate dehydrogenase preparations is markedly altered in the presence of various ions. At low ion concentrations there is a strong augmentation of catalytic activity, while at high concentrations there is an inhibition.

2. Anions are important in the activation process. The relative effectiveness of various anions for augmentation of catalytic rate is $F^- > PO_4^{\equiv} > Cl^- > Br^- > SO_4^{\equiv} > I^- > SCN^-$.

The concentration for maximum activation varies with each anion.

3. Cations also play a role in augmentation of finite catalytic rate. Calcium and magnesium ions are more effective than sodium or potassium ions.

4. The inhibition of *Zwischenferment* activity at high ion concentrations is apparently due to a competition with substrates glucose- 6-phosphate and TPN, for site on the enzyme surface.

5. Possible mechanisms for the augmentation of a finite catalytic rate by both anions and cations are discussed.

The marked influence of the ionic environment on physiological activity is usually explained in terms of ionic effects on enzymes in the biological system. Many purified enzyme preparations absolutely require a particular ion or closely related group of ions for catalytic activity; while the catalytic activity of many other enzyme preparations is influenced by ionic environment to a greater or lesser degree.

In cases where an absolute ionic requirement for enzyme activity has been demonstrated, specific monovalent and/or divalent metal ions have usually been implicated as the actual cofactor. The anionic species may usually be varied without observable effect. From this it has been inferred that the accompanying anionic species is relatively unimportant in the cases where a specific cationic requirement exists; and that the metal ions are intimately associated in the catalytic apparatus and are obligatorily involved in the catalytic process.

* U. S. Public Health Service Fellow, 1954—55. Present address, Division of Biochemistry, University of Illinois, Urbana, Illinois, USA.

There are in addition some observations which are more easily explained in terms of an augmentation of a finite catalytic rate. These effects may be the reflection of a general influence of ionic strength of the medium, or may be more specifically related to a particular cationic or anionic species. Of particular interest for the present discussion, for example, is the stimulation of the activity of the pancreatic and salivary α-amylases by chloride ions [1]; the augmentation of the catalytic activity of fumarase by polyvalent anions [2], the affects of both cationic and ionic species on the activity of β-galactosidase [3,4], and the influence of the ionic strength on the catalytic activity of urease [5].

The earlier observations from this laboratory concerning large effects of anions on certain flavoprotein systems [6,7] as well as with the reaction catalyzed by liver alcohol dehydrogenase [8] has prompted additional studies of ionic effects on other enzyme systems in order to ascertain, 1) the generality and magnitude of such effects, 2) the mechanism of stimulation, and, 3) the physiological significance of such phenomena.

The present paper presents the data which have been obtained in the *Zwischenferment* system *. It has been found that a variety of ions, including phosphate and the substrate glucose-6-phosphate stimulate enzymatic activity markedly. At high concentrations inhibition is observed. Possible mechanisms of ionic effects on the catalytic activity of this and other enzymes are discussed.

MATERIALS AND METHODS

Glucose-6-phosphate dehydrogenase (*Zwischenferment*) was prepared according to the procedures of Warburg and Christian [9], and of Kornberg [10]. The reaction was followed spectrophotometrically. The specific activity of these preparations is expressed as μmoles TPNH formed/min/mg protein under optimum assay conditions. The results obtained were independent of the preparation used. Crystalline barium glucose-6-phosphate (G-6-P) was converted to the sodium or potassium salt which in turn was used as the substrate.

The rates reported here are the initial rates when the reaction rate was zero order with respect to concentration of substrates. The experiments were performed at 23°C.

RESULTS

The initial experiments to be reported here concern the effects of certain ions on *Zwischenferment* activity. The addition of monovalent ions to the assay system is typified by the data presented in Fig. 1. In the presence of sodium chloride or sodium fluoride there was observed an increase in activity, especially on the acid side of the pH activity curve, and a change in the pH of optimum activity. It is noteworthy that fluoride and chloride did not elicit identical effects on catalytic activity. The strong role of the anion is indicated in the experiments summarized in Fig. 2 in which enzyme activity was measured as a function of anion concentration. A stimulation of activity was

* Abbreviations used in this manuscript are as follows: *Zwischenferment*, yeast glucose-6-phosphate dehydrogenase; G-6-P, glucose-6-phosphate; TPN, triphosphopyridine nucleotide; DPN, diphosphopyridine nucleotide; 6PGL, 6-phosphogluconolactone.

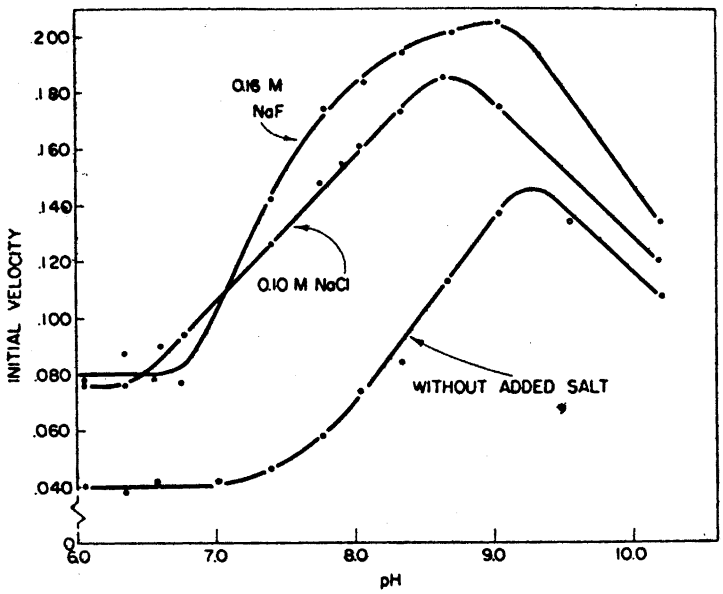


Fig. 1. Influence of ions on the *Zwischenferment* reaction as a function of pH. The reaction mixtures contained 6 μM G-6-P, 0.3 μM TPN, 100 μg *Zwischenferment* preparation, 100 μM buffer. (Histidine pH 0.6—7.0; glycyl-glycine pH 7.0—9.0, glycine pH 9.0—10.2) salt added when indicated, final volume 3.0 ml, temperature 23°C. Initial velocity is expressed in terms of change in optical density change at 340 mμ/min. The pH of each reaction was tested imediately after assay of enzymatic activity.

observed at low concentration and an inhibition at higher concentrations; the degree of stimulation and concentration required for stimulation and inhibition varied with the anionic species. The "effectiveness" of various anions in augmentation of *Zwischenferment* activity may be stated qualitatively $F^- > PO_4^{\equiv} > Cl^- > Br^- > SO_4^{\equiv} > I^- > SCN^-$; and for inhibition of catalytic rate $SCN^- > I^- > SO_4^{\equiv} > PO_4^{\equiv} > Br^- > Cl^- > F^-$. The position of $PO_4^{\equiv}$ in these series is noteworthy. The wide variation in effects elicited by anions precludes ionic strength as the sole cause of activation and inhibition phenomena. It is true, however, that certain of the data, for example the stimulation by low concentrations of phosphate, chloride, and fluoride may be so related. The finite activity observed without the further addition of ions does not represent activity of a salt free system, but that in the presence of 3×10^{-2} M glycylglycine buffer and 2×10^{-3} M glucose-6-phosphate. The ionic strength of the solution, therefore, was high enough to allow the possibility of an absolute requirement for added ions for enzyme activity. Suitable experiments with dialyzed preparations, however, showed that glycylglycine as well as versene and citrate give practically no activation or inhibition of this system. These observations make it unlikely that the activation by ions is due to the solvation of a contaminating inhibitory metal ion, and also emphasize the role of the anionic species in the activation process.

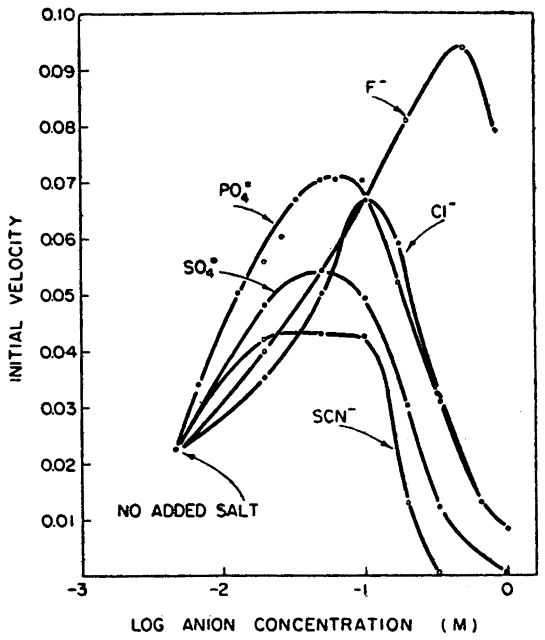


Fig. 2. Effect of anions on the rate of the *Zwischenferment* reaction.
The reaction mixtures contained 6 μM G-6-P, 0.3 μM TPN, 100 μg *Zwischenferment*, 100 μM glycyl-glycine pH 7.4, anions as indicated, water to 3.0 ml, temperature 23°C. All of the anions were added as the sodium salts.
The rate expressed as optical density change at 350 mμ/min.

Fig. 3 shows the effect of substrate concentration in the presence and absence of added ions. Glucose-6-phosphate does, itself, stimulate enzyme activity at concentrations higher than those needed to saturate the enzyme, but it is less effective than the simple inorganic anions. The presence of other anions markedly influences the apparent affinity of the enzyme for its substrate (*i. e.*, the K_m of the substrate). At a concentration of 0.5 M NaCl, for example, at least ten times more glucose-6-phosphate is required to obtain maximum activity than at 0.1 M NaCl. The early reports [11,12] concerning the phosphate inhibition of *Zwischenferment* activity, could, on the basis of the present investigation, be related to the concentrations of glucose-6-phosphate and/or TPN present in the assay system used.

Fluoride ions are more effective than chloride or other ions in augmenting the catalytic rate, especially at low substrate concentrations. The small size of the fluoride ion could conceivably allow more effective collisions of enzyme and substrate.

In Fig. 4 are presented Lineweaver-Burk plots of representative data on the interrelationship of ions and G—6—P in the *Zwischenferment* reaction at a constant TPN concentration. There is an apparent competitive relationship between ions and the substrate. The strong activation by high concentrations

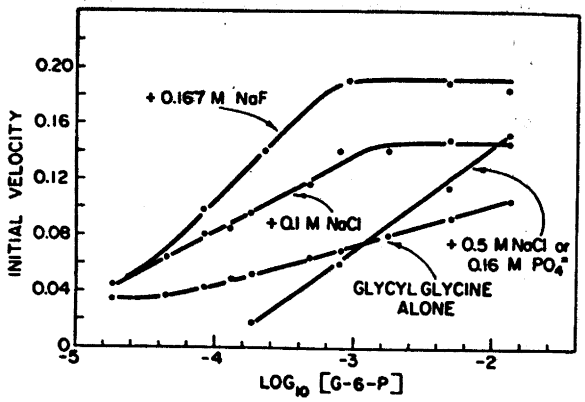


Fig. 3. Ion-glucose-6-phosphate interrelationships in the *Zwischenferment* reaction. The general reaction conditions are as indicated in Fig. 2. The molar G-6-P- concentration was varied as indicated. The sodium salts of anions were employed.

of the substrate is evidenced by the rather marked inflection in the curve. It is not possible to say definitely whether G—6—P itself is the activating ion, or whether contaminating ions (traces of sodium sulfate, *e. g.*, any sodium) are responsible for this effect.

Similar data concerned with the influence of ions on the reaction of *Zwischenferment* with TPN at constant glucose-6-phosphate concentration are

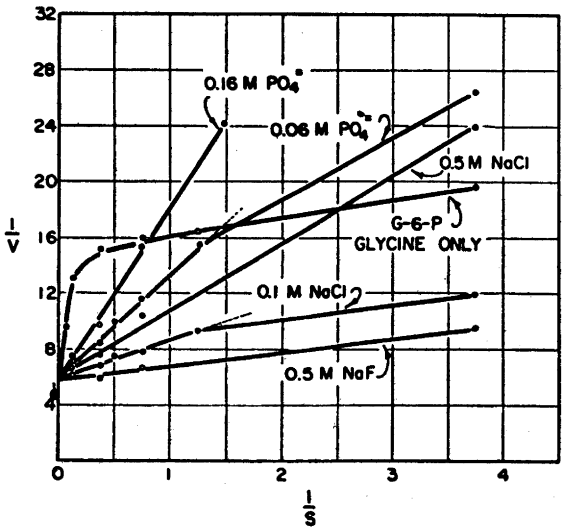


Fig. 4. Ion-glucose-6-phosphate relationships in the *Zwischenferment* reaction. The general reaction conditions are as indicated in Fig. 3. In these Lineweaver-Burk plots the units of reaction velocity are optical ensity change at 340 mμ/min and the units of substrate concentration are μM/ml reaction medium.

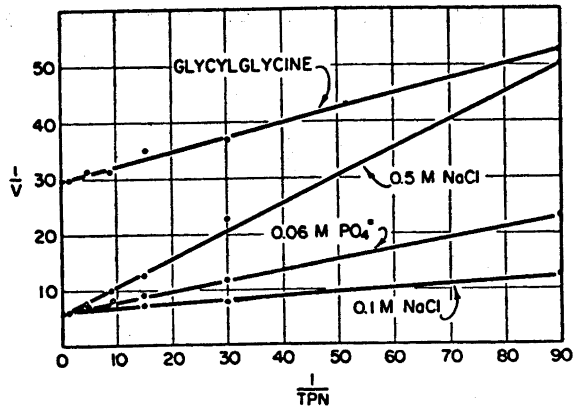


Fig. 5. Ion-TPN relationship in the *Zwischenferment* reactions.
General reaction conditions are as described in the legend of Fig. 2, 6 μM G-6-P present, and TPN concentration varied as indicated. In these Lineweaver-Burk plots, the units of reaction velocity are — O.D. 340 mμ/min, and units of TPN concentration μM/ml reaction medium.

presented in Fig. 5. Again there is a competitive relationship between TPN and the ions tested, presumably for a site on the enzyme surface. TPN in the concentrations used is not effective as an ion activator, and may be contrasted to glucose-6-phosphate in this respect.

The difference between the maximum velocities in the presence and absence of added ions is considered a point of some significance. At concentrations of G—6—P below those at which activation occurs (10^{-3} M) and in the absence of added activating ions, either a large fraction of total enzyme molecules are catalytically inactive, or, perhaps more likely, catalysis proceeds at all active sites of the enzyme population, but at a much slower rate. Some of the inflec-

Table 1. Effect of substrate and TPN in overcoming anion inhibition of glucose-6-phosphate dehydrogenase

In 0.5 molar NaCl Additions	Initial rate
1. 0.4 μmoles G-6-P 0.18 μmoles TPN	0.020
2. 10 μmoles G-P-6 0.18 μmoles TPN	0.030
3. 0.4 μmoles G-6-P 1.5 μmoles TPN	0.042
4. 10 μmoles G-6-P 1.5 μmoles TPN	0.042

Each reaction mixture contained 1.5 μmoles NaCl, 100 μg *Zwischenferment*, 100 μM glycyl glycine buffer, pH 7.4, and the concentration of G-6-P and TPN indicated above. The final volume was 3.0 ml., temperature 23°C.
The initial rate is expressed in terms of change in optical density.

Table 2. Effect of cations on *Zwischenferment* activity.

Ion	μ	% Stimulation
NaCl	0.02	87
	0.04	175
	0.10	312
	0.15	250
KCl	0.04	175
$CaCl_2$	0.02	300
	0.05	387
	0.07	425
	0.10	437
	0.15	437
	0.20	437
$MgCl_2$	0.02	287
	0.05	350
	0.10	400
	0.15	387
$MnCl_2$	0.02	312
	0.05	350
	0.10	300

Each reaction mixture contained 1 μmole G-6-P, 0.3 μmoles TPN, 100 μmole glycyl glycine, pH 7.4. 100 μg *Zwischenferment* (lyophilized preparation, original specific activity approximately 1.0). Ions added when indicated, final volume 3.0 ml, temperature 23°C. The figures represent stimulations of the rate observed in the absence of added ions (Δ O.D./min = 0.032).

tions in the Lineweaver-Burk curves in Fig. 4 (which have been consistently observed) may be the result of transitions between the two types of catalysis. The possibility that anions influence the dissociation of the enzyme-product complex will be considered in the discussion section.

Since the reaction of both G—6—P and TPN with the enzyme is inhibited in a competitive manner by a variety of ions, the question arises whether the binding of one substrate to the enzyme influences the binding of the other; that is whether the competitive inhibition by anions of the reaction of G—6—P with *Zwischenferment* is independent of TPN and vice versa. The experiment reported in Table 1 was performed to test this possibility. At high salt concentrations, increasing the concentration of either substrate (G—6—P or TPN) increases the reaction rate. This observation is most easily explained in terms of an increased affinity for the second substrate, when the enzyme is combined with the first substrate.

The fact that anions elicit more or less specific effects on the catalytic activity of *Zwischenferment* does not, of course, rule out a role of the cationic species. An experiment, therefore, was designed to test the effects of various chloride salts on enzyme activity. As shown in Table 2, the divalent metals ions, Ca^{++}, Mg^{++}, and Mn^{++} are more effective than sodium and potassium, especially at low ionic strengths *. Moreover, inhibition of the reaction by

* Dr. Hans Klenow, Universitetets Institut for Cytofysiologi, Copenhagen, Denmark, has independently observed a stimulation of *Zwischenferment* by certain ions (private communication).

chloride salts occurs according to the concentration of chloride ions, and is not, apparently, simply related to the overall ionic strength; thus at 0.1 M NaCl there is already a significant decrease in activity, while at this concentration of $MgCl_2$ and $CaCl_2$ maximum activity is still observed. The report of Kornberg [10] that magnesium ions stimulate *Zwischenferment* activity is thus confirmed, but it is emphasized that there is no apparent specific requirement for magnesium or other divalent metal ions in the system [13]. This is not to deny the possible existence of a non-dissociable metal ion in the enzyme itself. The possible role of divalent metal ions as non-specific activators will be considered in the discussion.

DISCUSSION

The ionic effects observed here are more easily interpreted in terms of an augmentation of catalytic rate, rather than an absolute requirement for added ion. It would not be wise, however, to suggest that there is not an absolute requirement for ions, since the H_3O^+ and OH^- ions of the solvent are doubtless contributory in the system. As a matter of fact, one explanation for the comparative lack of ionic effect in the basic portion of the pH activity curve, may be the increasing number OH^- ions in solution. The marked influence of ions on the catalytic rate cannot be a simple function of the ionic strength, since widely varying effects were observed with different ionic species at the same ionic strength. Any interpretation of the data must consider the role of both cationic and anionic species in the catalytic process.

Michaelis and Pechstein[14] have advanced a theory to explain ionic stimulation of enzymatic activity. According to their argument, enzymatic activity is related to both acidic and basic dissociable groups; the optimum catalytic activity being at that pH where maximum dissociation of both acidic and basic groups occurs. The presence of salts then may affect catalytic activity by altering the dissociation of these groups involved in the catalytic process. This theory extended by Alberty [15] has satisfactorily explained much of the data concerned with the effect of ions on enzymatic activity. The extensive studies on the influence of ions on fumarase activity by Massey [2], and Massey and Alberty [16], for example, suggest effects of anions on the dissociation of groups at, or near, the active center.

This type of explanation may at least in part have validity here. It is true that the apparent affinity (K_m) of the enzyme for G—6—P and TPN is markedly affected by the ionic environment. The strong stimulation of catalytic activity on the acidic side of the pH-activity curve would presumably be related to the influence of anions present, and the smaller but significant increase on the basic side of the curve, to the influence of cations.

There is, however, another interpretation of effects observed in this and in certain other cases. As is the case with any enzymatically catalyzed reaction which is presumed to proceed through the formation of an enzyme substrate complex, the catalytic process associated with *Zwischenferment* may be considered to be composed of several partial reactions: (a) the association of the enzyme with its substrates, (b) the catalytic process *per se*, and (c) the dissociation of the enzyme from the products of the reaction. For the *Zwischenfer-*

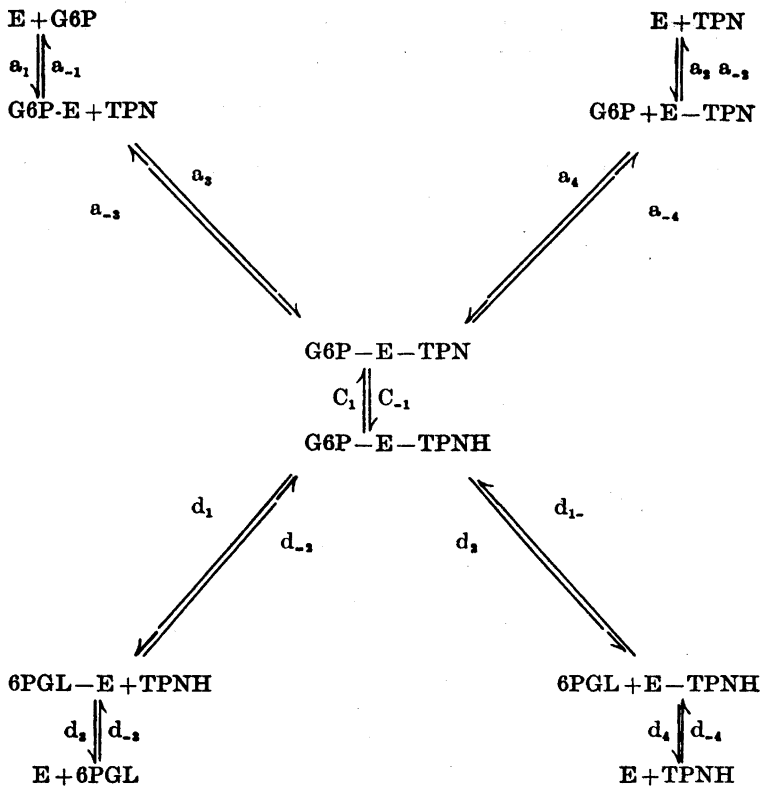


Fig. 6. Hypothetical kinetic mechanism for the *Zwischenferment* reaction.

ment system, the partial reactions formulated in Fig. 6 have been arbitrarily selected as an expression of the overall process. The actual catalytic reaction is represented by C, which is a composite constant of the partial reactions involved in this process. Clearly the observed overall rate of the reaction will be a function of the rate constants for the partial reactions, and in particular instances could, therefore, be a reflection of association of enzyme and substrates, the catalytic reaction, or of dissociation to enzyme and products, or combinations of these. If the formation of the enzyme-substrate complex can be considered according to the ion association theory, then at low dielectric constant (in the absence of salts), there would exist a greater tendency for the enzyme and substrate, to associate, and at higher dielectric constant (*i. e.*, at higher ionic strength), a greater tendency to dissociate since both charged species would then be solvated. The stimulatory effects of ions on *Zwischenferment* activity are explicable on this basis if it be assumed that the dissocia-

tion of products is rate limiting *. An increase in the anion concentration would simultaneously decrease the association reaction, and increase the dissociation reaction. The net result would be a stimulation of activity together with an increased K_m for the substrate. In the observations presented in this paper, note that at a given substrate concentration a stimulation of activity followed by an inhibition was observed as the ionic concentration increased. The degree of effectiveness of a particular anion, either as an activator or inhibitor, would then be related to its effectiveness in displacing the product from the complex, and the ease with which it in turn was displaced by the substrate. Thus, phosphate is especially effective as an activator at low concentrations, while sulfate inhibits at comparatively low concentrations presumably because it would be less readily displaced by the substrate. The increased effectiveness of the divalent metal ion can be easily visualized, since these cations would readily form an ion pair with the divalent phosphate groups on the product molecules, enhancing the rate of dissociation. The pH optimum of the enzyme in the absence of added ions then might be expected to be in the basic region where the hydroxyl ions could increase dissociation rate of enzyme product complex. The change in pH optimum with salt concentration could conceivably be a reflection of the relatively smaller effect of hydroxyl ions in the presence of salt. It would be expected that effects of added anions would be proportionally greater at lower pH values, as has been observed in these studies.

The argument presented provides a means of explaining the effect of ions on catalytic activity of glucose-6-phosphate dehydrogenase, and could be applied to other cases of ion stimulation and inhibition, especially when concomitant effects on the apparent affinity of the enzymes for the substrates are also observed.

It is not a novel idea that the rate limiting reaction of an enzymatic catalysis be the association or dissociation of enzyme-substrate complex. Theorell and Chance [19] have, for example, shown that in the reaction of ethanol with DPN catalyzed by alcohol dehydrogenase, the dissociation of Enzyme-DPNH is in all probability the limiting step.

The above treatment allows the qualitative prediction of this type of ionic effects on the rate constants in the catalytic process. For example, an increase in appropriate ion concentration should increase A_{-1}, A_{-2}, A_{-3}, A_{-4}, d_1, d_2, d_3, d_4, and decrease A_1, A_2, A_3, A_4, d_{-1}, d_{-2}, d_{-3}, d_{-4}, in the *Zwischenferment* system as written. It is conceivable that ionic affects of the type suggested, could be observed on the catalytic step C_1 and C_{-1}. In this case, however, the manner in which C_1 and C_{-1} would be affected would be considerably more difficult to predict.

* It is true in the present instance, that ionic effects observed might also be related to a conversion of the product, 6-phosphogluconolactone (6PGL) to a compound not involved in the reaction, namely, 6-phosphogluconic acid [14]. Since the observations were initial reaction rates, it is believed the large effects observed cannot be solely related to this additional reaction. The results also cannot be effects on the lactonizing enyme, since Ca++ ions stimulate the present reaction while magnesium, manganese, or cobalt ions are required for gluconolactonase; and in addition, fluoride ions are efficient activators of *Zwischenferment*, yet they inhibit gluconolactonase [15].

An effect of ions on the dissociation of groups involved in the combination of the substrate or products with the enzyme, or in the catalytic reaction itself could on the other hand alter the individual rate constants in either direction, depending on the chemical circumstances.

According to the nature of the reacting groups the present hypothesis provides an explanation for ionic effects on reactions involving groups which are completely ionized under the conditions imposed. It is an adjunct to the more often expostulated theory which concerns the effects of added ions on reactions involving groups which dissociate under the conditions imposed; together, they provide a general mechanism for the interpretation of cases in which there is a general ionic influence in catalytic activity, but no specific ion erquirement.

The author wishes to express appreciation to Prof. H. Theorell for his active interest in this work and for the gracious hospitality extended by him and other members of the Biochemical department.

REFERENCES

1. Bernfeld, P., Staub, A. and Fischer, C. H. *Helv. Chim. Acta* **31** (1948) 2165.
2. Massey, V. *Biochem. J.* **53** (1953) 67.
3. Cohn, M. and Monod, J. *Biochim. et Biophys. Acta* **7** (1951) 153.
4. Kuby, S. A. and Lardy, H. A. *J. Am. Chem. Soc.* **75** (1953) 890.
5. Kistiakowsky, G. B. and Shaw, W. H. A. *J. Am. Chem. Soc.* **75** (1953) 2751.
6. Theorell, H. and Nygaard, A. P. *Acta Chem. Scand.* **8** (1954) 877, 1649.
7. Walaas, E. and Walaas, O. *Acta Chem. Scand.* **10** (1956) 122.
8. Theorell, H., Nygaard, A. P. and Bonnichsen, R. *Acta Chem. Scand.* **9** (1955) 1148.
9. Warburg, O. and Christian, W. *Biochem. Z.* **254** (1932) 438.
10. Kornberg, A. *J. Bio.. Chem.* **182** (1950) 805.
11. Theorell, H. *Biochem. Z.* **275** (1953) 416.
12. Negelein, E. and Haas, E. *Biochem. Z.* **282** (1935) 206.
13. McNair-Scott, D. B. and Cohen, S. S. *Biochem. J.* **55** (1953) 23.
14. Michaelis, L. and Pechstein, H. *Biochem. Z.* **59** (1914) 77.
15. Alberty, R. A. *J. Am. Chem. Soc.* **76** (1954) 2494.
16. Massey, V. and Alberty, R. A. *Biochim. et Biophys. Acta* **12** (1954) 354.
17. Cori, O. and Lipmann, F. *J. Biol. Chem.* **194** (1952) 417.
18. Brodie, A. F. and Lipmann, F. *J. Biol. Chem.* **212** (1955) 677.
19. Theorell, H. and Chance, B. *Acta Chem. Scand.* **5** (1951) 1127.

Received July 6, 1957.

ACTA CHEMICA SCANDINAVICA 11 (1957) 1587—1593

Determination of Accurate Interplanar Spacings and Lattice Parameters from Guinier Powder Photographs

SVEN WESTMAN and ARNE MAGNÉLI

Institute of Inorganic and Physical Chemistry, University of Stockholm, Stockholm, Sweden

X-Ray powder photographs obtained in a Guinier type focusing camera of 80 mm diameter (transmission position) often permit the calculation of interplanar spacings and unit cell dimensions with considerable accuracy provided that an internal standard is admixed with the powder specimens. The procedure is rapid and simple. The high accuracy obtained in the low-angle region is particularly valuable when applying analytical methods for indexing powder patterns.

Accuracy in powder data is of great importance in many instances of X-ray diffraction studies, *e. g.* when indexing complicated patterns by analytical methods [1,2]. Access to accurate interplanar spacings and unit cell dimensions has been essential also in connection with studies carried out by members of the present research team on some series of closely related, discrete phases giving very similar X-ray patterns (homologous series of oxides of transition elements) [3,4]. The information thus needed has to a large extent been obtained from powder photographs.

The determination of interplanar spacings and unit cell dimensions with the highest degree of accuracy is a complicated task [1,2]. Quite often, however, a more modest degree of accuracy in the interplanar spacings values is required and for such cases the employment of a Guinier focusing camera[5] has been found to give, by a simple and rapid procedure, results satisfactory for most needs.

The two Guinier camera sets used in the present investigation were built according to a design by Professor G. Hägg, Uppsala, at the workshop of the Chemistry Department, Research Institute of National Defence (FOA 1) through the kind permission of the head of the Department, Professor G. Ljunggren. The delicate adjustment of the camera sets, which were designed for taking transmission photographs with Cu$K\alpha$ radiation, was carried out by Dr. J. Österlöf of this Institute. One of the cameras, intended for precision measurements, utilizes strictly monochromatized Cu$K\alpha_1$ radiation, while the

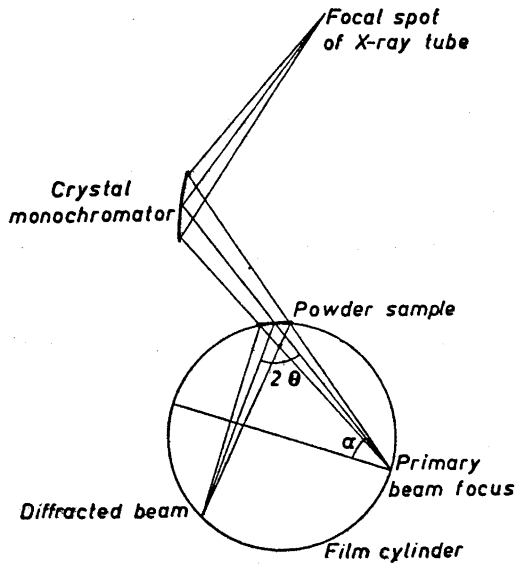


Fig. 1. Guinier focusing camera (transmission position).

other, used for ordinary work and with somewhat higher intensity, employs the Cu$K(\alpha_1 + \alpha_2)$ doublet. The diameter of the film cylinder is 80 mm. The exposure times are generally rather short, being about 30 min for substances of high symmetry and simple structure.

A condition for the camera to give sharp interference lines on the film is that the powder sample is situated on the cylinder defined by the film (*cf.* Fig. 1). In the actual procedure, the sample is stuck to a piece of thin Scotch tape which is attached to a flat metal ring rotated in a plane tangent to the focusing cylinder. A minor deviation of the sample from the correct site causes a slight broadening of the interference lines and considerable displacements of their positions on the film. Thus, if the sample is moved outwards Δa at right angles to the tangent plane, the position (s) of the interference line on the film will shift towards increasing s by an amount $\Delta s = F(\Theta,\alpha) \cdot \Delta a$, where Θ is the Bragg angle and α the angle between the incident beam and the normal to the powder specimen. Fig. 2 gives a representation of the quotient $\Delta s/\Delta a$ as a function of Θ when α is given the value, 35°, of the actual camera sets. It is obvious that, with this method of mounting the specimen, accurate Θ values for the reflexions cannot be obtained by straight-forward measurements of the distances s_{obs} between the positions on the film of the primary beam and the reflexions.

Admixture of an internal standard with accurately known lattice dimensions makes it possible to correlate for each individual exposure the readings on the film s_{obs} with the Θ values of the standard. This is advantageously done by determining for every reflexion of the standard substance the difference

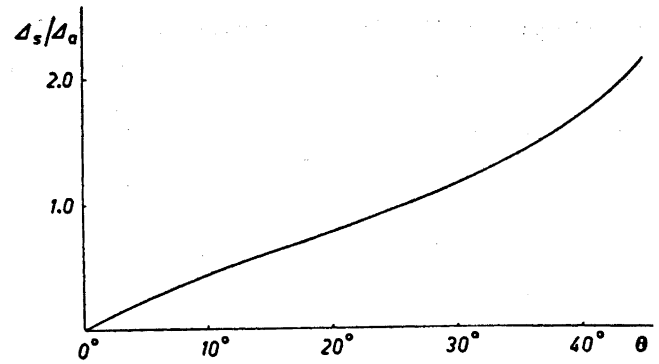


Fig. 2. Relation between line displacement (Δs) and sample displacement (Δa) as a function of diffraction angle (Θ).

$\Delta s = s^\circ - s_{obs}$, where s° represents the value calculated for a nominal value r° chosen for the camera radius. By plotting Δs against s_{obs}, a correction curve is obtained which is of a form analogous to that given in Fig. 2 if the camera is truly cylindrical and correctly adjusted. Within the limits given by the accuracy of the readings, this function corresponds to a line $\Delta s = \text{const} \times s_{obs}$.

The use of admixed standard substances in X-ray powder work has been discussed by Bacon [6], Andrews [7] and Parrish [8]. For the present investigation, use was generally made of a potassium chloride standard (Analar, British Drug Houses) the lattice parameter and linear expansion coefficient of which have been determined by Hambling [9], $a = 6.2930$ Å (25°C) and $\beta = 3.37 \times 10^{-5}$/°C. After grinding and recrystallization at 600°C for one hour, this substance gave powder interferences of good quality. Seven reflexions of suitable intensity and distribution appear within the diffraction range of the Guinier cameras used.

Other standard substances may be preferable for special purposes. Thus, when studying phases displaying solid solubility, addition of a pure component as a standard may make possible very accurate measurements of the changes of the lattice parameters accompanying the solution phenomenon, provided that the changes are large enough to give good resolution of corresponding lines. For very accurate determinations of absolute cell dimensions, it may sometimes be advisable to use a standard giving more reflexions than those obtained from potassium chloride in order to be able to fix the correction line $\Delta s = \text{const} \times s_{obs}$ more accurately.

When evaluating the films an automatic correction for film shrinkage was obtained according to Hägg [10] by printing a scale (graduated to 0.1 mm) on the film prior to development. The films were measured in a projection comparator obtained by slightly modifying an ordinary 35 mm "Prado" projector. The high quality of the Guinier photographs allowed a linear magnification as high as 7 or 8 times to be used.

Following a procedure introduced by Österlöf [11], the measurement of the reflexions was made not, as has usually been the case, on the maximum den-

Table 1. Guinier powder pattern of Hg_3TeO_6. CuKa_1 radiation. $a_{obs} = 13.3921 \pm 0.0013$ Å.

Intensity	Σh^2	$\sin^2\Theta_{obs}$	$\sin^2\Theta_{calc}$	$(\sin^2\Theta_{obs} - \sin^2\Theta_{calc}) \times 10^4$	$s^\circ - s_{calc}$ mm
m	14	0.046307	0.046312	− 5	−0.002
w	16	0.052964	0.052978	−14	−0.005
s	18	0.059541	0.059544	−3	−0.001
s	20	0.066188	0.066160	+28	+0.009
m	24	0.079411	0.079392	+19	+0.006
vw	30	0.099238	0.099240	− 2	−0.001
vw	34	0.112446	0.112472	−26	−0.006
vw	38	0.125692	0.125704	−12	−0.003
w	40	0.132321	0.132319	+ 2	±0.000
m	46	0.152170	0.152167	+ 3	+0.001
w	54	0.178701	0.178631	+70	+0.014
w	56	0.185184	0.185247	−63	−0.013
w	62	0.205118	0.205095	+23	+0.005
vw	64	0.211628	0.211711	−83	−0.016
w	66	0.218313	0.218327	−14	−0.003
w	68	0.225017	0.224943	+74	+0.014
vw	70	0.231582	0.231559	+23	+0.004
vw	78	0.258013	0.258023	−10	−0.002
w	80	0.264659	0.264639	+20	+0.004
vw	82	0.271316	0.271255	+61	+0.011
w	86	0.284484	0.284487	− 3	−0.001
vw	88	0.291125	0.291103	+22	+0.004
w	94	0.310940	0.310951	−11	−0.002
vw	96	0.317498	0.317567	−69	−0.012
w	104	0.344053	0.344031	+22	+0.004
vw	106	0.350618	0.350647	−29	−0.005
vw	110	0.363935	0.363879	+56	+0.009
vw	116	0.383669	0.383726	−57	−0.009
vw	118	0.390325	0.390342	−17	−0.003

sity but on the very sharp high-angle edge of the lines. Provided that the lines are of good quality and that their intensities are not very high or too low, this method has been found to give very good results. It is essential that the reflexions of the test substance and of the standard are similar in their sharpness.

The usefulness of the camera for accurate work was tested by studying the photographs of several substances. All the exposures were made at about 20°C. For several of the test substances, accurate lattice parameters at this temperature have been reported in the literature or could be calculated from data obtained at other temperatures and the values for the thermal coefficient.

Table 2. Lattice parameters for some cubic substances obtained from Guinier powder photographs.

Substance	a_{obs} (20°C)	a_{lit} (21°C)	Reference
Al	4.0492±0.0004 Å	4.04922	8, 14
$Pb(NO_3)_2$	7.8560±0.0012 Å	7.8562	8
TlBr	3.9846±0.0006 Å	3.98506	14
NaCl	5.6396±0.0008 Å	5.64006	8

Table 3. Guinier powder pattern of MoO_3. CuKa_1 radiation. Lattice parameters found

$a = 3.9628 \pm 0.0009$ Å
$b = 13.855 \pm 0.004$ Å
$c = 3.6964 \pm 0.0008$ Å

Intensity	*hkl*	$\sin^2\Theta_{obs}$	$\sin^2\Theta_{calc}$	$(\sin^2\Theta_{obs} - \sin^2\Theta_{calc}) \times 10^5$
w	020	0.01246	0.01236	+10
vs	110	0.04094	0.04087	+ 7
m	040	0.04948	0.04945	+ 3
m	120	0.05025	0.05014	+11
vs	021	0.05586	0.05578	+ 8
vw	130	0.06566	0.06560	+ 6
m	101	0.08122	0.08120	+ 2
s	111	0.08432	0.08429	+ 3
vw	041	0.09282	0.09287	− 5
vw	060	0.11122	0.11126	− 4
vw	150	0.11507	0.11505	+ 2
vw	141	0.13055	0.13065	−10
m	200	0.15113	0.15112	+ 1
m	210	0.15428	0.15421	+ 7
s	002	0.17361	0.17368	− 7
vw	022	0.18605	0.18605	± 0
w	221	0.20684	0.20691	− 7
m	112	0.21444	0.21456	−12
w	171	0.23264	0.23264	± 0
w	081	0.24122	0.24122	± 0
vw	062	0.28494	0.28495	− 1
vw	152	0.28880	0.28873	+ 7
vw	212	0.32787	0.32790	− 3
w	232	0.35259	0.35262	− 3
vw	023	0.40324	0.40315	+ 9

Table 4. Guinier powder pattern of Ti_8O_9. CuKa_1 radiation. Lattice parameters found

$a = 5.569$ Å, $b = 7.120$ Å, $c = 8.865$ Å
$\alpha = 97.55°, \beta = 112.34°, \gamma = 108.50°$

Intensity	*hkl*	$\sin^2\Theta_{obs}$	$\sin^2\Theta_{calc}$	$(\sin^2\Theta_{obs} - \sin^2\Theta_{calc}) \times 10^5$
vw	001	0.00973	0.00962	+11
w	$10\bar{1}$	0.02194	0.02189	+ 5
vw	100	0.02665	0.02664	+ 1
st	$10\bar{2}$	0.03643	0.03638	+ 5
vw	101	0.05063	0.05061	+ 2
v st	$1\bar{2}0$	0.05226	0.05224	+ 2
vw	$02\bar{1}$	0.05294	0.05294	± 0
w	020	0.05676	0.05674	+ 2
w	$12\bar{1}$	0.06091	0.06091	± 0
v st	$1\bar{2}1$	0.06278	0.06279	− 1
w	$02\bar{2}$	0.06841	0.06837	+ 4
v st	$10\bar{3}$	0.07010	0.07011	− 1
m	021	0.07986	0.07978	+ 8
st	$20\bar{1}$	0.08737	0.08744	− 7
vw	$12\bar{2}$	0.08886	0.08882	+ 4
st	$10\bar{2}$	0.09384	0.09382	+ 2
st	$12\bar{1}$	0.09633	0.09635	− 2
vw	$2\bar{2}0$	0.10081	0.10100	−19
m	$02\bar{3}$	0.10297	0.10303	− 6
w	200	0.10654	0.10654	± 0
w	$22\bar{2}$	0.10867	0.10887	−20

The cylindrical form and the adjustment of the camera were checked by means of the diagram obtained from mercuric tellurate, Hg_3TeO_6. According to Hägg and Holmberg [12], this substance is cubic with the cube edge equal to 13.4 Å. A sample prepared according to Hutchins [13] was kindly lent by Professor Hägg. The powder photograph (Table 1) indicated that the form and adjustment of the camera were perfect. The 29 observed reflexions give the relative value of the lattice parameter to ± 0.004 % (confidence limits for 95 % probability). The absolute value for the parameter, given in Table 1, lacks significance due to the inadequate knowledge of the purity of the sample. The differences between the s values corresponding to $\sin^2\Theta_{obs}$ and $\sin^2\Theta_{calc}$, given in the column $s^o - s_{calc}$ of Table 1, show that the error in the readings is of the magnitude of 0.01 mm. The use of a vernier for the film measurements thus seems warranted. However, it ought to be emphasized that the maximum error of the scale printed on the film is also of this magnitude [10].

Table 2 gives lattice parameters obtained for samples of aluminium (99.99% pure), thallous bromide (British Drug Houses), sodium chloride (Merck, Analytical reagent) and lead nitrate (Riedel — E. de Haën p.a.). The influence of refraction has been considered when warranted. The confidence limits are given for 95 % probability. The agreement with precision data reported in the literature is satisfactory. It is evident that the accuracy obtained is high enough to require that the temperature is maintained constant to within about $\pm$ 1°C during the exposure.

Lattice parameters may also be obtained with a considerable degree of accuracy for substances of symmetry lower than cubic. This is illustrated in Tables 3 and 4 which give the powder patterns of orthorhombic molybdenum trioxide (C. P., Baker's Analyzed) and triclinic pentatitanium enneaoxide (prepared from titanium metal and titanium dioxide, both of high purity) [4]. The very satisfactory agreement between observed and calculated values of $\sin^2\Theta$ clearly suggests the suitability of Guinier camera data for the analytical methods of indexing powder patterns.

The camera with $CuK(\alpha_1+\alpha_2)$ radiation has also been found to give data of rather high accuracy although it does not completely match the $CuK\alpha_1$ camera in this respect. The superposition or close vicinity of the α_1 and α_2 reflexions and the shift of their relative position ($\Theta_{\alpha_2}-\Theta_{\alpha_1}$ negative for $\Theta < 14.3°$ and positive for higher values of Θ) makes it somewhat difficult to apply the Österlöf measuring technique within extensive parts of the diffraction range. However, measurements of the sharp α_1 reflexion edge for Θ values below 14.3°, of the α_2 reflexion edge for unresolved doublets at higher values of Θ and of the edges of both components for well resolved doublets have been found to give results which compare favourably with those obtained from measurements on the maximum density of the lines.

Acknowledgements. The authors wish to express their sincere gratitude to Professor G. Hägg, Uppsala, and to Dr. J. Österlöf of this Institute for valuable information and discussions. Several members of the research staff have contributed to the results reported in this article by their observations and discussions of previous experiences. Thanks are especially due to Mr. Sten Andersson, Mr. Ulf Kuylenstierna, Mrs. Stina Nord and Docent Herbert Pestmalis.

REFERENCES

1. Klug, H. P. and Alexander, L. E. *X-Ray diffraction procedures for polycrystalline and amorphous materials.* John Wiley & Sons Inc., New York 1954.
2. Peiser, H. S., Rooksby, H. P. and Wilson, A. J. C. *X-Ray diffraction by polycrystalline materials.* The Institute of Physics, London 1955.
3. Magnéli, A., Blomberg-Hansson, B., Kihlborg, L. and Sundkvist, G. *Acta Chem. Scand.* **9** (1955) 1382.
4. Andersson, S. and Magnéli, A. *Naturwiss.* **43** (1956) 495.
5. Guinier, A. *X-Ray Crystallographic Technology.* Hilger & Watts Ltd., London 1952.
6. Bacon, G. E. *Acta Cryst.* **1** (1948) 337.
7. Andrews, K. W. *Acta Cryst.* **4** (1951) 562.
8. Parrish, W. *Technical Report* No. 68, Philips Laboratories (1953).
9. Hambling, P. G. *Acta Cryst.* **6** (1953) 98.
10. Hägg, G. *Rev. Sci. Instruments* **18** (1947) 371.
11. Österlöf, J. *To be published.*
12. Hägg, G. and Holmberg, K. E. *Unpublished experiments.*
13. Hutchins, E. B. *J. Am. Chem. Soc.* **27** (1905) 1157.
14. Smakula, A. and Kalnajs, J. *Phys. Rev.* **99** (1955) 1737.

Received July 8, 1957.

ACTA CHEMICA SCANDINAVICA 11 (1957) 1594—1598

The Crystal and Molecular Structure of β-Arabinose

SVEN FURBERG and ASBJØRN HORDVIK

Chemical Institute, University of Bergen, Bergen, Norway

The crystal and molecular structure of β-arabinose has been determined, mainly by means of the "multiplication rule". There is a *cis*-glycol grouping on C_1 and C_2, and the molecule has the structure 1*a*2*e*3*e*4*a*.

As the pyranose ring has the staggered "chair" form, there are according to Hassel [1] two possibilities for the molecular structure of each pyranose sugar, the one being formed from the other by conversion of the ring. For some sugars it is fairly evident which structure is the more stable one and to be expected in the crystalline state. In other cases, such as the present one, it would appear difficult to settle this question without determining the crystal structure. So far detailed structure analysis of two pyranose sugars, α-glucose and α-rhamnose monohydrate, have been reported in the literature (Beevers *et al.*[2,3]).

EXPERIMENTAL CRYSTAL DATA

A commercial sample of β-D-(−)-arabinose from Eastman Kodak Co. was used for the investigation. Good crystals were obtained by recrystallization from alcohol. They are needle-shaped and elongated along the *c*-axis. Weissenberg- and oscillation diagrams were taken about two axes, using filtered copper radiation. The crystals are ortorhombic, with unit cell dimensions $a = 6.50$ Å, $b = 19.41$ Å, and $c = 4.83$ Å (±0.5 %). The values agree well with those given by Cox [4]. The density is 1.627 g/cm³ and there are four molecules $C_5H_{10}O_5$ in the unit cell. The only systematic absences occur in the odd-order reflections $h00$, $0k0$ and $00l$, and the space group is therefore $P2_12_12_1$, as was also found by Cox [4].

The relative intensities were estimated visually from a series of Weissenberg photographs of the $hk0$ and $0kl$ zones. 93 of the 146 $hk0$ reflections and 100 of the 127 $0kl$ reflections accessible with Cu$K\alpha$ radiation were recorded with measurable intensity. The intensities were corrected for Lorentz and polarisation effects, but not for absorption, as small crystals of dimensions less than 0.2 mm were used. For the $0kl$ reflections a correction was also made for the "spot-shape" effect [5].

DETERMINATION OF THE STRUCTURE

Projections of the structure along the *c* and *a* axes were determined by Patterson projections, trial and error methods, the "multiplication rule", and

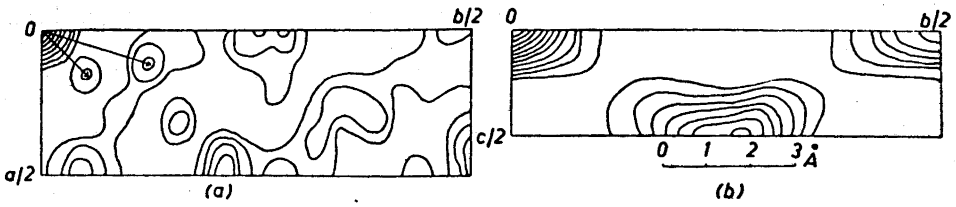


Fig. 1. Patterson projections on the (001) plane (a) and the (100) plane (b).

F_0 and $(F_0—F_c)$ refinement. As the *c* axis is the shortest one, this projection was first determined.

The c-projection. The Patterson synthesis is reproduced in Fig. 1a. The orientation of the six-membered ring could be derived from the two intramolecular vectors shown in the figure. Following the procedure described by Beevers [2], two possible positions of the centre of the ring were found, but attempts at further interpretation were not successful. A number of reasonable structures were then postulated by studying selected reflections by Bragg-Lipson charts. However, all attempts at Fourier refinement of these structures failed. It was then tried to deduce the signs of the strongest reflections by inequalities and the "multiplication rule" [6,7]. The intensities were put on an approximately absolute scale by Wilson's method [8]. The reflection 1,17,0 was found to have a unitary structure factor (U) as high as 0.68, and 26 reflections had unitary structure factors greater than 0.30. Negative signs were chosen for 1,17,0 and 4,11,0 ($U = 0.52$) and the signs of the reflections 240 ($U = 0.38$), 0,18,0 ($U = 0.55$), 2,17,0 ($U = 0.44$) and 3,12,0 ($U = 0.45$) were denoted by a, b, c and d, respectively. Only two additional signs could be deduced from simple inequality relations, but the "multiplication rule" led to the determination of the probable signs of 18 more structure factors in terms of the letter symbols. Furthermore, the relations d = b and bc = —a were strongly indicated. Twenty of the reflections could be divided in four groups whose signs were expressed by —1, a, c and ac, respectively. Six other strong reflections for which the signs were given in terms of b and ab, were not con-

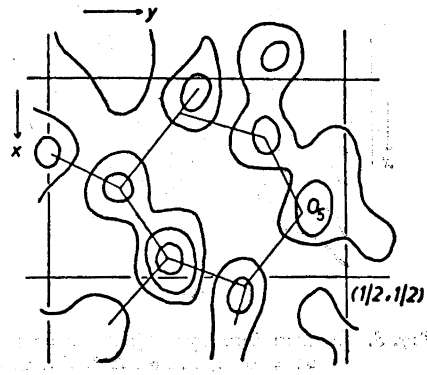


Fig. 2. The best electron density map obtained by permutation of the signs of groups of reflections. The postulated structure is shown.

sidered in order to limit the number of permutations. The Fourier synthesis of the reflections within each group was then calculated, and the electron density maps corresponding to the four possible combinations of the signs of the groups were derived. In one of the maps (Fig. 2) a six-membered ring was indicated, although not very clearly. Fourier refinement of a structure postulated on this basis led eventually to the correct structure. Three (F_0—F_c) refinements were also carried out. The final structure factors showed that two of the reflections used to calculate the map in Fig. 2 had the wrong sign, and that the values used for the unitary structure factors were about 35 % too high. The reliability factor $R = (\Sigma|F_0—F_c|)/\Sigma|F_0|$ is 0.18, and the corresponding electron density map is shown in Fig. 3a. The contributions from the hydrogen atoms were not included in the structure factors. The atomic scattering factors employed are those given by Berghuis *et al.*[9] A temperature factor exp. ($-3.5\sin^2\Theta/\lambda^2$) was used.

The a-projection. The Patterson synthesis (Fig. 1b) gave little information,

Table 1. Atomic coordinates as fractions of the corresponding cell edge.

Atom	x	y	z
C_1	0.486	0.418	0.189
C_2	0.431	0.347	0.302
C_3	0.253	0.320	0.130
C_4	0.091	0.369	0.144
C_5	0.150	0.442	0.048
O_1	0.562	0.411	0.918
O_2	0.603	0.302	0.273
O_3	0.190	0.253	0.237
O_4	0.005	0.377	0.430
O_5	0.328	0.462	0.209

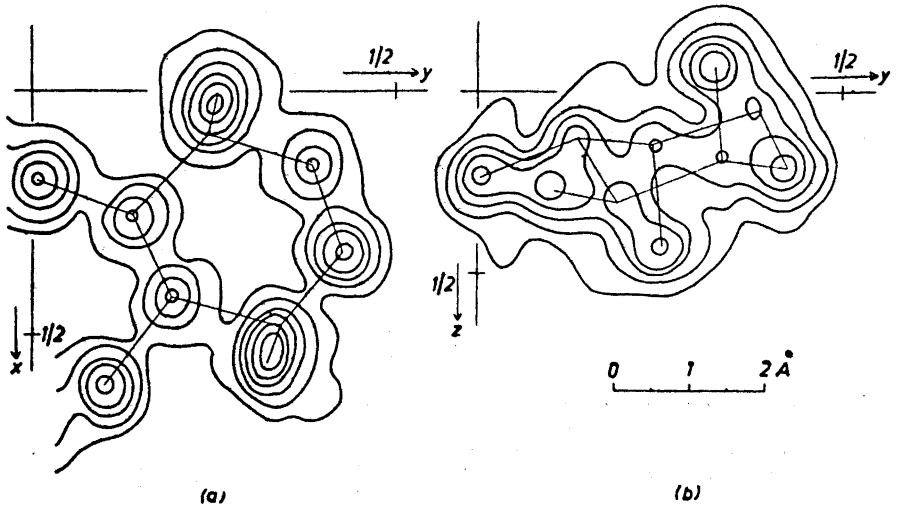


Fig. 3. Electron density projections on the (001) plane (a) and the (100) plane (b). Contours at 2, 4, 6, . . . e . Å^{-2}. Calculated at 1/60 of b and 1/30 of a and c.

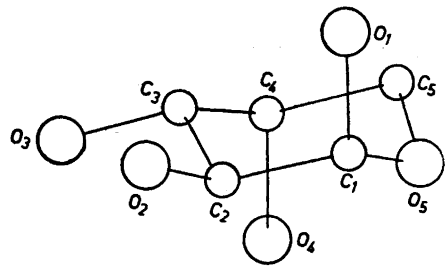


Fig. 4. The molecular structure of β-arabinose.

but confirmed that the "plane" of the molecule is nearly perpendicular to the *c*-axis. Approximate relative *z* coordinates were derived from the *c*-projection and known interatomic distances. The position of the molecule was deduced mainly by considering the possibilities for favourable hydrogen bond formation between neighbouring molecules. By Fourier and difference refinement satisfactory agreement between F_0 and F_c was finally obtained ($R = 0.16$). The electron density map is shown in Fig. 3b. In Table 1 the coordinates of the atoms are given.

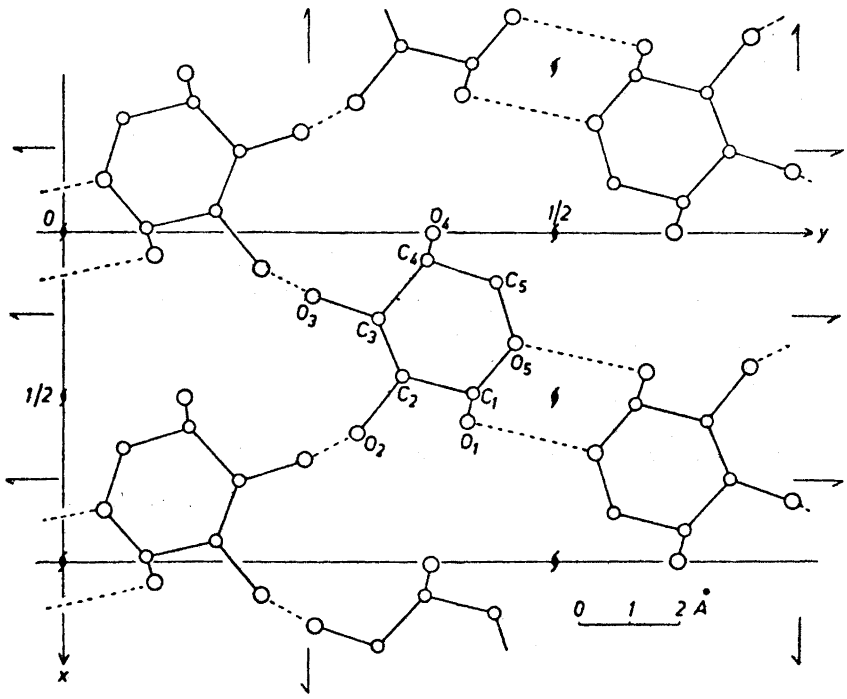


Fig. 5. The *c*-projection of the structure. Broken lines indicate hydrogen bonds.

DISCUSSION OF THE STRUCTURE

The electron density maps in Fig. 3 show that the molecule of β-arabinose has the structure given in Fig. 4. The ring has the staggered "chair" form, and the structure of the molecule is 1*a*2*e*3*e*4*a* (*a* = axial, *e* = equatorial). Thus β-arabinose has the "*cis*" configuration at atoms C_1 and C_2, as a study of its interaction with boric acid also indicates [10]. Its anomer α-arabinose consequently has the conformation 1*e*2*e*3*e*4*a* or 1*a*2*a*3*a*4*e*, probably the former.

The aim of the present investigation was to determine the molecular structure. Hydrogen atoms were neglected and the same temperature factor was used for all the atoms, although the $(F_0—F_c)$ synthesis indicates considerable differences. No great accuracy can therefore be claimed in the bond lengths and bond angles derived from the coordinates in Table 1. Values between 1.48 Å and 1.59 Å were found for the C—C bonds whereas the C—O bonds vary in length between 1.38 Å and 1.46 Å, in agreement with the expected values of 1.54 Å and 1.42 Å, respectively. As was found also for α-glucose and α-rhamnose [2,3], $C_1—O_1$ appears to be somewhat shorter than the other C—O bonds. Possibly this bond has some double bond character, a point which may be of considerable interest for the understanding of the reactions of pyranose sugars. The molecules are linked together by a system of hydrogen bonds, as shown in Fig. 5. The atoms O_1, O_2, O_3 and O_5 take part in hydrogen bonds of lengths between 2.65 Å and 2.75 Å. Surprisingly, the distance from O_4 to the nearest oxygen atom in a neighbouring molecule is as great as 3.0 Å. In order to decide whether or not this corresponds to a weak hydrogen bond, it would appear necessary to determine the position of the corresponding hydrogen atom.

A further refinement of the structure will be carried out by one of us.

REFERENCES

1. Hassel, O. and Ottar, B. *Acta Chem. Scand.* **1** (1947) 929
2. McDonald, T. R. R. and Beevers, C. A. *Acta Cryst.* **5** (1952) 654.
3. McGeachin, H. McD. and Beevers, C. A. *Acta Cryst.* **10** (1957) 227.
4. Cox, E. G. *J. Chem. Soc.* **1931** 2313.
5. Broomhead, J. M. *Acta Cryst.* **1** (1948) 324.
6. Sayre, D. M. *Acta Cryst.* **5** (1952) 60.
7. Zachariasen, W. H. *Acta Cryst.* **5** (1952) 68.
8. Wilson, A. J. C. *Acta Cryst.* **2** (1949) 318.
9. Berghuis, J., *et al. Acta Cryst.* **8** (1955) 478.
10. Bøeseken, J. *Advances in Carbohydrate Chem.* **4** (1949) 189.

Received July 2, 1957.

ACTA CHEMICA SCANDINAVICA 11 (1957) 1599—1603

The Composition of Ribonucleic Acids Isolated from Chloroplasts of *Lamium album* and *Symphytum officinale*

H. LEYON

Institute of Biochemistry, University of Uppsala, Sweden *

The purpose of this investigation was to analyze the nucleic acids of chloroplasts of some plant species to find, eventually, any indication of a species-specificity and of a difference between the RNA of the chloroplasts and that of the corresponding cytoplasm (microsomes).

Chloroplasts of *Lamium album* and *Symphytum officinale* were isolated and fragmented and these preparations were freed from protein by boiling at pH 8. The RNA of the solutions thus obtained was precipitated by means of acid ethanol and was purified by repeated redissolutions and precipitations in combination with centrifugations. After acid hydrolysis the preparations were analyzed quantitatively with respect to guanine, adenine, cytidylic and uridylic acids by means of paper chromatography and spectrophotometry in U.V.

Similar analyses were performed on preparations of sap of fragmented leaves freed from chloroplasts and nuclei.

The analytical data show a characteristic difference between *Lamium album* and *Symphytum officinale* with respect to the molar ratios of the components of the RNA of their chloroplasts. The data obtained for the chloroplasts also differed from those of the cytoplasm of the same species.

From data available by analytical techniques ribonucleic acid has been estimated to be present in chloroplasts and to form up to 2 % of their dry weight [2,3,5,6,10]. Histochemical techniques suggest that both DNA and RNA are to be found in chloroplasts [1,2,7]. There is some ambiguity, however, concerning the presence of DNA since highly polymerized RNA may be responsible for the colouring of the plastids by methyl green [4].

In purified preparations of chloroplasts no trace of DNA was detected but enough RNA could be obtained for analysis regarding its purine and pyrimidine bases.

* Present address: Klarinettgatan 15, *Järnbrott*, Sweden.

MATERIAL AND METHODS

In the autumn (September 1953) nucleoproteins were isolated from purified preparations of chloroplasts from several plant species. After treatment with acid ethanol most of this material was stored at —15°C for further investigations during the winter season. However, when this frozen material was investigated with respect to the composition of its RNA it was found that the material had obviously hydrolyzed and no reproducible data could be obtained. Thus the results reported here are from preliminary experiments made on fresh material immediately after the isolation of the chloroplasts.

Chloroplasts from different plants were found to vary considerably in their stability during the purification procedures. Species with the most stable chloroplasts were selected for further work. All preparative work was carried out in the cold room at about +4°C. Detached leaves were fragmented in a domestic mincing machine and the mass was pressed through cloth. The sap, about 700 ml from each preparation, was diluted immediately with 1/3 volume of 2 M sucrose solution. The suspension was freed from coarse material by filtration through a thin layer of glass wool and by a few minutes centrifugation at low speed. The sap was then centrifuged for 30 min at about 2 000 r. p. m. (radius approximately 10 cm). The green upper layers of the pellets were resuspended in about 50 volumes of cold 0.5 M sucrose solution and centrifuged until the supernatant liquid was clean. This washing was repeated once. During the purification samples were withdrawn occasionally for inspection under the microscope. In this way the chloroplast fragmentation process was observed carefully. Great care was taken to free the suspension from whole and fragmented nuclei. These were detected by the carmine-acetic acid method of Belling and Heitz [9]. It was found that nuclei could be removed by repeated washings and centrifugations as stated by Weier and Stocking [12] or by centrifugation of a chloroplast suspension superimposed on a 2 M sucrose solution in which case nuclei sedimented also through this concentrated solution of sucrose but most of the chloroplasts formed an intermediary layer above the layer of 2 M sucrose. Treatment with the ion exchange resin Amberlite IR 120 (Rohm & Haas, Philadelphia), also removed nuclei effectively.

To obtain an effective extraction of nucleoprotein from the chloroplasts it was found necessary to disintegrate the chloroplasts thoroughly. This was achieved by resuspending the pellet of purified chloroplasts in distilled water (about 30 ml per preparation) to which a few drops of xylene had been added and shaking with glass beads over night in the cold room. By ordinary microscopy and electron microscopy it was found that the fragmentation was very effective. Only small parts of chloroplasts could be seen in the electron micrographs.

The pH of the suspension was raised to 8 by adding some sodium hydroxide solution, traces of sodium chloride was also added after which the solution was kept in boiling water for 10 min. During this procedure there was a fall of pH of 0.4—0.8 units. The precipitate was removed by 45 min centrifugation. The clear supernatant fluid was diluted with an equal volume of ethanol and this mixture was acidified with HCl. The precipitated nucleic acid was sedimented in the centrifuge and then dissolved in distilled water to which a few drops of

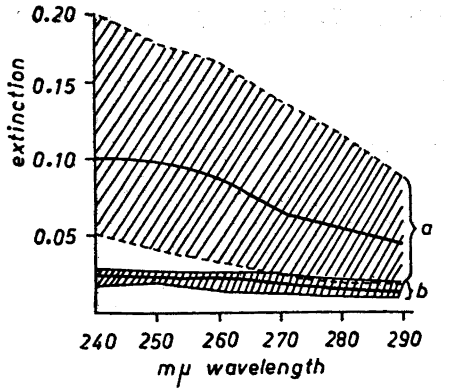


Fig. 1. Absorption in U.V. light of extracts from filter paper Whatman No. 1 before and after washing the paper with 0.1 N HCl. Circular pieces of the paper 2.5 cm in diameter were cut out and extracted each with 5 ml 0.1 N HCl. Heavy lines show average values of 10 measurements at each wave-length. The lined areas include all measurements; a) nontreated papers; b) papers washed in HCl and distilled water.

NaOH had been added. The solution was cleared by centrifugation for 1 h at 3 500 r. p. m. Such precipitation and redissolution of the nucleic acid was twice repeated. The preparation was then only slightly tinged with dark-coloured material.

The alcohol was evaporated from the precipitated nucleic acid in an evacuated vessel. 0.6 ml of 1 N HCl was added to 3 mg of the dry preparation and hydrolysis was performed at 100°C for 1 h. As shown by Smith and Markham [11] this hydrolysis gives guanine, adenine, and the nucleotides cytidylic acid and uridylic acid. The hydrolysis products were analyzed quantitatively by means of paper chromatography as recommended by Smith and Markham [11].

The paper was, however, first investigated with respect to its content of substances absorbing in ultraviolet light and extractable with 0.1 N HCl. For this purpose a series of 10 spots 2.5 cm in diameter were cut out from papers which had not been treated with any solvent. These paper samples were extracted with 5 ml 0.1 N HCl each for about 10 h and the absorption of the extracts in the ultraviolet region was measured. As shown in Fig. 1 the filter paper was rather heterogeneous with respect to its content of U.V.-absorbing material and could be freed from this material by washing with hydrochloric acid. Therefore papers to be used for chromatography were first treated with 0.1 N HCl over night and were then washed with water and dried.

Since a very acid solvent was used in the chromatographical analysis there would be an inherent tendency for the solvent front to remove most of the disturbing material from those areas of the paper where spots were located at the end of the run. However, the best results were obtained on papers which had been washed previously with hydrochloric acid and water.

A mixture which was 0.8 N with respect to HCl and contained 70 % by volume of *tert.* butanol, the remainder being water, was used as solvent during chromatography. Ascending fronts were run on paper Whatman No. 1 in glass vessels. Each spot contained 0.2 ml of the hydrolysate mentioned above. A length of flow of 20—25 cm was obtained after about 30 h at 18—20°C. The papers were dried at room temperature over a ventilating fan. By examining the fluorescence in ultraviolet light the spots could be located easily. The occupied parts of the paper were cut out and the hydrolysis products were extracted from these paper pieces by means of 0.1 N HCl over night in the cold

Table 1. Ultraviolet light absorption of hydrolysis products of rinonucleic acid from chloroplasts of *Lamium album.*

Preparation	Guanine		Adenine		Cytidyl. acid		Uridyl. acid	
	Extinction at 250 mμ	R_F	Extinction at 260 mμ	R_F	Extinction at 280 mμ	R_F	Extinction at 260 mμ	R_F
1	0.372	0.19	0.392	0.32	0.283	0.49	0.201	0.76
2	0.382	0.24	0.378	0.37	0.279	0.54	0.190	0.80
3	0.388	0.24	0.387	0.34	0.284	0.54	0.196	0.77
Concentration,* average, Mol. · 10^{-3}	36.3±1.0		29.7±0.8		29.6±0.6		19.8±0.6	

* Absorbancy coefficients according to Smith and Markham[11] and Ploeser and Loring[8] were used: guanine 10.6×10^3 at 250 mμ
adenine 13.0×10^3 „ 260 „
cytidylic acid 12.72×10^3 at 280 mμ
uridylic acid 9.89×10^3 „ 260 „.

room. The absorption in ultraviolet light of the four samples was measured in a Beckman spectrophotometer model DU against similar extracts of paper pieces cut out near the respective spots.

The R_F-values obtained for the four products were in good agreement with those reported by Smith and Markham and so were the wave-lengths of maximum absorption of the four curves.

In two separate runs the hydrolysate was investigated for amino acids by spraying with ninhydrin. No trace of amino acids was found.

Table 2. Composition of acid hydrolysates of ribonucleic acid from chloroplasts and the corresponding cytoplasms of *Lamium album* ans *Symphytum officinale.* Ratio of molar concentrations, adenine = 1.

Source of RNA	Guanine	Adenine	Cytidylic acid	Uridylic acid
L. album, chloropl.	1.30	1.00	1.00	0.67
L. album, cytopl.	1.17	1.00	0.75	0.35
S. officinale, chloropl.	1.26	1.00	0.76	0.65
S. officinale, cytopl.	1.43	1.00	0.85	0.55

RESULTS

In Table 1 values are collected from chromatograms of 3 preparations of nucleic acid isolated from chloroplasts of *Lamium album* and in Table 2 the molar ratios of guanine, adenine, cytidylic acid and uridylic acid in hydrolysates from nucleic acid preparations from chloroplasts and cytoplasm of *Lamium album* and *Symphytum officinale* are recorded.

There is a clear difference between the two kinds of chloroplasts with respect to cytidylic acid. There is also, within each species, a difference between the RNA from the chloroplasts and that from the cytoplasm. The values for the cytoplasmic RNA were obtained from only one analysis each, those for the chloroplasts represent average data each from three experiments (*cf.* Table 1).

REFERENCES

1. Chiba, Y. *Cytologia Tokyo* **16** (1951) 259.
2. Granick, S. *Handb. Pflanzenphysiol.* **1** (1955) 558.
3. Jagendorf, A. T. and Wildman, S. S. *Plant Physiol.* **29** (1954) 270.
4. Kurnick, N. B. *J. Gen. Physiol.* **33** (1950) 243.
5. Mc Clendon, J. H. *Am. J. Botany* **39** (1952) 275.
6. Menke, W. *Hoppe-Seylers Z. physiol. Chem.* **257** (1938) 43.
7. Metzner, H. *Naturwiss.* **39** (1952) 64.
8. Ploeser, J. Mc T. and Loring, H. S. *J. biol. Chem.* **178** (1949) 431.
9. Romeis, B. *Taschenbuch der mikroskopischen Technik*, München u. Berlin 1943.
10. Sisakyan, N. M. and Chernyak, M. S. *Doklady Akad. Nauk SSSR.* **87** (1952) 469.
11. Smith, J. D. and Markham, R. *Biochem. J.* **46** (1950) 509.
12. Weier, E. and Stocking, C. R. *Am. J. Botany* **39** (1952) 720.

Received July 6, 1957.

ACTA CHEMICA SCANDINAVICA 11 (1957) 1604—1612

Short Communications

Protein-bound Sialic Acids in Human, Hog and Horse Kidneys

ERIK MÅRTENSSON, AINO RAAL and LARS SVENNERHOLM

Department of Medical Biochemistry, University of Gothenburg, Gothenburg, Sweden

As part of an investigation of the protein-bound carbohydrates in mammalian kidneys, carried out by one of us (E.M.), the sialic acids were isolated from human, hog and horse kidneys. Blix *et al.*[1] have by the X-ray diagram pattern differentiated between four sialic acids, *viz.* ovine (N-acetylsialic acid), porcine (N-glycolylsialic acid), bovine and equine (N, O-diacetylsialic acid) sialic acids. All these acids were isolated from the submaxillary mucin of the animals. The procedure applied by Blix *et al.* is unsuitable for the isolation of sialic acids from organs with a low sialic acid content[2]. In such cases chromatography on anion exchange resins is to be preferred, but by this technique only N-acetylsialic acid and N-glycolylsialic acid can be isolated quantitatively as the labile O-acetyl group is partly split off in the course of the preparation. However, our main problem was to ascertain the possible occurrence of N-glycolylsialic acid, as at quantitative estimation it gives about 20 % higher molar absorbancy than N-acetylsialic acid and N,O-diacetylsialic acid[3,4]. The three species investigated were chosen because their submaxillary mucins contain different sialic acids.

Experimental. Materials. Human kidneys, from three young healthy persons killed by accidents, were removed as soon as possible after death (12—24 h) with intact blood vessels. The hog and horse kidneys were also dissected with intact vessels.

Isolation procedure. The kidneys were perfused with physiological saline through their renal artery until the perfusion solution was free from visible amounts of blood cells or pigments. Then the kidneys were homogenized in a Turmix blendor and extracted twice with four volumes of acetone at +4°C for 24 h. The remaining lipids were extracted with methanol-chloroform (2:1 v/v) in a Soxhlet apparatus for 24 h. The isolation of the sialic acids from the defatted kidney tissues was performed with the ion-exchange procedure earlier described[2]. The lyophilized sialic acids were rather impure and rechromatography on the resins was done as a routine. The yields of recrystallized sialic acids were 50—75 % (the lowest yield was obtained from horse kidney).

Identification. The specific optical rotation had the same value for the three specimens, $[\alpha]_D$ —31° ± 1. In paper partition chromatography[2] an elongated spot was given by hog and horse sialic acids, while the spot of the human acid was more round and distinct. The X-ray diffraction patterns (Fig. 1) of the sialic acids were all of the same type as the pattern of ovine sialic acid[1] (N-acetylsialic acid). No lines of the porcine sialic acid pattern were indicated. The determination of glycolic acid, performed according to Klenk and Uhlenbruck[5], showed that the human sialic acid contained no glycolic acid, while the other two contained about 3 % of glycolic acid (Table 1).

Discussion. Although the X-ray diffraction patterns only showed the occurrence of N-acetylsialic acid, the acids from hog

Table 1. Determination of glycolic acid in sialic acids.

Source of sialic acid	Glycolic acid, %	Calc. amount of N-glycolylsialic acid, %
Human kidney	0.1	0
Hog kidney	3.2	14
Horse kidney	2.6	11
Human serum	0.1	0
Hog submaxillary mucin	20.9	90



Fig. 1. X-Ray diffraction patterns of sialic acids isolated from (a) human, (b) hog and (c) horse kidneys.

and horse kidneys contained appreciable amounts of glycolic acid. The diversity of the results might be explained either by some unspecificity of the glycolic acid method or by lacking sensitivity of the X-ray method for rather large admixtures of a second sialic acid.

The first alternative seems rather unlikely as no glycolic acid could be indicated in sialic acids from human sources. The sialic acid isolated from hog submaxillary mucin contained 90 % of the theoretical value for N-glycolylsialic acid. In the resorcinol method [4] the sialic acids from hog and horse kidneys had some per cent higher molar absorbancy indices than our standard sample of N-acetylsialic acid. That is also a support of the occurrence of N-glycolylsialic acid, as the latter has about 20 % greater molar absorbancy index than N-acetylsialic acid.

Regarding the second alternative it might be possible that N-glycolylsialic acid is built into the crystal lattice of N-acetylsialic acid, as the two sialic acids only differ by the substitution of a hydrogen atom in the acetic acid moiety of N-acetylsialic acid with a hydroxyl group. We have also evidence that N-acetylsialic acid can be built into the crystal lattice of N-glycolylsialic acid. In a preparation of sialic acid from beef serum N-acetylsialic acid made out 60 % and N-glycolylsialic acid 40 %. The X-ray diffraction pattern was the same as that of porcine sialic acid (N-glycolylsialic acid). This may appear puzzling as the amount of N-glycolylsialic acid is lower than that of N-acetylsialic acid, but might be explained by the lower solubility of N-glycolylsialic acid.

Conclusion. The sialic acids from human, hog and horse kidneys were isolated. X-Ray diffraction patterns showed N-acetylsialic acid only, but the estimation of glycolic acid demonstrated that hog and horse sialic acids also contained N-glycolylsialic acid. It is concluded that the X-ray diffraction pattern is unsuitable as a criterion of the uniformity of a sialic acid.

Acknowledgement. The authors are indebted to Dr. S. Abrahamson, Kemiska Institutionen, Uppsala, for performing the X-ray diagrams.

1. Blix, G., Lindberg, E., Odin, L. and Werner, I. *Acta Soc. Med. Upsaliensis* **61** (1956) 1.
2. Svennerholm, L. *Acta Soc. Med. Upsaliensis* **61** (1956) 75.
3. Svennerholm, L. *Arkiv Kemi* **10** (1957) 577.
4. Svennerholm, L. *Biochim. et Biophys. Acta* **24** (1957) 604.
5. Klenk, E. and Uhlenbruck, G. *Hoppe-Seyler's Z. physiol. Chem.* **307** (1957) 266.

Received October 2, 1957.

Note on the Crystal Structure of Trititanium Pentoxide

STIG ÅSBRINK and ARNE MAGNÉLI

Institute of Inorganic and Physical Chemistry, University of Stockholm, Stockholm, Sweden

The crystal structure of trititanium pentoxide has been determined from single-crystal X-ray data using Fourier techniques. The oxide specimen was prepared by melting an appropriate mixture of titanium metal and titanium dioxide (both better than 99.97 % pure) in an electric arc furnace under argon atmosphere and subsequent annealing of the crushed sample for two weeks at 1 150°C in a sealed, evacuated silica tube. In this way black, prismatic crystals several hundredths of a millimeter in length were obtained. The composition of the sample after the heat-treatment was found to be $TiO_{1.667}$ (calculated for Ti_3O_5: $TiO_{1.667}$). Powder photographs of samples quenched in the electric arc furnace and of those annealed at 1 150°C were identical.

The following data were obtained for the monoclinic structure:

Unit cell dimensions (from Guinier powder photographs taken with Cu$K\alpha_1$ radiation using potassium chloride (a = 6.292 Å) as an internal standard)

a = 9.757 Å, b = 3.802 Å, c = 9.452 Å, β = 93°.11

Cell content: 4 Ti_3O_5 (observed density 4.20, calculated density 4.24).

Space-group: $C2/m$ (No. 12)

Arrangement of atoms: All atoms occupy four-fold positions 4(i):
(000, $\frac{1}{2}\frac{1}{2}$0) + x0z, $\bar{x}$0$\bar{z}$

4 Ti_1 with x = 0.129, z = 0.043
4 Ti_2 with x = 0.280, z = 0.268
4 Ti_3 with x = 0.053, z = 0.366
4 O_1 with x = 0.187, z = 0.063
4 O_2 with x = 0.236, z = 0.239
4 O_3 with x = 0.095, z = 0.337
4 O_4 with x = 0.454, z = 0.161
4 O_5 with x = 0.371, z = 0.442

The quotient $\Sigma||T_o|-|T_c||/\Sigma|T_o|$ is 0.14 (calculated for all reflexions $h0l$, $h1l$ and $h2l$ registered with Cu$K\alpha$ radiation).

Interatomic distances:
Ti—O 1.78—2.21 Å
O—O 2.55—3.25 Å

The structure is illustrated in Fig. 1. The titanium atoms are indicated by

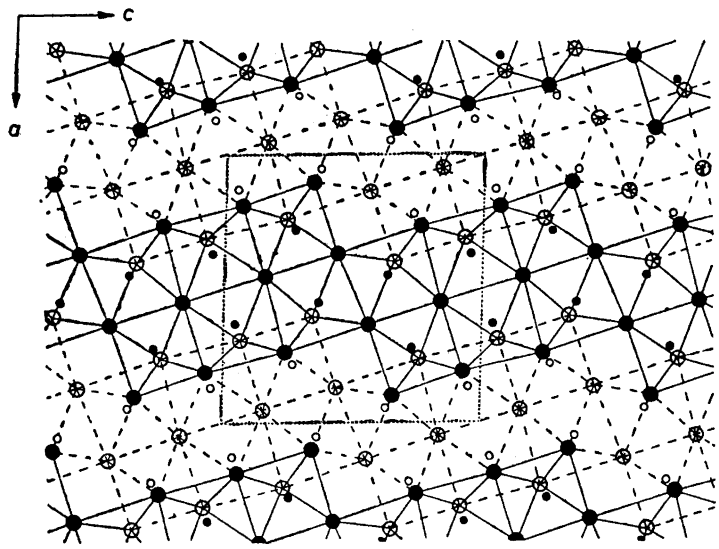


Fig. 1.

smaller rings and the oxygen atoms by larger ones. Open and filled circles represent atoms at $y = 0$ and $y = \frac{1}{2}$, respectively. The extension of the unit mesh is indicated by dotted lines. The titanium atoms are surrounded by six oxygen atoms to form TiO_6 octahedra which are joined by edges and corners. The coupling together of the octahedra is different from that found in anosovite (pseudobrookite structure) by Zhdanov and Rusakov [1]. Studies on the $(Ti_{1-x}, Fe_x)_3O_5$ system have shown the pseudobrookite-type structure to be present even at rather low contents of iron ($x < 0.05$)[2]. Further studies on the relationships between the Ti_3O_5 structure found in this investigation and the anosovite structure are in progress.

Full details on this investigation and a discussion of the structure will be given elsewhere.

This investigation forms part of a research programme on metal oxides and related compounds financially supported by the *Swedish Natural Science Research Council.*

1. Zhdanov, G. S. and Rusakov, A. A. *Trudy Inst. Krist., Akad. Nauk S.S.S.R.* **9** (1954) 165.
2. Åsbrink, S. *To be published.*

Received October 2, 1957.

Correction to: Refractometric Determination of Diffusion Constants in the Critical Region of Partly Miscible Liquids *

HANS LUDVIG LORENTZEN and BJØRN BERGSNOV HANSEN

Universitetets Kjemiske Institutt, Blindern-Oslo, Norway

In Fig. 4, p. 895 the figures of the ordinate scale should be one fifth of those shown.

Consequently, the inclination of the resultant straight line of Fig. 4, which is stated at the end of the text to be 0.37 cm² per day and °C, should in fact be one fifth of this amount, *i. e.*, 0.074 cm² per day and °C.

* *Acta Chem. Scand.* **11** (1957) 893.

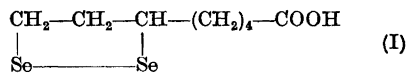
Received October 15, 1957.

The Selenium Analogue of 6-Thioctic Acid

GÖRAN BERGSON

Chemical Institute, University of Uppsala, Sweden

In connection with preparative and physico-chemical studies on organic disulphides and diselenides [1], particularly cyclic molecules [2], the author started a synthesis of the selenium analogue of 6-thioctic acid (α-lipoic acid) some months ago. The new acid (I), for which the name 6-selenoctic acid is proposed, has now been obtained in crystalline form, and investigations of its chemical and biochemical properties are in progress.



(I)

The primary aim of this investigation was twofold. First one could expect the 5-membered ring in 6-selenoctic acid to be more stable than the unsubstituted 1,2-diselena*cyclo*pentane, because it is known that substituents stabilize strained rings. Secondly, 6-selenoctic acid might possess interesting biological properties because of its similarity to 6-thioctic acid. When the present investigation was in progress, Schwarz and Foltz [3] reported the very remarkable discovery of a selenium-containing factor in casein and yeast. This factor ("factor 3") has been known for some years to be active against dietary necrotic liver degeneration and other diseases [3,4], but only recently Schwarz and Foltz showed that the biological action was connected with a low molecular weight organic selenium compound of unknown structure. Since pyruvic acid and lactic acid are accumulated in the blood of factor 3 deficient animals it seems possible to the present author that factor 3 is a cofactor in the oxidative decarboxylation of pyruvic acid. It is not impossible that 6-selenoctic acid might act as such a cofactor like 6-thioctic acid, and the hypothesis might be advanced that factor 3 is identical with or related to 6-selenoctic acid.

6-Selenoctic acid has been prepared in a way analogous to that used by Reed and

smaller rings and the oxygen atoms by larger ones. Open and filled circles represent atoms at $y = 0$ and $y = \frac{1}{2}$, respectively. The extension of the unit mesh is indicated by dotted lines. The titanium atoms are surrounded by six oxygen atoms to form TiO_6 octahedra which are joined by edges and corners. The coupling together of the octahedra is different from that found in anosovite (pseudobrookite structure) by Zhdanov and Rusakov [1]. Studies on the $(Ti_{1-x}, Fe_x)_3O_5$ system have shown the pseudobrookite-type structure to be present even at rather low contents of iron ($x < 0.05$)[2]. Further studies on the relationships between the Ti_3O_5 structure found in this investigation and the anosovite structure are in progress.

Full details on this investigation and a discussion of the structure will be given elsewhere.

This investigation forms part of a research programme on metal oxides and related compounds financially supported by the *Swedish Natural Science Research Council.*

1. Zhdanov, G. S. and Rusakov, A. A. *Trudy Inst. Krist., Akad. Nauk S.S.S.R.* **9** (1954) 165.
2. Åsbrink, S. *To be published.*

Received October 2, 1957.

Correction to: Refractometric Determination of Diffusion Constants in the Critical Region of Partly Miscible Liquids *

HANS LUDVIG LORENTZEN and BJØRN BERGSNOV HANSEN

Universitetets Kjemiske Institutt, Blindern-Oslo, Norway

In Fig. 4, p. 895 the figures of the ordinate scale should be one fifth of those shown.

Consequently, the inclination of the resultant straight line of Fig. 4, which is stated at the end of the text to be 0.37 cm² per day and °C, should in fact be one fifth of this amount, *i. e.*, 0.074 cm² per day and °C.

* *Acta Chem. Scand.* **11** (1957) 893.

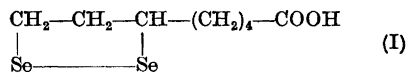
Received October 15, 1957.

The Selenium Analogue of 6-Thioctic Acid

GÖRAN BERGSON

Chemical Institute, University of Uppsala, Sweden

In connection with preparative and physico-chemical studies on organic disulphides and diselenides [1], particularly cyclic molecules [2], the author started a synthesis of the selenium analogue of 6-thioctic acid (α-lipoic acid) some months ago. The new acid (I), for which the name 6-selenoctic acid is proposed, has now been obtained in crystalline form, and investigations of its chemical and biochemical properties are in progress.

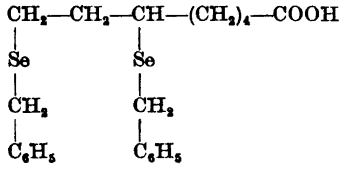


(I)

The primary aim of this investigation was twofold. First one could expect the 5-membered ring in 6-selenoctic acid to be more stable than the unsubstituted 1,2-diselena*cyclo*pentane, because it is known that substituents stabilize strained rings. Secondly, 6-selenoctic acid might possess interesting biological properties because of its similarity to 6-thioctic acid. When the present investigation was in progress, Schwarz and Foltz [3] reported the very remarkable discovery of a selenium-containing factor in casein and yeast. This factor ("factor 3") has been known for some years to be active against dietary necrotic liver degeneration and other diseases [3,4], but only recently Schwarz and Foltz showed that the biological action was connected with a low molecular weight organic selenium compound of unknown structure. Since pyruvic acid and lactic acid are accumulated in the blood of factor 3 deficient animals it seems possible to the present author that factor 3 is a cofactor in the oxidative decarboxylation of pyruvic acid. It is not impossible that 6-selenoctic acid might act as such a cofactor like 6-thioctic acid, and the hypothesis might be advanced that factor 3 is identical with or related to 6-selenoctic acid.

6-Selenoctic acid has been prepared in a way analogous to that used by Reed and

Ching-I Niu [5] in the preparation of 6-thioctic acid. Ethyl 6,8-dichlorooctanoate was allowed to react with the sodium salt of benzylselenol in absolute alcoholic solution, after which the ester was saponified and 6,8-dibenzylselenoloctanoic acid (II) isolated. This acid was treated with sodium



(II)

in liquid ammonia, and the product oxidized with air. From the reaction mixture 6-selenoctic acid was isolated. It consists of brownish-red crystals melting at 88—90.5°. The UV-absorption of 6-selenoctic acid has a maximum at 440 mμ. This is a good proof for the existence of the 5-membered ring and it shows that the substance is monomer [2]. The IR-absorption in the region 2—15 μ has been recorded and it is in accord with formula I. The molecular weight as determined by the Rast camphor method is 326 (calc. 300).

Experimental: 6,8-Dibenzylselenoloctanoic acid (II). 1.56 g of sodium is dissolved in 50 ml of abs. ethanol and 11.59 g of benzylselenol and 8.17 g of ethyl 6,8-dichlorooctanoate [5] is added. The mixture is stirred and refluxed in nitrogen atm. for 5 h. After cooling to room temperature 3.80 g of potassium hydroxide is added, and the mixture stirred at room temperature for 20 h. The reaction mixture is poured into 175 ml of water, acidified with 6 N HCl, and the product extracted with 2 × 50 ml ether. The combined etherial extracts are dried with sodium sulphate and the ether removed in vacuum. The crude acid solidifies at room temperature. It can be purified by dissolving it in a mixture of ether and petroleum ether and allowing the ether to evaporate slowly. In this way a fine crystalline almost white powder was obtained. Melting point 54—57°. (Equiv. wt: Found 477; calc. 482. % Se: Found 33.0; calc. 32.8).

6-Selenoctic acid (I): 0.35 g of sodium was dissolved in about 50 ml of liquid ammonia and 2.41 g (0.005 mole) of II in 10 ml toluene was added dropwise. A little more sodium was added to complete the reaction, and the ammonia was allowed to evaporate slowly. The residue was extracted with 70 ml of water, and the pH of this solution was adjusted to 7—8. A trace of $FeCl_3$ was added and a rapid stream of air passed through the solution. When excess hydrochloric acid was added a dark oil separated which was taken up in 50 ml of chloroform. The extract was dried with sodium sulphate, and when the solvent was removed in vacuum the crude 6-selenoctic acid solidified. The substance was purified by recrystallization from *n*-hexane, which gave a dark brownish-red crystalline powder m.p. 87—90°. (Equiv.wt: Found 298; calc. 300. Mol. wt: Found 326; calc. 300. % Se: Found 51.9; calc. 52.6).

A small sample was recrystallized again from *n*-hexane. The product consisted of brownish-red crystal flakes, m.p. 88—90.5°. The exact yield of the syntheses described above cannot be specified at present, but it exceeds 50 %.

I wish to express my gratitude to Professor Arne Fredga for his stimulating interest and much helpful advice. I am also indebted to Dr. Lennart Schotte for many important discussions and for his kind interest in this work. A grant from the *Swedish Natural Science Research Council* is gratefully acknowledged.

1. Bergson, G. *Arkiv Kemi* **9** (1956) 121.
2. Bergson, G. and Claeson, G. *Acta Chem. Scand.* **11** (1957) 911.
3. Schwarz, K. and Foltz, C. M. *J. Am. Chem. Soc.* **79** (1957) 3292.
4. Schwarz, K. *Proc. Soc. Exptl. Biol. Med.* **80** (1952) 319; *Ann. N. Y. Acad. Sci.* **57** (1954) 878.
5. Reed, L. J. and Ching-I Niu. *J. Am. Chem. Soc.* **77** (1955) 416.

Received October 4, 1957.

Optically Active α-(2-Naphthyl)-ethylamine as Resolving Base

ARNE FREDGA, BERNDT SJÖBERG and RUNE SANDBERG

Chemical Institute, University of Uppsala, Uppsala, Sweden

The number of bases available for optical resolution of racemic acids is rather restricted. To be suitable for this purpose, a base must be optically active, chemically stable and not too expensive. In addition, its salts must have good crystallisation properties. About ten commercially available natural alkaloids fulfil these conditions. A few synthetic bases, *e. g.* α-phenylethylamine and α-phenyl*iso*propylamine [1] (benzedrine), for which both antipodes are available, have also been used with good success. In recent years, quaternary alkaloid salts [2] and *iso*thiuronium salts [3] have been recommended, especially for weak acids. The purpose of this paper is to draw attention to α-(1-naphthyl)-ethylamine and α-(2-naphthyl)-ethylamine, especially to the latter compound.

The synthesis and resolution of these bases were first described by Samuelsson in 1923 [4]. The preparation of the methyl naphthyl ketones used as starting materials was, however, very tedious in those days and to our knowledge the amines have not found practical use for stereochemical purposes. For some years the ketones have been commercially available and the optically active bases are now as easily accessible as the active phenylethylamines. The salts of the 2-naphthyl derivative especially crystallise very readily and we have found this base suitable for the resolution of several acids, *e. g.* terpenylic acid and α-(2-thianaphthenyl)-propionic acid. For the resolution of the latter acid, ten different bases were tried but only α-(2-naphthyl)-ethylamine yielded the levorotatory acid [5]. In the case of terpenylic acid, this amine had far better resolving power than any other base tried [6].

The resolution of the racemic α-(2-naphthyl)-ethylamine was carried out according to the method of Samuelsson. We have found, however, that a slight modification in the amount of solvent is advisable to ensure the best resolution. A brief description is given here; for details the original paper of Samuelsson should be consulted.

Experimental. Racemic α-(2-naphthyl)-ethylamine was prepared according to Organic Reactions [7].

Resolution. A mixture of 128.4 g (0.075 mole) of the racemic amine and 112.6 g (0.075 mole) of tartaric acid is dissolved in 5.0 l of hot water. After standing at room temperature over-night, the crystals are filtered off. This procedure gives about 120 g salt of the (+)-amine. The base is liberated with dilute sodium hydroxide and taken up in ether. The ether solution is transferred to a 5-l beaker and 95 ml (0.19 mole) of 2 M sulphuric acid is added with vigorous stirring. The salt obtained is recrystallised twice from the necessary amount of boiling water, yielding the sulphate of the pure (+)-amine with the composition $(C_{12}H_{13}N)_2 \cdot H_2SO_4 \cdot 2H_2O$ and the m. p. 261—263°.

From the mother liquor after the first crystallisation of the tartrate the partially resolved (—)-amine is liberated and treated in the same way.

The yield of each antipode is 50—60 % of the theoretical.

The amines are best stored as sulphates. The free bases have the m. p. 53° and $[\alpha]_D = \pm 19°$ (in ethanol solution).

1. Matell, M. *Acta Chem. Scand.* **7** (1953) 698.
2. Wolf, D. E., Mozingo, R., Harris, S. A., Anderson, R. C. and Folkers, K. *J. Am. Chem. Soc.* **67** (1945) 2100.
3. Klötzer, W. *Monatsh.* **87** (1956) 346.
4. Samuelsson, E. *α- und β-Naphtäthylamin.* Diss. Lund 1923.
5. Sjöberg, B. *To be published.*
6. Fredga, A. and Sandberg, R. *To be published.*
7. *Organic Reactions*, Vol. *V*, New York 1949, p. 320.

Received October 16, 1957.

Inhibition of *Lactobacillus leichmannii* 313 by Purine Nucleotides

ARNE E. BOLINDER

Division of Food Chemistry, Royal Institute of Technology, Stockholm 70, Sweden

Plate assays for vitamin B_{12}-factors, deoxyribosides, and deoxyribotides as well as bioautography of these growth factors have been carried out in this laboratory using *Lactobacillus leichmannii* 313 ATCC 7830 as the test organism [1,2]. This paper deals with the growth inhibitory activity of several purine nucleotides, notably adenine ribotides, in the *Lb. leichm.* 313 cup plate assay for vitamin B_{12}, deoxyribosides, and deoxyribotides. A report is also given on the usefullness of *Lb. leichm.* 313 for the cup plate assay and bioautography of the growth inhibitory purine nucleotides.

Large plates were used, each containing 150 ml of agar medium inoculated with *Lactobacillus leichmannii* 313 ATCC 7830. The media contained high concentrations of vitamin B_{12}, deoxyribosides, or deoxyribotides, in order to obtain heavy growth in the plates and thereby give a more pronounced appearance of growth inhibition. For the cup plate assays, 0.03 ml aliquots of the test solutions were pipetted into cups, 6 mm in diameter and the plates were incubated over night at 37° C. A detailed report of the preparation of these plates will be published later in this journal.

A series of plate experiments were first made, using *Lb. leichm.* 313 in two types of media which contained: 1) 150 mμg of vitamin B_{12} and 2) 150 μg of thymidine per plate. When tested in the cup plate assay the following purine nucleotides formed clear (or almost clear) inhibition zones: AMP-3'*, adenylic acid (mixture of AMP-2' and AMP-3'), AMP-c2'3' [b], AMP 5' [b], DAMP-5' [c], IMP-5' [d].

Table 1. The inhibitory activity of purine nucleotides in *Lb. leichmannii* 313 ATCC 7830 plates with media containing either vitamin B_{12} (150 mμg per plate) or thymidine (150 μg per plate).

Compound tested	Concentration μg/ml	Inhibition zone diameter in mm [a] *Lb. leichm.* 313 medium containing: Vit. B_{12}	Thymidine
AMP-3' [b]	10	12.0	12.0
	30	14.7	14.8
	100	18.0	18.0
	300	21.5	21.3
	500	23.2	23.0
Adenylic acid [b] (mixture of AMP-2' and AMP-3')	30	13.0	13.3
	100	16.0	16.4
	300	19.0	19.3
	1 000	23.2	23.2
AMP-c2'3' [b]	30	14.0	14.2
	100	17.0	17.2
	300	20.0	20.7
	1 000	25.0	24.8
AMP 5' [b]	10	12.3	13.2
	30	15.4	15.6
	100	18.8	19.0
	300	22.0	22.2
	1 000	25.5	25.7
DAMP-5' [c]	30	14.5	13.9
	100	17.8	17.0
	300	21.0	20.1
	1 000	24.4	23.1
IMP-5' [d]	30	12.7	12.5
	100	14.4	14.0
	300	15.7	15.6
	1 000	16.9	17.2

[a] Each figure for the inhibition zone diameter represents the average reading obtained from twelve cups, evenly distributed in three plates.

[b] Forms sharp edged and completely clear inhibition zones.

[c] Forms well defined and almost clear inhibition zones.

[d] Forms somewhat fainter inhibition zones than those formed by DAMP-5'.

* The following abbreviations are used in this paper: AMP-2', AMP-3' and AMP-c2'3' for the 2'-, 3'-, and the cyclic 2'3'-monophosphates of adenosine; AMP-5', DAMP-5', IMP-5', GMP-5', and DGMP-5' for the 5'-monophosphates of adenosine, deoxyadenosine, inosine, guanosine, and deoxyguanosine; ADP, IDP, ATP, and ITP for the 5'-di- and -tri-phosphates of adenosine and inosine.

and AMP-3′), AMP-c2′3′, AMP-5′, DAMP-5′, and IMP-5′. The sizes of the inhibition zones formed by these compounds are given in Table 1. Bioautography using five different solvent systems showed that the UV-absorbing spot of each of AMP-3′, AMP-c2′3′, AMP-5′, DAMP-5′, and IMP-5′ always corresponded to the growth inhibition spot. Bioautography of adenylic acid revealed that its growth inhibitory activity was due only to AMP-3′; AMP-2′ was inactive.

Very faint and diffuse inhibition zones were formed by DGMP-5′, GMP-5′, and guanylic acid (mixture of the 2- and 3′-phosphates) when these compounds were tested in high concentrations.

When high concentrations of AMP-2′ and ADP were tested in the *Lb. leichm.* 313 plates small inhibition zones were formed, but bioautography revealed that these growth inhibitory effects were due to trace contamination by AMP-3′ and AMP-5′, resp. Similarly the low inhibitory activity of high concentrations of IDP and ITP were probably due to trace contamination by IMP-5′.

No inhibition zones could be detected in the plates when the following compounds were tested separately at concentrations of 1 mg/ml: (a) the ribosides of cytosine, uracil, adenine, guanine, xanthine, and hypoxanthine, (b) uridylic acid and cytidylic acid (mixtures of the 2′- and 3′-phosphates), (c) the 2′- and the 3′-phosphates of cytidine, (d) the 5′-phosphates of uridine and cytidine, (e) the cyclic 2′3′-phosphates of uridine and cytidine, (f) ATP, and (g) yeast nucleic acid (also tested in 10 mg/ml).

As can be seen from Table 1, the two types of *Lb. leichm.* 313 plates gave almost the same size of inhibition zones for each of the strongly growth-inhibitory purine nucleotides. The straight-line relationship between the logarithm of the concentration of the test solutions in the cups and the mean zone diameter normally found in cup plate assays, was obtained for all these compounds. Already after 3—4 h of incubation at 37° C the inhibition zones produced by the purine nucleotides could be seen against the faint background growth in the *Lb. leichm.* 313 plates. These inhibition zones were almost the same size as those formed after the routine incubation time of 16—18 h, when heavy background growth was obtained in the plates. Prolonged incubation of the plates to 48 h did not have any influence on the inhibition zones already formed.

Using these *Lb. leichm.* 313 plates as little as 0.1 μg of either AMP-3′, AMP-c2′3′, or AMP-5′, or 0.5 μg of DAMP-5′ could be detected bioautographically, whereas about 2—3 μg was required for the detection of these compounds by inspection in UV-light. Only amounts larger than 1 μg of IMP-5′ could be detected bioautographically.

In another series of inhibition experiments *Lb. leichm.* 313 plates were made using media containing 150 μg per plate of one of the following nine compounds: deoxyadenosine, DAMP-5′*, deoxyguanosine, DGMP-5′, deoxyinosine, deoxycytidine, deoxycytidylic acid, deoxyuridine, and thymidylic acid. In all these nine different plates the same inhibition patterns for the purine nucleotides were observed as for the two types of plates previously used in which the media contained either vitamin B_{12} or thymidine.

Turbidimetric tube tests with *Lb. leichm.* 313 showed that only early growth of this organism was inhibited by the adenine ribotides. Merely prolonged incubation was sufficient to overcome growth inhibition, in contrast to the plate tests mentioned above.

Inhibition experiments were also made with *Lactobacillus leichmannii* 327 ATCC 7831 plates containing vitamin B_{12} 150 mμg, thymidine 150 μg, or thymidylic acid 150 μg per plate. The same inhibition pattern for the adenine nucleotides was obtained as in the *Lb. leichm.* 313 plates. However, no inhibition zones were formed by IMP-5′ in the *Lb. leichm.* 327 plates.

Some additional inhibition plate experiments were made with other test organisms. However, none of the purine nucleotides which were found to be inhibitory in the plate tests with the two *Lb. leichm.* strains had any inhibitory effect on the growth of the following organisms: *Thermobacterium acidophilus* R-26 ATCC 11506, (grown with large amounts of thymidine or thymidylic acid), *Escherichia coli* 113—3 ATCC 1105 (grown with large quantities of vitamin B_{12} or methionine),

* At the low concentration of 1 μg/ml in the plate medium, DAMP-5′ showed only growth promoting activity. When tested at concentrations of 10 μg/ml and above, DAMP-5′ formed inhibition zones in the cup plate assay.

Streptococcus faecalis ATCC 8043 (grown with large amounts of folic acid or thymidine), and *Pediococcus cerevisiae (Leuconostoc citrovorum)* ATCC 8081 (grown in a high concentration of folinic acid or thymidine).

Some earlier reports in the literature have dealt with the growth inhibitory activity of adenylic acids on certain vitamin B_{12} requiring lactobacilli. Using tube assay procedures Skeggs *et al.* have studied this effect on *Lb. acidophilus (Lb. bifidus)* ATCC 4963 [3-5] and on *Lb. leichm.* 326 ATCC 4797 [6]. The specific growth inhibitory activity of several purine nucleotides in the *Lb. leichm.* 313 plate assay for vitamin B_{12}, deoxyribosides, and deoxyribotides as observed here, needs further investigation before any conclusions can be drawn concerning the mechanism of these inhibitions.

Several of the nucleotides were kindly supplied by Dr. P. Reichard, Karolinska Institutet, Stockholm.

1. Lundin, H. *European Brewery Conv. Proc. 4th Congr. Nice*, **1953** 9.
2. Bolinder, A., Kurz, W. and Lundin, H. *J. Inst. Brewing* **62** (1956) 497.
3. Skeggs, H. R., Spizizen, J. and Wright, L. D. *J. Am. Chem. Soc.* **72** (1950) 811.
4. Skeggs, H. R., Wright, L. D., Valentik, K. A., Nepple, H. and Spizizen, J. *Federation Proc.* **9** (1950) 228.
5. Skeggs, H. R., Nepple, H. M., Spizizen, J. and Wright, L. D. *J. Bacteriol.* **61** (1951) 41.
6. Skeggs, H. R., Nepple, H. M., Valentik, K. A., Huff, J. W. and Wright, L. D. *J. Biol. Chem.* **184** (1950) 211.

Received October 26, 1957.

ACTA CHEMICA SCANDINAVICA 11 (1957) 1613—1621

N-Substituted Alkyltriaminosilanes

I. On the Reaction of *n*-Propyltrichlorosilane with Primary and Secondary Amines

LEWI TANSJÖ

Department of Organic Chemistry, University of Lund, Lund, Sweden

As a part of an investigation on aminosilanes the synthesis of N-substituted *n*-propyltriaminosilanes from *n*-propyltrichlorosilane and various primary and secondary amines was studied.

Observations were made which indicate a probable influence by the steric and electric properties of the amines on the reaction between *n*-propyltrichlorosilane and amines.

The preparation of thirty compounds which have not earlier been reported in the literature is described.

During the last ten years a great number of organosilicon compounds in which silicon is bound to one or more amino-nitrogen atoms have been described in the literature. Among these, however, there are only a few [1-3] with three silicon-nitrogen bonds and one silicon-carbon bond. In this work there will be reported the synthesis of some new aminosilanes of this type, containing the trifunctional silicon group n-$C_3H_7Si{\equiv}$.

It is well known that the silicon-chlorine bond reacts readily with ammonia and primary and secondary amines. If all the chlorine atoms in *n*-propyltrichlorosilane are exchanged, the reaction in the case of a primary amine takes part according to the formula

$$n\text{-}C_3H_7SiCl_3 + 6\ RNH_2 \rightarrow n\text{-}C_3H_7Si(NHR)_3 + 3\ RNH_3Cl \qquad (A)$$

Amine hydrochlorides containing silicon were not obtained, and tertiary amines (trimethylamine, triethylamine, and pyridine) did not react with *n*-propyltrichlorosilane to give quaternary salts. Nor did they under the conditions employed give addition compounds, n-$C_3H_7SiCl_3{:}xR_3N$, of the type which was proposed by Trost [4] to be formed between silicon tetrachloride and tertiary amines.

When *n*-propyltrichlorosilane in ether or benzene solution reacted with an amine with a small R-group, the above reaction proceeded rapidly with

evolution of considerable heat, giving the calculated amount of hydrochloride which could be filtered from the reaction mixture.

However, when an ether or benzene solution of *n*-propyltrichlorosilane was added to an excess of *tert.*-butylamine or diethylamine in ether or benzene, only two chlorine atoms — and in the case of di-*iso*propylamine or di-*cyclo*hexylamine only one chlorine atom — were replaced even after several hours at the boiling point of the reaction mixture. Even on prolonged heating of the compounds in a steel-bomb at 160°C, with excess of amine, no more amine hydrochloride was formed. This illustrates the great resistance against further replacement of chlorine atoms. It is most likely due to the steric effects of the bulky groups in these amines, since the residual chlorine atoms reacted readily with ammonia and after refluxing even with *iso*propylamine.

Aniline gave after refluxing for some hours in benzene or ether solution complete reaction with the chlorine in *n*-propyltrichlorosilane, but it did not react so readily as *cyclo*hexylamine, thus indicating that not only the size but also the electric properties of the amine influences reaction (A). The fact that N-methylaniline in ether or benzene reacted even with the second chlorine atom only to a small extent then may be explained as a result of both the steric properties and the low base strength of N-methylaniline as compared to aliphatic amines. The influence of the electric properties of the amine on reaction (A) is also supported by the fact that diphenylamine did not react at all with *n*-propyltrichlorosilane at room temperature, while di-*iso*propylamine and di-*cyclo*hexylamine under the same conditions readily reacted with one of the chlorine atoms. This is in agreement with observations made on the reaction of silicon tetrachloride with diphenylamine and di-*iso*propylamine [5].

It is interesting to note that while diethylamine reacted with only two chlorine atoms in *n*-propyltrichlorosilane even after prolonged heating in benzene solution, piperidine after refluxing for about 5 h in the same solvent gave total replacement. This difference in behaviour between these two amines can hardly be explained by the small difference in base strength (for piperidine $K_b = 16 \times 10^{-4}$ at 25°C, and for diethylamine $K_b = 12.6 \times 10^{-4}$ at 25°C). It may, however, be caused by the difference in free rotation around the carbon-nitrogen bonds: in diethylamine the free rotation is not hindered, but in the case of piperidine it is prevented because of the ring structure of this amine. This difference must obviously diminish the steric requirement of piperidino groups as compared to that of diethylamino groups. The observed difference between the reactivity of diethylamine and piperidine is in full analogy with the fact that diethylamine in benzene solution reacted with only three chlorine atoms in silicon tetrachloride, while piperidine gave total replacement [6].

*Cyclo*hexylamine reacted more readily than *sec.*-butylamine with *n*-propyltrichlorosilane. This difference may be explained as a result of the difference in free rotation around the carbon-carbon bonds in these amines, but, of course, the difference in this case was much less.

The following compounds have been prepared (the Arabic figures refer to the numbering in the experimental part):

I	(1)	n-$C_3H_7Si(NHCH_3)_3$
II	(2)	n-$C_3H_7Si[N(CH_3)_2]_3$
III	(3)	n-$C_3H_7Si(NHC_2H_5)_3$
IV	(4)	n-$C_3H_7Si(NHC_3H_7\text{-}n)_3$
V	(5)	n-$C_3H_7Si(NHC_3H_7\text{-}i)_3$
VI	(6)	n-$C_3H_7Si(NHC_4H_9\text{-}n)_3$
VII	(7)	n-$C_3H_7Si(NHC_4H_9\text{-}i)_3$
VIII	(8)	n-$C_3H_7Si(NHC_4H_9\text{-}s)_3$
IX	(9)	n-$C_3H_7Si(NHC_6H_{11})_3$
X	(10)	n-$C_3H_7Si(NHC_6H_5)_3$
XI	(11)	n-$C_3H_7Si[N(CH_2)_5]_3$
XII	(13)	n $C_3H_7Si(NHC_4H_9\text{-}t)_2NH_2$
XIII	(14)	n-$C_3H_7Si(NHC_4H_9\text{-}t)_2(NHC_2H_5)$
XIV	(15)	n-$C_3H_7Si(NHC_4H_9\text{-}t)_2(NHC_3H_7\text{-}i)$
XV	(19)	n-$C_3H_7Si[N(C_2H_5)_2]_2NH_2$
XVI	(20)	n-$C_3H_7Si[N(C_2H_5)_2]_2(NHC_3H_7\text{-}i)$
XVII	(31)	n-$C_3H_7Si[N(CH_3)(C_6H_5)]_2(NHC_3H_7\text{-}i)$
XVIII	(17)	n-$C_3H_7Si(NHC_4H_9\text{-}t)(NHC_3H_7\text{-}i)_2$
XIX	(22)	n-$C_3H_7Si[N(C_2H_5)_2](NHC_3H_7\text{-}i)_2$
XX	(24)	n-$C_3H_7Si[N(C_3H_7\text{-}i)_2](NHC_3H_7\text{-}i)_2$
XXI	(26)	n-$C_3H_7Si[N(C_6H_{11})_2](NHC_3H_7\text{-}i)_2$
XXII	(29)	n-$C_3H_7Si[N(CH_3)(C_6H_5)](NHC_3H_7\text{-}i)_2$
XXIII	(12)	n-$C_3H_7Si(NHC_4H_9\text{-}t)_2Cl$
XXIV	(18)	n-$C_3H_7Si[N(C_2H_5)_2]_2Cl$
XXV	(30)	n-$C_3H_7Si[N(CH_3)(C_6H_5)]_2Cl$
XXVI	(16)	n-$C_3H_7Si(NHC_4H_9\text{-}t)Cl_2$
XXVII	(21)	n-$C_3H_7Si[N(C_2H_5)_2]Cl_2$
XXVIII	(23)	n-$C_3H_7Si[N(C_3H_7\text{-}i)_2]Cl_2$
XXIX	(25)	n-$C_3H_7Si[N(C_6H_{11})_2]Cl_2$
XXX	(28)	n-$C_3H_7Si[N(CH_3)(C_6H_5)]Cl_2$

The assigned structural formulas for these compounds have been based on the way of the syntheses (amount of amine hydrochloride formed), and the silicon content and neutralization equivalents have been determined to confirm the composition of the expected compounds.

The prepared compounds are all colourless, water-insoluble liquids, soluble in organic solvents. Some of their reactions will be described in a later part of this work. Physical constants and analyses are given in Tables 1 and 2.

The author wishes to thank Professor E. Larsson for his kind interest in this work.

EXPERIMENTAL

The n-propyltrichlorosilane used for the syntheses was a sample of technical grade from Hopkins and Williams Ltd., England, which was fractionated before use (B.p. 123°C).

All experiments were performed with carefully dried reagents and solvents and precautions were taken to exclude moisture from the reaction vessels.

The aminosilanes were distilled at reduced pressure in a glass-helix packed column of a length of 15 cm.

Analyses

Silicon analyses were performed according to Smith [7].

The equivalent weights of the compounds containing three aliphatic or alicyclic amino groups could be determined by direct titration with standard hydrochloric acid using methyl red as the indicator, if a weighed sample was dissolved in a water-alcohol mixture

Table 1. Physical constants and analyses of compounds with three silicon-nitrogen bonds.

No.	M	B.p. °C	Pressure mm Hg	n_D^{20}	d^{20}	MR_D	% Si		Equiv. wt.	
							found	calc.	found	calc.
I	161.33	101	50	1.4427	0.8884	48.11	17.5	17.4	54.6	53.8
II	203.40	72–74	13	1.4423	0.8695	61.93	13.8	13.8	69.1	67.8
III	203.40	90	12	1.4380	0.8545	62.49	13.8	13.8	68.4	67.8
IV	245.48	120	11	1.4436	0.8545	76.25	11.5	11.4	82.3	81.8
V	245.48	101–02	12	1.4339	0.8332	76.69	11.4	11.4	82.1	81.8
VI	287.56	117–19	2	1.4474	0.8527	90.17	9.8	9.8	96.8	95.9
VII	287.56	140–41	12	1.4424	0.8466	89.94	9.8	9.8	96.5	95.9
VIII	287.56	130–31	12	1.4436	0.8473	90.08	9.9	9.8	96.2	95.9
IX	365.67	187–89	2	1.4916	0.9478	111.85	7.8	7.7	122.3	121.9
X	347.52	235	3				8.0	8.1	115.4	115.8[a]
XI	323.58	172–75	2	1.5007	0.9696	98.27	8.6	8.7	109.5	107.9
XII	231.46	104	15	1.4414	0.8539	71.64	12.0	12.1	78.0	77.2
XIII	259.51	109–10	12	1.4415	0.8471	80.98	10.8	10.8	86.5	86.5
XIV	273.53	118–19	14	1.4404	0.8430	85.58	10.2	10.3	93.4	91.2
XV	231.46	108–09	15	1.4489	0.8684	71.48	12.1	12.1	77.7	77.2
XVI	273.53	125–26	15	1.4494	0.8595	85.43	10.2	10.3	93.0	91.2
XVII	341.56	204–05	10	1.5608	1.0155	108.89	8.2	8.2	113.2	113.9[a]
									344.0	341.6
XVIII	259.51	105–07	11	1.4375	0.8385	81.16	10.8	10.8	86.6	86.5
XIX	259.51	111–12	13	1.4412	0.8469	80.95	10.7	10.8	87.8	86.5
XX	287.56	131–32	15	1.4480	0.8564	89.89	9.7	9.8	96.3	95.9
XXI	367.68	188–89	8	1.494			7.5	7.6	126.0	122.6
XXII	293.52	153	10	1.5030	0.9352	92.78	9.6	9.6	96.8	97.8[a]
									148.0	146.8

a) *In non-aqueous medium*

containing sufficient alcohol to give a homogeneous system throughout the titration (about 25 ml 96 % alcohol were used for 10 ml 0.1 N hydrochloric acid). With considerably less alcohol the solution became turbid during the titration and too high an equivalent weight resulted. In such a case an excess of hydrochloric acid had to be added and after digesting for several hours back-titration with standard base gave the expected equivalent weight, *i.e.*, $M/3$ (M = molecular weight).

In an analogous way compounds of the types n-$C_3H_7Si(NHR)_2Cl$ and n-$C_3H_7Si(NHR)Cl_2$ gave equivalent weights = M, the first type with standard hydrochloric acid and the second type with standard base.

For the trianilino compound (X) a titration in a non-aqueous solvent had to be used. A weighed sample was dissolved in glacial acetic acid and titrated with standard perchloric acid in glacial acetic acid using methyl violet (violet to blue green) as the indicator giving an equivalent weight = $M/3$.

Compounds with aromatic amino groups and unexchanged chlorine atoms (XXV and XXX) were titrated in water. After agitating a weighed sample of the compounds in an excess of base and digesting for some hours back-titration with standard hydrochloric acid gave the expected equivalent weights.

For compounds with both aliphatic and aromatic amino groups (XVII and XXII) titration in water-alcohol mixture with standard hydrochloric acid and methyl red indicator gave equivalent weights corresponding to the aliphatic amino groups = M or $M/2$, and a non-aqueous titration as above gave equivalent weights = $M/3$, corresponding to the sum of amino groups.

Beside the analyses the following data are given in the tables: Boiling points, refractive indices (determined with an Abbe refractometer), densities (determined with an Ostwald-Sprengler pycnometer of a volume of 1.5 ml) and molecular refractivities (calculated from Lorenz-Lorentz formula).

Table 2. Physical constants of compounds containing silicon-chlorine bonds.

No.	M	B.p. °C	Pressure mm Hg	n_D^{20}	d^{20}	MR_D	% Si		Equiv. wt.	
							found	calc.	found	calc.
XXIII	250.89	118–19	15	1.4468	0.9153	72.89	11.1	11.2	251.5	250.9
XXIV	250.89	121	17	1.4530	0.9323	72.74	11.0	11.2	253.0	250.9
XXV	318.92	195–97	11	1.5675			8.8	8.8	319.9	318.9
XXVI	214.22	73–74	11				13.0	13.1	217.0	214.2
XXVII	214.22	86–88	17				13.1	13.1	213.9	214.2
XXVIII	242.26	105	15	1.4557	1.0192	64.58	11.5	11.6	244.0	242.3
XXIX	322.39	180–81	10	1.499			8.7	8.7	326.0	322.4
XXX	248.23	125	11				11.4	11.3	123.0	124.1

Syntheses

All the reactions were performed in a three-necked flask equipped with a mechanical stirrer, a dropping funnel and a reflux condenser. The amine hydrochloride formed was filtered from the mixture on a fine-porous glass-filter in an atmosphere of dry air and was carefully washed with the solvent and dried before the weighing. The complete separation of amine hydrochloride sometimes caused considerable difficulty. If it was not completely removed, it contaminated the aminosilanes, subliming with them during the distillation. After the filtration the filtrate and wash-liquid were combined, and the solvent was removed at atmospheric pressure before distillation of the aminosilane at reduced pressure.

1. n-*Propyltri-(methylamino)-silane (I)*. To an ice-cooled, vigorously stirred solution of about 30 g (1.0 mole) of methylamine in 150 ml of ether a solution of 17.8 g (0.1 mole) of *n*-propyltrichlorosilane in 50 ml of ether was added dropwise. After all had been added the stirring was continued, and the temperature was slowly raised by the removal of the ice-bath. Finally the stirred mixture was heated to reflux temperature for 2 h to remove the excess of methylamine. Filtration of the cooled mixture left 20.2 g (calc. 20.3 g) of methylamine hydrochloride on the filter. Distillation of the filtrate gave 14.2 g (88 %) of I.

2. n-*Propyltri-(dimethylamino)-silane (II)*. Under exactly the same conditions as above 45 g (1.0 mole) of dimethylamine and 17.8 g (0.1 mole) of *n*-propyltrichlorosilane gave only 23.6 g (calc. 24.5 g) of dimethylamine hydrochloride, and 18 g of a product with an equivalent weight of 74 (calc. for II 67.8) was obtained. When this was again heated for 2 h in benzene containing dimethylamine, more amine hydrochloride was obtained; distillation gave 15.0 g (74 %) of II with the data given in Table 1. The observed difference in reactivity between dimethylamine and methylamine must be ascribed to the greater steric requirement of the former one.

3. n-*Propyltri (ethylamino) silane (III)*. As described for the methylamine compound 44.4 g (0.25 mole) of *n*-propyltrichlorosilane in 50 ml of ether and about 90 g (2.0 moles) of ethylamine in 250 ml of the same solvent gave 61.2 g (calc. 61.2 g) of ethylamine hydrochloride and 47.2 g (93 %) of III.

4. n-*Propyltri*-(n-*propylamino*)-*silane (IV)*. 17.8 g (0.1 mole) of *n*-propyltrichlorosilane in 50 ml of benzene were added to 53 g (0.9 mole) of *n*-propylamine in 100 ml of benzene. The mixture was refluxed for 2 h. Thereafter the excess of *n*-propylamine was distilled off. Filtration left 28.7 g (calc. 28.7 g) of *n*-propylamine hydrochloride on the filter, and fractionation of the filtrate gave 22.1 g (90 %) of IV.

5. n-*Propyltri-(iso propylamino)-silane (V)*. In the same way 8.9 g (0.05 mole) of *n*-propyltrichlorosilane in 50 ml of ether and 30 g (0.5 mole) of *iso*propylamine in 75 ml of the same solvent gave 14.4 g (calc. 14.4 g) of *iso*propylamine hydrochloride and 10.5 g (86 %) of V.

6. n-*Propyltri*-(n-*butylamino*)-*silane (VI)*. 8.9 g (0.05 mole) of *n*-propyltrichlorosilane in 75 ml of benzene were added to 37 g (0.5 mole) of *n*-butylamine in 100 ml of the same solvent. After refluxing for 2 h and cooling, filtration left 16.0 g (calc. 16.4 g) of *n*-butylamine hydrochloride on the filter; fractionation of the filtrate gave 11.1 g (77 %) of VI.

7. n-*Propyltri-(isobutylamino)-silane (VII).* In the same way 8.9 g (0.05 mole) of *n*-propyltrichlorosilane in 75 ml of benzene and 37 g (0.5 mole) of *iso*butylamine in 100 ml of the same solvent gave 16.4 g (calc. 16.4 g) of *iso*butylamine hydrochloride and 11.7 g (81 %) of VII.

8. n-*Propyltri-(sec.-butylamino)-silane (VIII).* 7.1 g (0.04 mole) of *n*-propyltrichlorosilane in 50 ml of ether were added to 21.9 g (0.3 mole) of *sec.*-butylamine in 50 ml of the same solvent. After refluxing for 1.5 h and cooling, filtration left 11.1 g (calc. 13.2 g) of *sec.*-butylamine hydrochloride on the filter. A little more *sec.*-butylamine was added to the filtrate, and the mixture was refluxed for 6 h. On cooling, filtration left 2.0 g of amine hydrochloride; distillation gave 7.8 g (68 %) of VIII.

9. n-*Propyltri-(cyclohexylamino)-silane (IX).* In exactly the same way 29.8 g (0.3 mole) of *cyclo*hexylamine gave already after refluxing for 1 h the calculated amount of *cyclo*hexylamine hydrochloride (16.3 g). From the filtrate 11.3 g (77 %) of IX were obtained.

10. n-*Propyltrianilinosilane (X).* 17.8 g (0.1 mole) of *n*-propyltrichlorosilane in 50 ml of ether were added dropwise to 70 g (0.75 mole) of aniline in 125 ml of the same solvent. The mixture was refluxed for 2 h. After cooling, filtration left 34.2 g (calc. 38.9 g) of aniline hydrochloride on the filter. After removal of the ether from the filtrate by distillation, the residual mixture was heated at about 100°C for 2 h. On cooling and addition of 150 ml of ether, filtration left another 4.6 g of amine hydrochloride on the filter. Fractionation gave 29.5 g (85 %) of X as a colourless, very viscous syrup, which soon achieved the yellow tint, which aniline usually has.

In another experiment the reactivity of aniline and *cyclo*hexylamine was studied as follows. A mixture of 1.78 g (0.01 mole) of *n*-propyltrichlorosilane and 5.59 g (0.06 mole) of aniline in 25 ml of benzene was agitated for 15.0 min at room temperature and filtered. 1.95 g of aniline hydrochloride were left on the filter, which makes 50.1 % of the calculated amount according to formula (A). After standing for 12 h, 1.05 g more aniline hydrochloride were obtained, yielding a total of 77.1 %.

5.95 g (0.06 mole) of *cyclo*hexylamine under exactly the same conditions gave 3.38 g (82.3 %) of *cyclo*hexylamine hydrochloride and after 12 h 0.59 g. This makes a total of 97.5 % of the calculated amount. Therefore it must be concluded that *cyclo*hexylamine reacts more readily than aniline with *n*-propyltrichlorosilane.

11. n-*Propyltripiperidinosilane (XI).* 17.8 g (0.1 mole) of *n*-propyltrichlorosilane in 50 ml of benzene were added to 60 g (0.7 mole) of piperidine in 100 ml of the same solvent, and the mixture was refluxed for 5 h. Filtration of the cooled mixture left 34.0 g (calc. 36.5 g) of piperidine hydrochloride. The filtrate was again refluxed for 5 h, and filtration then gave 2.3 g more amine hydrochloride. From the filtrate 22.0 g (68 %) of XI were obtained.

12. n-*Propyldi-(tert.-butylamino)-chlorosilane (XXIII).* In the same way 17.8 g (0.1 mole) of *n*-propyltrichlorosilane and 55 g (0.75 mole) of *tert.*-butylamine after refluxing for 2 h gave 22.5 g of *tert.*-butylamine hydrochloride. This is in agreement with the calculated amount for the replacement of only two of the chlorine atoms in *n*-propyltrichlorosilane (21.9 g). The filtrate did not give more amine hydrochloride even when refluxed for 10 h. On fractionation of the mixture 20.5 g (81 %) of XXIII were obtained.

12.5 g (0.05 mole) of XXIII were heated with 11 g (0.15 mole) of *tert.*-butylamine and 50 ml of benzene in a steel-bomb at about 160°C for 8 h. Only traces of amine hydrochloride were formed, and XXIII could be recovered by distillation. Thus it must be concluded that *n*-propyltri-(*tert.*-butylamino)-silane cannot be obtained in this way.

13. n-*Propyldi-(tert.-butylamino)-aminosilane (XII).* 10.0 g (0.04 mole) of XXIII in 50 ml of ether were added dropwise to about 50 ml of liquid ammonia, cooled in a dry ice and acetone bath. The temperature was slowly raised to room temperature, and the mixture was at last refluxed for 1 h to remove the excess of ammonia. Filtration left 2.1 g (calc. 2.1 g) of ammonium chloride on the filter, and distillation of the filtrate gave 6.5 g (70 %) of XII.

14. n-*Propyldi-(tert.-butylamino)-(ethylamino)-silane (XIII).* 5.0 g (0.02 mole) of XXIII dissolved in 15 ml of ether were added to an ether solution containing excess of ethylamine. After stirring at room temperature for about half an hour, the excess of ethylamine was removed. Filtration left 1.6 g (calc. 1.6 g)of ethylamine hydrochloride on the filter, and on fractionation of the filtrate 4.6 g (89 %) of XIII were obtained.

15. n-*Propyldi-(*tert.-*butylamino)-(iso*propylamino*)-silane (XIV).* 10.0 g (0.04 mole) of XXIII in 25 ml of benzene were added to 7 g (0.12 mole) of *iso*propylamine in 40 ml of the same solvent. No amine hydrochloride precipitated until the mixture had been heated for a while. After refluxing for 1.5 h and removal of the excess of *iso*propylamine, filtration left only 1.8 g (calc. 3.8 g) of *iso*propylamine hydrochloride on the filter. 7 g of *iso*propylamine were added to the filtrate, and the mixture was refluxed for 15 h. The excess of *iso*propylamine was again distilled off. Filtration now left another 1.9 g, and from the filtrate 8.0 g (73 %) of XIV were obtained.

n-Propylamine and *n*-butylamine gave immediately a heavy precipitate of amine hydrochloride when XXIII, dissolved in benzene, was added to their benzene solutions. The low reactivity of *iso*propylamine may be attributed to its steric properties.

16. n-*Propyl-(*tert.-*butylamino)-dichlorosilane (XXVI).* This compound was obtained by the addition dropwise of 36.5 g (0.5 mole) of *tert.*-butylamine in 75 ml of ether to 44.4 g (0.25 mole) of *n*-propyltrichlorosilane in 75 ml of the same solvent and refluxing for 1.5 h. Filtration left 27.3 g (calc. 27.4 g) of *tert.*-butylamine hydrochloride, and distillation of the filtrate gave 36.0 g (67 %) of XXVI.

17. n-*Propyl-(*tert.-*butylamino)-di-(iso*propylamino*)-silane (XVIII).* 10.7 g (0.05 mole) of XXVI in 50 ml of benzene were added to 15 g (0.25 mole) of *iso*propylamine in 50 ml of the same solvent. After refluxing for 1.5 h and removal of the excess of *iso*propylamine, filtration left 9.6 g (calc. 9.6 g) of *iso*propylamine hydrochloride. Thus it is seen that the chlorine is more easily replaced by *iso*propylamine in XXVI than in XXIII. From the filtrate 9.9 g (76 %) of XVIII were obtained.

18. n-*Propyldi-(diethylamino)-chlorosilane (XXIV).* 17.8 g (0.1 mole) of *n*-propyltrichlorosilane in 50 ml cf benzene were added to 59 g (0.8 mole) of diethylamine in 75 ml of the same solvent. Thereafter the mixture was refluxed for 4.5 h. After the excess of diethylamine had been removed by distillation, filtration left 22.4 g of diethylamine hydrochloride on the filter. This corresponds with the calculated amount for the replacement of only two chlorine atoms in *n*-propyltrichlorosilane (21.9 g), and no more amine hydrochloride precipitated on further refluxing with diethylamine in benzene. Fractionation gave 18.5 g (73 %) of XXIV. The resistance of this compound against further reaction with diethylamine was illustrated in the same way as for XXIII.

19. n-*Propyldi-(diethylamino)-aminosilane (XV).* This substance was prepared as described for XII from 5.0 g (0.02 mole) of XXIV giving 1.1 g (calc. 1.1 g) of ammonium chloride and 3.2 g (69 %) of XV.

20. n-*Propyldi-(diethylamino)-*iso*propylaminosilane (XVI).* 8.3 g (0.033 mole) of XXIV were refluxed with 12 g (0.2 mole) of *iso*propylamine in 50 ml of benzene for 20 h, and then the excess of *iso*propylamine was removed. Filtration left 3.1 g (calc. 3.2 g) of *iso*propylamine hydrochloride on the filter, and from the filtrate 5.8 g (64 %) of XVI were obtained.

21. n-*Propyl-(diethylamino)-dichlorosilane (XXVII).* This substance was prepared as described for XXVI from 35.5 g (0.2 mole) of *n*-propyltrichlorosilane in 90 ml of benzene and 30 g (0.41 mole) of diethylamine in 100 ml of the same solvent. Filtration left 21.4 g (calc. 21.9 g) of diethylamine hydrochloride and 31.0 g (72 %) of XXVII were obtained.

22. n-*Propyl-(diethylamino)-di-(iso*propylamino*)-silane (XIX).* As described for the preparation of XVIII, 10.7 g (0.05 mole) of XXVII and 15 g (0.25 mole) of *iso*propylamine gave 9.5 g (calc. 9.6 g) of *iso*propylamine hydrochloride and 10.7 g (82 %) of XIX.

23. n-*Propyl-(di-*iso*propylamino)-dichlorosilane (XXVIII).* 60.7 g (0.6 mole) of di-*iso*propylamine in 75 ml of benzene were added dropwise to 53.3 g (0.3 mole) of *n*-propyltrichlorosilane in 100 ml of the same solvent. The mixture was then refluxed for 1 h. Filtration left di-*iso*propylamine hydrochloride on the filter, which even after ordinary washing contained some grams of a material containing silicon (total weight 45.2 g; calc. for the replacement of one of the chlorine atoms in *n*-propyltrichlorosilane 41.3 g). From the filtrate 38.3 g (53 %) of XXVIII were obtained. When this substance was refluxed for several hours with di-*iso*propylamine in benzene, only a very small amount of amine hydrochloride was formed.

In another experiment 18.2 g (0.075 mole) of XXVIII and 20 g (0.2 mole) of di-*iso*propylamine in 50 ml of benzene were heated to about 170°C for 15 h in a steel-bomb. Only 0.4 g of amine hydrochloride was formed. — Therefore it must be concluded that *n*-propyldi-(di-*iso*propylamino)-chlorosilane cannot be obtained in reasonable yield in this way.

24. n-*Propyl-(di-*iso*propylamino)-di-(*iso*propylamino)-silane (XX).* 9.7 g (0.04 mole) of XXVIII and 18 g (0.3 mole) of *iso*propylamine in 50 ml of ether were refluxed for 1 h. Filtration of the cooled mixture left 6.0 g (calc. for total replacement 7.7 g) of *iso*propylamine hydrochloride. The ether was distilled off from the filtrate, and 50 ml of benzene containing about 10 g of *iso*propylamine were added to the rest. After refluxing for about 5 h and removal of the excess of *iso*propylamine, a new filtration left the expected amount of *iso*propylamine hydrochloride (1.6 g). From the filtrate 6.5 g (57 %) of XX were obtained.

25. n-*Propyl-(di-*cyclo*hexylamino)-dichlorosilane (XXIX).* 35.5 g (0.2 mole) of *n*-propyltrichlorosilane in 75 ml of benzene were added dropwise to 81.6 g (0.45 mole) of di-*cyclo*hexylamine in 100 ml of benzene. Amine hydrochloride was immediately formed. After refluxing for 5 h, filtration left 44.0 g (calc. 43.6 g) of di-*cyclo*hexylamine hydrochloride on the filter. On fractionation of the filtrate 44.1 g (68 %) of XXIX were obtained. 16.1 g (0.05 mole) of this substance were refluxed with 22 g (0.12 mole) of di-*cyclo*hexylamine in 100 ml of benzene for 8 h, but no more amine hydrochloride was formed. Thereafter the benzene was distilled off and the rest was heated at 180°C for 12 h, but even now only traces of amine hydrochloride were formed. Thus it is seen that *n*-propyldi-(di-*cyclo*hexylamino)-chlorosilane cannot be obtained in reasonable yield in this way.

26. n-*Propyl-(di-*cyclo*hexylamino)-di-(*iso*propylamino)-silane (XXI).* A mixture of 16.1 g (0.05 mole) of XXIX and 24 g (0.4 mole) of *iso*propylamine in 100 ml of benzene were refluxed for 15 h, and then the excess of *iso*propylamine was removed. Filtration of the cooled mixture left 9.3 g (calc. 9.6 g) of *iso*propylamine hydrochloride, and from the filtrate 14.0 g (77 %) of XXI were obtained.

27. n-*Propyltrichlorosilane and diphenylamine.* 8.9 g (0.05 mole) of *n*-propyltrichlorosilane in 25 ml of benzene were added to 34 g (0.2 mole) of diphenylamine in 100 ml of the same solvent. No reaction could be observed at room temperature, so it is evident that the reactivity of diphenylamine is much less than that of di-*iso*propylamine and di-*cyclo*hexylamine. Since the steric properties of these amines are of about the same order, the difference may be attributed to the difference in their base strength. Even after refluxing for 8 h and cooling no solid precipitated, and on fractionation more than 8 g of the *n*-propyltrichlorosilane could be recovered.

28. n-*Propyl-(N-methylanilino)-dichlorosilane (XXX).* 8.9 g (0.05 mole) of *n*-propyltrichlorosilane in 25 ml of benzene were added to 27 g (0.25 mole) of N-methylaniline in 50 ml of benzene. The precipitate of N-methylaniline hydrochloride, which was first formed, dissolved on heating of the mixture to reflux. After refluxing for 4.5 h and cooling of the mixture, filtration left 6.4 g (calc. for the replacement of one of the chlorine atoms in *n*-propyltrichlorosilane 7.2 g). The filtrate was again refluxed for 20 h, and filtration now left 1.2 g of amine hydrochloride. Reflux of the filtrate for another 22 h caused the formation of only about 0.5 g of amine hydrochloride, so it is evident that the second chlorine atom in *n*-propyltrichlorosilane is difficultly replaced by N-methylaniline. If the benzene is distilled off and the residue is heated to reflux of the N-methylaniline for several hours, more amine hydrochloride is formed and *n*-propyldi-(N-methylanilino)-chlorosilane (XXV) can be obtained in reasonable yield from the reaction mixture.

In another experiment 43 g (0.4 mole) of N-methylaniline in 50 ml of ether were added dropwise to 35.5 g (0.2 mole) of *n*-propyltrichlorosilane in 100 ml of ether. After refluxing for 2.5 h, filtration of the cooled mixture left 22.9 g (calc. 28.7 g) of N-methylaniline hydrochloride on the filter. The ether was distilled off from the filtrate, and the residue was heated to about 100°C for 2 h. After cooling the ether was again added, and filtration now left 2.0 g of amine hydrochloride. The ether was again distilled off, and refluxing for about 5 h now left 3.1 g of amine hydrochloride on the filter (totally 28.0 g). Distillation of the filtrate gave 32.1 g (65 %) of XXX.

29. n-*Propyl-(N-methylanilino)-di-(*iso*propylamino)-silane (XXII).* 12.4 g (0.05 mole) of XXX in 50 ml of benzene were added to 24 g (0.4 mole) of *iso*propylamine in 50 ml of benzene. After refluxing for 8 h and removal of the excess of *iso*propylamine, filtration left 9.5 g (calc. 9.6 g) of *iso*propylamine hydrochloride on the filter. From the filtrate 12.0 g (82 %) of XXII were obtained.

30. n-*Propyldi-(N-methylanilino)-chlorosilane (XXV).* 21 g (0.2 mole) of N-methylaniline were added to 20.0 g (0.089 mole) of XXX in 100 ml of ether. After refluxing for 3 h, only traces of N-methylaniline hydrochloride had precipitated. Therefore the ether

was distilled off, and the residual mixture was heated to about 100°C for 8 h. When the ether was again added to the cooled mixture, 3.5 g of amine hydrochloride were obtained on filtration. After repeating the same procedure, 2.5 g of amine hydrochloride were left on the filter. On fractionation of the filtrate about 4 g of XXX and 5.1 g (20 %) of XXV were obtained.

31. n-*Propyldi-(N-methylanilino)-(iso*propylamino*)-silane (XVII).* 4.2 g (0.013 mole) of XXV and 9 g (0.15 mole) of *iso*propylamine in 50 ml of benzene were refluxed for 10 h, and the excess of *iso*propylamine was removed. Filtration left 1.2 g (calc. 1.3 g) of *iso*propylamine hydrochloride, and from the filtrate 3.5 g (78 %) of XVII were obtained.

32. n-*Propyltrichlorosilane and tertiary amines.* When *n*-propyltrichlorosilane was added to absolutely dry trimethylamine, triethylamine or pyridine in ether or benzene solution, no reaction was observed in any case and the *n*-propyltrichlorosilane could be recovered by distillation.

REFERENCES

1. Anderson, H. H. *J. Am. Chem. Soc.* **73** (1951) 5802.
2. Anderson, H. H. *J. Am. Chem. Soc.* **74** (1952) 1421.
3. Chugunov, V. S. *Zhur. Obshchei Khim.* **23** (1953) 777.
4. Trost, W. R. *Can. J. Chem.* **29** (1951) 877.
5. Breederveld, H. and Waterman, H. I. *Research London* **7** (1954) S 5—6.
6. Breederveld, H. and Waterman, H. I. *Research London* **5** (1952) 537.
7. Smith, B. *Kiselorganiska studier* (Diss.) Chalmers University of Technology, Gothenburg 1951.

Received July 9, 1957.

ACTA CHEMICA SCANDINAVICA 11 (1957) 1622—1634

Studien über Metallcyanate

ERIK SÖDERBÄCK

Chemisches Institut der Universität Uppsala, Schweden

Es wurden vorher unbekannte Cyanate von Cadmium und von ein- und zweiwertigem Kupfer synthetisiert und von beiden letzteren Doppelcyanate mit Alkalimetallen.

Ein katalytischer Effekt der Cuprocyanate bei der Einführung der *Iso*cyanatgruppe in einen Benzolkern nach Sandmeyer wurde entdeckt und als Beispiel die Synthese von *o*-Tolylisocyanat durchgeführt.

Neue Methoden für die Darstellung von Mercuricyanat sind ausgearbeitet worden; diese Substanz wurde näher studiert und Ähnlichkeiten mit dem Mercurichlorid nachgewiesen. Eine neue bequeme Methode für die Darstellung von Bariumcyanat ist angegeben und die Löslichkeit des Salzes in Wasser bestimmt worden.

Die Leitfähigkeitbestimmungen und einige der Analysen sind im hiesigen Centralanalytischen Laboratorium, Vorstand Dr. F. Nydahl, ausgeführt worden. Für diese sowie für Debye-Scherrer-Aufnahmen durch Herrn Privatdozent Dr. I. Lindqvist bin ich sehr zu Dank verpflichtet.

Die Metallcyanate sind im Verhältnis zu den Metallrhodaniden recht wenig untersucht worden, und viele einfache Cyanate von gewöhnlichen Metallen sind noch unbekannt. Der Grund dafür ist hauptsächlich die relative Schwäche und Unbeständigkeit der Cyansäure in wässriger und alkoholischer Lösung. Die Säure wird in wässriger Lösung rasch zu Ammoniak und Kohlensäure hydrolysiert, in alkoholischer sind Urethane und Allophansäureester die Reaktionsprodukte.

Das Cyanation wird häufig als ein Analogon der Hypohalogenitionen, z.B. des Hypochloritions betrachtet, weil es durch Hydrolyse des Dicyans in alkalischer Lösung nebst Cyanidion gebildet wird. Diese Übereinstimmung ist aber ausschliesslich formal, da keine Übereinstimmung in Eigenschaften besteht; die Cyanate haben z.B. keine oxydierende Wirkungen. Das Cyanation zeigt vielmehr gewisse Ähnlichkeiten mit den Halogenidionen, namentlich mit dem Chloridion, und diese sind besonders bei gewissen Schwermetallcyanaten hervorstechend. So ist z.B. schon längst ein Kaliumchloroplatinatcyanat $K_2Pt(OCN)Cl_5H_2O$ bekannt [1].

Das Cyanation besitzt indessen eine mehr ausgeprägte Neigung zur Bildung von schwerlöslichen Doppelcyanaten als das Chloridion zu Bildung von Doppel-

chloriden, was bei der Darstellung einfacher Metallcyanate manchmal Schwierigkeiten macht *. Es ist mir gelungen die einfachen Cyanate von Cadmium und Kupfer darzustellen und Doppelsalze von ein- und zweiwertigem Kupfer mit Alkalicyanaten. Ferner sind neue Methoden zur Darstellung von Mercuricyanat aufgefunden worden, ein Salz das grosse Ähnlichkeiten mit dem Chlorid aufweist.

Cadmiumcyanat

Versetzt man eine nicht zu verdünnte Wasserlösung von einem normal ionisierten Cadmiumsalz mit Kaliumcyanat, kristallisiert das Salz $KCd(OCN)_3$ rasch aus [3]. Die Bereitung des einfachen Cyanats als Hydrat bietet indessen keine grössere Schwierigkeiten; es kann, wie ich gefunden habe, entweder durch Umsatz von Cadmiumsulfat mit Bariumcyanat in verdünnter wässriger Lösung und Konzentrieren der Lösung durch Vakuumdestillation bis zur eintreten der Kristallisation oder durch Reaktion von Cadmiumjodid in Acetonlösung mit der genau äquivalenten Menge Silbercyanat und Auslagen des Gemenges von AgJ und $Cd(OCN)_2$ mit Wasser gewonnen werden. Das aus Wasser kristallisierte Cyanat ist immer etwas von basischem Salz verunreinigt und löst sich deshalb nicht klar in Wasser, es kann aber leicht durch Waschen mit verdünnter Essigsäure ** gereinigt werden und ist dann analysenrein. Die Zusammensetzung entspricht der Formel $2Cd(OCN)_2 \cdot 5H_2O$, der Wassergehalt ist also derselbe als für Cadmiumchlorid ***. Das Salz ist in Methanol und Äthanol ziemlich löslich.

Die Löslichkeiten in Wasser von Cadmiumsalzen der zusammengesetzten Halogene $(OCN)_2$, $(SCN)_2$ und $(SeCN)_2$ sind nicht besonders gross. Nach von mir ausgeführten Messungen sind sie bei 20° für $2Cd(OCN)_2 \cdot 5H_2O$ $9{,}1 \times 10^{-2}$, für $Cd(SCN)_2$ $4{,}8 \times 10^{-2}$ und für $Cd(SeCN)_2$ $2{,}3 \times 10^{-2}$ M. Die beiden letzten Salze kristallisieren anhydrisch und können aus konzentrierten $Cd(NO_3)_2$-Lösungen durch KSCN bezw. KSeCN gefällt werden. Der Grund für die relative Schwerlöslichkeit dieser Salze in Vergleich mit $CdCl_2$, $CdBr_2$ und CdJ_2 dürfte in Autokomplexbildung zu suchen sein.

Mercuricyanat

Von Birckenbach und Kolb [6] sind eine Reihe von Doppelcyanaten von Quecksilber(II) hergestellt und studiert worden, von welchen durch Ramananalyse einige als O-Cyanate andere als N-Cyanate zu formulieren seien. Die Verhältnisse sind indessen sehr verwickelt, und die Strukturen können kaum als endgültig geklärt betrachtet werden. Von denselben Autoren ist auch das einfache Mercuricyanat $Hg(OCN)_2$ dargestellt worden durch Umsetzung von $HgCl_2$ mit AgOCN in Methanol und Verdampfen des Lösungsmittels. Die Struktur soll nach Ramanaufnahmen der Ket-Imidformel entsprechen, was

* Bei den mit den Cyanaten isomeren Fulminaten ist diese Tendenz noch stärker ausgeprägt.

** Über die relative Stärke von Essigsäure und Cyansäure, siehe weiter unten.

*** Das bei Zimmertemperatur aus wässriger Lösung kristallisierte Cadmiumchlorid ist nach Untersuchungen von Cohen [4] und Dietz [5] das Hydrat $2CdCl_2.5H_2O$. Diese Tatsache ist seit Ende des vorigen Jahrhunderts bekannt. Nichts destoweniger wird das käufliche Chlorid von chemischen Fabriken als Dihydrat formuliert.

an und für sich nicht unwahrscheinlich ist. Methanol dürfte indessen kein geeignetes Solvenz für Mercuricyanat sein wegen mangelnder Stabilität des Salzes in diesem Lösungsmittel. Um es rein zu erhalten muss es sehr schnell aus der Lösung isoliert werden. Wie ich gefunden habe, ist es viel besser Äther als Solvenz zu verwenden, in welchem die Reaktion glatt verläuft. Es wird zwar von Birckenbach und Kolb behauptet, dass $Hg(OCN)_2$ in Äther wenig löslich sei; nach meinen eigenen Messungen ist die Löslichkeit bei 20° 1,3 g per 100 ml, eine Löslichkeit die ausreicht um das Salz mit Äther gut extrahieren zu können. Bei Abdestillieren des Äthers kristallisiert $Hg(OCN)_2$ in analysenreiner Form aus. Es dürfte dies die beste Darstellungsmethode sein.

Mercuricyanat kann ferner, wie ich gefunden habe, durch Neutralisation von gelbem HgO mit Cyansäure in Äther gewonnen werden. Die Reaktion muss aber einen möglichst rapiden Verlauf haben, weil sonst durch eine sekundäre Reaktion zwischen HgO und $Hg(OCN)_2$ letzteres in eine weisse schwerlösliche Substanz verwandelt wird, die nicht durch HOCN in normales Cyanat umgewandelt wird. Das HgO muss deshalb höchstreaktiv, in der Kälte dargestellt sein. Die Cyansäure lässt sich sehr bequem durch Umsatz von AgOCN mit HCl in trocknem Äther darstellen *. Die Isolierung des $Hg(OCN)_2$ geschieht wie oben beschrieben, und die Ausbeuten sind befriedigend. Keine Unterschiede zwischen dem aus HgO und dem aus $HgCl_2$ in Methanol synthetisierten $Hg(OCN)_2$ konnten bei Debye-Scherreraufnahmen im hiesigen Institut durch Lindqvist beobachtet werden.

Das Mercuricyanat lässt sich auch nach einer dritten Methode gewinnen und zwar durch Erhitzen von Mercurocyanat $Hg_2(OCN)_2$ mit Wasser, wobei jenes in Quecksilber und $Hg(OCN)_2$ zerfällt. Es stellen sich Gleichgewichte ein, die sich mit der Temperatur stark verschieben; bei Zimmertemperatur wird die Reaktion quantitativ rückgängig. Durch Erneuerung der Wasserphase kann die Dissoziation von $Hg_2(OCN)_2$ leicht vollständig gemacht werden. Durch möglichst rasches Einengen der abgekühlten Wasserextrakte mittelst Vakuumdestillation wird das Cyanat fraktioniert auskristallisiert und durch Umlösen in Äther gereinigt. Es konnten in dieser Weise Ausbeuten von etwa 80 % erreicht werden.

Das Mercuricyanat kristallisiert aus Äther in prismatischen Kristallen, die sich in Licht etwas gräulich färben und deshalb im Dunkeln aufzubewahren sind. Die Löslichkeit in Äther nimmt mit dem Wassergehalt des Äthers zu, was auch für Quecksilberchlorid gilt. Während in trocknem Äther die Löslichkeit bei 20° 1,3 g/100 ml beträgt, steigt sie für einen Äther, dessen Wassergehalt 0,1 M ist zu 1,8 g und für 0,25 M zu 2,7 g. Diese Löslichkeiten wurden durch Wägen des Verdampfungsrückstandes eines abgemessenen Volumens gesättigter Lösung bestimmt. $Hg(OCN)_2$ ist wie $HgCl_2$ leicht löslich in einer Menge von organischen Solvenzien, in Methanol und Äthanol, in aliphatischen Nitrilen wie Acetonitril, in den verschiedensten aliphatischen Ketonen, wie Aceton, Methyläthylketon und *Cyclo*hexanon. Es ist ferner beträchtlich löslich in Wasser. 100 ml lösen bei 20° 7,5 g $Hg(OCN)_2$ ** und 5,7 g $HgCl_2$. Bei 0°

* Ganz analog lässt sich eine ätherische Rhodanwasserstofflösung durch Umsatz von AgSCN mit HCl bereiten.

** Die Löslichkeit von $Hg(ONC)_2$ in Wasser ist bei 18° 0,74 g in 100 ml.

sinkt die Löslichkeit für das Cyanat zu 3,7 g und für das Chlorid zu 3,6 g. Eben wie $HgCl_2$ ist $Hg(OCN)_2$ in Wasser anomal wenig ionisiert. Alkalicarbonate erzeugen keinen Niederschlag von HgO, wohl aber Alkalihydroxyde. $AgNO_3$ fällt nicht; aus Lösungen von $HgCl_2$ wird bekanntlich AgCl partiell gefällt. Es ist dazu zu bemerken, dass das Löslichkeitsprodukt von AgCl, 2×10^{-10} nicht unwesentlich kleiner ist als dasjenige von AgOCN, $\sim 10^{-7}$. Dass $Hg(OCN)_2$ anomal wenig ionisiert ist, geht aus der Tabelle 1 hervor, wo die molekularen Leitfähigkeiten Λ bei 25° in reciprok. Ohm für 4 verschiedene Verdünnungen angeführt sind. Die letzte Kolumne enthält die Leitfähigkeiten für $HgCl_2$ bei denselben Verdünnungen nach Ley [7]. Die Zeiten Z sind von dem Augenblick, wo das Salz mit dem Lösungsmittel in Berührung kam, gerechnet.

Es geht aus der Tabelle hervor, dass die Leitfähigkeit von $Hg(OCN)_2$ von derselben Grössenordnung wie diejenige von $HgCl_2$ ist *. Sie steigt mit der Zeit, offenbar durch eine Reaktion des Salzes mit Wasser. Die wässrigen Lösungen von $Hg(OCN)_2$ sind nämlich nicht stabil, sondern setzen allmählich gelblich gefärbte Niederschläge ab unter gleichzeitiger Entwicklung von CO_2. Über die Art dieser Reaktion kann gegenwärtig nichts bestimmtes gesagt werden. Auch in wasserhaltigem Äther wird $Hg(OCN)_2$ allmählich zersetzt.

Die Mercurisalze der elementaren Halogene sowie diejenige der zusammengesetzten $(SCN)_2$ und $(SeCN)_2$ werden bei Zimmertemperatur in Wasser oder organischen Solvenzien leicht und quantitativ durch Quecksilber zu den entsprechenden Mercurosalzen reduziert und derselben Reaktion unterliegt auch das Mercuricyanat. Es wurden Versuche in Wasser und Äther angestellt. Das Abschliessen der Reaktion konnte leicht durch Ausbleiben der Ausfällung von HgO bei Zusatz von Alkalihydroxyd, im Falle Äther auch durch das Verschwinden von Eindampfungsrückstand festgestellt werden, da Mercurocyanat in Äther sehr schwerlöslich ist. Die Identität des Reaktionsproduktes mit $Hg_2(OCN)_2$ konnte dadurch gezeigt werden, dass beim Aufkochen mit Wasser $Hg(OCN)_2$ ausgelöst wurde und wie oben beschrieben, isoliert werden konnte.

Das Mercuricyanat gibt genau wie $HgCl_2$ die Edersche Reaktion d.h. es wird in wässriger Lösung bei Gegenwart von $(NH_4)_2C_2O_4$ durch Belichtung zu $Hg_2(OCN)_2$ reduziert unter gleichzeitiger Bildung von CO_2

$$2Hg(OCN)_2 + (NH_4)_2C_2O_4 + h\nu \longrightarrow Hg_2(OCN)_2 + 2NH_4OCN + 2\,CO_2$$

Bei einem derartigen Versuch wurden 16,6 g $Hg(OCN)_2$ in einer Lösung von 17 g $(NH_4)C_2O_4$ in 400 ml Wasser aufgelöst mit einer Quarzquecksilberlampe mehrere Tage belichtet. Es wurden dabei 12,7 g $Hg_2(OCN)_2$ ausgefällt = 89 %. Das Präparat war durch kleine Mengen von ausreduziertem Hg etwas gräulich gefärbt.

Von Interesse ist, dass die Doppelverbindungen Hlg · HgOCN (Hlg = Cl, Br oder J) eben wie die entsprechenden Rhodanide und Selenocyanide Phototropie zeigen. Die Empfindlichkeit steigt von Cl zu J an [8].

Wie schon erwähnt, ist Mercuricyanat in Methanol, Äthanol und aliphatischen Ketonen leichtlöslich. Wenn eine Lösung von anhydrischem Cupri-

* Das mit Mercuricyanate isomere Fulminat hat eine Leitfähigkeit die nicht merkbar grösser als diejenige von Wasser ist.

Tabelle 1.

64 l		128 l		256 l		512 l		$HgCl_2$	
Z	*A*	*Z*	*A*	*Z*	*A*	*Z*	*A*	*v*	*A*
13′	1,56	19′	2,12	20,5′	3,00	22′	4,56	64 l	3,77
19′	1,67	38′	2,18	30′	3,02	33′	4,61	128 l	4,91
23′	1,69	53′	2,23	50′	3,20	55′	4,66	256 l	7,54
43′	1,83	83′	2,47	81′	3,32	79′	4,92	512 l	12,0
53′	1,84								
16 St.	4,08								

bromid in Methanol oder Äthanol mit einer äquivalenten Menge von $Hg(OCN)_2$ in demselben Solvenz versetzt wird, so schlägt die braune Farbe der $CuBr_2$-Lösung sofort in grün um. Der Farbenwechsel ist durch eine Umsetzung von $CuBr_2$ in $Cu(OCN)_2$, welch letzteres in alkoholischer Lösung grün ist, bedingt. Gleichzeitig wird $HgBr_2$ gebildet. Wenn bei der Reaktion Aceton oder Methyläthylketon als Lösungsmittel gebraucht werden, so fällt das gebildete $Cu(OCN)_2$ zum grössten Teil aus und kann nach Waschen mit den Ketonen und schliesslich mit Äther als lichtgrünes mikrokristallines Pulver isoliert werden. Das reinste Produkt wurde aus Aceton erhalten. In dieser Weise ist das aus wässriger oder alkoholischer Lösung wegen solvolytischer Zersetzung nicht gewinnbare Cyanat leicht darstellbar. Wie von Naumann [9] beobachtet worden ist, setzt sich $HgCl_2$ mit $CuBr_2$ in Aceton um, wobei zunächst $CuCl_2$ gebildet, aber allmählich zu CuCl reduziert wird. Wie ich selbst konstatiert habe, tritt in Methanol und Äthanol derselbe momentane Farbenumschlag ein wie mit $Hg(OCN)_2$.

Das Mercurichlorid wirkt bekanntlich auf viele organische Verbindungen merkurierend, wobei Quecksilber an Kohlenstoff fixiert wird. Die Ähnlichkeit zwischen Chlorid und Cyanat lässt vermuten, dass wenigstens in gewissen Fällen das Chlorid bei solchen Reaktionen durch das Cyanat vertreten werden kann. So wird, wie ich festgestellt habe, *Pyrrol* in Wasser glatt durch $Hg(OCN)_2$ zu einer Verbindung $C_4H_2NH(HgOCN)_2$ merkuriert unter gleichzeitiger Entwicklung von Cyansäure. *Thiophen* wird von einer acetatgepufferten Wasserlösung von $Hg(OCN)_2$ eben wie von $HgCl_2$ langsam angegriffen. Isoliert wurden durch Extraktion mit Aceton ein Monomerkurierungsprodukt und ein dimerkuriertes, deren Untersuchung jedoch noch nicht abgeschlossen ist. Ersteres, welches durch seine Ätherlöslichkeit leicht von letzterem separiert werden kann, kristallisiert aus Äther in Prismen von Schmelzp. 105°.

Mercurocyanat

Mercurocyanat scheint erstmalig von Wöhler [10] dargestellt zu sein, er gewann es durch Umsetzen von $Hg_2(NO)_2$ mit $Ba(OCN)_2$. Das Salz ist sehr wenig untersucht worden. Von Knoll & Co.[11] ist es für Darstellung von α-Brom*iso*-

valerylharnstoff gebraucht worden und von Rao und Watson [8] für die Synthese von Br · Hg(OCN) und J · Hg(OCN). Wie ich festgestellt habe, kann das Salz durch Fällen einer halbmolaren mit HNO_3 angesäuerten Wasserlösung von $Hg_2(NO_3)_2$ mit NaOCN in einigem Überschuss in 95 %-iger Ausbeute und von grosser Reinheit erhalten werden. Es ist in heissem Wasser etwas löslich und daraus bei Abkühlen als kleine Nadeln erhältlich. Seine Dissoziation in Wasser in der Wärme sowie die umgekehrte Reaktion bei Zimmertemperatur sind schon erwähnt worden, ebenso seine Bildung nach der Ederschen Reaktion. Wässriges NH_3 bewirkt sofortige Schwärzung durch Bildung von met. Hg.

Kupfercyanate

Normale Cyanate von Kupfer waren meines Wissens bis jetzt unbekannt *, woran die leichte Hydrolysierbarkeit hauptsächlich die Schuld trug. Wie *Cupricyanat* aus Acetonlösung darzustellen ist, wurde oben mitgeteilt. Ein Doppelsalz mit Kaliumcyanat kann aber in Wasser dargestellt werden; es fällt bei Vermischen einer konzentrierten $Cu(NO_3)_2$-Lösung mit KOCN in Überschuss als ein voluminöser Kristallniederschlag aus. Das Salz, welches die Formel $KCu(OCN)_3$ hat, löst sich in Wasser mit blauer Farbe, die Löslichkeit beträgt bei 20° 5,2 g pro 100 ml (durch Cu-Analyse einer abgewogenen Menge gesättigter Lösung bestimmt). In absolutem Alkohol ist die Löslichkeit so gering, dass der Alkohol farblos bleibt. Aceton löst kleine Mengen mit hellgrüner Farbe. Die Verbindung kann nur kurze Zeit in Wasserlösung aufbewahrt werden, da sie rasch unter Bildung von basischem Cyanat zersetzt wird. Versuche ein entsprechendes Natriumsalz zu bereiten scheiterten, wahrscheinlich wegen einer zu grossen Löslichkeit des Salzes in Wasser.

Die Fähigkeit Doppelcyanate zu bilden ist auch für das *Cuprocyanat* CuOCN eigentümlich. Wenn eine Wasserlösung von Kupfersulfat oder Nitrat mit überschüssigem Kaliumcyanat und dann mit Kaliumbisulfit versetzt wird, tritt bald Ausfällung von glänzenden farblosen Kristallblättern ein, und gleichzeitig beginnt eine ziemlich lebhafte Entwicklung von CO_2. Die Zusammensetzung der Kristalle ist $KCu_3(OCN)_4$. Bei später ausgeführten Synthesen wurde immer als Cu^{2+}-Salz das Nitrat verwendet und das Bisulfit gegen eine frisch bereitete Lösung von SO_2 in Wasser ausgetauscht. Die Lösung muss dann um die Auskristallisation zu beschleunigen gepuffert werden. Die Pufferung ist auch dadurch geboten, dass die Zersetzung der bei der Reduktion gebildeten Cyansäure in CO_2 und NH_4-Salz unbedingt verhindert werden muss um Komplikationen durch Doppelsalzbildung von NH_4OCN mit CuOCN zu vermeiden. Als Puffer wurde Kaliumacetat benutzt, wodurch die CO_2-Bildung praktisch vollständig zurückgedrängt werden konnte. Nach neuesten Messungen von Amell [12] ist die thermodynamische Dissoziationskonstante der Cyansäure bei 20° $2{,}0 \times 10^{-4}$, diejenige von Essigsäure ist bekanntlich ungefähr ein Zehntel von diesem Wert.

* In Williams, H. E. *Cyanogen Compounds*, 2. Aufl. s. 73, wird Cupricyanat als eine grüne in Wasser unlösliche Verbindung beschrieben. Wie ich festgestellt habe, handelt es sich hier um ein basisches Cyanat von der Formel $Cu(OH)_2 \cdot Cu(OCN)_2$.

Dieselbe Zusammensetzung wie das Kaliumsalz hat das in analoger Weise dargestellte Rubidiumsalz, also $RbCu_3(OCN)_4$, während diejenige der Natriumverbindung der Formel $NaCu_4(OCN)_5$ gehorcht. Auch dieses Salz kristallisiert in Tafeln *. Selbstverständlich ist bei Synthesen der Na- und Rb-Verbindungen Na- bezw. Rb-Acetat als Puffer zu verwenden.

Die Komplexizität dieser in Wasser schwerlöslichen Doppelcyanate ist schwach; sie werden z.B. von Wasser unter Bildung von gelbem Cu_2O hydrolytisch zersetzt.

Die abweichende Formel des Na-Salzes gab mir den Anlass, auch die Darstellung eines Lithiumsalzes zu versuchen. Bei Zusatz von Lithiumcyanat zu einer Mischung von $Cu(NO_3)_2$, LiOAc und SO_2 trat in einigen Fällen keine, in anderen eine geringfügige Kristallisation ein, bei Einleiten von SO_2 jedoch eine reichliche. Die Analyse der gewaschenen und getrockneten prismatischen Kristalle zeigte, dass sie alkalifrei waren und die Formel CuOCN hatten. LiOCN ist also zur Bildung von schwerlöslichem Doppelcyanat unfähig, und damit war also eine Methode zur Darstellung von CuOCN gefunden.

Das Cuprocyanat ist in seinem chemischen Verhalten Cuprochlorid sehr ähnlich. Es wird wie dieses leicht von Wasser under Gelbfärbung hydrolysiert und in feuchtem Zustand leicht durch den Luftsauerstoff unter Grünfärbung oxydiert. Dieses ist auch bei seinen Doppelverbindungen der Fall, weshalb das Abfiltrieren und Auswaschen in einer Stickstoffatmosphäre auszuführen ist. Brom in Wasser bewirkt sofortige Auflösung zu $CuBr_2$, und $Cu(OCN)_2$, $(SCN)_2$ in einem organischen Solvenz schwärzt unter Bildung von $Cu(SCN)_2$. Konzentrierte Wasserlösungen von KOCN lösen CuOCN zu einer leicht oxydablen Lösung. Längeres Aufbewahren geschieht am besten in Vakuum unter Ausschluss von Tageslicht. CuOCN wirkt ferner als Katalysator nach Sandmeyer bei Einführung von einer *Iso*cyanatgruppe in den Benzolkern, wovon weiter unten die Rede sein wird.

Die für die Synthesen von $RbCu_3(OCN)_4$ und CuOCN erforderlichen Rb- bezw. Li-Cyanate sind aus den entsprechenden Sulfaten durch Umsatz mit Bariumcyanat und Konzentrieren der filtrierten Lösung durch Vakuumdestillation erhältlich. Die Methoden der Literatur zur Herstellung von $Ba(OCN)_2$ sind wenig befriedigend; das Salz kann aber, wie ich gefunden habe, sehr bequem durch Fällen einer gesättigten wässrigen Lösung von Natriumcyanat mit einer äquivalenten Menge von Bariumrhodanid- oder Perchlorat in Methanol gewonnen werden **. Das Cyanat kristallisiert anhydrisch in kleinen Prismen von neutraler Reaktion, seine Löslichkeit in Wasser bei 20° wurde durch Ba-Analyse der gesättigten Lösung zu 10,6 g pro 100 ml = 0,45 M bestimmt.

Wie schon oben erwähnt, zeigt sich die Halogenähnlichkeit der Cyanatgruppe auch darin, dass CuOCN als Sandmeyerkatalysator bei der Einführung von einer *Iso*cyanatgruppe in den Benzolkern wirken kann. Für eine solche Reaktion via ein Diazoniumsalz war man früher auf Katalyse nach Gattermann [14] also mit metallischem Cu hingewiesen.

---

* Von Wöhler und Berthmann [13] sind Natriumcuprofulminate der Formeln $NaCu(ONC)_2$ und $Na_2Cu(ONC)_3 3H_2O$ dargesteilt worden.

** Versuche analog das Strontiumcyanat aus dem Rhodanid und NaOCN zu gewinnen scheiterten, wahrscheinlich wegen einer zu grossen Löslichkeit des Salzes in Methanol-Wasserlösung.

Wird zu einer diazotierten Lösung von Anilinhydrosulfat KOCN gesetzt und dann sofort $KCu_3(OCN)_4$ oder $NaCu_4(OCN)_5$, tritt unmittelbar eine lebhafte Stickstoffentwicklung ein, und es scheidet sich C_6H_5NCO als Öltropfen ab, die mit einem passenden Solvenz wie Benzol, Chloroform oder Tetrachlorkohlenstoff aufgenommen werden können. Die Reaktion ist wegen der Wasserempfindlichkeit des Isocyanats etappenweise auszuführen; der Katalysator ist in Portionen zuzusetzten und das Reaktionsprodukt jedesmal zu extrahieren. Die Ausbeuten sind aus dem genannten Grunde nicht besonders gut, auch nicht bei möglichst rapidem Arbeiten. Etwas bessere Ausbeuten, bis auf 30 %, sind mit *o*-Toluidin erhalten worden, was wohl hauptsächlich der geringeren Wasserempfindlichkeit des *o*-Tolyl*iso*cyanats zuzuschreiben ist.

Das durch Fraktionieren isolierte Reaktionsprodukt wurde durch kurzes Erwärmen mit *o*-Kresol identifiziert, wobei in fast quantitativer Ausbeute der *o*-Tolylester der *o*-Tolyl-Carbaminsäure entstand.

EXPERIMENTELLER TEIL

Das für die folgenden Versuche benutzte Kaliumcyanat war Bakers' Analyzed ebenso das Cuprinitrat; das Natriumcyanat war von Hopkin und Williams geliefert.

Cadmiumcyanat aus Sulfat und Bariumcyanat

12,82 g $3CdSO_4 \cdot 8H_2O$ wurden in 100 ml H_2O gelöst und zu dieser Lösung eine solche von 11,09 g $Ba(OCN)_2$ in 150 ml H_2O gesetzt. Um alles $Cd(OCN)_2$ in Lösung zu bringen, wurde auf ein Volumen von 550 ml verdünnt. Das Reaktionsgemisch blieb über Nacht bei Zimmertemperatur stehen, wonach der Niederschlag von $BaSO_4$ auf einem grossen Jenaer Glasfilter G4 abfiltriert wurde. Durch Vakuumdestillation wurde dann die Lösung sofort auf ein Volumen von 55 ml konzentriert, wobei Kristallisatiou in seideglänzenden Blättern eintrat. Nach etwa zweistündigem Kühlen in Eisbad wurde die Mutterlauge abgesogen, die Kristalle zunächst mit Aceton und dann mit Äther gewaschen und kurz an der Luft getrocknet. Gewicht 10,0 g statt theor. 12,0. Das so präparierte Salz war mit etwas basischem Salz gemengt und löste sich nicht klar in Wasser. Zwecks Reinigung wurden 2,2 g in 100 ml H_2O gelöst und soviel einer 0,25 M Essigsäurelösung zugesetzt, dass die Trübung verschwand. Es wurde nun sofort durch Vakuumdestillation mit einer Badtemperatur, die nicht 50° überstieg, auf ein Volumen von 25 ml eingeengt und dann nach Zugabe von 3 ml 0,25 M HOAc in Eisbad der Kristallisation überlassen. Nach etwa 3 Stunden Abfiltrieren, Waschen und Trocknen, wie oben angegeben. Ausbeute 1,6 g = 73 %.

Das Cd wurde als Oxid bestimmt, C und H nach Liebig (Gef. Cd 46,64; C 9,96; H 2,08. Ber. für $2Cd(OCN)_25H_2O$ [482,92]: Cd 46,55; C 9,94; H 2,08; für $Cd(OCN)_22H_2O$ (232,45): Cd 48,35; C 10,32; H 1,73). Bei Aufbewahren in Vakuum über konz. H_2SO_4 gibt das Salz langsam sein Kristallwasser ab.

Cadmiumcyanat aus Jodid und Silbercyanat

21,976 g CdJ_2 wurden in 100 ml reinem Aceton suspendiert und zu der Lösung 17,988 g AgOCN in Portionen gesetzt. Beide Präparate waren von hochgradiger Reinheit. Reaktion unter Wärmeentwicklung. Das Gemisch blieb während 2 Tagen bei Zimmertemperatur unter zeitweiligem Umschütteln stehen. Dann wurde der Niederschlag abfiltriert, in Vakuum getrocknet, pulverisiert und dann wieder in die Acetonlösung hineingebracht. Nach weiteren 2 Tagen war die Lösung jodidfrei, der Niederschlag wurde abfiltriert, mit Äther gewaschen und in Vakuum getrocknet. Gewicht 41,7 statt 39,9 g. Zwecks Gewinnung des Cyanats wurden 6,66 g des Gemenges von AgJ und anhydrischem $Cd(OCN)_2$ mit 115 ml Wasser digeriert, die Wasserlösung abgesogen, und der Niederschlag mit

2 × 10 ml Wasser gewaschen. Gewicht nach Trocknen 4,73 statt 4,70 g. Durch Konzentrierung der Lösung wie oben angegeben auf ein Volumen von 25 ml und nachfolgender Kühlung konnten 1,43 g Ag-freies Cyanat isoliert werden.

Darstellung von Mercuricyanat aus $HgCl_2$ und AgOCN in Äther

27,25 g gepulvertes $HgCl_2$ wurden in 600 ml trocknem Äther gelöst und 33 g reines AgOCN zugesetzt (theor. 30,0). Das Reaktionsgemisch wurde während einer Stunde geschüttelt und dann während eines Tages sich selbst überlassen. Die Lösung war dann chlorfrei. Nach Filtrieren wurde der Äther abdestilliert, wobei Kristallisation von $Hg(OCN)_2$ eintrat. Der von AgCl, AgOCN und $Hg(OCN)_2$ bestehende Niederschlag wurde dann erschöpfend mit Äther extrahiert, wodurch insgesamt 27 g reines $Hg(OCN)_2$ erhalten wurden. Das Präparat ist in einer trocknen Atmosphäre, am besten in Vakuum aufzubewahren. Bei der Analyse wurde Hg als HgS bestimmt, N nach Kjeldahl und C auf nassem Wege durch Verbrennung mit einem Gemisch von H_2SO_4, CrO_3, H_3PO_4 und KJO_3. (Gef. Hg 70,66; N 9,80; C 8,36. Ber. für $Hg(OCN)_2$ (284,61): Hg 70,49; N 9,84; C 8,44). Die Dichte wurde pyknometrisch bei 20° zu 4,35±0,01 mit Brombenzol als Sperrflüssigkeit bestimmt.

Darstellung von Mercuricyanat aus Quecksilberoxyd und Cyansäure

In 75 ml eisgekühltem trocknem Äther wurden 8,9 g trocknes HCl eingeleitet und zu der Lösung in Portionen 47 g AgOCN gegeben (theor. 36,9). Reaktion unter Wärmeentwicklung. Nach Umschütteln unter Kühlung während etwa 1,5 Stunden wurde der Niederschlag auf einem Glasfilter G3 mit 65 ml Äther in Portionen ausgewaschen und zu der Lösung sofort 24,4 g gelbes, in der Kälte ausgefälltes, mit Wasser, Alkohol und Äther gewaschenes HgO in Portionen unter Umschütteln gesetzt. Reaktion unter einiger Wärmeentwicklung, weshalb anfänglich etwas mit kaltem Wasser gekühlt wurde. Beim Stehen wurde die gelbe Farbe des Bodenkörpers allmählich blasser und war nach 12 Stunden gelblich weiss. Der stechende Geruch von HOCN war nun verschwunden. Der Bodenkörper wurde abfiltriert, mit etwas Äther gewaschen und in Vakuum getrocknet. Gewicht 23,4 g. Die Mutterlauge wurde durch Abdestillieren des Äthers konzentriert, wobei Kristallisation eintrat. Die Kristalle wurden sofort von dem wasserhaltigen Äther abfiltriert und in Vakuum getrocknet. Die 23,4 g Bodensubstanz wurden mit Äther erschöpfend extrahiert und insgesamt konnten nach Konzentrieren der Lösungen 21,7 g $Hg(OCN)_2$ isoliert werden. (Gef. Hg 70,41; N 9,24 (Kjeldahl). Ber. Hg 70,49; N 9,84).

Als Kontrolle der Reinheit von $Hg(OCN)_2$ kann die restlose Auflösung in Äther oder Aceton benutzt werden. Wenn sich eine Probe nicht vollständig löst, ist eine Umlösung in Äther für die Reinigung genügend.

Darstellung von Mercurocyanat

56,1 g (0,1 Mol) $Hg_2(NO_3)_2 \cdot 2H_2O$ wurden in einer Mischung von 150 ml H_2O und 20 ml 2 M HNO_3 bei gelinder Wärme aufgelöst, die Lösung mit Eis gekühlt und sofort mit einer Lösung von 17,5 g NaOCN in 200 ml H_2O gemischt, Die Menge von NaOCN war so bemessen, dass sie ausser zur Ausfällung von $Hg_2(OCN)_2$ auch zur Pufferung der überschüssigen HNO_3 ausreichte. Es entstand sofort ein rein weisser Niederschlag, der sich ziemlich rasch absetzte. Nach einer Viertelstunde wurde der Niederschlag auf einem grösseren Jenaer Glasfilter G3 abfiltriert, durch Umrühren mit eiskaltem Wasser viermal ausgewaschen, dann zweimal mit Alkohol und Äther und zuletzt in Vakuum über H_2SO_4 getrocknet. Gewicht 46,2 statt 48,5 g = 95 %. (Gef. Hg 82,90. Ber. für $Hg_2(OCN)_2$ (485,22): Hg 82,68).

Dissoziation von Mercurocyanat durch Erhitzen mit Wasser

41,9 g $Hg_2(OCN)_2$ wurden mit 200 ml siedeheissem Wasser kurz umgeschüttelt, wobei der Niederschlag sich sofort grau färbte. Die warme Lösung wurde durch ein grosses Glasfilter G3 filtriert und sofort gekühlt, wobei eine kleine Menge einer in kleinen Nadeln anschiessenden Substanz sich absetzte, ($Hg_2(OCN)_2$). Das Digerieren wurde nun mit neuen Portionen von 200 ml heissem Wasser fortgesetzt, bis bei Ankühlen keine weitere Kristallisation von $Hg_2(OCN)_2$ eintrat. Der rückständige Niederschlag konnte nach Trocknen praktisch vollständig zu flüssigem Hg zusammengerieben werden. Gewicht 15,8 statt 16,9 g. Die vereinigten völlig klaren Wasserextrakte, deren Volumen etwa 1 Liter betrug, wurden möglichst rasch durch Vakuumdestillation konzentriert, wobei Kristallisation allmählich eintrat. Die Kristalle wurden fraktioniert aufgesammelt und in Vakuum getrocknet, und die Konzentrierung der Mutterlauge bis zu wenigen ml getrieben. Insgesamt konnten 20,2 g Substanz statt theor. 24 g isoliert werden und daraus nach Umlösen in Äther 18,4 g reines $Hg(OCN)_2$.

Reduktion von $Hg(OCN)_2$ zu $Hg_2(OCN)_2$

Lösungsmittel Wasser. 2,84 g $Hg(OCN)_2$ wurden in 50 ml H_2O gelöst und während einer Stunde mit 33 g met. Hg geschüttelt. Probe auf Hg^{2+} mit NaOH gab dann keinen Niederschlag von HgO. Nach Absaugen der Wasserlösung wurde mit Wasser, Alkohol und Äther gewaschen und luftgetrocknet. 29 g Hg wurden entfernt und der Rückstand fünfmal mit je 25 ml siedeheissem Wasser ausgelaugt, der wässrige Extrakt eisgekühlt, wobei 0,11 g $Hg_2(OCN)_2$ ausfiel. Die Mutterlauge wurde durch Vakuumdestillation eingetrocknet und dabei ein Salzrückstand von 2,33 g erhalten. Dieser löste sich bei Digerieren mit 170 ml Äther mit einem äusserst kleinen gelben Rückstand. 1,82 g $Hg(OCN)_2$ wurden aus der Ätherlösung isoliert.

Lösungsmittel Äther. 4,40 g $Hg(OCN)_2$ wurden in 100 ml Äther suspendiert und mit 125 g met. Hg geschüttelt. Die Reduktion war nach 2 Stunden beendet, da die Probe mit NaOH einen negativen Ausfall hatte. Der Niederschlag wurde abfiltriert, wie oben beschrieben gewaschen und getrocknet und mit 3×50 ml heissem Wasser ausgelaugt. Beim Einengen der filtrierten Lösung konnten 3,0 g Mercuricyanat isoliert werden. Die Ätherlösung, wo die Reduktion ausgeführt wurde, gab keinen Eindampfungsrückstand, was also zeigt dass der Reaktionsverlauf ein quantitativer war.

Cupricyanat

6,2 g $Hg(OCN)_2$ wurden in 50 ml Aceton gelöst und zu der Lösung 4,46 g anhydrisches $CuBr_2$ gesetzt. Unter gelinder Wärmeentwicklung geht das Bromid in Lösung und reagiert mit dem Cyanat unter Ausfällung eines hellgrünen Niederschlags. Die Umsetzung ist nach wenigen Minuten beendet *. Nach stundenlangem Stehen bei Zimmertemperatur wird der Niederschlag unter Ausschluss von Feuchtigkeit abfiltriert, dreimal mit kleinen Mengen des Ketons unter Umrührung und dreimal mit trocknem Äther gewaschen und dann in Vakuum über P_2O_5 bis zu Gewichtskonstanz getrocknet. Ausbeute 2,6 g statt theor. 2,95. (Gef. Cu 42,34; C 16,62. Ber. für $Cu(OCN)_2$ (147,59): Cu 43,08; C 16,27).

$Cu(OCN)_2$ ist leicht und vollständig löslich in Wasser zu einer blauen Lösung, die aber bald unlösliches basisches Salz absetzt. In Methanol und Äthanol sowie in Aceton ist es mit grüner Farbe etwas löslich. Diese Lösungen sind bei längerem Aufbewahren auch nicht stabil. Die Dichte wurde bei 20° pyknometrisch mit Xylol als Sperrflüssigkeit zu 2,45± 0,01 bestimmt.

* In rigorös getrocknetem Aceton ist die Reaktion träger

Kaliumcupricyanat

Eine Lösung von 8,2 g KOCN in 25 ml H_2O wurde durch Zusatz von 0,2 g $Ba(NO_3)_2$ und Abfiltrieren des Niederschlags von Carbonat befreit, und die eisgekühlte Lösung mit einer ebenfalls eisgekühlten Lösung von 6,0 g $Cu(NO_3)_2 \cdot 3H_2O$ in 15 ml H_2O gemischt. Es entstand sofort ein aus feinen Nadeln bestehender hellgrüner Kristallbrei. Nach etwa 30 Min wurden die Kristalle auf einem Glasfilter G3 aufgesammelt, mit 10 ml eiskaltem Wasser und dann mit Alkohol und Äther unter Umrühren gewaschen und in Vakuum über konz. H_2SO_4 getrocknet. Ausbeute 4,2 g. Bei der Analyse wurde K als Sulfat und Cu als Rhodanur bestimmt. (Gef. K 16,51; Cu 27,74. Ber. für $KCu(OCN)_3$ (228,62): K 17,09: Cu 27,86).

Kaliumcuprocyanat

12,0 g $Cu(NO_3)_2 \cdot 3H_2O$ wurden in 50 ml Wasser gelöst und dazu 50 ml einer 1,3 M Lösung von SO_2 in Wasser gesetzt. Bei Zugabe von 9,8 g KOAc in 50 ml H_2O entstand ein gelbgrüner Niederschlag der sich sofort auflöste, wenn eine Lösung von 8,1 g KOCN in 50 ml H_2O zugegeben wurde. Die grüne Farbe der Lösung wurde rasch abgeblasst, und Ausfällung von glänzenden Kristallblättern setzte sofort ein. Das Gemisch wurde 45 Min im Eisbad gekühlt und dann die Kristalle auf ein Glasfilter von mittlerer Feinheit aufgesammelt, mit 0,2 M SO_2-Lösung dreimal unter Umrührung gewaschen, dann zweimal mit Alkohol und dreimal mit Äther und dann sofort in Vakuum über H_2SO_4 getrocknet. Ausbeute 5,4 statt theor. 6,6 g. Abfiltrierung und Auswaschen sind in einer N_2-Atmosphäre auszuführen, und bevor der Zugabe von Alkohol ist das SO_2 mit N_2 zu verjagen, da alkoholisches SO_2 mit CuOCN eine braune Färbung gibt.

Bei der Analyse wurde K als Sulfat nach Entfernen des Cu mit H_2S als Cu_2S bestimmt. Für die Cu-Analyse wurde die Probe in Wasser suspendiert; soviel Brom wurde zugesetzt, dass vollständige Auflösung eintrat, und dann nach Zugabe von SO_2 wurde Cu als CuSCN ausgefällt und gewogen. (Gef. K 9,42; Cu 47,37; C 12,29; H 0,19. Ber. für $KCu_3(OCN)_4$ (397,85): K 9,83; Cu 47,94; C 12,07).

Natriumcuprocyanat

12,1 g $Cu(NO_3)_2 \cdot 3H_2O$ in 25 ml H_2O + 50 ml einer 1,4 M SO_2-Lösung + 17 g $NaOAc \cdot 3H_2O$ in 50 ml + 6,5 g NaOCN in 75 ml. Auskristallisation etwas langsamer als beim Kaliumsalz. Kristallisationszeit 1 Stunde. Auswaschen und Trocknen wie oben beschrieben mit der Ausnahme, dass statt mit Alkohol mit einer 0,1 M Lösung von HOAc in Alkohol gewaschen wurde. Ausbeute 4,5 g statt 6,1. Ziemlich grosse rein weisse Blätter. Das Na wurde als Sulfat, Cu als CuSCN bestimmt. (Gef. Na 4,68; Cu 51,80. Ber für $NaCu_4(OCN)_5$ (487,32): Na 4,72; Cu 52,12).

Rubidiumcuprocyanat

Zu einer Lösung von 6,0 g $Cu(NO_3)_2 \cdot 3H_2O$ in 15 ml H_2O wurde eine Lösung von RbOAc, aus 6,52 g Rb_2CO_3 und 3,25 ml Eisessig in 25 ml H_2O dargestellt, gesetzt und dann eine Lösung von RbOCN, die aus 6,52 g Rb_2SO_4 und 5,4 g $Ba(OCN)_2$ in 100 ml H_2O bereitet und dann durch Vakuumdestillation auf ein Volumen von 25 ml konzentriert worden war. Kleine Mengen eines hellgrünen Niederschlages entstanden, die aber bei Zusatz von 25 ml einer 1,5 M SO_2-Lösung sofort verschwanden. Rasches Ausfallen eines weissen Niederschlags von kleinen Schuppen. Nach halbstündigem Stehen in Eisbad Abfiltrieren und Waschen wie bei der Na-Verbindung und Trocknen in Vakuum. Gewicht 3,3 g, theor. 3,9 g. Die Mutterlauge setzte bei Stehen noch etwa 0,1 g Substanz als grössere Tafeln mit rhombischer Begrenzung ab. Bei der Analyse wurde Rb als Perchlorat und Cu als CuSCN bestimmt. (Gef. Rb 18,89; Cu 43,19. Ber. für $RbCu_3(OCN)_4$ (444,23): Rb 19,24; Cu 42,93).

Cuprocyanat

24,2 g $Cu(NO_3)_2 \cdot 3H_2O$ in 25 ml H_2O + 0,3 Mol LiOAc in 60 ml H_2O, wobei eine dunkelblaue Lösung entstand. Zu dieser wurde eine Lösung von 0,2 Mol LiOCN gegossen, aus 0,1 Mol $Li_2SO_4 \cdot H_2O$ + 0,1 Mol $Ba(OCN)_2$ dargestellt und durch Vakuumdestillation auf

ein Volumen von 50 ml konzentriert.* Die Farbe der Lösung wurde dabei etwas dunkler. Nun wurde 100 ml einer 1,4-M SO_2-Lösung zugesetzt, was einen Farbenumschlag in grün bewirkte. Bald setzte unter Abblassen der Farbe Kristallisation ein, und es wurde nun während 30 Min SO_2 in die Lösung eingeleitet. Die Kristalle wurden wie vorher beschreiben abfiltriert und gewaschen und in Vakuum unter Lichtausschluss getrocknet und aufbewahrt. Ausbeute 9,3 g = 88 %. Kleine Prismen von der Dichte 3,13 ± 0.01 bei 20°, pyknometrisch mit Brombenzol und Xylol als Sperrflüssigkeiten bestimmt. Bei der Analyse wurden Cu als CuSCN und N nach Kjeldahl bestimmt. (Gef. Cu 60,15; N 13,29; Ber. für CuOCN (105,58): Cu 60,23; N 13,27).

Darstellung von Bariumcyanat

Zu einer Lösung von 13,0 g NaOCN in 115 ml H_2O wurden 0,3 g $Ba(ClO_4)_2$ (Anhydrid) gesetzt und der kleine Niederschlag von $BaCO_3$ abfiltriert. Ferner wurden 33,6 g $Ba(ClO_4)_2$ in 115 ml reinem Methanol gelöst und die beiden Lösungen gemischt. Auskristallisieren setzte fast sofort ein. Nach Aufbewahren über Nacht in Kälteschrank, wurden die Kristalle abfiltriert mit Methanol und Äther gewaschen und in Vakuum getrocknet. Ausbeute 15,8 g = 71 %. (Gef. Ba 62,35. Ber. für $Ba(OCN)_2$ (221,38) Ba 62,04). Das Salz ist auch wiederholt aus Methanollösungen von $Ba(SCN)_2$ mit ungefähr derselben Ausbeute dargestellt worden.

Darstellung von *o*-Tolyl*iso*cyanat

Zu einer Lösung von 10,8 ml konz. H_2SO_4 in 100 ml H_2O wurden 10,7 ml *o*-Toluidin gesetzt und das Gemisch bis zur vollständigen Auflösung der Base gewärmt. Die eisgekühlte Lösung wurde nun mit 7,5 g $NaNO_2$ in 10 ml H_2O diazotiert. Farbe der Lösung blassgelb. Zusatz einer Lösung von 10 g KOCN in 15 ml H_2O und sofort 5 g $KCu_3(OCN)_4$. Ein braunes Addukt von Katalysator und Diazoniumsalz endstand sofort und bei dessen Zersetzung lebhafte Stickstoffentwicklung und Abscheiden einer Flüssigkeit. Sofortiges Ausschütteln mit 70 ml eisgekühltem Chloroform, das stark braun gefärbt wurde. Das ganze wurde durch ein grosses Glasfilter G2 filtriert und die Chloroformschicht schnell abseparіert. Zu der lichtgrünen Wasserlösung wurden weitere 3 g des Katalysators gesetzt, wobei nochmals Gasentwicklung eintrat, jedoch schwächer als vorher. Erneutes Ausschütteln mit $CHCl_3$, das sich diesmals schwächer braun färbte. Die Prozedur wurde ein drittes Mal mit 3 g Katalysator wiederholt, wobei kaum Gasentwicklung stattfand und das Chloroform fast farblos blieb. Die vereinigten Chloroformextrakte wurden sofort mit P_2O_5 getrocknet und das Lösungsmittel in Vakuum bei einer Badtemperatur unter 40° abdestilliert. Gewicht des flüssigen Rohprodukts von 3 solchen Synthesen 37 g. Zunächst wurde in Vakuum fraktioniert, wobei als Mittelfraktion 16 g Flüssigkeit gewonnen wurden. 30 g derart dargestelltes Präparat lieferten bei einer zweiten Fraktionierung unter gewöhnlichem Druck 21 g zwischen 183° und 187° siedendes *Iso*cyanat = 28 %.

Die Synthese des *o*-Tolyl*iso*cyanats ist auch mit Benzol als Extraktionsmittel ausgeführt worden. Die Abtrennung der Benzolschicht geht jedoch langsamer, was sich in einer verschlechterten Ausbeute kundgibt.

Wie ich gefunden habe, enthält das mit $CHCl_3$ oder CCl_4 extrahierte Tolyl*iso*cyanat immer kleine Mengen von Chlor, und dies gilt auch für das durch Katalyse nach Gattermann hergestellte. Das *o*-Tolyl*iso*cyanat ist wie Phenyl*iso*cyanat zu Tränen reizend, jedoch nicht so stark, dass Arbeiten damit eigentliche Unannehmlichkeiten mitführt.

o-Tolylcarbaminsäure-*o*-Tolylester aus *o*-Tolyl*iso*cyanat

In 6,0 g wie oben beschrieben dargestelltes $CH_3C_6H_4NCO$ wurden 4,87 g *o*-Kresol gelöst, was unter Temperaturerniedrigung geschah. Die Lösung wurde auf dem Wasserbade gewärmt, wobei der Inhalt des Kolbens bald zu einem Kristallkuchen erstarrte.

* Eine Wasserlösung von LiOCN kann ebensowenig wie die Lösungen von Li-Halogeniden durch Destillation konzentriert werden ohne durch Hydrolyse alkalisch zu werden. Diese Tatsache wirkt aber in diesem Falle kaum belästigend, da die Lösung bei Zusatz von SO_2 sauer wird.

Nach etwa 7 Stunden wurde das Reaktionsprodukt pulverisiert. Gewicht 10,70 g statt theor. 10,87. Die Substanz, die nicht mehr nach *Iso*cyanat roch, wurde zwei Stunden bei Zimmertemperatur mit 50 ml Benzin digeriert, dieses scharf abgesogen, die Kristalle mit etwas Benzin gewaschen und in Vakuum getrocknet. Gewicht 9,34 g. 2 g der Substans wurden nun aus 5 ml warmen Eisessig kristallisiert, wobei 1,34 g zurückgewonnen wurden. Schmelzp. 115—118°. Durch zwei weitere Kristallisationen aus Eisessig konnte der Schmelzpunkt auf 124—126° erhöht werden aber nicht weiter. Prismen aus Eisessig. Von Gattermann wurde als Schmelzpunkt 126° gefunden.

LITERATUR

1. Clarke, F. W. und Owens, M. E. *Am. Chem. J.* **3** (1881—82) 350.
2. Graf, R. *Chem. Ber.* **89** (1956) 1071.
3. Ripan, R. *Bul. Soc. Stiinte Cluj.* **4** (1928) 144; *Chem. Zentr.* **1929 I** 2905.
4. Cohen, E. Z. physik. Chem. **14** (1894) 71; *Gmelin Handb. d. anorg. Chem.* 8. Aufl. Bd 32—33, S. 85.
5. Dietz, R. *Z. anorg. Chem.* **20** (1899) 253.
6. Birckenbach, L. und Kolb, H. *Ber.* **68** (1935) 895.
7. Ley, H. Z. *physik. Chem.* **30** (1899) 247.
8. Rao, S. V. R. und Watson, H. E. *J. Phys. Chem.* **32** (1928) 1354.
9. Naumann, A. *Ber.* **37** (1904) 4335.
10. Wöhler, L. *Gilberts Annalen* **73** 166.
11. Knoll & Co. D. R. P. 275200; *Chem. Zentr.* **1914 II** 277.
12. Amell, A. R. *J. Am. Chem. Soc.* **78** (1956) 6234.
13. Wöhler, L. und Berthmann, A. *Ber.* **62** (1929) 2754.
14. Gattermann, L. und Cantzler, A. *Ber.* **23** (1890) 1225; **25** (1892) 1086.

Eingegangen am 9. Juli 1957.

ACTA CHEMICA SCANDINAVICA 11 (1957) 1635—1640

Metal-Metal Bonding in Some Transition Metal Dioxides

BENGT-OLOV MARINDER and ARNE MAGNÉLI

Institute of Inorganic and Physical Chemistry, University of Stockholm, Stockholm, Sweden

Short metal-metal distances found in the rutile-type phases in the systems $(Ti,V)O_2$ and $(V,Mo)O_2$ indicate the presence of bonds between the metal atoms. There is a close relation between the axial ratio of these compounds and the number of free valence electrons available per bond. A comparison is made with the bonds observed in the dioxides of MoO_2-type and in orthorhombic rhenium dioxide and also in some complex ions containing transition metals of valence numbers lower than their maximum ones.

In the dioxides of MoO_2-type, *i.e.* vanadium, molybdenum, wolfram, technetium and rhenium dioxide, and in the orthorhombic modification of the latter, short metal-metal distances have been observed which indicate the presence of bonds between the metal atoms. All these oxides contain metal atoms with valence numbers lower than their maximum ones, which implies that there are valence electrons not engaged in metal-oxygen bonding. It has been pointed out in previous articles that there exists a qualitative relation between the metal-metal bond distances and the number of free electrons available per bond [1,2].

In order to throw further light on this relationship a few systems of mixed transition metal dioxides have been studied [3]. These systems have contained representatives of the structure types mentioned above and titanium dioxide (rutile type). A surprising result of this investigation was the occurrence of extended regions of rutile-type structure not only in pseudobinary systems containing titanium dioxide as a component, *e.g.* TiO_2-VO_2, but also in systems that did not contain a component of rutile structure, *e.g.* VO_2-MoO_2.

The structure types of rutile, molybdenum dioxide and orthorhombic rhenium dioxide are alike in being built up of metal-oxygen octahedra joined by corners and by edges. The short metal-metal distances are associated with the octahedra sharing edges. For the rutile type this distance is simply equal to the length of the *c* axis of the unit cell, while the calculation of the metal-metal distances for the two other structure types requires the knowledge of the actual values of the metal atom parameters.

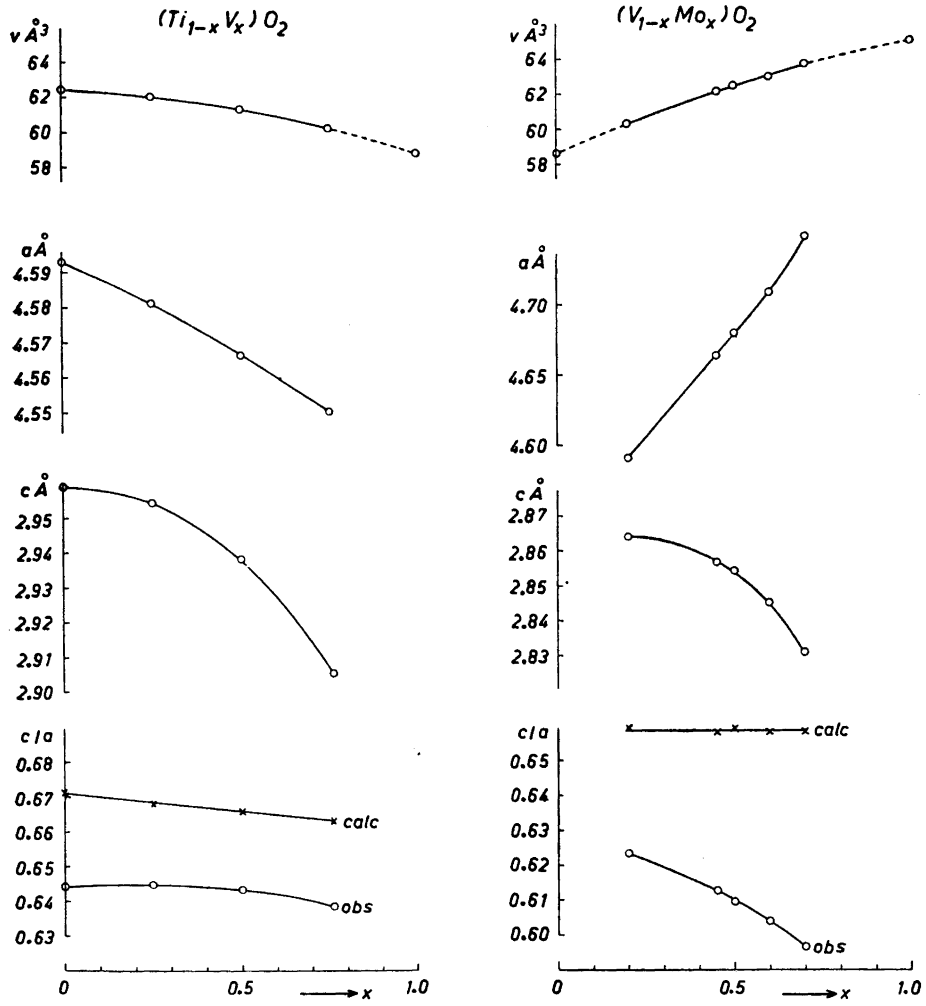


Fig. 1. Lattice parameters of the rutile-type phases in the systems (Ti,V)O_2 and (V,Mo)O_2.

The factors determining the length of the close metal-metal approach may be rather complicated in nature but for a simplified discussion the following factors will be considered:

1) The geometrical relations connected with the ratio of the metal and oxygen atom radii.
2) The repulsive forces caused by the charges of the atoms.
3) The bonding forces between the metal atoms.

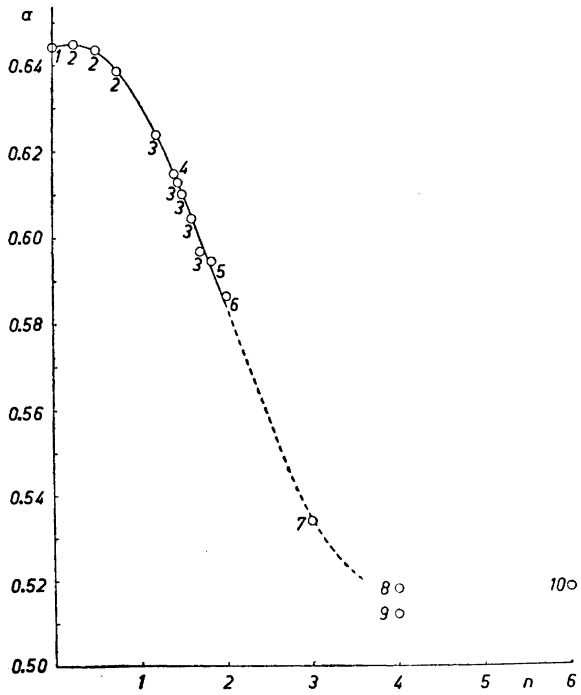


Fig. 2. Axial ratios of rutile-type phases and equivalent quantities for other types of transition metal dioxides (a) *versus* number of valence electrons available per metal-metal bond (n). The figures correspond to the following samples: 1-TiO_2, 2-$(Ti,V)O_2$, 3-$(V,Mo)O_2$, 4-$(Re,V)O_2$, 5-$(Re,Mo,V)O_2$, 6-VO_2, 7-ReO_2 (orthorhombic), 8-MoO_2, 9-WO_2, 10-TcO_2 and ReO_2 (MoO_2-type).

The lattice parameters of the rutile-type phases in the systems $(Ti_{1-x},V_x)O_2$ and $(V_{1-x},Mo_x)O_2$ are represented in Fig. 1 as functions of the composition. The decrease with increasing x of the volume per formula unit (v) of the former is in accordance with the formula volumes of the pure components. The same is true for the increase with x of the volume of the $(V_{1-x},Mo_x)O_2$ rutile phase.

For $(Ti,V)O_2$ both the a and c axes decrease with increasing x. At about $x = 0.4$ the shortening of c seems to be slightly accelerated. For $(V,Mo)O_2$ the increase of the a axis with x parallels the change of the formula volume, while the c axis shows a simultaneous shortening. The results indicate the presence in $(V,Mo)O_2$ of considerable attractive forces between neighbouring metal atoms, increasing in strength with the molybdenum content. They also suggest the possibility of slight attraction in $(Ti,V)O_2$ for high vanadium contents.

Pauling [4] has given an expression for the axial ratio of rutile-type crystals considering the influence of the ratio of the atomic radii and of the anion-anion repulsive forces. The metal-metal interaction was considered negligible.

Fig. 1 also shows the axial ratio derived by this formula, c/a (calc), and those obtained from the experimental data, c/a (obs). For $(Ti,V)O_2$ the calculated and experimental ratios differ by approximately the same amount as that found by Pauling for pure titanium dioxide. The deviating slope of the observed ratios for $(V,Mo)O_2$ indicates that a contracting force acts between the metal atoms in the c direction and that this effect increases with increasing molybdenum content.

It appears that the axial ratio may provide a suitable "normalized" measure of the metal bond length present in these phases. Fig. 2 gives the values of c/a (obs) for the various samples of $(Ti,V)O_2$ and $(V,Mo)O_2$ as a function of the number of valence electrons available per metal-metal bond, *i.e.* the number of valence electrons not engaged in metal-oxygen bonding divided by the number of short metal-metal distances. The corresponding data for two samples of rutile structure obtained in the $(V,Re)O_2$ and $(V,Mo,Re)O_2$ systems also fit the smooth curve.

Fig. 2 also contains data for the various dioxides of MoO_2-type (deformed rutile structure) and for the orthorhombic rhenium dioxide. For these substances a different normalized bond length had to be chosen instead of the axial ratio used for the rutile-type structures. Thus, for the monoclinic MoO_2-type compounds, the quotient $d/\sqrt{bc\sin\beta}$ was adopted as an appropriate equivalent of c/a (rutile). In this expression, d denotes the length of the metal-metal bonds which extend approximately parallel to the a axis of the unit cell, this direction corresponding to that of the unique axis of the ideal rutile lattice. For the orthorhombic rhenium dioxide where the bonds form zig-zag strings through the structure, the bond length was analogously divided by the square root of the unit mesh area projected parallel to the bond direction.

It must be emphasized that the bond lengths of the pure dioxides are less accurately known than those present in the rutile-type structures. This is especially so for the technetium and rhenium dioxides. The d values for these two compounds have thus been roughly estimated assuming the metal atom positions to be the same as those found for molybdenum dioxide.

The change of direction of the curve for high number of electrons is very likely associated with the considerable electrostatic repulsion between the metal atoms at the very short metal-metal distances present in these compounds which are significantly shorter than those occurring in the metals.

It seems probable that similar but not identical curves may be given by other mixed oxide systems. Thus niobium dioxide, the structure of which is a superstructure of the rutile type [5], gives an axial ratio of the subcell falling considerably below the curve given in Fig. 2. This may indicate the existence of stronger bonds in this compound than those found in the present investigation. On the other hand tantalum dioxide of rutile structure [6] shows an axial ratio rather close to that of titanium dioxide, which may be an indication of weak or no bonding between the tantalum atoms. Similar values of the axial ratio (0.642—0.673) are also shown by several rutile-type structures found by Brandt [7] among mixed oxides of antimony, niobium or tantalum with aluminium, gallium or transition elements which are likely to be present in a trivalent state (chromium, iron and rhodium). The group of trirutile structures, studied by Byström, Hök and Mason [8], and comprising mixed

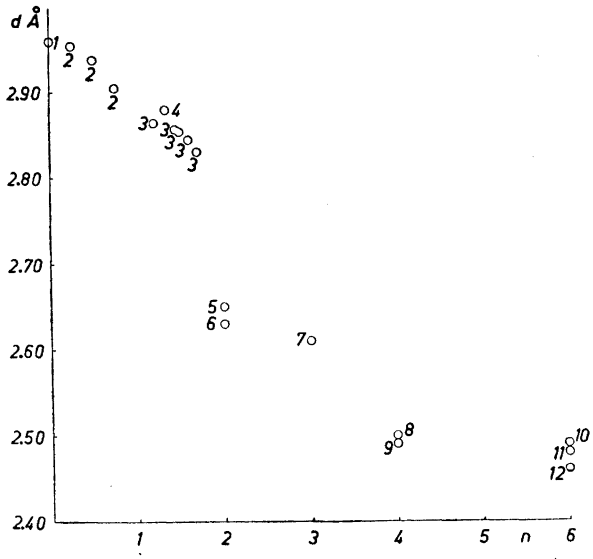


Fig. 3. Metal-metal bond lengths for various transition metal compounds (d) *versus* number of valence electrons available per bond (n). The figures denote the following substances: 1-TiO_2, 2-(Ti,V)O_2, 3-(V,Mo)O_2, 4-$(Ta_6Cl_{12})^{2+}$, $(Ta_6Br_{12})^{2+}$ and $(Nb_6Cl_{12})^{2+}$, 5-VO_2, 6-$(Mo_6Cl_8)^{4+}$, 7-ReO_2 (orthorhombic), 8-MoO_2, 9-WO_2, 10-ReO_2 (MoO_2-type), 11-TcO_2, 12-$(W_2Cl_9)^{3-}$.

oxides ASb_2O_6 and ATa_2O_6, where A is magnesium, zinc, iron, cobalt or nickel, likewise gives high values for the ratio $c/3a$ (0.645—0.665). X-Ray studies on further systems of mixed transition metal dioxides are in progress. It is also planned to start magnetic investigations of these substances in the near future.

Very short metal-metal distances have also been found in other transition metal compounds, *e.g.* the ions $W_2Cl_9^{3-}$ and $Mo_6Cl_8^{4+}$ studied by Brosset [9–11] and the ions $Nb_6Cl_{12}^{2+}$, $Ta_6Br_{12}^{2+}$ and $Ta_6Cl_{12}^{2+}$ investigated by Vaughan, Sturdivant and Pauling [12]. The geometrical conditions present in these compounds are of course quite different from those in the dioxides. It is, however, interesting to note that the rough qualitative relation found to connect the metal-metal distances with the number of valence electrons available per metal-metal bond in the dioxides also seems to be valid for these complex ions (*cf.* Fig. 3).

These studies form part of a research program on metal oxides and related compounds supported by the *Swedish Natural Science Research Council.*

REFERENCES

1. Magnéli, A. and Andersson, G. *Acta Chem. Scand.* **9** (1955) 1378.
2. Magnéli, A. *Acta Chem. Scand.* **11** (1957) 28.
3. Marinder, B.-O. and Magnéli, A. *To be published.*

4. Pauling, L. *Z. Krist.* **67** (1928) 377.
5. Magnéli, A., Andersson, G., and Sundkvist, G. *Acta Chem. Scand.* **9** (1955) 1402.
6. Schönberg, N. *Acta Chem. Scand.* **8** (1954) 240.
7. Brandt, K. *Arkiv Kemi, Mineral. Geol.* **17A** (1943) No. 15.
8. Byström, A., Hök, B., and Mason, B. *Arkiv Kemi, Mineral. Geol.* **15B** (1941) No. **4.**
9. Brosset, C. *Arkiv Kemi, Mineral. Geol.* **12A** (1935) No. 4.
10. Brosset, C. *Arkiv Kemi, Mineral. Geol.* **20A** (1945) No. 7.
11. Brosset, C. *Arkiv Kemi, Mineral. Geol.* **22A** (1946) No. 11.
12. Vaughan, P. A., Sturdivant, J. H., and Pauling, L. *J. Am. Chem. Soc.* **72** (1950) 5477.

Received July 13, 1957.

ACTA CHEMICA SCANDINAVICA 11 (1957) 1641—1652

Phase Analysis Studies on the Titanium-Oxygen System

STEN ANDERSSON, BENGT COLLÉN, ULF KUYLENSTIERNA and ARNE MAGNÉLI

Institute of Inorganic and Physical Chemistry, University of Stockholm, Stockholm, Sweden

The titanium-oxygen system has been studied by means of X-ray powder photographs of preparations quenched after annealing at various temperatures. A number of phases not previously described has been observed, *viz.*

Ti_2O, TiO (low-temperature modification), Ti_4O_7, Ti_5O_9, Ti_6O_{11}, Ti_7O_{13}, Ti_8O_{15}, Ti_9O_{17} and $Ti_{10}O_{19}$.

The extensions of the homogeneity ranges have been determined for the phases with variable composition.

The first phase analysis by means of X-ray methods on the titanium-oxygen system was carried out by Ehrlich [1,2], who reported the existence of three intermediary oxides and a high solubility of oxygen in the hexagonal titanium modification. Subsequent investigations by other authors have been numerous and comprise in addition to X-ray studies the employment of other techniques, *e.g.* microscopy and thermal measurements. These studies have contributed some modifications and added further details to the general conception of the titanium oxides established by Ehrlich but the results are not consistent throughout.

A phase diagram for the titanium-oxygen system constructed on the basis of data published up to 1954 has been given by De Vries and Roy [3]. The uncertainty in several respects was emphasized by these authors who actually characterized the diagram as a "not-impossible" phase diagram.

As there seemed to be reasons for considering the knowledge of the titanium-oxygen system as inadequate it was thought worth-while to undertake a comprehensive phase analysis. The results obtained so far will be reported in this article. X-Ray diffraction data for the various phases will be published seperately [4]. Crystal structure studies on several of the oxides are in progress.

STARTING MATERIALS

Starting materials for the syntheses were titanium metal, titanium dioxide and intermediary titanium-oxide preparations of known compositions. The metal was "Matthey Titanium Sponge" (Johnson, Matthey & Co., Ltd), the principal impurities of which were stated by the manufacturer to be 0.01 % magnesium, 0.01 % iron and 0.003 % silicon. A determination according to Kjeldahl of the nitrogen content gave the result < 0.01 %. The titanium dioxide was of "Baker Analyzed" quality, the principal impurities being zinc (0.01 %), lead (0.006 %) and iron (0.008 %). The X-ray diffraction pattern showed that the sample consisted of the anatase modification.

The samples of intermediary titanium oxides used in the syntheses were prepared by melting mixtures of titanium metal and dioxide in an electric arc furnace. The products were analyzed in the way described below.

PREPARATION METHODS

The samples used in the present investigation were obtained by heat-treating appropriate mixtures of the starting materials. The heating was carried out in three different ways, *viz.* in an electric arc furnace under argon atmosphere, in an electric resistance furnace in a stream of argon and finally with the samples sealed in evacuated silica tubes. In order to accelerate the attainment of equilibrium, samples intended for heat-treatment at lower temperatures were generally premelted in the arc furnace.

The electric arc furnaces employed were of a design by Hägg and Kiessling [5]. The arc (DC) is formed between a negative wolfram electrode and the specimen in the form of a pressed tablet or pellet (positive electrode), which rests on a strongly water-cooled copper base. In this way no reaction occurs with the base, nor is there any transport of material from the wolfram electrode to the specimen. The cooling rate of the sample after disconnecting the arc is very high. The argon pressure within the furnace was for the actual preparations kept at about 0.5 at. When needed, the tablets were remelted once or twice in order to obtain a complete reaction. Due to segregation the samples prepared in the arc furnace were often not in a complete state of equilibrium — this was indicated by the relatively diffuse powder photographs given by these specimens.

For the syntheses in an argon stream, a horizontal electric resistance furnace (maximum temperature 1 200°C) with a Pythagoras mass tube was used. The specimen tablets were kept in an alumina boat. For low contents of oxygen a superficial reaction was found to occur between the specimens and the boat. The reaction product, however, stuck to the boat and thus did not contaminate the titanium oxide samples. For high contents of oxygen no appreciable attack on the boat was observed. The argon was purified by passing it at about 770°C over finely divided uranium, obtained according to Kiessling [6] by thermal decomposition of partially hydrogenated uranium chips. The titanium oxide samples were allowed to cool in the furnace under argon, the cooling rate thus being rather slow.

Most of the annealing operations were carried out with the specimen tablets sealed in evacuated silica tubes, which were heated in vertical, electric resistance furnaces. All the samples treated in this way were quickly quenched in water. For the lowest heating temperatures applied (400° and 600°C) no reaction was found to occur between the silica and the samples. Specimens low in oxygen only slightly affected the silica when heated for long periods of time at 800°C. At 1 150°C preparations with oxygen contents below about $TiO_{1.5}$ attacked the tubes to an extent that made annealing under these conditions impracticable. Samples richer in oxygen did not react in a serious way with the silica at this temperature. In order to prevent a reaction with the silica tube at the beginning of the heating, it was found necessary to avoid as far as possible the use of titanium metal or low oxides as components in the sample.

CHEMICAL ANALYSIS

The oxygen contents of all samples prepared by arc-melting and by heating in an argon stream and of several of those heated in silica tubes were determined by the increase of weight when oxidized to titanium dioxide. Weighed samples of 0.3—0.5 g were heated in silica boats in an oxygen stream at 1 000°C for periods ranging from one hour for specimens of high oxygen content to some ten hours for those low in oxygen. Following Ehrlich [1] the latter specimens were admixed with a known amount of titanium dioxide in order to avoid spitting. Only the rutile form (preheated at high temperatures) could be used for this purpose since anatase was found to cover the specimen grains with rigid shells of rutile, thus preventing complete oxidation. The reproducibility of the analyses was found to be good. The difference between starting composition and the analytically found composition after the various heat-treatments was small in most cases.

X-RAY METHODS

The phase analysis was performed by means of X-ray powder photographs taken in a Guinier focusing camera of 80 mm diameter with strictly monochromatized Cu$K\alpha_1$ radiation. In order to depress the back-ground fogging caused by the fluorescence radiation from the titanium content of the samples, an aluminium filter foil of 35 μ thickness was placed in contact with the photographic film. The registration and evaluation of the patterns were carried out in the way described in a previous article [7]. Thus an internal standard (potassium chloride, British Drug Houses, Analar, $a = 6.2919$ Å at 20°C [8]) was added to the powder specimens. Photographs of samples without admixture were used to reveal superpositions of lines. The effect of film shrinkage was overcome according to Hägg by printing a scale on the film prior to development [9]. Following Österlöf the measurement of the reflexions was made on the sharp, high-angle edge of the lines [10]. In this way it was generally possible to determine the line positions to within $\pm$ 0.01 mm.

The single-crystal photographs were taken in a Weissenberg camera using CuK radiation.

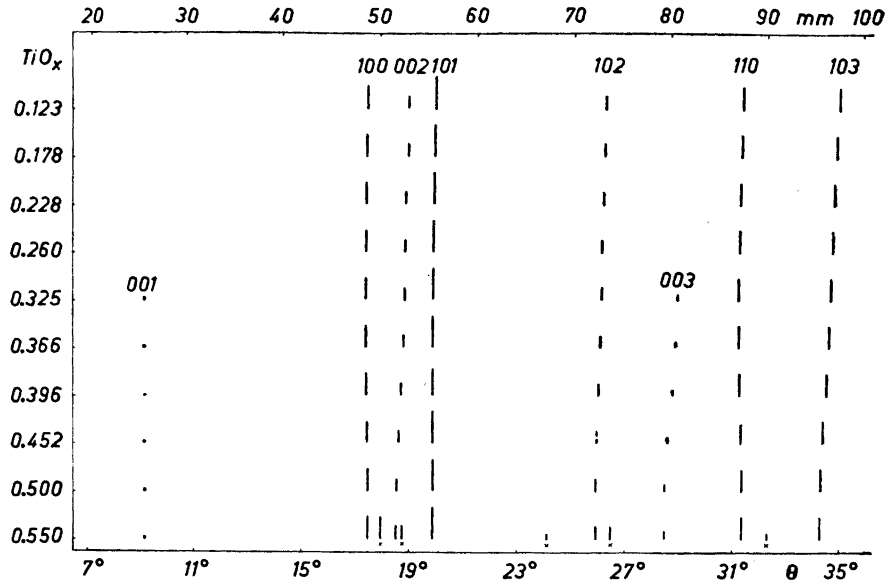


Fig. 1. Powder patterns of preparations $TiO_{0.12}$-$TiO_{0.55}$ annealed at 400°C. The lines marked with an X in $TiO_{0.55}$ belong to the δ-oxide.

RESULTS OF THE PHASE ANALYSIS

On account of the experimental difficulties mentioned above the phase analysis studies have so far been restricted to a few temperature regions. Thus samples low in oxygen have been mostly studied after quenching from annealing temperatures of 800°, 600° and 400°C. The composition range $TiO_{0.5-1.5}$ has also been investigated by means of specimens quenched from the melting temperature (about 1 800°C). For higher oxygen contents, samples heat-treated at 1 150°C have been studied.

The results obtained for the various regions of composition will be discussed in the following.

The composition range $TiO_{0-0.5}$.

Data on the solubility of oxygen in α-titanium have been given by several authors [11]. They all give values for the maximum oxygen content of this phase, corresponding to the approximate formula $TiO_{0.5}$, and the oxygen atoms are supposed to occur randomly distributed in the octahedral interstices of the hexagonally close-packed titanium lattice. The c-axis is said to increase over the whole composition range while the a axis, which is only slightly affected by the incorporation of the oxygen atoms, reaches a maximum value at about $TiO_{0.25}$ and then remains constant with increasing oxygen content.

The powder patterns of several samples within this composition range heat-treated at 400°C for 6 weeks are represented in Fig. 1. Photographs of samples annealed for several weeks at 600° and 800°C and of specimens quench-

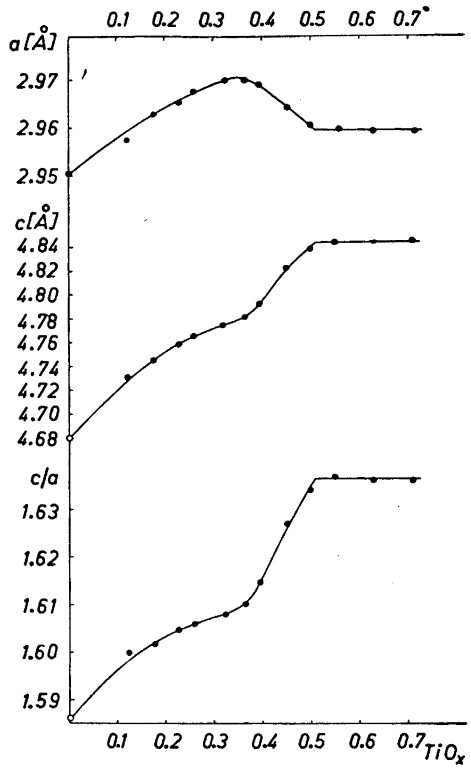


Fig. 2. Lattice parameters and axial ratios of the hexagonal specimens α-Ti-$TiO_{0.5}$.

ed in the arc furnace are all in full agreement with those shown in Fig. 1 ecxept for the fact that the reflexions 001 and 003 are not always present (*v. infra*).

Fig. 2 shows the variation of the lattice parameters with the oxygen content. The dimensions for pure titanium are those given by Szántó [12], which, however, do not differ considerably from recent values reported by other authors [11]. The maximum solubility of oxygen corresponds closely to $TiO_{0.50}$ and this value is evidently valid irrespective of the heat-treatment. The length of the a axis goes through a maximum at about $TiO_{0.35}$ and the steady increase of the c axis is suddenly accelerated at the same composition.

The lines 001 and 003, both of very low intensity, are incompatible with an hexagonal close-packed titanium structure containing randomly distributed oxygen atoms. The value of the axis ratio ($c/a = 1.637$) reached at the composition $TiO_{0.5}$ is evidently not connected with the presence of an almost perfect hexagonal close-packing of the atoms (ideal value of $c/a = 1.633$). For samples heat-treated at 400°C, the extra lines 001 and 003 occur in $TiO_{0.33}$ and specimens higher in oxygen. This is close to the composition where anomalous changes of the lattice parameters have been found to occur. For preparations annealed at 600° and 800°C and quenched in the arc furnace, however,

the minimum compositions for the appearance of these two lines are about $TiO_{0.40}$, $TiO_{0.45}$ and $TiO_{0.50}$, respectively. In the patterns of the high-temperature samples the two lines are slightly diffuse.

The two extra lines may be accounted for if the oxygen atoms are assumed to be arranged in every second layer of octahedral interstices extending normally to the hexagonal axis of the titanium host lattice. Simultaneously the oxygen atoms force the adjacent titanium atom layers somewhat apart. The transition from the random TiO_{0+x} to the ordered Ti_2O_{1-y} arrangement will be further studied. Details for the Ti_2O structure will appear elsewhere.

Ehrlich's observation [2] that samples $TiO_{\sim 0.2}$ are remarkably volatile has been confirmed by experiments in sealed, evacuated silica tubes and also in an argon stream at about 1 000°C. Further studies on this phenomenon are in progress.

The composition range $TiO_{0.5-1.4}$

According to Ehrlich [1] titanium monoxide is of the NaCl type with randomly distributed vacancies in both the titanium and oxygen lattices. The range of homogeneity extends from between $TiO_{0.58}$ and $TiO_{0.69}$ to between $TiO_{1.25}$ and $TiO_{1.33}$. All the titanium positions are occupied at the lower limit and all the oxygen sites are filled at the higher limit. At the composition $TiO_{1.00}$, 15 % of both atomic positions are vacant. Similar ranges of homogeneity have been reported by subsequent authors for samples prepared at high temperatures.[11]

Naylor [13] found, from heat capacity measurements, indications of a phase transition in TiO at 991°C. Jenkins [14] reported that the powder photograph of $TiO_{1.00}$ heat-treated at 870°C is composed of the patterns of two distinct bodycentered cubic structures. Wang and Grant [15] and also two of the present authors [16] found that TiO (NaCl type) when annealed at 925° and 800°C transforms giving a phase of the stoichiometric composition TiO and a complicated powder pattern.

The existence of a phase of a composition close to Ti_3O_2 or Ti_4O_3 formed by annealing below 925°C was reported by Bumps, Kessler and Hansen [17].

In the present investigation, arc-melted samples of compositions between $TiO_{0.64}$ and $TiO_{1.25}$ were found to give powder photographs showing exclusively the pattern of a NaCl-type phase. The lines were very sharp. No superstructure reflexions could be observed. Samples outside this composition region gave powder patterns showing an additional phase (α-Ti or Ti_2O_3). The homogeneity range of TiO (NaCl-type) derived from the observed unit cell dimensions extends from $TiO_{0.64}$ to $TiO_{1.26}$ (*cf.* Fig. 3). Table 1 lists the observed densities for the various TiO samples and the corresponding values for the occupancy of the atomic positions. The data confirm the results reported by Ehrlich[1].

Samples TiO_x ($0.5 < x < 1$) annealed at 900°C for 2 weeks gave powder photographs showing the pattern of Ti_2O and a great number of extra lines which appeared alone at the composition $TiO_{1.00}$. No reflexions of the NaCl-type oxide were present. The powder pattern of $TiO_{1.00}$ could not be accounted for by assuming the coexistence of two cubic phases as suggested by Jenkins [14]. Annealing at 800°C for two weeks was also performed for preparations with x values ranging from 0.55 to 1.40. For oxygen contents x below 1 the patterns were found to contain all those lines observed in the 900°C samples and in addition a considerable number of extra ones. The specimens annealed at

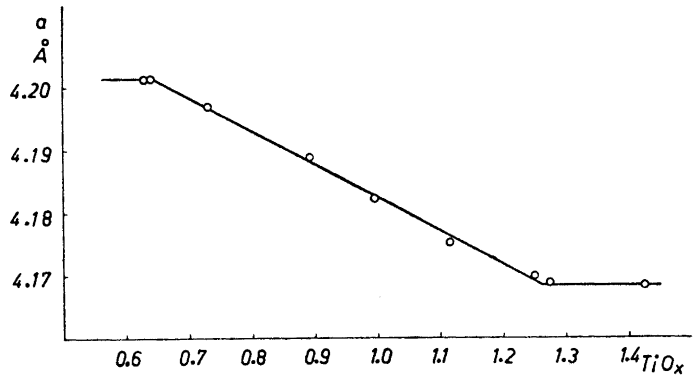


Fig. 3. Lattice parameter of TiO_x (NaCl type).

800°C were not in a state of equilibrium. The same three sets of X-ray reflexions were also found to occur in preparations heated for several weeks at 600°C.

Specimens TiO_x ($1 < x < 1.15$) annealed at 800°C gave powder patterns containing the lines found in the sample $TiO_{1.00}$ and those of TiO (NaCl-type). The latter pattern appeared alone in samples around $TiO_{1.20}$ and mixed with a corundum-type pattern (Ti_2O_3) at higher contents of oxygen. None of the systems of reflexions observed for the preparations heat-treated at 900—600°C showed any indication of line displacement with varying oxygen content.

The results may be accounted for in the following way. At 800°C there exist the phases Ti_2O, an oxide of the approximate composition $TiO_{0.65}$, not prepared in a pure state, TiO (low-temperature modification of stoichiometric composition), TiO (NaCl-type with a very narrow range of homogeneity and the approximate composition $TiO_{1.20}$) and Ti_2O_3. The $TiO_{\sim 0.65}$ phase, the powder pattern of which is similar to that given by Bumps, Kessler and

Table 1. Occupancy of the atomic positions in TiO_x (defective NaCl-type)

x	a Å	Density		Occupancy	
		obs	calc for $4TiO_x$/cell	% Ti	% O
(0.637	4.201_6	5.00	5.20	96.2	61.3)
0.716	4.196_6	5.01	5.33	94.0	67.3
0.892	4.188_9	4.96	5.62	88.3	78.8
0.995	4.182_2	4.95	5.79	85.5	85.1
1.116	4.175_2	4.89	6.00	81.5	91.0
1.195	4.172_5	4.83	6.13	78.8	94.2
1.250	4.169_9	4.77	6.22	76.7	95.9
(1.275	4.168_9	4.80	6.26	76.7	97.8)

Hansen [17] for the δ-phase, forms also at 600°C but not at 900°C. The low-temperature TiO is stable also at 900°C.

It has been pointed out [15,16] that the densities of TiO (low-temperature form) and $TiO_{1.00}$ (NaCl-type) are very nearly the same, *viz.* 4.91 and 4.95, respectively, and that there seems to be a pronounced relationship between the powder patterns of these two phases. This may indicate close structural kinship and it may be that the random atomic vacancies present in TiO (NaCl-type) occur in an ordered way in the low-temperature form.

The composition range $TiO_{1.4-1.7}$

The phases reported by previous authors within this range of composition are Ti_2O_3 and Ti_3O_5. The former, which according to Zachariasen [18] has the corundum structure, was said by Ehrlich [1] to have an extended range of homogeneity, $TiO_{1.46-1.56}$. A compound said to be Ti_3O_5 has been studied by Rusakov and Zhdanov [19] who found this substance to be isomorphous with pseudobrookite.

The phase conditions within this range of composition were studied by means of samples heat-treated at 1 150°C for four days. A slight variation was found for the lattice parameters of Ti_2O_3 (corundum type), the limiting values being reached in the preparations $TiO_{1.49}$ ($a = 5.160$ Å, $c = 13.60$ Å) and $TiO_{1.51}$ ($a = 5.147$ Å, $c = 13.64$ Å). The range of homogeneity thus lies within the limits $TiO_{1.49-1.51}$.

The powder pattern of a phase appearing pure at the composition $TiO_{1.67}$ (Ti_3O_5) is independent of the oxygen content. This pattern (*cf.* Fig. 4) is incompatible with the one reported by Rusakov and Zhdanov [19] for Ti_3O_5. Single crystals have been obtained in the electric arc furnace and a structure determination using Weissenberg photographs is in progress. The single crystal data have made it possible to interpret the powder pattern and the following dimensions have been obtained for the monoclinic unit cell:

$$a = 9.757 \text{ Å}, \qquad b = 3.802 \text{ Å}, \qquad c = 9.452 \text{ Å}, \qquad \beta = 93.11°$$

The observed density of 4.20 is in good agreement with the one calculated for a cell content of four formula units of Ti_3O_5 (4.24). The results of the structure determination will be published elsewhere [20].

It is of interest to note that studies on the system $(Ti_{1-x}, Fe_x)_3O_5$ have revealed the existence of a phase of pseudobrookite type for iron contents down to $x = 0.03$ [21]. It may be that the crystal studied by Rusakov and Zhdanov, which was obtained from slag, contained impurities stabilizing the pseudobrookite structure.

The composition range $TiO_{1.7-1.9}$

Previous authors have reported the existence in this region of a phase with an extended homogeneity range, *viz.* $TiO_{1.70-1.80}$ (Ehrlich [1]) and $TiO_{1.80-1.83}$ (Filonenko, Kudryavtsev and Lavrov [22]).

The samples used in the present studies were with few exceptions annealed at 1 150°C for three days. Specimens quenched in the arc furnace showed the same phases as those obtained at 1 150°C, but were found less suitable

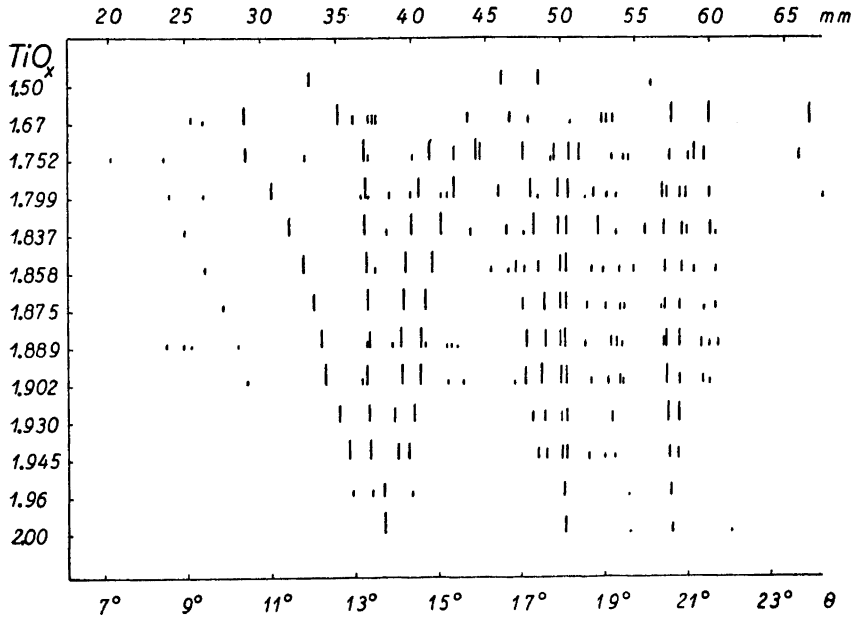


Fig. 4. Powder patterns of preparations $TiO_{1.50}$-$TiO_{2.00}$.

for X-ray studies because they gave less distinct powder lines. The reaction rate at 1 000°C was too low for equilibrium to be reached within a reasonable period of time.

Samples slightly higher in oxygen than $TiO_{1.70}$ still showed the presence of Ti_3O_5 but at about the composition $TiO_{1.75}$ the powder pattern showed only the reflexions of a new phase. With increasing oxygen content the pattern changed but was always of a similar general character (*cf.* Fig. 4). A detailed analysis, however, showed that this change was not a continuous one but that there was a periodic alternation of single-phase and two-phase regions of composition. This is demonstrated in Fig. 5 which shows the reflexions observed within a narrow range of Θ. The reflexions at low Θ angles provide the most sensitive test for the identification of these phases.

In order to find the compositions of the various phases, samples TiO_x were used with x values varied stepwise down to 0.002. Fairly large quantities were employed for the annealing in order to minimize the influence of the reaction with the silica. Chemical analyses performed on several of the samples confirmed that the compositions did not change during the heat-treatment.

The compositions of the phases thus derived are, within the limits of accuracy, in accordance with the general formula Ti_nO_{2n-1} (*cf.* Table 2). Phases were thus identified with all values of n from 4 to 10. The formula Ti_5O_9 has been verified by means of the unit cell dimensions obtained from

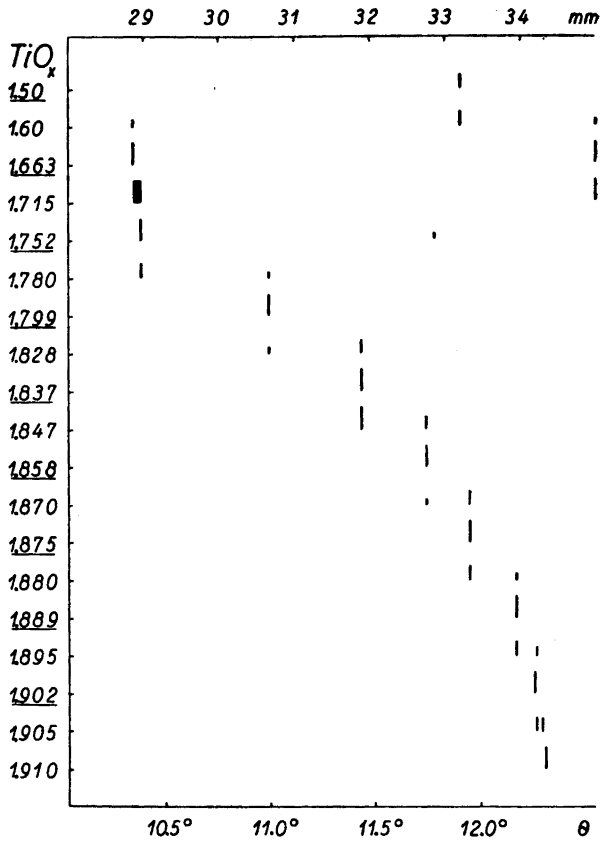


Fig. 5. Powder patterns within a narrow range of Θ of preparations $TiO_{1.50}$-$TiO_{1.91}$, demonstrating alternation of single-phase and two-phase regions of composition. Underlined x values correspond to single-phase photographs.

Table 2. Comparison between experimentally obtained compositions TiO_x and ideal compositions corresponding to a series Ti_nO_{2n-1}.

x_{obs}	n	$2n-1$	$x_{calc}=\frac{2n-1}{n}$	Ti_nO_{2n-1}
1.752	4	7	1.750	Ti_4O_7
1.799	5	9	1.800	Ti_5O_9
1.837	6	11	1.833	Ti_6O_{11}
1.858	7	13	1.857	Ti_7O_{13}
1.875	8	15	1.875	Ti_8O_{15}
1.889	9	17	1.889	Ti_9O_{17}
1.902	10	19	1.900	$Ti_{10}O_{19}$

single crystal data (triclinic symmetry) and density measurement. (The cell parameters were incorrectly given in a preliminary communication [23].)

$a = 5.569$ Å $\quad b = 7.120$ Å $\quad c = 8.865$ Å
$\alpha = 97.55°$ $\quad \beta = 112.34°$ $\quad \gamma = 108.50°$

The observed density is 4.29 in good agreement with the value 4.31 calculated for a cell content of two formula units of Ti_5O_9.

The general appearance of the X-ray patterns suggests that the oxides Ti_nO_{2n-1} form a homologous series of structurally interrelated compounds based on the rutile-type structure [23,24].

The composition range $TiO_{1.9-2}$

Several authors have reported on an extended homogeneity range of TiO_2 [11]. There are, however, no statements as to changes of the unit cell dimensions.

For higher oxygen contents than $TiO_{1.90}$ the powder patterns (samples annealed at 1 150°C) are still of the same type (*cf.* Fig. 4), which may suggest the existence of still higher members of the homologous series. It has, however, not been possible to prove the existence of two-phase regions above $TiO_{1.90}$. The difference between the powder patterns of consecutive homologues decreases with increasing n and it may be that the resolving power of the camera does not suffice to reveal the coexistence of two phases. Indications in favour of the supposition of distinct homologues above $Ti_{10}O_{19}$ are the considerable line displacements, which are not easily accounted for assuming a mechanism of solid solubility, and, especially, a periodical appearance of line broadenings with varying x. Anyhow, it is at present not possible to judge whether distinct phases Ti_nO_{2n-1} exist up to the limit of the two-phase region towards rutile or whether the series ends with a phase of variable composition. It is worth mentioning that equilibrium conditions are not easily reached in this border region.

The first trace of TiO_2 (rutile) was observed at the composition $TiO_{1.95}$. The lattice parameters of TiO_2 in the two-phase region differ slightly but significantly from those of pure rutile. The data obtained for the latter

$a = 4.593$ Å $\quad c = 2.959$ Å

are in good agreement with figures recently reported in the literature [25,26]. For the lower oxygen limit (sample quenched from 1 150°C) the corresponding values obtained were:

$a = 4.603$ Å $\quad c = 2.960$ Å

The data do not permit any accurate estimation of the width of the homogeneity range. The minimum content of oxygen is, however, higher than $TiO_{1.96}$.

When melted in the arc furnace, TiO_2 (rutile) was found to loose considerable amounts of oxygen. Thus, in one case, the composition of the sample after melting was found to be $TiO_{1.90}$. The powder photograph of this sample was diffuse. It showed no rutile lines but a pattern similar to that of the phases of the homologous series.

Acknowledgements. This investigation has been greatly facilitated by the support and assistance given by members of the research staff and representatives of other institutions. Thanks are due to Professor A. Ölander for his kind interest and for placing laboratory facilities at our disposal. Mrs. Stina Nord, Mr. G. Kruuse and Docent H. Pestmalis have given valuable assistance in the experimental and computational work.

Professor G. Hägg, Uppsala, and Docent R. Kiessling, AB Atomenergi, have given valuable information and advice in connection with the building of the electric arc furnace. In addition, Professor Hägg allowed the arc furnace of the Institute of Chemistry, University of Uppsala, to be used for the preparative work during the early stages of the investigation. This preparative work was carried out by Mr. S. Wahlgren.

Mr. H. Brynielsson, managing director, and Docent R. Kiessling of the AB Atomenergi kindly placed the uranium metal at our disposal.

These studies form part of a research program on metal oxides and related compounds financially supported by the *Swedish Natural Science Research Council.*

REFERENCES

1. Ehrlich, P. *Z. Elektrochem.* **45** (1939) 362.
2. Ehrlich, P. *Z. anorg. Chem.* **247** (1941) 53.
3. De Vries, R. C. and Roy, R. *Am. Ceram. Soc. Bull.* **33** (1954) 370.
4. Andersson, S., Collén, B., Kruuse, G., Kuylenstierna, U., Magnéli, A., Pestmalis, H., and Åsbrink, S. *Acta Chem. Scand.* **11** (1957) 1653.
5. Hägg, G. and Kiessling, R. *IVA* **26** (1955) 105.
6. Kiessling, R. *Private communication.*
7. Westman, S. and Magnéli, A. *Acta Chem. Scand.* **11** (1957) 1587.
8. Hambling, P. G. *Acta Cryst.* **6** (1953) 98.
9. Hägg, G. *Rev. Sci. Instr.* **18** (1947) 371.
10. Österlöf, J. *To be published.*
11. McQuillan, A. D. and McQuillan, M. A. *Titanium*, London 1956, p. 250.
12. Szántó, I. *Acta Tech. Acad. Sci .Hung.* **13** (1955) 363.
13. Naylor, B. F. *J. Am. Chem. Soc.* **68** (1946) 1077.
14. Jenkins, A. E. (Discussion of Ref. [17]). *Trans. Am. Soc. Metals* **45** (1953) 1025.
15. Wang, C. C. and Grant, N. J. *J. Metals 8* AIME Trans **206** (1956) 184.
16. Kuylenstierna, U. and Magnéli, A. *Acta Chem. Scand.* **10** (1956) 1195.
17. Bumps, E. S., Kessler, H. D., and Hansen, M. *Trans. Am. Soc. Metals* **45** (1953) 1008.
18. Zachariasen, W. H. *Skrifter Norske Videnskaps-Akad. Oslo I. Mat. Naturv. Kl.* **Nr 4** (1928) 165S, S21.
19. Rusakov, A. A. and Zhdanov, G. S. *Doklady Akad. Nauk. SSSR* **77** (1951) 411.
20. Åsbrink, S. and Magnéli, A. *Acta Chem. Scand.* **11** (1957) 1606.
21. Åsbrink, S. *To be published.*
22. Filonenko, N. E., Kudryavtsev, V. I. and Lavrov, I. V. *Doklady Akad. Nauk. SSSR* **86** (1952) 561.
23. Andersson, S. and Magnéli, A. *Naturwiss.* **43** (1956) 495.
24. Andersson, S. *To be published.*
25. Legrand, C. U. J. and Delville, C. R. *Compt. rend.* **236** (1953) 944.
26. Baur, W. H. *Acta Cryst.* **9** (1956) 515.

Received July 13, 1957.

ACTA CHEMICA SCANDINAVICA 11 (1957) 1653—1657

Identification of Titanium Oxides by X-Ray Powder Patterns

STEN ANDERSSON, BENGT COLLÉN, GEORG KRUUSE, ULF KUYLENSTIERNA, ARNE MAGNÉLI, HERBERT PESTMALIS and STIG ÅSBRINK

Institute of Inorganic and Physical Chemistry, University of Stockholm, Stockholm, Sweden

X-Ray powder data are given for fifteen phases occurring in the titanium-oxygen system.

Recent phase analysis studies carried out at this Institute on the titanium-oxygen system have revealed the existence of several previously unknown titanium oxide phases [1]. The analysis was performed by means of X-ray powder patterns, which were found to provide a powerful tool for the identification of the various oxides, both when occurring pure as well as in mixtures with each other.

The powder patterns were obtained using a Guinier focusing camera (80 mm diameter) with strictly monochromatized Cu$K\alpha_1$ radiation. Reflexions could be registered within the diffraction range $1.25° < \Theta < 43.5°$, the lower limit corresponding to a "cut-off" spacing of 35 Å. Potassium chloride (Analar, British Drug Houses, lattice parameter $a = 6.2919$ Å at 20°C [2]) was added to the powder specimens as an internal standard. The back-ground fogging caused by the fluorescence radiation from titanium was effectively depressed by means of an aluminium foil (35 μ) covering the photographic film. The techniques employed in evaluating the photographs have been described in a previous article [3].

The oxides were prepared from starting materials of high purity, *viz.* titanium metal (99.97 %) and titanium dioxide (99.98 %) by methods described previously [1]. The latter substance was found to be of the anatase form and was consequently used for registering the powder pattern of this modification of the dioxide.

All the synthesized oxides were obtained in a pure state except the so-called δ-phase ($TiO_{\sim 0.65}$) which always appeared together with Ti_2O and TiO (low-temperature form). The tables list parts of the powder patterns suitable for identification purposes, ranging from the lower "cut-off" limit

Table 1. α-Ti and Ti_2O. The hexogonally close-packed structure of α-Ti can dissolve considerable amounts of oxygen in a random distribution. At an oxygen content of about $TiO_{0.3}$, a transition occurs to an ordered arrangement of the oxygen atoms. The maximum solubility of oxygen corresponds to the composition Ti_2O, the powder pattern of which is given below. Reflexions indicating the ordered state are indicated by asterisks. The unit cell dimensions for Ti_2O are $a = 2.959_3$ Å and $c = 4.845_4$ Å.

I	$\sin^2\Theta_{obs}$	hkl	$\sin^2\Theta_{calc}$
vvw	0.02536	001*	0.02527
m	0.09028	100	0.09033
m	0.10108	002	0.10108
v st	0.11568	101	0.11560
st	0.19135	102	0.19141
vw	0.22740	003*	0.22743
st	0.27092	110	0.27099
m	0.31785	103	0.31776
vw	0.36141	200	0.36132
m	0.37215	112	0.37207
m	0.38666	201	0.38659
w	0.40429	004	0.40432
w	0.46240	202	0.46240

Table 2. δ-Titanium oxide ($TiO_{\sim 0.65}$).

I	$\sin^2\Theta_{obs}$
st	0.09526
st	0.10332
w	0.16678
m	0.19858
m	0.28590
w	0.29385
w	0.38136

Table 3. TiO (low-temperature form)

I	$\sin^2\Theta_{obs}$
w	0.01906
w	0.02997
w	0.03466
m	0.04206
st	0.05392
m	0.06826
m	0.07613
m	0.07723
w	0.09946
st	0.10183
st	0.10377
st	0.13475
v st	0.13862
vw	0.15741
vw	0.16814
vw	0.19160
w	0.20472
vw	0.20835
w	0.21542
w	0.22115
w	0.22590

Table 4. TiO (NaCl-type). At temperatures above 1 000°C this phase has a very wide homogeneity range which, however, decreases considerably at lower temperatures. At 800°C the phase only exists at a composition very close to $TiO_{1.20}$. The pattern given below corresponds to the sample $TiO_{1.00}$, the cube edge of which is $a = 4.182_2$ Å.

I	$\sin^2\Theta_{obs}$	hkl	$\sin^2\Theta_{calc}$
st	0.10172	111	0.10176
v st	0.13578	200	0.13568
v st	0.27137	220	0.27136
m	0.37305	311	0.37312
m	0.40704	222	0.40704

Table 5. Ti_2O_3. The phase has a very narrow range of homogeneity. The actual sample was of the composition $TiO_{1.500}$ with the lattice parameters of the hexagonal structure, $a = 5.155$ Å, $c = 13.607$ Å.

I	$\sin^2\Theta_{obs}$	hkl	$\sin^2\Theta_{calc}$
m	0.04262	102	0.04258
m	0.08095	014	0.08104
m	0.08929	110	0.08929
w	0.11808	113	0.11813
vvw	0.13202	202	0.13187
w	0.17035	204	0.17032
v st	0.20452	116	0.20465
vw	0.22116	212	0.22116
w	0.25966	214	0.25961
m	0.26787	300	0.26787

Table 6. Ti_3O_5. Dimensions of the monoclinic unit cell: $a = 9.757$ Å, $b = 3.802$ Å, $c = 9.452$ Å and $\beta = 93.11°$.

I	$\sin^2\Theta_{obs}$	hkl	$\sin^2\Theta_{calc}$
vw	0.00669	001	0.00666
vvw	0.02662	002	0.02664
m	0.03239	201	0.03236
v st	0.04736	110	0.04729
vw	0.05025	$20\bar{2}$	0.05024
w	0.05302	202	0.05304
w	0.05359	$11\bar{1}$	0.05360
w	0.05426	111	0.05430
m	0.05995	003	0.05995
vw	0.07323	$11\bar{2}$	0.07323
m	0.08284	$20\bar{3}$	0.08284
w	0.08706	203	0.08704
w	0.10497	311	0.10500
w	0.10615	$11\bar{3}$	0.10618
w	0.10793	401	0.10806
st	0.12375	$40\bar{2}$	0.12384
st	0.13429	204	0.13436
st	0.16415	020	0.16415
m	0.20796	314	0.20805

Table 7. Ti_4O_7

I	$\sin^2\Theta_{obs}$
vw	0.01559
w	0.02143
st	0.03248
w	0.04166
v st	0.05192
w	0.05288
w	0.06135
v st	0.06504
m	0.07011
v st	0.07481
st	0.07560
st	0.08576
vw	0.09210
st	0.09316
st	0.09671
st	0.10109
w	0.10748

Table 8. Ti_5O_9. Dimensions of the triclinic unit cell: $a = 5.569$ Å, $b = 7.120$ Å, $c = 8.865$ Å, $\alpha = 97.55°$, $\beta = 112.34°$, $\gamma = 108.50°$

I	$\sin^2\Theta_{obs}$	hkl	$\sin^2\Theta_{calc}$
vw	0.00973	001	0.00962
w	0.02194	$10\bar{1}$	0.02189
vw	0.02665	100	0.02664
st	0.03643	$10\bar{2}$	0.03638
vw	0.05063	101	0.05061
v st	0.05226	$1\bar{2}0$	0.05224
vw	0.05294	$02\bar{1}$	0.05294
w	0.05676	020	0.05674
w	0.06091	$\bar{1}21$	0.06091
v st	0.06278	$1\bar{2}1$	0.06279
w	0.06841	$02\bar{2}$	0.06837
v st	0.07010	$10\bar{3}$	0.07011
m	0.07986	021	0.07978
st	0.08737	$20\bar{1}$	0.08744
vw	0.08886	$\bar{1}22$	0.08882
st	0.09384	102	0.09382
st	0.09633	$12\bar{1}$	0.09635
vw	0.10081	$2\bar{2}0$	0.10100
m	0.10297	$02\bar{3}$	0.10303
w	0.10654	200	0.10654
w	0.10867	$\bar{2}22$	0.10877

Table 9. Ti_6O_{11}

I	$\sin^2\Theta_{obs}$
w	0.02410
st	0.03915
v st	0.05224
w	0.05638
st	0.06115
v st	0.06722
w	0.07372
m	0.08212
vw	0.08601
st	0.08841
st	0.09399
st	0.09586
st	0.10421
vw	0.10903

Table 10. Ti_7O_{13}

I	$\sin^2\Theta_{obs}$
w	0.02676
vw	0.03932
st	0.04144
v st	0.05260
w	0.05432
st	0.06028
vw	0.06121
v st	0.06545
w	0.06734
vw	0.07844
vw	0.08233
m	0.08415
w	0.08598
m	0.08955
st	0.09432
st	0.09597
w	0.10264
w	0.10539
w	0.10961

Table 11. Ti_8O_{15}

I	$\sin^2\Theta_{obs}$
w	0.02915
st	0.04311
v st	0.05288
st	0.05966
v st	0.06409
m	0.08548
st	0.09037
st	0.09450
st	0.09590
w	0.10147
w	0.10623

Table 12. Ti_9O_{17}

I	$\sin^2\Theta_{obs}$
vw	0.02380
vw	0.03139
st	0.04453
w	0.05277
st	0.05310
w	0.05777
st	0.05927
st	0.06311
vw	0.06414
st	0.08661
st	0.09091
st	0.09464
st	0.09590
w	0.10071
m	0.10736
m	0.10903

Table 13. $Ti_{10}O_{19}$

I	$\sin^2\Theta_{obs}$
vw	0.03295
v st	0.04516
w	0.05155
v st	0.05271
v st	0.05959
v st	0.06308
vw	0.06890
vw	0.07223
vw	0.08370
st	0.08646
st	0.09019
st	0.09479
st	0.09616
m	0.10238
m	0.10670
m	0.10968

Table 14. TiO_2 *(rutile).* Narrow range of homogeneity. The pattern refers to a sample of stoichiometric composition. Dimensions of the tetragonal unit cell: a = 4.593 Å, c = 2.959 Å.

I	$\sin^2\Theta_{obs}$	hkl	$\sin^2\Theta_{calc}$
st	0.05623	110	0.05626
m	0.09589	101	0.09588
vw	0.11260	200	0.11252
w	0.12399	111	0.12401
w	0.14070	210	0.14065
st	0.20835	211	0.20840
m	0.22501	220	0.22504
w	0.27114	002	0.27102
w	0.28122	310	0.28130
w	0.32093	301	0.32092
vw	0.32716	112	0.32728

Table 15. TiO_2 (anatase). Dimensions of the tetragonal unit cell: $a = 3.786$ Å, $c = 9.517$ Å.

I	$\sin^2\Theta_{obs}$	hkl	$\sin^2\Theta_{calc}$
v st	0.04798	101	0.04795
vw	0.10030	103	0.10035
st	0.10482	004	0.10480
vw	0.10891	112	0.10900
st	0.16558	200	0.16560
m	0.20522	105	0.20515
m	0.21347	211	0.21355
vw	0.26599	213	0.26600
m	0.27043	204	0.27040
vw	0.31878	116	0.31860
vw	0.33116	220	0.33120
m	0.37075	215	0.37075

and upwards. The phases are of stoichiometric composition if not otherwise stated in the tables.

The effectiveness of the powder patterns for the identification of the titanium oxides may be illustrated by the following example, encountered when analyzing the composition region around the phase Ti_6O_{11}. Photographs of samples TiO_x differing in composition from that of the pure phase by $\Delta x = \pm 0.002$ clearly showed weak extra reflexions which were identified as the strongest lines of the neighbouring phases ($\sin^2\Theta = 0.07011$ of Ti_5O_9 and $\sin^2\Theta = 0.06545$ of Ti_7O_{13}, respectively). The approximate amounts of the extra phases were thus about 5 % of the sample. The exposure times used for these photographs were of normal length, *viz.* one hour. Since the background of the films was quite low, considerably longer exposure times might have been applied, which would correspondingly increase the sensitivity of the method for the identification of minute amounts of extra phases.

Thanks are due to Mrs. Stina Nord for her valuable assistance in preparing the majority of the X-ray photographs.

This work forms part of a research program on metal oxides and related compounds financially supported by the *Swedish Natural Science Research Council.*

REFERENCES

1. Andersson, S., Collén, B., Kuylenstierna, U. and Magnéli, A. *Acta Chem. Scand.* **11** (1957) 1641.
2. Hambling, P. G. *Acta Cryst.* **6** (1953) 98.
3. Westman, S. and Magnéli, A. *Acta Chem. Scand.* **11** (1957) 1587.

Received July 13, 1957.

ACTA CHEMICA SCANDINAVICA 11 (1957) 1658—1662

Paper Chromatography and Colorimetric Determination of Free and Esterified Cholesterol in Very Small Amounts of Blood

PREBEN W. HANSEN and HENRIK DAM

Department of Biochemistry and Nutrition, Polytechnic Institute, Copenhagen, Denmark

A simple and rapid method for paper chromatography and colorimetric determination of cholesterol and total cholesterol esters in very small amounts of blood is described.

Cholesterol and cholesterol esters are separated within 20 min on paper with *iso*octane as mobile phase.

The quantitative determination after elution of the spots on the chromatogram is based on a modification of Zlatkis' color reaction. Equivalent amounts of cholesterol and cholesterol esters show the same optical density.

Total amounts of cholesterol and esters as low as 2.5 μg can be determined with an accuracy of 5 %.

In 1953 Zlatkis, Zak and Boyle [1] described a rapid and simple method for the determination of total cholesterol in blood. By the present modification of this method it is possible to determine cholesterol and its esters in amounts from 2.5 μg to 25 μg per 0.5 ml of reaction mixture.

The method of Zlatkis *et al.* is less specific than the methods of Liebermann-Burchard and Tschugaeff and frequently gives too high cholesterol values when used directly on plasma [2, 3].

We have, therefore, combined our modification of the method with a new and rapid paper chromatographic separation of cholesterol and its esters from other components which might interfere with the colorimetric determination.

EXPERIMENTAL

Reagents and Solvents

1. Standard cholesterol solution: 25.0 mg in 100 ml of chloroform.
2. Standard cholesterylacetate solution: 27.75 mg in 100 ml of chloroform.
3. Standard cholesterylpalmitate solution: 40.40 mg in 100 ml of chloroform.
4. Ferric chloride solution: 1.0 g in 10 ml of 99.5 % glacial acetic acid. (This solution can be kept for weeks).

5. Color reagent: 0.5 ml of the ferric chloride solution diluted to 25 ml with concentrated sulfuric acid. (The reagent has to be prepared just before the colorimetric determination is carried out).
6. Acetone-ethanol 1:1 (v/v).
7. 2,2,4-Trimethylpentane ("*iso*octane").
8. Chloroform.
9. Phosphotungstic acid solution: 10 % in ethanol.

Procedures

A. Preparation of sample for chromatography: 20 µl of plasma is pipetted by means of a constriction pipette (Carlsberg pipette [4]) into 300 µl of warm acetone-ethanol reagent in a 4.5 ml polyethylene-stoppered centrifuge tube. (In case the cholesterol is expected to be high the ratio of plasma taken to volume of extract should be reduced.) The tube is stoppered and placed for 5 min in a water bath at 80—85°C and then shaken violently for 1 min in a shaking apparatus (Microid Flask Shaker, Griffin & George Ltd., England). The tube is then centrifuged (approximately 1 min) and the supernatant liquid applied to the paper with a constriction pipette as described below. The precipitate is re-extracted twice with 100 µl acetone-ethanol reagent, every extract being applied to the paper.

B. Paper chromatography. Schleicher & Schüll 2043 b paper is cut out in sheets 15 cm long and 24.7 cm wide. Parallel to the longer edge of the paper three pencil lines are drawn at distances of 1, 2, and 12 cm from this edge. Between the 1 and 12 cm lines the paper is divided by means of a scalpel into 8 strips separated from each other by 1 mm open spaces.

The sheets are washed with *iso*octane by placing them for 5 min in the solvent in a glass bowl under slow motion. After drying the sheets are treated with chloroform in the same way.

By means of a constriction pipette the solution containing the cholesterol and cholesterol esters (from 2.5 to 25 µg) is applied as 1.5 cm streaks along the 2 cm line on each of the 6 strips in the middle. The first strip serves as a blank, whereas 100 µl from the cholesterol standard solution and 100 µl from one of the ester standard solutions are applied to the last strip. During application warm air is blown upward against the starting lines.

The paper is placed in the tank containing the mobile phase on the bottom. The tank must be completely saturated with vapor of *iso*octane before the chromatogram is started. Therefore, precaution must be taken to avoid vapor from escaping when the paper is brought into the tank. The chromatogram is started 5 min later and is run until the solvent front reaches the upper end of the strips. This requires about 20 min.

C. Elution of cholesterol and cholesterol esters. After chromatography the paper is removed from the tank and allowed to dry at room temperature for 1 min. The last strip is cut out and the spots are made visible by spraying with a solution of phosphotungstic acid (10 % in ethanol) followed by drying at 100°C for about 1 min. The zones on the other strips, including the blank, corresponding to the spots on the last strip, are cut out, placed in weighing glasses and extracted with 1.0 ml chloroform under gently shaking. The chloroform extracts are transferred to 1.5 ml test tubes with a constriction pipette, and the chloroform is evaporated by placing the tubes in a water bath at 70—80°C. The extraction procedure is repeated twice with 0.5 ml of chloroform.

While the chloroform extracts are evaporated, 20 µl of the cholesterol standard solution is pipetted into two test tubes and dried simultaneously with the eluates from the chromatogram. When dry the tubes are allowed to cool to room temperature, and subsequently 0.30 ml of glacial acetic acid is added. The tubes are stoppered and carefully shaken.

D. The colorimetric determination. From a Krogh-syringe [5] (mounted in a burette holder) 0.20 ml of the color reagent is added to the first of the tubes, and after rapid mixing with a small glass rod the tube is placed in a boiling water bath for exactly 1 min. The remaining tubes are treated similarly.

After cooling to room temperature in ice water the reaction mixtures are transferred to micro cuvettes with 1 cm light path and the optical density is measured at 530 mµ in a Beckman spectrophotometer.

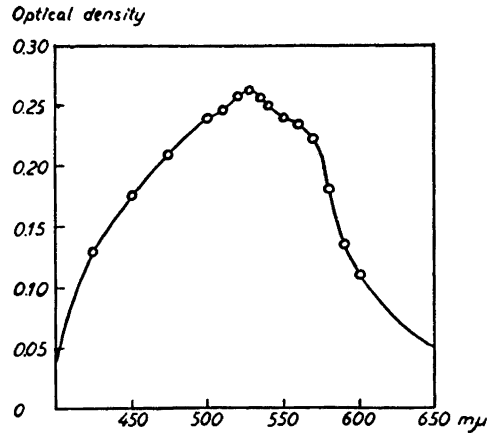


Fig. 1. Absorption curve for 5 μg cholesterol (free or esterified) per 0.5 ml reaction mixture.

DISCUSSION OF THE METHOD

The method of Zlatkis *et al.* consists in mixing a solution of cholesterol in 3 ml of glacial acetic acid with 2 ml of the color reagent, whereby a light brown color appears which changes to purple within a minute. This color shows a maximum at 560 mμ.

During our attempts to modify the method for determination of cholesterol and its esters in amounts from 2.5 μg to 25 μg per 0.5 ml (total) reaction mixture it was observed that by mixing the reagents as described by Zlatkis *et al.*, only the light brown color appeared. The temperature of the reaction mixture did not, because of the small volume, reach the level required for full development of the color (60—65°C)[6].

By placing the reaction mixture in a boiling water bath the light brown color changed to purple within a few seconds. After one minute in the boiling water bath followed by cooling in ice water the color obtained showed a maximum at 530 mμ for cholesterol as well as for cholesterol esters as shown in Fig. 1.

The color follows Beer's law in the concentration range examined, and equivalent amounts of cholesterol, cholesterylacetate and cholesterylpalmitate show the same optical density as it appears from Table 1.

The method of Zlatkis *et al.* was originally used on serum directly, but several authors [2,3] have stated that in this way the method often shows too high cholesterol values because of the interference of other compounds with the development of the color. It might be expected that combination of the method with a paper chromatographic separation of cholesterol and its esters from the interfering compounds would eliminate this error.

Several methods for paper chromatographic separation of cholesterol and its esters have been published [7-9], but most of these methods employ as mobile or stationary phase solvents which are difficult to remove from the

Table 1. Optical density at 530 mμ obtained with cholesterol and cholesterol esters per 0.5 ml reaction mixture (the total volume of the mixture).

Compound	μg/0.5 ml	Density	Density/μg cholesterol
Cholesterol	2.50	0.127	0.051
	5.00	0.260	0.052
	10.00	0.520	0.052
	15.00	0.782	0.052
	20.00	1.040	0.052
	25.00	1.320	0.053
Cholesterylacetate	2.78	0.130	0.052
	5.55	0.254	0.051
	11.10	0.512	0.051
	16.65	0.740	0.049
	22.20	0.995	0.050
	27.80	1.275	0.051
Cholesterylpalmitate	4.04	0.128	0.051
	8.08	0.255	0.051
	16.16	0.514	0.051
	24.24	0.762	0.051
	32.32	1.040	0.052
	40.40	1.290	0.052

Table 2. Recovery of cholesterol and cholesterol esters after chromatography of mixtures

Amounts in μg applied to the paper			Recovery			
Free cholesterol	Cholesterol as acetate	Cholesterol as palmitate	Cholesterol		Cholesterol as esters	
			μg	%	μg	%
2.5	10.0	15.0	2.49	99.6	25.08	100.3
5.0	10.0	10.0	4.98	99.6	19.50	97.5
10.0	5.0	10.0	9.87	98.7	14.33	95.6
15.0	5.0	5.0	14.60	97.4	9.55	95.5
20.0	0.0	5.0	19.12	95.7	5.15	103.1
25.0	2.5	0.0	24.75	98.9	2.59	103.9

Table 3. Comparison of the Sperry-Webb method with the present method.

Method of Sperry and Webb			Our method		
Free cholesterol	Esterified cholesterol	Total cholesterol	Free cholesterol	Esterified cholesterol	Total cholesterol
mg/100 ml					
46.00	91.20	137.20	43.35	89.30	132.65
39.30	69.90	109.20	35.50	67.35	102.85
47.80	75.50	123.30	45.40	75.00	120.40

paper after chromatography. When the chromatogram is eluted with chloroform these solvents will pass into solution and interfere with the development of the color.

We therefore tried to find a paper chromatographic procedure by which cholesterol and its esters could be separated on untreated paper and with a mobile phase which is easy to remove from the paper after chromatography. *Iso*octane fulfills this requirement, and with this solvent we were able to obtain clear separation of cholesterol and total cholesterol esters in 20 min. On Schleicher & Schüll 2043 b paper the R_F values for cholesterol and cholesterol esters were 0.35 and 0.80, respectively.

Table 2 shows the recovery after chromatography of mixtures of cholesterol, cholesterylacetate and cholesterylpalmitate.

Table 3 shows the results obtained with hamster plasma by the present method (0.02 ml plasma) and by the method of Sperry and Webb [10] (0.2 ml plasma).

By the present method determination of free and esterified cholesterol in plasma from 6 animals can be carried out within 5 h, whereas the same determination by the Sperry-Webb method requires 2 days.

REFERENCES

1. Zlatkis, A., Zak, B. and Boyle, A. J. *J. Lab. Clin. Med.* **41** (1953) 486.
2. Lovern, J. A. *Proc. Nutrition Soc. (Engl. and Scot.)* **15** (1956) 46.
3. Best, M., Van Loon, E. J., Wathen, J. D. and Seger, A. J. *Am. J. Med.* **16** (1954) 601.
4. Linderstrøm-Lang, K., and Holter, H. in Bamann, E. and Myrbäck, K. *Die Methoden der Fermentforschung*, Thieme, Leipzig, 1940. I p. 1132.
5. Krogh, A. *Ind. Eng. Chem., Anal. Ed.* **7** (1935) 130.
6. Fürst, V., Jr. and Lange, R. *Scand. J. Clin. Lab. Invest.* **6** (1954) 60.
7. Harrison, E. G. *Paper Chromatographic Study of Adrenal Cholesterol*, (Thesis) University of Illinois 1949.
8. Michalec, C. *Biochim. et Biophys. Acta* **19** (1956) 187.
9. See Michalec, C. *Naturwiss.* **42** (1955) 509.
10. Sperry, W. M. and Webb, M. *J. Biol. Chem.* **187** (1950) 97.

Received July 29, 1957.

ACTA CHEMICA SCANDINAVICA 11 (1957) 1663—1670

The Effect of Ions on the Catalytic Activity of Enzymes: The Old Yellow Enzyme

WILLIAM J. RUTTER* and BRITA ROLANDER

Medicinska Nobelinstitutet, Biokemiska avdelningen, Stockholm, Sweden

The present communication is concerned with a study of the effect of ions on the activity of the old yellow enzyme system. In addition to a general inhibitory effect by anions, certain specific effects were observed. Fe^{3+} ions can, for example, act as the electron acceptor in the reaction, and in fact, with chelated iron compounds as the electron acceptor, the reaction rate increases markedly. The old yellow enzyme, as isolated, is apparently not a metallo flavoprotein.

The implications of the date with regard to the physiological activity of the old yellow enzyme are discussed.

The old yellow enzyme (OYE) ** facilitates the oxidation of TPNH (and to a lesser extent DPNH) according to equations (1) and (2).

$$\text{TPNH} + \text{H}^+ + \text{yellow enzyme} \rightleftharpoons \text{TPN}^+ + \text{leuco enzyme} \qquad (1)$$

$$\text{leuco enzyme} + \text{oxygen or dye} \rightarrow \text{H}_2\text{O}_2 \text{ or leuco dye} + \text{yellow enzyme} \qquad (2)$$

This enzyme was discovered by Warburg and Christian [1], and later purified extensively and studied by Theorell [2]. It has recently been crystallized by Theorell and Åkesson [3].

OYE preparations are characterized by a low turnover number in oxygen (approximately 35 moles O_2/min/mole enzyme at 30°C for the crystalline enzyme [3]), and also a very slow reaction rate with cytochrome c. Under aerobic conditions [4] reaction with oxygen takes precedence over reaction with cytochrome c. On this basis, OYE could be considered the TPN counterpart to the diaphorases.

---

* U. S. Public Health Service Fellow, 1954—55. Present address, Division of Biochemistry, University of Illinois, Urbana, Illinois, USA.

** Abbreviations used in this paper are OYE, old yellow enzyme; TPN, TPNH, oxidized and reduced triphosphopyridine nucleotide, respectively; Zwischenferment, yeast glucose-6-phosphate dehydrogenase; EDTA, ethylene diamine tetraacetic acid.

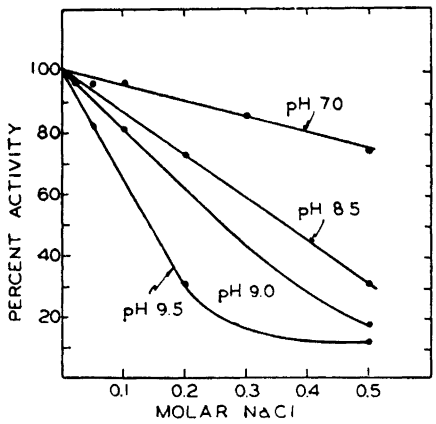


Fig. 1. Inhibition of activity of the Zwischenferment OYE system by sodium chloride. The measurements were made in conventional Warburg apparatus, each flask contained 15 μM glucose-6-phosphate; 0.5 μM TPN; 2 mg *Zwischenferment* (activity under optimal conditions, 1 μM TPNH formed/min/mg); 334 μg OYE; 29 mμM catalase; 100 μM buffer (glycine, pH 9.0, 9.5; glycylglycine, pH 8.5, 7.0); salts were added to the final concentration indicated; total volume 3.0 ml. Under these conditions 4.2 μM O_2 disappeared in 10 min, in control flasks at pH 8.5.

Theorell and Nygaard [5-7] have studied in a thorough manner the reaction of the old yellow protein, and the prosthetic group, FMN:

$$FMN + \text{old yellow enzyme apoprotein} \rightleftharpoons \text{old yellow enzyme} \qquad (3)$$

It was found that the ionic environment, especially the anionic species, influenced the reaction markedly.

METHODS

The old yellow enzyme was prepared by a modification of methods used for some time in the laboratory of Professor Theorell. A preparation having a β 280/β 465 ratio of 12.8 corresponding to 80 % purity was used in these experiments. Glucose-6-phosphate dehydrogenase (*Zwischenferment*) was prepared by the method of Warburg and Christian [8] and a modification of the procedure of Kornberg [9].

TPN, 90 % pure, was procured from Sigma Company. Oxygen consumption by the glucose-6-phosphate dehydrogenase — old yellow enzyme system was measured in the conventional Warburg apparatus. TPNH oxidation was followed spectrophotometrically or by the decrease in the intensity of fluorescence [10].

RESULTS

Effects of anions on the Zwischenferment— old yellow enzyme system. The influence of anions on the coupled Zwischenferment-old yellow enzyme system was studied using O_2 as the electron acceptor. Because of the experience already gained with Zwischenferment reaction [11], it was possible to keep this enzyme activity in considerable excess. The TPN concentration was

Table 1. Inhibition of the activity of the Zwischenferment—OYE system by ions.

Salt	pH	Molar concentration for 50 % inhibition
Fluoride	9.5	0.25*
	9.0	**
Chloride	9.5	0.14
	9.0	0.25
	8.5	0.37
Bromide	9.5	0.13
	8.5	0.24
Iodide	9.5	0.05
	8.5	0.08
Phosphate	9.5	0.04
Nitrate	9.0	0.14
Sulfate	9.5	0.07
Carbonate	9.5	0.03
Formate	9.5	0.14
Citrate	9.5	0.05
EDTA	9.5	0.01
Cholate	9.5	0.005

* 0.2 M NaF produces 40 % inhibition, higher concentrations produce no greater inhibtion
** only 10 % inhibition at 0.5 M NaF

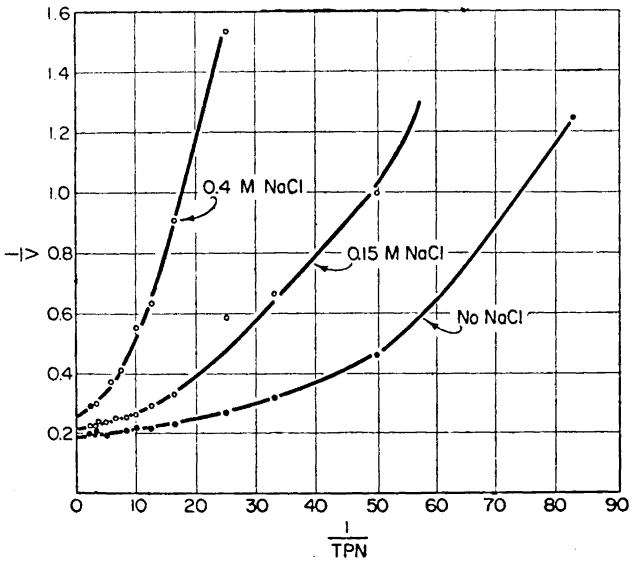


Fig. 2. Effect of TPN concentration on the inhibition of activity of the Zwischenferment OYE system by salts. Experimental conditions are essentially those described under Fig. 1; salt concentration, and TPN concentration varied as indicated.

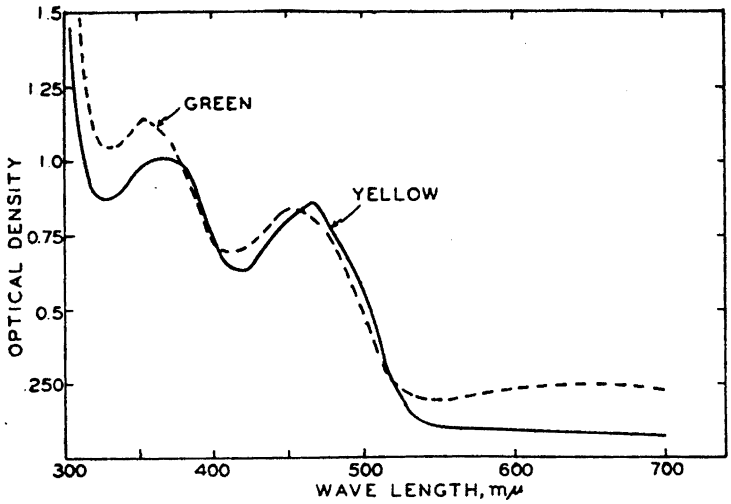


Fig. 3. Absorption spectra of OYE in acidic and basic ammonium sulfate solutions. OYE used in these experiments was approximately 80 % pure, spectra were taken in approximately 0.50 saturated $(NH_4)_2SO_4$, pH 10.2 (by addition of concentrated ammonium hydroxide, and in the same solution after bubbling with N_2.)

kept at a level of several times required to saturate the system under control conditions. Under these conditions the pH of optimal activity was 8.3 It was found that various salts inhibited oxygen uptake by the system, especially on the alkaline side of the pH activity curve. The inhibitory effect of sodium chloride, for example, as a function of pH, is presented in Fig. 1. Similar data were obtained with other salts. The degree of inhibition was in large measure a reflection of the anionic species present. Table 1 summarizes the data obtained with various salts. The inorganic salts may be placed in the order of decreasing effectiveness PO_4, CO_3, $I > SO_4$, $NO_3 > Br > Cl > F$.

The possibility that the inhibitory effects were simply related to a decreased affinity of the system for TPN was tested. The inhibition could be partly reversed by the addition of additional TPN to the system. As shown in Fig. 2, the saturation of the system with TPN was a function of the ions present in the assay system. A substantial inhibition remained, however, even after extrapolation to infinite TPN concentration. It was also confirmed that additional Zwischenferment and glucose-6-phosphate did not affect the inhibition. These observations suggested that some of the inhibitory effects might be on the catalytic process associated with the old yellow enzyme. This result was interesting in view of the effects of anions on the dissociation of the old yellow enzyme observed by Theorell and Nygaard. Addition of large amounts of FMN did not, however, increase the reaction rate in the presence of salts, and calculations from their data show that dissociation as measured by appearance of fluorescence is still much too small to account for inhibition by salts in the presence of excess TPN.

The solubility of oxygen in the medium is not significantly altered by salts at the concentrations used in these experiments, but the reaction of the old yellow enzyme with oxygen may be markedly affected.

Of particular interest was the strong inhibition observed with divalent anions and especially with EDTA.

The transformation of the old yellow enzyme into a green-colored protein. It was observed that addition of saturated ammonium sulfate solutions, adjusted to pH 10—10.5 with ammonium hydroxide, to solutions of the old yellow enzyme produced greenish solution. This did not reflect a complete dissociation of FMN from the protein, since OYE could be precipitated in this green form, redissolved in buffer (becoming yellow instantly) and reprecipitated in the green form without leaving absorption at 465 mμ. It was found that if the ammonia were removed, by bubbling a gas through the solution, for example, the yellow color would also reappear. Fig. 3 presents the absorption spectra of the green compound, and the spectra of the same solution after bubbling with oxygen. There was less than 4 % difference in the fluorescence of the solutions of the yellow and green proteins. It would not, however, be wise to conclude that the green form of OYE is nonfluorescent as is the yellow form, since the high concentrations of NH_4^+, $SO_4^=$, and NH_3 might effectively quench fluorescence, if present.

Several cycles of conversion from the green to the yellow form did not influence the catalytic activity of the enzyme.

Metal ion content of old yellow enzyme preparations. The strong inhibition of activity of old yellow enzyme preparations by EDTA (see Table 1) prompted an examination of the relationship of various metal ions to this catalysis. The effect of prolonged dialysis against chelating agents and subsequent addition of metal ions was studied, and in addition, the metal content of OYE preparations was assayed by emission spectroscopic and chemical methods.

Table 2. Effect of metal ions on oxygen consumption by Zwischenferment—OYE system. Conditions essentially the same as those described in the legend of Figure 1. Glycylglycyl buffer, pH 7.8, 200 μgm OYE (dialyzed against 0.001 M versene), metal ions were added at the concentration listed, as their chloride or sulfate salts.

		μM O_2/10 min	% Activity
1.	Control	2.01	100
2.	» + 10^{-3} M Mg^{2+}	2.02	100
3.	» + 10^{-2} M Mg^{2+}	1.08	54
4.	» + 10^{-3} M Cu^{2+}	1.93	95
5.	» + 10^{-2} M Cu^{2+}	0.81	40
6.	» + 10^{-5} M Mn^{2+}	2.11	105
7.	» + 10^{-4} M Mn^{2+}	1.94	97
8.	» + 10^{-3} M Mn^{2+}	0.48*	24
9.	» + 10^{-5} M Fe^{3+}	2.03	100
10.	» + 10^{-4} M Fe^{3+}	2.01	100
11.	» + 10^{-3} M Fe^{3+}	0.47	23
12.	» + 10^{-2} M Fe^{3+}	0.06	3

* Visible precipitate formed

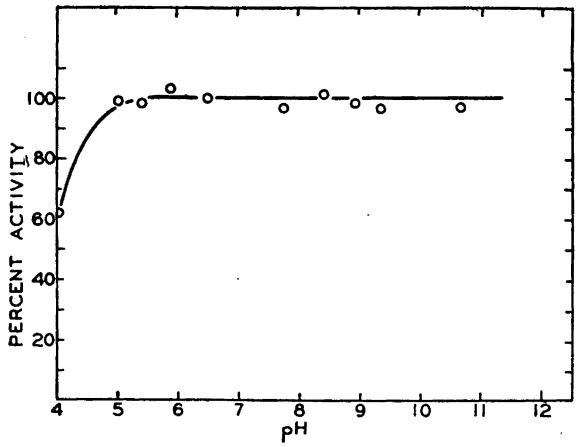


Fig. 4. Oxidation of TPNH by OYE as a function of pH. Each reaction mixture contained 50 μg OYE β 280/β 464 = 12.8 (~80 % pure), 0.15 μM TPNH, 100 μM buffer (acetate pH 4.0, 5.0; histidine, pH 5.4, 5.8; phosphate, pH 6.4, 6.7, 7.2; glycylglycine, pH 7.4, 7.8, 8.3; glycine pH 8.7, 9.1, 10.2, 10.7), total volume 3 ml. 100 % activity under these conditions represented an optical density change at 340 mμ of 0.045.

Prolonged dialysis against EDTA at pH 9.4, 7.5, and 5.0 did not decrease the specific activity; in fact, when most of the EDTA was removed by dialysis against triple-distilled water, the specific activity consistently increased 10—15 %.

The metal content of OYE preparations dialyzed against dilute buffer, and against EDTA solutions was measured in cooperation with Kandidat Molt, of Sveriges Geologiska Undersökning, Geokemiska avdelningen. Emission spectroscopic assays were made for the presence of Zn, Fe, Mn, Cu, Mg and Ca. Fairly large and variable quantities of Mg and Ca and insignificant amounts of Fe, Mn, Cu, Zn were found. The zinc and iron content of OYE preparations was also assayed by chemical methods with a similar result. In addition, a preparation of OYE of approximately 80 % purity which had

Table 3. Fe^{3+} and oxidation of TPNH by OYE. The control reaction mixture contained 0.1 μM TPNH, 50 μg OYE, 100 μM glycylglycine, pH 8.2, total volume, 3.0 ml. The experimental cuvettes contained in addition $FeCl_3$ in the amount indicated, and 1 μM *a,a'*-dipyridyl when indicated. Measurements were made spectrophotometrically at 340 mμ with appropriate correction for absorption of other materials.

		TPNH Oxidized μM/min
1.	Control	0.0212
2.	» + 10^{-3} M Fe^{3+}	0.0249
3.	» + 10^{-4} M Fe^{3+}	0.024
4.	» + *a,a'*-dipyridyl	0.023
5.	» + 10^{-4} M Fe^{3+} + *a,a'*-dipyridyl	0.030

been dialyzed against dilute ammonia buffer, was kindly assayed by Professor B. L. Vallee of Harvard University. Only traces of Zn, Fe, Cu, and Mn were found, in all cases less than 0.1 mole metal/mole protein.

It is concluded that the old yellow enzyme, as isolated at least, is not a metallo flavoprotein involving Fe, Zn, Cu, or Mn. Mg and Ca are commonly present in many enzyme preparations, and it is presumed, though not proved, that these cations are contaminants not involved in the catalytic function of OYE.

Effect of metal ions on the catalytic activity of old yellow enzyme. The effect of metal ions on the activity of the Zwischenferment-OYE system assayed by measurement of oxygen uptake was studied. As shown in Table 2, it was found that no significant stimulation of activity occurred under the conditions employed, but that concentrations of Mn^{2+} or Fe^{3+} higher than 10^{-4} M caused marked inhibition. Since a visible precipitate accompanied Mn^{2+} inhibition, but none occurred with Fe^{3+} inhibition, further studies of this inhibitory phenomena were made primarily with Fe^{3+} ions. At 10^{-3} M, Fe^{3+} did not markedly influence the activity of isolated Zwischenferment, nor did increased TPN concentration influence the inhibition of oxygen uptake of the coupled system. It was, therefore, likely that the inhibition of oxygen uptake by Fe^{3+} concerned the activity of OYE itself. Experiments on the activity of OYE were carried out by measuring the oxidation of added TPNH spectrophotometrically. Fig. 4 presents the remarkable relationship between pH and activity for this reaction; essentially full activity is measured over the range from pH 5.0 to pH 10.

The Fe^{3+} ions did not inhibit TPNH oxidation by OYE in the concentration ranges 10^{-5} to 10^{-1} M, but instead acted as an electron acceptor. The formation of Fe^{2+} during the reaction was detected by spectrophotometric measurement of its complex with α,α'-dipyridyl. Table 3 presents the results of these experiments. The apparent inhibition of the Zwischenferment system by Fe^{3+} is likely a result of its competition with oxygen for electrons. Since the solubility of oxygen is 10^{-3} M, these data suggest Fe^{3+} to be a more efficient electron acceptor than oxygen for OYE.

Table 4. Effect of various electron acceptors on TPNH oxidation by OYE. The control reaction mixture contained 0.5 μM TPNH, 50 μg OYE, 100 μM glycylglycine, pH 8.2, total volume 3.0 ml. The experimental cuvettes contained, in addition when indicated: DCPIP (2,6-dichlorophenolindophenol); ferricyanide at a final concentration of 4×10^{-4} M; H_2O_2, 0.05 ml 30 % solution; catalase, 50 μg crystalline beef liver preparation. Measurements were made spectrophotometrically at 340 mμ; corrections for absorption of other materials were made when necessary.

		TPNH oxidized μM/min
1.	Control	0.022
2.	» + DCPIP	0.032*
3.	» + H_2O_2 + catalase	0.12*
4.	» + 4×10^{-4} M Fe $(CN)^{3-}$	0.18*
5.	» + 10^{-4} M Fe^{3+} + H_2O_2 + catalase	0.13

* Corrected for endogenous TPNH oxidation which occurred at a slow rate in the absence of substrate.

Table 4 presents a typical experiment in which different electron acceptors were used. Coupling to the dye dichlorophenolindophenol did not alter the rate markedly, but the presence of a chelated iron compound $Fe(CN)_6$ stimulated the catalytic rate 8 to 10-fold over the rate observed under ordinary conditions. The addition of H_2O_2 and catalase also caused a substantial increase in rate. This might be the reflection of an increased oxygen tension, although rates could not be obtained by bubbling oxygen through the solutions. It is possible that a more specific reaction is involved.

Attempts to find in bottom yeast a system which would stimulate oxidation of TPNH by OYE preparation have thus far been unsuccessful.

DISCUSSION

Although the old yellow enzyme is present in high concentration in yeast (1 mg OYE/g dry weight) and although the enzyme has been studied extensively, its physiological role is yet unclear (like the majority of flavoprotein enzymes). Its turnover number with oxygen or cytochrome c as electron acceptor is very low. Several experimental observations are consistent with the postulate that the old yellow enzyme has been separated from its appropriate acceptor during the course of purification. Haas [12] has shown that the reduction of OYE by TPNH according to equation (1) occurs at 60 times the rate of the oxidation of the leuco enzyme by oxygen. The present experiments indicate that appropriate electron acceptors indeed allow a much faster rate. It is not surprising that Fe^{3+} acts as an electron acceptor. Kaplan *et al.*[13] have recently shown that this is perhaps a general phenomenon with flavoprotein enzymes. It is pertinent, however, that Fe^{3+} is a more efficient electron acceptor than oxygen, and that with ferricyanide very considerable increases in catalytic rates are obtained. It would be unwise to conclude from this that the biological electron acceptor system for OYE is mediated through Fe^{3+} or another suitable metal ion, but the attractiveness of this possibility is manifest. The possible role of metals in the activity of flavoprotein enzymes has been recently discussed by Mahler [14].

The authors wish to thank Prof. H. Theorell for his active interest in this work. W. J. R. wishes to express his appreciation for the gracious hospitality extended by him and other members of the Biochemical Department.

REFERENCES

1. Warburg, O. and Christian, W. *Biochem. Z.* **266** (1933) 377.
2. Theorell, H. *Biochem. Z.* **288** (1936) 317.
3. Theorell, H. and Åkeson, Å. *Arch. Biochem. and Biophys.* **65** (1956) 439.
4. Theorell, H. *Nature* **138** (1936) 687.
5. Theorell, H. and Nygaard, A. P. *Acta Chem. Scand.* **8** (1954) 877.
6. Theorell, H. and Nygaard, A. P. *Acta Chem. Scand.* **8** (1954) 1649.
7. Nygaard, A. P. and Theorell, H. *Acta Chem. Scand.* **9** (1955) 1587.
8. Warburg, O. and Christian, W. *Biochem. Z.* **254** (1932) 438.
9. Kornberg, A. *J. Biol. Chem.* **182** (1950) 805.
10. Theorell, H., Nygaard, A. P. and Bonnichsen, R. *Acta Chem. Scand.* **9** (1955) 1148.
11. Rutter, W. J. and Rolander, B. *Acta Chem. Scand. In press.*
12. Haas, E. *Biochem. Z.* **298** (1938) 378.
13. Weber, M. N., Lenhof, H. M. and Kaplan, N. O. *J. Biol. Chem.* **220** (1956) 93.
14. Mahler, H. *Advances in Enzymol.* **17** (1956) 233.

Received July 15, 1957.

ACTA CHEMICA SCANDINAVICA 11 (1957) 1671—1676

A New Volumetric Method for Determination of Tin Beside Antimony

JOHN V. VILLADSEN and KNUD G. POULSEN

Chemistry Department A, Technical University of Denmark, Copenhagen, Denmark

A volumetric method is described for the determination of tin in the presence of antimony. The antimony is at first titrated with bromate according to Györy and afterwards precipitated with thioacetamide and filtered off, while keeping tin in solution as oxalate complexes. After oxidizing the oxalate, tin is reduced to the stannous state and titrated with bromate in an inert atmosphere (CO_2). The complete time required for an analysis was 2—2½ h and the accuracy was 0.2 %.

The well-known determination of tin [7-9] based upon its reduction to the stannous state by means of some metal, *e.g.* lead, iron or aluminium, and subsequent titration with bromate in an inert atmosphere has for a long time been used in this laboratory, where the procedure, described by Kühnel Hagen *et al.*[12] has been followed. In connection with the Györy [10] titration of antimony it has been our standard method in the analysis for tin and antimony in "white metal" alloys. The method has the advantage of being a rapid one and is accurate as long as the ratio antimony/tin is low.

When, however, this ratio increases above 1 : 3, the method involves increasing difficulties for the accurate determination of the tin content due to interference from the large amount of solid antimony then suspended in the solution. The present work has been carried out in order to improve the accuracy while trying to maintain the rapidity of the previous procedure.

The suggestion by Barber and Grezekowiak [6] of using thioacetamide instead of hydrogen sulphide in quantitative analysis has been developed by Musil, Flaschka and their coworkers to valuable gravimetric methods for most of the heavy metals, including also tin and antimony [3,5]. The antimony is for example precipitated and weighed as Sb_2S_3, giving excellent results [2,5]. The quantitative precipitation of tin by means of thioacetamide is more difficult, but Flaschka [1] gives details of a procedure where the results are only slightly low, the weighing form being SnO_2. Flaschka, Musil and coworkers [1] point out, however, that no difficulties are encountered in the quantitative precipitation of tin when thioformamide is used instead of thioacetamide. Musil and co-

workers [4] describe a procedure for determination of arsenic, antimony and tin, in which arsenic and antimony are titrated with bromate and thereupon separated by precipitation with thioformamide in 6 N hydrochloric acid for arsenic and in weak acid solution for antimony. The tin is kept in solution as oxalate complexes and determined by electrolysis or gravimetrically as SnO_2. The method we propose below combines the advantages of the method of Musil and coworkers for the separation of antimony from tin (arsenic is not considered in the present paper) with that of the volumetric determination of tin.

PROCEDURE

The solution, which should contain the metals as Sn^{4+} and Sb^{3+} or Sb^{5+}, respectively, the latter being the case if the alloy is dissolved in hot sulfuric acid and subsequently titrated with bromate according to Györy to determine the antimony content. Aliquots containing approx. 0.15 g Sn are pipetted off from the titrated solution, and 7.5 g oxalic acid and 20 ml conc. hydrochloric acid added whereafter the aliquot is diluted to 100 ml with water. The solution is heated to boiling and 0.3 g of thioacetamide dissolved in 3 ml water is added for each 0.1 g antimony present. During the addition of the thioacetamide the solution is well stirred, and the stirring is continued while 100 ml hot water is added. After cooling to 50°C the crystalline red precipitate of Sb_2S_5 is filtered off on a G 4 glass-filter, which is washed beforehand with a 1 % solution of oxalic acid to avoid separation of SnS_2 in the collector flask. The precipitate is washed with warm 0.1 % oxalic acid. The filtrate is transferred to a 1 liter beaker or a 500 ml Erlenmeyer flask and sufficient ammonium persulfate (17 g) is added to oxidize all oxalic acid. The flask is warmed on a gas burner or an electric heater for 15–20 min in order to destroy all persulfate. After cooling 50 ml conc. hydrochloric acid, 10 ml conc. sulfuric acid and 200 ml of water are added. The tin can now be determined according to one of the well-known procedures. We usually add a sheet of high purity aluminium to reduce the tin to metallic state. After the aluminium (*ca.* 3 g) has been added, the flask is fitted with a stopper with 3 holes, one of which is fitted with a glass tube to the bottom and is used to pass a stream of carbon dioxide into the solution. The second is fitted with a long glass tube as a refluxer and the third is available for the burette tip but is initially closed by a glass rod. With the concentration of acid used the aluminium is slowly dissolved while the tin separates as a spongy mass. After 20 min the flask is heated without boiling and the tin and a possible rest of aluminium is dissolved. When all is dissolved the flask is cooled, while the flow of carbon dioxide is temporarily increased.

In a test tube 0.5 g KI and 5 ml of a 0.5 % starch solution are mixed with 0.5 ml diluted sulfuric acid, a little $NaHCO_3$ is added to expel dissolved oxygen. This mixture is added with a pipette to the analysis and the burette tip is introduced through the third hole. Bromate solution is added until one drop gives a pertaining blue colour.

Chemicals

Tin solutions were made by dissolving pure tin in hot sulfuric acid and diluting to known volumes. Tin was either "AnalaR" or in some cases "Banka Tin" of unknown manufacture.

Antimony solutions were made from "AnalaR" $SbCl_3$ and were analyzed by titration with potassium bromate according to Györy.

Potassium bromate solutions were made from Merck potassium bromate *p.a.* dried at 150°C. Weighed amounts were dissolved in water to known volumes. The solutions were also standardized on tin, and the usual corrections of the titer found by weighing off the potassium bromate were +0.4 % and 0.2 % compared to "AnalaR" tin and "Banka" tin, respectively. The titers used for calculation of "mg tin found" are the ones based on "AnalaR" tin.

Thioacetamide and ammonium persulfate were "Merck" products.

Table 1. Analysis of tin solution without antimony. Standard procedure, no oxalate or persulfate added.

Expt. No.	mg Sn taken	mg Sn found	Deviation mg	Deviation %
1	150.1	150.3	0.2	0.1
2	150.1	150.1	0	0
3	150.1	150.2	0.1	0.1
4	150.1	150.5	0.4	0.3
5	150.1	150.1	0	0
6	150.1	150.1	0	0
7	150.1	150.1	0	0

Table 2. Analysis of samples containing tin and antimony.

Expt. No.	mg Sb taken	mg Sn taken	mg Sn found	Deviation mg	Deviation %
8	38.71	104.8	104.9	0.1	0.1
9	79.41	104.8	104.9	0.1	0.1
10	79.41	104.8	104.6	−0.2	−0.2
11	119.2	104.8	104.1	−0.7	−0.7
12	119.2	104.8	104.0	−0.8	−0.8
13	238.4	104.8	104.8	0	0
14	238.4	104.8	104.9	0.1	0.1
15	101.1	147.1	147.1	0	0
16	101.1	147.1	146.9	−0.2	−0.2
17	101.1	147.1	147.0	−0.1	−0.1

Table 3. Analysis of samples containing only tin, but treated as the filtrate from Sb_2S_3. The destruction of excess persulfate is carried out in a 1 liter beaker.

Expt. No.	mg Sn taken	mg Sn found	Deviation mg	Deviation %
18	150.1	149.5	−0.6	−0.4
19	150.1	149.4	−0.7	−0.5
20	150.1	149.4	−0.7	−0.5
21	150.1	149.3	−0.8	−0.6
22	150.1	149.4	−0.7	−0.5
23	150.1	149.5	−0.6	−0.4
24	150.1	149.5	−0.6	−0.5
25	150.1	149.6	−0.5	−0.3
26	150.1	149.1	−1.0	−0.7
27	147.1	147.3	0.2	0.1
28	147.1	147.2	0.1	0.1
29	147.1	147.2	0.1	0.1

The aluminium sheet used for reduction was known to be 99.9 % pure.

Carbon dioxide was taken from cylinders which had been used for some time, so that the small amount of oxygen present in freshly filled cylinders had escaped.

Sulfuric and hydrochloric acids were chemically pure products.

All volumetric glasswares were calibrated before use.

The oxalic acid ($H_2Ox,2H_2O$) was a high grade "Merck".

RESULTS

The results given in Table 1 are obtained by pipetting off 20 ml samples from the stock solution of pure tin and analyzing the aliquots according to the nor-

mal procedure, *e.g.* reducing with aluminium and titration with potassium bromate. An average error of less than 0.1 % is found. When these results are compared with those in Tables 2 and 3, it is seen that the last two show a tendency to lower values. The samples in Tables 2 and 3 were both analyzed according to the procedure described above. In Table 3 no antimony was present, but the procedure was followed except that no thioacetamide was added. The somewhat higher error found when the sample was treated for antimony can evidently not be due to co-precipitation of tin when antimony sulfide is precipitated.

In order to see whether some tin escaped as $SnCl_4$ during the oxidation of oxalate with persulfate, we have carried out the experiments in Table 4. The procedure was changed such that the heating for destruction of oxalate and persulfate was carried out in the Erlenmeyer flask later to be used for the titration of tin. This flask was fitted with a stopper with a long glass tube acting as a refluxer. The results seem rather to indicate an increase than a decrease in the error.

That no tin seems to disappear during the heating to nearly 100°C for 20 min is in accordance with qualitative tests made in the following way: the tube otherwise used as a refluxer was bent downwards just above the stopper and the vapour now distilled was collected in dilute sodium hydroxide solution. After heating for 25 min, when approx. 10 % of the volume had distilled, the basic solution was neutralized and tested for tin with dithiol and mercaptoacetic acid, according to Charlot and Gauguin [11]. In four experiments no tin at all could be found with this very sensitive reaction. Experiments with prolonged heating (120 min) showed the same results.

It is important that all persulfate is destroyed during the heating, since the experiments show that persulfate remaining in the solution after the heating was not reduced completely by the aluminium and therefore invalidated the tin titration. We therefore made some experiments to find the time of heating necessary for the complete destruction of the excess of persulfate when different kinds of glassware were used: 1) a 1 liter beaker, 2) the 500 ml Erlenmeyer flask used as in Table 4. To the analysis containing 7.5 g oxalic acid and 15 g ammonium persulfate were added a few drops of a 0.1 N titanium chloride. The presence of peroxide is indicated by the formation of the yellow peroxytitanate ion when the solution is heated. With electrical heating of the solutions in the beaker the destruction temperature of the persulfate excess was measured to 80°C and somewhat higher (85—90°) in the Erlenmeyer flask owing to the higher partial pressure above the latter solution. Complete destruction, indicated by the sudden disappearance of the yellow colour, was obtained after 8 min in 1) and after 13 min in 2). The importance of a relatively long time of heating, when no catalyst is present, is emphasized by the results given in Table 5, where larger excess of persulfate has been combined with shorter time of heating with remarkable results.

That heating on a steam bath requires more time than heating by a free flame or electrical heating was realized from results obtained when 24 g (10.4 g excess) ammonium persulfate was used to oxidize 7.5 g oxalic acid and heating on a steam bath for 15 min. The average of 5 tin determinations was 4 % lower than calculated.

Table 4. As in Table 3 but using 500 ml Erlenmeyer flask and refluxer when destroying persulfate.

Expt. No.	mg Sn taken	mg Sn found	Deviation mg	Deviation %
30	150.1	148.8	−1.3	−0.9
31	150.1	148.9	−1.2	−0.8
32	150.1	148.8	−1.3	−0.9
33	150.1	148.8	−1.3	−0.9
34	150.1	148.8	−1.3	−0.9
35	150.1	148.7	−1.4	−0.9
36	150.1	148.6	−1.5	−1.0
37	150.1	148.5	−1.6	−1.1
38	150.1	148.5	−1.6	−1.1

The deviations are seen to be somewhat larger compared to the results of Table 3 when the Erlenmeyer flask is used.

Table 5. The influence of time of heating on excess of persulfate.

Expt. No.	mg Sn taken	mg Sn found	Deviation mg	gram per-sulfate used	Time of heating, min	°C
39	150.1	81.9	−68.2	24	5	
40	150.1	149.5	− 0.6	24	30	90−95
41	150.1	147.4	− 2.7	17	5	
42	150.1	144.4	− 5.6	17	5	

The experiments show that the treatment of the tin solution with persulfate will cause some lowering of the tin content found. The small — constant — deviation can easily be determined in the individual case (for other chemicals used). No tin seems to escape from the containers and excess persulfate is evidently completely removed by 20 min heating. It is likely then that the tin is to some extent transformed to a state not easily reduced. Experiments, where small glass pellets were introduced in order to increase the surface, showed no increase in error, which excludes the possible adhering of some tin to the walls of the containers. The error is, however, almost negligible when traces of antimony as in Table 2 are present, probably owing to catalytic effects.

We have finally made a few experiments using $KMnO_4$ as oxidizing agent instead of $(NH_4)_2S_2O_8$. When due care is taken to the vigorous evolution of CO_2 when adding $KMnO_4$ to the hot solution, this method has some advantages over the method described above, *i.e.* the destruction of excess oxidizing agent is avoided as the end point is easily visible and dissolving of the tin is very quickly accomplished due to catalytic effects ($Mn^{+2} \rightleftharpoons Mn^{+1}$). The theoretical amount of $KMnO_4$ for 7.5 g $H_2Ox,2H_2O$ is 3.76 g. Deviations with $KMnO_4$ as destructing agent for the oxalic acid were 0.1—0.3 %, and the complete analysis is accomplished in 2 h.

The dissolution of the spongy tin may be a rather tedious process when no traces of other metals are present (Table 1). The time for dissolution can be

reduced to less than 1 h by adding a few drops of a very diluted Pd solution. Owing to the same kind of catalytic effects as obtained by using a Pd (or Au) catalyst we have obtained considerably lower dissolution times in the experiments with both Sn and Sb where minute traces of Sb are still present at this stage. The time of dissolution should, however, not be shortened by adding more acid as the reaction will tend to be too vigorous with foaming and even splashing (thus invalidating the determination).

The method gives results with an average deviation of ± 0.2 % when the titer of the potassium bromate is increased by 0.3 %. The time required for a complete analysis was 2—2 ½ h.

REFERENCES

1. Flaschka, H. and Jacobljevich, H. *Anal. Chim. Acta* **5** (1951) 60.
2. Flaschka, H. and Jacobljevich, H. *Anal. Chim. Acta* **4** (1950) 247.
3. Flaschka, H. *Z. anal. Chem.* **137** (1952) 112.
4. Musil, A., Gagliardi, E. and Reischl, K. *Z. anal. Chem.* **140** (1953) 346.
5. Musil, A., Gagliardi, E. and Reischl, K. *Z. anal. Chem.* **137** (1952) 252.
6. Barber, H. H. and Grezekowiak, E. *Anal. Chem.* **21** (1949) 192.
7. Biltz, H. *Z. anal. Chem.* **81** (1930) 88.
8. Hillebrand, W. F. and Lundell, G. E. F. *Applied Inorg. Analysis*, New York 1929, p. 237.
9. Scott, W. *Standard Methods of Chem. Analysis*, 4' ed. New York 1925, p. 533.
10. Györy, S. *Z. anal. Chem.* **32** (1893) 415.
11. Charlot, G. et Gauguin, R. *Dosages Colorimétriques*, Paris 1952, p. 153.
12. Kühnel Hagen, S., Hofman-Bang, N. and Gjertsen, P. *Acta Chem. Scand.* **2** (1948) 343.

Received May 21, 1957.

ACTA CHEMICA SCANDINAVICA 11 (1957) 1677—1691

Spectroscopic Conformational Analysis of Some 1,2-Dihalogeno *Cyclo*hexanes

PETER KLÆBOE, JOHAN J. LOTHE and K. LUNDE

Sentralinstitutt for Industriell Forskning og Universitetets Kjemiske Institutt. Blindern-Oslo, Norway

The infrared spectra of the *trans* 1,2-dichloro- and *trans* 1,2-dibromo-*cyclo*hexanes are highly dependent on the dielectric properties of the solvents. This suggests a method of determining the conformational equilibrium ratio. The mole fractions of the *ee*-conformations were calculated to 0.34 and 0.19 for the dichloro- and dibromo-compound, respectively, when dissolved in *cyclo*hexane and 0.71 and 0.63 when dissolved in nitromethane.

Trans 1,2-dichloro*cyclo*hexane crystallizes in the *ee*-conformation whereas *trans* 1,2-dibromo*cyclo*hexane crystallizes in the *aa*-conformation.

A discussion of some of the steric factors which may be important for the conformational equilibrium is presented.

Using some assumptions concerning the relative intensities of the infrared carbon-halogen stretching bands of the monohalogeno *cyclo*hexanes, the mole fraction of the *e*-conformation was calculated to 0.8 for the chloro compound and 0.85 for the bromo compound.

A previous paper [1] reported on a conformational investigation of some monohalogenated *cyclo*hexanes using infrared and Raman spectra. It was concluded that both the *e*- and the *a*- conformation of the monochloro- and the monobromo*cyclo*hexane were present in the liquid state, the *e*-conformation preponderating in both compounds. In the anisotropic modification of the crystalline state only the *e*-conformation of the two compounds could be detected, whereas in the semisolid cubic modification of the chloro compound both conformations were present.

The conformational equilibrium of the *trans* 1,2- dihalogeno *cyclo*hexanes has previously been given a quantitative treatment by some authors [2–5] measuring the dipole moments of the *cyclo*hexane compounds dissolved in carbon tetrachloride and benzene. Kozima and co-workers [2] were able to draw certain semiquantitative conclusions about the conformational equilibrium by considering the Raman spectra. From an investigation of the infrared spectra Larnaudie [6] concluded that both conformations were present in the liquid state.

Table 1. Raman and infrared spectra of *trans* 1,2-dichloro*cyclo*hexane.

Raman spectrum liquid (20°C)			Infrared spectra liquid (25°C)		Solid (−70°C)	Conformation
$\Delta\nu$ cm^{-1}	I	ϱ	ν cm^{-1}	I	ν cm^{-1}	
3 130						
3 050		0.52				
2 957	10	0.45				
2 907	5		2 909	8		
2 868	8	0.16				
			2 838	6		
			2 655	2		
			1 716	1		
			1 521	1		
1 451	5	0.68	1 450	1	1 450	
1 437	2					
			1 426	3	1 426	
			1 357	4		*aa*
1 345	6	0.49				
			1 338	6	1 338	
			1 318	2	1 318	
1 287	2					
1 275	3	0.50	1 276	5	1 276	
			1 267	4		
			1 255	10	1 255	
			1 222	0	1 222	
			1 212	10		*aa*
1 207	2	0.60	1 202	9	1 202	*ee*
1 132	1		1 138	4		*aa*
1 127	1	0.53	1 121	2	1 121	
1 107	1	0.19	1 103	1	1 103	
			1 079	1	1 079	
			1 064	1	1 064	
1 055	2	0.60				
1 045	2	0.75	1 048	1	1 048	
			1 039	0	1 039	
			1 031	1		*aa*
			1 005	9		*aa*
989	2					
984	2	0.66	980	9	980	*ee*
			957	1	957	
			940	1	940	
911	1	0.19	909	9	909	
874	1	0.49	sh	0	874	
			864	4		*aa*
848	2	0.01	844	8	844	*ee*
830	3	0.62	827	7		*aa*
			821	9	821	*ee*
803	3	0.11	805	2	805	
749	3		746	10	746	*ee*
738	7	0.23	738	10	738	*ee*
703	7	0.70				*aa*
			692	9		*aa*
621	1		613	7	not	
516	2		520	4	recorded	
520	3	0.13	498	1		
			462	1		*aa*

Table 1. Continued.

451	3	0.20	446	2	*ee*
388	9	0.25	383	4	
379	3		372	1	*ee*
			362	1	*aa*
331	1	0.70	331	1	*ee*
309	5	0.22	303	1	
286	2	1.05			
236	2	0.91			
186	3	0.55			

Table 2. Raman and infrared spectra of *trans* 1,2-dibromo*cyclo*hexane.

Raman spectrum liquid (20°C)			Infrared spectra liquid (25°C)		Solid (−70°C)	Conformation
$\Delta\nu$ cm^{-1}	I	ϱ	ν cm^{-1}	I	ν cm^{-1}	
3 047	3					
2 991	6					
2 949	10	0.37				
2 900	6	0.23	2 909	8		
2 864	5	0.70				
2 844	2		2 838	7		
			2 665	2		
			2 478	1		
			2 380	1		
			2 260	1		
			2 172	2		
			2 126	1		
			2 074	1		
			1 716	7		
1 445	4	0.76				
1 429	4	0.75	1 426	6	1 426	
1 362	1		1 357	5	1 357	
1 339	1	0.43	1 342	4	1 342	
1 331			1 334	4		*ee*
			1 318	3	1 318	
1 303	2	0.29	1 302	0	1 302	
1 279	2		1 282	1		*ee*
1 269	3	0.60	1 269	3	1 269	
1 259	4	0.34	1 258	3	1 258	
1 202	8	0.32	1 198	4	1 198	
1 181	7		1 177	9	1 177	*aa*
1 161	1		1 160	6		*ee*
1 138	2	0.71	1 135	2	1 135	
1 122	1		1 124	2		
			1 117	2	1 117	
			1 067	0	1 067	
1 060	2	0.52	1 059	1	1 059	
1 048	2		1 048	1		*ee*
1 034	4	0.80	1 032	2	1 032	
1 002	2		999	8	999	*aa*
971			973	5		*ee*
906	1	0.56	904	7	904	
868	4	0.34	861	6	861	*aa*
843	2	0.33	841	3		*ee*
815	5	0.39	814	5	814	*aa*
804	5	0.50				

Table 2. Continued.

			710	0	710	
699	4	0.76	693	6		*ee*
686	4	0.21	684	6		*ee*
			663	6	663	*aa*
652	10	0.21	651	0	651	*aa*
541	3	0.58	539	9		
			495	3		
477	6	0.22	476	2	not	
441	1		441	2	recorded	
365	2	0.45				
341	2					
324	2		322	3		
308	6	0.17	308	5		
			282	1		
238	7	0.17				
223	3	0.60				
179	6	0.34				
145						

The present paper is concerned with an examination of the conformational equilibrium of some 1,2-dihalogeno *cyclo*hexanes using the infrared and the Raman spectra. A quantitative determination of the conformational equilibrium ratio, using data from the infrared spectra of the compounds in solvents of different dielectric constant is proposed. The method, although involving several assumptions, is believed to present a good approximation, and has been applied to the *trans* 1,2-dichloro- and the *trans* 1,2-dibromo-*cyclo*hexane in 10 solvents of different polarity.

EXPERIMENTAL

Preparations. Trans 1,2-dichloro*cyclo*hexane was prepared by bubbling chlorine gas through *cyclo*hexene in the darkness as reported by Carrol *et al.*[7] The *trans* configuration of this compound has been confirmed in different ways [8,9].

Trans 1,2-dibromo*cyclo*hexane was prepared by adding a solution of bromine in carbon tetrachloride to *cyclo*hexene at −5°C [10]. It was found necessary to remove hydrochloric and hydrobromic acid from the products by shaking with an alcoholic solution of potassium hydroxide, because traces of these acids catalyze the decomposition of the halogenated *cyclo*hexanes during the Raman exposures.

Cis 1,2-dichloro*cyclo*hexane was a sample prepared by Stevens and Grummit [11].

The purity of the three 1,2-dihalogeno *cyclo*hexanes was checked by their refractive indices and melting points.

Infrared spectra. Infrared spectra of the two *trans* 1,2-dihalogeno *cyclo*hexanes and the cis 1,2-dichloro*cyclo*hexane were recorded in the pure liquid state using sealed cells of 0.05 mm thickness in the sodium chloride region, and demountable cells of approximately the same thickness in the caesium bromide region. The position of the infrared bands of the three compounds are given in Tables 1, 2 and 3, their intensities being indicated with numbers from 0 to 10.

The infrared data used for calculating the conformational equilibrium of the two *trans* 1,2-dihalogeno *cyclo*hexanes were obtained on solutions of concentrations below 5 % in 0.5 mm cells. In order to allow comparison of the extinction values of the bands, the different solution spectra were obtained using the same split program, program 3 on the Perkin-Elmer Model 21 double beam spectrophotometer, which was used for all the recordings. Apparent molar extinction values for the strong and the medium bands of the three compounds were calculated from the infrared spectra by subtracting the back-

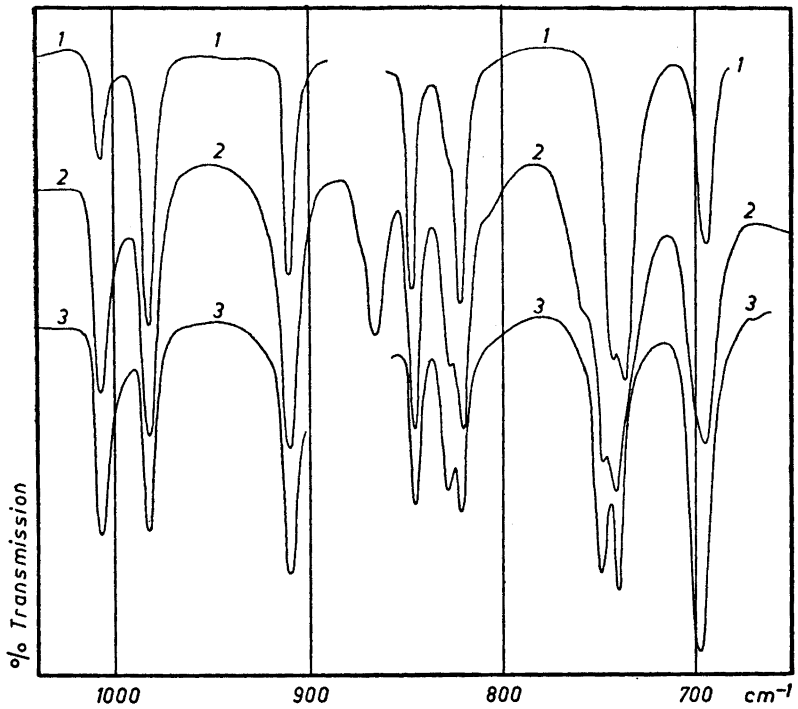


Fig. 1. Infrared spectra of *trans* 1,2-dichloro*cyclo*hexane. 1.—15% solution in nitromethane. 2. — pure liquid. 3. — 15 % solution in *cyclo*hexane. The open spaces indicate regions where the solvents have strong bands.

ground and making allowance for the concentrations and the specific gravity of the solutions. Correction for stray radiation in the region below 900 cm^{-1} was carried out using a calcium fluoride plate.

The infrared spectra of the three *cyclo*hexane compounds were also run in the solid state at —50°C. (Tables 1, 2 and 3).

Raman spectra. The Raman lines and the polarization data for the two *trans* 1,2-dihalogeno *cyclo*hexanes are reproduced in Tables 1 and 2 for the chloro and the bromo compound, respectively. The frequencies of the Raman lines are in good agreement with those reported by Kozima [2] and by Bastiansen [12]. For the *trans* 1,2-dibromo-*cyclo*hexane we have found some lines not reported by Kohlrausch [13]. The polarization data represent the average from three and four exposures of the dichloro and dibromo derivatives, respectively, and seem to be much more complete than the results from an earlier investigation by Canals [14].

The amount of *cis* 1,2-dichloro-*cyclo*hexane available was not sufficient for Raman investigations.

The Raman spectrograph was described in the previous paper [1].

THE CONFORMATIONAL EQUILIBRIUM

Effect of solvents

The most striking difference between the *cis* and the *trans* 1,2-dihalogeno *cyclo*hexanes is that while the infrared spectra of the first one is practically

unaffected by the solvent, the extinction values of some of the bands belonging to the *trans* compounds are quite sensitive to the dielectric constant of the solvent (Fig. 1). It was possible to make the following rough classification of the bands of the *trans* dihalogeno *cyclo*hexanes: Class 1 — extinction value increases with increasing polarity of the solvent; Class 2 — extinction value decreases with increasing polarity, and Class 3 — no apparent variation of the extinction value with change of polarity. The solvents were selected to give a large range of dielectric constants, with the extremes *cyclo*hexane ($D = 2.05$) and nitromethane ($D = 39.4$).

The different effect of solvents on the spectra of the *cis* and the two *trans* 1,2-dihalogeno *cyclo*hexanes can most likely be explained by the fact that the *trans* compounds [9,15] appear in two different conformations, *ee* and *aa*, interconvertible by inversion of the carbon ring, whereas only one, the *ea*-conformation, is possible for the *cis* compound.

While the *aa*-conformation of the *trans* 1,2-dihalogeno *cyclo*hexanes has a dipole moment of zero, or because of induced moments very near zero, the *ee*-conformation has, according to Tulinskie [3], a dipole moment very near the moment of the *cis* 1,2-dihalogeno *cyclo*hexanes which was found to be 3.1 *D* for both the chloro and the bromo compound [4]. Taking into account a dipole theory by Onsager [16] the conformational equilibrium of the *trans* compounds would be expected to be displaced toward the polar *ee*-conformation in solvents of high dielectric constant.

It may be concluded that the three classes of infrared bands of the *trans* 1,2-dihalogeno *cyclo*hexanes, found to increase (Class 1), decrease (Class 2), and to undergo no significant variation (Class 3) on going from unpolar to more polar solvents, should be assigned respectively to specific *ee*-bands, *aa*-bands and bands common to both conformations. This assignment seems justified as the relative intensity of the bands of the *cis* compound did not change with the solvent, and it is in accordance with the dipole theory of Onsager that the *ee*-conformation of the *trans* compound is stabilized by solvents of high dielectric constant.

Quantitative treatment of the equilibrium

Having divided the bands into classes belonging to one or both of the two conformations of the *trans* 1,2-dihalogeno *cyclo*hexanes, the infrared spectra give directly qualitative information about the relative displacement of the conformational equilibrium with change of the solvent. It is, however, also possible to gain quantitative values for the equilibrium ratio from the infrared spectra provided the following set of assumptions is accepted:

1. The bands assigned to the *ee*-conformation (Class 1) and the *aa*-conformation (Class 2) are not contaminated with bands from the other conformation.

2. The apparent molar extinction coefficients for the selected *ee*-and *aa*-bands are independent of the solvent.

3. Beer's law is valid for the concentration range investigated.

Let us assume that two bands have been selected, belonging to the *ee*- and the *aa*-conformation, respectively. Measurement of the extinction values

of these bands in two solvents, one of low the other of high dielectric constant, leads to the following set of equations:

$$E'_{ee} = \varepsilon_{ee} c'_{ee} d \quad (1)$$

$$E'_{aa} = \varepsilon_{aa} c'_{aa} d \quad (2)$$

$$E''_{ee} = \varepsilon_{ee} c''_{ee} d \quad (3)$$

$$E''_{aa} = \varepsilon_{aa} c''_{aa} d \quad (4)$$

$$C' = c'_{ee} + c'_{aa} \quad (5)$$

$$C'' = c''_{ee} + c''_{aa} \quad (6)$$

where E'_{ee}, E''_{ee}, and E'_{aa}, E''_{aa} are the measured extinction values of the *ee*- and *aa*-bands in the two solvents. ε_{ee} and ε_{aa} are the molar extinction coefficients of the *ee*- and the *aa*-bands.

C' and C'' are the total concentrations of the *trans* 1,2-dihalogeno *cyclo*hexane in the two solvents.

c'_{ee}, c''_{ee} and c'_{aa}, c''_{aa} are the concentrations of the *ee*- and *aa*-conformation in the two solvents.

d is the thickness of the cell.

Eliminating the unknown quantities ε_{ee}, ε_{aa}, c''_{ee}, and c''_{aa} from these equations, one obtains the following expression for the mole fraction, X_{ee}, of the *ee*-conformation in one solvent

$$X'_{ee} = \frac{c_{ee}}{C'} = \frac{E'_{ee}}{C'} \cdot \frac{C''E'_{aa} - C'E''_{aa}}{E''_{ee}E'_{aa} - E''_{aa}E'_{ee}} \quad (7)$$

It is thus possible to calculate the conformational equilibrium ratio in one solvent from the measured extinction values of the selected pair of bands in two solvents of different dielectric constant.

Tables 4 and 5 give the values of the mole fraction, X_{ee}, of the *ee*- conformation of the *trans* 1,2-dichloro- and the *trans* 1,2-dibromo-*cyclo*hexane in ten different solents. The data were obtained by applying eqn. 7 to the measured extinction values of several pairs of band.

The calculations are based on the validity of Beer's law. Furthermore, the contribution of solute to the dielectric properties of the solutions at higher concentrations also makes the use of low concentrations preferable. This requires consequently the use of rather thick absorption cells, about 0.5 mm. Especially the choice of polar organic solvents will for this reason be highly limited as these solvents usually display strong absorption bands in infrared. It was, however, found that both acetonitrile ($D = 38.8$) and nitromethane ($D = 39.4$) were sufficiently transparent to permit the use of 0.5 mm cells for the quantitative determination of the extinction values of several bands.

The specific *ee*- and *aa*-bands, selected for the determination of the equilibrium ratio, were mostly neighbour bands (Tables 4 and 5). This makes the construction of the background line, a necessary correction before obtaining the extinction values, less ambiguous. In some cases the *ee*- and *aa*-bands were somewhat overlapping, and it was necessary to apply a correction for

Table 3. Infrared spectra of *cis* 1,2-dichloro*cyclo*hexane in the liquid (25°C) and solid state (−70°C) [a]

ν cm^{-1}	I	ν cm^{-1}	I
2 943		1 131	(2)
2 854		1 083	(2)
1 564		1 079	(2)
1 430		1 056	(2)
1 400		1 025	(1)
1 376		986	(10)
1 354	(4)	907	(7)
1 345	(3)	878	(1)
1 333	(3)	835	(7)
1 312	(4)	818	(8)
1 297	(5)	744	(10)
1 272	(9)	696	(10)
1 266	(5)	655	(7)
1 227	(5)	512	(6)
1 216	(4)	370	(1)
1 193	(3)	346	(4)

a) The infrared spectra in the liquid and solid state were identical.

the contribution of one band to the extinction at band maximum of the other conformation. This was carried out by drawing a Gauss' curve by hand. It is obvious that this correction is somewhat ambiguous and the corresponding calculated mole fractions should be regarded with some reservation. This is especially the case with the pair of bands at 1 212 and 1 202 cm^{-1} of Table 4, and the pair 1 177 and 1 160 cm^{-1} of Table 5.

It is evident from eqn. 7 that the highest accuracy for the mole fraction is achieved when the extinction values in unpolar solvents are compared with

Table 4. Mole fractions of *trans* 1*e*—2*e*-dichloro*cyclo*hexane in several solvents calculated from different pair of bands.

Solvent	Diel. const.	Band pairs in wavenumbers [a] 1 212 / 1 202	1 005 / 980	864 / 844	827 / 821	692 / 738	Mean value
*Cyclo*hexane	2.05	0.35[b]	0.34		0.35	0.32	0.34
Carbon tetrachloride	2.24	0.32[b]	0.34		0.36	0.35	0.35
Carbon disulphide	2.65	0.42[b]	0.38	0.39	0.43	0.30	0.40
Pure liquid		0.43[b]	0.47	0.50	0.48	0.57	0.50
Chloroform	5.05		0.48	0.53			0.50
Benzene	2.28	0.43[b]	0.50	0.50			0.50
*Cyclo*hexanone	18.2		0.59				0.59
Benzaldehyde	18.0		0.61				0.61
Acetone	21.4		0.63	0.65	0.68	0.71	0.67
Acetonitrile	38.8	0.55[b]		0.66	0.68	0.74	0.69
Nitromethane	39.4	0.55[b]	0.70	0.70	0.70	0.75	0.71

a) The *aa*-bands are given in the first line, the *ee*-bands in the second line.
b) Not included in the mean value.

Table 5. Mole fractions of *trans* 1*e*—2*e*-dibromo*cyclo*hexane in several solvents calculated from different pair of bands.

Solvent	Diel. const.	Band pairs in wavenumbers [a] 1 177 / 1 160	999 / 973	861 / 841	663 / 684	Mean value
*Cyclo*hexane	2.05	0.19[b]	0.21		0.18	0.19
Carbon tetrachloride	2.24	0.20[b]	0.21	0.23	0.19	0.21
Carbon disulphide	2.65	0.26[b]	0.27	0.31	0.22	0.28
Pure liquid		0.44[b]	0.44	0.39	0.33	0.39
Chloroform	5.05	0.31[b]	0.40	0.39		0.39
Benzene	2.28	0.31[b]	0.42			0.42
*Cyclo*hexanone	18.2	0.39[b]	0.51	0.55		0.53
Benzaldehyde	18.0		0.53			0.53
Acetone	21.4	0.48[b]	0.56	0.56	0.50	0.54
Acetonitrile	38.8		0.62	0.59	0.59	0.60
Nitromethane	39.4	0.49[b]	0.63			0.63

a) The *aa*-bands are given in the first line, the *ee*-bands in the second line.
b) Not included in the mean value.

those in highly polar solvents. The results in Tables 4 and 5 were consequently obtained in the following way. The mole fractions in the unpolar solvents *cyclo*hexane, carbon tetrachloride, and carbon disulfide were first calculated by combining the measured extinction values in these solvents with those from the highly polar acetonitrile and nitromethane. The results were the basis for the calculation of the molar extinction coefficients of the *ee*- and *aa*-band. The mole fraction in the other solvents, including the pure liquid, was thereupon easily calculated from the extinction coefficients and the measured extinction values. It is highly gratifying to note the close agreement in Tables 4 and 5 between the mole fractions calculated from different pairs of bands. This agreement seems partially to justify the assumptions 1—3 upon which the calculations are based.

Unfortunately, it is not possible to estimate a confidence limit for the mole fractions of Tables 4 and 5. It is believed that the data represent qualitatively the actual situation, that is the displacement of the equilibrium with solvent and the relatively higher stability of the *aa* conformation of the bromo compound than that of the chloro compound. The absolute values of the mole fractions may, however, be wrong by several per cent relative. A possible source of error would be the non-constancy of the molar extinction coefficient of the bands of any one configuration in the different solvents. It has actually been observed on some systems [17] that bands are broader and lower in polar solvents than in nonpolar, and that consequently the integrated extinction values are a better measure of the concentration. Careful examination of the infrared bands of the two *trans* halogeno *cyclo*hexanes in solvents of different polarity did not indicate any increase in half-width of the bands on going towards polar solvents. Only the carbon-halogen stretching frequencies around 700 cm^{-1} showed a slight increase in half-width. The increase was too small, however, to be of any significance to the calculated mole fractions.

Another source of error would be the contamination of the bands, assumed to be pure *ee*- and *aa*-bands, with bands from the other conformation. The use of several band pairs for the calculations should minimize this source of error.

It may be added that the selected pair of bands of Tables 4 and 5 may probably be assigned to the same type of vibration in the two conformations. The fact that these pair of bands occur in the same spectral region in both compounds, but somewhat displaced to shorter wave numbers in the bromo compound, strongly suggests such an assignment. It is obvious, however, that the validity of the calculations made from eqn. 7 is quite independent of this assumption.

DISCUSSION

The data of Tables 4 and 5 show that the equilibrium values for both compounds in the pure liquid state are close to the values in chloroform. This is quite reasonable as in the liquid state there will be an appreciable interaction between neighbour molecules some of which are in the polar * *ee*-conformation. The result would be the same as if the compounds were dissolved in solvents of medium polarity like chloroform. The calculated equilibrium ratios of the *trans* 1,2-dihalogeno *cyclo*hexanes indicate the presence of 50 % of the *ee*-conformation of the chloro-derivative and 40 % of the bromo-derivative in the pure liquid state at room temperature. Transition from one conformation to the other is assumed to take place through a very low energy barrier. From Tables 4 and 5 the difference in energy between the two conformations, calculated by applying the Boltzmann distribution law, is found to be less than 0.8 kcal/mole at room temperature in the dielectric area investigated.

It seems reasonable to assume that the conformational equilibrium ratio in the unpolar solvents, like *cyclo*hexane, should approach the equilibrium ratio in the vapour phase, the *ee*-conformation being only slightly more favoured in the non-polar solvents than in the vapour phase. An infrared spectrum of *trans* 1,2-dichloro*cyclo*hexane, run in an 1 meter gas cell, seemed to verify this statement. It should be pointed out, however, that the calculated mole fraction of the *ee*-conformation of the *trans* 1,2-dichloro- and the *trans* 1,2-dibromo*cyclo*hexane dissolved in *cyclo*hexane (0.34 and 0.19, respectively) do not agree at all with the electron diffraction data (0.5 and 0.6, respectively) [9,15] obtained on the vapour phase.

The infrared bands found in the solid state of *cis* 1,2-dichloro*cyclo*hexane at −50°C are the same as those found in the liquid state. This is in agreement with the existence of only one conformation of this compound, (*ae*). In the two *trans* derivatives, however, a set of bands appearing in the liquid state spectra are absent in the solid state ones, but on the other hand, all bands in the solid state spectra are present in the liquid. The bands which disappear in the solid spectra, are just the same as those assigned to *aa* and *ee* in the chloro- and bromo-compound, respectively. The conclusion must be drawn that *trans* 1,2-dichloro*cyclo*hexane exsist in *ee* and that *trans* 1,2-dibromo-

* Polar points here to polarity and not to the old designation p — polar for an *axial* (*a*) substituent.

Table 6. The unfavourable distances between the halogen substituents (X) and other atoms in the *trans* 1,2-dihalogeno *cyclo*hexanes compared with the sum of the appropriate van der Waals radii.

Distance	*trans* 1,2-dichloro-*cyclo*hexane		*trans* 1,2-dibromo-*cyclo*hexane		Multiplicity
	calculated	van der Waals	calculated	van der Waals	
$X_1(a)-H_3(a)$	2.61	3.0	2.67	3.15	4
$X_1(a)-H_2(e)$	2.89	3.0	3.04	3.15	4
$X_1(e)-H_2(e)$	2.89	3.0	3.04	3.15	2
$X_1(e)-H_2(a)$	2.89	3.0	3.04	3.15	4
$X_1(a)-H_1(e)$	2.38	3.0	2.56	3.15	2
$X_1(e)-H_1(a)$	2.38	3.0	2.56	3.15	2
$X_1(e)-X_2(e)$	3.21	3.6	3.42	3.9	1

The calculations are based on the following distances that apply to *cyclo*hexane derivatives [30]

C—C = 1.54 Å
C—Cl = 1.78—1.79 Å
C—Br = 1.98—1.99 Å
C—H = 1.09 Å

and no distortion from tetrahedral angles.

*cyclo*hexane exist in *aa* in the solid state. Kozima *et* al.[2] suggested the same conformations on the basis of a Raman investigation. It will indeed be gratifying if these findings can be verified through an X-ray crystallographic investigation which we know is under way [18].

The interaction between the halogen substituents and the carbon and hydrogen atoms of the *cyclo*hexane ring may explain the difference in energy between the conformations [19]. If the distance between non-bonded atoms is less than the sum of the van der Waals radii a repulsion between the respective atoms will occur. A kind of stressing or deformation of the *cyclo*hexane ring with increase of the energy will probably be the result. By electron diffraction methods a certain amount of deformation of the valence angles in several substituted *cyclo*hexanes has been reported [20].

Provided that there is no such deformation, Table 6 gives the unfavourable distances within the molecule as compared to the normal van der Waals distances as well as the number of occurrences of these within the same molecule.

We assume that the most important factor for evaluating the relative stability of two possible conformations are the unfavourable atomic distances which are specific for each conformation. It will appear from Table 6 that the most unfavourable distances are $Hal_1(a) - H_3(a)$ and $Hal_1(e) - Hal_2(e)$. The first one will favour the formation of the *ee*-conformation, the latter will countercurrently favour the formation of the *aa*-conformation. The question is: Which effect is the stronger? There can be but little doubt that the $Hal_1(a) - H_3(a)$ distance represents a very strong steric hindrance. Hassel and Bastiansen have calculated the distortion of the appropriate valence angles to approximately 7°. This distance also has the high multiplicity of 4.

On the other hand it seems reasonable to assume that a still stronger steric hindrance arises from the $Hal_1(e) - Hal_2(e)$ configuration. In this case there is a marked violation of the normal van der Waals distance between the two strongly electronegative halogen atoms, whereas the repulsion between the electronegative halogen atoms and the electropositive hydrogen atom would be assumed to be of a weaker character.

It is interesting to note that in the monohalogeno derivatives of *cyclo*hexane only the $Hal_1(a) - H_3(a)$ repulsion is present, and the equilibrium is highly displaced towards the *e*-conformation [1]. In the *trans* 1,2-dihalogeno *cyclo*hexanes, however, where both effects are active, the equilibrium in the pure liquid state is found to be equally distributed between both conformations in the chloro compound, but displaced somewhat towards *aa* in the bromo compound. It seems probable that by increasing the atomic radii in going from the chloro to the bromo derivative, the $Hal_1(e) - Hal_2(e)$ repulsion will increase more than the $Hal_1(a) - H_3(a)$ repulsion and make the *aa* conformation energetically more favourable. The fact that the dichloro- and dibromo compound crystallize in the *ee* and *aa* conformation, respectively, seems to support this assumption, even if the forces involved in the crystal lattice may be important in this respect.

It must be pointed out, however, that the result of X-ray crystallographic [21,22] and electron diffraction measurements [23] of the 1,2-dichloro-4,5-dibromo*cyclo*hexane (*aa-ee* — *ee-aa*) revealed the compound to be present entirely in the *aa-ee* conformation in the solid and vapour state. The conclusions drawn for the 1,2-dichloro-4,5-dibromo*cyclo*hexane [24] seem at the present state to be quite inconsistent with the conclusions which can be drawn for the *trans* 1,2-dihalogeno *cyclo*hexanes.

By measuring the dipole moments of *trans* 1,2-dichloro- and *trans* 1,2-dibromo*cyclo*hexane dissolved in carbon tetrachloride or benzene, several authors [2–5] have calculated the conformational equilibrium. They find smaller dipole moments of the bromo than of the chloro compound, and conclude that the equilibrium is more displaced towards the unpolar conformation *aa* in the bromo compound than in the chloro compound. This is in agreement with the results in the present paper. The absolute values for the equilibrium ratio calculated from the dipole moment measurements indicate, however, a conformational equilibrium displaced more towards the *ee* conformations than the results from our investigation. The calculations made by these authors are based upon severe assumptions concerning the dipole moments of each conformation. It must be admitted, however, that the present work also is based upon several assumptions.

Carbon-halogen stretching frequencies

Among the normal vibrations of the 1,2-dihalogeno *cyclo*hexanes the vibrations dominated by stretching of the highly polar carbon-halogen bond can easily be assigned to specific bands near 700 cm^{-1} in the infrared and Raman spectra.

In the *trans* compounds one would expect two vibrations for each conformation, one symmetric and one asymmetric. A consideration of models

Table 7. Apparent molar extinction coefficients in infrared, and relative intensities in Raman of the carbon-halogen stretching frequencies.

trans 1,2-dichloro-*cyclo*hexane				*trans* 1,2-dibromo-*cyclo*hexane				Vibration type	Conformation
IR		Raman		IR		Raman			
ν cm^{-1}	ε	$\Delta\nu$ cm^{-1}	I	ν cm^{-1}	ε	$\Delta\nu$ cm^{-1}	I		
746	117	749	1.0	693	70	699	1.0	asym.	*ee*
738	117	738	2.4	684	70	686	1.9	sym.	*ee*
		703	2.8			652	12.4	sym.	*aa*
692	94			663	58			asym.	*aa*

of the *trans* 1*a*—2*a*-dihalogeno *cyclo*hexanes shows that the symmetric carbon-halogen stretching vibration should not, to the first approximation, involve a change of the dipole moment of the molecule. The corresponding infrared bands would correspondingly be weak. In the Raman spectra, however, the symmetric stretching vibration would be expected to give a rather strong and polarized line. This is indeed observed. The much higher intensity of the symmetric Raman line for the bromo- than for the chloro-compound is striking. It is probable that the normal vibration is better defined as a carbon-halogen stretching vibration with the heavier bromo atoms than with the lighter chloro atoms where possibly other parts of the molecule takes part in the normal vibration. The asymmetric stretching of the carbon-halogen bonds of the *trans* 1*a*—2*a*-dihalogeno *cyclo*hexanes should give a strong band in the infrared spectra and probably only a weak line in the Raman spectra. Again, this is found to be true (Table 7).

A similar description of the two carbon-halogen stretching vibrations of the *trans* 1*e*—2*e*-dihalogeno *cyclo*hexanes is more difficult. Models indicate that both the symmetric and the asymmetric stretching vibrations should involve a change of dipole moment. Any prediction as to the relative intensity of the bands in the infrared spectra would be somewhat dubious. Correspondingly, two carbon-halogen bands, belonging to the *ee*-conformation are observed in the 700 cm^{-1} region. The bands are of approximately equal intensity.

In the *cis* 1,2-dichloro*cyclo*hexane one chlorine atom is in the *e*- the other in the *a*-position. The carbon-chlorine bonds make an angle of about 70°. Because of repulsion between the chlorine atoms the angle may be somewhat larger. If the bonds made an angle of 90° one might assume the stretching vibrations of the two carbon-halogen bonds not to be coupled. Two frequencies should be observed, characteristic of the stretching of the *equatorial* and the *axial* bonds. In the infrared spectra of the *cis* 1,2-dichloro*cyclo*hexane the carbon-chlorine stretching bands are found at 744 and 696 cm^{-1}, values that are very near those observed for the stretching vibrations of the *e*, respectively the *a*-conformation of monochloro*cyclo*hexane [1]. This may in fact suggest only a weak coupling of the two carbon-chlorine stretching vibrations of the *cis* 1,2-dichloro*cyclo*hexane. The 744 cm^{-1} vibration should then involve mainly a stretching of the *equatorial* carbon-chlorine bond, and the 696 cm^{-1}

vibration a stretching of the *axial* bond. The two bands have very near the same intensity.

In the previous paper [1] on the monohalogenated *cyclo*hexanes it was not possible to calculate the conformational equilibrium value from the intensities of the characteristic frequencies because the molar extinction coefficients were unknown. According to the discussion above the two carbon-chlorine stretching vibrations of the *cis* 1,2-dichloro*cyclo*hexane are probably characteristic of the *equatorial* and the *axial* bond, respectively. As the intensity of the corresponding infrared bands are nearly the same, one may assume that the molar extinction coefficients of the characteristic *e* and *a* stretching bands are approximately equal. On this basis one calculates the mole fraction of the *e*-conformation to 0.78 for the monochloro*cyclo*hexane and to 0.85 for the monobromo*cyclo*hexane. It must be admitted that the assumptions upon which these calculations are based, are somewhat drastic. The results are, however, not inconsistent with those obtained from electron diffraction measurements [25].

For monosubstituted *cyclo*hexanes and steroids it has been pointed out by several authors [26-29] that the stretching motion of an *equatorial* substituent induces a higher vibrational frequency than the stretching motion of the corresponding *axial* substituent. This empirical rule is substantiated by the data of Table 7, which shows that the rule holds even for disubstituted *cyclo*hexanes.

The authors desire to express their sincerest thanks to Professor O. Hassel for helpful discussions and encouragement during the work. One of the authors (K.L.) wishes to thank *Norges Almenvitenskapelige forskningsråd* for financial support.

REFERENCES

1. Klæboe, P., Lothe, J. and Lunde, K. *Acta Chem. Scand.* **10** (1956) 1465.
2. Kozima, K., Sakashati, S. and Maeda, S. *J. Am. Chem. Soc.* **76** (1954) 1965.
3. Tulinskie, A., Giacomo, A. and Smyth, C. P. *J. Am. Chem. Soc.* **75** (1953) 3552.
4. Kwestroo, W., Meijer, F. A. and Havinga, E. *Rec. trav. chim.* **T73** (1954) 717.
5. Bender, P., Flowers, D. and Goering, H. L. *J. Am. Chem. Soc.* **77** (1955) 3463.
6. Larnaudie, J. M. Thesis Paris 1953. *Compt. rend.* **235** (1952) 154; **236** (1953) 909.
7. Carrol, B., Kubler, D., Davis, H. and Whaley, A. *J. Am. Chem. Soc.* **73** (1951) 5382.
8. Mousseron, M., Granger, R. and Valette, J. *Bull. soc. chim. France* **1946** 244.
9. Bastiansen, O., Hassel, O. and Munthe-Kaas, A. *Acta Chem. Scand.* **8** (1954) 872.
10. Blatt, A. *Org. Syntheses. Coll. Vol. 2*, 171–173.
11. Stevens, H. C. and Grummit, O. *J. Am. Chem. Soc.* **74** (1952) 4876.
12. Bastiansen, O. *Private communications.*
13. Kohlrausch, K. W. P. and Stockmair, W. *Z. physik. Chem.* **31** (1936) 500.
14. Canals, E., Mousseron, M., Granger, R. and Gaustaud, I. *Bull. soc. chim. France* **4** (1937) 2048.
15. Bastiansen, O. and Hassel, O. *Tidskr. Kjemi Bergvesen Met.* **8** (1946) 96.
16. Onsager, L. *J. Am. Chem. Soc.* **58** (1936) 1486.
17. Whiffen, D. H. *Trans. Faraday Soc.* **49** (1953) 878.
18. Norman, N. *To be published shortly.*
19. Hassel, O. *Research* **3** (1950) 504.
20. Hassel, O. and Wang Lund, E. *Acta Cryst.* **2** (1949) 309.
21. Hassel, O. and Wang Lund, E. *Acta Chem. Scand.* **6** (1952) 238.
22. Hassel, O., Wang Lund, E. and Lunde, K. *Acta Chem. Scand.* **6** (1952) 426.
23. Bastiansen, O. and Hassel, O. *Acta Chem. Scand.* **5** (1951) 1404.

24. Lunde, K. *Acta Chem. Scand.* **10** (1956) 690.
25. Hassel, O. and Viervoll, H. *Tidsskrift Kjemi Bergvesen Met.* **3** (1943) 35.
26. Corey, E. J., Sneen, R. A., Danaher, M. G., Young, R. L. and Rutledge, R. L. *Chemistry & Industry* **1954** 1294.
27. Page, J. E. *J. Chem. Soc.* **1955** 2017.
28. Barton, D. H. R., Page, J. E. and Shoppee, C. W. *J. Chem. Soc.* **1956** 331.
29. Cole, A. R. H., Jones, R. N. and Dobriner, K. *J. Am. Chem. Soc.* **74** (1952) 5571.
30. Hassel, O. *Private communication.*

Received July 20, 1957.

ACTA CHEMICA SCANDINAVICA 11 (1957) 1692—1694

On the Preparation of Cholesterol Labelled with Tritium at Carbon Atoms 24 and 25 (Cholesterol-24,25-T_2)

Bile Acids and Steroids 54

S. BERGSTRÖM, S. LINDSTEDT and D. SEN*

Department of Physiological Chemistry, University of Lund, Lund, Sweden

Cholesterol-24,25-T_2 has been prepared by electrolysis of 3β-hydroxychol-5-enic acid and *iso*valeric acid-2,3-T_2 obtained by reduction of 3,3-dimethylacrylic acid with tritium gas.

In order to study the metabolism of cholesterol we have synthesized cholesterol labelled with tritium mainly at carbon atoms 24 and 25.

Cholesterol has been obtained by anodic (Kolbe) synthesis from 3β-hydroxychol-5-enic acid and *iso*valeric acid. With a 25-fold excess of *iso*valeric acid a 17 % yield of cholesterol calculated on the amount of bile acid used has been obtained (*cf.* Ref.[1]).

Adsorption chromatography on alumina followed by reversed phase partition chromatography had to be used to obtain a pure product from the reaction mixture.

Tritium labelled *iso*valeric acid was obtained by reducing 3,3-dimethylacrylic acid with tritium gas in dioxan solution in presence of platinum catalyst. The isotope is presumably located at carbon atoms 2 and 3 of the *iso*valeric acid but according to the experience of reduction with tritium gas in other cases, some isotope might also be located in the terminal methyl groups.

EXPERIMENTAL

All melting points were taken on an electrically heated aluminum block and are corrected. The radioactivity was estimated in a Tracerlab gas flow counter in an "infinitely thin" layer.

Δ^5-3β-Hydroxycholenic acid. An impure sample of the acid was purified by chromatography of its methyl ester on alumina. We are indebted to Ciba Ltd., Basel, for a generous sample of this acid. Electrolysis was carried out in wide test tubes (i.d. 35—38 mm)

* Present adress: Department of Applied Chemistry, University College of Science and Technology, Calcutta 9, India.

in which 3 platinum electrodes (20 × 26 mm) were fixed parallel to and at distances of 2 mm from each other. The middle one served as anode and the two outer ones as cathode. The current used was 2.2 A.

262 mg (0.7 mmole) of 3β-hydroxychol-5-enic acid, 2 ml (1.80 mmole) of isomer-free *iso*valeric acid and 42 mg (1.87 mmole) of sodium was dissolved in a mixture of 26 ml methanol and 9 ml dry pyridine. (The cholenic acid did not dissolve in methanol alone.)

The vessel was cooled in an ice-salt mixture and the solution was also cooled by dipping into it a glass tube through which cold water was circulated. The temperature of the reaction mixture remained between 35° and 45° during the electrolysis that was continued until pH 7.5 was reached. The solution was then taken to dryness *in vacuo*. 20 ml of 2 N hydrochloric acid was added and extracted with four 50 ml portions of ether. The ethereal solution was washed with 2 N hydrochloric acid, water, 10 % sodium hydroxide solution and water, and then taken to dryness *in vacuo*. The residue weighed 230 mg.

Chromatography. The residue was dissolved in benzene and brought onto a column (i.d. of tube 15 mm) of 20 g aluminum oxide (alkali free [2]), prepared with benzene. The column was eluted as shown in Table 1, fractions of 40 ml being collected.

Table 1.

Fraction	Eluent	Eluate		
1	Benzene	—		
2,3	Benzene/ether 19:1 v/v	11 mg oil		
4—13	»	small amount of oil in each		
14	Benzene/ether 17:3 v/v	5.9 mg, oily		
15	»	8.0 mg, crystalline		
16	»	10.1 mg	»	
17	»	12.6 mg	»	m.p. 95—105°
18	»	14.2 mg	»	m.p. 119—30°
19	»	21.6 mg	»	m.p. 126—32°
20	»	28.3 mg	»	m.p. 130—135°
21	»	27.7 mg	»	m.p. 128—34°
22	»	12.1 mg	»	m.p. 127—30°
23	»	4 mg	»	
24	»	2 mg	»	

Similar chromatograms were also obtained in the preparation of active cholesterol.

Fractions 19, 20 and 21 after one crystallization from methanol yielded 71 mg of crystals of m.p. 133—37°. 23.6 mg of this was mixed with 1 mg of cholesterol-4-^{14}C and

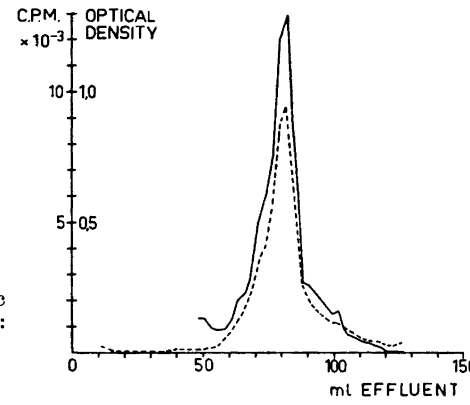


Fig. 1. Partition chromatogram of synthetic cholesterol. Full line: c.p.m. Broken line: cholesterol color reaction [4].

subjected to reversed phase partition chromatography at 23° on hydrophobic Supercel (4.5 g) with 55 % *iso*propanol in water as the mobile phase and chloroform/heptane (1:4) (4 ml) as the stationary phase as described by Danielsson [3].

Fractions of about 2 ml were collected with a fraction-collector. Aliquot parts of the fractions were taken and the radioactivity estimated by plating and counting. The total cholesterol was determined with the Tschugaeff's reaction [4]. The results are shown in Fig. 1.

The substance (17 mg) was collected from the fractions between 66 and 90 ml effluent. One crystallization from methanol gave 14.0 mg of crystals, m.p. 147–48°. A mixed melting point determination with authentic cholesterol gave no depression.

3,3-Dimethylacrylic acid was prepared by oxidation of mesityl oxide [5].

Isovaleric acid-2,3 T. The hydrogenation was carried out in a high vacuum apparatus similar to that described by Glascock [6]. The reaction vessel had a volume of 2.9 ml and was connected to the vacuum line with a balljoint. We have also found it convenient to introduce a 15 mm long gold-plated iron rod as a magnetic stirrer. By this technique the long reaction time described by Glascock can be much reduced.

2 mg of platinum oxide suspended in 0.1 ml dry dioxan was reduced with inactive hydrogen in the reaction vessel. 5 mg of dimethylacrylic acid in 0.15 ml of dioxan was then added. The apparatus was evacuated with the reaction vessel cooled in liquid air and 0.208 ml of tritium gas (0.5 C) pumped into the reaction space with the Toepler pump. After 1 h 95 % of the tritium gas had been taken up. 0.5 ml of inactive hydrogen was then pumped into the vessel. This gas was consumed in 2 h and the reduction then brought to completion with a further portion of inactive hydrogen.

Cholesterol-24,25-T. The labelled *iso*valeric acid was dissolved in 5 ml dioxan and added to the same mixture as described above and was then electrolysed and worked up as before. 230 mg of residue was obtained.

Chromatography on alumina followed by partition chromatography yielded in all 46 mg cholesterol (m.p. 147–48°), *i.e.* a 17 % yield calculated on the amount of 3β-hydroxychol-5-enic acid used.

REFERENCES

1. Bergström, S. and Krabisch, L. *Acta Chem. Scand.* **11** (1957) 1067.
2. Reichstein, T. and Schoppee, C. W. *Discussions Faraday Soc.* **7** (1949) 305.
3. Danielsson, H. *Biochim. et Biophys. Acta. In press.*
4. Hanel, H. K. and Dam, H. *Acta Chem. Scand.* **9** (1955) 677.
5. Smith, L. I., Prichard, W. W. and Spillane, L. J. *Org. Syntheses* **23** (1946) 27.
6. Glascock, R. F. *Isotopic gas analysis for biochemists.* Academic Press, N.Y. 1954.

Received August 6, 1957.

ACTA CHEMICA SCANDINAVICA 11 (1957) 1695—1697

Synthesis of the Tritiated 25-Methyl Homologues of 3α,7α,12α-Trihydroxy Coprostane and Coprocholic Acid

Bile Acids and Steroids 55

SUNE BERGSTRÖM, URS GLOOR and LENNART KRABISCH

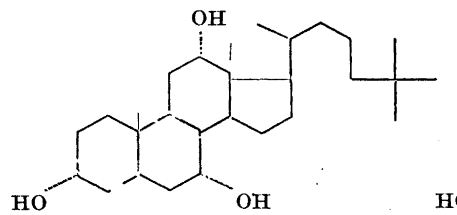
Department of Physiological Chemistry, University of Lund, Lund, Sweden

The compounds have been prepared through electrolysis of tritiated cholic acid together with *tert.* butyl acetic acid, respectively the monoester of 2,2-dimethylsuccinic acid.

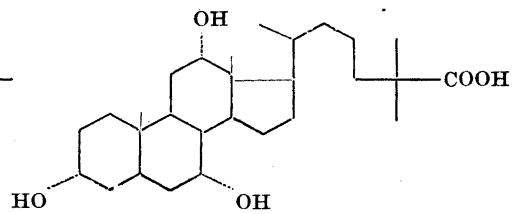
Previous work at this institute has shown that the hydroxylating enzyme systems involved in the transformation of cholesterol into bile acids have very exacting requirements as far as the structure of the side chain is concerned.

A 12α-hydroxyl is introduced resulting in the formation of cholic acid when labelled cholesterol (*cf.* Summary [1]), 3α,7α-dihydroxycoprostane [2] or 7α-hydroxycholesterol [3] is administered. If the side chain contains a carboxyl at the end of the C_5-cholanic or the C_8-"coprocholanic" side chain, however, the molecule is hydroxylated at other positions. Furthermore the 7α-hydroxylating enzyme system present in rat liver microsomes that transforms taurodeoxycholic acid into taurocholic acid does not work on free deoxycholic acid [1] *in vitro*.

As a step in the investigation of the influence of the side chain structure on the hydroxylating system and on the taurine conjugating system and also as a useful substrate in studying the ω- or methyloxidation we have prepared 3α,7α,12α-trihydroxy-25-methylcoprostane (I), *i.e.* a coprostane with the stable cholic acid structure in the ring system and a tertiary butyl group at the end of the side chain, thus blocking any β-oxidation after a possible ω-oxidation.



I



II

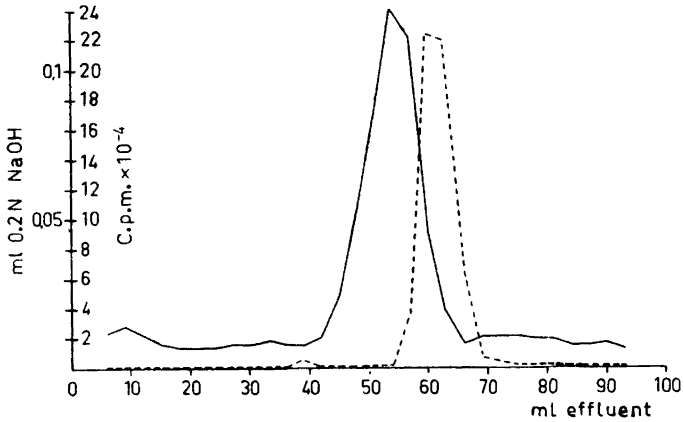


Fig. 1. Reversed phase partition chromatography of deoxycholic acid (solid line) and [T]-25-methyl-coprocholic acid (<0.1 mg) (broken line, cpm) in 55 % aqueous methanol/chloroform-heptane 9:1, *cf.* Ref.[1]

We have also prepared the corresponding possible metabolite that would be formed if one of the terminal methyl groups was oxidized to a carboxyl, *i.e.* 3α,7α,12α-trihydroxy-25-methylcoprocholanic acid (II).

The preparation of these two compounds (I and II) from tritium labelled cholic acid is described in this publication. Some data on the metabolism of these compounds are given in a separate communication.

EXPERIMENTAL

3,7,12-Trihydroxy-25-methylcoprostanic acid (25-methyl-coprocholic acid). Tritiated cholic acid (250.8 mg) was dissolved in methanol (50 ml) and 2,2-dimethyl-succinic acid mono-methyl ester (tertiary) (2.33 g) and sodium (35 mg in one ml of methanol) was added.

The solution was electrolyzed as described earlier [4] until a pH of about 7.5 had been reached. The solution was then taken to dryness *in vacuo* and the residue distributed between ether and water. The ether phase was washed neutral with carbonate and brought to dryness leaving a residue of 884 mg.

The crude product was dissolved in methylene chloride and chromatographed on a column of silicic acid (dried at 120° for 24 h) and Hyflo Supercel. The material eluted with 6 % methanol in methylene chloride. The centre of the material eluted with this solvent was saponified in 2 N potassium hydroxide for 4 h at 130°.

Of the free acid recovered (129 mg) 70 mg was subjected to reversed phase partition chromatography on hydrophobic Kieselguhr (18 g) with 60 % aqueous methanol as mobile phase and chloroform-heptane as stationary phase [5].

The well defined peak between 100 and 180 ml effluent was combined and crystallized from aqueous acetone. The product melted at 224—226°C. (Found: C 72.8; H 10.5. Calc. for $C_{28}H_{48}O_5$: C 72.4; H 10.4).

A sample of the acid was also run with deoxycholic acid in a system of 55 % aqueous methanol and chloroform-heptane 9:1.

As seen in Fig. 1 the peak of the labelled material appeared at 60—65 ml effluing slightly after the deoxycholic acid (55 ml) whereas coprocholic acid has been found to appear at 40—45 ml and cholic acid at 20—25.

The addition of three carbons to the side chain of cholic acid thus does not quite counterbalance the effect of one hydroxyl in this system, whereas the further addition of one methyl group makes the acid less polar than deoxycholic acid.

3,7,12-Trihydroxy-25-methylcoprostane. Tritiated cholic acid (50 mg) was dissolved in methanol (5 ml). Tertiary butylacetic acid (316 mg) was added together with sodium methylate (7 mg). The platinum electrodes were 5×7 mm at a distance of 2 mm from each other and the electrolysis was run as indicated above. The neutral product was chromatographed on silicic acid and the material eluted with methylene chloride containing 2 % of methanol, combined and recrystallized from aqueous acetone yielding 14 mg of a product melting at 203°. (Found: C 77.3; H 11.7. Calc. for $C_{28}H_{50}O_3$: C 77.4; H 11.6).

We are very grateful to Dr. S. Lindstedt for supplying us with cholic acid labelled with tritium through catalytic exchange essentially according to the method of Trenner *et al.*[6]

REFERENCES

1. Bergström, S. *Record Chem. Progr. Kresge-Hooker Sci. Lib.* **16** (1955) 63.
2. Bergström, S. and Lindstedt, S. *Biochim. et Biophys. Acta* **19** (1956) 556.
3. Lindstedt, S. *Acta Chem. Scand.* **11** (1957) 417.
4. Bergström, S. and Krabisch, L. *Acta Chem. Scand.* **11** (1957) 1067.
5. Bergström, S. and Sjövall, J. *Acta Chem. Scand.* **5** (1951) 1267.
6. Trenner, N. R., Pfluger, H. L., Neustead, E. T., Jones, S. L. and Sutton, C. T. *J. Am. Chem. Soc.* **76** (1954) 1196.

Roceived August 6, 1957.

ACTA CHEMICA SCANDINAVICA 11 (1957) 1698—1705

Bifunctional Amines and Ammonium Compounds

VI.* Further Homologs and Analogs of bis-Choline Ether Salts

JØRGEN FAKSTORP and JYTTE CHRISTIANSEN

Aktieselskabet Pharmacia, Copenhagen-Vanløse, Denmark

As an extension of earlier work twelve aliphatic bis-alkylammonium alkyl ethers, representing different chain-lengths, distribution and size of N-substituents, and chain branching, are reported together with twenty-four quaternary salts. Six aromatic ethers are reported along with eight bis-quaternary and three mono-quaternary salts derived therefrom. Transformation to non-halide salts is discussed. Alkylation of bis-(2-dimethyl-2'-diethyl)-aminoethyl ether with various alkyl halides gave ten different quaternary salts, which are reported.

In the current investigations on the relation of structure to pharmacological activity in an extended series of bis-ammonium salts, the need arose for salts representing further extensions on the structural theme exemplified by bis-choline ether. A number of such variations have been reported earlier from this laboratory [1-4].

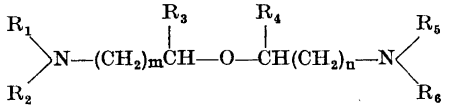
The present paper reports twelve additional bis-tertiary aliphatic ethers, representing variations in chain-length, degree of asymmetry, size of N-substituents and chain-branching (Table 1). These ethers were obtained essentially as described earlier [1]. They were prepared, in most cases, from known aminoalcohols or aminoalkylhalides, respectively.

This paper further presents six bis-tertiary ethers having an aromatic ring system in the chain (Table 2). The bis-tertiary ethers have been transferred to their corresponding methiodides and ethobromides or ethiodides, respectively. The twenty-four salts corresponding to the aromatic ethers are shown in Table 4. The quaternary salts were obtained by conventional procedures.

The substituted choline phenyl ethers are formed with considerable difficulty, and in several cases only the mono-quaternary salt (retaining the tertiary amino group on the aromatic ring) was obtained. Three such mono-quaternary salts are shown in Table 5.

* Part V. *Acta Chem. Scand.* 10 (1956) 15.

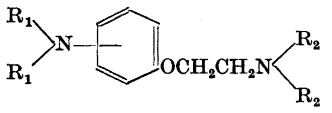
Table 1.



Code No.	R_1	R_2	R_3	R_4	R_5	R_6	m	n	B.p. °C	Press. mm Hg	Yield %	Emp. formula	M	Analysis, % Calc. C	Calc. H	Calc. others	Found C	Found H	Found others
Asa- 85	CH_3	CH_3	CH_3	CH_3	CH_3	CH_3	1	1	82—85	12	37	$C_{10}H_{24}N_2O$	188.31	63.78	12.85	N 14.88	63.04	12.21	N 14.13
Asa-120	CH_3	C_2H_5	H	H	CH_3	CH_3	1	1	81—82	8	64	$C_9H_{22}N_2O$	174.28	62.02	12.72	N 16.08	60.55	12.64	N 14.87
																			E 99.8 a)
Asa-121	CH_3	C_2H_5	H	H	C_2H_5	C_2H_5	1	1	103	8	12	$C_{11}H_{26}N_2O$	202.33	65.29	12.95	N 13.85	64.35	12.45	N 12.29
																			E 100.3
Asa-122	C_4H_8 b)		H	H	CH_3	CH_3	1	1	121—124	25	40	$C_{10}H_{22}N_2O$	186.29	64.47	11.90	N 15.04	64.33	11.97	N 14.68
Asa-123	C_4H_8		H	H	C_2H_5	C_2H_5	1	1	140—144	25	30	$C_{12}H_{26}N_2O$	214.34	67.24	12.23	N 13.07	67.01	12.22	N 12.70
Asa-124	C_4H_8		H	H	C_4H_8		1	1	150—151	15	22	$C_{12}H_{24}N_2O$	212.33	67.88	11.39	N 13.19	67.90	11.32	E 100.6
Asa-135	C_2H_5	n-C_3H_7	H	H	CH_3	HC_3	1	1	106—110	12	12.3	$C_{11}H_{26}N_2O$	202.33	65.29	12.95	N 13.85	—	—	E 97.3
Asa-136	C_2H_5	n-C_4H_9	H	H	CH_3	CH_3	1	1	115—118	13	11.5	$C_{12}H_{28}N_2O$	216.36	66.61	13.04	N 12.95	—	—	E 98.6
Asa-165	CH_3	CH_3	H	H	CH_3	CH_3	1	2	89	18	55	$C_9H_{22}N_2O$	174.28	62.02	12.72	N 16.08	61.70	12.82	E 98.2
Asa-166	C_2H_5	C_2H_5	H	H	CH_3	CH_3	1	2	110—111	17	59	$C_{11}H_{26}N_2O$	202.33	65.29	12.95	N 13.85	64.70	12.54	E 99.4
Asa-167	CH_3	CH_3	H	H	CH_3	CH_3	2	2	115—120	25—30	42.1	$C_{10}H_{24}N_2O$	188.31	63.78	12.85	N 14.89	63.79	12.91	N 14.49
Asa-178	CH_3	CH_3	H	H	C_2H_5	C_2H_5	2	2	95	2	37.9	$C_{12}H_{28}N_2O$	216.36	66.61	13.04	N 12.95	66.40	12.83	N 12.95

a) E: Percent base by perchloric acid titration.
b) pyrrolidino.

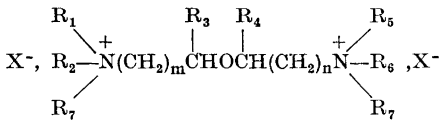
Table 2.



Code No.	R_1	R_2	Position	B.p. °C	Press. mm Hg	Yield %	Emp. formula	M	Analysis, % Calc. C	Calc. H	Calc. others	Found C	Found H	Found others
Asa-129	C_2H_5	CH_3 a)	*m*	155	2	69.9	$C_{14}H_{24}N_2O$	236.35	71.14	10.24	N 11.85	71.14	10.13	N 11.26
Asa-130	C_2H_5	C_2H_5 b)	*m*	158	2.5	62.1	$C_{16}H_{28}N_2O$	264.40	72.68	10.66	N 10.60	72.21	10.27	N 10.61
Asa-133	CH_3	C_2H_5	*p*	140	2	42.1	$C_{14}H_{24}N_2O$	236.35	71.14	10.24	N 11.85	—	—	N 11.89
Asa-134	CH_3	CH_3	*p*	169—73	18	48.9	$C_{12}H_{20}N_2O$	208.30	69.19	9.68	N 13.45	—	—	N 12.35
Asa-142	CH_3	CH_3	*m*	178—80	20	70	$C_{12}H_{20}N_2O$	208.30	69.19	9.68	N 13.45	69.35	9.63	N 11.35
														E 96.7
Asa-143	CH_3	C_2H_5	*m*	185—86	18	32	$C_{14}H_{24}N_2O$	236.35	71.14	10.24	N 11.85	70.90	10.22	N 9.93
														E 99.65

a) bis-HCl(As-12935), m.p. 184°C. Found Cl 23.01; calc. for $C_{14}H_{26}N_2OCl_2$ (309.28) Cl 22.93
b) bis-HCl(As-13036), m.p. 187°C. Found Cl 21.32; calc. for $C_{16}H_{30}N_2OCl_2$ (337.33) Cl 21.02.

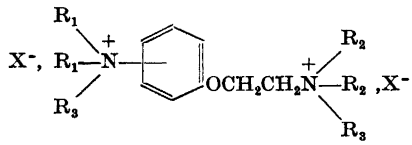
Table 3



Code No.	R_1	R_2	R_3	R_4	R_5	R_6	R_7	X^-	m	n	M.p. °C	Crystall. from [a]	Yield %	Emp. formula	M	Analysis, % Calc.		Found	
As-8558	CH_3	CH_3	CH_3	CH_3	CH_3	CH_3	CH_3	I	1	1	128—130	dil. A	84	$C_{12}H_{30}N_2OI_2$	472.21	I	53.76	I	52.10
As-8559	CH_3	CH_3	CH_3	CH_3	CH_3	CH_3	C_2H_5	Br	1	1	98—100	E-A	61	$C_{14}H_{34}N_2OBr_2$	406.27	Br	39.34	Br	38.06
As-12045	CH_3	C_2H_5	H	H	CH_3	CH_3	CH_3	I	1	1	290	E-W	66	$C_{11}H_{28}N_2OI_2$	458.18	I	55.40	I	55.09
As-12046	CH_3	C_2H_5	H	H	CH_3	CH_3	C_2H_5	Br	1	1	270—272	E-W	51	$C_{13}H_{32}N_2OBr_2$	392.24	Br	40.75	Br	40.87
As-12117	CH_3	C_2H_5	H	H	C_2H_5	C_2H_5	CH_3	I	1	1	268	A	48	$C_{13}H_{32}N_2OI_2$	486.24	I	52.20	I	52.91
As-12118	CH_3	C_2H_5	H	H	C_2H_5	C_2H_5	C_2H_5	Br	1	1	245	A	48	$C_{15}H_{36}N_2OBr_2$	420.29	Br	38.03	Br	37.15
As-12203	C_4H_8		H	H	CH_3	CH_3	CH_3	I	1	1	260—262	dil. A	98	$C_{12}H_{28}N_2OI_2$	470.19	I	53.99	I	53.55
As-12204	C_4H_8		H	H	CH_3	CH_3	C_2H_5	Br	1	1	255—256	—	87	$C_{14}H_{32}N_2OBr_2$	404.25	Br	39.56	Br	39.45
As-12305	C_4H_8		H	H	C_2H_5	C_2H_5	CH_3	I	1	1	263—266	dil. A	98	$C_{14}H_{32}N_2OI_2$	498.25	I	50.95	I	50.58
As-12306	C_4H_8		H	H	C_2H_5	C_2H_5	CH_3	Br	1	1	233	—	46	$C_{16}H_{36}N_2OBr_2$	432.30	Br	36.97	Br	36.90
As-12487	C_4H_8		H	H	C_4H_8		CH_3	I	1	1	244—246	—	100	$C_{14}H_{30}N_2OI_2$	496.20	I	51.16	I	50.33
As-12488	C_4H_8		H	H	C_4H_8		C_2H_5	Br	1	1	223—225	A-E	69	$C_{16}H_{34}N_2OBr_2$	430.29	Br	37.15	Br	36.91
As-13569	C_2H_5	n-C_3H_7	H	H	CH_3	CH_3	CH_3	I	1	1	196	E	65	$C_{13}H_{32}N_2OI_2$	486.24	I	52.20	I	52.40
As-13570	C_2H_5	n-C_3H_7	H	H	CH_3	CH_3	C_2H_5	Br	1	1	172—180	E-A-EE	47	$C_{15}H_{36}N_2OBr_2$	420.29	Br	38.03	Br	36.54
As-13671	C_2H_5	n-C_4H_9	H	H	CH_3	CH_3	CH_3	I	1	1	205	E	52	$C_{14}H_{34}N_2OI_2$	500.26	I	50.74	I	50.67
As-13672	C_2H_5	n-C_4H_9	H	H	CH_3	CH_3	C_2H_5	Br	1	1	163—166	E-A-EE	37	$C_{16}H_{38}N_2OBr_2$	434.32	Br	36.80	Br	34.88
As-16575	CH_3	CH_3	H	H	CH_3	CH_3	CH_3	I	1	2	204—206	—	82	$C_{11}H_{28}N_2OI_2$	458.18	I	55.40	I	54.76
As-16576	CH_3	CH_3	H	H	CH_3	CH_3	C_2H_5	Br	1	2	217—219	—	87	$C_{13}H_{32}N_2OBr_2$	392.24	Br	40.75	Br	40.12
As-16677	C_2H_5	C_2H_5	H	H	CH_3	CH_3	CH_3	I	1	2	244—246	—	91	$C_{13}H_{32}N_2OI_2$	486.23	I	52.21	I	51.40
As-16678	C_2H_5	C_2H_5	H	H	CH_3	CH_3	C_2H_5	Br	1	2	195—196	—	72	$C_{15}H_{36}N_2OBr_2$	420.29	Br	38.03	Br	37.88
As-16701	CH_3	CH_3	H	H	CH_3	CH_3	CH_3	I	2	2	233	E-W	62	$C_{12}H_{30}N_2OI_2$	472.21	I	53.76	I	53.50
As-16702	CH_3	CH_3	H	H	CH_3	CH_3	C_2H_5	Br	2	2	254—256	E-A	30	$C_{14}H_{34}N_2OBr_2$	406.27	Br	39.34	Br	38.67
As-17842	CH_3	CH_3	H	H	C_2H_5	C_2H_5	CH_3	I	2	2	144—145	E	70	$C_{17}H_{34}N_2OI_2$	500.26	I	50.74	I	50.31
As-17843	CH_3	CH_3	H	H	C_2H_5	C_2H_5	C_2H_5	I	2	2	201—202	E	66	$C_{16}H_{38}N_2OI_2$	528.31	I	48.05	I	46.11

[a] A: acetone; E: ethanol; W: water; dil. A. 70 % acetone dil.w.water; EE: ethyl ether; M: methanol; iso-Pr: *iso*propyl alcohol.

Table 4.



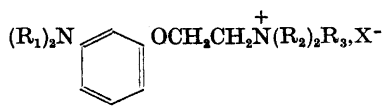
Code No.	R_1	R_2	R_3	X	Position	M.p. °C	Yield %	Emp. formula	M	Analysis, % Calc.	Found
As-12982	C_2H_5	CH_3	CH_3	I	*m*	186	80	$C_{16}H_{30}N_2OI_2$	520.26	I 48.79	I 48.31
As-13030	C_2H_5	C_2H_5	CH_3	I	*m*	158	40	$C_{18}H_{34}N_2OI_2$	548.31	I 46.29	I 45.28
As-13345	CH_3	C_2H_5	CH_3	I	*p*	200	83	$C_{16}H_{30}N_2OI_2$	520.26	I 48.79	I 48.03
As-13346	CH_3	C_2H_5	C_2H_5	I	*p*	188—90	77	$C_{18}H_{34}N_2OI_2$	548.31	I 46.29	I 45.75
As-14235	CH_3	CH_3	CH_3	I	*m*	188—94	67	$C_{14}H_{26}N_2OI_2$	492.20	I 51.57	I 50.25
As-14213	CH_3	CH_3	C_2H_5	I	*m*	115	48	$C_{16}H_{30}N_2OI_2$	520.26	I 48.79	I 48.75
As-14340	CH_3	C_2H_5	CH_3	I	*m*	175—76	74	$C_{16}H_{30}N_2OI_2$	520.26	I 48.79	I 48.23
As-14310	CH_3	C_2H_5	C_2H_5	I	*m*	153—56	—	$C_{18}H_{34}N_2OI_2$	548.31	I 46.29	I 46.17

Among the bis-quaternary salts described in the second paper of the series [1], high ganglion blocking activity was found in the asymmetric compound N,N,N,N'-tetraethyl-N',N'-dimethyl-3-oxa-pentane-1,5-diammonium di-bromide (As-4179) [5]. Because of the toxic nature of the bromide anion, it was of importance to study other salts of the biologically active ion. A number of such salts have been prepared or their preparation attempted. Most of them were not useful in that they were either deliquescent, or contained toxic anions (Table 6). One of the few salts which seemed to be of interest, was the acid tartrate (As-4137) *. This salts has been the basis of further pharmacological and clinical work [6,7].

The tartrate and the other salts were available by addition of the appropriate acid to a solution of the free alkyl ammonium hydroxide. A number of methods for the transformation of the direct products of quaternization, bromide, iodide or alkyl sulfate, into salts of any given anion have been in-

* 'Oxaditon' (Regd. Trade Mark).

Table 5.



Code No.	R_1	R_2	R_3	X	M.p. °C	Emp. formula	M	Analysis % Calc.	Found
As — 12932	C_2H_5	CH_3	CH_3	I	190	$C_{15}H_{27}N_2OI$	378.3	I 33.55	I 33.36
As — 12933	C_2H_5	CH_3	C_2H_5	Br	98	$C_{16}H_{29}N_2OBr$	345.3	Br 23.14	Br 23.05
As — 13031	C_2H_5	C_2H_5	C_2H_5	Br	135	$C_{18}H_{33}N_2OBr$	373.4	Br 21.35	Br 21.37

Table 6.

Code No.	Anion	M.p. °C	Crystall. from a)	Emp. formula	M	Analysis	Remarks
As-4194	maleate	164	M-A	$C_{22}H_{40}O_9N_2$	476.3	Ep: 94.24 b)	deliquescent
As-4193	carboxymethyl-theophyllin	210	not	$C_{32}H_{52}O_9N_{10}$	720.5	N calc. 19.52 found 19.41	decomposes when recryst.
As-4120	cinnamate	110—114	M-A	$C_{32}H_{48}O_5N_2$	540.7	—	oil after recryst.
As-4127	retene-3-sulfonate	115	E-A	$C_{50}H_{74}O_7N_4$	871.2	N calc. 3.2 found 3.05	
As-4182	bis-OH-naphthoate	272 d	not	$C_{38}H_{60}O_{13}N_2$	618.4	Ep: 100.6	
As-4176	perchlorate	220 d	EW	$C_{14}H_{34}O_9N_2Cl_2$	445.1	N calc. 6.30 found 6.19	
As-4101	D-camphorate	200	—	$C_{34}H_{64}O_5N_2$	588.6	Ep: 94.45	deliquescent
As-4122	fumarate	230	—	$C_{22}H_{40}O_9N_2$	476.3	Ep: 93.80	oil after recryst.
As-4178	monohydrogen tartrate	184	E-W	$C_{22}H_{44}O_{13}N_2,2H_2O$	580.2	C calc. 45.51 found 45.66 H calc. 7.63 found 8.18 N calc. 4.83 found 5.07	

a) *cf.* footnote to Table 3.
b) Purity % by perchloric acid titration.

vestigated. This examination shows the need for still better methods, when commercial production is contemplated and yield and other operational factors become critical. The hydroxide solution can be had by ion exchange, using a strongly basic resin (*e.g.* "Amberlite IRA-400") *, by hydrolysis of etho-

* Regd. Trade Mark of Rohm & Haas Co., Philadelphia, Penn. U.S.A.

Table 7.

$X^-,R(CH_3)_2\overset{+}{N}CH_2CH_2OCH_2CH_2\overset{+}{N}(C_2H_5)_2R,X^-$

Code No.	R	X	M.p. °C	Recryst. from a)	Yield %	Emp. formula	M	Analysis, Found	Analysis, Calc.
As-4144	CH_3	CH_3SO_4	143	E-EE	70	$C_{14}H_{36}N_2O_9S_2$	40.56	N 6.15	N 6.36
As-4124	C_2H_5	$C_2H_5SO_4$	88—90	*iso*-Pr-EE	75	$C_{18}H_{44}N_2O_9S_2$	496.67	N 5.63	N 5.64
As-4107	*n*-C_3H_7	Br	164—66	E-A(1:1)	26	$C_{16}H_{38}N_2OBr_2$	434.28	Br 36.36	Br 36.80
As-4101	*n*-C_4H_9	Br	138—40	E-A(1:1)	13	$C_{18}H_{42}N_2OBr_2$	462.37	Br 34.82	Br 34.57
As-4147	*n*-C_5H_{11}	Br	110	E-EE	20	$C_{20}H_{46}N_2OBr_2$	490.23	Br 32.21	Br 32.60
As-4148	*n*-C_6H_{13}	Br	158—60	A-E(5:1)	10	$C_{22}H_{50}N_2OBr_2$	518.47	Br 30.20	Br 30.83
As-4149	*n*-C_7H_{15}	Br	120	E-EE	14	$C_{24}H_{54}N_2OBr_2$	546.52	Br 28.90	Br 29.25
As-4159	C_2H_4OH	Br	194	E	50	$C_{14}H_{34}N_2O_3Br_2$	438.26	Br 36.18	Br 36.47
As-4182 II	C_3H_5	Br	118—24	E-A(2:1)	56	$C_{16}H_{34}N_2OBr_2$	430.27	Br 36.67	Br 37.15
As-4182 IV	$CH_2C_6H_5$	Cl	185—86	—	21	$C_{24}H_{38}N_2OCl_2$	441.47	Cl 15.98	Cl 16.06

a) *cf.* footnote to Table 3.

sulfate according to Barber and Gaimster [8], by addition of propylene oxide to an aqueous solution of the quaternary bromide and the desired acid (*cf.* Sackur [9]). A special method for transformation into chloride is that of Phillips and Baltzley [10]. The use of double decomposition with salts of aromatic acids was also explored. Since the sodium salt of retene-3-sulfonic acid is soluble, while the potassium salt is not, it was hoped that an insoluble salt of the bis-quaternary ion would form with this acid. This was, however, not the case. Similarly no sparingly soluble salt is formed with 2,2'-dihydroxy-1,1-dinaphthylmethane-3,3'-dicarboxylic acid (Barner and Gaimster's [11] "embonic acid"). Sparingly soluble salts were obtained, however, with 2,2'-dihydroxy-1,1'-dinaphthyl-3,3'-dicarboxylic acid ("bis-hydroxy-naphtoic acid" [11]) and with 4,4'-diamino-stilbene-2,2'-disulfonic acid as disclosed by Slack [12]. Tartaric acid expels these weak acids from their salts in the form of the insoluble free acid.

In view of the interesting pharmacological results obtained with the simple quaternary salts of the asymmetric base, bis-(2-diethylamino-2'-dimethylamino)-ethyl ether (Asa 41), it appeared of interest to prepare some salts containing higher alkyls as N-substituents. These salts were obtained in conventional fashion and are shown in Table 7.

Attempts to prepare the "totally asymmetric" 2-trimethylammonium-ethyl-2'-triethylammoniumethyl ether by various routes were unsuccessful. In several cases N-dialkyl morpholinium ions, however, were obtained from the reaction mixtures.

EXPERIMENTAL *

Bis-tertiary *amino ethers.* With the exceptions mentioned below these substances were obtained simply by Williamson ether condensation of the appropriate tertiary amino alcohols resp. amino halides as described earlier [1].

Bis-(2-ethylmethyl-2'-dimethyl)-aminoethyl ether

a) Bis-(2-ethyl-2'-dimethyl)-aminoethyl ether. Twenty-three grams of sodium (1 mole) was dissolved by heating in a solution of 90 g of N-ethylethanolamine in 800 ml dry toluene. Condensation with N-dimethyl-aminoethyl chloride prepared *in situ* from 144 g (1 mole) of the corresponding hydrochloride. After removal of sodium chloride and toluene the residue is distilled in vacuum to give 10 g of oil, b.p. 87—95°C/20 mm Hg. (Found: N 16.41. Calc. for $C_8H_{20}N_2O$ (160.6): N 17.48). Purity (by perchloric acid titration) 98.0 %.

b) Methylation of (a) (Eschweiler-Hess procedure) (Asa 120). To 49 g (0.3 mole) of the amine in a flask is added 45 g of 85 % formic acid (0.6 mole) at such a rate that the temperature never exceeds 60°C. After cooling to room temperature 11 g of 37 % formalin is added at once. The mixture is heated to approximately 60° at which temperature an exothermic evolution of CO_2 begins. After this has subsided the mixture is refluxed for 3 h. The mixture is made just acid with 4 N HCl and air blown through for 1 h for removal of volatile products. More HCl is added and the mixture is evaporated in vacuum till the residue is semisolid. After addition of a large excess of NaOH extraction with ether, 200 ml, three times. The residue from the dried ether is distilled. Yield: 34 g (64 %). See Table 1 for analytical data.

Bis-(2-ethylmethyl-2'-diethyl)-aminoethyl ether is obtained in essentially similar fashion from the intermediate bis(2-ethyl-2'-diethyl)-amino ethyl ether (b.p. 120°C at 20 mm Hg).

* All melting and boiling points are uncorrected. The nitrogen and halogen values are semi-micro determinations by Mrs. G. Speggers and her staff. Carbon and hydrogen values are micro determinations by Messrs. W. Egger and P. Hansen, University of Copenhagen.

Bis-(2-ethyl-*n*-propyl-2'-dimethyl)-aminoethyl ether (Asa-135)

From 32 g (0.2 mole) of bis-(2'-ethyl-2'-dimethyl)-aminoethyl ether and 25 g of *n*-propylbromide in *iso*propanol. Yield 5 g (12 %). See Table 1 for analytical data.

By substituting 27.4 g of *n*-butylbromide for the propyl bromide in the procedure given immediately above one obtains the corresponding *bis-(2-ethyl-n-butyl-2'-dimethyl)-aminoethyl ether (Asa-136)*. Yield 6 g (11 %). See Table 1 for analytical data.

Acknowledgement. The authors are pleased to acknowledge a gift of retene-3-sulfonic acid from professor H. Lund, University of Århus, Denmark, and a generous sample of N-ethylaminoethanol from Carbide & Carbon Chemicals Corporation, Geneve, Switzerland.

REFERENCES

1. Fakstorp, J., Christiansen, J. and Pedersen, J. G. A. *Acta Chem. Scand.* **7** (1953) 134.
2. Fakstorp, J. and Christiansen, J. *Ibid.* **8** (1954) 346.
3. Fakstorp, J. and Christiansen, J. *Ibid.* **8** (1954) 356.
4. Fakstorp, J. *Ibid.* **10** (1956) 15.
5. Fakstorp, J. and Pedersen, J. G. A. *Acta Pharmacol. & Toxicol.* **10** (1954) 7.
6. Fakstorp, J., Poulsen, E., Richter, W. and Schilling, M. *Ibid.* **11** (1955) 319.
7. Harvald, B. *Ugeskrift. Laeger* **117** (1955) 580.
8. Barber, H. J. and Gaimster, K. *J. Pharm. and Pharmacol.* **3** (1951) 663.
9. Sackur, O. *Bull. Soc. Chim.* [5] **19** (1952) 796.
10. Phillips, A. P. and Baltzley, R. *J. Am. Chem. Soc.* **14** (1952) 5231.
11. Barber, H. J. and Gaimster, K. *J. Appl. Chem. London* **2** (1952) 565.
12. Slack, R. Swedish Patent No. 153262.

Received August 14, 1957.

ACTA CHEMICA SCANDINAVICA 11 (1957) 1706—1723

Initial Steady State Velocities in the Evaluation of Enzyme-Coenzyme-Substrate Reaction Mechanisms

KEITH DALZIEL*

Biochemistry Department, Nobel Medical Institute, Stockholm, Sweden

The initial rate equations for a number of possible reaction sequences for enzyme-coenzyme-substrate reactions deduced by the steady state treatment are compared and contrasted.

For certain mechanisms the initial rate equations may be considered to be derived from a common equation which is most conveniently and simply expressed in terms of four kinetic coefficients. In this equation the reciprocal rate is linearly related to the reciprocal of each substrate concentration. A method for determining the kinetic coefficients from initial rate measurements, as slopes and intercepts of double plots, is described.

The distinctive Haldane relations between kinetic and equilibrium constants which exist for certain mechanisms [5] are a consequence of differences between the initial rate equations: either there are distinctive relations between the kinetic coefficients or certain of the coefficients are equal to zero. These mechanisms can sometimes be rejected on the basis of initial rate data alone, with greater certainty than by the Haldane relations.

Certain more complex mechanisms are considered which make provision for deviations from the linear reciprocal form of initial rate equation at high concentrations of one substrate. Substrate inhibition of various types may be distinguished experimentally, and a possible explanation of substrate activation is also considered.

From initial overall velocity measurements in the steady state, Theorell, Nygaard and Bonnichsen [1] were able to calculate all six rate constants in the mechanism proposed by Theorell and Chance [2] for the liver alcohol dehydrogenase reaction. There was reasonably good agreement between two of the rate constants so obtained and values determined in single reaction steps [2], and also between the equilibrium constant for the overall reaction calculated from the six rate constants and the value obtained from equilibrium measurements [3].

* Rockefeller Fellow, 1955—57; present address, Biochemistry Department, (Radcliffe Infirmary), University of Oxford.

The importance of such comparison of kinetic and equilibrium data as a test of the suitability of a postulated reaction sequence [4] was emphasized by Alberty [5], who discussed a number of possible mechanisms for enzyme-coenzyme-substrate reactions, and showed that for some the Haldane relation between the overall equilibrium constant and initial rate parameters (maximum rate and Michaelis constants) assumes a distinctive form. Theorell *et al.*[3] and Nygaard and Theorell [6] tested their data for liver and yeast alcohol dehydrogenases by means of these relations, and found the Theorell-Chance mechanism to be satisfactory for the liver enzyme but not for the yeast enzyme, and that certain other reaction sequences could be rejected in both cases.

Further kinetic studies of liver alcohol dehydrogenase [7,8] have revealed deviations from the Theorell-Chance mechanism under certain conditions. It is the purpose of the present paper to describe in general terms the theoretical basis and design of those experiments, to extend the discussion by Alberty [5] of possible mechanisms for enzyme-coenzyme-substrate reactions and of the manner in which initial rate data may be used to distinguish them, and to consider more complex reaction sequences which might account for substrate inhibition. The distinctive Haldane relations deduced by Alberty result from differences between the initial rate equations for certain mechanisms, and initial rate data alone can be used, with advantage, to distinguish these alternatives. It is of course essential that the appropriate Haldane relation also be fulfilled by the data if a particular reaction sequence is to be accepted as a satisfactory hypothesis. The relations are simplified by an alternative formulation of the initial rate equations, analogous to that of Lineweaver and Burk [9] for single-substrate reactions, but not employing Michaelis constants.

THE STEADY STATE METHOD

The steady state method [10] of deriving the relation between the initial rate, the total enzyme concentration and the initial substrate concentrations is preferable to the more restrictive equilibrium method [11] and except for one mechanism has been used throughout this paper. The assumptions involved are (i) that the enzyme concentration is small compared with the substrate concentrations (ii) that the rate of change of concentration of all enzyme-substrate complexes is zero. For initial rates the product concentrations are set equal to zero, a proceeding which has been widely adopted [4,5] if not theoretically justified [12]. To the succinct description of the steady state method given by Alberty [5] it needs only be added that in deducing the initial rate equation it is simpler to disregard all reactions involving products in setting up the rate equations for the enzyme-substrate complexes than to obtain the general rate equation and then set the product concentrations equal to zero. For single-substrate reactions, the deduction of the initial rate equation is equivalent to using the Michaelis-Menten formulation, $E + S \rightleftharpoons EX \rightarrow E + S'$, ignoring the reverse of the second step. For reactions involving a coenzyme and a substrate, however, it is not desirable to group together all steps after the formation of the ternary complex as a single step [13] as the rates of breakdown of binary enzyme-product complexes enter into the steady state expression for the initial rate, and in some cases can be evaluated from initial rate data.

THE THEORELL-CHANCE MECHANISM

Theorell and Chance [2] proposed that in the liver alcohol dehydrogenase reaction, binary compounds of enzyme and coenzyme (diphosphopyridine nucleotide) react with the substrate (alcohol or acetaldehyde) without the intervention of a rate-limiting ternary complex. If the overall reaction of coenzyme and substrate is represented in general by $S_1 + S_2 \rightleftharpoons S_1' + S_2'$, the Theorell-Chance mechanism may be written:

$$\begin{aligned} E + S_1 &\underset{k_2}{\overset{k_1}{\rightleftharpoons}} ES_1 \\ ES_1 + S_2 &\underset{k_3'}{\overset{k_3}{\rightleftharpoons}} ES_1' + S_2' \qquad \text{II (iii)} \\ ES_1' &\underset{k_1'}{\overset{k_2'}{\rightleftharpoons}} E + S_1' \end{aligned}$$

Both the coenzyme, S_1, and the substrate, S_2, will be referred to as substrates. Steady state treatment [2] yields the following relations, for the forward and reverse reactions respectively, between the total enzyme concentration e, the initial rate v_0, and the initial substrate concentrations:

$$\frac{e}{v_0} = \frac{1}{k_2'} + \frac{1}{k_1[S_1]} + \frac{1}{k_3[S_2]} + \frac{k_2}{k_1k_3[S_1][S_2]} \qquad 1(a)$$

$$\frac{e}{v_0'} = \frac{1}{k_2} + \frac{1}{k_1'[S_1']} + \frac{1}{k_3'[S_2']} + \frac{k_2'}{k_1'k_3'[S_1'][S_2']} \qquad 1(b)$$

Because of the symmetry of the mechanism and of the numbering of the rate constants, the forward and reverse initial rate equations 1(a) and 1(b) are interchangeable by the insertion or deletion of primes on the rate constants, and this will be true throughout. The reciprocal initial rate is linearly related to the reciprocal concentration of each substrate, so that if either substrate concentration is varied whilst the other is kept constant, plots according to Lineweaver and Burk [9] should be linear. If each substrate concentration is varied in turn whilst the other is kept at a sufficiently high level, the last term and either the second or third terms of the above equations will be negligible, and therefore all 6 rate constants could be determined from the slopes and intercepts of four Lineweaver-Burk plots for the forward and reverse reactions. This was in principle the method used by Theorell *et al.*[1], but because a sufficiently great concentration of the constant partner could not be used in every case, some corrections were necessary. Moreover, elimination of the last terms of 1(a) and 1(b) neglects the important relation between the last three terms of each equation and the first term of the other.

The initial rate eqns. (1) may be written in a general form:

$$\frac{e}{v_0} = \Phi_0 + \frac{\Phi_1}{[S_1]} + \frac{\Phi_2}{[S_2]} + \frac{\Phi_{12}}{[S_1][S_2]} \qquad (2)$$

for the forward reaction; for the reverse reaction, the coefficients will be distinguished by primes. Comparison of eqns. (1) and (2) shows that there are complementary relationships between the kinetic coefficients of the forward and reverse reactions:

$$\Phi_0' = \Phi_1\Phi_2/\Phi_{12} \qquad 3(a)$$

$$\Phi_0 = \Phi_1'\Phi_2'/\Phi_{12}' \qquad 3(b)$$

These relations distinguish the Theorell-Chance mechanism from others which conform to (2). To test them, all 4 coefficients for the forward and reverse reaction must be determined; the determination of Φ_{12} and Φ_{12}' requires initial rate measurements with low concentrations of both substrates.

It can be shown that the overall equilibrium constant is equal to two functions of the kinetic coefficients (Haldane relations):

$$K_{Eq} = \Phi_{12}'/\Phi_{12} \qquad (4)$$

$$K_{Eq} = \Phi_0'\Phi_1'\Phi_2'/\Phi_0\Phi_1\Phi_2 \qquad (5)$$

Other mechanisms which conform to (2) also conform to (4), but (5) is distinctive for the Theorell-Chance mechanism (*cf.* Alberty [5], eqn. 9) and is a consequence of relations 3(a) and 3(b) between the coefficients. If experimental data conform to (4) but not to (5), either 3(a) or 3(b), or both, will not be satisfied. These latter relations are a more sensitive test than (5) because they involve fewer experimental quantities, do not involve separate equilibrium measurements, and are independent of one another, whereas (5) is a resultant of both of them.

GENERAL FORM OF THE INITIAL RATE EQUATION

It will be seen that the initial rate equations for a number of other mechanisms may also be considered as special cases of eqn. (2), and that certain of these mechanisms may be distinguished by the fact that one or more of the kinetic coefficients is equal to zero, or, as in the case of the Theorell-Chance mechanism, by a relation between the coefficients.

Initial rate equations are usually, but not always [13], formulated in terms of Michaelis constants, defined as the concentration of the substrate which gives half the maximum rate approached asymptotically with increase of substrate concentration [4]. With this definition, the steady state treatment [10,4] of single-substrate reaction mechanisms in which one or two intermediate enzyme-substrate compounds are postulated gives the same initial rate equation as the equilibrium teatment, *viz.* the Michaelis-Menten equation. For two-substrate reactions, the Michaelis constant for each substrate varies with the concentration of the other [4,2]. Alberty [5] defines the Michaelis constant in this case as the concentration which gives half the maximum rate approached with increase of *both* substrate concentrations, and obtains by steady state treatment of several possible mechansims an initial rate equation analogous to that of Michaelis and Menten [11]:

$$v_0 = \frac{V}{1 + \frac{K_1}{[S_1]} + \frac{K_2}{[S_2]} + \frac{K_{12}}{[S_1][S_2]}} \qquad (6)$$

V is the maximum rate and K_1 and K_2 are the Michaelis constants for S_1 and S_2. K_{12} is a new kinetic constant [5]. This equation is equivalent to eqn. (2).

The Michaelis constant has its original theoretical significance as the dissociation constant of a compound of the substrate with the enzyme only when the relative reaction rates are such that the compound can be assumed to be in equilibrium throughout with the free substrate and enzyme. This is true for two-substrate reactions also, the dissociation in this case being from the ternary complex [13] (Mechanism I below). With the less restrictive steady state assumption, the Michaelis constant has no obvious physical significance. For a single-substrate reaction in which one intermediate enzyme complex is postulated, it is still a simple function of rate constants relating to the substrate and its enzyme compound [10]. When more than one intermediate enzyme compound is postulated [4] and for two-substrate reaction mechanisms in general [5], the Michaelis constant of a substrate is a more or less complex function of several rate constants, some of which relate to reaction steps not involving either the free or bound substrate [2,14]. In the initial rate equation for one mechanism discussed by Alberty, and considered to be a special case of (6), V, K_1, and K_2 do not conform to the definitions given above, and this seems to have led to an erroneous formulation of the kinetic expression for the equilibrium constant (Alberty [5]: mechanism I (6), eqns. (11) and (12)).

Equation (2) is analogous to that of Lineweaver and Burk [9] for single-substrate reactions, which could be written $e/v_0 = \Phi_0 + (\Phi_1/[S_1])$. The coefficients are simpler functions of the rate constants than are Michaelis constants, and can be determined as slopes and intercepts by an extension of the Lineweaver-Burk plot (*vide infra*). Φ_0 has the dimension of a reciprocal first order rate constant, and is equal to the reciprocal of the maximum rate with unit enzyme concentration, or the reciprocal of the maximum turnover number. Φ_1 and Φ_2 are equivalent to reciprocal second-order rate constants, and are related to the Michaelis constants, as defined by Alberty [5], by $\Phi_1/\Phi_0 = K_1$ and $\Phi_2/\Phi_0 = K_2$. Φ_{12} has the dimension of a third order rate constant, and $\Phi_{12}/\Phi_0 = K_{12}$ in Alberty's equation.

EXPERIMENTAL DETERMINATION OF THE KINETIC COEFFICIENTS

Rearrangement of eqn. (2) gives:

$$\frac{e}{v_0} = \Phi_0 + \frac{\Phi_2}{[S_2]} + \left(\Phi_1 + \frac{\Phi_{12}}{[S_2]}\right)\frac{1}{[S_1]}$$

If a series of initial rate measurements is made with a constant initial concentration of S_2 (not necessarily large) and different concentrations of S_1, a plot [9] of e/v_0 against $1/[S_1]$ should give a straight line, with both slope and intercept linear functions of $1/[S_2]$. If several such series of initial rate measurements are made, each with a different constant value of $[S_2]$, the slopes and intercepts of the primary plots may be plotted against $1/[S_2]$, to give the 4 coefficients directly as slopes and intercepts, thus:

Secondary plots of intercepts: slope $= \Phi_2$, intercept $= \Phi_0$.
Secondary plots of slopes: slope $= \Phi_{12}$, intercept $= \Phi_1$.

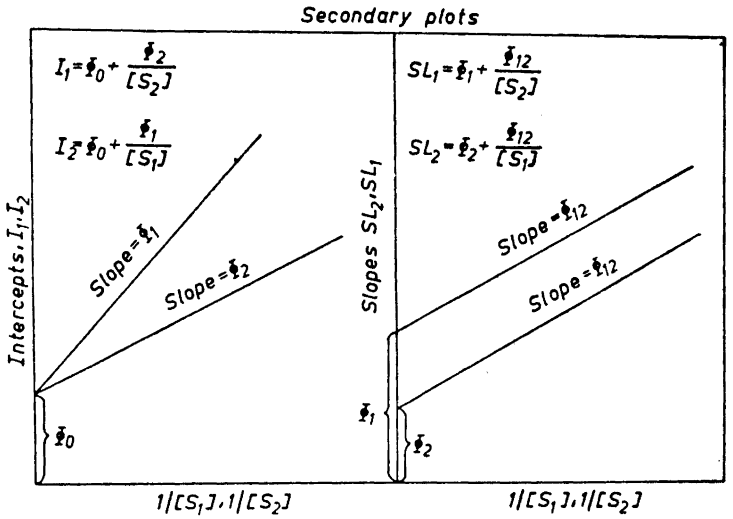


Fig. 1. Illustration of the determination of the kinetic coefficients of eqn. (2) by secondary plots of slopes and intercepts of primary Lineweaver-Burk plots.

The initial rate eqn. (2) is symmetrical in $[S_1]$ and $[S_2]$, and $[S_2]$ could equally well be chosen as the variable in the primary plots, and $[S_1]$ as the variable in the secondary plots. If say 5 different concentrations of both substrates are used, the 25 initial rate measurements may be plotted in both ways, thereby grouping them in different sets of 5 for the primary plots. Two sets of values for the 4 coefficients will be obtained from the secondary plots, as illustrated in Fig. 1.

This procedure seems to make the best use of the data, and is a generalisation of those described by Schwert and Hakala [15], Hakala, Glaid and Schwert [16] and Alberty [5]. It has the advantage of giving all the coefficients in the initial rate equation directly, but it depends upon initial rate measurements with low concentrations of both substrates. Accurate data can only be obtained under these conditions if a sensitive method of analysis is available, so that small enzyme concentrations can be used and measurements made over a small fraction of the total reaction to equilibrium.

DISCUSSION OF MECHANISMS CONFORMING TO EQUATION (2)

The most obvious general mechanism for an enzyme-catalysed reaction $S_1 + S_2 \rightleftharpoons S_1' + S_2'$ is one in which both substrates form binary compounds with the enzyme, providing two alternative pathways for the formation of a ternary complex, which undergoes intramolecular transformation (see I, below). The steady state treatment of this mechanism does not give an initial rate equation of the simple form of (2)[13]. Less complex mechanisms which do [5] may be divided into four types according to the simplifying assumptions. The coefficients in the initial rate eqn. (2) in terms of the rate constants or equilibrium constants for the cases to be discussed are given in Table 1,

Table 1. Initial rate equations (steady state) and Haldane relations for possible mechanisms for an enzyme-catalysed reaction $S_1+S_2 \rightleftharpoons S_1'+S_2'$.

General initial rate equation: $\frac{e}{v_0} = \Phi_0 + \frac{\Phi_1}{[S_1]} + \frac{\Phi_2}{[S_2]} + \frac{\Phi_{12}}{[S_1][S_2]}$

(For description of mechanisms, see text. Only the kinetic coefficients for the forward reactions are given; those for the reverse reaction, denoted by primes, are obtained by inserting or deleting primes on the rate constants.)

Mechanism	Kinetic coefficients				Relations between coefficients	Haldane relation
	Φ_0	Φ_1	Φ_2	Φ_{12}		K_{Eq}
I(a)	$\frac{1}{k}$	$\frac{K_4}{k}$	$\frac{K_3}{k}$	$\frac{K_1K_3}{k}$		$\frac{\Phi_{12}'}{\Phi_{12}}$
I(b)	$\frac{1}{k}$	$\frac{K_4}{k}$	$\frac{K_3}{k}$	$\frac{K_3K_4}{k}$	$\frac{\Phi_1\Phi_2}{\Phi_{12}} = \Phi_0$	$\frac{\Phi_{12}'}{\Phi_{12}} = \frac{\Phi_0\Phi_1'\Phi_2'}{\Phi_0'\Phi_1\Phi_2}$
II(i)	$\frac{1}{k_2'}+\frac{1}{k_4'}+\frac{1}{k}+\frac{k'}{kk_4'}$	$\frac{1}{k_1}$	$\frac{k_4k_4'+k_4k'+k_4'k}{k_3k_4'k}$	$\frac{k_2(k_4k_4'+k_4k'+k_4'k)}{k_1k_3k_4'k}$	$\frac{\Phi_1\Phi_2}{\Phi_{12}} < \Phi_0'$	$\frac{\Phi_{12}'}{\Phi_{12}}$
II(ii,a)	$\frac{1}{k_2'}+\frac{1}{k_4'}$	$\frac{1}{k_1}$	$\frac{k_4+k_4'}{k_3k_4'}$	$\frac{k_2(k_4+k_4')}{k_1k_3k_4'}$	$\frac{\Phi_1\Phi_2}{\Phi_{12}} < \Phi_0'$	$\frac{\Phi_{12}'}{\Phi_{12}}$
II(ii,b)	$\frac{1}{k_2'}$	$\frac{1}{k_1}$	$\frac{k_4+k_4'}{k_3k_4'}$	$\frac{k_2(k_4+k_4')}{k_1k_3k_4'}$	$\frac{\Phi_1\Phi_2}{\Phi_{12}} = \Phi_0'$	$\frac{\Phi_{12}'}{\Phi_{12}} = \frac{\Phi_0'\Phi_1'\Phi_2'}{\Phi_0\Phi_1\Phi_2}$
II(iii)	$\frac{1}{k_2'}$	$\frac{1}{k_1}$	$\frac{1}{k_3}$	$\frac{k_2}{k_1k_3}$	$\frac{\Phi_1\Phi_2}{\Phi_{12}} = \Phi_0'$	$\frac{\Phi_{12}'}{\Phi_{12}} = \frac{\Phi_0'\Phi_1'\Phi_2'}{\Phi_0\Phi_1\Phi_2}$
III	$\frac{1}{k_4'}$	0	0	$\frac{k_4+k_4'}{k_3k_4'}$	—	$\frac{\Phi_{12}'}{\Phi_{12}}$
IV(i)	$\frac{1}{k_2'}+\frac{1}{k_4'}$	$\frac{k_2+k_2'}{k_1k_2'}$	$\frac{k_4+k_4'}{k_3k_4'}$	0	—	$\frac{\Phi_1'\Phi_2'}{\Phi_1\Phi_2}$
IV(ii)	0	$\frac{1}{k_1}$	$\frac{1}{k_2}$	0	—	$\frac{\Phi_1'\Phi_2'}{\Phi_1\Phi_2}$

together with the Haldane relations between the kinetic coefficients and the overall equilibrium constant, and in some instances relations between the kinetic coefficients themselves. Only the forward initial rate coefficients are given; the expressions for the reverse coefficients are obtained by inserting or deleting primes on the rate constants.

Type I. Four binary and two ternary enzyme complexes are in rapid equilibrium with the free substrates, so that the intramolecular reaction of the ternary complex is the rate-limiting step:

$$\begin{array}{llll} E + S_1 \rightleftharpoons ES_1 & (K_1) & ES_1' \rightleftharpoons E + S_1' & (K_1') \\ E + S_2 \rightleftharpoons ES_2 & (K_2) & ES_2' \rightleftharpoons E + S_2' & (K_2') \\ ES_1 + S_2 \rightleftharpoons ES_1S_2 & (K_3) & ES_1'S_2' \rightleftharpoons ES_1' + S_2' & (K_3') \\ ES_2 + S_1 \rightleftharpoons ES_1S_2 & (K_4) & ES_1'S_2' \rightleftharpoons ES_2' + S_1' & (K_4') \end{array} \qquad \text{I}$$

$$ES_1S_2 \underset{k'}{\overset{k}{\rightleftharpoons}} ES_1'S_2'$$

The equilibrium treatment of Michaelis and Menten [11] will be valid and gives the initial rate in terms of the dissociation constants of the enzyme complexes and the rate constants of the intramolecular reaction (Table 1).

(a) In the general case, there are 6 independent dissociation constants, since $K_1K_3 = K_2K_4$, and $K_1'K_3' = K_2'K_4'$. All 8 dissociation constants and the two rate constants may be calculated if the 8 kinetic coefficients for the forward and reverse reactions are determined. The Haldane relation $K_{Eq} = \Phi_{12}'/\Phi_{12}$ is common to this and several other mechanisms, but for this mechanism there is no relation between the coefficients themselves. Since this is the most complicated mechanism considered here, it would only be adopted if all the others had to be rejected. Mechanisms *II* (i) and II (ii, a) differ from it only in that they require the limiting relations $\Phi_0' > \Phi_1\Phi_2/\Phi_{12}$ and $\Phi_0 > \Phi_1'\Phi_2'/\Phi_{12}'$. The conclusion of Alberty [5] that these three mechanisms cannot be distinguished by initial rate data alone is valid only if these limiting relations are fulfilled.

The maximum rates are $1/\Phi_0 = k$ and $1/\Phi_0' = k'$, and the condition that this mechanism give linear reciprocal plots is that these rates be small compared with those of the other reaction steps. If one of the latter is accessible to direct measurement, it may be possible to test this condition; for example, the spectral shift, which accompanies the combination of reduced diphosphopyridine nucleotide with liver alcohol dehydrogenase [3] made it possible to study this step in isolation [2]. Also, the results of ultracentrifuge studies of enzyme-substrate compounds [17] may be compared with the apparent dissociation constants calculated from initial rate measurements [18].

(b) In the special case that the combination of the enzyme with one substrate does not influence its affinity for the other[19], then $K_1 = K_4$, $K_2 = K_3$, *etc.*, and there are only 4 independent dissociation constants. There is then a relation between the 4 kinetic coefficients for the reaction in each direction, $\Phi_0 = \Phi_1\Phi_2/\Phi_{12}$, which distinguishes the mechanism from all the others considered, and can be used to test the forward and reverse reactions separately. In consequence also, there is an additional distinctive Haldane relation, $K_{Eq} = \Phi_0\Phi_1'\Phi_1'/\Phi_0'\Phi_1\Phi_2$.

Type II. Only one of the substrates, in each direction, forms a binary enzyme compound, so that there is a compulsory order of reaction.

(i) Two ternary complexes:

$$\begin{array}{c} \mathrm{E} + \mathrm{S_1} \underset{k_2}{\overset{k_1}{\rightleftharpoons}} \mathrm{ES_1} \\ \mathrm{ES_1} + \mathrm{S_2} \underset{k_4}{\overset{k_3}{\rightleftharpoons}} \mathrm{ES_1S_2} \underset{k'}{\overset{k}{\rightleftharpoons}} \mathrm{ES_1'S_2'} \underset{k_3'}{\overset{k_4'}{\rightleftharpoons}} \mathrm{ES_1'} + \mathrm{S_2'} \\ \mathrm{ES_1'} \underset{k_1'}{\overset{k_2'}{\rightleftharpoons}} \mathrm{E} + \mathrm{S_1'} \end{array} \qquad \text{II(i)}$$

This and the following mechanisms give an initial rate equation of the form of (2) by steady state treatment. The expressions given by Alberty [5] for Michaelis constants and maximum rates in terms of the rate constants in the

mechanism are incorrect. The 10 rate constants cannot all be calculated from the 8 kinetic coefficients for the forward and reverse reactions.

(ii) One ternary complex:

$$\begin{gathered} E + S_1 \underset{k_2}{\overset{k_1}{\rightleftharpoons}} ES_1 \\ ES_1 + S_2 \underset{k_4}{\overset{k_3}{\rightleftharpoons}} EXY \underset{k_3'}{\overset{k_4'}{\rightleftharpoons}} ES_1' + S_2' \qquad \text{II(ii)} \\ ES_1' \underset{k_1'}{\overset{k_2'}{\rightleftharpoons}} E + S_1' \end{gathered}$$

(a) In the general case the 8 rate constants could all be calculated from the kinetic coefficients. This mechanism was the basic one assumed by LuValle and Goddard [20] in their discussion of enzyme oxidation-reduction mechanisms.

(b) In the special case that $k_4 \gg k_2$ and $k_4' \gg k_2'$, the maximum rate becomes equal to the rate of the last step *i.e.* $\Phi_0 = 1/k_2'$, $\Phi_0' = 1/k_2$, and there are relations between the kinetic coefficients identical with those for the Theorell-Chance mechanism. But Φ_2 remains a function of k_3, k_4 and k_4', although these rate constants cannot now be separately evaluated from the coefficients.

(iii) No ternary complex. This is the Theorell-Chance mechanism described previously.

These mechanisms of Type II have the following features in common.

1. The Haldane relationship, $K_{Eq} = \Phi_{12}'/\Phi_{12}$.
2. The rate constants for the formation and dissociation of the binary complex are given by $k_1 = 1/\Phi_1$ and $k_2 = \Phi_{12}/\Phi_1\Phi_2$, and its dissociation constant by Φ_{12}/Φ_2.
3. Φ_0' cannot be less than $\Phi_1\Phi_2/\Phi_{12}$, since the maximum rate cannot exceed the rate of the last step.

These three mechanisms are not in fact alternatives in a practical sense. Cases (i) and (ii, a) cannot be distinguished, and the second with 8 calculable rate constants would be preferred. Case (iii), in which no ternary complex is included, cannot be distinguished by initial rate measurements of the type considered here from (ii, b), in which the dissociation rate of the ternary complex is fast enough not to limit the maximum rate. The postulate of Theorell and Chance [2] was not intended to explicitly exclude a ternary complex. There is no direct evidence for the formation of a ternary enzyme complex, but it has generally been thought likely [20], and the recent work of Vennesland and Westheimer [21] makes it probable in the dehydrogenase reactions involving diphosphopyridine nucleotide. Case (ii, b) would therefore be a preferable hypothesis to (iii), although it is not possible to calculate k_3 and k_3' individually, but only as functions of k_4 and k_4' (Table 1). Recently Alberty [22] has shown that it may be possible to distinguish mechanisms (ii,b) and (iii) by initial rate measurements with product S_2' present at the start.

Type III. There are no binary complexes; a ternary complex is formed by a termolecular reaction:

$$E + S_1 + S_2 \underset{k_4}{\overset{k_3}{\rightleftharpoons}} EXY \underset{k_3'}{\overset{k_4'}{\rightleftharpoons}} E + S_1' + S_2'$$

Two of the terms in the initial rate eqn. (2) are zero. The intercepts of Lineweaver-Burk plots are independent of the concentration of the constant partner. The mechanism can therefore be distinguished from the others considered, although there is no distinctive Haldane relation. All the rate constants can be calculated from initial rate measurements in both directions.

Type IV. The enzyme reacts with each substrate in turn to form a product, itself undergoing intermediate chemical change, *e.g.* oxidation and reduction. Such a mechanism is in principle open to direct test with stoichiometric proportions of enzyme and one substrate.

(i) Binary enzyme-substrate compounds are formed:

$$E + S_1 \underset{k_2}{\overset{k_1}{\rightleftharpoons}} EX \underset{k_1'}{\overset{k_2'}{\rightleftharpoons}} E' + S_1'$$

$$E' + S_2 \underset{k_4}{\overset{k_3}{\rightleftharpoons}} E'Y \underset{k_3'}{\overset{k_4'}{\rightleftharpoons}} E + S_2' \qquad \text{IV(i)}$$

In recent practical considerations of this mechanism [5,1,6] the fact that it is distinguished from the preceding ones by the absence of the last term of equation (2) from the initial rate equation, as well as by a distinctive Haldane relationship, seems to have been overlooked. The Haldane relationship differs from those for Mechanisms I(b), II(ii, b) and II(iii) only by the ratio Φ_0'/Φ_0 or its reciprocal, so that these mechanisms cannot be distinguished by the Haldane relationship when the forward and reverse maximum rates are about the same.

(ii) No enzyme-substrate compounds:

$$E + S_1 \underset{k_1'}{\overset{k_1}{\rightleftharpoons}} E' + S_1'$$

$$E' + S_2 \underset{k_2'}{\overset{k_2}{\rightleftharpoons}} E + S_2' \qquad \text{IV (ii)}$$

Since there are no enzyme-substrate compounds, the initial rate increases indefinitely with increase of substrate concentration. The slopes of Lineweaver—Burk plots will be independent of the concentration of the constant partner. The intercepts will be inversely proportional to the concentration of the constant partner, and the secondary plots of the intercepts will therefore pass through the origin. The Haldane relation given by Alberty [5], which apparently distinguishes this case from the preceding one, is indeterminate. The correct Haldane relation is the same as that for the preceding case.

APPLICATION

Sufficient experimental data for the application of the principles discussed appears to be available for only three enzymes. Two of these will be considered briefly; the third, liver alcohol dehydrogenase, will be discussed in detail elsewhere [8].

Yeast alcohol dehydrogenase. Application of the Haldane relations of Alberty [5] to initial rate and equilibrium data at pH 6.0 and pH 7.15 enabled Nygaard and Theorell [6] to show that the rapid equilibrium mechanism I(a) was a satisfactory hypothesis for the yeast alcohol dehydrogenase relation, and that the special case of this mechanism, I(b) and the Theorell-Chance mechanism, could be rejected. As regards the "enzyme oxidation" mechanism IV(i), it was considered that the discrepancy of 60 % between the value of the equilibrium constant calculated from the appropriate Haldane relationship, and the direct value, was not outside the possible combined experimental error in the kinetic constants involved, but this mechanism was rejected on other grounds. The preceding discussion permits extension of these arguments.

Values for the kinetic coefficients and a distinctive function of the coefficients (Table 1) are shown in Table 2. Mechanism IV(i) requires $\Phi_{12} = \Phi_{12}' = 0$, so that this possibility can be rejected from the kinetic data alone. The Theorell-Chance mechanism can be rejected by discrepancies from the required relations between the kinetic coefficients $\Phi_0 = \Phi_1'\Phi_2'/\Phi_{12}'$ and $\Phi_0' = \Phi_1\Phi_2/\Phi_{12}$ (primes denote coefficients for the DPN + C_2H_5OH reaction).

Mechanism I(a) was satisfactory as regards the values of $K_{Eq} = 0.81$ and 1.1×10^{-11} M, calculated from the appropriate Haldane relationship, which agree well with the directly determined value of 0.9×10^{-11} M, but the same Haldane relation is also fulfilled by the simpler mechanisms II(i) and II(ii) (*cf.* Table 1) which were not considered by Nygaard and Theorell [6]. The data of Table 2 show, however, that $\Phi_0 < \Phi_1'\Phi_2'/\Phi_{12}'$ at both the pH values, which is contrary to the requirements of Mechanisms II(i) and II(ii). This same discrepancy from the requirements of all Type II mechanisms has recently been observed with liver alcohol dehydrogenase at pH 7.15 [7, 8].

The special case of the rapid equilibrium mechanism, I(b), was rejected because the appropriate Haldane relation gave values of $K_{Eq} = 4.5$ and 18×10^{-11}. This mechanism also requires that $\Phi_0' = \Phi_1'\Phi_2'/\Phi_{12}'$ and $\Phi_0 =$

Table 2. Kinetic coefficients for yeast alcohol dehydrogenase, 23°C, calculated from the data of Theorell and Nygaard [6]

Substrates	Φ_0 sec.	Φ_1 μM sec.	Φ_2 μM sec.	Φ_{12} μM^2 sec.	$\Phi_1\Phi_2/\Phi_{12}$ sec.
pH 6.0					
DPNH, CH_3CHO (Φ)	0.0027	0.063	0.79	3.4	0.014
DPN, C_2H_5OH (Φ')	0.026	4.2	2.6×10^3	4.2×10^5	0.026
pH 7.15					
DPNH, CH_3CHO (Φ)	0.002	0.077	1.12	11.2	0.008
DPN, C_2H_5OH (Φ')	0.016	0.94	2.95×10^2	6.9×10^4	0.004

$\Phi_1\Phi_2/\Phi_{12}$. At pH 6.0 the first of these relations is satisfied, but the second is not and accounts for the whole of the discrepancy of a factor of 5 in the Haldane relation. Thus, Mechanism I(b) is satisfactory for the alcohol-DPN reaction, but not for the aldehyde-DPNH reaction, *i.e.* if mechanism I(a) is accepted, it can also be assumed that at pH 6 the combination of the enzyme with either DPN or alcohol does not affect its affinity for the other. At pH 7.15 this additional assumption is not valid.

Lactic dehydrogenase. From tests of initial rate data with the Haldane relations of Alberty, Hakala *et al.*[16] concluded that the Theorell-Chance mechanism and the enzyme oxidation mechanism could be rejected, and that any of the ternary complex mechanisms I, II(i) and II(ii, a) were satisfactory. Examination of their data shows that the limiting relations between the kinetic coefficients required by mechanisms II(i) and II(ii, a) are also satisfied, so that no further conclusions can be drawn, except that the special case I(b) is not satisfactory for either the forward or reverse reactions.

SUBSTRATE INHIBITION

Deviations from the linear reciprocal form of initial rate equation at high substrate concentrations are common. Liver alcohol dehydrogenase [1,2] and lactic dehydrogenase [16] show substrate inhibition with high concentrations of alcohol and pyruvate, respectively. With yeast alcohol dehydrogenase on the other hand, deviation towards higher activity occur at high alcohol concentrations [6]. In cases such as lactic dehydrogenase where the reaction conforms, at low substrate concentrations, to the requirements of a Type II mechanism, in which there is a compulsory order of reaction of the two substrates with the enzyme, inhibition at high concentrations of the second substrate might be accounted for by combination of the latter with the enzyme and/or with the active ternary complex to form inactive compounds. It will be seen that the effects of such substrate inhibition on Lineweaver-Burk plots with respect to the first substrate are to a large extent analogous to the effects of inhibition in single-substrate reactions, and competitive, uncompetitive and non-competitive types may be distinguished. At present there does not appear to be sufficiently detailed data available to test these mechanisms, but the treatment may serve as a guide in the planning of further experiments.

Competitive substrate inhibition. The second substrate forms an inactive binary complex with the enzyme:

$$\mathrm{E} + \mathrm{S}_2 \rightleftharpoons \mathrm{ES}_2 \quad (K_I)$$

$$\mathrm{E} + \mathrm{S}_1 \underset{k_2}{\overset{k_1}{\rightleftharpoons}} \mathrm{ES}_1$$

$$\mathrm{ES}_1 + \mathrm{S}_2 \underset{k_3'}{\overset{k_3}{\rightleftharpoons}} \mathrm{ES}_1' + \mathrm{S}_2'$$

$$\mathrm{ES}_1' \underset{k_1'}{\overset{k'_2}{\rightleftharpoons}} \mathrm{E} + \mathrm{S}_1'$$

$$\mathrm{ES}_2' \rightleftharpoons \mathrm{E} + \mathrm{S}_2'$$

The last step will not influence the initial rate of the forward reaction, nor the first step that of the reverse reaction.

Steady state treatment gives for the forward reaction:

$$\frac{e}{v_0} = \frac{1}{k_2'} + \left(1 + \frac{[S_2]}{K_I}\right)\frac{1}{k_1[S_1]} + \frac{1}{k_3[S_2]} + \left(1 + \frac{[S_2]}{K_I}\right)\frac{k_2}{k_1k_3[S_1][S_2]} \quad (7)$$

$$= \Phi_0 + \left(1 + \frac{[S_2]}{K_I}\right)\frac{\Phi_1}{[S_1]} + \frac{\Phi_2}{[S_2]} + \left(1 + \frac{[S_2]}{K_I}\right)\frac{\Phi_{12}}{[S_1][S_2]} \quad (8)$$

$$= \left(\Phi_0 + \frac{\Phi_2}{[S_2]}\right) + \left(1 + \frac{[S_2]}{K_I}\right)\left(\Phi_1 + \frac{\Phi_{12}}{[S_2]}\right)\frac{1}{[S_1]} \quad (8a)$$

Intercept Slope

The Φ coefficients have the same significance in terms of rate constants as in the simple Theorell-Chance mechanism (Table 1, II (iii)), and K_I is the dissociation constant of the inactive complex. If one or two ternary complexes are postulated, eqn. (8) is also valid, and the Φ coefficients are identical with those for mechanisms II(i) and II(ii), respectively. If the inhibition factor is replaced by $\left(1 + \frac{[I]}{K_I}\right)$, eqn. (8) is quite general [13] for an inhibitor which competes with S_1 and includes the case when product S_1' (but not S_2') is present at the start [22].

With low concentrations of S_2 such that (i) $[S_2]/K_I \ll 1$, eqn. (8) reduces to eqn. (2), and initial rate data will conform to the requirements of the corresponding Type II mechanism. Plots of e/v_0 against $1/[S_2]$ will be linear only when (i) holds, and at some higher value of $[S_2]$ which will depend upon $[S_1]$, e/v_0 will pass through a minimum. Plots of e/v_0 against $1/[S_1]$ will be linear for all values of $[S_2]$ (eqn. 8a), and as in Lineweaver-Burk plots for a single-substrate reaction with competitive inhibition, the slope is increased by the inhibition factor but the intercept is unaffected. Φ_0 and Φ_2 can therefore be determined by a secondary plot of the intercepts against $1/[S_2]$. The slope is not a linear function of $1/[S_2]$ except when (i) holds, and will have a minimum value when (ii) $[S_2]^2 = \Phi_{12}K_I/\Phi_1$, as shown by differentiation. Theoretically Φ_1 and Φ_{12} can be obtained in the usual way by a secondary plot of the slope against $1/[S_2]$ for low values of $[S_2]$ such that (i) holds, and K_I can then be calculated from the value of $[S_2]$ at which the slope is minimum by (ii). However, the upper limit imposed on $[S_2]$ by (i) will make it difficult to get accurate values of Φ_1 in this way unless $\Phi_1 > \Phi_{12}/K_I$ (*i.e.* $K_I > k_2/k_3$), since otherwise Φ_1 will be negligible compared with $\Phi_{12}/[S_2]$ over the whole linear range. If the expression for the slope of equation (8a) is rearranged thus,

$$\text{Slope} = \Phi_1 + \frac{\Phi_{12}}{K_I} + \frac{\Phi_1[S_2]}{K_I} + \frac{\Phi_{12}}{[S_2]}$$

it is seen that a plot of the reciprocal of the slope against $-\log [S_2]$ over a wide range of the latter should give a bell-shaped curve, from which Φ_1, Φ_{12} and K_I could be determined by the method employed by Alberty and Massey [23]

to calculate the acid dissociation constants of an enzyme-substrate complex and the pH-independent maximum velocity [24].

When the inhibitor is not a substrate, the determination of the kinetic coefficients and the inhibition constant is obvious. The case in which S_1' is present at the start, when $K_I = k_2'/k_1'$, is discussed by Alberty [22].

Uncompetitive substrate inhibition. In single-substrate reactions, the effect of an inhibitor which combines with the enzyme-substrate complex but not with the free enzyme is to increase the intercept of the Lineweaver-Burk plot without affecting the slope, and this type of inhibition has been termed uncompetitive [25]. Haldane [4] discussed substrate inhibition of this kind, in which a second molecule of the substrate combines with the enzyme-substrate complex to form an inactive compound. An analogous situation in two-substrate systems would be the combination of a second molecule of one substrate with the ternary complex in mechanism II(ii) to give an inactive compound:

$$E + S_1 \underset{k_2}{\overset{k_1}{\rightleftharpoons}} ES_1$$

$$ES_1 + S_2 \underset{k_4}{\overset{k_3}{\rightleftharpoons}} EXY$$

$$EXY + S_2 \rightleftharpoons EXYS_2 \quad (K_I')$$

$$EXY \underset{k_3'}{\overset{k_4'}{\rightleftharpoons}} ES_1' + S_2'$$

$$ES_1' \underset{k_1'}{\overset{k_2'}{\rightleftharpoons}} E + S_1'$$

Steady state treatment of this mechanism gives, for the forward reaction

$$\frac{e}{v_0} = \frac{1}{k_2'} + \left(1 + \frac{[S_2]}{K_I'}\right)\frac{1}{k_4'} + \frac{1}{k_1[S_1]} + \frac{k_4+k_4'}{k_3k_4'[S_2]} + \frac{k_2(k_4+k_4')}{k_1k_3k_4'[S_1][S_2]} \quad (9)$$

$$= \Phi_0 + \frac{[S_2]}{K_I'k_4'} + \frac{\Phi_1}{[S_1]} + \frac{\Phi_2}{[S_2]} + \frac{\Phi_{12}}{[S_1][S_2]} \quad (10)$$

$$= \left(\Phi_0 + \frac{[S_2]}{K_I'k_4'} + \frac{\Phi_2}{[S_2]}\right) + \left(\Phi_1 + \frac{\Phi_{12}}{[S_2]}\right)\frac{1}{[S_1]} \quad (11)$$

The Φ coefficients are identical with those for mechanism II (ii,a), (Table 1) and K_I' is the dissociation constant of the inactive complex. With low concentrations of S_2, such that $[S_2]/K_I'k_4' \ll \Phi_0$, the initial rate data will conform to the requirements of mechanism II(ii). With higher concentrations of S_2, plots of e/v_0 against $1/[S_2]$ will pass through a minimum. As for competitive substrate inhibition, plots of e/v_0 against $1/[S_1]$ will be linear for all values of $[S_2]$. In contrast to the preceding case, however, the slope is not affected by the inhibition term, and will yield values of Φ_1 and Φ_{12} by a secondary plot against $1/[S_2]$, whilst the intercept is no longer linear in $1/[S_2]$. A secondary

plot of the intercept against $1/[S_2]$ for low values of $[S_2]$, such that $[S_2]/K_I'k_4' \ll \Phi_0$, would give Φ_0 as intercept and Φ_2 as slope and at higher values of $[S_2]$ there will be a minimum value of the intercept when $[S_2]^2 = \Phi_2 K_I'k_4'$, from which $K_I'k_4'$ could be calculated. Alternatively, a plot of the reciprocal of the intercept against $-\log[S_2]$ should give a bell-shaped curve from which Φ_0, Φ_2 and $K_I'k_4'$ could be determined [4,23]. Since k_4' can be calculated from the coefficients for the forward and reverse reactions taken together ($\Phi_0 = (k_2' + k_4'/k_2'k_4'$; $k_2' = \Phi_{12}'/\Phi_1'\Phi_2'$), K_I' can be evaluated.

In contrast to the analogous single-substrate case, the whole maximum rate term in eqn. (11) is not multiplied by an inhibition factor. Only one of the two terms comprising Φ_0 is affected (eqn. 9), namely $1/k_4'$. If $k_4' \gg k_2'$, *i.e.* if the data at low S_2 concentrations conform to the special case II(ii, b), k_4' and K_I' cannot be separately evaluated, and also substrate inhibition will be deferred to much higher values of $[S_2]$.

Non-competitive substrate inhibition. If the second substrate can combine with both the free enzyme and the ternary complex to give inactive compounds, it is obvious from the preceding discussion that the initial rate equation will be

$$\frac{e}{v_0} = \left(\Phi_0 + \frac{[S_2]}{k_4'K_I'} + \frac{\Phi_2}{[S_2]}\right) + \left(1 + \frac{[S_2]}{K_I}\right)\left(\Phi_1 + \frac{\Phi_{12}}{[S_2]}\right)\frac{1}{[S_1]} \quad (12)$$

Again the plot of e/v_0 against $1/[S_1]$ should be linear for all values of $[S_2]$ but neither the slope nor the intercept will be linear in $1/[S_2]$. The kinetic coefficients and the inhibition constants may be determined as in the two previous cases.

The term non-competitive inhibition has usually been applied to single-substrate reactions in which the dissociation constants of the inactive compounds of the inhibitor with the free enzyme and the enzyme-substrate complex are equal, in which case the slope and the intercept of Lineweaver-Burk plots are multiplied by the same inhibition factor. It would seem to be logical to extend the use of the term to the more general case in which the dissociation constants are unequal, and the slope and intercept are affected to different extents. This is true of eqn. (12) even when $K_I = K_I'$.

SUBSTRATE ACTIVATION

Steady state treatment of Type I mechanisms in which there are alternative pathways for the overall reaction yields complex initial rate equations [26] which would be difficult to deal with experimentally. Such mechanisms yield the linear reciprocal rate eqn. (2) only if it is assumed that all steps except one are in equilibrium. It is evident, however, that if the enzyme has a much greater affinity for one substrate than for the other, the reaction may be effectively confined to one pathway over a certain range of substrate concentrations, and initial rate data would conform to the requirements of a Type II mechanism. It is of interest to consider under what conditions the initial rate equation obtained by steady state treatment of a mechanism of Type I will reduce to eqn. (2) over a reasonably wide range of substrate con-

centrations, and what kind of deviations might be observed outside this range. A simple case is an extension of the Theorell-Chance mechanism in one direction:

$$E + S_1 \underset{k_1}{\overset{k_2}{\rightleftharpoons}} ES_1$$

$$E + S_2 \underset{l_2}{\overset{l_1}{\rightleftharpoons}} ES_2$$

$$ES_1 + S_2 \underset{k_3'}{\overset{k_3}{\rightleftharpoons}} ES_1' + S_2'$$

$$ES_2 + S_1 \underset{l_3'}{\overset{l_3}{\rightleftharpoons}} ES_1' + S_2'$$

$$ES_1' \underset{k_1'}{\overset{k_2'}{\rightleftharpoons}} E + S_1'$$

The same rate constants as before are used for the preferred pathway, and l_1 *etc.* are the rate constants for the alternative pathway which will be assumed to be important only when $[S_2]/[S_1]$ is large. There is a compulsory relation between the equilibrium constants for the alternative reactions (i) $l_1l_3/l_2l_3' = k_1k_3/k_2k_3'$.

(a) For the forward reaction, steady state treatment gives:

$$\frac{e}{v_0} = \frac{1}{k_2'} + \frac{k_1[S_1](l_3[S_1]+l_2)+(l_3[S_1]+l_2)(k_3[S_2]+k_2)+l_1[S_2](k_3[S_2]+k_2)}{[S_1][S_2]\{k_1k_3(l_3[S_1]+l_2)+l_1l_3(k_3[S_2]+k_2)\}} \quad (13)$$

If $l_1 = 0$, this mechanism reduces to the Theorell-Chance mechanism, and if $l_1 \neq 0$ but $l_3 = 0$ it reduces to the competitive substrate inhibition type. Accordingly, substitution of $l_1 = 0$ and $l_3 = 0$, respectively, in (9) gives eqns. (1a) and (7). If (ii) $k_1k_3l_2 \gg l_1l_3k_2$, eqn. (13) approximates to

$$\frac{e}{v_0} = \frac{1}{k_2'} + \left(\frac{A}{A+l_3l_1[S_2]/k_1}\right)\frac{\Phi_2}{[S_2]} + \left(\frac{A+l_1[S_2]}{A+l_3l_1[S_2]/k_1}\right)\left(\frac{\Phi_1}{[S_1]} + \frac{\Phi_{12}}{[S_1][S_2]}\right) \quad (14)$$

where the Φ coefficients have the same significance as in the Theorell-Chance mechanism, and $A = l_3[S_1] + l_2$. If the first factors of the second and third terms of eqn. (14) are equal to unity, this equation reduces to the Theorell-Chance equation. This will be true if $l_1[S_2] \ll A$ and $l_1[S_2] \ll k_1A/l_3$. Conditions favouring these requirements are high values of k_1/l_1, l_2/l_1 and l_3/l_1, which are compatible with (ii). Thus, this mechanism may conform to the requirements of the Theorell-Chance mechanism over a wide range of substrate concentrations, even when k_3 and l_3 are of the same order of magnitude, if the complex ES_2 has a large dissociation constant and is formed much more slowly than ES_1. With sufficiently high values of $[S_2]/[S_1]$, Lineweaver-Burk plots against both $1/[S_1]$ and $1/[S_2]$ will be non-linear. Consider the

plot of e/v_0 against $1/[S_2]$ with a fixed concentration of S_1. The second term of eqn. (14) does not contain $[S_2]$ in the numerator, and with high concentrations of S_2 will produce deviations in the linear reciprocal plot towards higher activity. This will be true also of the third term if $l_3 > k_1$, and with this condition, therefore, substrate activation should be observed at high concentrations of S_2, regardless of the value of the fixed concentration of S_1. If $l_3 < k_1$, the third term of eqn. (14) will produce deviations towards lower activity, and the effects of the second and third terms will be opposed. Whether activation or inhibition occurs at high values of S_2 will depend upon the relative values of these two terms. High values of the fixed concentration of S_1 will make the third term smaller compared to the second, and therefore favour substrate activation. This situation provides a possible explanation of substrate activation by alcohol in the yeast dehydrogenase reaction, which occurs only with high concentrations of the coenzyme [6].

(b) For the reverse reaction, steady state treatment gives:

$$\frac{e}{v_0} = \frac{B}{k_2} + \frac{1}{k_1'[S_1']} + \frac{1}{(k_3'+l_3')[S_2']} + \frac{k_2'}{k_1'(k_3'+l_3')[S_1'][S_2']} \quad (15)$$

$$= B\Phi_0' + \frac{\Phi_1'}{[S_1']} + \frac{\Phi_2'}{[S_2']} + \frac{\Phi_{12}'}{[S_1'][S_2']} \quad (16)$$

The Φ coefficients have the same significance as in the Theorell-Chance mechanism except that, in Φ_2' and Φ_{12}', k_3' is replaced by $k_3' + l_3'$; and $B = \left(1 + \frac{l_3'k_2}{k_3'l_2}\right) \Big/ \left(1 + \frac{l_3'}{k_3'}\right)$. Corollaries of assumption (ii) in the preceding section, together with the compulsory relation (i), however, are that $l_3' \ll k_3'$ and $B \doteq 1$. Therefore under conditions for which it has been possible to show that the forward reaction will conform to the Theorell-Chance mechanism over a wide range of substrate concentrations, the reverse reaction will also conform to that mechanism.

Although mechanisms of this type, with alternative pathways, do not lend themselves readily to experimental evaluation, these considerations of a simple case emphasize the fact that, under less restrictive conditions than are assumed in the equilibrium treatment, such mechanisms may conform to the linear reciprocal initial rate eqn. (2), and provide a possible explanation of complex types of deviation at extremes of substrate concentration.

Acknowledgement. I wish to thank Professor Hugo Theorell for stimulating discussions and encouragement during this work.

REFERENCES

1. Theorell, H., Nygaard, A. P. and Bonnichsen, R. *Acta Chem. Scand.* **9** (1955) 1148.
2. Theorell, H. and Chance, B. *Acta Chem. Scand.* **5** (1951) 1127.
3. Theorell, H. and Bonnichsen, R. *Acta Chem. Scand.* **5** (1951) 1105.
4. Haldane, J. B. S. *Enzymes*, Longman's Green & Co., London 1930.
5. Alberty, R. A. *J. Am. Chem. Soc.* **75** (1953) 1928.
6. Nygaard, A. P. and Theorell, H. *Acta Chem. Scand.* **9** (1955) 1300.
7. Dalziel, K. and Theorell, H. *Biochem. J.* **66** (1957) 34 P.

8. Dalziel, K. and Theorell, H. *In preparation.*
9. Lineweaver, H. and Burk, D. *J. Am. Chem. Soc.* **56** (1934) 658.
10. Briggs, G. E. and Haldane, J. B. S. *Biochem. J.* **19** (1925) 338.
11. Michaelis, L. and Menten, M. L. *Biochem. Z.* 49 (1913) 333.
12. King, E. L. and Altman, C. *J. Phys. Chem.* **60** (1956) 1375.
13. Segal, H. L., Kachmar, J. F. and Boyer, P. D. *Enzymologia* **15** (1952) 187.
14. Chance, B. in McElroy, W. D. and Glass, B. *The Mechanism of Enzyme Action*, Johns Hopkins Press, Baltimore 1954.
15. Schwert, G. W. and Hakala, M. T. *Arch. Biochem. and Biophys.* **38** (1952) 55.
16. Hakala, M. T., Glaid, A. J. and Schwert, G. W. *J. Biol. Chem.* **221** (1956) 191.
17. Hayes, J. E. and Valick, S. F. *J. Biol. Chem.* **207** (1954) 225.
18. Nygaard, A. P. and Theorell, H. *Acta Chem. Scand.* **9** (1955) 1551.
19. Laidler, K. L. and Socquet, I. M. *J. Phys. & Colloid Chem.* **54** (1950) 530.
20. LuValle, J. E. and Goddard, D. R. *Quart. Rev. Biol.* **23** (1948) 197.
21. Vennesland, B. and Westheimer, F. H. in McElroy, W. D. and Glass, B. *The Mechanism of Enzyme Action*, Johns Hopkins Press, Baltimore 1954.
22. Alberty, R. A. *J. Am. Chem. Soc. In press.*
23. Alberty, R. A. and Massey, V. *Biochim. et Biophys. Acta* **13** (1954) 347.
24. Alberty, R. A. *Personal communication.*
25. Ebersole, E. R., Guttentag, C. and Wilson, P. W. *Arch. Biochem.* **3** (1944) 399.
26. King, E. L. *J. Phys. Chem.* **60** (1956) 1378.

Received July 26, 1957.

ACTA CHEMICA SCANDINAVICA 11 (1957) 1724—1737

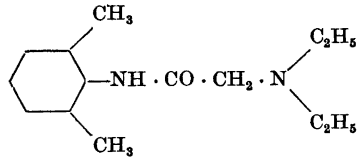
Studies on Local Anesthetics XVI*

NILS LÖFGREN, CLAËS TEGNÉR and BERTIL TAKMAN

Institute of Organic Chemistry and Biochemistry, University of Stockholm, Stockholm, Sweden

Twentyfour new compounds, closely related to xylocaine **, have been synthesized and studied pharmacologically, especially for their surface anesthetic action on the rabbit cornea. Some conclusions have been drawn as to the relation between corneal anesthetic activity and chemical constitution.

As an extension of previous works on local anesthetics by Löfgren *et al.* twentyfour new analogues of xylocaine



Xylocaine

have been synthesized and tested pharmacologically. The compounds are of the general type

$$\text{Ar-NH} \cdot \text{CO} \cdot \underset{\displaystyle \text{R}}{\text{CH}}\text{-Am}$$

in which Ar is phenyl, 2-methylphenyl, 2,6-dimethylphenyl, or 2,4,6-trimethylphenyl, R hydrogen or methyl, and Am alkylamino, dialkylamino, *cyclo*-hexylamino, pyrrolidino, piperidino, or 2-methylpiperidino. The combinations

* For paper XV of this series see Lindström [1].
** Registered trade mark.

of the groups Ar, R, and Am are evident from Table 1 where the compounds (I—XXIV) are listed.

To synthesize these compounds, the arylamines ($Ar \cdot NH_2$) were first converted to the corresponding halogenoacylated compounds by reaction with a halogenoacyl halide (chloroacetyl chloride or α-bromopropionyl bromide) in an aqueous acetate buffer, the general directions of Löfgren [2] being followed. Thus the following N-(halogenoacyl) arylamines were prepared as intermediates for the synthesis of compounds I—XXIV, *viz.* for I: α-chloroacetanilide; II: α-chloro-2-methylacetanilide; III—V: α-chloro-2,6-dimethylacetanilide; VI—XI: α-bromo-2,6-dimethylpropionanilide; XII—XIX: α-chloro-2,4,6-trimethylacetanilide; XX—XXIV: α-bromo-2,4,6-trimethylpropionanilide. The halogeno derivatives produced were then heated with an excess of the necessary primary or secondary amine to give the products desired. In the reactions where primary amines were involved, a high excess of amine (5 moles of amine per mole of halogeno compound) was used to avoid the formation of compounds of the alkylimino-bis(N-acyl-arylamine) type:

$$\text{Alkyl-N}\begin{matrix}\diagup\ \text{acyl} \cdot \text{NH} \cdot \text{Ar} \\ \diagdown\ \text{acyl} \cdot \text{NH} \cdot \text{Ar}\end{matrix}$$

The compounds were tested for their local anesthetic action on the rabbit cornea and compared with xylocaine, the technique of Wiedling [3] being followed (*cf.* also Löfgren and Tegnér [4]). Xylocaine and all the other compounds were used as solutions of their hydrochlorides containing 0.85 % sodium chloride.

As a measure of the potency *relative activity* (RA) was used, *i.e.* the activity which is found by dividing the molarity of a standard xylocaine solution by the molar concentration of the actual compound at which the duration of anesthesia is the same as that of the xylocaine standard. The molarity of the latter was 0.0738 (= 2 % xylocaine · HCl solution). Before measuring the duration of anesthesia for the solution of the actual compound and that for xylocaine, both solutions were adjusted to the same pH, usually 6.0 *.

In the toxicity investigations the LD_{50} values were obtained from subcutaneous injections in white mice and calculated (a) as grams of the base per

* For a few compounds, test solutions of lower pH — but in no case lower than 5.3 — had to be prepared since the solubilities were too low at pH 6.0. These solutions were then compared with the 0.0738 M xylocaine solution adjusted to the same lower pH value. There is no reason to believe that the RA values originating from measurements of such solutions differ significantly from those which would have been obtained from a comparison of solutions of pH 6.0. Thus, for several of our compounds of which test solutions can be prepared at pH 6.0, solutions were made at various pH values between 5 and 6 and RA values were obtained by comparison with a 0.0738 M xylocaine solution of the same pH. No significant difference in the RA values could be found; *cf.* also Löfgren and Tegnér [4].

Table 1. Chemical data of xylocaine analogues I—XXIV. Melting points corrected unless ether of b.p. 40—60°; Dibut.eth., di-*n*-butyl ether; benz.,

	Compound AR—NH · CO · CH(R)—Am			
	Name	Ar	R	Am
I	α-(2-Methyl-1-piperidyl)acetanilide	C_6H_5	H	2-CH_3 · C_5H_9N
II	α-(*n*-Amylamino)-2-methylacetanilide	2-CH_3 · C_6H_4	»	NH-*n*-C_5H_{11}
III	α-*Iso*amylamino-2,6-dimethylacetanilide	2,6-$(CH_3)_2$ · C_6H_3	»	NH-*i*-C_5H_{11}
IV	α-(1-Pyrrolidyl)-2,6-dimethylacetanilide	»	»	C_4H_8N
V	α-(2-Methyl-1-piperidyl)-2,6-dimethylacetanilide	»	»	2-CH_3 · C_5H_9N
VI	α-Ethylamino-2,6-dimethylpropionanilide	»	CH_3	NHC_2H_5
VII	α-(*n*-Propylamino)-2,6-dimethylpropionanilide	»	»	NH-*n*-C_3H_7
VIII	α-*Iso*propylamino-2,6-dimethylpropionanilide	»	»	NH-*i*-C_3H_7
IX	α-(*n*-Butylamino)-2,6-dimethylpropionanilide	»	»	NH-*n*-C_4H_9
X	α-*Iso*butylamino-2,6-dimethylpropionanilide	»	»	NH-*i*-C_4H_9
XI	α-Dimethylamino-2,6-dimethylpropionanilide	»	»	$N(CH_3)_2$
XII	α-(*n*-Propylamino)-2,4,6-trimethylacetanilide	2,4,6-$(CH_3)_3$ · C_6H_2	H	NH-*n*-C_3H_7
XIII	α-*Iso*propylamino-2,4,6-trimethylacetanilide	»	»	NH-*i*-C_3H_7
XIV	α-(*n*-Butylamino)-2,4,6-trimethylacetanilide	»	»	NH-*n*-C_4H_9
XV	α-*Iso*butylamino-2,4,6-trimethylacetanilide	»	»	NH-*i*-C_4H_9
XVI	α-*Iso*amylamino-2,4,6-trimethylacetanilide	»	»	NH-*i*-C_5H_{11}
XVII	α-*Cyclo*hexylamino-2,4,6-trimethylacetanilide	»	»	$C_6H_{11}NH$
XVIII	α-Dimethylamino-2,4,6-trimethylacetanilide	»	»	$N(CH_3)_2$
XIX	α-(1-Piperidyl)-2,4,6-trimethylacetanilide	»	»	$C_5H_{10}N$
XX	α-Ethylamino-2,4,6-trimethylpropionanilide	»	CH_3	NHC_2H_5
XXI	α-(*n*-Propylamino)-2,4,6-trimethylpropionanilide	»	»	NH-*n*-C_3H_7
XXII	α-*Iso*propylamino-2,4,6-trimethylpropionanilide	»	»	NH-*i*-C_3H_7
XXIII	α-(*n*-Butylamino)-2,4,6-trimethylpropionanilide	»	»	NH-*n*-C_4H_9
XXIV	α-*Iso*butylamino-2,4,6-trimethylpropionanilide	»	»	NH-*i*-C_4H_9

a) Uncorrected value.
b) Purified *via* the hydrochloride, see Table 2.
c) Titration of the base in 30 % ethanol with 0.1 N HCl; mixed indicator methylene blue — methyl red.

kilogram of body weight and (b) as moles per kilogram of body weight ("molar" LD_{50} value).

The ratio of the *molar* LD_{50} value for xylocaine to the corresponding value for one of the other compounds is called here the *relative toxicity* (RT) of the compound. For the quotient RA/RT we use the term *anesthetic index* (Q).

To determine the RA value of a compound, 10—30 animals were used. In general, the maximum error in the RA values is about 20 %. The error in the RT values is much less. The results of the pharmacological measurements are collected in Table 3. The material allows a study of the relationship between the chemical constitution and the pharmacological properties. Thus we

otherwise stated, boiling points uncorrected. Abbreviations for solvents: Pet., petroleum benzene; Xyl., xylene; Lgr., ligroin of b.p. 90—120°.

Empirical formula	Yield %	B.p., °C uncorr.	M.p., °C corr.	Solvent for recrystallization	Euqivalent weight c)		Analyses C		Analyses H	
					Calc.	Found	Calc.	Found	Calc.	Found
$_{14}H_{20}N_2O$	77	—	74—75	Pet.	232.3	230	72.4	72.1	8.68	8.55
$_{14}H_{22}N_2O$	90	162—163 0.3 mm	—	—	234.3	—	71.8	72.0	9.46	9.38
$_{15}H_{24}N_2O$	83	—	42—43	Dibut.eth.	248.4	250	72.5	72.5	9.74	9.58
$_{14}H_{20}N_2O$	73	—	82—83	Pet. — Dibut.eth.	232.3	—	72.4	72.1	8.68	8.55
$_{16}H_{24}N_2O$	90	—	118—120a)	Xyl.	260.4	262	73.8	73.7	9.29	9.11
$_{13}H_{20}N_2O$	90	—	86—88	Pet. — Dibut.eth.	220.3	221	—	—	—	—
$_{14}H_{22}N_2O$	89	—	76—77	Dibut.eth.	234.3	234	71.8	71.6	9.46	9.38
$_{14}H_{22}N_2O$	87	—	86—87	Dibut.eth.	234.3	—	71.8	71.8	9.46	9.35
$_{15}H_{24}N_2O$	80	—	40—42	Pet.	248.4	248	—	—	—	—
$_{15}H_{24}N_2O$	93	—	65—66	Dibut.eth.	248.4	—	72.5	72.6	9.74	9.70
$_{13}H_{20}N_2O$	93	—	70—72	Dibut.eth.	220.3	219	70.9	70.8	9.15	9.13
$_{14}H_{22}N_2O$	86	175 0.6 mm	60—61	Pet. — Dibut.eth.	234.3	234	71.8	71.6	9.46	9.33
$_{14}H_{22}N_2O$	65	163—164 0.4 mm	81—83	— b)	234.3	—	71.8	71.7	9.46	9.50
$_{15}H_{24}N_2O$	67	180—181 0.6 mm	59—60a)	Pet. — dibut.eth.	248.4	248	72.5	72.3	9.74	9.61
$_{15}H_{24}N_2O$	94	—	73—74	Dibut.eth.	248.4	—	72.5	72.4	9.74	9.53
$_{16}H_{26}N_2O$	87	—	58—60a)	Dibut.eth.	262.4	263	73.2	73.1	9.99	9.90
$_{17}H_{26}N_2O$	83	—	71—72	Dibut.eth.	274.4	276	74.4	74.7	9.55	9.52
$_{13}H_{20}N_2O$	77	—	73—74a)	Lgr.	220.3	222	70.9	70.6	9.15	9.03
$_{16}H_{24}N_2O$	72	—	111—114	Dibut.eth.	260.4	261	73.8	73.8	9.29	9.22
$_{14}H_{22}N_2O$	88	—	100—101	Dibut.eth.	234.3	236	71.8	71.8	9.46	9.34
$_{15}H_{24}N_2O$	93	—	67—70	Pet.	248.4	250	72.5	72.7	9.74	9.62
$_{15}H_{24}N_2O$	85	158—159 0.3 mm	92—94	Pet. — Benz.	248.4	248	72.5	72.1	9.74	9.62
$_{16}H_{26}N_2O$	88	—	67—69	— b)	262.4	—	73.2	73.3	9.99	9.94
$_{16}H_{26}N_2O$	78	—	65—67a)	— b)	262.4	261	—	—	—	—

are able to analyse the influence on RA, RT and Q of certain variations in the groups R_1, R_2 and R_3 in the structure shown in Table 4. The change in RA, RT and Q is indicated by factors f_A, f_T and f_Q, respectively. In this connection, it should be emphasized that, in the following, an increase or a decrease in RA, RT or Q always means a proportional, and not an absolute, increase or decrease. The results may be summarized as follows:

1. A straight lengthening of a *normal* alkyl group R_1 by a single carbon atom (*cf.* Table 4: A) increases the activity RA ($1.2<f_A<2.5$) as well as the toxicity RT ($1.7<f_T<4.6$) — the increase of the latter being, however, greater so that the anesthetic index Q changes unfavourably ($0.5<f_Q<0.9$). The

Table 2. Chemical data of salts prepared (hydrochlorides, methanesulphonates and perchlorates). Melting points corrected unless otherwise stated. Abbreviations for solvents: *n*-Prop., *n*-propanol; Me.et.ket., methyl ethyl ketone; Aq., water; Al., ethanol; Diox., dioxan; Dibut.eth., di-*n*-butyl ether; *i*-But., *isobutanol; *n*-But., *n*-butanol.

	Salt	Empirical formula	M.p., °C corr.	Solvent for recrystallization	Analyses					
					C		H		Cl	
					Calc.	Found	Calc.	Found	Calc.	Found
II	hydrochloride	$C_{14}H_{23}ClN_2O$	218—219[a]	*n*-Prop.	62.1	62.1	8.56	8.52	—	—
II	methanesulphonate	$C_{15}H_{28}N_2O_4S$	124—125	Me.et.ket.	54.5	54.7	7.93	7.82	—	—
III	hydrochloride	$C_{15}H_{25}ClN_2O$	211—213	Al. — Aq.	—	—	—	—	12.45	12.38
VI	»	$C_{13}H_{21}ClN_2O$	248—250	*n*-Prop.	60.8	60.7	8.24	8.13	—	—
VII	»	$C_{14}H_{23}ClN_2O$	200—201	Me.et.ket. — *n*-Prop.	62.1	61.8	8.56	8.50	—	—
IX	»	$C_{15}H_{25}ClN_2O$	153—157	Me.et.ket.	63.3	63.4	8.85	8.68	—	—
XI	»	$C_{13}H_{21}ClN_2O$	196—198	Diox. — *n*-Prop.	—	—	—	—	13.81	13.82
XII	»	$C_{14}H_{23}ClN_2O$	277—278[a]	Aq.	—	—	—	—	13.09	13.02
XIII	»	$C_{14}H_{23}ClN_2O$	218—220	Me.et.ket.	62.1	61.9	8.56	8.44	—	—
XIV	»	$C_{15}H_{25}ClN_2O$	237—238[a]	Aq.	—	—	—	—	12.45	12.39
XVI	»	$C_{16}H_{27}ClN_2O$	236—238	Al. — Aq.	—	—	—	—	11.87	11.86
XVII	»	$C_{17}H_{27}ClN_2O$	261—262	Dibut.eth. — Al.	—	—	—	—	11.41	11.49
XIX	»	$C_{16}H_{25}ClN_2O$	197—199	*n*-Prop. — Dibut.eth.	—	—	—	—	11.95	12.06
XX	»	$C_{14}H_{23}ClN_2O$	145—146	*n*-But.	—	—	—	—	13.09	13.13
XXI	»	$C_{15}H_{25}ClN_2O$	236—239 (decomp.)	*i*-But.	63.3	63.3	8.85	8.67	—	—
XXII	»	$C_{15}H_{25}ClN_2O$	212—214	Me.et.ket.	63.3	63.0	8.85	8.53	—	—
XXIII	»	$C_{16}H_{27}ClN_2O$	203—208	Diox.	63.3	63.3	8.85	8.84	—	—
XXIV	perchlorate	$C_{16}H_{27}ClN_2O_5$	212—213	Al.	53.0	53.3	7.52	7.62	—	—

a) Uncorrected value.

greatest increase in RA and also in RT is obtained by substituting a *n*-butyl group for the *n*-propyl group in XXI ($R_1 = n\text{-}C_3H_7$, $R_2 = R_3 = CH_3$), *i.e.* by transition from XXI to XXIII ($f_A = 2.5$, $f_T = 4.6$, $f_Q = 0.5$).

2. The introduction of a methyl group at the penultimate carbon atom of a *normal* alkyl group R_1, *i.e.* the transition from a *normal* alkyl group R_1 to the

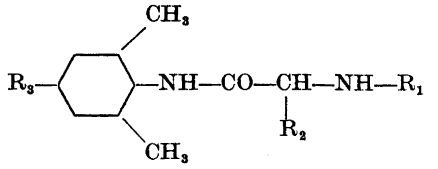
Table 3. Local anesthetic activity (rabbit cornea) and toxicity (white mouse) of compounds I—XXIV. For the terms relative anesthetic activity and relative toxicity, see p. 1725.

Compound	Relative anesthetic activity (RA) xylocaine = 1	Toxicity, LD_{50}		Relative toxicity (RT) xylocaine = 1	RA / RT
		g base/kg	moles/kg·10^3		
Xylocaine	1.0	0.34	1.4	1.0	1.0
I	~0.5	0.85	3.7	0.38	~1.3
II	<0.2	—	—	—	—
III	3.3	0.35	1.4	1.0	3.3
IV	~0.2	0.56	2.4	0.58	~0.3
V	~1.6	0.075	0.29	4.8	~0.3
VI	1.1	0.44	2.0	0.70	1.6
VII	1.7	0.27	1.2	1.2	1.4
VIII	0.9	0.26	1.1	1.3	0.69
IX	3.1	0.094	0.38	3.7	0.84
X	1.8	0.089	0.36	3.9	0.46
XI	~0.3	0.52	2.4	0.58	~0.5
XII	1.9	0.56	2.4	0.58	3.3
XIII	0.9	0.47	2.0	0.70	1.3
XIV	2.3	0.29	1.2	1.2	1.9
XV	1.7	0.35	1.4	1.0	1.7
XVI	4.8	0.42	1.6	0.87	5.5
XVII	16	0.11	0.40	3.5	4.6
XVIII	~0.1	0.52	2.4	0.58	~0.2
XIX	2.4	0.34	1.3	1.1	2.2
XX	1.9	0.54	2.3	0.61	3.1
XXI	2.6	0.26	1.0	1.4	1.9
XXII	1.7	0.50	2.0	0.70	2.4
XXIII	6.4	0.058	0.22	6.4	1.0
XXIV	3.5	0.20	0.76	1.8	1.9

next higher homologous *iso*alkyl group (*cf.* Table 4: B), sometimes increases and sometimes decreases the activity ($0.8<f_A<1.3$) — the change in no case being great — whereas the toxicity increases in all five cases ($1.1<f_T<3.25$), the increase being considerable in three of them ($1.7<f_T<3.25$). In these three cases the anesthetic index is altered very unfavourably ($0.3<f_Q<0.5$). In the other two, *i.e.* by replacing (a) the ethyl group in XX ($R_1 = C_2H_5$, $R_2 = R_3 = CH_3$) by an *i*-propyl group and (b) the *n*-propyl group in XXI ($R_1 = n\text{-}C_3H_7$, $R_2 = R_3 = CH_3$) by an *i*-butyl group, the anesthetic index remains approximately constant ($f_Q = 0.8$ and 1.0).

3. During the discussions in *1* and *2* we have at the same time obtained an idea of what would happen on replacing a *normal* alkyl group R_1 by an isomeric *iso*alkyl group. Direct information on this point is obtained by comparing the isomers available (comparison not tabulated), *i.e.* VII with VIII, IX with X, XII with XIII, XXI with XXII, and XXIII with XXIV. These comparisons show that the replacement of a *normal* alkyl group R_1 by an isomeric *iso*alkyl group in all five cases definitely decreases the activity ($0.5<f_A<0.7$). The toxicity increases slightly in three cases (VII→VIII, IX→X, XII→XIII; $1.05<f_T<1.2$), while in the other two, *i.e.* by replacing (a) the *n*-propyl group

Table 4. Change in relative anesthetic activity (RA), relative toxicity (RT) and anesthetic index (Q) when varying the groups R_1, R_2 and R_3 (*cf.* formula).



R_1 = {C_2H_5, *n*-C_3H_7, *i*-C_3H_7, *n*-C_4H_9, *i*-C_4H_9 or *i*-C_5H_{11}

R_2 or R_3 = H or CH_3

Factors f_A, f_T and f_Q indicate the change in RA, RT and Q, respectively; *cf.* also text on pp, 1725–1727.

Compound No.	R_1	R_2	R_3	RA	f_A	RT	f_T	$Q (=\frac{RA}{RT})$	f_Q
A. Introduction of a methyl group at the end of a *normal* alkyl group R_1 (straight lengthening of a *normal* alkyl group R_1 by a single carbon atom).									
VI	C_2H_5	CH_3	H	1.1	1.5	0.70	1.7	1.6	0.9
VII	*n*-C_3H_7	CH_3	H	1.7		1.2		1.4	
VII	*n*-C_3H_7	CH_3	H	1.7	1.8	1.2	3.1	1.4	0.6
IX	*n*-C_4H_9	CH_3	H	3.1		3.7		0.84	
XII	*n*-C_3H_7	H	CH_3	1.9	1.2	0.58	2.1	3.3	0.6
XIV	*n*-C_4H_9	H	CH_3	2.3		1.2		1.9	
XX	C_2H_5	CH_3	CH_3	1.9	1.4	0.61	2.3	3.1	0.6
XXI	*n*-C_3H_7	CH_3	CH_3	2.6		1.4		1.9	
XXI	*n*-C_3H_7	CH_3	CH_3	2.6	2.5	1.4	4.6	1.9	0.5
XXIII	*n*-C_4H_9	CH_3	CH_3	6.4		6.4		1.0	
B. Introduction of a methyl group at the penultimate carbon atom of a *normal* alkyl group R_1 (transformation of a *normal* alkyl group R_1 into the next higher homologous *iso*alkyl group).									
VI	C_2H_5	CH_3	H	1.1	0.8	0.70	1.9	1.6	0.4
VIII	*i*-C_3H_7	CH_3	H	0.9		1.3		0.69	
VII	*n*-C_3H_7	CH_3	H	1.7	1.1	1.2	3.25	1.4	0.3
X	*i*-C_4H_9	CH_3	H	1.8		3.9		0.46	
XII	*n*-C_3H_7	H	CH_3	1.9	0.9	0.58	1.7	3.3	0.5
XV	*i*-C_4H_9	H	CH_3	1.7		1.0		1.7	
XX	C_2H_5	CH_3	CH_3	1.9	0.9	0.61	1.1	3.1	0.8
XXII	*i*-C_3H_7	CH_3	CH_3	1.7		0.70		2.4	
XXI	*n*-C_3H_7	CH_3	CH_3	2.6	1.3	1.4	1.3	1.9	1.0
XXIV	*i*-C_4H_9	CH_3	CH_3	3.5		1.8		1.9	
C. Introduction of a methyl group at the *α* position of the amide chain (change of R_2 from H to CH_3).									
XII	*n*-C_3H_7	H	CH_3	1.9	1.4	0.58	2.4	3.3	0.6
XXI	*n*-C_3H_7	CH_3	CH_3	2.6		1.4		1.9	
XIV	*n*-C_4H_9	H	CH_3	2.3	2.8	1.2	5.3	1.9	0.5
XXIII	*n*-C_4H_9	CH_3	CH_3	6.4		6.4		1.0	
XIII	*i*-C_3H_7	H	CH_3	0.9	1.9	0.70	1.0	1.3	1.8
XXII	*i*-C_3H_7	CH_3	CH_3	1.7		0.70		2.4	
XV	*i*-C_4H_9	H	CH_3	1.7	2.1	1.0	1.8	1.7	1.1
XXIV	*i*-C_4H_9	CH_3	CH_3	3.5		1.8		1.9	

Table 4, contd.

D. Introduction of a methyl group at the position of the nucleus which is *para* to the amide nitrogen (change of R_3 from H to CH_3).

III	i-C_5H_{11}	H	H	3.3	1.5	1.0	0.9	5.3	1.7
XVI	i-C_5H_{11}	H	CH_3	4.8		0.87		5.5	
VI	C_2H_5	CH_3	H	1.1	1.7	0.70	0.9	1.6	1.9
XX	C_2H_5	CH_3	CH_3	1.9		0.61		3.1	
VII	n-C_3H_7	CH_3	H	1.7	1.5	1.2	1.2	1.4	1.4
XXI	n-C_3H_7	CH_3	CH_3	2.6		1.4		1.9	
VIII	i-C_3H_7	CH_3	H	0.9	1.9	1.3	0.5	0.69	3.5
XXII	i-C_3H_7	CH_3	CH_3	1.7		0.70		2.4	
IX	n-C_4H_9	CH_3	H	3.1	2.1	3.7	1.7	0.84	1.2
XXIII	n-C_4H_9	CH_3	CH_3	6.4		6.4		1.0	
X	i-C_4H_9	CH_3	H	1.8	1.9	3.9	0.5	0.46	4.1
XXIV	i-C_4H_9	CH_3	CH_3	3.5		1.8		1.9	

in XXI ($R_1 = n$-C_3H_7, $R_2 = R_3 = CH_3$) by an i-propyl group and (b) the n-butyl group in XXIII ($R_1 = n$-C_4H_9, $R_2 = R_3 = CH_3$) by an i-butyl group, the toxicity is decreased more ($f_T = 0.5$ and 0.3) than the activity ($f_A = 0.7$ and 0.5), *i.e.* the anesthetic index is altered unfavourably in three cases ($0.4 < f_Q < 0.5$) and favourably in two ($f_Q = 1.3$ and 1.9).

4. By introducing a methyl group at the α-position of the amide-chain (*cf.* Table 4: C) the activity increases in all four available cases ($1.4 < f_A < 2.8$). In the first two of these (see Table), the toxicity increases more than the activity and, therefore, the anesthetic index is altered unfavourably ($f_Q = 0.6$ and 0.5). Introduction of the methyl group into XIII ($R_1 = i$-C_3H_7, $R_2 = H$, $R_3 = CH_3$), *i.e.* the third case, does not alter the toxicity and, since the increase in activity is considerable, the anesthetic index is changed favourably ($f_Q = 1.8$). In the fourth case, *i.e.* introduction of the methyl group in XV ($R_1 = i$-C_4H_9, $R_2 = H$, $R_3 = CH_3$), the toxicity increases ($f_T = 1.8$) approximately in the same ratio as the activity ($f_A = 2.1$) so that the anesthetic index remains practically unchanged ($f_Q = 1.1$). It should be emphasized that, due to the limited material at present available, the above examination includes only the introduction of a methyl at the α-position in such molecules that have their nuclear position *para* to the amide nitrogen occupied by a methyl group ($R_3 = CH_3$).

5. The introduction of a methyl group *para* to the amide nitrogen * (*cf.* Table 4: D) is in all six cases accompanied by an increased activity ($1.5 < f_A < 2.1$). The toxicity may increase, decrease or remain practically unchanged ($0.5 < f_T < 1.7$) and, since the increase is in no case greater than the corresponding increase in activity, the anesthetic index is in all cases improved ($1.2 < f_Q < 4.1$). In two cases, *i.e.* introduction of the methyl group in VIII ($R_1 = i$-C_3H_7, $R_2 = CH_3$, $R_3 = H$) and X ($R_1 = i$-C_4H_9, $R_2 = CH_3$, $R_3 = H$), the activity is increased to about double its value whereas the toxicity is decreased to about half its value so that the anesthetic index is increased greatly, *viz.* approximately four times.

* In the following this position is called the *p* position.

6. The discussions in *4* and *5* suggest that a transfer of a methyl group from the α position to the p position would lead to an improved anesthetic index. Direct information on this point can be obtained by comparing the isomers available (comparison not tabulated), *i.e.* VII with XII, VIII with XIII, IX with XIV, and X with XV. An examination shows that the said transfer in three of the four cases (VII→XII, VIII→XIII, X→XV) causes no appreciable change in the activity ($0.9<f_A<1.1$) and in one case (IX→XIV) decreases it slightly ($f_A = 0.7$). The toxicity decreases in all cases considerably ($0.3<f_T<0.5$). Accordingly, the anesthetic index changes favourably in all cases and calculation shows that the improvement throughout is considerable ($1.9<f_Q<3.7$).

In addition to what has been said under *1—6*, it should be emphasized that a certain structural change in one of the groups R_1, R_2 and R_3 is followed by an alteration in activity and/or toxicity which, as expected, is sometimes greatly dependent on the nature of the two other groups remaining unchanged. Thus, for instance, if in VII (R_1 = *n*-C_3H_7, R_2 = CH_3, R_3 = H), XII (R_1 = *n*-C_3H_7, R_2 = H, R_3 = CH_3) and XXI (R_1 = *n*-C_3H_7, $R_2 = R_3$ = CH_3) the *n*-propyl group is replaced by a *n*-butyl group (*cf.* Table 4:A) an increase in activity as well as toxicity will occur which in the last case is much greater than in the other two cases. In other words, if the α and p positions are *both* occupied by methyl groups and if a *n*-propyl group at the amino-end of the molecule is replaced by a *n*-butyl group, then this change is accompanied by an accentuated increase in activity and toxicity. Other examples: If the structure is changed in such a way that the resulting molecule is furnished with an *iso*alkyl group R_1 at the amino-end and with a methyl group in the α position as well as in the p position, *i.e.* a change which involves (a) the transformation of a *normal* alkyl group R_1 into the next higher homologous *iso*alkyl group (α and p positions with $R_2 = R_3 = CH_3$ kept unchanged; *cf.* Table 4:B) or (b) isomerization of R_1 from a *normal* alkyl group into an *iso*alkyl group (α and p positions with $R_2 = R_3 = CH_3$ kept unchanged; available examples: XXI → XXII and XXIII → XXIV; *cf.* also section *3*, p. 1729) or (c) introduction of a methyl group at the α position (p position occupied by a methyl group, R_1 being an *iso*alkyl group; *cf.* Table 4:C) or (d) introduction of a methyl group at the p position (α position occupied by a methyl group, R_1 being an *iso*alkyl group; *cf.* Table 4:D), then it is seen from the eight cases available that such a change is never accompanied by a marked decrease in anesthetic index. Thus, there is only one case of transformation (XX→XXII) which is associated with a slight decrease in the index ($f_Q = 0.8$) whereas, in the other seven cases, the index remains unchanged or is increased. In four of the cases (XIII→XXII, XXIII→XXIV, VIII→XXII, X→XXIV) the increase is very pronounced ($1.8<f_Q<4.1$).

The following comparison which does not fall within the above types of examination can also be made:

7. Replacement of the ethylamino group in VI (α-ethylamino-2,6-dimethylpropionanilide) by the isomeric dimethylamino group, *i.e.* the transformation of VI into XI, results in a considerable decrease in activity ($f_A \sim 0.3$) and a moderate decrease in toxicity ($f_T = 0.8$).

8. By cyclization of the diethylamino group in xylocaine to the pyrrolidino group, *i.e.* by transformation of xylocaine into IV, the activity is strongly decreased ($f_A \sim 0.2$). The toxicity is also decreased, though less ($f_T = 0.6$).

It should be realised that what has been said under *1—8* concerning the chemical structure and the pharmacological properties must be regarded as limited to the material treated here and great care chould be taken when trying to extend the results to other structures — even those which are closely related to the ones considered here.

Judged by the results hitherto obtained, fourteen of the compounds were considered worthy of a further study in subcutaneous anesthesia on man. These tests were undertaken merely from a clinical point of view and were thus restricted to the usual clinical technique, *i.e.* solutions of the same percentage concentration were made and, after injection of equal volumes, the duration was measured. The comparison with xylocaine was made in the presence as well as in the absence of epinephrine.

Solutions containing 0.5 % of the hydrochloride and a physiological NaCl content (0.85 %) * were prepared. From these solutions another series was made up by adding epinephrine to a strength of 1 : 100 000. The pH of the solutions was in both series adjusted to 4.0 **. Together with xylocaine, 3 or 4 compounds were compared at the same time on each individual in a group of twelve persons. The individuals in this group varied from time to time. The amount injected was always 0.5 ml and the injections were made on the volar side of the forearm, each compound being applied to the right as well as to the left arm. Thus, for each of the 3 or 4 compounds, two average values (presence or absence of epinephrine) were obtained, which were comparable with the corresponding values for xylocaine.

The following compounds were tested: III, VI, VII, XII—XVII, XIX—XXII and XXIV. With the exception of VI and XIII, each of these fourteen compounds has a RA value which is significantly larger than the corresponding value for xylocaine, most of the compounds having very high activities compared with xylocaine (*cf.* Table 3). Compounds VI and XIII have values (1.1 and 0.9, respectively) which are approximately equal to that of xylocaine (= 1.0). All fourteen compounds have Q values which are greater than the corresponding value for xylocaine.

Because of the RA values of these fourteen compounds, one could expect that all of them, with the exception of XIII and possibly VI, would, when injected under the above conditions, give greater durations than that of xylo-

---

* When preparing the solution of XVII glucose (5.5 %) was added instead of NaCl. The hydrochloride of this compound is so slightly soluble in water that the presence of NaCl lowered its solubility to such a degree that a 0.5 % solution could not be prepared.

** When a local anesthetic is used for infiltration anesthesia, the pH of its solution may be varied within wide limits without affecting the duration. This has been demonstrated by various investigators (*cf.* Adriani [5], Tainter, Throndson and Moose [6], Björn and Huldt [7], Huldt [8]). Investigations just on 0.5 % xylocaine · HCl solutions have been made by Löfgren and Lundqvist [9]. In a fairly large number of subcutaneous wheal experiments, the durations of 0.5 % xylocaine· HCl solutions (NaCl concn. = 0.85 %, epinephrine concn. = 1 : 100 000), adjusted to different pH values between 4 and 7, were measured and no significant differences between the values could be found.

caine *. The results from the measurements do not, however, support such a conclusion.

In the test series where no epinephrine had been added, only three of the fourteen compounds gave durations which were greater than that of xylocaine, the order of magnitude being as follows: XXI>XIII ≅ XXII>xylocaine ≅ III, VI, VII, XV, XVI and XXIV>XII ≅ XVII and XX>XIV>XIX. The most active compound in this series, *i.e.* XXI, has a duration approximately 60 % larger than that of xylocaine whereas the compound with the lowest action, *i.e.* XIX, has a duration about 70 % smaller. It is particularly notable that compound XIII, which one might expect to have the lowest duration, is one of those three which have durations higher than that of xylocaine and that XVII, which has the highest relative activity on the cornea, *viz.* no less than 14 (= the RA value 16 multiplied by a conversion factor (0.87); *cf.* above), is inferior to xylocaine.

In the test series where epinephrine was added, none of the fourteen compounds showed a duration significantly greater than that of xylocaine. The order of magnitude was: Xylocaine ≅ VII, XIII, XV, XX and XXI>III ≅ XXII and XXIV>VI ≅ XIV and XVII>XII ≅ XVI and XIX. The least active compounds in this series, *i.e.* XII, XVI and XIX, all show durations about 45 % less than that for xylocaine. It should be emphasized that, also in this series, XIII belongs to the most active of the compounds — here it has approximately the same duration as xylocaine — and that XVII belongs to those which are inferior to xylocaine.

There is therefore a great discrepancy between the durations which were found by the topical application to the rabbit cornea and those which were found by subcutaneous injection in man. This kind of discrepancy has been noticed previously [4,10].

In a special series of subcutaneous injections in man, the fourteen compounds were investigated as to their irritant action **. Here, the above-described solutions containing epinephrine were used. On each of 12 persons, 2 or 3 of the compounds together with xylocaine were tested at the same time by subcutaneous injection of 2 ml of their solutions on the *dorsum*. The reaction of the skin was observed after 16 h. To judge from these screening tests, VII, XVI, XVII, XX, XXII and XXIV did not seem to differ very much from xylocaine, *i.e.* they were considered harmless to the tissues, whereas the other compounds gave evidence of more or less irritating properties. However, XX was later tried topically as an anesthetic in bronchoscopy and it was then found that this compound can produce severe tissue reactions.

* Consideration has here been given to the facts that (a) the RA values — valid for surface anesthetic potency — refer to a quotient of *molarities* with equal durations (= the duration of a 0.0738 M xylocaine solution) and (b) in the subcutaneous anesthesia, the evaluated durations refer to the same amount by weight of the *hydrochlorides* (= 0.5 ml of 0.5 % hydrochloride solutions). To make the RA values valid for a mutual comparison on the gram scale of the hydrochlorides, we thus have to multiply each RA value by a factor equal to the quotient of the molecular weight of xylocaine hydrochloride and the molecular weight of the hydrochloride of the compound.

** In the subcutaneous tests which were performed for the evaluation of anesthesia durations (*cf.* above), the injected amount was so small that only very limited information about the irritant action was obtained.

From what has been discovered about these fourteen compounds selected for studies in infiltration anesthesia, it can be stated that two of them, *viz.* VII and XXII, should be regarded as possible competitors to xylocaine. For this reason, a summary of the observed characteristic features of VII and XXII together with some additional experiments made in order to obtain a clearer picture of their possible clinical value in infiltration anesthesia is given:

By LD_{50} measurements on white mice (*cf.* Table 3) it was found that VII is about 25 % more toxic and XXII approximately 30 % less toxic than xylocaine *. The subcutaneous tests in man showed that xylocaine, VII and XXII do not differ greatly as to their durations. This was found to be the case in the presence as well as in the absence of epinephrine. Concerning irritant properties the screening tests described above were negative and the present authors could not find any irritant action when these two compounds and xylocaine were later compared in block anesthesia of the fingers. In these experiments all three compounds were used in form of their 1 % hydrochloride solutions containing epinephrine (1 : 100 000) and the physiological amount of sodium chloride. From a considerable number of such block anesthesias, it was found that, in comparison with xylocaine, both compounds were somewhat inferior in duration, the value for both being approximately 20 % lower than that of xylocaine. The latency time of VII was about 100 % greater than that of xylocaine whereas XXII gave approximately the same rapid onset as xylocaine.

Since VII has a higher toxicity and a much greater latency time than xylocaine, the compound was not considered to merit clinical trials in infiltration anesthesia. Compound XXII, in view of its properties, was submitted to clinical tests in dental anesthesia (therminal anesthesia, mandibular block)**. These experiments were made in the presence of epinephrine (1 : 80 000). As compared with xylocaine, XXII gave a somewhat shorter duration and the incidence of anesthesia was somewhat lower.

EXPERIMENTAL

Preparation of N-(halogenoacyl)arylamines. Of these derivatives prepared as intermediates in the synthesis of compounds I—XXIV, α-chloro-2-methylacetanilide, α-chloro-2,6-dimethylacetanilide and α-chloro-2,4,6-trimethylacetanilide were made as described previously by Löfgren [2] and α-bromo-2,6-dimethylpropionanilide as described by Löfgren and Lundquist [11], *i.e.* all these compounds were prepared by coupling a halogenoacyl halide (chloroacetyl chloride or α-bromopropionyl bromide) with an arylamine in an aqueous sodium acetate buffer according to the general method described by Löfgren [2]. The same method was used for the preparation of α-chloroacetanilide and α-bromo-2,4,6-trimethylpropionanilide (*cf.* below).

α-Chloroacetanilide. Prepared from chloroacetyl chloride and aniline in accordance with the method mentioned above. The yield of white microcrystalline powder was 86 %. On recrystallization from ligroin the compound was obtained as needles. M.p. 134 – 135° (uncorr.), in agreement with the value given by Meyer [12] who previously synthesized the compound by reacting aniline and chloroacetyl chloride in dry ether.

* In the subcutaneous experiments, the durations refer to the amount of hydrochloride used (0.5 ml of 0.5 % hydrochloride solution). Therefore, in this comparison of the toxicities of VII, XXII and xylocaine, the LD_{50} values of their *hydrochlorides* are considered. (In Table 3 the LD_{50} values are those of the bases.)

** Experiments performed by S. Ekmanner.

α-Bromo-2,4,6-trimethylpropionanilide. Prepared from α-bromopropionyl bromide and mesidine (*cf.* above). Yield of white microcrystalline powder 88 %. Needles from di-*n*-butyl ether. M.p. 188–190° (uncorr.). (Found: C 53.5; H 5.99. Calc. for $C_{12}H_{16}BrNO$ (270.2): C 53.3; H 5.97.)

Preparation of compounds I–XXIV (*cf.* Table 1). For the synthesis of I, IV, V, XI, XVIII and XIX, which are all *tertiary* bases, a mixture of 0.10 mole of the appropriate N-(halogenoacyl)arylamine (*cf.* p. 1725), 0.26 mole of the secondary amine (*cf.* Table 1) and 70 ml of dry benzene was boiled under reflux for 5 h (for I, IV, V and XIX) or heated for 5 h at a temperature of 80° in an autoclave (for XI and XVIII). When cool the mixture, including a possible water-soluble precipitate of the hydrochloride of the starting amine, was extracted in a separating funnel twice with 4 N hydrochloric acid, first with 75 ml and then with 40 ml. The combined aqueous extracts were washed with ether and then made alkaline with concentrated ammonia. The liberated base was extracted with ether and the solution thus obtained was dried over anhydrous sodium sulphate. The ether and the residual amount of starting amine were removed by distillation, first at atmospheric pressure, and then at water pump *vacuum* with a bath temperature of 100°. From the residue the desired base was purified either by recrystallization or by distillation under reduced pressure (*cf.* Table 1).

To synthesize II, III, VI–X, XII–XVII, and XX–XXIV, which are all *secondary* bases, a mixture of 0.10 mole of the appropriate N-(halogenoacyl)arylamine (*cf.* p. 1725), 0.50 mole of the primary amine (*cf.* Table 1) and 100 ml of absolute alcohol was refluxed for 5 h (for II, III, IX, XIV–XVII, XXIII, and XXIV) or heated for 5 h at a temperature of 100° in a pressure bottle or an atuoclave (for VI–VIII, X, XII, XIII, and XX–XXII). From the mixture obtained, the alcohol and the excess starting amine were distilled off, first at atmospheric pressure and then at water pump *vacuum* with a bath temperature of 100°. To the residue, 125 ml of 4 N hydrochloric acid was added. The resulting mixture was kept at 50° for half an hour under mechanical stirring and then allowed to cool. If the mixture contained a solid, *i.e.* a hydrochloride which may be contaminated with a small quantity of a halogenoacylarylamine, then it was filtered off by suction. The solid was dried and washed with benzene. The acid filtrate was purified by extracting twice with ether. The solid hydrochloride was combined with the acid filtrate. The base was liberated from this mixture with a sufficient amount of 5 N sodium hydroxide solution, mechanical stirring being applied for half an hour. The alkaline mixture was extracted sufficiently with chloroform and the solution dried over anhydrous sodium sulphate. (If no hydrochloride had appeared after the addition of hydrochloric acid (*cf.* above), the mixture was filtered. The filtrate was extracted twice with ether and from the aqueous solution the base was liberated and treated as described above.) The chloroform was distilled off and the base was isolated from the residue by either recrystallization or distillation.

The bases thus produced were analysed by determining the equivalent weight * or by usual elementary analyses or by both methods. Further analytical characterization was obtained from elementary analyses of the salts prepared (*cf.* below).

Yields, melting and boiling points, solvents for recrystallization, and analytical data are shown in Table 1.

Preparation of salts. Hydrochlorides of all the compounds, except I, IV, V, VIII, X, XV, XVIII and XXIV, were made. The methanesulphonate of II and the perchlorate of XXIV were also prepared. The salts were made by dissolving the compound in dry ether and adding the required amount of dry acid dissolved in dry ether **. The colourless microcrystalline precipitate was then recrystallized from a suitable solvent.

Melting points, solvents for recrystallization, and analytical data are shown in Table 2.

The authors are indebted to Dr S. Wiedling of the Biological Department of A.-B. Astra, Södertälje, Sweden for performing the activity tests on the rabbit cornea and the toxicity measurements on white mice and also to Dr T. Edlund of the Institute of Pharmacology, University of Uppsala, Uppsala, Sweden for carrying out the subcutaneous tests in man.

* Titration of the base in 30 % ethanol with 0.1 N HCl; mixed indicator methylene blue — methyl red.

** When perchloric acid was used, the commercial 73 % acid was dissolved in absolute ether.

REFERENCES

1. Lindström, S. *Acta Chem. Scand.* **11** (1957) 962.
2. Löfgren, N. *Studies on Local Anesthetics. Xylocaine a New Synthetic Drug.* Dissertation, Stockholm 1948.
3. Wiedling, S. *Acta Pharmacol. Toxicol.* **8** (1952) 117.
4. Löfgren, N. and Tegnér, C. *Acta Chem. Scand.* **8** (1954) 1806.
5. Adriani, J. *The Chemistry of Anesthesia.* Charles E. Thomas Publ., Springfield, 1946, p. 440.
6. Tainter, M. L., Throndson, A. H. and Moose, S. M. *J. Am. Dental Assoc. and Dental Cosmos* **24** (1937) 376; *ibid.* **25** (1938) 1321; *J. Am. Dental Assoc.* **26** (1939) 920.
7. Björn, H. and Huldt, S. *Svensk Tandläkare Tidskrift* **40** (1947) 831.
8. Huldt, S. *Acta Odontol. Scand.* **11** (1953) Supplementum 13, p. 69.
9. Löfgren, N. and Lundqvist, B. *Unpublished experiments.*
10. Löfgren, N. and Takman, B. *Acta Chem. Scand.* **6** (1952) 1010.
11. Löfgren, N. and Lundqvist, B. *Svensk Kem. Tidskr.* **58** (1946) 206.
12. Meyer, P. *Ber.* **8** (1875) 1153.

Received August 13, 1957.

ACTA CHEMICA SCANDINAVICA 11 (1957) 1738—1744

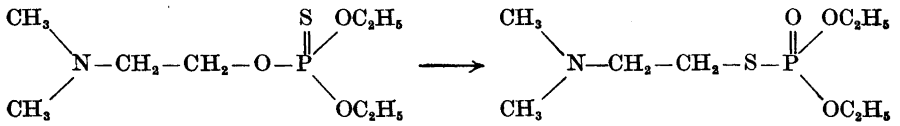
Isomerisation of ω-Dimethylaminoethyl-diethyl-thionophosphate

L.-E. TAMMELIN

Research Institute of National Defence, Dept. 1, Sundbyberg 4, Sweden

The structures of ω-dimethylaminoethyl-diethyl-thionophosphate and the thiolo isomer S,ω-dimethylaminoethyl-diethyl-thiolophosphate, have been studied by infrared spectra. Some spectra of related compounds are given. Isomerisation of the thiono compound has been shown by means of infrared spectrophotometry and paper chromatography to yield S,ω-dimethylaminoethyl-diethyl-thiolophosphate. The reaction rate at 100°C of the isomerisation has been studied. Two tentative reaction mechanisms are given for the isomerisation.

Organophosphorus compounds containing an ω-dimethylaminoeththio group as, *e.g.*, S,ω-dimethylaminoethyl-diethyl-thiolophosphate have been described as potent insecticides and cholinesterase inhibitors [1, 2]. Reports have been given about their synthesis [1-3] and among the methods is isomerisation at elevated temperature of ω-dialkylaminoethyl-diethyl-thionophosphate [3].



Few details, however, have been given about the rearrangement from thiono to thiolo ester and no evidence has been given for the position of the sulfur atom. Since this reaction seems interesting both in connection with the syntheses of compounds of this type and with the confirmation of their structures, it was decided to study the reaction rate semiquantitatively with spectrophotometry and to investigate the reaction products qualitatively with paper chromatography. Infrared spectrophotometry seemed to be an applicable method for the kinetic studies as well as for a confirmation of the structures in general. It was thus decided to record spectra of S,ω-dimethylaminoethyl-diethyl-thiolophosphate and related compounds.

METHODS

Synthesis of dimethylaminoethyl-diethyl-thionophosphate

One mole of diethoxy-thionophosphorylchloride and one mole of sodium dimethylaminoethanolate are mixed in benzene at room temperature. The sodium chloride formed is filtered off, and the filtrate is fractionated under reduced pressure by distillation. Yield 60 %. B.p. 90°/0.1 mm $n_D^{20} = 1.4590$.

The compound was purified as the oxalate. One mole of dimethylaminoethyl-diethyl-thionophosphate (25 % solution in methanol) and 1.05 moles of oxalic acid (10 % solution in methanol) were mixed and the methanol evaporated. Recrystallisation from acetone gives colorless crystals M.p. 132°C (Kofler Heizbank). (Found: C 36.1; H 6.6. Calc. for $C_{10}H_{22}NO_7PS$ (331.3): C 36.3; H 6.7).

The oxalate of ω-dimethylaminoethyl-diethyl-thionophosphate was titrated in 0.10 M KCl with sodium hydroxide as described for analogous compounds in an earlier paper [2]. The mixed dissociation constant, as pK'_a, was determined by the curve fitting method [4]. The calculated amount of sodium hydroxide was found to be consumed. The thermodynamic dissociation constant, was estimated as in the earlier paper [2].

Infrared spectra and photometry

Spectra of ω-dimethylaminoethyl-diethylthionophosphate, S-ω-dimethylaminoethyl-diethyl-thiolophosphate and related compounds were determined with a Perkin and Elmer Mod. 21 spectrophotometer. The spectra were obtained using the following solvents: carbon tetrachloride between 2 and 12 μ, benzene between 12 and 14 μ and carbon tetrachloride between 14 and 15 μ. The solutions were 0.3 M.

In order to study the rearrangement of ω-dimethylaminoethyl-diethyl-thionophosphate, samples were taken at different lengths of time after the preparation of the pure compound, which was stored at 100°C. These samples were studied spectrophotometrically between 6 and 9 μ. Transmittance was determined at 7.95 μ. The refractive index of each sample was determined by an Abbe refractometer. Standard curves for the correlation of concentrations to I.R. transmittance ($T_{7.95}$) and to refractive index (n_D^{20}) were determined by mixing S,ω-dimethyl-aminoethyl-diethyl-thiolophosphate [2] with ω-dimethylaminoethyl-diethyl-thionophosphate in different proportions. The spectrophotometer was used with a sodium chloride prism, resolution = 927, response = 2 : 1170, gain = 5, speed = 1 μ/min, suppression = 3 and scale 5 cm/μ. The thickness of the cell was 0.116 mm.

Paper chromatography of the thiolo and thiono ester

Solvent [5]: *n*-butanol 8, ethanol 2, acetic acid 2 and water 3 parts by volume.
Reagent [5]: 0.2 g of dipicrylamine is dissolved in 50 ml of acetone and 50 ml of water (Reacts with the amino group).
Paper: Whatman 1. Height 35 cm.

Procedure: Spots of 10 μl of about 1 % solution of the samples were dried with hot air. The paper was equilibrated with air in equilibrium with the solvent for 1 h. An ascending technique was used at 25°C for 17 h. After drying with hot air the paper was sprayed with the reagent.

Paper chromatography of hydrolysis products

An approximately 10 % solution of S,ω-dimethylaminoethyl-diethyl-thiolophosphate was hydrolyzed at 50°C overnight in 0.1 M sodium hydroxide solution. The same experiment was done with the isomerized thiono compound. The hydrolysis products together with ω-dimethylaminoethanthiol were investigated as follows.

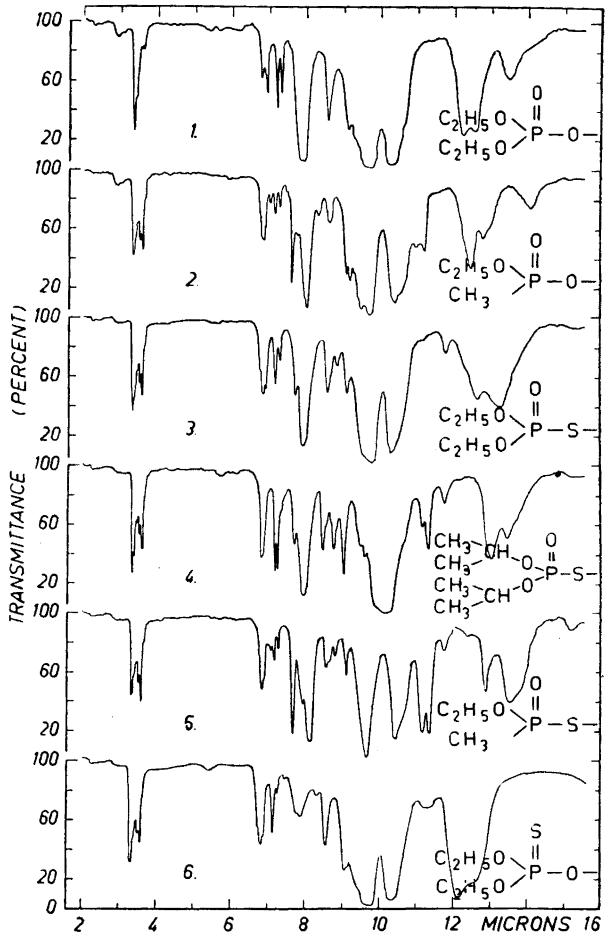


Fig. 1. Infrared spectra of ω-dimethylaminoethyl esters of organophosphorus acids.

Solvent: *n*-butanol 8, ethanol 2, acetic acid 1 and water 3 parts by volume.
Reagent: Grotes reagent [9] (SH-reagent).
Paper: Whatman 1. Height 35 cm.

Procedure: Spots of 10 μl of about 10 % solution of the three samples were dried with hot air. The paper was equilibrated with air in equilibrium with the solvent for 1 h. An ascending technique was used at 25°C for 17 h. After drying with hot air the paper was sprayed with the reagent. The papers were kept at 100°C for 5 min. Parallel tests were performed and developed by the dipicrylamine reagent [5] which colors amino groups.

Determination of the cholinesterase inhibiting effect (pI_{50})

The cholinesterase inhibiting effect of ω-dimethylaminoethyl-diethyl-thionophosphate was determined by means of an electrometric method. All conditions were identical with

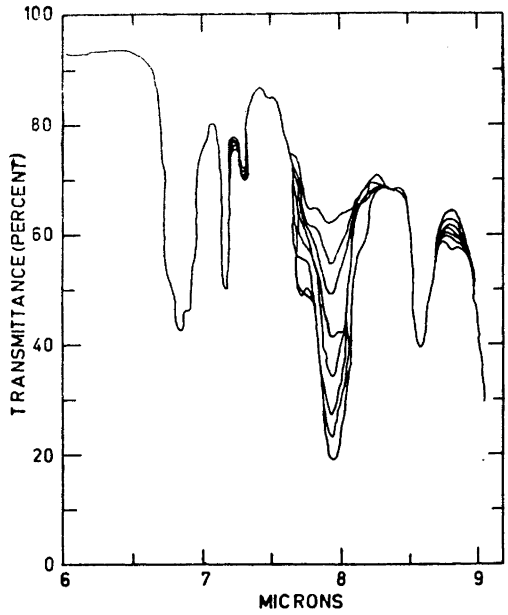


Fig. 2. Infrared spectra showing the isomerisation at 100°C of ω-dimethylaminoethyl-diethyl-thionophosphate. Samples taken at different times show increasing phosphoryl concentration by the decreased transmittance at 7.95 microns.

those in experiments with the thiolo ester [2]. Human erythrocytes and plasma were used as enzyme sources and acetylcholine as substrate. The results are expressed as the negative logarithm of the inhibitor concentration which decreases enzyme activity to 50 % (pI_{50}).

RESULTS

The infrared spectra obtained (Fig. 1) are in good agreement with those obtained from related compounds in earlier literature [6, 7]. They thus need few comments. However, at 11.76 μ the thiolo compounds show a weak absorption which seems characteristic. It has not been possible to correlate this band with some special part of the molecular structure. The phosphoryl group, as seen in Fig. 1, gives a strong absorption near 8 μ [6-8] which is not found in the thiono compounds, although a weak absorption in this region indicates contamination with thiolo isomer presumably formed during the distillation. Spectrophotometric measurements made in this region during the reaction were used for the study of the rearrangement. The result of the kinetic investigation is shown in Fig. 2 where the increasing concentration of a phosphoryl group is demonstrated and in Fig. 3 which shows the reaction rate. The specific change in the infrared spectra shown in Fig. 2 and the relatively good agreement of the results from different methods shown in E (Fig. 3) demonstrate that the reaction product is rather homogeneous. If the process is allowed to proceed for more than 5 h at 100°C, side reactions become obvious. The

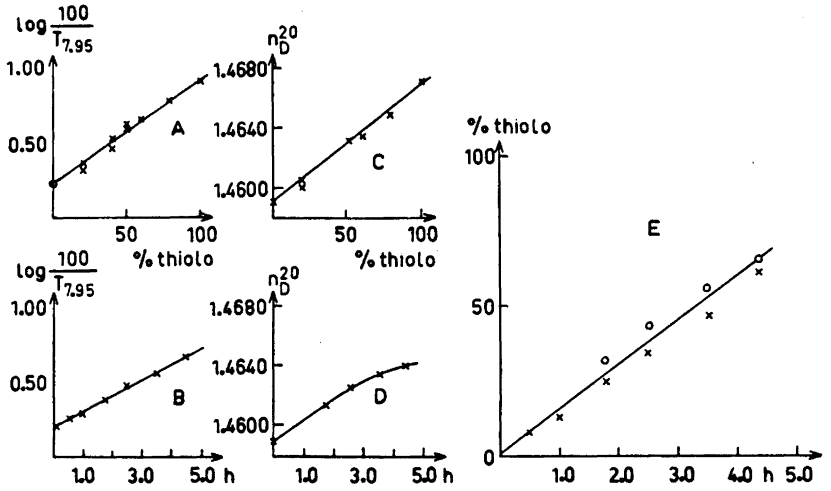


Fig. 3. The diagrams show the time dependence of the isomerisation of ω-dimethylaminoethyl-diethyl-thionophosphate to S,ω-dimethylaminoethyl-diethyl-thiolophosphate at 100°C. A and C are standard curves showing transmittance at 7.95 microns ($T_{7.95}$) and refractive index (n_D^{20}) as functions of the composition of the isomeric mixture. B and D show the primary results. E shows the velocity of the isomerisation at 100°C. The points O are from refractive index measurements and × from I.R. transmittance.

refractive index/time diagram (D, Fig. 3) bends against the time axis. A precipitate of white crystals with salt character is formed in the reaction vessel, and an unidentified absorption band at about 5.5 μ is found in the infrared spectrum. The precipitate has approximately the same percent composition as the original compound (C 34.9; H 8.3) but has not been investigated further. Tests with isomerisation at 70°C gave a slower reaction, but side reactions were not avoided.

Infrared spectra of S,ω-dimethylaminoethyl-diethyl-thiolophosphate prepared by direct synthesis and of the isomerized product show, on the whole, identical patterns, which seems to justify the conclusion that the main product of isomerisation is identical with the reference compound. However, at 8 μ and in the region between 12 and 15 μ the transmittance differs at the coinciding absorption maxima. This is probably caused by a residue of thiono component in the isomerized compound but might also be due to the other components in the reaction mixture.

The paper chromatogram obtained from a sample of dimethylaminoethyl-diethyl-thionophosphate which had been incubated at 100°C for 4 h gave only two tailless spots with $R_F = 0.76$ and $R_F = 0.87$. A mixture of oxalates of the thiono and thiolo [2] compounds which had been synthesized with direct methods gave two spots with $R_F = 0.74$ and $R_F = 0.87$. Separate experiments with thiolo compound as free amine gives $R_F = 0.75$ and thiono compound as oxalate (see syntheses) gives $R_F = 0.86$. The paper chromatography in order to study the hydrolysis products shows three identical spots ($R_F = 0.37$) corresponding to ω-dimethylaminoethanthiol, hydrolysates of S,ω-dimethyl-

aminoethyldiethyl-thiolophosphate and isomerized thionophosphate, respectively. The dimethylaminoethanthiol spot was obtained with both reagents [5,9]. Three other spots were obtained. Two of them were developed by both reagents and could be identified by their R_F values as unhydrolyzed thiono and thiolo compounds. The third spot, $R_F = 0.5$, was only developed by the sulfhydryl reagent [9] and might be caused by O,O-diethyl-thiophosphate. This result shows that ω-dimethylaminoethanthiol is among the main products of hydrolysis of the isomerized compound as well as of the S,ω-dimethylaminoethyl-diethyl-thiolophosphate. *These experiments together with the infrared spectrophotometric studies show that S,ω-dimethylaminoethyl-diethyl-thiolophosphate is the main product of isomerisation of ω-dimethylaminoethyl-diethyl-thionophosphate and exclude considerable formation of an ethyl thiolo isomer.*

The pK_a and pI_{50} values of the thio isomers and a related oxygen compound [2] are given in Table 1. The low pI_{50} value of the thiono ester compared to the thiolo ester emphasizes the specific role of a P—S—C structure in cholinesterase inhibitors.

Table 1.

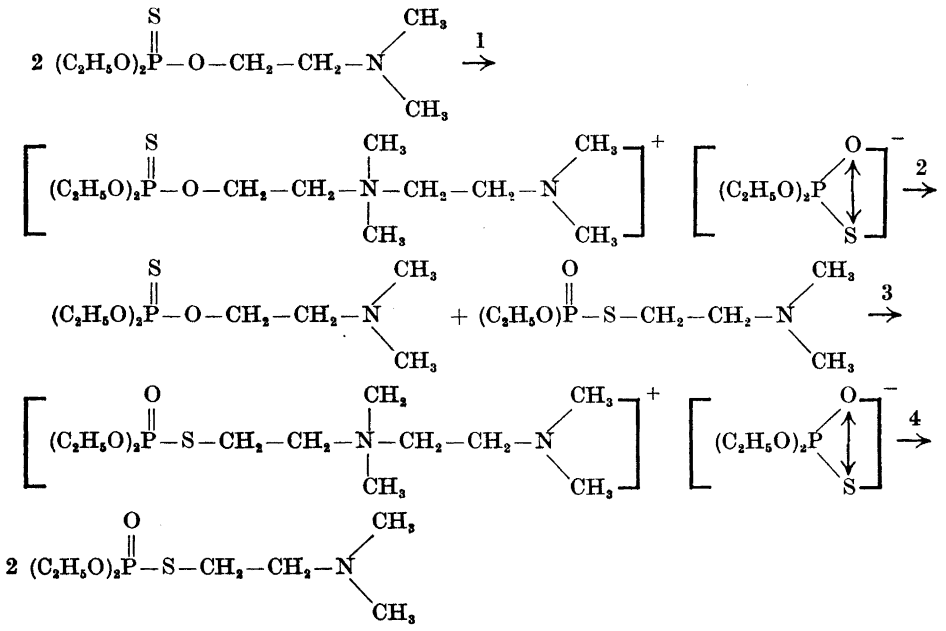
	X = $-CH_2-CH_2-N(CH_3)_2$		
	$(EtO)_2\overset{O}{\overset{\|}{P}}-S-X$	$(EtO)_2\overset{S}{\overset{\|}{P}}-O-X$	$(EtO)_2\overset{O}{\overset{\|}{P}}-O-X$
pK_a	7.73	8.12	8.03
pI_{50}			
erythrocytes	7.9	4.4	4.6
plasma	8.0	5.5	4

DISCUSSION

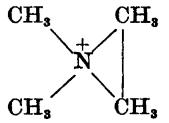
The mechanism of the rearrangement from thiono to thiolo isomer is not elucidated by the present experiments. However, some conclusions can be drawn from the results which may permit the postulation of a tentative reaction scheme.

The rate of the isomerisation is unexpectedly independent of the time, giving a picture (Fig. 3) which seems characteristic of a zero order reaction. During prolonged heating, an impurity with approximately the same composition as the starting compound but of salt character, which might be a quaternary ammonium compound, precipitates in considerable amounts. The isomerisation yields only one of the two possible thiolo isomers, the S,ω-dimethylaminoethyl-phosphoryl compound. These facts may be explained dy the following reaction scheme.

If steps 2 and 4 are rate determining (with saturated solutions of the salts as an added condition) the zero order reaction is explained by the scheme, which also excludes formation of other isomers than the S,ω-dimethylaminoethyl-diethyl-thiolophosphate. The quaternary ammonium compounds should be



the precipitate observed upon prolonged heating. Other types of possible quaternary ammonium ions than the one proposed above might be formed, *e.g.*



but formation of the dialkoxy-thiophosphate ion seems very probable.

Addendum: While this paper was in press a paper by Fukuto and Stafford [10] has appeared which gives strong experimental support to the idea that an immonium ion is formed during the process of isomerisation.

REFERENCES

1. Ghosh, R. and Newman, J. F. *Chem. & Ind. London* **1955** 118.
2. Tammelin, L.-E. *Acta Chem. Scand.* **11** (1957) 1340.
3. Ghosh, E. *Brit. Pat.* 738839.
4. Sillén, L. G. *Acta Chem. Scand.* **10** (1956) 186.
5. Augustinsson, K. B. *Acta Chem. Scand.* **7** (1953) 906.
6. Mc Ivor, R. A., Grant, G. A. and Hubley, C. E. *Can. J. Chem.* **34** (1956) 1611.
7. Harvey, R. B. and Mayhood, J. E. *Can. J. Chem.* **33** (1955) 1552.
8. Bellamy, L. J. *The Infra-Red Spectra of Complex Molecules*, Methuen, London 1954.
9. Block, R. J., Durrum, E. L. and Zwerg, G. *A Manual of Paper Chromatography and Paper Electrophoresis*, Academic Press Inc., N.Y. 1955, p. 96.
10. Fukuto, T. R. and Stafford, E. M. *J. Am. Chem. Soc.* **79** (1957) 6083.

Received August 27, 1957.

ACTA CHEMICA SCANDINAVICA 11 (1957) 1745—1751

The Heats of Hydrolysis of Some Alkyl Thiolesters

INGEMAR WADSÖ

Thermochemistry Laboratory, University of Lund, Lund, Sweden

The heats of hydrolysis of some alkyl thiolesters have been determined at 25°. For the idealized, isothermal hydrolysis reactions

$$RSAc(l) + H_2O(l) \rightarrow RSH(l) + HOAc(l)$$

the changes in enthalpy at 25°C were found to be:
-0.95 ± 0.06 kcal.mole^{-1} for R = Et; -0.93 ± 0.06 kcal.mole^{-1} for *n*-Pr; -1.09 ± 0.06 kcal.mole^{-1} for *n*-Bu; -1.39 ± 0.07 kcal.mole^{-1} for *i*-Pr; -3.00 ± 0.07 kcal.mole^{-1} for *t*-Bu.

The interest which biochemists show towards S-acyl compounds today is fully evident. The role played by coenzyme A and its acyl derivatives in acyl transfer processes has stressed the importance of studying the energy relationships between different acylated compounds containing O-acyl, N-acyl and S-acyl bonds. The present investigation continues a research program which began with the study of the hydrolysis of thiolacetic acid [1], and aims at a mapping out of the enthalpy changes accompanying different types of trans-acylation processes.

EXPERIMENTAL

Materials

Preparation of the esters. The esters were synthesized in two different ways:

1. Acylation of the corresponding thiol [2]. This method was used to prepare EtSAc from EtSH and Ac_2O, and *t*-BuSAc from *t*-BuSH and AcCl.

2. Reaction between thiolacetic acid and the appropriate alkyl bromide [3]. The reaction was carried out in a 500 ml flask with a reflux condenser. To a solution of 0.5 mole of KOH in 150 ml 96 % ethanol was added 0.5 mole of HSAc. The mixture was cooled to room temperature and 0.5 mole of alkyl bromide was slowly added. After a few minutes the solution became warm and KBr precipitated. After one hour the mixture was poured into 2 l of water. The oil was separated and the water phase extracted twice with ether. The oil and the extract were combined, and washed with 2.5 N H_2SO_4, saturated $NaHCO_3$ solution and twice with water. The product was dried overnight with anhydrous Na_2SO_4. After removing the ether, the residue was fractionated. Yield *ca.* 80 %. This method was used to prepare *n*-Bu, *n*-Pr and *i*-Pr thiolacetates. The method is convenient and the use of evil-smelling thiols is avoided. Attempts to prepare *t*-BuSAc by this method failed.

Purity of the esters. The esters were purified by distillation through a 10-plate column. Purities were >99.5 %, as judged by measurements of their equivalent weights. The

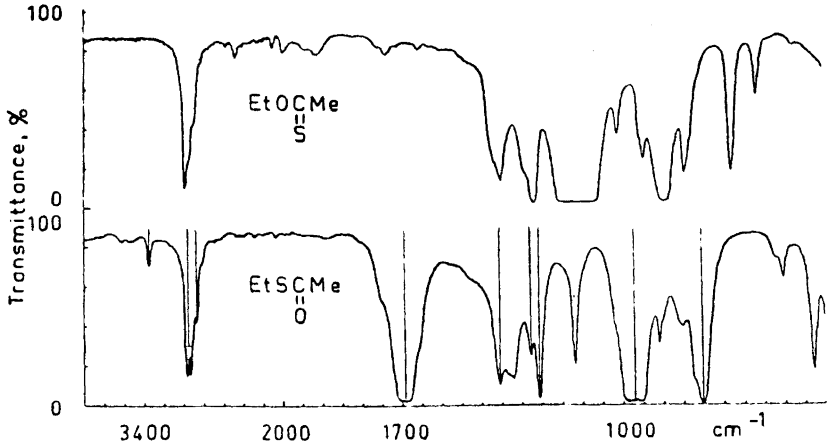


Fig. 1. Infrared spectra of ethyl thionester and ethyl thiolester.

esters showed a neutral reaction, and did not absorb iodine. The equivalent weights were determined after alkaline hydrolysis by titration of both RSH and HOAc.

Determination of RSH. The hydrolysing liquid consisted of an alcoholic NaOH solution (0.5 N NaOH in 50 % ethanol; 10 moles per mole of ester). In this medium the hydrolysis was quantitative within 10 min. However, the thiol formed is very sensitive to air oxidation at high pH values. The reaction was therefore carried out in a nitrogen atmosphere in a long-necked flask with glass stopper. A thinwalled glass ampoule containing 3 mmoles of ester was dropped into the flask and broken by shaking. After about 10 min the solution was cooled to *ca.* −10°C and an excess of glacial acetic acid added. The thiol was titrated with 0.1 N iodine solution in 90 % alcohol. It is well-known that *t*-BuSH cannot be titrated quantitatively with iodine [4].

Determination of HOAc. The hydrolysis was carried out as described above but in a weakly alkaline medium (2 moles NaOH per mole of ester). After leaving overnight the sample was titrated with 0.1 N HCl to pH 7. The thiol was then blown off with CO_2-free air and the solution was titrated to pH 10. Equivalent weight, density and refractive index for the thiolesters synthesized are listed in Table 1.

Table 1. Equivalent weight, density and refractive index for the synthesized thiolesters, RSAc.

R	Equivalent weight			d_4^{25}	n_D^{25}
	RSH	HOAc	Theoretical		
Et	104.6	104.9	104.17	0.9728	1.4568
n-Pr	118.5	118.5	118.19	0.9532	1.4580
n-Bu	132.9	132.9	132.22	0.9390	1.4590
i-Pr	118.1	118.3	118.19	0.9368	1.4510
t-Bu	—	132.3	132.22	0.9207	1.4511

Infrared spectra of the esters. The infrared spectra for the thiolesters have been determined and compared with that of ethyl thionester. It was found that the thiolesters did not contain any detectable amount of thion isomer. Fig. 1 shows the spectra of EtOCSMe and EtSCOMe. The vertical lines indicate the absorption maxima common to all the thiol esters. They are characterized mainly by the C = O stretching bond vibration frequency at 1 700 cm^{-1} and its overtone at 3 400 cm^{-1}.

Auxiliary substances. The thiols used were freshly distilled before their heats of solution were determined. The estimated purity (from determinations of equivalent weights) was better than 99 % except for EtSH which was 98.0 % pure. The density and refractive index for *t*-BuSH was d^{25}_4 0.7942; n_D^{25} 1.4205 in good agreement with values from the literature [5]. The acetic acid was purified by freezing out three times. The purity was found to be 99.5 % (titration with NaOH).

Apparatus

The reactions were carried out in an isothermal calorimeter which will be described in detail elsewhere. The system consisted of a steel reaction vessel with a combined stirrer and ampoule holder and a heating element. The vessel was surrounded by a thick-walled copper jacket. The space between the vessel and the jacket was evacuated to 0.1 mm Hg. The temperature change was determined by use of a thermistor (Stantel U 236120).

Calibration

The determination of the heat capacity of the calorimeter was carried out by passing a known current for a known time through the calibration resistance in the calorimeter. The overall error in the calibration measurements was ± 0.16 %. The calibrations were carried out on the system after the hydrolysis. Owing to the different behaviour towards oxygen of *t*-BuSH compared with other thiols the slope of the resistance-time curve was different in the two cases. Therefore, the hydrolyses were carried out at slightly different temperatures. In order to minimize errors from small variations in ε with temperature, two series of calibration experiments were performed, namely between the thermistor resistances 2 125 and 2 085 Ω (heat capacity ε_1) and between 2 155 and 2 115 Ω (heat capacity ε_2). Experiments corresponding to reactions III and IV (below) and reactions I and II for R = *t*-Bu were carried out in the latter temperature interval, reactions I and II where R = Et, *n*-Pr, *i*-Pr, *n*-Bu were performed between 2 125 and 2 085 Ω. A check on the accuracy of the heat capacity values was obtained by the determination of the heat of solution of KCl in water. The values obtained agreed within the limits of error with those in the literature.

Procedures

The calorimeter was charged with 90 ml of 0.8 N sodium hydroxide solution in water-ethanol (2 : 3). The sealed glass ampoule contained about 3 mmoles of ester (thiol, glacial acetic acid or water). After equilibration, the reaction was started by breaking the ampoule. The hydrolysis was quantitative within 5 min and the duration of the reaction period was 7 min. Thereafter, a linear time-temperature relationship was established. The short reaction period makes the corrections for heat exchange with the surroundings very small and the initial and final thermistor resistances (R_i and R_f, respectively) could thus be obtained graphically.

The large excess of alkali (*ca.* 25 times) greatly speeds up the hydrolysis reaction and is also favorable from another point of view since the degree of protolysis of the sodium mercaptides formed in the reaction becomes independent of small variations in the amount of ester hydrolyzed. As stated above, the thiols are extremely easily oxidized in an alkaline medium and the heat of oxidation is appreciable. Attempts to free the reaction system completely from oxygen were unsuccessful. Therefore, it was impossible to avoid a false slope of the time-temperature curve during the after period, leading to erroneous values of the heat leakage. Also, the oxidation occurring during the reaction period introduced a considerable error. The same errors, however, occurred in the determinations of the heats of solution of the thiols, and to some extent, these errors cancelled out in the final results. In order to ascertain that no errors should be introduced from variations in oxygen content of the calorimeter liquid, and also to ensure complete cancellation in the final results, 4 mmoles of the appropriate thiol were added prior to beginning the experiment. Thus, the oxidation occurred also in the initial period. The limiting factor on the rate of oxidation was the availability of oxygen as the thermal leakage values obtained were identical with those obtained in experiments without thiol present.

Corrections to standard states

The ideal isothermal hydrolysis reaction V is obtained from eqns. I to IV, corresponding to the reactions taking place under actual experimental conditions.

I	$RSAc(l) + H_2O(l) = RSH(soln) + HOAc(soln)$	ΔH_1
II	$RSH(l) = RSH(soln)$	ΔH_2
III	$HOAc(l) = HOAc(soln)$	ΔH_3
IV	$H_2O(l) = H_2O(soln)$	ΔH_4
V	$RSAc(l) + H_2O(l) = RSH(l) + HOAc(l)$	$\Delta H°$

$$\Delta H° = \Delta H_1 - \Delta H_2 - \Delta H_3 + \Delta H_4$$

Units of measurement

The results of the calorimetry experiments are expressed in terms of the defined calorie equal to 4.1840 abs. joules and refer to the isothermal process at 25° and to the true mass. The molecular weights were computed from the 1951 table of international atomic weights [6].

RESULTS

The experimental results are summarized in Tables 2 to 5. Table 2 gives two series of calibration experiments, one performed in the interval 2 125 to 2 085 Ω, the second between 2 155 and 2 115 Ω (ε_1 and ε_2, respectively). The first column gives the input of electrical energy, the second the expression proportional to the temperature increase and the third the value of the heat capacity in calories per unit in $\log(R_i/R_f)$.

Table 2. Calibration experiments.

q, cal.	$\log(R_i/R_f) \times 10^4$		$E \times 10^{-2}$
48.59	82.25		59.08
48.45	82.29		58.87
48.26	81.77		59.02
49.48	84.19		58.77
		Mean	58.93 ± 0.06
48.11	82.07		58.62
47.62	81.53		58.41
48.69	83.37		58.40
48.21	82.31		58.57
		Mean	58.50 ± 0.06

In Table 3 the first column gives R in RSAc, the second column the amount of ester hydrolyzed (corrected to 100 % purity). The fourth column gives the amount of heat evolved during the experiment and the last column ΔH_1 in kcal.mole^{-1}.

Table 3. Determinations of heats of hydrolysis of a number of alkyl thiolesters, RSAc.

R	mmoles	$\log(R_i/R_t) \times 10^4$	q, cal	$-\Delta H$ kcal.mole^{-1}
Et	3.230	94.85	55.84	17.29
	3.278	96.09	56.57	17.26
	3.245	95.03	55.95	17.24
	3.154	92.27	54.32	17.22
			Mean	17.25±0.02
n-Pr	2.813	80.20	47.22	16.79
	2.870	81.64	48.07	16.75
	2.946	83.37	49.09	16.66
	2.936	83.40	49.10	16.72
			Mean	16.73±0.02
n-Bu	2.931	81.91	48.27	16.47
	3.106	86.92	51.22	16.49
	2.987	83.59	49.26	16.59
	3.010	84.60	49.85	16.56
			Mean	16.50±0.02
i-Pr	3.293	97.51	57.41	17.43
	3.096	92.36	54.38	17.56
	2.925	87.04	51.25	17.52
	2.958	87.86	51.73	17.49
			Mean	17.50±0.02
t-Bu	3.086	98.95	57.88	18.76
	3.136	100.08	58.54	18.67
	3.167	101.09	59.14	18.67
	3.106	99.05	57.94	18.65
			Mean	18.69±0.02

Table 4 contains the pertinent heats of solution measurements.

Table 5 contains a summary of the observed data and the heat of hydrolysis of the idealized reaction V.

DISCUSSION

In biochemical literature the thiolesters are often spoken of as being "energy-rich" [7,8]. This expression is meant to imply that a large amount of standard free energy, $\Delta F°$, is released when the S-acyl bond is broken *i.e.* by hydrolysis. Quantitatively, it is sometimes stated that, if $-\Delta F°$ exceeds 8 kcal.*, the compound contains an "energy-rich" bond.

* See for example Fruton, J.S. and Simmonds, S. *General Biochemistry*, John Wiley & Sons, Inc., New York 1954, p. 355.

Table 4. Heats of solution measurements.

Substance	mmoles	$\log(R_i/R_f) \times 10^4$	q, cal	$-\Delta H$ kcal.mole^{-1}
EtSH	3.503	30.38	17.74	5.06
	3.596	31.15	18.19	5.06
	3.588	30.90	18.05	5.03
			Mean	5.05±0.02
n-PrSH	3.215	25.40	14.84	4.62
	3.024	23.34	13.64	4.51
	3.192	24.77	14.47	4.53
			Mean	4.55±0.02
n-BuSH	3.007	21.53	12.58	4.18
	3.249	23.16	13.53	4.16
	3.154	22.36	13.07	4.14
			Mean	4.16±0.02
i-PrSH	3.047	25.40	14.84	4.87
	2.930	24.12	14.09	4.81
	3.345	28.08	16.40	4.90
			Mean	4.86±0.02
t-BuSH	2.852	21.68	12.67	4.44
	3.058	23.31	13.63	4.46
	3.306	25.01	14.62	4.42
			Mean	4.44±0.02
HOAc	3.298	63.79	37.55	11.39
	2.836	55.37	32.59	11.49
	3.020	58.84	34.63	11.47
	3.473	68.07	40.07	11.54
			Mean	11.47±0.03
H_2O	3.168	1.17	0.69	0.22
	2.934	1.10	0.64	0.22
			Mean	0.22±0.02

The equation relating a change in standard free energy, $\Delta F°$, to changes in standard entropy, $\Delta S°$, and standard enthalpy, $\Delta H°$, is

$$\Delta F° = \Delta H° - T\Delta S°$$

Table 5. Summary of experimental data and values of heats of hydrolysis of the idealized reaction RSAc(l) + H_2O(l) = RSH(l) + HOAc(l).

R	$-\Delta H_1$	$-\Delta H_2$	$-\Delta H_3$	$-\Delta H_4$	$-\Delta H°$ at 25°C
Et	17.25	5.05	11.47	0.22	0.95
n-Pr	16.73	4.55	11.47	0.22	0.93
n-Bu	16.50	4.16	11.47	0.22	1.09
i-Pr	17.50	4.86	11.47	0.22	1.39
t-Bu	18.69	4.44	11.47	0.22	3.00

A large $\Delta F°$ value may be traced back either to a large $\Delta H°$-term or to a large $T\Delta S°$-term or to both terms, $\Delta H°$ and $\Delta S°$ in this case having different signs.

The present investigation shows that the value of $-\Delta H°$ for simple alkyl thiolesters is only from 1 to 3 kcal.mole^{-1}. Therefore, if $-\Delta F°$ is to be large, a large increase in entropy must occur during the hydrolysis.

The close analogy between the hydrolysis of an alkyl ester and an alkyl thiol ester

$$\mathrm{ROAc} + \mathrm{H_2O} \rightleftharpoons \mathrm{ROH} + \mathrm{HOAc}$$
$$\mathrm{RSAc} + \mathrm{H_2O} \rightleftharpoons \mathrm{RSH} + \mathrm{HOAc}$$

makes it unlikely that the hydrolysis of the S-acyl compounds should be accompanied by a large change in $\Delta S°$. It is known that $\Delta H°$ and $\Delta F°$ for the hydrolysis of an O-ester have nearly the same values, both being *ca.* 0—2 kcal.mole^{-1}. The change in entropy is therefore small. From known values of entropies of alcohols and thiols on one hand, and non-hydrogen bonding compounds like ethers on the other, it is likely that the $T\Delta S°$-term for the hydrolysis of a thiolester is *ca.* 1—1.5 kcal.mole^{-1}. It is therefore very probable that simple alkyl thiolesters are not "energy-rich" in the sense referred to above.

Acknowledgement. The author wishes to thank Professor B. Bak and co-workers, University of Copenhagen, for determining the infrared spectra. This investigation has been supported by the *Swedish Natural Science Research Council* and the *State Council of Technical Research.*

REFERENCES

1. Sunner, S. and Wadsö, I. *Trans. Faraday Soc.* **52** (1956) 1088.
2. Rylander, P. N. and Tarbell, D. S. *J. Am. Chem. Soc.* **72** (1950) 3021.
3. Brinzinger, H., Pfannenstill, K. and Kling, K.-E. *Chem. Ber.* **83** (1950) 87.
4. Barltrop, J. A., Hayes, P. M. and Calvin, M. *J. Am. Chem. Soc.* **76** (1954) 4359.
5. Mathias, S. *J. Am. Chem. Soc.* **72** (1950) 1897.
6. Wichers, E. *J. Am. Chem. Soc.* **74** (1952) 2447.
7. Wieland, Th. and Bokelmann, E. *Ann.* **576** (1952) 20.
8. Lynen, F. *Angew. Chem.* **67** (1955) 463.

Received July 31, 1957.

ACTA CHEMICA SCANDINAVICA 11 (1957) 1752—1756

The Preparation of 6-Chloro-*ortho*cresol and 4,6-Dichloro-*ortho*cresol and the Corresponding *Ortho*toloxyacetic acids

SVEN NORD and BERTIL SJÖBERG

Research Laboratories, Skoghallsverken, Uddeholms AB., Skoghall, Sweden

From a mixture of the closeboiling *o*-cresol and 6-chloro-*o*-creso pure 6-chloro-*o*-cresol has been prepared over the corresponding acetates. From the 6-chloro-*o*-cresol pure 4,6-dichloro-*o*-cresol was obtained by chlorination. 6-Chloro-*o*-toloxyacetic acid and 4,6-dichloro-*o*-toloxyacetic acid have been synthesized and the infrared spectra of these compounds and *o*-toloxyacetic acid have been recorded.

In an earlier paper [1] describing the determination of chloro-2-methylphenoxyacetic acid by infrared spectrophotometry the preparation of 6-chloro-*o*-cresol (2-methyl-6-chlorophenol) and 4,6-dichloro-*o*-cresol (2-methyl-4,6-dichlorophenol) and the corresponding *o*-toloxyacetic acids was briefly mentioned. As an answer to many inquiries we now give the details about the preparation and further physical data.

By the chlorination of *ortho*cresol with an equivalent amount of chlorine the reaction product usually has the following composition: 5—10 % *ortho*-cresol, 57—60 % 4-chloro-*ortho*cresol, 22—26 % 6-chloro-*ortho*cresol and 3—7 % 4,6-dichloro*ortho*cresol. The boiling points of these compounds given in the literature are shown in Table 1.

Table 1. The boiling points of *o*-cresol and chlorinated *o*-cresols.

Compound	Boiling point, °C at 760 mm Hg
o-Cresol	191
6-Chloro-*o*-cresol [2]	189
4-Chloro-*o*-cresol [3]	220—225
4,6-Dichloro-*o*-cresol [4]	226.5

At the distillation of the crude chlorination product the first run will contain the low-boiling *o*-cresol and 6-chloro-*o*-cresol. These two compounds can hardly be separated by further distillation on account of their close boiling points. Neither can in the higher boiling fraction 4-chloro-*o*-cresol and 4,6-dichloro-*o*-cresol conveniently be separated by distillation.

In order to obtain better separation we transformed the mixture of *o*-cresol and 6-chloro-*o*-cresol from the distillation of the crude chlorination product into the corresponding acetates. *o*-Cresylacetate has previously been prepared by v. Auwers, Lechner and Bundesmann [5], who found a boiling point of 87°C at 12 mm Hg and by Raschig [6], who reports a boiling point of 212.5°C at 760 mm Hg. 6-Chloro-*o*-cresylacetate does not seem to have been prepared before. In the present investigation we found that 6-chloro-*o*-cresylacetate had an about 30°C higher boiling point than *o*-cresylacetate and that the two acetates could effectively be separated by fractional distillation. During the distillation we checked the purity of the fractions by means of infrared spectrographic analysis. The physical data of the carefully purified acetates are given in Table 2.

The pure 6-chloro-*o*-cresylacetate was hydrolyzed with dilute sodium hydroxide solution and from the alkaline solution 6-chloro-*o*-cresol was liberated with sulfuric acid. The cresol was distilled in vacuum and further purified by fractional freezing. In the pure 6-chloro-*o*-cresol no traces of other cresols could be found by vapor chromatography.

By chlorination of the pure 6-chloro-*o*-cresol with less than the equivalent amount of chlorine we obtained a 4,6-dichloro-*o*-cresol that could be purified by distillation and recrystallization. The physical data for 6-chloro-*o*-cresol and 4,6-dichloro-*o*-cresol are given in Table 2.

Table 2. Physical data

	Boiling point °C/mm Hg	Melting point °C	d_4^{20}	n_D^{20}	MR_D Calc.[10]	MR_D Found
o-Cresylacetate	63.5/1.5 210.7—210.9/774		1.0482	1.4998	41.82	42.12
6-Chloro-*o*-cresyl acetate	78/1.2 238.4—239.0/753		1.1778	1.5134	46.68	47.14
6-Chloro-*o*-cresol	191.0—192.3/757	1.5—2.0	1.1966	1.5452	37.32	37.68
4,6-Dichloro-*o*-cresol	231.6—231.9/739	52.5—52.7				
6-Chloro-*o*-toloxy-acetic acid		109.5—109.8				
4,6-Dichloro-*o*-toloxy-acetic acid		187.9—188.2				
o-Toloxyacetic acid		154.8—154.9				

From the cresols we prepared 6-chloro-*o*-toloxyacetic acid and 4,6-dichloro-*o*-toloxyacetic acid [7, 8] by reaction with monochloro-acetic acid in an alkaline solution as has been described earlier [1, 9]. The acids were carefully purified by recrystallization from benzene (physical data in Table 2). The infrared spectra of the acids were recorded (Figs. 1 and 2). As a comparison we also recorded the infrared spectrum of *o*-toloxyacetic acid (Fig. 3).

From the comparison of the spectra it is obvious that the acids are not contaminated with each other.

EXPERIMENTAL

Preparation of o-cresylacetate and 6-chloro-o-cresylacetate. 900 g of a mixture of about 22 % cresol and 78 % 6-chloro-*o*-cresol, obtained from the distillation of chlorinated

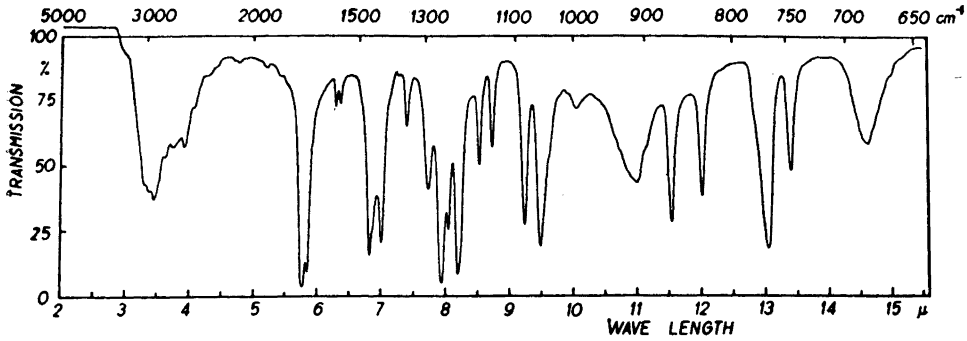


Fig. 1. The infrared spectrum of 6-chloro-*o*-toloxyacetic acid in KBr.

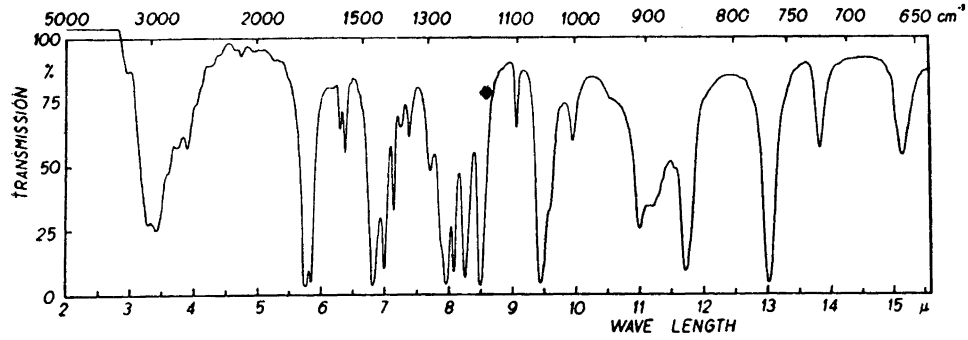


Fig. 2. The infrared spectrum of 4,6-dichloro-*o*-toloxyacetic acid in KBr.

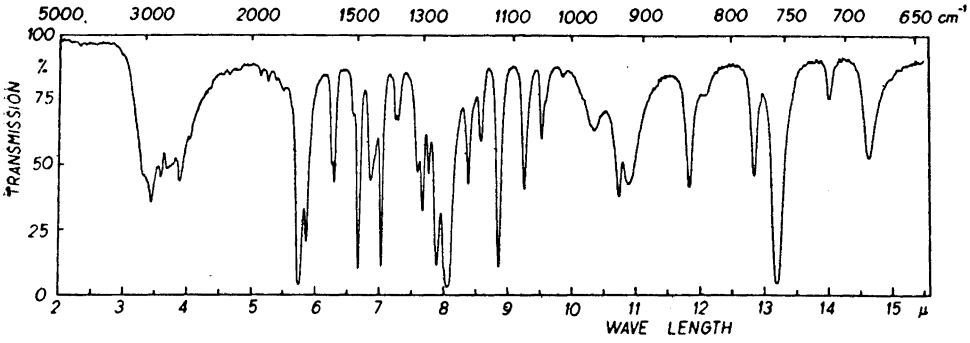


Fig. 3. The infrared spectrum of *o*-toloxyacetic acid in KBr.

o-cresol, was heated with reflux with 900 g acetic acid anhydride and 2 ml konc. sulfuric acid for about 2 h. From the reaction product most of the remaining anhydride and the acetic acid formed was distilled off at 100 mm Hg. The rest was fractionated in vacuum with an 1.5 m highly effective column. At about 90°C and 10 mm Hg we obtained 236 g *o*-cresylacetate and at about 105°C and 10 mm Hg 813 g 6-chloro-*o*-cresylacetate. The acetates were carefully purified by further distillation and the purity checked by infra-

red spectrometry. o-*Cresylacetate* (Found: C 71.4; H 6.74. Calc. for $C_9H_{10}O_2$: C 72.0; H 6.71). *6-Chloro*-o-*cresylacetate* (Found: C 58.3; H 4.79; Cl 19.26. Calc. for $C_9H_9ClO_2$: C 58.6; H 4.91; Cl 19.21).

Preparation of 6-chloro-o-*cresol:* 200 g sodium hydroxide dissolved in 500 ml water was heated to 110°. With good agitation 386 g 6-chloro-*o*-cresylacetate was added in about half an hour. After cooling to room temperature the reaction product was acidified with 300 ml sulfuric acid (50 %). The separated oil was washed with a saturated solution of sodium bicarbonate and distilled in vacuum. To prevent oxidation carbon dioxide was led through the capillary in the distillation pot. At 76°C and 10 mm Hg we obtained 285 g 6-chloro-*o*-cresol (yield 95 %). The cresol was redistilled and purified by fractional freezing. The purity of the 6-chloro-*o*-cresol was checked with vapor chromatography. We used a Perkin Elmer chromatograph, model 154 B with column C at a temperature of 190°C. No traces of other cresols could be found in the purified 6-chloro-*o*-cresol. *6-Chloro*-o-*cresol* (Found: C 58.4; H 4.87; Cl 24.99. Calc. for C_7H_7ClO: C 59.0; H 4.95; Cl 24.87).

Preparation of 4,6-dichloro-o-*cresol.* 150 g 6-chloro-*o*-cresol (1.05 mole) was heated to 50—60°C in a round bottom flask equipped with agitator and reflux condenser. At this temperature the cresol was reacted with 71 g chlorine which was slowly introduced during about 5 h. The reaction product was distilled in vacuum. After a forerun of 37 g, mainly containing unchlorinated 6-chloro-*o*-cresol we obtained 111 g 4,6-dichloro-*o*-cresol boiling between 111 and 113°C at 16 mm Hg (yield 60 %). The cresol was further purified by recrystallization from petroleum ether. *4,6-Dichloro*-o-*cresol* (Found: C 47.6; H 3.46; Cl 40.25. Calc. for $C_7H_6Cl_2O$: C 47.5; H 3.42; Cl 40.06).

Preparation of 6-chloro-o-*toloxyacetic acid.* 71 g 6-chloro-*o*-cresol (0.5 mole) and 27 ml sodium hydroxide solution (35 %) were charged in a round bottom flask equipped with agitator, two separating funnels as charging means, a reflux condenser, an antimony electrode with a calomel reference electrode and a heating device. The solution was heated to about 100°C. Then 57 g monochloroacetic acid (0.6 mole) dissolved in 15 ml water was added from one of the separating funnels in the course of about one hour. Through the other separating funnel sodium hydroxide solution of 35 % strength was simultaneously added to keep the solution during the whole reaction at a pH value of 10.5 as measured by means of the antimony electrode. Altogether 80 ml sodium hydroxide solution was added. After 3 h at 100°C the reaction mixture was cooled to room temperature and adjusted with acid to pH 7.0. Nonreacted 6-chloro-*o*-cresol was extracted with ether. The solution was then acidified to complete precipitation of the acid, which was filtered, washed and dried. Yield 92 g or 92 %. The acid was purified by recrystallization from benzene. *6-Chloro*-o-*toloxyacetic acid* (Found: C 53.8; H 4.46; Cl 17.69. Calc. for $C_9H_9ClO_3$: C 53.9; H 4.52; Cl 17.68).

Preparation of 4,6-dichloro-o-*toloxyacetic acid.* 80 g 4,6-dichloro-*o*-cresol (0.45 mole) was reacted with 52 g monochloroacetic acid (0.55 mole) in alkaline solution in the same way as described for 6-chloro-*o*-toloxyacetic acid. We obtained 89 g 4,6-dichloro-*o*-toxyacetic acid (yield 84 %) which was purified by recrystallization from benzene. *4,6-Dichloro*-o-*toloxyacetic acid* (Found: C 45.9; H 3.36; Cl 30.30. Calc. for $C_9H_8Cl_2O_3$: C 46.0; H 3.43; Cl 30.17).

The infrared spectra. The infrared spectra were recorded with a Perkin-Elmer spectrometer, Model 21a, with a rock-salt prism. Slit schedule 927, corresponding to program 4. Speed: 3 min/μ. The frequencies of the absorption bands are given below in cm^{-1}.

6-Chloro-toloxyacetic acid (Fig. 1). 1.4 mg/0.35 g KBr. At 2 500—3 100 broad band with peaks at 2 920, 2 774, 2 685 and 2 561, 1 741(s), 1 717 (m), 1 594(w), 1 576(w), 1 470(s), 1 432(s), 1 354(w), 1 296(w), 1 262(s), 1 245(w), 1 223(s), 1 174(w), 1 146(w), 1 084(m), 1 057(s), 996(w), 910(m), 868(m), 833(m), 767(s), 747(m) and 685(m).

4,6-Dichloro-o-*toloxyacetic acid* (Fig. 2). 1.8 mg/0.35 g KBr. At 2 500—3 100 broad band with peaks at 3 044, 2 920, 2 677 and 2 574, 2 107(w), 1 738(s), 1 714(m), 1 589(w), 1 569(m), 1 470(s), 1 430(m), 1 400(m), 1 378(w), 1 356(w), 1 296(w), 1 257(s), 1 237(m), 1 210(s), 1 177(s), 1 103(w), 1 060(s), 1 006(w), 910(m) 854(s) 768(s), 723(m) and 661 (m).

o-*Toloxyacetic acid* (Fig. 3). 1.6 mg/0.35 g KBr. At 2 500—3 100 broad band with peaks at 2 928, 2 805, 2 714 and 2 587, 1 744(s), 1 711(m), 1 601(w), 1 592(m), 1 503(s), 1 461(m), 1 426(s), 1 380(w), 1 373(w), 1 320(w), 1 306(m), 1 289(w), 1 268(s), 1 243(vs), 1 194(m), 1 166(w), 1 130(s), 1 082(m), 1 051(w), 1 017(vw), 965(w), 932(m), 918(m), 845(m), 825(vw), 779(m), 758(s), 713(w) and 684(m).

The authors gratefully acknowledge the assistence of ing. Sven Lundgren and ing. Bengt Axelsson (synthetic work), ing. Bengt Berglund (infrared spectrometry) and ing. Esse Zetterqvist (chemical analyses).

REFERENCES

1. Sjöberg, B. *Acta Chem. Scand.* **4** (1950) 798.
2. Huston, R. C. and Neely, A. H. *J. Am. Chem. Soc.* **57** (1935) 2177.
3. Sah, P. P. T. and Anderson, H. N. *J. Am. Chem. Soc.* **63** (1941) 3165.
4. Bures, E. *Chem. listy* **21** (1927); *Chem. Abstracts* **22** (1928) 63.
5. v. Auwers, K., Lechner, M. and Bundesmann, H. *Ber.* **58B** (1925) 41.
6. Raschig, F. in *Beilsteins Handbuch der organischen Chemie*, IV. Aufl., Bd. **6** (1923) **355.**
7. Haskelberg, L. *J. Org. Chem.* **12** (1947) 426.
8. Hansch, C. and Crosby, D. G. *J. Am. Chem. Soc.* **71** (1949) 3851.
9. Sjöberg, B. and Lundgren, S. Brit. pat. 697.468.
10. Eisenlohr, F. *Z. physik. Chem.* **75** (1910) 585; **79** (1912) 129.

Received August 13, 1957.

ACTA CHEMICA SCANDINAVICA 11 (1957) 1757—1760

The Heat of Hydrolysis of *i*-Propenyl Acetate and *m*-Cresyl Acetate and the Heat of Enolization of Acetone

S. SUNNER

Thermochemistry Laboratory, University of Lund, Lund, Sweden

The heats of hydrolysis of *i*-propenyl acetate and of *m*-cresyl acetate were measured at 25°C in a reaction calorimeter. The experimental data yielded for the reaction

$$CH_2 = CMe \cdot OAc(liq) + H_2O(liq) \rightarrow Me_2CO(liq) + HOAc(liq)$$

the value $\Delta H°_r = -14.39 \pm 0.06$ kcal.mole^{-1} and for the reaction

$$m\text{-}MeC_6H_4 \cdot OAc(liq) + H_2O(liq) \rightarrow m\text{-}MeC_6H_4OH(liq) + HOAc(liq)$$

the value $\Delta H°_r = -4.39 \pm 0.07$ kcal.mole^{-1}. A comparison between these two reactions yielded for the enolization reaction of acetone

$$Me_2CO(liq) \rightarrow CH_2 = CMeOH(liq)$$

a value of the enthalpy change of $\Delta H° = 7$ kcal.mole^{-1} in excellent agreement with a value derived from the measurement of the equilibrium between acetone and *i*-propenol, made by Schwarzenbach and Wittwer [9].

EXPERIMENTAL

Apparatus, calibration and procedure have been described elsewhere [1]. The calorimeter was charged with 90 ml of 60 % by volume ethanol containing 0.8 equiv. of sodium hydroxide per liter. The sample of the ester was enclosed in a sealed glass ampoule.

Materials. i-Propenyl acetate (Eastman Kodak) was purified by distillation through a 75 cm packed column; the main fraction had a b.p. of 96.7°C at 749 mm Hg (corr.). The equivalent weight was determined by hydrolysis in 90 % ethanol containing twice the required amount of NaOH. Equiv. wt found: 100.2, 100.2, 100.0 and 99.7; mean value 100.05±0.10; calculated 100.11.

m-Cresyl acetate was synthesized [2] from *m*-cresol, distilled twice (b.p. 76° at 2 mm Hg and 102° at 22 mm Hg) and the resulting main fraction was frozen out four times (m.p. 9.8°, corr.). The purity was checked by alkaline hydrolysis. Neither the use of indicators and reference solutions nor of potentiometric titrations gave a sharp end point. The potentiometric titrations showed an equivalent weight 0.3 % too low.

Acetone, analytical reagent grade, was purified according to Vogel (method a) [3].

m-Cresol (B.D.H. Laboratory Reagent 98/100 %) was distilled and the main fraction (b.p. 71° at 3 mm Hg) was frozen out three times (m.p. 11.1°, corr.).

RESULTS

Calibration and heat of reaction measurements. The determinations of the heat equivalent of the calorimeter and of the heat of hydrolysis of *i*-propenyl acetate and *m*-cresyl acetate are summarized in Tables 1, 2 and 3, respectively.

The first column in all tables gives the number of the experiment. In Table 1, the second column shows the temperature increase, expressed as $^{10}\log R_i/R_f$, where R_i is the resistance of the thermistor at the initial temperature and R_f that at the final temperature of the reaction period. The third column gives the input of electrical energy in calories and the fourth column shows the value obtained for the proportionality constant, k, in the expression $q(\text{cals.}) = k \times {}^{10}\log R_i/R_f$.

In Tables 2 and 3 the second column gives the number of mmoles of acetate hydrolyzed, the fourth column the amount of heat evolved and the last column the increase in enthalpy on a molar basis.

Table 1. The heat equivalent of the calorimeter. Initial temperature 24.5° and final temperature 25.5°C. The current was passed for 570 sec, the duration of the reaction period was 11 min.

No.	$10^4 \times \log R_i/R_f$	q, cal	$k \times 10^{-2}$ cal
1 565	139.153	81.242	58.38
1 567	140.946	82.217	58.33
1 569	141.724	82.559	58.25
1 571	141.030	82.148	58.25
		Mean:	$(58.30 \pm 0.30) \times 10^{-2}$

Table 2. The heat of hydrolysis of *i*-propenyl acetate. Duration of the reaction period 7 min. $k = 0.5830$.

No.	mmoles	$10^4 \times \log R_i/R_f$	q, cal	$-\Delta H_1$ kcal.mole^{-1}
1 566	3.0262	131.157	76.464	25.27
1 568	3.1667	137.565	80.200	25.33
1 570	3.0230	131.277	76.534	25.32
1 572	3.2487	141.083	82.251	25.32
			Mean:	25.31 ± 0.015 kcal.mole^{-1}

Table 3. The heat of hydrolysis of *m*-cresyl acetate. Duration of the reaction period 10 min. $k = 0.7219$ (1 577), 0.7207 (1 579), 0.6965 (1 588).

No.	mmoles	$10^4 \times \log R_i/R_f$	q, cal	$-\Delta H_1$ kcal.mole^{-1}
1 577	2.968	83.894	60.563	20.41
1 579	3.022	85.762	61.809	20.45
1 588	3.006	88.400	61.571	20.48
			Mean:	20.45 ± 0.02 kcal.mole^{-1}

Correction to standard states. The actual reaction taking place in the calorimeter is represented by eqn. (1). In order to obtain the isothermal, ideal hydrolysis reaction (5), it is necessary to substract eqns. (2) and (3) from (1) and to add eqn. (4).

$$CH_2 = CMe \cdot OAc(liq) + OH^-(soln) \rightarrow Me_2CO(soln) + AcO^-(soln) \quad (1a)$$
$$MeC_6H_4 \cdot OAc(liq) + OH^-(soln) \rightarrow MeC_6H_4OH(soln) + AcO^-(soln) \quad (1b)$$
$$Me_2Co(liq) \rightarrow Me_2CO(soln) \quad (2a)$$
$$MeC_6H_4OH(liq) \rightarrow MeC_6H_4OH(soln) \quad (2b)$$
$$HOAc(liq) + OH^-(soln) \rightarrow AcO^-(soln) + H_2O(soln) \quad (3)$$
$$H_2O(liq) \rightarrow H_2O(soln) \quad (4)$$

$$CH_2 = CMe \cdot OAc(liq) + H_2O(liq) \rightarrow CH_3COCH_3(liq) + HOAc(liq) \quad (5a)$$
$$MeC_6H_4 \cdot OAc(liq) + H_2O(liq) \rightarrow MeC_6H_4OH(liq) + HOAc(liq) \quad (5b)$$

The heat of solution of acetone and *m*-cresol in a liquid phase of proper composition, eqn. (2), had to be determined in separate experiments. The heat of solution of glacial acetic acid, eqn. (3), and the heat of dilution of the liquid, eqn. (4), have been previously determined.

The heat of hydrolysis of the idealized reaction (5) at 25°C is then

$$\Delta H_r^\circ = \Delta H_1 - \Delta H_2 - \Delta H_3 + \Delta H_4$$

ΔH_2 was determined to be 0.498 ± 0.003 kcal.mole^{-1} (acetone) and -4.643 ± 0.007 kcal.mole^{-1} (*m*-cresol). ΔH_3 and ΔH_4 were found to be -11.61 ± 0.03 and -0.19 ± 0.01 kcal.mole^{-1}, respectively [4]. Thus

$$-\Delta H_r^\circ(liq) = 14.39 \pm 0.06 \text{ kcal.mole}^{-1} \quad (5a)$$
$$-\Delta H_r^\circ(liq) = 4.39 \pm 0.07 \text{ kcal.mole}^{-1} \quad (5b)$$

In order to calculate the heat of hydrolysis when both reactants and reaction products are in the gaseous state it is necessary to know the heats of vaporization for all the compounds at 25°C.

The heat of vaporization of acetic acid to form monomer gaseous molecules was calculated by Parks and Huffman [5] to be 12.5 kcal.mole^{-1}. The heat of vaporization of acetone [5] and water [6] have been determined to be 7.59 and 10.52 kcal.mole^{-1}, respectively. For *i*-propenyl acetate and *m*-cresyl acetate, the heat of vaporization was estimated from Klages equation [7] to be 8.9 and 13.2 kcal.mole^{-1}, respectively. For *m*-cresol the heat of vaporization was calculated from Stull's vapor pressure data [8] to be 12.0 kcal.mole^{-1}.
Thus, for the reaction,

$$CH_2 = CMe \cdot OAc(g) + H_2O(g) \rightarrow CH_3COCH_3(g) + HOAc(g) \quad (6a)$$
$$\Delta H_r^\circ(g) = -13.7 \text{ kcal.mole}^{-1}$$

and for the reaction

$$CH_3C_6H_4 \cdot OAc(g) + H_2O(g) \rightarrow CH_3C_6H_4OH(g) + HOAc(g) \quad (6b)$$
$$\Delta H_r^\circ(g) = -3.6 \text{ kcal.mole}^{-1}$$

THE HEAT OF ENOLIZATION OF ACETONE

The hydrolysis of *i*-propenyl acetate to acetone, (6a), may be split into two consecutive steps, *viz.* the hydrolysis to *i*-propenol, (6a 1) and the protomeric isomerization of *i*-propenol to acetone, (6a 2):

$$CH_2 = CMe \cdot OAc + H_2O \rightarrow CH_2 = CMeOH + HOAc \quad (6a\ 1)$$
$$CH_2 = CMeOH \rightarrow Me_2CO \quad (6a\ 2)$$

A knowledge of the value of the heat of reaction (6a 1) makes it possible to obtain a value for the heat of reaction (6a 2), which is the reverse of the enolization reaction of acetone.

Reaction (6a 1) is of course not experimentally accessible; it is therefore necessary to estimate the accompanying change in enthalpy indirectly. This has been achieved by a comparison of the hydrolysis of *i*-propenyl acetate with that of *m*-cresyl acetate. By subtracting eqn. (6a 1) from (6b) one gets

$$m\text{-}MeC_6H_4 \cdot OAc + CH_2 = CMeOH \rightarrow m\text{-}MeC_6H_4OH + CH_2 = CMe \cdot OAc \quad (7)$$

The complete symmetry in eqn. (7) suggests that $\Delta H_7 = \Delta H_{6b} - \Delta H_{6a\,1} = 0$. Thus $\Delta H_{6a\,1} = -3.6$ kcal.mole^{-1} and the heat of enolization of acetone in the gaseous state becomes $-\Delta H_{6a\,2} = +10$ kcal.mole^{-1}.

The heat of vaporization of acetone [5] is 7.6 kcal.mole^{-1} and that of *i*-propenol was estimated to 10.5 kcal.mole^{-1} from a comparison between saturated and unsaturated compounds. The heat of enolization of acetone in the liquid state is therefore equal to 7.0 kcal.mole^{-1}.

Schwarzenbach and Wittwer [9] determined experimentally the equilibrium between acetone and *i*-propenol in solution and found the change in standard free energy to be about 8 kcal.mole^{-1}. The change in entropy accompanying the isomerization can be estimated in the following way.

For the dehydrogenation reaction

$$Me_2CHOH(g) \rightarrow Me_2CO(g) + H_2(g) \quad (8)$$

the entropy change at 25°C is $\Delta S_8^\circ = 29.80$ e.u.[5] A comparison between different gaseous compounds of the two types RCH = CMe . R' and RCH_2—CHMeR' and with known values of ΔS° shows that the unsaturated compound has an entropy value which is in average 0.3 kcal. less than that of the saturated compound. This value combined with the known ΔS° value for gaseous hydrogen [6], 31.2 e.u., gives $\Delta S^\circ = -1$ e.u. for the isomerization *i*-propenol(g)→acetone(g). From estimated values of the vapor pressure (20 mm) and heat of vaporization (10.5 kcal.) of *i*-propenol at 25°C and those data of acetone [5], the entropy change for the isomerization in the liquid state was calculated to +3 e.u. Thus, the heat of enolization of acetone to *i*-propenol in the liquid state becomes 7 kcal.mole^{-1} in excellent agreement with the result from the present thermochemical investigation.

Acknowledgement. This investigation has been supported by the *Swedish Natural Sciences Research Council* and the *State Council of Technical Research.*

REFERENCES

1. Sunner, S. and Wadsö, I. *Acta Chem. Scand.* **12** (1958) *In press.*
2. Vogel, A. I. *Practical Organic Chemistry* Longmans, Green and Co., London 1948, p. 639.
3. Ref.[2] p. 170.
4. Wadsö, I. *Acta Chem. Scand.* **11** (1957) 1745.
5. Parks, G. S. and Huffman, H. M. *The Free Energies of Some Organic Compounds.* The Chemical Catalog Co., Inc., New York 1932.
6. *Selected Values of Chemical Thermodynamic Properties* (SVCTP), *Natl. Bur. Standards Circ.* 500, Washington 1950.
7. Klages, F. *Chem. Ber.* **82** (1949) 358.
8. Stull, D. R. *Ind. Eng. Chem.* **39** (1947) 517.
9. Schwarzenbach, G. and Wittwer, Ch. *Helv. Chim. Acta* **30** (1947) 669.

Received August 27, 1957.

ACTA CHEMICA SCANDINAVICA 11 (1957) 1761—1765

The Heat of Oxidation of Arsenious Oxide to Arsenic Oxide in Aqueous Solution

LARS BJELLERUP, STIG SUNNER and INGEMAR WADSÖ

Thermochemistry Laboratory, University of Lund, Lund, Sweden

The heat of reaction, $-\Delta H$, at 25°C and at a constant pressure of 1 atm, for the reaction of liquid bromine with arsenious oxide solution was measured with a glass Dewar calorimeter.

The experimental data yielded for the reaction

$$[As_2O_3 + 2H_2O](aq) + 2Br_2(liq) \rightarrow [As_2O_5 + 4HBr](aq)$$

the value $\Delta H_{25°C} = -56.92 + 0.12$ kcal/mole. Combination of this datum with established heat of formation data for aqueous hydrogen bromide and liquid water yielded for the reaction

$$As_2O_3(aq) + O_2(g) \rightarrow As_2O_5(aq)$$

$\Delta H_{25°C} = -78.0 \pm 0.1$ kcal/mole.

In connection with bomb calorimetric work on organic bromine compounds [1] an accurate value for the heat of reaction, $-\Delta H$, at 25°C and constant pressure for the reaction

$$As_2O_3(aq) + O_2(g) \rightarrow As_2O_5(aq) \quad (1)$$

was needed. Since a direct determination of this heat effect could not be undertaken a review was made of available experimental thermochemical data from which the required datum could be calculated. As a result of this review it was decided necessary to make a redetermination of the heat of reaction, $-\Delta H$, at 25°C and constant pressure of 1 atm, for the reaction

$$[As_2O_3 + 2H_2O](aq) + 2Br_2(liq) \rightarrow [As_2O_5 + 4HBr](aq) \quad (2)$$

This paper described the measurement of the mentioned datum. The heat capacity for the arsenious oxide solution used in the heat of reaction experiments was also determined.

EXPERIMENTAL

Apparatus. The calorimetric system [2] consisted of a silvered glass Dewar vessel, capacity 100 ml, mounted in a thermostat. The inner parts, stirrer, thermometer, heating coil and sample ampoule were mounted in a size 34 cone, fitting in the Dewar vessel. The temperature was measured with a small Beckmann thermometer.

Calibration. The energy equivalent of the calorimetric system at 25°C was determined electrically by passing a constant current through the heating coil for a measured length of time (about 180 sec). The resistance of the heating coil was known to within 0.05 % and the current was measured with the aid of a standard resistor in series with the heating coil. The potential drop across the standard resistor was measured by comparing it with a standard cell to within 0.02 %. The temperature readings of the after period were started 15 min from the end of the heating period in order to secure thermal equilibrium. The thermal leakage was calculated by the Regnault-Pfaundler method.

In the calibration experiments the calorimeter contained 75.00 ml of a 0.0624 M arsenious oxide solution. Two series of calibration experiments were performed — one with a temperature increase of the calorimeter, ΔT, of about 0.9 deg and one with a ΔT of about 0.45 deg, corresponding to the two different amounts of bromine used in the heat of reaction measurements.

Procedure. The calorimeter was charged with 75.00 ml of 0.0624 M arsenious oxide solution and with a sealed glass ampoule containing a known amount of bromine. At the end of the fore period the reaction was started by breaking the thinwalled glass ampoule by pushing it against the bottom of the calorimeter vessel. The reaction was completed within 5 min but the after period — as in the calibration experiments — was not started until 15 min after the completion of the heat evolution. In order to detect possible systematic errors, two different amounts of bromine were used, about 0.25 and 0.50 g, respectively. All measurements were made at 25°C.

Materials. The bromine used was a Merck, Darmstadt, *pro analysi* grade. In order to remove the small amount of chlorine known to be present in the commercial sample the bromine was stored over finely ground potassium bromide (Coleman & Bell's C.P. grade) for two days with occasional shaking. The bromine was then distilled from the mixture under vacuum at about 20°C. The distillate was free from chlorine.

The arsenious oxide was a Merck, Darmstadt, *pro analysi* grade and was used without further purification. Arsenious oxide solution was prepared by dissolving the substance in boiling water.

The concentration of the arsenious oxide solution was determined by potentiometric titration with potassium permanganate and was found to be $C_{As_2O_3} = 0.0625$ M. The density at 25°C of this solution was $d_4^{25} = 1.0067$ g/ml.

RESULTS

Calibration. Data obtained in the two series of calibration experiments are given in Tables 1 and 2.

The following quantities are listed in the tables:

q	amount of heat evolved in the calorimetric system,
ΔT	temperature increase in the calorimeter,
ε	energy equivalent at 25°C of the calorimetric system.

Heat of reaction measurements. The data obtained in the heat of reaction experiments with various amounts of bromine are given in Table 3.

The ε-values given in the table are the means from Table 1 and Table 2, respectively, to which have been added the heat capacities of the glass ampoule and the bromine used in the various experiments.

Of the dissolved substances participating in the reaction $HBr \cdot nH_2O$ is the only one for which heat of dilution data are available. Therefore, by

Table 1. Calibration experiments with arsenious oxide solution in the calorimeter and ΔT = *ca.* 0.9 deg

q cal	ΔT deg	ε cal/deg
71.94	0.7921	90.82
85.44	0.9418	90.72
85.54	0.9355	91.44
83.47	0.9136	91.36
83.03	0.9134	90.90
82.89	0.9138	90.71

Mean: $\varepsilon = 90.99 \pm 0.13$ * cal/deg

* All uncertainties given are the standard deviation of the mean

Table 2. Calibration experiments with arsenious oxide solution in the calorimeter and ΔT = *ca.* 0.45 deg

q cal	ΔT deg	ε cal/deg
41.67	0.4592	90.74
41.63	0.4564	91.21
41.65	0.4624	90.07
41.56	0.4628	89.80
41.51	0.4551	91.21
41.50	0.4591	90.39
41.27	0.4484	91.98

Mean: $\varepsilon = 90.77 \pm 0.29$ cal/deg

Table 3. Data from heat of reaction experiments

Amount of bromine g	ΔT deg	ε cal/deg	$q_{\text{dil HBr}}$ cal	$q + q_{\text{dil HBr}}$ cal	$-\Delta H_{25°C}$ (reaction 2) kcal/mole
0.5603	1.0827	91.11	0.86	99.50	56.77
0.4544	0.8794	91.10	0.64	80.76	56.81
0.2316	0.4505	90.87	0.25	41.18	56.84
0.2247	0.4413	90.87	0.24	40.34	57.38
0.2251	0.4438	90.86	0.24	40.56	57.60
0.2568	0.5023	90.87	0.29	45.93	57.17
0.4845	0.9310	91.09	0.70	85.51	56.42
0.4910	0.9411	91.09	0.72	86.44	56.28
0.5005	0.9709	91.10	0.74	89.19	56.96
0.2297	0.4506	90.84	0.24	41.18	57.30
0.2754	0.5328	90.85	0.32	48.72	56.55

Mean: $\Delta H_{25°C}$ (reaction 2) $= -56.92 \pm 0.12$ kcal/mole

addition of the term $q_{\text{dil HBr}}$ to the experimentally determined q-value ($q = \varepsilon \cdot \Delta T$), all data have been reduced to a uniform final concentration of HBr, corresponding to infinite dilution.

Heat capacity measurements. In order to obtain a value for the heat capacity of the 0.0624 M arsenious oxide solution used in the heat of reaction experiments an electrical "calibration" of the calorimetric system was done with the calorimeter containing 75.00 ml of water instead of arsenious oxide solution. The data obtained are given in Table 4.

Table 4. "Calibration" with water in the calorimeter

q cal	ΔT deg	ε cal/deg
73.52	0.8074	91.06
73.41	0.8108	90.54
73.82	0.8088	91.27
85.37	0.9398	90.84
85.43	0.9351	91.36
83.00	0.9095	91.26
82.55	0.9025	91.47

Mean: $\varepsilon = 91.11 \pm 0.12$ cal/deg

Table 5. Comparison of results from various investigations

Investigators	$\Delta H_{25°C}$ (reaction 1) kcal/mole
Thomsen [5]	−78.2
Berthelot [6]	−76.2
Smith and Sunner [7]	−77.9
This work	-78.0 ± 0.1

Combination of the mean ε-values from Tables 1 and 4 with the value 0.99707 g/ml for the density of water at 25°C, the value 0.99892 cal/g deg for the heat capacity of water at 25°C and the value 1.0067 g/ml for the density of 0.0624 M arsenious oxide water solution at 25°C yielded the value 0.988 ± 0.002 cal/g deg for the heat capacity of 0.0624 M arsenious oxide solution at 25°C.

DISCUSSION OF RESULTS

Combination of reaction 2 with reaction 3

$$4\text{HBr(aq)} + \text{O}_2\text{(g)} \rightarrow 2\text{H}_2\text{O(liq)} + 2\text{Br}_2\text{(liq)} \qquad (3)$$

yielded reaction 1. From the standard enthalpies of formation $\Delta Hf°_{25°C}$ [HBr(aq)] = −28.90 kcal/mole[3] and $\Delta Hf°_{25°C}$[H_2O(liq)] = −68.3174 kcal/mole [4] the standard enthalpy change associated with reaction 3 was calculated to be

$\Delta H°_{25°C}$ (reaction 3) = —21.03 kcal/mole. Combination of this datum with the experimental value $\Delta H_{25°C}$ (reaction 2) = —56.92±0.12 kcal/mole yielded for reaction 1

$$\Delta H_{25°C} \text{ (reaction 1)} = -78.0+0.1 \text{ kcal/mole.}$$

Results from previous experimental investigations leading to ΔH-values for reaction 1 have been summarized in Table 5 for comparison with the result of this work. With the aid of certain approximations all data have been recalculated to apply to a temperature of 25°C.

As is seen from Table 5 the only discordant value is that of Berthelot. It should be mentioned that calculation of $\Delta H°_{25°C}$ (reaction 1) from the heat of formation compilations of Bichowsky and Rossini [8] and of the National Bureau of Standards [3] give the values —77.3 and —74.9 kcal/mole, respectively.

REFERENCES

1. Bjellerup, L. *Trans. Faraday Soc.* **52** (1956) 1153.
2. Sunner, S. and Wadsö, I. *To be published.*
3. Rossini, F. D., Wagman, D. D., Evans, W. H., Levine, S. and Jaffe, I. *Selected Values of Chemical Thermodynamic Properties, Circular of the National Bureau of Standards 500*, U.S. Government Printing Office, Washington 1952.
4. Wagman, D. D., Kilpatrick, J. E., Taylor, W. J., Pitzer, K. S. and Rossini, F. D. *J. Research Natl. Bur. Standards* **34** (1945) 143.
5. Thomsen, J. *Thermochemische Untersuchungen*, Barth, Leipzig 1882, Zweiter Band p. 236.
6. Berthelot, M. *Thermochimie*, Gauthier-Villars, Paris 1897, Tome II, p. 117.
7. Smith, L. and Sunner, S. *The Svedberg*, Almqvist & Wiksells Boktryckeri AB, Uppsala 1944, p. 352.
8. Bichowsky, F. R. and Rossini, F. D. *The Thermochemistry of the Chemical Substances*, Reinhold Publishing Corporation, New York, 1936.

Received August 27, 1957.

ACTA CHEMICA SCANDINAVICA 11 (1957) 1766—1770

Reactions between Hydrazine, Thiocyanic Acid and Oxo-compounds

IV. Heats of Combustion and Derived Data for some Compounds Related to Thiosemicarbazide

S. SUNNER

Thermochemistry laboratory, University of Lund, Lund, Sweden

The heat of combustion was determined and the heat of formation at 20° was calculated for the following compounds: hydrazinium thiocyanate ΔHf(s) = 9.2±0.7 kcal · mole^{-1} and ΔHf(aq) = 17.1±0.8 kcal · mole^{-1}; thiosemicarbazide ΔHf(s) = 5.7±0.5 kcal · mole^{-1} and ΔHf(aq) = 13.5±0.7 kcal · mole^{-1}; acetaldehyde thiosemicarbazone ΔHf(s) = 15.0±0.8 kcal · mole^{-1}; acetone thiosemicarbazone ΔHf(s) = 4.6±0.8 kcal · mole^{-1} and compound A ($C_6H_{10}N_4S_2$) ΔHf(s) = 32.7± 1.6 kcal · mole^{-1}.

The thermochemical data have been used further to discuss the equilibrium between hydrazinium thiocyanate and thiosemicarbazide, to calculate the resonance energy of thiosemicarbazones and to compare the exothermicities of the reactions between hydrazinium thiocyanate and oxo-compounds.

THE EQUILIBRIUM BETWEEN HYDRAZINIUM THIOCYANATE AND THIOSEMICARBAZIDE

From a kinetic study at 100° of the isomerization of hydrazinium thiocyanate to thiosemicarbazide and of the reverse reaction in 0.4 M solution it was concluded that the equilibrium is composed of *ca.* 40 % thiosemicarbazide and 60 % hydrazinium thiocyanate *. Using an approximation of activity equal to molarity, one gets for the reaction

$$N_2H_5NCS \underset{k_{-1}}{\overset{k_1}{\rightleftharpoons}} NH_2 \cdot NH \cdot CS \cdot NH_2$$

$$\Delta F^\circ = -RT \ln K = 0.3 \text{ kcal} \cdot \text{mole}^{-1}$$

* Ref.[1] From the data given in Table 2 the velocity constant, k_1 for the first order forward reaction, assuming $k_1/k_{-1} = 2/3$, was found to be 0.0016, 0.0016 and 0.0017 hour^{-1}. The data for the reverse reaction do not obey a simple first order rate equation.

From heat of combustion and solution data, the heat of formation of hydrazinium thiocyanate and thiosemicarbazide in aqueous solution at 20° was found to be 17.1 and 13.5 kcal · mole^{-1}, respectively. Thus, $\Delta Hr = -3.6 \pm 1.1$ kcal · mole^{-1}. Assuming ΔHr to be independent of temperature between 20 and 100°, the equilibrium constant at 20° is calculated to be 4.6, which gives $\Delta F° = -0.56$ kcal · mole^{-1}. At 20° the equilibrium mixture therefore consists of about 80 % thiosemicarbazide and 20 % hydrazinium thiocyanate. Thus, the position of the equilibrium at room temperature is favourable for the synthesis of thiosemicarbazide from hydrazinium thiocyanate; however, the reaction was found to be too slow to be utilized for this purpose [1].

It is of interest to compare this reaction with the isomerization of hydrazinium cyanate to semicarbazide. Baker and Gilbert [2] investigated this reaction and found $k_1/k_{-1} = 200\,000$ at 15° and 30 000 at 25°. Thus 95 % of a 0.5 M hydrazinium cyanate solution should isomerize within 11 min.

THE RESONANCE ENERGY OF THIOSEMICARBAZONES

The resonance energy of thiosemicarbazide was recently estimated [3] to be 28 kcal · mole^{-1}. It is of interest to compare this value with estimated values of the resonance energy of the thiosemicarbazones. For the purpose of calculating these quantities we computed the change in enthalpy of the reactions:

$$NH_2NHCSNH_2(g) + CH_3CHO(g) \rightarrow CH_3CH{=}N \cdot NHCSNH_2(g) + H_2O(g) \quad (1)$$

$$NH_2NHCSNH_2(g) + (CH_3)_2CO(g) \rightarrow (CH_3)_2C{=}N \cdot NHCSNH_2(g) + H_2O(g) \quad (2)$$

The following data were used for the computation: thiosemicarbazide [3] $\Delta Hf(g) = +24.7$ kcal · mole^{-1}; acetaldehyde [4] $\Delta Hf(g) = -39.76$ kcal · mole^{-1}; acetone [5] $\Delta Hf(g) = -52.6$ kcal · mole^{-1}; water [4] $\Delta Hf(g) = -57.80$ kcal · mole^{-1}.

The heats of sublimation of the thiosemicarbazones were related to that of thiosemicarbazide. A comparison between different amines and their corresponding aldehyde and ketone derivatives (aniline — anils; phenyl hydrazine — phenyl hydrazones; methoxamine — methyl oximes; ethoxamine — ethyl oximes; hydrazine — hydrazones — azines) showed that the boiling points of the aldehyde compounds are in average 5° lower, and of the acetone compounds in average 20° higher than those of the corresponding amines. Using Klages equation [6], the differences between the heats of sublimation of the aldehyde and acetone compounds and the parent amine was calculated to be -0.2 kcal · mole^{-1} and $+0.7$ kcal · mole^{-1}, respectively. The heat of sublimation of thiosemicarbazide [3] was estimated to be 19 kcal · mole^{-1} and thus for acetaldehyde thiosemicarbazone $\Delta Hf(g) = 33.8$ kcal · mole^{-1} and for the acetone compound $\Delta Hf(g) = 24.3$ kcal · mole^{-1}. This gives

$$\Delta Hr_1 = -9 \text{ kcal} \cdot \text{mole}^{-1} \text{ and } \Delta Hr_2 = -6 \text{ kcal} \cdot \text{mole}^{-1} \text{ *}$$

*. The thermochemical bond energy term value of the C = O double bond is 3 kcal larger for ketones than it is for aldehydes [8].

These values may be compared with the heat of reaction for

$$Me_2CH \cdot CHO(g) + H_2N \cdot n\text{-}Bu(g) \rightarrow Me_2CH \cdot CH = N \cdot Bu(g) + H_2O(g) \quad (3)$$

The heat of combustion of the aldimine was determined by Coates and Sutton [7]; for n-$BuNH_2$ a value is found in Kharasch's compilation [5].

The heat of combustion of *iso*butyraldehyde can be computed from known data [5] for heptaldehyde, (ΔHc(liq) = −1 062.4 kcal · mole^{-1}), methyl n-propyl ketone, (−735.6 kcal · mole^{-1}) and methyl i-propyl ketone, (−733.9 kcal · mole^{-1}), by adjustment to the gaseous phase [6] and utilizing the known CH_2-increment from values of heats of combustion of a homologue series [9], −154.6 kcal · mole^{-1}. Thus, for *iso*butyraldehyde $\Delta Hc(g)$ = −607.3 kcal · mole^{-1}. The formation of the aldimine is therefore accompanied by a change in enthalpy of ΔHr_3 = −9.5 kcal.

Thus, within the limits of error, the resonance energy for the thiosemicarbazones is the same as it is for the thiosemicarbazide.

REACTIONS BETWEEN HYDRAZINIUM THIOCYANATE AND OXO-COMPOUNDS

When a solution of hydrazinium thiocyanate reacts with acetone, acetone thiosemicarbazone is formed in good yield; the reaction with acetaldehyde is much more complex and a compound with a bicyclic structure is formed [10]. From the thermochemical data [5,4] the following values of the heats of reaction are calculated:

$$N_2H_5NCS(aq) + Me_2CO(aq) \rightarrow Me_2C = N \cdot NHCSNH_2(s) + H_2O(liq) \quad (4)$$
$$\Delta Hr_4 = -18.5 \text{ kcal} \cdot \text{mole}^{-1}$$
$$2N_2H_5NCS(aq) + 2MeCHO(aq) \rightarrow C_6H_{10}N_4S_2(s) + 2H_2O(liq) + N_2H_4(aq) \quad (5)$$
$$\Delta Hr_5 = -31 \text{ kcal} \cdot \text{mole}^{-1}$$

This reaction, however, is much better carried out in an acid, where an additional decrease in enthalpy of 10 kcal · mole^{-1} occurs due to the neutralization reaction:

$$N_2H_4(aq) + HCl(aq) \rightarrow N_2H_5Cl(aq) \quad (6)$$

The competing process (which does not occur):

$$N_2H_4NCS(aq) + CH_3CHO(aq) \rightarrow CH_3CH = N \cdot NHCSNH_2(s) + H_2O(liq) \quad (7)$$

is accompanied by a ΔHr_7 = 21 kcal · mole^{-1} which is almost the same value as in reactions 5 to 6 counted on a molar basis. The explanation for the easiness of formation of the more complex reaction product cannot therefore be sought in an extra stabilization of compound A ($C_6H_{10}N_4S_2$) but must be caused by different rates of reaction for the competing mechanisms.

HEATS OF COMBUSTION * AND SOLUTION

Materials. The samples of the substances were purified by repeated recrystallizations from at least two different solvents, pulverized and carefully dried. The purity was check-

* Dr. Lars Bjellerup made the combustions. I am very grateful for his kind co-operation.

ed by elementary analyses and titrimetric determinations [1]. From the analyses the lower limits of the purity of the substances were estimated and are given below.

Hydrazinium thiocyanate: m.p. 77.5°. Purity better than 99.8 % .
Acetaldehyde thiosemicarbazone: m.p. 146°. Purity better than 99 %.
Acetone thiosemicarbazone: m.p. 179°. Purity better than 99 %.

Compound A (tetrahydro-3,7-dimethyl-s-triazolo(a)-s-triazol-1,5-dithione) [10]: m.p. (decomp.) 170°. The purity could not be estimated from the analyses. The method of synthesis and the low solubility make a good reason for the belief, that the purity is fairly high.

Apparatus and method. The calorimeter and experimental procedure was described in a previous communication [11].

Units of measurement and auxiliary quantities. The results of the combustions are expressed in terms of the 15° calorie in which unit the certified heat of combustion of the benzoic acid (Kahlbaum, 6 324 cal/g "auf den luftleeren Raum bezogen") was given. Unfortunately, the conditions are not precisely known under which this value was obtained. Therefore, the reduction to standard conditions can be slightly uncertain, a value of 6 319 cal/g mass was used. The observed values for the heat of the bomb process were corrected to obtain values for the idealized combustion reaction in which all the reactants and products are in their standard states at 20° and no external work is performed [12].

The accuracy of the obtained results. The combustion experiments referred to in this paper were performed several years ago. At that time the method for the determination of heats of combustion of organo-sulfur compounds was not very well established. The results are therefore not as accurate as they may be obtained to-day, but are believed to be accurate to within 3 to 5 parts in a thousand. The internal consistency, however, is higher and probably about one part in a thousand. For this reason, the usual practice of giving primary data for the combustion experiments was considered of no real use and only the final results will be given.

Energy equivalent of the calorimeter: 4 707.7, 4 709.1, 4 708.7 and 4 712.2, average 4 709.5±1.4 (average deviation) cal/degree.

Heat of combustion of paraffin oil: 10 986, 10 976, 10 969, 10 971, and 10 988, average 10 978±7 cal/g mass.

Heat of combustion of rhombic sulfur: 4 559, 4 570, 4 540, 4 587, average 4 562±15 cal/g mass.

For the reaction

$$S(\text{rhombic}) + 1.5\ O_2(g) + 10\ 001\ H_2O(\text{liq}) = H_2SO_4, 10\ 000\ H_2O$$
$$\Delta Ec\ (293°) = 146.3 \pm 0.4\ \text{kcal} \cdot \text{mole}^{-1}$$

Recalculated to the formation of H_2SO_4, 115 H_2O the value becomes

$$\Delta Ec\ (293°) = 143.3 \pm 0.4\ \text{kcal} \cdot \text{mole}^{-1}$$

which is almost identical to that obtained when the method became better established [12].

Heats of combustion: Hydrazinium thiocyanate: 4 605, 4 615, 4 628, 4 608, average 4 614 cal · g mass^{-1}

Thiosemicarbazide: 4 578, 4 562, 4 582, 4 576 ,average 4 574 cal · g mass^{-1}
Acetaldehyde thiosemicarbazone: 5 821, 5 827, 5 825, average 5 824 cal · g mass^{-1}
Acetone thiosemicarbazone: 6 365, 6 358, 6 345, 6 362, average 6 358 cal · g mass^{-1}
Compound A: 6 100, 6 083, 6 084, 6 069, average 6 084 cal · g mass^{-1}
These values are valid for the formation of gaseous carbon dioxide, liquid water and H_2SO_4, 10 000 H_2O at 20° and constant volume.

Heats of formation. By use of the obtained value for the heat of combustion of rhombic sulfur to H_2SO_2, 10 000 H_2O, $\Delta Ec(293°) = 146.3$ kcal · mole^{-1}, and the known heats of formation of carbon dioxide and water $\Delta Hf(293°) = 94\ 050$ and 68 355 cal · mole^{-1}, respectively, the following values for the heats of formation from graphite, gaseous hydrogen, oxygen and nitrogen and rhombic sulfur were derived:

$C(graphite) + 2\frac{1}{2}\ H_2(g) + 1\frac{1}{2}\ N_2(g) + S(rhombic) = N_2H_5SCN(s)$
$\Delta Hf\ (293°) = +9.2 \pm 0.7$* kcal · mole^{-1}
$C(graphite) + 2\frac{1}{2}\ H_2(g) + 1\frac{1}{2}\ N_2(g) + S(rhombic) = NH_2NHCSNH_2(s)$
$\Delta Hf\ (293°) = +5.7 \pm 0.5$ kcal · mole^{-1}
$3\ C(graphite) + 3\frac{1}{2}\ H_2(g) + 1\frac{1}{2}\ N_2(g) + S(rhombic) = CH_3CH = NNHCSNH_2(s)$
$\Delta Hf\ (293°) = +15.0 \pm 0.2$ kcal · mole^{-1}
$4\ C(graphite) + 4\frac{1}{2}\ H_2(g) + 1\frac{1}{2}\ N_2(g) + S(rhombic) = (CH_3)_2C = NNHCSNH_2(s)$
$\Delta Hf\ (293°) = +4.6 \pm 0.8$ kcal · mole^{-1}
$6\ C(graphite) + 5\ H_2(g) + 2\ N_2(g) + 2S(rhombic) = C_6H_{10}N_4S_2(s)$
$\Delta Hf\ (293°) = +32.7 \pm 1.7$ kcal · mole^{-1}

Heats of solution. The heats of solution of hydrazinium thiocyanate and thiosemicarbazide were determined in an "isothermal" reaction calorimeter of the Dewar-type. The pulverized sample of the crystalline material was dissolved in distilled water and the temperature decrease was read on a Beckmann thermometer. The accuracy of the determinations was better than 1 %. The strengths of the final solutions were 1 % (hydrazinium thiocyanate) and 0.4 % (thiosemicarbazide).

$N_2H_5NCS(c) = N_2H_5NCS(aq)$; $\Delta H = +7.9$ kcal · mole^{-1}
$NH_2NHCSNH_2(c) = NH_2NHCSNH_2(aq)$; $\Delta H = +7.7$ kcal · mole^{-1}

REFERENCES

1. Sunner, S. *Kgl. Fysiograf. Sällskap Lund Förh.* **18** (1948) Nr 9.
2. Baker, E. M. and Gilbert, E. C. *J. Am. Chem. Soc.* **64** (1942) 2777.
3. Sunner, S. *Acta Chem. Scand.* **9** (1955) 847.
4. *Selected Values of Chemical Thermodynamic Properties. Natl. Bur. Standards Circ.* 500, Washington 1950.
5. *International Critical Tables.* McGraw-Hill Book Company, New York 1926—1933.
6. Klages, F. *Chem. Ber.* **82** (1949) 358.
7. Coates, G. E. and Sutton, L. E. *J. Chem. Soc.* **1948** 1187.
8. Cottrell, T. L. *The Strengths of Chemical Bonds.* Butterworths Sci. Publ., London 1954.
9. Prosen, E. J. and Rossini, F. D. *J. Research Natl. Bur. Standards* **34** (1945) 263.
10. Sunner, S. *Svensk Kem. Tidskr.* **64** (1952) 121.
11. Sunner, S. *Svensk Kem. Tidskr.* **58** (1946) 71.
12. Sunner, S. *Diss.* Lund 1949.

Received September 5, 1957.

* Average error from the determinations of heat of combustion of the substances, all errors in common are not included. When comparing these values with those obtained in other laboratories the total error should be calculated and used.

ACTA CHEMICA SCANDINAVICA 11 (1957) 1771—1786

Studies on the Extraction of Metal Complexes

XXX. The Dissociation, Distribution and Dimerization of Di-*n*-butyl Phosphate (DBP)

DAVID DYRSSEN

Research Institute of National Defence, Dept. 1 (FOA 1), Sundbyberg 4, Sweden

The solubility and acidity of DBP in water and the distribution of DBP between chloroform or hexone (methyl *iso*butyl ketone) and $HClO_4$—$NaClO_4$ solutions has been studied at 25°C. The distribution of DBP has been chiefly measured with DBP labelled with radioactive ^{32}P. It was thus possible to measure q, the net distribution ratio of DBP, at very low concentrations of DBP and to determine the very high dimerization constant, k_2, in chloroform.

From the data, the following constants were calculated by fitting the normalized curve, $\log y = \log (x+1)$ (*cf.* Refs. [17, 18]).

Dissociation of DBP in 0.1 M and 1 M $HClO_4$-$NaClO_4$

$$pk_a = 1.00 \pm 0.01$$

Distribution of DBP between chloroform or hexone and 0.1 M $HClO_4$-$NaClO_4$

$$\log k_d = 0.34 \pm 0.01 \text{ (chloroform)}$$
$$\log k_d = 1.36 \pm 0.01 \text{ (hexone)}$$

Dimerization of DBP in

chloroform (wet): $\log k_2 = 4.48 \pm 0.04$
hexone (wet): $\log k_2 = 1.19 \pm 0.03$
water (sat.soln.): $\log k_2 = 1.11 \pm 0.07$

Complex formation of DBP and TBP in chloroform

$$\log k_B = 1.6$$

These constants are discussed together with data for some carboxylic acids, and it is shown that the dimerization of DBP is much more pronounced than for these acids. Furthermore it is possible to calculate the distribution constant, k_D, for some of the dimers.

Di-*n*-butyl phosphate (DBP) has been shown to be a very suitable complexing agent for the extraction of elements such as scandium [1], yttrium [2, 3], zirconium [3], lanthanum [1], hafnium [1] and uranium [1, 4, 5]. It is also known that

DBP interfers with TBP extractions in reactor fuel processes [6]. In order to obtain a more complete understanding of the reactions of DBP in these systems it was necessary to determine the dissociation constant and partition coefficients of DBP. During these studies we found that DBP had a pronounced tendency to dimerize, and the values of the association constants in chloroform, hexone (methyl *iso*butyl ketone) and water were determined. Previously the dissociation constants for some dialkyl phosphates have been determined by van Hove [7], Drushel and Felty [8], and Kumler and Eiler [9]. Recently Peppard *et al.*[10] have reported that dialkyl phosphates in benzene solution are dimeric, and in measurements of the infrared spectra of DBP in non-polar solvents [11] it has not been possible to find any evidence of free hydroxyl-group absorption.

Symbols and formulas

$[\ ]$ or $[\ ]_{aq}$	concentrations in the aqueous phase
$[\ ]_{org}$	concentrations in the organic phase
C_A	initial total concentration of DBP in the organic phase
C_{org}, C_{aq}	equilibrium total concentrations of DBP
HA	di-*n*-butyl phosphate (DBP), $(C_4H_9O)_2PO(OH)$
H_2A_2	dimer of DBP
B	solvent molecule
$k_a = [H^+][A^-]/[HA]$	stoichiometric acid dissociation constant
$k_B = [HA \cdot B]_{org}/[HA]_{org}[B]_{org}$	association constant of HA and B
$k_d = [HA]_{org}/[HA]$	distribution constant for HA
$k_D = [H_2A_2]_{org}/[H_2A_2]$	distribution constant for H_2A_2
$k_2 = [H_2A_2]_{org}/[HA]^2_{org}$	dimerization constant in the organic phase
$k'_2 = [H_2A_2]/[HA]^2$	dimerization constant in the aqueous phase
q	net distribution ratio of DBP
V_{org}, V_{aq}	phase volumes

The experimental errors given were estimated from the fit obtained between the normalized curve $\log y = \log (x+1)$ and the experimental points.

REAGENTS AND APPARATUS

Our general experimental techniques have been described previously by other papers in this metal extraction series (*cf.* Ref. [12]). The DBP was kindly supplied by Albright & Wilson Ltd., London. Titration with alkali and analysis for C (Found: 45.0. Calc. for $C_8H_{19}PO_4$: 45.7) and H (Found: 8.7. Calc: 9.1) showed the compound to be at least 99 % pure. DBP labelled with radioactive ^{32}P was purchased from Radiochemical Centre, Amersham, England. This product was free of any non-acidic ^{32}P-products (*e.g.* TBP or pyrophosphate, TBPP). The specific activity was 4.7 mc per gram of DBP. The chloroform was washed three times with twice the volume of water to remove the 1 % alcohol. The hexone and TBP were washed with alkali, acid, and finally with water.

The radioactivity of $DB^{32}P$ was measured in 10 ml liquid counter tubes (type **M6**, 20th Century Electronics) with an approximate wall-thickness of 35 mg/cm^2. In order to determine the influence of the solvent on the counting rate, solutions were made of 0.5 ml of acetone with $DB^{32}P$ and 9.5 ml of different solvents. These values are given in Table 1

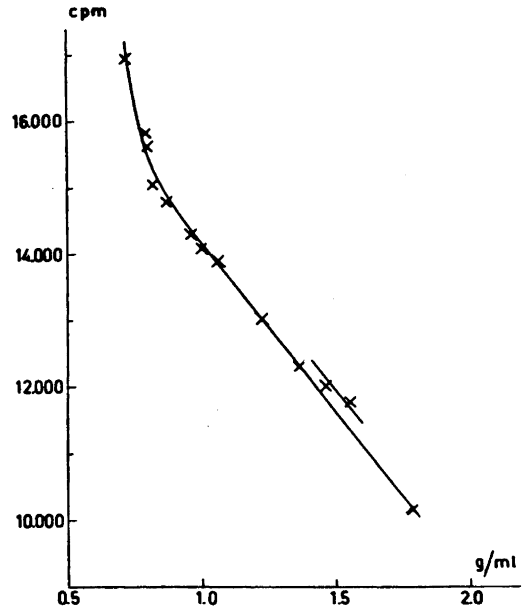


Fig. 1. Effect of solvent density on the counting rate of ^{32}P in a liquid counter.

and plotted in Fig. 1. The values of chloroform and carbon tetrachloride fall above the curve because of the comparatively low electron density of these two solvents. Similar results have been reported earlier [13, 14].

All experiments were carried out at 25°C, and all counting rates given are corrected for background activity and resolving time. Measurements of the hydrogen ion concentration were carried out with a Radiometer pHM3i valve potentiometer, equipped with a Radiometer glass electrode G 100 and a calomel electrode K 100. The two-phase titrations [15] were performed with the same potentiometer but with other types of glass and calomel electrodes.

THE SOLUBILITY AND ACIDITY OF DBP IN WATER

The solubility of DBP in water at 25°C was found to be 0.0818 M by titration with alkali. The pH of the saturated solution was 0.022 units higher than for a solution of 0.05 M $HClO_4$+0.05 M $NaClO_4$. If we use values of the activity coefficients given by Kielland [16] and the value of $pk_a = 1.00$ in 0.1 M ClO_4^-, which was determined in other experiments reported here, we may calculate the following values for the saturated aqueous solution of DBP.

$$-\log [H^+] = 1.340$$

$$[H^+] = [A^-] = 0.0457 \text{ M}$$

$$pk_a = 1.036 = \log [HA] - \log [H^+] - \log [A^-]$$

$$[HA] = 0.0227 \text{ M}$$

$$[H_2A_2] = \tfrac{1}{2}(0.0818 - 0.0227 - 0.0457) = 0.0067 \text{ M}$$

Table 1. The effect of the solvent on the counting rate of DB^{32}P for a Century Electronics M6 liquid counter tube.

Solvent	Density g/ml	Density of DB^{32}P solution [a]	I [b] cpm
Ether	0.714	0.72	16 964
Acetone	0.792	0.792	15 830
Hexone	0.802	0.80	15 623
Kerosene	0.82	0.82	15 054
Benzene	0.879	0.87	14 793
TBP	0.973	0.96	14 304
0.1 M $NaClO_4$	1.006	1.00	14 089
1 M $NaClO_4$	1.076	1.06	13 897
4.32 M H_2SO_4	1.252	1.23	13 033
7.11 M H_2SO_4	1.395	1.36	12 307
Chloroform	1.498	1.46	12 022
Carbon tetrachloride	1.595	1.55	11 770
18 M H_2SO_4	1.836	1.78	10 164

[a] 2.5×10^{-5} M DBP, 5 % acetone
[b] Corrected for the decay of ^{32}P. Standard error approx. ± 130 cpm.

The assumption, that DBP dimerizes also in water, will explain the low value of [HA] that is obtained from the value of pk_a found in distribution experiments with radioactive DBP. The association constant may then be calculated as

$$k'_2 = [H_2A_2]/[HA]^2 = 13 \pm 2$$

THE ACIDITY IN THE AQUEOUS PHASE AS A FUNCTION OF THE CONCENTRATION OF DBP IN THE ORGANIC PHASE

Solutions of DBP (conc. C_A) in chloroform or hexone were shaken with an equal volume of 0.1 M $NaClO_4$, and the value of $-\log [H^+]$ was measured in the aqueous phase (the potentiometer was set to pH = 2.000 for a solution of 0.01 M $HClO_4$ + 0.09 M $NaClO_4$). The results are given in Figs. 2 and 3. With chloroform there seemed to be mainly dimers present in the concentration range studied (10^{-4} to 1 M). The following equations are valid in these experiments.

$$C_A = C_{org} + C_{aq} \quad (1)$$

$$C_{org} = 2[H_2A_2]_{org} + [HA]_{org} \quad (2)$$

$$C_{aq} = [HA] + [A^-] \quad (3)$$

$$[A^-] = [H^+] \quad (4)$$

Additional results were obtained by a two-phase titration [12, 15] of 0.5 mmoles of DBP in 75 ml chloroform or hexone. From these titrations C_{org} and $[H^+][A^-]$ were calculated.

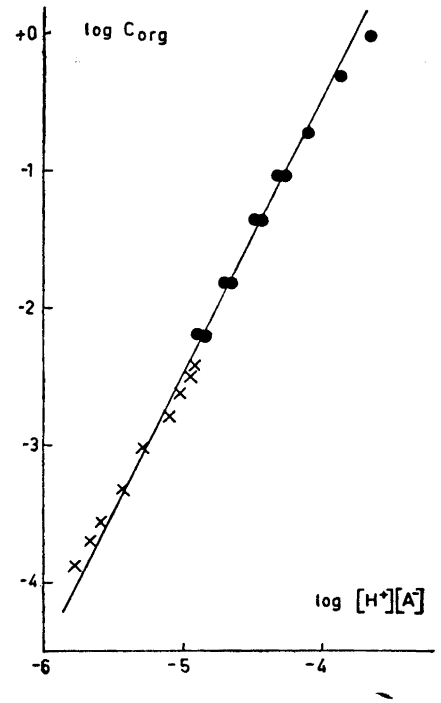


Fig. 2. Distribution of DBP between chloroform and 0.1 M $NaClO_4$ ● $[H^+]$ measured in the aqueous phase after equilibration and separation of the two phases. × $[H^+]$ measured in a two-phase titration.

From eqn. (2) and the definitions of k_2, k_d and k_a given above, the following equation may be derived

$$C_{org} = 2k_2(k_d/k_a)^2[H^+]^2[A^-]^2+(k_d/k_a)[H^+][A^-] \quad (5)$$

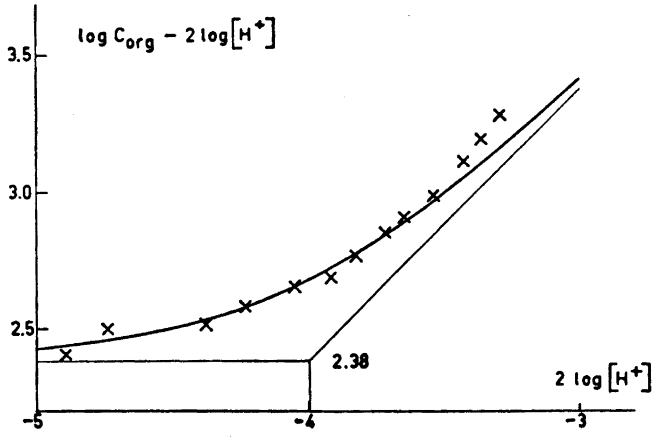


Fig. 3. Distribution of DBP between hexone and 0.1 M $NaClO_4$. $[H^+]$ measured in the aqueous phase. Position of horizontal asymptote ($pk_a+\log k_d = 2.38$) determined from a two-phase pH-titration.

Table 2. Distribution of DB^{32}P between chloroform and 0.1 M perchloric acid for different conc. of DBP. $V_{org} = V_{aq} = 15$ ml.

C_A M	I_{org} cpm	I_{aq} cpm	log q [a]	log C_{org} [b]
0.987	7 800	57	+2.210	−0.009
0.500	8 003	75	+2.102	−0.305
0.333	7 289	64	+2.130	−0.481
0.200	8 074	78	+2.089	−0.703
0.133	7 530	95	+1.980	−0.880
0.100	8 000	128	+1.869	−1.006
0.0500	7 739	159	+1.761	−1.309
0.0200	7 969	250	+1.577	−1.710
0.0100	7 470	325	+1.435	−2.016
0.00501	7 747	468	+1.293	−2.322
0.00201	7 070	672	+1.096	−2.730
0.00101	6 495	877	+0.943	−3.043
5.13×10^{-4}	6 029	1 106	+0.810	−3.352
2.13×10^{-4}	5 521	1 571	+0.620	−3.765
1.13×10^{-4}	4 890	1 912	+0.481	−4.071
5.33×10^{-5}	18 285	9 418	+0.362	−4.430
2.67×10^{-5}	7 258	5 330	+0.224	−4.777
1.33×10^{-5}	13 120	9 918	+0.195	−5.088
6.67×10^{-6}	1 867	1 590	+0.143	−5.412

[a] $q = I_{org} \cdot 1.186/I_{aq}$
[b] $C_{org} = C_A \cdot q/(1+q)$

For chloroform (Fig. 2) the points follow a straight line with a slope equal to 2 when log C_{org} is plotted against log $[H^+][A^-]$. This means that the monomer HA in the chloroform phase can be neglected (last term in eqn. (5)). From this line we obtained

$$\log k_2(k_d/k_a)^2 = +7.22 \pm 0.05$$

Table 3. Distribution of DB^{32}P between hexone and 0.1 M perchloric acid for different conc. of DBP. $V_{org} = V_{aq} = 15$ ml.

C_A M	I_{org} cpm	I_{aq} cpm	log q [a]	log C_{org} [b]
0.973	8 631	118	+1.825	−0.018
0.500	8 665	159	+1.698	−0.310
0.200	9 046	249	+1.521	−0.712
0.100	9 078	317	+1.418	−1.017
0.0500	8 638	404	+1.291	−1.322
0.0200	8 315	511	+1.173	−1.727
0.0100	8 290	567	+1.126	−2.032
0.00503	8 157	580	+1.109	−2.332
0.00203	8 131	666	+1.048	−2.730
0.001027	7 957	661	+1.043	−3.027
1.33×10^{-5}	11 741	950	+1.053	−4.912

[a] $q = I_{org} \cdot 0.915/I_{aq}$
[b] $C_{org} = C_A \cdot q/(1+q)$

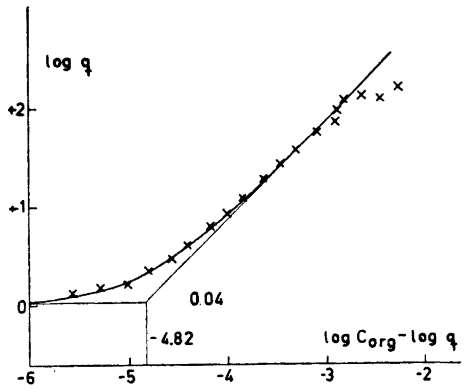


Fig. 4. The distribution ratio of $DB^{32}P$ between chloroform and 0.1 M perchloric acid as a function of the DBP conc. in the chloroform phase.

For hexone a plot (Fig. 3) of log C_{org} — 2log $[H^+]$ against 2log $[H^+]$ does not give a straight line. The normalized curve log y = log $(x+1)$ (*cf.* Refs. [17, 18]) fits the data except for the highest DBP concentrations (0.5 and 1 M). The horizontal asymptote (log y = 0) to the curve was obtained from a two-phase titration

$$pk_a + \log k_d = +2.38 \pm 0.01$$

The point of intersection of the two asymptotes (log y = 0 and log y = log x) gives

$$\log 2k_2k_d/k_a = +4.00 \pm 0.03$$

$$i.e., \log k_2 = +1.32 \pm 0.04$$

THE DISTRIBUTION OF DBP AS A FUNCTION OF THE CONCENTRATION OF DBP IN THE ORGANIC PHASE

In these experiments the distribution of DBP was measured by means of DBP labelled with radioactive ^{32}P. The results for chloroform and hexone are given in Tables 2 and 3 and in Figs. 4 and 5. The aqueous phase was 0.1 M

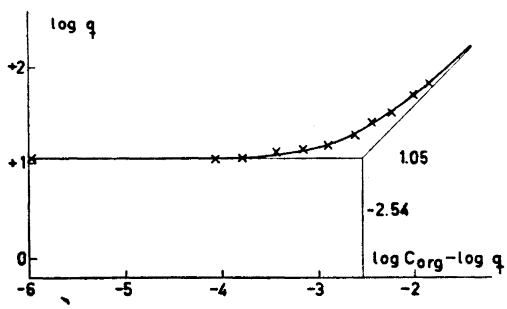


Fig. 5. The distribution ratio of $DB^{32}P$ between hexone and 0.1 M perchloric acid as a function of the DBP conc. in the hexone phase.

perchloric acid. Eqns (1)—(3) given above are also valid here. As C_{aq} is always low any formation of dimers in the aqueous phase can be neglected. The net distribution ratio is

$$q = C_{org}/C_{aq} \quad (6)$$

and from eqns. (2), (3), and (6) and the definitions of k_2, k_d and k_a follows that

$$q = 2k_2(k_d/\varphi)^2 C_{org}/q + k_d/\varphi \quad (7)$$

where φ is a constant in these experiments

$$\varphi = 1 + k_a/[H^+] \quad (8)$$

In Figs. 4 and 5 log q is plotted against log C_{org}—log q.

The normalized curve log y = log $(x+1)$ fits the data very well except for 0.5 and 1 M DBP in chloroform. The horizontal asymptote (log $y = 0$) gives

$$\log k_d/\varphi = +0.04 \pm 0.02 \text{ for chloroform (Fig. 4)}$$

$$\text{and} \quad \log k_d/\varphi = +1.05 \pm 0.01 \text{ for hexone (Fig. 5)}$$

and the point of intersection between the two asymptotes gives

$$\log 2k_2k_d/\varphi = +4.82 \pm 0.02 \text{ for chloroform}$$
$$\log 2k_2k_d/\varphi = +2.54 \pm 0.02 \text{ for hexone}$$

i.e., log $k_2 = +4.48 \pm 0.04$ (chloroform) and $+1.19 \pm 0.03$ (hexone).

The latter value for hexone is definitely lower than the value of 1.32 obtained in the previous part.

If we use the value of $k_a = 10^{-1.00 \pm 0.01}$ that was obtained in the experiments reported below, φ will be equal to 2.00 ± 0.02 (eqn. 8). The distribution coefficient of the monomeric form HA may then be calculated as

$$\log k_d = +0.34 \pm 0.02 \text{ for chloroform}$$

$$\log k_d = +1.35 \pm 0.01 \text{ for hexone}$$

For comparison with the results obtained from the acidity measurements with inactive DBP (given in brackets), the following values may be calculated

$$\log k_2(k_d/k_a)^2 = +7.16 \pm 0.06 \text{ for chloroform } (7.22 \pm 0.05)$$

$$pk_a + \log k_d = +2.35 \pm 0.02 \text{ for hexone } (+2.38 \pm 0.01)$$

$$\log 2k_2k_d/k_a = +3.84 \pm 0.04 \text{ for hexone } (+4.00 \pm 0.03)$$

Except for the value of log k_2 for hexone the agreement seems to be rather good. We consider the value of log k_2 obtained with radioactive DBP to be more reliable.

THE DISTRIBUTION OF DBP AS A FUNCTION OF THE ACIDITY IN THE AQUEOUS PHASE

These experiments were carried out in order to determine both the distribution coefficients and the acidity constant of DBP. The distribution of DBP was again measured with radioactive DB^{32}P. The results for chloroform and

Table 4. Distribution of DB^{32}P between chloroform and $HClO_4$-$NaClO_4$ solutions. Initial conc. of DBP in the chloroform layer 1.33×10^{-5} M.

Ionic strength M	I_{org} cpm	I_{aq} cpm	log q [a]	$-\log [H^+]$	log q_{corr} [b]
0.1	13 281	10 011	+0.196	1.00	+0.06
	10 510	12 500	−0.002	1.30	−0.13
	8 180	13 953	−0.158	1.48	−0.27
	6 226	17 203	−0.368	1.70	−0.43
	3 573	21 154	−0.699	2.00	−0.76
	2 084	23 601	−0.980	2.30	−1.01
	795	24 131	−1.408	2.70	−1.43
	307	9 211	−1.404	2.72	−1.42
1	6 145	3 854	+0.265	0.00	+0.12
	6 832	3 582	+0.349	0.30	+0.19
	6 615	3 645	+0.321	0.48	+0.16
	6 426	3 917	+0.277	0.70	+0.13
	5 733	4 443	+0.173	1.00	+0.03
	4 850	5 728	−0.011	1.30	−0.16
	3 333	7 388	−0.283	1.70	−0.38

[a] $q = I_{org} \cdot 1.186/I_{aq}$ for 0.1 M ionic strength and $q = I_{org} \cdot 1.154/I_{aq}$ for 1 M.
[b] corrected for the increase of q due to the formation of dimers in the chloroform phase.

hexone with both 0.1 and 1 M ionic strength ($HClO_4$-$NaClO_4$) in the aqueous phase are given in Tables 4 and 5 and in Figs. 6 and 7.

Even though the initial conc. of DBP in the chloroform layer was only 1.33×10^{-5} M we had to correct for the increase in q due to the formation

Table 5. Distribution of DB^{32}P between hexone and $HClO_4$-$NaClO_4$ solutions. Initial conc. of DBP in the hexone layer 1.33×10^{-5} M.

Ionic strength M	I_{org} cpm	I_{aq} cpm	log q [a]	$-\log [H^+]$
0.1	11 740	953	+1.052	1.00
	11 308	1 317	+0.895	1.30
	10 748	1 731	+0.754	1.48
	10 244	2 449	+0.583	1.70
	8 567	3 774	+0.318	2.00
	6 657	5 535	+0.042	2.30
	3 771	8 230	−0.377	2.70
1	11 298	368	+1.436	0.00
	10 281	327	+1.446	0.30
	10 618	388	+1.387	0.48
	10 541	430	+1.339	0.70
	10 344	6 622	+1.170	1.00
	10 119	899	+1.001	1.30
	8 450	1 651	+0.658	1.70

[a] $q = I_{org} \cdot 0.915/I_{aq}$ for 0.1 M ionic strength and $q = I_{org} \cdot 0.890/I_{aq}$ for 1 M.

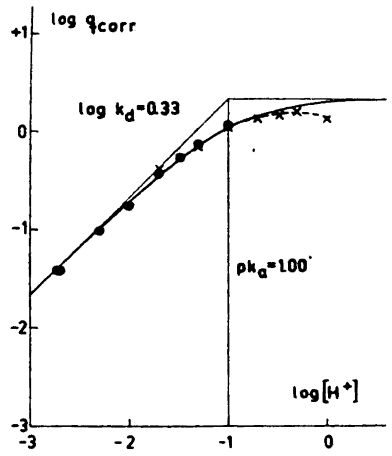


Fig. 6. Distribution of DB^{32}P between chloroform and $HClO_4$-$NaClO_4$ solutions. × = 1 M ionic strength. ● = 0.1 M ionic strength.

of dimers in the organic phase; for hexone no correction was needed. In these experiments the net distribution of DBP is given by

$$q = \frac{[HA]_{org}}{[HA]+[A^-]} \tag{9}$$

From the definitions of k_a and k_d it follows that

$$q = k_d/(1+k_a[H^+]^{-1}) \tag{10}$$

The same normalized curve, $\log y = \log (x+1)$, is thus valid for these experimental data if $\log q$ is plotted against $\log [H^+]$. The horizontal asymptote ($\log y = 0$) gives $\log k_d$ and the point of intersection of this asymptote with the asymptote $\log y = \log x$ gives $pk_a = -\log [H^+]$. From Figs. 6 and 7 we obtained the following values by fitting the normalized curve (*cf.* Refs. [17, 18]) to the data

$$pk_a = 1.00 \pm 0.01 \text{ for } 0.1 \text{ and } 1 \text{ M } ClO_4^-$$

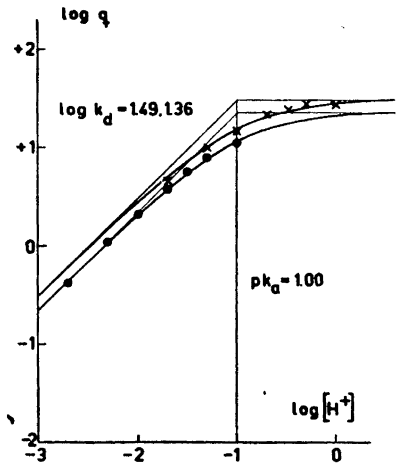


Fig. 7. Distribution of DB^{32}P between hexone and $HClO_4$-$NaClO_4$ solutions. × = 1 M ionic strength. ● = 0.1 M ionic strength.

Other acids, *e.g.* HCl and $HClO_4$ (*cf.* Ref. [16] p. 75), also have approximately the same mean activity coefficients in 0.1 M and 1 M solutions at 25°C.

$$\log k_d = 0.33 \pm 0.02 \text{ for chloroform/0.1 and 1 M } ClO_4^-$$
$$\log k_d = 1.36 \pm 0.02 \text{ for hexone/0.1 M } ClO_4^-$$
$$\log k_d = 1.49 \pm 0.02 \text{ for hexone/1 M } ClO_4^-$$

The values of $\log k_d$ for 0.1 M ClO_4^- agree with those found in the previous part.

For chloroform the more acid 1 M $HClO_4$-$NaClO_4$ solutions show a salting-in effect. Using activity coefficients given by Kielland [16] the thermodynamic dissociation constant may be calculated

$$pk_a = 1.00 + 0.17 = 1.17$$

This value is definitely lower than the value of 1.72 reported by Kumler and Eiler [9]. However, their results on other dialkyl phosphates are about 0.4—0.6 units higher than dissociation constants given by van Hove [7] and by Drushel and Felty [8].

THE DISTRIBUTION OF DBP AS A FUNCTION OF THE CONCENTRATION OF TBP IN THE CHLOROFORM PHASE

If DBP reacts with TBP (tri-*n*-butyl phosphate) in the chloroform phase the net distribution ratio will increase according to

$$q = \frac{k_d}{\varphi}(1 + k_B[B]_{org}) \qquad (11)$$

Table 6. Distribution of $DB^{32}P$ between chloroform and 1 M $HClO_4$ for different concentrations of TBP in the chloroform phase. Initial conc. of DBP in the chloroform layer 3.33×10^{-5} M. $V_{org} = V_{aq} = 15$ ml.

ml TBP · H_2O per 15-v ml $CHCl_3$	$[TBP]_{org}$ M	I_{org} cpm	I_{aq} cpm	A	log q [a]
15	3.44	5 667	73.4	0.966	1.873
14.5	3.32	8 682	98.6	0.972	1.932
9	2.06	7 396	144	1.041	1.728
5	1.145	8 929	277	1.091	1.546
5	1.145	4 897	126	1.091	1.627
4	0.918	4 935	123	1.104	1.647
3	0.687	6 832	185	1.116	1.614
3	0.687	4 819	145	1.116	1.569
2.5	0.572	7 691	253	1.123	1.534
1	0.229	8 248	582	1.141	1.208
0.45	0.1031	6 778	739	1.148	1.022
0.2	0.0458	7 272	1 419	1.151	0.771
0.1	0.0229	5 805	1 352	1.153	0.695
0.05	0.01145	5 388	1 520	1 153	0.612
0.02	0.00458	4 957	1 569	1.154	0.562
0.01	0.00229	4 946	1 629	1.154	0.545
0	0	4 873	1 721	1.154	0.514
0	0	4 032	1 420	1.154	0.515

[a] $q = I_{org} \cdot A / I_{aq}$

where φ is given by eqn. (8) and k_B is defined by

$$k_B = [HA \cdot B]_{org}/[HA]_{org}[B]_{org} \quad (12)$$

In a plot log q against log $[TBP]_{org}$ (= log $[B]_{org}$) the data would then follow the normalized curve log y = log $(x+1)$. With a high value of φ or a very high specific activity of the radioactive DBP we could have made the conc. of DBP dimers negligible. But with 1 M $HClO_4$ ($\varphi = 1.10$) and an initial conc. of DBP equal to 3.33×10^{-5} M, TBP has to compete with the dimerization of DBP. The expression for q will therefore contain an additional term.

$$q = \frac{k_d}{\varphi}(1+2k_2 \frac{k_d}{\varphi} \cdot \frac{C_A}{1+q} + k_B[B]_{org}) \quad (13)$$

With this expression we calculated for $(TBP)_{org} < 0.4$ M

$$k_B = 40$$

As aspected the tendency for DBP to dimerize ($k_2 = 3 \times 10^4$) is much stronger than the tendency to associate with TBP. However, the effective concentration of TBP in chloroform may be lower than $[B]_{org}$ as TBP is known to associate both with H_2O and $CHCl_3$ according to McKay *et al.*[19] and Kosolapoff and McCullough [20] (*cf.* also Ref.[21]).

CONCLUSIONS AND DISCUSSION

From the experiments carried out the following data may be summarized:
Dissociation of DBP in 0.1 M and 1 M $HClO_4$-$NaClO_4$

$$pk_a = 1.00 \pm 0.01 \ (pK_a = 1.17)$$

Dimerization (association) of DBP in

chloroform (wet): log $k_2 = 4.48 \pm 0.04$

hexone (wet): log $k_2 = 1.19 \pm 0.03$

water (sat.soln.): log $k_2 = 1.11 \pm 0.07$

Distribution of DBP between

chloroform	and 0.1 M $HClO_4$-$NaClO_4$:	log k_d =	0.34 ± 0.01
hexone	and 0.1 M $HClO_4$-$NaClO_4$:	log k_d =	1.36 ± 0.01
hexone	and 1 M $HClO_4$-$NaClO_4$:	log k_d =	1.49 ± 0.02
TBP	and 1 M $HClO_4$:	log k_d =	1.87

Association (complex formation) of DBP and TBP in chloroform

$$\log k_B = 1.60$$

According to Drushel and Felty [8] and the result obtained by us the lower dialkyl phosphates are definitely stronger acids (10—20 times) than phosphoric acid ($pK_a = 2.12$). It might be suggested that H_3PO_4 is stabilized by three

Table 7. Summary of some dimerization constants in chloroform calculated from distribution measurements at 25°C.

Acid	pK_a	log k_d	log k_2	Ref.
Acetic	4.76	−1.36	1.05	22, 23
Propionic	4.87	−0.80; −0.75	1.50; 1.44	22, 24
n-Butyric	4.82	−0.27	1.68	22
n-Valeric	4.80	+0.32	1.73	22
Cinnamic	4.44	+1.20	2.22	26
Phenyl acetic	4.31	+0.46	1.75	22
Lactic	3.86	−1.81	2.33	22
Chloracetic	2.87	−1.84	2.38; 3.10	22, 23
Benzoic	4.20	+0.53; +0.58	1.96; 1.87	22, 25
m-Nitrobenzoic	3.49	+0.39	1.99	22
3,5-Dinitrobenzoic	2.80	+0.18	no ass.	26
Salicylic	2.98	+0.48; +0.64	1.62; 1.22	26, 25
o-Chlorbenzoic	2.92	+0.89	1.04	22
o-Methoxybenzoic	4.09	+1.60	no ass.	22, 27
DBP	1.17	+0.34	4.48	this work

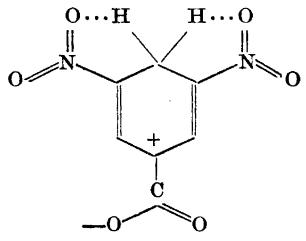
internal hydrogen bonds while the hydrogen bonding in the dialkyl phosphates is disturbed by the free rotation of the two ester groups. The degree of hydration is probably also different for the two acid-base pairs, H_3PO_4—$H_2PO_4^-$ and $(RO)_2PO(OH)$ — $(RO)_2PO_2^-$.

The tendency for a dialkylphosphoric acid or a carboxylic acid to associate to double molecules depends on the tendency of the $P\langle^{O}_{OH}$ and $C\langle^{O}_{OH}$ groups to form hydrogen bonds. The dimerization is, however, very dependent on the solvent. Hitherto only the carboxylic acids have been investigated [23–33]. Usually very large dimerization constants are obtained in hexane, benzene and carbon tetrachloride. Smaller values (about 10 times) are obtained with chloroform, which is a weak donor for hydrogen bonds. The dimerization of carboxylic acids is very slight [25, 26] in oxygen-containing solvents like ethers and ketones, which are good acceptors for hydrogen bonds. Finally the dimerization is almost negligible [31–33] in hydroxyl-containing solvents such as water. From Table 7 it may be seen that the dimerization constant for DBP is much larger than for any of the carboxylic acids. It is therefore not astonishing that a considerable dimerization also takes place in hexone and water. There seems to be a general trend for k_2 to increase with K_a and k_d. However, many of the k_2-values in Table 7 are not very accurate. One of the reasons for this is that the aqueous phase has been unbuffered. Furthermore, the correction for ionization becomes too large when $K_a > 10^{-3}$. This emphasizes the necessity of measuring the distribution with constant ionic and acidity strength in the aqueous phase and carrying out the analysis of the acids, *e.g.* spectrophotometrically [26] or radiometrically as in this work. Table 7 shows furthermore the lowering effect on k_2 of OH, Cl and OCH_3 groups in the *ortho*-

Table 8. Distribution constants of some monomers and dimers.

Organic phase/acid	log k_d		log k_D	
	found	calc.	found	calc.
Chloroform/acetic	−1.36	−1.36	−0.39	−0.16
Chloroform/propionic	−0.76	−0.76	+1.22	+1.04
Chloroform/*n*-butyric	−0.27	−0.16	+2.18	+2.24
Chloroform/*n*-valeric	+0.32	+0.44	—	+3.44
Chloroform/DBP	+0.34	—	+4.05	—
Hexone/DBP	+1.36	—	+2.80	—

position of benzoic acid: Cl and OCH_3 act as acceptors for the carboxylic hydrogen while the OH group in salicylic acid can act both as a donor and acceptor. Careful work [26] on 3,5-dinitrobenzoic acid has revealed no evidence of association. This result has surprised us, especially when compared with *m*-nitrobenzoic acid. The result suggests that the carboxylic hydrogen is bound intramolecularly, *e.g*, as follows



The dimerization in water, which could be estimated from our measurements of the acidity of DBP in water, has been calculated for some fatty acids [31–33]. Thus, if the dimerization constants in both the organic and aqueous phases and the distribution constant of the monomer are known, it is possible to calculate the distribution constant of the dimer

$$k_D = [H_2A_2]_{org}/[H_2A_2] = k_2k_d^2/k_2' \qquad (14)$$

Some values of k_D are given in Table 8. Some estimations of k_d and k_D for the fatty acids can be made. Collander [34] found in his investigations of the distribution of organic compounds between ether and water that k_d increases 2 to 4 times when a CH_2 group is added in a homologous series; this factor is here denoted with m. Furthermore it is reasonable to assume that the dimerization makes the carboxylic groups less hydrophilic, *i.e.* increases k_d by a factor n regardless of the length of the hydrocarbon chain. If the distribution constant k_d for acetic acid is a, the values of log k_d and log K_D for the fatty acids will increase as log a, log am, log am^2 and log anm, log $anmm^2$, log $anmm^4$. The values calculated in Table 8 have been obtained with $m = n = 4$ and $a = 0.044$. The deviation from the rather uncertain experimental values is not too serious. The assumptions made here lead also to the following relation

$$k_2/k_2' = k_D/k_d^2 = mn/a = 16/0.044$$

In fact k_2 ans k_2' do not vary much for the fatty acids (for k_2' see Ref.[32]) and the ratio k_2/k'_2 is thus rather constant. If the values in Table 8 for DBP with chloroform and hexone are compared, it may be seen that the increase of the distribution constant on dimerization is much larger for chloroform (5 100 times) than for hexone (27 times). This is also in agreement with Collander [35], who found that the distribution constants differed much less for *iso*butanol than for ether.

The association between chloroform and DBP is presumably rather weak (*cf.* Ref.[28]). The lowering of k_2 in hexone may then be ascribed to complex formation between hexone and DBP according to eqn. (12). This can also explain the larger value of k_d for hexone. For comparison with k_B for TBP we may then calculate k_B for hexone as

$$k_B = \frac{10^{\frac{1}{2}(4.48-1.19)}}{[\mathrm{B}]_{\mathrm{org}}} = 5.5$$

The complex formation is thus somewhat lower for hexone than for TBP ($k_B = 40$). The tendency for DBP to dimerize is however much stronger. It would be interesting to know if the eight-membered dimer ring is planar or not (*cf.* Ref.[36]).

The dimerization constant of DBP in chloroform is very large (3×10^4) and should be still larger in non-polar solvents such as carbon tetrachloride. This means that DBP will exist as dimers even at very low concentrations. Thus no shifts can probably be detected in the infra-red spectra within a measurable concentration range (*cf.* Ref.[11]). The dimerization constant in carbon tetrachloride may however be determined with radioactive DBP if a larger value of φ in eqn. (7) (higher pH) or a higher specific activity of DBP than in the experiments reported here is used.

The dimerization constant for water, k_2', has been determined with the distribution method for acetic acid [33]. This method could probably be also used for the lower dialkyl phosphates (*e.g.* dimethyl phosphate). For DBP k_d and k_2 are too large, and the concentration of DBP in water will be too low.

The author wishes to thank the head of FOA 1, Professor Gustaf Ljunggren, for his interest in our work, and Fil.kand. Bengt Carlsson and Mr. Ebbe Johansson for their technical assistance. Sincere thanks are due to Professor Lars Gunnar Sillén for his criticism of the manuscript and to Dr. Stuart Tobias for revising the English text.

REFERENCES

1. Dyrssen, D. *To be published. Cf. Paper VI-10, XVth Int. Congr. of Pure and Applied Chemistry*, Lisbon 1956.
2. Dyrssen, D. *Acta Chem. Scand.* **11** (1957) 1277.
3. Scadden, E. M. and Ballou, N. E. *Anal. Chem.* **25** (1953) 1602.
4. Hyde, E. K. *Int. Conf. on Peaceful Uses of Atomic Energy*, Geneva 1955, Vol. **7**, p. 290.
5. Stewart, D. C. and Bently, W. C. *Science* **120** (1954) 50.
6. *Process Chemistry*, Vol. 1, *Progress in Nuclear Chemistry*, Series III, Pergamon Press Ltd, London 1956, Cf. index.
7. van Hove, T. *Bull. Acad. Roy. Belgique, Classe de Sciences* **1909** 282.
8. Drushel, W. A. and Felty, A. R. *Am. J. Sci.* **4**, **43** (1917) 57.

9. Kumler, W. D. and Eiler, J. J. *J. Am. Chem. Soc.* **65** (1943) 2355.
10. Peppard, D. F., Ferraro, J. R. and Mason, G. W. *J. Inorg. & Nuclear Chem.* **4** (1957) 371.
11. Bellamy, L. J. and Beecher, L. *J. Chem. Soc.* **1952**, 1701.
12. Dyrssen, D. *Svensk Kem. Tidskr.* **68** (1956) 212.
13. Chiang, R. S. and Willard, J. E. *Sciencc* **112** (1950) 81.
14. Rose, G. and Emery, E. W. *Nucleonics* **9** (1951): 1, 5.
15. Dyrssen, D. *Svensk Kem. Tidskr.* **64** (1952) 213.
16. Conway, B. E. *Electrochemical Data*, Elsevier Publishing Co., London 1952.
17. Dyrssen, D. and Sillén, L. G. *Acta Chem. Scand.* **7** (1953) 663.
18. Sillén, L. G. *Acta Chem. Scand.* **10** (1956) 186.
19. Alcock, K., Grimley, S. S., Healy, T. V., Kennedy, J. and McKay, H. A. C. *Trans. Faraday Soc.* **52** (1956) 39.
20. Kosolapoff, G. M. and McCullough, J. F. *J. Am. Chem. Soc.* **73** (1951) 5392.
21. Halpern, E., Bouck, J., Finegold, H. and Goldenson, J. *J. Am. Chem. Soc.* **77** (1955) 4472.
22. Seidell, A. *Solubilities of Organic Compounds*, D. van Nostrand Co. Inc., New York 1941.
23. Brown, C. P. and Mathieson, A. R. *J. Phys. Chem.* **58** (1954) 1057.
24. Davies, M., Jones, P., Patnaik, D. and Moelwyn-Hughes, E. A. *J. Chem. Soc.* **1951** 1249.
25. Davies, M. and Griffiths, D. M. L. *J. Chem. Soc.* **1955** 132.
26. Hök-Bernström, B. *Svensk Kem. Tidskr.* **65** (1953) 182.
27. Hök-Bernström, B. *Acta Chem. Scand.* **10** (1956) 174.
28. Barrow, G. M. and Yerger, E. A. *J. Am. Chem. Soc.* **76** (1954) 5248.
29. Barton, B. C. and Kraus, C. A. *J. Am. Chem. Soc.* **73** (1951) 4561.
30. Wideqvist, S. *Arkiv Kemi* **7** (1954) 381.
31. Katchalsky, A., Eisenberg, H. and Lifson, S. *J. Am. Chem. Soc.* **73** (1951) 5889.
32. Cartwright, D. R. and Monk, C. B. *J. Chem. Soc.* **1955** 2500.
33. Davies, M. and Griffiths, D. M. L. *Z. physik. Chem.* [*N.F.*] **2** (1954) 353.
34. Collander, R. *Acta Chem. Scand.* **3** (1949) 717.
35. Collander, R. *Acta Chem. Scand.* **4** (1950) 1085.
36. Bastiansen, O., Finbak, C. and Hassel, O. *Tidskr. Kjemi, Bergvesen, Met.* **4** (1944) :9, 81.

Received September 7, 1957.

ACTA CHEMICA SCANDINAVICA 11 (1957) 1787—1796

Short Communications

A New Procedure for the Preparation of *Iso*nicotinic Acid Hydrazide

H. B. THOMASEN

Laboratory of Messrs. Dumex Private Ltd., Bombay, India

A well-known preparative method for aliphatic amides consists in the thermal decomposition of the ammonium salts of the acids. A simple example is the formation of acetamide from ammonium acetate by heating. Similarly the hydrazonium salts of the acids on heating give rise to the hydrazides. The preparation of acyl hydrazides by this method, though less well-known has been reported in the literature [1].

The reactions may be represented as follows:

$$R-COONH_4 \xrightarrow{\text{heat}} R-CONH_2 + H_2O$$

$$R-COONH_3-NH_2 \xrightarrow{\text{heat}} R-CONH-NH_2 + H_2O$$

If R is aromatic the reaction generally fails and the hydrazide can only be prepared *via* the corresponding ester, acid chloride or the anhydride. This involves an extra step in the process and it was, therefore, considered worthwhile to investigate the possibility of a direct conversion of the hydrazonium salt to the acid hydrazide.

In the last few years, *iso*nicotinic acid hydrazide has come into prominence as a valuable remedy against tuberculosis. The hydrazide is usually manufactured by the condensation of the ethyl ester of *iso*nicotinic acid or the acid chloride with hydrazine hydrate [2,3].

During, the study undertaken in our laboratory, it was realised that the reaction

$$R-COONH_3-NH_2 \rightleftharpoons R-CONH-NH_2 + H_2O$$

could be made to proceed to the right if the water formed in the reaction is constantly and almost completely removed.

Such a dehydration may be performed by azeotropic distillation with the help of a suitable water entrainer. Many such media are available but the choice is restricted as a certain temperature is also required to obtain a workable rate of reaction. It has been found that immiscible water entrainers having boiling points above 120° are most suitable, *e. g.* amyl alcohol, hexyl alcohol, or octyl alcohol, and hydrocarbons, *e. g.* toluene, xylene or mesitylene. It has thus been described how maleic anhydride can be prepared from the acid by an azeotropic removal of water by the use of xylene [4].

It is likely that the reaction mechanism is not as simple as represented above but perhaps passes through an ester stage where an alcohol is used as water entrainer or through the anhydride where a hydrocarbon is used. The experimental procedures finally worked out are described in the experimental section.

Experimental. Procedure 1. Normal amyl alcohol (60 ml) was added to a solution of *iso*nicotinic acid (30 g) in 60 % hydrazine hydrate (27 ml). The reaction mixture was slowly distilled when a mixture of amyl alcohol and dilute solution of hydrazine hydrate distilled over. A further quantity of dry amyl alcohol (40 ml) was added and the distillation continued till water ceased to appear in the distillate. The mixture was then refluxed for 3 h, the water formed at this stage removed by distillation, and the refluxing continued for another 3.5 h. The reaction product was cooled to 0° when crude *iso*nicotinic acid hydrazide crystallised out. The product was purified by recrystallisation from a small amount of ethyl alcohol yielding *iso*nicotinic acid hydrazide, m.p. 170—172°, and a purity of 98.5—99.0 %, when assayed by the B.P. procedure. Yield 24 g.

The amyl alcoholic mother liquor was acidified with hydrochloric acid to a pH 3.5 when the unreacted *iso*nicotinic acid (4—5 g) precipitated. Taking into consideration the recovered material, an yield of 86.5 % was obtained.

The mother liquor, after the precipitation of *iso*nicotinic acid, in the previous step, con-

tained some dissolved hydrazide besides other condensation products formed by side reactions. Further quantity of the acid was recovered by hydrolysing these products. The mother liquor was boiled under reflux with an excess of sodium hydroxide, acidified to a pH 3.5 and the precipitated acid collected by filtration. The total yield of the hydrazide, taking into consideration the recovered *iso*-nicotinic acid in both the steps amounted to over 90 % of the theory.

Procedure 2. To a solution of *iso*nicotinic acid (30 g) in 60 % hydrazine hydrate (27 ml), xylene (100 ml) was added and the mixture was heated in an oil bath at 170°. A mixture of xylene and hydrazine hydrate distilled over slowly during the first 2 h. The temperature of the oil bath was now lowered to 150° and maintained at this point for the next 4 h. During this period the last traces of xylene and a strong solution of hydrazine hydrate distilled over. The reaction product was cooled somewhat, water (20 ml) was added and the resulting solution filtered at a temperature between 70—75°. The filtrate was cooled to —3° when crude *iso*nicotinic acid hydrazide crystallised out; yield 24—25 g.

Recovery of *iso*nicotinic acid was carried out as described under procedure 1.

1. Curtius, T. and Franzen, H. *Ber.* **3** (1902) 3239.
2. Urbanski, T. *Roczniki Chem.* **27** (1953) 161.
3. Ororbia, M. A. M. *Ion* **15** (1955) 421.
4. Ohsol, E. O., Sussky, W. C. and Beach, L. K. *U. S. 2,729,599* (1956).

Received September 30, 1957.

A New Synthesis of 4-*O*-Methyl-D-Glucose

HANS O. BOUVENG, BENGT LINDBERG and OLOF THEANDER

Träkemiska avdelningen, Svenska Träforskningsinstitutet, Stockholm, Sweden

The unambiguous synthetic routes leading to 4-*O*-methyl-D-glucose [1-3] are rather tedious and give low yields. As we required this substance and its methyl β-pyranoside we sought for other methods of preparing them. Bearing in mind the ease with which acyl migration takes place from the 4- to the 6-position, we investigated the direct methylation of the easily available methyl 2,3,4-tri-*O*-acetyl-β-D-glucopyranoside with methyl iodide and silver oxide. The alkalinity of the silver oxide we believed would probably be sufficient to effectively catalyse the acyl migration. This reaction has already been investigated in the α-series by Haworth, Hirst and Teece[4]. They found that methylation took place in the 2-position. On the other hand, Helferich and Lang [5] prepared methyl 2,3,6-tri-*O*-acetyl 4-*O*-methyl-β-D-glucopyranoside by the Purdie methylation of methyl 2,3,6-tri-*O*-acetyl-β-D-glucopyranoside. These results show that acyl migration is rather unpredictable and may proceed by several paths.

By methylation of methyl 2,3,4-tri-*O*-acetyl-β-D-glucopyranoside with methyl iodide and silver oxide in dimethylformamide, according to the method of Kuhn *et al.*[6], we have now obtained crystalline methyl 2,3,6-tri-*O*-acetyl-4-*O*-methyl-β-D-glucopyranoside in a yield of 45 %. A hydrolysate of the mother liquors contained 4-*O*-methyl-D-glucose as the main product, contaminated by glucose and by some methyl glucoses. 2-*O*-Methyl-D-glucose, which has almost the same electrophoretic mobility as 4-*O*-methyl-D-glucose but a higher R_F-value, was only present in traces. The pure, acetylated glucoside was converted by standard procedures to the crystalline methyl 4-*O*-methyl-β-D-glucopyranoside and to the amorphous 4-*O*-methyl-D-glucose. Paper chromatographic and paper electrophoretic examination of this latter product showed it to be indistinguishable from an authentic sample of 4-*O*-methyl-D-glucose but to be readily distinguishable from the other mono-*O*-methyl-D-glucoses. The values of the m.p. and optical rotations of the crystalline products were in good agreement with those previously recorded [1,2]. As comparatively few steps are needed, and as the yields are fairly good, this is probably the most convenient synthesis of 4-*O*-methyl-D-glucose and of its methyl-β-pyranoside.

Experimental. Methyl 2,3,6-tri-O-acetyl-4-O-methyl-β-D-glucopyranoside. Methyl 2,3,4-tri-*O*-acetyl-β-D-glucopyranoside (4.0 g) was dissolved in dimethylformamide (50 ml) and to this solution methyl iodide (12 ml) was added. Silver oxide (8.0 g) was added in four portions during 30 min under vigorous stirring and

tained some dissolved hydrazide besides other condensation products formed by side reactions. Further quantity of the acid was recovered by hydrolysing these products. The mother liquor was boiled under reflux with an excess of sodium hydroxide, acidified to a pH 3.5 and the precipitated acid collected by filtration. The total yield of the hydrazide, taking into consideration the recovered *iso*-nicotinic acid in both the steps amounted to over 90 % of the theory.

Procedure 2. To a solution of *iso*nicotinic acid (30 g) in 60 % hydrazine hydrate (27 ml), xylene (100 ml) was added and the mixture was heated in an oil bath at 170°. A mixture of xylene and hydrazine hydrate distilled over slowly during the first 2 h. The temperature of the oil bath was now lowered to 150° and maintained at this point for the next 4 h. During this period the last traces of xylene and a strong solution of hydrazine hydrate distilled over. The reaction product was cooled somewhat, water (20 ml) was added and the resulting solution filtered at a temperature between 70—75°. The filtrate was cooled to —3° when crude *iso*nicotinic acid hydrazide crystallised out; yield 24—25 g.

Recovery of *iso*nicotinic acid was carried out as described under procedure 1.

1. Curtius, T. and Franzen, H. *Ber.* **3** (1902) 3239.
2. Urbanski, T. *Roczniki Chem.* **27** (1953) 161.
3. Ororbia, M. A. M. *Ion* **15** (1955) 421.
4. Ohsol, E. O., Sussky, W. C. and Beach, L. K. *U. S. 2,729,599* (1956).

Received September 30, 1957.

A New Synthesis of 4-*O*-Methyl-D-Glucose

HANS O. BOUVENG, BENGT LINDBERG and OLOF THEANDER

Träkemiska avdelningen, Svenska Träforskningsinstitutet, Stockholm, Sweden

The unambiguous synthetic routes leading to 4-*O*-methyl-D-glucose [1-3] are rather tedious and give low yields. As we required this substance and its methyl β-pyranoside we sought for other methods of preparing them. Bearing in mind the ease with which acyl migration takes place from the 4- to the 6-position, we investigated the direct methylation of the easily available methyl 2,3,4-tri-*O*-acetyl-β-D-glucopyranoside with methyl iodide and silver oxide. The alkalinity of the silver oxide we believed would probably be sufficient to effectively catalyse the acyl migration. This reaction has already been investigated in the α-series by Haworth, Hirst and Teece[4]. They found that methylation took place in the 2-position. On the other hand, Helferich and Lang [5] prepared methyl 2,3,6-tri-*O*-acetyl 4-*O*-methyl-β-D-glucopyranoside by the Purdie methylation of methyl 2,3,6-tri-*O*-acetyl-β-D-glucopyranoside. These results show that acyl migration is rather unpredictable and may proceed by several paths.

By methylation of methyl 2,3,4-tri-*O*-acetyl-β-D-glucopyranoside with methyl iodide and silver oxide in dimethylformamide, according to the method of Kuhn *et al.*[6], we have now obtained crystalline methyl 2,3,6-tri-*O*-acetyl-4-*O*-methyl-β-D-glucopyranoside in a yield of 45 %. A hydrolysate of the mother liquors contained 4-*O*-methyl-D-glucose as the main product, contaminated by glucose and by some methyl glucoses. 2-*O*-Methyl-D-glucose, which has almost the same electrophoretic mobility as 4-*O*-methyl-D-glucose but a higher R_F-value, was only present in traces. The pure, acetylated glucoside was converted by standard procedures to the crystalline methyl 4-*O*-methyl-β-D-glucopyranoside and to the amorphous 4-*O*-methyl-D-glucose. Paper chromatographic and paper electrophoretic examination of this latter product showed it to be indistinguishable from an authentic sample of 4-*O*-methyl-D-glucose but to be readily distinguishable from the other mono-*O*-methyl-D-glucoses. The values of the m.p. and optical rotations of the crystalline products were in good agreement with those previously recorded [1,2]. As comparatively few steps are needed, and as the yields are fairly good, this is probably the most convenient synthesis of 4-*O*-methyl-D-glucose and of its methyl-β-pyranoside.

Experimental. Methyl 2,3,6-tri-O-acetyl-4-O-methyl-β-D-glucopyranoside. Methyl 2,3,4-tri-*O*-acetyl-β-D-glucopyranoside (4.0 g) was dissolved in dimethylformamide (50 ml) and to this solution methyl iodide (12 ml) was added. Silver oxide (8.0 g) was added in four portions during 30 min under vigorous stirring and

with external cooling with tap water. The stirring was continued for 6 h, then the solution was filtered. The silver salts were washed with some dimethylformamide and, after chloroform (100 ml) had been added to the combined filtrate and washings, the solution was washed with 6 % aqueous potassium cyanide (100 ml). After washing the aqueous phase with chloroform (2 × 25 ml), the chloroform layers were combined and were washed with water (2 × 50 ml), dried over calcium chloride and concentrated. The remaining dimethylformamide was removed by co-distillation with butanol. The crystalline residue was recrystallised from ethanol, and this, together with the material obtained by working up the mother liquors, gave a total of 1.90 g having m.p. 104—105°. After further crystallisations the product had m.p. 110—111° (corr.) and $[\alpha]_D^{21}$ —35° (c = 1, in chloroform).

Methyl 4-O-methyl-β-D-glucopyranoside. By deacetylation of the above acetate the glycoside was obtained. After crystallisation from ethyl acetate it had m.p. 102—103° (corr.), $[\alpha]_D^{20}$ —18° (c = 1, in water).

4-O-Methyl-D-glucose. Acid hydrolysis of the glycoside yielded 4-*O*-methyl-D-glucose. $R_{Glucose}$ 2.40 (in butanol-ethanol-water, 10:3:5). M_G 0.17 (in 0.1 M borate buffer of pH 10). The corresponding values for 2-. 3- and 6-*O*-methyl-D-glucose were $R_{Glucose}$ 2.78, 2.67 and 2.47 and M_G, 0.17, 0.80 and 0.75, respectively.

The authors are indebted to Professor J. K. N. Jones for a gift of 4-*O*-methyl-D-glucose.

1. Bourne, E. J. and Peat, S. *Advances in Carbohydrate Chem.* **5** (1950) 145.
2. Mc Gilvray, D. I. *J. Chem. Soc.* **1952** 3648.
3. Gorin, P. A. J. *Can. J. Chem.* **35** (1957) 595.
4. Haworth, W. N., Hirst, E. L. and Teece, E. G. *J. Chem. Soc.* **1931** 2858.
5. Helferich, B. and Lang, O. *J. prakt. Chem.* **132** (1932) 321.
6. Kuhn, R., Trischmann, H. and Löw, I. *Angew. Chem.* **67** (1955) 32.

Received December 6, 1957.

Preliminary Calculations of Mean Amplitudes of Vibration in *Cyclo*propane

O. BASTIANSEN and S. J. CYVIN

Institutt for teoretisk kjemi, Norges tekniske høgskole, Trondheim, Norway

Reinvestigations on the structures of the *cyclo*alkanes are in progress[1]. From the radial distribution curve of *cyclo*propane the root mean square amplitude of vibration (u) has been calculated for the C—H and C—C bond distances. Least square calculations were applied to fit Gaussian shaped peaks to the peaks of the radial distribution curve. It was observed that there was a reproducible deviation from the symmetric form due to anharmonicity[2,3]. However, this effect will not be discussed here. The electron diffraction results for values of u are listed in Table 1.

Table 1. Mean amplitudes of vibration in *cyclo*propane (Å units).

Distance	El.diff.	Spectr.
C—H	0.0784 ± 0.0015	0.0770
Distance	El.diff.	Spectr.
C—C	0.0480 ± 0.0015	0.0489

It is of interest to compare these values with theoretical ones calculated from spectroscopic data. Some simple, approximate methods, which yield data of sufficient accuracy for this purpose, shall be reported in this communication.

The C—H distances. The four C—H stretching fundamental frequencies have been separated from the remaining fundamentals. Thus an explicit approximate formula for the mean square amplitude could be evaluated, the result being[4]

$$u^2_{C-H} = h\ (\mu_H + \mu_C)^{1/2} / 4\pi k^{1/2}$$

where only the principal C—H stretching force constant (k) appears. μ_H and μ_C are the inverse masses of the H and C atoms. From the experimental fundamentals[5] (A_1') 3 029, (E') 3 024.4, (A_2'') 3 103.0 and (E'') 3 080 cm^{-1}, the value

with external cooling with tap water. The stirring was continued for 6 h, then the solution was filtered. The silver salts were washed with some dimethylformamide and, after chloroform (100 ml) had been added to the combined filtrate and washings, the solution was washed with 6 % aqueous potassium cyanide (100 ml). After washing the aqueous phase with chloroform (2 × 25 ml), the chloroform layers were combined and were washed with water (2 × 50 ml), dried over calcium chloride and concentrated. The remaining dimethylformamide was removed by co-distillation with butanol. The crystalline residue was recrystallised from ethanol, and this, together with the material obtained by working up the mother liquors, gave a total of 1.90 g having m.p. 104—105°. After further crystallisations the product had m.p. 110—111° (corr.) and $[\alpha]_D^{21}$ —35° (c = 1, in chloroform).

Methyl 4-O-methyl-β-D-glucopyranoside. By deacetylation of the above acetate the glycoside was obtained. After crystallisation from ethyl acetate it had m.p. 102—103° (corr.), $[\alpha]_D^{20}$ —18° (c = 1, in water).

4-O-Methyl-D-glucose. Acid hydrolysis of the glycoside yielded 4-*O*-methyl-D-glucose. $R_{Glucose}$ 2.40 (in butanol-ethanol-water, 10:3:5). M_G 0.17 (in 0.1 M borate buffer of pH 10). The corresponding values for 2-. 3- and 6-*O*-methyl-D-glucose were $R_{Glucose}$ 2.78, 2.67 and 2.47 and M_G, 0.17, 0.80 and 0.75, respectively.

The authors are indebted to Professor J. K. N. Jones for a gift of 4-*O*-methyl-D-glucose.

1. Bourne, E. J. and Peat, S. *Advances in Carbohydrate Chem.* **5** (1950) 145.
2. Mc Gilvray, D. I. *J. Chem. Soc.* **1952** 3648.
3. Gorin, P. A. J. *Can. J. Chem.* **35** (1957) 595.
4. Haworth, W. N., Hirst, E. L. and Teece, E. G. *J. Chem. Soc.* **1931** 2858.
5. Helferich, B. and Lang, O. *J. prakt. Chem.* **132** (1932) 321.
6. Kuhn, R., Trischmann, H. and Löw, I. *Angew. Chem.* **67** (1955) 32.

Received December 6, 1957.

Preliminary Calculations of Mean Amplitudes of Vibration in *Cyclo*propane

O. BASTIANSEN and S. J. CYVIN

Institutt for teoretisk kjemi, Norges tekniske høgskole, Trondheim, Norway

Reinvestigations on the structures of the *cyclo*alkanes are in progress[1]. From the radial distribution curve of *cyclo*propane the root mean square amplitude of vibration (u) has been calculated for the C—H and C—C bond distances. Least square calculations were applied to fit Gaussian shaped peaks to the peaks of the radial distribution curve. It was observed that there was a reproducible deviation from the symmetric form due to anharmonicity[2,3]. However, this effect will not be discussed here. The electron diffraction results for values of u are listed in Table 1.

Table 1. Mean amplitudes of vibration in *cyclo*propane (Å units).

Distance	El.diff.	Spectr.
C—H	0.0784 ± 0.0015	0.0770
Distance	El.diff.	Spectr.
C—C	0.0480 ± 0.0015	0.0489

It is of interest to compare these values with theoretical ones calculated from spectroscopic data. Some simple, approximate methods, which yield data of sufficient accuracy for this purpose, shall be reported in this communication.

The C—H distances. The four C—H stretching fundamental frequencies have been separated from the remaining fundamentals. Thus an explicit approximate formula for the mean square amplitude could be evaluated, the result being[4]

$$u^2_{C-H} = h\ (\mu_H + \mu_C)^{1/2} / 4\pi k^{1/2}$$

where only the principal C—H stretching force constant (k) appears. μ_H and μ_C are the inverse masses of the H and C atoms. From the experimental fundamentals[5] (A_1') 3 029, (E') 3 024.4, (A_2'') 3 103.0 and (E'') 3 080 cm^{-1}, the value

$k = 5.120 \times 10^5$ dyn cm^{-1} have been computed, yielding the u value listed in Table 1.

The C—C distances. An approximate calculation of the mean amplitude of vibration of the C—C distances have been worked out by adopting the equilateral triangle model $(CH_2)_3$ for *cyclo*propane. The following explicit formula has been derived

$$u^2_{C-C} = (h\mu_X^{1/2} / 4\pi 3^{1/2}) \, [(k + 2\,k')^{-1/2} + 2^{1/2} \, (k - k')^{-1/2}]$$

k denotes here the principal C—C stretching force constant and k' the interaction force constant between two C—C stretches. μ_X is the inverse mass of CH_2. In this case it did not affect the result appreciably when the interaction constant was made equal to zero. Consequently, the formula could be simplified to

$$u^2_{C-C} = h\mu_X^{1/2} \, (1 + 2^{1/2}) / 4\pi(3k)^{1/2}$$

From the fundamentals [5] (A_1') 1 189 and (E') 868 cm^{-1}, the value $k = 4.064 \times 10^5$ dyn cm^{-1} have been obtained, and the resulting u value is listed in Table 1.

It is planned to perform more rigorous calculations of u-values in *cyclo*propane, including also the other C—H distances as well as the H—H distances.

1. Almenningen, A., Bastiansen, O. and Fernholt, L. *Unpublished.*
2. Bartell, L. *J. Chem. Phys.* **23** (1955) 1219.
3. Almenningen, A. and Bastiansen, O. *Research Correspondence* **9** (Sept. 1956).
4. Cyvin, S. J. *Acta Chem. Scand.* **12** (1958). *In press.*
5. Herzberg, G. *Infrared and Raman Spectra of Polyatomic Molecules*, N.Y. 1945.

Received October 31, 1957.

A Photoactivated Polymerization of Hexabromoethane

K. TAUGBØL and J. B. DAHL

Joint Establishment for Nuclear Energy Research, Kjeller, Norway

Investigations of the photoactivated exchange reaction of bromine between hexabromoethane and free bromine in carbon tetrachloride solution by means of the radioactive isotope ^{82}Br, indicated a polymerization reaction occurring coincident with the exchange reaction.

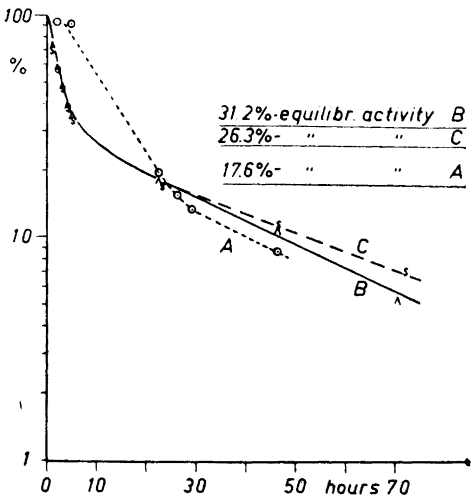


Fig. 1. Activity in organic phase as percentage of activity at zero time.

Curve A: $[C_2Br_6^*] = 1.04$ mmole/l, $[Br_2] = 14.56$ mmole/l. In air, 50°C.
Curve B: $[C_2Br_6^*] = 1.39$ mmole/l, $[Br_2] = 9.18$ mmole/l. In carbon dioxide atm, 20°C.
Curve C: $[C_2Br_6^*] = 1.39$ mmole/l, $[Br_2] = 11.50$ mmole/l. In nitrogen atm, 20°C.

A condensation of carbon tetrabromide to hexabromoethane has been described earlier [1], but this work did not indicate any polymerization of the hexabromoethane.

Procedure: Free bromine and hexabromoethane were irradiated in the pile, dissolved in carbon tetrachloride solutions and irradiated by an electric bulb. The solutions were in turn kept in a closed glass flask filled with dry, purified nitrogen or carbon dioxide.

The apparatus was placed in a thermostatic bath, and filling and removing of aliquots could take place without letting air into the system. Aliquots were taken at different times and free bromine extracted with reducing, aqueous solutions of sodium bisulphite. The organic phases containing the hexabromoethane were washed with distilled water, and the radioactivity measured with a scintillation counter.

The hexabromoethane was prepared according to the method of Mouneyrat [2] and recrys-

$k = 5.120 \times 10^5$ dyn cm^{-1} have been computed, yielding the u value listed in Table 1.

The C—C distances. An approximate calculation of the mean amplitude of vibration of the C—C distances have been worked out by adopting the equilateral triangle model $(CH_2)_3$ for *cyclo*propane. The following explicit formula has been derived

$$u^2_{C-C} = (h\mu_X^{1/2} / 4\pi 3^{1/2}) \, [(k + 2\,k')^{-1/2} + 2^{1/2} \, (k - k')^{-1/2}]$$

k denotes here the principal C—C stretching force constant and k' the interaction force constant between two C—C stretches. μ_X is the inverse mass of CH_2. In this case it did not affect the result appreciably when the interaction constant was made equal to zero. Consequently, the formula could be simplified to

$$u^2_{C-C} = h\mu_X^{1/2} \, (1 + 2^{1/2}) / 4\pi(3k)^{1/2}$$

From the fundamentals [5] (A_1') 1 189 and (E') 868 cm^{-1}, the value $k = 4.064 \times 10^5$ dyn cm^{-1} have been obtained, and the resulting u value is listed in Table 1.

It is planned to perform more rigorous calculations of u-values in *cyclo*propane, including also the other C—H distances as well as the H—H distances.

1. Almenningen, A., Bastiansen, O. and Fernholt, L. *Unpublished.*
2. Bartell, L. *J. Chem. Phys.* **23** (1955) 1219.
3. Almenningen, A. and Bastiansen, O. *Research Correspondence* **9** (Sept. 1956).
4. Cyvin, S. J. *Acta Chem. Scand.* **12** (1958). *In press.*
5. Herzberg, G. *Infrared and Raman Spectra of Polyatomic Molecules*, N.Y. 1945.

Received October 31, 1957.

A Photoactivated Polymerization of Hexabromoethane

K. TAUGBØL and J. B. DAHL

Joint Establishment for Nuclear Energy Research, Kjeller, Norway

Investigations of the photoactivated exchange reaction of bromine between hexabromoethane and free bromine in carbon tetrachloride solution by means of the radioactive isotope ^{82}Br, indicated a polymerization reaction occurring coincident with the exchange reaction.

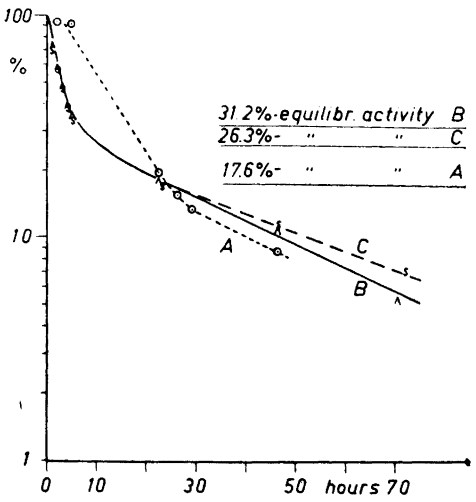


Fig. 1. Activity in organic phase as percentage of activity at zero time.

Curve A: $[C_2Br_6^*] = 1.04$ mmole/l, $[Br_2] = 14.56$ mmole/l. In air, 50°C.
Curve B: $[C_2Br_6^*] = 1.39$ mmole/l, $[Br_2] = 9.18$ mmole/l. In carbon dioxide atm, 20°C.
Curve C: $[C_2Br_6^*] = 1.39$ mmole/l, $[Br_2] = 11.50$ mmole/l. In nitrogen atm, 20°C.

A condensation of carbon tetrabromide to hexabromoethane has been described earlier [1], but this work did not indicate any polymerization of the hexabromoethane.

Procedure: Free bromine and hexabromoethane were irradiated in the pile, dissolved in carbon tetrachloride solutions and irradiated by an electric bulb. The solutions were in turn kept in a closed glass flask filled with dry, purified nitrogen or carbon dioxide.

The apparatus was placed in a thermostatic bath, and filling and removing of aliquots could take place without letting air into the system. Aliquots were taken at different times and free bromine extracted with reducing, aqueous solutions of sodium bisulphite. The organic phases containing the hexabromoethane were washed with distilled water, and the radioactivity measured with a scintillation counter.

The hexabromoethane was prepared according to the method of Mouneyrat [2] and recrys-

tallized repeatedly from carbon disulphide solutions. The carbon tetrachloride was purified by irradiation in the presence of chlorine and chlorine dioxide, followed by fractional distillations [3].

Results: In several experimental series the radioactivity in the hexabromoethane was found to fall far below the calculated exchange equilibrium values. Fig. 1 shows some typical results corrected for radioactive decay. Corresponding series in darkness at 20°C and 50°C showed no exchange in organic bound activity after 50 h.

Solutions containing radioactive hexabromoethane with no free bromine added, were irradiated 45 h and 48 h, respectively, with no change in organic bound activity. One of the solutions was then treated with dry chlorine gas and again exposed to light. This caused a continuous fall in organic bound activity followed for 143.5 h. The activity had fallen to 4.8 % of the original activity.

The other solution was kept in light over night. The reaction had then started, and the solution was coloured by free bromine. Similar results were obtained in other runs. Some free bromine, however, up to 20—30 % of the total activity, depending on the pile flux, is always present in the hexabromoethane due to recoil reactions. In all series the reaction was followed by a marked increase in pressure owing to liberated bromine.

Different samples of the reaction products were isolated. One sample was prepared from a nearly saturated solution of hexabromoethane in 70 ml of carbon tetrachloride. 3 ml of bromine were added. The solution was irradiated in nitrogen atmosphere for one week, and the reaction was followed by a manometer. A white, flaky material was then floating on the surface. The solution was carefully evaporated to dryness, and the residue washed with alcohol. Another sample was prepared in a similar way, but with chlorine instead of bromine. The product was a similar, white and light material, with low solubility in carbon tetrachloride and *cyclo*hexane.

Microscopical examinations showed no distinct crystals. The materials turned dark at about 140°C and charred later without melting and without visible evolution of bromine or chlorine gas. Hexabromoethane decomposes at 210—215°C and gives off free bromine. Infrared spectra of the two samples showed the materials to be high-symmetric, saturated,

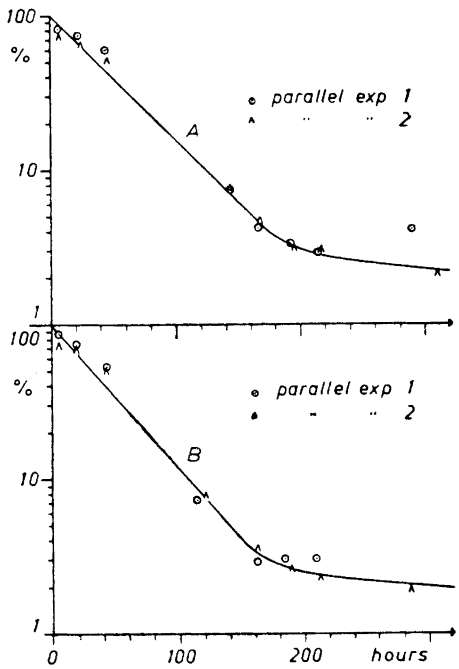


Fig. 2. Activity in organic phase as percentage of activity at zero time.

Curve A: $[C_2Br_6^*] = 1.24$ mmole/l, $[Br_2] = 28.2$ mmole/l.
Curve B: $[C_2Br_6^*] = 1.24$ mmole/l, $[Br_2^*] = 0.58$ mmole/l.

containing C—C bonds and to a small extent C—Br and C—Cl bonds, respectively. In the case of chlorine this has consequently exchanged with the organic bound bromine. There were no oxides, no C—H bonds and no functional groups.

To study the reaction without complications from the exchange reaction, hexabromoethane and free bromine were irradiated in the pile in two different ampulles placed in the same container to get the same specific activities. Different series of measurements with different concentrations of free bromine were carried out.

Fig. 2 shows two typical runs at 20°C in nitrogen atmosphere for two different bromine concentrations. In either case, two parallel experiments were carried out.

Fig. 2 shows that the reactions are represented by nearly straight lines on a semi-logarithmic scale. The slopes seem

nearly independent of the amount of free bromine in this region of concentration.

Runs with free iodine instead of bromine or chlorine gave no reaction.

An experiment with symmetric tetrabromethane and free chlorine gave a marked reaction. A yellow, viscous oil was isolated.

A rough test with radioactive free chlorine and inactive hexabromoethane showed an uptake of chlorine activity in the organic phase, later falling off again.

The curves, Fig. 2, show that the organic bound activities fall to at least 2 % of the original activities. Setting aside isotope effect, this may indicate a polymer consisting of some system of condensed carbon rings.

Further investigations are in progress.

1. Seely, L. B., Jr. and Willard, J. E. *J. Am. Chem. Soc.* **69** (1947) 2061.
2. Mouneyrat, X. *Bull. soc. chim.* **19** (1898) 177.
3. Dickinson, R. G. and Leermakers, J. A. *J. Am. Chem. Soc.* **54** (1932) 3853.

Received November 6, 1957.

The Precipitation of Neutral Polysaccharides by Cationic Detergents

HANS PALMSTIERNA, J. E. SCOTT* and S. GARDELL

Depts. of Chemistry and Bacteriology Karolinska institutet, Stockholm, Sweden

During an investigation on the charged polysaccharide luteic acid, described by Raistrick and collaborators in 1931 [1], the method of Scott was used as one step in the purification of it. It has been shown [2] that it is possible to use detergents for the precipitation and separation of mixtures of charged polysaccharides (and desoxyribonucleic acid). For obvious reasons neutral polysaccharides cannot be precipitated directly by the use of detergents such as cetylpyridinium chloride (C.P.C.) or cetyltrimethylammonium bromide (C.T.A.B.). If, however, the neutral polysaccharide is coupled to borate and C.P.C. is added, complete precipitation can be achieved. Since the work in this paper was carried out a short communication has appeared also recording this fact [3]. The precipitates are soluble in salt solutions, dilute acids and glycerol and galactose solutions.

To eliminate the effect of buffer salts on the precipitate, cetyl-trimethyl ammonium borate (C.T.A. Borate) was prepared and used as the precipitant. The pH dependance of the reaction was marked, as was observed by Barker *et al.*[3] Rat liver glycogen was not precipitated by C.T.A. borate, which had a pH of 8.5, but the addition of a few drops of ammonia resulted in good precipitation. Yeast mannan and ivory nut mannan were precipitated immediately without the addition of ammonia. Inulin, dextran and starch were not precipitated even in the presence of ammonia, but only on adding an appreciable concentration of potassium hydroxide. This latter type of precipitation in potassium hydroxide also took place in the absence of borate, and although the precipitates were soluble in salt solutions they were resistant to solvent action by glycerol or galactose.

It is therefore clear that there are two possibilities of precipitating neutral polysaccharides with amphipathic cations, due to the acquiring of polyanionic properties:

(1) by formation of borate complexes, and

(2) by the ionisation of hydroxyl groups at high pH.

The possibility of salt fractionation, such as is available with acidic polysaccharides [2], coupled with the differential solubilities of the precipitates in glycerol and galactose solutions, suggest that this reaction has great potential practical value. The following experiment describes a simple test of its utility (see also Barker *et al.*[3]).

The test system used was glycogen from *Escherichia coli* B alone or in combination with luteic acid. It was possible to separate these polysaccharides by precipitating the luteic acid directly with C.P.C. The glycogen was then precipitated by making the solution 0.01 M with regard to borate, adjusting the pH to 9.2 with KOH and finally adding C.P.C. to complete precipitation. This last operation should be finished within an hour, since the solution may otherwise be discoloured due to slight decomposition of C.P.C. in alkaline solutions. The supernatant contained hardly detectable amounts of polysaccharide.

* Present address. Institute of Pathology and Tropical Medicine, R. A. F. Halton Bucks, England.

nearly independent of the amount of free bromine in this region of concentration.

Runs with free iodine instead of bromine or chlorine gave no reaction.

An experiment with symmetric tetrabromethane and free chlorine gave a marked reaction. A yellow, viscous oil was isolated.

A rough test with radioactive free chlorine and inactive hexabromoethane showed an uptake of chlorine activity in the organic phase, later falling off again.

The curves, Fig. 2, show that the organic bound activities fall to at least 2 % of the original activities. Setting aside isotope effect, this may indicate a polymer consisting of some system of condensed carbon rings.

Further investigations are in progress.

1. Seely, L. B., Jr. and Willard, J. E. *J. Am. Chem. Soc.* **69** (1947) 2061.
2. Mouneyrat, X. *Bull. soc. chim.* **19** (1898) 177.
3. Dickinson, R. G. and Leermakers, J. A. *J. Am. Chem. Soc.* **54** (1932) 3853.

Received November 6, 1957.

The Precipitation of Neutral Polysaccharides by Cationic Detergents

HANS PALMSTIERNA, J. E. SCOTT* and S. GARDELL

Depts. of Chemistry and Bacteriology Karolinska institutet, Stockholm, Sweden

During an investigation on the charged polysaccharide luteic acid, described by Raistrick and collaborators in 1931 [1], the method of Scott was used as one step in the purification of it. It has been shown [2] that it is possible to use detergents for the precipitation and separation of mixtures of charged polysaccharides (and desoxyribonucleic acid). For obvious reasons neutral polysaccharides cannot be precipitated directly by the use of detergents such as cetylpyridinium chloride (C.P.C.) or cetyltrimethylammonium bromide (C.T.A.B.). If, however, the neutral polysaccharide is coupled to borate and C.P.C. is added, complete precipitation can be achieved. Since the work in this paper was carried out a short communication has appeared also recording this fact [3]. The precipitates are soluble in salt solutions, dilute acids and glycerol and galactose solutions.

To eliminate the effect of buffer salts on the precipitate, cetyl-trimethyl ammonium borate (C.T.A. Borate) was prepared and used as the precipitant. The pH dependance of the reaction was marked, as was observed by Barker *et al.*[3] Rat liver glycogen was not precipitated by C.T.A. borate, which had a pH of 8.5, but the addition of a few drops of ammonia resulted in good precipitation. Yeast mannan and ivory nut mannan were precipitated immediately without the addition of ammonia. Inulin, dextran and starch were not precipitated even in the presence of ammonia, but only on adding an appreciable concentration of potassium hydroxide. This latter type of precipitation in potassium hydroxide also took place in the absence of borate, and although the precipitates were soluble in salt solutions they were resistant to solvent action by glycerol or galactose.

It is therefore clear that there are two possibilities of precipitating neutral polysaccharides with amphipathic cations, due to the acquiring of polyanionic properties:

(1) by formation of borate complexes, and

(2) by the ionisation of hydroxyl groups at high pH.

The possibility of salt fractionation, such as is available with acidic polysaccharides [2], coupled with the differential solubilities of the precipitates in glycerol and galactose solutions, suggest that this reaction has great potential practical value. The following experiment describes a simple test of its utility (see also Barker *et al.*[3]).

The test system used was glycogen from *Escherichia coli* B alone or in combination with luteic acid. It was possible to separate these polysaccharides by precipitating the luteic acid directly with C.P.C. The glycogen was then precipitated by making the solution 0.01 M with regard to borate, adjusting the pH to 9.2 with KOH and finally adding C.P.C. to complete precipitation. This last operation should be finished within an hour, since the solution may otherwise be discoloured due to slight decomposition of C.P.C. in alkaline solutions. The supernatant contained hardly detectable amounts of polysaccharide.

* Present address. Institute of Pathology and Tropical Medicine, R. A. F. Halton Bucks, England.

The glycogen was easily dissociated from the borate-C.P.C. complex by lowering the pH to neutrality. This was followed by a dialysis against tap water. The luteic acid was separated from the C.P.C. by the following procedure [2].

The complex was dissolved in a solvent consisting of methanol 20 % v/v, saturated sodium chloride 30 % v/v and water to 100 %. This solution was treated with Lloyds reagent and the disappearance of the C.P.C. was followed spectrophotometrically.

It should be pointed out the method cannot be used when large amounts of protein contaminate the polysaccharide solution, because the proteins tend to form highly viscous cakes with detergents, thus enclosing the polysaccharides.

In microbiological work extracellular polysaccharides can in many instances be isolated by the above methods if the salt concentration of the medium is not too high. When the salt content is high it is advisable to dilute the medium or to dialyse it before precipitation with C.P.C.

1. Raistrick, H. *et al. Phil. Trans. Roy. Soc. London, Ser. B* **220** (1931).
2. Scott, J. E. *Chemistry & Industry* **1955** 1568; *Biochem. J.* **62** (1956) 31P.
3. Barker, S. A. *et al. Chemistry & Industry* **1957** 330.

Received November 13, 1957.

Isolation of Oestradiol-17α from Bovine Meconium

WEIERT VELLE

Department of Sexual Physiology and Sexual Pathology, Veterinary College of Norway, Oslo, Norway

Investigations on oestrogens in the newborn calf have shown that significant amounts of oestrone and oestradiol-17α are excreted with the urine during the first days of life [1]. These observations led to investigations on the oestrogen contents of meconium in this species.

In this preliminary communication results are presented which strongly indicate the presence of significant quantities of oestradiol-17α in meconium from calves.

Experimental. Meconium was obtained from normal, healthy, newborn calves of both sexes and the analyses were undertaken immediately.

Reagents were of the same grade and manufacture as those used in a previous investigation [2]. The material was examined for the contents of both free and conjugated oestrogens:

a. For determination of free oestrogens specimens of meconium were suspended in distilled water and disintegrated in an "Ato-Mix" blender. The suspensions were then extracted repeatedly with ether. The combined ether extracts were processed as described in the following.

b. For determination of conjugated oestrogens the water phase from a. was freed from ether by evaporation, and concentrated HCl added to a final concentration of 10 %. Fitted with reflux condenser, the flask was kept at 100° C for 1 h. After cooling ether extraction was performed as before. The combined ether extracts were analysed according to the following procedures:

1. The chemical method for determination of urinary oestrogens, described by Brown [3] was applied with minor modifications [2]. This method is based on the chromatographic separation of the 3-methyl ethers of the oestrogens, using standardized alumina as adsorbent.

2. Chromatographic separation of the unaltered oestrogens were performed according to the method of Stimmel [4] as modified by Kakusjkina and Orlova [5].

3. The *cis-trans* test for the 17-hydroxy group of oestradiol was performed according to Kägi and Miescher [6], omitting the addition of bromine.

4. Absorption spectra of the isolated fractions were examined from 400—600 mμ using the Kober reagent described by Bauld [7], and from 240—500 mμ using fuming sulphuric acid according to Axelrod [8]. The registered spectra were compared with those of pure compounds. All readings were made in a Beckman Model DU spectrophotometer supplied with photomultiplier.

Results and discussion. Using the modified Brown procedure, a strongly reacting Kober chromogen was found present in the oestradiol fractions from both a. and b., indicating that the substance is partly excreted in free and partly in conjugated form. Considerably greater quantities were observed in the "conjugated" fractions.

In the oestriol and oestrone fractions no trace of Kober chromogen could be detected.

The glycogen was easily dissociated from the borate-C.P.C. complex by lowering the pH to neutrality. This was followed by a dialysis against tap water. The luteic acid was separated from the C.P.C. by the following procedure [2].

The complex was dissolved in a solvent consisting of methanol 20 % v/v, saturated sodium chloride 30 % v/v and water to 100 %. This solution was treated with Lloyds reagent and the disappearance of the C.P.C. was followed spectrophotometrically.

It should be pointed out the method cannot be used when large amounts of protein contaminate the polysaccharide solution, because the proteins tend to form highly viscous cakes with detergents, thus enclosing the polysaccharides.

In microbiological work extracellular polysaccharides can in many instances be isolated by the above methods if the salt concentration of the medium is not too high. When the salt content is high it is advisable to dilute the medium or to dialyse it before precipitation with C.P.C.

1. Raistrick, H. *et al. Phil. Trans. Roy. Soc. London, Ser. B* **220** (1931).
2. Scott, J. E. *Chemistry & Industry* **1955** 1568; *Biochem. J.* **62** (1956) 31P.
3. Barker, S. A. *et al. Chemistry & Industry* **1957** 330.

Received November 13, 1957.

Isolation of Oestradiol-17α from Bovine Meconium

WEIERT VELLE

Department of Sexual Physiology and Sexual Pathology, Veterinary College of Norway, Oslo, Norway

Investigations on oestrogens in the newborn calf have shown that significant amounts of oestrone and oestradiol-17α are excreted with the urine during the first days of life [1]. These observations led to investigations on the oestrogen contents of meconium in this species.

In this preliminary communication results are presented which strongly indicate the presence of significant quantities of oestradiol-17α in meconium from calves.

Experimental. Meconium was obtained from normal, healthy, newborn calves of both sexes and the analyses were undertaken immediately.

Reagents were of the same grade and manufacture as those used in a previous investigation [2]. The material was examined for the contents of both free and conjugated oestrogens:

a. For determination of free oestrogens specimens of meconium were suspended in distilled water and disintegrated in an "Ato-Mix" blender. The suspensions were then extracted repeatedly with ether. The combined ether extracts were processed as described in the following.

b. For determination of conjugated oestrogens the water phase from a. was freed from ether by evaporation, and concentrated HCl added to a final concentration of 10 %. Fitted with reflux condenser, the flask was kept at 100° C for 1 h. After cooling ether extraction was performed as before. The combined ether extracts were analysed according to the following procedures:

1. The chemical method for determination of urinary oestrogens, described by Brown [3] was applied with minor modifications [2]. This method is based on the chromatographic separation of the 3-methyl ethers of the oestrogens, using standardized alumina as adsorbent.

2. Chromatographic separation of the unaltered oestrogens were performed according to the method of Stimmel [4] as modified by Kakusjkina and Orlova [5].

3. The *cis-trans* test for the 17-hydroxy group of oestradiol was performed according to Kägi and Miescher [6], omitting the addition of bromine.

4. Absorption spectra of the isolated fractions were examined from 400—600 mμ using the Kober reagent described by Bauld [7], and from 240—500 mμ using fuming sulphuric acid according to Axelrod [8]. The registered spectra were compared with those of pure compounds. All readings were made in a Beckman Model DU spectrophotometer supplied with photomultiplier.

Results and discussion. Using the modified Brown procedure, a strongly reacting Kober chromogen was found present in the oestradiol fractions from both a. and b., indicating that the substance is partly excreted in free and partly in conjugated form. Considerably greater quantities were observed in the "conjugated" fractions.

In the oestriol and oestrone fractions no trace of Kober chromogen could be detected.

The elution pattern of the methylated substance appearing in the oestradiol fraction closely followed the elution pattern of the 3-methyl ether of oestradiol-17α.

Oestradiol fractions isolated according to the modified Stimmel procedure showed intense pink colour and green fluorescence when subjected to the test of Kägi and Miescher. An identical reaction was shown by oestradiol-17α, while oestradiol-17β showed only a faint colour reaction.

The absorption spectra of the methylated oestradiol fractions, using the modified Kober reagent, closely followed the one of oestradiol-17α-3-methyl ether with the absorption maximum at 524 mμ.

The absorption spectra of the non-methylated oestradiol fractions, using fuming sulphuric acid as reagent, closely followed the one of oestradiol-17α, with distinct maxima at 300 and 430 mμ.

The Kober reaction is known to be highly specific to the oestrogenic hormones. Using the Brown method for isolation of the oestrogens, both the β- and α-isomer of oestradiol will appear in the oestradiol fraction. No other Kober chromogen is known to appear in this fraction. The conformity between the absorption spectra of the methylated and non-methylated substance isolated in the oestradiol fractions, and the absorption spectra of oestradiol-17α-3-methyl ether and oestradiol-17α * respectively, and the results of the *cis-trans* test for the 17-hydroxy group, support the validity of the concept that the Kober chromogen isolated from meconium of calves is identical to oestradiol-17α.

The quantities found is of the order of magnitude of 20 mg/kg in unconjugated, and 25—35 mg/kg in conjugated form, both figures representing free oestradiol-17α. There seems to be no significant difference between the sexes as regards the amounts present. This would indicate that the substance is of maternal origin.

As far as the present author is aware, the only previous paper reporting the presence of oestrogens in similar material is the one presented by Kinsella *et al.*[9], who in 1956 isolated oestriol from human meconium. No other oestrogen was present in this material.

Isolation of greater quantities of oestradiol-17α from bovine meconium is being carried out. The work shows that the substance is easily crystallized from ethanol-water mixtures.

* Gift from Ciba, Basel.

A detailed report of the work in progress will be published later.

Added in proof: By use of infrared spectroscopy it has now been definitely established that the isolated substance is identical with oestradiol-17α.

This investigation was financially supported by the *Agricultural Research Council of Norway.*

1. Velle, W. *To be published.*
2. Velle, W. *Acta Endocrinol.* **27** (1958) **64.**
3. Brown, J. B. *Biochem. J.* **60** (1955) 185.
4. Stimmel, B. F. *J. Biol. Chem.* **162** (1946) 99.
5. Kakusjkina, E. A. and Orlova, V. G. *Biochimia (Moskva)* **21** (1956) 26.
6. Kägi, M. and Miescher, K. *Helv. Chim. Acta* **22** (1939) 683.
7. Bauld, W. S. *Biochem. J.* **63** (1956) 488.
8. Axelrod, L. R. *Recent Progr. in Hormone Research* **9** (1954) 69.
9. Kinsella, R. A., Francis, F. E., Thayer, S. A. and Doisy, E. A. *J. Biol. Chem.* **219** (1956) 265.

Received October 27, 1957.

Carbohydrates in a Cold Water Extract of a Pine Forest Soil

E. ALVSAKER and K. MICHELSEN

Chemical Institute, University of Bergen, Bergen, Norway

In a preliminary communication Haworth *et al.*[1] state that levans have been isolated from polysaccharides obtained by extraction of soil with buffer solutions. We have not, however, been able to find any information about the existence of free fructose in soil. Forsyth[2] mentions the occurrence of small amounts of free glucose, xylose, rhamnose, and galactose in water extracts of several types of soil, but no details are given about methods of identification. Hot (85°C) water soluble soil polysaccharides have been investigated by Duff[3,4]. In the polysaccharide hydrolysates several aldoses could be identified by chromatographic methods.

An attempt was made to isolate levans from the uppermost layer (F-layer) of a pine forest soil from Western Norway, according to the experimental conditions described by Haworth, but the attempt

The elution pattern of the methylated substance appearing in the oestradiol fraction closely followed the elution pattern of the 3-methyl ether of oestradiol-17α.

Oestradiol fractions isolated according to the modified Stimmel procedure showed intense pink colour and green fluorescence when subjected to the test of Kägi and Miescher. An identical reaction was shown by oestradiol-17α, while oestradiol-17β showed only a faint colour reaction.

The absorption spectra of the methylated oestradiol fractions, using the modified Kober reagent, closely followed the one of oestradiol-17α-3-methyl ether with the absorption maximum at 524 mμ.

The absorption spectra of the non-methylated oestradiol fractions, using fuming sulphuric acid as reagent, closely followed the one of oestradiol-17α, with distinct maxima at 300 and 430 mμ.

The Kober reaction is known to be highly specific to the oestrogenic hormones. Using the Brown method for isolation of the oestrogens, both the β- and α-isomer of oestradiol will appear in the oestradiol fraction. No other Kober chromogen is known to appear in this fraction. The conformity between the absorption spectra of the methylated and non-methylated substance isolated in the oestradiol fractions, and the absorption spectra of oestradiol-17α-3-methyl ether and oestradiol-17α * respectively, and the results of the *cis-trans* test for the 17-hydroxy group, support the validity of the concept that the Kober chromogen isolated from meconium of calves is identical to oestradiol-17α.

The quantities found is of the order of magnitude of 20 mg/kg in unconjugated, and 25—35 mg/kg in conjugated form, both figures representing free oestradiol-17α. There seems to be no significant difference between the sexes as regards the amounts present. This would indicate that the substance is of maternal origin.

As far as the present author is aware, the only previous paper reporting the presence of oestrogens in similar material is the one presented by Kinsella *et al.*[9], who in 1956 isolated oestriol from human meconium. No other oestrogen was present in this material.

Isolation of greater quantities of oestradiol-17α from bovine meconium is being carried out. The work shows that the substance is easily crystallized from ethanol-water mixtures.

* Gift from Ciba, Basel.

A detailed report of the work in progress will be published later.

Added in proof: By use of infrared spectroscopy it has now been definitely established that the isolated substance is identical with oestradiol-17α.

This investigation was financially supported by the *Agricultural Research Council of Norway.*

1. Velle, W. *To be published.*
2. Velle, W. *Acta Endocrinol.* **27** (1958) **64.**
3. Brown, J. B. *Biochem. J.* **60** (1955) 185.
4. Stimmel, B. F. *J. Biol. Chem.* **162** (1946) 99.
5. Kakusjkina, E. A. and Orlova, V. G. *Biochimia (Moskva)* **21** (1956) 26.
6. Kägi, M. and Miescher, K. *Helv. Chim. Acta* **22** (1939) 683.
7. Bauld, W. S. *Biochem. J.* **63** (1956) 488.
8. Axelrod, L. R. *Recent Progr. in Hormone Research* **9** (1954) 69.
9. Kinsella, R. A., Francis, F. E., Thayer, S. A. and Doisy, E. A. *J. Biol. Chem.* **219** (1956) 265.

Received October 27, 1957.

Carbohydrates in a Cold Water Extract of a Pine Forest Soil

E. ALVSAKER and K. MICHELSEN

Chemical Institute, University of Bergen, Bergen, Norway

In a preliminary communication Haworth *et al.*[1] state that levans have been isolated from polysaccharides obtained by extraction of soil with buffer solutions. We have not, however, been able to find any information about the existence of free fructose in soil. Forsyth[2] mentions the occurrence of small amounts of free glucose, xylose, rhamnose, and galactose in water extracts of several types of soil, but no details are given about methods of identification. Hot (85°C) water soluble soil polysaccharides have been investigated by Duff[3,4]. In the polysaccharide hydrolysates several aldoses could be identified by chromatographic methods.

An attempt was made to isolate levans from the uppermost layer (F-layer) of a pine forest soil from Western Norway, according to the experimental conditions described by Haworth, but the attempt

failed. A cold water soluble polysaccharide complex could be isolated from the soil in question; by means of chromatographic analysis the same aldoses as those reported by Duff could be identified in the polysaccharide hydrolysate, but also in this case no ketoses could be detected.

On the other hand it was possible to identify fructose and other free sugars in a cold water extract. For identification of the chromatographically separated fructose a simple X-ray method has been devised [5]. The various sugars eluted from the paper chromatograms were also determined quantitatively according to Giri and Nigam [6]: Glucose 0.22, arabinose 0.04, fructose 0.035, xylose 0.03_5, galactose 0.02_5, and ribose <0.001, expressed as a percentage of dry (105°C) soil organic matter.

Experimental. 700 g samples of air-dry soil were first extracted with ether and then with water, both extractions carried out at room temperature (20°C). The water extract was concentrated *in vacuo* (maximum 40°C), and after precipitation of polysaccharides by means of ethanol the further concentrated filtrate was de-ionized with ion exchangers [7] and subjected to chromatographic analysis. Circular chromatograms on Whatman filter paper No. 1, obtained by the multisector and multiple development techniques described by Giri and Nigam [6], revealed several sugar bands. One of these bands reacted to colour tests in the following manner: Positive triphenyl tetrazolium bromide and α-naphthylamine phosphoric acid tests [6], negative aniline hydrogen phthalate test [8]. These reactions indicate the presence of ketoses and the absence of aldoses. The distance moved on the chromatogram corresponded to authentic fructose spotted on the same paper. As the R_F values of natural ketohexoses are very nearly identical, additional information is necessary for identification. It was not possible to obtain the eluted sugar in a crystalline state. Nor was it possible to analyze fructose derivatives precipitated direct from the water extract by the usual methods, because they were contaminated by considerable amounts of "humic matter". A larger sample was therefore prepared by means of a cellulose column [9]. The column eluates were examined by paper chromatography; one of the fractions revealed only one band, and this band reacted positively to ketose and negatively to aldose colour tests. A micro method for preparation of the osazone was successful, and the osazone could be identified by means of its powder diffraction pattern [5]. The sensitivity of this method also proved sufficient for identification of fructose eluted from paper chromatograms.

The other sugars mentioned could be completely separated on paper, and identified by colour reactions [6,8] combined with the distances moved as compared with those of authentic sugars on the same chromatogram. These distances were identical in three different developers (*n*-butanol-pyridine-water [6], ethyl acetate-pyridine-water [10], ethyl acetate-acetic acid-water [11]).

The authors wish to express their thanks to *Norges Almenvitenskapelige Forskningsråd* for a grant.

1. Haworth, W. N., Pinkard, F. W. and Stacey, M. *Nature* **158** (1946) 836.
2. Forsyth, W. G. C. *Chemistry & Industry* **1948** 515.
3. Duff, R. B. *J. Sci. Food Agr.* **3** (1952) 140.
4. Duff, R. B. *Chem. & Ind. London* **1952** 1104.
5. Michelsen, K. and Alvsaker, E. *Acta Chem. Scand.* **11** (1957) 1795.
6. Giri, K. V. and Nigam, V. N. *J. Indian Inst. Sci.* **36** (1954) 49.
7. Williams, K. T. and Bevenue, A. *J. Assoc. Offic. Agr. Chemists* **36** (1953) 969.
8. Partridge, S. M. *Nature* **164** (1949) 443.
9. Hough, L., Jones, J. K. N. and Wadman, W. H. *J. Chem. Soc.* **1949** 2511.
10. Fisher, F. G. and Dörfel, H. *Z. physiol. Chem. Hoppe-Seyler's* **297** (1954) 164.
11. Jermyn, M. A. and Isherwood, F. A. *Biochem. J.* **44** (1949) 402.

Received November 18, 1957.

A Simple X-Ray Method for Identification of Chromatographically Separated Fructose

K. MICHELSEN and E. ALVSAKER

Chemical Institute, University of Bergen, Bergen, Norway

Minute amounts of crystalline fructose may be identified by means of the X-ray diffraction pattern [1]. It may, however, be difficult to obtain small sugar amounts in a crystalline state, and we therefore considered it an advantage if it would be possible to convert the sugar into a derivative that could easily be prepared and was suitable for X-ray analysis. The osazone acted up to these requirements.

failed. A cold water soluble polysaccharide complex could be isolated from the soil in question; by means of chromatographic analysis the same aldoses as those reported by Duff could be identified in the polysaccharide hydrolysate, but also in this case no ketoses could be detected.

On the other hand it was possible to identify fructose and other free sugars in a cold water extract. For identification of the chromatographically separated fructose a simple X-ray method has been devised [5]. The various sugars eluted from the paper chromatograms were also determined quantitatively according to Giri and Nigam [6]: Glucose 0.22, arabinose 0.04, fructose 0.035, xylose 0.03_5, galactose 0.02_5, and ribose <0.001, expressed as a percentage of dry (105°C) soil organic matter.

Experimental. 700 g samples of air-dry soil were first extracted with ether and then with water, both extractions carried out at room temperature (20°C). The water extract was concentrated *in vacuo* (maximum 40°C), and after precipitation of polysaccharides by means of ethanol the further concentrated filtrate was de-ionized with ion exchangers [7] and subjected to chromatographic analysis. Circular chromatograms on Whatman filter paper No. 1, obtained by the multisector and multiple development techniques described by Giri and Nigam [6], revealed several sugar bands. One of these bands reacted to colour tests in the following manner: Positive triphenyl tetrazolium bromide and α-naphthylamine phosphoric acid tests [6], negative aniline hydrogen phthalate test [8]. These reactions indicate the presence of ketoses and the absence of aldoses. The distance moved on the chromatogram corresponded to authentic fructose spotted on the same paper. As the R_F values of natural ketohexoses are very nearly identical, additional information is necessary for identification. It was not possible to obtain the eluted sugar in a crystalline state. Nor was it possible to analyze fructose derivatives precipitated direct from the water extract by the usual methods, because they were contaminated by considerable amounts of "humic matter". A larger sample was therefore prepared by means of a cellulose column [9]. The column eluates were examined by paper chromatography; one of the fractions revealed only one band, and this band reacted positively to ketose and negatively to aldose colour tests. A micro method for preparation of the osazone was successful, and the osazone could be identified by means of its powder diffraction pattern [5]. The sensitivity of this method also proved sufficient for identification of fructose eluted from paper chromatograms.

The other sugars mentioned could be completely separated on paper, and identified by colour reactions [6,8] combined with the distances moved as compared with those of authentic sugars on the same chromatogram. These distances were identical in three different developers (*n*-butanol-pyridine-water [6], ethyl acetate-pyridine-water [10], ethyl acetate-acetic acid-water [11]).

The authors wish to express their thanks to *Norges Almenvitenskapelige Forskningsråd* for a grant.

1. Haworth, W. N., Pinkard, F. W. and Stacey, M. *Nature* **158** (1946) 836.
2. Forsyth, W. G. C. *Chemistry & Industry* **1948** 515.
3. Duff, R. B. *J. Sci. Food Agr.* **3** (1952) 140.
4. Duff, R. B. *Chem. & Ind. London* **1952** 1104.
5. Michelsen, K. and Alvsaker, E. *Acta Chem. Scand.* **11** (1957) 1795.
6. Giri, K. V. and Nigam, V. N. *J. Indian Inst. Sci.* **36** (1954) 49.
7. Williams, K. T. and Bevenue, A. *J. Assoc. Offic. Agr. Chemists* **36** (1953) 969.
8. Partridge, S. M. *Nature* **164** (1949) 443.
9. Hough, L., Jones, J. K. N. and Wadman, W. H. *J. Chem. Soc.* **1949** 2511.
10. Fisher, F. G. and Dörfel, H. *Z. physiol. Chem. Hoppe-Seyler's* **297** (1954) 164.
11. Jermyn, M. A. and Isherwood, F. A. *Biochem. J.* **44** (1949) 402.

Received November 18, 1957.

A Simple X-Ray Method for Identification of Chromatographically Separated Fructose

K. MICHELSEN and E. ALVSAKER

Chemical Institute, University of Bergen, Bergen, Norway

Minute amounts of crystalline fructose may be identified by means of the X-ray diffraction pattern [1]. It may, however, be difficult to obtain small sugar amounts in a crystalline state, and we therefore considered it an advantage if it would be possible to convert the sugar into a derivative that could easily be prepared and was suitable for X-ray analysis. The osazone acted up to these requirements.

Experimental. Approximately 50 μg fructose dissolved in 15 μl water is placed on a watch glass (diameter 4 cm) by means of a micro pipette. 4 μl phenylhydrazine reagent (phenylhydrazine, acetic acid, water 3:3:10 by volume) and 2 drops acetic acid are added. The watch glass is placed between two larger, matched watch glasses, and heated on a boiling water bath. The two larger watch glasses have been preheated, and the undermost has been wetted with a few drops of water in order to reduce evaporation. After 3—5 min the small glass is withdrawn and examined under the microscope. It is neither necessary nor suitable to the purpose to recrystallize or otherwise purify the product. The tough mass in which the crystals are imbedded is non-crystalline, and acts as an excellent adhesive when the specimen is to be mounted on the glass fiber. The mounting is easily done in the following manner: A small quantity of the material is collected with a spatula to a globe and then formed between thumb and forefinger with a light squeeze. The glass fiber is brought into contact with the specimen, and by rolling between the fingers the desired magnitude and shape are readily obtained.

For X-ray powder diffraction data (Table 1) nickel-filtered copper-radiation and a camera 11.46 cm in diameter have been used. The intensities have been visually estimated. Identical diffraction pattern is obtained for fructosazone prepared by the usual macro method. The osazones of fructose, glucose, and mannose being identical, additional information is necessary to distinguish between these sugars (chromatographic separation, colour reactions).

Table 1. X-Ray powder diffraction data for fructosazone.

d, Å	I/I_1	d, Å	I/I_1
17.02	0.37	3.22	0.37
8.86	0.50	3.12	0.08
6.10	0.08	3.04	0.08
5.78	0.25	2.94	0.30
5.16	0.25	2.84	0.20
4.94	0.63	2.72	0.20
4.52	1.00	2.66	0.25
4.40	0.15	2.60	0.08
4.20	0.50	2.58	0.08
3.96	0.37	2.42	0.05
3.72	0.30	2.38	0.15
3.60	0.50	2.32	0.02
3.40	0.50	2.28	0.10
3.32	0.25		

The method proved successful for fructose quantities as small as 18 μg; this figure, however, probably does not represent the lower limit for the practical applicability of the method. The sensitivity is sufficient for identification of fructose eluted from paper chromatograms [2].

The fructosazone prepared by the micro method has an appearance that differs from the usual crystal aggregates obtained by macro methods: The crystal needles are always arranged radially, thus forming spherulites about 0.05 mm in diameter.

1. Werner, I. *Mikrochemie ver. Mikrochim. Acta* **39** (1952) 133.
2. Alvsaker, E. and Michelsen, K. *Acta Chem. Scand.* **11** (1957) 1794.

Received November 18, 1957.